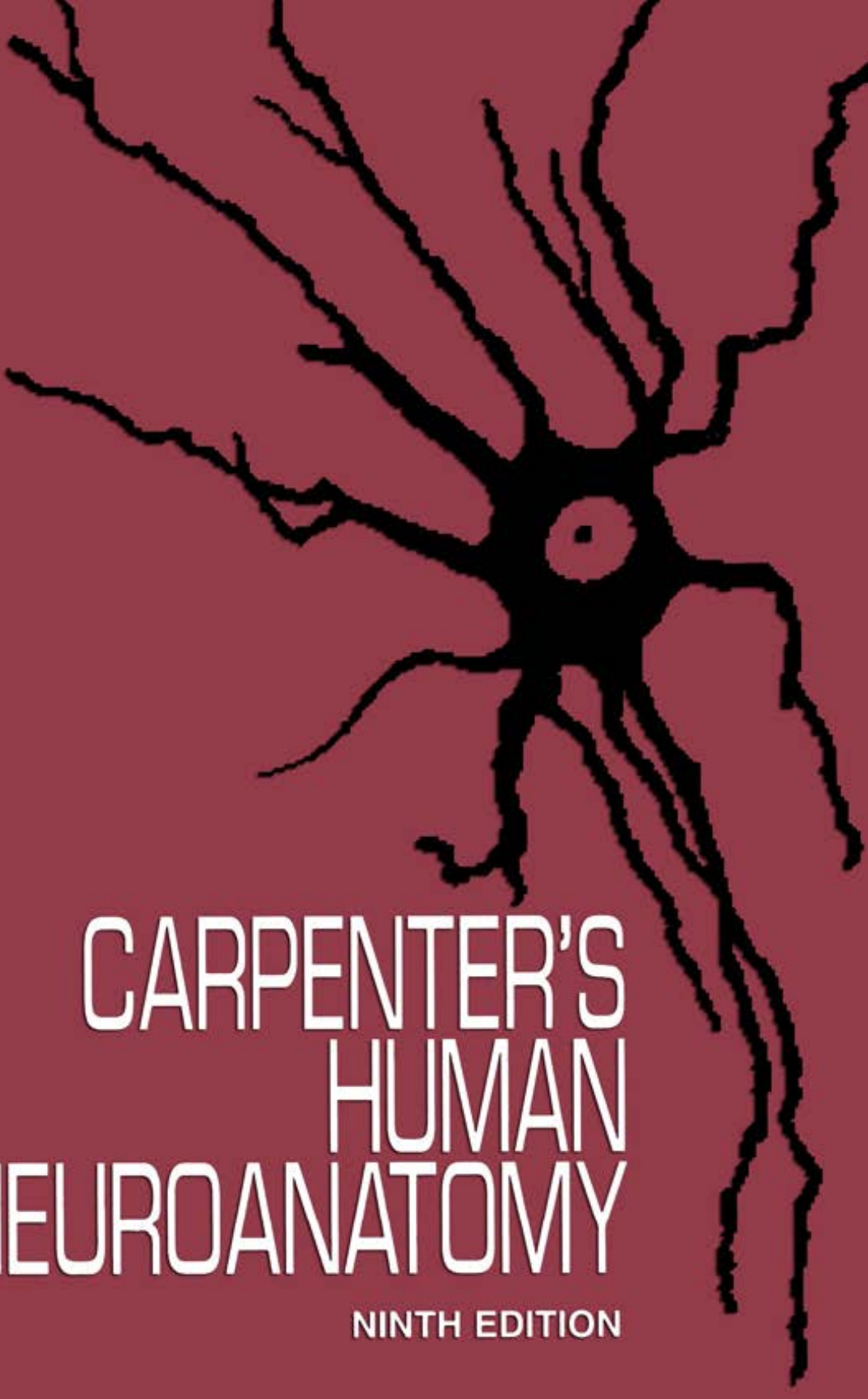


CARPENTER'S HUMAN NEUROANATOMY

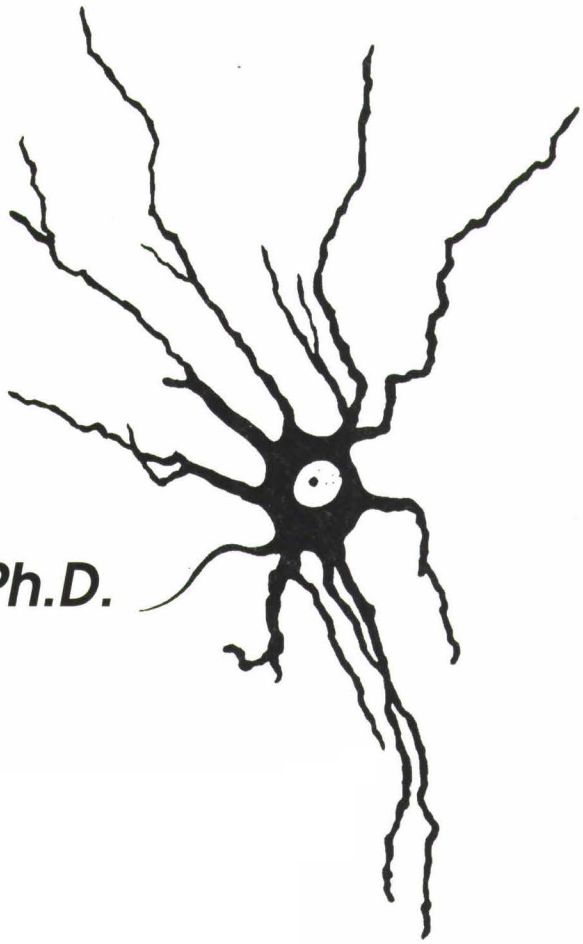
NINTH EDITION

ANDRÉ PARENT

CARPENTER'S HUMAN NEUROANATOMY *Ninth Edition*

CARPENTER'S HUMAN NEUROANATOMY

Ninth Edition



André Parent, Ph.D.

Departement d'Anatomie
Faculté de Médecine
Université Laval
Quebec, Canada

Williams & Wilkins

BALTIMORE • PHILADELPHIA • HONG KONG
LONDON • MUNICH • SYDNEY • TOKYO

A WAVERLY COMPANY
1996



Editor: Patricia Coryell
Managing Editor: Linda S. Napora
Copy Editor: Richard H. Adin
Designer: Wilma Rosenberger
Illustration Planner: Ray Lowman
Production Coordinator: Marette Magargle

Copyright © 1996
Williams & Wilkins
Rose Tree Corporate Center, Building II
1400 N. Providence Rd.
Suite 5025
Media, PA 19063-2043



All rights reserved. This book is protected by copyright. No part of this book may be reproduced in any form or by any means including photocopying, or utilized by any information storage and retrieval system without written permission from the copyright owner.

Accurate indications, adverse reactions, and dosage schedules for drugs are provided in this book, but it is possible that they may change. The reader is urged to review the package information data of the manufacturers of the medications mentioned.

Printed in the United States of America

First Edition 1943

Library of Congress Cataloging-in-Publication Data

Parent, André, 1944–
Human neuroanatomay / André Parent.—9th ed.
p. cm.
Rev. ed. of: Human neuroanatomy / Malcolm B. Carpenter, Jerome Sutin. 8th ed. c1983.
Includes bibliographical references and index.
ISBN 0-683-06752-4
1. Neuroanatomy. I. Carpenter, Malcolm B. Human neuroanatomy. II. Title.
[DNLM: 1. Nervous System—anatomy & histology. WL 101 P228h 1995]
QM451.T7 1995
611'.8—dc20
DNLM/DLC
for Library of Congress 94-40506
CIP

96
1 2 3 4 5 6 7 8 9 10

To my late father, Lucien Parent, who, with very little means, taught me that knowledge is our destiny.

Et quant à la cognoissance des faicts de nature, je veux que tu t' y adonne curieusement: qu' il n' y ait mer, rivière, n' y fontaine, dont tu ne cognoisse les poissons; tous les oiseaux de l'air, tous les arbres, les arbustes et fructices des forêts . . . Par fréquente anatomies, acquiers toy parfaicte cognoissance. . . . Je voye un abysme de science . . . Mais science sans conscience n'est que ruine de l' âme.

François Rabelais, 1554

And as for knowledge of the facts of nature, I want you to devote yourself with curiosity: let there be no sea, river nor fountain of which you do not know its fish; all the birds in the air, all the trees, all the shrubs and fruits of the forests . . . By frequent dissections, acquire perfect knowledge . . . I feel a well of science . . . But science without conscience is nothing but ruin of the soul.

François Rabelais, 1554

Preface

In the midst of the *Decade of the Brain*, attempts to summarize the current state of knowledge about the anatomical and functional organization of the nervous system has become a gigantic task. Several thousand researchers around the world are currently applying ever more powerful neurobiological tools to unravel the complexities of the brain. The approach is frankly multidisciplinary, involving techniques that range from genetics and molecular biology to behavioral analyses and neuropathology. Initiatives combining neurosciences and informatics, such as *The Human Brain Project*, have helped to acquire, store, manipulate, analyze, integrate and, above all, share data derived from brain and behavioral experiments. The joint effort of neuroscientists throughout the world has yielded a wealth of knowledge whose detailed coverage would be well beyond the scope of this book. This knowledge has given rise to novel concepts about neural organization and function, and has also opened new therapeutic avenues for some of the most devastating afflictions of the brain and spinal cord. In the nervous system, however, structural organization is central to most functional concepts, and this is what this book is all about.

The Ninth Edition of *Human Neuroanatomy* is an attempt to provide medical students, as well as graduate students in neuroscience and neurology/neurosurgery residents, with a general guide to the structural and functional organization of the nervous system. The book describes the major neuronal systems that compose the brain, spinal cord, and peripheral nervous system in the light of the most recent concepts about neural organization. In contrast to most other neuroscience texts, where there is a clear tendency toward reductionism, I have tried as much as possible to provide more general and systematic views of the organization of the nervous system so as to maximally help those students with clinical concerns.

There have been major changes in both the format and content of the book over the previous edition published 12 years ago. Each chapter has been entirely revised and updated with the addition of more than 500 new references. Most of the references to classic studies have been retained, however, largely because of their historical importance and also because they can no longer be found in any current textbook. Thus, *Human Neuroanatomy* represents a unique repository of over 3000 references to both historically significant contributions and recent breakthroughs in the neurosciences. Furthermore, the chapters have been regrouped in distinct sections with new subheadings that emphasize the content and major conclusion of each section. Over 180 new or revised illustrations have been added, many in the form of computer-generated diagrams or drawings, which students have found very useful in the past. New sections on the molecular aspect of neuronal and glial functions have also been added as this type of information is essential to understand properly the various basic neuronal functions in both normal and pathological conditions. Information concerning the localization and roles of neurotransmitters and their highly specific receptors in the nervous system has been given a high priority in this book because a proper knowledge of chemical anatomy has become essential to understand the current views about neural functions. Finally, an effort was made to add as many clinical notes and functional correlations as possible to emphasize the importance of a proper knowledge of neuroanatomy. In this context, particular attention was paid to neuropathological studies of normal aging versus neurodegenerative diseases, such as Alzheimer's, Hutington's, and Parkinson's diseases, because these investigations have shed new light on how the nervous system works in both health and disease.

I am immensely indebted to the previous authors who have contributed to Human Neuroanatomy since its inception in May of 1943. Among those are Professors Adolph Elwyn, Oliver S. Strong, Raymond Truex, Jerome Sutin, and, above all, Malcom B. Carpenter, Professor and Chairman Emeritus, Department of Anatomy, F. Edward Hebert School of Medicine, Services University of

Health Science, Bethesda, Maryland. Despite a very active career in both research and teaching, Dr. Carpenter has contributed significantly to *Human Neuroanatomy*, which has become the most important reference book in the field under his expert guidance.

I also want to express my deep gratitude to several colleagues from various American and Canadian Universities, including a fair number of neuroscientists from the Neurobiology Research Center at Laval University, who have generously supplied illustrations for this edition. Their names and specific contributions are indicated in appropriate sections of the text. Thanks are also due to my graduate students: Ali Charara, Pierre-Yves Côté, Luc De Bellefeuille, Céline Desjardins, Lili-Naz Hazrati, Brigitte Lavoie, and Abbas Sadikot, from whom I borrowed various photomicrographs and drawings.

Many of the superb illustrations from Professor Fred A. Metler's *Neuroanatomy*, published in 1948, were made by Mr. Ivan Summers and are still reproduced in the present edition of *Human Neuroanatomy*. The same applies to the beautiful drawings made by Mr. Robert J. Desmarest who worked for many years in close collaboration with Dr. M.B. Carpenter. Most of the new illustrations for this edition were prepared by Mrs. Louise Bertrand of the Neurobiology Research Center at Laval University. Her skill, talent, and total devotion to her work are greatly acknowledged.

Thanks are also due to the unfailing support of Mrs. Carole Emond who was responsible for many aspects of the production of this book, including the preparation of photographic illustrations, proof reading and text scanning. I also acknowledge the secretarial help of Mrs. Suzanne Bilodeau and of my wife, Doris Parent. Finally, I express my deep gratitude to Williams & Wilkins and especially to Pat Coryell and Linda Napora, for their patience, support, and expert handling of this vast project.

Contents

Section I ***Regional Anatomy, Development, and Blood Supply of the Neuraxis***

1 Meninges and Cerebrospinal Fluid 3
- Meninges 3
- Cerebrospinal Fluid 14
- Barriers Related to the Brain 16
- Circumventricular Organs 21

2 Regional Anatomy of the Brain 25
- Subdivisions of the Brain 25
- Cerebral Hemispheres 25
- Basal Ganglia 41
- Lateral Ventricles 42
- Brainstem 45
- Diencephalon 50
- Cerebellum 52
- Brain Imaging 54

3 Development of the Nervous System 65
- Determination and Differentiation 65
- Formation of Neural Tube 65
- Neural Crest 67
- Histogenesis of Neural Tube 69
- Neurons 69
- Glial Cells 73
- Spinal Cord 73
- Brain 77
- Congenital Anomalies 90

4 Blood Supply of the Central Nervous System 93
- Blood Supply of the Spinal Cord 94
- Blood Supply of the Brain 98
- Basal Ganglia, Internal Capsule and Diencephalon 112
- Vertebral Basilar System 113
- Arteries of the Dura Mater 119
- Cerebral Veins and Venous Sinuses 120

Section II ***Neurohistology and Neurocytology***

5 Neurons 131
- Neurons as Signaling Unit 131
- Neurobiological Tools 134
- Neuronal Diversity 144
- Neuronal Cytoskeleton 146
- Nerve Cell Body 148
- Synthesis of Neuronal Proteins 157
- Signaling Molecules 159
- Axons 162
- Synapses 172
- Axoplasmic Transport 181

Degeneration of Nerve Fibers 183
Regeneration and Plasticity 186

6 Neuroglia 199
Changing Concept of Neuroglia 199
General Features and Cell Lineage 200
Astrocytes 203
Oligodendrocytes 211
Microglia 214
Ependyma 218
Choroid Epithelium 224

Section III ***Peripheral Nervous System***

7 Receptors and Effectors 235
Sensory Receptors 235
Receptors' Diversities 237
Sensory Receptors and Sensory Modalities 252
Effectors 255

8 Spinal Nerves and Peripheral Innervation 262
Peripheral Nervous System 262
Segmental Innervation 268
Peripheral Innervation 273
Functional Considerations 287

9 Autonomic Nervous System 293
Tripartite Integrated System 293
Pre- and Postganglionic Neurons 296
Sympathetic System 299
Parasympathetic System 301
Enteric System 302
Visceral Afferent Fibers 303
Structure of Autonomic Ganglia 304
Chemical Anatomy 306
Denervation Sensitization 311
Central Autonomic Pathways 314
Functional Considerations 315

Section IV ***Spinal Cord***

10 Spinal Cord: Regional Anatomy and Internal Structure .. 325
Topographic Organization 325
Internal Structure 329
Primary Afferent Fibers 351
Chemoarchitecture 352
Functional Considerations 359

11 Spinal Cord: Fiber Tracts 368
Ascending Spinal Tracts 368
Descending Spinal Tracts 383
Intrinsic Spinal Fibers 400
Upper and Lower Motor Neurons 402
Spinal Cord Lesions 405

Section V ***Brainstem and Cerebellum***

12 Medulla 421
Spinomedullary Transition 421

Inferior Olivary Complex 432
Medullary Reticular Formation 434
Ascending and Descending Tracts 436
Inferior Cerebellar Peduncle 437
Cranial Nerves of the Medulla 437
Corticobulbar Fibers 451
Chemical Anatomy 454
Medullary-Pontine Junction 461

13 Pons 469
Caudal Pons 469
Vestibulocochlear Nerve 474
Facial Nerve 495
Abducens Nerve 498
Trigeminal Nerve 500
Rostral Pons-Isthmus Level 509
Reticular Formation 519

14 Midbrain 527
Caudal Midbrain 527
Rostral Midbrain 534
Midbrain Tegmentum 549
Substantia Nigra 557
Crus Cerebri 572

15 Cerebellum 583
Regional Organization 583
Cerebellar Cortex 585
Cerebellar Nuclei 600
Somatotopic Organization 605
Cerebellar Connections 606
Functional Organization 616
Clinical Considerations 617

Section VI ***Forebrain***

16 Thalamus 633
Regional Organization of the Diencephalon 633
Midbrain-Thalamic Junction 633
Epithalamus 635
Topographical Organization of the Thalamus 639
Nuclear Organization of the Thalamus 640
Chemical Anatomy of the Thalamus 673
Thalamic Radiations and Internal Capsule 682
Visual Pathways 685
Functional Considerations 691

17 Hypothalamus 706
Hypothalamic Nuclei 707
Hypothalamic Connections 715
Hypophysial Portal System 728
Hypophysiotrophic Agents 729
Functional Considerations 732

18 Limbic System 744
Limbic Lobe Versus Limbic System 744
Olfactory System 748
Anterior Commissure 759
Hippocampal Formation 760

Amygdala 773
Substantia Innominata 786

19 Basal Ganglia 795
Nomenclature 795
Striatum 798
Globus Pallidus 828
Subthalamic Region 838
Ventral Striatopallidal Complex 844
Functional Considerations 846

20 Cerebral Cortex 864
Structure of the Cortex 864
Chemical Anatomy of the Cortex 873
Cortical Areas 882
Sensory Areas of the Cortex 886
Motor Areas of the Cortex 909
Nonpyramidal Corticofugal Fibers 916
Association Fibers 918
Functional Considerations 919

Section VII ***Atlas of the Human Brain***

Figure and Table Credit List 945

Index 947

Section I

Regional Anatomy, Development, and Blood Supply of the Neuraxis

1
Meninges and Cerebrospinal Fluid

MENINGES

The brain and spinal cord, which together form the neuroaxis, are delicate semisolid structures requiring protection and support. Major protection is ensured by the skull for the brain and by the vertebral column for the spinal cord. Additionally, the brain and spinal cord are surrounded by three membranes or meninges: (a) the thick *dura* mater externally, (b) the delicate *arachnoid* lining the inner surface of the dura, and (c) the thin *pia mater* internally, which accurately follows every contour of the brain and spinal cord. The dura mater is also termed pachymeninx (thick membrane), whereas the arachnoid and the pia mater, which have a similar structure, may be combined under the heading pia-arachnoid or leptomeninges (slender membranes). The space between the arachnoid and the pia mater, the subarachnoid space, is filled with cerebrospinal fluid (CSF). The main supportive and protective functions of the meninges come from the dura mater and the CSF, which serve as a cushion between the brain and the rigid skull.

A proper knowledge of the topographic organization of the meninges and their relationships to the brain and CSF is essential for understanding the physiopathology of different clinical conditions such as head trauma, intracranial hemorrhages, central nervous system infection, and hydrocephalus.

Dura Mater

The cranial dura consists of (a) an outer *periosteal layer*, which is rich in blood vessels and nerves and is adherent to the inner surface of the cranium, and (b) an inner *meningeal layer* that is closely attached to the underlaying arachnoid. At certain sites, these layers are separated and form large venous sinuses such as the superior sagittal sinus (Fig. 1.1, see Chapter 4). Cranial meninges in humans do not include a subdural space (23, 42). The erroneous macroscopic impression of a subdural space results from an extraordinary lack of cohesion within the dura-arachnoid interface layer. Subdural lesions are believed to form within a sheet of torn dural border cells and not within a preexistent tissue compartment (42).

The meningeal layer gives rise to several septa which divide the cranial cavity into various compartments. The largest of these septa is the sickle-shaped *falx cerebri*, which extends in the midline from the crista galli to the internal occipital protuberance (Fig. 1.2). Posteriorly this septum is continuous with a transverse dural reflection from the superior crest of the petrous portion of the temporal bone—the *tentorium cerebelli*—which covers the dorsal surface of the cerebellum. As illustrated in Figures 1.2 and 1.3, the various dural reflections divide the cranial cavity into (a) a large, paired *supratentorial compartment* which contains the cerebral hemispheres, and (b) a smaller, single *infratentorial compartment* containing the cerebellum and the brainstem. The infratentorial compartment corresponds to the *posterior cranial fossa*, whereas the supratentorial compartment comprises an *anterior cranial fossa* for the frontal lobes and a *middle cranial fossa* for the temporal lobes. The occipital lobes lie on the superior surface of the tentorium cerebelli whose free borders form the *tentorial incisure* (or notch), the only opening between the supratentorial and infratentorial compartments (Figs. 1.2 and 1.3). The brainstem passes through the tentorial notch (Fig. 1.4) where it can be severely compressed and damaged in cases of expanding brain lesions. The occipital lobes lie on the superior surface of the tentorium. A small midsagittal septum below the tentorium forms the *falx cerebelli* (Fig. 1.2) which partially separates the cerebellar hemispheres. The *diaphragma sellae* roofs over the pituitary fossa and is perforated by the infundibulum (see Chapter 2).

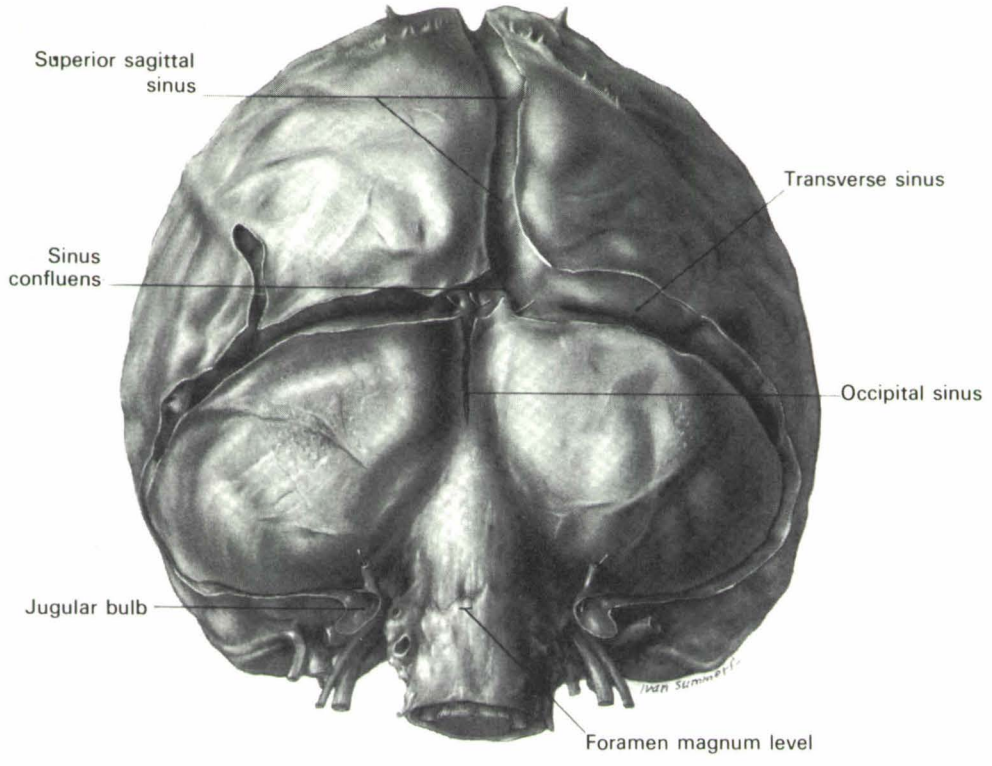


Figure 1.1. Posterior view of the dura surrounding the brain. Prominent dural sinuses have been opened. The periosteal layer of the dura has been cut at the margins of the foramen magnum.

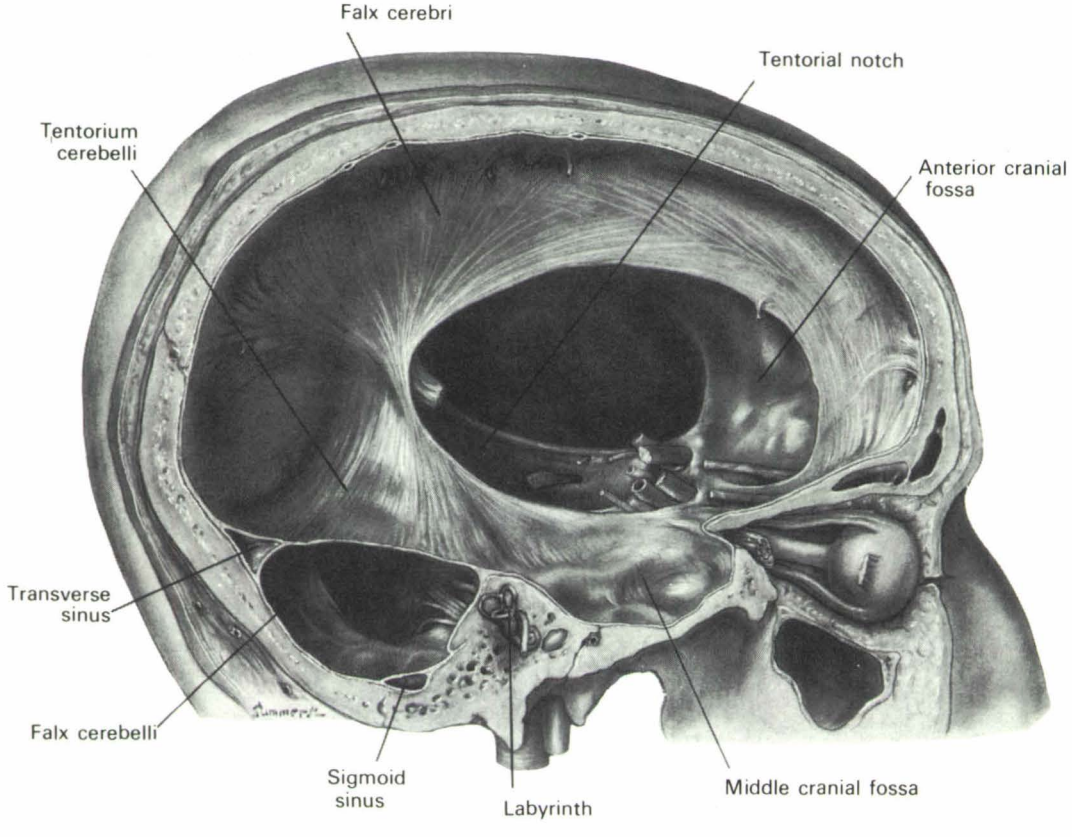


Figure 1.2. Sagittal section of the head showing the falx cerebri, the tentorium cerebelli, and the falx cerebelli.

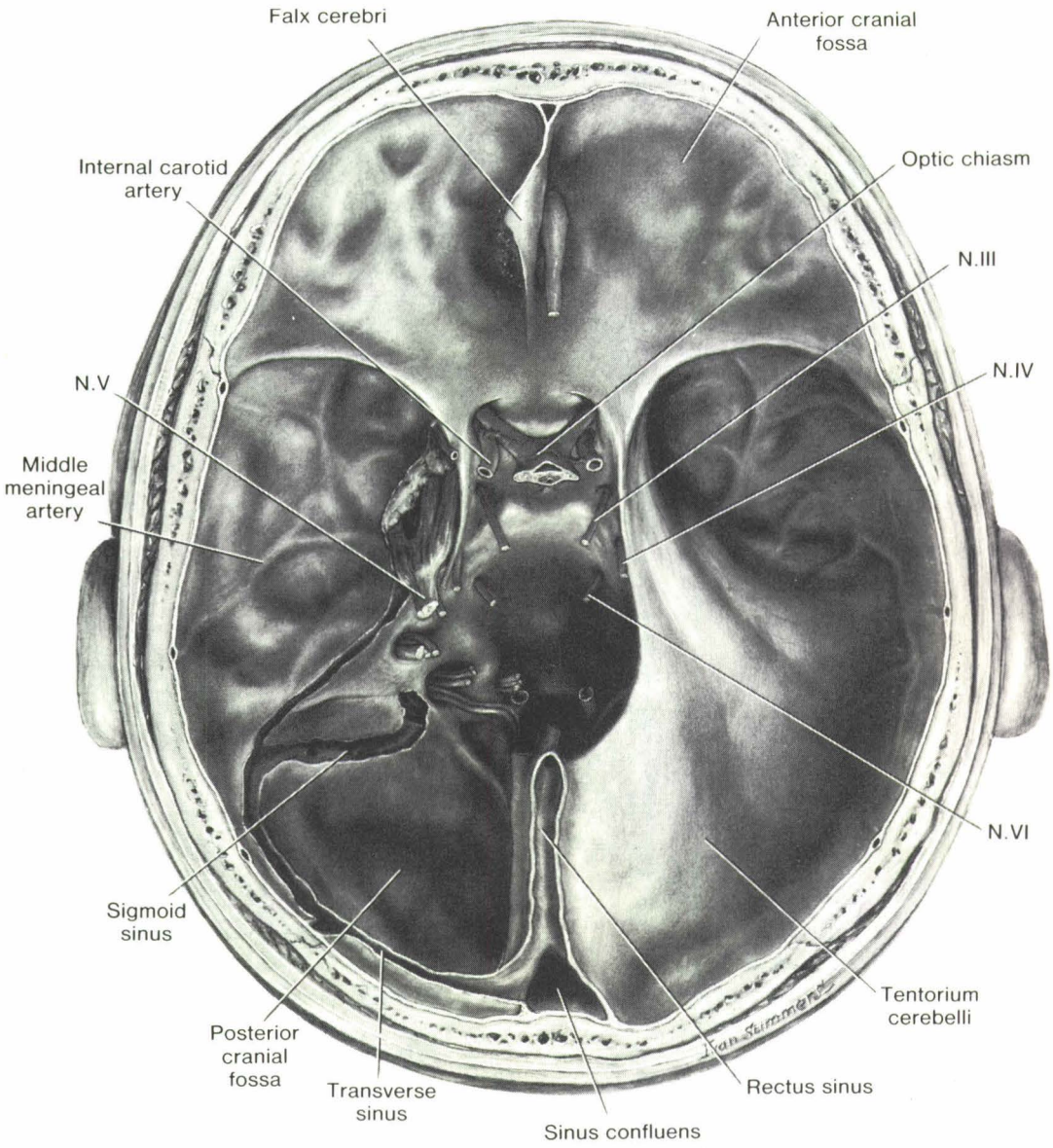


Figure 1.3. Base of the skull with dura mater. The falx cerebri has been removed and the tentorium cerebelli has been cut away on the left to expose the posterior fossa.

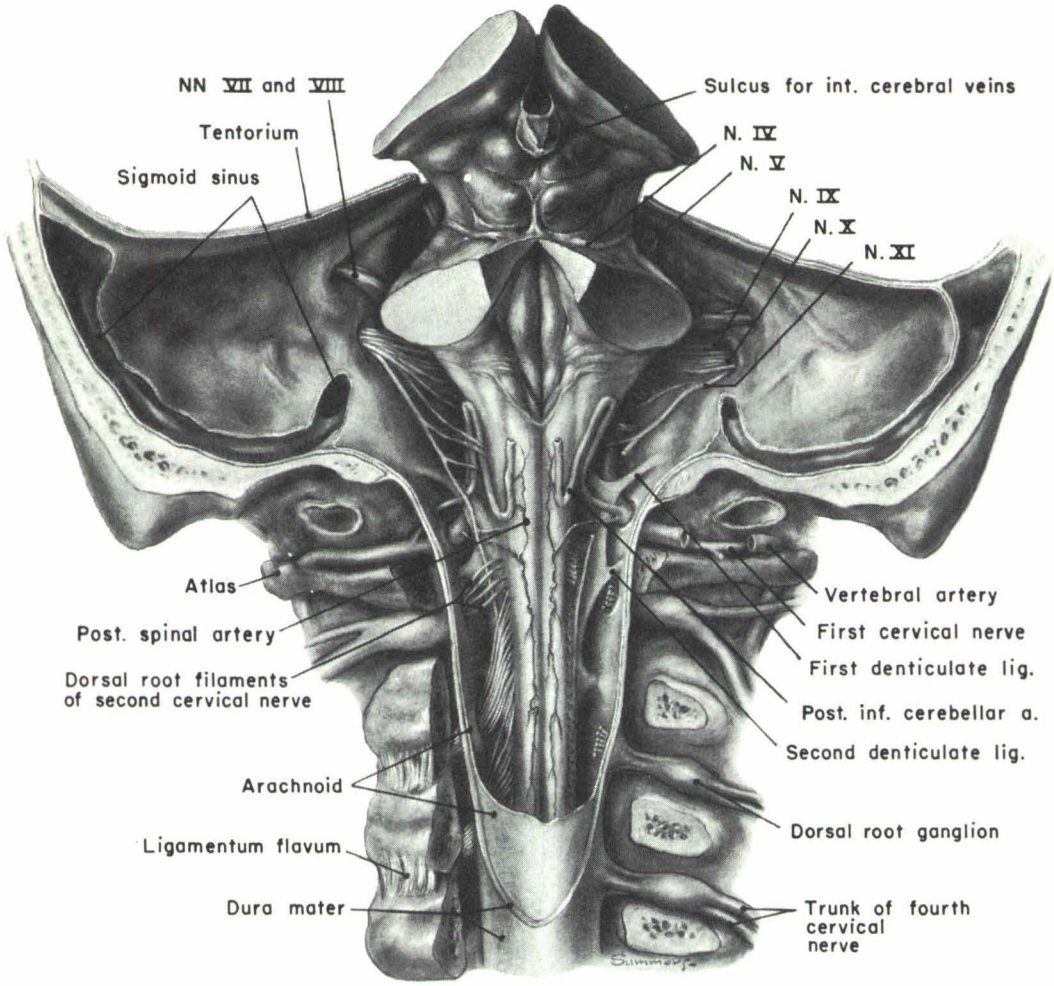


Figure 1.4. Posterior view of the brainstem, upper cervical spinal cord and meninges.

The major blood supply for the dura is provided by the middle meningeal artery, a branch of the maxillary artery, which enters the skull via the foramen spinosum (28) (Figs. 1.3 and 4.4). The ophthalmic artery gives rise to anterior meningeal branches and the occipital and vertebral arteries provide posterior meningeal branches. Skull fractures lacerating these meningeal arteries produce space occupying epidural hemorrhages between the skull and the dura that require prompt surgical intervention.

The supratentorial dura is innervated by branches of the trigeminal nerve (N. V), whereas the infratentorial dura is supplied by branches of the upper cervical spinal nerves and the vagus nerve (N. X). Stimulation of the supratentorial dura by a space-occupying lesion located anywhere in the anterior fossa will produce pain radiating toward the forehead on the lesion side. The pain from a similar lesion in the posterior fossa will be felt more diffusely in the occipital and neck region.

The innermost layer of the dura is composed of flattened fibroblasts that are in close contact with the arachnoid, suggesting that the *subdural space* is a potential space rather than an actual space (11, 23, 42). The *spinal dura* is a continuation of the meningeal layer of the cranial dura (Figs. 1.4 and 1.5). The periosteum of the vertebrae corresponds to the outer (periosteal) layer of the cranial dura. Inner and outer surfaces of the spinal dura are covered by flattened fibroblasts, and the dense membrane is separated from

the periosteum by a narrow *epidural space.* The spinal epidural space contains areolar tissue and the internal vertebral venous plexuses (Fig. 4.3). This actual space is largest at the level of the second lumbar vertebra where it is nearly half the diameter of the spinal canal. Clinically the epidural space is used to inject a local anesthetic to produce an extensive paravertebral nerve bloc known as *epidural anesthesia.* The epidural space can be distinguished because it has a negative pressure. *Caudal anesthesia,* used in obstetrics, is a form of epidural anesthesia in which the anesthetic agent is injected into the epidural space via the sacral canal.

The spinal dura extends as a closed tube from the margins of the foramen magnum to the level of the second sacral vertebra (Fig. 1.6). At the caudal termination of the dural sac the dura invests the filum terminale to form a thin fibrous cord, the *coccygeal ligament* (Fig. 1.6). This ligament extends caudally to the coccyx where it becomes continuous with the periosteum. The spinal cord ends at the lower border of the first lumbar vertebra. Extensions of the dura passing laterally around the spinal nerve roots form dural root sleeves (Figs. 1.5 and 1.7).

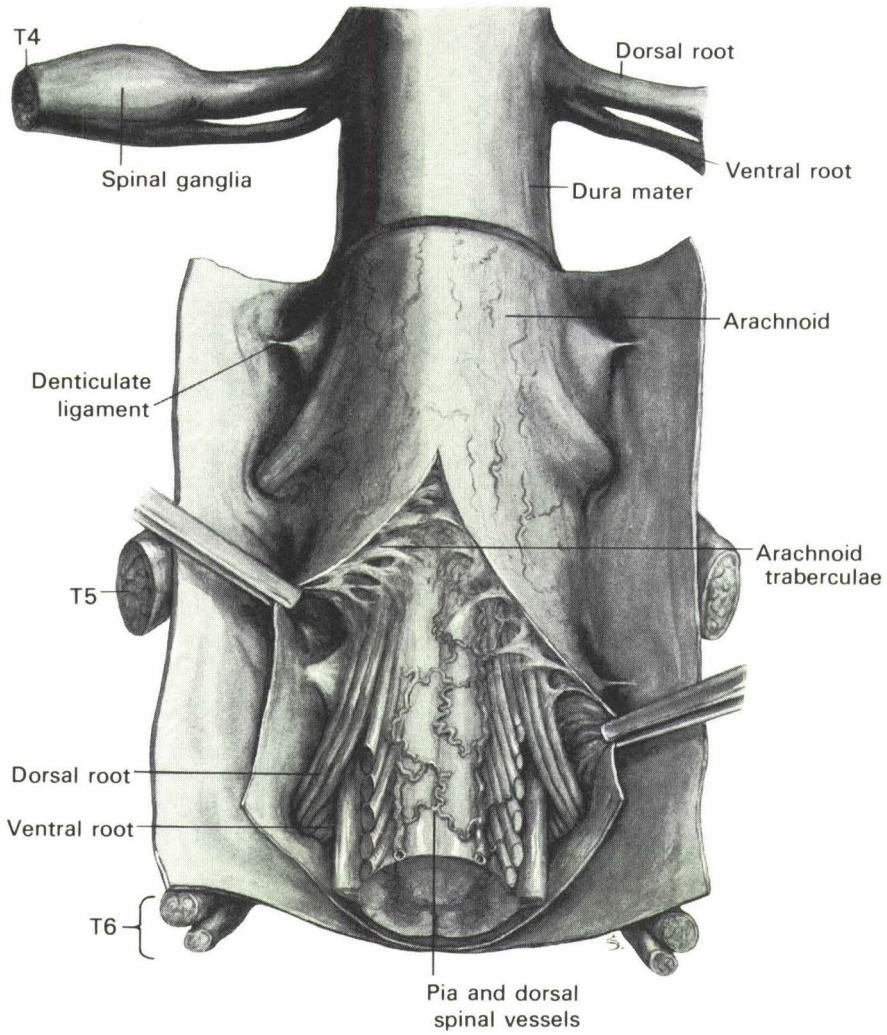


Figure 1.5. Posterior view of part of the upper thoracic spinal cord. The dura and arachnoid have been split at the midline to expose the spinal cord and pial vessels. Above the intact dura covers the spinal cord and spinal nerve roots.

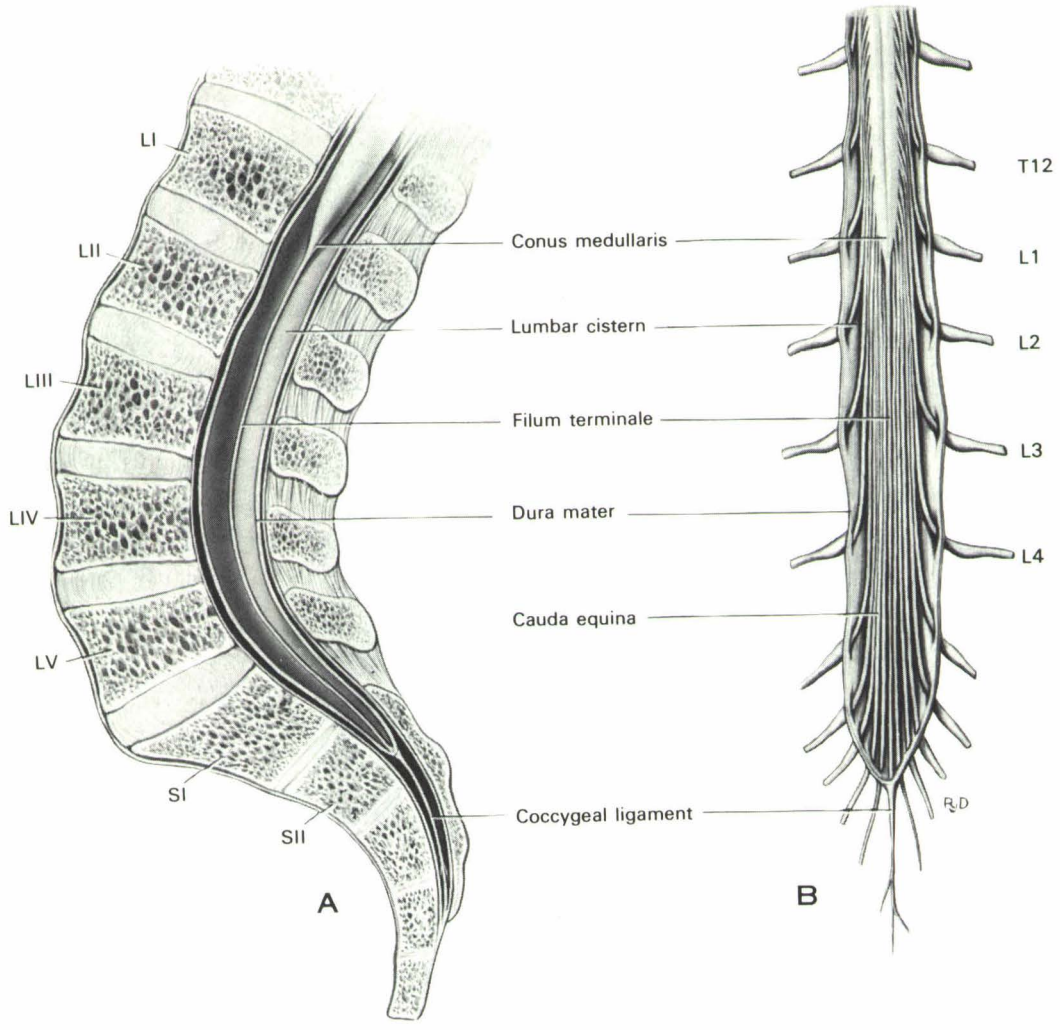


Figure 1.6. Diagrammatic representation of the caudal part of the spinal cord and lumbar cistern. **A.** Sagittal view of the conus medullaris, lumbar cistern, and lumbosacral vertebrae. **B.** Posterior view of the cauda equina and nerve roots.

Pia Mater

This thin and translucent vascular membrane is composed of an inner membranous layer, the *intima pia*, and a more superficial *epipial layer*. The intima pia, adherent to underlying nervous tissue, follows its contours closely and is composed of fine reticular and elastic fibers. Where blood vessels enter and leave the central nervous system, the intima pia is invaginated forming a perivascular space (Fig. 1.12). The intima pia, like the arachnoid, is avascular and derives its nutrients by diffusion from the cerebrospinal fluid and the underlying nervous tissue (11, 12, 29). The epipial layer is formed by a meshwork of collagenous fiber bundles continuous with the arachnoid trabeculae. The blood vessels of the spinal cord lie within the epipial layer. Over the convex surface of the cerebral cortex, the epipial layer is absent and the large cerebral vessels lie on the intima pia where they are anchored by fine arachnoid trabeculae. The pia mater is made up of leptomeningeal cells virtually indistinguishable from those of the arachnoid. Subpial astrocytes form a continuous sheath of underlying cytoplasm; between the pia and subpial astrocytic layer is an osmiophilic basement membrane separated from the plasma mem-

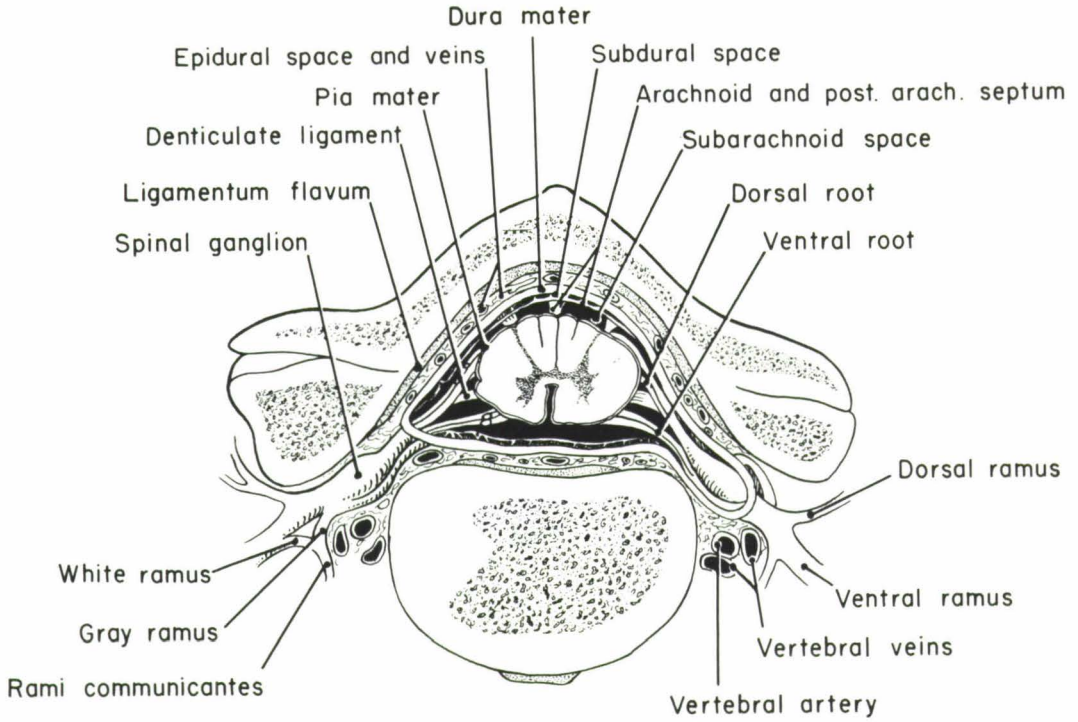


Figure 1.7. Spinal cord and its meningeal coverings in cross-section. Note the continuities of the pia mater with the denticulate ligament, and of the dura mater with the epineurium of the spinal nerves.

branes. The spinal cord is attached to the dura mater by a series of (18 to 24) lateral flattened bands of epipial tissue known as the *denticulate ligaments* (Figs. 1.4, 1.5, and 1.7). In the region of the conus medullaris, epipial tissue forms a covering of the filum terminale (Fig. 1.6).

In the region of the ventricles, the brain wall is formed by a single layer of ependymal cells, the outer surface of which is firmly adherent to the pia mater. In the roof of the third ventricle (Figs. 1.9, 1.10, and 2.29**B**), in the lower part of the roof of the fourth ventricle (Figs. 1.9 and 1.10), and on the medial wall of the inferior horn of the lateral ventricle (choroid fissure), the intima pia blends with the ependymal layer to form the *tela choroidea* (Fig. 6.17). The tela choroidea anchors the choroid plexuses to the walls of the ventricles. It has a triangular shape in the roof of the third and fourth ventricles and is horseshoe-shaped in the lateral ventricles as it follows the choroidal fissure (Figs. 2.29**B**, 18.12, and 18.13). The two layers of the pia mater in the transverse cerebral fissure, below the splenium of the corpus callosum and above the pineal body, form the *velum interpositum* (Fig. 2.29**B**). The internal cerebral veins, branches of the posterior cerebral artery, and arteries to the choroid plexuses of the third and lateral ventricles, lie between these two layers (Figs. 4.26 and 4.27).

Arachnoid

The arachnoid is a delicate nonvascular membrane between the dura and the pia mater which passes over the sulci without following their contours (Figs. 1.11 and 1.12). This membrane also extends along the roots of the cranial and spinal nerves. Arachnoid trabeculae extend from the arachnoid to the pia. The space between the arachnoid and the pia mater, filled with cerebrospinal fluid (CSF), is called the *subarachnoid space* (Figs. 1.11 and 1.12). Most cranial nerves are surrounded by a subarachnoid space (11, 12, 47). A small subarachnoid space also surrounds the spinal nerve roots in the root sleeves (Fig. 1.7). In the spinal regions, fewer arachnoid trabeculae are concentrated into several subarachnoid septa; hence the spinal subarach-

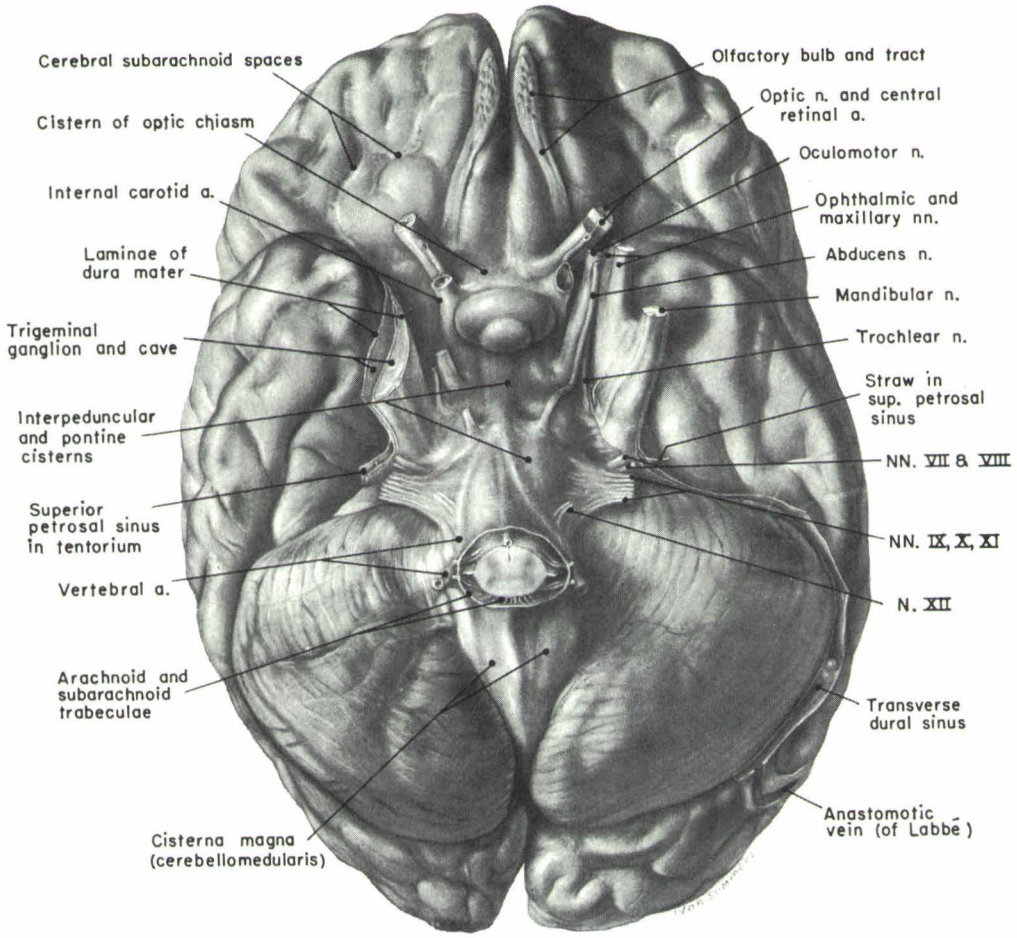


Figure 1.8. Inferior view of the brain, cranial nerves, and meninges showing locations of subarachnoid cisterns.

noid space is a more continuous cavity and the spinal arachnoid a more distinct membrane (Fig. 1.7). The arachnoid membrane is made up of leptomeningeal cells with a watery cytoplasm which forms long, irregular pseudopods that interdigitate with those of adjacent cells. These cells form a protoplasmic layer which may be several cells thick and exhibit great irregularity. When certain substances are injected into the subarachnoid space, these cells may swell and participate in phagocytic activity by ingesting particles of the foreign material. They may also become detached and form free macrophages.

The extent of the subarachnoid space surrounding the brain shows local variations. Over the convexity of the cerebral hemisphere this space is narrow, except in the depths of the sulci. At the base of the brain and around the brainstem the pia and the arachnoid often are widely separated, creating *subarachnoid cisternae* (Figs. 1.8 and 1.9). The largest cistern is found between the medulla and the cerebellum and is called the *cerebellomedullary cistern* (cisterna magna). Other cisterns of considerable size are the *pontine cistern*, the *interpeduncular cistern*, the *chiasmatic cistern*, and the *superior cistern* (Fig. 1.9). The superior cistern, surrounding the posterior, superior, and lateral surfaces of the midbrain, is referred to clinically as the cisterna ambiens (47). This cistern is of great importance because it contains the great vein of Galen, and the posterior cerebral and superior cerebellar arteries. Most of these cisterns can be visualized by special radiographic techniques (such as pneumoencephalography or computerized tomography). The *lumbar cistern* extends from the conus medullaris (lower border of the first lumbar vertebra) to about the level of the second sacral vertebra (Fig. 1.6). It contains the filum terminale and nerve roots of the cauda equina. It is from this cistern that CSF is withdrawn in a lumbar spinal tap.

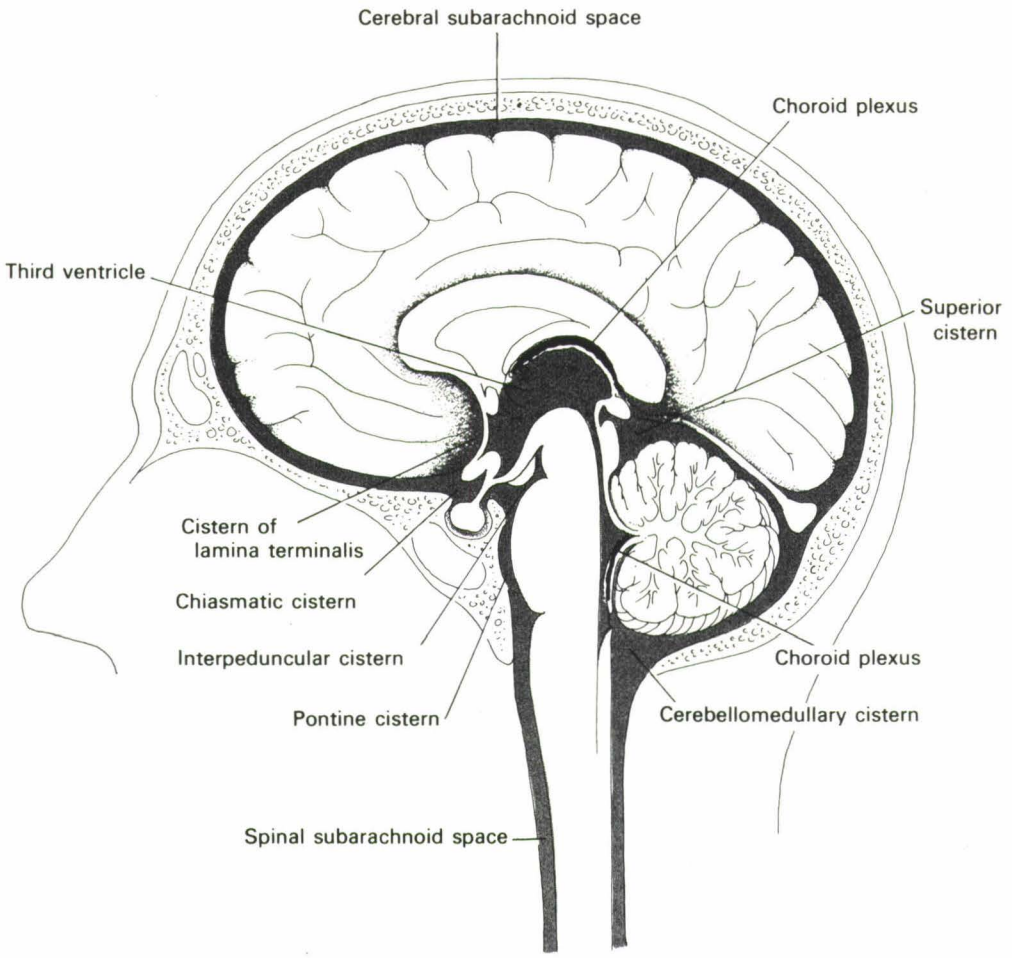


Figure 1.9. Subarachnoid cisterns as seen in a midsagittal view. The superior cistern is referred to clinically as the cisterna ambiens. The choroid plexus in the roof of the third ventricle and in the fourth ventricle is shown in *red*.

In regions adjacent to the superior sagittal sinus (Figs. 1.1, 4.22, and 4.25), the cerebral pia-arachnoid gives rise to tufted prolongations termed *arachnoid granulations* which protrude through the meningeal layer of the dura into the superior sagittal sinus (Figs. 1.10 and 1.11). These granulations are variable in number and location and each consists of numerous arachnoid villi. These villi have a thin outer limiting membrane beneath which are bundles of collagenous and elastic fibers. Cells similar to those of the pia-arachnoid are scattered among the fibers, and small oval epithelial cells cap the surface of the villi. Arachnoid granulations frequently are surrounded by a venous lacuna along the margin of the superior sagittal sinus. With advancing age the arachnoid granulations become larger and more numerous and tend to become calcified. Although arachnoid villi are most numerous in relation to the superior sagittal sinus, they are also found along the other intracranial venous sinuses. Arachnoid villi also have been described in the spinal arachnoid and along the optic nerves. In both the spinal and cerebral arachnoid, cell clusters are sometimes formed which become attached to the dura. These growths may become calcified or, under abnormal conditions, form the sites where tumors arise.

Arachnoid granulations and villi are the major site of fluid transfer from the subarachnoid space to the venous system. In the upright position, venous pressure is less than the hydrostatic pressure of the CSF so that fluid moves from the subarachnoid space to the venous dural sinuses. When venous pressure exceeds CSF pressure, the valves close and blood cannot enter the CSF. Arachnoid granulations appear to function as passive, pressure-dependent, one-way-flow valves whose membranes are readily permeable to

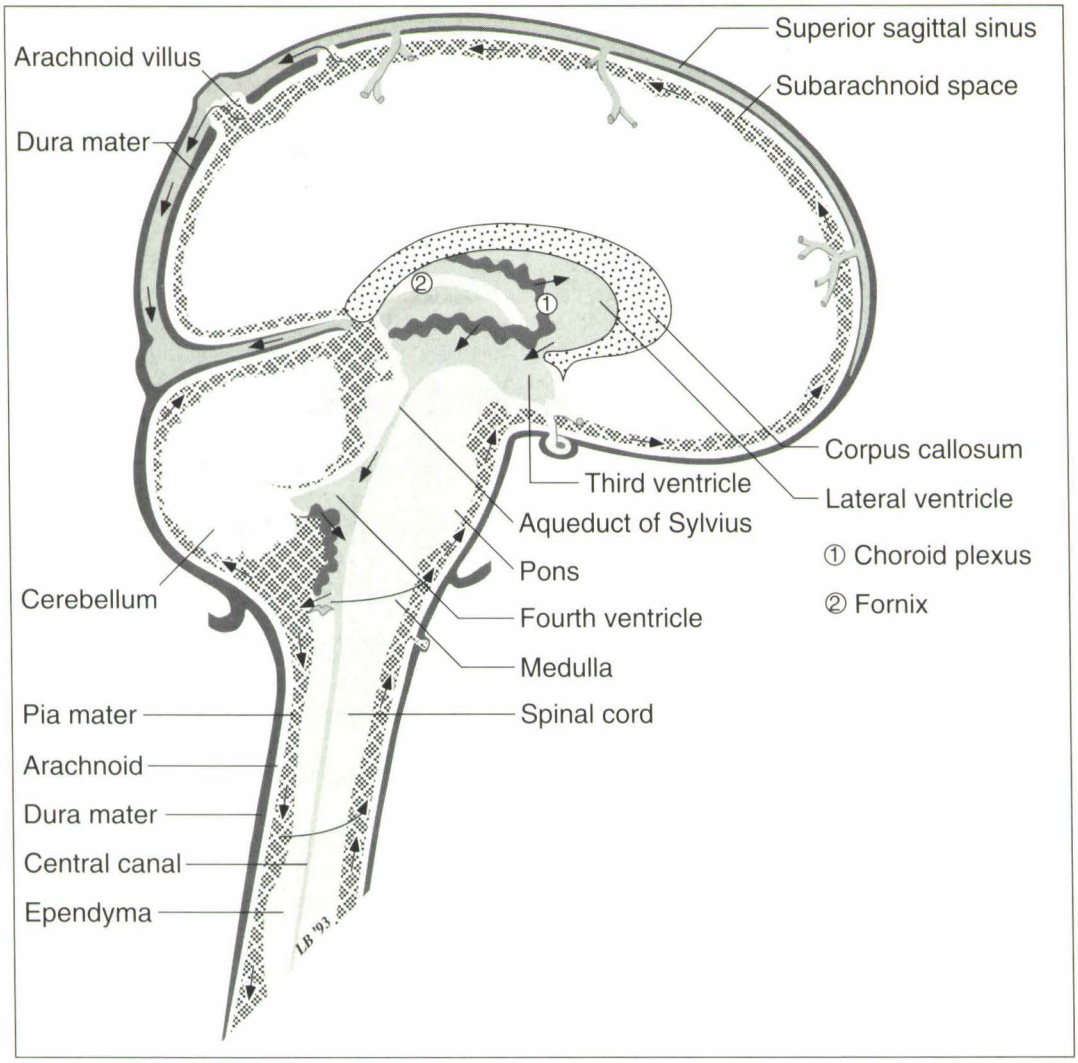


Figure 1.10. Sagittal view of the brain and spinal cord to illustrate the circulation of the cerebrospinal fluid. The direction of the CSF flow is indicated by *arrows*.

metabolites, Prussian blue reagents, and even large molecular weight substances. These valves are spongy tissue containing a series of interconnecting tubes approximately 6 μm in diameter. The tubes remain open only when the CSF flows from the subarachnoid space into venous blood under a pressure head (18, 19, 22). When the pressure of venous blood exceeds that of the CSF, the tubes collapse (51). The surface of an arachnoid villus has a layer of overlapping endothelial cells. In the absence of pressure differences between the CSF and venous blood, the membranes of these cells are folded and have numerous microvilli. When CSF pressure exceeds venous pressure, the microvilli disappear, the cells are stretched and CSF flows into the venous sinuses. Bulk volume flow of CSF occurs through the arachnoid tubular system and between stretched endothelial cells. Flow of CSF into the venous sinuses is proportional to the increase in CSF pressure but does not begin until it exceeds venous pressure by 3–6 cm of water.

Pia-Glia and the Perivascular Spaces

The intima pia or pia-glia is regarded as the external limiting membrane of the central nervous system (CNS) whereas the

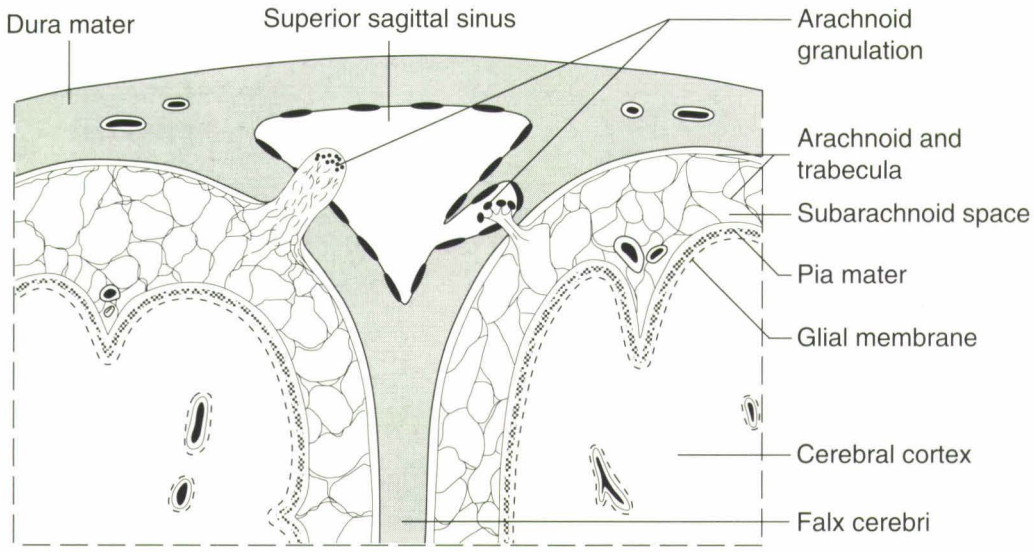


Figure 1.11. Meningeal-cortical relationships. Arachnoid granulations may penetrate dural sinuses or terminate in a lateral lacuna of a sinus. The pia is firmly anchored to cortex by the glial membrane.

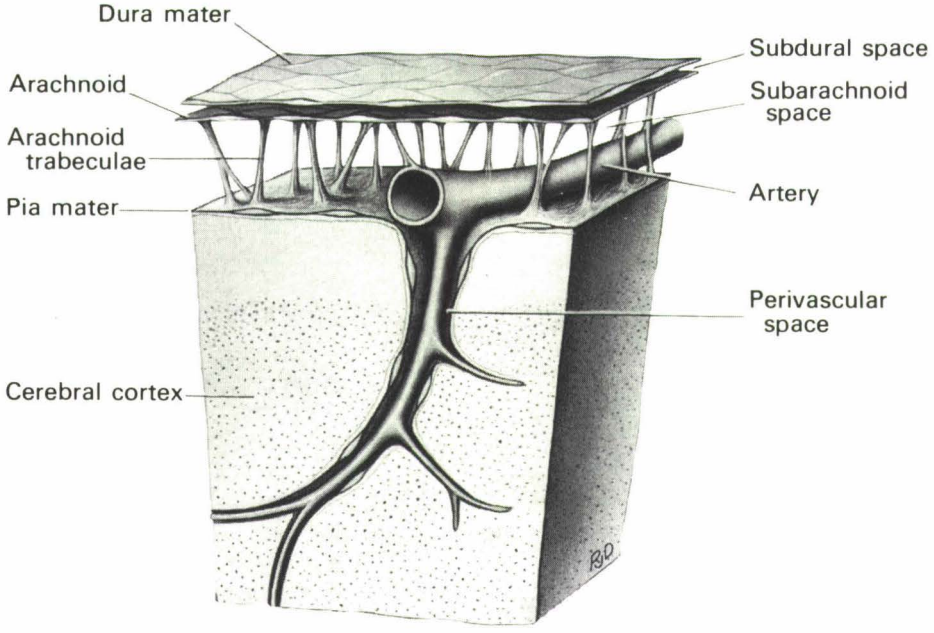


Figure 1.12. Meninges showing relationship of the membranes to the subarachnoid and perivascular spaces.

ependyma can be considered as the internal limiting membrane. It has been suggested that the intima pia arises from ectoderm (29). The arachnoid membrane which represents the principal physiologic barrier that protects the CNS and separates it from the surrounding connective tissue also has been considered to be of ectodermal origin (11, 12). The parenchyma of the CNS, the glia, the ependyma, and the leptomeninges arise from ectoderm, while the blood vascular system and the dura mater are of mesodermal origin. As blood vessels enter and leave the nervous tissue, they carry with them arachnoid and pia-glia which form a cuff around the vessel. The space between the blood vessel and its "adventitial sheath" has been called the *Virchow-Robin space.* It was suggested that these spaces might permit the flow of cerebrospinal fluid from the subarachnoid spaces into the depths of the tissue. Electron microscopic studies indicate that as blood vessels penetrate neural tissue from the subarachnoid space, reflections of the intima pia and arachnoid which form the "adventitial sheath" are carried with it. In the CNS, however, these two layers become continuous and there is no real space between them. When the smallest veins and capillaries are reached, no adventitial elements surround them. Only processes of astrocytes surround the basement membranes of the capillary endothelium.

CEREBROSPINAL FLUID

The CSF is a clear, colorless liquid that fills the ventricles of the brain and subarachnoid spaces. Approximately 70% of the CSF is produced by secretion at the choroid plexus located in the walls of the lateral ventricles and in the roof of the third and fourth ventricles (Figs. 1.10, 2.21, and 2.29). The remaining 30% of the CSF is derived from the capillary bed of the brain and metabolic water production (36, 40, 41). Estimates of metabolic water production, based on the assumption of complete oxidation of glucose for a 1500 g human brain, suggest a net contribution of about 12% of the total CSF. Approximately 18% of the CSF is derived from extrachoroidal sources, presumably as a capillary ultrafiltrate. In humans, the total volume of CSF has been estimated to be about 140 ml, of which 23 ml are contained within the ventricles. The net production of CSF in humans appears to be between 0.35 and 0.37 ml per minute which leads to the formation of over 400 ml per day (11, 12). These data suggest a CSF turnover rate of 0.25% per minute (9, 10).

The CSF is formed at a hydrostatic pressure head of 15 ml of H_2O which is sufficient to drive it through the ventricular system and into the arachnoid spaces surrounding the brain and spinal cord. Pulsation of the choroid plexus also probably contributes to the movement of CSF within the ventricular system. These pulsations reflect the presence of several arteries in the choroid plexus and are not due to some intrinsic pulsatile characteristic of the plexus itself.

The CSF formed in the lateral ventricles enter the third ventricles through the interventricular foramen (of Monro) and then pass via the cerebral aqueduct (of Sylvius) into the fourth ventricle (Fig. 1.10). The fluid enters the cerebellomedullary cistern via a *median aperture* (foramen of Magendie) located in the posterior medullary velum, and two *lateral apertures* (foramina of Luschka) in the lateral recesses of the fourth ventricle (Figs. 1.10 and 2.21). The fluid then circulates in the subarachnoid spaces surrounding both the brain and the spinal cord. The bulk of the CSF is passively returned to the venous system via the arachnoid villi (Fig. 1.10). The hydrodynamic permeability of the arachnoid villi is large compared with that of the peripheral capillaries. Large protein molecules leave the CSF by passage through the arachnoid villi at roughly the same rate as smaller molecules.

The composition and pressure of the CSF may vary in different pathologic conditions, thus the analysis of this liquid can give us important clues to establish a diagnosis (15). Under normal conditions, the CSF is clear, mostly devoid of blood cells, and contains only small amounts of protein, glucose, and potassium, but relatively large amounts of sodium chloride. In acute bacterial meningitis, however, the white blood cell count may reach 5000/ml and cultures of CSF may be used to identify the infectious agent. Usually, cell number increases only moderately in cases of viral infections or in response to cerebral infarction, brain tumor, or other cerebral tissue damage. The concentration of glucose in the CSF is decreased in acute bacterial infection, but rarely in viral infection. An increase in the protein content of the CSF may be found in several pathologies of the CNS, probably because of changes in the vascular

permeability. For instance, protein content greater than 500 mg/dl is often indicative of a tumor or other compressive lesion blocking the spinal subarachnoidal space. In multiple sclerosis, a slowly progressive CNS disease characterized by disseminated patches of demyelination in the brain and spinal cord, the γ-globulins increase to more than 13% of the total protein content in the CSF (15).

The CSF serves to support and cushion the CNS against trauma. The buoyancy of CSF is indicated by the fact that a brain weighing 1500 g in air weighs only 50 g when immersed in CSF (25). Buoyancy reduces the momentum and acceleration of the brain when the cranium is suddenly displaced, thereby reducing concussive damage (31). Because the brain is nearly incompressible within the skull, the combined volumes of brain, CSF, and intracranial blood must be maintained at a constant level. The volume of any of these components can be increased only at the expense of one or both of the others. For instance, any space-occupying lesion such as a tumor or hematoma usually results in an increase in intracranial pressure that may severely damage the brain. Brain tumors and hematomas usually cause an increase in CSF pressure, which can be used as a guide to intracranial pressure. The normal CSF pressure measured at the lumbar cistern is about 100–150 mm of H_2O in the recumbent position, and varies between 200 and 300 mm H_2O in the sitting position. An excessive amount of CSF can, itself, markedly elevate the intracranial pressure, if not compensated by increased absorption or decreased formation. This pathologic condition, known as *hydrocephalus*, is encountered frequently in infants. It is also observed in adults pursuant to tumors, vascular lesions, and other pathologic conditions. Hydrocephalus is characterized by an enlargement of the ventricles, a thinning of neural tissue, and changes in the morphology of the skull. Such increases in CSF may result from an overproduction of fluid, an obstruction to its flow, or inadequate absorption. In most instances, hydrocephalus results from obstruction within the ventricular system, particularly the cerebral aqueduct. Removal of the choroid plexus from one lateral ventricle usually causes the ventricle to collapse, while obstruction of one interventricular foramen results in dilatation of the ipsilateral ventricle.

In cases of senile atrophy of the brain, there is often an accumulation of CSF within the subarachnoid spaces, a condition referred to as external hydrocephalus. Obstruction of the CSF flow through the tentorial notch around the midbrain results in a combination of *internal (intraventricular) hydrocephalus* and subtentorial *external hydrocephalus*. This pathologic condition is known as *communicating hydrocephalus*. Hydrocephalus resulting from a tumor obstructing the CSF flow can usually be treated by surgical removal of the causative factor. In the other cases, the overflow of CSF can be diverted to a new site of absorption by means of ventricular-atrial, ventricular-peritoneal, or lumbar-peritoneal surgical shunts.

The CSF also removes waste products of neuronal metabolism, drugs, and other substances which diffuse into the brain from the blood. As the CSF streams over the ventricular and pial surfaces of the brain, it drains away solutes and carries them through the arachnoid villi into venous blood. Additionally, some drugs, such as penicillin, and certain neurotransmitters, like serotonin and norepinephrine and their metabolites, are rapidly removed from the CSF by the choroid plexus (1). The 30% of the CSF derived from extrachoroidal sources may contribute to the bulk volume movement within normal brain parenchyma. The CSF also plays an important role in integrating brain and peripheral endocrine functions in that hormones or hormone-releasing factors from the hypothalamus are secreted into the extracellular space or directly into the CSF. These hormones, which include hormone-releasing factors, are carried via CSF to the median eminence in the floor of the third ventricle, from which site they are transported by specialized ependymal cells (i.e., tanycytes) into the hypophysial portal system (Figs. 17.18 and 17.19). The CSF also influences the microenvironment of neurons and glial cells because there is no diffusion barrier between CSF at either the ependymal lining of the ventricles or at the pia-glial membrane. Changes in CSF calcium, potassium, and magnesium ion concentrations may affect blood pressure, heart rate, vasomotor reflexes, respiration, muscle tone, and the emotional state of animals (24).

The CSF has been regarded as an ultrafiltrate of the blood plasma because of their resemblance, except for huge differences in protein concentration (plasma, 6500 mg/100 g; CSF, 25 mg/100 g). The characteristic dis-

tribution of the number of ions and nonelectrolytes in CSF and plasma, however, is such that the CSF cannot be described as a simple filtrate or dialysate of the blood plasma. In general the CSF has higher Na^+, Cl^-, and Mg^{2+} concentrations, and lower K^+, Ca^{2+}, and glucose concentrations than would be expected in a plasma dialysate. Finally, the osmotic pressure relationships are not sufficient to produce a virtually protein-free fluid from the blood plasma (11, 12).

The choroid plexus is a villous structure extending from the ventricular surface like coral fronds into the CSF. The plexus consists of a single layer of cuboidal epithelium with basal infoldings on the choroidal stroma and apical microvilli in contact with the CSF (45). The cuboidal epithelial cells of the plexus rest on a basement membrane enclosing an extensive capillary network embedded in a connective tissue stroma (Fig. 1.16). The choroid plexus regulates a large part of the production, as well as, the composition of the CSF. A Na^+-K^+ exchange pump, catalyzed by Na^+-K^+-ATPase, drives Na^+ toward the ventricular surface of the plexus and K^+ in the opposite direction. Thus, the concentration of K^+ is lower and the concentration of Na^+ is higher in the choroidal secretion than in serum or in an ultrafiltrate of the plasma (30, 45). These data suggest that K^+ is transported out of the CSF, while Na^+ is actively transported into it. The choroid plexus also plays a role in the regulation of Mg^{2+} and Ca^{2+} in the CSF. Fluid secreted by the choroid plexus contains a higher concentration of Mg^{2+} and a lower concentration of Ca^{2+} than does an ultrafiltrate of the plasma. Considerable controversy concerns the manner in which water, the largest constituent of the CSF, moves across the choroidal epithelium. The hypothesis, based upon hydrostatic pressure, is supported by data indicating that modifications of choroidal blood flow can increase or decrease the CSF secretion rate (50). Approximately 25% of the volume of blood flowing to the choroid plexus normally is secreted as CSF. The other theory concerning the water content of the CSF, suggests that water moves across the choroidal epithelium under a standing osmotic gradient established by the active transport of Na^+. This hypothesis is based upon the observation that movement of water into the CSF is quantitatively coupled to the active transport of Na^+ (48). Water secretion is reduced proportionally to the inhibition of the enzyme Na^+-K^+-ATPase which catalyzes the Na^+ pump.

BARRIERS RELATED TO THE BRAIN

The functional capacity of all neurons of the brain and spinal cord is dependent upon the nature of the chemical milieu which surrounds them. To maintain the physiochemical composition of the microenvironment of neurons, axons, and glia within the narrow limits of neuron survival requires a unique regulatory mechanism. The system that regulates the transport of chemical substances between arterial blood, the CSF, and brain tissue is the blood-brain barrier, a series of regulatory interfaces between blood and the nervous system. The blood-brain barrier separates the two major compartments of the CNS, the brain and the CSF, from a third compartment, the blood. The sites of the barrier are the interfaces between the blood and these two compartments of the CNS. These interfaces regulate diffusion at cerebral capillaries and the exchange of metabolites and metabolic products between blood and brain. Two separate barriers, a *blood-CSF barrier* and a *blood-brain barrier*, have been distinguished to explain why intravascular substances enter the CSF and the brain at different rates (11, 12). When substances such as glucose or urea are injected intravascularly, they diffuse rapidly and come to equilibrium with extracellular or interstitial fluids of most tissues. The observation that the transport of substances from the blood to the CSF requires hours instead of minutes gave rise to the concept of the blood-CSF barrier. Injections of certain dyes, such as trypan blue, into the blood, stains most body tissue quickly, but does not enter the CSF. Early studies indicated important differences between CSF and the interstitial fluid of most body tissues and further established that this barrier is not absolute, but selectively permeable. The kinetic aspects of the passage of substances from blood into brain are included under the term blood-brain barrier, by analogy with the blood-CSF barrier. The concept of the restriction of the passage of dissolved substances from blood to brain dates back to 1885, when Paul Ehrlich demonstrated that intravenous injections of many vital dyes stained practically all body tissues, except the brain (13). These blood-brain and blood-CSF barriers differ greatly in surface area. The surface area

of the blood-brain barrier has been estimated to be 5000 times greater than that of the blood-CSF barrier (33).

Overall, the blood-brain barrier appears to be principally in charge of transporting those substances that the brain consumes rapidly and in large quantities (e.g., glucose, amino acids, lactate, and ribonucleosides). In contrast, the choroid plexus controls the transfer of different micronutrients—substances that are essential to the brain but only needed in relatively small amounts over extended periods (e.g., vitamin C, folates, deoxyribonucleosides, and vitamin B_6) (45).

The brain barriers develop at the time when blood vessels invade the brain, and evidence suggests that the adult barriers react differently to the electrical charges of various vital dyes. The blood-brain barrier is more permeable to basic (positively charged) dyes, whereas the blood-CSF barrier is more permeable to acid (negatively charged) dyes. Such interfaces are structural and functional entities which dynamically control the transfer of chemical substances into and out of the three fluid compartments of the brain (i.e., extracellular or interstitial, intracellular, and CSF).

The ependymal surfaces of the cerebral ventricles and the pia-glial membrane on the surface of the brain do not impede the exchange of substances between the CSF and brain and do not constitute a sub-barrier. The walls of the cerebral ventricles and the spinal canal are lined by a single layer of epithelial cells whose cilia beat synchronously to cause local mixing of CSF. Ependymal cells are not connected by tight junctions and do not hinder macromolecular exchange between the CSF and the brain. Ferritin and the enzymatic marker horseradish peroxidase (HRP) injected into CSF of the ventricles diffuse between ependymal cells and enter the extracellular space of the brain (4). Additionally, these tracers are found in pinocytotic vesicles within ependymal cells. Drugs injected into the cerebral ventricles easily cross the ependymal lining and produce immediate pharmacologic and behavioral effects. A schematic diagram of relationships between the blood-brain barrier, the blood-CSF barrier, and the brain-CSF interface is shown in Figure 1.14. Excellent reviews of the brain barriers consider this subject in depth (2, 3, 16, 17, 37).

Blood-Brain Barrier

It is important to realize that for any chemical compound the efficacy of the blood-brain barrier is determined by two major sets of factors: (a) the morphologic and functional characteristics of brain capillaries that are different from those of the capillaries found elsewhere in the body, and (b) the biochemical and biophysical characteristics of the compound, among which molecular size, lipid solubility, and existence of carrier-mediated transport systems play the most crucial role.

The blood-brain barrier comprises three major components: (a) the endothelial cells forming the wall of brain capillaries, (b) the continuous and homogeneous basement membrane of these endothelial cells, and (c) the multiple processes of the astrocytes covering much of the surface of brain capillaries (Fig. 1.13). These three elements are all that separate the plasma in blood vessels from the

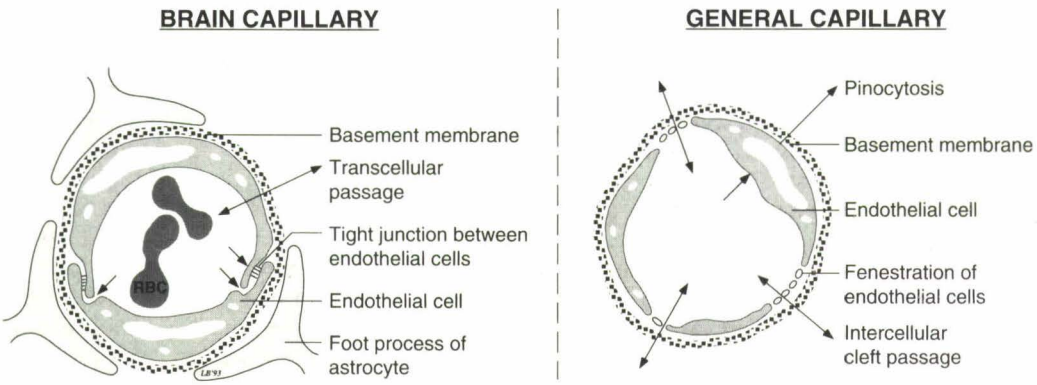


Figure 1.13. Differences between the structure of capillaries in the brain (*left*) and those in the general circulation (*right*).

extracellular (i.e., interstitial) space within the CNS.

In all parts of the body, the exchanges between blood and tissue take place in the capillary bed. The brain is no exception to this generalization, but there are some significant differences. A capillary is distinguished from an arteriole and a venule by the absence of a well-defined muscular coat. The wall of a capillary consists only of flattened endothelial cells resting on a basement membrane surrounded by a thin adventitial layer made up of cells and fibers. These latter cells, referred to as *pericytes*, are often enclosed within parts of the basement membrane (12). Capillaries within the CNS contain a continuous inner layer of endothelial cells connected by tight junctions (Fig. 1.13). Similar capillaries are found in the retina, the iris, the inner ear, and within the endoneurium of peripheral nerves. Tissue with capillaries of this type are derived totally or partially from neuroectoderm (20). The morphologic and enzymatic properties of capillaries in tissue derived from neuroectoderm are controlled by specific angiogenic substances released by neural tissue. When iris tissue is transplanted to the brain it is vascularized with capillaries that do not contain monoamine oxidase or dopa-decarboxylase. Embryonic brain tissue transplanted in the anterior chamber of the eye is vascularized from the iris, but the capillaries contain these brain enzymes. The tight junctions between endothelial cells of cerebral capillaries restrict intercellular diffusion (Fig. 1.15). The presence of high-resistance tight junctions between adjacent brain endothelial cells, and the paucity of pinocytosis or capillary fenestrations, means that circulating substances in the cerebral vascular system can enter the brain only via carrier mediation or lipid mediation (33). The tight junctions that connect capillary endothelial cells form, in essence, a continuous cell layer that has the permeability properties of a plasma membrane. The basement membrane surrounds the endothelial cells and approximately 85% of its surface is covered by glial cells. The tight junctions between endothelial cells prevent the transfer of $La(OH)_3$, microperoxidase, HRP, and ferritin (5, 6, 38). The capillary surface area in 1 g of brain has been estimated to be 240 cm^2 (8).

Cerebral blood vessels have neither a well-developed small pore system for diffusion nor a vesicular transport system such as that found in the capillaries of skeletal and cardiac muscles. Pinocytotic vesicles are rare in endothelial cells of cerebral capillaries or venules, but are occasionally seen in arterioles. Additionally, endothelial cells of cerebral vessels do not contain contractile protein as seen in peripheral capillaries, and capillary permeability does not increase in response to histamine, serotonin, or norepinephrine (52). The capillary endothelial cells in the central nervous system are metabolically active with respect to both oxidative and hydrolytic enzymes. Enzymes within these cells regulate the transport of amines and amino acids. An example of this regulation is seen in Parkinson's disease (paralysis agitans) in which there is a deficiency of dopamine, a neurotransmitter synthesized in the substantia nigra and conveyed by axons to specific portions of the striatum. Because dopamine cannot cross the blood-brain barrier, the precursor L-dopa is given to correct this metabolic defect. L-dopa crosses the blood-brain barrier and is decarboxylated in the capillary endothelium to dopamine, a biogenic amine that is therapeutically effective (Fig. 1.15). Although it has been suggested that active transport mechanisms exist across cerebral capillaries, their precise role is difficult to distinguish from that of the choroid plexus.

The blood-brain barrier in the central nervous system is not everywhere complete. In certain regions of the brain, the continuous capillary endothelia are replaced by capillaries with fenestrated endothelia. These regions with capillary fenestrations provide specific sites for the transfer of proteins and solutes irrespective of molecular size and lipid solubility. Regions of the brain devoid of a blood-brain barrier include the pineal body (or pineal gland), the neurohypophysis, the area postrema, the subfornical organ, the organum vasculosum of the lamina terminalis (or supraoptic crest), and the median eminence of the hypothalamus. All of these regions are highly vascular, and many are known or suspected of having a secretory function. The blood-brain barrier, except in the special regions noted earlier, functions as a differential filter that permits the selective exchange of many substances from blood to the *extracellular compartment* (i.e., interstitial fluid). It appears to be impermeable to many substances (e.g., vital dyes).

It has been suggested that the blood-brain barrier in the fetus and newborn is immature

because blood-borne dyes stain these brains more extensively than adult brains. Electron microscopic evidence indicates that tight junctions surrounding epithelial cells of the choroid plexus of the rat at early developmental stages do not differ qualitatively from the adult (32). However, the water content of the cerebral cortex and white matter of the brain of the rhesus monkey progressively diminishes during fetal development and postpartum maturation (44). An expanded extracellular space in the brains of the newborn appears to provide a greater volume for the distribution of extracellular markers (e.g., inulin). This increased extracellular space appears to account for the observation that trypan blue, given intravenously, stains the brain of an immature animal. Although the dye enters the brain only at the nonbarrier sites, it extends further in the extracellular space than in the mature brain.

Unconjugated bilirubin, a breakdown product of hemoglobin, can stain the brain of the newborn if severe jaundice results from accelerated destruction of red cells, as occurs in erythroblastosis fetalis associated with Rh incompatibility. This condition, known as *kernicterus,* results in a yellow staining of the brain, especially the nuclei of the basal ganglia. Unconjugated bilirubin is very lipid-soluble and crosses the lipoid membranes of capillary endothelia in both the adult and immature brain. In the adult, bilirubin is bound to serum albumin and does not enter the brain. The immature liver of the neonate cannot conjugate large quantities of bilirubin and unconjugated bilirubin passes the blood-brain barrier to stain the brain nuclei yellow. The mortality in kernicterus is high and infants that survive have a high incidence of motor disorders and mental retardation (26).

Certain regions outside the CNS have neural tissue in direct contact with the extracellular fluid. Regions without an intervening barrier include (a) the terminals of peripheral nerves, (b) sensory ganglia, (c) the olfactory epithelium, and (d) the optic nerve where it penetrates the sclera. The absence of a barrier at these sites represent loci where protein, including toxins and viruses, may enter the extracellular space. In some diseases, the blood-brain barrier may break down and substances that are normally excluded may enter the brain. This is the case with penicillin, an important antibiotic used to treat some forms of meningitis. Normally, penicillin does not reach the brain in large amounts mostly because of its large size (in plasma, penicillin is bound to albumin) and low degree of lipid solubility. This is fortunate because penicillin is toxic to the nervous tissue. In meningitis, however, the blood-brain barrier becomes much less effective and the antibiotic enters the brain in sufficient amounts to exert a therapeutic effect. In cases of focal brain lesion such as tumor and abscess, the breakdown of the blood-brain barrier is often limited to the lesion site and this has important practical implications. For instance, albumin labeled with radioactive iodine can be used as a tracer to locate the lesion site, since this protein will reach only the lesion area and not the normal parts of the brain where the blood-brain barrier has remained intact. The accumulation of radioactivity in a restricted brain area can then be localized by external detectors or can serve to enhance computerized images of the brain.

Neurons and neuroglial cells comprise the *intracellular fluid compartment* of the brain (Fig. 1.14). Passage of substances into and out of glial cells and neurons takes place from the extracellular space through cell membranes. Estimates of the total extracellular space between neurons, neuroglia, and capillaries of the brain vary widely, but some data suggest that it equals approximately 18% of wet brain weight (14).

In some pathologic processes, increased permeability of brain capillary endothelial cells may lead to important augmentation of the volume of the extracellular fluid, a condition referred to as brain edema. Brain edema may be local, as in areas surrounding contusion, infarct, or tumor, or general, as in head injury, lead encephalopathy, and meningitis. Local brain edema may cause herniation of brain tissue. For instance, the cingulate gyrus may be forced to protrude beneath the falx cerebri on one side, whereas the uncus of the temporal lobe may engage itself across the tentorium cerebelli and the cerebellar tonsils through the foramen magnum. All these herniations cause severe damage to the brain tissue. Functional manifestations of more generalized brain edema comprise focal neurologic deficits, a slowing of the electroencephalogram, and impaired consciousness. Glucocorticoids and hypertonic solutions of urea, mannitol, or glycerol are the most commonly used compounds to treat brain edema.

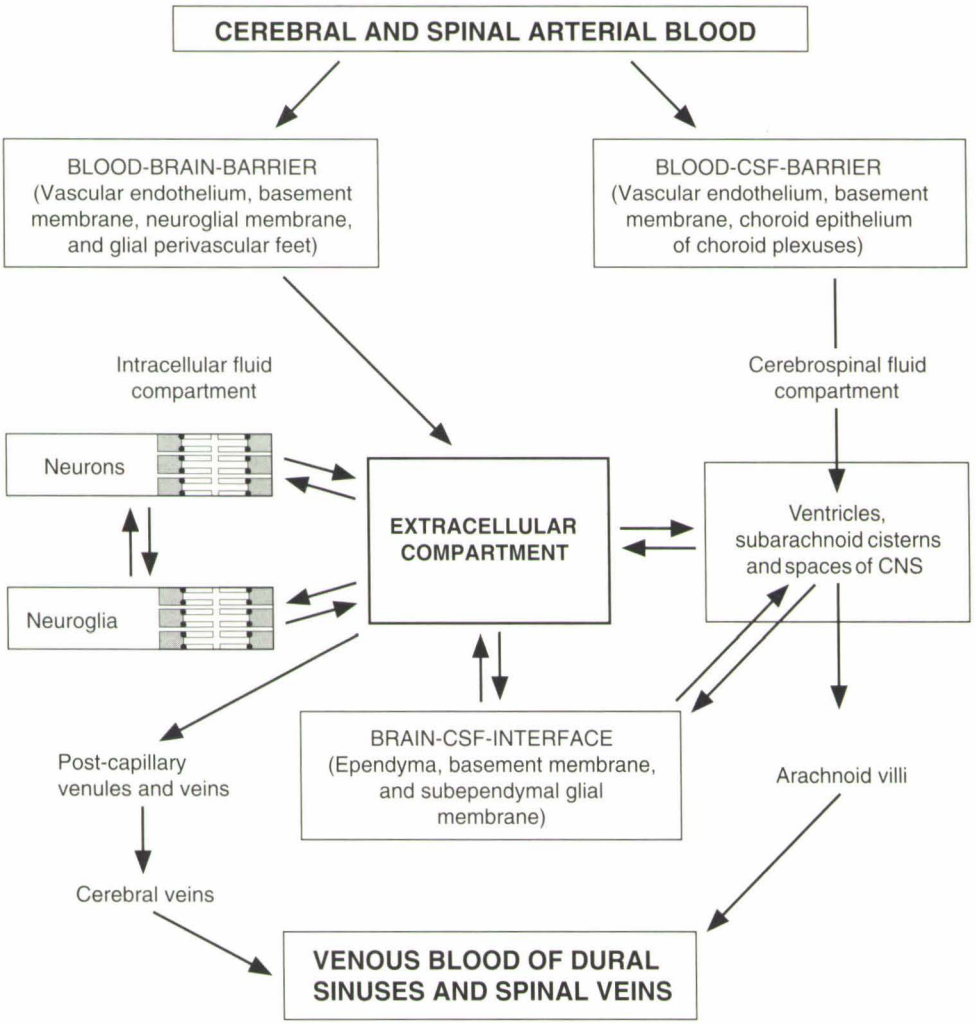


Figure 1.14. Blood-brain barrier, the blood-CSF barrier, and the brain-CSF interface that separate the brain and CSF from the cerebral vascular compartment. The blood-brain barrier is a series of interfaces between arterial blood, CSF, and neural tissue that regulate the transport of chemical substances. Tight junctions between endothelial cells (Figs. 1.13 and 1.15) of cerebral capillaries (the blood-brain barrier) and a paucity of pinocytosis restrict the passage of solutes from the blood into the extracellular compartment (i.e., interstitial fluid). The blood-CSF barrier is formed by tight junctions surrounding apical regions of the cuboidal epithelium of the choroid plexus. The brain-CSF interface, consisting of the ependymal lining of the cerebral ventricles and the pia-glial membrane on the external surface of the brain, does not impede the exchange of solutes between the CSF and the brain. The extracellular compartment has been estimated to constitute about 18% of wet brain weight.

Blood-Cerebrospinal Fluid Barrier

The epithelium and adnexa of the choroid plexuses of the lateral, third, and fourth ventricles actively secrete CSF. Evidence that they are an effective barrier is attested to by the relatively higher concentration of sodium and chloride ions in CSF than in the plasma. In composition, the CSF is the same as that of the interstitial fluid of the brain. The barrier to passive exchange of proteins and small hydrophilic solutes between blood and CSF is not at the choroidal capillaries as they have fenestrated endothelia that permit exchange of solutes (Fig. 1.16). The blood-CSF barrier is located at tight junctions which surround and connect the cuboidal epithelial cells on the surface of the choroid plexus. Protein tracers like Evans blue-albumin, injected intravascularly, stain the stroma of the choroid plexus but do not enter the CSF. Similarly, HRP passes through pores of choroidal capillaries

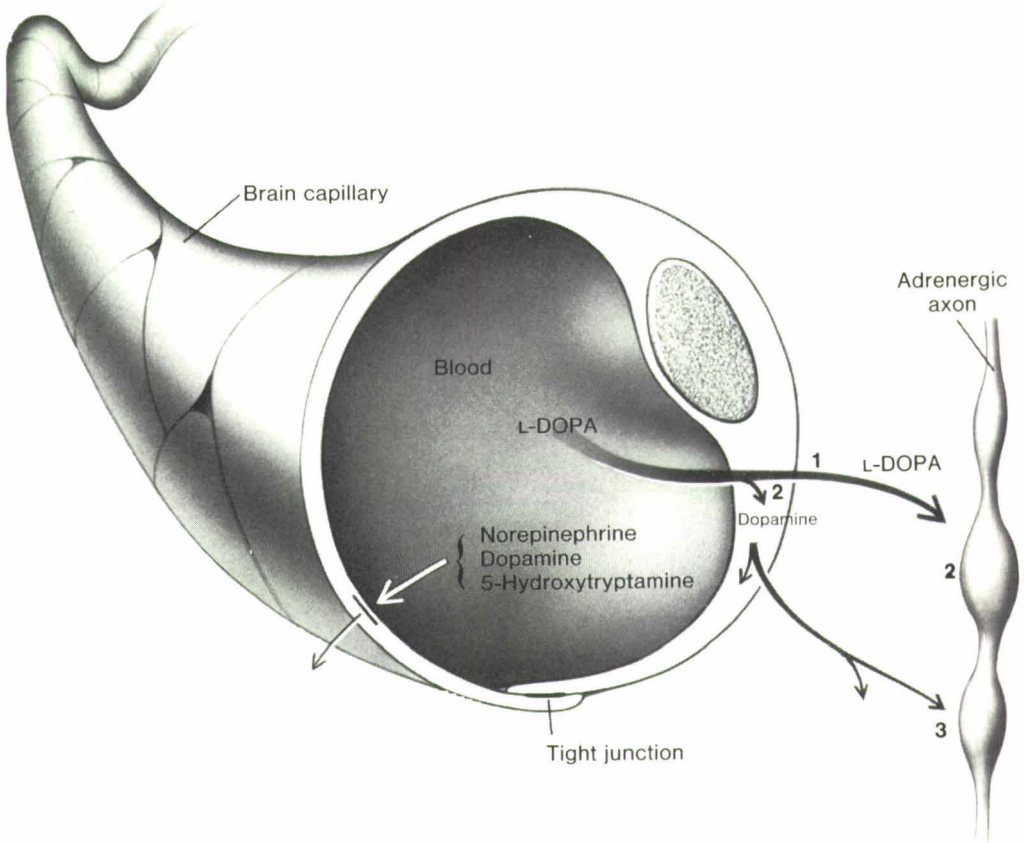


Figure 1.15. Brain capillary demonstrating a tight junction between endothelial cells that constitute part of the blood-brain barrier. Endothelial cells of brain capillaries contain enzymes that regulate the specific transport of biogenic amines (norepinephrine, dopamine, and 5-hydroxytryptamine) and amino acids. Dopa passes the blood-brain barrier (*1*), is decarboxylated to dopamine in the capillary endothelium (*2*) and enters neural tissue (*3*), where it is degraded by monoamine oxidase. Decarboxylation of L-dopa to dopamine (*2*) also occurs after its incorporation into axonal varicosities of aminergic neurons.

to fill the connective tissue stroma but does not pass beyond the tight junctions which surround the apical regions of epithelial cells of the choroid plexus (6). The surface area of the blood-CSF barrier is only about 0.02% of the surface area of the blood-brain barrier. Despite great quantitative differences in surface area, it is probable that some circulating substances enter the brain via the blood-CSF barrier (33). Available evidence suggests that some circulating peptides (e.g., insulin) and plasma proteins (e.g., prealbumin) may be selectively transported into the CSF via the blood-CSF barrier. The ependymal surface of the cerebral ventricles and the pia-glial membrane on the surface of the brain do not impede exchanges between the CSF and the brain. Molecules with a relatively high plasma/CSF ratio (compared with inulin) are transported across the blood-CSF barrier in a selective and limited fashion.

CIRCUMVENTRICULAR ORGANS

The circumventricular organs are areas of specialized tissue located at strategic positions in the midline ventricular system (Fig. 1.17). Included under this designation are (a) the subfornical organ, (b) the organum vasculosum of the lamina terminalis (or supraoptic crest), (c) the median eminence, (d) the neurohypophysis, (e) the pineal body, (f) the subcommissural organ, and (g) the area postrema (27, 49). With the exception of the area postrema, located along the caudal margins of the fourth ventricle (Figs. 1.17 and 12.11), all circumventricular organs are unpaired, occupy midline positions, and are re-

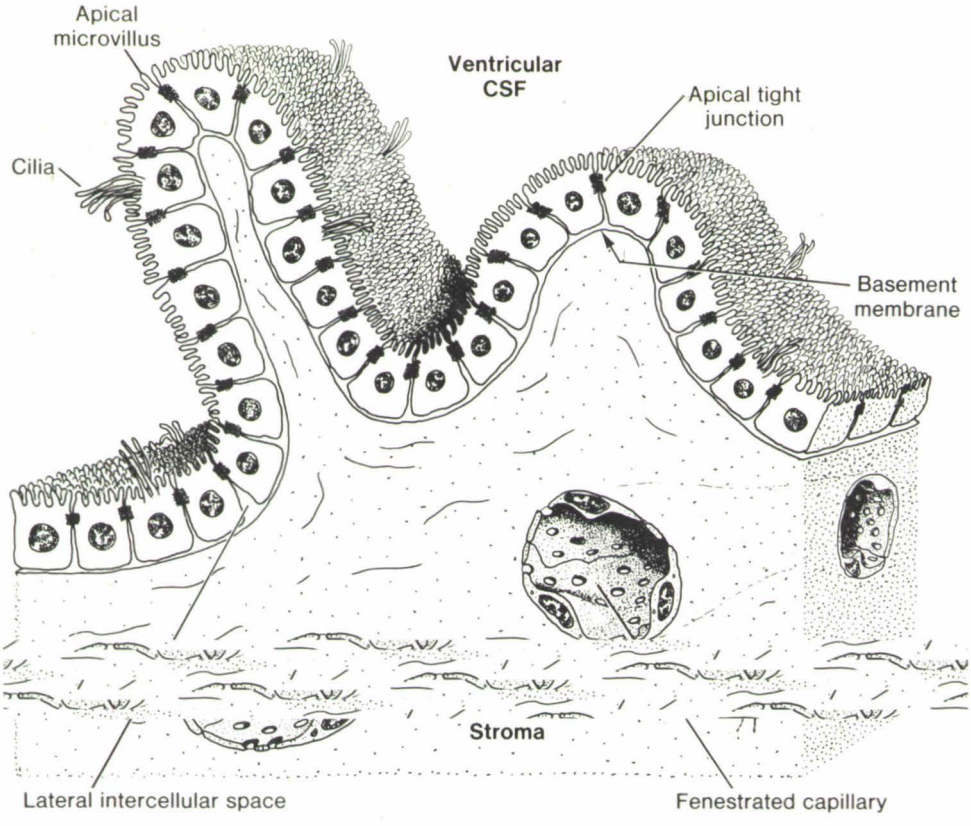


Figure 1.16. Choroid plexus villus covered by a single layer of cuboidal epithelium with apical microvilli protruding into the ventricular CSF. The base of these cells rests upon a basement membrane. Tight junctions connecting apical regions of the epithelial cells constitute the blood-CSF barrier. The underlying connective tissue stroma contains capillaries with fenestrations.

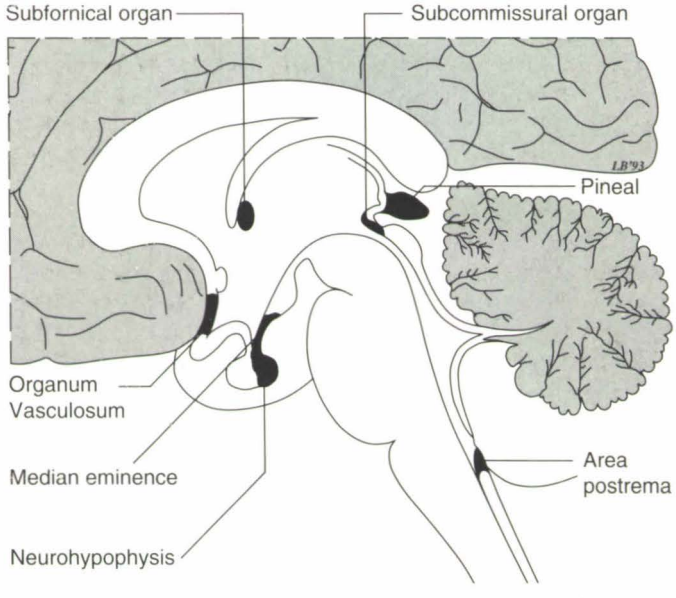


Figure 1.17. Midsagittal section of the human brain indicating the locations of the circumventricular organs. All of these structures, except the area postrema, are unpaired, situated in the midline, and related to diencephalic structures. All, except the subcommissural organ, are highly vascularized and lack a blood-brain barrier. Neuropeptides have limited transport across the blood-brain barrier, but can enter and leave the brain, via the CSF, in regions of the circumventricular organs. The organum vasculosum of the lamina terminalis (OVLT) resembles the median eminence, but its function is not yet clarified. This structure, particularly prominent in rodents, is also designated as the supraoptic crest. The median eminence serves as a neuroendocrine transducer and the final common pathway by which releasing factors are discharged into the hypophysial portal system.

lated to portions of the diencephalon. All of these structures, except the subcommissural organ, are highly vascularized and contain fenestrated capillary loops surrounded by perivascular connective tissue spaces. The circumventricular organs, with the exception of the subcommissural organ, lack a blood-brain barrier. The absence of this barrier, demonstrated by permeability to HRP, suggests that these tissues are permeable to proteins and peptides.

The *neurohypophysis* is a well-known target of various peptidergic neuroendocrine neurons. Fibers from the magnocellular hypothalamic nuclei terminate in the neural lobe of the hypophysis around fenestrated capillaries. These terminal fibers contain neurophysin, vasopressin, and oxytocin, which are stored and released into the general circulation from the neural lobe of the hypophysis. The *organum vasculosum of the lamina terminalis* (OVLT) appears to be a vascular outlet for luteinizing hormone releasing hormone (LHRH) and somatostatin, which inhibits the release of somatotropin (growth hormone) (49). The OVLT may serve not only as a neurohemal outlet for hypothalamic peptides, but also as a hemoneural function whereby certain peptides, proteins, and amines in the blood are sensed by neurons with receptor properties. The *median eminence,* recognized as a circumventricular organ, serves as a neuroendocrine transducer that translates bioelectrical activity in the central nervous system into blood-borne signals in the form of releasing factors (43). The final common pathway of neuroendocrine control of the anterior pituitary by the hypothalamus is a pool of neurosecretory neurons whose axons terminate upon fenestrated portal capillaries in the median eminence, and discharge releasing factors into the hypophysial portal system (Fig. 17.18). The *subfornical organ,* located between the interventricular foramina, has connections with the choroid plexus and its vascular permeability suggests that it may regulate body fluids (46, 49). The *pineal body* (pineal gland or epiphysis) contains specialized cells known as pinealocytes and produces the hormone melatonin under the influence of light deprivation. The *subcommissural organ* (SCO) is located beneath the posterior commissure at the junction of the third ventricle and the cerebral aqueduct (Fig. 14.12). Cells of SCO are not highly vascularized, but secrete a mucopolysaccharide into the CSF which forms filaments that converge as Reissner's fiber. This curious fiber can be traced from the cerebral aqueduct through the fourth ventricle to the caudal end of the central canal of the spinal cord. The function of this structure is unknown. The *area postrema,* located at the junction of fourth ventricle and spinal canal, has a structure similar to that of the subfornical organ (Fig. 12.11). It is surrounded by fields of terminal fibers containing neurophysin, oxytocin, and vasopressin, although none of these peptides can be identified within the area postrema. The area postrema is considered a chemoreceptor that triggers vomiting in response to circulating emetic substances (i.e., apomorphine and digitalis glycosides).

Recent evidence of the widespread distribution of peptides in the CNS suggests that the CSF may be a route by which these substances modulate neuronal function in different regions of the brain (21). Although neural peptides have limited access to the CNS across the blood-brain barrier, hypothalamic hormones have been detected in high concentrations in the circumventricular organs. The peptides which have been identified in the CSF include (a) thyroid releasing hormone (TRH), (b) luteinizing hormone releasing hormone (LHRH), (c) somatostatin (SRIF), (d) opioid peptides, (e) cholecystokinin (CCK), (f) angiotensin II, (g) substance P (SP), (h) adenohypophysial hormones, and (i) neurohypophysial hormones. There is some evidence that neural peptides in the CSF may be altered by neurologic diseases. These data raise the interesting possibility that measurements of neural peptides in the CSF might provide a sensitive "marker" for the anatomic localization of pathologic processes in specific regions of the CNS (21).

In nonmammalian vertebrates, the circumventricular organs are highly developed and comprise a multitude of small monoaminergic cells provided with a short clublike process floating freely within the CSF of the third ventricle (34). In mammals, many of the circumventricular organs, particularly the OVLT, SCO, and subfornical organ, are densely innervated by serotonin-containing fibers originating in the raphe nuclei of the midbrain (7, 35). Other serotoninergic fibers pierce the ependymal wall of the cerebral ventricles and form a relatively dense and extended supraependymal plexus, as demonstrated in different mammals, including humans (39). These recent findings led to the suggestion that serotonin may act as a neurohormone in these circumventricular organs and supraependymal fibers (7).

References

1. Barany EH. Inhibition of hippurate and probenecid of in vitro uptake of iodipamide and o-iodohippurate: a composite uptake system for iodipamide in choroid plexus, kidney cortex and anterior uvea of several species. Acta Physiol Scand 1972; 86:12–27.
2. Bradbury MWB. The concept of a blood-brain barrier. New York: John Wiley & Sons, 1979.
3. Bradbury MWB. The structure and function of the blood-brain barrier. Fed Proc 1984;43:186–190.
4. Brightman MW. The distribution within the brain of ferritin injected into cerebrospinal fluid compartments. I. Ependymal distribution. J Cell Biol 1965;26:99–123.
5. Brightman MW, Reese TS. Junctions between intimately apposed cell membranes in the vertebrate brain. J Cell Biol 1969;40:648–677.
6. Brightman MW, Reese TS, Feder N. Assessment with the electronmicroscope of the permeability to peroxidase of cerebral endothelium and epithelium in mice and sharks. In: Crone C, Lassen NA, eds. Capillary permeability. New York: Academic Press, 1970:468–476.
7. Calas A, Bossler O, Arluison M, Bouchaud C. Serotonin as a neurohormone in circumventricular organs and supraependymal fibers. In: Scott DE, Kozlovsky GP, Wiendl A, eds. Brain-endocrine interaction. III. Neural hormones and reproduction. Basel: Karger, 1978:238–250.
8. Crone C. The permeability of capillaries in various organs as determined by use of the "indicator diffusion" method. Acta Physiol Scand 1963;58:292–305.
9. Cutler RWP, Lorenzo AV, Barlow CF. Changes in blood-brain permeability during pharmacologically induced convulsions. Prog Brain Res 1967;29:367–384.
10. Cutler RWP, Spertel RB. Cerebrospinal fluid: a selective review. Ann Neurol 1982;11:1–10.
11. Davson H. Physiology of the cerebrospinal fluid. Boston: Little, Brown and Company, 1967.
12. Davson H. The blood-brain barrier: review lecture. J Physiol (Lond) 1976;255:1–28.
13. Ehrlich P. Das sauerstoff-bedürfnis des organismus. Eine farbenalytische studie. Berlin: Herschwald, 1885:69–72.
14. Fenstermacher JD, Rall DP. Physiology and pharmacology of cerebrospinal fluid. In: Fenstermacher JD, Rall DP, eds. Pharmacology of the cerebral circulation. Vol. 1. Oxford: Pergamon Press, 1973:35–79.
15. Fishman RA. Cerebrospinal fluid in diseases of the nervous system. Philadelphia: W.B. Saunders, 1980.
16. Ford DH. Blood-brain barrier: a regulatory mechanism. Ann Rev Neurosci 1976;2:1–42.
17. Goldstein GW, Betz AL. The blood-brain barrier. SciAm 1986;255: 74–93.
18. Gomez DG, Chambers AA, DiBenedetto AT, Potts DG. The spinal cerebrospinal fluid absorptive pathways. Neuroradiology 1974a;8:61–66.
19. Gomez DG, Potts DG, Deonarine J. Arachnoid granulations of sheep: structural and ultrastructural changes with varying pressure differences. Arch Neurol 1974b;30: 169–175.
20. Hamilton WJ, Mossman, HW. Human embryology. Baltimore: Williams & Wilkins, 1972.
21. Jackson IMD. Neural peptides in the cerebrospinal fluid. Adv Biochem Psychopharmacol 1981;28:337–356.
22. Jayatilaka ADP. An electron microscopic study of sheep arachnoid granulations J Anat 1965;99: 635–649.
23. Kawano N, Endo M, Saito M, Yada K. Origin of the capsule of a chronic subdural hematoma—an electron microscopy study. No Shinkei Geka 1988;16:747–752.
24. Leusen I. Regulation of cerebrospinal fluid composition with reference to breathing. Physiol Rev 1972;52:1–56.
25. Livingston RB. Mechanics of cerebrospinal fluid. In: Ruch TC, Patton HD, eds. Physiology and biophysics. Ch. 47. Philadelphia: W.B. Saunders, 1964:935–940.
26. Merritt HH. A textbook of neurology. Philadelphia: Lea & Febiger, 1979.
27. Mestres P. Old and new concepts about circumventricular organs: an overview. Scan Electron Micros 1978;2:137–143.
28. Mettler FA. Neuroanatomy. 2d ed. St. Louis: C.V. Mosby, 1948.
29. Millen JW, Woollam DHM. Observations on the nature of the pia mater. Brain 1961;84:514–520.
30. Miner LC, Reed DJ. Composition of fluid obtained from choroid plexus tissue isolated in a chamber in situ. J Physiol (Lond) 1972;227:127–139.
31. Ommaya AK, Corrao P, Letcher FS. Head injury in the chimpanzee. I. Biodynamics of traumatic unconsciousness. J Neurosurg 1973;39: 152–166.
32. Pappas GD, Tennyson JM. An electron microscopic study of the passage of colloidal particles from the blood vessels of the ciliary processes and choroid plexus of the rabbit. J Cell Biol 1962;15:227–239.
33. Pardridge WM, Frank HJL, Cornford EM, Braun LD, Crane PD, Oldendorf WH. Neuropeptides and the blood brain barrier. Adv Biochem Psychopharmacol 1981;28:321–328.
34. Parent A. Anatomical organization of monoamine- and acetylcholinesterase-containing neuronal systems in the vertebrate hypothalamus. In: Morgane PJ, Panksepp J, eds. Handbook of the hypothalamus. Vol. 1. Anatomy of the hypothalamus. New York: Marcel Dekker, 1979:511–554.
35. Parent A, Descarries L, Beaudet A. Organization of ascending serotonin systems in the adult rat brain. A radioautographic study after intraventricular administration of [^{3}H]5-hydroxytryptamine. Neuroscience 1981;6:115–138.
36. Pollay M, Curl F. Secretion of cerebrospinal fluid by the ventricular ependyma of the rabbit. Am J Physiol 1967;213:1031–1038.
37. Rapoport SI. Blood-brain barrier in physiology and medicine. New York: Raven Press, 1976.
38. Reese TS, Karnovsky MJ. Fine structural localization of a blood-brain barrier to exogenous peroxidase. J Cell Biol 1967;34:207–217.
39. Richards JG, Lorez HP, Colombo VE, Guggenheim R, Kiss D, Wu JY. Demonstration of supra-ependymal 5-HT nerve fibres in human brain and their immunohistochemical identification in rat brain. J Physiol (Paris) 1981;77:219–224.
40. Sahar A. Choroidal orgin of cerebrospinal fluid. Isr J Med Sci 1972;8:594–596.
41. Sato O, Bering EA. Extra-ventricular formation of cerebrospinal fluid. Brain Nerve (Tokyo) 1967;19: 883–885.
42. Schachenmayr W, Friede R. The origin of subdural membranes: I. Fine structure of the dura-arachnoid interface in man. Amer J Pathol 1978;92:53–68.
43. Scott DE, Krobisch-Dudley G. Ultrastructural analysis of the mammalian median eminence. In: Knigge KM, Scott DE, Kobayashi H, Ishii S, eds. Brain-endocrine interaction II. Basel: Karger, 1975:29–39.
44. Selzer ME, Myers RE, Holstein SB. Maturational changes in brain water and electrolytes in rhesus monkey with some implications for electrogenesis. Brain Res 1972;45:193–204.
45. Spector R, Johanson CE. The mammalian choroid plexus. Sci Am 1989;261:68–74.
46. Summy-Long JY, Keil LC, Severs WB. Identification of vasopressin in the subfornical organ region: effects of dehydration. Brain Res 1978; 140:241–250.
47. Taverras JM, Wood EH. Diagnostic neuroradiology. Baltimore: Williams & Wilkins, 1976.
48. Vates TS, Bonting SL, Oppelt WW. Na-K activated adenosine triphosphatase formation of cerebrospinal fluid in the cat. Am J Physiol 1964;206:1165–1172.
49. Weindl A, Sofroniew MV. Relation of neuropeptides to mammalian circumventricular organs. In: Martin JB, Reichlin S, Bick KL, eds. Advances in biochemical psychopharmacology. Vol 28. Neurosecretion and brain peptides. New York: Raven Press, 1981;303–320.
50. Welch K. Secretion of cerebrospinal fluid by choroid plexus of the rabit. Am J Physiol 1963;205:617–624.
51. Welch K, Friedman J. The cerebrospinal fluid valves. Brain 1960;83:454–469.
52. Westergaard E, Brightman, MW. Transport of proteins across normal cerebral arterioles. J Comp Neurol 1973;152:17–44.

2
Regional Anatomy of the Brain

SUBDIVISIONS OF THE BRAIN

The nervous system is composed of two parts, the central nervous system (CNS) and the peripheral nervous system (PNS). The *peripheral nervous system* consists of the spinal and cranial nerves, while the *central nervous system* is represented by the brain and spinal cord. The autonomic nervous system, often considered as a separate functional entity, is part central and part peripheral.

The human brain is a relatively small structure weighing about 1400 g and constituting about 2% of total body weight. The brain is regarded as the organ solely concerned with thought, memory, and consciousness, but these are only a few of its complex and varied functions. All information we have concerning the world about us is conveyed centrally to the brain by an elaborate sensory system. Receptors of many kinds act as transducers which change physical and chemical stimuli in our environment into nerve impulses which the brain can read and give meaning to. The ability to discriminate between stimuli of the same and different types forms one of the bases for learning. Attention, consciousness, emotional experience, and sleep are all central neural functions. Such higher functions as memory, imagination, thought, and creative ability are poorly understood, but must be related to complex neuronal activity. The brain is also concerned with all kinds of motor activity, with the regulation of visceral, endocrine and somatic functions, and with the receptive and expressive use of symbols and signs that underlie communication. While the gross features of the human brain are not especially impressive, its versatility, potential capabilities, efficiency, and self-programming nature render it unique among all organs of the human body.

The brain consists of four subdivisions, the cerebral hemispheres, the brainstem, the diencephalon, and the cerebellum (Figs. 2.1–2.4, 2.9, 2.25, 2.27, and 2.30). The massive paired *cerebral hemispheres* are derived from the *telencephalon*, the most rostral cerebral vesicle. The brainstem proper consists of three distinct parts: (a) the *mesencephalon*, (b) the *metencephalon*, and (c) the *myelencephalon* (Fig. 2.1). A fourth subdivision, the *diencephalon*, which is considered by some authors as the most rostral segment of the brainstem (Figs. 2.25 and 2.26), acts as an anatomic and functional interface between the brainstem and the forebrain (i.e., telencephalon). The mesencephalon, or midbrain, is the shortest division of the brainstem. The metencephalon (pons) and myelencephalon (medulla) together constitute the *rhombencephalon* or hindbrain. The cerebellum is a derivative of the metencephalon that develops from ectodermal thickening about the rostral borders of the fourth ventricle, known as the rhombic lip (Figs. 2.27, 2.30, 2.31, 3.11**A**, and 3.14).

CEREBRAL HEMISPHERES

The paired cerebral hemispheres consist of a highly convoluted gray cortex (pallium or mantle), an underlying white matter of considerable magnitude and a collection of deeply located neuronal masses, known as the basal ganglia (7,13) (Figs. 2.4–2.7, 2.9, and 2.10). The cerebral hemispheres are partially separated from each other by the *longitudinal fissure*. This fissure *in situ* contains the falx cerebri (Fig. 1.2). In frontal and occipital regions, the separation of the hemispheres is complete, but in the central region the fissure extends only to fibers of the broad interhemispheric commissure, the corpus callosum (Figs. 2.4–2.7, 2.9, and 2.10). Each cerebral hemisphere is subdivided into lobes, most of which are named after the bones of the skull overlying them (Figs. 2.2–2.4). Although the boundaries of the various lobes as seen in the gross specimen are somewhat arbitrary, multiple cortical areas in each lobe are histologically distinctive. The gray cellular mantle of

MAJOR SUBDIVISIONS OF THE CENTRAL NERVOUS SYSTEM

MAJOR COMPONENTS		EMBRYONIC SUBDIVISIONS		ADULT DERIVATIVES	CAVITIES
Brain (Encephalon)	Cerebrum	Prosencephalon (Forebrain)	Telencephalon (Endbrain)	Cerebral hemispheres (Cortex, white matter, and basal ganglia)	Lateral ventricles
			Diencephalon (Interbrain)	Diencephalon (Thalamus, subthalamus and hypothalamus)	Third ventricle
	Brainstem	Rhombencephalon (Hindbrain)	Mesencephalon (Midbrain)	Midbrain (tectum, tegmentum and crura cerebri)	Cerebral aqueduct (of Sylvius)
			Metencephalon (Afterbrain)	Pons and Cerebellum	Fourth ventricle (Rhomboid fossa)
			Myelencephalon (Medula)	Medulla oblongata	
Spinal cord (Medulla spinalis)		Neural tube (Caudal portion)		Spinal cord	Central canal

Figure 2.1. Principal subdivisions of the human central nervous system, their embryonic origin and major derivatives in adults, as well as the corresponding ventricular compartments.

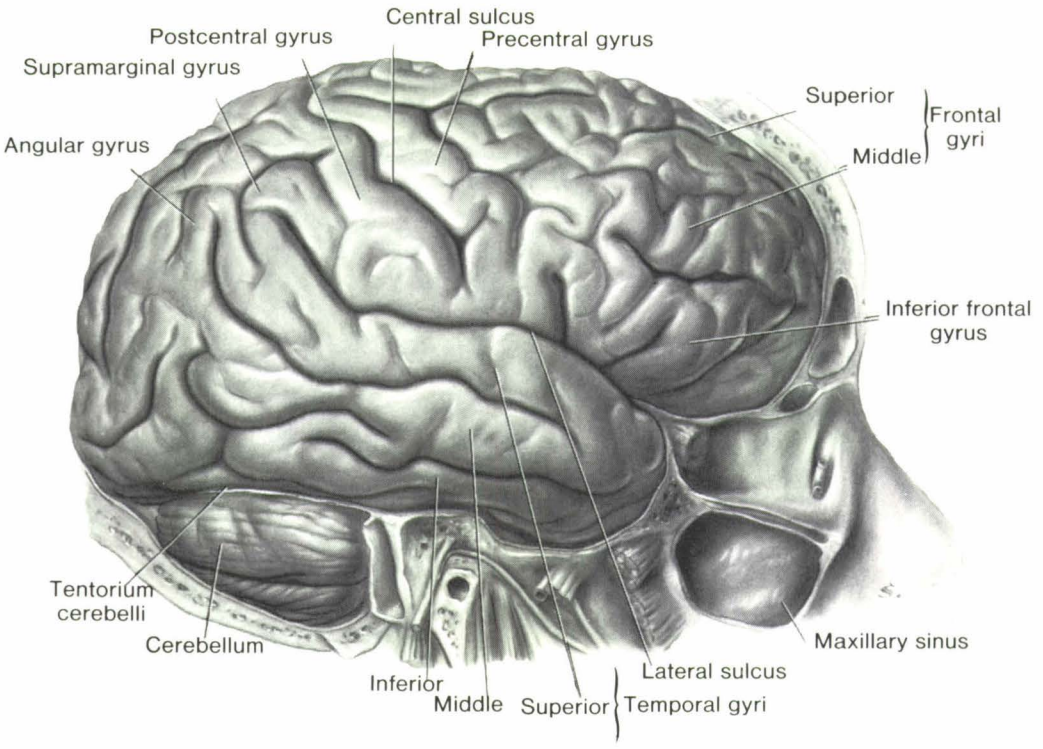


Figure 2.2. Lateral view of the brain exposed in the skull to show topographic relationships.



1. Sup. frontal gyrus
2. Middle frontal gyrus
3. Inf. frontal gyrus
4. Precentral gyrus
5. Postcentral gyrus
6. Supramarg. gyrus
7. Angular gyrus
8. Lateral occipital gyrus
9. Sup. temporal gyrus
10. Middle temporal gyrus
11. Inf. temporal gyrus
12. Cerebellum

Figure 2.3. Lateral surface of the brain.

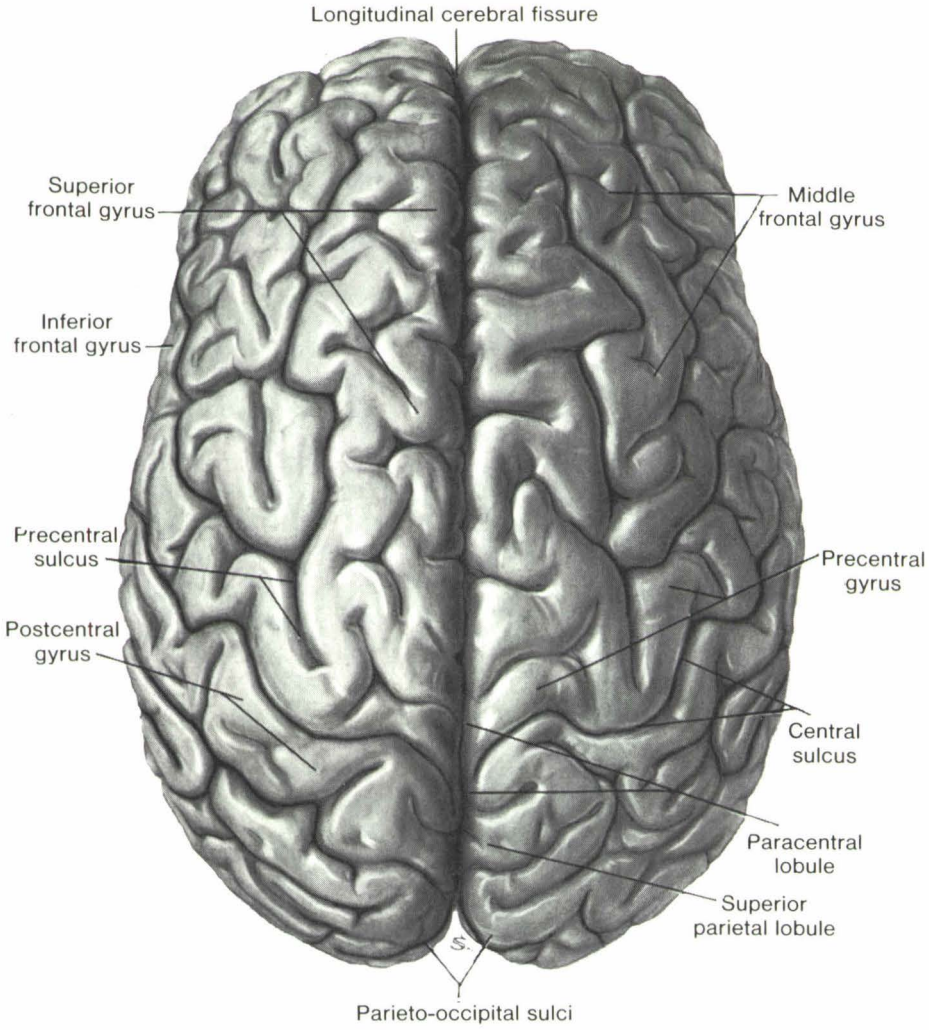


Figure 2.4. Superior view of the brain indicating the main sulci and gyri.

the cerebral cortex in humans is highly convoluted. The crest of a single convolution is referred to as a *gyrus*. *Sulci* (fissures) separate the various gyri, producing a pattern with more or less constant features. On the basis of the more constant sulci and gyri, the cerebrum is divided into six so-called lobes: (a) frontal, (b) temporal, (c) parietal, (d) occipital, (e) insular, and (f) limbic. Neither the insula nor the limbic lobe is a true lobe. The insula is a cortical area buried in the depths of the lateral sulcus (Figs. 2.8, 2.11, and 2.14). The limbic lobe is a highly heterogeneous entity on the medial aspect of the hemisphere consisting of portions of the frontal, parietal, occipital, and temporal lobes which surround the upper part of the brainstem (Fig. 18.1).

Lateral Surface

The two most important sulci for topographic orientation on the lateral convexity of the hemisphere are the lateral and central sulci (Figs. 2.2 and 2.3). The *lateral* sulcus begins inferiorly in the Sylvian fossa and extends posteriorly, separating the frontal and temporal lobes. Caudally this sulcus separates portions of the parietal and temporal lobes. The terminal ascending ramus of the sulcus extends into the inferior part of the parietal lobe. Portions of the frontal, parietal, and temporal lobes, adjacent to the lateral sulcus, which overlie the insular region, are referred to as the *opercular portions* of these lobes (Fig. 2.8). The *central sulcus* is a promi-

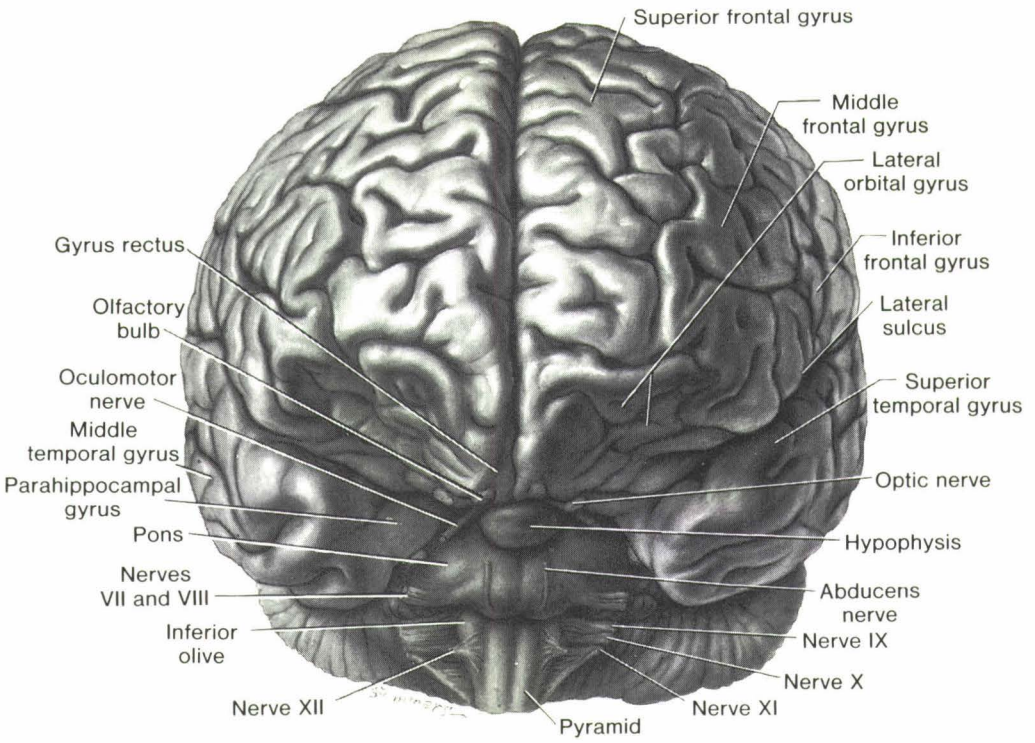


Figure 2.5. Frontal view of the rostral aspect of the brain.

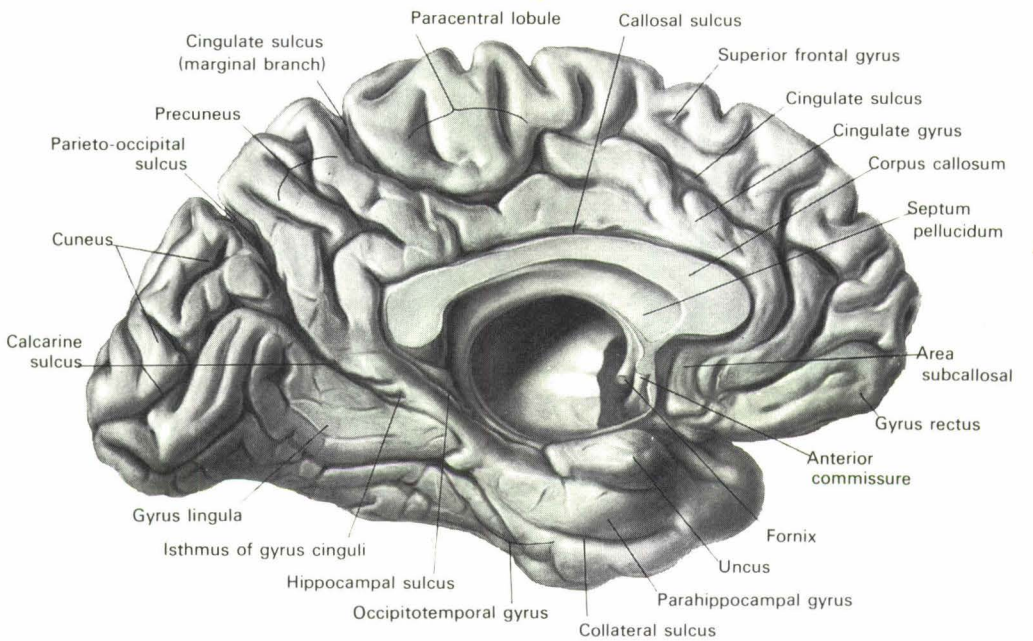


Figure 2.6. Medial surface of the cerebral hemisphere with diencephalic structures removed.

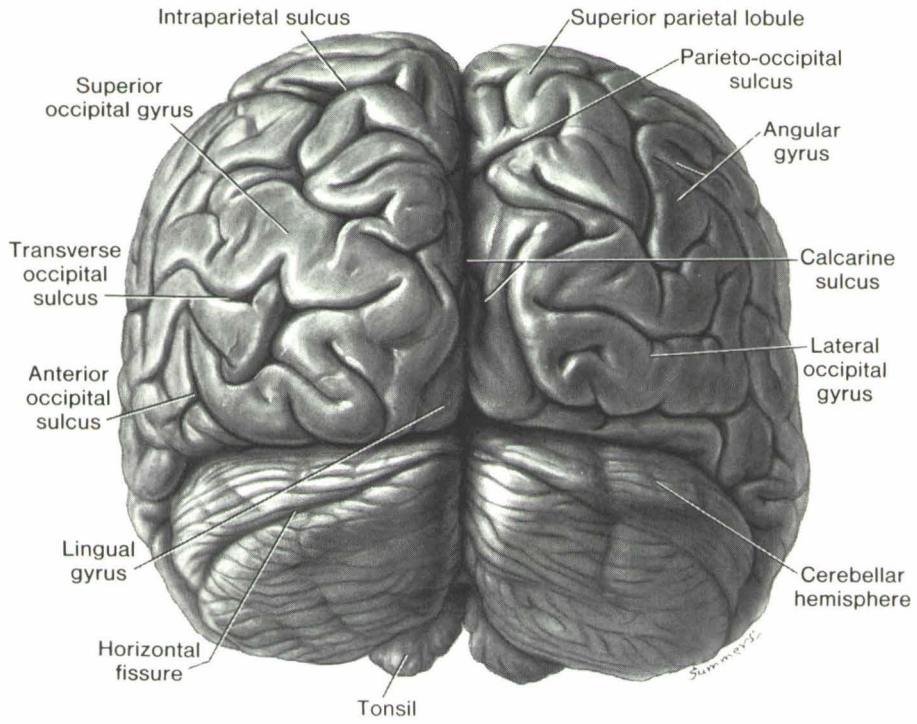


Figure 2.7. Posterior view of the cerebral hemispheres and cerebellum.

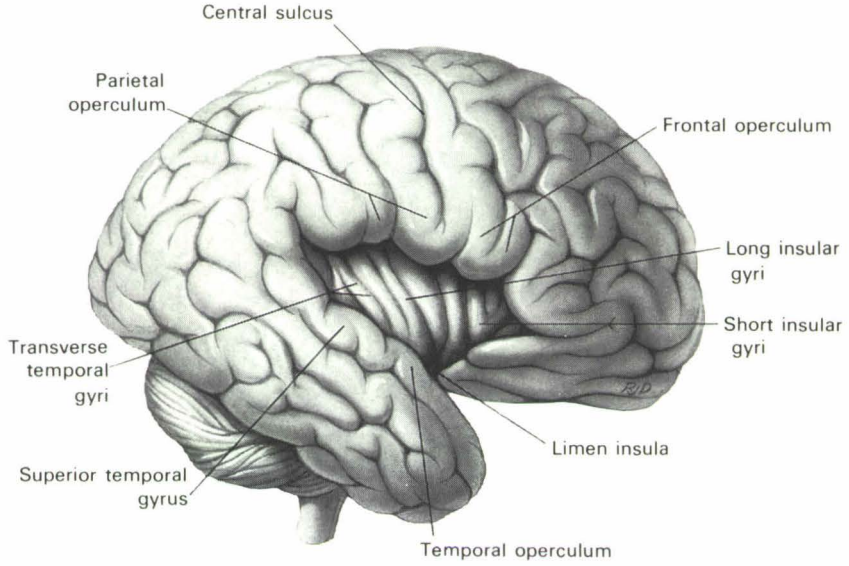


Figure 2.8. Right cerebral hemisphere with the banks of the lateral sulcus drawn apart to expose the insula.

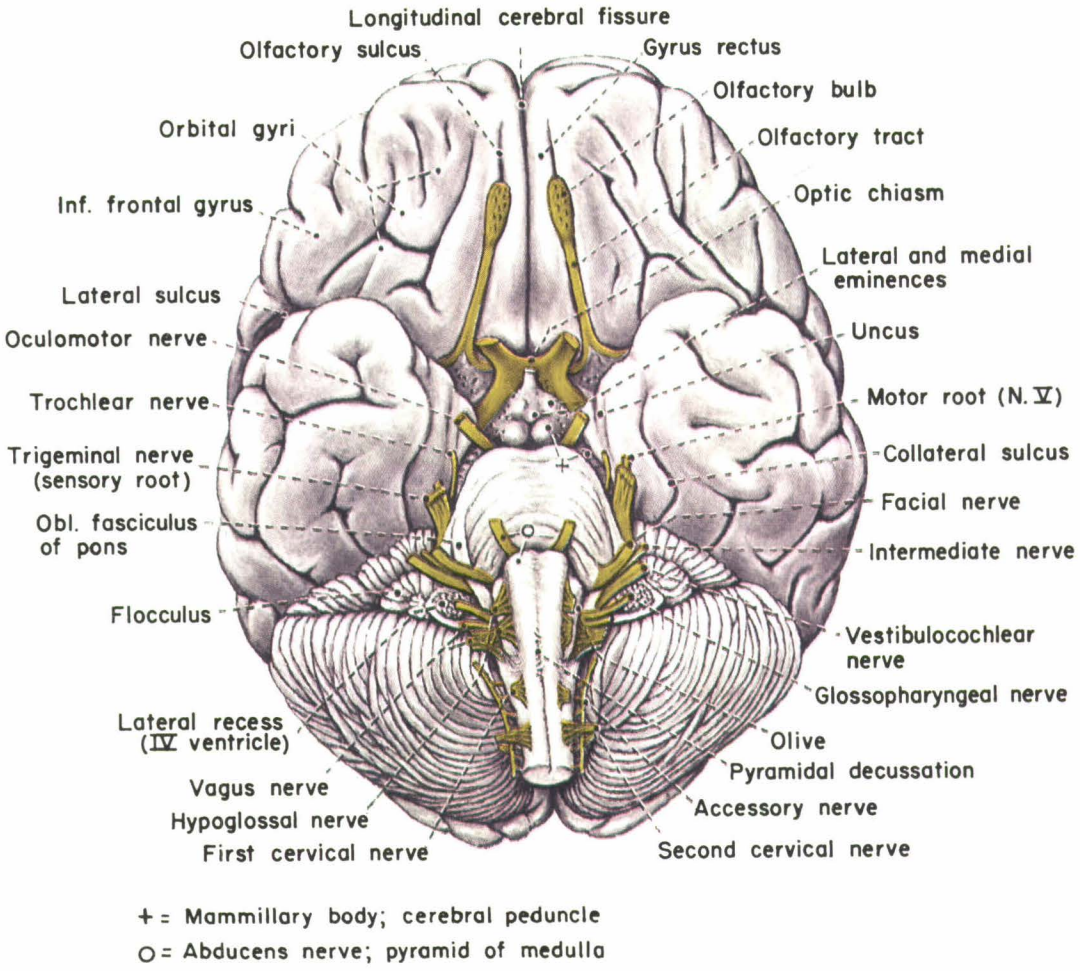


Figure 2.9. Inferior surface of the brain showing the cranial nerves.

nent sulcus running from the superior margin of the hemisphere downward and forward toward the lateral sulcus (Figs. 2.2 and 2.3). Usually, this sulcus is bowed in two locations, and superiorly it does not extend onto the medial surface of the hemisphere for any distance. The depths of the sulcus constitute the boundary between the frontal and parietal lobes.

FRONTAL LOBE

It is the largest of all the lobes of the brain, comprising about one-third of the hemispheric surface. Its large size represents one of the most characteristic morphologic features of the human brain. The frontal lobe extends rostrally from the central sulcus to the frontal pole; its inferior lateral boundary is the lateral sulcus. The convexity of the frontal lobe has four principal convolutions: (a) a *precentral* gyrus that parallels the central sulcus, and (b) three horizontally oriented convolutions, the *superior, middle,* and *inferior frontal gyri* (Figs. 2.2 and 2.3). The anterior boundary of the precentral gyrus is the *precentral sulcus.* The precentral gyrus and the anterior bank of the central sulcus comprise the *primary motor area,* where all parts of the body are represented in a distorted but topographic manner (Fig. 20.18). Regions of the frontal lobe rostral to the primary motor area are referred to as *premotor* and *prefrontal* areas. The broad middle frontal gyrus often is divided by a shallow horizontal sulcus into upper and lower tiers (Figs. 2.2 and 2.3). The inferior frontal gyrus is divided by anterior and horizontal rami (limbs) of the lateral sulcus into three parts: (a) *pars orbitalis,* (b) *pars triangularis,* and (c) *pars opercularis.* The pars triangularis

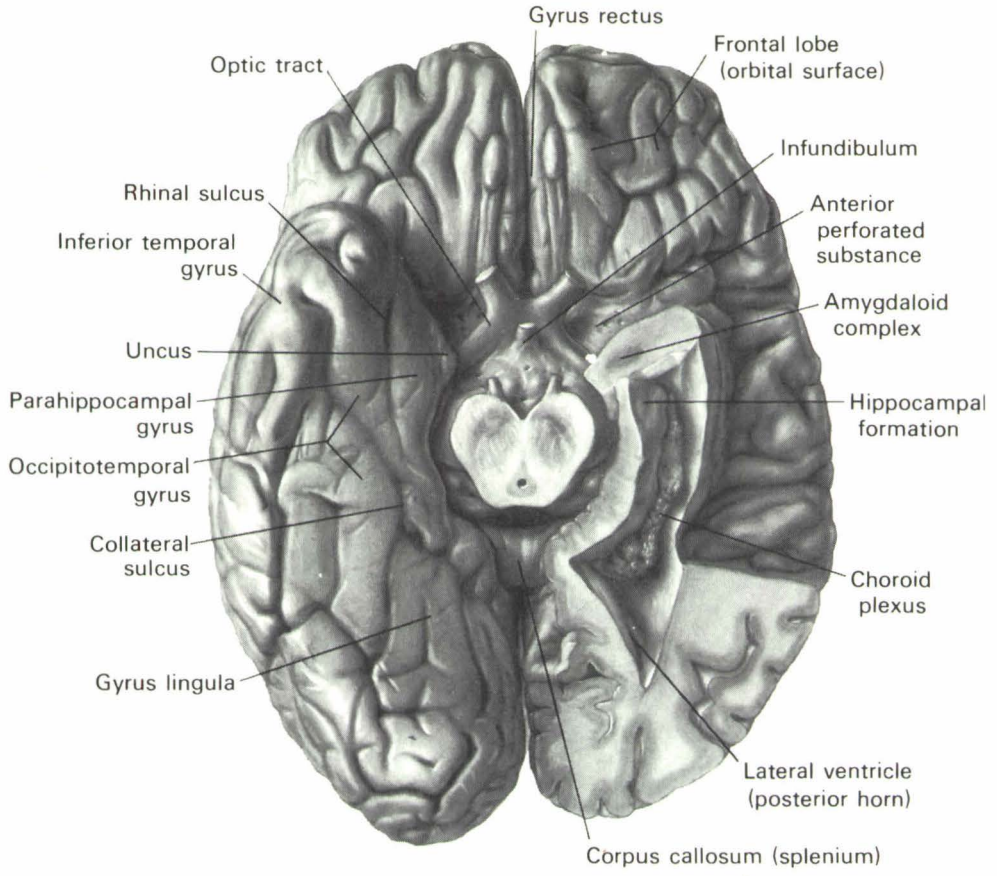


Figure 2.10. Inferior surface of the brain following transection of the midbrain. The inferior and posterior horns of the left lateral ventricle have been opened and portions of the temporal and occipital lobes have been removed.

and opercularis in the dominant hemisphere (usually the left in right-handed individuals) are referred to as *Broca's speech area*, a region concerned with the motor mechanisms of speech formulation. The inferior surface of the frontal lobe lies on the superior surface of the orbital part of the frontal bone and is concave (Figs. 2.4, 2.9, and 2.10). The olfactory bulb and tract lie in a sulcus near the medial margin of the hemisphere known as the *olfactory sulcus*. The *gyrus rectus* lies medial to the olfactory sulcus and the medial orbital gyrus is located lateral to this sulcus. The orbital gyri occupy the concave lateral area.

PARIETAL LOBE

The boundaries of this lobe are not precise, except for its anterior border on the lateral convexity formed by the central sulcus and its posterior border on the medial aspect of the hemisphere *(parieto-occipital sulcus)* (Figs. 2.3 and 2.6). On the convexity of the hemisphere, the posterior boundary is arbitrarily considered as an imaginary line projected from the superior limit of the parieto-occipital sulcus to the small indentation on the inferior surface known as the *preoccipital notch* (Fig. 2.3). Three parts of the parietal lobe are distinguished: (a) a *postcentral gyrus* running parallel and caudal to the central sulcus, (b) a *superior parietal lobule*, and (c) an *inferior parietal lobule*. The postcentral gyrus, usually not continuous but broken into superior and inferior segments, lies between the central and postcentral sulci. The posterior bank of the central sulcus and the postcentral gyrus constitute the *primary somesthetic area*, the cortical region where impulses concerned with tactile and kinesthetic sense from superficial and deep receptors converge and are somatotopically represented. The majority of cortical neurons in the postcentral gyrus are concerned with fixed receptive fields on the con-

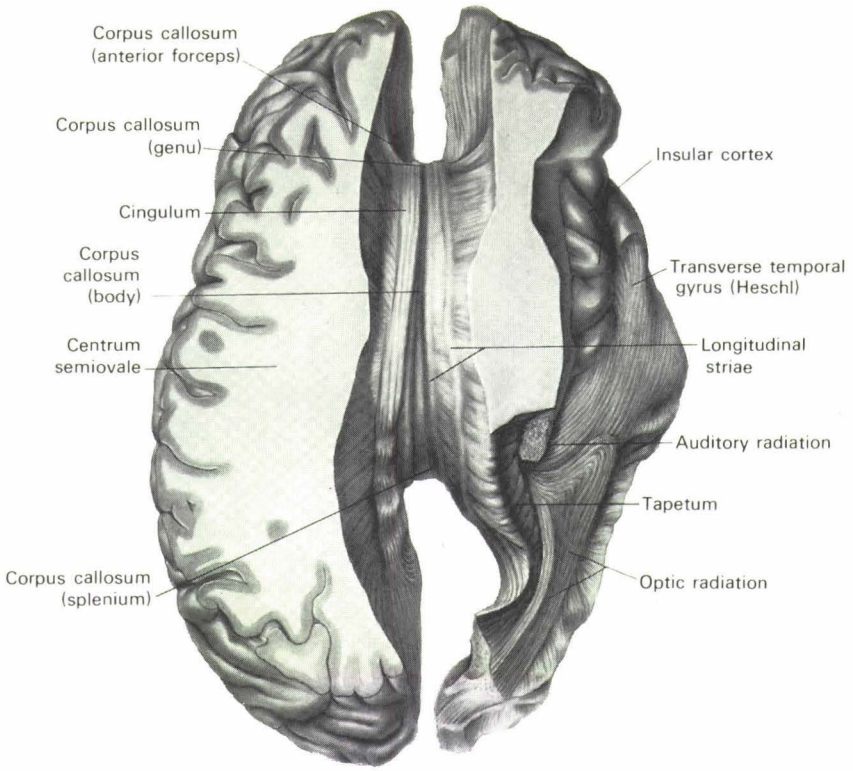


Figure 2.11. Dissection of the superior surface of the hemispheres exposing the corpus callosum, cingulum, longitudinal striae, and the optic and auditory radiations.

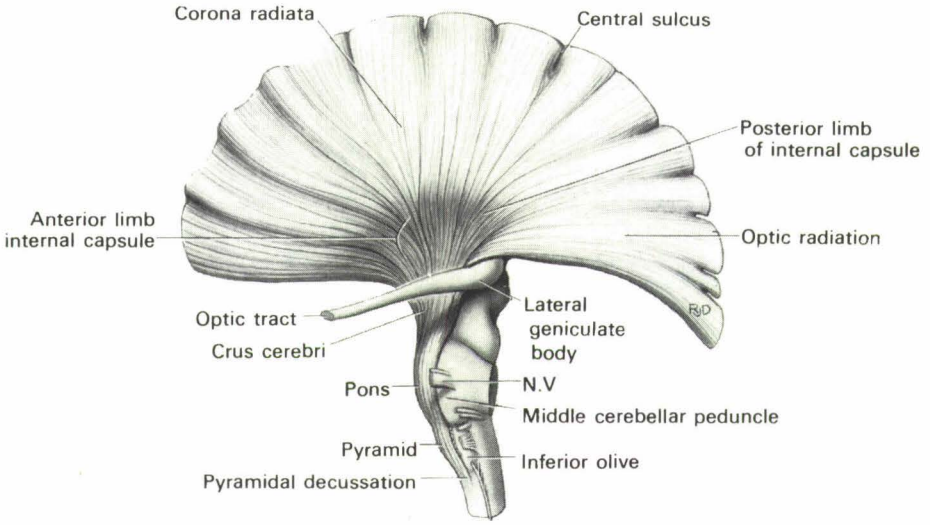


Figure 2.12. Dissection demonstrating the continuity and relationships of the corona radiata, the internal capsule, the crus cerebri, and the medullary pyramid.

tralateral side of the body that are place-specific, modality-specific, and related to discriminative aspects of sensation. The *intraparietal sulcus*, a horizontally oriented sulcus, divides portions of the parietal lobe caudal to the postcentral gyrus into superior and inferior parietal lobules (Fig. 2.3). The *inferior parietal lobule* consists of two gyri, the *supramarginal gyrus*, arching along both banks of an ascending ramus of the lateral sulcus, and the *angular gyrus*, which surrounds the ascending terminal part of the superior temporal sulcus (Figs. 2.2 and 2.3). The inferior parietal lobule represents a cortical association area where various multisensory perceptions of a higher order from adjacent parietal temporal and occipital regions overlap. This region is especially concerned with mnemonic constellations that form the basis for understanding and interpreting sensory signals. This is one region of the cortex where different disturbances occur as a consequence of lesions in the dominant and nondominant hemisphere.

TEMPORAL LOBE

This large lobe lies ventral to the lateral sulcus and on its lateral surface displays three obliquely oriented convolutions, the *superior, middle,* and *inferior temporal gyri* (Figs. 2.2 and 2.3). The *superior temporal sulcus* courses parallel to the lateral sulcus and its ascending ramus terminates in the angular gyrus. On the inner bank of the lateral sulcus, several short, oblique convolutions form the transverse gyri of Heschl. These gyri constitute the primary *auditory cortex* in humans (Figs. 2.8 and 2.11). The inferior surface of the temporal lobe, which lies in the middle fossa of the skull, reveals part of the *inferior temporal gyrus,* the broad *occipitotemporal gyrus,* and the *parahippocampal gyrus* (Figs. 2.9 and 2.10). The parahippocampal gyrus and its most medial protrusion, the *uncus,* are separated from the occipitotemporal gyrus by the collateral sulcus (Fig. 2.6). The rostral part of the parahippocampal gyrus, the uncus, and the lateral olfactory stria constitute the pyriform (pear-shaped) lobe, parts of which constitute the *primary olfactory cortex* (Figs. 2.6, 2.7, and 2.10).

OCCIPITAL LOBE

This small lobe rests on the tentorium cerebelli (Figs. 2.2 and 2.7). The rostral boundary of this lobe is the parieto-occipital sulcus on the medial aspect of the hemisphere (Fig. 2.6). The lateral surface of the occipital lobe is poorly delimited from the parietal lobe and is composed of a number of irregular *lateral occipital gyri* which are separated into groups by the *lateral occipital sulcus.* (Figs. 2.3 and 2.6). On the medial aspect of the hemisphere, the occipital lobe is divided by the *calcarine sulcus* into the *cuneus* and the *lingual gyrus* (Figs. 2.6 and 2.7). The calcarine sulcus joints the parieto-occipital sulcus rostrally in a Y-shaped formation. The cortex on both banks of the calcarine sulcus represents the *primary visual cortex* (i.e, the striate cortex). The visual cortex in each hemisphere receives impulses from the temporal half of the ipsilateral retina and the nasal half of the contralateral retina, and is concerned with perception from the contralateral half of the visual field.

INSULA

The insula is a cortical area that lies buried in the depths of the lateral sulcus; it can be seen only when the temporal and frontal lobes are separated. This "lobe" is, in fact, a triangular cortical area, the apex of which is directed forward and downward to open into the lateral fossa (Figs. 2.8, 2.11, and 2.14). The surface is covered by the *gyri breves* and *longus* (short and long gyri) which course nearly parallel to the lateral sulcus. The relationships of this region can be appreciated in transverse and horizontal sections of the hemisphere (Figs. 2.13–2.16). The opening leading to the insular region is called the *limen insula.* The temporal, frontal, and parietal opercular regions cover the insula.

Medial Surface

Convolutions on the medial surface can be studied in a hemisected brain. These convolutions are somewhat flatter than those on the convexity. The most prominent structure on the medial surface is the massive interhemispheric commissure, the *corpus callosum* (Figs. 2.6, 2.11, 2.20, 2.22, and 2.28). This structure, composed of millions of myelinated fibers, reciprocally interconnects broad regions of the two hemispheres. Different parts of the corpus callosum are referred to as the *rostrum, genu, body,* and *splenium* (Figs. 2.11 and 2.20). Fibers in this structure spread out as a mass of radiations to nearly all parts of the

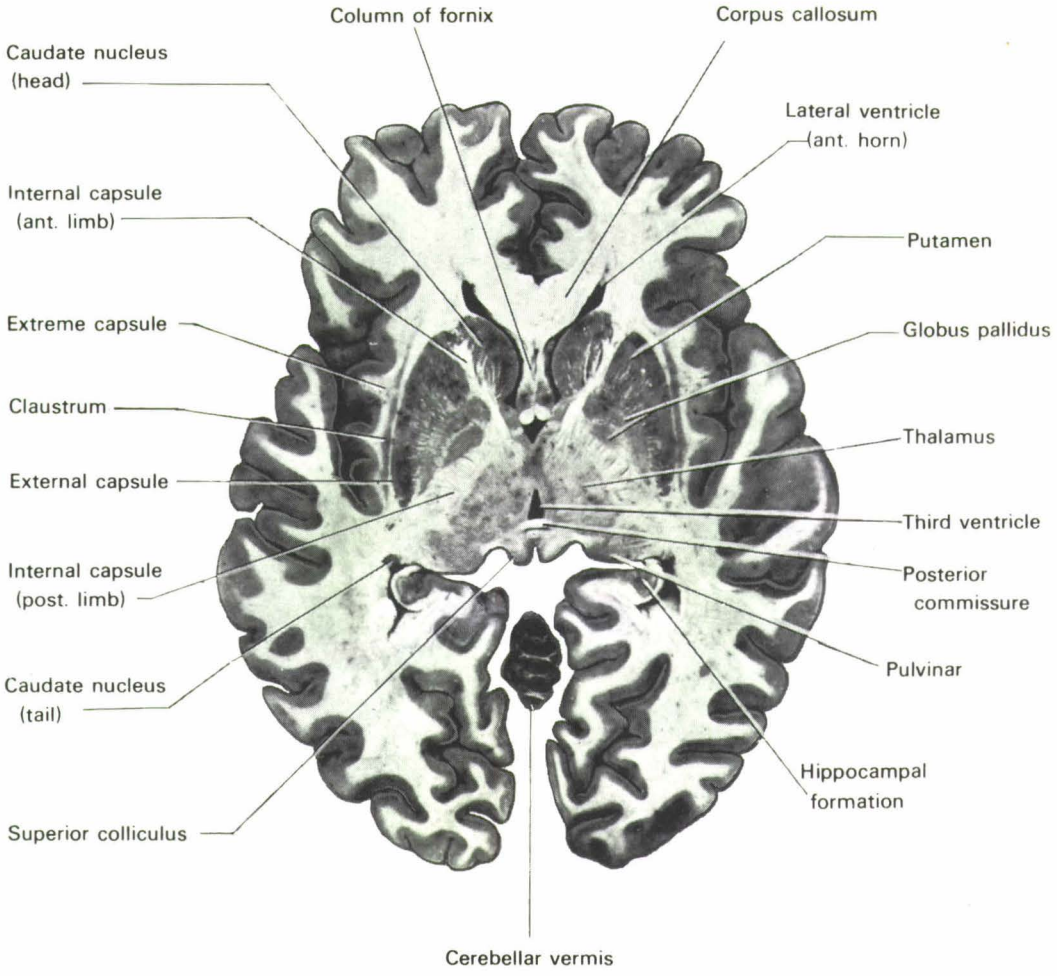


Figure 2.13. Horizontal section through the cerebral hemispheres showing relationships of internal structures to the internal capsule.

cortex. Callosal fibers, projecting to parts of the frontal and occipital lobes, form the so-called *anterior* and *posterior forceps*, which are best appreciated in horizontal sections of the brain (Fig. 2.11). The corpus callosum forms the floor of the longitudinal fissure, as well as a good part of the roof of the lateral ventricle. It plays an important role in interhemispheric transfer of learned discriminations, sensory experience, and memory. Although surgical section of the corpus callosum in humans produces little disturbance of ordinary behavior, temperament, or intellect, information received exclusively by the nondominant hemisphere (usually the right) cannot be communicated in speech or writing (4, 5). In these same patients there was no impairment of speech or writing when information was processed in the dominant hemisphere (left). These studies conclude that linguistic expression and analytic functions are organized almost exclusively in the dominant hemisphere. The nondominant hemisphere is concerned with spatial concepts, recognition of faces, and some musical ability. The *callosal sulcus* separates the corpus callosum from the cingulate gyrus. Posteriorly, this sulcus curves around the splenium to be continued into the temporal lobe as the *hippocampal sulcus* (Fig. 2.6). The *cingulate gyrus*, dorsal to the callosal sulcus, encircles the corpus callosum and consists of two tiers. The *cingulate sulcus*, dorsal to the cingulate gyrus, runs parallel to the callosal sulcus, but near the splenium turns dorsally as the *marginal sulcus*. The anterior portion of cortex dorsal to the cingulate gyrus is the medial surface of the superior frontal gyrus. The *paracentral lobule* is formed by the precentral and postcentral gyri and is notched in its middle portion by the central

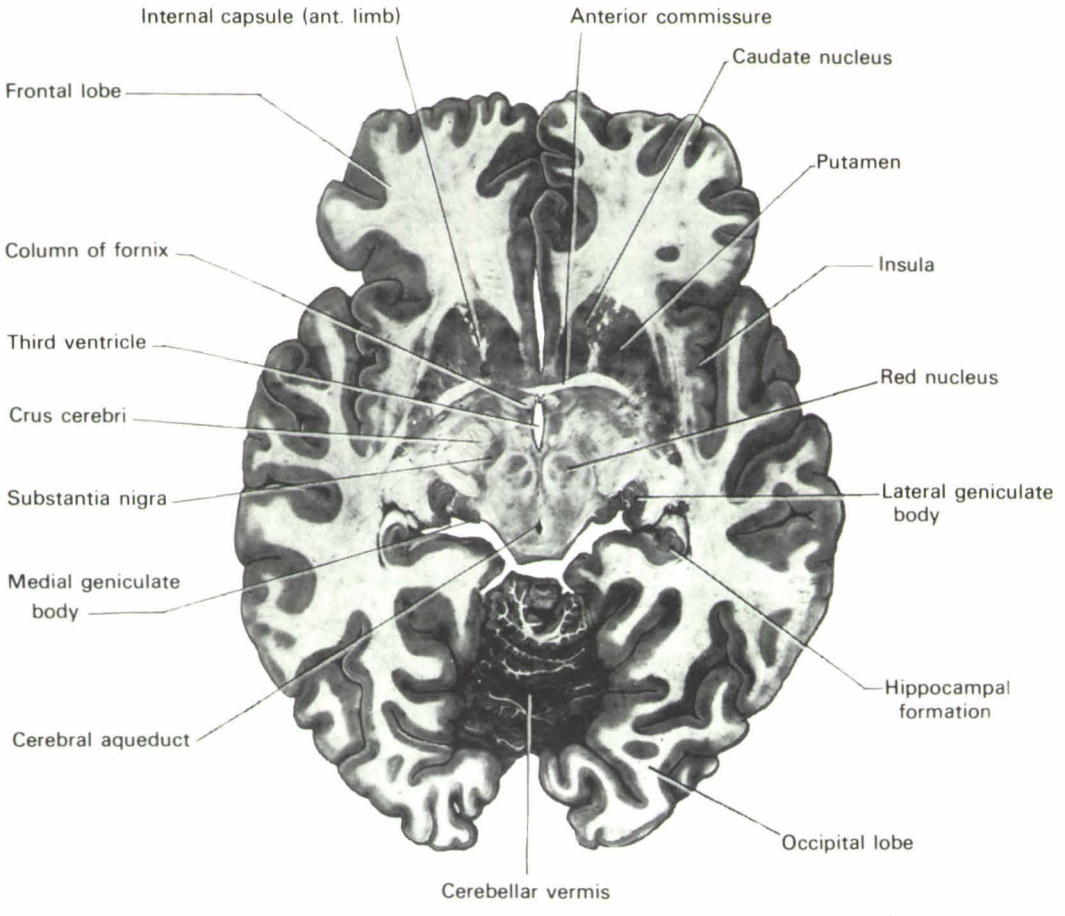


Figure 2.14. Horizontal section through the cerebral hemispheres passing through the anterior commissure and the crus cerebri.

sulcus (Fig. 2.6). The *paracentral sulcus* forms the rostral border of this lobule, while the *marginal sulcus* forms the caudal border. The portion of the parietal lobe caudal to the paracentral lobule is known as the *precuneus*. This lobule lies immediately rostral to the parieto-occipital sulcus previously discussed.

LIMBIC LOBE

The limbic lobe consists of large cortical convolutions on the medial aspect of the hemisphere which surround the rostral part of the brainstem and the interhemispheric commissure (Fig. 18.1). As originally defined by the French anatomist Paul Broca in 1878 (1), the limbic lobe includes the *subcallosal*, *cingulate*, and *parahippocampal gyri*, as well as primitive cortical derivatives, the *hippocampal formation* and the *dentate gyrus*, which in the course of development have become invaginated within the temporal lobe (Fig. 2.10). The parahippocampal gyrus is directly continuous with the cingulate gyrus by a narrow strip of cortex, posterior and inferior to the splenium, known as the *isthmus of the cingulate gyrus* (Fig. 2.6). The parahippocampal gyrus, the most medial convolution of the temporal lobe, is bounded laterally by the *rhinal* and *collateral sulci* and superiorly and medially by the *hippocampal sulcus* (Figs. 2.9 and 2.10). Rostrally, the parahippocampal gyrus hooks around the hippocampal sulcus to form a medially protruding convolution, the *uncus*. The proximity of the uncus to the cerebral peduncle should be noted. There are differences of opinion concerning what should be lumped together as the so-called "limbic lobe" (2). While all of these structures appear early in phylogenesis, physiologic evidence suggests that wide functional differences exist between various components and separate functions are expressed by distinctive neural mechanisms.

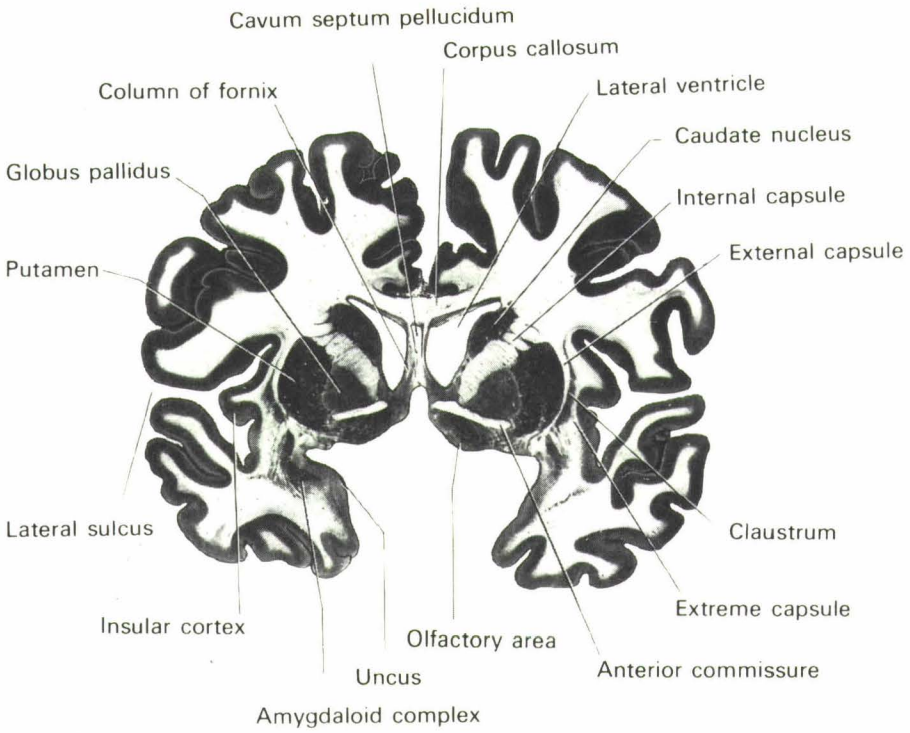


Figure 2.15. Frontal section of the brain passing through the columns of the fornix and the anterior commissure.

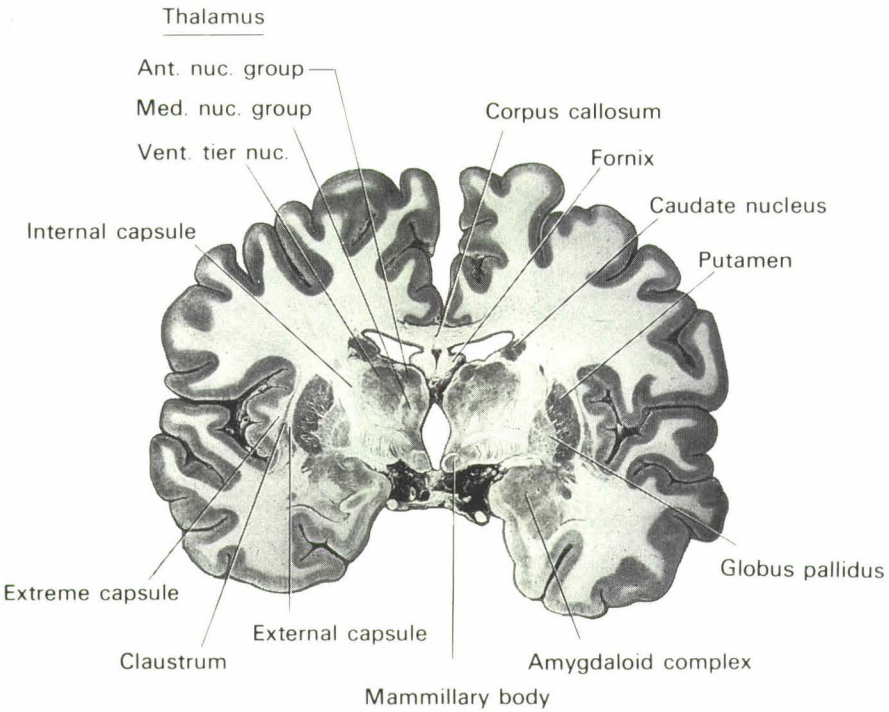


Figure 2.16. Frontal section of the brain at the level of the mammillary bodies. In this section, the main nuclear groups of the thalamus are identified and portions of all components of the basal ganglia are present. The amygdaloid nuclear complex lies in the temporal lobe internal to the uncus and ventral to the lentiform nucleus.

Inferior Surface

The inferior surface of the hemisphere consists of two parts: (a) a larger posterior portion, representing the inferior surfaces of the temporal and occipital lobes, and (b) the orbital surface of the frontal lobe (Figs. 2.5, 2.9, and 2.10). The inferior surface of the occipital lobe and the posterior part of the temporal lobe lie on the tentorium cerebelli (Figs. 1.2 and 2.2), while rostral parts of the temporal lobe lie in the middle cranial fossa. Gyri present in this posterior part include (a) the lingual gyrus, (b) the extensive occipitotemporal gyrus, and (c) the parahippocampal gyrus and uncus (Fig. 2.10). Part of the inferior temporal gyrus may be seen lateral to the occipitotemporal gyrus. A small part of the isthmus lies medially posterior to the splenium of the corpus callosum (Fig. 2.6). The orbital surface of the frontal lobe has a deep, straight sulcus medially, the olfactory sulcus, which contains both the olfactory bulb and tract (Figs. 2.5, 2.9, and 2.10). The *gyrus rectus* lies along the ventromedial margin of the hemisphere medial to the olfactory sulcus. The region lateral to the olfactory sulcus contains the orbital gyri whose convolutional patterns are variable (Figs. 2.5 and 2.10). Posteriorly, the olfactory tract divides into *medial* and *lateral olfactory striae* (Figs. 2.9 and 2.10). Caudal to this is the olfactory trigone and the *anterior perforated substance*, a region studded with small openings through which numerous small blood vessels pass to deep regions (Figs. 2.9, 2.10, 2.24, and 4.11).

White Matter

The massive white matter of the cerebral hemisphere forms the medullary core of the cortical convolutions and contains basically three types of fibers in prodigious quantity. Fibers within the white matter are classified as (a) *projection fibers* that convey impulses either from the cortex to distant loci, or from distant loci to the cortex, (b) *association fibers* that interconnect various cortical regions of the same hemisphere, and (c) *commissural fibers* that interconnect corresponding cortical regions of the two hemispheres. The white matter extends from the cortex to the basal ganglia and the ventricular system. The common central mass of the white matter, containing commissural, association, and projection fibers, has an oval appearance in horizontal sections of the brain and is termed the *semioval center* (or centrum semiovale) (Fig. 2.11).

PROJECTION FIBERS

Afferent and efferent fibers conveying impulses to and from the entire cerebral cortex enter the white matter and are arranged as radiating bundles that converge toward the brainstem (Figs. 2.12 and 2.19). These radiating projection fibers are known as the *corona radiata*. Near the upper part of the brainstem these fibers form a compact band known as the *internal capsule*, which is flanked medially and laterally by nuclear masses (Figs. 2.13, 2.15, 2.16, and 2.19). Three distinct parts of the internal capsule are evident in horizontal sections of the hemispheres: (a) an anterior limb, (b) a posterior limb, and (c) a genu (Fig. 2.13). The *anterior limb* partially separates two of the largest components of the basal ganglia, the caudate nucleus, and the putamen (Figs. 2.13, 2.14, and 2.15). Fibers in the anterior limb of the internal capsule are directed horizontally, obliquely, laterally, and upwards toward the frontal lobe, and in horizontal sections of the hemisphere appear to be cut in the longitudinal axis of the fiber bundles (Figs. 2.12, 2.13, 2.14, and 2.19). In horizontal sections, the anterior and posterior limbs of the internal capsule meet at an obtuse angle with the apex directed medially. The larger and longer *posterior limb* of the internal capsule is flanked medially by the diencephalon and laterally by a part of the basal ganglia known as the lentiform nucleus (Figs. 2.13, 2.16, and 2.19). The region of junction between the anterior and posterior limbs of the internal capsule is referred to as the *genu*. Fibers in the posterior limb of the internal capsule course in nearly a vertical plane toward the brainstem, and in horizontal sections fibers appear to be cut transversely (Fig. 2.13). The most posterior component of the posterior limb of the internal capsule contains fibers, radiating toward the calcarine sulcus, known as the *optic radiation* (Figs. 2.11, 2.12, 2.19, and 2.36). Afferent fibers in the internal capsule arise mainly from the thalamus and project to nearly all regions of the cortex; these fibers are referred to as *thalamocortical radiations* (Fig. 2.19). Efferent fibers in the internal capsule arise from cells in various regions of the cerebral cortex and project to specific nuclear masses in the brainstem and spinal cord. These fibers are categorized as corticothalamic, corticopontine, corticobul-

bar, and corticospinal. Cortical fibers projecting to the brainstem and spinal cord traverse the internal capsule and enter the crus cerebri, its equivalent at midbrain levels (Figs. 2.12, 2.14, 2.24, and 2.26). The continuity of projection fibers in the internal capsule, the crus cerebri, and the medullary pyramid is shown in Figure 2.12.

ASSOCIATION FIBERS

Association fibers are divided into long and short groups. *Short association fibers* arch through the floor of each sulcus to connect adjacent convolutions and course transversely to the long axis of the sulci (Fig. 2.17). *Long association fibers*, interconnecting cortical

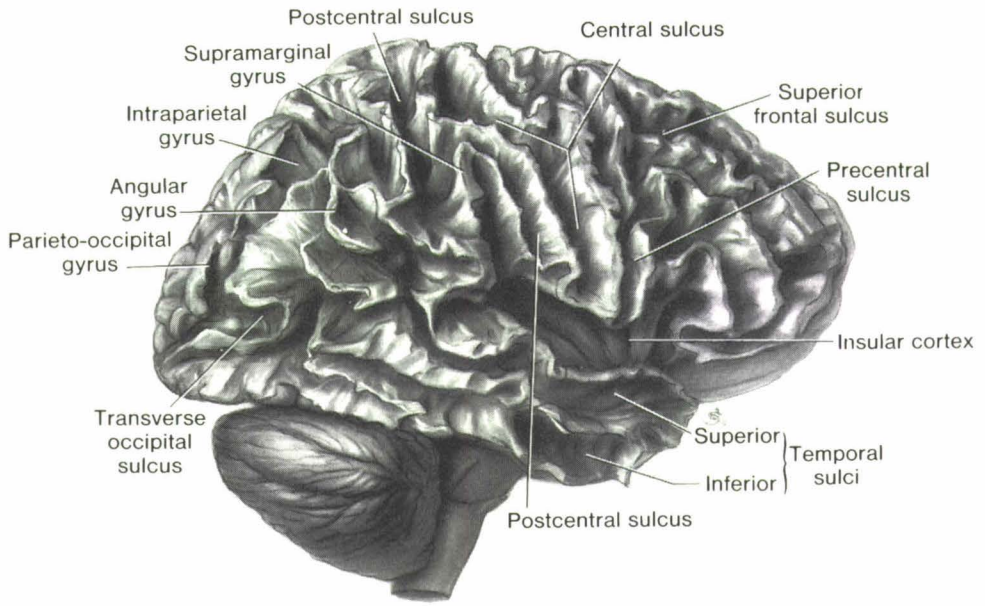


Figure 2.17. Lateral view of the brain after removal of the cortical gray matter. The medullary laminae and short association fibers of major gyri are indicated.

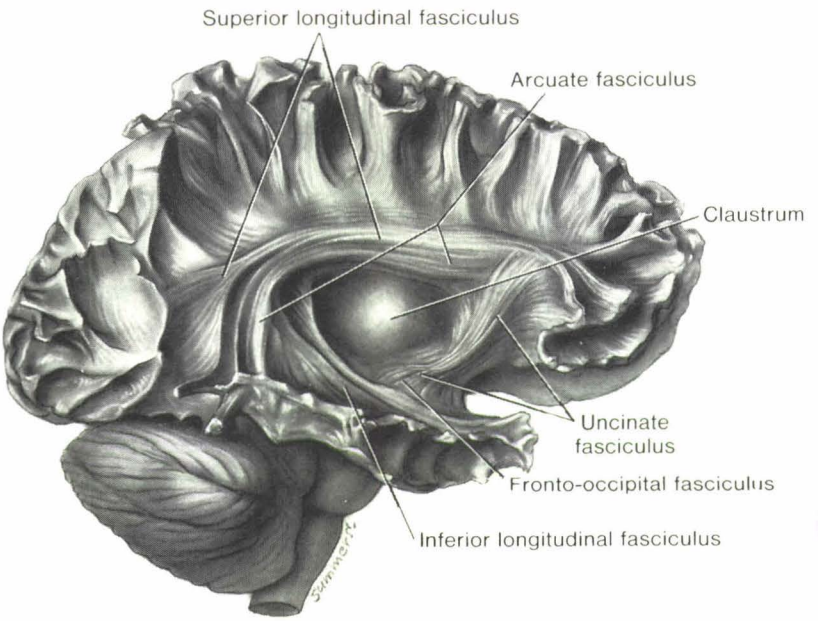


Figure 2.18. Dissection of the lateral surface of the hemisphere revealing the long association fibers interconnecting cortical regions in different lobes.

regions in different lobes within the same hemisphere, form three main bundles: (a) the uncinate fasciculus, (b) the arcuate fasciculus, and (c) the cingulum (Figs. 2.18 and 2.20).

The *uncinate fasciculus* is a compact bundle between the limen insula which connects the orbital frontal gyri and parts of the inferior and middle frontal gyri with anterior portions of the temporal lobe (Figs. 2.18 and 2.19). A deeply placed part of this fasciculus is thought to connect the frontal and occipital lobes (i.e., inferior occipitofrontal fasciculus). The *arcuate fasciculus* sweeps dorsally around the insular region and its fan-shaped ends

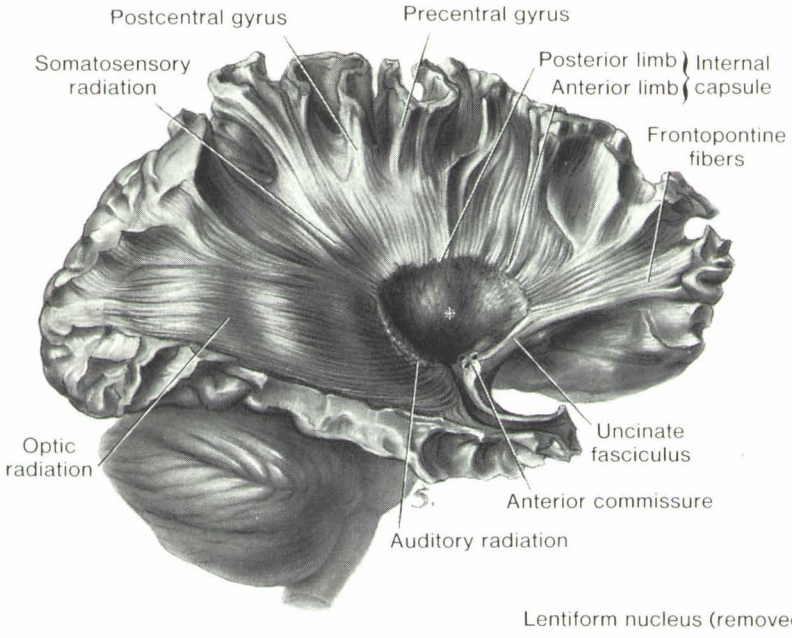


Figure 2.19. Dissection of the lateral aspect of the cerebral hemisphere to reveal the corona radiata and the optic radiation. The lentiform nucleus (*asterisk*) has been removed.

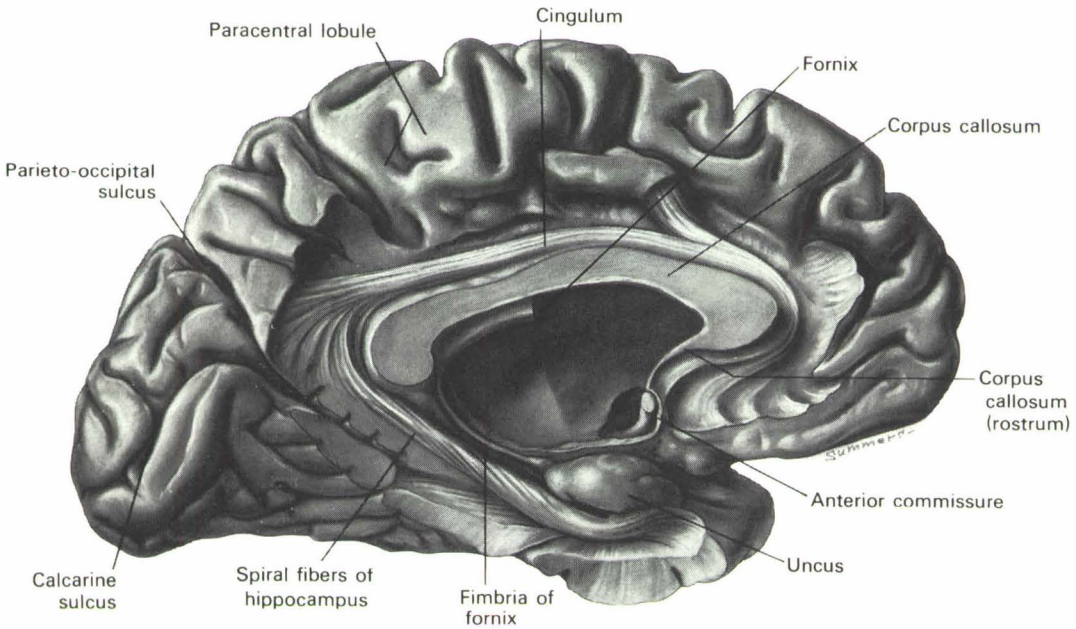


Figure 2.20. Dissection of the medial surface of the left cerebral hemisphere exposing the cingulum. The diencephalon has been removed.

connect the superior and middle frontal gyri with parts of the temporal lobe. A group of superiorly situated fibers in this bundle, extending caudally into portions of the parietal and occipital lobe, is known as the *superior longitudinal fasciculus* (Fig. 2.18).

The *cingulum*, the principal association bundle on the medial aspect of the hemisphere, lies in the white matter of the cingulate gyrus (Fig. 2.20). This bundle contains fibers of variable length which connect regions of the frontal and parietal lobes with parahippocampal gyrus and adjacent temporal cortical regions (Figs. 2.11 and 2.20). The cortical area deep to the insula contains association fibers in the *extreme* and *external capsules* (Figs. 2.13, 2.15, and 2.16). These capsules are two thin layers of white matter separated by a sheet of gray matter, known as the *claustrum*. All three of these structures overlie the lateral aspect of the basal ganglia.

COMMISSURAL FIBERS

Commissural fibers are represented principally by two structures: (a) the corpus callosum and (b) the anterior commissure. The *corpus callosum* is a broad, thick plate of dense myelinated fibers that reciprocally interconnect broad regions of the cortex in all lobes with corresponding regions of the opposite hemisphere (Figs. 2.6, 2.11, and 2.20). These fibers traverse the floor of the hemispheric fissure, form most of the roof of the lateral ventricles, and fan out in a massive callosal radiation as they are distributed to various cortical regions (Fig. 2.22). As mentioned earlier, the various parts of the corpus callosum are designated as (a) rostrum, (b) genu, (c) body, and (d) splenium. The genu contains fibers interconnecting rostral parts of the frontal lobes. Fibers from the remaining parts of the frontal lobe and the parietal lobe traverse the body of the corpus callosum. Fibers traversing the splenium relate regions of the temporal and occipital lobes. Fibers in the splenium of the corpus callosum, which sweep inferiorly along the lateral margin of the posterior horn of the lateral ventricle and separate the ventricle from the optic radiation, form the *tapetum* (Figs. 2.11 and 2.22).

The *anterior commissure* is a small compact bundle which crosses the midline rostral to the columns of the fornix, which is the major efferent bundle of the hippocampal formation (Figs. 2.6, 2.14, 2.15, and 2.20). This commissure consists of two parts that cannot be distinguished in the gross specimen (Fig. 18.12). A small anterior part of the commissure interconnects olfactory structures on the two sides (Fig. 18.8), while the larger posterior part mainly interconnects regions of the middle and inferior temporal gyri.

BASAL GANGLIA

Basal ganglia are large subcortical nuclear masses derived mostly from the telencephalon (Figs. 2.13–2.16). Structures composing the basal ganglia are the *caudate nucleus*, the *putamen*, the *globus pallidus*, and the *amygdaloid nuclear complex*. The caudate nucleus and putamen constitute the *striatum*. The term *lentiform nucleus* (lenticular nucleus) refers to the putamen and the globus pallidus. The lentiform nucleus, with the size and shape of a Brazil nut, appears in transverse sections as a wedge with the apex directed medially. This nuclear mass lies between the internal and the external capsules. A slightly curved vertical lamina of white matter divides the lentiform nucleus into an outer portion, the putamen, and an inner portion, the globus pallidus.

Putamen

This structure is the largest and most lateral component of the basal ganglia, lying between the external medullary lamina of the globus pallidus and the external capsule (Figs. 2.13–2.16). It is traversed by numerous fascicles of myelinated fibers directed ventromedially toward the globus pallidus, but these are seen clearly only in stained sections. The rostral part of the putamen is continuous with the head of the caudate nucleus (Fig. 19.5).

Globus Pallidus

The globus pallidus forms the most medial part of the lentiform nucleus and consists of two segments separated by the internal medullary lamina of the globus pallidus (Figs. 2.13, 2.15, and 2.16). The globus pallidus appears pale and homogeneous in freshly sectioned brains. Its medial border is formed largely by the fibers of the posterior limb of the internal capsule.

Caudate Nucleus

The caudate nucleus is an elongated, arched gray mass related throughout its ex-

tent to the lateral cerebral ventricle (Figs. 2.13–2.16 and 19.5). It consists of an enlarged rostral part, called the *head* of the caudate nucleus, which protrudes into the anterior horn of the lateral ventricle. The *body* of the caudate nucleus lies dorsolateral to the thalamus near the lateral wall of the lateral ventricle. The *tail* of the caudate nucleus follows the curvature of the inferior horn of the lateral ventricle and enters the temporal lobe (Fig. 2.13). The tail of the caudate nucleus terminates in the region of the amygdaloid nuclear complex (Fig. 2.16).

Amygdaloid Nuclear Complex

The amygdaloid nuclear complex is a gray mass in the dorsomedial part of the temporal lobe which underlies the uncus (Figs. 2.10, 2.15, and 2.16). This complex lies dorsal to the hippocampal formation and rostral to the tip of the inferior horn of the lateral ventricle. The amygdaloid complex gives rise to fibers of the *stria terminalis*, which arch along the entire medial border of the caudate nucleus and are especially evident near the junction of the caudate nucleus and thalamus (Figs. 2.25 and 2.29**B**). The terminal vein lies near the stria terminalis. Despite its close topographic relationship with the caudate nucleus, the amygdaloid complex appears to be functionally more closely related to the so-called limbic system than to the basal ganglia.

LATERAL VENTRICLES

The ependyma-lined cavities of the cerebral hemisphere constitute the lateral ventricles. The arched-shaped lateral ventricles contain cerebrospinal fluid and conform to the general shape of the hemispheres (Fig. 2.21). The lateral ventricles can be divided into five parts: (a) the anterior (frontal) horn, (b) the ventricular body, (c) the collateral (atrium) trigone, (d) the inferior (temporal) horn, and (e) the posterior (occipital) horn. Each lateral ventricle communicates with the slit-shaped, midline third ventricle by a short channel, known as the interventricular foramen (of Monro). These foramina serve as a basic reference point and are of great importance in radiographic studies.

Anterior Horn

The anterior horn portion of the lateral ventricle lies rostral to the intraventricular foramen, has a triangular shape in frontal section, and extends forward, laterally and ventrally, to end in a rounded termination in the white matter of the frontal lobe (Figs. 2.13, 2.15, and 2.21). The roof and rostral wall of this horn are formed by the corpus callosum, while its medial wall is the *septum pellucidum* which separates the ventricles of the two hemispheres (Fig. 2.6). The lateral wall of the ventricle is formed by the head of the caudate nucleus whose surface bulges convexly into the cavity (Figs. 2.13–2.15 and 2.29**A**).

Body of the Lateral Ventricle

The body of the lateral ventricle extends caudally from the interventricular foramen to an ill-defined point near the splenium of the corpus callosum. This narrow arched part of the ventricle continues until the ventricle begins to widen into the collateral trigone (referred to by neuroradiologists as the atrium). The *collateral trigone* composes that part of the lateral ventricle near the splenium of the corpus callosum where the body of the lateral ventricle is confluent with the temporal and occipital horns (Fig. 2.21).

Inferior Horn

The inferior horn portion of the lateral ventricle curves downward and forward around the posterior aspect of the thalamus, and extends rostrally into the medial part of the temporal lobe to end approximately 3 cm from the temporal pole (Fig. 2.10). The roof and lateral wall of this horn are formed by the tapetum (Figs. 2.11 and 2.22) and the optic radiation; the floor contains the *collateral eminence* caused by the deep collateral sulcus (Fig. 2.10). The inferior horn of the lateral ventricle contains the *hippocampal formation* in the medial wall of the horn which extends from the region of the splenium to the temporal tip of the ventricle (Figs. 2.10, 2.13, and 2.14). The hippocampal formation becomes folded into the ventricle along the hippocampal sulcus during development. Along the superior and medial surfaces of the hippocampus is a flattened band of fibers, known as the fimbria, which extends from the region of the uncus toward the splenium of the corpus callosum. The fimbria continues under the corpus callosum and becomes the fornix (Figs. 2.10, 2.20, 2.27, and 2.28).

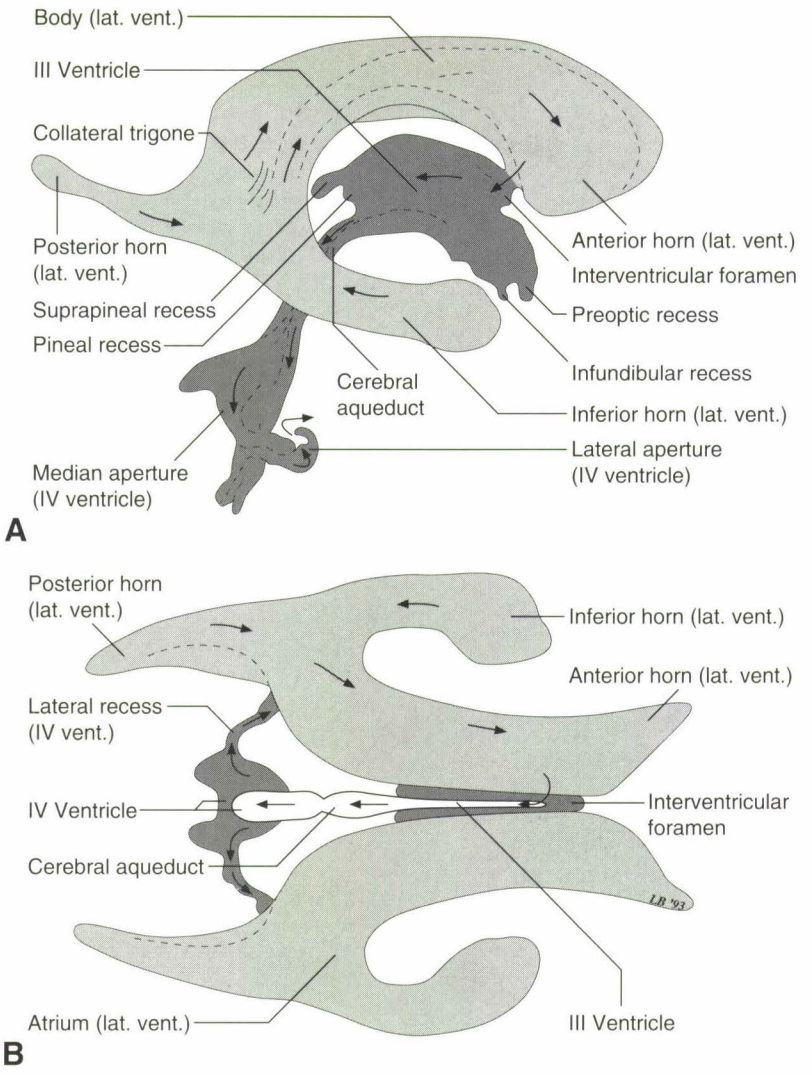


Figure 2.21. Ventricular system in lateral (**A**) and superior (**B**) views. *Arrows* indicate direction of CSF flow.

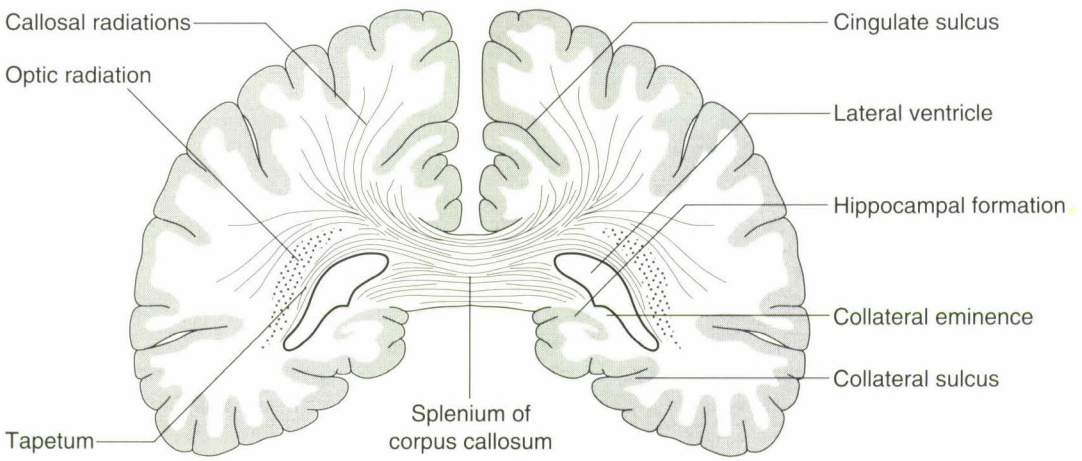


Figure 2.22. Frontal section at the level of the splenium of the corpus callosum. Callosal fibers lateral to the ventricle are known as the tapetum. The optic radiations lie lateral to the tapetum.

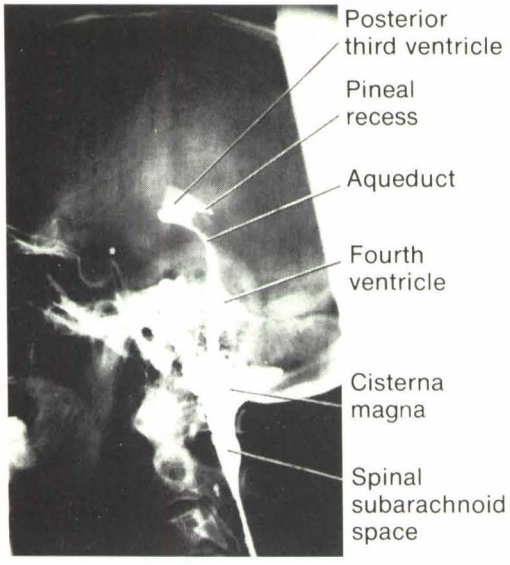


Figure 2.23. Positive contrast ventriculography clearly outlining the fourth ventricle, cerebral aqueduct, and the posterior part of the third ventricle. In this lateral view radiopaque material also fills part of the cisterna magna and part of the spinal subarachnoid space.

Posterior Horn

The posterior horn part of the lateral ventricle extends from the collateral trigone into the occipital lobe. This horn exhibits a high degree of variability in appearance and is often rudimentary. The occipital horn has frequently the appearance of a small fingerlike projection with a rounded tip. The roof and lateral wall of this horn are formed by tapetal fibers of the corpus callosum, whereas its floor is the white matter of the occipital lobe (Fig. 2.22). The *calcar avis*, a longitudinal prominence, is produced by the deep penetration of the calcarine sulcus.

Portions of the lateral ventricles contain *choroid plexus*, formed by the invagination of the ependymal roof plate into the ventricular cavities. The choroid plexus develops at sites where the ependyma and the pia mater containing blood vessels come together. This plexus is present in the body, collateral trigone, and in the inferior horn of the lateral ventricle, and extends through the interven-

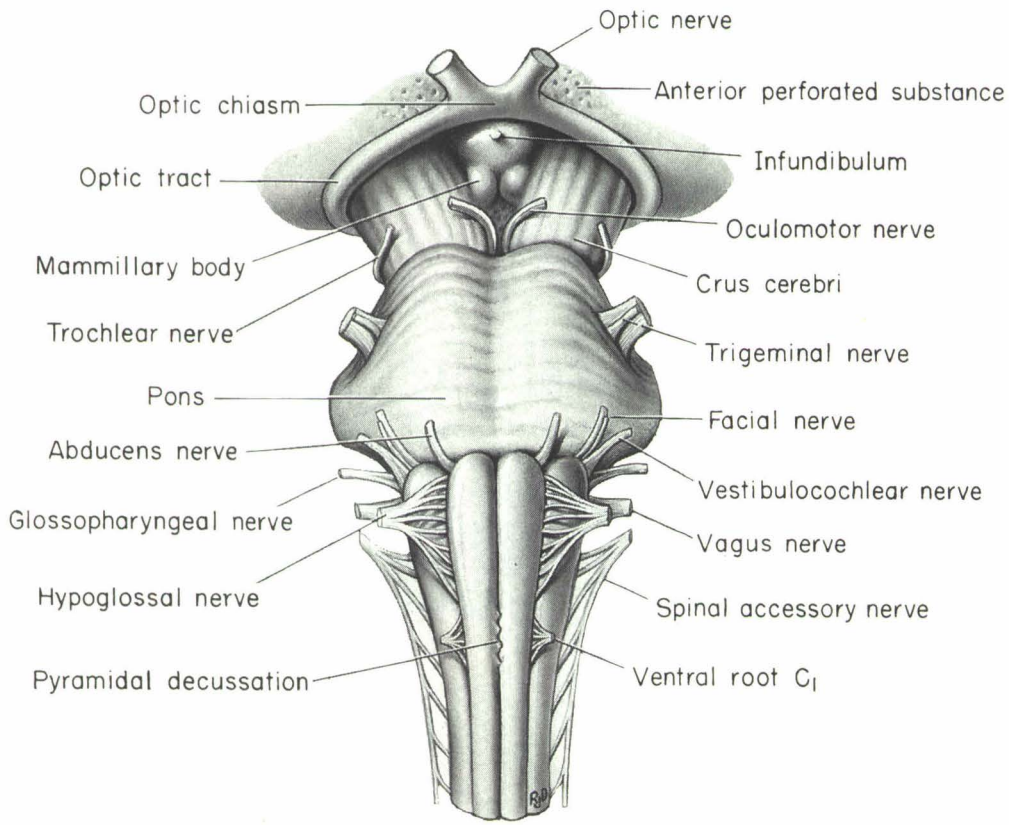


Figure 2.24. Anterior surface of the brainstem showing the emergence and entrance of most of the cranial nerves.

tricular foramen to lie in the roof of the third ventricle (Fig. 2.29).

BRAINSTEM

In the intact brain, only the anterior surface of the brainstem can be seen throughout its extent, because the cerebral hemispheres and cerebellum overlap its lateral and posterior surfaces. On the anterior surface of the brainstem, the medulla, pons, midbrain, and part of the *hypothalamus* (a component of the diencephalon) can be identified (Figs. 2.5, 2.9, and 2.24). The diencephalon is surrounded by hemispheric structures on all sides except for a small region of the hypothalamus between the *optic chiasm* and the *mammillary bodies*. The midbrain appears very small, but root fibers of the oculomotor nerve (N. III) can be seen emerging between two massive fibers bundles, the *crura cerebri* (Figs. 2.9, 2.10, and 2.24). The ventral surface of the pons produces a convex protrusion covered by transversely coursing fiber bundles which disappear laterally in the substance of the cerebellum. The medulla, caudal to the pons, reveals the large *medullary pyramids* medially and the oval *olivary eminences* ventrolaterally. The transition from medulla to spinal cord is characterized by the disappearance of the medullary pyramids, the development of the anterior median fissure of the spinal cord, a conspicuous reduction in size, and the appearance of paired spinal nerves.

Removal of the cerebral hemispheres and cerebellum reveals the posterior and lateral surfaces of the brainstem (Figs. 2.25 and 2.26). The expanded diencephalon appears as paired oval nuclear masses on each side of a vertical slitlike third ventricle (Fig. 2.25). The *thalamus* and *epithalamus*, seen in the posterior view of the brainstem, lie between the fibers

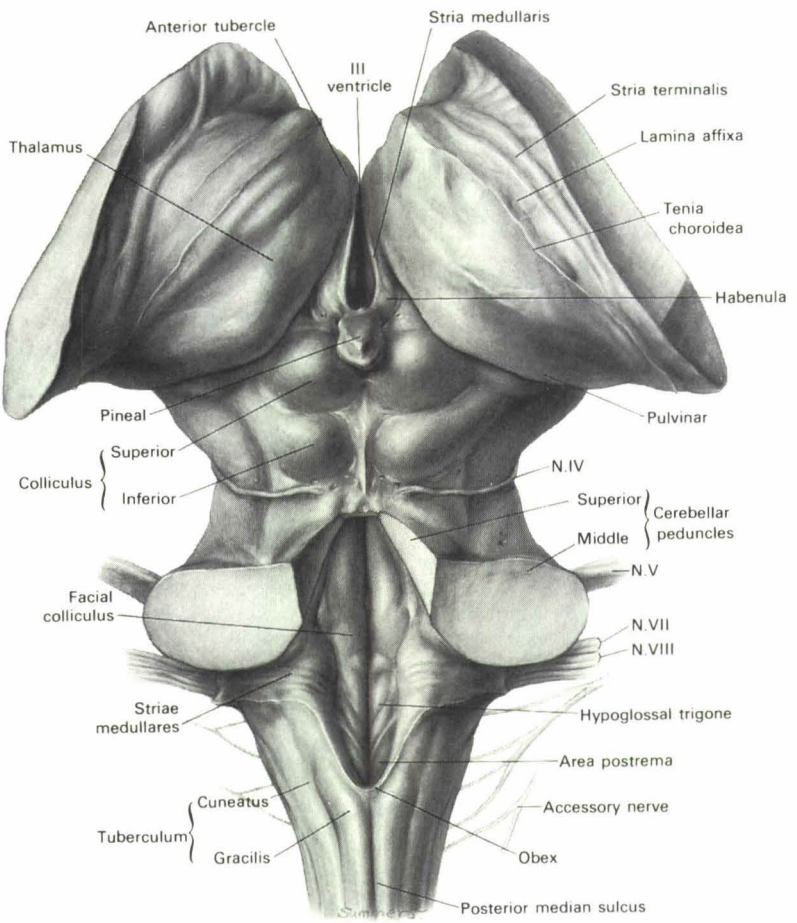


Figure 2.25. Posterior surface of the brainstem and diencephalon with the cerebellum removed.

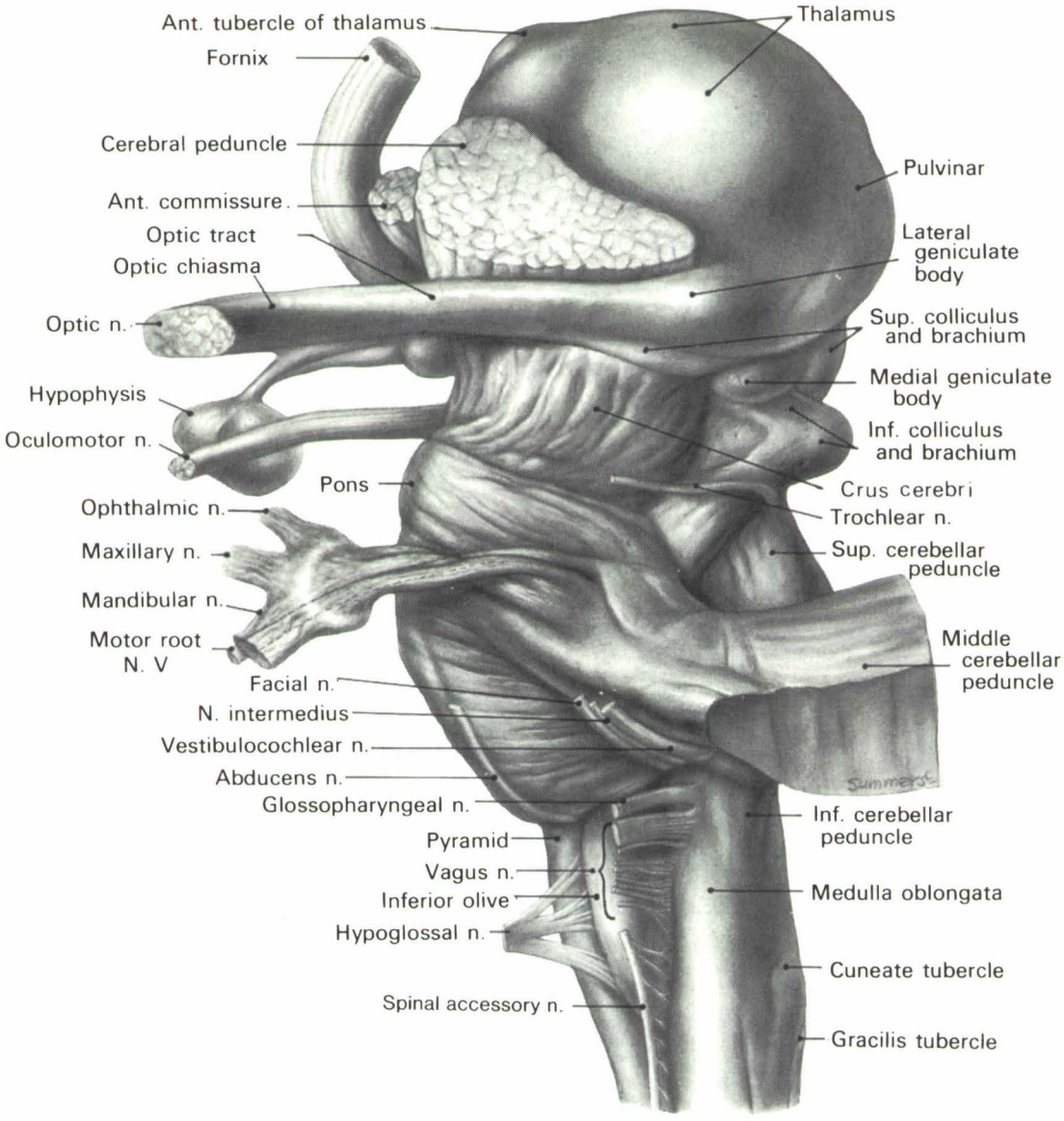


Figure 2.26. Lateral view of the brainstem and diencephalon with the cerebellum removed showing the sites of emergence and entrance of most of the cranial nerves.

of the internal capsule and are flanked dorsolaterally by the body and tail of the caudate nucleus. Along the dorsomedial margin of the thalamus is the *stria medullaris*, a band of fibers coursing posteriorly toward the habenula and the base of the pineal gland.

The dorsal aspect of the midbrain reveals the *superior* and *inferior colliculi* and their *brachia*, which relate these structures to particular parts of the thalamus. The trochlear nerve (N. IV) emerges from the dorsal part of the midbrain caudal to the inferior colliculus (Figs. 2.25 and 2.26). The dorsal aspects of the hindbrain are revealed by removing the cerebellum (Fig. 2.25). This discloses the rhomboid fossa, an unpaired symmetric ventricle that overlies the pons and medulla. The rhomboid-shaped fourth ventricle is surrounded by three paired cerebellar peduncles, which relate the three brainstem segments to the cerebellum. The fourth ventricle contains several eminences which overlie nuclear masses, the most evident of which are the *facial colliculus* and the *hypoglossal eminence*. Caudal to the fourth ventricle on the dorsal surface of the medulla are nuclear masses related to ascending spinal systems, namely, the *cuneate* and *gracilis tubercles* (Fig. 2.25).

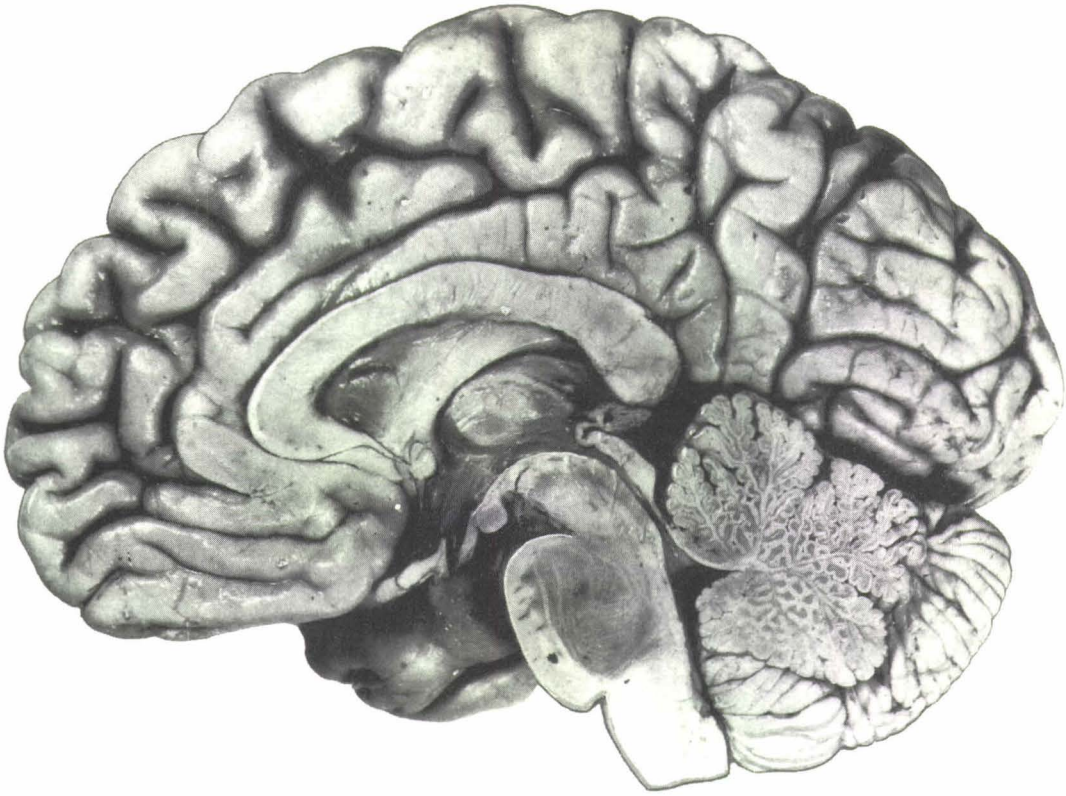


Figure 2.27. Midsagittal section of the brainstem and diencephalon. Structures are identified in Figure 2.28.

Structurally, the brainstem consists of three distinctive parts: (a) a roof plate dorsal to the ventricular system, (b) a central core of cells and fibers beneath the ventricular system known as the tegmentum, and (c) a massive collection of ventrally located fibers derived from cells of the cerebral cortex (Figs. 2.27 and 2.28). The *roof plate* of the midbrain is represented by the *tectum* or *quadrigeminal plate*, consisting of the superior and inferior colliculi. In the hindbrain, the roof plate is more elaborate and comprises the *cerebellum* and the *tela choroidea*. The *tegmentum* of the midbrain, pons, and medulla contains the brainstem *reticular formation*, a large collection of cells and intermingled fibers that subserve multiple functions, as well as several more precisely delineated nuclei. The *cortically derived ventral fiber system* forms the *crus cerebri* at midbrain levels, one of the principal constituents of the *ventral* or *basilar part* of the pons, and the *medullary pyramids* of the medulla (Fig. 2.26). Both the reticular formation and the cortically derived ventral fiber system are continuous within the brainstem, but undergo change and modification at various levels (Fig. 2.12).

Medulla

The medulla (myelencephalon), the most caudal basic subdivision of the brainstem, extends from the level of the foramen magnum to the caudal border of the pons. The transition from spinal cord to medulla is gradual and characterized by (a) the obliteration of the anterior median fissure ventrally and the decussation of the medullary pyramids, (b) the appearance of the gracilis and cuneate tubercles dorsally, (c) the disappearance of spinal nerves and the appearance of cranial nerves, and (d) the development of the fourth ventricle (Figs. 2.23–2.26). The full development of the medullary pyramids, the appearance of the inferior olivary eminence, the widening of the fourth ventricle, and the gradual increase in size of the restiform body, which is the larger component of the inferior cerebellar peduncle, give the medulla its characteristic configuration (Figs. 2.24 and 2.25). Cranial nerves associated with the medulla are (a) the hypoglossal (N. XII) whose fibers emerge through the preolivary fissure located ventrolaterally between the pyramid and the inferior olivary complex, (b)

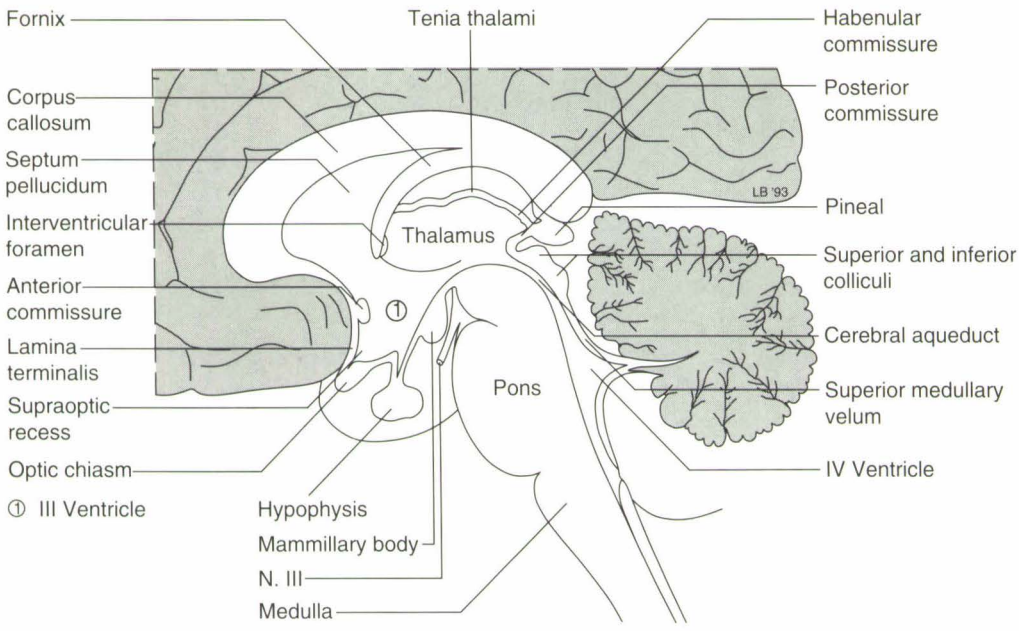


Figure 2.28. Midsagittal section of the brainstem and diencephalon identifying some of the structures shown in Figure 2.27.

the accessory (N. XI), the vagus (N. X), and the glossopharyngeal (N. IX) whose fibers emerge from the postolivary sulcus, and (c) the vestibulocochlear nerve (N. VIII) whose separate components enter the brainstem at the junction of the pons and medulla (Fig. 2.26). Auditory fibers are located dorsally and partially arch over the lateral aspect of the inferior cerebellar peduncle.

Fourth Ventricle

The fourth ventricle is a broad, shallow, rhomboid-shaped cavity overlying the pons and medulla that extends from the central canal of the upper cervical spinal cord to the cerebral aqueduct of the midbrain (Figs. 2.21, 2.23, and 2.25). Its roof is the cerebellum and the *superior* and *inferior medullary veli*, which extend toward an apex within the cerebellum known as the *fastigium* (Figs. 2.21, 2.27, 2.28, and 2.33). The superior medullary velum forms the roof of the pontine part of the ventricle, while the inferior medullary velum and the *tela choroidea* form the roof over the medullary part of this ventricle. The *choroid plexus* from the tela choroidea projects into the caudal part of the ventricle. The widest part of the fourth ventricle is immediately caudal to the *middle cerebellar peduncles*. In this region, there is a *lateral recess* on each side, which extends over the surface of the inferior cerebellar peduncle to open into the *lateral cerebellomedullary* (or *inferior cerebellopontine*) *cistern* (Figs. 1.8 and 1.9). These small lateral recesses contain choroid plexus that protrudes through the *foramina of Luschka* into the subarachnoid space (Figs. 2.9 and 2.21). A small median aperture in the caudal part of the ventricle is known as the *foramen of Magendie*. Through these three apertures cerebrospinal fluid flows from the ventricular system into the subarachnoid spaces (see Chapter 1). Using positive contrast ventriculography the fourth ventricle, cisterna magna and cerebral aqueduct can be viewed in detail (Fig. 2.23).

The *rhomboid fossa*, which forms the floor of the fourth ventricle, is divided by the *median sulcus* into symmetric halves. The sulcus limitans divides each half into a *medial eminence* and a lateral region known as the *vestibular area* (Fig. 12.14). The vestibular nuclei lie beneath the vestibular area. The *facial colliculus* and the *hypoglossal trigone* lie within the medial eminence, with the latter near the caudal border of the ventricle. Transversely coursing fibers of the *striae medullares* run from the region of the lateral recess toward the midline and disappear in the median sulcus (Fig. 2.25). These strands of myelinated fibers lie rostral to the hypoglossal trigone. The *vagal trigone* lies lateral to the hypoglossal trigone. The most caudal end of the rhomboid fossa resembles a pen and is called the *calamus scriptorius*. The point of caudal junc-

tion of the walls of the fourth ventricle is known as the *obex* (Fig. 2.25). Immediately rostral to the obex on each side of the fourth ventricle is a slightly rounded eminence, the *area postrema*.

Pons

The pons (metencephalon), representing the rostral part of the hindbrain, is well-delimited on the anterior surface of the brainstem (Figs. 2.24, 2.26 and 2.27). The massive pontine protuberance covered by broad bands of transversely oriented fibers is separated from the crus cerebri of the midbrain by the superior pontine sulcus and from the anterior surface of the medulla by the inferior pontine sulcus. The predominantly transverse fibers in the ventral part of the pons form the *middle cerebellar peduncle* (Figs. 2.26 and 2.32). An anterior median depression, the *basilar sulcus*, indicates the position occupied by the basilar artery (Figs. 2.24 and 4.11).

Transverse sections of the pons reveal its basic organization (Fig. 13.1). The pons consists of a massive *ventral part* composed of (a) longitudinal descending fiber bundles, (b) pontine nuclei, (c) transversely oriented fibers projecting to the cerebellum, and (d) a smaller dorsal part, known as the tegmentum. The tegmental portion contains aggregations of cells and fibers which form a central core known as the pontine reticular formation. The pontine tegmentum is continuous with the reticular formation of the medulla and midbrain.

Cranial nerve nuclei, ascending sensory systems and descending motor pathways are found within the tegmentum. Cranial nerves associated with the pons are the trigeminal (N. V), abducens (N. VI), facial (N. VII), and the two components of the vestibulocochlear nerve (N. VIII). The *abducens nucleus* lies in the floor of the fourth ventricle and is partially encircled by fibers of the facial nerve (N. VII). Facial nerve fibers and cells of the abducens nucleus underlie the *facial colliculus* seen in the floor of the fourth ventricle (Fig. 2.25). Fibers of the abducens nerve emerge from the ventral surface of the brainstem at the junction of the pons and medulla (Fig. 2.26). The facial and vestibulocochlear nerves emerge and enter the lateral surface of the pons at the *cerebellopontine angle*, formed by the junction of pons, medulla, and cerebellum (Figs. 2.26 and 13.6). The trigeminal nerve (N. V), consisting of motor and sensory fibers, passes through rostral parts of the middle cerebellar peduncle to reach nuclei in the dorsolateral pontine tegmentum (Fig. 2.26). The *middle cerebellar peduncle* consists of a large number of fibers, arising from the pontine nuclei, which project to the cerebellum; this is the largest of the three cerebellar peduncles (Figs. 2.25 and 2.26). Ventral to the root of the trigeminal nerve is the basilar pons while dorsal to the root of this nerve is the middle cerebellar peduncle.

Midbrain

The midbrain (mesencephalon) is the smallest part of the brainstem (Figs. 2.10, 2.25–2.27). It consists of (a) the *tectum*, represented by the superior and inferior colliculi, (b) the *tegmentum*, ventral to the cerebral aqueduct, and (c) the massive *crura cerebri* (Figs. 2.24, 2.26, and 14.1). The tegmentum and crura cerebri are separated by a large pigmented nuclear mass, the *substantia nigra* (Fig. 2.14). The superior colliculus and a region immediately rostral to it, known as the *pretectum*, are important relays in the visual system. The inferior colliculus relays auditory impulses to thalamic nuclei that in turn project to specific cortical areas.

Two cranial nerves are associated with the midbrain, the oculomotor (N. III) and the trochlear (N. IV). The oculomotor nerve emerges from the *interpeduncular fossa*, between the massive crura cerebri (Figs. 2.9, 2.10, and 2.26). The slender trochlear nerve exits from the dorsal surface of the brainstem, caudal to the inferior colliculus. Fibers of this nerve cross in the superior medullary velum and course anteriorly around the brainstem (Figs. 2.25 and 2.26). The fibers of the *superior cerebellar peduncle*, seen on each side of the upper part of the fourth ventricle (Figs. 2.25 and 2.26), decussate completely in the caudal midbrain tegmentum. Crossed fibers of this peduncle traverse and surround a large nuclear mass in the tegmentum called the *red nucleus* (Fig. 2.14).

The crus cerebri on the ventral surface of the midbrain are collections of fibers originating in broad areas of the cerebral cortex that pass through the internal capsule (Figs. 2.12 and 2.24). These fibers project to (a) spinal cord (i.e., corticospinal), (b) pontine nuclei (i.e., corticopontine), and (c) specific regions of the lower brainstem (i.e., corticobulbar). A large part of the corticobulbar fibers project to parts of the reticular formation. The pigmented substantia nigra, rich in dopamine and other neurotransmitters, is the largest

single nuclear mass in the midbrain. It has connections with parts of the basal ganglia, thalamus, and superior colliculus, and is considered to subserve a motor function (Fig. 2.14).

DIENCEPHALON

The diencephalon is a paired structure on each side of the third ventricle (Figs. 2.13, 2.16, and 2.25–2.28). The lateral ventricles, corpus callosum, fornix, and velum interpositum lie superior to the diencephalon (Fig. 2.29). Fibers of the posterior limb of the internal capsule and the body of the caudate nucleus constitute its lateral border. Caudally, the diencephalon appears continuous with the tegmentum of the midbrain; the posterior commissure is the junctional zone between the diencephalon and mesencephalon (Figs. 2.13 and 2.28). The rostral boundary of the diencephalon is near the interventricular foramen, but portions of the hypothalamus extend almost to the *lamina terminalis* (Figs. 2.27 and 2.28). The diencephalon consists of four parts: (a) the epithalamus, (b) the thalamus, (c) the hypothalamus, and (d) the subthalamus (Figs. 2.27–2.29).

Epithalamus

The epithalamus forms the dorsal part of the diencephalon and consists of (a) the pineal body or gland (epiphysis), (b) the habenular nuclei, (c) the stria medullares, and (d) the tenia thalami.

Thalamus

The thalamus represents the largest and most central portion of the diencephalon. The thalamus appears as an oblique, egg-shaped nuclear mass at the rostral end of the brainstem (Figs. 2.13, 2.16, and 2.25–2.29). This nuclear complex lies between the interventricular foramen and the posterior commissure, and extends from the third ventricle to the medial border of the posterior limb of the internal capsule. The thalamus lies dorsal to the hypothalamic sulcus, a shallow groove on the lateral wall of the third ventricle. The lateral and caudal parts of the thalamus overlie midbrain structures. The superior surface of the thalamus is covered by a thin layer of fibers known as the *stratum zonale*. A narrow lateral strip of the superior surface, adjacent to the body of the caudate nucleus, is covered by ependyma and forms part of the floor of the lateral ventricle. This strip is called the *lamina affixa* (Fig. 2.25). The *stria terminalis* and the *terminal vein* lie dorsally at the junction of thalamus and caudate nucleus. The *stria medullaris* extends along the dorsomedial margin of the thalamus near the roof of the third ventricle. The medial surfaces of thalami on each side of the third ventricle are partially fused in about 80% of human brains. This place of fusion is called the *interthalamic adhesion* or *massa intermedia*.

Although most subdivisions of the thalamus are not evident in gross specimens, the *anterior tubercle* of the thalamus is discernible rostrally as a distinct swelling (Fig. 2.26). The expanded posterior portion of the thalamus is known as the *pulvinar* (Figs. 2.13 and 2.25). The *medial* and *lateral geniculate bodies*, important relay nuclei concerned with audition and vision, lie ventral to the pulvinar (Fig. 2.26). Together, these structures are referred to as the *metathalamus*. The thalamus is divided into anterior, lateral, medial, and ventral nuclear groups by a thin layer of myelinated fibers, known as the *internal medullary lamina* of the thalamus, which can be seen grossly in transverse sections of the brain (Figs. 2.16 and 2.29). Nuclear groups within the internal medullary lamina are collectively referred to as the *intralaminar thalamic nuclei*. The largest of the intralaminar nuclei is the centromedian nucleus (Fig. 2.29**B**).

The thalamus is regarded as the neural structure whose relationship with other parts of the neuraxis provides the key to understanding the organization of the central nervous system. This part of the diencephalon is concerned with (a) distributing most of the afferent inputs to the cerebral cortex, (b) the control of the electrocortical activity of the cerebral cortex, and (c) the integration of motor functions by providing the relays through which impulses from the basal ganglia and cerebellum can reach the motor cortex. Through influences that modify electrocortical activities, the thalamus plays important roles in arousal, consciousness, and sleep mechanisms.

Hypothalamus

The hypothalamus portion of the diencephalon lies ventral to the hypothalamic sulcus. It forms the inferior and lateral walls of the third ventricle (Figs. 2.27–2.29 and 17.1) and extends from the region of the optic chi-

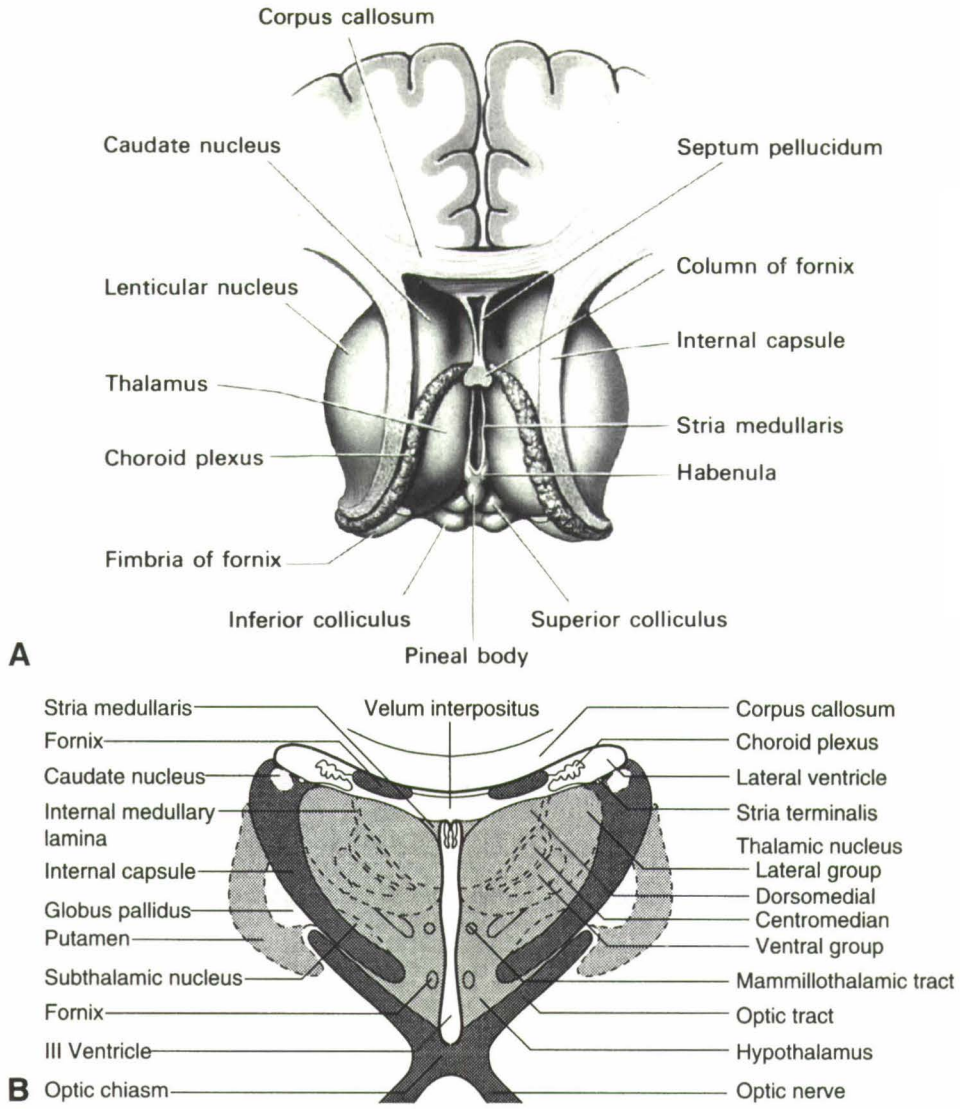


Figure 2.29. **A.** Posterior view of the diencephalon and related structures. **B.** Frontal section through the diencephalon and adjacent structures indicating some of the major nuclear groups of the thalamus. The hypothalamus lies on both sides of the third ventricle below the hypothalamic sulcus.

asm to the caudal border of the mammillary bodies. The gross structures visible on the ventral surface include the *optic chiasm, infundibulum, tuber cinereum,* and *mammillary bodies* (Figs. 2.9, 2.10, 2.24, 2.27, and 2.28). The hypothalamus is divided into medial and lateral nuclear groups by fibers of the fornix which mainly end in the mammillary body. Three rostrocaudal regions of the hypothalamus are recognized: (a) a supraoptic region, dorsal to the optic chiasm, (b) a tuberal region centrally, and (c) a mammillary region caudally (Fig. 17.1). The hypothalamus is continuous with the pituitary gland (hypophysis) through the infundibulum and pituitary stalk. It has a rostrocaudal extent of about 10 mm. This subdivision of the diencephalon is concerned with visceral, endocrine, and metabolic activity, as well as with temperature regulation, sleep, and emotion.

Subthalamus

The subthalamus portion of the diencephalon is a transitional zone ventral to the thalamus and lateral to the hypothalamus. It is bounded by the thalamus dorsally, the hypothalamus medially, and the internal capsule laterally (Fig. 2.29). The largest discrete nuclear mass is the *subthalamic nucleus,* a lens-

shaped structure on the inner aspect of the internal capsule (Fig. 16.6). This region is traversed by many important fiber systems in their projection to thalamic nuclei. A small, relatively clear area, known as the *zona incerta*, serves as an important landmark in distinguishing certain fiber bundles (Fig. 16.6). The subthalamic nucleus and pathways traversing this region are concerned with the integration of somatic motor function.

CEREBELLUM

The cerebellum overlies the posterior aspect of the pons and medulla and extends laterally under the tentorium to fill the greater part of the posterior fossa (Figs. 2.2, 2.7, 2.9, and 2.27). The superior surface is somewhat flattened, while the inferior surface is convex. A shallow *anterior cerebellar incisure* is present superiorly. A deeper and narrower *posterior cerebellar incisure* contains a fold of dura mater, the *falx cerebelli* (Fig. 1.2).

The cerebellum consists of a midline portion, the *vermis*, and two lateral lobes or *hemispheres*. This structure is essentially wedge-shaped, having a superior surface covered by the tentorium, a posterior surface in the suboccipital region, and an inferior surface which overlies the fourth ventricle. On the superior surface the distinction between vermis and hemispheres is not sharp (Fig. 2.30), whereas on the inferior surface two deep sulci clearly separate the vermis from the

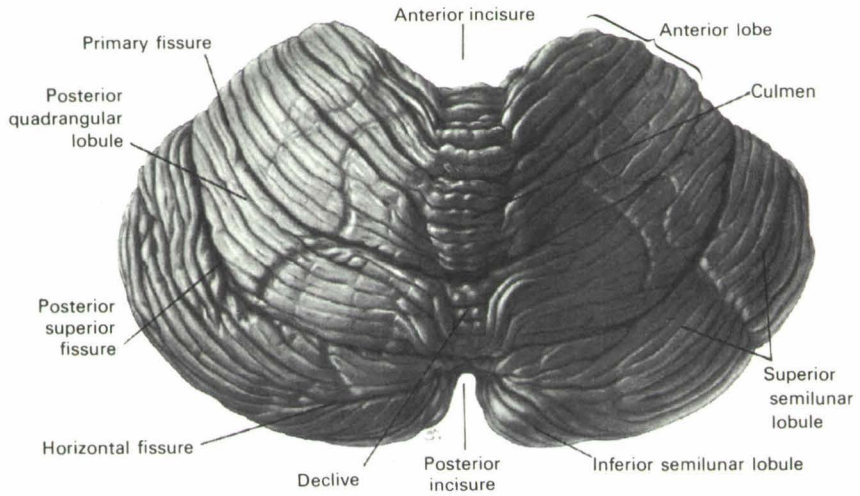


Figure 2.30. Superior surface of cerebellum.

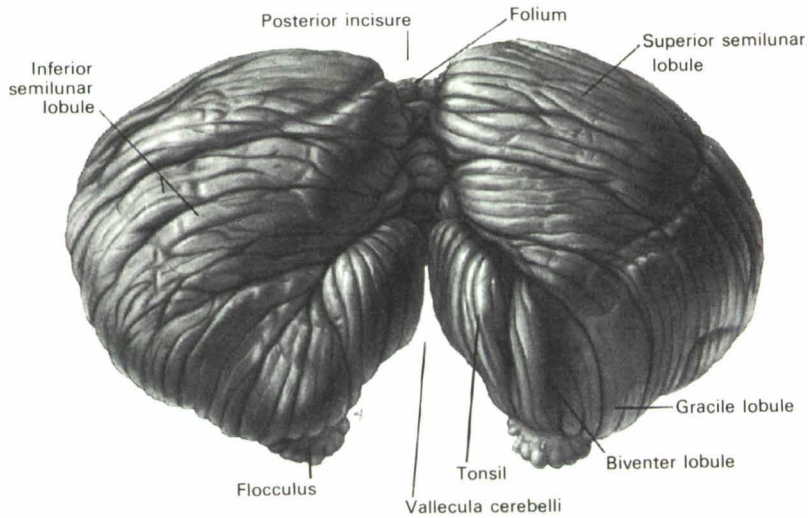


Figure 2.31. Posteroinferior view of the cerebellum.

hemispheres. Inferiorly, a deep median fossa, the *vallecula cerebelli,* is continuous with the posterior incisure. The floor of this fossa is formed by the inferior vermis (Fig. 2.31).

Structurally, the cerebellum consists of a gray cortical mantle, the cerebellar cortex, a medullary core of white matter, and four pairs of intrinsic nuclei. Three paired cerebellar peduncles connect the cerebellum with the three segments of the brainstem (Figs. 2.25, 2.26, and 2.32). The cerebellar cortex consists of a large number of narrow leaflike laminae known as cerebellar folia. Cerebellar folia are nearly parallel with each other and for the most part are oriented transversely. Each lamina contains several secondary and tertiary folia. Five transversely oriented fissures divide the cerebellum into lobes and lobules (Fig. 15.1). These fissures, and the various lobular subdivisions, can be identified on the isolated cerebellum or in midsagittal section (Fig. 2.33). On the superior surface of the cerebellum two fissures can be identified: (a) the *primary* and (b) the *posterior superior* fissures (Fig. 2.30). The *horizontal fissure,* one of the most distinctive, roughly divides the cerebellum into superior and inferior halves. The *prepyramidal* and *posterolateral fissures* are found on the inferior surface (Fig. 2.33).

The cerebellar vermis is the key to understanding the gross organization of the cerebellum, but in this part there is no median raphe and the midline is difficult to establish. Portions of the cerebellum rostral to the primary fissure constitute the *anterior lobe of the cerebellum* (Figs. 2.30 and 15.1). In the vermis, the lobules consist of the lingula, the central lobule, and the culmen (Fig. 2.33). In the hemisphere, the lingula has no corresponding part, but the *alar central lobule* and the *anterior quadrangular lobule* correspond to the central lobule and the culmen.

The *posterior lobe* of the cerebellum, between the primary and posterolateral fissures, represents the largest subdivision of the cerebellum (Figs. 2.33 and 15.1). Vermal parts of the posterior lobe in sequence are (a) the *declive,* (b) the *folium and tuber,* (c) the *pyramis,* and (d) the *uvula* (Fig. 2.33). The *simple lobule,* between the primary and posterior superior fissures, corresponds to the declive of the vermis (Fig. 15.1). The *ansiform lobule* is that part of the cerebellar hemisphere between the posterior superior fissure and the *gracile lobule.* The horizontal fissure divides the ansiform lobule into the *superior semilunar lobule* (crus I) and the *inferior semilunar lobule* (crus II). Vermal, counterparts of the ansiform lobule, are the folium and tuber. Between the prepyramidal and posterolateral fissures are the *pyramis* and *uvula* in the vermis, and the *biventer lobule* and the *cerebellar tonsil* in the hemisphere (Figs. 2.32 and 2.33). The *flocculonodular lobule* lies rostral to the posterolateral fissure and consists of the vermal nodulus and the paired flocculi (Fig. 2.32). The *nodulus* lies immediately caudal to the inferior medullary velum (Fig. 2.33).

In the midsagittal section, the relationships of the cerebellum to the brainstem are evident (Fig. 2.27). The complex branching of the medullary core, and the treelike appearance of the laminae and folia, have given rise to the descriptive term, *arbor vitae* (Figs. 2.27, 2.28, and 2.33). The intrinsic nuclei of

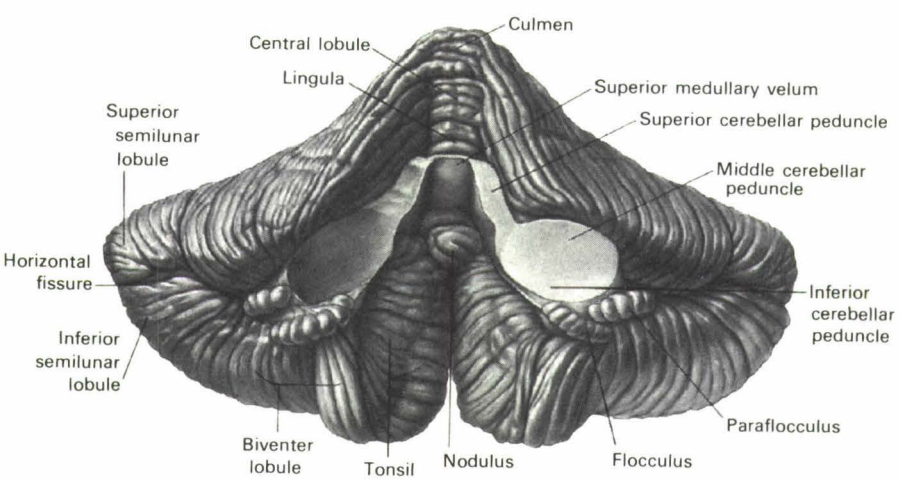


Figure 2.32. Inferior surface of cerebellum removed from brainstem by transection of cerebellar peduncles.

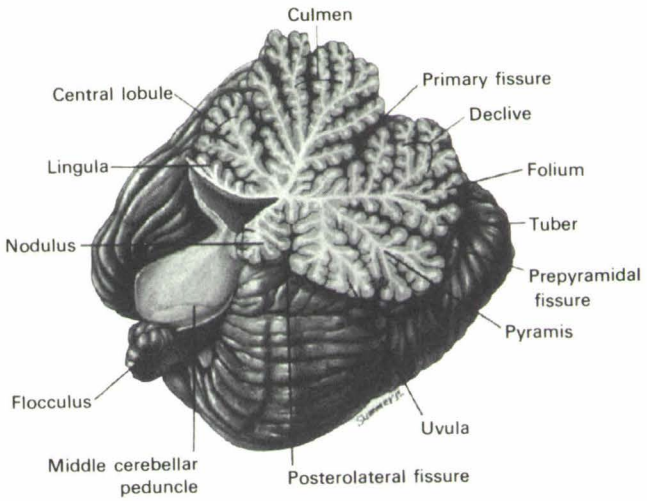


Figure 2.33. Sagittally sectioned cerebellum showing the lobules of the cerebellar vermis. The primary fissure is the deepest of all cerebellar fissure. (See Fig. 15.1.)

the cerebellum can be seen only in sections. These nuclei are the dentate (most lateral), the emboliform, the globose, and the fastigial (Figs. 15.17 and 15.19). The fastigial nuclei, commonly called the roof nuclei, lie in the roof of the fourth ventricle.

Although the cerebellum is derived from the metencephalon, this portion of the neuraxis functions in a suprasegmental manner. Therefore, it is not considered part of the brainstem. It is concerned primarily with coordination of somatic motor function, control of muscle tone, and equilibrium. The cerebellum receives input directly or indirectly from virtually all sensory receptors, including the organs of special sense, but this sensory information does not enter the conscious sphere. This structure functions as a special kind of computer that automatically processes, organizes, and integrates sensory input and provides prompt responses that contribute to smooth and effective control of somatic motor function. The output systems of the cerebellum arise largely from the cerebellar nuclei and their influences upon motor function are mediated through brainstem nuclei at multiple levels.

BRAIN IMAGING

Standard x-ray techniques for visualizing gross structures in and around the brain have been used for many years for diagnostic purposes. However, under ordinary circumstances, the soft tissues within the cranium are so nearly homogeneous in radiodensity that the brain is almost completely invisible on plain x-ray films of the head. All living tissue, except bone, fall within a narrow band of photon absorption coefficients that prevents discrimination of different tissue densities by conventional x-ray radiographic techniques. Additionally, when an x-ray beam penetrates the head, it superimposes the densities of all structures in its path with the composite density recorded on the x-ray film. One of the x-ray techniques that is successfully used is based upon the introduction of air (or various contrast media) into the subarachnoid space at spinal cord level to produce an image of the ventricular system termed a *pneumoencephalogram* (Fig. 2.23). In contrast to bone, air absorbs very little x-ray photons and appears dark in radiographs. Although useful for diagnostic purpose, this method is painful and, in some cases, can be dangerous for the patient. The same limitations apply to another procedure which consists of injecting intraarterially or intravenously a radiopaque dye to produce an image of the cerebral vasculature called an *angiogram* (Figs. 4.3, 4.9, 4.15, and 4.16). The blood vessels of the brain and brainstem can be studied in detail from carotid and vertebral angiograms, which first reveal the arteries and later the filling of the veins. Normal intracranial structures are not readily visualized with cerebral angiography, although some abnormalities can be inferred from distortion in the appearance of the brain vasculature. This procedure, however, clearly reveals highly vascularized tumors and vascular lesions such as aneurysms and arteriovenous malformations (see Chapter 4).

In the past decade, there was a true revolution in the field of brain imaging. Three extremely powerful and noninvasive techniques, computerized tomography (CT), magnetic resonance imaging (MRI), and

positron emission tomography (PET) (3, 6, 12), were developed to study the regional anatomy of the living brain with a high degree of spatial resolution.

Computerized Tomography

A system theoretically capable of producing a cross-sectional display of discontinuities of radiodensity within an irregular object, such as the head, was described by Oldendorf (9–11). He used a γ-ray source and a collimated scintillation counter to detect discontinuities in a rotating model. *Computerized tomography*, a technique capable of presenting an image of a cross section of the brain or body, is a remarkable method for x-ray examination of soft tissue. It was developed by Godfrey Hounsfield and Allan Cormack, who were awarded the Nobel Prize for Physiology and Medicine in 1979 for the importance of their contribution. This system utilizes scintillation counters as the primary detector, rather than x-ray film, and the information is fed into a computer capable of direct imaging. Using scintillation counters to detect photon attenuation (i.e., absorption coefficients) instead of x-ray film increases the sensitivity of the method by two orders of magnitude (6, 8). This procedure uses an x-ray tube, which gives off a series of narrow, highly-collimated beams of radiation, and photon detectors (sodium iodide crystals and photomultipliers) accurately aligned with the x-ray source to provide a detailed plot of the x-ray absorption coefficients in the scanned cross section of the body. The x-ray beam and the photon detectors scan the head in a linear fashion allowing 160 readings of photon transmission. The scanning unit is then rotated 1° around the head and the process is repeated; 180 scans are taken, each with the apparatus rotated an additional 1°. This results in 28,800 readings of photon detectors which are processed by a computer capable of calculating 6400 absorption values for each brain slice. From the computer calculations, a picture of the brain slice is constructed in the form of a matrix (80×80) of 6400 picture points (or pixels), each indicating an absorption coefficient value. Considerably greater definition is supplied by newer instruments using a 160×160 (25,600 pixels) or 320×320 (102,400 pixels) matrix. Currently available CT equipment can produce scans that have a resolution of less than 1 mm. Hence, even though gray and white matter do not differ in radiodensity by more than 2%, they can be distinguished from each other in CT scans.

Although CT scans or computerized tomograms can be taken in a horizontal plane parallel to the anatomic baseline of Reid (a line joining the inferior orbital margin and the top of the auditory meatus), such scans do not permit visualization of all posterior fossa structures (Fig. 2.34). An example of a computerized tomogram in the horizontal plane and a corresponding section of the head and brain in the same plane are shown in Figures 2.35 and 2.36. To visualize the largest number of intracranial structures, including those in the posterior fossa, computerized tomograms usually are taken in parallel planes at angles of 25–30° with reference to the orbitomeatal baseline (Fig. 2.34). Another advantage of choosing such an angle is that the eye does not become involved and the whole brain can be scanned with a minimum amount of radiation.

Computerized x-ray tomography provides a pictorial cross-section of the intracranial contents and brain at multiple levels which cannot be obtained by any other radiologic technique. The method is entirely noninvasive and has the capacity to reveal differential densities in the components of the brain (e.g., gray and white matter). Certain contrast agents containing iodine can be used to enhance the contrast of tomograms, especially when lesions or neoplasms show increased vascularity.

Magnetic Resonance Imaging

Magnetic resonance imaging (MRI), previously called nuclear magnetic resonance (NMR), creates very detailed images of the brain and other body organs without using x-rays. First developed to measure the atomic constituent of chemical samples, it was recently combined with CT for spatial localization of atomic nuclei, and this combination has produced an imaging technique much more powerful than CT itself. This method is based on the *resonance* of certain atomic nuclei, such as hydrogen, when placed in a strong, static, and homogeneous magnetic field. The magnetic field used is as much as 60,000 times as strong as that of the earth and is produced by several powerful electromagnets supercooled by helium. To obtain an MRI signal, a brief pulse of radio waves at a given frequency is used to perturb the alignment of the spinning nuclei along the strong

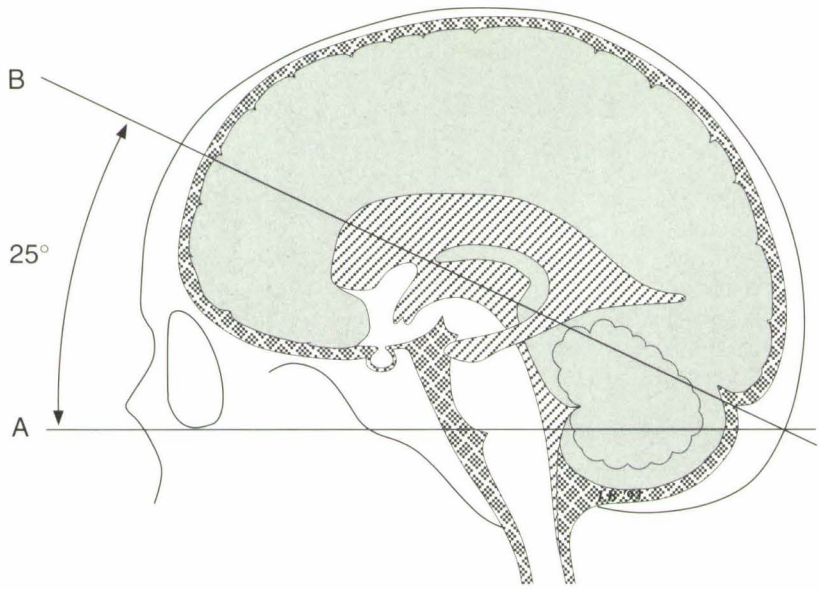


Figure 2.34. Head and brain demonstrating tomographic planes. The zero degree plane (*A*) corresponds to the orbitomeatal baseline which passes through the inferior margin of the orbit and the external auditory meatus. Tomograms taken in parallel planes at an angle of 25° to the baseline (*B*) provide more information about structures in the posterior fossa.

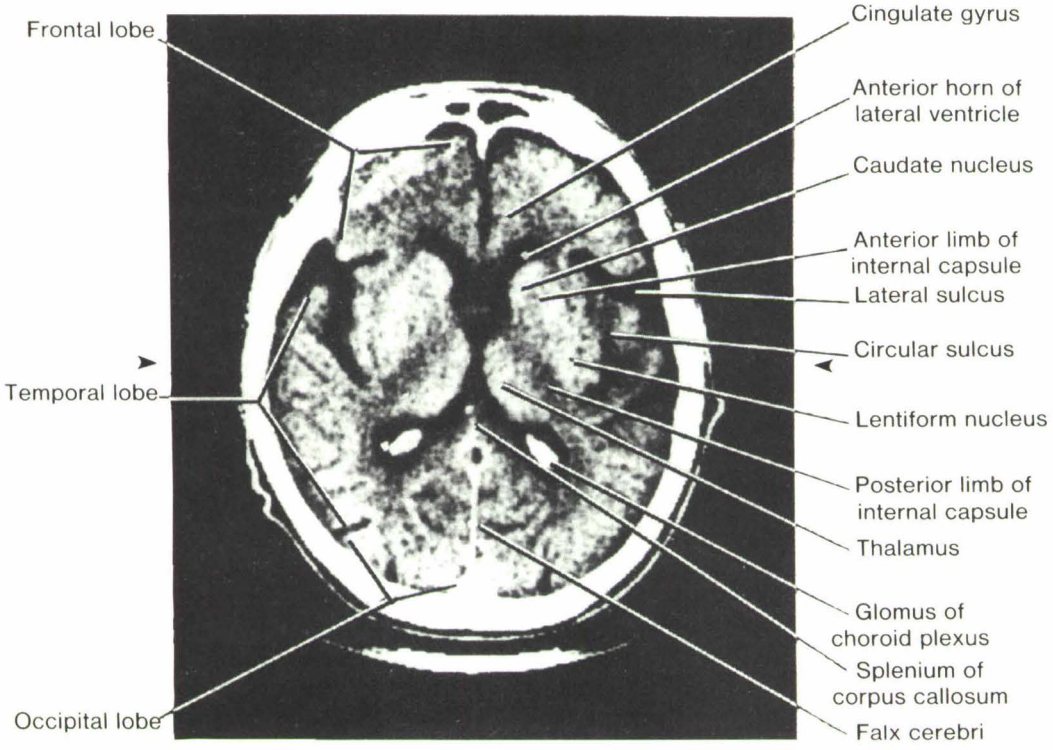


Figure 2.35. Computerized tomogram taken parallel to the zero degree plane through the thalamus internal capsule and basal ganglia.

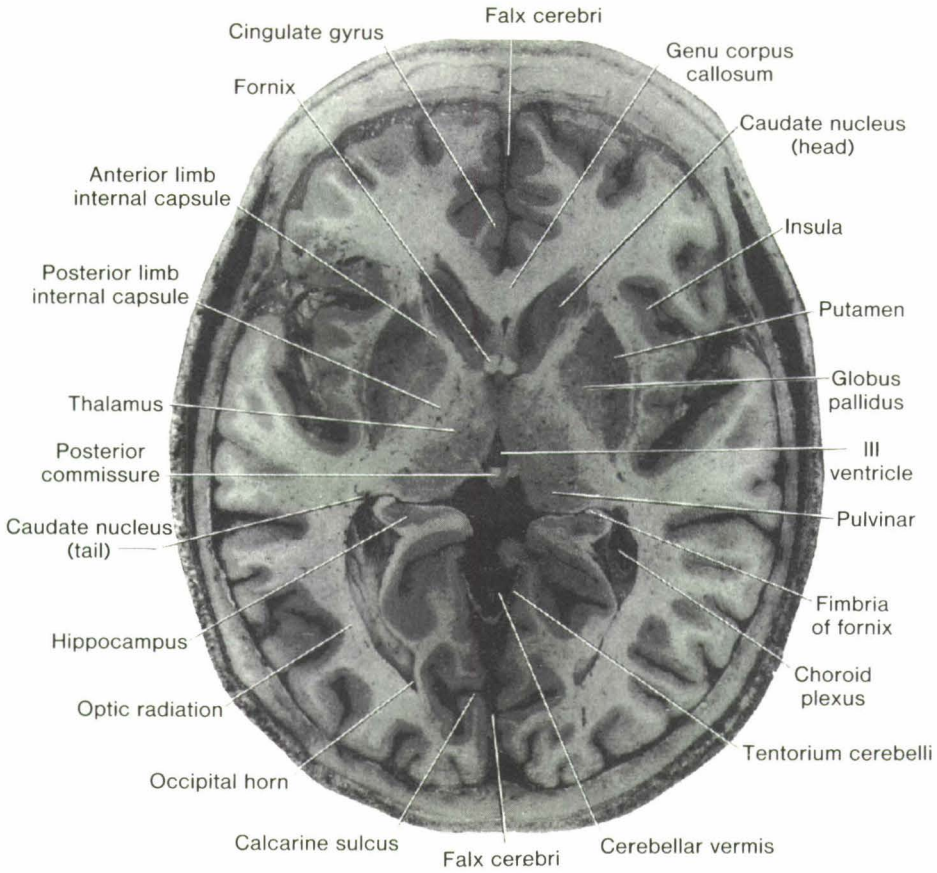


Figure 2.36. Section of the head and brain in the same horizontal plane as the computerized tomogram shown in Figure 2.35.

magnetic field. When this pulse is turned off, the nuclei tend to return to their original orientation, and in doing so release energy in the form of faint radio waves that are used to construct the images (6, 12).

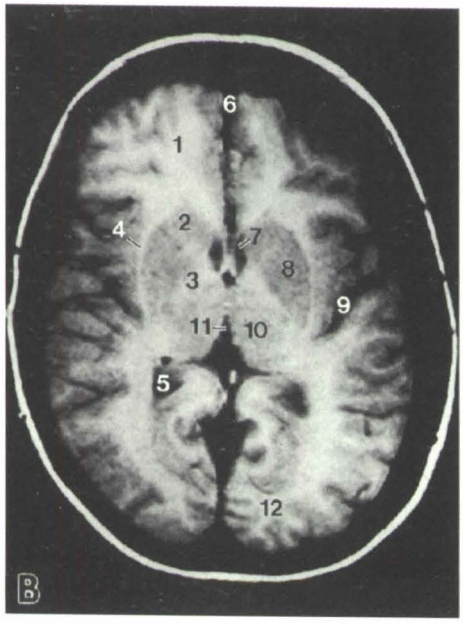
The radiofrequencies emitted are different for each atom and the strength of the radio wave at each frequency is proportional to the number of atomic nuclei of each kind in the sample. The rate at which a group of nuclei return from an excited to a lower energy state is termed *relaxation* and is usually expressed by its time constant (T). Two types of relaxation are of particular importance: spin-lattice relaxation (T_1) and spin-spin relaxation (T_2). Relaxation times are influenced by local tissue conditions so that images emphasizing either T_1 or T_2 help in discriminating between normal tissues of various compositions and pathologic processes.

The hydrogen atom, whose nucleus comprises a single proton, is a particularly good candidate for MRI scanning because of its abundance in the body and its prominent magnetic qualities. Hydrogen largely reflects water content, which varies from one brain region to the other (e.g., there is more water in gray than in white matter). Therefore, by manipulating the radiofrequency signal to which the tissue is exposed, the relaxation time of protons in water can be enhanced and a strikingly differentiated image of a section of the brain can be produced by MRI. In contrast to soft tissues, bones contain little free water so that their image in MRI scans of the head is usually faint and does not compromise the visualization of brain structures. In fact, due to its ability to clearly distinguish between white and gray matter, the images obtained in a living brain with MRI reveal almost as many details as one can obtain with fixed and sectioned anatomic material (Figs. 2.37–2.39).

MRI can greatly facilitate clinical diagnosis. The analysis of relaxation times, which varies and depends on local tissue conditions, enables clinicians to detect pathologic processes such as small infarctions, tumors, or the plaques of multiple sclerosis (Fig. 2.40).

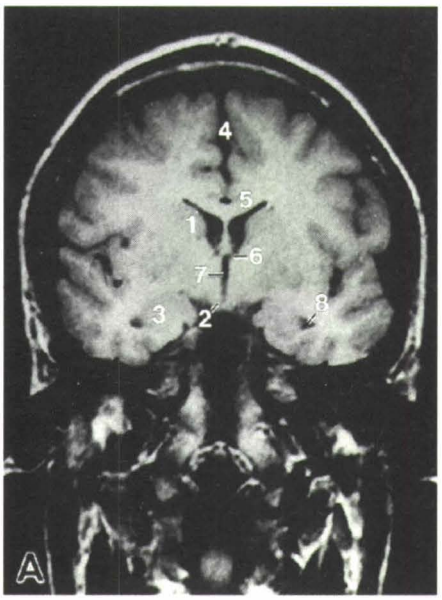


1- Optic nerve
2- Crus cerebris
3- Inferior colliculus
4- Vermis of cerebellum
5- Temporal Horn
6- Cerebral aqueduct
7- Occipital lobe

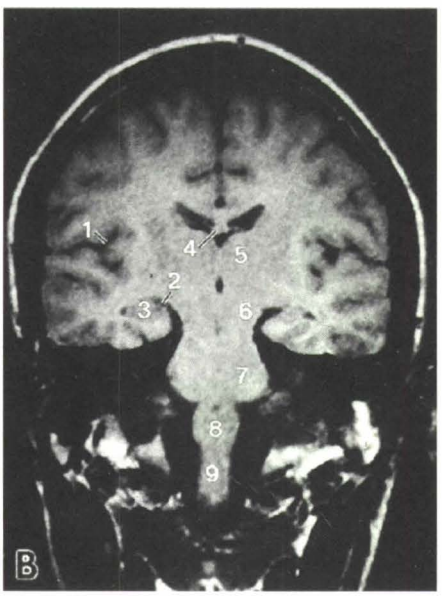


1- Frontal lobe
2- Caudate nucleus
3- Internal capsule
4- External capsule
5- Trigone
6- Interhemispheric fissure
7- Frontal horn
8- Lentiform nucleus
9- Lateral fissure
10- Thalamus
11- Third ventricle
12- Occipital lobe

Figure 2.37. Magnetic resonance imaging (MRI) of two horizontal sections (or slices) of the brain parallel to the orbitomeatal line in a healthy human subject. **A.** A ventral section passing through the midbrain. **B.** A more dorsal section passing through the basal ganglia. T_1-weighted images (TR 500 msec, TE 30) carried out with 1.5 Tesla Philips gyroscan unit.

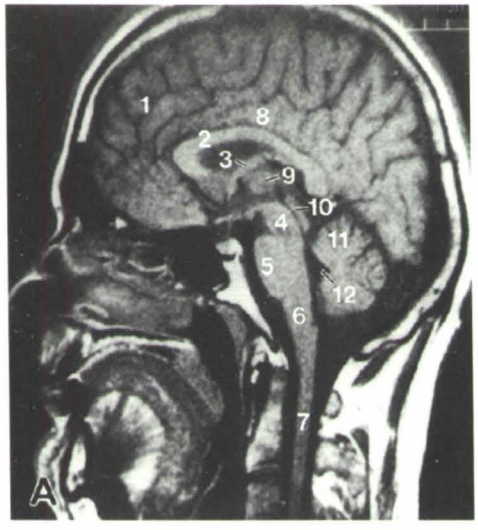


1- Caudate nucleus
2- Mammillary body
3- Amygdala
4- Interhemispheric fissure
5- Corpus callosum
6- Interventricular foramen
7- Third ventricle
8- Temporal horn

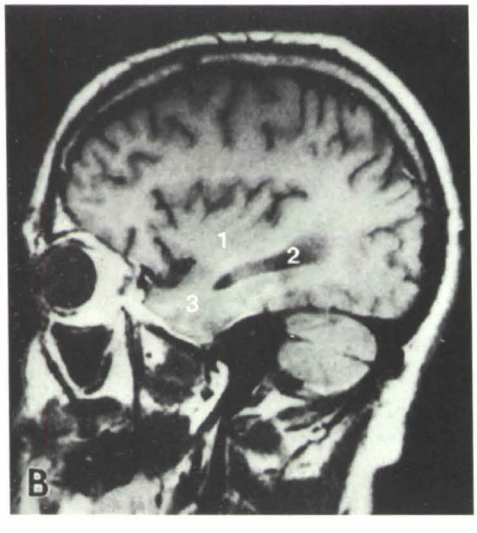


1- Lateral fissure
2- Choroidal fissure
3- Hippocampal gyrus
4- Fornix
5- Thalamus
6- Crus cerebri
7- Pons
8- Medulla
9- Spinal cord

Figure 2.38. MRI images of two frontal sections of the same subject as in Figure 2.37. **A.** A somewhat rostral section, passing through the basal ganglia and rostral pole of the temporal lobe. **B.** A more caudal section showing the brainstem and the thalamus. T_1-weighted images (TR 500 msec, TE 30) carried out with 1.5 Tesla Philips gyroscan unit.



1- Frontal lobe
2- Corpus callosum
3- Fornix
4- Midbrain tegmentum
5- Pons
6- Medulla
7- Spinal cord
8- Gyrus cingulis
9- Massa intermedia
10- Quadrigeminal plate
11- Vermis of cerebellum
12- Fourth ventricule



1- Insula
2- Temporal horn
3- Temporal lobe

Figure 2.39. MRI images of two parasagittal sections of the same subject as in Figures 2.37 and 2.38. **A.** Section along the midline showing the medial surface of the hemisphere and the entire brainstem. **B.** A more lateral section depicting the insula and part of the temporal lobe. T_1-weighted images (TR 500 msec, TE 30) carried out with 1.5 Tesla Philips gyroscan unit.

Research is under way to develop MRI scanners that detect other elements, such as sodium or phosphorus, whose altered properties could provide early warning signs of cerebral infarction or metabolic diseases. However, sodium and phosphorus imaging requires a magnetic field that is even stronger than that used for hydrogen imaging.

Positron Emitting Tomography

Positron emitting tomography (PET) is a technique that combines CT with radioisotope imaging and allows exploration of various functions of the living brain. In contrast to CT, which depends on transmission tomography, PET images depict the distribution in the tissue of injected or inhaled isotopes that emit positrons (positively charged electrons). The most commonly used positron-emitting isotopes are ^{11}C, ^{13}N, ^{15}O, and ^{18}F. Any one of these radioisotopes can be bound to compounds of biologic interest, such as water, glucose, neurotransmitters, or ligands that bind to particular receptors on neuronal membranes, so that it becomes pos-

sible to map the distribution of these various compounds within the brain (3, 6).

These positron-emitting isotopes have relatively short half-lives (minutes to hours) so that they must be generated shortly before their use. Hence, they are usually made on site by accelerating protons in a small, low-energy cyclotron at very high rates until they collide into the stable nuclei of nitrogen, oxygen, carbon, and fluorine. In their normal state, these nuclei contain protons and neutrons in equal numbers and incorporation of an extra proton produces an unstable isotope. To regain stability, the proton is broken down into a neutron and a positron. The neutron remains within the nucleus because a stable nucleus can accept extra neutrons. In contrast, the positron is an unstable particle, which tends to travel away from the site where it was generated. Along its course, the positron eventually collides with an electron and this event leads to the annihilation of the two particles and the release of a burst of energy in the form of two γ-rays. These rays are emitted precisely at 180° from each other and are simultaneously detected by crystal photomultipliers that surround the patient's head. A computer records the precise location of the site of γ-ray emission and uses this information to construct the image.

One of the most interesting possibilities of PET scanning is the mapping of regional brain activities through the monitoring of local variations in neuronal glucose metabolism. It is possible to map glucose metabolism by using *2-deoxyglucose*, an analogue of glucose. This compound is readily taken up by neurons and phosphorylated by hexokinase in the same manner as glucose. Unlike glucose, however, phosphorylated deoxyglucose cannot be further metabolized nor can it exit from neurons by traversing the cell membrane. Therefore, 2-deoxyglucose accumulates within active neurons where it can be visualized with PET scanning if, prior to its intravenous injection, the compound has been tagged with the positron-emitting isotope of fluorine (^{18}F). Assuming that the uptake of ^{18}F-deoxyglucose into neurons is directly proportional to the degree of activity of these neurons, active brain areas will appear more heavily labeled than inactive ones in PET images.

Figure 2.41**A** shows PET scans of 14 brain sections, each section being 14 mm apart from each other and aligned parallel to the orbitomeatal line. In this case, the isotope ^{18}F-deoxyglucose was used to measure glucose metabolism in various brain areas in a normal person at rest. The resolution (4–8 mm) of current PET scanners is modest by comparison to those of MRI and CT scanners. Yet,

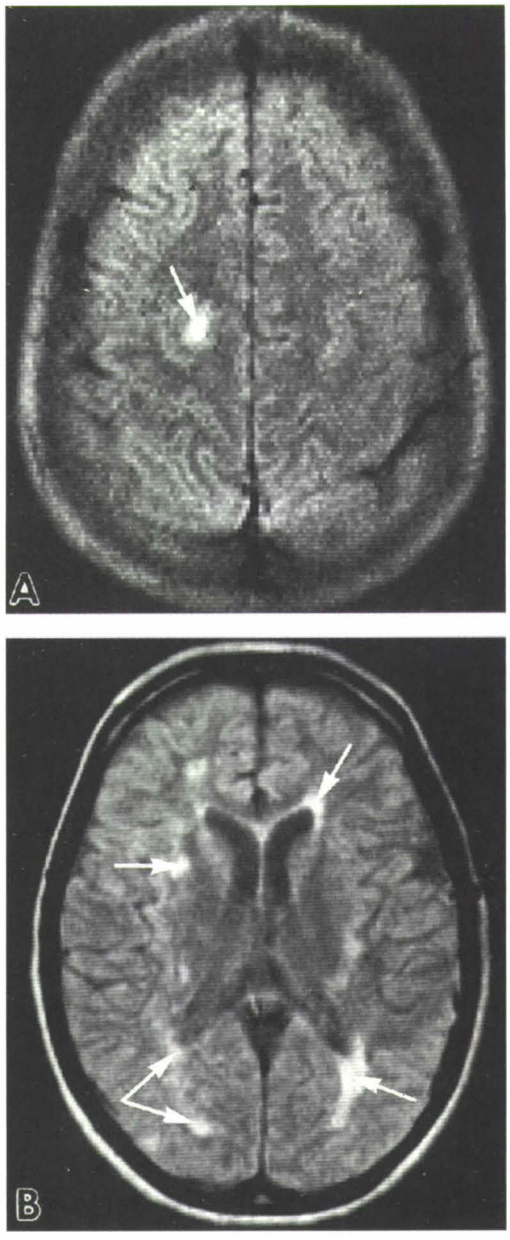


Figure 2.40. Spin-echo MRI images from patients with multiple sclerosis. **A.** Axial (horizontal) section high in the brain showing a single lesion (*arrow*) in a neurologically unimpaired patient with multiple sclerosis. **B.** Axial (horizontal) section through the basal ganglia depicting multiple lesions (*arrows*) in the brain of a moderately impaired patient with long standing multiple sclerosis.

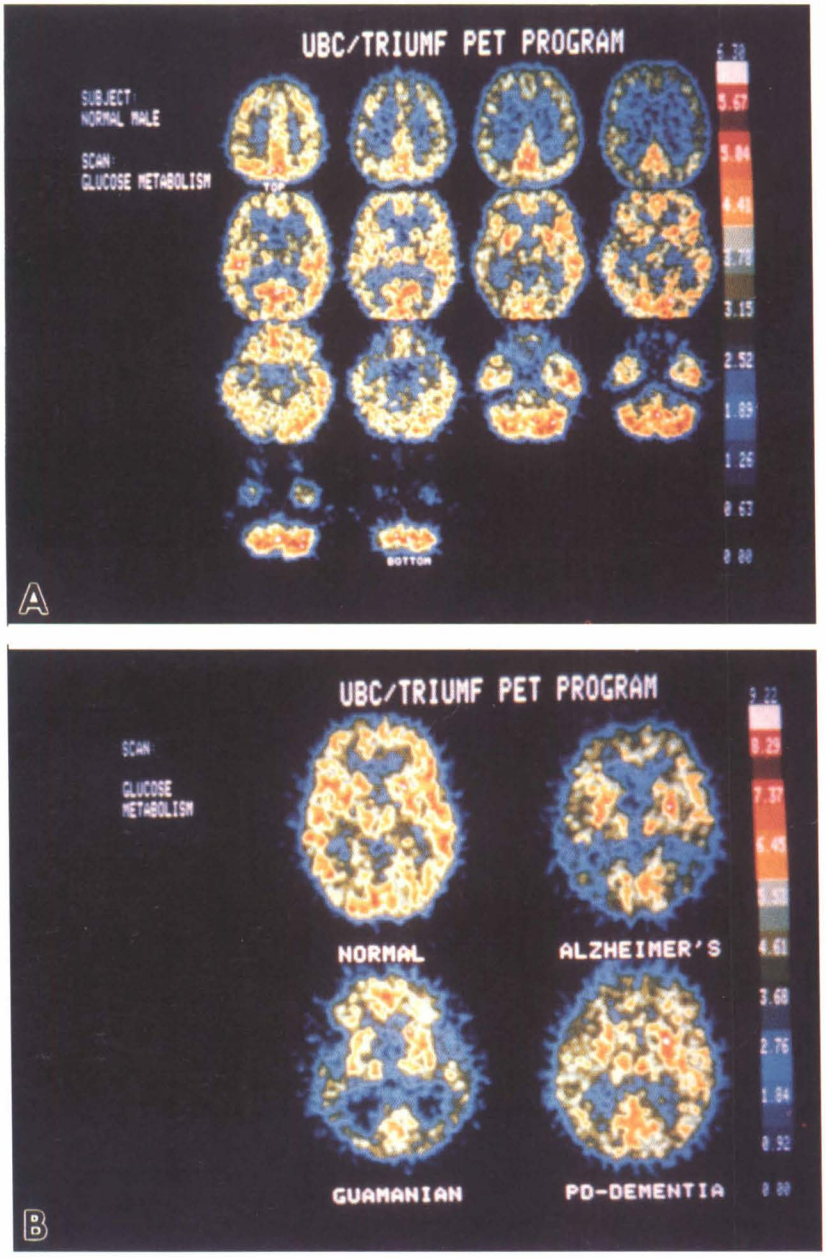


Figure 2.41. Positron emission tomography (PET) images. **A.** Fourteen interleaved PET axial slice images of regional cerebral glucose metabolism, as measured by fluorodeoxyglucose (^{18}F-2-fluoro-2-deoxy-D-glucose), in a normal human brain, with the highest brain slice at the top left and the lowest at bottom right. The slice thickness varies with radius from 10–16 mm, and the in-plane resolution is 8–9 mm. **B.** Four PET axial slice images through the basal ganglia showing regional cerebral glucose metabolism as measured with ^{18}F-deoxyglucose in the brains of a normal subject and subjects suffering from Alzheimer's disease, the Guamanian ALS-Parkinson's-dementia complex, and dementia associated with Parkinson's disease.

despite this relatively poor spatial resolution, one can clearly see the contours of various gyri and sulci, as well as subcortical structures such as the thalamus and the basal ganglia, in these PET scans. PET scans can also reveal major disturbances in glucose metabolism in certain diseases, such as dementia of the Alzheimer's type and dementia present in patients suffering from the Guamanian amyotrophic lateral sclerosis-Parkinson's-dementia complex or Parkinson's disease (Fig. 2.41**B**). The Guamanian syndrome is a complex disease characterized by motor deficiencies resulting from a combined lesion of vari-

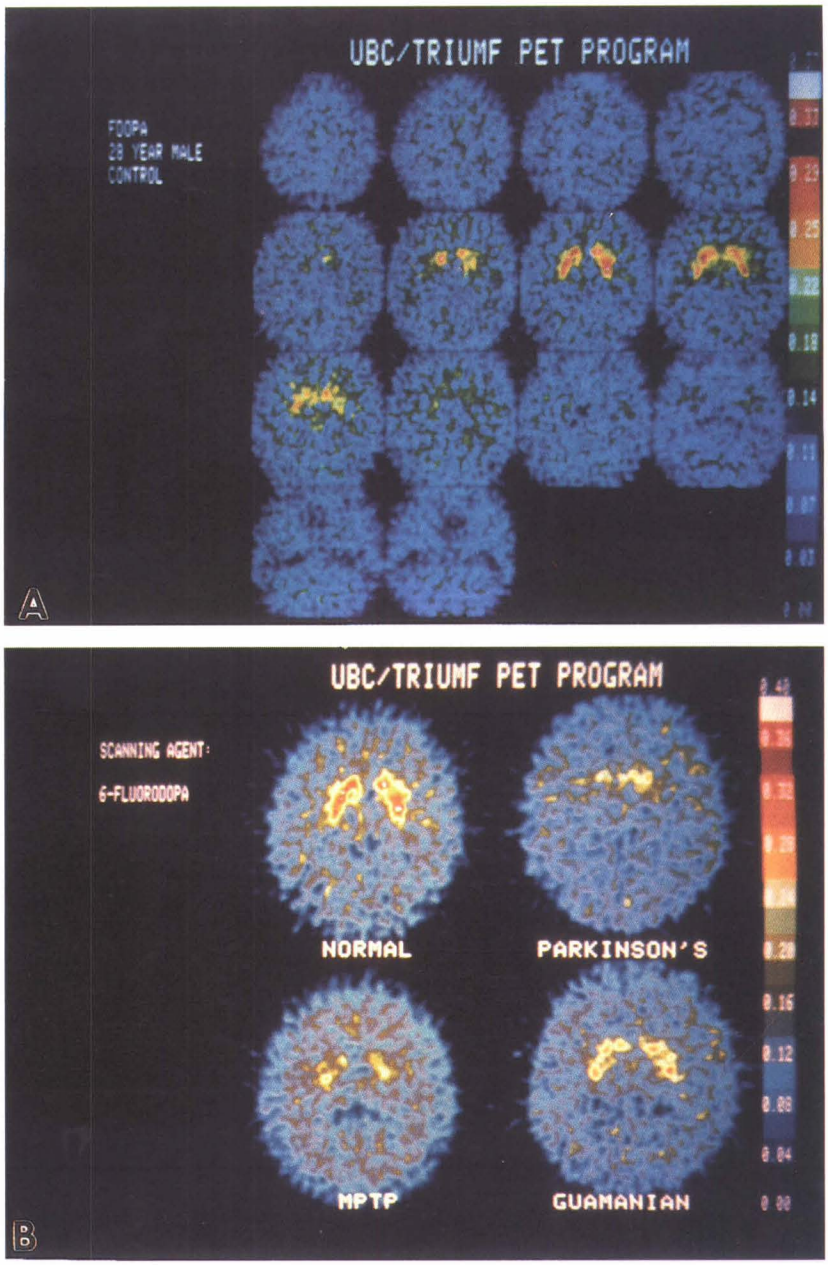


Figure 2.42. Positron emission tomography (PET) images. **A.** Fourteen interleaved PET axial slice images of fluorodopa (^{18}F-6-fluorodopa) uptake in the brain of a normal subject. Slice locations and thickness are similar to those in Figure 2.41A. **B.** Four PET axial slice images through the basal ganglia showing ^{18}F-6-fluorodopa uptake in the brains of a normal subject, one suffering from early Parkinson's disease, an asymptomatic subject known to have ingested MPTP neurotoxin, and one suffering from the Guamanian ALS-Parkinson's-dementia complex.

ous portions of the pyramidal motor tract and motoneurons at spinal cord level (amyotrophic lateral sclerosis or ALS), together with the cardinal signs of Parkinson's disease (akinesia, rigidity, and tremor) and an impairment of higher mental functions (dementia). Although present in all parts of the world, this disease is particularly frequent on the island of Guam, from which it derives its name.

PET scan can also be used to probe the functional status of various neurotransmitter systems in the living brain. This is the case with the neurotransmitter dopamine, which

is produced by neurons of the substantia nigra at midbrain level and acts principally within the striatum at telencephalic level. Areas of the brain containing high concentrations of dopamine can be visualized with PET scans by using the isotope fluorodopa (^{18}F-dopa). L-dopa, the immediate metabolic precursor of dopamine, is preferred to dopamine because it crosses the blood-brain barrier much more easily than the neurotransmitter (Fig. 1.15). Figure 2.42**A** displays PET scans of 14 brain sections (slices) obtained with ^{18}F-dopa. At the spatial resolution of these scans, we can see that the most heavily labeled areas of the brain correspond to the basal ganglia and particularly to the striatum, which can be visualized on both sides of the brain on sections 6 to 9 from top to bottom.

Lesions of the nigrostriatal dopaminergic system resulting in a marked depletion of striatal dopamine is believed to be the major cause of Parkinson's disease. A decrease in striatal dopamine concentration is readily detected with PET scans, as illustrated in Figure 2.42**B**. This Figure shows four brain sections through the basal ganglia in a normal subject, one suffering from early Parkinson's disease, an asymptomatic subject known to have ingested the neurotoxin MPTP, and one suffering from the Guamanian ALS-Parkinson's-dementia complex. The compound MPTP (1-methyl-4-phenyl-1,2,3,6-tetrahydropyridine) is a synthetic analogue of the narcotic analgesic meperidine (Demerol). When administered systemically it produces a marked degeneration of dopaminergic cell bodies of the substantia nigra, which rapidly leads to severe Parkinson's disease, as observed in young adults who injected themselves with this drug on the street. This neurotoxin is currently used to produced animal models of Parkinson's disease in nonhuman primates.

In addition to neurotransmitters and their precursors, molecules that bind to specific neurotransmitter receptors on the surface of neurons have been labeled with positron-emitting isotopes and used successfully with PET scans. For example, ^{11}C-N-methylspiperone, a ligand that preferentially binds to dopaminergic receptors, has been used to map receptor locations in the living brain. Additionally, subclinical impairment of the dopaminergic nigrostriatal system can be detected with PET scan by combining the use of ^{18}F-dopa and ^{11}C-nomifensine. In such a case, the kinetics of ^{18}F-dopa uptake gives an indication of the dopamine storage capacity of the striatum, whereas ^{11}C-nomifensine allows to assess the integrity of the dopamine re-uptake sites in the same structure. Because of its ability to reveal the distribution of specific neurotransmitters as well as metabolic substrates, PET permits a more functional approach to the anatomic study of the human brain. This cell-biologic approach may soon lead to major revisions of our basic concepts of the anatomy and physiology of the nervous system.

References

1. Broca P. Anatomie comparée des circonvolutions cérébrales: le grand lobe limbique et la scissure limbique dans la série des mammifères. Rev Anthropol (Ser. 2) 1878;1:384–498.
2. Brodal A. Neurological anatomy in relation to clinical medicine. 3rd ed. New York: Oxford University Press, 1981.
3. Brownell GL, Budinger TF, Lauterbur PC McGeer PL. Positron tomography and nuclear magnetic resonance imaging. Science 1982;215: 619–626.
4. Gazzaniga MS. The bisected brain. New York: Appleton-Century-Crofts, 1970.
5. Gazzaniga MS, Sperry RW. Language after section of the cerebral commissures. Brain 1967;90: 131–148.
6. Martin JH, Brust JCM, Hilal S. Imaging the living brain. In: Kandel ER, Schwartz JH, Jessell TM, eds. Principles of neural science. Ch. 22. Amsterdam: Elsevier, 1991:309–324.
7. Mettler FA. Neuroanatomy. 2d ed. St. Louis: C.V. Mosby, 1948.
8. New PFJ, Scott WR. Computer tomography of the brain and orbit (EMI scanning). Baltimore: Williams & Wilkins, 1975.
9. Oldendorf W, Oldendorf W Jr. MRI primer. New York: Raven Press, 1991.
10. Oldendorf WH. Isolated flying spot detection of radiodensity discontinuities—displaying the internal structural pattern of a complex object. IRE Trans Biomed Electron 1961;8:68–72.
11. Oldendorf WH. The quest for an image of brain: computerized tomography in the perspective of past and future imaging methods. New York: Raven Press, 1980.
12. Pykett IL. NMR imaging in medicine. Sci Am 1982;246:78–88.
13. Truex RC, Kellner CE. Detailed atlas of the head and neck. New York: Oxford University Press, 1948.

3
Development of the Nervous System

DETERMINATION AND DIFFERENTIATION

The central nervous system (CNS) is a segmented entity whose complexity increases markedly as it develops. Part of this complexity derives from the fact that the various segments of the CNS do not develop at the same rate and that each segment acquires its adult form by going through a succession of highly specific developmental events. The development of the nervous system, like that of any other system or organ of the body, proceeds according to two fundamental sequences—*determination* and *differentiation*. Determination refers to the event whereby a certain cell population of the embryo gives rise to cells of the nervous system (neurons and glia), whereas differentiation alludes to the cellular processes which ensures that the cells arising from the determined population will be the source of subpopulations of neurons and glial cells that are specific to each region of the CNS. The term differentiation thus applies to the complex mechanisms whereby neurons will proliferate and migrate to appropriate locations within the nervous system, and ultimately make highly specific connections with their targets. Neuronal differentiation is, in fact, the result of elaborated interactions between the developing neuron and its microenvironment, that is between intrinsic (genetic) and extrinsic (epigenetic) factors (5, 13, 21, 33). Such poorly understood interactions are currently the subject of active researches in developmental neurobiology whose aim is to elucidate the molecular basis of neuronal development. The present chapter describes the major developmental events that lead to the formation of the nervous system in humans. A proper knowledge of these events will greatly facilitate the understanding of the anatomical organization of the CNS and the comprehension of various malformations of the CNS.

FORMATION OF NEURAL TUBE

The fertilized ovum undergoes a period of cell division until it reaches the uterus. At this time, the spherical ball of cells develops a cavity, forming the blastula. A bilaminar layer of cells, called the embryonic disk, develops a few days after the blastula and becomes implanted into the uterine wall (Fig. 3.1). During the third week of development, the embryonic disk becomes trilaminar, and at this stage the three primary tissues of the embryo, ectoderm, endoderm, and mesoderm, can be distinguished. Additionally, a cord of mesodermal cells, the *notochord*, lies directly beneath the most dorsal portion of the ectoderm.

The interaction between the notochord and its overlying ectoderm is of utmost importance because the notochord will induce the ectoderm to form the hollow *neural tube* which will differentiate into the brain and spinal cord (13). The action by which the notochord instructs the ectoderm to become the neural tube is called *primary embryonic induction* or, more specifically, *neural induction*. The cellular response by which the flat layer of ectoderm cells is transformed into a hollow tube is called *neurulation*. Early in development, neural induction imposes a regional specificity along the rostrocaudal axis of the ectoderm (or neuroectoderm) and this specificity is irreversible. As a result, the major subdivisions of the CNS (forebrain, midbrain, hindbrain, and spinal cord) are already specified in the neuroectoderm and this specification appears to be irreversible (5, 21, 33).

Neurulation is a highly complex and multifactorial process resulting from forces both intrinsic and extrinsic to the neuroectoderm. It is driven by changes in neuroectodermal cell shape, as well as other form-shaping events, in which microtubules, microfilaments, and other elements of the cytoskeleton are involved (50). The first stage of neurula-

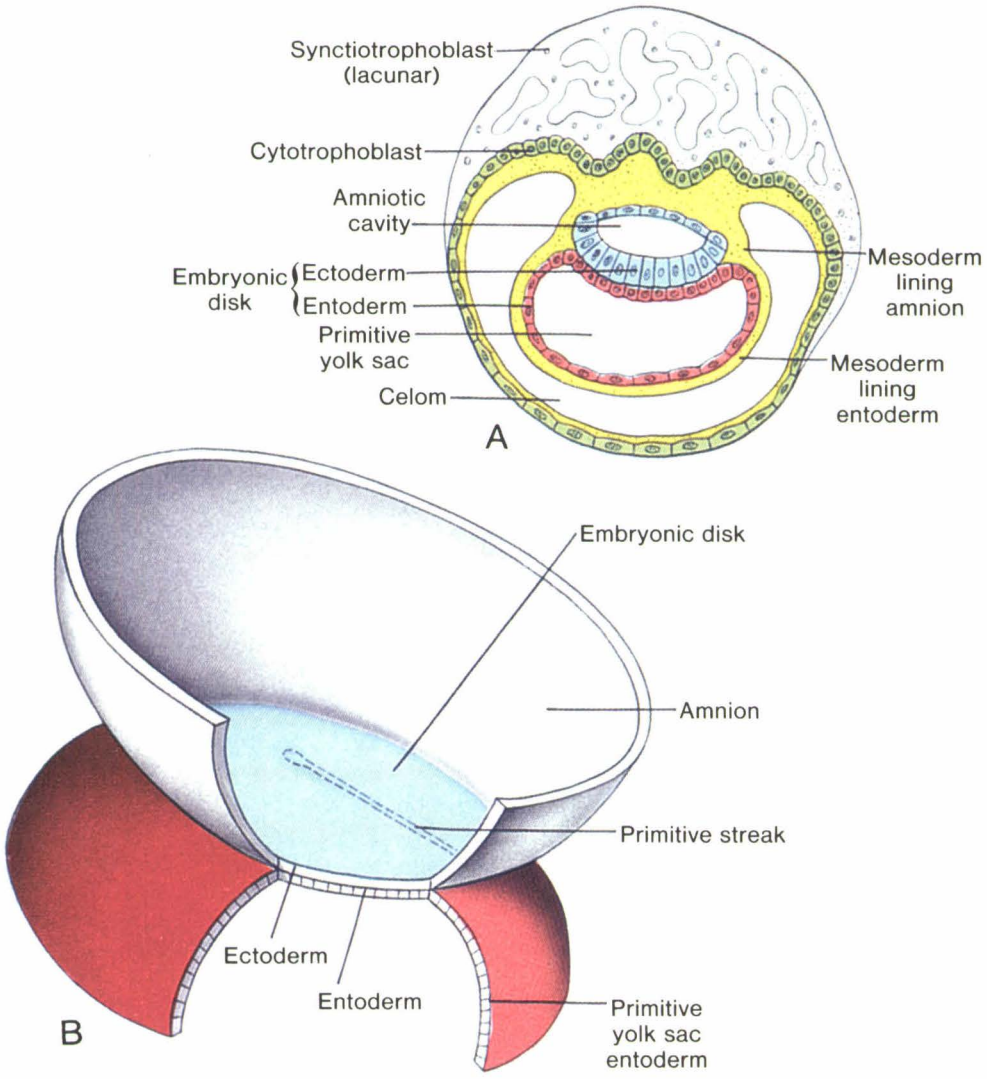


Figure 3.1. **A.** Embryonic disk in a blastocyst at the end of the second week of development: cytotrophoblasts are *green*; mesoderm is *yellow*; ectoderm is *blue*; and endoderm is *light red*. **B.** Schematic diagram of the embryonic disk viewed from the amniotic cavity. The appearance of the primitive streak indicates the start of gastrulation.

tion is characterized by the formation of a thickened plate of neuroectoderm known as the *neural plate*, which first appears late in the third week of fetal life and contains about 125,000 cells. As much as 50% of the ectoderm is included in this plate (13). Initially, the neural plate lies dorsally, rostral to the primitive streak and Hensen's node (7, 20, 32,) (Fig. 3.2), and consists of a single layer of cells. This neuroectoderm undergoes rapid proliferation and becomes stratified. The growth rate near the margins of the plate exceeds that in the midline, causing the formation of a *neural groove*, which is bounded on each side by an elevated *neural fold* (Fig. 3.3). As the primitive neuroectodermal cells proliferate, the neural groove deepens, and the neural folds thicken, become more prominent, and ultimately fuse dorsally to form the neural tube. Closure of the neural tube begins in the region of the fourth somite (i.e., future cervical region) and proceeds in both cranial and caudal directions. During the formation of the neural tube its lumen has temporary cranial and caudal connections with the amniotic cavity via the *anterior (rostral)* and *posterior (caudal) neuropores* (Fig. 3.2). The anterior neuropore which represents the most rostral opening of the embryonic neural tube closes in embryos of 18 to 20 somites and the zone of closure ulti-

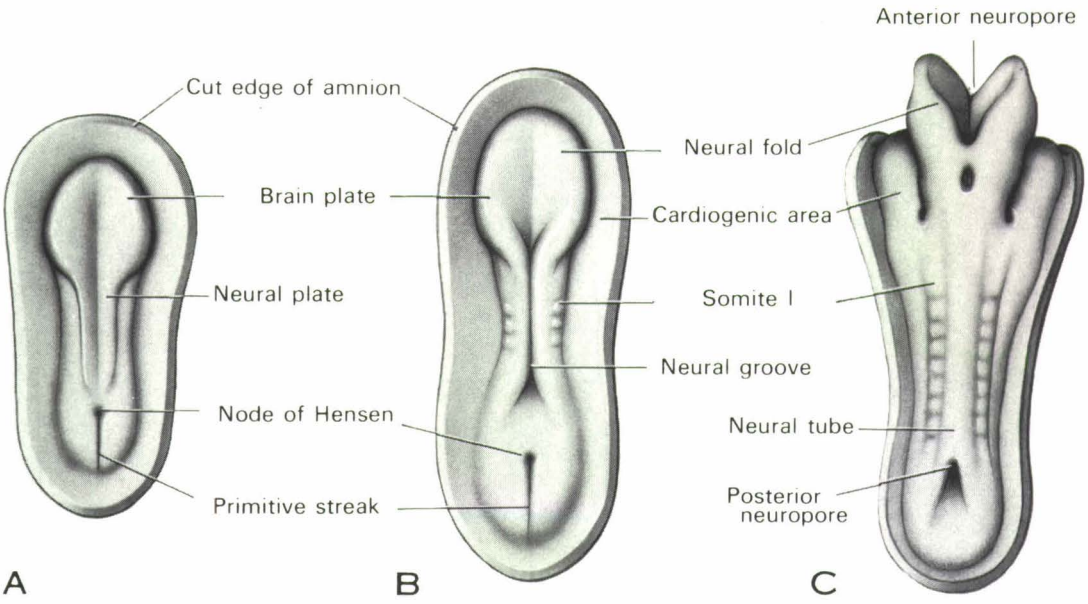


Figure 3.2. Early development of the human nervous system. **A.** Late presomite and early neural plate stage. **B.** Early somite and neural groove stage. **C.** Eight-somite and early neural tube stage.

mately becomes the *lamina terminalis*. The posterior neuropore usually closes later when the embryo has reached the 25 to 26 somite stage. At early stages in the formation of the neural tube, before closure is complete, rostral portions of the neural tube are enlarged and indicate the formation of primary brain vesicles. Three primary brain vesicles are evident by the time the neural tube is completely closed (19) (Fig. 3.10). The brain is formed from these primary vesicles. Caudal portions of the neural tube which remain relatively small in diameter form the spinal cord. The appearance of the neural folds heralds the segmentation of bilateral strips of paraxial mesoderm into somites (Figs. 3.2 and 3.3). New somites continue to be formed in a craniocaudal sequence and at the end of the fourth week 40 somites normally are present.

NEURAL CREST

The lateral margins of the neural plate are thinner and continuous with the general body ectoderm. The thinned lateral margins of the neural plate (neural crest cells) are approximated as the neural folds meet and fuse. Neural crest cells form a temporary intermediate layer between the neural tube and the surface ectoderm (Fig. 3.3). This temporary layer extends from the level of the mesencephalon to the caudal somites and, is for a time, continuous across the midline. Neural crest cells migrate laterally, then divide and become segmented into cell clusters between the neural tube and the somites (Fig. 3.3). These clusters of neural crest cells give rise to the primary sensory neurons of the dorsal root ganglia of spinal nerves. Similar cell clusters in the hindbrain give rise to sensory neurons which form cranial nerve ganglia (N. V, VII, VIII, IX, and X), but these are not segmentally arranged (Fig. 3.10). The neural crest has a temporary existence as its cells migrate widely in the body and undergo various differentiations in different tissues (30). All of the sensory cells of the peripheral nervous system (with a few exceptions), and most of the peripheral cells of the autonomic nervous system, are derived from the neural crest. Thus, the neural crest gives rise to the unipolar spinal ganglion cells and their equivalent in the sensory ganglia of cranial nerves V, VII, IX, and X. Some elements persisting as bipolar cells form the auditory nerve. Other derivatives of the neural crest include (a) the neurolemmal sheath cells of all peripheral nerves, (b) capsule cells in ganglia, (c) sympathetic ganglia, (d) chromaffin cells, and (e) pigment cells (30).

Cells of the sympathetic ganglia and the chromaffin cells of the adrenal medulla produce high levels of specific amines such as norepinephrine (noradrenaline) or epineph-

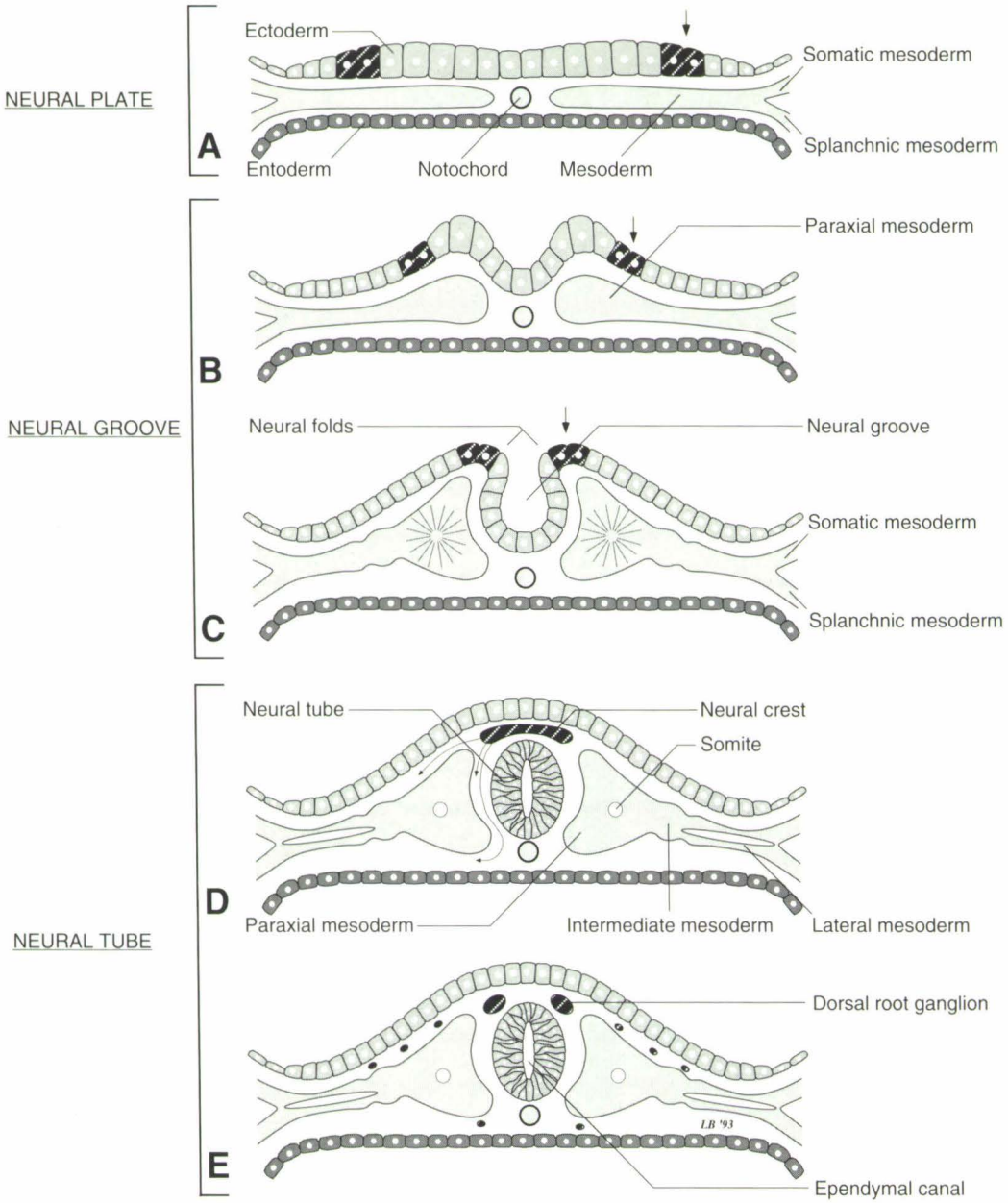


Figure 3.3. Transverse sections of embryos at different ages to show development of the spinal cord. **A.** Neural plate stage. **B.** Early neural groove stage. **C.** Late neural groove stage. **D.** Early neural tube and neural crest stage. **E.** Neural tube and dorsal root ganglion stage.

rine (adrenaline). Other cells that contain high concentrations of amines are found throughout the gut and its associated glands. These have been termed APUD (amine precursor uptake and decarboxylation) cells. APUD cells can be recognized with fluorescent histochemical techniques. Some of the polypeptide hormone-producing cells in the pancreas, stomach, and other parts of the gut also show a fluorescent histochemical reaction, but it cannot be assumed that these cells are of neural crest origin (41).

It is also important to realize that cells of the neural crest, as well as any other neurons, are influenced by the local environment during their migration. The target of the migrating crest cells plays a crucial role in their differentiation. For instance, analysis of sympathetic neurons developing in cell culture show that neurons normally utilizing

norepinephrine as a neurotransmitter (i.e., noradrenergic neurons) can be changed to neurons using acetylcholine (i.e., cholinergic neurons) under the influence of soluble factors released by nonneuronal cells normally present in the local environment (30). A similar switch in the expression of neurotransmitter phenotype has been shown to occur during the normal development of the sweat glands in the rat (27). In this particular case, neurons that innervate developing sweat glands are noradrenergic at the time of innervation, but as the glands and their innervation mature, cholinergic properties appear. The finding that targets can retrogradely specify the transmitter phenotype of neurons that innervate them provides important insight into the role that neuronal targets can play during development. For example, it is well-established that targets can determine the final number of surviving neurons during the development of the vertebrate CNS. Furthermore, targets can influence the morphologic phenotype of the neurons that survive. For instance, the size of sympathetic neuron cell bodies and the extent of branching of their dendritic arbors is influenced by the size of the target that they innervate during development (27). Likewise, peripheral targets of sensory neurons, such as skin or muscle, may determine the nature and specificity of their central connections as well as that of the neurotransmitter they contain.

HISTOGENESIS OF NEURAL TUBE

The histogenetic changes whereby the columnar neuroectoderm is converted to nervous tissue occur in characteristic areas of the neural tube called *germinal zones*. In most regions of the CNS, these germinal zones are located near the lumen of the central canal, which will later form the ventricular system of the brain. The recently closed neural tube consists of only one type of cell, the undifferentiated *neuroepithelial cell* or *stem cell*. In the germinal zone, the neuroepithelial cells form a pseudostratified epithelium which extends from the *internal limiting membrane* to the *external limiting membrane* (Fig. 3.4). Each neuroepithelial cell is wedge-shaped and possesses cytoplasmic processes which reach the internal limiting membrane and are attached to adjacent cells by *terminal bars*. Nuclei of neuroepithelial cells that will divide undergo characteristic oscillatory movements (12, 49). First, the nucleus of an actively dividing cell migrates toward the external limiting membrane and then moves back toward the internal limiting membrane. Deoxyribonucleic acid (DNA) replication occurs only when the nucleus is near the external limiting membrane (in the so-called synthetic zone). Once DNA replication is complete, the nucleus moves toward the lumen of the neural tube (in the so-called mitotic zone) and the cell loses its contact with the external limiting membrane. Cells undergo mitosis only when the nucleus has reached the innermost zone, and daughter cells remain attached by the terminal bars at the internal limiting membrane. After division the cells elongate and their nuclei migrate toward the external limiting membrane where further DNA synthesis occurs. After several divisions, the stem cells lose their ability to divide. The postmitotic cells then leave the germinal zone of the ependymal layer and migrate to their appropriate position in the so-called mantle layer. The migrating cells are either immature neurons (*neuroblasts*) or glial cells precursors (*glioblasts*). In contrast to most neuroblasts, the glioblasts retain their capability to divide. Having reached their appropriate position in the mantle layer, the neuroblasts tend to send their processes into the outermost layer called the *marginal layer* (24) (Fig. 3.5).

NEURONS

The differentiation of neurons from primitive neuroepithelial cells involves three phases: (a) proliferation and generation of specific classes of neurons, (b) migration of cells to a specific position, and (c) maturation of cells and establishment of specific connections. Neuroblasts arising from division of neuroepithelial cells in germinal zones migrate into the mantle layer of the neural tube and increase in number as neuroepithelial cells continue to proliferate. These cells form rounded *apolar neuroblasts* (Fig. 3.6), which further differentiate into *bipolar neuroblasts* with two cytoplasmic processes on opposite sides of the cell body. One cytoplasmic process elongates to form a *primitive axon*, whereas the other cytoplasmic process develops numerous small outgrowths which arborize and form the *primitive dendrites*. At this stage, the cell becomes a *multipolar neuroblast*. Further growth and differentiation results in the formation of an adult nerve cell or *neuron*. The intense bursts of neuroblast proliferation that occur early in neurogenesis result in an

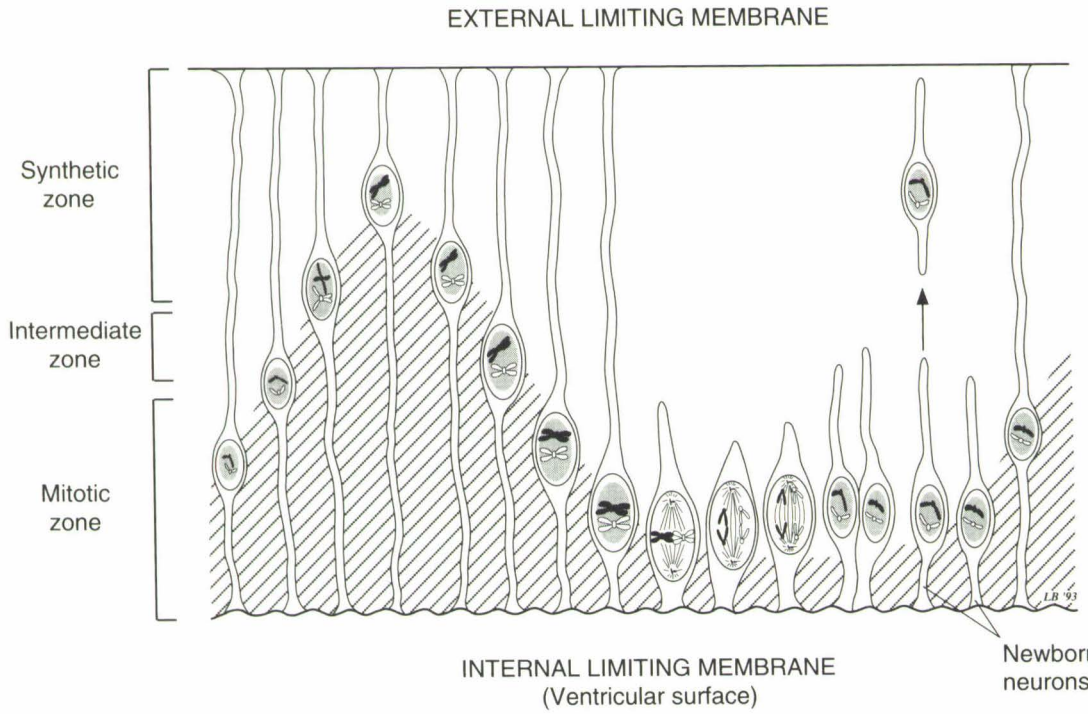


Figure 3.4. Characteristic oscillatory movement of the nuclei of the actively dividing cells in the germinal zone of the primitive neural tube. At the beginning of the cycle, the cells have long cytoplasmic processes that span the entire width of the germinal zone and their nuclei lie near the ventricular surface. The nuclei then migrate toward the external limiting membrane, into the synthetic (or marginal) zone, where DNA synthesis occurs. The nuclei then migrate back toward the ventricular surface, into the mitotic (or ventricular) zone, retract their processes from the outer surface, and undergo mitosis. The daughter cells can either resume the mitotic activity and enter a second phase of the cycle or stop dividing and migrate away from the ventricular surface.

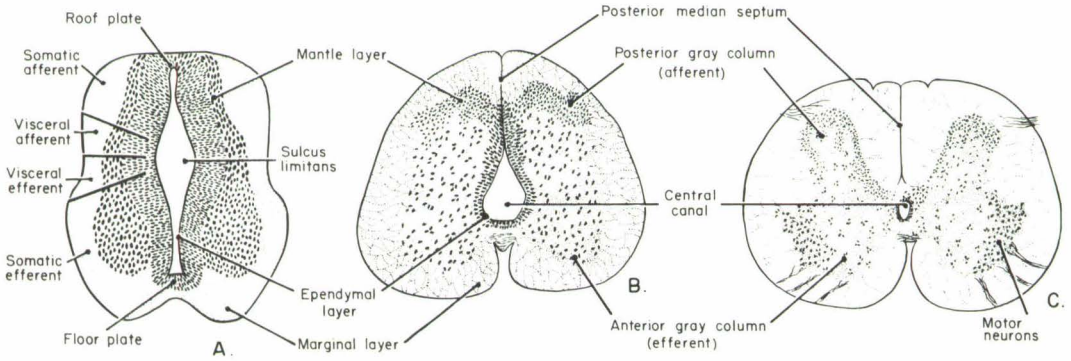


Figure 3.5. Differentiating layers of the spinal cord. **A.** Section through spinal cord of a 5-week human embryo. **B.** Cervical spinal cord of an 8-week human embryo. **C.** Cervical spinal cord of a 10-week human embryo.

overproduction of neurons. Neurons, however, that are not properly located in the various regions of the CNS, or those which have not established appropriate connections, will eventually die, so that the total number of neurons is reduced to the final normal population size. In fact, there appears to be a fierce competition between neuroblasts to reach their target and establish proper connections. This finding has lead Gerald Edelman to propose the interesting concept of "neuronal Darwinism" based upon the survival of neurons which are successful in contacting their target (11).

Maturing neuroblasts do not establish synapses randomly (23). Instead, they are at-

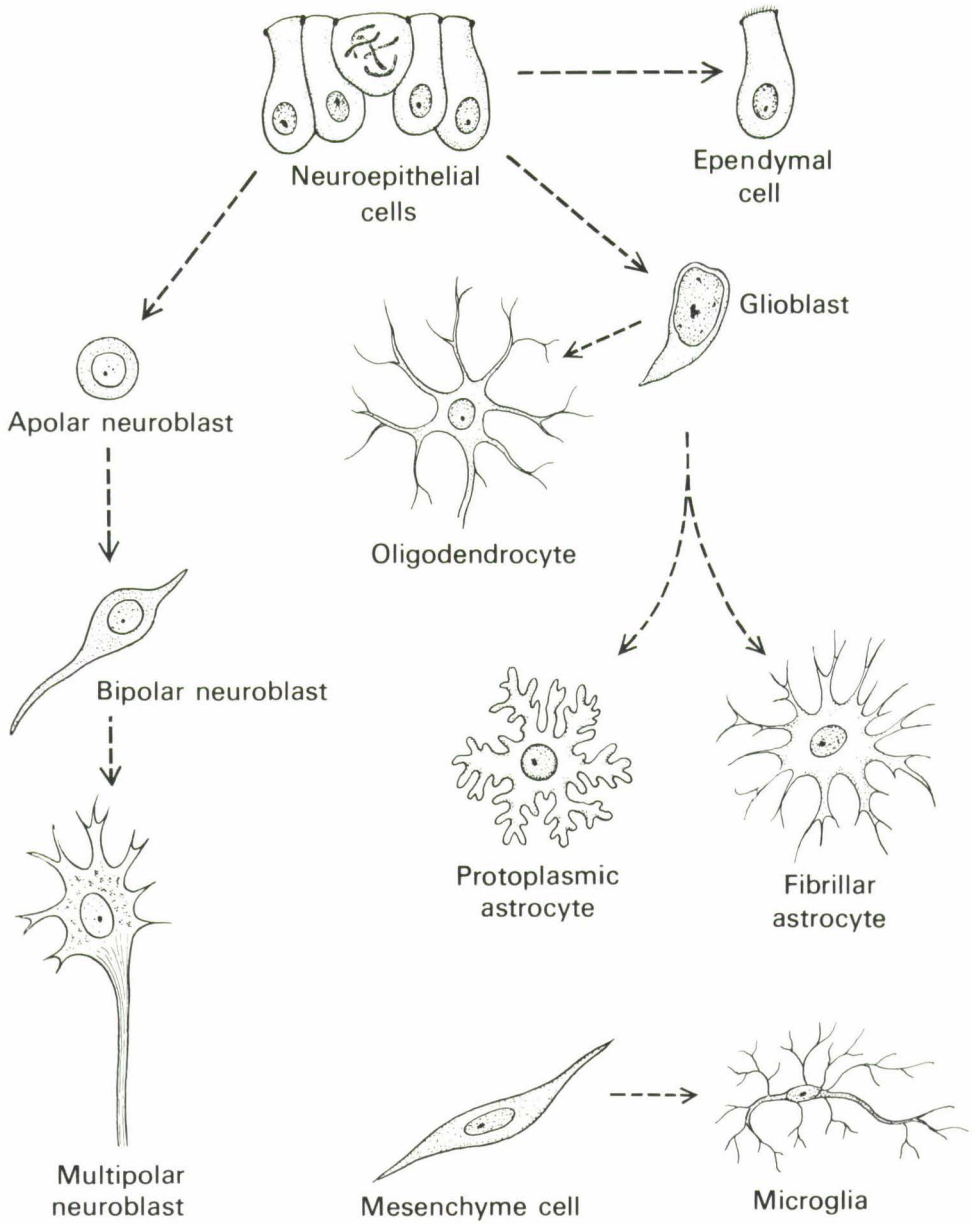


Figure 3.6. Histogenesis of neurons and neuroglial cells. Neuroblasts, glioblasts, and ependymal cells originate from neuroepithelial cells. The origin of the oligodendrocyte is obscure, but both protoplasmic and fibrillar astrocytes are derived from gliobasts. The microglia are considered to arise from mesenchyme.

tracted in a very specific manner to particular groups of target cells. Many years ago, the elegant experiments conducted by Roger Sperry on the visual system of frogs, salamanders, and goldfish (52), lead to the suggestion that chemical gradients or specific chemical affinities enabled axons to establish synaptic contacts only with appropriate postsynaptic neurons. The movement of axons is determined by expansions of the growing axons called *growth cones*. The growth cones provide the mechanical force that pull an axon forward through cycles of protrusion, adhesion, and contraction of filopodia. It is likely that the physical substrate over which an axon grows contributes mechanical and chemical cues, particularly molecules controlling cell adhesiveness, that guide the growth cone to its target. Proteins that promote the aggregation of neurons in specific portions of the brain have been isolated (38) and cell surface proteins, such as *N*-acetyl-D-galac-

tosamine have been implicated in adhesion between specific pre- and postsynaptic elements (15). These molecules, called *cell adhesion molecules* (CAM), or, in the present case, nerve cell adhesion molecules (N-CAM), are sizable glycoproteins with molecular weights of 180–250 kD that contain large amounts of the ionically charged sugar, sialic acid (10). The various forms of N-CAM that characterize the different regions of the CNS apparently can be differentiated from one another by their sugar residues. Besides N-CAM, substrate adhesion molecules (SAM) were also studied intensively. These molecules, which include laminin, fibronectin, chodronectin, and certain types of procollagen located in the extracellular matrix, play a key role in the migration of neuroblasts outside the CNS (e.g., neural crest cells), but their role within the CNS is still uncertain (3).

Experiments in developing amphibians, in which an eye is transplanted into the spinal cord, show that factors other than cell surface recognition sites are also involved in the specification of neural connections. Axons from the ectopic (spinal) eye reach the optic tectum and form synapses only when the embryo's own eyes are removed (14), suggesting that some afferent axons may mask cellular recognition sites or render them ineffective. Among the various pathfinding mechanisms which may explain how axons find their way over such great distances are those involving the presence of different growth factors. Of all the putative growth factors that have been identified up to now, the *nerve growth factor* (NGF) is certainly the most well-characterized (31). NGF is a protein that is synthesized in target cells as part of a larger prohormone. It has a molecular weight of 130 kD and contains three subunits: α, β, and γ. The biologic activity of NGF depends on the β subunit, which is a 26 kD dimer similar in amino acid sequence to insulin, another growth-enhancing hormone. Although its exact mode of action is still not known, the presence of NGF appears essential for the development and maintenance of certain neuronal populations, such as the sympathetic neurons and the sensory neurons of the dorsal root ganglia (31). NGF can be taken up from the target cells by pinocytic activity of neuron terminals and then carried back by axonal retrograde transport to the cell body, where it acts by altering gene expression. When injected into the brain, NGF will cause axons of sympathetic neurons to proliferate into the brain. These axons, which normally do not invade the CNS, will do so, apparently by following chemical tracks created by diffusion of NGF (31). Recently, a specific receptor for NGF was identified in the nervous tissue and antibodies against this receptor were produced. Immunohistochemical mapping studies with these antibodies revealed the presence of NGF receptors in several neuronal populations of the adult human brain, such as the cholinergic neurons of the basal forebrain. Antibodies against NGF itself were also produced and administration of these antibodies to newborn animals causes sympathetic ganglia to atrophy (*immunosympathectomy*).

The direction of growth cones and, hence, the establishment of neuronal connections, appears to be influenced by a wide variety of clues ranging from (a) simple mechanical differences in the texture of the extracellular matrix (e.g., adhesiveness), (b) signals from recognition molecules on the cell membrane (e.g., N-CAM), and (c) molecular information provided by a distant source via the production of a diffusible compound (e.g., NGF). The final step in the making of a neuronal connection involves a highly complex set of events that lead to the formation and stabilization of synapses. This set of events comprises two major series of interactions between the outgrowing fiber and its target. First, there is a matching of the size of the population of presynaptic neurons and their target which is accomplished by cell death, synapse retraction, and competition for growth substance. Second, there is a fine tuning of the connections that results from the competition between various outgrowing fibers and the activity of both the pre- and postsynaptic elements. The influence of the external environment on the developing brain is crucial for the fine tuning, maintenance, and strength regulation of neuronal connections. Although the structures of the brain are largely specified by genetic and developmental processes, the pattern of interconnections between neurons is also influenced by experience. In fact, studies during the last decade revealed that the brain is remarkably plastic; it can readily change its performance, and even its strategies, as a result of experience. The influence of experience on the brain is particularly important at early stages of development, when the integrative action of the brain and even its structural organization is dependent on its interaction with the environment.

GLIAL CELLS

Some of the neuroepithelial cells differentiate into primitive *glioblasts* which form supporting cells. The majority of glioblasts are generated after the production of neuroblasts has ceased (28). Glioblasts become spindle-shaped bipolar cells that extend the entire thickness of the neural tube. Their large nuclei are placed close to the lumen and their processes are attached to both the internal and external limiting membranes of the neural tube. Some glioblasts retain this position and become transformed into ependymal cells (Fig. 3.6). During maturation most ependymal cells lose their attachment to the external limiting membrane and their processes extend only a short distance from the central canal to become anchored in a subependymal glial membrane (Fig. 6.13). Ependymal cells in the adult form the lining of the central canal of the spinal cord and the ventricular surfaces of the brain. Epithelial cells of the choroid plexus (Fig. 6.15) are believed to be modified ependymal cells.

Other glioblasts in the mantle layer lose their attachments with the limiting membrane and assume apolar or unipolar appearances. In later stages of development, these detached stem cells send out new processes and are transformed ultimately into fibrous and protoplasmic astrocytes (Fig. 3.6). Smaller glial cells, the oligodendrocytes, are also thought to be derived from glioblasts. These cells are found mainly in the marginal layer and play a role in developing myelin sheaths (Fig. 6.9).

In addition to the macroglia, the adult central nervous system contains *microglia*, considered by Del Rio-Hortega to be of mesodermal origin (8). These cells do not appear in the central nervous system until it is invaded by blood vessels and their perivascular adventitia. Despite many descriptions of microglia in light microscopy, there is uncertainty regarding their identification in the electron microscope (40). Microglia are considered to serve a phagocytic function and may be derived from blood histiocytes. In tissue culture, neurons develop better if they are embedded in dense glia. Glial cells retain a certain degree of motility in the adult, whereas neurons are immobile beyond the neuroblast stage. Glial cells also can divide and increase in number, while neurons do not divide after birth and remain in permanent interphase throughout life (1). The latter is a significant point because the maintenance of specific neural pathways and reflexes, as well as the storage of learned information, all require a metabolically stable and permanent set of neurons. Structural and functional features of the neuroglial elements are presented in Chapter 6.

SPINAL CORD

In the spinal cord continued cell proliferation produces an anterior and a posterior thickening in the mantle layer. The anterior thickening forms the larger *basal plate*, which gives rise to the anterior (motor) gray horn in the adult spinal cord. The smaller posterior thickening constitutes the *alar plate*, from which the future posterior (sensory) gray horn of the spinal cord is formed. A longitudinal groove, the *sulcus limitans*, marks the lateral junction of basal and alar plates (Fig. 3.5). The sulcus limitans extends the length of the primitive spinal cord and continues into the brainstem and remains as a prominent sulcus in the floor of the fourth ventricle in the adult brain (Fig. 12.14). In transverse sections of the neural tube, the lumen is rhomboid-shaped with relatively thin *roof* and *floor plates* (Fig. 3.5). The roof and floor plates furnish only glioblastic elements at spinal cord levels.

Neuroblasts of the basal plates become the efferent peripheral neurons. Their axons penetrate the marginal layer and the external limiting membrane and emerge from the spinal cord as ventral root fibers (Figs. 3.7 and 3.9). Fibers of the ventral root pass directly to skeletal muscles or to autonomic ganglia for the innervation of visceral structures (Figs. 3.9 and 10.23). Neuroblasts of the basal plates also give rise to local circuit neurons. Cells of the alar plate have axons that remain within the central nervous system. Part of these axons arch anteriorly, cross through the basal plate to the opposite side, and reach the marginal layer, where they ascend or descend for variable distances (Fig. 3.7). Some of these axons ascend as far as supraspinal levels (e.g., spinothalamic, spinoreticular, and spinocerebellar pathways). Other axons remain on the same side and ascend or descend in the marginal layer. These neurons, whose processes are entirely confined to the central nervous system, constitute the *central*, or *intermediate, cells*. Those whose axons remain on the same side are

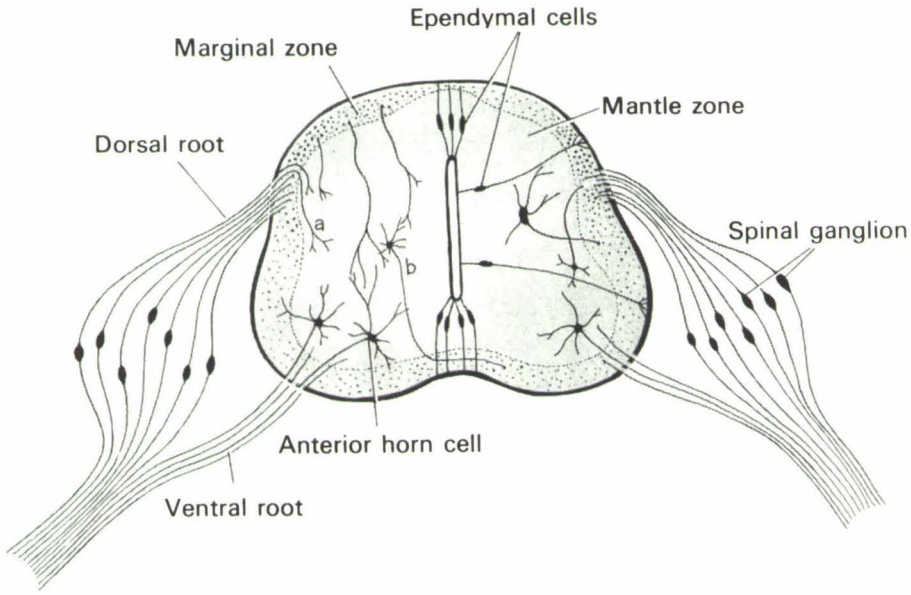


Figure 3.7. Transverse section of spinal cord and spinal ganglia of a chick embryo. The mantle zone becomes the butterfly gray matter of the adult spinal cord, while the marginal zone develops into the white matter containing ascending and descending fiber tracts: *a* indicates afferent fiber with collaterals; *b* represents a column cell that projects contralaterally. Based upon silver impregnation.

known as *association cells*, whereas those whose axons cross to the opposite side are *commissural cells*.

As development proceeds, the proliferation of the germinal cells gradually decreases and ultimately stops altogether. As more and more stem cells are transformed into neuroblasts, the germinal zone progressively diminishes in size and ultimately is reduced to a single layer of columnar ependymal cells. In certain places, as in the anterior commissure of the spinal cord, some of the ependymal cells may retain their embryonic glioblast character and extend the whole thickness of the neural wall (Fig. 3.7). On the other hand, the mantle layer progressively increases in size and becomes the gray matter of the spinal cord. It is surrounded by an expanding marginal layer which contains the descending and ascending axons of the central cells. At a much later period, most of the axons become myelinated and the marginal layer assumes the white, glistening appearance characteristic of the white matter of the adult spinal cord. The expansion of the alar plates in a medial direction brings these plates into close apposition. The posterior *median septum*, formed of glial processes and intima pia, marks the line of junction in the adult (Figs. 3.5 and 10.6). In the floor plate region, an invagination forms the *anterior median fissure* (Figs. 3.5 and 10.7). As a consequence of all these changes, the size of the central canal is greatly reduced and the embryonic neural tube is transformed into the spinal cord.

The spinal cord has a long cylindrical shape and is curved in the embryonic axis. There is an acute ventral flexure, *the cervical flexure*, at the junction of the spinal cord and hindbrain (rhombencephalon). Until the beginning of the third month, the spinal cord extends the entire length of the vertebral canal. After this time, the mesodermal elements which have formed the cartilages and bones of the vertebral column grow more rapidly than the spinal cord, so that at birth the most caudal part of the spinal cord, the *conus medullaris*, lies at the level of the third lumbar vertebra. The sites of emergence of spinal nerves do not change, but there is a lengthening of root filaments between the intervertebral foramina and the spinal cord which is most marked for lumbar and sacral spinal roots. The lengthening of root filaments is the result of the differential growth rate between the vertebral column and the spinal cord. The large number of nerve roots surrounding the *filum terminale* (Fig. 1.6) constitute the *cauda equina*. In the adult, the conus medullaris lies between the Ll and L2 vertebrae, and the spinal cord occupies only the upper two-thirds of the vertebral canal (Fig. 10.3).

Neuron Differentiation in Ganglia

In the spinal ganglia, derived from the neural crest, a similar differentiation takes place. Many of the original polygonal or round cells become spindle-shaped and bipolar with the development of two neurofibrillar processes, one central and one peripheral (Figs. 3.7 and 5.10). The central processes enter the spinal cord as dorsal root fibers and there bifurcate into ascending and descending arms which contribute collaterals to the mantle layer or gray matter (Figs. 3.7 and 10.23). In human embryos with a crown-to-rump length of 25 mm, many of the neuro blasts have attained the bipolar stage. A few neurons with greater amounts of cytoplasm and distinct neurofilaments appear transitional in shape and are referred to as pseudounipolar cells (Fig. 5.10). The cytoplasm of the cell body elongates, and the two processes become approximated. Ultimately, the elongated cell cytoplasm forms the single stem of a T-like structure, while the top of the T is formed by the thin central and thicker peripheral processes (53). Many neurons are of the unipolar type in spinal ganglia of human 100 mm fetuses, and most of the spinal ganglia cells are true unipolar neurons in the newborn human infant. An occasional bipolar neuron, or those in transitional stages, may, at times, be observed in the adult dorsal root ganglia. It is interesting to note that a large number of ganglionic neuroblasts may be produced initially. Embryonic dorsal root and sympathetic ganglia appear to have an overabundance of neuroblasts when compared to the number of fully differentiated ganglion cells present at birth. For example, total cell counts of the submandibular ganglia in a graded series of human fetuses showed a progressive reduction from 12,128 cells at 17 weeks of gestation to 5,988 at full term (6). As in the CNS, cell death appears to be a normal event in the course of embryonic development of peripheral ganglia. It is estimated that 25–75% of the original neuronal population in autonomic ganglia lies in neonatal life (43).

Not all of the cells in the spinal ganglia differentiate into neuroblasts. Some develop into *capsule* or *satellite cells* which form a capsule around the bodies of the spinal ganglion cells (Fig. 5.2**A**). Others wander out along the course of the growing peripheral nerve fibers, envelop them, and ultimately become *Schwann cells*. These cells play an active role in the formation of myelin and may be considered as a peripheral type of neuroglia, perhaps most closely related to oligodendrocytes.

Besides the spinal ganglia, there are other peripheral aggregations of nerve cells known as *autonomic* or *sympathetic ganglia* (Figs. 3.9 and 9.2). Arising mainly from the neural crest, these cells form two ganglionic chains on the anterolateral aspect of the vertebral column (vertebral sympathetic ganglia). Others migrate further to form the ganglia of the mesenteric plexuses (collateral or prevertebral ganglia), while some actually invade the walls of the viscera, or settle close to them, as the terminal or peripheral autonomic ganglia (Figs. 3.8 and 9.1). Here, too, differentiation occurs in several directions. Some cells enlarge to form the multipolar sympathetic ganglion cells, whose axons terminate in visceral effectors, smooth muscle, heart muscle, and glandular epithelium (Fig. 5.10). Others, as in the case of the spinal ganglia, give rise to satellite cells, which envelop the bodies of one or several ganglion cells. Finally, some differentiate into the chromaffin cells found in the adrenal medulla, carotid bodies, and other portions of the body.

Segmental Arrangement of Peripheral Nerve Elements

With the differentiation of the various types of nerve cells in early stages of development, a neuronal mechanism adequate for complete, if simple, reflex arcs is established. Such arcs consist of afferent, intermediate, and efferent neurons, and their peripheral extensions. However, the synaptic junctions of these cells, which make such reflex arcs functional, are as yet unformed. In embryos of about 10 mm, the various components of the peripheral nervous system already are laid down and may be recognized in a transverse section of any typical body segment (Fig. 3.9). The central processes of the spinal ganglion cells form the *dorsal roots*, whereas the *ventral root* is composed of axons from cells in the anterior gray matter of the spinal cord (mantle layer). Distal to the ganglion, the ventral root unites with the peripheral processes of the spinal ganglion cells to form a mixed *spinal nerve* (Figs. 3.9 and 8.1). Each spinal nerve containing afferent and efferent fibers divides into a *dorsal* and a *ventral ramus* and also sends a fiber bundle known as the *ramus communicans*

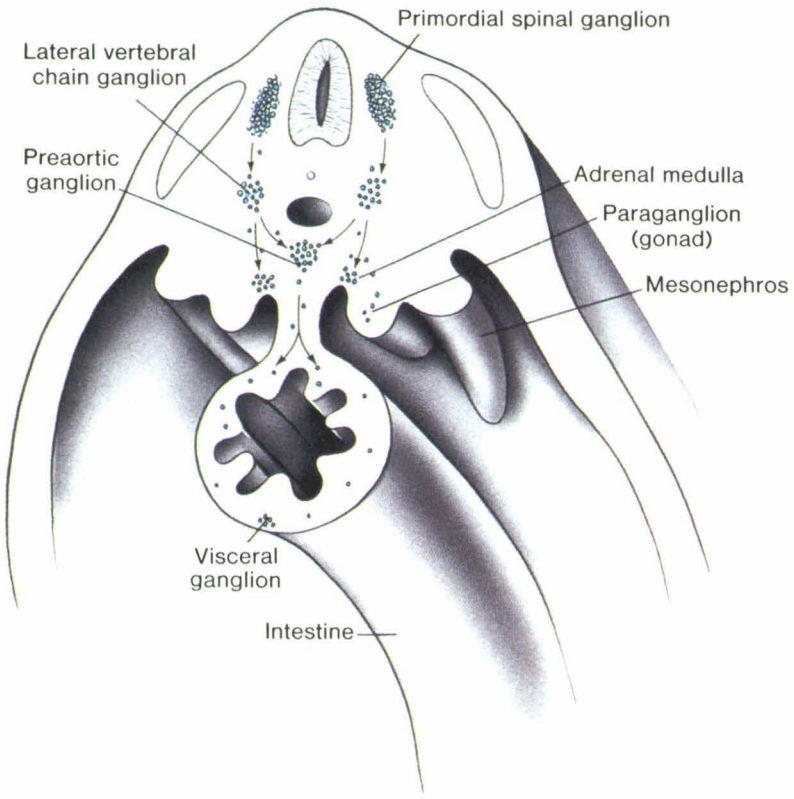


Figure 3.8. Neural crest cells differentiate to form the primordial spinal ganglia. Sympathetic neuroblasts migrate ventrally where clusters of cells differentiate further to form sympathetic ganglia, preaortic ganglia, chromaffin cells of the adrenal medulla, and autonomic neurons of the alimentary tract.

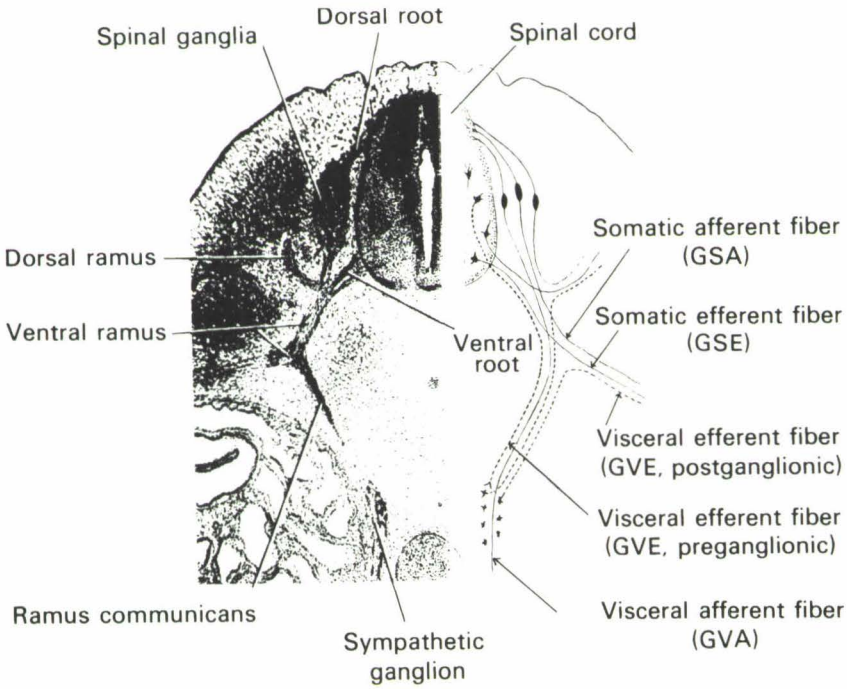


Figure 3.9. Transverse section of 14-mm pig embryo. The functional categories of spinal nerve fibers are indicated on the *right* (Bielschowsky's silver stain).

to the vertebral sympathetic chain. The dorsal ramus supplies the muscles and skin of the back, whereas the larger ventral ramus goes to the ventrolateral parts of the body wall. Four functional types of peripheral nerve fibers may be distinguished: *general somatic afferent* (GSA), *general visceral afferent* (GVA), *general somatic efferent* (GSE), and *general visceral efferent* (GVE). The efferent innervation of visceral structures differs from that of the somatic muscles by the fact that two neurons are always involved in the conduction of impulses from the central nervous system to the effector organs (Figs. 3.9 and 9.2). The fibers of these two neurons are referred to as pre- and postganglionic fibers. The arrangement of these various type of fibers that constitute the peripheral nervous system are described in detail in Chapters 8 and 9.

As in the CNS, cell death is a normal process during development of the peripheral nervous system. Somewhat later in development, there is a change in synapses formed by motor neurons upon striated muscle and by parasympathetic preganglionic axons upon postganglionic cells (43). In newborn animals, both muscle fibers and ganglion cells are innervated by several different axons, but in the adult each cell is usually innervated by a single axon (9). In the case of ganglion cells, the number of synaptic terminals per cell may actually increase, but the number of cells innervated by a single axon decreases. As we have seen, target structures influence the outgrowing neurons and play a fundamental role in the establishment of synaptic contacts. Conversely, outgrowing neurons can markedly influence their targets as exemplified by the effect of activity in motoneurons on the properties of skeletal muscles. The motoneuron exerts its effect on skeletal muscles by using acetylcholine as a neurotransmitter. Acetylcholine acts upon specific receptors normally confined to the end-plate region where their density exceeds $20{,}000/\mu m^2$. The density of acetylcholine receptors is much lower in other regions of the muscle fiber. However, if motoneuron fibers are sectioned and degenerate, acetylcholine receptors are no longer confined to the end-plate, but occur all over the muscle fiber. These numerous extrajunctional receptors, which are the result of a synthesis of new receptors and their insertion into the membrane, will disappear if the muscle is reinnervated. Likewise, embryonic muscles are first diffusely sensitive to acetylcholine. However, once the muscle fiber becomes innervated, its sensitivity to the neurotransmitter is progressively restricted to the end-plate region. These findings suggest that the restriction of chemosensitivity, which occurs when synapse formation has started, may be one means of preventing other nerve axons from forming synapses on the muscle (22).

BRAIN

As soon as the anterior neuropore is closed, the rostral cavity of the neural tube shows three dilatations or brain vesicles. These three early subdivisions are the *prosencephalon* or forebrain, the *mesencephalon* or midbrain, and the *rhombencephalon* or hindbrain (Figs. 2.2 and 3.10**A**). The constricted region between the mesencephalon and rhombencephalon is known as the *isthmus*. The brain vesicles maintain many of the fundamental morphologic features seen in more caudal parts of the embryonic neural tube in that each has roof and floor plates and alar and basal plates. Although the walls of these vesicles are thin, the sulcus limitans is present at the junction of alar and basal plates in caudal brain vesicles (rhombencephalon and mesencephalon). The large dilated cavities within each brain vesicle are the forerunners of the ventricular system. They are destined to undergo extensive alterations in size, shape, and extent as a consequence of cell proliferation, growth, and various brain flexures. These ventricular cavities are continuous with the central canal of the spinal cord. The lateral margins of the prosencephalon develop shallow depressions, the optic sulci, which subsequently becomes evaginated to form the optic vesicle (Fig. 3.10**B** and **C**). Each optic vesicle becomes modified to form an *optic cup* which is joined to the prosencephalon by a hollow optic stalk.

Two prominent brain flexures appear at an early embryonic stage. The *cervical flexure* develops at the junction of rhombencephalon and spinal cord, with its concavity directed ventrally. A second ventral flexure, the *cephalic flexure*, occurs at the junction of mesencephalon and rhombencephalon (Fig. 3.10**B** and **D**). Rapid changes in the brain occur in the fourth and fifth week of development. In the sixth week, a third impressive flexure with a dorsal concavity develops in the rhombencephalon and divides it into two

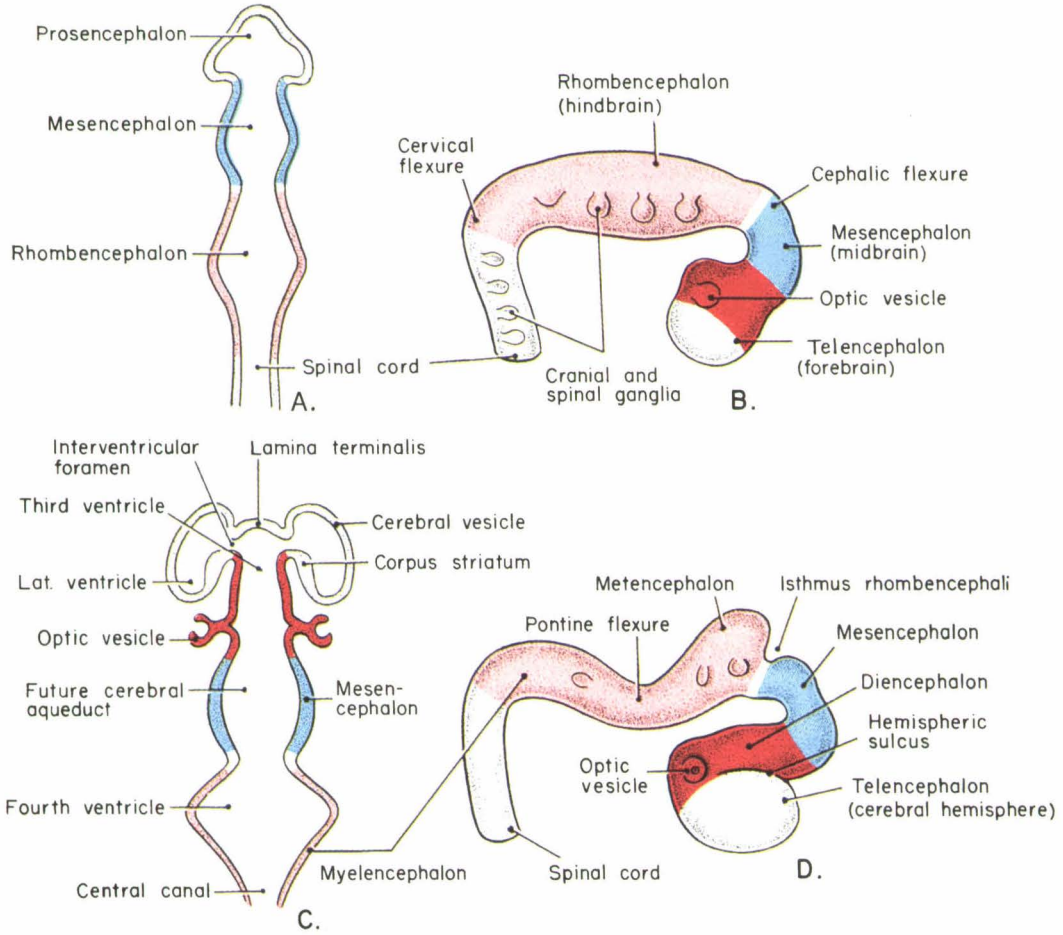


Figure 3.10. Developing brain vesicles and ventricular system. **A, B.** Three-brain vesicle stage of a 4-week embryo. **C, D.** Five-brain vesicle stage of a 6-week human embryo. The prosencephalon, telencephalon, and spinal cord are stippled. The diencephalon is shown in *dark red*, while the mesencephalon is *blue*. The derivatives of the rhombencephalon (pons and medulla) are in *light red* and the isthmus is *white*.

segments, the *metencephalon* and the *myelencephalon*. This prominent *pontine flexure* creates the *transverse rhombencephalic sulcus* on the dorsal surface of the brainstem (Figs. 3.10**D** and 3.11**A**). A relatively shallow hemispheric sulcus on each side of the forebrain divides the prosencephalon into a cephalic *telencephalon*, or *endbrain*, and a caudal part, the *diencephalon*. The optic stalks and optic vesicles are attached to the diencephalon. It has been assumed that bending of the developing neural tube results from differences in the rate of cell proliferation (50). In chick embryos, cyclic adenosine monophosphate can act as a stimulus for axial bending of the embryo which is caused, at least in part, by cell movement (48).

The basic pattern of the ventricular system of the brain is evident in early stages of development (Fig. 3.11**B**). The caudal roof of the rhombencephalon is extremely thin and the underlying cavity (*fourth ventricle*) appears as a shallow, diamond-shaped depression called the *rhomboid fossa* (42, 55) (Figs. 2.26, 3.11**B**, 3.14, and 3.16). With continued growth, the lumen of the midbrain will become narrowed to form the *cerebral aqueduct*. Medial growth and expansion of the diencephalon also reduce the lumen of this segment of the brain to a thin vertical cleft, the *third ventricle*. A large opening (*interventricular foramen*) behind the lamina terminalis provides continuity between the third ventricle and the cavity of the laterally expanding cerebral hemisphere. The primitive *lateral ventricle* within each cerebral hemisphere will become altered extensively by subsequent development (Figs. 3.10 and 3.15). Five distinctive subdivisions of the developing brain are established at this stage, and each subdivision undergoes elaborate, and sometimes unique, development as growth continues (Fig. 3.11). The five basic

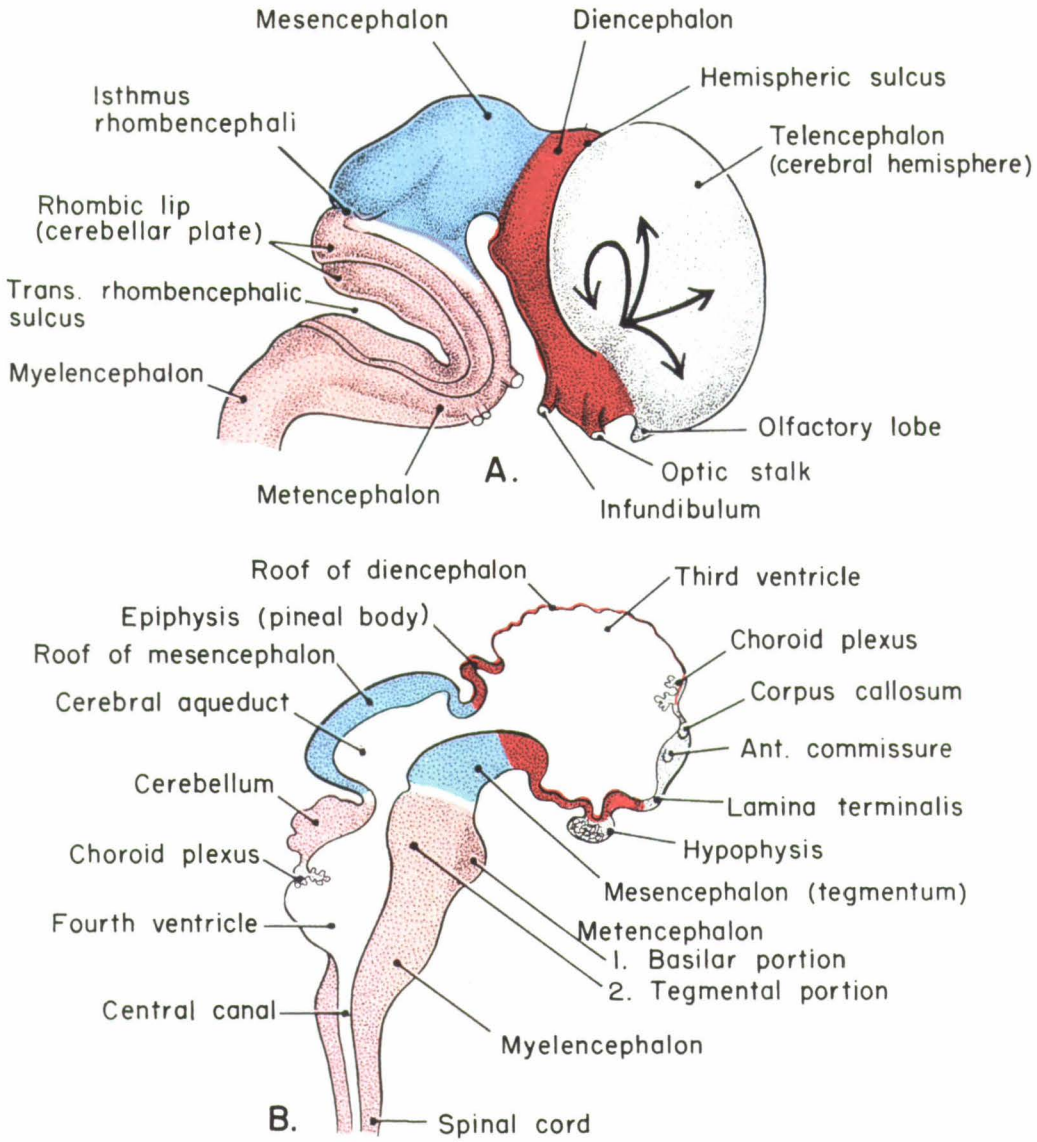


Figure 3.11. Developing brain vesicles and ventricular system. **A.** Lateral view of cerebral vesicle and developing brainstem in human embryo of 8 weeks. *Arrows* indicate directions of growth and expansion of cerebral hemisphere. **B.** Sagittal section through the brainstem of a 12-week human fetus. The telencephalon is stippled, the diencephalon is *dark red*, and the mesencephalon is *blue*. Rhombencephalic derivatives (metencephalon and myelencephalon) are *light red*, while the isthmus is *white*.

subdivisions of the brain are (a) the *telencephalon*, (b) the *diencephalon*, (c) the *mesencephalon*, (d) the *metencephalon*, and (e) the *myelencephalon* (Fig. 2.1). The development of each subdivision is considered separately, even though the embryologic events described occur simultaneously.

Myelencephalon

The *medulla*, the most caudal brain segment, is derived from the myelencephalon. This brain segment extends from levels of the first spinal nerve of the cervical cord to the beginning of the pontine flexure (Fig. 3.11). As the future medulla oblongata, it differs from the spinal cord in that the walls (alar portions of the neural tube in the rhombencephalon) are shifted laterally at higher levels by the expanding fourth ventricle and also by the development of the cerebellum dorsal to the medulla and pons. As a result of the expansion of the roof plate, the alar plate is displaced laterally to the basal plate. The sulcus limitans continues to mark the boundary between these alar and the basal plates as can

be seen in both gross and microscopic specimens (Figs. 3.12 and 12.14). Derivatives of the basal plate form the motor nuclei of cranial nerves, and come to occupy positions in the floor of the fourth ventricle medial to the sulcus limitans (Fig. 3.12). The most medial cell column gives rise to general somatic efferent (GSE) fibers that form the hypoglossal nerve (N. XII). The more laterally located cell columns are associated with special (SVE) and general efferent (GVE) fibers. The SVE cell column issues fibers from the nucleus ambiguous, that forms components of cranial nerves IX, X, and XI (Fig. 12.14). The GVE cell column, also medial to the sulcus limitans, represented by the dorsal motor nucleus of vague nerve (N. X) and inferior salivatory nucleus (N. IX), gives rise to preganglionic parasympathetic fibers that are widely distributed.

Derivatives of the alar plate form sensory relay nuclei lateral to the sulcus limitans. The most lateral of these nuclei are the auditory and vestibular (special somatic afferent (SSA) cranial nerve components), and those of the trigeminal complex (general somatic afferent (GSA)). General and special visceral afferent (GVA and SVA) cell columns, represented by the solitary nuclei, lie medial to the this group (Fig. 3.13). Caudally, near the junction between the myelencephalon and the spinal cord, cell groups of the alar lamina differentiate into the nuclei gracilis and cuneatus (general somatic afferent, GSA). More rostrally, some cells derived from the alar lamina migrate ventrally from the inferior rhombic lip to form portions of the *inferior olivary complex*, the largest cerebellar relay nucleus of the medulla (Fig. 12.11). Fibers forming the medullary pyramids are cortically derived,

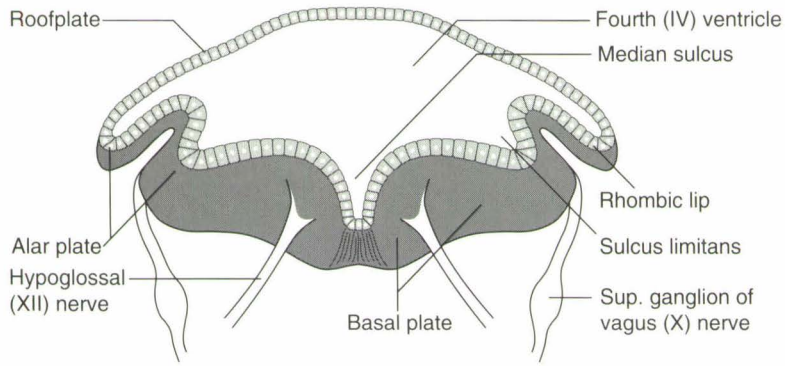


Figure 3.12. Medulla of a 5-week human embryo. Note the prominent sulcus limitans separating structures derived from the basal and alar plates.

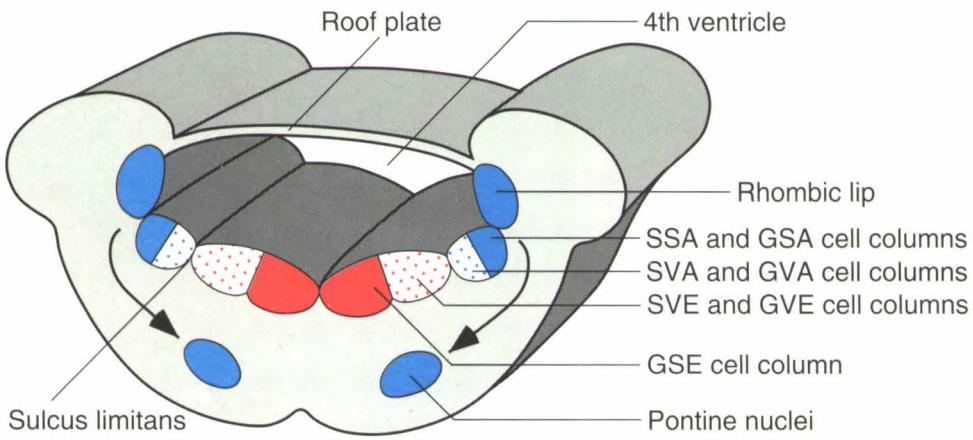


Figure 3.13. Caudal metencephalon showing the cell columns of the cranial nerve nuclei with respect to the sulcus limitans. Cell groups derived from the alar plate are shown in *blue*, while those from the basal plate are *red*. Both the superior rhombic lip (cerebellum) and the pontine nuclei develop from the alar plate. Cells of the pontine nuclei migrate ventrally (*arrows*). *Dark blue*, superior rhombic lip, special (SSA), general somatic afferent (GSA) cell columns, and the pontine nuclei; *blue stipple*, special (SVA) and general visceral afferent (GVA) cell columns; *red stipple*, special (SVE) and general visceral efferent (GVE) cell columns; *red*, general somatic efferent (GSE) cell column.

late in appearance and occupy ventromedial regions near the midline.

In the region of the fourth ventricle, the roof plate consists of a single layer of ependymal cells covered by a thin layer of pia mater. These two layers form the tela choroidea, and prolongations project into the ventricle in the region of the transverse rhombencephalic sulcus to form the choroid plexus (Fig. 6.17). Openings in the roof plate appear (4 to 5 months) which establish continuity between the fourth ventricle and the subarachnoid space surrounding the brainstem. Two lateral apertures (foramina of Luschka) connect the lateral recesses of the fourth ventricle with the pontine cistern. A single median aperture (foramen of Magendie) in the lower roof connects the fourth ventricle with the dorsal cerebellomedullary cistern.

Metencephalon

This rostral portion of the hindbrain, extending from the pontine flexure to the rhombencephalic isthmus, develops into two elaborate and distinctive components of the neuraxis—the pons and the cerebellum (Figs. 3.13 and 3.14). The *pons* consists of two parts: (a) a dorsal portion lying in the floor of the fourth ventricle, referred to as the pontine tegmentum, and (b) a ventral portion in which some cortical efferent fibers terminate while others continue to more caudal regions. The *pontine tegmentum* is derived from the basal plate (Fig. 3.13). A medial general somatic efferent (GSE) cell column gives rise to fibers of the abducens nerve (N. VI). An intermediate and interrupted cell column of typical motor neurons gives rise to special visceral efferent (SVE) fibers that form cranial nerves V and VII, and respectively innervate the musculature of the first and second branchial arches. General visceral efferent (GVE) cells contained in the superior salivatory nucleus supply preganglionic parasympathetic innervation for the submandibular, sublingual, and lacrimal glands. Cells of the basal plate also contribute to the pontine reticular formation (Fig. 3.13).

Ventromedial portions of the alar plate form cell groups similar to those described for the medulla (28). These cell groups are concerned with (a) the vestibulocochlear nerve (SSA), (b) the trigeminal nuclear complex (GSA), and (c) the solitary nucleus (SVA and GVA). The *pontine nuclei* which form massive cell collections in the ventral portion of the pons originate from the alar plate of both the metencephalon and myelencephalon (Fig. 3.13). Corticofugal fibers which develop later end, in part, upon these nuclei. The pontine nuclei give rise to a massive collection of fibers which cross the midline and enter the opposite cerebellar hemisphere. Fibers in this bundle form the *middle cerebellar peduncle* (Figs. 2.26 and 2.33). The *cerebellum* is derived mainly from the dorsolateral portions of the alar plates which bend posteriorly and medially to form the *rhombic lips* (Figs. 3.11 and 3.14). The rhombic lips are at first widely sep-

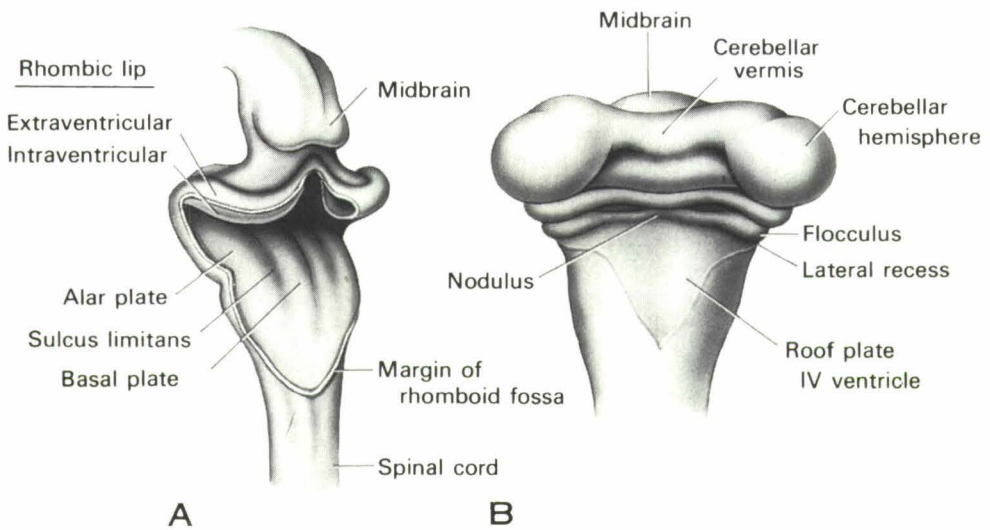


Figure 3.14. Developing cerebellum and hindbrain. **A.** Posterior oblique view of human embryo at 6 weeks. **B.** Posterior view of human fetus at 4 months of gestation.

arated from each other, and each lip projects partly into the fourth ventricle (intraventricular portion) and partly on the surface of the metencephalon above the roof plate. Further deepening of the transverse rhombencephalic sulcus at the pontine flexure causes the cerebellar rudiments of both sides to fuse in the midline caudal to the roof of the mesencephalon. Fusion of the rhombic lips forms the transverse *cerebellar plate.* At 3 months these cerebellar primordia have a dumbbell-shaped appearance (Fig. 3.14) in which the unpaired central part represents the *vermis* and the two large lateral knobs represent the *hemispheres.* Near the end of the fourth month fissures begin to develop on the cerebellar surface. The first fissure to appear is the *posterolateral* (prenodular) *fissure* which separates the *nodulus* from other parts of the vermis and the *flocculus* from the rest of the cerebellar hemisphere. The *flocculonodular lobe (archicerebellum),* phylogenetically the oldest part of the cerebellum, has the most extensive connections with the vestibular system (29). The portion of the cerebellar plate between the posterolateral fissure and the isthmus represents the rudiment of the *corpus cerebelli.* The first fissure to become visible in the corpus cerebelli is the *primary fissure.* The primary fissure is the deepest of all cerebellar fissures, and it separates the anterior and posterior lobes (Figs. 2.33 and 15.1). All parts of the cerebellum rostral to the primary fissure constitute the *paleocerebellum* (anterior lobe), whereas the *neocerebellum* (posterior lobe) lies between the primary and posterolateral fissures. The neocerebellum is subsequently divided into lobules by three transverse fissures, the prepyramidal, the horizontal, and the posterior superior.

Studies of the neurogenesis of the cerebellar cortex have revealed developmental features that are general and apply to other cortical structures, including the neocortex of the cerebral hemispheres. Cerebellar primordia initially consist of a germinal zone at the surface of the fourth ventricle (ependymal layer) and a marginal zone at the pial surface. The germinal zone gives rise first to the large Purkinje and Golgi-II cells that migrate outward from the ependymal layer to form the Purkinje cell layer. The Purkinje cells are the principal projection neurons of the cerebellar cortex. The germinal zone of the fourth ventricle also produces neuroblasts that migrate to the pial surface where they form a second germinal zone called the *external granular layer* (17, 37, 45, 51). After their migration, these neuroblasts proliferate and produce the three main types of interneurons of the cerebellar cortex: the basket and stellate cells of the molecular layer, and the granule cells of the granular layer. The production of interneurons of the molecular layer is completed at birth, whereas that of the granule cells continues for periods ranging from 6 months to 2 years after birth in primates. In contrast to the basket and stellate cells, which remain superficially located, the newly formed granule cells must migrate from the external granular layer across the molecular and Purkinje cell layers to reach their final destination in the granular layer. The guidance for the migrating granule cells is provided by a particular type of glial process, the *radial glial fibers,* which are extensions of *Bergman astrocytes.* These peculiar glial cells are generated in the ventricular germinal zone. Their cell bodies are located just beneath the Purkinje cell layer and they send radially oriented fibers to the pial surface. The Bergman glial fibers can be readily identified by their content in glial fibrillary acidic protein (GFAP) against which specific antibodies have been raised (32). It is along these fibers that the migrating granule cells move until they reach the granular layer (44, 45). Absence or aberrant orientation of the radial glial fibers leads to degeneration of granule cells and severe malfunctions of the cerebellum, as seen in the *weaver* mutant mice (46). After completion of the granule cell migration, the network of radial glial fibers disappear. The Bergman glia appear to transform into astrocytes, ependymal cells, and, possibly, oligodendroglial cells (4). Although cells of the transient external granular layer migrate inward, their axonal processes, which will become the *parallel fibers,* remain in the *molecular layer* where synaptic contacts are established with outgrowing dendrites of the Purkinje cells.

The *cerebellar nuclei,* which are also generated relatively early, are considered to be derived from neuroblasts located close to the ventricular surface of the cerebellum. The largest and most lateral of these nuclei, the *dentate nucleus,* has a convoluted appearance (Fig. 15.17) which becomes evident during the fifth month (29). The *roof nuclei* (the fastigial nuclei) develop near the midline and have profuse connections with the vestibular

nuclei. In some species, the *globose* and *emboliform nuclei* are not clearly separated and are referred to as the *interposed nuclei.* Cranial and caudal portions of the thin metencephalic roof plate persist in the adult as the superior and inferior medullary veli (Fig. 2.28).

Mesencephalon

The *mesencephalon* is the smallest brain vesicle and ultimately forms the shortest division of the brainstem. The alar and basal plates are separated by a well-defined sulcus limitans. The cavity of this vesicle is greatly reduced during development and ultimately becomes the cerebral aqueduct. The portion of the midbrain ventral to the aqueduct consists of the *midbrain tegmentum,* dorsally, and the *crus cerebri* ventrally. These structures are separated by the *substantia nigra* (Fig. 14.1). Motor neurons derived from the basal plates form the general somatic efferent (GSE) cell columns that compose the oculomotor complex (N. III) and what must be regarded as a caudal appendage to it, the trochlear nuclei (N. IV). These cranial nerves, together with the abducens nerve, innervate the extraocular muscles derived from the preotic somites. A smaller lateral cell group from the basal plate migrates dorsal to the somatic cell columns of cranial N. III to form the visceral component (GVE) of this nuclear complex. The marginal layer of each basal plate eventually is invaded by massive collections of corticofugal fibers which form the crus cerebri. These are corticospinal, corticopontine, and corticobulbar fibers largely destined for more caudal regions of the neuraxis.

The alar plates of the mesencephalon proliferate and produce two longitudinal eminences separated by a median depression dorsal to the aqueduct. These eminences form the *quadrigeminal plate* (Fig. 3.16). A later developing transverse depression divides each longitudinal eminence into a *superior* and *inferior colliculus* (Fig. 2.26). Neuroblasts forming the inferior colliculus produce a central homogeneous cell mass surrounded by a narrow cortical rim. The superior colliculus is a more complex stratified structure formed by waves of migrating neuroblasts. Its development resembles that of the cerebral cortex in that cell migrations follow an "inside-out" sequence (12), which means that cells forming the deeper layers appear first and those destined for the superficial layers must pass through the deep layers. The inferior colliculus serves as a major relay complex in the auditory system, whereas the superior colliculus serves as a subcortical integrative center for the visual system.

The exact origin and patterns of formation of the *midbrain reticular formation*, the *red nucleus,* and the *substantia nigra* are still poorly understood. As to the substantia nigra, however, recent evidence from the rat embryo suggests that most of the nigral neurons originate from a specific region of the basal plate located at the junction between the mesencephalon and the isthmus of the metencephalon (36). Cells of the pars compacta of the substantia nigra do not contain melanin pigment at birth; appreciable pigmentation does not develop until the fourth or fifth year. In the rabbit, neurons of the substantia nigra have been found to contain dopamine on the nineteenth day of gestation (54).

Diencephalon

The prosencephalon comprises the diencephalon and the telencephalon, both subdivisions forming the entire central nervous system rostral to the midbrain (Figs. 3.1 and 3.10). The *diencephalon* develops from the thickened lateral walls of the caudal portion of the original prosencephalic vesicle. It is considered to be derived only from the alar plates. The prosencephalon is caudally continuous with the mesencephalon, and at an early embryonic stage optic cups, formed from the optic vesicles, are attached to the lateral walls of the diencephalon. The cavity of the prosencephalon becomes narrowed to form the third ventricle. The *posterior commissure* is considered to mark the caudal limit of the diencephalon (Fig. 2.13), whereas the *interventricular foramen* delineates its boundary with the telencephalon (Fig. 3.15). The *lamina terminalis,* representing the membrane formed by the closure of the anterior (rostral) neuropore, is a telencephalic derivative, but its ventral part gives rise to a matrix in which the *optic chiasm* ultimately develops.

The roof plate of the diencephalon becomes very thin and rostral parts of it invaginate to form the *choroid plexus* of the third ventricle (Figs. 3.11 and 3.15). Caudal portions of the roof plate thicken medially and evaginate posteriorly to form the *pineal gland.* This gland which develops at about the seventh week, functions as a neuroendocrine

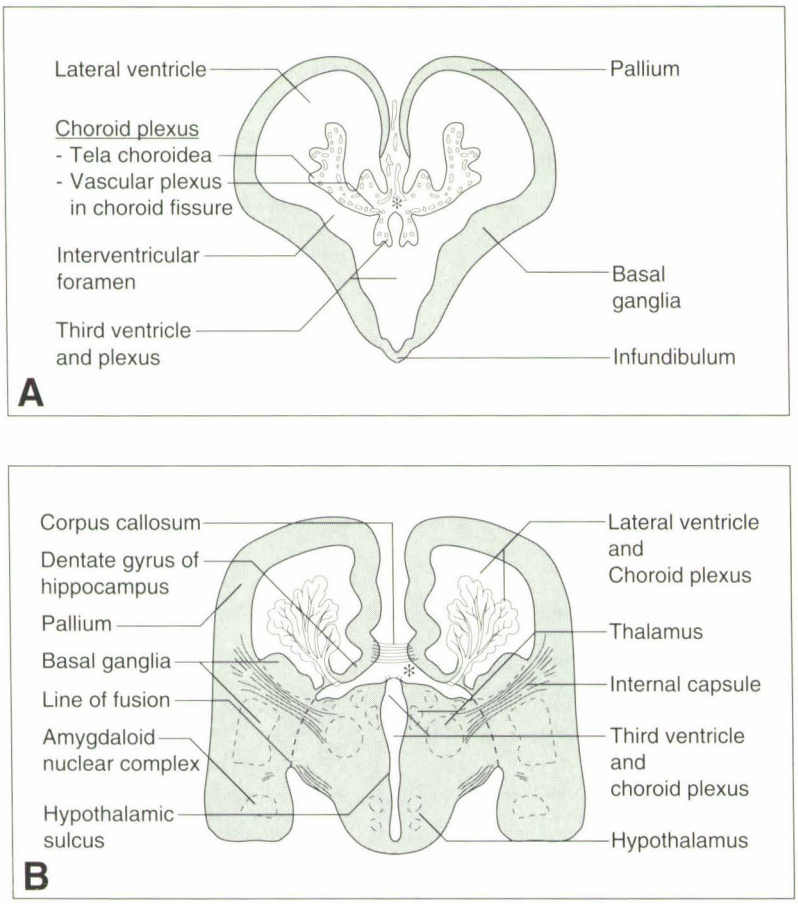


Figure 3.15. Frontal sections through diencephalon, ventricular system, and choroid plexuses of the developing brain. **A.** Invagination of choroid plexuses into lateral and third ventricles. **B.** Choroid plexuses and secondary fusion of telencephalon with diencephalon. The transverse cerebral fissure is indicated in both A and B by an *asterisk*.

transducer. It produces melatonin, a hormone which is secreted into the bloodstream with a 24-hour periodicity, providing the body with a circulating "clock" which is under the direct control of lighting environment. Melatonin appears to exert inhibitory effects on gonadal and thyroid function. After puberty the gland has a tendency to calcify and because it lies in the midline dorsal to the posterior commissure, it serves as an important landmark on x-ray films of the skull. The roof plate of the diencephalon may form another evagination in the region of the interventricular foramen, known as the *paraphysis*. This epithelial sac may persist into adult life as a paraphysial cyst and produce intermittent blockages in the flow of cerebrospinal fluid. Other epithalamic structures, considered to be derived from the roof plate, or adjacent parts of the alar plate, are the *habenular nuclei* and *habenular commissure*. These structures lie dorsally, immediately rostral to the posterior commissure. The habenular nuclei, which receives fibers of the *stria medullaris* and gives rise to the *fasciculus retroflexus*, links the septal nuclei with the midbrain reticular formation.

The proliferative activity of the germinal zone of the third ventricle is used to subdivide the diencephalon into five longitudinal zones: (a) the hypothalamus, (b) the subthalamus, (c) the pars ventralis thalami, (d) the pars dorsalis thalami, and (e) the epithalamus, comprising the pineal gland and the habenular nuclei. Contemporaneously, the lateral walls of the third ventricle develop distinct longitudinal sulci on the surfaces facing the lumen. One of these depressions is the *hypothalamic sulcus* which serves to divide the major part of the diencephalon into the *thalamus* and *hypothalamus* (Figs. 3.15 and 16.6). Some authors have suggested that the hypothalamic sulcus may be the diencephalic equivalent of the sulcus limitans, but this is uncertain since it does not mark either the division of alar and basal plates or the bound-

ary between sensory and motor regions. Active proliferation and cell differentiation produces an expansion of thalamic regions dorsal to the hypothalamic sulcus which greatly narrows the third ventricle. The thalamic nuclear masses of each side approach the midline and fuse in an *interthalamic adhesion* in about 80% of human brains. Cell growth in the thalamus proceeds rapidly and results in the formation of thalamic nuclear groups, some of which are clearly separated by medullary laminae (Figs. 2.16 and 2.29**B**). The principal nuclear groups of the thalamus are the anterior, the medial, the ventral, and the dorsal nuclear groups. The *medial* and *lateral geniculate bodies* (metathalamus) represent a caudal extension of the ventral nuclear group which function in part as relay nuclei. In general, the dorsal nuclear group serves as association nuclei. Thalamic nuclear groups readily detectable in gross specimens include the anterior and medial groups, as well as the geniculate bodies and the pulvinar, which are part of the posterior group.

The germinal zone that lies ventral to the hypothalamic sulcus (Figs. 3.11 and 3.15) on both sides of the third ventricle gives rise to the hypothalamus. Cells in this region differentiate into a number of separate nuclear groups which subserve visceral, endocrine, and regulatory functions. The most prominent nuclear group forms the *mammillary body*, a rounded protuberance on the ventral surface of the hypothalamus (Figs. 2.9 and 2.10). A small evagination in the floor of the diencephalon caudal to the optic chiasm forms the primordium of the *infundibulum*, which gives rise to the *posterior lobe* of the *hypophysis* or *neurohypophysis*. The *anterior lobe* of the hypophysis derives from an ectodermal diverticulum of the mouth cavity (stomodeum) known as *Rathke's pouch*, which superiorly comes in contact with the infundibulum. Rathke's pouch loses its pharyngeal attachment and differentiates into the anterior lobe of the hypophysis or *adenohypophysis* (Fig. 3.11).

Other hypothalamic derivatives include the subthalamic nucleus and the inner part of the globus pallidus. These structures are described in the next section.

Telencephalon

This most rostral segment of the developing brain is composed of the two evaginating *cerebral vesicles* and their median connection, the *lamina terminalis* (Figs. 3.10 and 3.11). Each cerebral vesicle is in wide communication with the third ventricle via the interventricular foramen (Fig. 3.15) and expands upward, forward, and backward. Through this caudal expansion, the telencephalic vesicles cover the diencephalon dorsally and laterally. The region where the cerebral vesicle is attached to the roof of the diencephalon becomes very thin. Here the single layer of ependymal cells and the vascular mesenchyme in the roof of the third ventricle become continuous with similar layers in the lateral ventricle that form the choroid plexus. The line of invagination which first appears at the level of the interventricular foramen is called the *choroidal fissure*. Thus, the choroid plexus of the third and lateral ventricles is continuous through the interventricular foramina along the line of vesicle evagination, the choroid fissure. A small horizontal cleft persists between the cerebral vesicle and the diencephalon (Fig. 3.15). This narrow triangular space dorsal to the thalamus is lined with a double layer of pia mater and filled with loose mesenchyme (velum interpositum, Fig. 2.29**B**). This space represents the most rostral extension of the *transverse cerebral fissure* (Fig. 3.15**A** and **B**). The lower pial layer of this fissure, as observed in frontal section, forms the roof of the diencephalon and becomes invaginated as the choroid plexus of the third ventricle (Figs. 2.29**A** and 3.15). The adult cerebral hemisphere also is separated from the cerebellum by the transverse cerebral fissure. The tentorium cerebelli occupies part of the transverse fissure and separates the inferior surfaces of the hemispheres from the superior surface of the cerebellum (Fig. 2.3).

Immediately above the choroid fissure the medial wall of the cerebral vesicle becomes thickened and forms the *hippocampal ridge* (Figs. 3.15 and 3.17). This ridge bulges into the lateral ventricle as a longitudinal elevation, the *hippocampal formation*. As the cerebral hemispheres expand, the hippocampal formation extends posteriorly and is finally carried downward into the temporal lobe. The medial surface of the hemisphere develops a corresponding groove, the *hippocampal fissure*, which runs parallel to the choroid fissure throughout its extent. The hippocampal formation and the dentate gyrus together constitute the *archipallium*, which is believed to be the most phylogenetically ancient portion of the cerebral cortex.

The walls of the primitive telencephalic vesicle consist of germinal, mantle, and marginal layers, and represent only the alar plates. The mantle layer ventrolaterally undergoes relatively rapid thickening as a consequence of cell proliferation, and creates a cell mass that protrudes into the lumen of the vesicle. This thickened basal region is known as the *striatal portion* because it ultimately gives rise to the *striatum* and other components of the *basal ganglia* (Fig. 3.15). The thinner and more dorsal wall of the brain vesicle is referred to as the *suprastriatal portion*. This part of the cerebral hemisphere gives rise to the *cerebral cortex*.

BASAL GANGLIA AND INTERNAL CAPSULE

The thickened basal ganglia region appears in the telencephalon at the level of the interventricular foramen (Fig. 3.15). With the expansion of the cerebral hemispheres back over the diencephalon, part of the striatal ridge is carried in the wall of the lateral ventricle dorsal to the lateral border of the thalamus and down into the roof of the inferior horn of the lateral ventricle. Large numbers of developing corticofugal and corticopetal fibers projecting from, and to, the developing cerebral cortex incompletely divide the basal ganglia into a dorsomedial portion which bulges into the lateral ventricle and a ventrolateral portion medial to the insular region. The paraventricular striatal tissue medial to these fibers forms the *caudate nucleus* which throughout most of its extent is closely related to the lateral ventricle (Figs. 2.15 and 2.29**B**). The *amygdaloid nuclear complex* arises from the same medial primordium. The portion of the basal ganglia lateral to these cortical fiber systems, which collectively form the *internal capsule*, constitutes the *lentiform nucleus* (Fig. 3.15). The lentiform nucleus is divided into two parts: (a) a larger lateral part known as the *putamen*, and (b) a smaller inner part, the *globus pallidus*.

Although the basal ganglia are classically regarded as subcortical telencephalic nuclei, some authors (25, 26, 47) consider parts, or all, of the globus pallidus to be derived from portions of the hypothalamus. Indeed, the entopeduncular nucleus of the rat, considered homologous to the internal segment of the primate globus pallidus, was shown to arise from a germinal zone that is closely associated with the hypothalamic sulcus (35). The *subthalamic nucleus*, a small nucleus of the subthalamic region that is closely connected with the globus pallidus, also is considered a hypothalamic derivative. More precisely, it is generated in a germinal zone lying in the supramammillary recess of the third ventricle (34). The internal capsule, formed by fibers projecting to and from the cerebral cortex, has a complex development (18), but ultimately forms two major limbs—an *anterior limb* which partially separates the head of the caudate nucleus and the putamen, and a larger *posterior limb* between the thalamus and the globus pallidus (Fig. 2.13).

The *cerebral hemispheres* grow and expand rapidly, first forward to form the frontal lobe area, then laterally and upward to form the future parietal lobe (Figs. 3.11, 3.16, and 3.17). Posterior and inferior expansions soon produce the occipital and temporal lobes. The expansions of the cerebral hemispheres cover the diencephalon and posterior surface of the midbrain. The anterior, posterior, and inferior expansions during development explain the curved shape and the relations of several internal telencephalic structures in the adult brain (e.g., lateral ventricle, choroid plexus, caudate nucleus, and fornix). The cortex covering the lenticular nucleus remains as a fixed area, the insula (Fig. 3.18). This region becomes buried in the floor of the lateral sulcus by the subsequent overgrowth of adjacent lobes (Fig. 3.17).

CEREBRAL CORTEX

The suprastriatal portion of the early telencephalic vesicle appears to be composed of three concentric zones during its smooth-surfaced (lissencephalic) stage. A *germinal* or *matrix zone* surrounds the lateral ventricle. Most of the cells of this zone migrate outwards to become nerve and glial cells upon maturation. However, some cells remain in this zone to form the internal limiting membrane, ependyma, and the subependymal glial layer. The pale *intermediate zone* becomes the white matter of the cerebral hemispheres. It has many radiating fibers and is traversed by neuroblasts and glioblasts migrating from the matrix zone to the more superficial layer. An outer *cortical zone* or *plate* represents the prospective neopallium (isocortex). This zone has two distinct layers. The deeper pyramidal layer has many cells and will form layers II to VI of the adult six-layered cortex (Fig. 20.1). The marginal layer is composed mostly of fibers and becomes the molecular (plexiform)

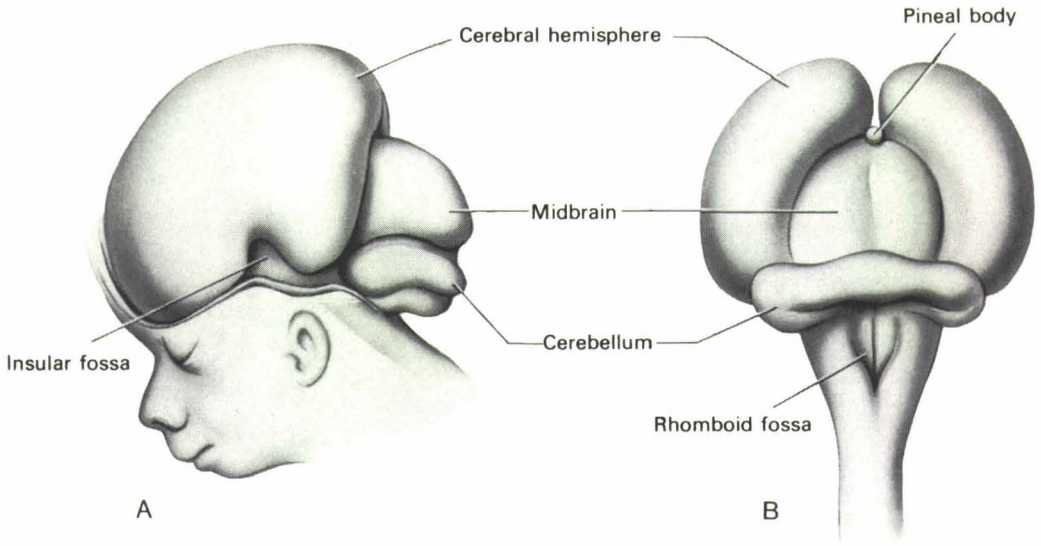


Figure 3.16. Cerebral vesicle and brainstem in the 12-week human fetus. **A.** Lateral view. **B.** Posterior view.

or most superficial layer (layer I). In areas of the olfactory cortex (allocortex), the six layers are not present. In these regions, the migrating neuroblasts and glioblasts enter the cortical zone and form a thin nuclear layer close to the surface.

It is now well-established that the cortical cell layers develop in an inverted fashion, so that cells in the deeper layers (i.e., layer VI) develop first (2, 45, 51). Hence, cells destined to the superficial layers must migrate past older cells to reach their final position. As in the cerebellar cortex, the migration of neuroblasts is guided from an early stage by a system of radial glial fibers that extends the width of the thickening telencephalon. The perikarya of the radial glial cells lie in the ventricular and subventricular zones. In the human fetus, this process takes place, for the greater part, between 7 and 16 weeks gestational age. However, the presence of radial glial fibers has been noted in the human telencephalon beyond 16 weeks, raising the possibility that migration does not end sharply at this time. In addition to the system of radial glial fibers, other organizing principles may be involved, such as the thalamocortical afferents that already exist before the beginning of migration to the cortical plate (3).

In humans, the cortical zone becomes highly cellular due to massive neuroblast migrations in the twelfth week. Differentiation of neuroblasts into neuronal classes characteristic of each cortical layer is accomplished after the completion of migration. This differentiation involves both the shape of the perikaryon (pyramidal versus nonpyramidal) and its connections. The commitment of a neuron to differentiate into a certain morphologic class appears to depend mostly on the order in which it is generated, rather than on its final position within the cortex. In support of this view is the evidence gathered in the murine *reeler* mutant that suffers from an inherited neuronal migration disorder which specifically affects the intracortical migration of the pyramidal neurons. In this mutant, the neuroblasts migrate to faulty positions but nevertheless differentiate into neurons whose perikaryal shapes are characteristic of each layer (3). At birth the human neopallium has assumed a stratified appearance as a result of neuron differentiation and laminae formation by the incoming and outgoing nerve fibers.

In the early weeks of gestation, the surfaces of the cerebral hemispheres are lissencephalic (smooth). The developing commissures form conspicuous bundles on the cut medial surfaces (Figs. 3.15 and 3.17). During the sixth and seventh months, the surfaces of the hemispheres grow rapidly and develop convolutions (gyri) separated by shallow or deep furrows (*sulci*). As a result of such surface folds, two-thirds of the cerebral cortex becomes buried in the walls and floor of the sulci when the brain attains its adult size. Fetal sulci appear in an orderly sequence: the phylogenetically older sulci appear first, and more recently acquired sulci

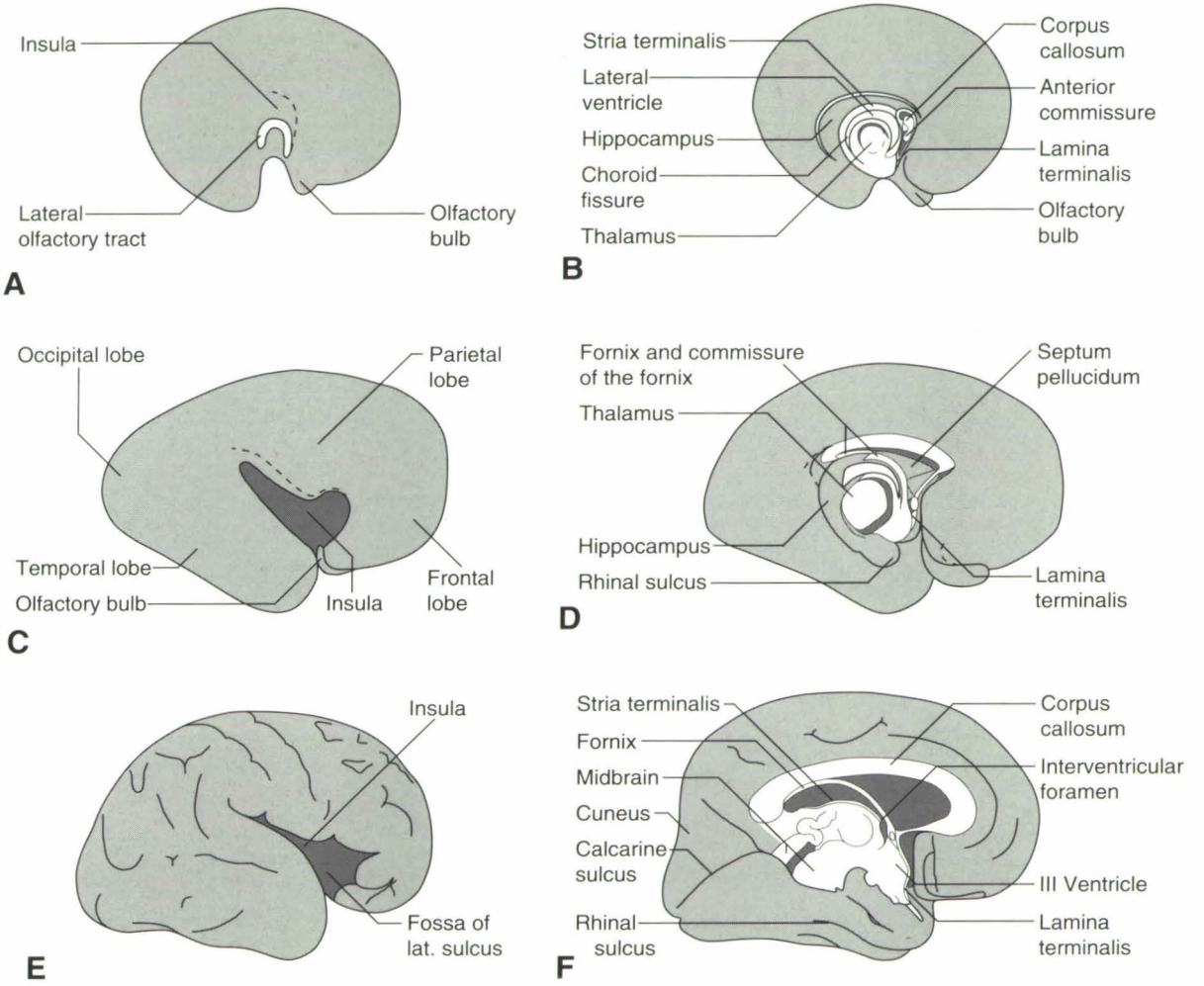


Figure 3.17. Development of human cerebral hemisphere. **A, B.** Lateral and medial surfaces of the hemisphere in a fetus of 3 months. **C, D.** Lateral and medial surfaces of the hemisphere in a fetus at the beginning of the fifth month. **E, F.** Lateral and medial surfaces of the hemisphere at the end of the seventh month.

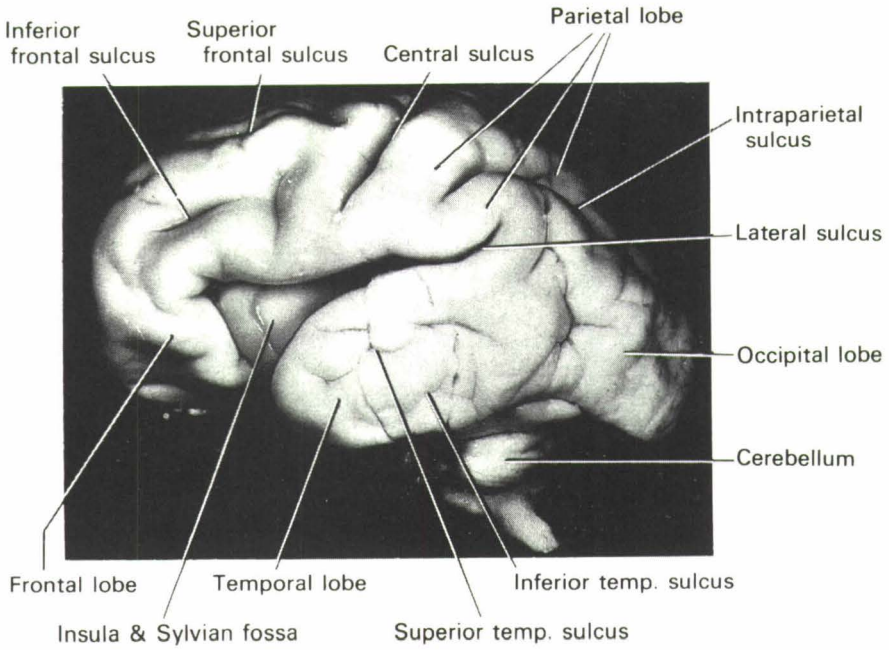


Figure 3.18. Lateral view of the brain of a 7-month human fetus. Note the primitive sulcal pattern and the exposure of the insular cortex.

appear later (Figs. 3.17**E**, **F** and 3.18). The principal sulci and gyri that form the characteristic pattern of the human cerebral cortex all can be identified in the full-term infant.

COMMISSURES

The medially placed *lamina terminalis* represents the cephalic end of the early neural tube and extends from the roof plate of the diencephalon to the optic chiasm (Figs. 3.11 and 3.17). This primitive midline telencephalic structure provides the only bridge whereby nerve fibers can pass from one cerebral hemisphere to the other. The first fibers to cross between the two hemispheres *(commissural fibers)* are within the *anterior commissure*. This structure appears in the lower portion of the lamina terminalis by the third month. It connects the olfactory bulb and portions of the temporal lobe of one side with the same structures of the opposite hemisphere (Figs. 18.8 and 18.12). The small *commissure of the fornix* (psalterium) is the second to appear in the lamina terminalis close to the roof of the diencephalon (Fig. 3.17**D**). Its fibers connect portions of the hippocampal formation with each other.

The largest and most important commissure to cross in the lamina is the *corpus callosum*. The first fibers of the corpus callosum, connecting nonolfactory cortical areas of the two hemispheres, appears as a small bundle rostral to the commissure of the fornix. The size of the corpus callosum parallels the rapid growth and expansion of the neopallium. It first extends anteriorly to connect the frontal lobes and then enlarges posteriorly as the parietal lobes develop. As the constituent fibers increase in number, the corpus callosum arches back over the thin roof of the diencephalon (Fig. 3.17). The superior and rostral portions of the hippocampal formation undergo regressive changes in association with development of the corpus callosum, but these parts persist in the adult as the *indusium griseum* or *supracallosal gyrus* (Fig. 18.11). The area between the corpus callosum and the fornix becomes very thin and forms the *septum pellucidum*. These commissures and septum pellucidum develop within, and represent prolongations of, the embryonic lamina terminalis. The fibers of the *optic chiasm* cross in the junctional zone between the lamina terminalis and the rostral wall of the diencephalon (Figs. 2.29 and 3.17).

After the neural tube has been formed, it lies deep to the overlying ectoderm and is surrounded on all sides by primitive mesoderm (or mesenchyme). This embryonic relationship is shown in Figure 3.9, where the more darkly stained mesenchyme is seen to

the left of the spinal nerve and neural tube. Recent evidence in birds suggests that much of this mesenchyme has most likely a neural crest origin (30). From the surrounding mesenchyme the muscles, blood vessels, cartilage, bone, and connective tissue of the body are derived. This mesenchyme thus gives rise to several supporting structures of the nervous system (e.g., skull, vertebrae, meninges (dura mater), intervertebral discs, ligaments, sheaths of peripheral nerves, blood vessels, and microglia). These mesodermal structures are of paramount importance, for they provide not only support, but protection and nourishment to the nervous system.

Supporting tissues are, under some circumstances, responsible for serious damage to the nervous system. For example, an artery may rupture with extensive hemorrhage, or the lumen of a vessel may be occluded suddenly and produce anoxia in the area of its neural distribution. Tumors commonly arise from the meninges, from the connective tissue sheaths along peripheral nerves, or from glioblasts. An intervertebral disc may rupture posteriorly into the vertebral canal and compress the spinal cord or spinal nerves. Also, fractures of the skull and vertebrae often compress the underlying brain or spinal cord.

CONGENITAL ANOMALIES

A detailed discussion of malformations of the developing neural tube or changes in brain development resulting from malnutrition are beyond the scope of this textbook. Some malformations involving both the developing neural tube and the vertebral column will serve as examples. Defects in the development and fusion of the dorsal arch of one or more vertebrae produce a condition referred to as *spina bifida*. There are many variations of such a condition, including some in which the meninges and/or the

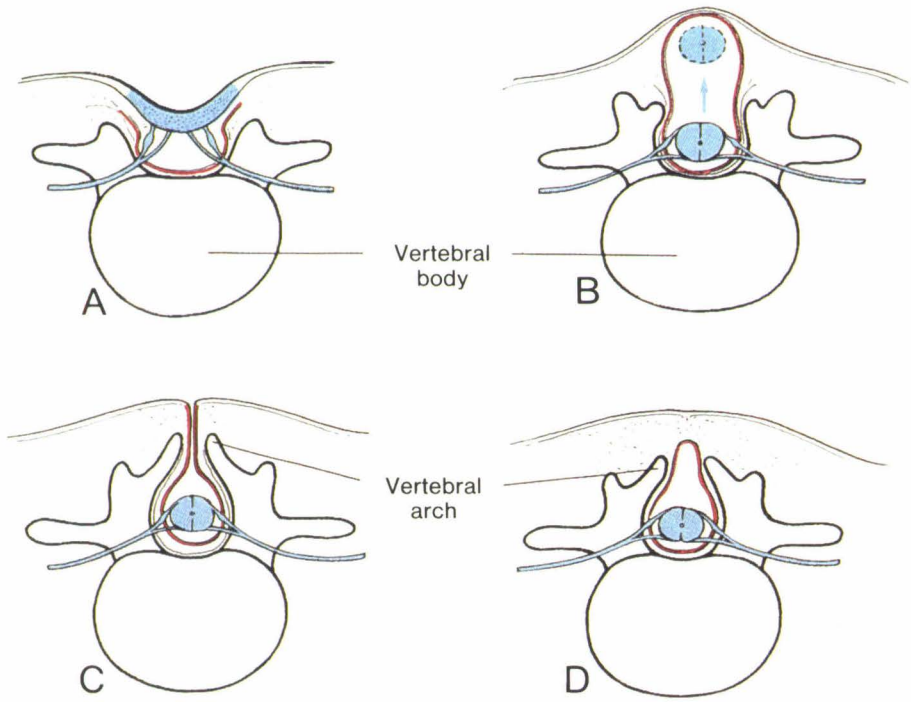


Figure 3.19. One type of spinal malformation is called *spina bifida*. In this condition, there is a failure of closure of the posterior arch of one or more vertebrae and in some types there is a failure of development of the neural tube. **A** illustrates failure of closure of both neural tube and the vertebral arch. In **B**, the neural tube develops normally, but the meninges and the subarachnoid space extend dorsally through the defect in the vertebrae to produce a *meningocele*. If the spinal cord forms part of the subcutaneous herniation (*arrow*), it is called a *meningocele*. **C** represents a minor defect in the vertebral arch in which a dermal sinus extends from the skin to the subarachnoid space. This sinus may close secondarily. **D** represents *spina bifida occulta*, in which the meningeal herniation does not extend far above the defect in the vertebral arch. Skin overlying the vertebral defect may contain a dense tuft of hair. Nerves and neural tissue are in *blue;* the meninges are in *red*.

spinal cord may be involved. For instance, an unclosed posterior arch of the vertebra may result in herniation of the dura and arachnoid membranes dorsally, forming a translucid cystlike expansion of the subarachnoid space filled with cerebrospinal fluid. This condition, which occurs most often in the lumbosacral region, is called a *meningocele* (Fig. 3.19**B**). Meningocele is often associated with other congenital malformations, such as hydrocephalus that sometimes can be cured only after the resection of the protruding meningeal sac. When the spinal cord is displaced dorsally into the cyst, the condition is termed a *meningomyelocele*. Neurologic complications, such as motor, sensitive, and sphincteral deficits, often accompany meningomyelocele. If the meningeal sac does not extend far enough into the subcutaneous tissue to form a cyst, there may be no protrusion of the overlying skin (Fig. 3.19**D**). This relatively asymptomatic condition is termed *spina bifida occulta* and is often marked by a tuft of hair on the overlying skin. In some cases, the caudal neuropore may not close completely, forming a channel or fibrous cord extending from a dimple on the surface of the skin to the meninges (Fig. 3.19**C**). This abnormality is referred to as *congenital dermal sinus*. A more serious defect involves failure of the neural groove to close and form the neural tube. The neural tissue then remains exposed to the outside and the subsequent differentiation of neurons is arrested. This is termed spina bifida with *myeloschisis*, or simply *rachischisis*, a condition that is accompanied by severe neurologic deficits (Fig. 3.19**A**).

References

1. Altman J. Proliferation and migration of undifferentiated precursor cells in the rat during postnatal gliogenesis. Exp Neurol 1966;16: 263–278.
2. Angevine JB Jr, Sidman RL. Autoradiographic study of cell migration during histogenesis of the cerebral cortex in the mouse. Nature 1961; 192:766–768.
3. Barth PG. Disorders of neuronal migration. Can J Neurol Sci 1987; 14:1–16.
4. Choi BH, Lapham LW. Evolution of Bergman glia in developing human fetal cerebellum: a Golgi, electronmicroscopic and immunofluorescence study. Brain Res 1980;190: 369–383.
5. Cowan WM. The development of the brain. Sci Am 1979;241:112–133.
6. Crouse GS, Cucinotta AJ. Progressive neuronal differentiation in the submandibular ganglia of a series of human fetuses. J Comp Neurol 1965;125:259–272.
7. Davis CL. Description of a human embryo having 20 paired somites. Contrib Embryol 1923;15:1–51.
8. Del Rio-Hortega P. El Tercer elemento de los centros nerviosus. Histogenesis y evolucion normal: exoda y distribucion regional de microglia. Mem R Soc Espan Hist Nat 1921;11:213–268.
9. Dennis J. Development of the neuromuscular junction: Inductive interactions between cells. Annu Rev Neurosci 1981;4:43–68.
10. Edelman GM. Cell-adhesion molecules in neural histogenesis. Annu Rev Physiol 1986;48:417–430.
11. Edelman GM. Neural Darwinism. The theory of neuronal group selection. New York: Basic Books, 1987.
12. Fujita S. Analysis of neuron differentiation in the central nervous system by tritiated thymidine autoradiography. J Comp Neurol 1964;122: 311–327.
13. Gilbert SF. Developmental biology. Sunderland, MA: Sinauer Associates, 1988.
14. Giorgi PP, van Der Loos H. Axons from eyes grafted in Zenopus can grow into the spinal cord and reach the optic tectum. Nature 1978;275: 746–748.
15. Gottlieb DI, Glaser L. Cellular recognition during neural development. Annu Rev Neurosci 1980; 3:303–318.
16. Hamilton WJ, Boyd JD, Mossman HW. Human embryology. Prenatal development of form and function. Ch. XII. Baltimore: Williams & Wilkins, 1962:315–388.
17. Hanaway J. Formation and differentiation of the external granular layer of the chick cerebellum. J Neurol Sci 1967;131:1–14.
18. Hewitt W. The development of the human internal capsule and lentiform nucleus. J Anat 1961;95: 191–199.
19. Hochstetter F. Beiträge zur Entwicklungsgeschichte des menschlichen Gehirns. Vol. I. Vienna and Leipzig: F. Deutcke, 1919.
20. Ingalls NW. A human embryo at the beginning of segmentation with special reference to the vascular system. Contrib Embryol 1920;11: 61–90.
21. Jacobson M. Developmental neurobiology. New York: Plenum Press, 1978.
22. Jessell TM. Neuronal survival and synapse formation. In: Kandel ER, Schwartz JH, Jessell TM, eds. Principles of neural science. Ch. 59. Am-sterdam: Elsvier, 1991:929–944.
23. Kalil RE. Synapse formation in the developing brain. Sci Am 1989; 261:76–85.
24. Keibel F, Mall FP. Manual of Human Embryology, Vol. II, Ch. XIV. Philadelphia: J.P. Lippincott, 1912:1–144.
25. Kuhlenbeck H. The central nervous system of vertebrates. Vol. 5, Part I. Derivatives of the prosencephalon: diencephalon and telencephalon. Basel: Karger, 1977.
26. Kuhlenbeck H, Haymaker W. The derivatives of the hypothalamus in the human brain: their relation to the extrapyramidal and autonomic-systems. Milit Surg 1949;105:26–52.
27. Landis SC. Target regulation of neurotransmitter phenotype. Trends in Neurosci 1990;13:344–350.
28. Langman J. Medical embryology. 4th ed. Baltimore: Williams & Wilkins, 1981.
29. Larsell O, Jansen J. The comparative anatomy and histology of the cerebellum: the human cerebellum, cerebellar connections and cerebellar cortex. Minneapolis: University of Minnesota Press, 1972.
30. Le Douarin N. The Neural Crest. Cambridge, UK: Cambridge University Press, 1982.
31. Levi-Montalcini R, Calissano P. The nerve-growth factor. Sci Am 1979;240:68–77.
32. Levitt P, Rakic P. Immunoperoxydase localization of glial fibrilary acidic protein in radial glial cells and astrocytes of the developing rhesus monkey brain. J Comp Neurol 1980;193:417–448.
33. Lund RD. Development and plasticity of the brain. New York: Oxford University Press, 1978.
34. Marchand R. Histogenesis of subthalamic nucleus. Neuroscience 1987;21:183–195.
35. Marchand R, Lajoie L, Blanchet C. Histogenesis at the level of the basal forebrain: the entopeduncular nucleus. Neuroscience 1986, 17: 591–607.
36. Marchand R, Poirier LJ. Isthmic origin of neurons of the rat substantia nigra. Neuroscience 1983;9:373–381.

37. Miale IL, Sidman RL. An autoradiographic analysis of histogenesis in the mouse cerebellum. Exp Neurol 1961;4:277–296.
38. Moscona AA, Hausman RE. Biological and biochemical studies on embryonic cell recognition. In: Lash JW, Burger MB, eds. Cell and tissue interactions. New York: Raven Press, 1977:173–186.
39. Payne F. General description of a 7-somite human embryo. Contrib Embryol 1924;16:115–124.
40. Peters A, Palay SL, Webster H de F. The fine structure of the nervous system: the neurons and supporting cells. Philadelphia: W.B. Saunders Co., 1976.
41. Pictet RL, Rall LB, Phelps P, Rutter WJ. The neural crest and the origin of the insulin-producing and other gastrointestinal hormone-producing cells. Science 1976;191:191–192.
42. Prentiss CW, Arey LB. A laboratory manual and textbook of embryology. Ch. XII. Philadelphia: W.B. Saunders Company, 1920:321–352.
43. Purves D, Lichtman JW. Formation and maintenance of synaptic connections in autonomic ganglia. Physiol Rev 1978;58:821–862.
44. Rakic P. Neuron-glia relationship during granule cell migration in developing cerebellar cortex. A Golgi and electron microscopic study in *Macacus rhesus*. J Comp Neurol 1971;141:283–312.
45. Rakic P. Neuronal-glial interaction during brain development. Trends in Neurosci 1981;4:184–187.
46. Rakic P, Sidman RL. Weaver mutant mouse cerebellum: defective neuronal migration secondary to abnormality of Bergman glia. Proc Natl Acad Sci (USA) 1973;70:240–244.
47. Richter E. Die Entwicklung des Globus Pallidus und des Corpus Subthalamicum. Berlin: Springer-Verlag, 1965.
48. Robertson A, Gingle AR. Axial bending in the early chick embryo by a cyclic adenosine monophosphate source. Science 1977;197: 1078–1079.
49. Sauer FC. Mitosis in the neural tube. J Comp Neurol 1935;62:377–405.
50. Schoenwolf GC, Smith JL. Mechanisms of neurulation: traditional viewpoint and recent advances. Development 1990;109:243–270.
51. Sidman RL, Rakic P. Neuronal migration, with special reference to developing human brain: a review. Brain Res 1973;62:1–35.
52. Sperry RW. Chemoaffinity in the orderly growth of nerve fiber patterns and connections. Proc Natl Acad Sci (USA) 1963;50:703–710.
53. Tennyson VM. Electron microscopic study of the developing neuroblast of the dorsal root ganglion of the rabbit embryo. J Comp Neurol 1965;124:267–318.
54. Tennyson VM, Barrett RE, Cohen G, Côté L, Heikkila R, Mytilineou C. Correlation of anatomical and biochemical development of the rabbit neostriatum. In: Ford D, ed. Neurobiological aspects of maturation and aging. Progress in brain research. Vol. 40. Amsterdam: Elsevier, 1973:203–217.
55. Tuchman-Duplessis H, Auronx M, Haegel P. Illustrated human embryology. Vol. 3. Nervous system and endocrine glands (translated from French). New York: Springer-Verlag, 1974.

4
Blood Supply of the Central Nervous System

Metabolically, the central nervous system is one of the most active systems of the body. Although the brain constitutes only about 2% of the body weight, it requires 17% of the cardiac output and 20% of the oxygen utilized by the body. Estimates of cerebral blood flow based on the nitrous oxide method (39) indicate a normal blood flow of about 50 ml/100 g of brain tissue per minute. Thus, a brain of average weight has a normal blood flow of about 750 ml/minute and a mean oxygen consumption of about 3.3 ml/100 g of brain tissue per minute (about 46 ml/min for the entire brain).

The brain is not a homogeneous organ and metabolic activity in various regions reflect the functional activity of distinct brain regions. This differential functional activity of neuronal systems under various conditions can be demonstrated autoradiographically and mapped quantitatively by injections of 2[^{14}C]-deoxyglucose (2-DG) technique, which uses a glucose analogue, that passes the blood-brain barrier, is partially metabolized by functionally active neurons, and is trapped in the neurons (37, 38, 53). This technique has revealed surprisingly detailed features of neuronal activity under controlled conditions, as illustrated in Chapter 20 (Figs. 20.24 and 20.25).

Positron emission tomography (PET) provides images of brain functions in living individuals, and the introduction of the PET scan technology has revolutionized the study of human cognitive processes, as well as that of psychiatric and neurologic diseases. One powerful application of this noninvasive method makes use of deoxyglucose to visualize the metabolic activity of various cortical regions and subcortical nuclei. By covalently bonding the positron-emitting isotope of fluorine-18 to deoxyglucose to make ^{18}F-labeled deoxyglucose, it is possible to assess glucose utilization in small regions of the brain. This approach is very useful for detecting any brain areas deprived of glucose following the occlusion of cerebral arteries (55).

The term *stroke*, or *cerebrovascular accident*, refers to the neurologic symptoms and signs, usually focal and acute, that result from diseases involving blood vessels. Strokes are either *occlusive* (due to closure of a blood vessel) or *hemorrhagic* (due to bleeding from a blood vessel). The term *ischemia* refers to insufficiency of blood supply. In cases of brief or temporary ischemia, neurologic symptoms and signs may disappear rapidly, without leaving traces of tissue damage. Severe and prolonged ischemia, however, deprives brain tissue not only of oxygen but also of glucose, and, moreover, prevents the removal of potentially toxic metabolites such as lactic acid (9). It usually leads to the death of neurons and glial cells in the ischemic zone, a condition referred to as *infarction*. Diseases of the blood vessels are among the most frequent serious neurologic disorders, ranking third as a cause of death in the adult population of the United Sates and probably first as a cause of chronic functional incapacity (9).

Even brief interference with cerebral circulation can cause neurologic or mental disturbances. Neural tissue deprived of an adequate blood supply undergoes necrosis. Impairment of local or regional blood supply constitutes the most common cause of central nervous system lesions. Vascular lesions most commonly result from arteriosclerosis of cerebral and cervical (i.e., internal carotid artery) vessels, which reduce blood flow and can lead to thrombosis. Vascular occlusions also may result from emboli (i.e., fragments of blood clots, fat, and tumors or air bubbles) (5, 12). Hemorrhage into brain tissue, the brain ventricles, or the meninges may result from vascular lesions. Probably the most common cause of spontaneous hemorrhage into the brain and subarachnoid space is rupture of cerebral aneurysms (abnormal sacculations), most of which are of congenital origin. Neural

lesions resulting from interruptions of the blood supply often can be localized to specific cerebral arteries on the basis of characteristic sensory and motor deficits (8, 9).

BLOOD SUPPLY OF THE SPINAL CORD

The spinal cord is supplied by (a) branches of the *vertebral arteries* that descend, and (b) multiple *radicular arteries* derived from segmental vessels (7) (Fig. 4.1). As the vertebral arteries ascend along the anterolateral surfaces of the medulla, each gives rise to two paired descending vessels: (a) the posterior spinal artery, and (b) the anterior spinal artery.

Posterior Spinal Arteries

Paired posterior spinal arteries descend on the posterior surface of the spinal cord medial to the dorsal roots (Fig. 4.1**B**). These vessels receive variable contributions from the posterior radicular arteries and form two longitudinal plexiform channels near the dorsal root entry zone. At certain sites these spinal arteries become so small that they appear discontinuous. These arteries and their small branches supply the posterior third of the spinal cord (67).

Anterior Spinal Arteries

The paired anterior spinal arteries unite to form a single descending midline vessel that supplies midline rami to the lower medulla and sulcal branches that enter the anterior median fissure of the spinal cord (Figs. 4.1**A** and 4.2). The continuity of the anterior spinal artery is dependent upon anastomotic branches that it receives from the anterior radicular arteries (63). The anterior radicular arteries join the anterior spinal artery by branching gently upward or sharply downward. Where two anterior radicular arteries reach the same level of the spinal cord, a diamond-shaped arterial configuration results.

The anterior and posterior spinal arteries form anastomotic channels that extend the entire

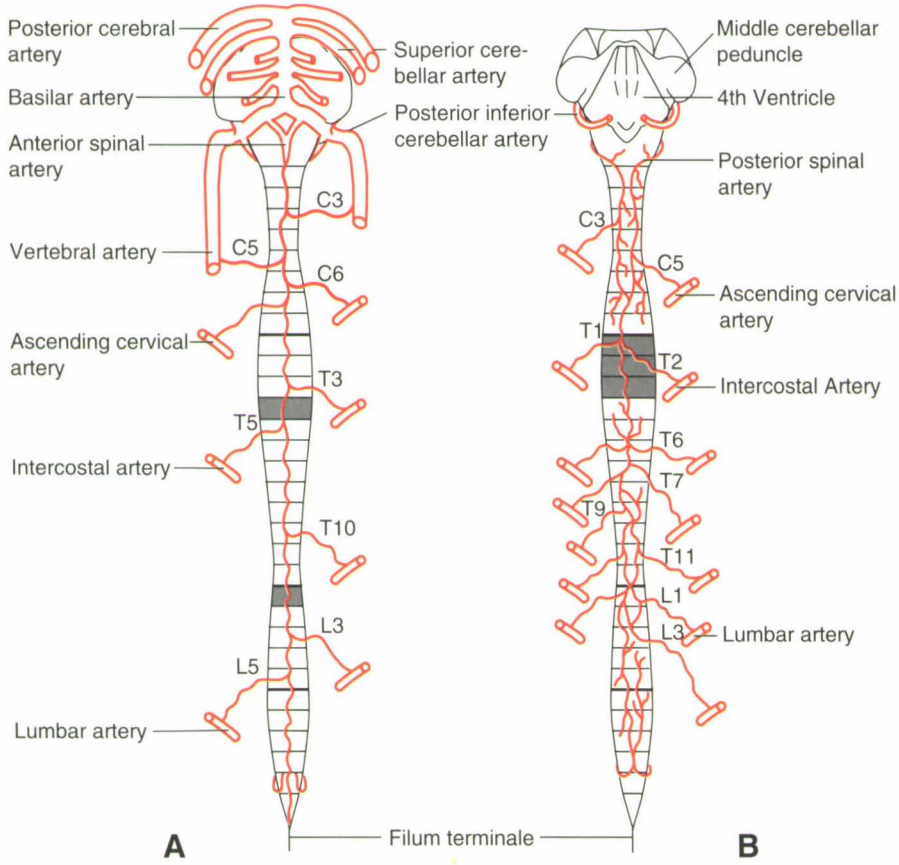


Figure 4.1. Arterial supply of the spinal cord. **A.** Anterior surface and arteries. **B.** Posterior surface and arteries. Vulnerable segments of the spinal cord are stippled. Letters and numbers indicate most important radicular arteries.

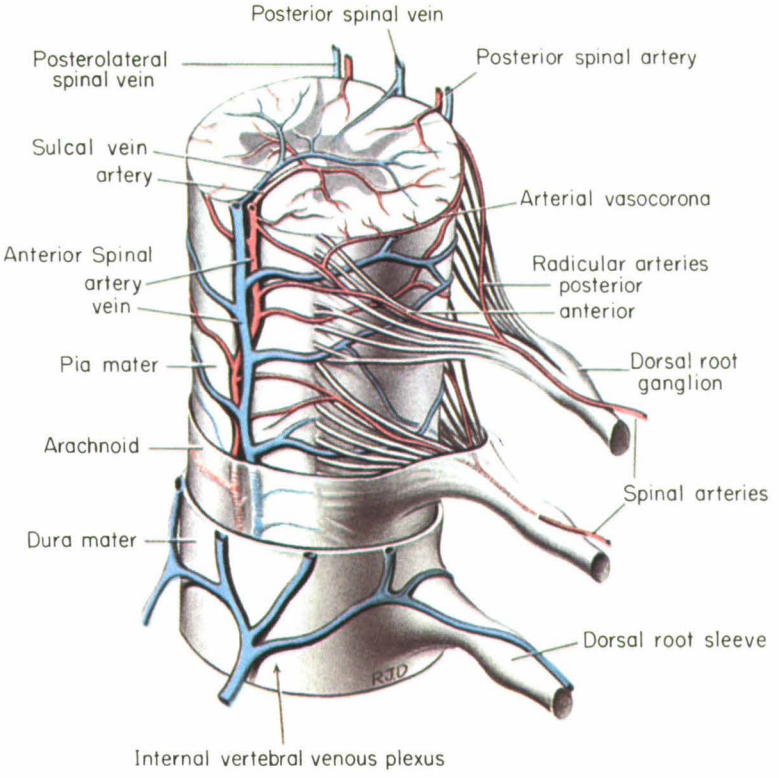


Figure 4.2. Blood supply and venous drainage of the spinal cord shown with respect to the meninges and internal structure.

length of the spinal cord and receive branches from the radicular arteries. Branches of the vertebral arteries provide the principal blood supply of virtually the entire cervical spinal cord. In the thoracic region, the anterior spinal artery narrows to such an extent that it may not form a functional anastomosis if the radicular arteries are occluded above or below. An arterial ring encircling the conus medullaris communicates with the most caudal part of the anterior spinal artery.

Radicular Arteries

Radicular arteries are derived from segmental vessels (i.e., ascending cervical, deep cervical, intercostal, lumbar, and sacral arteries) that pass through the intervertebral foramina and divide into anterior and posterior radicular arteries. These arteries provide the principal blood supply of thoracic, lumbar, sacral, and coccygeal spinal segments (Figs 4.1 and 4.2). Radicular arteries are most frequently on the left side in the thoracic and lumbar regions of the spinal cord, while cervical spinal cord segments are supplied equally from both sides. Radicular arteries course along the ventral surface of the spinal root they accompany (Fig. 4.2). Where the epineurium blends with the dura mater, the radicular arteries enter the subarachnoid space. A single radicular artery may become either an anterior or posterior radicular artery, or divide to form both (67). Small twigs leave the arteries to supply the dura mater and the spinal roots they accompany.

The *anterior radicular arteries* contributing to the anterior spinal artery vary from 2 to 17, but most commonly number between 6 and 10 arteries. The cervical spinal cord receives up to six anterior radicular arteries, while the thoracic cord receives two to four and the lumbar cord has one or two. One anterior radicular artery in the lumbar region, appreciably larger than all others, is known as the *artery of Adamkiewicz* or the artery of the lumbar enlargement (41). In 75% of cases, this artery originates at the level of the vertebral segments T9 to T12. This radicular artery travels with a lower thoracic or upper lumbar spinal root most frequently on the left side. Thoracic spinal segments have the greatest length between radicular arteries, which means that occlusion of one radicular artery

may seriously compromise its circulation (5, 12, 32). Certain spinal regions which receive their blood supply from more than one source are particularly vulnerable if they are suddenly deprived of blood from one of these sources (Fig. 4.1). The upper thoracic (T1-T4) and first lumbar spinal segments are among the most vulnerable regions of the spinal cord. The intercostal arteries do not interconnect with other arteries in the same extensive fashion as the other extraspinal arteries in the cervical and lumbosacral regions. Occlusion of one intercostal artery in a vulnerable region can result in a spinal cord infarction. This clinical picture is seen with dissecting aneurysms of the aorta or as a result of surgery on the aorta where more than one intercostal artery may be occluded. Spinal cord segment L1 is another vulnerable region, where the anterior aspect of the cord is susceptible to vascular insult (Fig. 4.1) (5, 12).

The *posterior radicular arteries*, numbering between 10 and 23, divide on the posterolateral surface of the spinal cord and join the paired posterior spinal arteries. Although these vessels are more often on the left side, left predominance is not as evident as with the anterior radicular arteries.

The *anterior spinal artery* gives rise to a number of sulcal branches that enter the anterior median fissure and alternately pass to the right or left, except for an occasional sulcal artery that divides into right and left branches (23) (Fig. 4.2). Central branches arising from the anterior spinal artery are numerous and of larger caliber in the cervical and lumbar regions of the spinal cord (28). Sulcal branches of the anterior spinal artery supply the anterior horn, the lateral (intermediate) horn, the central gray matter, and the basal part of the posterior horn. Additionally, these branches supply the anterior and lateral funiculi. Peripheral portions of the lateral funiculi receive branches from the *arterial vasocorona*. The posterior spinal arteries supply the posterior horns and the posterior funiculus (Fig. 4.2).

The blood supply of the spinal cord may be jeopardized in certain transitional regions where its arterial supply is derived from more than one source. For example, the cervical segments are supplied primarily by branches of the vertebral artery and to a lesser extent by small branches of the ascending cervical artery. The upper segments of the thoracic spinal cord, on the other hand, are dependent upon the radicular branches of the intercostal arteries. If one or more of the parent intercostal vessels are compromised by injury or ligature, spinal cord segments T1 to T4 could not be adequately maintained by the small sulcal branches of the anterior spinal artery (Fig. 4.1**A**). For this reason, thoracic segments T1 to T4, particularly T4, are considered vulnerable areas in the distribution of the anterior spinal artery (70). The occlusion of several intercostal arteries in a vulnerable region can result in spinal cord infarction. This clinical picture may be seen in association with dissecting aneurysms of the aorta or as a complication of surgery on the aorta where more than one intercostal artery has been occluded (5, 12, 68). Spinal cord segment L1 is another vulnerable region. The posterior surface of the cord most susceptible to vascular insult is also in segments T1 to T4 (Fig. 4.1**B**). Such vascular injuries may result in necrosis of an entire segment and produce neurologic symptoms comparable to complete cord transection.

Spinal Veins

Veins draining the spinal cord have a general distribution similar to that of spinal arteries. Anterior longitudinal venous trunks consist of anteromedian and anterolateral veins (Fig. 4.2). Sulcal veins entering the anteromedian vein drain anteromedial portions of the spinal cord; each sulcal vein drains regions on both sides of the spinal cord. Anterolateral regions of the spinal cord drain into anterolateral veins and into the *venous vasocoronal*. The *anteromedian* and *anterolateral spinal veins* are drained by 6 to 11 anterior radicular veins that empty into the epidural venous plexus. One large radicular vein in the lumbar region is referred to as the *vena radicularis magna* (63); other smaller radicular veins are distributed along the spinal cord.

Posterior longitudinal venous trunks, consisting of a *posteromedian vein* and paired *posterolateral veins*, drain the posterior funiculus, the posterior horns (including their basal regions), and the white matter in the lateral funiculi adjacent to the posterior horn (Fig. 4.2). The posterior longitudinal veins are drained by 5 to 10 posterior radicular veins that enter the epidural venous plexus. The longitudinal veins are connected with each other by coronal veins (venous vasocorona) that encircle the spinal cord.

The *internal vertebral venous plexus* (epidural venous plexus), located between the dura mater and the vertebral periosteum (Fig. 4.3), consists of two or more anterior and posterior longitudinal venous channels that are interconnected at many levels from the clivus to the sacral region (Fig. 4.23) (13). At each intervertebral space there are connections with thoracic, abdominal, and intercostal veins, as well as with the external vertebral venous plexus. Since there are no valves in this spinal venous network, blood flowing in these channels may pass directly into the systemic venous system. When intra-abdominal pressure is increased, venous blood from the pelvic plexus passes upward in the internal vertebral venous system. When the jugular veins are obstructed, blood leaves the skull via this plexus. The continuity of this venous plexus with the prostatic plexus is believed to be a route whereby neoplasms may metastasize (6). Epidural

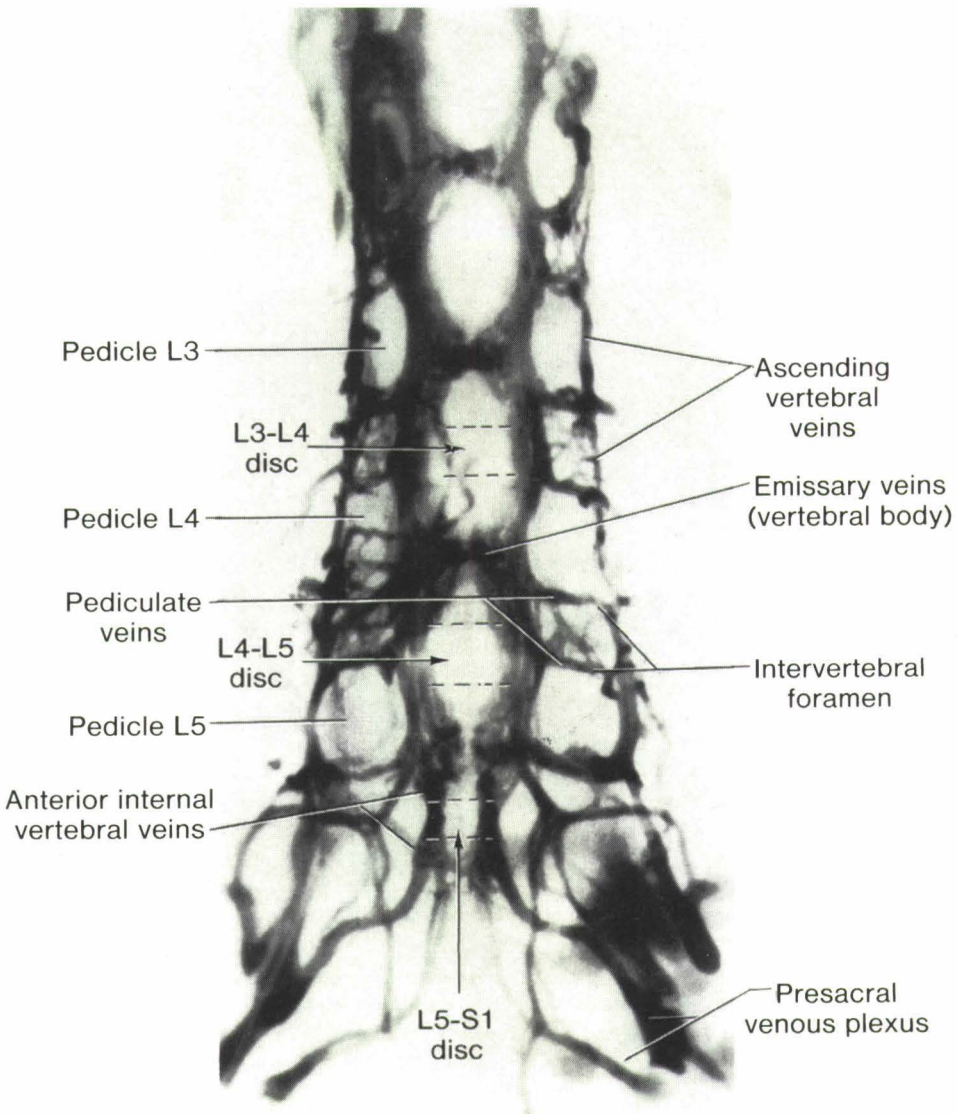


Figure 4.3. Epidural venogram done retrograde from one ascending lumbar vein. Venogram reveals details of the internal vertebral venous plexus, including ascending vertebral veins, emissary veins from vertebral body pediculate veins at the superior and inferior margins of the intervertebral foramina, the anterior internal vertebral veins, and the presacral venous plexus. The pedicles of L3, L4, and L5 vertebrae are well-outlined, and the approximate position of the intervertebral discs at three levels are indicated by *dashed lines*.

venograms reveal many details of the internal vertebral venous plexus and usually fill the pediculate veins which outline the superior and inferior margins of the intervertebral foramina (Fig. 4.3).

BLOOD SUPPLY OF THE BRAIN

The entire brain is supplied by two pairs of arterial trunks, the internal carotid arteries and the vertebral arteries. On the left, the common carotid artery arises directly from the aortic arch; the right common carotid is one of the two branches which arises from the bifurcation of the brachiocephalic artery. The common carotid artery bifurcates at the upper level of the thyroid cartilage forming the internal and external carotid arteries.

Internal Carotid Artery

This artery can be divided into four segments: cervical, intrapetrosal, intracavernous, and cerebral (supraclinoid). The intracavernous and cerebral portions of this artery are referred to as the "carotid siphon" because of their characteristic configuration (65). The *intracavernous segment* of the internal carotid artery lies close to the medial wall of the cavernous sinus, courses nearly horizontally, and bears important relationships to cranial nerves III, IV, VI, and portions (divisions I and II) of nerve V, which is located along the wall of the sinus (Fig. 4.24). The abducens nerve (N. VI) lies immediately adjacent to the internal carotid artery within the cavernous sinus (Fig. 4.6). The *cerebral segment* begins as the artery emerges from the cavernous sinus and passes medial to the anterior clinoid process (Fig. 4.4). This portion of the artery, extending upward and backward, gives rise to all major branches of the internal carotid artery. The *cervical segment* extends from the bifurcation of the common carotid to the carotid canal in the petrous bone and has no branches. The *intrapetrosal segment* of this vessel is surrounded by dense bone. Small branches given off from the intrapetrosal and *intracavernous segments* pass into the tympanic cavity and the cavernous and inferior petrosal sinuses, as well as the trigeminal ganglion and the meninges of the middle cranial fossa.

Major branches of the internal carotid artery are the ophthalmic, posterior communicating, and anterior choroidal arteries (66) (Figs. 4.4 and 4.5). The *ophthalmic artery* enters the orbit through the optic foramen, ventral and lateral to the optic nerve (N. II). The *posterior communicating artery* arises from the dorsal aspect of the carotid siphon and passes posteriorly and medially to join the posterior cerebral artery (Fig. 4.5). The *anterior choroidal artery* usually arises from the internal carotid artery distal to the posterior communicating artery and passes backward across the optic tract and then laterally to enter the choroidal fissure in the temporal lobe (Figs. 4.5 and 4.11) (10). Lateral to the optic chiasm, the internal carotid artery divides into its two terminal branches—the smaller *anterior cerebral artery* and the larger *middle cerebral artery*, which is regarded as the direct continuation of the internal carotid artery.

Most of the arterial blood within the internal carotid artery is distributed by the more mobile branches of the anterior and middle cerebral arteries. The rostral parts of the brain normally supplied by these two arteries are the anterior half of the thalamus, the basal ganglia, the corpus callosum, most of the internal capsule, the medial and lateral surfaces of the frontal and parietal lobes, and the lateral surface of the temporal lobe (Figs. 4.5, 4.7, and 4.8).

Vertebral Artery

The vertebral arteries arises as the first part of the subclavian artery, traverse the foramen of the sixth cervical vertebra, and ascend though the transverse foramina of all higher cervical vertebrae. The artery pierces the atlanto-occipital membrane and the dura mater to enter the posterior cranial fossa through the foramen magnum (Fig. 4.15). Thin radicular branches of the vertebral artery pass through the intervertebral foramina to supply the meninges and portions of the cervical spinal cord (Fig. 4.1). The relationships of the two vertebral arteries to the anterior and posterior surfaces of the caudal brainstem are shown in Figures 1.4, 1.8, 4.1, and 4.5. The two vertebral arteries course along the anterolateral surface of the medulla and unite at the caudal border of the pons to form the basilar artery (Figure 4.16). Cervical portions of the vertebral artery give rise to spinal (radicular) and muscular branches.

Intracranial branches of the vertebral and basilar arteries supply the cervical spinal cord (via anterior and posterior spinal arteries), the medulla, pons, midbrain, cerebellum, posterior parts of the diencephalon, and parts

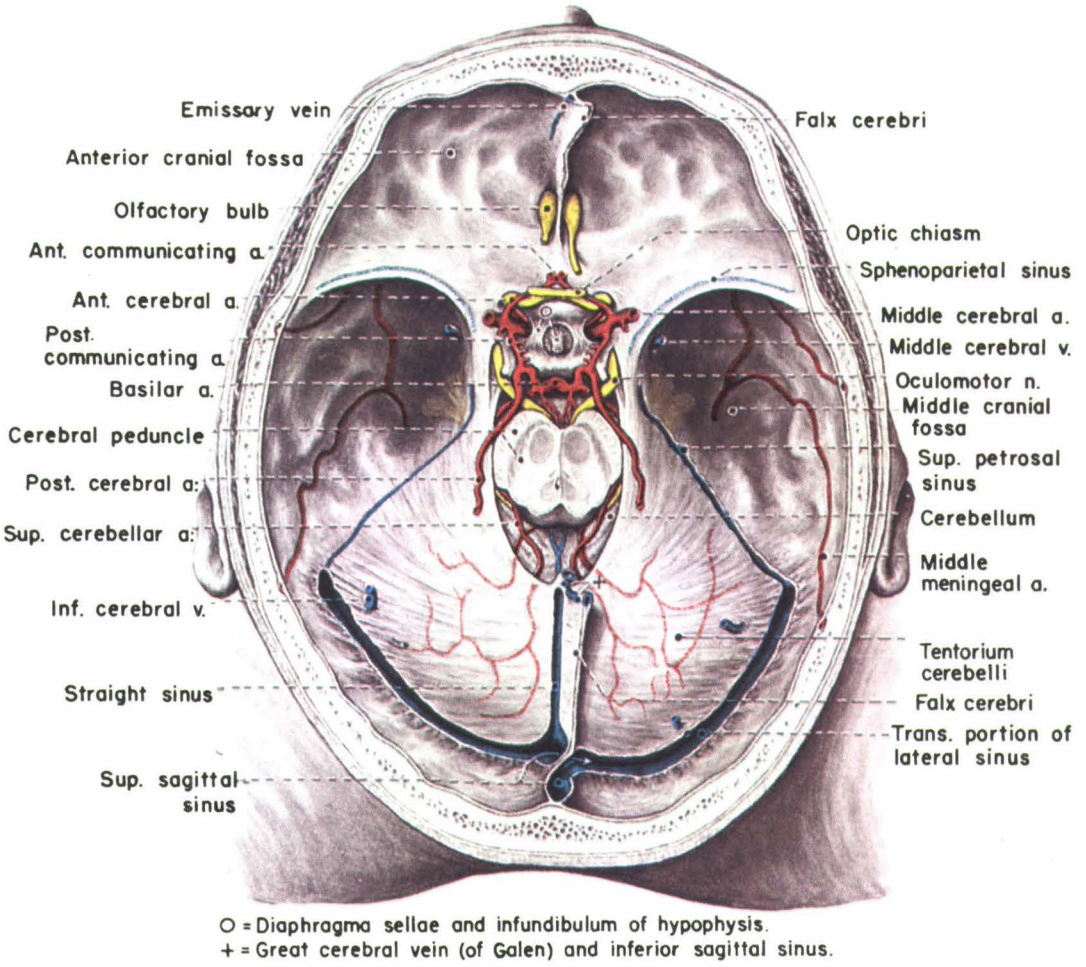


Figure 4.4. Cranial cavity after brain was removed to demonstrate relationship of the cerebral arterial circle, adjacent neural structures, and reflections of the dura mater.

of the occipital and temporal lobes of the brain (Fig. 4.5). A labyrinthine branch of the basilar artery supplies the cochlea and vestibular apparatus (Fig. 4.5).

Cerebral Arterial Circle

The cerebral arterial circle (of Willis) is an arterial wreath encircling the optic chiasm, the tuber cinereum, and the interpeduncular region formed by anastomotic branches of the internal carotid artery and the most rostral branches of the basilar artery (Figs. 4.4, 4.5, and 4.11). This arterial circle is formed by anterior and posterior communicating arteries, and proximal portions of the anterior, middle, and posterior cerebral arteries. The *anterior cerebral arteries* run medially and rostrally toward the interhemispheric fissure. In front of the optic chiasm, these two arteries are joined by a connecting vessel, the *anterior communicating artery*. The *posterior communicating arteries* arise from the internal carotid arteries, run caudomedially, and anastomose with proximal portions of the posterior cerebral arteries (Fig. 4.11). The *posterior cerebral arteries* are formed by the bifurcation of the basilar artery at the rostral border of the pons (Figs. 4.5 and 4.7). The posterior cerebral arteries give rise to numerous small branches that enter the interpeduncular fossa and hypothalamus, while the main vessels pass laterally, rostral to the root fibers of the oculomotor nerve (N. III), and encircle part of the midbrain before passing above the tentorium cerebelli (Figs. 4.4 and 4.5). The cerebral arterial circle formed by the anastomoses of these vessels is said to equalize blood flow to various parts of the brain, but normally there is little exchange of blood between the right and left halves of the arterial circle because of the equality of blood pressure. Alterations of

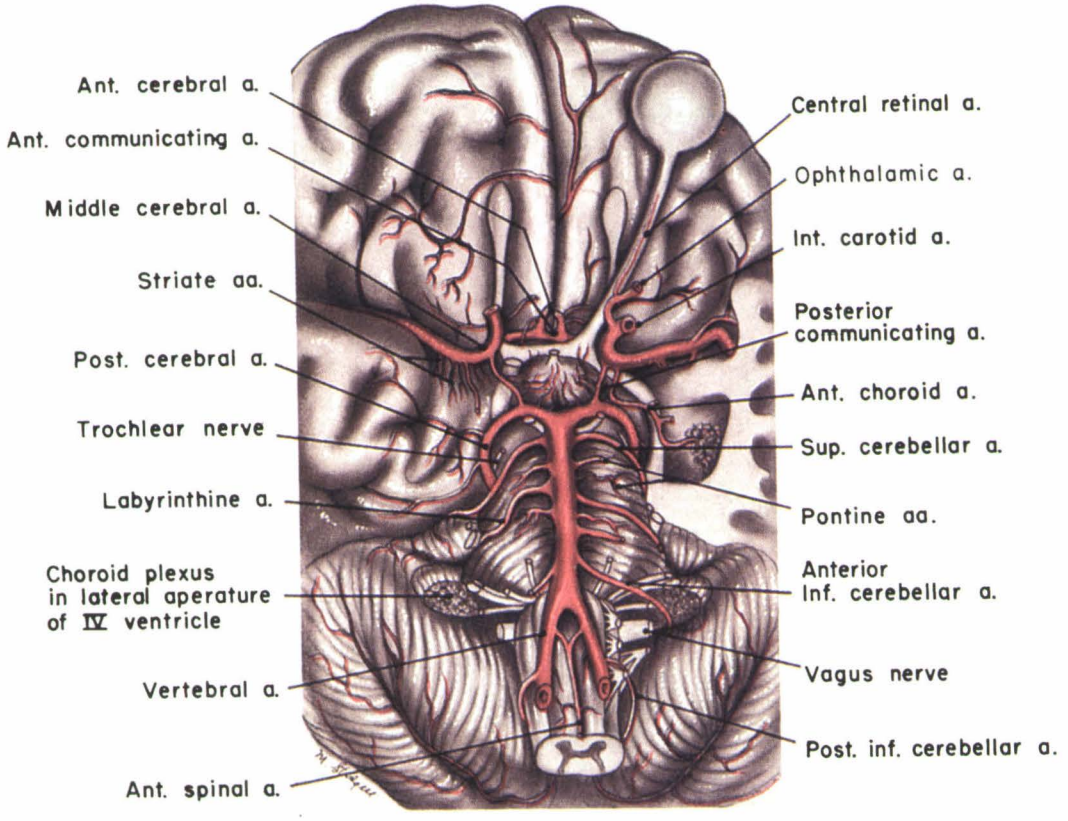


Figure 4.5. Formation and branches of the arterial circle on the inferior surface of the brain. The relationships of the arterial circle to structures on the base of the skull are shown in Figure 4.4.

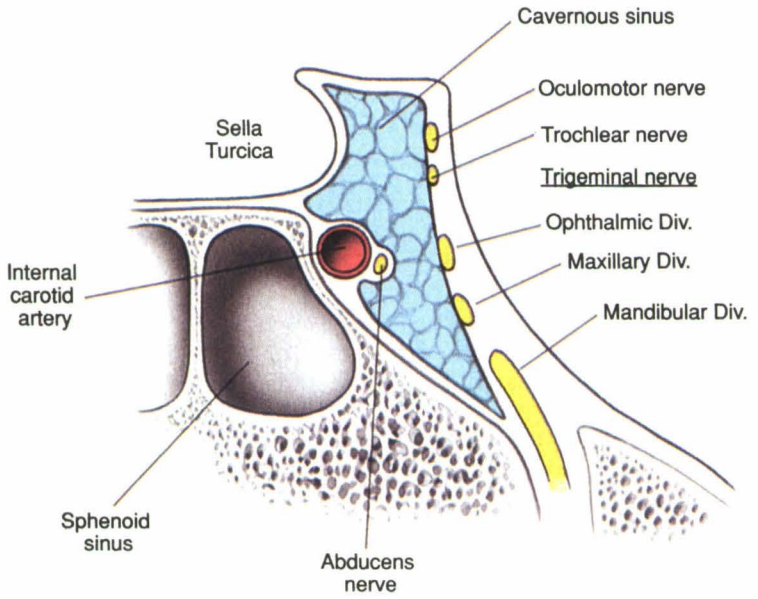


Figure 4.6. Oblique coronal section through the cavernous sinus viewed from behind showing the relationships of this venous sinus to the sella turcica, the sphenoid sinus, and the locations of cranial nerves in the wall of the sinus. The abducens nerve lies adjacent to the internal carotid artery.

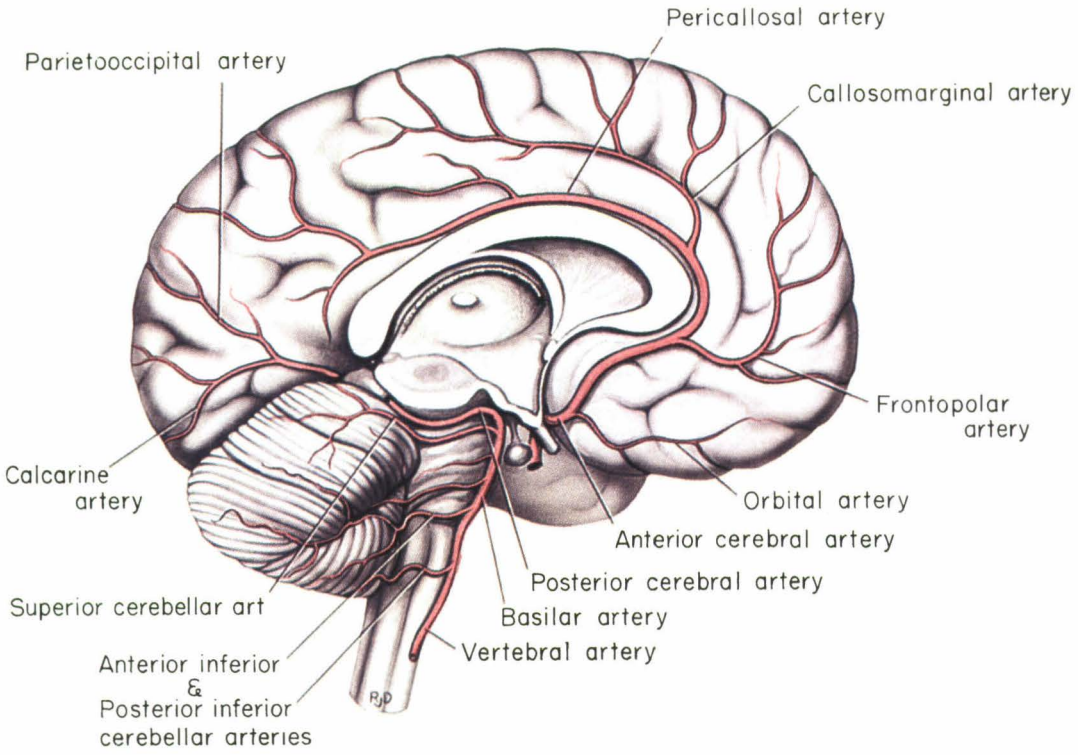


Figure 4.7. Principal arteries on the medial surface of the brain shown together with the arteries of the brainstem and cerebellum.

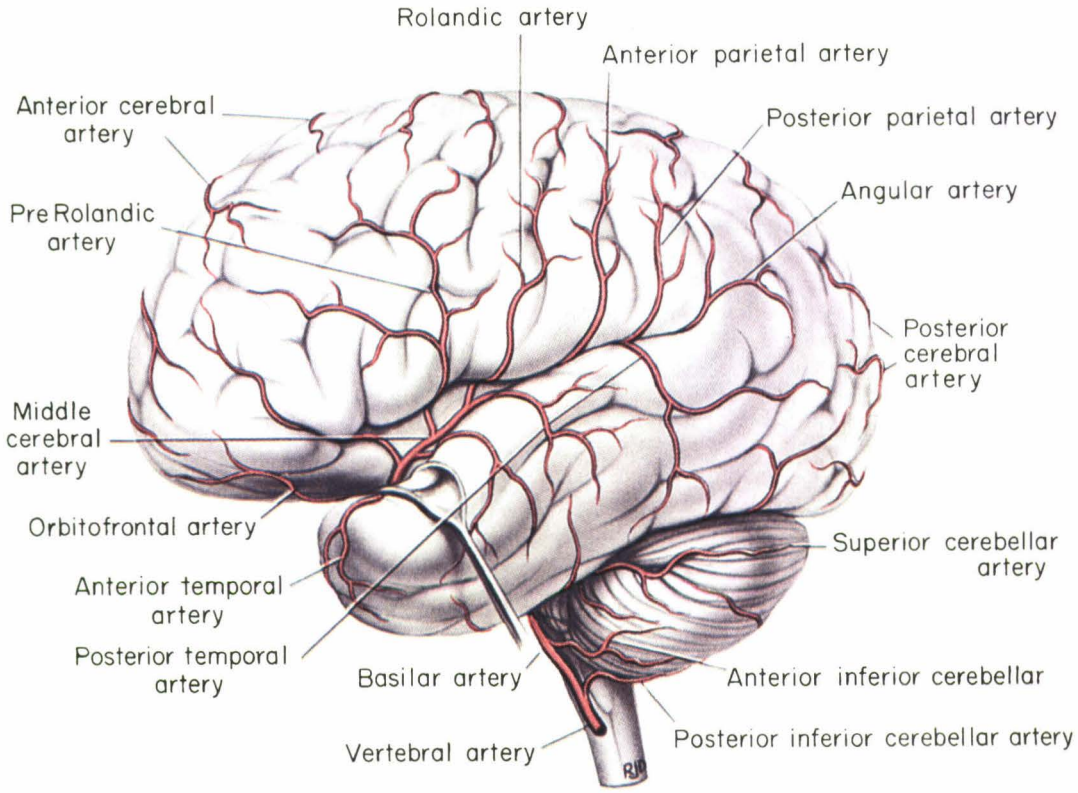


Figure 4.8. Principal arteries on the lateral surface of the brain and cerebellum.

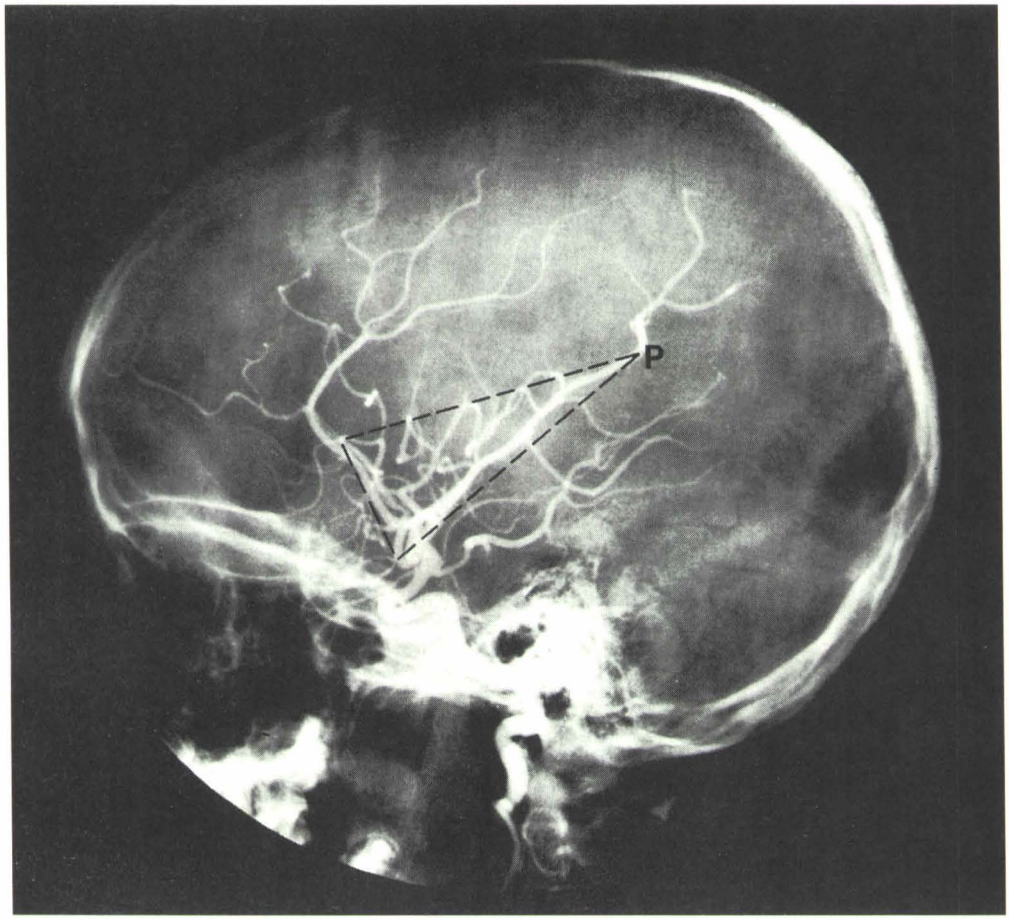


Figure 4.9. Cerebral angiogram demonstrating the Sylvian triangle. There are 5 to 8 branches of the middle cerebral artery on the surface of the insula. As they course upward, they reach the deepest portion of the sulcus formed by the junction of the insula and the frontoparietal operculum. Upon reaching this point, the middle cerebral branches change direction and proceed downward a short distance to emerge from the lateral sulcus (Sylvian fissure). The points of reversal can be identified in the angiogram, and a line drawn from the most anterior to the most posterior point (*P*) forms the upper margin of the Sylvian triangle. The inferior margin of the triangle is a line from the most posterior point (the angiographic Sylvian point, *P*) to the anterior extremity of the middle cerebral artery. The anterior border is a line drawn from the rostral extremity of the middle cerebral artery to the first turn of the opercular branch. The triangle contains branches of the middle cerebral artery as they are disposed on the insula.

blood flow in the arterial circle undoubtedly occur following occlusion of one or more of the arteries contributing to the circle. However, the communicating arteries of the arterial circle often form functionally inadequate anastomoses, which account for the high incidence of serious disturbances in blood flow following unilateral occlusion or compression of the internal carotid artery, especially in elderly individuals (5, 12).

The circle of Willis is a common site for saccular cerebral aneurysms. High blood turbulence and congenital defects in the wall of blood vessels are major factors involved in the development of aneurysms. The commonest sites of occurrence of saccular cerebral aneurysms are at the origin of the anterior communicating artery or the posterior communicating artery (Fig. 4.17). Other sites include the bifurcation of the middle cerebral artery, the cavernous carotid artery, the internal carotid bifurcation, and various loci on the vertebrobasilar arteries. Rupture of these aneurysms leads to subarachnoid hemorrhages, which often result in serious neurological impairment. Treatment is neurosurgical application of an occlusive clip resulting in eclusion of the aneurysm from the parent circulation.

Relationships of the arterial circle and its branches to the inferior surface of the brain and the origins of the respective cranial

nerves are shown in Figures 4.5 and 4.11. The *in situ* surgical relationships of the arterial circle to the base of the skull, following removal of the brain, can be appreciated by comparing Figure 4.4 with the relationships illustrated in Figure 4.5.

From the arterial circle and the principal cerebral arteries, two types of branches arise, central and cortical, which form two distinct systems.

The *central (ganglionic) arteries* arise from the circle of Willis and the proximal portions of the three cerebral arteries, dip perpendicularly into the brain substance, and supply the diencephalon, basal ganglia, and internal capsule (Fig. 4.11). For a long time, these penetrating vessels have been referred to as terminal or end arteries. Earlier studies by Scharrer (57) indicate that the vast majority of arteries in the brains in nonprimates are end arteries, but in the human brain there are no end arteries. Precapillary anastomoses have been observed in humans and nonprimates, but these anastomoses usually are not sufficient to maintain adequate circulation if a major vessel is occluded suddenly. Occlusion of one of these arteries produces a softening in the area deprived of an adequate blood supply. The anterior and posterior choroidal arteries, which are respectively branches of the internal carotid and posterior cerebral arteries, may be included in this group.

The larger *cortical (circumferential) branches* of each cerebral artery enter the pia mater, where they form a superficial plexus of more or less freely anastomosing vessels, which in some places may be continuous with the plexuses derived from the other main arteries. From these plexuses arise the smaller terminal arteries that enter the brain substance at right angles and run for variable distances. The shorter ones arborize in the cortex, while the longer ones supply the more deeply placed medullary substance of the hemisphere. Owing to the anastomoses of the larger cortical branches, the occlusion of one of these vessels is compensated to a variable extent by the blood supply from neighboring branches, although such collateral circulation is often not sufficient to prevent brain damage. The great majority of vascular occlusions occur in the cerebral vessels before they enter the substance of the brain. Areas of the cerebral cortex, internal capsule, or basal ganglia that lie between the territorial distributions of two primary arteries are the sites most severely involved after vascular injury (5, 12, 46). Brain damage to these areas, which are referred to as *watershed zones* may occur with hypotension; the resulting condition is termed *borderzone infarction*. The degree of brain damage is variable and depends upon several factors, including site of injury, amount of vascular overlap, confluence, and the rapidity with which an occlusion will develop.

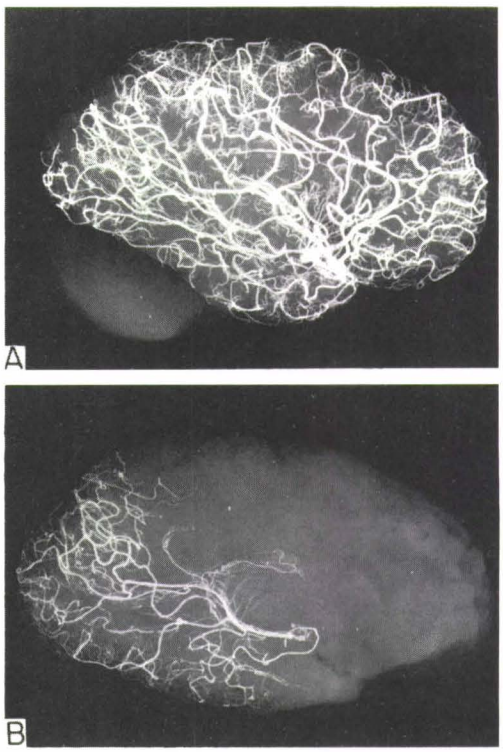


Figure 4.10. X-rays of fresh cadaver brains in which cerebral vessels have been injected with radiopaque material. **A.** Injections of the anterior, middle, and posterior cerebral arteries. **B.** Injection of the posterior cerebral artery. Note the filling of the thalamoperforating branches.

Cortical Branches

The cortical branches of the cerebral hemisphere are derived from the anterior, middle, and posterior cerebral arteries.

ANTERIOR CEREBRAL ARTERY

This artery originates at the bifurcation of the internal carotid artery lateral to the optic chiasm and nerve (Fig. 4.5). The anterior cerebral artery passes rostromedially, dorsal to the optic nerve, and approaches the corre-

sponding artery of the opposite side with which it connects via the anterior communicating artery (Figs. 4.5 and 4.11). The artery enters the interhemispheric fissure, passes upward on the medial surface of the hemisphere, curves around the genu of the corpus callosum, and continues posteriorly on the superior surface of the corpus callosum. The anterior cerebral artery gives rise to the (a) medial striate artery, (b) orbital branches, (c) frontopolar artery, (d) callosomarginal artery, and (e) pericallosal artery.

The *medial striate artery* (recurrent artery of Heubner) may arise proximal or distal to the anterior communicating artery (40, 50, 51). In the majority of the cases (78%), the artery originates just distal to the anterior communicating artery; in 14% of the cases it arises proximal to the anterior communicating artery; and in 8% of cases it arises at the level of the anterior communicating artery. The medial striate artery courses caudally and laterally, doubles back on its parent vessel, and undergoes significant branching prior to entering the anterior perforated substance as multiple vessels (Figs. 2.10, 4.11, and 18.2). In some cases it terminates in the sylvian fissure lateral to the anterior perforated substance or in the inferior frontal lobe. This artery supplies the anteromedial part of the head of the caudate nucleus, adjacent parts of the internal capsule and putamen, and parts of the septal nuclei (1) (Figs. 4.11, 4.13, and 4.14). The medial striate artery is said to anastomose with the lenticulostriate arteries and surface branches of the anterior and middle cerebral arteries (34), and frequently gives rise to several branches supplying the inferior surface of the frontal lobe (51, 52).

Orbital branches of the anterior cerebral artery, arising from the ascending portion of this vessel ventral to the genu of the corpus callosum, extend forward to supply the orbital and medial surfaces of the frontal lobe (Figs. 4.5 and 4.7).

A *frontopolar branch* is given off as the anterior cerebral artery curves around the genu of the corpus callosum (Fig. 4.7). Branches of this artery supply medial parts of the frontal lobe and extend laterally on reaching the convexity of the hemisphere.

The *callosomarginal artery*, a major branch

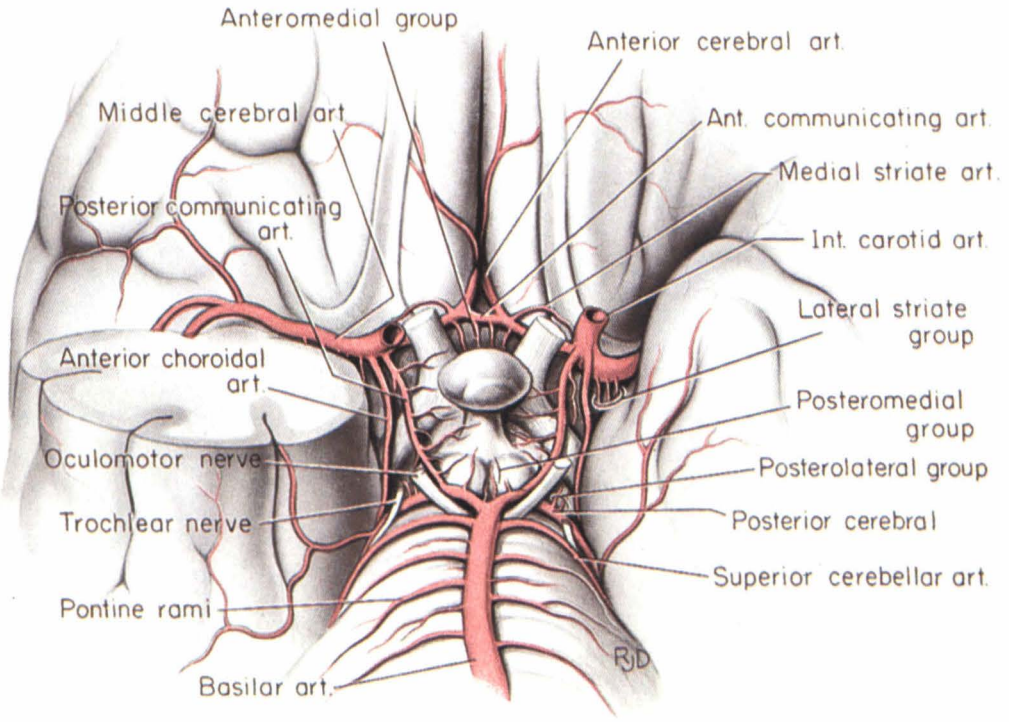


Figure 4.11. The cerebral arterial circle at the base of the brain, showing the distribution of the ganglionic branches. These vessels form anteromedial, posteromedial, posterolateral, and lateral striate arterial groups. The medial striate and anterior choroidal arteries also are shown.

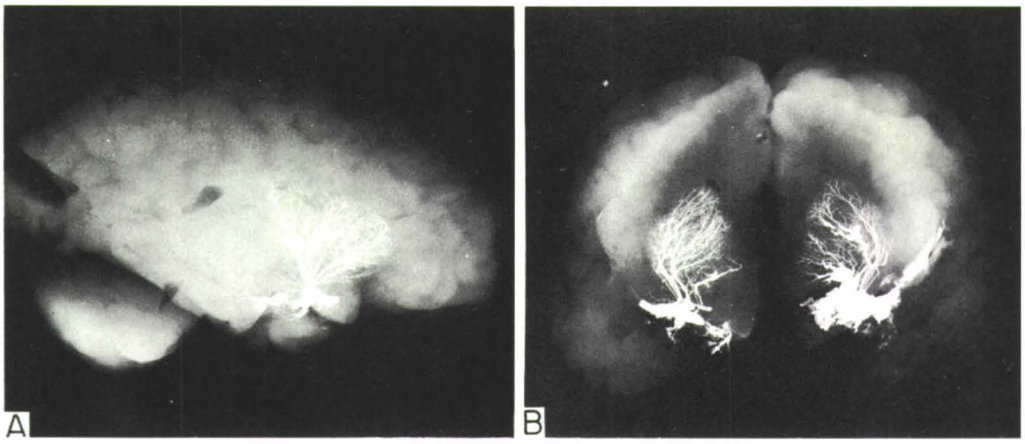


Figure 4.12. X-rays of fresh cadaver brains in which individual arteries have been injected with radiopaque material. **A** and **B** are lateral and frontal views, respectively, of the deep ganglionic branches of the middle cerebral artery that penetrate the brain in the anterior perforated substance.

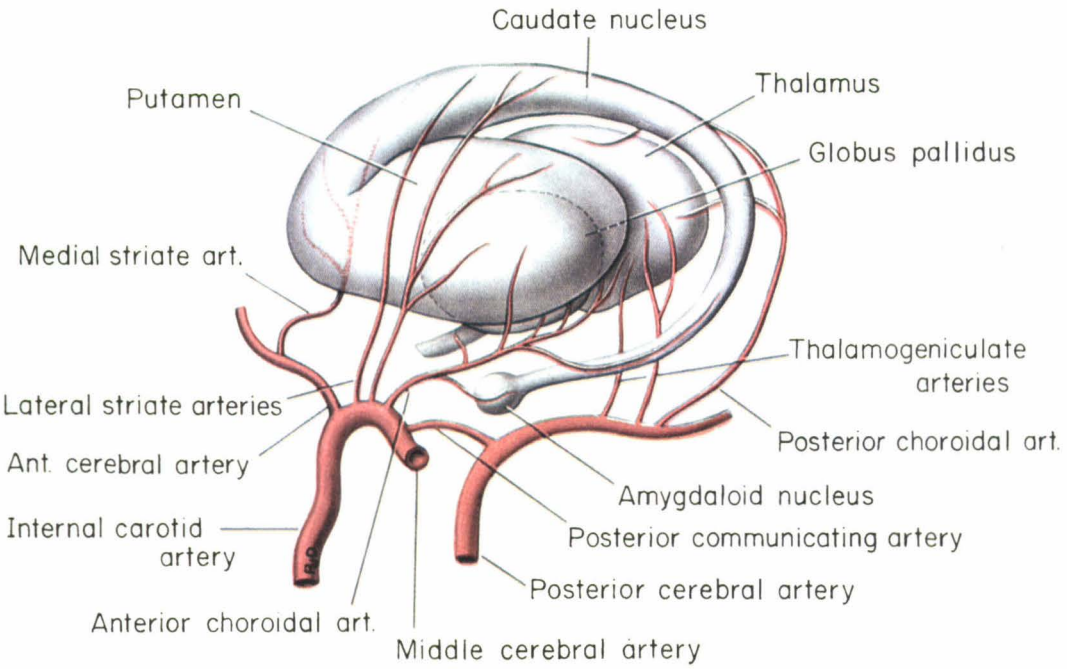


Figure 4.13. Arterial supply of the basal ganglia and thalamus.

of the anterior cerebral artery, arises distal to the frontopolar artery and passes caudally in the callosomarginal sulcus, dorsal to the cingulate gyrus (Fig. 4.7). Branches of this artery supply the paracentral lobule and parts of the cingulate gyrus (40).

The *pericallosal artery*, regarded as the terminal branch of the anterior cerebral artery, courses caudally along the dorsal surface of the corpus callosum and supplies the medial surface of the parietal lobe, including the precuneus (Fig. 4.7) (56).

Anomalies of the anterior cerebral artery occur in about 25% of brains and include unpaired arteries and instances where branches are given off to the contralateral hemisphere (4, 51, 52). Occlusion of the trunk of one anterior cerebral artery produces contralateral muscle weaknesses and sensory losses, which are greatest in distal lower limbs. The main sensory modalities affected are discriminative sensation, such as stereognosis and two-point discrimination, and proprioception. Pain, temperature, and light touch sensation

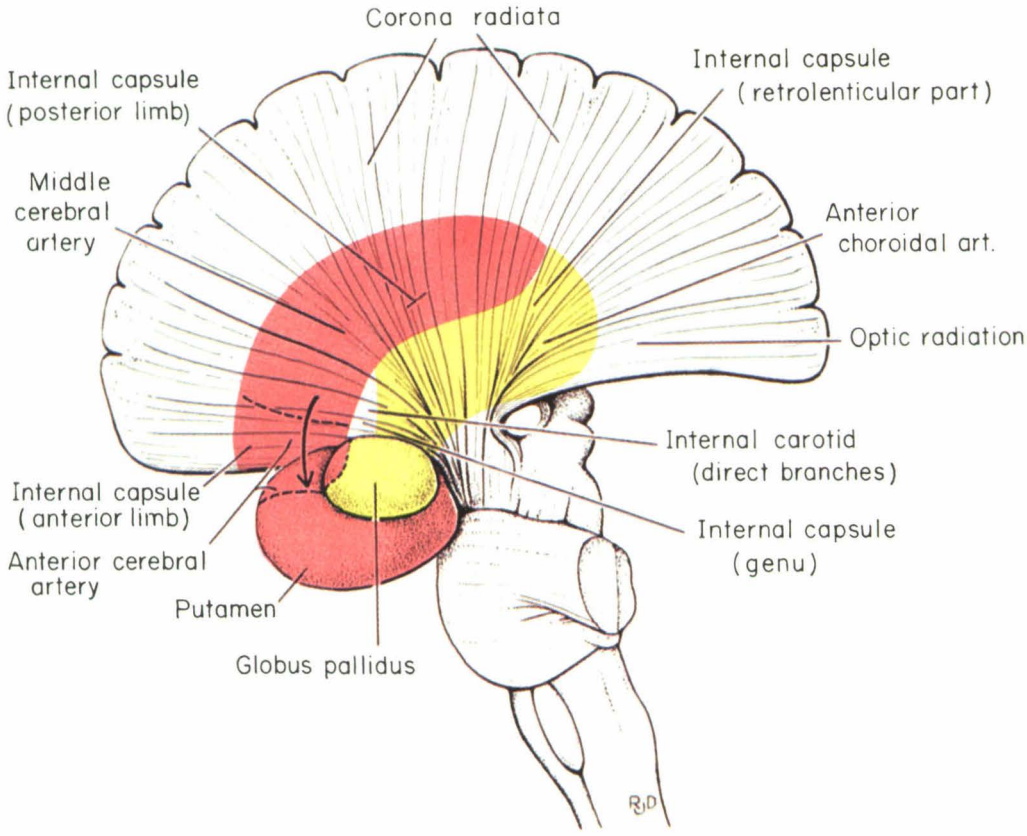


Figure 4.14. Blood supply of the internal capsule and basal ganglia. The putamen and globus pallidus are shown rotated ventrally away from the internal capsule. Regions supplied by branches of the middle and anterior cerebral arteries are shown in *red*; portions of the internal capsule and basal ganglia supplied by the anterior choroidal artery are in *yellow*. Direct branches of the internal carotid artery supply the genu of the internal capsule.

are relatively spared. Very proximal occlusion of the anterior cerebral artery may compromise blood supply to the internal capsule, with additional weakening of the contralateral arm and face. Obstruction of both anterior cerebral arteries is associated with bilateral paralysis, especially in the lower limbs, and impaired sensation that mimics a spinal cord lesion (5, 12). Additionally, bilateral medial prefrontal damage may result in motor and psychomotor abnormalities, including bradykinesia, rigidity, abulia, and a variety of other emotional or intellectual impairments (8).

MIDDLE CEREBRAL ARTERY

Beyond the origin of the anterior cerebral artery, the middle cerebral artery passes laterally over the anterior perforated substance to enter the lateral cerebral fossa between the temporal lobe and the insula (Figs. 4.5 and 4.8). This artery, the largest and most complex of the cerebral arteries, divides into a number of large branches, which course upward and backward. As these arteries reach the uppermost portions of the insula, they loop abruptly downward toward the lateral sulcus (22). The course of the branches of the middle cerebral artery in the insular region is of great importance in the interpretation of cerebral angiograms (65). In the insular region, five to eight branches of the middle cerebral artery lie within what is called the Sylvian triangle (Fig. 4.9). The Sylvian point (or apex) is established angiographically by the most posterior branch of the middle cerebral artery to emerge from the lateral sulcus. The inferior margin of the Sylvian triangle is formed by the lower branches of the middle cerebral artery, while the superior margin is formed by looping branches of this artery that are reversing their course (Fig. 4.9). Displacement of branches of the middle cerebral artery in the Sylvian triangle by mass lesions can be detected readily in cerebral angio-

grams, and the direction of displacement provides important information concerning the localization of these lesions.

Branches of the middle cerebral artery emerge from the lateral sulcus and are distributed in a "fanlike" fashion over the lateral convexity of the hemisphere. These cortical branches supply lateral parts of the orbital gyri, the inferior and middle frontal gyri, most of the precentral and postcentral gyri, the superior and inferior parietal lobules, and the superior and middle temporal gyri, including the temporal pole (Fig. 4.8). The largest cortical branches appear to supply the temporo-occipital and angular areas (22). The cortical arteries arise from stem arteries and supply individual cortical regions. In general, one or two cortical arteries pass to each cortical region supplied. The cortical branches to the frontal, anterior temporal, and anterior parietal regions are smaller than those to the posterior parietal, posterior temporal, and temporo-occipital regions, but are more numerous.

Branches of the middle cerebral artery include (a) the lenticulostriate arteries, (b) the anterior temporal artery, (c) the orbitofrontal artery, (d) pre-Rolandic and Rolandic branches, (e) anterior and posterior parietal branches, and (f) a posterior temporal branch, which extends caudally to supply lateral portions of the occipital lobe (Fig. 4.8).

The lenticulostriate arteries, the first branches to arise from the middle cerebral artery, enter the anterior perforated substance (Figs. 4.11 and 18.2). These vessels are considered with the central or ganglionic branches. The next branches to arise from the middle cerebral artery are the anterior temporal artery and the orbitofrontal artery (Fig. 4.8). The *anterior temporal artery* frequently anastomoses with temporal branches of the posterior cerebral artery, while the *orbitofrontal artery* may anastomose with the frontopolar branch of the anterior cerebral artery. Ascending branches of the middle cerebral artery, given off more distally, include *pre-Rolandic branches*, a *Rolandic branch*, an *anterior parietal* (or post-Rolandic) branch, and a *posterior parietal branch*. A *posterior temporal branch* extends backwards to supply lateral portions of the occipital lobe. The angular branches supplying the angular gyrus constitute the terminal part of the middle cerebral artery.

The extensive and functionally important region supplied by the middle cerebral artery includes the motor and premotor areas, the somesthetic and auditory projection areas, and large regions of the association cortex. Occlusion of the middle cerebral artery near the origin of its cortical branches may produce (a) a contralateral hemiplegia, most marked in the upper extremity and face, (b) a contralateral loss of position and discriminative tactile sense, and (c) severe aphasia, when the dominant hemisphere is involved (5, 8, 9, 12).

POSTERIOR CEREBRAL ARTERY

This artery, formed by the bifurcation of the basilar artery, passes laterally around the crus cerebri (Figs. 4.5 and 4.7). After receiving anastomoses from the posterior communicating arteries, it continues along the lateral aspect of the midbrain, and then passes dorsal to the tentorium to course on the medial and inferior surfaces of temporal and occipital lobes (Figs. 4.15 and 4.16). Branches of the posterior cerebral artery extend onto the lateral surfaces of the hemisphere to supply parts of the inferior temporal gyrus, variable portions of the occipital lobe, and parts of the superior parietal lobule (Figs. 4.7, 4.8, 4.15, and 4.16). Branches of the posterior cerebral artery also are distributed to the brainstem, the choroid plexus of the third and lateral ventricles, and to regions of the cerebral cortex (69).

The posterior cerebral artery divides into two main branches: (a) the posterior temporal artery, and (b) the internal occipital arteries.

The *posterior temporal (temporo-occipital) artery* gives off an anterior temporal branch (Fig. 4.16), which supplies the inferior surface of the temporal lobe anteriorly, and frequently anastomoses with branches of the anterior temporal artery (Figs. 4.7 and 4.10**B**). The largest branches of the posterior temporal artery reach the lateral surface of the hemisphere immediately anterior to the preoccipital notch (69). More posterior branches of this vessel supply the occipitotemporal and lingual gyri.

The *internal occipital artery* divides into the *parieto-occipital artery* and the *calcarine artery*, which supply different regions on the medial aspect of the occipital lobe and portions of the splenium of the corpus callosum (Figs. 4.7 and 4.15). The cortical branches of the posterior cerebral artery supply the medial and in-

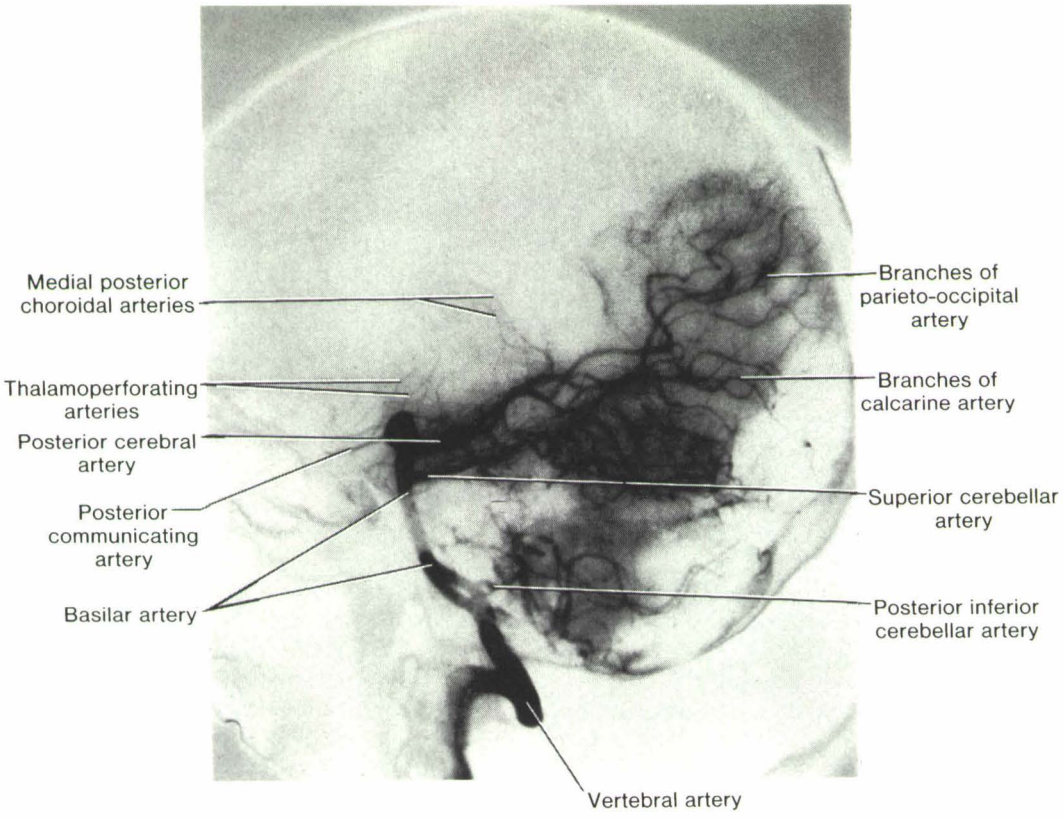


Figure 4.15. Lateral projection of a vertebral angiogram demonstrating major branches of the vertebral basilar system.

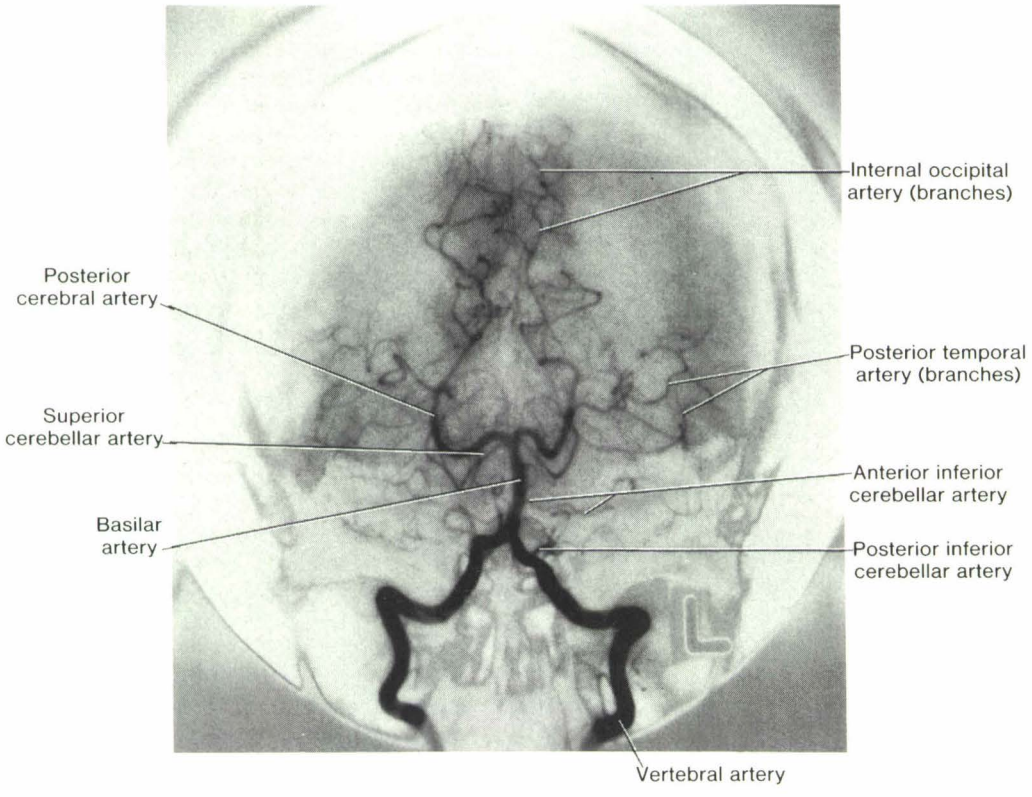


Figure 4.16. Vertebral angiogram as seen in the Towne projection using a subtraction technique.

ferior surfaces of the occipital lobe and the inferior surface of the temporal lobe, except for the temporal pole (Figs. 4.7 and 4.10**B**). Branches of these arteries extend onto the lateral surface of the brain and supply the inferior temporal gyrus and variable portions of the lateral occipital region. Some of the branches from the medial surface supply a considerable part of the superior parietal lobule. In these regions, branches of the posterior cerebral artery anastomose with marginal branches of the anterior and middle cerebral arteries (Fig. 4.8). The calcarine branch of the posterior cerebral artery is of major importance because it supplies the primary visual cortex (Figs. 4.7 and 4.15). The extensive anastomoses appear to explain why occlusion of the posterior cerebral artery rarely produces softening (encephalomalacia) in the total distribution of this vessel. Occlusion of the posterior cerebral artery produces a contralateral homonymous hemianopsia (Fig. 16.43), frequently with sparing of macular vision. Anastomoses between branches of the middle and posterior cerebral arteries in the region of the occipital pole probably account for the preservation of macular vision.

Cerebral angiography, a technique based on the injection of radiopaque solutions into cerebral vessels, followed by serial x-rays photography at about 1-second intervals (48, 49), reveal not only the position and configuration of the cerebral vessels, but also the phases of filling and emptying of vessels by the radiopaque solutions (Fig. 4.18). This radiographic technique shows the contrast medium in progressive stages of passage through the arterial tree and venous return. This method is particularly useful in localizing cerebral aneurysms and vascular malformations (Figs. 4.17 and 4.18). Additionally, it often provides information concerning occlusive vascular disease and space-occupying intracranial masses. While cerebral angiography provides invaluable diagnostic information, it is usually not possible to visualize the small terminal arteries. The larger cerebral vessels also can be demonstrated by computerized axial tomography (CT) after injection of a contrast medium. Brain hemorrhages usually can be seen clearly in CT scans. Images of brain vasculature also can be obtained by a procedure called MRI angiography, which uses magnetic resonance imaging technology (see Chapter 2). This method employs paramagnetic compounds synthesized with gadolium. The intravascular injection of such gadolium substances outlines brain vasculature and intracranial structures that have no blood-brain barrier (55).

Cerebral *aneurysms* are mostly of congenital origin and appear to arise frequently from vessels on the inferior surface of the brain (Fig. 4.17). Although it has been stated that aneurysms arise only at the point of bifurcation of an artery, Dandy (14) found that many aneurysms were not associated with arterial branching. Vascular malformations also involved arteriovenous malformations, an abnormal nest of blood vessels in which there are direct anastomoses of arteries and veins (Fig. 4.18). Cerebral angiography is important in diagnosing occlusive vascular disease in the internal carotid (both cervical and intracranial portions) and in the vertebral and basilar arteries, as well as in the trunk of the middle cerebral artery (Figs. 4.9, 4.15, and 4.16). It is more difficult to ascertain the presence of vascular occlusions in the distal branches of the anterior, middle, and posterior cerebral arteries (64) because of direct end-to-end anastomoses between branches of these vessels on the surface of the brain. While intracerebral hemorrhage cannot be distinguished angiographically from cerebral edema or other avascular space-occupying lesions, they sometimes can be localized on the basis of occlusion of certain vessels and displacement of cerebral vessels. Certain highly vascular brain tumors may produce what is called a "tumor stain" in the cerebral angiogram (5, 8, 9, 12).

While cerebral angiography provides invaluable diagnostic information, it is unusual for the contrast medium to permeate the very small terminal arteries (Fig. 4.10). Injection of the internal carotid artery usually permits visualization of the main branches of the anterior and middle cerebral arteries on the side of the injection. A radiographic technique for studying individual cerebral vessels and their branches in fresh cadaver brains has been developed by Kaplan (33–35) and has been used extensively to study cerebral vessels (56). The exquisite detail which can be obtained by this method is demonstrated in Figures 4.10 and 4.12.

Central Branches

CENTRAL OR GANGLIONIC ARTERIES

Central or ganglionic arteries arise from proximal portions of the major cerebral and communicating arteries and supply the dien-

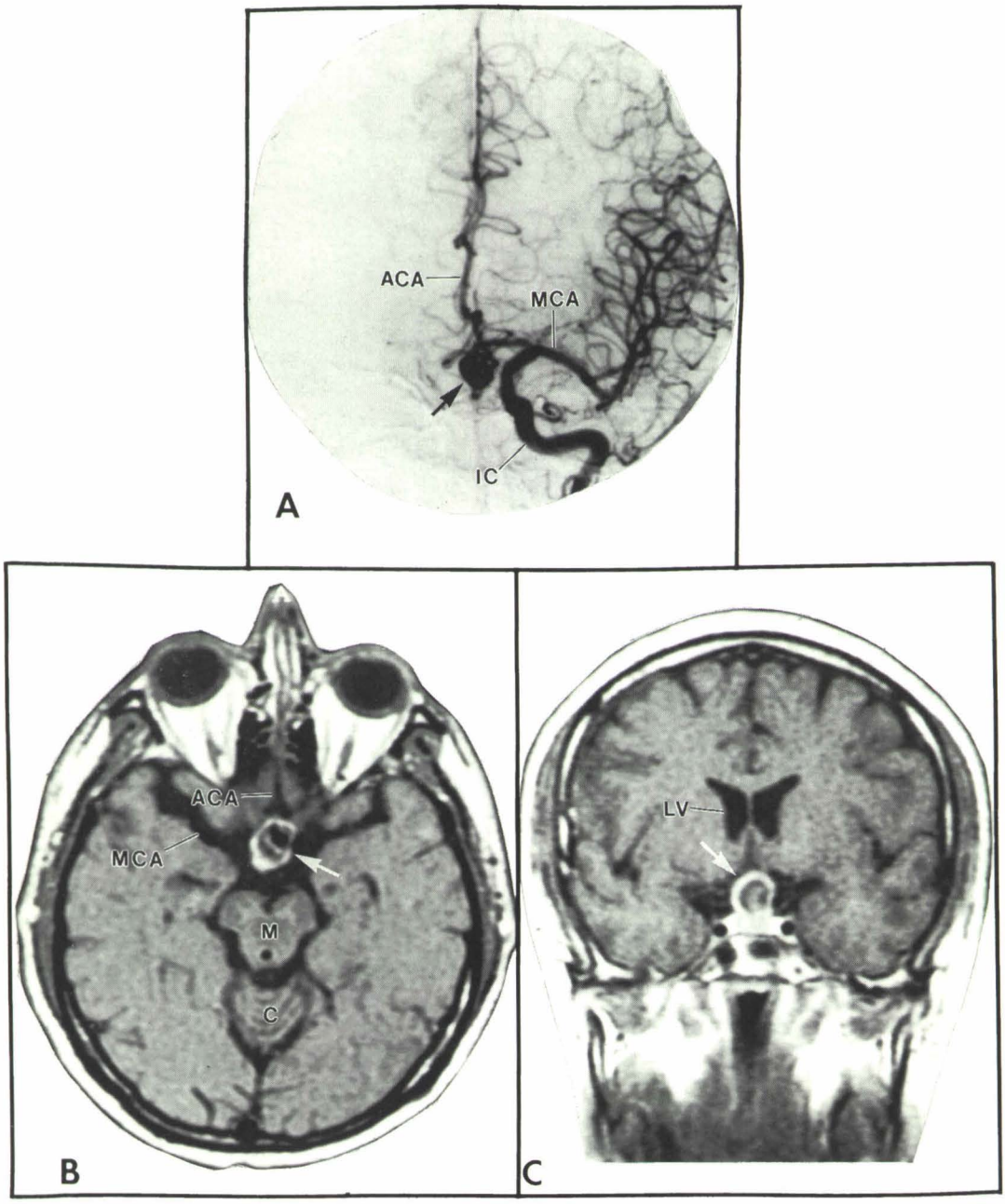


Figure 4.17. Aneurysm of the anterior communicating artery in a 40-year-old man, as seen with both angiography (**A**) and magnetic resonance imaging (MRI) (**B**, **C**). **A.** Lateral view of internal carotid injection on early arterial phase. Note the aneurysm (*arrow*) arising from the anterior communicating artery. The internal carotid (*IC*), middle (*MCA*), and anterior (*ACA*) cerebral arteries are also clearly visible. **B, C.** This partially trombosed aneurysm (arrow) can be seen on MRI scans (**B**: axial view; **C**: coronal view). The location of the middle and anterior cerebral arteries, as well as that of the midbrain (*M*), cerebellum (*C*) and lateral ventricles (*LV*) is also indicated.

cephalon, basal ganglia, and internal capsule. Penetrating ganglionic arteries are arranged in four groups, designated as anteromedial, anterolateral, posteromedial, and posterolateral (Fig. 4.11).

The *anteromedial arteries* arise from the anterior cerebral and anterior communicating arteries, but some twigs come directly from the terminal portion of the internal carotid (Fig. 4.11). They enter the most medial part of the anterior perforated substance, and are distributed to the anterior hypothalamus, including the preoptic area, and supraoptic regions.

The *posteromedial arteries* which enter the tuber cinereum, mammillary bodies, and interpeduncular fossa are derived from the most proximal portion of the posterior cerebral, and from the whole extent of the posterior communicating arteries (Fig. 4.11). Some twigs come directly from the internal carotid artery just before its bifurcation. A rostral and caudal group may be distinguished. The rostral group supplies the hypophysis, infundibulum and tuberal regions of the hypothalamus. A number of vessels, the *thalamoperforating arteries,* penetrate more deeply and are distributed to the anterior and medial portions of the thalamus (Figs. 4.12**B**, 4.13, and 4.15). The caudal group supplies the mammillary region of the hypothalamus, the subthalamic region, and sends small branches to the medial nuclei of the thalamus. Other vessels from the caudal group are distributed to medial regions of the midbrain tegmentum and crus cerebri.

The *posterolateral arteries* arise from the posterior cerebral arteries, lateral to its anastomosis with the posterior communicating artery (Figs. 4.11 and 4.13). These penetrating branches supply the caudal half of the thalamus (i.e., the lateral geniculate body, pulvinar, lateral nuclear group, and large parts of the ventral tier thalamic nuclei). These branches of the posterior cerebral artery are referred to as the *thalamogeniculate arteries* (Fig. 4.13). Occlusion of these arteries results in the *thalamic syndrome* of Dejerine and Roussy. This syndrome includes variable degrees of motor loss, sensory loss, pain, and hyperpathia in the contralateral face, body, or extremities (15).

The *anterolateral arteries,* commonly referred to as the *striate arteries,* arise primarily from proximal portions of the middle cerebral artery and, to a lesser extent, from the anterior cerebral artery (Figs. 4.5 and 4.11). The medial striate artery (Heubner), which derived from the anterior cerebral artery, belongs to this group (Fig. 4.13). These arteries enter the anterior perforated substance and supply portions of the basal ganglia and internal capsule (Figs. 4.13 and 4.14). The medial striate artery supplies the rostroventral part of the head of the caudate nucleus and adjacent portions of the putamen and internal capsule. The lateral striate arteries, derived from the middle cerebral artery, supply remaining portions of the striatum (i.e., caudate

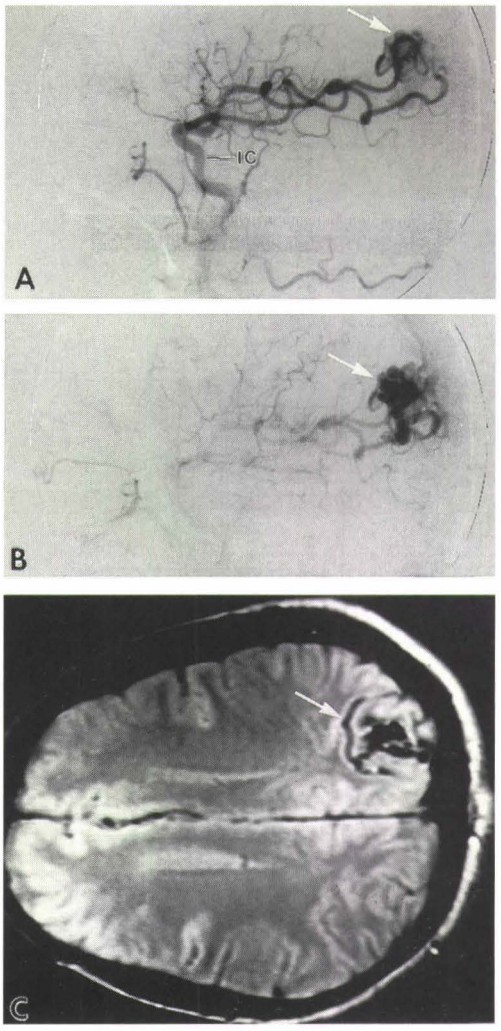


Figure 4.18. Angiograms (**A**, **B**) and MRI scan (**C**) of the brain of a 55-year-old man with hemorrhage from an anteriovenous malformation in the occipital lobe. **A**, **B.** Lateral view of internal carotid (*IC*) injection in the early (**A**) and late (**B**) arterial phase showing the malformation (*arrow*), which is fed by both the posterior and middle cerebral arteries. **C.** MRI scan (axial view) showing the resulting tissue damage (*arrow*) in the occipital lobe.

nucleus and putamen), except for extreme caudal parts of the putamen and the tail of the caudate nucleus (Fig. 4.12). These arteries also nourish the lateral part of the globus pallidus, the anterior limb of the internal capsule, and dorsal portions of the posterior limb of the internal capsule. While it appears doubtful that the striate arteries supply parts of the thalamus, vessels, referred to as lenticulo-optic arteries, have been described. The central perforating branches arising from the middle cerebral artery are shown radiographically in injected specimens in Figure 4.12.

CHOROIDAL ARTERIES

The anterior and posterior choroidal arteries may be regarded as distinctive central branches (Figs. 4.5, 4.11, 4.13, and 4.14).

The *anterior choroidal artery* usually arises from the internal carotid artery distal to the origin of the posterior communicating artery, but it also may arise from the middle cerebral artery (10). This artery, characterized by its long subarachnoid course and its relatively small caliber, passes caudally across the optic tract, and then laterally toward the rostromedial surface of the temporal lobe (Figs. 4.11 and 4.13). It enters the inferior horn of the lateral ventricle through the choroidal fissure. The artery enters the choroidal fissure at a point that is identified radiologically as the *choroid point*. Structures supplied by this artery, in addition to the choroid plexus, include the hippocampal formation, portions of both segments of the globus pallidus (i.e., lateral parts of the medial pallidal segment and medial parts of the lateral pallidal segment), ventrolateral parts of the posterior limb of the internal capsule, and the entire retrolenticular portion of the internal capsule (Fig. 4.14). Small branches of this artery supply parts of the amygdaloid nuclear complex, ventral parts of the tail of the caudate nucleus, extreme posterior parts of the putamen, and ventrolateral parts of the thalamus. The anterior choroidal artery is often considered as a vessel highly susceptible to thrombosis because of its long subarachnoid course and its relatively small caliber (36). It appears significant that the globus pallidus and hippocampal formation, two of the most vulnerable structures of the brain, are both supplied by this artery. Interestingly, surgical occlusion of the proximal portion of the anterior choroidal artery was used for the treatment of Parkinsonian tremor and rigidity (11).

The *posterior choroidal arteries*, arising from the posterior cerebral artery (Fig. 4.13), consist of one medial posterior and at least two lateral choroidal arteries (20). The *medial posterior choroidal artery* arises from the proximal part of the posterior cerebral artery, curves around the midbrain to reach the region of the pineal body. It gives off branches to the tectum, the choroid plexus of the third ventricle, and the superior and medial surfaces of the thalamus (Fig. 4.10**B**). The *lateral posterior choroidal arteries* arise from the posterior cerebral artery. They encircle the brainstem, enter the choroidal fissure, and supply the choroid plexus of the lateral ventricle. Some branches anastomose with branches of the anterior choroidal artery (10, 16).

BASAL GANGLIA, INTERNAL CAPSULE, AND DIENCEPHALON

Striatum

The striatum is nourished mainly by the lateral striate arteries derived from the middle cerebral artery (Figs. 4.13 and 4.14). Rostromedial parts of the head of the caudate nucleus are supplied by the medial striate artery (Heubner), while the tail of the caudate nucleus and caudal parts of the putamen receive branches of the anterior choroidal artery. The lateral segment of the globus pallidus is supplied by branches of both the lateral striate and anterior choroidal arteries (47). The lateral part of the medial pallidal segment receives branches from the anterior choroidal artery, and branches of the posterior communicating artery nourish the most medial parts of this pallidal segment.

Internal Capsule

Both anterior and posterior limbs of the internal capsule are supplied primarily by the lateral striate branches of the middle cerebral artery (Fig. 4.14). The medial striate artery supplies rostromedial parts of the anterior limb of the internal capsule. The genu of the internal capsule receives direct branches from the internal carotid artery (2), while ventral parts of the posterior limb and its entire retrolenticular part are supplied by branches of the anterior choroidal artery (56).

Thalamus

The thalamus is nourished mainly by branches of the posterior cerebral artery

(Figs. 4.10**B**, 4.11, and 4.13). *Thalamoperforating branches*, referred to as the posteromedial arteries, course dorsally and medially to supply chiefly medial and anterior regions of the thalamus (17, 56). These arteries, arising from the most medial part of the posterior cerebral artery and from the terminal part of the basilar artery, course dorsally into the diencephalon and nourish paraventricular regions of the hypothalamus and medial regions of the thalamus (21, 24). Perforating branches of these arteries, visualized in vertebral angiograms (Fig. 4.15), may be displaced, deformed, or stretched by space-occupying lesions or enlargement of the third ventricle. *Thalamogeniculate branches*, referred to as the posterolateral arteries, supply the pulvinar and the lateral nuclei of the thalamus. These arteries arise from the posterior cerebral artery as it winds around the crus cerebri, and the choroidal arteries (10, 42). The *medial posterior choroidal artery* supplies the choroid plexus of the third ventricle and superior and medial portions of the thalamus. The *inferior thalamic arteries* arise from the posterior communicating artery and the bifurcation of the basilar artery. These arteries course rostrally and dorsally and enter inferior portions of the thalamus (42). The inferior thalamic arteries supply regions of the thalamus rostral to the territory of the thalamoperforating arteries.

Hypothalamus

The anterior hypothalamus and preoptic region receive their blood supply from the anteromedian ganglionic arteries. Caudal parts of the hypothalamus and the subthalamic region are supplied by branches of the posteromedian group derived from the posterior cerebral and posterior communicating arteries (Fig. 4.11).

VERTEBRAL BASILAR SYSTEM

With the exception of the most rostral portions of the crus cerebri, the entire blood supply of the medulla, pons, midbrain, and cerebellum is derived from the vertebral basilar system.

Vertebral Artery

The intracranial part of each vertebral artery gives rise to (a) a *posterior spinal artery*, (b) an *anterior spinal artery*, (c) a *posterior inferior cerebellar artery*, and (d) a *posterior meningeal artery*. The two vertebral arteries unite to form the basilar artery at the caudal border of the pons. This large vessel passes rostrally in the basilar sulcus and bifurcates at the upper border of the pons, forming the posterior cerebral arteries (Figs. 4.1, 4.5, 4.7, 4.15, and 4.16).

Basilar Artery

Branches of the basilar artery include (a) the *anterior inferior cerebellar arteries*, (b) the *labyrinthine arteries*, (c) *numerous paramedian* and *circumferential pontine rami*, (d) the *superior cerebellar arteries*, and (e) the *posterior cerebral artery* (Figs. 4.1, 4.5, 4.7, and 4.11). The posterior cerebral arteries, representing the terminal branches of the basilar artery, furnish branches that supply parts of the midbrain, thalamus, and large regions of the temporal and occipital lobes (Figs. 4.7 and 4.16). The labyrinthine arteries do not supply the brainstem, but pass laterally through the internal auditory meati to the inner ear (Fig. 4.5).

Vertebral angiography is more difficult to perform than carotid angiography because this artery is smaller and contained within a bony canal. Many of the branches of the vertebral and basilar arteries are small and difficult to identify angiographically, but the posterior inferior cerebellar, the anterior inferior cerebellar, the superior cerebellar, and the posterior cerebral arteries usually can be seen. Both posterior cerebral arteries are filled by contrast media following injection of one vertebral artery (Figs. 4.15 and 4.16).

Medulla and Pons

These portions of the brainstem are supplied by the anterior and posterior spinal arteries, the posterior inferior cerebellar arteries, and branches of the vertebral and basilar arteries. The anterior inferior and superior cerebellar arteries make smaller contributions (Fig. 4.5). There is great variation in the extent of the areas supplied by individual vessel and considerable overlap in some regions. These variations are due in part to the different levels of origin of the anterior spinal arteries, and to the varying level of fusion of the two vertebral arteries into the basilar artery. One or another artery may be entirely missing, and its place taken by a vessel supplying the adjacent territory. Since the vascular supply of this region has considerable clinical im-

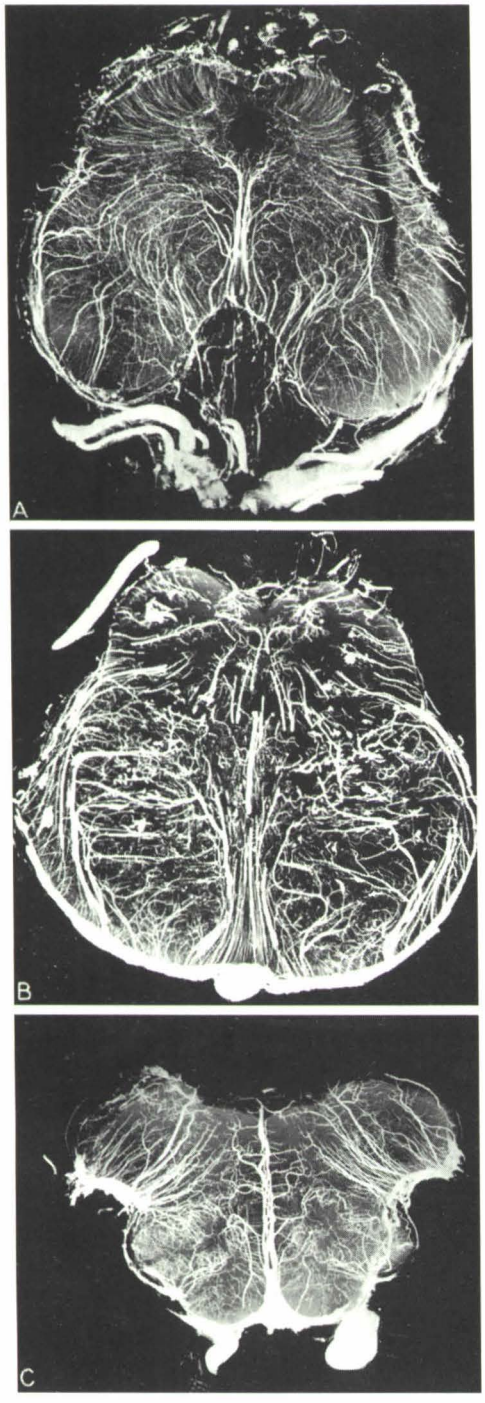


Figure 4.19. Microangiograms of the blood supply of the midbrain, pons, and medulla made from 4 mm-thick injected specimens. In the midbrain (**A**) the tegmentum is supplied mainly by branches of the posterior cerebral and superior cerebellar arteries, but it also receives contributions from the paramedian and both long and short circumferential arteries. The upper pons (**B**) receives paramedian and circumferential branches from the basilar artery, as well as branches of the superior cerebellar artery distributed to dorsal regions. The vascular pattern in the upper medulla (**C**) should be compared with the diagram of Figure 4.20.

portance, the main structures normally supplied by the various arteries are summarized briefly (Figs. 4.19 and 4.20).

The *posterior spinal artery* supplies the gracile and cuneate fasciculi and their nuclei, and the caudal and dorsal portions of the inferior cerebellar peduncle (62) (Figs. 4.1 and 4.20). There are numerous anastomoses between branches of the posterior spinal and the posterior inferior cerebellar arteries (16). When the posterior spinal artery on one side is small, or even missing, its territory is supplied by the posterior inferior cerebellar artery. Branches of the posterior spinal artery also supply parts of the nucleus of the solitary fasciculus and vagal nuclei, and portions of the spinal trigeminal nucleus. Small branches of this artery with a superficial course may penetrate the taenia to supply the area postrema.

The *anterior spinal artery* supplies a paramedian region of the medulla which includes the pyramids, the medial lemniscus, medial longitudinal fasciculus, most of the hypoglossal nucleus (except its most cephalic portion), caudal parts of the solitary nucleus and dorsal motor nucleus of the vagus nerve (N. X), and the medial accessory olive (Fig. 4.20). Medullary branches arising from the anterior spinal artery increase in size and number from caudal to rostral levels. The larger and longer branches pass in the medial raphe between the medial lemnisci (Fig. 4.20**C**), and their terminal rami reach the floor of the fourth ventricle. Smaller, shorter branches of the anterior spinal artery run obliquely through the medial lemnisci to enter the medial reticular formation and medial parts of the inferior olivary nuclear complex (16). In the upper medulla, the distribution of the anterior spinal artery is reduced gradually, and it is replaced by branches of the vertebral and basilar arteries (62) (Fig. 4.20).

Occlusion of one anterior spinal artery is associated with a medullary lesion producing an *inferior alternating hemiplegia* characterized by ipsilateral paralysis of the tongue and a contralateral hemiplegia. Such lesions sometimes involve portions of the medial lemniscus which result in contralateral sensory deficits.

The *bulbar branches of the vertebral artery* arise as a series of rami that enter the brainstem in relation to rootlets of the glossopharyngeal (N. IX), vagus (N. X), and accessory nerves (N. XI). The most densely vascularized lateral medullary region lies dorsal to the infe-

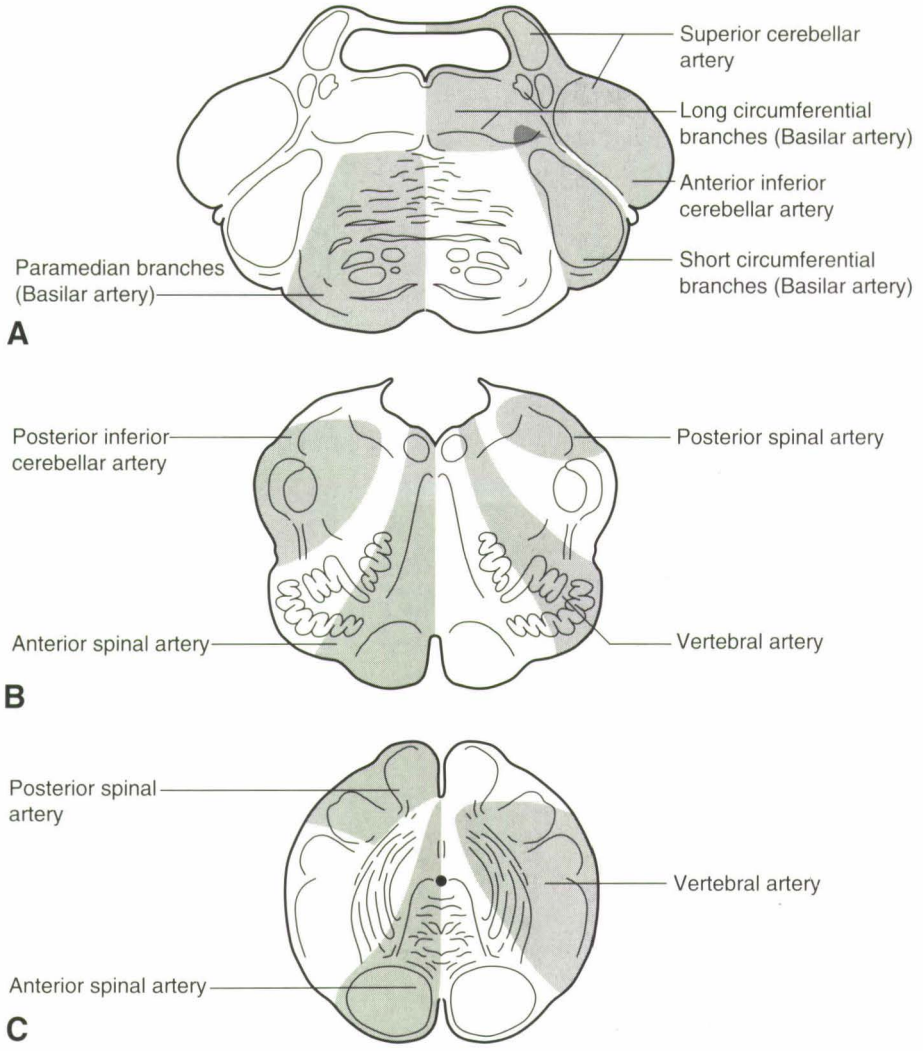


Figure 4.20. Arterial supply of the medulla and pons. The pons (**A**) is supplied by paramedian and circumferential branches of the basilar artery. Medullary levels shown are through the posterior column nuclei (**C**) and the inferior olivary nuclear complex (**B**). The pons (**A**) is supplied by paramedian and circumferential branches of the basilar artery.

rior olivary complex. This region contains numerous small arteries and veins on the surface that penetrate deeply into the medulla (Fig. 4.20**B**). The inferior rami arise directly from the vertebral artery, enter the medulla between the rootlets of the accessory nerve, and supply the region between the inferior olivary nuclear complex and the inferior cerebellar peduncle (Figs. 4.19**C** and 4.20**C**). A larger and more important group of rami enter the lateral surface of the medulla in relation to the glossopharyngeal and vagus nerves. These direct branches of the vertebral artery normally supply the pyramids at the lower border of the pons, the most cephalic part of the hypoglossal nucleus, and large parts of the inferior olivary nucleus, including the dorsal accessory olive. These arteries also supply olivocerebellar fibers traversing the reticular formation, portions of the dorsal motor nucleus of the vagus, and the solitary nucleus and fasciculus. At the level of the pyramidal decussation the most caudal branches are distributed to practically the whole lateral region of the medulla lying between the pyramids and the fasciculus cuneatus. Two types of arteries enter the medulla—short arteries supply small branches to the spinal trigeminal, spinothalamic, and spinocerebellar tracts, while long arteries supply deeper regions. Some of the long arteries reach the floor of the fourth ventricle (Fig. 4.19**C**).

The *posterior inferior cerebellar artery* supplies the lateral medullary region rostral to that supplied by direct bulbar branches of the vertebral artery (Fig. 4.19). This retro-olivary region contains the spinothalamic tracts, the spinal trigeminal nucleus and tract, the emerging fibers from nucleus ambiguous, the dorsal motor nucleus of the vagus nerve, as well as the ventral part of the inferior cerebellar peduncle (Fig. 4.20). Autonomic fibers are found in this area of the medulla and pons. The *lateral medullary syndrome* (or *Wallenberg's syndrome*), produced by sudden occlusions of the posterior inferior cerebellar artery or bulbar branches of the vertebral artery, is associated with lesions in the dorsolateral part of the medulla. Such lesions are characterized by (a) loss of pain and thermal sense in the face (ipsilaterally) and over the body (contralaterally), (b) ipsilateral paralysis of the pharynx and larynx, and (c) an ipsilateral Horner's syndrome (3, 5, 12, 60). Disturbances of equilibrium usually are transient.

The ventral portion of the pons receives arterial blood from three series of branches, all derived from the *basilar artery* (Figs. 4.19–4.21). These arterial branches are grouped as (a) paramedian, (b) short circumferential, and (c) long circumferential.

Paramedian arteries leave the dorsal surface of the parent vessel to supply a medial pontine area that includes the pontine nuclei and the corticopontine, corticospinal, and corticobulbar tracts. Smaller arterial twigs also penetrate dorsally to supply ventromedial parts of the pontine tegmentum, including a portion of the medial lemniscus.

Short circumferential arteries supply the adjacent anterolateral part of the pons, and variable parts of overlying tegmentum (Fig. 4.22). Neural structures in this intermediate area of the pons include a variable number of fibers of the corticospinal tract and medial lemniscus, the pontine nuclei and pontocerebellar fibers, and part of the nuclei and fibers of the trigeminal and facial nerves. Some of the circumferential branches may ascend to supply part of the superior cerebral peduncle.

Long circumferential arteries course laterally over the anterior surface of the pons and anastomose with smaller branches of the anterior inferior cerebellar and superior cerebellar arteries (Figs. 4.19 and 4.20). The long circumferential and *anterior inferior cerebellar arteries* supply most of the tegmentum in the caudal portion of the pons, whereas the long circumferential and *superior cerebellar arteries* supply a similar area in the more rostral levels of the pons. Important neural structures within this area of vascular distribution are the nuclei of oculomotor to vestibulocochlear cranial nerves (N. III to VIII), the spinal trigeminal nucleus and tract, the medial longitudinal fasciculus, the medial lemniscus, the spinothalamic and spinocerebellar tracts, the superior cerebellar peduncle, and the reticular formation.

Sudden occlusion of paramedian branches of the basilar artery on one side usually produces lesions in the basilar part of the pons



Figure 4.21. Microangiogram of a 4-mm midsagittal section of the midbrain, pons, and medulla made from an injected specimen. Paramedian arteries form different angles with the basilar artery at various levels. In the caudal midbrain and upper pons, they are inclined caudally; in the upper medulla and caudal pons, these vessels are inclined rostrally.

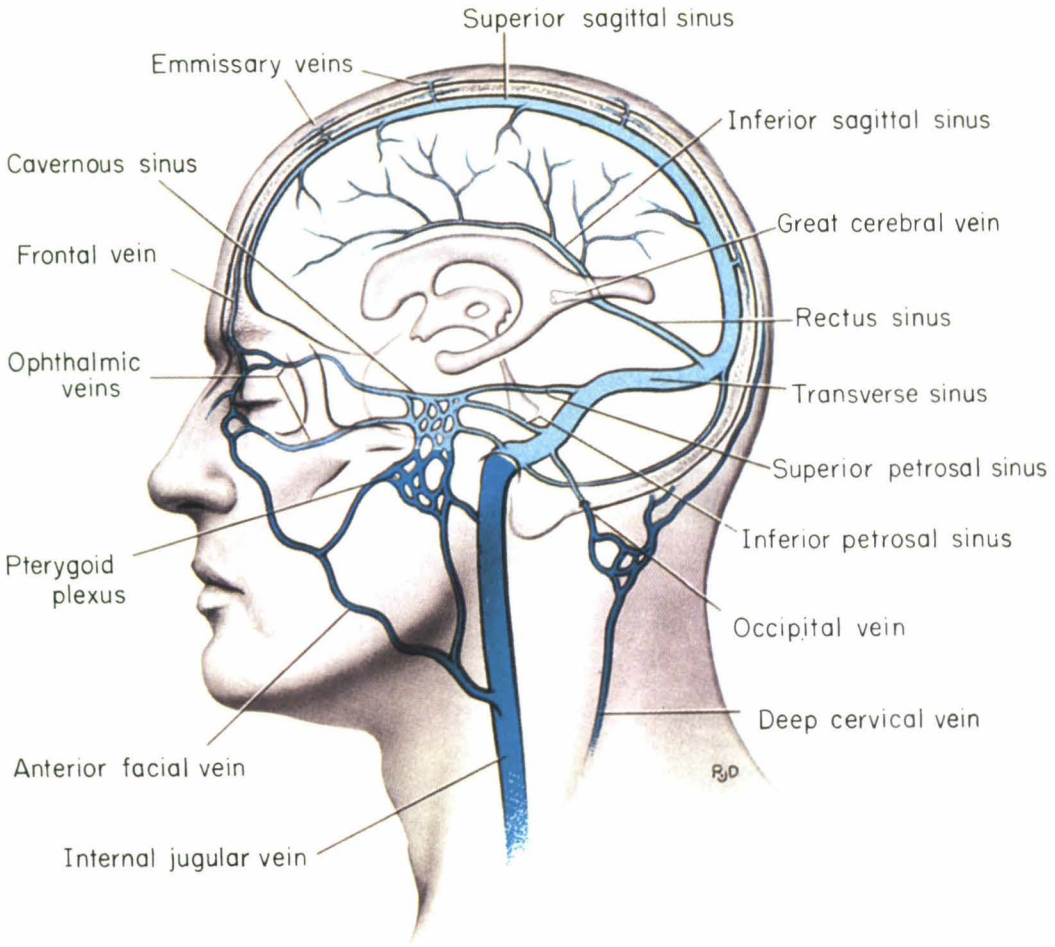


Figure 4.22. The dural sinuses and their principal connections with extracranial veins. Intracranial venous sinuses and veins are *light blue*; extracranial veins are *dark blue*.

that result in a contralateral hemiparesis and damage to the root fibers of the ipsilateral abducens nerve (5, 12, 18, 44). *Middle alternating hemiplegia* is a classic example of such a lesion. Obstruction of the short circumferential arteries on one side usually results in ipsilateral cerebellar and autonomic disturbances and impairment of contralateral sensation. Occlusion of the long circumferential arteries and other arteries supplying the pontine tegmentum produces cranial nerve disturbances, paresis of conjugate eye movements, contralateral hemianesthesia, ipsilateral cerebellar disturbances, and frequently nystagmus. Complete or partial thrombosis of the basilar artery may produce precipitous loss of muscle tone, dilated or pinpoint pupils that do not react to light, and bilateral Babinski responses (31). Neurologic disturbances usually are bilateral but may be asymmetric and exhibit fluctuations.

In the so-called *lock-in syndrome*, paralysis prevents communication with gesture or voice. The patient may have full comprehension of his or her environment, but can only communicate using vertical eye movements or blinking. Basilar artery occlusion is a common cause of lock-in syndrome (54).

Midbrain

Most of the blood supply of the midbrain is derived from branches of the basilar artery, although branches of the internal carotid may also contribute (Figs. 4.15, 4.19, and 4.21). Arteries supplying this part of the brainstem include branches of (a) the posterior cerebral artery, (b) the superior cerebellar artery, (c) the posterior communicating artery, and (d) the anterior choroidal artery (Figs. 4.1, 4.4, 4.5, 4.7, and 4.11). Branches of these arteries, like those supplying the pons, can be

grouped into (a) paramedian arteries, which nourish structures on both sides of the midline, and (b) long and short circumferential arteries, which wind laterally around the crus cerebri and supply lateral and dorsal regions of the midbrain (Fig. 4.19**A**).

Paramedian arteries, derived from the posterior communicating artery and from proximal portions of the posterior cerebral arteries, form an extensive plexus in the interpeduncular fossa (Fig. 4.11), enter the brainstem in the posterior perforated substance, and supply the raphe region, the oculomotor complex, the medial longitudinal fasciculus, the red nucleus, and medial parts of the substantia nigra and crus cerebri. Vascular lesions involving paramedian arterial branches at midbrain levels frequently produce a *superior alternating hemiplegia*, characterized by ipsilateral oculomotor disturbances and a contralateral hemiplegia (Weber's syndrome). This syndrome results from lesions involving portions of the crus cerebri and fibers of the oculomotor nerve (N. III). A less frequent lesion in the paramedian tegmental zone destroys portions of the red nucleus, the superior cerebellar peduncle, and intra-axial rootlets of the oculomotor nerve (Benedikt's syndrome).

Short circumferential arteries, arising from the interpeduncular plexus and proximal portions of the posterior cerebral and superior cerebellar arteries, supply central and lateral parts of the crus cerebri, the substantia nigra, and lateral portions of the midbrain tegmentum (Fig. 4.19). In the rostral mesencephalon, some branches of the anterior choroidal artery are distributed to the interpeduncular fossa.

Long circumferential arteries arise primarily from the posterior cerebral artery. The most important of these, the *quadrigeminal* or *collicular artery*, encircles the brainstem and supplies the superior and inferior colliculi. The tectum also is supplied by branches of the medial posterior choroidal artery and the superior cerebellar artery.

Angiographic studies (30) of the arterial pattern of the human brainstem clearly demonstrate the distribution of paramedian and circumferential arteries in the upper pons and midbrain (Figs. 4.19 and 4.22). Sagittal sections show that paramedian arteries that enter the brainstem at various levels do so at different angles. At the junction of pons and medulla, these vessels are directed forward at an oblique angle, while at rostral pontine levels these vessels course obliquely in a caudal direction (Fig. 4.21).

Brainstem Venous Drainage

The venous drainage of the hindbrain has been demonstrated by stereomicroangiography (29). The paramedian veins which run near the midline to the ventral surface of the brainstem are inclined caudally in the upper pons, but are nearly perpendicular to the axis of the brainstem in more caudal regions. At the junction of pons and medulla, a conspicuously large vein consistently drains the floor of the fourth ventricle. Veins draining ventral portions of the pons usually empty into paired longitudinal venous plexuses several millimeters lateral to the basilar artery. However, in some instances these veins enter a single unpaired vein situated between the basilar artery and the brainstem parenchyma. In the lower medulla, posterior veins are larger than the anterior veins and penetrate deeper regions. Although the veins of the hindbrain seldom accompany the arterial branches in the same vascular sheath, the intraparenchymatous venous angioarchitecture resembles the arterial pattern. Anastomoses between intraparenchymatous veins occur mainly at the capillary level. Large veins draining the choroid plexus of the fourth ventricle, most of the pons, and the upper medulla, empty into the sigmoid sinus, or the superior or inferior petrosal sinuses. Veins draining caudal parts of the medulla empty into the anterior and posterior spinal veins (29).

Numerous veins of the mesencephalon arise from capillaries and, in general, run near the arteries but not directly with them. These veins form an extensive peripheral plexus in the pia and are collected by the basal veins, which drain into either the great cerebral vein (Galen) or the internal cerebral veins (Figs. 4.26 and 4.27).

Cerebellum

Each half of the cerebellum is supplied by three arteries: (a) the superior cerebellar, (b) the anterior inferior cerebellar, and (c) the posterior inferior cerebellar (Figs. 4.7 and 4.15).

The *posterior inferior cerebellar artery*, derived from the vertebral artery, courses rostrolaterally along the surface of the medulla

where small perforating rami supply the dorsolateral region of the medulla. From this locus the artery curves upward onto the inferior surface of the cerebellum, where branches supply the inferior vermis, especially the uvula and nodulus, the cerebellar tonsil, and the inferolateral surface of the cerebellar hemisphere (Fig. 4.7). Medial branches of this artery supply portions of the choroid plexus of the fourth ventricle.

The *anterior inferior cerebellar artery* is usually the most caudal large vessel arising from the basilar artery (Fig. 4.5), but it is highly variable both in its origin and area of distribution (36). This artery most frequently arises as a single vessel, courses caudally and laterally around the pons toward the cerebellopontine angle, and comes into close relationship with both the facial and vestibulocochlear nerves (N. VIII) (43). After crossing the nerves in the cerebellopontine angle, the artery courses laterally above the flocculus to reach the inferior surface of the cerebellum where it supplies the pyramis, tuber, flocculus, and portions of the inferior surface of the cerebellar hemisphere. Penetrating branches supply portions of the dentate nucleus and the surrounding white matter. Smaller branches of this artery contribute to choroid plexus of the fourth ventricle. In some cases, the flocculus and portions of the tonsil and biventer lobule may be supplied by an inconstant middle inferior cerebellar artery. Nerve-related branches of the anterior inferior cerebellar artery frequently supply tumors and arteriovenous malformations arising in the cerebellopontine angle. An internal auditory artery arising from this vessel appears quite constant, and occlusion of the anterior inferior cerebellar artery frequently produces nausea, vomiting, deafness, facial paralysis, and cerebellar disturbances (43).

The *superior cerebellar artery* arises from the rostral part of the basilar artery, encircles the brainstem near the pontomesencephalic junction, and passes onto the superior surface of the cerebellum (Fig. 4.11). This vessel runs caudal to the oculomotor (N. III) and trochlear (N. IV) nerves and rostral to the trigeminal (N. V) nerve. In its proximal portion, the artery courses medial to the free edge of the tentorium cerebelli (Fig. 4.4), but distally it passes beneath the tentorium, making it the most rostral of the infratentorial arteries (Fig. 4.7). The superior cerebellar artery gives off perforating, precerebellar, and cortical branches (25). Perforating branches of the artery penetrate the interpeduncular fossa, the crus cerebri, and portions of the superior and middle cerebellar peduncles. Precerebellar branches supply the colliculi (midbrain tectum) and the superior medullary velum. The cortical branches are divided into vermian, hemispheric, and marginal arteries. These branches supply the superior (tentorial) and petrosal surfaces of the cerebellum and, in some instances, the region of the horizontal fissure (marginal branches). The hemispheric arteries give rise to numerous branches that extend deeply into the cerebellum. These vessels supply the middle and superior cerebellar peduncles, the deep cerebellar nuclei, the superior medullary velum, and the corpus medullary velum. Smaller branches supply portions of the choroid plexus of the fourth ventricle.

Cerebellar veins have a course similar to that of the arteries. A superior and an inferior median vein drain respective portions of the vermis, paravermal regions, and the deep cerebellar nuclei. The superior vein terminates in the *great cerebral vein* (Galen), while the inferior vein empties into the rectus and transverse sinuses (Fig. 4.27). Superior and inferior lateral veins drain respective portions of the cerebellar hemispheres and empty into the superior and petrosal sinuses (Fig. 4.22).

ARTERIES OF THE DURA MATER

The cranial dura mater is supplied by a number of meningeal arteries derived from several sources. The largest and most important is the *middle meningeal artery,* which supplies most of the dura and practically its entire calvarial portion. It is a branch of the maxillary artery, which enters the cranial cavity through the foramen spinosum and then divides into an anterior and a posterior branch (Figs. 1.3 and 4.4). Each branch runs outward and upward and extends toward the superior sagittal sinus, giving off numerous branches which run forward and backward. A small *accessory meningeal artery,* which may arise from the maxillary artery or the middle meningeal artery, enters the middle fossa through the foramen ovale. This vessel supplies the dura of the middle fossa and the trigeminal ganglion. Meningeal branches from the intracavernous portion of the internal carotid artery also supply the dura of the middle fossa.

The dura of the anterior and the posterior fossae also receives a number of arteries, known respectively as the *anterior* and *posterior meningeal rami* or *arteries*. The anterior meningeal rami, usually two in number, are branches of the anterior and posterior ethmoidal arteries. The dura of the posterior fossa is supplied by a variable number of posterior meningeal arteries and include (a) one or more meningeal branches from the occipital artery entering through the jugular and hypoglossal foramina, (b) meningeal branches of the vertebral artery reaching the posterior fossa through the foramen magnum, and (c) several branches of the ascending pharyngeal artery entering through the foramen lacerum and hypoglossal canal.

CEREBRAL VEINS AND VENOUS SINUSES

Venous Sinuses of the Dura Mater

The cerebral veins of the brain do not run together with the arteries. Emerging as fine branches from the substance of the brain, they form a pial plexus from which the larger venous channels or cerebral veins arise. These veins run in the pia for a variable distance, pass through the subarachnoid space, and empty into a system of intercommunicating endothelium-lined channels, the *dural venous sinuses*. The dural venous sinuses are located between the meningeal and periosteal layers of the dura (Figs. 1.1–1.4 and 4.4). The walls of these sinuses, unlike those of other veins, are composed of the tough fibrous tissue of the dura, and exhibit a greater tautness and do not collapse when sectioned. The various venous sinuses converge at the internal occipital protuberance into two transverse sinuses (Figs. 1.1 and 1.3), one for each side, which enter the sigmoid sinuses, and eventually the jugular foramina, to form the internal jugular veins. Besides draining the blood from the brain, the venous sinuses communicate with the superficial veins of the head by a number of small vessels that perforate the skull as *emissary veins*.

The *superior sagittal sinus* extends from the foramen cecum to the internal occipital protuberance, lying along the superior border of the falx cerebri. It progressively increases in caliber as it proceeds caudally (Figs. 1.1 and 4.22). In its middle portion, it gives off a number of lateral diverticula, the *venous lacunae*, into which the arachnoid villi protrude (Fig. 1.11).

The *inferior sagittal sinus* extends caudally along the free border of the falx cerebri. On reaching the anterior border of the tentorium, it is joined by the *great cerebral vein* (Galen), which drains the deep structures of the brain, and the two veins form the *straight sinus* (or *sinus rectus*) (Figs. 1.3 and 4.22). The straight sinus runs backward and downward along the line of attachment of the falx and tentorium and joins the superior sagittal sinus near the internal occipital protuberance (45) (Figs. 4.4 and 4.23).

The two *transverse sinuses* arise from the confluens sinuses and pass laterally and forward in a groove in the occipital bone (Figs. 1.3 and 4.4). At the occipitopetrosal junction, each sinus curves downward and backward as the sigmoid sinus. The *sigmoid sinus* is drained by the internal jugular vein (Fig. 4.22).

The confluens of sinuses is formed by the union of the superior sagittal, straight, and transverse sinuses. A small unpaired *occipital sinus* from the region to the foramen magnum ascends along the margin of the falx cerebelli (Figs. 1.1 and 4.23) and joins the confluens. The confluens is asymmetric and shows many individual variations (Figs. 1.3 and 4.4). In relatively few cases is there an actual union of the four sinuses. Most often, the superior sagittal sinus turns to the right to become continuous with the right transverse sinus, while the straight sinus bends to the left as the left transverse sinus (Fig. 1.1). In general, the venous blood of the superior cerebral veins and the superior sagittal, right transverse, and right sigmoid sinuses is drained by the right internal jugular vein. Most of the venous blood of the Galenic vein, the straight sinus, left transverse, and left sigmoid sinuses usually is drained by the left internal jugular vein.

The *cavernous sinus* is a large irregular space located on each side of the sphenoid sinus, sella turcica, and pituitary gland that extends from the superior orbital fissure to the petrous portion of the temporal bone (26). It is a network of intercommunicating venous channels enclosing the internal carotid artery and the abducens nerve (N. VI) (Fig. 4.24). The oculomotor (N. III), trochlear (N. IV), and the ophthalmic division of the trigeminal nerve (N. V1) lie between dural leaves of the lateral wall of the cavernous sinus. The abducens nerve (N. VI) lies within the sinus, adjacent to the intracavernous portion of the carotid artery. The cavernous sinus of each

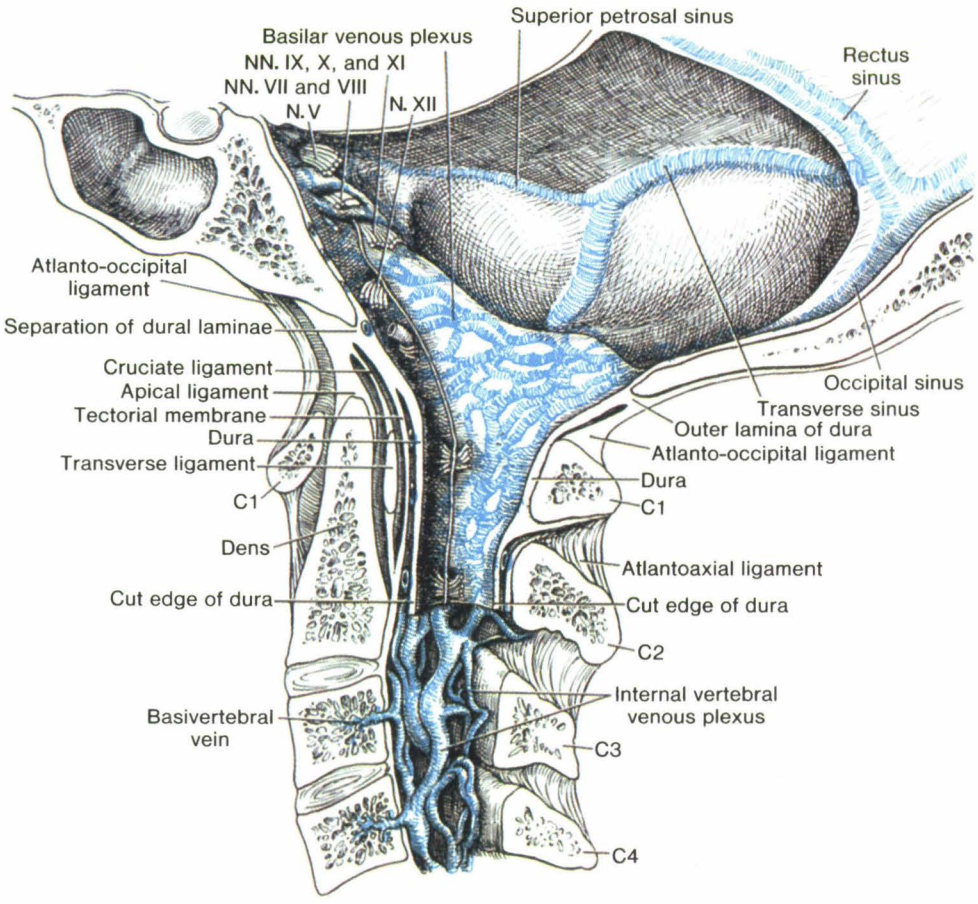


Figure 4.23. Sagittal view of the base of the skull and upper cervical vertebrae, showing ligaments, the dural venous sinuses, and the internal vertebral venous plexus at the foramen magnum. Communications of the internal vertebral venous plexus with the basilar plexus are indicated.

side is connected with the other by venous channels that pass anterior and posterior to the hypophysis, and by the *basilar venous plexus* (Figs. 4.23 and 4.24). The latter venous plexus extends along the basilar portion of the occipital bone as far caudally as the foramen magnum where it communicates with the venous plexuses of the vertebral canal (Figs. 4.23 and 4.24). The venous ring, surrounding the hypophysis and composed of the two cavernous sinuses and their connecting channels, often is designated as the *circular sinus*. Each cavernous sinus likewise may be regarded as a confluens of sinuses. Rostrally it receives the two ophthalmic veins through the superior and inferior orbital fissures and the small *sphenoparietal sinus*, which runs along the under surface of the lesser wing of the sphenoid (Figs. 4.4 and 4.24). Posteriorly, it empties into the superior and inferior petrosal sinuses, through which it is connected, respectively, with the transverse sinus and the bulb of the internal jugular vein (Figs. 4.23 and 4.24).

In the adult, the sphenoid air sinus separates the cavernous sinuses on the two sides and, in addition, separates the pituitary gland from the nasal cavity. The increasing use of the transsphenoidal approach to tumors of the sellar region has created a need for detailed anatomy of this region (19). Three structures producing prominent bulges in the lateral wall of the sphenoid sinus are (a) the optic nerves (N. II), (b) the internal carotid arteries, and (c) the maxillary branches of the trigeminal nerve (N. V2). The bone in the lateral wall of the sphenoid sinus, separating it from the internal carotid artery and the cavernous sinus, is thin, and extreme care must be taken to avoid injury to this region, which offers the potential for neural and arterial damage.

The dural sinuses communicate with the extracranial veins by a number of emissaries (Fig. 4.22). Thus, the superior sagittal sinus is connected with the frontal and nasal veins and the emissaries of the foramen cecum (Fig. 4.4). It also sends a *parietal emissary* to the superficial temporal vein. The confluens of sinuses usually gives off an *occipital emissary* to

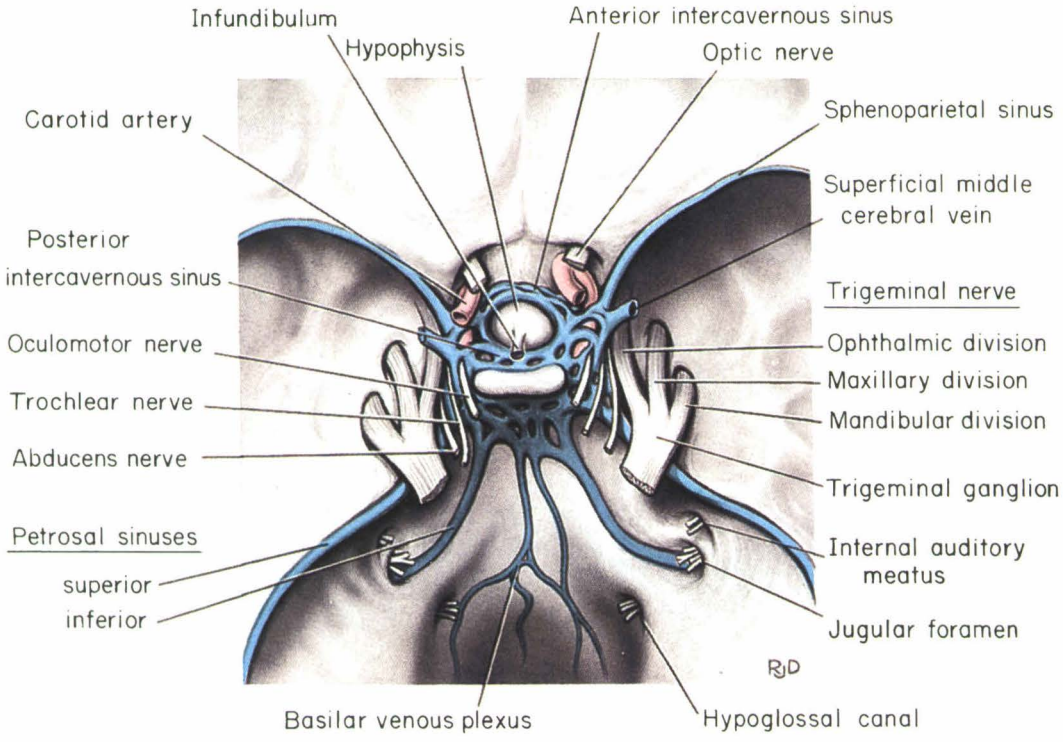


Figure 4.24. The cavernous sinus, its venous connections, and related structures.

the occipital vein, which is connected also with the transverse sinus by the larger *mastoid emissary* (Fig. 4.22). Smaller emissaries from the sigmoid sinus pass through the condyloid and hypoglossal foramina and communicate with vertebral and deep cervical veins. The cavernous sinus, besides receiving the ophthalmic veins, is connected with the internal jugular vein and with the pterygoid and pharyngeal plexuses by fine venous nets that pass through the foramen ovale, spinosum, lacerum, as well as the carotid canal and jugular foramen.

Cerebral Veins

The cerebral veins consist of superficial and deep groups and, like the dural sinuses, are devoid of valves. Superficial veins draining the blood from the cortex and subcortical white matter empty into the superior sagittal or basal sinuses (i.e., cavernous, petrosal, and transverse) (Fig. 4.25). The deep cerebral veins, draining the choroid plexus, periventricular regions, diencephalon, basal ganglia, and deep white matter, empty into the internal cerebral and the great cerebral veins (Figs. 4.26 and 4.27). These two groups of veins are interconnected by numerous anastomotic channels, both intracerebral and extracerebral.

Thus, large surface areas can be drained through the great cerebral vein (Galen). Conversely, territories supplied by deep cerebral veins may be drained, when necessity arises, by surface vessels. This anastomotic venous arrangement facilitates the drainage of capillary beds by shifting the blood from one area to another and readily equalizes regional increases in pressure due to occlusion or other factors. As a result, the occlusion of even a large vein, if not too rapid, will produce only slight transitory effects. When occlusion or increase in pressure occurs suddenly, there will be marked hyperemia and often extensive hemorrhages, as in birth injuries and, occasionally, in cases of thrombosis in adults (58, 59).

SUPERFICIAL CEREBRAL VEINS

Superficial cerebral veins arise from the cortex and subcortical white matter, anastomose freely in the pia, and form larger veins that empty into the dural sinuses. The larger veins include the superior and inferior cerebral veins and the superficial middle cerebral vein.

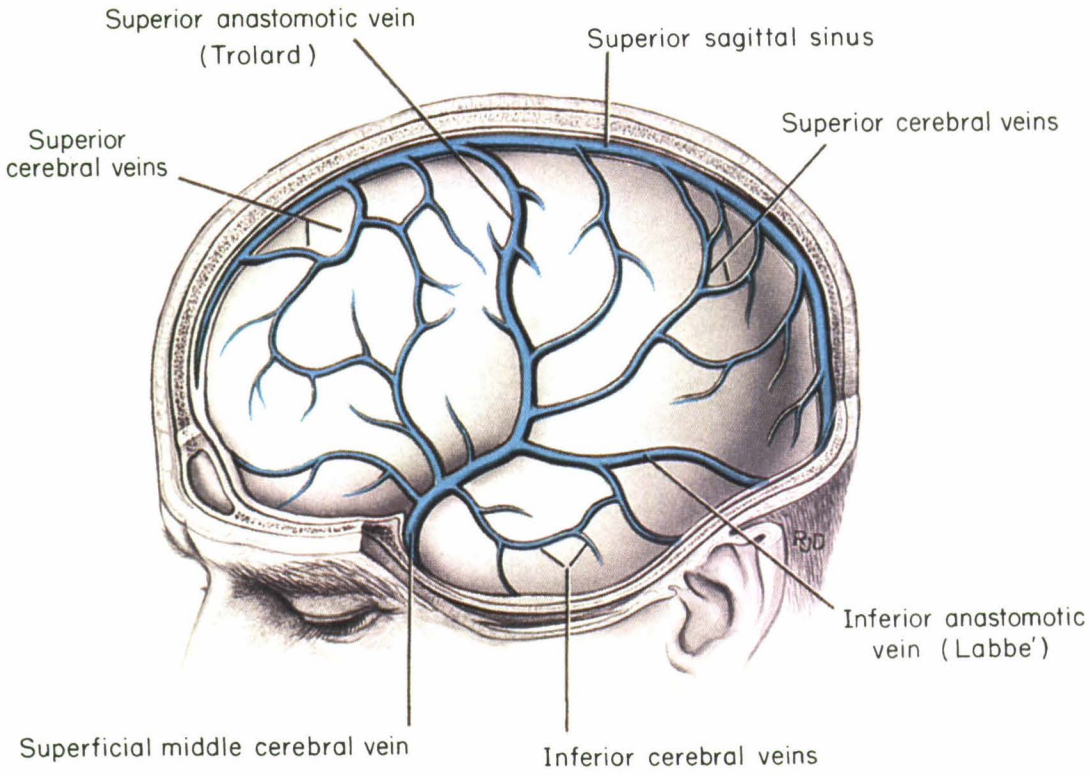


Figure 4.25. The external cerebral veins on the convexity of the hemisphere.

The *superior cerebral veins,* collecting blood from the convex and medial surfaces of the cerebral hemisphere drain into the superior sagittal sinus. These veins, 10 to 15 in number, enter the sinus by coursing obliquely forward. Blood flow in these veins, as they enter the sinus, is opposite to that in the sinus. Some veins on the medial surface of the hemispheres drain into the inferior sagittal sinus, or its venous lacunae (Fig. 4.25). Many of them, especially the larger posterior ones, run obliquely forward through the subarachnoid space and enter the sinus.

The *inferior cerebral veins* drain the basal hemispheric surface and ventral parts of the lateral surface. Inferior cerebral veins on the basal surface of the hemisphere empty into the basal sinuses. In rostral regions, these veins enter the cavernous and sphenoparietal sinuses (Figs. 4.4, 4.24, and 4.25); caudally, they empty into the petrosal and transverse sinuses.

The *superficial middle cerebral vein* courses along the lateral sulcus and receives smaller veins on the lateral surface of the hemisphere (Fig. 4.25). This large vein empties into the cavernous sinus (Fig. 4.24). The superficial middle cerebral vein also receives anastomotic branches, the most constant and prominent of which are the *superior anastomotic* (Trolard) and the *inferior anastomotic* (Labbé) veins. These anastomotic veins connect the superficial middle cerebral vein respectively with the superior sagittal and transverse sinuses.

On the inferior surface, the small inferior cerebral veins, arising from extensive pial plexuses, drain in part into the basal sinuses. Those from the tentorial surface of the hemisphere empty into the transverse and superior petrosal sinuses (Figs. 4.4 and 4.24). Veins from the anterior temporal lobe and from the interpeduncular regions drain partly into the cavernous and sphenoparietal sinuses, while some veins from the orbital region join the superior or the inferior sagittal sinus.

Large cortical regions on the inferior and medial surfaces of the brain are drained by a number of vessels that empty into the great cerebral vein (Figs. 4.26 and 4.27). Anastomotic channels connecting the superficial and deep veins, include the occipital vein, the basal vein (Rosenthal), and the posterior callosal vein (Figs. 4.26 and 4.27). Veins of this group are best considered in relation to the deep cerebral veins.

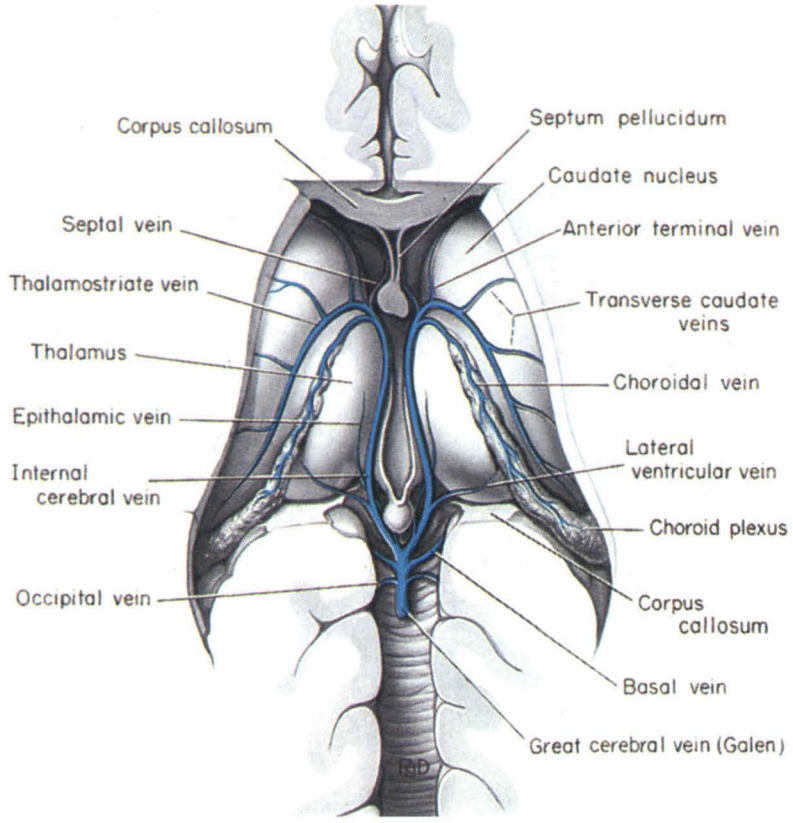


Figure 4.26. The internal cerebral veins and their tributaries.

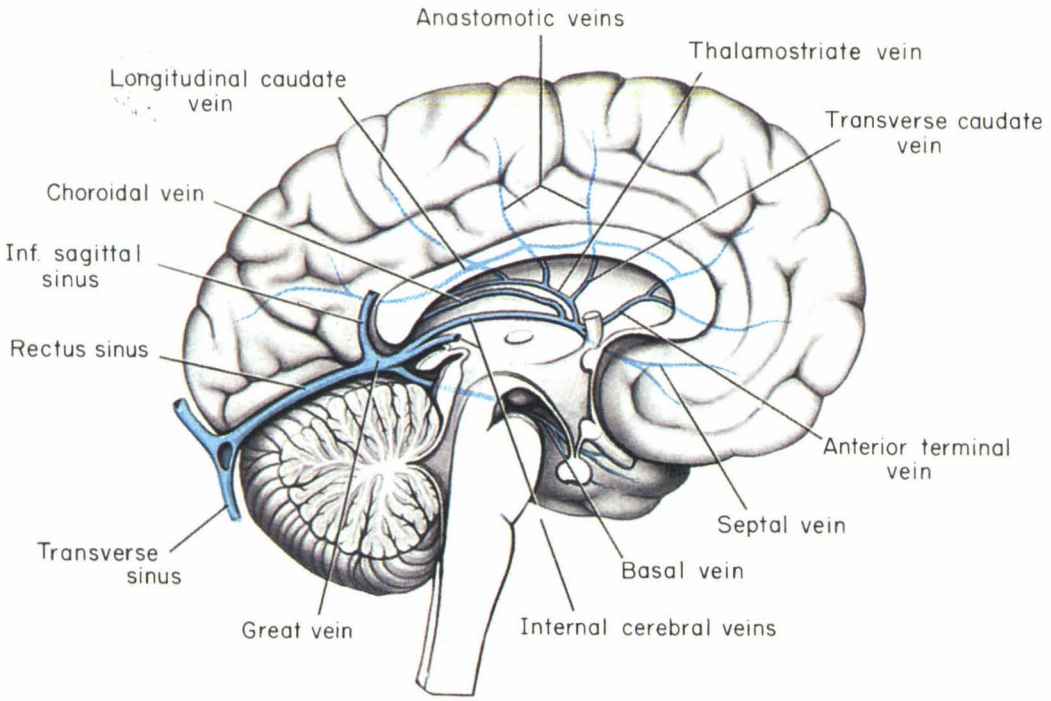


Figure 4.27. Midsagittal view of the internal cerebral veins showing the relationship of the great vein to the rectus sinus.

DEEP CEREBRAL VEINS

The deep cerebral veins of major importance are (a) the internal cerebral veins, (b) the basal veins (Rosenthal), and (c) the great cerebral vein (Galen) (27).

The *internal cerebral veins* (paired) are located near the midline in the tela choroidea of the roof of the third ventricle (velum interpositum) (Figs. 4.26 and 4.27). They extend caudally from the region of the interventricular foramina over the superior and medial surface of the thalamus. In the rostral part of the quadrigeminal cistern, these paired veins join to form the great cerebral vein (Galen). The internal cerebral vein on each side receives (a) the thalamostriate vein (terminal vein), (b) the choroidal vein, (c) the septal vein, (d) the epithalamic vein, and (e) the lateral ventricular vein (Fig. 4.26).

The *thalamostriate vein* runs forward in the terminal sulcus at the junction of the thalamus and caudate nucleus. This vein receives the *anterior terminal vein*, which drains the ventricular surface of the head of the caudate nucleus. Numerous *transverse caudate veins* join the thalamostriate vein throughout its course (Figs. 4.26 and 4.27). Distally the transverse caudate veins enter the white matter adjacent to the lateral angle of the lateral ventricle; their smaller tributaries in this region form the *longitudinal caudate veins* (Fig. 4.27). The latter veins divide at acute angles into a number of branches that fan out into the white matter by coursing with the fibers of the corpus callosum (Figs. 4.27–4.29). Some of the shorter branches drain the deep capillary plexuses of the white matter. Longer branches of these veins, extending almost to the cortex, may be regarded as intracerebral anastomotic channels connecting ventricular and surface veins. Additionally, the transverse and longitudinal caudate veins give rise to another group of branches known as the *superior striate veins* (Figs. 4.29 and 4.30). These veins pass ventrally through and around the caudate nucleus, perforate the internal capsule, and break into a number of smaller vessels that drain the dense capillary plexus of the lentiform nucleus (Fig. 4.29). This capillary plexus is drained from below by the *inferior striate veins*, which converge upon the anterior perforated substance and enter the deep middle vein.

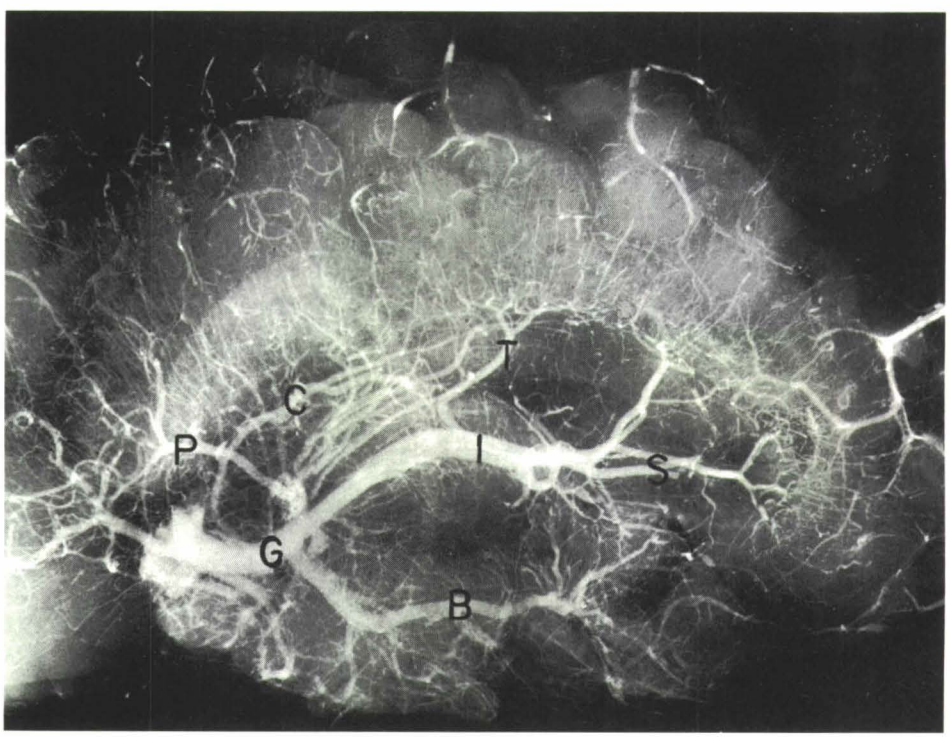


Figure 4.28. Angiographic appearance of the deep venous system in one intact cerebral hemisphere. Abbreviations: *S*, septal vein; *T*, thalamostriate vein; *I*, internal cerebral vein; *B*, basal vein; *C*, choroidal vein; *G*, great cerebral vein (Galen); and *P*, occipital vein (vein of the posterior horn).

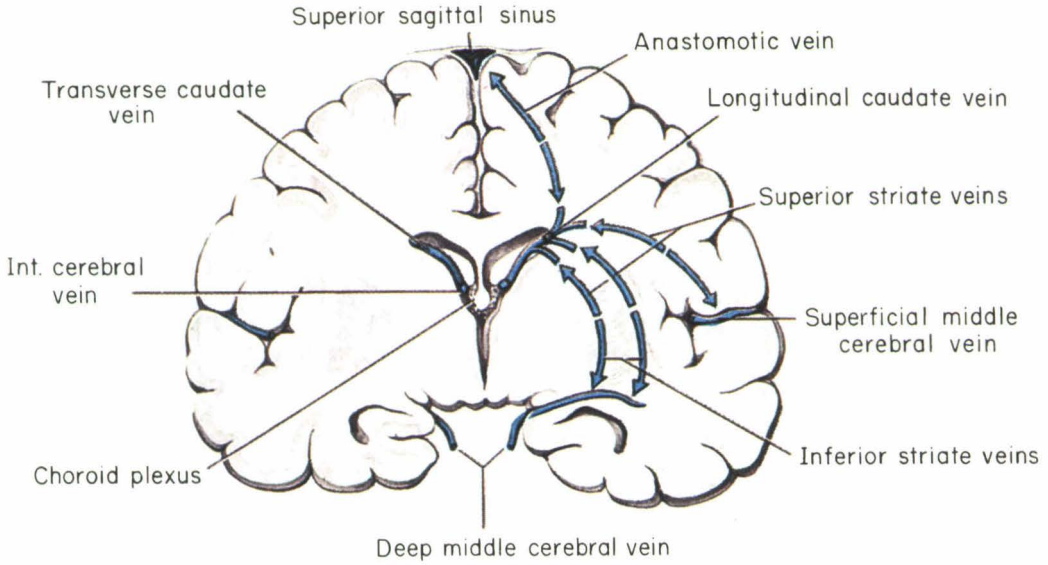


Figure 4.29. Transverse section through the brain of the rhesus monkey, showing the connections between deep and superficial veins.

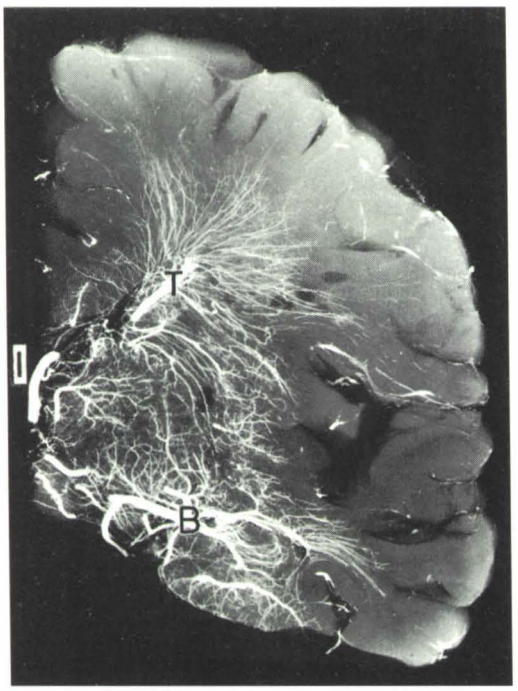


Figure 4.30. Angioarchitecture of the deep cerebral venous system as shown in a 1-cm-thick coronal section. Anastomoses between deep and superficial veins are evident. Abbreviations: *T*, terminal vein; *B*, basal vein; *I*, internal cerebral vein.

The *choroidal vein* runs along the lateral border of the choroid plexus and distally extends into the inferior horn of the lateral ventricle (Fig. 4.26). This tortuous vessel drains portions of the choroid plexus and adjacent hippocampal regions. The choroid plexus also is drained by the choroidal branch of the basal vein and, to a lesser extent, through the lateral ventricular vein.

The *septal vein* drains the septum pellucidum and rostral portions of the corpus callosum. Distally, branches of this vein extend beneath the head of the caudate nucleus into the white matter at the base of the frontal lobe (Figs. 4.26 and 4.27). The septal vein joins the internal cerebral vein in the region of the interventricular foramen.

The *epithalamic vein* is a small vessel that drains the dorsal part of the diencephalon. This vein enters the internal cerebral vein, or the great cerebral vein, near their junction. Blood from ventral portions of the thalamus and from the hypothalamus is drained by vessels that pass ventrally into the pial venous plexus of the interpeduncular fossa. From this plexus venous blood is conveyed into the cavernous or sphenoparietal sinuses or into tributaries of the basal vein.

The *lateral ventricular vein* courses over the superior caudal surface of the thalamus (Fig. 4.25) and enters the internal cerebral vein as this vessel joins the great cerebral vein. Occasionally, this vein terminates directly in the great cerebral vein. Distally the lateral ventricular vein extends over the surface of the thalamus and the tail of the caudate nucleus and enters the medullary substance near the angle of the lateral ventricle. Small branches

of this vein arise from the choroid plexus and from the white matter of the parahippocampal gyrus.

The *basal vein* (Rosenthal) arises near the medial part of the anterior temporal lobe (Figs. 4.27 and 4.28). This vein receives (a) the anterior cerebral vein, (b) the deep middle cerebral vein, and (c) the inferior striate veins.

The *anterior cerebral vein* accompanies the anterior cerebral artery and drains the orbital surface of the frontal lobe, anterior portions of the corpus callosum, and rostral portions of the cingulate gyrus. The *deep middle cerebral vein*, located in the depths of the lateral sulcus, drains insular and adjacent opercular cortex. The *inferior striate veins* drain ventral portions of the basal ganglia, emerge through the anterior perforated substance, and empty into the deep middle cerebral vein (Figs. 4.28–4.30). In the region of the anterior perforated substance, these veins unite with the basal vein which courses caudally around the crus cerebri to join the great cerebral vein. The basal vein receives additional tributaries from the interpeduncular region, the midbrain, and the inferior horn of the lateral ventricle. The hypothalamus and ventral portions of the thalamus also are drained by the basal veins.

The *great cerebral vein* (Galen) receives the paired basal internal cerebral veins, the paired internal cerebral veins, the paired basal veins, the paired occipital veins, and the posterior callosal vein (Figs. 4.26–4.28). This short vein passes caudally beneath the splenium of the corpus callosum and empties into the rectus sinus. The paired *occipital veins* drain inferior and medial surfaces of the occipital lobe and adjacent parietal regions. The *posterior callosal vein* drains the splenium of the corpus callosum and adjacent medial surfaces of the brain.

Angiographic studies (65) of cerebral veins made by serial x-rays reveal that the superficial frontal veins fill slightly before the parietal veins. The deep veins usually are the last to fill, and they retain sufficient concentrations of radiopaque material to be visualized for a longer time. From the standpoint of diagnostic radiology, the deep cerebral veins are more important than the superficial veins which exhibit extremely variable configurations. Visualization of the thalamostriate vein and some of its major tributaries can provide information concerning the position and size of the lateral ventricle.

The deep veins are concerned primarily with the drainage of the ventricular surface, the choroid plexuses, the deep medullary substance, the caudate nucleus, and the dorsal portions of the lentiform nucleus and thalamus. All these structures also can be drained by surface vessels through numerous intracerebral and extracerebral anastomotic veins.

References

1. Aitken HF. A report on the circulation of the lobar ganglia made to Dr. James B. Ayer (with a postscript by JB Ayer, MD). Boston Med Surg J 1909;160(Suppl):18.
2. Alexander L. The vascular supply of the striopallidum. Proc Assoc Res Nerv Ment Dis 1942;21:77–132.
3. Baker AB. Cerebrovascular disease. IX. The medullary blood supply and the lateral medullary syndrome. Neurology 1961;11:852–861.
4. Baptista AP. Studies on the arteries of the brain. II. The anterior cerebral artery: some anatomic features and their clinical implication. Neurology 1963;13:825–835.
5. Barnett HJM. Cerebrovascular diseases. In: Wyngaarden JB, Smith LH, eds. Cecil texbook of medicine. 18th ed. Philadelphia: W.B. Sanders, 1988:21–59.
6. Batson OV. The function of the vertebral veins and their role in the spread of metastases. Ann Surg 1940;112:138–149.
7. Bolton B. The blood supply of the human spinal cord. J Neurol Psychiatry 1939;2:137–148.
8. Brust JCM. Cerebral infarction. In: Rowland LP, ed. Merrit's textbook of neurology. 8th ed. Philadelphia: Lea & Febiger, 1989:206–214.
9. Brust JCM. Cerebral circulation: Stroke. In: Kandel ER, Schwartz JH, Jessel TM, eds. Principles of neural science. Appendix B. New York: Elsevier, 1991:1041–1049.
10. Carpenter MB, Noback CR, Moss ML. The anterior choroidal artery. Its origins, course, distribution and variations. Arch Neurol Psychiatry 1954;71:714–722.
11. Cooper IS. Surgical occlusion of the anterior choroidal artery in Parkinsonism. Surg Gynocol Obst 1954;99:207–219.
12. Coronna JJ. Cerebrovascular diseases. Textbook of internal medicine. 2d ed. Philadelphia: J.B. Lippincott, 1991:2161–2168.
13. Crock HV, Yoshizawa H. The blood supply of the vertebral column and spinal cord in man. Berlin: Springer-Verlag, 1977.
14. Dandy WE. Intercranial arterial aneurysms. Ithaca, NY: Comstock Publishing Company, 1947.
15. Dejerine J, Roussy G. Le syndrome thalamique. Rev Neurol (Paris) 1906;14:521–532.
16. Duvernoy HM. Human brainstem vessels. Berlin: Springer-Verlag, 1978.
17. Foix C, Hillemand J. Les artères de l'axe encéphalique jusqu'au diencéphale inclusivement. Rev Neurol (Paris) 1925;44:705–739.
18. Frantzen E, Olivarius BIF. On thrombosis of the basilar artery. Acta Psychiatr Neurol Scand 1957;32:431–439.
19. Fujii K, Chambers SM, Rhoton AL Jr. Neurovascular relationships of the sphenoid sinus—a microsurgical study. J Neurosurg 1979;50:31–39.
20. Galloway JR, Greitz T. The medial and lateral choroid arteries: an anatomic and roentgenographic study. Acta Radiol (Stockh) 1960;53:353–356.
21. George AE, Salamon G, Kricheff IN. Pathologic anatomy of the thalamoperforating arteries in lesions of the third ventricle: Part II. Am J Roentgenol Radium Ther Nucl Med 1975;124:231–240.
22. Gibs H, Carver CC, Rhoton AL, Lenkey C, Mitchell RJ . Microsurgical anatomy of the middle cerebral artery. J Neurosurg 1981;54:151–169.
23. Gillilan LA. The arterial blood supply of the human spinal cord. J Comp Neurol 1958;110:75–103.

24. Hara K, Fujino Y. The thalamoperforate artery. Acta Radiol 1966;5: 192–200.
25. Hardy DG, Peace DA, Rhoton AL. Microsurgical anatomy of the superior cerebellar artery. Neurosurgery 1980;6:10–27.
26. Harris FS, Rhoton AL Jr. Anatomy of the cavernous sinus: a microsurgical study. J Neurosurg 1976;45: 169–180.
27. Hassler O. Deep cerebral venous system in man: a microangiographic study on this areas of drainage and its anastomoses with the superficial cerebral veins. Neurology 1966;16: 505–511.
28. Hassler O. Blood supply to the human spinal cord. Arch Neurol 1966;15:302–307.
29. Hassler O. Venous anatomy of human hindbrain. Arch Neurol 1967;16:404–409.
30. Hassler O. Arterial pattern of human brain stem. Normal appearance and deformation in expanding supratentorial conditions. Neurology 1967;17:368–375.
31. Haugsted H. Occlusion of the basilar artery. Diagnosis by vertebral angiography during life. Neurology 1956;6:823–828.
32. Herren RY, Alexander L. Sulcal and intrinsic blood vessels of human spinal cord. Arch Neurol Psychiatry 1939;41:678–687.
33. Kaplan HA. Arteries of the brain. Acta Radiol (Stockh) 1956;46: 364–370.
34. Kaplan HA. Vascular supply of the base of the brain. In: Fields WS, ed. Pathogenesis and treatment of Parkinsonism. Ch. 6. Springfield, IL: Charles C. Thomas, 1958:138–155.
35. Kaplan HA. Collateral circulation of the brain. Neurology 1961;11:9–15.
36. Kaplan HA, Ford DH. The brain vascular system. Amsterdam: Elsevier, 1966.
37. Kennedy C, Des Rosiers MH, Jehle JW, Reivich M, Sharp F, Sokoloff L. Mapping of functional neural pathways by autoradiogaphic survey of local metabolic rate with [^{14}C] deoxyglucose. Science 1975;187: 850–853.
38. Kennedy C, Des Rosiers H, Sakurada O, et al. Metabolic mapping of the primary visual system of the monkey by means of the autoradiographic [^{14}C] deoxyglucose technique. Proc Natl Acad Sci (USA) 1976;73:4230–4234.
39. Kety SS, Schmidt CF. The nitrous oxide method for the quantitative determination of cerebral blood flow in man: theory, procedure and normal values. J Clin Invest 1948;27:484–492.
40. Lazorthes G, Gouszé A, Salamo, G. Vascularisation et Circulation de l'Encéphale. Paris: Masson et Cie, 1976.
41. Lazorthes G, Poulhes J, Bastide G, Rolleau J, Chancholle AR. Recherche sur la vascularisation artérielle de la moelle: application à la pathologie médullaire. Bull Acad Natl Med 1957;141:464–477.
42. Lazorthes G, Salamon G. The arteries of the thalamus: an anatomical and radiological study. J Neurosurg 1971;34:23–26.
43. Martin RG, Grant JL, Peace D, Theiss C, Rhoton AL. Microsurgical relationships of the anterior inferior cerebellar artery and the facial-vestibulocochlear nerve complex. Neurosurgery 1980;6:483–507.
44. Masucci EF. Bilateral ophthalmoplegia in basilar-vertebral artery disease. Brain 1965;88:97–106.
45. Mettler FA. Neuroanatomy. St. Louis: C.V. Mosby Co., 1948.
46. Mettler FA, Cooper IS, Liss H, Carpenter MB, Noback CR. Patterns of vascular failure in the central nervous system. J Neuropathol Exp Neurol 1954;13:528–539.
47. Mettler FA, Liss HR, Stevens GH. Blood supply of the primate striopallidum. J Neuropathol Exp Neurol 1956;15:377–383.
48. Moniz E. Diagnostic des Tu-meurs Cérébrales et Epreuve de l'Encéphalographie Artérielle. Paris: Masson et Cie, 1931.
49. Moniz E. L'Angiographie Cérébrale, ses Applications et Résultats en Anatomie, Physiologie et Clinique. Paris: Masson et Cie, 1934.
50. Ostrowski AZ, Webster JE, Gurdjian ES. The proximal anterior cerebral artery: an anatomic study. Arch Neurol 1960;3:661–664.
51. Perlmutter D, Rhoton AL. Microsurgical anatomy of the anterior cerebral-anterior communicating-recurrent artery complex. J Neurosurg 1976;45:259–272.
52. Perlmutter D, Rhoton AL. Microsurgical anatomy of the distal anterior cerebral artery. J Neurosurg 1978;49:204–228.
53. Plum F, Gjedde A, Samson FE. Neuroanatomical functional mapping by radioactive 2-deoxy-d-glucose method. Neurosci Res Program Bull 1976;14:457–518.
54. Plum F, Posner JB. The diagnosis of stupor and coma. 3rd ed. Philadelphia: Davis, 1966.
55. Reichle ME. Circulatory and metabolic correlates of brain function in normal humans. In: Plum F, ed. Handbook of physiology. Vol. V. Higher functions of the brain. Part 2; Section I: The nervous system. Bethesda, MD: American Physiological Society, 1987:643–674.
56. Salamon G, Lazorthes G. Atlas of the arteries of the human brain. Paris: Sandoz, 1971.
57. Scharrer E. The blood vessels of the nervous tissue. Q Rev Biol 1944; 19:308–318.
58. Schlesinger B. Venous drainage of the brain, with special reference to galenic system. Brain 1939;62: 274–291.
59. Schwartz P, Fink L. Morphologie und Entstehung der geburstraumatischen Blutungenim Gehirn und Schädel des Neugeborenen. Z Kinder heilk 1926;40:427–474.
60. Stephens RB, Stilwell DL. Arteries and veins of the human brain. Springfield, IL: Charles C. Thomas, 1969.
61. Stopford JSB. The arteries of the pons and medulla oblongata. Part I. J Anat Physiol 1915;50:131–164.
62. Stopford JSB. The arteries of the pons and medulla oblongata. Part II. J Anat Physiol 1916;51:255–280.
63. Suh TH, Alexander L. Vascular system of the human spinal cord. Arch Neurol Psychiatry 1939;41:659–677.
64. Taveras J. Angiographic observation in occlusive cerebrovascular disease. Neurology 1961;11:86–90.
65. Taveras JM, Wood EH. Diagnostic neuroradiology. 2d ed. Baltimore: Williams & Wilkins, 1976.
66. Truex RC, Kellner CE. Detailed atlas of the head and neck. New York: Oxford University Press, 1948.
67. Turnbull IM. Blood supply of the spinal cord. In: Vinken PJ, Bruyn GW, eds. Handbook of clinical neurology. Vol. 12. Amsterdam: North-Holland Publishing Company, 1972:478–491.
68. Turnbull IM. Blood supply of the spinal cord: normal and pathological considerations. Clin Neurosurg 1973;20:56–84.
69. Zeal AA, Rhoton AL. Microsurgical anatomy of the posterior cerebral artery. J Neurosurg 1978;48:534–559.
70. Zülch KJ. Mangeldurchblutung an der Grenzzone zweier Gefässgebiete als Ursache bisher ungeklärter Rückenmarksschädigungen. Dtsch Z Nervenheilk 1954;172:81–101.

Section II

Neurohistology and Neurocytology

5
Neurons

NEURONS AS SIGNALING UNITS

A proper knowledge of the histologic organization of the nervous tissue is required to understand how the nervous system works and to fully appreciate its uniqueness. The tissue of the central nervous system is made up of two classes of cells that may be broadly categorized as neurons and neuroglia. Neuroglia will be discussed in Chapter 6. Despite great variability in size and shape, all neurons share common morphologic features, which are those of the key elements of a highly complex communication network.

Typically neurons have several processes, called *dendrites*, radiating from a central portion of the cell, known as the *soma* or *perikaryon*. They also possess a single process, the *axon*, which extends for variable distances from the soma and breaks out into a multitude of *axon terminals* that establish specialized junctional contacts, called *synapses*, upon the dendrites and cell bodies of other neurons. The axon is capable of conveying information over great distances by propagating in an all-or-none fashion a transient electrical signal termed the *action potential*. The axon arises from a specialized region of the cell body called the axon hillock, where the action potential is initiated once a critical threshold is reached.

The neuron is a dynamically polarized cell that serves as the major signaling unit of the nervous system. It comprises four functionally distinct components: (a) an input or receptive component (usually the dendrites and part of the soma), (b) an integrative component (usually the axon hillock), (c) a conductile component (the axon), and (d) an output or secretory component (the axon terminals). The human brain is known to contain about 10^{11} neurons, each being able to contact at least 10,000 other neurons (3). Despite their large number, all the neurons in the central nervous system share the common features noted earlier and appear as rather simple basic units. In terms of information processing, the complexity of the human brain derives not from the contribution of its individual components, but from the highly ordered connections that exist between these innumerable elements. It is through the specific wiring of its individual elements, which is established during development and can be modified by learning, that the human brain can generate the most complex forms of behavior.

The fact that each neuron is a structural and functional unit is known as the *neuron doctrine*. It was proposed late in the 19th century in opposition to the then prevailing view that nerve cells form a syncytium or continuous reticulum. The neuron doctrine or theory was popularized by Waldeyer (197), but had its foundation in the embryologic investigations of Wilhem His in Germany, the neuropathologic works of August Forel in Switzerland, and, particularly, the extensive histologic studies of Ramón y Cajal in Spain (175). This theory was perfectly congruent with the cell theory formulated by Jacob Schleiden and Theodor Schwann in the 1930s, which holds that cells are the structural units of all living matter.

The neuron doctrine states that the individual nerve cell (neuron) constitutes the genetic, anatomic, trophic, and functional unit of the nervous system. All neural pathways, circuits, and reflex arcs are composed of individual neurons arranged in simple or complex patterns.

A variety of staining techniques have revealed the principal features of the neuron and the manner in which individual neurons are interrelated. The electron microscope and cytochemical techniques provided a new insight into the fine structure and the functional roles of specific organelles that occur within the neuron. All the recent data acquired with these techniques support the neuron doctrine. However, some of these recent findings have shown that the interactions between

neurons are much more complex and subtle than previously thought. For instance, some neurons are known to communicate through ultramicroscopic channels formed by special proteins in regions referred to as gap junctions. Therefore, it must be realized that most of the unique properties of the nervous tissue stem from the highly differentiated interactions that exist between billions of distinct cellular units.

A generalized concept of neurons based upon the site of impulse origin, rather than the location of the cell body, was proposed by Bodian (15). In such a scheme, the term *"dendritic zone"* is used to denote the receptor membrane of a neuron (Fig. 5.7), which may be cytoplasmic extensions (i.e., dendrites), portions of the cell soma, or specialized receptors which act as transducers. The cell body (soma) remains the focal point of embryonic outgrowth of dendrites and axons and of axonal regeneration. It also maintains the trophic aspects of neuronal activity. The position of the soma is irrelevant as far as the major electrochemical functions of the neuron are concerned. Its position is related to the outgrowth of processes and to metabolic maintenance, rather than to the polarized conduction of the neuron.

This functional concept recognizes the site of impulse origin as the pivotal position in the neuron. This site may not necessarily be a fixed point in a particular neuron. Furthermore, all surfaces bearing synapses (dendrites, cell body, and axon) are related to response-generating functions. In these functional terms, the axon may be said to arise from any response-generating structure, such as a dendrite, the cell body, or a sensory receptor. The functional role of the axon is to conduct signals away from the response-generating region. In peripheral sensory neurons, the response-generating zone is the distal tip of the axon which is usually associated with a connective tissue capsule or other receptor of epithelial or mesodermal origin. The action potential generally occurs at or near the origin of the axon and conducts the nerve impulse away from the "dendritic zone." Axons are ensheathed by neuroglial or Schwann cells. Both axon diameter and sheath differentiation are related to the rate of impulse conduction. The branched and variously differentiated terminals of axons are sometimes called *telaxons* or *telodendria*. They may show membrane and cytoplasmic differentiations related to synaptic transmission or neurosecretory activity (Fig. 9.8). Mitochondrial concentrations, synaptic vesicles, or secretory granules are commonly present in their bulblike terminals, which release chemical compounds known as neurotransmitters. The telaxons transmit electrical or chemical signals capable of producing generator potentials in the dendritic zones of other neurons and in muscle, or they can induce stimulatory effects in innervated glands. The terms axon, dendrite, and cell body, used in this text, are in accordance with the functional concepts earlier described.

Intercellular and intracellular communication in the nervous tissue is accomplished through both electrical and chemical mechanisms (Fig. 5.1). Electrical communication is a property of the neuronal surface membrane, whereas chemical communication results from a specialization of the secretory nature of neurons. While in this chapter the detailed biophysical or chemical aspects of cellular communication in the nervous system is not considered, some introduction to general concepts is provided for students who have not yet studied neuronal physiology. In a "resting" neuron, the interior of the cell is 60–70 mV negative with respect to the extracellular fluid. This *resting membrane potential* reflects steady-state ionic concentration gradients resulting from the selective permeability properties of the cell membrane. Inside the cell there is a high potassium concentration (about 50 times higher than outside) and a low sodium concentration (about 10 times lower than outside). Potassium ions move freely through the membrane, and the resting membrane potential is due largely to the distribution of potassium ions needed to balance the charge of impermeant anions.

In the resting neuron, the surface membrane is effectively impermeable to sodium ions because of a unidirectional transport mechanism called the sodium pump. When a neuron becomes active, the permeability of the membrane to sodium and other ions changes. This movement of ions, termed *conductance*, is inversely proportional to the resistance of the membrane. In axons, the conductance change has a duration of approximately 1 millisecond (msec) and is called an *action potential*. In dendrites and soma, the conductance change has a duration varying from a few to more than 100 msec. These longer duration changes are called

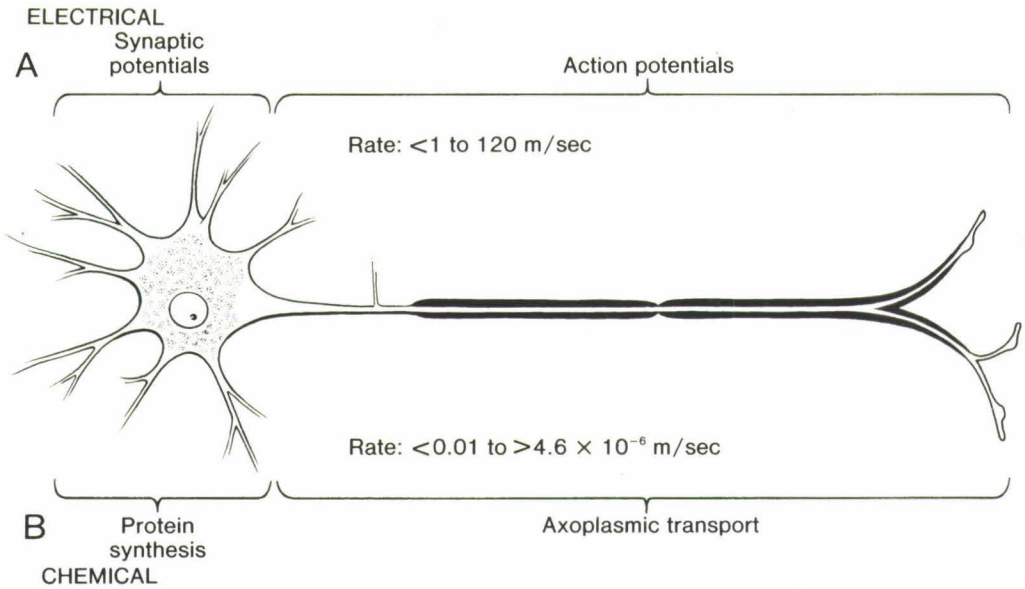


Figure 5.1. Comparison of major type of intra- and intercellular communications in neurons. The dendrites and soma of the cell are shown toward the *left*, the axon and synaptic terminals toward the *right*. **A.** Two regions of the neuron concerned with intracellular electrical communication are shown. One zone (the dendrosomatic domain) sustains graded, nonpropagated synaptic potentials, and the other (axon and axon terminal domain) sustains all or nonpropagated action potentials. **B.** The rates of chemical (axoplasmic) transport between the soma and synaptic terminals are shown for comparison with rates of electrical communication by action potentials.

synaptic potentials and are graded in amplitude. In contrast to synaptic potentials, action potentials are always of the same amplitude once the threshold has been exceeded. A potential change which causes the inside of a cell to become less negative with respect to the extracellular fluid is termed a *depolarizing potential*. An increased negativity of the interior of the cell is termed a *hyperpolarizing potential*. Synaptic potentials may be either depolarizing or hyperpolarizing, while action potentials are always depolarizing. Hyperpolarization decreases a cell's ability to generate an action potential and is therefore *inhibitory*, whereas depolarization does exactly the inverse and is *excitatory*.

Action potentials are usually generated in the soma at the region of the emergence of the axon and propagated along the axonal membrane to its terminal (Fig. 5.1). The action potential can be regarded as a means of transferring a signal from the soma, along the axon, to the synaptic terminals, where the process of intercellular communication is initiated (105). The rate of propagation of action potentials depends upon the diameter of the axon and its associated myelin sheath and can range from less than 1 to about 120 meters per second (m/sec) (Fig. 5.1). At the terminal, the depolarization of the surface membrane as it is invaded by the action potential leads to an influx of calcium ions, which in turn causes the release of a chemical called a neurotransmitter. The frequency of action potentials usually determines the amount of transmitter that is released. Thus, the frequency of action potentials (digital signal) is transformed into a graded amount of transmitter (analog signal) at the level of axon terminals. Many of the neurotransmitter substances are synthesized and stored in the synaptic terminals of the axon. However, their synthesis depends upon enzymes which are synthesized in the cell body and moved by a process called axoplasmic transport along the axon to the terminal (Fig. 5.1). In contrast to the rapid rate of propagation of action potentials, rates of axoplasmic transport range from less than 0.01 to more than 4.6×10^{-6} m/sec. Intercellular communication, for the most part, is accomplished through the release of a neurotransmitter at the synapse (Fig. 5.34). The transmitter diffuses across the small extracellular space between the membrane of the synaptic terminal and the surface membrane of the adjacent neuron.

The membrane of the dendrite and soma

of the postsynaptic cell contains specific molecular binding sites for the transmitter. When these binding sites can be shown to be associated with a response in the postsynaptic neuron, they are called receptors. These receptors may be part of an ion conductance channel, so that the transmitter-receptor interaction results in an opening or closing of a channel for a specific ion. In some cases, the transmitter-receptor interaction leads to the activation of enzymes and a sequence of chemical reactions in the postsynaptic cell. When these reactions result, over time, in changes in the number of receptors or transmitter synthetic enzyme molecules in the postsynaptic cell, it is said to be a trophic effect (Fig. 5.33). Several of these physiologic and chemical properties of neurons are at the basis of some of the most currently used neuroanatomic methods.

NEUROBIOLOGIC TOOLS FOR STUDYING NEURONAL MORPHOLOGY

Histologic Techniques

Although unstained fresh nervous tissue, or nervous tissue grown in tissue culture, may be studied with the phase microscope, the customary method is to use stained preparations. It is essential that fresh nervous tissue be fixed in a solution which kills bacteria, inactivates autolytic enzymes, and produces minimal shrinkage, swelling, or distortion. Appropriate fixatives also make components of the nerve cell receptive to suitable dyes or permeable to colloidal solutions. The most common fixatives for neural tissue are aldehydes and alcohols. These fixatives often are used in conjunction with a variety of chemicals, such as chloral hydrate, ammonia, pyridine, glacial acetic acid, and mercuric chloride. In experimental studies in animals, excellent fixation of neural tissue is achieved by perfusion techniques, but obviously this is not possible in humans. Since several hours usually intervene between death and autopsy, it is rarely possible to obtain perfectly fixed human neural tissue. Appropriate fixation renders many components of the nerve cell, such as chromatin, receptive to suitable dyes (i.e., cresyl violet) (Fig. 5.2**E**), or neurofilaments more permeable to colloidal silver solutions (Fig. 5.2**A** and **B**).

Formalin fixation followed by a mordanting in potassium dichromate preserves the normal lipids of myelin, and enhances the appearance of the myelin sheaths when stained with hematoxylin (e.g., Weigert method) (Fig. 10.17). Primary fixation in potassium dichromate, followed by an osmic acid solution, selectively stains the fatty acids of degenerating myelin black, while the normal myelin remains a yellow-brown color (Marchi method) (Fig. 11.4). When the initial fixative contains solvents (e.g., alcohol, ether, chloroform), lipids of myelin are removed and only a clear space remains (Fig. 5.3**A** and **B**). If such solvents are avoided, the lipids of the normal myelin sheath are readily stained by osmic acid (Fig. 5.3**C-E**) and Luxol fast blue (Fig. 5.3**F** and **H**). Positive results with the Marchi technique may be obtained several years after degeneration has occurred and in specimen stored in paraformaldehyde for long periods. Despite its limitation in defining the exact site of termination of fiber bundles, this method can be successfully applied to trace degenerating fiber tracts in human postmortem material.

The nervous tissue has a strong affinity for weak silver solutions (*argyrophilia*). Blocks of nervous tissue are impregnated with silver salts for several days, and then placed in suitable reducing solutions. This action results in the deposit of silver particles within the nerve cell and its processes. The reduced silver particles in nonneural tissue are removed by subsequent solutions, so that the neurons and their processes appear golden brown or black against a light yellow background. The Ramón y Cajal (155) and Ranson (156) techniques both permit bulk staining of tissue blocks and are still used to elucidate the structural features of the central and peripheral nervous system (Fig. 5.2**C**).

Other methods have been developed which permit the staining of mounted sections. In the Bodian (14) method, the slides are placed in a silver protein solution (protargol) with metallic copper and incubated at 3°C. Again, the silver is reduced as in the bulk method. The silvered sections are then passed through a solution of gold chloride. Since gold has a higher atomic number and atomic weight than silver, gold replaces the silver particles in the nerve tissue of the section. The sections then are developed in oxalic acid, and the nonneural gold particles are removed. Nerve cells, their nuclei and processes are all beautifully visualized by this method (Fig. 5.2**A** and **B**).

The Golgi technique is based on the phenomenon of silver impregnation of neurons which was accidentally discovered by the

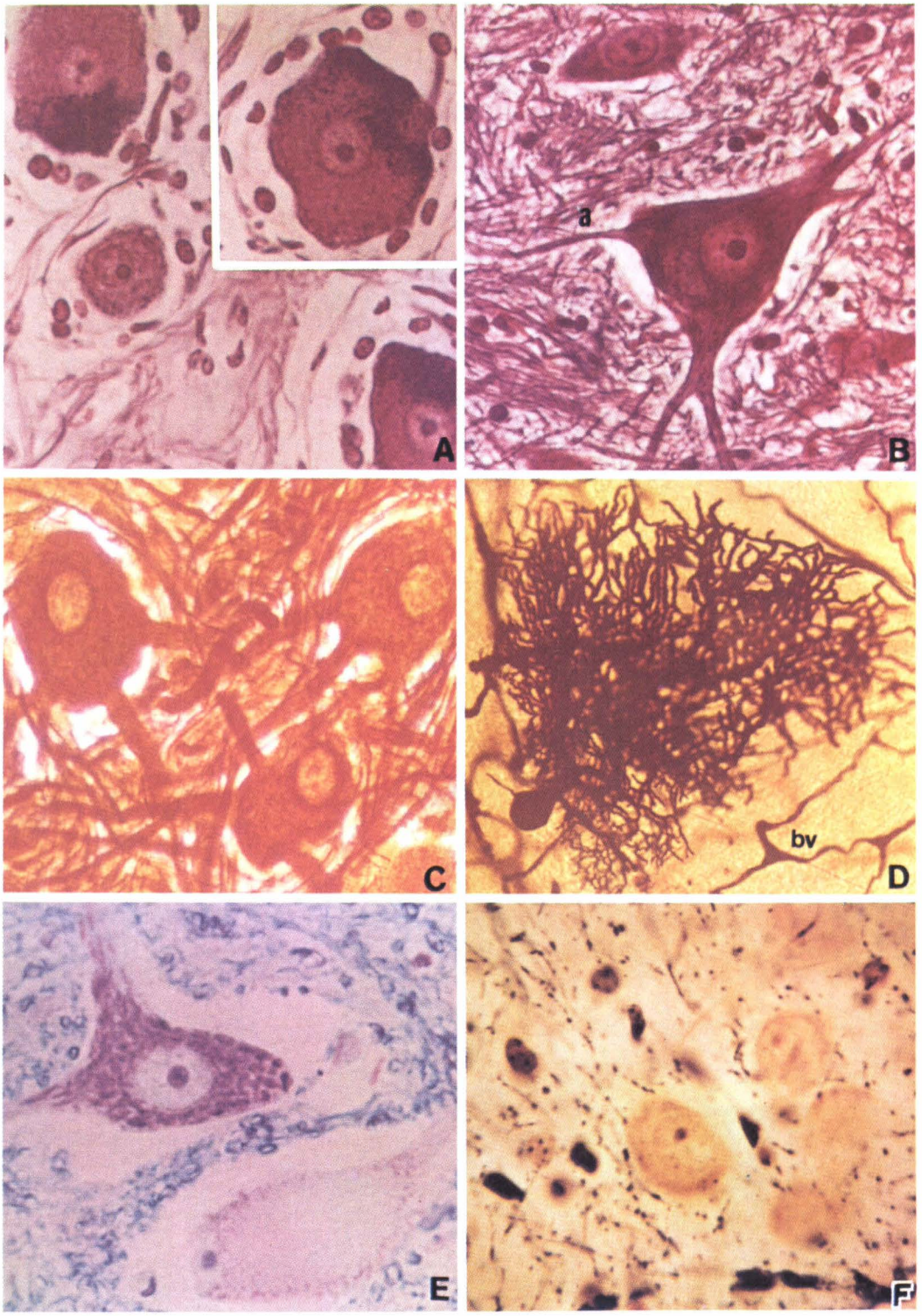


Figure 5.2. Shape, size, and appearance of nerve cells stained by different techniques. (×370 except **D** which is ×125.) **A.** Unipolar neurons of dorsal root ganglion. Three larger cells contain melanin granules (silver protargol technique). **B.** Multipolar neurons of reticular formation. An area of cytoplasmic lopofuscin pigment appears between the nucleus and axon (*a*) of the large cell (silver protargol technique). **C.** Multipolar neurons of sympathetic ganglion with interlacing of dendrite and small axons (Ramón y Cajal silver nitrate technique). **D.** Purkinje cell of cerebellar cortex whose dendritic branches are studded with small gemmules. Adjacent blood vessels (*bv*) are identified in this preparation (Golgi technique). **E.** Cytoplasmic chromatin and nuclear appearance of normal (*above*) and injured (*below*) anterior horn cell of spinal cord. The small eccentric nucleus and depleted chromatin pattern (chromatolysis) resulted from earlier axonal destruction (Luxol-fast-blue and cresyl violet technique). **F.** Terminal degeneration in the ventral nucleus of the thalamus following a localized lesion in the internal segment of the globus pallidus. Degenerated pallidothalamic fibers appear as black beaded and dots near the soma and dendrites of thalamic neurons (Wiitanen's silver technique).

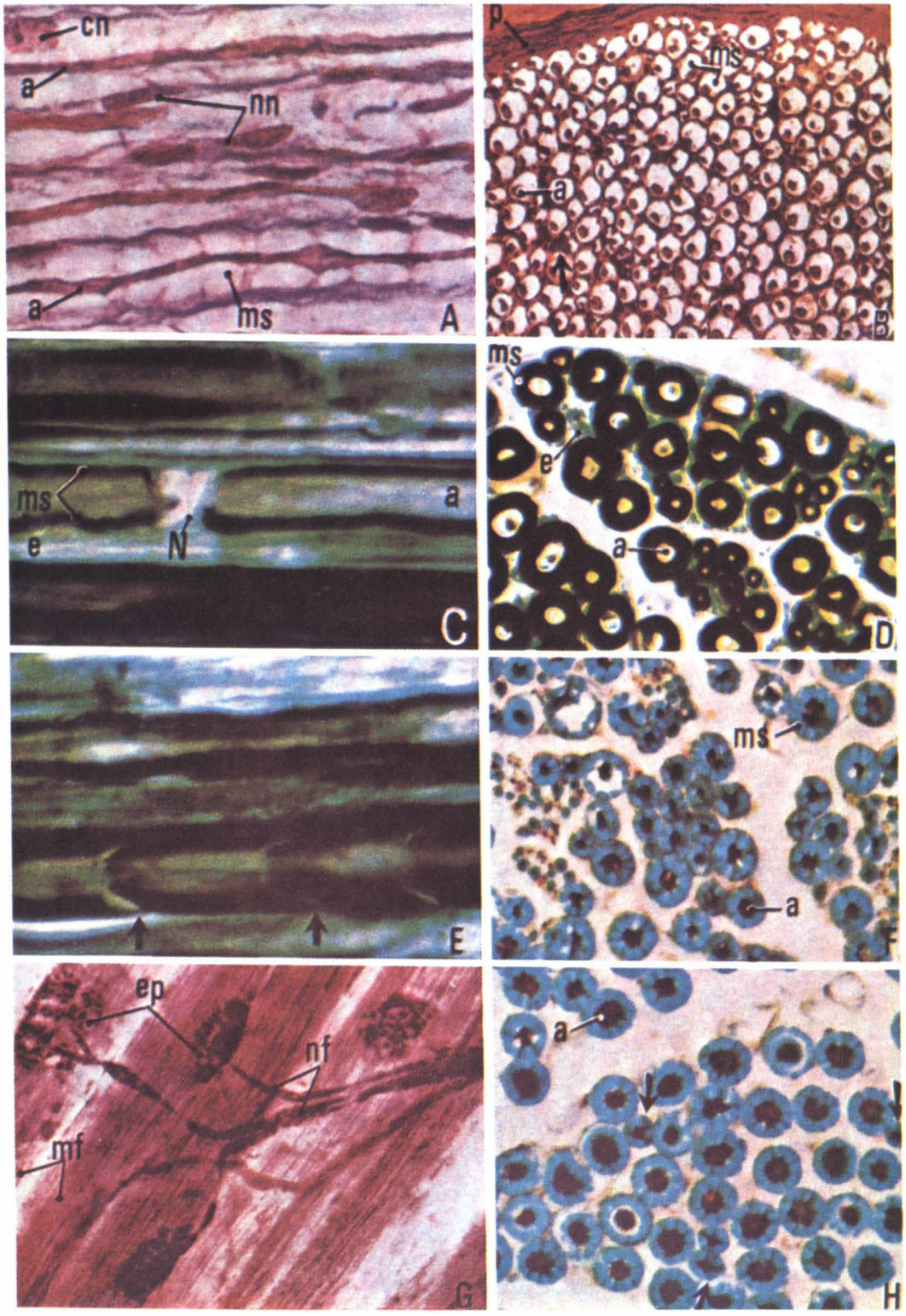


Figure 5.3. Size and appearance of nerve fibers stained by different techniques. **A.** Longitudinal section of femoral nerve stained with silver protargol. Axons (*a*), Schwann cell (*nn*) and connective tissue (*cn*) nuclei are identified. The myelin sheath (*ms*) is dissolved and remains as a clear space in such silver preparation (×370). **B.** Cross-section of sciatic nerve stained with silver nitrate. Axons (*a*), myelin space (*ms*), and connective tissue of perineurorium (*p*) are identified. Small black dots between larger fibers are axons of nonmyelinated fibers (*arrows*) (×130). **C.** Longitudinal section of myelinated nerve fiber and node of Ranvier (*N*) stained with osmic acid and *light green*. Myelin sheath (*ms*) stained *black*, axon (*a*) is unstained, and connective tissue of endoneurium (*e*) is *green* (×370). **D.** Cross-section of lumbar nerve in caudal equina with osmic acid and *light green*. Endoneurium (*e*) derived from pia mater is *green*,

Italian histologist Camillo Golgi in the late 19th century (69). This technique and its numerous variants are among the oldest and most widely used methods for studying neurons and neuroglia (154). The Golgi methods are based on a pretreatment of the tissue with potassium dichromate, followed by exposure to silver nitrate, which produces a black deposit that literally fills the cell bodies and processes of many neurons. Although only a fraction of the total number of neurons and neuroglia are stained black, these often are revealed in great detail against a nearly colorless background (Fig. 5.2**D**).

In addition to neurons and neuroglia, the blood vessels also may be stained by the Golgi methods. The methods are empirical and the results are uncertain, but magnificent neuronal and neuroglial details are revealed in successful preparations (Figs. 6.2 and 15.6). The advantage of the Golgi methods are that they provide a three-dimensional view of the cellular elements of the nervous tissue and are invaluable for both qualitative and quantitative studies of the nervous system (147, 205). They have been extensively used to evaluate the extent and analyze the architecture of the dendritic ramifications. (See Ambrogi (5) and Culling (34) for further details on these classical neurologic stains.)

Much of our recent knowledge of neuron cytology has resulted from the use of the electron microscope and the freeze-etch apparatus. The short wave length of a beam of electrons from a high voltage source permits a greater resolution of biologic structures than that obtained from electromagnetic radiation in the visible spectrum (the light microscope has a limit of resolution of about 0.2 μm). Electron density is imparted to the specimen by impregnating it with compounds of metal of high atomic number, such as osmium, lead, and uranium. The electron microscope methods reveal the detail of the internal structure of the neurons and the specializations that exist at synaptic junctions (Figs. 5.13, 5.17, 5.18). However, electron microscopy requires very thin tissue sections, less than 50 nm, and the preparation of such sections calls for special attention to fixation and embedding. The necessity of using ultrathin sections renders difficult the three-dimensional reconstruction of a whole neuron in electron microscopy. Today, electron microscopic methods are used in combination with histochemical or immunocytochemical methods to visualize neurotransmitters (60), or with anterograde and retrograde axonal tracing methods to define the connections of the neurons under study (182).

Tract-Tracing Methods

The study of connectivity, or the relation of one part of the nervous system with another, requires tracing of the long axonal processes of neurons. This was first done by placing lesions in the brain and visualizing the degenerating axons with specific stains (Fig. 5.2**F**). One method which proved valuable in the past, the Nauta-Gygax reduced silver impregnation technique (136, 137), results in a selective silver impregnation of degenerating axons. Staining of normal nerve fibers and endings is suppressed and these have a golden yellow appearance (Fig. 10.25). Thick, as well as thin, degenerating axons of injured neurons appear as discontinuous black droplets or beaded segments arranged in an orderly linear fashion (degeneration "en passage"). Arborizing degenerating axons, observed in close proximity to nerve cells, represent "terminal" fiber degeneration. Selective staining of the terminal end-feet of nerve processes (synaptic knobs, boutons terminaux) upon the dendrite or cell body of another neuron also is accomplished by the use of modified silver methods (Fig. 5.28). Several variants of the original Nauta-Gygax method have been developed (54, 202) and used in numerous studies to localize terminal fibers or pathways within the central nervous system (Fig. 5.2**F**).

Instead of being dependent on degenerative changes that occur in neurons following lesions, the current tract-tracing methods uti-

myelin (*ms*) is *black*, while axons (*a*) are unstained (×270). **E.** Longitudinal section of two myelinated nerve fibers with osmic acid and *light green*. Lower fibers with thicker myelin sheath exhibit Schmidt-Lantermann clefts (*arrows*) (×370). **F.** Cross-section of intradural dorsal root sensory fibers with combined Holmes' silver and Luxol blue techniques. Axons (*a*) appear *dark brown*, and myelin sheath (*ms*) is *blue*. Note variation in size of myelinated and nonmyelinated axons (×270). **G.** Longitudinal section of nerve fibers (*nf*) terminating as motor end-plates (*ep*) on extrafusal skeletal muscle fibers (*mf*) (gold chloride technique, ×145). **H.** Cross-section of intradural ventral root motor fibers stained as in **F**. Larger fibers (*a*) terminate as motor-end plates on extrafusal muscle fibers, while smaller γ-efferent fibers (*arrows*) end on intrafusal muscle fibers of neuromuscular spindle (×270).

lize some of the recently discovered physiologic properties of neurons. For instance, the fact that there exists a constant and active intracellular movement of molecules along the axon (axonal flow) was extensively exploited to study neuronal connections. In the case of the *autoradiographic tracing method*, radioactively labeled amino acids are injected into a small region of the brain where they are taken up by nerve cell bodies, incorporated into cellular protein, and transported in an anterograde (orthograde) direction from the cell body to the axon terminals. Autoradiographs are prepared by coating the slides with a nuclear emulsion. After several weeks of exposure, the emulsion is developed and fixed to reveal tracks of silver grains overlying labeled axons and terminals (Fig. 5.6). A major advantage of this technique over silver impregnation methods (Nauta-Gygax and Fink-Heimer methods) is that fibers of passage which do not originate at the site of the injection will not take up the tritiated amino acids and thus will not be labeled (32).

In contrast, the *horseradish peroxidase* (HRP) *method* is based on the retrograde transport of material from axon terminals to the cell body. When this large glycoprotein enzyme (molecular weight of about 40,000) is injected into the nervous tissue, it is incorporated into neurons by the process of micropinocytosis (endocytosis). This is most marked at axon terminals where the HRP is engulfed primarily into multivesicular endosomes and transported back to the cell body where it is ultimately degraded. By reacting the tissue with an appropriate substrate such as tetramethyl benzidine, an insoluble polymer is formed wherever the enzyme is located (Fig. 5.4) (109, 111, 126, 127). The same marker can also be used in *intracellular labeling methods* (103). When HRP is injected into individual neurons through a micropipette, the whole neuron, including dendrites and axonal projections, can be stained in a Golgilike fashion. This technique can serve to study the morphology of a neuron whose functional characteristics have been first investigated by electrophysiologic recording techniques.

In current tract-tracing studies, the enzyme HRP is no longer used alone, but conjugated to the lectin wheat germ agglutinin (WGA). Lectins are naturally occurring proteins or glycoproteins that bind to cell membranes and stimulate micropinocytosis. The presence of WGA molecules greatly enhances HRP uptake by neurons, so that WGA-HRP is readily taken up by both cell bodies and axon terminals at the site of injection. This compound is now widely used as both anterograde and retrograde tracer. Certain lectins, such as the leucoagglutinin extracted from kidney beans (*Phaseolus vulgaris*), are very efficient anterograde tracers. In optimal conditions, anterograde labeling studies with *Phaseolus vulgaris*-leucoagglutinin (PHA-L) display the terminal arborization of axons with as much detail as those obtained for the dendritic arborization with the Golgi methods (Fig. 5.4) (67, 68). PHA-L is visualized by using a highly specific antibody raised against this lectin, and the immunoprecipitate can be observed at both light and electron microscopic levels.

Biocytin is a compound of biotin and lysine (molecular weight 372.48) that can be used as either an intracellular marker (Fig. 5.5) (103) or an extracellular tracer (101). When utilized as an extracellular tracer, biocytin gives results that are as good as those obtained with PHA-L. Because of its biotin moiety, biocytin can readily bind to any probes that are conjugated to avidin, so that its visualization does not require the use of specific antibodies, as is the case for PHA-L. Furthermore, since both biocytin and PHA-L are equally sensitive, they can easily be combined (*anterograde double-labeling methods*) so that the organization of two different axonal projection systems can be investigated simultaneously (84, 179). This approach is particularly useful to establish the degree of convergence or divergence of two afferent projections upon a given neuronal population. Both biocytin and PHA-L can be visualized at the electron microscopic level and can be used in combination with immunocytochemical methods to reveal neurotransmitters (Fig. 5.4).

Fluorescence retrograde double-labeling methods make use of the principle of retrograde axonal transport of several fluorescent dyes (e.g., nuclear yellow, fast blue, fluorogold). When different dyes are injected into various brain loci, neurons whose axons provide collaterals to these brain regions can be identified by the double, or even triple, labeling that occurs in their cell bodies (8, 106, 194). Therefore, retrograde double-labeling methods allow investigation of both the cellular origin and degree of axonal collateralization of central nervous system pathways (Fig. 5.4).

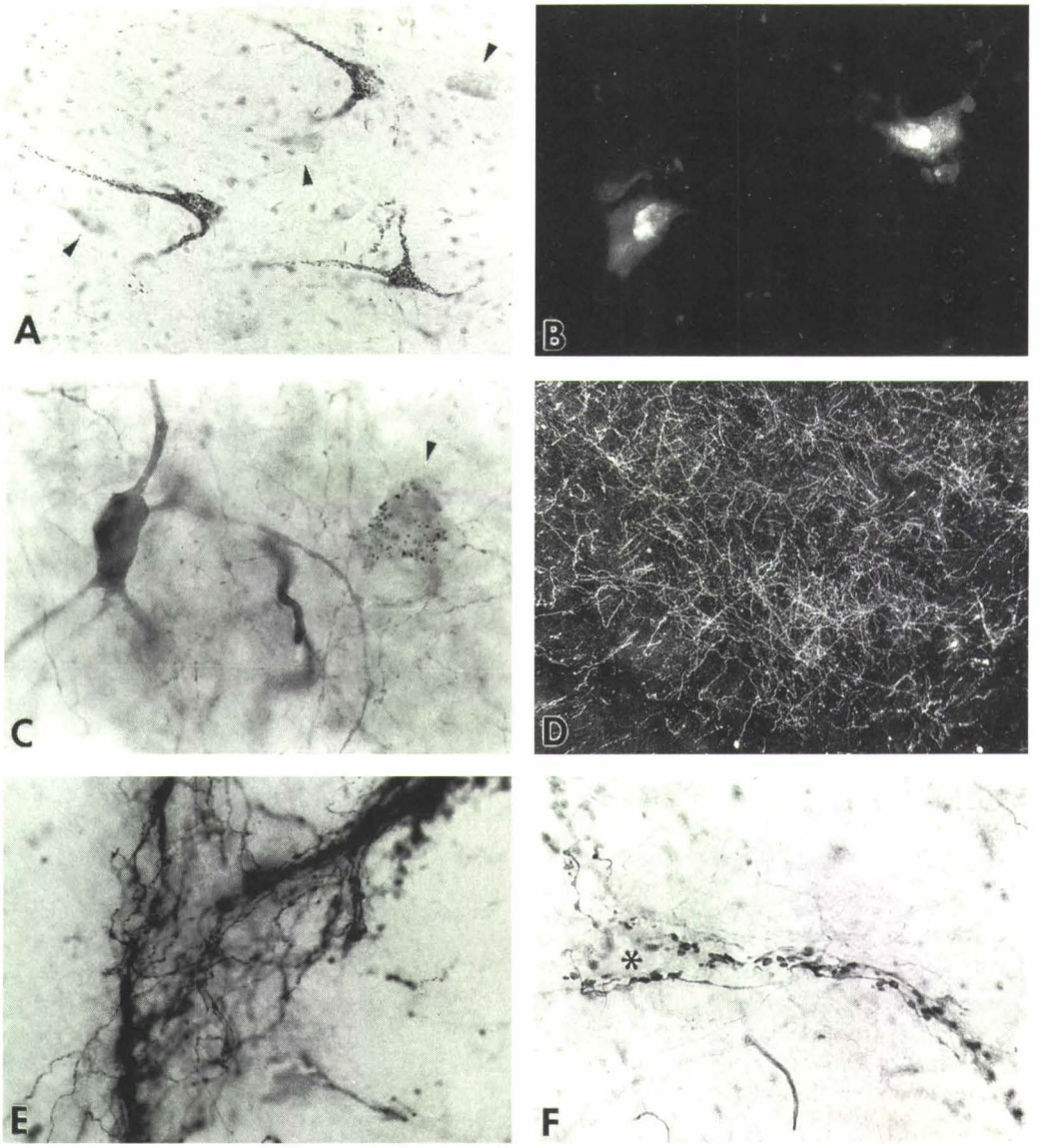


Figure 5.4. Examples of retrograde (**A-C**) and anterograde (**D-F**) neuronal labeling obtained with various tract-tracing methods in the squirrel monkey (*Saimiri sciureus*). **A.** Three brainstem neurons retrogradely labeled after injections of wheat germ agglutinin-horseradish peroxidase conjugate (WGA-HRP) into the thalamus. The *arrowheads* indicate unlabeled neurons that are visible because the section has been counterstained with neutral red (×300). **B.** Two double-labeled neurons occurring in the internal segment of the globus pallidus after injections of fast blue into the anterior portion of the thalamus and nuclear yellow into the upper region of the brainstem. These two retrograde tracers fluoresce at the same wavelength, but can be differentiated from each other by color and because they occupy different cellular compartments. Fast blue is sequestered within the cytoplasm and proximal dendrites and yields a rather weak blue fluorescence, whereas nuclear yellow is confined to the nucleus, which displays a very bright yellowish fluorescence when examined under dark-field illumination (×350). **C.** Immunocytochemical techniques can be easily combined with retrograde tracing methods as exemplified in this photomicrograph which shows a striatal neuron displaying immunoreactivity for the neuropeptide Y (NPY) adjacent to another striatal neuron (*arrowhead*) that is neuropeptide Y-negative but contains HRP granules following injection of WGA-HRP into the globus pallidus. This result indicates that striatal NPY-immunoreactive neurons do not project outside the striatum and thus should be considered as interneurons (×350). **D.** Dark-field photomicrograph showing a dense field of anterogradely labeled fibers in the anterior portion of the globus pallidus after microiontophoretic injections of the tracer *Phaseolus vulgaris*-leucoagglutinin (PHA-L) into the striatum (×200). **E.** Similar striatopallidal PHA-L-labeled fibers occur more caudally in the globus pallidus and closely surround dendrites of pallidal neurons. Note that many of these fibers display characteristic varicosities suggestive of terminal boutons (×400). **F.** Fibers anterogradely labeled with biocytin that was microiontophoretically delivered into the lateral segment of the globus pallidus. These markedly varicose fibers closely surround the cell body (*asterisk*) and proximal dendrite of a neurons of the reticular nucleus of the thalamus. (×400).



Figure 5.5. Pyramidal neuron of the hippocampal formation of the rat. This neuron has been electrophysiologically characterized by in vivo recording and then intracellularly injected with biocytin at the end of the electrophysiologic recording period. Note that only part of the profuse dendritic arborization of this neuron is visible in this plane of section. The axon (*arrowheads*) of this particular neuron could be followed as far as 4 mm from its point of origin. (×450).

A major disadvantage of this procedure, however, is that most fluorescent dyes fade rapidly and are not amenable to electron microscopic examination.

Histochemistry and Immunocytochemistry

In addition to the general morphology of neurons, it is important to be able to study the cellular localization of specific chemical substances. In recent years, a number of histochemical and immunocytochemical techniques have been developed to visualize neurotransmitters and neurosecretory products. In general, these methods are based upon formation of (a) a colored, insoluble precipitate (e.g., the histochemical method for the visualization of acetylcholinesterase), (b) a compound with characteristic fluorescence when excited by ultraviolet light (e.g., the histofluorescence procedure for the localization of biogenic amines), or (c) a complex with a labeled antibody (i.e., the immunocytochemical approach that allows cellular localization of neurotransmitters and related compounds).

The introduction in the early 1960s of the paraformaldehyde-induced fluorescence technique by Falck and Hillarp (50, 51) for the visualization of biogenic amines, particularly catecholamines and indolamines, kindled interest in the anatomic localization of other biochemically definable neurons or *chemospecific neuronal systems*. Since the early 1980s, the histochemical techniques have been largely superseded by the immunocytochemical approach, which allows a more sensitive and specific visualization of neurotransmitters and related substances. The widespread use of immunocytochemical techniques has given a strong impetus to a field of research that is often referred to as *chemical neuroanatomy*.

The immunocytochemical methods are based on the immunologic concept of antigen-antibody reaction which requires that the substance to be localized is antigenic. Small molecules, such as serotonin and dopamine, can be rendered antigenic by conjugating them to large immunogenic protein by aldehydes (Fig. 5.19). Incubation of a tis-sue section in an antibody-containing solution leads to the development of an immunochemical bound between the specific antibody and the antigen in its original *in vivo* location. In turn, the transmitter-specific antibody (primary antibody) can be visualized either directly or indirectly after incubation with a second antibody raised in a different species. The use of a proper marker facilitates the visualization of the immunologically bound antibody and antigen. The two markers that are most frequently used are fluorescein isothiocyanate (FITC) and horseradish peroxidase (HRP), the latter allowing visualization of the antigen-antibody labeled complex at the ultrastructural level. Another method uses antibodies linked to electron-dense gold particles. Antibodies that are currently available include those that were raised against (a) neuroactive peptides (e.g., substance P, somatostatin, enkephalin, neurotensin), (b) enzymes involved in the synthesis of neurotransmitters (e.g., tyrosine hydroxylase, dopamine-β-hydroxylase, glutamate decarboxylase), (c) neurotransmitter themselves (e.g., serotonin, dopamine, γ-aminobutyric acid or GABA, glutamate), and

(d) neurotransmitter receptors (e.g. cholinergic, dopaminergic, and serotoninergic receptors) (33).

Furthermore, it is now possible to identify histochemically neurons in which the gene for a particular neurotransmitter enzyme or peptide precursor is active by localizing the messenger ribonucleic acid (mRNA) that encodes the molecule. Most methods for detecting mRNA are based on the phenomenon of nucleic acid hybridization, which implies that single strands of a nucleic acid polymer will pair if the sequence of bases is complementary or homologous. This approach can be applied to the nervous tissue via a technique called *in situ hybridization*. This method uses radiolabeled copied deoxyribonucleic acid (cDNA) encoding the peptide of interest, which is applied to tissue sections under conditions suitable for hybridizing with endogenous mRNA. If the probes are radiolabeled, autoradiography reveals the location of neurons that contain the complex formed between the labeled cDNA and the homologous mRNA (Fig. 5.6) (26, 152). Quantitative methods (autoradiographic grain counting) can also be used to study the variations in the expression of a given peptide under specific experimental conditions. These very powerful techniques, which can be combined with retrograde fluorescent tract-tracing methods (28), allow a molecular biology approach to the study of the nervous tissue.

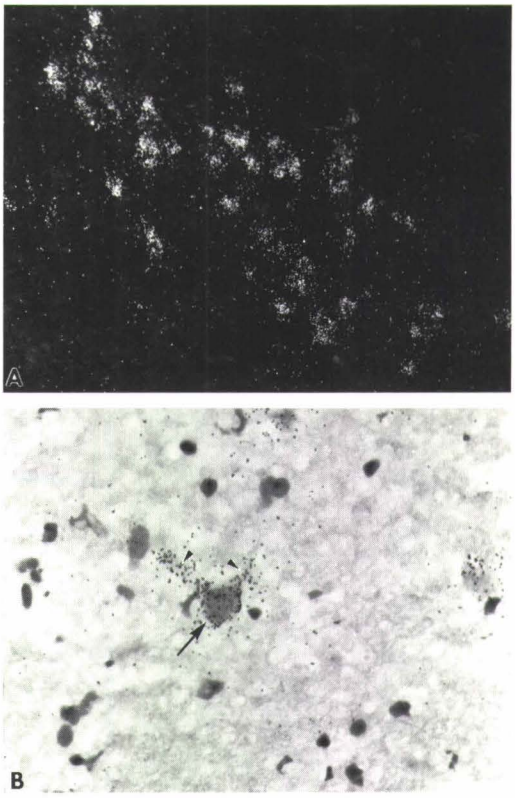


Figure 5.6. **A.** Dark-field photomicrograph of autoradiographically labeled neurons (clusters of silver grains) in the substantia nigra pars compacta of the rat. These dopaminergic neurons have been visualized with in situ hybridization using a molecular probe for tyrosine hydroxylase mRNA (×350). **B.** Bright-field photomicrograph of a neuron autoradiographically labeled in the substantia nigra pars compacta with a tyrosine hydroxylase riboprobe as in A. The cell body (*arrow*) and proximal dendrites (*arrowheads*) are covered by a high number of silver grains indicating a wide distribution of this mRNA in dopaminergic neurons (×550).

Receptor Localization

Receptors for various neurotransmitters can be visualized by autoradiography, immunocytochemistry, and *in situ* hybridization methods. Receptor autoradiography involves the identification of receptors in tissue sections with the use of pharmacologic binding techniques. Frozen sections are incubated with specific tritium-labeled ligands and apposed to sheets of x-ray sensitive film in the dark room. The x-ray films are exposed for the appropriate amount of time and developed. Densitometric measurements are made over regions of the autoradiographs, as well as the appropriate coexposed calibrated standards. The data are then expressed as binding site density per unit weight of tissue. Results obtained from receptor autoradiographic studies have complemented our knowledge of brain functional anatomy derived from tract-tracing, immunocytochemistry, and 2-deoxyglucose autoradiographic studies (65).

Recently, the molecular biology approach was used to isolate and clone several transmitter receptors, such as the dopaminergic receptors (186). Since the amino acid sequences of these proteins were deciphered, cDNA or cRNA probes and specific antibodies are available to study the distribution of these receptors with *in situ* hybridization and immunocytochemistry.

Metabolic Methods

Since there is a general correlation between glucose metabolism and functional activity of neurons, a method has been devel-

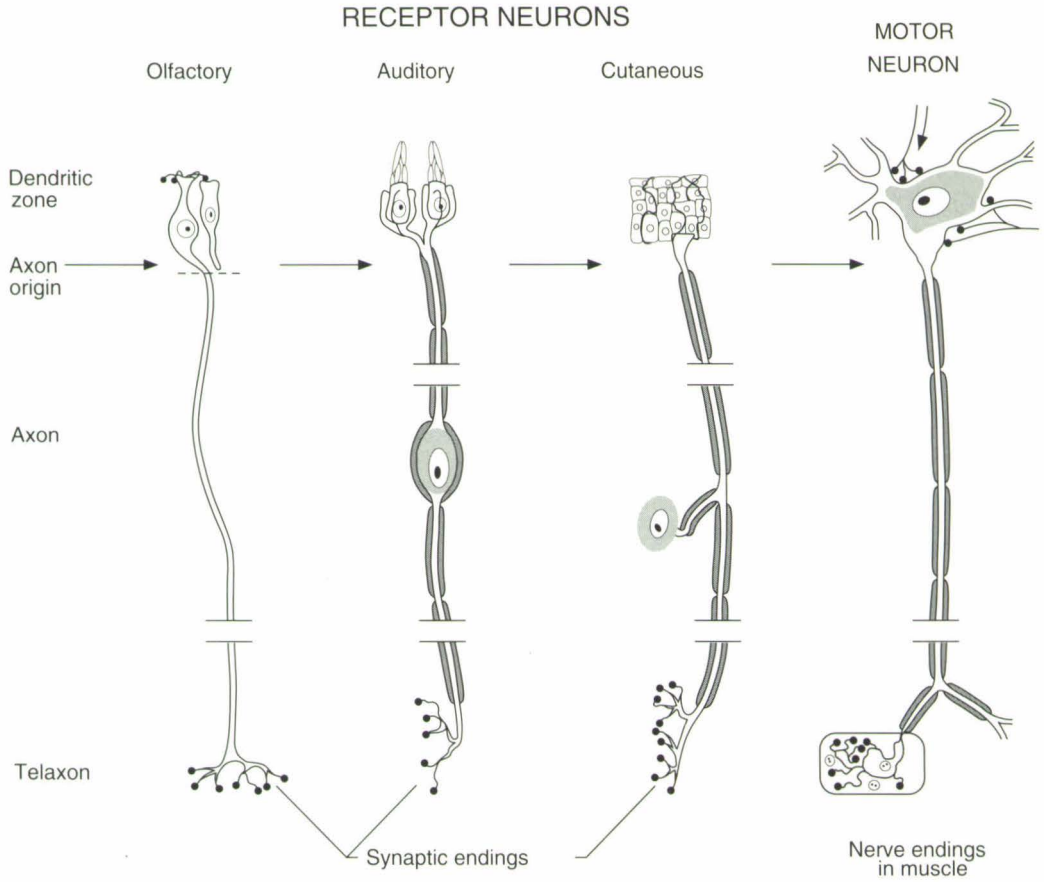


Figure 5.7. Three sensory neurons and a motor neuron based on the site of impulse origin rather than location of cell body. Dendritic zone is concerned with the generator potential in a receptor, as well as excitatory and inhibitory input of synaptic endings (dotted lines on motor neurons) on another nerve cell. The axon and its terminals are related to the conduction and synaptic transmission of the generated nerve impulse. The perikaryon of a neuron is the trophic center primarily concerned with the outgrowth and maintenance of processes, and their metabolic functions other than membrane activity. Note that the cell body may be located either in the dendritic zone or the region of the axon.

oped to study regional variations in energy metabolism based upon the autoradiographic analysis of [^{14}C] 2-deoxyglucose (2-DG) incorporation (181). This chemical compound is an analog of glucose which is transported from blood to neurons where it is taken up as if it was glucose and phosphorylated to 2-deoxyglucose-6-phosphate (2-DG-6P0_4). In contrast to glucose, however, 2-DG-6P0_4 is not metabolized further, and its accumulation in neurons is related to the rate of glucose utilization of the cell. The *2-deoxyglucose method* has proved useful in studying cellular and synaptic regions active following specific forms of sensory stimulation or during repetitive movements. However, in terms of anatomic localization, the 2-DG method has a relatively poor degree of resolution.

Another means of monitoring the neuronal activity is to visualize the expression of some early onset genes, such as the proto-oncogene c-*fos*, which acts as a nuclear transcription factor and is often considered as a "third messenger." This proto-oncogene and its protein product Fos can be activated in certain neuronal systems by various stimuli and under specific experimental conditions. For instance, dopaminergic agonists produce a rapid and transient increase in Fos protein levels in the striatum and cerebral cortex (157). Likewise, exposure of rodents to light or noxious stimuli can induce the expression of different early onset genes, including c-*fos*, in the cells of the different brain nuclei specifically concerned with the processing of visual and nociceptive information (55, 162). The levels of c-*fos* in the nuclei of neurons that are activated by various stimuli can be estimated by immunocytochemistry with antibodies raised against the Fos protein, or by *in situ*

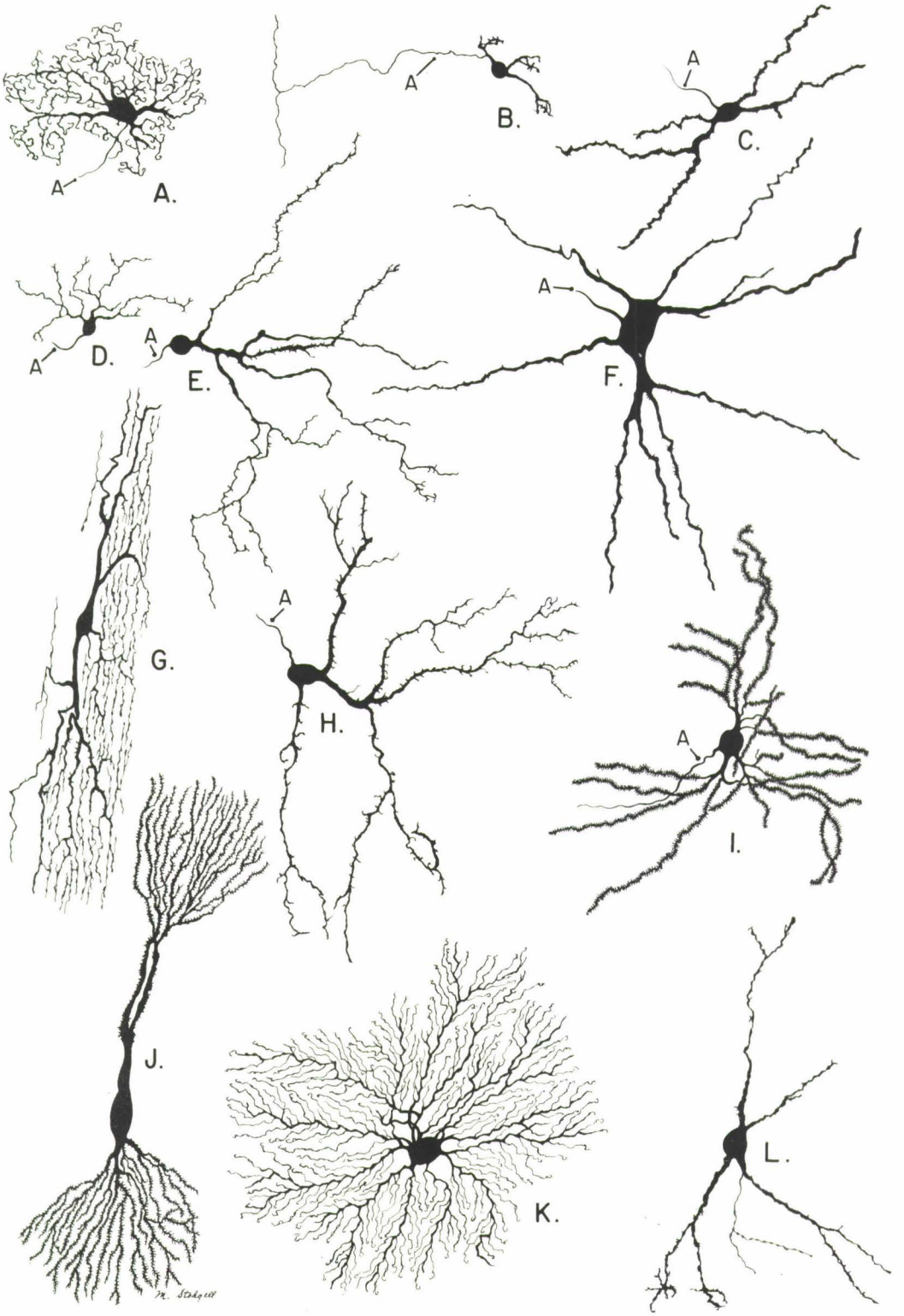


Figure 5.8. Characteristic neurons whose axons (*A*) and dendrites remain within the central nervous system. **A.** Neuron of inferior olivary nucleus. **B.** Granule cell of cerebellar cortex. **C.** Small cell of reticular formation. **D.** Small gelatinosa cell of the spinal trigeminal nucleus. **E.** Ovoid cell of nucleus tractus solitarius. **F.** Large cell of reticular formation. **G.** Spindle-shaped cell of substantia gelatinosa of spinal cord. **H.** Large cell of spinal trigeminal nucleus. **I.** Neuron of putamen. **J.** Double pyramidal cell in Ammon's horn of hippocampal formation. **K.** Cell from thalamic nucleus. **L.** Cell from globus pallidus. (Golgi preparations, macaque monkeys.)

hybridization with cRNA or cDNA probes for *c-fos*.

NEURONAL DIVERSITY

Functionally, neurons of the central nervous system can be grouped into three broad categories: afferent, motor, and interneurons. Afferent or sensory neurons convey information from the periphery to the central nervous system, whereas motor neurons send commands to muscles and glands. The remaining cells—the interneurons—are by far the most abundant signaling elements in the central nervous system. Their role is to either process the information locally or to convey the information from one region of the central nervous system to another (97). The first type of interneurons is variably termed *local interneurons*, internuncial *neurons, local circuit neurons*, or simply *interneurons*, and corresponds to the short axon type II neurons as defined by Golgi (70, 71). The second type of interneurons is termed either *relay, principal*, or *projection neurons* and correspond to the long axon Golgi type I neurons. In most regions of the central nervous system, the Golgi type II neurons greatly outnumber the Golgi type I neurons.

Neurons belonging to each of these three categories display a wide variation in size and an infinite variety in the arrangement of their processes. However, nerve cells serving a similar function or located in a given region of the nervous system often resemble each other structurally (Figs. 5.2, 5.8, and 5.10). Thus, *bipolar neurons* are sensory in function and transmit impulses generated by olfactory, visual, vestibular, and auditory receptor endings (Fig. 5.10**A**). The T-shaped *unipolar neurons* are characteristic of the spinal ganglia and mesencephalic nucleus of the trigeminal nerve (N. V) (Figs. 5.2**A** and 5.10**B-D**). These cells are occasionally referred to as *pseudo-*

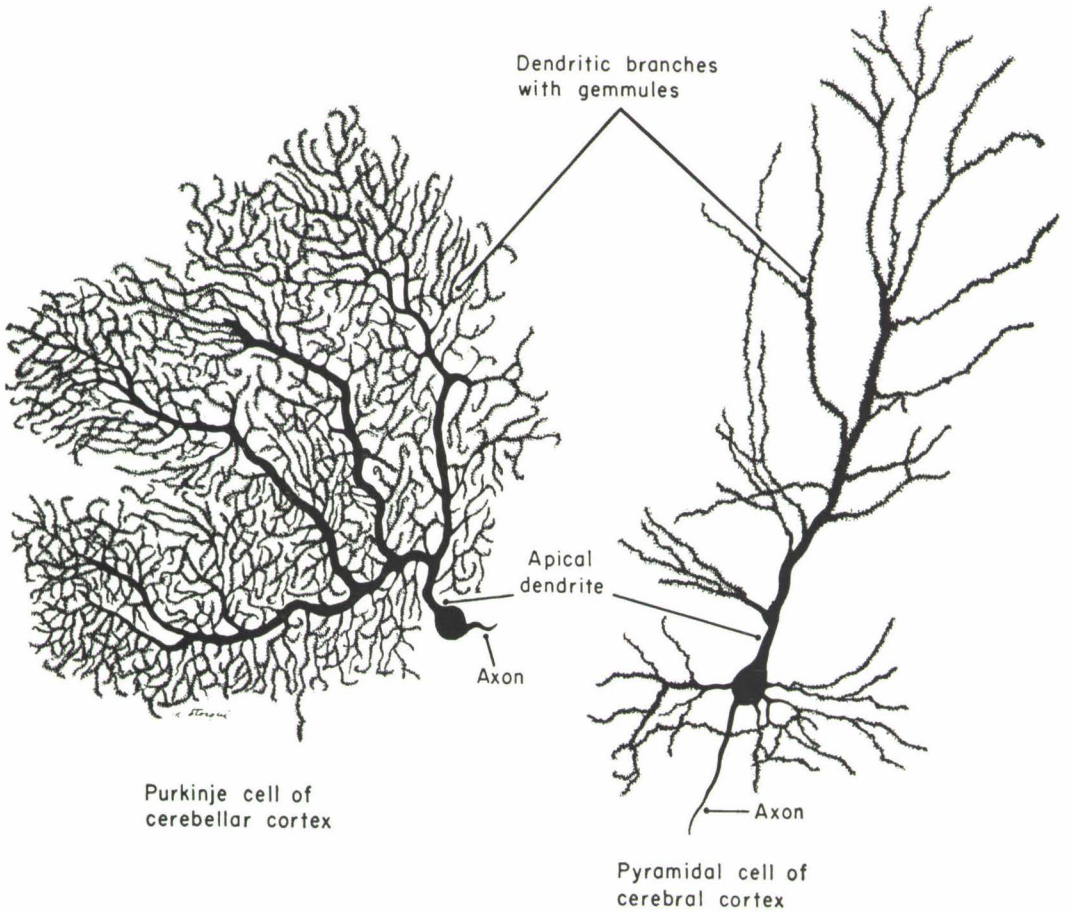


Figure 5.9. Two principal cell types in cerebellar and cerebral cortex. Dendritic branches provide extensive area for synaptic terminals of many cortical and subcortical neurons (Golgi preparations, macaque monkeys.)

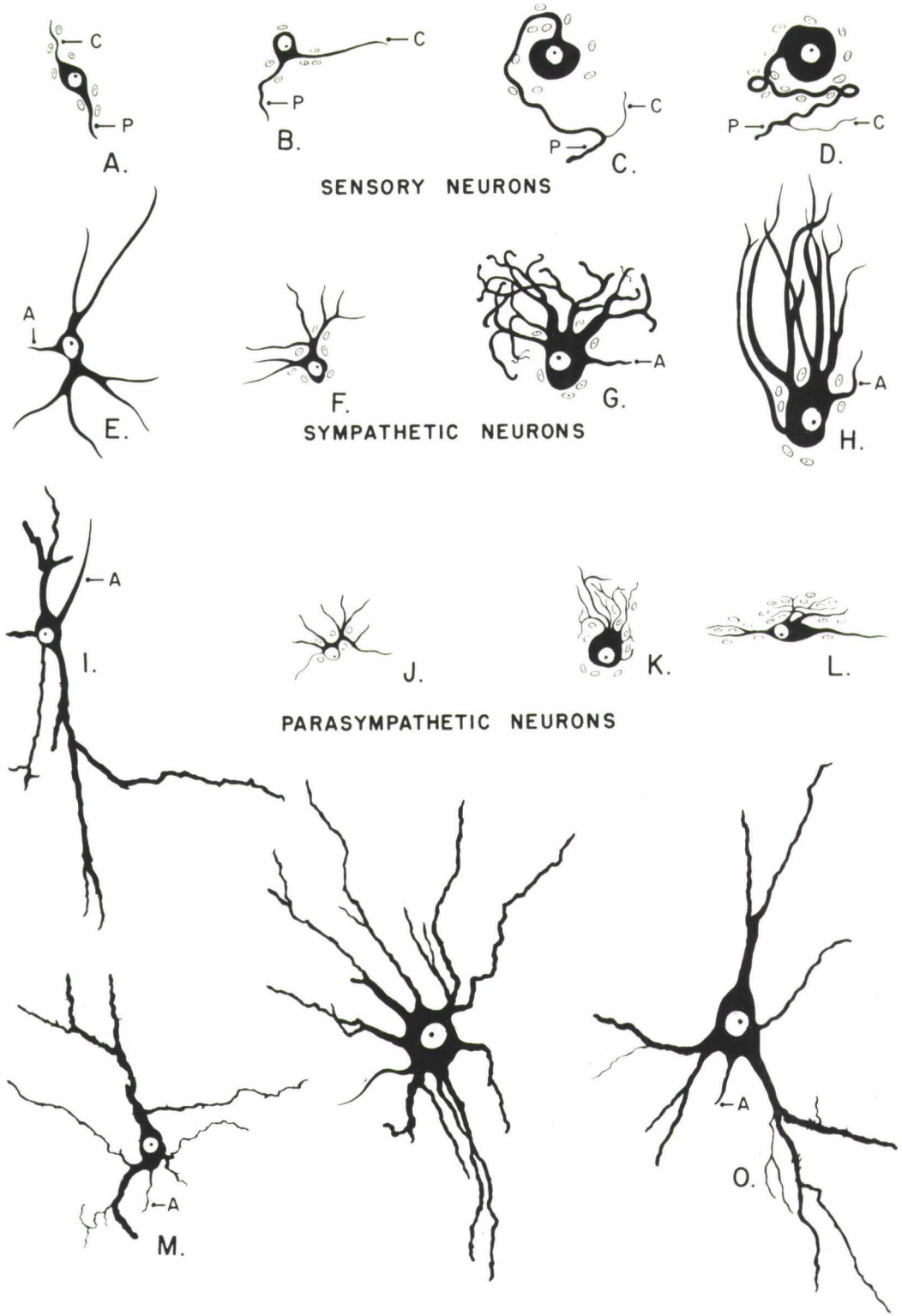


Figure 5.10. Representative neurons whose axons (*A*) are distributed in the peripheral nervous system of humans. Capsular nuclei are shown around all ganglion cells. The central (*C*) and peripheral (*P*) processes of the sensory neurons are identified. **A.** Bipolar neuron of nodose ganglion (newborn). **B.** Pseudo-unipolar neurons of nodose ganglion (newborn). **C.** Unipolar neuron of dorsal root ganglion (newborn). **D.** Unipolar neuron of trigeminal ganglion (newborn). **E.** Multipolar neuron of intermediolateral nucleus of spinal cord. **F.** Neuron of superior cervical ganglion (newborn). **G** and **H.** Stellate ganglion neurons. **I.** Neuron of dorsal motor nucleus of vagus nerve. **J.** Ciliary ganglion neuron (newborn). **K.** Intracardiac ganglion neuron. **L.** Myenteric ganglion neuron. **M.** Nucleus ambiguus neuron. **N.** Neuron of hypoglossal motor nucleus. **O.** Anterior horn cell.

unipolar because they develop from bipolar neurons, in which the initial portion of the two processes approximate and eventually fuse. Such sensory neurons convey nerve impulses from a variety of specialized and nonspecialized receptors. *Multipolar neurons* transmit both sensory and motor nerve impulses, and are characteristic of the brain, spinal cord, and peripheral autonomic nervous system (Figs. 5.2**B-F**, 5.8, and 5.10). The primary, secondary, and tertiary dendritic branches of some multipolar neurons may be elaborate and enormously increase its synaptic surface (Figs. 5.8 and 5.9). A Purkinje cell of the cerebellar cortex serves as an illustrative example.

The dendrites of Purkinje cells are wide at the base, and taper rapidly. The primary, secondary, and tertiary branches have a smooth surface, while the more distal dendritic branches are studded with thornlike processes called *dendritic spines* or *gemmules* (Fig. 5.9). The length of the spiny dendritic branches of a single Purkinje cell was estimated to be 40,700 μm, whereas these dendritic branchlets with their 61,000 spines have a combined synaptic surface area of 222,000 μm^2 (57). These estimates of the spiny branchlets are now believed to be too conservative, and probably should be doubled (58). This extremely large receptive field is known to receive approximately 150,000 synaptic contacts.

Arborizations of neurons in other parts of the central nervous system are less extensive, yet they reveal a characteristic pattern of branching. For example, nerve cells of the inferior olivary nuclear complex in the medulla (Fig. 5.8**A**) have radiating dendrites with curly branches, whereas neurons of the thalamus (Fig. 5.8**K**) have long radiating dendrites with numerous branches. The cells of the *substantia gelatinosa* of the spinal cord, best seen in stained longitudinal sections, demonstrate only a few large dendrites that issue chiefly from one side of the cell (Fig. 5.8**G**). Smaller branches of these dendrites form a compact zone of fine parallel fibers.

It is instructive to compare the profuse dendritic branches of the central sensory and integrating neurons (Fig. 5.8**A**, **B**, **D**, **E**, and **G-K**) with the robust dendrites of motor neurons (Figs. 5.8**C**, **F**, **L**, and 5.10**M-O**). This comparison is even more striking if one contrasts the two principal cell types of the cerebellar and cerebral cortex—the Purkinje and the pyramidal cell (Fig. 5.9). The brushlike spread of dendrites of the Purkinje cell is similar to that of other central integrating neurons (Fig. 5.8**A** and **I-K**), yet each has individual characteristics. The large pyramidal cell (Fig. 5.9) also has an extensive dendritic spread and tiny dendritic spines. However, its basic structure more closely resembles that of a motor neuron (Figs. 5.8**F** and **L**, and 5.10**I** and **M-O**). Successful Golgi preparations permit following the processes of a neuron for considerable distances. Studies using this method provide clearer concepts of neuron structure, dendritic ramification, and axonal distribution (167).

The somatic and visceral neurons of the central and peripheral nervous systems of humans can be compared in Figure 5.10. The peripheral processes and axons of such neurons form the peripheral, cranial, and spinal nerves. Nerve cells of the sensory and autonomic ganglia are surrounded by a thin, nucleated capsule.

Although nerve cells in most regions of the central nervous system do not undergo mitotic division after birth, they probably increase in size as their axons and dendrites grow in length. The length of some nerve axons is quite remarkable. Giant pyramidal cells of the cerebral cortex may send axons to the caudal tip of the spinal cord, that is from the top of the head to the lumbar region of the spinal cord (Fig. 11.13). Axons of motor neurons in the spinal cord may extend the length of the lower extremity to terminate in muscle fibers of the toes. A sensory unipolar neuron situated in the first sacral spinal ganglion may send a peripheral fiber to one of the toes, while its central fiber may ascend the length of the spinal cord and terminate in the medulla (Fig. 11.1). The total length of such a neuron would be from the toe to the nape of the neck. The size of the cell body fluctuates within wide limits, from a diameter of 4 μm in the smallest granule cells of the cerebellum (Fig. 5.8**B**) and cerebral cortex to well over 100 μm in the largest motor cells of the spinal cord. In general, the size of the cell body is proportional to the length, thickness, richness of branchings, and terminal arborizations of its dendrites and axon.

NEURONAL CYTOSKELETON

The shape of the neuron is generated and maintained largely by a multitude of fibril-

lary proteins that form complex and dynamic networks extending throughout the neuronal cytoplasm. These long polypeptide chains undergo profound changes during aging in certain neurodegenerative disorders, such as in Alzheimer's and Parkinson's diseases. These major constituents of the neuronal cytoskeleton differ from one another by their thickness and molecular composition. They can be grouped into three broad categories: microtubules, neurofilaments, and microfilaments, together with their associated proteins (171).

Microtubules

These are the thickest cytoskeletal fibrillary components with an outer diameter of 25.28 nm. They consist of a ring of 13 protofilaments with a clear lumen, which has a rod-like structure in its center (150). Each protofilament is formed by the polymerization of α- and β-tubulin dimers (molecular weight 100,000), which are encoded by a multigene family comprising at least six genes. Microtubules have an inherent polarity because their tubulin subunits are arranged in a specific orientation in the polymer. Their two ends differ and grow at different rates. In the axon, microtubules are oriented longitudinally with polarity always in the same direction, an arrangement that appears important for the directional specificity of the two forms of fast axonal transport. All microtubules in axons are oriented with their (+) ends (fast growing ends) away from the cell body, whereas in dendrites comparable numbers are found with the (+) ends and the (−) ends distally oriented. Recent evidence indicates that the orientation of microtubule polarity may play a crucial role in the differential routing of organelles in dendrites and axons (13). For instance, the microtubule polarization could explain why ribosomes and Golgi elements are present in dendrites, but are absent from axons. In the axoplasm of peripheral and central nerves, one usually can see microtubules, as well as strands of canaliculi, vesicles of endoplasmic reticulum, and a few ribosomes (Fig. 5.23).

Microtubules are highly labile molecules that are sensitive to specific antimitotic drugs, such as colchicine. Colchicine, an alkaloid extracted from the meadow saffron, is used in experimental animals to increase the level of certain neuroactive peptides in the cell body to facilitate their visualization. Each molecule of colchicine binds tightly to one tubulin molecule and thus prevents its polymerization. By disturbing the complex dynamics of microtubules assembly, colchicine blocks the axonal transport and causes an accumulation in the cell body of neurotransmitters and other molecules that are normally conveyed to the distal ends of the axon through axonal flow.

Two major classes of microtubule-associated proteins (MAPs) have been isolated from the brain: high-molecular-weight proteins (*HMW proteins*), which have molecular weights of 200,000–300,000 or more, and *tau proteins*, with molecular weights of 40,000–60,000 (3). High-molecular-weight MAPs, particularly MAP-2, abound in cell bodies and dendrites, whereas *tau* proteins and MAP-3 tend to be segregated in the axon. Thus, certain MAPs can specifically label axons and dendrites, and such molecular markers are very useful in differentiating axonal from dendritic profiles in developing neurons, both *in vitro* and *in vivo*. MAPs regulate the stability of microtubules and promote their oriented polymerization or assembly. *Tau* binds to several tubulin molecules simultaneously, enhancing their polymerization. Other MAPs also enhance microtubule polymerization, but differ in being composed of two domains, one that binds to the microtubules and another that extends outward and is likely to be involved in cross-linking microtubules to other cellular components. Furthermore, MAP-2 and *tau* can serve as substrates for both the cAMP-dependent and the Ca^{2+}/calmodulin-dependent protein kinases. Phosphorylation of MAPs decreases their ability to promote assembly and produces depolarization of the microtubules. Such a phenomenon is greatly exacerbated in aging neurons and in neurons involved in degenerative processes.

Neurofilaments

These are the most abundant fibrillary components in the axon, being three to ten times more numerous than microtubules. The neurofilaments are about 10 nm in diameter and represent the bones of the cytoskeleton (Fig. 5.40). The neurofilaments observed in electron microscopy become aggregated during some types of fixation and form the *neurofibrils*, which were observed with the light microscope for the first time by the German

neurologist Robert Remak in the midst of the 19th century (Fig. 5.16). These neurofibrils are the neuronal elements that retain silver nitrate used in Golgi stains. They are built with fibers that twist around each other to produce complex coiled structures of increasing thickness (10). Neurofilaments are biochemically related to the intermediate filaments of other cells, all of which belong to a family of proteins termed *cytokeratins*, which includes vimentin, glial fibrillary acidic protein, desmin, and keratin (3, 172). In contrast to microtubules, neurofilaments are rather stable and remain totally polymerized in the cell. Neurofilaments are among the most phosphorylated neuronal proteins, and this phosphorylation has direct implications for neurofilament function in normal neurons and disease states characterized by neurofibrillary pathology. For instance, in Alzheimer's disease and in other neurodegenerative disorders, these fibrillary proteins are modified and form the so-called *neurofibrillary tangles* (104).

Microfilaments

Microfilaments are the thinnest of all fibrillary components of the cytoskeleton, with a diameter of 3–5 nm. They are composed of two strands of polymerized globular (G) *actin* monomers arranged in a helix. Actins, a major constituent of all cells, are encoded by a gene family that includes, in addition to the α-actin of skeletal muscles, at least two other forms (β and γ). Neural actin is a mixture of β and γ species, which differs from α-actin at only a few amino acid residues. Microfilaments are attached to the plasma membrane by several associated proteins linked to actin (spectrin, ankyrin, vinculin, and talin), although the major anchoring protein in neurons as in other cells is *fondrin* or neural spectrin (3, 171)

Dynamics of Polymerization

It is important to realize that, in contrast to the bones that form the body skeleton, the various elements of the neuronal cytoskeleton vary constantly in size and are in a state of continuous flux in the neurons. Three major processes of polymerization are recognized: self-assembly, treadmilling, and dynamic instability. *Self-assembly* is the simplest way all fibrillary proteins polymerize. It depends on an equilibrium between the concentration of monomers and polymers, the latter being more stable than free monomers. *Treadmilling* is a process of directional polymerization that requires the energy of a nucleotide triphosphate to occur. This process can induce the rapid growth or disappearance of microtubules, and thus can play a crucial role in the growth and extension of neurites during development. *Dynamic instability* is another complex energy-dependent process whereby microtubules can abruptly change their length. In this case, any microtubule that happens to encounter a structure that caps its free (+) end will be selectively stabilized, while other microtubules will depolarize (3, 20, 171). This dynamic instability of microtubules is said to provide an organizing principle for neuronal morphogenesis. In fact, dynamic instability plays a crucial role in the constant remodeling of cytoskeleton architecture, which is necessary for axonal growth and guidance, signal transduction, and many other fundamental aspects of neuronal function.

NERVE CELL BODY

The nerve cell body or soma consists of a nucleus surrounded by a mass of cytoplasm whose surface layer forms a delicate plasma membrane. It is the trophic center of the neuron, and the function and survival of the axon and dendrites, which constitute more than 90% of the total volume of the neuron, are dependent on the integrity of the cell body. This was first appreciated by the English physiologist Augustus Waller who, in 1861, referred to the cell body of the neuron as "a centre of nutritive energy." The soma of the neuron appears as a fine structure in stained sections when viewed with the light microscope (Figs. 5.2 and 5.11). When observed with the electron microscope, the plasma membrane, or plasmalemma (Fig. 5.13), has a three-layered appearance similar to that of most tissue cells. It delimits sharply the cytoplasm of the neuron (neuroplasm) from adjacent processes of other nerve cells and from neuroglial and connective tissue cells and fibers. The composition of the neuronal cell membrane is of particular importance because of its role in the initiation and propagation of action potentials. The plasma membrane is formed by two layers of phospholipid molecules whose hydrophobic hydrocarbon chains are all directed toward the middle. Numerous protein

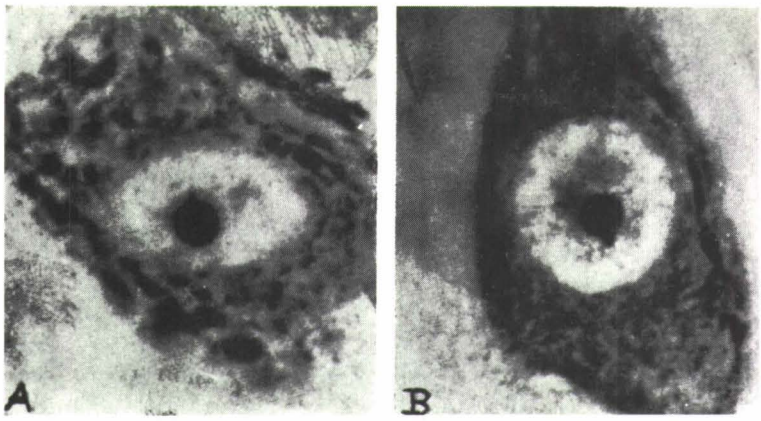


Figure 5.11. **A.** Nucleolar satellite in motor cell of spinal cord. **B.** Betz cell of motor cortex (female cat, cresyl violet, ×1200).

molecules are embedded in this structure and some of them extend throughout the entire width of the membrane providing hydrophilic channels through which inorganic ions may enter and leave the cell. Other proteins have side chains bearing carbohydrate groups that form, on the external surface, the outermost layer of the cell membrane known as the glycocalyx or cell coat. Action potentials are propagated through ionic changes that occur along the cell membrane of the neuronal surface.

The cytoplasm of a neuron in a routinely stained section appears basophilic and has a large, pale nucleus with a prominent nucleolus. After appropriate staining procedures, one also can demonstrate, within the cytoplasm of nerve cells, neurofibrils, chromophilic substance (Nissl bodies), Golgi apparatus, mitochondria, at times a central body, and various inclusions such as pigment and lipids (Fig. 5.12). Neurofibrils are characteristic of nerve cells, whereas the other cytoplasmic constituents are observed in other tissue cells. The cytoplasm extends throughout the confines of the cell and all of its processes and, in the axon, is often called axoplasm. As observed by light microscopy, the cytoplasm appears open and somewhat dispersed, whereas it has a compact and crowded appearance in electron micrographs (Fig. 5.13). Many of the neuronal structures seen by light microscopy require specific stains (e.g., neurofibrils, mitochondria, Golgi apparatus, Nissl bodies, and lipids), while most of these constituents are visualized simultaneously with the electron microscope.

Nucleus

This spherical structure has a diameter that varies from 3–18 μm. It is usually centrally located and its size is generally proportional to the size of the neuron (Fig. 5.10). Because mature neurons cannot divide, the chromosomes are not arranged in compact structures. Instead, small aggregates of deoxyribonucleic acid (DNA) are scattered in a somewhat homogeneous nucleoplasm and account for the pale appearance of the nucleus, even when viewed in the electron microscope (Figs. 5.2 and 5.13). Usually, one deeply staining nucleolus occupies a prominent position in the nucleus. The nuclear membrane seen with the light microscope appears sharp and continuous, while electron micrographs reveal it as a double-layered membrane, periodically interrupted by nuclear pores (Fig. 5.13) through which nucleic acid materials can migrate. The two leaflets of the nuclear membrane are continuous only at the margin of the nuclear pores; the outer leaflet is continuous with the highly folded membranes of the endoplasmic reticulum. The nuclear pores have a diameter of 65 nm and are arranged in rows with a center-to-center spacing of approximately 150 nm. The nuclei of Purkinje cells have a nuclear membrane that is wrinkled or puckered on the side facing the origin of the dendritic tree (144). This irregular depression in the nucleus, stuffed with granular or rough endoplasmic reticulum (Fig. 5.14), has been called the nuclear cap region. This region appears to contain more nuclear pores than the smooth

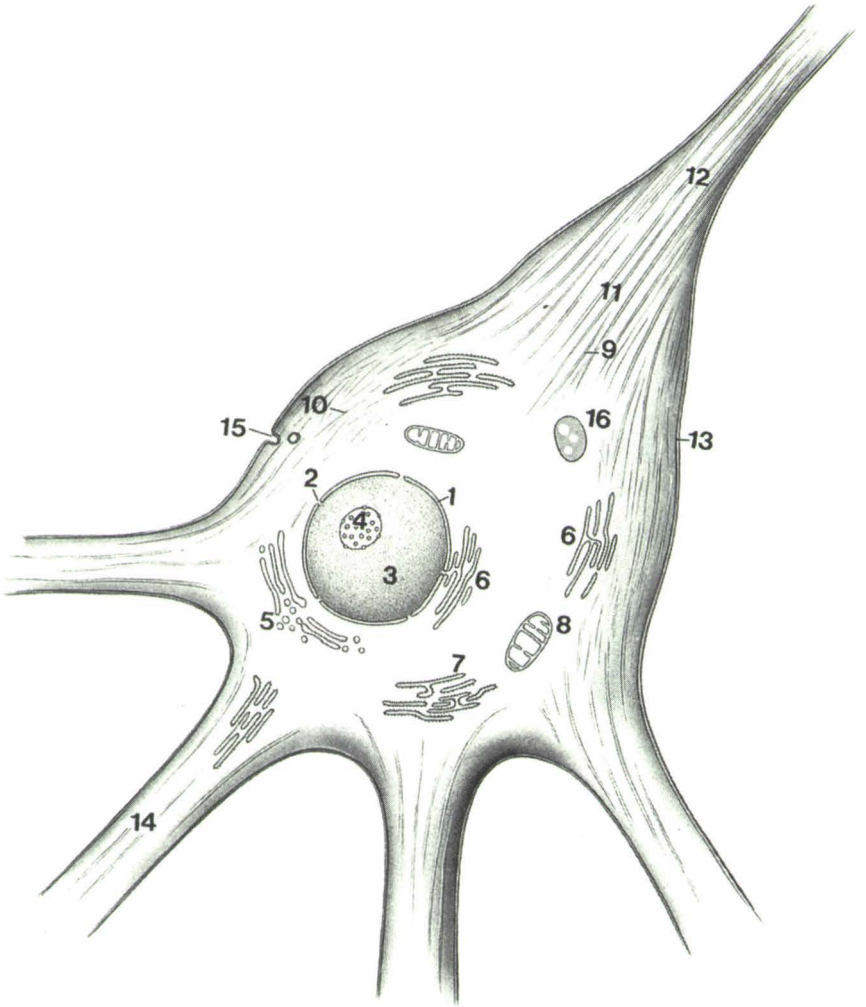


Figure 5.12. Neuronal cell body showing major organelles as seen in electron micrographs. (*1*) Nuclear membrane, (*2*) pores in nuclear membrane, (*3*) interior of nucleus, (*4*) nucleolus, (*5*) Golgi apparatus, (*6*) smooth endoplasmic reticulum, (*7*) granular or rough endoplasmic reticulum, (*8*) mitochondrion, (*9*) microtubules, (*10*) neurofilaments, (*11*) axon hillock, (*12*) initial segment of axon, (*13*) soma (perikaryon) of cell, (*14*) dendrites, (*15*) pinocytotic vesicles, (*16*) lipofuscin granule.

portions of the nuclear membrane. For a more detailed description of nuclear ultrastructure, the student is referred to the studies of Palay and Chan-Palay (144) and Peters, et al. (150).

Nucleolus

This basophilic structure contains a large amount of RNA, as well as a diffuse coating of DNA. It also includes a specific portion of DNA encoding the RNA of future ribosomes (rRNA), which are complex cytoplasmic particles that serve as templates for protein synthesis. The nucleolus stains more intensely than the rest of the nucleus with basic dyes because it contains many repetitive sequences of DNA and RNA that display a more compact organization than the rest of the chromosomes, which remain in a dormant or uncoiled state for most of the life of the neuron. It is known to have positive histochemical reactions for several enzyme systems associated with respiration, energy production, and the synthesizing functions of the cell. It is particularly related to the production of nucleic acid and protein in nerve cells. In most electron micrographs, the nucleolus shows no limiting membrane and the structure has a dense granular appearance. A "nucleolar satellite" 1 μm or less in diameter may be found closely apposed to the nucleus in nerve

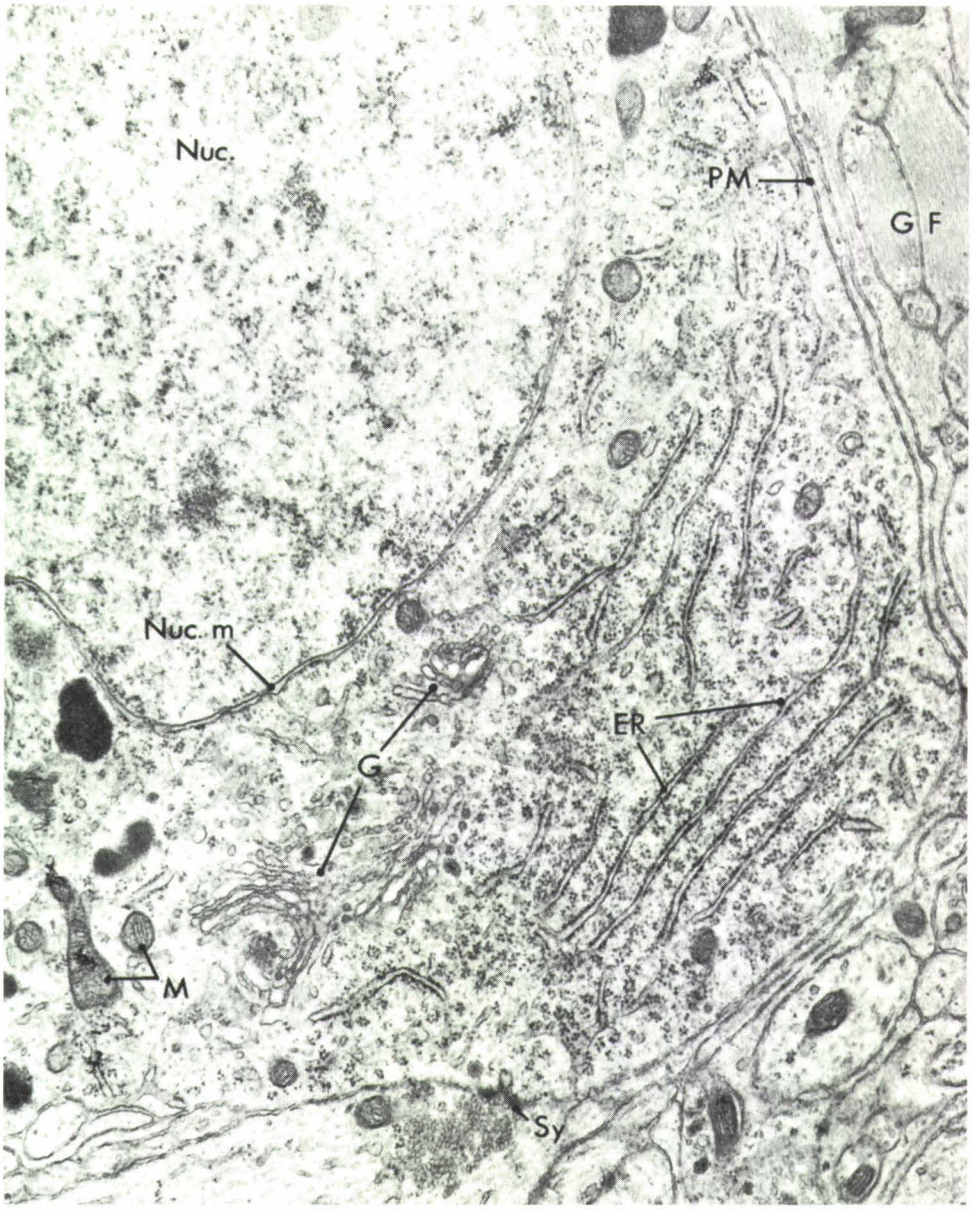


Figure 5.13. Part of a neuron in the posterior gray column (cat). The plasma membrane (*PM*) separates cytoplasmic structures from glial fibers (*GF*) and a synapse (*sy*) which are identified in the adjacent neuropil. Part of the pale nucleus (*Nuc.*) and the nuclear membrane (*Nuc. m*) appear to the *upper left*. The cytoplasm demonstrates pouches and vesicles of the Golgi complex (*G*), mitochondria (*M*), and an array of individual ribonucleoprotein particles. Some appear as clumps or rosettes (polysomes), while some ribosomes are attached to the outer surface membranes. The parallel stacks of cisternae of the granular or rough endoplasmic reticulum (*ER*) are characteristic of Nissl bodies (×75,000).

cells from female specimens (sex chromatin) (7) as shown in Figure 5.11.

Chromophilic Substance

There are two main types of nucleic acid in the cell: (a) ribonucleic acid (RNA: the sugar of the nucleotide is a ribose-pentose), and (b) deoxyribonucleic acid (DNA: the sugar is a deoxyribose-deoxypentose). Cytochemical methods indicate that nucleoproteins of the deoxyribose type are found chiefly in the chromatin, which forms the spireme and chromosomes in mitosis and, during the intermitotic period, is partly represented by chromatin bodies known as karyosomes. De-

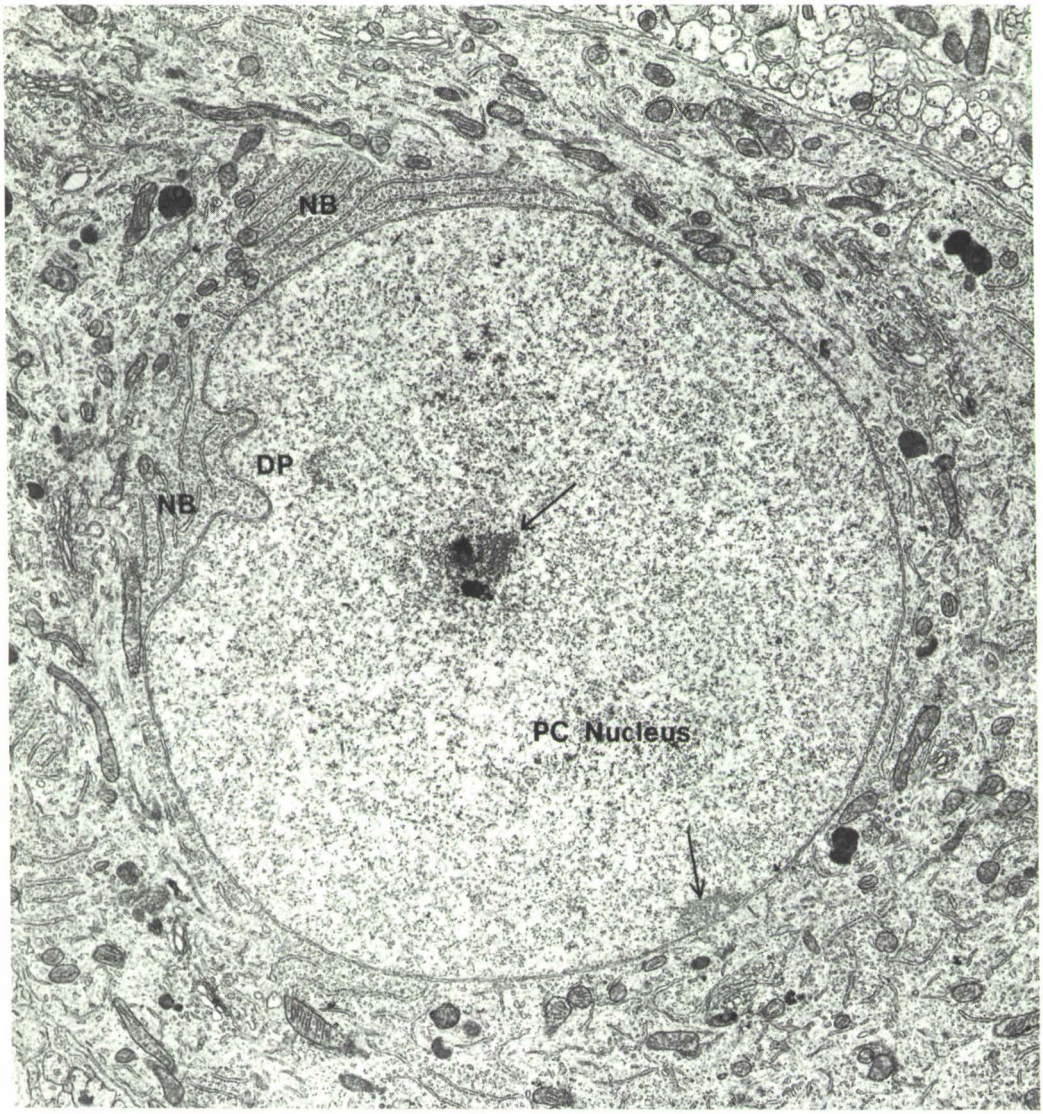


Figure 5.14. Purkinje cell nucleus in the rat. The nuclear chromatin is thinly and uniformly distributed throughout the nucleus, except for two sites indicated by *arrows*. The dendritic pole (*DP*) of the nucleus is wrinkled and capped by a small Nissl body (*NB*) (×14,000).

oxyribonucleic acid is also found in the nucleolar satellite and in small quantities within the mitochondria (Fig. 5.12). Conversely, the true nucleolus is, as a rule, a dense, spherical, optically homogeneous body that is rich in ribonucleic acid. Similar ribonucleoproteins are found in the cytoplasm, and there is good evidence for the assumption that the nucleolus plays an important part in cytoplasmic protein synthesis.

In preparations stained with basic aniline dyes (e.g., cresyl violet, toluidine blue, thioneine), the *chromophilic substance* appears in the form of deeply staining granules or clumps of granules known as *Nissl (tigroid) bodies*, after the German neuropathologist Franz Nissl (Fig. 5.2E). These staining procedures are often called *Nissl stains*. The Nissl bodies are found in the cell bodies and dendrites of all large, and many of the smaller, cells, but are absent in the axon and in the axon hillock from which that process arises. They are most abundant and sharply defined in the larger cells, whose clear vesicular nucleus contains practically no basichromatin (Figs. 5.2 and 5.11). The Nissl bodies are larger in motor than in sensory cells. Attempts have been made to distinguish the

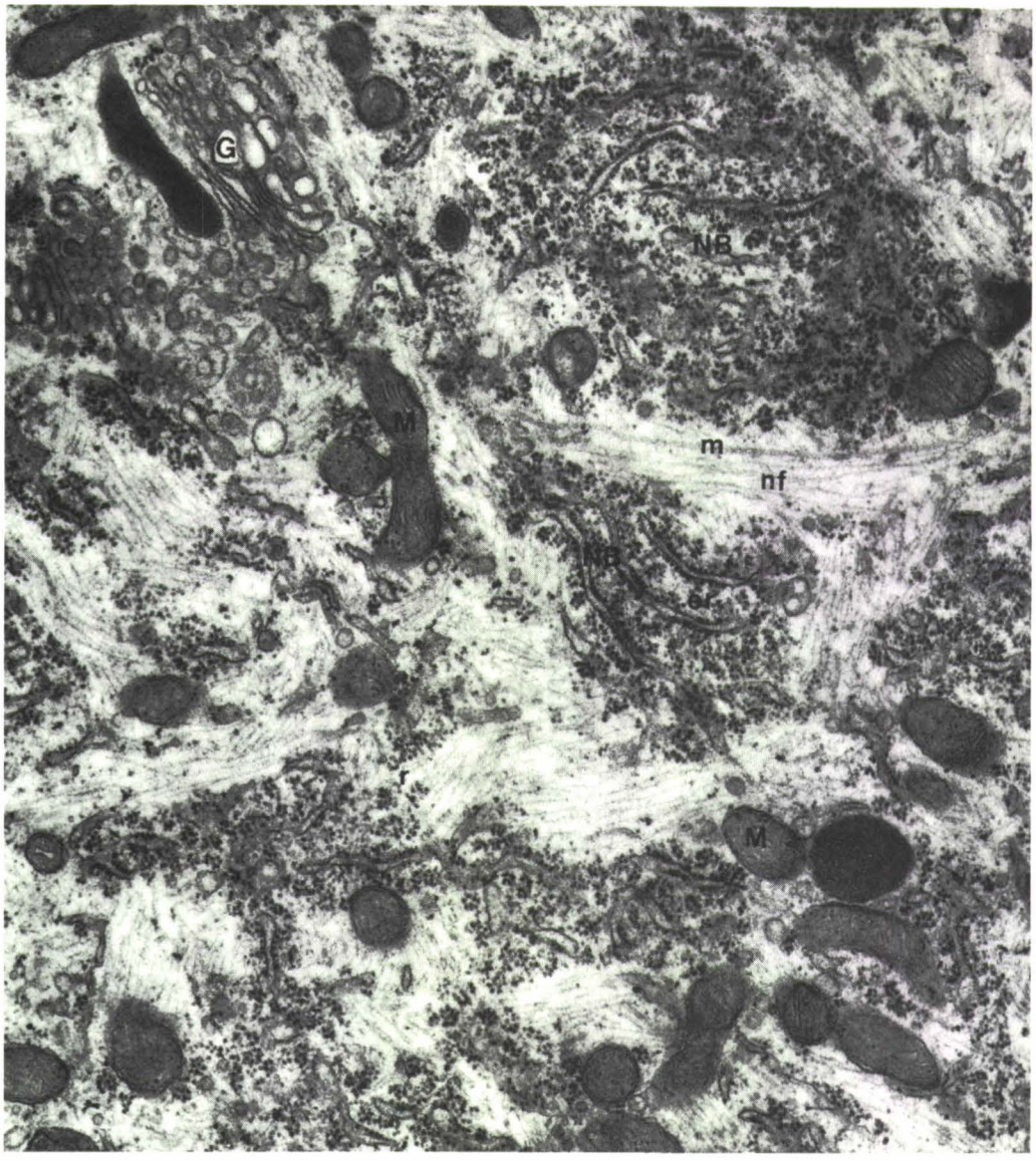


Figure 5.15. Cytoplasm of a dorsal root ganglion cell. The cytoplasm contains well-defined Nissl bodies (*NB*) separated by spaces containing microtubules (*m*) and neurofilaments (*nf*). Some ribosomes in the Nissl bodies are arranged in rows attached to the outer surfaces of cisternae of the granular or rough endoplasmic reticulum (*er*), while others lie free (*r*) in the cytoplasmic matrix. Free ribosomes appear in rosettes of six or more members (polysomes). *G* in the *upper left* indicates part of the Golgi apparatus (×46,000).

many neuron types by the size, shape, distribution, and staining capacity of the chromophilic granules.

The electron microscopic study of Palay and Palade (145) identified Nissl bodies as masses of granular or rough endoplasmic reticulum (RER). Clusters of punctate RNA granules 10–30 nm in diameter, called ribosomes, were oriented upon and between the cisterns, tubules, and vesicles to form a series of flattened, anastomosing, parallel-arranged sheets or membranes (Figs. 5.13 and 5.15). Dispersed free ribosomes also can be observed within the neuron cytoplasm. Free and membrane bound ribosomes are loci for active protein synthesis (Fig. 5.12). Neurons, like most cells, produce proteins which are used within the cell for both structural and metabolic purposes. A number of brain-specific proteins have been isolated biochemically, purified, and their cellular localization studied by immunocytochemical techniques

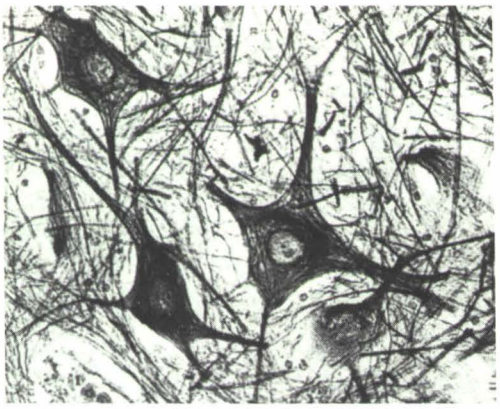


Figure 5.16. Large motor neurons from infant spinal cord showing neurofibrillary structures. Portions of dendrites and axons of other neurons fill the field (Ramón y Cajal silver method).

(119). Additionally, most neurons synthesize neuroactive peptide or transmitters which are secreted at the axon terminal. Following section of the axon, alterations in the discrete structure of the Nissl bodies can be demonstrated when stained by basic dyes and viewed with light microscopy (Fig. 5.2**E**). Nissl bodies in the cytoplasm about the nucleus appear dispersed or dissolved, a phenomenon termed *chromatolysis* (see section on retrograde degeneration).

Mitochondria

Granular or filamentous mitochondria are scattered throughout the entire cell body, dendrites, and axon (Figs. 5.13, 5.17, and 5.27). These organelles occur even in the smallest ramifications and terminals of the neuron and are prominent electron microscopic features wherever intense metabolic activity occurs, such as at synapses and at sensory and motor endings (145). These widely distributed cytoplasmic organelles are involved in glycolysis, biosynthesis, and cell respiration, but their most important function is to serve as a source of energy for the cell. During cell respiration the enzymatic breakdown of carbohydrates and amino acids yields CO_2, water, and energy. The energy, bound in adenosine triphosphate (ATP), is utilized in the transport of ions across cell membranes and protein synthesis. The mitochondria (Figs. 5.13–5.15, 5.27, and 5.30) are recognized easily in most electron micrographs. The growing tips of dendrites often exhibit varicosities or swellings which are filled with mitochondria (183). Mitochondria in these varicosities are long and slender, and are arranged either parallel to the long axis of the dendrite or form gentle swirls (Fig. 5.17).

Mitochondria, which are about the size of a bacterial cell, contain 2–10 copies of a small, double-stranded circular DNA molecule that is exclusively maternally transmitted. Human mitochondrial DNA (mtDNA) has been entirely sequenced. The 16.6 kilobase mtDNA encodes information for mitochondrial transfer RNAs (tRNA) and rRNAs, which differ from those of the rest of the cell, and form a small number of mitochondrial proteins. The rest of the mitochondrial proteins are encoded by nuclear genes, synthesized on cytoplasmic ribosomes, and then incorporated into mitochondria. From a clinical point of view, it is worth noting that major deletions and mutations of mtDNA may be responsible for several human abnormal conditions or diseases, such as chloramphenicol resistance and mitochondrial myopathies and encephalopathies (83).

Peroxisomes

These small organelles (diameter of about 0.25–0.5 μm) are bounded by a single membrane and represent a highly concentrated source of oxidative enzyme, such as catalase, which form up to 40% of its total protein content. Microsomes (also called microbodies) do not contain DNA or ribosome, and thus resemble the endoplasmic reticulum in being a self-replicating membrane-bounded organelle that exists without a genome of its own. They sometimes stand out in electron micrographs because of the presence of a "crystalloid" core composed of urate oxidase. Like mitochondria, peroxisomes are a major site of oxygen utilization. They are believed to play a role in detoxification through peroxidation reactions, and in preventing accumulation of strong oxidizing agents, such as hydrogen peroxide (H_2O_2) which is believed to be involved in the complex metabolic cascade leading to neurodegeneration in certain diseases. It has been hypothesized that peroxisomes are a vestige of an ancient organelle that carried out all the oxygen metabolism in the primitive ancestors of eukaryotic cells (3).

Centrosome

A microcentrum often is demonstrated in neuroblasts. It consists of one or two granules surrounded by a clear cytoplasmic area. In



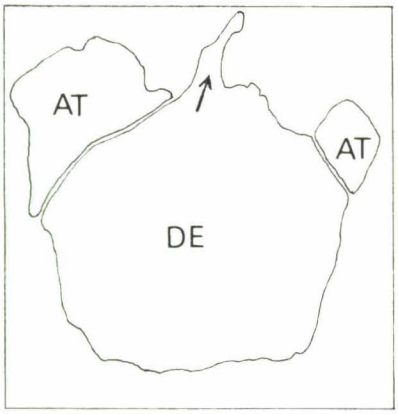


Figure 5.17. Dendritic expansion (*DE*) filled with mitochondria (*mit*) and glycogen (*gly*) granules. This growing dendritic tip shows a filopodia-like expansion (*arrow*) and has two axon terminals (*AT*) synapsing upon its surface. Dendritic profiles of this type are abundant in the dorsal part of the lateral vestibular nucleus of the rat (×39,000).

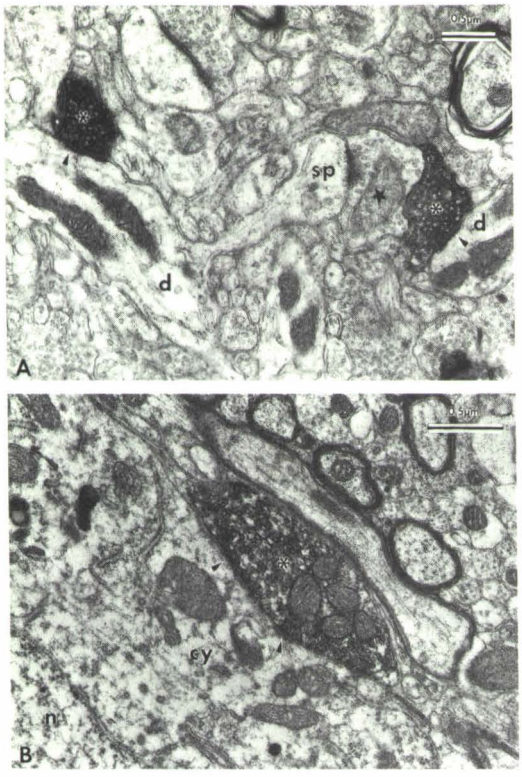


Figure 5.18. Different types of terminal boutons. **A.** Two PHA-L-labeled terminal boutons (*asterisks*) forming asymmetric synapses (*arrowheads*) with dendrites (*d*) of striatal neurons after injection of this anterograde tracer into the parafascicular thalamic nucleus in the squirrel monkey. The presence of the anterograde tracer is indicated by a dense immunoprecipitate in the terminal boutons and the asymmetric nature of the synaptic contacts is revealed by the abundant electron-dense material lying along the postsynaptic membrane. Note the presence of an unlabeled terminal bouton (*star*) containing several small electron-lucent vesicles. This bouton forms a synapse with the head of a spine (*sp*) that is in direct continuity with a dendrite (*d*) contacted by one of the PHA-L-labeled terminal bouton. **B.** Large PHA-L-labeled terminal bouton (*asterisk*) forming a symmetric synapse (*arrowheads*) with the perikarya of a neuron of the subthalamic nucleus following injection of the anterograde tracer into the globus pallidus of the rat. Note the absence of abundant electron-dense material at the postsynaptic membrane level in this case. *cy*: cytoplasm; *n*: nucleus.

some instances, fine wavy fibrils may radiate from the clear area of cytoplasm. The significance of the centrosome is puzzling, for adult neurons are incapable of cell division. However, Murray and Stout (131) demonstrated that adult human sympathetic ganglia could survive, migrate, and occasionally divide mitotically in tissue culture. As is the case in many nonneuronal cells, the centrosome may also act as a microtubule-organizing center in nerve cells.

Golgi Apparatus

The Golgi complex, a specialization of the agranular or smooth endoplasmic reticulum (SER), is highly developed in nerve cells (Fig. 5.12). In electron micrographs, the Golgi apparatus appears as stacks of closely packed agranular membranous cisternae associated with vacuoles and vesicles. Their close packing (Fig. 5.15) and the absence of ribosomes, either free or attached, distinguish the Golgi apparatus from the agranular or smooth endoplasmic reticulum and the Nissl substance (150). In glandular epithelial cells, the Golgi apparatus is involved in the segregation of secretory proteins into membrane bound vesicles. In the region of the Golgi apparatus, sugars are added to protein to form glycoproteins. It is possible that different cisternae within the Golgi complex may perform different functions. The innermost Golgi cisternae contain acid phosphatase and the "alveolate vesicles" of this region are enriched in hydrolytic enzymes (150). Thus, the Golgi apparatus may be associated with the production of lysosomes, which contain hydrolases that break down protein, carbohydrates and nucleic acids (94).

Inclusion Bodies

In addition to the organelles described earlier, some nerve cells demonstrate dense cytoplasmic bodies and pigment granules. Most of the larger adult nerve cells contain a yellowish auto-fluorescent pigment known as *lipochrome* or *lipofuscin*. The amount found within nerve cells increases with age, and appears in the form of granules which are usually aggregated in a dense mass in some part of the cell body (Fig. 5.2**B**). Occasionally, they may be dispersed throughout the cell. They are insoluble in the usual lipoid solvents and are blackened by osmic acid. The cells of the newborn do not contain the pigment, which appears about the 6th year in the spinal ganglia, a few years later in the spinal cord, and after the 20th year in the cerebral cortex. Pigments increase in number with age, and during senescence may occupy a large part of the cytoplasm of some neurons (189). Both histochemical and ultrastructural evidence suggest that lipofuscin granules are a form of lysosome (49). Other histochemical studies indicate there are really three types of granules in the autonomic cells, namely, pigmented, nonpigmented, and neurosecretory

(132). Granules of a blackish pigment known as *melanin* or *neuromelanin* are found in the substantia nigra, locus coeruleus, and certain other pigmented cells scattered through the brainstem. Neuromelanin is also found in spinal and sympathetic ganglion cells (Fig. 5.2**A**). Melanin appears at the end of the first year and increases in amount until puberty, after which it apparently remains constant through senescence.

SYNTHESIS OF NEURONAL PROTEINS

Like in any other cells of the body, the information for the synthesis of proteins in neurons is encoded in the DNA of chromosomes within the nucleus. This information can be processed in two major ways: *heredity* and *gene expression*. Heredity refers to the process whereby the genetic information is passed from parent to daughter cell during cellular division, whereas gene expression alludes to the multistep procedure through which a selected portion of the genetic information is *transcribed* into RNA and then *translated* into proteins. In contrast to other tissues, cell division is not possible in the adult nervous system, so that in neurons genetic expression can only occur through gene expression. Except for the few proteins encoded by the mitochondrial genome, virtually all the macromolecules of the neuron are made in the cell body from messenger ribonucleic acids (mRNA) that are transcribed and spliced into the nucleus. The various types of mRNAs are then exported from the nucleus to other regions of the cell body by passing through the pores of the nuclear membrane. The mRNAs that encode the different proteins form either free polyribosomes (*polysomes*) that are attached to the endoplasmic reticulum. The mRNAs are translated on these polysomes. It must be mentioned that the brain expresses more of the total genetic information encoded in DNA than does any other organ in the body (171). This probably accounts for the extreme structural and functional diversity encountered in the brain compared to other organs.

The various mRNAs species are differentially distributed in the neuron. Indeed, recent *in situ* hybridization studies revealed that, although the majority of neuronal mRNAs are confined to the cell body, two mRNA species are prominent in dendrites. These two mRNAs are (a) the mRNA encoding the high molecular weight form of the cytoskeletal protein MAP-2, a protein considered to be a marker for the dendritic cytoskeleton, and (b) the mRNA encoding of the α subunit of the Ca^{2+}/calmodulin-dependent protein kinase (CaM kinase II) (185). It was also demonstrated conclusively that dendrites exhibit local protein synthesis and have translationally competent mRNA present in the form of polyribosomes. In light of these results, it becomes crucial to know how neurons target these specific mRNAs to cellular microdomains at a distance from the nucleus.

Recent studies by Steward and Banker (185) revealed three previously unknown processes that can account for the differential distribution of mRNAs within neurons. These are (a) a sorting mechanism that determines whether particular mRNAs will be transported into dendrites or will remain in the cell body, (b) a mechanism for transporting mRNAs selectively into dendrites and, presumably, into the initial segments of axons, and (c) a mechanism that docks mRNAs and associated translational machinery (ribosomes) at postsynaptic sites (185). Much of the structural and functional differences that exist between the various neuronal compartments (dendrites, soma, axon, and axon terminals) heavily rely on these three fundamental intracellular transport mechanisms. The molecular base of these transport mechanisms has not yet been fully worked out.

The multitude of proteins in a neuron can be grouped into three major categories: (a) proteins that are synthesized in the cytosol and remain there, (b) proteins that are synthesized in the cytosol but are later incorporated into the nucleus, mitochondria, or peroxisomes, and (c) proteins that are synthesized in association with the cell membrane system. In addition to encoding the primary sequence of the proteins, the mRNAs contain information that, when translated into polypeptide sequences, targets the new protein to its final destination. Cytosolic proteins are by far the most abundant proteins in the neuron. They comprise the fibrillary elements that form the cytoskeleton and numerous soluble enzymes that catalyze the various metabolic reactions of the neuron. The nuclear, mitochondrial, and peroxisomal proteins are targeted to the proper organelles soon after their synthesis by a mechanism called posttranslational importation. This mechanism relies on specific receptors around nuclear pores that bind and translo-

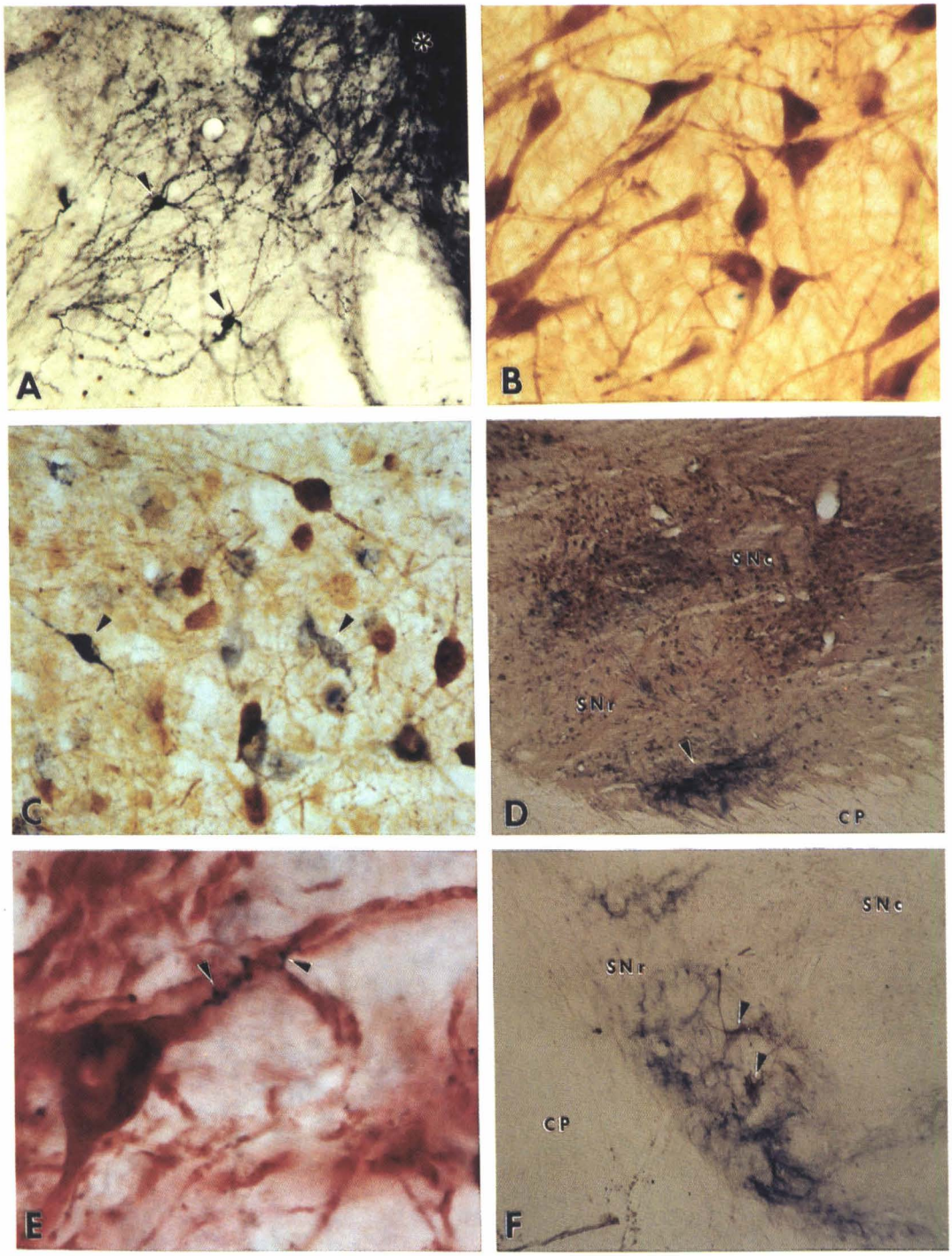


Figure 5.19. Results that can be obtained with immunocytochemistry alone or in combination with retrograde and anterograde tract-tracing methods in the squirrel monkey. **A.** PHA-L injection site in the putamen. Note the presence near the core of the injection site (*asterisk*) of a few striatal neurons (*arrowheads*) that have actively taken up the tracer and display a Golgi-like appearance (×200). **B.** Dopaminergic neurons of the substantia nigra as visualized by immunocytochemistry with a highly specific monoclonal antibody raised against dopamine itself (×300). **C.** Serotoninergic neurons (*brown*) of the dorsal raphe nucleus intermingled with a few neurons retrogradely labeled with cholera toxin B subunit (*dark blue, arrowheads*) injected into the globus pallidus. Both serotonin and cholera toxin were visualized immunocytochemically and immunoprecipitates were revealed by the chromogen diaminobenzidine (*DAB*) and nickel-intensified diaminobenzidine (*NiDAB*), respectively (×300). **D.** Striatonigral fibers anterogradely labeled with PHA-L injected into the caudate nucleus. A small contingent of these fibers (*arrowhead*) arborize within the substantia nigra pars reticulata (*SNr*) along the dorsal surface of the cerebral peduncle (*CP*). The presence of the dopaminergic neurons of the substantia nigra pars compacta (*SNc*) was also revealed immunocytochemically in the

cate these newly synthesized polypeptide chains (171). Membrane proteins, which includes secretory proteins, are of three types: membrane-spanning (or integral), anchored, and associated. The names of these proteins reflect the strength of their link with the membrane system of the neuron. The different receptors that are found on the surface of the neuronal membrane are typical membrane-spanning or integral proteins (see the section on the synapses later).

Proteins are polypeptides or polymers of amino acids, with one end having a free amino (N-terminal) group and the other a carboxyl (C-terminal) group. Translation of the polypeptide chain always begins at the N-terminal end. Cytosolic proteins are little modified or processed compared to membrane proteins. In proteins destined to be modified, the modification can occur either during or after the polypeptide chain is synthesized. These modifications are respectively called *cotranslational* and *posttranslational*. An example of important cotranslational modifications is N-acetylation, the transfer of an acetyl group to the N-terminus of the nascent polypeptide. An example of important posttranslational modifications is the addition of other functional groups to specific amino acid residues, such as *phosphorylation* and *ubiquitination*. Phosphorylation, which is reversible and involves protein kinases, is the most common mechanism for altering the biochemical function of a protein in any cell. Ubiquitination consists of adding *ubiquitin*, a highly conserved protein with 77 amino acid residues, to specific amino acid residues throughout the protein molecule. Ubiquitination is believed to be a mechanism for tagging proteins for degradation by special proteases. It is a very important mechanism for protein turnover in neurons. Ubiquitination is said to be greatly exacerbated in certain neurodegenerative disorders, such as Alzheimer's disease.

SIGNALING MOLECULES

One of the characteristics of most nerve cells is that they communicate with each other through the release of specific chemical messengers or signaling molecules at synaptic level. The concept of chemical transmission is derived from the classical experiments performed by Otto Loewi (121). Loewi demonstrated chemical transmission by transferring the ventricular fluid of a stimulated frog heart onto a nonstimulated frog heart, showing that the effects of the nerve stimulus were reproduced by the chemical activity of the solution flowing onto the second heart (30). In that particular case, the neurotransmitter involved was acetylcholine, which was released by the vagus nerve innervating the heart. The pharmacologic studies of Henri Dale on cholinergic and adrenergic transmission were also instrumental in the formulation of the chemical transmission concept (36).

To be accepted as neurotransmitters, a putative chemical messenger must fulfill four criteria: (a) it must be synthesized in the neuron, (b) it must be present in the presynaptic terminal and released in sufficient amount to exert its supposed action on the postsynaptic neuron or the effector organ, (c) when applied exogenously in sufficient concentration, it must mimic exactly the action of the endogenously released transmitter, and (d) a specific mechanism for removing the presumed neurotransmitter from its site of action must exist (30, 172). The demonstration that a suspected chemical messenger indeed fulfills most of these criteria is extremely difficult, particularly for a molecule that is presumed to act as a neurotransmitter at a specific region in the central nervous system. Nevertheless, the recent development of new and powerful methods to localize and pharmacologically characterize putative chemical messengers has greatly helped the identification of synaptic transmitters. At present,

same section with an antibody raised against the enzyme tyrosine hydroxylase (*TH*). PHA-L immunoreactivity was revealed with *NiDAB* (dark blue precipitate), whereas TH was visualized with DAB (brown precipitate) (×200). **E.** Striatonigral fibers anterogradely labeled with PHA-L and displaying varicosities (*arrowheads*) in close contact with the proximal dendrite of a TH-immunoreactive neuron of SNc. In this case, PHA-L immunoreactivity was revealed with *NiDAB*, whereas TH-immunoreactivity was visualized with the new chromogen 3-amino-9-ethyl-carbazole (AEC), which appears red (×500). **F.** Double anterograde labeling experiment involving injections of PHA-L and biocytin in two adjacent areas of the putamen. The two types of anterogradely labeled fibers form terminal fields in the substantia nigra that can be distinguished from one another by their color: the PHA-L-labeled fibers are *dark blue (NiDAB)*, whereas the biocytin-labeled fibers (*arrowheads*) are *brown* (DAB) (×200).

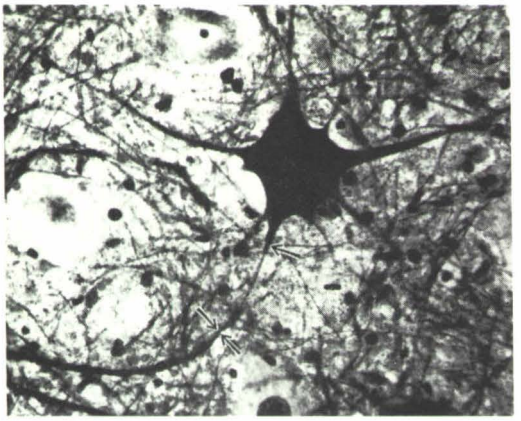


Figure 5.20. Large motor neuron in the anterior gray horn of an infant's spinal cord revealing several dendrites and the origin of the axon. The axon arises from the lower side of the cell body, tapers to a thin thread for a short distance, and thickens at the point where the myelin sheath develops. Small neuroglial nuclei are stained black (modified Weigert's stain).

there is a multitude of presumed neurotransmitters, but these various signaling molecules conveniently can be grouped into two broad categories—small-molecule transmitter substances and neuroactive peptides (172).

Small signaling molecules

There are only eight low-molecular-weight chemical messengers that are actually recognized as transmitter substances. These signaling molecules share many biochemical similarities since they all are amines, and seven of them are amino acids or their derivatives. They are small, charged molecules that are synthesized through relatively short metabolic pathways from precursors that ultimately derive from carbohydrate substrates of intermediary metabolism. These transmitters are (a) acetylcholine, (b) the biogenic amines, comprising the catecholamines (dopamine, norepinephrine, and epinephrine), serotonin, and histamine, and (c) the amino acids γ-aminobutyric acid (GABA), glycine, and glutamate.

Acetylcholine was one of the first neurotransmitters to be identified. Yet, it was only after the recent application of immunocytochemical procedures making use of antibodies able to recognize its synthesizing enzyme—choline acetyltransferase (ChAT)—that a proper knowledge of the anatomic organization of brain cholinergic system began to emerge (128). In the human brain, the number of cholinergic neurons is surprisingly small. These chemospecific neurons are largely confined to various basal forebrain nuclei, including the nucleus basalis of Meynert that projects widely to the cerebral cortex. Acetylcholine is also the neurotransmitter used by the spinal cord motor neurons whose axon terminate at the nerve-skeletal muscle junction, and by all preganglionic neurons of the autonomic nervous system, as well as by the postganglionic neurons of the parasympathetic system.

Biogenic amines, also called monoamines, includes the catecholamines (dopamine, norepinephrine, and epinephrine), that derive from the amino acid tyrosine, and the indolamine serotonin (or 5-hydroxytryptamine), that derives from the amino acid tryptophan. As their names imply, catecholamines possess a catechol nucleus, a 3,4-dihydroxylated benzene ring, and are part of a common biosynthetic pathway with tyrosine hydroxylase as the rate-limiting enzyme. Serotonin belongs to a group of aromatic compounds called indoles, which is characterized by a five-membered ring containing nitrogen joined to a benzene ring. Tryptophane hydroxylase is the rate limiting enzyme in the synthesis of serotonin. Histamine is an imidazole derived from the amino acid histidine. Although its biochemistry is remote from that of catecholamines and serotonin, it is often referred to as a biogenic amine. Biogenic amines have been first visualized with the help of the formaldehyde-induced fluorescence method developed by Falck and Hillarp in Sweden (50, 51). They can now be studied in more detail with immunocytochemical procedures and antibodies that have been raised against either the neurotransmitters themselves (Fig. 5.15) or the different enzymes involved in their synthesis (91, 138). All three catecholamines and serotonin occur in specific brainstem nuclei, whereas histamine is concentrated in certain neuronal populations of the hypothalamus (30). At the periphery, norepinephrine is the neurotransmitter used by postganglionic neurons of the sympathetic nervous system.

In contrast to acetylcholine and biogenic amines, which are synthesized only in certain neurons, the amino acid transmitters GABA, glutamate, and aspartate are intermediates in general biochemical pathways. For instance, glycine and glutamate are among the 20 common amino acids incorporated into proteins in all cells. Furthermore, glutamate is the im-

mediate metabolic precursor of GABA. It is thus surprising to see that the same amino acid may act as transmitter in certain neurons and be mostly involved in intermediary metabolism in others. This dichotomy of function calls for a compartmentalization of the two types of amino acids, that is the transmitter amino acids must somehow be kept separate from metabolic amino acids (30, 172). In the brain, glutamate is the major excitatory transmitter and GABA the major inhibitory transmitter. Glycine, which is probably derived from serine, acts as an inhibitory transmitter in the spinal cord interneurons.

Neuroactive Peptides

Small-molecule transmitter substances can be synthesized in all parts of the neurons, including axon terminals (180). In contrast, neuroactive peptides derive from the processing of secretory proteins that are only formed in the cell body, so that neuroactive peptides must be transported to terminals within vesicles by fast axonal transport. Another major difference between the two classes of chemical messengers is that neuroactive peptides are much more numerous and diversified than small-molecule transmitter substances. More than 50 neuroactive peptides have been found to be pharmacologically active (Table 5.1). Interestingly, several of these peptides are also known to act as hormones outside the brain (e.g., angiotensin and gastrin) or as products of neurosecretion (e.g., oxytocin, vasopressin, and somatostatin). Despite their diversity, neuroactive peptides can be grouped into about 10 large families whose members are structurally related and often derived from a common large precursor protein (polyprotein). These large polyproteins are subsequently processed within vesicles and several neuroactive peptides are produced through specific proteolytic cleavages. Specific functions, such as modulation of pain (substance P and enkephalin) and control of emotional states (adrenocorticotropin and β-endorphin) have been attributed to certain neuroactive peptides. This topic is dealt with in subsequent chapters.

Because they are synthesized locally in the terminals, the small-molecule transmitters can be released very rapidly, whereas neuroactive peptides are released more slowly. Peptides and small-molecule transmitters can coexist in the same neuron and even be coreleased at the same axon terminals, as is the case for acetylcholine and vasoactive intestinal peptide (25, 92, 93). In such a case, the small signaling molecule usually acts much more rapidly than the neuroactive peptide, which often exerts a slow modulatory effect on the postsynaptic element. Since specific postsynaptic receptors exist for these two classes of transmitters, cotransmission allows for a great diversity in the transfer of information (172).

Neurosecretion

Certain neurons in the nervous system of both vertebrates and invertebrates act as neurohormonal transducers. These neurosecretory neurons, which are particularly abundant at the level of the hypothalamo-hypophysial system, transform the action potential and chemical signaling they received into hormone secretion (9, 61, 142, 143, 164–166). Thus, neurosecretory neurons can be said to bridge the gap between the nervous and endocrine systems. Morphologically, these neurons possess all the organelles that are present in other neurons, but also display some differences. For example, the neurofilaments in the axon and its preterminal region appear different from those found in other neurons. The microtubules may be as thick as 30–50 nm in diameter, and the axons also display multilamellate bodies (9). Neurosecretory neurons have unusually electron-dense material associated with Golgi membranes and a very prominent endoplasmic reticulum. Secretory proteins are synthesized on polyribosomes attached to the endoplasmic reticulum and then move to the Golgi apparatus where it is conjugated to a carrier protein, such as neurophysin in the case of oxytocin and vasopressin hormones. The hormones and the carrier protein are packaged in dense core vesicles that are transported along the axon by fast axonal transport from the cell body to the axon terminals. Large masses of secretory material (*Herring bodies*) are observed along the axons of these neurons. The axon terminals containing neurosecretory vesicles are unique in that they abut a perivascular space rather than another neuron or effector cell. Their secretory product is released by exocytosis into the perivascular space from where it can reach its distant target sites through the blood (150). A typical example of such a system is the neurons of the supraoptic and paraventricular hypothal-

Table 5.1.

PARTIAL LIST OF BRAIN NEUROACTIVE PEPTIDES

HYPOTHALAMIC-RELEASING HORMONES	AMINO ACIDS	FUNCTIONS
Thyrotropin-releasing hormone	(3)	Control of thyroid hormone
Gonadotropin-releasing hormone	(10)	Stimulation of gonadotropic cells
Somatostatin	(14)	Inhibition of secretion of GH
Corticotropin-releasing hormone	(41)	Inhibits gonadotropic cells
Growth hormone releasing hormone	(44)	Stimulation of secretion of GH
Luteinizing hormone releasing hormone	(8)	Regulates release of luteinizing hormone
NEUROHYPOPHYSEAL HORMONE		
Vasopressin	(9)	Influences blood pressure
Oxytocin	(9)	Stimulates reproductive system
PITUITARY PEPTIDES		
Adrenocorticotropic hormone	(39)	Stimulates adrenal steroid biosynthesis
β-Endorphin	(31)	Analgesia, emotion
α-Melanocyte-stimulating hormone	(13)	Unknown in mammals
Prolactin	(199)	Synthesis of milk proteins
Luteinizing hormone	(96)	Maturation of reproductive cells
Growth hormone	(191)	Skeletal and soft tissue growth
HEART-DERIVED PEPTIDE		
Atrial natriuretic peptide	(28)	Control of salt and water intake

amic nuclei (Fig. 17.18), which produce the nonapeptides vasopressin and oxytocin (6) (see also Figs. 17.2 and 17.4). Vesicles containing these hormones can be visualized at both light and electron microscopic levels in material prepared according to specific histochemical stains (e.g., chromhematoxylin-phloxine stain).

In mammals, there is another important neurosecretory system in the hypothalamus represented by the arcuate nucleus and the median eminence. Nerve fibers originating from the arcuate nucleus course into the median eminence and terminate in relationship to the perivascular spaces, as described for the supraoptico-hypophysial neurosecretory system (Figs. 17.1 and 17.18). Granule-containing vesicles in these nerve endings are smaller and of at least two types. The median eminence is involved in the elaboration and control of various releasing hormones (e.g., tyrotropin-releasing hormone and somatostatin), which regulate the adenohypophysis. Some of the small clear vesicles containing dense granules encountered in the nerve terminals that occur in the median eminence resemble those found in adrenergic nerve terminals. This system is discussed further in Chapter 17.

AXONS

The axon is a slender, usually long process which arises from a conical mass of specialized protoplasm known as the axon hillock. It is distinguished from the cell body and dendrites by the complete absence of Nissl bodies, which also are lacking in the axon hillock.

Table 5.1.—*continued*

PARTIAL LIST OF BRAIN NEUROACTIVE PEPTIDES (Continued)

GASTROINTESTINAL PEPTIDES	AMINO ACIDS	FUNCTIONS
Vasoactive intestinal peptide	(28)	Relaxation of smooth muscle, stimulation of exocrine and endocrine secretion
Cholecystokinin octapeptide	(8)	Induces satiety
Gastrin	(34)	Stimulation of gastric acid secretion
Calcitonin	(32)	Inhibits gastric acid secretion
Calcitonin gene-related peptide	(37)	Inhibits gastric acid secretion
Substance P	(11)	Stimulates gastrointestinal motility
Neurotensin	(13)	Inhibits gastric acid secretion
Methionin-enkephalin	(5)	Analgesia
Leucine-enkephalin	(5)	Analgesia
Insulin	(51)	Induces hypoglycemia
Glucagon	(29)	Induces hyperglycemia
Bombesin	(14)	Stimulation of many gastrointestinal peptides
Secretin	(27)	Stimulates water secretion
Somatostatin	(28)	Nociception and pain signals
Motilin	(22)	Initiates myoelectric discharges (gastric tract)
Neuropeptide Y	(36)	Inhibits gastric and pancreatic secretion
Polypeptide Y	(36)	Inhibits gastric and pancreatic secretion
Pancreatic polypeptide	(36)	Stimulates gastric and pancreatic secretion
OTHERS		
Angiotensin II	(8)	Influences blood pressure
Bradykinin	(9)	Stimulates contraction of smooth muscle
Carnosine	(2)	Sensory information
Dynorphin A	(17)	Analgesia

In smaller neurons, an axon hillock is not easily identified in light microscopic preparations. The reason suggested by electron microscopy is that in these small cells there is little difference between the cytoplasm of the axon hillock and that of the neuronal cell body (150). As the axon hillock narrows into the initial axonal segment, there is a gradual diminution in the number of ribosomes, but no abrupt change as suggested by light microscopic descriptions. Beyond the initial segment the axon contains mitochondria, neurofilaments, microtubules, agranular endoplasmic reticulum, vesicles, and multivesicular bodies. No granular endoplasmic reticulum or ribosomes are present. Distally, each axon breaks up into simple or extensive terminal arborizations, the telaxon. The latter may be synaptic endings on other neurons (e.g., sensory neurons), or effector endings in muscle and glands (Figs. 5.3**G**, 5.7, and 10.23).

In the central nervous system, axons may be *myelinated* or *unmyelinated*. The former possess a sheath of myelin for at least a portion of their course, whereas the latter are completely devoid of such a sheath. The oligodendrocyte forms and maintains the myelin sheath within the brain and spinal cord, while the Schwann cell plays the same role at the periphery. In the peripheral nervous system, both myelinated and unmyelinated fibers have, in addition, an outer delicate nucleated membrane, the *sheath of Schwann*. The peripheral myelinated fiber is structurally the most differentiated, consisting of axon (axis cylinder), myelin, and sheath of Schwann. The myelin sheath is not continuous, but is interrupted at fairly regu-

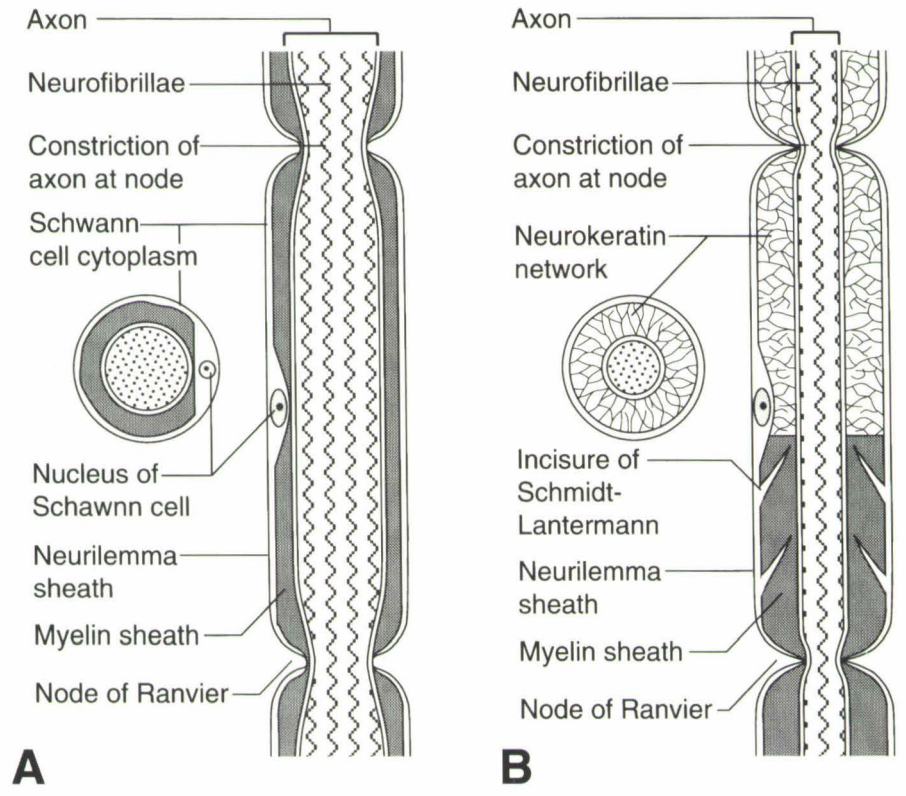


Figure 5.21. **A.** and **B.** Peripheral myelin sheaths based on studies of living nerve fibers. Cross-sections of different fixed preparations of the myelinated fibers are shown in the central portion of each drawing. The cross membrane is not shown.

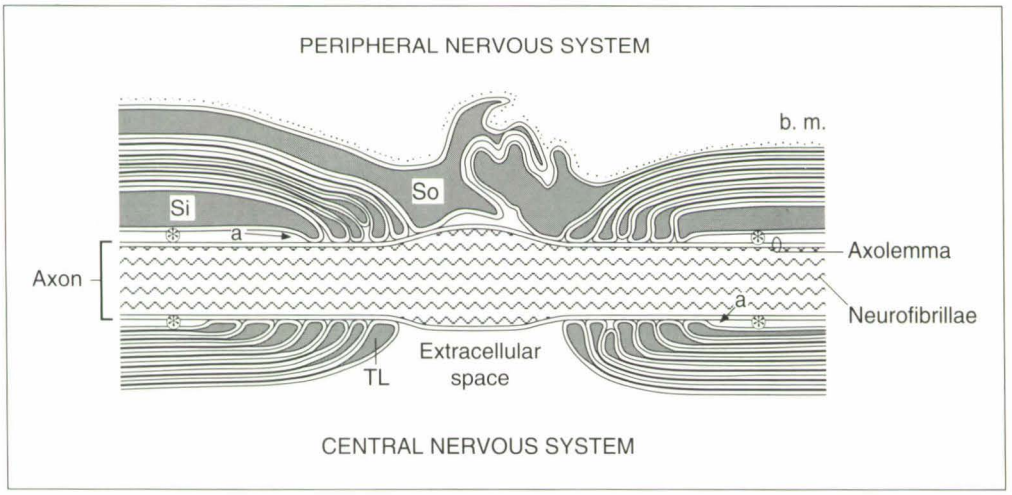


Figure 5.22. Nodal regions from peripheral (*PNS*) (*above*) and central nervous system (*CNS*) (*below*). In the PNS the Schwann cell provides both an inner collar (*Si*) and an outer collar (*So*) of cytoplasm in relation to the compact myelin. The outer collar (*So*) is extended into the nodal region as a series of loosely interdigitating processes. Terminating loops of the compact myelin come into close apposition to the axolemma in region near the node, apparently providing some barrier (*arrow at "a"*) for movement of material into or out of the periaxonal space (*asterisks*). The Schwann cell is covered externally by a basement membrane. In the CNS the myelin ends similarly in terminal loops (*tl*) near the node, and there are periodic thickenings of the axolemma where the glial membrane is applied in paranodal region. These may serve as diffusion barriers and thus confine the material in the periaxonal space (*asterisks*) so that movement in the direction of the arrow at "a" would be restrained. At many CNS nodes there is considerable extracellular space (*ECS*). Compare with CNS node shown in Figure 5.21.

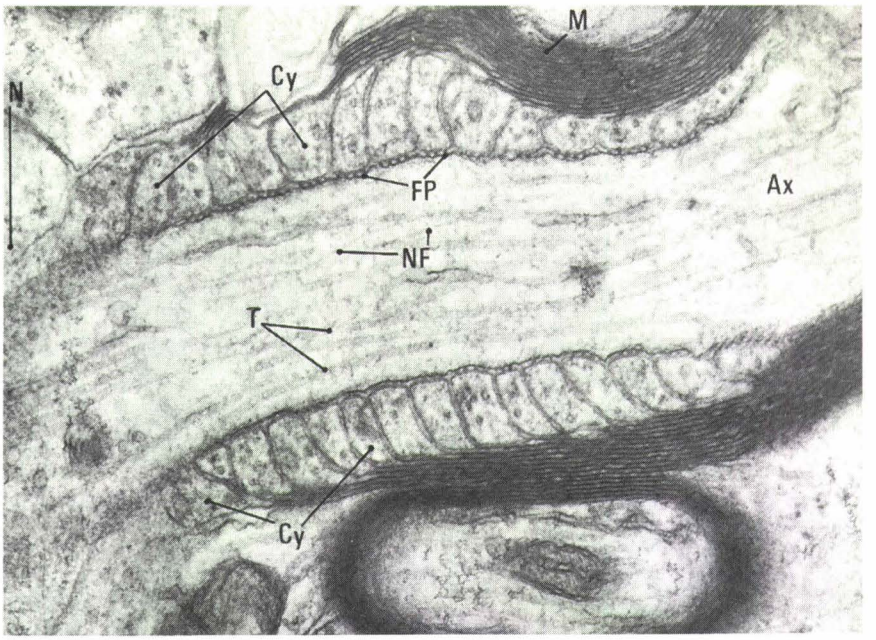


Figure 5.23. Node of Ranvier on nerve of spinal cord (cat). The oligoglial cytoplasm (*CY*) forms loops of myelin (*M*) around the axon (*Ax*) and the node (*N*). Fusion points (*FP*) between the myelin and axon membranes are also shown. Neurotubules (*T*) and neurofilaments (*NF*) are identified in the axoplasm (×70,000).

lar intervals. The parts of the fiber free from myelin appear as constrictions known as the nodes of Ranvier, named after the French pathologist Louis Antoine Ranvier who first described them at the end of the 19th century (Figs. 5.3C and 5.21). In the fresh condition, the semifluid axon is homogeneous in appearance and occasionally shows faint longitudinal striations. In silver stained preparations, it consists of closely packed, parallel-running neurofibrils embedded in a scanty amount of homogeneous axoplasm. In most fixatives, the axon usually shrinks to a thin axial thread. With special methods of fixation and tissue embedding, its normal size may be more nearly approximated.

Between the axon and myelin sheath there is a delicate layer or membrane known as the *axolemma* (Fig. 5.22). Although difficult to demonstrate histologically, the membrane may be seen in ultraviolet photographs of the living nerve fiber, since the axolemma shows a much greater ultraviolet absorption than the axon or the myelin sheath. The axolemma is part of the neuron plasma membrane, and possesses a similar structure and specialized properties. It is easily identified in high magnification electron micrographs as a delicate membrane surrounding the axon (Figs. 5.22 and 5.23).

Myelin

STRUCTURAL ORGANIZATION

The myelin sheath starts at a short distance from the cell body (Fig 5.20), the proximal portion of the axon, including the axon hillock, being as a rule unmyelinated. The sheath is of varying thicknesses and is composed of a semifluid, doubly refracting substance known as *myelin*, which in the fresh state has a glistening white appearance. Physical techniques have provided data concerning the orderly arrangement of lipoproteins that form myelin (168, 178). Studies based upon polarized light, x-ray diffraction, and electron microscopy have yielded a high degree of correlation and indicate that the myelin sheath is composed of concentric layers in which protein and lipid alternate. Lipid molecules are radially oriented in their layers, while protein molecules are arranged tangentially. Myelin is composed of a fundamental, radially arranged repeating unit membrane with a spacing of 17–18.5 nm. The repeating unit membrane is formed of two subunits, each consisting of a bimolecular lipid leaflet sandwiched between monolayers of protein. Each of these subunits corresponds to a single layer of plasma membrane

derived from the myelin-forming cell (Figs. 5.24 and 5.27).

With the limited magnification of light microscopy, it was presumed that peripheral myelinated nerves were enclosed by two separate layers, the myelin and Schwann cell sheaths. The histologic appearances of myelinated nerves in cross-section, when stained by the osmic acid and silver nitrate methods, are shown in Figure 5.3**B** and **D**. Electron microscopy studies revealed that myelin was formed primarily by a double-layered infolding of the Schwann cell membrane, which became wrapped spirally around the axon in concentric layers (66, 158, 159).

Four stages in the "jelly-roll theory" of myelin formation are depicted in Figure 5.25. In the peripheral nervous system, the myelin sheath represents concentric layers of the Schwann cell, while the oligodendrocyte assumes the role of myelin formation within the central nervous system (20). In the latter case, one oligodendrocyte may form a myelin layer on more than one axon (Fig. 6.9). Note that the inner surfaces of the plasma membranes come into apposition and fuse to form *major dense lines* which are approximately 3 nm thick. Between each major dense line is a less dense *intraperiod line* formed by the union of the outer surfaces of the plasma mem-

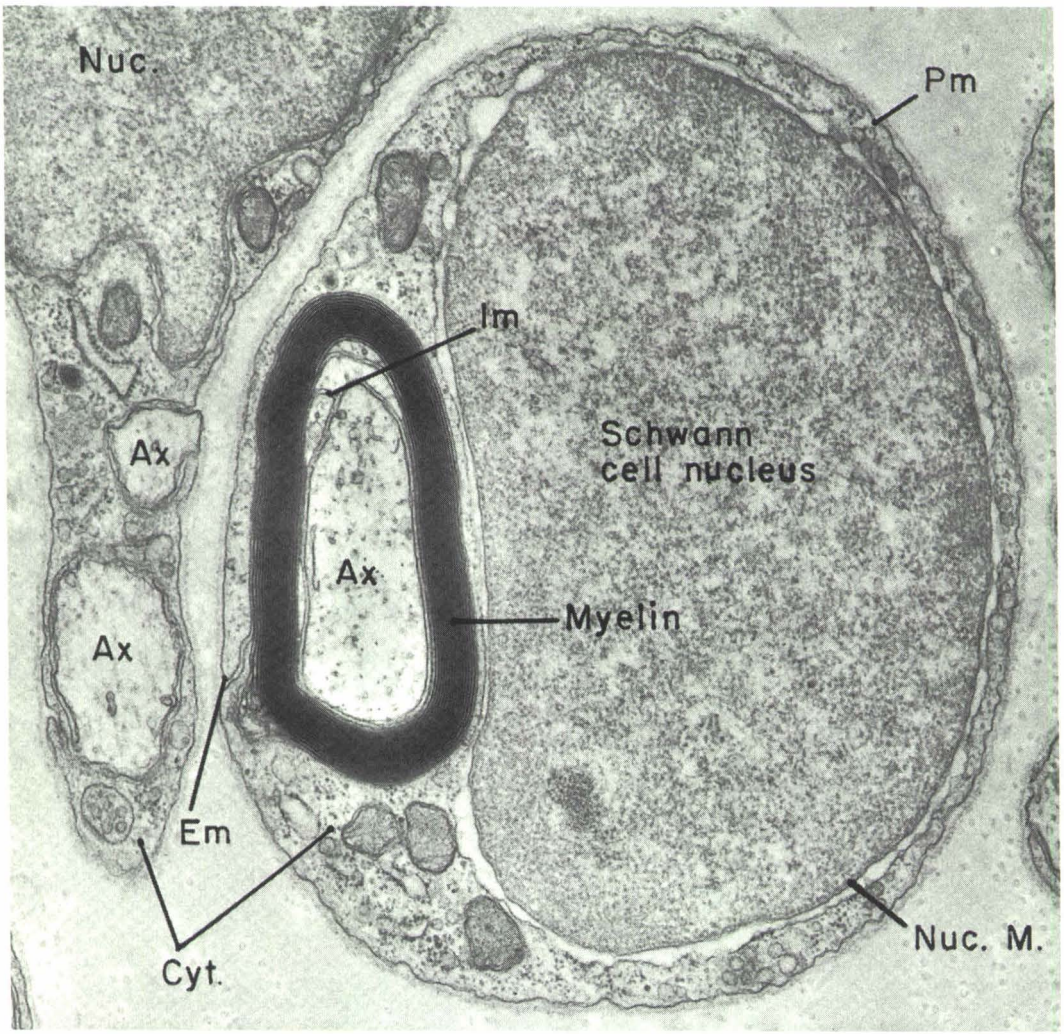


Figure 5.24. Small myelinated nerve fibers from rat dorsal root ganglion matured in tissue culture. The infolding plasma membrane (*PM*) of the Schwann cell forms an external mesaxon (*EM*) continuous with the outermost lamella of the myelin sheath. An internal mesaxon (*Im*) surrounds the axon (*Ax*) and is continuous with the most internal lamella of the myelin sheath. Note the small amount of Schwann cell cytoplasm (*Cyt*) between the nuclear (*Nu. M.*) and plasma membranes. At the *left* are two unmyelinated axons associated with another Schwann cell (×27,000).

branes (Fig. 5.25). This fusion of membranes, accompanied by a reduction in cell cytoplasm, results in the repeating series of light and dark lines observed in electron micrographs (Figs. 5.24 and 5.27). Cytoplasmic remnants of the Schwann cell infolding may at times be identified at the axon-myelin junction (Fig. 5.27**A**). The primary infolding of the Schwann cell membrane is often present as an *internal mesaxon* (Fig. 5.24). Continuity between the most superficial lamellae of the myelin sheath and the Schwann cell plasma membrane forms the *external mesaxon* (Fig. 5.24).

These intimate relations of Schwann cell and myelin are further amplified by the tissue culture observations of several investigators (29, 151, 161) who found that myelination began in isolated segments near the Schwann cell nucleus and extended along the fiber to a node of Ranvier. Remyelination of experimentally injured axons of the cat spinal cord appears to resemble the mechanism of myelination observed along peripheral nerves and in tissue culture (18).

MOLECULAR ORGANIZATION

In the peripheral nervous system, Schwann cells express a *myelin-associated glycoprotein* (MAG) early during myelination. This protein becomes only a minor component of mature (compact) myelin, but may play a crucial role in the initiation of the myelination process. It is primarily found at the margin of the myelin sheath just adjacent to the axon. Its cellular location, structural similarity to other surface recognition molecules, and early expression in development favor the view that MAG is important for the initiation of myelination. There are two isoforms of MAG with molecular weights of 68,900 and 64,000 generated from a single gene through alternative RNA splicing. MAG belong to a superfamily of proteins related to immunoglobulins and includes several cell-surface proteins, such as the neural cell adhesion molecule (NCAM), whose role is important in cellular recognition (see Chapter 3).

Myelin in both the central and peripheral nervous system is composed of the same group of proteins originally called *myelin basic protein*. Recent gene cloning methods revealed that this group of proteins, previously consid-

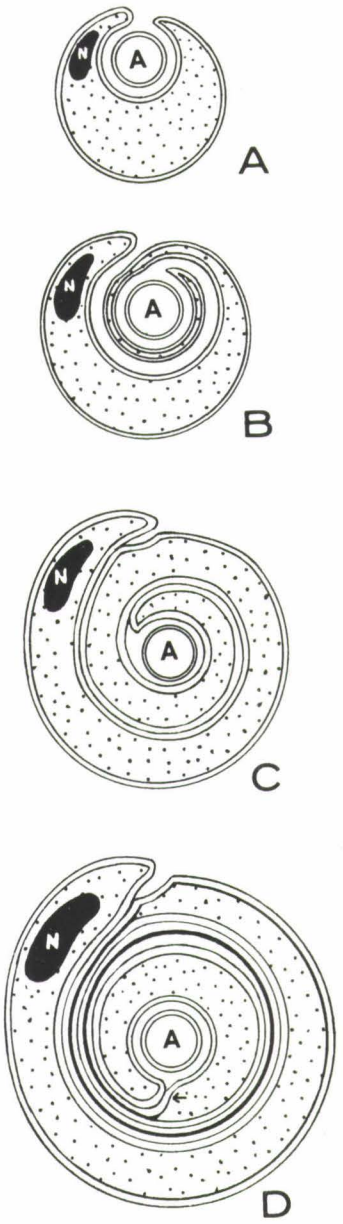


Figure 5.25. A-D. Stages in the development of the myelin sheath about the axon (*A*). Cytoplasm of the Schwann cell is stippled and its nucleus is indicated (*N*). After the initial phase of ensheathment (**A**), additional layers of cell cytoplasm become wrapped around the axon (**B** and **C**). The cytoplasm is then reduced in amount and the double layered plasma membrane comes into apposition (**D**). The outer membrane unit of the Schwann cell will become the future intraperiod line of myelin. The dark line (*major dense line*) represents the apposition of the inner (cytoplasmic) surfaces of the unit membrane as shown in **D**. The internal mesaxon is also indicated (*arrow* in **D**).

ered as a single entity, consists of at least seven related proteins with molecular weights ranging from 14,100–21,400. These proteins are apparently produced by a single gene through alternative RNA splicing. These myelin basic proteins are all highly antigenic and, when injected into animals, produce a cellular autoimmune response called experimental allergic encephalomyelitis. This syndrome is characterized by focal inflammation and demyelination in the central nervous system, and has been used by some investigators as an animal model for human *multiple sclerosis*.

Ranvier Nodes, Schmidt-Lantermann Clefts, and Schwann Sheaths

NODES OF RANVIER

The myelin sheath is interrupted by constrictions at varying intervals on both central and peripheral axons. These areas, which are called *nodes of Ranvier*, are identified in both the light and electron microscopes as regions where the myelin sheath is deficient (Figs. 5.3**C** and 5.23). At the nodal gap of peripheral nerves, the axolemma is ensheathed by a fine basement membrane and small fingerlike processes of the Schwann cell. As shown in Figure 5.22, there are some characteristic differences between the nodes of central and peripheral axons. The internodal distance and nodal gap are both shorter on central axons. Such nodes also lack both interdigitating glial processes and a basement membrane. Thus, the nodes of Ranvier in the central nervous system have a greater extracellular space in the nodal region. The blunt spiral ends of the glial processes appear to fuse with the axolemma adjacent to a central node, as shown in Figures 5.22 and 5.23. Paranodal terminations of myelin loops, on each side of the node, provide close apposition of plasma membranes rather than complete obliteration of the extracellular space about the axon (Fig. 5.22). The length of the internodal segment varies considerably and is proportional to the diameter of the fiber, the thinner fibers having the shorter internodes. For example, in the peroneal nerve of the rabbit the internodes on fibers with a diameter of 3–18 μm range from 400–1500 μm (195), and these figures probably apply to other mammals and humans. Electron microscopy has provided essential information on the fine structure of the node (see references 20, 129, 148, 149, 160, and 190 for additional details).

In unmyelinated axons, the propagation of the action potential is a continuous process. In peripheral myelinated axons with regularly spaced nodes of Ranvier, the action potential appears to "jump" from node to node rather than proceed at a uniform velocity along the axon membrane between nodes. This is called "saltatory" conduction and is the result of the electrical resistance and capacitance properties of the myelin sheath. The basic conductance mechanism of the action potential conduction along the surface membrane of myelinated and unmyelinated axons is the same.

SCHMIDT-LANTERMANN CLEFTS

The myelin sheath of each internode is divided at intervals into conical segments by the so-called *Schmidt-Lantermann clefts*. They consist of oblique, funnel-shaped clefts, which extend to the axon. These are best seen in preparations treated with osmic acid, but are also visible in the living fiber when it is viewed in polarized light. Several cone-shaped indentations may occur in a myelin segment between two nodes, while the myelin sheaths of adjacent axons may be devoid of such clefts for long distances. Although long regarded as artifacts, the clefts have been observed in electron microscopic studies as shearing defects in the lamellae of the myelin sheath (19, 159). Such clefts were shown to be areas of local separation of the spirally wrapped myelin lamellae which are, nevertheless, continuous across the incisure (Fig. 5.26). The light appearing regions between the lamellae consist of Schwann cell cytoplasm. In other preparations, the myelin sheath may exhibit a delicate trabecular reticulum, the *neurokeratin network* (31) (Fig. 5.21). The network probably represents a precipitated protein residue of the myelin sheath rather than a true cytoplasmic reticulum. The myelin sheath ends at or near the point where the terminal arborizations are given off. No structure similar to the Schmidt-Lantermann clefts has been identified in myelin sheaths in the central nervous system.

SHEATH OF SCHWANN

The *sheath of Schwann* consists of a layer of flattened cells that form the myelin of larger fibers. It also provides a thin, attenuated cytoplasmic investment on nonmyelinated fibers of the cranial and spinal nerves (Figs. 5.24

and 5.27). Schwann cells, like neurons, are of ectodermal origin (neural crest and neural tube; see Chapter 3). Each Schwann cell has a flat, oval nucleus surrounded by a thin rim of cytoplasm which contains a Golgi complex and mitochondria (Fig. 5.24). The Schwann cells of both myelinated and nonmyelinated nerve fibers are surrounded by a typical basement membrane approximately 25 nm in thickness (Fig. 5.22). This is separated from the plasma membrane of the Schwann cell by an interval of 25 nm. Ultrastructural studies indicate that the Schwann cell plasma membrane, with its surrounding basement membrane, correspond to the so-called *neurolemma sheath* that was described earlier on the basis of light microscopic observations (24, 188). Nathaniel and Pease (135) regard only the granular basement membrane surrounding the Schwann cell as equivalent to the neurolemma.

One Schwann cell may have extensive cytoplasmic processes as it presides over, and maintains the integrity of, the segment of myelin between two nodes of Ranvier. If an ultrathin section were cut through a small myelinated nerve fiber to include the nucleus of a Schwann cell, it would reveal ultrastructural relations similar to those shown in Figure 5.24. A longitudinally cut nerve fiber with a thicker myelin sheath is shown in Figure 5.27**A**. Electron micrographs of adult unmyelinated nerves may reveal several axons lying within recesses of one Schwann cell (Figs. 5.24 and 5.27**B**). The plasma membrane of the Schwann cell is closely apposed to the axon except for a small periaxonal space of 15–20 nm (20). However, at some point around the circumference of each unmyelinated axon, the plasma membrane is reflected and extends superficially to form the mesaxon (Fig. 5.27**B**).

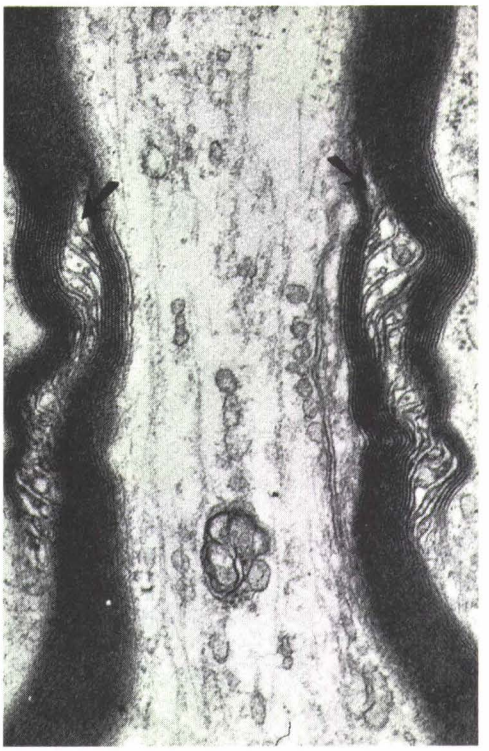


Figure 5.26. Schmidt-Lantermann cleft (*arrows*). Clear areas consist of Schwann cell cytoplasm.

Connective Tissue Sheaths

In addition to the foregoing structures, peripheral nerve fibers are surrounded by protective sheaths formed by connective tissue. These sheaths vary in thickness depending on the number of nerve fibers involved. They can be grouped into three different types: endoneurium, perineurium, and epineurium.

ENDONEURIUM

The *endoneurium* (sheath of Henle, or of Key and Retzius), is a reinforcing sheath of delicate connective tissue that surrounds individual peripheral nerve fibers. It is composed of delicate collagenous fibers, disposed longitudinally for the most part, a homogeneous ground substance, and an occasional flattened fibroblast. A close contact between the endoneurial collagen and the basement membrane of Schwann cells is an inevitable consequence of the ensheathing of nerve fibers in collagen. Actual "collagen pockets" surrounded by Schwann cells have been observed along nonmyelinated axons. Thin bundles of collagen usually can be observed within the typical basement membrane surrounding a Schwann cell (63). The endoneurium is continuous with the more abundant connective tissue of the perineurium, which envelops both small and large bundles of fibers within a peripheral nerve trunk.

PERINEURIUM

The outermost layers of the perineurium are composed of dense concentric layers of mostly longitudinally arranged strands of collagen. A few fibroblasts and macrophages

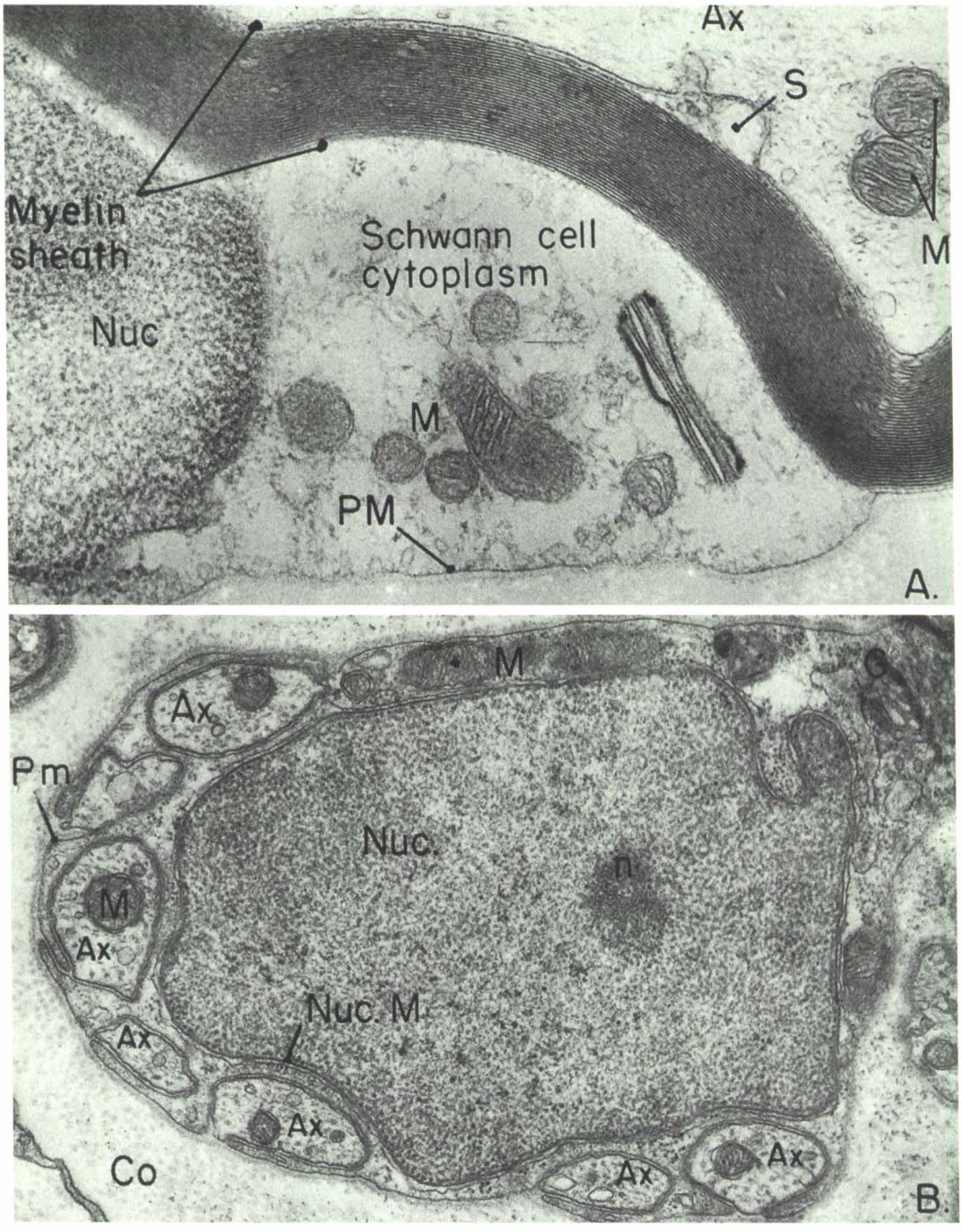


Figure 5.27. **A.** Part of a myelinated nerve fiber in cross section. The Schwann cell cytoplasm and axoplasm (*Ax*) both contain mitochondria (*M*). Note the alternation of dense lamellae with less dense intermediate layers in the myelin sheath. This sheath is composed of thinned out Schwann cell cytoplasm wrapped concentrically around the axon (*Ax*). The innermost layer of the myelin sheath displays a local swelling (*S*). The plasma membrane (*PM*) of the Schwann cell envelops the entire structural complex (mouse sciatic nerve, ×39,000). **B.** Electron micrograph showing the relationship of several unmyelinated axons (*Ax*) to the plasma membrane (*Pm*) of a Schwann cell. The nuclear membrane (*Nuc. M*), the nucleus (*Nuc*), and the nucleolus (*n*) are identified. Mitochondria (*M*) and the Golgi complex (*G*) can be seen within the cytoplasm, while fine collagen fibrils (*Co*) surround the Schwann cell (mouse sciatic nerve, ×26,000).

are also present among the strands. Perineurial tissue is somewhat unique in that it consists of fibroblasts and smooth lamellae that resemble mesothelium (41). The deeper concentric layers of flattened cells have prominent basement membranes, often with closed contacts. The flattened cells also have a slightly granular cytoplasm with scattered mitochondria and rough-walled vesicles. Large molecular dyes, silver nitrate, toxins, and [^{131}I]-labeled proteins have been used to investigate the blood-nerve barrier in animals (196). The peripheral nerve of the rabbit has an effective nerve barrier, interpreted as due to the vascular endothelium rather than the mesothelial cells that accompany the endoneurial connective tissue.

EPINEURIUM

This dense, collagenous layer forms an external connective tissue ensheathment for all peripheral nerve trunks. It is continuous centrally with the dura mater of cranial and spinal nerves. Its fibrous nature reinforces the toughness of peripheral nerve trunks. The collagen strands are disposed mainly longitudinally, and the component fibers have diameters between 70 and 85 nm. A few elastic fibers and fibroblasts with elongated processes are scattered throughout the epineurium. Axial arteries to peripheral nerves are derived from the large arteries adjacent to nerve trunks. Arteries that provide nourishment to a peripheral nerve penetrate the epineurium and give off several branches. The smaller arterioles pursue proximal or distal courses within the perineurium of the nerve trunk. Most of the capillaries supplying the peripheral nerve fibers are located in the endoneurium.

Grouping of Nerve Fibers

The unmyelinated peripheral nerve fibers consist of slender axons enveloped by the thin Schwann cell sheath, its basement membrane, and fine strands of collagen (Figs. 5.24 and 5.27**B**). The critical point for fiber myelination of an axon in tissue culture is reported to be a diameter of 1 μm (19). Axons of thicker diameters always are invested with a myelin sheath. The peripheral axons of most postganglionic sympathetic neurons and many cells of the spinal ganglia are unmyelinated (47). Numerous unmyelinated fibers are also found in the gray and white matter of the spinal cord and brain. Here they appear as fine naked axons embedded in glial cell processes with relationships similar to that of the Schwann cells on the peripheral unmyelinated fibers (18, 122, 123).

Myelinated fibers vary greatly in size. The fine fibers have a diameter from 1–4 μm; those of medium size from 5–10 μm; and the largest from 11–20 μm. Collaterals or branches are given off by most fibers of the central nervous system. They are usually of finer caliber than the parent stem, extend at right angles, and often arise from the proximal unmyelinated part of the axon. In the myelinated portion they are given off at the nodes of Ranvier and become myelinated themselves. In the peripheral nervous system, the fibers of somatic motor neurons, which supply skeletal muscle, branch repeatedly at acute angles before reaching the muscle. Within the muscle, the branching may be very extensive, and a single nerve fiber may furnish motor terminals to many muscle fibers. Sensory fibers probably branch in a similar manner since their terminal arborizations extend over a considerable area. A single myelinated fiber may supply sensory endings to more than 300 hair follicle groups.

Myelinated fibers conduct more rapidly than unmyelinated ones. Speed of conduction is proportional to the diameter of the fiber and, especially, to the thickness of the myelin sheath. The myelin sheath may be regarded as insulation, while the extracellular space at the nodes of Ranvier and the periaxonal space provide ready avenues for ionic diffusion.

When an axon is excited, a finite length of the axonal membrane is depolarized. This zone of depolarization is propagated along the length of the axon and is known as a nerve impulse or action potential. An impulse consists of a large negative voltage deflection of short duration, the *spike potential*, which is usually followed by two longer, but much smaller, voltage shifts known as the *negative and positive after-potentials*. The speed with which the spike potential travels over the nerve fiber constitutes the *conduction velocity* of the nerve impulse, and the number of successive potentials traversing the fiber per unit time represents the frequency of the impulses (Fig. 5.1).

As early as 1937, Erlanger and Gasser demonstrated that different fibers in a nerve trunk conduct at varying velocities (48). As mentioned earlier, the speed of conduction is

proportional to the diameter of the fiber and of the myelin sheath. Each nerve has a characteristic pattern of velocities corresponding to an analogous pattern of fiber diameters in the nerve trunk. As a result of extensive physiologic investigations supported by histologic studies, nerve fibers have been grouped into three main classes, A, B, and C (Table 5.2). The A group includes several subdivisions, designated A_α, A_β, A_γ and A_δ. Criteria for the classification are fiber diameter, conduction velocity, threshold to electrical stimulation, and patterns of electrical signaling (11, 64, 81, 82, 87, 120, 146, 153).

The type A fibers are myelinated, range in diameter from 1–22 μm and conduct at rates of 5–120 m/sec. The more finely myelinated B fibers have a diameter up to 3 μm and a conduction rate of about 3–15 m/sec, although a higher velocity has been observed in some fibers of this group. The C fibers are unmyelinated and conduct very slowly, about 0.6–2 m/sec. There is a certain amount of overlap so that a fiber of 2 μm could belong to either the A or B group, but certain features of the electrical signaling permit a definite classification. The duration of the spike potential is always much longer in type B fibers than in type A fibers, and the type B fibers lack a negative afterpotential.

Studies on various types of nerves (muscular, cutaneous, and autonomic) indicate a general functional grouping of the three classes of fibers. This grouping must not be regarded as rigid, since many fibers serving the same function may have widely different calibers. The type A fibers comprise several subdivisions. The largest and most rapidly conducting fibers (conduction velocity 70–120 m/sec in humans) transmit motor impulses to skeletal muscles, while other type A fibers convey afferent impulses from stretch receptors in muscle. The rest of the type A fibers, varying considerably in diameter and speed of conduction, carry afferent impulses from cutaneous receptors. Fibers of intermediate size are related to touch and pressure. The finest fibers transmit impulses associated with pain, and some of these fibers conduct thermal and tactile impulses.

Type B fibers are associated mainly with visceral innervation and are both efferent and afferent. All the preganglionic autonomic fibers belong to this group, as well as the postganglionic fibers from the ciliary ganglion, which are partly or wholly myelinated. The more rapidly conducting type B fibers transmit afferent impulses from viscera. The unmyelinated type C fibers comprise the efferent postganglionic autonomic fibers and afferent fibers which are believed to conduct impulses of poorly localized pain from the viscera and the periphery (Table 5.2).

The classification of axons in peripheral nerves on the basis of conduction velocity reveals certain correlations with function. When sensory physiologists studied the organization of dorsal root fibers activated by natural stimuli, it was convenient to use a classification that applied specifically to sensory neurons, and they identified axons as belonging to groups I, II, III, and IV. Each group is activated by particular types of sensory stimulation and contains fibers of a particular size range. These are shown in Table 5.2 along with the corresponding conduction velocity classification.

SYNAPSES

The simplest segmental reflex requires at least two neurons. The action potential, initiated in a peripheral sensory nerve ending, passes centrally along the axon of a dorsal root ganglion cell into the spinal cord. There it activates a motor neuron, whose action potential travels along the motor fiber and causes a group of muscle fibers to contract (Fig. 10.23). Even simple reactions have, as a rule, a central neuron interposed between the afferent and efferent cells (Fig. 10.24). In the more complicated neural circuits, the number of such *interneurons*, or *internuncial* central neurons, may be very large. All neural pathways therefore consist of chains of neurons related to each other so as to make possible the continuity of signal transfer over the complete circuit. The point of junction of neurons, that is the region where the axonal arborizations of one neuron come in contact with the cell body or dendrites of another, is known as the *synapse*. The synapse is not a site of cytoplasmic continuity between neurons, but a functional interface between two neurons. Axons terminating upon the dendrite of another neuron form *axodendritic synapses*, whereas axons terminating upon the cell soma or perikaryon form *axosomatic synapses*. Less frequently, axon terminals of one neuron may be located directly on other axonic terminals, or on the initial segment of the axon of another neuron *(axoaxonic synapses)*. The

Table 5.2.

PERIPHERAL NERVE FIBER CLASSIFICATION				
FIBER TYPE		FUNCTION	SIZE (μm)	CONDUCTION Velocity (m / sec)
Aα	Ia	Proprioception, stretch, Primary muscle spindle afferents Motor efferent to muscles (extrafusal)	12 - 22	70 - 120
Aα	Ib	Contractile force: Golgi tendon organ afferents	12 - 22	70 - 120
Aβ	II	Mechanoreception: discriminative touch, pressure, joint rotation Secondary muscle spindle afferents	5 - 12	30 - 70
Aγ	II	Muscle spindle (intrafusal) efferents	2 - 8	15 - 30
Aδ	III	Mechanoreception: touch Nociception: discriminative pain	1 - 5	5 - 30
B	-	Sympathetic preganglionic axons	< 3	3 - 15
C	IV	Nociception: in inflammatory or visceral pain, thermal sense	0.1 - 1.3	0.6 - 2.0

term "synapse," coined by Sherrington at the turn of this century (176), may be expanded to include the functional contacts between two neurons and those between neurons and effector cells, such as muscle cells.

Synaptic junctions show many structural variations (Fig. 5.28) (174). Commonly, the axon terminals end in small bulblike expansions *(end feet, boutons terminaux)*. In terms of cytoskeletal elements, each terminal consists of a neurofibrillary loop embedded in perifibrillary substance; sometimes there are simply small neurofibrillary rings. A large motor neuron in the spinal cord may receive as many as 10,000 such endings, most of them 1–2 μm in diameter. Approximately 8000 of these synapses are located on dendrites and 2000 on the soma of the motor neuron. In another type of synapse, the delicate axon terminals do not form end feet but come in lengthwise apposition with the dendrites or cell body, often for considerable distances. The most striking example is the climbing fibers of the cerebellum (Figs. 15.4 and 15.5). In some cases, unmyelinated axons run at right angles to the dendrites and come in contact with the spiny-excrescences or *gemmules* with which the dendrites are beset (Fig. 5.9). Dendritic spines are, in fact, major sites of synaptic contacts. One axon may convey impulses to many neurons, and, conversely, one neuron (e.g., anterior horn cell) may receive impulses from many other neurons, some of which are widely separated in the neuraxis.

Ultrastructural Characteristics

The first electron microscope studies of the synapses in the 1960s (37, 75–77, 124) showed that all synapses in the vertebrate nervous system are composed of three basic elements: the presynaptic axon terminal, the postsynaptic target site, and the minute synaptic cleft that separates them. The presynaptic element of the synaptic complex possesses the necessary metabolic machinery for the synthesis, stocking, release, and inactivation of the neurotransmitter. This is evidenced by the presence of mitochondria, neurofilaments, and numerous synaptic vesicles. In contrast, the postsynaptic element is specialized for the reception of the neurotransmitter. Its plasma membrane, which often displays electron-dense specializations, contains complex pro-

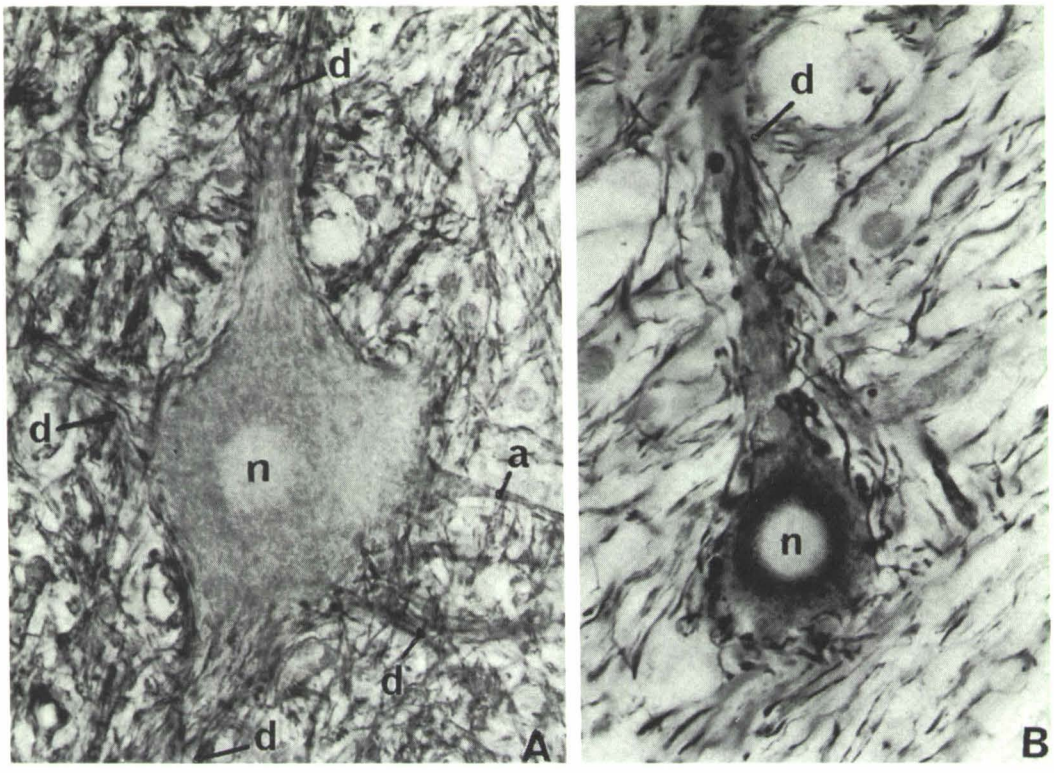


Figure 5.28. Synaptic endings on human CNS neurons after silver impregnation and observed by light microscopy. Note numerous terminal boutons on the dendrites (*d*, axodendritic synapses) and some on the cell body (axosomatic synapses). The axon (*a*) and nucleus (*n*) are identified in **A** (×650). The smaller neurons shown in **B** are magnified ×920.

teins that act as a receptor for the neurotransmitter. The synaptic cleft that separates the pre- and postsynaptic elements is usually 20–40 nm in width (Figs. 5.30 and 5.31).

Two major types of synapses can be recognized on the basis of morphologic criteria. These are referred to as Gray type I and type II, after the investigator who first described them (75). In type I synapses, the cleft is approximately 30 nm, the presynaptic zone is 1–2 μm^2 in area, and dense projections, the presumed release sites for the vesicles, are prominent. The synaptic vesicles are mostly round, although this varies according to the fixative used for electron microscopy. Amorphous dense basement membrane material exists in the synaptic cleft and the postsynaptic membrane displays a markedly dense region, which gives to this type of synapse a typical asymmetric appearance (75–77). These type I, or *asymmetric synapses*, are often associated with glutamatergic excitatory synapses (Fig. 5.18). In type II synapses, the cleft is 20 nm wide, the active zone is small (less than 1 μm^2), there is little or no basement membrane material in the cleft, and the postsynaptic membrane specializations and dense projections are not obvious. The last feature gives this type of synapse a more symmetric appearance in comparison to the type I synapses (Fig. 5.18). The type II, or *symmetric synapses*, are often associated with the GABAergic inhibitory synapses. Despite that the notion of symmetric and asymmetric synapses is used in contemporary studies of the synaptologic organization of the central nervous system, it must realized that these two forms of synapses may represent the two extremes of a morphologic continuum.

Electrical Synapses

There was a considerable debate during the first half of this century as to whether neural transmission is electrical, as proposed by the physiologic school led by John Eccles, or chemical, as advocated by the pharmacologic school led by Henry Dale (36, 45).

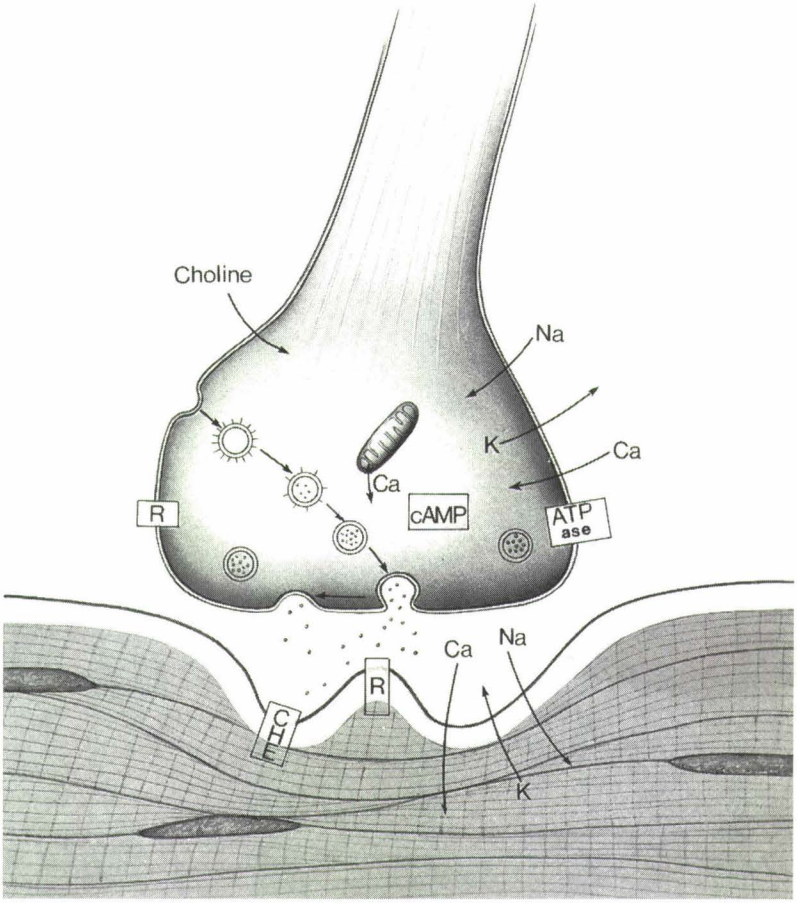


Figure 5.29. Motor nerve terminal and muscle end plate showing the major biochemical and biophysical events in neuromuscular transmission. (*ATPase*) adenosine triphosphate, (*cAMP*) cyclic adenosine monophosphate, (*CHE*) acetylcholinesterase, (*Ca*) calcium ions, (*Na*) sodium ions, (*K*) potassium ions, (*R*) transmitter receptor.

Today, we know that both electrical and chemical synapses exist in the central nervous system.

The term *electrical synapse* refers to a form of neuronal signaling that consists of current flow through *gap junction* channels that directly connect the cytoplasm of both neurons, which are separated from one another by only 3.5 nm. Gap junction channels consist of paired hemicylinders in the membrane of each interconnected cell that are permeable to small molecules and some second messengers. Electrical synapses can be either unidirectional (rectifying) or bidirectional (nonrectifying), and are the most rapid form of synaptic transmission. They allow for rapid and synchronous firing of interconnected cells. Electrical synapses are abundant in invertebrates, but occur only in specific locations in the mammalian central nervous system. Their two major properties, speed and synchrony, render this type of synaptic connection ideal for fast, simple, and stereotyped behaviors.

Chemical Synapses

The *chemical synapse* is by far the most common form of neuronal signaling in the mammalian central nervous system. Chemical transmission is strictly unidirectional and slower than electrical transmission. This is because the presynaptic neuron must release a transmitter, which then diffuses across the synaptic cleft and binds to a receptor in the postsynaptic cell membrane (37–40, 201). However, chemical transmission has the advantage that a single action potential can induce the release of thousands of transmitter molecules, allowing amplification of the

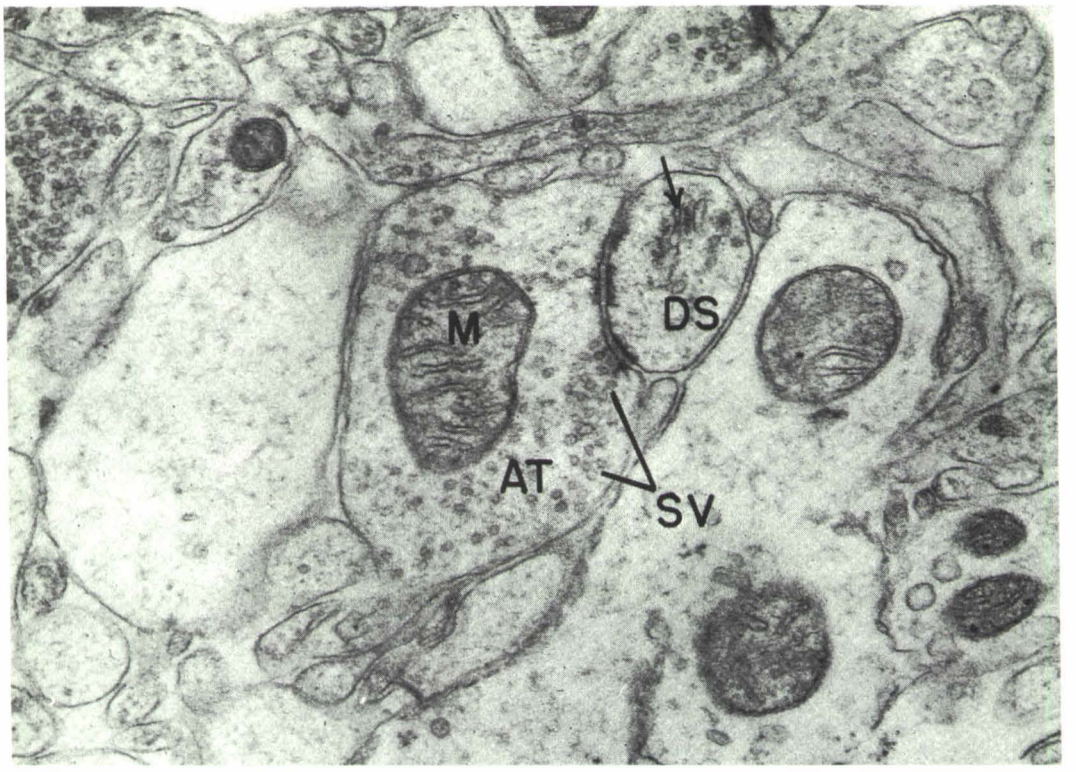


Figure 5.30. Axodendritic synapse in the human cerebral cortex. The saclike enlargement comprising the axon terminal (*AT*) contains a mitochondrion (*M*) and numerous vesicles (*SV*). The axon terminal is indented by the dendritic spine (*DS*). Profiles of the spine apparatus (*arrow*) are seen *above*, while to the *left* the postsynaptic membrane of the dendritic spines is thickened in three places (×38,500). Compare with synapse shown in Figure 5.28.

synaptic response. Perhaps because of its multistep process, chemical transmission is said to be more easily modified than electrical transmission. Its plasticity renders chemical synapses more suitable than electrical synapses for complex behaviors, such as learning, which involves stabilization and reinforcement of neuronal circuits (98).

In chemical synapses, neurotransmitters are largely sequestered within synaptic vesicles in the presynaptic element. In the case of cholinergic neurons, each electron-lucent synaptic vesicle is considered to contain a quantum of acetylcholine which is released when an action potential arrives at the synapse (38, 99, 201, 208). At the neuromuscular junction, quanta of acetylcholine, released a few at a time during quiescence, are associated with miniature end plate potentials (52, 100). The most commonly occurring synaptic vesicles are about 40 nm in diameter, are roughly spherical and have clear centers (Figs. 5.30 and 5.31). Vesicles of this type are found in axon terminals at neuromuscular junctions, throughout the central nervous system, and in some sympathetic nerve endings. In cholinergic autonomic neurons, each synaptic vesicle contains an estimated 1600 molecules of acetylcholine (203). The vesicles also contain 1 molecule of ATP for every 4 molecules of transmitter. Furthermore, several proteins (e.g., caldesmin, synapsins, annexins, and synaptophysin) associated with the membranes of synaptic vesicles are believed to be involved in the mobilization of synaptic vesicles from a general pool in the axon terminal to the docking sites at the presynaptic membrane. Some of these proteins are also involved in the Ca^{2+}/dependent mechanisms underlying the fusion and the recycling of vesicle membranes.

Vesicle Recycling

As the nerve impulse invades the terminal, there is an influx of calcium ions which leads to the exocytosis of synaptic vesicles and the release of transmitter into the synaptic cleft (184) (Fig. 5.29). The transmitter molecules diffuse across the cleft and bind to receptor mole-

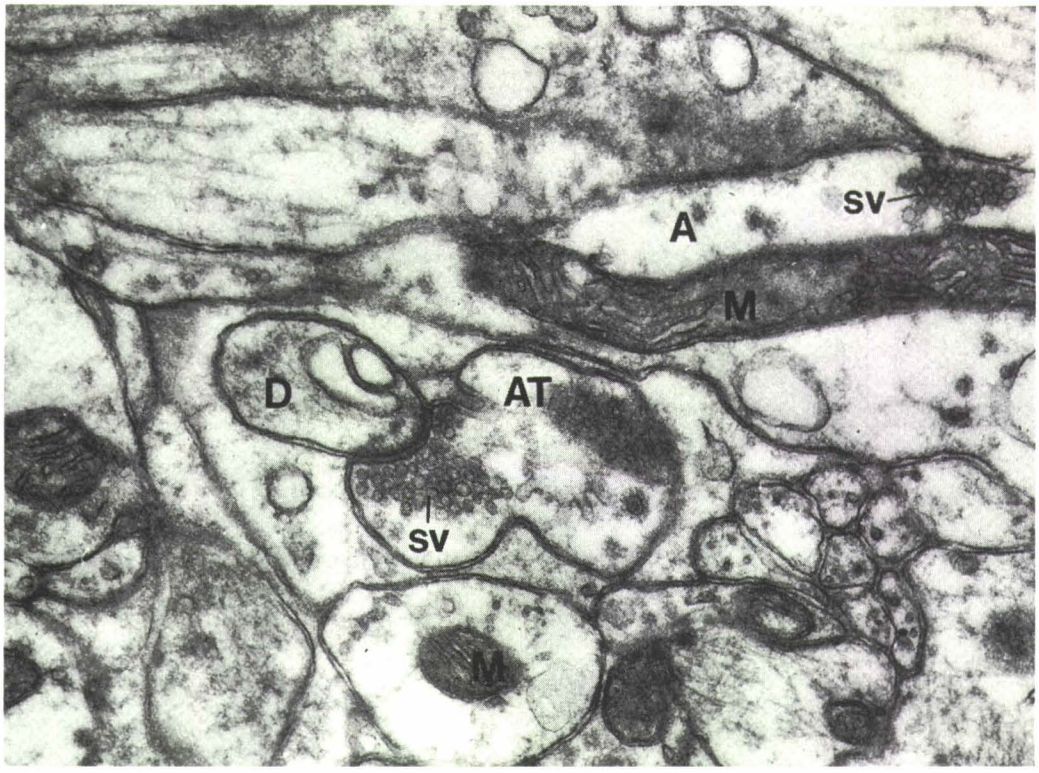


Figure 5.31. Axodendritic synapse in monkey cerebellar cortex. Synaptic vesicles (*SV*) are present in the axon terminal (*AT*) and in the axon (*A*) in the *upper right*. Other organelles are dendrites (*D*) with spine apparatus, and mitochondria (*M*) (×48,000).

cules in the postsynaptic membrane. Transmitter molecules that are not bound to receptors are either inactivated in the synaptic cleft region by degrading enzymes (e.g., acetylcholinesterase for acetylcholine and monoamine oxidase for biogenic amines) or returned back into the presynaptic ending through a highly specific and very powerful reuptake mechanism. This mechanism involves the use of highly specific protein complexes known as *transmitter transporters*. When a transmitter is released from vesicles by exocytosis, the membrane of the discharged vesicles becomes incorporated into the surface membrane of the presynaptic terminal. If no process compensates for exocytosis, the membrane of a synaptic terminal would enlarge as a result of nerve activity, because vesicle membrane would be continuously added to the plasmalemma. This does not happen, however, because new synaptic vesicles are continuously generated in the terminals through the process of *endocytosis* that occurs in the presynaptic membrane. Other synaptic vesicles are recycled at a certain distance from the site where they were originally. This recycling process is called *transcytosis* and involves the retrograde transport of membrane material within endosomes. New synaptic vesicles are also formed at even further distances from the active zone by the endoplasmic reticulum (88, 89). In fact, the total amount of membrane in vesicles, cisternae, and plasma membrane in the axon terminal remains constant, indicating that membrane is indeed recycled from the plasmalemma into the internal organelles.

Receptors

It is extremely important to realize that, in the process of chemical transmission, it is the receptor, not the transmitter, that determines whether the synaptic response is excitatory or inhibitory. Indeed, the action of transmitters depends on the properties of the receptors, not on the chemical nature of the transmitter. For example, acetylcholine produces synaptic excitation at the neuromuscular junction by acting upon a nicotinic receptor, whereas it slows the heart by acting on a muscarinic inhibitory receptor. The notion of receptor was

introduced in the late 19th century by the German biochemist Paul Ehrlich to explain the action of various toxins and the specificity of immunologic reactions (46). This concept was substantiated by the work of the English pharmacologist John Langley and two of his students, Henri Dale and Eliot Smith, on curare and nicotine.

Receptors are essentially large membrane-spanning (integral) proteins that allow the signaling molecule to exert its effect upon the target cell. More specifically, they consist of complex macromolecules containing several protein subunits that form the recognition element and the ion channel. Channels can be distinguished from one another by their ion selectivity and the factors that control their opening and closing, or gating. Ion selectivity is achieved by physical and chemical interactions between the ion and various amino acid residues that line the wall of the pore. Gating involves a conformational change of the channel in response to various external stimuli, particularly voltage and ligands (177). There are two major classes of receptor proteins that derive from two distinct gene families: receptors that gate ion channel directly and receptors that gate ion channel indirectly by initiating a second messenger cascade.

Receptors that gate ion channel directly, such as the cholinergic receptor at the neuromuscular junction, consist of a single macromolecule that comprises both the recognition element and the ion channel. When bound to a transmitter, such *inotropic receptor* undergoes a conformational change that opens the channel. In the brain, the actions of glutamate, GABA, and glycine are mediated by receptors of this type (98). Receptors that gate ion channel indirectly, such as those for norepinephrine and serotonin in the cerebral cortex, are called *metabotropic receptors*. They involve separate recognition elements and ion channels that communicate through guanosine triphosphate (GTP)-binding proteins (G-proteins). These G-proteins couple the receptor to effector enzymes that produce intracellular second messengers, like 3′, 5′-adenosine monophosphate (cAMP) and diacylglycerol. The second messengers can act on the channel directly, but more commonly they activate protein kinases, which induce conformational changes by phosphorylating either the channel protein or a regulatory protein that acts on the channel (113). G-proteins can also interact directly with the ion channel, without the intervention of second messengers.

Directly-gated transmission is only slightly slower than electrical transmission since it is mediated by receptors that are part of the ion channel molecule. This form of chemical signaling allows for fast synaptic actions that are in the millisecond range. In contrast, indirectly-gated transmission, which involves formation of second messengers, is much slower, lasting seconds and even minutes. This form of chemical signaling serves to modulate behavior by altering the excitability of neurons and the strength of synaptic connections (98).

The cortical noradrenergic synapse is good example of indirectly-gated transmission. When norepinephrine binds to the postsynaptic metabotropic receptor on the surface of cortical neurons, the enzyme adenylate cyclase is activated. Adenylate cyclase then catalyzes the conversion of adenosine triphosphate (ATP) to cAMP. In the cytoplasm, cAMP may activate one or several protein kinases, which in turn may regulate phosphorylation of either plasma membrane proteins (56) or acidic nuclear proteins (Fig. 5.32). A lesion of the noradrenergic fibers innervating the cortex or a pharmacologic blockage of the noradrenergic transmission will lead to an increased number and/or sensitivity of adrenergic receptors in postsynaptic cells (130). This *upregulation* of adrenergic receptors accounts for the phenomenon called *denervation supersensitivity*.

In addition to the directly- and indirectly-gated transmission, transmitters, acting through second messengers, can phosphorylate transcriptional regulatory proteins, altering gene expression. Through their action via second-messenger kinases, transmitters can induce the synthesis of new proteins, a phenomenon that could be involved in the regulation of receptor molecules themselves, as well as the induction of rate-limiting enzymes available for the synthesis of new transmitters in postsynaptic cells (Fig. 5.33). In the case of catecholaminergic neurons, denervation results in lowered levels of cAMP in the postsynaptic cell. This decrease in cAMP leads to an increase in the amount of tyrosine hydroxylase (2). These *genomic transmitter effects* appear to be part of a mechanism whereby neurons attempt to adjust their input/output sensitivity to compensate for a reduced number of afferent axons.

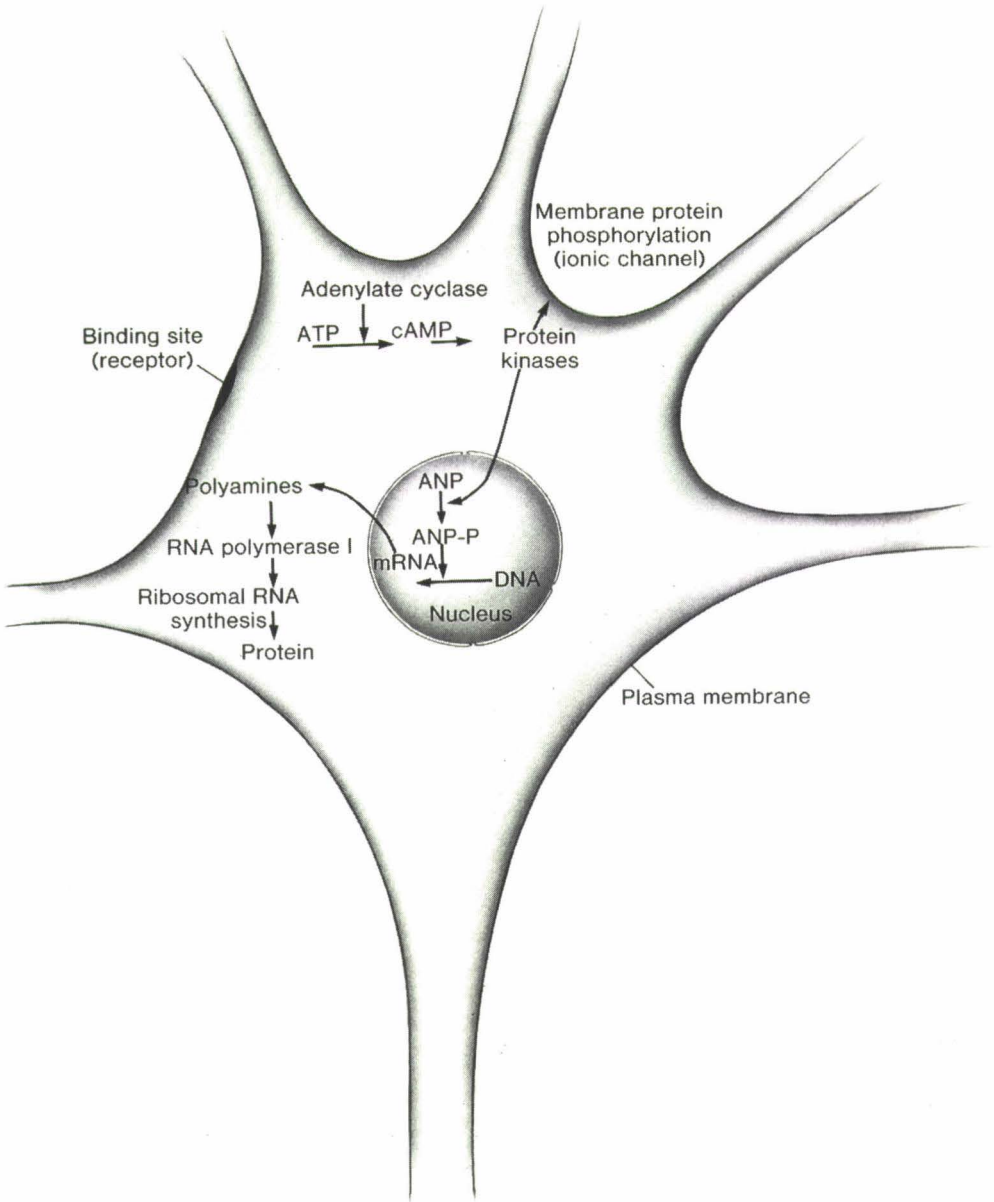


Figure 5.32. How cyclic AMP may participate in synaptic transmission and also initiate trophic changes. A transmitter receptor site in the surface membrane is shown in the *upper left*. When the catecholamine transmitter binds to the receptor, adenylate cyclase becomes available to form cyclic adenosine monophosphate (*cAMP*). cAMP activates protein kinases, some of which phosphorylate surface membrane proteins presumed to be associated with ionic channels. Other protein kinases may migrate to the nucleus initiating a chain of events ultimately resulting in increased protein synthesis. (*ATP*) adenosine triphosphate, (*ANP*) acidic nuclear protein, (*ANP-P*) phosphorylated acidic nuclear proteins, (*DNA*) deoxyribonucleic acid, (*mRNA*) messenger ribonucleic acid.

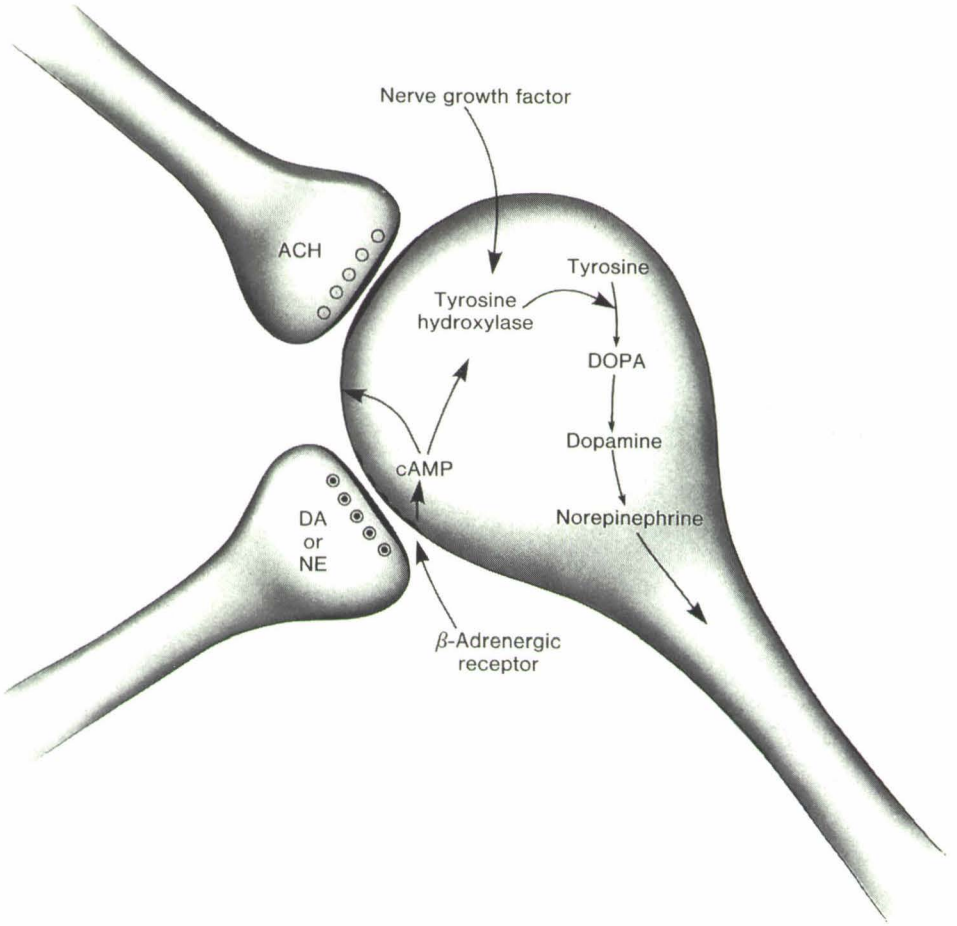


Figure 5.33. Cholinergic (*ACH*) and catecholaminergic (dopamine (*DA*) or norepinephrine (*NE*)) synapse upon a noradrenergic cell of the superior cervical ganglion. The level of the enzyme tyrosine hydroxylase, the rate limiting enzyme in the synthesis of DA and NE, is regulated by the level of cAMP. Prolonged periods of increased cAMP levels results in reduced amounts of tyrosine hydroxylase.

The enduring synthesis of new proteins by transmitter genomic action is important because, among other things, it appears to be involved in the complex phenomenon whereby a given chemospecific afferent can regulate the concentration of another transmitter in a postsynaptic target cell (Fig. 5.34). Such a regulation occurs in the superior cervical ganglion where the amount of norepinephrine synthesized is regulated transynaptically through synaptic receptors in response to the activity of cholinergic afferents. If the activity of the cholinergic presynaptic neurons is sufficiently prolonged, the released acetylcholine will induce relatively long-term changes on the postsynaptic cell, including an increase in the supply of norepinephrine through an increase in tyrosine hydroxylase. These genomic regulatory mechanisms also occur in catecholaminergic cells of the central nervous system (96, 98). Many of these effects are mediated through cAMP and cGMP (Fig. 5.34). The specific effects of cAMP and cGMP are not known, but it is hypothesized that each cyclic nucleotide phosphorylates different membrane proteins (78, 79).

In recent years, there has been great interest in the role of a calcium-binding protein called *calmodulin*. The calmodulin/calcium complex may regulate some of the enzymes related to cyclic nucleotide formation or degradation (27). Calmodulin is a highly conserved protein with a molecular weight of 17,000. In the presence of calcium, this protein binds reversibly to many enzymes and other proteins, thereby regulating their function. For additional details on the anatomic and functional organization of the synaptic complex the reader is referred to the studies of Peters, et al. (150), and Kandel, et al. (98).

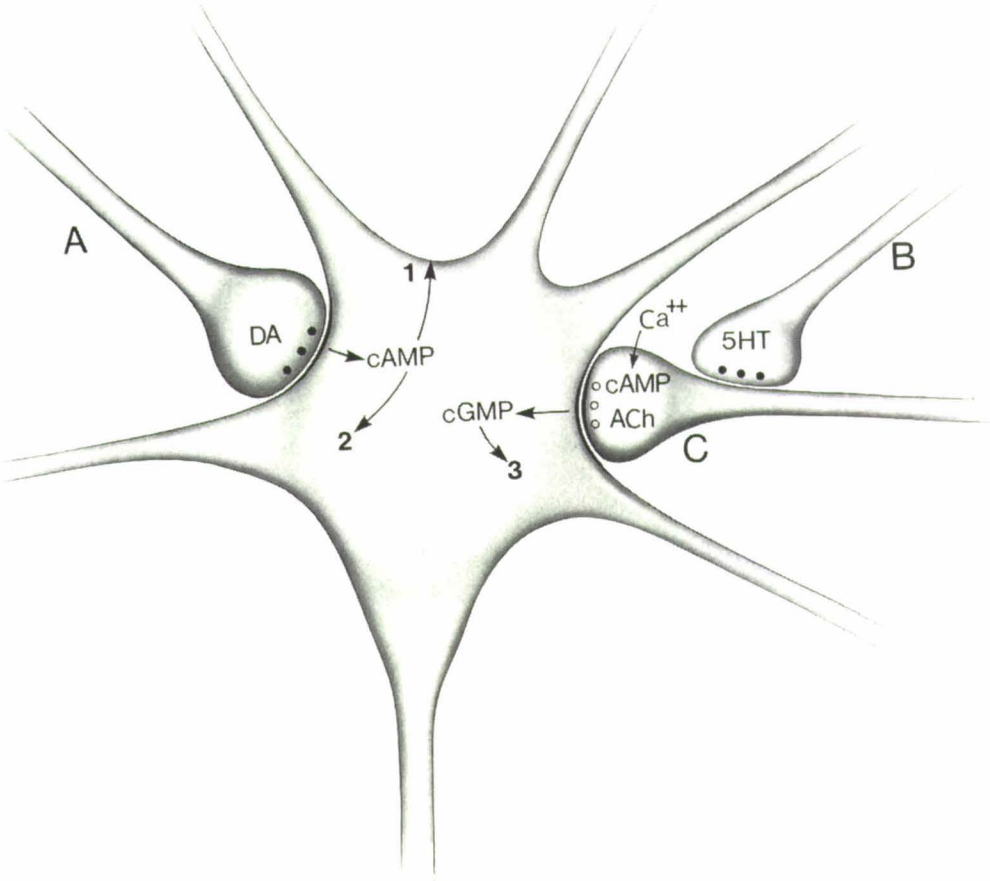


Figure 5.34. Ways in which synaptic actions might be mediated by a second messenger. This model is based upon observations of the nervous system in invertebrates and vertebrates. *Cell A* is dopaminergic and controls the level of 3',5'-adenosine monophosphate (cAMP) in the postsynaptic cell. cAMP may (*1*) phosphorylate a membrane protein to alter membrane ionic permeability and/or (*2*) alter synthesis of a rate limiting enzyme for transmitter synthesis. *Cell B* is serotoninergic and increases cAMP in the presynaptic terminal of *cell C*, resulting in an increased calcium permeability and transmitter exocytosis. *Cell C* is cholinergic and increase 3',5'-guanosine monophosphate (cGMP) in the postsynaptic cell. Increased cGMP (*3*) may phosphorylate a different specific membrane protein.

AXOPLASMIC TRANSPORT

Axoplasmic transport refers to the movement of proteins and other substances along the axon. The movement occurs in both directions: *anterograde*, from cell body toward axon terminal, and *retrograde*, from terminal toward cell body (Fig. 5.40). Axonal transport is extremely important for the growth and maintenance of neurons. Indeed, virtually all of the protein synthesis in neurons occurs in the cell body, with only minor amounts detected in axons, terminals, and distal dendrites. The growth and subsequent maintenance of long axonal and dendritic processes must require some mechanism for moving newly synthesized structural protein and enzymes throughout the neuron.

Two early observations led to the concept of axoplasmic flow. It was found that constriction of an axon by a ligature led to a buildup of material on the proximal side (199, 200), and that proteins migrated along axons in both the peripheral and central nervous system (42) (Fig. 5.41**B**). Isotopically labeled amino acids injected near the cell body are transported into the cell and become incorporated into newly synthesized proteins. The movement of the labeled proteins along the axon can be measured by either scintillation counting or autoradiographic methods. A method was also devised which permits direct labeling of cellular protein (53). More recently, direct observation made with video-enhanced microscopy (4) has shown that large particles move in a stop-and-go (salta-

tory) fashion in both the anterograde and retrograde directions in the axon. Anterograde transport has been found to occur at two different rates, termed fast and slow. Furthermore, the slow axonal transport has fast and slower components.

Anterograde Transport

The fast anterograde transport predominantly serves to export membrane bound vesicles derived from the Golgi apparatus and endoplasmic reticulum, including membrane bound neurotransmitters, from the cell body to the axon and axon terminals (Fig. 5.40) (35, 74, 107, 108, 141). This component has a mean rate of about 400 mm/day (43, 140). The fast anterograde transport depends on oxidative metabolism, is not affected by inhibitors of protein synthesis, and is independent of the cell body. It is largely based on microtubules that provide stationary tracts on which organelles move in a saltatory fashion (171, 191). Fast transport can be blocked by the alkaloids colchicine or vinblastine, which bind to tubulin and disrupt microtubules, while slow transport is much less impaired.

The slower component of slow axonal transport occurs at rates of 0.2–2.5 mm/day and principally involves cytosol elements, that is, soluble enzymes and filamentous proteins that make up microtubules and neurofilaments, which is approximately 75% of all proteins transported in the slower component (Table 5.3) (72). Neurofilaments and microtubules move in a polymerized form as a network with regulatory and cross-linking proteins tightly associated with them. The faster component of the slow transport moves twice as fast as the slower component. Its protein composition is rather complex, involving cytoskeletal proteins such as actin, myosinlike protein, clathrin, calmodulin, as well as enzymes of the intermediary metabolism formed on free ribosomes. Clathrin is a protein that has a molecular weight of 180,000 and forms a highly ordered polyhedral coat around synaptic vesicles that are destined to be recycled. This protein plays an important role in the recycling of synaptic vesicle membrane.

The motor molecule for anterograde transport is believe to be *kinesin*, an ATPase that consists of two large subunits (α) each with a molecular weight of 125,000, and two small subunits (β). More than 20 years ago, cross-bridges between microtubules and vesicular particles that were believed to play a role in the transport of vesicles were observed at the electron microscopic level. Kinesin is most likely the protein that formed these bridges. Kinesin appears to contain a pair of globular heads that bind to microtubules and a fan-shaped tail that binds the organelles to be moved. Similarities between kinesin and muscle myosin has led to the hypothesis that organelles movement during axoplasmic transport is produced by the sliding of kinesin molecules along microtubular tracts (90).

Retrograde Transport

In addition to anterograde axoplasmic transport from cell body to distal processes, it was found that some substances can be taken up by axonal terminals or distal dendrites and transported back to the cell body (Fig. 5.40). The retrograde transport proceeds at a rate that ranges from one-half to two-thirds that of the fast anterograde axonal transport. Endocytosis (or micropinocytosis), which is the reverse of exocytosis, seems to be an important mechanism for incorporating within the axon terminal vesicles and various types of adsorbed and unadsorbed materials that are transported to the cell body and degraded within the system of lysosomal organelles (17). Retrograde transport may be studied by placing the glycoprotein horseradish peroxidase (HRP) in the vicinity of nerve endings. The enzyme marker adheres to the membrane of the axon terminal which is pinocytosed and transported back to the cell body for lysosomal degradation (110). The enzyme can be visualized by histochemical treatment using a substrate that is converted into a colored insoluble polymer.

The retrograde transport system has mainly a scavenger function. However, it can also inform the cell body about events that occur at the distant end of axonal processes. It also has the capability of taking up and transporting to the cell body important molecules, such as nerve growth factor (NGF), which can induce long-lasting metabolic changes in neurons. Furthermore, some viruses and toxins (e.g., *Herpes simplex*, rabies, polio viruses, and tetanus toxin) can reach the central nervous system by ascending from peripheral nerve terminals to the cell body by retrograde transport. The retrograde trans-

Table 5.3.

AXOPLASMIC TRANSPORT	
TYPE	SUBSTANCE TRANSPORTED
I. Anterograde transport	
a) Fast component (400 mm / day)	Noncytosolic material; principally bound vesicles deriving from Golgi apparatus and endoplasmic reticulum: neuroactive peptides, bound small transmitter molecules and some degradative enzymes.
b) Slow component (1-5 mm / day)	Cytosolic material: principally cytoskeletal proteins and various soluble enzymes including those necessary for transmitter synthesis.
II. Retrograde transport (200-300 mm / day)	Aging cytoplasmic organelles, endocytotic organelles (including vesicle membrane to be recycled), absorbed and unabsorbed exogenous material: viruses, toxins and various growth promoting and inhibiting factors.

port of some of these viruses or toxins may rapidly lead to various functional impairments.

The molecular mechanisms of retrograde transport are not as well understood as those of anterograde transport (170, 171). However, there is recent evidence suggesting that the motor molecule in retrograde transport is a form of dynein, which is also a microtubule-associated ATPase (MAP-1c). Dynein is a large protein complex containing two or three globular heads with an ATPase activity. It is involved in the beating of cilia in various unicellular organisms, as well as in the movement of chromosomes during cell division (3).

DEGENERATION OF NERVE FIBERS

The cell body is the trophic center of the neuron, and any process detached from it disintegrates. Crushing injuries or interruption of an axon produces detectable changes in the cell body (chromatolysis), as well as in the central and distal stumps of the injured fiber. When an axon is sectioned, degenerative changes of a traumatic character first affect the cut edges. In the proximal portion of the fiber, which is attached to the cell body, the degenerative changes (retrograde degeneration) extend only a short, although variable distance, depending on the nature of the injury. In a clean section, only one or two internodes may be involved. In more severe injuries, such as gunshot wounds or inflammatory processes, the retrograde degeneration may extend as much as 2 or 3 cm. However, the degeneration is soon succeeded by reparative processes leading to the formation of new axonal sprouts from the central stump.

Anterograde Degeneration

In the distal portion, the axon and myelin sheath completely disintegrate, and degeneration occurs throughout the length of the fiber, including its terminal arborization. This process is known as *secondary* or *Wallerian degeneration* (Figs. 5.35 and 5.36). The changes, as a rule, appear simultaneously along the length of the nerve fiber distal to the injury. Functional failure of the nerve also is abrupt down the length of the distal nerve trunk, as shown by Novak and Salafsky (139) and Salafsky and Jasinski (163). These electrophysiologic studies revealed that muscle responses to distal nerve stimulation ceased 54–72 hours after sciatic nerve section, depending on whether nerve injury occurred in the thigh or at the level of the knee. Axonal changes begin almost at once. Electron micrographs of the sciatic nerve following crush injury demonstrate that the initial change is an accumulation of mitochondria in the axoplasm at the nodes of Ranvier (Fig. 5.41**A**). This is followed by a breakdown of the axoplasm and mitochondria (198). Twelve hours after injury, the axon is swollen and irregular in shape. Within a few days, it begins to break into fragments. However, the breaking process may continue for a considerable time in some fibers, and fragments of degenerating axons have been found as late as 3–4 weeks after the injury. The synaptic terminals are affected similarly, and synaptic transmission is rapidly lost. Degenerating synaptic terminals become filled with electron-dense products of degeneration, including whorls of neurofilaments that surround swollen and disrupted mitochondria. The myelin sheath likewise degenerates. Two or three days after section, constrictions appear that fragment the myelin into elongated ellipsoid segments, which in turn break into smaller ovoid or spherical droplets or granules (Figs. 5.35 and

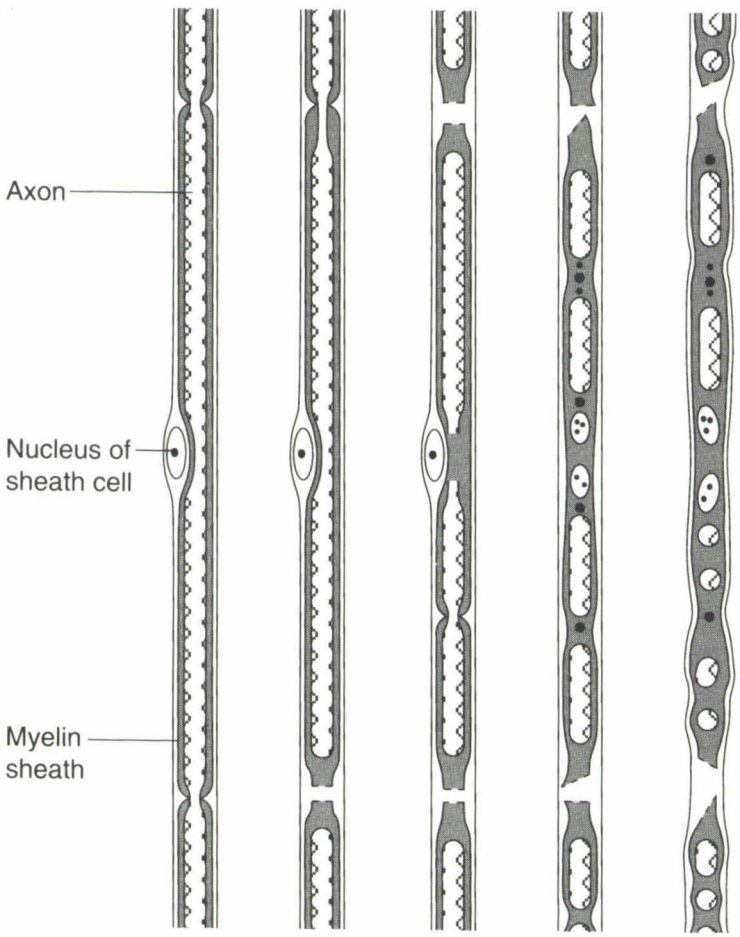


Figure 5.35. Breakup of myelin and axon during nerve degeneration. Note increase in sheath cell protoplasm and division of the nucleus.

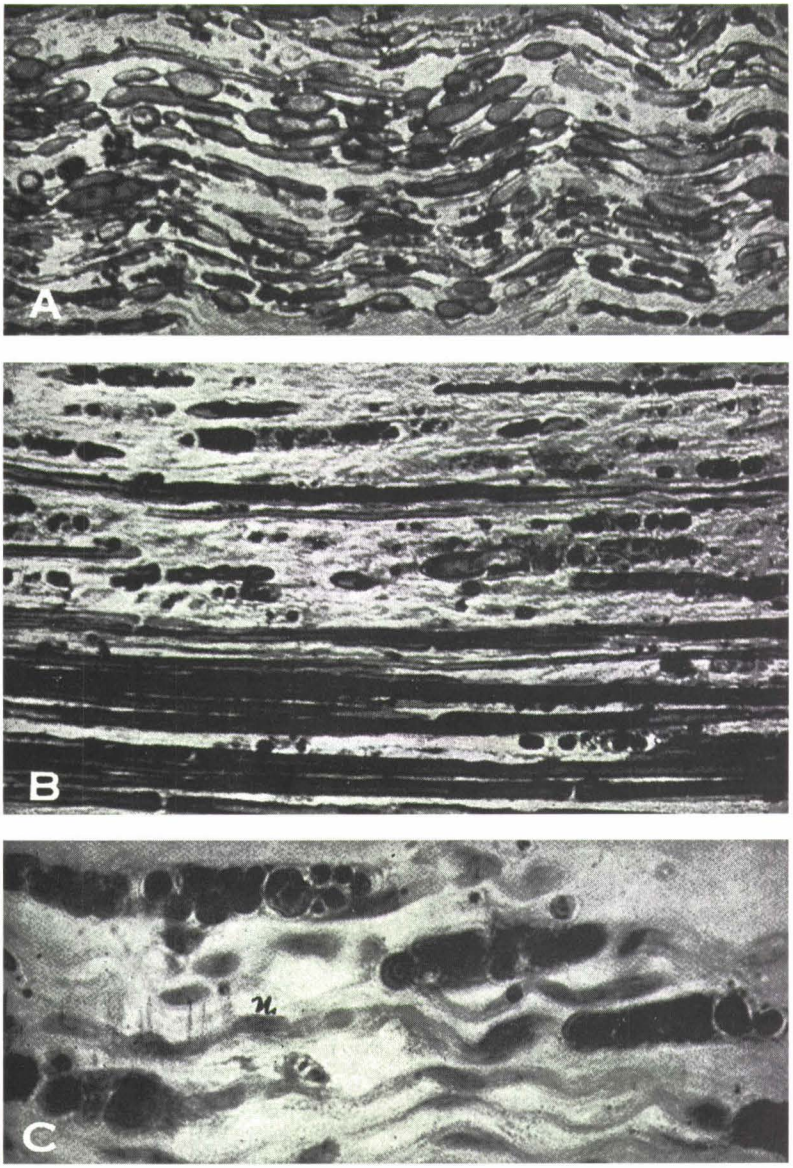


Figure 5.36. **A.** Distal stump of a nerve cut 3–5 days previously (osmic acid). **B.** Distal stump of a nerve partly cut 12–15 days previously (osmic acid). Normal fibers and two nodes of Ranvier are shown at the bottom. **C.** Distal stump of a nerve cut 12–15 days previously (osmic acid and iron hematoxilin). In addition to the clumps or islands of degenerating myelin, several bands of fibers and their nuclei (*n*) are shown.

5.36). The whole process resembles the breakup of a liquid column under surface tension and is ascribed to the fact that the fiber is no longer kept in a turgid condition by neuroplasmic pressure emanating from the cell body (206, 207).

The myelin changes, at first purely physical, are followed by chemical changes as well. The myelin breaks into simpler intermediate substances, which react to the Marchi stain. Ultrastructural studies provide information about the degenerative process. Nineteen hours after peripheral nerve injury there is a loosening of the myelin lamellae (112). Myelin disintegration is evident at 4 days in Schwann cells and well-advanced 96 hours after crushing dorsal roots of the cauda equina as shown by Nathaniel and Pease (134).

These authors have elucidated the key roles of the Schwann cell and its basement membrane in both degeneration and regeneration. Schwann cells undergo hypertrophy, demonstrate unusual numbers of ribosomes,

multiply in number, become mobile, and form elaborate basement membranes. These cells are almost exclusively responsible for the removal of axon remnants and autodigestion of disintegrated myelin. There is no connective tissue response in the endoneurium, and leucocytes do not appear to participate in the phagocytosis of neuronal debris. The only endoneurial response is a slow accumulation, and slight increase, in the amount of collagen adjacent to the basement membranes. Newly formed and hypertrophied Schwann cells have extensive tapering and overlapping cytoplasmic processes, which in light microscopy were interpreted as multinucleated syncytial cords (band fibers).

Nuclear division of the Schwann cells begins around the 4th day and continues actively to about the 25th day, mitosis occurring over the whole length of the fiber. The increase in the number of nuclei is considerable, in some instances as much as 13 times the original population (1). During degeneration, the Schwann cell plasma and basement membranes become separated from each other to markedly increase the extent and complexity of the extracellular spaces (134). The reactive Schwann cells form new, elaborately folded and successive basement membranes, one inside the other. These Schwann cells and basement membranes form numerous extracellular compartments or tubes surrounded by collagen of the endoneurium. Regenerating axonal sprouts from regions above the injury later enter these extracellular compartments or "tubes" between the basement membrane and Schwann cell. If no axonal sprouts enter the tube, it shrinks considerably and the walls thicken, due to the increase in the collagen content of the endoneurium.

Retrograde Degeneration

The neuronal cell body whose axon is injured likewise shows marked degenerative changes (Figs. 5.2**E** and 5.37). The cell body swells and becomes distended, the nucleus is displaced toward the periphery and the Nissl bodies undergo dissolution. Nissl body breakdown begins in the center of the cell and spreads outward (*central chromatolysis*) (73). With light microscopy the fixed Nissl material appears to undergo lysis (Fig. 5.37). Cytochemical and electron microscopic studies indicate that there is an increase in the total quantity of RNA in the perikaryon, and suggest that the cisternae and ribosomes are dispersed and less concentrated. That these cells imbibe water results in a tremendous increase of their volume. Ultrastructural changes also have been observed in many neuronal organelles (e.g., mitochondria, endoplasmic reticulum, Golgi apparatus, ribosomes, and lysosomes) following nerve section or x-ray irradiation of ganglion cells in tissue culture (94, 102, 125). Histochemical changes occur in a number of oxidative and hydrolytic enzymes within chromatolytic and regenerating neurons (133). Such changes reflect a reduction, or an increase, in glucose metabolism, a breakdown of Golgi bodies or increased RNA, and nucleoprotein synthesis.

The extent and rapidity of these changes depend on the type of neuron involved, on the nature of the lesion, and, especially, on the location of the injury. A lesion of the axon near the cell body produces a greater central effect than one more distant. The effect depends upon the percentage of the neuron destroyed. If the lesion is near the cell body, the latter may ultimately die and the proximal portion of the nerve fiber attached to it degenerates. Chromatolysis in the cell body reaches its maximum 12–14 days following injury to the axon. This retrograde alteration of Nissl material has been employed extensively in earlier neuroanatomic research to locate the cells of origin of axons in central tracts, or in a peripheral nerve (Figs. 5.2**E** and 5.37).

REGENERATION AND PLASTICITY

Regeneration in the Peripheral Nervous System

If the neuron survives injury, *regeneration* takes place in the peripheral nervous system. Recovery in the cell body begins at about the 3rd week and is characterized by the appearance of Nissl bodies around the nuclear membrane. The swelling of the perikaryon gradually subsides, the nucleus returns to its central position, and the Nissl bodies are restored to the normal amount and distribution. Full recovery may take from 3–6 months, the time depending on the mass of axon to be reconstituted. While this is going on, regenerative processes appear in the axons of the central stump. As early as the 10th hour, the axon terminals begin to swell.

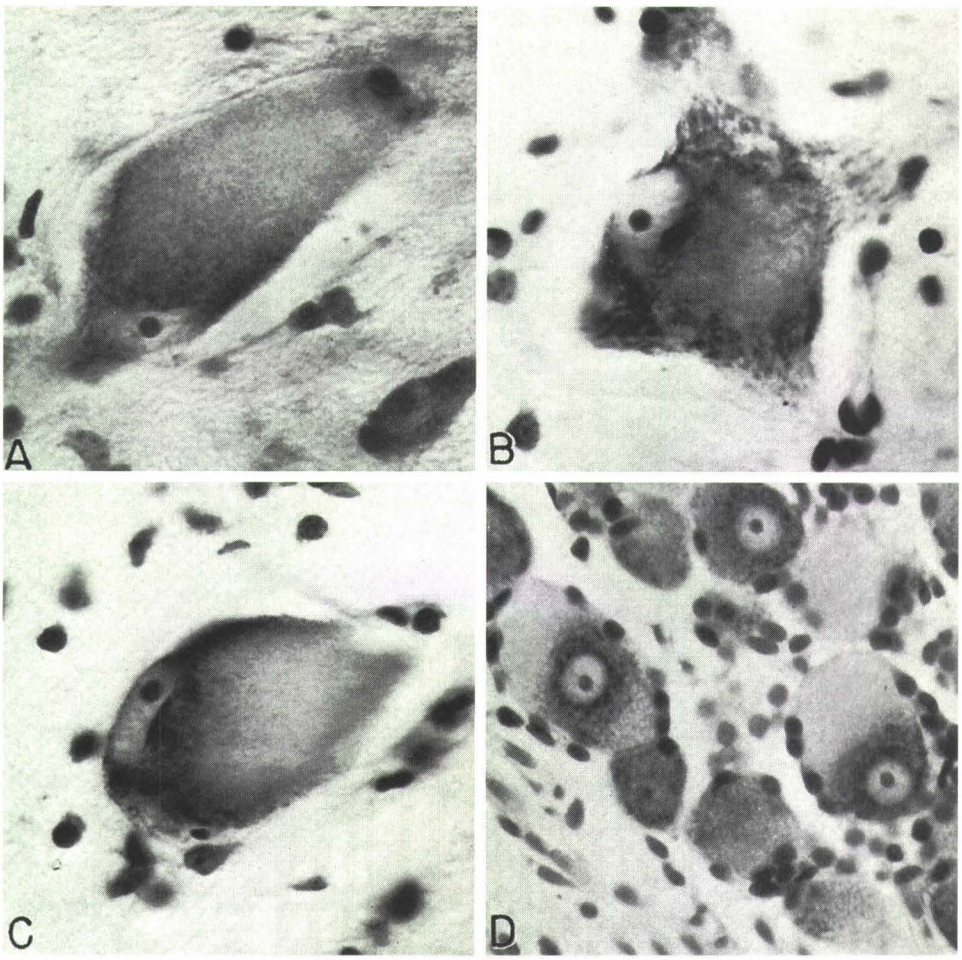


Figure 5.37. Four examples of central chromatolysis in the monkey. **A** and **B.** Neurons in the brainstem reticular formation following section of the reticulospinal tract (cresyl violet, ×600, ×500). **C.** Retrograde cell change in lateral vestibular nucleus (cresyl violet, ×500). **D.** Retrograde cell change in the superior vagal ganglion (cresyl violet, ×500).

Each axon splits into numerous fine strands or fibers (Figs. 5.38 and 5.39) that traverse the scar formed at the site of the injury and reach the Schwann tubes of the degenerating stump. Many of these fibers enter a single tube where they are disposed peripherally (Fig. 5.38). Later, some of them move to a more central position and become completely surrounded by the plasma membrane of the sheath cells (Fig. 5.39). Along or within the bands, the regenerating axons grow distally for long distances to their peripheral destinations. Nathaniel and Pease (135) have found that regenerating axonal sprouts reach the extracellular spaces of the membrane envelope as early as 4 days after a lesion. Although many sprouts initially may occupy the spaces and gutters of the Schwann tube, only one persists and becomes remyelinated. This is usually the largest one (Fig. 5.39). The elimination of excess fibers may take considerable time, and some of them may still be seen in tubes 3 or 4 months after section. The enlargement of one fiber and the elimination of the others, occur only if the regenerating axons make sensory or motor contact with appropriate receptor or effector endings in the periphery.

The thin regenerating axons, at first about 0.5–3 μm in diameter, gradually enlarge; the increase in diameter advances progressively down the tube, as if propelled by some centrifugal force from the central stump. When the fiber reaches the periphery, growth in length ceases, but the increase in diameter continues until the original thickness is ap-

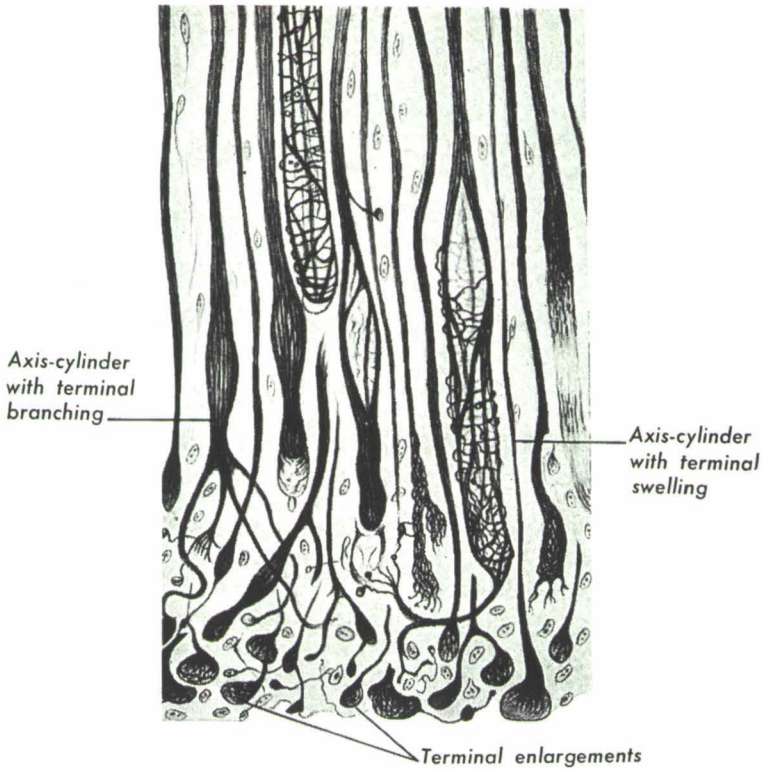


Figure 5.38. Regenerating axons in the central stump of a cat's sciatic nerve 2.5 days after section of the nerve.

proximated. Myelination may occur as early as the 2nd or 3rd week in some fibers. It likewise advances in a proximodistal direction, and the process becomes somewhat slower in the more distal regions of the fiber. The myelin is at first laid down as a thin continuous sheath which subsequently becomes broken up into short internodal segments, about 150–700 μm in length. In fully regenerated nerve fibers, the internodes are shorter and more numerous, and there is no longer any definite relation between internodal length and diameter because fibers of varying thickness may possess similar internodal lengths. The time course of the events in degeneration and regeneration overlap each other. As noted earlier, regeneration of new axonal sprouts occurs before the disintegration of the axon and myelin sheath is completed in the distal segments of injured nerves. In a similar fashion, regenerating axonal sprouts may traverse Schwann tubes which still contain degeneration debris (135).

The growth processes observed during regeneration are remarkable (155). A slender axonal filament ultimately is transformed into a mature fiber whose volume in some instances may be several hundred times the volume of the original filament (Fig. 5.41**A**). The manner in which this new axoplasm is formed has been investigated by Weiss and Hiscoe (200) in a series of ingenious experiments. They fashioned small arterial rings which, when distended, could be slipped over the end of a cut nerve and placed in the desired position. The subsequent contraction of these rings produced localized constrictions with consequent reduction in the diameter of the individual fiber tubes (Fig. 5.41**B**). The reduction in the lumen of the tube does not at first interfere with the advance of the slender regenerating axon, which passes through the constricted zone and makes contact with the periphery. But when the fiber, as it continues to enlarge, attains the dimensions of the constricted zone, a remarkable difference appears between those parts lying at the distal and proximal sides of the narrow neck. The distal segment ceases to grow and remains permanently undersized, while the proximal segment not only continues to enlarge, but near the entrance of the constricted

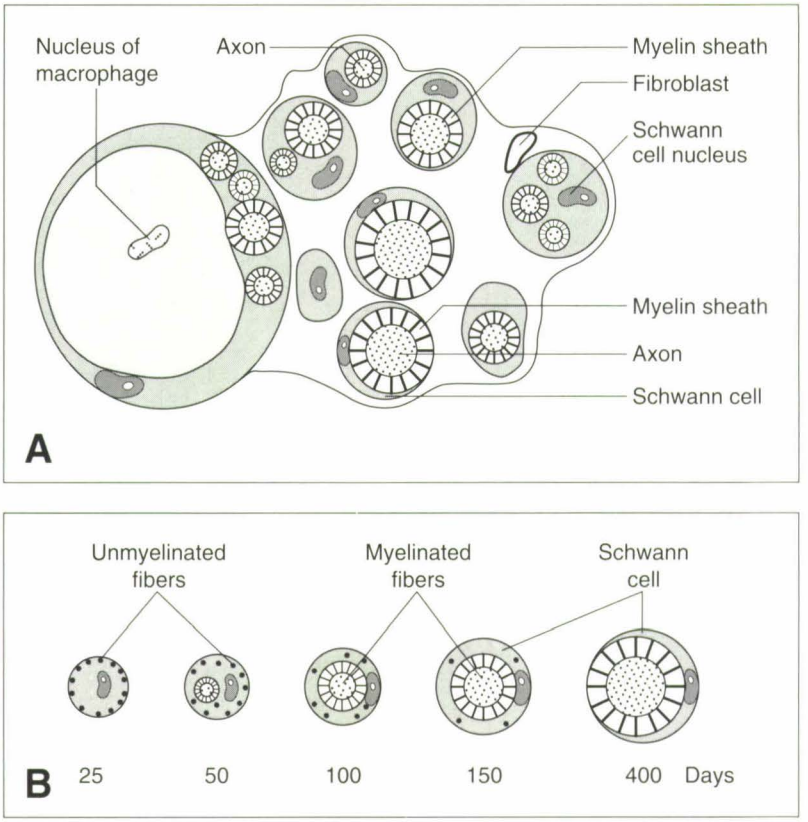


Figure 5.39. **A.** Transverse section of peripheral stump of rabbit peripheral nerve severed 150 days previously. The stumps were left unsutured, but union was established by outgrowth. Most of the tubules contain one or more myelinated nerve fibers which are surrounded by protoplasm of the Schwann cells. **B.** Diagram of the progress of regeneration within Schwann tubule distal to a good nerve suture at different time intervals (days). At 25 days there are many fibers near the edge of the tube; at 50 days one or two fibers are enlarged and surrounded by Schwann cell cytoplasm; at 100 days one large myelinated fiber occupies the center of the tube, while other smaller fibers are peripheral. At approximately 400 days excess fibers disappear and a single large fiber attains its normal diameter.

zone, enlarges excessively (200). It was concluded that the axoplasm exerts pressure in a distal direction and becomes dammed where the channel narrows (Fig. 5.41). The damming increases in intensity with time, and varies with the amount of constriction and the size of the fiber. Morphologically, it is expressed in several ways, such as ballooning, beading, telescoping, and coiling of the fibers. On release of the constriction, some of the dammed axoplasm flows into the distal portion, which consequently increases in thickness (Fig. 5.41). The authors concluded that the formation of new axoplasm, that is growth in volume, occurs only in the cell body, and that this axoplasm maintains a constant proximodistal motion that causes the elongation and enlargement of the regenerating fiber.

A knowledge of the mode of nerve regeneration is important as a basis for surgical treatment. If a nerve is severed, it is desirable to surgically approximate the cut ends promptly. If some time has elapsed since the injury, it is necessary to resect surrounding scar tissue and the neuroma on the proximal nerve stump before the nerve can be sutured. This subject is discussed further in Chapter 8.

Regeneration in the Central Nervous System

Fiber degeneration in the central nervous system is similar to that observed in the peripheral nerves. However, the degeneration proceeds at a slower pace, and the removal of neural debris by glial cells takes a longer

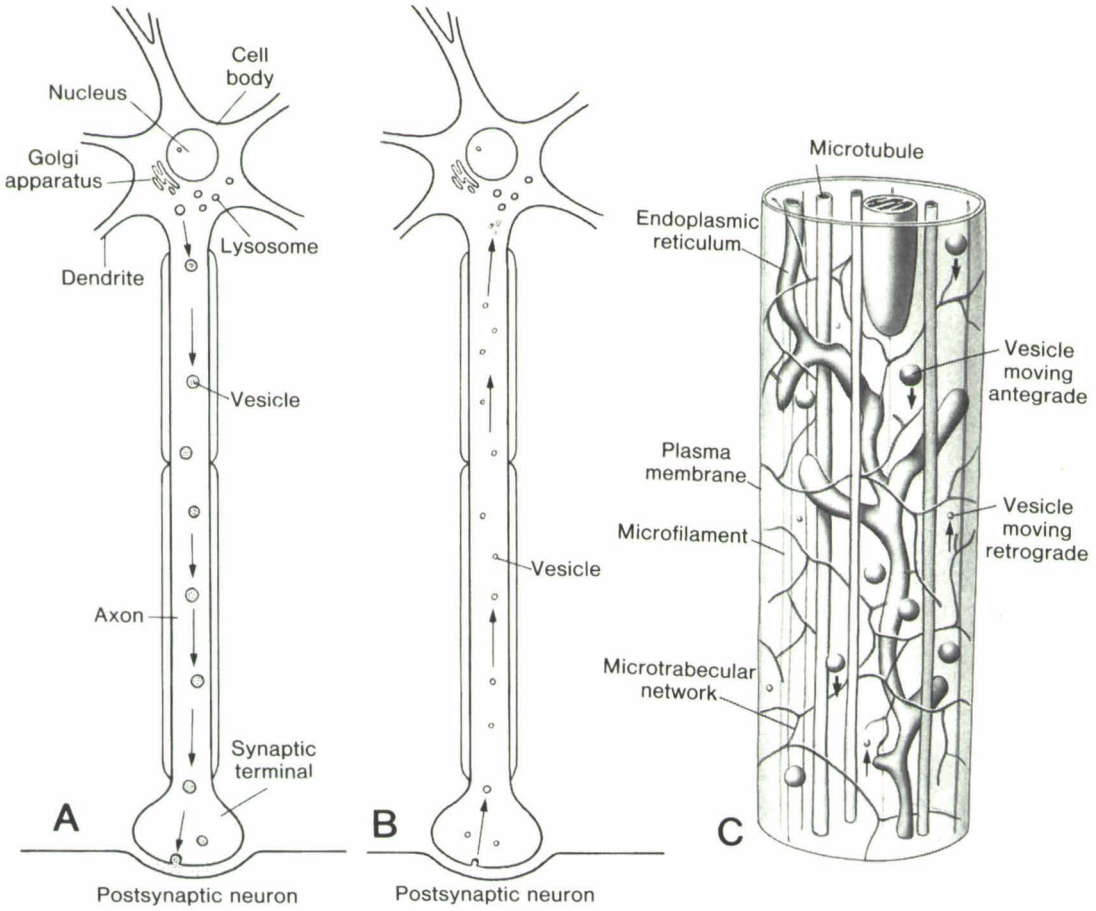


Figure 5.40. Some of the major features of anterograde and retrograde axonal transport. **A.** The major components of anterograde axonal transport are filamentous proteins and vesicles originating from the Golgi apparatus and endoplasmic reticulum. **B.** Retrograde axonal transport involves movement toward the cell body of smaller vesicles formed by micropinocytosis (endocytosis) at the synaptic terminal. In the cell body, the vesicles coalesce and become incorporated into lysosomes for degradation. **C.** Organelles that are thought to be associated with axoplasmic transport. Microtubules form an essential anatomical substrate for the transport of organelles, which are linked to these cytoskeleton components by microtubule-associated proteins (MAPs).

time. It is known that the large fibers of the corticospinal tract and optic nerve degenerate faster than the fibers of small size (192, 193). Such studies indicate that fibers of equal size tend to possess equal resistance to secondary degeneration. The large fibers degenerate faster, but are resorbed more slowly. Hence the debris of total degeneration in the central nervous system is in evidence for several months.

Compared to neurons in the peripheral nervous system, neurons in the central nervous system have only limited capacity to regenerate their axon. Regeneration within the central nervous system of mammals has been studied with both anatomic and physiologic techniques since the second half of this century (22, 23, 59, 173, 204). Such studies indicate that the central axons of injured nerve cells make abortive attempts to regenerate across an experimental gap in the spinal cord. Factors that influence and often hamper central regeneration are similar to those influencing regeneration in the peripheral nervous system (e.g., length of gap between severed stumps, hemorrhage, and scar formation). Central regeneration is further thwarted by the absence of sheath cells to guide the regenerating axonal sprouts. As early as 1940, Sugar and Gerard found evidence of functional regeneration in adult rats whose thoracic spinal cords had been transected with care to prevent injury to the blood supply (187). No significant return of function has

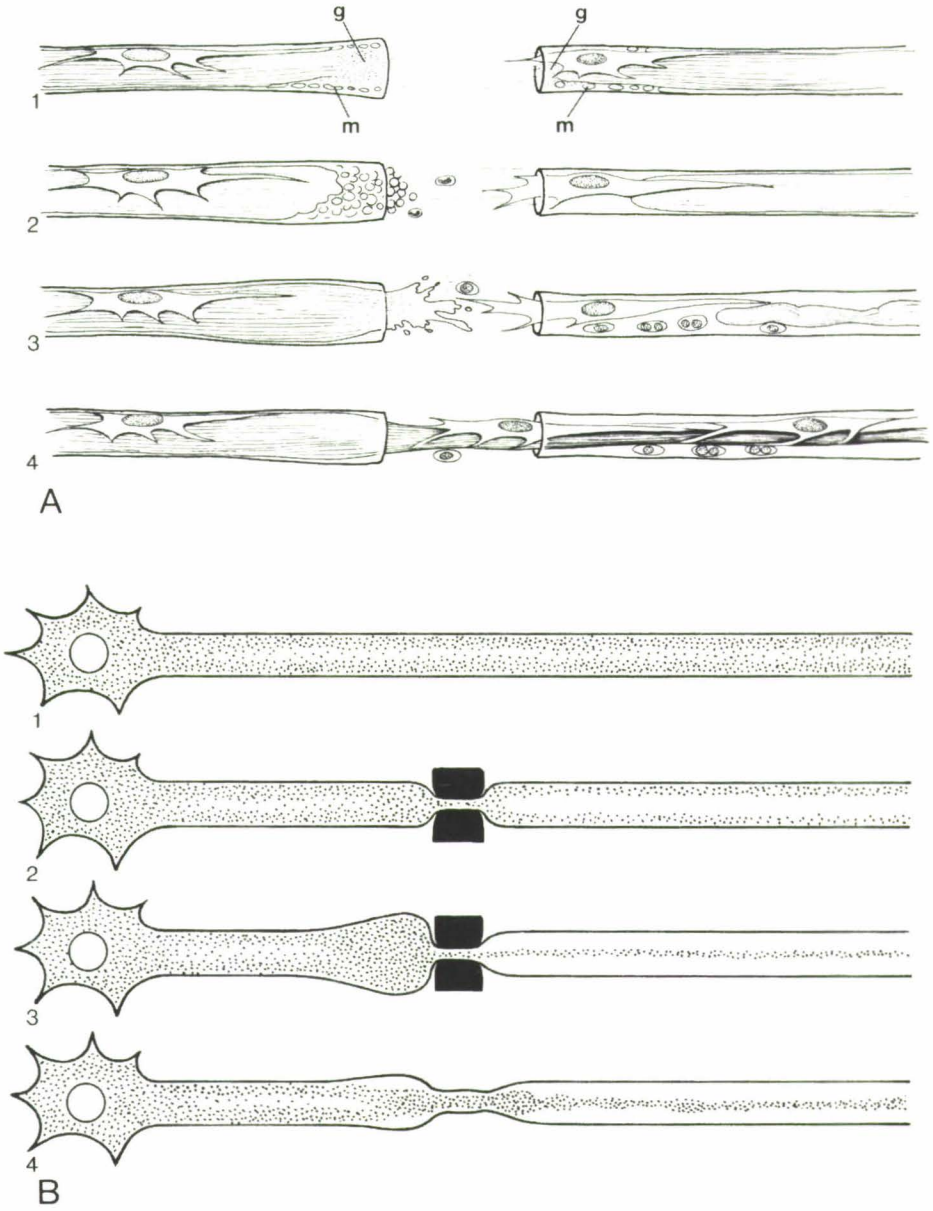


Figure 5.41. Stages of nerve regeneration (**A**) and the consequences of nerve constriction (**B**). Following severance of a nerve (**A-1**) a fibrin clot forms a bridge between the cut ends, and for a short distance in both stumps, the myelin (*m*) breaks into droplets and the axon breaks into granules (*g*). During the first few days following nerve section, the axon forms multiple sprouts (**A-2**, **A-3**) which later enter the distal Schwann cell tube (**A-4**). **B-1** depicts a normal nerve fiber, and **B-2** and **B-3** show the proximal accumulation of cytoplasm which occurs gradually over a period of several weeks following application of a constricting cuff. After removal of the cuff (**B-4**), the swelling of the axon diminishes as axoplasmic transport is restored in the distal segment of the fibers.

been noted in the higher mammals following complete transection of the spinal cord. It was shown that remyelination of experimentally injured axons of the spinal cord can take place in the cat (18).

Peripheral and Central Grafting Experiments

Recent experiments by Albert Aguayo and his colleagues demonstrated that peripheral nerve grafts promote the growth of central axons. For example, these investigators replaced central nervous tissue of the optic nerve of adult rats with segments of the peripheral sciatic nerve. The cut axons of ganglion neurons in the adult retina, which do not normally regenerate into the optic nerve, were able to regrow into the graft and reinnervate their targets in the superior colliculus. At this level, the newly formed axon terminals resemble normal presynaptic terminals and appear to be functional and permanent (16). These experiments demonstrate that if regenerating axons in the central nervous system are able to reach their target area they are capable of forming functional synaptic connections.

Another approach developed by Anders Björklund and colleagues consists of transplanting cells from fetal or neonatal animals into adult brain to alleviate experimentally induced behavioral deficits in rats. For example, movement disorders induced by lesions of the dopaminergic input to the basal ganglia can be prevented by grafts of fetal midbrain dopaminergic neurons into the denervated striatum (Fig. 5.42). The mechanisms of

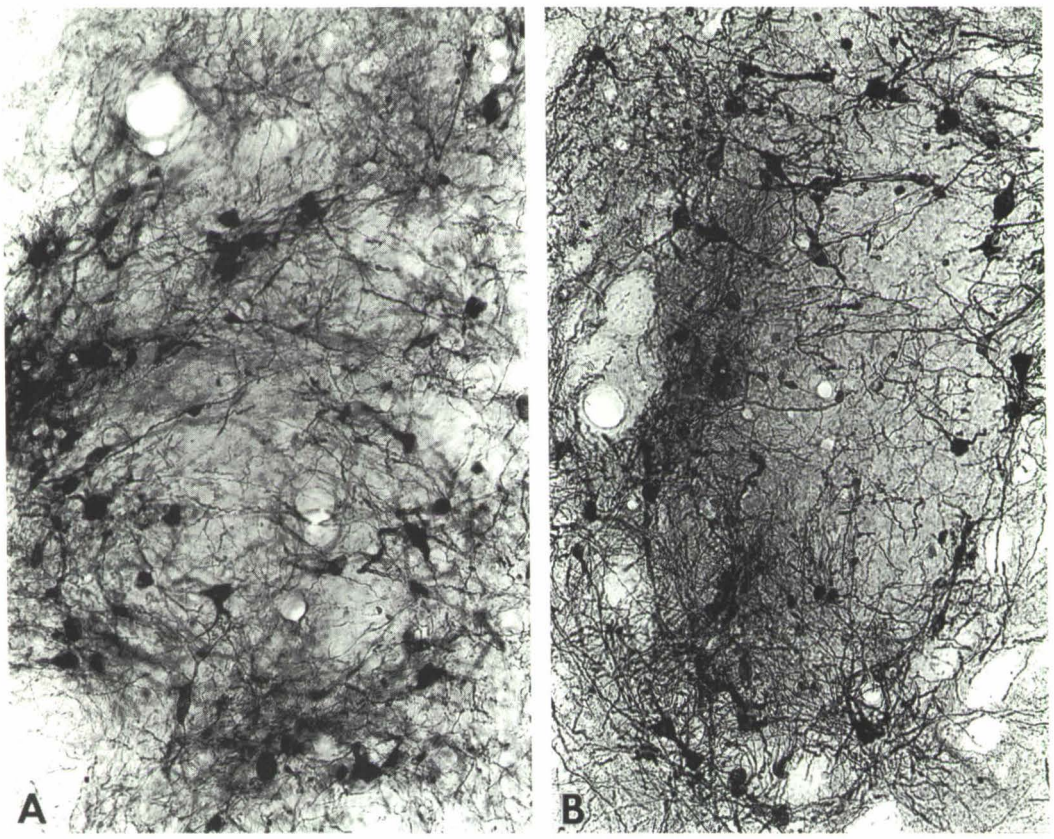


Figure 5.42. **A** and **B.** Two examples of fetal dopaminergic nigral cells implanted into the striatum of adult rats whose nigrostriatal dopaminergic pathway had been previously lesioned with the neurotoxin 6-hydroxydopamine (6-OHDA). These fetal dopaminergic cells have produced numerous processes that display TH immunoreactivity and arborize profusely within the dennervated striatum. The arborization of the implanted dopaminergic neurons is particularly obvious in **B** where numerous TH-immunoreactive processes can be seen not only within the confines of the graft, which corresponds to the area containing the cell bodies, but also in the adjacent striatal areas where the density of the dopaminergic innervation appears similar to that found in normal animals. The motor deficits caused by the 6-OHDA dopaminergic denervation of the striatum in these two animals were largely alleviated by the grafts (×250).

action of such neural grafts are not fully understood. The grafts may release transmitters that act at distance upon target cells and/or release some trophic factors that influence cells in the damaged brain. The fetal surface adhesion molecules of the grafted cells may also provide a suitable microenvironment within which damaged host neurons can reconnect with their targets (12, 62, 95, 118). This approach was recently used to treat motor disorders in Parkinsonian patients. Although promising, the results of these preliminary clinical trials clearly call for further improvement of the transplantation approach, as well as more detailed animal experiments (12). The fetal cell transplant approach was also used in rats to partially restore cognitive function deficits, such as maze learning problems, induced by cortical lesions or by lesions of the cortically projecting cholinergic neurons of the septum and basal forebrain (44, 85).

Growth Promoting and Inhibiting Factors

Over the years, various chemical compounds were used in an attempt to stimulate the growth of neurons and their processes. One of the best characterized molecules that can promote nerve regeneration is the nerve growth factor (NGF) (114–117). NGF plays a crucial role in the development of the nervous system, as seen in Chapter 3. However, recent studies revealed that NGF can also act as a potent neurotrophic agent in specific regions of the adult brain. For example, NGF has been used successfully to promote regeneration of basal forebrain cholinergic neurons whose cortically projecting axons had been experimentally lesioned in the rats (85, 86, 128). These cholinergic neurons possess specific NGF receptors on their surface. Cortically applied NGF is apparently able to prevent the cell loss of experimentally damaged basal forebrain cholinergic neurons, as well as allow recovery of memory function, which is altered in these animals. On the basis of these animal experiments, the use of NGF is presently envisaged as a possible treatment for Alzheimer's disease, which is characterized by a marked dysfunction of cortically-projecting basal forebrain cholinergic neurons.

Since the discovery of NGF, several other molecules with growth promoting capability were isolated and characterized. For example, neurons that are insensitive to NGF were shown to be dependent on other trophic factors, such as *brain-derived neurotrophic factor* (BDNF), *ciliary neurotrophic factor* (CNF), and *fibroblast growth factor* (FGF) (169). Furthermore, Schwann cells contribute to the regeneration of peripheral axons. In addition to providing an anatomic substrate for the support and guidance of regenerating axons, the proliferating Schwann cells secrete several extracellular proteins, such as *laminin*, which promote axon extension. Laminin, together with fibronectin, are glycoproteins that occur in large concentrations in the extracellular matrix in both the central and peripheral nervous systems early in neural development. These two proteins persist in the periphery, but are absent in the adult brain and spinal cord. This may explain, at least in part, the marked difference between central and peripheral neurons in their capability of regenerating their axon. Developing axons, themselves, contain intracellular proteins associated with active growth. One of these proteins, *GAP-43*, which has a molecular weight of 43,000, disappears from the axons of most adult central neurons, but is present in many adult peripheral neurons. Although the exact function of this protein is not known, it is interesting to note that it is expressed in some adult brain neurons that have the capacity to sprout axons after injury, such as the neurons of the hippocampus.

Conversely, recent biochemical and cell biologic studies by Martin Schwab showed the existence of two membrane proteins localized exclusively on oligodendrocytes and central myelin and which exert a powerful inhibitory effect on neurite growth. These two *neurite growth inhibitory proteins* (NI) have a molecular weight of 33,00–35,000 (NI-35) and 250,000 (NI-250), respectively, and are normal constituents of myelin in the central nervous system. Specific antibodies raised against these two proteins, and applied to rats with complete transection of the corticospinal tract, greatly helped regeneration of the corticospinal axons. Similar results were obtained in rats lacking myelin and oligodendrocytes in the spinal cord (169). These results raise the interesting possibility that the difference between central and peripheral neurons in regeneration capability does not result from a lack of trophic factor but from the presence of inhibitory factors in the central nervous system.

References

1. Abercrombie M, Johnson ML. The effect of reinnervation on collagen formation in degenerating sciatic nerves of rabbits. J Neurol Neurosurg Psychiatry 1947;10:89–92.
2. Acheson AL, Zigmond MJ, Stricker M. Compensatory increase in tyrosine hydroxylase activity in rat brain after intraventricular injections of 6-hydroxydopamine. Science 1980;207:537–540.
3. Alberts B, Bray D, Lewis J, Raff M, Roberts M, Watson JD. Molecular biology of the cell. 2d ed. New York: Garland, 1989.
4. Allen RD. New directions and refinements in video-enhanced microscopy applied to problems in cell motility. Prog Clin Biol Res 1985;196:3–11.
5. Ambrogi LP. Manual of histologic and special staining technics. 2d ed. New York: McGraw-Hill, 1960:157–174.
6. Bargmann W. Neurosecretion. Int Rev Cytol 1966;19:183–201.
7. Barr ML, Bertram LF, Lindsay HA. The morphology of the nerve cell nucleus according to sex. Anat Rec 1950;107:283–297.
8. Bentivoglio M, Kuypers HGJM, Catsman-Berrevoets CE, Loewe H, Dann O. Two new fluorescent retrograde neuronal tracers which are transported over long distances. Neurosci Lett 1980;18:25–30.
9. Bern, HA, and Knowles, FGW. Neurosecretion. In: Martini LM, Ganong WF, eds. Neuroendocrinology. Ch. 5. New York: Academic Press, 1966;139–186.
10. Bershadsky AD, Vasiliev JM. Cytoskeleton. New York: Plenum Press, 1988.
11. Bishop TW, Heinbecker P, O'Leary JL. The function of non-myelinated fibers of the dorsal roots. Am J Physiol 1933;106:647–669.
12. Björklund A. Neural transplantation—an experimental tool with clinical possibilities. Trends Neurosci 1991;14:319–322.
13. Black MM, Baas PW. The basis of polarity in neurons. Trends Neurosci 1989;12:211–214.
14. Bodian D. A new method for staining nerve fibers and nerve endings in mounted paraffin sections. Anat Rec 1936;65:89–97.
15. Bodian D. The generalized vertebrate neuron. Science 1962; 137:323–326.
16. Bray GM, Vllegas-Pérez MP, Vidal-Sanz M, Aguayo AJ . The use of peripheral nerve grafts to enhance neuronal survival, promote growth and permit terminal reconnections in the central nervous system of adult rats. J Exp Biol 1987;132:5–19.
17. Broadwell RD, Oliver C, Brightman MW. Neuronal transport of acid hydrolases and peroxidase within the lysosomal system of organelles: involvement of agranular reticulum-like cisterns. J Comp Neurol 1980;190:519–532.
18. Bunge MB, Bunge RP, Ris H. Ultrastructural study of remyelination in an experimental lesion in adult cat spinal cord. J Biophys Biochem Cytol 1961;10:67–94.
19. Bunge MB, Bunge RP, Peterson ER, Murray MR. A light and electron microscope study of long term organized cultures of rat dorsal root ganglia. J Cell Biol 1967;32:439–466.
20. Bunge MB. The axonal cytoskeleton: Its role in regenerating and maintaining cell form. Trends Neurosci 1986;9:477–487.
21. Bunge RP. Glial cells and the central myelin sheath. Physiol Rev 1968;48:197–251.
22. Campbell JB, Bassett CAL, Husby J, Noback CR. Regeneration of adult mammalian spinal cord. Science 1957;126:929.
23. Campbell JB, Bassett CAL, Husby J, Noback CR. Axonal regeneration in the transected adult feline spinal cord. Surg Forum, Clin Cong Am Coll Surgeons 1958;8:528–532.
24. Causey G. The cell of Schwann. Edinburgh: Livingston, 1960.
25. Chan-Palay V, Palay SL. Coexistence of neuroactive substances in neurons. New York: John Wiley & Sons, 1984.
26. Chesselet M-F, ed. In situ hybridization histochemistry. Boca Raton, FL: CRC Press, 1990.
27. Cheung, WY. Calmodulin plays a pivotal role in cellular regulation. Science 1980;207:19–27.
28. Chronwall BM, Lerois ME, Schwaber JS, O'Donohue TL. In situ hybridization combined with retrograde fluorescent tract tracing. In: Heimer L, Zaborsky L, eds. Neuroanatomical tract-tracing methods 2. Ch. 10. New York: Plenum Press, 1989:265–297.
29. Chu LW. Cytological study of anterior horn cells isolated from human spinal cord. J Comp Neurol 1954;100:381–413.
30. Cooper JR, Bloom RE, Roth RH. The biochemical basis of neuropharmacology. 6th ed. New York: Oxford University Press, 1991.
31. Copenhaver WM, Bunge RP, Bunge MB. Bailey's textbook of histology. 16th ed. Baltimore: Williams & Wilkins, 1971.
32. Cowan WM, Gottlieb DL, Hendrickson AE, Price JL, Woolsey TA. The autoradiographic demonstration of axonal connections in the central nervous system. Brain Res 1972;37:21–51.
33. Cuello AC. Immunohistochemistry. IBRO handbook series: Methods in the neurosciences. Vol. 3. New York: John Wiley & Sons, 1983.
34. Culling CFA. Handbook of histopathological techniques. 2d ed. London: Butterworths, 1963: 348–375.
35. Dahlström A. Regional distribution of brain catecholamines and serotonin. Neurosci Res Program Bull 1971;9:197–205.
36. Dale H. Pharmacology of nerve-endings. Proc R Soc Med (Lond) 1935;28:319–332.
37. De Robertis E. Synaptic complexes and synaptic vesicles as structural and biochemical units of the central nervous system. In: Rodahl K, Issekuts B Jr, eds. Nerve as a tissue. New York: Harper & Row, 1966:88–115.
38. De Robertis E. Ultrastructure and cytochemistry of the synaptic region. Science 1967;156:907–914.
39. De Robertis E, Bennett HS. Submicroscopic vesicular component in the synapse. Fed Proc 1954;13:35.
40. De Robertis E, De Iraldi AP, De Lores R, Arnaiz G, Salganicoff L. Cholinergic and non-cholinergic nerve endings in rat brain. I. Isolation and subcellular distribution of acetylcholine and acetylcholinesterase. J Neurochem 1962; 9:23–35.
41. Denny-Brown D. Importance of neural fibroblasts in the regeneration of nerve. Arch Neurol Psychiatry 1946;55:171–215.
42. Droz B, Leblond CP. Axonal migration of proteins in the central nervous system and peripheral nerves as shown by radioautography. J Comp Neurol 1963; 121:325–346.
43. Droz B, Rambourg A, Koenig HL. The smooth endoplasmic reticulum: structure and role in the renewal of axonal membrane and synaptic vesicles by fast axonal transport. Brain Res 1975;93:1–13.
44. Dunnett S. Cholinergic grafts, memory and ageing. Trends Neurosci 1991;14:371–376.
45. Eccles JC. The physiology of synapses. Berlin: Springer-Verlag, 1964.
46. Ehrlich P. On immunity with special reference to cell life. Croonian Lecture Proc R Soc (Lond) 1900; 66:424–448.
47. Elfvin LG. The ultrastructure of unmyelinated fibers in the splenic nerve of the cat. J Ultrastruct Res 1958;1:428–454.
48. Erlanger J, Gasser HS. Electrical signs of nervous activity. Philadelphia: University of Pennsylvania Press, 1937.
49. Essner E, Novikoff AB. Human hepatocellular pigments and lysosomes, J Ultrastruct Res 1960; 3:374–391.
50. Falck B. Observations of the possibilities of the cellular localization of monoamines by a fluorescence method. Acta Physiol Scand 1962; 56(Suppl 197):1–25.
51. Falck B, Hillarp NA, Thieme G, Torp A. Fluorescence of catechol amines and related compound condensed with formaldehyde. J Histochem Cytochem 1962;10: 348–354.
52. Fatt P, Katz B. Spontaneous sub-

threshold activity of motor nerve endings. J Physiol (Lond) 1952; 117:109–128.
53. Fink DJ, Garnor H. Axonal transport of proteins: a new view using in vivo covalent labeling. J Cell Biol 1980;85:175–186.
54. Fink RP, Heimer L. Two methods for selective silver impregnation of degenerating axons and their synaptic endings in the central nervous system. Brain Res 1967; 4:369–374.
55. Fitzgerald M. C-Fos and the changing face of pain. Trends Neurosci 1990;13:439–440.
56. Forn J, Greengard P. Depolarizing agents and cyclic nucleotides regulate the phosphorylation of specific neuronal proteins in rat cerebral cortex slices. Proc Natl Acad Sci USA 1978;75:5195–5199.
57. Fox CA, Barnard JW. A quantitative study of the Purkinje cell, dendritic branchlets and their relationship to afferent fibres. J Anat 1957;91:299–313.
58. Fox CA, Hillman DE, Siegesmund KA, Dutta CR. The primate cerebellar cortex: a Golgi and electron microscope study. In: Fox CA, Snider RS, eds. The cerebellum, progress in brain research. Vol. 25. Amsterdam: Elsevier, 1967: 174–225.
59. Freeman LW. Return of function after complete transection of the spinal cord of the rat, cat and dog. Am Surg 1952;136:193–205.
60. Freund T, Somogyi P. Synaptic relationship of Golgi-impregnated neurons as identified by electrophysiological or immunocytochemical techniques. In: Heimer L, Zaborsky L, eds. Neuroanatomical tract-tracing methods 2. Ch. 8. New York: Plenum Press, 1989; 201–238.
61. Gabe M. Neurosecretion. (Crawford R, trans.) Oxford: Pergamon, 1966:427–736.
62. Gage FH, Fisher LJ. Intracerebral grafting: a tool for the neurobiologist. Neuron 1991;6:1–12.
63. Gamble HJ. Comparative electronmicroscopic observations on the connective tissues of a peripheral nerve and a spinal nerve root in the rat. J Anat 1964;98:17–25.
64. Gasser HS, Grundfest H. Axon diameters in relation to the spike dimensions and the conduction velocity in mammalian A fibers. Am J Physiol 1939;127:393–414.
65. Geary WA II, Wooten GF. Receptor autoradiography. In: Heimer L, Zaborsky L, eds. Neuroanatomical tract-tracing methods 2. Ch. 12. New York: Plenum Press, 1989; 311–330.
66. Geren BB. The formation from the Schwann cell surface of the myelin in peripheral nerves of chick embryos. Exp Cell Res 1954;7:558–562.
67. Gerfen CR, Sawchenko PE. An anterograde neuroanatomical tracing method that shows the detailed morphology of neurons, their axons and terminals: immunohistochemical localization of an axonally transported plant lectin, Phaseolus vulgaris—leucoagglutinin (PHA-L). Brain Res 1984; 290:219–238.
68. Gerfen CR, Sawchenko PE, Carlsen J. The PHA-L anterograde axonal tracing method. In: Heimer L, Zaborsky L, eds. Neuroanatomical tract-tracing methods 2. Ch. 3. New York: Plenum Press, 1989: 19–47.
69. Golgi C. Sulla fine anatomia degli organi centrali del sistems nervoso. Riv Sper Frenia Med Leg 1882–1885;8:165–195, 361–391; 9:1–17, 161–192, 385–402; 11:72–123, 193–220.
70. Golgi C. Untersuchungen über den feineren Bau des centralen und peripherischen Nervensystems. Jena: Gustav Fischer, 1894.
71. Golgi C. Sur la structure des cellules nerveuses. Arch Ital Biol 1898;30:60–71.
72. Grafstein B. Axonal transport: the ultracellular traffic of the neuron. In: Kandel ER, ed. Handbook of physiology. Section I: The nervous system. Vol. I: Cell biology of neurons, Part I. Washington, DC: American Physiological Society, 1977;691–717.
73. Grafstein B. Chromatolysis reconsidered: a new view of the reaction of the nerve cell body to axon injury. In: Seil FJ, ed. Nerve, organ, and tissue regeneration: research perspectives. New York: Academic Press, 1983:37–50.
74. Grafstein B, Miller JA, Ledeen RW, Haley J, Specht SC . Axonal transport of phospholipid in goldfish optic system. Exp Neurol 1975; 46:261–281.
75. Gray EG. Electron microscopy of presynaptic organelles in the spinal cord. J Anat 1963; 97:101–106.
76. Gray EG, Guillery RW. The basis for silver staining of synapses of the mammalian spinal cord: a light and electron microscope study. J Physiol (Lond) 1961;157:581–588.
77. Gray EG, Guillery RW. Synaptic morphology in the normal and degenerating nervous system. Int Rev Cytol 1966;19:111–182.
78. Greengard P. Possible role for cyclic nucleotides and phosphorylated membrane proteins in postsynaptic actions of neurotransmitters. Nature 1976;260:101–108.
79. Greengard P. Cyclic nucleotides, phosphorylated proteins and neuronal structure. New York: Raven Press, 1978.
80. Greengard P. Cyclic nucleotides, phosphorylated proteins and the nervous system. Fed Proc 1979; 38:2208–2217.
81. Grundfest H. The properties of mammalian B fibers. Am J Physiol 1939;127:252–262.
82. Grundfest H. Bioelectric potentials. Annu Rev Physiol 1940;2:213–242.
83. Harding HA. Neurological disease and mitochondrial genes. Trends Neurosci 1991;14:132–138.
84. Hazrati L-N, Parent A. Convergence of subthalamic and striatal efferents at pallidal level in primates: an anterograde double-labeling study with biocytin and PHA-L. Brain Res 1992; 569: 336–340.
85. Hefti F. Nerve growth factor promotes survival of septal cholinergic neurons after fimbrial transections. J Neurosci 1986;6:603–616.
86. Hefti F, Wainer WJ. Nerve growth factor and Alzheimer's disease. Ann Neurol 1986;20:275–281.
87. Heinbecker P, Bishop GH, O'Leary JL. Functional and histologic studies of somatic and autonomic nerves of man. Arch Neurol Psychiatry 1936;35:1233–1255.
88. Heuser JE, Reese TS. Structure of the synapse. In: Kandel ER, ed. Handbook of physiology, cellular biology of neurons. Vol. 1, Part 1. Washington, DC: American Physiological Society, 1977;261–294.
89. Heuser JE, Reese TS. Structural changes after transmitter release at the frog neuromuscular junction. J Cell Biol 1981;88:564–580.
90. Hirokawa N, Pfister KK, Yorifuji H, Wagner MC, Brady ST, Bloom GS. Submolecular domains of bovine brain kinesin identified by electron microscopy and monoclonal antibody decoration. Cell 1989;56:867–878.
91. Hökfelt T, Björklund A. Handbook of chemical neuroanatomy. Vol. 3: Classical transmission and the transmitter receptors in the CNS. Part 2. Amsterdam: Elsevier, 1985.
92. Hökfelt T, Fuxe K, Pernow P. Coexistence of neuronal messengers: a new principle in chemical transmission, progress in brain research. Vol. 68. Amsterdam: Elsevier, 1986.
93. Hökfelt T, Johansson O, Ljungdahl A, Lundberg JM, Schultzberg M. Peptidergic neurones. Nature 1980;284:515–521.
94. Holtzman E, Novikoff AB, Villaverde H. Lysosomes and GERL in normal and chromatolytic neurons of rat ganglion nodosum. J Cell Biol 1967;33:419–435.
95. Jessell TM. Reactions of neurons to injury. In: Kandel ER, Schwartz JH, Jessell TM, eds. Principles of neural science. Ch. 18. New York: Elsevier, 1991;258–269.
96. Kandel E. Cellular insights into behavior and learning. In: The Harvey Lectures, series 73. New York: Academic Press, 1979:19–92.
97. Kandel ER. Nerve cells and behavior. In: Kandel ER, Schwartz JH, Jessell TM, eds. Principles of neural science. Ch. 2. New York: Elsevier, 1991:18–32.
98. Kandel ER, Siegelbaum SA, Schwartz JH. Synaptic transmission. In: Kandel ER, Schwartz JH, Jessell TM, eds. Principles of

neural science. Ch. 9. New York: Elsevier, 1991:123–134.
99. Katz B. Nerve, Muscle and synapse. New York: McGraw-Hill, 1966.
100. Katz B. The release of neural transmitter substances. Springfield, IL: Charles C. Thomas, 1969.
101. King MH, Louis PM, Hunter BE, Walker DW. Biocytin: a versatile anterograde neuroanatomical tract-tracing alternative. Brain Res 1990; 497:361–367.
102. Kirkpatrick JB. Chromatolysis in the hypoglossal nucleus of the rat: an electron microscopic analysis. J Comp Neurol 1968;132:189–212.
103. Kitai ST, Penny GR, Chang HT. Intracellular labeling and immunocytochemistry. In: Heimer L, Zaborsky L, eds. Neuroanatomical tract-tracing methods 2. Ch. 7. New York: Plenum Press, 1989; 173–199.
104. Kosik KS. Alzheimer plaques and tangles: advances on both fronts. Trends Neurosci 1991;14:218–219.
105. Kuffler SW, Nicholls JG, Martin AR. From neurons to brain. 2d ed. Sunderland, MA: Sinauer, 1984.
106. Kuypers HGJM, Bentivoglio M, Catsman-Berrevoets CE, Bharos AT. Double retrograde neuronal labeling through divergent axon collaterals, using two fluorescent tracers with the same excitation wavelength which label different features of the cell. Exp Brain Res 1980;40:383–392.
107. Lasek RJ. Protein transport in neurons. Int Rev Neurobiol 1970; 13:289–324.
108. Lasek RJ. Axonal transport: a dynamic view of neuronal structures. Trends Neurosci 1980;3:87–91.
109. LaVail JH, LaVail MM. Retrograde axonal transport in the central nervous system. Science 1972; 176: 1416–1417.
110. LaVail JH, LaVail MM. The retrograde intraaxonal transport of horseradish peroxidase in the chick visual system: a light and electron microscopic study. J Comp Neurol 1974;157:303–358.
111. LaVail JH, Winston KR, Tish A. A method based on retrograde intraaxonal transport of protein for identification of cell bodies of origin of axons terminating within the CNS. Brain Res 1973;58:470–477.
112. Lee JCY. Electron microscopy of Wallerian degeneration. J Comp Neurol 1963;120:65–79.
113. Lefkowitz RJ, Caron MG, Stiles GL. Mechanisms of membrane-receptor regulation. N Engl J Med 1984;310:1570–1574.
114. Levi-Montalcini R, Angeletti PV. Growth control of the sympathetic system by a specific protein factor. Q Rev Biol 1961;36:99–108.
115. Levi-Montalcini R, Angeletti PV. Essential role of the nerve growth factor in the survival and maintenance of dissociated sensory and sympathetic embryonic nerve cells in vitro. Dev Biol 1963;7:653–659.
116. Levi-Montalcini R, Hamburger V. Selective growth stimulating effects of mouse sarcoma on the sensory and sympathetic nervous system of the chick embryo. J Zool (Lond) 1951;116:321–362.
117. Levi-Montalcini R, Meyer H, Hamburger V. In vitro experiments on the effects of mouse sarcomas 180 and 37 on the spinal and sympathetic ganglia of the chick embryo. Can Res 1954;14:49–57.
118. Lindvall O. Prospects of transplantation in human neurodegenerative diseases. Trends Neurosci 1991;14:376–384.
119. Livett BG. Immunohistochemical localization of nervous system specific proteins and peptides. Int Rev Cytol 1978;7:53–237.
120. Lloyd DPC. Conduction and synaptic transmission of reflex response to stretch in spinal cats. J Neurophysiol 1943;6:317–326.
121. Loewi O. Über humorale Übertragbarkeit der Herznervenwirkung. Pfluegers Arch 1921;189:239–248.
122. Luse SA. Electron microscopic observations of central nervous system. J Biophys Biochem Cytol 1956a;2:531–542.
123. Luse SA. Formation of myelin in the central nervous system of mice and rats, as studied with the electron microscope. J Biophys Biochem Cytol 1956b;2:777–783.
124. McLennan H. Synaptic transmission. Philadelphia: W.B. Saunders, 1963:3–15.
125. Masurovsky EB, Bunge MB, Bunge RP. Cytological studies of organotypic cultures of rat dorsal root ganglia following x-irradiation in vitro. I. Changes in neurons and satellite cells. J Cell Biol 1967; 32:467–496.
126. Mesulam M-M. Tetramethylbenzidine for horseradish peroxidase neurohistochemistry: a non-carcinogenic blue reaction-product with superior sensitivity for visualizing neural afferents and efferents. J Histochem Cytochem 1978; 26:106–117.
127. Mesulam M-M, ed.. Tracing neural connections with horseradish peroxidase. IBRO handbook series: methods in the neurosciences. Vol. 1. New York: John Wiley & Sons, 1982.
128. Mesulam M-M, Geula C, Bothwell MA, Hersch LB. Human reticular formation: cholinergic neurons of the pedunculopontine and laterodorsal tegmental nuclei and some cytochemical comparisons to forebrain cholinergic neurons. J Comp Neurol 1989;281:611–633.
129. Metuzals, J. Ultrastructure of the nodes of Ranvier and their surrounding structures in the central nervous system. Z Zellforsch Mikrosk Anat 1965;65:719–759.
130. Minneman KP, Dibner MD, Wolfe BB, Molinoff PB. β1- and β2-adrenergic receptors in rat cerebral cortex are independently regulated. Science 1979;204:866–868.
131. Murray MR, Stout AP. Adult human sympathetic ganglion cells cultivated in vitro. Am J Anat 1947;80:225–273.
132. Mytilineou C, Issidorides M, Shanklin WM. Histochemical reactions of human autonomic ganglia. J Anat 1963;97:533–542.
133. Nandy K. Histochemical study of chromatolytic neurons. Arch Neurol 1968;18:425–434.
134. Nathaniel EJH, Pease DC. Degenerative changes in rat dorsal roots during Wallerian degeneration. J Ultrastruct Res 1963a;9:511–532.
135. Nathaniel EJH, Pease DC. Regenerative changes in rat dorsal roots following Wallerian degeneration. J Ultrastruct Res 1963b;9:533–549.
136. Nauta WJH, Gygax PA. Silver impregnation of degenerating axons in the central nervous system: a modified technic. Stain Technol 1954a;29:91–93.
137. Nauta WJH, Gygax PA. Silver impregnation of degeneration axon terminals in the central nervous system. I. Technic; II. Chemical notes. Stain Technol 1954b;26:5–11.
138. Nieuwenhuys R. Chemoarchitecture of the brain. Berlin: Springer-Verlag, 1985.
139. Novak J, Salafsky B. Early electrophysiological changes after denervation of slow skeletal muscle. Exp Neurol 1967;19:388–400.
140. Ochs S. Rate of fast axoplasmic transport in mammalian nerve fibers. J Physiol (Lond) 1972; 227:627–645.
141. Ochs S, Ranish N. Characteristics of the fast transport system in mammalian nerve fibers. J Neurobiol 1969;1:247–261.
142. Ortmann R. Neurosecretion. In: Field J, ed. Handbook of physiology, neurophysiology. Vol. II, Ch. 40. Washington, DC: American Physiological Society, 1960;1039–1065.
143. Palay SL. Neurosecretion. VII. The preopticohypophysial pathway in fishes. J Comp Neurol 1945; 82:129–143.
144. Palay SL, Chan-Palay V. Cerebellar cortex: cytology and organization. Berlin: Springer-Verlag, 1974.
145. Palay SL, Palade GE. The fine structure of neurons. J Biophys Biochem Cytol 1955;1:69–88.
146. Patton HD. Special properties of nerve trunks and tracts. In: Ruch TC, ed. Neurophysiology. Ch. 3. Philadelphia: W.B. Saunders, 1961: 66–95.
147. Percheron, G, Yelnik, J, and Francois, C. A Golgi analysis of the primate globus pallidus. III. Spatial organization of the striato-pallidal complex. J Comp Neurol 1984; 227:214–227.
148. Peters A. The formation and structure of myelin sheaths in the central nervous system. J Biophys Biochem Cytol 1960;8:431–446.
149. Peters A. The node of Ranvier in the central nervous system. Q J Exp Physiol 1966;51:229–236.

150. Peters A, Palay SL, Webster H deF. The fine structure of the nervous system: neurons and their supporting cells. 3rd ed. New York: Oxford University Press, 1991.
151. Peterson ER, Murray MR. Myelin sheath formation in cultures of avian spinal ganglia. Am J Anat 1955;96:319–355.
152. Polack JM, McGee OD. In situ hybridization. Principles and practice. Oxford: Oxford University Press, 1990.
153. Quensel W. Über die Faserspezifität in sensiblen Hautnerven. Pflügers Arch. Gesamte Physiol Menschen Tiere 1944;248:1–20.
154. Ramón y Cajal, S. Histologie du Systeme Nerveux de l'Homme et des Vertébrés. (Azoulay L, trans.) Paris: Maloine, 1909, 1911 (Reprinted, Consejo Superior de Investigaciones Cientificas, Instituto Ramón y Cajal, Madrid, 1972).
155. Ramón y Cajal, S.. Degeneration and regeneration of the nervous system. (May RM, trans. and ed., 1959). New York: Hafner, 1928.
156. Ranson SW. The tract of Lissauer and the substantia gelatinosa Rolandi. Am J Anat 1914;16: 97–126.
157. Robertson HA, Paul ML, Moratalla R, Graybiel AM. Expression of the immediate early gene c-fos in basal ganglia: induction by dopaminergic drugs. Can J Neurol Sci 1991;18:380–383.
158. Robertson JD. Ultrastructure of adult vertebrate peripheral myelinated nerve fibers in relation to myelinogenesis. J Biophys Biochem Cytol 1955;1:271–278.
159. Robertson JD. The ultrastructure of Schmidt-Lantermann clefts and related shearing defects of the myelin sheath. J Biophys Biochem Cytol 1958;4:39–46.
160. Robertson JD. Preliminary observations on the ultrastructure of nodes of Ranvier. Z Zellforsch Mikrosk Anat 1959;50:553–560.
161. Ross LL, Bornstein MB, Lehrer G. Electron microscope observations of rat and mouse cerebellum in tissue culture. J Cell Biol 1962; 14:19–30.
162. Rusak B, Robertson HA, Wisden W, Hunt SP. Light pulses that shift rhythms induce gene expression in the supraoptic nucleus. Science 1990;248:1237–1240.
163. Salafsky B, Jasinski D. Early electrophysiological changes after denervation of fast skeletal muscle. Exp Neurol 1967;19:375–387.
164. Scharrer B. Recent progress in the study of neuroendocrine mechanisms in insects. Arch Anat Microscop Morphol Exp 1965;54: 331–342.
165. Scharrer E, Scharrer B. Secretory cells within the hypothalamus. Proc Assoc Res Nerv Ment Dis 1940;20:170–194.
166. Scharrer E, Scharrer B. Neurosecretion. Physiol Rev 1945;25:171–181.
167. Scheibel ME, Scheibel AB. Neurons and neuroglial cells as seen with the light microscope. In: Windle WF, ed. Biology of neuroglia. Springfield, IL: Charles C. Thomas, 1958:5–23.
168. Schmitt FO, Bear RS, Palmer KJ. X-ray diffraction studies on the structure of the nerve myelin sheath. J Cell Comp Physiol 1941;18:31–42.
169. Schwab ME. Myelin-associated inhibitiors of neurite growth and regeneration in the CNS. Trends Neurosci 1990;13:452–456.
170. Schwartz JH. Axonal transport: components, mechanisms and specificity. Annu Rev Neurosci 1979;2:467–504.
171. Schwartz JH. Synthesis and trafficking of neuronal proteins. In: Kandel ER, Schwartz JH, Jessell TM, eds. Principles of neural science. Ch. 4. New York: Elsevier, 1991:49–65.
172. Schwartz JH. Chemical messengers: small molecules and peptides. In: Kandel ER, Schwartz JH, Jessell TM, eds. Principles of neural science. Ch. 14. New York: Elsevier, 1991:213–224.
173. Scott D Jr, Clemente CD. Mechanism of spinal cord regeneration in the cat. Fed Proc 1952;11:143–144.
174. Shepherd GM. The synaptic organization of the brain. 3rd ed. New York: Oxford University Press, 1990.
175. Shepherd GM. Foundation of the neuron doctrine. New York: Oxford University Press, 1991.
176. Sherrington C. The integrative action of the nervous system. 2d ed. New Haven: Yale University Press, 1947.
177. Siegelbaum SH, Koester J. Ion channels. In: Kandel ER, Schwartz JH, Jessell TM, eds. Principles of neural science. Ch. 5. New York: Elsevier, 1991:66–79.
178. Sjöstrand FS. The structure and formation of the myelin sheath. In: Rose AS, Pearson CM, eds. Mechanisms of demyelination. New York: McGraw-Hill, 1963:1–43.
179. Smith Y, Bolam JP. Convergence of synaptic inputs from the striatum and the globus pallidus onto identified nigrocollicular cells in the rat: a double anterograde labeling study. Neuroscience 1991;44:45–73.
180. Snyder SH. Brain peptides as neurotransmitters. Science. 1980; 209: 976–983.
181. Sokoloff L. Relation between physiological function and energy metabolism in the central nervous system. J Neurochem 1977; 29: 13–26.
182. Somogyi P, Freund T. Immunocytochemistry and synaptic relationships of physiologically characterized HRP-filled neurons. In: Heimer L, Zaborsky L, eds. Neuroanatomical tract-tracing methods 2. Ch. 9. New York: Plenum Press, 1989:239–264.
183. Sotelo C, Palay SL. The fine structure of the lateral vestibular nucleus in the rat. I. Neurons and neuroglial cells. J Cell Biol 1968;36:151–179.
184. Standaert FG, Dretchen KL. Cyclic nucleotides and neuromuscular transmission. Fed Proc 1979; 38:2183–2192.
185. Steward O, Banker GH. Getting the message from the gene to the synapse: sorting and intracellular transport of RNA in Neurons. Trends Neurosci 1992;15:180–186.
186. Strange PE. Interesting times for dopamine receptors. Trends Neurosci 1991;14:43–45.
187. Sugar O, Gerard RW. Spinal cord regeneration in the rat. J Neurophysiol 1940;3:1–19.
188. Thomas PK. The connective tissue of peripheral nerve: an electron microscope study. J Anat 1963; 97:35–44.
189. Truex RC. Morphological alterations in the Gasserian ganglion cells and their association with senescence in man. Am J Pathol 1940;16:255–268.
190. Uzman BG, Nogueira-Graf G. Electron microscope studies of the formation of nodes of Ranvier in mouse sciatic nerves. J Biophys Biochem Cytol 1957;3:589–598.
191. Vallee RB, Bloom GS. Mechanisms of fast and slow axonal transport. Annu Rev Neurosci 1991;14:59–92.
192. Van Crevel H, Verhaart WJC. The rate of secondary degeneration in the central nervous system. I. The pyramidal tract of the cat. J Anat 1963a;97:429–449.
193. Van Crevel H, Verhaart WJC. The rate of secondary degeneration in the central nervous system. II. The optic nerve of the cat. J Anat 1963b;97:451–464.
194. Van der Kooy D, Kuypers HGJM, Catsman-Berrevoets CE. Single mammillary cell bodies with divergent axon collaterals. Demonstration by a simple, fluorescent retrograde double labeling technique in the rat. Brain Res 1978;150:189–196.
195. Vizoso AD, Young JZ. Internode length and fibre diameter in developing and regenerating nerves. J Anat 1948;82:110–134.
195. Waksman BH. Experimental study of diphtheritic polyneuritis in the rabbit and guinea pig. III. The blood nerve barrier in the rabbit. J Neuropathol & Exp Neurol 1961;20:35–77.
197. Waldeyer W. Ueber einige neuere Forschungen im Gebiete der Anatomie des Centralnervensystems. Dtsch Med Wochenschr 1891; 17:1213–1218, 1244–1246, 1267–1269, 1287–1289, 1331–1332, 1352–1356.
198. Webster H deF. Transient, focal accumulation of axonal mitochondria during the early stages of Wallerian degeneration. J Cell Biol 1962;12:361–377.
199. Weiss P. Neuronal dynamics and neuroplasmic flow. In: Schmidt FD, ed. The neurosciences. Second study program. New York: Rock-

feller University Press, 1970; 840–850.
200. Weiss P, Hiscoe HB. Experiments on the mechanism of nerve growth. J Exp Zool 1948;107: 315–396.
201. Whittaker VP. The application of subcellular fractionation techniques to the study of brain function. Prog Biophys Chem 1965; 15:39–96.
202. Wiitanen JT. Selective silver impregnation of degenerating axons and axon terminals in the central nervous system of the monkey (Macaca mulatta). Brain Res 1969;14:546–548.
203. Wilson WS, Schulz RA, Cooper JR. The isolation of cholinergic synaptic vesicles from bovine superior cervical ganglion and estimations of their acetylcholine content. J Neurochem 1973;20:659–667.
204. Windle WF, Chambers WW. Regeneration in the spinal cord of the cat and dog. J Comp Neurol 1950; 93:241–257.
205. Yelnik J, Percheron G, Francčois C. A Golgi analysis of the primate globus pallidus. II. Quantitative morphology and spatial orientation of dendritic arborization. J Comp Neurol 1984;227: 200–213.
206. Young JZ. The functional repair of nervous tissue. Physiol Rev 1942; 23:318–374.
207. Young JZ. Factors influencing the regeneration of nerves. Adv Surg 1949;1:165–220.
208. Zimmerman H. Vesicle recycling and transmitter release. Neuroscience 1979;4:1773–1804.

6
Neuroglia

CHANGING CONCEPT OF NEUROGLIA

As seen in Chapter 5, the central nervous system is made up of only two cell types, neurons and neuroglia, the latter being far more numerous than the former in all regions of the brain and spinal cord and in all species. Neuroglia (nerve-glue) occur first during ontogeny, but the bulk of glial cells do not arise until the majority of neurons have developed, that is around the time of birth or in the early postnatal period (12). Cell counts made in different species suggest that the neuroglia/neurons ratio has steadily increased during phylogeny (104). Indeed, the numerical preponderance of glia over neurons, already obvious in rodents, markedly increases in primates and reaches its peak in humans. Of all living species, the human appears to possess the brain that has, both in relative and absolute terms, the greatest number of glial cells (95, 104).

It is, therefore, surprising to see that, compared to neurons, relatively little is known of the roles of neuroglia. In fact, until recently, the only functions attributed to neuroglia were those already postulated by the first neuroanatomists that discovered and characterized these elements in the first half of the 19th and the beginning of the 20th century (27, 43, 98, 99 129, 130). The neuroglia was left with the rather passive role of supporting and protecting neurons during the performance of their noble functions, upon which the entire complexity of the human brain was thought to rely. This rather simplistic view of the brain has lost much of its original significance and the role and status of neuroglia has been reappraised in the light of new data gathered during the last decade.

The supporting and protecting role of neuroglia was confirmed, particularly through a multitude of very detailed light and electron microscopic studies of glial cells. These studies provide a clear picture of the immense diversity of this cell population. Another important clue about glial function came from the description of their behavior in diseases or injuries. These cells were found to be extremely sensitive to disturbance, modifying their shape and location in response to the most minor changes in brain tissue (95). At the beginning of the 1970s, careful studies by Pasko Rakic and others (96) revealed the fundamental role that neuroglia play during embryonic development in guiding the migration of neurons from the neuroepithelium to their adult location (see Chapter 3). More recent studies confirmed and greatly extended this view by showing the very active role of glial cells in establishing and maintaining the fundamental patterns of neuronal circuits (33, 68, 93).

During the last decade, the application of technical approaches as diverse as tissue culture, immunology, patch-clamp electrophysiology, receptor localization, and molecular biology have radically changed our view of neuroglia. Biochemical and immunologic investigations produced, among other things, highly specific biochemical markers for studying the neuroglia cell lineage. Electrophysiologic investigations revealed that glial cells possess different voltage-dependent ions channels that can be activated by specific transmitter receptors located on their membrane (55, 73, 77, 121). Some glial cells were also shown to play a crucial role in the maintenance of the homeostasis of the microenvironment (71, 132) and the immunologic response to various infectious or toxic agents (122). Neuroglia is now known to produce various growth and trophic factors, which makes it a key element in central nervous system regeneration and plasticity (85). It is also thought to be directly involved in the basic mechanisms underlying certain neurodegenerative diseases (31, 48, 65).

It is clear that glial cells are now viewed in a much more dynamic way than previously. These central nervous system elements are now believed to be much more closely associ-

ated with neuronal functions. The various changes through which the concept of neuroglia went since the discovery of these cells in the middle of the 19th century are certainly unique in the history of neurobiology. First thought of as a sort of "glue" or simple connective tissue, then later regarded as supporting and protective tissue, neuroglia is now believed to play a key role in association with neurons in the overall functioning of the central nervous system. It seems that we have now entered the era of "neurogliobiology" (86).

GENERAL FEATURES AND CELL LINEAGE

The discovery of neuroglia is attributed to the German pathologist Rudolph Virchow, who first called it Bindesubstanz (connective tissue) and later Nervenkitt (nerve-cement) (55, 95, 116, 136). Early investigators recognized that neuroglia separated neural elements from blood vessels and regarded neuroglia as an interstitial material in which characteristic stellate and spindle-shaped cells were suspended. Although peripheral nerves have a supporting framework formed by connective tissue, this is lacking in the central nervous system. In the brain and spinal cord, connective tissue is limited to the membranes which surround and envelop them, the meninges, and small extensions of these membranes which accompany blood vessels that penetrate neural tissue (see Chapter 1). At the light microscopic level the structural features of neuroglia are difficult to demonstrate except by complex selective staining methods. In ordinary preparations stained with basophilic dyes, usually only the nuclei are seen. Sections impregnated by the metallic techniques of Golgi (43), Ramón y Cajal (97,98, 99), and Del Rio Hortega (27, 28) reveal the different cell types, their processes and their relationships to neurons and blood vessels (Figs. 6.1–6.4, and 6.7). In the first half of the 20th century, the morphologic characteristics of neuroglia as observed in the light microscope were described by several authors: Penfield (87), Del Rio Hortega (30), Glees (42), Scheibel and Scheibel (109), Windle (135), and Polak (91). Electron microscopic studies indicate that the interstitial material of the central nervous system is composed only of neuroglia (40, 90). Thus the central nervous system is composed almost entirely of two elements, neurons and neuroglia, which are separated from each other by extracellular fluid contained in a space 10–20 nm in width (32, 84).

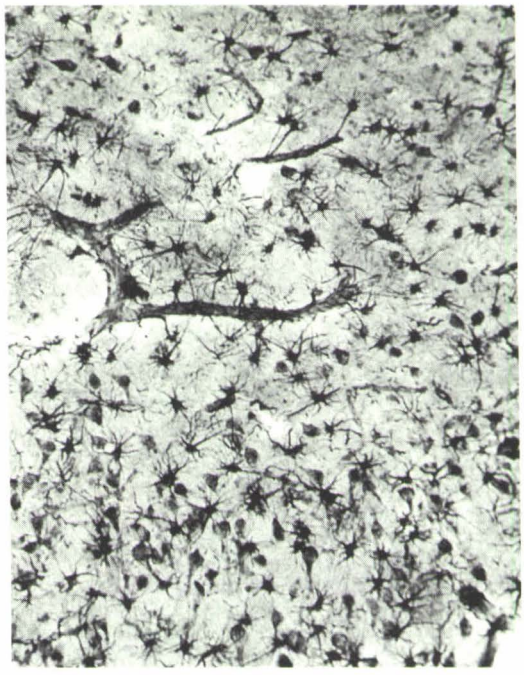


Figure 6.1. Astrocytes showing their radially arranged processes and "end feet" (Ramón y Cajal gold-sublimate method, ×150).

In contrast to other epithelial tissues, there is relatively little extracellular space in the central nervous system. Electron microscopic studies indicate that neurons and neuroglia are tightly packed in the central nervous system with spaces no greater than 20 nm wide between individual cells. However, measurements of the extracellular space, based upon equilibration with sucrose, suggest that the small size of the extracellular space in electron micrographs of conventionally processed tissue is an artifact probably due to cellular swelling resulting from asphyxia (67). In fact, the real extracellular space in mature brain appears to be approximately 15–20% in volume (25, 67).

Information concerning the volume, the nature of the fluid filling the extracellular space, and the possibilities for controlling both its composition and volume is of great practical significance in relation to cerebral edema. Electron microscopic investigations suggest that experimental and clinical edema in the gray matter of the brain may be due to swelling of glial cells, particularly astrocytes

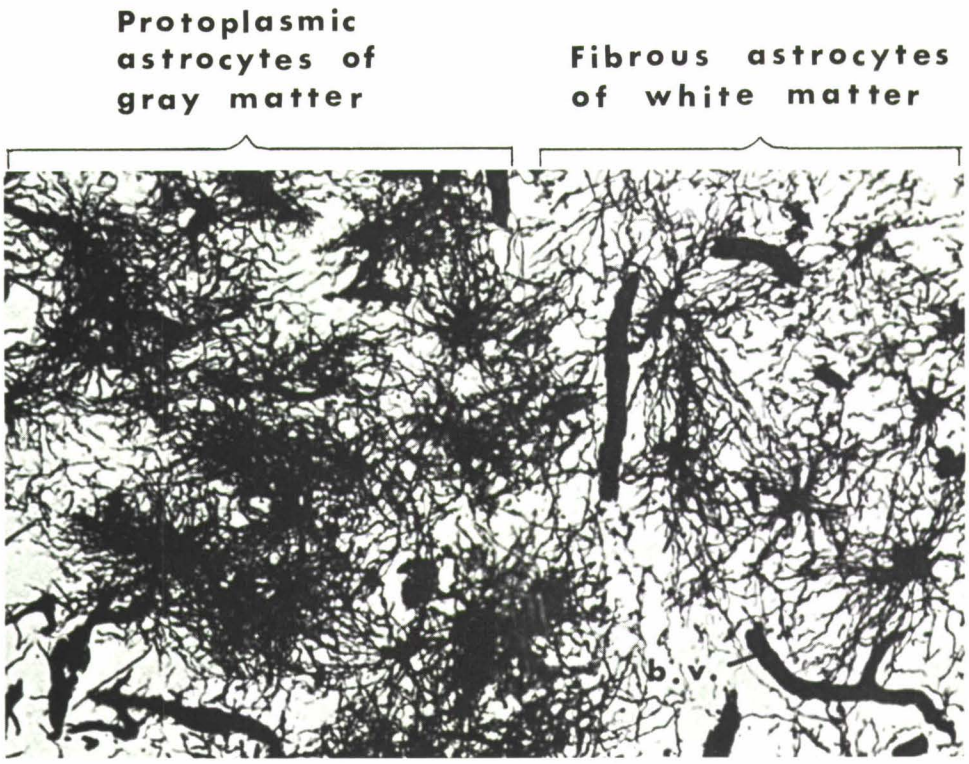


Figure 6.2. Distribution and appearance of astrocytes in gray and white matter of human spinal cord. Smaller nerve cell bodies are often obscured by profuse branches of protoplasmic astrocytes. Blood vessels (*b.v.*) also are stained in such preparations and receive vascular end feet from adjacent astrocytes (Golgi stain, ×175).

(26). In the white matter, where edema is more severe, the enlargement is primarily in the extracellular region with marked widening of the 20 nm extracellular space (128). It is apparent that cerebral edema is not a uniform reaction in neural tissue.

In mammals, neuroglial cells outnumber nerve cells 10:1 and form about half of the total volume of the human brain. Their counterparts also are a constant feature of the peripheral nervous system. Similar supportive cells are present in all vertebrate nervous systems and in some invertebrate nervous tissue as well (14, 22, 37, 61). The wide distribution of this class of cells throughout the animal kingdom suggests that their functional role must be of great importance. Glial cells of the mammalian brain are difficult to study because of their inaccessibility. For this reason information has been sought concerning neuroglia in invertebrates and nonmammalian vertebrates (37, 56, 57, 61), as well as in tissue culture studies (41, 74, 75, 78, 92). Among the most widely accepted functions of neuroglia is the role of glial cells (oligodendrocytes in the central nervous system and Schwann cells in the peripheral nervous system) in the formation of myelin sheath (16, 17).

Classically, two categories of glial cells are recognized in the central nervous system, macroglia and microglia (Fig. 6.3). The *macroglia,* comprising astrocytes and oligodendrocytes, are derived from ectoderm, have only one type of cytoplasmic process, do not generate action potentials, and have not been observed to provide or receive synapses. In contrast to macroglia, there is still a debate about the origin of microglia. *Microglia* are considered by some authors to be of mesodermal origin and to derive from monocytes (macrophage precursor cells) that infiltrate the embryonic brain and spinal cord when these developing structures are penetrated by blood vessels (Fig. 6.3). However, a neuroectodermal origin was proposed recently by Federoff and his colleagues, based on the appearance of macrophages in culture derived from a mouse brain before vascularization (45). Whichever turns out to be true, microglia have more in common with periph-

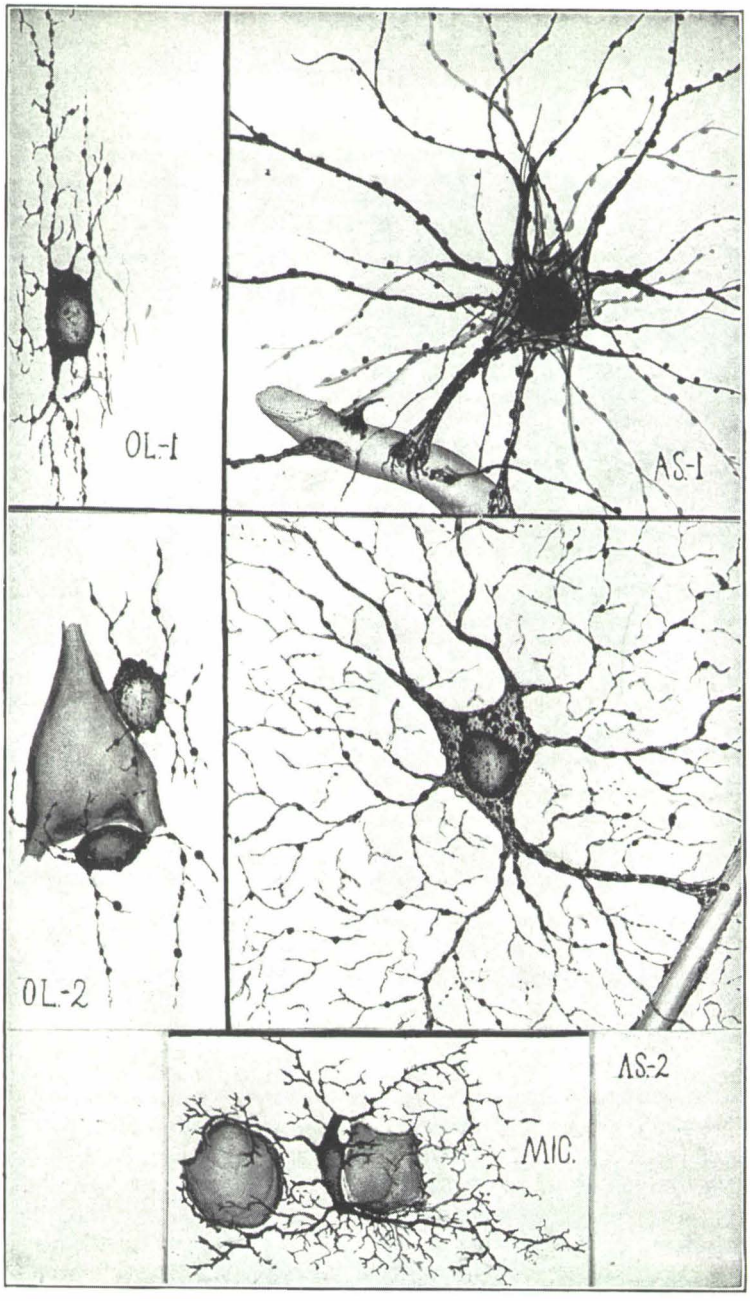


Figure 6.3. Various types of neuroglia cells. *AS-1,* Fibrous astrocyte with one or two processes forming foot plates against a neighboring blood vessel; *AS-2,* protoplasmic astrocyte with foot plate containing gliosomes (dark granules) in its body and processes; *MIC,* microglial cell whose delicate spiny processes embrace the bodies of two neurons; *OL-1,* oligodendrocyte in the white matter (interfascicular form); *OL-2,* two oligodendrocytes lying against a nerve cell (perineuronal satellites).

eral macrophages than with other cells in the nervous system, both in the molecule they express and in their behavior when activated (2).

In the broadest sense, neuroglia, often referred to simply as glia, should include the ependyma, the neurilemma cells (Schwann cells), and the satellite cells of peripheral sensory ganglia, in addition to the macroglia and microglia. Ependymal, neurilemma and satellite cells are all derived from ectoderm; neurilemma and satellite cells are derivatives of the neural crest. Unlike neurons, neuroglia retain the ability to divide throughout life.

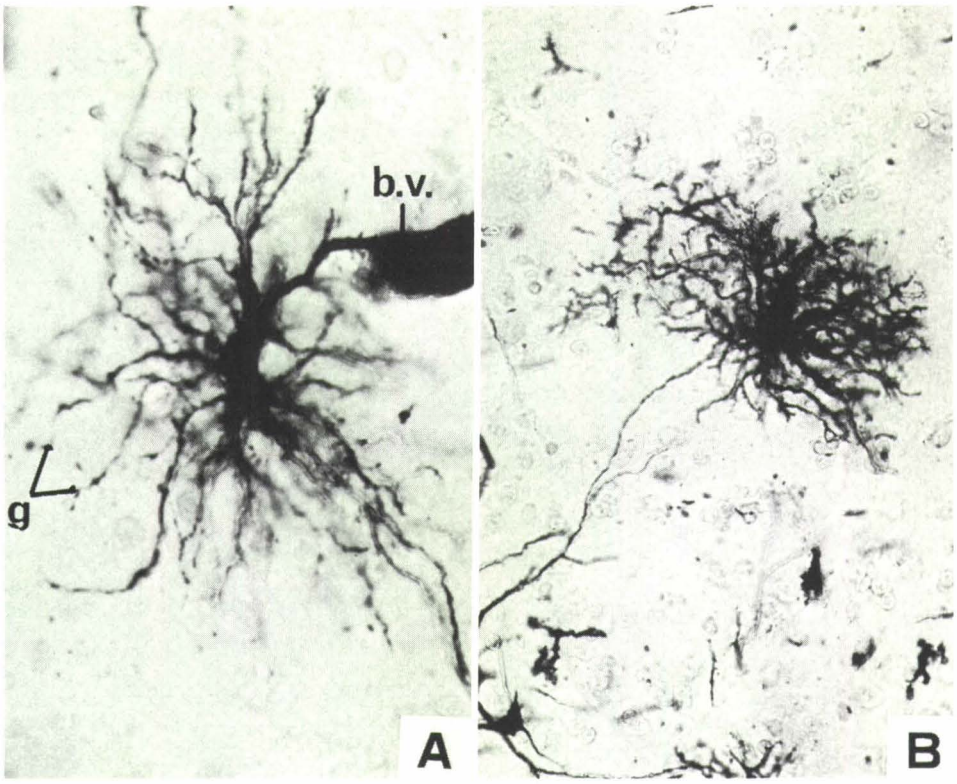


Figure 6.4. (**A.**) Fibrous and (**B.**) protoplasmic astrocytes in white matter of adult cerebral cortex. Note numerous gliosomes (*g*) in the processes of the fibrous astrocyte and vascular end foot on blood vessel (*b.v.*) (Golgi-stain, ×550).

Proliferation of macroglia occurs particularly in response to injury in the nervous system (58, 68, 112, 118).

No morphologic classification of neuroglia is entirely satisfactory, for there may be many intermediate forms between oligodendrocytes and astrocytes (21, 42, 62, 63, 93, 100, 105, 111, 133), and some authors do not consider microglia to be true neuroglial cells (90). In fact, considerable evidence for glial heterogeneity exists and there are many examples of regional variations in the phenotypic expression of glial cells (21, 93, 101, 133). The development of macroglia has been studied extensively in cell culture of the developing rat optic nerve, which has served as a very useful model for the study of complex cell-to-cell interactions that underlie macroglial differentiation (41, 94). Such cultures were shown to contain three antigenically distinct types of macroglial cells: oligodendrocytes and two types of astrocytes (type-1 and type-2). These three cell types appear to arise from two separate lineages: type-1 astrocytes develop from one type of precursor cells, whereas oligodendrocytes and type-2 astrocytes develop from a common, bipotential precursor called the *O-2A progenitor cells*. The O-2A progenitor cells differentiate autonomously into oligodendrocytes in culture, while their differentiation into type-2 astrocytes requires two or more inducing factors produced by other cells as well as extracellular matrix signals. Two of the effective inducing factors are the ciliary neurotrophic factor (CNTF) and the platelet-derived growth factor (PDGF), which are produced by type-1 astrocytes and/or mesenchymal cells (41). The existence of the type-2 astrocyte in the mature central nervous system is still a matter of controversy (41). These results suggest that glial cells, like neurons, defy rigid classification because of their remarkable phenotypic plasticity in response to changes in their environment.

ASTROCYTES

Astrocytes are the largest, most numerous, and most elaborate of all the glial elements.

They are recognized by their stellate-shaped cell body and their many processes which extend into the surrounding neuropil (Figs. 6.1 and 6.2). Some of the long, branched processes from each cell form expansions that are applied to the surface of blood vessels, where they form the so-called *end feet*, a major component of the blood-brain barrier (see Chapter 1). Processes of astrocytes extending to the surface of the central nervous system form similar expansions that constitute the superficial glial membrane (*glia limitans*) beneath the pia mater. Each neuron has a specific relationship with the astrocytic processes in its vicinity, ranging from complete encapsulation to none at all (83, 89). Astrocytes form a continuous lining separating brain from mesenchymal structures—capillaries, meninges, and vascular adventitia enclosing the Virchow-Robin (perivascular) spaces. A basal lamina is invariably interposed between astrocytes and mesenchyma (see Chapter 1).

The astrocytes are densely packed within the neuropil of the nervous system (Fig. 6.2), and reduce the extracellular space to a series of irregular and interlacing small clefts. With the Golgi stain, these glial cells show a delicate, but pervasive, framework in which the neural elements appear to be suspended (Fig. 6.2). In sharp contrast to this somewhat rigid configuration, astrocytes in tissue culture show flowing veil-like expansions in all directions, and migrate with a slow, gliding motion (39, 40, 74).

Astrocytes form a highly heterogeneous cell population in the central nervous system (39, 40, 93). In fact, astrocytes belong to a large family of cells displaying various morphologic and functional phenotypes, as well as regional specificity. The family comprises radial glia, the probable precursor of fibrous and protoplasmic astrocytes (131), ependymal cells, Bergmann glia in the cerebellum, Müller glia in the retina, tanycytes in the hypothalamus, and specialized glial cells that are found in the posterior lobe of the hypophysis (pituicytes) and in the pineal gland (pinealocytes). It also contains a relatively large number of cell subpopulations that can be differentiated from one another by their receptors, ionic channels, and antigenicity (21, 93, 133). These cells all share common features, including (a) interactions with neurons, (b) close contacts with either the glia limitans, perivascular walls, or with ventricular walls, (c) being coupled with gap-junctions, and (d) most express glial fibrillary acidic protein (GFAP) at one specific timeframe during their development (121).

Fibrous and Protoplasmic Astrocytes

Two main types of astrocytes can be distinguished in both light and electron microscopy. The *fibrous astrocyte* (spider cell) is characterized by its thin, poorly branched processes, which radiate from the cell body for considerable distances. These glial elements are often interposed between neurons and adjacent blood vessels and have prominent perivascular end feet (9)(Figs. 6.1, 6.3 and 6.4). Fibrous astrocytes are most numerous in the white matter (Fig. 6.2). With appropriate stains the cell body and processes are seen to contain many delicate fibrils. Each intracellular gliofilament is 10 nm in width and of various length. Such filaments correspond to the thicker fibrils observed in muscle and epithelial cells (i.e., myofibrils and tonofibrils) and are part of the group of intermediate filaments, which form neurofilaments in neurons (see the section entitled *Neuronal Cytoskeleton* in Chapter 5). In the larger processes, they are arranged in straight parallel bundles and can be followed for considerable distances. Such gliofibrils are much less numerous in the protoplasmic astrocytes described later. Another feature common to both types of astrocytes are small granular swellings along the processes called *gliosomes* (Figs. 6.3 and 6.4). They occur in the cell body as well, and in electron micrographs they are seen to be clumps of mitochondria which contain a dense matrix material.

The *protoplasmic astrocytes* (mossy cells) are most numerous and easy to identify in the gray matter (Fig. 6.2). They have numerous freely branching processes, perivascular end feet, and often are observed in close proximity to neuronal soma and dendrites. If fibrous and protoplasmic astrocytes are examined in Golgi preparations (Fig. 6.4), one can find sharp distinctive cells in each category. In the same sections, one can also observe a host of intermediate and transitional cells that defy a precise morphologic classification. Electron microscopic studies suggest that they may represent different forms of the same cell (69, 90). Variations in cell type may in part be a reflection of the cytoarchitectural differences that exist between the gray and white matter

of the brain and spinal cord. Electron microscopic features common to both types of astrocytes (Fig. 6.5) are the usual cytoplasmic organelles: dense mitochondria, scanty rough and smooth endoplasmic reticulum, gliofilaments, and an abundant watery cytoplasm. The nucleus is finely granular and only moderately dense, and nuclear pores have been identified, as shown by Palay (82) and Maxwell and Kruger (69). Fine structural characteristics that identify the astrocyte alone were described by the latter authors. These include a watery cytoplasm that contains gliofilaments and dense glycogen granules 15–40 nm in diameter. Furthermore, recent intracellular HRP experiments by Sasaki and colleagues have shown that gray matter and white matter astrocytes possess distinctive morphologic features. Their camera lucida reconstructions clearly show the difference between the very long, threadlike processes of fibrous astrocytes in the white matter compared with the shorter, sinuous processes with clusters or lamellar appendages of protoplasmic astrocytes in gray matter (107).

Specific Biochemical Markers

The various astrocytes can be distinguished from one another by different molecular characteristics, including specific endogenous proteins and cell-surface antigens. For example an acidic protein, with a molecular weight of 24,000, and termed S-100 because of its solubility in saturated ammonium sulfate,

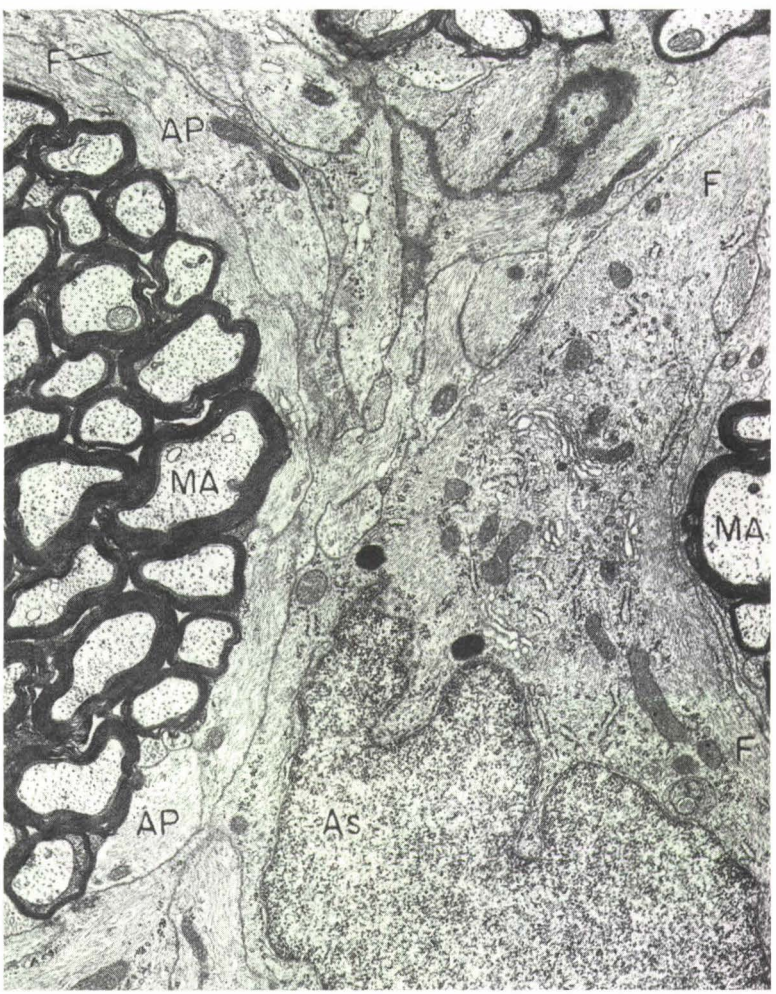


Figure 6.5. Fibrous astrocyte (*As*) from normal, adult rat optic nerve. The astrocytic cell body contains numerous filaments (*F*), as do the astrocytic processes (*AP*) which subdivide the myelinated axons (*MA*) of the optic nerve into bundles (×12,000).

is found mainly in glial cells in the adult rat (70). However, one of the most widely used astrocytic markers is *glial fibrillary acidic protein* (GFAP), which differs from S-100 in amino acid sequence and electrophoretic mobility, and also differs from the fibrillary proteins tubulin and filarin found in neurons (6) (Fig. 6.20). GFAP is the subunit of the intermediate filaments in astrocytes. In immature skeletal muscle, 10-nm filaments were first called "intermediate" because their diameter was between that of thin actin and thick myosin filaments. The term is now applied to all 10-nm filaments regardless of their location. In all nonmuscle cells, the term intermediate refers to filaments with a diameter ranging from that of microfilaments and microtubules. Intermediate filaments have a similar appearance in most cells, but their protein subunits are regarded as highly specific and can be used as a taxonomic criterion to differentiate the major cells of the body: epithelia (keratins), mesenchyma (vimentin), muscle (desmin), astroglia (GFAP), and neurons (neurofilament proteins; see Chapter 4) (4). Because of the large number of intermediate filaments in fibrous astrocytes, compared to protoplasmic astrocytes, GFAP is closely associated with fibrous astrocytes in both normal and pathologic brain tissue (5), and with embryonic radial glial cells (60). Of high clinical relevance is that increased production of GFAP is one of the most sensitive indicators of central nervous system damage (Fig. 6.20).

Another biochemical marker for astrocytes is *glutamine synthetase*, the enzyme responsible for the formation of glutamine from glutamate, ATP, and ammonia. In the brain, this enzyme is exclusively found in astrocytes. It is involved in the regulation of glutamate and GABA pools in the microenvironment. Astrocytes can also be readily identified by the monoclonal antibody A_2B_5 (35), which recognizes specific gangliosides that are express at the cell surface of astrocytes. This monoclonal antibody is extensively used as an astrocytic marker, particularly in tissue culture studies (41). Since astrocytes possess other distinctive features, such as specific receptors and ionic channels, other biochemical markers or electrophysiologic properties can be used to identify the various types of astrocytes.

Homeostasis and Ionic Channels

One of the major functions of astrocytes is to ensure the stability of the central nervous system microenvironment. Because of their close contacts with neurons, astrocytes are ideally located for this purpose. Furthermore, due to the presence of gap junctions, astrocytes form a functional syncytium so that changes in the concentration of ions and small solutes can be rapidly equilibrated (71). It is worth noting that, because of the high synaptic activity, the homeostasis requirements are particularly stringent in the gray matter. The maintenance of adequate extracellular concentrations of potassium (K^+) and glutamate are two examples of the role of astrocytes in the control of the microenvironment.

Potassium concentration [K^+] is much lower in the extracellular than in the intracellular space. The membrane of both astrocytes and neurons are permeable to potassium and this, together with the large concentration gradient, is the reason for their negative membrane potential (see Chapter 5). Although the amount of potassium release during neuronal signaling is relatively small, it nevertheless produces a significant increase in extracellular [K^+]. Increase of extracellular [K^+] depolarizes neurons and astrocytes due to the decrease of concentration gradients. To avoid excessive neuronal depolarization (spreading depression) due to high extracellular [K^+], potassium needs to be buffered in some way. Dispersal of this ion through the astrocyte syncytium, a phenomenon called *spatial buffering*, is one of the most effective mechanisms for extracellular [K^+] regulation. The astrocytes membrane is more permeable to potassium than the neuronal membrane. Increase in extracellular [K^+] results in more potassium influx in astrocytes than in neurons. If the increase of extracellular [K^+] is local, potassium will be redistributed to distant areas where extracellular [K^+] is lower via the astrocyte syncytium. This remarkable mechanism allows for a return of extracellular [K^+] to normal values without loss of potassium from the brain. This is important because the cerebral capillary endothelium is relatively impermeable to potassium (132).

The regulation of extracellular [K^+] is possible because of numerous ionic pumps present within the membrane of astrocytes. In a first step, potassium ions enter into the astrocyte through passive, voltage-independent channels. However, if the intracellular [K^+] increases significantly, this will activate potassium and sodium ATPase-dependent pumps, as well as various transport systems for potassium chloride (KCl) and sodium

chloride (NaCl) (79). The potassium influx transforms the astrocyte into a polarized cell whose surface expresses voltage-dependent potassium, sodium, chloride, and calcium ionic channels. Compared to neurons, voltage-dependent ionic channels are relatively few in astrocytes and this may explain why astrocytes do not generate action potentials. The roles of the voltage-dependent ionic channels in astrocytes remain to be determined.

Astrocytes also control the extracellular concentrations of glutamate, GABA, and biogenic amines. It appears that the segregation of glutamate and GABA within glial and neuronal compartments is one of the major mechanisms involved in the control of these two amino acids transmitters. Astrocytes possess the highly specific uptake mechanisms for these two transmitters, as well as the entire enzymatic machinery to metabolize them (3, 36, 48). Despite some regional differences, the uptake capacity of glutamate is much higher in astrocytes than in neurons, whereas the reverse is true for GABA. Glutamate is released in large amounts at excitatory synapses in the central nervous system, where it binds to specific neuronal receptors (see Chapter 5). Those molecules that did not bind to the appropriate receptors or the ones that are liberated from the receptors after they exerted their action are actively taken up by astrocytes and metabolized into glutamine by glutamine synthetase, an enzyme that is specific to astrocytes. Since glutamate, like other acidic amino acids, is neurotoxic in large concentration (excitotoxins), a failure in the astrocytic glutamate uptake and metabolic mechanisms is believed to be a factor contributing to neuronal necrosis in status epilepticus and anoxia. Furthermore, since astrocytic glutamine synthetase uses ammonia and ATP to transform glutamate into glutamine, astrocytes are thought to play an important role in brain ammonia detoxification. After diffusion into the extracellular space, glutamine may be taken up by neurons and hydrolyzed back to glutamate by glutaminase, which is mainly a neuronal enzyme.

GABA is synthesized from glutamate by the enzyme glutamate decarboxylase (GAD). It is released in large amounts at the level of inhibitory synapses in the central nervous system (see Chapter 5). After its release in the synaptic cleft, GABA may be taken up partly by neurons and partly by astrocytes. Within astrocytes, GABA is first metabolized to glutamate by the enzyme glutamate transaminase (GABA-T) and then to glutamine by the enzyme glutamine synthetase. Glutamine is again exported into the extracellular space where it can be taken up by neurons and transform into glutamate and/or GABA (121). Large concentrations of GABA in the microenvironment can induce lethargic states, whereas lack of this major inhibitory transmitter can produce convulsions. Therefore, the role that astrocytes play in the control of extracellular concentrations of glutamate and GABA is a perfect example of the importance of glial-neuronal interactions in the control of homeostasis in the central nervous system.

Transmitter Receptors

Astrocytes display a high degree of phenotypic plasticity since they are able to respond to various stimuli by changing their form, functional state, and even their rate of multiplication. Among these various stimuli are several small-molecule transmitters and neuroactive peptides, which can bind to astrocytes via specific cell membrane receptors (73, 119). Specific astrocytic receptors exist for a large number of molecules, including epinephrine (α- and β-adrenergic receptors), histamine, dopamine, serotonin, substance P, bradykinin, secretin, adenosine, vasoactive intestinal peptide, and calcitonin (134). These receptors are, like their neuronal homologues, often coupled to second messengers.

The physiologic responses to the activation of many of these receptors are not yet known. However, it is well-established that the activation of β-adrenergic, vasoactive intestinal peptide, and serotonin astrocytic receptors induces glycogenolysis. It must remembered that glycogen particles are one of the distinguishing features of astrocytes, allowing their identification especially where intermediate filaments are few in number (e.g., in the neocortex) (4). In addition to noradrenaline, several substances released by neurons during depolarization, such as adenosine and potassium, stimulate glycogenolysis. It is thus possible that one function of the astrocytic is to provide energy to active neurons (66). In turn, astrocytes have been found to release arachidonic acid derivatives, such as prostaglandins and leucotrienes, as well as other vasorelaxing factors with properties similar to nitrous oxide. Furthermore, activation of β-adrenergic, va-

soactive intestinal peptide, and serotonin astrocytic receptors, coupled to cAMP or phosphoinositides, can produce significant changes in the phosphorylation of GFAP. Therefore, through their action on the major astrocytic cytoskeletal elements, neurotransmitters can modify the shape of astrocytes (59, 64, 121).

Catecholamines released normally at synaptic junctions, as well as neurotrophic viruses, endogenous toxins, and interferon γ released at the level of cerebral lesions, can activate specific astrocytic genes and induce the expression of the encoded proteins. This is the case of NGF, as well as other factors, such as interleukins and cytokins (121). Active astrocytes can also release interferon α/β and become associated with lymphocyte T to induce the expression of class II major histocompatibility antigens. They also secrete factors capable of affecting the survival and maturation of microglia, and modulating inflammatory and immunologic responses (121).

Neuronal Development and Plasticity

The role of radial glia for the guidance of migrating neurons, first suggested by Ramón y Cajal, was convincingly demonstrated by the work of Pasko Rakic and his collaborators, which showed the close apposition of migrating neuroblasts to radial glia in the cerebral hemispheres and to Bergman radial glia in the cerebellar cortex (96, 118). However, note that not all neuronal migrations occur along radial glial fibers. Heynes and collaborators showed that neuroblasts forming the germinal layer of the cerebellum migrate from the caudolateral margin of the fourth ventricle to the surface of the cerebellum while remaining in close contact with preexisting axonal bundles (49). It appears that migrating neuroblasts can use different surfaces as long as they lead to the right direction.

Astrocytes are also involved in various recognition systems that guide axon elongation during development. Among these recognition systems, astrocytes are simply in those comprising either cell interactions mediated through cell adhesion molecules (CAM) or interactions with the extracellular matrix mediated by integrins and other matrix glycoproteins (see Chapter 3). The role of astrocytes in neuronal development is not restricted to the support and guidance of growing neurons, but these glial cells appear also involved in the control of neuronal morphogenesis. This is exemplified by the now classic experiment of Prochiantz and Mallat (93), which showed that neurons of the substantia nigra developed dendrites when grown in culture with astrocytes from this nucleus, whereas they developed axons in the presence of astrocytes from the striatum, which they are supposed to meet *in situ* only at the end of their axogenesis. Furthermore, it was shown that the shape of substantia nigra dopaminergic neurons, or, especially, the extent of their dendritic arborization, depends in large part from the local astrocyte population (33). It remains to be seen whether astrocytes affect neuronal shape by providing a suitable substrate for dendritic growth or by secreting appropriate soluble trophic factors. Through all these effects on neuronal migration, axogenesis, and neuronal morphogenesis, astrocytes appear to provide much of the basic pattern for the establishment of the major neuronal circuits.

Blood-Brain Barrier

The endothelium of brain microvessels constitutes a highly specialized, metabolically active barrier responsible for the stable environment of the central nervous system. The passage of different substances across the blood-brain barrier into cerebral interstitial fluid is regulated by this endothelial layer, which possesses several structural and biochemical properties distinct from those of noncerebral capillaries. Among other things, the end feet of astrocytes and their basal lamina are believed to be major components of the blood-brain barrier (see Chapter 1). Endothelial cells of brain capillaries are linked by tight junctions that form a continuous belts around contiguous endothelial cells (76). This elaborate junctional network is considered a major structural component of the blood-brain barrier to macromolecules. The ability of brain endothelial cells to form a barrier depends on the environment in which they grow. If a developmental, postnatal increase in the ensheathment of endothelium by astroglia occurs, there appears to be a related maturation of the blood-brain barrier. Furthermore, the astrocytic processes that envelope the brain capillaries appear to alter the capillaries' passive permeability by modulating the formation of tight junctions between the endothelial cells. A close interaction be-

tween endothelium and astroglia was demonstrated by allowing permeable vessels from nonneuronal tissue to grow into embryonic avascular brain fragments *in vivo*. Upon entering the brain, the permeable vessels became impermeable to circulating tracers (117). The component of the brain environment responsible for this permeability change appears to be astroglia. Indeed, when dissociated astrocytes are grafted to the anterior chamber of the eye, the permeable vessels of the iris become impermeable as they penetrate the astrocytic domain (51). This hypothesis was confirmed and further extended by experiments involving the insertion of fetal cerebellar tissue into the anterior chamber of the eye in the rat (76). Thus, astrocytes induce the formation of the blood-brain barrier *in vivo* and the organization of the tight junction *in vitro*, but the nature of the inductive factor(s) remains to be discovered (76). The involvement of astrocytes in the formation of the blood-brain barrier reveals that these glial cells actively interact not only with neurons, but with other elements of the central nervous system as well.

Pathologic Conditions

The most common astrocyte reactions to injury are hypertrophy and the production of intermediate filaments, that is, *fibrillary gliosis*. Numeric increase of astrocytes due to cell division is also part of the response, but is probably less important compared to hypertrophy and fibrillogenesis in scar formation (4). The increase in fibrillogenesis can be easily monitored with GFAP immunocytochemistry since the production of this protein is greatly enhanced in case of central nervous system damage (Fig. 6.20).

Astrocytic reactions vary considerably depending on the type and extent of injury (Fig. 6.6). In case of severe brain injury, such as in ischemic necrosis (infarct) involving blood vessel damage at the surface of the brain, protein-rich fluid pours out from the necrotic brain tissue causing severe white matter edema. Reactive astrocytes rapidly surround the infarct with a thick mesh of fibrils, demarcating the necrotic tissue from viable brain and probably preventing the spread of edema. Finally, the glial scar covered by a basal lamina forms the new surface of the brain. The cyst resulting from the absorption of the necrotic tissue by blood-born macrophages is now part of the subarachnoid space. If the infarct is deeper into the brain, like in the basal ganglia, the resulting cyst is then part of the perivascular space. Thus, as in normal conditions, astrocytes always form the boundary between central and noncentral nervous tissue in pathologic conditions (4). The astrocyte scar resulting from severe brain damage is called *anisomorphic gliosis* because of the irregular arrangement of the glial fibrils with no preservation of the preexisting structure. In cases of more selective brain injuries, such as the loss of a given neuronal population following anoxia or retrograde degeneration of nerve fibers, the reactive astrocytes retain their normal architecture and the resulting scar is called *isomorphic gliosis*.

Protoplasmic astrocytes undergo characteristic changes in *hepatic encephalopathy*. These consist of swelling and vacuolation of astrocytic nuclei and mitochondria, most prominent in cerebral cortex and basal ganglia. As seen earlier, astrocytes play a role in ammonia detoxification, but the relation between this astrocytic function and the morphologic changes seen in protoplasmic astrocytes in the hyperammonemia condition that is characteristic of hepatic encephalopathy is still uncertain. However, it is worth noting that cerebral cortex and basal ganglia, where nuclear swelling is most severe, are among the brain regions with the highest concentrations of glutamine synthetase.

Astrocytes are also thought to be involved in some forms of Parkinsonism and Huntington's disease. The drug 1-methyl-phenyl-1,2,3,6-tetrahydropyridine (MPTP) is known to cause clinical symptoms and neuropathologic signs that are indistinguishable from those occurring in idiopathic Parkinson's disease. Furthermore, it has been established that astrocytes convert MPTP into its toxic metabolite 1-methyl-4-phenylpiridinium ion (MPP^+). The toxic metabolite appears to be produced by the enzyme monoamine oxydase B (MAOB) which, in the brain, is predominantly located in astrocytes (102).

Studies of the pathogenesis of Huntington's disease have shed new light on the function of the reactive astrocytes. Huntington's disease is characterized by a massive neuronal loss in the caudate nucleus and putamen (striatum) resulting in a marked atrophy of both structures. The important neuronal depletion is accompanied by a marked astrocytes hypertrophy together with increase of filaments and GFAP (*reactive gliosis*) in the striatum. Recent findings suggest that

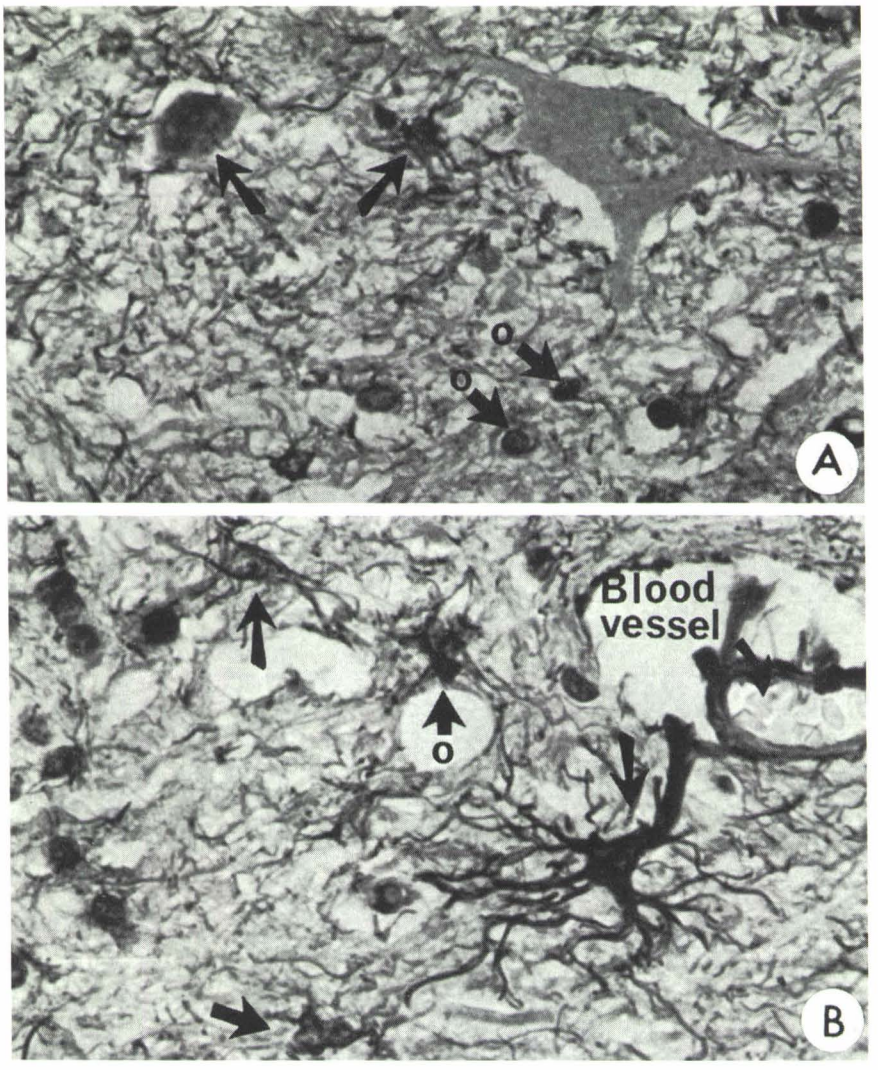


Figure 6.6. Reactive astrocytes in gray matter of adult human spinal cord 4 weeks after a spinal stereotaxic lesion. **A.** Anterior horn cell with adjacent oligodendrocytes (*o*) and swollen astrocytes (*arrows*). **B.** A prominent and bizarre astrocyte with enlarged vascular end foot. Several smaller astrocytes with gliofibrils are indicated by *arrows*. The cell body of an oligodendrocyte (*o*) is identified for comparison of relative sizes. (Holzer stained sections, ×550.)

reactive gliosis may play a role in the pathogenesis of Huntington's disease. Lesions similar to those observed in Huntington's disease can be experimentally produced by intrastriatal injection of various exogenous amino acids (excitotoxins) (e.g., kainic and ibotenic acid). Quinolinic acid, an endogenous metabolite of tryptophan metabolism, can produce changes similar to those of exogenous excitotoxins (7) and this suggests that it could play a role in the pathogenesis of Huntington's disease. The marked increase of the anabolic enzyme for quinoline in both experimental excitotoxic lesions and in Huntington's disease, suggests that astrocytes are primarily involved in the production of quinolinic acid since they are the main cell population that remains intact and even proliferates in these conditions.

Most primary brain tumors are *gliomas* and most gliomas derive from astrocytes as shown by GFAP immunocytochemistry (4). In various organs of the body, local spread of malignant tumors mainly occurs through lymphatic and interstitial tissue spaces. However, the brain is different in that lymphatics are missing and interstitial tissue spaces are sealed. Therefore, metastatic carcinomas are not able to infiltrate brain tissue and grow as solid nodes. Astrocytomas are different in

that the cells forming the tumor are able to infiltrate brain tissue because of their organization in the form of a functional syncytium. The extent of infiltration depends on the malignancy of the tumor. It is possible that the characteristic patterns resulting from astrocytoma infiltration in the brain are relevant to the question of glial migration in development.

OLIGODENDROCYTES

The term oligodendroglia was introduced by Ramón y Cajal's student Pio Del Rio Hortega (29) to describe small neuroglial cells with relatively few processes. The delicate slender processes of oligodendrocytes radiate only a short distance from a spherical or pear-shaped cell body (Figs. 6.3 and 6.7). In sections stained with basic dyes, the nuclei of oligodendrocytes are smaller, more regular, and more chromophilic than astrocytic nuclei. These glial cells differ from astrocytes in that (a) their nuclei are smaller, rounder, and more dense, (b) the cell body is smaller and gives rise to fewer processes, and (c) their cytoplasm is more dense, containing chiefly ribosomes, mitochondria, and microtubules. The dense chromatin of the nucleus has light patches adjacent to numerous nuclear pores, while the cytoplasm has a crowded appearance, due to large quantities of free ribosomes and rough endoplasmic reticulum. Other distinguishing features of their cytoplasm are prominent microtubules, dark and light multivesicular bodies, and granular inclusions. The cytoplasm has mitochondria and a Golgi apparatus, but contains neither fibrils nor glycogen granules (15, 54, 72). The plasma membrane of the oligodendrocyte makes close contact with adjacent myelin sheaths and the processes of adjacent glial cells (Fig. 6.8).

In contrast to astrocytes, oligodendrocytes are more numerous in the white matter than in the gray matter. They can also be differentiated from astrocytes by different morphologic, physiologic, and biochemical criteria. Oligodendrocytes' distinctive features include (a) the intracellular enzyme carbonic anhydrase, (b) the cell membrane surface molecule galactocerebroside, which can be recognized with specific antibodies, (c) myelin and the expression of mRNA for myelin basic proteins, and (d) weak electrotonic coupling through gap junctions (101).

Major Types of Oligodendrocytes

Two principal types of oligodendrocytes can be identified by their location and relationships with other elements of the central nervous system. *Perineuronal satellite cells* are closely apposed to neuron perikarya or their dendrites in the gray matter. This type is the most easily identified in adult material (Figs. 6.3 and 6.7). *Interfascicular cells* occur in the white matter and often appear in rows between the myelinated fibers (Fig. 6.3). The *interfascicular* oligodendrocytes are numerous in the white matter of the fetus and newborn. However, they rapidly diminish in number as myelination progresses. After the myelin sheath is formed, only the nucleus remains, so that in adult material their processes rarely are observed (Fig. 6.7**B**). As mentioned ear-

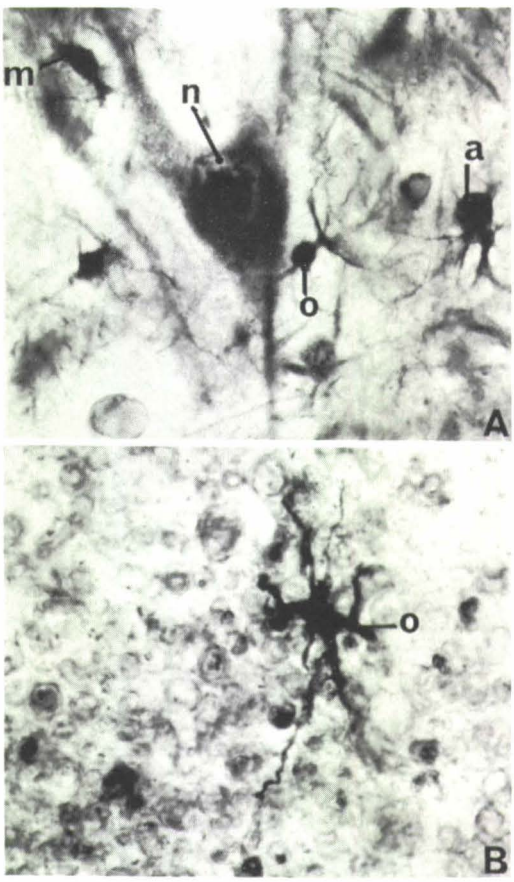


Figure 6.7. Oligodendrocytes in human spinal cord. **A.** Newborn gray matter to demonstrate relative size of a neuron cell body (*n*), perineuronal (satellite) oligodendrocyte (*o*), astrocyte (*a*), and microglial cell (*m*). (Ramón y Cajal gold sublimate stain, ×565). **B.** Posterior white column of adult cord with oligodendrocyte (*o*). (Golgi stain, ×550).

lier, all oligodendrocytes appear to derive from the bipotential O-2A progenitor cells.

Myelination

One of the major function of oligodendrocytes is to form and maintain myelin sheaths in the central nervous system (Fig. 6.8). The fine structural continuity of the plasma membrane of oligodendrocytes with the myelin sheath (23)(Fig. 6.9), and their active participation in remyelination, has been reported in detail (15, 18, 44, 47), and the mechanisms of myelination were discussed in Chapter 5. As in the peripheral nervous system, the myelin sheath in the central nervous system allows saltatory action potential conduction, since nerve impulse jumps from one periodic interruption of the myelin sheath at the node of Ranvier to the next, instead of spreading continuously along the axon. This is why myelinated axons conduct faster than nonmyelinated axon of the same size.

In terms of myelination, the efficiency of oligodendrocytes far exceeds that of the Schwann cells because a single oligodendrocyte can myelinate from 7 to 70 axons, depending on the brain region or the species (44). Oligodendrocytes are not only involved in myelination during development, but also play an important role in the maintenance of myelin in the adult. Oligodendroglia are particularly involved in the process called *spontaneous remyelination*, which refers to the rapid and spontaneous repair of myelin that sometimes occurs in the adult brain in response to acute or chronic demyelination conditions, such as those found in multiple

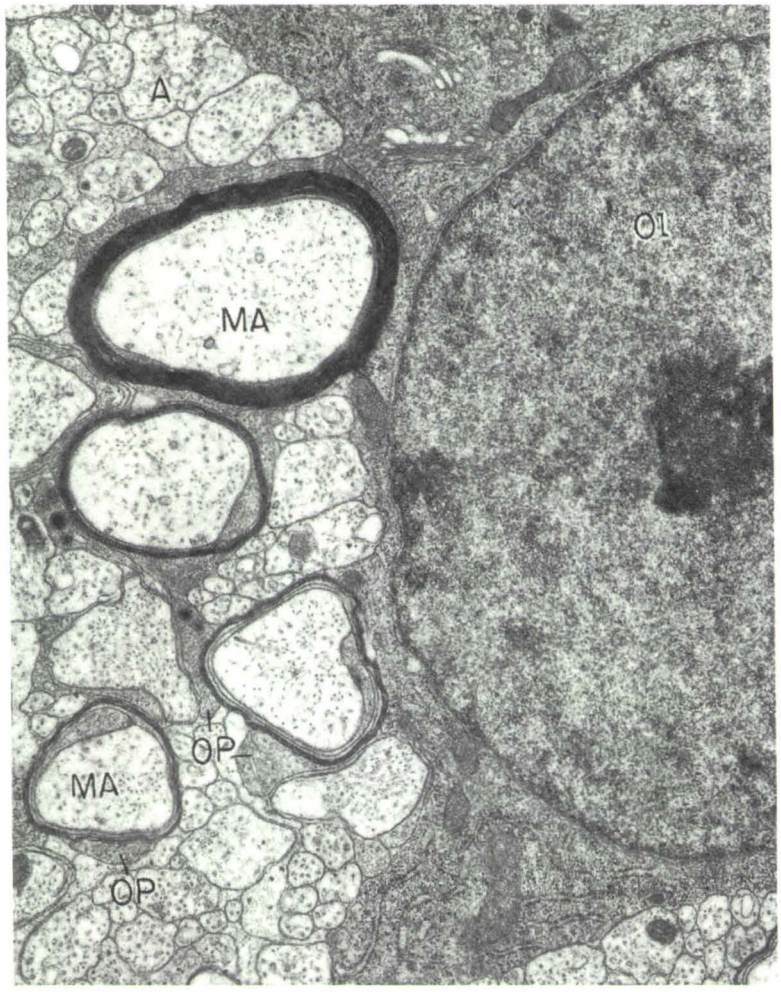


Figure 6.8. Myelin-forming oligodendrocyte (*ol*) in a 6-day postnatal rat. Specimen is taken in the ventrolateral funiculus of the spinal cord near unmyelinated axons (*A*) and axons (*MA*) exhibiting different stages of myelination. Oligodendrocytic processes (*OP*) are closely associated with several newly formed myelin sheaths (×16,000).

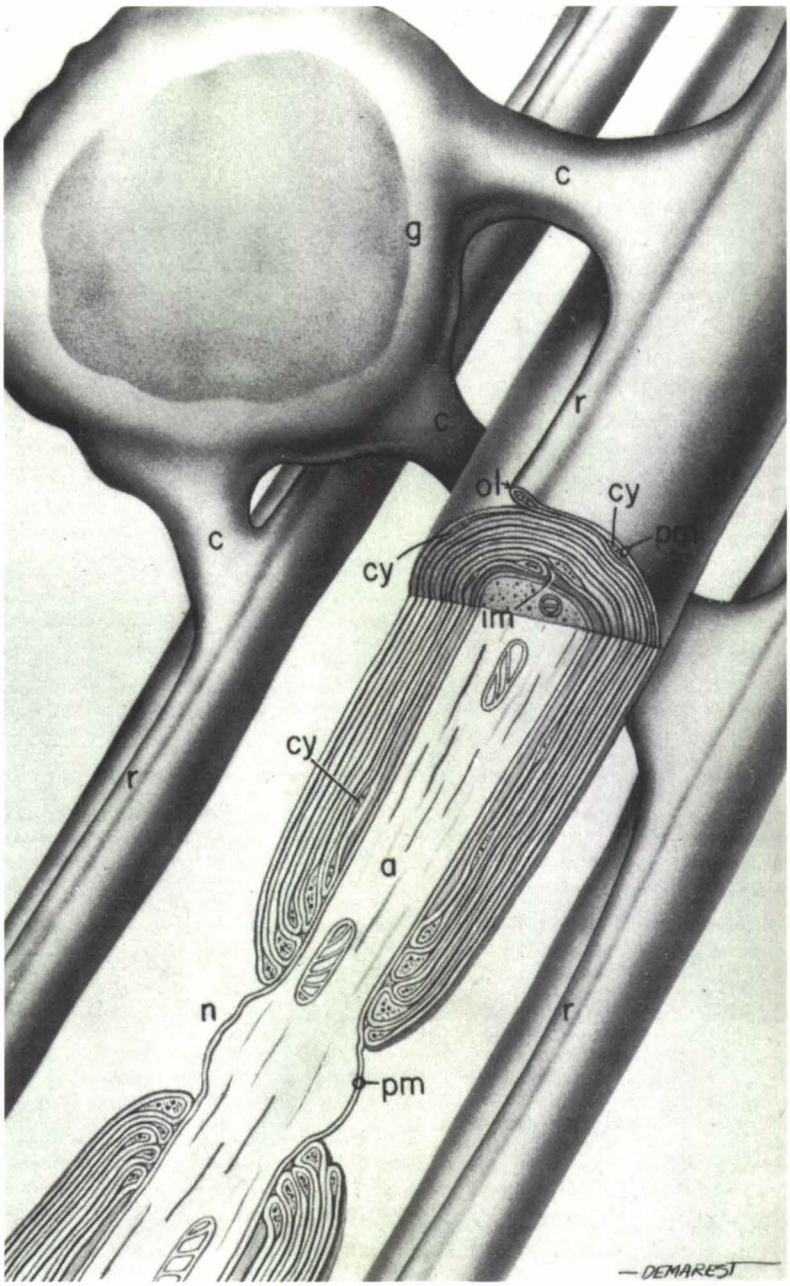


Figure 6.9. Relationship of the oligodendrocyte to the central myelin sheath. The trilaminar plasma membrane (*pm*) is designated by two lines, separated by a space, except in the mitochondrion, where it is represented by a single line. The inner mesaxon (*im*), formed as a glial process, completes the initial turn around the axon (*a*) and starts a second turn; it is retained after myelin formation is complete. Some cytoplasm of the glial process is trapped occasionally (*cy*) and some is also retained on the fully formed sheath exterior. In transverse sections, this cytoplasm is confined to a loop (*ol*), but along the internode length it forms a ridge (*r*) continuous with the glial cell body (*g*) at the level of glial processes (*c*). Viewed transversely, the sheath components form a spiral with only the innermost and outermost layers ending in loops. In the longitudinal plane, every myelin unit terminates in a separate loop near a node (*n*). Glial cytoplasm is retained within these loops.

sclerosis. Experiments with different animal models of demyelinating diseases have revealed that spontaneous remyelination is a general rule rather than an exception in the central nervous system. Since the formation of the myelin sheath is viewed as the last step in oligodendrocyte maturation (115), the mechanisms whereby mature oligodendrocytes can be mobilized and reengaged in the myelination process appear complex and are still not fully understood. They most likely necessitate the recruitment and activation of the bipotential O-2A progenitor cells, which are still present in the mature central nervous system. Spontaneous remyelination is a well-documented phenomenon that may explain the sudden clinical improvements occasionally seen in different demyelinating diseases, such as multiple sclerosis and lateral amyotrophic sclerosis. It must be realized, however, that spontaneous remyelinization does not, in any way, allow for complete recovery from demyelinating diseases. Use of grafts of oligodendrocyte precursors, or even more mature oligodendrocytes, as a therapeutic tool to improve symptoms in demyelinating diseases is a very active field of research (44).

pH Regulation and Ionic Channels

The appropriate regulation of pH in the central nervous system is crucial because of the large number of pH-sensitive processes that occur in this tissue. In excitable cells like neurons, changes in intracellular pH modify various ionic conductances, and the electrical coupling between adjacent cells is blocked by decreased intracellular pH. In addition to its effects on other ionic conductances, H^+ might, itself, act as a carrier through H^+-specific channels (110). The control of extracellular space pH has been studied extensively in the central nervous system. It has been shown that this pH decreases during neuronal activity, often after an alkaline shift. For example, peripheral noxious stimuli and direct stimulation of the nervous tissue induce a significant decrease of the extracellular pH. More dramatic changes in the extracellular pH were observed in pathologic conditions.

The mechanisms involved in pH control in the central nervous system are complex and not fully understood. Data derived from studies of the invertebrate nervous system indicate that glial cells enriched with the enzyme carbonic anhydrase, which correspond with mammalian oligodendrocytes, can control the acid-base equilibrium through several mechanisms involving acid extruders and acid loaders (110). Among the acid extruders that contribute to pH regulation are (a) Na^+-HCO_3^- cotransport, (b) Na^+-dependent Cl^-/HCO_3^- exchange, and (c) Na^+/H^+ exchange across the glial membrane. In contrast, pH recovery from alkalosis involves at least one acid loader, which is Na^+-independent Cl^-/HCO_3^- exchange (110).

Like astrocytes, oligodendrocytes precursor cells express a defined set of voltage- and ligand-dependent ionic channels, but the expression of the channels changes markedly during development (52). Voltage-gated channels that occur in oligodendrocyte precursor cells include potassium channels, sodium channels, and calcium channels. More mature oligodendrocytes also possess pH-activated channels, as well as GABA and glutamate receptors, whose expression is greatly reduced in more advanced stages. It was suggested that during their development certain chemospecific neurons (e.g., GABAergic neurons) may be able to regulate both the rate of differentiation and the function of glial cells by releasing their transmitter at the axon growth cone level (52). The transmitter would exert its action by binding to specific astrocytic membrane receptors that are only expressed at a certain time during astrocyte development.

These data reveal that the electrical properties of oligodendrocytes change markedly during development. The transition from the bipotential precursor cell, which can still develop into astrocytes and oligodendrocytes, into an oligodendrocyte, results in a marked change in the ion channel pattern. During this transition, voltage-activated Na^+ and several types of K^+ currents disappear, whereas a comparatively passive, inwardly rectifying K^+ current becomes dominant. GABA receptor-mediated Cl^- currents and a pH-activated Na^+ current are down-regulated at this transition, but still present at all developmental stages. These changes in the receptors and ionic channels repertoire during oligodendrocytes development are at variance with the situation in astrocytes, where the various receptors and channels are still fully expressed in mature cells.

MICROGLIA

Microglia were first recognized as distinctive glial elements by Del Rio Hortega (27, 30)

when he introduced his silver carbonate staining method (Fig. 6.3). These cells are small in comparison to astrocytes, have elongated or triangular nuclei which stain deeply with basic dyes, and have wavy, branching processes that give off spinelike projections. Microglia are found in both white and gray matter, but are more abundant in gray matter (Figs. 6.10 and 6.11). Approximately 10% of glial cells are classified as microglia in light microscopic preparations of the cerebral cortex (2, 13). Although microglial cells appear inactive in normal adult brain tissue, inflammatory or degenerative processes activate these cells which undergo rapid proliferation and migrate toward the site of injury. Histiocytes from the meninges and blood vessel walls behave similarly if they reach the central nervous tissue. Both types of cells become macrophages and phagocytize debris.

Small numbers of microglia in white matter have processes that wind along or follow myelinated fibers in a remarkably tortuous manner (20). A microglial cell has an irregu-

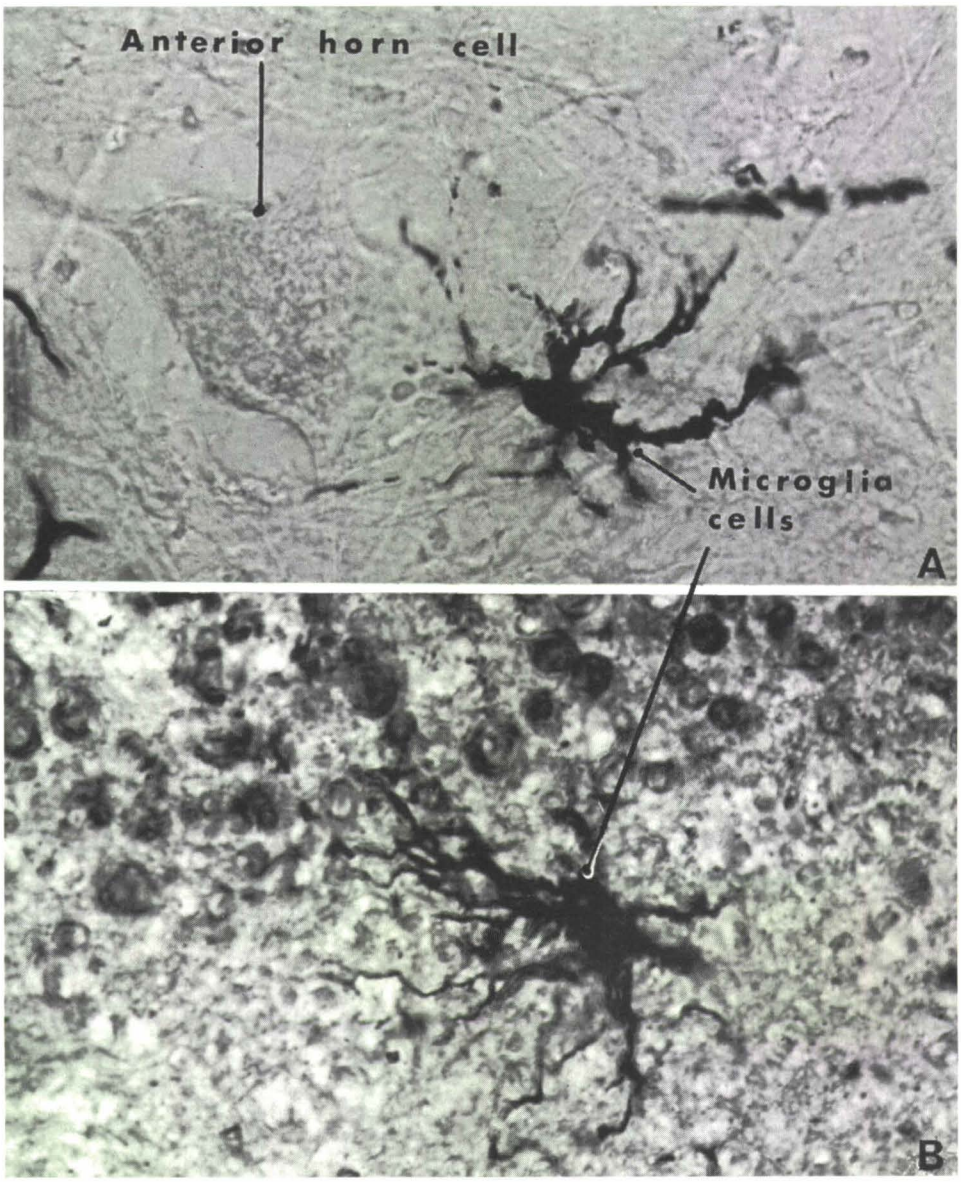


Figure 6.10. Microglial cells in gray and white matter of adult human spinal cord 3 weeks after a spinal stereotaxic lesion. Note thickened and stubby processes extending toward an adjacent anterior horn cell (**A**) and a knobby angular processes of microglial cell extending into the dark zone of degenerating fibers above (**B**). (Golgi stain, ×555.)

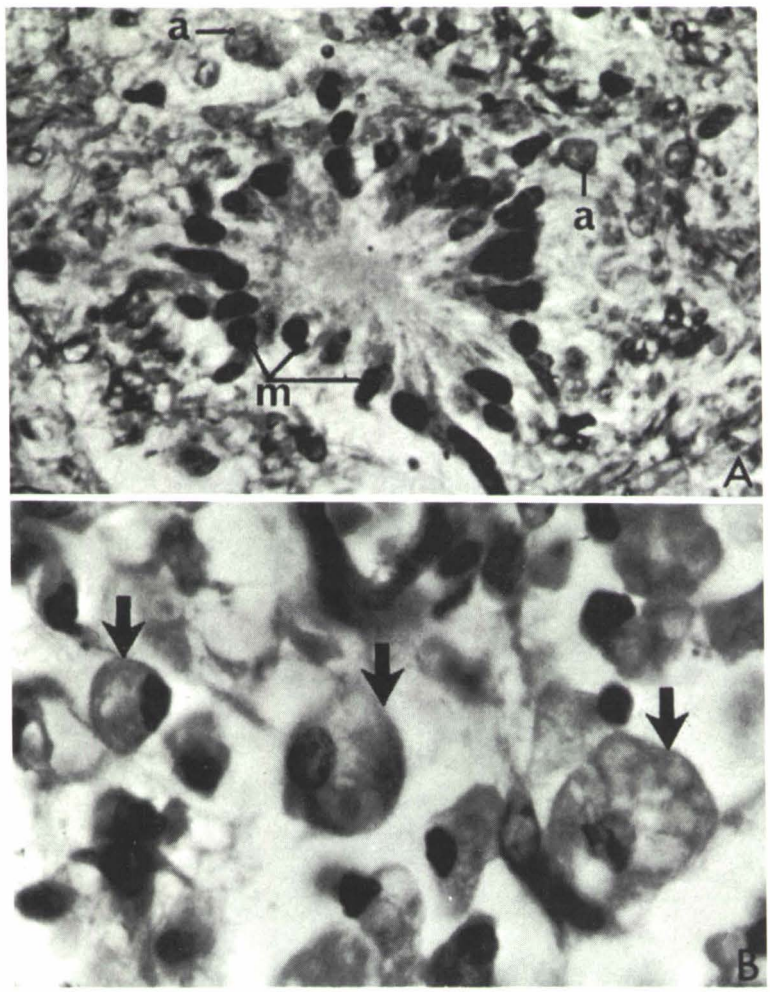


Figure 6.11. **A.** Carousel formed by numerous microgliocytes (*m*) closely surrounding a degenerating anterior horn cell 4 weeks after injury of its axon. Two astrocyte nuclei also are identified (*a*). Adult human spinal cord (Luxol fast blue-cresyl violet stain, ×555). **B.** Three stages (*arrows*) in the formation of a microglial phagocyte (gitter cell). White matter of adult human spinal cord, 4 weeks after a stereotaxic lesion (Luxol fast blue-cresyl violet stain, ×655).

lar perikaryon and a few thick processes which often appear to take off from each pole of the cell body. These large antler-like processes divide after variable distances into many smaller branches. Each branch then pursues an irregular and tortuous course either to adjacent neurons, or, less often, to a blood vessel wall. The nucleus is ovoid or elongated, which aids in distinguishing the microglia from oligodendrocytes. The cytoplasm is pervaded by a myriad of minute vacuoles, which often gives the cell, or some of its processes, a sievelike appearance (Fig. 6.10**A**). Despite many descriptions of microglia in the light microscopic literature, this cell is still difficult to identify in electron microscopic preparations (90). Criteria for identification of microglial cells initially were arrived at by a process of elimination (38, 46, 72, 111). The cell thought to correspond with the microglia was small with a dark nucleus, dark cytoplasm, and compact organelles.

Microglia have long been considered the scavengers of the nervous system. They were presumed to be pleomorphic cells capable of (a) metamorphosis into a macrophage, (b) undergoing mitotic division and migrating at will through the already formed neuropil, and (c) autolyzing or phagocytizing neuronal and other debris (30, 87).

Brain Macrophages

Our conception of microglia recently changed because of the introduction of various immunocytochemical techniques with

lectin binding and monoclonal antibodies recognizing complement receptors and other surface antigens common to both microglial cells and macrophages outside the central nervous system (88). Microglia are currently referred to as *resident brain macrophages*. Evidence for the existence of resident macrophages in the central nervous system with properties indistinguishable from those of peripheral macrophages, was obtained by Streit and Kreutzberg (120). Their experiment involved a mechanic and/or toxic lesion of the facial nerve, which induced retrograde neuronal damage without any increase in the permeability of the blood-brain barrier, thus excluding invasion by blood-borne macrophages. In cases where facial motor neurons did degenerate because of the retrograde transport of the toxin along their axon, resident microglia were capable of phagocytosis (neuronophagia) and behavior like blood-born macrophages in viral poliomyelitis. In cases where facial motor neurons did not degenerate despite lesion of their axon, resident microglia surrounding the neuronal perikarya underwent mitosis and hypertrophy, but did not phagocytize the neurons (120).

Macrophage-like cells in the brain can be subdivided into three types: (a) those found in the parenchyma (the microglia proper); (b) those found in the choroid plexus and circumventricular organs, where there is no blood-brain barrier; and (c) the perivascular cells. Unlike the second and third type, which are always in an activated state, parenchymal microglia have resting and activated forms (2).

Great numbers of discretely arranged microglial cells have been observed in the regions of injury and edema in other experimental conditions (106). Such cellular mobilizations occur as early as 24 hours after cold injury (−50°C) and persist for days. Schultz and Pease (112) observed a similar accumulation of microglial elements in the acute phase, 24 hours after stab wounds of the cerebral cortex. The microglia underwent a remarkable transformation within this period. They exhibited a rounded appearance as the cytoplasmic volume increased and became less dense so that the nuclei became more prominent. In about 1 week, these changes culminated in the formation of typical macrophages with pale cytoplasm and no definite processes. An enlarged macrophage in the central nervous system with a foamy cytoplasmic appearance and ingested material is called a *gitter cell* (Fig. 6.11**B**). As the cytoplasm of the macrophages became packed with ingested material, the nucleus was often pushed to the cell periphery. Such phagocytosed particles included myelin and lipoid droplets. Gitter cells abounded in the lesion area for the first week, then decreased in number until 90 days at which time only an occasional phagocyte was seen (Fig. 6.11). A similar mobilization is observed in the human nervous system after neuron injury (Fig. 6.11**A**). Three stages in the formation of a gitter cell are indicated by arrows in Figure 6.11**B**. These large vacuolated macrophages may assume a gigantic size and a bloated appearance. When suitable fat stains are used, the vacuolated gitter cells display an unusual number of fat droplets of varying size. These lipid droplets are formed by cholesterol esters which persist for long periods of time in the tissue.

Macrophages rapidly remove degenerated myelin in peripheral nerves, whereas this process is very slow in the central nervous system. This difference is surprising because resident microglia and peripheral macrophages are believed to have similar properties. Since central and peripheral myelin have different biochemical compositions, it is possible that some constituents of central myelin act as repellents for resident macrophages. Indeed, the occurrence of central myelin proteins that inhibit axonal growth was reported by Schwab and his collaborators (19). Another possibility, suggested by Bignami (4), is that the hyaluronate-protein complex forming the extracellular matrix of the white matter prevents phagocytosis either by "masking" degenerated myelin, or by interfering with microglial migration from their predominantly perivascular location.

Neuronal Shaping

Resident microglia are particularly abundant during certain phases of neuronal development, particularly those involving "regressive" events such as neuronal cell death and axon collateral elimination, in which they play a very active role (68). During these regressive events, the phagocytic activity of resident macrophages is not limited to the elimination of neuronal debris. These glial cells actively participate in the shaping of neuronal circuits as exemplified by their selective

involvement in collateral elimination. This phenomenon is very specific in that it must not affect the viability of the rest of the neuron. Electron microscopic studies reveal that resident macrophages are able to transiently sequester specific portions of the axonal arbor within their cytoplasmic extensions (50). Phagocytic activity of glial cells can also help to shape neurons and neuronal circuits in the mature central nervous system, as shown by the study undertaken by Raisman and his collaborators (95) of synaptic plasticity after denervation. These authors observed that the process of presynaptic terminal replacement involves the essential intermediate stage of engulfment by a glial process. This glial process must act in a very concerted way, because after phagocytosis of a degenerating terminal, the glial process must be able to recognize and give way to the ingrowth of a newly forming axon terminal, as well as discriminate among different types of neuronal inputs competing for the same target (95). The occurrence of transmitter receptors on glial cells may explain how such specificity may be obtained.

Phagocytosis is not the only way whereby resident macrophages can shape neuronal morphology. Indeed, evidence for a facilitatory action of resident microglia on neuronal growth and survival in the central nervous system have been documented. For example, brain macrophages can produce interleukins (1 and 6) which, in turn, can modulate the intracerebral concentration of nerve growth factor (NGF) (68). Interleukin-1 can be detected biochemically in various brain regions where transient expression of brain macrophages has occurred. When injected into the cerebral ventricles, interleukin-1 induces a marked increase of the expression of the mRNA that encodes NGF within the hippocampus, as well as in the cerebral cortex. Furthermore, *in vitro* studies revealed that interleukins-1 and -6 stimulate NGF production by astrocytes, and that brain macrophages can, themselves, produce NGF following lipopolysaccharide stimulation (68). Taken together, these results clearly indicate that microglia (as well as astriglia) play a very active role in shaping developing neurons and in the constant remodeling of brain neuronal architecture.

Pathologic Conditions

Apart from contributing to inflammation and necrosis, microglia seem to be implicated in several pathologic processes in specific ways. They are the only cell type in the brain known to be infected by the HIV virus, and thus might be crucial to the development of the acquired immunodeficiency syndrome (AIDS)-dementia complex. The extent of neurodegeneration in AIDS-dementia seems to correlate well with microglial density (2). In Alzheimer's disease, microglia are being implicated in the transformation of soluble amyloid precursor protein (βA4) into insoluble fibrils and the inflammatory processes within senile plaques. In demyelinating conditions such as multiple sclerosis, microglia act both as antigen-presenting cells and, to some extent, to degrade myelin debris.

Microglia can be imaged *in vivo* by positron emitting tomography (PET) scanning. Activated microglia express the peripheral benzodiazepine receptor, for which there is a ligand suitable for PET scanning. This is being used in humans to study microglial activation after stroke. Works on multiple sclerosis in humans show high activation in the thalamus and correlation of the receptor binding with hot spots detected with magnetic resonance imaging (MRI) using gadolinium (see Chapter 2).

EPENDYMA

The ependyma lines the central canal of the spinal cord and the ventricles of the brain. In the embryo, the ependymal processes traverse the entire thickness of the neural tube to become attached to the pia mater and superficial glial membrane (glia limitans) by terminal expansions. Most of the processes retract, so that at birth these processes reach only the pia where the neural wall is thin, as in the basal plate region (Fig. 6.12). In fetal life, the ependyma consists of several layers of nuclei, and one can see the large pale nuclei of the germinal cells, as well as mitotic cells (Fig. 6.13**A**). Cilia are observed in only the embryologic stages of humans, but persist in some adult animals, such as the rabbit and dog (Figs. 6.13**C**, 6.14, and 6.16).

Ependymal cells also have numerous microvilli on their ventricular surface (Fig. 6.16). The surface morphology of ependymal cells varies over white and gray matter. In scanning electron microscope studies of rabbit ependymal cells, those covering myelinated structures, such as the corpus callosum, have fewer microvilli and cilia than ependymal cells covering neuropil (81). Additional dif-

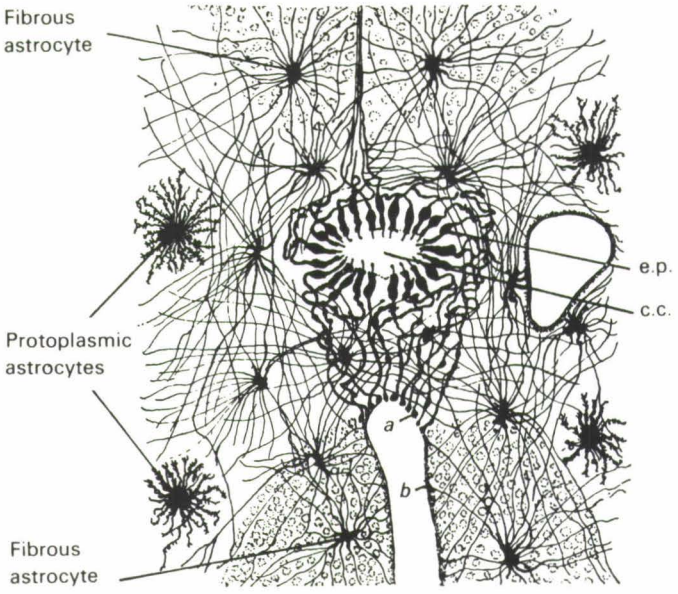
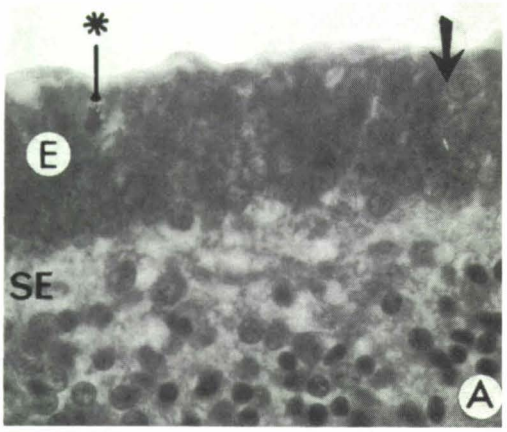


Figure 6.12. Ependyma and neuroglia lining the central canal of the spinal cord of an infant 8 days old (Golgi impregnation). *a*, Terminal foot plate of ependymal cell; *b*, terminal foot plate of fibrous astrocyte; *cc*, central canal; *e.p.*, ependymal cell.



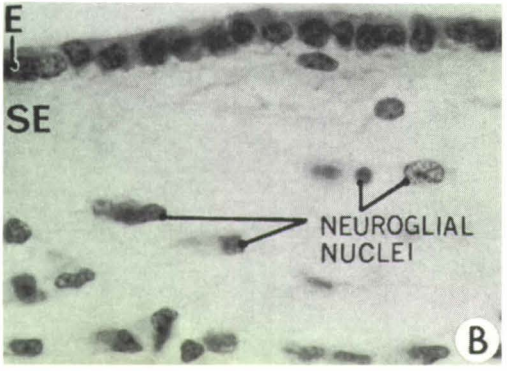


Figure 6.13. Ependyma of human and rabbit brains. **A.** Ependymal cells (*E*) and subependymal glial membrane (*SE*) in a human fetus of 80 mm crown-rump (*C-R*) length. Mitotic figures (*asterisks*) and pale germinal cell nuclei (*arrow*) are indicated (Luxol fast blue-cresyl violet stain). **B.** Ependymal cell lining adult human third ventricle (Luxol fast blue-cresyl violet stain). **C.** Ciliated ependymal cells lining adult rabbit fourth ventricle (Bodian stain).

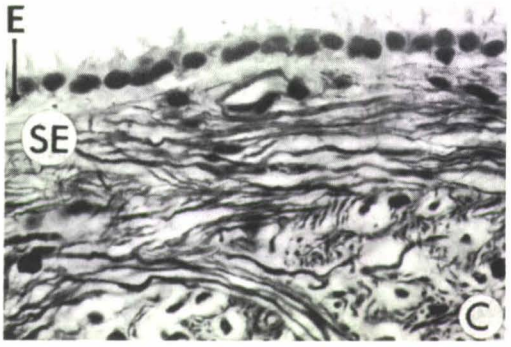




Figure 6.14. Ependymal cells with long basal processes (*P*) lining the aqueduct of the dog. The apical surface may exhibit short microvilli (*Mv*) and cilia (*C*), or may be relatively smooth. Rows of desmosomal-like plaques (*arrows*) join adjacent cells apically. Most of the mitochondria (*M*) in the cells are scattered randomly, but they are also aligned in rows close to the junctions. The Golgi complex (*G*) is usually in a supranuclear position. The nucleus (*N*) may be ovoid or indented and sometimes a nucleolus is seen. Fine filaments (*F*), similar to those found in the subependymal astrocytic processes (*As*), are present in the ependymal processes (×7,800).

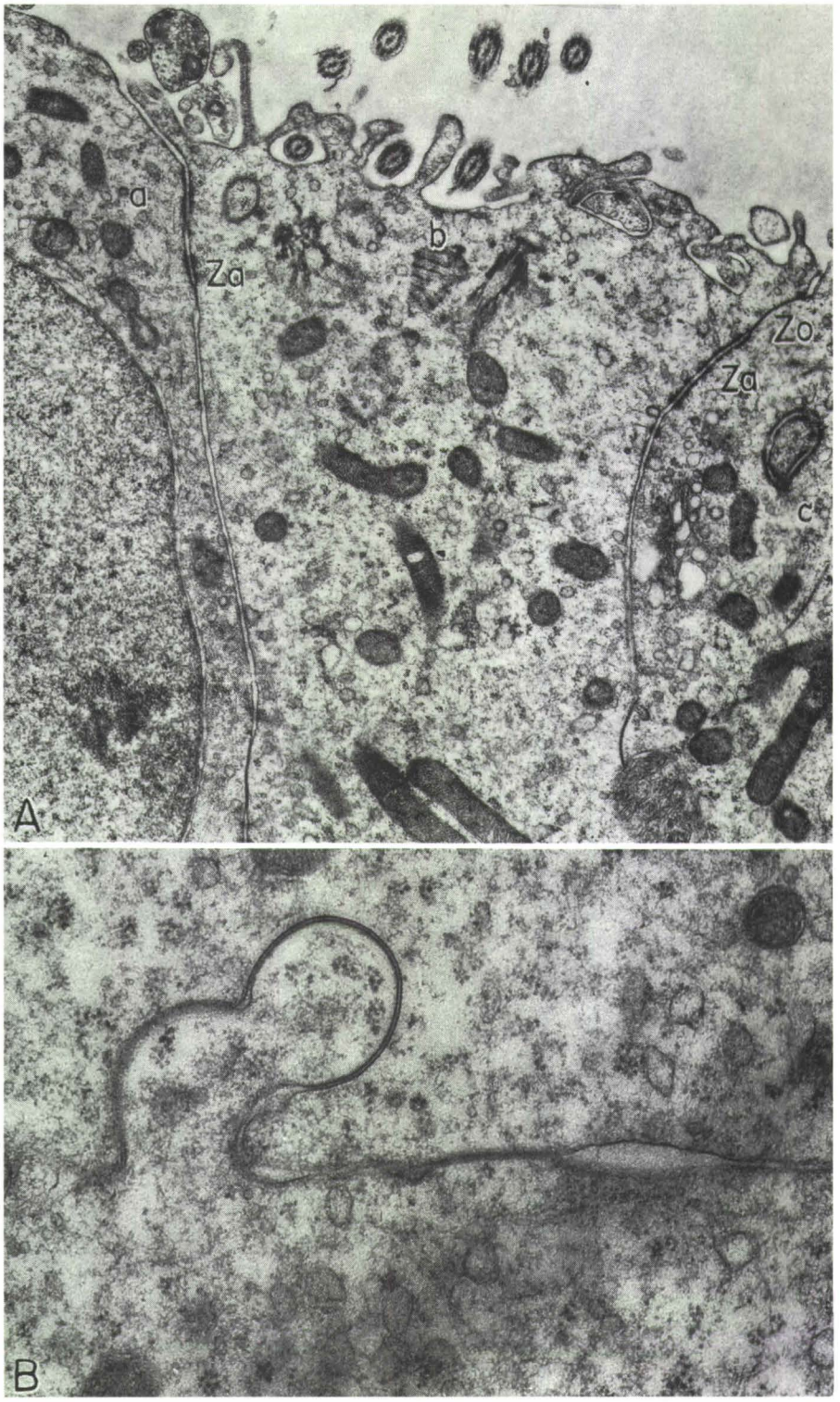


Figure 6.15. Features of ependymal cells. **A.** The apical cytoplasm of three contiguous ependymal cells (*a, b,* and *c*). The luminal surfaces of cells are joined by the zonula occludens (*zo*) which is directly continuous with a zonula adhaerens (*za*) (×21,000). **B.** A zonula occludens forms a dovetail type junction between the base of two ependymal cells. The interval between the two dense, parallel membranes can be compared with the usual intercellular space at the right (×49,000).

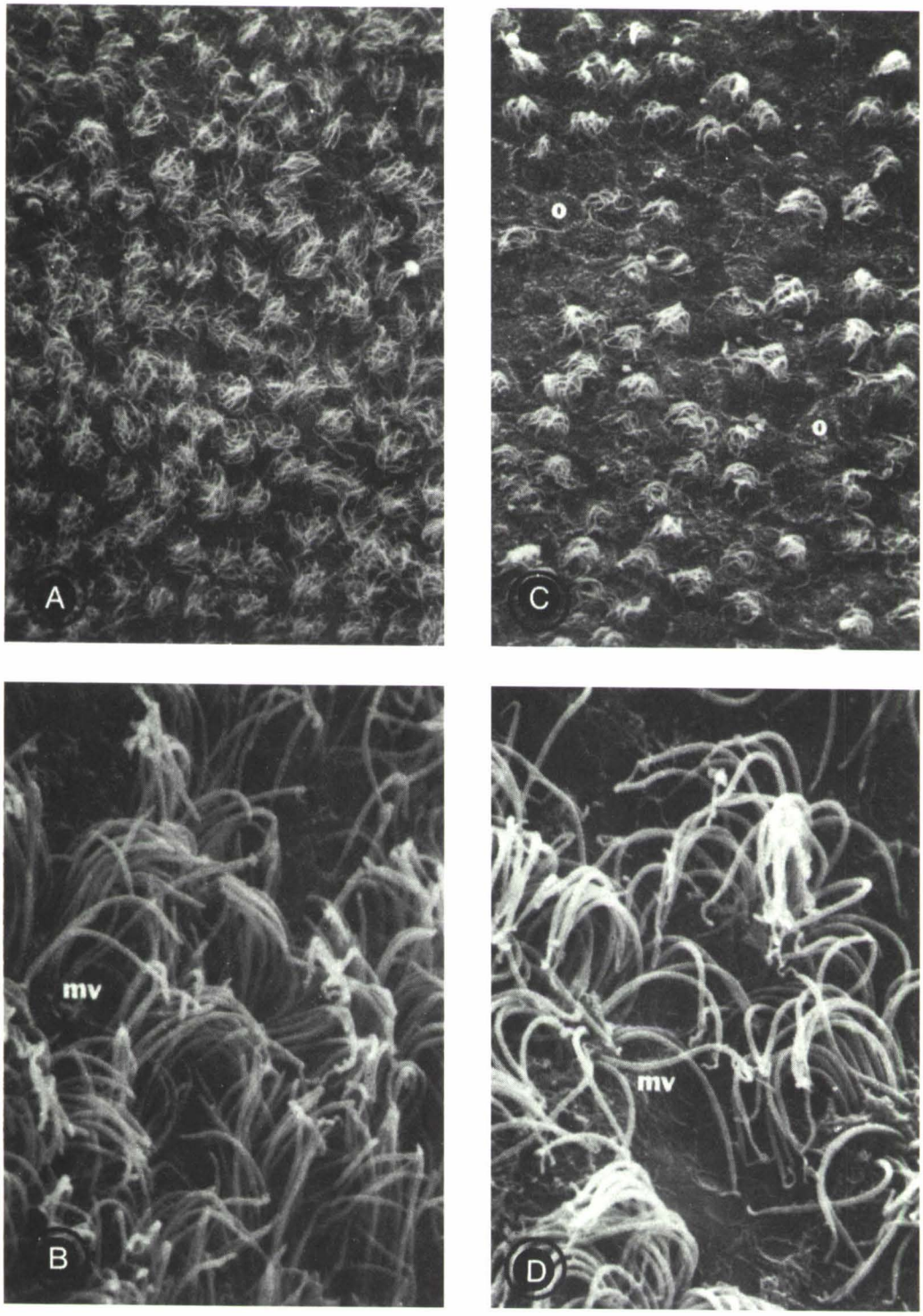


Figure 6.16. Scanning electron micrographs of the ependyma in the rabbit in various locations. **A.** Over the caudate nucleus showing clusters of surface cilia (×200). **B.** Over the caudate nucleus showing microvilli (*mv*) between ciliary clusters (×2000). **C.** Over periventricular white matter where cilia are more widely separated and nonciliated cells (*o*) are outlined by aggregates of microvilli (×200). **D.** Over periventricular white matter where cilia arise in clusters and microvilli (*mv*) aggregate at cell boundaries (×2000).

ferences are seen in the arrangement of intercellular clefts and junctional specializations of ependymal cells in the two regions. These morphologic differences may account for the selective changes observed in ependymal cells over periventricular white matter in experimentally induced hydrocephalus (80).

In the human adult, the single layer of ependymal cells is cuboidal, while their retracted processes are entwined in the packed astrocytic processes of the *subependymal* (Fig. 6.13) or internal limiting *glial membrane*. There are few places in the nervous system where typical astrocytes and their processes are as concentrated as in this subependymal limiting membrane. During development, the pia-arachnoid pushes a layer of ependymal cells ahead of it, and invaginates into each of the primitive brain ventricles to form the tufted choroid plexuses (Figs. 3.11 and 3.15). The points of attachment, composed of pia mater and the cuboid ependymal cells, form the *tela choroidea* of the third, fourth, and lateral ventricles (Fig. 6.17). These points of junction or reflection are observable in gross brain specimens after the choroid plexus is removed. The macroscopic torn edge of the ependyma is referred to as the *tenia choroidea* (Fig. 2.25).

Electron micrographs (Fig. 6.14) reveal that the ependymal cell cytoplasm contains small slender mitochondria, vesicles of ergastoplasm, a smooth endoplasmic reticulum, a Golgi complex, and compact bundles of intermediate filaments (82, 126). Histochemically, the ependymal epithelium exhibits high oxidative activity as reflected by its enzyme content, which comprises acid and alkaline diphosphatase and adenosine triphosphatase. Both structural and chemical reactions reflect the secretory and absorptive functions attributed to the ependymal cells and choroid epithelium (1).

Specialized ependymal cells called *tanycytes* (elongated cells) are found in the base of the third ventricle. Tanycyte processes extend for some distance into the neuropil where they are juxtaposed to blood vessels and neurons. Indirect evidence suggests that these

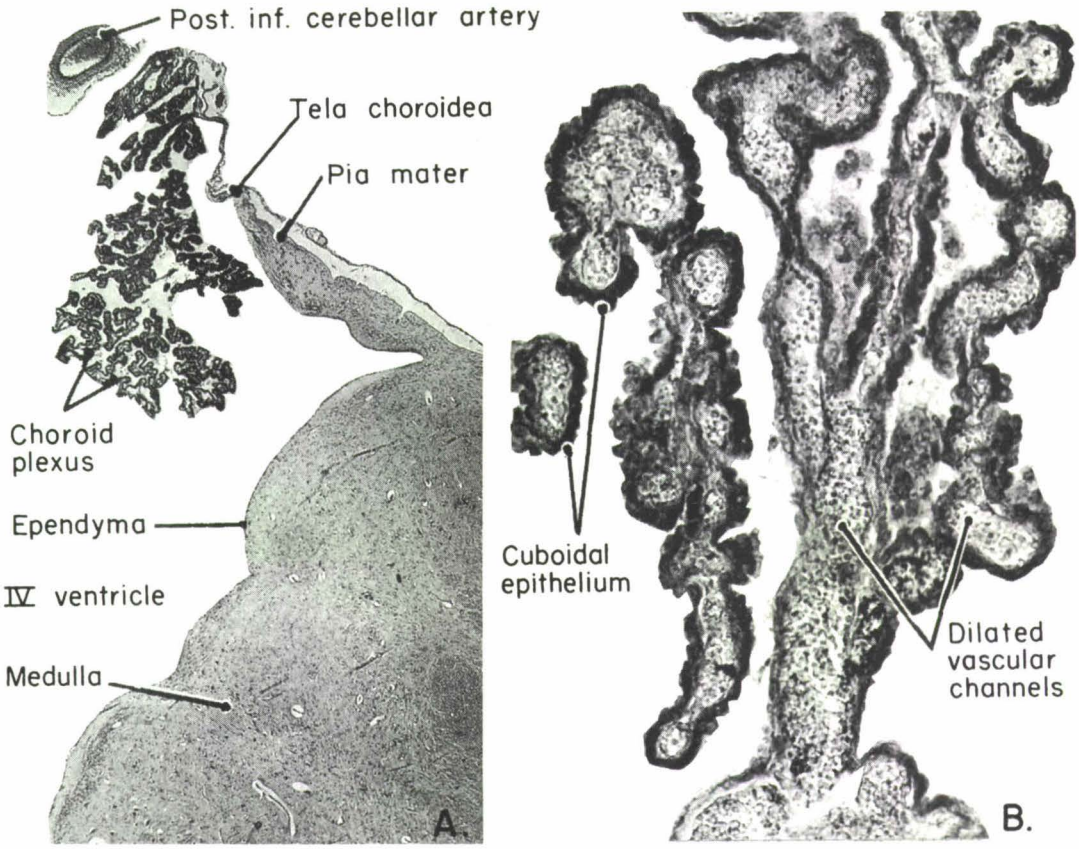


Figure 6.17. Human choroid plexus at (**A**) low magnification to show topography and relations of the plexus in the fourth ventricle, and at (**B**) higher magnification to demonstrate the epithelium and vascularity of two choroid villi.

cells selectively transport molecules from the cerebrospinal fluid (CSF) to diencephalic neurons concerned with the regulation of gonadotropic hormone release from the anterior lobe of the pituitary gland (8, 53).

The surface layer of ependymal cells and subjacent astrocytes (i.e., subependymal glial membrane) constitute a brain-cerebrospinal fluid interface (Fig. 1.14). The lateral cell surfaces of ependymal cells are comparatively simple without elaborate folds or interdigitations. Near the apices of contiguous cells, the apposed surface membranes contribute to the formation of complex intercellular junctions, which in light microscopy are called terminal bars. Electron microscopic studies of the ependyma in the rat brain indicate that the lateral portions of the plasmalemma of contiguous cells are fused at discrete sites to form five-layered junctions, referred to as *zonulae occludens*, which obliterate the intercellular space (11). These fusions occur at some distance below the free surface (Fig. 6.15). Another type of intercellular junction, the *zonula adhaerens*, occurs near the apices of contiguous cells. Segments of the plasmalemma comprising this junction are characterized by their increased density, and the interspace of the junction contains filamentous material. This structural arrangement forms the brain-cerebrospinal fluid interface. Neither the ependymal surfaces of the cerebral ventricles nor the pial-glial membrane on the surface of the brain impede the exchange of substances between the CSF and the brain (103). Thus the brain-CSF interface does not constitute a subbarrier (Fig. 1.14).

CHOROID EPITHELIUM

The choroid plexuses, whose major role is to secrete the cerebrospinal fluid (CSF), are formed as a result of the invagination of the ependymal roof plate into the ventricular cavities by the blood vessels of the pia mater (see Chapter 3). In human embryos, the primordia of all the choroid plexuses develop during the second month of gestation. A mesenchymal invagination into the thin roof area of the fourth ventricle first appears at 6 weeks. The primordia of the telencephalic choroid plexuses becomes visible in the 7th week, followed in the 8th week by an invagination into the roof of the third ventricle. It is not surprising that extensive structural alterations in shape and microscopic appearances accompany the different stages of choroid plexus development. Four stages have been described (113). For our purpose, it suffices to note that each primordium enlarges, becomes lobulated, and each lobule later demonstrates frondlike expansions (Fig. 6.17). In still later stages, many villi develop on the surface. The entire lobulated, vascularized mass remains attached by a broad stalk at the point of the original invagination. The covering cells are at first pseudostratified tall epithelial cells, 50–60 μm in thickness, with a brush border on the luminal surface. At 11 weeks, the choroid plexus fills 75% of the lateral ventricle, and the covering, tall, columnar cells have an abundance of cytoplasmic glycogen (Fig. 6.18). At this stage the mesenchyme of the underlying connective stroma becomes extremely loose and accumulates a large amount of mucin. In the interval between 15 and 17 weeks of gestation, the entire plexus gradually decreases in size and the primary villi are better developed. The epithelium changes from low columnar to cuboidal and

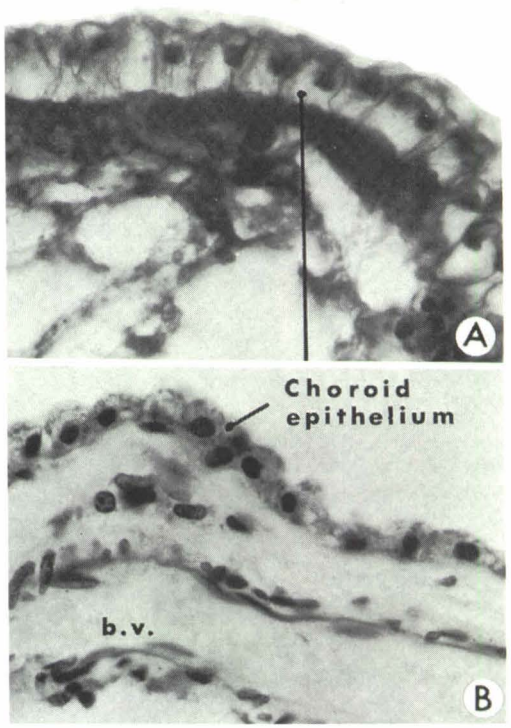


Figure 6.18. Choroid epithelium in humans. **A.** Tall columnar choroid cells in a human fetus of 100 mm crown-rump length (Holmes' silver with hematoxylin counterstain). **B.** Cuboidal choroid cells of an adult human brain. A subjacent blood vessel (*b.v.*) is identified (Luxol fast blue-cresyl violet stain) (×655).

measures 15×15 μm. The loose underlying mesenchyme decreases in amount, while distinct connective tissue fibers (mostly collagen) make their appearance in the stroma. Between 29 weeks and full term the large cuboidal cells are replaced by smaller ones which are 10×10 μm. The cytoplasm loses its glycogen, while meningocytes, foamy cells, and fat-laden macrophages are scattered through the stroma. Once removed, the glycogen never reappears as a normal constituent of the adult choroid epithelium. Such disappearance of glycogen after birth, or at the beginning of aerobic oxidation, suggests that the developing nervous tissue uses energy released by the anaerobic metabolism of glycogen.

Epithelial indentations lining the interlobular clefts may become buried in the stroma during early development and form the colloid cysts observed in the adult human brain (113). They appear red due to the blood in the stromal vessels, and the fine, leaflike projections endow the choroid plexus with a shaggy surface appearance. Hardened bodies composed of concentric rings of calcium carbonate, calcium, and magnesium phosphate also occur in the adult choroid plexus (*psammoma bodies*). They are generally spherical and originate around a group of degenerated cells (108). Psammomatous bodies are usually of small diameter (0.01–0.15 μm) and appear to increase in number with age. Studies of morphologic and histochemical alterations of the choroid plexus with age, indicate that the height of the cuboidal epithelium gradually decreases, proliferated cells eventually desquamate, and cytoplasmic vacuoles increase in number (114). It seems likely that lipids in the cytoplasm of desquamated choroidal epithelial cells may be one source of lipids in the cerebrospinal fluid.

The histologic appearance of the adult choroid epithelial cells after routine staining is shown in Figures 6.17 and 6.18**B**. They are low cuboidal cells with round and basally located nuclei. The bases of the cells are moderately smooth, while the lateral boundaries interdigitate with adjacent cells and demonstrate terminal bars. Tight junctions surrounding and connecting apical regions of epithelial cells of the choroid plexus constitute the blood-CSF barrier (Figs. 1.16 and 6.19; see Chapter 1 for further details). Small inpocketings can be seen on surfaces of the cell *(pinocytosis)* and are regarded as a mechanism whereby surface solutes can be taken into the cell.

An occasional cilium may occur on the apical surface of adult choroid cells. Each cell is bounded by a dense continuous cell membrane. On the ventricular surface, each cell is thrown into elaborate, finger-like extensions 80–90 nm in diameter, which contain cytoplasmic cores. These elements appear to correspond to the striated or brush border observed in light microscopic studies or to the microvilli seen with the electron microscope. Microvilli in this instance are a structural device to increase the cell surface and enhance its secretory and possibly absorptive functions (Fig. 6.19).

Electron microscopic studies on the developing choroid plexus of the rabbit by Tennyson and Pappas suggest such a *dual secretory-absorptive* role (123–125, 127). Their ultrastructural observations also confirm and greatly extend the embryologic data of light microscopy. As shown in one electron micrograph (Fig. 6.19), the adult choroidal cell contains numerous mitochondria, a Golgi complex, cisternal and tubular elements of the endoplasmic reticulum, numerous small vesicles, dense bodies with a heterogeneous content, and occasional cilia. These investigators also called attention to the *pores* present in the capillaries of the newborn and adult choroid plexus. They found no evidence that thorium dioxide, when injected intravenously, traversed these pores to enter the connective tissue stroma. However, other investigators showed that protein tracers (Evans blue-albumin and HRP) injected intravascularly pass through the choroid capillary pores and stain the connective tissue stroma, but do not pass beyond the tight junctions which surround apical regions of the epithelial cells of the choroid plexus (10, 103).

Histochemical demonstration of phosphatase activity in choroid cells, particularly the intracellular location of adenosine triphosphatase and acid phosphatase, should be noted. These hydrolytic enzymes play key roles in metabolically active cells; adenosine triphosphatase participates in the ionic transport at membrane surfaces, and in oxidative phosphorylation within mitochondria. Acid phosphatase is an important constituent of the lysosomes (dense bodies of electron micrographs) which appear to play an important part in transcellular transport and diges-

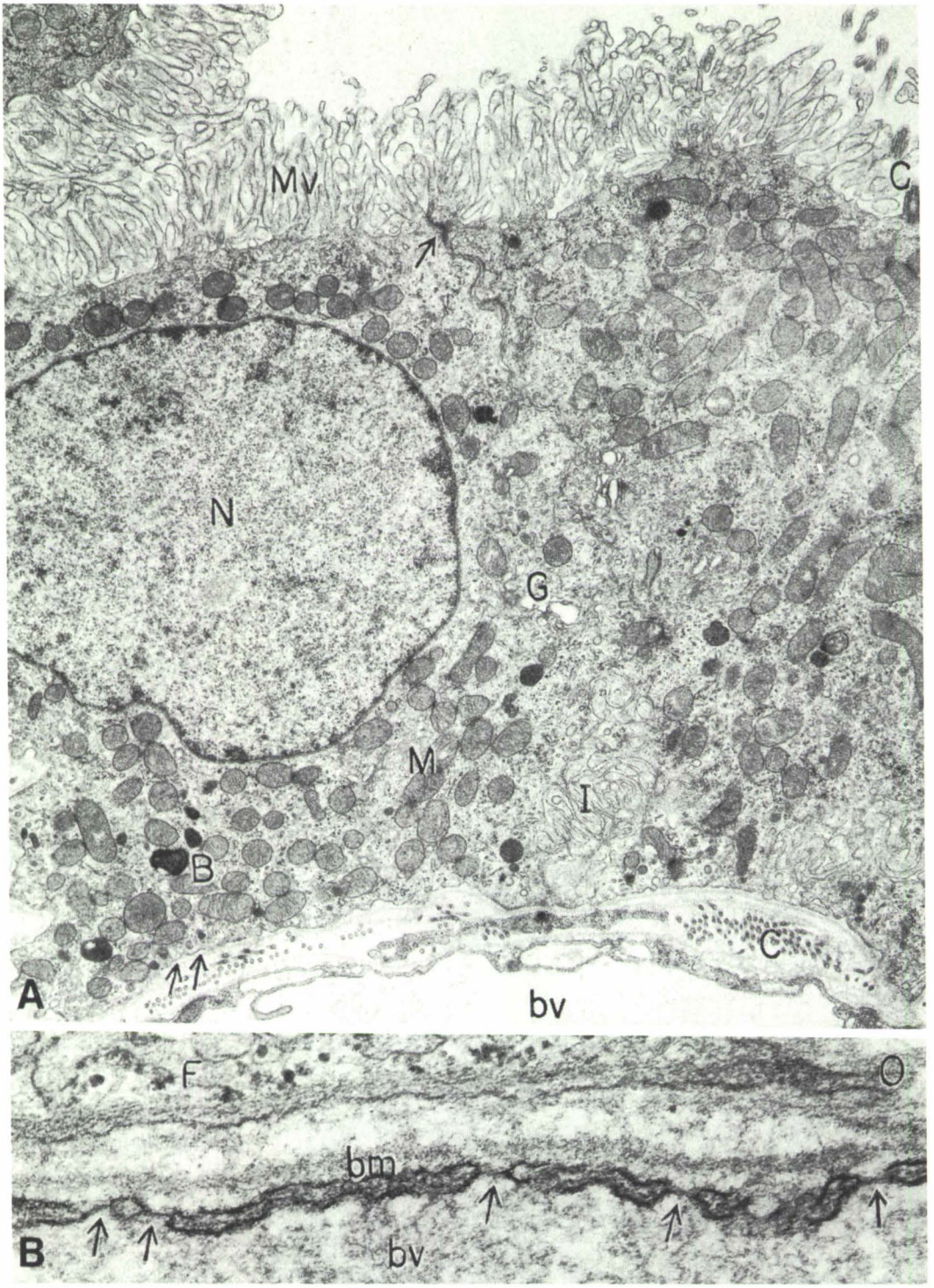


Figure 6.19. Adult rabbit choroid plexus of the fourth ventricle. **A.** The cuboidal epithelial cells have a large nucleus (*N*). An occasional cilium (*C*) and polypoid microvilli (*Mv*) line the ventricular surface. Apically, a tight junction seals adjacent cells (*arrow*); near their base, elaborate infoldings (*I*) of the cell surfaces occur. A paranuclear Golgi complex (*G*), numerous mitochondria (*M*), heterogeneous dense bodies (*B*), and vesicles are present in the cytoplasm. A basement membrane (*double arrows*) separates the choroidal epithelial cells from the connective tissue which contains collagen (*C*), processes of fibroblasts, and other interstitial cells and blood vessels (*bv*). The thin wall of this choroidal capillary is typical (×8,000). **B.** The thin capillary wall is interrupted by "pores," which exhibit a diaphragm (*arrows*) between the lumen (*bv*) and the interstitial space. A basement membrane (*bm*) coats the surface of the capillary. Fibroblast (*F*) (×66,000).

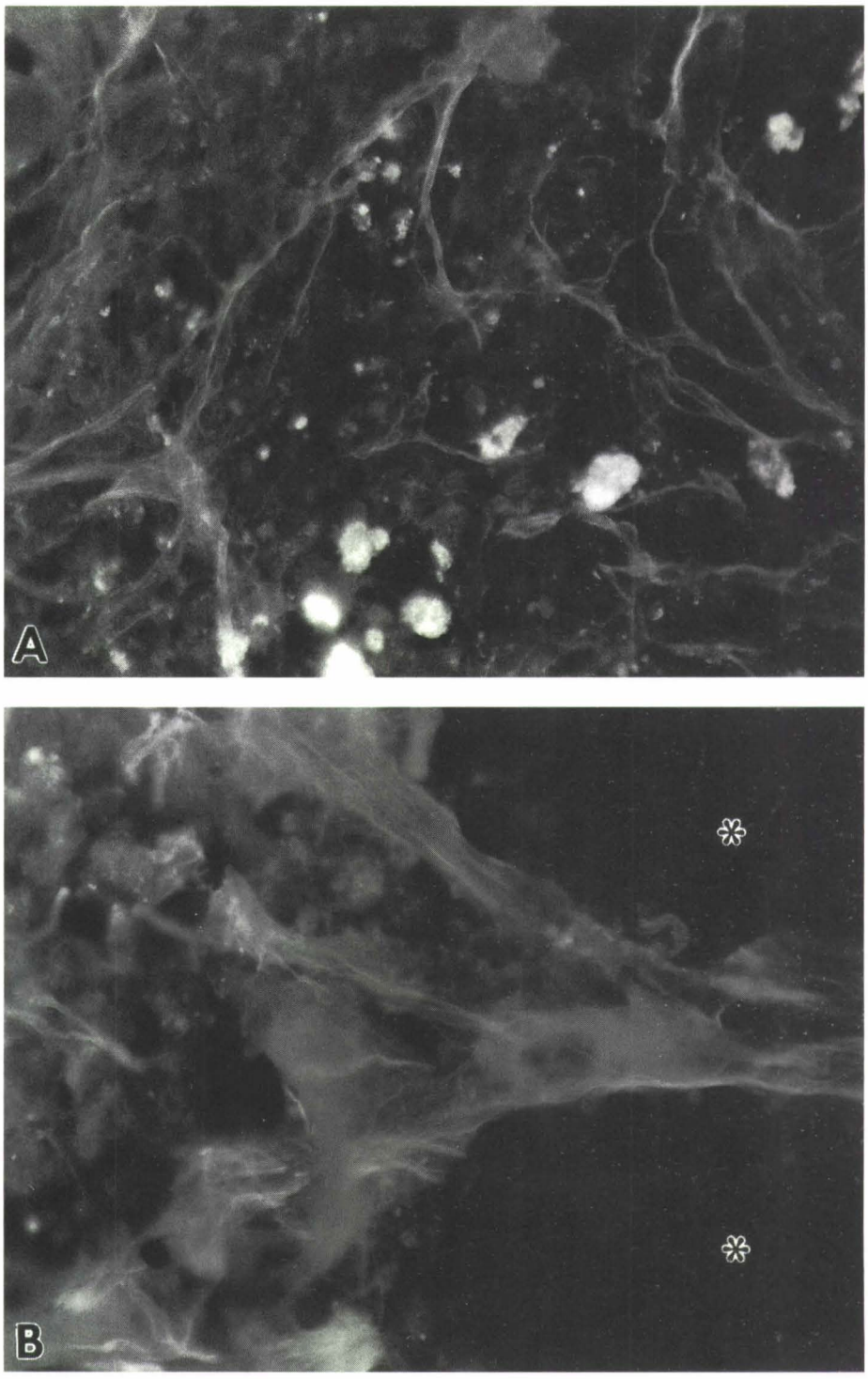


Figure 6.20. **A** and **B**. Dark-field photomicrographs showing astrocytic processes displaying immunoreactivity for the glial acidic fibrillary protein (GFAP) in the vicinity of a lesion site in the spinal cord of the rat. These GFAP-positive fibers invade the injection site which harbors an artificial collagen-chondroitin sulfate biomatrix implanted 6 months earlier to favor axonal regeneration. In **B**, several GFAP-positive fibers are clustered together to form a fascicle that directly penetrates the biomatrix (*asterisks*). The small round and brightly fluorescent profiles in the lower part of **A** most probably represent macrophages. The GFAP-positive fibers were visualized with the immunofluorescence method using fluorescein isothiocyanate (FITC) as a marker.

tion, as well as phagocytosis, necrosis, and autolysis (1). Additional information concerning structure and function of the choroid plexus is available in reviews (24, 34).

The tight junctions surrounding and connecting apical regions of the cuboidal epithelial cells of the choroid plexus (Fig. 6.19) act as an effective barrier which prevents large molecular substances from entering the CSF (e.g., serum proteins, inulin, and fluorescent dyes). However, such substances injected into the ventricles can pass through the ependyma and subependymal glia to enter the extracellular space of the brain which is guarded by astrocytes (Fig. 1.14; see Chapter 1). Thus, all the neuroglial elements must be considered not only as an impressive structural skeleton, but also as dynamic units that regulate the chemical milieu of nerve cells and probably their metabolism.

References

1. Adams CWM. Disorders of neurons and neuroglia. In: Adams CWM, ed. Neurohistochemistry. Ch. 10. Amsterdam: Elsevier, 1965:403–436.
2. Altman J. Microglia emerge from the fog. Trends Neurosci 1994; 17:47–49.
3. Bardakdjian J, Tardy M, Pimoule C, Gonnard P. GABA metabolism in cultured glial cells. Neurochem Res 1979;4:519–529.
4. Bignami A. Glial cells in the central nervous system. In: Magistretti PJ, ed. Discussions in the neuroscience. Vol. 8. Amsterdam: Elsevier, 1991:11–45.
5. Bignami A, Dahl D. Astrocyte-specific protein and neuroglial differentiation: an immunofluorescence study with antibodies to the glial fibrillary acidic protein. J Comp Neurol 1974;153:27–38.
6. Bignami A, Eng LF, Dahl D, Uyeda CT. Localization of the glial fibrillary acidic protein in astrocytes by immunofluorescence. Brain Res 1972;43:429–435.
7. Björklund A, Olson L, Dahl D, Schwarcz R. Short- and long-term consequences of intracranial injections of the excitotoxin quinolinic acid, as evidenced by GFAP immunohistochemistry of astrocytes. Brain Res 1986;371:267–277.
8. Bleier R. The relations of ependyma to neurons and capillaries in the hypothalamus: a Golgi-Cox study. J Comp Neurol 1971;142:439–462.
9. Bodian D. Neurons, circuits and neuroglia. In: Quarton GC, Melnechuk T, Schmitt FO, eds. The neuroscience. A study program. New York: Rockefeller University Press, 1967:6–24.
10. Brightman MW, Reese TS, Feder N. Assessment with the electron microscope of the permeability to peroxidase of cerebral endothelium and epithelium in mice and sharks. In: Crone C, Lassen NA, eds. Capillary permeability. New York: Academic Press, 1970: 468–476.
11. Brightman MW, Palay SL. The fine structure of ependyma in the brain of the rat. J Cell Biol 1963; 19:415–439.
12. Brizee KR, Vogt J, Kharetchko X. Postnatal changes in glial/neurons index with a comparison of methods of cell enumeration in the white rat. In: De Robertis EDP, Carreas R, eds. Biology of the neuroglia, progress in brain research. Vol. 4. Amsterdam: Elsevier, 1964: 136–149.
13. Brownson RH. Perineuronal satellite cells in the motor cortex of aging brains. J Neuropathol Exp Neurol 1956;15:190–195.
14. Bullock TH, Horridge GA. Structure and function in the nervous systems of invertebrates. Vols. 1 and 2. San Francisco: W.H. Freeman, 1965.
15. Bunge RP. Glial cells and central myelin sheath. Physiol Rev 1968; 48:197–251.
16. Bunge RP, Bunge MB, Eldridge CF. Linkage between axonal ensheathment and basal lamina production by Schwann cells. Ann Rev Neurosci 1986;9:305–328.
17. Bunge RP, Bunge MB, Kleitman N. Role of peripheral extracellular matrix in Schwann cell function and in neurite regeneration. Dev Neurosci 1989;11:348–360.
18. Bunge MB, Bunge RP, Ris H. Ultrastructural study of remyelination in an experimental lesion in adult cat spinal cord. J Biophys Biochem Cytol 1961;10:67–94.
19. Cadelli DS, Schwab ME. Myelin-associated inhibitors of neurites outgrowth and their role in CNS regeneration. In: Abbott NJ, ed. Glial-neuronal interaction. Ann NY Acad Sci 1991;633:234–240.
20. Cammermeyer J. Histiocytes, juxtavascular mitotic cells and microglia cells during retrograde changes in the facial nucleus of rabbits of varying age. Ergeb Anat Entwickl-Gesch 1965;38:195–229.
21. Cholewinski AJ, Hanley MR, Wilkin GP. A phosphoinositide-linked peptide response in astrocytes: evidence for regional heterogeneity. Neurochem Res 1988; 13:389–394.
22. Coggeshall RE, Fawcet DW. The fine structure of the central nervous system of the leech, Hirudo medicinalis. J Neurophysiol 1964; 27:229–289.
23. Copenhaver WM, Bunge RP, Bunge MB. Bailey's textbook of histology. 16th ed. Baltimore: Williams & Wilkins, 1971.
24. Cserr HF. Physiology of the choroid plexus. Physiol Rev 1971; 51:273–311.
25. Davson H, Bradbury M. The extracellular space of the brain. In: De Robertis EDP, Carreas R, eds. Biology of the neuroglia, progress in brain research. Vol. 15. Amsterdam: Elsevier, 1965:124–134.
26. De Robertis EDP. Some new electron microscopical contributions to the biology of neuroglia. In: De Robertis EDP, Carreas R, eds. Biology of the neuroglia, progress in brain research. Vol. 15. Amsterdam: Elsevier, 1965:1–11.
27. Del Rio Hortega P. El "tercer elemento" de los centros nerviosus. Bol Soc Espan Bio 1919;9:69–120.
28. Del Rio Hortega P. El tercer elemento de los centros nerviosus. Histogenesis y evolucion normal: exoda y distribucion regional de microglia. Mem R Soc Espan Hist Nat 1921a;11:213–268.
29. Del Rio Hortega P. Estudios sobre la neuroglia. La glia de escasas radiaciones (oligodendroglia). Bol R Soc Espan Hist Nat 1921b;21:63–92.
30. Del Rio Hortega P. Microglia. In: Penfield WG, ed. Cytology and cellular pathology of the nervous system. Vol. II. New York: Paul B. Hoeber, 1932:483–534.
31. Delacourte A. General and chromatic glial reaction in Alzheimer brains. Neurol 1990;40:33–37.
32. Dempsey EW, Luse S. Fine structure of the neuropil in relation to neuroglia cells. In: Windle WF, ed. Biology of neuroglia. Springfield, IL: Charles C. Thomas, 1958: 99–108.
33. Denis-Donini S, Glowinski J, Prochiantz A. Glial heterogeneity may define the three-dimensional shape of mouse mesencephalic dopaminergic neurons. Nature 1984;307:641–643.
34. Dohrmann GJ. The choroid plexus: a historical review. Brain Res 1970;18:197–218.
35. Eisenbarth GS, Walsh FS, Nirenberg M. Monoclonal antibody to a plasma membrane antigen of neurons. Proc Natl Acad Sci (USA) 1979;76:4913–4917.
36. Erecinska M, Troeger MB, Wilson DF, Silver IA. The role of glial cells in regulation of neurotransmitter aminoacids in the external environment. Brain Res 1986; 369: 203–214.
37. Evans PD, Reale V, Merzon RM, Villegas J. Mechanisms of axon-Schwann cell signaling in the squid

nerve fiber. In: Abbott NJ, ed. Glial-neuronal interaction. Ann NY Acad Sci Vol 1991;633:434–447.
38. Farquhar MG, Hartmann JF. Neuroglial structure and relationships as revealed by electron microscopy. J Neuropathol Exp Neurol 1957;16:18–39.
39. Federoff S. From neuroepithelium to mature astrocytes. In: Althaus HH, Seifert W, eds. Glial-neuronal communication in development and regeneration. Berlin: Springer-Verlag, 1987:4–25.
40. Federoff S, Vernadakis A, eds. Astrocytes. Vol. I–III. New York: Academic Press, 1986.
41. Fulton BP, Burne JF, Raff MC. Glial cells in the rat optic nerve. In: Abbott NJ, ed. Glial-neuronal interaction. Ann NY Acad Sci 1991; 633:27–34.
42. Glees P. Neuroglia, morphology and function. Springfield, IL: Charles C. Thomas, 1955.
43. Golgi C. Sulla fine anatomia degli organi centrali del sistema nervoso. Riv Sper Freniat Med Leg 1882–1885;8:165–195, 361–391; 9: 1–17, 161–192, 385–402; 11:72–123, 193–220.
44. Gumpel M, Tourback A, Baron-Van Evercooren A. La réparation myélinique dans le système nerveux central des mammifères. Médecine/Sciences 1991;7:782–789.
45. Hao C, Richardson A, Federoff S. Macrophage-like cells originate from neuroepithelium in culture: characterization and properties of the macrophage-like cells. Int J Dev Neurosci 1990;9:1–14.
46. Herndon RM. The fine structure of the cerebellum. II. The stellate neurons, granule cells and glia. J Cell Biol 1964;23:277–293.
47. Herndon RM, Price DL, Weiner LP. Regeneration of oligodendroglia during recovery from demyelinating disease. Science 1977; 195:693–694.
48. Hertz L. Is Alzheimer's disease an anterograde degeneration, originating in the brainstem, and disrupting metabolic and functional interactions between neurons and glial cells? Brain Res 1989; 514: 335–353.
49. Heynes RO, Patel R, Miller RH. Migration of neuroblasts along preexisting axonal tracts during prenatal cerebellar development. J Neurosci 1986;6:867–876.
50. Innocenti GM, Clark S, Koppel H. Transitory macrophages in the white matter of the developing visual cortex. II. Development and relations with axonal pathways. Dev Brain Res 1983;11:55–66.
51. Janzer RC, Raff MC. Astrocytes induce blood-brain barrier properties in endothelial cells. Nature 1987;325:253–257.
52. Kettenmann H, Blankenfeld GV, Trotter J. Physiological properties of oligodendrocytes during development. In: Abbott NJ, ed. Glial-neuronal interaction. Ann NY Acad Sci 1991;633:64–77.
53. Knigge K, Joseph SA, Sladek JR Jr, Hoffman G, Scott DE . Structure and function of the endocrine hypothalamus. In: Morgane PJ, Panksepp J, eds. Physiology of the hypothalamus. New York: Marcel Dekker, 1980.
54. Kruger L, Maxwell DS. Electron microscopy of oligodendrocytes in normal rat cerebrum. Am J Anat 1966;118:411–436.
55. Kuffler SW, Nicholls JG, Martin AR. From neuron to brain: a cellular approach to the function of the nervous system. 2d ed. Sunderland, MA: Sinauer, 1984.
56. Kuffler SW, Nicholls JG, Orkand RK. Physiological properties of glial cells in the central nervous system of amphibia. J Neurophysiol 1966;29:768–787.
57. Kuffler SW, Potter DD. Glia in the leech central nervous system: physiological properties and neuron-glia relationships. J Neurophysiol 1964;27:290–320.
58. Laywell ED, Steindler DA. Boundaries and wounds, glial and glucoconjugates. In: Abbott NJ, ed. Glial-neuronal interaction. Ann NY Acad Sci 1991;633:122–141.
59. Le Prince G, Copin MC, Hardin H, Belin MF, Bouilloux JP, Tardy M. Neuron-glia interactions: effect of serotonin on the astroglial expression of GFAP and its encoding message. Exp Brain Res 1990; 51:295–290.
60. Levitt P, Rakic P. Immunoperoxidase localization of glial fibrillary acidic protein in radial glial cells and astrocytes of the developing rhesus monkey brain. J Comp Neurol 1980;193:815–840.
61. Lieberman EM. Role of glutamate in axon-Schwann cell signaling in the squid. In: Abbott NJ, ed. Glial-neuronal interaction. Ann NY Acad Sci 1991;633:448–457.
62. Luse SA. Electron microscopic observations of central nervous system. J Biophys Biochem Cytol 1956;2:531–432.
63. Luse SA. Ultrastructure of reactive and neoplastic astrocytes. Lab Invest 1958;7:401–417.
64. McCarthy KD, Salm H, Lera LS. Astroglial receptors and their regulation of intermediate filament protein phosphorylation. In: Kimelberg HK, ed. Glia cells, receptors. New York: Raven Press, 1988:1–22.
65. McGeer PL, Itagaki S, McGeer EG. Expression of the histocompatibility glycoprotein HLA-DR in neurological disease. Acta Neuropathol 1988;78:550–557.
66. Magistretti PJ, Hof PR, Martin J-L. Adenosine stimulates glycogenolysis in mouse cerebral cortex: a possible coupling mechanism between neuronal activity and energy metabolism. J Neurosci 1986;6: 2558–2562.
67. Malhotra SK, Shnitka TK, Elbrink J. Reactive astrocytes—a review. Cytobiol 1990;61:133–160.
68. Mallat M, Chamak B, Théry C. Les macrophages cérébraux: Rôle dans les remaniements morphologiques et la dégénérescence des neurones. Médecine/Sciences 1991;7:768–774.
69. Maxwell DS, Kruger L. The fine structure of astrocytes in the cerebral cortex and their response to focal injury produced by heavy ionizing particles. J Cell Biol 1965;25:141–157.
70. Moore BW. Brain-specific proteins. In: Schneider DJ, ed. Proteins of the nervous system. New York: Raven Press, 1973:1–12.
71. Mugnaini E. Cell junctions of astrocytes, ependyma, and related cells in the mammalian cerebral nervous system, with emphasis on the hypothesis of a generalized functional syncytium of supporting cells. In: Federoff S, Vernadakis A, eds. Astrocytes. Vol. 1. New York: Academic Press, 1986: 329–371.
72. Mugnaini E, Walberg F. Ultrastructure of neuroglia. Ergeb Anat Entwickl-Gesch 1964;37:194–236.
73. Murphy S, Pearce B. Functional receptors for neurotransmitters on astroglial cells. Neuroscience 1987; 22:381–394.
74. Murray MR. Response of oligodendrocytes to serotonin. In: Windle WF, ed. Biology of neuroglia. Springfield, IL: Charles C. Thomas, 1958:176–180.
75. Murray MR. Nervous tissue in vitro. In: Wilmer EN, ed. Cells and tissues in culture. Vol. 2. Methods, biology and physiology. New York: Academic Press, 1965; 373–455.
76. Nagy L, Martinez K. Astrocytic induction of endothelial tight junctions. In: N.J. Abbott, ed. Glial-neuronal interaction. Ann NY Acad Sci 1991;633:395–404.
77. Newman EA. Regulation of potassium levels by glial cells in the retina. Trends Neurosci 1985; 7:156–199.
78. Noble M, Ataliotis P, Barnett SC, et al. Development, regeneration, and neoplasia of glial cells in the central nervous system. In: Abbott NJ, ed. Glial-neuronal interaction. Ann NY Acad Sci 1991;633:34–47.
79. Orkand, RK. Glial electrophysiology and transport. In: Abbott NJ, ed. Glial-neuronal interaction. Ann NY Acad Sci 1991;633:245–247.
80. Page RB, Rosenstein JM, Dovey BJ, Leure-DuPree AE. Ependymal changes in experimental hydrocephalus. Anat Rec 1979a; 194: 83–104.
81. Page RB, Rosenstein JM, Leure-DuPree AE. The morphology of extrachoroidal ependyma overlying gray and white matter in the rabbit lateral ventricle. Anat Rec 1979b; 194:67–82.
82. Palay SL. An electron microscopical study of neuroglia. In: Windle WF, ed. Biology of neuroglia.

Springfield, IL: Charles C. Thomas, 1958:24–38.
83. Palay SL. The role of neuroglia in the organization of the central nervous system. In: Rodahl K, Issekutz B Jr, eds. Nerve as a tissue. New York: Harper & Row, 1966: 3–10.
84. Palay SL, Palade GE. The fine structure of neurons. J Biophys Biochem Cytol 1955;1:69–88.
85. Patel AJ, Hunt A. Regulation of production by primary cultures of rat forebrain astrocytes of a trophic factor important for the development of cholinergic neurons. Neurosci Lett 1989;99:223–228.
86. Peschanski M. Le temps venu de la "neurogliobiologie." Médecine/Science 1991;7:766–767.
87. Penfield W. Neuroglia, normal and pathological. In W.G. Penfield, ed. Cytology and cellular pathology of the nervous system. Vol. II. New York: Paul B. Hoeber, 1932;423–479.
88. Perry VH, Gordon S. Macrophages and microglia in the nervous system. Trends Neurosci 1988;11: 273–277.
89. Peters A, Palay SL. An electron microscope study of the distribution and patterns of astroglial processes in the central nervous system. J Anat 1965;99:419.
90. Peters A, Palay SL, Webster H deF. The fine structure of the nervous system: neurons and their supporting cells. 3rd ed. New York: Oxford University Press, 1991.
91. Polak M. Morphological and functional characteristics of the central and peripheral neuroglia (light microscopic observations). In: De Robertis EDP, Carreas R, eds. Biology of the neuroglia, progress in brain research. Vol. 15. Amsterdam: Elsevier, 1965:12–34.
92. Pomerat CM. Functional concepts based on tissue culture studies of neuroglia cells. In: Windle WF, ed. Biology of neuroglia. Springfield, IL: Charles C. Thomas, 1958: 162–175.
93. Prochiantz A, Mallat M. Astrocytes diversity. Ann NY Acad Sci 1988;540:52–63.
94. Raff MC. Glial cell diversification in the rat optic nerve. Science 1989;243:1450–1455.
95. Raisman G. Glia, neurons, and plasticity. In: Abbott NJ, ed. Glial-neuronal interaction. Ann NY Acad Sci 1991;633:209–213.
96. Rakic P. Guidance of neurons migrating to the fetal monkey neocortex. Brain Res 1971;33:471–476.
97. Ramón y Cajal S. Histologie du Système Neveux de l'Homme et des Vertébrés. (Azoulay L, trans.) Paris: Maloine, 1909, 1911. (Reprinted, Consejo Superior de Investigaciones Cientificas, Instituto Ramón y Cajal, Madrid, 1972.)
98. Ramón y Cajal S. Sobre un nuevo proceder de impregnacion de la neuroglia y sus resultados in los centros nerviosos del hombre y animales. Trab Lab Invest Biol Univ Madrid 1913;11:219–237.
99. Ramón y Cajal S. El proceder del oro-sublimado para la coloracion de la neuroglia. Trab Lab Invest Biol Univ Madrid 1916;14:155–162.
100. Ramon-Moliner E. A tungstate modification of the Golgi-Cox method. Stain Technol 1958;33: 19–29.
101. Ransom BR. Vertebrate glial classification, lineage, and heterogeneity. In: Abbott NJ, ed. Glial-neuronal interaction. Ann NY Acad Sci 1991;633:19–26.
102. Ransom BR, Kunis DM, Irwin I, Langston JW. Astrocytes convert the Parkinsonism inducing neurotoxin, MPTP, to its active metabolite, MPP+. Neurosci Lett 1987; 75:323–328.
103. Rapoport SI. Blood-brain barrier in physiology and medicine. New York: Raven Press, 1976.
104. Reichenbach A. Glia/neurons index: review and hypothesis to account for different values in various mammals. Glia 1989;2:71–77.
105. Robertson DM, Vogel FS. Concentric lamination of glial processes in oligodendrogliomas. J Cell Bio 1962;15:313–334.
106. Rubinstein LJ, Klatzo I, Miquel J. Histochemical observations on oxidative enzyme activity of glial cells in a local brain injury. J Neuropathol Exp Neurol 1962;21: 116–136.
107. Sasaki H, Sato F, Mannen H. Morphological analysis of single astrocytes of the adult cat central nervous system visualized by HRP microinjection. Brain Res 1989;501: 339–354.
108. Schaltenbrand G. Plexus und Meningen. Saccus vasculosus. In: von Möllendorff W, ed. Handbuch der mikroskopische Anatomie des Menschen. Vol. 4, part 2. Berlin: Springer-Verlag, 1955:94–98.
109. Scheibel ME, Scheibel AB. Neurons and neuroglial cells as seen with the light microscope. In: Windle WF, ed. Biology of neuroglia. Springfield, IL: Charles C. Thomas, 1958:5–23.
110. Schlue W-R, Dörner R, Rempe L, Riehl B. Glial H+ transport and control of pH. In: Abbott NJ, ed. Glial-neuronal interaction. Ann NY Acad Sci 1991;633:287–305.
111. Schultz RL, Maynard EA, Pease DC. Electron microscopy of neurons and neuroglia of cerebral cortex and corpus callosum. Am J Anat 1957;100:369–407.
112. Schultz RL, Pease DC. Cicatrix formation in the rat cerebral cortex as revealed by electron microscopy. Am J Pathol 1959;35:1017–1041.
113. Shuangshoti S, Netsky MG. Histogenesis of choroid plexus in man. Am J Anat 1966;118:283–316.
114. Shuangshoti S, Netsky MG. Human choroid plexus: morphologic and histochemical alterations with age. Am J Anat 1970;128: 73–96.
115. Skoff RP, Knapp PE. Lineage and differentiation of oligodendrocytes in the brain. In: Abbott NJ, ed. Glial-neuronal interaction. Ann NY Acad Sci 1991;633:48–55.
116. Somjen GG. Nervenkitt: notes on the history of the concept of neuroglia. Glia 1988;1:2–9.
117. Stewart PA, Wiley MJ. Developing nervous tissue induces formation of blood-brain barrier characteristics in invading endothelial cells. Dev Biol 1981;84:183–192.
118. Stitt TN, Gasser UE, Hatten ME. Molecular mechanisms of glial-guided neuronal migration. In: Abbott NJ, ed. Glial-neuronal interaction. Ann NY Acad Sci 1991;633: 113–121.
119. Stone EA, Ariano MA. Are glial cells targets of central noradrenergic system? A review of the evidence. Brain Res Rev 1989;14: 297–309.
120. Streit WJ, Kreutzberg GW. The response of endogenous glial cells to motor neuron degeneration induced by toxic ricin. J Comp Neurol 1988;268:248–263.
121. Tardy M. Astrocytes et homéostasie. Médecine/Sciences 1991;7:799–804.
122. Tedeschi B, Barret JN, Keane RW. Astrocytes produce interferon that enhances the expression of H-2 antigens on a subpopulation of brain cells. J Cell Biol 1986; 102:2248–2252.
123. Tennyson VM. The differences in fine structure of the myelencephalic and telencephalic choroid plexuses in the fetuses of man and rabbit, and a comparison with the mature stage. In: Walker AE, Arana-Iniguez R, eds. Cerebrospinal fluid in health and disease. Acta Neurol Lat Am 1971; 17:(Suppl 1):11–52.
124. Tennyson VM, Pappas GD. Electron microscope studies of the developing telencephalic choroid plexus in normal and hydrocephalic rabbits. In: Fields W, Desmond M, eds. Disorders of the developing nervous system. Ch. 12. Springfield, IL: Charles C. Thomas, 1961:267–318.
125. Tennyson VM, Pappas GD. Fine structure of the developing telencephalic and myelencephalic choroid plexus of the rabbit. J Comp Neurol 1964;123:379–412.
126. Tennyson VM, Pappas GD. Some aspects of the fine structure of the ependyma. In: Minckler J, ed. Pathology of the nervous system. Vol. 1. New York: McGraw-Hill, 1968a;518–531.
127. Tennyson VM, Pappas GD. The fine structure of the choroid plexus: Adult and developmental stages. In: Lajtha A, Ford DH, eds. Brain barrier systems, progress in brain research. Vol. 29. Amsterdam: Elsevier, 1968b;63–86.
128. Terry RD. Electron microscopy of the central nervous system. In: Bailey OT, Smith DE, eds. The

central nervous system. Baltimore: Williams & Wilkins, 1968:335–346.
129. Virchow R. Über das granulierte Ansehen der Wandungen der Gerhirnventrikel. Allg Zeitschchr Psychiatr 1846;3:242–250.
130. Virchow R. Cellular pathology. (Translated from the 2nd German edition by F. Chance.) London: Churchill, 1860.
131. Voigt T. Development of glial cells in the cerebral wall of ferrets: direct tracing of their transformation from radial glia to astrocytes. J Comp Neurol 1989;289:74–88.
132. Walz W. Role of glial cells in the regulation of the brain ion neuroenvironment. Prog Neurobiol 1989;33:309–333.
133. Wilkin GP, Marriott DR, Cholewinski AJ Astrocytes heterogeneity. Trends Neurosci 1990;13:43–46.
134. Wilkin GP, Marriott DR, Cholewinski AJ, et al. Receptor activation and its biochemical consequences in astrocytes. In: Abbott NJ, ed. Glial-neuronal interaction. Ann NY Acad Sci 1991;633: 475–489.
135. Windle WF, ed. Biology of neuroglia. Springfield, IL: Charles C. Thomas, 1958.
136. Young JZ. The concept of neuroglia. In: Abbott NJ, ed. Glial-neuronal interaction. Ann NY Acad Sci 1991;633:1–18.

Section III

Peripheral Nervous System

7
Receptors and Effectors

SENSORY RECEPTORS

All information we have concerning the world about us is conveyed to the brain by an elaborate sensory system. This input, initiated from the external world, reaches the central nervous system via first order sensory nerve fibers. Sensory receptors and sensory endings act as transducers, which change physical and chemical stimuli in our environment into coded nerve impulses the brain can decode. A *sensory unit* consists of a single peripheral neuron, located in a spinal or cranial nerve ganglion, its peripheral and central ramifications, and, in certain instances, the nonneural transducer cells with which the distal end of the peripheral nerve fiber may be associated. Information conveyed centrally by sensory units provides an ongoing, constantly changing global picture of the external environment and the stimuli which it presents. From this massive barrage of sensory impulses generated in many different types of receptors and nerve endings, the central nervous system derives precise information concerning the quality, the intensity, the locus, and the spatial and temporal patterns of stimuli.

Stimuli in our environment elicit sensory experiences that, within certain limits, can be recognized, described and classified. Each more or less unique sensory experience is referred to as a *sensory modality*. Sensations of color compose a single modality, as do those of tones. General somatic sensibility consists of several sensory modalities that differ in quality and can be distinguished readily as touch-pressure, pain, warmth, cold, and sense of position or movement of limbs at joints. Certain substances can be readily differentiated by the way they taste, and the capacity of humans and animals to distinguish and discriminate a great diversity of odors is well-known. The spatial position of a tactile stimulus can be located with considerable accuracy, especially on certain surfaces of the body, such as the hand or face (23). Certain forms of sensation arising in abdominal and thoracic viscera are poorly localized, difficult for the patient to describe, and sometimes referred to false locations. *A peripheral receptive field* is the area within which a stimulus of appropriate quality and strength will cause an afferent neuron to discharge. The receptive field may represent an area of skin in which a mechanical stimulus will excite cutaneous receptors, the angle of joint rotation necessary to excite sensory units, or an area of the visual field in which a light stimulus will evoke discharges in retinal ganglion cells. Within a peripheral receptive field the threshold for adequate stimulation varies in that it is usually lowest in the central region where the density of receptor elements is highest. Peripheral branches of one sensory unit often overlap those of adjacent sensory units, and peripheral receptive fields on the body surface vary greatly in size. Cutaneous receptive fields on the digits of the hand are small in comparison to those on proximal portions of the limbs and on the trunk, but the central representation of these densely innervated areas in the cerebral cortex is massive.

Muller's "doctrine of specific energies," interpreted in modem physiologic terms, states that different sets of nerve fibers, when activated, elicit different sensations by virtue of their unique central connections (61–63). A particular sensory nerve fiber provokes an identical sensation regardless of how it is excited, that is, by a natural adequate stimulus or by an artificial stimulus. Within a receptive surface, such as the skin, different sets of nerve endings and receptors are distributed in a mosaic fashion. Why a particular set of nerve fibers that terminates in an area common to other receptive elements responds selectively to a stimulus of a particular quality is unknown. The modalities and qualities of sensation seem to depend upon the temporal and spatial patterns of activation, the specificity of the sensory endings, and the central

connections (24). The four elemental qualities of cutaneous sensibility are not distributed uniformly over an area of skin. Within a cutaneous area there is a local differential sensitivity to touch, warmth, cold, and pain (8). Each spot receives terminal branches from several afferent nerve fibers and a single nerve fiber may innervate several sensory spots. Regardless of how a particular spot is excited, only one elementary sensory experience is evoked, if the excitation is local. Variations of the elementary sensory experience can be produced by temporal and quantitative variations of the stimulus. The wide variety of complex sensory experiences are thought to be generated in the central nervous system from the combinations of activities evoked in afferent nerve fibers, each of which, when acting alone, is associated with a sensory quality of some purity (61–63).

The manner in which receptors behave in response to a continuing stimulus varies. Some receptors discharge only at the onset of a steady stimulus; these receptors are called *rapidly adapting*. Other receptors respond to a continuing stimulus with a high frequency discharge for its full duration; these receptors are called *slowly adapting*.

The transduction of mechanical, chemical, or electromagnetic energy into a train of nerve impulses is accomplished by receptors that develop in three distinct ways in the embryo (92) (Fig. 7.1). Some transducing elements, such as olfactory receptor cells in the nasal cavity, hair cells in the inner ear, and taste receptors, differentiate within localized thickenings of the cephalic surface ectoderm. Photoreceptors of the eye develop from the neural tube, and other sensory receptors arise from neural crest tissue. Many of the latter types of receptor cells may be in contact with a specialized ectodermal or mesodermal structure such as a layered capsule or a muscle fiber. The categorization of receptors on the basis of their embryology is important for comparative purposes, but a functional classification is most useful for the study of sensory mechanisms in mammals.

Sensory receptors may be regarded as

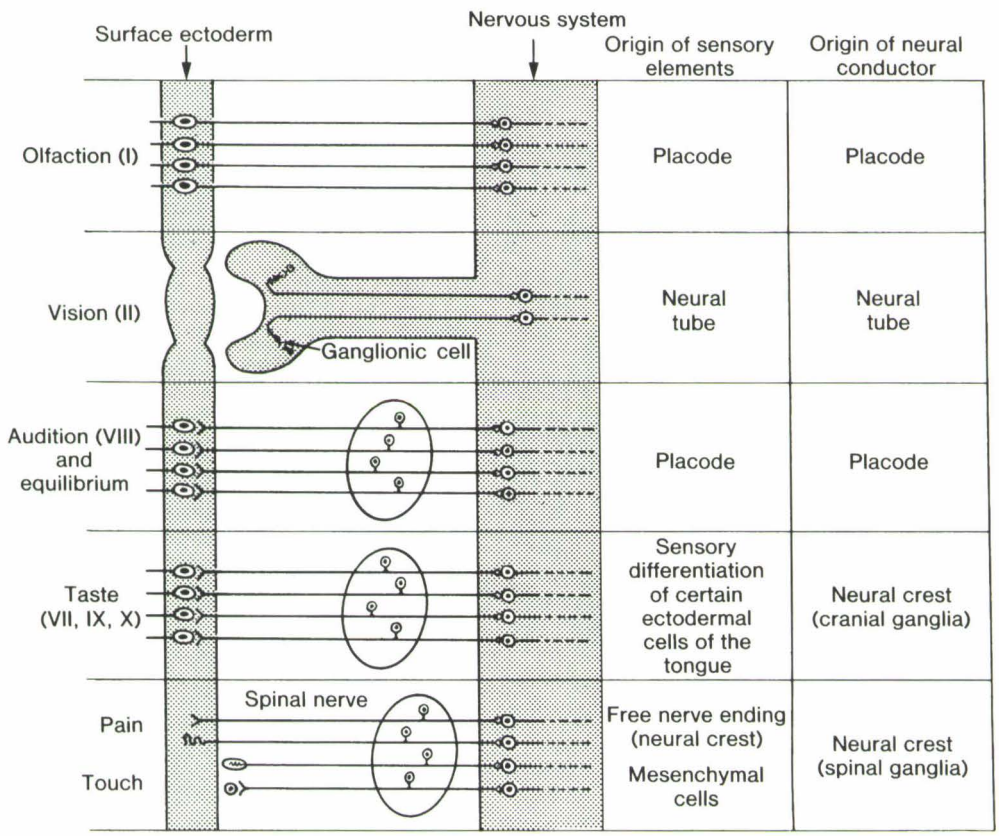


Figure 7.1. Classification of sensory receptor cells according to embryonic origin. All sensory cells are derived from surface ectoderm, except those associated with vision and touch. Sensory elements in the visual system are derived from the central nervous system (neural tube), but their nature, concentration, and specialization are similar to placodal cells. Touch receptors below the surface ectoderm are derived from mesenchymal cells.

miniature transducers capable of responding readily to appropriate forms of energy (adequate stimulus). An appropriate external stimulus applied to a receptor gives rise to a graded electrical response, known as a "receptor potential." The term "generator potential" is used to define the electrical potential that triggers the "all or none" response in the initial segment of the sensory nerve fiber. If the receptor potential is generated in the first sensory neuron, then it is also the generator potential (24, 33). Such physiologic events are demonstrated best in the Pacinian corpuscle (45–48).

Biochemical and electrophysiologic studies of sensory receptors revealed that the transduction of different types of stimulus energies into neural activity is based on various specific mechanisms, involving membrane channels and second-messenger systems. Mechanoelectric transduction is produced by direct mechanical interaction between the stimulus and membrane channels. Few channels are open in the unstimulated condition, whereas mechanical stimulation deforms the membrane and cause channels to open. Influx of Na^+ and K^+ causes the receptor terminal to depolarize locally producing the receptor potential. Chemoelectric transduction is similar, except that a receptor-ligand interaction produces channel opening. A second messenger mediates channel opening in olfactory receptors and certain gustatory receptors. Photoelectric transduction involves the absorption of light by photoreceptors. A photon-photopigment interaction on intracellular membrane produces a three-dimensional change in the photopigment. The resulting change in membrane permeability also involves a second-messenger system. For further details on the physiology, biochemistry, and molecular biology of sensory receptor the reader is referred to the excellent reviews by Shepherd (85), Martin (50), and Martin and Jessell (51).

Receptor endings have numerous mitochondria, microvesicles, neurofilaments, and even acetylcholinesterase in the case of nerve endings related to hairs. Other receptors are associated with supportive cells that demonstrate a variety of enzyme activities. Free nerve endings appear to be the receptors in fetal life, whereas encapsulated endings appear after birth (16). Throughout life receptors show a continuous cycle of breakdown, renewal, and reorganization (12). This observation accounts for the variable appearance of Pacinian and Meissner's corpuscles in older individuals. Different regions and tissues of the body have marked differences in the type and number of receptors. Detailed reviews of cutaneous innervation have been published (32, 33, 73, 87).

RECEPTOR'S DIVERSITY

No single classification of receptors has evolved which adequately correlates the principles of structural organization, distribution, and function. The three simple categories suggested by Miller and collaborators (58, 59) are the least elaborate and restrictive. They suggested that the entire body is served by a basic triad of sensory nerve endings which are either "free," "expanded-tip," or "encapsulated." Such designations are applicable to the endings in glabrous skin and the subpapillary dermis. These terms also apply to the endings observed in fascia, tendons, ligaments, periosteum, and synovial membranes (75) (Figs. 7.2 and 7.4). However, difficulty is encountered with such categories in hairy skin and muscle spindle receptors where free nerve and expanded-tip endings are also encapsulated.

Sherrington (86) classified all receptors into three main groups: *exteroceptors, proprioceptors,* and *interoceptors* (Fig. 10.23). Exteroceptors on the external body surface receive stimuli from the outside which may, or may not, result in somatic movements. They include touch, pressure, pain, temperature, smell, sight, and hearing. Some of these are *contact receptors;* others, such as smell, sight, hearing, and aspects of thermal sense, are activated by distant stimuli and are known as *teloreceptors.*

The proprioreceptors, which receive stim-



Figure 7.2. Sensory nerve terminations in corneal epithelium.

uli from the deeper portions of the body wall, especially from the joints, joint capsules, ligaments, and fascia, give rise to position sense and the sense of movement (i.e., kinesthesis). They are primarily concerned with the regulation of movement in response to exteroceptive stimuli. These receptors provide sensory information which is utilized in the cerebral cortex to generate a conscious awareness of bodily muscle activity and joint movements *(kinesthetic sense).* Most of the receptors related to the knee and temporomandibular joints are diffuse unencapsulated nerve terminals (30, 41). Other specialized receptors (spindles) in skeletal muscle and tendon are activated by muscle contraction and stretch. Their encoded signals regulate muscular activities, either at spinal cord levels (e.g., myotatic, flexor, and extensor reflexes), or they reflexively regulate muscle tone and coordination of muscle activities (i.e., synergy) via projections to specific parts of the cerebellum. Nerve endings in skin, joints, fascia, muscle, and tendons all transmit afferent nerve impulses from the soma or body wall. Hence exteroceptors, proprioceptors, and stretch receptors in muscles and tendons, are grouped together as somatic receptors.

The interoceptors (viscероceptors) are the visceral sense organs that receive and transmit poorly localized sensory impulses related to digestion, excretion, circulation, and respiration, which are primarily under the control of the autonomic nervous system. They give rise to sensations of visceral pain and contribute to forms of visceral sensibility such as hunger, thirst, and sexual feelings, and to the general feelings of well-being or malaise. Smell, although not interoceptive, has close visceral affiliations and may be considered partly visceral.

Sensibility may also be divided into *superficial* and *deep.* The former obviously coincides with exteroceptive sense and the latter comprises both interoceptive and proprioceptive sense, including deep pressure. A special form of sensation is the ability to recognize the vibrations of a tuning fork applied to bone or skin. This is known as *vibratory* sense, a form of mechanoreceptive sensibility dependent for its unique qualities upon the temporal pattern of the neural inputs. The perception of vibratory sense appears dependent upon two sets of primary afferents, one innervating the skin and one innervating deep tissue (64). Cutaneous afferents probably convey impulses from Meissner's corpuscles, and deep afferents probably end in Pacinian corpuscles.

In an analysis of clinical problems related to sensation, Head (35, 36) proposed that there are two different kinds of sensation subserved by dual sensory mechanisms at the periphery. This dual innervation was postulated to consist of a *protopathic* system and an *epicritic* system. Protopathic sensation was considered to be mediated by a primitive system subserving pain and extreme temperature differences which yield ungraded, diffuse impressions of a marked affective character. Epicritic sensation was thought to be mediated by a phylogenetically more advanced system sensitive to smaller temperature changes and concerned with the discriminative aspects of tactile sensation (i.e., precise localization and gradation of stimulus intensity). The concept of a duality of cutaneous sensations has been severely criticized (93), but it has been useful in studying pain in humans. It is likely that the two categories of pain reflect central rather than peripheral mechanisms. It also seems likely that the protopathic system may be anatomically related to free nerve endings of small diameter axons (81). Affective sensations are related primarily to reactions indirectly involving bodily welfare, and neuronal activities in the limbic cortex may play an important role in this form of sensation. Discriminative sensibility forms the basis for cognitive and complex associative reactions which involve the cerebral cortex; this form of sensation is regarded as *gnostic* or *cortical.* In a general way, pain, thermal, visceral sensibility, and certain aspects of touch are predominantly affective, while tactile sense, kinesthesis, and teloceptive sensibilities are predominantly discriminative.

Physiologically, receptors can be classified in terms of the form of energy to which they respond at the lowest stimulus intensity. *Mechanoreceptors,* responding to mechanical forces, include those that subserve touch-pressure in the skin, position sense, and kinesthesis (joints and joint capsules), as well as stretch receptors in muscle, visceral pressure receptors, and hair cells in the cochlea. *Thermoreceptors,* responding separately and differentially to warmth and cold, are distributed in spotlike fashion in the skin and vary greatly in their density in different parts of the body. *Photoreceptors* subserving vision respond to light, and *chemoreceptors* initiate impulses concerned with taste and olfaction.

Pain receptors are collectively referred to as *nociceptors* since pain can be produced by

different forms of energy (mechanical, chemical, or thermal). Pain, frequently a frightening sensory experience, is associated with noxious stimuli that injure tissue. Because almost all descriptions of pain come from studies in humans, many distinctive forms are recognized. Descriptions of particular kinds of pain guide the astute physician in his search to determine the nature and extent of the underlying pathologic process. Two aspects of pain are recognized: (a) the distinct sensation, and (b) the psychologic reaction to pain which depends upon many variables. Certain stimuli which commonly produce pain evoke other kinds of sensory experience at weaker intensities. Melzack and Wall (54) proposed that pain perception is modulated by both sensory feedback mechanisms and the influences of the central nervous system.

From a morphologic point of view, two main types of receptors are found: (a) the *free* and *diffuse endings*, which are always unencapsulated, and (b) the *encapsulated* endings or corpuscles, which are enclosed in a capsule of modified supporting cells.

Free Nerve Endings

Free nerve endings are the most widely distributed receptors in the body. They are most numerous in the skin, but also are found in the mucous and serous membranes, muscle, deep fascia, and the connective tissue of many visceral organs. The skin is supplied by many cutaneous nerve trunks composed of myelinated and unmyelinated fibers. Some of the large myelinated fibers are destined for the encapsulated organs, but the majority are of a relatively small caliber. The fibers of these small nerve trunks separate as they approach the epidermis, lose their myelin sheath, undergo branching, and form extensive unmyelinated plexuses in the deeper portion of the dermis and immediately beneath the epidermis (Fig. 7.3). From this subepithelial plexus, delicate fibers penetrate

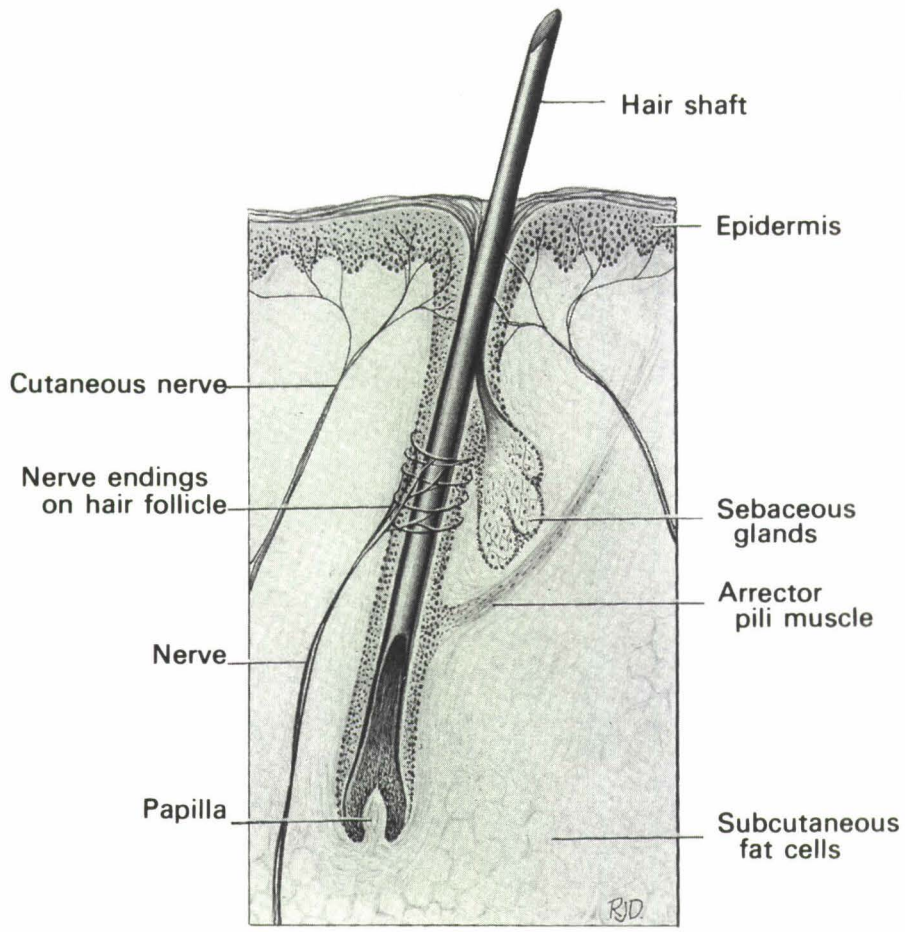


Figure 7.3. Nerves and nerve endings in skin and hair follicle.

the epithelium, divide repeatedly, and form terminal arborizations composed of delicate terminal fibrils, which wind vertically through the epidermis and end in small knoblike thickenings, upon the surface of the epithelial cells (Figs. 7.2 and 7.3). In the cornea, which has no horny layer, these intraepithelial endings may reach the surface, but in the skin they do not extend beyond the germinative layer. Intraepithelial endings also are found in mucous membranes lined by stratified epithelium, such as the esophagus and bladder. Similar endings may be seen in simple columnar epithelium as well.

Other nerve fibers form unmyelinated arborizations or terminal nets in the connective tissue of the dermis. There is some evidence that the intraepithelial endings are derived from fine myelinated fibers, while the subepidermal arborizations and plexiform nets are in the main terminals of unmyelinated nerve fibers (96). Such terminal unmyelinated fibers are never naked, but are always invested by Schwann cells (13). Diffuse nerve endings in the form of nerve nets, or arborizations of varying complexity, are distributed widely in visceral organs. They have been described in the serous membranes, heart, bronchial tree, alimentary canal, and blood vessels (11,25,89) (Fig. 7.4). Such endings also are found in the choroid plexuses of the brain and in skeletal muscle. For the most part, they are terminals of unmyelinated fibers. Complicated arborizations were found in the smooth muscle of the bronchi by Larsell and Dow (43) (Fig. 7.4). These visceral receptors are endings of

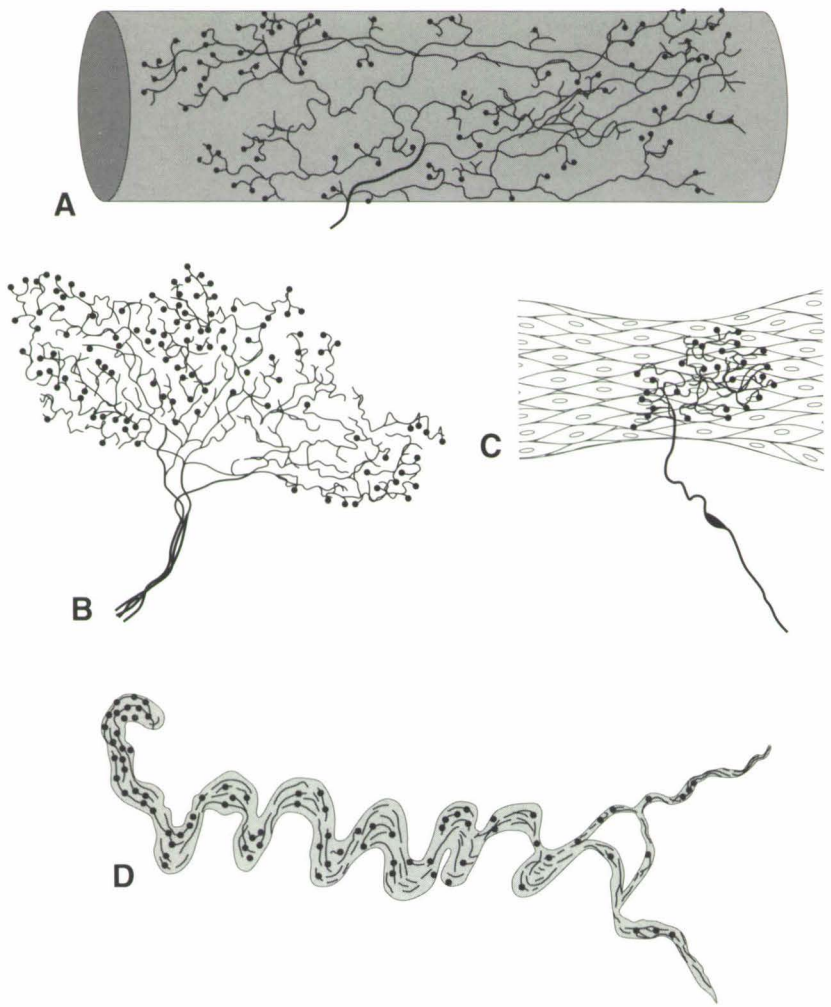


Figure 7.4. Afferent nerve endings in various visceral structures. **A.** On a large pancreatic blood vessel; **B.** In endocardium of dog; **C.** In bronchial musculature of child; and **D.** In longitudinal muscle coat of stomach of cat.

medium-sized or large myelinated fibers and may initiate proprioceptive bronchial reflexes.

An important type of diffuse cutaneous receptor is represented by the *peritrichal* endings of the hair follicles, which are activated by the movements of hairs (Fig. 7.3). They vary considerably in complexity and are best developed in the vibrissae of certain mammals. In the simpler forms, several myelinated fibers approach the hair follicle just below its sebaceous gland, lose their myelin sheath, and divide into several branches which encircle the outer root sheath (Fig. 7.3). From these branches numerous fine fibers run for a short distance upward and downward in the outer root sheath and terminate in flattened or bulbous endings. The smallest hair follicles have at least two stem nerve fibers which form an outer circular plexus and an inner palisading one formed by the longitudinally directed fibers. Larger follicles are supplied by 6 to 10 fibers, while the largest receive between 20 and 30. In the rabbit, each myelinated fiber sends branches to 4 to 120 hairs, and an average of 4 different dorsal root fibers supply each hair (94). Only free epidermal and dermal endings, and the fibers associated with hair follicles, are found in truly hairy skin.

Besides the intraepithelial endings, which end among or upon ordinary epithelial cells, the deeper portion of the germinative layer contains somewhat more specialized endings known as the *tactile discs* of Merkel (55) (Fig. 7.5). Each consists of a concave neurofibrillary disc or meniscus closely applied to a single epithelial cell of modified structure. A single epidermal nerve fiber may, by repeated branching, give rise to a number of such discs. These simple endings lie along the deeper sweat ridges between dermal papillae (Fig. 7.5). They are numerous at birth but gradually diminish with age. With the electron microscope, the Merkel cell of humans and opossums can be distinguished from epidermal cells (65, 66). The Merkel cell has a lobulated nucleus and a massive accumulation of secretory granules (glycoprotein) in the cytoplasm that is apposed to the neurite. Cauna (12) believes them to be touch receptors which respond to the lever movement that results from deformation of the surface epidermis. In areas of transition to glabrous skin, there is a gradual increase in the number of Merkel's discs and Meissner's corpuscles. In glabrous skin, such as the volar surface of the finger, the epidermis and dermal papillae contain a profuse array of free nerve endings, Merkel's discs, and the encapsulated Meissner's corpuscle (Fig. 7.5). The subpapillary dermis under such skin contains a wide variety of endings including the end bulbs of Ruffini, Krause, and Pacinian corpuscles.

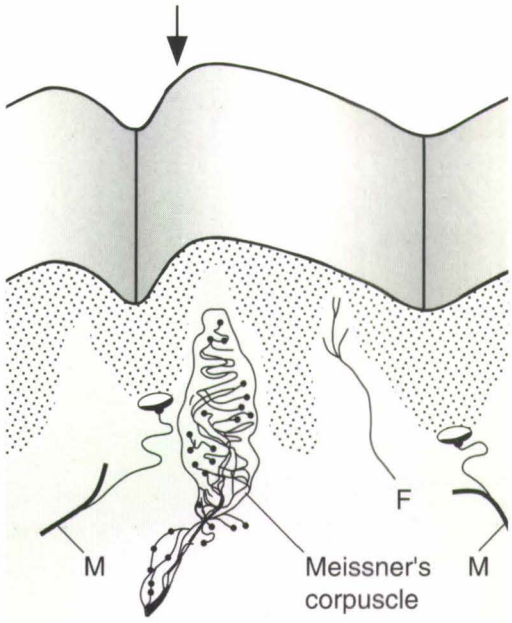


Figure 7.5. Papillary ridge in glabrous skin showing Meissner's corpuscle in a dermal papilla and Merkel's discs (*M*) on the deep edges of the sweat ridges. A free nerve ending (*F*) is shown in adjacent papilla. *Arrow* indicates direction of most effective epidermal stimulation to elicit touch and tactile two point discrimination.

The tendency toward modification of epithelial cells receiving sensory nerve endings is found in various *neuroepithelial* cells which have special forms and show staining affinities similar to nerve cells. The specific cells of the taste buds (Fig. 7.6), olfactory mucosa, and hair cells in the sensory epithelia of the cochlear and vestibular apparatus, are examples of such neuroepithelial cells. These supportive cells, as well as those forming the lamellae of encapsulated endings, have surrounding basement membranes. It remains to be determined whether they are modified epithelial or transformed Schwann cells.

Diffuse Endings

The deep somatic structures of the human body have unencapsulated sensory endings that are more profuse than those observed in

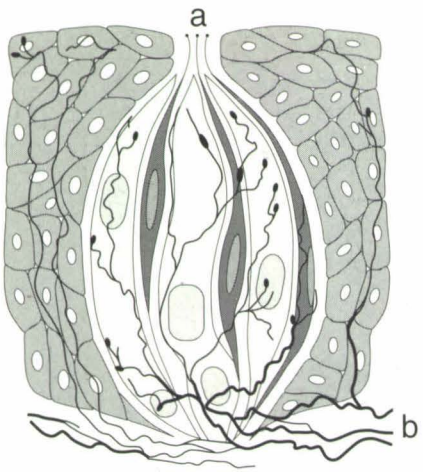


Figure 7.6. Taste bud from circumvallate papilla of tongue. *a*, Taste pore; *b*, nerve fiber entering taste bud and ending upon neuroepithelial cells. On either side are some free intraepithelial endings.

visceral structures (Fig. 7.4). Elaborate nerve endings have been disclosed by Ralston and collaborators (74) in the tendons, ligaments, joint capsules, deep fascia, and periosteum of man (Fig. 7.7). Ruffini (83) originally described an encapsulated fusiform end organ in the skin and adipose tissue. Although long considered as a corpuscle, its morphology is vague and most investigators have failed to verify its abundant distribution in humans. It may well represent a variation of the diffuse, expanded-tip, unencapsulated endings described by Miller, et al (59). Encoded messages from these diffuse unencapsulated receptors appear to be an important component of impulses carried by the axons of the posterior white columns. Proprioceptive nerve impulses from these deep receptors play an important role centrally in that they make us aware of the numerous localized body changes that occur during locomotion, standing or sitting.

When recordings are made from single primary afferent neurons innervating the general body surface, cutaneous receptors sensitive to mechanical stimuli can be classified into 11 groups. The characteristics used for classification include: (a) conduction velocity, (b) distance the central axon ascends in the spinal cord, and (c) pattern of action potentials generated by defined stimuli (38) (Table 7.1).

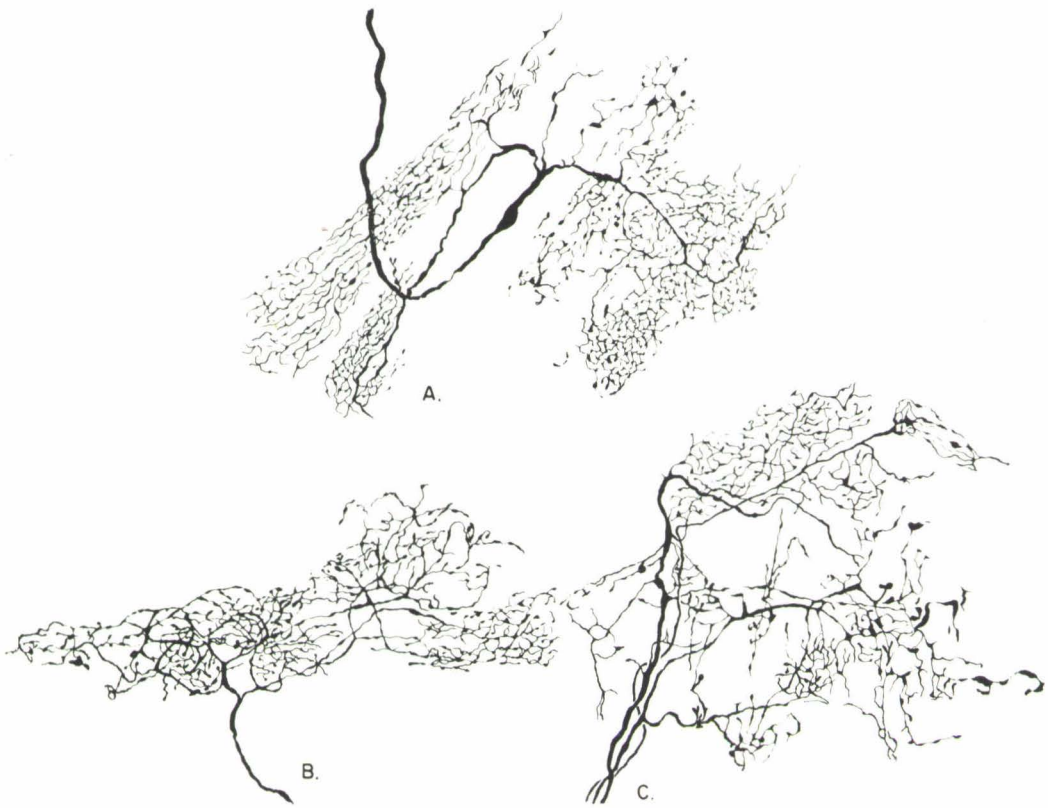


Figure 7.7. Unencapsulated nerve endings in deep somatic tissues of humans. **A.** Patellar ligament. **B.** Capsule of knee joint. **C.** Periosteum of femur.

Encapsulated Endings

Encapsulated endings include the *tactile corpuscles of Meissner*, the *end bulbs*, the *Pacinian corpuscles*, the *Golgi-Mazzoni corpuscles*, the *neuromuscular spindles*, and the *neurotendinous organs of Golgi*.

CORPUSCLES OF MEISSNER

The *tactile corpuscles of Meissner* are elongated ovoid bodies, 90–120 μm in length, found in the dermal papillae, close to the epidermis (Figs. 7.5 and 7.8). Each corpuscle is surrounded by a thin, nucleated connective tissue sheath, while the interior consists of many flattened epithelioid cells whose nuclei are placed transversely to the long axis of the corpuscle. From one to four myelinated nerve fibers supply each corpuscle. As each fiber enters, its connective tissue sheath becomes continuous with the fibrous capsule. The myelin sheath disappears and the naked axon winds spirally among the epithelioid cells, giving off numerous branches which likewise spiral, show numerous varicosities, and end in flattened neurofibrillary expansions. Besides the myelinated fibers, the corpuscles also may receive one or more fine unmyelinated fibers. Meissner corpuscles occur mainly in the hairless portion of the skin and are most numerous on the volar surface of the fingers, toes, hands, and feet. They are found in lesser numbers in the lips, eyelids, tip of the tongue, and volar surface of the forearm (60). Meissner's corpuscles are formed in excess of adult requirements, and those that survive possess a capacity for continuous growth and reorganization (12, 59). In young persons, nearly every dermal papilla contains a small Meissner corpuscle, 25 μm in length. In older individuals, only a few papillae contain corpuscles which are larger and of more irregular arrangement. These endings always are associated with the papillary ridge which plays an essential role in their stimulation. Their relationship is designed so that the nerve endings are stimulated effectively through one surface elevation of the epidermis, which is in line with the long axis of the corpuscle (Fig. 7.5). This arrangement makes the Meissner corpuscle particularly suitable for tactile two-point discrimination (12).

END BULBS

End bulbs resemble the tactile corpuscles in structure and are spherical or ovoid bodies

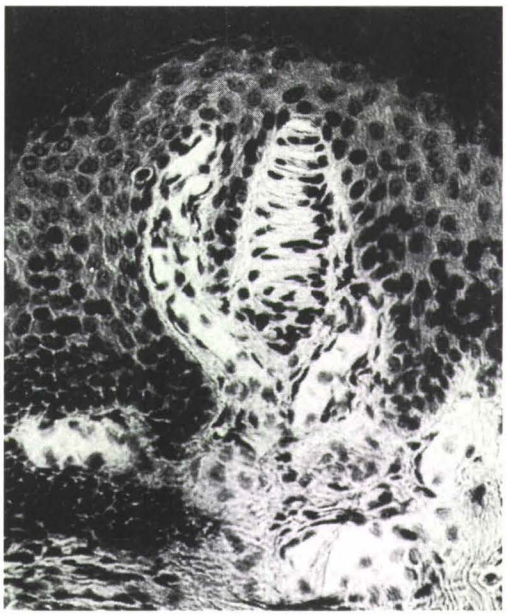


Figure 7.8. Meissner's corpuscle in a dermal papilla of human finger tip.

which vary greatly in dimension. The simplest and smallest ones are found in the conjunctiva (68); the largest in the connective tissue of the external genitalia, where they are known as *genital corpuscles*. In its simplest form (26)(Fig. 7.9**A**), the end bulb consists of a nucleated capsule enclosing a soft gelatinous core in which nuclei may often be seen. One or more myelinated fibers lose their myelin on entering the capsule, and give off numerous lateral branches which form a complicated terminal arborization. Some end bulbs may be compound. End bulbs of various forms have a wide distribution, being found in the conjunctiva, mouth, tongue, epiglottis, nasal cavity, peritoneum (and other serous membranes), lower end of rectum, and external genitalia, especially the glans penis and clitoris. They also are found in tendons, ligaments, synovial membranes, and in the connective tissue of nerve trunks.

PACINIAN CORPUSCLES

The *Pacinian (Vater-Pacini) corpuscles* are the largest and most widely distributed of the encapsulated receptors (Fig. 7.10). They are laminated, elliptical structures of whitish color, and each is supplied by a large myelinated fiber. They differ from the other encapsulated organs mainly in the greater development of their perineural capsule. This capsule is formed by a large number of concentric

Table 7.1. Properties of Cutaneous Axons Responding to Mechanical Stimulation of the Skin[a]

MECHANO-RECEPTOR TYPE	MEAN PERIPHERAL CONDUCTION VELOCITY (m/sec)	LEVEL AT WHICH MOST FIBERS LEAVE THE FASCICULUS GRACILIS	MEAN SLOPE OF TUNING CURVES	PLATEAU RESPONSE	TYPE OF RAMP RESPONSE: ON vs. OFF SENSITIVITY[b]	PROBABLE OR POSSIBLE RECEPTOR STRUCTURE
C	< 2	—	Does not follow above 2 Hz	< 20 sec	V/D; little or no off, but has an after discharge	Free nerve ending?[c]
Aδ	20	Lower lumbar	−0.4[d]	Little or none	V; on = off	Free nerve endings in skin or around hair follicles?[c]
G_2 hair	50	1/2 upper lumbar, 1/2 nucleus gracilis	−0.2	Little	V/D; on > off	
GI hair	65	Nucleus gracilis	−0.4	None	V; on ≥ off	Lanceolate, pallisade or circular endings of follicle[e]
G_1 Hair	75	Nucleus gracilis	−1	None	V/A; on = off	
F_2 field	50	1/2 upper lumbar, 1/2 nucleus gracilis	−0.15	< 20 sec	V/D; little or no off	
FI field	55	1/2 upper lumbar, 1/2 nucleus gracilis	−0.25	None	V; on > off	Sparsely laminated corpuscles (such as Meissner's corpuscles, Krause end bulbs, Golgi-Mazzoni organs)?[f]
F_1 field	65	Nucleus gracilis	−0.6	None	V; no off	
Ruffini	55	Nucleus gracilis	0	Persists	D; no off	Ruffini endings

Haarschiebe	65	Upper lumbar	0	Persists	D/V; no off	Merkel cells
Pacinian corpuscle	65	Nucleus gracilis	−2	None	A; on = off	Pacinian corpuscles

[a] A classification scheme for mechanoreceptors that is based upon the morphology of receptors in the skin of cats and their physiologic properties. The scheme derived from primary afferent neurons which ascend in the dorsal column of the spinal cord. The free ending of Aδ (delta) axons are exquisitely sensitive to slight movement of the skin and act as velocity detectors. On hairy skin, two types of hair follicles are distinguished. Fine "down" hairs emerge in groups from a follicle and the larger "guard" hairs emerge singly. Receptors associated with guard hair follicle are designed type G. Receptors responding to stimulation of the skin between hairs or movement of clumps of hairs are field receptors (type F). F receptors are also found in glabrous skin. "Haarschiebe" is the term given to small, fairly evenly spaced protuberances on the surface of the skin. Field (F) and guard (G) receptors are subdivided according to their phasic. (F_1, G_1), tonic (F_2, G_2), or intermediate (FI,GI) response patterns.

[b] A = acceleration response; D = displacement response; V = velocity response; FI = intermediate field receptors; GI = intermediate guard hair receptors.

[c] Receptor identification uncertain and based on supposition.

[d] Estimated.

[e] It is not known to what extent G_1 endings differ in structure from G_2, if at all. Both G_1 and G_2 can innervate the same hair.

[f] Receptor identification based on reasonable likelihood.

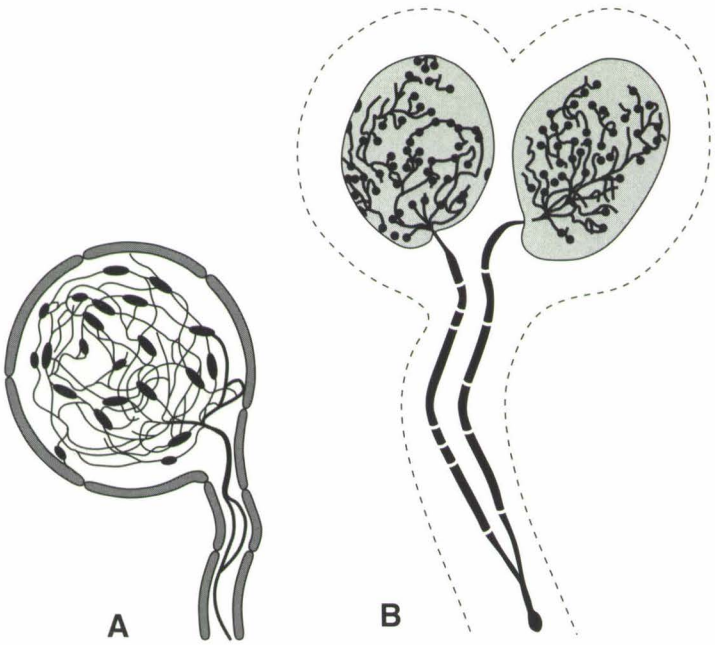


Figure 7.9. **A.** End bulb of Krause from conjunctiva. **B.** Compound corpuscle of Golgi-Mazzoni from the subcutaneous tissue of the finger tip.

lamellae. Each lamella of the outer bulb consists of a single continuous layer of flattened cells, and is supported by fine collagen fibrils of the interlamellar spaces. The interlamellar spaces contain a network of fine fibers, blood vessels, and some free cells in a semifluid substance. Blood vessels accompany the nerve fiber to the capsule, but ramify only in the outer bulb. At birth the Schwann cell and myelin sheaths are lost as the large nerve fiber enters the inner bulb. However, the capsule continues to grow and enlarge, so that in the human adult both the Schwann cell and myelin elements can at times be identified within the inner bulb (14, 15). No fine nerves enter the inner bulb with the large fiber. Cauna and Mannan found that the average length of the corpuscle at birth ranges from 500–700 μm. The size increases gradually throughout life to become 3–4 mm in the adult. In persons over 70 years of age, the corpuscles are less numerous, show regressive changes, and are smaller and more irregular. The entire length of the unmyelinated fiber within the corpuscle is sensitive to deformation, and can initiate "all or none" responses, as shown by Ozeki and Sato (69, 70). These investigators removed the surrounding capsule and found the mechanoreceptor function was still intact. They concluded that the short-lasting receptor potential, obtained from intact corpuscles, must be attributed to properties of the lamellae. In addition to pressure, the Pacinian corpuscle deep in the limbs may be sensitive to vibratory stimuli. The corpuscles are found in subcutaneous tissue, especially of the hand and foot, in the peritoneum, pleura, mesenteries, penis, clitoris,

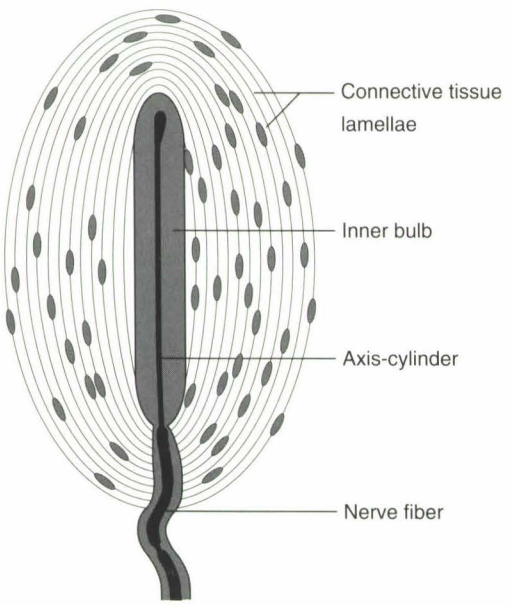


Figure 7.10. Human Pacinian corpuscle.

urethra, nipple, mammary glands, and pancreas, and in the walls of many viscera. They are especially numerous in the periosteum, ligaments, and joint capsules, and they also occur in muscular septa and occasionally in the muscle itself.

CORPUSCLES OF GOLGI-MAZZONI

The lamellated *corpuscles of Golgi-Mazzoni*, found in the subcutaneous tissue of the fingers and on the surface of tendons, are related to the Pacinian corpuscles (Fig. 7.9**B**). They are ovoid bodies with lamellated capsules of varying thickness and a central core of granular protoplasm in which the single myelinated fiber forms a rich arborization with varicosities and terminal expansions.

Stretch Receptors

Among the most highly specialized encapsulated end organs are the stretch receptors, represented by the neuromuscular spindles and neurotendinous organs.

NEUROMUSCULAR SPINDLES

The *neuromuscular spindles* (muscle spindles) are fusiform in shape and widely scattered in the fleshy bellies of skeletal muscles. Each spindle consists of 2 to 10 slender striated muscle fibers, enclosed within a thin connective tissue capsule, and attached at both ends to the epimysium or ordinary striated muscle (Fig. 7.11). These slender muscle fibers are known as *intrafusal fibers* and are small compared with the *extrafusal fibers* that produce contractile tension within a muscle. In nonmammalian species, muscle spindles are innervated by collateral branches of axons which supply extrafusal striated muscle fibers. In mammals, muscle spindles are largely supplied by an independent group of motor axons, called fusimotor or γ-axons. It is now recognized that mammals have a significant number of muscle spindles innervated by collaterals of axons also innervating the extrafusal muscle fibers. These axons, which show the innervation pattern previously associated exclusively with nonmammalian species, are called, beta (β)-axons to distinguish them from exclusively skeletomotor alpha (α)-axons and exclusively fusimotor gamma (γ)-axons (1, 6, 42). Fusimotor axons are of two types—dynamic and static. The dynamic γ-axons increase the sensitivity of the spindle primary endings to changes of muscle length. Static γ-axons reduce spindle afferent sensitivity to changes of muscle length, but increase spindle afferent firing at a constant length.

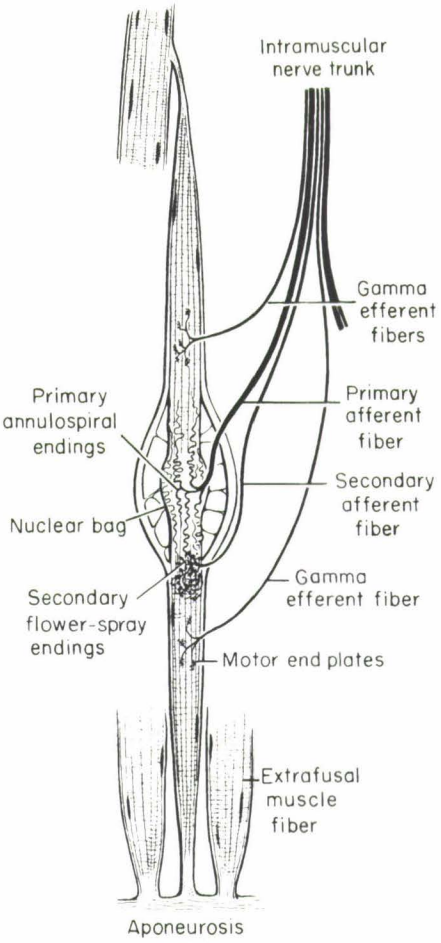


Figure 7.11. Nuclear bag intrafusal muscle fiber within a neuromuscular spindle. The intrinsic sensory and motor nerve endings on the spindle fiber are identified, and the polar and equatorial regions are indicated on the left. Normally there are 2–10 small and large intrafusal fibers within each neuromuscular spindle.

Intrafusal muscle fibers are of two distinct sizes. One is of smaller diameter (10–12 μm), is shorter in length (3–4 mm), and has a single chain of central nuclei. The second, or larger, spindle fibers are about 25 μm in diameter, are 7–8 mm in length, and in the equatorial region are enlarged to accommodate an area of numerous small nuclei ("nuclear bag" of Barker) (3). The small intrafusal fibers are known as "nuclear chain fibers," and the larger ones are designated "nuclear bag fibers" (5, 9, 10). The ends of the nuclear chain fibers are attached to the polar parts of

the longer nuclear bag fibers. There are usually two of the longer fibers and five of the smaller fibers in each spindle, but these numbers are variable. A nuclear bag fiber with its capsule and associated sensory and motor nerve endings is shown in Figures 7.11 and 7.12. Two or more myelinated afferent fibers enter each spindle. A thick primary afferent fiber forms a spiral, branching and reticulated ending within the nuclear bag area (primary, annulospiral, or nuclear bag ending). Silver-stained primary and secondary sensory end-

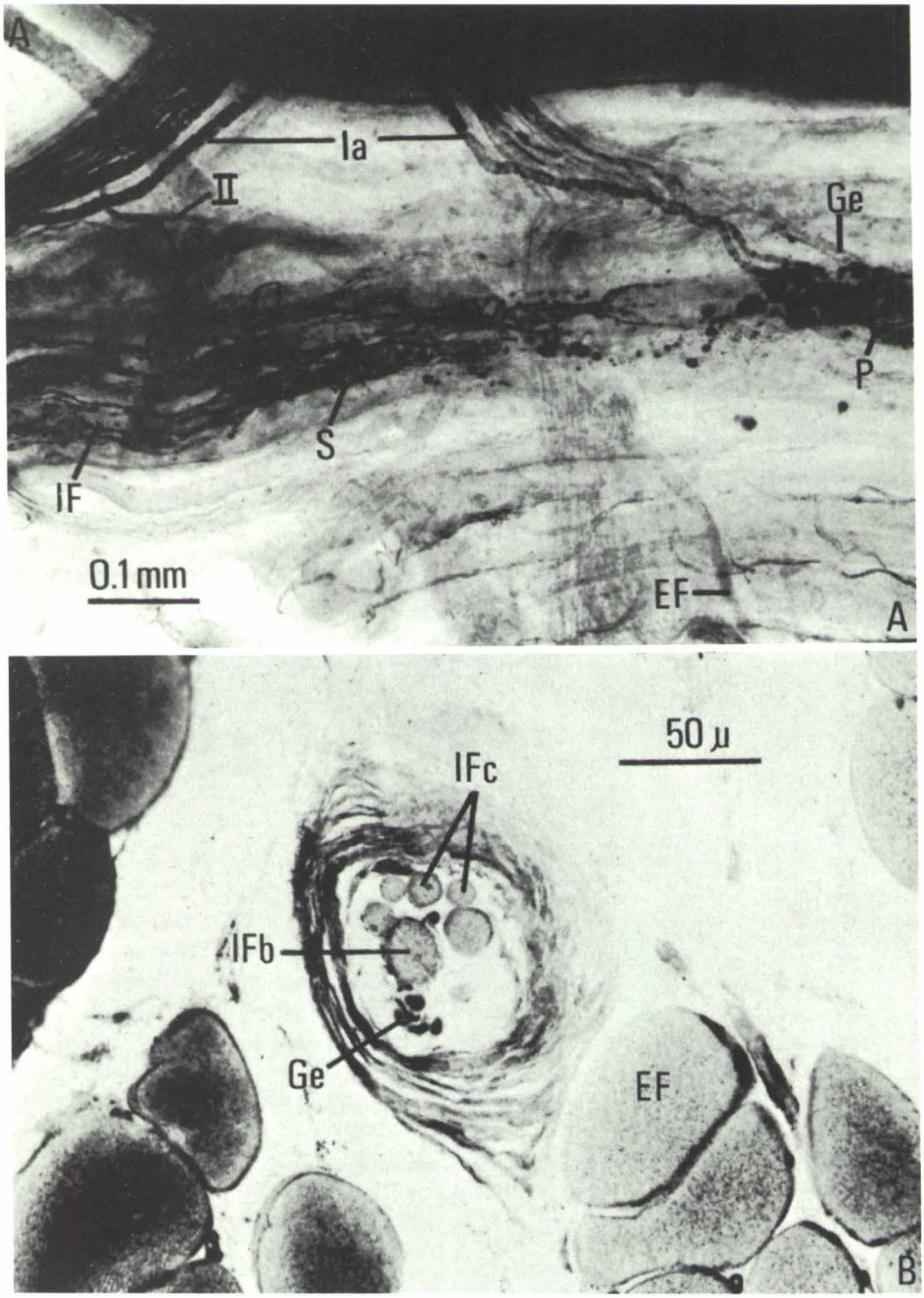


Figure 7.12. Human intercostal neuromuscular spindle. **A.** Longitudinal squashed preparation showing sensory and motor neural elements related to the intrafusal muscle fibers (*IF*). Compare diameters of sensory fibers (*Ia*) related to primary (*P*, annulospiral) ending, sensory fiber (*II*) of secondary (*S*, flower-spray) ending, and γ-efferent (*Ge*) fiber. An adjacent extrafusal muscle fiber (*EF*) and artery (*A*) are identified. **B.** Cross-section of muscle spindle demonstrating its multilayered capsule and the diameters of the nuclear bag (*IFb*) and nuclear chain (*IFc*) intrafusal fibers. γ-Efferent axons (*Ge*) and extrafusal (*EF*) muscle fibers are identified (modified De Castro silver stain).

ings on intrafusal muscle fibers are shown in Figure 7.13. The primary receptor has a low threshold to stretching of the muscle or its tendon, and also discharges a volley of impulses when the intrafusal fiber contracts as a result of stimulation by a γ-efferent motor axon (Figs. 7.11). The neuromuscular spindle is arranged parallel to the extrafusal or contractile fibers of the muscle. Tension on the spindle is relaxed and afferent volleys from the annulospiral endings cease during active muscle contraction (i.e., the spindle is un-

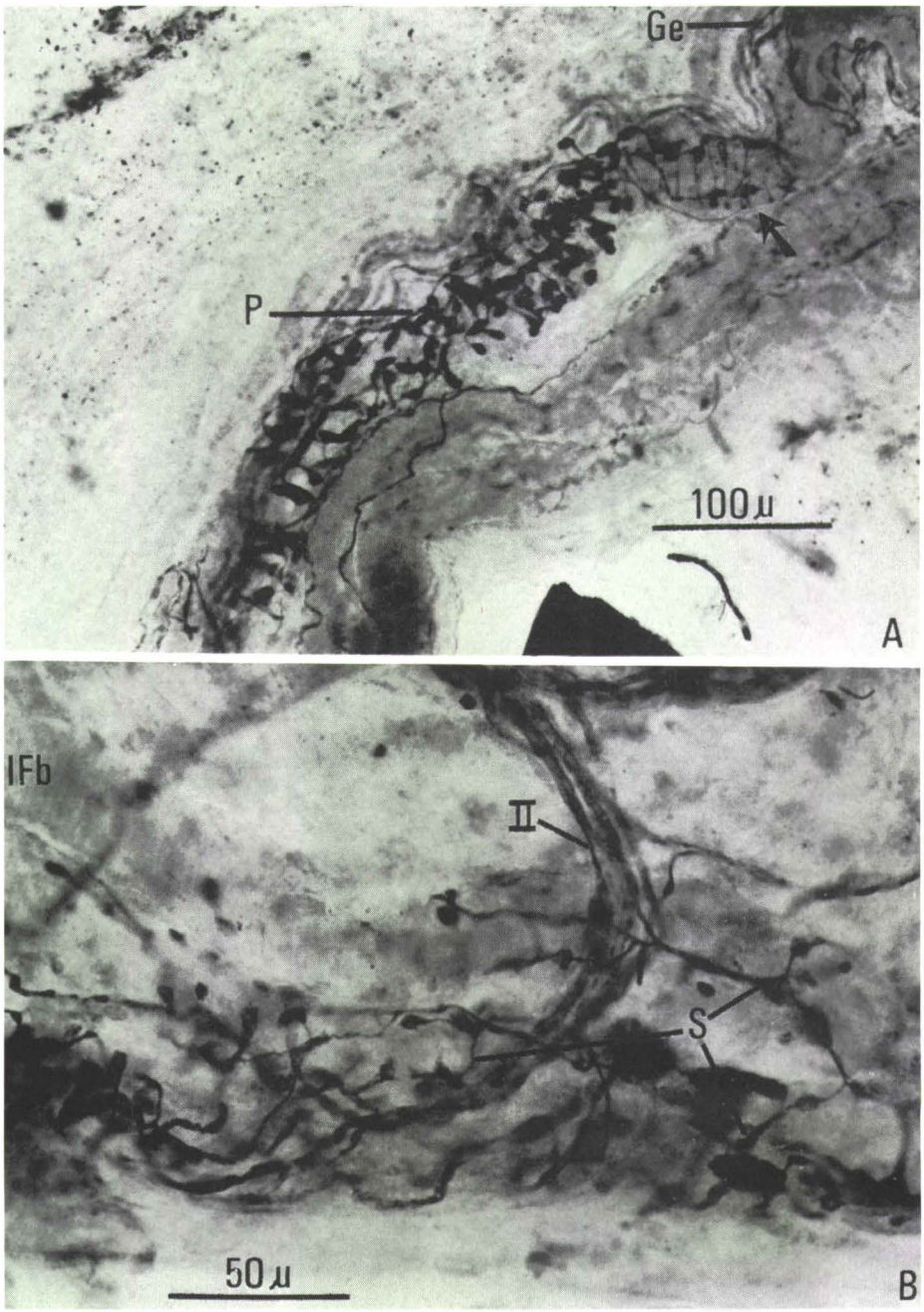


Figure 7.13. Human intercostal neuromuscular spindles with two types of sensory endings. **A.** Primary (*P*, annulospiral) ending on each intrafusal muscle fiber has a thick axon with many side branches and terminal enlargements. The slender coil (*arrow*) is not seen on all primary endings. Adjacent efferent axons (*Ge*) are identified. **B.** secondary (*S*, flower-spray) endings found on both bag and chain intrafusal muscle fibers (*IFb*). Architecture is similar to that of primary ending except for the slender, delicate nature of the branches. The axon related to this secondary ending is identified (*II*) (modified De Castro silver stain).

loaded, and its receptors are silent). The primary afferent fibers (*Ia* in Fig. 7.12**A**) are 8–12 μm in diameter, have fast conduction velocities, and their central processes within the spinal cord participate in the monosynaptic stretch (myotatic) reflex that regulates muscle tone (Figs. 10.29 and 10.30).

The myelinated secondary afferent fibers (Fig. 7.13**B**), with diameters of 6–9 μm also enter the spindle to form small rings, coils, and spraylike varicosities on both sides of the nuclear bag area. These are called secondary, flower-spray, or myotube endings (Figs. 7.11 and 7.13**B**). Secondary endings are the principal sensory terminals associated with nuclear chain fibers (5, 9, 10). Both the primary and secondary endings are terminals of sensory fibers, for they degenerate after section of appropriate dorsal roots.

Small fusimotor fibers (γ-efferents), 3–7 μm in diameter, enter each spindle and terminate. Two kinds of γ-fiber endings upon

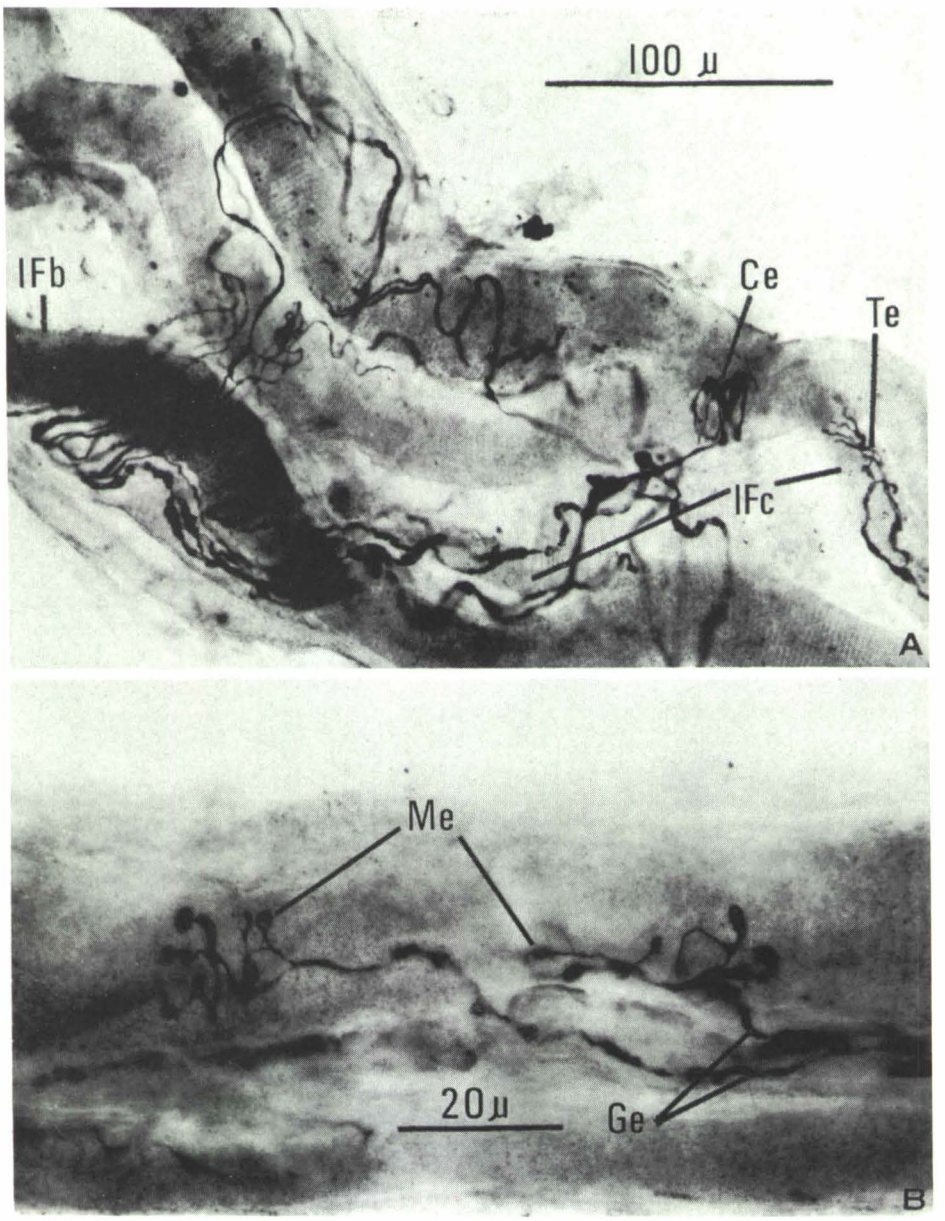


Figure 7.14. Human intercostal neuromuscular spindle. **A.** γ-Efferent axons near sensory area that demonstrate trail (*Te*) and coiled (*Ce*) endings. In other sections, these axons and endings are found on bag (*IFb*) and chain (*IFc*) intrafusal muscle fibers. **B.** γ-Efferent (*Ge*) motor endplates (*Me*) found toward capsular pole of spindle. Pairs of endplates occur frequently. Here two endplates are seen on one bag fiber (modified De Castro silver stain).

the intrafusal muscle fibers have been described. Some end as diffuse, multiterminal "trail fibers," while others terminate in miniature "endplates" (Fig. 7.14). Barker (4) maintains that both nuclear bag and nuclear chain muscle fibers usually receive each type of γ motor endings. Boyd (9) pretends that nuclear bag intrafusal fibers usually receive "plate endings," and nuclear chain muscle fibers usually receive "trail endings."

The contraction of intrafusal muscle fibers by γ-efferent nerves induces discharges in the afferent nerves from the spindle. The fusimotor fibers thus reset the spindle mechanism, thereby regulating the sensitivity of the receptor. Contraction of the spindle fibers contributes nothing *per se* to the contractile tension of the muscle (72). Additionally, the neuromuscular spindles receive a variable number of fine unmyelinated fibers which appear to be vasomotor to the small vessels within the spindle. Other fine nerve fibers ramify in the capsule and probably mediate pain impulses.

The recorded dimensions of human muscle spindles vary enormously, the extremes for length being 0.05 and 13 mm. The usual length is 2–4 mm. Spindles have been found in practically all muscles but they are most numerous in the muscles of the extremities. They are especially abundant in the small muscles of the hand and foot. Fewer muscle spindles are present in the extraocular muscles (20, 21, 34, 56). Cells in part of the trigeminal ganglion convey afferent impulses from muscle spindles in the extraocular muscles (49).

Information conveyed centrally from the neuromuscular spindles play a major role in the reflex regulation of muscle tonus. Ascending impulses from these receptors are conveyed via nuclei in the spinal cord and medulla mainly to the cerebellum, and are secondarily concerned with conscious sensory experience. Responses of primary and secondary endings to mechanical stimuli differ in that the primary ending is more sensitive to the dynamic component of the stimulus. Thus, primary endings measure both velocity of stretching and length, while secondary endings measure mainly length. Collaterals from these sensory fibers have monosynaptic junctions with α-motor neurons (Figs. 10.23 and 10.30). More than one internuncial neuron is interposed between these collaterals and the γ-efferent neurons as shown in Figure 10.23. If the primary fiber (Ia) from the annulospiral ending is stimulated, there is a central delay of 2 msec before the efferent fiber response is recorded. Hence, the annulospiral collaterals use central internuncial neurons to influence γ-efferent neurons, and such connections are polysynaptic (52).

NEUROTENDINOUS ORGANS

Neurotendinous organs (Golgi tendon organs) are encapsulated spindle-shaped receptors found at the junction of muscle and tendon, and occasionally in muscular septa and sheaths. They have been demonstrated in practically all muscles. The capsule of the Golgi tendon organs is approximately 8–10 times longer than it is wide, and consists of several concentric lamellae that form cytoplasmic sheets closely applied to each other (57). Cells of one lamella extensively overlap adjacent cells in the same concentric lamella. The outer lamina appears as typical squamous epithelium without fenestrations, and the extensive overlap of neighboring cell processes suggests that intracapsular fluids are not easily exchanged with extracapsular fluids. The cells which form the capsule of the neurotendinous organs resemble those of the perineural epithelial sheath surrounding nerve trunks, and the capsule is regarded as a direct continuation of the perineural sheath.

The capsule of the Golgi tendon organ exhibits four morphologically distinct levels (84). At the proximal opening, several loosely organized cellular lamellae surround entering muscle fibers. At a slight distance below the capsule opening is the proximal collar, where collagen bundles of the muscle fibers are tightly enveloped by capsule cells so as to provide an effective seal between intracapsular and extracapsular fluids (Fig. 7.15). Distally there also is a capsular collar from which collagen bundles leave their capsular investments in a staggered fashion to join the central tendon. The receptor body, occupying nearly 80% of the length of the Golgi tendon organ, lies between the proximal and distal collars. The capsule wall of the receptor body is uninterrupted except for an opening near the midpoint through which the primary afferent fiber (Ib) enters the lumen of the capsule. The lumen of the receptor body is divided by thin cytoplasmic processes into longitudinally oriented compartments which in cross section have a honeycombed appearance. Cells and their processes which parti-

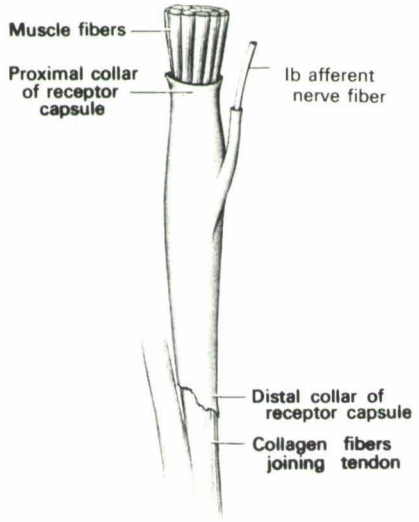


Figure 7.15. Golgi tendon organ. Muscle fibers converge as they enter the proximal opening of receptor capsule, below which is a slight constriction known as the proximal collar. Ib afferent fiber emerges from the central region of the receptor capsule in a connective tissue sleeve. Near the distal collar of the capsule collagen bundles emerge, and at staggered levels join the fibrils of the central tendon.

tion the lumen are termed septal cells. These cells resemble fibroblasts and probably originate from lamellae of the capsule wall. In the greater part of the receptor body, compartments contain a mixed assortment of collagen fibrils from muscle fibers (Fig. 7.16). A large number of collagen fibers appear to terminate within the capsule lumen in an undetermined manner.

The primary afferent fiber (Ib) enters the capsule lumen in the equatorial region of the receptor body and divides into major ascending and descending branches. Unmyelinated collaterals from the major branches project radially through openings between septal cells to penetrate peripherally located compartments containing longitudinal collagen bundles derived from muscle fibers. Preterminal nerve fibers branch extensively and spiral around discrete collagen bundles. Attempted serial reconstructions of the Golgi tendon organ indicate that collagen bundles spiral about one another like the strands of a rope and often split to entrap smaller nerve fibers and terminals (Fig. 7.16). Evidence suggests that the mechanical component of the transducer process must involve physical distortion of the axonal membranes during an increase in tensile forces along the collagen strands. It has been suggested that contraction, or passive muscle stretch, will tighten the braided strands of collagen in the neurotendinous organ, reduce the size of the septal spaces, and pinch nerves laced between them (84).

The afferent nerve fibers from tendon organ receptors are large fibers of about 12 μm diameter. The neurotendinous organs are relatively insensitive to passive stretch because they lie in series with the contractile muscle that absorbs most of the stretch and prevents elongation of the tendon. Muscle contraction causes the tendon organs to discharge proportional to the tension developed. Contractions which shorten the muscle without developing much tension produce only weak excitation of the tendon organ. If the contraction shortens the muscle, lengthens the tendon, and develops tension, the tendon organs fire vigorously (Fig. 10.29) (37). If the stimulus is appropriate, the tendon organ is an extremely sensitive receptor. Contractions produced by stimulation of an isolated motor unit can easily cause individual tendon organs lying in series with it to discharge (39).

Afferent nerve fibers from the muscle spindle (primary) and the Golgi tendon organs are large and conduct impulses centrally at rapid rates. To distinguish between these two subgroups, the annulospiral afferent nerves are designated as Ia, while the tendon organ afferents are referred to as Ib nerve fibers. While stretch receptors in muscle furnish some information which enters the conscious sphere signaling the position of a limb or joint, these receptors function mainly in the automatic control of muscle tone.

Besides the neuromuscular and neurotendinous organs, muscle and tendon have a variety of other sensory structures—free nerve endings, end bulbs, and Pacinian corpuscles. The latter are especially numerous in tendons.

SENSORY RECEPTORS AND SENSORY MODALITIES

Overall View

It is generally maintained, although not proven, that each type of receptor is activated by only one kind of physical or chemical change and is associated with only one kind of sensory modality. The problem of relating the various receptors to specific sensory modalities has been exceedingly difficult and many important details remain unknown

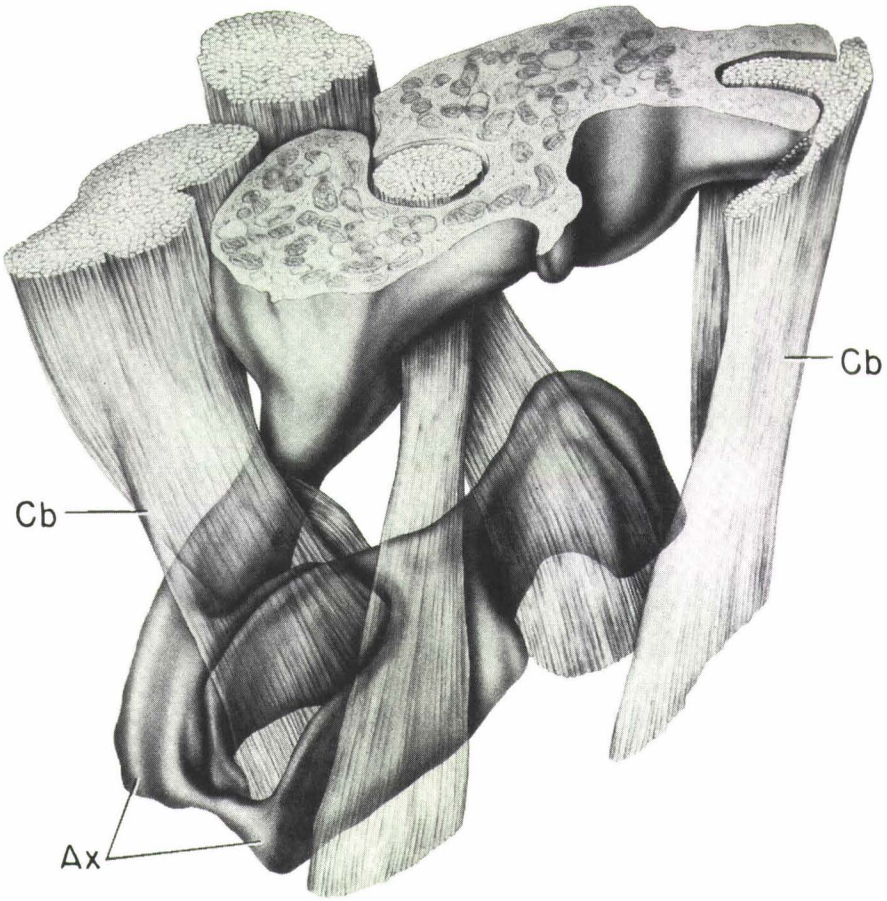


Figure 7.16. Three-dimensional reconstruction of relationships between axonal branches (*Ax*) and longitudinally oriented collagen bundles (*Cb*) in a septal cell compartment of a Golgi tendon organ. The spiraling axon threads its way through the collagen bundles. Most collagen bundles do not run a straight parallel course through the lumen of the Golgi tendon organ, but twist like the strands of a braided rope. Increasing tensile forces on the collagen strands cause them to straighten and twist which results in pinching of the axonal branches trapped between them.

(87). It seems probable that painful stimuli are received by the diffuse, cutaneous end arborizations. Not only would their universal presence and unspecialized terminals indicate this, but also their sole presence in places where stimuli give rise only to pain (e.g., the tympanic membrane of the ear and the pulp of the teeth). Touch is represented by the endings in hair follicles, Meissner's corpuscles, and probably by tactile discs and some other intraepithelial endings. The peritrichal endings, stimulated by movements of the hair, give rise to a delicate and discriminative sensibility with a marked affective tone. Shaving greatly reduces sensibility to touch. On the hairless part of the body, tactile stimuli are received primarily by the corpuscles of Meissner, which are probably the chief sense organs of discriminative touch. The receptors for temperature are not well-known, but they are probably end bulbs of various kinds. Possibly, some are diffuse endings. It is known that the margin of the cornea is sensitive only to cold and pain, and is provided only with diffuse endings and end bulbs of Krause. Hence the latter and similar subcutaneous end bulbs are believed to be receptors for cold. In the same way, the diffuse unencapsulated nerve endings are believed to be related to warmth.

The different parts of the body surface vary considerably as to their capacity for affective and discriminative sensibility. The skin of the hand and fingers is particularly sensitive, and provides a variety of exteroceptive impulses that are integrated in the cerebral cortex. In other regions, such as the back, abdomen, and especially the genitalia, affective sensibility predominates, to the partial exclusion of discriminative aspects of sensation.

The Pacinian corpuscles, found in both deep subcutaneous and visceral structures, appear physiologically to be pressure transducers, but there is no evidence that they subserve steady pressure, or that pressure sensitivity is particularly acute in regions where Pacinian corpuscles are found. The rapidly adapting nature of the Pacinian corpuscle suggests that it may be particularly sensitive to vibration. This receptor may play a role in the threshold detection of tactile stimuli, despite its deep position, because it has a lower threshold for short mechanical stimuli than more superficial intracutaneous receptors (44).

The proprioceptive senses of position and movement are initiated by the constant or varying tension states of the skeletal muscles, and their tendons, and by the movements of the joints. The changes in tension and pressure are received by the Pacinian and unencapsulated corpuscles found in the joint capsules, ligaments, and periosteum (Fig. 7.7). Such afferent inputs are transmitted to cortical levels where they are utilized in the formulation of kinesthetic sense (conscious proprioception or kinesthesis). Proprioceptive impulses from neuromuscular spindles are used for regulation of the spinal myotatic reflex, or project via cerebellar pathways to regulate muscle tonus and synergy (i.e., such sensory inputs are for subcortical reflex control of skeletal muscle). The subcortical regulation of muscle tone and posture provides a background of muscle tone upon which discrete cortical (voluntary) activity, such as locomotion and fine finger movements, is based.

There is much that is still obscure about visceral sensibility. It is known that the viscera are insensitive to many mechanical and chemical stimuli, yet they may be the source of intense pain, as well as contribute to the sensations of hunger, thirst, etc. Visceral pain is due mainly to either distension or spasm of the muscle coats. Diffuse intramuscular nerve endings appear to be the receptors for these stimuli (Fig. 7.4). The blood vessels also may give rise to painful sensation, which is likewise due to spasms in their muscular walls and to the resulting stimulation of similar diffuse endings. The totality of stimuli, constantly received by these diffuse visceral receptors during normal and abnormal function, probably gives rise to the general affective sensibility of internal well-being or of malaise.

Referred Pain

One peculiarity of visceral pain is that painful visceral stimuli are often "felt" in the corresponding somatic segment, or segments, of the body wall, a phenomenon known as "referred pain." Centrally, the receptive nuclei for somatic and visceral pain impulses are associated closely within the dorsal gray column of the spinal cord. Referred pain is most likely due to central mechanisms within the spinal cord, although the precise neurons involved have not been ascertained. A common explanation is that the constant bombardment of pain impulses, from a diseased viscus, lowers the threshold of stimulation of adjacent central (somatic) relay neurons. Normally these relay neurons are concerned with somatic sensations and not with transmission of visceral pain. As a result, normal incoming somatic sensory impulses that terminate in this "sensitized" neuron pool are relayed to higher centers, where they are misinterpreted as painful stimuli coming from body surfaces.

Sinclair and collaborators have suggested that the production of referred pain may be due to the branching of the sensory fibers which conduct pain impulses (88). One limb of a branched axon goes to the visceral site where the disturbance originates, while others go to the peripheral area to which the pain is referred.

Pain referred to the skin from a viscus tends to be "felt" in a relatively small circumscribed area, usually, but not always, within the dermatome of the same spinal segment that supplies the viscus. This pain rarely occupies the whole, or even the major part, of the corresponding dermatome. In the reference zone, there may be changes in the quality of sensation in response to stimuli and alterations of threshold (87). Pain is the only sensory modality commonly referred to in this manner. Thus, referred pain has a dermatomal distribution corresponding to the spinal nerves. Some classical examples of a diseased viscus that causes pain to be referred to the overlying body wall and corresponding dermatomes are: diaphragm referred to dermatome C4; heart referred to dermatomes C8–T8; bladder referred to dermatomes T1–T10; stomach referred to dermatomes T6–T9; intestine referred to dermatomes T7–T10; testes, prostate, and uterus referred to dermatomes T10–T12; kidneys referred to dermatomes T11–L1; and rectum re-

ferred to dermatomes S2–S4 (Figs. 8.1, 8.11, and 8.12).

EFFECTORS

The endings of the peripheral fibers in the effector organs of the body fall into two groups: somatic efferent and visceral efferent. The somatic efferent terminations represent the motor terminals of myelinated axons whose cell bodies are located in the anterior gray horn of the spinal cord. These fibers go directly to the skeletal muscles. The visceral endings are terminals of unmyelinated fibers which arise from cells of the various autonomic ganglia. These fibers supply the heart (cardiomotor), visceral muscle (visceromotor), blood vessels (vasomotor), hair (pilomotor), salivary and digestive glands (secretory), and sweat glands (sudomotor).

During development, cholinergic axons form a specialized synapse, the myoneural or neuromuscular junction, with skeletal muscle fibers which already contain acetylcholine receptors distributed over the whole of the muscle membrane. As the neuromuscular junction is formed, acetylcholine receptors cluster in the muscle membrane at the site of axon contact and gradually disappear from the extrajunctional membrane (7). In the case of sympathetic motor neurons, differentiation to become either cholinergic or noradrenergic is made relatively late in development and depends both on the local environment of the neurons and their activity (71).

Somatic Effectors

The somatic efferent fibers terminate upon the skeletal muscle fibers in small, flattened, oval expansions, the *motor endplates*, or neuromuscular junction (Figs. 5.3**G** and 7.14). Motor endplates are located in narrow zones in a given muscle. Each endplate always lies in the midportion of the fiber it supplies. Larger muscle fibers have larger endplates, and in the rabbit and monkey the diameters of endplates differ in "red" and "white" muscle fibers (18). For example, in red extrafusal fibers the endplates are significantly larger. These muscle fibers are known to be slow reacting and capable of sustained contraction. According to Coers (17), the mean diameter of adult human limb motor endplates is 32.2 μm. In humans, most of the endplates have a length of 40–60 μm. The myelinated fibers, in their course to the muscle, repeatedly divide, and branch even more extensively as they spread out within the fleshy belly of the muscle. In this manner, a single motor nerve fiber provides endplates to a variable number of the large extrafusal muscle fibers (Fig. 5.3**G**). Each terminal nerve branch loses its myelin sheath as it approaches the sarcolemma of a muscle fiber, while the Schwann cell sheath continues to invest even the smallest terminals. Electron microscopy has confirmed and elucidated many of the structural features of the motor endplate (22, 76–79, 97). The axoplasm of the small nerve branches contains numerous mitochondria, vesicles, round and oval profiles, small granular elements, and tubular-appearing components of the endoplasmic reticulum. Such nerve terminals do not lie within the sarcoplasm of the muscle fiber, as believed previously, but occupy troughs which are hollowed out by infoldings of the sarcolemma (Fig. 7.17). The floor of the trough is usually corrugated by numerous secondary invaginations of the sarcoplasm (junctional folds). The entire depressed area is called a "synaptic gutter." Within the gutter, the axon membrane and sarcolemma remain as discrete structures separated by a gap, or synaptic cleft. The whole ending is covered over by Schwann cell cytoplasm. The membranes of the Schwann cell, axon, and sarcolemma are all separated from each other by a thin layer of moderately electron dense material (basal lamina) which also extends out into the extracellular space around the entire ending.

The synaptic vesicles within the axon terminals of the endplate are presumed to represent the storage sites of acetylcholine (Fig. 7.17). With the arrival of a nerve impulse, numerous quanta of acetylcholine are released through the presynaptic membrane into the synaptic gutter. The liberated acetylcholine binds to postsynaptic receptor sites, and alters the permeability of the postsynaptic (sarcolemmal) membrane of the muscle fiber. Acetylcholine receptors and acetylcholinesterase were localized to the sarcolemma at the apical portions of the junctional folds (29) (Fig. 7.17). Depolarization and a muscle action potential result from this series of events.

When a foreign motor nerve is implanted into an adult rat soleus muscle and the nerve normally providing innervation severed, changes in four molecular components of the newly formed neuromuscular junctions can be followed. Within 2 days, acetylcholine re-

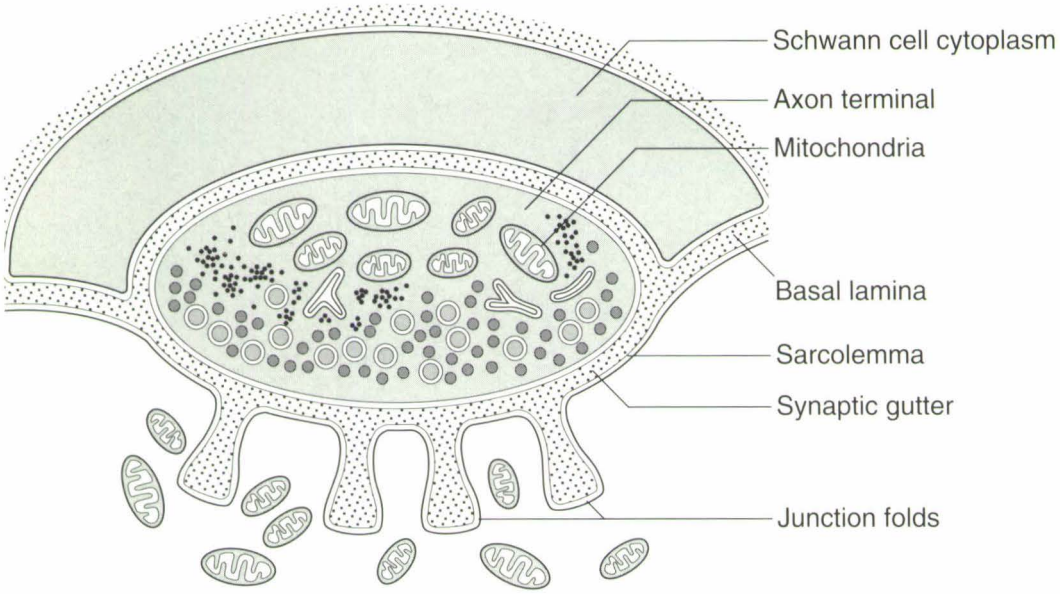


Figure 7.17. Motor ending on a skeletal muscle fiber as seen in transverse section by electron microscopy. The mitochondria are presumed to play an active role in the synthesis of acetylcholine, whereas the numerous smaller vesicles shown here represent a stored state of acetylcholine. Small clusters of dark granules are also found in the axon terminal. Note the separation of axon, Schwann cell, and muscle membranes by the basal lamina.

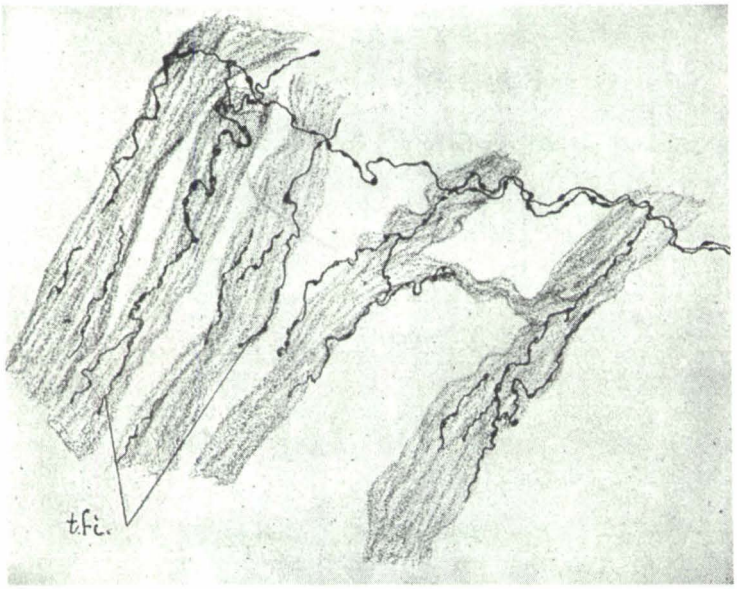


Figure 7.18. Motor nerve terminations in the smooth muscle bands of a bronchus (rabbit); *tfi*, terminal fibrils.

ceptors appear in clusters in the new endplate region. The clusters continue to grow in size and receptor number over the next 30 days. About 2 weeks following reinnervation, an endplate-specific form of the enzyme acetylcholinesterase is present. Specific antigens of the synaptic basal lamina appear slightly earlier and accumulate with a time course paralleling that for acetylcholinesterase. The maturation of the synaptic basal lamina appears to occur only after acetylcholine receptors form clusters (95). A large number of microscopic histochemical techniques have been used to localize the enzymes of the motor endplate in

humans and numerous animals. These have been reviewed extensively by McLennan (53) and Zacks (97), and more recently by Cooper, et al. (19), and by Kandel and Siegelbaum (40). If an inadequate amount of acetylcholine is produced (or if it is destroyed too rapidly by acetylcholinesterase), muscle contraction is altered and the involved muscles are prone to early fatigue (Fig. 7.19). If the enzyme acetylcholinesterase is inactivated by anticholinesterase drugs (e.g., by neostigmine), the endogenous acetylcholine is preserved at the endplate for longer periods.

The excitation of a striated muscle fiber by a motor neuron can be blocked in several ways by naturally occurring toxins. These toxins are useful tools for analyzing mechanisms of nerve conduction and transmitter release (Fig. 7.19). Tetrodotoxin blocks Na^+ channels in the axon membrane, thereby preventing the generation of action potentials. Botulinum toxin blocks the release of acetylcholine from synaptic vesicles. α-Bungarotoxin, derived from the venom of a snake, binds irreversibly to the acetylcholine receptor, blocking access of the transmitter. These three toxins block neuromuscular transmission through different mechanisms.

The number of muscle fibers innervated by a single motor neuron varies greatly depending on the function of the particular muscles. In muscles that control fine movements, such as those of the ocular muscles and the small muscles of the hand, motor units comprise only 3 to 6 muscle fibers. In contrast, there are about 2000 muscle fibers in each motor unit of the gastrocnemius, the muscle that flexes the foot in the movement of walking (82). Namba and collaborators have described two kinds of motor endings in the extraocular muscles of humans. The superior rectus muscles had both *en plaque* and *en grappe* endings. The levator palpebrae had only *en plaque* terminals with a mean diameter of 27 μm. As many as 12 *en grappe* endings were found on superior rectus fibers 10–20 μm thick. *En grappe* endings had a mean diameter of only 9.6 μm (67).

In 1925, Edward Liddell and Charles Sherrington introduced the term *motor unit* to designate the basic unit of motor function, that is a motor neuron and the group of muscle fibers it innervates. The motor unit comprises four functional components: (a) the cell body of the motor neurons located in the ventral horn of the spinal cord, (b) the axon of the motor neuron that emerges from the ventral spinal root and runs in the peripheral nerve, (c) the neuromuscular junction, and (d) the muscle fibers innervated by that motor neuron (82). A muscle with many motor units for a given number of muscle fibers is capable of more precise movements than a muscle with a few motor units for the same number of muscle fibers. It also follows that only a few motor units are required to maintain reflex muscle tone during periods of rest or sleep. However, many or all motor units may be called into operation when demands are made upon the muscle for maximal contraction.

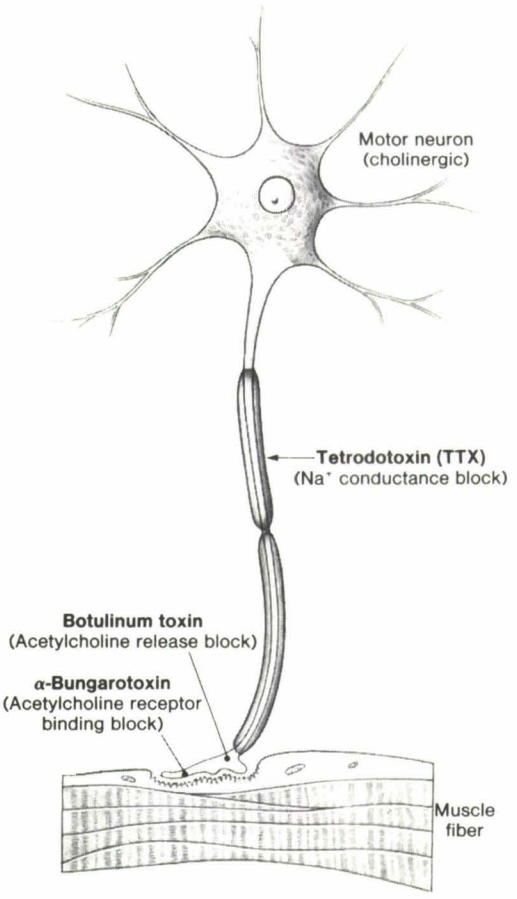


Figure 7.19. Examples of sites of action of some animal and bacterial neurotoxins. Tetrodotoxin (*TTX*), obtained from the ovaries of the puffer fish, prevents the influx of Na^+ ions, thereby blocking the propagation of the action potential along the axon. Botulinum toxin, of bacterial origin, blocks the release of acetylcholine from the synaptic terminal. The venom of the Formosan krait, α-bungarotoxin, binds almost irreversibly to acetylcholine receptors at the muscle end-plate, thereby preventing acetylcholine (*ACh*) from initiating an action potential in the muscle fiber.

Myasthenia Gravis

Most diseases of the motor unit cause weakness and wasting of skeletal muscles. The distinguishing features of these diseases depend upon which of the four components of the motor unit is primarily affected. Pathologic changes affecting markedly central nerve cell bodies or peripheral nerves and only slightly muscle fibers, are characteristics of neurogenic diseases, or neuropathies (e.g., *central motor neuron diseases* or *peripheral neuropathies*). In contrast, advanced degeneration of muscle fibers with little change in motor neurons or their axons are characteristics of myopathic diseases, or myopathies (e.g., muscular dystrophies). Myasthenia gravis (severe muscle weakness), which was first described by the famous English anatomist Thomas Willis in 1672, involves mainly cranial muscles (eyelids, eye muscles, and oropharyngeal muscles) as well as limb muscles (2). It is a very peculiar myopathy since, unlike any other diseases of muscle or nerve, the severity of weakness varies markedly in time and there are no clinical signs similar to those that characterize disorders of the motor unit, such as loss of tendon reflex or atrophy of muscle. This disease is particularly interesting in that it affects specifically the transmission of information between the two major components of the motor unit, the nerve and muscle. More specifically, it is an autoimmune disorder which alters the cholinergic transmission at the neuromuscular junction. Detailed physiologic and immunologic studies of this human disease helped understanding of the basic mechanisms involved in the synaptic transmission.

The first evidence that myasthenia is a disorder of the neuromuscular transmission came from the demonstration that acetylcholinesterase inhibitors, such as physostigmine and neostigmine, which amplify the action of acetylcholine at the neuromuscular junction, reverse the symptoms of myasthenia gravis. Indications that it may be an autoimmune disease came from observations that about 15% of adult patients with myasthenia had a benign tumor of the thymus and removal of such thymosas results in a reduction of the symptoms. However, the major breakthrough came after the identification of antibodies to the nicotinic acetylcholine receptors of the neuromuscular junction (27, 82). The cholinergic receptors at the neuromuscular junction were isolated and purified with the help of the highly specific cholinergic receptor ligand α-bungarotoxin. The injection of purified cholinergic receptor into rabbits to produce specific antibodies was accompanied by the onset of myasthenia-like symptoms in the injected animals, and these symptoms could be alleviated by the use of acetylcholinesterase inhibitors. These findings led to the production of useful animal models of this human disease, which greatly helped unravel the molecular basis of the autoimmune reaction involved in myasthenia.

The autoimmune reaction depends on 3 molecules: (a) the antigen, the immunogenic peptide of the cholinergic receptor, or a peptide that mimics the receptor, (b) an antigen-specific T (thymus) cell receptor, and (c) class II molecules of the major histocompatibility complex (MHC) expressed on the antigen presenting cells. In myasthenia, the T cells become reactive against cholinergic receptor for a reason that is still not known. One possibility is an infection in which a viral protein includes a peptide homologous to one in the cholinergic receptor, a form of molecular mimicry (82). For whatever reason, antibodies directed against nicotinic acetylcholine receptors occur in the serum of patients with myasthenia and can serve as a reliable marker for the disease.

The symptoms of myasthenia can be alleviated to a certain extent with anticholinesterase drug therapy or thymectomy. However, the recent discovery of the immunologic basis of this disease leads to even more promising approaches. For example, the use of either antibodies against the anticholinergic receptor antibodies (anti-idiotype antibodies) or peptide competitors for cholinergic receptors that might block T-cell reaction, are therapeutic tools that are currently being tested in animal models of myasthenia (82).

The history of the work on myasthenia gravis is particularly instructive, as it shows the crucial role that interactions between clinical and basic research play in the understanding of human disorders. It must be realized that the therapeutic effect of thymectomy was discovered by clinicians long before the immunologic role of thymus was known. In turn, basic scientists have deciphered the major immunologic and molecular mechanisms involved in the pathogenesis of myasthenia gravis, providing new therapeutic approaches for the treatment of this disease.

Visceral Effectors

The unmyelinated autonomic fibers which supply visceral muscle either end in simple arborizations, or first form extensive intramuscular plexuses from which the terminals arise. The terminal fibrils wind between the smooth muscle cells and end in small neurofibrillary thickenings, or delicate loops on the surface of the muscle fibers (Fig. 7.18). Similar terminals arise from delicate plexuses which surround the tubules or acini of glands, pass between the cells and terminate upon the plasma membrane of the glandular cells. Terminal endings occupy small troughs in the plasma membranes of both cardiac and smooth muscle fibers, sometimes for long distances. However, no endplates, or specialized endings, have been observed on visceral muscle by either light or electron microscopy. Groups of tiny axons surrounded by Schwann cell cytoplasm do come into intimate contact with single smooth muscle cells of the small intestine (multiaxonal junctions). In the large intestine, single axons diverge from nerve bundles and come to lie, free of the Schwann sheath, in shallow grooves in the muscle cell. It is likely that one muscle cell has several widely separated single axon contacts (80). Axon terminals have either a predominance of granular or agranular vesicles and numerous mitochondria.

A plethora of fine nerve fibers and plexuses have been demonstrated about blood vessels and in a variety of tissues by the paraformaldehyde-induced fluorescence technique developed by Hillarp, Falck, and collaborators for the visualization of monoamines (28). This technique, as well as the more recent immunocytochemical procedures (see Chapter 5), reveals an exquisite array of adrenergic nerve fibers and their terminals and has been used to study the course and relations of adrenergic nerve fibers to the smooth muscle within several organs. The meticulous studies of Thaemert (90, 91) are equally informative. He has made three-dimensional montages from serial section electron micrographs to demonstrate the intricate nerve muscle fiber relationships in both smooth and cardiac muscle. The gut contains a population of intrinsic neurons termed the "enteric nervous system." Some of these cells are serotoninergic interneurons which probably act upon other cholinergic and purinergic intrinsic neurons that control smooth muscle (31).

References

1. Adal MN, Barker D. Intramuscular branching of fusimotor fibres. J Physiol (Lond) 1965;177:288–299.
2. Adams RD, Bradley WG. Myasthenia gravis and episodic muscular weakness. In: Isselbacher KJ, Adams RD, Braunwald E, Petersdorf RG, Wilson JD, eds. Harrison's principles of internal medicine. 9th ed. Section 14: Disease of striated muscle. New York: McGraw-Hill, 1980: 2064–2068.
3. Barker D. The innervation of the muscle-spindle. QJ Microscop Sci 1948;89:143–186.
4. Barker D. The innervation of mammalian skeletal muscle. In: de Reuck AVS, Knight J, eds. Myotatic, kinesthetic and vestibular mechanisms. Boston: Little, Brown and Company, 1967:3–15.
5. Barker D, Cope M. The innervation of individual intrafusal muscle fibres. In: Barker D, ed. Symposium on muscle receptors. Hong Kong: Hong Kong University Press, 1962:263–269.
6. Bessou P, Emonet-Denand F, LaPorte Y. Occurrence of intrafusal muscle fibre innervation by branches of slow A motor fibres in the cat. Nature 1963;198:594–595.
7. Bevan S, Steinbach JH. The distribution of α-bungarotoxin binding sites on mammalian skeletal muscle developing in vivo. J Physiol (Lond) 1977;267:195–213.
8. Blix M. Experimentelle Beiträge zur Lösung der Frage über die specifische Energie der Hautnerven. Z Biol (München) 1884;20:141–156.
9. Boyd IA. The nuclear-bag fibre and nuclear-chain fibre systems in the muscle spindles of the cat. In: Barker D, ed. Symposium on muscle receptors. Hong Kong: Hong Kong University Press, 1962a:185–190.
10. Boyd IA. The structure and innervation of the nuclear-bag fibre system and the nuclear-chain fibre system in mammalian muscle spindles. Phil Trans R Soc Lond (Biol) 1962b; 245:81–136.
11. Carpenter FW. Nerve endings of sensory type in the muscular coat of the stomach and small intestine. J Comp Neurol 1918;29:553–560.
12. Cauna N. The effects of aging on the receptor organs of the human dermis. In: Montagna W, ed. Advances in biology of skin. Vol. 6. Aging. New York: Pergamon Press, 1965: 63–69.
13. Cauna N. Fine structure of the receptor organ and its probable functional significance. In: DeReuck AVS, Knight J, eds. Touch, heat and pain. Ciba Foundation Symposium. Boston: Little, Brown and Company, 1966:117–127.
14. Cauna N, Mannan G. The structure of human digital Pacinian corpuscles (Corpuscula lamellosa) and its functional significance. J Anat 1958; 92:1–20.
15. Cauna N, Mannan G. Development and postnatal changes of digital Pacinian corpuscles (Corpuscula lamellosa) in the human hand. J Anat 1959;93:271–286.
16. Cauna N, Mannan G. Organization and development of the preterminal nerve pattern in the palmar digital tissues of man. J Comp Neurol 1961;117:309–328.
17. Coers C. Les variations structurelles normales et pathologiques de la jonction neuromusculaire. Acta Neurol (Belg) 1955;55:741–866.
18. Coers C, Woolf AL. The innervation of muscle: a biopsy study. Oxford: Blackwell Scientific Publications, 1959.
19. Cooper JR, Bloom RE, Roth RH. The biochemical basis of neuropharmacology. 6th ed. New York: Oxford University Press, 1991.
20. Cooper S, Daniel PM. Muscle spindles in human extrinsic eye muscles. Brain 1949;72:1–24.
21. Cooper S, Daniel PM, Whitteridge D. Muscle spindles and other sensory endings in the extrinsic eye muscles: the physiology and anatomy of these receptors and their connections with the brainstem. Brain 1955;78:564–583.
22. Couteaux R. Morphological and cytochemical observations on the

postsynaptic membrane at motor endplates and ganglionic synapses. Exp Cell Res 1958;5:294–322.
23. Darian-Smith I. Touch in primates. Annu Rev Psychol 1982;33:155–194.
24. Davis H. Some principles of sensory receptor action. Physiol Rev 1961; 41:391–416.
25. De Castro F. Contribution à la connaissance de l'innervation du pancréas. Y a t-il des conducteurs spécifiques pour les ilots de Langerhans, pour les acini glandulaires et pour les vaisseaux. Trav Lab Rech Biol Univ Madrid 1923; 21:423–457.
26. Dogiel AS. Die Nervenendkörperchen (Endkolben. W. Krause) in der Cornea und Conjunctiva Bulbi des Menschen. Arch Mikrosk Anat Entwickl-Gesch 1891;37:602–619.
27. Drachman DB, ed. Myasthenia gravis. Biology and treatment. Ann NY Sci 1987;505:1–914.
28. Falck B, Hillarp NA, Thieme G, Torp A. Fluorescence of catecholamines and related compounds condensed with formaldehyde. J Histochem Cytochem 1962;10:348–354.
29. Fertuck HC, Salpeter MM. Quantitation of junctional and extrajunctional acetylcholine receptors by electron microscope autoradiography after ^{125}I γ-bungarotoxin binding at mouse neuromuscular junctions. J Cell Biol 1976;69:144–158.
30. Gardner E. The distribution and termination of nerve fibers in the knee joint of the cat. J Comp Neurol 1944;80:11–32.
31. Gershon MD, Dreyfus CF. Serotonergic neurons in the mammalian gut. In: Brooks FP, Evers PW, eds. Nerves and the gut. Thorofare, NJ: Charles B. Slack, 1977:197–206.
32. Granit R. Receptors and sensory perception. Yale New Haven, CT: University Press, 1955.
33. Gray, JAB. Initiation of impulses at receptors. In: Field J, ed. Handbook of physiology. Section I, Vol. 1, Ch. 4. Washington, DC: American Physiological Society, 1959:123–145.
34. Greene J, Jampel R. Muscle spindles in the extraocular muscles of the Macaque. J Comp Neurol 1966;126: 547–550.
35. Head H. The afferent nervous system from a new aspect. Brain 1905; 28:99–116.
36. Head H. Studies in neurology. Oxford: Oxford University Press, 1920.
37. Henneman E. Peripheral mechanisms involved in the control of muscle. In V.B. Mountcastle, ed. Medical physiology. Ch. 73. St. Louis: C.V. Mosby Company, 1968: 1697–1716.
38. Horch KW, Tuckett RP, Burgess PR. A key to the classification of cutaneous mechanoreceptors. J Invest Dermatol 1977;69:75–82.
39. Houk J, Henneman E. Responses of tendon organs to active contractions of the soleus muscle of the cat. J Neurophysiol 1967;30:466–481.
40. Kandel ER, Siegelbaum SA. Directly-gated transmission at the nerve-muscle synapse. In: Kandel EC, Schwartz JH, Jessell TM, eds. Principles of neural science. Chap. 10. New York: Elsevier, 1991: 135–152.
41. Keller JH, Moffett BC Jr. Nerve endings in the temporomandibular joint of the Rhesus macaque. Anat Rec 1968;160:587–594.
42. LaPorte Y, Emonet-Denand F, Jami L. The skeleto-fusimotor or innervation of mammalian muscle spindles. Trends Neurosci 1981;4:97–99.
43. Larsell O, Dow RS. Innervation of the human lung. Am J Anat 1933; 52:414–438.
44. Lindblom U, Lund L. The discharge from vibration-sensitive receptors in the monkey foot. Exp Neurol 1966; 15:401–417.
45. Loewenstein WR. The generation of electric activity in a nerve ending. Ann NY Acad Sci 1959;81:367–387.
46. Loewenstein WR. Biological transducers. Sci Am 1960;203:99–108.
47. Loewenstein WR. Mechano-electric transduction in the Pacinian corpuscle: initiation of sensory impulses in mechanoreceptors. In: Loewenstein WR, ed. Principles of receptor physiology. Ch. 9. Berlin: Springer-Verlag, 1971:269–290.
48. Loewenstein WR, Altamirano-Orrego R. The refractory state of the generator and propagated potentials in a Pacinian corpuscle. J Gen Physiol 1958;41:805–824.
49. Manni E, Bortolami R, Desole C. Eye muscle proprioception in the semilunar ganglion. Exp Neurol 1966; 16:226–236.
50. Martin JH. Coding and processing of sensory information. In: Kandel EC, Schwartz JH, Jessell TM, eds. Principles of neural science. Chap. 23. New York: Elsevier, 1991: 329–340.
51. Martin JH, Jessell TM. Modality coding in the somatic sensory system. In: Kandel EC, Schwartz JH, Jessell TM, eds. Principles of neural science. Chap. 24. New York: Elsevier, 1991:341–352.
52. Matthews PBC. Muscle spindles and their motor control. Physiol Rev 1964;44:219–288.
53. McLennan H. Synaptic transmission. Philadelphia: W.B. Saunders, 1963:3–15.
54. Melzack R, Wall PD. Pain mechanisms: A new theory. Science 1965; 150:971–979.
55. Merkel F. Tastzellen und Tastkörperchen beiden Hausthieren und beim Menschen. Arch Mikrosk Anat Entwick Mech 1975;11:636–652.
56. Merrillees N, Sunderland S, Hayhow W. Neuromuscular spindles in the extraocular muscles in man. Anat Rec 1950;108:23–30.
57. Merrillees NCR. Some observations on the fine structure of a Golgi tendon organ of a rat. In: Barker D, ed. Symposium on muscle receptors. Hong Kong: Hong Kong University Press, 1962:199–206.
58. Miller MR, Ralston HJ, Kasahara M. The pattern of cutaneous innervation of the human hand. Am J Anat 1958;102:183–218.
59. Miller MR, Ralston HJ, Kasahara M. The pattern of cutaneous innervation of the human hand, foot, and breast. In: Montagna W, ed. Advances in biology of skin. Vol. I: Cutaneous innervation. New York: Pergamon Press, 1960:1–47.
60. Montagna W. Morphology of cutaneous sensory receptors. J Invest Dermatol 1977;69:4–7.
61. Mountcastle VB. Sensory receptors and neural encoding: Introduction to sensory processes. In: Mountcastle VB, ed. Medical physiology. Vol. I. St. Louis: C.V. Mosby, 1974: 285–306, 348–381.
62. Mountcastle VB. Sensory receptors and neural encoding: Introduction to sensory process. In: Mountcastle VB, ed. Medical physiology. 14th ed. Vol. 1. St. Louis: C.V. Mosby, 1980:327–347.
63. Mountcastle VB. Central nervous mechanisms in mechanoreceptive sensibility. In: Darian-Smith I, ed. Handbook of physiology. Section 1: The nervous system. Vol. 3: Sensory processes, part 2. Bethesda, MD: American Physiological Society, 1984:789–878.
64. Mountcastle VB, Talbot WH, Darian-Smith I, Kornhuber HH. The neural base for the dense vibration. Science 1967;155:597–600.
65. Munger BL. The intraepidermal innervation of the snout skin of the opossum: a light and electron microscope study, with observations of the nature of Merkel's Tastzellen. J Cell Biol 1965;26:79–97.
66. Munger BL. Discussion of fine structure of the receptor organs and its probable functional significance. In: De Reuck AVS, Knight J, eds. Touch, heat, and pain. Ciba Foundation Symposium. Boston: Little, Brown and Company, 1966:129–130.
67. Namba T, Nakamura T, Grob D. Motor nerve endings in human extraocular muscle. Neurology 1968; 18:403–407.
68. Oppenheimer DR, Palmer E, Wedell G. Nerve endings in the conjunctiva. J Anat 1958;92:321–352.
69. Ozeki M, Sato M. Initiation of impulses at the non-myelinated terminal in Pacinian corpuscles. J Physiol (Lond) 1964;170:167–185.
70. Ozeki M, Sato M. Changes in the membrane potential and the membrane conductance associated with a sustained compression of the non-myelinated nerve terminal in Pacinian corpuscles. J Physiol (Lond) 1965;180:186–208.
71. Patterson PH. Environmental determination of autonomic neurotransmitter functions. Annu Rev Neurosci 1978;1:1–17.
72. Patton HD. Reflex regulation of movement and posture. In: Ruch TC, ed. Neurophysiology. Ch. 6. Philadelphia: W.B. Saunders, 1961: 167–198.
73. Quilliam TA. Unit design and array

patterns in receptor organs. In: De Reuck AVS, Knight J, eds. Touch, heat and pain. Ciba Foundation Symposium. Boston: Little, Brown & Company, 1966:86–112.
74. Ralston HJ III, Miller MR, Kasahara M. Nerve endings in human fasciae, tendons, ligaments, periosteum, and joint synovial membrane. Anat Rec 1960;136:137–148.
75. Ramón y Cajal S. Histologie du Système Nerveux de l'Homme et des Vertébrés. (Azoulay L, trans.) Paris: Maloine, 1909, 1911. (Reprinted, Consejo Superior de Investigaciones Cientificas, Instituto Ramón y Cajal, Madrid, 1972.)
76. Reger JF. Electron microscopy of the motor endplate in rat intercostal muscle. Anat Rec 1955;122:1–10.
77. Reger JR. The ultrastructure of normal and denervated neuromuscular synapses in mouse gastrocnemius muscle. Exp Cell Res 1957;12: 661–665.
78. Robertson JD. The ultrastructure of a reptilian myoneural junction. J Biophys Biochem Cytol 1956;2: 381–394.
79. Robertson JD. Electron microscopy of the motor end-plate and the neuromuscular spindle. Am J Phys Med 1960;39:1–43.
80. Rogers DC, Burnstock G. Multiaxonal autonomic junctions in smooth muscle of the toad (Bufo Marinus). J Comp Neurol 1966;126:625–652.
81. Rose JE, Mountcastle VB. Touch and kinesthesis. In: Fields J, ed. Handbook of physiology. Section I, Vol. I: Neurophysiology. Ch. 17. Washington, DC: American Physiological Society, 1959:387–429.
82. Rowland LP. Diseases of chemical transmission at the nerve-muscle synapse: myasthenia gravis. In: Kandel EC, Schwartz JH, Jessell TM, eds. Principles of neural science. Chap. 16. New York: Elsevier, 1991: 235–243.
83. Ruffini A. Sur un nouvel organe nerveux terminal et sur la présence des corpuscules Golgi-Mazzoni dans le conjonctif sous-cutané de la pulpe des doigts de l'homme. Arch Ital Biol 1894;21:249–265.
84. Schoultz TW, Swett JE. The fine structure of the Golgi tendon organ. J Neurocytol 1972;1:1–26.
85. Shepherd GM. Neurobiology. 2d ed. Oxford: Oxford University Press, 1988.
86. Sherrington CS. The integrative action of the nervous system. New York: Charles Scribner's Sons, 1906. (Reprinted, New Haven, CT: Yale University Press, 1947.)
87. Sinclair DC. Cutaneous sensation. New York: Oxford University Press, 1967:35–80.
88. Sinclair DC, Weddell G, Feindel WH. Referred pain and associated phenomena. Brain 1948;71:184–211.
89. Smirnow A. Über die sensiblen Nervenendigungen im Herzen bei Amphibien und Saügetieren. Anat Anz 1895;10:737–749.
90. Thaemert JC. Ultrastructural interrelationships of nerve processes and smooth muscle cells in three dimensions. J Cell Biol 1966a;28:37–49.
91. Thaemert JC. Ultrastructure of cardiac muscle and nerve contiguities. J Cell Biol 1966b;29:152–162.
92. Tuchmann-Duplessis H, Auronx M, Haegel P. Illustrated human embryology. Vol. 3: Nervous system and endocrine glands (translated from French) New York: Springer-Verlag, 1974.
93. Walshe FMR. The anatomy and physiology of cutaneous sensibility: a critical review. Brain 1942;65: 48–114.
94. Weddell G, Taylor DA, Williams CM. Studies on the innervation of skin. III. The patterned arrangement of the spinal sensory nerves to the rabbit ear. J Anat 1955;89:317–342.
95. Weinberg C, Sanes JR, Hall Z. Formation of neuromuscular junctions in adult rats: accumulation of acetylcholine receptors, acetylcholinesterase, and components of the synaptic basal lamina. Dev Biol 1981;84:255–266.
96. Woollard HH. Observations on the terminations of cutaneous nerves. Brain 1935;58:352–367.
97. Zacks SI. The motor endplate. Philadelphia: W.B. Saunders, 1964.

8
Spinal Nerves and Peripheral Innervation

PERIPHERAL NERVOUS SYSTEM

The peripheral nervous system comprises the cerebrospinal and autonomic groups of nerves, as well as their associated ganglia, together with the cellular and connective tissue elements which ensheathe them. All these structures lie peripheral to the pial envelope which covers the central nervous system and through which the central and peripheral nervous fibers are continuous at many points. The peripheral nervous system is composed of *somatic* and *autonomic* divisions. The somatic division includes sensory neurons of the dorsal root and cranial ganglia that innervate the skin, muscles, and joints, and provide sensory information about the environment outside the body. The axons of somatic motor neurons innervate skeletal muscles and are currently considered part of the somatic division, although their cell bodies lie within the central nervous system. The autonomic division of the peripheral nervous system can be viewed as the sensorimotor system for the viscera, the smooth muscles, and the exocrine glands. It has three spatially segregated components: the *sympathetic* system, the *parasympathetic* system, and the *enteric* nervous system (13). The sympathetic and parasympathetic systems act in concert to maintain homeostasis. The enteric nervous system exerts a local action to control the activity of smooth muscles at the level of the gastrointestinal tract. The organization and function of these three components of the autonomic nervous system are described in detail in Chapter 9. The present chapter principally focuses on the organization of the somatic division of the peripheral nervous system.

Spinal Nerve

GENERAL ORGANIZATION

Each spinal nerve arises from a region of the spinal cord by two roots, a dorsal sensory-afferent root and a ventral motor-efferent root. The two roots traverse the dural sac, penetrate the dura, and reach the intervertebral foramen, where the dorsal root swells into the spinal ganglion that contains the cell bodies of origin of the sensory-afferent fibers (Figs. 5.2**A** and 8.1). Distal to the ganglion, the dorsal and ventral roots unite and emerge from the intervertebral foramen as a *mixed spinal nerve* or *common nerve trunk*, containing both sensory-afferent and motor-efferent fibers. There are usually 31 pairs of segmentally arranged spinal nerves, which receive and distribute fibers to various parts of the body. In most individuals these nerves are grouped as: cervical, 8; thoracic, 12; lumbar, 5; sacral, 5; and coccygeal, 1. The abbreviations C, T, L, S, and Co, followed by the appropriate number, are commonly used to identify the individual nerves. The first cervical nerve (the suboccipital nerve) emerges from the vertebral canal between the atlas (C1) and the occipital bone (Fig. 1.4). The eighth cervical nerve emerges from the intervertebral foramen between C7 and T1. All more caudal spinal nerves emerge from the intervertebral foramina caudal to the vertebrae of the corresponding number (Fig. 10.3).

DORSAL ROOTS

The dorsal roots contain most fibers that convey somatic and visceral sensory information to the central nervous system (Fig. 10.23). These fibers are the central processes of the dorsal ganglion cells. As a rule, the dorsal roots are thicker than the ventral ones and their size varies with that of their respective ganglia. The first cervical and the first coccygeal nerves represent exceptions in that the dorsal root fibers are absent in many individuals. About 1 million dorsal root fibers have been found on each side in the human adult. Considering the fact that about two-thirds of the afferent fibers may be unmyelinated, a more realistic number of dorsal root fibers should be 2–2.5 million (35).

The size of the myelinated and unmyelinated nerve fibers that form each dorsal root varies from 0.5–20 μm. The larger myelinated fibers (10–20 μm) convey sensory impulses to the spinal cord from elaborate receptors located in the dermis, subcutaneous connective tissue, muscles, tendons, joint capsules, ligaments, periosteum, and deep fasciae (see Chapter 7). Large afferent fibers conduct rapidly (5–120 m/sec) and, by virtue of their several physiologic properties, are classified as the *A fiber* component of peripheral nerves. Smaller myelinated nerve fibers in dorsal roots (0.5–10 μm) convey sensory information to the cord from less specialized receptors, and from free nerve endings in the skin, viscera, muscles, and connective tissues of the body. Small, unmyelinated, slow-conducting sensory fibers of the dorsal roots are classified physiologically as *C fibers*. The diameter spectra of the fibers within a dorsal root are shown in Figure 8.6.

VENTRAL ROOTS

The major portion of the ventral root of a spinal nerve is composed of myelinated axons with a diameter that ranges from 3–13 μm. The vast majority are the axons (9–13 μm) of large anterior horn cells (general somatic efferent, GSE) of the spinal cord (Figs. 8.6**B** and 10.19). They conduct rapidly and have functional properties similar to the large sensory A fibers of the dorsal root. Each large A alpha (α) fiber in the ventral root enters a peripheral nerve and supplies motor impulses to a variable number of *extrafusal skeletal muscle fibers* (Fig. 5.3**G**). Smaller myelinated fibers, 3–6 μm in diameter, form a second component of the ventral root (gamma (γ) efferent fibers). These finer axons arise from smaller multipolar neurons scattered among the larger cells of the anterior gray horn (Figs. 10.19 and 10.23). Such small motor axons of ventral roots and motor nerves are designated as "γ-efferents," and they innervate the *intrafusal skeletal muscle fibers* of the neuromuscular spindle (Figs. 7.11 and 10.23). A third fiber component is found only in the ventral roots of spinal nerves T1 to L2 and S2 to S4. These myelinated fibers range from 3–10 μm in diameter and are the preganglionic axons of visceral motor neurons (general visceral efferent, GVE) located in the intermediolateral cell column of the spinal cord. Preganglionic visceral efferent fibers from spinal levels T1 to L2 leave the ventral root to enter the ganglia of the sympa-

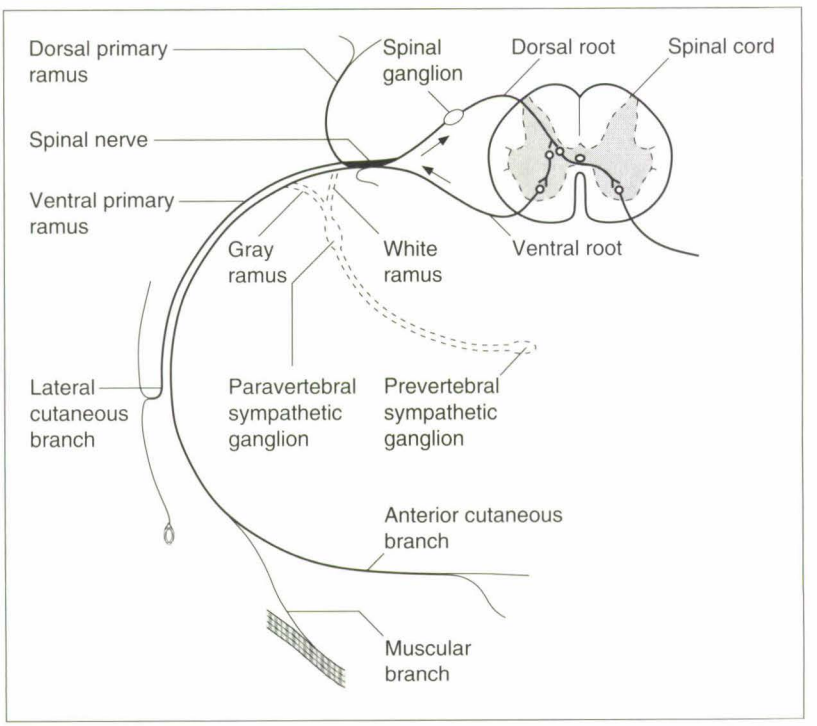


Figure 8.1. Typical thoracic spinal nerve and its branches.

thetic trunk through a white communicating ramus (Figs. 8.1, 9.1, 9.2, and 10.23). Similar preganglionic visceral efferent fibers (parasympathetic) are found in the ventral roots of sacral nerves (S2, S3, and S4). The preganglionic visceral components of the ventral spinal roots conduct more slowly (3–15 m/sec). They are concerned with visceral reflexes and are designated as *B fibers*.

In recent years, it became evident that there are a large number of sensory fibers in certain ventral roots (47). Electron microscopic studies have revealed a surprisingly large number of unmyelinated fibers in the ventral roots of several mammals including humans (9). Approximately 28% of the axons in the ventral root in humans are unmyelinated. Additionally, there are a small number of myelinated sensory fibers in the ventral root (48). Evidence that these fibers were afferent originally was based upon the observation that following ventral root section, some fibers distal to the cut survived, while proximal root fibers degenerated (10). Retrograde transport techniques provided more conclusive evidence in that horseradish peroxidase (HRP) injected into the spinal cord after dorsal root section (proximal to the ganglion) resulted in labeling of spinal ganglion neurons (28). Additionally, physiologic recording from fine filaments of the ventral roots provided information that support the existence of unmyelinated sensory fibers (7, 11). An important question, not entirely resolved, is whether these unmyelinated sensory ventral root fibers enter the spinal cord directly, or whether they curve back and enter the spinal cord via the dorsal root. At least some of these fibers enter the spinal cord directly through the ventral root. As yet, no special sensory mechanism has been demonstrated for the ventral root afferents (47). Since their large numbers were only recently demonstrated, their precise function is not yet established. These observations suggest that complete deafferentation cannot be accomplished by dorsal root section (rhizotomy) alone.

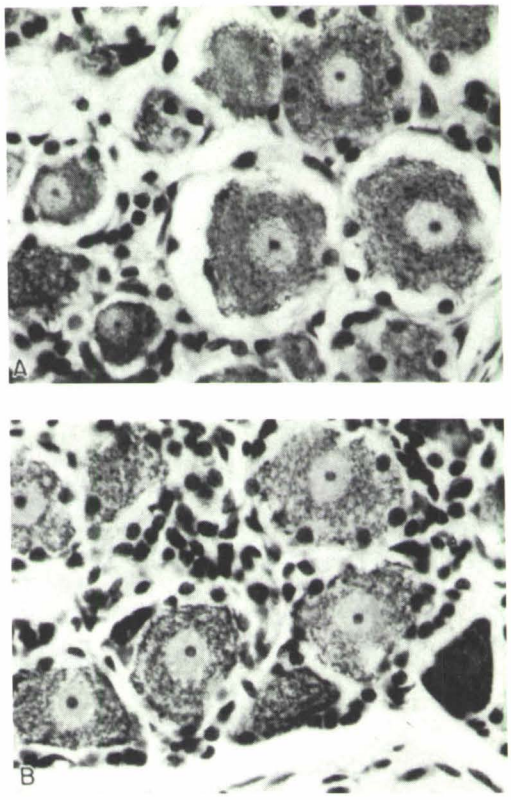


Figure 8.2. Photomicrographs of normal cells in lumbar spinal ganglion (**A**) and the superior glossopharyngeal ganglion (**B**) of macaque monkeys. Note variations in ganglion cell size and small dark nuclei of the capsule cells (cresyl violet stain, ×500).

Spinal Ganglia

The spinal and autonomic ganglia are part of the peripheral nervous system. Almost all of the sensory-afferent fibers, both somatic and visceral, have their cell bodies in the spinal ganglia. These aggregations of unipolar nerve cells form spindle-shaped swellings on the dorsal roots (Figs. 1.4, 1.5, 8.1, and 9.1) and are commonly referred to as *dorsal root ganglia*. The dorsal root ganglia are usually located in the intervertebral foramina, immediately lateral to the sites where the nerve roots perforate the dura mater. However, the C1 and C2 ganglia lie on the vertebral arches of the atlas and axis, those of the sacral nerves are inside the vertebral canal, and that of the coccygeal nerve is usually within the dura mater. The C1 ganglia are missing in some individuals.

Each spinal ganglion is surrounded by a connective tissue capsule that is continuous with the epineurium of the spinal nerves. Cells of the spinal ganglia have a peripheral location beneath the capsule, and bundles of nerve fibers entering and leaving the ganglia form a central core. In the trigeminal ganglion, the cells and fibers are more loosely arranged. In dorsal root ganglia, the interneural spaces contain large and small axons, satellite cells, Schwann cells, and

blood vessels. Studies of the topographic organization of cells in dorsal root ganglia of the cat indicate that cells in medial and caudal regions project processes into the most caudal rootlets, while cells in rostral parts of the ganglia project fibers into rostral rootlets (4). Cells in the trigeminal ganglion also have a topographic arrangement in that cells contributing fibers to the ophthalmic division are located anteromedially and those distributing fibers to the mandibular division are situated posterolaterally (24).

The spinal ganglia are derived from the embryonic neural crest (see Chapter 3) and are populated by typical unipolar neurons whose cell body is ovoid or spherical and often has indentations on its surface (Fig. 5.1**A**). The cell diameters range from 20 to over 100 μm. Sensory ganglion cells grown in tissue culture and studied by electron microscopy have all the cytoplasmic organelles possessed by other neurons (3, 31, 43). However, these sensory neurons have less prominent Nissl bodies and scattered cytoplasmic chromatin, and each cell has a variable number of satellite cells. The unipolar ganglion cells give rise to a single process (sometimes termed dendroaxonal process) which bifurcates at a T-junction into a peripheral and a central branch. In the case of myelinated fibers, such a junction occurs at a node of Ranvier. The proximal portion of this process often follows a highly convoluted course and is referred to as the glomerular segment or *initial glomerulus*. The peripheral process terminates in a sensory ending. Although this process is functionally an elongated dendrite, it possesses all the morphologic and physiologic characteristics of a peripheral axon. Recently, it was suggested that a single ganglion cell may give rise to more than one peripheral and central branch. Although not yet firmly established (8, 34), the possible branching of peripheral axons is clinically highly relevant since it bears on the problem of referred pain (8).

On the basis of their staining properties two types of ganglion cells were described in the light microscope. The larger cells are lighter, while smaller cells often appear dark (obscure cells) (Fig. 8.3) (32). Bunge, et al. (3), observed light and dark cells in tissue culture and believed this appearance depended on the amount of cytoplasmic neurofilaments. Angular and indented surface margins of the perikaryon represent interdigitations with

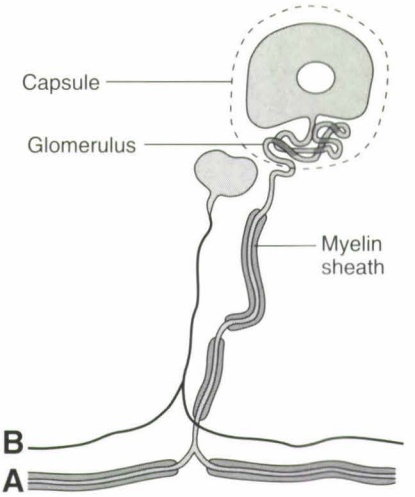


Figure 8.3. Two cells from vagus ganglion of cat. **A.** Large clear cell. **B.** Small "obscure" cell with deeply staining cytoplasm (Ehrlich's methylene blue).

the processes of surrounding satellite cells. Such ultrastructural extensions of the perikaryon explain the surface spines and excrescences observed in Golgi, silver, and methylene blue preparations. These typical, and often bizarre, sensory neurons commonly are observed in ganglia from older individuals (Fig. 8.4). The numerous processes may divide repeatedly or terminate as elaborate end bulbs within the capsule. Sensory neurons with such supernumerary processes have been mistaken by some as multipolar (motor) neurons. However, no one has yet reported vesicle-containing axon terminals or morphologic evidence of synaptic contacts within the spinal or trigeminal ganglia. A more detailed study of the sensory ganglia and neuronal variations that accompany aging can be found in the literature (14, 33, 39, 44–46). Furthermore, attempts have been made recently to better characterize the morphologic and neurochemical phenotypes of the two major populations of ganglion cells with the help of physiologic, anatomic, and immunocytochemical techniques (12, 26, 27, 30).

Satellite cells, variously termed capsular nuclei, capsular cells, or amphicytes, are also derived from the embryonic neural crest and, in the adult, form a concentric layer which closely invests the perikaryon and its unmyelinated axonic coils (49). The round or elongated nuclei of the satellite cells are more dense than the adjacent perikaryon, and are

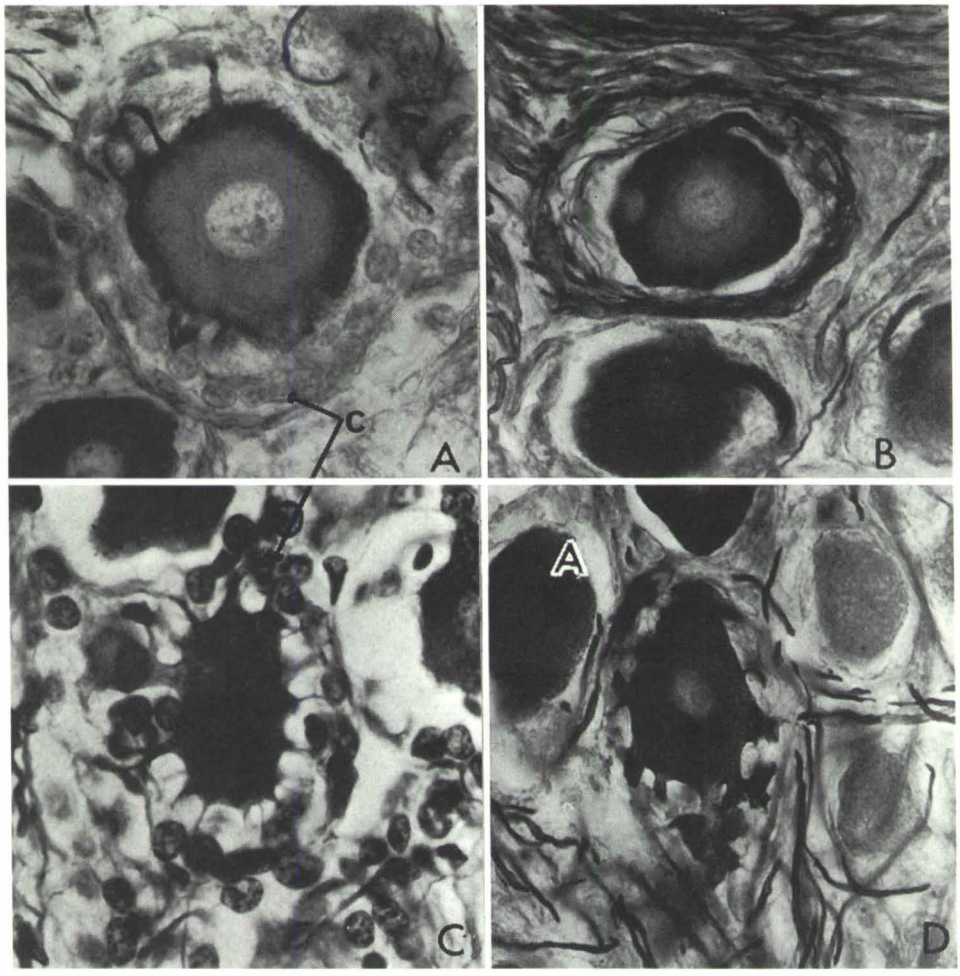


Figure 8.4. Photomicrographs of atypical sensory neurons of adult human trigeminal ganglion. **A.** Fenestrated cell with three looped processes on surface of perikaryon. Satellite and capsular nuclei are identified (*c*). **B.** Pericellular plexus of nerve fibers surrounding a unipolar ganglion cell. **C.** Frayed cell (of Ramón y Cajal) with multiple short processes most of which terminate in the surrounding capsule. The preparations were counterstained with hematoxylin to demonstrate capsular nuclei (*c*). **D.** Erethized or irritated cell (of DeCastro). Note thick, palm-leaf expansions or supernumerary processes that issue from perikaryon and axon. Types shown in **A**, **C**, and **D** are often observed in sensory ganglia of older individuals (Ramón y Cajal silver stain, all photographs, ×650).

identified easily with the light microscope (Figs. 5.2**A**, 8.2, and 8.4). They show ultrastructural features that distinguish them from Schwann cells. Satellite cells display plasma membrane redundancy in the form of folds on the surface that faces the neuron. Such folds and processes may form several layers and interdigitate with the surface evaginations of the perikaryon. The outer surface of the satellite cell is invested with a basal lamina which is continuous with that investing the myelin at the first internode (31). The capsule of satellite cells separates the perikarya from adjacent ganglionic capillaries, and must be involved in fluid transport mechanisms. They can increase in number after birth, and may play a role in the metabolism of the ganglion cells.

Studies of cell changes in sensory ganglia, spinal and cranial, in the monkey indicate that (a) the section of the nerve proximal to the ganglia produces no cellular changes but causes centrally projecting fibers to degenerate, and (b) the section of sensory nerves distal to the ganglia produces profuse chromatolytic changes in the cells of all sizes and types within the ganglia (Fig. 8.5), but no central degeneration (5). Severance of nerve fibers distal to sensory ganglia appears to eliminate peripheral neurotrophic influences necessary for the growth and maintenance of the ganglion cell. The integrity of this influ-

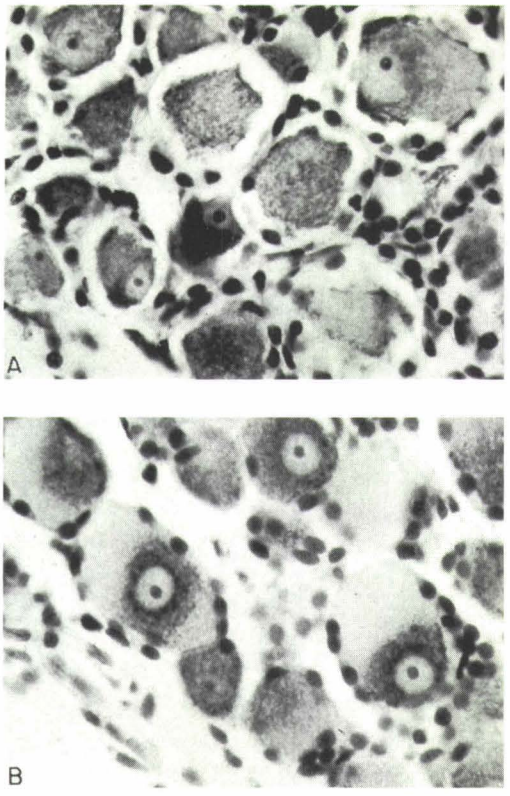


Figure 8.5. Photomicrographs of chromatolytic cells in lumbar spinal ganglion (**A**) and the superior vagal ganglion (**B**) of macaque monkeys after section of the nerve fibers distal to the ganglia. Although lesions of this type produce classic retrograde cell changes, they do not induce degeneration in the centrally projecting fibers (cresyl violet stain, ×500).

ence is sufficient to sustain sensory ganglion cells after their central processes have been sectioned.

Mixed Nerve

After union of the dorsal and ventral roots, the common nerve trunk divides into four branches or rami—dorsal ramus, ventral ramus, meningeal ramus, and ramus communicans (Figs. 3.9 and 8.1). The *dorsal rami* (or posterior primary rami) supply the deep muscles and skin of the back. The larger *ventral rami* innervate the ventrolateral portion of the body wall and all the extremities, as well as all the superficial muscles of the back. The *ramus communicans* connects the common spinal trunk with the sympathetic ganglia and consists of white and gray portions (Fig. 9.2). The former contains the myelinated preganglionic fibers passing from the spinal cord to the sympathetic ganglion, while the gray rami contain the unmyelinated postganglionic fibers which rejoin the dorsal and ventral rami to be distributed to the body wall. The white rami also contain afferent fibers from the viscera whose cell bodies are situated in the spinal ganglia (Fig. 10.23). The *meningeal ramus* is a small nerve trunk which usually arises as several twigs from both the common trunk and the ramus communicans (Fig. 8.1). It reenters the intervertebral foramen to supply the meninges, blood vessels and vertebral column.

The dorsal and ventral rami divide into superficial (cutaneous) and deep (muscular) peripheral nerves. These nerve trunks branch repeatedly and become progressively smaller as they extend peripherally. Ultimately, these branches break up into individual nerve fibers which terminate in receptors or effectors. The cutaneous nerves are composed mainly of sensory fibers of various size, but they also contain efferent vasomotor, pilomotor and secretory fibers for the blood vessels, hair and glands of the skin. In muscle nerves there also is a mixture of sensory and motor fibers. Both somatic α and γ efferent fibers go to the skeletal muscle fibers, while numerous large (**A**) and small afferent fibers pass centrally from receptors in the neuromuscular spindles and tendon organs. Small pain afferents and postganglionic vasomotor (**C**) fibers to the blood vessels also are found in the nerves that enter each muscle. In each peripheral nerve there are fibers of various categories: myelinated and unmyelinated, large and small, visceral and somatic, sensory and motor (Fig. 8.6).

With the exception of the thoracic nerves, which retain their segmental distribution, the cervical and lumbosacral ventral rami branch and anastomose to form the cervical, brachial, and lumbosacral plexuses (Figs. 8.14, 8.15, 8.19, and 8.20). In these plexuses a regrouping of fibers occurs, so that each of the peripheral nerves which arises from the plexus contains contributions from two, three, or even four ventral rami. The peripheral nerves are therefore "mixed" in a double sense—they consist not only of afferent and efferent fibers, but also of fibers which come from several spinal cord segments.

Connective Tissue Sheaths

Morphologically, each peripheral nerve consists of parallel-running nerve fibers invested by a thick sheath of rather loose connective tissue, the *epineurium* (Fig. 8.7). From

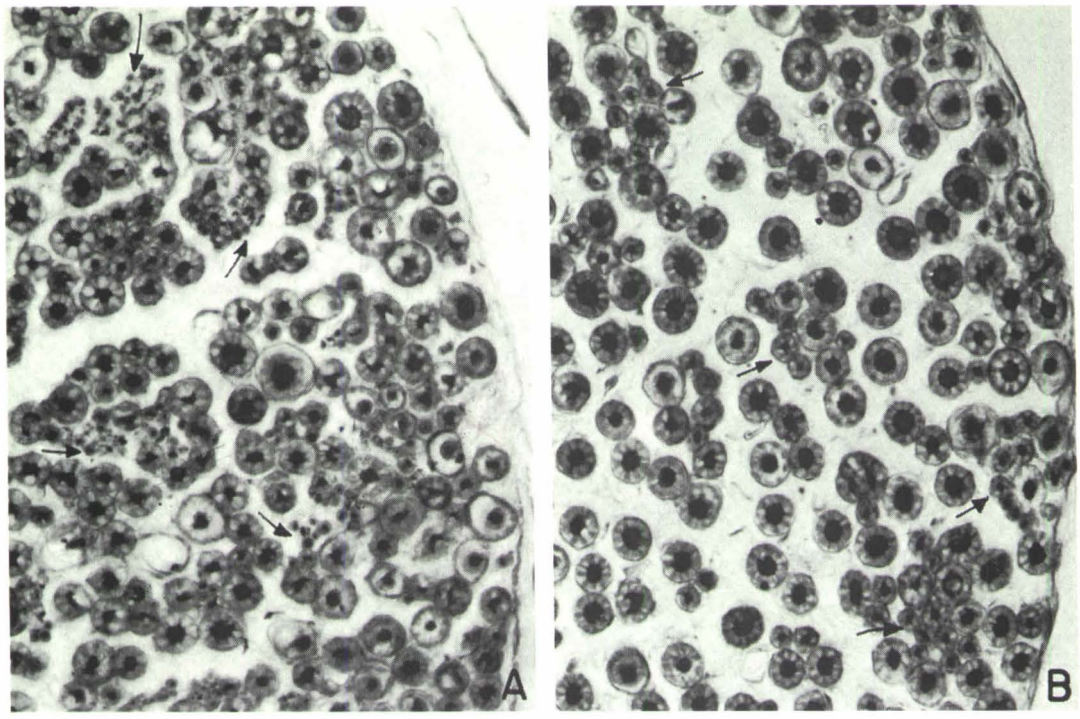


Figure 8.6. Photomicrographs of nerve fibers of dorsal and ventral roots. **A.** Cross-section of L4 dorsal root within the dura mater. *Arrows* indicate groups of unmyelinated C fibers. **B.** Cross-section of L4 ventral root within the dura mater. *Arrows* indicate axons of smaller γ-efferent neurons to spindle muscle fibers. Larger α axons supply groups of skeletal muscle fibers (Holmes' silver-Luxol fast blue stain, photograph, ×275).

this sheath septa extend into the interior and divide the fibers into bundles or *fascicles* of varying size, each of which is surrounded by a fairly distinct perifascicular sheath or *perineurium*. These fascicles do not run like isolated cables but repeatedly divide and join adjacent fascicles in an interchange of fibers (Fig. 8.7). As a result, the fascicular arrangement at different levels varies greatly in portions of the same nerve.

From the perineurium delicate strands invade the bundle as intrafascicular connective tissue or *endoneurium*. This tissue separates the fibers into smaller and smaller bundles and ultimately invests each fiber as a delicate tubular membrane. In the epineurial and perineurial connective tissue, blood vessels and endothelial lined spaces communicate with lymph channels within smaller fascicles.

On emerging from the spinal cord, the dorsal and ventral roots receive an investment of connective tissue as they pass through the pia. This tissue is reinforced by additional connective tissue as the roots pass through the arachnoid and dura, the latter becoming continuous with the epineurium of the spinal nerve (root sleeve) (Fig. 10.2).

SEGMENTAL INNERVATION

The external segmentation of the spinal cord produced by the spinal nerves corresponds to the general metamerism of the body. Each pair of spinal nerves innervates symmetrically arranged paired somites (metamere). The embryonic somites formed from paraxial mesoderm differentiate into (a) a *myotome*, which give rise to muscle, (b) a *sclerotome*, concerned with the development of the axial skeleton, and (c) a *dermatome*. Efferent fibers in the ventral roots innervate somatic musculature (myotomes) and some ventral roots contain preganglionic autonomic fibers which pass to autonomic ganglia which in turn give rise to postganglionic fibers that innervate blood vessels, smooth muscle, and glandular epithelium. The dorsal roots contain most afferent fibers, somatic and visceral (Fig. 9.28). The cutaneous area supplied by the sensory fibers from a single dorsal root and its ganglion is called a *dermatome* (Figs. 8.8, 8.9, and 8.11–8.13).

In the adult, the correspondence between neural and body metameres is recognized readily in the trunk region, where each spinal

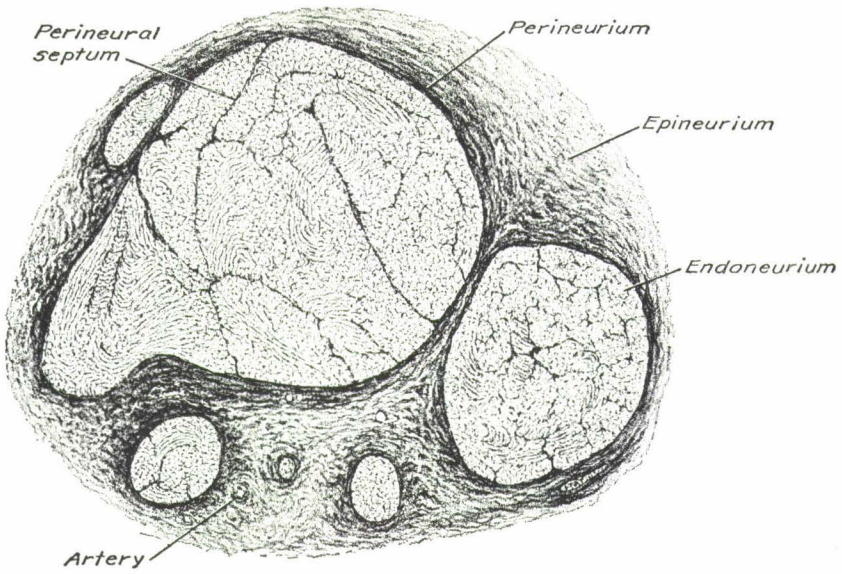


Figure 8.7. Drawing of a cross-section of sciatic nerve of macaque monkeys.

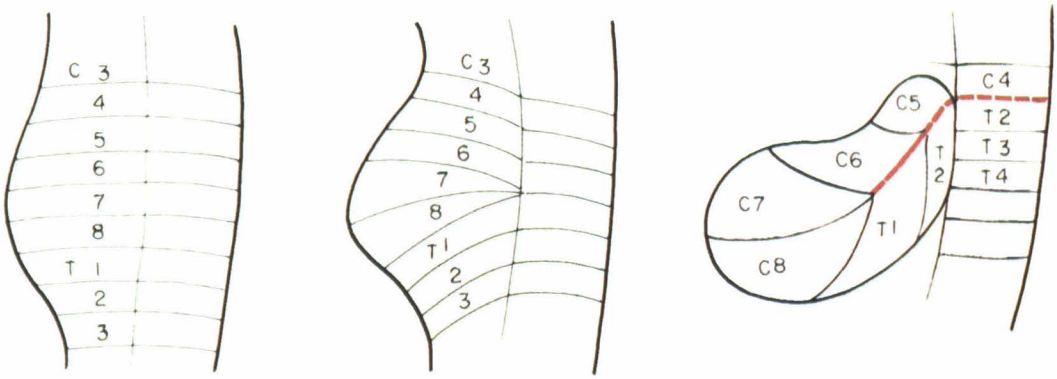


Figure 8.8. Diagram of various stages in the development of the limb bud for the upper extremity. Dermatomes C5, C6, and C7 occupy the preaxial part of the limb bud, while dermatomes C8, T1, and T2 are postaxial. The axial line is indicated by a *red dashed line*.

nerve supplies the musculature and cutaneous area of its own segment. In this region, the dermatomes follow one another consecutively, each forming a band encircling the body from the midposterior to the midanterior line (Figs. 8.11 and 8.12). In the extremities, the dermatomes have a more complex arrangement. During development, the metameres migrate distally into the limb buds and arrange themselves parallel to the long axis of the future limb (Fig. 8.8). In each extremity, consecutive segments which have migrated peripherally are arranged about an axial line (Figs. 8.8 and 8.9). As a consequence of limb development, the C4 dermatome comes to lie adjacent to the T2 dermatome, and the dermatomes of C5 through T1 lie in the upper extremity (Figs. 8.8, 8.9, 8.11, and 8.12). For similar reasons, the dermatomes of L2 and S3 are adjacent posteriorly (Figs. 8.9 and 8.12). The intervening segments migrated peripherally to form the more distal dermatomes of the lower extremity. This migration of metameres in the formation of limbs and the rotation of the lower extremity appears to explain the more complex arrangement of dermatomes in the extremities (Fig. 8.8). In each extremity, an axial line is formed along which are placed a number of consecutive segments which have wandered out from the axial portions.

As early as 1893, Sir Charles Scott Sherrington, the English physiologist, demonstrated experimentally the cutaneous areas

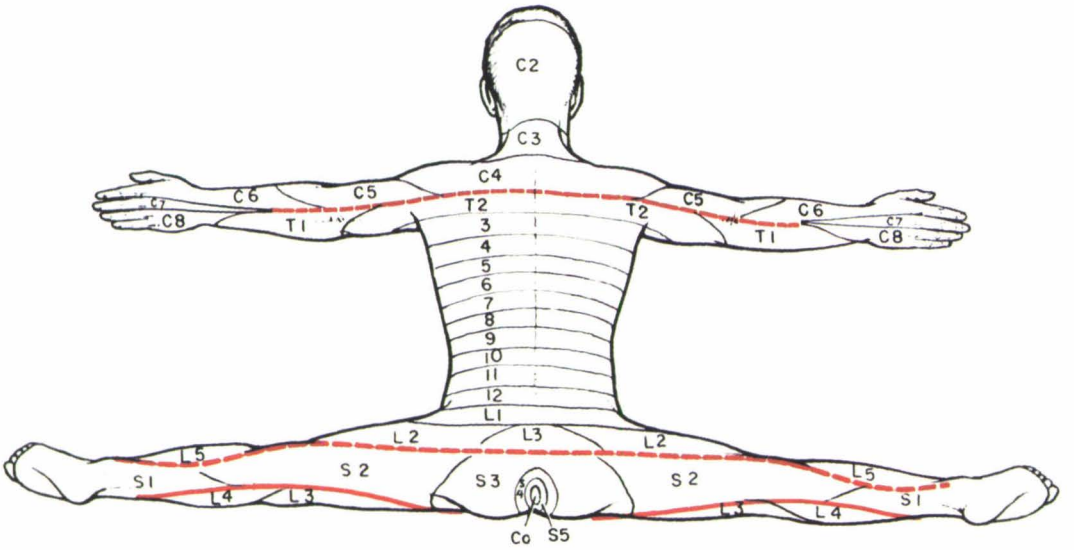


Figure 8.9. Position of the posterior (*red dashed lines*) and anterior (*red line*) axial lines. In the upper extremity, the axial lines extend down the middle of the corresponding surfaces of the limb. In the lower extremity, the posterior axial line (*red dashed line*) courses down the more lateral part of the leg to the region of the ankle. The anterior axial line (*red*) begins in the pubic region and winds around the inner aspect of the thigh to reach the posterior surface of the thigh. The pattern of dermatomes is shown with respect to the axial lines.

supplied by the various dorsal roots in the monkey (37). Because section of a single root did not produce a detectable anesthesia anywhere, he selected a specific root for study and cut two or three adjacent roots above and below. He found that each dermatome overlapped the sensory cutaneous areas of adjacent roots, being coinnervated by the one above and the one below (Fig. 8.10). Hence, at least three contiguous dorsal roots had to be sectioned to produce a region of complete anesthesia. Findings similar to those of Sherrington were obtained by the French physiologist Dusser de Barenne (15) who irritated single spinal roots or ganglia with strychnine and noted the resulting hypersensitive areas.

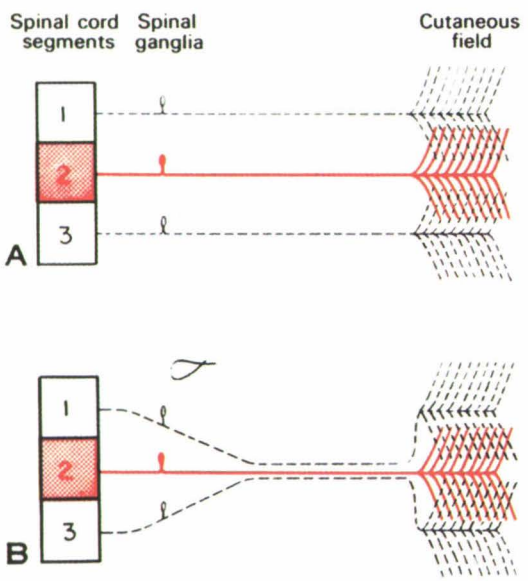


Figure 8.10. Overlap of cutaneous fields of segmental innervation. **A.** Three intercostal nerves are shown. **B.** The analogous arrangement is shown for a peripheral nerve in an extremity. The cutaneous distribution of fibers from the spinal ganglion associated with segment 2 of the spinal cord is shown in red in both **A** and **B**. Because of the extensive overlap, the section of one spinal dorsal root produces virtually no loss in cutaneous sensibility.

Dermatomes in humans were first outlined by mapping the areas of cutaneous eruption and hyperalgesia occurring in association with herpes zoster (shingles), a virus which often affects a single ganglion (23). Foerster (17, 18) furnished a remarkably complete map of human dermatomes based upon surgical section of various dorsal roots for the alleviation of spastic conditions, and cases of root injury due to tumors or other causes. His dermatomal maps correspond closely to those of Head (23), and show the same overlap described by Sherrington (37) in monkeys. Most dermatomes are supplied by fibers of three, occasionally four, dorsal roots.

The distribution of the three principal divisions of the trigeminal nerve and the cervical spinal nerves innervating cutaneous regions of the head and neck are shown in Figure 8.13. The only spinal root whose section produces an area of complete anesthesia is C2. Neither C3 nor branches of the trigeminal

nerve supply cutaneous regions in the back of the head. There also is virtually no overlap in the areas supplied by the three divisions of the trigeminal nerve, in sharp contrast to the overlap demonstrated for spinal dermatomes. In spinal dermatomes, the overlap is greater for tactile sense than for pain and thermal sense. The distribution of the human dermatomes is shown in Figures 8.11 and 8.12.

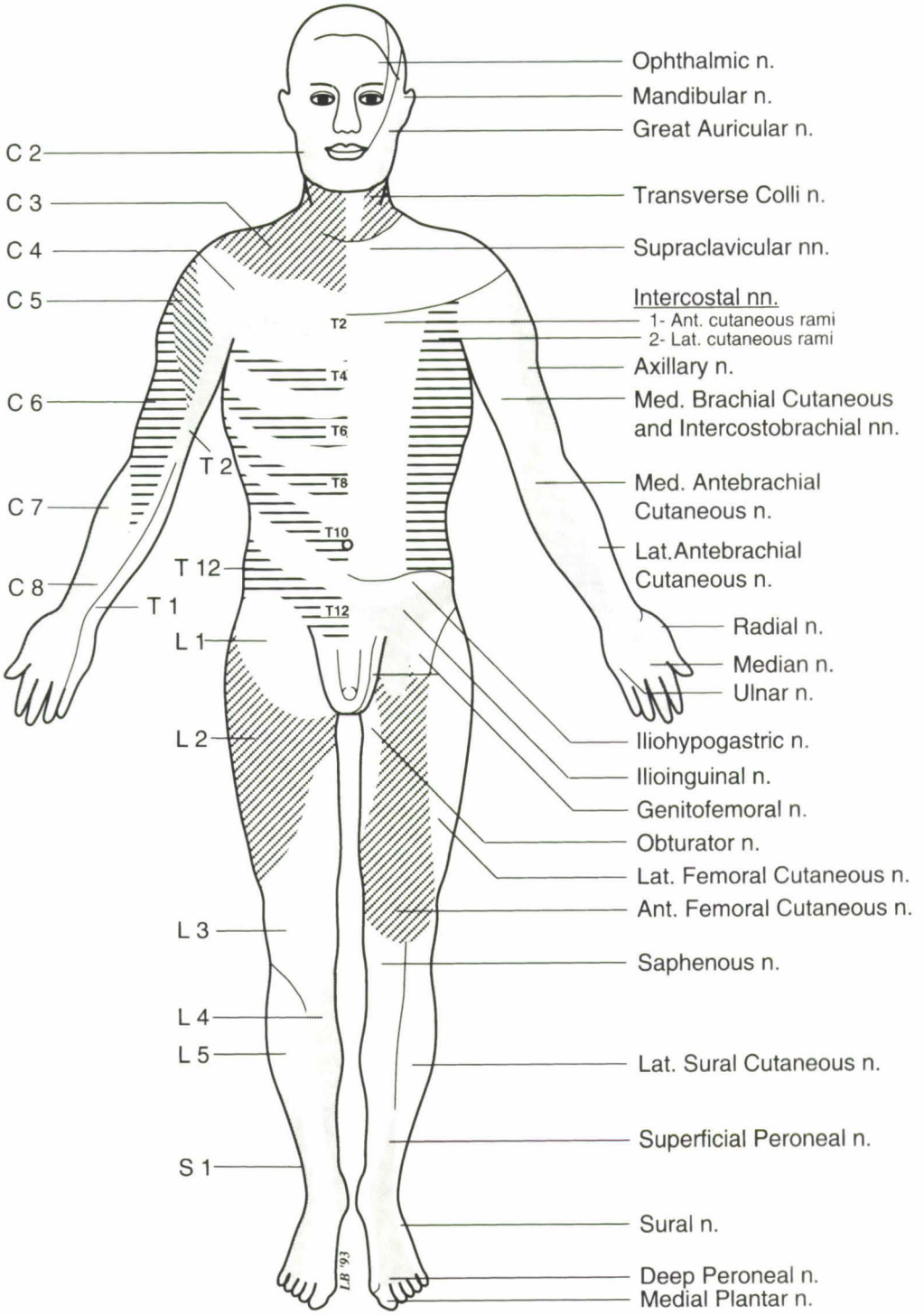


Figure 8.11. Anterior view of dermatomes (*left*) and cutaneous areas supplied by individual peripheral nerves (*right*).

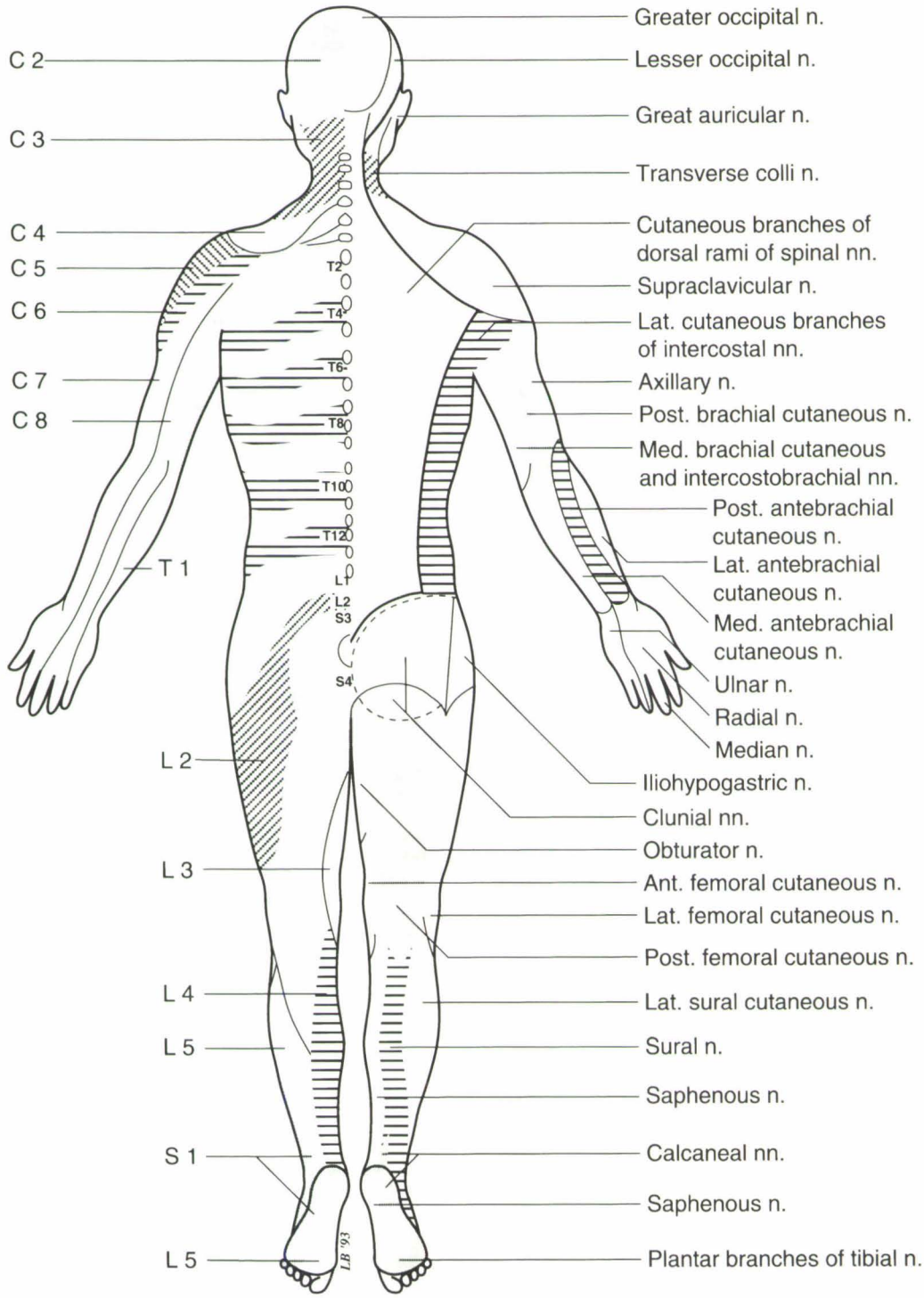


Figure 8.12. Posterior view of dermatomes (*left*) and cutaneous areas supplied by individual peripheral nerves (*right*).

In individuals with sensory loss of the segmental type, it is important to determine the level of the lesion. Diagrams such as those shown in Figures 8.11 and 8.12 are useful for reference, but certain features of the dermatomal maps are worth remembering: (a) the nipple is located in the region of T4 or T5 dermatome, (b) the umbiculus lies in the T9 or T10 dermatome, and (c) the inguinal region corresponds to L1 dermatome. The anogenital region is supplied by the S3 to S5 sacral nerve roots.

The segmental innervation of the skeletal musculature (myotomes) has been worked out in humans and animals by (a) selective stimulation of the ventral roots; (b) study of the pathologic changes which occur in the anterior horn cells when a ventral root or motor nerve is cut (Figs. 5.2E, 10.19, and 10.23); or (c) study of secondary degeneration of peripheral nerve fibers to muscle after central and peripheral lesions. As in the dermatomes, the majority of the muscles, especially those of the extremities, are innervated by two or three, and occasionally four, ventral roots. Hence injury to a single ventral root may only weaken a muscle or have no apparent effect. Only the very short muscles of the trunk and spinal column and a few others, such as the abductor pollicis, are formed from single myotomes and retain a monosegmental innervation. The peripheral projection of fibers from individual spinal cord segments to a specific muscle thus provides a clue to the myotonic origin of skeletal muscle. The segmental motor supply to the major trunk and extremity muscles is shown graphically in Figures 8.16–8.18. Because this information is essential to a full appreciation of muscle physiology, these figures are included for reference.

Following is a list of some of the important reflex and visceral and motor activities with the locations in the spinal cord of the anterior horn cells that carry them out.

Movements of the head (by muscles of neck), C1 to C4.
Movements of diaphragm (phrenic center), C3 to C5.
Movements of upper extremity, C5 to T1.
Biceps tendon reflex (flexion of forearm on percussion of biceps tendon), C5 and C6.
Triceps tendon reflex (extension of forearm on percussion of triceps tendon), C6 to C8.
Radial periosteal reflex (flexion of forearm on percussion of distal radius), C7 and C8.
Wrist tendon reflexes (flexion of fingers on percussion of wrist tendons), C8 to T1.
Movements of trunk, T1 to T12.
Abdominal superficial reflexes (ipsilateral contraction of subjacent abdominal muscles on stroking the skin of the upper, middle, and lower abdomen); upper (epigastric), T6 and T7; middle T8 and T9; lower, T10 and T12.
Movements of lower extremity, L1 to S2.
Cremasteric superficial reflex (elevation of scrotum on stroking skin on the inner aspect of the thigh), T12 to L2.
Genital center for ejaculation, L1 and L2 (smooth muscle); S3 and S4 (skeletal muscles).
Vesical center for retention of urine, T12 to L2.
Patellar tendon reflex or knee jerk (extension of leg on percussion of patellar ligament), L2 to L4.
Gluteal superficial reflex (contraction of glutei on stroking skin over glutei), L4 to S1.
Plantar superficial reflex (flexion of toes on stroking sole of foot), L5 to S2.
Achilles tendon reflex or ankle jerk (plantar flexion of foot on percussion of Achilles tendon), L5 to S2.
Genital center of erection, S2 to S4.
Vesical center for evacuation of bladder, S3 to S5.
Bulbocavernosus reflex (contraction of bulbocavernosus muscle on pinching penis), S3 to S4.
Anal reflex (contraction of external rectal sphincter on stroking perianal region), S4, S5, and coccygeal.

PERIPHERAL INNERVATION

Dorsal and Ventral Rami

Although each spinal nerve supplies its own body segment, there is considerable intermixing and anastomosing of adjacent nerve trunks before they reach their peripheral termination. The primary dorsal rami remain relatively distinct, but interconnections are common in the cervical and sacral regions (29). The ventral rami form more elaborate connections. Except for the thoracic nerves, which largely retain their segmental distribution, the cervical and lumbosacral rami innervating the extremities anastomose and branch to form extensive plexuses in which a radical regrouping of fibers occurs. Each of the peripheral nerves arising from these

plexuses contains fibers contributed by two, three, four, or five ventral rami. As a result the cutaneous areas supplied by the peripheral nerves do not correspond with the cutaneous areas supplied by the individual dorsal roots (dermatomes). The peripheral and dermatomal distributions of sensory nerve fibers are contrasted in the anterior and posterior body views in Figures 8.11 and 8.12. Similarly, several ventral roots may contribute fibers to a single muscle, and, conversely, several muscles may receive fibers from a single ventral root. A knowledge of the cutaneous and muscular distribution of the peripheral nerves is of importance to the neurologist in determining the level of peripheral nerve injuries; hence, the more important morphologic features are presented briefly. A more complete account is found in textbooks of anatomy and clinical neurology.

DORSAL RAMI

The dorsal rami of the spinal nerves innervate the intrinsic dorsal muscles of the back and neck, and the overlying skin from vertex to coccyx (Figs. 8.11 and 8.12). In the middle of the back, the cutaneous area roughly corresponds to that of the underlying muscles, but in the upper and lower portions of the trunk it widens laterally to reach the acromial region above and the region of the greater trochanter below. With certain exceptions the dorsal rami have a typical segmental distribution, the field of each overlapping with that of the adjacent segments above and below (Fig. 8.10). Each ramus usually divides into a medial and a lateral branch, both of which may contain sensory and motor fibers, although the lateral branches of the cervical rami are purely motor. Deviations are found in the upper two cervical nerves (Fig. 8.13) and in the lumbosacral rami. The first or *suboccipital* nerve is purely motor and terminates in the short posterior muscles of the head (rectus capitis and obliquus capitis). The main branch of the second cervical ramus, known as the *greater occipital* nerve, ascends to the region of the superior nuchal line, where it becomes subcutaneous, and supplies the scalp on the back of the head to the vertex, occasionally extending as far as the coronal suture (Figs. 8.12 and 8.13). This nerve is joined by a filament from the third cervical ramus. The lateral branches of the upper three lumbar and upper three sacral rami send cutaneous twigs which supply the upper part of the gluteal area, extending laterally to the region of the great trochanter. These branches are known as the *superior* (lumbar) and *medial* (sacral) *clunial nerves* (Fig. 8.12).

VENTRAL RAMI

The ventral rami of the spinal nerves supply the ventrolateral muscles and the skin of the trunk, as well as the extremities (Figs. 8.1 and 8.9). With the exception of most thoracic nerves, the ventral rami of adjacent nerves unite and anastomose to form the cervical, brachial and lumbosacral plexuses.

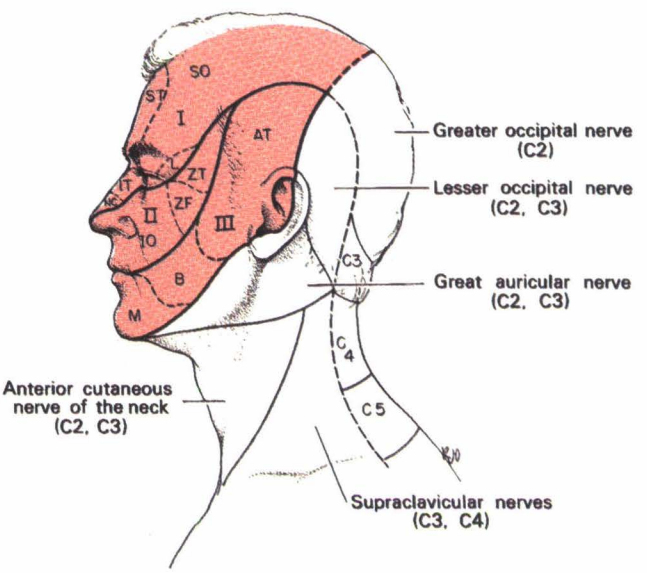


Figure 8.13. Diagram of cutaneous fields of the head and neck. The distribution of the three peripheral divisions of the trigeminal nerve are shown in *red* (I, ophthalmic division; II, maxillary division; III, mandibular division). Abbreviations indicate the following nerves within the trigeminal divisions: *AT*, auriculotemporal; *B*, buccal; *IO*, infraorbital; *IT*, unfratrochlear; *L*, lacrimal; *M*, mental; *NC*, nasociliary (external branch); *SO*, supraorbital; *ST*, supratrochlear; *ZF*, zygomaticofacial; *ZT*, zygomaticotemporal. There is no dermatomal overlap between the three divisions of the trigeminal nerve. Branches of cervical spinal nerves innervate cutaneous regions over the back of the head and in the neck.

Cervical Plexus

The cervical plexus is formed from the ventral rami of the four upper cervical nerves. It furnishes cutaneous nerves for the ventrolateral portions of the neck and shoulder and for the lateral portions of the back of the head. The muscular branches supply the deep cervical muscles of the spinal column, the infrahyoid muscles, and the diaphragm. They also contribute to the innervation of the trapezius (nerves C1 to C4) and sternocleidomastoid, which are chiefly supplied by the accessory nerve (N. XI).

The *lesser occipital nerve* (C2 and C3) is distributed to the upper pole of the pinna and to the lateral area on the back of the head, overlapping only slightly the field of the greater occipital nerve (Figs. 8.12 and 8.13). The *great auricular nerve* (C2 and C3) supplies the larger, lower portion of the pinna and the skin over the angle of the mandible. The *transverse colli* (C2 and C3) innervates the ventral and lateral parts of the neck from chin to sternum (supra- and infrahyoid region). The *supraclavicular nerves* (C3 and C4), which have a variable number of branches, are distributed to the shoulder, the most lateral regions of the neck and the upper part of the breast, where their terminal branches overlap those of the second intercostal nerve (Figs. 8.11–8.13).

The major muscular nerve of the cervical plexus, the *phrenic* nerve, supplies the diaphragm and is derived mainly from C4, but receives smaller contributions from C3 or C5, or from both (Fig. 8.15). It frequently receives an anastomotic branch from the subclavian nerve of the brachial plexus, which enters the phrenic at a variable height. Hence in high lesions of the phrenic nerve, paralysis of the diaphragm may not be complete. The deep cervical muscles are innervated by direct segmental branches from the ventral rami, as indicated in Figure 8.16.

The hyoid muscles, except those supplied by the cranial nerves, are innervated by twigs from C1 to C3. These twigs unite into a common trunk known as the *ansa cervicalis*. The geniohyoid and thyrohyoid are supplied entirely from C1. The sternohyoid, sternothyroid, and omohyoid are innervated from C2 and C3 by motor twigs from the ansa cervicalis. The cervical plexus also aids in the innervation of the sternocleidomastoid and trapezius. The sternocleidomastoid is supplied mainly by the spinal root of the accessory nerve, with sensory fibers that join it through a branch of C2. The trapezius receives major motor contributions from the spinal accessory nerve, and additional motor fibers from C2, C3 and C4. Brendler (2) has demonstrated that C1 may contribute motor fibers to the trapezius, while the spinal accessory nerve sends most of the motor fibers to the middle and lower portions of the muscle. These motor and sensory fibers form one or more bundles, and may be intermixed with the supraclavicular nerves.

Paralysis as a result of injury of the short segmental nerves is rare and usually associated with involvement of the spinal cord. However, the trapezius and sternocleidomastoid frequently are involved as a result of penetrating stab and bullet wounds of the posterior triangle of the neck which injure the spinal accessory nerve. These muscles are superficial and palpable so that their respective muscle actions are of diagnostic value. The sternocleidomastoid and trapezius may be involved along with axial and limb muscles in diseases of the basal ganglia. One particularly troublesome disorder is the condition known as *torticollis*. Due to spasm, the contracted sternocleidomastoid muscle stands out as a large cord, and the head usually is involuntarily rotated toward the opposite side. This awkward position may be maintained for long periods. Spasmodic torticollis may be associated with neuroses. In the latter cases, it is often difficult to distinguish between a functional disorder and organic disease. Emotional stress usually aggravates these involuntary muscle movements.

Brachial Plexus

The nerves supplying the upper extremity and forming the brachial plexus are derived as a rule from the ventral rami of the four lower cervical and the first thoracic nerves, with a small contribution from the fourth cervical nerve (Figs. 8.14 and 8.15). However, considerable variations are not uncommon. If the contribution from the fourth cervical nerve is strong and that of the first thoracic negligible, the plexus is referred to as the *prefixed* type. It is called *postfixed* when the fourth cervical does not participate at all but the first thoracic makes a significant contribution and the second thoracic sends a branch. Between these extremes there are many intermediate conditions, depending on the degree of participation of the fourth cervical, on the

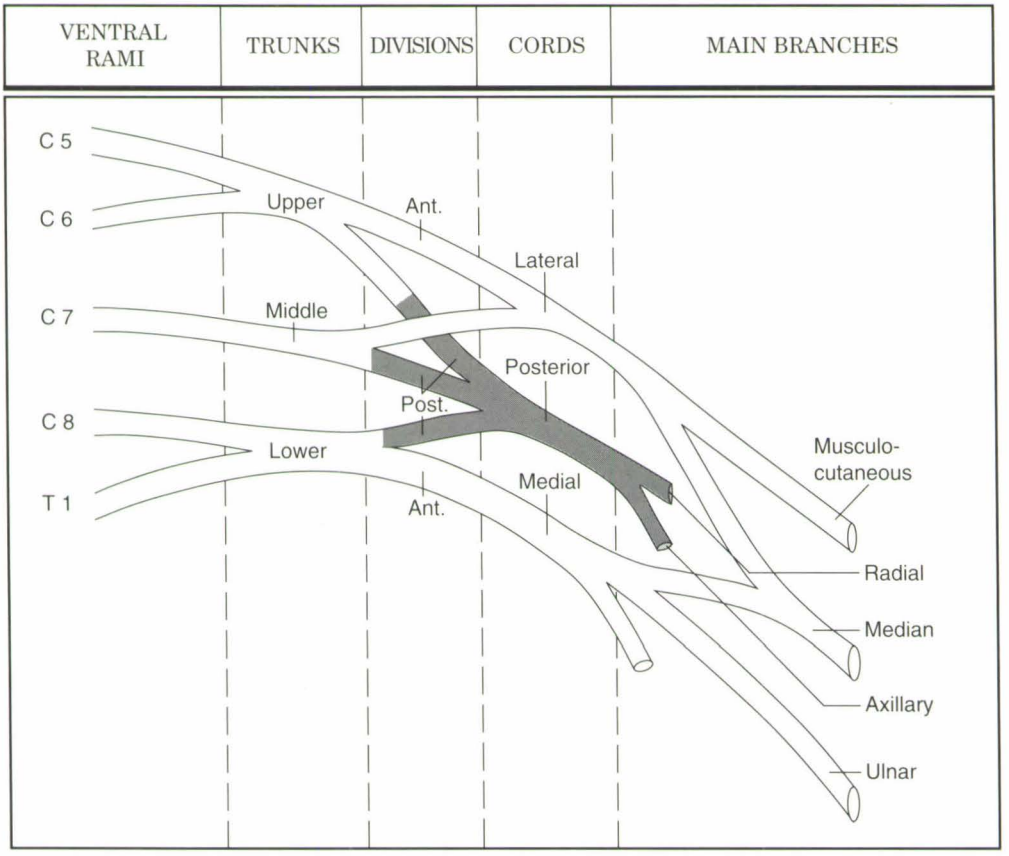


Figure 8.14. Formation of the brachial plexus, indicating ventral rami, trunks, divisions, cords, and main branches. The posterior divisions and the posterior cord are shaded.

one hand, and the second thoracic, on the other. These variations are dependent on embryologic factors. The limb buds of both arms and legs may vary in longitudinal extent and especially in their relative position to the neuraxis. The more cephalic the position of the limbs, the more cephalic will be the nerves contributing to the plexus, and vice versa.

The ventral rami supplying the plexus give rise to three *primary trunks;* C5 and C6 unite to form the *superior (upper) trunk;* C8 and T1 form the *inferior (lower) trunk;* and C7 is continued as the *middle trunk* (Fig. 8.14). Each trunk splits into a posterior and an anterior division. The posterior divisions of all three trunks fuse to form the *posterior cord,* situated behind the axillary artery. The anterior divisions of the superior and middle trunk form the *lateral cord,* while the anterior division of the inferior trunk is continued as the *medial cord* (Fig. 8.14).

Many of the nerves supplying the shoulder muscles are given off directly from the ventral rami, or from the primary trunks and their branches before these unite to form the secondary cords. Thus the *dorsal scapular* nerve supplying the rhomboid muscles arises from the dorsal surface of C5, and the *long thoracic* nerve to the serratus anterior muscle arises from the dorsal surface of C5, C6, and C7. From the superior trunk the *suprascapular* nerve (C4, C5, and C6) for the supraspinatus and infraspinatus muscles emerges dorsally, and the small nerve to the subclavius muscle (C5 and C6) arises ventrally. The roots of the *medial and lateral pectoral* nerves (C5 to T1), which innervate the pectoralis major and minor muscles, arise in part from the ventral surface of the superior and medial trunks, and in part from the medial cord (Fig. 8.15).

The three large peripheral nerves of the forearm (radial, median and ulnar) are formed in the following manner. The posterior cord, which receives contributions from all the plexus nerves, gives off the *thoracodorsal* (C6 to C8) and the *subscapular* nerves (C5 to C8), the former supplying the latissimus dorsi muscle, and latter innervating the teres

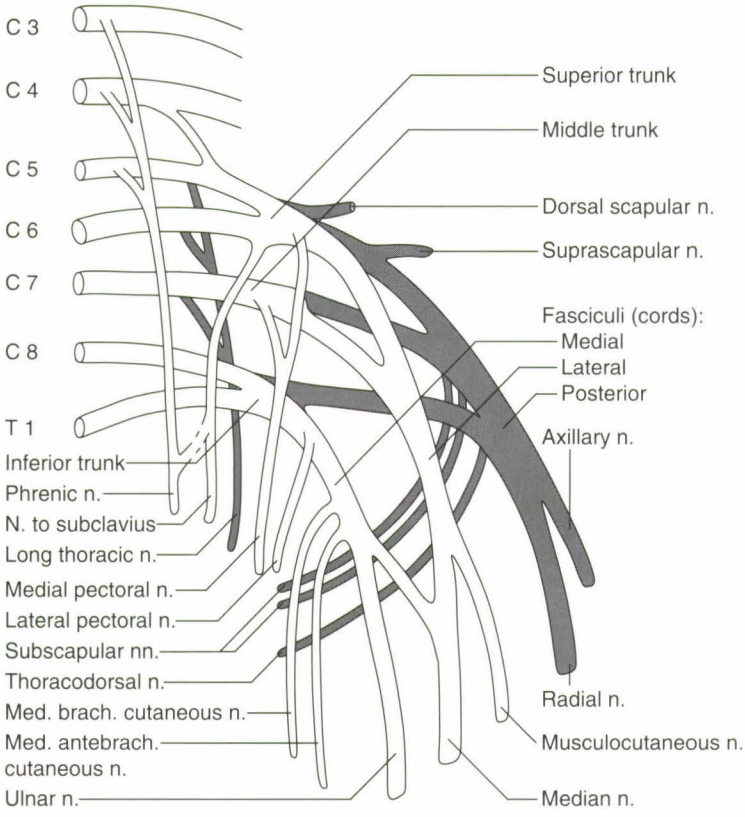


Figure 8.15. Brachial plexus. The posterior divisions, posterior cords, and peripheral nerves formed from the posterior divisions are shaded. Cords and peripheral nerves formed from the anterior divisions of the ventral primary rami are in white.

major and subscapularis muscles (Fig. 8.15). Then the posterior cord splits into its two terminal branches, the larger *radial* nerve and the smaller *axillary* nerve. The lateral and medial cords each split into two branches, thus forming four nerves (Fig. 8.14). The two middle branches, one from the lateral cord and one from the medial cord, unite to form the *median* nerve. The outer branch, derived from the lateral cord, becomes the *musculocutaneous nerve*. The large innermost branch, derived from the medial cord, gives off the purely sensory *medial brachial cutaneous* and *medial antebrachial cutaneous* nerves, and its continuation becomes the *ulnar nerve* (Fig. 8.15).

A brief reference to embryology aids in explaining the formation of the plexus. During early development the primitive muscle mass of the limb is split into posterior and anterior layers, which are separated by the anlage of the humerus. The primary ventral nerve rami invading the limb split into posterior and anterior branches to supply corresponding muscles and the overlying skin. Within the primitive musculature, many simple muscles fuse to form larger and more complex ones innervated by two or more spinal nerves (Figs. 8.17 and 8.18). Such fusion usually occurs within either the posterior or the anterior musculature, and the muscles are innervated, respectively, by posterior or anterior divisions of the nerves. At the cephalic (preaxial) and the caudal (postaxial) borders of the limb, some muscles may be derived from both the posterior and the anterior musculature. These muscles are supplied by nerve fibers from both posterior and anterior divisions. A well-known example is the brachialis muscle, which receives branches from the radial and musculocutaneous nerves. Thus, the primitive plexus shows a division into posterior and anterior plates. The posterior plate innervates the posterior or extensor half of the arm and the posterior shoulder muscles; the anterior plate supplies the volar or flexor half of the arm and the anterior muscles of the shoulder. The nerves arising from the posterior plate are the dorsal scapular, long thoracic, suprascapular, sub-

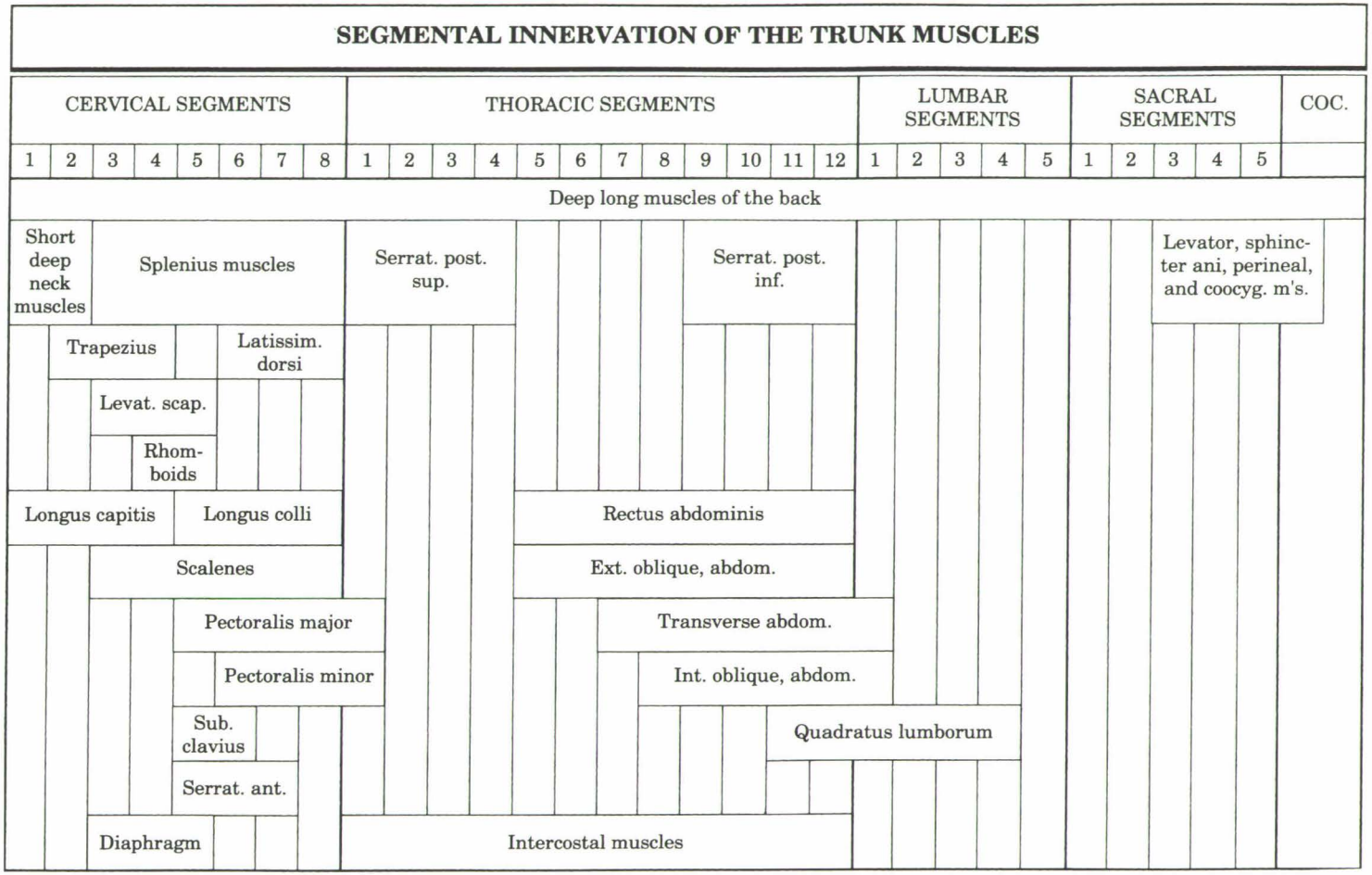


Figure 8.16. Segments of spinal cord that contribute somatic motor nerve fibers to individual trunk muscles.

SEGMENTAL INNERVATION OF MUSCLES OF THE UPPER LIMB

	CERVICAL SEGMENTS					THORACIC SEGMENTS
	4	5	6	7	8	1
SHOULDER	Supraspinatus					
	Teres minor					
		Deltoid				
	Infraspinatus					
		Subscapular				
		Teres major				
ARM		Biceps brachii				
		Brachialis				
		Coracobrachialis				
			Triceps brachii			
				Anconeus		
FOREARM		Brachioradialis				
		Supinator				
			Extensor carpi radialis			
			Pronator teres			
			Flexor carpi radialis			
			Flexor pollicis longus			
				Abductor pollicis longus		
					Extensor pollicis brev.	
				Extensor pollicis longus		
				Extensor digitorum communis		
				Extensor indicis proprius		
				Extensor carpi ulnaris		
				Extensor digiti minimi		
					Flexor digitorum sublimis	
					Flexor digitorum profondus	
					Pronator quadratus	
					Flexor carpi ulnaris	
					Palmaris longus	
HAND					Abductor pollicis brevis	
					Flexor pollicis brevis	
			Opponens pollicis			
					Flexor digiti minimi	
					Opponens digiti minimi	
					Abductor pollicis	
					Palmaris brevis	
					Abductor digiti minimi	
					Lumbricals	
					Interossei	

Figure 8.17. Segments of spinal cord that contribute somatic motor nerve fibers to the individual muscles of the shoulder and upper extremity.

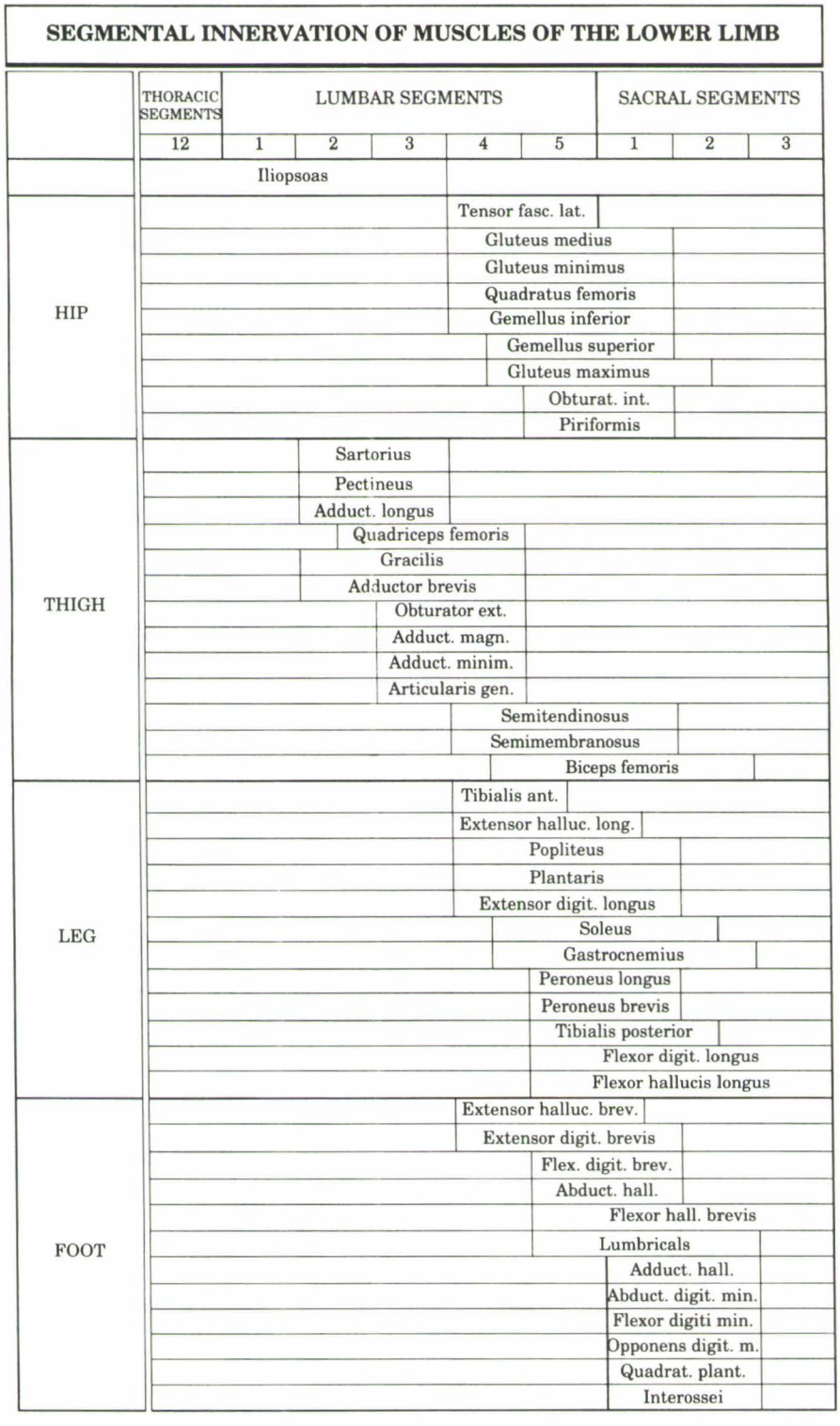


Figure 8.18. Segments of spinal cord that contribute somatic motor nerve fibers to individual muscles of the hip and lower extremity.

scapular, thoracodorsal, axillary, and radial nerves (*black* in Fig. 8.15). Those from the anterior plate include the subclavius, pectoral, musculocutaneous, median, and ulnar, as well as the purely sensory medial brachial and medial antebrachial cutaneous nerves.

A summary of the peripheral distribution of the principal nerves of the upper extremity follows. The cutaneous areas innervated by each nerve are shown in Figures 8.11 and 8.12. In their peripheral courses, some of the nerves of both the upper and lower extremity are particularly prone to trauma, or entrapment by fibrous tissue related to either muscles, tendons, ligaments, or fascia (25). Sensory and motor symptoms that accompany such neuropathies depend on whether the nerves are primarily motor or sensory.

AXILLARY NERVE

This nerve (C5 and C6) innervates the deltoid and teres minor muscles and sends the *lateral brachial cutaneous* nerve to the skin of the upper outer surface of the arm, mainly in the deltoid region. After complete section of the axillary nerve, the deltoid muscle is paralyzed and abduction without external rotation is practically impossible. In time, deltoid atrophy leads to loss of the round contour normally present at the shoulder. The sensory loss is less extensive, owing to the overlap of neighboring cutaneous nerves.

RADIAL NERVE

This nerve (C5 to C8) supplies motor branches to the triceps muscle and all of the extensor muscles of the elbow, hands, and fingers, and to the brachioradialis, supinator and abductor pollici longus. Additionally, it usually sends a twig to the brachialis muscle. Its cutaneous branches, distributed to the posterior surface of the extremity, are the *posterior brachial cutaneous nerve* to the arm, the *posterior antebrachial cutaneous* nerve to the forearm, and the *superficial radial* nerve which innervates the radial half of the dorsum of the hand and fingers as far as the distal interphalangeal joints (Fig. 8.12). The segmental innervation of the muscles supplied by the radial nerve is indicated in Figure 8.17.

Injuries of the radial nerve give variable symptoms which depend upon the location of the lesion. Complete section of the nerve above all its branches produces inability to extend the elbow, wrist, fingers, and thumb, with wrist drop being the most striking feature. The sensory loss is most marked on the dorsum of the hand and thumb in the territory supplied by the superficial radial nerve. Anesthesia in the arm is negligible, but usually is present in a narrow strip on the dorsal surface of the forearm from the elbow to the wrist. The limited sensory loss is due to overlap by adjacent cutaneous nerves. The most vulnerable parts of the radial nerve lie adjacent to the middle third of the humerus and over the lateral epicondyle. The radial nerve is frequently injured in fractures of the humerus and those involving the elbow. The nerve also may be compressed against the humerus during sleep, especially when the patient is anesthetized or intoxicated.

MUSCULOCUTANEOUS NERVE

This nerve (C5 to C7) sends muscular branches to the coracobrachialis, biceps, and brachialis muscles, and continues as the *lateral antebrachial cutaneous* nerve to supply the radial half of the forearm, on both posterior and volar surfaces (Figs. 8.11 and 8.12). In complete lesions of the nerve, flexion and supination of the forearm are weakened. The lateral portion of the brachialis muscle may be spared since it receives, as a rule, a branch from the radial nerve, and forearm flexion can still be produced by the brachioradialis muscle. The sensory loss is variable in extent. It is poorly defined posteriorly, due to overlap with the posterior antebrachial cutaneous nerve (a branch of the radial nerve). On the volar side, sensory loss is more extensive and approximates the territory supplied by the lateral antebrachial cutaneous nerve (Fig. 8.11).

MEDIAN NERVE

This nerve (C6 to T1, and sometimes C5) supplies all the muscles on the volar surface of the forearm except the flexor carpi ulnaris and the ulnar head of the flexor digitorum profundus. In the hand, its branches innervate the outer lumbricals (I and II) and the muscles of the thenar eminence, except for the adductor pollicis brevis. The sensory innervation is limited to the hand. It comprises the volar surface of the thumb, index, and middle fingers, the radial half of the fourth finger, and corresponding portions of the palm (Fig. 8.11). Posteriorly, the nerve supplies the distal phalanx of the index and mid-

dle fingers and the radial half of the fourth finger. An inconstant *palmar* branch is distributed to the radial half of the volar surface of the wrist, but usually this area is completely overlapped by the lateral antebrachial branch of the musculocutaneous nerve. The flexor and pronator muscles supplied by the motor branches of the median nerve have a segmental innervation, as indicated in Figure 8.17.

Injury to the nerve along its course in the arm affects all its branches. Complete interruption causes severe impairment of pronation of the forearm and weakens flexion at the wrist. The wasting of the thenar eminence and the abnormal position of the thumb give the hand a characteristic appearance after median nerve injury (*simian hand*). Normally, the thumb is partially rotated and its metacarpal bone is in a more volar plane than the other metacarpals. In injury of the median nerve, this rotation is lost, and the flexion of the terminal phalanx is completely lost, as are abduction and opposition. Makeshift movements of opposition, without abduction and rotation, can still be affected by the abductor pollicis and the deep head of the flexor brevis muscle (pseudo-opposition). The motor defects are brought out readily in attempts to make a fist. The fourth and fifth fingers flex, but the thumb and index finger, and to a variable degree the middle finger, remain partially extended.

Sensory loss following a lesion of the median nerve is somewhat variable. Usually it is less extensive than the area supplied by the nerve (Figs. 8.11 and 8.12), and it is most constant on the volar surface of the index and middle finger. Loss of appreciation of light touch generally is more constant and extensive than appreciation of pinprick, and extends from the radial border of the thumb to the base of the thenar eminence and across the palm to include the palmar aspects of the ring finger on the radial side. On the dorsum of the hand it includes the radial side of the terminal two-thirds of the ring finger and the middle and index fingers as far proximal as the middle of the proximal phalanges. Deep sensibility usually is lost in the terminal phalanges of the index and middle fingers. The median nerve is prone to injury in deep cuts at the wrist and to entrapment as it passes beneath the transverse carpal ligament with the flexor tendons, a condition referred to as the *carpal tunnel syndrome*. Nerve compression may follow fractures (carpal and distal radial bones) or occur without external stress. Injuries here, as well as lesions of the nerve anywhere along its course, may be accompanied by secondary autonomic system overactivity. Following incomplete regeneration of the nerve, an intense, persistent "burning pain" may be found over one or more points in the distal course of the nerve (*causalgia*). The median nerve is commonly involved in causalgia.

ULNAR NERVE

This nerve (C8 and T1) supplies the flexor carpi ulnaris and the ulnar head of the flexor digitorum profundus in the forearm. In the hand, it innervates the adductor pollicis, the deep head of the flexor pollicis brevis, the interossei, the two inner lumbricals, and the muscles of the hypothenar eminence. It gives off three cutaneous branches. The *palmar cutaneous* branch supplies the ulnar half of the volar surface of the wrist, an area extensively overlapped by the medial antebrachial cutaneous nerve (Fig. 8.11). The posterior branch innervates the ulnar half of the dorsum of the hand, all of the little finger, and the proximal phalanx of the ulnar half of the ring finger. The *superficial volar* branch supplies the volar surface of the fifth digit, and the ulnar half of the fourth finger, and the corresponding ulnar portion of the palm (hypothenar region) (Figs. 8.11 and 8.12). The segmental innervation of muscles supplied by the ulnar nerve is indicated in Figure 8.17.

As in the case of the median nerve, injury to the ulnar nerve in the arm affects its whole distribution. Flexion of the wrist is weakened, as are flexion of the fourth and fifth fingers and adduction of the thumb. There is marked wasting of the hypothenar and interossei muscles. The paralysis of these small muscles is particularly disturbing, for it makes execution of the finger movements required for writing, sewing, and other skilled activities exceedingly difficult. The interossei flex the basal phalanges and extend the middle and distal ones. Hence paralysis of the interossei results in (a) overextension of the basal phalanges by the extensor digitorum communis muscle, and (b) flexion of the middle and distal phalanges by the flexor digitorum sublimis muscle (*claw hand*). Sensory disturbances are variable and depend upon the level of nerve injury. Total anesthesia as a rule is limited to the little finger and the hypothenar region. The ulnar nerve is prone to trauma as it crosses the medial epicondyle of

the humerus, and to entrapment as it passes from the wrist to the hand.

MEDIAL ANTEBRACHIAL CUTANEOUS NERVE

This nerve (C8 and T1) supplies the medial half of the forearm, on both posterior and volar surfaces (Figs. 8.11 and 8.12). The extent of the sensory deficits caused by injury to this nerve varies in individual cases. On the volar side it often reaches to the middle of the arm. On the posterior surface the sensory deficit is somewhat smaller than the area of supply shown in Figure 8.12.

MEDIAL BRACHIAL CUTANEOUS NERVE

This nerve (T1) usually is associated with the *intercostobrachial* nerve derived from the second, and often from the third, thoracic (intercostal) nerve. These two nerves supply the axillary region and the inner surface of the arm, the area being considerably larger on the volar surface than on the posterior surface (Figs. 8.11 and 8.12). The area is overlapped extensively by adjacent cutaneous nerves. Injury to one of the nerves produces negligible symptoms. In injuries of both, the region of anesthesia is limited to the axillary region and medial surface of the upper arm.

Injuries of the Brachial Plexus

The motor and sensory deficits of the brachial plexus lesions vary considerably, depending on the extent of the injury and its location. In injury of the trunks, the symptoms are segmental in character, and two main syndromes may be recognized. One syndrome affects the upper (superior) trunk and the other the lower (inferior) trunk. The upper trunk syndrome (*Duchenne-Erb syndrome*) involves the muscles supplied by C5 and C6, namely the deltoid, biceps, brachialis, brachioradialis, supinator, teres major, teres minor, supraspinatus, and infraspinatus. In this syndrome there is difficulty in elevation and external rotation of the arm, accompanied by a severe loss of flexion and supination of the forearm. Owing to the overlap of adjacent roots, the sensory deficit is as a rule limited to the deltoid region and lateral aspect of the arm.

The lower (inferior) trunk syndrome (*Klumpke* or *Duchenne-Aran syndrome*) is relatively rare and affects primarily the small muscles of the hand innervated by C8 and T1 (Fig. 8.17). The palmaris longus and the long digital flexors usually are involved, with the chief disabilities being in finger and wrist movements. The sensory loss is along the medial aspects of the arm, forearm, and hand. If preganglionic sympathetic fibers of the first thoracic root are included in the injury, there is drooping of the eyelid, diminution in the size of the pupil, and narrowing of the palpebral fissure (*Horner's syndrome*) (see Fig. 11.30).

Injuries of the cords of the brachial plexus produce symptoms similar to those of peripheral nerves, except that they are multiple and often incomplete. A lesion of the posterior cord involves the radial and axillary nerves and often the thoracodorsal and subscapular nerves (Fig. 8.15). Interruption of the lateral cord affects the musculocutaneous and the lateral portion of the median nerve. Injury to the medial cord involves the ulnar and the medial portion of the median nerve, as well as the medial brachial and antebrachial cutaneous nerves.

Lumbosacral Plexus

The plexus innervating the lower extremity is, as a rule, formed by the primary ventral rami of L1 to S2 and the larger portion of S3. Frequently, there is a small contributing branch from T12 (Figs. 8.19 and 8.20). As in the case of the brachial plexus, anatomic variations occur. The plexus is *prefixed* when it is supplied by T12 to S2, and *postfixed* when it is formed from roots L2 to S4. There are also many intermediate forms, but the maximum shift in either direction rarely exceeds the extent of a single spinal nerve. These conditions are determined by the individual variations in the position of the limb buds during development. According to Foerster (16), prefixed lumbosacral plexuses are rare. The lumbosacral plexus, excluding the pudendal and coccygeal portions, which are not distributed to the leg, is conveniently subdivided into an upper *lumbar* and a lower *sacral* plexus.

The *lumbar plexus,* formed by L1, L2, L3, and the larger part of L4, usually receives a communicating branch from T12 (Fig. 8.19). The larger *sacral plexus* is supplied by the smaller portion of L4 (furcal nerve), which joins L5 to form the large lumbosacral trunk, and by S1, S2, and the greater portion of S3 (Fig. 8.20). Except for the uppermost portion supplied mainly by L1, where the conditions are somewhat obscure, both plexuses show

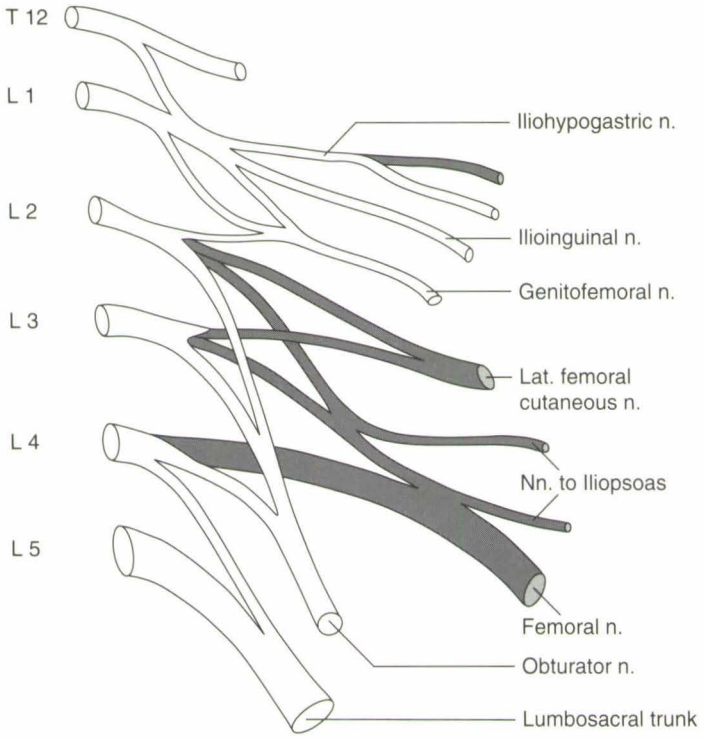


Figure 8.19. Lumbar plexus. Peripheral nerves formed by anterior divisions of ventral primary rami are *white;* nerves formed by posterior divisions of ventral primary rami are *gray.*

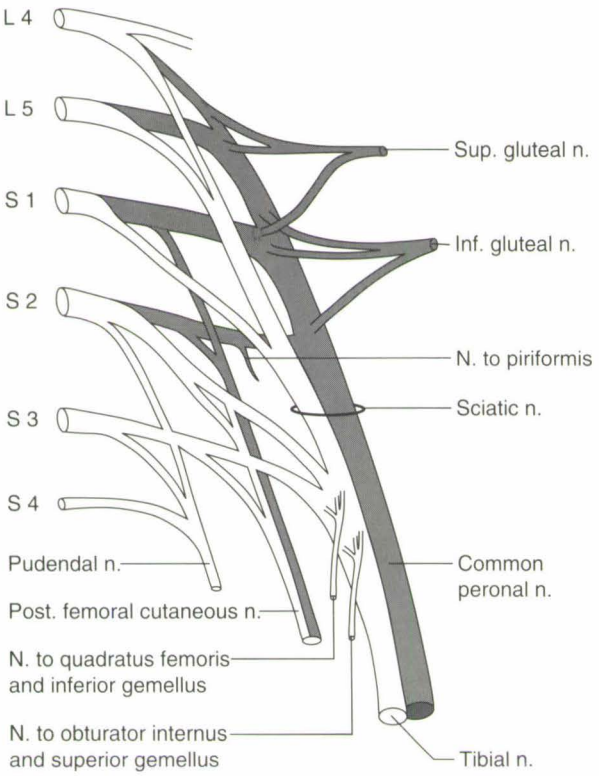


Figure 8.20. Lumbosacral plexus. Peripheral nerves formed by anterior divisions of ventral primary rami are *white;* nerves formed by posterior divisions of ventral primary rami are *gray.*

an organization into posterior and anterior divisions, and the arrangement is simpler than in the brachial plexus. The undivided lumbosacral primary rami do not form interlacing trunks but split directly into posterior and anterior divisions related, respectively, to the primitive posterior and anterior musculature of the leg. The peripheral nerves to the extremity are formed by the union of a variable number of either posterior or anterior divisions (Figs. 8.19 and 8.20). In the lumbar plexus, the anterior divisions give rise to the *iliohypogastric* (anterior branch), *ilioinguinal*, *genitofemoral*, and *obturator* nerves. The posterior divisions give rise to the *iliohypogastric* (posterior branch), *iliopsoas*, *femoral*, and *lateral femoral cutaneous* nerves.

In the *sacral plexus*, the anterior divisions furnish the *tibial* nerve and the nerves to the hamstring, quadratus femoris, obturator internus, and gemelli muscles. The posterior divisions form the *common peroneal* and the *superior* and *inferior gluteal* nerves. The *posterior femoral cutaneous* nerve, which supplies the back of the thigh, receives fibers from both posterior and anterior divisions. As in the case of the arm, muscles derived from both the posterior and the anterior primitive musculature are innervated by both posterior and anterior divisions. Thus the biceps femoris receives branches from the tibial, as well as peroneal portions of the sciatic nerve. Following is a summary of the peripheral distribution of the principal nerves of the lower extremity. The cutaneous areas supplied by these nerves are shown in Figures 8.11 and 8.12.

OBTURATOR NERVE

The obturator nerve (L2 to L4) supplies the adductor muscles of the thigh and the gracilis muscle. It sends an inconstant branch to the pectineus muscle, which more often is innervated by the femoral nerve. Its cutaneous branch is distributed to the inner surface of the thigh (Figs. 8.11 and 8.12), the area being extensively overlapped by adjacent cutaneous nerves. The segmental innervation of the muscles supplied by the obturator nerve is indicated in Figure 8.18. In injury of this nerve, adduction of the thigh is weakened severely, but not lost, since the adductor magnus muscle also receives some fibers from the sciatic nerve. The sensory defects usually involve only a small triangular area of the anatomic field. The obturator nerve is vulnerable to entrapment by the obturator membrane as it passes through the obturator canal.

FEMORAL NERVE

The femoral nerve (L2 to L4) sends motor branches to the extensors of the leg, the iliopsoas, the sartorius, and also the pectineus. Occasionally, a branch may go to the adductor longus. The cutaneous branches are the *anterior femoral cutaneous* nerves for the thigh and the *saphenous* nerve for the leg and foot (Figs. 8.11 and 8.12). The former supply the anterior and anteromedial surface of the thigh, comprising a relatively large autonomous sensory field. The saphenous nerve sends an infrapatellar branch to the skin in front of the kneecap and then is distributed to the medial side of the leg, and the lowermost branches are distributed from the medial margin of the foot to the proximal phalanx of the great toe. The segmental innervation of the quadriceps femoris, iliopsoas, sartorius, and pectineus muscles is shown in Figure 8.18.

Injury of the femoral nerve causes inability to extend the leg. If the lesion is high enough to involve the iliopsoas, flexion of the thigh at the hip is severely impaired. Sensory disturbances are manifested throughout the field of supply, and there are relatively large areas of total anesthesia. If the thigh nerves alone are involved, the anesthesia is most extensive on the anterior surface of the thigh above the knee. In isolated lesions of the saphenous nerve, the anesthetic field extends on the inner surface of the leg from below the knee to the medial margin of the foot. The femoral nerve may become involved secondary to an abscess in the psoas muscle. The terminal sensory branch of the femoral (saphenous nerve) is subject to entrapment as it leaves the subsartorial canal.

LATERAL FEMORAL CUTANEOUS NERVE

The lateral femoral cutaneous nerve (L2 and L3) supplies the lateral half of the thigh, from the lateral buttock region to the knee (Figs. 8.11 and 8.12). In spite of overlap by adjacent cutaneous nerves, injury of this nerve produces a considerable area of anesthesia on the lateral aspect of the thigh. The cutaneous areas supplied by the *iliohypogastric* (L1), *ilioinguinal* (L1), and *genitofemoral* (L1 and L2) nerves are shown in Figures 8.11 and 8.12. The iliohypogastric and ilioinguinal nerves

also send motor fibers to the internal oblique and transverse abdominal muscles. Sensory loss due to injury to one of these nerves is relatively small or may be absent, but such lesions may cause neuralgia.

SCIATIC NERVE

The sciatic (ischiadic) nerve (L4 to S3), the largest nerve in the body, is the chief continuation of all the roots of the sacral plexus. It is composed of two parts, the *tibial* nerve and the *common peroneal* nerve, enclosed for a variable distance within a common sheath (Fig. 8.20). Emerging from the greater sciatic foramen, or while still within it, the nerve sends branches to the main external rotators of the thigh, namely, the obturator internus, the gemelli and the quadratus femoris (L4 to S1). Lesions of these nerves are comparatively rare, and only external rotation is weakened, since other external rotators are available. In the region of the thigh, branches are given off to the flexors of the knee (hamstring muscles) and to the adductor magnus, the latter being innervated also by the obturator nerve. These branches, all derived from the tibial portion of the sciatic nerve, often spring from a common trunk, which either runs independently or is loosely incorporated in the medial side of the sciatic nerve. An additional branch from the common peroneal nerve supplies the short head of the biceps femoris muscle. In injuries of the hamstring nerves flexion of the knee is impaired severely, but weak flexion still may be produced by the action of the gracilis and sartorius muscle. The sciatic nerve splits into its two terminal nerves at varying levels in the thigh. The muscular branches of the common trunk provide motor and sensory fibers to the quadratus femoris, the obturator internus, the gemelli, the semitendinosus, the semimembranosus, and the biceps femoris.

Normal peripheral nerve can be damaged by excessive stretch, as may occur in the roots and cords of the brachial plexus following undue angulation of the head and shoulder, or arm traction, during delivery. Reaction to stretch in an injured or irritated nerve with a long course, such as the sciatic, often produces pain, and paresthesias. One of the best known nerve stretching mechanisms is the straight leg-raising test (*sign of Lasègue*). In a person lying supine with the legs extended, elevation of one extended (straightened) leg by flexion of the thigh at the hip causes stretching of the sciatic nerve. Stretching of the sciatic nerve in the presence of meningitis, intervertebral disc disease, peripheral neuritis, or nerve trauma, produces pain in the distribution of the nerve. The patient usually attempts to relieve the pain by automatically flexing the leg at the knee (*Kernig's sign*). This nerve is accompanied by the popliteal artery and vein, as well as a large number of postganglionic sympathetic fibers. Injuries of this nerve, like the median nerve described earlier, are particularly prone to be followed by causalgia.

TIBIAL NERVE

The tibial nerve (L4 to S3) supplies the posterior calf muscles concerned with (a) plantar flexion and inversion of the foot, and (b) plantar flexion of the toes. It also supplies the intrinsic muscles of the sole, which aid in maintaining the arch of the foot. One cutaneous branch given off in the thigh, the *sural* nerve, is distributed to the posterior and medial surface of the calf, where it is overlapped extensively by branches of the saphenous and lateral sural (peroneal) nerves. Terminal branches of the sural nerve *(lateral calcaneal)* supply the outer margin of the heel and a triangular area on the outer surface of the foot which extends to the lower portion of the Achilles tendon (Fig. 8.12). Other cutaneous branches of the tibial nerve *(medial calcaneal* and *plantar)* supply the back and medial margin of the heel, the plantar surface of the foot and toes, and the dorsal phalanges (Figs. 8.11 and 8.12). The terminal branches of the tibial nerve are the *medial* and *lateral plantar* nerves. The segmental innervation of the calf and plantar muscles supplied by the tibial nerve is indicated in Figure 8.18.

Complete interruption of the tibial nerve above all its branches abolishes plantar flexion of the foot and toes and severely impairs inversion of the foot. Atrophy of the plantar muscles increases the concavity of the plantar arch (pes cavus). Sensory disturbances are negligible in the calf region, in which only a narrow strip may show reduced sensitivity. Total anesthesia is found on the sole of the foot, the plantar surface of the toes, the heel, and often in a triangular area on the outer surface of the foot. This nerve is vulnerable to fractures and dislocations of the medial malleolus, calcaneus, and astragalus bones. It also can be compressed as it passes through the osseofibrous canal with three tendons,

deep to the flexor retinaculum or deltoid ligament (*tarsal tunnel syndrome*).

COMMON PERONEAL NERVE

The common peroneal nerve (L4 to S2) supplies the lateral and anterior muscles of the leg and the dorsal muscles of the foot, effecting dorsal flexion and eversion of the foot and dorsal flexion of the toes. The chief cutaneous nerves are the *lateral sural cutaneous* and the *superficial peroneal* nerve (Fig. 8.11). The former, given off in the thigh, is distributed to the outer side of the leg from the knee region to nearly the outer margin of the sole, where it invades the territories of the superficial peroneal and sural nerves. The superficial peroneal nerve supplies the dorsum of the foot and toes to the distal phalanges and a portion of the anterior surface of the leg. A small cutaneous branch of the deep peroneal nerve is distributed to the cleft between the adjacent surfaces of the great and second toe (Fig. 8.11). The common peroneal nerve divides into its superficial and deep branches as it passes to the lateral side of the neck of the fibula under cover of the peroneus longus muscle. The segmental innervation of the peronei, tibialis anterior, and extensor muscles on the dorsum of the foot is indicated in Figure 8.18.

Complete section of the peroneal nerve causes paralysis of dorsal flexion and eversion of the foot and paralysis of dorsal flexion (extension) of the toes. The most striking feature is inability to elevate the foot and toes (foot drop). If the condition is prolonged, shortening of the Achilles tendon will produce a permanent plantar hyperflexion and the foot will assume an equinovarus deformity. Sensory defects will be found on the dorsum of the foot, the outer part of the leg, and between the great and second toe. The extent of the sensory loss is much smaller than the anatomic field, since cutaneous areas on both, foot and leg, are overlapped extensively by the adjacent cutaneous nerves. The common peroneal nerve is subject to injury both by compression and fracture at the neck of the fibula. A terminal branch of the deep peroneal nerve is frequently injured as it crosses the dorsum of the foot. The terminal sensory fibers of the superficial peroneal nerve may become entrapped as they pierce the deep fascia at the distal and lateral part of the leg.

GLUTEAL NERVES

The *superior gluteal* nerve (L4 to S1) supplies the gluteus medius, gluteus minimus, and tensor fasciae latae muscles, which abduct the hip and rotate it internally. These movements are impaired by injury to the nerve. The *inferior gluteal* nerve (L5 to S2) is distributed to the gluteus maximus, the strongest extensor of the hip. Injury causes wasting of the buttock. There is difficulty in rising from a sitting position, walking uphill, or climbing stairs, where powerful contraction of the muscle is required for raising the body.

POSTERIOR FEMORAL CUTANEOUS NERVE

The posterior femoral cutaneous nerve (S1 to S3) gives off several branches *(inferior clunial)* which supply lower portions of the buttocks. These nerves overlap branches of the lumbar and sacral dorsal rami (superior and medial clunial nerves) (Fig. 8.12). Another small branch *(perineal)* goes to the lower innermost part of the buttock, the dorsal surface of the scrotum (or labia majora) and reaches the inner surface of the thigh. The main nerve supplies the posterior aspect of the thigh, often extending below the knee and widely overlapping the territories of adjacent nerves. Injuries produce a relatively broad strip of anesthesia on the posterior surface of the thigh from the buttocks to the knee.

FUNCTIONAL CONSIDERATIONS

Spinal Roots and Nerves

Knowledge of the origin, size, course, and relations of the spinal nerves to their respective vertebrae (Figs. 10.1 and 10.3) is clinically highly relevant. Meninges, intervertebral discs, size of the intervertebral foramina, and vertebral mobility often can be correlated anatomically with a variety of spinal nerve root syndromes. For example, a ruptured or herniated intervertebral disc may lead to compression of spinal nerve roots as they approach the intervertebral foramen, or the foramina may be narrowed due to osteoarthritis. Effects of stress and strain on the erect spine appear first at the weakest points. Here motion occurs and the mechanical impacts of postural strain and trauma usually are recorded (i.e., cervical and lumbar regions). Dorsal roots, except for C1, are nearly

three times larger than ventral roots. However, the spinal roots vary in size in different regions. The largest nerve roots are those that participate in the formation of the nerve plexuses that supply the limbs. The sixth cervical is the largest of the cervical nerves and from this point upward the roots diminish in size. Root size in relation to bony foramina have some interesting correlations with attendant liability to mechanical irritation or compression. Cervical roots occupy only one-fourth of their respective intervertebral foramen. In contrast, from the first lumbar nerve downward, the size of the nerve roots increase in relation to the size of the foramen. The first to third lumbar nerves never completely fill the foramina, and the fourth root rarely does, whereas the fifth lumbar nerve root frequently fills the intervertebral foramen. This suggests a possible explanation for the high incidence of compression of the fibers of the fifth lumbar nerve root.

Nerve compression by disease or injury can result in a variety of root symptoms, usually associated with pain of short duration (*radicular* or *root pain*). Pain often dominates the clinical picture, but the patient may also complain of numbness, tingling, and prickly sensations (*paresthesias*) localized to the dermatome supplied by the affected dorsal roots. If the ventral roots are involved, muscle spasm, weakness, and vasomotor disturbances may accompany the pain. A knowledge of the radicular (segmental) distribution of the spinal nerves is helpful in evaluating root lesions which may lie in and around the vertebra of a given region.

Injury to the spinal nerves or their peripheral branches causes disturbances of both sensation and movement. Section of a dorsal root rarely produces a loss of sensation (*anesthesia*), although it may impair reflexes (*hyporeflexia*) initiated by appropriate stimuli in the areas supplied by that root. Owing to the overlapping distribution of fibers of adjacent roots, anesthesia will not be detectable unless several contiguous roots are injured or cut (Fig. 8.10). The hyporeflexia involves superficial and deep reflexes and it is associated with a diminution of tone (*hypotonia*) in the affected muscles.

It is clinically important to clearly distinguish the deficits which occur as a consequence of lesions in spinal segments from those that occur in spinal roots, mixed spinal nerves, and peripheral nerves. A lesion in ventral root fibers usually produces the same motor deficits as those resulting from destruction of anterior horn cells (discussed later). However, at certain levels (i.e., thoracolumbar and sacral), section of ventral root fibers produces additional autonomic deficits which may not accompany lesions of the anterior horn cells. Section of a single ventral root, for example C5, would produce weakness in the supraspinatus, infraspinatus subscapularis, biceps brachii, and brachioradialis, but not complete paralysis of any of these muscles. This pattern of distribution is unique to the C5 ventral root and different from that of any single peripheral nerve.

Lesions of mixed spinal nerves produce motor and sensory deficits that correspond to those of combined dorsal and ventral root lesions. While the motor deficits correspond almost exactly to those seen with pure lesions of the ventral root, sensory deficits follow a dermatomal distribution and tend to be less extensive because of the overlapping innervation characteristic of dermatomes (Fig. 8.10). If only one mixed spinal nerve were injured, for example C5, the motor weakness (paresis) would be the same as described earlier, but no sensory loss would be detectable. Involvement of several contiguous mixed spinal nerves would produce marked weakness or paralysis in the muscles innervated by those spinal segments and detectable sensory loss in at least one dermatome, usually the one innervated by the intermediate nerves.

These findings are in sharp contrast to the motor and sensory deficits associated with peripheral nerve lesions. With a peripheral nerve lesion, the muscle paralysis and the sensory loss correspond to the peripheral distribution of the particular nerve.

Lower Motor Neuron

The behavioral expression of central nervous system activities involved a convergence of various central neuronal systems onto projection neurons, whose axons reach peripheral effector organs belonging to either the somatic or visceral components of the peripheral nervous system. For example, the large α motor neurons of the anterior horn of the spinal cord give rise to axons which emerge via the ventral root and innervate striated muscles. The α motor neurons and their axons constitute anatomic and physiologic units, referred to as the final common

pathway or the *lower motor neurons* (38). The concept of the lower motor neuron is not limited to the spinal cord, even though it is frequently used in that context. Cells of the motor cranial nerve nuclei (nerves III to VII, IX to XI, and XII), which innervate the muscles of the head and neck, also must be classified as lower motor neurons. Lesions selectively involving the cell bodies of lower motor neuron in the spinal cord, or their axons in the ventral root or in a peripheral nerve, produce complete or partial loss of motor function (*paralysis* or *paresis*), complete or partial loss of muscle tone (*atonia* or *hypotonia*), loss of reflex activity (*areflexia* or *hyporeflexia*), and muscle atrophy. All of these changes are confined to the affected muscles (6). Atrophy as a consequence of a lower motor neuron lesion develops gradually and in time is obvious on inspection.

Since the anterior horn cells that innervate a single muscle extend longitudinally through several spinal segments, and since several such cell columns exist at each spinal level, a lesion confined to one spinal segment will cause weakness, but not complete paralysis, in all muscles innervated by this segment. Complete paralysis will occur only when the lesion involves the column of cells in several spinal segments that innervate a particular muscle, or the ventral root fibers that arise from these cells. Because most appendicular muscles are innervated by fibers arising from parts of three spinal segments (Figs. 8.16–8.18), complete paralysis of a muscle implies a central lesion involving anterior horn cells in several spinal segments, or a lesion involving ventral root fibers from several spinal segments (Figs. 10.19 and 10.23). Since neighboring cell columns are likely to be affected at each level, such lesions usually produce paralysis in muscle groups rather than individual muscles.

The denervated muscle also shows certain changes in its reaction to electrical stimulation. Healthy muscle responds to stimulation by both the faradic (interrupted) and galvanic (continuous) current. In faradic stimulation, the response lasts as long as the stimulus is applied. In galvanic stimulation, the response occurs only on closing or opening the circuit. Normally it is the application of the negative pole or cathode which produces the strongest contraction on closing the current. In the complete *reaction of degeneration*, which appears 10–14 days after nerve injury, the muscle no longer responds to stimulation of its motor nerve. However, the muscle still responds to direct stimulation with slow wavelike contractions, but it is the positive pole or anode which induces the strongest response on closing the circuit. If preganglionic visceral fibers are involved by a lesion, as in the case of the thoracic and upper lumbar roots, there are sudomotor, vasomotor, and atrophic disturbances expressed by dryness and smoothness of the skin.

In certain diseases of the lower motor neuron, the muscles exhibit small, localized spontaneous contractions known as *fasciculations*. These muscle twitches, visible under the skin, represent the discharge of squads of muscle fibers innervated by nerve fibers arising from lower motor neurons. Fasciculations occur asynchronously in different parts of various muscles and are thought to be triggered by motor unit discharges that occur within the cell body of the degenerating motor neuron. Fasciculations commonly are seen in *amyotrophic lateral sclerosis* (Fig. 11.28), occasionally in acute inflammatory lesions of peripheral nerves (i.e., *polyneuritis*), and generally do not occur when the anterior horn cells are rapidly destroyed (i.e., acute poliomyelitis). The term *fibrillations*, frequently misused as the equivalent of the term fasciculations, refers to small (10–20 μV) potentials of 1–2 msec duration that occur irregularly and asynchronously in electromyograms of denervated muscle. These spontaneous discharges cannot be observed under the skin and produce no detectable shortening of muscles. These potentials represent the spontaneous activation of individual muscle fibers.

Regeneration of Injured Peripheral Nerves

Our knowledge of the processes of degeneration and regeneration has been greatly increased in recent years by investigations on mammalian nerves under various experimental conditions. Valuable information was obtained by clinical and surgical studies of the peripheral nerve injuries during World War II (21, 22). Seddon (36) distinguished three types of nerve injury: (a) complete anatomic division; (b) crush or compression injuries in which the continuity of the nerve fibers is broken but the sheaths and supporting tissue remain intact; and (c) temporary

impairment or nerve block. Nerve section nearly always demands surgical intervention to reestablish continuity. The recovery is more or less successful, but never complete, since many of the regenerating fibers fail to reach their respective end organs. After nerve crush there also is complete degeneration of the severed nerve fibers. Both nerve section and nerve crush are followed by loss of sensation and movement, wasting of muscles, and degenerative reaction. However, the damaged nerve fibers and their sheaths are in close anatomic contiguity after nerve crush, and subsequent regeneration usually leads to a nearly complete recovery. In mild compression or block, there are varying degrees of paralysis, but electrical excitability remains normal. Because the nerve fibers are not severed, there is no peripheral degeneration. Recovery is more rapid. It begins in a few weeks and usually is completed within 2 or 3 months. These three types of nerve injury may appear as separate entities or in various combinations. Since the clinical symptoms after nerve section and crush are the same until regeneration is completed, surgical exploration usually is indicated to determine the nature of the injury (40).

In a simple crush, although the continuity of the axons is interrupted, the endoneurium and other supporting tissues remain essentially intact. As a result, regenerating nerve fibers from the central stump can grow distally, traverse the minimal scar tissue between the severed axonal ends, and enter appropriate Schwann cell tubes of the distal stump. After complete anatomic severance, the conditions are quite different at the site of injury. The cut ends are separated by a gap of variable extent which becomes filled with connective tissue and sheath cells, so that a scar of union is formed between the stumps. Hemorrhage and the vascular mesenchyme contribute cells to the scar tissue. These cellular elements in the lesion area seriously impede the growth of fine sprouts of regenerating axons from the proximal stump of the nerve. An enlarged heterogeneous mass at the cut end of a previously injured nerve is known as a *traumatic neuroma* (amputation or pseudoneuroma). It consists of Schwann cells, connective tissue cells and fibers, macrophages, and an abundance of tangled aberrant nerve fibers. Such a skein of "lost" nerve fibers in scar tissue can be a most serious complication following peripheral nerve section or injury. Many of these fibers are "functional" processes of dorsal root ganglion cells, and these tangled ends can transmit nerve impulses into the spinal cord. Such neuromas explain why a patient may have localized *phantom pain* and/or paresthesias in a previously amputated hand or foot.

The behavior of the Schwann cells after anatomic severance is especially significant. About the 4th day, they become elongated and migrate out of the stumps into the scar, coming mainly from the peripheral stump but, to a lesser extent, also from the central one. These cells arrange themselves end-to-end, and form strands which traverse the fibrous tissue of the scar and establish continuity between the intact axons and the degenerating tubes of the peripheral stump. In some animals, under suitable conditions, gaps of 2 cm have been naturally bridged in this manner. In humans, gaps of several millimeters may be similarly bridged. Under most circumstances, however, the mass of scar tissue is too extensive to be handled by the sheath cells themselves and surgical intervention is required. Scar tissue must be removed from both ends of the severed nerve, and these ends must be approximated and maintained by epineural sutures. The central axonal tips swell and produce a number of fine branches which enter the injured area by the 3rd day. At first they appear free in the connective tissue. Soon they apply themselves to the surface of the sheath cell strands and are led to the peripheral stump, where many of the branches enter the old Schwann cell tubes (Figs. 5.38 and 5.39). However, the number of fibers entering the distal tubes is always smaller after section of the nerve than after crush. Moreover, many nerve fibers enter tubes which are structurally unsuitable for full functional maturation. Once the fibers have entered the distal tubes, the processes of growth and maturation are the same as after crush. These are described in Chapter 5.

The rate of nerve regeneration has been studied by a number of investigators. After primary suture of the peroneal nerve in the rabbit, it takes about 7 days for the growing axon tips of the central stump to traverse the scar of the gap and reach the peripheral stump (19, 20, 42). After crush the "scar" delay was about 5 days. Then the fastest axonal tips grew at the rate of 3.5 mm a day after suture, and 4.4 mm after a crush. Most of the axons grow distally at 3 mm a day after

the peroneal nerve is crushed, and 2 mm a day after nerve section and suture. When the fine regenerated axons attain the periphery they increase in diameter and most of them ultimately become remyelinated. If a sufficient number of such fibers reach and successfully reestablish contact with appropriate sensory and motor end organs, there will be an eventual return of function. The total latent period in the rabbit between nerve regeneration and functional recovery was 20 days following nerve crush and 36 days after nerve suture.

In the longer nerves of humans, the process is slower, although a rate of 4.4 mm a day for growing axons was found after a crush of one of the digital nerves (1). The rate of functional regeneration falls off with the distance traversed, since increases in diameter and myelinization occur more slowly in the distal portions of the fiber. A justifiable assumption for axonal growth in humans under ideal conditions is about 3 mm/day. The average latent period until functional maturity after distal nerve injuries is 20 days after crush and 50 days after suture.

Regeneration can occur when two stumps are sutured after being left apart for a considerable period of time. However, it is generally agreed that functional recoveries after long-delayed sutures usually are unsatisfactory. The difficulties occasioned by long delay are due to a number of factors which interfere with the regenerative processes, and these effects become progressively more serious. Some of the factors are briefly mentioned. After a long delay, the distal stump atrophies and the outgrowth of sheath cells is reduced or ceases. Hence good apposition of the cut nerve ends is difficult, and many axons fail to reach the degenerated atrophic Schwann cell tubes of the distal stump. The tubes themselves are greatly shrunken and receive fewer fibers, so that the chances for reestablishing appropriate peripheral connections are reduced. Myelinization is delayed and increase in diameter of the nerve fiber is restricted by the thickened endoneurium, which forms a large portion of the tube.

Of special importance is the progressive atrophy of the muscles and end organs. In early stages, where the motor end plates remain intact and connected with the Schwann cell tubes, new fibers can enter directly and restore the original pattern. In later stages, these channels become occluded and the end organs may completely disintegrate. The regenerating fibers often fail to enter the old sensory and motor endings or their previous locations. These fibers wander along the muscle fibers, ultimately forming new motor end plates of a more primitive character, whose distribution is irregular and different from the original pattern of innervation. All studies favor early nerve suture, perhaps 3 or 4 weeks after injury. At this time sheath cell activity is at its height and the somewhat thickened perineurium permits easier surgical apposition of the injured nerve stumps (50). Delays of 6 months or more before suture may seriously interfere with the reparative processes but failure is not necessarily encountered in all cases. Good recovery is possible after long-delayed suture if enough axons reach appropriate Schwann cell tubes and the muscles are maintained in good condition by appropriate therapy. Sunderland (41) has reported good restoration of function in human hand and finger muscles which had been denervated for 12 months.

Recent experimental studies have underlined the importance of various growth factors and other molecules in the nerve regeneration processes. Several procedures, including the use of peripheral nerve grafts to promote axonal growth, have also been developed. These novel approaches to the problem of nerve regeneration are reviewed in Chapter 5.

References

1. Bowden REM, Gutmann E. Denervation and re-innervation of the human voluntary muscle. Brain 1944;67:273–313.
2. Brendler SJ. The human cervical myotomes: functional anatomy studies at operation. J Neurosurg 1968;28:105–111.
3. Bunge MB, Bunge RP, Peterson ER, Murray MR. A light and electron microscope study of long-term organized cultures of rat dorsal root ganglia. J Cell Biol 1967;32:439–466.
4. Burton H, McFarlane JJ. The organization of the seventh lumbar spinal ganglion in the cat. J Comp Neurol 1973;149:215–232.
5. Carmel PW, Stein BM. Cell changes in sensory ganglia following proximal and distal nerve section in the monkey. J Comp Neurol 1969; 135:145–166.
6. Carpenter MB. Upper and lower motor neurons. In: Downey JA, Darling RC, eds. Physiological basis of rehabilitation medicine. Ch. 1. Philadelphia: W.B. Saunders, 1971: 3–27.
7. Clifton GL, Coggeshall RE, Vance WH, Willis WD. Receptive fields of unmyelinated ventral root afferent fibres in the cat. J Physiol (Lond) 1976;256:573–600.
8. Coggeshall RE. Nonclassical features of dorsal root ganglion cell organization. In: Yaksh L, ed. Spinal

afferent processing. New York: Plenum, 1986:83–96.
9. Coggeshall RE, Applebaum ML, Frazen M, Stubbs TB III, Sykes MT. Unmyelinated axons in human ventral roots, a possible explanation for the failure of dorsal rhizotomy to relieve pain. Brain 1975;98:157–166.
10. Coggeshall RE, Coulter JD, Willis WD. Unmyelinated axons in the ventral roots of the cat lumbosacral enlargement. J Comp Neurol 1974;153:39–58.
11. Coggeshall RE, Ito H. Sensory fibers in ventral roots L7 and S1 in the cat. J Physiol (Lond) 1977;267:215–235.
12. Dodd J, Jessell TM. Lactoseries carbohydrates specify subsets of dorsal root ganglion neurons projecting to the superficial dorsal horn of rat spinal cord. J Neurosci 1985; 5:3274–3278.
13. Dodd J, Role LW. The autonomic nervous system. In: Kandel ER, Schwartz JH, Jessell TM, eds. Principles of neural science. Ch. 18. New York: Elsevier, 1991:258–269.
14. Dogiel AS. Der Bau der Spinalganglien des Menschen und der Säugetiere. Jena: Gustav Fisher, 1908.
15. Dusser de Barenne JG. Experimental researches on sensory localization in the cerebral cortex of the monkey. Proc R Soc Lond (Biol) 1924;96: 272–291.
16. Foerster O. Die Leitungsbahnen des Schmerzgefühles und die chirurgische Behandlung der Schmerzzustände. Berlin: Urban and Schwarzenberg, 1927.
17. Foerster O. The dermatomes in man. Brain 1933;56:1–39.
18. Foerster O. Sensible cortical Felder. In: Bumke O, Foerster O, eds. Handbuch der Neurologie. Vol. 6. Berlin: Julius Springer, 1936:358–448.
19. Gutmann E, Guttmann L, Medawar PB, Young JZ. Rate of regeneration of nerve. J Exp Biol 1942;19:14–44.
20. Gutmann E, Young JZ. The re-innervation of muscle after various periods of atrophy. J Anat 1944; 78:15–43.
21. Haymaker W. Bing's local diagnosis in neurological diseases. St. Louis: C.V. Mosby, 1956:52; 105–112.
22. Haymaker W, Woodhall B. Peripheral nerve injuries: principles of diagnosis. Philadelphia: W.B. Saunders, 1945.
23. Head H. Studies in Neurology. London: Oxford University Press, 1920.
24. Kerr FWL, Lysak WR. Somatotopic organization of trigeminal-ganglion neurons. Arch Neurol 1964;11: 593–602.
25. Kopell HP, Thompson WAL. Peripheral entrapment neuropathies. Baltimore: Williams & Wilkins, 1963.
26. Lawson SN, Harper EI, Harper AA, Garson JA, Coakham HB, Randle BJ. Monoclonal antibody 2C5: a marker for a subpopulation of small neurons in rat dorsal root ganglia. Neuroscience 1985;16:365–374.
27. Lawson SN, Wadell PJ, McCarthy PW. A comparison of the electrophysiological and immunocytochemical properties of rat dorsal ganglion neurons with A and C fibers. In: Schmidt RF, Schaible HG, Vahle-Hinz C, eds. Fine afferent nerve fibers and pain. Weinheim and New York: VCH Publisher, 1987:193–203.
28. Maynard CW, Leonard RB, Coulter JD, Coggeshall RE. Central connections of ventral root afferents as demonstrated by the HRP method. J Comp Neurol 1977;172:601–608.
29. Pearson AA, Sauter RW, Buckely TW. Further observations on the cutaneous branches of the dorsal primary rami of the spinal nerves. Am J Anat 1966;118:891–904.
30. Philippe E, Garosi M, Droz B. Influence of peripheral and central targets on subpopulations of sensory neurons expressing calbindin immunoreactivity in the dorsal root ganglion of the chick embryo. Neuroscience 1988;26:225–232.
31. Pineda A, Maxwell DS, Kruger L. The fine structure of neurons and satellite cells in the trigeminal ganglion of cat and monkey. Am J Anat 1967;121:461–488.
32. Ramón y Cajal S. Histologie du Système Nerveux de l'Homme et des Vertébrés. (Translated by L. Azoulay), Paris: Maloine, 1909, 1911. (Reprinted, Consejo Superior de Investigaciones Cientificas, Instituto Ramón y Cajal, Madrid, 1972.)
33. Ranson SW. The structure of the spinal ganglia and of the spinal nerves. J Comp Neurol, 1912;22: 159–175.
34. Schmalbruch H. The number of neurons in dorsal root ganglia L4-L6 of the rat. Anat Rec 1987;219: 315–322.
35. Schoenen J, Grant G. Spinal cord: connections. In: Paxinos G, ed. The human nervous system. Ch. 4. New York: Academic Press, 1990:77–92.
36. Seddon HJ. Three types of nerve injury. Brain 1943;66:237–288.
37. Sherrington CS. Experiments in examination of the peripheral distribution of the fibers of the posterior roots of some spinal nerves. Phil Trans R Soc Lond (Biol) 1893; 184:641–763.
38. Sherrington CS. The integrative action of the nervous system. New York: Charles Scribner's Sons, 1906. (Reprinted, Yale University Press, New Haven, 1947.)
39. Sosa JM, DeZorrilla NB. Spinal ganglion cytological responses to axon and to dendrite sectioning. Acta Anat (Basel) 1966;65:236–255.
40. Stookey B, Scarff J. Injuries of peripheral nerves. In: National Research Council Committee on Surgery. Neurosurgery and thoracic surgery. Philadelphia: W.B. Saunders, 1943:81–184.
41. Sunderland S. Capacity of reinnervated muscles to function efficiently after prolonged denervation. Arch Neurol Psychiatry 1950;64:755–771.
42. Sunderland S. Factors influencing the course of regeneration and the quality of the recovery after nerve suture. Brain 1952;75:19–54.
43. Tennyson VM. Electron microscopic study of the developing neuroblast of the dorsal root ganglion of the rabbit embryo. J Comp Neurol 1965;124:267–318.
44. Truex RC. Morphological alterations in the Gasserian ganglion cells and their association with senescence in man. Am J Pathol 1940;16:255–268.
45. Truex RC. Degenerate versus multipolar neurons in sensory ganglia. Am J Pathol 1941;17:211–218.
46. Warrington WB, Griffith F. On the cells of the spinal ganglia and on the relationship of their histological structure to axonal distribution. Brain 1904;27:297–326.
47. Willis WD, Coggeshall RE. Sensory mechanisms of the spinal cord. New York: Plenum Press, 1978.
48. Windle WF. Neurons of the sensory type in the ventral roots of man and other mammals. Arch Neurol Psychiatry 1931;26:791–800.
49. Wyburn GM. The capsule of spinal ganglion cells. J Anat 1958;92: 528–533.
50. Young JZ. Factors influencing the regeneration of nerves. Adv Surg 1949;1:165–220.

9
Autonomic Nervous System

TRIPARTITE INTEGRATED SYSTEM

The portions of the central and peripheral nervous system that are concerned primarily with the regulation and control of visceral functions are termed collectively the *visceral, vegetative,* or *autonomic nervous system* (Fig. 9.1). The vegetative nervous system is said to have been first recognized in 1807 by the German anatomist Johann Christian Reil (113). Nearly 90 years later, John Newport Langley, the English physiologist, introduced the term "autonomic nervous system" to include the cranial and spinal components of the vegetative nervous system. While doing so he commented:

> "the word 'autonomic' does suggest a much greater degree of independence of the central nervous system than in fact exists, except perhaps in that part which is in the walls of the alimentary canal. But it is, I think, more important that new words should be used for new ideas than that the word should be accurately descriptive" (69).

In 1921, Langley proposed a subdivision of the autonomic nervous system that is still widely used today. In this partitioning, neurons of the autonomic system are classified in three groups (a tripartite integrated system) according to the origin of the preganglionic input: (a) sympathetic neurons, with preganglionic input from nerve cell bodies located in the thoracolumbar region of the spinal cord; (b) parasympathetic neurons, with preganglionic input from neurons located either in the brainstem (cranial parasympathetic outflow) or in the sacral region of the spinal cord (sacral parasympathetic outflow); and (c) enteric neurons, with little or no preganglionic input from the central nervous system (53). In the present account, the terms sympathetic and parasympathetic are not restricted to postganglionic neurons. They are applied to both the pre- and postganglionic elements of the thoracolumbar and craniosacral subdivisions of the autonomic nervous system, which are viewed as closely interrelated systems working in a highly concerted fashion.

Visceral sensory-afferent signals are initiated mainly by internal changes that activate visceroceptors. Visceral reactions processed by the central nervous system are usually vague, poorly localized and predominantly of an affective character. Tactile sensibility is practically absent, and temperature sense is appreciated only in certain places, such as the esophagus, the stomach, the colon, and the rectum. On the other hand, distension or spasms of the muscular walls of hollow viscera or blood vessels may produce severe distress or acute pain. As defined by Langley (70), the *autonomic system* was purely a visceral motor system consisting of "visceral efferent cells and fibers that pass to tissues other than the skeletal muscle." This rigid definition, which is still used in some recent textbooks (39), limits the term autonomic to a two neuron visceral efferent system and excluded visceral afferent fibers. Yet, sensory fibers accompany most visceral motor fibers and form the afferent links of most visceral reflex arcs. Recent clinical studies underline the importance of visceral afferent mechanisms in functional disorders of various viscera (81). Visceral afferent fibers have their cells of origin in the spinal and specific cranial nerve ganglia (Figs. 9.2 and 10.23). They, like the higher brain centers, play a constant and dynamic role in the regulation of autonomic activities.

During the years that have followed the pioneering studies of Walter Hess (60), the foregoing limited concept has been liberalized to make the term "autonomic" more synonymous with "visceral," and to include both peripheral and central neural structures. It behooves all concerned with visceral function to remember that central neurons and visceral afferent neurons are vital and integral parts of the autonomic system, regardless of arbitrary definitions. In similar fashion, no attempt should be made to sharply

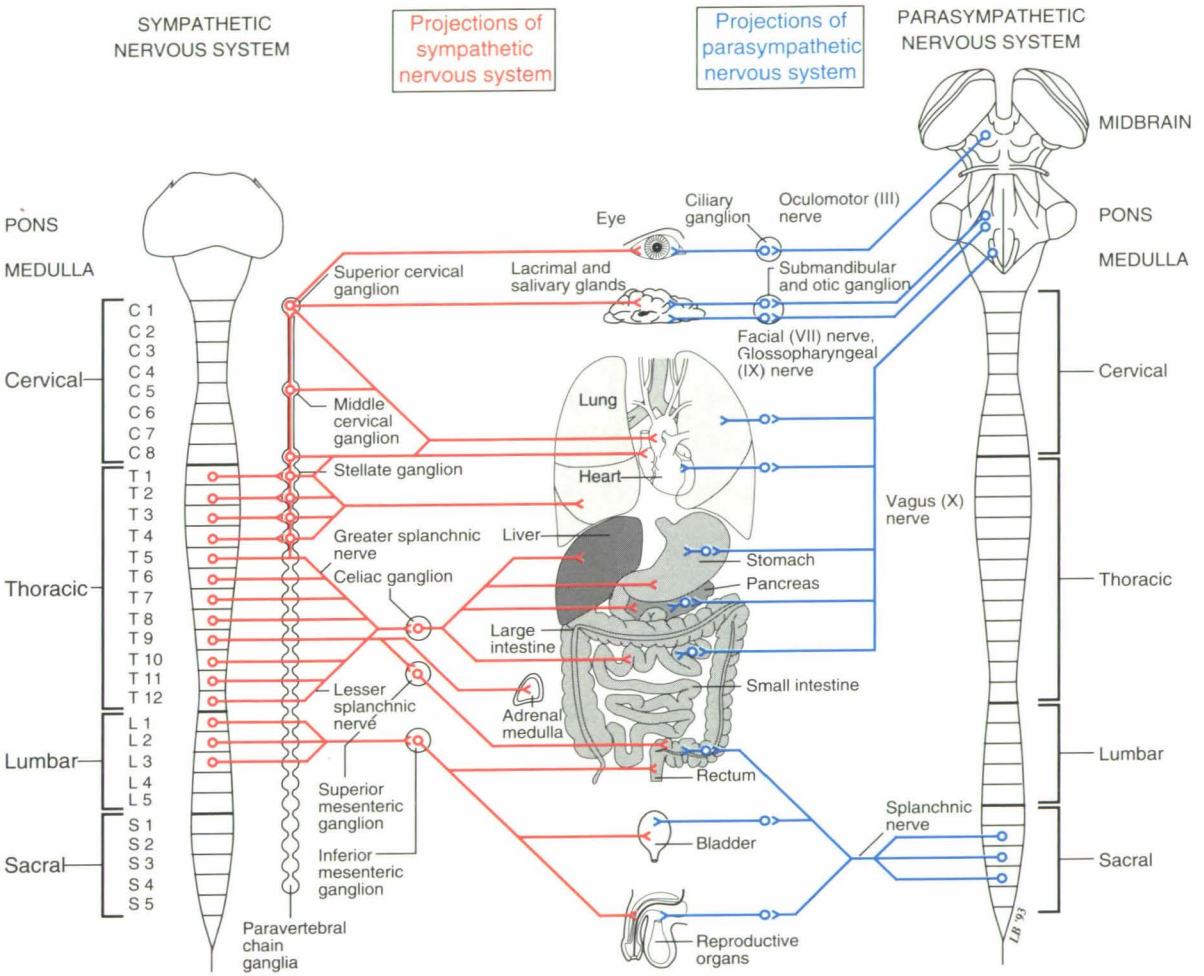


Figure 9.1. General arrangement of the autonomic system. The sympathetic components are shown in *red*, while the parasympathetic components are in *blue*. For clearness the sympathetic fibers to the blood vessels, hair, and sweat glands are shown separately in Figure 8.2.

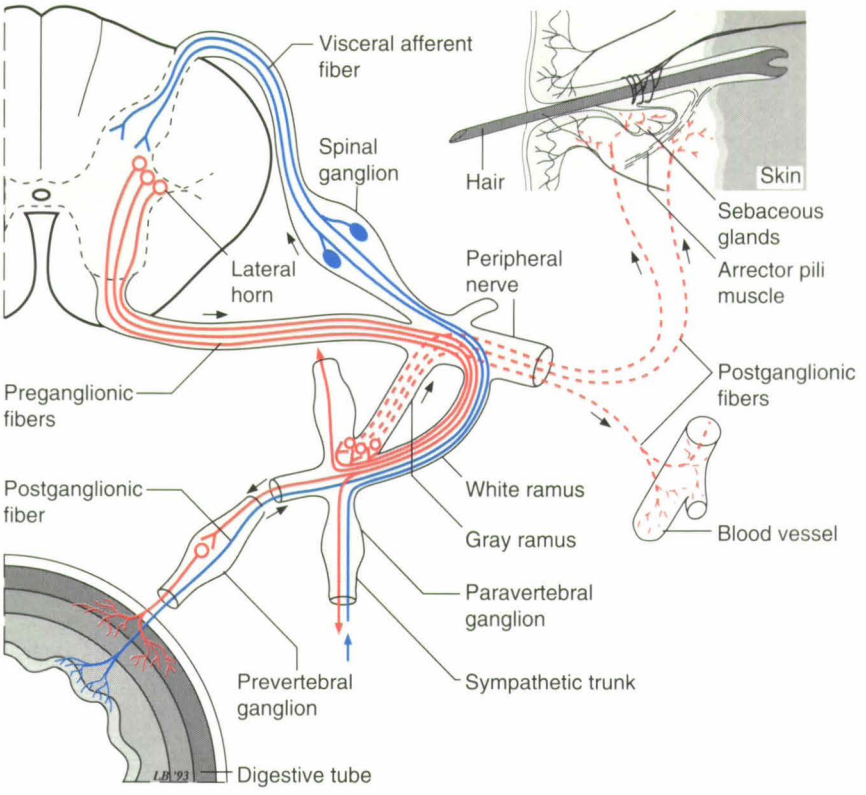


Figure 9.2. Neural reflex arcs of the sympathetic system.

delineate the nervous system into somatic and visceral portions. This is a convenient physiologic subdivision, but the two are merely different parts of a single integrated neural mechanism. The higher brain centers regulate both somatic and visceral functions, and throughout the neuraxis there is intermingling and association of visceral and somatic neurons. Moreover, visceral reflexes may be initiated by impulses passing through somatic afferent fibers from any receptor, and, conversely, visceral changes may give rise to somatic activities. Through some mechanism, as yet unexplained, stimulation of peripheral visceral efferent neurons also can alter the activity of somatic sensory receptors. Also of interest are the results of a recent immunohistochemical study of the embryonic development of the enzyme choline acetyltransferase (ChAT) in thoracic spinal motor neurons of the rat, which suggests that both somatic and autonomic neurons at this level are derived from a common cellular group (93).

Interposed in the efferent peripheral pathway between the central nervous system and the visceral structures are aggregations of nerve cells known as the *autonomic ganglia*. The cells of these peripheral ganglia are in synaptic relation with fibers from the spinal cord or brainstem, and they send out axons which terminate in the visceral effectors: smooth muscle, heart muscle, and glandular epithelium. There are fundamental differences in the innervation of striated and smooth muscle. In striated muscle, each muscle fiber is innervated by a single axon, but a single motor neuron may send axons to many muscle fibers. Furthermore, the efferent pathway to striated skeletal muscle is *monosynaptic*; the central motor neuron, whose cell body resides in the ventral horn of the spinal cord, projects directly to the striated muscle. The nerve-muscle junction in striated fibers has a characteristic morphology and is called the motor end plate or the neuromuscular junction.

In smooth muscle, the efferent axon has numerous swellings or varicosities which constitute sites of transmitter storage and release. There may be no specialized structure on the postjunctional membrane of the smooth muscle fiber, and not all muscle cells are innervated. Smooth muscle cells are often

electrotonically coupled through gap junctions, so it is not necessary for each muscle fiber to be directly contacted by the axon (25, 125). Peripheral autonomic neurons usually discharge at low frequencies, and may produce their maximal effect at rates of 4–10 Hz (55). The visceral motor system also differs from the somatic voluntary motor system in that its efferent pathway to the target is *disynaptic*; a synapse in the peripheral autonomic ganglion is always interposed between the efferent neuron in the central nervous system and the target organ in the periphery. Another important difference concerns the mechanisms by which motor output is inhibited. Since all somatic motor neurons are excitatory, inhibition can only be obtained by acting directly onto the motor neuron. Thus, relaxation of the striated muscle is achieved not by inhibiting the muscle directly but by inhibiting the motor neurons in the spinal cord that excite the striated muscle. In contrast, smooth muscle typically receive inhibitory, as well as excitatory, inputs from different autonomic postganglionic neurons. This organization allows the autonomic nervous system to respond to environmental changes in a highly ordered fashion.

PRE- AND POSTGANGLIONIC NEURONS

The transmission of impulses from the central nervous system to the viscera is disynaptic; it always involves two different neurons (Figs. 9.1 and 9.3). The first neuron, the *preganglionic* neuron, is situated in the brainstem or spinal cord and sends a thinly myelinated fiber to an autonomic ganglion where it synapses with one or more *postganglionic* cells. Preganglionic fibers of the cranial and spinal nerves are approximately 3 μm in diameter, have slow conduction velocities (3–15 m/sec), and are designated as the B fibers of peripheral nerves (91). The usually unmyelinated axons of postganglionic neurons (autonomic ganglion cells) then pass to visceral effectors (Fig. 10.23). Postganglionic autonomic axons have smaller diameters (0.3–1.3 μm), possess slower conduction velocities (0.7–2.3 m/sec), and are usually classified as C fibers in peripheral nerves (Table 5.2). Therefore, even the simplest visceral reflex arc will involve at least three neurons: (a) visceral afferent, (b) preganglionic visceral efferent, and (c) postganglionic visceral efferent (Figs. 9.2 and 10.23). Quantitative studies of midthoracic communicating rami in the cat show that about 10% of the axons in the white rami are sensory. About half of the sensory axons are unmyelinated. In the gray rami, less than 1% of the axons are sensory (28, 29). While the number of afferent axons in the sympathetic rami is small, they will need to be considered in functional studies relating to visceral sensation.

The autonomic ganglia, which have a wide distribution in the visceral periphery, may be classified in three groups: (a) *paravertebral*, (b) *prevertebral (collateral)*, and (c) *terminal*. Paravertebral ganglia are arranged in a segmental fashion along the anterolateral surface of the vertebral column and are connected with each other by longitudinal fibers to form the two ganglionated cords called *sympathetic trunks* (Fig. 9.1). The prevertebral ganglia are irregular aggregations of cells found in the mesenteric neural plexuses surrounding the abdominal aorta and its larger visceral branches. The terminal ganglia are parasympathetic and are located within, or close to, the structures they innervate. These ganglia show extreme variations in size and compactness. Some are organized into distinct, anatomically encapsulated structures, as in the case of the sympathetic trunks and the autonomic ganglia of the head. Others form extensive plexuses of nerve cells and fibers, as in the intramural intestinal plexuses. Small ganglionic masses (microganglia) or scattered cell groups are found within, or near, the walls of visceral structures (e.g., heart, bronchi, pancreas, and urinary bladder).

The outflow of preganglionic fibers from the central nervous system, which establishes synaptic connections with peripheral autonomic ganglia, arises from three well-defined regions. The *cranial outflow* originates from visceral cell groups (nuclei) of the brainstem associated with the oculomotor (N. III), facial (N. VII), glossopharyngeal (N. IX), and vagus (N. X) nerves, and emerges from the brainstem in association with these cranial nerves *(blue* in Fig. 9.1). These preganglionic fibers are parasympathetic and terminate either in cranial autonomic ganglia (ciliary, pterygopalatine, submandibular, or otic), or in terminal ganglia within the walls of thoracic or abdominal viscera (e.g., heart, lungs, esophagus, and stomach). The *thoracolumbar outflow* arises from cells of the intermediolateral cell column in all thoracic and the upper two or three lumbar spinal cord segments. The peripheral ax-

	SYMPATHETIC		PARASYMPATHETIC	
Structure supplied	Preganglionic Cell Bodies in CNS Nuclei	Postganglionic Cell Bodies in Peripheral Ganglia	Preganglionic Cell Bodies in CNS Nuclei	Postganglionic Cell Bodies in Peripheral Ganglia
Iris of eye	intermediolateral nuc. in cord segments C8 - T2 (3)	sup. cervical ganglion and scattered along carotid plexus	Edinger-Westphal nuc. of midbrain	ciliary ganglion
Lacrimal gland	intermediolateral nuc. in cord segments T1 - 2	sup. and middle cervical symp. ganglia	sup. salivatory nuc. in pons	pterygopalatine ganglion
Submandibular and sublingual glands	intermediolateral nuc. in cord segments T1 - 3 (4)	sup. and middle cervical symp. ganglia	sup. salivatory nuc. in pons	submandibular ganglion
Parotid gland	intermediolateral nuc. in cord segments T1 - 3 (4)	sup. and middle cervical symp. ganglia	inf. salivatory nuc. in medulla	otic ganglion
Sweat glands of head and neck	intermediolateral nuc. in cord segments T1 - 3	3 cervical sympathetic ganglia		
Lungs and bronchi	intermediolateral nuc. in cord segments T1 - 5	inf. cervical and thoracic (T1 - 5) symp. ganglia	dorsal motor nuc. N. X	ganglia of pulmonary plexi
Heart	intermediolateral nuc. in cord segments T1 - 5 (6, 7)	3 cervical and thoracic (T1 - 6) symp. ganglia	dorsal motor nuc. N. X	intra-cardiac ganglia of atria
Esophagus	intermediolateral nuc. in cord segments T1 - 6	thoracic symp. T(1 - 3) 4 -6 ganglia	dorsal motor nuc. N. X	myenteric and submucous plexi
Stomach, small intestine; ascending and transverse colon	intermediolateral nuc. in cord segments T5 - 11	celiac and sup. mesenteric ganglia	dorsal motor nuc. N. X	myenteric and submucous plexi
Descending colon and rectum	intermediolateral nuc. in cord segments T12 - L3	lumbar and inf. mesenteric symp. ganglia	autonomic nuc. of intermediate gray in cord segments S2 - 4	ganglia of hemorrhoidal myenteric and submucous plexi
Sex organs	intermediolateral nuc. in cord segments T10 - L2	lumbar, sacral and inf. mesenteric symp ganglia	autonomic nuc. of intermediate gray in cord segments S2 - 4	Ganglia along branches of aorta and int. iliac arteries (e.g. ovarian, uterine)
Urinary bladder	intermediolateral nuc. in cord segments T12 - L2	lumbar and inf. mesenteric symp. ganglia	autonomic nuc. of intermediate gray in cord segments S2 - 4	ganglia along visceral branches of int. iliac artery
Sweat glands and blood vessels of lower extremity	intermediolateral nuc. in cord segments L1 - 2	lumbar and sacral symp. ganglia		

Figure 9.3. Location of preganglionic and postganglionic autonomic neurons in relation to important visceral structures.

onal processes of these cells form the preganglionic sympathetic fibers which emerge from the spinal cord via the ventral roots of the thoracic and upper lumbar spinal nerves (*red* in Fig. 9.1). Peripherally, these fibers leave the mixed spinal nerve and contribute to the *white rami communicantes*, or communicating branches, which appear white because they are composed of myelinated fibers. The fibers then enter the sympathetic trunk and terminate upon cells in the paravertebral ganglia or pass through the trunk to synapse in prevertebral ganglia (Fig. 9.2). Although the thoracolumbar outflow arises from a cell column in a restricted region of the spinal cord (T1 to L3), it represents the total sympathetic output for the entire body. This is possible because some preganglionic sympathetic fibers ascend and descend in the sympathetic trunk for considerable distances before terminating upon post-

ganglionic neurons. The *sacral outflow* arises from preganglionic visceral neurons in the intermediate gray matter of the second, third, and fourth sacral segments of the spinal cord. These preganglionic parasympathetic fibers emerge from sacral spinal segments via their corresponding ventral roots and pass to terminal ganglia within the walls of pelvic viscera (*blue* in Fig. 9.1).

Although preganglionic neurons are located in three distinct regions of the central nervous system, they are regrouped in two main divisions: (a) the *sympathetic* or *thoracolumbar system* and (b) the *parasympathetic* or *craniosacral system* (Figs. 9.1 and 9.2). In spite of the restricted central origins of preganglionic sympathetic and parasympathetic fibers, most viscera receive a double autonomic innervation. Notable exceptions are the glands of the skin and peripheral blood vessels, which receive only a sympathetic innervation. Peripherally fibers of the two divisions of the autonomic nervous system often are intermingled, but they retain their functional independence, which usually is antagonistic but closely integrated. The thoracolumbar outflow provides sympathetic innervation for all visceral structures of the body via synaptic articulations with postganglionic sympathetic neurons in peripheral autonomic ganglia. The cranial portion of the parasympathetic system supplies specific visceral structures in the head via postganglionic parasympathetic fibers from autonomic ganglia, and thoracic and abdominal viscera via the vagus nerve, and postganglionic fibers from terminal ganglia. Pelvic viscera are innervated by the parasympathetic sacral outflow and postganglionic fibers from terminal ganglia.

The investigation of the origin of autonomic preganglionic axons using horseradish peroxidase (HRP) retrograde tracing methods is leading to some revision of the classical view. For example, there is evidence that some sympathetic fibers to the small intestine arise in the cervical sympathetic ganglia and reach the gut by traveling in the vagus nerve (75). Where it was once thought that distinct portions of the gut were innervated by vagal and sacral parasympathetic fibers, it now appears that there is overlap in the descending colon and rectum (108). There is some species difference in autonomic innervation of the heart, the cornea and other peripheral structures (30, 51, 80).

Experimental studies with powerful tract-tracing techniques have revealed new information regarding the organization of the autonomic nervous system in different species. For example, studies with retrograde tracers such as wheat germ agglutinin conjugated to HRP (WGA-HRP), cholera toxin subunit B, or fluorogold, revealed with great detail the cellular origin of the sympathetic innervation of various structures, including the adrenal medulla and the aorticorenal ganglion (65), the elbow and knee joints (131), the cornea (80), the spleen (105), and the lumbar visceral nerves (7). Other studies have used WGA-HRP as an anterograde tracer to label entirely the terminal plexus of sympathetic nerve fibers innervating the cerebral arterial system (58). This investigation has detected differences in the distribution pattern of the nerve plexus. These differences appear clinically relevant as they may account for the variations in the strength and quality of the sympathetic-induced vasoconstriction at various points along the cerebral arterial system (58). Furthermore, the use of two different retrograde tracers (double retrograde labeling techniques; see Chapter 5), have revealed that the sympathetic preganglionic neurons are organized according to a highly ordered pattern (65, 123). For example, despite their similar segmental distribution (T2 to L2), the preganglionic sympathetic neurons projecting to the adrenal gland and the adjoining aorticorenal ganglion belong to separate populations (65). On the other hand, intracellular injections of HRP have provided detailed views of the preganglionic sympathetic neurons, particularly its dendritic tree (47).

One of the most promising tools for the anatomic study of the autonomic nervous system, and perhaps of the central nervous system as well, is the pseudorabies virus, which can be used as a retrograde transneuronal cell body marker (104, 119, 120). Results from recent studies designed to identify central nervous system cell groups regulating the sympathetic outflow to the adrenal gland in the rat exemplify the usefulness of this marker (119, 120). When injected directly into the adrenal medulla, the pseudorabies virus induces retrograde viral infections of the ipsilateral sympathetic neurons (T4 to T13) and causes retrograde transneuronal cell body infections in several areas of the brain, including the caudal raphe nuclei, various portions of the medulla, and the paraventricular nu-

cleus of the hypothalamus. In the spinal cord, the segmental distribution of virally infected neurons is the same as the retrograde cell labeling that can be observed following fluorogold injection in the adrenal medulla, except that there is almost a 300% increase in the number of labeled cells (120). Furthermore, this retrograde labeling method can be easily combined with standard immunohistochemical procedures so that neurotransmitter(s) used by central neurons regulating the sympathoadrenal outflow can be identified. Indeed, the combination of these two approaches has revealed that neurons in the medullary raphe nuclei that project to the sympathetic preganglionic neurons innervating the adrenal medulla display immunoreactivity for either serotonin, substance P, thyrotropin-releasing hormone, met-enkephalin, or somatostatin (120). Virally infected neurons lying in other portions of the medulla, or in the hypothalamus, were found to be either adrenergic or noradrenergic, while others displayed immunoreactivity for neuropeptide Y, substance P, and somatostatin. Future studies with such powerful techniques should greatly increase our knowledge of the anatomic and functional organization of the autonomic nervous system.

SYMPATHETIC SYSTEM

Topographic Organization

The sympathetic trunks are two ganglionated cords symmetrically placed along the anterolateral aspects of the vertebral column that extend from the base of the skull to the coccyx. The cervical portion contains three ganglia formed by the fusion of the original eight segmental ganglia. The *superior cervical ganglion,* the largest of the paravertebral ganglia, is situated near the second and third cervical vertebrae. It is about 2.5–3.0 cm long and contains more than 1 million neurons (92). The small *middle cervical ganglion* is present only in about 60% of the individuals. It is about 0.7–0.8 cm long and lies near the sixth cervical vertebra, just superior to the inferior thyroid artery. In some cases, the middle cervical ganglion fuses to the inferior pole of the superior cervical ganglion to form a combined mediosuperior cervical ganglion up to 4.5 cm long (53). The *inferior cervical ganglion* lies at the lower border of the seventh cervical vertebra, behind the subclavian artery. This ganglion frequently fuses with the first thoracic ganglion to form the *stellate ganglion* (Fig. 9.1). The stellate ganglion may extend up to 2.8 cm. In the thoracic, lumbar, and sacral regions, the ganglia are segmentally arranged. There are 11 or 12 thoracic, 3 or 4 lumbar, and 4 or 5 sacral ganglia. In the sacral portion, the two trunks gradually approach each other and fuse at the coccyx in the unpaired coccygeal ganglion. Sometimes, the stellate and all the thoracic ganglia down to the fourth segment are fused. The thoracic and lumbar sympathetic ganglia are relatively small, each containing about 50,000–100,000 nerve cell bodies.

The prevertebral ganglia are irregular ganglionic masses lying in complex plexuses associated with the abdominal aorta and its major arterial branches. The largest prevertebral ganglia are the paired celiac ganglia embedded within the celiac plexus, which surrounds the proximal segment of the celiac artery and the root of the superior mesenteric artery. The celiac ganglion has two major poles, each about 20–25 mm by 10–15 mm, and about 3–5 mm thick. Together, they contain approximately 1,800,000 cell bodies. Other prevertebral ganglia are the aorticorenal, the phrenic and the superior and inferior mesenteric. These ganglia are closely interconnected by numerous nerve fibers (Fig. 9.1) and are described in relation to the celiac and subsidiary plexuses.

The sympathetic ganglia receive preganglionic fibers from the lateral horn of the spinal cord through the ventral roots of all the thoracic and the upper two lumbar nerves (95, 114, 115). These fibers leave the ventral roots, pass through the white rami communicantes, and enter the sympathetic trunk to reach either the paravertebral or prevertebral ganglia. The fibers that terminate in the paravertebral sympathetic ganglia either end in the first one entered, or pass up or down in the sympathetic trunk giving off collaterals, and finally terminate in ganglia above or below the level of their entrance (Fig. 9.1). The preganglionic fibers from the upper five thoracic segments pass mainly upward, those from the middle thoracic segments (T7 to T10) pass up or down, while those of the lowest thoracic and lumbar segments pass only downward. The preganglionic fibers that terminate in the prevertebral ganglia do not synapse in the paravertebral ganglia, but merely pass through them and emerge as the

splanchnic nerves (Figs. 9.1 and 9.2). While the sympathetic pathway from the spinal cord to the viscera always involves two neurons, there are never more than two. Thus, synapses between pre- and postganglionic neurons occur either in the paravertebral or prevertebral ganglia, but not in both.

While the white rami communicantes are limited to the thoracic and upper lumbar nerves, each spinal nerve receives a *gray ramus communicans* from the sympathetic trunk (Fig. 9.2). The gray ramus consists of unmyelinated postganglionic fibers which innervate the blood vessels, arrector pili muscles, and glands of the body wall. The cervical sympathetic ganglia receive ascending preganglionic fibers from the white rami of the upper thoracic nerves, most of which go to the superior cervical ganglion.

Cervical Ganglia and Related Fibers

The *superior cervical ganglion* gives rise to postganglionic fibers distributed as gray rami to (a) the lower four cranial nerves, (b) the upper three or four cervical nerves, (c) the pharynx, (d) the external and internal carotid arteries, and (e) the superior cervical cardiac nerve. Postganglionic sympathetic fibers passing to the external and internal carotid arteries form plexuses about these vessels and their branches (83). From these vascular plexuses the postganglionic fibers pass through cranial autonomic ganglia to join branches of the cranial nerves. Such sympathetic postganglionic fibers supply the dilator muscle of the iris, the smooth muscle portion of the levator palpebrae, the orbital muscle of Müller, the blood vessels, sweat glands, hair of the head and face, and the lacrimal and salivary glands (Fig. 9.3). The superior cervical cardiac nerve passes to the cardiac plexus.

The *middle cervical ganglion*, when present, supplies gray rami to cervical nerves C5 and C6, and sometimes also to C4 and C7, and contribute to the esophageal, tracheal, and aortic plexuses. When this ganglion is absent the cervical spinal nerves C5 and C6 receive gray rami from the sympathetic trunk.

The *inferior cervical ganglion* furnishes gray rami to spinal nerves C7, C8, and T1 (Fig. 9.3). Thus a single ganglion may supply two or more of the lower cervical nerves, and a single nerve may be supplied by two ganglia. Potts (96) has found that the lower four cervical nerves may each receive three gray rami derived from the sympathetic trunk, and from the middle and inferior cervical ganglia. Additionally, the middle and inferior cervical ganglia give off, respectively, the middle and inferior cardiac nerves, which take part in the formation of the cardiac plexus (Fig. 9.1).

Spinal Ganglia and Related Nerves

The thoracic, lumbar, and sacral ganglia furnish gray rami to the remaining spinal nerves. Delicate branches from the upper four or five thoracic ganglia go to the cardiac plexuses as the thoracic cardiac nerves. Other fibers from the inferior cervical ganglion reach the pulmonary plexuses to innervate the bronchial musculature and blood vessels of the lungs (Fig. 9.3). Shorter mediastinal branches from both the thoracic and lumbar ganglia form plexuses around the thoracic and abdominal aorta. In addition to these, there are two, sometimes three, important branches known as the *splanchnic nerves* which arise from the thoracic portion of the sympathetic trunk, pierce the diaphragm, and terminate in the prevertebral ganglia of the mesenteric plexuses (Fig. 9.1). Although the splanchnic nerves appear to be branches of thoracic ganglia, they represent axons of preganglionic neurons which merely pass through paravertebral ganglia and the sympathetic trunk en route to the celiac and mesenteric ganglia. Thus, the splanchnic nerves correspond to white rami communicantes. The *greater splanchnic* nerve arises by roots from the fifth to the ninth thoracic ganglia and goes to the celiac plexus. The *lesser splanchnic* nerve usually arises by two roots from the tenth and eleventh ganglia, and either unites with the greater splanchnic, or continues as an independent nerve to that portion of the celiac plexus which surrounds the roots of the renal arteries and terminates in the aorticorenal ganglion (83). The *smallest splanchnic* nerve, when present, arises from the last thoracic ganglion and goes to the renal plexus. Often this nerve is represented by a branch from the lesser splanchnic nerve.

The *celiac plexus*, the largest of all autonomic plexuses, surrounds the celiac and superior mesenteric arteries. This asymmetric paired plexus extends cranially to the diaphragm, caudally to the renal arteries and laterally to the suprarenal bodies. It becomes continuous below with the abdominal aortic plexuses. From the main plexus, paired and unpaired subsidiary plexuses are given off which accompany the branches of the celiac

and superior mesenteric arteries as well as other branches of the abdominal aorta. The paired plexuses include the phrenic, suprarenal, and spermatic (or ovarian) plexuses. The gastric, hepatic, splenic, and superior mesenteric plexuses are unpaired. Within the celiac plexus are found two relatively large ganglionic masses, the *celiac ganglia,* lying on either side of the celiac artery and connected with each other by delicate fiber strands. Occasionally, the two may be so close as to form a single unpaired ganglion encircling the artery. Other ganglionic masses found in the plexus include the paired aorticorenal ganglia and the *superior mesenteric ganglion* lying near the roots of their respective arteries. All these ganglia receive preganglionic fibers from the splanchnic nerves.

Caudally the celiac plexus becomes continuous with the abdominal aortic plexuses lying on either side of the aorta. From these plexuses nerve strands pass to the root of the inferior mesenteric artery and form the inferior mesenteric plexus, which surrounds that artery and its branches. Within this plexus, and lying close to the root of the artery, is another prevertebral ganglionic mass, the *inferior mesenteric ganglion* (Figs. 9.1 and 9.11). Further caudally, the abdominal aortic plexuses are continued into the unpaired *hypogastric* or *pelvic plexus,* which also receives strands from the inferior mesenteric plexus. On entering the pelvis the plexus breaks up into a number of subsidiary plexuses adjacent to the rectum, bladder, and accessory genital organs (Figs. 9.9 and 9.11). The preganglionic fibers supplying the pelvic organs come from the white rami of the two upper lumbar nerves and from the lowest thoracic nerve. They pass through the corresponding ganglia of the sympathetic trunk, and terminate in the inferior mesenteric ganglion (Fig. 9.1). The cells of this ganglion then send their postganglionic axons by way of the inferior mesenteric and hypogastric plexuses to the pelvic viscera (Fig. 9.11).

PARASYMPATHETIC SYSTEM

The preganglionic fibers of the craniosacral division form synaptic relations with postganglionic neurons in cranial autonomic, or terminal, ganglia. Thus, most parasympathetic preganglionic fibers are longer than the sympathetic preganglionic fibers, which terminate in the more proximal paravertebral and prevertebral ganglia.

Cranial Region

Central neurons whose axons form parasympathetic preganglionic fibers of cranial nerves VII, IX, and X in the rodent brain have been analyzed using retrograde tracing methods (31). The preganglionic cell bodies form a column extending from the level just below the obex to the level of the seventh cranial nerve in the pons. The column is rather compact and is located medial to the nucleus of the solitary tract and dorsolateral to the hypoglossal nucleus. At more rostral levels, the cell column is located progressively more laterally until the level of the facial nucleus. One group of cells sending axons in the greater superficial petrosal nerve (lacrimal neurons) is located lateral to the facial nucleus while neurons sending axons to the chorda tympani nerve or the otic ganglion are distributed more widely through the lateral tegmentum at the pontomedullary junction (31).

In the cranial region four ganglia are related topographically to the branches of the trigeminal nerve (Fig. 9.1). The *ciliary ganglion* lying against the lateral surface of the optic nerve receives preganglionic fibers from the visceral nuclei of the oculomotor complex (N. III) and sends postganglionic fibers (short ciliary nerves) to the sphincter of the iris and the smooth muscle of the ciliary body. The *pterygopalatine ganglion,* in the pterygopalatine fossa, and the *submandibular ganglion,* lying over the submandibular gland, receive fibers from the superior salivatory nucleus via the intermediate portion of the facial nerve (N. VII) (Figs. 9.1 and 13.23). The preganglionic fibers pass by way of the major petrosal nerve to the pterygopalatine ganglion, and by way of the chorda tympani nerve to the submandibular ganglion. The latter usually is broken into submandibular and sublingual portions. The pterygopalatine ganglion sends postganglionic fibers to the lacrimal glands and to the blood vessels and glands of the mucous membranes of the nose and palate. Postganglionic fibers from the submandibular ganglion go to the submandibular and sublingual salivary glands and also to the mucous membranes of the floor of the mouth. The *otic ganglion* is situated medial to the mandibular nerve as it leaves the oval foramen. It receives preganglionic fibers from the inferior salivatory nucleus of the glossopharyngeal nerve (N. IX) by way of the minor petrosal nerve and sends postganglionic fibers to the parotid gland

(Fig. 9.1). All of these cranial autonomic ganglia receive sympathetic fibers from the superior cervical ganglion, passing by way of the internal and external carotid plexuses. These fibers do not synapse with the ganglionic cells, but merely pass through the cranial parasympathetic ganglia to furnish sympathetic innervation to blood vessels, smooth muscle and glands.

The largest source of preganglionic parasympathetic fibers is the dorsal motor nucleus of the vagus nerve (N. X), which supplies practically all the thoracic and abdominal viscera except those in the pelvic region (Figs. 9.1, 9.3, and 12.21). In the thorax, these preganglionic fibers enter the pulmonary, cardiac, and esophageal plexuses to be distributed to the terminal (intrinsic) ganglia of the heart and bronchial musculature. Short postganglionic fibers then go to the heart and bronchial muscle. In the abdomen, the parasympathetic fibers of the vagus nerve go to the stomach, and pass through the celiac and its subsidiary plexuses, to end in the terminal ganglia of the intestine, liver, pancreas, and probably the kidneys. In the gastrointestinal tract, these terminal ganglia form the extensive ganglionated plexuses of Auerbach (myenteric) and of Meissner (submucosal), which are part of the enteric system (discussed later). The alimentary innervation of the vagus extends as far as the descending colon (Figs. 9.1 and 9.3).

Sacral Region

The *sacral* preganglionic parasympathetic fibers exit from the spinal cord via the second, third, and fourth sacral nerves which form the *pelvic* nerve (N. erigentes) and go to the terminal ganglia of the pelvic plexuses, as well as to the myenteric and submucosal plexuses of the descending colon and rectum (Fig. 9.1). Postganglionic fibers from terminal ganglia supply the urinary bladder, descending colon, rectum, and accessory reproductive organs. These sacral parasympathetic fibers innervate viscera not supplied by the vagus nerve (N. X) (Figs. 9.3 and 9.11).

ENTERIC SYSTEM

The enteric system is a highly complex neuronal network extending over the full extent of the gastrointestinal tract. It is composed of local sensory neurons capable of recording variations in the tension of the gut wall and the chemical environment, as well as interneurons and motor neurons that control the muscles of the gut wall, together with the vasculature and the secretory activity of the mucosa (48). Although the activity of the enteric neurons can be modified by inputs from the central nervous system, much of the control of the gastrointestinal function can be achieved by the enteric system independent of central influences. The complex intrinsic neuronal circuits of the enteric system regulate gastrointestinal motility, mucosal secretion and absorption, and local blood flow, largely as a result of activating intrinsic reflexes (53). As such, the enteric system plays a crucial role in the maintenance of homeostasis. It is important to realize that enteric neurons outnumber by far all the rest of the autonomic neurons. There are probably over 100 million neurons in the enteric system of humans (49, 52, 66). Furthermore, the anatomic and functional complexity of the enteric nervous system is second only to the central nervous system (53). Most enteric neurons are multipolar. Some have relatively short dendrites with irregular shapes and a prominent axon (type I neurons of Dogiel), whereas others have several long processes which cannot be identified easily as axons or dendrites (type II neurons of Dogiel) (53). Numerous putative neurotransmitters have been localized in the different classes of enteric neurons. These transmitters, which include acetylcholine, a vast array of neuroactive peptides, and probably serotonin and γ-aminobutyric acid (GABA), are colocalized in combinations that are specific for particular populations of neurons with well-defined shapes, projections, and functions (39, 49, 53). Interestingly, the enteric nervous system shares some neuroactive peptides with the central nervous system. Such "brain-gut" peptides include cholecystokinin, vasoactive intestinal peptide, substance P, neurotensin, and somatostatin (see Chapter 5).

The neurons of the enteric system are arranged in interconnected plexuses that extend over much of the gastrointestinal tract and also invest the pancreas and the gall bladder. The plexuses, which comprise ganglia and interconnecting nerve fibers, are situated between the various layers of muscle and endothelium. The two major intrinsic plexuses are the *myenteric* (or Auerbach's) and the *submucous* (or Meissner's) plexuses.

The myenteric plexus lies between the external longitudinal and circular smooth muscle layers while the submucosal plexus lies within the connective tissue of the submucosa between the circular muscle and the mucosa (Fig. 9.4). Although the myenteric plexus extends virtually the full length of the gastrointestinal tract, the submucosal ganglia are rare or absent in the esophagus and stomach.

The enteric system is regulated to some extent by parasympathetic and sympathetic inputs. Parasympathetic preganglionic neurons project directly to enteric ganglia of the stomach, colon, and rectum through the vagus and the pelvic splanchnic nerves. The sympathetic input comes principally from the postganglionic fibers of the prevertebral sympathetic ganglia and, to a lesser extent, the cervical paravertebral chain. These ganglia project to plexuses embedded in the wall of the stomach, the small intestine, and the colon. This extrinsic innervation of the gut by the parasympathetic and sympathetic components of the autonomous nervous system provides a second level of control of motility and secretion, but also can override intrinsic enteric activity in cases of emergency or stress.

VISCERAL AFFERENT FIBERS

There are numerous receptors in the viscera whose afferent fibers, myelinated or unmyelinated, travel centrally by way of the autonomic nerves, both sympathetic and parasympathetic. The largest myelinated fibers come principally from Pacinian corpuscles, while the smaller myelinated and the unmyelinated ones come from the more numerous diffuse visceral receptors (Fig. 7.4). Sensory fibers from the thoracic, abdominal, and pelvic viscera traverse sympathetic and splanchnic nerves to reach the sympathetic trunk. They pass uninterrupted through the trunk and white communicating rami to their perikarya of origin in the dorsal root ganglia (Figs. 9.2, 9.11, and 10.23). The parasympathetic nerves likewise contain many visceral afferent fibers. The visceral afferent fibers of the vagus nerve, whose cell bodies are in the inferior (nodose) ganglion, and are distributed peripherally to the heart, lungs, and other viscera. Similar fibers from the bladder, rectum, and accessory genital organs pass by way of the pelvic nerves and enter the spinal cord through the second, third, and fourth

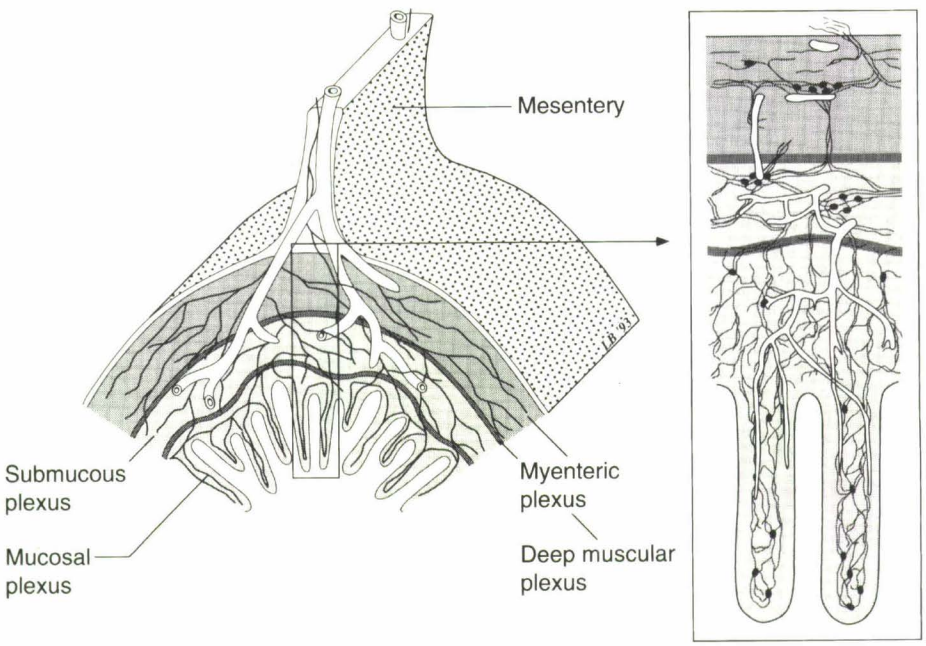


Figure 9.4. Cross-section through the intestinal wall showing the location of the mucosal, submucosal, and myenteric plexuses, which form the essential portion of the enteric nervous system. The nerve fibers are *black* and the blood vessels are *white*. The insert provides a more detailed view of this highly complex neuronal network.

sacral dorsal roots (Fig. 9.11). Their cell bodies are located in corresponding sacral spinal ganglia. Visceral sensory fibers from the bladder also enter the spinal cord through the lower thoracic and lumbar spinal nerves (Fig. 9.11). The sacral visceral afferent fibers, which convey impulses from stretch receptors in the wall of the urinary bladder, play a dominant role both in reflex control and the mediation of vesical pain impulses. These afferents accompany the sacral parasympathetic outflow and convey the sensory impulses that signal bladder distension. The sensation of a distended bladder is abolished by anesthetic block of the pelvic nerves, resection of these nerves, or the cutting of dorsal roots S2, S3, and S4. Visceral afferents from the bladder and adjacent viscera which ascend to the lumbar and lower thoracic dorsal root ganglia appear to play a minor role in the regulation of the bladder. Resection of the presacral nerve and hypogastric plexus in humans produces little or no alteration of vesical function.

The afferent visceral fibers are important in the initiation of various visceral and viscerosomatic reflexes mediated through the spinal cord and brainstem. Many of these reactions remain at a subconscious level, but afferent impulses also give rise to visceral pain or distress, nausea, hunger, and other poorly localized visceral sensations. It is the constant stream of afferent visceral impulses that is responsible for the general feeling of internal well-being or of malaise.

Visceral pain from most abdominal and pelvic organs is carried chiefly by the sympathetic nerves. Vagal sensory fibers are concerned with specific visceromotor, vasomotor, and secretory reflexes, most of which do not reach consciousness. It should be recalled that pain carried by visceral afferent fibers from diseased or inflamed organs may be "referred" to skin areas supplied by somatic afferent fibers of the same segment (see Chapter 8). The sense of taste is mediated by afferent fibers of the vagus, glossopharyngeal, and facial nerves, while impulses giving rise to the sensation of hunger probably are carried by the vagus.

Up to 30% of the axons in lower lumbar and upper sacral ventral roots in some spinal cord segments are unmyelinated afferent fibers. The cell bodies of these axons are located in the dorsal root ganglion. Unlike most sensory fibers, the central process of these afferent neurons does not enter the cord through the dorsal root. Instead, the axon takes a recurrent course and enters the ventral root, finally terminating in the gray matter of the spinal cord (see Chapter 8). About one-third of the ventral root afferent fibers carry information from somatic structures, while the remaining two-thirds are visceral sensory afferents with receptive fields in the lower bowel and pelvis (26, 27, 135).

STRUCTURE OF AUTONOMIC GANGLIA

The autonomic ganglia are aggregations of multipolar neurons of varying size and shape, each surrounded by a loosely organized connective tissue capsule. Trabeculae extending from the capsule form an internal framework which contains numerous, often pigmented, perikarya, between which are irregular plexuses of myelinated and unmyelinated fibers (Fig. 9.5). Besides these ganglia, isolated autonomic cells or nonencapsulated aggregations of such cells are found widely distributed throughout the viscera.

The diameter of autonomic cells ranges from 20–60 μm, and the number and length of their branching dendrites is exceeding variable. The morphology of the dendritic tree of autonomic ganglia neurons has been studied in detail in recent studies making use of intracellular HRP injections (47). There may be as few as 3 or 4 on some perikarya, and as many as 20 on others. In the thoracic segments of the rat, the average total dendritic length for preganglionic sympathetic neurons is 2343 μm (47). In humans, the number of dendrites and their degree of branching increase with age. The cell bodies have a clear ovoid, and often eccentric, nucleus, delicate neurofibrils, and fine chromophilic bodies. Binucleated or even multinucleated cells are not uncommon. Most of the cells are surrounded by cellular capsules that share some similarities with those surrounding spinal ganglion cells (Figs. 5.10 and 8.2). Electron microscopic studies of autonomic ganglion cells reveal large pigmented granules, numerous small dense bodies, and the usual perikaryonal components. Neuronal processes are readily identified as they emerge from cells or, when viewed without this continuity, by the striking number of synaptic and presynaptic junctions with which they are studded (59, 94). Synapses directly on the nerve cell bodies are rare.

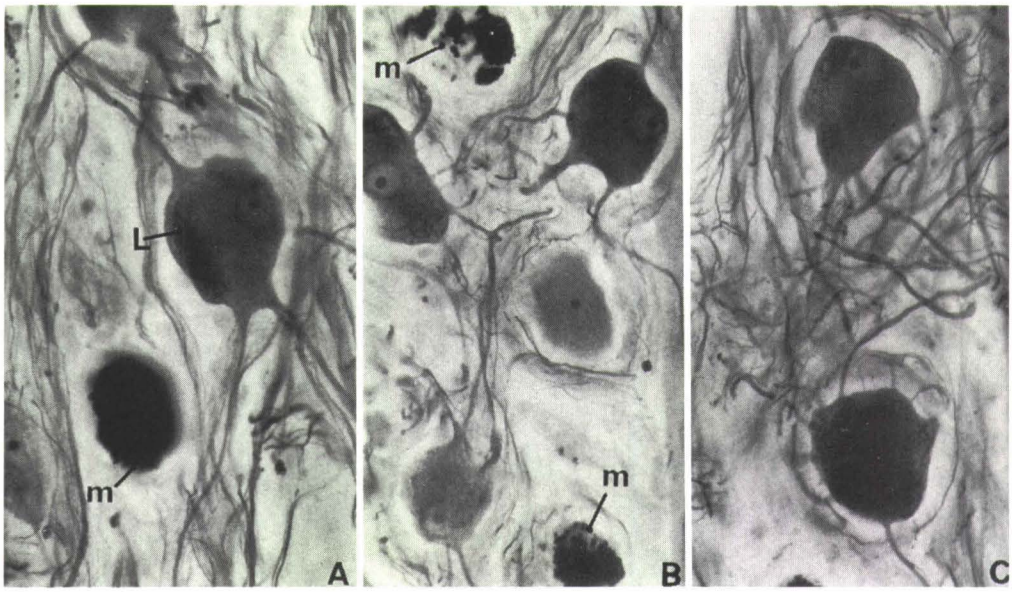


Figure 9.5. Adult human sympathetic neurons. Interdigitating dendrites often form a complex pericellular plexus. Perikarya frequently show eccentric nuclei, melanin granules (*m*), and lipofuscin granules (*L*). The nuclei of the capsule cells are not stained (Ramón y Cajal silver stain, ×490).

Processes filled with Nissl substance, mitochondria, large inclusion bodies, and pigment particles usually are considered to be dendrites. Neuronal processes containing only neurofilaments and some smooth vesicles are regarded as axons, but the distinction between dendrites and axons on the basis of the presence or absence of Nissl substance is not easy to make. Furthermore there are no reliable morphologic criteria for distinguishing between cells and fibers belonging to the sympathetic and parasympathetic systems.

Some of the cells have short dendrites which ramify within the capsules. These are numerous in the autonomic ganglia of humans (Fig. 9.5). Others have long, slender dendrites which pierce the capsule and run for varying distances in the intercellular plexuses. Still other cells possess both short and long processes. The long dendrites may branch considerably and bear varicose terminations that form "dendritic nests" enclosing other ganglion cells within a single capsule. Commonly, the long branching dendrites from several nearby cells intermingle to form complex "dendritic glomeruli" (98) (Fig. 9.6**A**). Such cells probably receive common terminal arborizations of preganglionic fibers. The shorter dendrites usually end as fine tapering processes, but often terminate with bulbous expansions (53). Axons usually arise from the proximal portion of a large dendrite and do not emit collaterals within the ganglia.

Preganglionic fibers end in synaptic relation with dendrites of many postganglionic cells (99) (Fig. 9.6**B**). They branch repeatedly within the ganglion and form pericellular arborizations. Some of the terminals contain neurofibrillary rings or loops. More common are the axodendritic synapses where the preganglionic fibers end in diffuse arborizations about the intracapsular and extracapsular dendrites. These ganglia are not simple relays transmitting impulses between preganglionic and postganglionic neurons (62). Small cells interpreted as internuncial neurons have been described (133). Depending upon the species examined, these interneurons contain dopamine or norepinephrine. When visualized with the paraformaldehyde- or glyoxylic acid-induced fluorescence techniques (see Chapter 5), the cell fluoresces brightly. Consequently these interneurons are known as small, intensely fluorescent, or SIF, cells (134).

The capsule cells of the autonomic ganglia are known to contain a variety of enzymes (1, 124). They are considered as homologous to the oligodendrocytes by Schwyn (111), to satellite and Schwann cells of dorsal root ganglia by Barton and Causey (9), or as connective tissue fibroblasts and interstitial cells. These supportive cells show a marked hyper-

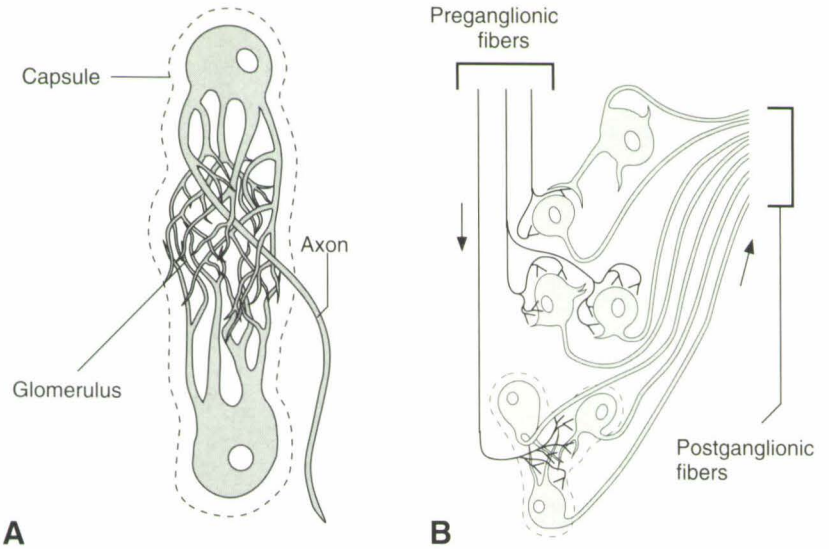


Figure 9.6. **A.** Glomerulus formed by dendrites of two sympathetic ganglion cells. **B.** Relationship between preganglionic fibers and sympathetic ganglion cells. One preganglionic fiber may come into synaptic relationships with several sympathetic postganglionic cells.

plasia following stimulation of the preganglionic fibers for periods of 105–180 minutes (111). Thus, like neuroglia in the central nervous system (see Chapter 7), these cells are likely to play a role that is much more complex than that of simple supportive tissue.

CHEMICAL ANATOMY

Cholinergic Transmission

The investigations of Dale (35), Loewi (72, 73), Cannon (19), and many others demonstrated that autonomic effects are mediated by transmitter molecules that are liberated at preganglionic and postganglionic nerve terminals. The principal transmitter molecule in the autonomic nervous system is acetylcholine (ACh). This small-molecule transmitter acts in conjunction with one or more neuroactive peptides. It is present in all preganglionic autonomic fibers, all postganglionic parasympathetic fibers, and in postganglionic sympathetic nerve fibers innervating sweat glands. Norepinephrine (NE) is the principal small-molecule transmitter in postganglionic sympathetic neurons, except those destined to the sweat glands. Dale was the first investigator to propose a functional classification of neurons based on their chemospecificity:

"Feeling the need of terms to describe nerve-fibres, or their impulses, in terms of a chemical function, which we can no longer regard as corresponding to their anatomical origin, I suggested the term 'cholinergic' to describe those which transmit their action by release of acetylcholine, and 'adrenergic' for those which employ a substance resembling adrenaline" (36).

Nerve impulses conveyed by cholinergic fibers produce rapid, localized responses of short duration in postjunctional effectors. Acetylcholine (ACh) is the transmitter at various peripheral junctions, including the neuromuscular junction, but does not always have the same physiologic effect on the postsynaptic membrane. This is due to the existence of two different postjunctional receptor molecules to which ACh can bind to initiate a postsynaptic response. The action of ACh on one type of receptor is mimicked by the drug nicotine and on the other by the drug muscarine; hence, the two receptor types are called nicotinic and muscarinic (see Chapter 5). Atropine blocks all muscarinic responses to ACh and related cholinomimetic drugs. Nicotinic receptors in autonomic ganglia and skeletal muscle are not identical in that tetraethylammonium and hexamethonium selectively block ganglionic transmission, and *d*-tubocurarine blocks transmission at both the somatic motor end plates and at autonomic ganglia, although its action at the motor end plate predominates. These differences could be related to the fact that, unlike the ACh receptors of skeletal muscle, neu-

ronal ACh receptors contain only two types of subunits, termed alpha (α) and beta (β). Expression of different combinations of the several neuronal α-subunits with any of the different β-subunits are likely to result in ACh receptor-channels with distinct conductance, kinetics, and pharmacology.

Stimulation of presynaptic fibers destined to an autonomic ganglia induces the release of ACh and evokes a fast excitatory synaptic potential (EPSP) that is mediated by nicotinic receptors. This fast EPSP is often large enough to generate an action potential in the postganglionic neuron. In addition to the fast nicotinic excitation, all sympathetic, and some parasympathetic ganglia exhibit slow synaptic potentials that can modulate the firing of the principal neurons. There is a slow EPSP and a slow IPSP (inhibitory postsynaptic potential) mediated by ACh, and a slow EPSP mediated by peptides. The slow ACh-mediated EPSP is produced by muscarinic receptors opening NA^+ and Ca^{2+} channels while closing the K^+ channel. The slow ACh-mediated IPSP is produced by activation of muscarinic receptors that open K^+ channels. This inhibition does not suppress action potentials elicited by fast nicotinic EPSPs but inhibits repetitive firing initiated by the slow peptidergic EPSP (39).

At cholinergic junctions a specialized enzyme, *acetylcholinesterase* (AChE), which readily hydrolyzes free acetylcholine to choline and acetate, is found in both the synaptic terminal and in the postsynaptic cell. Thus, AChE serves to terminate the transmitter action of ACh at postsynaptic sites and at effector junctions. Drugs which inhibit or inactivate AChE cause ACh to accumulate at cholinergic sites and produce effects equivalent to continuous stimulation of cholinergic fibers. Physostigmine (eserine) and neostigmine are "reversible" anticholinesterase drugs useful in treating myasthenia gravis, glaucoma, and atony of smooth muscle. Anticholinesterase compounds of the "irreversible" type, such as those of the organophosphate group (e.g., di-isopropyl fluorophosphate, DFP) form the basis for "nerve gases," which are among the most potent synthetic toxic agents known (68). Recovery of neuronal AChE activity after intoxication with DFP or similar drugs occurs primarily, if not exclusively, by synthesis of new enzyme molecules. Such *de novo* synthesis takes place first in the cell body, and the newly synthesized enzyme is then transported throughout neuronal processes. This feature allowed the development of a pharmacohistochemical procedure that improves the visualization of AChE-containing neurons, particularly in those regions of the brain where intense AChE-positive neuropil tends to obscure the neuronal somata and proximal processes (16, 90).

A monoclonal antibody was raised against neural AChE (13). When injected systemically in rats, this antibody causes a permanent destruction of presynaptic fibers in sympathetic ganglia and adrenal medulla. This results in a syndrome consisting of ptosis, hypotension, and bradycardia. In sympathetic ganglia, AChE activity disappears from the neuropil but not from nerve cell bodies. Ultrastructurally defined synapses and ChAT activity are also lost at the ganglionic level. Electrical stimulation of presynaptic fibers to the superior cervical ganglion ceases to evoke end organ responses. On the other hand, direct ganglionic stimulation remains effective, and the postsynaptic adrenergic system appears intact. Motor performance and ChAT content of skeletal muscle are preserved, as is parasympathetic (vagal) function (13). This new animal model of selective cholinergic autoimmunity is a novel and potent tool for autonomic physiology, and may be relevant to the pathogenesis of various human disorders involving the autonomic nervous system.

Adrenergic Transmission

The majority of postganglionic sympathetic nerves release noradrenaline (norepinephrine, NE) and are classified as noradrenergic, although the older term, adrenergic, is still widely used (20, 21, 32, 77, 88, 126, 127). The widespread distribution of sympathetic nerves and the demonstration of monoaminergic neurons in the central nervous system suggest that monoaminergic mechanisms are important. The paraformaldehyde-induced fluorescence histochemical method (44, 45), and, more recently, the immunohistochemical procedures, allow anatomic localization of monoamines and investigations of problems related to the synthesis, storage, release, and metabolism of the amines in neurons and their terminals (Figs. 5.19, 9.7, 13.35, and 14.20). Pioneering observations with the histofluorescence method

have indicated that in postganglionic sympathetic nerves, NE is present not only in synaptic terminals, but in the entire sympathetic neuron (43, 88, 126, 127). The noradrenergic fibers are markedly varicose and each varicosity appears to be enriched with NE. Axonal varicosities form a ground plexus in close contact with effector cells, and, according to Hillarp (61), the transmitter is released along the entire length of the terminals (Fig. 9.7).

Evidence indicates that the norepinephrine content of the terminals can be depleted by electrical stimulation (79, 88). Thus, there is little doubt that the varicosities are specialized structures involved in the storage and release of the transmitter. Histochemical studies have shown that the transmitter is stored in special granules within the adrenergic neurons and electron microscopic observations indicate that the small "dense-cored" vesicles (Figs. 9.7 and 9.8) are the storage granules (128, 136, 139). In addition to NE, these storage vesicles contain dopamine-β-hydroxylase, ATP, and a characteristic-binding protein termed chromogranin (32). These storage granules have several functions: (a) they bind and store NE, thereby retarding its diffusion out of the neuron and protecting it from degradation by monoamine oxidase, (b) they serve as a depot of NE that may be released following appropriate stimuli, and (c) they oxidize dopamine to NE (32). All parts of the sympathetic noradrenergic neuron contain norepinephrine, but the terminals contain the highest concentrations (126). Transmitter granules in adrenergic neurons are formed in the cell body, transported peripherally in the axon, and stored in terminal varicosities (32–34, 88).



Figure 9.7. Normal rat iris. Strands of the adrenergic ground plexus over the dilator muscle are demonstrated by formaldehyde-induced fluorescent technique. Several axons are markedly varicose (×250).

It is important to realize that NE axonal varicosities in the autonomic nervous system do not display the usual synaptic junctional features typical of central nervous system synapses (see Chapter 5). This phenomenon suggests that NE released from axonal varicosities may diffuse over a rather large territory and can influence vast neuronal populations. Interestingly, noradrenergic fibers in certain brain areas also appear to lack junctional specializations (10, 112). It is presumed that such central noradrenergic fibers exert a rather diffuse influence over large neuronal assemblies in a manner similar to that found in the autonomic nervous system.

In the adrenal medulla the release of ACh by preganglionic sympathetic fibers and its combination with receptors on chromaffin cells is followed by the liberation of epinephrine into the extracellular fluid which ultimately enters the circulation. Osmophilic granules have been isolated from the adrenal medulla which contain high concentrations of catecholamines and collectively represent a major storage site of epinephrine.

The adrenergic neuron also contains mechanisms for the inactivation of the transmitter substance, but these are not as rapid and efficient as those involved in the breakdown of ACh. Monoamine oxidase (MAO) is an intraneuronal enzyme involved in regulating the amine level within the neuron (22). The adrenergic transmitter released at synaptic junctions is inactivated by several mechanisms: (a) diffusion, (b) the enzyme catechol-*o*-methyl-transferase (COMT), which occurs extraneuronally, and (c) binding to extraneuronal sites not involved in nerve conduction. The inactivating mechanism of greatest physiological importance is the powerful transmitter reuptake mechanism present at adrenergic terminals. This uptake occurs at the neuronal cell membrane by an active mechanism involving specific transporter enzymes. It is of historic interest to note that NE was the first monoamine for which a presynaptic transporter system was implicated in neurotransmission (4), and that 20 years later the human NE transporter was the first monoamine transporter to be cloned (89). Monoamine transporters play a crucial role in the regulation of monoaminergic transmission. Additionally, monoamine transporters

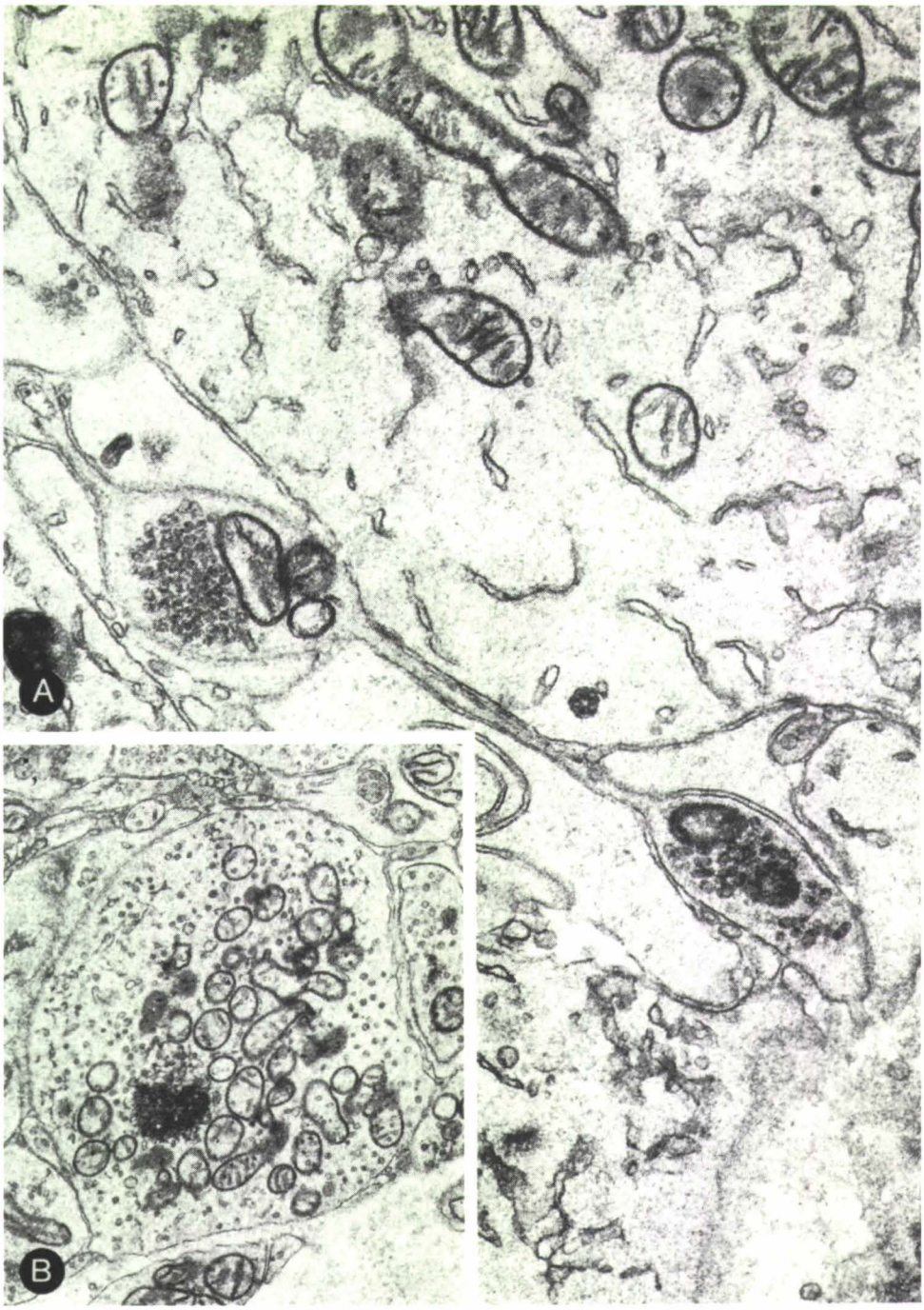


Figure 9.8. **A.** A noradrenergic axon from the enteric nervous system of a mouse. The tissue has been fixed with $NaMnO_4$ to specifically reveal this axonal subtype. Note that the axon is varicose. Two varicosities appear in the field. Varicosities are thought to be points where neurotransmitter is released. They are distinguished by their swollen appearance and content of 50 nm synaptic vesicles that, after permanganate fixation, contain characteristic dense cores. Note that the varicosities seem to lack synaptic membrane specializations and that no preferential distribution of synaptic vesicles or an active zone can be discerned. The varicosities also contain accumulations of mitochondria. The narrow intervaricose segment between the two varicosities contains few organelles, and no synaptic vesicles or mitochondria. At the *lower right,* the noradrenergic terminal appears to end on the basal lamina that surrounds this portion of the enteric nervous system and that separates it from the smooth muscle of the gut (×28,600). **B.** (*inset*) A section through a noradrenergic varicosity is shown. The tissue was fixed with $NaMnO_4$ 1 hour following injection of a mouse with the neurotoxin, 6-hydroxydopamine. Noradrenergic axons actively take up and concentrate norepinephrine. 6-Hydroxydopamine is specifically taken up and concentrated by these axons because its chemical structure resembles that of norepinephrine sufficiently well for it to be subject of the norepinephrine transport mechanism. The 50 nm dense cored vesicles permit the varicosity to be identified as noradrenergic. The accumulation of dense material in the cytosol of the varicosity is an early degenerative change due to uptake of 6-hydroxydopamine. Note that the varicosity is apposed to the basal lamina. This is typical of autonomic postganglionic axon terminals and makes it necessary for the transmitter to act across a wide synaptic gap.

appear to be major action sites of drugs such as cocaine and antidepressants. Thus, the study of these molecules furthers our knowledge of the complex mechanisms involved in neurotransmission, and helps elucidate the molecular basis of addictive and mental disorders.

Smooth muscle can be either excited or inhibited by norepinephrine or epinephrine, depending upon the site of action and the concentration of the transmitter. Norepinephrine excites smooth muscle, isoproterenol inhibits smooth muscle, and epinephrine can both excite and inhibit. Ahlquist (2) postulated two types of adrenergic receptors: α-receptors associated with excitatory responses and β-receptors associated with inhibition. There are two major exceptions to this: (a) stimulation of β-receptors in cardiac muscle produces excitatory effects and (b) stimulation of either α- or β-receptors in the gastrointestinal tract produces inhibitory responses that are additive. Synthetic compounds which structurally resemble naturally occurring catecholamines can combine with α- or β-receptors and produce sympathomimetic effects. The term *adrenergic blocking agent* is used for compounds that interfere with binding of the transmitter to postsynaptic receptors. Pharmacologic studies with blocking agents have allowed further differentiation of adrenergic receptor into α_1-, α_2-, β_1-, and β_2-subtypes (82, 86). Genes for these subtypes of adrenergic receptors were cloned, showing that these receptors are members of a larger family of hormone receptors whose activity is mediated through G-proteins (32).

Dale's Principle

Early studies of the autonomic nervous system, followed by many years of attempts to characterize neurons on the basis of their neurotransmitter content, led to this important generalization: *A neuron makes use of the same transmitter molecule at all of its synapses.* This concept was first suggested by Sir Henry Dale:

> "It is to be noted, further, that in the cases for which direct evidence is already available, the phenomena of regeneration appear to indicate that the nature of the chemical function, whether cholinergic or adrenergic, is characteristic for each particular neurone, and unchangeable. When we are dealing with two different endings of the same sensory neurone, the one peripheral and concerned with vasodilatation and the other at a central synapse, can we suppose that the discovery and identification of a chemical transmitter of axon-reflex vasodilatation would furnish a hint as to the nature of the transmission process at a central synapse? The possibility has at least some value as a stimulus to further experiment" (36).

This generalization was formulated as a principle in 1957 by Sir John Eccles who was studying the spinal motor neuron, which was then known to form a cholinergic synapse at the neuromuscular junction. Eccles correctly predicted, on the basis of Dale's works on autonomic cholinergic and adrenergic neurons, that the synapse formed by the recurrent collateral of the same spinal motor neuron onto the Renshaw cell of the spinal cord would also be cholinergic. Since most of the neurons examined at that time were found to use only one transmitter, Dale's principle was interpreted to mean that neurons use only one transmitter molecule. However, developing neurons have been shown to synthesize and release more than one transmitter. Furthermore, numerous mature neurons, including those of the autonomic nervous system, were found to contain more than one putative chemical messenger. Such a coexistence of several transmitters almost always involved a low-molecular-weight transmitter and a neuroactive peptide. In autonomic ganglia, for example, noradrenergic neurons often contain neuropeptide Y while cholinergic neurons are frequently enriched with vasoactive intestinal peptide. Thus, Dale's principle might better be reformulated to state that: *A neuron makes use of the same combination of chemical messengers at all of its synapses* (110).

A wide variety of neuroactive peptides occur in autonomic neurons and are thought to be coreleased with ACh and NE. In addition to neuropeptide Y and vasoactive intestinal peptide, one can note bombesin, cholecystokinin, dynorphin, enkephalin, gastrin-releasing hormone, luteinizing hormone-releasing hormone, neurotensin, somatostatin, substance P, calcitonin gene-related peptide, and peptide histidine isoleucine (53, 67). These peptides appear to be distributed with either ACh or NE in a highly ordered fashion in the different regions of the autonomic nervous system. For example, about 75% of the neurons in lumbar sympathetic ganglia are noradrenergic. Approximately half of these neurons also contain neuropeptide Y (76), while a small proportion of them also contain somatostatin (64). The remaining 25% are devoid of NE and represent the

cholinergic elements of the ganglia. Some of these NE-negative neurons contain the vasoactive intestinal peptide as well as the calcitonin gene-related peptide (6, 118). In addition to neuroactive peptides, various small-molecule transmitters other than ACh and NE are believed to play an active role in the function of the autonomic nervous system. Particularly convincing evidence exists for the involvement of serotonin, dopamine, GABA, and glutamate (52, 53, 71, 132).

One of the major functions of neuroactive peptides in autonomic ganglia is to alter neuronal excitability and thereby modulate the effectiveness of cholinergic and noradrenergic synaptic transmissions. In contrast to the fast nicotinic-mediated effect of ACh, the action of peptides on ganglionic neurons is slow, lasting up to several minutes. This delay is probably due to the fact that these peptides bind to receptors that are coupled to guanine nucleotide-binding regulatory proteins (G-proteins) (see Chapter 5). The results of several recent pharmacologic studies are in keeping with the idea that peptides in autonomic ganglia act more like neuromodulators than transmitters. For example, the neuropeptides vasoactive intestinal polypeptide, neuropeptide Y, and peptide histidine isoleucine modulate the release of tritiated NE from the sympathetic nerves in the choroid plexus of the rat (87).

In the excerpt quoted earlier, Dale alludes to the phenomenon of regeneration as indicating that the nature of the chemical function is characteristic for each particular neuron, and is also *unchangeable*. Although basically true, particularly for mature neurons, this assertion must be modulated to account for recent experimental evidence of a remarkable degree of neuronal plasticity in both the central and peripheral nervous systems. Of particular interest in the present context are the results of an experiment dealing with the development of the innervation of the sweat gland and the parotid gland in the rat (109). In this experiment, the sweat gland, a target of the cholinergic sympathetic neurons, was replaced with the parotid gland, a target of noradrenergic sympathetic neurons, in neonatal rats. This transplantation paradigm allowed sympathetic neurons that would normally innervate the sweat glands and develop a cholinergic phenotype to innervate the parotid gland instead. The neurons innervating the transplanted parotid gland did not develop a cholinergic phenotype, as assessed by measurements of ChAT activity and histochemical visualization of AChE, but continued to express intense catecholamine fluorescence. Additionally, immunoreactivity for vasoactive intestinal peptide, normally expressed by the sympathetic neurons that innervate the sweat glands but not by those innervating the parotid, was observed in only a small percentage of the parotid-associated fibers (109). These findings suggest that cellular interactions between neurons and their targets play an important role in the differentiation of chemical messenger phenotype *in vivo*.

The terms "adrenergic" and "cholinergic" do not correspond completely with "sympathetic" and "parasympathetic," respectively. For instance, the postganglionic fibers to the sweat glands (sudomotor fibers), although anatomically part of the sympathetic system, are cholinergic. Moreover they react to certain drugs, such as pilocarpine and atropine, in the same way as parasympathetic fibers. It should be recalled that the upper and lower extremities have no parasympathetic nerve fibers. In these regions, the sympathetic postganglionic fibers are of two distinct types—most are adrenergic, but those to the sweat glands are cholinergic (130) (Figs. 9.9 and 9.10). There are other instances of mixed autonomic nerves. For example, the splanchnic nerves contain both adrenergic and cholinergic fibers. The latter are destined for the adrenal medulla, where acetylcholine is the transmitter substance. Overactivity of both adrenergic and cholinergic fibers is indicative of either autonomic imbalance, irritating lesions, or abnormal regeneration along the course of the fibers. These may be expressed as excessive or abnormal sweating and salivation, alterations in gastrointestinal motility, or increased peripheral vasoconstriction as in hypertension. Appropriate drugs can either enhance or inhibit impulses at the sympathetic and parasympathetic ganglionic synapses, or block the membrane receptor sites upon which the neurotransmitter substances produce their effects (e.g., muscle, heart, glands, blood vessels).

DENERVATION SENSITIZATION

If the superior cervical ganglion (Fig. 9.1) is isolated by section of all incoming preganglionic fibers, the postganglionic perikarya do not degenerate. The isolated postganglionic perikarya may decrease slightly in di-

FUNCTION	SYMPATHETIC	PARASYMPATHETIC
Iris	dilates the pupil (mydriasis)	Constricts the pupil (miosis)
Lacrimal gland	little or no effect on secretion	stimulates secretion
Salivary glands	secretion reduced in amount and viscid	secretion increased in amount and watery
Sweat glands of head, neck, trunk, and extremities	stimulates secretion (cholinergic fibers) nerve fibers	little or no effect on secretion
Bronchi	dilates lumen	constricts lumen
Heart	accelerates rate, augments ventricular contraction	decreases heart rate
GI motility and secretion	inhibits	stimulates
GI sphincters	constricts	relaxes
Sex organs	contraction of ductus deferens, seminal vesicle, prostatic and uterine musculature; vasoconstriction	vasodilatation and erection
Urinary bladder	little or no effect on bladder	contracts bladder wall, promotes emptying
Adrenal medulla	stimulates secretion (cholinergic nerve fibers)	little or no effect
Blood vessels of trunk and extremities	constricts	no effect

Figure 9.9. Sympathetic and parasympathetic actions upon visceral structures.

ameter and show alterations of Nissl substance, endoplasmic reticulum, and mitochondria, but they survive. In such a condition, the perikarya do not demonstrate transneuronal degeneration (9, 56). However, following section of postganglionic axons of the cervical and ciliary ganglia, the perikarya show central chromatolysis and changes in their electrophysiologic properties (9, 63, 129).

Although postganglionic perikarya and their processes can survive to a section of their preganglionic fibers, such a section results in increased sensitivity of the isolated neurons and the tissues they supply to circulating adrenaline. At least a part of the denervation hypersensitivity is due to an increase in the number of adrenergic receptor sites on the postsynaptic cell membrane and/or to an increase in the degree of affinity of the receptors for the transmitter molecule. This phenomenon is often referred to by pharmacologists as "up-regulation." The receptor molecules are proteins and their synthesis is under genetic control, which in turn is influenced by diminished transmitter availability

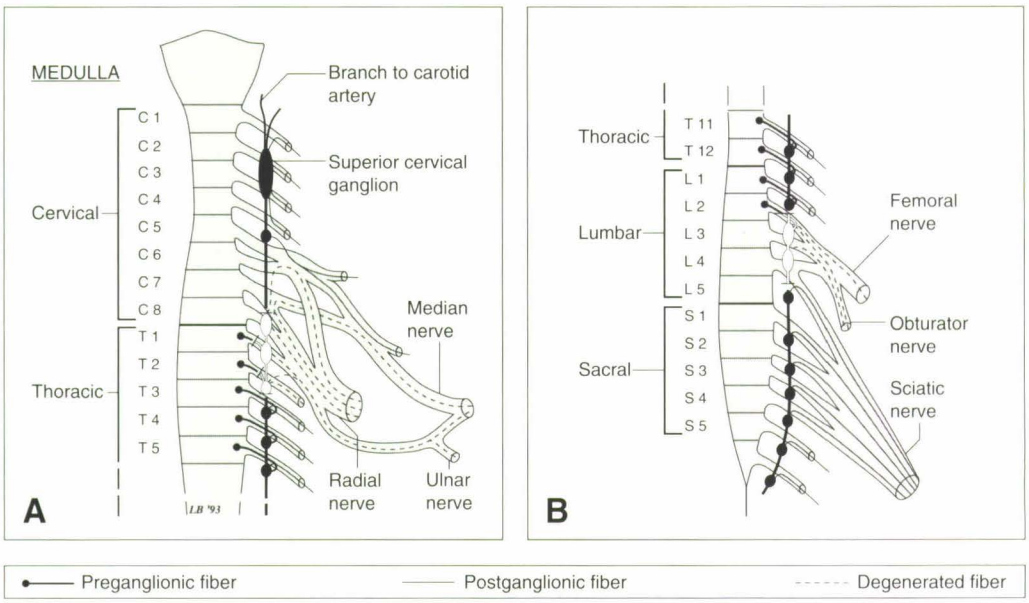


Figure 9.10. Anatomic course of preganglionic and postganglionic sympathetic vasoconstrictor fibers projecting to the upper and lower extremities. **A.** After cervicothoracic ganglionectomy (inferior cervical ganglion, T1 and T2, white) all of the postganglionic fibers to the hand degenerate. **B.** Resection of sympathetic ganglia L2 and L3 (white) interrupts only descending preganglionic fibers to lower lumbar and sacral sympathetic ganglia. Postganglionic fibers in the sciatic nerve to the foot region do not degenerate.

over a period of several weeks (see Chapter 5). This form of trophic/genomic interaction between pre- and postsynaptic neurons has been observed in many regions of the central and peripheral nervous system. It was observed that complete section of the postganglionic fibers to an organ or region resulted in far greater sensitization to adrenaline than that which followed complete preganglionic nerve section. Hampel (57) observed the qualitative responses of the nictitating membrane of the cat to adrenaline on successive days after denervation. He found that the response reached a maximum about 8 days after preganglionic denervation. Postganglionic denervation resulted in sensitization responses that were twice as great as those that followed preganglionic section. Similar responses are observed in most other tissues supplied by the adrenergic fibers. Increased sensitivity has been observed as well in structures supplied by the cholinergic fibers (e.g., lacrimal, sweat, and salivary glands). The latter become sensitive to ACh, which is equally true of denervated skeletal muscle. This peculiar phenomenon often is referred to as Cannon's (19) law of denervation: *When in a series of efferent neurons a unit is destroyed, an increased irritability to chemical agents develops in the isolated structure or structures. The effect being maximal in the part directly denervated.* Such denervation accounts for the increased sensitization of the superior cervical ganglion cells to acetylcholine which occurs after severance of its preganglionic fibers.

The paralysis after denervation of smooth muscle is very different from that seen in skeletal muscle where there is a persisting flaccid paralysis. Restoration of smooth muscle tone is due in part to the sensitization of the neuroeffector mechanism to circulating epinephrine. The anatomic arrangement of the preganglionic and postganglionic sympathetic vasoconstrictor fibers to the hand and foot serves as an excellent example to illustrate this point (Fig. 9.10). In Reynaud's disease, the small arteries and arterioles of the upper extremities, usually the hands, undergo episodic vasoconstriction in response to cold. As a result, the extremity demonstrates pallor and reactive hyperemia (i.e., an increased amount of blood in a part or congestion). In chronic cases, trophic changes develop with atrophy of the skin and subcutaneous tissues. Long-standing cases may develop skin ulceration or even ischemic gangrene. Removal of the inferior cervical, first and second thoracic sympathetic ganglia,

eliminates the vasoconstriction but destroys both the preganglionic as well as the postganglionic fibers to the forearm and hand (Fig. 9.10**A**). The smooth muscle of the arteries and arterioles will, in time, regain some vascular tone since the smooth muscle is also highly sensitized by removal of the postganglionic cells and fibers. Better results usually are obtained in the foot following removal of the second and third lumbar sympathetic ganglia (Fig. 9.10**B**). Here the partial sympathectomy interrupts the preganglionic outflow but leaves intact the postganglionic cells and fibers in the lower lumbar and sacral ganglia, which reach the foot through the sciatic nerve and its branches. Thus the vessels of the leg and foot regions are less sensitized to neurohumoral catecholamines.

CENTRAL AUTONOMIC PATHWAYS

Visceral structures innervated by the autonomic nervous system normally maintain a constant internal environment within the organism (homeostasis). Preganglionic neurons in the central nervous system (Figs. 9.1 and 9.3) are maintained in a continuous, but quantitatively variable state of activity by a multitude of segmental and suprasegmental mechanisms. Regulation from higher levels is accomplished by multiple neuronal pathways. This regulation appears to be mediated, in part, by a series of synaptic relays between several interposed neurons located at successively lower levels of the brainstem and forming a somewhat diffuse multisynaptic descending system.

The hypothalamus commonly is regarded as the principal locus of central autonomic integration. Simply stated, the most voluminous afferent connections of the hypothalamus originate from the hippocampal formation, the amygdaloid nuclear complex, and the olfactory cortex, and indirectly from cortical regions that are part of the limbic system (85, 97, 106). Many of these structures are involved in a neural circuitry that begins in the septal region and extends in a paramedian zone through the preoptic region and hypothalamus into the rostral mesencephalon (Fig. 17.14). In this view, the hypothalamus is the central part of a continuum that has been termed the "septo-hypothalamo-mesencephalic continuum" (85). There are a great number of reciprocal connections between structures within this subcortical continuum and phylogenetically older derivatives of the forebrain.

Most brain regions involved in the control of the autonomic nervous system outflow exert their influence by way of the hypothalamus, which may be considered as the head ganglion of the autonomic nervous system. The hypothalamus regulates the autonomic nervous system in two ways. First, it projects to the brainstem and spinal cord nuclei that act on preganglionic autonomic neurons to control temperature, heart rate, blood pressure, and respiration. The nucleus of the solitary tract is one of the brainstem nuclei that are actively involved in the regulation of cardiovascular and respiratory functions. Second, the hypothalamus acts on the endocrine system to release hormones that influence autonomic function.

Investigations using silver impregnation methods for degenerating axons indicated no direct descending connections from the hypothalamus that extended beyond the mesencephalic tegmentum (54, 97, 137). Later studies with newer tract-tracing and immunohistochemical methods, showed that hypothalamic neurons project directly to medullary autonomic nuclei and the spinal cord (11, 106, 107, 121) (Figs. 11.23, 12.24, and 17.17). Mesencephalic structures receive an input from the hypothalamus via (a) a descending component of the medial forebrain bundle, (b) the mammillary bodies (mamillotegmental tract), and (c) descending projections in the periventricular gray (Fig. 17.16). Hypothalamic impulses conveyed to the mesencephalon are transmitted to more caudal parts of the neuraxis via numerous synaptic relays within the brainstem reticular formation, as well as the smaller number of direct projections (84). It is presumed that reticular neurons convey impulses to visceral motor nuclei in the brainstem and spinal cord.

In the midbrain and upper pons, these descending tracts are located dorsally and medially near the central gray matter and floor of the fourth ventricle (12, 24, 117, 137). In most mammals that have been studied, including humans, the fibers descending into the upper midbrain stream through the prerubral field and region above the red nucleus. Stereotaxic surgery for dyskinesia in this area of the human brain has resulted in widespread autonomic deficits (23). These deficits include ptosis (drooping) of the eyelid, miosis (constriction) of the pupil, and a loss of

sweating (hemianhydrosis) on the same side (ipsilateral) of the body as the lesion. In humans, these descending fibers are uncrossed below the level of the red nucleus. These fibers are located more laterally in the pontine tegmentum and reticular formation of the medulla. Through this descending fiber system, the hypothalamus and other suprasegmental structures contribute to the regulation of a variety of visceral reflex activities (e.g., blood pressure, body temperature, sweating, secretion, eye, vesicle, rectal, and sexual reflexes). Lesions of these descending central tracts can result in a complete loss, or altered control, of visceral activities at lower segmental levels. For example, lesions in the lateral reticular formation of the medulla interrupt the fibers regulating sympathetic control of the smooth muscle of the eye and may result in a Horner's syndrome.

Familial dysautonomia or *Riley-Day syndrome* is an unusual clinical entity that affects children of Jewish extraction (101, 102). It can serve as an excellent example of the disseminated and abnormal functional activities of central descending autonomic fibers. This syndrome is characterized by deficiency of lacrimation, transient and extreme elevation in blood pressure induced by mild anxiety, excessive sweating and drooling of saliva, and the occurrence of sharply demarcated, bilateral and symmetric erythematous blotches on the skin. A central, possibly congenital, diencephalic dysfunction has been postulated to account for these symptoms. Subsequent studies revealed other disturbances, including postural hypotension, feeding difficulties from birth onward, a relative indifference to pain, erratic control of body temperature, emotional lability, loss of corneal reflexes, corneal anesthesia, loss of deep tendon reflexes, abnormal pupillary response to methacholine, and an abnormal intradermal response to histamine. Hypotonus, poor motor coordination, and developmental retardation may accompany the mentioned symptoms. The precise pathologic causes remain unknown, but lesions have been found in the thalamus, reticular formation of pons and medulla, spinal cord, sympathetic ganglia, and the myenteric plexus (102).

Bilateral lesions of the lateral white funiculi may result in altered sweating in regions supplied by the cord segments below the level of such lesions. Control of the bladder and rectum also may be lost. After spinal cord transection the autonomic reflexes are at first depressed (spinal shock), temperature regulation and sweating are absent, and blood pressure falls profoundly. Weeks later, after spinal shock has waned, segmental reflexes caudal to the lesion reappear. Somatic segmental reflexes in time become exaggerated, but visceral reflexes usually are sluggish.

FUNCTIONAL CONSIDERATIONS

Antagonistic Effects of Sympathetic and Parasympathetic Systems

Gaskell (50) pointed out that when a visceral structure is innervated by both sympathetic and parasympathetic fibers, the effects of the two are as a rule antagonistic. The sympathetic neurons dilate the pupil, accelerate the heart, inhibit intestinal movements, and contract the vesical and rectal sphincters. The parasympathetic neurons constrict the pupil, slow the heart, further peristaltic movement, and relax the vesical and rectal sphincters (Fig. 9.9). The apparently haphazard effects on smooth and cardiac muscle produced by each autonomic division in different organs (contraction in one, inhibition in another) are more readily explained when the *overall* activities of the two systems are taken into consideration. The parasympathetic deals primarily with anabolic activities concerned with the restoration and conservation of bodily energy and the resting of vital organs. In the words of Cannon:

> "A glance at these various functions of the cranial division reveals at once that they serve for bodily conservation; by narrowing the pupil they shield the retina from excessive light; by slowing the heart rate they give the cardiac muscle longer periods for rest and invigoration; and by providing for the flow of saliva and gastric juice, and by supplying the necessary muscular tone for the contraction of the alimentary canal, they prove fundamentally essential to the processes of proper digestion and absorption, by which energy-yielding material is taken into the body and stored. To the cranial division belongs the great service of building up reserves and fortifying the body against times of need and stress" (18).

The sacral division supplements the cranial by ridding the body of intestinal and urinary wastes.

On the other hand, stimulation of the sympathetic component equips the body for the intense muscular action required in offense

and defense. It is a mechanism that quickly mobilizes the existing reserves of the body during emergencies or emotional crises. The pupils dilate, respiration is deepened, and the rate and force of the cardiac contractions are increased. The blood vessels of the viscera and the skin are constricted, the blood pressure is raised and an ample blood supply is made available to the skeletal muscles, lungs, heart, and brain. The peaceful activities are slowed or stopped, blood is drained from the huge intestinal reservoir, peristalsis and alimentary secretion are inhibited, and the urinary and rectal outlets are blocked by contraction of their sphincters.

The two systems are reciprocal and their dual activities are integrated into coordinated responses ensuring the maintenance of an adequate internal environment to meet the demands of any given situation. The parasympathetic activities are initiated primarily by internal changes in the viscera themselves. The sympathetic system is in considerable part activated by exteroceptive impulses that pass over somatic afferent fibers and are initiated by favorable or unfavorable changes in the external environment.

The preganglionic fibers of the sympathetic system arise from a continuous cell column in the spinal cord, and a single fiber may form synaptic relations with many cells in different paravertebral or prevertebral ganglia (Fig. 9.6**B**). Both types of ganglia are placed at considerable distances from the organs innervated, and from them postganglionic fibers are distributed to extensive visceral areas (Figs. 9.1 and 9.11). Such a mechanism permits a wide radiation of impulses. The NE released at most sympathetic terminals further enhances the widespread and prolonged effects of sympathetic stimulation. Thus, stimulation of a thoracic ventral root, or white ramus, causes piloerection and vasoconstriction in five, six, or even more segmental skin areas.

In the parasympathetic system the preganglionic neurons are represented by more isolated cell groups whose fibers pass out in separate nerves and go directly to the terminal ganglia within or near the organs. Each preganglionic parasympathetic fiber enters into synaptic relations with fewer postganglionic neurons than is the case in the sympathetic division. Thus, in the superior cervical ganglion of the cat, the ratio of preganglionic fibers to postganglionic neurons is about 1:15 or more, while in the ciliary ganglion the ratio is only 1:2 (138). Parasympathetic action is more discrete and is limited to the portion of the target that is stimulated. The liberation and rapid hydrolysis of acetylcholine by the parasympathetic postganglionic fibers is compatible with such localized autonomic responses. Thus, stimulation of the glossopharyngeal nerve (N. IX) increases parotid gland secretion, while stimulation of the oculomotor nerve constricts the pupil, in each case without the appearance of other parasympathetic effects. These data indicate that the sympathetic system is much more divergent than the parasympathetic system.

Autonomic Innervation of the Eye and Salivary Glands

The functions of the two subdivisions of the autonomic system are most easily understood by contrasting the individual structures innervated and noting the reciprocal actions of their dual nerve supply (Fig. 9.9). The autonomic fibers to the eye provide an excellent example of this dual innervation. The sympathetic division stimulates the smooth muscle fibers of the dilator muscle of the iris, the tarsal muscle and the orbital muscle (of Müller). The tarsal muscle extends from the levator palpebrae muscle to the tarsal plate of the upper lid and aids in full elevation of the upper eyelid. The orbital muscle, at least in nonprimate species, keeps the ocular bulb forward in the bony orbit. Lesions in either the central or peripheral sympathetic pathways to the eye produce a triad of symptoms known as *Horner's syndrome*. As a result of sympathetic injury, the parasympathetic innervation is unopposed, and results in constriction of the ipsilateral pupil (miosis), dropping of the upper eyelid (pseudoptosis), and an apparent sinking in of the eyeball (enophthalmos) (46). Vasodilation and dryness of the skin of the face also may be evident. Sympathetic fibers destined for the eye follow the internal carotid artery, while those to sweat glands on the face course along the branches of the external carotid artery. This dichotomy of postganglionic fibers from the cervical ganglia explains the altered patterns of autonomic function that can occur after injuries of the face, deep neck, or within the skull. There may be loss of sweating on the face with preservation of sympathetic innervation to the eye or vice versa. Lesions of the cervical sympathetic trunk, inferior cervical ganglion, or ventral roots of the upper tho-

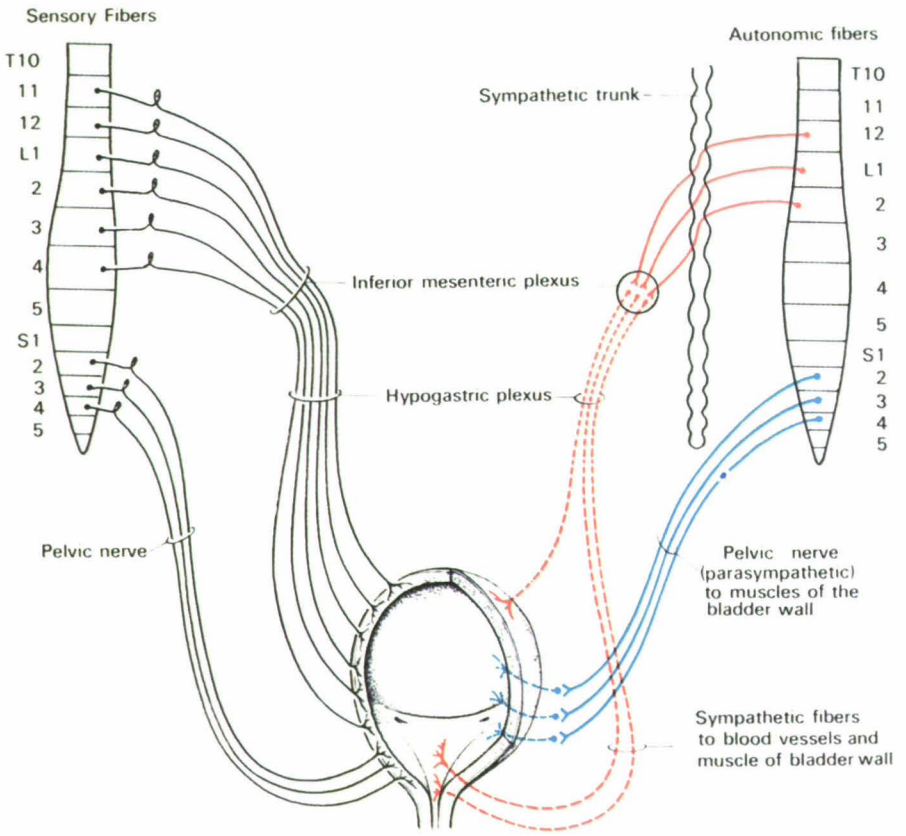


Figure 9.11. Sensory and autonomic innervation of the urinary bladder. Preganglionic parasympathetic visceral motor (*purple*) fibers from S2, S3, and S4 pass to terminal ganglia which give rise to postganglionic fibers that induce contractions of the detrusor muscle. Afferent impulses from stretch receptors (*black*) in the bladder wall enter upper lumbar and lower thoracic spinal segments via the hypogastric plexus, and S2, S3, and S4 spinal segments via the pelvic nerve. Descending sympathetic fibers (*red*) synapse in the inferior mesenteric plexus and travel in the hypogastric nerves and plexus. Somatic motor fibers from S2, S3, and S4 spinal segments (not shown) innervate the external vesicle sphincter. Relaxation of the external sphincter and contraction of the detrusor muscle are essential for micturition.

racic nerves interrupt the fibers before they divide to follow separate courses.

Parasympathetic fibers to the eye stimulate the sphincter muscle of the iris and bring about constriction of the pupil. These axons also stimulate the ciliary muscle. Contraction of the circular fibers of the ciliary muscle causes relaxation of the ciliary zonule and thereby decreases the tension of the lens capsule. As a result of such parasympathetic activity, the pupil is constricted and the convexity of the lens is increased for near vision (accommodation).

Innervation of the salivary glands was long believed due solely to secretory fibers in the cranial parasympathetic nerves (Fig. 9.9). Many differences have been found between the several glands of the different species studied, but both parts of the autonomic system send secretory fibers to the salivary glands. Sympathetic fibers provide for vasoconstriction of blood vessels, contraction of the myoepithelial cells of the ducts, and secretory fibers to the demilune gland cells (5). Stimulation of the human sympathetic trunk in the neck, or the injection of adrenaline into the salivary duct, evokes a flow of saliva from the submandibular, but not from the parotid gland. The secretory response to sympathetic stimulation is of short duration when compared to the long-acting response that follows parasympathetic stimulation (42). Parasympathetic fibers in cranial nerves VII and IX provide for vasodilation of the blood vessels and secretory fibers to the alveolar and acinar cells of the parotid, submandibular sublingual, and retrolingual glands. The vagus nerve (N. X) contains secretory fibers to the glands of the trachea and upper digestive tract. For additional details on the innervation of the

salivary glands the reader is referred to the classic reviews by Babkin (5), Lundberg (74), Burgen and Emmelin (15), and Emmelin (41).

Autonomic Innervation of the Urinary Bladder

The innervation of the urinary bladder and the control of micturition represent a complex and specific autonomic function of great practical importance (Fig. 9.11). The smooth muscle of the urinary bladder exhibits two types of activity: (a) intermittent contractions which occur as the organ adapts its capacity to an increasing volume, and (b) sustained contractions associated with relaxation of the external sphincter which occur during micturition. These activities are controlled by the interplay not only of sympathetic and parasympathetic neurons but also of somatic motor neurons. All three systems are activated by reflexes that are regulated at both spinal and supraspinal levels (39). However, the various neuronal events involved in the control of micturition are not fully understood and the subject is still a matter of some controversy.

Most investigators agree that the excitatory input to the bladder wall that causes contraction and promotes emptying is parasympathetic. Cholinergic axons originating in the intermediolateral region of the spinal cord (S2 to S4) leave the sacral nerves, and, as the *pelvic nerve*, course to the lateral wall of the bladder where the fibers terminate in the pelvic ganglion plexus, whose neurons are dispersed near to and within the bladder wall. Short postganglionic parasympathetic fibers to the bladder musculature induce contraction of the detrusor smooth muscle by releasing ACh, which acts on muscarinic receptors (116) (Fig. 9.11). The parasympathetic neurons are quiescent during initial bladder filling, but bladder distension initiates impulses in visceral afferents that course in the pelvic nerve to the sacral spinal cord and activate parasympathetic preganglionic neurons.

While there is a general consensus about the role of the parasympathetic system in micturition, the involvement of the sympathetic system is much debated. The major problem stems from the fact that the sympathetic innervation of the bladder appears to be largely restricted to the muscle fibers of the vesical trigone, including the orifices of the ureters and the urethra. The trigone muscles are believed to be concerned principally with vasomotor control and the mechanism of ejaculation. However, recent anatomic and pharmacologic studies led to the idea that the sympathetic outflow to the bladder counteract, and even control, the activity of the parasympathetic system (39). In humans, the sympathetic innervation of the bladder arises from the thoracic and lumbar segments (T12 to L2) of the spinal cord. Preganglionic fibers reach the inferior mesenteric ganglion or plexus and from there postganglionic fibers travel in the hypogastric nerve to the pelvic ganglion, the bladder wall, and the internal urethral sphincter muscle. It should be noted, however, that the internal sphincter is probably not a distinct anatomic entity. It is more likely formed by a continuation of the longitudinal detrusor fibers around the bladder outlet. This sympathetic outflow can be stimulated by the activity of sensory afferents responding to tension in the bladder wall (stretch receptors). These sensory afferents travel through the pelvic nerve or, if the bladder is greatly distended, by way of the hypogastric nerves and plexus to arborize at the level of spinal segments T10 to T12. Stimulation of the sympathetic outflow results in an α-adrenergic inhibition of parasympathetic activity in the pelvic ganglion, relaxation of the muscles of the bladder wall (mediated by β-adrenergic receptors), and excitation of the internal sphincter muscle (14, 39). Thus, during the bladder filling, the sympathetic system promotes bladder wall relaxation directly, and also indirectly through inhibition of the parasympathetic activity (37), and causes closure of the internal urethral sphincter.

The somatic motor neurons that participate in the control of bladder function are located in the ventral horn at the sacral spinal segments 2, 3, and 4. Their axons become incorporated in the pudendal (pudic) nerve, and, via a branch of that nerve, the perineal nerve, innervate the external urethral sphincter and cause contraction. These motor neurons are stimulated by the activity in visceral afferents to low levels of bladder distension. At high levels of distension, supraspinal neurons that inhibit both the sympathetic and the somatic motor neurons are activated so that the sympathetic inhibition of the parasympathetic activity is released and both sphincters relax, allowing bladder contraction and urination (39).

It should be noted that the desire to urinate is dependent upon intravesical pressure

rather than fluid-volume content. The vesical capacity and frequency of urination vary with age and are influenced by reflex, psychic, and local irritative factors. In children 8–10 years of age, the initial desire to void occurs with an intravesical pressure of 9–11 cm of water (bladder volume 80–100 ml of urine). In adults with a fluid capacity of 140–180 ml, an intravesical pressure of 15–16 cm of water induces the desire to void (17).

Sensory information about the status of the bladder reaches conscious level through long and poorly defined multisynaptic pathways. It was suggested that these pathways lie in the dorsal half of the lateral funiculus (8, 78, 103). Facilitating and inhibiting suprasegmental influences upon spinal mechanisms concerned with micturition suggest that regions in the pontine and midbrain tegmentum are involved (122). Additionally, the cerebral cortex appears to exert some control over bladder function. Clinical studies indicate that portions of the superior frontal gyrus on the medial surface of the hemisphere may be specially concerned with control of micturition and defecation (3). Lesions in this region, involving one or both frontal lobes, may cause urgency, frequency of micturition, or incontinence. Such lesions are also associated with lack of awareness of all vesical events, including the sensation of the desire to micturate and the sensation that micturition is imminent. Disturbances of bladder function associated with spinal cord injury are described in Chapter 11.

Clinical Notes

A familiarity with the information in Figure 9.9 proves useful in evaluating the overall functional status of the autonomic nervous system. Vital body processes such as circulation, secretion, digestion, and excretion, are essentially autonomic reflex responses. The autonomic nervous system also participates in many somatic-visceral and visceral-somatic reflexes which involve either cranial or spinal nerves (e.g., respiration, pupillary, lacrimal, palatal, pharyngeal, sneeze, cough, swallowing, vomiting, carotid sinus, vasomotor, sudomotor, pilomotor, vesicle, genital, and emotional reflexes). Some of these reflexes are presented as individual nerves are discussed. Metabolic or mechanical irritations of autonomic nerve fibers in the periphery may cause exaggerations of some of the sympathetic and parasympathetic functions included in Figure 9.9. Partial or complete lesions of autonomic fibers may occur in either the central or the peripheral nervous system (Fig. 11.28). An appreciation of the nuclei, fiber pathways, and resulting reflex deficits from injuries are useful as a diagnostic aid in exploring the diffuse distribution of the autonomic system. In the periphery, the postganglionic sympathetic fibers that rejoin spinal nerves (Fig. 9.2) have a distribution which compares closely to that of the sensory dermatomes (38, 100). Hence changes in cutaneous sudomotor and vasomotor reflexes, changes in skin temperature, and increased skin resistance to passage of a minute electric current indicate the involvement of sympathetic nerve fibers. A knowledge of dermatomal and peripheral nerve distributions (Figs. 8.11, 8.12, and 8.16–8.18), correlated with the segmental nuclear origins of autonomic neurons (Figs. 9.1 and 9.3), often can provide additional evidence to substantiate both the location and level of a nerve injury.

References

1. Adams CWM. Disorders of neurons and neuroglia. In: Adams CWM, ed. Neurohistochemistry. Ch. 10. Amsterdam: Elsevier, 1965:403–436. (See also Chs. 1–8: 1–332.)
2. Ahlquist RP. A study of the adrenotropic receptors. Am J Physiol 1948;153:586–600.
3. Andrew J, Nathan PW. Lesions of the anterior frontal lobes and disturbances of micturition and defecation. Brain 1964;87:233–262.
4. Axelrod J. Noradrenaline: fate and control of its biosynthesis. Science 1971;173:598–606.
5. Babkin BP. Significance of the double innervation of the salivary glands. In: Babkin BP, ed. Secretory mechanism of the digestive glands. 2d ed. Ch. 27. New York: P.B. Hoeber, 1950:733–766.
6. Baldwin C, Sasek CA, Zigmond RE. Evidence that some preganglionic sympathetic neurons in the rat contain vasoactive intestinal peptide- or peptide histidine isoleucine amide-leke immunoreactivities. Neuroscience 1991;40: 175–184.
7. Baron R, Jänig, W. Afferent and sympathetic neurons projecting into lumbar visceral nerves of the male rat. J Comp Neurol 1991; 314:429–436.
8. Barrington FJF. The relation of the hind brain to micturition. Brain 1921;44:23–53.
9. Barton AA, Causey G. Electron microscopic study of the superior cervical ganglion. J Anat 1958;92: 399–407.
10. Beaudet A, Descarries L. The monoaminergic innervation of rat cerebral cortex; synaptic and nonsynaptic axon terminals. Neuroscience 1978;3:851–860.
11. Björklund A, Skagerberg G. Evidence for a major spinal cord projection from the diencephalic A 11 dopamine cell group in the rat using transmitter-specific fluorescent retrograde tracing. Brain Res 1979;177:170–175.
12. Bradley WE, Conway CJ. Bladder representation in the pontine-mesencephalic reticular formation. Exp Neurol 1966;16:237–249.
13. Brimijoin S, Lennon VA. Selective destruction of preganglionic sympathetic nerves by antibodies to

acetylcholinesterase. J Neurol Transm 1991;34:139–145.
14. Brindley GS. Autonomic control of the pelvic organs. In: Bannister R, ed. Autonomic failure. 2d ed. London and New York: Oxford University Press, 1988:223–237.
15. Burgen ASV, Emmelin NG. Innervation of the glandular elements. In: Burgen ASV, Emmelin NG, eds. Physiology of the salivary glands. Ch. 3. Baltimore: Williams & Wilkins, 1961:38–71.
16. Butcher LL, Talbot K, Bilezikjian L. Acetylcholinesterase neurons in dopamine-containing regions of the brain. J Neural Transm 1975;38:137–153.
17. Campbell MF. Neuromuscular uropathy. In: Campbell MF, ed. Principles of urology. Ch. 9. Philadelphia: W.B. Saunders, 1957: 337–378.
18. Cannon WB. Bodily changes in pain, hunger, fear and rage. An account of recent researches into the function of emotional excitement. New York: Appleton, 1929.
19. Cannon WB. A law of denervation. Am J Med Sci 1939;98:737–750.
20. Cannon WB, Rosenblueth A. Studies on activity in endocrine organs: sympathin E and sympathin I. Am J Physiol 1933;104:557–574.
21. Cannon WB, Rosenblueth A. Autonomic neuro-effector systems. New York: Macmillan, 1937.
22. Carlsson A. Drugs which block the storage of 5-hydroxytryptamine and related amines. In: Eichler O, Farah A, eds. Handbuch der experimentellen Pharmakologie. Vol. 19. Heidelberg: Springer, 1965: 529–592.
23. Carmel PW. Sympathetic deficits following thalamotomy. Arch Neurol 1968;18:378–387.
24. Cheatham ML, Matzke HA. Descending hypothalamic medullary pathways in the cat. J Comp Neurol 1966;127:369–380.
25. Cobb JLS, Bennett T. A study of plexuses in visceral smooth muscle. J Cell Biol 1969;41:287–297.
26. Coggeshall RE, Applebaum ML, Frazen M, Stubbs TB III, Sykes MT. Unmyelinated axons in human ventral roots, a possible explanation for the failure of dorsal rhizotomy to relieve pain. Brain 1975;98:157–166.
27. Coggeshall RE, Coulter JD, Willis WD. Unmyelinated axons in the ventral roots of the cat lumbosacral enlargement. J Comp Neurol 1974;153:39–58.
28. Coggeshall RE, Galbraith SL. Categories of axons in mammalian rami communicantes, part II. J Comp Neurol 1978;181:349–360.
29. Coggeshall RE, Hancock MB, Applebaum ML. Categories of axons in mammalian rami communicantes. J Comp Neurol 1976; 167:105–124.
30. Coil JD, Norgren R. Cells of origin of motor axons in the subdiaphragmatic vagus of the rat. J Auto Nerv Syst 1979;1:203–211.
31. Contreras RJ, Gomez MM, Norgren R. Central origins of cranial nerve parasympathetic neurons in the rat. J Comp Neurol 1980; 190:373–394.
32. Cooper JR, Bloom FE, Roth RH. The biochemical basis of neuropsychopharmacology. 6th ed. New York: Oxford University Press, 1991.
33. Dahlström A. Observation on the accumulation of noradrenaline in the proximal and distal parts of peripheral adrenergic nerves after compression. J Anat 1965;99: 677–689.
34. Dahlström A, Carlsson A. Making visible the invisible. In: Parnham MJ, Bruinvels J, eds. Pharmacology methods, receptors and chemotherapy. Vol 3. Amsterdam: Elsevier, 1986;97–125.
35. Dale HH. The action of certain esters and ethers of choline, and their relation to muscarine. J Pharmacol Exp Ther 1914;6:147–190.
36. Dale H. Pharmacology and nerve endings. Proc R Soc Med 1935; 28:319–332.
37. De Groat WC, Steers WD. Neural control of the urinary bladder and sexual organs. In: Bannister R, ed. Autonomic failure. 2d ed. London and New York: Oxford University Press, 1988;196–222.
38. DeJong RN. The neurological examination. 4th ed. New York: Harper & Row, 1979.
39. Dodd J, Role LW. The autonomic nervous system. In: Kandel ER, Schwartz JH, Jessell TM, eds. Principles of neural science. Ch. 49. New York: Elsevier, 1991:761–775.
40. Eccles JC. The physiology of nerve cells. Baltimore: Johns Hopkins Press, 1957.
41. Emmelin N. Nervous control of salivary glands. In: Code CF, ed. Handbook of physiology. Vol. II: Secretion. Sec. 6. Ch. 37. Washington, DC: American Physiological Society, 1967:595–632.
42. Emmelin N, Stromblad BCR. A method of stimulating and inhibiting salivary secretion in man. Acta Physiol Scand 1954;31(Suppl 114): 12–13.
43. Falck B. Observations on the possibilities of the cellular localization of monoamines by a fluorescence method. Acta Physiol Scand 1962;56(Suppl 197):1–25.
44. Falck B, Hillarp NA, Thieme G, Torp A. Fluorescence of catecholamines and related compounds condensed with formaldehyde. J Histochem Cytochem 1962; 10:348–354.
45. Falck B, Torp A. A new evidence for localization of noradrenaline in adrenergic nerve terminals. Med Exp (Basel) 1962;6:169–172.
46. Fields CR, Barker FM 2d. Review of Horner's syndrome and a case report. Optom Vis Sci 1992;69: 481–485.
47. Forehand CJ. Morphology of sympathetic preganglionic neurons in the neonatal rat spinal cord: an intracellular horseradish peroxidase study. J Comp Neurol 1990; 298:334–342.
48. Furness JB, Costa M. Types of nerves in the enteric nervous system. Neuroscience 1980;5:1–20.
49. Furness JB, Costa M. The enteric nervous system. Edinburg: Livingstone, 1987.
50. Gaskell WH. The involuntary nervous system. London: Longmans & Green, 1916.
51. Geis GS, Wurster RD. Horseradish peroxidase localization of cardiac vagal preganglionic somata. Brain Res 1980;182:19–31.
52. Gershon MD. The enteric nervous system. Annu Rev Neurosci 1981; 4:227–272.
53. Gibbins I. Peripheral autonomic nervous system. In: Paxinos G, ed. The human nervous system. Ch. 5. New York: Academic Press, 1990: 93–123.
54. Guillery RW. Degeneration in the hypothalamic connexions of the albino rat. J Anat 1957;91:91–115.
55. Haefely W, Hürlimann A, Thoenen H. Relations between the rate of stimulation and the quantity of noradrenaline liberated from the sympathetic nerve endings in the isolated perfused spleen of the cat. J Physiol (Lond) 1965;181:48–58.
56. Hamlyn LH. The effect of preganglionic section on the neurons of the superior cervical ganglion in rabbits. J Anat 1954;88:184–191.
57. Hampel CW. The effect of denervation on the sensitivity to adrenaline of the smooth muscle in the nictitating membrane of the cat. Am J Physiol 1935;61:611–621.
58. Handa Y, Caner H, Hayashi M, Tamamaki N, Nojyo Y. The distribution of the sympathetic nerve fibers to the cerebral arterial system in rat as revealed by anterograde labeling with WGA-HRP. Exp Brain Res 1990;82:493–498.
59. Hervonen A, Pelto-Huikko M, Helén P, Halho H. Electron microscopic localization of enkephalin-like immunoreactivity in axon terminals of human sympathetic ganglia. Histochemistry 1980;70: 1–6.
60. Hess WR. Die Funktionelle Organisation des Vegetativen Nervensystems. Basel: Schwabe, 1948.
61. Hillarp N-A. The construction and functional organization of the autonomic innervation apparatus. Acta Physiol Scand 1959;46(Suppl 157):1–38.
62. Hillarp N-A. Peripheral autonomic mechanisms. In: Field J, ed. Handbook of physiology. Vol. II. Sec. I: Ch. 38. Washington, DC: American Physiological Society, 1960:979–1006.
63. Hunt CC, Riker WK. Properties of

frog sympathetic neurons in normal ganglia and after axon section. J Neurophysiol, 1966;29:1096–1114.
64. Järvi R, Pelto-Huikko M, Helén P, Hervonen A. Somatostatin-like immunoreactivity in human sympathetic ganglia. Cell Tissue Res 1987;249:1–5.
65. Jensen I, Pilowsky PM, Llewellyn-Smith IJ, Minson JB, Chalmers JP. Sympathetic preganglionic neurons projecting to the adrenal medulla in the rabbit. Brain Res 1992;586:125–129.
66. Johnson LR, ed.. Physiology of the gastrointestinal tract. 2d ed. New York: Raven Press, 1987.
67. Karczmar AG, Koketsu K, Nishi S, eds. Autonomic and enteric ganglia: transmission and its pharmacology. New York: Plenum Press, 1986.
68. Koelle GG. Anticholinesterase agents. In: Goodman LS, Gilman A, eds. The pharmacological basis of therapeutics. Ch. 22. New York: Macmillan, 1970:442–465.
69. Langley JN. On the union of cranial autonomic (visceral) fibres with the nerve cells of the superior cervical ganglion. J Physiol (Lond) 1898;23:240.
70. Langley JN. The autonomic nervous system. Vol. I. Cambridge: Heffer & Sons, 1921.
71. Llewellyn-Smith IJ, Phend KD, Minson JB, Pilowsky PM, Chalmers JP. Glutamate-immunoreactive synapses on retrogradely-labelled sympathetic preganglionic neurons in the rat thoracic spinal cord. Brain Res 1992;581: 67–80.
72. Loewi O. Über humorale Übertragbarkeit der Herznervenwirkung. Arch Gesamte Pysiol Menschen Tiere 1921;189:239–242.
73. Loewi O. Chemical transmission of nerve impulses. Sci Prog 1945; 4:98–119.
74. Lundberg A. Electrophysiology of the salivary glands. Physiol Rev 1958;38:21–40.
75. Lundberg JM, Dahlström A, Larsson I, Petersson G, Ahlman H, Kewenter J. Efferent innervation of the small intestine by adrenergic neurons from the cervical sympathetic and stellate ganglia, studied by retrograde transport of peroxidase. Acta Physiol Scand 1978; 104:33–42.
76. Lundberg JM, Terenius L, Hökfelt T, et al. Neuropeptide Y (NPY)-like immunoreactivity in peripheral noradrenergic neurons and effects of NPY on sympathetic function. Acta Physiol Scand 1982;116: 477–480.
77. McLennan H. Synaptic transmission. Philadelphia: W.B. Saunders, 1963.
78. McMichael J. Spinal tracts subserving micturition in a case of Erb's spinal paralysis. Brain 1945;68:162.
79. Malmfors T. Release and depletion of the transmitter in adrenergic terminals produced by nerve impulses after the inhibition of noradrenaline synthesis of reabsorption. Life Sci 1964;3:1397–1402.
80. Marfurt CF, Kingsley RE, Echtenkamp SF. Sensory and sympathetic innervation of the mammalian cornea. A retrograde tracing study. Invest Ophthalmol 1989;30:461–472.
81. Mayer EA, Raybould HE. Role of visceral afferent mechanisms in functional bowel disorders. Gastroenterology 1990;99:1688–1704.
82. Minneman KP, Pittman RN, Molinoff PB. β-adrenergic receptor subtypes: properties, distribution and regulation. Ann Rev Neurosci 1981;4:419–461.
83. Mitchell GAG. Anatomy of the autonomic nervous system. Edinburgh: Livingstone, 1953.
84. Nauta WJH. Hippocampal projections and related neural pathways to the midbrain in the cat. Brain 1958;81:319–340.
85. Nauta WJH. The central visceromotor system: a general survey. In: Hockman CH, ed. Limbic system mechanisms and autonomic function. Ch. 2. Springfield, IL: Charles C. Thomas, 1972:21–33.
86. Nickerson M. Drugs inhibiting adrenergic nerves and structures innervated by them. In: Goddman LS, Gilman A, eds. The pharmacological basis of therapeutics. Ch. 26. New York: Macmillan, 1970; 549–584.
87. Nilsson C, Kannisto P, Lindvall-Axelsson M, Owman C, Rosengren E. The neuropeptides vasocative intestinal polypeptide, peptide histidine isoleucine and neuropeptide Y modulate [^{3}H] noradrenaline release from sympathetic nerves in the choroid plexus. Eur J Pharmacol 1990;181:247–252.
88. Norberg KA. Transmitter histochemistry of the sympathetic adrenergic nervous system. Brain Res 1967;5:125–170.
89. Pacholczyk T, Blakeley RD, Amara SG. Expression cloning of a cocaine- and antidepressant-sensitive human noradrenaline transporter. Nature 1991;350:350–354.
90. Parent A, Poirier LJ, Boucher R, Butcher LL. Morphological characteristics of acetylcholinesterase-containing neurons in the CNS of DFP-treated monkeys. Part 2. Diencephalic and medial telencephalic structures. J Neurol Sci 1977;32:9–28.
91. Patton HD. Reflex regulation of movement and posture. In: Ruch TC, ed. Neurophysiology. Ch. 6. Philadelphia: W.B. Saunders, 1961:167–198.
92. Pearson J, Pytel B. Quantitative sudies of sympathetic ganglia and spinal cord intermedio-lateral gray columns in familial dysautonomia. J Neurol Sci 1978;39:47–59.
93. Phelps PE, Barber RP, Vaughn JE. Embryonic development of choline acetyltransferase in thoracic spinal motor neurons: somatic and autonomic neurons may be derived from a common cellular group. J Comp Neurol 1991;307:77–86.
94. Pick J. The autonomic nervous system. Philadelphia: J.B. Lippincott, 1970.
95. Pick J, Sheehan D. Sympathetic rami in man. J Anat 1946;80:12–20.
96. Potts TK. The main peripheral connections of the human sympathetic nervous system. J Anat 1924; 59:129–135.
97. Raisman G. Neural connexions of hypothalamus. Br Med Bull 1966; 22:197–201.
98. Ramón y Cajal S. Histologie du Système Nerveux de l'Homme et des Vertébrés. (Azoulay L, Trans.) Paris: Maloine, 1909, 1911. (Reprinted, Consejo Superior de Investigaciones Cientificas, Instituto Ramón y Cajal, Madrid, 1972.)
99. Ranson SW, Billingsley PR. The superior cervical ganglion and the cervical portion of the sympathetic trunk. J Comp Neurol 1918;29: 313–358.
100. Richter CP, Woodruff BG. Lumbar sympathetic dermatomes in man determined by the electrical skin resistance method. J Neurophysiol 1945;8:323–338.
101. Riley CM. Familial autonomic dysfunction. JAMA 1952;149:1532–1535.
102. Riley CM, Moore RH. Familial dysautonomia differentiated from related disorders. Pediatrics 1966; 37:435–446.
103. Root WS. Physiology of micturition: a specific autonomic function. In: Mountcastle VB, ed. Medical physiology. 12th ed. Ch. 79: St. Louis: C.V. Mosby, 1969:1831–1838.
104. Rotto-Percelay DM, Wheeler JG, Osorio FA, Platt KB, Loewy AD. Transneuronal labeling of spinal interneurons and sympathetic preganglionic neurons after pseudorabies virus infections in the rat medial gastrocnemius muscle. Brain Res 1992;574:291–306.
105. Saito H. Innervation of the guinea pig spleen studied by electron microscopy. Am J Anat 1990;189: 213–235.
106. Saper CB. Hypothalamus. In: Paxinos G, ed. The human nervous system. Ch. 15. New York: Academic Press, 1990;389–413.
107. Saper CB, Loewy AD, Swanson LW, Cowan WM. Direct hypothalamo-autonomic connections. Brain Res 1976;117:305–312.
108. Satomi H, Yamamoto T, Ise H, Takatama H. Origins of the parasympathetic preganglionic fibers to the cat intestine, as demonstrated by the horseradish peroxidase method. Brain Res 1978;151:571–578.
109. Schotzinger RJ, Landis SC. Acquisition of cholinergic and peptidergic properties by sympathetic in-

nervation of rat sweat glands requires interaction with normal target. Neuron 1990;5:91–100.
110. Schwartz JH. Chemical messengers: small molecules and peptides. In: Kandel ER, Schwartz JH, Jessell TM, eds. Principles of neural science. Ch. 14. New York: Elsevier, 1991:213–224.
111. Schwyn RC. An autoradiographic study of satellite cells in autonomic ganglia. Am J Anat 1967;121: 727–740.
112. Séguéla P, Watkins KC, Geffard M, Descarries L. Noradrenaline axon terminals in adult rat neocortex: an immunocytological analysis is serial thin sections. Neuroscience 1990;35:249–264.
113. Sheehan D. Discovery of the autonomic nervous system. Arch Neurol Psychiatry 1936;35:1081–1115.
114. Sheehan D. Spinal autonomic outflows in man and monkey. J Comp Neurol 1941;75:341–370.
115. Sheehan D. The autonomic nervous system. Annu Rev Physiol 1941;3:399–448.
116. Sjögren C, Andersson K-E, Husted S, Mattiasson A, Moller-Madsen B. Atropine resistance of transmurally stimulated isolated human bladder muscle. J Urol 1982; 128:1368–1371.
117. Smith OA Jr, Clarke NP. Central autonomic pathways: a study in functional neuroanatomy. J Comp Neurol 1964;122:399–406.
118. Sternini C, Anderson K. Calcitonin gene-related peptide-containing neurons supplying the rat digestive system: differential distribution and expression pattern. Somatosen Mot Res 1992;9:45–59.
119. Strack AM, Loewy AD. Pseudorabies virus: a highly specific transneuronal cell body marker in the sympathetic nervous system. J Neurosci 1990;10:2139–2147.
120. Strack AM, Sawyer WB, Platt KB, Loewy AD. CNS cell groups regulating the sympathetic outflow to adrenal gland as revealed by transneuronal cell body labeling with pseudorabies virus. Brain Res 1989;491:274–296.
121. Swanson LW, McKellar S. The distribution of oxytocin-and neurophysin-stained fibers in the spinal cord of the rat and monkey. J Comp Neurol 1979;188:87–106.
122. Tang PC, Ruch TC. Localization of brain stem and diencephalic areas controlling the micturition reflex. J Comp Neurol 1956;106:213–26.
123. Tollefson L, Bulloch K. Dual-label retrograde transport: CNS innervation of the mouse thymus distinct from other mediatinum viscera. J Neurosci Res 1990;25:20–28.
124. Truex RC. The sympathetic ganglions of hypertensive patients. AMA Arch Pathol 1951;51:186–191.
125. Uehara Y, Burnstock G. Demonstration of gap junctions between smooth muscle cells. J Cell Biol 1970;44:215–217.
126. Von Euler US. Noradrenaline. Springfield, IL: Charles C. Thomas, 1956.
127. Von Euler US. Neurotransmission in the adrenergic nervous system. The Harvey Lectures, Ser. 55. New York: Academic Press, 1961:43–65.
128. Von Euler US. Catecholamines in nerve and organ granules. In: Von Euler US, ed. Mechanism of release of biogenic amines. New York: Pergamon, 1966:211–222.
129. Warwick R. The ocular parasympathetic nerve supply and its mesencephalic sources. J Anat 1954; 88:71–93.
130. White JC, Okelberry AM, Whitelaw GP. Vasomotor tonus of the denervated artery. Arch Neurol and Psychiatry 1936;36:1251–1276.
131. Wiberg M, Widenfalck B. An anatomical study of the origin of sympathetic and sensory innervation of the elbow and knee joint in the monkey. Neurosci Lett 1991; 127:185–188.
132. Wiley JW, Lu YX, Owyang C. Evidence for a glutamatergic neural pathway in the myenteric plexus. Am J Physiol 1991;261: 693–700.
133. Williams TH. Electron microscopic evidence for an autonomic interneuron. Nature 1967;214:309–310.
134. Williams TH, Black AC, Chiba T, Jew JY. Species differences in mammalian SIF cells. In: Costa E, Gessa GL, eds. Advances in biochemical psychopharmacology. Vol. 16. New York: Raven Press, 1977:505–511.
135. Willis W. Visceral pain. In: Brooks FP, Evers PW, eds. Nerves and the gut. Thorofare, NJ: C.B. Slack, 1977:350–364.
136. Winkler H. Occurrence and mechanism of exocytosis in adrenal medulla and sympathetic nerve. In: Trendelenberg U, Weiner N, eds. Handbook of experimental pharmacology. Vol. 90. Part II. Berlin: Springer Verlag, 1988: 43–118.
137. Wolf G, Sutin J. Fiber degeneration after lateral hypothalamic lesions in the rat. J Comp Neurol 1966;127:137–156.
138. Wolf GA Jr. The ratio of preganglionic neurons to postganglionic neurons in the visceral nervous system. J Comp Neurol 1941; 75:235–243.
139. Wolfe DE, Potter LT, Richardson KC, Axelrod J. Localizing tritiated norepinephrine in sympathetic axons by electron microscopic autoradiography. Science 1962;138: 440–442.

Section IV

Spinal Cord

10
Spinal Cord: Regional Anatomy and Internal Structure

TOPOGRAPHIC ORGANIZATION

The spinal cord is the least modified portion of the embryonic neural tube and the only part of the adult nervous system in which the primitive segmental arrangement clearly is preserved. It is a long, cylindrical structure, invested by meninges, which lies in the vertebral canal. It extends from the foramen magnum (Fig. 1.4), where it is continuous with the medulla, to the lower border of the first lumbar vertebra (Fig. 1.6). The spinal cord has two enlargements, cervical and lumbar or lumbosacral, each associated with nerve roots which innervate, respectively, the upper and lower extremities (Fig. 10.1). The spinal cord has a conical termination, the *conus medullaris* (Figs. 1.6 and 10.1). A condensation of pia mater, extending caudally from the conus medullaris, forms the *filum terminale*. The latter structure joins the dural tube at levels of the second sacral vertebra, becomes invested by dura, and continues as the coccygeal ligament to the posterior surface of the coccyx (Fig. 1.6).

While the spinal cord is a continuous unsegmented structure, the 31 pairs of spinal nerves associated with localized regions produce an external segmentation (Fig. 10.1). On the basis of this external segmentation, the spinal cord is considered to consist of 31 segments, each of which receives and furnishes paired dorsal and ventral root filaments (Fig. 10.2). The spinal cord is divided into the following segments: 8 cervical, 12 thoracic, 5 lumbar, 5 sacral, and 1 coccygeal. Up to the 3rd month of fetal life the spinal cord occupies the entire length of the vertebral canal, but after that time the differential rate of growth of the vertebral column exceeds that of the spinal cord. At birth, the conus medullaris is located near the L3 vertebra; in the adult it is between the L1 and L2 vertebrae, and the spinal cord occupies only the upper two-thirds of the vertebral canal (Fig. 10.3). The sites of emergence of the spinal nerves do not change, but there is a lengthening of root filaments between the intervertebral foramina and the spinal cord. This is most marked for the lumbar and sacral spinal roots. These roots descend for a considerable distance within the dural sac before reaching their respective intervertebral foramina. The large number of lumbosacral roots surrounding the filum terminale is known as the *cauda equina* (Fig. 10.1). Spinal nerves emerge from the vertebral canal via the intervertebral foramina. The first cervical nerve emerges between the atlas and the occiput (Fig. 1.4). The eighth cervical root emerges from the intervertebral foramen between C7 and T1; all more caudal spinal nerves emerge from the intervertebral foramina beneath the vertebrae of their same number (Fig. 10.3). Dorsal root fibers usually are absent in the first cervical and the coccygeal roots, and there are no corresponding dermatomes for these segments.

The length of the spinal cord from its junction with the medulla to the tip of the conus medullaris is about 45 cm in the male and 43 cm in the female. In contrast, the length of the vertebral column is about 70 cm. The weight of the spinal cord is about 35 g. In the midthoracic region, the transverse and sagittal diameters of the spinal cord are about 10 mm and 8 mm, respectively; in the cervical enlargement (sixth cervical), 13–14 mm and 9 mm; in the lumbar enlargement (third lumbar), about 12 mm and 8.5 mm (see Fig. 10.5).

When freed from its meninges, the surface of the cord shows a number of longitudinal furrows (Figs. 10.1, 10.2, 10.6, and 10.7). On the anterior surface, an *anterior median fissure*, penetrating the cord for a depth of some 3 mm, contains an epipial fold with sulcal branches of the anterior spinal artery and vein (Fig. 4.2). On the posterior surface is the shallow *posterior median sulcus*. This sulcus is continuous with a delicate glial partition, the *posterior median septum*, which extends into the cord and reaches the deeplying gray matter. Lateral to the midline

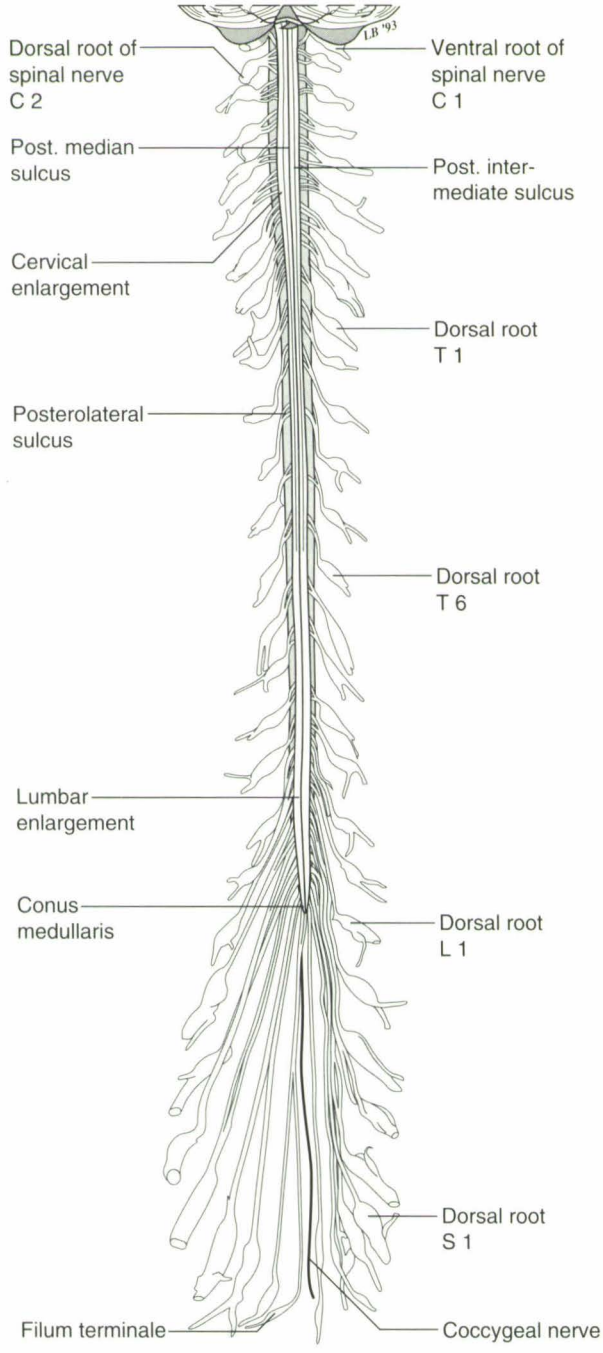


Figure 10.1. Posterior view of the spinal cord showing attached dorsal root filaments and spinal ganglia. Letters and numbers indicate corresponding spinal nerves.

posteriorly are two less distinct sulci associated with spinal roots. The *posterolateral sulcus* is a shallow furrow into which filaments of the dorsal roots enter the spinal cord (Fig. 10.6). The *anterolateral sulcus* marks the site of emergence of ventral root fibers. Since ventral filaments emerge at less regular intervals and are less numerous than dorsal roots, the anterolateral sulcus may be more difficult to distinguish. In cervical and upper thoracic spinal segments, the *posterior intermediate sulcus* indents the spinal cord between the poste-

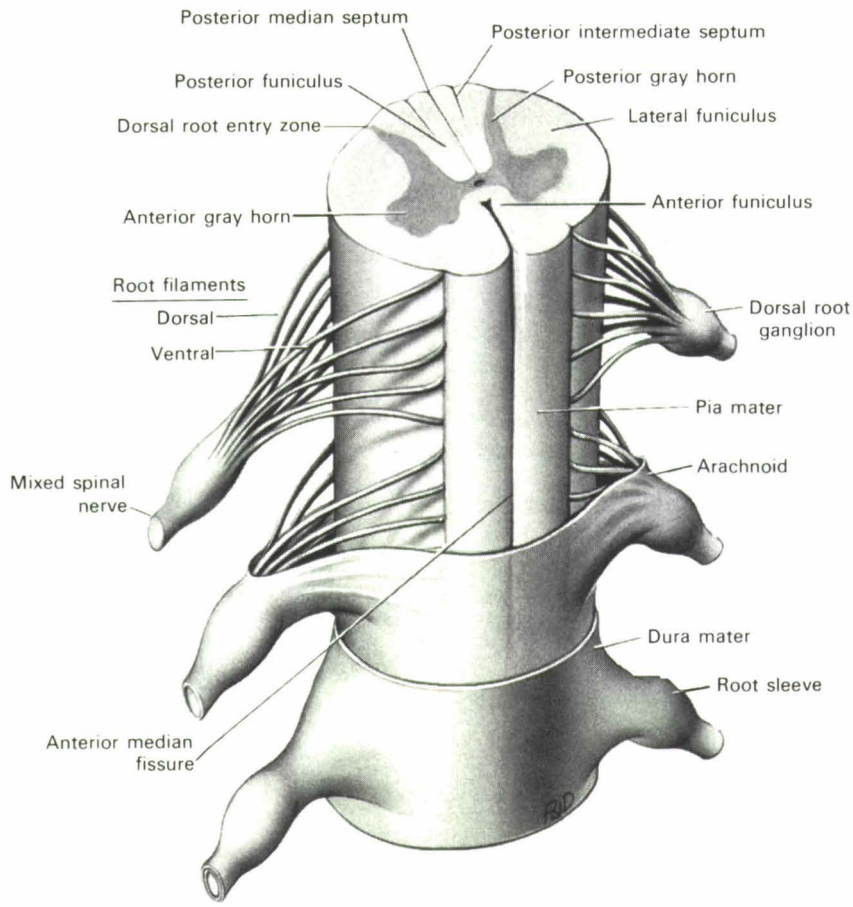


Figure 10.2. Spinal cord, nerve roots, and meninges. The blood supply and venous drainage of the spinal cord are shown in Figures 4.1 and 4.2.

rior median and posterolateral sulci (Figs. 10.2 and 10.6). This sulcus is associated with a glial partition, the *posterior intermediate septum*, that extends internally toward the spinal gray matter (Figs. 10.2 and 10.6). The anterior median fissure and posterior median septum divide the cord into incompletely separated halves connected by a narrow midline commissure, composed of gray and white matter.

Although the spinal cord is a symmetric structure, it is not uniform in diameter. It contains two enlargements, cervical and lumbosacral, associated with the largest nerve roots which innervate the extremities. The *cervical enlargement*, consisting of the four lowest cervical segments and the first thoracic segment, gives rise to the nerve roots that form the *brachial plexus* (Figs. 10.1 and 10.3) and provide innervation for the upper extremity (Figs. 8.14 and 8.15). The *lumbar or lumbosacral enlargement* (Figs. 10.1 and 10.3) gives rise to fibers that form the *lumbar plexus* (L1 to L4) and the *sacral plexus* (L4 to S2). Spinal segments vary in cross-sectional diameters and in length. Thoracic spinal segments have the longest length while sacral segments have the shortest length. The tapered terminal portion of the spinal cord, the *conus medullaris* provides cutaneous innervation to the saddle area, motor innervation for the sphincters, and parasympathetic innervation for the bladder (Fig. 9.11). The *filum terminale* extending caudally from the conus medullaris lies in the lumbar cistern surrounded by lumbosacral nerve roots forming the *cauda equina* (Figs. 1.6 and 10.1).

In transverse section the spinal cord consists of (a) a butterfly-shaped central gray matter composed of collections of cell bodies and their processes, and (b) a surrounding mantle of white matter composed of bundles of myelinated fibers, most of which are either

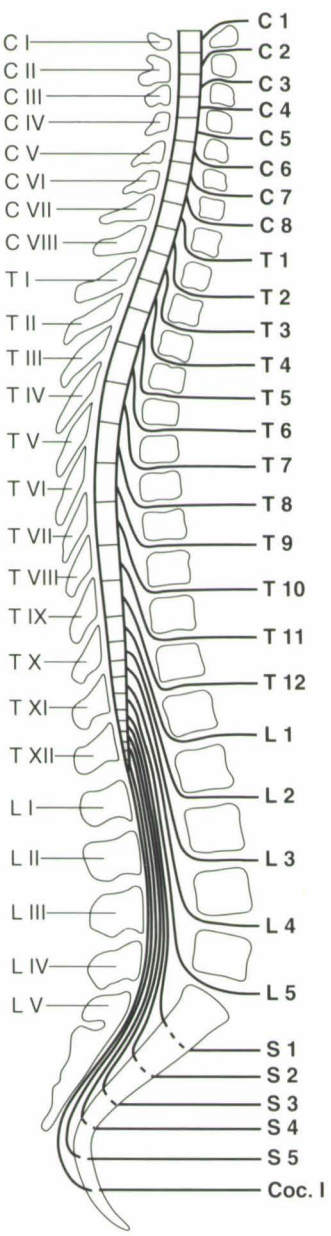


Figure 10.3. Position of the spinal cord segments with reference to the bodies and spinous processes of the vertebrae.

ascending or descending (Figs. 10.2 and 10.7). The symmetric butterfly-shaped gray consists of cell columns, some of which extend the length of the spinal cord, and vary in configuration at different levels (Figs. 10.5 and 10.6).

Each half of the spinal cord has a *posterior (dorsal) gray column* or *horn* which extends posterolaterally almost to the surface near the root entry zone. An *anterior (ventral) gray column* or *horn* extends anteriorly but does not reach the surface. Thoracic spinal segments are characterized by a small, pointed *lateral horn* near the base of the anterior horn (Fig. 10.7). *Gray anterior* and *posterior commissure*, connecting the gray matter of the two sides, encompasses the central canal (Fig. 10.4). Surrounding the central canal is a light granular area composed mainly of neuroglia, known as the central gelatinous substance (substantia gliosa). Anterior to the gray commissure is a bundle of transverse fibers, the *anterior (ventral) white commissure*, composed of crossing fibers arising from nerve cells in the gray matter (Figs. 10.4 and 10.7).

Ascending and descending fibers occupying particular regions of the white matter of the spinal cord are organized into more or less distinct bundles (Figs. 10.6 and 10.13). Fiber bundles having the same, or similar, origin, course and termination are known as *tracts* or *fasciculi*. The white matter of the spinal cord is divided into three paired *funiculi*: posterior, lateral, and anterior. The *posterior funiculus* lies between the dorsal horn and the posterior median septum (Fig. 10.2). In upper thoracic and cervical regions, a small *posterior intermediate septum* divides each posterior funiculus into two white columns. The *lateral funiculus* lies between the dorsal root entry zone and the site where ventral root fibers emerge from the spinal cord. The *anterior funiculus* lies between the anterior median fissure and the emerging ventral root filaments. The posterior funiculus is the largest and is composed almost exclusively of long ascending and short descending fibers that arise from cells in the spinal ganglia.

The *cervical enlargement*, consisting of the four lowest cervical segments and the first thoracic segment, gives rise to nerve roots which form the *brachial plexus* (Figs. 8.14 and 8.15). The *lumbar (or lumbosacral) enlargement* (Figs. 8.19 and 8.20) gives rise to fibers that form the *lumbar plexus* (L1 to L4) and the *sacral plexus* (L4 to S2).

Although the spinal cord constitutes only 2% of the central nervous system by weight, its functions are tremendously important since it (a) receives afferent inputs via the dorsal roots from somatic and visceral receptors in most parts of the body, (b) gives rise to ascending pathways which transmit impulses to higher levels of the neuraxis, (c) gives rise to fibers emerging in the ventral roots that in-

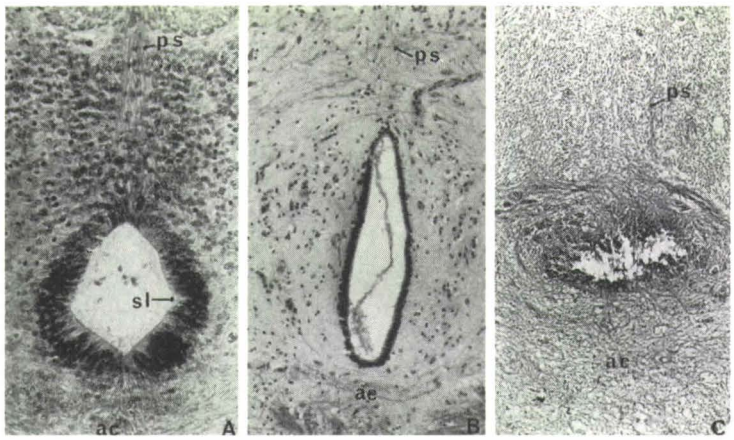


Figure 10.4. Ependymal cells and central canal of embryonic and adult human spinal cord. The sulcus limitans (*sl* in **A**) becomes lost in the adult. Processes of the ependymal cells entering the posterior median septum (*ps*) can be seen and the fibers of the anterior white commissure are identified (*ac*) **A.** Holmes silver stain, ×263. **B.** Luxol fast blue-cresyl violet, ×112. **C.** Holmes silver-cresyl violet, ×108.

nervate somatic and visceral effectors, (d) conveys descending pathways from higher levels of the nervous system, and (e) participates in a variety of somatic and autonomic reflexes. Meninges surrounding the spinal cord and nerve roots are described in Chapter 1 and the blood supply of the spinal cord is discussed in Chapter 4.

INTERNAL STRUCTURE

The microscopic appearance of the adult spinal cord is vastly altered from the three-layered embryonic neural tube (Fig. 3.5). The incoming and outgoing processes of ganglion cells and intrinsic neurons produce marked changes in the embryonic marginal and mantle layers. The embryonic layers become longitudinal columns of gray and white matter in the adult spinal cord, each having microscopic landmarks and subdivisions (Figs. 10.2 and 10.6). Individual segments of the spinal cord show variations at different levels, for there is great variation in the size and number of fibers in the individual spinal nerves (Fig. 10.1).

Gray and White Matter

The gray and white matter (or substance) are composed of neural elements supported by an interstitial neuroglial framework. The mesodermal structures comprise the blood vessels and their contents. The larger vessels are accompanied by prolongations of pial connective tissue. The gray matter contains the nerve cells, dendrites, portions of myelinated and unmyelinated nerve fibers, and glial cells. These fibers are axons of nerve cells located in the gray matter which pass into the white matter, or portions of the axons in the white matter which enter the gray matter to terminate there. The preponderance of neurons, neuroglia, and capillaries imparts a firm consistency to the butterfly- or H-shaped gray matter (Fig. 10.7). This density is enhanced further by a multitude of fine glial processes, fibrils, synaptic terminals, and dendrites, which invests neurons in an intricate meshwork, or *neuropil*. In sections stained with either hematoxylin and eosin or cresyl violet, the gray matter has a highly cellular appearance, while the fibrous elements of the neuropil are unstained. In such sections only the neuronal perikarya, glial, and endothelial nuclei are apparent. The enormous dendritic plexus of the neurons and their synaptic endings remain unstained (Fig. 5.28). Lorente de Nó (74) estimated that the soma of the perikaryon forms only 6% of the surface of a neuron. Hence the neuropil of the gray matter, which is not visible in Nissl-stained sections, is where most dendritic plexuses are located. The central canal, surrounded by ependymal cells, is located in the crossbar of the H-shaped gray matter (Figs.

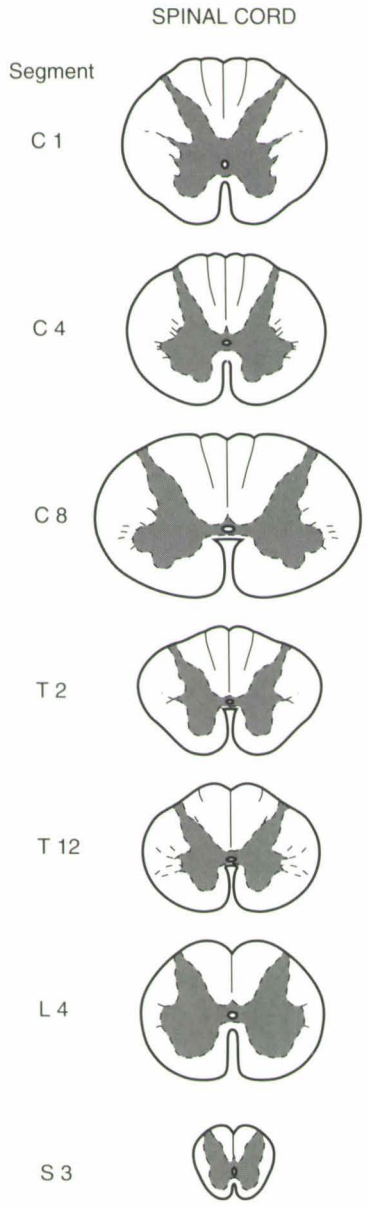


Figure 10.5. Selected spinal cord segments at different levels showing the variations in size, shape, and topography of gray and white matter.

10.4 and 10.7). A sharply delineated central canal is seen only in fetal and newborn spinal cords. In the adult, the ependymal lining often is discontinuous and the lumen may contain debris, round cells, macrophages, and neuroglial processes (Fig. 10.4**C**). Surrounding the central canal are clumps of fibrous astrocytes rarely seen in other parts of the gray matter (Figs. 6.2 and 6.12). The two slender bands of gray matter above and below the central canal form the posterior and anterior gray commissures. The anterior commissure is much more massive than the posterior commissure, which is composed only of a small group of myelinated fibers.

The white matter contains few neurons or dendrites, but is composed of ascending and descending myelinated and unmyelinated nerve fibers. The longitudinally arranged fiber bundles and their supportive neuroglial cells surround the gray matter as the posterior, lateral, and anterior white funiculi. Numerous myelinated axons can be observed entering or leaving the white funiculi as dark fibers in sections stained by the Weigert method (Figs. 10.7 and 10.10). The structure and distribution of the glial cells are presented in Chapter 6. The processes of astrocytes form a *superficial glial membrane* which is adherent to the deep surface of the pia mater.

Segmental Variations

The different segments of the spinal cord vary (a) in size and shape, (b) in the relative amounts of gray and white matter, and (c) in the disposition and configuration of the gray matter (Fig. 10.5). Cervical spinal segments contain the largest number of fibers in the white matter because (a) descending fiber systems have not yet contributed fibers to lower segmental levels and (b) ascending fiber systems at each successively rostral segment reach their maximum. The gray cell columns are maximal in the cervical and lumbar enlargements which are associated with the larger nerves that innervate the extremities. Lumbosacral segments contain large amounts of gray matter, relative to both the size of the cord segments and the amount of white matter (Figs. 10.16 and 10.17).

CERVICAL SEGMENTS

These segments are characterized by their relatively large size, relatively large amounts of white matter, and oval shape (Figs. 10.5, 10.8–10.10). The transverse diameter exceeds the anteroposterior diameter at nearly all levels. On each side, the posterior funiculus is divided by a prominent posterior intermediate septum into a *fasciculus gracilis* (medial) and a *fasciculus cuneatus* (lateral). In the lower cervical segments (C5 and below) related to the brachial plexus, the posterior (dorsal) horns are enlarged, and well-developed ante-

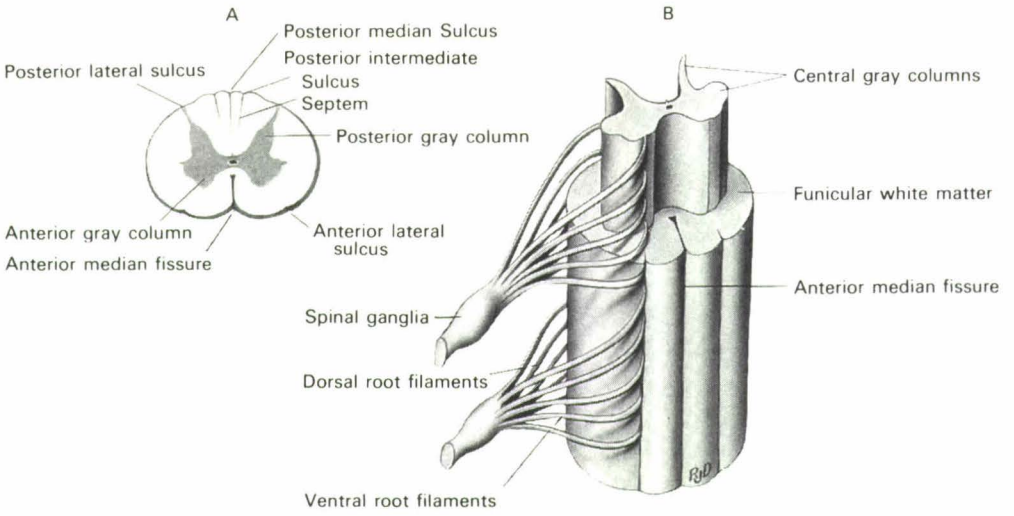


Figure 10.6. **A.** Internal arrangement of gray and white matter of the spinal cord. **B.** External and internal topography of cervical spinal cord.

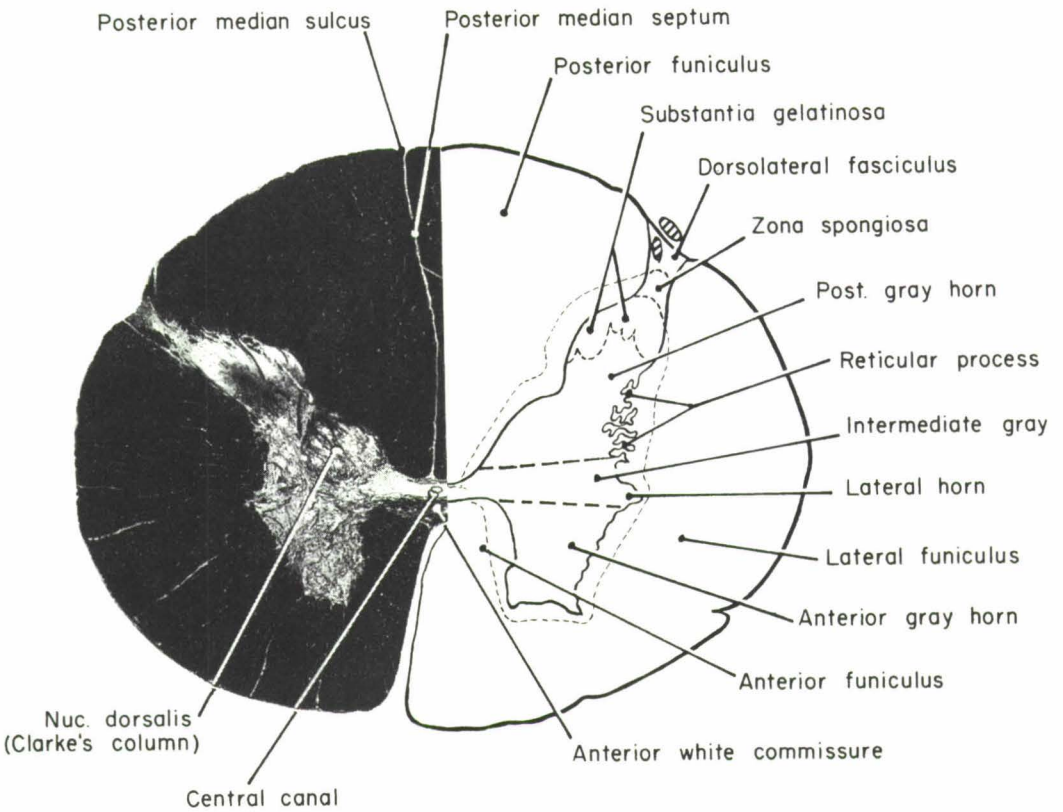


Figure 10.7. Section through a lower thoracic segment of adult human spinal cord to demonstrate subdivisions of the gray and white matter. Photograph of Weigert's myelin stain on *left* and schematic drawing on *right*. Area surrounding the gray matter, and limited peripherally by the *dotted line*, is composed of shorter ascending and descending fibers of the fasciculus proprius system.

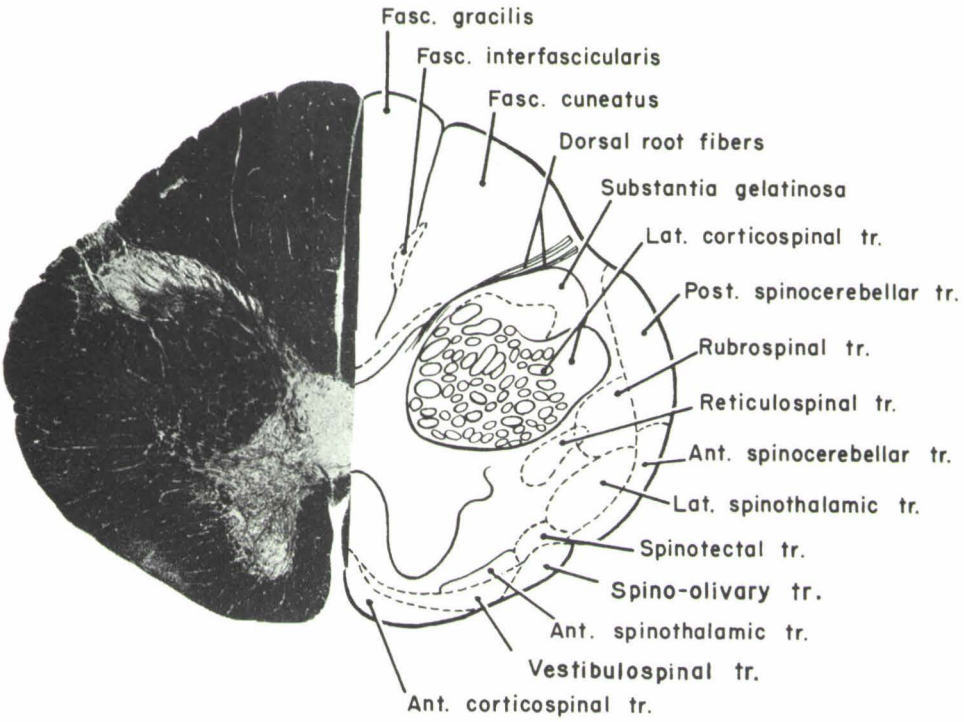


Figure 10.8. Photomicrograph (*left*) and drawing (*right*) of a section through upper portion of first cervical segment of adult human spinal cord. Some of the important fiber tracts are identified (Weigert's myelin stain).

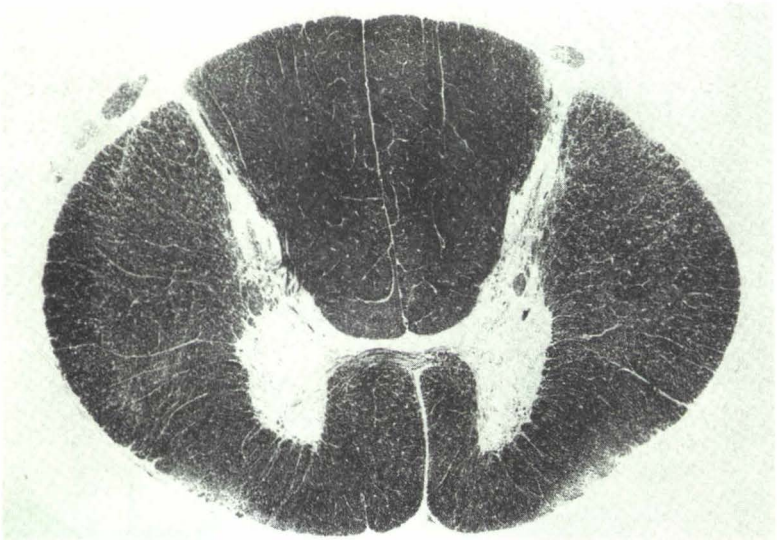


Figure 10.9. Transverse section through the second cervical segment of the adult human spinal cord. Note the narrowness of the anterior and posterior gray horns and the abundant white matter. Cell groups are identified in Figure 10.11 (Weigert's myelin stain).



Figure 10.10. Transverse section through the fourth cervical segment of the adult human spinal cord demonstrating entering dorsal root fibers. At this level the substantia gelatinosa is larger and a well-developed lateral process of the anterior gray horn is seen. Cell groups in the spinal gray are identified in Figure 10.11 (Weigert's myelin stain).

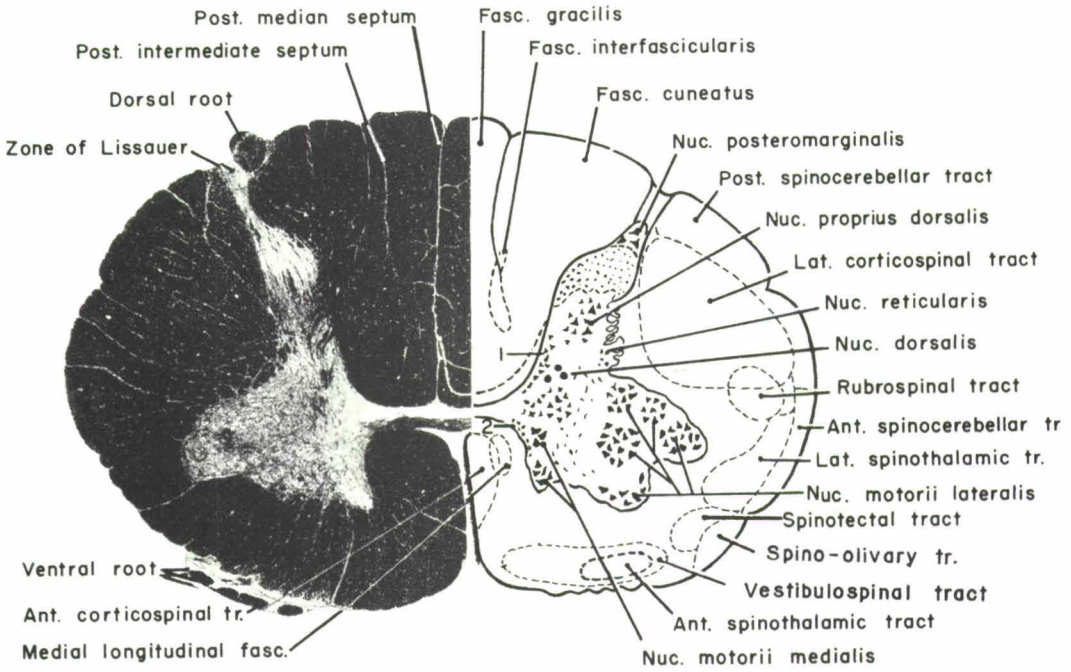


Figure 10.11. Section through eighth cervical segment of adult human spinal cord. The important cell groups and fiber tracts are identified. *1*, Nucleus cornucommissuralis posterior; *2*, nucleus cornucommissuralis anterior (Weigert's myelin stain).

rior (ventral) horns extend into the lateral funiculi (Figs. 10.11 and 10.12**A**). Near the neck of the posterior horn is a serrated cellular area known as the *reticular process* (reticular nucleus); this process is present in all cervical segments. In upper cervical segments (C1 and C2), the dorsal horn is enlarged, but the anterior (ventral) horn is relatively small (Figs. 10.8–10.10). The transverse diameter of the most rostral cervical spinal segment is about 12 mm, while it is 13–14 mm at C8.

THORACIC SEGMENTS

These segments show variations at different levels (Figs. 10.5, 10.7, 10.13, and 10.15). Both the fasciculi gracilis and cuneatus are present in upper thoracic segments (T1 to T6), while only the fasciculus gracilis is seen in the posterior funiculus at more caudal levels (below about T6). In general, the anterior (ventral) and posterior (dorsal) horns are small and somewhat tapered. The first thoracic segment is an exception in that it forms the lowest segment of the cervical enlargement and contributes to the brachial plexus. A prominent, but small, lateral horn is present at all thoracic levels and contains the intermediolateral cell column which gives rise to preganglionic sympathetic fibers (Figs. 10.12**B** and 10.13). At the base of the medial aspect of the posterior horn is a rounded collection of large cells, the *dorsal nucleus of Clarke* (Figs. 10.7, 10.12**B**, 10.13, and 10.15). While this nucleus is present in all thoracic segments it is particularly well-developed at T10 through T12. The large cells of this nucleus have a characteristic appearance in that their large vesicular nuclei often are eccentric, and chromophilic material is distributed peripherally in the perikaryon.

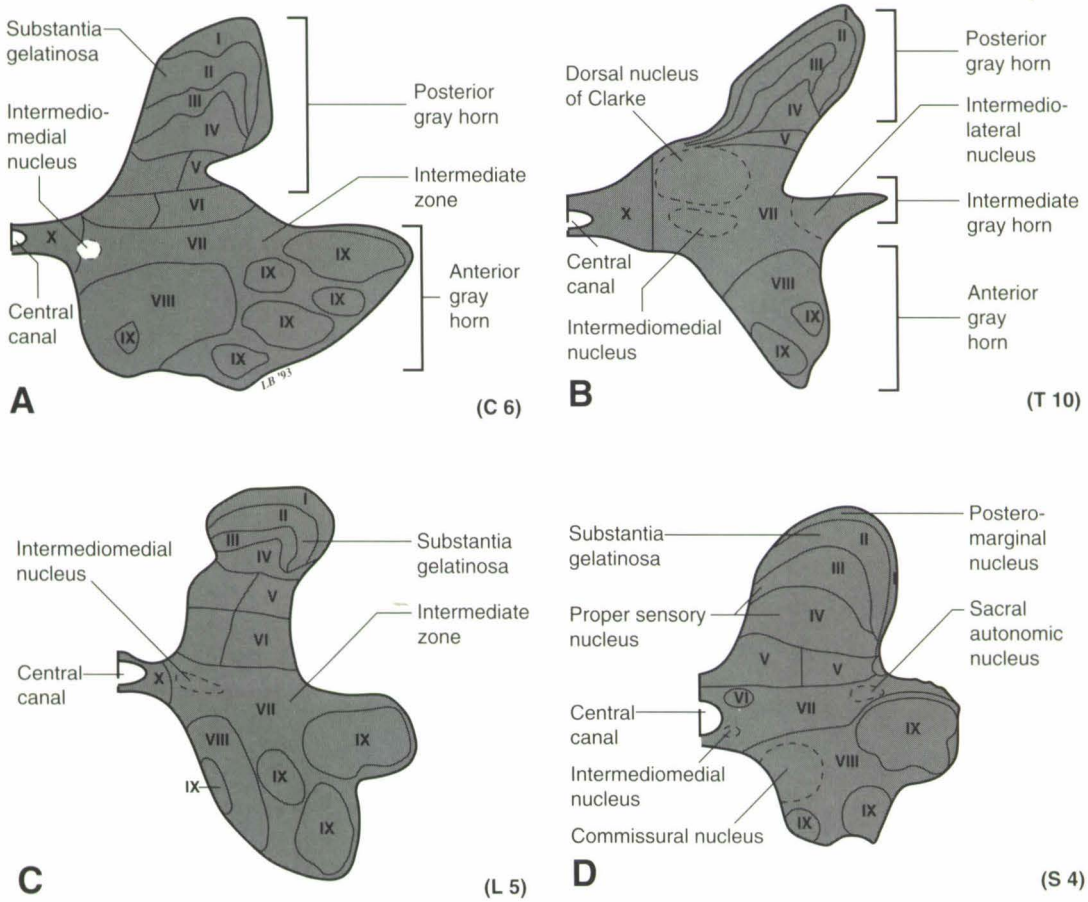


Figure 10.12. Structural lamination of human spinal cord segments at C6 (**A**), T10 (**B**), L5 (**C**), and S4 (**D**). Additionally, the laminae of Rexed, several distinct nuclei, and structures are identified, including the central canal. The drawings are derived from analyses of thick human spinal cord sections stained with thionin.

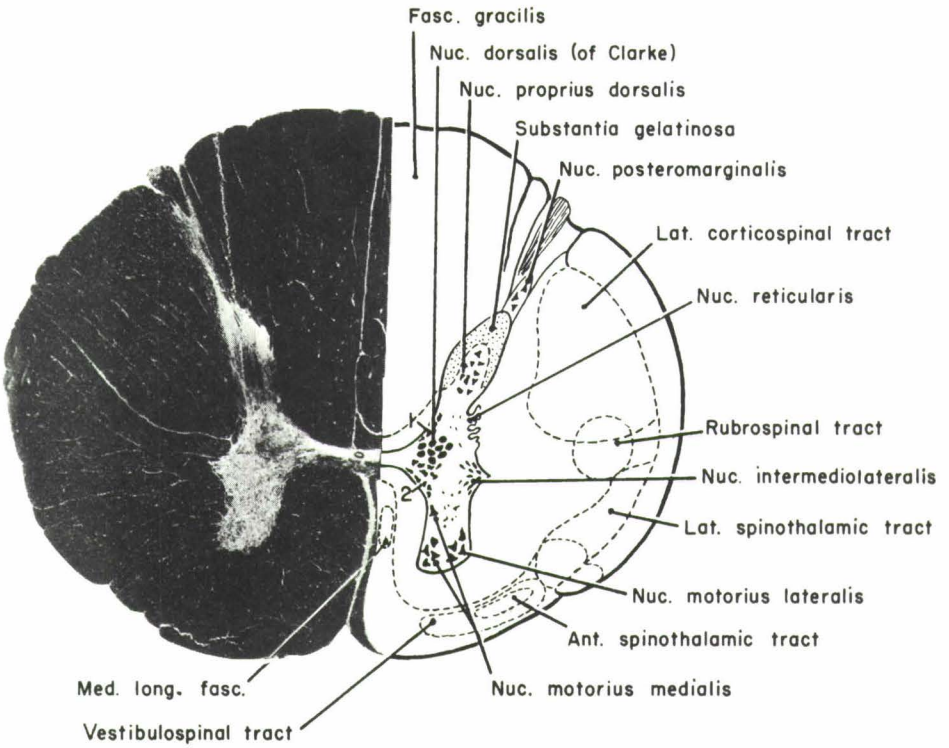


Figure 10.13. Photomicrograph (*left*) and drawing (*right*) of a section through the fifth thoracic segment of adult human spinal cord. Important cell groups and fiber tracts are identified. *1*, Nucleus cornucommissuralis posterior; *2*, nucleus cornucommissuralis anterior (Weigert's myelin stain).

Upper thoracic spinal nerves, except for T1, supply motor innervation only to axial musculature (i.e., the back and intercostals). Lower thoracic nerves supply the same muscles and the abdominal musculature. Thus, the anterior horns of lower thoracic spinal segments are a little larger. The small diameter of the thoracic segments is due primarily to the marked reduction of gray matter (Fig. 10.13).

LUMBAR SEGMENTS

These segments are nearly circular in transverse section, have massive anterior (ventral) and posterior (dorsal) horns, and contain relatively and absolutely less white matter than cervical segments (Figs. 10.5, 10.12**C**, and 10.16). The fasciculi gracilis which compose the posterior funiculus are not as broad as at higher levels, especially near the gray commissure, and have a highly characteristic configuration (Fig. 10.16). The well-developed anterior (ventral) horns have a blunt process that extends into the lateral funiculi. Motor cells in this process in segments L3 through L5 innervate large muscle groups in the lower extremities. Upper lumbar levels (L1 and L2) resemble lower thoracic spinal segments (Figs. 10.7 and 10.15) in that they contain the dorsal nucleus of Clarke and the intermediolateral cell column. The dorsal nucleus of Clarke is especially well-developed at L1 and L2. The transition between T12 and L1 is subtle, and these levels are difficult to identify precisely.

SACRAL SEGMENTS

These segments are characterized by their small size, relatively large amounts of gray matter, relatively small amounts of white matter, and a short, thick gray commissure (Figs. 10.5, 10.12**D**, and 10.17). The anterior (ventral) and posterior (dorsal) horns are large and thick, but the anterior horn is not bayed out laterally as in lumbar spinal segments. In caudal sequence, sacral segments conspicuously diminish in overall diameter but retain relatively large proportions of gray matter. The substantia gelatinosa is particularly well-developed in sacral segments, and

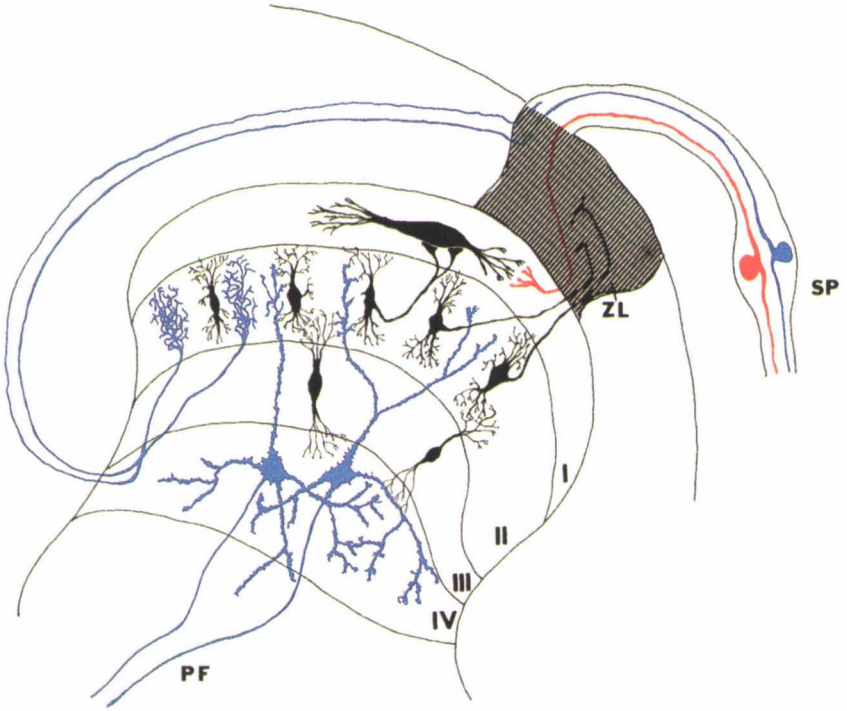


Figure 10.14. Cutaneous input into the posterior gray horn. Roman numbers *I, II, III,* and *IV* represent laminae of Rexed, *SP* is the spinal ganglion, and *ZL* (*shaded area*) is the zone of Lissauer. Primary nociceptive afferents (*red*) enter lateral parts of the root entry zone, traverse the zone of Lissauer, and synapse upon distal dendrites of larger cells in the posteromarginal nucleus (lamina I). Gelatinosa neurons in lamina II provide axons, or axon collaterals, that synapse on the soma of cells in lamina I, and longer axons that ascend/or descend in the zone of Lissauer to ultimately return to lamina II at other levels. Nonnociceptive primary afferents (*blue*) enter as part of the medial division of root fibers by either passing medial to or through the superficial gray laminae. These larger caliber fibers enter lamina II from its ventral aspect and arborize near gelatinosa neurons and in relation to dendrites of large cells of the proper sensory nucleus in lamina IV. Large cells in lamina IV (*blue*) give rise to projection fibers (*PF*), some of which cross in the anterior white commissure and project to the thalamus.

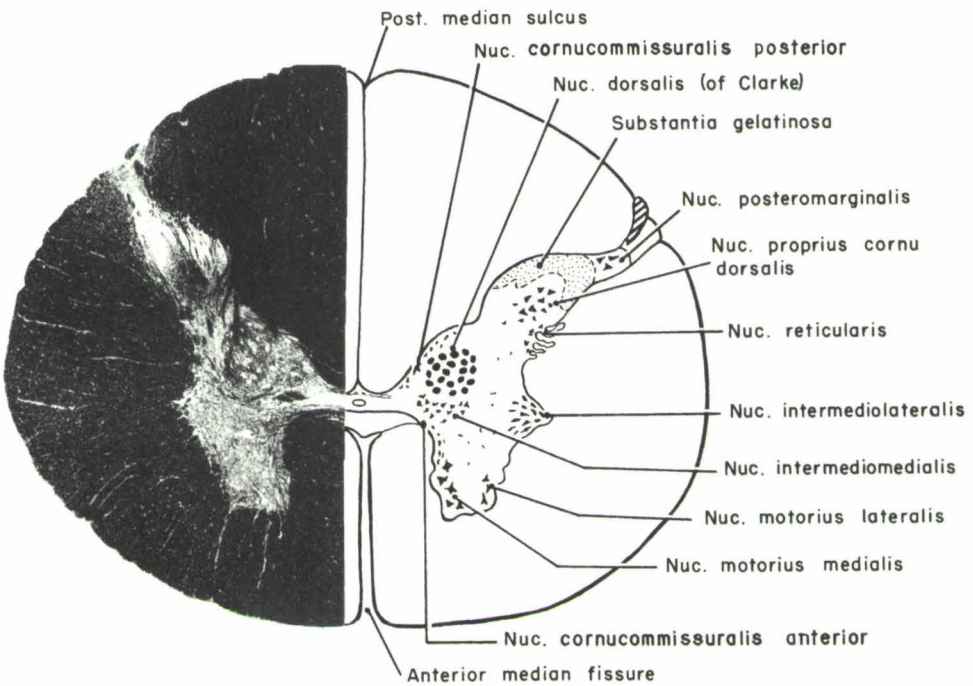


Figure 10.15. Photomicrograph (*left*) and drawing (*right*) of a section through the twelfth thoracic segment of the adult human spinal cord. Important cell groups are identified on the right (Weigert's myelin stain).

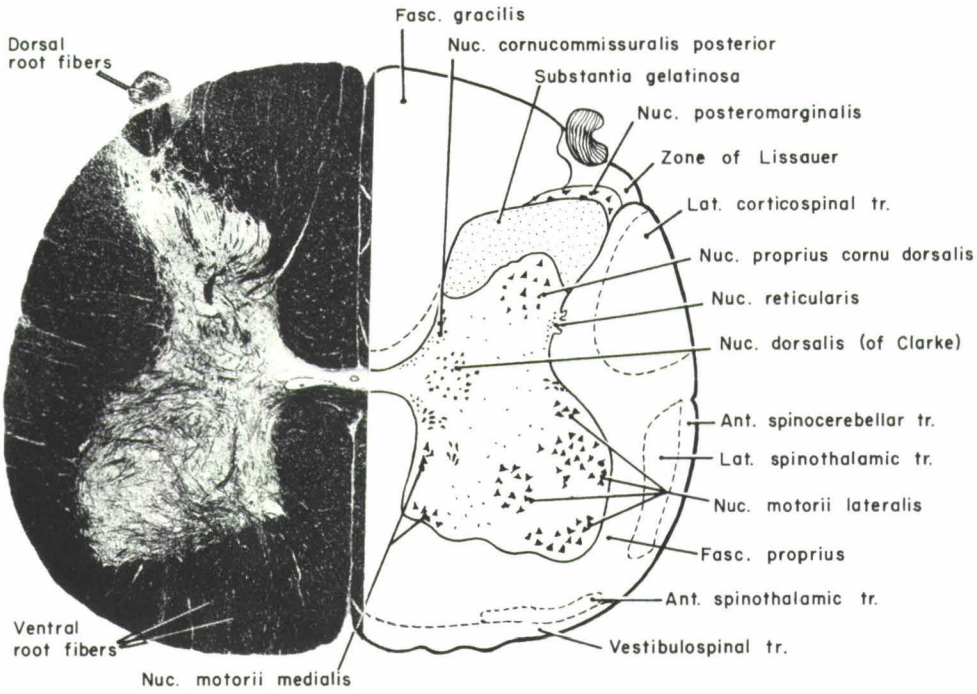


Figure 10.16. Photomicrograph (*left*) and drawing (*right*) of a section through the fourth lumbar segment of adult human spinal cord. The important cell groups and fiber tracts are identified (Weigert's myelin stain).

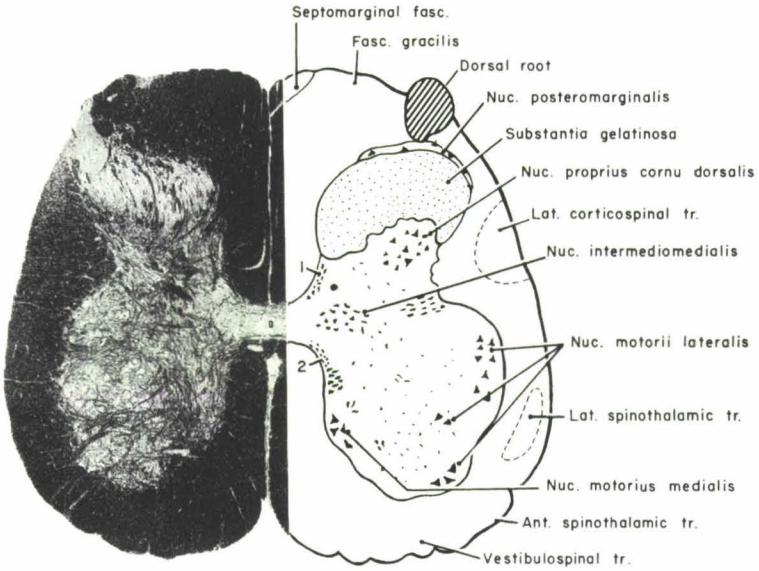


Figure 10.17. Photomicrograph (*left*) and drawing (*right*) of a section through the third sacral segment of adult human spinal cord. The important cell groups and fiber tracts are identified. *1*, Nucleus cornucommissuralis posterior; *2*, nucleus cornucommissuralis anterior (Weigert's myelin stain).

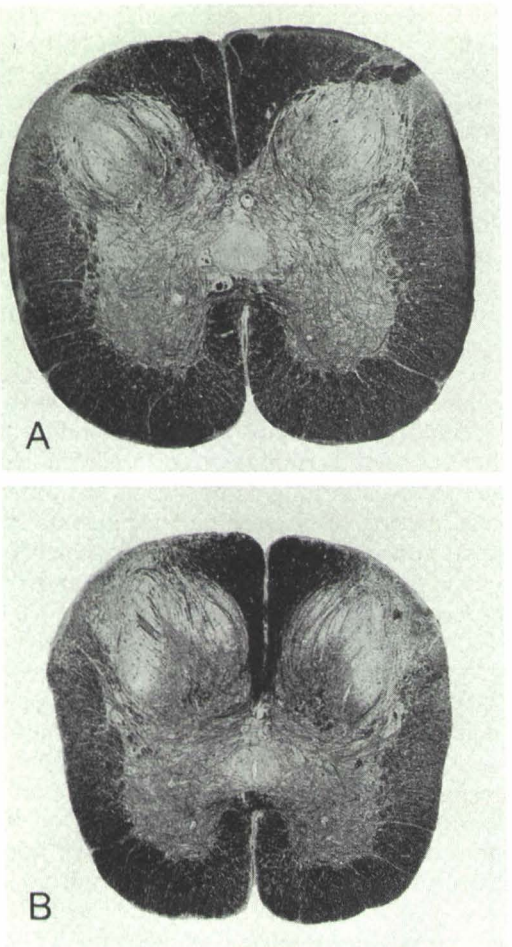


Figure 10.18. Transverse sections through (**A**) the fifth sacral and (**B**) first coccygeal spinal segments of the adult human spinal cord. Note the abundance of spinal gray in the anterior and posterior horns, the thickness of the gray commissures, the size of the gray surrounding the central canal, and the configuration of fasciculus gracilis (Weigert's myelin stain).

this accounts for the thickened posterior gray column (Figs. 10.17 and 10.18**A**). Coccygeal segments resemble lower sacral spinal segments but are reduced in size (Fig. 10.18**B**). The posterior gray horn and especially the substantia gelatinosa are greatly increased in size, while the anterior gray horn becomes smaller.

Cytoarchitectural Lamination

A variety of eponyms and inconsistent terminologies have long been used to describe the nuclear groups in the spinal gray matter. Terminology has been based largely upon cytologic features (i.e., cell size, shape, processes, and appearance) and the topographic location of cells within the spinal gray matter, but this scheme has been rather crude. While some believe that the terminology should be based upon synaptology (according to synaptic connections of neurons), this suggestion appears overly complex. The most satisfactory terminology is based upon the cytoarchitectural lamination of the spinal gray matter as observed in thick sections (80–100 μm) of the spinal cord stained with cresyl violet. In a series of papers, Rexed (118–120) described an architectural organization of neurons in the cat spinal cord that has proven to be valuable in research and has gradually become the accepted standard. His several zones have been corroborated and used by many investigators to describe terminal arborizations of fibers within the spinal gray matter. It is generally accepted that a similar lamination or zoning of the gray matter exists in all mammals. A preliminary report by Truex and Taylor (150) mentioned that the cytoarchitectural laminae described by Rexed in the cat are also present in humans. This has been confirmed by a detailed study of the cytoarchitecture, dendroarchitecture, and myeloarchitecture of the spinal cord in the newborn and adult human (131). This lamination of cell populations within the spinal gray matter has become the most precise and most widely used method for describing cell groups within the mammalian spinal cord.

Studies of the *cytoarchitectonic organization* of the spinal gray matter recognize 10 distinct cellular laminae in most regions, which are represented by Roman numerals (Rexed's laminae I to X) (Fig. 10.12). Lamina X refers to the gray matter surrounding the central canal. It is present in all segments and appears fairly uniform throughout the spinal cord.

Drawings taken from thick frozen sections of the human spinal cord from different segmental levels are shown in Figure 9.12**A-D**. The sections were stained with a combined Weigert-Nissl method to demonstrate neurons and delineate the boundaries of Rexed's laminae. There are differences in laminar configuration at various segmental levels of the spinal cord. The laminae constitute regions with characteristic properties, but their boundaries are zones of transition, where changes may occur either gradually or abruptly. Only the principal features of indi-

vidual lamina are included in this brief presentation. Some of the laminae correspond to recognized cell columns and nuclei, while others are regional admixtures of cells.

LAMINA I

This lamina is, in the words of Rexed (118), "a thin veil of gray substance" that caps the surface of the posterior horn and bends around its margins. It does not have a uniform thickness, being thicker at the level of the Lissauer tract and on the lateral border of the posterior horn. The lamina has a spongy appearance and is penetrated by small and large fiber bundles (Figs. 10.12**C** and 10.16). The neuronal density is low and most cells are found in its dorsolateral part. It contains small and medium-sized cells with scant cytoplasm and scattered, fairly large, spindle-shaped cells oriented parallel to the convex surface of the posterior horn (Figs. 10.14, 10.16, and 10.17). The cytoplasm of the large cells (the marginal cells of Waldeyer) is rich in granular endoplasmic reticulum and other organelles (107, 108). The majority of dendrites are oriented tangentially to the edge of the posterior horn. However, besides their disc-like dendritic domain being restricted to the tangential plane (127), most cells also possess ventrally oriented dendrites, which impinge deeply into lamina II and can even reach laminae III and IV (129, 131). The dendrites of lamina I neurons are poorly branched and moderately covered with sessile or pedicled spines, which appear more numerous on the ventral dendrites. The complex array of nonmyelinated axons, small dendrites, and synaptic knobs that lies within this lamina corresponds to the *posteromarginal nucleus*. In light microscopic preparations, it is best identified in sections through the lumbar enlargement (Figs. 10.16 and 10.17).

Studies in the rat, cat, and monkey, in which horseradish peroxidase (HRP) has been used to trace anterograde projections of dorsal root fibers into the spinal cord, indicate that thin fibers of the lateral division end principally in lamina I and the outer part of lamina II (67). The high density of terminals in lamina I (marginal zone) and in the outer part of lamina II indicate that these parts of the spinal gray matter receive a major afferent input (Fig. 10.14). Physiologic observations further demonstrate that lamina I and the outer zone of lamina II receive direct projections from cutaneous nociceptors but have no direct input from cutaneous receptors responding to innocuous stimuli (68). Iontophoretically injected HRP into single neurons of lamina I has revealed the dendritic arborizations, spines, and terminal varicosities of these neurons (69). No correlation could be made between cell size, configuration, or dendritic arborizations and distinct physiologic characteristics of those neurons. Other evidence indicates that axons of fibers in the dorsolateral fasciculus of Lissauer end upon neurons in lamina I (58). A large proportion of axons in the dorsolateral fasciculus arise from cells of the substantia gelatinosa (lamina II). An electron microscopic study has shown that axons of neurons in lamina II end axosomatically upon cells in lamina I, while primary afferent fibers terminate axodendritically (89). Almost all evidence suggests that neurons of lamina I respond specifically to nociceptive and thermal stimuli (Fig. 10.14). The suggestion that cells of lamina I contribute some fibers to the spinothalamic tract is based upon (a) retrograde cell changes following spinothalamic tractotomies for relief of pain in humans (64), and (b) antidromic stimulation and retrograde labeling with HRP indicating that cells of lamina I project axons to the thalamus (63, 148, 161, 162).

In humans, spinothalamic cells in lamina I represents only a small percentage of the total cell population (130). Input to this lamina is chiefly from peripheral nociceptors through Aδ and C fibers (13, 76). These afferents form a dense tangentially oriented terminal plexus which covers almost entirely the disc-like dendritic domains of lamina I neurons. There is evidence that lamina I also contains polymodal neurons, that is cells responding to noxious as well as to innocuous stimuli conveyed by Aβ fibers (159, 160). The latter are distributed mainly in the deeper laminae of the posterior horn (76). There is also the possibility that Aβ fibers might contact lamina I neurons on their ventral dendrites, which are particularly obvious in humans. These ventral dendrites lie within the rich plexus of lamina II, where part of the control exerted by the substantia gelatinosa on nociceptor-driven projection neurons may be localized (131).

Other evidence indicates that some cells, or dichotomizing axons of cells, in lamina I give rise to descending propriospinal projec-

tions extending for 8 or more spinal segments (9). These descending fibers may influence motor neurons involved in withdrawal reflexes, or be part of an indirect input to other ascending systems.

LAMINA II

This lamina which forms a well-delimited band around the apex of the posterior horn is readily identified in both myelin sheath and cell stains (Figs. 10.8, 10.11, 10.15–10.17). This fairly broad band is covered dorsally and dorsolaterally by lamina I, but its medial border is the posterior funiculus. Lamina II is composed of tightly packed small cells, corresponds to the *substantia gelatinosa* of Rolando, and is the oldest cytoarchitectonic region delimited in the spinal cord (118). Although found at all spinal levels, it is massive in the cord enlargements. In the cat lamina II consists of a dorsal or *outer zone* and a ventral or *inner zone*. In the outer zone, about one-quarter of the thickness of the whole lamina, cells are slightly smaller and more tightly packed than in the inner zone. In humans, the separation between the outer and the inner zone is much less clear (131).

Neurons in lamina II are round or elongated with their long axis oriented radially to the surface of the lamina (Fig. 10.14). The spindle-shaped cell bodies are hardly larger than the nucleus and give rise to rich dendritic trees from one or both poles of the soma (143). Based on dendritic geometry and axonal course, neurons in human lamina II were classified into four types: (a) islets cells, present in the central part of the lamina, (b) filamentous cells, located either in the outer or inner portion of the lamina, (c) curly cells, generally located in the outer substantia gelatinosa, and (d) stellate cells, preferentially found in the inner portion of the lamina (131). Although the dendritic architecture of these neurons varies from simple (e.g., stellate cells) to highly complex (e.g., curly cells), the main axes of the dendritic arborizations in most cases are radial (i.e., perpendicular to the curved lamina). At the ultrastructural level, cells of lamina II show a striking paucity of granular endoplasmic reticulum which is correlated with the absence of discrete Nissl bodies in light microscopy (106, 111). Thus, the cytoplasm of cells in lamina II is unusually pale in comparison with other spinal neurons. The most characteristic feature of the substantia gelatinosa is the presence of numerous small unmyelinated axons grouped in bundles running parallel to the long axis of the spinal cord, or perpendicular to that axis. Large myelinated axons representing primarily dorsal root fibers, pass through lamina II into deeper regions of the spinal gray matter. Myelinated fibers, frequently in bundles, are especially common in the medial half of lamina II.

Afferent fibers to lamina II are derived from collaterals in (a) the dorsolateral fasciculus, (b) the posterior funiculus, and (c) parts of the lateral funiculus adjacent to the posterior horn (143). Collateral fibers from these sources enter the substantia gelatinosa in a radial fashion and form flame-shaped terminal arborizations which establish synaptic contact with large numbers of neurons (Fig. 10.14). Fibers entering from the posterior funiculus traverse medial parts of laminae I and II, penetrate parts of laminae IV and V, and recurve dorsally and laterally to enter lamina II from its ventral surface. Terminal arborizations within lamina II have a columnar arrangement with little overlap. Synaptic profiles with round synaptic vesicles were found to be the dominant type in lamina I and the outer zone of lamina II (109, 110, 117).

Anterograde transport of HRP via spinal dorsal roots reveal that the outer zone of lamina II receives terminations from the very finest afferent fibers, while the inner zone of this lamina receives endings from some of the finest fibers, as well as from small myelinated fibers (32, 67). Physiologic observations on morphologically identified cells in laminae I and II suggest that thinly myelinated primary afferents from nociceptors end mainly in lamina I, while unmyelinated afferents from nociceptors, thermoreceptors, and mechanoreceptors terminate predominantly in lamina II (69). Soma location could not always be correlated with afferent input, but cell bodies of nociceptive and thermoreceptive neurons tended to be in lamina I, or the outer zone of lamina II, while innocuous mechanoreceptive neurons tended to be in the inner zone of lamina II (Fig. 10.14).

The majority of neurons in lamina II send axons into the dorsolateral fasciculus, or into the adjacent lateral fasciculus proprius, although some cells give rise to fine axonal plexuses retained within this lamina (25, 143). Cells in medial parts of lamina II give rise to commissural fibers that can be followed into

the contralateral substantia gelatinosa. Axons originating from cells of lamina II have always been traced back into this same lamina at different levels. None of these axons have been followed into other structures which might forward impulses to known sensory pathways. Thus, lamina II has been regarded as a "closed system," although it can influence larger neurons in deeper laminae whose dendrites are embedded in lamina II (Fig. 10.14). Because neurons in lamina II appear organized to exert their main synaptic influences upon the larger cells in laminae III and IV, whose dendrites lie within lamina II, it has been postulated that the substantia gelatinosa may function as a controlling system modulating synaptic transmission from primary sensory neurons to secondary sensory systems (59, 60, 69, 83, 143, 156).

LAMINA III

This lamina forms a band across the posterior horn parallel with laminae I and II, except that the lateral bend is not so sharp (Figs. 10.12**A-D**). The neurons of this lamina are not so closely packed as in lamina II, but are similarly round or spindle-shaped. Cells show more variations in size and, in general, are larger than those in lamina II. Most of the cells are oriented transversely to the lamina and vertically to its surface (Fig. 10.14). Occasionally, an exceptional large cell may be seen, but such cells properly belong to lamina IV. The border between lamina II and III is well-defined due to the presence of large numbers of medium-sized and small axons in lamina III which form a meshwork of fibers running longitudinally (109, 110). Neurons of lamina III have a large light-staining nucleus, relative scant cytoplasm, and small amounts of Nissl substance (106, 118).

Golgi-stained reconstructions of neurons in lamina III reveal that they belong to two neuronal types (131). The majority of impregnated neurons possess an asymmetric dendritic in that the dorsal branches are more developed. These branches ascend vertically from the soma (30–50 μm in diameter) and penetrate deeply into the overlying lamina II, reaching up to 400 μm in length (78). The ventral dendrites are few and short. The second neuronal type is characterized by a radial dendritic tree and a smaller perikarya (20 μm or less). In both cases, the dorsally directed dendrites radiate into the substantia gelatinosa over a considerable rostrocaudal distance. Axons of these neurons emerge from the proximal part of one ventral dendrite, bifurcate a number of times, and the collaterals form a dense plexus in laminae III and IV. Although the length of these axons is great they appear to ramify entirely within the gray matter and have been regarded primarily as interneurons transmitting impulses from incoming afferent fibers to the cells of origin of sensory tracts. Most of the primary afferent fibers to cells in lamina III are intermediate to thick fibers that follow a recurving course to enter the ventral aspect of the lamina II (67, 109, 110). Ultrastructural studies indicate diverse synaptic populations in the posterior horn derived from difference sources. The round synaptic profiles, dominant in laminae I and II, decline in numbers in lamina III, where flattened synaptic vesicles predominate (109, 117). Thus, most cells in lamina III appear anatomically organized to function as interneurons. Although a few of the larger neurons in this lamina may contribute to ascending sensory pathways, most of the long ascending sensory fibers originate from cells of laminae I, IV, and V (1, 148, 149, 161).

LAMINA IV

This lamina is the thickest of the first four laminae of the posterior horn. It extends straight across the gray column (Fig. 10.12**C**, **D**). The borders of this lamina are sometimes diffuse and its cells, which vary greatly in size, give it a less compact appearance than lamina III. Most cells of this lamina are round, triangular, or multipolar with a diameter ranging from 25–40 μm. Some very large cells (50–75 μm) also occurs. The cytoplasm of these cells is more abundant than in the cells of lamina III and the plentiful Nissl substance in the large cells appears as fine evenly distributed granules (118). The dendrites of cells in lamina IV radiate upward into the substantia gelatinosa in a candelabra fashion parallel to the primary afferent fibers (111, 143). These dendrites have well-developed spines and it seems likely that a large part of the dendritic surface is covered with synaptic contacts of larger primary afferent fibers (Fig. 10.14). Primary afferents terminating on the somata of these neurons are rare (57, 60). Neurons of lamina IV respond to low intensity stimuli, such as light touch, and their discharge frequency parallels the stimulus inten-

sity (103). Because of these properties they have been referred to as "wide dynamic range neurons." Cells in laminae III and IV correspond to the *proper sensory nucleus* (nucleus proprius cornu dorsalis) of the older terminology (Figs. 10.13 and 10.15–10.17).

In Golgi preparations, and in degeneration studies, there is no evidence that the axons of cells in lamina IV give rise to axons that cross in the anterior white commissure and enter the anterolateral funiculus (143). Nevertheless studies using antidromic stimulation and the retrograde transport of HRP indicate that axons of some of these cells cross at spinal levels and ascend to thalamic levels (1, 148, 149). These cells and others in laminae I and V thus contribute fibers to the spinothalamic tracts (Figs. 10.14 and 11.6).

LAMINA V

This lamina is a broad zone extending across the neck of the posterior horn, which is divided into medial and lateral subdivisions, except in the thoracic region (Fig. 10.12**B**). In humans, this mediolateral subdivision is not as obvious as in cats, so that lamina V and lamina VI, which are cytologically similar, are sometimes considered as a single entity (i.e., lamina V-VI) (131). Many fiber bundles pass through the lateral zone of lamina V, giving it a reticulated appearance. The lateral part of lamina V gives rise to a reticular process (i.e., reticular nucleus), prominent at cervical levels (Figs. 10.9–10.11). The dorsal and ventral boundaries of this lamina are diffuse. Neurons of lamina V are highly variable in size and shape, and commonly are triangular or multipolar, although spindle-shaped neurons are seen. Cells have large clear nuclei, relatively large amounts of cytoplasm and fine Nissl granules; coarse Nissl granules occur only in the largest cells. Dendrites of some neurons in lamina V extend dorsally in lamina II in the same manner as the majority of cells in lamina IV (143). The ventral dendrites may extend as far down as lamina VII. The dendritic domain of lamina V neurons has a preferential verticotransverse orientation. Dorsal root fibers synapse upon dendrites of cells in lamina V in the substantia gelatinosa, and descending suprasegmental fiber systems (e.g., corticospinal and rubrospinal fibers) appear to establish synaptic contacts upon cells and their processes within lamina V. Neurons in lamina V, like those in lamina IV, contribute fibers that enter the spinothalamic tracts on the opposite side of the spinal cord (1, 148, 149).

LAMINA VI

This lamina is a broad layer at the base of the posterior horn and extends across its width. It is present only in the cord enlargements (Figs. 10.1 and 10.5). There is no lamina VI between T4 and L2 (Figs. 10.12**B**, **D**) where lamina V forms the dorsal boundary of lamina VII. Like lamina V, it is divided into medial and lateral regions (Figs. 10.12**A**, **C**), although such a division is less obvious in humans (131). The smaller, more compact, medial region contains numerous dark-staining medium and small-sized cells. The larger lateral region contains triangular or stellate neurons. Many dorsal root group I muscle afferents terminate in the medial zone of layer VI while descending pathways are known to project to cells in the lateral zone. Physiologic studies indicate functional differences between laminae in the posterior horn (155). Cutaneous afferents are distributed more dorsally than those concerned with proprioceptive sense or kinesthesis, but, with few exceptions, no lamina can be related to particular sensory modalities (32). There is some evidence that a group of cells in lamina VI in the cervical enlargement, designated as the *centrobasal nucleus* gives rise to an uncrossed tract projecting to the cerebellum (80, 98). These cells are considered as the origin of the rostral spinocerebellar tract. The centrobasal nucleus is a major terminus of dorsal root fibers (134).

LAMINA VII

This lamina occupies a large heterogeneous region anterior to laminae V and VI, extending across the spinal gray matter on each side. This region, also known as the *zona intermedia* (intermediate gray matter), has boundaries which vary at different spinal levels (Fig. 10.7). In the cervical and lumbosacral enlargements lamina VII extends laterally and ventrally into the anterior (ventral) horn and contains cell groups of lamina IX embedded in it. In the thoracic region lamina VII occupies the zona intermedia and the base of the anterior horn. Lamina VIII, which forms its ventral border, is arched dorsally (Figs. 10.7 and 10.12**B**). Lamina VII gives a fairly

homogeneous appearance with evenly distributed light-staining nerve cells, a large number of which are local interneurons (internuncial). The dendritic tree of these neurons extends mainly along the mediolateral plane. In particular, regions with well-defined cell columns are readily recognized. These well-defined cell columns are the dorsal nucleus of Clarke, the intermediolateral nucleus, and the intermediomedial nucleus.

Lamina VII and adjacent parts of laminae V and VI also give rise to crossed fibers that ascend in the anterior spinocerebellar tract (80, 93). Many of these cells receive nonsynaptic excitation and disynaptic inhibition from ipsilateral group Ib muscle afferents.

LAMINA VIII

This lamina includes a zone at the base of the anterior horn, but its size and shape differs at various spinal levels. In the spinal enlargements, this lamina occupies only the medial part of the anterior horn (Figs. 10.12**A**, **C**, **D**). At other levels it extends across the base of the anterior horn under lamina VII (Fig. 10.12**B**). Cells of this lamina vary greatly in size but are mostly triangular and stellate-shaped. The cells have relatively large amounts of cytoplasm and contain large Nissl granules. The larger multipolar neurons differ from motor neurons only by the finer appearance of their Nissl bodies. The dendritic tree of lamina VIII neurons is predominantly vertically oriented. These dorsal dendrites are directed toward the anterior gray commissure without crossing the midline, or toward lamina VII. Ventral dendrites run toward the ventromedial tip of the posterior horn (131). Axons of some medially located neurons are considered to cross the midline in the anterior white commissure. This lamina constitutes an entity of importance since specific descending fiber systems terminate upon cells in this region. Descending spinal tracts terminating, in part, within lamina VIII include the vestibulospinal, the medial longitudinal fasciculus, the pontine reticulospinal, and the tectospinal (Figs. 10.8 and 11.25).

LAMINA IX

This lamina consists of several distinct groups of somatic motor neurons (Figs. 10.8, 10.11, 10.12, 10.15–10.17). In thoracic regions of the cord, several islands of motor neurons occupy the ventromedial part of the anterior gray horn, but in the cord enlargements greatly increased numbers of motor neurons form larger groups. Anterior horn cells of this lamina are large multipolar neurons (30–70 μm in diameter) regarded as the prototype of motor neurons. These cells have large central vesicular nuclei, coarse Nissl bodies, multiple dendrites, and large axons which contribute to the ventral root. Somatic efferent neurons are largest in size and number in the cervical and lumbar enlargements where the cell groups spread both laterally and dorsally (Figs. 10.11 and 10.16). The total number of motor neurons in segments L1 to S5 is about 52,000–62,000, with segment L5 frequently containing the largest number of cells (around 10,000) and segment S1 showing the highest density of motor neurons per section. The number of motor neurons decreases with age. It has been estimated that after 60 years of age, about 200 lamina IX neurons are lost per decade (131).

There has been numerous qualitative and quantitative studies of the dendritic arborization of spinal motor neurons performed with either the Golgi method or the intracellular HRP injection procedures (10, 56, 87, 127, 128, 130, 152). These studies have led to various classifications and groupings of motor neurons on the basis of the morphologic organization of their dendritic tree. One interesting characteristic of the dendrites of motor neurons is their tendency to gather into bundles. The exact function of these dendritic bundles is not known, but it has been suggested that they play a role in certain aspects of the execution of motor programs (127).

At the levels of the cervical and lumbar enlargements, the lateral groups of motor neurons are always sharply delimited. Within each nuclear group both large and small perikarya are rich in Nissl bodies. The smaller medial nuclear masses often are less sharply defined and share a diffuse border with lamina VIII (Figs. 10.12**B**, **C**).

The large somatic motor cells of the anterior (ventral) horn which innervate striate muscle are referred to as alpha (α) motor neurons. Scattered among these large motor cells are a number of smaller gamma (γ) neurons which give rise to efferent fibers. These emerge via the ventral root and supply the contractile elements of the muscle spindle (i.e., intrafusal muscle fibers). γ-Efferent fibers play an essential role in the mainte-

nance of muscle tone and bring the muscle spindle under spinal and supraspinal controls (Fig. 10.30). Studies of the retrograde transport of HRP from muscle to spinal neurons in the anterior horn indicate qualitative differences between α and γ motor neurons (142). The γ motor neurons, most of which are less than 37 μm in average somal diameter, exhibited the heaviest and largest intracytoplasmic granules. Cells in the α motor neuron range (i.e., somal diameters greater than 37 μm) showed less intensely stained, smaller HRP granules. While it is suggested that γ neurons may take up and transport more HRP per unit cell volume than α motor neurons, this difference may be due to a variety of qualitative features that distinguish these cells.

In addition to the α and γ motor neurons, the anterior (ventral) gray horn contains a large population of local interneurons which have been studied with both anatomic and electrophysiologic techniques. One group of these interneurons is the *Renshaw cells*, discovered by Birdsey Renshaw in the early 1940s. Renshaw cells have attracted much attention because they are known to receive recurrent collaterals of α motor neurons and exert inhibitory influences upon adjacent motor neurons (26, 27, 114–116, 128, 163, 164). These interneurons make synaptic connections with several populations of motor neurons, including the motor neurons that send collaterals to the same interneurons. Renshaw cells are part of a negative feedback loop, which regulates the firing rate of the motor neurons via a phenomenon termed *recurrent inhibition* (100). If the firing rate of the motor neuron increases, recurrent inhibition of the motor neuron increases, limiting the changes in firing rate. Decreases in motor neuron firing rate lead to less inhibition and increase the net excitability of the motor neuron. Recurrent inhibition stabilizes the motor neuron firing rate by counteracting large transient changes (37). Renshaw cells also make inhibitory connections with the Ia inhibitory interneurons that act on antagonistic motor neurons. Thus, when they fire they do not only inhibit certain motor neurons, they also disinhibit antagonistic motor neurons. Renshaw cells receive significant synaptic input from descending pathways, which can change the excitability of these cells and adjust the sensitivity of motor neurons to other descending inputs or to afferent peripheral inputs. Recurrent collaterals of a motor neurons and their relationship with Renshaw

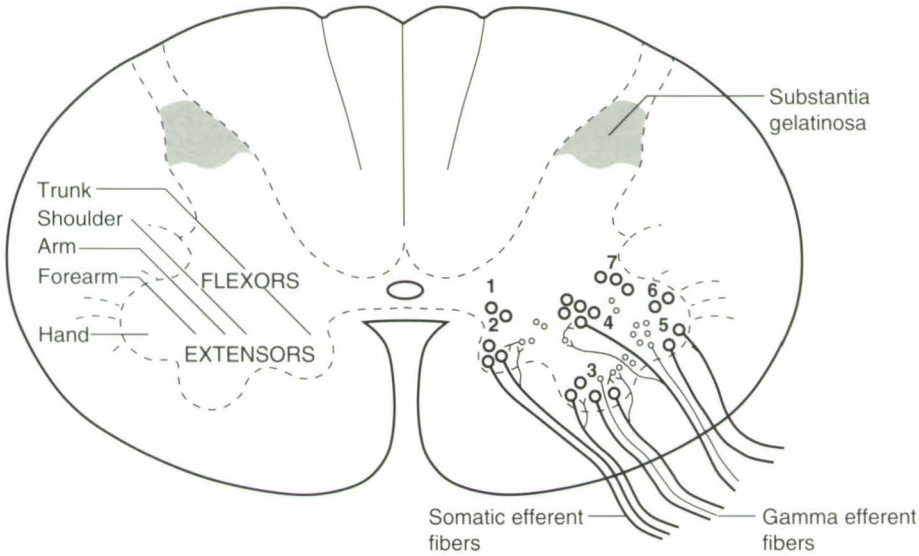


Figure 10.19. Motor nuclei in anterior gray horn of a lower cervical segment of spinal cord. On the *left* is shown the general location of anterior horn cells that send motor axons to specific muscle groups of the upper extremity. Motor nuclei indicated on the *right* are: *1*, posteromedial; *2*, anteromedial; *3*, anterior; *4*, central; *5*, anterolateral; *6*, posterolateral; *7*, retroposterolateral. Smaller anterior horn cells send axons (γ-efferents) to supply small muscle fibers of neuromuscular spindle (Fig. 10.30). Note the collaterals from somatic efferent axons that return to gray matter and synapse on small medially placed Renshaw cells. Smaller cells appearing as the dotted zone in the intermediate gray indicate the area of the internuncial neuron pool.

cells are schematically diagrammed in Figure 10.19.

Recently, two types of physiologically identified Renshaw cells were visualized after intracellular HRP labeling (33). In addition to the common multipolar neurons, a distinctive group of fusiform interneurons occurs in the anterior horn. These neurons may represent a subset of Renshaw cells having separate function and/or synaptic transmitter. Furthermore, light and electron microscopic studies involving the intracellular staining of both Renshaw cells and α motor neurons in the cat (34) revealed that, in contrast to the synapses made by Ia inhibitory interneurons, Renshaw cell synapses on motor neurons are located on dendrites and not on the cell body. This finding raises the possibility that the recurrent inhibitory pathway selectively inhibits particular dendritic inputs.

Somatic Efferent Neurons

Motor nuclei in the anterior horn have been subdivided and named on the basis of their location in the gray matter (Fig. 10.19). As shown in Figure 10.19, there is a topographic distribution of perikarya whose axons supply the different muscle groups of the extremity. The somatic efferent neurons are referred to as α motor neurons. They contribute axons to the ventral roots of respective spinal nerves and are organized into named nuclear groups, which may vary from segment to segment (Figs. 10.11, 10.13, 10.16, and 10.17). Large multipolar neurons have 3 to 20 dendrites with ramifications which extend into laminae VII and VIII. Some longitudinally oriented dendrites may enter adjacent spinal segments (128, 140). Axons of α motor neurons arise primarily from the axon hillock, are quite thin in the initial unmyelinated segment (i.e., 3.5 μm), exhibit a variable course in the gray matter, and increase in diameter as they enter the white matter (18). A large number of these axons give off multiple collaterals in the gray matter which become myelinated and ramify among α motor neurons (Fig. 10.20) upon which some terminals make direct synaptic contact (18, 19). Each cell has a large central vesicular nucleus and coarse Nissl bodies in the cytoplasm (Figs. 5.2**E** and 5.11**A**). These somatic efferent neurons are largest in the lumbar and cervical enlargements and smaller in the thoracic segments of the spinal cord (Fig. 10.12**B**). Scattered among the large anterior horn (α motor neurons) cells are γ neurons whose axons are destined for the muscle spindles (Fig. 10.30).

Several ways of regrouping the large motor neurons of the anterior horn have been proposed (131). However, these subdivisions

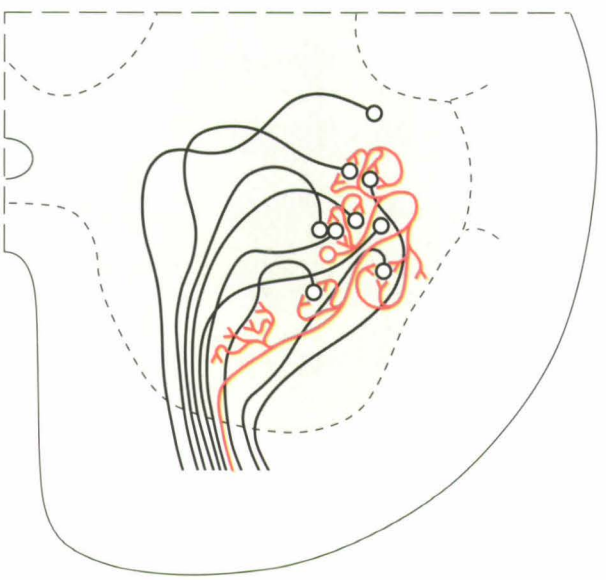


Figure 10.20. Transverse reconstructions of the trajectories of axons of motor neurons injected intracellularly with horseradish peroxidase (HRP). One α motor neuron (*red*) demonstrates recurrent collaterals that establish direct synaptic contacts with other α motor neurons. Axon collaterals of α motor neurons are not restricted to the ventromedial region of the anterior horn referred to as the Renshaw cell area.

are somewhat arbitrary and only the most obvious medial and lateral groups, each with their several subdivisions, are retained here.

MEDIAL NUCLEAR GROUP

This cell group or column is divisible into a posteromedial and anteromedial group. The latter extends throughout the whole cord and is most prominent in C1, C2, C4, T1, T2, L3, L4, S2, and S3. The nucleus of the hypoglossal nerve in the medulla appears to be a rostral continuation of this column. The posteromedial group is smaller and most distinct in the cervical and lumbar enlargements (Fig. 10.19). It may be missing in the sacral portions of the cord. The medial motor cell column innervates the short and long muscles attached to the axial skeleton.

LATERAL NUCLEAR GROUP

This motor cell group innervates the rest of the body musculature. In the thoracic segments, it is small and undivided and innervates the intercostal and other anterolateral trunk muscles (Fig. 10.13). In the cervical and lumbar enlargements, it is increased and a number of subgroups may be distinguished. The group is especially prominent in those segments which participate in the innervation of the most distal portions of the extremities. Here may be distinguished anterolateral, posterolateral, anterior, central, and retroposterolateral groups (Figs. 10.16 and 10.19). The exact innervation of individual muscles in the extremities by each of these groups has not been completely worked out, but, in general, the more distal muscles are supplied by the more lateral cell groups. Passing from the most medial part of the anterior horn to its lateral periphery, α motor neurons successively innervate muscles of the trunk, shoulder and pelvic girdle, upper leg and arm, and lower leg and arm (Fig. 10.19). The retroposterolateral group supplies the muscles of the hand and foot. Experimental denervation studies in animals have produced variable results. Sectioning of specific peripheral motor nerves of the cat produced central chromatolysis in discrete anterior horn cells. Cell columns that supplied nerve fibers to the dorsal divisions of the ventral primary ramus were located anterolaterally. Cell groups placed posteromedially contributed fibers to the ventral division of the ventral primary ramus (123).

Multipolar neurons found along the lateral and medial borders of the anterior gray horn in the thoracic, lumbar, and sacral segments of the spinal cord are known as spinal border cells (16). These border cells form the *nucleus pericornualis anterior*, considered to contribute fibers to the anterior spinocerebellar tracts. Similar neurons have been identified in the posterior and intermediate regions of the anterior gray horn of the monkey (138).

Data based upon retrograde cell changes following sectioning and crushing of peripheral nerves in various combinations indicate that motor neurons supplying flexor limb muscles are aligned longitudinally in dorsolateral regions of the lateral cell column, while extensor motor neurons lie ventral to flexor motor neurons (141). A schematic rep-

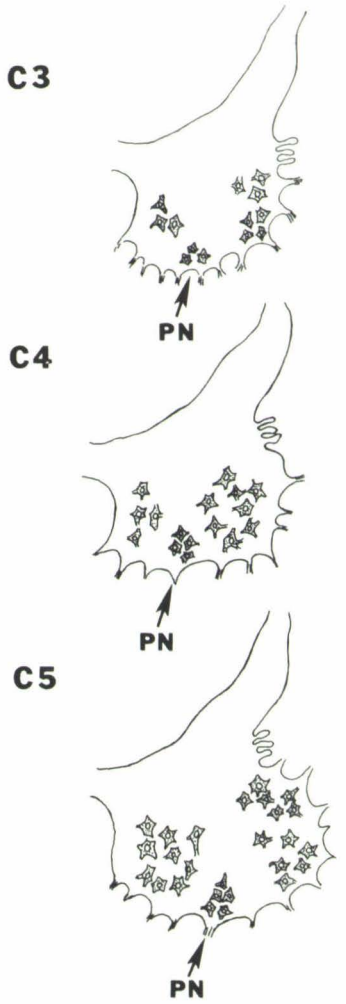


Figure 10.21. Cell groups in the anterior gray horn in cervical segments C3, C4, and C5. Phrenic nerve motor neurons (*PN*) lie ventrally between medial and lateral somatic cell columns.

resentation of α motor neurons innervating the muscles of the upper extremity is depicted in Figure 10.19. Neurons in the most ventral portion of the anterior horn between the medial and lateral cell columns in cervical segments C3, C4, and C5 give rise to axons which form the phrenic nerve (Fig. 10.21) (141). Dendrites of these neurons display a striking longitudinal orientation.

Neurons embedded in a tract of unmyelinated fibers in the most ventral part of the sacral spinal cord form the *nucleus of Onuf*. The axons emerging from this nucleus contribute to the pudendal nerve (roots S2 to S4), and supply muscles in the pelvic floor, including the striated muscle sphincters that contribute to urinary and fecal incontinence. The Onuf nucleus also contributes fibers to the ischiocavernous and bulbospongiosus muscles, and contains more neurons in men than in women.

Visceral Efferent Neurons

Axons of these neurons pass by way of the ventral roots and white rami communicantes to the various sympathetic ganglia. They are small ovoid or spindle-shaped cells with thin, short dendrites, vesicular nuclei, and fine chromophilic bodies (Figs. 5.10**E** and 10.12**B**). They range in size from 12 to 45 μm, and may be divided into two groups.

INTERMEDIOLATERAL NUCLEUS

This nucleus (Figs. 10.12**B** and 10.13) is located in Rexerd's lamina VII and consists of several adjacent cell columns. The most lateral apical cell group constitutes the lateral horn, which is characteristic of thoracic levels. The nucleus begins in the lower portion of C8 and extends caudally through L2 or L3. Neurons of this nucleus are considerably smaller than somatic motor neurons and their cell bodies are either spindle-shaped or ovoid with vesicular nuclei and fine Nissl granules (Figs. 10.12**B**, 10.13, and 10.15). Axons of neurons in the intermediolateral nucleus leave the cord in the ventral roots of spinal nerves T1 and L3 (8, 99) to reach the ganglionated sympathetic chain or, in more peripheral ganglia, along the aorta via the white rami communicantes (Figs. 9.1 and 10.23). Each preganglionic axon has synaptic endings upon the dendrites and cell bodies of many postganglionic neurons in outlying sympathetic ganglia.

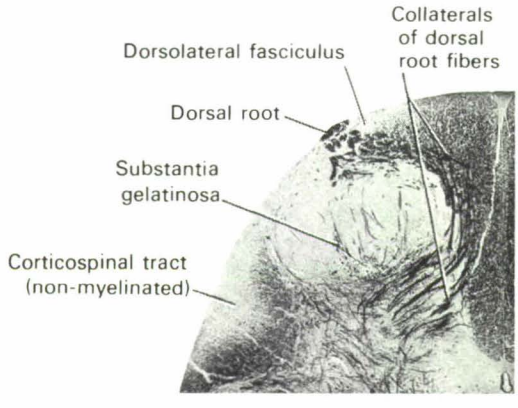


Figure 10.22. Transverse section of the lumbar spinal cord in an infant showing entrance of dorsal root fibers and collaterals (Weigert's myelin stain).

SACRAL AUTONOMIC NUCLEI

Scattered small neurons are found along the lateral surface at the base of the anterior gray horn in sacral segments S2, S3, and S4 (Fig. 10.17). Such cells bear a striking resemblance to those found in the intermediolateral nucleus and occupy a corresponding position in the lateral part of lamina VII (133), even though no lateral horn is present (Fig. 10.17). Axons of these scattered cells leave the cord in the corresponding ventral roots as preganglionic (sacral) parasympathetic fibers that form the pelvic nerves. These fibers, in turn, have multiple synapses with many postganglionic cells located in or near the wall of the pelvic viscera (Fig. 9.1).

Posterior Horn

The posterior (dorsal) horn is composed of neurons that belong to laminae I to VI and whose cytologic features were examined earlier. These neurons and their processes are confined entirely to the central nervous system. They receive collaterals or direct terminations of dorsal root fibers. In turn, they send their axons either directly to anterior horn cells of the same segments or to the white matter, where, by bifurcating, they become ascending and descending longitudinal fibers, forming intersegmental tracts of varying length (Fig. 10.24). The cells vary in size, form, and internal structure. Some are organized into definite cell groups that are easily distinguished in transverse sections, others are scattered irregularly in the gray matter. Among the most clearly defined cell groups

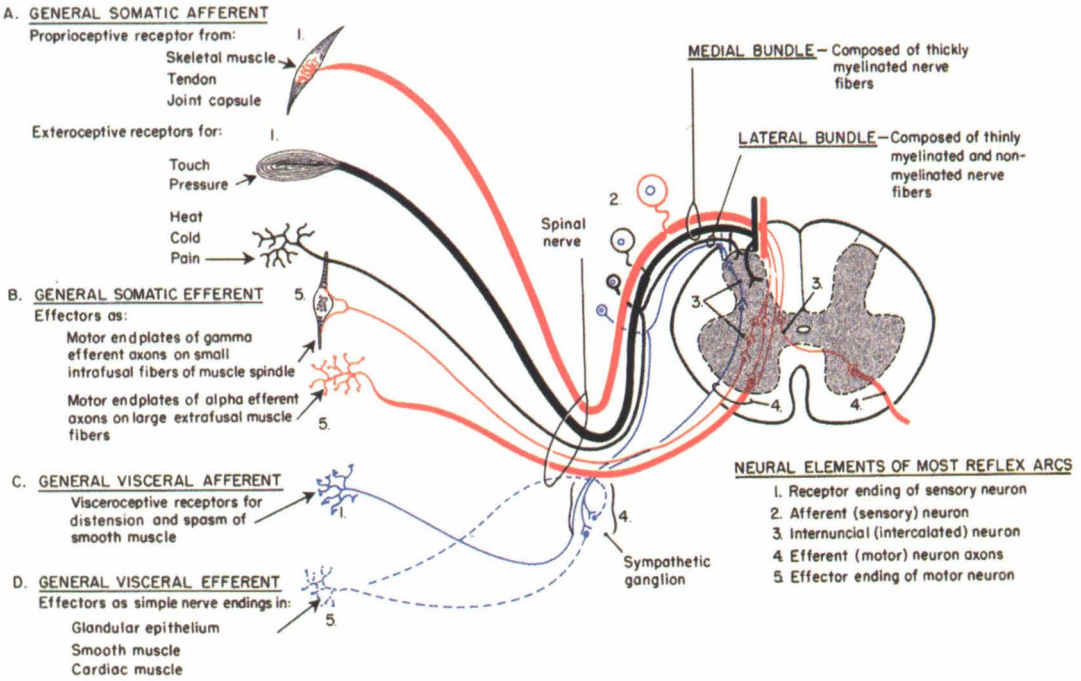


Figure 10.23. Functional components of a thoracic spinal nerve, and the arrangement of dorsal root fibers as they enter the spinal cord. Skeletal muscle afferent and efferent fibers are indicated in *red*. Visceral afferent and efferent fibers are shown in *blue*. An afferent fiber from a Pacinian corpuscle (*black*) and a thin pain fiber (*black*) also are shown. *Numbers* correspond to neural elements that form reflex arcs.

of the posterior horn are (a) the posteromarginal nucleus, (b) the substantia gelatinosa, and (c) proper sensory nucleus.

POSTEROMARGINAL NUCLEUS

This nucleus is situated in lamina I and forms a thin layer of cells covering the tip of the posterior (dorsal) horn (Figs. 10.12**B**, 10.13, 10.14, and 10.17). It is composed of large, tangentially arranged stellate or spindle-shaped cells reaching a diameter of over 50 μm. Cells of the posteromarginal nucleus receive axons of primary afferent fibers conveying impulses related to nociceptive and thermal stimuli and axons from cells in the substantia gelatinosa (Fig. 10.14) (68, 89). Axons of cells in this nucleus contribute fibers to the contralateral spinothalamic tract (159, 160, 162) and give rise to descending propriospinal projections that may influence motor neurons (9). Cells of this nucleus are found throughout the cord, and are most numerous in the lumbosacral segments.

SUBSTANTIA GELATINOSA

This structure, forming the outer cap-like portion of the head of the posterior horn, is present at all spinal levels and is best developed in the enlargements and in the first two cervical spinal segments (Figs. 10.8, 10.11, 10.14, and 10.16). It corresponds to Rexed's lamina II. Variations in size and configuration of the substantia gelatinosa are related to the size of the respective dorsal roots and the spinal level. The nucleus is composed of tightly packed, spindle-shaped cells oriented radially that give rise to rich dendritic arborizations. Small unmyelinated axons course longitudinally in the substantia gelatinosa and bundles of myelinated dorsal root fibers pass through this lamina to deeper regions of the spinal gray matter. Afferent fibers project to the substantia gelatinosa in a radial fashion from the dorsolateral fasciculus, the posterior funiculus and parts of the lateral funiculus. The organization of these fibers, as well as other details about the morphology of the substantia gelatinosa, were discussed earlier with the anatomic characteristics of lamina II.

PROPER SENSORY NUCLEUS

This nucleus occupies the head and neck of the posterior horn and corresponds to Rexed's laminae III and IV as seen in Figures

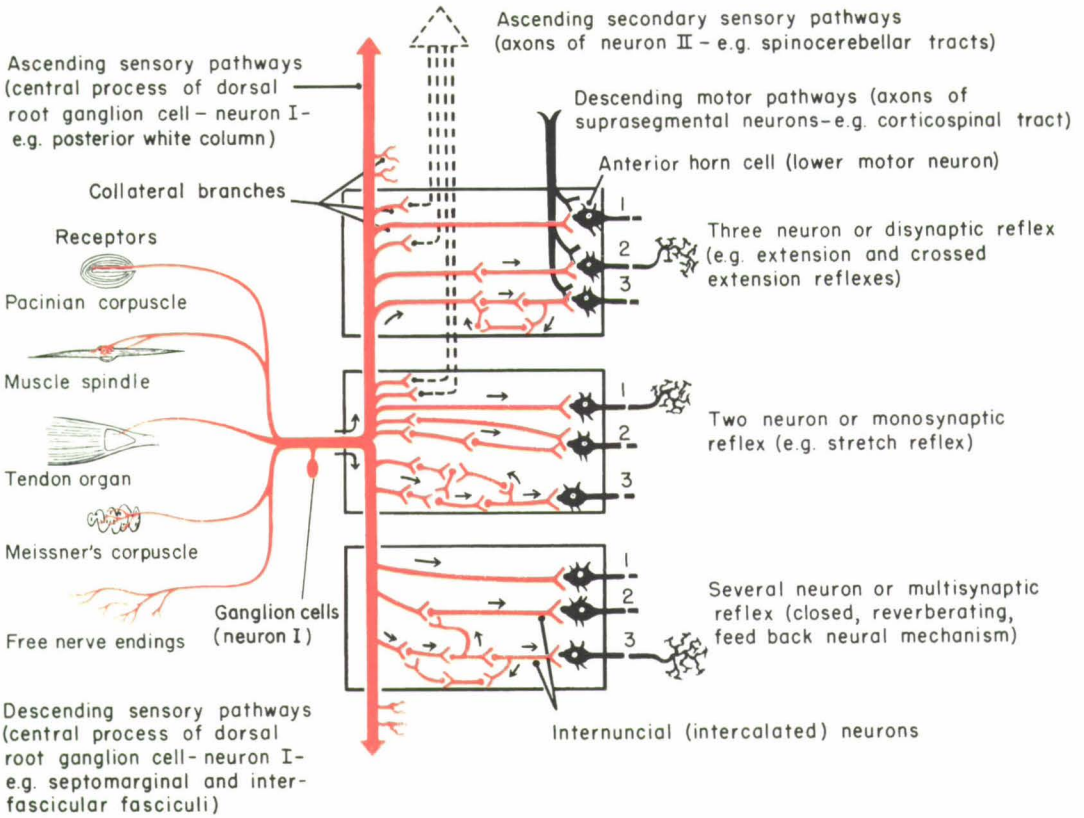


Figure 10.24. Major branches and collaterals of dorsal root ganglion cells within three spinal cord segments. On the *left* are various receptors that generate impulses in response to different kinds of stimuli. Impulses from muscle spindles initiate the myotatic or stretch reflex involving two neurons (monosynaptic reflex). Impulses from the tendon organ initiate disynaptic reflex circuits involving inhibitory mechanisms. Other reflex circuits may involve many neurons (multisynaptic). Also indicated are ascending and descending branches of dorsal root fibers in the posterior white column and collateral pathways that project fibers to the cerebellum (see Chapter 11).

10.11 and 10.13–10.16. Cells of this nucleus are of mixed types. Round or spindle-shaped cells which predominate dorsally are oriented vertically, while in deeper parts of the nucleus, round, triangular, and polygonal cells with abundant Nissl substance are conspicuous. Dendrites of cells in the proper sensory nucleus radiate into the substantia gelatinosa where they make synaptic contact with primary afferent fibers (Fig. 10.14). Axons of larger cells in this nucleus cross in the anterior white commissure and contribute fibers to the spinothalamic tracts (Fig. 10.16) (1, 148). Cells composing this poorly defined cell column are found at all spinal levels but are most numerous in lumbosacral segments. Lateral to the nucleus proprius the reticular process of the posterior horn protrudes finger-like extensions into the lateral funiculus (Figs. 10.9 and 10.11). Cells of this process are part of lamina V and are called the *reticular nucleus*. The reticular process is most evident in cervical spinal segments.

Intermediate Gray Zone

Neurons of the intermediate gray zone belong to Rexed's lamina VII. As those of the dorsal horn, neurons of the intermediate gray zone and their processes are confined to the central nervous system and receive collaterals or direct terminations of dorsal root fibers. They form several distinct nuclear masses, including (a) the dorsal nucleus of Clark, (b) the intermediomedial nucleus, (c) the central cervical nucleus, (d) the intermediolateral nucleus, and (e) the sacral autonomic nuclei. The latter two groups of nuclei were discussed earlier in the section on visceral efferent neurons.

DORSAL NUCLEUS OF CLARKE

This nucleus forms a prominent round or oval cell column in the medial part of lamina VII that extends throughout thoracic and upper lumbar segments (Figs. 10.7, 10.12**B**,

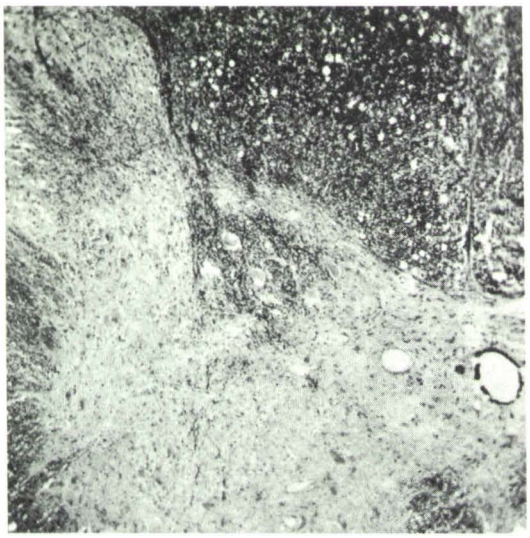


Figure 10.25. Degenerated dorsal root fibers in the rhesus monkey projecting directly to the dorsal nucleus of Clarke at L2. Lumbar dorsal roots were sectioned proximal to the dorsal root ganglia (Nauta-Gygax stain, ×80).

10.13, and 10.15). It begins to be well-defined in C8 and extends through the thoracic and upper lumbar segments, being most prominent in T10, T12, and L1 (Figs. 10.12**B** and 10.15). Below L3 it becomes indistinguishable, although occasional cells may be found. Collaterals of dorsal root afferents establish secure synapses upon cells of this nucleus at their levels of entrance and at adjoining levels which exhibit extensive overlap (38). The large cells of the dorsal nucleus give rise to the uncrossed fibers of the posterior spinocerebellar tract.

INTERMEDIOMEDIAL NUCLEUS

This nucleus, unlike other cell columns in lamina VII, extends virtually the entire length of the spinal cord (Figs. 10.12**A-D** and 10.15). It is not as sharply outlined as the intermediolateral nucleus occupying the lateral horn. This nucleus consists of a group of small- and medium-sized cells, 10–24 μm in size, with a triangular shape that lie in the most medial part of lamina VII, lateral to the central canal. The nucleus consistently receives a small number of fibers from the dorsal root at all levels (12, 134). It has been suggested that the intermediomedial nucleus may receive visceral afferent fibers and serve as an intermediary relay in transmission of impulses to visceral motor neurons (97).

CENTRAL CERVICAL NUCLEUS

This nucleus is located in the upper four cervical spinal segments and forms an inter-

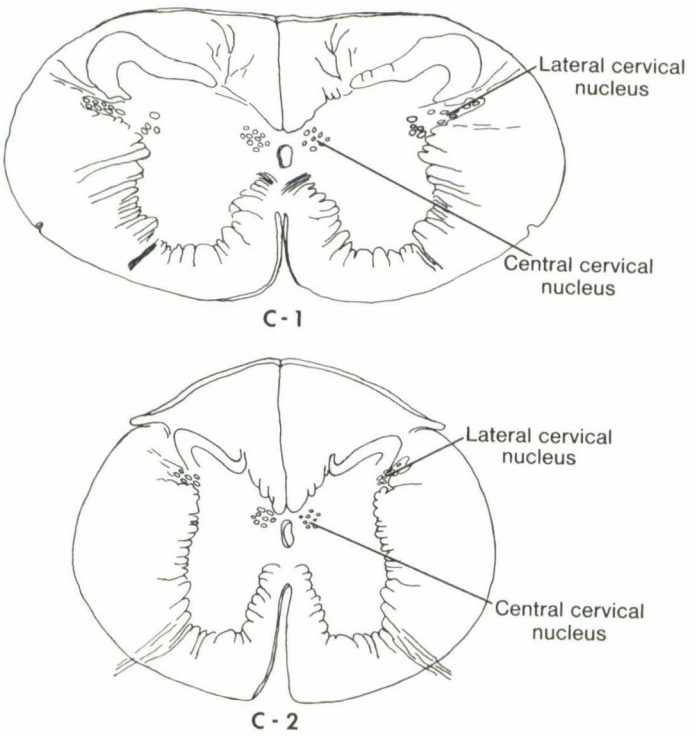


Figure 10.26. First two cervical spinal segments in a dog showing the locations of the central cervical nucleus.

rupted cell column consisting of a series of discrete cell groups (Fig. 10.26). Cells are fairly large, polygonal in shape, and resemble motor neurons. This group of cells lies lateral to the intermediomedial nucleus (20, 119). Cells of the central cervical nucleus receive direct projections from dorsal root ganglion cells (97, 134) and give rise to a crossed spinocerebellar tract (20, 79).

Two less distinct cell columns extending the length of the cord are the *nuclei cornucommissurales posterior* and *anterior* (Fig. 10.17). The former, in section, is a thin strip of cells occupying the medial margin of the posterior horn and extending along the border of the posterior gray commissure. It lies over the column of Clarke when the latter is present. The anterior nucleus is a similar cell group along the medial surface of the anterior horn and anterior gray commissure. These nuclei consist of small- and medium-sized spindle-shaped cells whose axons probably form intersegmental tracts in the posterior and anterior white funiculi, respectively.

PRIMARY AFFERENT FIBERS

Topographic Organization

Central processes of cells in the spinal ganglia enter the dorsolateral aspect of the spinal cord in small fascicles over a considerable distance (Fig. 10.2). The dorsal roots break up into a number of filaments, or rootlets, which enter the spinal cord in a linear manner. Peripheral processes of spinal ganglion cells convey impulses centrally from various somatic and visceral receptors. As central processes of spinal ganglion cells approach the dorsal root entry zone, small fine fibers become segregated in lateral portions of the rootlets and enter lateral parts of the posterior horn and the dorsolateral fasciculus directly (32, 58, 60, 67, 111–113, 127, 131, 137). Larger fibers, shifting medially in the rootlets, enter the posterior (dorsal) columns directly or traverse medial parts of the posterior horn in passage to deeper laminae of the spinal gray matter (Figs. 10.22 and 10.23). Thick myelinated fibers of the *medial bundle* are described as representing the central processes of spinal ganglion cells conveying impulses from large encapsulated somatic receptors, such as neuromuscular spindles, neurotendinous organs, Pacinian corpuscles, and Meissner's corpuscles (Fig. 10.23). The smaller, less conspicuous *lateral bundle*, composed of thinly myelinated fibers, is described as representing the central processes of smaller ganglion cells related to free nerve endings tactile, thermal, and other somatic and visceral receptors.

Upon entering the spinal cord, central processes of each spinal ganglion cell divide into ascending and descending branches (112), which in turn give rise to numerous collaterals (Fig. 10.24). Most of the collateral branches are given off in the segment of entry, where they either relay impulses to second order neurons, or participate in intrasegmental reflexes (Fig. 10.24). Primary ascending and descending branches extending into adjacent spinal cord segments, together with their collaterals, constitute the anatomic basis of intersegmental reflexes, and the relay of impulses to secondary sensory pathways (Figs. 10.23 and 10.24). The longer ascending primary branches of the medial bundle enter the ipsilateral posterior funiculus, and many of these ascend without synapse as far as the medulla. Fine, thinly myelinated and unmyelinated fibers of the lateral bundle of the dorsal root, conveying impulses related to pain, thermal, and light tactile sense, enter the medial part of the *zone of Lissauer (fasciculus dorsolateralis)* and terminate directly in portions of laminae I and II (67, 68) (Figs. 10.7, 10.14, and 10.16). Physiologic data coupled with detailed anatomic studies indicate that lamina I and the outer zone of lamina II receive direct projections from cutaneous nociceptors, but have no direct input from cutaneous receptors responding to innocuous stimuli (68). Primary afferent fibers terminating in the inner zone of lamina II are a mixture of fine and small myelinated fibers related physiologically to innocuous mechanoreceptive neurons (69).

Zone of Lissauer

This zone is composed of (a) fine myelinated and unmyelinated dorsal root fibers, which enter medial parts of the bundle, and (b) a large number of endogenous propriospinal fibers, which interconnect different levels of the substantia gelatinosa (25, 32, 113, 127, 131, 143). According to Chung and Coggeshall (15), 80% of the axons in the dorsolateral fasciculus are unmyelinated in the cat and approximately 50% of the axons represent primary afferent fibers derived from the entering dorsal roots. In Golgi preparations, axons of cells in laminae I, II, and III have been followed into lateral parts of the zone of Lissauer and most of these fibers

have been traced back to lamina II at other levels. Because few, if any, of the axons of cells in the substantia gelatinosa appear to relay impulses into known sensory pathways and the dendrites of larger sensory neurons in laminae III and IV extend radially into lamina II, this structure is regarded as a modulator of synaptic transmission from primary to secondary sensory neurons (59, 60, 83, 143).

Most of the primary afferent fibers entering laminae III and IV are intermediate to thick fibers that pass through or around lamina II and, after a recurving course in the gray matter, approach cells in the proper sensory nucleus from a ventral direction (Fig. 10.14). Primary afferent fibers largely terminate on dendrites of these neurons. Most of the neurons of lamina IV appear to respond to low intensity stimuli such as light touch (103). Cells in laminae I, IV, and V have been identified as giving rise to fibers that form the crossed spinothalamic tracts (1, 32, 148, 149).

Other Sites of Termination

One of the principal sites of termination of large myelinated dorsal root fibers is the dorsal nucleus of Clarke (Fig. 10.25). Clarke's nucleus receives fibers from all ipsilateral spinal roots except the upper cervical roots (38, 134). Studies of dorsal root afferents to Clarke's nucleus (38, 71) indicate (a) the greatest number of fibers come from dorsal roots of the hindlimb, (b) there is considerable overlap of different dorsal root fibers distributed to the nucleus, and (c) fibers enter the nucleus via both ascending and descending collateral branches of the dorsal root. Synapses of dorsal root afferents upon the cells of Clarke's nucleus appear unique in that terminal fibers have long parallel contact with the dendrites of Clarke's neurons, and unusually large terminal boutons are partially buried in depressions on the cell surface (144). These "giant synapses" between dorsal root fibers and cells of the dorsal nucleus are said to be larger than any other spinal cord synapses. Anatomic observations are in agreement with physiologic studies (72) which show that selective stimulation of group I afferent fibers establish secure synaptic relationships with the cells of Clarke's nucleus.

Collateral branches of dorsal root fibers also are distributed to parts of the anterior horn (Figs. 10.23 and 10.30). According to Sprague (139) and Sprague and Ha (140), dorsal root fibers become concentrated especially in the central part of lamina VI, and from this region fibers pass in numerous small bundles into lamina IX where they arborize about the soma and dendrites of large motor neurons. Dorsal root fibers also give off collaterals which pass into lamina VIII. Since collaterals of dorsal root fibers passing to laminae VIII and IX traverse broad regions of lamina VII, it is likely that many fibers, or collaterals, end upon interneurons in this lamina, as well as on dendrites of motor nuclei which extend beyond the limits of Rexed's lamina IX. Dorsal root fibers from group Ia afferent fibers projecting to lamina IX are involved in the monosynaptic myotatic reflex (Figs. 10.29 and 10.30). Group Ib and group II afferent fibers also generate synaptic potentials in central parts of laminae V, VI, and VII (140).

The central course of major branches and collaterals of dorsal root ganglion cells within three spinal segments are diagrammed schematically in Figure 10.24. This simplified diagram summarizes information concerning sensory pathways and certain spinal reflexes.

CHEMOARCHITECTURE

During the last decade, immunohistochemistry, receptor autoradiography, and refined biochemical methods have been applied the study of the spinal cord in experimental animals and, less extensively, in humans. These studies have significantly increased our knowledge of the anatomic and functional organization of the spinal cord. Interesting information regarding transmitter alterations in various spinal cord diseases also has been gathered. The following is a brief survey of the major small-molecule transmitters and neuroactive peptides that are thought to play a role in the function of the spinal cord. Before proceeding, however, a word of caution. Much of the data that is reviewed here derive from experimental studies in animals. Because of considerable species differences in the distribution of transmitters, care should be taken in extrapolating the results of animal experiments to humans. Thus, when available, results derived from human materials are emphasized in the present account.

Acetylcholine

Acetylcholine (ACh) is one of the key transmitters at spinal cord levels. However,

because of the lack of straightforward methods for visualizing ACh, much of our knowledge about the localization of spinal cholinergic neurons relies on indirect methods, such as the histochemical procedures for ACh hydrolyzing enzyme, acetylcholinesterase (AChE), or the immunohistochemical method for ACh synthesizing enzyme, choline acetyltransferase (ChAT). While ChAT is believed to occur only in neurons that synthesize ACh, AChE is known to be present in both neurons that uses ACh as a neurotransmitter (cholinergic neurons) and in neurons that receive a cholinergic input (cholinoceptive neurons). Hence, ChAT is considered a more reliable marker than AChE for cholinergic neurons (3). Cholinergic neurons in the central nervous system also can be demonstrated by *in situ* hybridization of choline acetyltransferase mRNA (92). The principal cholinergic neurons in the spinal cord are the large α motor neurons (Fig. 10.27**C**, **D**), which use ACh as a transmitter at the neuromuscular junction peripherally and at the synapse of its recurrent collaterals with Renshaw cells centrally. At both sites the ACh effect is mediated through nicotinic receptors. The other major collection of spinal cholinergic neurons is in the intermediolateral cell column at thoracolumbar levels (Fig. 10.27**B**). These are the preganglionic sympathetic neurons that project to noradrenergic neurons in the paravertebral or prevertebral ganglia.

In addition to nicotinic receptors, muscarinic cholinergic receptors also occur in the spinal cords. They are particularly abundant in laminae II and IX (126, 153). As is the case in the rat, muscarinic receptors in the human spinal cord are predominantly of the M1 type in lamina II, but significant densities of both M1 and M2 receptor subtypes are found over the columns of motor neurons in the anterior horn (153). These results indicate that, in addition to using ACh as a neurotransmitter, motor neurons receive a prominent cholinergic input whose effect is mediated through muscarinic receptors. The marked reduction in AChE and ChAT activities and the decrease in the number of muscarinic receptors in the anterior horn following degeneration of spinal motor neurons encountered in amyotrophic lateral sclerosis are consistent with the concept that motor neurons use ACh as a neurotransmitter and also receive a cholinergic innervation. The latter is most likely provided by recurrent collaterals of motor neurons and/or supraspinal and propriospinal afferents (132). Furthermore, the high density of M1 receptors in human lamina II, contrasting with the mixed population of M1 and M2 receptor subtypes in the anterior horn, suggests that M1 and M2 may be differentially involved in sensory and motor function in the human spinal cord (153).

Monoamines

The monoaminergic innervation of the spinal cord in animals is well-known and has been reviewed elsewhere (51, 70, 147). This innervation was studied first with histofluorescence methods (21), and subsequently with immunohistochemical techniques using antibodies against synthesizing enzyme or against the transmitters themselves. It is commonly admitted that the noradrenergic fibers arborizing in the anterior horn derive from the locus coeruleus and subcoeruleus, whereas those terminating in the posterior horn originate from neurons located in the lateral portion of the pontomedullary tegmentum, that is, groups A5 and A7, according to the nomenclature of Dahlström and Fuxe (21). However, some conspicuous species variations of this scheme have been noted in rodents (47, 136). It must also be mentioned that in the cat about 70% of the noradrenergic coeruleospinal neurons exhibit enkephalin immunoreactivity (165), whereas approximately 20% display neuropeptide Y immunoreactivity (31).

The noradrenergic fibers terminate preferentially in the deeper layers of the posterior horn, in the intermediolateral column, in the motor neuron region, and in lamina X around the central canal. At the ultrastructural level, they make conventional synapses with dendrites in the motor neuron region and in the intermediolateral column, and contact posterior horn neurons probably via nonjunctional synapses (105). This finding suggests that noradrenergic fibers may exert a direct influence on somatic and autonomic motor neurons via conventional synapses, whereas they may diffusely modulate the activity of posterior horn neurons through nonconventional synapses.

A direct dopaminergic input to the spinal cord arising mainly from the diencephalic group A11 was described in rodents (70). This diencephalospinal dopaminergic system arborizes principally in the intermediolateral column and less abundantly in the superficial laminae of the posterior horn, including the

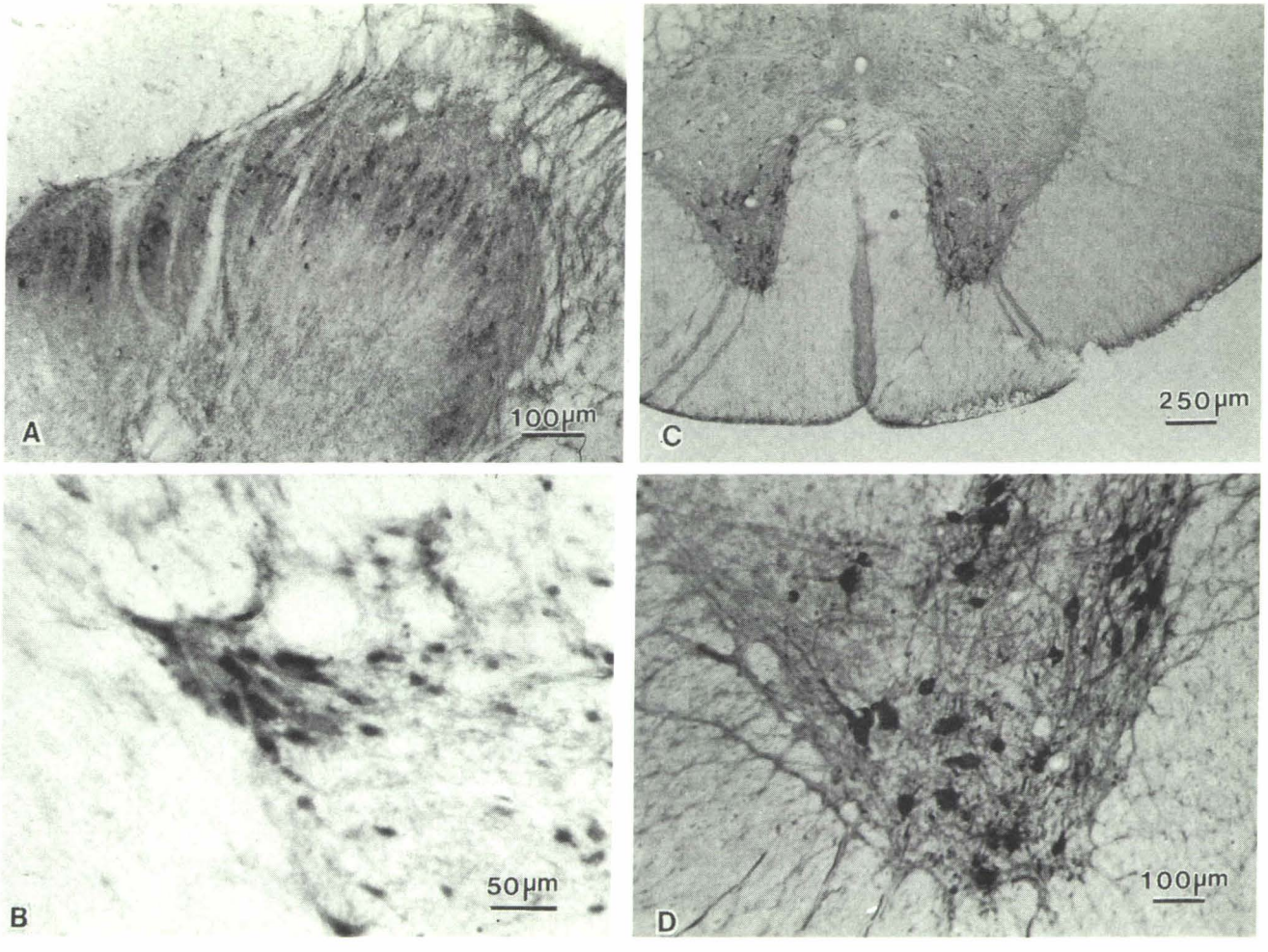


Figure 10.27. Immunocytochemical staining of spinal neurons in a macaque monkey. **A.** Neurons in deep portions of lamina II at C1 immunoreactive to leucine enkephalin. **B.** Visceral neurons in the intermediolateral cell column at thoracic level immunoreactive to choline acetyltransferase (ChAT). **C** and **D.** Spinal motor neurons in the anterior horn immunoreactive to ChAT.

reticular nucleus, and in lamina X. Also worth noting is the demonstration of a subpopulation of catecholaminergic, probably dopaminergic, neurons in the dorsal root ganglion in the rat (104). This finding indicates that, although the catecholaminergic innervation of the spinal cord arises in large part from suprasegmental regions, part of the dopaminergic input may come from primary peripheral afferents.

There is also evidence in rodents and nonhuman primates for a brainstem catecholaminergic afferent to the spinal cord that uses epinephrine (adrenaline) as a neurotransmitter (11). This adrenergic projection arises from medullary neurons of the C1 group, according to the nomenclature of Hökfelt (45), and terminates preferentially in the intermediolateral cell column, the superficial laminae of the posterior horn, the intermediate gray matter, and lamina X. This adrenergic input may directly influence the cholinergic autonomic motor neurons and may also contribute to the modulation of nociceptive processing at spinal cord level (11, 45). These effects are most probably mediated by α-adrenergic receptors, which are particularly abundant in lamina II and in the intermediolateral cell column in both rodents and humans (151). The density of β-adrenergic receptors is weak in the spinal cord.

The serotoninergic innervation of the spinal cord arises chiefly from nuclei raphe pallidus, magnus, and obscurus (groups B1 to B3, according to Dahlström and Fuxe) (21), whose neurons are scattered from caudal medulla to middle pons (91, 147). Most fibers descend in the lateral funiculi and terminate chiefly in laminae I and II, in the intermediolateral cell column, and in the primary motor neuron region. The serotoninergic fibers form a dense pericellular network around the somata and proximal dendrites of somatic and autonomic motor neurons. These pericellular plexuses are more prominent in primates than in rodents (91). Neurons of the serotoninergic bulbospinal system display varying combinations of neuroactive peptides (40, 41). In rodents, somatostatin is the peptide that coexists most frequently with serotonin, followed by substance P, enkephalins, and thyrotropin-releasing hormone (14). Moreover, many raphe neurons that project to the spinal cord are immunoreactive for two or more peptides. In addition to these supraspinal serotoninergic projections, local serotonin-containing nerve cell bodies have been visualized in lamina X of the monkey spinal cord (65), but similar neurons have not been identified in human material (132).

The prominent serotoninergic pericellular innervation of primary motor neurons suggests that serotonin plays an important role in the control of motor functions. Indeed, systemic injections of 5-hydroxytryptophan, the immediate precursor of serotonin, facilitates spinal reflexes and locomotor activity. On the other hand, the dense serotoninergic innervation of the superficial laminae of the posterior horn favors the idea of a direct involvement of serotonin and its accompanying peptides in the processing of sensory information, particularly nociception (6). Furthermore, the serotoninergic bulbospinal system is thought to play a role in the control of various aspects of autonomic function, including the regulation of blood pressure (17).

Amino Acids

GLUTAMATE AND ASPARTATE

These two amino acids are the major excitatory transmitters in the central nervous system and experimental studies in animals reveal that they play a crucial role in the functional organization of the spinal cord. The presence of glutamate has been detected in neurons of the dorsal root ganglion as well as in their afferent fibers terminating in the superficial laminae of the posterior horn (7). In these dorsal root neurons, substance P is coexpressed with glutamate (22). At the ultrastructural level, the central boutons of the primary afferent fibers in the substantia gelatinosa, as well as the giant terminals formed by the Ia muscle spindle afferents in the Clarke's column, were found to be enriched with glutamate (81, 82). A detailed ultrastructural analysis in the rat revealed that glutamate and aspartate immunoreactivity in laminae I to III are displayed by distinct sets of neuronal profiles (86). Glutamate-containing profiles are about 10 times more numerous than the aspartate-immunoreactive profiles, and these two types of profiles are distinct from those displaying GABA immunoreactivity. These results suggest that both glutamate and aspartate are neurotransmitters used by separate, non-GABAergic neuronal populations. The same study also revealed that glutamate is often coexpressed with either substance P

or calcitonin gene-related peptide in terminal boutons. In such a case, the immunoreactivity for glutamate is found in small clear vesicles, whereas that for the peptide occurs in larger dense-cored vesicles (86).

In humans, the three major types of glutamate receptors (i.e., NMDA, quisqualate, and kainate receptors) abound in lamina II (52), a finding consistent with electrophysiologic and pharmacologic data indicating that glutamate is a transmitter of primary afferent terminals in the spinal cord. Recently, the metabolism of excitatory amino acids, particularly that of glutamate, was shown to be altered in patients suffering of amyotrophic lateral sclerosis (124). This finding raises the possibility that such an alteration in glutamate metabolism may play a role in motor neuron loss.

GLYCINE

This amino acid is believed to be the major inhibitory transmitter in the spinal cord. Light and electron microscopic analysis combined with electrophysiologic recording has provided convincing evidence that Renshaw cells are glycinergic (35). As seen, these cells project principally on α motor neurons, but also on Ia interneurons and other Renshaw cells. Ia interneurons, which inhibit antagonistic motor neurons when activated by Ia afferent coming against muscles, might also use glycine as a transmitter. Glycinergic inhibition at the spinal cord level, however, may not be entirely derived from local interneurons. Indeed, recent neuroanatomic evidence in the rat suggest the existence of a glycinergic projection that arises in the ventromedial portion of the lower brainstem (at levels of the inferior olive and caudal facial nucleus) and terminates directly on motor neurons (48). In the human spinal cord, glycine is detected biochemically at appreciable levels in the anterior horn (132).

γ-AMINOBUTYRIC ACID

γ-Aminobutyric acid (GABA) is an inhibitory transmitter that has been implicated in presynaptic inhibition in the spinal cord. Indeed, the GABAergic nature of the presynaptic inhibition that occurs between intrinsic GABAergic neurons in laminae I and II and the incoming afferents of the Aδ type has been demonstrated convincingly in cats and monkeys (2). Immunohistochemical studies in the rat with antibodies raised against GABA itself or its synthesizing enzyme glutamic acid decarboxylase (GAD) have revealed the presence of GABAergic cell bodies in all regions of the spinal cord except lamina IX (4, 145). This widespread distribution suggests that GABAergic neurons in the spinal cord may exert diverse functions. As a rule, GABAergic neurons are smaller in dorsal laminae of the spinal gray matter than in ventral laminae. In some neurons in the superficial laminae of the superior gray horn in the rat, GABA was found to be coexpressed with the peptides methionine enkephalin or neurotensin (102, 146). In addition to the large number of intrinsic GABAergic neurons, evidence for a spinal GABAergic input of suprasegmental origin was recently reported in the rat (46). This projection arises from the ventromedial region of the lower brainstem tegmentum and synapses directly on the primary dendrites of motor neurons. It is likely to exert a powerful inhibitory effect on spinal motor neurons capable of counteracting the facilitation produced by the bulbospinal serotoninergic projection that arises from the same brainstem area.

In the human spinal cord, autoradiographic binding studies have revealed that both $GABA_A$ and $GABA_B$ receptors are highly concentrated in lamina II (132, 154). Both $GABA_A$ and $GABA_B$ receptors are scarce in the human inferior horn, but they exist in appreciable amounts in lamina X. Benzodiazepine receptors, which are linked to the $GABA_A$ receptor-chloride ionophore, are very dense in lamina II, particularly in its inner zone (132, 154). This highly specific distribution, together with physiologic evidence from animal experiments, suggests that benzodiazepines act by enhancing GABA-mediated presynaptic inhibition on primary dorsal root afferent terminals (39, 132).

Neuroactive Peptides

SUBSTANCE P

In humans, all spinal laminae contain substance P-immunoreactive fibers (132). However, these fibers are particularly abundant and densely packed in lamina I and in the inner portion of lamina II. In the inferior horn, some substance P-positive terminals are in close association with motor neurons. Cell

bodies immunoreactive for substance P occur in lamina III. Their dendrites are mostly confined to the sagittal plane, suggesting that they correspond to the "radial" cell type described in Golgi material (132).

Substance P-immunoreactive cell bodies and axonal profiles have also been visualized in different regions of the spinal cord of various animal species (Fig. 10.28) and the cellular localization of this peptide has been studied in detail in the rat (42, 43). Substance P-positive fibers and terminals are particularly abundant in the posterior horn where they are thought to play an important role in transmission and/or modulation of noxious information (55). In this regard, it is interesting to note that there is a marked decrease in substance P immunoreactivity in lamina II in postmortem tissue from patients suffering from familial dysautonomia (Riley-Day syndrome) and who had a profound analgesia (94).

Some substance P-immunoreactive cell bodies and axon terminals in laminae I-III in the rat also contain methionine enkephalin (122), suggesting that these neurons may release one or the other peptide depending on physiologic conditions. In addition to its role in nociception, substance P could also be involved in the modulation of both somatic and autonomic motor neurons.

OPIOID PEPTIDES

The spinal cord is one of the major sites of action of opioid peptides. In humans, numerous leucine enkephalin- and methionine enkephalin-immunoreactive fibers and axon terminals occur in most laminae of the spinal cord. However, enkephalin fibers are heterogeneously distributed at this level. Their density is highest in lamina II, particularly in its outer zone, and lowest in laminae IV, VII, and VIII (Fig. 10.27**A**) (132). Lamina X and the intermediolateral cell column also receive a dense enkephalinergic innervation. A substantial number of enkephalin fibers is found in lamina IX, where some of them closely surround the soma and proximal dendrites of motor neurons. Some enkephalin cell bodies occur in laminae I and II. The positive cells in lamina II are bipolar, dorsoventrally oriented, and appear to correspond to stellate cells that can be seen in Golgi material.

The high concentration of enkephalin immunoreactivity in laminae I and II closely matches the distribution of opiate receptors in the human spinal cord. Opiate receptor were found to be located mainly within laminae I, II and III of the posterior (dorsal) horn and in Lissauer's tract, with the highest density of receptors in the inner zone of lamina II (28, 132). These receptors appear to be princi-



Figure 10.28. Monkey spinal cord revealing the localization of substance P in lamina I and parts of lamina II. Tissue has been treated by immunocytochemical techniques with antibodies specific for substance P, which is present only in laminae of the dorsal horn that receive peripheral pain fibers. The morphine-like peptide enkephalin, also present in lamina I, may regulate the input of painful stimuli by modulating (i.e., inhibiting) the release of substance P.

pally of the kappa (κ) type (28). The pattern of distribution of both enkephalin and opiate receptors in humans is strikingly similar to that described in various animal species (66).

Numerous fibers displaying dynorphin immunoreactivity occur in the rat spinal cord. Dynorphin-immunoreactive fibers and terminals abound principally in the lumbar anterior horn and appear to arise largely from intrinsic neurons. Some dynorphin-positive fibers were found to closely surround the cell bodies and proximal dendrites of a subpopulation of motor neurons that innervate flexor muscles (61). Electrical stimulation of primary afferent fibers of the C type, but not of the A type, causes a decrease in dynorphin immunoreactivity in the anterior horn. This finding underlines the fact that dynorphin neurons are well-positioned to modulate nociceptive inputs as well as to act as interneurons in somatic motor reflexes. The decrease in dynorphin immunoreactivity observed after stimulation of the C fibers or after intense nociceptive stimuli may be the trigger for the upregulation of dynorphin expression that occurs in animal models of chronic pain states (61).

Physiologic and pharmacologic studies in animals have revealed that the effects of endogenous opioids (i.e., enkephalins, but also β-endorphin, dynorphin, and α-neoendorphin), the most powerful agents in alleviating pain, are largely mediated by opiate receptors in laminae I and II of the spinal cord (95). Part of the enkephalin action in nociception appears to be mediated by its inhibitory action on the release of substance P (53). In this regard, it is interesting to note that experimental nerve injuries and inflammation in animals induce an upregulation of the opioid gene expression (24). This is consistent with the increase of enkephalin immunoreactivity that occurs in laminae I and II in patients after limb amputation (132).

CHOLECYSTOKININ

Cholecystokinin fibers are present in all laminae of the spinal cord in humans. Their distribution is comparable to that of substance P, except for a heavier innervation of laminae VII and VIII. The innervation is densest in lamina I, the lateral part of laminae V and VI, in lamina VIII, and in the intermediolateral cell column. It is weakest in the outer zone of lamina I, and in laminae III, IV, and IX (132). The exact role of cholecystokinin in the spinal cord remains to be established. However, the fact that cholecystokinin fibers are particularly abundant in lamina VIII may be taken as an indication that this peptide modulates the activity of neurons that are specific to this region, including interneurons, propriospinal neurons, and long-projection neurons involved in the control of axial musculature.

CALCITONIN GENE-RELATED PEPTIDE

In humans, fibers demonstrating the calcitonin gene-related peptide are confined to laminae I to IV of the posterior horn, lamina X, the intermediolateral column, and the sacral parasympathetic nuclei. Fibers containing the calcitonin gene-related peptide are particularly abundant in laminae I and II, whereas they are scarce in the entire inferior horn. This peptide is the only one identified so far in motor neurons (36). Only weak immunoreactivity can be found in motor neurons of the human spinal cord. Receptor binding sites for this peptide are particularly numerous in laminae II and X, and in the intermediolateral column (132).

NEUROPEPTIDE Y AND SOMATOSTATIN

Neuropeptide Y-immunoreactive fibers are found in all laminae of the human spinal cord (132). Dot-like immunoreactivity characterizes the superficial posterior horn, whereas long and varicose fibers occur in other laminae. Lamina I, the outer zone of lamina II, and the intermediolateral column receive the densest innervation. It is also worth recalling that some of the brainstem noradrenergic descending fibers also express neuropeptide Y.

In humans, somatostatin-immunoreactive fibers are confined to the three superficial laminae of the posterior horn, the motor neuron cell column, lamina X, and the sacral autonomic nuclei. As is the case with many other peptides, the greatest number of somatostatin-positive fibers is found in lamina II, chiefly in its inner zone, where they form a dense longitudinal reticulum (132). A large number of somatostatin-positive cell bodies are found in lamina II in humans. The organization of their dendritic tree suggests that they belong to the islet cell type identified in Golgi material. Animal studies have also revealed the presence of numerous somato-

statin-positive nerve cell bodies, axons and terminal boutons in the superficial laminae of the superior horn. Ultrastructural evidence suggests that there may be two morphologically distinct somatostatin systems in the substantia gelatinosa in the rat (121).

THYROTROPIN RELEASING HORMONE, OXYTOCIN, AND VASOPRESSIN

Thyrotropin releasing hormone immunoreactivity is confined to laminae II, VII, IX, and X, as well as the intermediolateral column in humans. Some of the immunoreactive fibers are closely apposed to the perikarya or primary dendrites of lamina VII neurons, suggesting that this peptide may modify the excitability of somatic and autonomic motor neurons by acting at the level of the pool of interneurons in lamina VII. Experiments in rats reveal that a significant proportion of the bulbospinal neurons that contain thyrotropin-releasing hormone make direct synaptic contact with the autonomic motor neurons in the intermediolateral column (101). In humans, receptor binding sites for this peptide are abundant in lamina II, but much less so in lamina IX (77).

Oxytocin-immunoreactive fibers are scarce in human spinal cord and are confined to laminae I, III, IV, and IX. The immunoreactivity in lamina IX is chiefly concentrated in the dorsolateral portion of the motor neuron cell column. Scattered vasopressin-immunoreactive are restricted to laminae II, III, IV, and the medial portion of laminae V and VI (132). Oxytocin receptor binding sites in human cervical spinal cord and lower brainstem were found to be particularly numerous in the substantia gelatinosa of the caudal spinal trigeminal nucleus and in the dorsal portion of the superior horn (75).

These three different peptides are likely to originate in large part from suprasegmental centers. Indeed, examination of lumbar enlargements in patients with spinal cord transection at upper cervical or upper thoracic levels (C7-T2) has revealed that the immunoreactivity for both oxytocin and vasopressin was absent, whereas that for thyrotropin-releasing hormone was reduced (131). In contrast, the immunoreactivity for somatostatin, substance P, cholecystokinin, and enkephalins was virtually unchanged. Thus, the latter peptides appear to be present in neurons that are intrinsic to the spinal cord and/or in peripheral neurons that provide input to the spinal cord.

FUNCTIONAL CONSIDERATIONS

Pain Mechanisms

Pain is one of the most common complaints in medicine. Yet, because it is so dependent on personal experience and because it is influenced by emotion and the environment, pain is a very difficult clinical problem. Its nature is unresolved and is the subject of great controversy. Pain has been described as a sensory experience evoked by stimuli that injure or threaten to destroy tissue, which is defined introspectively by every human (88). More specifically, pain can be defined as the *perception* of an aversive or unpleasant sensation that originates from a specific region of the body. It should not be confused with *nociception*, which refers to the neural mechanisms involved in signaling and modulating noxious stimuli (54).

Pain in humans is mediated by different classes of nociceptive afferent fibers. Thermal or mechanical nociceptors convey impulses through the small-diameter, thinly myelinated Aδ fibers that conduct at about 5–30 m/s, whereas polymodal receptors responding to mechanical, chemical and thermal stimuli use the small diameter, unmyelinated C fibers that conduct slowly at 0.5–2.0 m/s. These two types of nociceptive fibers terminate primarily in lamina I (marginal zone) and lamina II (substantia gelatinosa) of the posterior horn. Both Aδ and C fibers use amino acids and neuroactive peptides as transmitters. Ultrastructural studies of nociceptive terminals in the superficial posterior horn suggest that the excitatory amino acid and the peptide are stored in small electron-translucent and dense-cored vesicles, respectively. Glutamate and substance P represent the most common combination of small-molecule transmitters and neuroactive peptides encountered in primary afferent fibers (125). The release of glutamate and the release of substance P evoke, respectively, fast and slow excitatory postsynaptic potentials (EPSPs) in nociceptive neurons of the posterior horn. After complex, local processing in the posterior horn, nociceptive signals are conveyed to higher brain centers through projection neurons whose axons segregate into several ascending fiber systems (see Chapter 11).

Activation of neurons in the superficial laminae of the posterior horn by noxious stimuli was elegantly demonstrated by the use of the proto-oncogen c-*fos*, which can be used as a reliable marker of neuronal activity (85). Both noxious stimuli and joint stimulation have been shown to induce the expression of c-*fos* in neurons primarily located in lamina I, the outer portion of lamina II, the lateral neck of the posterior horn, and in laminae VII, VIII, and X. Injection of retrograde tracers in thalamic and brainstem regions concerned with the processing of nociceptive signals, combined with c-*fos* immunohistochemistry, revealed that a significant proportion of the posterior horn neurons that are activated by noxious stimuli project to the thalamus and brainstem (85).

Early neurophysiologic studies revealed that stimulation of low-threshold myelinated primary afferent fibers decreases the response of posterior horn to unmyelinated nociceptors, whereas blockade of conduction in myelinated fibers enhances the response of posterior horn neurons. Thus, the firing of nociceptive posterior (dorsal) horn neurons appears dependent on the balance of activity between the unmyelinated nociceptors and the myelinated afferents not directly involved in pain transmissions (54). This idea was introduced by Patrick Wall and Ronald Melzack as the *gate control theory of pain* (83). According to this theory, the neurons involved in modifying the output of posterior horn neurons form a simple basic circuit that comprises (a) low-threshold Aα/Aβ myelinated and unmyelinated C fibers, (b) the posterior horn neurons that relay the incoming signals to the brain, and (c) an inhibitory interneuron that presynaptically inhibits the projection neuron. As seen earlier, the projection neuron can be directly activated by both the low-threshold myelinated and the unmyelinated fibers. However, the postulated difference between these two types of inputs is that the myelinated fibers also activated the inhibitory interneuron, whereas the unmyelinated fibers inhibit the interneuron. Thus, when low-threshold myelinated fibers are activated, the activity of the projection neuron (and ultimately the perception of pain) is reduced (84, 156, 157). Clinical application of the gate control concept demonstrated that transcutaneous stimulation of large caliber peripheral nerves raises the threshold of central neurons by increasing inhibition which may relieve pain in patients with peripheral nerve disease (73, 90, 158).

It is also important to realize that pain can be controlled by central mechanisms. Indeed, there is ample evidence that various brain centers and their descending projections to the spinal cord modulate the excitability of neurons that transmit signals initiated by noxious stimuli (5, 6). For example, electrical stimulation of certain brain regions, such as the periventricular gray matter, in experimental animals results in profound anesthesia. In humans, stimulating electrodes placed for therapeutic reasons in the periventricular gray region, the ventrobasal nuclei of the thalamus, or the internal capsule, can significantly reduce the severity of pain (54). Conversely, the occurrence of spontaneous lesions at various levels along central nociceptive pathways may produce chronic intractable pain. Such is the case with lesions in the ventrobasal nuclei of the thalamus, which may result in pain condition called the *thalamic syndrome* (23). All these findings point to the existence of descending pathways that may modulate the activity of nociceptor neurons in the spinal cord. Among such important descending pathways are the serotoninergic and the noradrenergic bulbospinal systems described earlier.

The most important advance in the understanding of pain mechanisms has been the identification of opiate receptor binding sites which are concentrated upon synaptic membranes (96). Because these binding sites mediate all pharmacologic effects of opiate alkaloids, which are universally regarded as the most powerful agents in alleviating pain, opiate receptors must play a dominant role in the control of nociception. While most regions of the central nervous system have some opiate receptors, their density varies greatly; only the white matter and the cerebellum appear totally devoid of opiate receptors (62). In the spinal gray matter, opiate receptors are primarily concentrated in laminae I and II, which were identified as containing neurons responding to nociceptive stimuli (44, 66, 68, 69).

The central nervous system contains endogenous opioids, the enkephalins (methionine and leucine), whose distribution in the spinal cord parallels that of opiate receptors (49, 135). Other endogenous opioids that can induce analgesia have been identified, including β-endorphin, dynorphin and α-

neoendorphin (29). Although enkephalin and β-endorphin exhibit similar opiate receptor binding activity, β-endorphin is more potent, has a longer period of action, and produces behavioral disturbances as well as analgesia (50). Thus, the opiate receptors and endogenous opioids, such as enkephalin and β-endorphin, compose an intrinsic "pain suppression system" that modulates sensory processes at multiple levels of the neuraxis (95). The opiate receptors concentrated in laminae I and II probably represent the first level at which these suppressor mechanism act to modulate pain. Pharmacologic studies indicate that opiates and opioid peptides regulate nociceptive transmission in part by presynaptically inhibiting the release of glutamate, substance P, and other transmitters from the sensory neurons. Transmitter release is suppressed by activation of opiate receptors on the sensory neurons, which decreases Ca^{2+} entry into the sensory terminal, either indirectly by activating K^+ conductances or directly by decreasing Ca^{2+} conductance (53, 54).

It must be remembered, however, that opiate receptors are widely distributed throughout the central nervous system, suggesting that endogenous opioid systems may act at various supraspinal levels and may also have functions other than pain modulation.

Spinal Reflexes

The five essential elements required for most spinal reflexes are (a) peripheral receptors, (b) sensory neurons, (c) local interneurons, (d) motor neurons, and (e) terminal effectors. The *myotatic* or *stretch reflex* is a monosynaptic reflex dependent upon two neurons. Stretch-sensitive proprioceptive endings located in muscle (muscle spindle) and tendon (Golgi tendon organ) are the receptors stimulated by a sudden brisk stretch

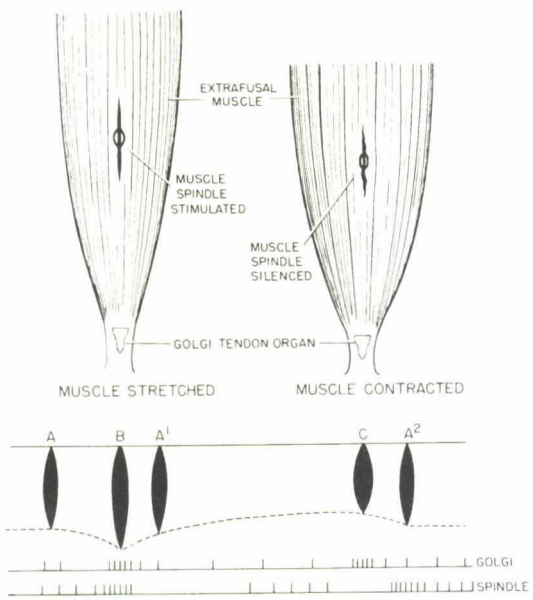


Figure 10.29. Anatomic and functional relationships of the muscle spindle and the Golgi tendon organ to extrafusal muscle fibers. The muscle spindles are arranged "parallel" with the extrafusal muscle fibers, so that stretching the muscle causes the spindles to discharge. Contraction of the muscle tends to "unload" or "silence" the muscle spindles. The Golgi tendon organs are arranged in "series" with respect of the extrafusal muscle fibers. Thus, the Golgi tendon organs can be discharged by either a stretch of the tendon or a contraction of the muscle. The threshold of the Golgi tendon organ is relatively higher than that of the muscle spindle. The *lower* diagram summarizes the functional characteristics of the muscle spindle and Golgi tendon in relation to changes in muscle length. At *A*, the muscle is shown at its resting length, and the slow spontaneous discharge of the tendon organ and muscle spindle is indicated. At *B*, the muscle is stretched and both receptors discharge, though the adaptation of the muscle spindle is more rapid. At *A1*, the muscle resumes its original length and tension, and there is a temporary reduction in the frequency of spontaneous firing of the muscle spindle. At *C*, where the muscle is contracted and shortened, the muscle spindle is silenced, but the rate of discharge of the tendon organ is increased. At *A2*, the muscle is stretched out to its resting length, and the muscle spindles are therefore discharged, while the tendon organs are silenced by the drop in tension.

of muscle. The *muscle spindle*, consisting of bundles of specialized slender muscle fibers (intrafusal fibers) surrounded by a connective tissue capsule, is attached to the endomysium of extrafusal muscle fibers (Fig. 7.11). Stretching of the noncontractile nuclear bag region (equatorial region) of the muscle spindle constitutes the mechanical stimulus required to fire the annulospiral or primary afferent fiber (group Ia) of this receptor. The γ-efferent fibers from the smaller anterior horn cells terminating in the polar (contractile) portions of the muscle spindle (intrafusal muscle fibers) bring this receptor under the control of spinal and supraspinal influences.

Golgi tendon organs are found in tendons

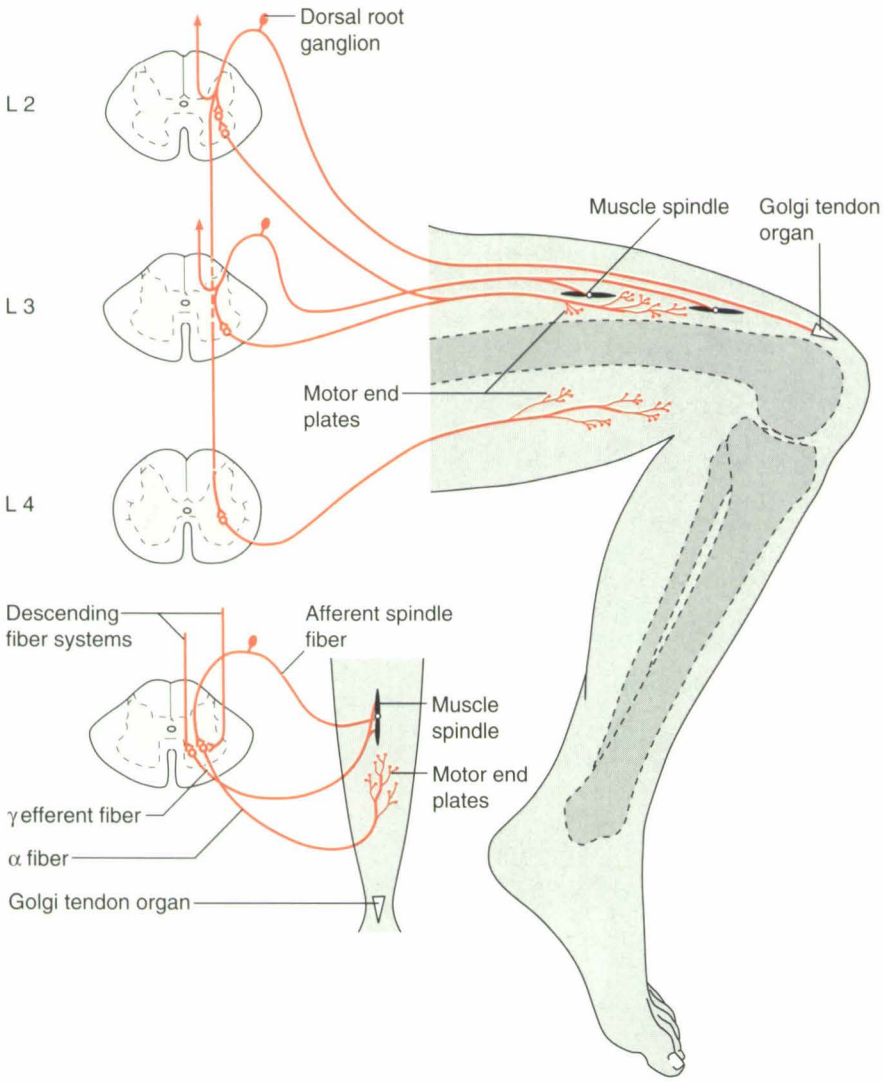


Figure 10.30. Patellar tendon reflex. Motor and sensory fibers of the femoral nerve associated with spinal segments L2, L3, and L4 mediate this myotatic reflex. The principal receptors are the muscle spindles, which respond to a brisk stretching of the muscle effected usually by tapping the patellar tendon. Afferent fibers from muscle spindles are shown entering only the L3 spinal segment, while afferent fibers from the Golgi tendon organ are shown entering only the L2 spinal segment. In this monosynaptic reflex, afferent fibers entering spinal segments L2, L3, and L4, and efferent fibers issuing from the anterior horn cells of these levels complete the reflex arc. Motor fibers shown leaving the L4 spinal segment and passing to the hamstring muscles demonstrate the pathway by which inhibitory influences are exerted upon an antagonistic muscle group during the reflex. The small diagram below illustrates the γ loop. γ-Efferent fibers pass to the polar portions of the muscle spindle. Contractions of the intrafusal fibers in the polar parts of the spindle stretch the nuclear bag region and thus cause an afferent impulse to be conducted centrally. The afferent fibers from the spindle synapse upon an α motor neuron, whose peripheral processes pass to extrafusal muscle fibers, thus completing the loop. Both α and γ motor neurons can be influenced by descending fiber systems from supraspinal levels. These are indicated separately.

close to their muscular attachments (Figs. 7.15 and 7.16). As first pointed out in early studies by Fulton and Pi-Suñer (30), the muscle spindle is arranged in "parallel" with extrafusal fibers, so that stretching of a muscle causes the spindle to discharge, while contraction of the extrafusal fibers tends to "unload" the spindle. The Golgi tendon organ is in "series" with extrafusal muscle fibers and thus can be caused to discharge by either a stretch or a contraction of the muscle (Fig. 10.29). Current physiologic belief, based largely upon indirect evidence, indicates that the low threshold muscle spindles are the prime receptors involved in the stretch reflex. However, γ-efferent fibers to the muscle spindle can exert potent influences upon the activity of this receptor. The myotatic reflex can be elicited in almost any muscle by sharply tapping either the muscle or its tendon in such a way as to produce a brief sudden stretch of the muscle. Thus, striking the tendon of the quadriceps femoris muscle provokes a forceful contraction of the stretched muscle and a quick extension of the leg at the knee (Fig. 10.29). In this example, both the sensory and motor nerve fibers leave and enter the quadriceps muscle as constituents of the femoral nerve. It will be recalled that parts of two, three, or more myotomes are incorporated in each muscle, and that two, three, or more spinal nerves and cord segments provide sensory and motor fibers. The femoral nerve is composed of sensory and motor fibers from spinal nerves L2, L3, and L4. Thus, the synapses between these sensory and motor fibers must be within spinal cord segments L2, L3, and L4. The myotatic reflex is clinically useful in determining the levels of motor integrity of the nervous system, and also may reveal evidence of release of higher control.

Afferent fibers from Golgi tendon organs (group Ib) have disynaptic inhibitory influences upon α motor neurons (Fig. 10.30). Although Golgi tendon organs have a higher threshold than the muscle spindles, afferent discharge of Ib fibers can exert inhibitory influences upon a motor neurons which reduce muscle tone. Unlike the muscle spindle, the Golgi tendon organ does not receive efferent fibers from the central nervous system. As shown in Figure 10.24, other spinal reflexes have one or more internuncial neurons interposed between sensory and motor neurons, and some of these may form complex circuits. An anterior horn cell (lower motor neuron) thus may be facilitated, or inhibited, by the sum total of all the impulses that play upon it through literally thousands of synaptic terminals. Such synaptic endings may be terminals of incoming sensory fibers, interneurons, or several of the descending motor pathways arising from higher levels of the neuraxis. This is the basic organization of the spinal cord segment and its attached spinal nerves.

References

1. Albe-Fessard D, Levante A, Lamour Y. Origin of spinothalamic tract in monkeys. Brain Res 1974;65:503–509.
2. Alvarez FJ, Kavookjian AM, Light AR. Synaptic interactions between GABA-immunoreactive profiles and the terminals of functionally defined myelinated nociceptors in the monkey and cat spinal cord. J Neurosci 1992;12:2901–2917.
3. Barber RP, Phelps PE, Houser CR, Crawford GD, Salvaterra PM, Vaughn JE. The morphology and distribution of neurons containing choline acetyltransferase in the adult rat spinal cord: an immunocytochemical study. J Comp Neurol 1984;229:329–346.
4. Barber RP, Vaughn JE, Roberts E. The cytoarchitecture of GABAergic neurons in rat spinal cord. Brain Res 1982;238:305–328.
5. Basbaum AR, Fields HL. Endogenous pain control systems: brainstem spinal pathways and endorphin circuitry. Annu Rev Neurosci 1984;7:309–338.
6. Basbaum AI, Ralston DD, Ralston HJ. Bulbospinal projections in the primate: a light and electron microscopic study of a pain modulating system. J Comp Neurol 1986;250:311–323.
7. Battaglia G, Rustioni A. Coexistence of glutamate and substance P in dorsal root ganglion neurons of the rat and monkey. J Comp Neurol 1988;277:302–312.
8. Bok ST. Das Rückenmark. In: von Molendorff W, ed. Handbuch der mikroskopischen Anatomie des Menschen. Berlin: Julius Springer, 1928:478–578.
9. Burton H, Loewy AD. Descending projections from the marginal cell layer and other regions of the monkey spinal cord. Brain Res 1976;116:485–491.
10. Cameron WD, Averill DB, Berger AJ. Morphology of cat phrenic motoneurons as revealed by intracellular injection of horseradish peroxidase. J Comp Neurol 1983; 219:70–80.
11. Carlton SM, Honda CN, Willcockson WS, et al. Descending adrenergic input to the primate spinal cord and its possible role in modulation of spinothalamic cells. Brain Res 1991;543:77–90.
12. Carpenter MB, Stein BM, Shriver JE. Central projections of spinal dorsal roots in the monkey. II. Lower thoracic, lumbosacral and coccygeal dorsal roots. Am J Anat 1968;123:75–118.
13. Cervero F, Iggo A. The substantia gelatinosa of the spinal cord. A critical review. Brain 1980;103: 711–772.
14. Chiba T, Masuko S. Coexistence of varying combinations of neuropeptides with 5-hydroxytryptamine in neurons of the raphe pallidus et obscurus projecting to the spinal cord. Neurosci Res 1989;7:13–23.
15. Chung K, Coggeshall RE. Primary afferent axons in the tract of Lissauer in the cat. J Comp Neurol 1979;186:451–464.
16. Cooper S, Sherrington CS. Gower's tract and spinal border cells. Brain 1940;63:123–143.
17. Coote JH. Bulbospinal serotonergic pathways in the control of blood pressure. J Cardiovasc Pharmacol 1990;15(Suppl 7):35–41.

18. Cullheim S, Kellerth J-O. Morphological study of the axons and recurrent axon collaterals of cat sciatic α motoneurons after intracellular staining with horseradish peroxidase. J Comp Neurol 1978; 178:537–558.
19. Cullheim S, Kellerth J-O, Conradi S. Evidence for direct synaptic interconnections between cat spinal gamma-motoneurons via the recurrent axon collaterals: A morphological study using intracellular injection of horseradish peroxidase. Brain Res 1977;132: 1–10.
20. Cummings JF, Petras JM. The origin of spinocerebellar pathways. I. The nucleus cervicalis centralis of the cranial cervical spinal core. J Comp Neurol 1977;173:655–692.
21. Dahlströlm A, Fuxe K. Evidence for the existence of monoamine-containing neurons in the central nervous system. I. Demonstration of monoamines in the cell bodies of brainstem neurons. Acta Physiol Scand 1964;62(Suppl 232):1–55.
22. DeBiasi S, Rustioni A. Glutamate and substance P coexist in primary afferent terminals in the superficial laminae of spinal cord. Proc Natl Acad Sci USA 1988;85:7820–7824.
23. Dejerine J, Roussy G. Le syndrome thalamique. Rev Neurol 1906; 14:521–532.
24. Draisci G, Kajander KC, Dubner R, Bennett GJ, Iadarola MJ. Up-regulation of opioid gene expression in spinal cord evoked by experimental nerve injuries and inflammation. Brain Res 1991;560:186–192.
25. Earle KM. The tract of Lissauer and its possible relation to the pain pathway. J Comp Neurol 1952;96: 93–111.
26. Eccles JC, Eccles RM, Iggo A, Lundberg A. Electrophysiological investigations on Renshaw cells. J Physiol (Lond) 1961;159:461–478.
27. Eccles JC, Fatt P, Koketsu K. Distribution of recurrent inhibition among motoneurons. J Physiol (Lond) 1954;126:524–562.
28. Faull RLM, Villiger JW. Opiate receptors in the human spinal cord: a detailed anatomical study comparing the autoradiographic localization of ^{3}H-diprenorphine binding sites with the laminar pattern of substance P, myelin and Nissl staining. Neuroscience 1987;20: 395–407.
29. Fields HL. Pain. New York: McGraw-Hill, 1987.
30. Fulton JF, Pi-Suñer J. A note concerning the probable function of various afferent end-organs in skeletal muscle. Am J Physiol 1927;83:554–562.
31. Fung SJ, Zhuo H, Manzoni D, Reddy VK, Barnes CD. Coeruleospinal cells containing neuropeptide Y in the cat. Peptides 1991;12: 739–743.
32. Fyffe REW. Afferent fibers. In: Davidoff RA, ed. Handbook of the spinal cord. Ch. 3. New York: M. Dekker, 1984:79–136.
33. Fyffe REW. Evidence for separate morphological classes of Renshaw cells in the cat's spinal cord. Brain Res 1990;536:301–304.
34. Fyffe REW. Spatial distribution of recurrent inhibitory synapses on spinal motoneurons in the cat. J Neurophysiol 1991;65:1134–1149.
35. Fyffe REW. Glycine-like immunoreactivity in synaptic boutons of identified inhibitory interneurons in the mammalian spinal cord. Brain Res 1991; 547:175–179.
36. Gibson SJ, Polak JM, Bloom SR, et al. Calcitonin gene-related peptide (CGRP)-immunoreactivity in the spinal cord of man and of eight species. J Neurosci 1984;4: 3101–3111.
37. Gordon G. Spinal mechanisms of motor coordination. In: Kandel ER, Schwartz JH, Jessell TM, eds. Principles of neural science. Ch. 38. New York: Elsevier, 1991:581–595.
38. Grant G, Rexed B. Dorsal spinal root afferents to Clarke's column. Brain 1958;81:567–576.
39. Haefely W, Pole P, Pieri L, Schaffner R, Laurent JP. Biological basis of the therapeutic effects of benzodiazepines. In: Costa E, ed. The benzodiazepine: from molecular biology to clinical practice. New York: Raven Press, 1983: 21–66.
40. Hökfelt T, Fuxe K, Pernow B, eds. Coexistence of neuronal messengers—a new principle in chemical transmission. Advances in brain research. Vol. 68. New York: Elsevier, 1986.
41. Hökfelt T, Johansson O, Ljüngdahl A, Lundberg JM, Schültzberg M. Peptidergic neurones. Nature 1980;284:515–521.
42. Hökfelt T, Kellerth JO, Nilsson G, Pernow B. Substance P: localization in the central nervous system and in some primary sensory neurons. Science 1975;190:889–890.
43. Hökfelt T, Kellerth J-O, Nilsson G, Pernow B. Experimental immunohistochemical studies on the localization and distribution of substance P in cat primary sensory neurons. Brain Res 1975;100: 235–252.
44. Hökfelt TA, Ljüngdahl A, Terenius L, Elde R, Nilsson G. Immunohistochemical analysis of peptide pathways possibly related to pain and analgesia: enkephalin and substance P. Proc Natl Acad Sci USA 1977;74:3081–3085.
45. Hökfelt T, Martensson R, Björklund A, Kleinau S, Goldstein M. Distributional maps of tyrosine-hydroxylase-immunoreactive neurons in the rat brain. In: Björklund A, Hökfelt T, eds. Handbook of chemical neuroanatomy. Vol. 2. Classical transmitters in the CNS, Part I. Ch. 6. Amsterdam: Elsevier, 1984:277–379.
46. Holstege JC. Ultrastructural evidence for GABAergic brain stem projections to spinal motoneurons in the rat. J Neurosci 1991; 11:159–167.
47. Holstege JC, Bongers CM. A glycinergic projection from the ventromedial lower brainstem to spinal motoneurons. An ultrastructural double labeling study in rat. Brain Res 1991;566:308–315.
48. Holstege JC, Bongers CM. Ultrastructural aspects of the coeruleospinal projection. Prog Brain Res 1991;88:143–156.
49. Hughes J. Isolation of an endogenous compound from the brain with pharmacological properties similar to morphine. Brain Res 1975;88:295–308.
50. Hughes J. Intrinsic factors and the opiate receptor system. Neurosci Res Program Bull 1978;16:141–147.
51. Hunt SP. Cytochemistry of the spinal cord. In: Emson PC, ed. Chemical neuroanatomy. New York: Raven Press, 1983:53–84.
52. Jansen KL, Faull RLW, Dragunow M, Waldvogel H. Autoradiographic localisation of NMDA, quisqualate and kainic acid receptors in human spinal cord. Neurosci Lett 1990;108:53–57.
53. Jessell TM, Iversen LL. Opiate analgesics inhibit substance P release from rat trigeminal nucleus. Nature 1977;268:549–551.
54. Jessell TM, Kelly DD. Pain and analgesia. In: Kandel ER, Schwartz JH, Jessell TM, eds. Principles of neural science. Ch. 27. New York: Elsevier, 1991:385–399.
55. Kellstein DE, Price DD, Hayes RL, Mayer DJ. Evidence that substance P selectively modulates C-fiber-evoked discharges of dorsal horn nociceptive neurons. Brain Res 1990;526:291–298.
56. Kernell D, Zwaagstra B. Dendrites of cat's spinal motoneurones: relationship between stem diameter and predicted input conductance. J Physiol (Lond) 1989;413:255–269.
57. Kerr FWL. The organization of primary afferents in the subnucleus caudalis of the trigeminal: a light and electron microscopic study of degeneration. Brain Res 1970; 23:147–165.
58. Kerr FWL. Neuroanatomical substrates of nociception in the spinal cord. Pain 1975;1:325–356.
59. Kerr FWL. Pain: a central inhibitory balance theory. Mayo Clin Proc 1975;50:685–690.
60. Kerr FWL. Segmental circuitry of the spinal cord and nociception. Neurosci Res Program Bull 1978; 16:51–65.
61. Klein CM, Sorkin LS, Chung K, Coggeshall RE. Unmyelinated primary afferent fiber stimulation depletes dynorphin A (1–8) immunoreactivity in rat ventral horn. Brain Res 1991;566:70–76.
62. Kuhar MJ, Pert CB, Snyder SH. Regional distribution of opiate recep-

tor bindings in monkey and human. Nature 1973;245:447–450.
63. Kumazawa TE, Perl ER, Burgess PR, Whitehorn D. Ascending projections from marginal zone (lamina I) neurons of the spinal dorsal horn. J Comp Neurol 1975; 162:1–12.
64. Kuru M. Sensory paths in the spinal cord and brainstem of man. Tokyo: Sogenska, 1949:675–713.
65. La Motte CC, Johns DR, de Lanerolle NC. Immunohistochemical evidence of indoleamine neurons in monkey spinal cord. J Comp Neurol 1982;206:359–370.
66. La Motte CC, Pert CB, Snyder SH. Opiate receptor binding in primate spinal cord: distribution and changes after dorsal root section. Brain Res 1976;112:407–412.
67. Light AR, Perl ER. Reexamination of the dorsal root projection to the spinal dorsal horn including observations on the differential termination of coarse and fine fibers. J Comp Neurol 1979;186:117–132.
68. Light AR, Perl ER. Spinal terminations of functionally identified primary afferent neurons with slowly conducting myelinated fibers. J Comp Neurol 1979;186:133–150.
69. Light AR, Trevino DL, Perl ER. Morphological features of functionally defined neurons in the marginal zone and substantia gelatinosa of the spinal dorsal horn. J Comp Neurol 1979; 186:151–172.
70. Lindvall O, Björklund A. Dopamine- and norepinephrine-containing neuron systems: their anatomy in the rat brain. In: Emson PC, ed. Chemical neuroanatomy. New York: Raven Press, 1983;229–256.
71. Liu CN. Afferent nerves to Clarke's and the lateral cuneate nuclei in the cat. Arch Neurol Psychiatry 1956;75:67–77.
72. Lloyd DPC, McIntyre AK. Dorsal column conduction of group I muscle afferent impulses and their relay through Clarke's column. J Neurophysiol 1950;13:39–54.
73. Long DM, Hagfors N. Electrical stimulation in the nervous system: the current status of electrical stimulation of the nervous system for the relief of pain. Pain 1975; 1:109–124.
74. Lorente de Nó R. Symposium discussion. In: Malcolm JL, Gray JAB, eds. The spinal cord. Ciba Foundation Symposium. Boston: Little, Brown & Company, 1953:40–41.
75. Loup F, Tribollet E, Dubois-Dauphin M, Pizzolato G, Dreifuss JJ. Localization of oxytocin binding sites in the human brainstem and upper spinal cord: an autoradiographic study. Brain Res 1989; 500:223–230.
76. Lynn B, Hunt SP. Afferent C-fibers: physiological and biochemical correlations. Trends Neurosci 1984; 7:186–188.
77. Manaker S, Winokur A, Rhodes CH, Rainbow TC. Autoradiographic localization of thyrotropin-releasing hormone (TRH) receptors in human spinal cord. Neurology 1985;35:328–332.
78. Mannen H, Sugiura Y. Reconstruction of neurons of dorsal horn proper using Golgi-stained sections. J Comp Neurol 1976; 168:303–312.
79. Matsushita M, Ikeda M. The central cervical nucleus as cell origin of a spinocerebellar tract arising from the cervical cord: a study in the cat using horseradish peroxidase. Brain Res 1975;100:412–417.
80. Matsushita M, Ikeda M. Projections from the lateral reticular nucleus to the cerebellar cortex and nuclei in the cat. Exp Brain Res 1976;24:403–422.
81. Maxwell DJ, Christie WM, Ottersen OP, Storm-Mathisen J. Terminals of group Ia primary afferent fibers in Clarke's column are enriched with L-glutamate-like immunoreactivity. Brain Res 1990;510:346–350.
82. Maxwell DJ, Christie WM, Short AD, Storm-Mathisen J, Ottersen OP. Central boutons of glomeruli in the spinal cord of the cat are enriched with L-glutamate-like immunoreactivity. Neuroscience 1990;36:83–104.
83. Melzack R, Wall PD. Pain mechanisms: a new theory. Science 1965;150:971–979.
84. Melzack R, Wall PD. The challenge of pain. New York: Basic Books, 1983.
85. Menétrey D, Gannon A, Levine JD, Basbaum AI. Expression of c-fos protein in interneurons and projection neurons of the rat spinal cord in response to noxious somatic, articular, and visceral stimulation. J Comp Neurol 1989;285:177–195.
86. Merighi A, Polak JM, Theodosis DT. Ultrastructural visualization of glutamate and aspartate immunoreactivities in the rat dorsal horn, with special reference to the co-localization of glutamate, substance P and calcitonin-gene related peptide. Neuroscience 1991; 40:67–80.
87. Moschovakis AK, Burke RE, Fyffe RE. The size and dendritic structure of HRP-labeled gamma motoneurons in the cat spinal cord. J Comp Neurol 1991;311:531–545.
88. Mountcastle VB. Sensory receptors and neural encoding: Introduction to sensory processes. In: Mountcastle VB, ed. Medical physiology. Vol. I. St. Louis: C.V. Mosby, 1974:285–306, 348–381.
89. Narotzky RA, Kerr FWL. Marginal neurons of the spinal cord. Brain Res 1978;139:1–20.
90. Nathan PW, Wall PD. Treatment of post-herpetic neuralgia by prolonged electric stimulation. Br Med J 1974;3:645–647.
91. Nieuwenhuys R. Chemoarchitecture of the brain. Berlin: Springer-Verlag, 1985.
92. Oh JD, Woolf NJ, Roghani A, Edwards RH, Butcher LL. Cholinergic neurons in the rat central nervous system demonstrated by *in situ* hybridization of choline acetyltransferase mRNA. Neuroscience 1992; 47:807–822.
93. Oscarsson O. Functional organization of spinocerebellar paths. In: Iggo A, ed. Handbook of sensory physiology. Vol. 2. Berlin: Springer-Verlag, 1973:339–380.
94. Pearson J, Brandeis L, Cuello AC. Depletion of substance P-containing axons in substantia gelatinosa of patients with diminished pain sensitivity. Nature 1982;295: 61–63.
95. Pert CB. Opiate receptors and pain pathways. Neurosci Res Program Bull 1978;16:133–141.
96. Pert CB, Snyder SH. Opiate receptor demonstration in nervous tissue. Science 1973;179:1011–1014.
97. Petras JM, Cummings JF. Autonomic neurons in the spinal cord of the Rhesus monkey: a correlation of the findings of cytoarchitectonics and sympathectomy with fiber degeneration following dorsal rhizotomy. J Comp Neurol 1972;146:189–218.
98. Petras JM, Cummings JF. The origin of spinocerebellar pathways. II. The nucleus centrobasalis of the cervical enlargement and the nucleus dorsalis of the thoracolumbar spinal cord. J Comp Neurol 1977;173:693–716.
99. Poliak S. Die Strukureigentümlichkeiten des Rückenmarkes bei den Chiroptern. Zugleich ein Beitrag zu der Frage über die spinalen Zentren des Sympathetic-us. Z Anat Entwickl-Gesch 1924;74:509–576.
100. Pompeiano O. Recurrent inhibition. In: Davidoff RA, ed. Handbook of the spinal cord. Ch. 11. New York: M. Dekker, 1984: 461–557.
101. Poulat P, Marlier L, Rajaofetra N, Privat A. 5-Hydroxytryptamine, substance P and thyrotropin-releasing hormone synapses in the intermediolateral cell column of the rat thoracic spinal cord. Neurosci Lett 1992;136:19–22.
102. Powell JJ, Todd AJ. Light and electron microscope study of GABA-immunoreactive neurones in lamina III of rat spinal cord. J Comp Neurol 1992;315:125–136.
103. Price DD, Mayer DJ. Physiological laminar organization of dorsal horn of *M. Mulatta*. Brain Res 1974;79:321–325.
104. Price J, Mudge AW. A subpopulation of rat dorsal ganglion neurons is catecholaminergic. Nature 1983; 301:241–243.
105. Rajaofetra N, Ridet JL, Poulat P, et al. Immunocytochemical mapping of noradrenergic projections to the rat spinal cord with an antiserum

against noradrenaline. J Neurocytol 1992;21:481–494.
106. Ralston HJ III. The organization of the substantia gelatinosa Rolandi in the cat lumbosacral spinal cord. Z Zellforsch Mikrosk Anat 1965; 67:1–23.
107. Ralston HJ III. The fine structure of neurons in the dorsal horn of the cat spinal cord. J Comp Neurol 1968;132:275–302.
108. Ralston HJ III. Dorsal root projections to the dorsal horn neurons in the cat spinal cord. J Comp Neurol 1968;132:303–330.
109. Ralston HJ III. The fine structure of laminae I, II, and III of the macaque spinal cord. J Comp Neurol 1979;184:619–642.
110. Ralston HJ III, Ralston DD. The distribution of dorsal root axons in laminae I, II and III of the macaque spinal cord: a quantitative electron microscope study. J Comp Neurol 1979;184:643–684.
111. Ramón y Cajal S. Histologie du Système Nerveux de l'Homme et des Vertébrés. (Azoulay L, Trans.) Paris: Maloine, 1909, 1911. (Reprinted, Consejo Superior de Investigaciones Cientificas, Instituto Ramón y Cajal, Madrid, 1972.)
112. Ranson SW. The course within the spinal cord of the non-myelinated fibers of the dorsal roots: a study of Lissauer's tract in the cat. J Comp Neurol 1913;23:259–281.
113. Ranson SW. The tract of Lissauer and the substantia gelatinosa Rolandi. Am J Anat 1914; 16:97–126.
114. Renshaw B. Activity in the simplest spinal reflex pathways. J Neurophysiol 1940;3:370–387.
115. Renshaw B. Influence of discharge of motoneurons upon excitation of neighboring motoneurons. J Neurophysiol 1941;4:167–183.
116. Renshaw B. Central effects of centripetal impulses in axons of spinal ventral roots. J Neurophysiol 1946;9:191–204.
117. Réthelyi M. Types of synaptic connections in the core of the spinal gray matter. In: Davidoff RA, ed. Handbook of the spinal cord. Ch. 5. New York: M. Dekker, 1984: 179–198.
118. Rexed B. The cytoarchitectonic organization of the spinal cord in the cat. J Comp Neurol 1952;96: 415–495.
119. Rexed B. A cytoarchitectonic atlas of the spinal cord in the cat. J Comp Neurol 1954;100:297–379.
120. Rexed B. Some aspects of the cytoarchitectonics and synaptology of the spinal cord. In: Eccles JC, Schadé JP, eds. Progress in brain research. Vol. II. Organization of the spinal cord. Amsterdam: Elsevier, 1964:58–92.
121. Ribeiro-da-Silva A, Cuello AC. Ultrastructural evidence for the occurrence of two distinct somatostatin-containing systems in the substantia gelatinosa of rat spinal cord. J Chem Neuroanat 1990; 3:141–153.
122. Ribeiro-da-Silva A, Pioro EP, Cuello AC,. Substance P-and enkephalin-like immunoreactivities are colocalized in certain neurons of the substantia gelatinosa of the rat spinal cord: an ultrastructural double-labeling study. J Neurosci 1991;11:1068–1080.
123. Romanes GJ. The motor cell columns of the lumbosacral spinal cord of the cat. J Comp Neurol 1951;94:313–363.
124. Rothstein JD, Tsai G, Kuncl RW, et al. Abnormal excitatory amino acid metabolism in amyotrophic lateral sclerosis. Ann Neurol 1990; 28:18–25.
125. Ruda MA, Bennett GJ, Dubner R. Neurochemistry and neural circuitry in the dorsal horn. Prog Brain Res 1986;66:219–268.
126. Scatton B, Dubois A, Javoy-Agid F, Camus A. Autoradiographic localization of muscarinic cholinergic receptors at various segmental levels of the human spinal cord. Neurosci Lett 1984;49:239–245.
127. Scheibel AB. Organization of the spinal cord. In: Davidoff RA, ed. Handbook of the spinal cord. Ch. 2. New York: M. Dekker, 1984: 47–77.
128. Scheibel ME, Scheibel AB. Spinal motoneurons, interneurons and Renshaw cells. Arch Ital Biol 1966;104:328–353.
129. Schoenen J. The dendritic organization of the human spinal cord: the dorsal horn. Neuroscience 1982;7:2057–2087.
130. Schoenen J. Dendritic organization of the human spinal cord: the motoneurons. J Comp Neurol 1982;211:226–247.
131. Schoenen J, Faull RLM. Spinal cord: cytoarchitectural, dendroarchitectural, and myeloarchitectural organization. In: Paxinos G, ed. The human nervous system. Ch. 2. New York: Academic Press, 1990:19–53.
132. Schoenen J, Faull RLM. Spinal cord: chemoarchitectural organization. In: Paxinos G, ed. The human nervous system. Ch. 3. New York: Academic Press, 1990:55–75.
133. Schnitzlein HN, Hoffman HH, Hamlett DM, Howell EM. A study of the sacral parasympathetic nucleus. J Comp Neurol 1963; 120:477–493.
134. Shriver JE, Stein BM, Carpenter MB. Central projections of spinal dorsal roots in the monkey. I. Cervical and upper thoracic dorsal roots. Am J Anat 1968;123:27–74.
135. Simantov R, Kuham JJ, Pasternak GW, Snyder SH. The regional distribution of a morphine-like factor enkephalin in monkey brain. Brain Res 1976;106:189–197.
136. Sluka KA, Westlund KN. Spinal projections of the locus coeruleus and the nucleus subcoeruleus in the Harlan and the Sasco Sprague-Dawley rat. Brain Res 1992;579: 67–73.
137. Snyder RL. The organization of dorsal root entry zone in cats and monkeys. J Comp Neurol 1977; 174:47–69.
138. Sprague JM. Motor and propriospinal cells in the thoracic and lumbar ventral horn of the Rhesus monkey. J Comp Neurol 1951; 95:103–124.
139. Sprague JM. The distribution of dorsal root fibers on motor cells in the lumbosacral spinal cord of the cat, and the site of excitatory and inhibitory terminals in monosynaptic pathways. Proc R Soc Lond (Biol) 1958;149:534–556.
140. Sprague JM, Ha H. The terminal fields of dorsal root fibers in the lumbosacral spinal cord of the cat, and the dendritic organization of the motor nuclei. In: Eccles JC, Schadé JP, eds. Progress in brain research. Vol. 2. Organization of the spinal cord. Amsterdam: Elsevier, 1964:120–152.
141. Sterling P, Kuypers HGJM. Anatomical organization of the brachial spinal cord of the cat. II. The motoneuron plexus. Brain Res 1967;4:16–32.
142. Strick PL, Burke RE, Kanda K, Kim CC, Walmsley B. Differences between alpha and gamma motoneurons labeled with horseradish peroxidase by retrograde transport. Brain Res 1976;113:582–588.
143. Szentagothai J. Neuronal and synaptic arrangement in the substantia gelatinosa Rolandi. J Comp Neurol 1964;122:219–239.
144. Szentagothai J, Albert A. The synaptology of Clarke's column. Acta Morphol Acad Sci Hung 1955;5:43–51.
145. Todd AJ, McKenzie J. GABA-immunoreactive neurons in the dorsal horn of the rat spinal cord. Neuroscience 1989;321:799–806.
146. Todd HJ, Spike RC, Russel G, Johnston HM. Immunhistochemical evidence that Met-enkephalin and GABA coexist in some neurons in rat dorsal horn. Brain Res 1992;584:149–156.
147. Törk I, Hornung J-P. Raphe nuclei and the serotoninergic system. In: Paxinos G, ed. The human nervous system. Ch. 30. New York: Academic Press, 1990:1001–1022.
148. Trevino DL, Carstens E. Confirmation of the location of spinothalamic neurons in the cat and monkey by the retrograde transport of horseradish peroxidase. Brain Res 1975;98:177–182.
149. Trevino DL, Coulter JD, Willis WD. Location of cells of origin of spinothalamic tract in lumbar enlargement of the monkey. J Neurophysiol 1973;36:750–761.
150. Truex RC, Taylor M. Gray matter lamination of the human spinal cord. Anat Rec 1968;160:502.
151. Unnerstall JR, Kopajtic TA, Kuhar MJ. Distribution of alpha-2 agonist

binding sites in the rat and human central nervous systems: analysis of some functional, anatomic correlates of the pharmacologic effects of clonidine and related adrenergic agents. Brain Res Rev 1984;7: 69–101.

152. Vanner SJ, Rose PK. Dendritic distribution of motoneurons innervating the three heads of the trapezius muscle in the cat. J Comp Neurol 1984;226:96–110.
153. Villiger JW, Faull RLM. Muscarinic cholinergic receptors in the human spinal cord: differential localization of ^{3}H-pirenzepine and ^{3}H-quinuclidinylbenzilate binding sites. Brain Res 1985;345:196–199.
154. Waldvogel HJ, Faull RLM, Jansen KL, et al. GABA, GABA receptors and benzodiazepine receptors in the human spinal cord. Neuroscience 1990;39:361–385.
155. Wall PD. The laminar organization of dorsal horn and effects of descending impulses. J Physiol (Lond) 1967;188:403–423.
156. Wall PD. The gate control theory of pain mechanisms: A re-examination and re-statement. Brain 1978; 101:1–18.
157. Wall PD, Melzack R, eds. Textbook of pain. 2d ed. Edinburgh: Churchill Livingstone, 1989.
158. Wall PD, Sweet WH. Temporary abolition of pain in man. Science 1967;155:108–109.
159. Willis WD. Nociceptive pathways: anatomy and physiology of nociceptive ascending pathways. Philos Trans R Soc (Biol) 1985; 308:253–268.
160. Willis WD, Coggeshall RE. Sensory mechanisms of the spinal cord. 2d ed. New York: Plenum, 1991.
161. Willis WD, Leonard RB, Kenshalo DR Jr. Spinothalamic tract neurons in the substantia gelatinosa. Science 1978;202:986–988.
162. Willis WD, Trevino DL, Coulter JD, Maunz RA. Responses of primate spinothalamic tract neurons to natural stimulation of hindlimb. J Neurophysiol 1974;37:358–372.
163. Willis WD, Willis JC. Location of Renshaw cells. Science 1964;204: 1214–1215.
164. Willis WD, Willis JC. Properties of interneurons in the ventral spinal cord. Arch Ital Biol 1966;104: 354–386.
165. Zhuo H, Fung SJ, Reddy VK, Barnes CD. Immunohistochemical evidence for coexistence of methionine-enkephalin and tyrosine hydroxylase in neurons of the locus coeruleus complex projecting to the spinal cord in the cat. J Chem Neuroant 1992;5:1–10.

11
Spinal Cord: Fiber Tracts

The motor and sensory information that flows along the spinal cord is conveyed through several, more or less distinct bundles lying within specific sectors of the white matter. Fiber bundles having the same origin, course, and termination are known as tracts or fasciculi. Information from the outside world and internal milieu reach suprasegmental levels of the neuraxis by coursing along various ascending spinal tracts, whereas motor and modulatory commands from higher brain centers reach their targets in the spinal cord by running along specific descending tracts. Additionally, local processing of information in the spinal cord is ensured by the presence of internuncial neurons and several fasciculi of varying lengths that serve as a link between different spinal segments. Since the white matter of the spinal cord is divided into three funiculi (see Chapter 10), all ascending and descending tracts lie in one or more funiculi. A funiculus may contain several different tracts conducting impulses in different directions. Certain spinal tracts are partially intermingled or overlap fibers in other tracts. In general, long tracts tend to be located peripherally in the white matter, while shorter tracts are found near the gray matter.

ASCENDING SPINAL TRACTS

Dorsal (posterior) root afferent fibers entering the spinal cord convey impulses from all general types of somatic and visceral receptors. The signals transmitted rostrally in the spinal cord are segregated so that impulses concerned with pain, thermal sense, touch, and kinesthesis (sense of movement and joint position) from various body segments ascend together in more or less specific tracts, sometimes widely separated from each other. Ascending tracts not only convey impulses concerned with specific sensory modalities that reach consciousness, but they also transmit impulses from stretch receptors and tactile receptors that project directly, or via relay nuclei, to the cerebellum. The cerebellum receives sensory inputs from all types of receptors but is not concerned with conscious sensory perception. Impulses projected to the cerebellum play an important role in the regulation of muscle tone and the coordination of motor function.

Posterior White Columns

A large proportion of heavily myelinated fibers of the dorsal root curve medially around the posterior horn and enter the posterior or dorsal funiculus. These fibers, arising from cells of spinal ganglia at all levels, bifurcate into long ascending and short descending branches. Ascending fibers from caudal segmental levels shift medially and dorsally as they ascend in the posterior funiculus. Branches of fibers from cervical dorsal roots ascend lateral to those of thoracic roots. This pattern of ascending fibers results in an overlapping laminar arrangement in which longer sacral fibers are most medial and posterior, shorter cervical fibers are most lateral, and thoracic fibers occupy intermediate positions (Figs. 11.1 and 11.2). The number of ascending fibers derived from a particular dorsal root bears a relationship to the size of the root, with dorsal roots of the cervical and lumbar (or lumbosacral) enlargements contributing the largest number of fibers.

The posterior funiculus on each side is divided by a posterior intermediate septum in the upper thoracic and cervical regions. This septum, which becomes discernible at about T6 (Fig. 10.5), separates the *fasciculus gracilis* medially from the *fasciculus cuneatus* laterally (Figs. 10.11 and 11.1). The fasciculus gracilis or gracile fascicle, present at all spinal levels, contains the long ascending branches of fibers from sacral, lumbar, and the lower six thoracic dorsal roots. The fasciculus cuneatus or cuneate fascicle first appears at about T6 and contains long ascending branches of the upper six thoracic and all cervical dorsal roots. Fibers in the fasciculus gracilis and cuneatus ascend ipsilaterally and terminate

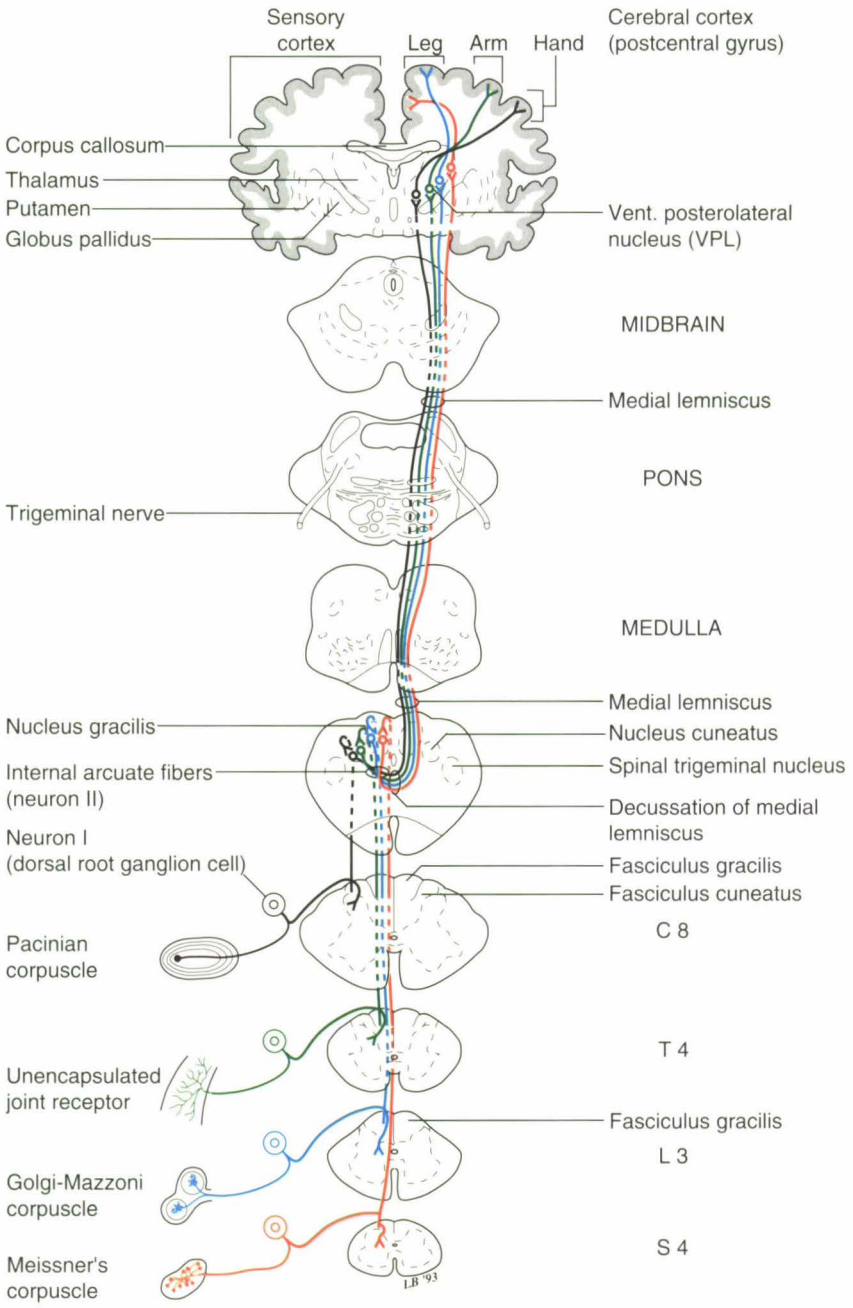


Figure 11.1. Formation and course of the posterior white columns in the spinal cord and the medial lemniscus in the brainstem. The posterior white columns are formed from uncrossed ascending branches of spinal ganglion cells. Fibers forming the medial lemniscus arise from cells of the nuclei gracilis and cuneatus, cross in the lower medulla, and ascend to the thalamus. Impulses mediated by this pathway largely concern discriminating tactile sense (touch and pressure) and kinesthetic sense (position and movement). Different receptors shown at various spinal levels on the left generate impulses conveyed centrally by this system. Spinal ganglia and afferent fibers entering the spinal cord at different levels (*red*, sacral; *blue*, lumbar; *green*, thoracic; *black*, cervical) are color coded. Letters and numbers indicate segmental levels of the spinal cord.

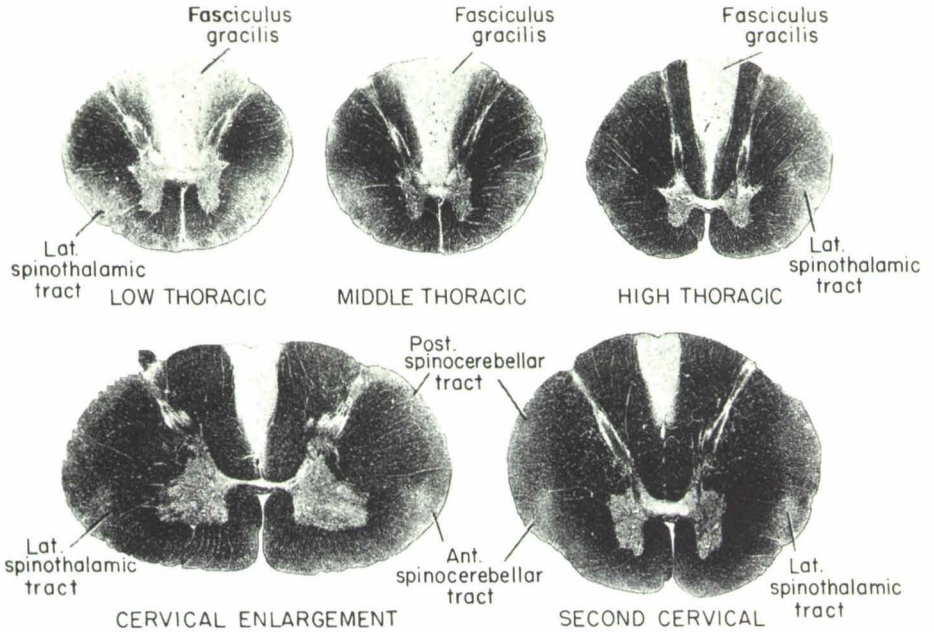


Figure 11.2. Transverse sections of human spinal cord accidentally crushed some time previously in the lumbosacral region. In this case, the antemortem neurologic signs and symptoms involved the lower extremities and the pelvis. In the posterior white columns, the progressive diminution of the degenerated area is due to passage into the gray matter of short and medium length ascending branches of lumbosacral dorsal root fibers. The progressive increase in normal fibers adjacent to the posterior horn is due to the addition of ascending branches of dorsal root fibers entering above the level of the injury (Weigert's myelin stain).

upon the posterior column medullary relay nuclei, namely, the *nuclei gracilis and cuneatus* (Fig. 11.1). Dorsal root fibers projecting to the nuclei gracilis and cuneatus terminate somatotopically (44, 203). The degree of overlap in the nucleus cuneatus is moderate, but that in the nucleus gracilis is more extensive.

The nuclei gracilis and cuneatus, collectively termed the posterior or dorsal column nuclei, give rise to second-order fibers, which sweep ventromedially, as *internal arcuate fibers*, decussate, and form a single compact bundle, the *medial lemniscus*. The medial lemniscus ascends through the contralateral half of the brainstem and its fibers terminate in the ventral posterolateral nucleus, pars caudalis (VPL_c), of the thalamus. These thalamic relay neurons emit third-order fibers, which ascend through the posterior limb of the internal capsule to terminate in the appropriate sensory areas of the cerebral cortex (Fig. 11.1). Thus, the posterior column system is a trisynaptic pathway whereby sensory information from the outside world can reach the cerebral cortex. In this highly ordered neuronal chain, the central processes of spinal ganglion cells that enter the spinal cord and ascend ipsilaterally in either the fasciculus gracilis or fasciculus cuneatus, depending on the level of ganglion, constitute the first-order neuron (neuron I). Fibers of the first order terminate upon second-order neurons (neuron II) in the posterior column nuclei (i.e., nuclei gracilis and cuneatus) of the caudal medulla. The second-order fibers originating in the posterior nuclei decussate in the caudal medulla, form the medial lemniscus, ascend, and terminate upon third-order neurons (neuron III) in the contralateral thalamus. As part of the thalamocortical projection system, the third-order fibers terminate somatotopically in the postcentral gyrus (somesthetic area) of the cerebral hemisphere (Fig. 11.1).

Ascending fibers in the posterior white columns and medial lemniscus convey impulses concerned primarily with touch-pressure and kinesthesis. These fibers constitute part of a large highly specific sensory pathway in which single elements are responsive to one or the other of these forms of physiologic stimuli but not to both (191). Fibers of this system are highly specific with respect to place and endowed with an exquisite capacity for temporal and spatial discrimination.

These fibers convey tactile impulses for precise localization and for two-point discrimination. Ascending impulses from receptors on joint surfaces and in joint capsules, which are excited by movement, convey information concerning the position of different parts of the body. Rapid successive stimuli perceived on bone or skin by Pacinian corpuscles result in a sense of vibration. "Vibratory sense" is not a specific sensory modality but a temporal modulation of tactile sense (39). Impulses concerned with this form of temporally modulated tactile sense are considered to ascend in both the posterior and lateral funiculi.

The dorsal column fibers system harbors several types of fibers other than the sensory axons described earlier. For example, the posterior columns contain group Ia muscle spindle afferents and group Ib Golgi tendon organ afferents. Most of the lower limb group I afferents ascending in the fasciculus gracilis project to the dorsal nucleus of Clark at L2 levels and above and do not reach the nucleus gracilis (203). Muscle spindle afferents (Ia) and Golgi tendons afferents (Ib) from the upper extremity enter the spinal cord rostral to the dorsal nucleus of Clarke. These afferents ascend in the fasciculus cuneatus and terminate somatotopically upon portions of the *accessory cuneate nucleus*. Cells of the accessory cuneate nucleus resemble those of Clarke nucleus and, like that nucleus, project fibers to the cerebellum (Figs. 11.9 and 12.8).

The descending branches of the dorsal root fibers in the posterior columns project for variable distances. These fibers terminate upon parts of the dorsal nucleus of Clarke and cells in medial parts of Rexed's lamina VI. Bundles of descending fibers in cervical and upper thoracic spinal segments are known as the *fasciculus interfascicularis* (comma tract of Schultze) and in the lumbar region as the *septomarginal fasciculus* (oval area of Flechsig) (Figs. 10.11 and 11.25). In the sacral region, the fibers of the septomarginal fasciculus occupy a small triangular area near the posteromedian periphery (triangle of Phillippe-Gombault) (Fig. 10.17). Besides the descending root fibers, the above named fascicles also contain descending fibers from cells of the posterior gray horn.

Anterograde and retrograde tract-tracing studies in animals indicate that cells in the nuclei gracilis and cuneatus give rise to descending axons which pass in the ipsilateral posterior columns (37). These cells, located largely in ventral regions of the posterior column nuclei, appear to project to all spinal levels but the terminal fields established for the cervical spinal segments are specific for Rexed's laminae IV and V, and possibly lamina I of the posterior horn. These descending pathways are regarded as part of a feedback mechanism which may regulate the flow of sensory information to higher levels of the neuraxis. The posterior column system also contains a significant number of long ascending unmyelinated primary afferent fibers (166). This finding suggests that fibers within the posterior columns may participate in the transmission of noxious stimuli. Other recent findings in the rat reveal that some neurons in the dorsal column nuclei project to the thalamus indirectly via a relay in the pretectal area of the midbrain (238). This is consistent with physiologic data suggesting a role for the pretectal area in sensorimotor integration.

Lesions involving the posterior columns diminish or abolish discriminating tactile and kinesthetic sense. Mere contact and pressure appear normal, but tactile localization is poor, and two-point discrimination and vibratory sense are lost or diminished. There is loss of appreciation of differences in weight and inability to identify objects placed in the hand by feeling them. These symptoms are most acute in the fingers and hand. Position and movement sense is severely affected, especially in the distal parts of the extremities. Small passive movements are not recognized as movements, but as touch or pressure. Even in long excursions the direction and extent of the movement may not be perceived. Loss of position sense greatly impairs the performance of voluntary motor function. This sensory loss causes movements to be clumsy, uncertain and poorly coordinated (posterior column ataxia).

The use of various tract-tracing methods has shed new light on the organization of the spinal tracts in experimental animals (198). In comparison, our knowledge of spinal pathways in humans is much more limited because these experimental methods cannot be applied to the study of human material. What is known about the arrangement of spinal tracts in humans is largely based on the examination of postmortem material from patients with lesions at different levels of the spinal cord. For example, since a fiber severed from its cell of origin degenerates, injury

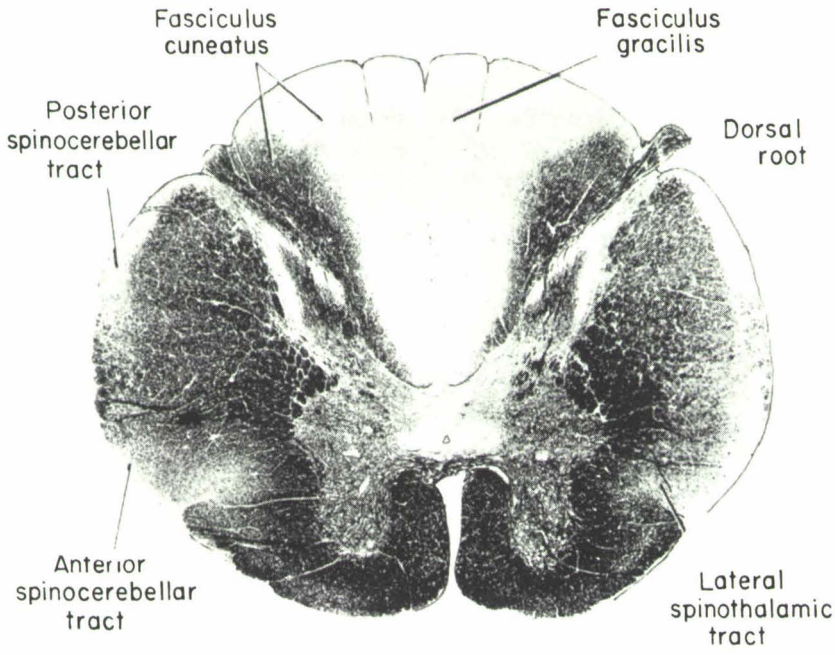


Figure 11.3. Section through the second cervical segment of a human spinal cord which had been accidentally crushed previously in the lower cervical region. The antemortem posterior column symptoms were far more extensive in this patient than in the one illustrated in Figure 11.2. Ascending branches of dorsal root fibers in the fasciculi gracilis and cuneatus are degenerated and demyelinated bilaterally, except for fibers in lateral parts of the fasciculi cuneatus which entered above the level of the lesion (about C6). This lesion also produced degeneration in most of the fibers of the spinocerebellar and spinothalamic tracts (Weigert's myelin stain).

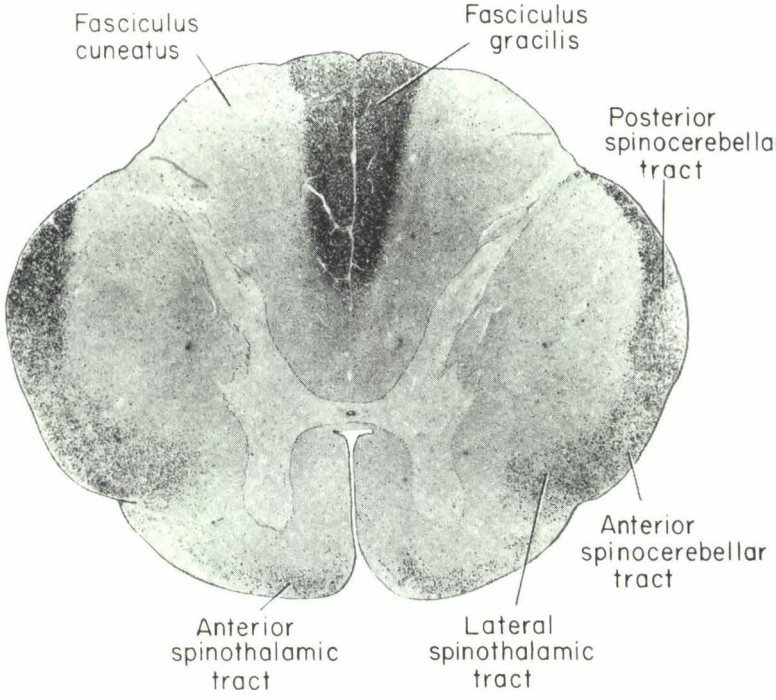


Figure 11.4. Section through the second cervical segment of a human spinal cord which had been crushed several weeks previously in the upper lumbar region. The ascending degeneration appears as black granules in fibers of the fasciculi gracilis, the anterior and posterior spinocerebellar tracts, and in the lateral and anterior spinothalamic tracts (Marchi stain).

to the fibers of the posterior white columns, or to dorsal root fibers proximal to the spinal ganglia, will cause degeneration in the posterior white columns in specific locations depending on the level of the lesion. Furthermore, the large myelinated fibers of the posterior columns are frequently involved in toxin-induced neuronal degeneration, as well as in demyelinating or metabolic diseases. Sections of human spinal cord can be processed according to various histologic methods that can reveal normal myelin (e.g., the Weigert method) as well as myelin that is undergoing degeneration (e.g., the Marchi procedure). A careful analysis of sections stained with such methods can yield useful information about the location and relative size of different spinal cord tracts in humans (Figs. 11.2–11.4). Evidence of degeneration in the posterior columns also can be detected in Nissl stained sections because relatively dense gliosis occurs in areas of degenerated fibers (Fig. 11.5). It must be realized, however, that the histologic methods that can be applied to the study of human material are much less powerful than the various experimental techniques that are currently used in animal studies. For instance, the Marchi method (126) does not provide information concerning the termination of degenerated fibers and often produces deceiving artifacts (see chapter 5).



Figure 11.5. Section through the fifth cervical spinal segment in a rhesus monkey following multiple cervical dorsal rhizotomies on the *right* and section of the C5 dorsal root on the *left*. Intense gliosis sharply outlines the fasciculus cuneatus on the *right*, while more restricted gliosis on the *left* occupies the area of degenerated C5 dorsal root fibers (Nissl stain).

Spinothalamic Tracts

The fibers that form the spinothalamic tracts differ from those in the posterior white columns in that they arise from cells within the spinal gray matter and cross within the spinal cord before ascending to the thalamus. The cells of origin of the spinothalamic tracts have been identified (a) physiologically by antidromic stimulation of the specific sensory relay nuclei of the thalamus and (b) anatomically by tracing the retrograde transport of the enzyme horseradish peroxidase (HRP). These data agree that the fibers of the spinothalamic tracts arise contralaterally in the spinal cord from cells in laminae I and V, and to a lesser extent from cells in laminae IV, VI, and VII of the posterior and intermediate horns (4, 215, 216). After large HRP injection in the monkey thalamus, the largest number of spinothalamic neurons is found in contralateral lower lumbar segments (9). For each region of the spinal cord, ipsilateral labeled spinothalamic neurons constitute about 10% of the total number of retrogradely labeled neurons. Neurons that form the spinothalamic tracts constitute a heterogeneous cell population that varies in size, shape, and number among the different segments and spinal laminae. Spinothalamic fibers cross in the anterior white commissure and collect contralaterally into three more or less distinct bundles termed *anterior spinothalamic*, *lateral spinothalamic*, and *spinocervicothalamic* tracts.

ANTERIOR SPINOTHALAMIC TRACT

Fibers forming the anterior spinothalamic tract ascend in the anterior and anterolateral funiculi and are somatotopically arranged, so that those arising from sacral and lumbar segments are most lateral and those from thoracic and cervical segments are most medial (Figs. 11.4 and 11.6). A small number of uncrossed fibers also occur, but these fibers are not illustrated in Figure 11.6. The anterior spinothalamic tract is reduced in size at medullary levels because some fibers, or collaterals, project to the nuclei of the reticular formation. The spinothalamic component of this tract becomes closely associated with the medial lemniscus in the pons and midbrain. At midbrain levels, the anterior spinothalamic tract consists of two components (98). Fibers of the larger lateral component terminate in caudal parts of the ventral posterolat-

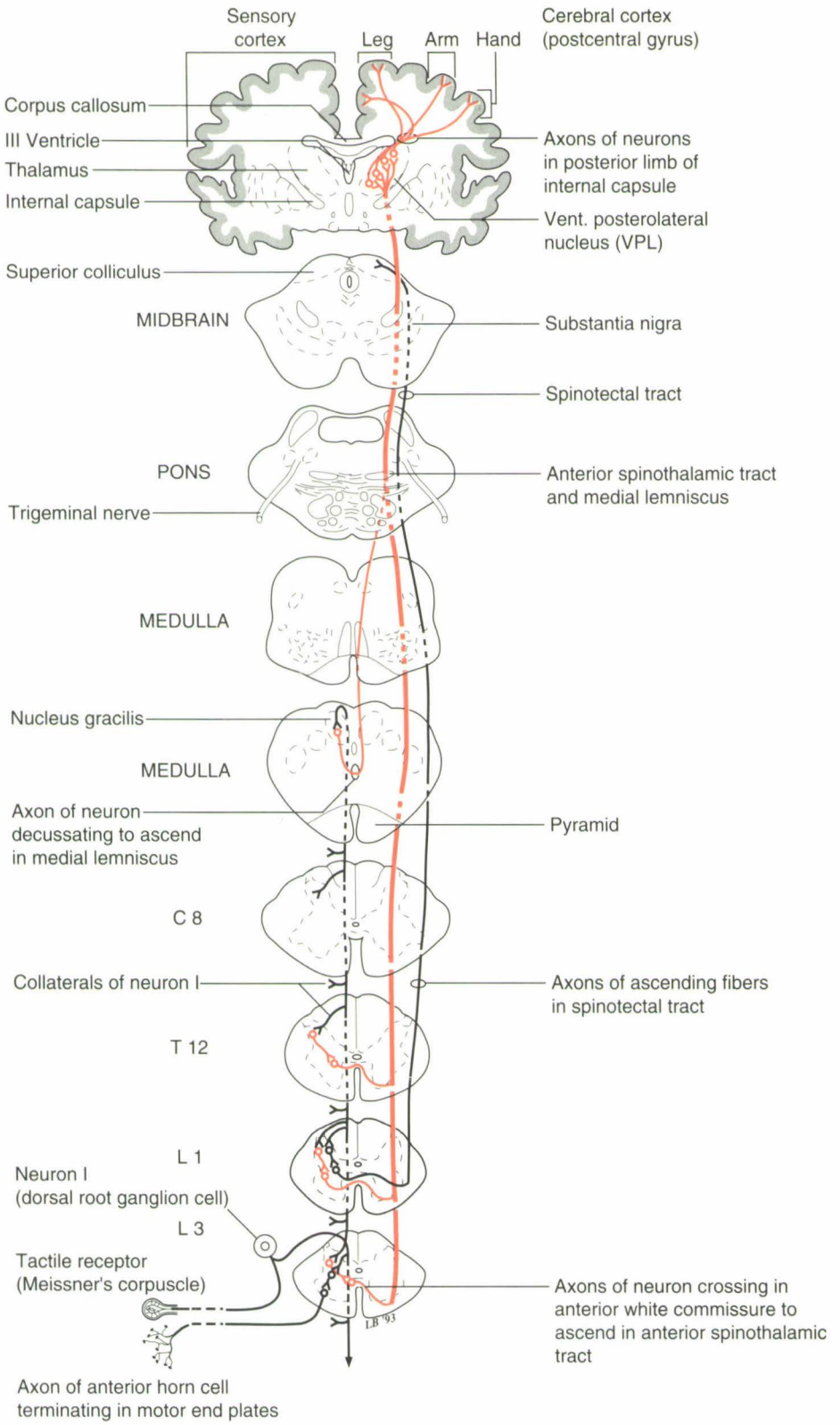


Figure 11.6. Anterior spinothalamic (*red*) and the spinotectal (*black*) tracts. These tracts arise from cells in multiple laminae of the spinal gray at all levels. The largest number of spinothalamic fibers appear to arise from cells in laminae I, IV, and V contralaterally. The anterior spinothalamic tract conveys impulses associated with "light touch," the sensation produced by stroking glabrous skin with a wisp of cotton. The spinotectal tract ascends in close association with the anterior spinothalamic tract, but terminates in deep layers of the contralateral superior colliculus and in parts of the periaqueductal gray. This tract conveys nociceptive impulses. Letters and numbers indicate segmental spinal levels.

eral, pars caudalis (VPL_c), thalamic nucleus. Fibers of the medial component of the tract project into the periaqueductal gray and bilaterally in the intralaminar thalamic nuclei. Axons reaching the VPL nucleus of the thalamus terminate somatotopically upon neurons which in turn project to the postcentral gyrus (somesthetic area) of the cerebral cortex.

Fibers of the anterior spinothalamic tract convey impulses associated with what is called "light touch," a sensation that is provoked by stroking skin, devoid of hair (glabrous skin), with a feather or wisp of cotton. This sensation supplements deep touch (pressure) and discriminative tactile sense conveyed in the posterior white columns. Because tactile sensation is transmitted centrally by both the posterior white columns and the anterior spinothalamic tracts, clinically this sensory modality is of limited value in localizing injuries of the spinal cord. In fact, injury to the anterior spinothalamic tract produces little, if any, disturbance in tactile sensibility.

LATERAL SPINOTHALAMIC TRACT

This tract is closely related to the anterior spinothalamic tract but is of greater clinical importance because it transmits impulses concerned with pain and thermal sense (Fig. 11.7). Its component fibers are more concentrated than those in the anterior spinothalamic tract, and it contains more fibers that project directly to the thalamus (97). Posterior horn neurons, principally those in laminae I and V, give rise to most of these fibers that first cross in the anterior white commissure before ascending in the contralateral lateral funiculus as the lateral spinothalamic tract (4, 215). Fibers of this tract cross obliquely to the opposite side, usually within one or two spinal segments. They lie medial to fibers of the anterior spinocerebellar tract (Figs. 11.4 and 11.25). They are somatotopically organized in a manner similar to those of the anterior spinothalamic tract. There is an incomplete segregation of fibers concerned with pain and thermal sense; fibers related to thermal sense tend to be posterior to those related to pain. In the brainstem, this tract sends branches into the reticular formation while the main fibers terminate in the VPL_c nucleus of the thalamus (Fig. 11.7).

Section of the spinothalamic tract (anterolateral cordotomy) in monkeys (29, 30, 135) indicates that the thalamic projections of the spinothalamic system are far more complex than classic descriptions suggest. Unilateral anterolateral cordotomy produces (a) ipsilateral degeneration in the VPL_c nucleus, (b) bilateral degeneration in certain intralaminar nuclei, and (c) bilateral degeneration in a posterior thalamic nucleus. These anatomical observations, confirmed by electrophysiologic studies (167, 173, 232), indicate that the body surface is represented in an orderly but distorted somatotopic fashion in the VPL_c nucleus and reveal that cells of the VPL_c nucleus are related to small contralateral receptive fields. In the posterior thalamic nucleus, cells are activated from large receptive fields, both ipsilaterally and contralaterally.

Recent anatomic investigations in various species, including nonhuman primates, have led to a more unified view of the spinothalamic afferents than the one presented earlier. These studies suggest that the spinothalamic tracts in the anterolateral quadrant of the spinal cord contain primarily axons of lamina V cells, which respond to both innocuous and noxious stimuli. Axons of lamina I cells, which respond to noxious mechanical or thermal stimuli, course more dorsally in the dorsolateral quadrant. The spinothalamic pathway in nonhuman primates is said to encompass a continuous fiber bundle that extends dorsally to include a region of the lateral funiculus where fibers project primarily to posterior thalamic nuclei (187). Whether or not the same organization prevails in humans remains to be determined.

Unilateral section of the lateral spinothalamic tract produces a complete loss of pain and thermal sense (analgesia and thermoanesthesia) on the opposite side of the body beginning about one or two segments below the level of the lesion (Fig. 11.27). The anesthesia involves the superficial and deep portions of the body wall, but not the viscera, which appear to be represented bilaterally. The anogenital region is not markedly affected with unilateral lesions. After a variable period there is often some return of pain and thermal sensibility, due perhaps to the presence of uncrossed spinothalamic fibers. Such pain impulses also may ascend by shorter relays along spinospinal and spinoreticular pathways.

In certain instances, bilateral surgical section of the lateral spinothalamic tracts (cordotomy) is performed at slightly different levels on selected patients to relieve pain and

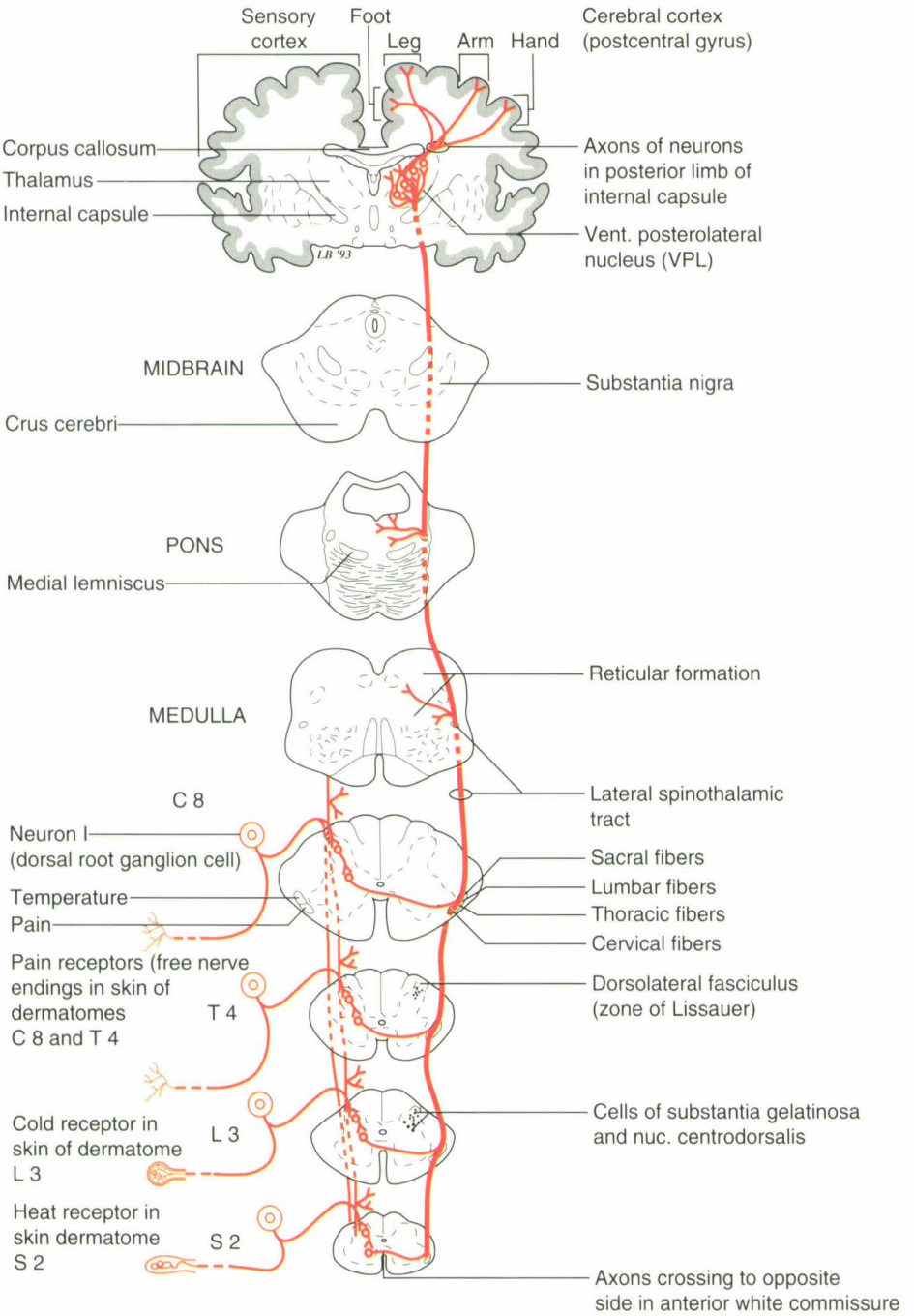


Figure 11.7. Lateral spinothalamic tract (*red*). The cells of origin of the lateral spinothalamic tract appear to be largely in laminae I, IV, and V of Rexed. Fibers of this tract usually cross to the opposite side within one segment in the anterior white commissure. The lateral spinothalamic tract has a more complex termination in the thalamus than indicated here, conveys impulses associated with pain and thermal sense, and has a somatotopic lamination. Letters and numbers indicate segmental spinal levels.

produce a complete and more enduring sensory loss. The spinothalamic and trigeminothalamic pathways both may be destroyed by one laterally placed lesion in the medulla or midbrain, where these two tracts occupy a superficial position (Figs. 11.7 and 13.30). Interruption of both tracts at medulla levels results in a loss of pain and thermal sense over the face contralaterally and over the body ipsilaterally, whereas mesencephalic tractotomy produces a thermoanalgesic loss over the face and body all on the side opposite to the lesion.

It is evident from the foregoing that the sensory impulses brought in by the dorsal roots are organized in the spinal cord into two main systems: discriminative (epicritic) and affective (vital, protopathic). The former are related to the long fibers of the posterior white columns and the latter to the shorter root fibers and the anterolateral white columns. Discriminative sensibility carried by the longest fibers remains uncrossed in the spinal cord. Pain and thermal impulses, initially conveyed by the short fibers in the *zone of Lissauer*, may synapse one or more times before reaching cells that give rise to fibers crossing in the anterior white commissure that form the lateral spinothalamic tract.

This distribution of afferent impulses accounts for the curious sensory dissociation occurring in the hemisection of the spinal cord (Brown-Séquard syndrome), where there is loss of pain and thermal sense on the opposite half of the body below the level of the lesion, while the sense of position and movement, two-point discrimination, and vibration are lost on the same side as the lesion (Fig. 11.27).

SPINOCERVICOTHALAMIC TRACT

Experimental studies in the cat, which appears to lack an uninterrupted spinothalamic tract terminating in the VPL_c nucleus of the thalamus (4, 25, 38), suggest that the spinocervicothalamic tract may serve as its homologue (58, 59, 139, 140, 210, 211). Cells in lamina IV of the posterior horn at all spinal levels give rise to uncrossed fibers that ascend in the dorsolateral funiculus (58, 210). These cells in the posterior horn are monosynaptically activated by dorsal root afferents that respond chiefly to low threshold cutaneous stimuli (108, 123). Spinocervical cells give off several collaterals before their axons enter the ipsilateral dorsolateral funiculus; other collaterals, which course back to the posterior horn, are emitted as the fibers ascend to the lateral cervical nucleus. The spinocervical fibers terminate in a profuse plexus of fine collaterals in the lateral cervical nucleus (Figs. 10.26 and 11.8). The *lateral cervical nucleus* is a longitudinal cell column, lateral to the posterior horn, in the lateral funiculus of the upper three cervical segments of the cat's spinal cord (189). This nucleus is present in a variety of species, including humans, although it is most prominent in carnivores (217). Cells of the lateral cervical nucleus are somatotopically organized (60). They give rise to fibers that cross in the ante-

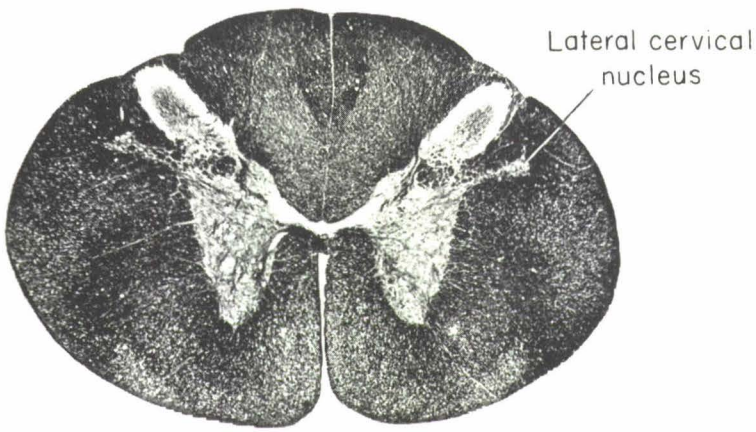


Figure 11.8. Section through the first cervical segment of the cat spinal cord demonstrating the lateral cervical nucleus. Cell of the lateral cervical nucleus receive fibers of the spinocervical tract, considered the feline equivalent of the spinothalamic tract. Fibers arising from cells in the lateral cervical nucleus cross in the upper cervical spinal segments and ascend to the thalamus in association with the medial lemniscus (cresyl violet stain).

rior white commissure at C1 and C2 levels and ascend in association with the medial lemniscus to the thalamus, where they end in a restricted part of the VPL nucleus (24, 59, 108, 137). Retrograde transport studies with HRP in the cat indicate that virtually all cells in the lateral cervical nucleus project to the contralateral thalamus and terminate somatotopically (59). In contrast, similar studies in monkeys indicate that only one-third of the cells in the lateral cervical nucleus project to the thalamus, the rest of the neurons sending their axons to the midbrain (205). There also are indications that the dorsal column-medial lemniscal pathway and the spinocervicothalamic projection may be functionally linked, because some spinocervical collaterals end in the dorsal column nuclei and some cells of the dorsal column nuclei project to the lateral cervical nucleus (58).

Impulses conveyed via the spinocervicothalamic tract reach the cortex earlier than those transmitted via the dorsal column-medial lemniscal pathway (148). Its integrity is essential for the earliest portion of the cortical evoked potential in somatic sensory areas I and II (7), and, according to Oscarsson and Rosén (163), this pathway also activates the motor cortex. Single units of the spinocervicothalamic tract show spontaneous activity and respond to hair movement and thermal stimuli with a uniformly low threshold. They are activated by tactile stimuli from relatively restricted receptive fields, but additional activation results from pressure and pinching the skin. The spinocervical tract, containing 2000–3000 fibers, 10–14 μm in diameter, is the most rapidly conducting pathway in the feline spinal cord. Anatomic studies suggest that the spinocervical tract may convey impulses related to painful stimuli and also plays a role in integration of motor functions.

Spinotectal Tract

Cells of origin of the spinotectal tract lie in laminae I and V of the posterior horn. Fibers of this crossed tract ascend in the anterolateral part of the spinal cord (Figs. 11.6 and 11.25) in close association with the spinothalamic fibers (8, 174). At midbrain levels fibers of the spinotectal tract project medially into the intermediate and deep layers of the superior colliculus and lateral regions of the periaqueductal gray. In the contralateral superior colliculus, the crossed spinal afferents terminate somatotopically in an orderly fashion in the caudal half of the colliculus (see Chapter 14). The functional significance of the spinotectal tract is unknown, but evidence suggests that it may be part of a multisynaptic pathway transmitting nociceptive impulses (135). The intermediate and deep layers of the superior colliculus receive multiple sensory inputs while projections to the superficial layers are all related to the visual system.

Cerebellar Afferents

POSTERIOR SPINOCEREBELLAR TRACT

This uncrossed tract, which ascends along the posterolateral periphery of the spinal cord (Figs. 11.3, 11.4, 11.9, and 11.25), arises from the large cells of the dorsal nucleus of Clarke. Posterior root afferent fibers reach the nucleus directly and after ascending and descending in the posterior columns (44, 77, 114, 203) (Fig. 10.25). The cells of the dorsal nucleus of Clarke give rise to large fibers that ascend in the posterolateral part of the lateral funiculus (i.e., lateral to the corticospinal tract). In the medulla, fibers of this tract become incorporated in the inferior cerebellar peduncle (Figs. 2.26 and 2.32), enter the cerebellum, and terminate in both rostral and caudal portions of the vermis (75). In the anterior vermis, fibers end in Larsell's lobules I to IV (Fig. 15.1); posteriorly, fibers terminate mainly in parts of the pyramis and paramedian lobule. These cerebellar cortical areas represent mainly the hindlimb. Thus, the posterior spinocerebellar tract, which conveys impulses from the periphery to the cerebellum, is an uncrossed disynaptic pathway formed by the axons of spinal ganglion cells (neurons I) and those of the dorsal nucleus of Clarke (neurons II).

Impulses relayed to the cerebellum via the posterior spinocerebellar tract arise from muscle spindles, Golgi tendons organs, and pressure receptors. Neurons of the dorsal nucleus of Clarke receive monosynaptic excitation mainly via group Ia, Ib, and group II afferents (159). The synaptic linkage between group I afferents and the dorsal nucleus of Clarke allows transmission of impulses at high frequency. Fibers of the posterior spinocerebellar tract have conduction velocities ranging from 30 to 110 m/sec (116, 159). Exteroceptive impulses, also transmitted via the posterior spinocerebellar tract, are related to touch and pressure receptors in skin and slowly adapting pressure receptors. The pos-

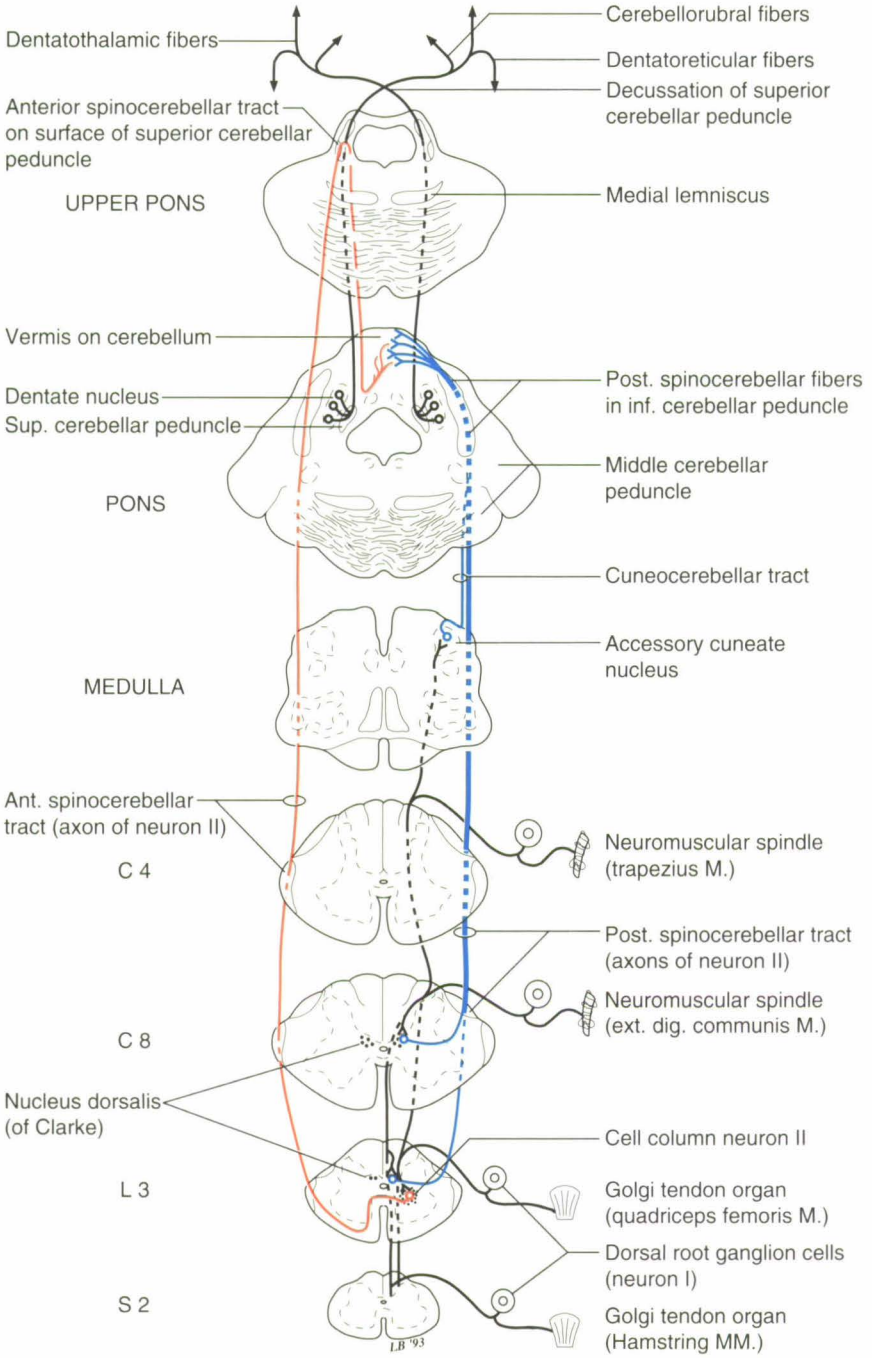


Figure 11.9. Anterior (*red*) and posterior (*blue*) spinocerebellar tracts and the cuneocerebellar tract (*black*). The posterior spinocerebellar tract arises from cells of the dorsal nucleus of Clarke and is uncrossed. It conveys impulses arising from muscle spindles and Golgi tendon organs. Fibers of the anterior spinocerebellar tract are crossed and arise from cells in parts of laminae V, VI, and VII. Fibers of this tract are activated by impulses from Golgi tendon organs. The cuneocerebellar tract, arising from cells of the accessory cuneate nucleus in the medulla, is considered the upper limb equivalent of the posterior spinocerebellar tract. This tract is uncrossed. An uncrossed rostral spinocerebellar tract (not shown) is considered the upper limb equivalent of the anterior spinocerebellar tract in the cat. Letters and numbers indicate spinal level.

terior spinocerebellar tract is somatotopically organized at spinal levels and in its cerebellar terminations (see Chapter 15). Recent double retrograde labeling studies in the rat have revealed that spinocerebellar projections arborizing in the anterior and posterior lobes of the cerebellum arise largely from the same neurons in the spinal cord (21). This high degree of axonal branching suggests that the rostral and posterior regions of the cerebellum receive common information from spinocerebellar fibers. None of the impulses conveyed by this tract reach conscious levels. Impulses transmitted by this tract are utilized in the fine coordination of posture and movement of individual limb muscles.

ANTERIOR SPINOCEREBELLAR TRACT

This tract ascends along the lateral periphery of the spinal cord anterior to the posterior spinocerebellar tract, and posterior to the site of emergence of ventral root fibers (Figs. 11.3, 11.4, and 11.9). The tract makes its first appearance in lower lumbar levels of the cord, but its cells of origin do not constitute a discrete entity such as the dorsal nucleus of Clarke. Fibers of the anterior spinocerebellar tract were considered by Cooper and Sherrington (50) to arise in lumbar spinal segments from cells in the periphery of the anterior horn, known as "spinal border cells" or the *nucleus pericornualis anterior*. Anatomic investigations in various species reveal that fibers of the anterior spinocerebellar tract arise from cells in part of the posterior (dorsal) and intermediate horns (laminae V, VI, and VII). Cells giving rise to this tract extend from coccygeal and sacral spinal segments as far rostrally as the L1 segment (76, 78, 87, 129, 236). Morphologically, these neurons are almost impossible to distinguish from motor neurons in Nissl preparations of normal spinal cord.

This pathway to the cerebellum is composed of two neurons: (a) neuron I in the spinal ganglia, and (b) neuron II in the scattered cell groups at the base of the anterior and posterior horns in lumbar, sacral, and coccygeal spinal segments. Fibers of neuron II cross in the spinal cord and ascend peripheral to the fibers of the lateral spinothalamic tract. At upper pontine levels, the tract enters the cerebellum by coursing along the dorsal surface of the superior cerebellar peduncle (Fig. 11.9). The majority of the fibers of this tract terminate contralaterally in the anterior cerebellar vermis in lobules I to IV (76, 165, 236). Experimental studies show that the majority of fibers of this tract in the cat terminate contralaterally, about 10% end ipsilaterally and about 15%, after branching, end both ipsilaterally and contralaterally. The axon terminals of the anterior spinothalamic tract in the anterior lobe of the cerebellum are concentrated in very characteristic longitudinal zones parallel to the midsagittal plane (236).

Fibers of the anterior spinocerebellar tract are less numerous than those of the posterior spinocerebellar tract, are uniformly large (11–20 μm), have conduction velocities of 70–120 m/sec, and are virtually all crossed. Like the posterior spinocerebellar tract, it is concerned with the transmission of impulses mainly from the lower extremity. Cells that give rise to the anterior spinocerebellar tract receive monosynaptic excitation from group Ib afferents from Golgi tendon organs whose receptive fields often include one synergic muscle group at each joint of the lower limb (159). Fibers of this system convey impulses concerned with coordinated movement and posture of the entire lower limb.

Clinically, it is virtually impossible to determine the effects of injury to the spinocerebellar tracts, because other spinal tracts usually are involved. No loss of tactile or kinesthetic sense results from such lesions, since the information projected to the cerebellum does not enter the conscious sphere.

CUNEOCEREBELLAR TRACT

The dorsal nucleus of Clarke is not present above C8 and dorsal root fibers above this level ascend ipsilaterally. These fibers, which convey impulses from muscle afferents (group Ia) and Golgi tendon organs (group Ib), terminate somatotopically upon cells of the *accessory cuneate nucleus*, a group of large cells in the dorsolateral part of the medulla with cytologic features similar to those of the dorsal nucleus of Clarke (Figs. 11.9 and 12.8). The accessory cuneate nucleus in the monkey receives afferents via the dorsal roots from T7 to C1 (203) which terminate in an overlapping systematic fashion. Cells of the accessory cuneate nucleus give rise to the cuneocerebellar tract, the upper limb equivalent of the posterior spinocerebellar tract. Fibers of this tract known as posterior external arcuate fibers, enter the cerebellum as a component of the inferior cerebellar peduncle, and terminate ipsilaterally in lobule V of the cerebellar

cortex. These cerebellar afferent fibers are distributed to the forelimb area of the intermediate zone in the anterior lobe and to forelimb areas of the pyramis and paramedian lobule (Fig. 15.1). As for the anterior spinocerebellar tract, there is a high degree of axonal collateralization of the cuneocerebellar fibers to both the anterior and posterior cerebellar regions (22). The cuneocerebellar tract is considered to be the upper limb equivalent of the posterior spinocerebellar tract.

OTHER SPINOCEREBELLAR TRACTS

In carnivores, another spinocerebellar pathway, the *rostral spinocerebellar tract*, has been described as the forelimb equivalent of the anterior spinocerebellar tract (159, 160, 162, 165). The cells of origin are rostral to the column of Clarke in the cervical spinal cord and they give rise to an uncrossed tract that ascends in the anterior part of the lateral funiculus and enters the cerebellum via both inferior and superior cerebellar peduncles. This tract appears to arise principally from the large neurons of the centrobasal nucleus located in lamina VI of the cervical enlargement (131, 169, 221). This tract resembles the anterior spinocerebellar tract, except that it is largely uncrossed. Fibers of the rostral spinocerebellar tract terminate more rostrally than those of the posterior and anterior spinocerebellar tracts. They arborize principally in lobules IV and V of the anterior lobe and in lobules VI and VII and the paramedian lobule (221).

Another, smaller, crossed *cervicospinocerebellar* pathway arises from an interrupted column of cells in the upper cervical spinal cord (C1 to C4), known as the central cervical nucleus (Fig. 10.26) (61, 132, 133). This pathway conveys impulses from upper cervical spinal segments to the cerebellum.

Thus, in addition to the posterior and anterior spinocerebellar tracts, related primarily to the hindlimbs and caudal parts of the body, there are two equivalent tracts, the cuneocerebellar and the rostral spinocerebellar, that relay sensory information from the forelimbs and rostral parts of the body (159). The posterior spinocerebellar and cuneocerebellar tracts are similar and convey information from muscle spindles, tendon organs and touch and pressure receptors in the skin. The anterior spinocerebellar and rostral spinocerebellar tracts are similar in that they convey impulses from tendon organ afferents and flexor reflex afferents, both with wide receptive fields.

The *spino-olivary pathways* appear to constitute another component of the spinocerebellar circuitry (36). The two best defined spino-olivary pathways have been designated as the posterior and anterior spino-olivary tracts (161, 162, 164). Fibers of the posterior spino-olivary tract ascend in the posterior white columns to the nuclei gracilis and cuneatus. The posterior column nuclei relay impulses to parts of the accessory olivary nuclei. The multiple anterior spino-olivary tracts ascend contralaterally in the anterior funiculus and terminate upon portions of the dorsal and medial accessory olivary nuclei. Fibers contributing to the spino-olivary tracts arise from all levels of the spinal cord, are somatotopically organized and are activated by cutaneous afferents and group Ib afferents from Golgi tendon organs. In the cat, the cells of origin of anterior spino-olivary tracts lie in laminae IV and V and in medial regions of laminae VII and VIII at lower lumbar levels (10). The accessory olivary nuclei which receive the spino-olivary systems, give rise to crossed olivocerebellar fibers which project mainly to the anterior lobe of the cerebellum. Brodal (34) has referred to these spino-olivary-cerebellar linkages as the *indirect spinocerebellar pathways*.

Spinoreticular and Other Ascending Fibers

SPINORETICULAR FIBERS

A considerable number of spinoreticular fibers, arising from cells in the posterior horn (31, 134, 141, 193), ascend in the anterolateral part of the spinal cord and are distributed to widespread regions of the brainstem reticular formation (Fig. 11.10). In the medulla, these fibers are predominantly uncrossed and terminate chiefly upon cells of the nucleus reticularis gigantocellularis and parts of the lateral reticular nucleus (186). The lateral reticular nucleus of the medulla (Fig. 12.7) is known to project to specific portions of the cerebellum, indicating that some fibers in this pathway are concerned with the transmission of exteroceptive impulses to the cerebellum. Large cells of the nucleus reticularis gigantocellularis project to spinal levels as well as to more rostral regions of the brainstem. Spinoreticular fibers passing to pontine levels are distributed bilaterally and are less numer-

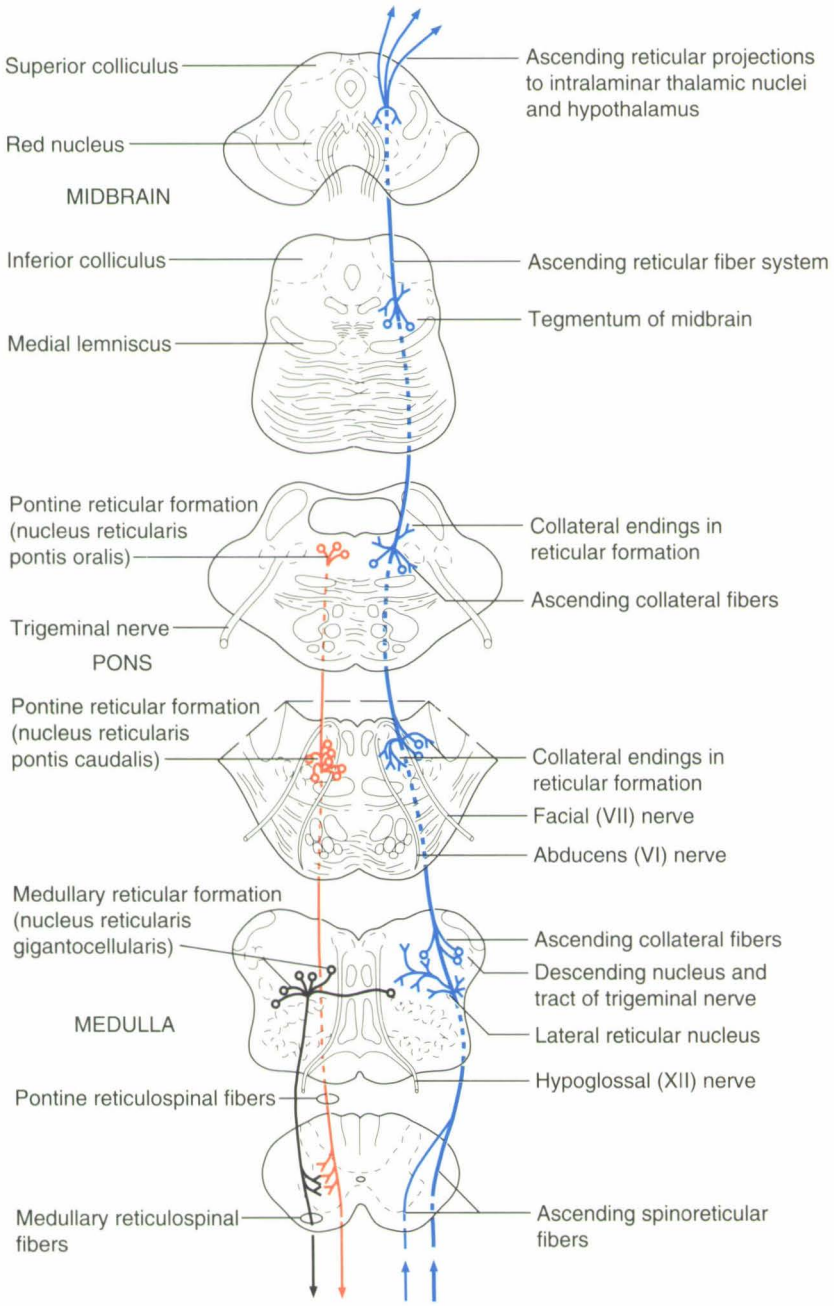


Figure 11.10. Ascending and descending reticular fibers systems. Ascending spinoreticular projections and collaterals are shown on the right (*blue*). In this system, collaterals are given off at various brainstem levels and the pathway is augmented by rostrally projecting reticular fibers. Pontine reticulospinal fibers (*red*) are uncrossed and originate largely from the nucleus reticularis pontis caudalis. Medullary reticulospinal fibers (*black*), predominantly uncrossed, arise from the nucleus reticularis gigantocellularis. Descending fibers from these sources are not topographically organized or sharply segregated in the spinal cord.

ous than those terminating in the medulla. Most of these fibers end in the nucleus reticularis pontis caudalis (32). A smaller number of spinoreticular fibers have been found in the reticular formation in the region of transition from pons to mesencephalon (155). Functionally, spinoreticular fibers represent a component of a polysynaptic system, which plays a significant role in behavioral awareness, modification of motor and sensory activities, and in the modulation of electrocortical activity.

OTHER ASCENDING FIBER SYSTEMS

In addition to the ascending fiber systems mentioned in preceding sections, several other ascending pathways have been described. While the existence of these anatomic pathways seems certain, relatively little is known of their functional significance. Among those are the *spinovestibular fibers*, which project largely upon the dorsal part of the lateral vestibular nucleus and to parts of the inferior vestibular nucleus that do not receive primary fibers. These fibers ascend ipsilaterally in the spinal cord from levels as far caudally as lumbar segments (180). Many fibers of this tract are partially intermingled with those of the posterior spinocerebellar tract. *Spinopontine fibers* have been described as terminating upon pontine nuclei. It has been suggested that these fibers may transmit exteroceptive impulses to the cerebellum (226).

DESCENDING SPINAL TRACTS

The descending spinal tracts are concerned with somatic and visceral motor function, the modification of muscle tone, segmental reflexes, and the modulation of central transmission of sensory impulses. The largest and most important tracts arise from the cerebral cortex; all other descending spinal tracts arise from localized cell groups in the three lowest segments of the brainstem.

Corticospinal System

These tracts consist of fibers that (a) arise from cells within the cerebral cortex, (b) pass through the medullary pyramid, and (c) descend into the spinal cord. They constitute the largest and most important descending fiber system of the human neuraxis (145). In humans, each tract is composed of over 1 million fibers of which some 700,000 are myelinated (109–111). Nearly 90% of these fibers are between 1–4 μm in diameter; remaining fibers range from 5–22 μm in diameter, but only about 3.5% of these are above 20 μm. Fibers of the corticospinal system arise from cells in the deeper part of lamina V in the precentral gyrus (area 4), the premotor area (area 6), the postcentral gyrus (areas 1, 2, 3a, 3b) and adjacent parietal cortex (area 5) (52, 92). The corticospinal tract is a complex fiber system arising from multiple cortical areas, and only a small part of it originates from the giant pyramidal cells of Betz in the precentral gyrus (area 4 of Brodmann) (Fig. 20.10). These cells have been estimated to number between 34,000 and 40,000 in one hemisphere. They are a major source of large fibers (10–20 μm) in the corticospinal tract (109, 112). The more numerous finer fibers come largely from cortical regions other than the primary motor cortex. The premotor areas collectively comprise more than 60% of the cerebral cortex of the frontal lobe that projects to the spinal cord in nonhuman primates (64). Like the primary motor cortex, each of the premotor areas contains local regions that have a high density of corticospinal neurons. These findings indicate that a substantial component of the corticospinal system originates from the premotor areas in the frontal lobe. Through their direct access to the spinal cord, each of these premotor areas has the potential to influence the generation and control of movement independently of the primary motor cortex. These findings raise questions about the utility of viewing the primary motor cortex as the "upper motor neuron" for the central control of movement (64).

Cells of origin of the corticospinal system are arranged in strips or clusters that vary in size in different cortical areas (Fig. 11.11). The axons of these cells converge in the corona radiata, enter the internal capsule, and descend to form the crus cerebri at midbrain levels (Figs. 11.11 and 11.12). As this large tract descends in the ventral part of the infratentorial brainstem, its fibers pass close to the emerging root fibers of cranial nerves III, VI, and XII. In the medulla, the fibers form the massive pyramids. At the junction of the medulla and spinal cord, the corticospinal tract undergoes an incomplete decussation and divides into three separate tracts: (a) the large lateral corticospinal tract (crossed), (b) the small an-

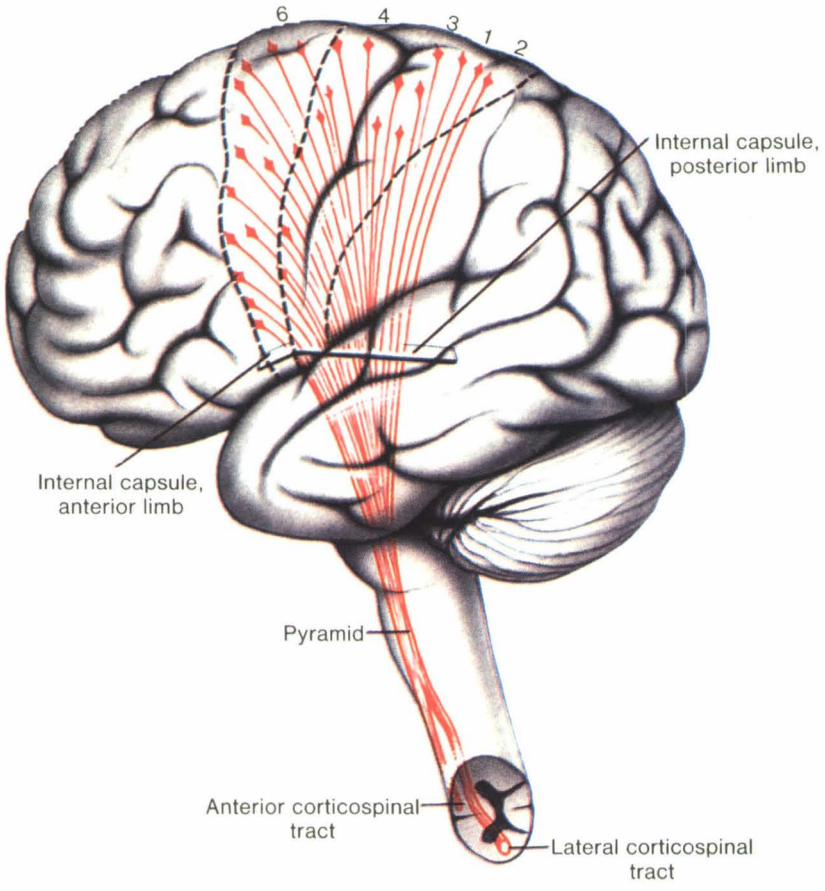


Figure 11.11. Lateral and anterior corticospinal tracts (*red*) showing their regions of origin and course. These tracts arise from cells of various sizes in the deep parts of lamina V.

terior corticospinal tract (uncrossed), and (c) the relatively minute uncrossed anterolateral corticospinal tract (Fig. 11.12). Between 75% and 90% of the fibers in the corticospinal tract decussate at caudal medullary levels and enter the posterior part of the lateral funiculus where they form the lateral corticospinal tract (Figs. 11.12–11.15). Fibers of this tract lie medial to the posterior spinothalamic tract and lateral to the fasciculus proprius (Figs. 11.15 and 11.16).

The *lateral corticospinal tract* descends the length of the spinal cord, gives off fibers to the spinal gray matter at all levels, and progressively diminishes in size at more caudal levels. In lower lumbar and sacral spinal segments, where the posterior spinocerebellar tract is absent, fibers of the lateral corticospinal tract reach the posterior (dorsal) surface of the spinal cord. Fibers of the crossed corticospinal tract enter the spinal gray matter in the intermediate zone and are distributed to part of laminae IV, V, VI, and VII. In monkeys, as well as in rats, a number of fibers synapse directly with anterior horn cells or their processes in lamina IX (12, 113).

The *anterior corticospinal tract* or direct corticospinal tract (bundle of Türk), formed from a smaller portion of pyramidal fibers, descends uncrossed into the spinal cord, and occupies an oval sector adjacent to the anterior median fissure (Figs. 11.11–11.15). This tract is distinguishable mainly in cervical segments. It is particularly well-developed in humans and apes, but shows considerable variation because the proportion of decussating pyramidal fibers is not constant (220). Most fibers of this tract cross at upper cervical spinal levels in the anterior white commissure and terminate bilaterally upon neurons in lamina VII. It appears chiefly concerned with motor neurons that innervate the muscles of the upper extremities and the neck.

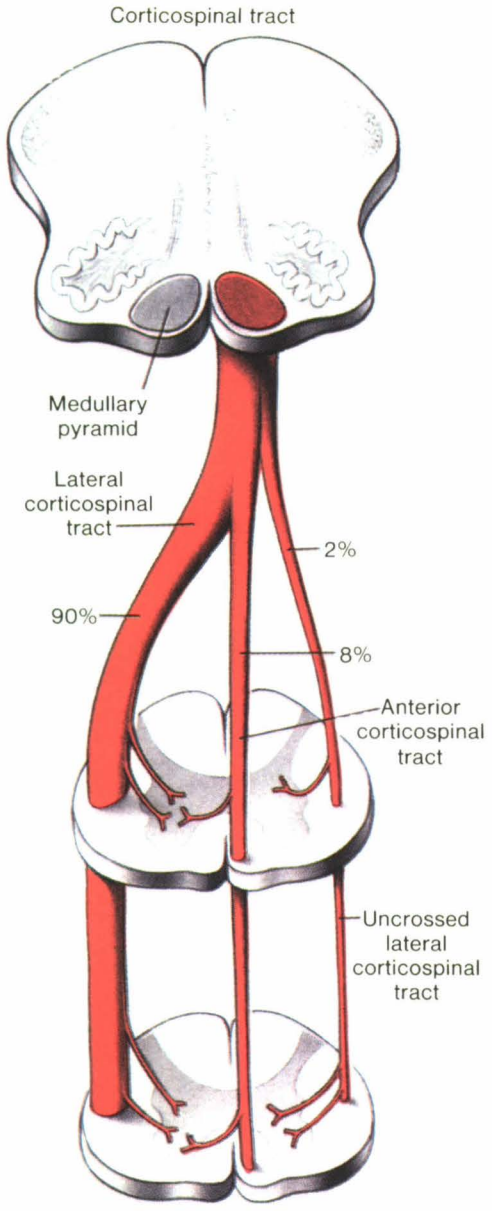


Figure 11.12. Decussation of the human corticospinal tract (*red*). Approximately 90% of the corticospinal tract crosses in the lower medulla to form the lateral corticospinal tract. Of the fibers which do not decussate in the medulla, approximately 8% form the anterior corticospinal tract which descends in the ventral funiculus. Most of these fibers cross in cervical spinal segments. The small number of fibers in the uncrossed lateral corticospinal tract remain uncrossed.

Fibers of the *anterolateral corticospinal tract* (15) are uncrossed, of fine caliber, and descend in a more ventral position in the lateral funiculus than those of the crossed lateral corticospinal tract (Fig. 11.12). These fibers remain uncrossed and terminate in the base of the posterior horn and the intermediate gray. Demyelination in the lateral corticospinal tract can be detected readily in Weigert-stained preparations (Figs. 11.14–11.16), but this stain is not sensitive enough to reveal the small number of fibers in the anterolateral corticospinal tract.

Tract-tracing studies with various tracers, including the lectin *Phaseolus vulgaris*-Leucoagglutin (PHA-L), indicate that fibers from the precentral motor cortex terminate extensively in lamina VII and in dorsolateral parts of lamina IX, while fibers from somatosensory cortex (areas 1, 2, 3, and 5) terminate in overlapping zones in parts of the posterior horn (12, 53, 113). Although the majority of corticospinal fibers terminate upon internuncial neurons in lamina VII, a significant number of fibers establish direct synaptic contact with motor neurons in the anterior horn (102, 113).

Corticospinal neurons in the motor cortex have multiple axonal branches that project to different spinal segments (3, 102, 113, 199, 202). Corticospinal neurons with axonal collaterals terminating at different spinal levels are distributed over wide areas of the motor cortex. Multiple collateral branches of the corticospinal axons explain (a) why a small HRP injection in the spinal gray matter retrogradely labels widely scattered projection neurons in the motor cortex, and (b) why a small lesion in the motor cortex produces corticospinal degeneration distributed over many segments. Collaterals of individual corticospinal axons project to multiple motor neuronal pools in the cervical and lumbar enlargements innervating different muscles. Corticospinal axons exert multiple influences upon different groups of spinal neurons in widely separated spinal segments. Interestingly, widely divergent corticospinal axons that branch to multiple motor neuronal pools have been shown to mediate activity in functionally related muscle groups (102). Such a divergence in the terminal arborization of corticospinal axons may play a crucial role in the coordinated control of specific subsets of muscles.

Cortical areas giving rise to the corticospinal tract also provide major inputs to other motor-related structures, such as the striatum, the pontine nuclei, and the red nucleus. The question as to whether single cortical neurons project to one or more of these sites is still a matter of controversy. Recent

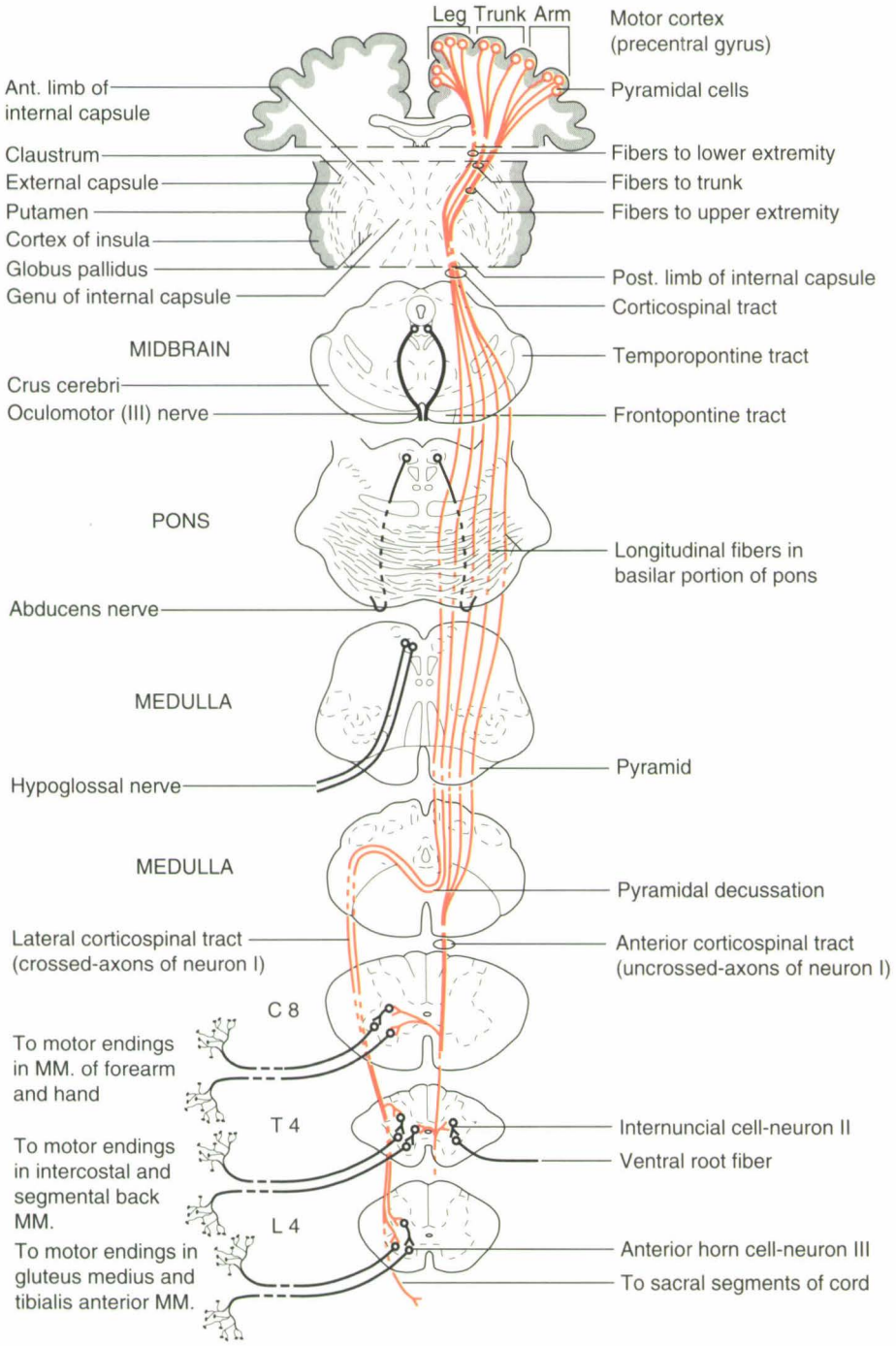


Figure 11.13. Lateral and anterior corticospinal tracts (*red*), which are the principal descending motor pathways concerned with skilled, voluntary motor activity. Letters and numbers indicate corresponding segments of the spinal cord.

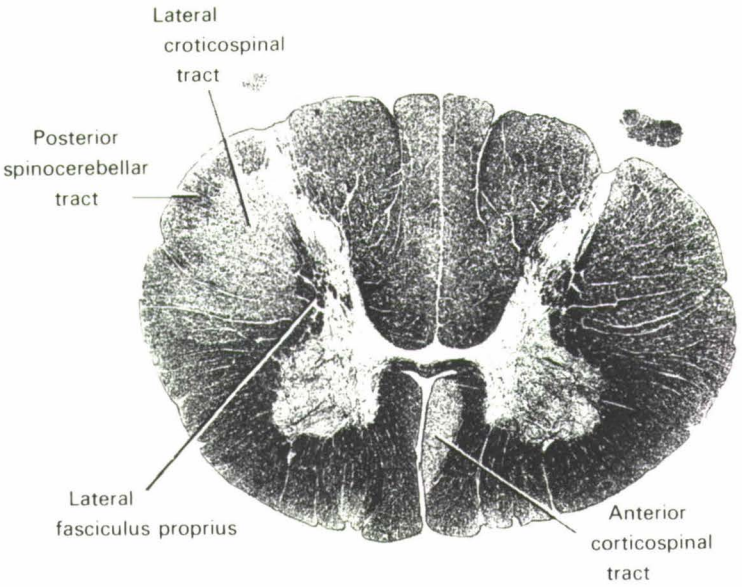


Figure 11.14. Transverse section through the cervical enlargement of an individual that has sustained a vascular lesion of one medullary pyramid. The lateral corticospinal tract on the left and the anterior corticospinal tract on the side of the lesion are degenerated and demyelinated (Weigert's myelin stain).

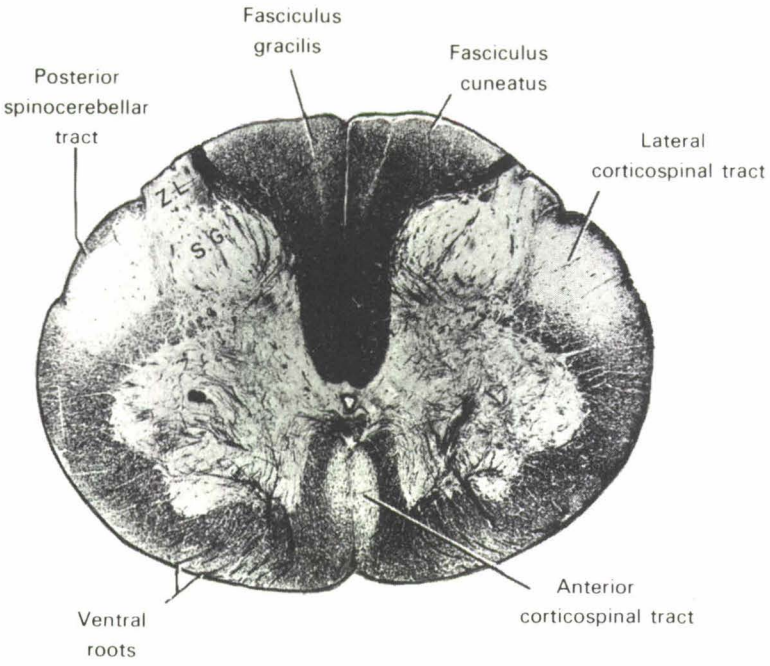


Figure 11.15. Section through the cervical enlargement of spinal cord of a 7–8-month human fetus. The corticospinal tracts are unmyelinated at this stage and hence are unstained. *S.G.*, substantia gelatinosa; *Z.L.*, zone of Lissauer (Weigert's myelin stain).

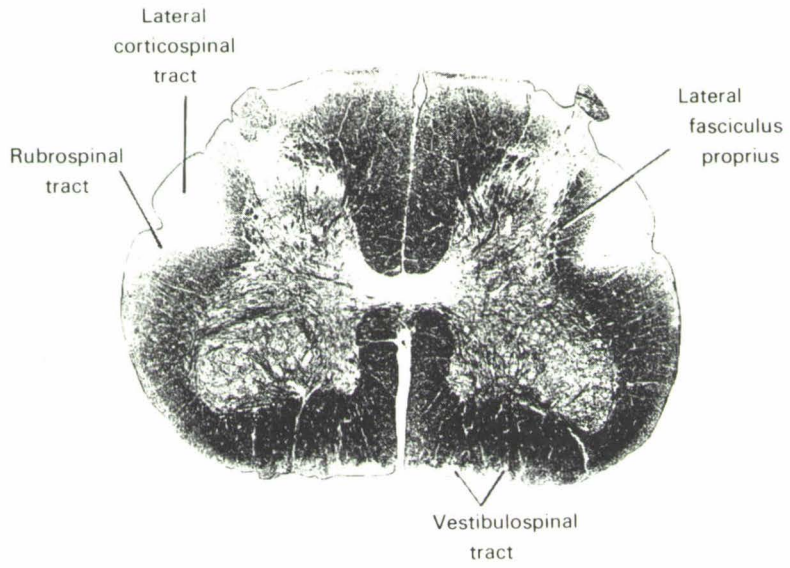


Figure 11.16. Section through the fourth lumbar segment of a human spinal cord that had been accidentally crushed in the lower cervical region some time before death. The degenerated long descending tracts are unstained. Note that the lateral corticospinal tract reaches the lateral periphery of the spinal cord at this level and the vestibulospinal tract lies on the anterior surface of the cord (Weigert's myelin stain).

tract-tracing studies in the rat reveal that there is a considerable overlap of cortical neurons projecting to these four sites (3). Furthermore, after injections of different retrograde tracers in the striatum, the pontine nuclei, the red nucleus, and the spinal cord, more than 98% of the cortical projection neurons were single-labeled while less than 2% were double-labeled. No triple- or quadruple-labeled neurons were observed (3). Hence, cortical motor neurons in the rat appear to project individual, rather than collateral, axons to these four motor-related structures. This finding indicates that the corticofugal motor system is highly ordered in rodents.

Some physiologic and anatomic studies suggest a somatotopical organization in the monkey in which fibers from the precentral gyrus pass to epi-axial motor neurons, but not axial motor neurons (20, 104, 105, 115, 182, 183). The contralateral projection is to neurons innervating distal (chiefly) and proximal limb muscles. The ipsilateral cortical projection is to motor neurons innervating proximal limb muscles. It has been estimated that about 55% of all pyramidal fibers end in the cervical cord, 20% in the thoracic, and 25% in the lumbosacral segments (229). The greater number of fibers terminating at cervical levels may reflect the fine control that the corticospinal system exerts upon the complex motor activity of the upper limbs compared to that of the lower limbs.

Immunocytochemical studies in the rat, combined with retrograde tracing methods, suggest that the amino acid glutamate and/or aspartate may be the excitatory transmitter in corticospinal neurons (73). Approximately 30% of identified corticospinal neurons in layer V were positive for either glutamate or aspartate, and 50% of these neurons were immunoreactive for both substances.

The corticospinal tract is universally regarded as the descending pathway most concerned with voluntary, discrete, skilled movement. Lesions destroying portions of this tract at any level result in variable degrees of paresis (i.e., paralysis). Such lesions usually are associated with (a) initial loss of muscle tone (atonia), (b) hyperactive deep tendons (myotatic) reflexes, (c) loss of superficial and cremasteric reflexes, and (d) the appearance of the Babinski sign. The *sign of Babinski* is an abnormal plantar response, which consists of extension of the great toe and fanning of the other toes on stroking the lateral or outer border of the sole of the foot with a blunt instrument (13). The normal plantar response is a brisk flexion of all toes. The Babinski sign is interpreted to mean injury of the corticospinal tract, but it is not an infallible sign, for it can be elicited in the

newborn, the sleeping or intoxicated adult, or following a generalized seizure. Likewise, the initial atonia seen after a lesion of the corticospinal tract is replaced after a period of days, or sometimes weeks, by spasticity. The affected muscles gradually become resistant to passive movement (see Chapter 20).

Paralysis of both arm and leg on the same side is termed *hemiplegia*. The term *paraplegia* denotes paralysis of both legs, while *quadriplegia* refers to paralysis of all four extremities.

Tracts Originating in Brainstem

All major descending spinal tracts, other than the corticospinal tract, arise from the brainstem. Three descending spinal tracts arise from the midbrain—the tectospinal, rubrospinal, and interstitiospinal tracts. The other tracts originating in the brainstem are the vestibulospinal and reticulospinal tracts, the medial longitudinal fasciculus, various autonomic descending projections, and the monoaminergic pathways. The fastigiospinal projection is also briefly reviewed in this section.

TECTOSPINAL TRACT

Fibers of this tract arise from neurons in the deeper layers of the superior colliculus, sweep anteromedially around the periaqueductal gray, cross in the *dorsal tegmental decussation*, and descend near the median raphe anterior to the medial longitudinal fasciculus (Figs. 11.17 and 11.18). At medullary levels, tectospinal fibers become incorporated in the medial longitudinal fasciculus. In the older literature, tectospinal fibers are referred to as the predorsal bundle. In the spinal cord, tectospinal fibers, located in the anterior funiculus near the anterior median fissure, descend only through cervical levels (Fig. 11.25). The

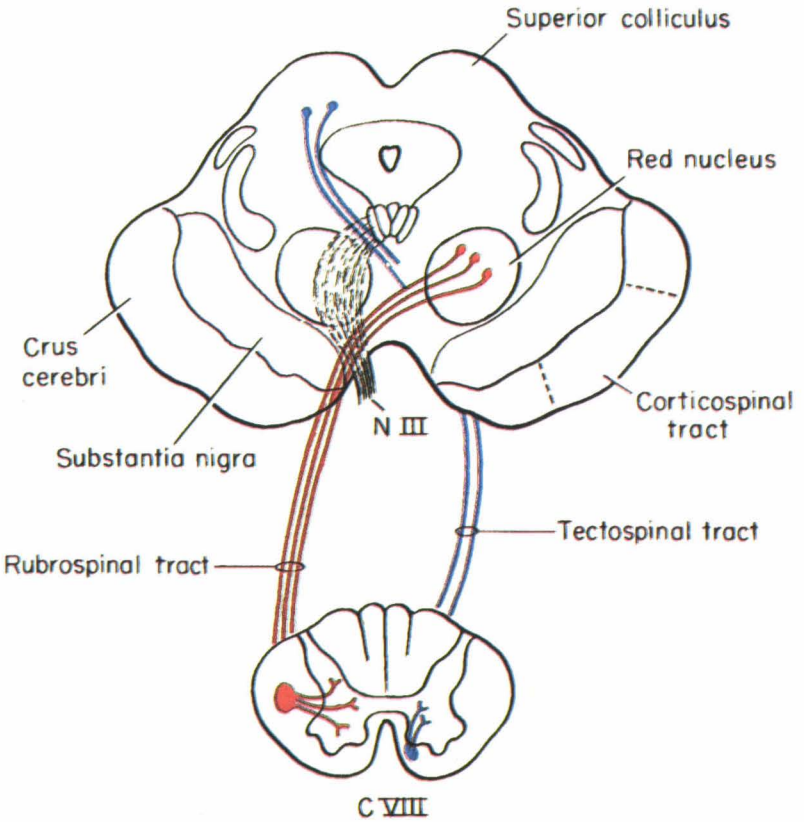


Figure 11.17. Rubrospinal (*red*) and the tectospinal (*blue*) tracts. The rubrospinal tract arises somatotopically from cells of the red nucleus, crosses in the ventral tegmental decussation, and descends to spinal levels where fibers terminate in parts of laminae V, VI, and VII of Rexed. Tectospinal fibers arise from cells in deep layers of the superior colliculus, cross in the dorsal tegmental decussation, and descend in association with the medial longitudinal fasciculus. Fibers of the tectospinal tract are distributed to parts of laminae VIII, VI, and VII only in cervical spinal segments.

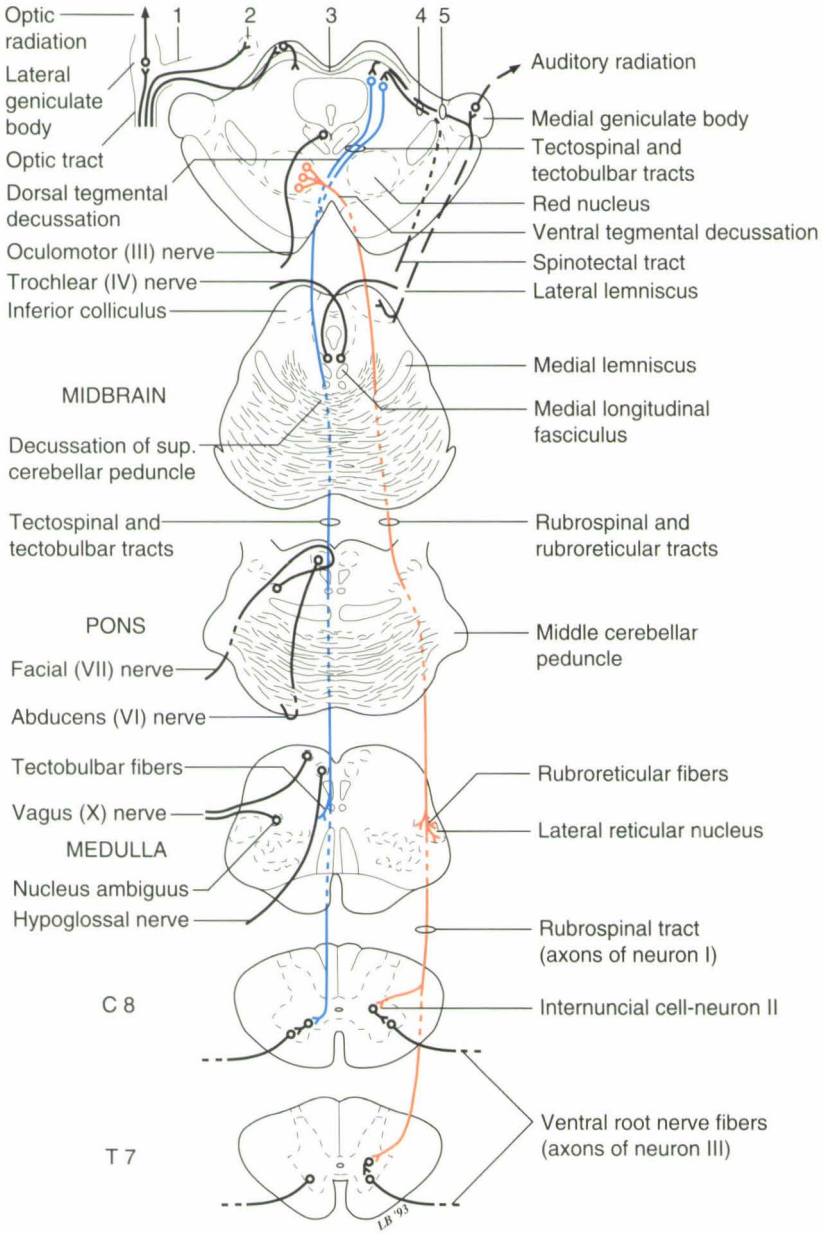


Figure 11.18. Course of the rubrospinal (*red*) and tectospinal (*blue*) tracts. Crossed rubrobulbar fibers project to parts of the facial nucleus (not shown) and to the lateral reticular nucleus of the medulla (rubroreticular fibers). Uncrossed rubrobulbar fibers (not shown) descend in the central segmental tract and terminate in the dorsal lamella of the ipsilateral principal olivary nucleus. Tectospinal fibers descend initially ventral to the medial longitudinal fasciculus. At medullary levels, these fibers become incorporated in the medial longitudinal fasciculus. Fibers of the tectospinal tract descend only to lower cervical spinal segments. Numbered midbrain structures include: *1*, the brachium of the superior colliculus; *2*, the pretectal area; *3*, commissure of the superior colliculus; *4*, spinotectal tract; and *5*, collicular fibers from the lateral lemniscus.

majority of the fibers terminate in the upper four cervical spinal segments in laminae VII, VIII, and parts of lamina VI (5, 151, 168). None of these fibers terminate directly upon alpha (α) motor neurons. The tectospinal tract mediates reflex postural movements in response to visual and, perhaps, auditory stimuli.

The superior colliculus also gives rise to fibers distributed bilaterally in the mesencephalic reticular formation and to medial regions of the contralateral pontine and medullary reticular formation (5). These fibers are referred to as *tectobulbar fibers* and their function is discussed in Chapter 14.

RUBROSPINAL TRACT

Fibers of this tract arise from cells of the red nucleus, a well-defined, oval-shaped structure in the central part of the midbrain tegmentum (Figs. 11.17, 11.18, 14.1, and 14.6). The red nucleus consists of a rostral parvicellular part and a caudal magnocellular part, which vary in size in different animals. In monkeys, three distinctive types of neurons are found in the red nucleus: (a) large giant neurons with coarse, evenly distributed, Nissl granules which characterize the magnocellular part, (b) medium-sized triangular neurons with prominent nucleoli and a Nissl substance that does not form distinct granules, which characterize the parvicellular part, and (c) small neurons, found in both magnocellular and parvicellular parts, which are achromatic and have scant cytoplasm (48, 99, 100, 188, 194). In the cat, the rubrospinal tract arises from cells of all sizes in the caudal three-fourths of the nucleus (179). In the monkey, the rubrospinal tract arises largely from the magnocellular region which occupies the caudal third of the red nucleus (96, 106, 128, 157, 175).

Rubrospinal fibers cross completely in the *ventral tegmental decussation*, and descend to spinal levels, where they lie anterior to, and partially intermingled with, fibers of the lateral corticospinal tract (Figs. 11.17, 11.18, and 11.25). Fibers of the rubrospinal tract are somatotopically organized, meaning that cells in particular parts of the nucleus project selectively to defined spinal levels (179). Fibers projecting to cervical spinal segments arise from dorsal and dorsomedial parts of the red nucleus, while fibers projecting to lumbosacral spinal segments arise from ventral and ventrolateral parts of the nucleus. Thoracic spinal segments receive fibers that originate from intermediate regions of the nucleus. Rubrospinal fibers descend the length of the spinal cord and terminate in the lateral half of lamina V, lamina VI, and dorsal and central parts of lamina VII (80, 151, 152, 200). These fibers terminate on somata and dendrites of large and small cells within these laminae (152). Since rubrospinal fibers do not end directly upon anterior horn cells, their facilitation of gamma (γ) motor neurons is mediated by spinal internuncial neurons.

In their descent through the brainstem, collateral fibers of the rubrospinal tract are given off to the cerebellum (56), the facial nucleus (54), and the lateral reticular nucleus of the medulla (54, 66, 80, 127, 138, 223). The parvicellular part of the red nucleus also gives rise to uncrossed rubrobulbar fibers (222) that project to dorsal parts of the principal inferior olivary nucleus (57, 66, 138, 175, 223).

The red nucleus receives fibers from the cerebral cortex and the cerebellum. In the cat and monkey, corticorubral fibers from the "motor" cortex project bilaterally to the parvicellular part of the nucleus and ipsilaterally to the magnocellular division (79, 106, 190, 218). These projections are somatotopically organized with respect to origin and termination. The synaptic linkage of corticorubral and rubrospinal fibers together constitute a somatotopically organized, disynaptic, nonpyramidal pathway between the motor cortex and particular spinal levels. All parts of the red nucleus receive crossed cerebellar efferent fibers via the superior cerebellar peduncle. Fibers from the interposed nucleus (equivalent to globose and emboliform nucleus in humans) relate portions of the cerebellar cortex somatotopically with the magnocellular part of the red nucleus (55, 69, 128). Stimulation of cells in the red nucleus (86, 176, 177, 196) produces excitatory postsynaptic potentials in contralateral flexor α motor neurons, and inhibitory postsynaptic potentials in extensor α motor neurons. The most important function of the rubrospinal tract concerns control of muscle tone in flexor muscle groups (128).

VESTIBULOSPINAL TRACT

The vestibular nuclei constitute a cytologic complex in the floor of the fourth ventricle of

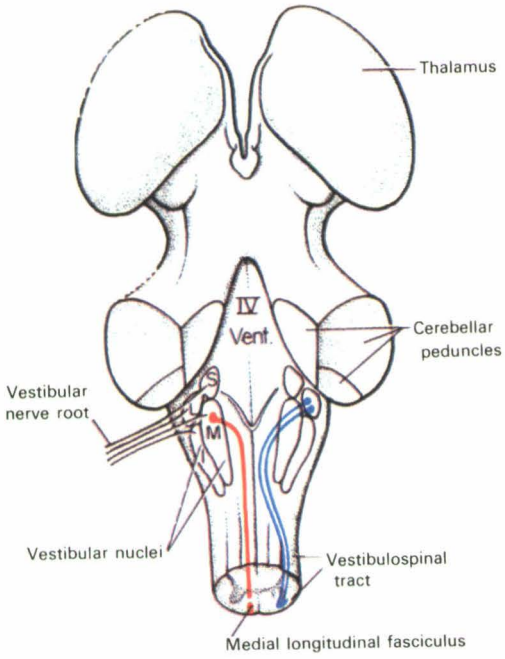


Figure 11.19. Spinal projections from the vestibular nuclei. The vestibulospinal tract (*blue*) arises only from cells of the lateral vestibular nucleus. This tract is uncrossed, somatotopically organized, and concerned with the facilitation of extensor muscle tone. Vestibular fibers descending in the medial longitudinal fasciculus (*red*) arise largely from the medial vestibular nucleus and are mainly uncrossed. *S*, indicates superior vestibular nucleus; *L*, indicates the lateral vestibular nucleus; and *I* and *M* indicate the inferior and medial vestibular nuclei.

both the pons and medulla. The four major nuclei of this complex (i.e., lateral, medial, superior, and inferior nuclei) (35) receive afferent fibers from the vestibular nerve and the cerebellum which are distributed differentially (Figs. 11.19, 11.21, and 13.18). The vestibulospinal tract, the principal descending spinal pathway from this complex, arises principally from the lateral vestibular nucleus (or Deiters' nucleus) (1, 33, 34, 41, 153). The *lateral vestibular nucleus* consists of a discrete collection of giant cells in the lateral part of the complex near the entry of the vestibular nerve root. Practically all cells of the lateral vestibular nucleus contribute fibers to the formation of this tract, which descends the length of the spinal cord in the anterior part of the lateral funiculus (Figs. 11.19–11.21).

The vestibulospinal tract, like the rubrospinal tract, is somatotopically organized (35, 181). Cells in dorsolateral parts of the vestibular nucleus project to lumbosacral spinal segments and cells in rostroventral regions project mainly to cervical spinal segments. Somatotopic features are somewhat blurred by the observation that fibers of the tract give off collaterals that innervate several spinal segments, particularly in the enlargements. The vestibulospinal tract has a three- to four-fold stronger influence on cervical

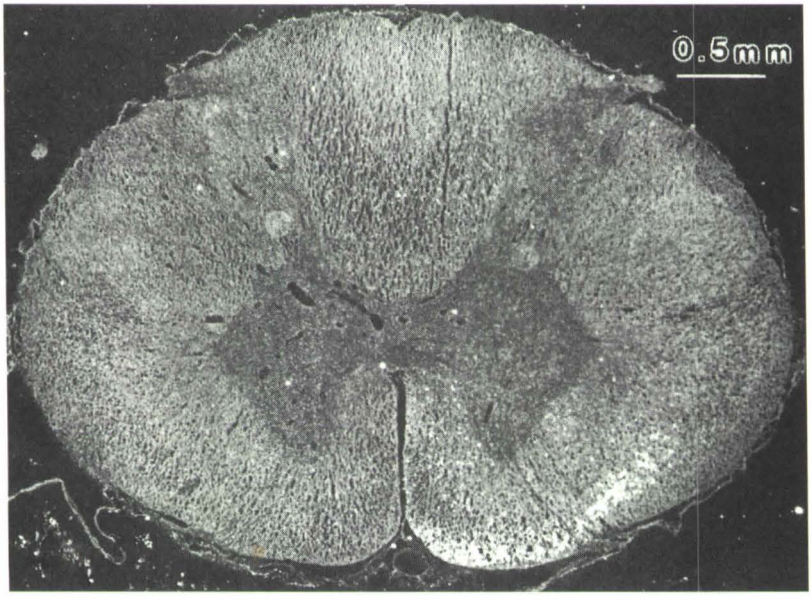


Figure 11.20. Section through the upper cervical spinal segments in a rhesus monkey demonstrating labeling of fibers (white area) in the vestibulospinal tract lying along the ventromedial border of the spinal cord. Autoradiographic tract-tracing method.

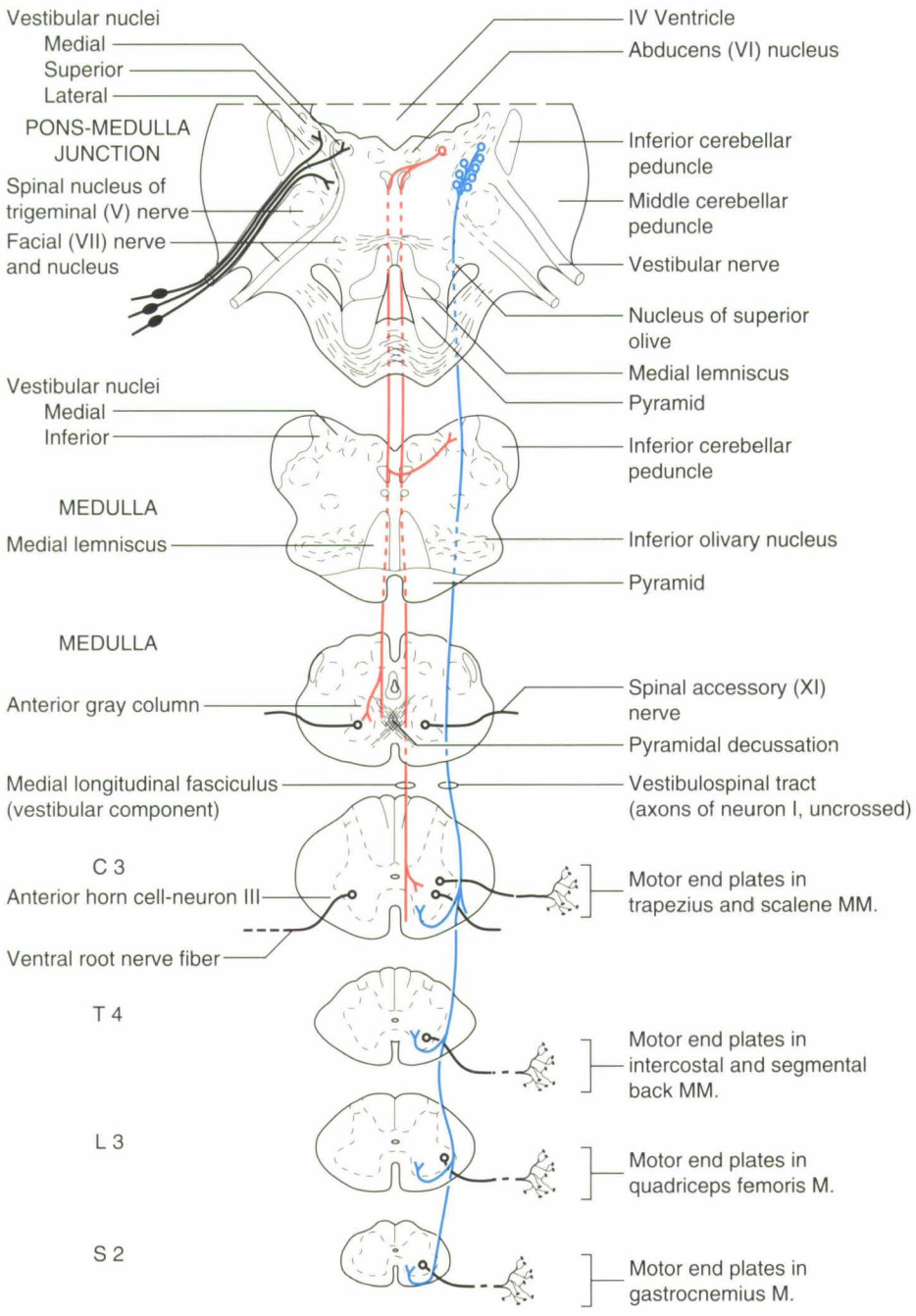


Figure 11.21. Vestibulospinal tract (*blue*) and descending vestibular fibers in the medial longitudinal fasciculus (*red*). Fibers of the vestibulospinal tract have a somatotopic origin in the lateral vestibular nucleus, descend the length of the spinal cord, and terminate predominantly in lamina VIII of Rexed. Descending vestibular fibers in the medial longitudinal fasciculus arise from the medial vestibular nucleus. In the lower brainstem, these fibers are bilateral, but in the cervical spinal cord they are ipsilateral. Letters and numbers indicate segmental spinal levels.

and lower lumbar segments than on thoracic spinal segments. Fibers of the vestibulospinal tract in cervical segments give off collaterals that enter laminae IX and adjacent parts of VII and VIII (153, 201). Synaptic contacts are made with interneurons and with proximal dendrites and somata of large motor neurons. Physiologic evidence indicates monosynaptic excitation of motor neurons in the lumbosacral region and direct connection with γ motor neurons.

Vestibular influences, and certain cerebellar influences, upon spinal cord activity are mediated by the vestibulospinal tract. Primary vestibular fibers terminate differentially and selectively upon cells in all four major divisions of the vestibular nuclear complex (208, 225). Projections to the lateral vestibular nucleus are restricted to its rostroventral part and represent predominantly input from the utricle. Electron microscopic findings indicate that primary vestibular fibers end upon perikarya and spines of proximal and distal dendrites of cells of all sizes in the lateral vestibular nucleus (144). The cerebellum provides a large number of afferent projections to the vestibular nuclear complex. These fibers are derived from (a) the "vestibular part" of the cerebellum (i.e., the nodulus, the uvula and the flocculus), (b) the fastigial nuclei, and (c) the anterior lobe of the cerebellum (143, 224, 227, 228). "Vestibular parts" of the cerebellum project fibers to regions of all vestibular nuclei in a pattern similar to that of primary vestibular fibers, except that the projection to the lateral vestibular nucleus is scant (33). Fastigial projections to the vestibular nuclei are crossed and uncrossed, nearly symmetric, and end mainly in ventral portions of the lateral and inferior vestibular nuclei (19). Cerebellovestibular fibers from the anterior lobe of the cerebellum, representing Purkinje cell axons, are somatotopically arranged and terminate only in dorsal parts of the lateral and inferior vestibular nuclei (143, 224). It is apparent that vestibular influences upon the spinal cord are mediated largely by the vestibulospinal tract.

The lateral vestibular nucleus exerts facilitatory influences upon the reflex activity of the spinal cord and spinal mechanisms which control muscle tone. This, perhaps, is best exemplified in experimental decerebrate animals by the reduction of rigidity which follows lesions in the lateral vestibular nucleus or interruption of the vestibulospinal tract in the spinal cord. It also has been shown that electrical stimulation of points in the lateral vestibular nucleus produces increases in extensor muscle tone which may be localized to forelimb or hindlimb, depending upon the position of the electrode within the nucleus (178). These physiologic findings confirm the anatomically described somatotopical origin of fibers in the lateral vestibular nucleus. Following stimulation of the lateral vestibular nucleus in the cat, excitatory postsynaptic potentials can be recorded intracellularly from extensor motor neurons, while the effects on flexor motor neurons are insignificant (197, 233). Excitatory vestibulospinal influences upon extensor muscles can be observed at rest and during locomotion (158). Stimulation of the lateral vestibular nucleus during locomotion enhances the activity of extensor muscles during the stance phase of the step. Modulation of vestibulospinal neurons with locomotor rhythm occurs only when the cerebellum is intact. Anatomic data suggest that these facilitatory effects are mediated both monosynaptically and disynaptically via interneurons in laminae VII and VIII that influence extensor α motor neurons, particularly those innervating limb muscles. The anterior lobe of the cerebellum inhibits neurons in the lateral vestibular nucleus and thus may exert a controlling influence upon labyrinthine activation.

Fibers from the medial vestibular nucleus project toward the midline and turn caudally in the *medial longitudinal fasciculus* of both sides. The fibers continue into the medial part of the anterior funiculus of the spinal cord. They influence cervical motor neurons so that the head moves in such a way as to assist in maintaining equilibrium and fixation of gaze. The medial longitudinal fasciculus is discussed in more detail later.

RETICULOSPINAL TRACTS

Two relatively large regions of the brainstem reticular formation give rise to fibers that descend to spinal levels. One of these regions is in the pontine tegmentum while the other lies in the medulla. Hence, it is proper to refer to these as the pontine and medullary reticulospinal tracts (Figs. 11.10 and 11.22).

The *pontine reticulospinal tract* arises from aggregations of cells in the medial pontine tegmentum referred to as the *nuclei reticularis pontis caudalis* and *oralis* (32, 34, 156, 213). The

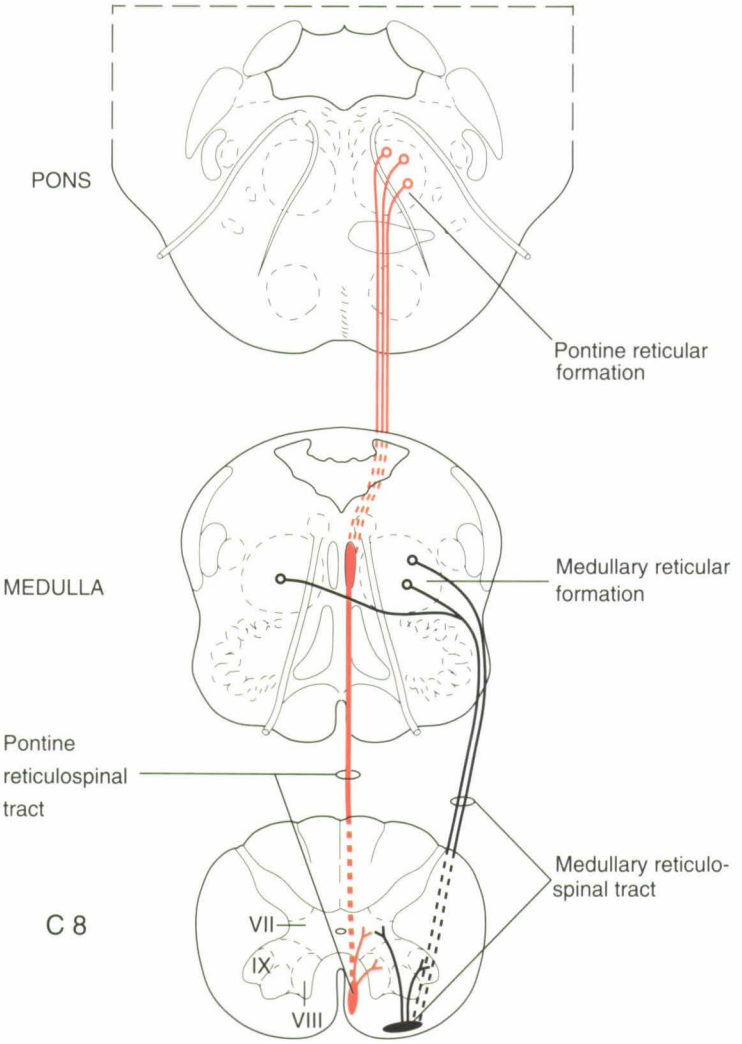


Figure 11.22. Reticulospinal tracts indicating their regions of origin, course, and terminations. Pontine reticulospinal fibers (*red*) terminate in lamina VIII and adjacent parts of lamina VII. Medullary reticulospinal fibers (*black*) terminate chiefly in laminae VII, but some end in lamina IX.

caudal pontine reticular nucleus begins in the caudal pontine tegmentum and extends rostrally to the level of the motor trigeminal nucleus. This nucleus contains a number of giant cells, in addition to various types of smaller cells. The oral pontine reticular nucleus occurs in more rostral parts of the medial pontine tegmentum and extends into the caudal mesencephalon. Giant cells are found only in the more caudal parts of this nucleus. Reticulospinal fibers arise from cells in all parts of the nucleus reticularis pontis caudalis, but only from the caudal part of the nucleus reticularis pontis oralis. More than half of the large cells in the caudal pontine reticular nucleus project fibers to spinal levels (213).

The pontine reticulospinal tract is almost entirely ipsilateral and descends chiefly in the medial part of the anterior funiculus (i.e., sulcomarginal area) (Fig. 11.22). Pontine reticulospinal fibers are more numerous than those arising in the medulla and descend the entire length of the spinal cord where they terminate in lamina VIII and adjacent parts of lamina VII (Fig. 11.22). A few pontine reticulospinal fibers cross at spinal levels in the anterior white commissure. A large proportion of pontine reticulospinal fibers give off collaterals to more than one level of the spinal cord, suggesting they are involved in activities at multiple spinal levels. Stimulation of the pontine reticulospinal pathway

evokes both monosynaptic and polysynaptic excitation of motor neurons supplying axial and limb muscles, with direct effects strongest upon axial muscles, particularly those in the neck.

The *medullary reticulospinal tract* arises from the medial two-thirds of the medullary reticular formation (32, 95). The largest number of fibers arise from the *nucleus reticularis gigantocellularis*, lying dorsal to the inferior olivary complex and lateral to the paramedian region (Fig. 11.22). As the name of this nucleus implies, it is composed of characteristic large cells, but, in addition, it contains many medium- and small-sized cells. Fibers of the medullary reticulospinal tract project bilaterally (both crossed and uncrossed) to spinal levels and mainly descend in the anterior part of the lateral funiculi (Figs. 11.10 and 11.22). Fibers crossing to the opposite side do so in the medulla (17) and are less numerous than uncrossed fibers. Some fibers of the medullary reticulospinal tract descend the entire length of the spinal cord. Reticulospinal fibers from the pons and medulla are not sharply segregated in the spinal cord. Medullary reticulospinal fibers terminate chiefly in lamina VII and, to a lesser extent, in laminae VIII and IX (17, 150, 151) (Fig. 11.22). Medullary reticulospinal fibers terminate in parts of the gray spinal laminae that also receive fibers from the rubrospinal and corticospinal tracts. Two components of the medullary reticulospinal tract have been identified physiologically: (a) long projections that provide collaterals to multiple spinal levels, and (b) short projections to cervical segments arising mainly from dorsolateral regions of the nucleus reticularis gigantocellularis.

Reticulospinal fibers, arising in both the pons and medulla, largely terminate upon the somata and dendrites of internuncial neurons, although some medullary projections end directly upon motor neurons. Most impulses from the reticular formation that influence γ motor neurons probably are mediated at segmental levels by internuncial neurons in laminae VII and VIII (67, 68). Anatomically, neither the pontine nor the medullary reticulospinal tract are somatotopically organized, although physiologic data suggest that localized regions of the pontine and medullary reticular formation may exert their major influence at particular spinal levels. Regions in which pontine reticulospinal fibers terminate are similar to those in which vestibulospinal fibers end; both of these systems are considered to convey facilitatory impulses. Likewise, medullary reticulospinal fibers terminate in portions of the spinal gray laminae that also receive fibers from corticospinal and rubrospinal tracts.

Experimental studies indicate that stimulation of the brainstem reticular formation can (a) facilitate or inhibit voluntary movement, cortically induced movement, and reflex activity; (b) influence muscle tone via the γ motor system; (c) affect phasic activities associated with respiration; (d) exert pressor or depressor effects on the circulatory system; and (e) exert facilitating and inhibiting influences on the central transmission of sensory impulses. Areas of the medullary reticular formation from which medullary reticulospinal fibers arise, correspond to regions from which inhibitory effects have been obtained (6, 32, 171, 172, 213). Facilitatory effects are obtained from far larger rostral regions of the reticular formation. The reticular formation can influence muscle tone by acting upon γ motor neurons, which innervate the contractile portions of the muscle spindle (68, 74). It is largely by this mechanism that the reticulospinal systems modify tendon reflex activity.

The brainstem reticular formation receives inputs from many sources, but direct corticoreticular projections are particularly abundant. Corticoreticular fibers arise from widespread areas of the cortex although the greatest number originate from the "motor area." These fibers terminate in two fairly restricted regions of the reticular formation, one in the pons and one in the medulla (192). Corticoreticular fibers are distributed bilaterally with some crossed preponderance. The termination within the reticular formation corresponds to those regions that give rise to the reticulospinal tract. Thus, the synaptic linkage of corticoreticular and reticulospinal fibers forms a pathway from the cortex to spinal levels. There is no evidence of a somatotopic arrangement within this system (32), whose function is examined in Chapters 12 and 13.

MEDIAL LONGITUDINAL FASCICULUS

The posterior part of the anterior funiculus contains a composite bundle of descending fibers that originates from different nuclei at

various brainstem levels. This composite bundle is known as the *medial longitudinal fasciculus* (MLF). Spinal portions of this bundle represent only a part of the brainstem tract designated by the same name. Descending fibers in the spinal medial longitudinal fasciculus arise from the medial and inferior vestibular nuclei (vestibulospinal fibers), the pontine reticular formation (reticulospinal fibers), the superior colliculus (tectospinal fibers), and the interstitial nucleus of Ramón y Cajal (interstitiospinal fibers). The medial longitudinal fasciculus forms a well-defined tract only in cervical spinal segments, but component fiber systems have been shown to descend to sacral levels (Figs. 11.19, 11.21, and 11.25). Fibers arising from the medial vestibular nucleus are predominantly ipsilateral in the spinal cord and terminate upon portions of laminae VII and VIII (33, 43, 124, 149). Physiologic studies suggest that these fibers convey monosynaptic inhibitory influences directly to upper cervical motor neurons (2, 235). This unusual direct pathway appears to play a role in the labyrinthine regulation of head position. The largest component of the spinal medial longitudinal fasciculus, the pontine reticulospinal tract, was described earlier (Fig. 11.22). The interstitiospinal tract arises from a small mesencephalic nucleus lateral to the medial longitudinal fasciculus and oculomotor complex. Fibers of this tract terminate in parts of laminae VII and VIII at all spinal levels. Fibers of the interstitiospinal tract are uncrossed, descend in the most posterior part of the anterior funiculus near the anteromedian fissure, and terminate in dorsal parts of lamina VIII and neighboring parts of lamina VII (151, 207).

FASTIGIOSPINAL FIBERS

Although the cerebellum has been considered to exert its influences upon spinal activities solely via relay nuclei in the brainstem, some evidence suggests that one of the deep cerebellar nuclei projects directly to cervical spinal levels (19, 72, 130, 212, 234). Fastigiospinal fibers arise from cells in all parts of the fastigial nucleus, cross the midline within the cerebellum and emerge via the uncinate fasciculus. Fibers descend ventral to the spinal trigeminal tract and are partially intermingled with fibers of the vestibulospinal tract at some levels. In the spinal cord, fibers descending in the ventral part of the lateral funiculus, project into the anterior gray horn. In the cat these fibers have been identified as far caudally as lower cervical spinal segments (234). Fastigial neurons projecting contralaterally to cervical spinal segments can be activated by labyrinthine and somatic stimuli, but the significance of this pathway in motor control remains unknown.

Autonomic Pathways

The spinal cord contains descending autonomic fibers that terminate upon visceral cell groups (i.e., intermediolateral cell column and sacral preganglionic cell groups) that innervate smooth muscle, cardiac muscle, and body viscera. The principal nuclei giving rise to descending autonomic fibers are (a) several regions of the hypothalamus, (b) visceral nuclei of the oculomotor complex, (c) the locus coeruleus and adjacent areas, and (d) portions of the nucleus of the solitary tract (Fig. 11.23). Additionally, some neurons in the reticular formation are concerned with visceral activities. These include some noradrenergic neuronal groups in the ventrolateral regions of the medulla and pons that receive inputs from rostral autonomic structures and project fibers to the spinal cord via a relay in the reticular formation. Hypothalamic neurons projecting to spinal levels include cells in (a) paraventricular nucleus, (b) lateral and posterior hypothalamic areas, (c) supramammillary nucleus, and (d) dorsomedian nucleus (94, 107, 195). Fibers from these hypothalamic nuclei project to visceral nuclei in the medulla as well as to the spinal cord (Fig. 11.23). Direct hypothalamic-spinal fibers descend in the lateral funiculus and terminate upon cells of the intermediolateral cell column in thoracic, lumbar, and sacral segments. These uncrossed fibers appear to directly influence preganglionic sympathetic and parasympathetic neurons. It should be noted that hypothalamic regions giving rise to spinal projections receive, in turn, a significant input from cells scattered in the spinal cord (23, 47, 93).

Although the visceral nuclei of the oculomotor complex project large numbers of preganglionic parasympathetic fibers into the third nerve, these neurons also project directly to spinal levels (120, 121, 195). Descending fibers from the Edinger-Westphal nucleus contribute fibers to the posterior col-

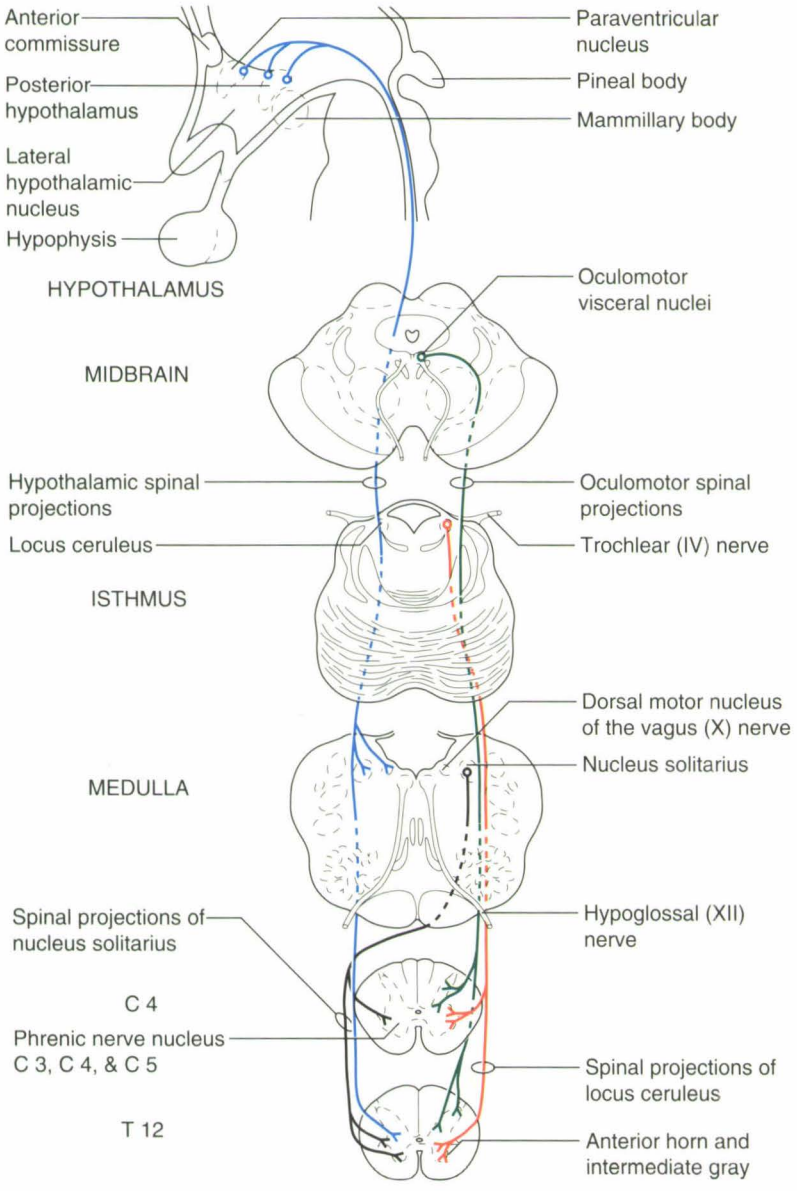


Figure 11.23. Descending autonomic projections to spinal cord. Projections from hypothalamic nuclei (parvicellular paraventricular nucleus, lateral and posterior hypothalamic areas) descend to terminate upon cells of the ipsilateral intermediolateral column in thoracic and upper lumbar spinal segments (*blue*). Hypothalamic nuclei are shown in a sagittal plane. Parasympathetic visceral neurons in the oculomotor supply intrinsic ocular structures and project fibers to the spinal cord that terminate in parts of laminae I and V (*green*). At isthmus levels, cells of the pigmented locus coeruleus give rise to descending noradrenergic fibers that reach the spinal cord and terminate in parts in the anterior horn and the intermediate gray (*red*). Cells in the ventrolateral part of the nucleus solitarius project crossed fibers to the phrenic nucleus (C3, C4, and C5) and to parts of the anterior horn in thoracic and spinal segments (*black*). Noradrenergic projections to the spinal cord from the ventrolateral pontine tegmentum (cell group A5) are shown in Figure 11.24.

umn nuclei and spinal projections that descend to lumbar levels (Fig. 11.23). In the spinal cord, these fibers course in the lateral funiculus and terminate in lamina I and parts of lamina V (121). It has been suggested that these descending spinal projections may modulate sensory input, especially that related to nociceptive stimuli.

Cells in the ventrolateral part of the solitary nucleus (Fig. 11.23) project to cervical and thoracic spinal segments (117). The solitariospinal tract is predominantly crossed

and terminates in the region of the phrenic motor neurons at C3-C5 levels and the anterior horn and intermediolateral cell column at thoracic levels (Fig. 10.21). Fibers of this tract provide excitatory inputs to phrenic and inspiratory motor neurons (45, 63, 65, 209).

Descending reticulospinal tracts that originate in regions of medullary and pontine reticular formation concerned with respiratory and cardiovascular control are also part of the autonomic pathways to the spinal cord (see Chapters 12 and 13).

Monoaminergic Systems

SEROTONINERGIC PROJECTIONS

Brainstem neurons which utilize serotonin (5-hydroxytryptamine, 5-HT) as a transmitter and project to the spinal cord are largely confined to nuclei raphe pallidus, obscurus and magnus in the caudal medulla (27). These nuclei correspond respectively to groups B1, B2, and B3 in the nomenclature of Dahlström and Fuxe (62). Additionally, axonal branches of a limited number of serotoninergic neurons in the dorsal raphe nucleus (group B7) and adjacent midbrain reticular formation also reach the cervical part of the spinal cord (28). The serotoninergic fibers originating in these nuclei descend principally in the lateral funiculus and arborize along the entire length of the spinal cord and in both the anterior (ventral) and posterior (dorsal) horn (17, 28, 147). In the posterior horn, serotoninergic fibers arborize more profusely in laminae I and II than in other laminae, and this dense innervation is particularly obvious at the levels of cervical and lumbar enlargements (147). In the anterior horn, a dense plexus of serotoninergic fibers occurs at the levels of the medial and lateral motor neuronal groups (lamina IX). These fibers form close pericellular contacts with the somata and proximal dendrites of the large motor neurons (101). In the intermediate gray of the spinal cord, serotoninergic fibers profusely arborize around, and synaptically contact sympathetic preganglionic neurons of the intermediolateral column (14).

In the lower medulla, serotoninergic neurons projecting to the spinal cord are intermingled with several other spinally-projecting neurons that contain different neurotransmitters. This chemically heterogeneous population of spinally-projecting cells comprises neurons that contain (a) amino acids, such as glycine (84), GABA (90, 91), aspartate, and glutamate (146), and (b) neuroactive peptides, such as thyrotropin releasing hormone (TRH) and substance P (11, 146). Furthermore, serotoninergic medullary raphe neurons that project to the spinal cord are known to coexpress several of these amino acids or neuroactive peptides.

The descending serotoninergic projections are believed to be involved in several spinal cord functions, such as control of motor neurons and autonomic activities (51), and modulation of pain (16, 18, 184).

CATECHOLAMINERGIC PROJECTIONS

A small pigmented nucleus in the upper pons, known as the locus coeruleus (Figs. 13.33–13.35) was demonstrated to synthesize, store, and release the neurotransmitter norepinephrine (also termed noradrenaline) (49). This relatively small nucleus, which corresponds to the catecholaminergic group A6 of Dahlström and Fuxe (62), distributes fibers widely in the neuraxis and is regarded as a principal source of norepinephrine. Data based upon axonal transport methods combined with immunocytochemistry brings detailed information on the organization of noradrenergic projections to the spinal cord. Noradrenergic fibers from the locus coeruleus and its ventral extension, the subcoeruleus area (group A6v), descend in the anterior and lateral funiculi, are largely uncrossed, and arborize in the anterior horn and the ventral half of the posterior horn (laminae IV, V, and VI) (Fig. 11.23) (154, 170, 185, 204, 230, 231). A large proportion of the coeruleospinal neurons in the cat coexpress the opiate peptide methionine-enkephalin (239). The noradrenergic cells of the locus coeruleus complex do not appear to project to the intermediolateral column (154, 231). In the anterior horn, noradrenergic coeruleospinal fibers form conventional synapses upon motor neurons (85) and are believed to augment the somatomotor output, at least in part, via an α-1-adrenoreceptor-mediated excitation of motor neurons (71).

Two other noradrenergic cell groups, one in the caudolateral portion of the pontine tegmentum (group A7) and the other in the ventrolateral region of the medullary reticular formation (group A5), give rise to fibers that descend to the spinal cord. Noradrenergic fibers from the A5 group form the *lateral*

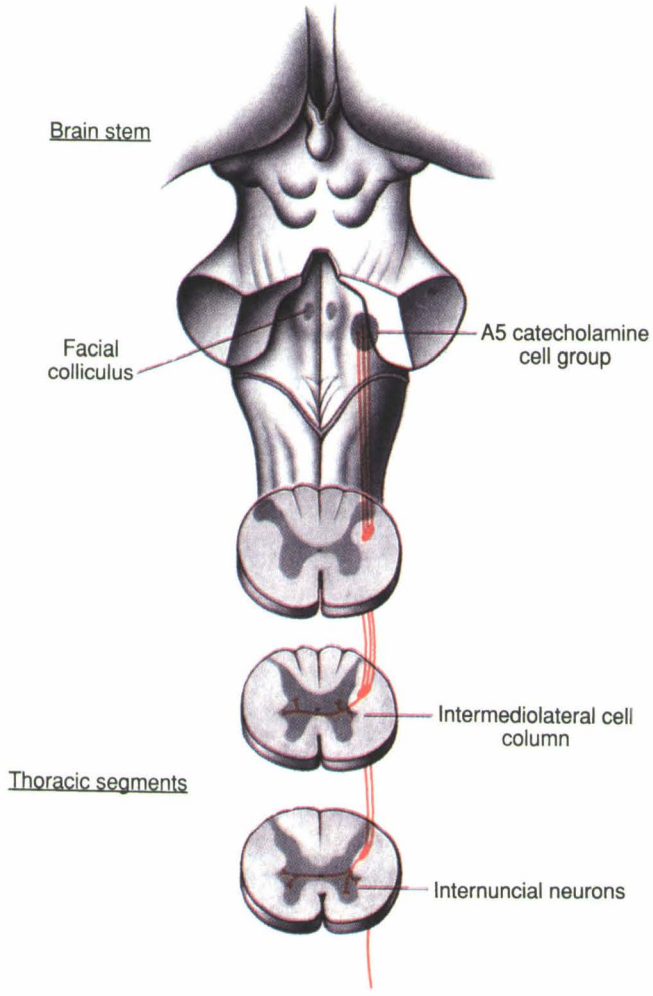


Figure 11.24. Spinal projections from the pontine catecholamine cell group A5. Noradrenergic fibers from this cell group descend ipsilaterally, but are distributed bilaterally to the intermediolateral cell column and internuncial neurons in thoracic spinal segments. Preganglionic and postganglionic sympathetic fibers project to the cardiovascular system.

tegmental system, which directly innervates cells of the intermediolateral column (46, 119, 122) (Fig. 11.24). Electrical stimulation of this neuronal group produces marked increases in arterial blood pressure (118). This nucleus is considered as part of a brainstem vasomotor center, whose effects on sympathetic preganglionic motor neurons are mediated via a noradrenergic synapse upon cells in the intermediolateral column (Fig. 11.24). In contrast, neurons of group A7 provide the major noradrenergic innervation of laminae I to IV in the posterior horn. Electrical stimulation of this nucleus has an antinociceptive effect that is mediated by spinally projecting noradrenergic neurons (237). These findings indicate that pontospinal noradrenergic neurons in the A7 group are important components of the descending neuronal system that modulates nociception (40, 89).

Other catecholaminergic inputs to the spinal cord derive from a group of adrenaline-producing neurons located in the ventrolateral portion of the caudal medulla and termed group C1 by Hökfelt and colleagues (82). These neurons project massively to cells of the intermediolateral column (83, 88), but their function remains unknown.

INTRINSIC SPINAL FIBERS

A certain number of dorsal root afferent fibers make monosynaptic connections with anterior horn cells (70, 81, 206). In most in-

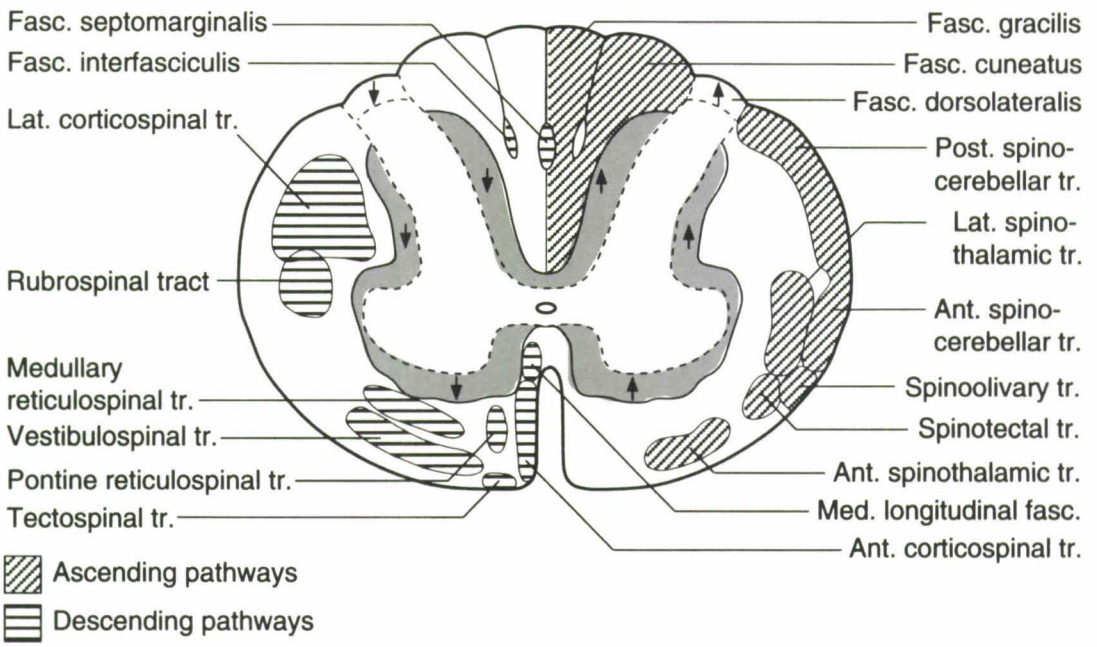


Figure 11.25. Ascending and descending pathways of the spinal cord. Two different types of *hatched areas* are used to differentiate ascending from descending pathways. The fasciculus proprius system (*shaded areas*) and dorsolateral fasciculus contain both ascending and descending nerve fibers.

stances, however, these first afferents synapse on central or internuncial neurons (interneurons) interposed between the afferent and efferent neurons. These interneurons then send their axons to the motor cells of the same segment, or to higher and lower segments, for the completion of various intersegmental reflex arcs. Axons of spinal interneurons ascend or descend in the white columns of the same side, or pass to the white matter of the opposite side. All these ascending and descending fibers, crossed and uncrossed, which begin and end in the spinal cord and connect its various levels, constitute the *fasciculi proprii* or *spinospinal fasciculi* of the spinal cord (Figs. 10.7 and 11.25). Long descending axons arise ipsilaterally from lamina I and bilaterally from laminae V, VII and VIII (131). The largest number of long descending fibers arise from cells in laminae VII and VIII. Fibers crossing to the opposite side decussate at levels of cell origin. Descending branches of axons in lamina I may be implicated in modulation of sensory input, while neurons in laminae VII and VIII may influence motor neurons at more caudal levels of the spinal cord.

The descending root fibers of the interfascicular and septomarginal bundles and the collaterals, and many terminals of ascending dorsal root fibers are also part of the spinospinal fiber system. Impulses entering the cord at any segment may travel along these fibers to higher or lower levels before synapsing directly or through internuncial neurons with the anterior horn cells (Fig. 10.24). These shorter fiber systems forming part of the intrinsic reflex mechanism of the spinal cord are of major importance in a variety of reflexes. Most long and myelinated spinospinal fibers are found in the interfascicular and septomarginal bundles, whereas unmyelinated, or group C, axons and some thin group A myelinated spinospinal axons occur in the *dorsolateral tract* (or *Lissauer's tract*).

The spinospinal fibers are found in all funiculi—posterior, anterior, and lateral. They occupy the area adjacent to the gray matter and lie between the gray matter and the peripherally placed long tracts. They are most numerous in the anterolateral white columns. In the posterior funiculus, they form a narrow zone along the posterior commissure and adjacent portions of the posterior horn. In general, the shortest fibers lie nearest the gray matter and connect adjacent segments while the longer fibers lie more peripherally. These tracts and the major ascending and de-

scending spinal pathways are diagrammed in Figure 11.25.

UPPER AND LOWER MOTOR NEURONS

One of the most important concepts in neurologic diagnosis rests upon distinguishing the abnormalities of motor function which result from pathologic involvement of, or injury to, the upper or lower motor neuron. This relatively simple, yet frequently puzzling, distinction forms one of the cornerstones of clinical neurology. The ability to distinguish upper and lower motor neuron lesions constitutes the first step in attempting to localize the site of a neural lesion that manifests itself by disturbances of normal motor function. Once the site of the neural lesion has been established, the clinician can begin to consider the pathologic processes which might be responsible (42).

Lower Motor Neurons

The anterior horn cells are regarded as the prototype for all motor neurons. These cells and their axons, which project via the ventral root to striated muscle, constitute the anatomic and physiologic unit commonly referred to as the final common motor pathway or the lower motor neuron. The concept of the lower motor neuron is not limited to the spinal cord, even though it is most frequently used in that context. Cells of the motor cranial nerve nuclei (N. III, IV, V, VI, VII, IX, X, XI, and XII), which provide innervation for skeletal muscles of the head and neck, also must be classified as lower motor neurons, even though these nuclei form discontinuous cell columns in the brainstem.

The segmental input to the lower motor neuron is profuse, both direct and indirect, and largely, but not exclusively, ipsilateral. Muscle spindle afferents (group Ia) project directly to the lower motor neuron (Figs. 10.23 and 10.30), while afferents from most other receptors, including the Golgi tendon organ (Fig. 10.30), influence the lower motor neuron indirectly via internuncial neurons. Afferent inputs from stretch receptors (i.e., muscle spindle and Golgi tendon organ) activate ipsilateral cell groups in the spinal cord, while afferent impulses from other sensory receptors are distributed by multisynaptic circuits to both sides of the spinal cord. The lower motor neuron also is under powerful indirect suprasegmental control by impulses transmitted via descending spinal systems (Fig. 11.25).

Injury or disease of the anterior horn cells or their projecting axons results in weakness or paralysis of the muscles innervated by these fibers, loss of muscle tone, and prompt atrophy of the denervated muscle. *Weakness* or *paralysis*, occurring in affected muscles, bears a direct relationship to the extent and severity of the lesion. Since the anterior horn cells that innervate a single muscle extend longitudinally through several spinal segments, and since several such cell columns exist at each spinal level, a lesion confined to one spinal segment will cause weakness, but not complete paralysis, in all muscles innervated by this segment. Complete paralysis will occur only when the lesion involves the column of cells in several spinal segments that innervate a particular muscle, or the ventral root fibers that arise from these cells. Because most of the appendicular muscles are innervated by fibers arising from parts of three spinal segments, complete paralysis of a muscle resulting from a central lesion in the anterior horn indicates involvement of several spinal segments. Furthermore, because neighboring cell columns are likely to be affected at each level, such a lesion usually produces paralysis in muscle groups, rather than in individual muscles.

Since the lower motor neuron consists of the anterior horn cells and their axons, which innervate striated muscle, it becomes necessary to distinguish the motor deficits that occur as a consequence of lesions in spinal segments from those which occur in ventral roots, spinal nerves and peripheral nerves. A lesion in ventral root fibers usually produces motor deficits similar to those resulting from destruction of anterior horn cells. At certain levels (i.e., thoracolumbar and sacral), section of the ventral root fibers produces additional autonomic deficits, which might not accompany anterior horn cell lesions at the same level (Fig. 11.26). Lesions of mixed spinal nerves produce motor and sensory deficits that correspond to those of combined dorsal and ventral root lesions. While the motor deficit corresponds almost exactly to that seen with pure lesions of the ventral root, sensory disturbances and loss follow a dermatomal distribution and tend to be less extensive because of overlapping innervation characteristic of dermatomes (Figs. 8.10–8.12).

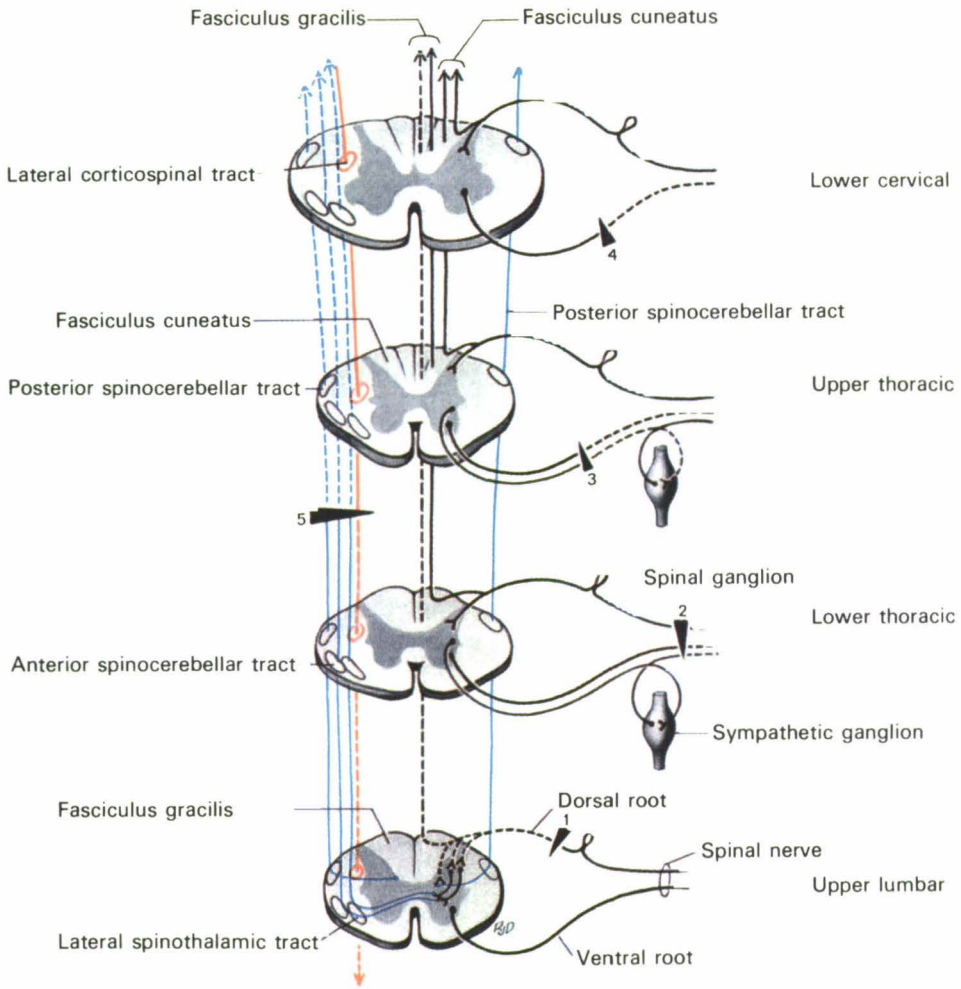


Figure 11.26. Degeneration resulting from certain lesions of the spinal nerves, spinal roots, and spinal cord. Sites of lesions are indicated by *small black wedges*. Dorsal and ventral root fibers, peripheral nerve fibers, fibers in the posterior white columns and short relays are in *black*; ascending spinal tracts are *blue*; and the corticospinal tract is *red*. A lesion of the dorsal root, *1*, at upper lumbar levels produces degeneration (*dashed lines*) in the posterior and anterior gray horns (not shown) and in parts of the fasciculus gracilis. No degeneration is present in other ascending spinal tracts because degeneration does not pass beyond the synapse. A lesion of a spinal nerve as at *2* produces peripheral degeneration (*dashed lines*) in somatic motor, sensory, and postganglionic sympathetic fibers. A lesion of the ventral root at site *3* produces degeneration in somatic motor and preganglionic sympathetic fibers. A lesion at *4* produces degeneration only in somatic motor fibers distal to the lesion. The lesion at *5* destroys the lateral funiculus and produces ascending degeneration (*dashed lines*) in the posterior and anterior spinocerebellar tracts (*blue*) and in the spinothalamic tracts (only the lateral spinothalamic tract (*blue*) is shown here) above the level of the lesion. This lesion also produces descending degeneration in the corticospinal tract (*red*) below the level of the lesion. Although other spinal tracts which would degenerate are not indicated, the same principle applies.

With a peripheral nerve lesion, the muscle paralysis and sensory loss correspond to the distribution of the particular nerve (Figs. 8.11 and 8.12).

Loss of muscle tone, *hypotonia*, is a characteristic and constant finding in lower motor neuron lesions. Flaccidity of the affected muscles is evidenced by greatly diminished resistance to passive movement. This reduction in muscle tone results from the withdrawal of streams of impulses transmitted to muscles that normally maintain a state of variable, but sometimes sustained, contraction in some of the muscle units. Reflexes in the affected muscles are diminished or lost *(areflexia)* in lower motor neuron lesions because the reflex arc is interrupted (Fig. 10.30). In this type of lesion, the effector mechanism is destroyed.

Although paralysis, hypotonia, and are-

flexia occur almost immediately following a lower motor neuron lesion, atrophy or muscle wasting does not become evident for 2 or 3 weeks. *Muscle atrophy* develops gradually, and in time is obvious on inspection. Why muscles deprived of their innervation atrophy and degenerate is not adequately understood. It seems likely that the morphologic and functional properties of muscle are dependent upon transmitter substances provided by the terminals of motor nerve fibers. Atrophy, of the type seen in lower motor neuron disease, does not result from depriving anterior horn cells of afferent impulses from either suprasegmental or segmental levels (214).

In certain diseases of the lower motor neuron, the muscles exhibit small, localized, spontaneous contractions known as *fasciculations*. These muscle twitches, visible through the skin, represent the discharge of groups of muscle fibers innervated by nerve fibers arising from a single lower motor neuron. Fasciculations occur asynchronously in different parts of various muscles and are thought to be due to a triggering of motor unit discharges that occur within the cell body of the motor neuron. Fasciculations of this type are interpreted as a disease process attacking the lower motor neurons in the anterior gray horn. Fasciculations commonly are seen in amyotrophic lateral sclerosis, occasionally in acute inflammatory lesions of peripheral nerves, but rarely when anterior horn cells are rapidly injured or destroyed, such as in acute poliomyelitis.

The term *fibrillation*, frequently misused as the equivalent of the term fasciculation refers to the small (10–200 μV) potentials of 1–2 msec duration that occur irregularly and asynchronously in electromyograms of denervated muscle. These spontaneous discharges cannot be observed through the skin and produce no detectable shortening of muscles.

Upper Motor Neurons

All of the descending fiber systems that can influence and modify the activity of the lower motor neuron constitute the system of upper motor neurons (Fig. 11.25). This is a more inclusive definition than that used by many clinicians who equate upper motor neurons solely with the corticospinal system. The narrower concept has become a rule of thumb because of the overwhelming clinical importance of the corticospinal system and the previously poorly defined functional influences of descending nonpyramidal fiber systems. Recent anatomic and physiologic data concerning descending nonpyramidal fiber systems make it necessary to modify this venerable rule of thumb and to consider the concept of the upper motor neuron in its broadest sense. Descending impulses, transmitted to spinal levels by a group of heterogeneous tracts, are concerned mainly with (a) mediation of somatic motor activity, (b) control of muscle tone (c) maintenance of posture and equilibrium, (d) suprasegmental control of reflex activity, (e) control of visceral and autonomic activities, and (f) modification of sensory input.

Lesions involving upper motor neurons, at a wide variety of locations and resulting from many different kinds of pathologic processes, produce paralysis, alterations of muscle tone, and reflex activity. Lesions destroying upper motor neurons are rarely selective, usually incomplete, and frequently involve adjacent pathways and nuclear structures. The degree of *paresis* (i.e., incomplete loss of muscle power) or paralysis does not bear a direct relationship to the size of the lesion, or to the extent of involvement of the corticospinal tract (110). Destruction of upper motor neurons may result from vascular disease, trauma, neoplasm, and infectious and degenerative diseases. Unilateral lesions in the cerebral hemisphere and brainstem produce contralateral paralysis, usually hemiplegia. Spinal lesions, most commonly the result of trauma, are usually bilateral, and either result in paraplegia or quadriplegia, depending upon the cord level involved.

Immediately after an upper motor neuron lesion in the cerebral hemisphere or brainstem, the paralyzed limbs contralateral to the lesion usually are flaccid and the myotatic reflexes are depressed or absent. After variable periods, the myotatic reflexes reappear in an exaggerated form in the paralyzed limbs. The superficial abdominal reflexes, elicited by stroking the skin over the abdomen, and the cremasteric reflexes in the male, disappear on the side of the paralysis. The plantar response, elicited by stroking the sole of the foot, becomes extensor (Babinski sign).

After a variable period of time, muscle tone in the affected limb gradually returns and ultimately exceeds that of the normal side. This exaggeration of muscle tone is referred to as *hypertonicity* or *spasticity*. The in-

crease in tone is not exhibited by all muscles of the affected limbs. Spasticity selectively involves the antigravity muscles. In the affected upper extremity, spasticity is present particularly in the adductors and internal rotators of the shoulder, in the flexors of the elbow, wrist, and digits, and in the pronators of the forearm. In the affected lower extremity, spasticity develops in the adductors of the hip, the extensors of the hip and knee, and in the plantar-flexors of foot and toes. *Spasticity* is relatively easy to describe but extremely difficult to define. Descriptively, spasticity is characterized by (a) increased resistance to passive movement, (b) extraordinarily hyperactive myotatic (deep tendon) reflexes that exhibit a low threshold, a large amplitude, an enlarged reflexogenous zone, and a briskness much greater than normal, and (c) the presence of clonus (125). *Clonus* is a manifestation of the exaggerated stretch reflex in which the contractions of one muscle group are sufficient to stretch antagonistic muscle groups and initiate myotatic responses in that muscle group. Clonus has a tendency to perpetuate itself in a synchronized manner. In some instances, the threshold for this extreme exaggeration of the myotatic reflex is so low that passively moving a limb may initiate it.

The paralysis, which may appear complete at the onset of an upper motor neuron lesion, tends to become less severe in time. Even the weakness tends ultimately to involve one limb more than the other. The motor functions affected most are those associated with fine, skilled movements. Gross movements, and those which involve a whole limb, are least affected and show considerable restitution. Atrophy of the type seen with lesions of the lower motor neuron does not occur with upper motor neuron lesions. However, after a period of years some atrophy of disuse becomes evident.

Many hemiplegic patients, in time, recover considerable motor function. Those that become ambulatory have a characteristic gait. The paralyzed leg is circumducted at the hip *en bloc* and swung forward, because of the difficulty in flexing the knee. The foot is plantar-flexed and the toe of the shoe is dragged in a characteristic circular fashion. The arm on the affected side is flexed at the elbow and wrist, the forearm is pronated, and the digits are flexed. The arm usually is held close to the body, but if the arm is swung at all in walking, it moves primarily at the shoulder. Upper motor neuron syndromes resulting from unilateral lesions in the brainstem or cerebral hemisphere produce contralateral disturbances of motor function. Unilateral brainstem lesions involving upper motor neurons frequently damage motor cranial nerves on the side of the lesion.

The concept of the upper and lower motor neuron constitute one of the basic corner stones of clinical neurology and the simple distinctions outlined above must be considered in the neurologic examination of every patient.

LESIONS OF THE SPINAL CORD AND NERVE ROOTS

Determination of the origin, course, and termination of most spinal cord pathways from the study of normal Weigert- and Nissl-stained sections is virtually impossible, but such preparations provide valuable information concerning spinal cord organization and cytoarchitecture. Secondary or Wallerian degeneration in nerve fibers (severe from cell bodies), studied in sections stained by the Marchi, Nauta, or other silver impregnation techniques, provided valuable information concerning the course and termination of fiber bundles in human materials (Fig. 11.26). Lesions in nerve fibers also produce alteration of the cell bodies giving rise to these fibers, and these changes can be detected in Nissl-stained sections within a few days. These cell changes, referred to as retrograde cell changes, are characterized by swelling and distortion of the perikaryon, eccentrically placed nuclei, and dissolution of Nissl substance. Retrograde cellular changes provide precise data concerning the cell of origin of particular fiber bundles. The most convincing data concerning spinal pathways, however, have been derived from tract-tracing studies undertaken in animals. These investigations were made possible with the advent of methods principally based on the physiologic principle of axoplasmic flow. The various neurobiologic tools currently available for studying neuronal morphology and connections were described in Chapter 5.

Root Lesions

DORSAL ROOT LESIONS

Section of the dorsal roots (dorsal rhizotomy) abolishes all input supplied by these roots and interrupts segmental reflex arcs

(Fig. 11.26). Because of extensive overlap of dermatomes in the periphery, destruction of one dorsal root does not result in detectable sensory loss. If multiple dorsal roots are sectioned, for example C5 to T1, cutaneous sensibility will be lost (anesthesia) or greatly impaired (hypoesthesia), in the C6, C7, and C8 dermatomes, but input from stretch receptors entering all five dorsal roots will be abolished. As a consequence, muscle tone and myotatic reflexes will be absent in most of the muscles of the upper extremity. Although the muscles can be contracted because the ventral root remains intact, the deafferented extremity is virtually useless due to loss of cutaneous and kinesthetic sense. Monkeys with such rhizotomies do not use the deafferented limb for walking, climbing, or grasping (142, 157, 219).

Spinal cord degeneration resulting from multiple dorsal rhizotomies (C5 to T1) is distributed more profusely at the level of the sectioned roots to portions of the posterior horn, to selected cell groups within lamina VII, and parts of lamina IX. Particularly profuse ascending and descending degeneration is present in the ipsilateral fasciculus cuneatus. No ascending degeneration is present in other ascending spinal tracts, because these tracts arise from cell groups within the spinal cord. In other words, degeneration is limited to the primary afferent fibers and does not involve intrinsic spinal neurons or their processes. A representation of degeneration resulting from section of a single lumbar dorsal root is shown at *1* in Figure 11.26.

VENTRAL ROOT LESIONS

Injury or section of the ventral root produces a lower motor neuron paralysis of the muscle units innervated by the particular root (*4*, in Fig. 11.26). If the lesion involved thoracic or upper lumbar ventral roots, preganglionic sympathetic fibers also would be interrupted (*3*, in Fig. 11.26). Thus, destruction of the C8 spinal ventral root would partly paralyze the small muscles of the hand (via median and ulnar nerves), whereas a lesion of both ventral roots C8 and T1 would produce a complete flaccid paralysis and atrophy of these muscles (Fig. 8.17). The inclusion of ventral root T1 in the injury would also interrupt many of the preganglionic visceral efferent fibers en route to the superior cervical sympathetic ganglion (Figs. 10.23 and 11.30). Loss of these visceral motor fibers to the smooth muscle of the eye and levator palpebrae muscle results in a triad of clinical symptoms known as *Horner's syndrome* (Chapter 9). This syndrome usually is accompanied by altered sweating on the face. In such a case, secondary (Wallerian) degeneration results in somatic and visceral efferent fibers; postganglionic neurons and their processes remain intact.

If a mixed nerve is injured distal to the junction of the dorsal and ventral root (*2*, in Fig. 11.26), the combined sensory and motor losses enumerated earlier will be present. It should be noted that if such combined nerve lesions are extensive, they may be followed by trophic changes in the skin (smoothness, dryness) and in capillary circulation (cyanosis). These trophic alterations presumably are due to the loss of peripheral vasomotor and afferent nerve fibers.

Spinal Cord Transection

COMPLETE SPINAL CORD TRANSECTION

Such a transection results in immediate loss of all neural functions below the level of the lesion. There is a complete loss below the level of the lesion of (a) all somatic sensation, (b) all motor function, (c) all visceral sensation, (d) all reflex activity, (e) all muscle tone, and (f) thermoregulatory control. This complete cessation of all neural function in the isolated spinal cord caudal to the lesion is called *spinal shock* and persists for 1–6 weeks (average 3 weeks) in humans. The termination of the period of spinal shock is heralded by the appearance of the Babinski sign. A fairly orderly sequence of events follows which vary in duration. The various phases involved in the recovery of function in the isolated human spinal cord have been carefully analyzed (103). These phases in recovery of neural function are (a) minimal reflex activity (3–6 weeks), (b) flexor spasms (6–16 weeks), (c) alternate flexor and extensor spasms (after 4 months), and (d) predominant extensor spasms (after 6 months). The phase of minimal reflex activity is characterized by weak flexor responses to nociceptive stimuli, which begin distally and progressively involve proximal muscle groups in the extremities. During this period the Babinski sign can be obtained bilaterally, but the muscles are flaccid and the deep tendon reflexes cannot be elicited.

The phase of *flexor muscle spasms* is charac-

terized by increasing tone in the flexor muscles and by stronger flexor responses to nociceptive stimuli, which progressively involve more proximal muscle groups. It is during this phase that the so-called *triple flexion response* of Sherrington is first seen. This involves flexion of the lower extremity at the hip, knee, and ankle in response to a relatively mild nociceptive stimulus. The most exaggerated form of this reaction is the *mass reflex* in which a relatively mild and sometimes nonspecific stimulus results in powerful bilateral triple flexion responses. These responses are characterized by repeated discharge of motor units throughout the caudal part of the spinal cord. The mass reflex appears to be due to the spread of afferent impulses from one cord segment to the next and dispersion of impulses in such a manner as to cause motor units to continue to fire after the exciting stimulus has been withdrawn. The mass reflex is distressing to the patient because it is almost impossible to control. This reflex becomes less severe about 4 months after spinal transection when extensor muscle tone gradually begins to increase. During this phase both flexor and extensor muscle spasms occur, but within a relatively short time extensor muscle tone predominates. It may be so great that the patient can momentarily support his weight in a standing position (103).

Examination of the patient 1 year after complete spinal cord transection reveals (a) marked extensor muscle tone, (b) spasticity, (c) hyperactive myotatic reflexes, (d) sustained clonus, (e) bilateral Babinski signs, (f) loss of the superficial abdominal and cremasteric (male) reflexes, and (g) loss of all sensation and voluntary motor function below the level of the lesion. Spasticity is characterized by increased tone in the antigravity muscles (extensors in the lower extremity and flexors in the upper extremity), increased resistance to passive movement, and a sudden reduction in tone as the limb is flexed or extended passively. The abrupt melting away of muscle tone, referred to as the *knife-clasp phenomenon*, is due to disynaptic inhibition of extensor or flexor motor neurons caused by stimulating Golgi tendon organs in passively stretching the involved muscles.

Bladder and bowel functions are disturbed in all transections of the cord, for they are no longer under voluntary control. Interruption of descending autonomic fibers, particularly those *en route* to parasympathetic nuclei in the sacral cord (S2, S3, S4), leads to loss of rectal motility. There are reflex spasms of the external anal sphincters and fecal retention. Defecation occurs involuntarily after long intervals. If cord segments S2, S3, and S4 are destroyed *(conus medullaris syndrome)*, there is a permanent paralysis of the external sphincter and fecal incontinence (Fig. 9.11). When these sacral segments are involved there is, in addition, paralytic incontinence and usually bladder distension, impotence, and perianal or saddle anesthesia. However, normal sensory and motor function is retained in the lower extremities. Bladder disturbances usually occur in three phases after cord transection. At the outset there is always urinary *retention*, due to paralysis of the muscular bladder wall (detrusor muscle), and spasm of the vesicle sphincter. Two or 3 weeks later (range 2 days to 18 months) the second phase or *overflow incontinence* is observed. An intermittent dribbling of urine during this phase is due to gradual hypertrophy of the detrusor smooth muscle. The muscle overcomes the resistance of the external sphincter for short periods of time. Continued hypertrophy of the bladder wall eventually permits the bladder to expel small amounts of urine automatically, providing bladder infections have not intervened. This is the third phase, known as *automatic micturition*. Such automatic activity of the bladder is poor if lumbar spinal cord segments are involved, and absent (paralytic incontinence) when the sacral segments are destroyed. The incontinence problem usually is handled by a system of tidal drainage, which automatically fills and empties the bladder at regular intervals.

Degeneration resulting from a complete transection of the spinal cord follows a well-established pattern. Above the level of the lesion ascending tracts will degenerate (Fig. 11.2) while, below the lesion level, they remain intact (Fig. 11.16). The reverse is seen in the descending tracts. Considerable degeneration usually is present in nearly all systems in the immediate vicinity of the lesion. By studying spinal cord sections above and below the level of the lesion, it is possible to predict fairly closely the level of the lesion.

SPINAL HEMISECTION

Spinal cord hemisection is less common than complete cord transection. When present it produces a *Brown-Séquard syndrome*, a

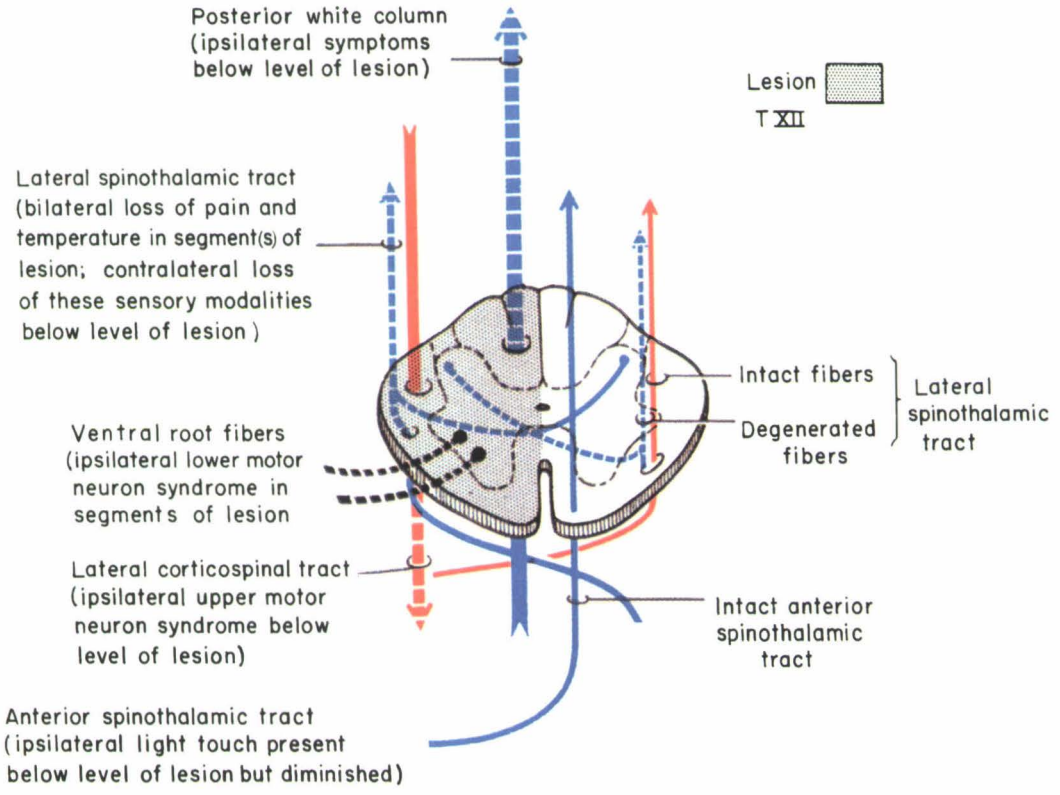


Figure 11.27. Degeneration associated with a spinal cord hemisection. Such a lesion produces the Brown-Séquard syndrome. The major degeneration occurs on the side of the lesion with ascending tracts degenerated above the lesion and descending tracts degenerated caudal to it. If the lesion involves only one spinal level, contralateral degeneration would be minimal and confined to crossed fibers arising from the involved segment. *Arrows* indicate direction of impulse conduction, while *broken lines* indicate degenerated tracts.

highly characteristic clinical entity which is instructive for teaching purpose (Fig. 11.27). This type of lesion is not associated with a period of spinal shock, and the neurologic disturbances are different. On the lesion side of the cord, the following are found below the lesion site: (a) an upper motor neuron syndrome, (b) greatly impaired discriminatory tactile sense, (c) loss of kinesthetic sense, and (d) reduced muscle tone. At the level of the lesion there usually is bilateral impairment of pain and thermal sense and variable degrees of lower motor neuron involvement dependent on the size of the lesion. Contralateral to the lesion there is loss of pain and temperature sensibility, usually beginning one or two segments below the level of the lesion. Sensory disturbances contralateral to the lesion are due to interruption of crossed ascending fibers of the spinothalamic tracts.

The spinal degeneration seen in the Brown-Séquard syndrome is almost entirely on the side of the lesion and conforms to the same principle as described for complete spinal cord transection (5, in Fig. 11.26 and Fig. 11.27). However, if the lesion involves several spinal segments, a small amount of degeneration may be detected in the contralateral spinothalamic tracts, and in the anterior spinocerebellar tract, if the lesion involves lumbar spinal segments.

Complete and incomplete transections of the human spinal cord may result from missile wounds or fracture-dislocation of vertebrae. Similar damage may follow ischemic necrosis due to occlusion or interruption of radicular arteries that supply the vulnerable upper thoracic segments (Fig. 4.1) of the spinal cord (26, 136, 240). Neoplasms also may compress the spinal cord and secondarily compromise the blood supply. In such spinal cord lesions, the symptoms are severe and the complications are numerous, regardless of the level of injury.

Spinal Cord Syndromes

AMYOTROPHIC LATERAL SCLEROSIS

This spinal cord disease involves both upper and lower motor neurons. It is a progressive degenerative disease of unknown etiology which occurs with greatest frequency in the 5th and 6th decades of life, and is characterized by degeneration and demyelination of the corticospinal tracts and degeneration of anterior horn cells bilaterally at some segmental levels. When degeneration of anterior horn cells begins in the cervical region (Fig. 11.28), the disease manifests itself by progressive muscular atrophy in the upper extremities, usually in the small intrinsic hand muscles, and spastic weakness of the muscles of the trunk and lower extremities. Muscular weakness usually is symmetric and becomes generalized in the terminal phases of the disease. Fasciculations (i.e., involuntary twitching of muscle fascicles) in affected muscles can be observed and felt by the patient and the examiner. Myotatic irritability of affected muscles persists until atrophy is complete. Late in the course of this progressive disease, functional disturbances of the bladder and bowel may appear due to injury of descending fibers en route to lumbar and sacral segments of the cord.

COMBINED SYSTEM DISEASE

This disease represents the neurologic manifestations of pernicious anemia. It involves degenerative changes in peripheral nerves and in the central nervous system. The anemia and the degenerative changes in the nervous system result from a deficiency of vitamin B12. A defect in gastric secretion de-

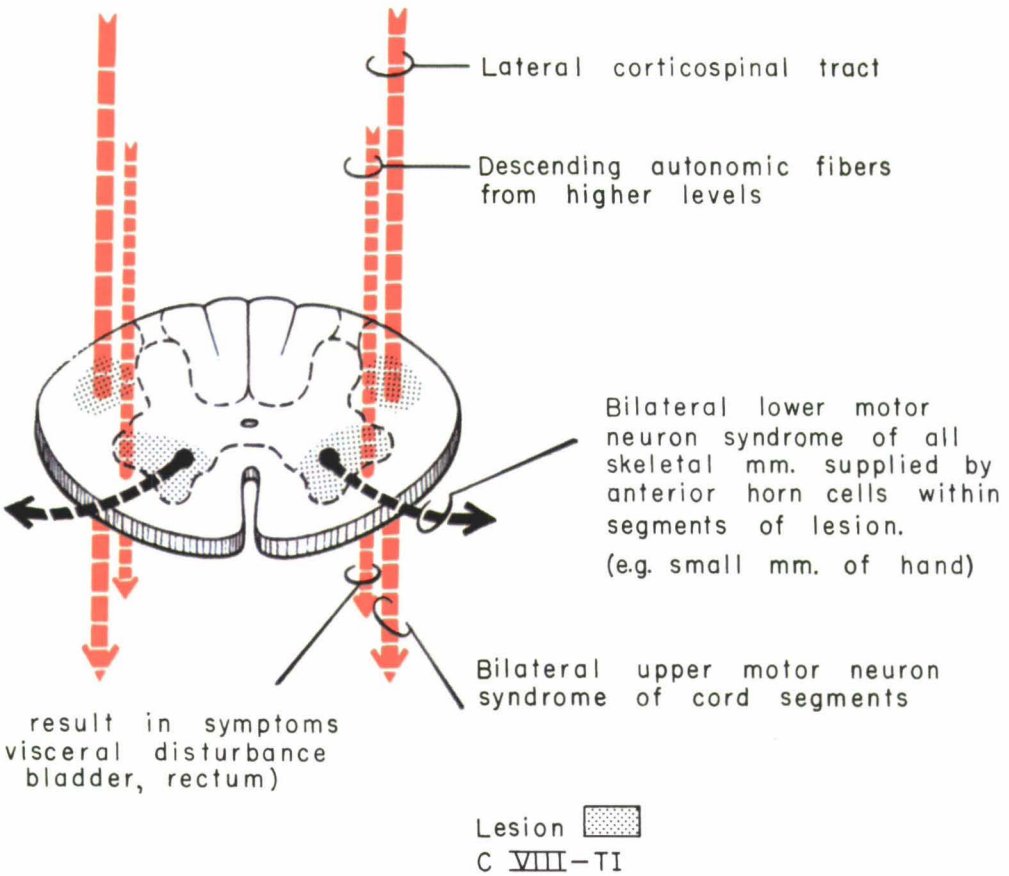


Figure 11.28. Spinal cord pathology in amyotrophic lateral sclerosis, a syndrome that involves both upper and lower motor neurons. Although the upper motor neuron lesion may involve all spinal levels, lower motor neuron involvement initially may be localized at particular levels. *Arrows* indicate direction of impulse conduction and *broken lines* indicate degenerated nerve fibers.

prives these patients of an enzyme specifically required for absorption of vitamin B12. Peripheral nerves and spinal tracts undergo varying degrees of degeneration. The degeneration in the spinal cord appears to affect especially the posterior white columns and the corticospinal tracts, but it is not confined to these systems (Fig. 11.29). Patients have both sensory and motor disturbances. The sensory disturbances include numbness and tingling, "pins and needles" sensation, loss of position sense, and loss of vibratory sense. These sensory disturbances are greatest in distal portions of the extremities and tend to be symmetric. There is little impairment of tactile, thermal, or pain sense. Weakness in the lower extremities is common, and the gait may be spastic and ataxic. The myotatic reflexes in the lower extremities usually are reduced while those in the upper extremity are normal. The sign of Babinski can be elicited bilaterally. Moderate muscular wasting usually occurs in the late stages of the disease.

SYRINGOMYELIA

This is a chronic disease characterized pathologically by long cavities, surrounded by glial elements, that develop in relationship to the central canal of the spinal cord. These cavities may extend into the medulla (syringobulbia). Syringomyelia probably is related embryologically to an abnormal closure of the central canal. Incomplete closure of the central canal may leave cavities around which a secondary gliosis develops. Characteristically syringomyelia involves the lower cervical and upper thoracic regions of the spinal cord. The affected region of the spinal cord is enlarged and transverse sections reveal a large irregular cavity containing a clear or yellow fluid.

The hallmark of this disease is an early impairment, or loss, of pain and thermal sense with preservation of tactile sense. This selective loss of pain and thermal sense, frequently noted first in the hands and forearms, results from interruption of decussating sen-

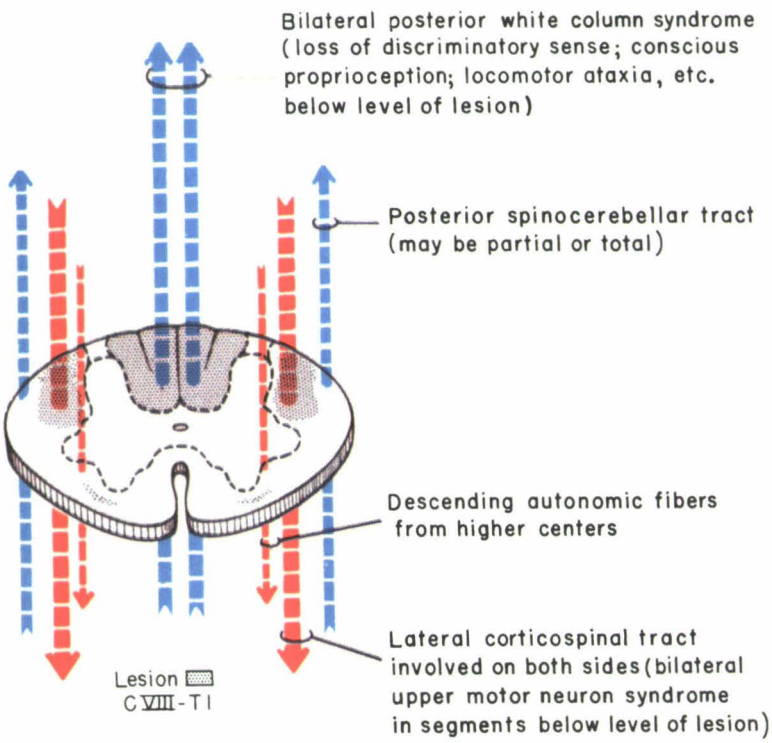


Figure 11.29. Spinal degeneration seen in combined system disease, a neurologic manifestation of pernicious anemia. Ascending fibers in the posterior columns and descending systems in the lateral funiculus are affected early but other tracts and peripheral nerves may be involved. Spinal degeneration is fairly symmetric. *Arrows* and *broken lines* indicate fiber systems which degenerate in the syndrome. The extent of degeneration in the posterior spinocerebellar tract is variable.

sory fibers (i.e., spinothalamic tracts) in several consecutive segments. This kind of sensory loss is referred to as a "dissociated sensory loss" because other forms of sensation are preserved. Later the cavity may enlarge in a lateral, posterior, cranial, or caudal direction, destroying adjacent fiber tracts or gray matter. An example of such a case is illustrated in Figure 11.30. Here the lesion interrupts the crossing fibers of the lateral spinothalamic tract in spinal segments C8 and T1. Axons distal to the lesion are separated from their cells or origin and undergo degeneration (*broken lines* in Fig. 11.30). Destruction of these crossing fibers from both sides of the spinal cord results in a bilateral loss of pain and thermal sense in the distribution of spinal nerves and dermatomes of C8 to T1. All pain and temperature fibers of T1 are destroyed, but some of the C8 fibers are spared inasmuch as a few fibers ascend in the dorsolateral tract (Lissauer's tract) and cross in the C7 spinal segment. This type of lesion results in a "dissociated sensory loss" as described earlier. The remainder of the lateral spinothalamic tract contains normal fibers that have crossed in spinal cord segments either above or below the area of the lesion. In this case, the lateral extension of the cavity also destroys the anterior (ventral) gray horn and nerve fibers passing through it (Fig. 11.30). A patient with such a lesion would have symptoms and signs of a unilateral lower motor neuron lesion and a Horner's syndrome, in addition to the classic sensory disturbances. These neurologic findings aid in localizing the lesion to spinal segments C8 and T1.

OTHER SPINAL SYNDROMES

There are many varieties of spinal cord lesions and syndromes in addition to those briefly described previously. *Tabes dorsalis* (locomotor ataxia) is a central nervous system form of syphilis which produces degeneration in the central processes of dorsal root ganglion cells. This results in extensive demyelination and degeneration of fibers in the fasciculus gracilis. There is no unanimity of opinion as to why the degenerative lesions in tabes dorsalis have this selective character. The principal

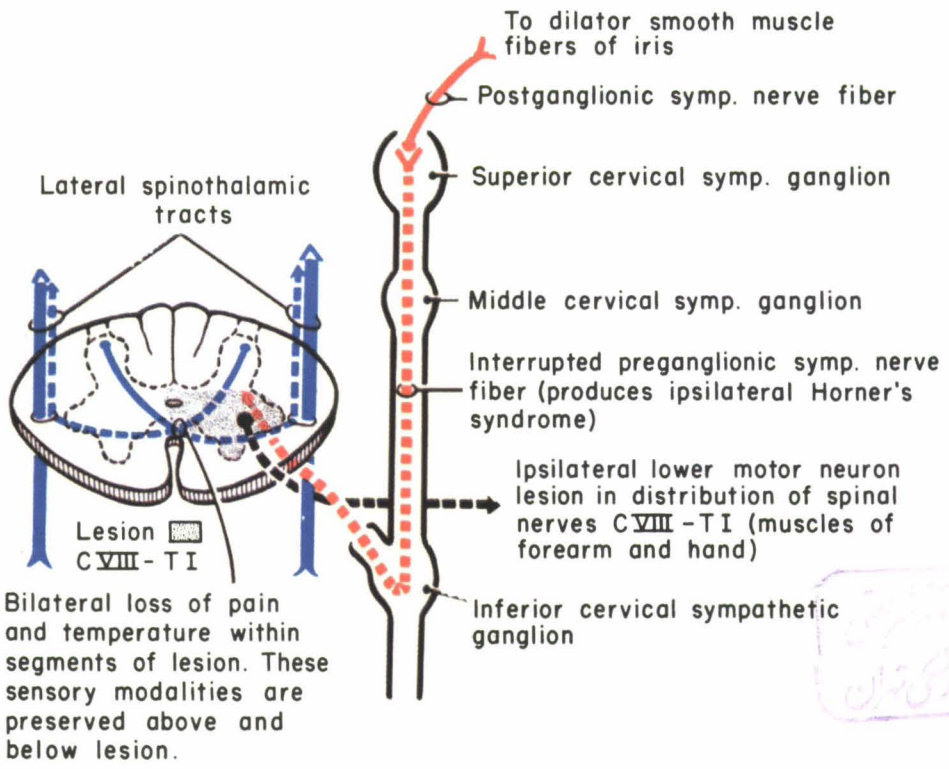


Figure 11.30. Syringomyelia with lateral extension of the cavity into anterior gray horn of spinal cord. *Arrows* show direction of impulse conduction and *broken lines* indicate degenerate nerve fibers.

symptoms of tabes are attributable to degeneration and irritation of dorsal root fibers. Sensory loss, impairment of position and vibratory sense, radicular pains, and paresthesias all are related to involvement of dorsal root fibers. Ataxia and difficulty in walking are related to loss of position and kinesthetic sense. The patient compensates for these deficits by walking on a broad base with eyes directed to the ground. Muscle tone is greatly reduced and the myotatic reflexes in the lower extremities are greatly diminished or absent.

Multiple sclerosis is a demyelinating disease of unknown etiology characterized by widely disseminated lesions in the central nervous system. This disease, which affects young adults, frequently involves the white matter of the brain and spinal cord, but there is nothing selective about the location of the lesions. Early manifestations of the disease are followed by conspicuous improvement, but relapses are a striking and constant feature of the disorder.

References

1. Akaike T. Neuronal organization of the vestibulospinal system in the cat. Brain Res 1983;259:217–227.
2. Akaike T, Fanardjian VV, Ito M, Ohno T. Electrophysiological analysis of vestibulospinal reflex pathways of rabbit. II. Synaptic actions upon spinal neurones. Exp Brain Res 1973;17:497–515.
3. Akintunde A, Buxton DF. Origins and collateralization of corticospinal, corticopontine, corticorubral and corticostriatal tracts: a multiple retrograde fluorescent tracing study. Brain Res 1992;586:208–218.
4. Albe-Fessard D, Levante A, Lamour Y. Origin of spinothalamic tract in monkeys. Brain Res 1974; 65:503–509.
5. Altman J, Carpenter MB. Fiber projections of the superior colliculus in the cat. J Comp Neurol 1961; 116:157–178.
6. Amoroso EC, Bell FR, Rosenberg H. The relationship of the vasomotor and respiratory regions in the medulla oblongata of the sheep. J Physiol (Lond) 1954;126:86–95.
7. Andersson S. Projection of different spinal pathways to the second somatic sensory area in cat. Acta Physiol Scand 1962;56(Suppl 194): 1–74.
8. Antonetty CM, Webster KE. The organization of the spinotectal projection: an experimental study in the rat. J Comp Neurol 1975;163:449–465.
9. Apkarian AV, Hodge CJ. Primate spinothalamic pathways: I. a quantitative study of the cells of origin of the spinothalamic pathway. J Comp Neurol 1989;288:447–473.
10. Armstrong DM, Schild RF. Spinoolivary neurons in the lumbosacral cord of the cat demonstrated by retrograde transport of horseradish peroxidase. Brain Res 1979;168:176–179.
11. Arvidsson U, Ulfhake B, Cullheim S, et al. Thyrotropin-releasing hormone (TRH)-like immunoreactivity in the grey monkey (*Macaca fascicularis*) spinal cord and medulla oblongata with special emphasis on the bulbospinal tract. J Comp Neurol 1992;322:293–310.
12. Asanuma H, Zarzecki P, Jankowska E, Hongo T, Marcus S. Projection of individual pyramidal tract neurons to lumbar motoneuron pool of the monkey. Exp Brain Res 1979;34:73–89.
13. Babinski J. Sur le reflexe cutané plantaire dans certaines affections organiques du système nerveux central. C R Soc Biol (Paris) 1896;48:207–208.
14. Bacon SJ, Zagon A, Smith AD. Electron microscopic evidence of a monosynaptic pathway between cells in the caudal raphe nuclei and sympathetic preganglionic neurons in the rat spinal cord. Exp Brain Res 1990;79:589–602.
15. Barnes S. Degenerations in hemiplegia: with special reference to a ventrolateral pyramidal tract, the accessory fillet and Pick's bundle. Brain 1901;24:463–501.
16. Basbaum AI, Clanton CH, Fields HL. Opiate and stimulus-produced analgesia: Functional anatomy of medullospinal pathways. Proc Natl Acad Sci USA 1976; 73:4685–4688.
17. Basbaum AI, Clanton CH, Fields HL. Three bulbospinal pathways from the rostral medulla of the cat: an autoradiographic study of pain modulating systems. J Comp Neurol 1978;178:209–224.
18. Basbaum AI, Ralston DD, Ralston HJ. Bulbospinal projections in the primate: a light and electron microscopic study of a pain modulating system. J Comp Neurol 1986;250:311–323.
19. Batton RR III, Jayaraman A, Ruggiero D, Carpenter MB. Fastigial efferent projections in the monkey: an autoradiographic study. J Comp Neurol 1977;174:281–306.
20. Bernhard CG, Bohm E. Cortical representation and functional significance of the cortico-motoneuronal system. Arch Neurol Psychiatry 1954;72:473–502.
21. Berretta S, Perciavalle V, Poppele RE. Origin of spinal projections to the anterior and posterior lobes of the rat cerebellum. J Comp Neurol 1991;305:273–281.
22. Berretta S, Perciavalle V, Poppele RE. Origin of cuneate projections to the anterior and posterior lobes of the rat cerebellum. Brain Res 1991;556:297–302.
23. Blomqvist A, Berkley KJ. A reexamination of the spino-reticulodiencephalic pathway in the cat. Brain Res 1992;579:17–31.
24. Boivie J. Terminations of the cervicothalamic tract in the cat: an experimental study with silver impregnation methods. Brain Res 1970;19:333–360.
25. Boivie J. The terminations of the spinothalamic tract in the cat: an experimental study with silver impregnation methods. Exp Brain Res 1971;12:331–353.
26. Bolton B. The blood supply of the human spinal cord. J Neurol Psychiatry 1939;2:137–148.
27. Bowker RM, Weslund KN, Coulter JD. Origins of serotonergic projections to the spinal cord in rat: an immunocytochemical-retrograde transport study. Brain Res 1981;226:187–199.
28. Bowker RM, Westlund KN, Coulter JD. Serotonergic projections to the spinal cord from the midbrain in the rat: an immunocytochemical and retrograde transport study. Neurosci Lett 1981;24:221–226.
29. Bowsher D. Termination of the central pain pathway: the conscious appreciation of pain. Brain 1957;80:606–622.
30. Bowsher D. The termination of secondary somatosensory neurons within the thalamus of *Macaca mulatta*: an experimental degeneration study. J Comp Neurol 1961; 177:213–227.
31. Brodal A. Spinal afferents to the lateral reticular nucleus of the medulla oblongata in the cat: an experimental study. J Comp Neurol 1949;91:259–295.
32. Brodal A.. The reticular formation of the brain stem. Anatomical aspects and functional correlations. Springfield, IL: Charles C. Thomas, 1957.
33. Brodal A. Anatomy of the vestibular nuclei and their connections. In: Kornhuber HH, ed. Handbook of sensory physiology: vestibular system. Vol. 6. Berlin: Springer-Verlag, 1974:239–352.
34. Brodal A. Neurological anatomy in relation to clinical medicine. 3rd

ed. New York: Oxford University Press, 1981.
35. Brodal A, Pompeiano O, Walberg F. The vestibular nuclei and their connections, anatomy and functional correlations. Springfield, IL: Charles C. Thomas, 1962.
36. Brodal A, Walberg F, Blackstad T. Termination of spinal afferents to inferior olive in cat. J Neurophysiol 1950;13:431–454.
37. Burton H, Loewy AD. Projections to the spinal cord from medullary somatosensory relay nuclei. J Comp Neurol 1977;173:773–792.
38. Busch HFM. An anatomical analysis of the white matter in the brain stem of the cat [Thesis]. University of Leiden. Leiden: Van Gorcum, 1961.
39. Calne DB, Pallis CA. Vibratory sense: a critical review. Brain 1966;89:723–746.
40. Carlton SM, Honda CN, Willcockson WS, et al. Descending adrenergic input to the primate spinal cord and its possible role in modulation of spinothalamic cells. Brain Res 1991;543:77–90.
41. Carpenter MB. Fiber projections from the descending and lateral vestibular nuclei in the cat. Am J Anat 1960;107:1–22.
42. Carpenter MB. Upper and lower motor neurons. In: Downey JA, Darling RC, eds. Physiological basis of rehabilitation medicine. Ch. 1. Philadelphia: W.B. Saunders, 1971:3–27.
43. Carpenter MB, Alling FA, Bard DS. Lesions of the descending vestibular nucleus in the cat. J Comp Neurol 1960;114:39–50.
44. Carpenter MB, Stein BM, Shriver JE. Central projections of spinal dorsal roots in the monkey. II. Lower thoracic, lumbosacral and coccygeal dorsal roots. Am J Anat 1968;123:75–118.
45. Caverson MM, Ciriello J, Calaresu FR. Direct pathway from cardiovascular neurons in the ventrolateral medulla to the region of the intermediolateral nucleus of upper thoracic cord: an anatomical and electrophysiological investigation in the cat. J Aut Nerv System 1983;9:451–475.
46. Clark FM, Proudfit HK. The projection of noradrenergic neurons in the A7 catecholamine cell group to the spinal cord in the rat demonstrated by anterograde tracing combined with immunocytochemistry. Brain Res 1991;547:279–288.
47. Cliffer KD, Burstein R, Giesler GJ Jr. Distributions of spinothalamic, spinohypothalamic, and spinotelencephalic fibers revealed by anterograde transport of PHA-L in rats. J Neurosci 1991;11:852–868.
48. Condé F, Condé H. Etude de la morphologie des cellules du noyau rouge du chat par la méthode de Golgi-Cox. Brain Res 1973; 53:249–271.
49. Cooper JR, Bloom FE, Roth RH. The biochemical basis of neuropharmacology. 6th ed. New York: Oxford University Press, 1991.
50. Cooper S, Sherrington CS. Gower's tract and spinal border cells. Brain 1940;63:123–134.
51. Coote JH. Bulbospinal serotonergic pathways in the control of blood pressure. J Cardiovasc Pharmacol 1990;15:35–41.
52. Coulter JD, Ewing L, Carter C. Origin of primary sensorimotor cortical projections to lumbar spinal cord of cat and monkey. Brain Res 1976;103:366–372.
53. Coulter JD, Jones EG. Differential distribution of corticospinal projections from individual cytoarchitectonic fields in the monkey. Brain Res 1977;129:335–340.
54. Courville J. Rubrobulbar fibers to the facial nucleus and the lateral reticular nucleus (nucleus of the lateral funiculus): an experimental study in the cat with silver impregnation methods. Brain Res 1966;1:317–337.
55. Courville J. Somatotopical organization of the projection from the nucleus interpositus anterior of the cerebellum to the red nucleus: an experimental study in the cat with silver impregnation methods. Exp Brain Res 1966;2:191–215.
56. Courville J, Brodal A. Rubrocerebellar connections in the cat: an experimental study with silver impregnation methods. J Comp Neurol 1966;126:471–485.
57. Courville J, Otabe S. The rubro-olivary projection in the Macaque: An experimental study with silver impregnation methods. J Comp Neurol 1974;158:494–497.
58. Craig AD Jr. Spinal and medullary input to the lateral cervical nucleus. J Comp Neurol 1978; 181:729–743.
59. Craig AD Jr, Burton H. The lateral cervical nucleus in the cat: Anatomical organization of cervicothalamic neurons. J Comp Neurol 1979;185:329–346.
60. Craig AD Jr, Tapper DN. Lateral cervical nucleus in the cat: Functional organization and characteristics. J Neurophysiol 1978; 41:1511–1534.
61. Cummings JF, Petras JM. The origin of spinocerebellar pathways. I. The nucleus cervicalis centralis of the cranial cervical spinal cord. J Comp Neurol 1977;173:655–692.
62. Dahlström A, Fuxe K. Evidence for the existence of monoamine-containing neurons in the central nervous system. I. Demonstration of monoamines in the cell bodies of brainstem neurons. Acta Physiol Scand 1964;62(Suppl 232):1–55.
63. Dampney RAL, Czachurski J, Dembowsky K, Goodchild AK, Seller H. Afferent connections and spinal projections of the pressor region in the rostral ventrolateral medulla of the cat. J Aut Nerv System 1987;20:73–86.
64. Dum RP, Strick PL. The origin of corticospinal projections from the premotor areas in the frontal lobe. J Neurosci 1991;11:667–689.
65. Duron B. Postural and ventilatory functions of intercostal muscles. Acta Neurobiol Exp (Warsz) 1973;33:355–380.
66. Edwards SB. The ascending and descending projections of the red nucleus in the cat: an experimental study using an autoradiographic tracing method. Brain Res 1972; 48:45–63.
67. Eldred E, Fujimori B. Relations of the reticular formation to muscle spindle activation. In: Jaspers HH, Proctor LD, Knighton RS, Noshay WS, Costello RT, eds. Reticular formation of the brain. Boston: Little, Brown and Company, 1958: 275–283.
68. Eldred E, Granit R, Merton PA. Supraspinal control of the muscle spindles and its significance. J Physiol (Lond) 1953;122:498–523.
69. Flumerfelt BA, Otabe S, Courville J. Distinct projections to the red nucleus from the dentate and interposed nuclei in the monkey. Brain Res 1973;50:408–414.
70. Foerster O, Gagel O, Sheeman D. Veränderungen an den Endösen im Rückenmark des Affen nach Hinterwurzeldurschschneidung. Z Anat Entwickl-Gesch 1933;101: 553–565.
71. Fung SJ, Manzoni D, Chan JY, Pompeiano O, Barnes CD. Locus coeruleus control of spinal motor output. Prog Brain Res 1991;88:395–409.
72. Fukushima K, Peterson BW, Uchino Y, Coulter JD, Wilson VJ. Direct fastigiospinal fibers in the cat. Brain Res 1977;126:538–542.
73. Giuffrida R, Rustioni A. Glutamate and aspartate immunoreactivity in corticospinal neurons of rats. J Comp Neurol 1989;288:154–164.
74. Granit R. Receptors and sensory perception. New Haven, CT: Yale University Press, 1955.
75. Grant G. Projection of the external cuneate nucleus onto the cerebellum in the cat: an experimental study using silver methods. Exp Neurol 1962;5:179–195.
76. Grant G. Spinal course and somatotopically localized termination of the spinocerebellar tracts: an experimental study in the cat. Acta Physiol Scand 1962;56(Suppl 193):1–45.
77. Grant G, Rexed B. Dorsal spinal root afferents to Clark's column. Brain 1958;81:567–576.
78. Ha H, Liu CN. Cell of origin of the ventral spinocerebellar tract. J Comp Neurol 1968;13:185–205.
79. Hartmann-von Monakow K, Akert K, Künzle H. Projections of the precentral and premotor cortex to the red nucleus and other midbrain areas in *Macaca fascicularis*. Exp Brain Res 1979;34:91–105.
80. Hinman A, Carpenter MB. Efferent fiber projections of the red nucleus in the cat. J Comp Neurol 1959;113:61–82.

81. Hoff EC. Central nerve terminals in the mammalian spinal cord and their examination by experimental degeneration. Proc R Soc Ser B 1932;111:175–188.
82. Hökfelt T, Fuxe K, Goldstein M, Johansson O. Immunohistochemical evidence for the existence of adrenaline neurons in the rat brain. Brain Res 1974;66:235–251.
83. Hökfelt T, Johansson O, Goldstein M. Central catecholamine neurons as revealed by immunohistochemistry with special reference to adrenaline neurons. In: Björklund A, Hökfelt T, eds. Handbook of chemical neuroanatomy. Vol. 2. Part 1: Classical transmitters in the CNS. Amsterdam: Elsevier, 1984;157–276.
84. Holstege JC, Bongers CM. A glycinergic projection from the ventromedial lower brainstem to spinal motoneurons. An ultrastructural double labeling study in rat. Brain Res 1991;566:308–315.
85. Holstege JC, Bongers CM. Ultrastructural aspects of the coeruleospinal projection. Prog Brain Res 1991;88:143–156.
86. Hongo T, Jankowska E, Lundberg A. The rubrospinal tract. I. Effects on alpha-motor-neurons innervating hindlimb muscles in cats. Exp Brain Res 1969;7:344–364.
87. Hubbard JI, Oscarsson O. Localization of the cell bodies of the ventral spinocerebellar tract in lumbar segments of the cat. J Comp Neurol 1962;118:199–204.
88. Jeske I, McKenna KE. Quantitative analysis of bulbospinal projections from the rostral ventrolateral medulla: Contribution of C1-adrenergic and nonadrenergic neurons. J Comp Neurol 1992; 324:1–13.
89. Jones SL. Descending noradrenergic influences on pain. Prog Brain Res 1991;88:381–394.
90. Jones SL, Light AR. Serotoninergic medullary raphespinal projection to the lumbar spinal cord in the rat: a retrograde immunohistochemical study. J Comp Neurol 1992; 322:599–610.
91. Jones BE, Holmes CJ, Rodriguez-Veiga E, Mainville L. GABA-synthesizing neurons in the medulla: their relationship to serotonin-containing and spinally projecting neurons in the rat. J Comp Neurol 1991;313:349–367.
92. Jones EG, Wise SP. Size, laminar and columnar distribution of efferent cells in the sensory-motor cortex of monkeys. J Comp Neurol 1977;175:391–438.
93. Katter JT, Burstein R, Giesler GJ Jr. The cells of origin of the spinohypothalamic tract in cats. J Comp Neurol 1991;303:101–112.
94. Kausz M. Distribution of hypothalamic neurons projecting to the thoracic and sacral spinal segments in the cat. J Hirnforsch 1990; 31;697–703.
95. Kausz M. Arrangement of neurons in the medullary reticular formation and raphe nuclei projecting to thoracic, lumbar and sacral segments of the spinal cord in the cat. Anat Embryol (Berlin) 1991; 183:151–163.
96. Keller AD, Hare WK. The rubrospinal tracts in the monkey: effects of experimental section. Arch Neurol Psychiatry 1934; 32:1253–1272.
97. Kerr FWL. Neuroanatomical substrates of nociception in the spinal cord. Pain 1975;1:325–356.
98. Kerr FWL. The ventral spinothalamic tract and other ascending systems of the ventral funiculus of the spinal cord. J Comp Neurol 1975;159:335–356.
99. King JS, Bowman MH, Martin GF. The red nucleus of the opossum (*Didelphis marsupialis virginiana*): a light and electron microscopic study. J Comp Neurol 1971; 143:157–184.
100. King JS, Schwyn RC, Fox CA. The red nucleus in the monkey (*Macaca mulatta*): a Golgi and an electron microscopic study. J Comp Neurol 1971;142:75–108.
101. Kojima M, Takeuchi Y, Goto M, Sano Y. Immunohistochemical study on the localization of serotonin fibers and terminals in the spinal cord of the monkey (*Macaca fuscata*). Cell Tissue Res 1983;229:23–36.
102. Kuang RZ, Kalil K. Branching patterns of corticospinal axon arbors in the rodent. J Comp Neurol 1990;292:585–598.
103. Kuhn RA. Functional capacity of the isolated human spinal cord. Brain 1950;75:1–51.
104. Kuypers HGJM. Central cortical projections to motor and somatosensory cell groups. Brain 1960;83:161–184.
105. Kuypers HGJM, Brinkman J. Precentral projections to different parts of the spinal intermediate zone in the rhesus monkey. Brain Res 1970;24:29–48.
106. Kuypers HGJM, Lawrence DG. Cortical projections to the red nucleus and the brain stem in the rhesus monkey. Brain Res 1967; 4:151–188.
107. Kuypers HGJM, Maisky VA. Retrograde axonal transport of horseradish peroxidase from spinal cord to brain stem cell groups in the cat. Neuroscience 1975;1:9–14.
108. Landgren S, Nordwall A, Wengström C. The location of the thalamus relay in the spino-cervico-lemniscal path. Acta Physiol Scan 1965;65:164–175.
109. Lassek AM. The human pyramidal tract. II. A numerical investigation of the Betz cells of the motor area. Arch Neurol Psychiatry 1940; 44:718–724.
110. Lassek AM. The pyramidal tract: its status in medicine. Springfield, IL: Charles C. Thomas, 1954.
111. Lassek AM, Evans JP. The human pyramidal tract. XII. The effect of hemispherectomies on the fiber components of the pyramids. J Comp Neurol 1945;83:113–119.
112. Lassek AM, Rasmussen GL. The human pyramidal tract: a fiber and numerical analysis. Arch Neurol Psychiatry 1939;42:872–876.
113. Liang FY, Moret V, Wiesendanger M, Rouiller EM. Corticomotoneuronal connections in the rat: Evidence from double-labeling of motoneurons and corticospinal axon arborizations. J Comp Neurol 1991;311:356–366.
114. Liu CN. Afferent nerves to Clarke's and the lateral cuenate nuclei in the cat. Arch Neurol Psychiatry 1956;75:67–77.
115. Liu CN, Chambers WW. An experimental study of the corticospinal system in the monkey (*Macaca mulatta*): the spinal pathways and preterminal distribution of degenerating fibers following discrete lesions of the pre- and postcentral gyri and bulbar pyramid. J Comp Neurol 1964;123:257–284.
116. Lloyd DPC, McIntyre AK. Dorsal column conduction of group I muscle afferent impulses and their relay through Clarke's column. J Neurophysiol 1950;13:39–54.
117. Loewy AD, Burton H. Nuclei of the solitary tract: efferent projections to the lower brain stem and spinal cord of the cat. J Comp Neurol 1978;181:421–450.
118. Loewy AD, Gregorie EM, McKellar S, Baker RP. Electrophysiological evidence that the A5 catecholamine cell group is a vasomotor center. Brain Res 1979; 178:196–200.
119. Loewy AD, McKellar S, Saper CB. Direct projections from the A5 catecholamine cell group to the intermediolateral cell column. Brain Res 1979;174:309–314.
120. Loewy AD, Saper CB. Edinger-Westphal nucleus: Projections to the brain stem and spinal cord in the cat. Brain Res 1978;150:1–27.
121. Loewy AD, Saper CB, Yamodis ND. Re-evaluation of the efferent projections of the Edinger-Westphal nucleus. Brain Res 1978;141:153–159.
122. Loewy AD, Wallach JH, McKellar S. Efferent connections of the ventral medulla oblongata in the rat. Brain Res Rev 1981;3:63–80.
123. Lundberg A. Ascending spinal hindlimb pathways in the cat. In: Eccles JC, Schadé JP, eds. Progress in brain research. Vol. 12. Physiology of spinal neurons. Amsterdam: Elsevier, 1964;135–165.
124. McMasters RE, Weiss AH, Carpenter B. Vestibular projections to the nuclei of the extraocular muscles: degeneration resulting from discrete partial lesions of the vestibular nuclei in the monkey. Am J Anat 1966;118:163–194.
125. Magoun HW, Rhines R. Spasticity: the stretch-reflex and extrapyramidal systems. Springfield, IL: Charles C. Thomas, 1947.

126. Marchi M, Algeri G. Sulle degenerazioni discendenti consecutive a lesioni sperimentale in diverse zone della corteccia cerebrale. Riv Sper Freniat Med Leg Alien Ment 1885;11:492–494.
127. Martin GF, Dom R. Rubrobulbar projections of the opossum (*Didelphia virginiana*). J Comp Neurol 1970;139:199–214.
128. Massion J. The mammalian red nucleus. Physiol Rev 1967;47:383–436.
129. Matsushita M. Spinocerebellar projections from the lowest lumbar and sacral-caudal segments in the cat, as studied by anterograde transport of wheat germ agglutinin-horse-radish peroxidase. J Comp Neurol 1988;274:239–254.
130. Matsushita M, Hosoya Y. The location of spinal projection neurons in the cerebellar nuclei (cerebellospinal tract neurons) of the cat: a study with the horseradish peroxidase technique. Brain Res 1978;142:237–248.
131. Matsushita M, Hosoya Y, Ikeda M. Anatomical organization of the spinocerebellar system in the cat as studied by retrograde transport of horseradish peroxidase. J Comp Neurol 1979;184:81–106.
132. Matsushita M, Ikeda M. The central cervical nucleus as cell origin of a spinocerebellar tract arising from the cervical cord: a study in the cat using horseradish peroxidase. Brain Res 1975;100:412–417.
133. Matsushita M, Ikeda M, Hosoya Y. The location of spinal neurons with long descending axons (long descending propriospinal tract neurons) in the cat: a study with the horseradish peroxidase technique. J Comp Neurol 1979; 184:63–80.
134. Mehler WR, Feferman ME, Nauta WJG. Ascending axon degeneration following anterolateral cordotomy in the monkey. Anat Rec 1956;124:332–333.
135. Mehler WB, Feferman ME, Nauta WJH. Ascending axon degeneration following anterolateral cordotomy: an experimental study in the monkey. Brain 1960;83:718–750.
136. Mettler FA. Neuroanatomy. St. Louis: C.V. Mosby, 1948.
137. Millar J. Topography and receptive fields of ventroposterolateral thalamic neurones excited by afferents projecting through the dorsolateral funiculus of the spinal cord. Exp Neurol 1973;41:303–313.
138. Miller RA, Strominger LN. Efferent connections of the red nucleus in the brain stem and spinal cord of the rhesus monkey. J Comp Neurol 1973;152:327–346.
139. Morin F. A new spinal pathway for cutaneous impulses. Am J Physiol 1955;183:245–252.
140. Morin F, Catalano JF. Central connections of a cervical nucleus (nucleus cervicalis lateralis) of the cat. J Comp Neurol 1955;103:17–32.
141. Morin F, Schwartz HG, O'Leary JL. Experimental study of the spinothalamic and related tract. Acta Psychiatr Neurol Scand 1951; 26:371–396.
142. Mott FW, Sherrington CS. Experiments upon the influence of sensory nerves upon movement and nutrition of the limbs. Proc R Soc 1895;57:481–488.
143. Mugnaini E, Walberg F. An experimental electron microscopical study on the mode of termination of cerebellar corticovestibular fibres in the cat lateral vestibular nucleus (Deiters' nucleus). Exp Brain Res 1967;4:212–236.
144. Mugnaini E, Walberg F, Haugli-Hanssen E. Observations on the fine structure of the lateral vestibular nucleus (Deiters' nucleus) in the cat. Exp Brain Res 1967;4:146–186.
145. Nathan PW, Smith MC. Long descending tracts in man. I. Review of present knowledge. Brain 1955;78:248–303.
146. Nicholas AP, Pieribone VA, Arvidsson U, Hökfelt T. Serotonin-, substance P- and glutamate/aspartate-like immunoreactivities in medullo-spinal pathways of rat and primate. Neuroscience 1992; 48:545–559.
147. Nieuwenhuys R. Chemoarchitecture of the brain. Berlin: Springer-Verlag, 1985.
148. Norrsell U, Voorhoeve P. Tactile pathways from the hindlimb to the cerebral cortex in cat. Acta Physiol Scand 1962;54:9–17.
149. Nyberg-Hansen R. Origin and termination of fibers from the vestibular nuclei descending in the medial longitudinal fasciculus: an experimental study with silver impregnation methods in the cat. J Comp Neurol 1964;122:355–368.
150. Nyberg-Hansen R. Sites and mode of termination of reticulospinal fibers in the cat: an experimental study with silver impregnation methods. J Comp Neurol 1965; 124:71–99.
151. Nyberg-Hansen R. Functional organization of descending supraspinal fibre systems to the spinal cord: anatomical observations and physiological correlations. Ergeb Anat Entwickl-Gesch 1966;39:1–48.
152. Nyberg-Hansen R, Brodal A. Sites and mode of termination of rubrospinal fibres in the cat: an experimental study with silver impregnation methods. J Anat 1964;98:235–253.
153. Nyberg-Hansen R, Mascitti TA. Sites and mode of termination of fibers of the vestibulospinal tract in the cat: an experimental study with silver impregnation methods. J Comp Neurol 1964;122:369–387.
154. Nygren LG, Olson L. A new major projection from the locus coeruleus: the main source of noradrenergic nerve terminals in the ventral and dorsal columns of the spinal cord. Brain Res 1977;132:85–93.
155. O'Leary JL, Kerr FWL, Goldring S. The relation between spinoreticular and ascending cephalic systems. In: Jaspers HH, Proctor LD, Knightton, RS, et al., eds. Reticular formation of the brain. Boston: Little, Brown and Company, 1958;187–201.
156. Olszewski J, Baxter D. Cytoarchitecture of the human brain stem. Philadelphia: J.B. Lippincott, 1954.
157. Orioli FL, Mettler FA. The rubrospinal tract in *Macaca mulatta*. J Comp Neurol 1956;106:299–318.
158. Orlovsky GN. Activity of vestibulospinal neurons during locomotion. Brain Res 1972;46:85–98.
159. Oscarsson O. Three ascending tracts activated from group I afferents in forelimb nerves of the cat. Prog Brain Res 1964;12:179–196.
160. Oscarsson O. Functional organization of the spino- and cuneocerebellar tracts. Physiol Rev 1965;45:495–522.
161. Oscarsson O. Termination and functional organization of a dorsal spino-olivocerebellar path. Brain Res 1967;5:531–534.
162. Oscarsson O. Functional organization of spinocerebellar paths. In: Iggo A, ed. Handbook of sensory physiology. Vol. 2. Berlin: Springer-Verlag, 1973:339–380.
163. Oscarsson O, Rosén I. Short-latency projections to the cat's cerebral cortex from skin and muscle afferents in the contralateral forelimb. J Physiol (Lond) 1966; 182:164–184.
164. Oscarsson O, Sjölund B. The ventral spino-olivocerebellar system in the cat. I. Identification of five paths and their terminations in the cerebellar anterior lobe. Exp Brain Res 1977;28:469–486.
165. Oscarsson O, Uddenberg N. Identification of a spinocerebellar tract activated from forelimb afferents in the cat. Acta Physiol Scand 1964;62:125–136.
166. Patterson JT, Chung K, Coggeshall RE. Further evidence for the existence of long ascending unmyelinated primary afferent fibers within the dorsal funiculus: Effects of capsaicin. Pain 1992;49:117–120.
167. Perl ER, Whitlock DG. Somatic stimuli exciting spinothalamic projections in thalamic neurons in the cat and monkey. Exp Neurol 1961;3:256–296.
168. Petras JM. Cortical, tectal and tegmental fiber connections in the spinal cord of the cat. Brain Res 1967;6:275–324.
169. Petras JM, Cummings JF. The origin of spinocerebellar pathways. II. The nucleus centrobasalis of the cervical enlargement and the nucleus dorsalis of the thoracolumbar spinal cord. J Comp Neurol 1977;173:693–716.
170. Pickel VM, Segal M, Bloom, FE. A radioautographic study of the efferent pathways of the nucleus locus coeruleus. J Comp Neurol 1974;155:15–42.

171. Pitts RF. The respiratory center and its descending pathways. J Comp Neurol 1940;72:605–625.
172. Pitts RF, Magoun HW, Ranson SW. Localization of the medullary respiratory centers in the cat. Am J Physiol 1939;126:673–688.
173. Poggio GF, Mountcastle VB. A study of the functional contributions of the lemniscal and spinothalamic systems to somatic sensibility. Bull Johns Hopkins Hosp 1960;106:266–316.
174. Poirier LJ, Bertrand C. Experimental and anatomical investigation of the lateral spinothalamic and spinotectal tracts. J Comp Neurol 1955;102:745–757.
175. Poirier LJ, Bouvier G. The red nucleus and its efferent nervous pathways in the monkey. J Comp Neurol 1966;128:233–244.
176. Pompeiano O. Sulle riposte posturali alla stimolazione elettrica del nucleo rosso nel gatto decerebrato. Boll Soc Ital Biol Sper 1956; 32:1450–1451.
177. Pompeiano O. Analisi degli effetti della stimolazione elettrica del nucleo rosso nel gatto decerebrato. Rend Accad Naz Lincei Cl Sci Fis Mat Nat 1957;22:100–103.
178. Pompeiano O. Organizzazione somatotopica delle risposte flessorie alla stimolazione elettrica del nucleo di Deiters nel Gatto cerebrato. Arch Si Biol (Bologna) 1960; 44:497–51.
179. Pompeiano O, Brodal A. Experimental demonstration of a somatotopical origin of rubrospinal fibers in the cat. J Comp Neurol 1957;108:225–251.
180. Pompeiano O, Brodal A. Spinovestibular fibers in the cat: an experimental study. J Comp Neurol 1957;108:353–382.
181. Pompeiano O, Brodal A. The origin of the vestibulospinal fibres in the cat: an experimental-anatomical study, with comments on the descending medial longitudinal fasciculus. Arch Ital Biol 1957; 95:166–195.
182. Preston JB, Whitlock DG. Precentral facilitation and inhibition of spinal motoneurons. J Neurophysiol 1960;23:154–170.
183. Preston JB, Whitlock DG. Intracellular potentials recorded from motoneurons following precentral gyrus stimulation in primate. J Neurophysiol 1961;24:91–100.
184. Proudfit HK, Anderson EG. Morphine analgesia: blockade by raphe magnus lesions. Brain Res 1975; 98:612–618.
185. Proudfit HK, Clark FM. The projections of locus coeruleus neurons to the spinal cord. Prog Brain Res 1991;88:123–141.
186. Rajakumar N, Hrycyshyn AW, Flumerfelt BA. Afferent organization of the lateral reticular nucleus in the rat: an anterograde tracing study. Anat Embryol (Berl) 1992;185:25–37.
187. Ralston HJ III, Ralston DD. The primate dorsal spinothalamic tract; evidence for a specific termination in the posterior nuclei (Po/SG) of the thalamus. Pain 1992; 48:107–118.
188. Reid JM, Gwyn DG, Flumerfelt BA. A cytoarchitectonic and Golgi study of the red nucleus of the rat. J Comp Neurol 1975;162:337–362.
189. Rexed B, Brodal A. The nucleus cervicalis lateralis: a spinocerebellar relay nucleus. J Neurophysiol 1951;14:399–407.
190. Rinvik E, Walberg F. Demonstration of a somatotopically arranged cortico-rubral projection in the cat: an experimental study with silver methods. J Comp Neurol 1963; 120:393–407.
191. Rose JE, Mountcastle VB. Touch and kinesthesis. In: Fields J, ed. Handbook of physiology. Sec. I, Vol. I: Neurophysiology. Ch. 17. Washington, DC: American Physiological Society, 1959:387–429.
192. Rossi GF, Brodal A. Corticofugal fibers to the brain stem reticular formation: an experimental study in the cat. J Anat 1956;90:42–62.
193. Rossi GF, Brodal A. Terminal distribution of spinoreticular fibers in the cat. AMA Arch Neurol Psychiatry 1957;78:439–453.
194. Sadun AA, Pappas GD. Development of distinct cell types in the feline red nucleus: a Golgi-Cox and electron microscopic study. J Comp Neurol 1978;182:315–366.
195. Saper CB, Loewy AD, Swanson LW, Cowan WM. Direct hypothalamo-autonomic connections. Brain Res 1976;117:305–312.
196. Sasaki K, Namikawa A, Hashiramoto S. The effect of midbrain stimulation upon alpha motoneurones in lumbar spinal cord. Nippon Seirugaku Zassi 1960; 3:303–316.
197. Sasaki K, Tanaka T, Mori K. Effects of stimulation of pontine and bulbar reticular formation upon spinal motoneurons of the cat. Jpn J Physiol 1962;12:45–62.
198. Schoenen J, Grant G. Spinal cord: connections. In: Paxinos G, ed. The human nervous system. Ch. 4. New York: Academic Press, 1990:77–92.
199. Shinoda Y, Arnold A, Asanuma H. Spinal branching of corticospinal axons in the cat. Exp Brain Res 1976;26:215–234.
200. Shinoda Y, Ghaz C, Arnold A. Spinal branching of rubrospinal axons in the cat. Exp Brain Res 1977;30:203–218.
201. Shinoda Y, Ohgaki T, Futami T. The morphology of single lateral vestibulospinal tract axons in the lower cervical spinal cord of the cat. J Comp Neurol 1986; 249:226–241.
202. Shinoda Y, Yamaguchi T, Futami T. Multiple axon collaterals of single corticospinal axons in the cat spinal cord. J Neurophysiol 1986;55:425–448.
203. Shriver JE, Stein BM, Carpenter MB. Central projections of spinal dorsal roots in the monkey. I. Cervical and upper thoracic dorsal roots. Am J Anat 1968;123:27–74.
204. Sluka KA, Westlund KN. Spinal projections of the locus coeruleus and the nucleus subcoeruleus in the Harlan and the Sasco Sprague-Dawley rat. Brain Res 1992; 579:67–73.
205. Smith MV, Apkarian AV. Thalamically projecting cells of the lateral cervical nucleus in monkey. Brain Res 1991;555:10–18.
206. Sprague JM, Ha H. The terminal fields of dorsal root fibers in the lumbosacral spinal cord of the cat, and the dendritic organization of the motor nuclei. In: Eccles JC, Schade JP, eds. Progress in brain research. Vol. 2. Organization of the spinal cord. Amsterdam: Elsevier, 1964;120–152.
207. Staal A. Subcortical projections on the spinal gray matter of the cat. The Hague: Koninkl Druk, Lankhout-Immig NV, 1961.
208. Stein BM, Carpenter MB. Central projections of portions of the vestibular ganglia innervating specific parts of the labyrinth in the rhesus monkey. Am J Anat 1967;120:281–318.
209. Sterling P, Kuypers HGJM. Anatomical organization of the brachial spinal cord of the cat. II. The motoneuron plexus. Brain Res 1967;4:16–32.
210. Taub A. Local, segmental and supraspinal interaction with a dorsolateral spinal cutaneous afferent system. Exp Neurol 1964; 10:357–374.
211. Taub A, Bishop PO. The spinocervical tract: Dorsal column linkage, conduction velocity, primary afferent spectrum. Exp Neurol 1965; 13:1–21.
212. Thomas DM, Kaufman RP, Sprague JM, Chambers WW. Experimental studies of the vermal cerebellar projections in the brain stem of the cat (fastigiobulbar tract). J Anat 1956;90:371–385.
213. Torvik A, Brodal A. The origin of reticulospinal fibers in the cat: an experimental study. Anat Rec 1957;128:113–137.
214. Tower SS. Function and structure in the chronically isolated lumbosacral spinal cord of the dog. J Comp Neurol 1937;67:109–131.
215. Trevino DL, Carstens E. Confirmation of the location of spinothalamic neurons in the cat and monkey by the retrograde transport of horseradish peroxidase. Brain Res 1975;98:177–182.
216. Trevino DL, Coulter JD, Willis WD. Location of cells of origin of spinothalamic tract in lumbar enlargement of the monkey. J Neurophysiol 1973;36:750–761.
217. Truex RC, Taylor MJ, Smythe MQ, Gildenberg PL. The lateral cervical nuclei of cat, dog and man. J Comp Neurol 1970;139:93–104.
218. Tsukahara N, Toyama K, Kosaka

K. Electrical activity of red nucleus neurones investigated with microelectrodes. Exp Brain Res 1967; 4:18–33.
219. Twitchell TE. Sensory factors in purposive movement. J Neurophysiol 1954;17:239–252.
220. Verhaart WJC, Kramer W. The uncrossed pyramidal tract. Acta Psychiat Neurol Scand 1952; 27:181–200.
221. Voogd J, Feirabend HKP, Schoen JHR. Cerebellum and precerebellar nuclei. In: Paxinos G, ed. The human nervous system. Ch. 14. New York: Academic Press, 1990:321–386.
222. Walberg F. Descending connections to the inferior olive: an experimental study in the cat. J Comp Neurol 1956;104:77–173.
223. Walberg F. On the termination of rubrobulbar fibers: experimental observations in the cat. J Comp Neurol 1958;110:66–73.
224. Walberg F. Cerebellovestibular relations: anatomy. Prog Brain Res 1972;37:361–376.
225. Walberg F, Bowsher D, Brodal A. The termination of primary vestibular fibers in the vestibular nuclei in the cat: an experimental study with silver methods. J Comp Neurol 1958;110:391–419.
226. Walberg F, Brodal A. Spinopontine fibers in the cat: an experimental study. J Comp Neurol 1953; 99:251–288.
227. Walberg F, Jansen J. Cerebellar corticovestibular fibers in the cat. Exp Neurol 1961;3:32–52.
228. Walberg F, Pompeiano O, Brodal A, Jansen J. The fastigiovestibular projection in the cat: an experimental study with silver impregnation methods. J Comp Neurol 1962; 118:49–75.
229. Weil A, Lassek A. A quantitative distribution of the pyramidal tract in man. Arch Neurol Psychiatry 1929;22:495–510.
230. Westlund KN, Bowker RM, Ziegler MG, Coulter JD. Origins and terminations of descending noradrenergic projections to spinal cord of monkey. Brain Res 1984;292:1–16.
231. Westlund KN, Coulter JD. Descending projections of the locus coeruleus and subcoeruleus/medial parabrachial nuclei in monkey: axonal transport studies and dopamine—hydroxylase immunocytochemistry. Brain Res Rev 1980;2:235–264.
232. Whitlock DG, Perl ER. Thalamic projections of spinothalamic pathways in monkey. Exp Neurol 1961;3:240–255.
233. Wilson VJ, Peterson BW. Peripheral and central substrates of vestibulospinal reflexes. Physiol Rev 1978;58:80–105.
234. Wilson VJ, Uchino Y, Susswein A, Fukushima K. Properties of direct fastigiospinal fibers in the cat. Brain Res 1977;126:543–546.
235. Wilson VJ, Yoshida M. Monosynaptic inhibition of neck motoneurons by the medial vestibular nucleus. Exp Brain Res 1969; 9:365–380.
236. Xu Q, Grant G. The projection of spinocerebellar neurons from the sacrococcygeal region of the spinal cord in the cat. An experimental study using anterograde transport of WGA-HRP and degeneration. Arch Ital Biol 1990;128:209–228.
237. Yeomans DC, Clark FM, Paice JA, Proudfit HK. Antinociception induced by electrical stimulation of spinally projecting noradrenergic neurons in the A7 catecholamine cell group of the rat. Pain 1992;48:449–461.
238. Yoshida A, Sessle BJ, Dostrovsky JO, Chiang CY. Trigeminal and dorsal column nuclei projections to the anterior pretectal nucleus in the rat. Brain Res 1992;590:81–94.
239. Zhuo H, Fung SJ, Reddy VK, Barnes CD. Immunohistochemical evidence for coexistence of methionine-enkephalin and tyrosine hydroxylase in neurons of the locus coeruleus complex projecting to the spinal cord of the cat. J Chem Neuroanat 1992;5:1–10.
240. Zülch KJ. Mangeldurchblutung an der Grenzzone zweer Gefässgebiete als Ursache bisher ungeklärter Rückenmarksschädigungen. Dtsch Z Nervenheilk 1954;172:81–101.

Section V

Brainstem and Cerebellum

12
Medulla

The medulla (myelencephalon), the most caudal segment of the brainstem, represents a conical, expanded continuation of the upper cervical spinal cord. Externally, the transition from the spinal cord to the lower medulla is gradual, without sharp demarcation. The caudal limit of the medulla is rostral to the highest rootlets of the first cervical spinal nerve at about the level of the foramen magnum. Above the level of transition, the medulla increases in size and its external features become distinctive. Changes in the external appearance of the medulla are due chiefly to structural rearrangement and development of structures peculiar to the medulla. The development of the fourth ventricle causes structures previously located posteriorly to be shifted posterolaterally, while the appearance of the pyramids on the anterior surface partially obliterates the anterior median fissure. The oval eminences posterolateral to the pyramids, produced by the inferior olivary nuclei, give the medulla above the zone of transition a characteristic configuration. The gross features of the brainstem are shown in anterior and posterior views in Figures 12.1 and 12.2.

Internally, changes in the transition from the spinal cord to the medulla are the following: (a) the development of the fourth ventricle, representing the rostral continuation of the central canal of the spinal cord, (b) the decussation of the medullary pyramids (decussation of the corticospinal tract), (c) the termination of the fasciculi gracilis and cuneatus upon their respective nuclei and the decussation of the internal arcuate fibers to form the medial lemniscus, (d) the replacement of butterfly-shaped central gray matter of the spinal cord by large cellular aggregations interlacing fibers constituting the reticular formation, (e) the termination of the ascending first order fibers contained in the fasciculi gracilis and cuneatus upon their respective nuclei, and the decussation of the internal arcuate fibers to form the second order medial lemniscus, (f) the gradual replacement of spinal fibers in the zone of Lissauer by fibers of the spinal trigeminal tract, and (g) the development of cranial nerve nuclei.

SPINOMEDULLARY TRANSITION

Transverse section at the junction of the spinal cord and the medulla (Fig. 12.3) resemble those of the upper cervical spinal segments. The substantia gelatinosa has increased in size, and coarse descending fibers of the spinal trigeminal tract, which replace spinal fibers in the zone of Lissauer, are found lateral to it. These fibers arise from cells of the trigeminal ganglion, enter the brainstem at pontine levels, and descend caudally in the posterolateral part of the brainstem as far as the second cervical segment (Fig. 12.9). The substantia gelatinosa gradually becomes the spinal trigeminal nucleus at high cervical levels, and this nucleus retains the same relative position and size throughout the medulla. Descending trigeminal fibers terminate directly, or by collaterals, in parts of the spinal trigeminal nucleus.

A conspicuous increase in the gray matter surrounding the central canal is evident (Figs. 12.3 and 12.4). The lateral corticospinal tract has become clearly separated from the medial longitudinal fasciculus by its passage into the posterior part of the lateral funiculus. It is broken into a number of obliquely or transversely cut bundles, between which are strands of gray matter. A few fibers of the spinal portion of the spinal accessory nerve can be seen arching posterolaterally to emerge from the lateral aspect of the spinal cord between the dorsal and ventral roots (Fig. 12.3). Axons of somatic motor neurons in the anterior horn emerge as ventral root fibers of the first cervical spinal nerve. Rostrally these cells extend into the lower medulla (Fig. 12.6) where they constitute the *supraspinal nucleus* (89). Fiber tracts in the white matter have the same arrangement as in cervical spinal segments.

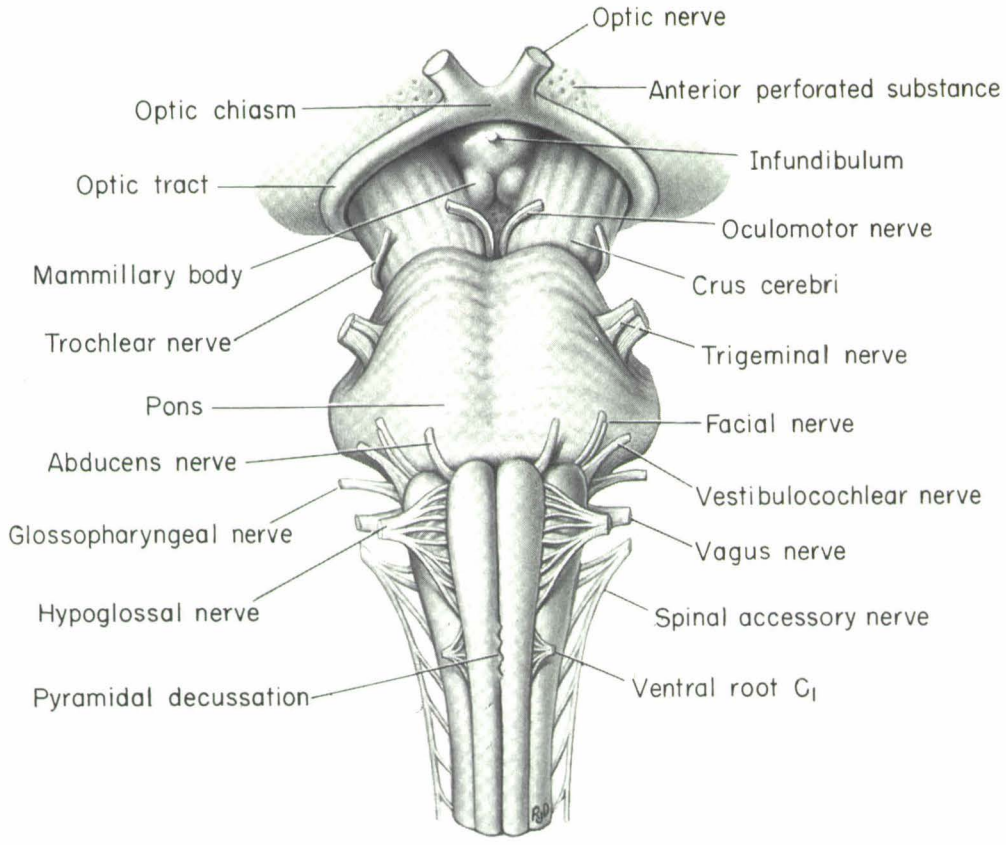


Figure 12.1. Anterior aspect of the medulla, pons, and midbrain.

Corticospinal Decussation

The most conspicuous features of the spinomedullary transition (Figs. 12.4 and 12.5) are the decussation of the corticospinal tracts, the first appearance of the nuclei of the posterior columns, and the development of the medullary reticular formation. The central gray matter has increased in size and lies mostly dorsal to the central canal.

Fibers in the medullary pyramid cross the midline in large fascicles anterior to the central gray matter and project posterolaterally across the base of the anterior horn. Interdigitating bundles, often of unequal size, project downward and posteriorly so that in transverse sections most of the bundles are cut obliquely. The crossed fibers of the corticospinal tract, which account for as much as 90% of all corticospinal fibers, descend as the lateral corticospinal tract in the posterior part of the lateral funiculus (Figs. 11.11–11.13). Fibers of the anterior corticospinal tract retain their original position and project uncrossed into the anterior funiculus of the spinal cord (Figs. 11.12 and 11.14). In a graded series of ascending sections, the corticospinal decussation is seen in reverse sequence.

The corticospinal decussation forms the anatomic basis for the voluntary motor control of one-half of the body by neuronal signals from the contralateral cerebral cortex. Injury of this tract anywhere above the decussation may cause upper motor neurons paralysis of the contralateral extremities. For reasons that will be clear when the motor cortex is studied, the consequences of lesions confined to axons of the corticospinal tract in the medullary pyramid have been of great interest. Due to the nature of the blood supply of the region, it is rare in humans to encounter a lesion limited to the pyramid, and the motor deficit is usually a contralateral paresis sparing the face (medial medullary syndrome). In those rare cases with relatively little damage beyond the pyramid, the paresis usually is accompanied by spasticity after an initial period of flaccidity (165). In monkeys, it is pos-

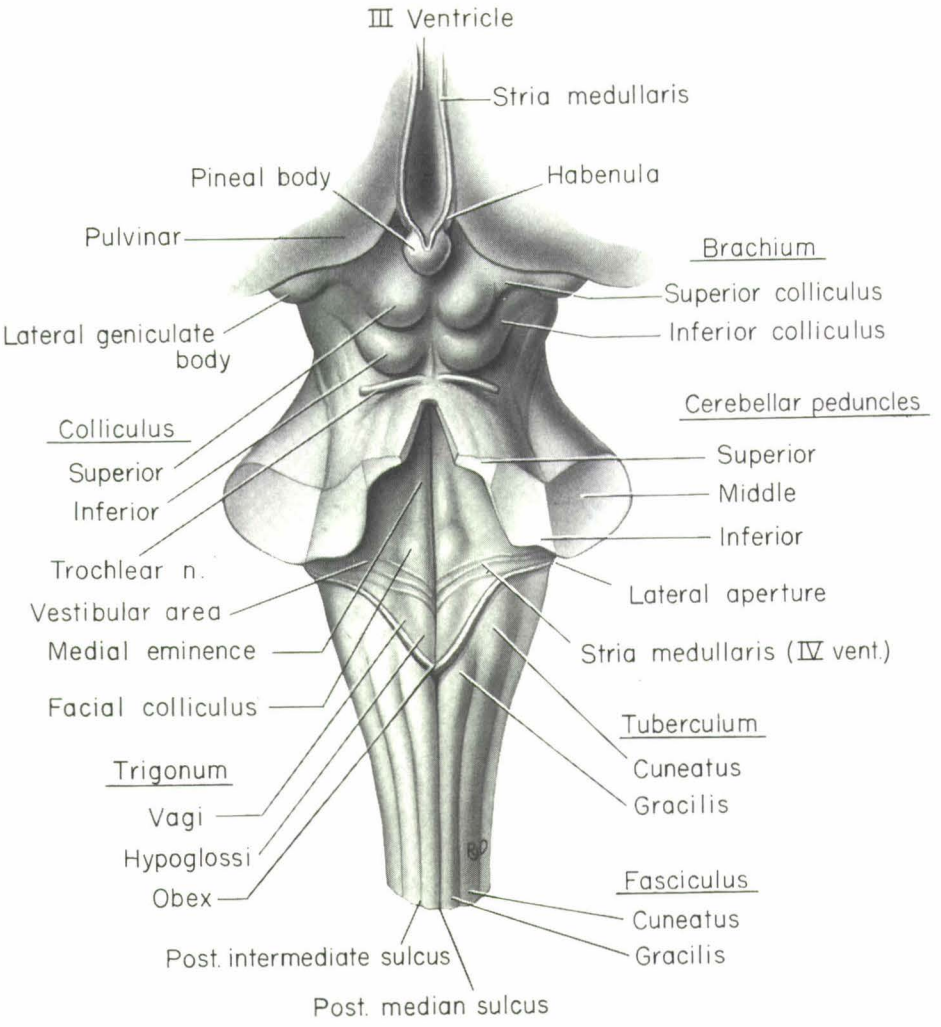


Figure 12.2. Posterior aspect of the brainstem with the cerebellum removed.

sible surgically to interrupt the pyramid with minimal damage to the adjacent medulla (65,195, 208). In these studies, there was a modest impairment of contralateral limb movement, most noticeable in the distal limb joints, and hypotonia. The major deficit was inability to individually move the fingers of the contralateral upper limb to pick up small objects. However, if about 30% of the pyramidal tract fibers remain intact, it is possible with time and retraining to overcome the deficits of finger movement. The enduring deficit is loss of hand contact orienting responses and reflex sensory-motor adjustments (175).

At the spinomedullary transition, the substantia gelatinosa of the cervical spinal cord becomes the *spinal trigeminal nucleus* (Figs. 12.4–12.7). This nucleus is capped dorsolaterally by descending fibers of the *spinal trigeminal tract*, which terminate in corresponding parts of this nucleus. The anterior horn, still recognizable at this level, contains groups of motor neurons which contribute fibers to the first cervical and the spinal accessory nerves. On the medial border of the anterior horn lies the medial longitudinal fasciculus, which is shifted laterally by the fibers of the corticospinal decussation (Figs. 12.4 and 12.5). On the ventral and lateral borders of the anterior horn are fibers of the vestibulospinal tract. The gray matter between the spinal trigeminal nucleus and the anterior horn has lost its definite continuity and consists of a few cells scattered among fiber bundles. Fibers present in this area are corticospinal fibers and short

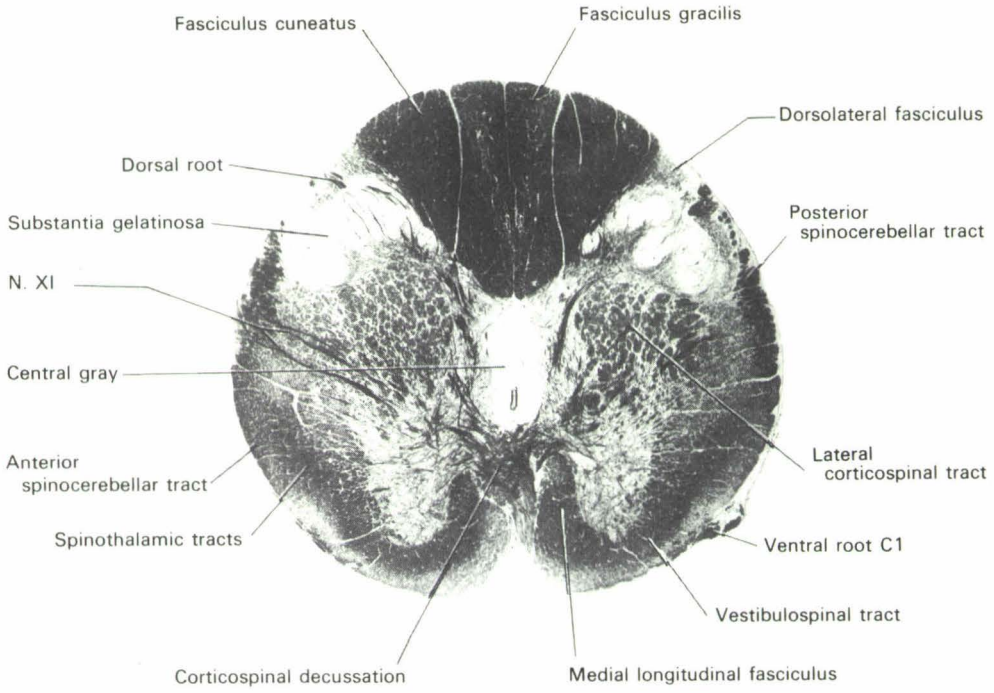


Figure 12.3. Transverse section through the junction of spinal cord and medulla. Some of the most caudal decussating fibers of the corticospinal tract can be seen passing into the posterior part of the lateral funiculus. The structure labeled substantia gelatinosa also contains cell groups of the spinal trigeminal nucleus (Weigert's myelin stain).

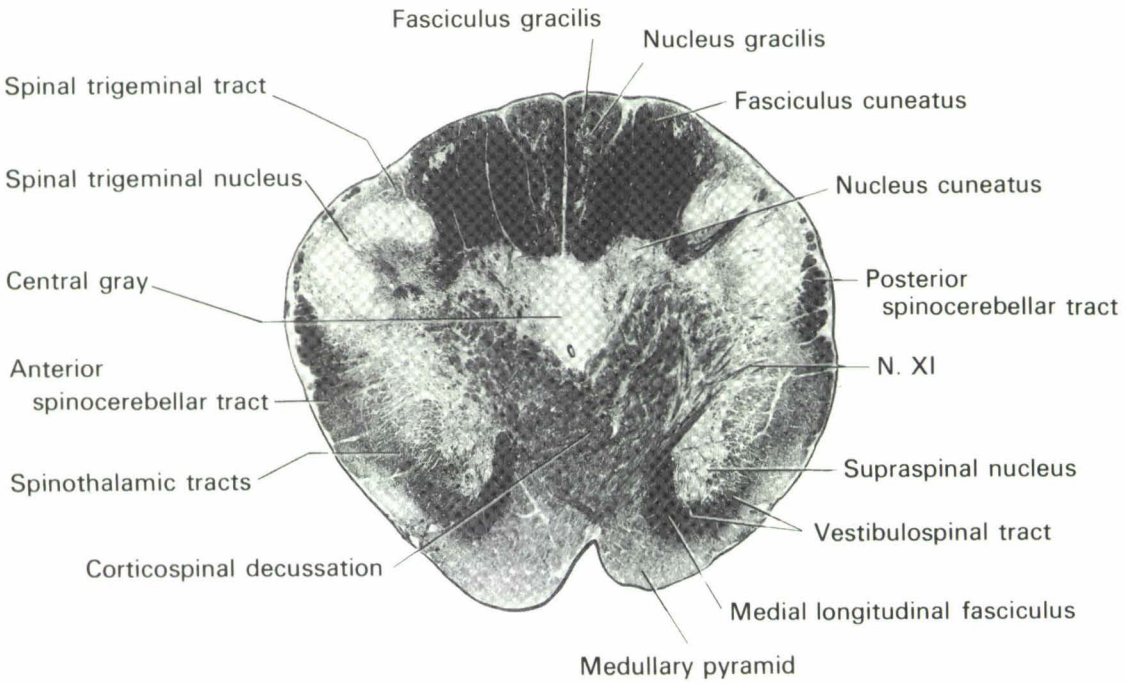


Figure 12.4. Transverse section of the medulla through the decussation of the corticospinal tract (Weigert's myelin stain).

intersegmental fibers, comparable to those in the fasciculi proprii. This area of intermingled gray and white matter is the most caudal part of the brainstem reticular formation.

Posterior Column Nuclei

In the posterior white columns, nuclear masses have appeared in the fasciculi gracilis and cuneatus. These are the nuclei of the posterior funiculi, known respectively as the *nucleus gracilis* and *nucleus cuneatus*. The long ascending branches of the cells in the dorsal root ganglia, coursing in the posterior funiculus (clinically called the posterior columns), terminate upon these nuclei (Figs. 11.1 and 12.2). At these levels, the fasciculus cuneatus is massive and only a small caudal part of the nucleus cuneatus protrudes into the ventral part of the fasciculus (Figs. 12.4 and 12.5). The nucleus gracilis is larger, occupies a more central position and is capped dorsally and laterally by fibers of the fasciculus gracilis. At progressively higher levels, increasing numbers of fibers terminate in these nuclei. The nuclei increase in size (Fig. 12.6) while the fasciculi correspondingly decrease (Fig. 12.7). At levels through the caudal part of the inferior olivary complex, the entire fasciculus gracilis and most of the fasciculus cuneatus were replaced by their respective nuclei (Figs. 12.7 and 12.8).

The overall appearance of the posterior (dorsal) column nuclei in humans (144, 151) is similar to that observed in macaque monkeys (62, 63). In both, the middle regions contain discrete clusters of neurons outlined by bands of myelinated fibers. Studies with histochemical methods for the mitochondrial enzyme cytochrome oxidase show that the cell clusters have more of the enzyme and, presumably, higher metabolic activity than the surrounding regions. The details of the parcellation pattern of the nuclei in humans and

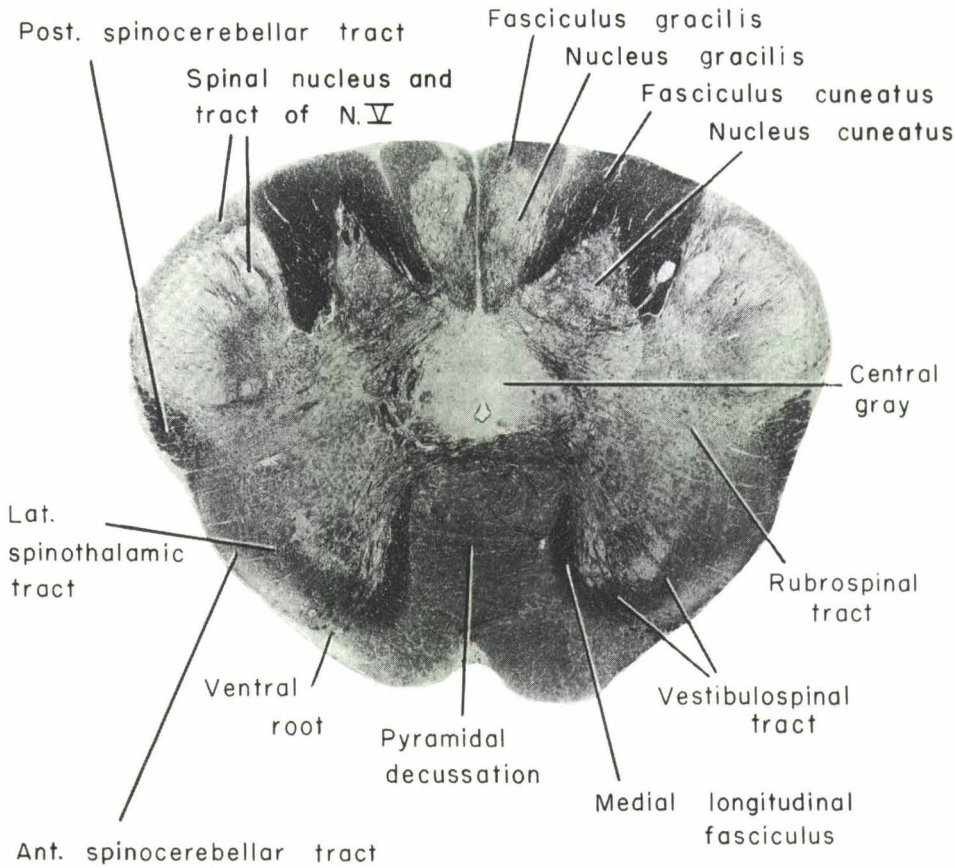


Figure 12.5. Transverse section of the medulla through the upper part of the corticospinal decussation (Weigert's myelin stain).

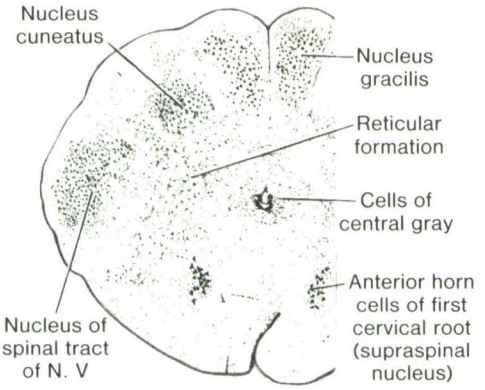


Figure 12.6. Transverse section through the medulla of 1-month infant at about same level as in Figure 12.4 (cresyl violet stain, with cell groups blocked in).

monkeys are quite comparable, suggesting the significance of the parcellation is the same (97).

In the nucleus gracilis, three cytologically distinct regions have been recognized: (a) a reticular region rostral to the obex characterized by a loose organization of cells, (b) a "cell nest" region caudal to the obex characterized by cell clusters, and (c) a caudal region characterized by scattered cells occurring singly or in small clusters (117, 161, 187). Ascending dorsal root fibers project somatotopically to the nucleus gracilis (38, 56, 60, 77, 204). According to Hand (77), lumbosacral dorsal root fibers exhibit a somatotopic lamination chiefly in the "cell nest" region, while terminations in the reticular region are diffuse with intersegmental overlap (97). Certain physiologic studies in the cat suggest that neurons in the nucleus gracilis exhibit rostrocaudal differences with respect to the size of the peripheral receptive fields, which supply afferent input (72, 124), and segregation of sensory modality (56, 70, 109, 153, 207). Rostral portions of the nucleus (i.e., reticular region) are said to be related to deep pressure and joint movement, while the "cell nest" and caudal regions of the nucleus are related to hair and skin receptors.

Other physiologic data (108), based upon single neuron analysis of posterior column nuclei, provide no evidence of rostrocaudal differentiation in terms of either somatotopy or modality segregation. The latter finding supports experimental studies (134, 157) which indicate that (a) the somatotopic orga-

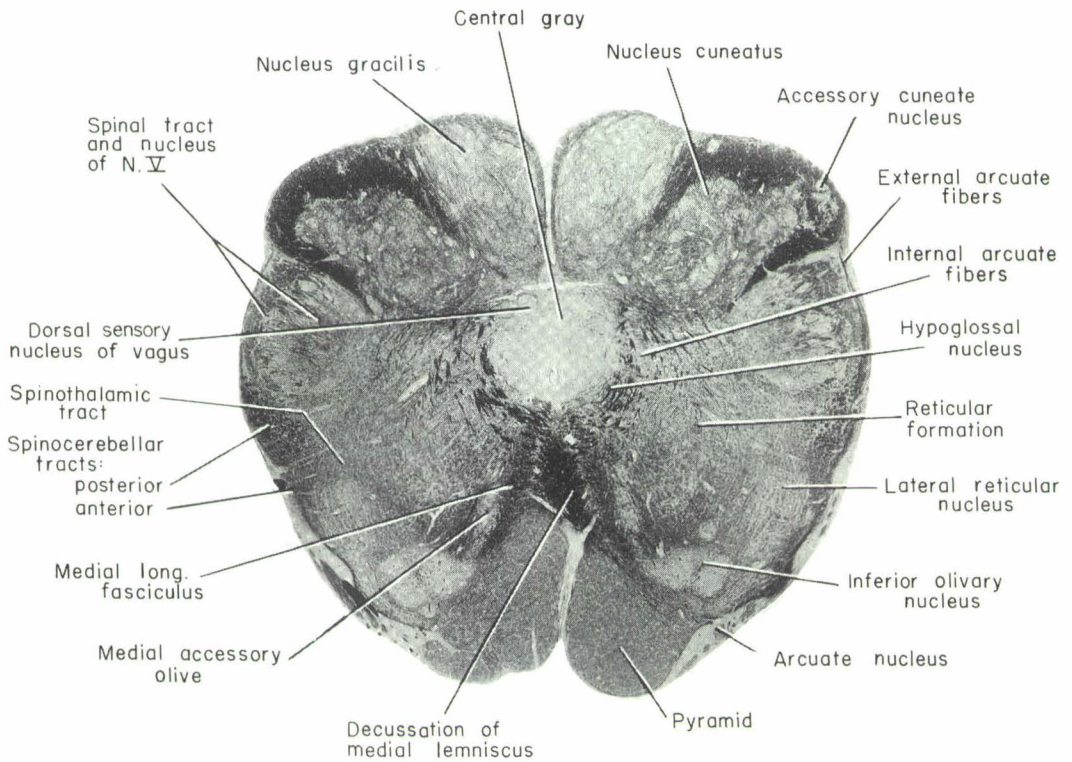


Figure 12.7. Transverse section of the medulla through the decussation of the medial lemniscus (Weigert's myelin stain).

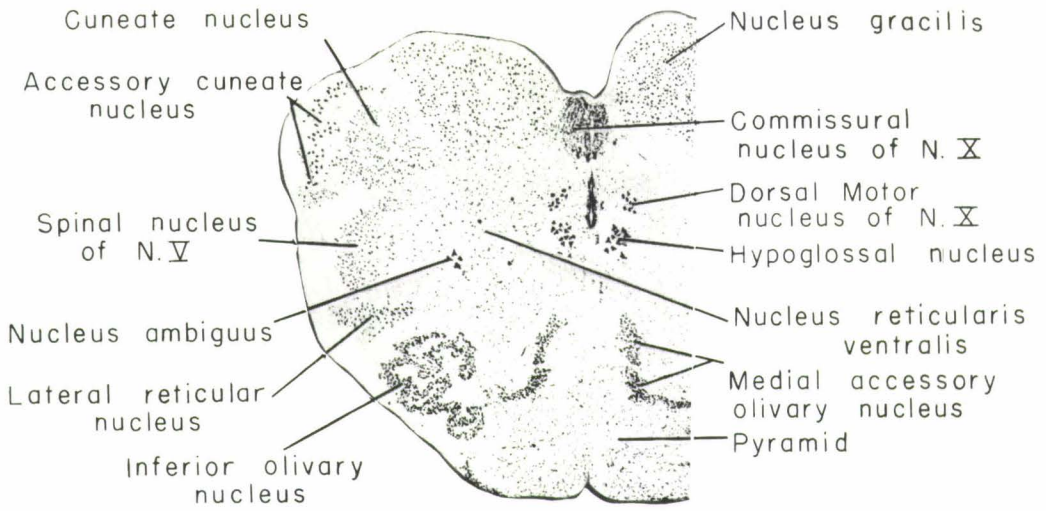


Figure 12.8. Transverse section through medulla of 1-month infant about the same level as in Figure 12.7 (cresyl violet stain, with cell groups blocked in).

nization of the posterior columns and the medial lemniscus is maintained at the level of the posterior column nuclei, and (b) neural elements devoted to kinesthesis and tactile sense are intermingled in a single and mutual somatotopic pattern. Studies in the monkey indicate that lower thoracic, lumbar, and sacrococcygeal dorsal roots project in overlapping somatotopic fashion throughout the rostrocaudal extent of the nucleus gracilis (38). Zones of the nucleus gracilis receiving terminals from fibers of the dorsal roots are organized so that (a) roots of the lumbar enlargement project to irregular-shaped areas in the central core of the nucleus; (b) lower thoracic and upper lumbar roots project in serial fashion to narrow, oblique laminae lateral to the core region; and (c) sacral and coccygeal dorsal roots project in serial fashion to crescent-shaped laminae in dorsomedial parts of the nucleus. The areas of terminal arborization in the nucleus gracilis are related to the size of the dorsal root and the number of ascending fibers they contribute to the fasciculus gracilis.

The nucleus cuneatus also exhibits regional differences in its cytoarchitecture (129, 144). Dorsal areas of the cuneate nucleus contain clusters of round cells with bushy dendrites, while basal areas contain triangular, multipolar, and fusiform cells with long, sparse dendrites (117). The round cell clusters are believed to receive afferents principally from distal parts of the body and to be related to small cutaneous receptive fields (117). Triangular and multipolar cells receive afferents primarily from proximal parts of the limb and trunk, and appear related to larger cutaneous receptive fields. These studies suggested that dorsal root fibers have a dual termination with some fibers ending in cell clusters and others among basal triangular cells.

A systematic study of dorsal root projections to the cuneate nucleus in the monkey has shown that (a) fibers from spinal segments C1 through T1 terminate in both exclusive and overlapping zones, (b) fibers from spinal segments C5 through C8 terminate in a central core region about which other dorsal root fibers terminate in oblique serial laminae, (c) fibers from upper cervical spinal segments (C1 through C4) terminate in ventrolateral regions of the nucleus, and (d) fibers from lower spinal segments (T1 through T7) terminate in dorsomedial regions of the nucleus (177). Comparisons of the patterns of dorsal root terminations in the two dorsal column nuclei in monkeys suggest that overlapping terminations are more extensive and irregular in the nucleus gracilis, and that there is less autonomous terminal representation of individual dorsal root fibers in the nucleus gracilis than in the nucleus cuneatus (38).

Decussation of the Medial Lemniscus

In transverse sections of the medulla above the corticospinal decussation (Figs. 12.7 and 12.8), the nucleus gracilis reaches its

greatest extent, and practically all fibers of the fasciculus gracilis have terminated in portions of the nucleus. A considerable number of fibers of the fasciculus cuneatus remain dorsal to the nucleus. From the nuclei gracilis and cuneatus, myelinated fibers arise which sweep ventromedially around the central gray matter. These fibers, known as *internal arcuate fibers*, cross the median raphe and form a well-defined ascending bundle, the *medial lemniscus* on the contralateral side. This large ascending fiber bundle can be readily followed through the brainstem to its termination in the ventral posterolateral nucleus (VPL_c) of the thalamus (Fig. 11.1). The medial lemniscus constitutes the second neuron of the posterior column pathway conveying kinesthetic sense and discriminative tactile sense to higher levels of the neuraxis. The decussation of the medial lemniscus provides part of the anatomic basis for sensory representation of half of the body in the contralateral cerebral cortex. Consequently, injury to the medial lemniscus causes characteristic kinesthetic and tactile deficits on the opposite side of the body.

The *accessory cuneate nucleus*, located lateral to the cuneate nucleus at slightly more rostral levels, is composed of large cells similar to those of the dorsal nucleus of Clarke (Figs. 11.9, 12.7, and 12.8). This nucleus is considered the medullary equivalent of the dorsal nucleus (25, 150, 176). The two nuclei share these anatomic and functional features: (a) cells are morphologically similar with eccentric nuclei, (b) afferent fibers are derived from dorsal root ganglia, (c) both nuclei give rise to uncrossed cerebellar afferent fibers, and (d) both nuclei relay impulses from muscle spindles, Golgi tendon organs, type II muscle afferents, and cutaneous afferents (145, 146). Ascending fibers conveyed by the fasciculus cuneatus and terminating in the accessory cuneate nucleus are derived from the same dorsal root ganglia as those projecting to the cuneate nucleus, namely those of cervical and upper thoracic spinal segments. Ascending fibers in the fasciculus cuneatus terminate somatotopically in the accessory cuneate nucleus (119, 177), and the pattern of termination is similar to that disclosed in the cuneate nucleus (177). Fibers from dorsal roots in cervical and upper thoracic spinal segments that terminate in the accessory cuneate nucleus end in both exclusive and overlapping zones; fibers from one dorsal root partially overlap the territory of the next highest root. Upper thoracic dorsal root fibers (other than T1) exhibit greater overlap and terminate in smaller zones in the lateral part of the nucleus.

Although fibers from parts of the fasciculus cuneatus terminate upon cells of the accessory cuneate nucleus, these cells do not contribute fibers to the formation of the medial lemniscus. Cells of the accessory cuneate nucleus give rise to uncrossed *cuneocerebellar fibers*, which enter the cerebellum via the restiform body, which is the major component of the inferior cerebellar peduncle (Fig. 11.9). The main cerebellar projection of the accessory cuneate nucleus is ipsilateral to paramedian parts in the anterior lobe. The cuneocerebellar tract is regarded as the upper limb equivalent of the posterior spinocerebellar tract.

Spinal Trigeminal Complex

SPINAL TRIGEMINAL TRACT

Afferent trigeminal root fibers, which enter the brainstem at midpontine levels, descend in the dorsolateral part of the brainstem as the spinal trigeminal tract (Figs. 12.4, 12.5, 12.7, 12.9, 12.11, 12.12, and 12.26). These fibers originating from cells of the trigeminal ganglion, have a definite topographic organization so that (a) fibers of the mandibular division are most dorsal, (b) fibers of the ophthalmic division are most ventral, and (c) fibers of the maxillary division are intermediate (Fig. 12.9). Some trigeminal root fibers from all divisions extend into upper cervical segments (100, 107, 164, 193) (Fig. 12.9). As this tract descends, it becomes progressively smaller as fibers leave the tract and terminate in the adjacent spinal trigeminal nucleus. The tract contains general somatic afferent fibers from the trigeminal nerve, as well as similar fibers from the vagus, glossopharyngeal, and facial nerves. These fibers descend in the dorsomedial part of the tract for a considerable distance before terminating in the magnocellular division of the caudal part of the spinal trigeminal nucleus (99, 101, 164, 193). A few visceral afferent fibers descending in the dorsal part of the spinal trigeminal tract project medially to terminate in ventrolateral parts of the nucleus solitarius (98, 100, 164, 193).

SPINAL TRIGEMINAL NUCLEUS

This nucleus, which lies along the medial border of the tract, extends from the level of

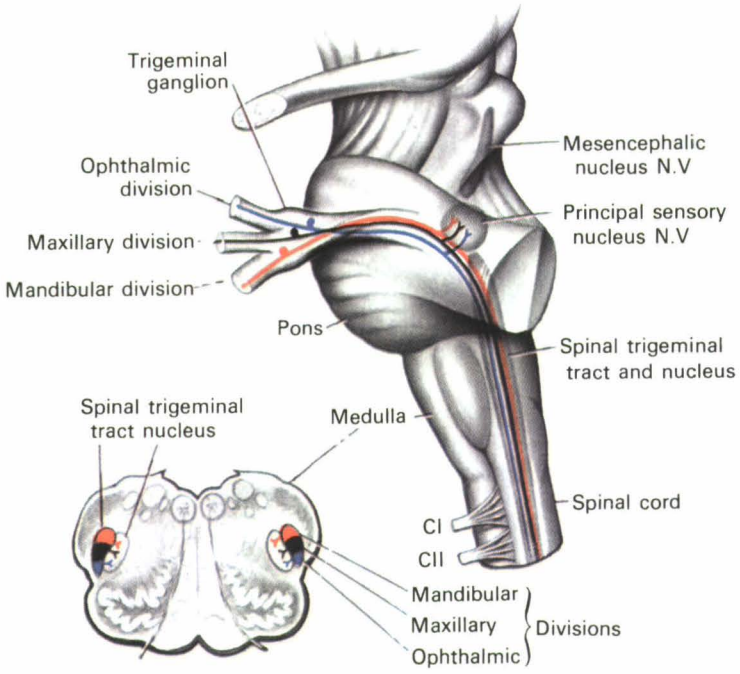


Figure 12.9. Topographic arrangement of fibers in the spinal trigeminal tract. Fibers with cell bodies in the trigeminal ganglion enter the upper pons and descend caudally as far as C2. Throughout the length of the tract, mandibular fibers are most dorsal and those of the ophthalmic division are most ventral. Fibers leave the spinal trigeminal tract to synapse upon cells in the spinal trigeminal nucleus.

entry of the trigeminal root in the pons to the second cervical spinal segment (Figs. 13.29–13.31). Fibers from the spinal trigeminal tract terminate upon cells of the nucleus throughout its extent. Cytoarchitecturally the spinal trigeminal nucleus is subdivided into three parts: (a) *pars oralis*, which extends caudally to the rostral pole of the hypoglossal nucleus; (b) *pars interpolaris*, which extends caudally to the level of the obex; and (c) *pars caudalis*, which begins near the level of the obex and extends caudally as far as the second cervical spinal segment (143). The caudal part of the spinal trigeminal nucleus has a cytologic lamination similar to that of the posterior horn of the spinal gray matter (Fig. 12.10). Four laminae are recognized: (a) lamina I, corresponding to the posteromarginal zone; (b) lamina II, corresponding to the substantia gelatinosa; and (c) laminae III and IV, which form the magnocellular layers (66–68, 106, 143). Fibers positive for substance P, as well as cells and fibers immunoreactive for enkephalin, are present in laminae I and II (Fig. 12.30).

Fibers in different parts of the spinal trigeminal tract terminate in corresponding

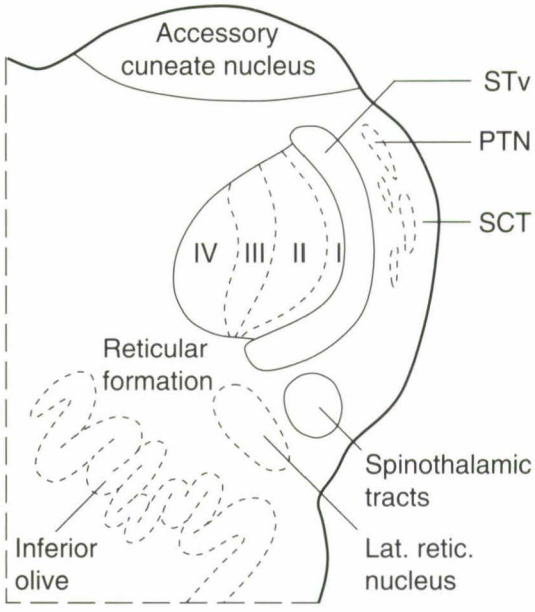


Figure 12.10. Laminar organization of the spinal trigeminal nucleus. Lamina I adjacent to the spinal trigeminal tract (*STv*) is called the marginal layer. Cells in lamina I resemble those of the posteromarginal nucleus at spinal levels. Laminae II corresponds to the substantia gelatinosa, and laminae III and IV form the magnocellular subdivision. *PTN* indicates the paratrigeminal nucleus and *SCT* the spinocerebellar tracts.

circumscribed sectors of the spinal trigeminal nucleus. Fibers conveying impulses from the mandibular division terminate in dorsal parts of the nucleus, while fibers of the ophthalmic division terminate in ventral parts of the nucleus. A number of descending trigeminal fibers pass beyond the spinal trigeminal nucleus to terminate in dorsal parts of the reticular formation and portions of the solitary nucleus. Many neurons of the spinal trigeminal nucleus give rise to an extensive axonal plexus of small fiber bundles which lie adjacent to the nucleus. These so-called "deep bundles" emit collaterals which effectively link different levels of the spinal trigeminal nucleus (69).

Fibers in the spinal trigeminal tract convey impulses concerned with pain, thermal, and tactile sense from the face, forehead, teeth, and mucous membranes of the nose and mouth (55, 57, 159) (Fig. 8.13). The spinal trigeminal tract and nucleus appear to be the only part of the trigeminal complex uniquely concerned with the perception of pain and thermal sense. Medullary trigeminal tractotomy (i.e., section of the spinal trigeminal tract) markedly reduces pain and thermal sense without impairing tactile sense (179). Physiologic studies (159) indicate that the spinal trigeminal nucleus, pars caudalis, encodes nociceptive information in the same manner as the dorsal horn of the spinal cord. Cells are found which respond solely to oral and facial nociceptive stimulation, as well as cells responding in a graded manner to a mechanical stimuli of increasing intensity. The cells responding to nociceptive stimulation are located within the nucleus and also in the subjacent reticular formation. Lesions in the dorsolateral region of the medulla involving the spinal trigeminal tract and adjacent spinothalamic tracts produce an alternating hemianalgesia and hemithermo-anesthesia of the face and the body. This condition, known as the *lateral medullary syndrome* (or Wallenberg's syndrome), is characterized by diminished pain and thermal sense in the face ipsilaterally (spinal trigeminal tract) and over the opposite side of the body and neck (*anterolateral system or ALS tracts*) (Fig. 13.30).

There appears to be little overlap between the terminal territories of the main branches of the trigeminal nerve in the spinal trigeminal nucleus. Evidence from clinical studies have led to an interesting model regarding the somatotopic representation in the trigeminal nuclei. This view surmises that afferents to the spinal trigeminal nucleus are distributed following a sort of "onion skin pattern" (26). In essence, this concept implies that axons from facial sensory regions near the midline, around the mouth and nose, project rostrally in the caudal nucleus, whereas those from successively more lateral regions of the face would supply more caudal parts of the nucleus. This scheme of organization has important clinical value for localizing lower medullary and upper cervical cord lesions.

Secondary trigeminal fibers arise from cells of the spinal trigeminal tract at multiple levels, cross through the reticular formation to the opposite side, and ascend to thalamic levels in association with the contralateral medial lemniscus (Fig. 13.30). These trigeminothalamic fibers constitute the second neuron in a sensory pathway from the face to the cortex. Other uncrossed fibers ascend and descend on the same side, forming reflex connections with the motor nuclei of the hypoglossal, vagus, facial, and other cranial nerves (Figs. 13.30 and 13.31). Other trigeminal fibers (a) terminate upon cells of the reticular formation, (b) project to the cerebellum via the inferior cerebellar peduncle (36), or (c) establish reflex connections with multiple motor cranial nerve nuclei.

Groups of cells located lateral to the spinal trigeminal tract and embedded in the fibers of the spinocerebellar tracts at the lateral edge of the medulla form the *paratrigeminal nucleus* (Fig. 12.10). Both cell bodies and fibers in the neuropil show substance P-like immunoreactivity. Additionally, the neuropil contains many serotonin (5-hydroxytryptamine 5-HT)-containing afferent axons (39, 40). The function of the paratrigeminal nucleus is not known. Since it receives afferent axons from the intermediate nerve (12) and nucleus of the solitary tract (11), and sends efferent fibers to the gustatory region of the thalamus, it has been thought to represent a rostral extension of the portion of the nucleus of the solitary tract concerned with taste.

The *arcuate nucleus* lies on the anterior aspect of the pyramid (Figs. 12.7 and 12.11–12.13). In rostral portions of the medulla, the nucleus enlarges considerably (nucleus precursorius pontis) and appears to become continuous with the nuclei of the pons. Afferent fibers to this nucleus are derived from the cerebral cortex, and its efferent

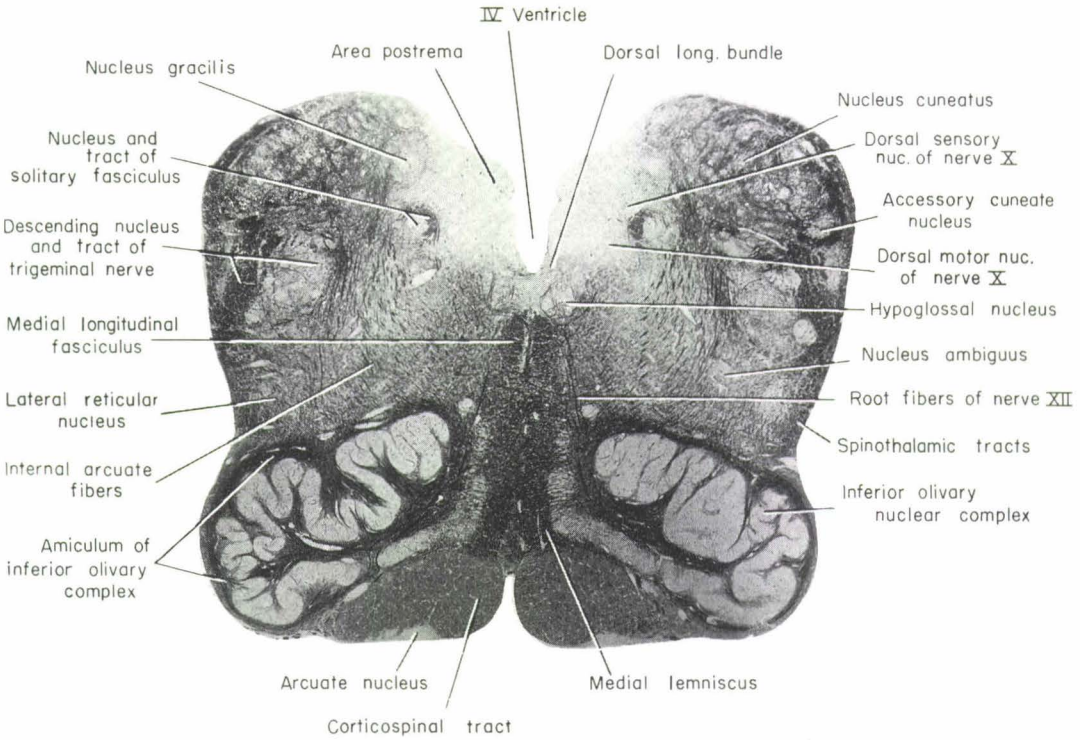


Figure 12.11. Transverse section of the medulla through the caudal part of the fourth ventricle, the area postrema and the lower part of the inferior olivary complex (Weigert's myelin stain).

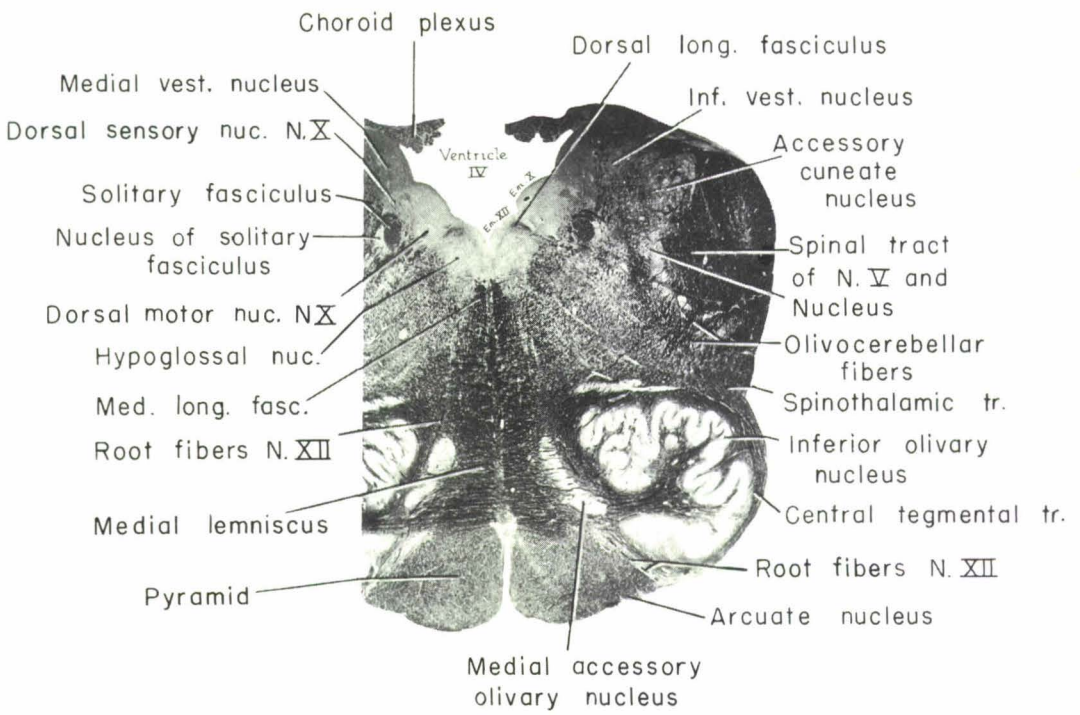


Figure 12.12. Transverse section of the medulla through the inferior olivary complex rostral to that shown in Figure 12.11. *Em. X,* eminentia vagi; *Em. XII,* eminentia hypoglossi (Weigert's myelin stain).

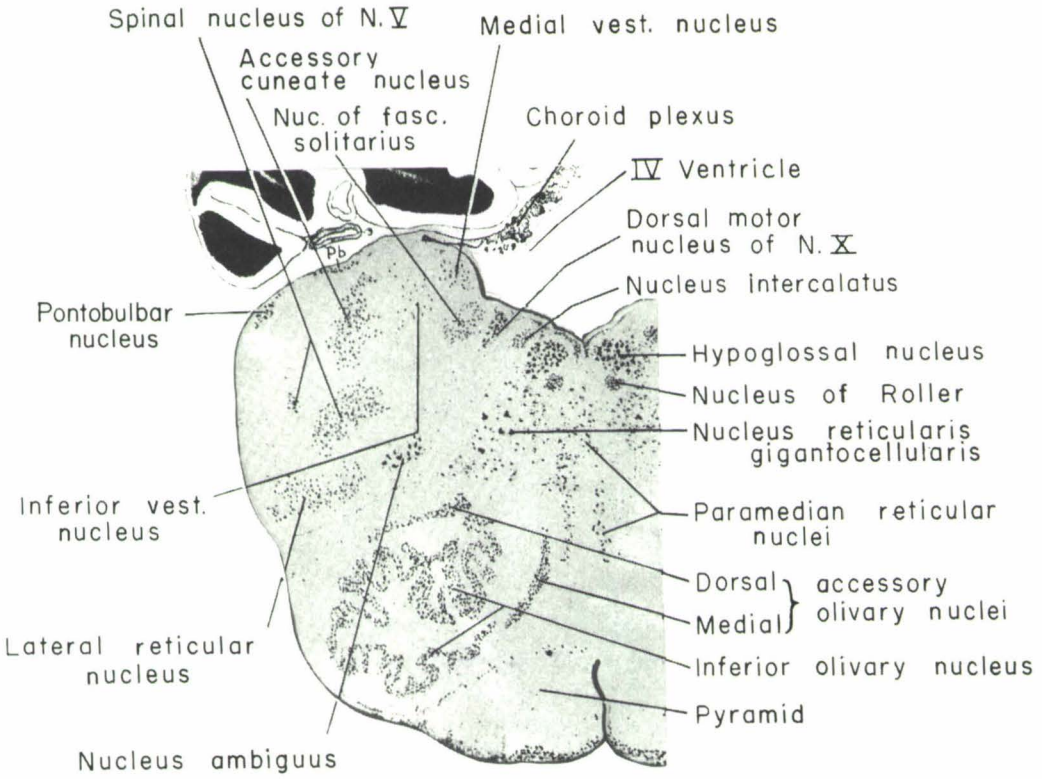


Figure 12.13. Transverse section through midolivary region of the medulla (cresyl violet stain, with schematic representation of the main cell groups).

fibers project as ventral external arcuate fibers to the cerebellum. Fibers from this small nucleus are thought to be crossed.

Area Postrema

Immediately rostral to the obex on each side of the fourth ventricle is a small rounded eminence, the *area postrema* (Fig. 12.11), containing astroblast-like cells, arterioles, sinusoids, and some apolar or unipolar neurons (20, 33). The area postrema is one of several specialized ependymal regions (104) that lie outside the blood-brain barrier, collectively referred to as circumventricular organs (Fig. 1.17). All the circumventricular organs, except the area postrema, are unpaired and related to portions of the diencephalon. Fibers of the solitary nucleus and spinal cord project to the area postrema, which also harbor axons and dendritic processes from nearby regions of the medulla (45, 132, 197). The chemical anatomy of the region is complex, and a number of putative transmitters have been identified (138). For example, fields of terminals surrounding this area contain neurophysin, oxytocin, and vasopressin, although these peptides cannot be demonstrated within the area postrema. The area postrema is an emetic chemoreceptor, sensitive to apomorphine and intravenous digitalis glycosides (16, 17). Electrical activity in the region of the area postrema is altered by intravenous administration of hypertonic solutions (46), and lesions result in altered Na^+/K^+ excretion ratios in urine, which suggest a transient potassium retention by the kidney (181).

INFERIOR OLIVARY COMPLEX

The most characteristic feature of the medulla is the inferior olivary complex (Figs. 12.8, 12.11, and 12.12). The central canal has opened into the fourth ventricle, and the roof of this ventricle is formed by the inferior medullary velum and the tela choroidea and choroid plexus. The floor of the fourth ventricle contains three eminences, which overlie cranial nerve nuclei. The most medial is the *hypoglossal eminence* (or *trigonum hypoglossi*), overlying the nucleus of the hypoglossal

nerve; an *intermediate eminence* (or *trigonum vagi*) overlies the vagal nuclei. The most medial of the vagal nuclei is the dorsal motor nucleus. The lateral part of the intermediate eminence overlies the nuclei of the solitary fasciculus. The sulcus limitans, often an indistinct sulcus, passes through the intermediate or vagal eminence. Cranial nerve cell columns medial to the sulcus are efferent, while those lateral to it are afferent (Fig. 12.14). The most *lateral eminence* overlies the vestibular nuclei and is referred to as the *area vestibularis*. (Figs. 12.2 and 12.13). Internal arcuate fibers sweep ventromedially through portions of the reticular formation, decussate, and enter the contralateral medial lemniscus. The medial lemnisci occupy triangular areas on each side of the median raphe, bounded ventrally by the pyramids and laterally by the inferior olivary nuclei. Dorsal to the medial lemnisci on each side of the median raphe are the medial longitudinal fasciculi (Figs. 12.11 and 12.12). The accessory cuneate nucleus lies dorsolaterally, posterior to the spinal trigeminal tract and nucleus.

The inferior olivary complex is a convoluted gray band of cells which consists of three parts: (a) the *principal inferior olivary nucleus*, appearing as a folded bag with the opening or hilus directed medially, (b) a *medial accessory olivary nucleus* located along the lateral border of the medial lemniscus, and (c) a *dorsal accessory olivary nucleus* located dorsal to the main nucleus (19, 151). These nuclei are composed of relatively small, round or pear-shaped cells with numerous short branching dendrites, and appear to have glutamate as their excitatory transmitter. Axons of cells in the inferior olivary complex cross the median raphe, sweep posterolaterally, and enter the cerebellum via the contralateral restiform body (part of the inferior cerebellar peduncle). Crossed olivocerebellar fibers constitute the largest single component of the restiform body (Figs. 12.25, 12.26, and 15.27). They project to all parts of the cerebellar cortex and to cerebellar nuclei (21). Fibers of this massive projection end as climbing fibers in the cerebellar cortex (50, 59, 76). Climbing fibers exert a powerful excitatory influence upon individual Purkinje cells, resulting in bursts of action potentials called complex spikes. Cells of the inferior olive have numerous gap junctions between dendrites (182) and are electrotonically coupled (120). This arrangement suggests that groups of cells in the inferior olive would tend to discharge synchronously.

The principal olivary nucleus is surrounded by a dense band of myelinated fibers, the *amiculum olivae*, composed largely of axons terminating in the nucleus. Descending fibers terminating upon cells of the inferior olivary complex arise from the cerebral cortex, the red nucleus, and the periaqueductal gray matter of the midbrain, the inferior vestibular nucleus, parts of the spinal trigeminal nucleus, and the contralateral cerebellar nuclei (131, 199, 203).

Cortico-olivary fibers arise from frontal, parietal, temporal, and occipital cortex, descend in most corticospinal fibers, and terminate bilaterally, primarily upon the ventral lamella of the principal olive. Rubro-olivary fibers and fibers arising from the periaqueductal gray matter of the midbrain enter a composite bundle known as the central tegmental tract, descend uncrossed, and terminate in different portions of the principal olive (Figs. 12.33, 13.1, and 13.4). Noradrenergic axons from the pons also reach the inferior olive (180). Rubro-olivary fibers end in the dorsal lamella while fibers from the periaqueductal gray matter, interstitial nucleus of Cajal, nucleus of Darkschewitsch, and nearby regions terminate in the rostral parts of the principal olivary nucleus, and in the medial and dorsal accessory nuclei (171, 203). Other brainstem projections to the olivary complex originate in the medial and inferior vestibular nuclei (170), caudal part of the spinal trigeminal nucleus, and the contralateral cerebellum (13, 14). Spinal projections to the inferior olivary complex terminate mainly in the accessory olivary nuclei. Fibers ascending in the anterior spino-olivary tract (anterior funiculus) synapse directly upon neurons in the dorsal and medial accessory olivary nuclei. More than half of these fibers cross in the medulla. Spino-olivary fibers, ascending in the posterior white columns, synapse upon cells in the rostral parts of the nuclei gracilis and cuneatus, which, in turn, project to the contralateral accessory olivary nuclei. All parts of the dorsal column nuclei send axons to the contralateral olivary complex, especially the dorsal accessory nucleus (13, 14). Spinal afferents to parts of the inferior olivary complex constitute a link in spinocerebellar circuitry resembling that of other spinocerebellar tracts.

Fiber tracts in ventrolateral parts of the

reticular formation are pushed dorsally by the olivary nuclei. The anterior spinocerebellar, rubrospinal, and spinothalamic tracts are located laterally between the restiform body and the olivary complex. Fibers of the vestibulospinal tract are scattered along the posterior surface of the inferior olive. Posteriorly on each side of the medial raphe lie the medial longitudinal fasciculi, containing at this level predominately descending fiber bundles of mixed origin. Descending fibers in this tract are derived from certain vestibular nuclei, portions of the brainstem reticular formation, and certain nuclei in the midbrain. The interstitial nucleus of Cajal (interstitiospinal tract) contributes a small number of fibers to the dorsomedial part of the medial longitudinal fasciculus. Tectospinal fibers from the superior colliculus form a loosely organized group of fibers in the ventral part of the bundle.

MEDULLARY RETICULAR FORMATION

Definition

The term "reticular formation" refers to portions of the brainstem core characterized structurally by a wealth of cells of various sizes and types, arranged in diverse aggregations, and enmeshed in a complicated fiber network. This structure is well-developed in all vertebrates (51), and it forms the core of the brainstem in humans. In a sense, the reticular formation constitutes a matrix within which "specific" nuclei and tracts are embedded. Anatomic studies indicate that the brainstem reticular formation, which extends from the medulla to the midbrain, can be subdivided into regions having distinctive cytoarchitecture, fiber connections, and intrinsic organization (24, 26, 127, 129, 144). Despite these features, various subdivisions cannot be regarded as entirely independent entities, because fiber connections provide innumerable possibilities for interaction between subdivisions.

Cytoarchitecture

Golgi studies indicate that almost all neurons in the reticular core project axons in both rostral and caudal directions (173). Primary bifurcating axons are oriented longitudinally, but collaterals pass in all directions and terminate in a variety of different endings. Many collaterals arborize about cells in both motor and sensory cranial nerve nuclei. The dendrites are usually long and radiating, characterizing the cells as being of the so-called isodendritic type (162). At one time, the reticular formation was thought to consist mainly of neurons with short axons. Golgi type II cells (i.e., cells with short axons) are, in fact, scarce in the reticular formation, a finding that suggests that polysynaptic transmission of impulses probably is due to dispersion of impulses along collateral fibers. The organizational pattern of the reticular formation suggests that single reticular neurons can convey impulses both rostrally and caudally, may exert influence locally and at a distance, and impulses can be conducted both rapidly (primary axon) and slowly (via synapsing collateral axons) (1, 173).

Major Subdivisions

The brainstem reticular formation begins in the caudal medulla rostral to the corticospinal decussation (Figs. 12.6 and 12.7). The lateral and ventral reticular nuclei are particularly well-delineated at this level. The *lateral reticular nucleus* lies ventrolaterally in the caudal medulla and extends rostrally up to midolivary levels (Figs. 12.8 and 12.11). It can be divided into three cytoarchitectonic parts: magnocellular, parvicellular, and subtrigeminal. The magnocellular part is oriented ventromedially within the nucleus, dorsal to the inferior olive, and the parvicellular part lies dorsolateral to it (110, 198). Cells in the lateral reticular nucleus project axons to specific portions of the cerebellar cortex and cerebellar nuclei via the ipsilateral restiform body (inferior cerebellar peduncle) (128). In turn, they receive a topographically organized and highly convergent input from the spinal cord via spinoreticular pathways (110). The lateral reticular nucleus also receives crossed descending rubrobulbar axons (80, 202). Most cells in the lateral reticular nucleus respond to stimulation over large peripheral receptive fields involving both fore- and hindlimbs (166). Medial to the lateral reticular nucleus and dorsal to the caudal half of the inferior olivary nucleus lies the *ventral reticular nucleus* (*nucleus reticularis ventralis*) (Fig. 12.8). By comparison to the lateral reticular nucleus, relatively little is known of the ventral reticular nucleus, except that it does not project to the cerebellum (26).

At midolivary levels, the gigantocellular reticular nucleus (*nucleus reticularis gigantocellularis* of Olszewski and Baxter (144)) occu-

pies the area medial and dorsal to the rostral half of the inferior olivary nucleus (Fig. 12.13). The latter nucleus is the rostral continuation of the nucleus reticularis ventralis. As its name implies, it has characteristic large cells, but it also contains many medium- and small-sized cells (Fig. 12.13). This nucleus occupies the medial two-thirds of the reticular formation and extends to the medullary-pontine junction. Descending fibers from the gigantocellular nucleus form the medullary reticulospinal tract, which exerts an inhibitory effect upon spinal neurons (see Chapter 11, and Figs. 11.10 and 11.22). The other major nuclei of the medullary reticular formation are the parvicellular nucleus (*nucleus reticularis parvicellularis*) and the paramedian nuclei.

The *parvicellular reticular nucleus* is a collection of small cells located posterolaterally, medial to the spinal trigeminal nucleus, and anterior to the vestibular nuclei. This nucleus, occupying roughly the lateral third of the medullary reticular formation, has been referred to as the sensory part because it receives collaterals from secondary sensory pathways (24, 26). The *paramedian reticular nuclei* consist of several small nuclear groups that lie close to, and sometimes among, fibers of the medial longitudinal fasciculus and the medial lemniscus (Fig. 12.13). These neurons project most of their fibers to the cerebellar vermis (23).

In essence, the medullary reticular formation consists of three principal nuclear masses: (a) a *paramedian reticular nuclear group*, (b) a *central group* (i.e., the ventral reticular and gigantocellular reticular nuclei), and (c) a *lateral nuclear group* consisting of the lateral reticular and parvicellular reticular nuclei. The raphe nuclei, consisting of several distinct groups of neurons, probably also belong to the reticular formation but, because they contain a multitude of serotoninergic neurons, they are described later with other chemospecific neuronal systems.

Afferent Fibers

The principal sources of afferents to the medullary reticular formation are (a) the spinal cord, (b) collateral fibers from second order neurons of sensory cranial nuclei, (c) the cerebral cortex, and (d) the cerebellar nuclei.

Spinoreticular fibers ascend in the anterolateral funiculus (130, 169), and terminate in the caudal and lateral portions of the medullary reticular formation. A considerable number of these fibers end in the caudal half of the nucleus reticularis gigantocellularis, though some project to more rostral portions of the reticular formation (Figs. 11.10 and 12.13). Collaterals of spinothalamic fibers terminate somatotopically upon cells of the lateral reticular nucleus, a cerebellar relay nucleus (22, 26). Physiologic data indicate that exteroceptive impulses are relayed to the cerebellum via this indirect spinocerebellar pathway (47).

Collateral fibers from second order sensory neurons of cranial nuclei, such as auditory, vestibular, trigeminal, and visceral (solitary fasciculus) nuclei, project to the parvicellular reticular nucleus. No collaterals of the medial lemniscus terminate in any part of the brainstem reticular formation. Except for a modest number of trigeminal fibers (36, 193), primary sensory fibers do not appear to terminate in the reticular formation.

Corticoreticular fibers originate from widespread areas of the cerebral cortex, but the majority of these fibers arise from sensorimotor areas (167). These fibers are both crossed and uncrossed, and most of them terminate in portions of the pons and medulla. Regions of the brainstem reticular formation receiving corticoreticular fibers are those which give rise to reticulospinal fibers. These regions encompass the *nucleus reticularis pontis oralis*, the *nucleus reticularis pontis caudalis*, and the *nucleus reticularis gigantocellularis* (Figs. 11.10, 11.22, and 12.13).

Cerebelloreticular fibers terminate mainly in the paramedian reticular nuclei. These reticular projections originate from the fastigial and dentate nuclei. Fibers from the fastigial nucleus reach the paramedian nuclei via the uncinate fasciculus (35, 189), while fibers from the dentate nucleus pass via the crossed descending division of the superior cerebellar peduncle (29, 37). Impulses from a wide variety of sources converge upon the reticular nuclei. The maximal overlap of afferent fibers from different sources occurs in the medullary reticular formation, which gives rise to a large number of long ascending and descending axons.

Efferent Fibers

They arise from the medial two-thirds of the medullary reticular formation, which corresponds to the gigantocellular reticular nucleus. This nuclear mass gives rise to both as-

cending and descending fibers. Ascending fibers course in the *central tegmental tract*, are uncrossed, and terminate mainly upon portion of the intralaminar and thalamic nuclei (136) (Fig. 13.4). This system plays an important role in the mechanism of arousal and sleep. Descending fibers from this medial region of the reticular formation form the medullary reticulospinal tracts, which are bilateral but predominantly uncrossed (194) (Figs. 11.10 and 11.22). Other fibers, originating in the paramedian and lateral reticular nuclei, project, uncrossed, to specific portions of the cerebellum. Fibers arising in the paramedian reticular nuclei terminate largely in the vermis of the anterior lobe (23), while those from the lateral reticular nucleus end in the vermis, hemisphere, and flocculonodular lobule.

The reticulospinal fibers have been the subject of numerous anatomic and physiologic studies, which yielded important information on the organizational features of the medullary reticular formation. For instance, anatomic studies of the origin of reticulospinal axons reveal both a rostrocaudal and dorsoventral topographic arrangement (103, 154, 155, 190, 210). In the spinal cord, reticulospinal axons from the pons form a medial tract in the ipsilateral ventromedial funiculus, and axons from the medulla form a lateral tract in the ipsilateral ventrolateral funiculus. Medullary reticulospinal axons reaching thoracic and lumbar spinal segments arise from cells in the caudal and ventral medullary reticular formation, while axons to cervical spinal segments originate from more rostrally located cells. Stimulation of the rostral and dorsal parts of the nucleus reticularis gigantocellularis and regions of the caudal pontine reticular formation produces monosynaptic excitatory postsynaptic potentials in motor neurons supplying the axial muscles of the neck and back (125, 150, 154, 155, 163, 183). Stimulation of the caudal and medial medullary reticular formation produces disynaptic and multisynaptic inhibitory postsynaptic potentials in motor neurons at all levels. The medullary reticular formation can be divided into a dorsolateral facilitatory region and a caudomedial inhibitory zone, which both constitute the "effector" area of the medullary reticular formation. This effector area receives projections from cells in the parvicellular reticular nucleus, which serve "receptive" or "associative" functions. The large effector area of the medullary reticular formation exerts its excitatory or inhibitory effects at both spinal and higher brainstem levels.

ASCENDING AND DESCENDING TRACTS

Ascending fibers of the medial lemniscus occupy an "L"-shaped area on each side of the median raphe posterior to the pyramid and medial to the inferior olivary complex (Figs. 12.11, 12.12, and 12.25). The spinothalamic tracts, which are part of the more global anterolateral system (ALS), have merged to form essentially a single entity in the retro-olivary area. These tracts appear considerably smaller than at spinal levels, because an appreciable number of fibers terminate in the lateral reticular nucleus and others have passed medially into the gigantocellular reticular nucleus. The posterior spinocerebellar tract has moved posteriorly at medullary levels and has become incorporated into the inferior cerebellar peduncle (Fig. 12.25). The anterior spinocerebellar tract maintains a retro-olivary position in the medulla, and ultimately enters the cerebellum by coursing along the dorsal surface of the superior cerebellar peduncle. About one-third of the fibers of the rostral spinocerebellar tract enter the cerebellum via the inferior cerebellar peduncle; all other fibers of this uncrossed tract enter the cerebellum in association with the superior cerebellar peduncle (145).

The medial longitudinal fasciculus lies anterior to the hypoglossal nucleus adjacent to the median raphe (Figs. 12.11, 12.12, and 12.25). Descending fibers in this complex bundle are derived from various brainstem nuclei. Vestibular fibers in this bundle arise from the medial and inferior vestibular nuclei. The pontine reticular formation contributes the largest number of fibers descending in the medial longitudinal fasciculus. Smaller groups of fibers arise from the interstitial nucleus of Cajal (interstitiospinal tract) and the superior colliculus (tectospinal tract).

Rubrospinal fibers, descending in retro-olivary position, project collaterals to the lateral reticular nucleus, a cerebellar relay nucleus. Uncrossed *rubrobulbar fibers*, arising from rostral parts of the red nucleus, descend in the central tegmental tract and end upon cells in the dorsal lamella of the principal inferior olivary nucleus. At midmedullary levels, fibers of the vestibulospinal tract are scattered in an area posterior to the inferior olivary complex. At more caudal levels, these

fibers form a more compact bundle located in the retro-olivary region. The medullary reticulospinal tract is not evident at these levels, but its cells of origin in the gigantocellular reticular nucleus are present posteromedial to the inferior olivary complex (Fig. 12.11). The spinal trigeminal tract and nucleus occupy the same location as at more caudal levels.

INFERIOR CEREBELLAR PEDUNCLE

This peduncle is a composite bundle that contains fibers arising from cell groups in the spinal cord and medulla that project to the cerebellum, as well as fibers interconnecting the vestibular nuclei and the cerebellum. The inferior cerebellar peduncle is composed of two major elements: (a) a large *restiform body*, which contains many afferent fibers from different sources (e.g., reticular formation, inferior olivary complex, trigeminal nuclei, nucleus cuneatus, and spinal cord), and (b) a smaller *juxtarestiform body*, which contains only cerebellovestibular and vestibulocerebellar fibers. The restiform body is the large bundle in the dorsolateral portion of the medulla that is often referred to as the inferior cerebellar peduncle. The term inferior cerebellar peduncle, however, should be restricted to the bundle that is formed at the base of the cerebellum by the confluence of both juxtarestiform and restiform bodies.

Fibers entering the inferior cerebellar peduncle assemble along the posterolateral border of the medulla, dorsal to the spinal trigeminal tract and lateral to the accessory cuneate nucleus. This bundle rapidly increases in size in the upper medulla by the addition of more fibers, and enters the cerebellum (Figs. 12.25, 12.26, and 12.33). The posterior spinocerebellar tract moves dorsally and enters the restiform body directly. Crossed olivocerebellar fibers, originating from all parts of the inferior olivary complex, constitute, quantitatively, the largest group of fibers that enter the inferior cerebellar peduncle (Figs. 12.25, 12.33, and 15.27). Other medullary nuclei projecting to the cerebellum via this peduncle are (a) the lateral reticular nucleus of the medulla, (b) the accessory cuneate nucleus, (c) the paramedian reticular nuclei, (d) the arcuate nucleus, and (e) the perihypoglossal nuclei (Figs. 12.13 and 12.25). Projections of the lateral reticular nucleus and the accessory cuneate nucleus are uncrossed; those from other relay nuclei are both crossed and uncrossed. At higher levels, the restiform body becomes covered laterally by fibers of the middle cerebellar peduncle (Figs. 12.33 and 13.2).

On the posterolateral aspect of the inferior cerebellar peduncle, a small group of closely packed, medium-sized cells can be seen (Fig. 12.13). These cells constitute the caudal portion of the *pontobulbar nucleus*. At more rostral levels, this cell column assumes a progressively more ventral position, and at the junction of the pons and medulla it forms a fairly large cell mass ventral to the restiform body and medial to the ventral cochlear nucleus (Figs. 12.26 and 12.32). The cells of this nucleus resemble those in the ventral portion of the pons and have been regarded as a caudal extension of the pontine nuclei.

CRANIAL NERVES OF THE MEDULLA

The schematic arrangement of the functional components of the cranial nerves of the medulla and the cell columns to which they are related are shown in Figure 12.14. This schema resembles that present in the spinal cord, although development of the fourth ventricle has shifted somatic and visceral afferent regions laterally. The functional components of a typical spinal nerve are four: (a) *general somatic afferent* (GSA), (b) *general visceral afferent* (GVA), (c) *general somatic efferent* (GSE), and (d) *general visceral efferent* (GVE). Functional components of the cranial nerves include the four types found in spinal nerves, plus three additional special categories: (a) *special somatic afferent* (SSA), (b) *special visceral afferent* (SVA), and (c) *special visceral efferent* (SVE). Somatic efferent fibers in both spinal and cranial nerves belong to the general component.

In the medulla, as in the spinal cord, the sulcus limitans divides afferent and efferent cell columns. Within the medulla special somatic afferent (SSA) cranial nerves in the medulla are represented by the auditory and vestibular components of the vestibulocochlear nerve (N. VIII). General somatic afferent (GSA) fiber components of cranial nerves V, VII, IX, and X enter the brainstem at different levels and descend in the spinal trigeminal tract. Fibers conveying taste (special visceral afferent (SVA)) and general visceral afferent (GVA) impulses from components of cranial nerves VII, IX, and X form a well-defined tract, the solitary fasciculus, which is embedded in the solitary nucleus

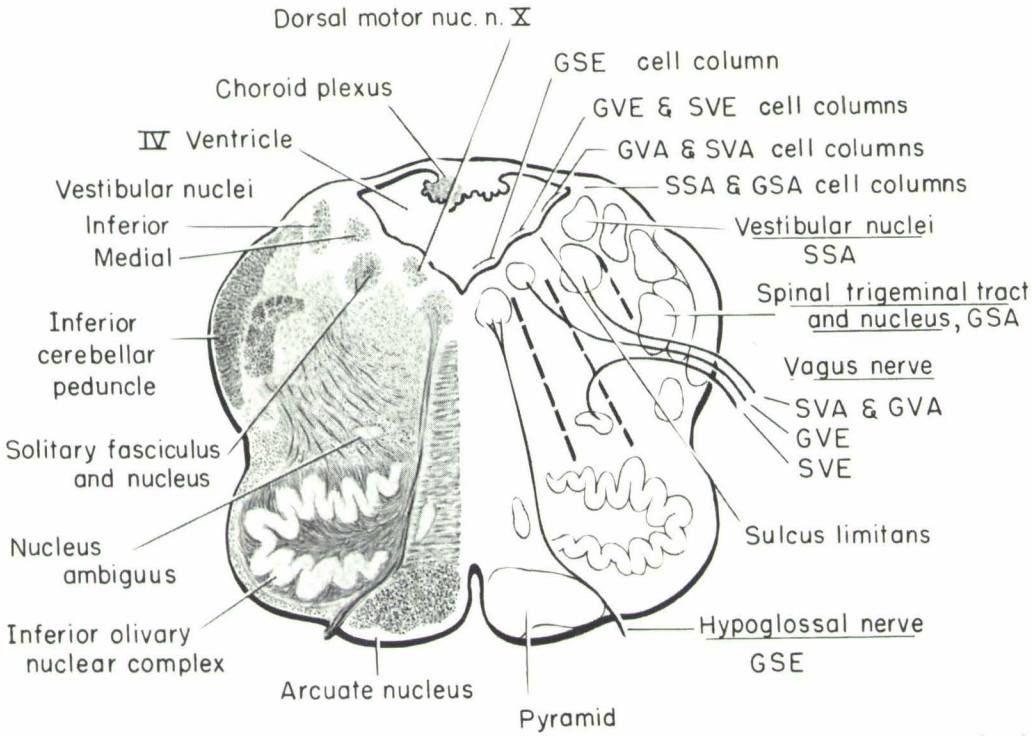


Figure 12.14. Transverse section of the medulla showing its basic features. Cell columns related to functional components of the cranial nerve are indicated on the right. Functional components of cranial nerves are both general and special. The vestibular nuclei shown at this level (and auditory nuclei at higher levels) form the special somatic afferent (SSA) cell columns. The spinal trigeminal nucleus forms the general somatic afferent (GSA) cell column and receives fibers from cranial nerves with this functional component (i.e., N. V, VII, IX, and X). Functional components of the vagus nerve (except GSA) are shown in relation to particular nuclei. The hypoglossal nucleus (and the nuclei of N. VI, IV, and III at higher brainstem levels) gives rise to general somatic efferent (GSE) fibers. *Heavy dashes* separate the nuclei of the various cell columns on the right side.

(Figs. 12.11, 12.12, 12.15, 12.16, and 12.18). All of the these cell columns lie lateral to the sulcus limitans (Fig. 12.14). Ventromedial to the sulcus limitans are the efferent cell columns. The dorsal motor nucleus of the vagus nerve and the inferior salivatory nucleus of the glossopharyngeal nerve give rise to general visceral afferent (GVE) fibers. Cells in the nucleus ambiguus, located in the ventrolateral reticular formation posterior to the inferior olivary nuclear complex, give rise to special visceral efferent (SVE) fibers that pass peripherally along cranial nerves XI, X, and IX (Figs. 12.15 and 12.16). These fibers innervate muscles of the pharynx and larynx derived from the third and fourth branchial arches (i.e., branchiomeric muscles). Other motor nuclei, having similar locations in the pons, supply special visceral efferent (SVE) fibers to muscles derived from the first and second branchial arches via cranial nerves V and VII, respectively (Figs. 12.15 and 12.16). The hypoglossal nucleus located in the floor of the fourth ventricle near the median raphe gives rise to general somatic efferent (GSE) fibers which innervate the muscles of the tongue. The general somatic efferent cranial nerve nuclei all lie near the median raphe and relatively close to the floor of the fourth ventricle or cerebral aqueduct. Other nuclei, at more rostral levels, belonging to this group are the abducens, trochlear, and oculomotor. Schematic color-coded diagrams showing these nuclei and the intramedullary course of their fibers (Figs. 12.15 and 12.16) help to understand the organization of cranial nerves and their various components. The general visceral efferent (GVE) components (parasympathetic) forming parts of cranial nerves III, VII, IX, and X are indicated in Figures 12.15 and 12.16.

Hypoglossal Nerve

The hypoglossal nerve (N. XII) is a *general somatic efferent* (GSE) cranial nerve that sup-

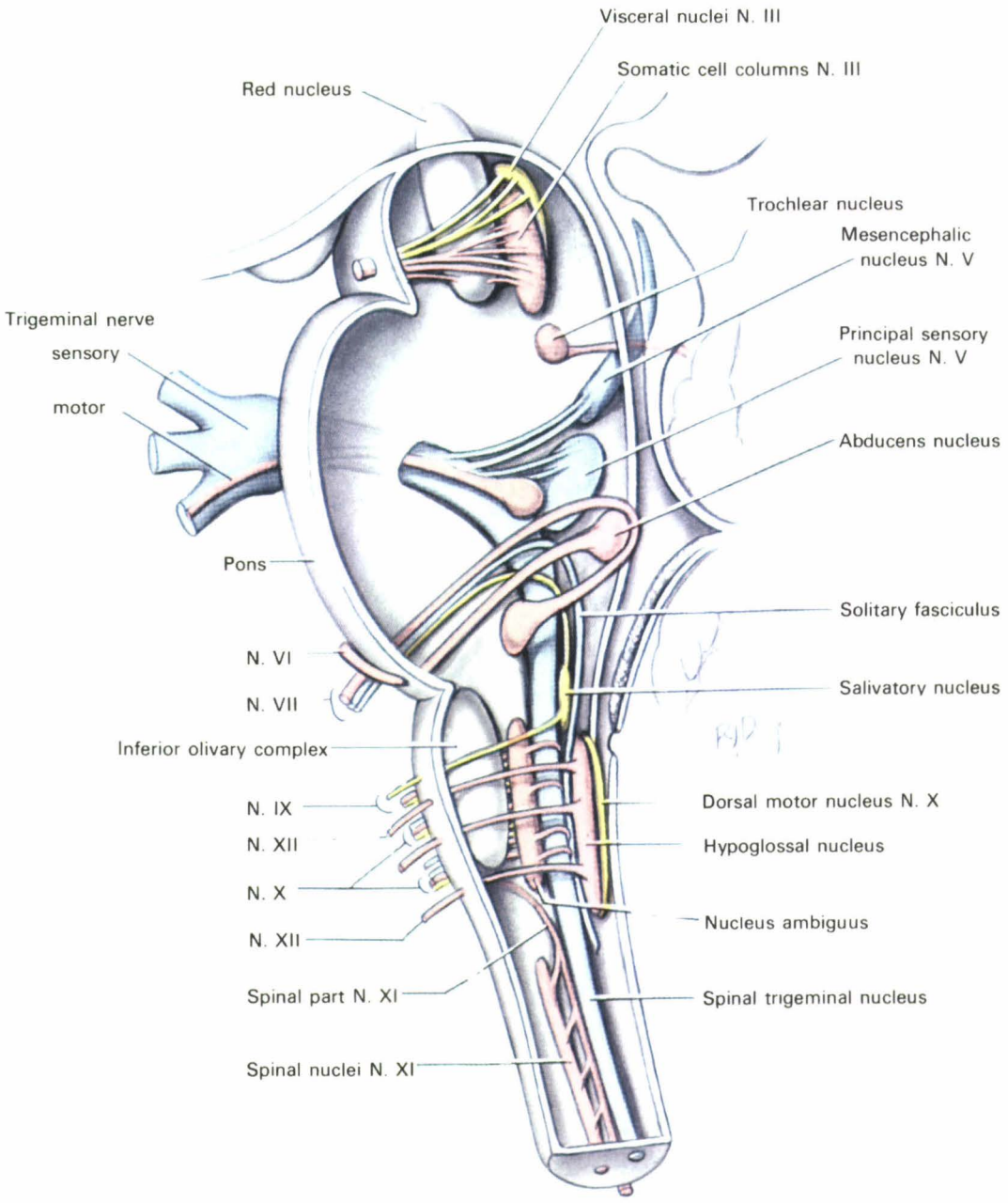


Figure 12.15. Intramedullary course of the cranial nerves in a midsagittal view. The brainstem is represented as a hollow shell except for cranial nerve components. General somatic (GSE) and special visceral (SVE) efferent components of cranial nerves innervating striated muscles are shown in *red*. General visceral efferent (GVE) components of cranial nerves III, VII, IX, and X, representing preganglionic parasympathetic fibers, are shown in *yellow*. General somatic (GSA), general visceral (GVA), and special visceral (SVA) afferent components of the cranial nerves are in *blue*.

کتابخانه دیجیتال دانشگاه علوم پزشکی تهران

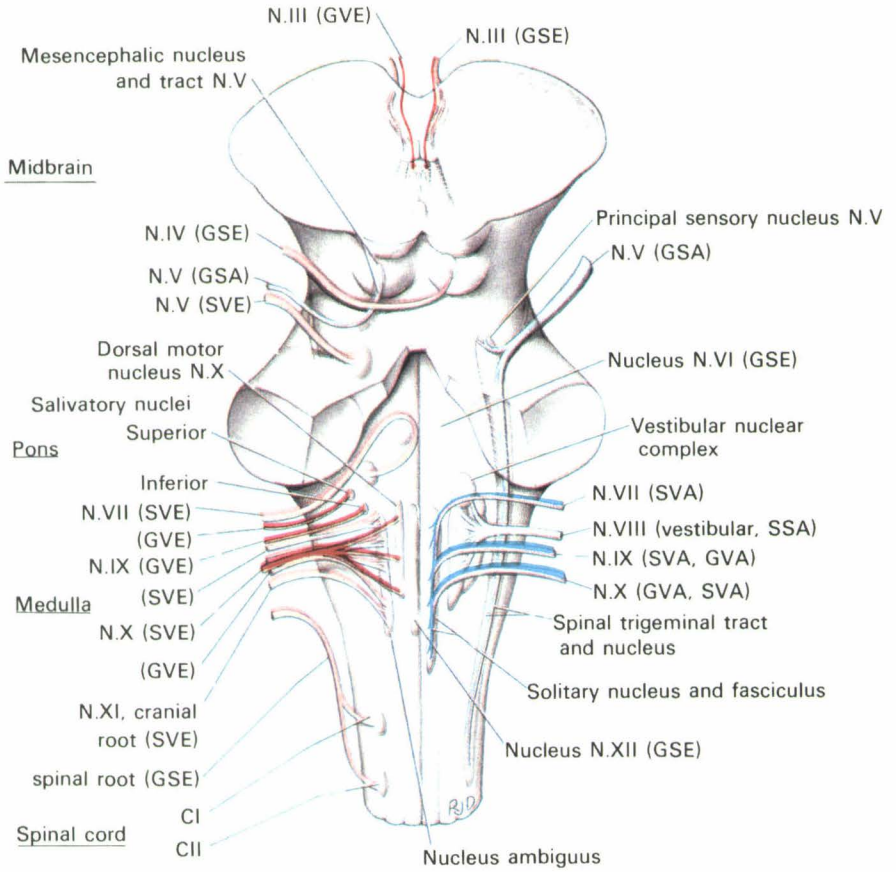


Figure 12.16. Infratentorial cranial nerves showing their nuclei of origin and termination, their intramedullary course, and their functional components. The cochlear nerve and nuclei are not shown. General somatic afferent (GSA) components of the trigeminal nerve (N. V) are shown in *light blue*. General and special visceral afferent (GVA, SVA) components of the facial (N. VII), glossopharyngeal (N. IX), and vagus (N. X) nerves are shown in *dark blue*. The vestibular nerve which differentially distributes special somatic afferent (SSA) fibers to the vestibular nuclear complex is *white*. Similarities in the intramedullary course of fibers in the spinal trigeminal tract, the vestibular nerve root and the solitary fasciculus are evident on the right. General somatic efferent (GSE) fibers from the oculomotor (N. III) and trochlear (N. IV) nuclei, and those of the spinal root of the accessory nerve (N. XI) are *light red*. Only contributions from the first and second cervical segments to the spinal root of the accessory nerve are shown. Root fibers of the abducens (N. VI) and hypoglossal (N. XII) nuclei, which exit ventrally and contain GSE fibers, are not shown. Special visceral efferent (SVE) fibers from the branchiomeric cranial nerves (N. V, VII, IX, X, and XI) are shown in *light red*. General visceral efferent (GVE) fibers, representing preganglionic parasympathetic components, of the oculomotor (N. III), facial (N. VII), glossopharyngeal (N. IX), and vagus (N. X) nerves are in *dark red*.

plies the somatic skeletal muscles of the tongue. It innervates the ipsilateral half of the tongue. The hypoglossal nucleus, composed of typical multipolar motor cells, forms a column about 18 mm long that is located internal to the trigonum hypoglossi. It begins caudal to the inferior olive and extends rostrally to the region of the striae medullares. Root fibers of this nerve emerge ventrally, pass along the lateral margin of the medial longitudinal fasciculus and the medial lemniscus, traverse medial parts of the inferior olivary complex, and exit from the medulla between the pyramid and the inferior olivary complex (Figs. 12.1, 12.11, and 12.12). The hypoglossal nucleus receives numerous crossed and uncrossed fibers from neurons in the medullary reticular formation that form delicate plexuses around the cells of the nucleus. It also receives direct projections from the "corticobulbar" fiber system, which plays a crucial role in the voluntary motor control of the tongue. Other inputs from secondary glossopharyngeal, vagal, and trigeminal fiber systems appear involved in reflex movements of the tongue in response to stimuli from lin-

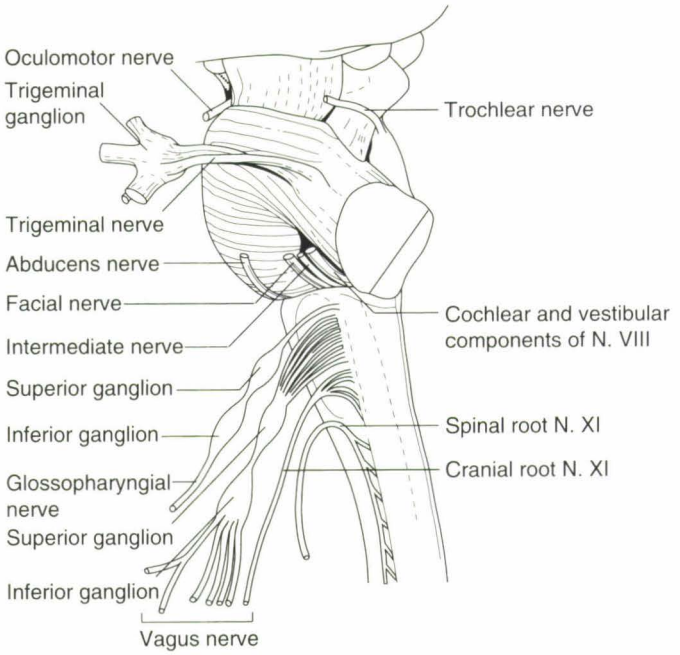


Figure 12.17. Brainstem and cranial nerves showing their peripheral ganglia.

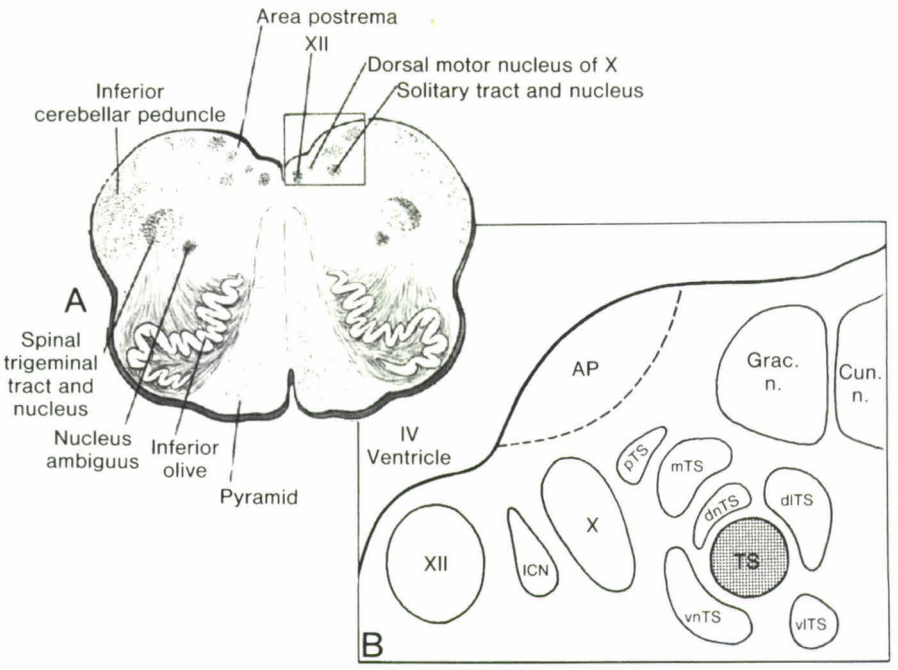


Figure 12.18. **A.** Major cell groups and tracts in the caudal medulla. The enclosed area in the dorsomedial portion of the diagram is shown in greater detail in B. **B.** Subnuclei forming the nucleus of the solitary tract which receive afferents from cranial nerves IX and X. *AP,* area postrema; *Cun. n.,* cuneate nucleus; *dlTs,* dorsolateral nucleus of solitary tract; *dnTS,* dorsal nucleus of solitary tract; *Grac. n.,* gracile nucleus; *ICN,* intercalated nucleus; *mTS,* medial nucleus of solitary tract; *pTS,* parvicellular nucleus of solitary tract; *TS,* solitary tract; *vlTS,* ventrolateral nucleus of solitary tract; *vnTS,* ventral nucleus of solitary tract; *X,* dorsal motor nucleus of vagus nerve; *XII,* hypoglossal nucleus.

gual, oral, and pharyngeal mucous membranes.

In the gray matter surrounding the hypoglossal nuclei are several discrete nuclear groups, collectively known as the perihypoglossal nuclei. These are the *nucleus intercalatus*, the *nucleus prepositus*, and the *nucleus of Roller* (Figs. 12.13, 12.25, and 12.26). The nucleus intercalatus, situated between the hypoglossal nucleus and dorsal motor nucleus of the vagus, is composed predominantly of small cells and a scattering of larger cells (Fig. 12.13). Rostral to the hypoglossal nucleus is the nucleus prepositus (Figs. 12.25 and 12.26), which extends from the oral pole of the hypoglossal nucleus almost to the abducens nucleus. It is composed of relatively large cells and a few smaller cells resembling those of the nucleus intercalatus, with which it is continuous at more caudal levels. The nucleus of Roller, composed of relatively large cells, lies ventral to the rostral pole of the hypoglossal nucleus and adjacent to its root fibers (Fig. 12.13). Immediately posterior to the hypoglossal nucleus is a small bundle of fibers in the periventricular gray matter known as the *dorsal longitudinal fasciculus* of Schütz (174) (Figs. 12.11 and 12.12). This composite bundle comprises both ascending and descending fibers and is considered to be visceral in nature (30, 87, 105, 136, 137).

Lesions of the hypoglossal nerve produce a lower motor neuron paralysis of the ipsilateral tongue muscles with loss of muscle tone and, ultimately, atrophy of the muscles. Due to the paralysis of the genioglossus muscle, a muscle that effects protrusion of the tongue, the tongue will deviate to the side of the lesion when protruded. The intrinsic muscles alter the shape of the tongue, while the extrinsic muscles alter its shape and position. Intramedullary lesions involving the pyramid and the hypoglossal nerve (e.g., in cases of vascular lesion of the anterior spinal artery) produce a combined upper and lower motor neuron syndrome referred to as *inferior* or *hypoglossal alternating hemiplegia*. This syndrome is characterized by (a) a contralateral hemiplegia (upper motor neuron), and (b) an ipsilateral paralysis of the tongue (lower motor neuron).

Spinal Accessory Nerve

The accessory nerve (N. XI) usually is divided into cranial and spinal portions which form, respectively, the internal and external branches of the nerve (Fig. 12.17). The *cranial part* of the nerve arises from cells in the caudal pole of the nucleus ambiguus. Axons of these cells emerge from the lateral surface of the medulla caudal to the lowest filaments of the vagus nerve. Fibers of the cranial part of the accessory nerve join the vagus nerve to form the inferior (recurrent) laryngeal nerve, which innervates the intrinsic muscles of the larynx. This component of the accessory nerve innervates branchiomeric musculature and is regarded as a special visceral efferent (SVE) component.

The *spinal portion* of the accessory nerve originates from a cell column in the anterior horn of the upper five (or six) cervical segments. Caudally cells of this column occupy a lateral process of the anterior horn, but at higher levels they tend to assume a more central position. Root fibers from these cells arch posterolaterally to emerge from the lateral aspect of the spinal cord between the dorsal and ventral roots (Fig. 12.3). Rootlets of the spinal portions of the accessory nerve from upper cervical segments unite to form a common trunk (external branch) that ascends posterior to the denticulate ligaments, enters the skull through the foramen magnum, and ultimately exits from the skull via the jugular foramen in association with the vagus and glossopharyngeal nerves (Fig. 12.17). The spinal part of the accessory nerve innervates the ipsilateral sternocleidomastoid and upper parts of the trapezius muscles. Although contractions of the sternocleidomastoid muscle turn the head to the opposite side, unilateral lesions of the spinal accessory nerve usually do not produce any abnormality in the position of the head. Weakness in turning the head to the opposite side against resistance, however, is obvious. Paralysis of the upper part of the trapezius muscle is evidenced by (a) downward and outward rotation of the upper part of the scapula, and (b) moderate sagging of the shoulder on the affected side.

Vagus Nerve

This complex mixed branchiomeric nerve (N. X) contains (a) *general somatic afferent* (GSA) fibers distributed to cutaneous areas back of the ear and in the external auditory meatus, (b) *general visceral afferent* (GVA) fibers from the pharynx, larynx, trachea, esophagus, and thoracic and abdominal vis-

cera, (c) *special visceral afferent* (SVA) fibers from taste buds in the region of the epiglottis, (d) *general visceral efferent* (GVE) fibers distributed to parasympathetic ganglia located near the thoracic and abdominal viscera, and (e) *special visceral efferent* (SVE) fibers that innervate the striated (branchiomeric) muscles of the larynx and pharynx.

General somatic afferent fibers of the vagus nerve arise from cells of the superior ganglion of the vagus nerve, located in, or immediately beneath, the jugular foramen (Fig. 12.17). Both general and special visceral afferent fibers of the vagus nerve arise from the larger inferior vagal ganglion (nodosal ganglion). Afferent vagal fibers enter the lateral surface of the medulla ventral to the inferior cerebellar peduncle by traversing the spinal trigeminal tract and nucleus (Fig. 12.14). Cutaneous afferent fibers enter the dorsal part of the spinal trigeminal tract along with similar general somatic afferents from other branchiomeric cranial nerves. More numerous visceral afferent fibers of the vagus nerve pass dorsomedially into the nucleus and tractus solitarius (Figs. 12.14–12.16). Fibers entering the solitary fasciculus bifurcate into short ascending and longer descending components. Descending vagal components in the solitary fasciculus gradually diminish in number as collaterals and terminals are given off to the solitary nucleus. Some vagal visceral fibers descend caudal to the obex, where the solitary nuclei of the two sides merge to form the *commissural nucleus* of the vagus nerve (Fig. 12.8). A number of descending vagal fibers decussate and enter the contralateral half of the commissural nucleus (95, 96, 164).

The *fasciculus solitarius* is formed by visceral afferent fibers contributed by the vagus, glossopharyngeal, and facial (intermediate) nerves (Figs. 12.15 and 12.16). Fibers conveying taste from the anterior two-thirds of the tongue (via the chorda tympani) and from the posterior third of the tongue (glossopha-

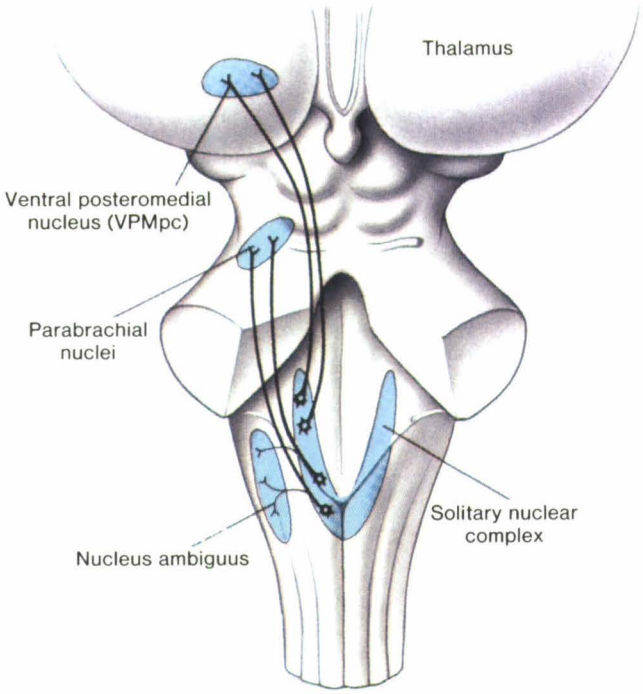


Figure 12.19. Ascending projections of the solitary nuclear complex superimposed upon a posterior view of the brainstem. The solitary nuclear complex receives special visceral afferent (SVA) fibers via the intermediate nerve and both special and general visceral afferent (SVA, SGA) fibers via the glossopharyngeal and vagus nerves. Cells in rostral parts of the nucleus solitarius project ipsilaterally via the central tegmental tract to the small-celled part of the ventral posteromedial (VPM_{pc}) nucleus of the thalamus. Caudal parts of the solitary nucleus which receive afferents largely from the glossopharyngeal and vagus nerves project fibers rostrally to caudal parts of the solitary nucleus and also project collaterals to the nucleus ambiguus. The solitary nuclear complex, the nucleus ambiguus, the parabrachial nuclei and VPM_{pc} are shown in *blue*.

ryngeal nerve) mainly terminate in rostral parts of the solitary nucleus. Portions of the solitary fasciculus at the level of entry of the vagus nerve, and caudal to it, contain mainly general visceral afferent fibers, largely from the vagus nerve (12).

The *nucleus solitarius* can be divided on cytoarchitectonic criteria into several parts: (a) a medial part, dorsolateral to the dorsal motor nucleus of the vagus; (b) dorsomedial, dorsolateral, and ventrolateral subnuclei, which surround the *tractus solitarius;* and (c) a parvicellular subnucleus lying between the medial nucleus and the area postrema (Fig. 11.18). Although there is some variation, this general arrangement has been observed in carnivores and nonhuman primates and humans (12, 95, 121, 192). Cells of the medial part extend rostrally slightly beyond the dorsal motor nucleus of the vagus (Figs. 12.20 and 12.21). This part of the nucleus also extends caudal to the fourth ventricle and merges with the corresponding cell column on the opposite side to form the commissural nucleus of the vagus nerve (Fig. 12.8) (193).

The lateral subnuclei form a column of larger cells which partially or completely surrounds the solitary fasciculus (Figs. 12.12, 12.18, and 12.20). This part of the nucleus parallels the fasciculus throughout most of its length. Rostrally it extends to the lower border of the pons, while caudally its cells diminish in number and are difficult to distinguish from reticular neurons. The enlarged rostral part of the solitary nucleus (i.e., the lateral part) receives mainly special visceral afferent (taste) fibers from the facial (intermediate) and glossopharyngeal nerves and is referred to as the *gustatory nucleus* (135, 164). The caudal and medial solitary nuclei receive most of the general visceral afferent fibers from the vagus nerve, along with some facial and glossopharyngeal fibers. Although visceral afferent axons to the solitary nuclear complex terminate over an extensive rostrocaudal portion of the structure, there is a viscerotropic pattern of endings within the subnuclei (96). Alimentary tract afferents end in the parvicellular nucleus (73), pulmonary afferents synapse in the ventrolateral subnu-

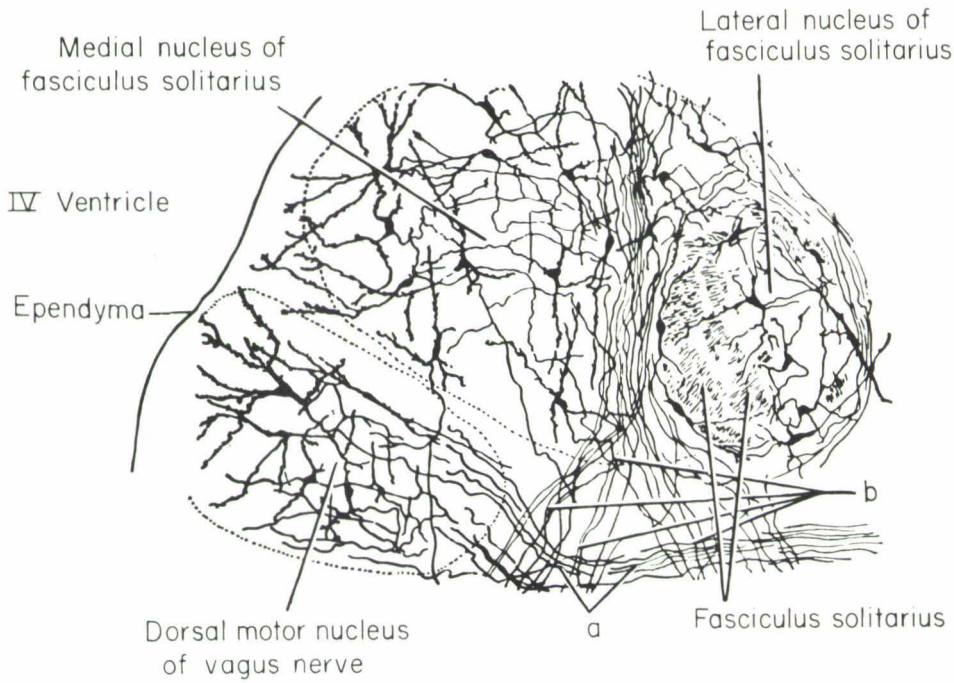


Figure 12.20. The vagal nuclei in the floor of the fourth ventricle based upon a drawing of a Golgi preparation of newborn cat. Efferent (preganglionic) fibers from the dorsal motor nucleus of the vagus nerve are indicated by *a*, while *b* indicates fibers from the medial and lateral (sensory) nuclei of the fasciculus solitarius forming secondary vagoglossopharyngeal pathways. The medial nucleus of the fasciculus solitarius extends caudally to the fourth ventricle and merges with corresponding cell group on the opposite side, forming the commissural nucleus of the vagus nerve (Fig. 12.8). The lateral nucleus of the fasciculus solitarius extends rostrally, increases in size and parallels the fasciculus solitarius throughout most of its length.

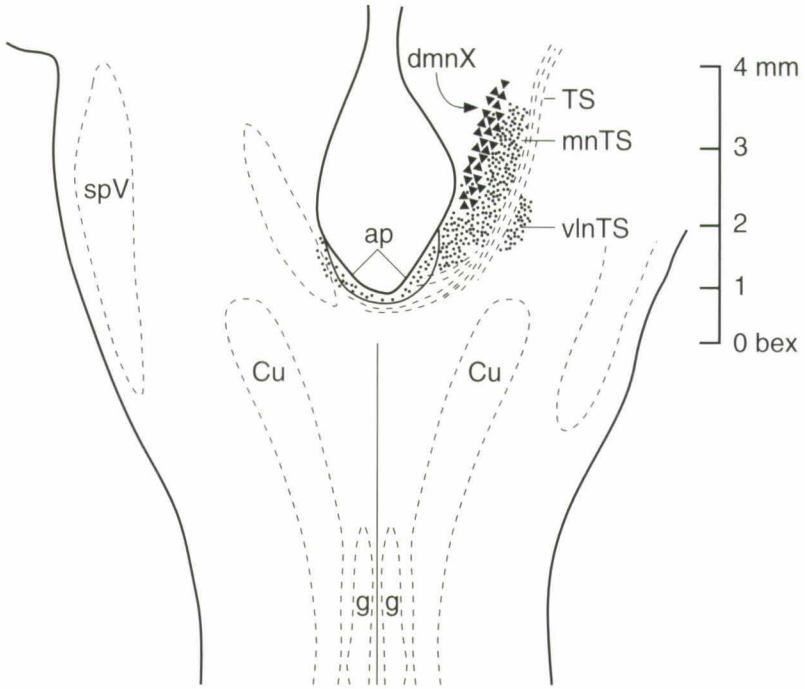


Figure 12.21. Horizontal section through the medulla showing the solitary tract (*TS*), medial, and ventrolateral nuclei of the solitary tract (*mnTS, vlTS*), dorsal motor nucleus of vagus (*dmnX*), and the area postrema (*ap*) labeled with horseradish peroxidase (HRP) following an injection into the right inferior (nodose) ganglion of X. Survival time was 48 hours. The right side of the medulla is on the right side of the diagram and rostral is upward. Interrupted lines represent the position of sensory and motor fibers of X labeled with HRP reaction product. *Dots* indicate terminals of afferent projections and solid triangles shown the location of retrogradely labeled cell bodies. *cu*, cuneate nucleus; *g*, gracile nucleus; *spV*, spinal trigeminal nucleus.

cleus (121), and carotid sinus afferent endings are concentrated in the medial and dorsomedial subnuclei (147) (Figs. 12.21 and 12.22).

In terms of neurotransmitters, the solitary nucleus is a highly heterogeneous structure. Neuropeptides identified within the various subdivisions of the solitary nucleus include enkephalin, somatostatin, substance P, cholecystokinin, and neuropeptide Y. These neuropeptides are present, sometimes in various combinations, in both cell bodies and afferent fibers. Cells in the solitary nucleus contain receptors for many neuropeptides. Many of the same neuropeptides have been identified in relay nuclei of ascending visceral and gustatory pathways at all levels of the neuraxis (138, 156). The largest numbers of cell bodies containing neuropeptides and catecholamine are located in the region of the solitary nucleus most concerned with visceral activities.

Secondary fiber systems originating from the solitary nucleus project ipsilaterally to (a) the nucleus ambiguus and the surrounding reticular formation, (b) the parabrachial nuclei in the rostral pons, and (c) the thalamic nucleus concerned with gustatory sensation, namely the ventral posteromedial nucleus, pars parvicellularis (VPM_{pc}) (11, 191) (Fig. 12.19). Other secondary fibers form the solitary nucleus projecting to the hypoglossal and salivatory nuclei mediate lingual and secretory reflexes. Projections from the solitary nucleus to the dorsal motor nucleus of the vagus nerve, the phrenic nerve nucleus (at spinal segments C3 to C5), and anterior horn cells of thoracic spinal segments are involved in coughing and vomiting reflexes. The solitary nucleus also appears to project directly to the hypothalamic paraventricular nucleus (42, 43). This projection may play a role in regulation of cardiovascular function, either by exerting control over vasopressin release from the neural lobe of the pituitary or by activating spinal sympathetic preganglionic neurons through axons of the paraventricular nucleus that reach thoracic spinal segments.

The solitary nucleus is a complex integration center subserving many diverse functions (191). As seen earlier, the rostral part of the nucleus is responsible for the processing

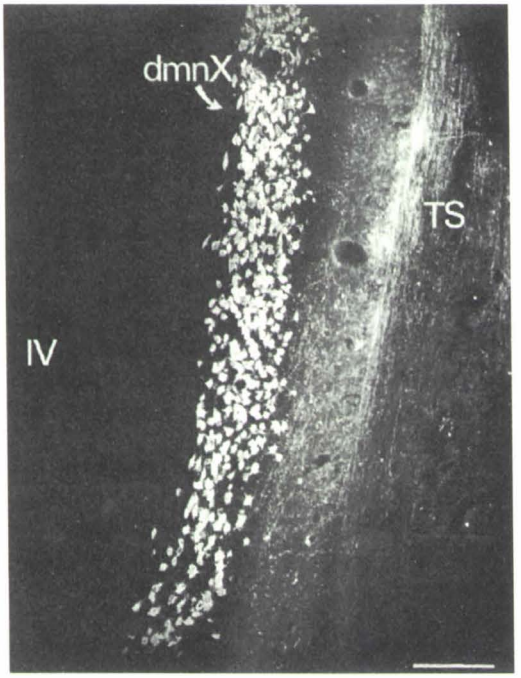


Figure 12.22. Medulla of a cat in which the inferior (nodose) ganglion of nerve X was injected with horseradish peroxidase. The medulla was sectioned in the horizontal plane. Rostral is toward the top, lateral is to the right. Survival time was 48 hours. Retrograde labeling is seen in perikarya of the dorsal motor nucleus of vagus (*dmnX*) and anterograde labeling occurs in the solitary nucleus and tract (*TS*). Notice labeled fibers leaving the caudal half of the solitary tract which is situated between *TS* and *dmnX* in the lower half of the Figure (calibration bar, 500 μm).

and relaying of gustatory sensations from the facial, glossopharyngeal, and vagus nerves (191, 206). Thus, the rostral pole of the solitary nucleus corresponds to the human gustatory nucleus of Nageotte (135) and the nucleus ovalis of Olszewski and Baxter (144) (see also 141). Furthermore, the nucleus of the solitary tract is coextensive with the physiologically defined dorsal medullary respiratory "center" (94), which includes the nucleus ambiguus and surrounding portions of the medullary reticular formation.

Additional brainstem regions important for the regulation of respiration are found in the pons. The medial parabrachial nucleus and the adjacent nucleus of Kölliker-Fuse constitute the functionally defined "pneumotaxic center." An apneustic center was also proposed, but has not been anatomically delineated. The parabrachial nuclei of the pons receive afferent connections from the solitary nucleus (94), and in turn project to both the dorsal and ventral respiratory centers (31, 188). An interesting feature of medullary cells projecting to the parabrachial nuclei is their orientation along the radial penetrating blood vessels (102).

Cells of the medullary "respiratory centers" are activated by vagal impulses and directly by changes in their chemical environment (CO_2 accumulation, etc.). A medullary vasomotor "center" consisting of separate pressor and depressor zones is also believed to be involved in the modulation of the cardiovascular function, but this "center" remains anatomically poorly defined. Recent emphasis has been on the distributed neural networks concerned with cardiovascular control. A group of noradrenergic neurons (designated A5) located in the caudal pons between the superior olive and roots of the facial nerve and projecting axons to the nucleus solitarius, the nucleus ambiguus, the dorsal motor nucleus of the vagus nerve, and preganglionic sympathetic neurons in the thoracic spinal cord, appears to be part of one of these neural networks (122, 138). Some of the projections of the A5 cell group to other brainstem structures are illustrated in Figure 12.24.

The *dorsal motor nucleus* of the vagus nerve is situated in the floor of the fourth ventricle posterolateral to the hypoglossal nucleus (Figs. 12.11, 12.13, and 12.14). This column of small spindle-shaped cells extends both rostrally and caudally beyond the hypoglossal nucleus. Some larger cells in the nucleus contain coarse chromophilic bodies and scattered melanin pigment. Cells of this nucleus give rise to preganglionic parasympathetic fibers (GVE) (Figs. 12.21 and 12.22). Axons of these cells traverse the spinal trigeminal nucleus and tract and emerge on the lateral surface of the medulla between the olive and the restiform body (Figs. A.4 and A.5 in the atlas of the human brain shown in Section VII). The dorsal motor nucleus contains relatively few myelinated fibers, indicating that most of the terminals entering it are unmyelinated. These are principally secondary fibers from the sensory nuclei of the glossopharyngeal and vagus nerves, and from visceral centers (Figs. 12.21–12.23). The dorsal motor nucleus of the vagus is the vagal secretory secretomotor center. Cells of the dorsal motor nucleus are strongly immunoreactive to choline acetyltransferase (ChAT) (Fig. 12.31). Destruction of this nucleus greatly reduces insulin-induced secretion of gastric acid.

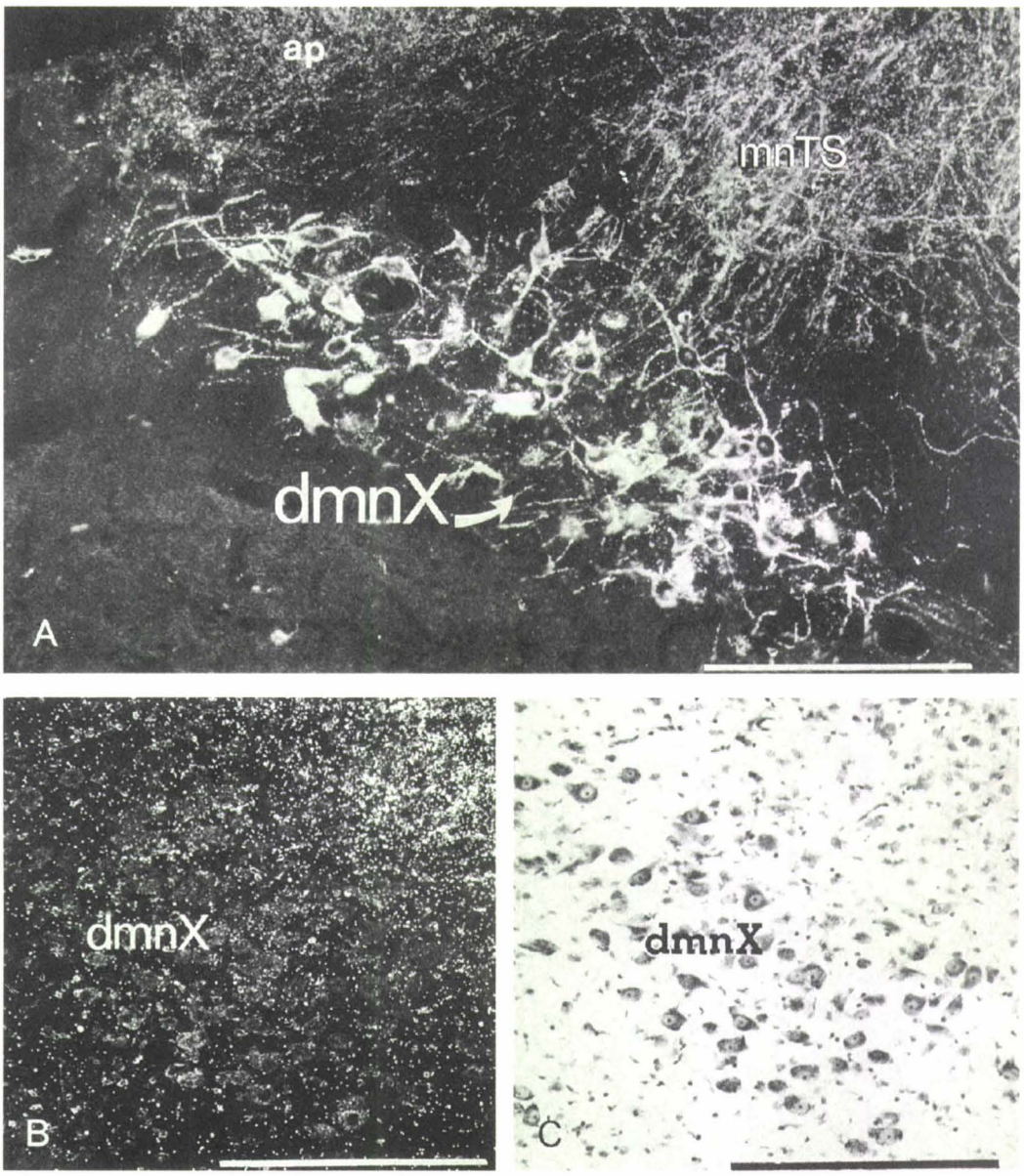


Figure 12.23. Medulla of cats in which the inferior (nodose) ganglion of nerve X was injected with either horseradish peroxidase or tritiated amino acid. The brain was sectioned transversally. Dorsal is toward the top and the midline to the left. In all photomicrographs, the rostrocaudal level is 1 mm rostral to the obex. **A.** Darkfield photomicrograph. The inferior ganglion was injected with horseradish peroxidase 48 hours before the animal was prepared for histologic examination. Retrograde labeling is seen in the dorsal motor nucleus of X (*dmnX*) and anterograde labeling is seen in the medial nucleus of the solitary tract (*mnTS*) as well as dorsomedially in the area postrema (*ap*). Afferents fibers from the *mnTS* are seen entering the *dmnX* and come into close contact with labeled perikarya (calibration bar, 250 μm). **B.** Darkfield photomicrograph. The inferior vagal ganglion was injected with tritiated amino acid 5 days prior to preparation for examination. In the *upper right*, the *mnTS* contains a high concentration of silver grains. The *dmnX* also contains a grain concentration that is above background level (calibration bar, 250 μm). **C.** Brightfield photomicrograph of exactly the same field as the one shown in B (calibration bar, 250 μm).

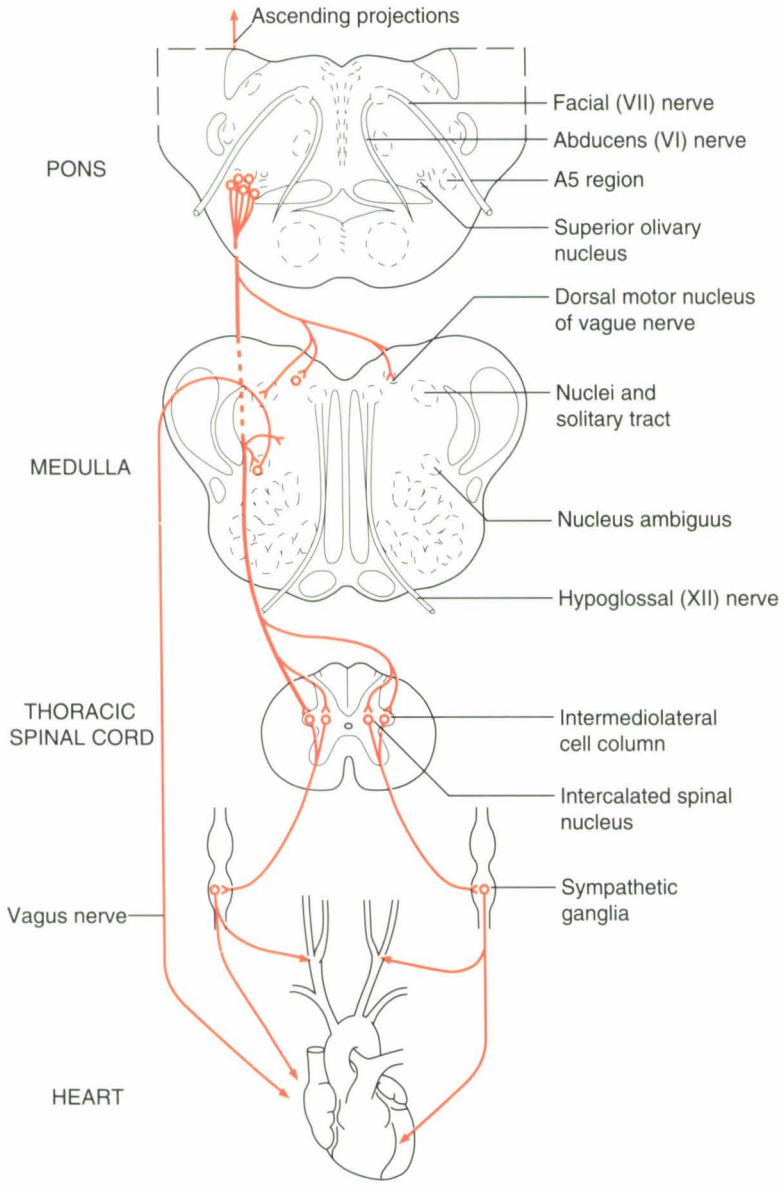


Figure 12.24. Descending projections of the A5 catecholamine cell group which lies lateral to the superior olivary nucleus and projects to (a) medullary vasomotor areas, (b) preganglionic sympathetic neurons, and (c) intercalated spinal neurons. Medullary nuclei receiving fibers from the A5 cell group include (a) the nuclei of the solitary tract, (b) the dorsal motor nucleus of the vagus nerve, (c) the nucleus ambiguus, and (d) the paramedian and medial medullary reticular formation. Inputs reaching cells of the intermediolateral cell column and intercalated spinal neurons project to postganglionic sympathetic neurons, which in turn project to the cardiovascular system. Electrical stimulation of the A5 cell group produces increases in systemic blood pressure and pulse pressure. Ascending projections from the A5 cell group have been described but not fully characterized.

The *nucleus ambiguus* is a column of cells in the reticular formation about halfway rostrocaudally between the spinal trigeminal nucleus and the inferior olivary complex (Figs. 12.8, 12.11, 12.13–12.16). This nucleus, extending from the level of the decussation of the medial lemniscus to levels through the rostral third of the inferior olivary complex, is composed of typical multipolar lower motor neurons. Fibers from the nucleus arch dorsally, join efferent fibers from the dorsal motor nucleus of the vagus nerve, and emerge from the lateral surface of the medulla dorsal to the inferior olivary complex (Figs. 12.14–12.16). Caudal parts of the nucleus ambiguus give rise to the cranial part of the spinal accessory

nerve, while rostral parts of this cell column give rise to glossopharyngeal special visceral efferent fibers (which innervate the stylopharyngeus muscle). Special visceral efferent fibers of the vagus nerve (and those from the cranial part of the accessory nerve which rejoin the vagus nerve) innervate the muscles of the pharynx and larynx (Figs. 12.14 and 12.16). The nucleus receives various projections, including corticobulbar (crossed and uncrossed) fibers involved in the voluntary control of swallowing and phonation (Fig. 12.27). The nucleus also receives impulses from receptors in the pharyngeal and laryngeal muscles, and from secondary vagal, glossopharyngeal, and trigeminal fibers. Fibers in these three nerves convey impulses from the oral, pharyngeal, and respiratory mucosa that mediate various reflexes, such as coughing, vomiting, and pharyngeal and laryngeal reflexes.

A unilateral lesion of the vagus nerve produces ipsilateral paralysis of the soft palate, pharynx, and larynx, which results in hoarseness, dyspnea, and dysphagia. During phonation, the soft palate is elevated on the normal side and the uvula deviates to the normal side. The palatal reflex is lost on the lesion side. Anesthesia of the pharynx and larynx results in an ipsilateral loss of the cough reflex, while destruction of visceral motor fibers of the vagus nerve abolishes the carotid sinus reflex ipsilaterally. As a rule, visceral disturbances are not marked following a unilateral lesion of the vagus nerve. A unilateral lesion of the recurrent laryngeal nerve will result in hoarseness of the voice and coughing attacks which in time diminish and disappear. The abductor muscles of the larynx are affected first.

Bilateral lesions of the vagus nerve causes complete paralysis of the pharynx and larynx, and will result in death due to asphyxia unless a tracheotomy is performed immediately. Paralysis and atonia of the esophagus and stomach produce pain and vomiting. The heart rate becomes rapid and irregular due to removal of vagal inhibition. This condition is associated with marked dysphagia and dysarthria.

Glossopharyngeal Nerve

This nerve (N. IX) is related closely to the vagus nerve, sharing common medullary nuclei and having similar functional components. Fibers of this nerve enter and emerge from the medulla at levels rostral to the rootlets of the vagus nerve, but like the vagus nerve, they traverse the spinal trigeminal tract and nucleus (Figs. 12.14, 12.25, and 12.26). The glossopharyngeal nerve is easier to identify than the vagus nerve, because its fibers form a single compact nerve root.

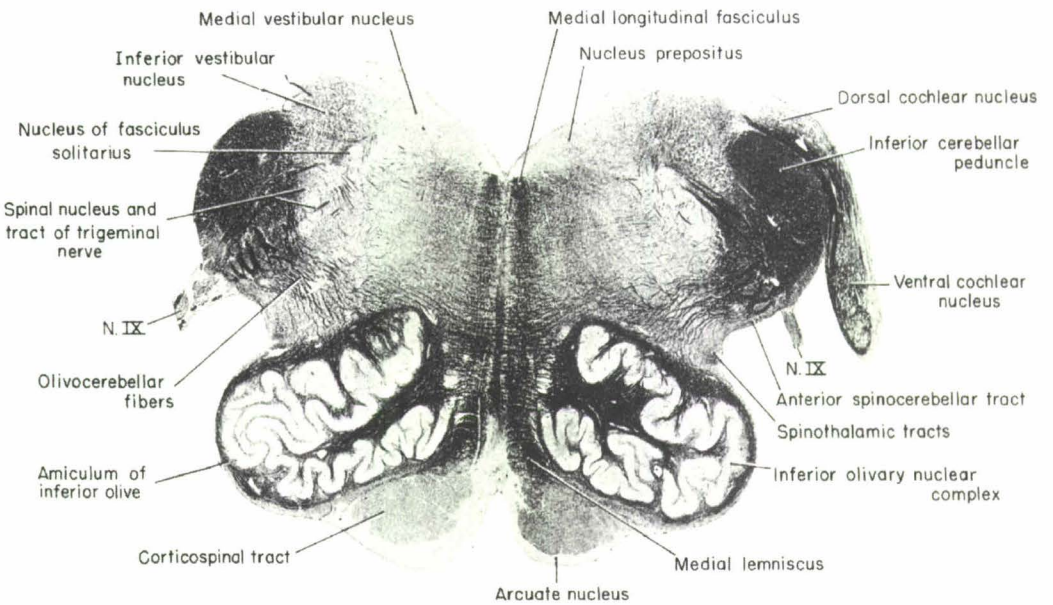


Figure 12.25. Transverse section of medulla of 1-month infant through the cochlear nuclei and ninth nerve (Weigert's myelin stain).

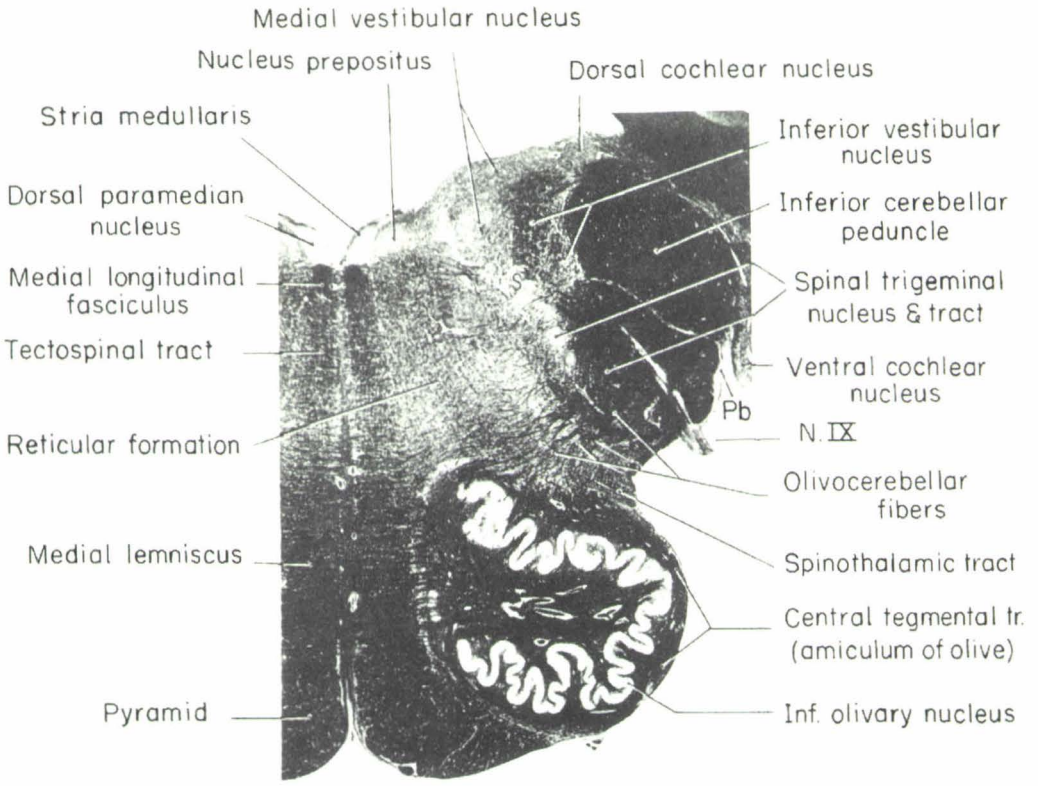


Figure 12.26. Transverse section through the upper medulla at the level of the cochlear nuclei and the root fibers of the glossopharyngeal nerve. *S*, lateral nucleus of the fasciculus solitarius; *Pb*, pontobulbar nucleus (Weigert's myelin stain).

Fibers of the vagus nerve enter and emerge from the brainstem by a number of small rootlets. The glossopharyngeal is a mixed branchiomeric cranial nerve with these functional components: (a) *general visceral afferent* (GVA) fibers, (b) *special visceral afferent* (SVA) fibers (taste), (c) a few *general somatic afferent* (GSA) fibers, (d) *general visceral efferent* (GVE) fibers, and (e) a small number of *special visceral efferent* (SVE) fibers. Like the vagus nerve, it has two sensory peripheral ganglia, a small *superior ganglion* in the jugular foramen, and a larger extracranial *inferior (petrosal) ganglion* (Fig. 12.17). The glossopharyngeal nerve also has a motor ganglion, the *otic ganglion*, situated below the foramen ovale and medial to the mandibular division of the trigeminal nerve.

Primary sensory neurons mediating general somatic sense (GSA) from cutaneous areas back of the ear lie in the superior ganglion. Central processes of these cells enter the spinal trigeminal tract and nucleus. Cell bodies of visceral afferent fibers lie in the inferior ganglion. General visceral afferent (GVA) fibers convey tactile sense, thermal sense, and pain from the mucous membranes of the posterior third of the tongue, the tonsil, the posterior wall of the upper pharynx, and the Eustachian tube. Special visceral afferent fibers convey taste sensation from the posterior third of the tongue. Visceral afferent fibers entering the posterolateral part of the medulla are distributed to rostral portions of the solitary fasciculus and its nucleus (Fig. 12.25). Rostral and lateral parts of the nucleus solitarius that receive fibers from the facial (intermediate) and glossopharyngeal nerves constitute the "gustatory nucleus."

The *carotid sinus nerve* conveys impulses from the carotid sinus, a baroceptor located at the bifurcation of the common carotid artery. Increases in carotid arterial pressure excite carotid sinus baroceptors and impulses are conveyed centrally by the glossopharyngeal nerve to the nucleus of the solitary tract (147). Second order neurons in the solitary nucleus, in turn, excite cells of the dorsal motor nucleus of the vagus nerve and bring about reductions in heart rate and arterial pressure

via cholinergic pre- and postganglionic vagal fibers that act upon the sinoatrial and atrioventricular nodes, as well as atrial heart muscle. The *carotid sinus reflex,* involving glossopharyngeal visceral afferents and vagal general visceral efferents, constitutes a mechanism for the regulation of arterial blood pressure.

General visceral efferent fibers, arising from the *inferior salivatory nucleus,* pass via the lesser petrosal nerve to the otic ganglion. Postganglionic fibers originating from the cells of the otic ganglion convey parasympathetic secretory impulses to the parotid gland. Cells of the inferior salivatory nucleus are scattered in lateral parts of the reticular formation and can be positively identified immunocytochemically by antiserum to ChAT.

Special visceral efferent fibers, as already described, arise from rostral portions of the nucleus ambiguus (Figs. 12.15 and 12.16). These fibers, small in number, innervate the stylopharyngeus muscle and perhaps portions of the superior pharyngeal constrictor muscle.

As the foregoing description indicates, the glossopharyngeal nerve is predominantly a sensory nerve and a nerve contributing preganglionic parasympathetic fibers to the otic ganglion. Isolated lesions of the glossopharyngeal nerve are rare. Disturbances associated with lesions of the nerve include (a) loss of the pharyngeal (gag) reflex, (b) loss of the carotid sinus reflex, and (c) loss of taste in the posterior third of the tongue. *Glossopharyngeal neuralgia* resembles trigeminal neuralgia in that the excruciating paroxysmal pain may be triggered by seemingly trivial stimuli such as coughing or swallowing. The pain associated with this syndrome radiates from the neck into regions behind the ear.

Swallowing, or deglutition, is a complex motor act which involves three identifiable neuroregulatory systems: (a) buccopharyngeal, (b) esophageal, and (c) gastroesophageal (58). The effector neurons lie in the motor nuclei of the trigeminal, facial, vagus (amibiguus), and hypoglossal nerves. Unlike spinal motor cells, neurons in the cranial motor nuclei have no recurrent collaterals which activate inhibitory interneurons. The neurons controlling the buccopharyngeal phase of deglutition are located in the medullary reticular formation close to the midline and dorsal to the inferior olive. These cells are found between the caudal border of the nucleus of the facial nerve and the rostral end of the inferior olive. The cells on each side of the midline can be considered "swallowing half-centers" which are coordinated through extensive interconnections.

Swallowing can be readily initiated by stimulation of the endings of the internal branch of the superior laryngeal nerve (part of the vagus nerve). Stimulation of the maxillary division of the trigeminal nerve and of the glossopharyngeal nerve can also trigger deglutition. Afferent neurons convey information from oropharyngeal receptive fields to neurons in the lateral subnuclei of the solitary complex. Projections from the solitary nucleus to all the cranial motor nuclei involved have not been demonstrated anatomically, but it is likely that interneurons within the reticular formation are part of the reflex circuit.

CORTICOBULBAR FIBERS

Corticofugal fibers projecting to, and terminating in, portions of the lower brainstem are referred to as *corticobulbar fibers.* These fibers arise mainly from cortex on both side of the central sulcus and project to (a) sensory relay nuclei, (b) parts of the reticular formation, and (c) certain motor cranial nerve nuclei.

Sensory relay nuclei receiving corticobulbar fibers include the nuclei gracilis and cuneatus, the sensory trigeminal nuclei, and the nucleus of the solitary fasciculus (28, 111–117, 193, 200, 211). Corticobulbar fibers to the posterior column nuclei leave the corticospinal tract and enter these nuclei by traversing the medial lemniscus or the reticular formation. After unilateral cortical lesions, degenerated terminal fibers are distributed bilaterally to the posterior column nuclei, but are most numerous contralaterally. There are suggestions of somatotopic projections between portions of the precentral and postcentral gyri and the nuclei gracilis and cuneatus, but considerable overlap also is evident (113). In rodents, projections from primary somesthetic cortex is organized so that fibers from the forelimb cortical area terminate in the nucleus cuneatus and those from the hindlimb area end in the nucleus gracilis (211). In carnivores, corticobulbar fibers are distributed preferentially to portions of the dorsal column nuclei that contain loosely organized cells. Few fibers from the cortex appear to terminate in "cell nest" regions, which receive ascending fibers

from spinal dorsal roots (117). Corticobulbar fibers projecting to all trigeminal sensory nuclei and the nucleus solitarius are derived from widespread cortical regions, with the largest number arising from the frontoparietal region (28). Corticofugal fibers to the nucleus solitarius terminate chiefly in its rostral part, near levels where facial and trigeminal afferents end.

Corticobulbar fibers, projecting to the posterior column and trigeminal sensory nuclei, are part of a complex mechanism whereby descending cortical impulses can modulate the transmission of ascending sensory impulses at the second neuron level. Both excitatory and inhibitory effects upon these sensory relay nuclei can be produced by stimulation of the cerebral cortex (70, 75, 79, 88). Excitatory and inhibitory actions appear to be exerted differentially upon portions of the nucleus gracilis that are distinguishable on the basis of the size of the receptive field and sensory modality represented (70, 71). Corticofugal inhibitory influences are principally exerted in middle portions of the nucleus, where individual cells responded to movement of hair, light touch to foot pads, pressure at the base of a claw, or subcutaneous pressure. These cells exhibited small receptive fields and were inhibited by stimuli applied outside the physiologic receptive field (i.e., surround inhibition). Corticofugal excitatory effects were found mainly in rostral and deep parts of the middle region of the nucleus, where individual cells responded principally to touch and pressure. These cells with rather large receptive fields do not display the phenomenon of surround inhibition.

Corticoreticular fibers projecting to the lower brainstem arise predominantly from the motor, premotor and somesthetic cortical areas (168). Fibers descend in association with the corticospinal tract, leave the tract at various levels, and enter the brainstem reticular formation. The bulk of these fibers terminate in two fairly circumscribed areas, one in the medulla and another in the pons. In the medulla, these fibers terminate in the area of the nucleus reticularis gigantocellularis; in the pons, most of the fibers end in the rostral pontine reticular formation (nucleus reticular pontis oralis). Corticoreticular fibers are distributed bilaterally but with a slight contralateral predominance (211). Regions of the reticular formation, receiving corticofugal fibers, give rise to (a) long ascending and descending projections (27, 194), (b) projections to the cerebellum (23, 47), and (c) projections to cranial nerve nuclei (173).

The *motor cranial nerve nuclei* innervating skeletal muscles receive impulses from the cerebral cortex via corticobulbar pathways. These fibers arise mainly from portions of the precentral gyrus and descend through the internal capsule and brainstem in association with the corticospinal tract (Figs. 2.12, 11.12, and 12.27). They constitute the upper motor neurons for the motor cranial nerve nuclei. Most of the so-called corticobulbar fibers conveying impulses to motor cranial nerve nuclei are actually corticoreticular fibers. Neurons in the reticular formation serve to relay impulses to motor cranial nerve nuclei. In nonprimate species, it has not been possible to trace corticobulbar fibers to direct terminations in motor cranial nuclei (111, 201, 211). In these animals, cortical influences upon motor cranial nerve nuclei are mediated by corticoreticular fibers and synaptically related reticular neurons projecting to the motor nuclei. This indirect system is supplemented in humans and nonprimates by corticobulbar fibers that project directly to particular motor cranial nerve nuclei. Nuclei receiving these direct corticobulbar projections are the trigeminal, facial, hypoglossal, and supraspinal (112). These fibers are bilateral and nearly equal, except for those passing to parts of the facial nucleus, which are more abundant contralaterally (Fig. 12.27). The more numerous corticoreticular fibers form the basis of an indirect corticobulbar system present in most mammalian species and in which neurons in the reticular core serve as internuncial elements. Direct corticobulbar fibers represent a parallel system that is particularly well-developed in humans and nonhuman primates.

The *supranuclear innervation of motor cranial nerve nuclei* is largely bilateral and more complex than that present at spinal levels. Corticobulbar projections are bilateral to those cranial nuclei that innervate muscle groups that, as a rule, cannot be contracted voluntarily on one side (Fig. 12.27). These include the laryngeal, pharyngeal, palatal, and upper facial muscles. The same principle applies to the muscles of mastication and the extraocular muscles. Because unilateral stimulation of the motor cortex produces isolated contraction of contralateral lower facial muscles, and unilat-

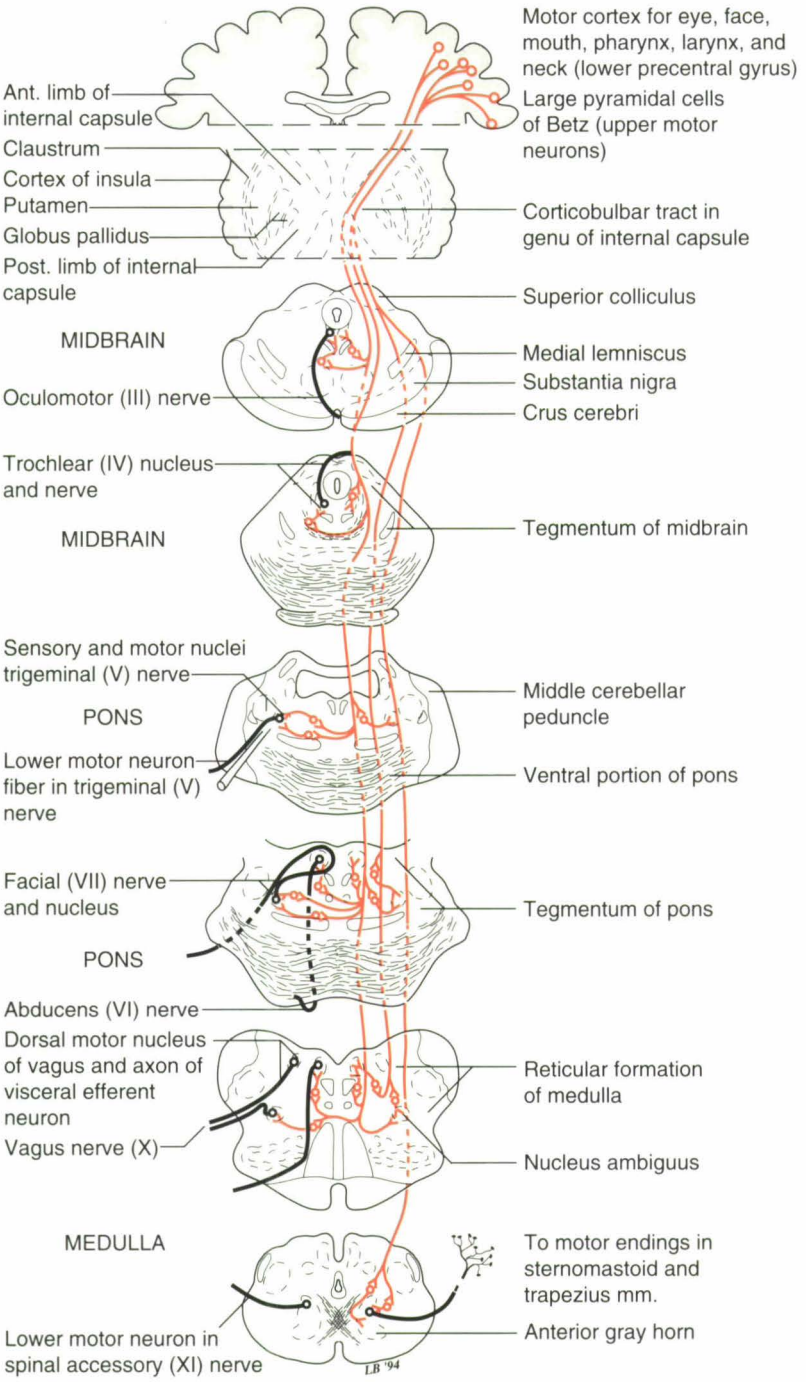


Figure 12.27. "Corticobulbar" pathways in the brainstem. Fibers of this upper motor neuron pathway to the motor cranial nerve nuclei arise in the cerebral cortex, pass caudally in the internal capsule, the crus cerebri, and the ventral portion of the pons, and are distributed largely to neurons in the reticular formation bilaterally. Reticular neurons conveying the impulses to the motor cranial nerve correspond to the intercalated on internuncial neurons found at spinal levels. In human and nonhuman primates, this indirect system is paralleled by direct corticobulbar fibers distributed to the motor nuclei of the trigeminal, facial and hypoglossal nerves.

eral lesions involving corticobulbar fibers produce paralysis only of contralateral lower facial muscles, cell groups of the facial nucleus innervating the lower facial musculature are regarded as receiving only crossed corticobulbar fibers. The fact that unilateral stimulation of the motor cortex causes turning of the head to the opposite side has been interpreted as indicating that corticofugal fibers to nuclei innervating the sternocleidomastoid muscle probably are uncrossed, because contraction of this muscle turns the head to the opposite side. It seems likely that some uncrossed corticospinal fibers (Figs. 11.13 and 11.14) project to spinal accessory cell groups innervating this muscle and the upper part of the trapezius muscle, although direct fibers to these cells appear meager (112). Eye movements elicited by electrical stimulation of the cerebral cortex are always conjugate, indicating that the supranuclear innervation of the nuclei of the extraocular muscles is bilateral.

Because the supranuclear innervation of the motor cranial nerve nuclei is largely bilateral, unilateral lesions interrupting corticobulbar fibers (upper motor neuron) produce comparatively mild forms of paresis. Only slight weakness of tongue (genioglossus muscle) and jaw movements (pterygoid muscles) contralateral to the lesions can usually be detected. These are seen as modest deviation of the tongue or jaw to the side opposite the lesion. However, marked weakness in the contralateral lower facial muscles is evident with such lesions. Weakness of lower facial muscles becomes obvious when the patient attempts to show the teeth, purse the lips, or puff out the cheeks.

Pseudobulbar palsy results from bilateral lesions involving corticobulbar fibers. This syndrome is characterized by weakness or paralysis of muscles involved in swallowing, chewing, breathing, and speaking, and may occur with relatively little paralysis in the extremities. Loss of emotional control, characterized by inappropriate outbursts of laughing and crying, form an important part of the syndrome. These symptoms appear as the physiologic expression of rather extensive bilateral lesions in the upper brainstem or at higher levels. Although there is marked paresis of the muscles of mastication and in the muscles of the face, tongue, pharynx, and larynx, these muscles do not atrophy, since the lower motor neurons remain intact. After prolonged periods of time, contractures may appear in the muscles of the lips, tongue, and palate (78). Cranial nerves V, VII, and IX through XII may be involved, together or in varying combinations, as a result of bilateral interruption of the corticobulbar tracts centrally (Fig. 12.27). Bilateral lesions involving "corticobulbar pathways" above pontine levels usually are the result of extensive demyelinating disease, vascular disease, thrombosis, or neoplasms.

CHEMICAL ANATOMY

As seen in Chapter 5, the functional organization of the central nervous system is dependent on transmitter molecules (neuromediators) to convey neural information across synapses. There are a large number of neuromediators recognized as having unique properties in certain neural circuits and probably a great many more that remain to be identified. There are two major types of neuromediators: (a) small-molecule transmitters, such as various amino acids, biogenic amines, and acetylcholine, and (b) neuroactive peptides belonging to different families, such as tachykinins, opioids, and pancreatic polypeptides (48). Small-molecule transmitters can rapidly turn the signals on or off as impulses arrive at the synapses, while neuroactive peptides can modify signals, act over a different time course, influence neuronal metabolism, or prepare cells for later neural events. A proper knowledge of the chemical coding of neurons and neuronal circuits is essential to understanding the anatomic and functional organization of the central nervous system, comprehension of a variety of neurologic diseases, and deciphering the nature of many drug actions. Immunohistochemical and *in situ* hybridization methods can reveal information concerning the site and level of synthesis and storage of known or suspected neuromodulators. Autoradiographic techniques can provide information concerning the localization of transmitter binding sites. Retrograde tract-tracing methods combined with immunocytochemistry make it possible to undertake detailed mappings of particular chemospecific neuronal systems in the brain.

In the medulla, neuromediators of particular interest are: (a) the indolamine serotonin (5-hydroxytryptamine or 5-HT), (b) various catecholamines, such as norepinephrine (or noradrenaline) and epinephrine (or adrena-

line), (c) acetylcholine, and (d) various neuroactive peptides, including substance P and enkephalin.

Serotonin and the Raphe Nuclei

Cell groups lying along the midline of the medulla, pons, and midbrain collectively are called the raphe nuclei. The major raphe nuclei of the brainstem are shown in Figure 12.28, a schematized midsagittal section of the brainstem. The raphe nuclei are not exclusively composed of neurons that use serotonin as a neurotransmitter. Neurons displaying immunoreactivity to amino acids, such as γ-aminobutyric acid (GABA) (41, 93) and glycine (85), as well as to neuropeptides, such as substance P, enkephalin, cholecystokinin, and thyrotropin-releasing hormone, occur within the confines of the raphe nuclei (18, 138, 185). Certain serotoninergic neurons in the raphe nuclei coexpress other neuromediators, particularly neuropeptides (3, 90), but also the excitatory amino acids aspartate and glutamate (139). Furthermore, although the bulk of serotoninergic neurons in the medulla lies within the raphe nuclei, some serotoninergic neurons are scattered more laterally among neurons of the reticular formation (40, 54, 92, 148, 149, 158, 184, 192). Fibers originating from cells in the raphe nuclei are distributed widely in the neuraxis and release serotonin, as well as other neuromodulators, at their terminals. Thus, the raphe nuclei may be viewed as a diffusely distributed multitransmitter system. The serotonin neuronal system can be considered as a component of the brainstem reticular formation, which has widespread and partly overlapping projections.

In the medulla, serotoninergic neurons lie in the nuclei raphe pallidus, raphe obscurus, and raphe magnus (Fig. 12.28). These nuclei correspond respectively to groups B1, B2, and B3 of Dahlström and Fuxe (54). They give rise principally to descending spinal projections. The raphe nuclei in the pons and midbrain are the sources of ascending projections that arborize profusely in the diencephalon and telencephalon. Cells in the nucleus raphe

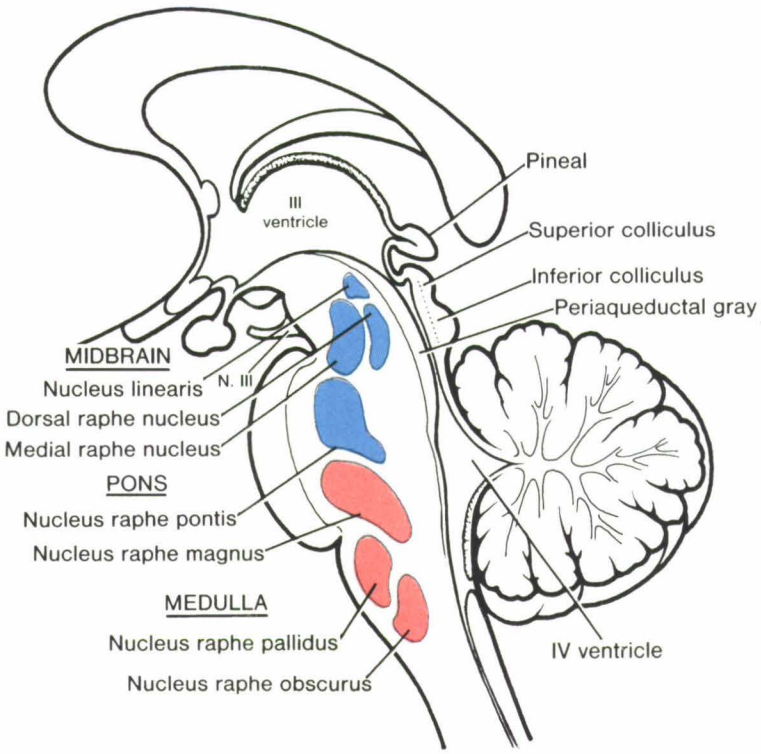


Figure 12.28. Midsagittal section of the brainstem indicating the positions of the raphe nuclei. Nuclei in *red* project to spinal levels, while those in *blue* have extensive projections to nuclei in the brainstem. Projections to diencephalic structures are most numerous from the dorsal and medial raphe nuclei and from the nucleus raphe pontis. The dorsal and medial raphe nuclei also project widely to telencephalic structures.

magnus give rise to bilateral spinal projections that descend in the dorsolateral funiculus and terminate principally in laminae I and II of the spinal posterior horn, and less abundantly in the intermediate gray matter and anterior horn (9) (Fig. 12.29). Portions of the motor nucleus of the facial nerve, the caudal part of the spinal nucleus of the trigeminal nerve, and the nucleus of the solitary tract receive a substantial serotonin innervation (184).

Stimulation of nucleus raphe magnus produces an analgesic effect by an inhibitory action upon nociceptive neurons in laminae I and II in caudal part of the spinal trigeminal nucleus and in the spinal cord (8, 10). Neuromediators involved in the mediation of pain probably are multiple and appear to act upon nociceptive interneurons, as well as neurons that give rise to pain pathways (i.e., anterolateral tract neurons).

Medullary raphe nuclei also synapse directly upon sympathetic preganglionic neurons in the intermediolateral column (5), and stimulation of medullary raphe nuclei produces inhibition of sympathetic preganglionic neurons (32). These findings indicate that the descending serotoninergic projec-

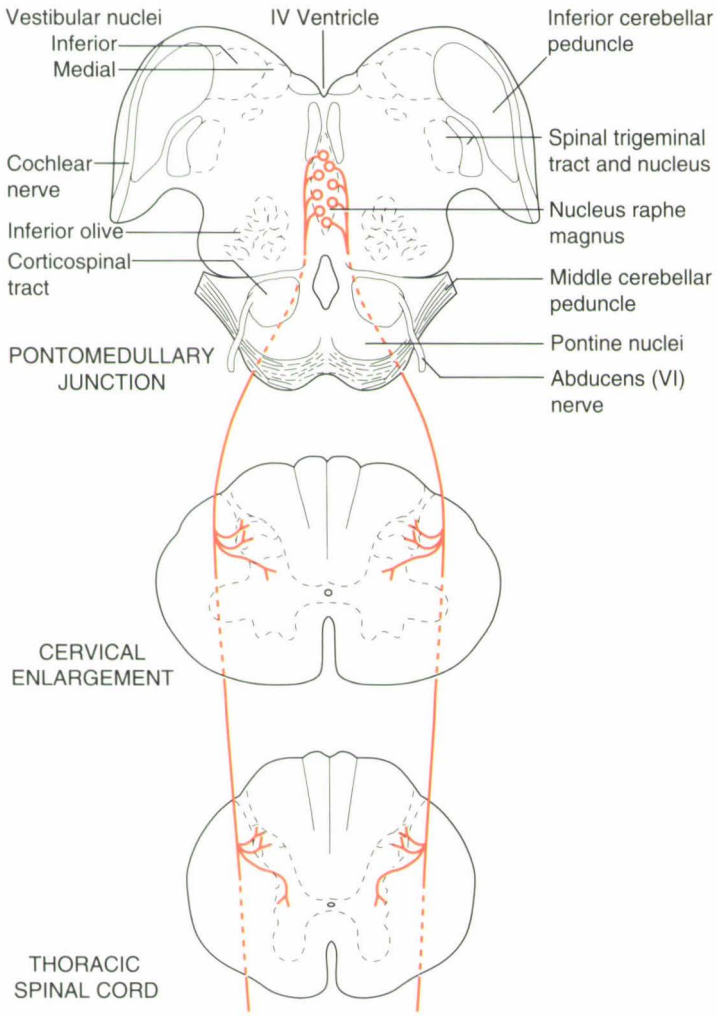


Figure 12.29. Spinal serotoninergic projections from the nucleus raphe magnus. These projections are bilateral, descend in the dorsal part of the lateral funiculus and terminate principally upon cells in spinal cord laminae I, II, and V, considered to receive nociceptive inputs. Large reticular neurons adjacent to the nucleus raphe magnus project fibers ipsilaterally to the same laminae in the posterior horn, but are not serotoninergic. Both of these pathways are considered links in an endogenous analgesia-producing system. Fibers from the nuclei raphe pallidus and obscurus (not shown) descend in the ventral quadrant of the spinal cord.

tions from the medullary raphe nuclei play a role in the control of various autonomic mechanisms, such as those involved in the maintenance of blood pressure (49).

Catecholaminergic Neurons

Catecholamines present in significant concentrations in the medulla are norepinephrine and epinephrine. The enzyme dopamine-β-hydroxylase (DBH) transforms dopamine to norepinephrine, while the enzyme phenylethanolamine-*n*-methyltransferase (PNMT) converts norepinephrine to epinephrine. Thus, DBH and PNMT are convenient markers for noradrenergic and adrenergic neurons, respectively, and antisera raised against each of these enzymes allow a clear visualization of these two types of catecholaminergic neurons. Specific antisera to norepinephrine and to epinephrine are also available, but their use requires particularly stringent technical conditions. Since most brainstem catecholaminergic cell groups in primates are pigmented, this feature has been used as a criteria for the identification of catecholaminergic neurons in human brainstem (15).

NORADRENERGIC CELL GROUPS

The locus coeruleus (group A6), a blue-black pigmented nucleus located at the upper pons levels, is the largest collection of noradrenergic neurons in the brain. This structure distributes noradrenergic fibers throughout the central nervous system (138). Neurons in the ventral part of the locus coeruleus and in the subcoeruleus area give rise to descending fibers that course in the lateral and ventral funiculi and arborize within nearly all segments of the spinal cord (85, 138, 160). The coeruleospinal noradrenergic fibers terminate in the ventral parts of the posterior horn (laminae IV, V, and VI), the intermediate gray matter, and the anterior horn. Through its noradrenergic spinal projections, the locus coeruleus is believed to be involved in such diverse functions as modulation of pain (91) and control of spinal motor output (64). Furthermore, the coeruleospinal noradrenergic fibers are likely to give collaterals to various medullary structures, such as the inferior olivary complex (180).

The locus coeruleus does not project significantly to the intermediolateral cell column and the superficial layers of the posterior horn of the spinal cord. These projections are ensured by noradrenergic neurons scattered throughout rostral regions of the lateral reticular nucleus and adjacent reticular formation (118). These ventrolaterally located noradrenergic neurons form the groups A5 and A7 of Dahlström and Fuxe (54). The A5 cell group, which lies lateral to the superior olivary complex, sends noradrenergic fibers to medullary vasomotor centers, the intermediolateral cell column at thoracic levels, and intercalated neurons at the same levels. These projections are collectively referred to as the lateral tegmental system. Medullary nuclei receiving noradrenergic fibers from the A5 cell group include (a) the dorsal motor nucleus of the vagus, (b) the nucleus ambiguus, (c) the nuclei of the solitary tract, and (d) portions of the medial medullary reticular formation. Descending projections to the spinal cord are relayed via preganglionic and postganglionic sympathetic neurons to cardiovascular structures (123). The A7 cell group lies in the ventrolateral portion of the pontine reticular formation medial to the lateral lemniscus and gives rise to descending noradrenergic fibers that terminate principally in the superficial layers of the posterior horn of the spinal cord (44). This descending noradrenergic system is believed to be involved in the modulation of nociception (209).

Noradrenergic cells found in the lower part of the medulla and have been designated groups A1 and A2 by Dahlström and Fuxe (54). Cells of group A1 surround the nucleus of the lateral funiculus and extend dorsomedially into the lateral part of the medullary reticular formation. Cells of this group project noradrenergic fibers to the solitary nucleus, the dorsal motor nucleus of the vagus nerve, the locus coeruleus, and the parabrachial nucleus in the pons. Cells of group A2 lie within the solitary nucleus, the dorsal motor nucleus of the vagus nerve, and the intervening areas. Numerous cells of the A2 group are found more caudally within the confines of the area postrema. This dorsal medullary group provides a heavy bilateral noradrenergic innervation to the solitary nucleus. Cells in the A1 and A2 groups also give rise to fibers that ascend toward the telencephalon (172).

In primates, the A1, A5, and A7 groups form a caudorostral continuum that extends throughout the lateral portion of the brain-

stem reticular formation (152). Caudal parts of this lateral tegmental nuclear complex are connected with group A2 by strands of noradrenergic cells. Rostrally, a comparable strand of noradrenergic cells forms a bridge between the locus coeruleus complex and the A5-A7 groups. These intervening cells lie partly within the confines of the medial parabrachial and Kölliker-Fuse nuclei, which are considered as a "pneumotaxic center" in the medulla. The axons emerging from this noradrenergic neuronal complex branch profusely throughout the entire rostrocaudal extent of the neuraxis (138).

ADRENERGIC NEURONS

Three groups of neurons displaying PNMT immunoreactivity occur in the lower portion of the medulla (83). By analogy with the nomenclature of Dahlström and Fuxe (54), these groups have been designated as C1, C2, and C3 (83). Cell group C1, the largest of the three, lies lateral to the inferior olivary complex and contains 69% of the total number of PNMT cells in the medulla. Cell group C2 is located partly within and partly adjacent to the solitary nucleus and comprises 22% of the total number of PNMT cells. Cell group C3, which contains the remaining 9% of the PNMT-immunoreactive cells, is composed of rather isolated elements interspersed among the fibers of the medial longitudinal fasciculus and scattered from the level of the hypoglossal nerve to that of the dorsal raphe nucleus (138). The C1 and C2 cell groups form a rostral continuation of groups A1 and A2, respectively.

Adrenergic fibers that emerge from the C1-C3 area ascend through the reticular formation to the hypothalamus, where they densely innervate the paraventricular nucleus (83, 138). The C1 and C2 nuclei also provide an adrenergic input to the ventral part of the locus coeruleus, the solitary nucleus, the dorsal motor nucleus of the vagus nerve, and the intermediolateral cell column in the spinal cord. Little is known of the central actions of the adrenergic cells in the medulla. The dense innervation of the hypothalamic paraventricular nucleus suggests that they might be involved in the control of oxytocin and vasopressin secretion, while the prominent input to the solitary nucleus, the dorsal motor nucleus of the vagus nerve, and the sympathetic preganglionic neurons indicate that they may play a role in the regulation of blood pressure and respiration. The medullary adrenergic neurons may also be involved in the modulation of spinothalamic cells (34).

Cholinergic Neurons

Neurons containing acetylcholine (ACh) can be identified immunocytochemically with antisera raised against choline acetyltransferase (ChAT), the enzyme that synthesizes ACh, or histochemically by visualizing the hydrolytic enzyme acetylcholinesterase (AChE) (151, 178). While there is a general correspondence between ChAT immunoreactivity and the presence of AChE, the hydrolytic enzyme also is present in noncholinergic neurons, nerve fibers, and terminals, and is not considered a specific marker of cholinergic neurons. As seen in previous chapters, ACh is released at the neuromuscular junction, as well as at the terminals of all preganglionic neurons. All motor cranial nuclei, all somatic spinal motor neurons, and all preganglionic autonomic neurons react positively to ChAT and are considered as cholinergic neurons. Postganglionic sympathetic neurons innervating the sweat glands also are cholinergic. In the medulla, cells of the hypoglossal nucleus, the dorsal motor nucleus of the vagus, and the nucleus ambiguus are all immunoreactive to ChAT (Fig. 12.31).

When thin sections of brain tissue are incubated with a radioactive ligand, which binds to ACh receptors with high specific activity, the general distribution of binding sites can be observed in autoradiographs. The highest density of muscarinic acetylcholine receptors is found in the nucleus of the hypoglossal nerve (cranial N. XII) and nucleus ambiguus (cranial N. IX and X), with somewhat lower densities in the solitary nucleus and lateral reticular nucleus. Still lower density is observed in the dorsal motor nucleus of the vagus nerve (205). In the medulla, nicotinic ACh receptors have their highest concentrations in the dorsal motor nucleus of the vagus nerve (2).

Neuroactive Peptides

OPIOID PEPTIDES

Immunocytochemical methods also have been used to visualize cell bodies and termi-

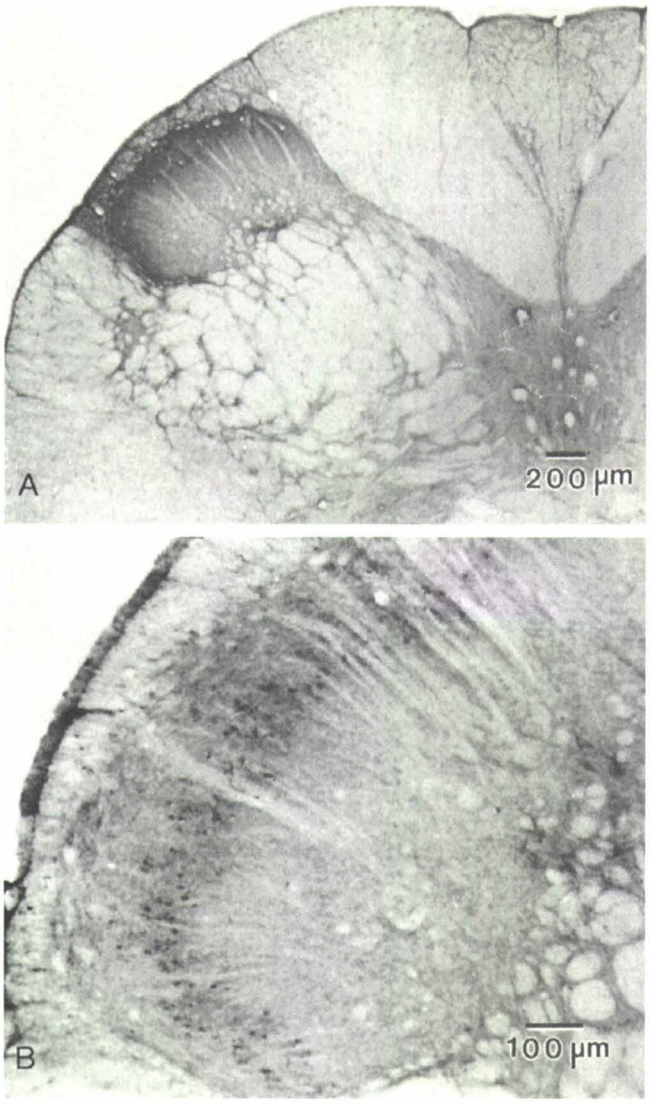


Figure 12.30. Immunocytochemical feature of the caudal spinal trigeminal tract and nucleus in a monkey. **A.** Fibers immunoreactive for substance P in the spinal trigeminal tract and in laminae I and II of the spinal trigeminal nucleus. **B.** Fibers and cells in the spinal trigeminal nucleus immunoreactive for leucine-enkephalin. Section were taken from the same animal.

nals containing the opiate peptides met- and leu-enkephalin (4, 61, 82, 84, 156, 196). In the medulla, cell bodies displaying enkephalin immunoreactivity occur in laminae II (substantia gelatinosa layer) and III of the caudal portion of the spinal nucleus of cranial N. V (Fig. 12.30). Other enkephalin-labeled cells are found in the solitary nucleus and in a ventral cluster lying lateral to nucleus raphe magnus. Axons and terminals containing enkephalins are generally seen in regions containing labeled cell bodies. Additionally, enkephalinergic fibers form moderately dense terminal plexuses in the motor nuclei of the facial and hypoglossal nerves and in parts of the reticular formation (156).

The study of the functional significance of enkephalinergic neuronal pathways is still incomplete. The morphine agonist properties of enkephalins (86) led to the analysis of the role of enkephalinergic descending projections in mechanisms of nociception and analgesia (7, 8, 10). Other studies have suggested that enkephalins and related peptides may have much broader functions, and it is now known that enkephalins and morphine bind to separate subclasses of opiate receptors. The organization of descending pain control systems is complex. Brainstem projections to the spinal cord other than those arising from enkephalin-containing neurons in the medulla have been shown to affect spinal neurons which respond to noxious stimulation (74, 81, 126, 142).

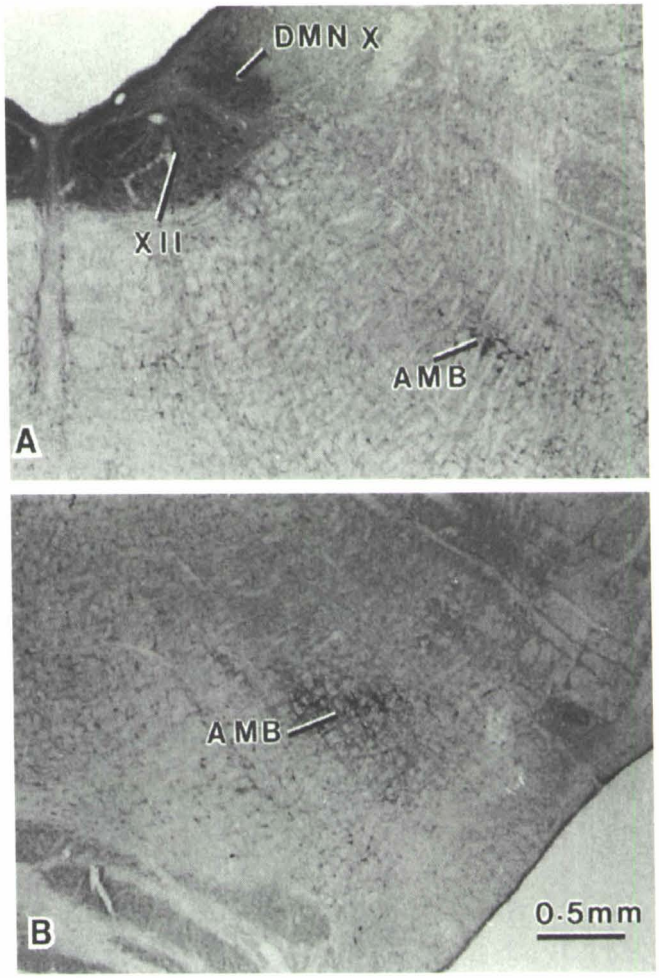


Figure 12.31. Transverse sections through the medulla of a monkey immunoreacted with antiserum raised against the enzyme choline acetyltransferase (ChAT), which is considered a reliable marker for cholinergic neurons. **A.** Cholinergic neurons in the hypoglossal nucleus (*XII*), the dorsal motor nucleus of the vagus (*DMN X*), and the nucleus ambiguus (*AMB*). **B.** Cholinergic neurons in the nucleus ambiguus.

SUBSTANCE P

Substance P is a peptide of 10 amino acids present in several neural systems. About 20% of the cell bodies in spinal ganglia contain substance P. Fibers of these cells project via dorsal root filaments to terminate in laminae I and II of the posterior horn (Fig. 12.30) (also see Chapter 10). Similar numbers of substance P-containing cell bodies are found in the trigeminal ganglion. Substance P-containing cell bodies are small, and give rise to small, poorly myelinated fibers that encode nociceptive information. Substance P produces a prolonged excitation of central neurons. In the medulla, terminals enriched with substance P are found in the superficial laminae of the caudal trigeminal nucleus, in the solitary nucleus, and in some cells of the raphe nuclei (52, 138, 156). Substance P also may coexist with other neuromediators in some neurons of the medulla.

OXYTOCIN AND VASOPRESSIN

A surprising finding emerging from studies of biologically important peptides in the brain, is the presence of posterior pituitary gland hormones in the brainstem and spinal cord. The nonapeptides oxytocin and vasopressin are synthesized by cells in discrete nuclei of the hypothalamus (see Chapter 17) and transported along axons to terminals in the posterior lobe of the pituitary. Double-labeling experiments have demonstrated that the hypothalamic nuclei which innervate the posterior pituitary gland contain separate subpopulations of cells with descending projections (186). The axons reaching the medulla contain mainly oxytocin and end in the solitary nucleus, dorsal motor nucleus of the vagus nerve, lateral reticular nucleus, and within lamina I (marginal layer) of the spinal nucleus of N. V (133, 140). When oxytocin is released into the circulation from the poste-

rior lobe of the pituitary gland, it acts upon smooth muscle of the uterus during parturition and upon myoepithelial cells of the mammary gland during milk letdown. The function of this peptide in the medulla is unknown, but it is interesting to note that oxytocin containing axon terminals are found in or near regions rich in catecholamine and enkephalin containing terminals.

MEDULLARY-PONTINE JUNCTION

The fourth ventricle reaches its maximum width at the level of the lateral recesses (Figs. 12.2, 12.32, and A.6). These lateral extensions of the fourth ventricle pass external to the inferior cerebellar peduncle and the cochlear nuclei (Fig. A.5). The lateral wall of each recess is formed by the *peduncle of the flocculus*, a part of the flocculonodular lobe of the cerebellum lying close to the lateral surface of the medulla (Fig. 12.32). The cochlear nerve and the *dorsal* and *ventral cochlear nuclei*, lie on the medial and rostroventral surfaces of the lateral recess. The restiform body has achieved its maximum size, and fibers of the cochlear nerve curve around its lateral and superior surfaces. At slightly more rostral levels, above the lateral recess, the inferior cerebellar peduncle enters the cerebellum by passing rostrodorsally. The fibers of this inferior cerebellar peduncle lie medial to the middle cerebellar peduncle (Fig. 12.33).

In the floor of the fourth ventricle, the nucleus prepositus lies medially in the position previously occupied by the hypoglossal nucleus. Lateral to this nucleus are the vestibular nuclei (Figs. 12.25 and 12.33). At this level, portions of the *medial* and *inferior vestibular nuclei* are seen. The inferior vestibular nucleus lies adjacent to the medial surface of the restiform body and is characterized by numerous, relatively coarse, myelinated fiber bundles which course through it. These fibers coursing longitudinally in the axis of the nucleus are descending primary vestibular fibers and cerebellar efferent fibers. The medial vestibular nucleus is highly cellular and contains finer fibers, most of which are not myelinated. In some preparations, myelinated fibers of the striae medullares of the medulla can be seen in the floor of the fourth ventricle dorsal to the nucleus prepositus and the vestibular nuclei. These fibers arise from the arcuate nucleus, pass dorsally in the raphe, and project laterally in the floor of the fourth ventricle to the cerebellum.

Root fibers of the *cochlear nerve*, conveying impulses from the organ of Corti in the cochlea, enter the posterolateral margin of the

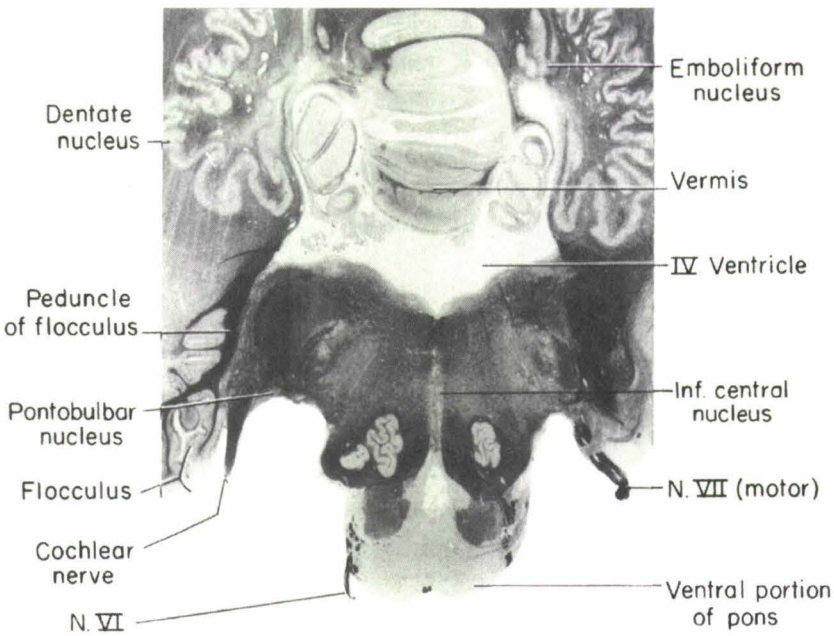


Figure 12.32. Transverse section through the junction of medulla and pons in a 1-month infant. Portions of the cerebellum containing large parts of the intracerebellar nuclei are attached. Structures in and around the tegmentum are identified in Figure 12.33 (Weigert's myelin stain).

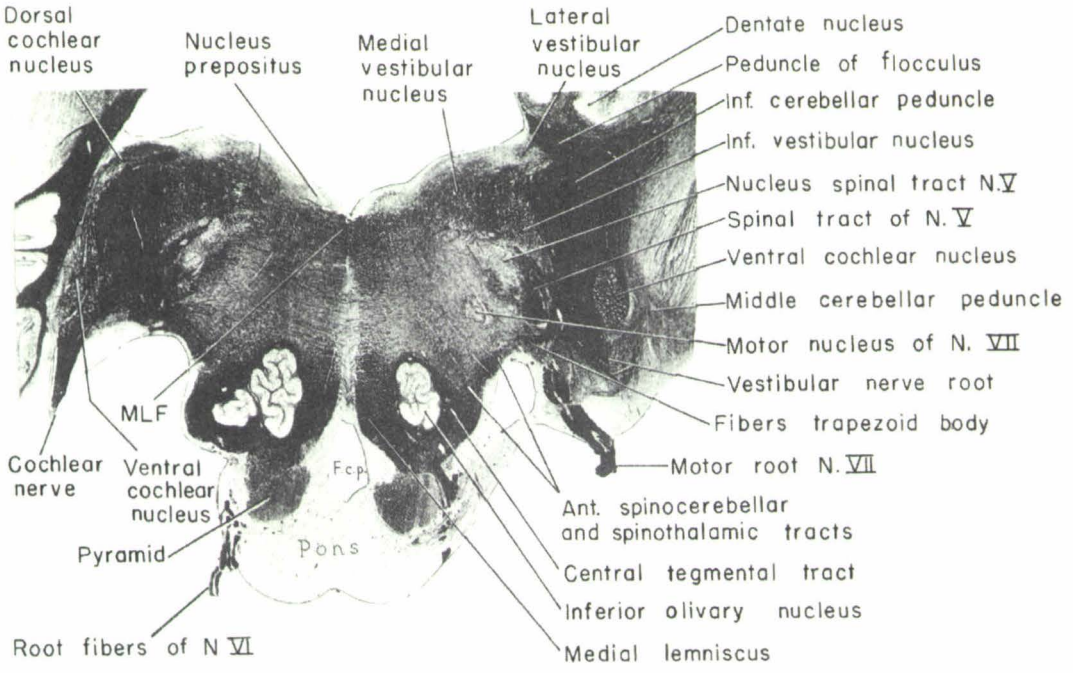


Figure 12.33. Transverse section of medulla of a 1-month infant through caudal border of pons. *F.c.p.*, Foramen cecum posterior; *MLF*, medial longitudinal fasciculus (Weigert's myelin stain).

upper medulla. Primary auditory fibers terminate upon two nuclear masses, the *ventral and dorsal cochlear nuclei*. The dorsal cochlear nucleus forms a prominence, the *tuberculum acusticum*, along the lateral border of the rhomboid fossa (Figs. 12.26, 12.33, and A.6). Cells of the dorsal cochlear nucleus are small, ovoid, and fusiform, while those of the ventral nucleus are large, round cells with a dark-staining cytoplasm. Secondary auditory fibers arising from the dorsal and ventral cochlear nuclei become apparent at more rostral brainstem levels.

The inferior olivary complex is reduced in size at the medullo-pontine junction, and the accessory olivary nuclei disappear (Fig. 12.32). Anterior to the olivary complex, the fibers of the pyramid are surrounded by pontine nuclei and some transverse fibers. The medial lemniscus and medial longitudinal fasciculus occupy the same positions as at more caudal levels, although they are slightly separated from the corresponding tract on the opposite side by more fully developed nuclei in the median raphe. Other ascending and descending tracts maintain the same relative positions as at lower medullary levels.

The junction of medulla and pons (Figs. 12.32 and 12.33) is characterized by (a) passage of the inferior cerebellar peduncle into the cerebellum, (b) reduction in size and, ultimately, disappearance of the inferior olivary complex, (c) incorporation of the corticospinal tract within the ventral part of the pons, (d) enlargement of the reticular formation, and (e) appearance of cranial nerve nuclei and root fibers typical of this higher level.

Cranial nerves present at the junction of medulla and pons are the abducens, cochlear, vestibular, and facial. The abducens nerve emerges at the lower border of the pons lateral to the pyramids. All other cranial nerves at this level are grouped together at the *cerebellopontine angle*, formed by the junction of medulla, pons, and cerebellum (Fig. 12.17). All of these nerves emerge from, or enter, the internal auditory meatus. The cochlear nerve is the most caudal and lateral, while the facial nerve is the most rostral and medial. The vestibular nerve lies between the cochlear and facial nerves. These cranial nerves are described and discussed in the next chapter.

In the upper medulla, the medial lemniscus reaches its full extent. It forms a vertical band of heavily myelinated fibers on either side of the raphe dorsal to the pyramids (Fig. 12.26). The formation and course of this tract are shown in Figure 11.1. The lateral and anterior spinothalamic tracts occupy a retro-olivary position (Fig. 12.26). Corticobulbar fibers

leave the pyramids and pass dorsally into the reticular formation (Fig. 12.27); intercalated neurons lying in the reticular formation, in turn, project upon motor cranial nerve nuclei (201). The medial longitudinal fasciculus, tectospinal, and tectobulbar tracts occupy an area dorsal to the medial lemniscus on each side of the median raphe. The tracts are partially separated by lighter-stained areas representing the raphe nuclei. At somewhat higher levels, this position is occupied by the inferior central nucleus (Figs. 12.32 and 13.4). Other descending tracts, such as the rubrospinal and vestibulospinal, are difficult to distinguish in Weigert-stained material.

As the inferior cerebellar peduncle enters the medullary core of the cerebellum, it is covered externally by the fibers of the middle cerebellar peduncle, which arise from the ventral part of the pons. The development of the ventral portion of the pons envelops the medullary pyramids. The blind end of the anterior median fissure, overhung by the pons, is known as the *foramen cecum posterior* (Fig. 12.33). The attenuated rostral pole of the inferior olivary nucleus is flanked laterally by the fibers of the central tegmental tract, and medially and ventrally by the medial lemniscus. The medial lemniscus gradually becomes flattened dorsoventrally and lies along the ventral border of the pontine tegmentum (Fig. 11.1). The light-staining area separating the medial lemnisci and the medial longitudinal fasciculi is occupied by raphe nuclei.

Lesions of the medulla or structures within it can be produced by a variety of causes, but those due to demyelinating diseases, neoplasms, and vascular pathology are the most common. Demyelinating diseases usually are disseminated and involve multiple systems at different sites. Neoplasms tend to extend in the longitudinal axis of the brainstem. Vascular lesions show great variation, but often give rise to characteristic syndromes. The vascular syndrome most commonly seen in the medulla is attributed to occlusion of the posterior inferior cerebellar artery (PICA), a vessel that supplies structures in the posterolateral region. While it seems likely that this syndrome may more frequently result from the involvement of the vertebral artery and its smaller branches (6), the symptoms and signs are similar and unmistakable. *Lateral medullary syndrome* (or *Wallenberg's syndrome*) is characterized by (a) loss of pain and thermal sense in the ipsilateral half of the face and the contralateral half of the body, (b) nausea, (c) vertigo, (d) disturbance of equilibrium, (e) persistent hiccup, and (f) dysphonia (hoarse voice) (53). Disturbances forming parts of this syndrome frequently can be correlated with the extent and precise location of the medullary lesion. Dorsolateral structures commonly involved in lateral medullary syndrome include (a) the spinal trigeminal tract and nucleus, (b) the spinothalamic tract, (c) efferent fibers of the vagus and glossopharyngeal nerves originating from the nucleus ambiguus, (d) parts of the inferior cerebellar peduncle, as well as fiber systems projecting toward this peduncle, and (e) variable portion of the inferior cerebellar cortex. The blood supply of the medulla is discussed in Chapter 4.

References

1. Adey WR, Segundo JP, Livingston RB. Corticofugal influences on intrinsic brain stem conduction in cat and monkey. J Neurophysiol 1957;20:1–16.
2. Arimatsu Y, Seto A, Amano T. An atlas of α-bungarotoxin binding sites and structures containing acetylcholinesterase in the mouse central nervous system. J Comp Neurol 1981;198:603–631.
3. Arvidsson U, Ulfhake B, Cullheim S, et al. Thyrotropin-releasing hormone (TRH)-like immunoreactivity in the grey monkey (*Macaca fascicularis*) spinal cord and medulla oblongata with special emphasis on the bulbospinal tract. J Comp Neurol 1992;322:293–310.
4. Atweh SF, Kuhar MJ. Autoradiographic localization of opiate receptors in rat brain. I. Spinal cord and lower medulla. Brain Res 1977;124:53–67.
5. Bacon SJ, Zagon A, Smith AD. Electron microscopic evidence of a monosynaptic pathway between cells in the caudal raphe nuclei and sympathetic preganglionic neurons in the rat spinal cord. Exp Brain Res 1990;79:589–602.
6. Baker AB. Cerebrovascular disease. IX. The medullary blood supply and the lateral medullary syndrome. Neurology 1961;11:852–861.
7. Basbaum AI, Clanton CH, Fields HL. Opiate and stimulus-produced analgesia: functional anatomy of medullospinal pathways. Proc Natl Acad Sci USA 1976;73:4685–4688.
8. Basbaum AI, Clanton CH, Fields HL. Three bulbospinal pathways from the rostral medulla of the cat: an autoradiographic study of pain modulating systems. J Comp Neurol 1978;178:209–224.
9. Basbaum AI, Fields HL. The origin of descending pathways in the dorsolateral funiculus of the spinal cord of the cat and rat: further studies on the anatomy of pain modulation. J Comp Neurol 1979;187:513–532.
10. Basbaum AI, Ralston DD, Ralston HJ. Bulbospinal projections if the primate: a light and electron microscopic study of a pain modulating system. J Comp Neurol 1986;250:311–323.
11. Beckstead RM, Morse JR, Norgren R. The nucleus of the solitary tract in the monkey: projections to the thalamus and brain stem nuclei. J Comp Neurol 1980;190:259–282.
12. Beckstead RM, Norgren R. An autoradiographic examination of the central distribution of the trigeminal, facial, glossopharyngeal and

vagal nerves in the monkey. J Comp Neurol 1979;184:455–472.
13. Berkley KJ, Hand PJ. Projections to the inferior olive of the cat. II. Comparisons of input from the gracile, cuneate and the spinal trigeminal nuclei. J Comp Neurol 1978;180:253–264.
14. Berkley KJ, Worden IG. Projections to the inferior olive of the cat. I. Comparisons of input from the dorsal column nuclei, the lateral cervical nucleus, the spino-olivary pathways, the cerebral cortex and the cerebellum. J Comp Neurol 1978;180:237–252.
15. Bogerts B. A brainstem atlas of catecholaminergic neurons in man, using melanin as a natural marker. J Comp Neurol 1981;197:63–80.
16. Borison HL, Wang SC. Functional localization of central coordinating mechanisms or emesis in cat. J Neurophysiol 1949;12:305–313.
17. Borison HL, Wang SC. Physiology and pharmacology of vomiting. Pharmacol Rev 1953;5:193–230.
18. Bowker RM, Westlund KN, Sullivan MC, Wilber JF, Coulter JD. Descending serotonergic, peptidergic and cholinergic pathways from the raphe nuclei: a multiple transmitter complex. Brain Res 1983; 288:33–48.
19. Bowman JP, Sladek JR. Morphology of the inferior olivary complex of the rhesus monkey (*Macaca mulatta*). J Comp Neurol 1973;152: 299–316.
20. Brizzee KR, Neal LM. A re-evaluation of the cellular morphology of the area postrema in view of recent evidence for a chemoreceptor function. J Comp Neurol 1954;100: 41–62.
21. Brodal A. Experimentelle Untersuchungen über die olivocerebellare Lokalisation. Z Gesamte Neurol Psychiatry 1940;169:1–153.
22. Brodal A. Spinal afferents to the lateral reticular nucleus of the medulla oblongata in the cat: an experimental study. J Comp Neurol 1949;91:259–295.
23. Brodal A. Reticulo-cerebellar connections in the cat: An experimental study. J Comp Neurol 1953; 98:113–153.
24. Brodal A. The reticular formation of the brain stem. Anatomical aspects and functional correlations. Springfield, IL: Charles C. Thomas, 1957.
25. Brodal A. Die Verbindungen des Nucleus cuneatus externus mit dem Kleinhirn beim Kaninchen und bei der Katze: Experimentelle Untersuchungen. Z Gesamte Neurol Psychiatry 1961 ;171:167–199.
26. Brodal A. Neurological anatomy in relation to clinical medicine. 3rd ed. New York: Oxford University Press, 1981.
27. Brodal A, Rossi GF. Ascending fibers in brain stem reticular formation of cat. Arch Neurol Psychiatry 1955 ;74:68–87.
28. Brodal A, Szabo T, Torvik A. Corticofugal fibers to sensory trigeminal nuclei and nucleus of solitary tract. J Comp Neurol 1956 ;106:527–555.
29. Brodal A, Szikla G. The termination of the brachium conjunctivum descendens in the nucleus reticularis tegmenti pontis: an experimental study in the cat. Brain Res 1972 ;39:337–351.
30. Burgi S, Bucher VM. Markhaltige Faserverbindungen im Hirnstamm der Katze. Berlin: Springer-Verlag, 1950.
31. Bystrzycka EK. Afferent projections to the dorsal and ventral respiratory nuclei in the medulla oblongata of the cat studied by the horseradish peroxidase technique. Brain Res 1980;185:59–66.
32. Cabot JB, Wild JM, Cohen DH. Raphe inhibition of sympathetic preganglionic neurons. Science 1979;203:184–186.
33. Cammermeyer J. Is the human area postrema a neuro-vegetative nucleus? Acta Anat (Basel) 1947; 2:294–320.
34. Carlton SM, Honda CN, Willcockson WS, et al. Descending adrenergic input to the primate spinal cord and its possible role in modulation of spinothalamic cells. Brain Res 1991;543:77–90.
35. Carpenter MB, Brittin GM, Pines J. Isolated lesions of the fastigial nuclei in the cat. J Comp Neurol 1958;109:65–90.
36. Carpenter MB, Hanna GR. Fiber projections from the spinal trigeminal nucleus in the cat. J Comp Neurol 1961;117:117–132.
37. Carpenter MB, Nova HR. Descending division of the brachium conjunctivum in the cat: a cerebelloreticular system. J Comp Neurol 1960;114:295–305.
38. Carpenter MB, Stein BM, Shriver JE. Central projections of spinal dorsal roots in the monkey. II. Lower thoracic, lumbosacral and coccygeal dorsal roots. Am J Anat 1968;123:75–118.
39. Chan-Palay V. Paratrigeminal nucleus. II. Identification and interrelations of catecholamine axons, indolamine axons and substance P immunoreactive cells in neuropil. J Neurocytol 1978;4:419–442.
40. Chan-Palay V. Morphological correlates for transmitter synthesis, transport, release, uptake and catabolism: a study of serotonin neurons in the nucleus paragigantocellularis lateralis. In: Fonnum F, ed. Amino acids as chemical transmitters. New York: Plenum Press, 1978:1–30.
41. Cho HJ, Basbaum A. GABAergic circuitry in the rostral ventral medulla of the rat and its relationship to descending antinociceptive controls. J Comp Neurol 1991; 303:316–328.
42. Ciriello J, Calaresu FR. Autoradiographic study of ascending projections from cardiovascular sites in the nucleus tractus solitarii in the cat. Brain Res 1980;180:448–453.
43. Ciriello J, Calaresu FR. Monosynaptic pathway from cardiovascular neurons in the nucleus tractus solitarii to the paraventricular nucleus in the cat. Brain Res 1980; 193:529–533.
44. Clark FM, Proudfit HK. The projection of noradrenergic neurons in the A7 catecholamine cell group to the spinal cord in the rat demonstrated by anterograde tracing combined with immunocytochemistry. Brain Res 1991;547: 279–288.
45. Clemente CD, van Breemen VL. Nerve fibers in the area postrema of cat, rabbit, guinea pig and rat. Anat Rec 1955;123:65–79.
46. Clemente CD, Sutin J, Silverstone JT. Changes in electrical activity of the medulla on the intravenous injection of hypertonic solutions. Am J Physiol 1957;188:193–198.
47. Combs CM. Bulbar regions related to localized cerebellar afferent impulses. J Neurophysiol 1956;19: 285–300.
48. Cooper JR, Bloom FE, Roth RH. The biochemical basis of neuropharmacology. 6th ed. New York: Oxford University Press, 1991.
49. Coote JH. Bulbospinal serotonergic pathways in the control of blood pressure. J Cardiovasc Pharmacol 1990;15:35–41.
50. Courville J, Faraco-Cantin F. On the origin of the climbing fibers of the cerebellum: an experimental study in the cat with an autoradiographic tracing method. Neuroscience 1978;3:797–809.
51. Cruce WLR, Newman DB. Evolution of motor systems—the reticulospinal pathways. Am Zool 1984;24:733–753.
52. Cuello AC, Kanazawa I. The distribution of substance P immunoreactive fibers in the rat central nervous system. J Comp Neurol 1978;178:129–156.
53. Currier RD, Giles CL, DeJong RN. Some comments on Wallenberg's lateral medullary syndrome. Neurology 1961;11:778–791.
54. Dahlström A, Fuxe K. Evidence for the existence of monoamine-containing neurons in the central nervous system. I. Demonstration of monoamines in the cell bodies of brain stem neurons. Acta Physiol Scand 1964;62(Suppl 232):1–55.
55. Dawson NJ, Hellon RF, Hubbard JI. Cell responses evoked by tooth pulp stimulation above the marginal layer of the cat's trigeminal nucleus caudalis. J Comp Neurol 1980;193:983–994.
56. Dykes RW, Rasmussan PD, Stretavan D, Rehaman NB. Submodality segregation and receptive field sequences in the cuneate, gracile, and external cuneate nuclei of the cat. J Neurophysiol 1982;47: 389–416.
57. Dostrovsky JO, Hellon RF. The representation of facial temperature in the caudal trigeminal nu-

cleus of the cat. J Physiol (Lond) 1978;277:29–48.
58. Doty RW. Neural organization of deglutition. In: Gode CP, ed. Handbook of physiology. Vol. IV, Sect. 6. Washington, DC: American Physiological Society, 1968:1861–1902.
59. Eccles JC, Ito M, Szentagothai J. The cerebellum as a neuronal machine. New York: Springer-Verlag, 1967.
60. Ferraro A, Barrera SE. Posterior column fibers and their terminations in the *Macacus rhesus*. J Comp Neurol 1935;62:507–530.
61. Finley JCW, Maderdrut JL, Petruz P. The immunocytochemical localization of enkephalin in the central nervous system of the rat. J Comp Neurol 1981;198:541–565.
62. Florence SL, Wall JT, Kaas JH. The somatotopic pattern of afferent projections from the digits to the spinal cord and cuneate nucleus in macaque monkeys. Brain Res 1988;452:388–392.
63. Florence SL, Wall JT, Kaas JH. Somatotopic organization of inputs from the hand to the spinal gray and cuneate nucleus of monkeys with observations on the cuneate nucleus of humans. J Comp Neurol 1989;286:48–70.
64. Fung SJ, Manzoni D, Chan JY, Pompeiano O, Barnes CD. Locus coeruleus control of spinal motor output. Prog Brain Res 1991; 88:395–409.
65. Gilman S, Marco LA. Effects of medullary pyramidotomy in the monkey. I. Clinical and electromyographic abnormalities. Brain 1971;94:495–514.
66. Gobel S. Golgi studies of the substantia gelatinosa neurons in the spinal trigeminal nucleus. J Comp Neurol 1975;162:397–416.
67. Gobel S. Golgi studies of the neurons in layer I of the dorsal horn of the medulla (trigeminal nucleus caudalis). J Comp Neurol 1978; 180:375–394.
68. Gobel S. Golgi studies of the neurons in layer II of the dorsal horn of the medulla (trigeminal nucleus caudalis). J Comp Neurol 1978; 180:395–414.
69. Gobel S, Purvis MB. Anatomical studies of the organization of the spinal V nucleus: the deep bundles and the spinal V tract. Brain Res 1972;48:27–44.
70. Gordon G, Jukes MGM. Dual organization of exteroceptive components of the cat's gracile nucleus. J Physiol (Lond) 1964;173:263–290.
71. Gordon G, Jukes MGM. Descending influences on the exteroceptive organization of the cat's gracile nucleus. J Physiol (Lond) 1964; 173:291–319.
72. Gordon G, Paine PH. Functional organization in nucleus gracilis of the cat. J Physiol (Lond) 1960; 153:331–349.
73. Gwyn DG, Leslie RA, Hopkins DA. Gastric afferent to the nucleus of the solitary tract in the cat. Neurosci Lett 1979;14:13–17.
74. Haber LH, Martin RF, Chatt AB, Willis WD. Effects of stimulation in nucleus reticularis gigantocellularis on the activity of spinothalamic tract neurons in the monkey. Brain Res 1978;153:163–168.
75. Hagbarth KE, Kerr DIB. Central influences on spinal afferent conduction. J Neurophysiol 1954;17: 295–307.
76. Hamori J, Szentagothai J. Identification under the electron microscope of climbing fibers and their synaptic contacts. Exp Brain Res 1966;1:65–81.
77. Hand PJ. Lumbosacral dorsal root terminations in the nucleus gracilis of the cat: some observations on terminal degeneration in other medullary sensory nuclei. J Comp Neurol 1966;126:136–156.
78. Haymaker W. Bing's local diagnosis in neurological diseases. St. Louis: C.V. Mosby, 1956:57–62; 105–112.
79. Hernandez-Peon R, Hagbarth KE. Interaction between afferent and cortically induced reticular responses. J Neurophysiol 1955; 18:44–55.
80. Hinman A, Carpenter MB. Efferent fiber projection of the red nucleus in the cat. J Comp Neurol 1959;113:61–82.
81. Hodge CJ, Apkarian AV, Stevens R, Vogel-Sang G, Wisnicki HJ. Locus coeruleus modulation of dorsal horn unit responses to cutaneous stimulation. Brain Res 1981;204:415–420.
82. Hökfelt T, Elde R, Johansson O, Terenius L, Stein L. The distribution of enkephalin immunoreactive cell bodies in the rat central nervous system. Neurosci Lett 1977;5:25–31.
83. Hökfelt T, Fuxe K, Goldstein M, Johansson O. Immunohistochemical evidence for the existence of adrenaline neurons in the rat brain. Brain Res 1974;66:235–251.
84. Hökfelt T, Terenius T, Kuypers HGJM, Dann O. Evidence for enkephalin immunoreactivity neurons in the medulla oblongata projecting to the spinal cord. Neurosci Lett 1979;14:55–60.
85. Holstege JC, Bongers CM. A glycinergic projection from the ventromedial lower brainstem to spinal motoneurons. An ultrastructural double labeling study in rat. Brain Res 1991;566:308–315.
86. Hughes J, Smith T, Kosterlitz H, Fothergill L, Morgan B, Morris H. Identification of two related pentapeptides from the brain with potent opiate agonist activity. Nature 1975;258:577–579.
87. Ingram WR. Nuclear organization and chief connections of the primate hypothalamus. Proc Assoc Res Nerv Ment Dis 1940;20: 195–244.
88. Jabbur SJ, Towe AL. Cortical excitation of neurones in dorsal column nuclei of cat, including an analysis of pathways. J Neurophysiol 1961;24:499–509.
89. Jacobsohn L. Über die Kerne des menschlichen Rüchenmarks. Abhandlungen des königl preuss. Akademie der Wissenschafte, 1908: 72.
90. Johansson O, Hökfelt T, Pernow B, et al. Immunohistochemical support for three putative transmitters in one neuron: coexistence of 5-hydroxytryptamine, substance P- and thyrotropin releasing hormone-like immunoreactivity in medullary neurons projecting to the spinal cord. Neuroscience 1981;6: 1857–1881.
91. Jones SL. Descending noradrenergic influences on pain. Prog Brain Res 1991;88:381–394.
92. Jones BE, Friedman L. Atlas of catecholamine perikarya, varicosities and pathways in the brainstem of the cat. J Comp Neurol 1983; 215:382–396.
93. Jones BE, Holmes CJ, Rodriguez-Veiga E, Mainville L. GABA-synthesizing neurons in the medulla: their relationship to serotonin-containing and spinally projecting neurons in the rat. J Comp Neurol 1991;313:349–367.
94. Kalia M. Neuroanatomical organization of the respiratory centers. Fed Proc 1977;36:2405–2411.
95. Kalia M, Mesulam M-M. Brain stem projections of sensory and motor components of the vagus complex in the cat. I. The cervical vagus and nodose ganglion. J Comp Neurol 1980;193:435–465.
96. Kalia M, Mesulam M-M. Brain stem projections of sensory and motor components of the vagus complex in the cat. II. Laryngeal, tracheobronchial, pulmonary, cardiac, and gastrointestinal branches. J Comp Neurol 1980;193:467–508.
97. Kaas JH. Somatosensory system. In: Paxinos G, ed. The human nervous system. Ch. 24. New York: Academic Press, 1990:813–844.
98. Kerr FWL. Structural relation of the trigeminal spinal tract to upper cervical roots and the solitary nucleus in the cat. Exp Neurol 1961;4:134–148.
99. Kerr FWL. Facial, vagal and glossopharyngeal nerves in the cat: afferent connections. Arch Neurol 1962;2:264–281.
100. Kerr FWL. The divisional organization of afferent fibers of the trigeminal nerve. Brain 1963;86: 721–732.
101. Kimmel DL, Kimmel CB, Zarkin A. The central distribution of afferent nerve fibers of the facial and vagus nerves in the guinea pig. Anat Rec 1961;139:245.
102. King GW. Topology of ascending brainstem projections to the nucleus parabrachialis in the cat. J Comp Neurol 1980;191:615–638.
103. Kneisley LW, Biber MP, LaVail JH. A study of the origin of brain stem projections to monkey spinal cord

using the retrograde transport method. Exp Neurol 1978;60:116–139.
104. Koella WP, Sutin J. Extra-blood-brain-barrier brain structures. Int Rev Neurobiol 1967;10:31–55.
105. Krieg WJS. The hypothalamus of the albino rat. J Comp Neurol 1932;55:19–89.
106. Kruger L. Functional subdivision of the brainstem sensory trigeminal nuclear complex. In: Bonica JJ, Liebeskind JC, Albe-Fessard DG, eds. Proceedings of the Second World Congress on pain: advances in pain research and therapy. Vol. 3. New York: Raven Press, 1979:197–211.
107. Kruger L, Michel F. A morphological and somatotopic analysis of single unit activity in the trigeminal sensory complex of the cat. Exp Neurol 1962;5:139–156.
108. Kruger L, Siminoff R, Witkovsky P. Single neuron analysis of dorsal column nuclei and spinal nucleus of trigeminal in cat. J Neurophysiol 1961;24:333–349.
109. Kuhn RA. Topographical pattern of cutaneous sensibility in the dorsal column nuclei of the cat. Trans Am Neurol Assoc 1949;74:227–230.
110. Künzle H. The topographical organization of spinal afferents to the lateral reticular nucleus of the cat. J Comp Neurol 1973;149: 103–117.
111. Kuypers HGJM. An anatomical analysis of corticobulbar connections to the pons and lower brain stem in the cat. J Anat 1958; 92:198–218.
112. Kuypers HGJM. Corticobulbar connections to the pons and lower brain-stem in man: an anatomical study. Brain 1958;81:364–388.
113. Kuypers HGJM. Some projections from the peri-central cortex to the pons and lower brain stem in monkey and chimpanzee. J Comp Neurol 1958;110:221–256.
114. Kuypers HGJM. Pericentral cortical projections to motor and sensory nuclei. Science 1958;128: 662–663.
115. Kuypers HGJM. Central cortical projections to motor and somatosensory cell groups. Brain 1960; 83:161–184.
116. Kuypers HGJM, Hoffman AL, Beasley RM. Distribution of cortical "feedback" fibers in the nuclei cuneatus and gracilis. Proc Soc Exper Biol Med 1961;108:634–637.
117. Kuypers HGJM, Tuerk JD. The distribution of cortical fibres within the nuclei cuneatus and gracilis in the cat. J Anat 1964;98:143–162.
118. Levitt P, Moore RY. Origin and organization of brainstem catecholamine innervation in the rat. J Comp Neurol 1979;186:505–528.
119. Liu CN. Afferent nerves to Clarke's and the lateral cuneate nuclei in the cat. Arch. Neurol. Psychiatry 1956;75:67–77.
120. Llinás R, Baker R, Sotelo C. Electrotonic coupling between neurons in cat inferior olive. J Neurophysiol 1974;37:560–571.
121. Loewy AD, Burton H. Nuclei of the solitary tract: efferent projections to the lower brain stem and spinal cord of the cat. J Comp Neurol 1978;181:421–450.
122. Loewy AD, McKellar S. The neuroanatomical basis of central cardiovascular control. Fed Proc 1980;39:2495–2503.
123. Loewy AD, Wallach JH, McKellar S. Efferent connections of the ventral medulla oblongata in the rat. Brain Res Rev 1981;3:63–80.
124. McComas AJ. Responses of the rat dorsal column system to mechanical stimulation of the hind paw. J Physiol (Lond) 1963;166: 435–445.
125. Magoun HW, Rhines R. An inhibitory mechanism in the bulbar reticular formation. J Neurophysiol 1946;9:165–171.
126. Martin RF, Haber LH, Willis WD. Primary afferent depolarization of identified cutaneous fibers following stimulation in medial brain stem. J Neurophysiol 1979;42: 779–790.
127. Martin GF, Holstege G, Mehler WR. Reticular formation of the pons and medulla. In: Paxinos G, ed. The human nervous system. Ch. 8. New York: Academic Press, 1990:203–220.
128. Matsushita M, Ikeda M. Projections from the lateral reticular nucleus to the cerebellar cortex and nuclei in the cat. Exp Brain Res 1976;24:403–422.
129. Meesen H, Olszewski J. A cytoarchitectonic atlas of the rhombencephalon of the rabbit. Basel: S. Karger, 1949.
130. Mehler WR, Feferman ME, Nauta WJG. Ascending axon degeneration following anterolateral cordotomy: an experimental study in the monkey. Brain 1956;83:718–750.
131. Mettler FA. The tegmento-olivary and central tegmental fasciculi. J Comp Neurol 1944;80:149–175.
132. Morest DK. Experimental study of the projections of the nucleus of the tractus solitarius and the area postrema in the cat. J Comp Neurol 1967;130:277–299.
133. Morris R, Salt TE, Sofroniew MW, Hill RG. Actions of microiontophoretically applied oxytocin, and immunohistochemical localization of oxytocin, vasopressin and neurophysin in the rat caudal medulla. Neurosci Lett 1980;18: 163–168.
134. Mountcastle VB, Powell TPS. Central nervous mechanisms subserving position sense and kinesthesis. Bull Johns Hopkins Hosp 1959; 105:173–200.
135. Nageotte J. The pars intermedia or nervus intermedius of Wrisberg, and the bulbo-pontine gustatory nucleus in man. Rev Neurol Psychiatry 1906;4:473–488.
136. Nauta WJH. Hippocampal projections and related neural pathways to the midbrain in the cat. Brain 1958;81:319–340.
137. Nauta WJH. The central visceromotor system: a general survey. In: Hockman CH, ed. Limbic system mechanisms and autonomic function. Ch. 2. Springfield, IL: Charles C. Thomas, 1972:21–33.
138. Nieuwenhuys R. Chemoarchitecture of the brain. Berlin: Springer-Verlag, 1985.
139. Nicholas AP, Pieribone VA, Arvidsson U, Hökfelt T. Serotonin-, substance P- and glutamate/aspartate-like immunoreactivities in medullo-spinal pathways of rat and primate. Neuroscience 1992;48:545–559.
140. Nilaver G, Zimmerman EA, Wilkins J, Michaels J, Hoffman D, Silverman A-J. Magnocellular hypothalamic projections to the lower brain stem and spinal cord of the rat. Neuroendocrinology 1980;30:150–158.
141. Norgren R. Gustatory system. In: Paxinos G, ed. The human nervous system. Ch. 25. New York: Academic Press, 1990:845–861.
142. Oliveras JL, Hosobuchi Y, Guilbaud G, Besson JM. Analgesic electrical stimulation of the feline nucleus raphe magnus: development of tolerance and its reversal by 5-HTP. Brain Res 1978;146:404–409.
143. Olszewski J. On the anatomical and functional organization of the spinal trigeminal nucleus. J Comp Neurol 1950;92:401–413.
144. Olszewski J, Baxter D. Cytoarchitecture of the human brain stem. Philadelphia: J.B. Lippincott, 1954.
145. Oscarsson O. Functional organization of the spino- and cuneocerebellar tracts. Physiol Rev 1965; 45:495–522.
146. Oscarsson O. Functional organization of spinocerebellar paths. In: Iggo A, ed. Handbook of sensory physiology. Vol. 2. Berlin: Springer-Verlag, 1973:339–380.
147. Panneton WM, Loewy AD. Projections of the carotid sinus nerve to the nucleus of the solitary tract in the cat. Brain Res 1980;191:239–244.
148. Parent A, Descarries L, Beaudet A. Organization of ascending serotonin systems in the adult rat brain. A radioautographic study after intraventricular administration of [^{3}H] 5-hydroxytryptamine. Neuroscience 1981;6:115–138.
149. Parent A, Poitras D, Dubé, L. Comparative anatomy of central monoaminergic systems. In: Björklund A, Hökfelt T, eds. Handbook of chemical neuroanatomy. Vol. 2. Part 1: Classical transmitters in the CNS. Amsterdam: Elsevier, 1984: 409–433.
150. Pass IJ. Anatomic and functional relationship of nuc. dorsalis (Clarke's column). Arch Neurol Psychiatry 1933;30:1025–1945.
151. Paxinos G, Törk I, Halliday G, Mehler WR. Human homologs to brainstem nuclei identified in other animals as revealed by acetyl-

cholinesterase activity. In: Paxinos G, ed. The human nervous system. Ch. 7. New York: Academic Press, 1990:149–302.
152. Pearson J, Halliday G, Sakamoto N, Michel J-P. Catecholaminergic neurons. In: Paxinos G, ed. The human nervous system. Ch. 31. New York: Academic Press, 1990: 1023–1049.
153. Perl ER, Whitlock DG, Gentry JR. Cutaneous projection to second-order neurons of the dorsal column system. J Neurophysiol 1962;25:337–353.
154. Peterson BW. Reticulo-motor pathways: their connections and possible roles in motor behavior. In: Asanuma H, Wilson VJ, eds. Integration in the nervous system. Tokyo: Igaku Shoin, 1979:185–200.
155. Peterson BW. Reticulospinal projections to spinal motor nuclei. Annu Rev Physiol 1979;41:127–140.
156. Pioro EP, Mai JK, Cuello AC. Distribution of substance P-and enkephalin-immunoreactive neurons and fibers. In: Paxinos G, ed. The human nervous system. Ch. 32. New York: Academic Press, 1990:1051–1094.
157. Poggio GF, Mountcastle VB. A study of the functional contributions of the lemniscal and spinothalamic systems to somatic sensibility. Bull Johns Hopkins Hosp 1960;106:266–316.
158. Poitras D, Parent A. Atlas of the distribution of monoamine-containing nerve cell bodies in the brain stem of the cat. J Comp Neurol 1978;179:699–718.
159. Price DD, Dubner R, Hu JW. Trigeminothalamic neurons in nucleus caudalis responsive to tactile, thermal and nociceptive stimulation of monkeys face. J Neurophysiol 1976;39:936–953.
160. Proudfit HK, Clark FM. The projections of locus coeruleus neurons to the spinal cord. Prog Brain Res 1991;88:123–141.
161. Ramón y Cajal S. Histologie du Système Nerveux de l'Homme et des Vertébrés. (Azoulay L, trans.), Paris: Maloine, 1909, 1911. (Reprinted, Consejo Superior de Investigaciones Cientificas, Instituto Ramón y Cajal, Madrid, 1972.)
162. Ramon-Moliner E, Nauta WJH. The isodendritic core of the brain stem. J Comp Neurol 1966;126: 311–335.
163. Rhines R, Magoun HW. Brainstem facilitation of cortical motor response. J Neurophysiol 1946;9: 219–229.
164. Rhoton AL, O'Leary JL, Ferguson JP. The trigeminal, facial, vagal and glossopharyngeal nerves in the monkey. Arch Neurol 1966; 14:530–540.
165. Ropper AH, Fisher CM, Kleinman GM. Pyramidal infarction in the medulla: a cause of pure motor hemiplegia sparing the face. Neurology 1979;29:91–95.
166. Rosén I, Scheid P. Patterns of afferent input to the lateral reticular nucleus of the cat. Exp Brain Res 1973;18:242–255.
167. Rossi GF, Brodal A. Corticofugal fibers to the brain stem reticular formation: an experimental study in the cat. J Anat 1956;90:42–62.
168. Rossi GF, Brodal A. Spinal afferents to the trigeminal sensory nuclei and the nucleus of the solitary tract. Confin Neurol 1956;16: 321–332.
169. Rossi GF, Brodal A. Terminal distribution of spinoreticular fibers in the cat. AMA Arch Neurol Psychiatry 1957;78:439–453.
170. Saint-Cyr JA, Courville J. Projection from the vestibular nuclei to the inferior olive in the cat: an autoradiographic and horseradish peroxidase study. Brain Res 1979; 165:189–201.
171. Saint-Cyr JA, Courville J. Sources of descending afferents to the inferior olive from the upper brain stem in the cat as revealed by the retrograde transport of horseradish peroxidase. J Comp Neurol 1981;198:567–581.
172. Sawchenko PE, Swanson LW. The organization of noradrenergic pathways from the brainstem to the paraventricular and supraoptic nuclei in the rat. Brain Res Rev 1982;4:275–325.
173. Scheibel ME, Scheibel AB. Structural substrates for integrative patterns in the brain stem reticular core. In: Jasper HH, Proctor LP, Knighton RS, et al., eds. Reticular formation of the brain. Ch. 2. Boston: Little Brown & Company, 1958:31–55.
174. Schütz H. Anatomische Untersuchungen über den Faserverlauf im zentralen Höhlengrau und den Nervenfaserschwund in demselben bei der progressiven Paralyse der Irren. Arch Psychiatr Nervenkr 1891;22:527–587.
175. Schwartzman RJ. A behavioral analysis of complete unilateral section of the pyramidal tract at the medullary level in *Macaca mulatta*. Ann Neurol 1978;4:234–244.
176. Sherrington CS. Note on the spinal portion of some ascending degenerations. J Physiol (Lond) 1893; 14:255–302.
177. Shriver JE, Stein BM, Carpenter MB. Central projections of spinal dorsal roots in the monkey. I. Cervical and upper thoracic dorsal roots. Am J Anat 1968;123:27–74.
178. Shute CCD, Lewis PR. Cholinesterase-containing systems of the brain of the rat. Nature 1963;199: 1160–1163.
179. Sjöqvist O. Studies on pain conduction in the trigeminal nerve: a contribution to surgical treatment of facial pain. Acta Psychiat Neurol Scand 1938;17(Suppl):1–139.
180. Sladek JR Jr, Bowman JP. The distribution of catecholamines within the inferior olivary complex of the cat and rhesus monkey. J Comp Neurol 1975;163:203–214.
181. Snyder RL Jr, Sutin J. Effect of lesions of the medulla oblongata on electrolyte and water metabolism in the rat. Exp Neurol 1961; 4:424–435.
182. Sotelo C, Llinás R, Baker R. Structural study of interior olivary nucleus of the cat: morphological correlates of electrotonic coupling. J Neurophysiol 1974;37:541–559.
183. Sprague JM, Chambers WW. Control of posture by reticular formation and cerebellum in the intact, anesthetized, unanesthetized and in the decerebrated cat. Am J Physiol 1954;176:52–64.
184. Steinbusch HWM. Distribution of serotonin-immunoreactivity in the central nervous system of the rat—cell bodies and terminals. Neuroscience 1981;6:577–618.
185. Steinbusch HWM, Nieuwenhuys R. The raphe nuclei of the rat brainstem: a cytoarchitectonic and immunohistochemical study. In: Emson PC, ed. Clinical neuroanatomy. New York: Raven Press, 1983:131–207.
186. Swanson LW, Kuypers HGJM. The paraventricular nucleus of the hypothalamus: cytoarchitectonic subdivisions and organization of projections to the pituitary, dorsal vagal complex, and spinal cord as demonstrated by retrograde fluorescence double-labeling methods. J Comp Neurol 1980;194:555–570.
187. Taber E. The cytoarchitecture of the brain stem of the cat. I. Brain stem nuclei of cat. J Comp Neurol 1961;116:27–70.
188. Takeuchi Y, Uemura M, Matsuda K, Matsushima R, Mizuno N. Parabrachial nucleus neurons projecting to the lower brain stem and the spinal cord: a study in the cat by the Fink-Heimer and the horseradish peroxidase methods. Exp Neurol 1980;70:403–413.
189. Thomas DM, Kaufman RP, Sprague JM, Chambers WW. Experimental studies of the vermal cerebellar projections in the brain stem of the (fastigiobulbar tract). J Anat 1956;90:371–385.
190. Tohyama M, Sakai M, Salvert D, Touret M, Jouvet M. Spinal projections from the lower brain stem in the cat as demonstrated by the horseradish peroxidase technique. I. Origins of the reticulospinal tracts and their funicular trajectories. Brain Res 1979;173:383–403.
191. Törk I, McRitchie DA, Rikard-Bell GC, Paxinos G. Autonomic regulatory centers in the medulla oblongata. In: Paxinos G, ed. The human nervous system. Ch. 9. New York: Academic Press, 1990:221–259.
192. Törk I, Hornung JP. Raphe nuclei and the serotonergic System. In: Paxinos G, ed. The human nervous system. Ch. 30. New York: Academic Press, 1990:1001–1022.
193. Torvik A. Afferent connections to the sensory trigeminal nuclei, the nucleus of the solitary tract and adjacent structures: an experimental

study in the rat. J Comp Neurol 1956;106:51–142.
194. Torvik A, Brodal A. The origin of reticulospinal fibers in the cat: an experimental study. Anat Rec 1957;128:113–137.
195. Tower SS. Pyramidal lesion in the monkey. Brain 1940;63:36–90.
196. Uhl GR, Goodman RR, Kuhar MJ, Childers SR, Snyder SH. Immunohistochemical mapping of enkephalin containing cell bodies, fibers and nerve terminals in the brain stem of the rat. Brain Res 1979; 166:75–94.
197. Vigier D, Rouvière A. Afferent and efferent connections of the area postrema demonstrated by the horseradish peroxidase method. Arch Ital Biol 1979;117:325–339.
198. Walberg F. Lateral reticular nucleus in medulla oblongata in mammals: comparative-anatomical study. J Comp Neurol 1952; 96:283–343.
199. Walberg F. Descending connections to the inferior olive: an experimental study in the cat. J Comp Neurol 1956;104:77–173.
200. Walberg F. Corticofugal fibres to the nuclei of the dorsal columns: an experimental study in the cat. Brain 1957;80:273–287.
201. Walberg F. Do the motor nuclei of the cranial nerves receive corticofugal fibres? An experimental study in the cat. Brain 1957; 80:597–605.
202. Walberg F. On the termination of rubrobulbar fibers: experimental observations in the cat. J Comp Neurol 1958;110:66–73.
203. Walberg F. Descending connections from the mesencephalon to the inferior olive: an experimental study in the cat. Exp Brain Res 1974;21:145–156.
204. Walker AE, Weaver TA Jr. The topical organization and termination of fibers of the posterior columns in *Macaca mulatta*. J Comp Neurol 1942;76:145–158.
205. Wamsley JK, Lewis MS, Young WS III, Kuhar MJ. Autoradiographic localization of muscarinic cholinergic receptors in rat brainstem. J Neurosci 1981;1:176–191.
206. Whitehead MC. Anatomy of the gustatory system in the hamster: synaptology of the facial afferent terminals in the solitary nucleus. J Comp Neurol 1986;244:72–85.
207. Winter DL. N. gracilis of cat: Functional organization and corticofugal effects. J Neurophysiol 1965; 28:48–70.
208. Woolsey CN, Gorska T, Wetzel A, Erickson TC, Earls FJ, Allman JM. Complete unilateral section of the pyramidal tract at the medullary level in *Macaca mulatta*. Brain Res 1972;40:119–124.
209. Yeomans DC, Clark FM, Paice JA, Proudfit HK. Antinociception induced by electrical stimulation of spinally projecting noradrenergic neurons in the A7 catecholamine cell group of the rat. Pain 1992; 48:449–461.
210. Zemlan FP, Pfaff DW. Topographical organization in medullary reticulospinal systems as demonstrated by the horseradish peroxidase technique. Brain Res 1979;174:161–166.
211. Zimmerman EA, Chambers WW, Liu CN. An experimental study of the anatomical organization of the cortico-bulbar system in the albino rat. J Comp Neurol 1964;123: 301–324.

13
Pons

The pons is the adult derivative of the metencephalon. It forms the rostral part of the hindbrain. This portion of the brainstem consists of two distinctive parts: (a) a dorsal *portion*, the pontine tegmentum, which is present in all mammalian species, and (b) a *ventral portion*, referred to as the pons proper, which is particularly well-developed in primates and becomes strikingly prominent in humans (Figs. 13.1 and 13.2). The pons also can be divided caudorostrally into three major segments: (a) the caudal pons, which is characterized by the presence of facial and abducens nerve and nuclei; (b) the midpons, including the trigeminal nerve and its chief sensory and motor nuclei, and (c) the rostral pons also referred to as the isthmus of the hindbrain.

CAUDAL PONS

Dorsal Portion

The pontine tegmentum is the rostral continuation of the medullary reticular formation. It contains cranial nerve nuclei, ascending and descending tracts, and reticular nuclei (Fig. 13.1). Cranial nerve nuclei found in the pons are those of cranial nerves V, VI, VII, and VIII. The ascending tracts in this part of the brainstem are similar to those found in the medulla, except for the medial lemniscus. The medial lemniscus, which is oriented vertically on each side of the median raphe in the medulla, now assumes a nearly horizontal position dorsal to the ventral part of the pons (Figs. 13.1 and 13.2). Crossing fibers of the trapezoid body traverse ventral parts of the bundle on each side. The medial longitudinal fasciculi (MLF) are situated dorsally on each side of the median raphe. The spinothalamic and anterior spinocerebellar tracts occupy positions in the anterolateral tegmentum. The spinal trigeminal tract and nucleus lie medial to the inferior cerebellar peduncle. The vestibular nuclei (i.e., medial and lateral) are present in the floor of the fourth ventricle throughout the caudal pons (Fig. 13.2).

The pontine reticular formation is more extensive than the medullary reticular formation, but occupies a similar region. The major part of the pontine reticular formation is represented by the pontine reticular nuclei (*nuclei reticularis pontis* (pars caudalis and pars oralis); Figs. 13.1 and 13.28) (31, 191). The *pars caudalis* replaces the gigantocellular reticular nucleus of the medulla and extends rostrally to the level of the trigeminal motor nucleus (Fig. 13.3). The *pars oralis*, present in more rostral pontine levels, extends into the caudal mesencephalon (Fig. 13.28). The pontine reticular nuclei give rise to the pontine reticulospinal tract (Figs. 11.10 and 11.22). Lateral to the pars caudalis is a small-celled reticular nucleus (parvicellularis) similar to that described in the medulla. The median raphe contains the inferior central nucleus, which is a rostral extension of the nucleus raphe magnus, and the subependymal area near the midline contains the nucleus of the *medial eminence* and the dorsal paramedian nucleus (Figs. 13.3 and 13.4).

The reticular formation posterolateral to the medial lemniscus contains a relatively large discrete bundle known as the *central tegmental tract* (Figs. 13.1 and 13.4). This is a composite tract consisting of descending fibers from midbrain nuclei that project mainly to the inferior olivary complex, and ascending fibers from the lower brainstem reticular formation that project to certain thalamic nuclei.

The *cerebellopontine angle*, formed laterally at the junction of pons, medulla, and cerebellum, contains root fibers of the vestibulocochlear and facial nerves (Figs. 13.2 and 13.6). Fibers of the cochlear nerve root pass dorsally, lateral to the inferior cerebellar peduncle, to terminate upon cells in all divisions of both the dorsal and ventral cochlear nuclei (Fig. 12.33). Vestibular root fibers, slightly medial and rostral to those of the

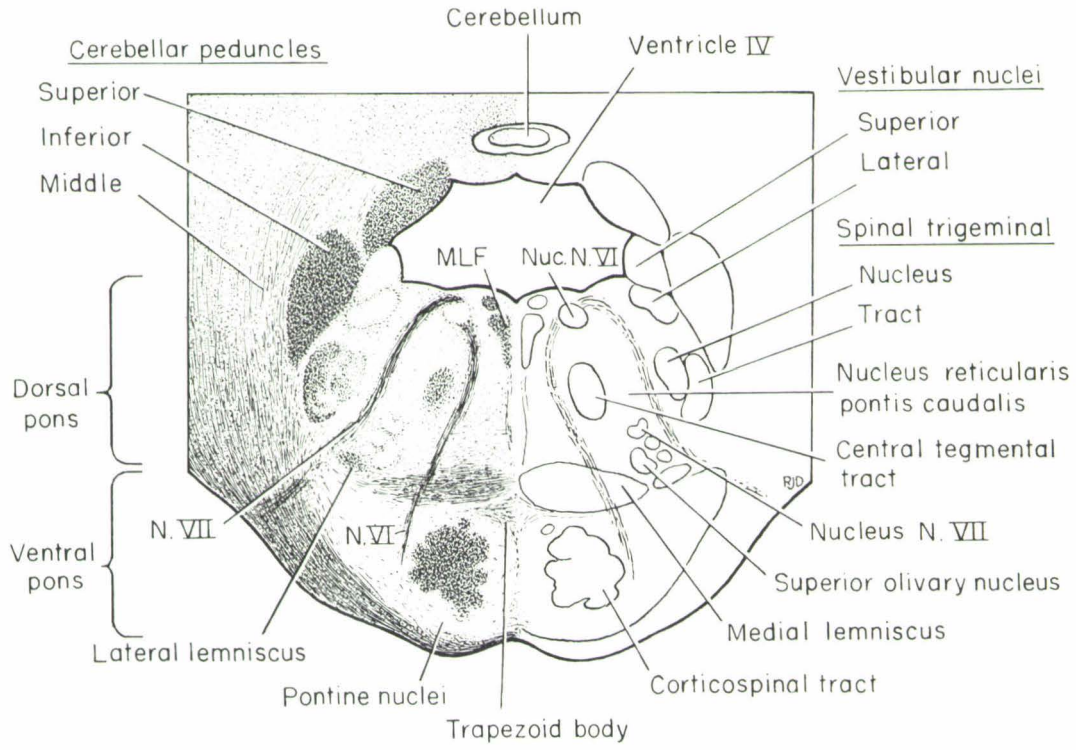


Figure 13.1. Transverse section of the pons at the level of the abducens nucleus. The dorsal portion of the pons, constituting the tegmentum, contains the reticular formation, cranial nerve nuclei, and ascending and descending tracts. The ventral portion of the pons contains the pontine nuclei, massive bundles of corticofugal fibers, and the transverse fibers of the pons which form the middle cerebellar peduncle.

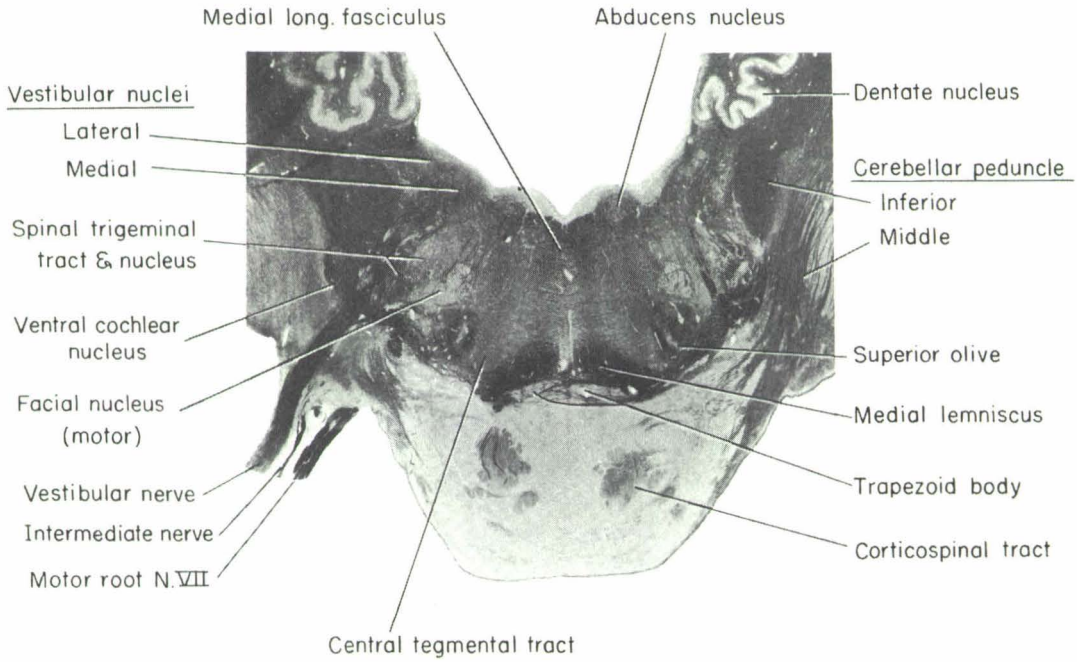


Figure 13.2. Slightly asymmetric transverse section through the pons of a 1-month infant. Root fibers of the vestibular and facial nerves are present on the left (Weigert's myelin stain).

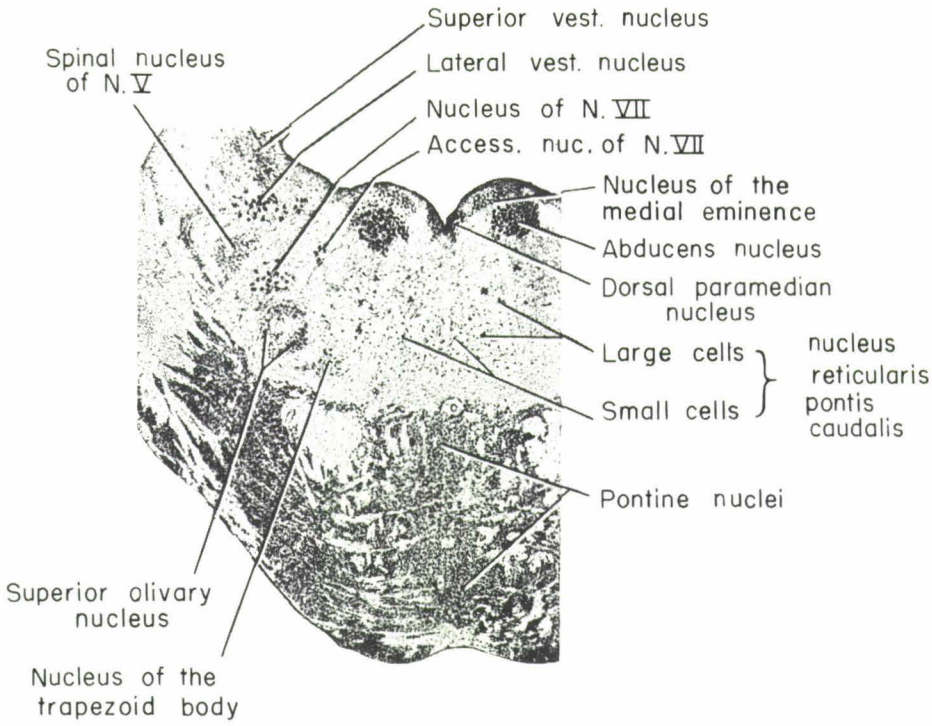


Figure 13.3. Transverse section through the pons and pontine tegmentum of 3-month infant at about same level as Figure 13.2 (Cresyl violet stain, with schematic representation of cell groups).

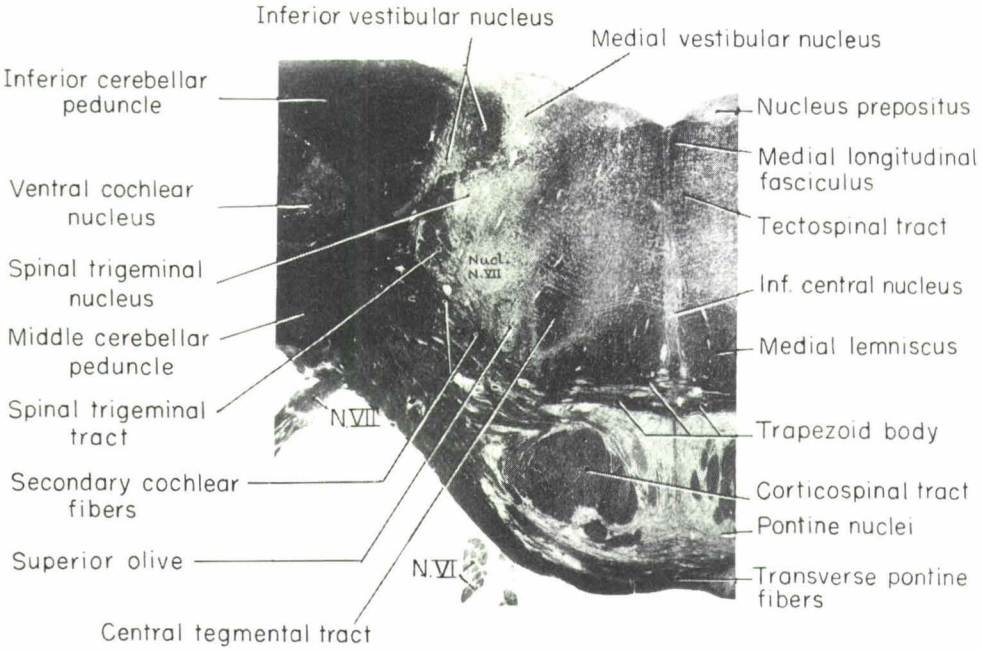


Figure 13.4. Transverse section of the adult pons at the level of the emergence of the facial nerve root (Weigert's myelin stain).

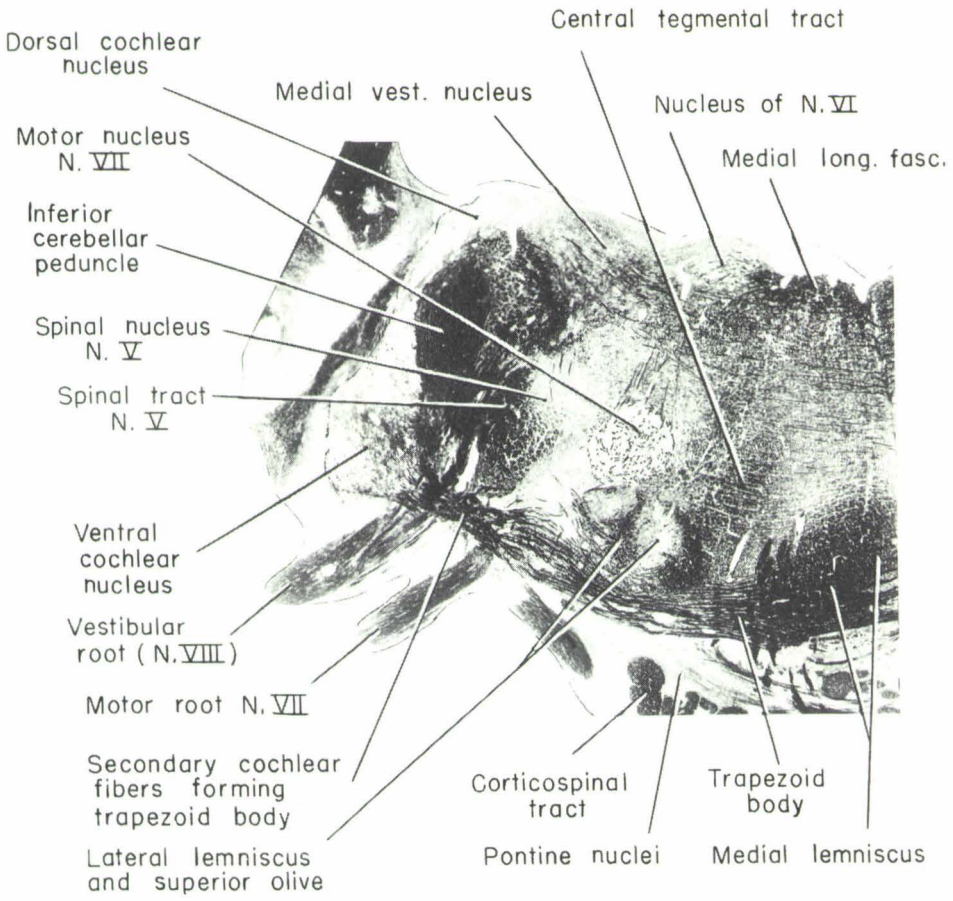


Figure 13.5. Transverse section of left half of the pons and pontine tegmentum of a 3-year-old child whose brain showed a complete absence of the left cerebellar hemisphere and middle cerebellar peduncle. The origin of the trapezoid fibers from the ventral cochlear nucleus is clearly shown. Note fibers of the dorsal acoustic stria passing into the tegmentum from the dorsal cochlear nucleus (Weigert's myelin stain).

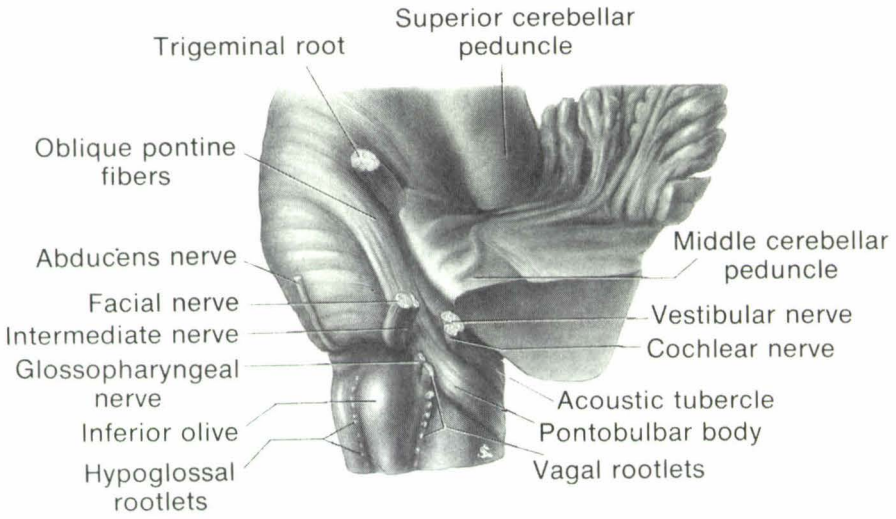


Figure 13.6. Lateral view of the cerebellopontine angle from a dissection of the brainstem and cerebellum.

cochlear nerve, enter caudal portions of the pons by passing between the restiform body and the spinal trigeminal tract (Figs. 13.2 and 13.5). Primary vestibular fibers are distributed differentially within the vestibular nuclear complex in the floor of the fourth ventricle. A moderate number of vestibular fibers project to specific parts of the cerebellum via the juxtarestiform body, which is part of the inferior cerebellar peduncle (Fig. 13.7). Ventral to the vestibular nerve are the intermediate and facial nerves (Figs. 13.2 and 13.5). The intermediate nerve contains mainly special visceral afferent (taste (SVA)) and general visceral efferent (parasympathetic (GVE)) fibers. The larger motor root of the facial nerve is the most rostral and medial cranial nerve in the cerebellopontine angle.

Ventral Portion

The massive ventral part of the pons consists of orderly arranged transverse and longitudinal fiber bundles intercalated between large collections of pontine nuclei (Figs. 13.1, 13.3, and 13.4). Longitudinal fiber bundles coursing through central regions of the ventral pons are (a) corticospinal, (b) corticobul-

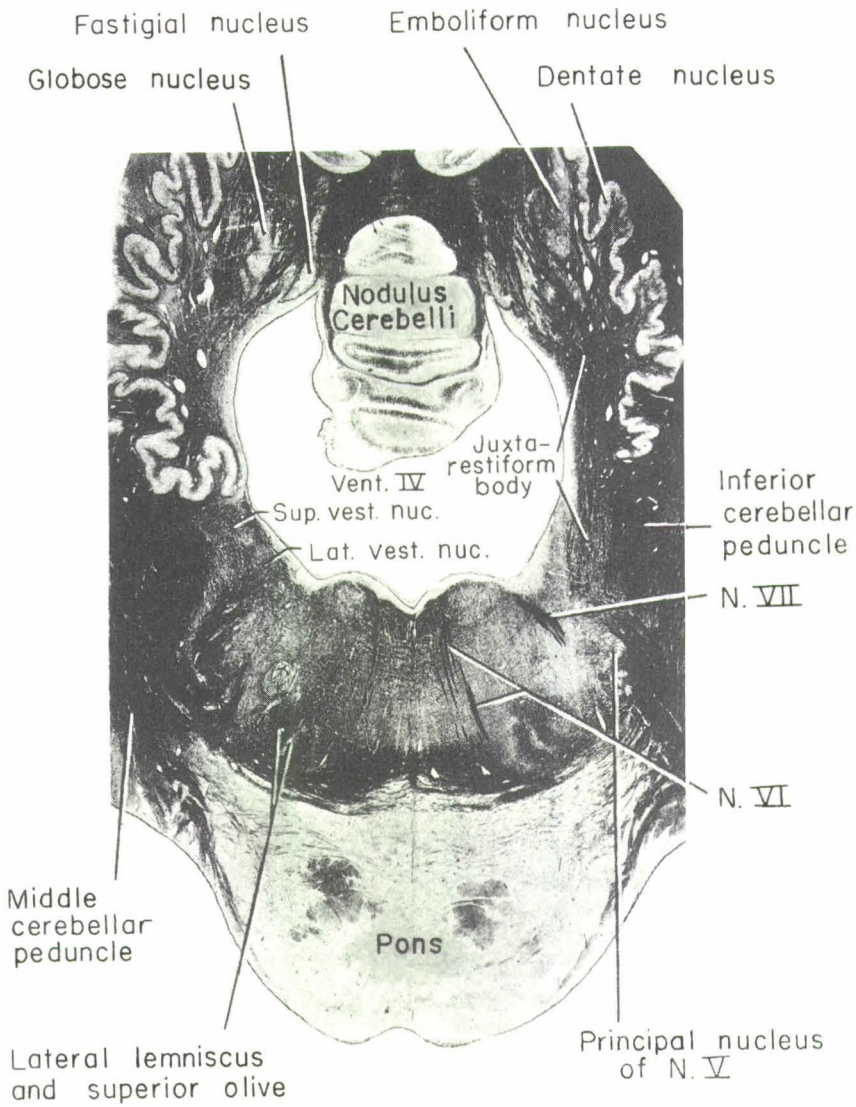


Figure 13.7. Transverse section of the pons, pontine tegmentum and portions of the cerebellum at the level of the abducens nuclei of a 1-month infant (Weigert's myelin stain).

bar, and (c) corticopontine (Figs. A.7–A.9 of the human brain atlas shown in Section VII).

Corticospinal fibers traverse the ventral part of the pons, and in sagittal sections can be traced into the medullary pyramids (Figs. 2.24, 2.26, 11.13, and A.28). These fibers display a compact arrangement at rostral and caudal pontine levels, but are broken into a number of small fascicles by transversely oriented pontine fibers in the middle regions of the pons.

Corticobulbar fibers separate from the corticospinal tracts and enter the pontine tegmentum. These fibers convey impulses that pass to the motor cranial nerve nuclei directly and via intercalated neurons.

Corticopontine fibers, arising from frontal, parietal, temporal, and occipital cortex, descend without crossing and terminate upon the pontine nuclei, between corticospinal and corticopontine tracts. Corticopontine fibers from the primary sensorimotor cortex appear to be somatotopically organized and end upon circumscribed regions of the pontine nuclei (42). Each part of the cerebral cortex so far studied appears to give off fibers to several well-defined areas within the pontine nuclei (43, 44). The pontine nuclei give rise to the transverse fiber bundles of the ventral pons, which cross the midline and enter the cerebellum via the middle cerebellar peduncle (Figs. 13.1 and 13.4). Transverse pontocerebellar fibers cross above (superficial layer) and below (deep layer) the fascicles of descending fibers. The ventral portion of the pons may be considered as a massive relay station in a disynaptic neuronal pathway whereby impulses from the cerebral cortex are transmitted to the contralateral cerebellar hemisphere. Additionally, a small number of fibers from the superior colliculus (tectopontine fibers) descend ipsilaterally to terminate upon dorsolateral pontine nuclei (8). These fibers, and fibers from the pontine nuclei, are considered to transmit optic impulses to restricted regions of the cerebellum.

The corticopontocerebellar pathway is quantitatively the most important route by which the cerebral cortex can influence the cerebellar cortex in a somatotopically organized manner. The corticopontine fibers are most numerous in the rostral pons, where they form bundles difficult to distinguish from the pyramidal tracts (Fig. 13.32). Their number gradually diminishes as fibers terminate in the pontine nuclei. The corticopontine fibers and the transverse pontocerebellar fibers do not become myelinated until some time after birth and are not distinguishable in brain sections of a 4-week infant stained by the Weigert technique (Fig. 13.2). They are shown in the adult pons in Figures 13.4, 13.27, and 13.32.

The pontine nuclei are large, closely packed cellular aggregations situated between the transverse and longitudinal fibers (Fig. 13.3). In caudal regions, the cells form a ring around the compact pyramidal tract, which more rostrally is broken into smaller bundles by islands of pontine cells. In a general way, the cells may be grouped into lateral, medial, dorsal, and ventral nuclear masses (Fig. 13.27). In the lateral groups, the polygonal cells are relatively large- or medium-sized; in the paramedian region, cells are smaller. Although the dendrites of these cells ramify around adjacent cell bodies, their axons are mainly crossed and form the middle cerebellar peduncle (or brachium pontis). Among these cells are found curiously shaped Golgi type II cells whose dendrites are beset with numerous hair-like processes and whose short, branching axons terminate in the vicinity of the cell body.

Certain nuclei in the pontine tegmentum, like the reticulotegmental nucleus, project fibers into the ventral part of the pons, which enter the cerebellum via the contralateral middle cerebellar peduncle (Figs. 2.26, 13.28, 13.33, A.8, and A.9). The reticulotegmental nucleus is regarded by some as a tegmental extension of the pontine nuclei (130).

VESTIBULOCOCHLEAR NERVE

The vestibulocochlear nerve (N. VIII) comprises two distinctive parts: (a) the cochlear part concerned with audition, and (b) the vestibular part conveying impulses concerned with equilibrium and orientation in three-dimensional space. These two components of the vestibulocochlear nerve run together from the internal auditory meatus to the cerebellopontine angle, where they enter the brainstem (Figs. 12.1 and 13.6). Each of these nerves has distinctive central nuclei and connections.

Cochlea and Related Nerve and Nuclei

COCHLEA

The cochlea consists of a fluid-filled coil tube of two and a half turns (Fig. 13.8) that serves as the auditory transducer (Fig. 13.9).

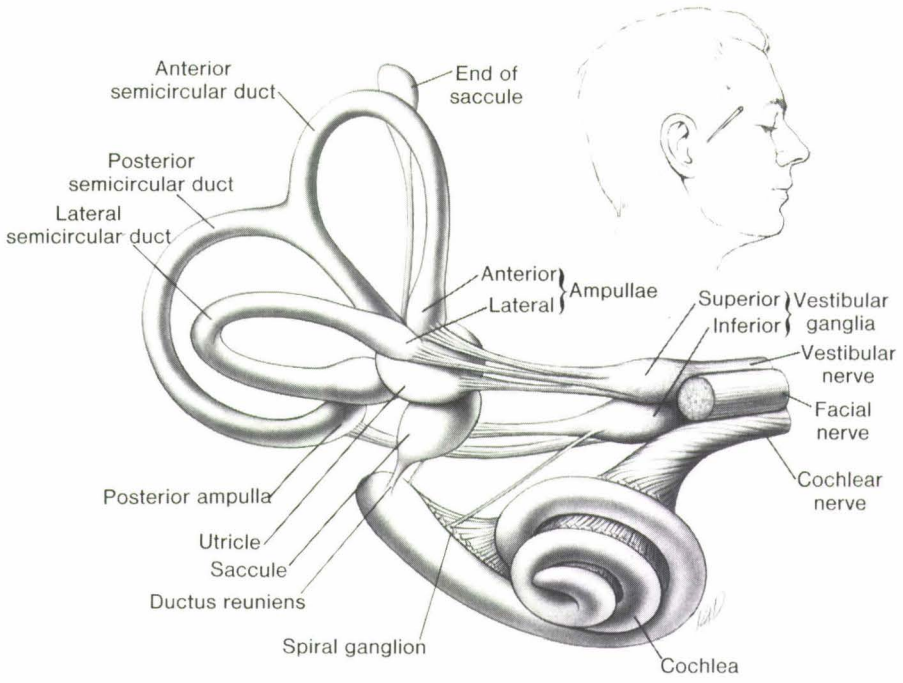


Figure 13.8. Labyrinthine and cochlear apparatus, their ganglia and nerves, with anatomic orientation. The cochlea has been rotated downward and laterally to expose the vestibular ganglia. The divisions of the vestibular nerve were separated by retracting the superior division proximal to its ganglion.

The basilar and vestibular (Reisner's) membranes partition the cochlea to form the scala vestibuli, the scala tympani, and the cochlear duct (scala media) (Figs. 13.9 and 13.10). Energy from sound reaching the tympanic membrane is transmitted via the ear ossicles to the scala vestibuli (oval window) by the foot plate of the stapes. The membrane covering the round window located at the base of the scala tympani accommodates to hydrostatic pressure changes. The *organ of Corti*, the auditory transducer, lies in the cochlear duct and consists of one row of inner hair cells and three rows of outer hair cells (223) (Figs. 13.9–13.11). The tectorial membrane, attached to the spiral limbus, overlies the hair cells (Fig. 13.10). The piston-like action of the stapes transmits the energy of the sound waves to the perilymph in the scala vestibuli. Energy transmitted to the perilymph produces traveling waves in the basilar membrane that moves from the base of the cochlea to its apex (273). Displacement of the basilar membrane in response to acoustic stimuli causes bending of hair cells in contact with the tectorial membrane. Maximum displacement of the basal membrane at different distances from the stapes can be correlated with specific sound frequencies. High frequencies are perceived at the base of the cochlea and low frequencies at its apex. The basilar membrane has a stiffness that varies 100-fold from one end to the other. It is narrowest and stiffest at the base of the cochlea and widest and most pliable near the helicotrema (118).

COCHLEAR NERVE AND NUCLEI

The cochlear nerve originates from cells of the *spiral ganglion* situated about the modiolus of the cochlea that use glutamate as their principal neurotransmitter (Figs. 13.9, 13.10, and 13.13). Peripheral processes of the bipolar cells of the spiral ganglion end in relation to the hair cells of the organ of Corti (Fig. 13.9). The central processes of ganglion cells form the cochlear nerve, which enters the brainstem lateral, dorsal, and slightly caudal to the vestibular nerve (Figs. 12.33 and 13.13). Fibers of the cochlear nerve terminate in two cell masses on the lateral surface of the inferior cerebellar peduncle, the ventral and dorsal cochlear nuclei (Figs. 12.25, 12.33, and 13.12). These nuclei represent a more or less continuous cell mass, but they have distinctive cells and cytoarchitecture.

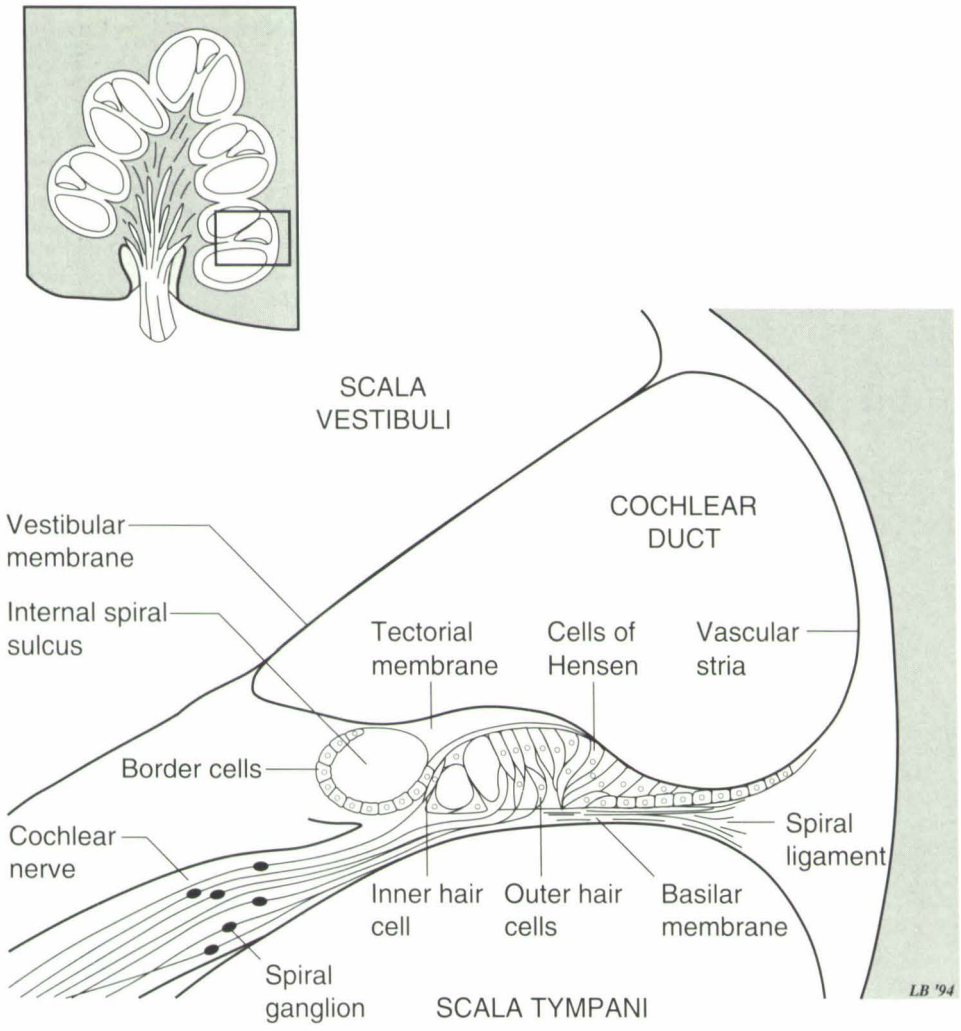


Figure 13.9. Radial section through the cochlea showing the cochlear duct, the basilar membrane, the organ of Corti, and the tectorial membrane. The small diagram in the *upper left* is an axial section of the cochlea. The area enclosed in the *rectangle* is reproduced in detail in the large drawing.

The *dorsal cochlear nucleus* forms an eminence on the most lateral part of the floor of the fourth ventricle, known as the *acoustic tubercle*. The acoustic tubercle lies dorsal to the restiform body and forms the floor of the lateral recess of the fourth ventricle (Figs. 13.5 and 13.12). Cells of the dorsal cochlear nucleus, in most mammals, are organized in three distinct layers: (a) molecular, (b) fusiform, and (c) polymorphic (30, 194, 216, 257). The *molecular layer*, beneath the ependyma of the lateral recess, contains small round neurons with scant cytoplasm which often are clustered in islands. The *fusiform layer* is composed of evenly distributed pyramidal cells oriented radially (i.e., with long axes perpendicular to the surface of the dorsal cochlear nucleus). This layer of conspicuous cells gives the dorsal cochlear nucleus its distinctive lamination. The *polymorphic layer*, the deepest and thickest of all three layers, contains a diverse population of cells, including small granule cells, pyramidal cells, multipolar cells, and occasional giant cells (193). In humans, these three layers are indistinct.

The *ventral cochlear nucleus* is subdivided into anteroventral and posteroventral nuclei on the basis of topography, cytology, and functional characteristics (Fig. 13.12). Each of these subdivisions is tonotopically organized and has an orderly sequential representation of the auditory spectrum (225, 226). The *anteroventral cochlear nucleus* lies in the most rostral part of the cochlear nuclear complex be-

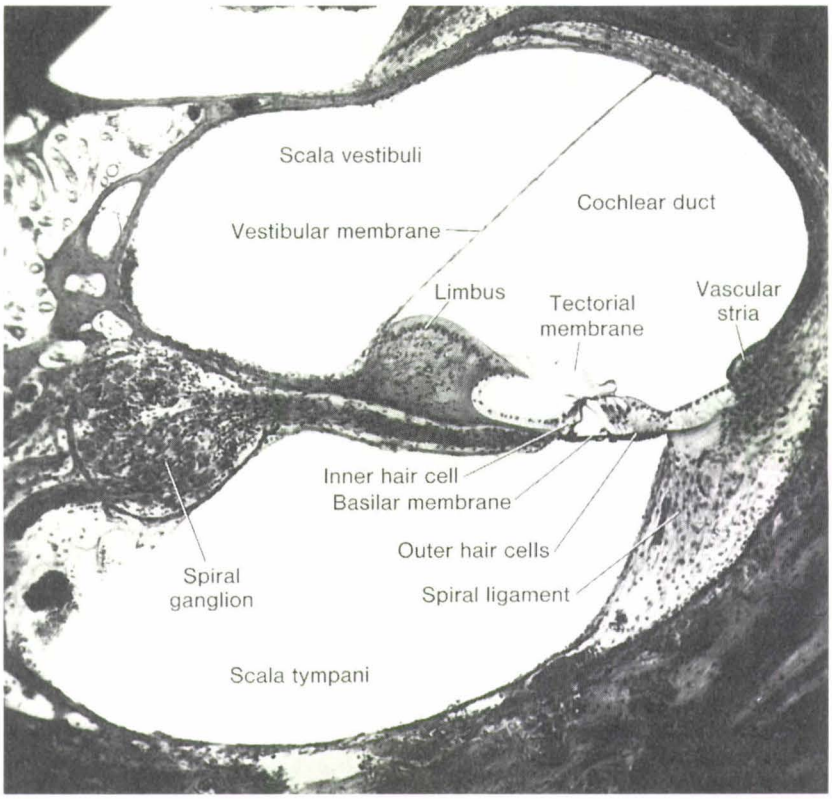


Figure 13.10. Radial section through the cochlea in human similar to Figure 13.9. Note the cells of the spiral ganglion.

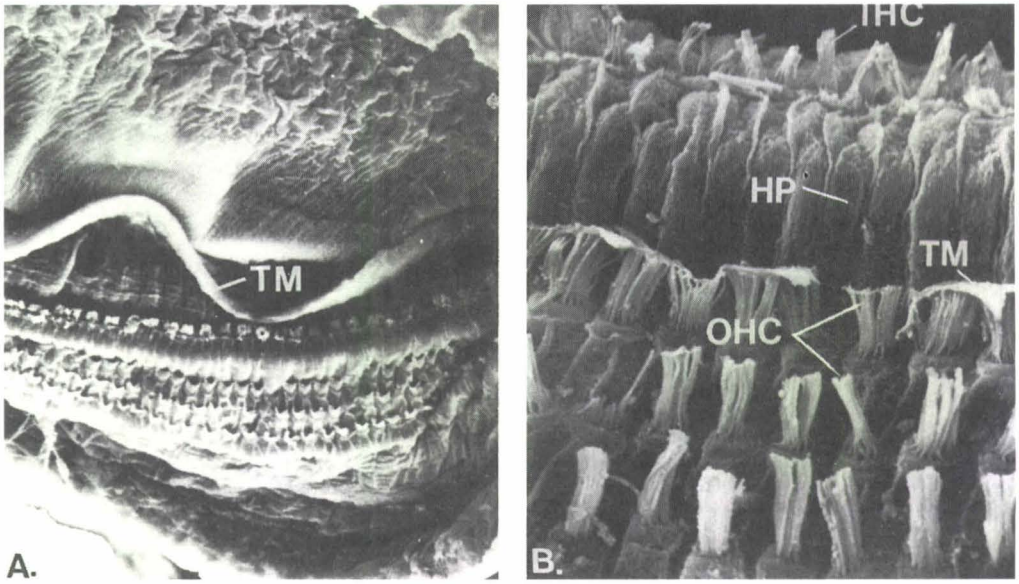


Figure 13.11. Cochlea of the rhesus monkey. **A.** View of the basal coil of the cochlea with the tectorial membrane (*TM*) reflected (×450). **B.** Surface view of the hair cells of the cochlea after removal of the tectorial membrane (*TM*), except for fragments attached to outer hair cells (*OHC*). *IHC*, inner hair cells; *HP*, head plate of inner pillar (×2100).

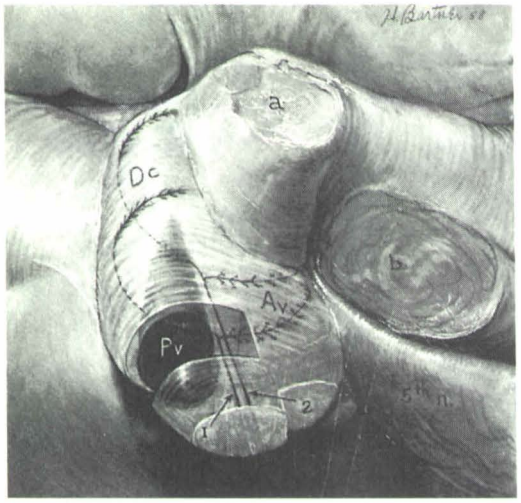


Figure 13.12. Cochlear nuclei from the lateral surface of the brainstem of a cat. Major divisions of the cochlear nuclei are indicated: *Dc*, dorsal cochlear nucleus; *Pv*, posteroventral nucleus; *Av*, anteroventral nucleus. Branches of central processes of the spiral ganglion cells are distributed to all divisions of cochlear nuclei and in each division neurons responding to higher frequencies are most dorsal. Fiber 1 is derived from the middle turn of the cochlea, while fiber 2 comes from the basal turn; *a* represents cut edges of the inferior and superior cerebellar peduncles; *b* is the cut edge of the middle cerebellar peduncle; 5th *n* is the trigeminal nerve root.

tween the vestibular nerve root and the peduncle of the flocculus. It is composed primarily of ovoid or spherical cells that are densely packed in rostral parts of the nucleus. In the posterior part of this nucleus, near the entry zone of the cochlear root, cells are more widely spaced and larger. This region also contains globular cells with eccentric nuclei which bulge on the cell surface (13, 30, 193).

The *posteroventral cochlear nucleus* begins at the level of entrance of the cochlear root into the brainstem and continues to the caudal tip of the cochlear complex, where it is capped posteriorly by the dorsal cochlear nucleus (30, 257) (Fig. 13.12). Although the posteroventral cochlear nucleus contains several distinct types of neurons, multipolar cells of various sizes predominate, especially rostrally (193). The caudal pole of this nuclear subdivision contains octopus cells, so-called because most of the dendrites are gathered together on one side of the cell body.

Auditory Fiber Systems

PRIMARY AUDITORY FIBERS

These fibers, representing the central processes of cells in the spinal ganglion, enter the cochlear nuclei, bifurcate in an orderly sequence, and are distributed to both dorsal and ventral cochlear nuclei (167). Primary auditory fibers arborize in all parts of the cochlear nuclear complex (178, 215, 289). Ascending branches of the auditory nerve root terminate in a rostrolateral to caudomedial gradient in the anteroventral cochlear nucleus chiefly upon spherical and globular cells. Descending branches of the root terminate in a ventral to dorsal pattern in the posteroventral and dorsal cochlear nuclei. Fibers in the posteroventral nucleus end upon globular, multipolar and octopus cells. Fibers to the dorsal cochlear nucleus terminate upon cells in the deep polymorphic layer and upon the deep dendrites of pyramidal cells.

One of the characteristic features of the auditory system is the pattern of tonotopic localization evident at various levels. In the cochlea, it has been shown that high tones are received in the basal coils, while the apical portion is sensitive to low frequencies (85, 263). Anatomic studies suggest that apical cochlear fibers terminate in ventral parts of the dorsal cochlear nucleus and in the ventral nucleus, while fibers from basal portions of the cochlea end in the dorsal part of the dorsal cochlear nucleus (162, 197). Physiologic evidence (224, 225), based upon microelectrode studies of neuron frequency sensitivity in the cochlear nuclear complex, indicates that each major division possesses its own frequency sequence and that each division seems to have a full tonal spectrum. The multiple tonotopic representation in all divisions of the cochlear nuclear complex is due to the orderly bifurcation and distribution of fibers throughout the complex. In all three divisions of the cochlear complex, neurons responding to higher frequencies are dorsal, while those responding to lower frequencies are ventral. Thus, the tonotopic localization in the cochlear nuclei is the reverse of that in the cochlea with high frequencies perceived in dorsal regions and low frequencies in ventral regions.

AUDITORY PATHWAYS

Secondary auditory pathways in the brainstem are complex, and many details concerning their composition are uncertain. Most of the available information regarding these pathways is based upon studies in animals (Fig. 13.13). Secondary auditory fibers arising from the three subdivisions of the cochlear nuclei are grouped into three acoustic striae:

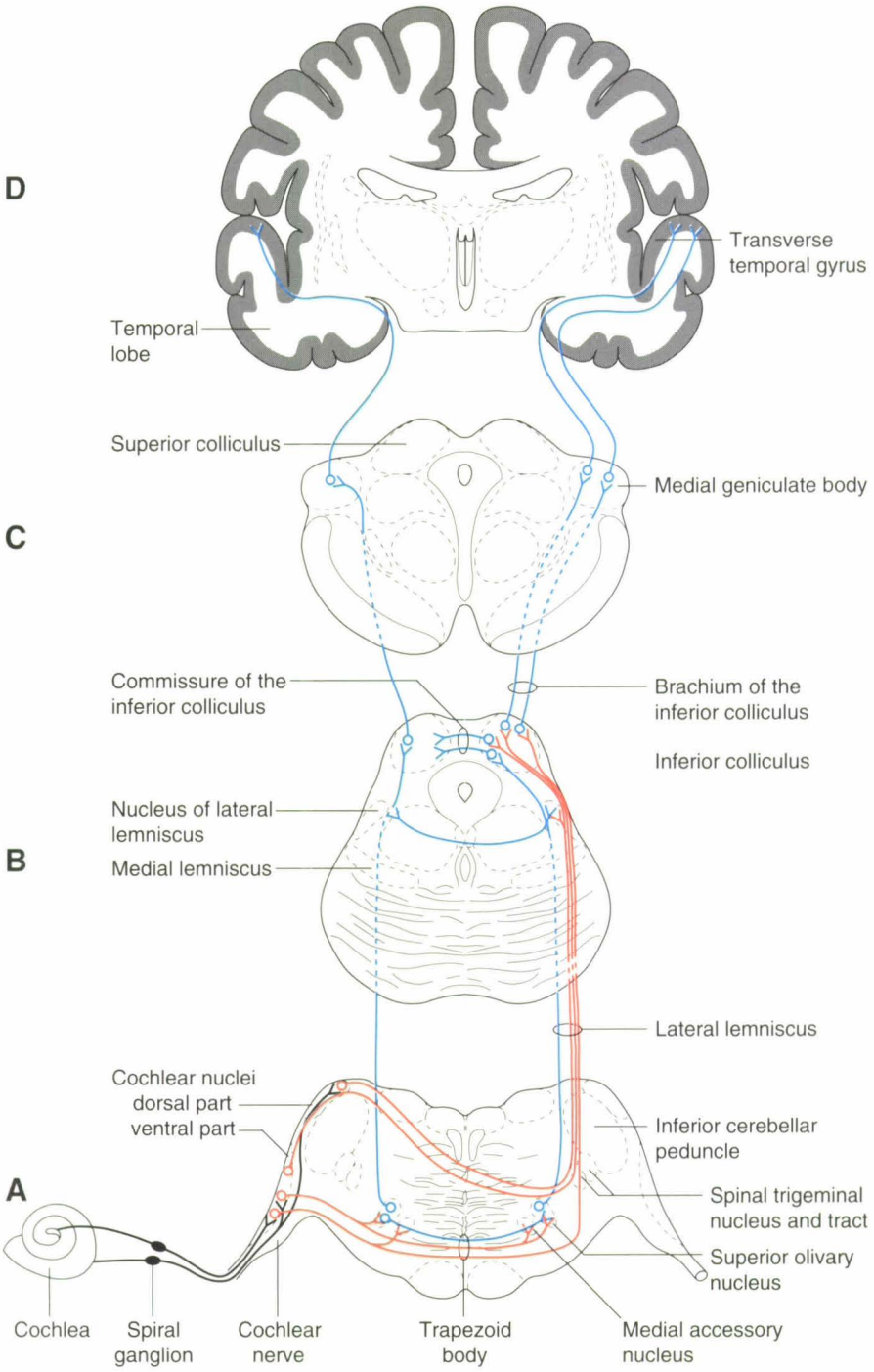


Figure 13.13. Auditory pathways. Primary auditory fibers arising from the spiral ganglion are in black. Secondary auditory fibers arising from the dorsal and ventral cochlear nuclei and forming the acoustic striae are in *red*. Auditory fibers arising from relay nuclei are in *blue*. *A*, medulla; *B*, level of inferior colliculus; *C*, level of superior colliculus and medial geniculate body; *D*, transverse section through the cerebral hemisphere.

(a) a dorsal acoustic stria, (b) a small intermediate acoustic stria, and (c) a ventral acoustic stria (15). The three acoustic striae project to auditory relay nuclei on both sides of the brainstem (i.e., nuclei of the superior olivary complex and trapezoid body) and also contribute fibers to the lateral lemniscus, the principal ascending auditory pathway in the brainstem.

The *dorsal acoustic stria* arises from the dorsal cochlear nucleus, arches medially around the superior surface of the inferior cerebellar peduncle, and crosses the median raphe ventral to the medial longitudinal fasciculus (256, 257). A few fibers in this stria appear to terminate in the contralateral lateral superior olivary nucleus, but the main bundle enters the opposite lateral lemniscus directly (Fig. 13.13). These fibers and their collaterals terminate in the contralateral ventral and dorsal nuclei of the lateral lemniscus and in the central nucleus of the inferior colliculus on the opposite side (256).

The *intermediate acoustic stria* arises from cells in the posteroventral cochlear nucleus, courses dorsally through parts of the dorsal cochlear nucleus and enters the tegmentum by passing around the inferior cerebellar peduncle (256). In the ipsilateral tegmentum, these fibers approach the dorsal aspect of the superior olivary complex where they are distributed to retro-olivary and periolivary nuclear groups. Fibers of the intermediate acoustic stria continue across the median raphe posterior to the trapezoid body to be distributed to retro-olivary and periolivary nuclei contralaterally (256, 257, 287). None of these fibers appears to terminate in the principal nuclei of the superior olivary complex. Other fibers in the intermediate acoustic stria reach the contralateral lateral lemniscus and terminate in the ventral nucleus of the lateral lemniscus and in the inferior colliculus (287). Because the retro-olivary and periolivary nuclei are known to give rise to fibers of the olivocochlear bundle that pass peripherally to make synaptic contact with outer hair cells, the posteroventral cochlear nucleus, which projects prominently to these nuclei, must play a significant role in this modulating feedback system (257, 287).

The *ventral acoustic stria* arises from the ventral cochlear nucleus (260, 286), and courses medially along the ventral border of the pontine tegmentum to form the trapezoid body (Figs. 13.5 and 13.13). Many of these fibers pass through or ventral to the medial lemniscus, cross the raphe, and reach the dorsolateral border of the opposite superior olive, where they turn upward to form a longitudinal ascending bundle known as the lateral lemniscus. Other trapezoid fibers terminate in the homolateral and contralateral nuclei of the superior olive and the trapezoid body, two nuclear masses interposed in the secondary cochlear pathway (Fig. 13.13). Fibers from these nuclei join the lateral lemniscus of the same or the opposite side.

The dorsal acoustic stria is larger than the intermediate stria and the ventral stria is larger than the other two combined. In their passage through the tegmentum, there is a diminution in the number of fibers in the various striae due to terminations in the reticular formation, the superior olivary nuclei, and the trapezoid nuclei. The superior olivary and trapezoid nuclei (Fig. 13.5) give rise to a number of tertiary auditory fibers which ascend mainly in the lateral lemniscus of the same side (193, 255, 289). The lateral lemniscus consists primarily of crossed secondary fibers contributed by the three auditory striae and tertiary fibers from the superior olive and trapezoid nuclei. No direct fibers from the cochlear nuclei ascend in the ipsilateral lateral lemniscus (15). The number of ascending fibers in the lateral lemniscus is small compared with the total number of fibers arising from the dorsal and ventral cochlear nuclei.

The *superior olivary complex* is a cellular column, about 4 mm long, extending from the level of the facial nucleus to the motor nucleus of the trigeminal nerve. It is in contact ventrally with the lateral portion of the trapezoid body (Figs. 13.3 and 13.5). It represents the most caudal relay in the auditory pathway where ascending fiber systems from the two sides converge (257). This nuclear complex is composed of (a) a large lateral (principal) superior olivary nucleus, (b) a small medial (accessory) superior olivary nucleus, and (c) a few cell aggregations referred to as preolivary, retro-olivary, and periolivary nuclei. From the region dorsal to the medial accessory olivary nucleus a bundle of fibers, the *peduncle of the superior olive*, passes dorsomedially toward the abducens nucleus (Figs. 13.2 and A.7). Binaural interaction in the superior olivary complex plays an important role in sound localization.

The *lateral superior olivary nucleus* has a

conspicuous S-shaped configuration in carnivores, but in monkeys and humans it is oval with dorsal and ventral indentations (Figs. 13.5 and 13.27). The lateral superior olive in humans consists of about six clusters of cells which do not present a sharply circumscribed configuration (258). The *medial superior olivary nucleus* forms a slender obliquely oriented cell column medial to the lateral superior olive, the dorsal tip of the cell column is closest to the midline. Spindle-shaped cells of the medial superior olivary nucleus emit dendrites from both poles of the neurons. In addition to the main nuclei, there are other smaller, diffusely arranged cell groups that belong to the superior olivary complex. Diffusely arranged cells ventral to the superior olivary complex are referred to as the *preolivary nuclei,* while cells dorsal to the main complex are designated as the *retro-olivary* cell group. The *periolivary nucleus* lies dorsal and medial to the medial superior olivary nucleus.

The *trapezoid body* forms a conspicuous bundle of transverse fibers in the ventral part of the pontine tegmentum (Figs. 13.4, 13.5, and 13.27). These fibers arise principally from the ventral cochlear nucleus and sweep medially in a gentle arc toward the median raphe. Most of these fibers cross to the opposite side, passing through or ventral to the medial lemniscus, and reach the ventrolateral portion of the tegmentum (Fig. 13.5). Here they turn sharply in a longitudinal direction to form the principal ascending auditory pathway, the lateral lemniscus (Fig. 13.13). The turn is made just dorsolateral to the *superior olivary* complex (Figs. 13.27 and A.29). Cell aggregations scattered among the trapezoid fibers constitute the *nuclei of the trapezoid body.*

The *lateral lemniscus,* the principal ascending auditory pathway in the brainstem, courses rostrally in the lateral part of the tegmentum. Initially, this bundle lies lateral to the superior olivary complex (Figs. 13.5 and 13.13), but at isthmus levels its position is more dorsal (Fig. 13.32). The lateral lemniscus ascends to midbrain levels, where the fibers terminate in the inferior colliculus. Interposed in the lateral lemniscus at isthmus levels are the *nuclei of the lateral lemniscus,* which receive and contribute fibers to the main bundle. Two nuclei are distinguished: a ventral nucleus and a dorsal nucleus. The *ventral nucleus of the lateral lemniscus,* a compact aggregation of cells in the ventrolateral tegmentum, appears immediately rostral to the lateral preolivary nuclei, and is surrounded ventrally and laterally by fibers of the lateral lemniscus. The *dorsal nucleus of the lateral lemniscus* appears at more rostral pontine levels and is composed of cell clusters located within fascicles of the lateral lemniscus (Fig. 13.32). The oral pole of the dorsal nucleus of the lateral lemniscus lies immediately ventral to the inferior colliculus. The dorsal and ventral nuclei of the lateral lemniscus of both sides receive inputs arising from the anteroventral cochlear nuclei (286). Other fibers ascending in the lateral lemniscus probably contribute terminals or collaterals to these nuclei. The extent to which the nuclei of the lateral lemniscus contribute to the principal ascending auditory pathway is unknown, but it probably is substantial. When the lateral lemniscus reaches the midbrain, most of its fibers terminate directly in the central nucleus of the inferior colliculus (259, 301). Some fibers may reach the colliculus of the opposite side through the commissure of the inferior colliculi. The inferior colliculus give rises to fibers that project to the medial geniculate body of the thalamus via the *brachium of the inferior colliculus* (Fig. 13.13).

Physiologic studies (228) suggest that some neurons of the inferior colliculus are sensitive to interaural time relationships of binaurally applied stimuli, while others are sensitive to small interaural intensity differences. These data indicate that certain neurons in the inferior colliculus are concerned with the localization of a sound source.

It is obvious from this description that the auditory pathway receives contributions from a number of intercalated nuclear masses and has a more complex composition than sensory systems considered heretofore. There is also a considerable ipsilateral ascending component consisting of ascending fibers arising mainly from the superior olivary complex. It is difficult to state the number of neurons involved in the auditory pathway from the periphery to the cortex, but the principal ones are (a) cells of the spiral ganglion whose central processes form the cochlear nerve, (b) secondary fibers from the dorsal and ventral cochlear nuclei which form the three auditory striae and contribute primarily crossed fibers to the lateral lemniscus, (c) the nuclei of the superior olivary complex and the trapezoid body that contribute to the lateral lemnisci, (d) the nuclei of the lateral lemniscus which

receive and contribute fibers to the bundle of the same name, (e) the inferior colliculus which receives fibers from the lateral lemniscus and projects via its brachium to the medial geniculate body, and (f) the medial geniculate body, which gives rise to geniculocortical fibers (auditory radiation) that project to the transverse temporal gyri of Heschl (Figs. 2.11 and 13.13). Some crossed fibers in the dorsal and intermediate acoustic striae may pass via the lateral lemniscus directly to the medial geniculate body (256, 259, 297).

Most of the auditory impulses reaching the auditory cortex are conveyed by higher order neurons. Physiologic studies indicate a definite tonotopic localization in the inferior colliculus (5, 176, 227, 289). Units of the central nucleus of the inferior colliculus are characterized by sharp tuning and binaural responses, while those in the pericentral and external nuclei are very broadly tuned (Fig. 14.4). There is a systematic representation of the cochlea within the pericentral nucleus and a highly ordered representation of the cochlea in the central nucleus of the inferior colliculus. Isofrequency contours in the central nucleus parallel cellular laminae with low frequencies represented dorsally and high frequencies represented ventrally. In the medial geniculate body, low frequencies are perceived laterally and high frequencies are represented medially in the principal division (3, 4, 289). Physiologic data concerning the tonotopic representation of auditory impulses at the cortical level are discussed in Chapter 20.

Because of the large number of intercalated nuclei in the course of the auditory pathway (i.e., superior olive, trapezoid nucleus, nucleus of the lateral lemniscus, inferior colliculus), the cochlear reflex connections are exceedingly complex. It seems likely that all of the relay nuclei along the auditory pathway are involved to some degree in reflex circuits by which various motor phenomena occur in response to cochlear stimulation. Experimental evidence suggests that a descending conduction system, from the auditory cortex to the cochlea (220), is associated with the classical ascending auditory system.

EFFERENT COCHLEAR BUNDLE

One of the most interesting cochlear reflex connections involves the *olivocochlear bundle* or the *efferent cochlear bundle* described by Rasmussen (218, 219). Crossed and uncrossed components of the olivocochlear bundle project peripherally from the brainstem to the cochlea and form a pathway by which the central nervous system may influence its own sensory input (108, 220). Electrical stimulation of the crossed olivocochlear bundle in the cat inhibits auditory nerve responses to acoustic stimuli (114). Fibers of the olivocochlear bundle originate from cholinergic neurons surrounding the principal and accessory superior olivary nuclei (Fig. 13.15). Cochlear efferent fibers are best defined on the basis of their cells of origin into medial and lateral systems (121, 291). The medial olivocochlear system originates from cells medial, ventral, and rostral to the medial superior olive (medial periolivary nucleus), is composed of myelinated fibers, and project bilaterally (with contralateral dominance) to the outer hair cell region of the cochlea. The lateral olivocochlear system arises from cells lateral to the medial superior olive (the lateral periolivary nucleus), contains unmyelinated fibers (264), and projects bilaterally (with ipsilateral dominance) to the inner cell region of the cochlea. Crossed fibers of the olivocochlear bundle project dorsomedially toward the facial genu, cross the midline, and are joined by uncrossed fibers (Fig. 13.14). Both crossed and uncrossed components of this efferent bundle emerge from the brainstem via the vestibular nerve root (168). In the inner ear, these efferent fibers enter the cochlear nerve via the vestibulocochlear anastomosis, pass to the organ of Corti (219), and make synaptic contact with hair cells (146, 239–241, 247–249). The efferent cochlear bundle suppresses auditory nerve activity by inhibiting the receptivity of the end organ.

Other feedback mechanisms in the auditory system involve relay nuclei in the auditory pathway (221). Fibers from the inferior colliculus, the nuclei of the lateral lemniscus, and the principal superior olive descend, or pass distally, to relay nuclei. These pathways differentially inhibit impulses concerned with certain frequencies of the auditory spectrum and in this way enhance frequencies not subject to central inhibition. This phenomenon is referred to as auditory sharpening.

Acoustic reflex mechanisms involve middle ear muscles, such as the stapedius and tensor tympani. The stapedius muscle, which serves to dampen the oscillations of the ear ossicles in response to high levels of acoustic stimuli, is innervated by the facial nerve. Auditory fibers from the superior olivary com-

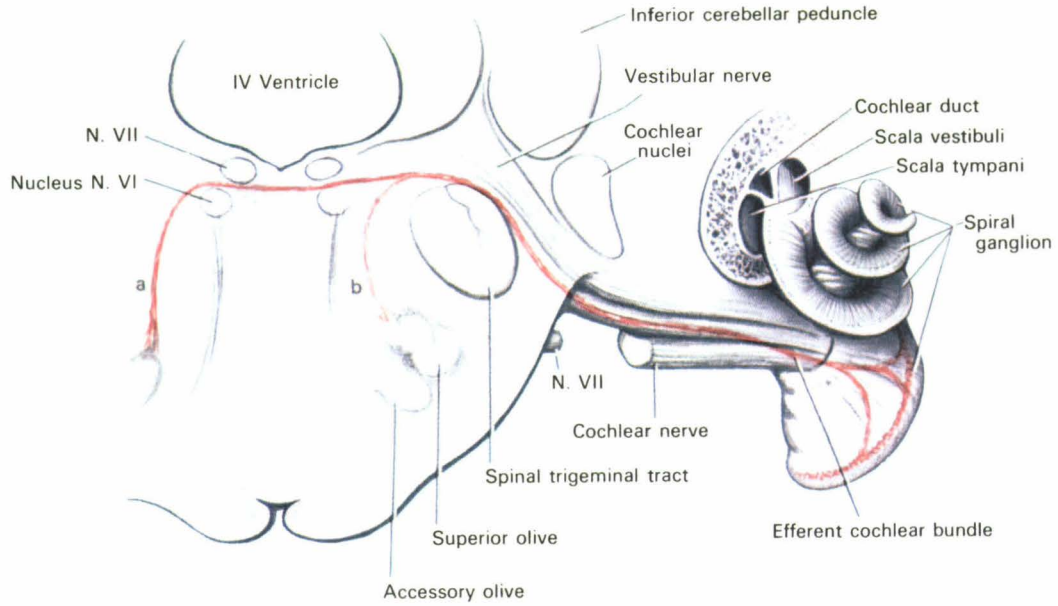
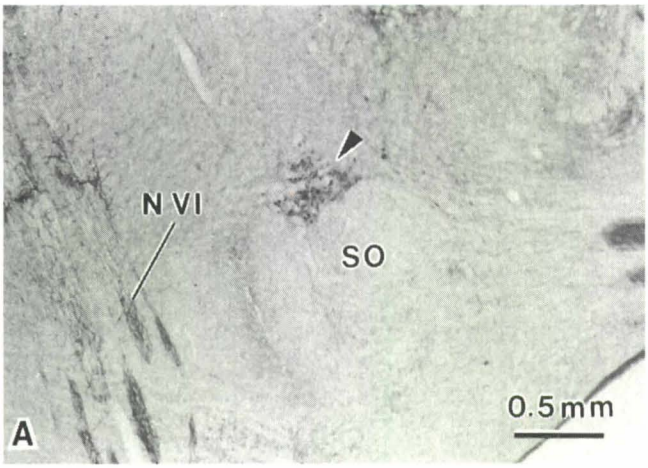


Figure 13.14. Efferent cochlear fibers in the cat. Crossed fibers of the olivocochlear bundle (*red, a*) arise from cells dorsal to the accessory superior olivary nucleus, pass dorsomedially toward the floor of the fourth ventricle, and cross to the opposite side. Uncrossed fibers of the olivocochlear bundle (*red, b*) arise from cells dorsal to the superior olivary nucleus, join the crossed fibers, and pass peripherally in association with the vestibular nerve. Peripherally, efferent cochlear fibers join the cochlear nerve via the vestibulocochlear anastomosis and are distributed to the hair cells of the cochlea.



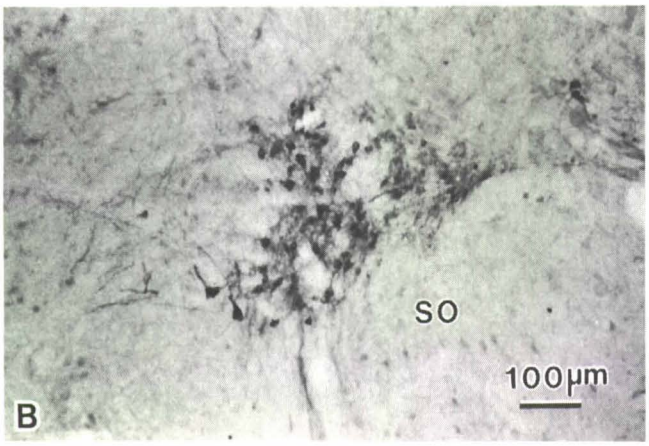


Figure 13.15. Cochlear efferent neurons identified by immunoreactivity to choline acetyltransferase (ChAT) in the rhesus monkey. **A.** A collection of ChAT-positive neurons (*arrowhead*) lying dorsal to the superior olivary nucleus (*SO*). **B.** The same group of cochlear efferent neurons seen at a higher magnification. *N. VI*, abducens nerve.

plex (27) project bilaterally to stapedius motor neurons. Contractions of the stapedius muscle, in response to loud sounds, serve to diminish amplitude. Contractions of the tensor tympani muscle, innervated by trigeminal nerve fibers, also are initiated by impulses from the superior olivary complex. The tensor tympani muscles diminish the sensitivity of the tympanic membrane to sound by tensing the membrane.

LESIONS OF THE AUDITORY SYSTEM

Destruction of the cochlear nerve or the cochlear nuclei causes complete deafness on the same side. Among the more common disorders is the so-called acoustic neurinoma, a perineural fibroblastoma that arises from cells of the Schwann sheath. Although this benign tumor probably originates from the vestibular portion of the eighth nerve, loss of hearing with, or without, tinnitus usually is the first symptom. Unilateral loss of hearing usually is gradual and may not be noticed by the patient until it is severe. In time, other cranial nerves almost invariably are involved, including the vestibular, trigeminal, and facial nerves. Since the secondary cochlear pathways are both crossed and uncrossed, lesions of one lateral lemniscus or of the auditory cortex cause a bilateral diminution of hearing (partial deafness) that is most marked in the contralateral ear. Removal of one temporal lobe causes an impairment of sound localization on the opposite side, especially as regards judgment of the distance from which the sound is coming (204).

Conduction deafness due to disease of the middle ear should be distinguished from nerve deafness. In conduction deafness, the ossicular chain fails to transmit vibrations from the tympanum to the oval window and to the scala vestibuli and scala media (i.e., cochlear duct) (Fig. 13.9). When the ossicular chain is broken, vibrations of the tympanum pass via the air of the middle ear to the round window. This is inefficient because it lacks the impedance matching of the ossicular chain and considerable sound energy is lost. Hearing loss due to interruption of the ossicular chain ranges from 30 decibels for low tones to 65 decibels in the middle range. Fixation of the ossicular chain resulting from middle ear infections, or otosclerosis, is more common than interruptions of the ossicular chain. In *otosclerosis*, air conduction is impaired because the membrane covering the oval window is thickened. Early in the course of the disease patients with otosclerosis have either a loss of appreciation of low tones, or a mild loss in the entire auditory range. Later there is a marked perceptual deficit for high tones. Tinnitus, without vertigo, is common, and many patients hear better in the presence of loud noises (*paracusis*).

Labyrinth and Related Nerve and Nuclei

LABYRINTH

The vestibular part of the inner ear consists of three *semicircular* ducts, the *utricle*, and the *saccule* (Figs. 13.8 and 13.16). These parts of the labyrinth are concerned with equilibrium and orientation in three-dimensional space, maintenance of equilibrium, and modification of muscle tone. The semicircular ducts, concerned with kinetic equilibrium, are arranged at right angles to each other and represent approximately the three planes of space. One end of each duct has a dilatation, the ampulla, containing a transversely oriented ridge, known as the *crista ampullaris*. Columnar epithelium of the *crista ampullaris* is composed of neuroepithelial hair cells that constitute the vestibular receptor (Fig. 13.20). Each crista is covered by a gelatinous *cupula* that moves across the hair cells in response of movement of the endolymphatic fluid. Angular acceleration causes displacement of endolymphatic fluid and movement of the cupula which stimulates the hair cells. Endolymphatic flow is greatest in the pair of semicircular ducts most nearly perpendicular to the axis of rotation.

The utricle and saccule together constitute the so-called "otolith organ." They have a similar patch of sensory epithelium known as the *macula*. The maculae are endowed with hair cells in contact with a gelatinous mass containing small calcareous concretions or particles, the *otoliths*. The utricular macula responds to changes in gravitational forces and to linear acceleration in the long axis of the body and convey impulses concerning the position of the head in space (i.e., static equilibrium). The macula of the saccule is less sensitive, but responds to linear acceleration in the ventrodorsal axis of the body.

Anatomic studies (167, 252) demonstrate that afferent nerve fibers from the saccular macula do not join the cochlear nerve and that they are distributed to the vestibular nu-

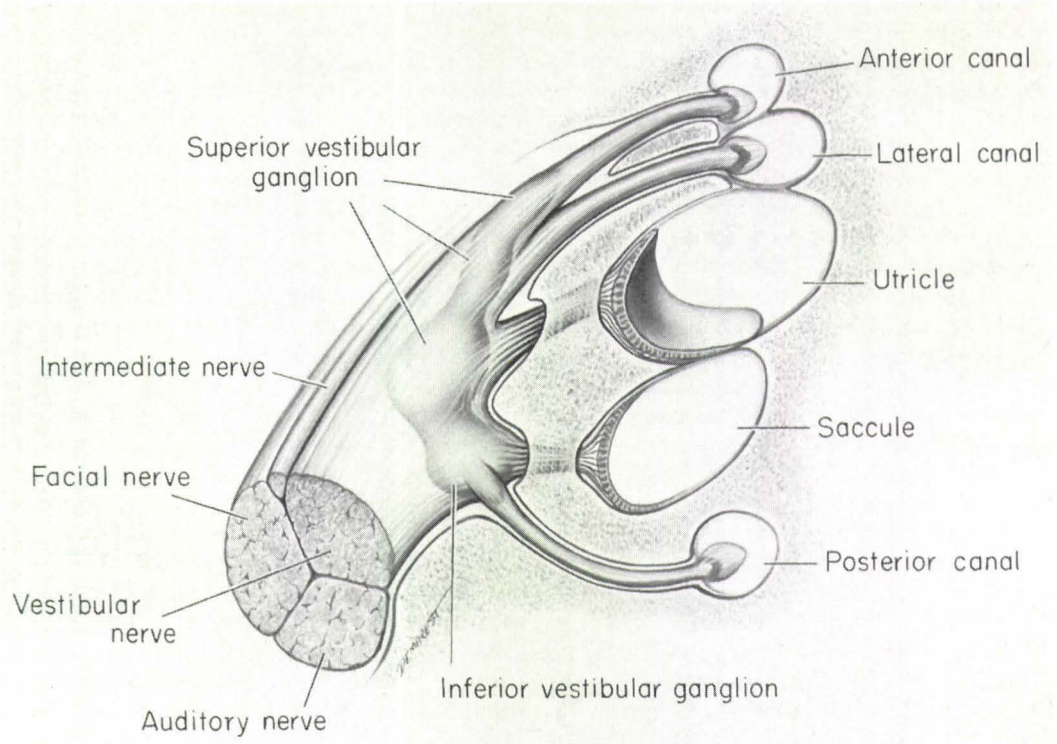


Figure 13.16. Vestibular ganglia and peripheral branches innervating distinct portions of the labyrinth. Cells in the superior vestibular ganglion are arranged in a spiral fashion. Cells in the superior and distal portion of this ganglion innervate the cristae of the anterior and lateral semicircular ducts. The broader proximal part of the superior vestibular ganglion contains cells which innervate the macula of the utricle. Cells of the inferior vestibular ganglion innervate the macula of the saccule and the crista of the posterior semicircular duct. The superior and inferior vestibular ganglia are joined by an isthmus of cells. The relationships between the facial, intermediate, vestibular, and auditory nerves are shown on the left.

clei in a manner similar to that of nerve fibers from the utricular macula and the semicircular ducts.

VESTIBULAR GANGLION AND NERVE

The maculae and cristae are innervated by cells of the vestibular ganglion (ganglion of Scarpa), an aggregation of bipolar cells located in the internal auditory meatus. Most cells of the vestibular ganglion have glutamate as their neurotransmitter, but over 20% of the cells contain substance P (58). This ganglion can be divided into superior and inferior vestibular ganglia, which are connected by a narrow isthmus (Figs. 13.8 and 13.16). The short peripheral processes of bipolar cells located in the ganglia go to the receptor cells of the maculae and cristae, while the longer central processes form the vestibular nerve. Cells of the superior vestibular ganglion innervate the cristae of the anterior and lateral semicircular ducts, and the macula of the utricle. Cells of the smaller inferior vestibular ganglion innervate the crista of the posterior semicircular duct, and the macula of the saccule (65, 144, 252). Vestibular root fibers enters the brainstem at the cerebellopontine angle where fibers pass between the inferior cerebellar peduncle and the spinal trigeminal tract. On entering the vestibular nuclear complex, the fibers bifurcate into short ascending and long descending branches that terminate in the vestibular nuclei (Figs. 12.16 and 13.17–13.19). Some primary vestibular fibers (i.e., root fibers) continue without interruption to particular parts of the cerebellum. These fibers reach the ipsilateral half of the cerebellum via the juxtarestiform body (Fig. 13.7) and project mainly to the cortex of the nodulus, uvula and flocculus (34, 65).

VESTIBULAR NUCLEI

The vestibular nuclei lie in the floor of the fourth ventricle and extend from levels ros-

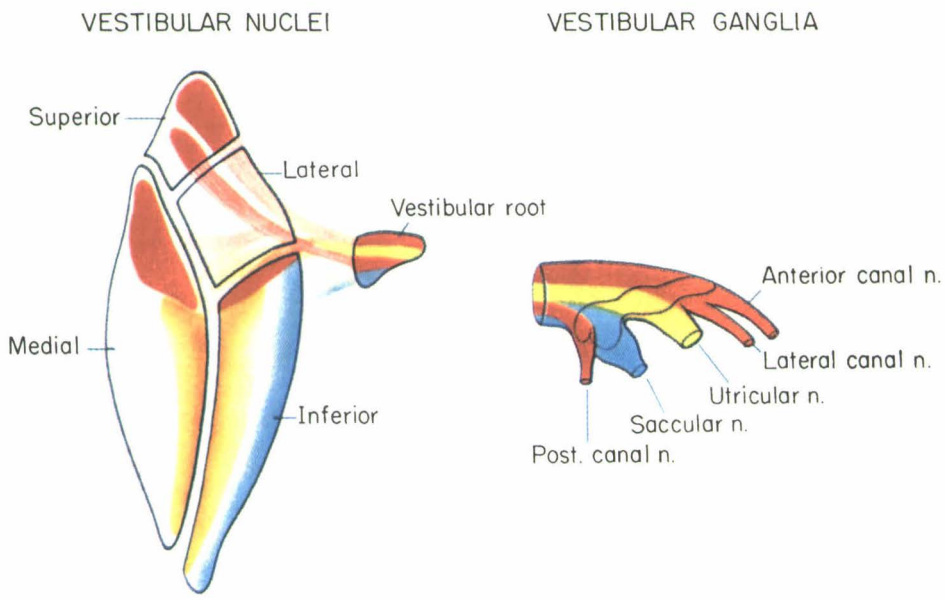


Figure 13.17. Relationship between portions of the vestibular ganglia and central fibers projecting to parts of the vestibular nuclear complex. The vestibular ganglia are shown in a modified transverse plane, while the vestibular nerve root and the vestibular nuclear complex are drawn in a stylized fashion, as they would appear in horizontal sections of the brainstem. Only the principal central projections of distinctive parts of the vestibular ganglia are shown. Portions of the vestibular ganglia innervating the cristae of the semicircular ducts (*red*) project primarily to the superior vestibular nucleus and rostral parts of the utricle project central fibers primarily to parts of the inferior and medial vestibular nuclei. Fibers from portions of the inferior vestibular ganglion innervating the macula of the saccule (*blue*), project mainly to dorsolateral parts of the inferior vestibular nucleus. Some cells in the vestibular ganglia project fibers to parts of an vestibular nuclei, so that each part of the labyrinth has a unique as well as common protection, within the vestibular nuclear complex.

tral to the hypoglossal nucleus to slightly beyond the level of the abducens nucleus. Nuclei of this complex are arranged into longitudinal columns. The lateral column consists of three distinctive nuclei: the inferior, lateral, and superior vestibular nuclei. The medial vestibular nucleus constitutes the medial cell column (115) (Figs. 13.17, 13.18, A.4, A.5, and A.6).

The *inferior vestibular nucleus* begins caudally in the medulla, medial to the accessory cuneate nucleus, and extends rostrally medial to the level of entrance of the vestibular nerve (Fig. 13.4). This nucleus is composed mostly of small- and medium-sized cells, except in its most rostral part, where large cells resemble those of the lateral vestibular nucleus. In the ventrolateral and caudal parts of the nucleus, a number of rather large cells form several densely packed groups. These cells (*group f* of Brodal and Pompeiano (36)) are of particular interest because they do not receive primary vestibular fibers and many of them project fibers to the cerebellum. In fiber-stained sections, the inferior vestibular nucleus is characterized by bundles of longitudinally oriented fibers, part of which are descending primary vestibular fibers. These descending fiber bundles facilitate the delineation of the inferior and medial vestibular nuclei (Figs. 12.26 and 13.4).

The *lateral vestibular nucleus* (Deiters' nucleus), located laterally in the ventricular floor at the level of entrance of the vestibular nerve, extends rostrally to the level of the abducens nucleus. This nucleus is composed of multipolar giant cells with coarse Nissl granules. Although most of the cells of this nucleus are regarded as giant cells, considerable variations in cell size are found (Fig. 13.3). The nucleus also contains varying types of smaller cells. Cells of all sizes are intermingled throughout the nucleus except in a small dorsolateral protrusion that consists only of medium-sized cells. There are some regional differences in the relative number and size of giant cells, which are most abundant in the caudal part of the nucleus. The giant cells in the lateral vestibular nucleus have numerous boutons on their soma, while small cells have

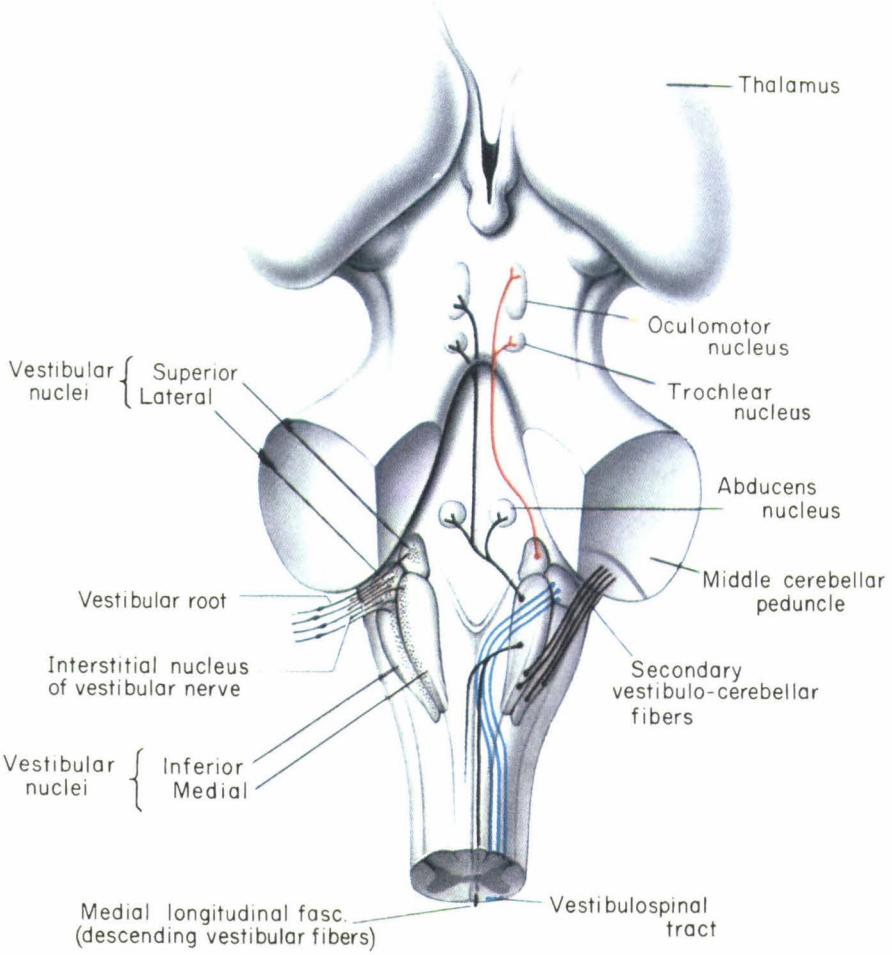


Figure 13.18. Principal fiber projections of the vestibular system. On the *left*, the relationships and spatial disposition of the four main vestibular nuclei are indicated. Among the afferent root fibers are the cells of the interstitial nucleus of the vestibular nerve. *Dotted areas* in the vestibular nuclei represent the regions of the nuclear complex which receive the largest number of primary vestibular fibers. These areas are (a) the ventral half of the lateral vestibular nucleus, (b) the lateral part of the medial vestibular nucleus, (c) the dorsomedial part of the inferior vestibular nucleus, and (d) the central part of the superior vestibular nucleus. On the *right*, secondary projections from some of the individual vestibular nuclei are shown. Fibers from the superior vestibular nucleus (*red*) ascend ipsilaterally in the medial longitudinal fasciculus (*MLF*) and terminate in parts of the trochlear and oculomotor nuclei. Ascending projections from the rostral part of the medial vestibular nucleus (*black*) to the nuclei of the extraocular muscles are predominantly crossed. A small number of uncrossed ascending fibers from lateral vestibular nucleus are not shown. Fibers from caudal parts of the medial vestibular nucleus descending in the MLF are shown in *black*. The somatotopically organized vestibulospinal tract (*blue*) arises only from the lateral vestibular nucleus. Secondary vestibulocerebellar fibers (*black*) arise from caudal parts of the inferior and medial vestibular nuclei.

relatively few boutons (180). Fibers of the vestibular root traverse ventral parts of this nucleus.

The *superior vestibular nucleus* lies dorsal and rostral to the lateral vestibular nucleus in the angle formed by the floor and the lateral wall of the fourth ventricle (Figs. 13.1 and 13.7). The superior cerebellar peduncle (or brachium conjunctivum) forms the dorsolateral border of the nucleus throughout most of its rostrocaudal extent. The mesencephalic and principal sensory nuclei of the trigeminal nerve are adjacent to the nucleus medially and ventrally, in its rostral two-thirds. The rostral pole of the nucleus is difficult to delimit. Cells in the central region of the nucleus are large, stellate, and form clusters (32), whereas those at the periphery are smaller, round or spindle-shaped, and more loosely distributed.

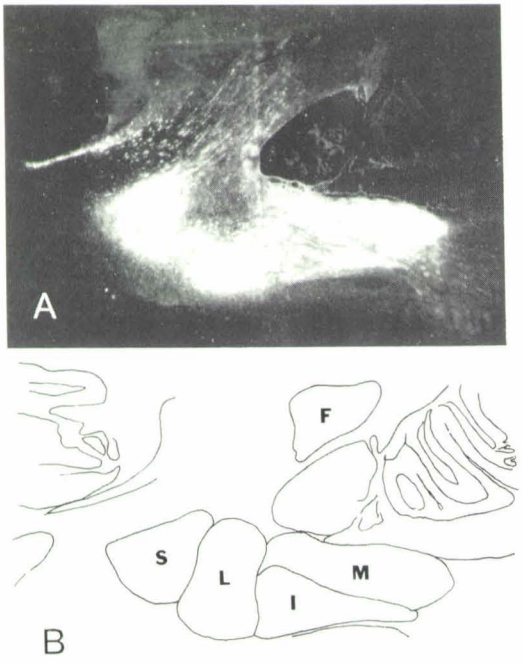


Figure 13.19. **A.** Saggital section through the brainstem in a rhesus monkey demonstrating transport of (^{3}H)-labeled amino acids from the labyrinth to the vestibular nuclei in an autoradiograph (Cresyl violet, dark field, ×20). **B.** Fastigial (*F*) and vestibular nuclei: *S,* superior vestibular nucleus; *L,* lateral vestibular nucleus; *I,* inferior vestibular nucleus; *M,* medial vestibular nucleus. Although primary vestibular afferents project to all ipsilateral vestibular nuclei, only the ventral half of the lateral vestibular nucleus receives terminals from this source.

The *medial vestibular nucleus*, the largest of all four vestibular nuclei, is located medial to the inferior and lateral vestibular nuclei in the floor of the fourth ventricle (Figs. 13.4 and 13.17). This nucleus extends from the oral pole of the hypoglossal nucleus to the abducens nucleus and rostrally fuses with the superior vestibular nucleus. It is composed of small- and medium-sized cells and contains relatively few fibers. Dorsolaterally, some larger cells resemble those of the lateral vestibular nucleus, although none are true giant cells. The medial and inferior vestibular nuclei can be readily distinguished at all levels in myelin-stained preparations because bundles of longitudinally coursing fibers are not present in the medial vestibular nucleus (Fig. 13.4).

Besides the main vestibular nuclei, there are several smaller accessory nuclei (32, 36, 115), one of which consists of strands of cells between the root fibers of the vestibular nerve (interstitial nucleus of the vestibular nerve) (Fig. 13.18).

Vestibular Fiber Systems

PRIMARY VESTIBULAR FIBERS

These fibers project to all four vestibular nuclei and to the interstitial nucleus of the vestibular nerve, a collection of cells between the entering vestibular root fibers. Upon entering the vestibular complex, virtually all fibers bifurcate into ascending and descending branches. Ascending branches project mainly to the superior, lateral, rostral parts of the medial vestibular nuclei (Fig. 13.17). Descending branches provides fibers to the inferior vestibular nucleus and collaterals to caudal parts of the medial vestibular nucleus (46, 47, 236, 252, 278). Primary vestibular fibers are distributed within all vestibular nuclei, but some regions of each nucleus contain fewer endings. In the superior vestibular nucleus, primary vestibular fibers terminate most profusely about large central cells but extend into all peripheral regions. In the lateral vestibular nucleus, primary vestibular fibers terminate only in the ventral regions (46, 47, 167, 252, 278) (Fig 13.19). These fibers establish synaptic contact primarily with the soma and dendritic stems of small cells; the giant cells receive fewer synaptic endings from primary vestibular fibers (180). The medial vestibular nucleus receives primary vestibular fibers throughout large regions of its rostral part, but caudally, terminations are mainly in lateral regions near the inferior vestibular nucleus (Fig. 13.17). Primary vestibular fibers in the inferior vestibular nucleus end more profusely in dorsal regions (Figs. 13.17 and 13.18). The cristae of the semicircular ducts give rise to fibers that project primarily to the superior vestibular nucleus and to rostral parts of the medial vestibular nucleus. Cells of the superior vestibular ganglion, which innervate the macula of the utricle, project almost exclusively to the ventral part of the lateral vestibular nucleus (Fig. 13.19). Cells of the inferior vestibular ganglion, which innervate the macula of the saccule, give rise to central fibers that descend and terminate mainly in dorsolateral portions of the inferior vestibular nucleus and in an accessory nucleus known as cell group "y" (46, 47, 59, 252). The interstitial nucleus of the vestibular nerve appears distinctive in that this nucleus receive fibers from all cell groups of the vestibular ganglia (Fig. 13.18).

A small number of primary vestibular

fibers enter the cerebellum via the juxtarestiform body. Most of these *primary vestibulocerebellar fibers* traverse portions of the lateral and superior vestibular nuclei and terminate in the cortex of the ipsilateral nodulus, uvula, and flocculus (34). In monkeys, cells in all parts of the vestibular ganglion project to the ipsilateral nodulus and uvula, where they end as mossy fibers in the granular layer of cerebellar cortex (65). Cells of the vestibular ganglion that innervate the cristae of the anterior and lateral ducts and the maculae of the utricle and saccule have distinctive regions of termination in the folia of the ipsilateral flocculus. Although a few primary vestibular fibers may end in the dentate nucleus, there is no conclusive evidence that such fibers terminate in the fastigial nucleus. At least one study suggests that primary vestibulocerebellar fibers are confined largely to the ipsilateral nodulus and flocculus and are relatively sparse (148).

AFFERENT PROJECTIONS TO THE VESTIBULAR NUCLEI

The vestibular nuclei receive a large number of afferent fibers from sources other than the vestibular ganglion (175). According to Brodal (32), vestibular afferents from the cerebellum outnumber those from any other source. Cerebellar projections to the vestibular nuclei arise from the following regions of the cerebellum: (a) the "vestibular part," (b) the "spinal part," and (c) the fastigial nucleus. The "vestibular part" of the cerebellum (or vestibulocerebellum), consisting of the flocculus, nodulus, and ventral portion of the uvula, projects ipsilaterally, chiefly to parts of the superior and medial vestibular nuclei (10). The lateral vestibular nucleus receives only a few afferents from this source. Projections from the "spinal part" of the cerebellum, represented mainly by the vermis of the anterior lobe, are ipsilateral to the dorsal part of the lateral vestibular nucleus and the dorsorostral part of the inferior vestibular nucleus (279). The latter projection somatotopically links the forelimb region of the anterior lobe with the forelimb region of the lateral vestibular nucleus. These fibers, representing axons of Purkinje cells, are known to have a monosynaptic inhibitory influence upon neurons of the lateral vestibular nucleus mediated by γ-aminobutyric acid (GABA) (68, 101, 128). Indirect projections from "spinal parts" of the cerebellum to the vestibular nuclei are relayed by the fastigial nuclei. The cortex of the cerebellar vermis projects upon the fastigial nucleus, which in turn gives rise to a vestibular projection. Fastigial efferent fibers follow a complex course, best described in relation to other efferent systems from the cerebellar nuclei (see Chapter 15). The fastigial nucleus projects bilaterally and nearly symmetrically upon ventral portions of the lateral and inferior vestibular nuclei (19, 55). Fastigial efferent projections have excitatory influences, probably mediated by glutamate.

The vestibular nuclei do not appear to receive descending fibers from the cerebral cortex, the corpus striatum, the superior colliculus, or the nuclei of the posterior commissure (214). Descending fibers from the interstitial nucleus of Cajal project via the medial longitudinal fasciculus to the medial vestibular nucleus. These fibers appear to be the only descending vestibular afferent fibers arising from cells within the brainstem.

Commissural projections from the contralateral vestibular nuclei, principally the superior and medial vestibular nuclei, have major influences on vestibular function (50, 94, 110, 157, 175, 235). Vestibular neurons receiving inputs from ganglion cells innervating the cristae of the semicircular ducts have inhibitory influences on contralateral vestibular neurons via commissural projections. Vestibular neurons with inputs from ganglion cells innervating the maculae of the otoliths exert contralateral excitatory influences via commissural projections.

SECONDARY VESTIBULAR FIBERS

The vestibular nuclei give rise to secondary fibers that project to specific portions of the cerebellum, to certain motor cranial nerve nuclei, and to all spinal levels. These fibers are more widely dispersed within the neuraxis than any other special sensory system, probably because the vestibular system is concerned with the maintenance of equilibrium and orientation in three-dimensional space.

Secondary vestibulocerebellar fibers arise mainly from caudal portions of the inferior and medial vestibular nuclei and project ipsilaterally to the cortex of the nodulus, uvula, and flocculus (41) (Fig. 13.18). Vestibulocerebellar fibers, both primary and secondary, enter the cerebellum via the juxtarestiform body. None of these fibers end in the fastigial nucleus, but this nucleus projects to the

vestibular nuclei in a selective manner (19, 49, 55, 265, 280).

Cells of the lateral vestibular nucleus give rise to the somatotopically organized, uncrossed vestibulospinal tract, which descends throughout the length of the spinal cord in the anterior and lateral funiculi (Figs. 11.19, 11.21, and 13.18). These fibers, arising from cells of all sizes within the nucleus, are somatotopically organized (213). In the medulla, the vestibulospinal tract is a loosely organized bundle extending obliquely from the region of the medial longitudinal fasciculus (MLF) to the retro-olivary area. The dorsal half of the lateral vestibular nucleus receives somatotopically organized inhibitory inputs from the Purkinje cells in the anterior lobe vermis, while ventral regions of the nucleus receive crossed and uncrossed excitatory influences from the fastigial nuclei (19, 55). Fibers from the fastigial nucleus do not appear to terminate upon large cells in the lateral vestibular nucleus (280), while fibers from the cerebellar vermal cortex end principally upon such cells (179, 279). Thus, the lateral vestibular nucleus receives impulses from the vestibular nerve and various parts of the cerebellum, and conveys impulses to spinal levels that mediate responses in axial and appendicular musculature (37). Impulses relayed to spinal levels via the vestibulospinal tract have facilitating influences upon extensor muscle tone.

MEDIAL LONGITUDINAL FASCICULUS (MLF)

Fibers from all of the vestibular nuclei pass medially in the region of the abducens nucleus and enter the MLF. Vestibular fibers in the MLF are both crossed and uncrossed, and many bifurcate into ascending and descending branches (Figs. 11.19 and 13.18).

Descending vestibular fibers in the MLF projecting to spinal levels arise primarily, if not exclusively, in the medial vestibular nucleus. These fibers, both crossed and uncrossed at medullary levels, descend in the MLF until they reach the pyramidal decussation, where they shift ventrolaterally to enter the sulcomarginal region of the anterior funiculus. In their course, they may project fibers into the lower brainstem reticular formation. Although these fibers are present bilaterally in the medulla, at spinal levels almost all fibers are ipsilateral. Some fibers may descend as far as upper thoracic segments, but most fibers end at cervical levels. Some vestibular fibers descending in the MLF synapse directly upon alpha (α) motor neurons. Experimental evidence indicates that these fibers exert direct inhibitory influences upon cervical motor neurons (295). The superior, lateral, and inferior vestibular nuclei do not appear to contribute descending fibers to the MLF that reach spinal levels (50, 187, 213).

The MLF at spinal levels also contains nonvestibular descending fibers from (a) the interstitial nucleus of Cajal (interstitiospinal tract), (b) the superior colliculus (tectobulbar and tectospinal tracts, sometimes referred to as the predorsal bundle), (c) the pontine reticular formation (reticulospinal tract), and (d) more rostral brainstem nuclei projecting to particular portions of the inferior olivary complex. The largest group of descending fibers in the MLF are the pontine reticulospinal fibers (Figs. 11.10 and 11.22). Other pontine reticulospinal fibers descend more ventrally to reach the anterior funiculus of the spinal cord (Fig. 11.25).

Ascending fibers in the MLF arise mainly from parts of the medial and superior vestibular nuclei (120, 251), are crossed and uncrossed, and project primarily to the nuclei of the extraocular muscles (i.e., the abducens, trochlear, and oculomotor) (52, 170). Ascending fibers from the medial vestibular nucleus reach (a) the abducens nucleus (bilateral), (b) the contralateral trochlear nucleus, (c) the contralateral intermediate cell column (i.e., inferior oblique muscle), and (d) the ipsilateral ventral nucleus (i.e., medial rectus muscle) of the oculomotor complex (Figs. 13.18 and 14.14). Large cells in central parts of the superior vestibular nucleus give rise to uncrossed ascending fibers in the MLF distributed to the trochlear and oculomotor nuclei. Smaller cells in peripheral parts of the superior vestibular nucleus project fibers to the oculomotor nucleus via a crossed ventral tegmental pathway (outside the MLF), which has major influences on cells innervating the opposite superior rectus muscle (56). Physiologically, crossed ascending vestibular projections to the nuclei of the extraocular muscles have excitatory effects, while uncrossed fibers exert inhibition (Fig 13.18).

Additionally, the MLF contains an impressive crossed ascending projection originating from the abducens internuclear neurons that terminate upon cells of the medial rectus subdivision of the oculomotor nuclear complex (14, 54, 56, 120, 243, 250, 251) (Fig. 13.25). This projection interrelates activities of the ab-

ducens nucleus neurons on one side with neurons of the oculomotor nucleus, which innervate the medial rectus muscle on the opposite side. This pathway provides a neural mechanism for simultaneous contractions of the lateral rectus muscle on one side and the medial rectus muscle on the opposite side, which are required for conjugate lateral gaze (Fig. 13.22).

A small number of ascending fibers in the MLF bypass the oculomotor nucleus to terminate in the interstitial nucleus of Cajal, a small group of neurons embedded in the MLF (Figs. 14.16–14.18). The medial vestibular nucleus project to the opposite interstitial nucleus, while the superior vestibular nucleus provides terminals to the ipsilateral interstitial nucleus.

Secondary vestibular projections to thalamic relay nuclei are bilateral, modest in number, and end about cell clusters in the ventral posterolateral (VPL_c) thalamic nucleus (24, 89–91, 158, 164). Thalamic nuclei receiving vestibular inputs also respond to somatosensory signals, suggesting there is no exclusive representation of vestibular sense at thalamic levels.

EFFERENT VESTIBULAR SYSTEM

Like the cochlea, the vestibular end organ receives an efferent innervation that arises bilaterally and symmetrically from brainstem neurons (112, 116, 288). These cholinergic efferent neurons lie along the lateral border of the abducens nucleus and give rise to fibers that pass peripherally with the vestibular nerve on each side to innervate hair cells in the cristae of the semicircular ducts and the maculae of the utricle and saccule (58) (Figs. 13.20 and 13.21). Efferent vestibular fibers have bilateral excitatory effects on each of the five end organs of the labyrinth. It has been postulated that the efferent vestibular fibers

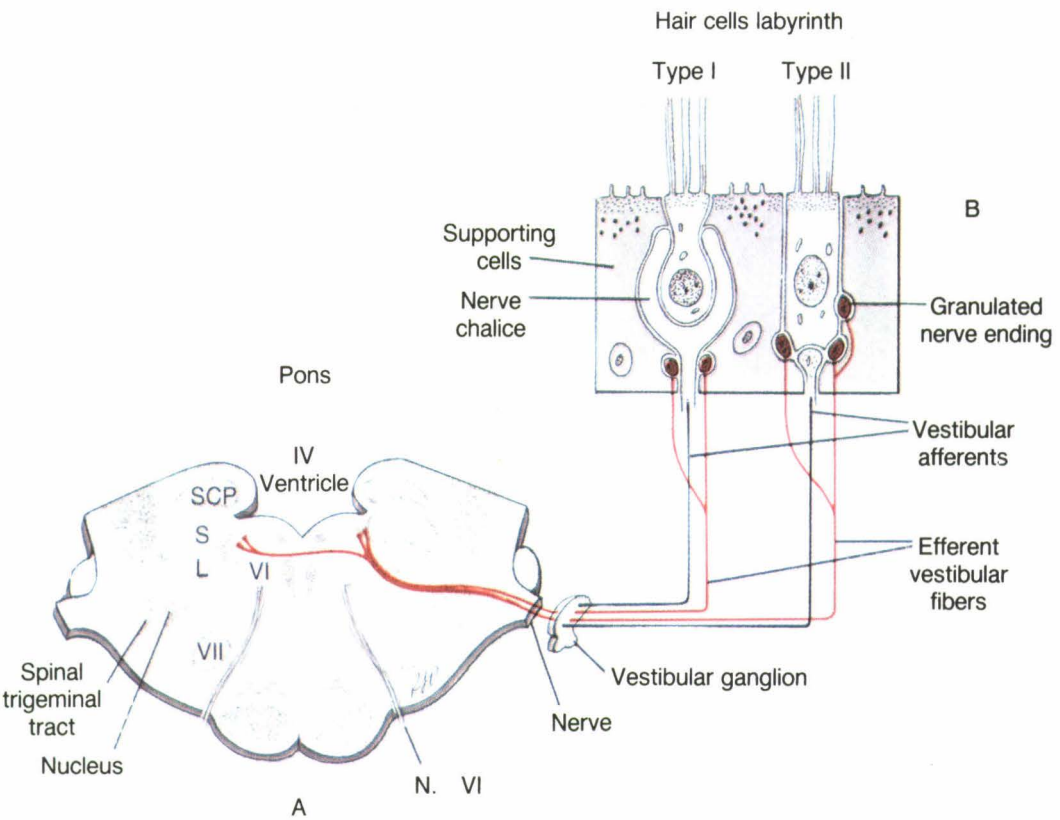


Figure 13.20. Efferent vestibular fibers (*red*) and their relationship to the hair cells of the labyrinth. Efferent cholinergic vestibular fibers arise bilaterally from small groups of neurons along the lateral border of the abducens nucleus (*VI*) (see Figure 13.21), emerge via the vestibular nerve, and terminate in granulated nerve endings at the base of type I and type II hair cells. **A.** Transverse section of the pons at level of abducens nuclei. **B.** Hair cells of the labyrinth. Efferent vestibular fibers exert excitatory influences upon the hair cells, which may modulate their dynamic range. *L*, lateral vestibular nucleus; *S*, superior vestibular nucleus; *SCP*, superior cerebellar peduncle.

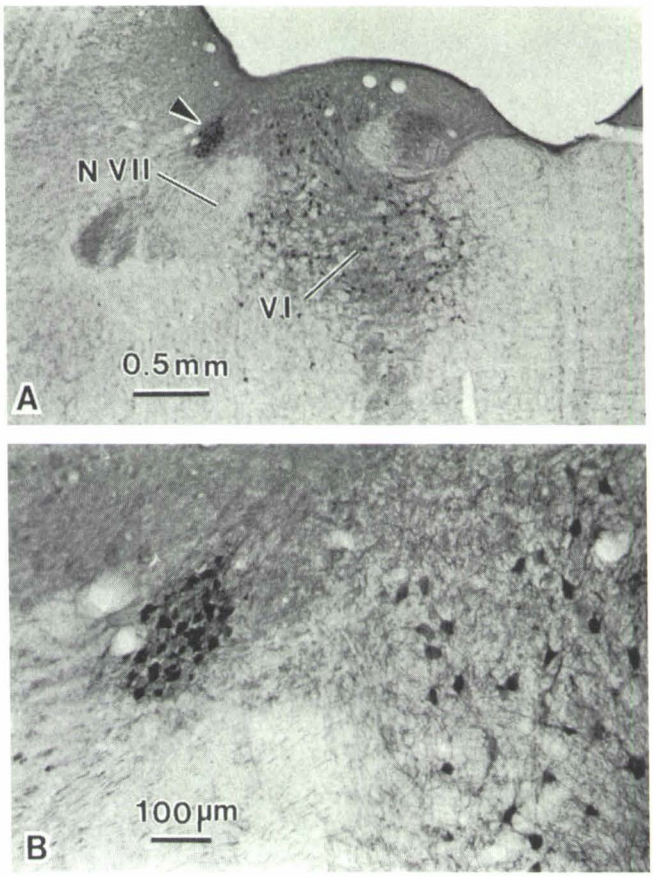


Figure 13.21. Vestibular efferent neurons identified by their immunoreactivity to choline acetyltransferase (ChAT) in a rhesus monkey. **A.** Vestibular efferent neurons (*arrowhead*) lying lateral to the cells of the abducens nucleus (*VI*). **B.** Higher magnification of the same section, showing vestibular efferent neurons and one population of cells in the abducens nucleus that are cholinergic.

may modulate the dynamic range of afferents to match expected acceleration. It is of interest that the efferent cochlear and vestibular neurons are both cholinergic, but efferent cochlear fibers are inhibitory and efferent vestibular fibers are excitatory (Figs. 13.15 and 13.21).

Functional Considerations

Secondary vestibular fibers contained in the MLF play an important role in conjugate eye movements (73, 74, 99, 261). Selective stimulation of the nerve from the ampulla of individual semicircular ducts produces specific deviations of both eyes that are regarded as primary responses. Stimulation of the ampullary nerve from the horizontal duct produces conjugate deviation of the eyes to the opposite side. Bilateral stimulation of the ampullary nerve of the anterior ducts produces upward movement of both eyes; similar bilateral stimulation of the ampullary nerve of the posterior ducts causes downward movements of the eyes. Section of the MLF rostral to the abducens nuclei abolishes these primary oculomotor responses, but nystagmus still results from labyrinthine stimulation (22, 165, 166, 244), suggesting that pathways essential for nystagmus probably pass via the reticular formation.

Labyrinthine stimulation, irritation, or disease cause vertigo, postural deviation, unsteadiness in standing and walking, deviations of the eyes, and nystagmus. In some instances, nausea, vomiting, vasomotor changes, and prostration occur. The term *vertigo* refers to a subjective sense of rotation, either of the individual or his environment. This term should not be regarded as a synonym for dizziness or giddiness. The most prominent objective signs of vestibular involvement is *nystagmus*, a rhythmic involuntary oscillation of the eyes characterized by alternate slow and rapid ocular excursions. By convention, the direction of the nystagmus is named for the rapid phase, even though the slow ocular excursion is the pri-

mary movement (the rapid phase is the automatic reflex correction). The nausea and vomiting which occur with motion sickness are mainly the result of stimulation of the utricle. Since the labyrinths are antagonistic to each other, the elimination of one causes the other to be overactive until accommodation takes place.

Tests for vestibular function are based on stimulation of the semicircular canals or vestibular nerve endings by (a) the rotating chair test (Bárány chair), (b) the caloric test (irrigation of the external auditory canal with water of temperatures appropriate to induce convection currents in the endolymphatic fluid), and (c) the galvanic test which stimulates nerve endings directly. Following a period of rotation in the Bárány chair, the chair is abruptly stopped, but the endolymphatic fluid continues to circulate for a time. In this postrotational phase, the slow phase of the nystagmus, the deviation of the eyes, postural deviation (standing), and past-pointing are all in the direction of the previous rotation and can be correlated with the direction of endolymphatic flow. The patient experiences a sensation of vertigo opposite to that of the prior rotation (92).

Lesions involving the MLF rostral to the abducens nuclei produce a disturbance of conjugate horizontal eye movements known as *internuclear ophthalmoplegia* (69, 72, 245, 246). The salient features of this syndrome in cases with a unilateral MLF lesion are (a) paresis of ipsilateral ocular adduction on attempted lateral gaze to the opposite side, (b) monocular horizontal nystagmus in the contralateral abducted eye, and (c) no impairment of ocular convergence. The paresis of ocular adduction on attempted lateral gaze to the opposite side occurs ipsilateral to unilateral lesions of the MLF (Fig. 13.22). Bilateral lesions of the MLF rostral to the abducens nuclei result in dissociated horizontal eye movements on attempted lateral gaze to both the right and left sides (22, 23, 233). In the bilateral syndrome, no ocular adduction is seen on attempted lateral gaze to either side. An adequate explanation for the monocular nystagmus seen in the abducting eye has eluded clinicians and basic science researchers. This syndrome has been produced in monkeys (62, 66) and occurs in humans, mainly as a consequence of brainstem vascular lesions or in association with demyelinating diseases, such as multiple sclerosis. The paresis of ocular adduction on attempted lateral gaze to the opposite size results from interruption of ascending fibers from the abducens internuclear neurons after they have crossed from the opposite side (54) (Fig. 13.22). Unilateral lesions of individual vestibular nuclei in the monkey do not produce dissociated (i.e., dysconjugate) eye movements (51, 170, 269).

Mechanisms governing equilibrium (i.e., maintenance of appropriate body position) and orientation in three-dimensional space are largely reflex in character and depend upon afferent inputs from several sources (294). The most important of these are (a) kinesthetic sense conveyed by the posterior column-medial lemniscal system from receptors in joints and joint capsules, (b) impulses conveyed centrally by spinocerebellar systems from stretch receptors in muscles and tendons, (c) the suprasegmental kinesthetic sense provided by the vestibular end organ, and (d) visual input from the retina. Among the sensory systems that contribute to the maintenance of equilibrium, the labyrinth constitutes a highly specialized receptor that is stimulated by the change of position or changes in position of the head. When the head is moved, either by contraction of the neck muscles or by shifting the body as a whole, the cristae are stimulated and effect compensatory reflex adjustments of the eyes and limb muscles needed for the particular movement (kinetostatic reflexes). As long as the position of the head remains unchanged, the new attitude is sustained by impulses originating in the macula of the utricle. The sustaining (static) reflexes are initiated by gravitational forces acting upon the macular hair cells.

The vestibulospinal tracts and descending fibers from the pontine reticular formation exert a strong excitatory influence upon muscle tone, particularly extensor muscle tone. Descending vestibular impulses in the MLF exert inhibitory influences upon cervical motor neurons (295). Normally, muscle tone is maintained by a balance of inhibitory and facilitatory influences from higher centers, a large part of which are mediated by the brainstem reticular formation. If the influences of higher centers are removed in an experimental animal, such as the cat, by transection of the brainstem at intercollicular level (i.e., between the superior and inferior colliculi), a condition known as *decerebrate rigidity* develops. This condition is character-

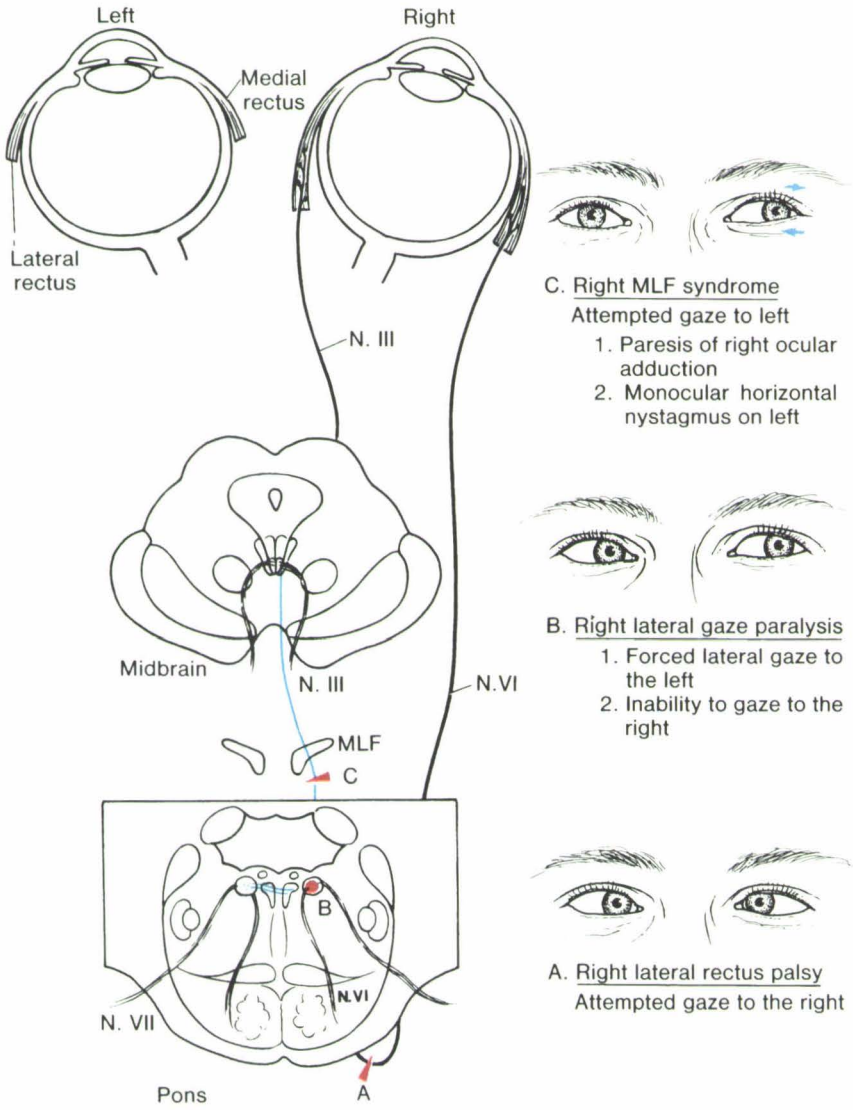


Figure 13.22. Lesions affecting conjugate horizontal gaze. The lesion at *A* (*red*), involving the right abducens nerve as it leaves the brainstem, produces a paralysis of the right lateral rectus muscle. In the eyes at *A*, the patient is attempting to gaze to the right. The right eye is somewhat adducted and the left eye is fully adducted. This patient would experience diplopia on attempted right lateral gaze. The lesion in the abducens nucleus (*B* (*red*)) would destroy lower motor neurons and abducens internuclear neurons whose axons enter the opposite MLF and ascend to the ventral nucleus (which innervates the medial rectus muscle) of the oculomotor complex. A patient with such a lesion would have a right lateral gaze paralysis and both eyes would be forcefully directed to the left field of gaze. A unilateral lesion (*red*) in the right MLF (*blue*) at *C* would interrupt axons of abducens internuclear neurons arising from the left abducens nucleus. This lesion would produce dissociated horizontal eye movements. On attempted gaze to the left, there would be a paresis of right ocular adduction (*C*) and monocular horizontal nystagmus in the left abducting eye, indicated by *arrows*.

ized by tremendously increased tone in the antigravity muscles, due to an increased firing rate of muscle spindles by gamma (γ) motor neurons. The increased firing rate of the muscle spindles afferents activates α motor neurons that maintain the tonic state (Fig. 10.30). In this experimental preparation, facilitatory pathways from the reticular formation and from the lateral vestibular nucleus (vestibulospinal tract) remain active, while inhibitory elements of the reticular formation no longer function. Inhibitory regions of the reticular formation are considered to be dependent upon descending impulses from higher levels, while facilitating regions of the reticular formation remain active. Midbrain

transection removes the input essential to the reticular inhibitory system but has little effect upon brainstem facilitating mechanisms. Decerebrate rigidity can be abolished, or diminished, by a variety of different lesions, including section of the vestibular nerve, destruction of the vestibular nuclei, or section of the vestibulospinal tract. Surgical section of several successive dorsal or ventral spinal roots will abolish the phenomenon segmentally because either will interrupt the gamma (γ) loop.

FACIAL NERVE

The facial nerve (N. VII) and the intermediate nerve usually are discussed together although they subserve separate functions (Figs. 13.1 and 13.2). Functional components of these nerves include (a) *special visceral efferent* (SVE, branchiomotor) fibers, (b) *general visceral efferent* (GVE, parasympathetic) fibers, (c) *special visceral afferent* (SVA, taste) fibers, and (d) a few *general somatic afferent* (GSA, sensory) fibers.

Special visceral efferent (SVE) fibers of the motor component innervate the muscles of facial expression, the platysma, the buccinator, and the stapedius muscles. The motor nucleus of nerve VII forms a column of cholinergic multipolar neurons in the ventrolateral tegmentum dorsal to the superior olivary nucleus and ventromedial to the spinal trigeminal nucleus (Figs. 13.1, 13.2, 13.23, and 13.24). The facial motor nucleus is subdivided into dorsomedial, ventromedial, intermediate, and lateral cell groups, each group innervating distinct facial muscles (84, 196, 276). The dorsomedial cell group gives rise to the posterior auricular nerve which innervates auricular muscles and the occipital muscle. The ramus colli which innervates the platysma muscle arises from be ventromedial cell group. Cells in the medial group are considered to innervate the stapedius muscle (27). The temporal and zygomatic branches of the facial nerve, related to the intermediate cell group, supply the frontalis, orbicularis oculi, the corrugator supercilli, and the zygomaticus. The lateral cell group gives rise to the buccal branches which innervate the buccinator muscle and the buccolabial muscles. Comparisons of the cell groups of the facial nucleus in animals and humans (276) reveal a

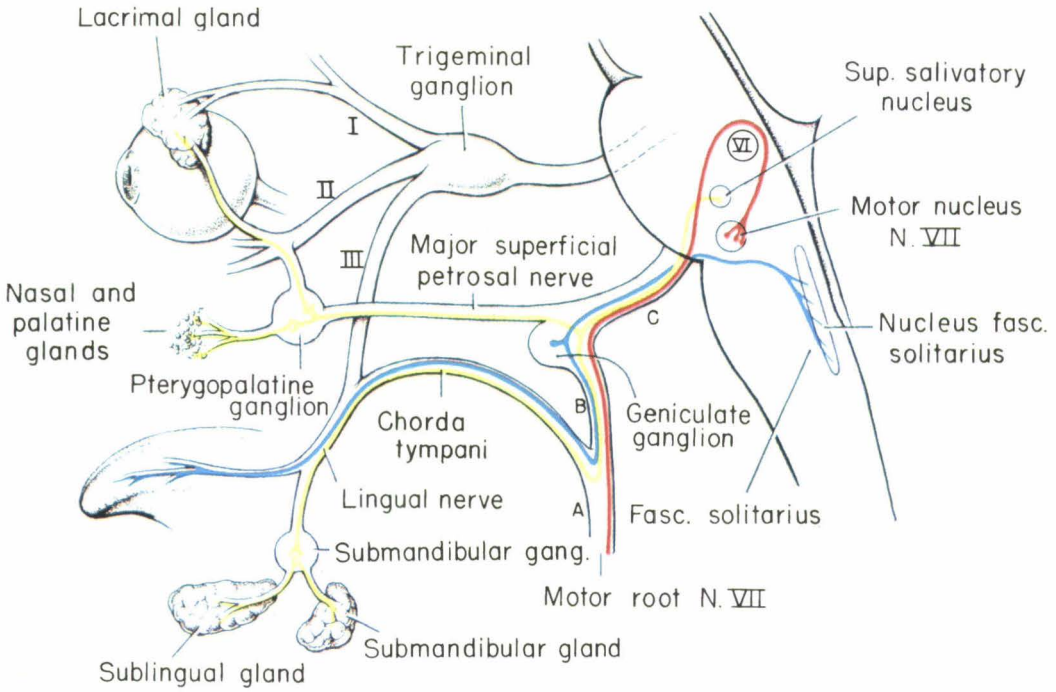


Figure 13.23. Functional components, organization, and peripheral distribution of the facial nerve. Special visceral efferent fibers (motor) are shown in *red*. General visceral efferent fibers (parasympathetic) are in *yellow*, and special visceral afferent fibers (taste) are in *blue*. *A*, *B*, and *C* denote lesions of the facial nerve at the stylomastoid foramen, distal to the geniculate ganglion, and proximal to the geniculate ganglion. Disturbances resulting from lesions at these locations are described in the text.

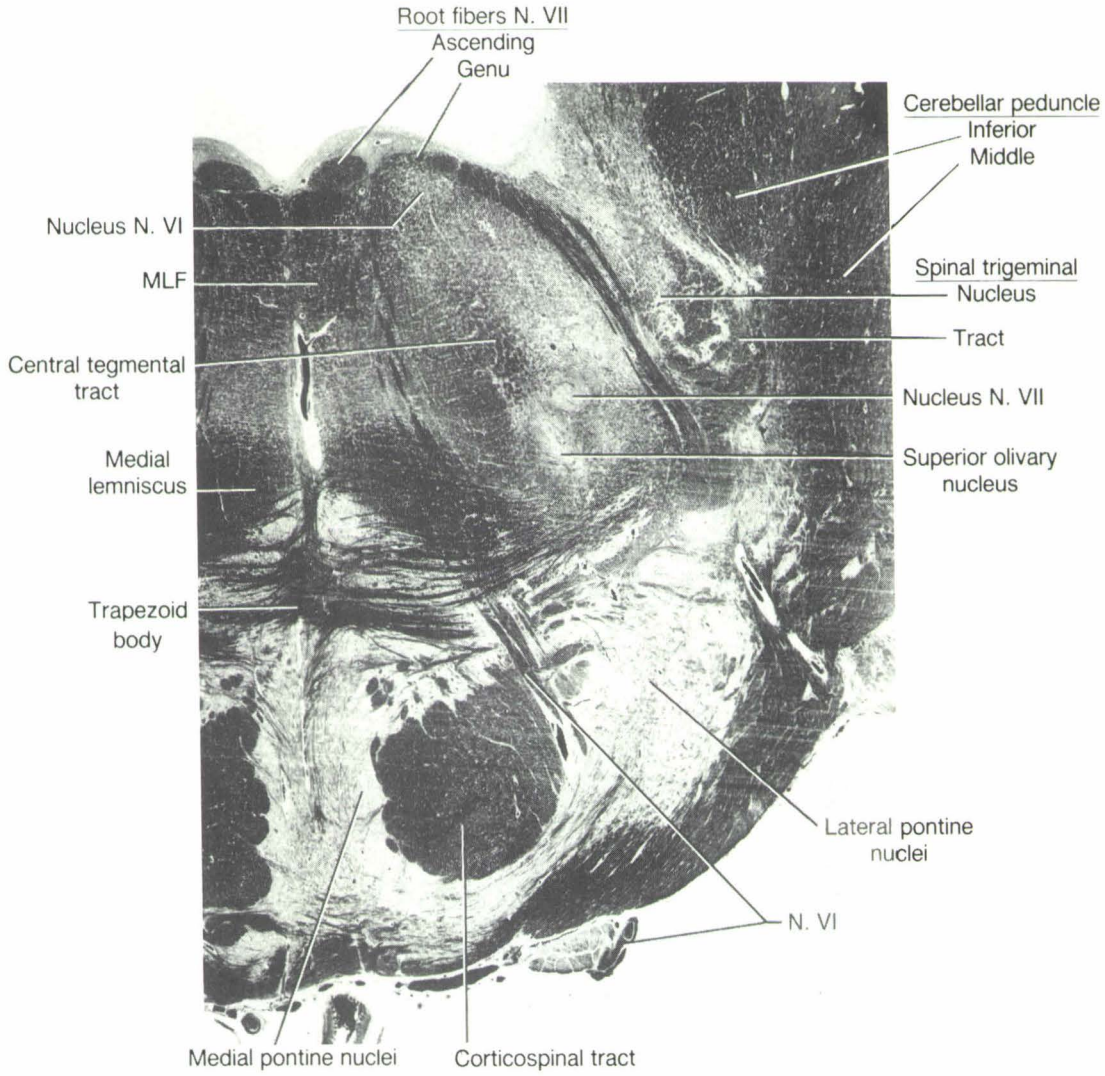


Figure 13.24. Transverse section of the adult pons through the abducens nucleus showing the root fibers of the abducens and facial nerves (Weigert's myelin stain).

close correspondence, except that in humans the lateral cell group (buccolabial muscles) is especially prominent while the medial cell group is very small. A few muscle spindles have been described in facial muscles (29, 275). The presence of muscle spindles suggests the existence of gamma (γ) efferent fibers, and leads to the assumption that gamma (γ) neurons are mixed with α neurons in the facial nucleus.

Efferent fibers from the facial motor nucleus (SVE fibers) emerge from its dorsal surface and project dorsomedially into the floor of the fourth ventricle. These fibers ascend longitudinally medial to the abducens nucleus and dorsal to the MLF (Fig. 13.24), but near the rostral pole of the abducens nucleus, they make a sharp lateral bend around the rostral border of the abducens nucleus and pass ventrolaterally. In their emerging course, these fibers pass medial to the spinal trigeminal complex, lateral to the superior olivary nucleus, and exit from the brainstem near the caudal border of the pons, at the cerebellopontine angle (Figs. 12.33, 13.1, 13.4, 13.6, and 13.7). Root fibers looping around the abducens nucleus form the *internal genu* of the facial nerve (Fig. 13.27).

The facial motor nucleus receives afferent fibers from a number of sources. Among these are (a) secondary trigeminal fibers from the spinal trigeminal nucleus (61, 217) in-

volved in corneal and other trigeminofacial reflexes, (b) direct corticobulbar fibers (Fig. 12.27), which project bilaterally, but with important regional differences (131, 152), (c) indirect corticobulbar fibers, which convey impulses to the facial nucleus via relays in the reticular formation (152, 153, 277), and (d) crossed rubrobulbar fibers (83), which project only to cell groups (i.e., dorsomedial and intermediate) innervating the upper facial muscles. Additionally, descending fibers from the mesencephalic reticular formation project ipsilaterally to portions of the facial nucleus (83). Secondary or tertiary auditory fibers, considered to reach the facial nucleus, are thought to mediate certain acousticofacial reflexes. These reflexes include closing of the eyes in response to a sudden loud noise, and contraction of the stapedius muscle to dampen the movements of the ear ossicles. Studies of the neuronal organization of acoustic middle ear reflexes indicate that pathways involved in the stapedius reflex comprise three or four neurons: (a) primary auditory neurons, (b) processes of cells of the ventral cochlear nucleus which form the trapezoid body, and (c) neurons in the ipsilateral and contralateral medial superior olivary nucleus, which project to facial motor neurons that innervate the stapedius muscle (27).

The *intermediate nerve* (of Wrisberg), which emerges at the cerebellopontine angle between the facial motor root and the vestibular nerve (Fig. 13.2), contains afferent and general visceral efferent fibers. Afferent fibers (SVA and GSA) arise from cells of the geniculate ganglion, located at the external genu of the facial nerve (Fig. 13.23). *Special visceral afferent* (SVA) *fibers* convey gustatory sense (taste) from the anterior two-thirds of the tongue via the chorda tympani nerve. Centrally, these fibers enter the solitary fasciculus and terminate upon cells in the rostral part of the solitary nucleus, sometimes referred to as the gustatory nucleus. *General somatic afferent* (GSA) *fibers* convey cutaneous sensory impulses from the external auditory meatus and the region back of the ear; centrally these fibers enter the dorsal part of the spinal trigeminal tract (20).

General visceral efferent (GVE) fibers in the intermediate nerve arise from the *superior salivatory nucleus*, which consists of scattered cholinergic cells in the dorsolateral reticular formation (Figs. 12.15, 12.16, and 13.23). These preganglionic parasympathetic neurons are part of an uninterrupted dorsal cell column that extends from the medulla to the pons (76). Cells of the dorsal motor nucleus of the vagus form the caudal portion of this column. Cells in more rostral regions are less compact and are distributed over a wide region of the reticular formation. In the pons, cells of this column lie between the nucleus of the solitary tract and the facial motor nucleus. The overlapping origins of neurons contributing to the glossopharyngeal and intermediate nerves raise a question concerning the appropriateness of a nomenclature that distinguishes separate salivatory nuclei as inferior and superior.

Preganglionic parasympathetic fibers from the superior salivatory nucleus pass peripherally as a component of the intermediate nerve, but near the external genu of the facial nerve they divide into two groups: (a) one group that passes to the pterygopalatine ganglion via the major superficial petrosal nerve, and (b) another group that projects via the chorda tympani and branches of the lingual nerves to the submandibular ganglia (Fig. 13.23). Synapses with postganglionic neurons occur in the pterygopalatine and submandibular ganglia. Postganglionic fibers from the pterygopalatine ganglion give rise to secretory and vasomotor fibers that innervate the lacrimal gland and the mucous membranes of the nose and mouth. Postganglionic parasympathetic fibers from the submandibular ganglion pass to the submandibular and sublingual salivary glands.

LESIONS OF THE FACIAL NERVE

Lesions of the facial nerve *(Bell's palsy)* produce paralysis of the ipsilateral facial muscles and other sensory and autonomic disturbances that depend upon the location and extent of the peripheral lesion. A complete lesion of the motor part of the facial nerve as it emerges from the stylomastoid foramen (*A* in Fig. 13.23) results in a complete paralysis of ipsilateral facial muscles. On the side of the lesion, the patient is unable to wrinkle the forehead, close the eye, show the teeth, purse the lips. The palpebral fissure is widened, the nasolabial fold is flattened, and the corner of the mouth droops. The corneal reflex is abolished on the side of the lesion, but corneal sensation remains. A lesion distal to the geniculate ganglion (*B* in Fig. 13.23) produces the deficits associated with a lesion at *A* but, in addition, produces impairment of

sublingual and submandibular salivary secretions, hyperacusis, and, frequently, loss of taste in the anterior two-thirds of the tongue ipsilaterally. Salivary secretions are impaired due to interruption of preganglionic parasympathetic fibers, and loss of taste is due to interruption of SVA fibers. *Hyperacusis* results from paralysis of the stapedius muscle, which serves to dampen the oscillations of the ear ossicles and causes sounds to be abnormally loud on the affected side. Lesions of the facial nerve proximal to the geniculate ganglion (*C* in Fig. 13.23) produce all of the disturbances described for lesions at *A* and *B* and, in addition, invariably result in complete loss of taste over the anterior two-thirds of the tongue and impairment of ipsilateral lacrimation. This lesion interrupts all SVA fibers as they course centrally and all preganglionic parasympathetic (GVE) fibers *en route* to both the pterygopalatine and submandibular ganglia. Following a complete lesion proximal to the geniculate ganglion, taste is permanently lost and no regeneration of sensory fibers takes place. Preganglionic parasympathetic fibers may regenerate, but this frequently occurs in an aberrant manner. Fibers that previously projected to the submandibular ganglion may regrow and enter the major superficial petrosal nerve. As a consequence of this aberrant regeneration, a salivary stimulus may produce lacrimation (syndrome of "crocodile tears"). The true etiology of Bell's palsy is poorly understood. It is assumed that most facial palsies of this type are due to compression of the nerve secondary to an unexplained swelling in the bony facial canal.

Central types facial palsies involve corticobulbar and corticoreticular fibers that directly and indirectly convey impulses to cells of the facial nucleus. Two types of central facial paralysis, voluntary and mimetic, are recognized. Voluntary central-type paralysis occurs contralateral to a lesion involving corticobulbar fibers and affects only the muscles of the lower half of the face, particularly those in the perioral region. Muscles of the upper facial region concerned with wrinkling the forehead, frowning, and closing the eyes are not affected. The accepted explanation of this upper motor neuron facial paralysis is that corticobulbar fibers projecting to cell groups of the facial nucleus innervating muscles of the upper face and forehead are distributed bilaterally, while those projecting to cell groups that innervate the lower part of the face are only crossed (131, 153). Thus, a unilateral lesion interrupting corticobulbar pathways results in paralysis of only the lower facial muscles contralaterally. A lesion involving corticobulbar and corticospinal fibers in the internal capsule produces a contralateral voluntary central type facial paralysis and a contralateral hemiplegia. Such a lesion never impairs taste, salivary or lacrimal secretions, or the corneal reflex.

Mimetic or emotional innervation of the muscles of facial expression may be preserved even in the presence of a voluntary central type facial palsy. In response to a genuine emotional stimulus, the muscles of the lower face will contract symmetrically. Mimetic or emotional innervation of facial muscles is involuntary and is mediated by pathways that are independent of those arising from the cerebral cortex. While it is recognized that these pathways are separate from those mediating voluntary facial expression, their origin and course are unknown. Thus, certain neural lesions can produce a mimetic facial paralysis without impairing voluntary facial contractions. More extensive lesions can produce combined voluntary and mimetic facial palsies.

ABDUCENS NERVE

The abducens nerve (N. VI) arises from a collection of typical motor cells that forms a column, about 3 mm in length, in the lateral part of the medial eminence of the fourth ventricle (Figs. 13.1, 13.7, and 13.27). Together with the internal genu of the facial nerve, it forms the rounded prominence in the ventricular floor known as the *colliculus facialis* (Figs. 13.1 and 13.24). This motor nerve (GSE) innervates the lateral rectus muscle, which serves to abduct the eye. Root fibers of the abducens nerve emerge from the medial aspect of the nucleus and pass ventrally through the pontine tegmentum lateral to the corticospinal tract (Figs. 13.1, 13.7, and 13.24). They emerge from the brainstem at the caudal border of the pons (Figs. 12.1, 12.15, and A.7). This slender nerve has a long intracranial course and traverses the cavernous sinus and the superior orbital fissure *en route* to the lateral rectus muscle. In the cavernous sinus, the abducens nerve lies close to the internal carotid artery.

The abducens nerve is unique among motor cranial nerves in that it contains two populations of neurons: (a) typical motor neurons that project fibers via the nerve root

to innervate the lateral rectus muscle, and (b) internuclear neurons whose axons (retained within the brainstem) cross the midline, ascend in the contralateral MLF, and terminate upon cells of the oculomotor nuclear complex that innervate the medial rectus muscle of the opposite side (14, 54, 55, 109, 120, 126, 243, 250, 251) (Fig. 13.25). Abducens internuclear neurons, constituting 25–30% of the nucleus (250), are distributed throughout the nucleus, and are virtually impossible to distinguish from motor neurons in common stain (243). Abducens motor neurons are immunocytochemically reactive to choline acetyltransferase (ChAT) (Fig. 13.21).

The abducens nucleus receives afferent inputs from the medial vestibular nucleus, the reticular formation, and the nucleus prepositus (111, 119, 171). Afferent fibers from the medial vestibular nucleus are predominantly ipsilateral and both populations of abducens neurons receive the same profile of disynaptic excitation and inhibition from the labyrinth (14). Abducens nucleus afferents from the *paramedian pontine reticular formation* (PPRF) and the nucleus prepositus hypoglossi are uncrossed. Corticobulbar fibers convey impulses bilaterally to the abducens nucleus via intercalated neurons in the reticular formation (Fig. 12.27).

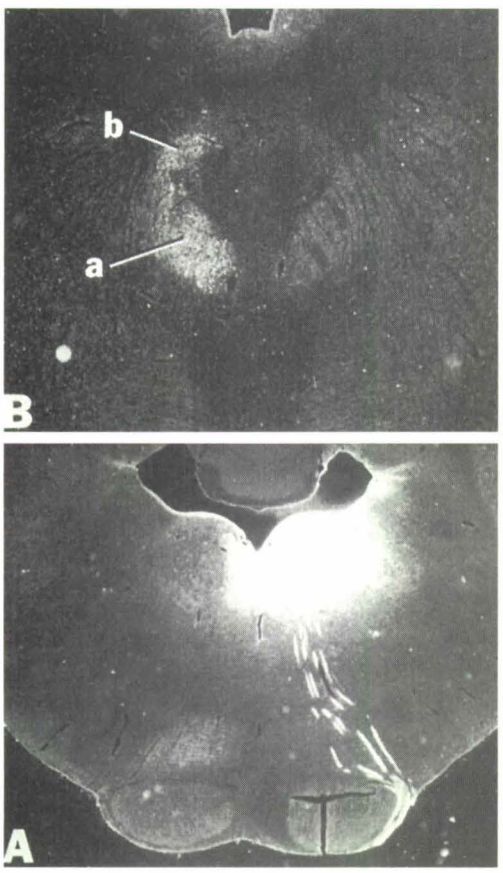


Figure 13.25. Dark-field photomicrographs of (^{3}H)-labeled amino acids injected into the right abducens nucleus in a rhesus monkey showing transport via abducens root fibers and the contralateral medial longitudinal fasciculus (**A**). Isotope transported from abducens internuclear neurons via the medial longitudinal fasciculus terminate in the medial rectus subdivision of the opposite oculomotor complex (**B**). The medial rectus subdivision in the caudal oculomotor complex are represented by cell groups designated *a* and *b*.

Lesions of the Abducens Nerve

Lesions of the abducens nerve in the brainstem, or in its long intracranial course, cause ipsilateral paralysis of the lateral rectus muscle (Fig. 13.22). Because contraction of the medial rectus muscle on the affected side is unopposed, the eye is strongly adducted. The contralateral eye is unaffected and can move in all directions. The patient has *diplopia* (double vision) on attempting to gaze to the side of the lesion. This impairment, called horizontal diplopia, results because light reflected by an object in the visual field does not fall upon corresponding points of the two retinae. The abducens nerve is the most frequently injured cranial nerve. An isolated lesion of the sixth nerve has no neurologic localizing value because of its long intracranial course. If the lesion produces ipsilateral horizontal diplopia and a contralateral hemiparesis, the lesion can be localized in the medial pons where it involves root fibers of the abducens nerve and part of the corticospinal tract. This resulting syndrome is known as *middle alternating hemiplegia* (Fig. 12.27). Ipsilateral horizontal diplopia combined with a facial paralysis on the same side indicates a lesion in the caudal pontine tegmentum involving root fibers of the abducens and facial nerves.

Lesions of the Abducens Nucleus

Discrete unilateral lesions of the abducens nucleus produce a paralysis of lateral gaze toward the side of the lesion. The syndrome of *lateral gaze paralysis* differs from paralysis of the lateral rectus muscle in that neither eye can be directed laterally toward the side of the lesion and that both eyes tend to be forcefully and conjugately deviated to the opposite side (Fig. 13.22). Ocular convergence usu-

ally is unaffected. Thus, the abducens nerve appears unique in that it is the only motor cranial nerve in which lesions of the root fibers and nucleus do not produce the same effect.

Lateral gaze paralysis, due to discrete lesions in the abducens nucleus, is caused by (a) destruction of motor neurons in the abducens nucleus, which results in paralysis of the ipsilateral lateral rectus muscle, and (b) destruction of internuclear neurons within the abducens nucleus, that give rise to ascending fibers that project via the opposite MLF to the medial rectus subdivision of the contralateral oculomotor complex (54, 55, 63) (Fig. 13.18). The paresis of ocular adduction in the contralateral eye (internuclear ophthalmoplegia), which forms part of the lateral gaze paralysis, appears to be due to destruction of abducens internuclear neurons that are intermingled with cells whose axons form the abducens nerve root (66) (Fig. 13.22). Another, and more common, cause of anterior internuclear ophthalmoplegia (as seen in multiple sclerosis), is a lesion of the contralateral ascending fibers in the medial longitudinal fasciculus originating from the PPRF and going to the cells of the oculomotor nuclear complex controlling movement of the contralateral medial rectus muscle. Experimental studies have shown that lesions limited to individual vestibular nuclei do not produce paresis of ocular adduction (170).

Horizontal and Vertical Eye Movements

All ocular movements, whether horizontal, vertical, or rotatory, require reciprocal activity in the extraocular muscles producing these movements. Conjugate lateral gaze requires simultaneous appropriate contractions of the lateral rectus muscle on one side and the medial rectus muscle of the opposite side. The central neural mechanisms underlying conjugate eye movements are just beginning to be understood (117). The observation that paralysis of vertical or horizontal eye movements can occur independently implies that there are separate anatomic sites at some distance from each other that generate vertical and horizontal eye movements. Many conjugate eye movements, however, have both vertical and horizontal components so precisely synchronized that centers controlling vertical and horizontal eye movements must be functionally connected and coordinated. Considerable evidence suggests that the pontine "center for lateral gaze" and the abducens nucleus probably constitute a single entity (53–55, 63, 117, 120, 243, 250).

The localized region most concerned with vertical eye movements lies in the tegmental area rostral to the oculomotor complex in the zone of transition between diencephalon and mesencephalon (45). This zone, which contains large cells lying among fibers of the MLF and is distinct from the interstitial nucleus of Cajal, are referred to as the *rostral interstitial nucleus of the MLF* (RiMLF). Centers for horizontal gaze (i.e., the abducens nucleus) and vertical (i.e., RiMLF) gaze are interrelated by a collection of physiologically defined neurons in the paramedian reticular formation rostral to the abducens nucleus, called the paramedian pontine reticular formation (PPRF). Stimulation of the caudal regions of the PPRF produces conjugate horizontal deviation of the eyes, while stimulation in rostral regions produces vertical eye movements. Caudal parts of the PPRF project fibers to the ipsilateral abducens nucleus—rostral regions of the PPRF project uncrossed fibers to the RiMLF, which ascend outside of the MLF (45). The RiMLF in turn project to the ipsilateral oculomotor nuclear complex. Lesions in the PPRF may cause paralysis of horizontal eye movements (caudal part), paralysis of vertical eye movements (rostral part), or both if extensive (21, 56).

TRIGEMINAL NERVE

The trigeminal nerve (N. V) is the largest of all cranial nerves and contains both sensory and motor components (Figs. 12.1 and 13.26). *General somatic afferent* (GSA) components convey both exteroceptive and proprioceptive impulses. Exteroceptive impulses of touch, pain, and thermal sense are transmitted from (a) the skin of the face and forehead (Fig. 8.13), (b) the mucous membranes of the nose and mouth, (c) the teeth, and (d) large portions of the cranial dura. Deep pressure and kinesthesis are conveyed from the teeth, periodontium, hard palate, and temporomandibular joint. Additionally, impulses are transmitted centrally from stretch receptors in the muscles of mastication. *Special visceral efferent fibers* (SVE, branchiomotor) innervate the muscles of mastication, the tensor tympani, the tensor veli palatini, the mylohyoid, and the anterior digastric muscles. Afferent fibers constitute the sensory root, while efferent fibers form the smaller motor root.

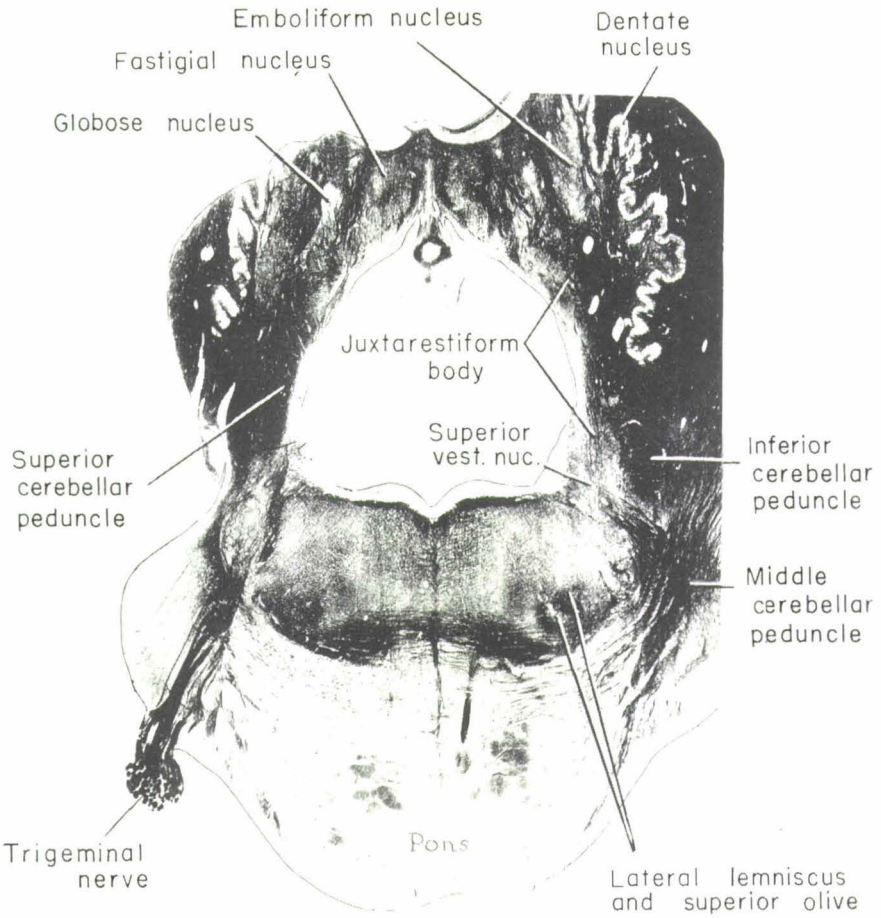


Figure 13.26. Transverse section through the pons, pontine tegmentum, and part of cerebellum at the level of the root of the trigeminal nerve in a 1-month infant (Weigert's myelin stain).

Trigeminal Ganglion

Afferent fibers, except those associated with pressure and stretch receptors, have their cell bodies in the large, flattened, crescent-shaped *trigeminal ganglion* (Figs. 1.8, 2.26, and 13.29). This semilunar-shaped ganglion, located in a dural cleft on the cerebral surface of the petrous bone in the middle cranial fossa, is composed of typical unipolar ganglion cells (268) (Fig. 13.31). Peripheral processes of these cells form the three main divisions of the trigeminal nerve: ophthalmic, maxillary, and mandibular (Fig. 13.30). The first two are wholly sensory, whereas the mandibular branch incorporates the entire motor root supplying the muscles of mastication. The ophthalmic branch innervates the forehead, upper eyelid, cornea, conjunctiva, dorsum of the nose, and mucous membranes of the nasal vestibule and the frontal sinus. The maxillary branch supplies the upper lip, lateral and posterior portions of the nose, upper cheek, anterior portion of the temple, and mucous membranes of the nose. It also innervates the upper jaw, upper teeth, and roof of the mouth to the palatopharyngeal arch. Sensory fibers of the mandibular branch are distributed to the lower lip, chin, posterior portions of the cheek, temple, external ear, lower jaw, lower teeth, cheeks, floor of the mouth, and anterior two-thirds of the tongue. All three divisions of the trigeminal nerve contribute sensory fibers to the dura. The dura of the posterior fossa is also innervated by fibers from the tenth cranial and the upper three spinal nerves (145, 205).

Central processes of trigeminal ganglion cells form the large sensory root of this nerve, which traverses the lateral part of the rostral pons, to enter the tegmentum where many fibers divide into short ascending and long

descending branches (Figs. 12.16 and 13.31). Other fibers descend or ascend without bifurcation (296). The short ascending fibers and their collaterals terminate in the principal sensory nucleus lying dorsolateral to the entering fibers. The long descending branches form the spinal trigeminal tract, whose longest fibers reach the uppermost cervical segments of the spinal cord; terminals and collaterals to the spinal trigeminal nucleus are given off *en route* (Fig. 13.31).

Spinal Trigeminal Tract and Nucleus

Root fibers entering the spinal trigeminal tract have a definite topographic organization (93, 142, 143, 298). Fibers of the ophthalmic division are most ventral, fibers of the mandibular division are most dorsal, and those of the maxillary division are intermediate (Fig. 13.29). This inverted laminar arrangement of fibers results from medial rotation of the trigeminal sensory root as it enters the brainstem and persists throughout the length of the tract. The tract extends from the level of the trigeminal root entry in the pons to the uppermost cervical spinal segments (Figs. 13.29 and 13.30). Fibers of the spinal trigeminal tract terminate upon cells of the spinal trigeminal nucleus, which forms a long cell column medial to the tract. Rostrally, the nucleus merges with the principal sensory nucleus, while caudally it blends into the substantia gelatinosa of the first two cervical spinal segments. Fibers of the spinal trigeminal tract project into that part of the spinal trigeminal nucleus immediately adjacent to it (87). There is a sharp segregation of terminal fibers within parts of the nucleus and virtually no overlap of fibers from the different divisions of the nerve (87, 93, 142, 149). The spinal trigeminal tract also contains small groups of GSA fibers from the facial, glossopharyngeal, and vagus nerves, which occupy dorsomedial regions (141, 222, 266).

Cytoarchitecturally the spinal trigeminal nucleus has been subdivided into three parts (190): (a) a *pars oralis* extending caudally to the rostral third of the inferior olivary nucleus, (b) a *pars interpolaris* extending from the pars oralis to the decussation of the pyramids, and (c) a *pars caudalis* extending caudally as far as the second cervical spinal segment. The laminar configurations within caudal parts of the spinal trigeminal nucleus consist of four layers and resemble those of the posterior gray horn at spinal levels. Cells in lamina I respond to nociceptive and thermal stimuli; lamina II correspond to the substantia gelatinosa; and laminae III and IV (magnocellular layers) correspond to the proper sensory nucleus. Fibers containing substance P terminate in lamina I and outer part of lamina II in the pars caudalis; cells positive for enkephalin are found in deeper parts of lamina II. Throughout the nucleus the face is represented in an upside down fashion, with the jaw dorsal and the forehead ventral (284). The pars oralis receives impulses predominantly from the internal structures of the nose and mouth. The pars interpolaris is related mainly to cutaneous facial regions, while the pars caudalis has large receptive fields over the forehead, cheek, and jaw. The peculiar "onionskin pattern" of termination of afferents to the spinal trigeminal nucleus and its relative clinical importance were alluded to in Chapter 12.

In addition to fibers of the trigeminal nerve and general somatic afferent fibers from other branchiomeric cranial nerves, the spinal trigeminal nucleus receives corticobulbar fibers (38, 93, 152, 156, 303). These fibers arise mainly from the frontal and parietal cortices and are predominantly crossed. Physiologic studies (88) indicate that corticobulbar fibers projecting to the pars oralis and pars caudalis mediate both inhibitory and excitatory effects. Observations suggest that inhibitory effects are presynaptic in nature.

Lesions of the spinal trigeminal tract result in loss or diminution of pain and thermal sense in areas innervated by the trigeminal nerve (95). Such lesions do not abolish tactile sense, because some neurons at all levels of the nucleus respond to tactile stimuli (149). Tactile sense may be mediated by fibers that bifurcate and send branches to both the spinal trigeminal nucleus and the principal trigeminal nucleus. Clinically, there is no doubt that pain and thermal sense are handled entirely by the spinal trigeminal tract and nucleus, principally the pars caudalis, while touch and two-point discrimination are in large part related to the principal sensory nucleus (Figs. 13.30 and 13.31). However, physiologic studies (150, 284) indicate that it is extremely difficult to isolate and identify neurons in the spinal trigeminal nucleus uniquely concerned with pain.

The composition, location, and relationships of the spinal trigeminal tract and nucleus are of considerable diagnostic and surgical importance. It should be noted that

virtually no overlap exists between the cutaneous areas supplied by the three peripheral divisions of the trigeminal nerve, in contrast to the extensive overlap characteristic of spinal dermatomes (Fig. 8.13). Trigeminal tractotomy (i.e., sectioning of the spinal trigeminal tract) can relieve various forms of facial pain including trigeminal neuralgia (*tic douloureux*) (237). This procedure eliminates or greatly reduces pain and thermal sense without impairing tactile sense. Corneal sensation remains, as does the corneal reflex, though it may not be as brisk (282, 290).

Principal, Mesencephalic and Motor Nuclei

PRINCIPAL SENSORY NUCLEUS

This nucleus lies lateral to the entering trigeminal root fibers in the upper pons (Figs. 13.27 and 13.31). Root fibers conveying impulses for tactile and pressure sense enter the principal sensory nucleus and are distributed in a manner similar to that described for the spinal trigeminal nucleus. Fibers of the ophthalmic division terminate ventrally, fibers of the maxillary division are intermediate, and fibers of the mandibular division are most dorsal (142, 143). Caudally this nucleus merges with the pars oralis of the spinal trigeminal nucleus and the level of transition is indistinct (Fig. 13.31). The principal sensory nucleus is populated by small to medium-sized, oval cells with relative large nuclei (Fig. 13.28). These cells have large receptive fields, show high spontaneous activity, and respond to a wide range of pressure stimuli with little adaptation (284).

MESENCEPHALIC NUCLEUS

This trigeminal nucleus forms a slender cell column near the lateral margin of the central gray matter of the upper fourth ventricle and cerebral aqueduct (Figs. 13.28–13.31). This nucleus, composed of large unipolar neurons, extends from the level of the trigeminal motor nucleus to the rostral midbrain. Most of its cells resemble those of the dorsal root ganglion but are encapsulated, often have more than one process, and lie within

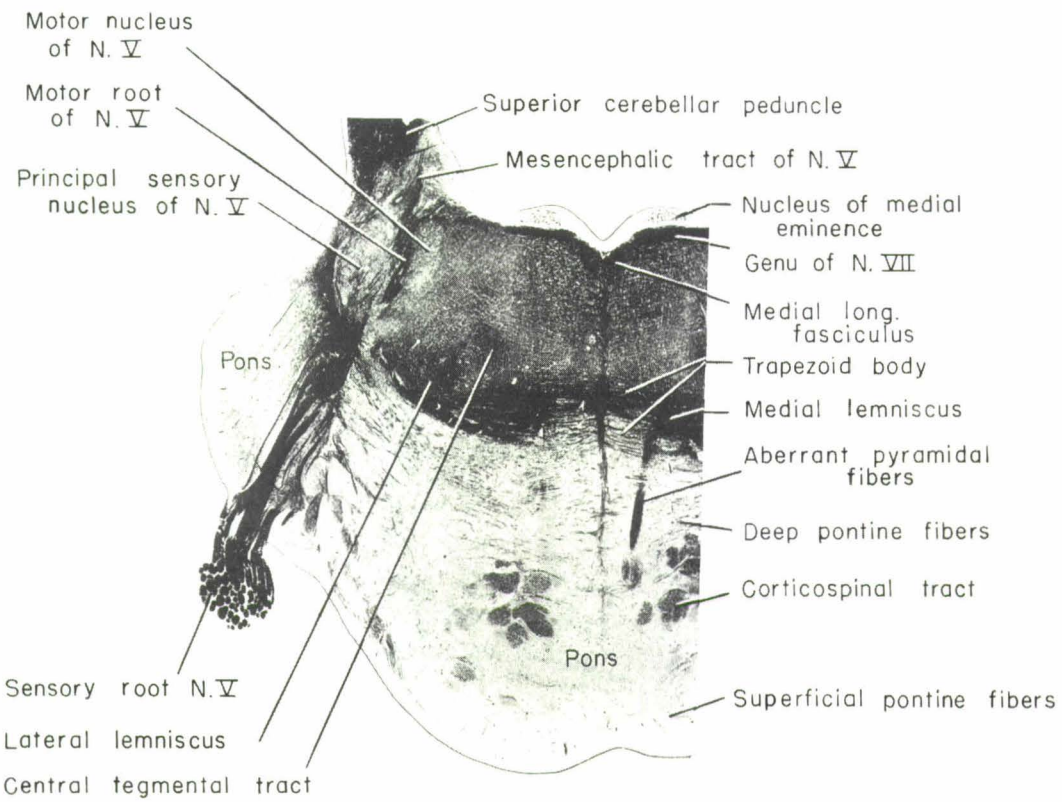


Figure 13.27. Transverse section through the pons and pontine tegmentum at the level of the entrance of the trigeminal nerve in a 1-month infant (Weigert's myelin stain).

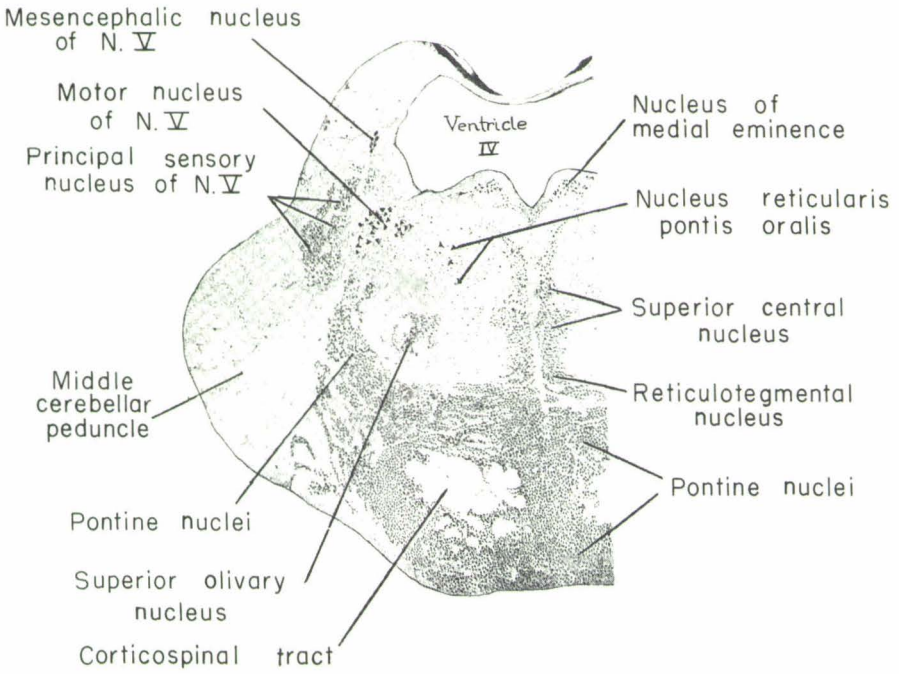


Figure 13.28. Transverse section through the pons and pontine tegmentum at about the same level as in Figure 13.27 in a 1-month infant (Cresyl violet stain, with cell groups blocked in).

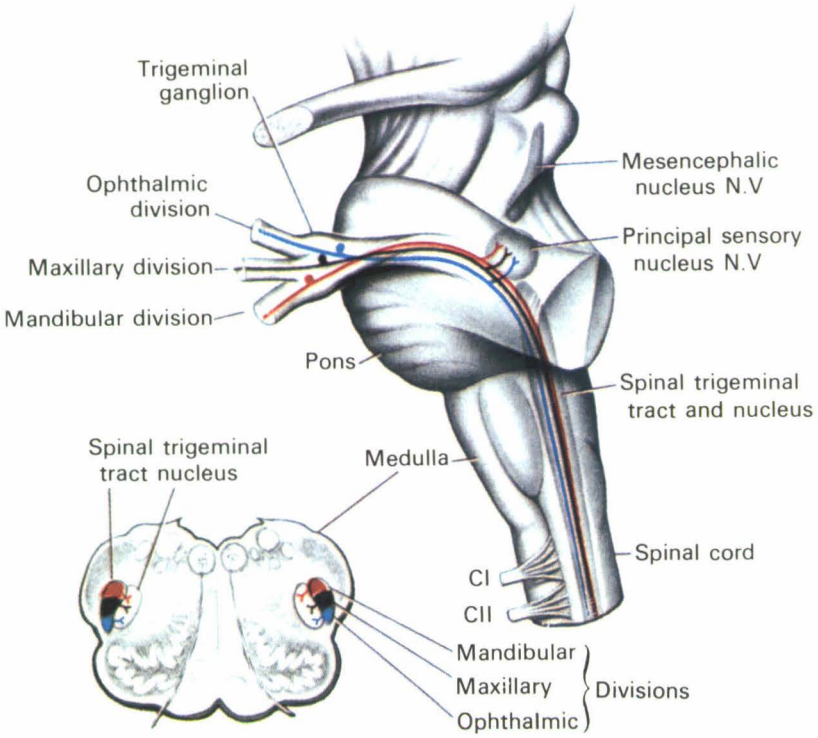


Figure 13.29. Topographic arrangement of the fibers in the spinal trigeminal tract. The laminar arrangement of fibers from the different divisions of the trigeminal nerve persists throughout its length, although fibers leave the tract at all levels to terminate upon cells of the spinal trigeminal nucleus.

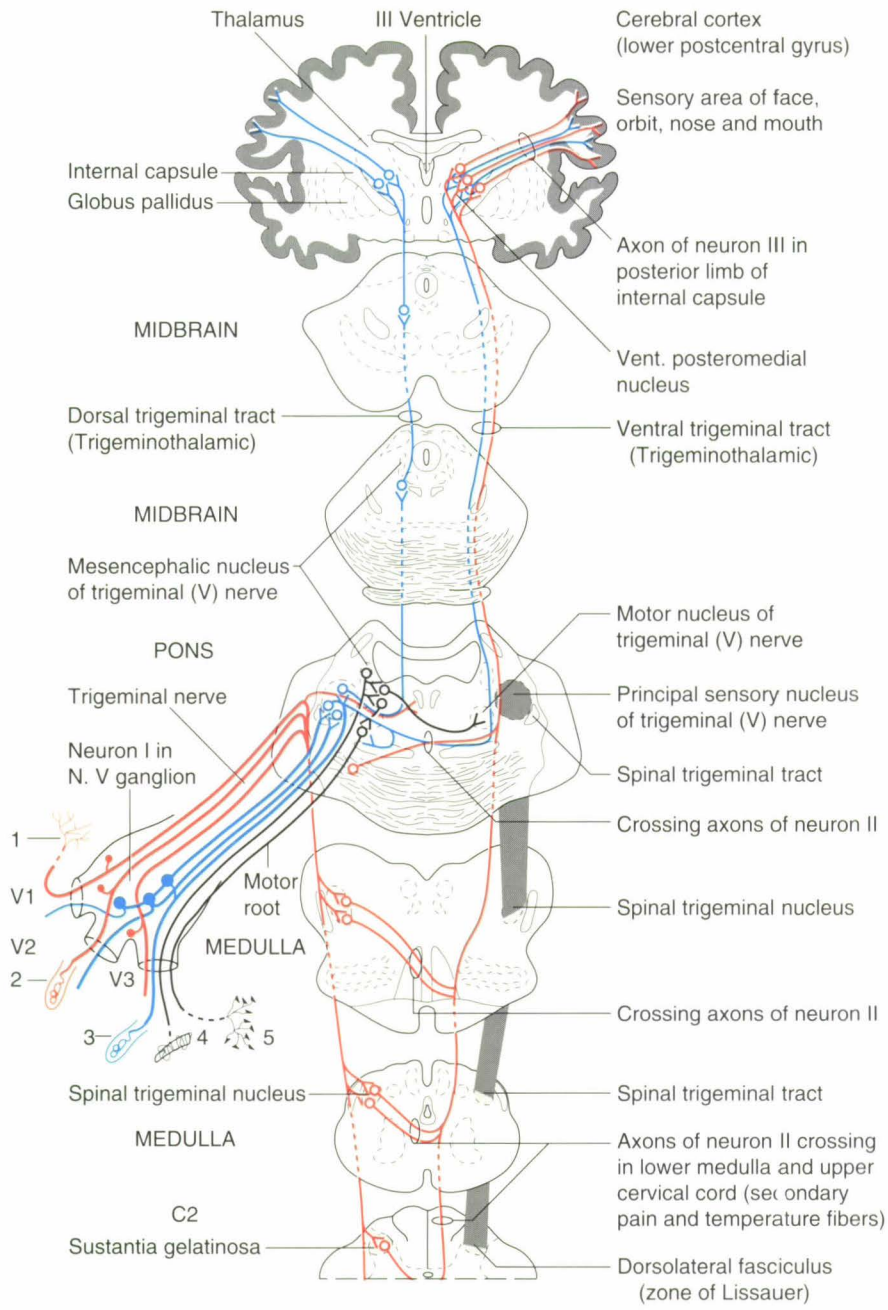


Figure 13.30. Secondary trigeminal tracts. The ventral trigeminal tract (*red*) conveys pain, thermal, and tactile sense. These fibers originate from the spinal trigeminal nucleus, cross at various locations in the lower brainstem, and ascend in association with the contralateral medial lemniscus. Secondary trigeminothalamic fibers from the principal sensory nucleus, conveying touch and pressure (*blue*) ascend by two separate pathways. Fibers from the ventral part of the principal sensory nucleus of the trigeminal nerve (N. V) cross and ascend in association with the contralateral medial lemniscus. Fibers from the dorsomedial part of the same nucleus ascend uncrossed as the dorsal trigeminal tract. Both the ventral and dorsal trigeminal tracts project to the ventral posteromedial nucleus of the thalamus. The brainstem location of the ascending lateral spinothalamic tract is indicated in *gray* on the right side. The ophthalmic (V1), maxillary (V2), and mandibular (V3) divisions of the trigeminal nerve are identified. *1*, Free nerve ending; *2*, thermal receptor; *3*, Meissner's corpuscle; *4*, neuromuscular spindle; *5*, motor end plate in muscle of mastication.

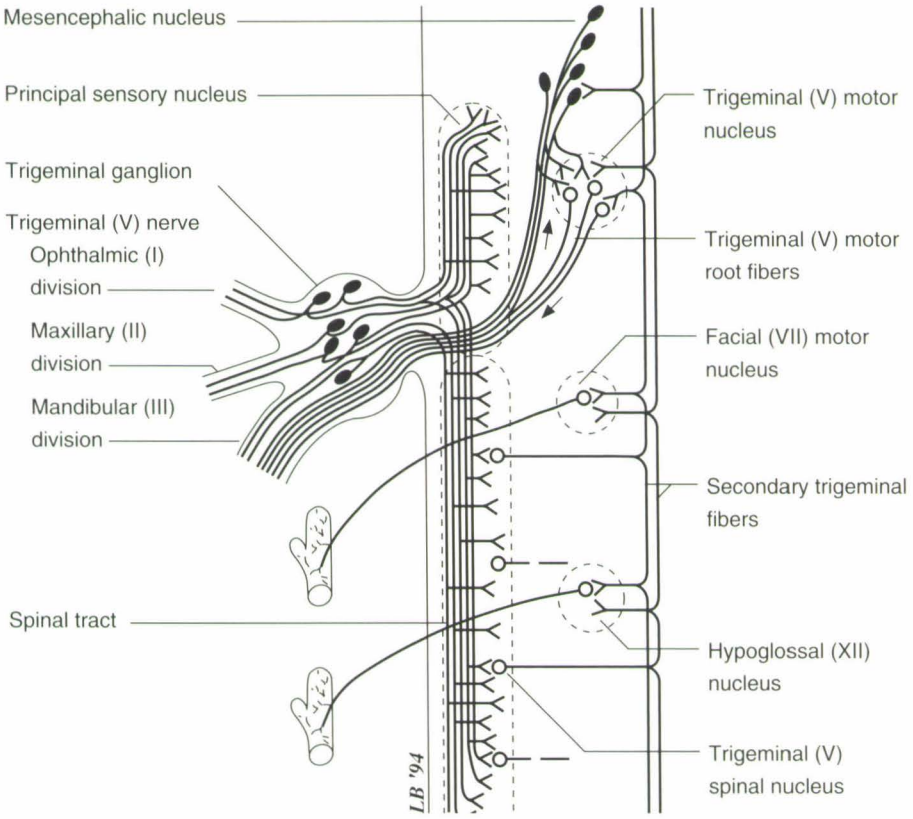


Figure 13.31. Trigeminal nuclei and some of the trigeminal reflex arcs.

the central nervous system (201, 202). The principal processes of these cells form a slender sickle-shaped bundle, the *mesencephalic tract of the trigeminal nerve* (Figs. 13.27, 13.32, and A.8), which descends to the level of the trigeminal motor nucleus. Collaterals of these processes enter the trigeminal motor nucleus, while the main fibers emerge as part of the motor root. Cells of this nucleus are considered to be primary sensory neurons that have been "retained" within the central nervous system.

Afferent fibers of the mesencephalic nucleus of the trigeminal nerve convey pressure and kinesthesis sense from the teeth, periodontium, hard palate, and joint capsules (6, 7, 81, 82, 208). These fibers appear concerned with the mechanisms that control the force of the bite. The mesencephalic nucleus also receives afferent impulses from stretch receptors in the muscles of mastication. Action potentials can be recorded in the mesencephalic nucleus in response to stretching the masticatory muscles (79, 82). Scattered ganglion cells found along the motor root appear related to the mesencephalic nucleus and are considered to convey impulses from stretch receptors in the mylohyoid and diagastric muscles. Although most afferent fibers of the mesencephalic nucleus course peripherally with fibers of the motor root, experimental evidence (81) indicates that some fibers from this nucleus pass peripherally in all three divisions of the trigeminal nerve.

Connections of the mesencephalic nucleus are more extensive than previously believed (201). Some fibers leave the mesencephalic tract and enter the white matter of the cerebellum, possibly connecting with the cerebellar nuclei. Other fibers have been traced to the roof of the cerebral aqueduct, the base of the cerebellum, and to the region of the superior colliculi.

It has been suggested that deep sensibility of the lingual, facial, and extraocular muscles is mediated by fibers of the fifth nerve (78, 79), and that impulses from muscle spindles in the extraocular muscles are conveyed by

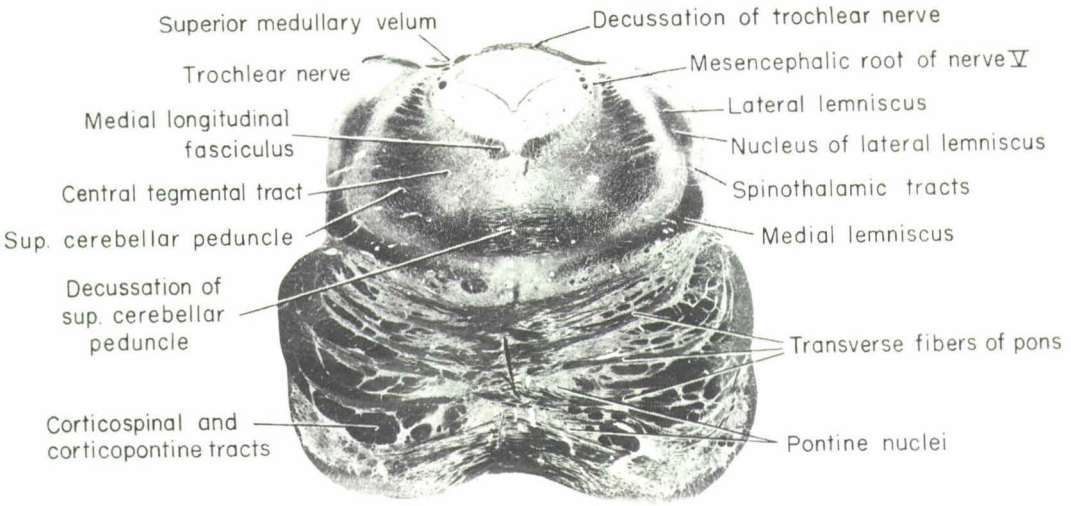


Figure 13.32. Transverse section through the upper pons (isthmus level) of an adult brain at the level of the decussation and exit of the trochlear nerve (Weigert's myelin stain).

the axons of specific cells in the trigeminal ganglion (173). Cells in a part of the ganglion that forms the ophthalmic division respond with a sustained increase in discharge rate when the extraocular muscles are stretched. These short latency responses are abolished by section of the ophthalmic division of the trigeminal nerve. Deep sensibility from the face also is considered to be mediated by the trigeminal nerve, but the possibility remains that this may be supplemented by facial nerve afferents.

MOTOR NUCLEUS

The motor nucleus of the trigeminal nerve forms an oval column of typical multipolar motor cells medial to the motor root and the principal sensory nucleus (Fig. 13.28). Fibers from this nucleus exit from the brainstem medial to the entering sensory root, pass underneath the trigeminal ganglion, and become incorporated in the mandibular division (Figs. 13.30 and 13.31). The motor nucleus receives collaterals from the mesencephalic root, which form a two-neuron arc for reflex control of the jaw muscles (jaw-jerk reflex). Secondary trigeminal fibers, both crossed and uncrossed, establish reflex connections between the muscles of mastication and cutaneous regions, as well as with lingual and oral mucous membranes. Some corticobulbar fibers terminate directly and bilaterally upon trigeminal motor neurons, while others pass to reticular neurons, which in turn project to the motor nucleus (Fig. 12.27).

Secondary Pathways and Trigeminal Reflexes

SECONDARY TRIGEMINAL PATHWAYS

These pathways originate from cells in the principal sensory and spinal trigeminal nuclei and project to higher levels of the brainstem, the cerebellum, and spinal cord. Collaterals of these fibers provide numerous projections to motor nuclei of the brainstem involved in complex reflexes (Fig. 13.31).

Trigeminothalamic projections arise largely from cells in laminae I and IV of the pars caudalis and interpolaris of the spinal trigeminal nucleus. Axons from cells in the spinal trigeminal nucleus project ventromedially into the reticular formation, cross the median raphe, and ascend in close association with the contralateral medial lemniscus (60, 183, 242, 281, 283) (Fig. 13.30). These secondary trigeminal fibers terminate in a selective manner about cells of the ventral posteromedial (VPM) nucleus of the thalamus (124). Crossed axons from cells of the spinal trigeminal nucleus that ascend in the brainstem with the contralateral medial lemniscus form the *ventral trigeminal tract* (ventral trigeminothalamic tract).

Secondary trigeminal fibers from the principal sensory nucleus are both crossed and

uncrossed. Cells in the dorsomedial part of the nucleus give rise to a small bundle of uncrossed fibers which ascends close to the central gray matter of the midbrain and enters the ipsilateral ventral posteromedial (VPM) nucleus of the thalamus (48, 267) (Fig. 13.30). These fibers form the *dorsal trigeminal tract* (197, 271, 274, 281, 297), and appear to be associated in a unique way with the mandibular division of the trigeminal nerve (142). Cells in the ventral part of the principal sensory nucleus of the trigeminal nerve give rise to a larger, entirely crossed bundle of trigeminothalamic fibers, which ascends in association with the contralateral medial lemniscus, in a manner similar to that described for the ventral trigeminal tract (197, 229, 267, 281, 285, 297). These crossed secondary trigeminal fibers also terminate in the VPM nucleus of the thalamus.

Trigeminocerebellar fibers arise from cells in lamina IV in all parts of the spinal trigeminal nucleus with the largest contribution originating from rostral parts of the nucleus (124). Additional trigeminocerebellar fibers come from cells in ventral portions of the principal sensory nucleus. These portions of the trigeminal nuclei project uncrossed fibers to the paramedian lobule, the simple lobule, and posterior part of crus II. A large number of these fibers enter the cerebellum via the inferior cerebellar peduncle.

As previously mentioned, the mesencephalic trigeminal nucleus is peculiar in that the primary sensory neurons that form this nucleus lie in a brainstem nucleus rather than in the trigeminal ganglion. While there is convincing evidence that fibers from this nucleus convey impulses from pressure, joint, and stretch receptors, the pathway by which these impulses are transmitted centrally remains obscure. It has been hypothesized that processes of cells in the mesencephalic nucleus may project to the cerebellum (201, 298). Since a significant part of the input to this nucleus comes from stretch receptors, and impulses from most stretch receptors in other parts of the body are relayed to the cerebellum, this hypothesis is plausible.

Trigeminospinal projections arise from cells in laminae I and III in all subdivisions of the spinal trigeminal nucleus. Fibers from pars caudalis and interpolaris are ipsilateral while those from pars oralis are bilateral (124). These descending projections may modulate incoming sensory information in the posterior horn, contribute to a variety of reflexes, and link receptors in the trigeminal distribution with somatic and visceral effectors in the spinal cord.

TRIGEMINAL REFLEXES

Although secondary trigeminal fibers are involved in a large number of reflexes, the corneal reflex is one of the most important. Stimulation of the cornea with a wisp of cotton produces bilateral blinking and closing of the eyes. The blinking and closing of the eyes is effected by impulses reaching the facial nuclei on both sides. This reflex is mediated by secondary trigeminal fibers projecting bilaterally to the facial nuclei. Following an injury to the ophthalmic division of the trigeminal nerve, corneal sensation and the corneal reflex are lost on that side because the afferent limb of the reflex arc has been destroyed. Corneal sensation, however, remains on the opposite side, and stimulation of that cornea will produce bilateral blinking and eye closure, indicating that the efferent limb (facial nucleus and nerve) of the reflex arc is intact. In patients with peripheral facial palsies, corneal sensation will be present on both sides, but no corneal reflex can be elicited on the side of the lesion because the efferent limb of the reflex arc has been destroyed. Stimulation of the cornea on the side of the lesion, however, will cause blinking and closure of the opposite eye (consensual response).

The numerous trigeminal secondary fibers that ascend and descend in the dorsolateral part of the reticular formation give off terminals or collaterals to various motor nuclei. These projections provide a substratum for specific reflexes initiated by stimulation of the skin of the face, the oral and nasal mucous membranes, and muscles, tendons, and bones of the jaw and face. Reflexes involving secondary trigeminal fibers that project impulses to cranial nerve nuclei include (a) the *lacrimal* or *tearing reflex*, in which corneal irritation initiates impulses via trigeminal nerve fibers that synapse upon neurons of the superior salivatory nucleus (parasympathetic) resulting in lacrimation; (b) *sneezing*, in which trigeminal impulses pass to the nucleus ambiguus, to respiratory centers in the reticular formation, and to cell groups in the spinal cord (i.e., phrenic nerve nuclei and anterior horn cells innervating the intercostal mus-

cles), which are paroxysmally activated; (c) *vomiting*, in which trigeminal impulses pass predominantly to vagal nuclei (i.e., dorsal motor, ambiguus and solitary); and (d) *salivary reflexes* in which secondary trigeminal fibers pass to the inferior salivatory nuclei. Secondary trigeminal fibers probably also pass to the hypoglossal nuclei and mediate reflex movements of the tongue in response to stimulation of the tongue and the mucous membranes of the mouth.

The *jaw-jerk*, or masseter reflex, is a monosynaptic myotatic reflex. This reflex is elicited by placing the examiner's index finger over the middle of the patient's chin (mouth slightly open) and tapping gently with a reflex hammer. The response is a bilateral contraction of the masseter and temporal muscles. This reflex involves stretch receptors in the muscles of mastication, the mesencephalic nucleus, and collaterals from this nucleus that terminate in the motor trigeminal nucleus. The jaw reflex is absent in peripheral lesions of the trigeminal nerve.

ROSTRAL PONS-ISTHMUS LEVEL

Tegmentum

Transverse sections through the upper pons at the level of the trigeminal nerve root (Figs. 13.26, 13.27, and A.8) reveal important changes when compared with sections at lower pontine levels (Figs. 13.2 and 13.4). The fourth ventricle is narrower, although its roof is still formed by the cerebellum. Within the cerebellum portions of all the cerebellar nuclei can be seen, and fibers of the inferior and middle cerebellar peduncles enter the cerebellum close to each other (Fig. 13.26). At slightly higher levels, the superior cerebellar peduncle forms the dorsolateral wall of the fourth ventricle (Fig. 13.27). The ventral portion of the pons is larger than at lower levels but still contains transverse and longitudinal fibers, as well as large masses of pontine nuclei. Corticospinal and corticopontine tracts consist of numerous fiber bundles less compactly arranged than in the caudal pons. Fibers within the raphe of the pons are probably reticulocerebellar fibers arising from cells in the pontine tegmentum.

In the dorsal part of the pons, the medial lemniscus is located ventrally and is traversed in part by the transverse fibers of the trapezoid body. Lateral to the medial lemniscus, and closely associated with fibers of the trapezoid body, is the rostral pole of the superior olivary nucleus (Fig. 13.26). Ventrolaterally, the lateral lemniscus is becoming a well-defined bundle (Fig. 13.27). The spinothalamic and anterior spinocerebellar tracts are located lateral to the medial lemniscus and the medial longitudinal fasciculus is located dorsally on each side of the median raphe. The central part of the pontine tegmentum contains the pontine reticular formation. Longitudinally cut fibers of the facial genu appear lateral to the medial longitudinal fasciculus. Fibers of the central tegmental tract form a fairly discrete bundle in the reticular formation dorsal to the lateral part of the medial lemniscus (Fig. 13.27).

The *isthmus rhombencephali* is situated rostral to the cerebellum and immediately caudal to the midbrain (Figs. 13.32, 13.33, and A.9). As in other parts of the brainstem, three regions are distinguished, namely, a roof plate, a tegmental region, and a ventral cortically dependent part. The roof consists of a thin membrane, the *superior medullary velum*. This thin membrane, containing the decussating fibers of the trochlear nerve, forms the roof of the most rostral part of the fourth ventricle.

The tegmental region, ventral to the fourth ventricle, is smaller than at caudal levels. The more abundant central gray matter resembles that seen at mesencephalic levels. The lateral border of the central gray matter contains the mesencephalic nucleus and tract of the trigeminal nerve. Ventral and medial to these structures is the relatively large collection of pigmented (melanin-containing) cells of the *locus coeruleus*. Lateral to the central gray matter are the fibers of the *superior cerebellar peduncle* that have passed into the tegmentum and are shifting ventromedially to undergo a complete decussation (Fig. 13.32). Cells of the *parabrachial nuclei* lie adjacent to the superior cerebellar peduncle. The lateral lemniscus lies near the lateral surface of the tegmentum, forming the major part of the external structure known as the *trigonum lemnisci*. Groups of cells among its fibers constitute the *nuclei of the lateral lemniscus*, which are part of several intercalated nuclei in the auditory pathway (Figs. 13.13, 13.32, and 13.33). Most fibers of the lateral lemniscus project rostrally and enter the inferior colliculus. The medial lemniscus is a flattened band of ascending fibers in the ventrolateral tegmentum. Fibers of the

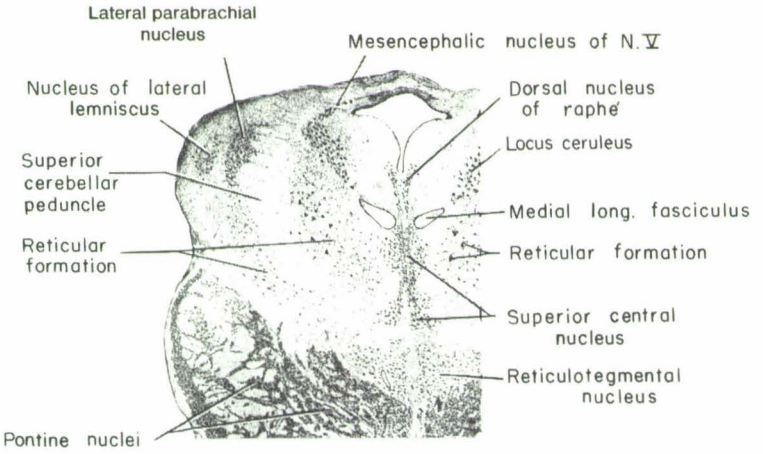


Figure 13.33. Transverse section through upper pons (isthmus level) of a 3-month infant (cresyl violet stain, with cell groups blocked in).

spinothalamic tract are located laterally near the junction of the medial and lateral lemnisci. Included in the medial lemniscus are the secondary trigeminal fibers. The dorsal trigeminal tract ascends in the dorsal part of the reticular formation, lateral to the medial longitudinal fasciculus (Fig. 13.30). Thus, at this level, the principal ascending sensory pathways form a peripheral shell of fibers that encloses most of the pontine tegmentum.

The ventral part of the pons at the isthmus level is larger than the tegmental part, but is not as impressive as at midpontine levels (Figs. 13.32, A.26, and A.27). Corticospinal and corticopontine tracts are broken up into numerous small bundles surrounded by pontine nuclei.

Superior Cerebellar Peduncle

The superior cerebellar peduncle (or brachium conjunctivum) arises from the dentate, emboliform, and globose nuclei, and forms the most important efferent fiber system of the cerebellum. Fibers of this large bundle ascend from the hilus of the cerebellar nuclei into the dorsolateral part of the rostral pontine tegmentum. It initially forms a crescent-shaped bundle dorsolateral to the fourth ventricle (Fig. 13.26), but at more rostral levels of the isthmus it lies medial to the lateral lemniscus (Fig. 13.32). The superior cerebellar peduncle decussates completely at midbrain levels (Figs. 13.32, 14.2, and 15.21). Some of its fibers end in the red nucleus; others continue directly to the ventral lateral nucleus of the thalamus (Figs. 15.21 and 16.13**A**). A relatively small number of fibers of the superior cerebellar peduncle descend lateral to the superior central nucleus and terminate in the pontine reticulotegmental nucleus and in the medullary paramedian reticular nuclei, which project back to the cerebellum (39, 64). Thus, these descending cerebellar fibers appear to be part of a cerebello-reticulo-cerebellar feedback loop (Fig. 15.21).

Fibers of the anterior spinocerebellar tract ascend in the lateral part of the reticular formation and accumulate on the lateral surface of the superior cerebellar peduncle at upper pons levels (Fig. 11.9). These fibers reverse their direction and enter the cerebellum by coursing within the superior medullary velum along the dorsolateral border of the superior cerebellar peduncle. The majority of the fibers cross to the opposite side within the cerebellum and terminate in the anterior lobe of the cerebellar vermis (Fig. 15.1).

As fibers of the superior cerebellar peduncle move ventromedially toward their decussation they divide the reticular formation into medial and lateral parts (Fig. 13.32). In the lateral part is a fairly dense collection of cells known as the *pedunculopontine tegmental nucleus* (i.e., the pedunculopontine nucleus). Cells of this nucleus are partially traversed by fibers of the superior cerebellar peduncle (Figs. 14.3 and 19.36), and some cerebellar axons give off collaterals that terminate within the pedunculopontine nucleus

itself (125). Compact and diffuse portions of this nucleus extend rostrally into the caudal midbrain (192). This nucleus receives cortical projections from the precentral gyrus (154), and descending fibers from the globus pallidus and substantia nigra (57, 67, 159, 184, 198). The efferent projections of the pedunculopontine nucleus are to the substantia nigra, the subthalamic nucleus, and the thalamus. This nucleus is known to play an important role in the functional organization of the basal ganglia and in the modulation of the thalamocortical neuronal system.

Parabrachial Nuclei

These nuclei consist of distinct groups of neurons that surround medial and lateral regions of the superior cerebellar peduncle. The *lateral parabrachial nucleus* receives input mainly from general visceral nuclei in caudal regions of the nucleus solitarius. The *medial parabrachial nucleus* receives afferents from the gustatory part of the nucleus solitarius. Afferents from the nucleus solitarius ascend uncrossed in the brainstem. The medial parabrachial nucleus projects to the thalamus, the hypothalamus, and the amygdala. The lateral parabrachial nucleus innervates nuclei in the hypothalamus and amygdala (105). The parabrachial nuclei are less densely populated in humans than in rodents, and it is not obvious that there are human homologues to the numerous subdivisions described in the rat (200). Cells in the parabrachial nuclei contain a large variety of neuromodulators. For example, cells and fibers displaying immunoreactivity to either enkephalin or substance P occur in both the medial and lateral parabrachial nuclei (211), and some of these peptidergic neurons were shown to project to the dorsal raphe nucleus (207). One group of large cells, ventral to the parabrachial nuclei, the *Kölliker-Fuse nucleus*, project to the nucleus of the solitary tract. These neurons are associated with central mechanisms involved in the control of respiration.

Locus Coeruleus

Near the periventricular gray matter of the upper part of the fourth ventricle is an irregular collection of pigmented cells referred to as the *locus coeruleus* or *nucleus pigmentosus pontis* (Figs. 13.33–13.35). The locus coeruleus in humans corresponds to group A6 disclosed in the rat by Dahlström and Fuxe (86). In humans, cells of this nucleus are partially intermingled with those of the mesencephalic nucleus of the trigeminal nerve, but the large globular neurons of the mesencephalic nucleus extend further dorsally and rostrally at the margin of the central gray matter (203)

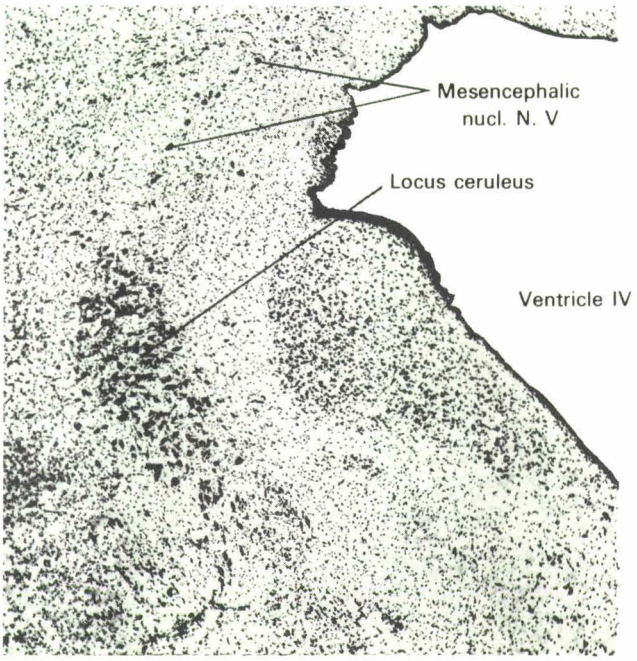


Figure 13.34. Cell groups surrounding the periventricular gray at isthmus levels. Cells of the locus coeruleus contain granules composed of melanin pigment and high concentrations of norepinephrine. Globular cells of the mesencephalic nucleus of the trigeminal nerve (N. V) are present along the dorsal border of the locus coeruleus and extend dorsally and rostrally at the margin of the central gray.

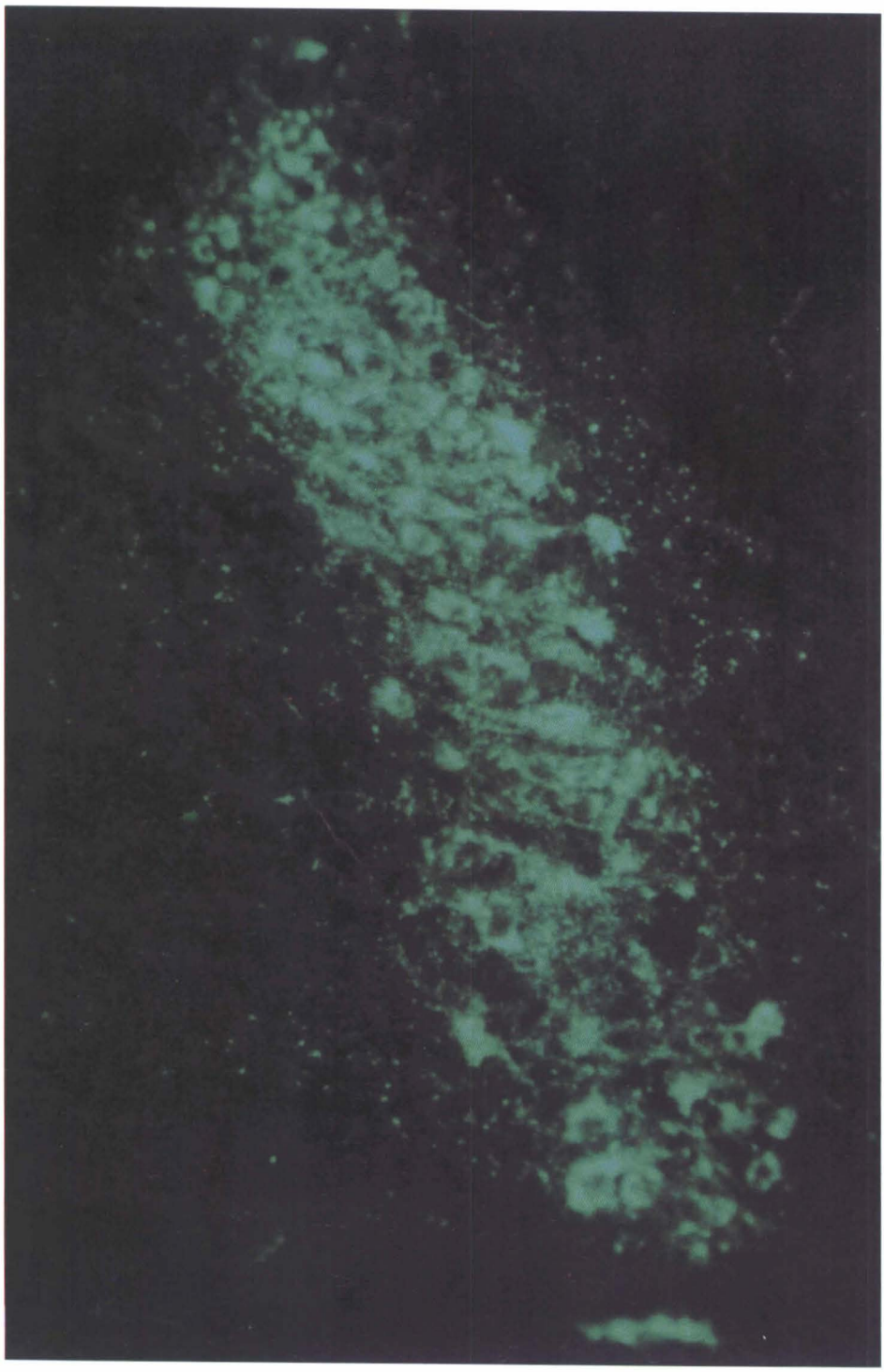


Figure 13.35. Neurons containing norepinephrine in the locus coeruleus of the rat. The norepinephrine-containing cells were reacted with glyoxylic acid which converts norepinephrine into a fluorescent chemical derivative that can be viewed under the fluorescence microscope.

(Figs. 13.29 and 13.34). Cells of the locus coeruleus are of at least two types: (a) medium-sized oval or round cells with eccentric nuclei and fairly large clumps of melanin pigment granules, and (b) small oval cells with scant cytoplasm and no pigment (192, 230). Ventrolateral to the locus coeruleus is a more diffuse collection of similar cells which forms the *nucleus subcoeruleus* (192).

Although the locus coeruleus is a relatively small structure, it can be identified readily in gross sections of the brainstem because of its characteristic pigmentation and location. The significance of this small, pigmented nucleus remained unknown until it was demonstrated by the formaldehyde-induced fluorescence method (96) that its cells contained catecholamines, nearly all of which were norepinephrine (Fig. 13.35) (9, 86, 151, 189, 270). Since then, the noradrenergic nature of the locus coeruleus neurons has been repeatedly confirmed with various techniques including immunocytochemical procedures (77, 203). Unlike other brainstem noradrenergic cells found as scattered neurons in the lateral tegmentum (groups A5 and A7 of Dahlström and Fuxe (86)), the locus coeruleus is a compact nucleus that projects fibers to portions of the telencephalon, diencephalon, midbrain, cerebellum, pons, medulla, and spinal cord. Information concerning the widespread projections of locus coeruleus and the nucleus subcoeruleus were obtained following studies undertaken in a wide range of mammalian species and with a combination of different anatomic, histochemical, immunocytochemical, biochemical, and pharmacologic methodologies (28, 97, 107, 127, 135, 137, 138, 161, 169, 172, 177, 186, 188, 189, 203, 209, 212, 270, 292).

Immunocytochemical studies revealed that noradrenergic cells of the locus coeruleus and subcoeruleus area are closely surrounded by, and partly intermingled with, neurons containing different types of neuromodulators, including acetylcholine and γ-aminobutyric acid (GABA) and various neuroactive peptides (100, 133, 211). Furthermore, a significant proportion of noradrenergic cells in the locus coeruleus and subcoeruleus are known to contain neuroactive peptides, such as enkephalin and neuropeptide Y (106, 304). Also of interest is the demonstration that noradrenergic cells in the locus coeruleus receive projections from adrenergic neurons in the lower medulla (groups C1 and C2) (140, 210) and from neighboring peptidergic neurons (195). These findings indicate that the locus coeruleus lies within an extremely complex neurochemical environment.

Major ascending projections from the locus coeruleus pass rostrally through the midbrain lateral to the medial longitudinal fasciculus and ventrolateral to the central gray matter. In the caudal diencephalon, the main ascending bundle of noradrenergic fibers enters the medial forebrain bundle via the mammillary peduncle and the ventral tegmental area. These fibers accompany the medial forebrain bundle to and through the lateral hypothalamus. This ascending pathway continues rostrally to levels of the anterior commissure where it divides into bundles innervating the diencephalic and telencephalic structures. The stria medullaris component turns caudally to innervate midline portions of the thalamus, while the stria terminalis component supplies the amygdaloid nuclear complex (Fig. 13.36). Other efferent fibers from the locus coeruleus pass via the fornix to the hippocampal formation and, as a component of the cingulum bundle, to the cingulate cortex, the subiculum, and the hippocampal formation. The most rostrally projecting fibers from the locus coeruleus pass from the medial forebrain bundle into the external capsule which distributes fibers to the rostral, dorsal, and lateral cortex of the frontal lobe. Smaller groups of fibers separating from the main bundle, which is referred to as the dorsal catecholamine pathway, project into the periaqueductal gray matter and the periventricular gray matter of the third ventricle. One of the most profuse projections is to the thalamus where terminals are found in the intralaminar thalamic nuclei, the anterior nuclear group, and the lateral geniculate body. In addition to these ipsilateral pathways, smaller numbers of fibers cross to the opposite side via the tegmental decussation, the posterior commissure, the supraoptic commissures, and the anterior commissure. After decussating, these noradrenergic pathways have a distribution similar to those on the ipsilateral side.

More than 10% of cells in the locus coeruleus innervate both the cerebral and cerebellar cortex. Noradrenergic fibers project to the cerebellar cortex via the superior cerebellar peduncle and terminate around Purkinje cell somata and in the lower third of the

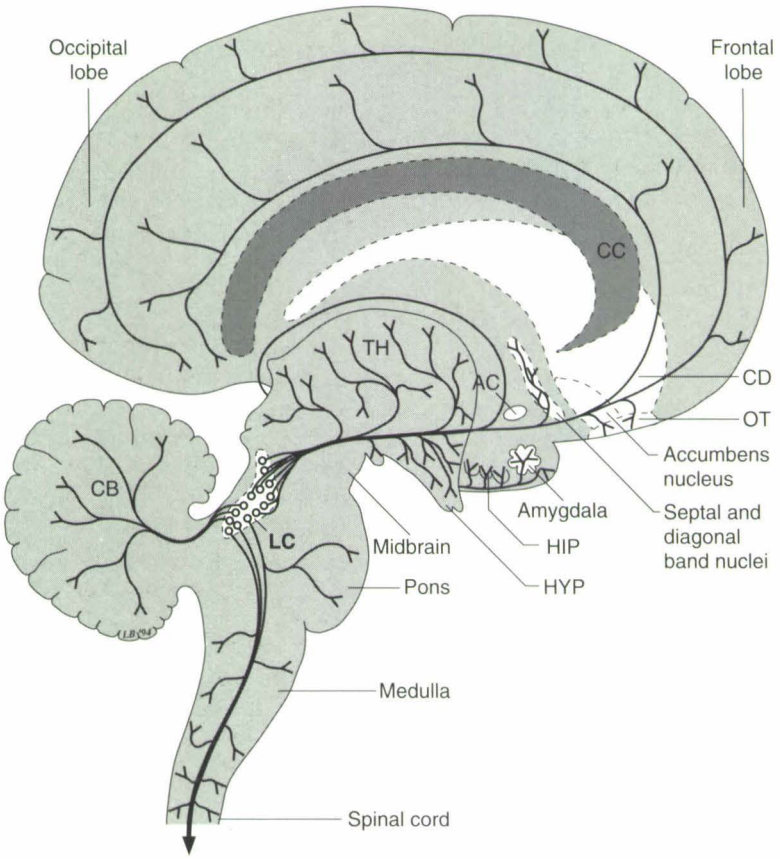


Figure 13.36. Parasagittal section of the human brain showing the widespread arborization of ascending and descending noradrenergic axons of the locus coeruleus. The locus coeruleus provides a noradrenergic innervation that covers the entire rostrocaudal extent of the neuraxis. *AC,* anterior commissure; *CB,* cerebellum; *CC,* corpus callosum; *CD,* caudate nucleus; *HIP,* hippocampal formation; *HYP,* hypothalamus; *LC,* locus coeruleus; *OT,* olfactory tubercle; *TH,* thalamus.

molecular layer (186, 209, 299). In the brainstem, the locus coeruleus innervates the inferior and superior colliculi, primary sensory, and association nuclei, as well as a portion of the pontine nuclei (103, 147, 186). Both the locus coeruleus and subcoeruleus project fibers to the spinal cord via the anterior and lateral funiculi, which innervate portions of the anterior and intermediate gray matter at all levels. A high percentage of these fibers cross at segmental levels (71, 104, 155, 186, 188, 238).

The remarkable feature of the locus coeruleus projection is its wide distribution throughout the neuraxis (Fig. 13.36). With the exception of the midbrain raphe serotonin projection system, no other cell group of the reticular formation has been shown to have such an extensive projection. The projection of the locus coeruleus directly to the cerebral cortex is unique in that it does not involve synaptic relays in the thalamus (138). Retrograde HRP studies based upon transport of the enzyme from a large number of sites within the neuraxis suggest a regional topography within the locus coeruleus (174). These data imply that the locus coeruleus is composed of several distinct subdivisions.

Noradrenergic neurons in the lower brainstem consist of smaller collections of cells and scattered neurons in the lateral tegmentum of the pons and medulla (e.g., groups A5 and A7). These cell groups have projections to regions of the central nervous system that do not receive fibers from the locus coeruleus. Thus, despite the widespread nature of their projections, the locus coeruleus and the lateral tegmental groups appear to form complementary and specific neuronal systems.

The locus coeruleus and its efferent projections are considered to play a role in paradoxical sleep, facilitation and inhibition of sen-

sory neurons, and control of cortical activation (11, 70, 134, 139, 163, 182, 231, 232). Additionally, descending noradrenergic fibers from the locus coeruleus may supply preganglionic sympathetic neurons in the intermediolateral cell column at thoracic and upper lumbar levels (122, 188).

Raphe Nuclei

Both the pons and the medulla contain cell groups in the median raphe which properly belong to the reticular formation (40, 262), but are the source of serotoninergic fiber systems widely distributed in the central nervous system. The raphe nuclei of the medulla (i.e., nucleus raphe obscurus, nucleus raphe pallidus, and nucleus raphe magnus) are smaller and less conspicuous than those seen in the pons (Figs. 12.28 and 12.29). The *inferior central nucleus* appears in the median raphe at the junction of pons and medulla (Fig. 13.4) and represents the rostral extension of the nucleus raphe magnus. The *nucleus raphe pontis* consists of several small cell groups, dorsal and rostral to the inferior central nucleus. Despite difficulties in reconciling data from cytoarchitectonic analysis with those from serotonin mapping studies, the nucleus raphe pontis appears largely homologous to group B5 of Dahlström and Fuxe (86). The rostral extension of the pontine raphe nuclei is the *superior central nucleus* (of Bechterew) (Figs. 13.28 and 13.33), a large aggregation of closely packed small- and medium-sized cells that encompass both groups B6 and B8 of Dahlström and Fuxe (86). This superior central nucleus is also known as the median nucleus of the raphe or, more simply, the *median raphe nucleus*. Decussating fibers of the superior cerebellar peduncle pass through portions of the superior central nucleus (Fig. 13.32). On each side of the midline, dorsal to the medial longitudinal fasciculus, is the *dorsal nucleus of the raphe* (Fig. 13.33). This paired nucleus corresponds to group B7 and lies within the anterior periaqueductal gray matter dorsomedial to the *dorsal tegmental nucleus* (of Gudden) (Fig. 14.3).

Serotoninergic (5-hydroxytryptamine or 5-HT) neurons, identified first by the Falck-Hillarp histofluorescence method and more recently with immunocytochemical procedures, are widely distributed in the raphe nuclei. The highest percentages of serotoninergic neurons are found in the dorsal raphe nucleus and the lowest percentage in the smaller raphe nuclei of the pons and medulla (254). Neurons in some raphe nuclei also contain noradrenaline, dopamine, GABA, enkephalin, somatostatin, and cholecystokinin (186). Furthermore, excitatory amino acids (e.g., glutamate and aspartate) and neuroactive peptides (e.g., substance P, enkephalin, and thyrotropin releasing hormone (TRH)) coexist with serotonin in some cells within the raphe (132, 185)

The principal ascending fibers arise from serotonin cell bodies located in the dorsal raphe nucleus and in the superior central nucleus (12, 25, 26, 75, 186, 270, 272). The major ascending pathway from the rostral raphe nuclei passes through the ventral tegmental area (of Tsai), medial parts of the fields of

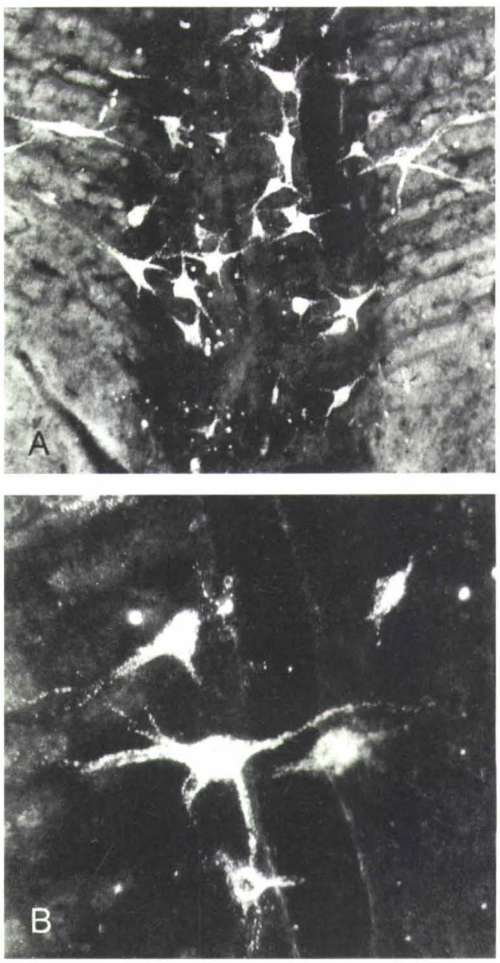


Figure 13.37. Dark-field photomicrographs of retrogradely labeled neurons in the nucleus raphe magnus after injection of horseradish peroxidase (HRP) at the level of the C2 spinal segment in a squirrel monkey (**A**, ×80; **B**, ×200).

Forel, and joins the medial forebrain bundle in the lateral hypothalamus. Fibers leaving this main ascending bundle enter the substantia nigra, the intralaminar thalamic nuclei, the stria terminalis, the septum, and the internal capsule. The most rostral projections terminate mainly in the frontal lobe, although some fibers are distributed throughout the cerebral cortex. The dorsal nucleus of the raphe selectively innervates the substantia nigra, the lateral geniculate body, the striatum, the pyriform lobe, the olfactory bulb, and the amygdaloid nuclear complex (12, 160, 199, 253) (Figs. 13.38 and 13.39). The superior central nucleus is particularly associated with serotonergic fibers projecting to the interpeduncular nucleus, the mammillary bodies, and the hippocampal formation. Other ascending fibers from these nuclei radiate into the mesencephalic reticular formation and the periventricular gray matter. Ascending projections from the caudal raphe nuclei are less numerous and distributed to the superior colliculus, the pretectum, and the nuclei of the posterior commissure. Ascending serotoninergic pathways from the superior central nucleus project mainly to mesolimbic structures, such as the hippocampus and septal nuclei, while the dorsal raphe nucleus has major projections to the basal ganglia, including the striatum and substantia nigra (12, 160) (Fig. 13.38). Ascending projections of cells in the raphe nuclei are mainly ipsilateral, but axons give rise to abundant collaterals with different terminations.

Descending projections of the dorsal raphe nucleus are modest, but they include fibers distributed to the locus coeruleus and the parabrachial nuclei (26). The superior central nucleus gives rise to descending projections to (a) the cerebellum via the middle cerebellar peduncle, (b) the locus coeruleus, and (c) large regions of the pontine reticular formation (Fig. 12.33). The mesencephalic and motor nuclei of the trigeminal nerve also receive serotoninergic afferents (80, 102). Nuclei raphe pontis and raphe magnus have diffuse projections in the brainstem and more specific projections to the spinal cord (Fig. 13.37). Autoradiographic studies have revealed that the nucleus raphe magnus projects primarily to structures concerned with nociceptive and/or visceral afferent input (17, 18). Structures receiving efferents from the nucleus raphe magnus, largely via the dorsal longitudinal fasciculus, include the dorsal motor nucleus of the vagus, the solitary nucleus, and the spinal trigeminal nucleus (pars caudalis). Spinal projections of this nucleus are bilateral and descend in the lateral funiculus (Figs. 11.23 and 12.29). These fibers terminate in the marginal zone (lamina I), the substantia gelatinosa (lamina II), and in parts of laminae V, VI, and VII of the spinal gray matter (see Chapter 12). Because electric stimulation of the nucleus raphe magnus inhibits the discharge of neurons associated with nociceptive sensory input, it was suggested that this nucleus is linked to endogenous analgesic mechanisms (16, 18, 98, 293). This thesis is strengthened by the close correspondence between the terminal projections of this nucleus and opiate receptor binding sites (206). Serotonin and the raphe nuclei also have been implicated in the regulation of diverse physiologic processes such as the regulation of sleep (139), aggressive behavior (234), and a variety of neuroendocrine functions (75, 302).

Structurally, the serotonin molecule is similar to a portion of the larger *d*-lysergic acid diethylamide (LSD) molecule in that both contain an indole nucleus. LSD is a hallucinogenic drug considered to be the prototype of a psychotomimetic drug (i.e., a drug whose effects mimic psychosis) (77, 113, 300). It was suggested that psychotic phenomenon might be due to either decreased amounts of brain serotonin or the synthesis of an endogenous compound that antagonized the action of serotonin in the brain. Microelectrode studies demonstrated that LSD produced a specific depression of activity in raphe neurons which contain serotonin (1, 123). These observations led to the hypothesis that LSD acts to depress the activity of serotoninergic neurons which through disinhibition, cause a release of activity in neurons in the visual system, the limbic system, and in many other brain areas (2). Destruction of serotonin neurons, inhibition of its synthesis, or blockade of its receptors consistently produces an animal that is hypersensitive to virtually all environmental stimuli and hyperactive in virtually all situations. By a general inhibitory action in the central nervous system, serotonin may serve to modulate and maintain behavior within specific limits. Studies indicate that as the overall level of motor activity or arousal increases, so does the activity of serotoninergic neurons. As an animal becomes quiescent and drowsy, the activity of these cells dimin-

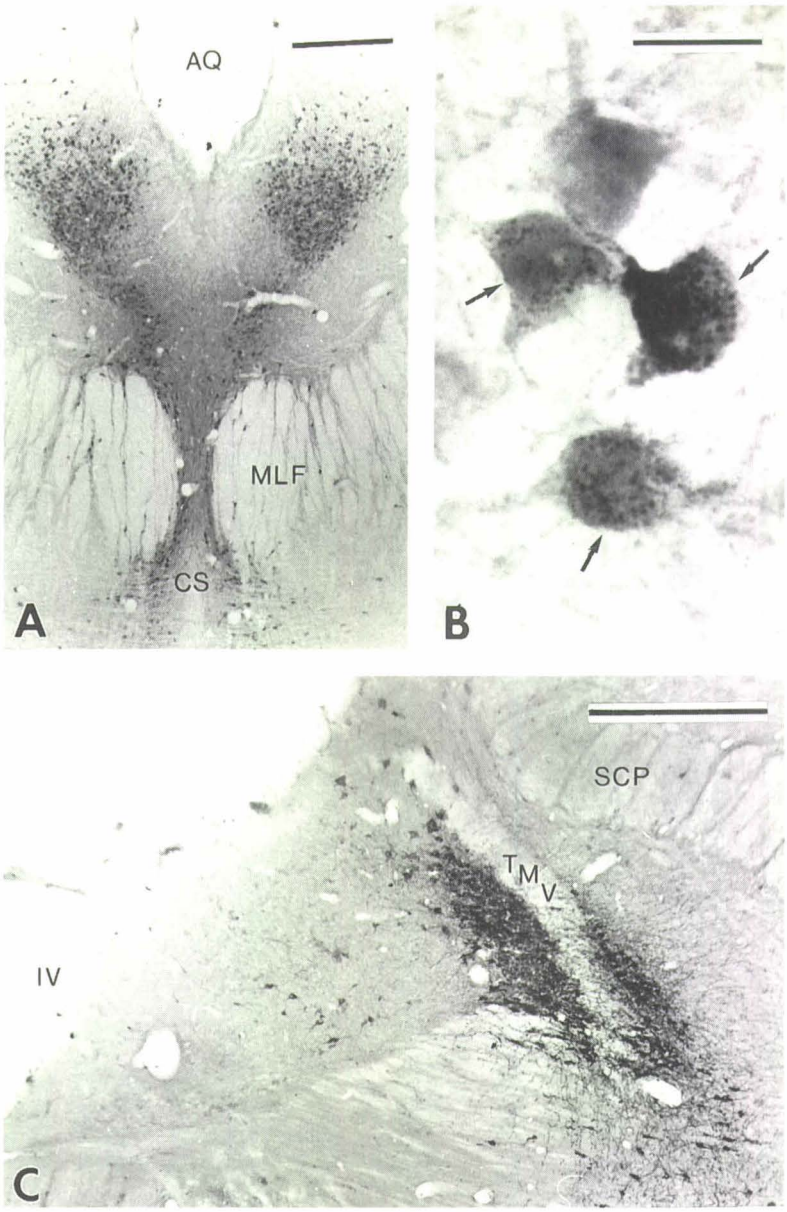


Figure 13.38. Serotonin-containing neurons in the dorsal raphe nucleus at low (**A**) and high (**B**) power magnifications, and noradrenaline-containing neurons in the locus coeruleus (**C**) of the squirrel monkey (*Saimiri sciureus*). The serotoninergic neurons were visualized immunohistochemically with an antibody directed against serotonin itself. The noradrenergic neurons of the locus coeruleus were identified on the basis of their immunoreactivity for tyrosine hydroxylase, the rate-limiting enzyme in the synthesis of primary catecholamines. Most serotoninergic neurons lie in between the cerebral aqueduct (*AQ*) and the medial longitudinal fasciculus (*MLF*). Some serotonin-immunoreactive neurons are also present in the central superior (median raphe) nucleus (*CS*). The locus coeruleus forms a compact cell group lying near the surface of the fourth ventricle (*IV*) and medial to the superior cerebellar peduncle (*SCP*). Fibers of the mesencephalic tract of the trigeminal nerve (*TMV*) traverse the locus coeruleus. The *arrows* in **B** point to some cells of the dorsal raphe nucleus that contain granular material indicating the presence of cholera toxin subunit B (CTb). This tracer was injected into the striatum and transported retrogradely to cell bodies in the dorsal raphe. Serotonin-immunoreactivity was revealed with diaminobenzidin (DAB), which gives a diffuse brown reaction, whereas CTb was visualized with a nickel intensification procedure (NiDAB), which gives a dark blue, granular reaction product. Scale bars: 500 μm (**A, C**) and 25 μm (**B**).

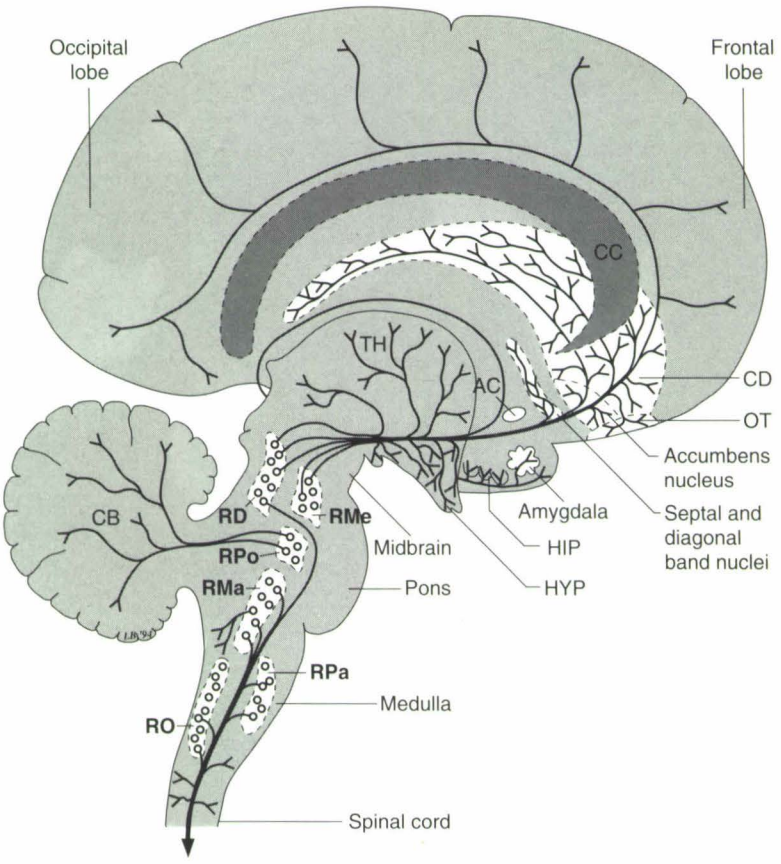


Figure 13.39. Parasagittal section of the human brain showing the widespread arborization of ascending and descending serotoninergic axons of the raphe nuclei. The caudally located raphe nuclei project primarily to lower medulla and spinal cord, while the rostrally located ones give rise to ascending projections that arborize profusely throughout the thalamus, hypothalamus, and cerebral hemispheres. *AC*, anterior commissure; *CB*, cerebellum; *CC*, corpus callosum; *CD*, caudate nucleus; *HIP*, hippocampal formation; *HYP*, hypothalamus; *OT*, olfactory tubercle; *RD*, nucleus raphe dorsalis; *RMa*, nucleus raphe magnus; *RMe*, nucleus raphe medianus; *RO*, nucleus raphe obscurus; *RPa*, nucleus raphe pallidus; *TH*, thalamus.

ishes. Neurons of the raphe fire slowly as an animal enters sleep, and during rapid eye movement (REM) sleep the cells stop firing. These findings suggest that, under the influence of hallucinogenic drugs, the individual is fully awake but the brain serotonin system is depressed and behaving as it does during sleep (129).

Investigations indicate that both serotonin and norepinephrine-containing neurons in the reticular formation play roles in the active mechanisms that control sleep states (139). Sleep is not a single phenomenon. Sleep states can be quantitatively measured and correlated with biochemical, pharmacologic, and structural alterations. Inhibition of serotonin synthesis, or total destruction of serotoninergic neurons in the raphe system, leads to insomnia. Serotonin seems to be involved in the mechanism of what is called *slow wave sleep*, a state characterized by the posture of sleep, myotic pupils, and cortical electrical activity (electroencephalogram or EEG) which displays spindles and slow waves. Additionally, serotoninergic neurons may have effects upon the cells of the locus coeruleus that trigger what is called *paradoxical sleep* (70, 139). Paradoxical sleep occurs intermittently after variable periods of slow wave sleep and is characterized by (a) abolition of antigravity muscle tone, (b) reductions in blood pressure, bradycardia, and irregular respiration, (c) bursts of REM, and (d) an EEG that resembles the waking state. Bilateral lesions of the locus coeruleus in animals cause a selective suppression of paradoxical sleep for about 2 weeks, after which it returns to nearly the normal range.

RETICULAR FORMATION

Two relatively large nuclear masses, the *nucleus reticularis pontis caudalis and oralis*, compose the bulk of the pontine reticular formation. The pars caudalis, which replaces the gigantocellular reticular nucleus of the medulla, extends rostrally to levels of the trigeminal motor nucleus. The pars oralis extends rostrally into the caudal mesencephalon where its precise boundary is indistinct (Fig. 13.28). Cells of the pontine reticular formation give rise to uncrossed reticulospinal fibers, which in the brainstem descend as a component of the MLF. Other cells give rise to fibers that ascend as part of the central tegmental tract (Fig. 13.32). Many cells have dichotomizing axons that project branches both rostrally and caudally. Ascending pontine reticular fibers project via the central tegmental tract to parts of the intralaminar thalamic nuclei. Impulses passing to these thalamic nuclei profoundly influence the electrical activity of broad areas of the cerebral cortex.

Other reticular nuclei present at pontine levels are the reticulotegmental and central superior nuclei (Figs. 13.28, 13.32, and 13.33). The reticulotegmental nucleus lies near the median raphe dorsal to the medial lemniscus and is regarded as a tegmentally displaced pontine nucleus (33) (Fig. 13.28). This nucleus receives projections from the cerebral cortex and the cerebellum (39, 64) and, in turn, projects massively to the cerebellum (35). Thus, the reticulotegmental nucleus is regarded as an important relay in cortical and cerebellar motor circuits. The superior central nucleus develops in the median raphe and enlarges at isthmus levels, where it is referred to as the median nucleus of the raphe (nucleus raphe medianus).

References

1. Aghajanian GK, Foote WE, Sheard H. Lysergic acid diethylamide: sensitive neuronal units in the midbrain raphe. Science 1968;161: 706–708.
2. Aghajanian GK, Haigler HJ, Bennett JL. Amine receptors in the CNS. III. 5–hydroxytryptamine in brain. In: Iverson LL, Iverson SD, Snyder SH, eds. Handbook of psychopharmacology. 6th ed. New York: Plenum Press, 1975:63–96.
3. Aitkin LM, Webster WR. Tonotopic organization in the medial geniculate body of the cat. Brain Res 1971;26:402–405.
4. Aitkin LM, Webster WR. Medial geniculate body of the cat: organization and responses to total stimuli of neurons in the ventral division. J Neurophysiol 1972;35: 365–380.
5. Aitkin LM, Webster WR, Veale JL, Crosby DC. Inferior colliculus. I. Comparison of response properties of neurons in central, pericentral and external nuclei of adult cat. J Neurophysiol 1975;38:1196–1207.
6. Allen, WF. Application of the Marchi method to the study of the radix mesencephalica trigemini in the guinea pig. J Comp Neurol 1919;30:169–216.
7. Allen WF. Identification of the cells and fibers concerned in the innervation of the teeth. J Comp Neurol 1925;39:325–343.
8. Altman J, Carpenter MB. Fiber projections of the superior colliculus in the cat. J Comp Neurol 1961; 116:157–178.
9. Andén N-E, Dahlström A, Fuxe K, Larsson K, Olson L, Ungerstedt U. Ascending monoamine neurons to the telencephalon and diencephalon. Acta Physiol Scand 1966;67:313–326.
10. Angaut P, Brodal A. The projection of the "vestibulocerebellum" onto the vestibular nuclei in the cat. Arch Ital Biol 1967;105:441–479.
11. Aston-Jones G, Chiang C, Alexinsky T. Discharge of noradrenergic locus coeruleus neurons in behaving rats and monkeys suggests a role in vigilance. Prog Brain Res 1991;88:501–520.
12. Azmitia EC, Gannon PJ. The primate serotoninergic system: a review of human and animal studies and a report on *Macaca fascicularis*. In: Fahn S, ed. Advances in neurology. Vol. 43. New York: Raven Press, 1986:407–468.
13. Bacsik RD, Strominger NL. The cytoarchitecture of the human anteroventral cochlear nucleus. J Comp Neurol 1973;147:281–290.
14. Baker R, Highstein SM. Physiological identification of interneurons and motoneurons in the abducens nucleus. Brain Res 1975;91:292–298.
15. Barnes WT, Magoun HW, Ranson SW. The ascending auditory pathway in the brain stem of the monkey. J Comp Neurol 1943;79: 129–152.
16. Basbaum AI. Opiate and stimulus-produced analgesia: functional anatomy of a medullospinal pathway. Proc Natl Acad Sci USA 1976;73:4685–4688.
17. Basbaum AI, Clanton CH, Fields HL. Three bulbospinal pathways from the rostral medulla of the cat: an autoradiographic study of pain modulating systems. J Comp Neurol 1978;178:209–224.
18. Basbaum AI, Ralston DD, Ralston HJ. Bulbospinal projections in the primate: a light and electron microscopic study of a pain modulating system. J Comp Neurol 1986;250:311–323.
19. Batton RR III, Jayaraman A, Ruggiero D, Carpenter MB. Fastigial efferent projections in the monkey: an autoradiographic study. J Comp Neurol 1977;174:281–306.
20. Beckstead RM, Norgren R. An autoradiographic examination of the central distribution of the trigeminal, facial, glossopharyngeal and vagal nerves in the monkey. J Comp Neurol 1979;184:455–472.
21. Bender MB, Shanzer S. Oculomotor pathways defined by electrical stimulation and lesions in the brain stem of the monkey. In: Bender MB, ed. The oculomotor system. New York: Harper and Row, 1964:81–140.
22. Bender MB, Weinsten EA. Effects of stimulation and lesion of the median longitudinal fasciculus in the monkey. Arch Neurol & Psychiatry 1944;52:106–113.
23. Bender MB, Weinstein EA. The syndrome of the median longitudinal fasciculus. Proc Assoc Res Nerv Ment Dis 1950;28:414–420.
24. Blum PS, Day MJ, Carpenter MB, Gilman S. Thalamic components of the ascending vestibular system. Exp Neurol 1979;64:587–603.
25. Bobillier P, Petitjean F, Salvert D, Ligier M, Seguin S. Differential projections of the nucleus raphe dorsalis and nucleus raphe centralis as revealed by autoradiography. Brain Res 1975;85:205–210.
26. Bobillier P, Seguin S, Petitjean F, Salvert D, Touret M Jouvet M. The raphe nuclei of the cat brain stem: a topographical atlas of their efferent projections as revealed by autoradiography. Brain Res 1976; 113:449–486.

27. Borg E. On the neuronal organization of the acoustic middle ear reflex: a physiological and anatomical study. Brain Res 1973;49: 101–123.
28. Bowden DM, German DC, Poynter WD. An autoradiographic, semistereotaxic mapping of major projections from locus coeruleus and adjacent nuclei in *Macaca mulatta*. Brain Res 1978;145:257–276.
29. Bowden REM, Mahran ZY. The functional significance of the pattern of innervation of the muscle quadratus labii superioris of the rabbit, cat and rat. J Anat 1956; 90:217–227.
30. Brawer JR, Morest DK, Kane EC. The neuronal architecture of the cochlear nucleus of the cat. J Comp Neurol 1974;155:251–300.
31. Brodal A. The reticular formation of the brain stem. Anatomical aspects and functional correlations. Springfield, IL: Charles C. Thomas, 1957.
32. Brodal A. Anatomy of the vestibular nuclei and their connections. In: Kornhuber HH, ed. Handbook of sensory physiology: vestibular system. Vol. 6. Berlin: Springer-Verlag, 1974:239–352.
33. Brodal A, Brodal P. The organization of the nucleus reticularis tegmenti pontis in the cat in the light of experimental anatomical studies of its cerebral cortical afferents. Exp Brain Res 1971;13:90–110.
34. Brodal A, Hoivik B. Site and mode of termination of primary vestibulo-cerebellar fibres in the cat. Arch Ital Biol 1964;102:1–21.
35. Brodal A, Jansen J. The ponto-cerebellar projection in the rabbit and cat. J Comp Neurol 1946;84:31–118.
36. Brodal A, Pompeiano O. The vestibular nuclei in the cat. J Anat 1957;91:438–454.
37. Brodal A, Pompeiano O, Walberg F. The vestibular nuclei and their connections, anatomy and functional correlations. Springfield, IL: Charles C. Thomas, 1962.
38. Brodal A, Szabo T, Torvik A. Corticofugal fibers to sensory trigeminal nuclei and nucleus of solitary tract. J Comp Neurol 1956;106:527–555.
39. Brodal A, Szikla G. The termination of the brachium conjunctivum descendens in the nucleus reticularis tegmenti pontis: an experimental study in the cat. Brain Res 1972;39:337–351.
40. Brodal A, Taber E, Walberg F. The raphe nuclei of the brain stem in the cat. II. Efferent connections. J Comp Neurol 1960;114:239–259.
41. Brodal A, Torvik A. Über den Ursprung der sekundären vestibulocerebellaren Fasern bei der Katze. Eine experimentell-anatomische Studie Arch Psychiatr 1957;195: 550–567.
42. Brodal P. The corticopontine projection in the cat. I. Demonstration of a somatotopically organized projection from the primary sensorimotor cortex. Exp Brain Res 1968;5:212–237.
43. Brodal P. The corticopontine projection from the visual cortex in the cat. I. The total projection and the projection from area 17. Brain Res 1972;39:297–317.
44. Brodal P. The corticopontine projection from the visual cortex in the cat. II. The projection from areas 18 and 19. Brain Res 1972;39:319–335.
45. Büttner U, Büttner-Ennever JA, Henn V. Vertical eye movement related unit activity in the rostral mesencephalic reticular formation of the alert monkey. Brain Res 1977;130:239–252.
46. Carleton SC, Carpenter MB. Afferent and efferent connections of the medial, inferior and lateral vestibular nuclei in the cat and monkey. Brain Res 1983;278:29–51.
47. Carleton SC, Carpenter MB. Distribution of primary vestibular fibers in the brain stem and cerebellum of the monkey. Brain Res 1984; 294:281–298.
48. Carpenter MB. The dorsal trigeminal tract in the rhesus monkey. J Anat 1957;91:82–90.
49. Carpenter MB. Lesions of the fastigial nuclei in the rhesus monkey. Am J Anat 1959;104:1–34.
50. Carpenter MB. Fiber projections from the descending and lateral vestibular nuclei in the cat. Am J Anat 1960;107:1–22.
51. Carpenter MB. The ascending vestibular system and its relationship to conjugate horizontal eye movements. In: Wolfson RJ, ed. The vestibular system and its diseases. Philadelphia: University of Pennsylvania Press, 1966:68–98.
52. Carpenter MB. Upper and lower motor neurons. In: Downey JA, Darling RC, eds. Physiological basis of rehabilitation medicine. Ch. 1. Philadelphia: W.B. Saunders, 1971:3–27.
53. Carpenter MB. Central oculomotor pathways. In: Bach-y-Rita P, ed. The control of eye movements. Ch. 4. New York: Academic Press, 1971:67–103.
54. Carpenter MB, Batton RR III. Abducens internuclear neurons and their role in conjugate horizontal gaze. J Comp Neurol 1980;189: 191–209.
55. Carpenter MB, Batton RR III. Connections of the fastigial nucleus in the cat and monkey. Exp Brain Res 1982;(Suppl 6):250–295.
56. Carpenter MB, Carleton SC. Comparison of vestibular and abducens projections to the medial rectus subdivision of the oculomotor complex in the monkey. Brain Res 1983;274:144–149.
57. Carpenter MB, Carleton SC, Keller JT, Conte P. Connections of the subthalamic nucleus in the monkey. Brain Res 1981;224:1–29.
58. Carpenter MB, Chang L, Pereira AB, Hersh LB, Bruce G, Wu JY. Vestibular and cochlear efferent neurons in the monkey identified by immunocytochemical methods. Brain Res 1987;408:275–280.
59. Carpenter MB, Cowie RJ. Connections and oculomotor projections of the superior vestibular nucleus and cell group "y." Brain Res 1985;336:265–287.
60. Carpenter MB, Hanna GR. Fiber projections from the spinal trigeminal nucleus in the cat. J Comp Neurol 1961;117:117–132.
61. Carpenter MB, Hanna GR. Effects of thalamic lesions upon cerebellar dyskinesia in the rhesus monkey. J Comp Neurol 1962;119:127–148.
62. Carpenter MB, McMasters RE. Disturbances of conjugate horizontal eye movements in the monkey. II. Physiological effects and anatomical degeneration resulting from lesions in the medial longitudinal fasciculus. Arch Neurol 1963;8: 347–368.
63. Carpenter MB, McMasters RE, Hanna GR. Disturbances of conjugate horizontal eye movements in the monkey. I. Physiological effects and anatomical degeneration resulting from lesions of the abducens nucleus and nerve. Arch Neurol 1963;8:231–247.
64. Carpenter MB, Nova HR. Descending division of the brachium conjunctivum in the cat: a cerebelloreticular system. J Comp Neurol 1960;114:295–305.
65. Carpenter MB, Stein BM, Peter P. Primary vestibulocerebellar fibers in the monkey: distribution of fibers arising from distinctive cell groups of the vestibular ganglia. Am J Anat 1972;135:221–250.
66. Carpenter MB, Strominger NL. The medial longitudinal fasciculus and disturbances of conjugate horizontal eye movements in the monkey. J Comp Neurol 1965;125:41–66.
67. Carpenter MB, Strominger NL. Efferent fibers of the subthalamic nucleus in the monkey: a comparison of the efferent projections of the subthalamic nucleus, substantia nigra and globus pallidus. Am J Anat 1967;121:41–72.
68. Chan-Palay V. Cerebellar dentate nucleus: organization, cytology and transmitters. Berlin: Springer-Verlag, 1977.
69. Christoff N, Anderson PJ, Nathanson M, Bender MB. Problems in anatomic analysis of lesions of the median longitudinal fasciculus. AMA Arch Neurol 1960;2:293–304.
70. Chu N-S, Bloom FE. Norepinephrine-containing neurons: changes in spontaneous discharge patterns during sleeping and waking. Science 1973;179:908–910.
71. Clark FM, Proudfit HK. The projection of locus coeruleus neurons to the spinal cord in the rat determined by anterograde tracing combined with immunocytochemistry. Brain Res 1991;538:231–245.
72. Cogan DG, Kubik CS, Smith WL.

Unilateral internuclear ophthalmoplegia: report of eight clinical cases with one postmortem study. Arch Opthalmol 1950;44:783–796.
73. Cohen B. Vestibulo-ocular relations. In: Bach-y-Rita P, ed. The control of eye movements. New York: Academic Press, 1971: 105–135.
74. Cohen B, Suzuki JI, Bender MB. Eye movements from semicircular nerve stimulation in the cat. Ann Otol Rhinol Laryngol 1964;73: 153–169.
75. Conrad LCA, Leonard CA, Pfaff DW. Connections of the median and dorsal raphe nuclei in the rat: an autoradiographic and degeneration study. J Comp Neurol 1974;156:179–206.
76. Contreras RJ, Gomez MM, Norgren R. Central origins of cranial nerve parasympathetic neurons in the rat. J Comp Neurol 1980; 190:373–394.
77. Cooper JR, Bloom FE, Roth RH. The biochemical basis of neuropharmacology. 6th ed. New York: Oxford University Press, 1991.
78. Cooper S, Daniel PM, Whitteridge D. Nerve impulses in the brainstem of the goat: short latency responses obtained by stretching the extrinsic eye muscles and the jaw muscles. J Physiol (Lond) 1953; 120:471–490.
79. Cooper S, Daniel PM, Whitteridge D. Nerve impulses in the brainstem of the goat: responses with long latencies obtained by stretching the extrinsic eye muscles. J Physiol (Lond) 1953;120:491–513.
80. Copray JC, Liem RS, Ter Horst GJ, van Willigen JD. Origin, distribution and morphology of serotonergic afferents to the mesencephalic trigeminal nucleus of the rat. Neurosci Lett 1991;121:97–101.
81. Corbin KB. Observations on the peripheral distribution of fibers arising in the mesencephalic nucleus of the fifth cranial nerve. J Comp Neurol 1940;73:153–177.
82. Corbin KB, Harrison F. Function of the mesencephalic root of the fifth cranial nerve. J Neurophysiol 1940; 3:423–435.
83. Courville J. Rubrobulbar fibres to the facial nucleus and the lateral reticular nucleus (nucleus of the lateral funiculus): an experimental study in the cat with silver impregnation methods. Brain Res 1966; 1:317–337.
84. Courville J. The nucleus of the facial nerve: the relation between cellular groups and peripheral branches of the nerve. Brain Res 1966;1:338–354.
85. Crowe SJ. Symposium on tone localization in the cochlea. Ann Otol Rhinol Laryngol 1935;44:737–837.
86. Dahlström A, Fuxe K. Evidence for the existence of monoamine-containing neurons in the central nervous system. I. Demonstration of monoamines in the cell bodies of brain stem neurons. Acta Physiol Scand 1964;62(Suppl 232):1–55.
87. Darian-Smith I, Mayday G. Somatotopic organization within the brain stem trigeminal complex of the cat. Exp Neurol 1960;2:290–309.
88. Darian-Smith I, Yokota T. Corticofugal effects of different neuron types within the cat's brain stem activated by tactile stimulation of the face. J Neurophysiol 1966; 29:185–206.
89. Deecke L, Schwarz DWF, Fredrickson JM. The vestibular thalamus in the Rhesus monkey. Adv Otorhinolaryngol 1973;19:210–219.
90. Deecke L, Schwarz DWF, Fredrickson JM. Nucleus ventroposterior inferior (VPI) as the vestibular thalamic relay in the Rhesus monkey. I. Field potential investigation. Exp Brain Res 1974;20:88–100.
91. Deecke L, Schwarz DWF, Fredrickson JM. Vestibular responses in the rhesus monkey ventroposterior thalamus. II. Vestibuloproprioceptive convergence at thalamic neurons. Exp Brain Res 1977;30: 219–232.
92. DeJong RN. The neurological examination. 4th ed. New York: Harper and Row, 1979.
93. Dodd J, Kelly JP. Trigeminal system. In: Kandel ER, Schwartz JH, Jessell TM, eds. Principles of neural science. 3rd ed. Ch. 45. New York: Elsevier, 1991:702–710.
94. Dow RS. The fiber connections of the posterior part of the cerebellum in the rat and cat. J Comp Neurol 1936;63:527–548.
95. Dubner R, Bennett GJ. Spinal and trigeminal mechanisms of nociception. Annu Rev Neurosci 1983;6: 381–418.
96. Falck B, Hillarp NA, Thieme G, Torp A. Fluorescence of catecholamines and related compounds condensed with formaldehyde. J Histochem Cytochem 1962;10:348–354.
97. Felten DL, Sladek JR Jr. Monoamine distribution in primate brain. V. Monoaminergic nuclei: anatomy, pathways and local organization. Brain Res Bull 1983;10:171–284.
98. Fields HL, Basbaum AI, Clanton CH, Anderson SD. Nucleus raphe magnus inhibition of spinal cord dorsal horn neurons. Brain Res 1977;126:441–454.
99. Fluur E. Influences of semicircular ducts on extraocular muscles. Acta Otolaryngol (Stockh) 1959;149: 1–46.
100. Fodor M, Görcs TJ, Palkovits M. Immunohistochemical study on the distribution of neuropeptides within the pontine tegmentum—particularly the parabrachial nuclei and the locus coeruleus of the human brain. Neuroscience 1992; 46:891–908.
101. Fonnum F, Walberg F. An estimate of the concentration of γ-aminobutyric acid and glutamate decarboxylase in the inhibitory Purkinje axons terminals in the cat. Brain Res 1973;54:115–127.
102. Fort P, Luppi PH, Sakai K, Salvert D, Jouvet M. Nuclei of origin of monoaminergic, peptidergic, cholinergic afferents to the cat trigeminal motor nucleus: a double-labeling study with choleratoxin as a retrograde tracer. J Comp Neurol 1990;301:262–275.
103. Fritschy JM, Grzanna R. Distribution of locus coeruleus axons within the rat brainstem demonstrated by *Phaseolus vulgaris* leucoagglutinin anterograde tracing in combination with dopamine-beta-hydroxylase immunofluorescence. J Comp Neurol 1990 ;293:616–31.
104. Fritschy JM, Grzanna R. Demonstration of two separate descending noradrenergic pathways to the rat spinal cord: evidence for an intragriseal trajectory of locus coeruleus axons in the superficial layers of the dorsal horn. J Comp Neurol 1990 ;291:553–82.
105. Fulwiler CE, Saper CB. Subnuclear organization of the efferent connections of the parabrachial nucleus in the rat. Brain Res Rev 1984;7:229–259.
106. Fung SJ, Zhuo H, Manzoni D, Reddy VK, Barnes CD. Coerulospinal cells containing neuropeptide Y in the cat. Peptides 1991;12:739–743.
107. Fuxe K. Evidence for the existence of monoamine neurons in the central nervous system. IV. Distribution of monoamine nerve terminals in the central nervous system. Acta Physiol Scand 1965;64(Suppl 247): 37–120.
108. Gacek RR. The efferent cochlear bundle in man. Arch Otolaryngol 1961;74:690–694.
109. Gacek RR. Location of brain stem neurons projecting to the oculomotor nucleus in the cat. Exp Neurol 1977;57:725–749.
110. Gacek RR. Location of commissural neurons in the vestibular nuclei of the cat. Exp Neurol 1978; 59:479–491.
111. Gacek RR. Location of abducens afferent neurons in the cat. Exp Neurol 1979;64:342–353.
112. Gacek RR, Lyon M. The localization of vestibular efferent neurons in the kitten with horseradish peroxidase. Acta Otolaryngol (Stockh) 1974;77:92–101.
113. Gaddum JH, Hameed KA. Drugs which antagonize 5-hydroxytryptamine. Br J Pharmacol 1954;9: 240–248.
114. Galambos R. Suppression of auditory nerve activity by stimulation of efferent fibers to cochlea. J Neurophysiol 1956;19:240–248.
115. Gerrits NM. Vestibular nuclear complex. In: Paxinos G, ed. The human nervous system. Ch. 26. New York: Academic Press, 1990;863–888.

116. Goldberg JM, Fernandez C. Efferent vestibular system in the squirrel monkey: an anatomical location and influence on afferent activity. J Neurophysiol 1980;43:986–1025.
117. Golberg ME, Howard ME, Gouras P. The ocular motor system. In: Kandel ER, Schwartz JH, Jessell TM, eds. Principles of neural science. 3rd ed. Ch. 43. New York: Elsevier, 1991;660–678.
118. Goldstein M. The auditory periphery. In: Mountcastle VB, ed. Medical physiology. 12th ed. Ch. 64. St Louis: C.V. Mosby, 1968;1465–1498.
119. Graybiel AM. Direct and indirect preoculomotor pathways of the brainstem: an autoradiographic study of the pontine reticular formation in the cat. J Comp Neurol 1977;175:37–78.
120. Graybiel AM, Hartwieg EA. Some afferent connections of the oculomotor complex in the cat: an experimental study with tracer techniques. Brain Res 1974;81:543–551.
121. Guinan JJ, Warr WB, Norris BE. Differential olivocochlear projections from the lateral versus medial zones of the superior olivary complex. J Comp Neurol 1983; 221:358–370.
122. Guyenet PG. Central noradrenergic neurons: the autonomic connection. Prog Brain Res 1991;88: 365–380.
123. Haigler HJ, Aghajanian GK. Lysergic acid diethylamide and serotonin: a comparison of effects on serotonergic neurons and neurons receiving serotonergic input. J Pharmacol Exp Ther 1974;188: 688–699.
124. Hayashi H, Sumino R, Sessle BJ. Functional organization of trigeminal subnucleus interpolaris: nociceptive and innocuous afferent inputs, projections to thalamus, cerebellum, and spinal cord, and descending modulation from periaqueductal gray. J Neurophysiol 1984;51:890–905.
125. Hazrati L-N, Parent A. Projection from the deep cerebellar nuclei to the pedunculopontine nucleus in the squirrel monkey. Brain Res 1992;585:267–271.
126. Highstein SM. Abducens and Oculomotor internuclear neurons: relation to gaze. In: Baker R, Berthoz A, eds. Control of gaze by brain stem neurons: developments in neuroscience. Vol. 1. Amsterdam: Elsevier, 1977;153–162.
127. Hökfelt T, Johansson O, Goldstein M. Central catecholamine neurons as revealed by immunohistochemistry with special reference to adrenaline neurons. In: Björklund A, Hökfelt T, eds. Handbook of chemical neuroanatomy. Vol. 2. Part 1: Classical transmitters in the CNS. Ch. 5. Amsterdam: Elsevier, 1984;157–276.
128. Ito M, Yoshida M. The cerebellar-evoked monosynaptic inhibition of Deiters neurones. Experientia 1964;20:515.
129. Jacobs BL, Trulson ME. Mechanisms of actions of LSD. Am Sci 1979;67:396–404.
130. Jacobsohn L. Über die Kerne des menschlichen Hirnstamms. Abhandlungen der königl. Preuss Akademie der Wissenschaften, 1909;1:1–70.
131. Jenny AB, Saper CB. Organization of the facial nucleus and corticofacial projection in the monkey: a reconsideration of the upper motor neuron facial palsy. Neurology 1987;37:930–939.
132. Johansson O, Hökfelt T, Pernow B, et al. Immunohistochemical support for three putative transmitters in one neuron: coexistence of 5-hydroxytryptamine, substance P- and thryrotropin releasing hormone-like immunoreactivity in medullary neurons projecting to the spinal cord. Neuroscience 1981;6: 1857–1881.
133. Jones BE. Noradrenergic locus coeruleus neurons: their distant connections and their relationship to neighboring (including cholinergic and GABAergic) neurons of the central gray and reticular formation. Prog Brain Res 1991;88:15–30.
134. Jones BE, Bobillier P, Pin C, Jouvet M. The effects of lesions of catecholamine-containing neurons upon monoamine content of the brain and EEG and behavioral waking in the cat. Brain Res 1973;58:157–177.
135. Jones BE, Friedman L. Atlas of catecholamine perikarya, varicosities and pathways in the brainstem of the cat. J Comp Neurol 1983; 215:382–396.
136. Jones BE, Halaris AE, McIlhany M, Moore RY. Ascending projections of the locus coeruleus in the rat. I. Axonal transport in central noradrenaline neurons. Brain Res 1977;127:1–22.
137. Jones BE, Harper ST, Halaris AE. Effects of locus coeruleus lesions upon cerebral monoamine content, sleep-wakefulness states and the response to amphetamine in the cat. Brain Res 1977;124:473–496.
138. Jones BE, Moore RY. Ascending projections of the locus coeruleus in the rat. II. Autoradiographic study. Brain Res 1977;127:23–53.
139. Jouvet M. Biogenic amines and the states of sleep. Science 1969; 163:32–41.
140. Kachidian P, Astier B, Renaud B, Bosler O. Adrenergic innervation of noradrenergic locus coeruleus neurons. A dual labeling immunocytochemical study in the rat. Neurosci Lett 1990;109:23–29.
141. Kerr FWL. Structural relation of the trigeminal spinal tract to upper cervical roots and the solitary nucleus in the cat. Exp Neurol 1961;4:134–148.
142. Kerr FWL. The divisional organization of afferent fibers of the trigeminal nerve. Brain 1963; 86:721–732.
143. Kerr FWL, Kruger LL, Schwassmann HO, Stern R. Somatotopic organization of mechanoreceptor units in the trigeminal nuclear complex of the monkey. J Comp Neurol 1968;134:127–144.
144. Kevetter GA, Perachio AA. Distribution of vestibular afferents that innervate the sacculus and posterior canal in the gerbil. J Comp Neurol 1986;254:410–424.
145. Kimmel DL. Innervation of the spinal dura mater and dura mater of the posterior cranial fossa. Neurology 1961;9:800–809.
146. Kimura R, Wersäll J. Termination of the olivo-cochlear bundle in relation to the outer hair cells of the organ of Corti in guinea pig. Acta Otolaryngol (Stockh) 1962;55: 11–32.
147. Klepper A, Herbert H. Distribution and origin of noradrenergic and serotonergic fibers in the cochlear nucleus and inferior colliculus of the rat. Brain Res 1991;557:190–201.
148. Korte GE, Mugnaini E. The cerebellar projection of the vestibular nerve in the cat. J Comp Neurol 1979;184:265–278.
149. Kruger L, Michel F. A morphological and somatotopic analysis of single unit activity in the trigeminal sensory complex of the cat. Exp Neurol 1962;5:139–156.
150. Kruger L, Michel F. Reinterpretation of the representation of pain based on physiological excitation of single neurons in the trigeminal sensory complex. Exp Neurol 1962;5:157–178.
151. Kuhar MJ, Roth RH, Aghajanian GK. Synthesis of catecholamines in the locus coeruleus from ^{3}H-tyrosine *in vivo*. Biochem Pharmacol 1972;21:2280–2282.
152. Kuypers HGJM. An anatomical analysis of cortico-bulbar connexions to the pons and lower brain stem in the cat. J Anat 1958; 92:198–218.
153. Kuypers HGJM. Corticobulbar connexions to the pons and lower brain-stem in man: an anatomical study. Brain 1958;81:364–388.
154. Kuypers HGJM, Lawrence DG. Cortical projections to the red nucleus and the brain stem in the rhesus monkey. Brain Res 1967;4: 151–188.
155. Kuypers HGJM, Maisky VA. Retrograde axonal transport of horseradish peroxidase from spinal cord to brain stem cell groups in the cat. Neuroscience Lett 1975;1:9–14.
156. Kuypers HGJM, Tuerk DJ. The distribution of cortical fibres within the nuclei cuneatus and gracilis in the cat. J Anat 1964;98:143–162.
157. Ladpli R, Brodal A. Experimental studies of commissural and reticular projections from the vestibular nuclei in the cat. Brain Res 1968;8:65–96.
158. Lang W, Büttner-Ennever JA, Büt-

tner U. Vestibular projections to the monkey thalamus: an autoradiographic study. Brain Res 1979; 177:3–17.
159. Larsen KD, McBride RL. The organization of feline entopeduncular nucleus projections: anatomical studies. J Comp Neurol 1979; 184:293–308.
160. Lavoie B, Parent A. Immunohistochemical study of the serotoninergic innervation of the basal ganglia in the squirrel monkey. J Comp Neurol 1990;299:1–16.
161. Levitt P, Moore RY. Origin and organization of brainstem catecholamine innervation in the rat. J Comp Neurol 1979;186:505–528.
162. Lewy FH, Kobrak H. Neural projection of cochlear spirals on primary acoustic centers. Arch Neurol Psychiatry 1936;35:839–852.
163. Lidbrink P. The effects of lesions of ascending noradrenaline pathways on sleep and waking in the cat. Brain Res 1974;74:19–40.
164. Liedgren SRC, Milne AC, Rubin AM, Schwarz DWF, Tomlinsen RD. Representation of vestibular afferents in somatosensory thalamic nuclei of the squirrel monkey (*Saimiri sciureus*). J Neurophysiol 1976;39:601–612.
165. Lorente de Nó R. Die Labyrinthreflexe auf die Augenmuskeln nach einseitiger Labyrinthextirpation nebst einer kurzen Angabe über den Nervenmechanismus der vestibulären Augenbewegungen. Vienna: Urban and Schwarzenberg, 1928.
166. Lorente de Nó R. Ausgewählte Kapitel aus der vergleichenden Physiologie des Labyrinthes: die Augenmuskelreflexe beim Kaninchen und ihre Grundlagen. Ergebn Physiol 1931;32:73–242.
167. Lorente de Nó R. Anatomy of the eighth nerve: the central projection of the nerve endings of the internal ear. Laryngoscope 1933;43:1–38.
168. Luk GD, Morest DK, McKenna NM. Origins of the crossed olivocochlear bundle shown by an acid phosphatase method in the cat. Ann Otol Rhinol Laryngol 1974; 83:382–391.
169. McBride RL, Sutin J. Projections of the locus coeruleus and adjacent pontine tegmentum in the cat. J Comp Neurol 1976;165:265–284.
170. McMasters RE, Weiss AH, Carpenter MB. Vestibular projections to the nuclei of the extraocular muscles: degeneration resulting from discrete partial lesions of the vestibular nuclei in the monkey. Am J Anat 1966;118:164–194.
171. Maciewicz RJ, Eagen K, Kaneko CRS, Highstein SM. Vestibular and medullary brain stem afferents to the abducens nucleus in the cat. Brain Res 1977;123:229–240.
172. Maeda T, Shimuzu N. Projections ascendantes du locus coeruleus et d'autres neurones aminergiques pontiques au niveau du prosencéphale du rat. Brain Res 1972; 36:19–35.
173. Manni E, Bortolami R, Desole C. Eye muscle proprioception in the semilunar ganglion. Exp Neurol 1966;16:226–236.
174. Mason ST, Fibiger HC. Regional topography within noradrenergic locus coeruleus as revealed by retrograde transport of horseradish peroxidase. J Comp Neurol 1979;187:703–724.
175. Mehler WR, Rubertone JA. Anatomy of the vestibular nucleus complex. In: Paxinos G, ed. The rat nervous system. Vol. 2. Chap. 9. Sydney, Australia: Academic Press, 1985:185–219.
176. Merzenich MM, Reid MD. Representation of the cochlea within the inferior colliculus of the cat. Brain Res 1974;77:397–415.
177. Moore RY, Card P. Noradrenaline-containing neuron systems. In: Björklund A, Hökfelt T, eds. Handbook of chemical neuroanatomy. Vol. 2. Part 1: Classical transmitters in the CNS. Ch. 4. Amsterdam: Elsevier, 1984:123–156.
178. Moskowitz N, Liu J-C. Central projections of the spiral ganglion of the squirrel monkey. J Comp Neurol 1972;144:335–344.
179. Mugnaini E, Walberg F. An experimental electron microscopical study on the mode of termination of cerebellar corticovestibular fibre in the cat lateral vestibular nucleus (Deiters' nucleus). Exp Brain Res 1967;4:212–236.
180. Mugnaini E, Walberg F, Brodal A. Mode of termination of primary vestibular fibres in the lateral vestibular nucleus: an experimental electron microscopical study in the cat. Exp Brain Res 1967; 4:187–211.
181. Mugnaini E, Walberg F, Hauglie-Hanssen E. Observations on the fine structure of the lateral vestibular nucleus (Deiters' Nucleus) in the cat. Exp Brain Res 1967; 4:146–186.
182. Nakai Y, Takaori S. Influence of norepinephrine-containing neurons derived from the locus coeruleus on lateral geniculate neuronal activities of cats. Brain Res 1974;71:47–60.
183. Nauta WJH, Kuypers HGJM. Some ascending pathways in the brain stem reticular formation. In: Jasper HH, Proctor LP, Knighton RS, et al., eds. Reticular formation of the brain. Henry Ford Hospital International Symposium. Ch. 1. Boston: Little, Brown and Company, 1958: 3–30.
184. Nauta WJH, Mehler WR. Projections of the lentiform nucleus in the monkey. Brain Res 1966;1: 3–42.
185. Nicholas AP, Pieribone VA, Arvidsson U, Hökfelt T. Serotonin, substance P- and glutamate/aspartate-like immunoreactivities in medullo-spinal pathways of rat and primate. Neuroscience 1992; 48:545–559.
186. Nieuwenhuys R. Chemoarchitecture of the Brain. Berlin: Springer-Verlag, 1985.
187. Nyberg-Hansen R. Origin and termination of fibers from the vestibular nuclei descending in the medial longitudinal fasciculus: an experimental study with silver impregnation methods in the cat. J Comp Neurol 1964;122:355–368.
188. Nygren LG, Olson L. A new major projection from the locus coeruleus: the main source of noradrenergic nerve terminals in the ventral and dorsal columns of the spinal cord. Brain Res 1977;132: 85–93.
189. Olsen L, Fuxe K. On the projections from the locus coeruleus noradrenaline neurons: the cerebellar innervation. Brain Res 1971;28: 165–171.
190. Olszewski J. On the anatomical and functional organization of the spinal trigeminal nucleus. J Comp Neurol 1950;92:401–413.
191. Olszewski J. Cytoarchitecture of the human reticular formation. In: Delafresnaye JF, ed. Brain mechanisms and consciousness. Oxford: Blackwell Scientific Publications, 1954;54–80.
192. Olszewski J, Baxter D. Cytoarchitecture of the human brain stem. Philadelphia: J.B. Lippincott, 1954.
193. Osen KK. The intrinsic organization of the cochlear nuclei in the cat. Acta Otolaryngol (Stockh) 1969;67:352–359.
194. Osen KK. Cytoarchitecture of the cochlear nuclei in the cat. J Comp Neurol 1969;136:453–484.
195. Pammer C, Görcs T, Palkovits M. Peptidergic innervation of the locus coeruleus cells in the human brain. Brain Res 1990;515:247–255.
196. Papez JW. Subdivisions of the facial nucleus. J Comp Neurol 1927; 43:159–191.
197. Papez JW, Rundles W. The dorsal trigeminal tract and the centre median nucleus of Luys. J Nerv Ment Dis 1937;85:509–519.
198. Parent A, De Bellefeuille L. Organization of efferent projections from the internal segment of the globus pallidus in primate as revealed by fluorescence retrograde labeling method. Brain Res 1982;245: 201–213.
199. Parent A, Descarries L, Beaudet A. Organization of ascending serotonin systems in the adult rat brain. A radioautographic study after intraventricular administration of [^{3}H] 5-hydroxytryptamine. Neuroscience 1981;6:115–138.
200. Paxinos G, Törk I, Halliday G, Mehler WR. Human homologs to brainstem nuclei identified in other animals as revealed by acetylcholinesterase activity. In: Paxinos G, ed. The human nervous system. Ch. 7. New York: Academic Press, 1990;149–302.

201. Pearson AA. The development and connections of the mesencephalic root of the trigeminal nerve in man. J Comp Neurol 1949;90:1–46.
202. Pearson AA. Further observations on the mesencephalic root of the trigeminal nerve. J Comp Neurol 1949;91:147–194.
203. Pearson J, Halliday G, Sakamoto N, Michel JP. Catecholaminergic Neurons. In: Paxinos G, ed. The human nervous system. Ch. 31. New York: Academic Press, 1990;1023–1049.
204. Penfield W, Evans J. Functional defects produced by cerebral lobectomies. Proc Assoc Res Nerv Ment Dis 1934;13:352–377.
205. Penfield W, McNaughton F. Dural headache and innervation of the dura mater. Arch Neurol Psychiatry 1940;44:43–75.
206. Pert CB, Kuhar MJ, Snyder SH. Autoradiographic localization of the opiate receptor in rat brain. Life Sci 1975;16:1849–1854.
207. Petrov T, Jhamandas JH, Krukoff TL. Characterization of peptidergic efferents from the lateral parabrachial nucleus to identified neurons in the rat dorsal raphe nucleus. J Chem Neuroanat 1992; 5:367–373.
208. Pfaffmann C. Afferent impulses from the teeth resulting from a vibratory stimulus. J Physiol (Lond) 1939;97:220–232.
209. Pickel VM, Segal M, Bloom FE. A radioautographic study of the efferent pathways of the nucleus locus coeruleus. J Comp Neurol 1974;155:15–42.
210. Pieribone VA, Aston-Jones G. Adrenergic innervation of the rat nucleus locus coeruleus arises predominantly from the C1 adrenergic cell group in the rostral medulla. Neuroscience 1991;41: 525–542.
211. Pioro EP, Mai JK, Cuello AC. Distribution of substance P- and enkephalin-immunoreactive neurons and fibers. In: Paxinos G, ed. The human nervous system. Ch. 32. New York: Academic Press, 1990;1051–1094.
212. Poitras D, Parent A. Atlas of the distribution of monoamine-containing nerve cell bodies in the brain stem of the cat. J Comp Neurol 1978;179:699–718.
213. Pompeiano O, Brodal A. The origin of the vestibulospinal fibres in the cat: an experimental-anatomical study, with comments on the descending medial longitudinal fasciculus. Arch Ital Biol 1957;95: 166–195.
214. Pompeiano O, Walberg F. Descending connections to the vestibular nuclei: an experimental study in the cat. J Comp Neurol 1957;108:465–502.
215. Powell TPS, Cowan WM. An experimental study of the projection of the cochlea. J Anat 1962;96: 269–284.
216. Powell TPS, Erulkar SD. Transneuronal cell degeneration in the auditory relay nuclei of the cat. J Anat 1962;96:249–268,
217. Ramón y Cajal S. Histologie du Système Nerveux de l'Homme et des Vertébrés. (Azoulay L, Trans.) Paris: Maloine, 1909, 1911. (Reprinted, Consejo Superior de Investigaciones Cientificas, Instituto Ramón y Cajal, Madrid, 1972.)
218. Rasmussen GL. The olivary peduncle and other fiber projections of the superior olivary complex. J Comp Neurol 1946;84:141–219.
219. Rasmussen GL. Further observations of the efferent cochlear bundle. J Comp Neurol 1953;99:61–74.
220. Rasmussen GL. Efferent fibers of the cochlear nerve and cochlear nucleus. In: Rasmussen GL, Windle WF, eds. Neural mechanisms of the auditory and vestibular systems. Ch. 8. Springfield, IL: Charles C. Thomas, 1960:105–115.
221. Rasmussen GL. Anatomic relationships of the ascending and descending auditory systems. In: Field WS, Alford BR, eds. Neurological aspects of auditory and vestibular disorders. Ch. 1. Springfield, IL: Charles C. Thomas, 1964:1–14.
222. Rhoton AL, O'Leary JL, Ferguson JP. The trigeminal, facial, vagal and glossopharyngeal nerves in the monkey. Arch Neurol 1966;14:530–540.
223. Rivera-Dominguez M, Agate FJ Jr, Noback CR. Scanning electron microscopy of the spiral organ of Corti of the adult rhesus monkey. Brain Res 1973;65:159–164.
224. Rose JE. Organization of frequency sensitive neurons in the cochlear complex of the cat. In: Rasmussen GL, Windle WF, eds. Neural mechanisms of the auditory and vestibular systems. Ch. 9. Springfield, IL: Charles C. Thomas, 1960:116–136.
225. Rose JE, Galambos R, Hughes JR. Microelectrode studies of the cochlear nuclei of the cat. Bull Johns Hopkins Hosp 1959;104: 211–251.
226. Rose JE, Galambos R, Hughes JR. Organization of frequency sensitive neurons in the cochlear complex of the cat. In: Rasmussen GL, Windle WF, eds. Neural mechanisms of the auditory and vestibular systems. Chap. 10. Springfield, IL: Charles C. Thomas, 1960; 116–136.
227. Rose JE, Greenwood DB, Golberg JM, Hind JE. Some discharge characteristics of single neurons in the inferior colliculus of the cat. I. Tonotopical organization, relation of spike-counts to tone intensity, and firing patterns of single elements. J Neurophysiol 1963;26: 293–320.
228. Rose JE, Gross NB, Geisler DC, Hind JE. Some neural mechanisms in the inferior colliculus of the cat which may be relevant to localization of a sound source. J Neurophysiol 1966;29:288–314.
229. Russell GV. The dorsal trigeminothalamic tract in the cat: reconsidered as a lateral reticulo-thalamic system of connections. J Comp Neurol 1954;101:237–264.
230. Russell GV. The nucleus locus coeruleus (dorsolateralis tegmenti). Tex Rep Biol Med 1955;13: 939–988.
231. Sakai K. Physiological properties and afferent connections of the locus coeruleus and adjacent tegmental neurons involved in the generation of paradoxical sleep in the cat. Prog Brain Res 1991; 88:31–45.
232. Sasa M, Takaori S. Influence of the locus coeruleus on transmission in the spinal trigeminal nucleus neurons. Brain Res 1973;55:203–208.
233. Shanzer S, Wagman IH, Bender MB. Further observations on the median longitudinal fasciculus. Trans Am Neurol Assoc 1959; 84:14–17.
234. Sheard MH. The effect of PCPA in behavior in rats: relation to brain serotonin and 5-hydroxyindoleacetic acid. Brain Res 1969;15: 524–528.
235. Shimazu H, Precht W. Inhibition of central vestibular neurons from the contralateral labyrinth and its mediating pathway. J Neurophysiol 1966;29:467–492.
236. Siegborn J, Grant G. Brain stem projections of different branches of the vestibular nerve. An experimental study by transganglionic transport of horseradish peroxidase in the cat. I. The horizontal ampullar and utricular nerves. Arch Ital Biol 1983;121:237–248.
237. Sjöqvist O. Studies on pain conduction in the trigeminal nerve: a contribution to surgical treatment of facial pain. Acta Psychiat Neurol Scand 1938;17(Suppl):1–139.
238. Sluka KA, Westlund KN. Spinal projections of the locus coeruleus and the nucleus subcoeruleus in the Harlan and the Sasco Sprague-Dawley rat. Brain Res 1992; 579:67–73.
239. Smith CA. Innervation of the organ of Corti. In: Iurato S, ed. Submicroscopic structure of the inner ear. Oxford: Pergamon, 1967:107–131.
240. Smith CA, Rasmussen GL. Recent observations on the olivo-cochlear bundle. Ann Otol Rhinol Laryngol 1963;72:489–507.
241. Smith CA, Rasmussen GL. Degeneration in the efferent nerve endings in the cochlea after axonal section. J Cell Biol 1965;26:63–77.
242. Smyth GE. The systemization and central connections of the spinal tract and nucleus of the trigeminal nerve. Brain 1939;62:41–78.
243. Spencer RF, Sterling P. An electron microscopic study of motoneurones and interneurones in the cat abducens nucleus identified by ret-

rograde intraaxonal transport of horseradish peroxidase. J Comp Neurol 1977;176:65–86.
244. Spiegel EA. Experimentalstudien am Nervensystem: XV. Der Mechanismus des labyrinthären Nystagmus. Z Hals-Nasen-Ohrenheilk 1929;25:200–217.
245. Spiegel EA, Sommer I. Neurology of the eye, ear, nose and throat. New York: Grune & Stratton, 1944:667.
246. Spiller WG. Ophthalmoplegia internuclearis anterior: a case with necropsy. Brain 1924;47:345–357.
247. Spoendlin HH. The organization of the cochlear receptor. Adv Otorhinolaryngol 1966;13:1–227.
248. Spoendlin HH. The innervation of the cochlear receptor. In: Moller AR, ed. Basic mechanisms in hearing. New York: Academic Press, 1973;185–234.
249. Spoendlin HH, Gacek RR. Electron microscopic study of the efferent and afferent innervation of the organ of Corti in the cat. Ann Otol Rhinol Laryngol 1963;72:660–686.
250. Steiger H-J, Büttner-Ennever J. Relationship between motoneurons and internuclear neurons in the abducens nucleus: a double retrograde tracer study in the cat. Brain Res 1978;148:181–188.
251. Steiger H-J, Büttner-Ennever JA. Oculomotor nucleus afferents in the monkey demonstrated with horseradish peroxidase. Brain Res 1979;160:1–15.
252. Stein BM, Carpenter MB. Central projections of portions of the vestibular ganglia innervating specific part of the labyrinth in the rhesus monkey. Am J Anat 1967;120:281–318.
253. Steinbusch HWM. Distribution of serotonin-immunoreactivity in the central nervous system of the rat—cell bodies and terminals. Neuroscience 1981;6:577–618.
254. Steinbusch HWM, Nieuwenhuys R. The raphe nuclei of the rat brainstem: a cytoarchitectonic and immunohistochemical study. In: Emson PC, ed. Chemical neuroanatomy. New York: Raven Press, 1983:131–207.
255. Stotler WA. An experimental study of the cells and connections of the superior olivary complex of the cat. J Comp Neurol 1953;98: 401–423.
256. Strominger NL. The origins, course and distribution of the dorsal and intermediate acoustic striae in the Rhesus monkey. J Comp Neurol 1973;147:209–234.
257. Strominger NL. The anatomical organization of the primate auditory pathways. In: Noback CR, ed. Sensory systems of primates. New York: Plenum Publishing Co., 1978;53–91.
258. Strominger NL, Hurwitz JL. Anatomical aspects of the superior olivary complex. J Comp Neurol 1976;170:485–498.
259. Strominger NL, Nelson LR, Doughterty WJ. Second order auditory pathways in the chimpanzee. J Comp Neurol 1977; 172:349–366.
260. Strominger NL, Strominger AI. Ascending brain stem projections of the anteroventral cochlear nucleus in the rhesus monkey. J Comp Neurol 1971;143:217–242.
261. Szentagothai J. The elementary vestibulo-ocular reflex arc. J Neurophysiol 1950;13:395–407.
262. Taber E, Brodal A, Walberg F. The raphe nuclei of the brain stem in the cat. I. Normal topography and cytoarchitecture and general discussion. J Comp Neurol 1960; 114:161–187.
263. Tasaki I. Nerve impulses in individual auditory nerve fibers of guinea pig. J Neurophysiol 1954; 17:97–122.
264. Terayama Y, Yamamoto K. Olivocochlear bundle in the guinea pig cochlear after central transection of the crossed bundle: Electron microscopic study on origin and distribution of unmyelinated efferent fibers by axonal degeneration. Acta Otolaryngol (Stockh) 1971:72: 385–396.
265. Thomas DM, Kaufman RP, Sprague JM, Chambers WW. Experimental studies of the vermal cerebellar projections in the brain stem of the cat (fastigiobulbar tract). J Anat 1956;90:371–385.
266. Torvik A. Afferent connections to the sensory trigeminal nuclei, the nucleus of the solitary tract and adjacent structures: an experimental study in the rat. J Comp Neurol 1956;106:51–142.
267. Torvik A. The ascending fibers from the main trigeminal sensory nucleus: an experimental study in the cat. Am J Anat 1957;100: 1–15.
268. Truex RC. Morphological alterations in the Gasserian ganglion cells and their association with senescence in man. Am J Pathol 1940;16:255–268.
269. Uemura T, Cohen B. Effects of vestibular nuclei lesions on vestibulo-ocular reflexes and posture in monkeys. Acta Otolaryngol (Stockh) 1973;315:1–71.
270. Ungerstedt U. Stereotaxic mapping of the monoamine pathways in the rat brain. Acta Physiol Scand 1971;367(Suppl):1–48.
271. Verhaart WJC. The tractus trigeminalis of Wallenberg. Acta Psychiat Neurol Scand 1954;290:269–279.
272. Vertes RP. A PHA-L analysis of ascending projections of the dorsal raphe nucleus in the rat. J Comp Neurol 1991;313:643–668.
273. Von Békésy G. Experiments in hearing. New York: McGraw-Hill, 1960.
274. Von Economo CF. Über dissoziierte Emphindungslähmung bei Ponstumoren und über die zentralen Bahnen des sensiblen Trigeminus. Jahrb Psychiat Neurol 1911;32:107–138.
275. Voss H. Zahl und Anordnung der Muskelspindeln in den oberen Zungenbeinmuskeln, im M. trapezius und M. latissimus dorsi. Anat Anz 1956;103:443–446.
276. Vraa-Jensen GF. The motor nucleus of the facial nerve, with a survey of the efferent innervation of the facial muscles [Thesis]. Copenhagen: Ejnar Munksgaard, 1942.
277. Walberg F. Do the motor nuclei of the cranial nerves receive corticofugal fibres? An experimental study in the cat. Brain 1957; 80:597–605.
278. Walberg F, Bowsher D, Brodal A. The termination of primary vestibular fibers in the vestibular nuclei in the cat: an experimental study with silver methods. J Comp Neurol 1958;110:391–419.
279. Walberg F, Jansen J. Cerebellar corticovestibular fibers in the cat. Exp Neurol 1961;3:32–52.
280. Walberg F, Pompeiano O, Brodal A, Jansen J. The fastigiovestibular projection in the cat: an experimental study with silver impregnation methods. J Comp Neurol 1962; 118:49–75.
281. Walker AE. The origin, course and terminations of the secondary pathways of the trigeminal nerve in primates. J Comp Neurol 1939;71:59–89.
282. Walker AE. Anatomy, physiology and surgical considerations of the spinal tract of the trigeminal nerve. J Neurophysiol 1939;2:234–248.
283. Walker AE. Somatotopic localization of spinothalamic and secondary trigeminal tracts in mesencephalon. Arch Neurol Psychiatry 1942;48:884–889.
284. Wall PD, Taub A. Four aspects of the trigeminal nucleus and a paradox. J Neurophysiol 1962;25: 110–126.
285. Wallenberg A. Die secondären Bahnen aus dem frontalen sensiblen Trigeminus Kerne des Kaninchens. Anat Anz 1905;26: 145–155.
286. Warr WB. Fiber degeneration following lesions in the anterior ventral cochlear nucleus of the cat. Exp Neurol 1966;14:453–474.
287. Warr WB. Fiber degeneration following lesions in the posteroventral cochlear nucleus of the cat. Exp Neurol 1969;23:140–155.
288. Warr WB. Olivocochlear and vestibular efferent neurons of the feline brain stem: their location, morphology and number determined by retrograde axonal transport and acetylcholinesterase histochemistry. J Comp Neurol 1975;161:159–182.
289. Webster WR, Garey LJ. Auditory system. In: Paxinos G, ed. The human nervous system. Ch. 27. New York: Academic Press, 1990:889–944.
290. Weinberger LM, Grant FC. Experi-

ences with intramedullary tractotomy. III. Studies in sensation. Arch Neurol Psychiatry 1942;48:355–381.
291. White JS, Warr WB. The dual origins of the olivocochlear bundle in the albino rat. J Comp Neurol 1983;219:203–214.
292. Wiklund L, Léger L, Persson M. Monoamine cell distribution in the cat brain stem. A fluorescence histochemical study with quantification of indolaminergic and locus coeruleus cell groups. J Comp Neurol 1981;203:613–647.
293. Willis WD, Haber LH, Martin RF. Inhibition of spinothalamic tract cells and interneurons by brainstem stimulation in the monkey. J Neurophysiol 1977;40:968–981.
294. Wilson VJ, Melvill Jones G. Mammalian vestibular physiology. New York: Plenum Press, 1979.
295. Wilson VJ, Yoshida M. Monosynaptic inhibition of neck motoneurons by the medial vestibular nucleus. Exp Brain Res 1969;9: 365–380.
296. Windle WF. Non-bifurcating nerve fibers of the trigeminal nerve. J Comp Neurol 1926;40:229–240.
297. Winkler C. Opera omnia. Vols. 1–10. Haarlem, The Netherlands: E.F. Bohn, 1918–1933.
298. Woodburne RT. A phylogenetic consideration of the primary and secondary centers and connections of the trigeminal complex in a series of vertebrates. J Comp Neurol 1936;65:403–501.
299. Woodward DJ, Moises HC, Waterhouse BD, Yeh HH, Cheun JE. The cerebellar norepinephrine system: inhibition, modulation, and gating. Prog Brain Res 1991;88: 331–341.
300. Wooley DW, Shaw E. A biochemical and pharmacological suggestion about certain mental disorders. Proc Natl Acad Sci USA 1954;40:228–231.
301. Woollard HH, Harpman JA. The connections of the inferior colliculus and dorsal nucleus of the lateral lemniscus. J Anat 1940; 74:441–458.
302. Wurtman RJ. Brain monoamines and endocrine function. Neurosci Res Program Bull 1971;9:177–297.
303. Zimmerman EA, Chambers WW, Liu CN. An experimental study of the anatomical organization of the cortico-bulbar system in the albino rat. J Comp Neurol 1964;123: 301–324.
304. Zhuo H, Fung SJ, Reddy VK, Barnes CD. Immunohistochemical evidence for coexistence of methionine-enkephalin and tyrosine hydroxylase in neurons of the locus coeruleus complex projecting to the spinal cord of the cat. J Chem Neuroanat 1992;5:1–10.

14
Midbrain

The midbrain, or mesencephalon, is the smallest and least differentiated division of the brainstem. Like other parts of the brainstem, the midbrain can be divided into three parts: (a) a dorsal part, the *tectum* or *quadrigeminal plate* , lying dorsal to the cerebral aqueduct, (b) a central part, the *tegmentum*, representing the rostral continuation of the pontine tegmentum, and (c) a ventral part, the massive *crura cerebri* or *cerebral peduncles*, containing descending cortical projections. The cerebral aqueduct, surrounded by the central gray substance (i.e., periaqueductal gray), separates the tectum from the tegmentum (Fig. 14.1), whereas the substantia nigra, a darkly pigmented nucleus, separates the midbrain tegmentum from the crus cerebri (Figs. 14.1, A.10, and A.27 in the Atlas of the Human Brain, Section VII). Two cranial nerve nuclei, the trochlear and the oculomotor, lie near the midline, ventral to the periaqueductal gray. The midbrain contains important relay nuclei of the auditory and visual systems, along with pathways interrelating higher and lower portions of the neuraxis. The principal nuclear masses and fiber pathways of the midbrain are described as they appear at caudal or inferior collicular level and at rostral or superior collicular level.

CAUDAL MIDBRAIN

The transition from the isthmus to the midbrain is associated with changes mainly in the tectum and tegmentum (Figs. 13.32, 13.33, 14.2, 14.3, A.9, and A.10). The major changes that characterize this transition can be summarized as follows: (a) the rostral fourth ventricle narrows and becomes the cerebral aqueduct, (b) the superior medullary velum is replaced by two rounded eminences, the inferior colliculi, (c) fibers of the superior cerebellar peduncles move ventromedially and begin to decussate, and (d) the tegmentum is reduced in size. The ventral part of the pons become smaller and at more rostral levels undergoes a reorganization as the massive crura cerebri appear (Figs. 14.3 and 14.6). In some sections, portions of the heavily pigmented substantia nigra are evident dorsal to the most rostral pontine nuclei. Fibers of the lateral lemniscus, located near the lateral surface of the tegmentum, migrate dorsally and enter the inferior colliculus. These fibers envelop the inferior colliculus and form its capsule (Figs. 14.2 and 14.3).

Inferior Colliculi

These paired ovoid cell masses of the caudal tectum can be divided into three parts: (a) an ovoid cell mass called the central nucleus, (b) a thin dorsal cellular layer, the pericentral nucleus, referred to as the cortex, and (c) an external nucleus that surrounds the central nucleus laterally and ventrally (126, 188, 269, 288, 342, 343).

The *central nucleus* of the inferior colliculus appears fairly homogeneous in Nissl and myelin stained preparations. In Golgi preparations, it can be subdivided into a smaller dorsomedial division composed of large cells and a large ventrolateral division of medium and small cells with a laminar arrangement (Fig. 14.4). In the ventrolateral division of the central nucleus, laminae form an overlapping onion-like series of concentric shells, most of which are incomplete except for those closest to the center of curvature. The thickness of the laminae is determined by the dendritic ramifications of fusiform and bitufted cells that represent the principal cell types in these layers (269, 288). These laminae provide the basis for the tonotopic organization of neurons in the central nucleus. Each of these laminae correspond to an isofrequency contour. Multipolar and large neurons have dendrites which cross one or more laminae and may form the basis for interactions between laminae (258, 348). A large proportion of neurons in the central nucleus are GABAergic (339).

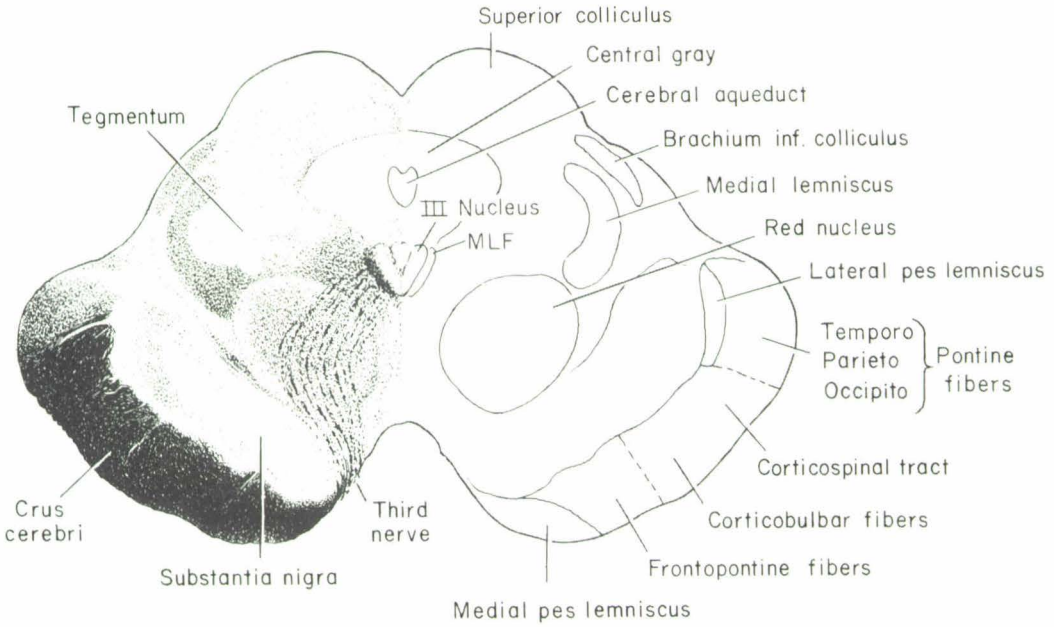


Figure 14.1. Transverse section through the rostral midbrain. *MLF*, medial longitudinal fasciculus.

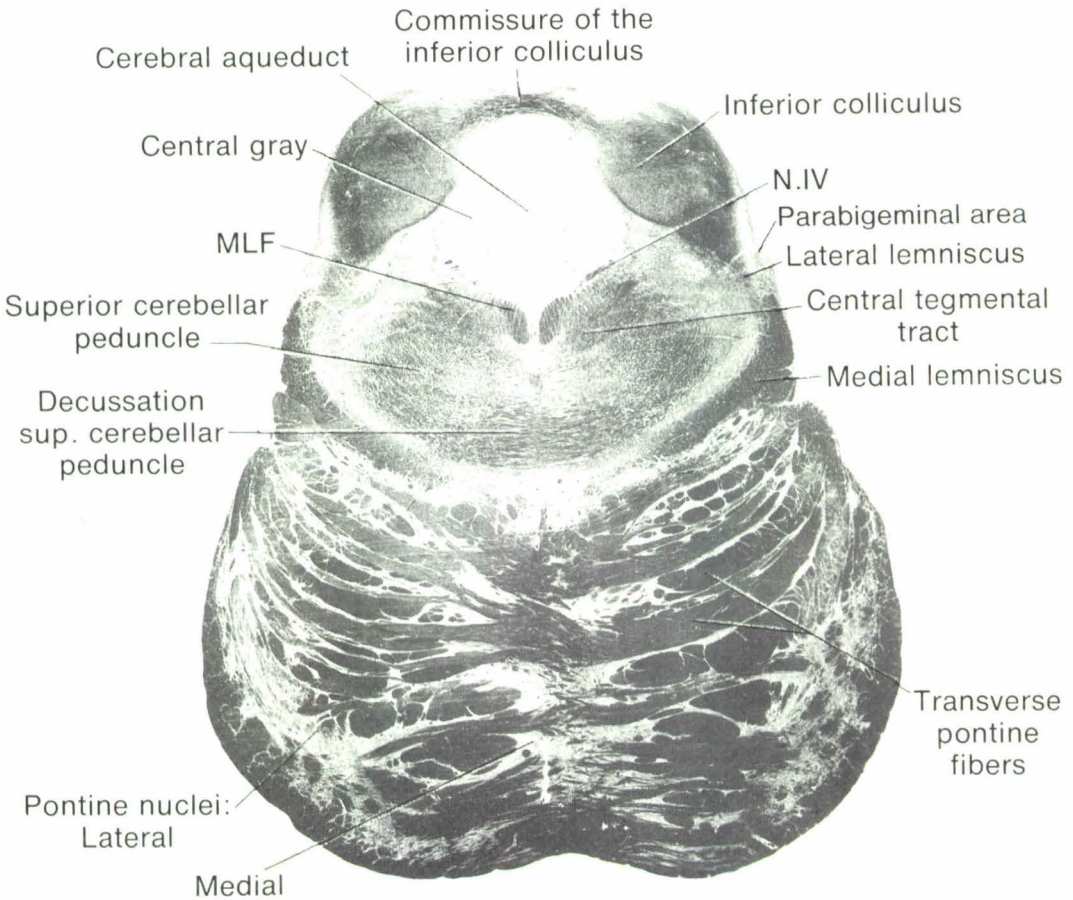


Figure 14.2. Transverse section of the adult midbrain through the inferior colliculus. Large fascicles of corticospinal and corticopontine fibers (unlabeled), cut in cross-section, are located among the bundles of transverse pontine fibers. (Weigert's myelin stain.)

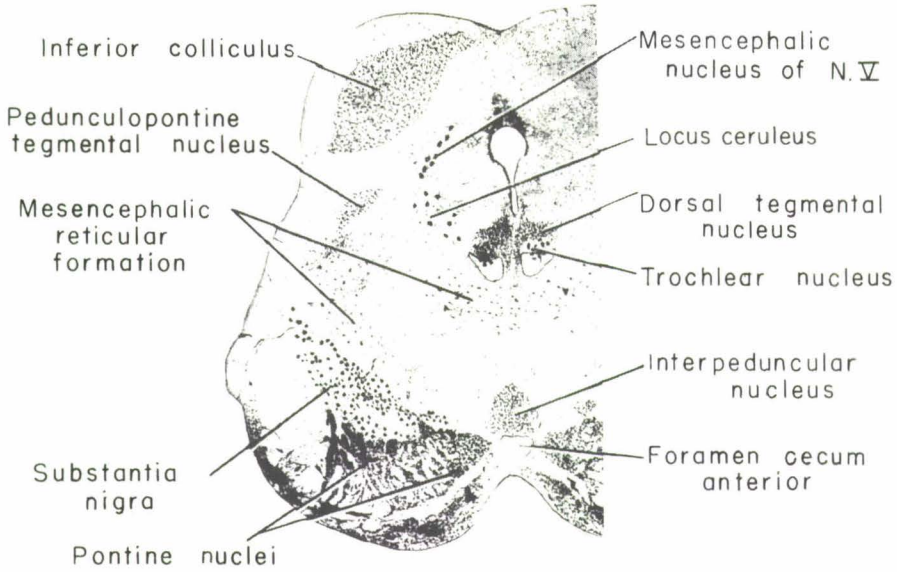


Figure 14.3. Transverse section through inferior colliculi of the midbrain in a 3-month infant. (Cresyl violet stain with schematic representation of main cell groups.)

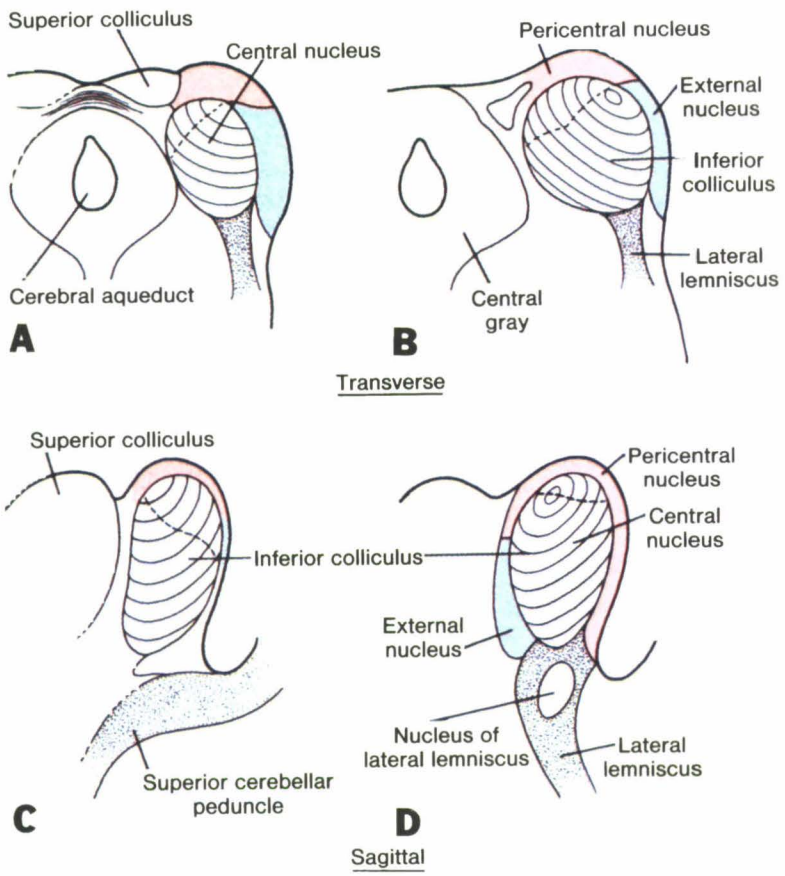


Figure 14.4. Transverse (**A** and **B**) and sagittal (**C** and **D**) sections through the inferior colliculus outlining the nuclear subdivisions. The pericentral nucleus is indicated in *red*, and the external nucleus in *blue*. The central nucleus in *white* shows contours of the laminae in the ventrolateral division. *Black dashes* indicate the division of the central nucleus into the large-celled dorsomedial part and the ventrolateral laminated part. Laminae in the central nucleus represent a given frequency band across the width of the nucleus and form the basis for the tonotopic organization of neurons. The disc-shaped laminae in dorsal regions are not as thick and represent the lower frequencies. High-frequency octaves are represented ventrally.

The *pericentral nucleus* is a thin sheet of densely packed cells extending over the dorsal and posterior surfaces of the inferior colliculus (Fig. 14.4). This nucleus overlies both major divisions of the central nucleus, and its lateral border is continuous with the external nucleus (343). Although the pericentral nucleus has been described as having a layered "cortical" structure, Golgi studies suggest only a predominance of certain cell types at different depths of the nucleus. This nucleus is composed of spiny and aspiny cells. Small spiny neurons are found at all depths in the pericentral nucleus, while large spiny neurons, overlying the large-celled division of the central nucleus, project axons into it. Large aspiny neurons are fusiform or multipolar; dendrites of multipolar neurons extend throughout the depth of the pericentral nucleus, and their axons project toward the brachium of the inferior colliculus. The largest cells are in deepest parts of the nucleus.

The *external nucleus* is composed of cells of various sizes, similar to those found in the central nucleus but less densely packed (342). This nucleus appears almost continuous with the pericentral nucleus but is traversed by fibers of the lateral lemniscus and the brachium of the inferior colliculus (Fig. 14.4). Physiologic studies indicate that the external nucleus is not an auditory relay nucleus like the central nucleus, but a nucleus related primarily to acousticomotor reflexes (4, 5).

The *inferior colliculus* is the major brainstem auditory relay, transmitting impulses from the lateral lemniscus to the medial geniculate body, which in turn projects to the primary auditory cortex. Ascending auditory fibers in the lateral lemniscus project to both dorsomedial and ventrolateral divisions of the central nucleus of the inferior colliculus. Fibers entering the ventromedial division of the inferior colliculus course along the length of each laminae following its curvature. As fibers traverse these laminae they establish synaptic contact with collicular neurons. The dorsomedial division of the central nucleus receives commissural connections from the corresponding region of the opposite inferior colliculus and bilateral projections from the auditory cortex. The pericentral nucleus also receives bilateral inputs from the auditory cortex and ascending projections from the dorsal nucleus of the lateral lemniscus. Cells of the pericentral nucleus project fibers into the central nucleus, which course parallel to its laminae.

Most cells of the inferior colliculus respond to binaural stimulation, and many cells encode information about sound localization with specific spatiotemporal discharge patterns. A definite tonotopic localization is present within the central and pericentral nuclei of the inferior colliculus (5, 258, 345). Neurons in the central nucleus of the inferior colliculus are arranged in a laminar pattern that represents different frequency bands. Isofrequency contours parallel the cellular laminae, which are tilted ventrally, laterally, and down rostrally. Most units respond to binaural stimuli. Advancement of an electrode from dorsal to ventral in the inferior colliculus consistently gives a sequence of frequencies from low to high in the central nucleus. The disc-shaped laminae representing the lowest frequencies (i.e., dorsal regions) are not as thick or as extensive as those representing middle and high frequencies (i.e., ventral region). The frequency representation in the central nucleus reflects the proportional representation of frequencies along the cochlear partition, in which low frequencies are perceived at the apex of the cochlea and high frequencies at the base. The central nucleus of the inferior colliculus is a tightly organized structure bearing specific relationships to the cochlea with elements sharply tuned to different frequencies. Small sections of the basilar membrane of approximately equal lengths are represented across individual anatomically defined cellular laminae within the nucleus (258). This tonotopic organization, which has been confirmed with anatomic, electrophysiologic, and metabolic (2-deoxyglucose) methods (417, 418), applies only to the ventrolateral division of the central nucleus.

The pericentral nucleus demonstrates some evidence of a tonotopic organization in which high frequencies are located externally and low frequencies are found near the margins of the central nucleus (5). This nucleus contains units with broad tuning characteristics, the majority of which receive only a contralateral monaural input. Axons of neurons in the pericentral nucleus project to areas around the ventral division of the medial geniculate body, which in turn project to nonprimary auditory cortex (370). The overall behavior of units in the pericentral nucleus and their monaural input suggest that cells in this

nucleus may serve to direct auditory attention. The external nucleus probably is not an auditory relay nucleus like the central nucleus of the inferior colliculus; this nucleus is related primarily to acousticomotor reflexes (4, 417).

Efferent fibers from the ventromedial division of the central nucleus of the inferior colliculus project via the brachium of the inferior colliculus to the ventral laminated part of the medial geniculate body (188, 219, 267, 322, 342, 417). Cells in the dorsal division of the central nucleus and in the pericentral nucleus send fibers to the dorsal part of the medial geniculate body. Thus, the dorsal division of the central nucleus and the pericentral nucleus of the inferior colliculus, which receive fibers from the auditory cortex but not from the lateral lemniscus, ultimately send impulses back to the secondary auditory cortex via the dorsal part of the medial geniculate body (219). Cells of the ventral part of the medial geniculate body project tonotopically upon the primary auditory cortex (51, 206).

Parabigeminal Area

Ventrolateral to the inferior colliculus and lateral to the lateral lemniscus is a fairly well-defined zone known as the *parabigeminal area* (Fig. 14.2). It is composed mainly of obliquely, or transversely, running fibers, among which are scattered groups of cells constituting the *parabigeminal nucleus*. This small oval nucleus in the lateral midbrain contain cholinergic neurons (group Ch 8 (260)) and receives a substantial projection from the superficial layers of the superior colliculus, which has a visuotopic organization (145, 148, 362). Cells of each parabigeminal nucleus project bilaterally upon superficial layers of the superior colliculi and show a regional organization. Rostral parts of the nucleus project contralaterally and cells in caudal parts of the nucleus project to the ipsilateral superior colliculus (97, 150). Cells of the parabigeminal nucleus respond briskly and consistently to visual stimuli, can be activated by both moving and stationary light spots, and have receptive fields similar to those of the superficial layers of the superior colliculus (362). The parabigeminal nucleus has a representation of the entire contralateral visual field and at least the central part of the ipsilateral field. This nucleus functions with the superior colliculus in processing visual information.

Trochlear Nerve

The nucleus of the trochlear nerve (N. IV) is a small compact cell group at the ventral border of the periaqueductal gray, which represents a small caudal appendage to the oculomotor complex indenting the dorsal surface of the medial longitudinal fasciculus (Figs. 14.3 and 14.5). Root fibers emerging from the nucleus curve dorsolaterally and caudally near the margin of the periaqueductal gray, decussate completely in the superior medullary velum, and exit from the dorsal surface of the brainstem caudal to the inferior colliculus (Figs. 2.25, 2.26, 12.2, 13.32, 14.2, 14.3, and A.9). Peripherally the slender nerve root curves around the lateral surface of the brainstem, passes between the superior cerebellar and posterior cerebral arteries, as do the fibers of the oculomotor nerve, and enters the cavernous sinus (Fig. 4.11). This cranial nerve innervates the superior oblique muscle that serves to intort the eye when abducted, and depress the eye when adducted (see Table 14.1). Lesions involving the trochlear nerve alone are unusual, and detection of resulting disturbances of extraocular movement by inspection is difficult. Diplopia resulting from such a nerve lesion is vertical and maximal on attempted downward gaze to the opposite side. Patients with trochlear nerve lesions complain especially of difficulty in walking downstairs. Tilting of the head to the opposite side, seen in some patients with trochlear nerve lesions, is a posture which compensates for the weakness of ocular intortion on the lesion side (76).

Tegmental and Interpeduncular Nuclei

The periaqueductal gray (PAG) surrounding the cerebral aqueduct contains several nuclear groups. The mesencephalic nucleus of the trigeminal nerve and the pigmented cells of the locus coeruleus occupy lateral regions at isthmus levels (see Chapter 13). The raphe region contains the *dorsal nucleus of the raphe* or *dorsal raphe nucleus*, which is greatly expanded at caudal midbrain levels. The dorsal raphe nucleus is flanked laterally by the *dorsal tegmental nucleus* (of Gudden) (Figs. 12.28, 13.33, and 14.3). This dorsal raphe nucleus, composed mainly of small cells dorso-

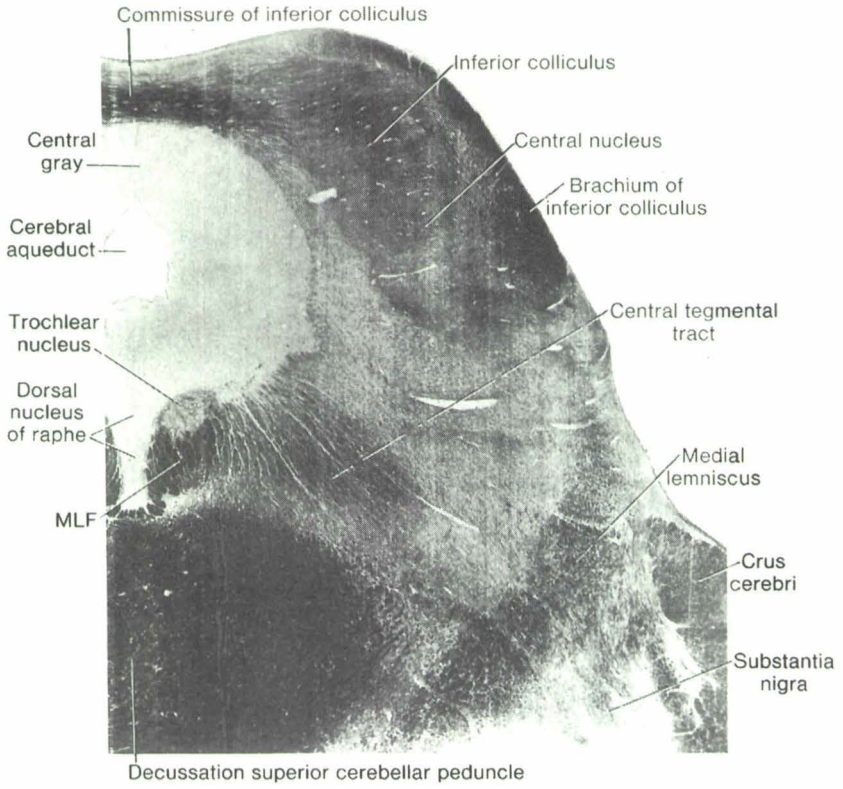


Figure 14.5. Right dorsal quadrant from a transverse section through the rostral part of the inferior colliculus. (Weigert's myelin stain.)

Table 14.1. Origin of Root Fibers to Extraocular Muscles

CRANIAL NERVE	MUSCLE SUPPLIED	COURSE OF FIBERS	ACTION OF MUSCLE
Oculomotor (III)	Medial rectus Inferior rectus Inferior oblique Superior rectus Levator palpebrae	Uncrossed Uncrossed Uncrossed Crossed Crossed and uncrossed	Adduct eye Depress eye when eye is abducted Elevate eye when eye is adducted Elevate eye when eye is abducted Raise upper eyelids
Trochlear (IV)	Superior oblique	Crossed	Depress eye when eye is adducted; intort eye when eye is abducted
Abducens (VI)	Lateral rectus	Uncrossed	Abduct eye

medial to, and between, the trochlear nuclei, has been called the supratrochlear nucleus (291). Although the dorsal nucleus of the raphe and the dorsal tegmental nucleus are adjacent to each other, only cells in the dorsal raphe nucleus utilizes serotonin as a neurotransmitter. Ventral to the medial longitudinal fasciculus and lateral to the raphe are the cells of the *ventral tegmental nucleus* (of Gudden). These cells appear as a rostral continuation of the *superior central nucleus* of the pons. These nuclei usually are designated together as the *superior central nucleus* or the *median raphe nucleus*. Fibers from both dorsal and ventral tegmental nuclei ascend to the mammillary bodies, the lateral hypothalamic areas, and the preoptic and septal areas (155, 280). These fibers travel in the *dorsal longitudi-*

nal fasciculus (of Schütz), a small but complex pathway in ventromedial PAG, the *mammillary peduncle*, and some continue rostrally in the medial forebrain bundle (Fig. 17.14).

As seen in Chapter 13, serotonin-containing neurons have been located in pontine and mesencephalic raphe nuclei (Fig. 13.38). These cell groups have been identified as the dorsal raphe nucleus (group B7), the median raphe nucleus (superior central nucleus, group B8), and the lateral cell group (B9) (86). Detailed anatomic and biochemical studies in various species, including nonhuman primates, reveal that cell groups B7 and B8 give rise to two distinct but overlapping ascending serotoninergic systems (16, 38, 39, 132, 198, 230, 231, 268, 289, 296, 379, 394). Despite several species variations in the organization of ascending serotoninergic systems (16, 198, 283, 398), there is a consensus regarding the respective contributions of the dorsal and median raphe nuclei to the serotoninergic innervation of the forebrain. The dorsal raphe nucleus projects to the periaqueductal gray and gives rise to fibers that ascend in the medial forebrain bundle and that project to the substantia nigra, the hypothalamus, the intralaminar thalamic nuclei, the lateral geniculate body, the striatum, the amygdaloid nuclear complex, and broad regions of the frontal cortex. The median raphe nucleus projects fibers to the midbrain reticular formation, the hypothalamus, including the mammillary bodies, the septal area, the entorhinal cortex, and the hippocampal formation. The median raphe nucleus and, to a lesser extent, the dorsal raphe nucleus, give rise to descending fibers projecting to the cerebellum, the locus coeruleus, the reticular formation of the lower brainstem, and the raphe nuclei of the pons and the medulla (39). The predominant postsynaptic action of serotonin in the forebrain is inhibition, although excitation is also frequently seen (198). These opposite effects of serotonin on forebrain neurons may be explained by the existence of a wide variety of serotoninergic receptors. Three major families of serotoninergic receptors (5-HT_1, 5-HT_2, and 5-HT_3) are now well-characterized, and other receptors are being discovered as a result of extensive application of molecular biology techniques to the cloning of new receptor families.

The *midbrain periaqueductal gray* (PAG) consists of dense collection of relatively small cells surrounding the cerebral aqueduct, which is functionally heterogeneous (24, 25). The region has been implicated in central analgesic mechanisms, vocalization, control of reproductive behavior, aggressive behavior, and mechanisms of upward gaze. Afferents to the periaqueductal gray arise from the hypothalamus, the brainstem reticular formation, the raphe nuclei, the locus coeruleus, and the spinal cord. Many of these regions receive reciprocal projection from the periaqueductal gray. Neurons in the periaqueductal gray are immunoreactive to enkephalin, substance P, dynorphin, cholecystokinin, neurotensin, serotonin, and somatostatin, and single neurons often contain several neuropeptides (283). The role of the periaqueductal gray in brainstem analgesic mechanisms received considerable attention. Ventrolateral regions of the periaqueductal gray appear the most effective sites for stimulation-produced analgesia. Microinjections of morphine in the ventral periaqueductal gray produce pronounced analgesia in rodents.

The *interpeduncular nucleus* is a collection of medium-sized, multipolar, slightly pigmented cells, that lie dorsal to the interpeduncular fossa (Fig. 14.3). This nucleus, which is prominent in most mammals but comparatively small in humans, receives fibers from the habenula via the fasciculus retroflexus (Figs. 16.5 and 17.14). A large proportion of the habenulo-interpeduncular fibers, particularly those terminating in the core of the interpeduncular nucleus, derive from the cholinergic neurons of the medial habenular nucleus (group Ch 7 (260)). In rodents, the interpeduncular nucleus is subdivided into multiple subnuclei whose neurons display various combinations of small-molecule neurotransmitters and neuroactive peptides, including substance P, enkephalin, cholecystokinin, vasoactive intestinal peptide, and somatostatin (163). Fibers of the fasciculus retroflexus, bypassing the interpeduncular nucleus, are distributed to the superior central nucleus, the dorsal tegmental nucleus, and the periaqueductal gray (279). The dorsal tegmental nucleus also receives fibers from the mammillary bodies via the mamillotegmental tract and is closely related to the dorsal longitudinal fasciculus (Fig. 17.16). Although the prevailing direction of conduction in this bundle appears to be ascending, it contains some descending elements, but few of these reach pontine levels. These pathways are part of a complex system whereby impulses related to the limbic sys-

tem, concerned primarily with visceral and behavioral functions, are projected to midbrain nuclei.

ROSTRAL MIDBRAIN

Transverse sections of the rostral midbrain appear strikingly different from those through the inferior colliculus in that (a) the flattened superior colliculi form the rostral part of the tectum (Figs. 14.6–14.8), (b) the oculomotor nuclei form a V-shaped complex ventral to the periaqueductal gray and root fibers of the oculomotor nerve emerge from the interpeduncular fossa (Figs. 14.1, 14.6, and 14.16), (c) the red nuclei, surrounded by fibers of the superior cerebellar peduncle, occupy the central tegmental region (Figs. 14.1, 14.6, and 14.13), and (d) the substantia nigrae achieve their maximum size ventral to the

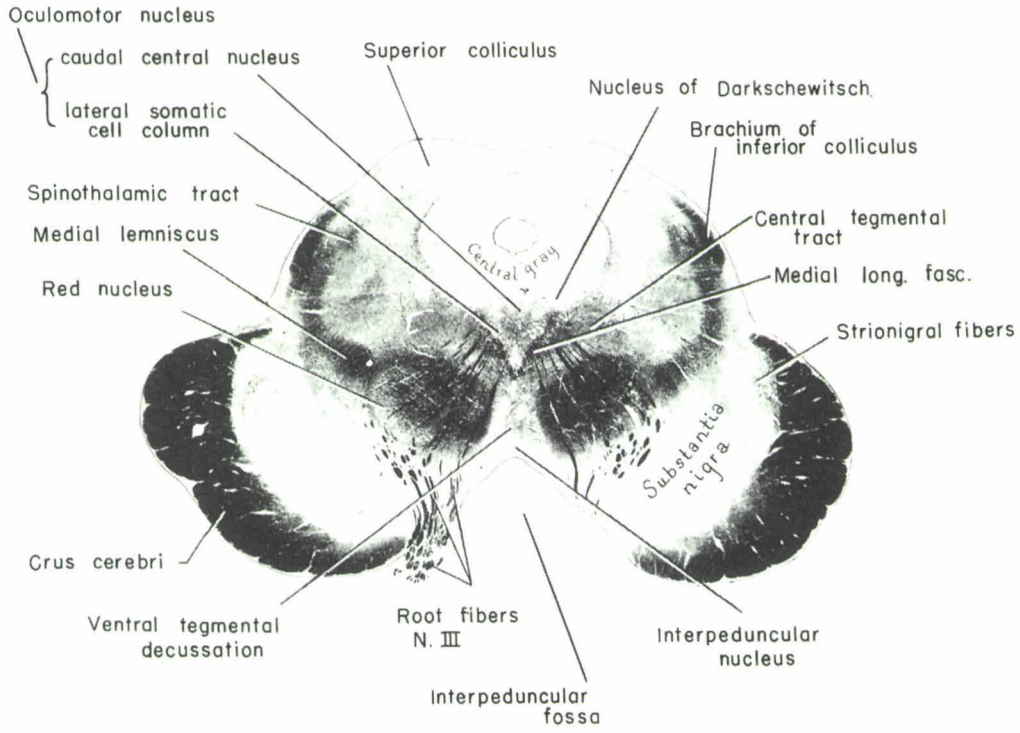


Figure 14.6. Transverse section of adult midbrain through the level of the oculomotor nerve. (Weigert's myelin stain.)

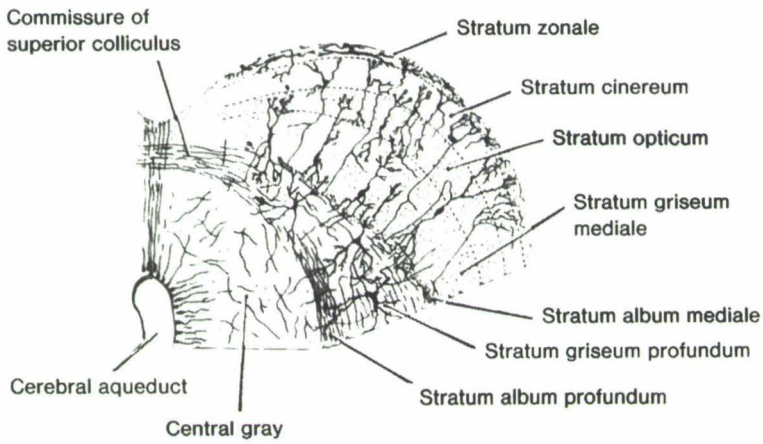


Figure 14.7. Cellular lamination and organization of the superior colliculus based upon Golgi preparations from a human fetus.

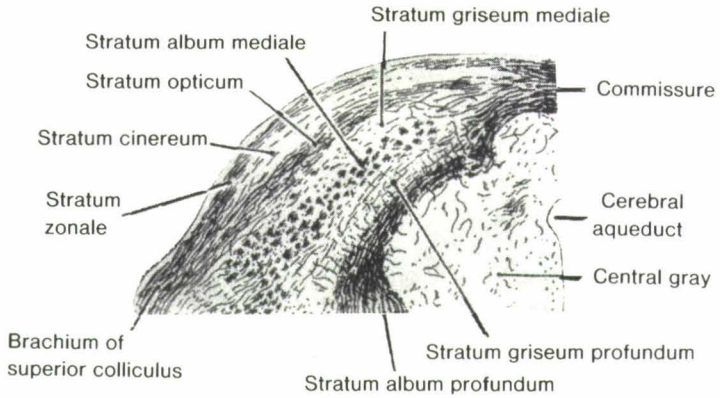


Figure 14.8. Myelinated fiber structure of the superior colliculus based upon Weigert-stained sections.

tegmentum and dorsal to the crura cerebri. Fibers of the brachium of the inferior colliculus lie on the lateral surface of the tegmentum at this level (Fig. 14.6). The medial lemniscus appears as a curved bundle dorsal to the substantia nigra and lateral to the red nucleus. Fibers of the spinothalamic and spinotectal tracts lie together medial to the most dorsal part of the medial lemniscus.

Superior Colliculi

The superior colliculi are flattened, laminated eminences that form the rostral half of the tectum (Figs. 2.25, 2.26, 14.6, and A.11). In nonmammalian vertebrates, the optic tectum, a structure homologous with the mammalian superior colliculus, has a complex laminated organization resembling that of the cerebral cortex and is the primary termination of the optic tract. Beginning with reptiles, the importance of the superior colliculus in visual discrimination progressively diminishes as an increasing number of optic fibers establish more extensive connections with the thalamus and cortex. In humans, the superior colliculi have become reduced in size and serve primarily as reflex centers, influencing the position of the head and eyes in response to visual, auditory, and somatic stimuli (142). The superior colliculus is concerned primarily with the detection of the direction of movement of objects in the visual fields (383), and facilitates visual orientation, searching, and tracking. Cells in deeper layers of the superior colliculus appear to respond to auditory, somatic, and visual stimuli, sometimes separately and sometimes in different combinations (142).

Each colliculus consists of alternate gray and white layers (Figs. 14.7 and 14.8). From the surface inward these layers are (a) the *stratum zonale* (mainly fibrous), (b) the *stratum cinereum* (outer gray layer), (c) the *stratum opticum* (superficial white layer), and (d) the *stratum lemnisci* consisting of middle and deep gray and white layers (stratum griseum medium, stratum album medium, stratum griseum profundum, and stratum album profundum) (Figs. 14.7 and 14.8). The stratum zonale is composed of fine nerve fibers arising mainly from the occipital cortex and entering through the brachium of the superior colliculus. Among the fibers are small, mostly horizontal cells with tangentially or centrally directed axons. The stratum cinereum consists of radially arranged cells whose dendrites pass peripherally and whose axons project inward. The larger cells lie deepest. The stratum opticum is composed mainly of fibers from the ganglion cells of the retina and corticotectal fibers arising from the visual cortex. These fibers enter the stratum opticum via the brachium of the superior colliculus and pass into the superficial and middle gray layers. Corticotectal fibers from the frontal lobe (Brodmann's area 8) reach superficial and middle layers of the superior colliculus via a transtegmental approach and are thought to participate in mechanisms related to saccadic eye movements (222, 223). The stratum lemnisci composed of medium- and large-sized stellate cells, receives heterogeneous inputs from diverse sources, most of which are somatosensory and auditory. These deep layers of the superior colliculus receive afferents from (a) the spinal cord (i.e., spinotectal tract), (b) somatosensory relay nuclei (i.e., nucleus cuneatus, lateral cervical nucleus, and spinal trigeminal nucleus), (c) cate-

cholaminergic and serotoninergic neurons in the locus coeruleus and raphe nuclei (272), (d) the inferior colliculus and a variety of auditory relay nuclei, (e) the cerebellar nuclei, and (f) the substantia nigra and various parts of the brainstem reticular formation (97, 124, 188, 201, 257).

The superficial layers of the superior colliculus receive most of their input from the retina and visual cortex, and are concerned with detection of movement of objects in the visual field, whereas the deep layers receive inputs from multiple sources and have anatomic and physiologic characteristics of the brainstem reticular formation. Superficial layers of the superior colliculus project primarily to vision related nuclei, while intermediate and deep layers project to diverse regions related to head and eye movements (8, 68, 124, 148, 169, 188). However, despite morphologic, connectional, and biochemical differences, the superficial and deep layers of the superior colliculus are intimately linked with each other in a spatial registration.

AFFERENT PROJECTIONS

The superior colliculus receives afferents from the retina, the cerebral cortex, brainstem nuclei, and the spinal cord.

Retinotectal fibers leave the optic tract rostral to its principal termination in the lateral geniculate body and project to the superior colliculus via its brachium. Fibers come from homonymous portions of the retina of each eye, but crossed fibers are most numerous. Thus, the contralateral homonymous halves of the visual field are represented in each superior colliculus (Fig. 14.9). Optic tract fibers project to all parts of the superior colliculus (85, 187). The upper quadrants of the contralateral visual field are represented in medial parts of the superior colliculus; the lower quadrants are related to lateral regions of this structure. The contralateral peripheral visual field is represented in the caudal two-thirds of the superior colliculus, while central regions of the visual field (i.e., within 10° of the fovea) are represented rostrally. The region of the retina corresponding to the optic disc (the blind spot) has been identified near the center of the superior colliculus (149, 168, 187, 188). Retinal ganglion cells projecting to the superior colliculus are of the Y and W cell types (see Chapter 16). In the superior colliculus, representation of the contralateral eye is dominant, a finding that contrasts with the equal representation of the two eyes in the lateral geniculate body and the striate cortex.

Corticotectal fibers arise from portions of the frontal, temporal, parietal, and occipital lobes. The most substantial and highly organized projection arises from the visual cortex and reaches the superior colliculus via the brachium of the superior colliculus (124, 125, 225, 420). These fibers enter the stratum opticum and pass into the superficial and middle gray layers. Fibers from the retina enter via the same route and appear to terminate in the same layers. Although retinal and visual cortical projections to the superior colliculus are similar, there are important differences: retinal projections are bilateral and greatest contralaterally, while striate cortical projections are unilateral. Anatomic data indicate that portions of the visual cortex and superior colliculus related to particular regions of the retina are interconnected. Thus, essentially the same cells of the superior colliculus receive distinct, but related, inputs from ganglion cells of the retina and the striate cortex (Fig. 14.9). Afferents to the superficial laminae also arise from the parabigeminal area.

Corticotectal fibers from the frontal lobe, particularly the frontal eye field (Brodmann's area 8), terminate in the middle gray layer, the stratum opticum, and the stratum zonale (223). These fibers reach the superior colliculus throughout via a transtegmental approach and are thought to participate in motor mechanisms related to eye movements. Cells in superficial layers respond to visual stimuli, while cells in the middle gray layers discharge prior to the onset of saccadic eye movements. The auditory cortex projects to deep layers in caudal parts of the superior colliculus that receive no visual input (90).

Brainstem afferents to the superior colliculus arise from the inferior colliculus and a number of auditory relay nuclei (97, 188, 322, 393). Projections to deep layers of caudal parts of the superior colliculus arise mainly from the external and pericentral nuclei of the inferior colliculus. Other auditory relay nuclei projecting fibers to the superior colliculus include the ventral nucleus of the lateral lemniscus and the nuclei of the trapezoid body. Commissural fibers coursing in the *commissure of the superior colliculus* (Figs. 14.7 and 14.8) primarily relate deep and intermediate gray layers in the rostral halves of the superior colliculi (96). Additionally, this bundle

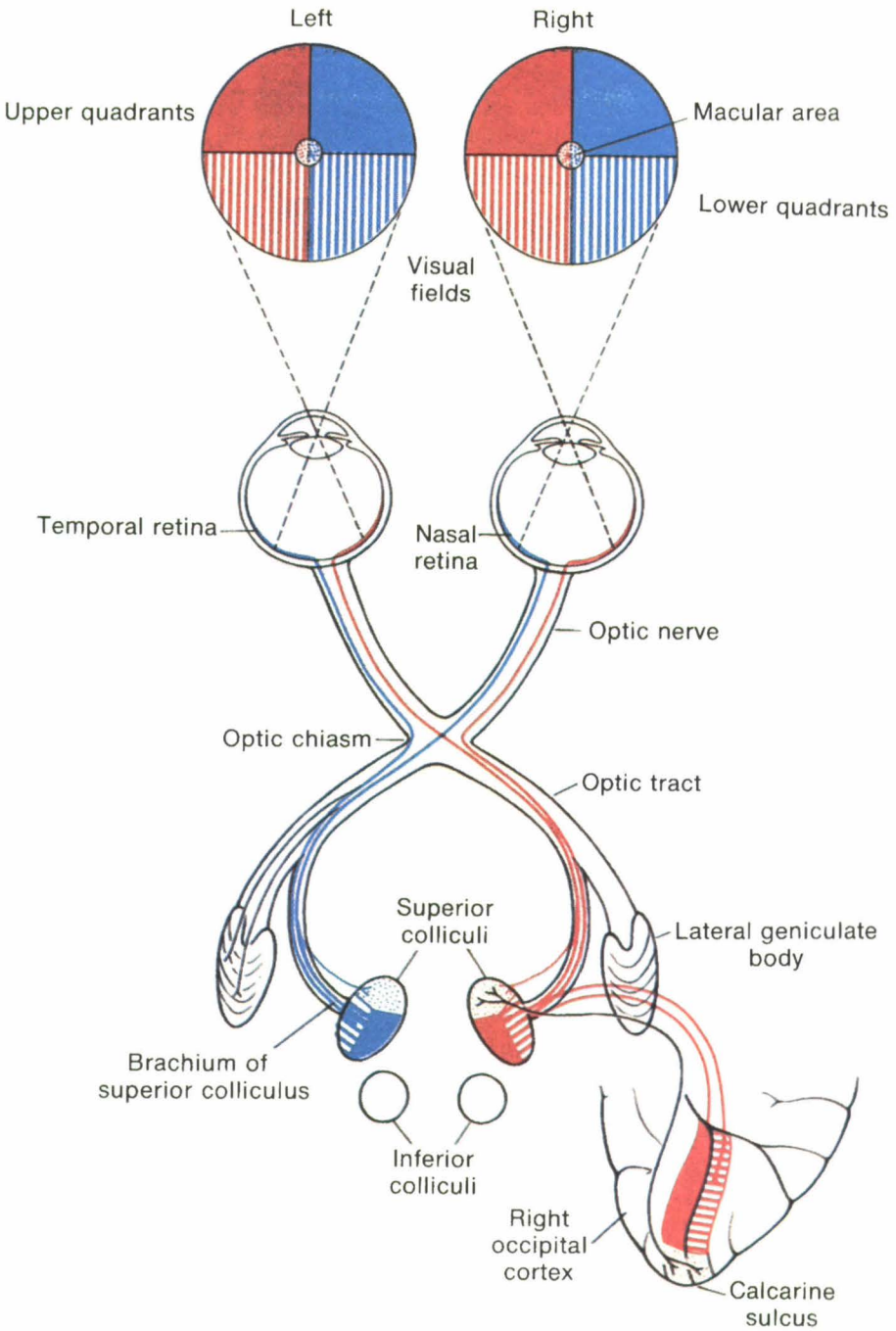


Figure 14.9. Projections of the retinae and striate cortex upon the superior colliculi in the rhesus monkey. Retinotectal fibers from the ipsilateral temporal and contralateral nasal halves of the retinae, which subserve the contralateral homonymous visual field, project to the superior colliculus. Cells in portions of the retinae concerned with the contralateral peripheral visual field project to the posterior two-thirds of the superior colliculus. Upper quadrants of the contralateral peripheral visual field (*solid blue* and *red*) are represented in medial region of caudal parts of the superior colliculus, while lower quadrants of the contralateral peripheral visual field (*blue* and *red stripes*) are represented in lateral regions. Portions of the retinae concerned with central vision (i.e., within 10° of the fovae centralis; *blue* and *red dots*) are represented in the rostral third of the superior colliculus. Although retinotectal fibers arise from portions of the retina of each eye, crossed fibers are most numerous. Corticotectal fibers from the striate cortex, shown on the *right*, project to all parts of the superior colliculus via its brachium. There is a correspondence in the superior colliculus of retinotectal and corticotectal terminations that represent both central and peripheral parts of the visual field.

contains some fibers projecting to noncorresponding areas of the colliculus and some decussating elements of both tectal and nontectal origin. The pars reticulata of the substantia nigra projects fibers to the deep and intermediate layers of the caudal two-thirds of the superior colliculus (58). Many of these GABAergic neurons have dichotomizing axons that also project to the thalamus (20, 30, 302). These connections appear related to motor functions, since all brainstem and spinal afferents arise from deep layers.

Spinotectal fibers projecting to the deep layers of the superior colliculus are not numerous. Although some somatosensory input to the superior colliculus arises from cells in the dorsal horn (lamina IV), the major inputs are from the posterior column nuclei (particularly the nucleus cuneatus) and all parts of the spinal trigeminal nuclear complex (97). Regardless of the locations of the cells of origin, somatosensory input to the deep layers of the superior colliculus is topographically organized with the head represented rostrally, the forelimbs posterolaterally, and the remainder of the body posteromedially (104, 378). The somatotopic representation is distorted in that regions related to the head and forelimb are unusually large.

As the preceding discussion indicates, the superior colliculus can be partitioned into two zones: (a) the superficial layers, which receive primarily visual afferents, and (b) deep layers, which receive a heterogeneous multimodal input. Although the superficial layers of the superior colliculus have projections distinct from that of all deeper layers, they also project to the deep layers (166).

EFFERENT PROJECTIONS

In general, the superficial layers give rise to ascending fibers and the deep layers project descending fibers to nuclei in the brainstem and spinal cord.

Tectothalamic fibers, arising from superficial layers of the superior colliculus, project ipsilaterally to the pulvinar, the dorsal and ventral lateral geniculate nuclei, and the pretectum (8, 26, 28, 68, 148, 169, 188). The pulvinar receives the most extensive projection from the superficial layers of the colliculus and, in turn, projects upon extrastriate cortical areas (areas 18 and 19) (27, 28, 140). Thus, the superficial layers of the superior colliculus give rise to tectothalamic fibers, part of which convey visual information to the extrastriate cortex via the pulvinar. It also has been shown that cells in the most superficial layers of the superior colliculus in primates project upon the dorsal lateral geniculate body (167) and to the parabigeminal nucleus (28). Most of the *tectogeniculate fibers* terminate in intralaminar geniculate regions adjacent to the magnocellular layers, which are thought to contain interneurons. Thus, visual pathways to the cortex via the superior colliculus and the lateral geniculate body are not entirely separate. The deep layers of the superior colliculus also give rise to ascending fibers that project to the posterior and intralaminar thalamic nuclei (169). Cells in the intermediate and deep collicular layers project to both motor and sensory nuclei. These collicular projections include the pretectum, the paramedian pontine reticular formation (PPRF), and the rostral interstitial nucleus of the medial longitudinal fasciculus (RiMLF) involved in subcortical control of eye movements.

Descending tectofugal fibers arising from intermediate and deep layers of the superior colliculus can be grouped into uncrossed tectopontine and tectobulbar tracts, and crossed tectobulbar and tectospinal projections.

Uncrossed tectopontine and *tectobulbar fibers* project to the ipsilateral dorsolateral pontine nuclei, the lateral part of the reticulotegmental nucleus, and the nucleus reticularis pontis oralis (8, 166, 169, 188, 210). Additionally, deep layers of the superior colliculus project fibers to the cuneiform nucleus and the external nucleus of the inferior colliculus. Superficial layers of superior colliculus give rise to a substantial ipsilateral projection to the parabigeminal nucleus, a structure that has bilateral regionally organized projections to the superior colliculus (150, 166). The dorsolateral region of the pontine nuclei, which receives fibers from the superior colliculus, also receives inputs from the visual and auditory cortex (48, 125). This collection of pontine nuclei projects to lobules VI and VII of the cerebellar vermis (46) and are responsive to visual, auditory, and somatosensory stimuli (359).

Tectoreticular fibers project profusely and bilaterally to dorsal regions of the midbrain reticular formation. Some tectofugal fibers enter the accessory oculomotor nuclei (i.e., the nucleus of Darkschewitsch and the interstitial nucleus of Cajal), but none appear to enter the oculomotor complex (8, 250, 292, 329, 392).

Crossed tectobulbar and tectospinal fibers decussate in the dorsal tegmental decussation at midbrain levels and descend near the median raphe (Fig. 11.18). At medullary levels these fibers become incorporated within the medial longitudinal fasciculus. Tectospinal fibers continuing to cervical spinal segments descend in the medial part of the anterior funiculus (Fig. 11.25). In the brainstem, this crossed projection is referred to as the *predorsal bundle*. Fibers from this bundle project to the reticulotegmental nucleus and to both rostral and caudal portions of the pontine reticular formation (166). At medullary levels, crossed tectobulbar fibers terminate in parts of the medial accessory olivary nucleus (i.e., nucleus β). Tectospinal fibers descending only to cervical spinal segments terminate in laminae VII and VIII (285).

FUNCTIONAL CONSIDERATIONS

Each superior colliculus receives a visual input related to the contralateral visual field. Additionally, it receives an ipsilateral projection from the visual cortex concerning only the contralateral visual field. These two systems are precisely and topographically organized at all levels. Unilateral lesions of the superior colliculus in a variety of animals produce (a) relative neglect of stimuli in the contralateral visual field, (b) deficits in perception involving spatial discriminations and tracking of moving objects, (c) heightened responses to stimuli in the ipsilateral visual field, and (d) no impairment of eye movements (374, 375). These disturbances undergo considerable attenuation in time, but indicate that the superior colliculus contributes to the coordination of head and eye movements used to localize and follow visual stimuli.

Physiologic studies in the cat indicate that the collicular receptive fields are two to four times larger than the receptive fields in the visual cortex. A receptive field in the visual system is defined as that region of the retina (or visual field) over which one can influence the firing of a particular ganglion cell (220). The receptive field consists of a central circular region and a concentric surround. Most collicular cells respond only to moving stimuli, and three-fourths of these cells show directional selectivity (85, 383). These cells respond well to movement in one direction, but poorly, or not at all, to movement in the opposite direction, and are nonresponsive to stationary stimuli flashed on and off within the receptive field. In the superior colliculus, the preferred directional selectivity is parallel to the horizontal meridian of the visual field and toward the periphery of the visual field. Thus, units in the left superior colliculus have receptive fields in the right visual field and respond best to stimuli moving from left to right. Cells in the superficial layers of the superior colliculus are most responsive to small moving objects.

In animals in which the visual cortex has been removed, cells of the superior colliculus lose their directional sensitivity to moving objects in the visual field (419). While in the normal animal cells in the superior colliculus can be driven by stimuli to either eye, following ablations of the visual cortex, these cells respond only to stimuli in the contralateral eye. Thus, the superior colliculus cannot perform its normal function as a detector of specific movements within the visual field when deprived of input from the visual cortex.

Stimulation of the superior colliculus results in contralateral conjugate deviations of the eyes (13, 384), even though this structure has no projections to the nuclei of the extraocular muscles. Part of these responses may be mediated by collicular projections to (a) the rostral interstitial nucleus of the medial longitudinal fasciculus (RiMLF), which projects to specific subdivisions of the ipsilateral oculomotor complex (61, 377), or (b) the pontine paramedian reticular formation (PPRF), which projects to the ipsilateral abducens nucleus (54) and the RiMLF. Although the PPRF has no direct connections with the oculomotor complex, impulses relayed via abducens internuclear neurons can influence subdivisions of the oculomotor nuclear complex (59).

Electrical stimulation of the superior colliculus in alert monkeys also elicits short-latency saccadic eye movements (340, 356). The amplitude and direction of these saccades are a function of the site stimulated within the superior colliculus. Medial regions of the colliculus are associated with upward components, while lateral regions have downward components (373). Chronic microelectrode recordings in the intermediate and deep layers of the superior colliculus have shown maximal discharges of neurons prior to eye movements in particular directions. These studies indicate that the superior colliculus is involved in coding the location of an object relative to the fovea and in eliciting

saccadic eye movements that produce foveal acquisition of the object (373). The GABAergic projections to the superior colliculus play a crucial role in the control of saccadic eye movements. The visuotopic order of the electrophysiologic response properties of neurons in the intermediate layers of the superior colliculus to which the substantia nigra projects, and the matching of visual receptive fields of superior colliculus neurons and nigral neurons that innervate them, suggest a visuotopic ordering of nigral neurons related to eye movements (178–181). The superficial laminae of the superior colliculus also play an important role in the extrageniculate visual pathways related to depth perception.

Pretectal Region

This region lies immediately rostral to the superior colliculus at levels of the posterior commissure (Figs. 14.10 and 16.4). Several distinctive cell groups within this region appear related to the visual system. The nuclei of the pretectal region include (a) the nucleus of the optic tract, (b) the sublentiform nucleus, (c) the nucleus of the pretectal area, (d) the pretectal olivary nucleus, and (e) the principal pretectal nucleus (14, 66, 208, 221). The nucleus of the optic tract consists of a plate of large cells along the dorsolateral border of the pretectum at its junction with the pulvinar (Fig. 14.10). The pretectal olivary nucleus (or olivary nucleus of the superior colliculus) forms a sharply delimited cell group at levels through caudal parts of the posterior commissure (Fig. 14.11), whereas the sublentiform nucleus forms a crescent-shaped group of small- and medium-sized cells medial to the nucleus of the optic tract. The nucleus of the pretectal area occupies a dorsomedial part of the pretectum throughout its extent, while the principal pretectal nucleus lies ventral to the sublentiform nucleus and its boundaries are difficult to distinguish.

The pretectal nuclei receive fibers from the optic tract, the lateral geniculate body, certain areas of the cortex, and probably from the

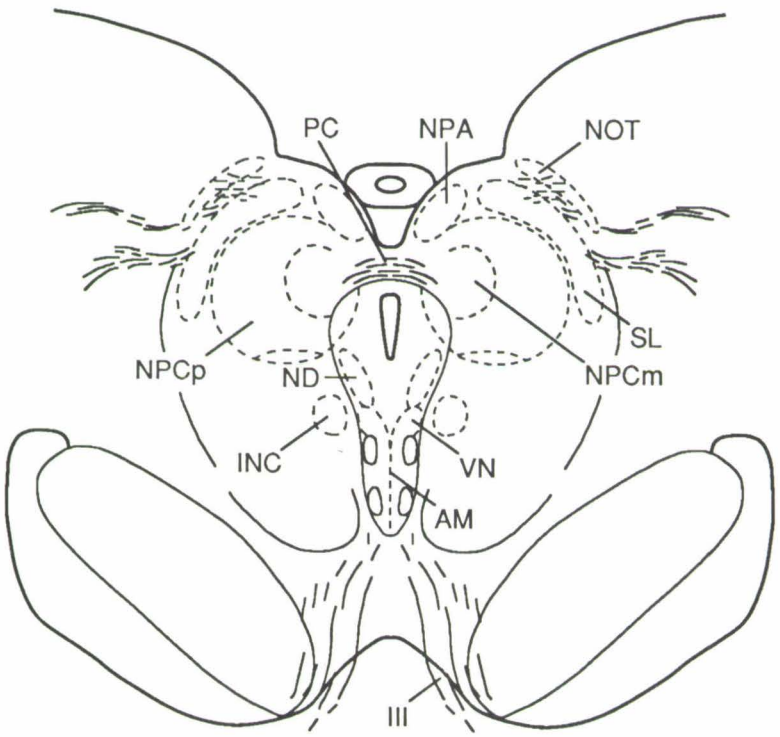


Figure 14.10. Brainstem transverse section through the most compact portion of the posterior commissure (*PC*). At this level, the nucleus of the optic tract (*NOT*), the sublentiform nucleus (*SL*), the nucleus of the pretectal area (*NPA*), and the nuclei of the posterior commissure (*NPC*) are well-developed. The anterior median nucleus (*AM*) is present, but the dorsal visceral nuclei (*VN*) of the oculomotor complex have not separated into medial and lateral cell columns. *INC*, interstitial nucleus of Cajal; *ND*, nucleus of Darkschewitsch; NPC_m, nucleus of posterior commissure, pars magnocellularis; NPC_p, nucleus of posterior commissure, pars principalis; *III*, oculomotor nerve.

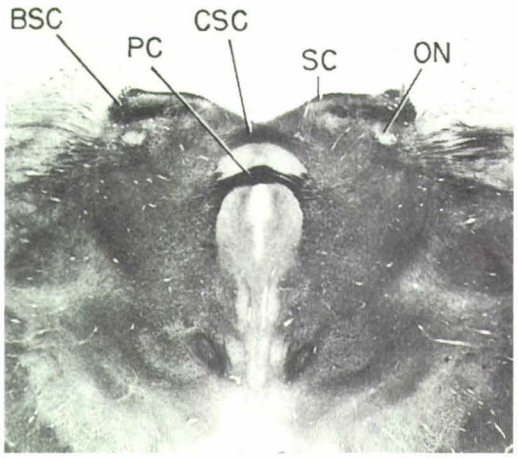


Figure 14.11. Myelin-stained section at junction of pretectum and superior colliculus in the rhesus monkey. *BSC*, brachium of the superior colliculus; *CSC*, commissure of the superior colliculus; *ON*, pretectal olivary nucleus; *PC*, posterior commissure; *SC*, superior colliculus (Weil stain.)

posterior thalamic nuclei (124, 125, 136, 137, 176, 190, 309, 353). The pretectal region is considered to be principal midbrain center involved in the *pupillary light reflex* (245, 246, 327).

Fibers from the pretectal olivary nucleus, which receives both crossed and uncrossed retinofugal fibers, cross in the posterior commissure and project to specific components of the visceral nuclei of the oculomotor complex (Fig. 14.16) (66, 377). Fibers from the nuclei of the posterior commissure, projecting bilaterally to other visceral nuclei, partially decussate ventral to the cerebral aqueduct (Fig. 14.16). Because of the complex crossed and uncrossed projections to the visceral nuclei of oculomotor nerve, only relatively large lesions involving multiple structures in the pretectum impair the pupillary light reflex.

Posterior Commissure

The transition from midbrain to diencephalon is marked dorsally by the *posterior commissure* (Figs. 2.28, 14.10, 14.11, 14.12**A**, and 14.15**B**). This small commissure lies dorsal to the periaqueductal gray and rostral to the superior colliculi at the point of transition between the cerebral aqueduct and the third ventricle. As fibers of the posterior commissure fan out laterally, they are surrounded by cells that collectively form the *nuclei of the posterior commissure* (Fig. 14.10) (64). Identified elements in the posterior commissure include fibers from (a) the pretectal nuclei, (b) the nuclei of the posterior commissure, (c) the interstitial nucleus of Cajal, and (d) the nucleus of Darkschewitsch (Fig. 14.17). Fibers from the pretectal olivary nucleus (Figs. 14.10 and 14.11) cross in the commissure to the same nucleus on the opposite side and give collaterals to the visceral nuclei of the oculomotor complex (Fig. 14.16). Lesions in the posterior commissure reduce, but not eliminate, the consensual pupillary light reflex (247) and do not affect the pupillary light reflex as measured in infrared pupillograms (66). Lesions in the nuclei of the posterior commissure, in-

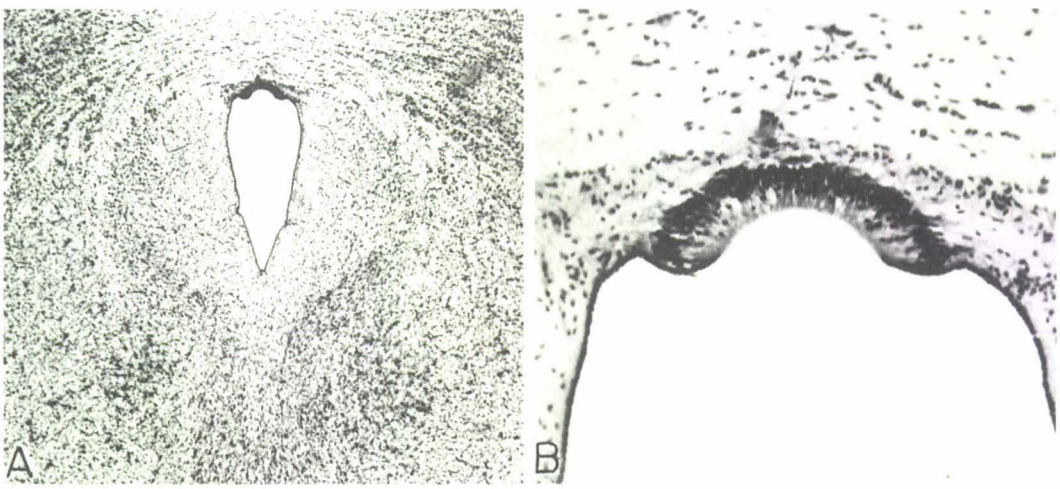


Figure 14.12. Subcommissural organ in the rhesus monkey. **A.** Position of the structure in the roof of the aqueduct beneath the posterior commissure. **B.** Difference between the tall columnar cells of the subcommissural organ and the cells of the ependyma. (Nissl stain, ×16; ×100.)

terrupting fibers from the interstitial nuclei of Cajal, produce bilateral eyelid retraction and impairment of vertical eye movements (61).

The *subcommissural organ* is a modified ependymal plate in the roof of the cerebral aqueduct immediately beneath the posterior commissure (Figs. 1.17 and 14.12). This periventricular organ, which is recognized as circumventricular and appears to have a secretory function, consists of ciliated columnar cells (421). The secretory product of these cells, in all species except human, is condensed to form a strand of proteinaceous material (Reissner's fiber) that extends through the aqueduct, the fourth ventricle and into the spinal canal. Cells of the subcommissural organ are different than the usual ependymal cells in that they have projections into the ventricular lumen covered with protruding microvilli, an abundance of rough endoplasmic reticulum and microtubules. These cells also show pinocytotic vesicles near the cell surface (77). These data, based upon scanning and transmission electron microscopy, suggest that cells of the subcommissural organ are active in secretion and possibly in absorbing substances from the cerebrospinal fluid. The function of this subcommissural organ in human is unknown, but it has been suggested that it may serve as a volume receptor (134), play an important role in control of salt and water balance (133, 253), and be concerned with thirst and water intake. The subcommissural organ is the only midbrain structure not included in the blood-brain barrier.

Oculomotor Nerve

OCULOMOTOR NUCLEAR COMPLEX

The oculomotor nuclear complex is a collection of cell columns and discrete nuclei that (a) innervate the inferior oblique and the superior, medial, and inferior rectus muscles, (b) supply the levator palpebrae muscle, and (c) provide preganglionic parasympathetic fibers to the ciliary ganglion (Fig. 14.14 and Table 14.1). Functional components of the nerve are categorized as *general somatic efferent* (GSE) and *general visceral efferent* (GVE). This complex lies ventral to the central gray matter in the midline in a V-shaped trough formed by the diverging fibers of the medial longitudinal fasciculus (MLF). It extends from the rostral pole of the trochlear nucleus to the upper limit of the midbrain (Figs. 14.6, 14.10, and 14.13). The nuclear complex con-

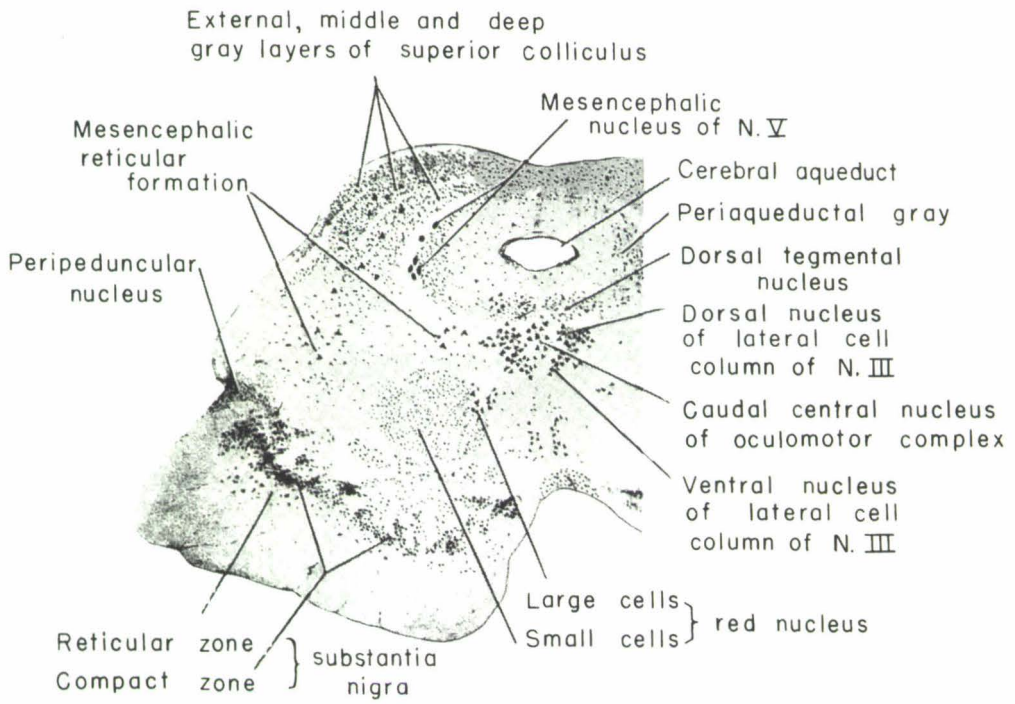


Figure 14.13. Transverse section through superior colliculi of midbrain in a 3-month infant. (Cresyl violet stain with the main cell groups schematically blocked.)

sists of paired lateral somatic cell columns, midline and dorsal visceral nuclei, and a discrete midline dorsal cell group called the caudal central nucleus.

The *lateral somatic cell columns* is composed of large motor-type neurons that innervate the extraocular muscles (413). The dorsal cell column (or nucleus) innervates the inferior rectus muscle, the intermediate cell column innervates the inferior oblique muscle, and the ventral cell column supplies fibers to the medial rectus muscle (Fig. 14.14 and Table 14.1). Although major representation of the medial rectus muscle is in the ventral cell column, a discrete collection of cells in dorsal regions also innervate this muscle. Root fibers arising from these cell columns are uncrossed. A cell column medial to both the dorsal and intermediate cell columns, referred to as the medial cell column, provides crossed fibers that innervate the superior rectus muscle.

The *caudal central nucleus* is a midline somatic cell group found only in the caudal third of the complex (414). This nucleus gives rise to crossed and uncrossed fibers that innervate the levator palpebrae muscle (Figs. 14.13 and 14.14).

Visceral nuclei of the oculomotor nuclear complex consist of two distinct nuclear groups, which are in continuity rostrally. The *Edinger-Westphal nucleus* (Figs. 14.10, 14.14, and 14.15**A**) consists of two slender columns of small cells dorsal to the rostral three-fifths of the somatic cell columns. In transverse sections through the middle third of the complex, each of these paired columns divides into two smaller cell columns, which taper and gradually disappear. Rostrally the cell column of the Edinger-Westphal nucleus merge in the midline dorsally and become continuous with the visceral cells of the *anterior median nucleus*. Cells of the anterior median nucleus lie in the raphe between por-

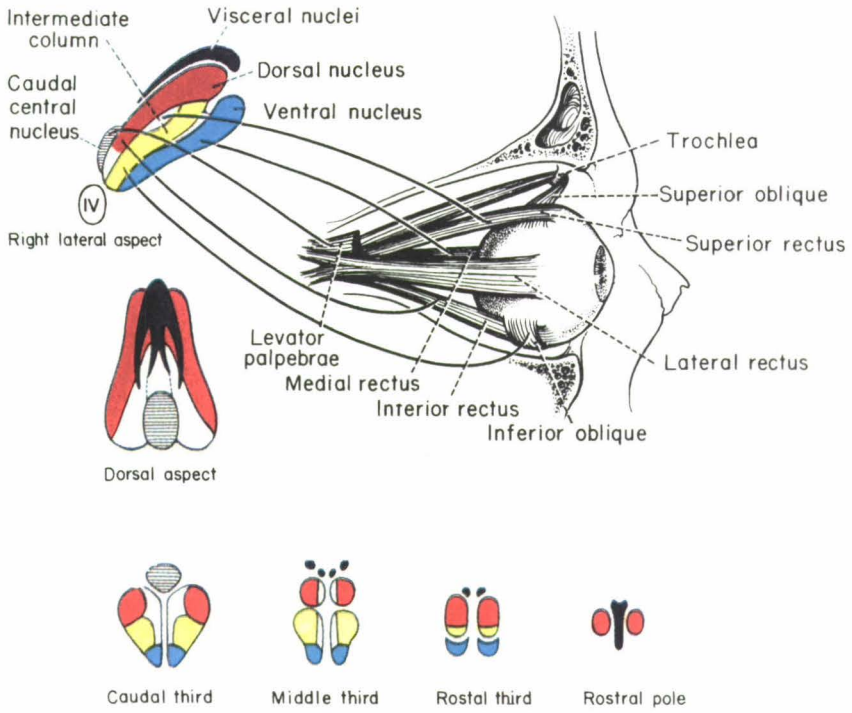


Figure 14.14. Localization of the extraocular muscles within the oculomotor nuclear complex, based upon studies in the rhesus monkey. Cell columns composing the complex are shown in lateral, dorsal, and transverse views through various levels. The visceral motor (parasympathetic) cell columns are shown in *black*. The ventral nucleus (*blue*) innervates the medial rectus muscle, while the dorsal nucleus (*red*) innervates the inferior rectus muscle. The intermediate cell column (*yellow*) innervates the inferior oblique muscle, while the cell column (*white*) medial to the dorsal and intermediate cell columns innervates the superior rectus muscle. The caudal central nucleus (*lined*) supplies fibers to the levator palpebrae superioris. Fibers innervating the medial rectus, inferior rectus, and inferior oblique muscles are uncrossed. Fibers supplying the levator palpebrae muscle are both crossed and uncrossed, while those to the superior rectus muscle are crossed. The drawing in the upper right shows the positions of the extraocular muscles in relation to the globe and the bony orbit.

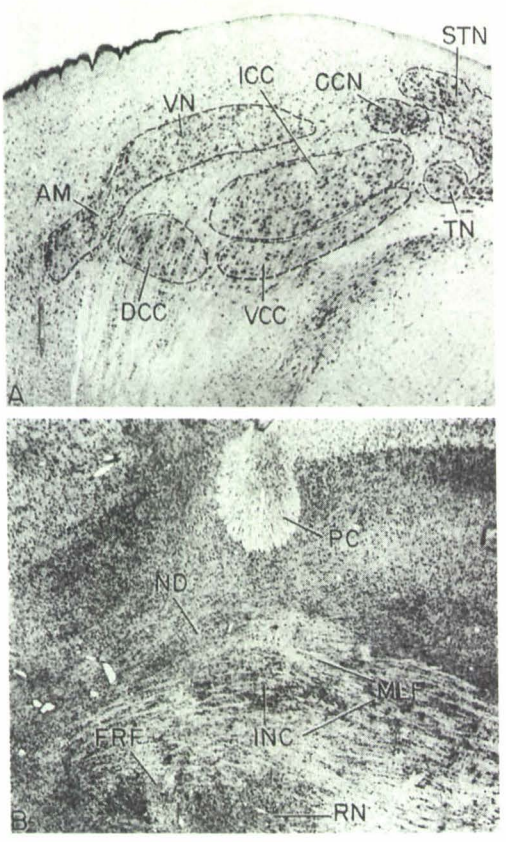


Figure 14.15. **A.** Sagittal section through the oculomotor complex slightly removed from the midline in a rhesus monkey. The continuity of the anterior median (*AM*) and dorsal visceral cell columns (*VN*) is evident. Other nuclei identified are: *DCC*, dorsal (somatic) cell column; *VCC*, ventral (somatic) cell column; *ICC*, intermediate (somatic) cell column; *CCN*, caudal central nucleus; *TN*, trochlear nucleus; and *STN*, supratrochlear (dorsal raphe) nucleus. (Nissl stain, ×20.) **B.** Parasagittal section through the posterior commissure (*PC*) and the medial longitudinal fasciculus (*MLF*), demonstrating the relationships between the nucleus of Darkschewitsch (*ND*), the interstitial nucleus of Cajal (*INC*), and the red nucleus (*RN*). *FRF* indicates fasciculus retroflexus. (Nissl stain, ×20.)

tions of the rostral lateral somatic cell columns (Figs. 14.10 and 14.16). Both the Edinger-Westphal and the anterior median nuclei give rise to uncrossed preganglionic parasympathetic fibers that emerge with somatic root fibers and project to the ciliary ganglion (50). The anterior median nuclei and the lateral visceral cell column receive fibers from the contralateral pretectal olivary nuclei which cross in the posterior commissure (377) (Fig. 14.16). The anterior median and medial visceral cell columns receive bilateral projections from the nuclei of the posterior commissure which partially decussate ventral to the aqueduct (66). Although the visceral nuclei of the oculomotor nuclear complex (i.e., the Edinger-Westphal and anterior median nuclei) have been considered to supply preganglionic parasympathetic fibers only to the ciliary ganglion, retrograde transport studies demonstrate that these visceral neurons also project to the lower brainstem, the cerebellum, and spinal cord (69, 226, 239, 240, 386). Descending fibers from distinctive visceral nuclei of the oculomotor complex project to the posterior column nuclei and Rexed's laminae I and V as far caudally as lumbar spinal segments (Fig. 11.23).

The so-called central nucleus of Perlia has been regarded as a midline cell group concerned with ocular convergence. There has been great difficulty in identifying this nucleus in humans and monkeys (74, 415, 416), and its function remains in doubt.

Root fibers of the oculomotor nerve pass ventrally in numerous small bundles, some of which traverse the red nucleus. Ventrally, the fibers converge and emerge from the interpeduncular fossa on the anterior aspect of the midbrain (Figs. 2.9, 2.26, and 12.1). Visceral fibers emerge with rootlets in the rostral part of the oculomotor nerve. Spreading of the root fibers through and around the red nucleus is an expression of the intraradicular expansion of the red nucleus during embryologic development (Fig. 14.6).

ACCESSORY OCULOMOTOR NUCLEI

Grouped under this designation are three nuclei closely associated with the oculomotor complex. These nuclei are the interstitial nucleus of Cajal, the nucleus of Darkschewitsch, and the nuclei of the posterior commissure.

The *interstitial nucleus* (of Cajal) is a small collection of multipolar neurons situated among, and lateral to, the fibers of the MLF in the rostral midbrain (326) (Figs. 14.10, 14.12**A**, 14.15**B**, and 14.18). In humans, the interstitial nucleus contains about 75% of small- to medium-sized polymorph cells and 25% of large polygonal neurons dispersed throughout the nucleus (35). The smaller neurons are believed to be key integrative elements while large neurons are thought of as projection elements. The interstitial nucleus receives projections from the superior and medial vestibular nuclei, the pretectum, the frontal eye fields, and the fastigial nucleus. Efferent fibers from the interstitial nucleus cross in the ventral part of the posterior commissure and

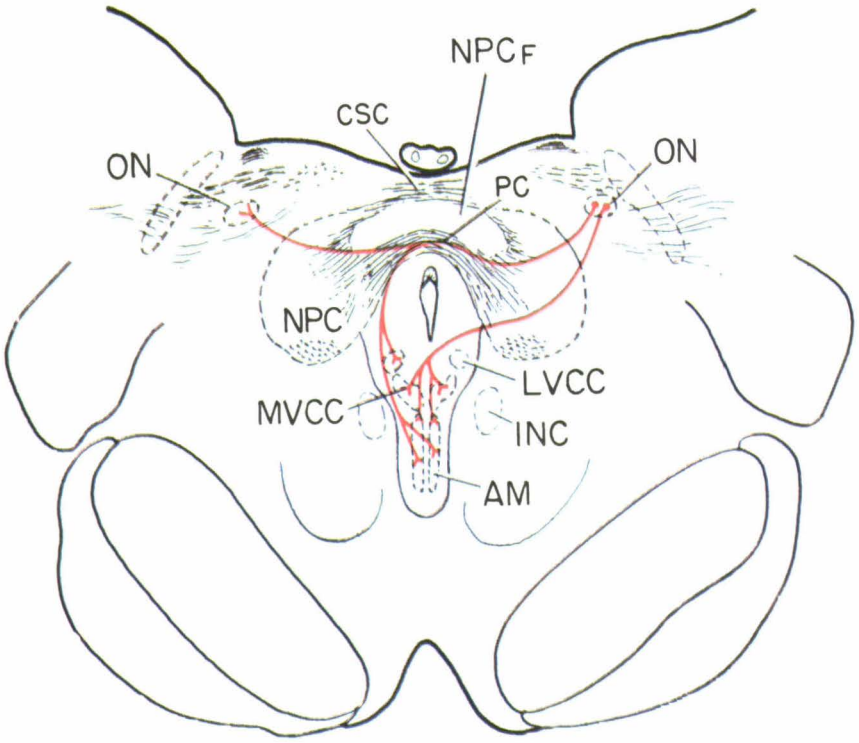


Figure 14.16. Transverse section of the midbrain through the posterior commissure, showing the course and terminations of afferents projecting to the visceral nuclei of the oculomotor complex. The pretectal olivary nucleus (*ON*) receives direct bilateral retinal projections. Projections of the pretectal olivary nucleus (*red*) partially cross ventral to the cerebral aqueduct and terminate in the medial visceral cell column (*MVCC*) and the anterior median nuclei (*AM*). Other efferents from the pretectal olivary nuclei cross in the posterior commissure and end in the lateral visceral cell column (*LVCC*) and the anterior median nuclei. Commissural connections interrelate the pretectal olivary nuclei. *CSC*, commissure of the superior colliculus; *INC*, interstitial nucleus of Cajal; *NPC*, nuclei of the posterior commissure; NPC_F, nucleus of the posterior commissure, pars infracommissuralis.

are distributed to all somatic cell columns of the contralateral oculomotor complex, except the ventral ones (61). Additionally, the nucleus projects fibers bilaterally to the trochlear nuclei and ipsilaterally to the medial vestibular nucleus (321) and spinal cord (i.e., interstitiospinal tract) (Fig. 14.17). This nucleus is concerned with slow rotatory and vertical eye movements and smooth pursuit eye patterns. It also plays a role in the control of head movements and posture (120).

The *nucleus of Darkschewitsch* is formed by small cells which lie inside the ventrolateral border of the central gray matter, dorsal and lateral to the somatic cell columns of the oculomotor complex (Figs. 14.10, 14.12**A**, 14.15**B**, and 14.18). The nucleus projects to the nuclei of the posterior commissure, but does also project fibers into the oculomotor nuclear complex or the lower brainstem (377).

The *nuclei of the posterior commissure* consist of collections of cells intimately associated with fibers of the posterior commissure, as mentioned earlier. Cells of these nuclei lie dorsolateral and dorsal to the central gray matter, and have connections with the pretectal and posterior thalamic nuclei. In the monkey, interruption of fibers in the posterior commissure in the midline does not impair the pupillary light reflex, but lesions involving the nuclei of the posterior commissure and crossing fibers from the interstitial nuclei of Cajal produce bilateral eyelid retraction and impairment of vertical eye movements.

AFFERENT CONNECTIONS OF THE OCULOMOTOR COMPLEX

Although no direct corticobulbar fibers reach the oculomotor complex, impulses from the cerebral cortex are conveyed to reticular neurons, which relay these impulses to the complex. Direct projections to the oculomotor nuclear complex arise from parts of the vestibular nuclei, the interstitial nucleus of Cajal, abducens internuclear neurons,

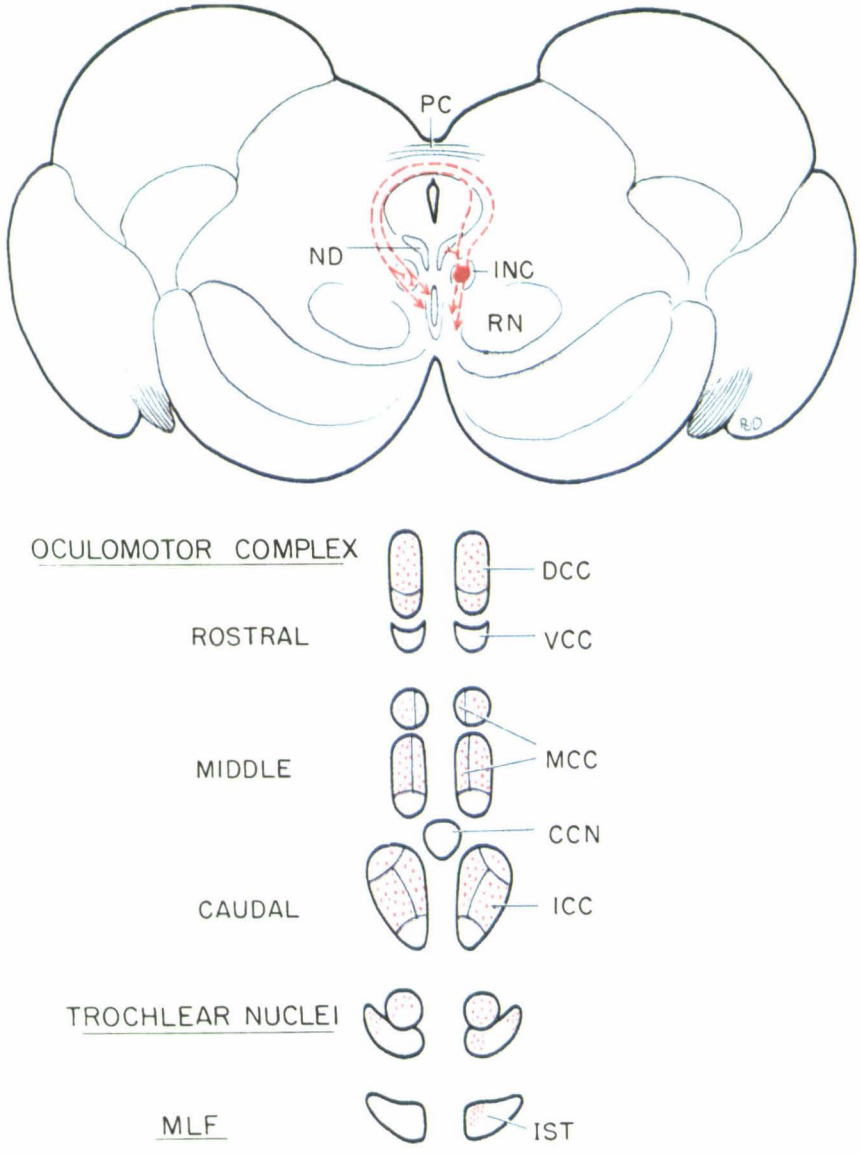


Figure 14.17. Degeneration resulting from a lesion (*red*) in the right interstitial nucleus of Cajal (*INC*). The lesion destroyed (a) cells which give rise to fibers that cross in the ventral part of the posterior commissure and fibers which descend in the ipsilateral MLF, and (b) fibers from the opposite interstitial nucleus which have crossed in the posterior commissure and traverse the lesion *en route* to the oculomotor complex. Fairly symmetric differential degeneration (*red stippling*) in the oculomotor complex was greatest in the intermediate (*ICC*) and medial cell columns (*MCC*), somewhat less profuse in the dorsal cell columns (*DCC*), and absent in the ventral cell columns (*VCC*) and in the caudal central nucleus (*CCN*). Degeneration in the trochlear nuclei was bilateral but was greatest ipsilaterally. Fibers of the interstitiospinal tract (*IST*) were concentrated in the dorsomedial part of the MLF. *ND*, nucleus of Darkschewitsch; *PC*, posterior commissure; *RN*, red nucleus.

parts of the perihypoglossal nuclei, the rostral interstitial nucleus of the MLF (RiMLF), and the pretectal olivary nucleus. The superior colliculus does not project directly to the oculomotor complex, but it innervates parts of the periaqueductal gray close to the oculomotor nuclei. The interstitial nucleus of Cajal gives rise to fibers that cross in the ventral part of the posterior commissure and pass to all somatic cell columns, except the ventral, on the opposite side (Fig. 14.17) (57, 61). Secondary fibers arising from the medial and superior vestibular nuclei project to the oculomotor nuclear complex via the MLF (377). Projections from the medial vestibular nucleus via the MLF are bilateral, while those

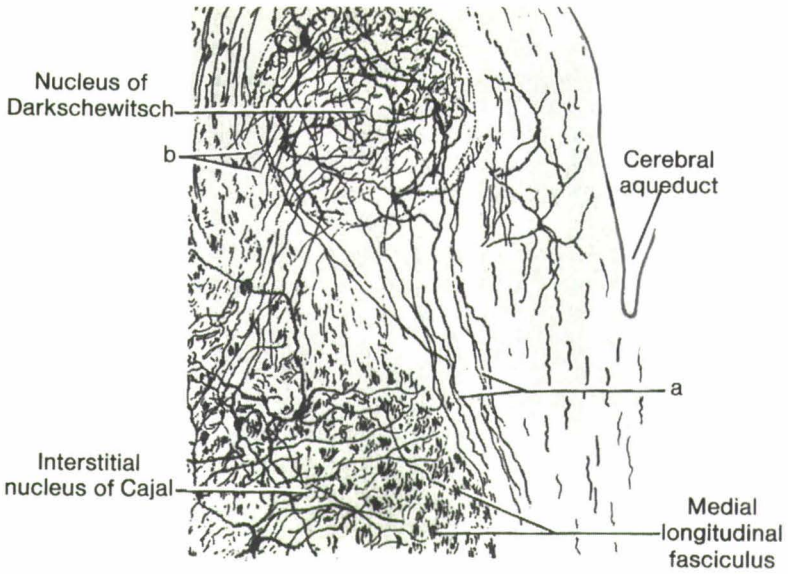


Figure 14.18. Relationships of the nucleus of Darkschewitsch and the interstitial nucleus of Cajal to the central gray matter (surrounding the cerebral aqueduct) and the medial longitudinal fasciculus (*b*, collateral fibers terminating in the nucleus of Darkschewitsch; *a*, fibers leaving this nucleus). Based upon Golgi preparations from a newborn kitten.

from the superior vestibular nucleus via this bundle are ipsilateral. Fibers from peripheral parts of the superior vestibular nucleus, not contained in the MLF, cross in the caudal midbrain and project to the superior rectus and inferior oblique subdivisions of the oculomotor complex. These vestibulo-oculomotor connections serve to integrate the receptor activities of the labyrinth and visual systems which provide information concerning orientation in three-dimensional space. Abducens internuclear neurons give rise to axons that ascend in the contralateral MLF and terminate selectively upon cells of the opposite medial rectus subdivision of the oculomotor complex (53, 59). These internuclear projections from the abducens to the oculomotor nucleus underlie the neural mechanism responsible for conjugate horizontal gaze.

The nucleus prepositus, which receives an input from the flocculus (7, 18, 118), projects ipsilaterally to the oculomotor nuclear complex (122, 151, 377), and may be concerned with vertical eye movements (18, 59, 118). Physiologically, the projection from the nucleus prepositus appears related to upward eye movements.

The rostral interstitial nucleus of the MLF (RiMLF), situated among the fibers of the MLF rostral to the oculomotor complex at the junction of the mesencephalon and the diencephalon, appears uniquely concerned with vertical eye movements, particularly in a downward direction. Cells in the RiMLF are activated in short bursts before vertical eye movements occur in response to vestibular or optokinetic stimuli. The RiMLF receives input from the superior vestibular nucleus via the MLF and uncrossed projections from the paramedian pontine reticular formation (PPRF), which ascend outside the MLF. Cells of the RiMLF project ipsilaterally to the oculomotor complex and terminate mainly in the inferior rectus subdivision. Thus, the PPRF projects fibers to both the principal center for conjugate horizontal eye movements, the abducens nucleus, and the established center for vertical eye movement, the RiMLF (52). These findings indicate that paralysis of conjugate horizontal and vertical eye movements can occur independently, yet a mechanism exists that integrates horizontal and vertical components of conjugate eye movements (141).

Pupillary Reflexes

Light shone on the retina of one eye causes both pupils to constrict. The response in the eye stimulated is called the *direct pupillary light reflex*, while that in the opposite eye is known as the *consensual pupillary light reflex*. Pathways involved in the pupillary light reflex are not entirely known but involve (a)

axons of retinal ganglion cells that pass via the optic nerve, optic tract, and brachium of the superior colliculus to the pretectal area; (b) axons of pretectal neurons that partially cross in the posterior commissure and terminate bilaterally in visceral nuclei of the oculomotor complex (Fig. 14.16); (c) preganglionic fibers from the visceral nuclei that course with fibers of the third nerve and synapse on cells in the ciliary ganglion (Fig. 9.1); and (d) postganglionic fibers from the ciliary ganglion that project to the sphincter of the iris. Cells of the pretectal olivary nucleus receive fibers of the optic tract and project bilaterally to the visceral nuclei of the oculomotor complex. In humans, direct and consensual pupillary light reflexes are equal (241). The term *anisocoria* is used to denote pupillary inequality. The principal central lesions producing anisocoria involve efferent pathways from the oculomotor complex.

The *accommodation-convergence reaction* occurs when gaze is shifted from a distant object to a near one. This reaction involves (a) contractions of both medial recti muscles for convergence; (b) contraction of the ciliary muscles, which relaxes the suspensory ligament of the lens and cause the lens to assume a more convex shape; and (c) pupillary constriction. In this reflex, retinal impulses must first reach the visual cortex and be relayed via corticofugal fibers to brainstem centers. Corticofugal fibers involved in this response reach the superior colliculus and pretectal region and are relayed to the oculomotor complex. Although under normal circumstances accommodation always is accompanied by pupillary constriction, certain central nervous system lesions can impair or abolish the pupillary light reflex without affecting accommodation. Such lesions occur with central nervous system syphilis (tabes dorsalis) in which the pupils are small (miosis) and do not react to light but react to accommodation. This is the *Argyll-Robertson* pupil. The precise location of the responsible lesion is unknown.

In intense illumination, contraction of the pupil may be accompanied by closure of the eyelids, lowering of the brow, and general contractions of the face, designed to shut out the maximal amount of light. In so far as they are not volitional, these reflex movements probably are mediated through the superior colliculi and the tectobulbar tracts.

The central pathways for pupillary dilatation are not entirely known, but dilatation occurs reflexly on shading the eyes, scratching the side of the neck, and in association with severe pain and extreme emotion. Impulses related to pain probably reach cells of the intermediolateral cell column in upper thoracic (C8 to T1) spinal segments (Fig. 11.23) that give rise to preganglionic sympathetic fibers that convey impulses to the superior cervical ganglion. Postganglionic fibers from the superior cervical ganglion pass via blood vessels to dilatator muscles fibers of the iris (Fig. 11.30).

A *Horner's syndrome* usually results from interruption of descending autonomic pathways that course in the dorsolateral tegmentum at all the brainstem levels caudal to the hypothalamus. This syndrome may also occur as a consequence of interrupting descending autonomic fibers in the brainstem or cervical spinal cord and with lesions involving either preganglionic or postganglionic sympathetic fibers to the superior cervical ganglion. The syndrome is characterized by miosis, pseudoptosis, apparent enophthalmos, and dryness of the skin over the face. If Horner's syndrome is the result of a brainstem lesion, the pupil shows relatively little dilatation to adrenaline. If the provocative lesion involves postganglionic sympathetic fibers, adrenaline produces mydriasis and eyelid retraction on the affected side due to denervation sensitivity (76).

LESIONS OF THE THIRD NERVE

Complete lesions of the third nerve produce an ipsilateral lower motor neuron paralysis of the muscles supplied by the nerve. There is a complete ptosis (dropping) of the eyelid, due to paralysis of the levator palpebral muscle. The eye is deviated laterally (external strabismus) due to paralysis of the oculomotor-innervated muscles and the unopposed action of the intact lateral rectus muscle. The pupil is fully dilated (mydriasis) and there is a loss of the pupillary light reflex as well as a loss of lens accommodation. Loss of the pupillary light reflex and accommodation results from the interruption of visceral efferent fibers. Lesions involving the oculomotor nerve and corticospinal fibers in the ventral part of the midbrain result in an ipsilateral oculomotor paralysis and a contralateral hemiplegia, which clinically are known as *Weber's syndrome*. This syndrome, also known as *superior alternating hemiplegia*, is a midbrain equivalent of similar syndromes occurring from lesions of the pons (i.e., middle

alternating hemiplegia) with involvement of the abducens nerve and the corticospinal tract and the medulla (i.e., inferior alternating hemiplegia) with involvement of the hypoglossal nerve and the pyramid.

MIDBRAIN TEGMENTUM

The midbrain tegmentum, the region ventral to the cerebral aqueduct and dorsal to the substantia nigra, contains the trochlear and oculomotor nuclei, the mesencephalic reticular formation, the red nuclei, and many scattered collections of cells. The most conspicuous structure in the midbrain tegmentum at the level of the superior colliculus is the red nucleus.

Red Nucleus

TOPOGRAPHY AND CYTOARCHITECTURE

The red nucleus is characterized by its pinkish-yellow color, due to its high degree of vascularization, its central position, and its capsule formed by fibers of the superior cerebellar peduncle. In transverse sections, the red nucleus appears oval, but in sagittal sections it has an elliptical shape with a blunt oral and a tapered caudal pole (Fig. 14.19). The nucleus extends from the caudal diencephalon to the decussation of the superior cerebellar peduncle. The red nucleus is traversed in its oral part by fibers of the fasciculus retroflexus (Fig. 16.4), in its central part by rootlets of the oculomotor nerve, and in its caudal and lateral regions by fibers of the superior cerebellar peduncle.

Since the classic comparative studies of Hatschek (172), it has been customary to recognize magnocellular and parvicellular portions of the red nucleus. The magnocellular part tends to occupy caudal parts of the structure, it is more extensive in lower mammals and has been considered as the cell group which gives rise to the rubrospinal tract. The small-celled, or parvicellular, portion forms the bulk of the nucleus (Fig. 14.13). Its development parallels the growth of the cerebellar nuclei, particularly the dentate nucleus. Between cells of the nucleus are numerous small bundles of myelinated fibers which give a punctate appearance to the nucleus in transverse sections. These are primarily fibers of the superior cerebellar peduncle which traverse the nucleus and terminate in parts of it.

Cytologic studies of the red nucleus in the monkey reveal three distinctive types of neurons (a) large multipolar neurons 50–90 μm

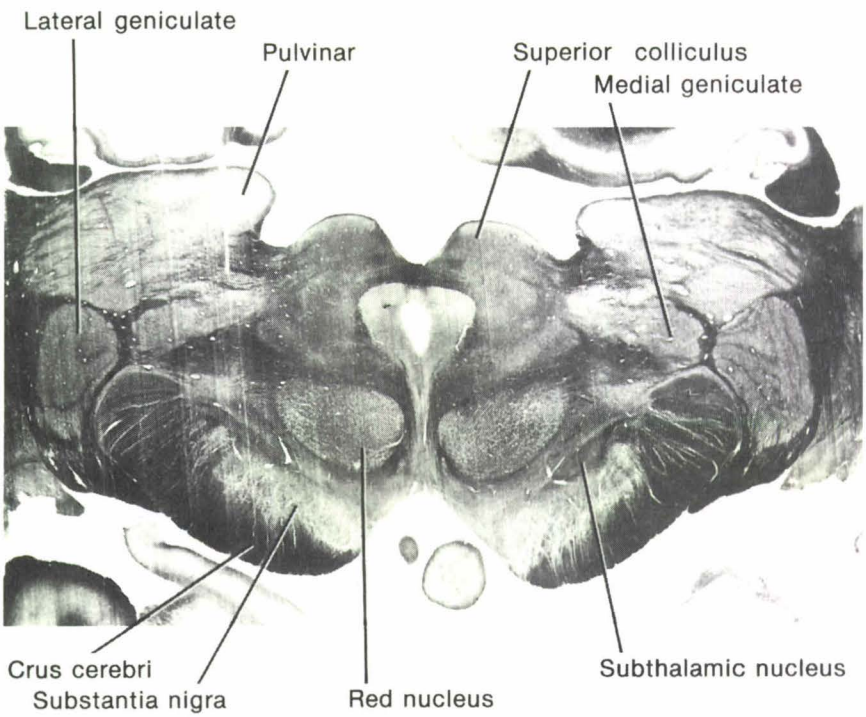


Figure 14.19. Transverse section through the rostral midbrain, demonstrating the manner in which diencephalic nuclei surround dorsal and lateral portions of the midbrain. (Weigert's myelin stain.)

in diameter with prominent nucleoli and a cytoplasm containing coarse Nissl granules (magnocellular part); (b) medium-sized cells, 20–30 μm in diameter, with a triangular or fusiform shape (parvicellular part); and (c) small achromatic neurons, 10–15 μm in diameter, found in all parts of the nucleus (214, 215). Golgi preparations in the monkey have provided details concerning these neurons. Giant neurons have star-shaped, ovoid, or elongated cell bodies with prominent somatic spines. Dendrites of these cells radiate in all directions and have a few isolated spines. Medium-sized neurons, largely representing cells of the parvicellular part of the nucleus, have shorter, less robust dendrites with branching collaterals. Small neurons have delicately branched dendrites and short axons.

CONNECTIONS

Afferent fibers projecting to the red nucleus are derived from two principal sources, the cerebellar nuclei and the cerebral cortex. Fibers from both of these sources terminate somatotopically within the red nucleus. Fibers of the superior cerebellar peduncle, arising from the dentate, emboliform, and globose nuclei, undergo a complete decussation in the caudal midbrain, and enter and surround the contralateral red nucleus. Fibers and collaterals from the dentate nucleus terminate in the rostral third of the red nucleus of the opposite side (parvicellular part) (81, 107), while fibers from the emboliform and globose nuclei (anterior and posterior interposed nuclei) project somatotopically upon the caudal two-thirds of the nucleus (Figs. 15.21 and 15.22). The latter connection links paravermial regions of the cerebellar cortex to the magnocellular part of the red nucleus that in turn project somatotopically to spinal levels (Fig. 11.18). Two decussations are involved, that of the superior cerebellar peduncle and that of the rubrospinal tract. The cerebellar afferent fibers form asymmetric synapses mainly with the soma and proximal dendrites in the red nucleus (276). Physiologic interrelationships between the cerebellar cortex, the interposed nuclei and the red nucleus indicate that excitatory influences of the interposed nuclei upon the large cells of the red nucleus are suppressed by stimulation of the cerebellar cortex. Cortical inhibition, mediated by Purkinje cell axons, is followed by enhanced excitability of interposed neurons whose discharges result in depolarization of red nucleus neurons (400). Cerebellar cortical inhibition is mediated via γ-aminobutyric acid (GABA) while the effect of cerebellar nuclei are likely to be mediated by the excitatory amino acid glutamate (78, 283).

Corticorubral projections arise from precentral and premotor cortex (106, 170, 203, 225, 276, 337). Both of these areas project somatotopically upon cells of the red nucleus. Projections from the medial part of area 6 (the supplementary motor area (M-II)) are crossed and end in the magnocellular region of the nucleus. Projections from the precentral motor cortex to the magnocellular part of the red nucleus are ipsilateral and correspond to the somatotopic origins of the rubrospinal fibers, as originally suggested by Pompeiano and Brodal (320). These fibers have a somatotopic linkage and, together with the rubrospinal tract (crossed), constitute a disynaptic pathway whereby impulses can be conveyed from the "motor" cortex to spinal levels. Corticorubral fibers form asymmetric synapses mainly with distal dendrites and dendritic spines in the red nucleus (203, 276). Electrophysiologic studies reveal that both cortical and cerebellar inputs converge upon the same rubrospinal neurons, where they exert a complementary influence (138, 139). Additionally, part of the cortical and cerebellar influence upon neurons of the red nucleus is mediated through a large pool of inhibitory interneurons that regulate the levels of excitability of rubrospinal neurons (325).

Descending rubral efferent fibers cross in the *ventral tegmental decussation* and project to (a) the interposed nuclei of the cerebellum, (b) the principal sensory and spinal trigeminal nuclei, (c) part of the facial nucleus, (d) several medullary relay nuclei, and (e) the spinal cord (80, 83).

Rubrobulbar projections are both crossed and uncrossed. Crossed rubrobulbar fibers project to the principal sensory nucleus of the trigeminal nerve, and some of these fibers extend caudally into the pars oralis of the spinal trigeminal nucleus (94, 252, 263). At more caudal levels, fibers separating from the rubrospinal tract enter the lateral aspect of the facial nucleus and terminate in dorsomedial and intermediate cell groups whose neurons innervate musculature of the upper part of the face (80, 82, 94, 263). Rubrobulbar fibers

ending upon motor neurons of the facial nucleus probably are not involved in the neural mechanism of mimetic facial innervation, since this phenomenon involves predominantly perioral facial muscles. In the medulla, crossed rubrobulbar fibers end in the lateral reticular nucleus, the accessory cuneate nucleus, and the nuclei gracilis and cuneatus (80, 94, 252, 412).

Rubrospinal fibers in the cat arise chiefly, but not exclusively, from cells of all sizes in the caudal three-fourths of the red nucleus (320, 341, 425). Cells in dorsomedial parts of the nucleus project fibers to cervical spinal segments, while cells in ventral and ventrolateral locations project to lumbosacral spinal segments. Fibers passing to thoracic regions of the spinal cord arise from intermediate parts of the red nucleus. Cervical spinal segments receive the largest number of rubrospinal fibers. In the monkey, rubrospinal fibers arise almost exclusively from the caudal magnocellular part of the nucleus (225). Recent electrophysiologic studies in the cat revealed the existence of direct monosynaptic effect of rubrospinal neurons upon spinal motor neurons innervating muscles of the forelimbs, whereas the same neurons do not receive such monosynaptic input from the cerebral cortex (119).

Uncrossed descending rubral efferents from the parvicellular part of the nucleus enter the central tegmental tract and project to the dorsal lamella of the principal inferior olivary nucleus. These fibers are referred to as *rubro-olivary* and constitute part of a feedback system to the cerebellum (94, 263, 314, 412). No fibers from the red nucleus project to thalamic nuclei.

NEUROTRANSMITTERS

Recent immunohistochemical studies have shed light on the neurotransmitters involved in the neuronal circuitry centered upon the red nucleus. For instance, there is strong evidence for the fact that afferents from both cerebral cortex and cerebellar nuclei excite rubral neurons by using excitatory amino acids, most likely glutamate, as a neurotransmitter (78, 182, 283). The excitatory influence of these two inputs are mediated, at least in part, by receptors of the *N*-methyl-D-aspartate (NMDA) type (36, 165). As mentioned earlier, however, input from the cerebellum terminate preferentially in the proximal somatodendritic domain, whereas that from the cerebral cortex terminates more distally. In respect to rubral neurons themselves, evidence from lesion experiments in rodents indicates that rubrospinal neurons also utilize an excitatory amino acid, most probably aspartate, as an excitatory transmitter (29). In contrast, local interneurons in the red nucleus appear to exert their inhibitory effect upon rubral projection neurons via GABA (325, 357). In fact, the strong motor impairment produced by injection of GABA antagonists into the red nucleus suggests an important functional role for the GABAergic interneurons. Principally under the control of cortical afferents, these GABAergic interneurons can modulate the level of activity of rubrospinal neurons and participate in the control of motor behavior (357).

FUNCTIONAL CONSIDERATIONS

Stimulation of the red nucleus in the decerebrate cat results in (a) excitatory postsynaptic potentials in the contralateral flexor α motor neurons, and (b) inhibitory postsynaptic potentials in contralateral extensor α motor neurons. These observations suggest that the rubrospinal tract transmits impulses that facilitate flexor muscle tone. Recent electrophysiologic evidence reveal that rubrospinal neurons may influence also the dynamic and static γ motor neurons (205). Because of somatotopic relationships between the interposed nuclei of the cerebellum and the red nucleus (81, 83), stimulation of these nuclei in decerebrate animals produces flexion in the ipsilateral limb muscles (242, 318, 319). These responses are ipsilateral because both fiber systems involved are crossed (i.e., the superior cerebellar peduncle and the rubrospinal tract) (Fig. 15.22). Thus, the red nucleus appears to act in close conjunction with the motor cortex and the cerebellum for the control of motor behavior (71, 254).

LESIONS OF THE RED NUCLEUS

Lesions involving the midbrain tegmentum and the red nucleus unilaterally produce (a) ipsilateral oculomotor disturbances, and (b) contralateral motor disturbances of an involuntary nature (i.e., tremor, ataxia, or choreiform movements). This combination of disturbances is known as the *syndrome of Benedikt*. Experimental evidence suggests the

contralateral abnormal involuntary motor activity is due primarily to involvement of crossed fibers of the superior cerebellar peduncle (55, 56, 195, 275, 324, 406).

Reticular Formation

CYTOARCHITECTONIC DIVISIONS

The midbrain reticular formation is less extensive than that of the pons. This term usually is used to designate structures dorsal and lateral to the red nucleus. According to detailed cytoarchitectonic studies (290, 291), the principal reticular nuclei of the midbrain reticular formation are (a) the nucleus tegmenti pedunculopontinus (pedunculopontine nucleus), (b) the nucleus cuneiformis, and (c) the nucleus subcuneiformis.

The *pedunculopontine nucleus* lies in the lateral part of the midbrain tegmentum ventral to the inferior colliculus (Fig. 14.3). The nucleus consists of two parts, a compact part located dorsolaterally and a small-celled diffuse part located ventrally (291). Fibers of the superior cerebellar peduncle traverse portions of the nucleus as they course ventromedially toward their decussation. The pedunculopontine nucleus appears to receive inputs from multiple sources that include (a) the cerebral cortex (170, 225), (b) the medial (or internal) pallidal segment (67, 213, 281, 295, 371), and (c) the pars reticulata of the substantia nigra (21, 60, 196, 265, 302). Projections of the pedunculopontine nucleus are mostly ascending, with the largest number of fibers projecting to the pars compacta of the substantia nigra and the subthalamic nucleus. A small number of fibers project to the medial pallidal segment (21, 60, 89, 161, 197, 234, 350, 372). A large proportion of the cells in the pedunculopontine nucleus are immunoreactive for choline acetyltransferase (ChAT). They correspond to the Ch5 group or sector, as defined by Mesulam, et al. (260), and are known to project to the thalamus (174, 293, 381, 422) and various basal ganglia components, particularly the substantia nigra (143, 234, 235, 259). Cells displaying immunoreactivity for other transmitters, including glutamate (75, 233, 235), are also present in the pedunculopontine nucleus. The pedunculopontine nucleus also lies in a region of the mesopontine tegmentum from which walking movements can be elicited on electrical stimulation (123). Furthermore, recent anterograde tract-tracing studies have revealed that collaterals from the superior cerebellar peduncle innervate cells of the pedunculopontine nucleus (173). This finding suggests that the pedunculopontine nucleus may act as a functional interface between the basal ganglia and the cerebellum for the control of motor behavior.

The *nuclei cuneiformis* and *subcuneiformis* lie ventral to the tectum and dorsal to the pedunculopontine nucleus. The nucleus cuneiformis extends throughout the rostrocaudal extent of the midbrain where it lies directly ventral to the superior and inferior colliculi (95). This nucleus increases in size at more rostral levels and merges with the pretectum. Most of the nucleus is composed of small- and medium-sized oval or fusiform cells. The nucleus subcuneiformis lies ventral to the nucleus cuneiformis. Descending fibers from the cuneiform nucleus cross in the ventral tegmental decussation and project to terminations in the reticulotegmental nucleus, the medial pontine and medullary reticular formation, the nucleus raphe magnus, and in parts of the facial nucleus (95). Some fibers also end in parts of the medial accessory olivary nucleus. Ascending projections of the cuneiform nucleus are to the pretectal nuclei, the nuclei of the posterior commissure, the posterior hypothalamus, the zona incerta, and the paraventricular and the caudal intralaminar thalamic nuclei (98). The widespread connections of the midbrain reticular formation are considered to mediate the varied somatic and visceral responses elicited by electrical stimulation of this region. These responses in the cat can be integrated into elaborate defense or attack behavior characterized by pupillary dilatation, widening of the palpebral fissures, flattening of the ears, and aggressive and vicious behavior (189, 361).

FUNCTIONAL CONSIDERATIONS

The anatomic organization of the brainstem reticular formation has been described regionally. In the medulla and pons, four zones are recognized: (a) a median zone containing nuclei of the raphe, (b) the paramedian reticular nuclei, (c) a medial zone regarded as an "effector" area, and (d) a smaller lateral region referred to as the "sensory" or "receptive" part because it receives collaterals from secondary sensory pathways. In the medulla, the paramedian reticular nu-

clei project mainly to the cerebellum. The "effector" zone, which is coextensive with the giant cell area of the reticular formation, gives rise to both ascending and descending fibers. The "sensory" zone, coextensive with the parvicellular area, projects its axons medially into the "effector" area. The pontine reticular formation has essentially the same zones, although the "sensory" portion is smaller and clearly evident only in the caudal pons.

The reticular formation comprises neurons that are not part of the major nuclear groups of the brainstem. It may be considered as a rostral extension of the interneuronal network of the spinal cord, but is considerably more extensive (344). It is composed of neurons whose axons are widely distributed within the neuraxis (355). The axon of reticular neurons not only descends to the spinal cord, but also ascends to the thalamus and hypothalamus. The brainstem reticular formation is involved in (a) regulation of muscles reflexes, (b) coordination of autonomic functions, (c) modulation of pain sensation, and (d) behavioral arousal.

Descending Reticular Neuronal Systems

Early experimental studies demonstrated that electrical stimulation of the caudal and medial "effector" zone of the medullary reticular formation inhibits most forms of motor activities, such as myotatic reflexes, flexion reflex, extensor muscle tone, and cortically induced movements (248, 249). Regions of the medullary reticular formation from which inhibitory responses are obtained correspond roughly to the area of the gigantocellular part that gives rise to medullary reticulospinal fibers (399). Stimulation of the rostral and dorsal part of the nucleus reticularis gigantocellularis produces monosynaptic excitatory postsynaptic potentials in motor neurons supplying axial muscles in the neck and back.

A far larger region of the brainstem reticular formation facilitates reflex activity and cortically induced movements. This facilitatory area extends rostrally from the upper medulla into caudal regions of the diencephalon. Bilateral facilitatory effects can be evoked throughout this extensive region of the reticular formation. The facilitatory region of the reticular formation includes many areas from which no direct reticulospinal projections arise. Facilitatory effects produced by stimulation of the rostral and dorsal parts of the nucleus reticularis gigantocellularis, or of the nuclei reticularis pontis caudalis and oralis, presumably could reach spinal levels by direct reticulospinal fibers originating in these nuclei. Descending polysynaptic pathways would appear to mediate facilitatory effects obtained from regions of the midbrain and diencephalon, which have no direct reticulospinal projections.

Descending influences of the brainstem reticular formation are not limited to inhibition and facilitation of somatic motor functions. Inspiratory and vasodepressor effects can be obtained from the gigantocellular region in the medulla, while expiratory effects are obtained from the parvicellular region. Vasopressor effects are evoked from lateral reticular regions that projects noradrenergic fibers to spinal levels (see Chapter 13). Although nearly all parts of the central nervous system are capable of exerting detectable influences upon the heart and blood vessels, the primary vasomotor control center is located laterally in the reticular formation of the pons and medulla. Transections of the brainstem as far caudal as the lower third of the pons have no significant effect upon arterial pressure. Successively more caudal transections produce (a) a drop in blood pressure and (b) a reduction in the discharge of cardiac accelerator impulses (19). The bulbar pressor and depressor areas constitute a central cardiovascular mechanism that reflexively regulates blood pressure and the parameters of the heart rate. In the intact animal, a normal arterial pressure is dependent on the bulbar pressor area. A group of noradrenergic neurons (group A7) (see chapter 12), located in the caudal pons and rostral medulla, sends axons to the nucleus of the solitary tract, the nucleus ambiguus, and preganglionic sympathetic neurons in the intermediolateral cell column of the thoracic spinal cord. These noradrenergic neurons are part of a neural network related to the regulation of the cardiovascular system.

The region surrounding the nucleus of the solitary tract is coextensive with the physiologically defined dorsal medullary respiratory "center." A ventral medullary respiratory "center" includes the nucleus ambiguus and the surrounding reticular formation. Additional brainstem regions important in the control of respiration are the "pneumotaxic center" found in the pons near the medial

parabrachial nucleus and an "apneustic center," which remains poorly defined. The parabrachial nuclei receive input from the nucleus of the solitary tract and, in turn, project to both dorsal and ventral respiratory "centers" in the medulla. The "pneumotaxic center" periodically releases the inhibition of the "apneustic center."

Stimulation of inhibitory and facilitatory regions of the reticular formation can decrease or increase the rates of discharges from the muscle spindles via γ-efferent fibers. A part of the effects exerted upon α motor neurons may result from the firing of γ-efferents, which indirectly influence these neurons through the γ-loop, as suggested by the pioneering studies of Granit and his colleagues (146) (Fig. 10.30). Granit and Kaada (147) demonstrated that repetitive electrical stimulation of the facilitating regions of the brainstem tegmentum increased the efferent discharge of γ motor neurons and increased the rate of discharge from the muscle spindle. On the other hand, inhibition of the γ discharge was produced by stimulating the medullary inhibitory region. These data suggest that a large part of the excitation of α motor neurons results from firing of the γ-efferents, which are actively controlled by the reticular formation. The inhibition of extensor muscle tone in a decerebrate animal by stimulation of the medullary reticular formation (395) is a dramatic example of this potent influence.

The discovery that the activity of the muscle spindle could be modified by descending reticular projections suggested that the reticular formation might affect the initiation and transmission of other sensory impulses. Hagbarth and Kerr (160) demonstrated that synaptic transmission of sensory impulses in the spinal cord could be depressed by stimulation of the reticular formation. Likewise, potentials evoked in the posterior column nuclei following stimulation of the posterior columns could be depressed or abolished by stimulation of the reticular formation. There is now ample evidence that this phenomenon occurs in the case of noxious stimuli, as described in Chapter 13.

Ascending Reticular Neuronal Systems

The seminal work of Giussepe Moruzzi and Horace Magoun in the late 1940s led to the discovery that the facilitatory region of the brainstem reticular formation also acts in an ascending direction to influence the electrical activity of the cerebral cortex (273). The pioneer investigations of Hans Berger (31, 32) indicated that in humans and other mammals wakefulness, sleep, alertness, and relaxation were characterized by strikingly different electroencephalographic patterns. Wakefulness and alertness are characterized by fast low-voltage activity, while at least one form of sleep is associated with the appearance of slow high-voltage waves.

Fundamental insight into the underlying brain mechanisms was provided by Frederic Bremer (43) who compared the electroencephalograms (EEG) of animals following high spinal transections *(encéphale isolé)* and decerebration (i.e., transection of the midbrain at the intercollicular level, *cerveau isolé).* In the encéphale isolé preparation, the EEG displayed the waking pattern, while in the cerveau isolé preparation, the EEG exhibited a pattern characteristic of the sleeping state. These experiments pointed to a potent ascending electrotonic influence generated in the lower brainstem. While it was well-known that a variety of different stimuli could change the EEG from a synchronized pattern (i.e., sleep state), to a desynchronized one (i.e., alert state), the puzzling feature was how impulses channeled in the classic ascending pathways could exert such broad and diffuse electrotonic changes in the cerebral cortex. The observations that stimulation of the brainstem reticular formation could activate and desynchronize the EEG and produce behavioral arousal without discharging the classic lemniscal pathways suggested the concept of a second ascending system (273). This second ascending system, exerting powerful influences upon broad regions of the cerebral cortex has become known as the ascending reticular activating system.

Interruption of the long ascending specific sensory pathways in the brainstem does not prevent impulses ascending in the reticular activating system from provoking their characteristic EEG arousal response (116, 273, 376). Lesions in the rostromedial midbrain tegmentum abolish the EEG arousal reaction elicited by sensory stimulation (115, 243, 244), even though long ascending sensory pathways are intact. Thus, two functionally distinct pathways must project to the diencephalon: (a) long ascending sensory pathways, the *lemniscal system,* concerned with specific sensory modalities (i.e., medial lem-

niscus, lateral lemniscus, spinothalamic tracts, and secondary trigeminal projections) that end upon specific thalamic nuclei, and (b) the *ascending reticular activating system*, which receives collaterals from the surrounding specific systems and conveys impulses via the reticular core. Physiologically, the ascending reticular activating system is regarded as a multineuronal, polysynaptic system within which collaterals conveying impulses of a "nonspecific" nature related to wakefulness and arousal.

It must be made clear, however, that the passive view of sleep as a functional deafferentation regulated by the ascending reticular activating system, which has dominated sleep research for many years, is no longer tenable. Experiments, conducted again by Morruzi and his colleagues in the late 1950s, questioned the unitary view of the nonspecific reticular activating system. These investigators showed that when brainstem transections are performed at midpontine level, just a few millimeters caudal to the midbrain cuts of Bremer, the animals could not sleep. This suggests that the rostral reticular formation contains a population of neurons whose activity is required for wakefulness, whereas the caudal brainstem reticular formation contains neurons that are necessary for sleep. Although there is still much uncertainty as to where exactly in the brainstem these two functionally opposite neuronal populations are located, electrophysiologic studies confirmed the existence of active sleep-inducing neurons in the brainstem reticular formation (382). Thus, sleep must be viewed as an active and rhythmic neural process.

The cerebral cortex also plays a role in altering the state of consciousness and alertness by influencing reticular neurons that mediate the arousal responses (44, 114, 200). Such a role has been suggested by the well-known arousal effect of psychic stimuli. Areas of the cerebral cortex from which the arousal responses can be obtained by nonconvulsive electrical stimulation include loci on the orbitofrontal surface, the frontal convexity, the sensorimotor cortex, the posterior parieto-occipital cortex, the superior temporal gyrus and the cingulate gyrus. Corticoreticular fibers, which originate from all parts of the cerebral cortex, convey excitatory impulses to the reticular neurons, whose ascending discharges participate in the arousal response. Corticoreticular fibers project most abundantly to two regions of the brainstem reticular formation: (a) the nucleus reticularis pontis oralis, and (b) the nucleus reticularis gigantocellularis (347).

Although physiologically the reticular formation behaves as if it consisted of a chain of neurons that fire successively, the reticular formation does not contain short-axoned, Golgi type II cells (355). Cells in the "effector" reticular regions that give rise to long ascending fibers in the reticular core appear to form the structural basis of the ascending reticular activating system (47). Rapidly conducted impulses in the reticular core are transmitted by the main long-ascending axons, while slowly conducted impulses are conveyed by collaterals or by multisynaptic pathways involving laterally dispersed collaterals. The main long-ascending pathway in the brainstem reticular formation appears to be the *central tegmental tract* (Figs. 13.4, 13.24, and 13.32), a large composite bundle that also contains descending fiber systems (45, 280). This bundle occupies a large part of the bulbar tegmentum, but at mesencephalic levels it is displaced dorsally so that its fibers occupy a position adjacent to the central gray and dorsal to the red nucleus (Fig. 14.6). At diencephalic levels, the central tegmental tract projects principally to the rostral intralaminar nuclei of the thalamus. Ascending projections from medial regions of the midbrain reticular formation projecting to the hypothalamus are distinct from those contained in the central tegmental tract (280). These projections are represented largely by three bundles: (a) the dorsal longitudinal fasciculus (of Schütz) situated ventrally in the central gray matter; (b) fibers of the mammillary peduncle, which originate in the medial tegmental region (Fig. 17.14) and terminate in the mammillary body and lateral hypothalamus (279); and (c) the medial forebrain bundle, which contains certain ascending components from several sources.

The central reticular core may be regarded as a common system of neurons with multiple relays, which are discharged equivalently by all sensory systems projecting collaterals to it. Such a common system is not involved in the conscious perception of any sensory modality, but is concerned with afferent functions common to all types of sensory experience, namely, alerting and attracting attention. The nonspecific sensory impulses ascending in the reticular activating system

appear to sharpen the attentive state of the cortex and create optimal conditions for the conscious perception of sensory impulses mediated by the classical pathways.

Clinical Notes

In humans, lesions of the brainstem often produce disturbances of consciousness that range from fleeting unconsciousness to deep and sustained coma. In all forms of disturbed consciousness due to brainstem lesions, there is a loss of crude awareness. With lesions of the lower brainstem, unconsciousness usually is accompanied by respiratory and cardiovascular disturbances and, often, increased muscle tone. The loss of consciousness frequently is sudden, and depression of vital functions leads to extreme states. Lesions of the upper brainstem most commonly produce hypersomnia characterized by muscular relaxation, slow respiration, and an EEG pattern showing large amplitude slow waves. The level of unconsciousness usually is not deep, and some patients can be aroused briefly. If the patient develops decerebrate rigidity, there is usually coma, but these phenomena are not always correlated. A variant of hypersomnia seen with upper brainstem lesions is referred to as *akinetic mutism* (coma vigil). In this variant, the EEG pattern resembles that associated with slow-wave sleep, but eye movements remain normal. Many patients with such lesions survive for months in this state.

It was once common to postulate a continuum of consciousness that ranged from attention, alertness, relaxation, and drowsiness, to sleep, stupor, and coma. It was generally believed that the level of excitation in the ascending reticular activating system determined the level of consciousness. As mentioned earlier, however, the discovery of the extraordinary amount of neural activity that characterizes sleep led to abandonment of the idea of a neurophysiologic continuum from quiescence to excitation (211). The lack of a direct continuity between the various states of consciousness is best exemplified by the differences that exist between sleep and coma. Sleep and coma differ behaviorally by their arousal threshold or relative reversibility. They can also be easily distinguished physiologically. Sleep is a highly active neurologic state during which cerebral oxygen uptake does not decline from normal waking levels. In contrast, cerebral oxygen uptake increases above normal during the rapid eye movement (REM) phase of sleep, whereas it decreases below normal resting levels in coma (212). Thus, coma may be defined as a nonsleep loss of consciousness that lasts for an extended period (211). Within the range of this definition, different levels of unconsciousness, including lethargy, loss of sensation, stupor, and coma, can be distinguished clinically based on the degree of indifference exhibited by the patient to various external stimuli. Stupor is a state in which someone is responsive only to shaking, shouting, or noxious stimuli, whereas coma refers to a state of total unresponsiveness (211).

At all levels of the brainstem, liability to unconsciousness is related to the rapidity with which the lesions develop. Lesions associated with hemorrhage produce sudden unconsciousness and coma. Slowly developing lesions, such as tumors, may not disturb consciousness for a considerable period of time (312). Although there is no center particularly concerned with consciousness, there are indications that the functional integrity of the brainstem reticular formation is essential for its maintenance. A healthy cerebral cortex cannot by itself maintain the conscious state.

Neurotransmitters

The brainstem reticular formation is a neurochemically highly heterogeneous structure. As described in Chapter 13, it harbors neurons that contain serotonin, noradrenaline, or acetylcholine. Additionally, many of these neurons coexpress other neuromediators, particularly neuroactive peptides. The noradrenergic neurons lie principally within lateral portions of the reticular formation, whereas serotoninergic neurons are mostly confined to the median raphe nuclei. The cholinergic neurons abound particularly within central portions of the reticular core. These three groups of chemospecific neuronal systems provide ascending projections to the thalamus, including projections that terminate within the intralaminar nuclei. Thus, the effects of the ascending reticular activating system is likely to be mediated by various neurotransmitters, whose complex interplay at target-site levels remains to be elucidated. Among these different neurotransmitters, serotonin has been the subject of innumerable studies (198, 199). This in-

dolamine is believed to play an important role in the modulation of various state-dependent behaviors mediated through both the ascending reticular activating system and the limbic system. Hallucinogenic drugs, such as lysergic acid diethylamide (LSD), depress the serotoninergic system and the release of inhibition results in hypersensitivity to environmental stimuli and hyperactivity in a brain otherwise behaving as if it were asleep. Numerous drugs used to treat psychoaffective disorders also act principally upon serotoninergic neurons of the reticular formation (78).

SUBSTANTIA NIGRA

Cytoarchitecture

The substantia nigra lies dorsal to the crus cerebri, ventral to the midbrain tegmentum, and extends throughout the length of the midbrain (Figs. 14.1, 14.3, 14.6, 14.13, and 14.19). It is rudimentary in fish and amphibians, makes its definite appearance in reptiles and birds, expands significantly in mammals, and reaches its greatest development in primates, particularly humans (294). Since the early studies of Mingazzini (264) and Sano (352), this structure is commonly divided into two parts: (a) the *pars compacta* (SNc), a cell-rich zone comprising numerous densely packed neurons that contain melanin pigments, and (b) the *pars reticulata* (SNr), a cell-poor zone whose neurons are enmeshed in the dense fiber network of the striatonigral fibers. A third part, the *pars lateralis* (SNl), comprising fibers and neurons dorsolateral and rostral in the most fibrous region of the substantia nigra, is also recognized by some authors (111, 113, 315). The pars compacta of the substantia nigra can be further divided into dorsal and ventral tiers (102). Neurons in the dorsal tier are few in number, have mediolaterally oriented dendrites, and merge medially with similar neurons in the *ventral tegmental area* (VTA), a tegmental region containing scattered cells of various sizes, many of which are pigmented. In contrast, neurons in the ventral tier are extremely abundant, have dorsoventrally oriented dendrites, and form typical cell columns that impinge deeply upon the underlying pars reticulata (Fig. 14.20**A**). Most pigmented cells occur in the ventral tier of the substantia nigra. The intensity of the pigmentation in primates is greater than in any other order and reaches maximum intensity in humans (42, 251, 405). In humans, pigmented cells do not appear in the substantia nigra until the fourth or fifth year of life and the amount of melanin within each neuron increases significantly with age. Caudally, neurons of the pars compacta extend as far as the *retrorubral area* (RRA) where they become intermingled with fibers of the lateral lemniscus. Lateral to the substantia nigra, a layer of small cells, the *peripeduncular nucleus*, caps the dorsal surface of the crus cerebri (Fig. 14.13).

The topographic relationship between the pars compacta and the pars reticulata of the substantia nigra varies greatly among species, and the exact boundary between the two major nigral subdivisions is not always easy to trace. In fact, the basis for subdividing the substantia nigra into two (or three) distinctive parts has been questioned in ultrastructural studies (334). Likewise, there is, at present, no consensus regarding classification of neurons of the substantia nigra in mammals. However, most investigators agree that this structure contains a certain proportion of small neurons (10–12 μm) with short axons, which are believed to be interneurons (Golgi type II cells) (112, 359), and a much larger number of projection (Golgi type I) neurons with medium-sized to large cell bodies. In rodents, the small interneurons are said to represent approximately 10% of the total neuronal population in the SNc and 40% of the SNr (156). The large output neurons (25–40 μm) abound in the SNr where they are embedded in a neuropil of fine unmyelinated fibers, whereas the medium-size (15–25 μm) projection neurons are closely grouped in the SNc but separated from one another by thin astrocytic sheaths.

In cats, all nigral neurons have a prominent rough endoplasmic reticulum and numerous free ribosomes, but the larger neurons are much richer in cytoplasmic organelles than the smaller ones (17, 334). In monkeys, nigral neurons display a wide variety of shape and sizes, with diameter ranging from 12–99 μm, and no significant difference has been noted between the large- and medium-sized neurons (359). Quantitative estimates reveal that the total number of neurons in the substantia nigra is much greater in macaque monkeys (N = 73,508) than in cats (N = 38,366) and rats (N = 22,532). The neurons of the SNc type are by far the most abun-

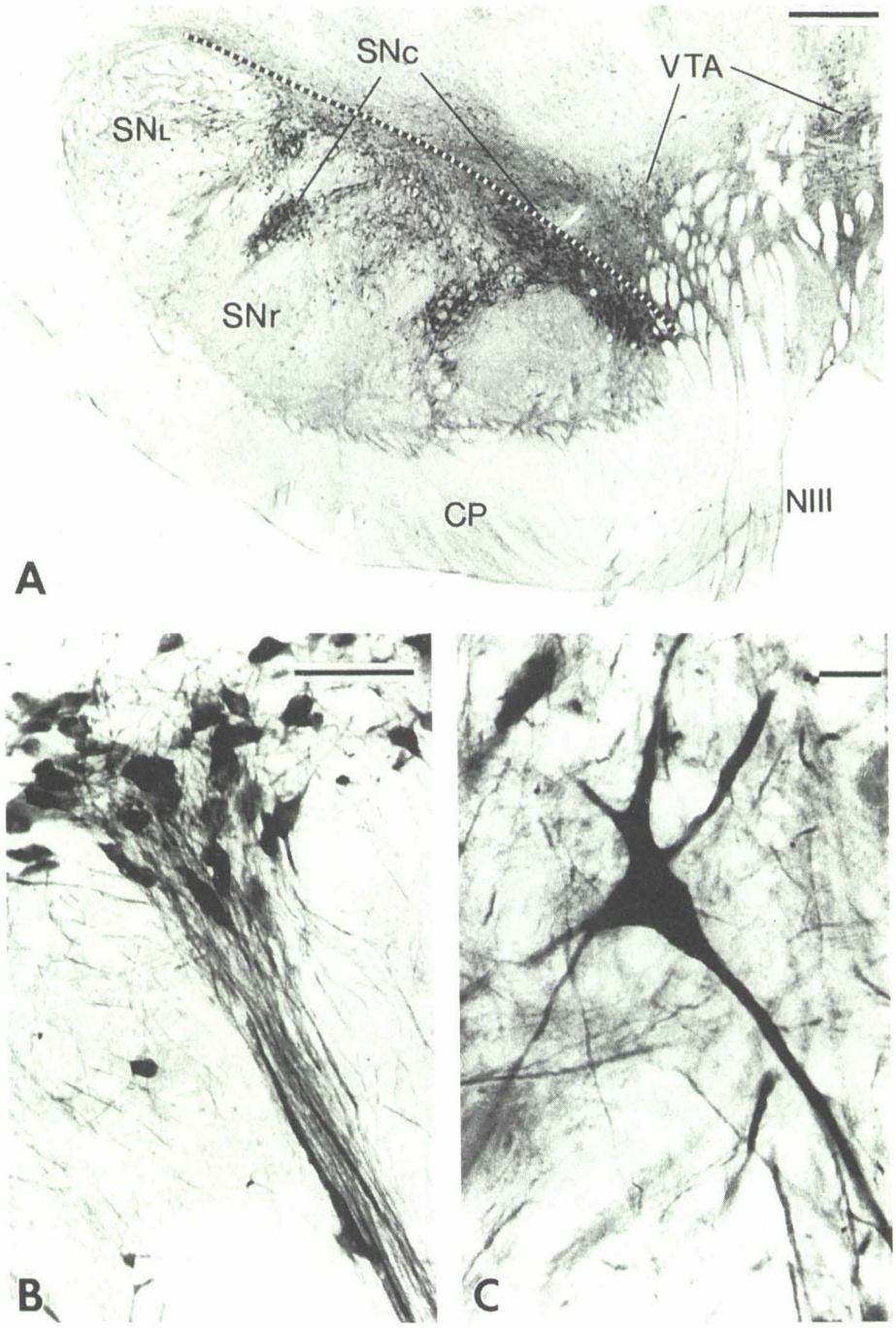


Figure 14.20. Dopamine-immunoreactive neurons of the substantia nigra pars compacta in the squirrel monkey. **A.** Low power view of the substantia nigra to illustrate the dopaminergic neurons in the ventral tegmental area (*VTA*) and in the substantia nigra pars compacta (*SNc*). The *dotted line* indicates the approximate limit between the dorsal and ventral tiers of the SNc. Note the columns of dopaminergic neurons belonging to the ventral tier of the SNc that impinge deeply upon the underlying the substantia nigra pars reticulata (*SNr*). The location of the substantia nigra pars lateralis (*SNl*) is also indicated. **B** and **C.** Higher power views of dopamine-immunopositive neurons lying in the ventral tier of the SNc. Note numerous long immunoreactive dendrites forming a dense bundle oriented dorsoventrally (*B*), and shorter dendrites arborizing in the viscinity of the cell body (*C*). *CP*, cerebral peduncle; *N III*, oculomotor nerve rootles. Scale bars equals 0.5 mm in **A**, 125 μm in **B**, and 25 μm in **C**.

dant, accounting for 85% of the total nigral population in monkeys, 58% in cats, and 44% in rats (315). In humans, the total number of SNc cells amounts to about one-half million (162, 405).

In Golgi preparations, nigral neurons display long radiating, smooth dendrites that branch infrequently (Fig. 14.20**B**, **C**). The dendritic fields of the SNc neurons are oriented primarily in a dorsoventral direction, while those of the SNr neurons have a rostrocaudal direction. The most ventral region of the SNr contains neurons with dendrites oriented mostly parallel to the crus cerebri. Furthermore, intracellular injections studies reveal that many SNc and SNr neurons give rise to dense collateral arborizations (294). The axons of nigral cells branch not only within the dendritic field of the parent cell but also in quite remote regions of the substantia nigra. The axon collaterals are one of the most important intrinsic features of the medium-sized and large nigral neurons, and may facilitate complex integration of neuronal output within the substantia nigra. Some of the intrinsic collaterals also terminate on dendrites of the parent cell, forming true *autaptic synapses*, or *autapses*, that could play an important role in the self-regulation of nigral neurons (294). The dendrites of nigral neurons are covered with boutons that increase in number with distance from the soma. The majority of these boutons are of type I, with pleomorphic vesicles and symmetric junction, and originate in the striatum (334, 359).

Chemoarchitecture

The two major divisions of the substantia nigra can be readily distinguished from one another on the basis of their neurotransmitter content. The neurons of the SNc contain high concentrations of dopamine (Fig. 14.20), as first demonstrated with histofluorescence techniques (9), whereas those of the SNr display GABA and GAD immunoreactivity (274, 286, 368).

Collections of dopaminergic neurons of the SNc, VTA, and RRA correspond respectively to groups A9, A10, and A8 of Dahlström and Fuxe (15) (86). Cells of the SNc and RRA give rise to the massive *nigrostriatal (mesostriatal) dopaminergic system*, whose fibers arborize profusely in most of the caudate nucleus and putamen, except their most ventral portions. Cells in the VTA give rise to the so-called *mesolimbocortical dopaminergic system*, whose fibers arborize principally in the ventral striatum, including the nucleus accumbens and the deep layers of the olfactory tubercle, the amygdala, and the prefrontal cortex (37, 236) (Fig. 14.21). Some dopaminergic neurons in the VTA and dorsal tier of the SNc also project directly to the pallidum, where they arborize principally within the internal pallidal segment (236, 366). Many of the dopaminergic neurons of the VTA contain the neuroactive peptide cholecystokinin (360), but midbrain dopaminergic neurons containing either dopamine and cholecystokinin appear to give rise to distinct projections to the prefrontal cortex in monkeys (287). Besides its action at striatal levels, dopamine can be released into the substantia nigra itself by dendrites of the nigrostriatal dopaminergic neurons (72, 238). Furthermore, electrotonic coupling is known to exist between nigrostriatal dopaminergic cells but not between SNr cells (144). Such electrical communication between SNc neurons appears to be involved in modulating burst firing and in synchronizing dopamine release.

The human substantia nigra contains numerous fibers and axon terminals displaying immunoreactivity for GABA, substance P, or enkephalin. Dynorphin is another neuroactive peptide that abounds at substantia nigra levels (128). The GABAergic fibers arborize profusely in the SNr, whereas fibers displaying immunoreactivity for either substance P or enkephalin are distributed in the SNr, as well as in the ventral tier, of the SNc (311). Substance P-positive fibers occur in large number in the substantia nigra of rats, cats, and primates, whereas enkephalinergic fibers are much more abundant in the substantia nigra of primates than in that of rats and cats (194) (Fig. 14.22). In humans, the distribution of enkephalinergic fibers is not as extensive as that of substance P-positive fibers, suggesting that specific peptidergic pathways differentially innervate the substantia nigra (157, 311). Peptidergic fibers at the substantia nigra levels display a typical arrangement termed "woolly" fibers (158). Woolly fibers are composed of an unstained core (the dendrite of a nigral cell) ensheathed in a dense plexus of thin beaded fibers (the substance P- or enkephalin-positive fibers) (157, 311). In accordance with experimental findings from animal studies, neuropathologic data clearly

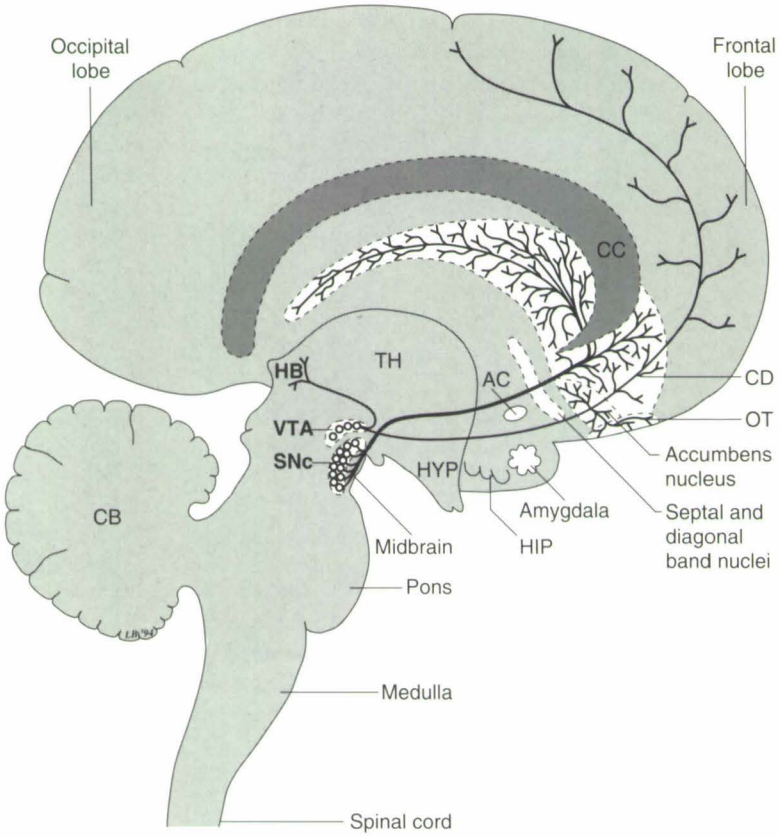


Figure 14.21. Comparison of the ascending projections arising from the dopaminergic neurons in the substantia nigra pars compacta (*SNc*) and in the ventral tegmental area (*VTA*) transposed on a parasagittal section of the human brain. *AC*, anterior commissure; *CB*, cerebellum; *CD*, caudate nucleus; *HIP*, hippocampal formation; *HYP*, hypothalamus; *HB*, habenula; *OT*, olfactory tubercle; *TH*, thalamus.

indicate that both substance P- and enkephalin-positive fibers in the human substantia nigra originate from the striatum. For example, in both striatopallidal infarction (310) and Huntington's disease (100, 330) there is a marked decrease of nigral peptidergic innervation. The substantia nigra also displays numerous serotonin-immunoreactive fibers and terminals, particularly in the SNr (230). The dorsal nucleus of the raphe appears to be the principal source of this serotoninergic innervation (49, 60, 92, 230).

Afferent Connections

Afferents to the substantia nigra arise mainly from the striatum (caudate nucleus and putamen), the lateral (or external) segment of the globus pallidus, the subthalamic nucleus, the dorsal raphe nucleus, the pedunculopontine nucleus, and the cerebral cortex. Quantitatively the largest numbers of nigral afferents arise from the caudate nucleus and the putamen and are known as striatonigral fibers.

STRIATONIGRAL FIBERS

These fibers (270, 349, 410) are topographically organized (Fig. 14.23), but their extensive nature, organization, and regions of termination were not appreciated until the anterograde degeneration studies of Voneida (411) and Szabo (387–389). These investigations indicated that, in primates, fibers from the head of the caudate nucleus project to the rostral third of the substantia nigra and have a mediolateral correspondence in primates. Fibers from the putamen project to the caudal two-thirds of substantia nigra, with dorsal regions of the putamen related to lateral parts of the nigra, and ventral regions related to medial parts of the nigra. More recent studies with highly sensitive anterograde tracers (127, 175, 298) have confirmed that there is an inverse topographic relationship between

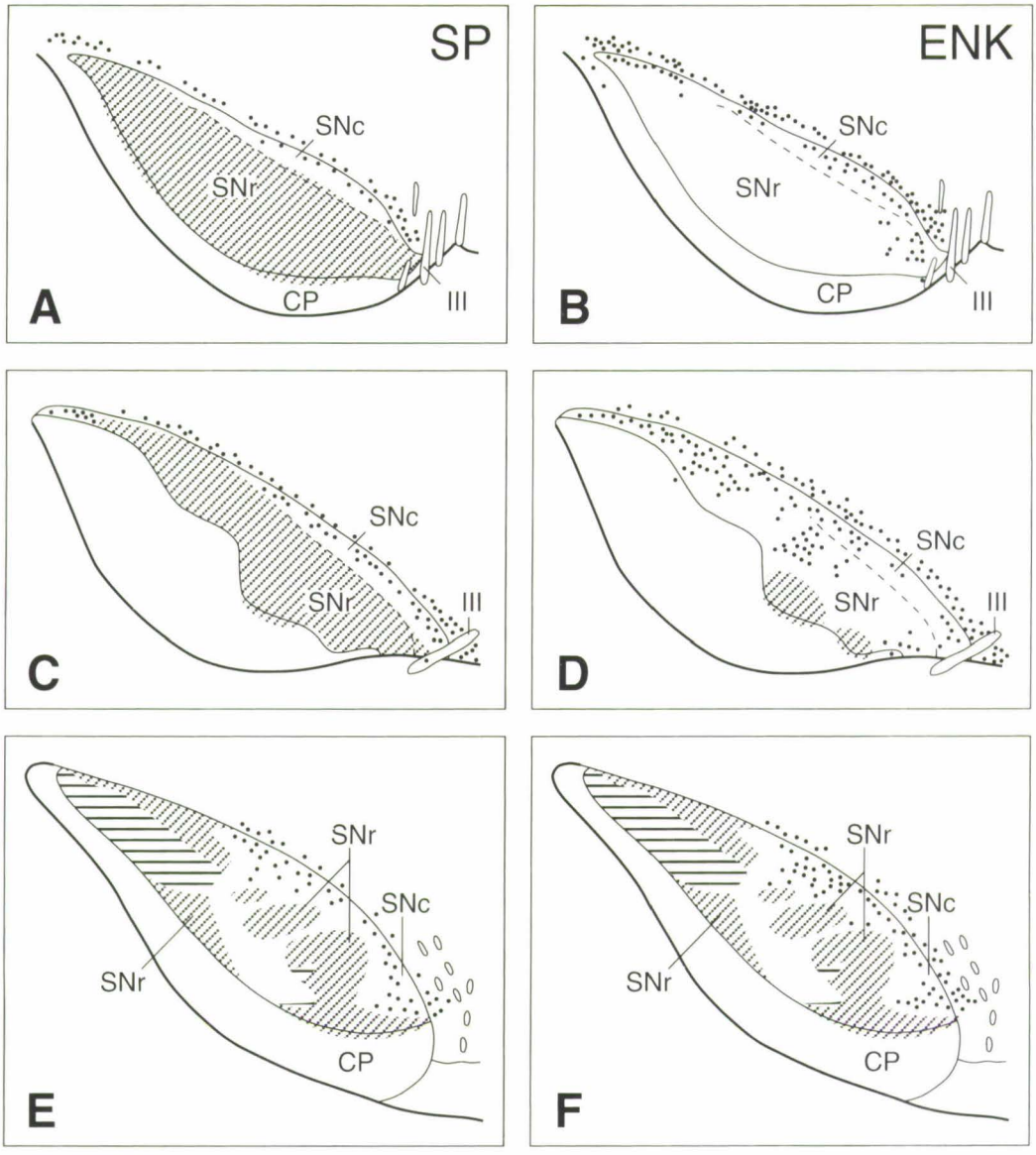


Figure 14.22. Transverse sections through the middle third of the substantia nigra in a rat, cat, and squirrel monkey comparing the distribution of substance P (*SP*)- and enkephalin (*ENK*)-immunoreactive fibers. The *hatched areas* represent dense networks of fine immunoreactive fibers; the *small dots* illustrate more scattered coarse fibers. *CP*, cerebral peduncle; *SNc*, substantia nigra pars compacta; *SNr*, substantia nigra pars reticulata; *III*, oculomotor nerve rootlets.

striatal cells of origin and their termination sites in the substantia nigra. They also revealed that fibers from both putamen and caudate nucleus form multiple terminal fiber plexuses that are distributed throughout the rostrocaudal and mediolateral extent of the substantia nigra (127, 298). Furthermore, neurons located in ventral portions of the striatum, including the nucleus accumbens and the deep layers of the olfactory tubercle, appear to project in a highly divergent manner onto neurons in most of the extent of the substantia nigra and ventral tegmental area (159). While most of the striatonigral fibers are regarded as terminating onto GABAergic neurons in the SNr, some striatal fibers terminate also onto dopaminergic neurons in the SNc. Even in the SNr, GABAergic and peptidergic striatal fibers synapse upon the long, ventrally oriented dendrites of the dopaminergic SNc neurons (41, 308). Striatonigral fibers arise from multitudinous medium-

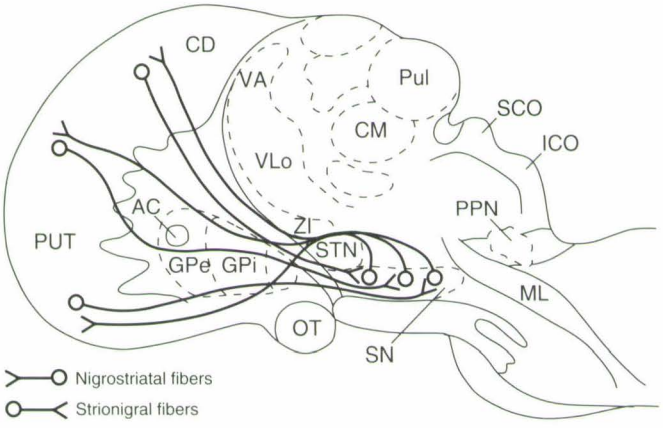


Figure 14.23. Striatonigral feedback system in a sagittal plane. Striatonigral fibers project topographically upon cells of the substantia nigra pars reticulata (*SNr*) and have γ-aminobutyric acid (GABA) as their neurotransmitter. Cells of the substantia nigra pars compacta (*SNc*) give rise to reciprocally arranged nigrostriatal fibers which convey dopamine to specific loci within the striatum. *AC*, anterior commissure; *CD*, caudate nucleus; *CM*, centromedian nucleus; *ICO*, inferior colliculus; *GPe*, external segment of globus pallidus; *ML*, medial lemniscus; *GPi*, internal segment of globus pallidus; *OT*, optic tract; *PPN*, pedunculopontine nucleus; *Pul*, pulvinar; *PUT*, putamen; *SCO*, superior colliculus; *SN*, substantia nigra; *STN*, subthalamic nucleus; *VA*, ventral anterior nucleus; *VLo*, ventral lateral thalamic nucleus, pars oralis; *ZI*, zona incerta.

sized (12–20 μm) neurons with spiny dendrites (medium spiny neurons) scattered throughout the caudate nucleus and putamen (49, 154), and establish symmetric types of synapses on the soma, dendritic trunks, or dendrites of nigral cells in the SNr. The striatonigral fibers use GABA as their major small-molecule transmitter, but also coexpress either substance P, enkephalin, and dynorphin, or a combination thereof (128, 294). While GABA is known to be inhibitory, substance P is considered to be excitatory. The precise role of opiate peptides at substantia nigra levels remains to be defined.

PALLIDONIGRAL FIBERS

These fibers were identified in a number of animals by retrograde transport studies (49, 154, 209). They are considered GABAergic and arise from the lateral (or external) pallidal segment. They terminate in the form of typical basket-like arrangements around the cell bodies of SNr neurons (299), with large terminal boutons making symmetric synapses. The pallidonigral projection appears particularly well-developed in rodents, and pallidonigral fibers were shown to converge with striatonigral fibers upon the same SNr neurons (364). The pallidonigral input appears to complement the striatonigral afferent in that pallidal fibers arborize mostly in the proximal somatodendritic domain, whereas striatal fibers terminate largely in the more distal dendritic domain of SNr neurons. Thus, the pallidonigral projection allows the striatum to influence the same SNr neurons by acting directly on their distal dendrites and indirectly on their cell bodies via a relay in the lateral (or external) pallidal segment (298).

SUBTHALAMONIGRAL FIBERS

These fibers were demonstrated by both anterograde and retrograde transport studies in primates (58, 277, 303, 365). They form several terminal fiber plexuses in the SNr (216), but the exact relationship with the multiple terminal plexuses formed by the striatonigral fibers remains to be established. Fluorescent double-labeling studies suggest that in the rat virtually all cells in the subthalamic nucleus project axons to both the substantia nigra and the globus pallidus (403). Similar studies in primates reveal that only about 10% of the subthalamic nucleus neurons project to both SNr and globus pallidus (297). Subthalamonigral fibers terminate in the form of large boutons that make asymmetric synapses with dendrites and cell bodies of SNr neurons and display glutamate immunoreactivity (336). Thus, the subthalamic nucleus appears to exert a glutamate-mediated excitatory influence upon SNr neurons which can serve to counteract the strong GABA-mediated action

of the striatonigral and pallidonigral fibers upon the same neurons.

RAPHE-NIGRAL FIBERS

These fibers use serotonin as their major neurotransmitter and arise principally from the dorsal raphe nucleus and less abundantly from the median (central superior) raphe nucleus of the midbrain (2, 16, 91, 121, 198, 230, 271, 296, 304, 379, 380). They arborize profusely in the SNr and much more lightly in the SNc (230). In rodents, the raphe-nigral projection is largely composed of collaterals of the raphe-striatal pathway (403), appears to be strictly ipsilateral (404), and contains a significant number of nonserotoninergic elements (88, 380). In primates, the exact cellular origin and the degree of collateralization of the raphe-nigral projection remain to be investigated. Ultrastructural studies in primates reveal that both synaptic and nonsynaptic axonal varicosities occur in the neuropil of the substantia nigra, although synapses with specific junctional appositions appear to predominate (271, 304). The axonal varicosities exhibiting junctional appositions were reported to be of the asymmetric type (177, 282, 304), and some of these serotoninergic synapses occur on dopaminergic neurons in both SNc (282) and VTA (177). These findings indicate that serotonin can alter the activity of nigrostriatal dopaminergic neurons by acting directly at the level of the SNc-VTA complex (230). Indeed, despite the fact that serotoninergic synapses at nigral levels are of the asymmetric type, which is usually indicative of excitatory effect, electrical stimulation of the dorsal nucleus of the raphe predominantly produces inhibition of spontaneous activity in single neurons of the substantia nigra (92). This discrepancy could be explained by the type(s) of receptors upon which serotonin acts at nigral levels. In primates, the action of serotonin at the substantia nigra level is likely to be mediated, in part, by 5-HT_1 receptors, which are the most abundant 5-HT receptors subtypes in this brain area (305, 306, 385).

PEDUNCULONIGRAL FIBERS

These fibers arise in the pedunculopontine nucleus and terminate principally in the SNc (197, 234, 265, 371, 396). There is ample evidence that the pedunculonigral projection is, at least in part, cholinergic, and that its terminals form asymmetric synaptic contacts with both cell bodies and proximal dendrites of SNc dopaminergic neurons (40, 143, 235, 255, 256, 259). An increase in the activity of the SNc cells is observed after either electrical stimulation of the pedunculopontine nucleus or exogenous application of acetylcholine and nicotine (284, 354). These results indicate that the substantia nigra is a site of cholinergic transmission and suggest that acetylcholine and dopamine interact at nigral levels as they do at striatal levels (235). In addition to ChAT-positive neurons, the pedunculopontine nucleus also contains neurons displaying immunoreactivity for glutamate (75, 233), and some of these glutamatergic neurons can be labeled following injection of retrograde tracers into the substantia nigra (235). Furthermore, recent studies in monkeys reveal that injection of anterograde tracers in the pedunculopontine nucleus label terminal boutons that form asymmetric synapses with dopaminergic SNc neurons and display glutamate immunoreactivity (70). These findings indicate that the pedunculonigral projection in primates has a dual cholinergic/glutamatergic nature (235).

CORTICONIGRAL FIBERS

These fibers have been a matter of much controversy over the years, their existence being alternatively demonstrated and denied, sometimes even by the same group of investigators (332, 338). However, recent retrograde and anterograde labeling studies provide rather convincing evidence for the existence of corticonigral fibers (49, 222, 351). These fibers arise principally from the prefrontal cortex and terminate preferentially within the ipsilateral SNc, with lighter innervation of the SNr, SNl, VTA, and RRA (351). Lesions of the frontal cortex in the cat produce a significant decrease of glutamate concentrations at nigral levels (218), which suggest that corticonigral fibers may use this excitatory amino acid as a neurotransmitter.

Efferent Connections

In respect to its efferent projections, the substantia nigra can be considered as a dual structure (294). Whereas the SNc is in some way locked in a closed reciprocal loop with the striatum (Fig. 14.23), the SNr has highly divergent projections and is considered, to-

gether with the medial (or internal) pallidal segment, as one of the major output nuclei of the basal ganglia (Fig. 14.24).

NIGROSTRIATAL FIBERS

They were first demonstrated by retrograde cellular degeneration in the substantia nigra following cerebral ablations that included portions of the striatum (407). Subsequent studies showed that the retrograde cell changes in the substantia nigra could be correlated with the extent of striatal injury (103, 262). Attempts to trace nigrostriatal fibers in Marchi preparations indicated that nigral efferent fibers ascended and entered both segments of the globus pallidus, but none could be followed into the caudate nucleus or putamen (261, 262, 328, 346). These data suggest that nigrostriatal fibers become poorly myelinated in the globus pallidus.

Even though the fluorescent histochemical technique clearly demonstrated nigrostriatal projections (10, 402), the Nauta silver impregnation method failed to provide evidence of a substantial projection (1, 62, 67). Investigations of nigral efferent projections using relatively short survival times and more sensitive silver impregnation techniques demonstrated nigrostriatal projections in both the cat and monkey (65, 266). Immunohistochemical studies with antibodies directed either against dopamine itself (15), or against tyrosine hydroxylase, the rate-limiting enzyme in the synthesis of dopamine (236), have revealed the organization of the ascending nigrostriatal dopaminergic system in primates. The nigrostriatal dopaminergic fibers arise from the cell bodies of the SNc, the RRA, and the lateral part of the VTA. These fibers accumulate dorsomedially to the rostral portion of the substantia nigra, where they form a massive bundle that courses through the prerubral field and ascend along the lateral aspect of the medial forebrain bundle in the lateral hypothalamus. Some ventrally located fibers run throughout the rostrocaudal extent of the preopticohypothalamic area and can be followed up to the olfactory tubercle, whereas other fibers turn laterodorsally to invade the caudate nucleus.

At more rostral levels in the lateral hypothalamus, many fiber fascicles detach themselves from the main bundle and sweep laterally to reach the globus pallidus and the putamen. At pallidal levels, most fibers destined to the striatum ascend within the internal and external medullary laminae, as well as along the inner border of the internal capsule, thus avoiding the core of the pallidal complex. In the striatum, the fibers break into a multitude of thin axonal varicosities that

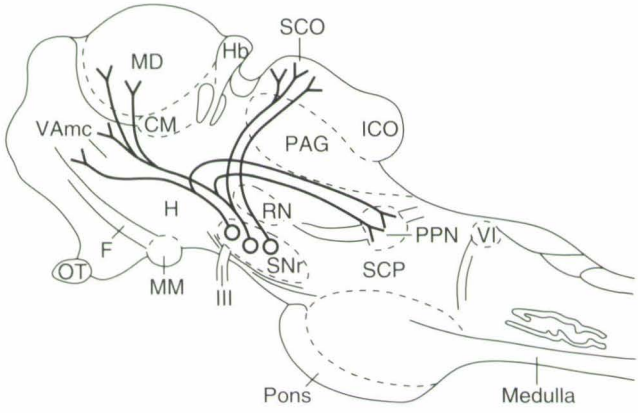


Figure 14.24. Efferent projections of the substantia nigra pars reticulata (*SNr*) as seen in sagittal sections. These GABAergic neurons give rise to nigrothalamic, nigrotectal, and nigrotegmental projections. Collectively, these fibers represent part of the output system of the basal ganglia by virtue of their input from spiny striatal neurons. Nigrothalamic fibers project to medial parts of the ventral lateral nucleus (*VLm*) (not shown), the magnocellular part of the ventral anterior nucleus (*VAmc*), and parts of the mediodorsal nucleus (*MD*). Of the fibers projecting to the middle and deep layers of the superior colliculus (*SCO*), 20–30% represent collaterals of nigrothalamic fibers. About 60% of the cells in the SNr projecting to the thalamus have collaterals that project to the pedunculopontine nucleus (*PPN*). *CM*, centromedian thalamic nucleus; *F*, fornix; *H*, Forel's field; *Hb*, habenular nucleus; *ICO*, inferior colliculus; *MD*, mediodorsal nucleus; *MM*, mammillary body; *OT*, optic tract; *PAG*, periaqueductal gray; *RN*, red nucleus; *SCP*, superior cerebellar peduncle; *VI*, abducens nucleus; *III*, oculomotor nerve.

are rather uniformly scattered along the rostrocaudal extent of the striatum, but appear slightly more numerous in the ventral striatum than in the dorsal striatum. Zones containing relatively few axonal varicosities embedded in a matrix of dense terminal labeling occur in the striatum, particularly in the head of the caudate nucleus (236). These zones of weak dopaminergic innervation appear to correspond to the striatal patches or "striosomes" that are embedded in a dense extrastriosomal matrix, both forming two anatomically and neurochemically distinct striatal compartments (152) (see Chapter 19 for further details).

Nigrostriatal dopaminergic fibers terminate upon striatal projection neurons, where they make symmetric synaptic contacts principally on the neck of dendritic spines (117). Thus, the striatal dopaminergic input appears ideally located to modulate the influence of the corticostriatal fibers, which terminate upon the head of the spines of medium-sized striatal projection neurons.

Until recently, it was believed that dopamine mediates its effects by interacting with two receptor subtypes, which have been designated D_1 and D_2 on the basis of different biochemical, electrophysiologic, and pharmacologic properties (84, 207, 331). The cloning of putative D_3, D_4, and D_5 receptor subtypes, however, implies that there is even greater heterogeneity within the dopamine receptor family (78). In general, D_1 and D_2 receptors have opposite effects on biochemical systems. For example, activation of D_1 receptor increases adenyl cyclase and cAMP production, whereas D_2 receptor inhibit, or have no effect on, this enzyme. These two receptor subtypes can interact to produce additive or synergistic effects, which may explain the wide variety of effects on behavior and movement-related functions noted with the use of different dopamine agonists. Recent evidence obtained in the rat suggests that D_2 receptors are preferentially located on striatal neurons that contain enkephalin and project to the lateral (or external) pallidal segment, while D_1 receptors abound on striatal neurons that project to the medial (or internal) pallidal segment and the SNr and contain substance P and dynorphin (128, 129). This concept of a differential distribution of dopamine receptors at striatal levels has important functional implications. Among other things, it raises the possibility of pharmacologically acting specifically upon one or the other type of striatal projection neurons with highly specific D_1 and D_2 receptor agonists and antagonists so as to develop more effective treatment for motor and psychoaffective disorders.

Striatonigral and nigrostriatal fibers appear to form a closed feedback loop in which striatonigral fibers form the afferent limb and nigrostriatal fibers constitute the efferent limb. This reciprocal arrangement is evident in that HRP injected into the striatum is transported retrogradely from the axon terminals to cells of the SNc, and anterogradely via striatal neurons to the SNr (278, 367) (Fig. 14.25). Retrograde transport studies of HRP in the cat and monkey provide data concerning the topographic organization of nigrostriatal projections (390, 391). The projections of the SNc to the striatum are organized in all principal planes. The rostral two-thirds of the substantia nigra is related to the head of the caudate nucleus, while neurons projecting to the putamen are located posteriorly. An inverse relationship exists dorsoventrally between the substantia nigra and the caudate nucleus, so that ventral parts of the pars compacta project to dorsal regions of the caudate nucleus and dorsally situated neurons in the nigra pass to ventral regions of the caudate nucleus. Lateral and posterior regions of the nigra are related to dorsal and lateral parts of the putamen. There is also a mediolateral correspondence between the cells of the substantia nigra and regions of fiber termination in the striatum.

Other levels of organization are superimposed upon this crude topographic arrangement. For example, fluorescent retrograde double-labeling studies in primates reveal that nigral projections to the caudate nucleus and to the putamen arise from separate neurons that form closely interdigitated clusters in the SNc (301) (Figs. 14.26 and 14.29). Other studies in rodents show that cells in the dorsal tier of the SNc and adjoining VTA project mainly the matrix compartment of the striatum, whereas those in the ventral tier project to the striatal patches or striosomes (see Chapter 19). In turn, neurons in the striatal matrix project principally to the SNr, while those in striatal patches innervate the dorsal tier of the SNc (128, 130). Neurons located in the dorsal tier of the SNc and projecting to the striatal matrix compartment are enriched with the calcium binding protein calbindin D-28k, whereas those lying in the ventral tier and projecting to the striosomes are largely devoid of such a protein (128). A similar, al-

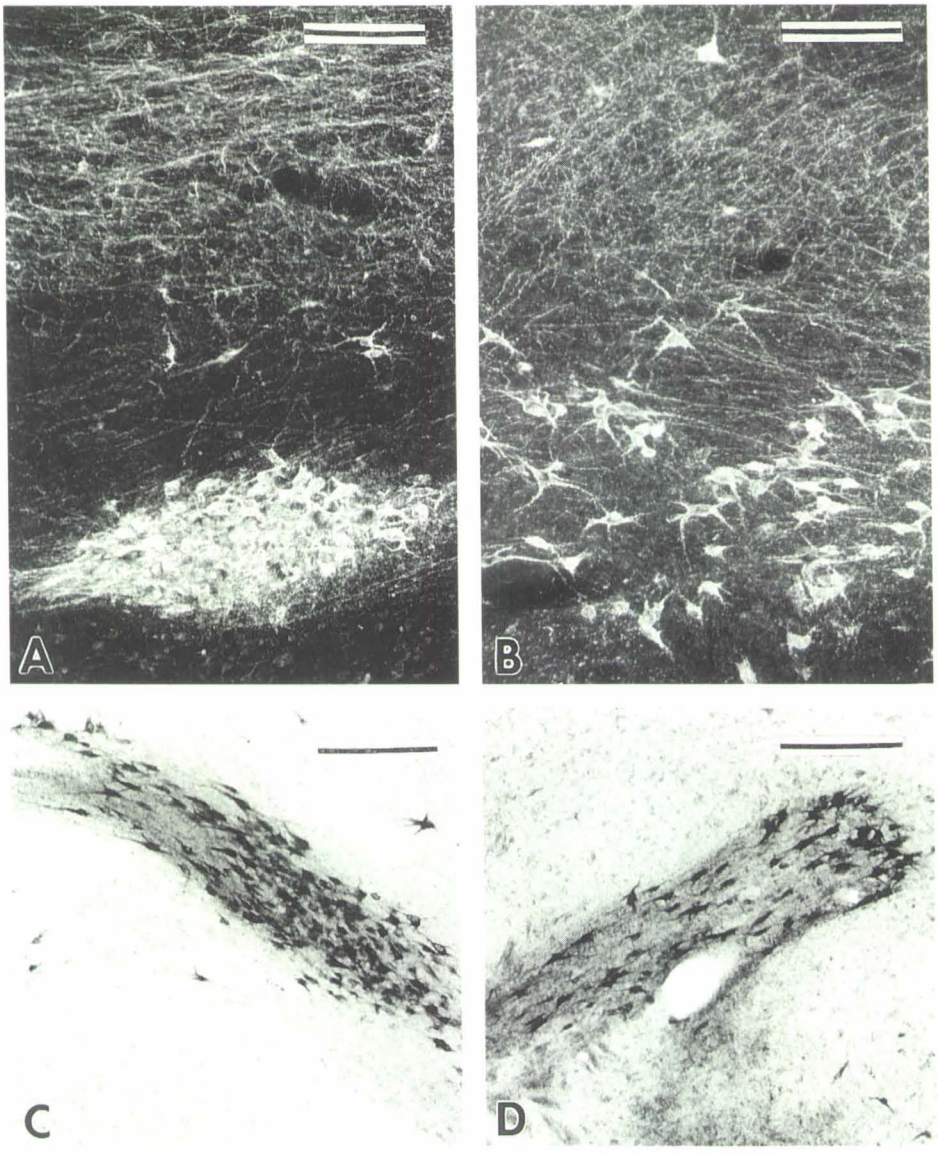
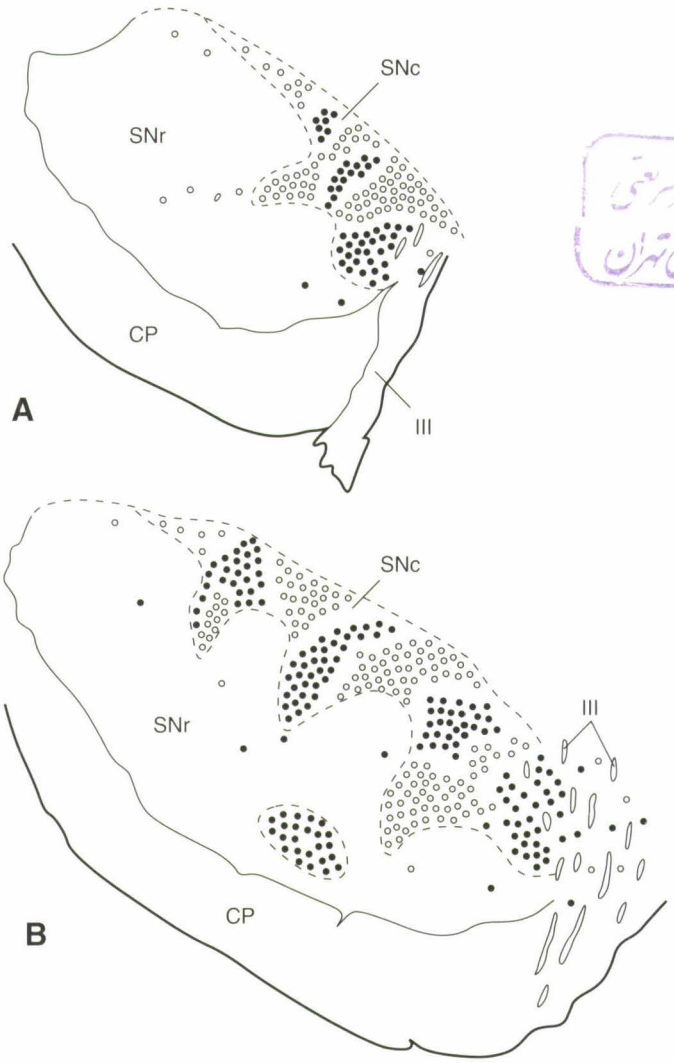


Figure 14.25. Features of the anterograde and retrograde labeling observed at the level of the substantia nigra after injection of wheat germ agglutinin-horseradish peroxidase conjugated (WGA-HRP) in the caudate nucleus on the right (**A**) and in the putamen on the left side (**B**, **C**, and **D**) in squirrel monkeys. **A** and **B**. Some retrogradely labeled nigral cells on the caudate-injected side (**A**) and putamen-injected side (**B**), as they appear under darkfield illumination. The bundle of anterogradely labeled nigrostriatal axons is partially visible in the upper portion of each photomicrograph. Note that labeled cells are more closely packed on the putamen-injected side (**B**) than on the caudate-injected side (**A**). **C** and **D**. Typical clusters of retrogradely labeled nigral cells lying within a dense terminal field of putamenonigral fibers, as seen under brightfield illumination. Scale bars equal 250 μm.

beit less distinct, arrangement appears to exist in primates (204, 227). These findings indicate that the striatonigrostriatal loop is not organized in a strict point-to-point manner.

NIGROTHALAMIC FIBERS

They arise from GABAergic cells of the SNr and project to the magnocellular part of the ventral anterior nucleus (VAmc) and the paralaminar part of the mediodorsal nucleus (MDpl) (58, 191, 193, 333). In their course, these fibers closely parallel the mammillothalamic tract (63, 65, 67). Cells of the SNr constitute an important component of the output system of the basal ganglia by virtue of their linkage with the striatonigral fibers. In primates, nigrothalamic fibers terminate in



کتابخانه بیمارستان دکتر شریعتی
دانشگاه علوم پزشکی تهران

Figure 14.26. Transverse sections through the rostral (**A**) and middle (**B**) third of the substantia nigra of the squirrel monkey illustrating the mosaic-like distribution of the pars compacta (*SNc*) neurons projecting to the caudate nucleus (*open circles*) and the putamen (*filled circles*), as seen after injection of one fluorescent retrograde tracer in the caudate nucleus (*CD*) and another in the putamen (*PUT*) on the same side of the brain. *CP*, cerebral peduncle; *SNr*, substantia nigra pars reticulata; *III*, oculomotor nerve rootlets.

thalamic motor nuclei, which do not receive afferents from any other part of the basal ganglia nor from the cerebellum (192, 193, 307). Fluorescent retrograde double-labeling studies indicate that nigrothalamic fibers have significant numbers of collaterals that project to the superior colliculus and the mesopontine tegmentum (20, 302) (Figs. 14.24, 14.28, and 14.29).

NIGROTECTAL AND NIGROTEGMENTAL FIBERS

Nigrotectal fibers arise only from cells of the SNr, particularly those located in the lateral portion of the SNr coextensive with the SNl, as defined by certain investigators (111). These neurons project to the middle gray layers of the caudal two-thirds of the ipsilateral superior colliculus, and appear topographically organized (153, 183, 201, 335) (Fig. 14.27). Projections of nigrotectal fibers are to portions of the superior colliculus that receive inputs not related to the visual system and contain large neurons giving rise to the tectospinal pathway. Electrophysiologic and fluorescent retrograde double-labeling studies reveal that a significant proportion of the SNr neurons projecting to the superior colliculus also project to the thalamus (11, 12, 20,

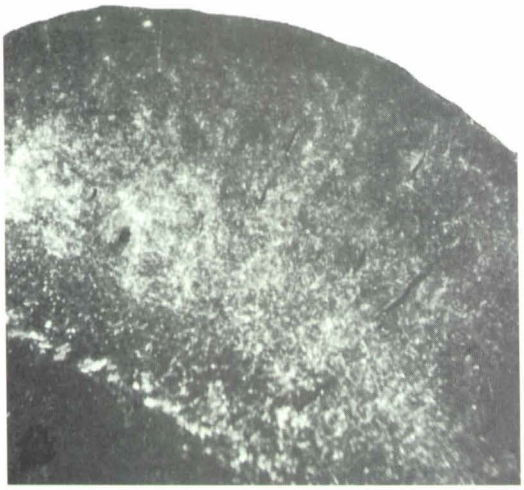


Figure 14.27. Darkfield photomicrograph of an autoradiograph demonstrating nigrotectal terminations. Nigrotectal fibers arise from cells in the substantia nigra pars reticulata (*SNr*) and terminate in the deep and middle gray layers of the superior colliculus.

302). Nigrotectal fibers play an important role in the control of oculomotor activities, particularly in the initiation of saccadic (rapid) eye movements (178–181).

Nigrotegmental fibers arise also from GABAergic neurons of the SNr and project principally to the pedunculopontine nucleus (21, 60). A large proportion of SNr neurons, up to 60%, project collaterals to both thalamus and pedunculopontine nucleus (20, 302). As mentioned, cells of the pedunculopontine nucleus receive inputs from multiple sources, including the cerebral cortex, the medial (or internal) pallidal segment, and the cerebellum. In turn, neurons of the pedunculopontine nucleus project back to the substantia nigra, where they terminate, not on GABAergic neurons of the SNr that innervate them, but on the dopaminergic nigrostriatal neurons of the SNc. Thus, the nigrotegmental fibers are part of a nigrotegmentonigral feedback loop that, as is the case for the nigrostriatonigral loop, involves the two major subdivisions of the substantia nigra.

Neuropathology

The substantia nigra is involved in some of the most prominent basal ganglia diseases, characterized by involuntary movements (dyskinesia), poverty or slowness of movement, and disorders of muscle tone and postural reflexes. These abnormal movements include (a) *tremor* (rhythmic, involuntary, oscillatory movements of a body part), (b) *athetosis* (slow, writhing movements involving primarily the distal part of the limb), (c) *chorea* (rapid, flick-like movements of the limbs and facial muscles), (d) *ballism* (violent, flailing movements primarily involving proximal parts of the limb), and (e) *dystonia* (a persistent posture of a body part that can result in grotesque movements and distorted positions of the body) (79). Parkinson's disease (paralysis agitans), one of the best characterized disorders of the basal ganglia, usually comprises (a) a rhythmic tremor at rest, (b) increased muscle tone or rigidity, and (c) a slowness in the initiation of movement (akinesia) as well as in the execution of movement (bradykinesia). The Parkinsonian syndrome may have different etiologies such as idiopathic Parkinson's disease, progressive supranuclear palsy, striatonigral degeneration, and postencephalitic Parkinsonism. However, idiopathic Parkinson's disease (PD) is by far the most common of all degenerative forms of Parkinsonism. Multisystem degeneration Parkinsonisms account only for about 15% of all forms (202).

The neuropathologic hallmark of Parkinson's disease is a massive loss of pigmented cells of the substantia nigra and ventral tegmental area first noted by Tretiakoff (401), and later confirmed by Foix (108), Foix and Nicolesco (109), and Hassler (171) (Fig. 14.30). The cell loss in the substantia nigra ranges from 50–85%, whereas it appears more variable in the ventral tegmental area (202). The nigral cell loss is currently accompanied by massive reactive gliosis. Furthermore, degenerating nigral neurons were found to display cytoskeletal abnormalities, such as cytoplasmic inclusion bodies first described by Lewy (237) and referred to as *Lewy bodies* (110). Since the pigmented dopaminergic cells are the major target of the neuronal degenerative processes involved in Parkinson's disease, the main biochemical feature of this disease is a marked decrease of striatal dopamine concentrations, as first observed by Oleh Hornykiewicz and his colleagues (99, 184–186). However, the dopaminergic neuronal systems do not degenerate to the same degree. The nigrostriatal (mesostriatal) systems is more severely affected than the mesolimbocortical system and the striatal dopaminergic denervation is more prominent

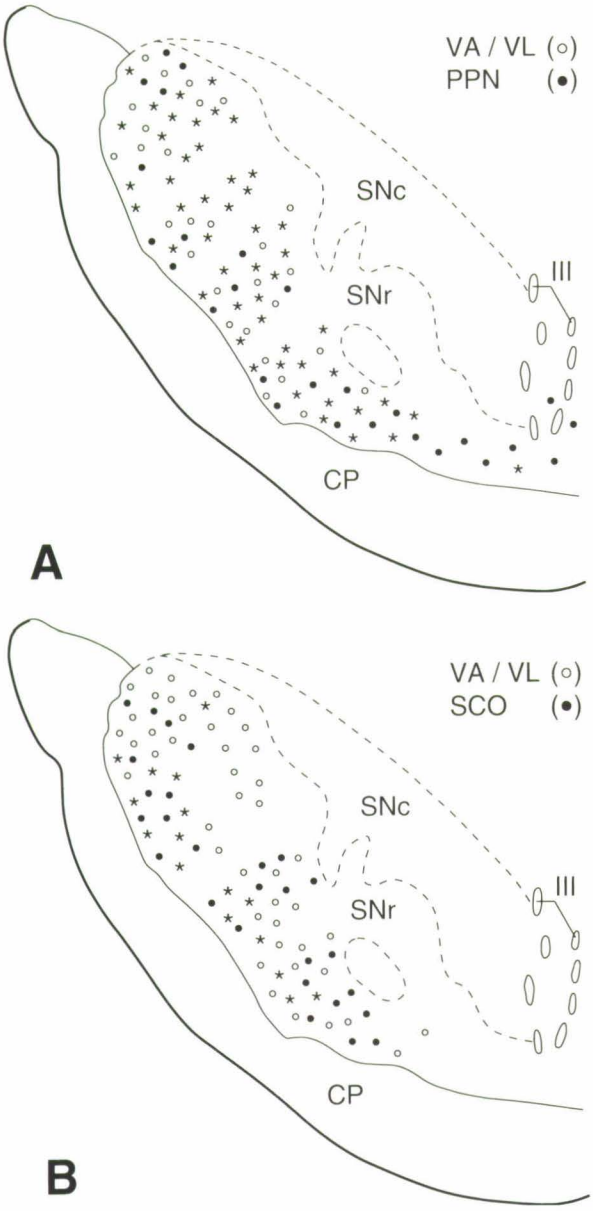


Figure 14.28. Transverse sections through the middle third of the substantia nigra in the squirrel monkey summarizing the distribution of retrogradely labeled neurons in two typical cases in a series of double-labeling experiments with retrograde fluorescent tracers. This study was designed to study the cellular origin and degree of axonal collateralization of the SNr efferent projections in primates. **A.** Results obtained after injections of one tracer in the ventral anterior/ventral lateral thalamic nuclei (*VA/VL*) and the other in the pedunculopontine nucleus (*PPN*). **B.** Results obtained after injections in the *VA/VL* nuclei and the superior colliculus (*SCO*). The double-labeled cells are represented by *asterisks*. *CP*, cerebral peduncle; *SNc*, substantia nigra pars compacta; *SNr*, substantia nigra pars reticulata; *III*, oculomotor nerve rootlets.

in the putamen than in the caudate nucleus (3, 99, 186). Overall, the striatal dopamine depletion is directly proportional to the cell loss in the substantia nigra (33).

An effective treatment for Parkinson's disease is the oral administration of large doses of L-dihydroxyphenylalanine (L-dopa or levodopa), a precursor of dopamine, which passes the blood-brain barrier. The effectiveness of L-dopa can be enhanced by the use of a peripheral decarboxylase inhibitor, which prevents systemic decarboxylation of L-dopa to dopamine. Thus, adequate L-dopa will be left unmetabolized systemically to enter the brain where the desired decarboxylation to dopamine can occur (Fig. 1.15). Although L-dopa therapy has been hailed as the most significant treatment of Parkinson's disease, this drug does not alter the course of the disease. Additionally, many patients become refractory or suffer side effects (e.g., hallucinations, nausea) after treatment with L-dopa for several years. Thus, new approaches have been used to overcome the limitations of L-dopa therapy. One involves the transplantation of fetal dopaminergic cells into the striatum (93,

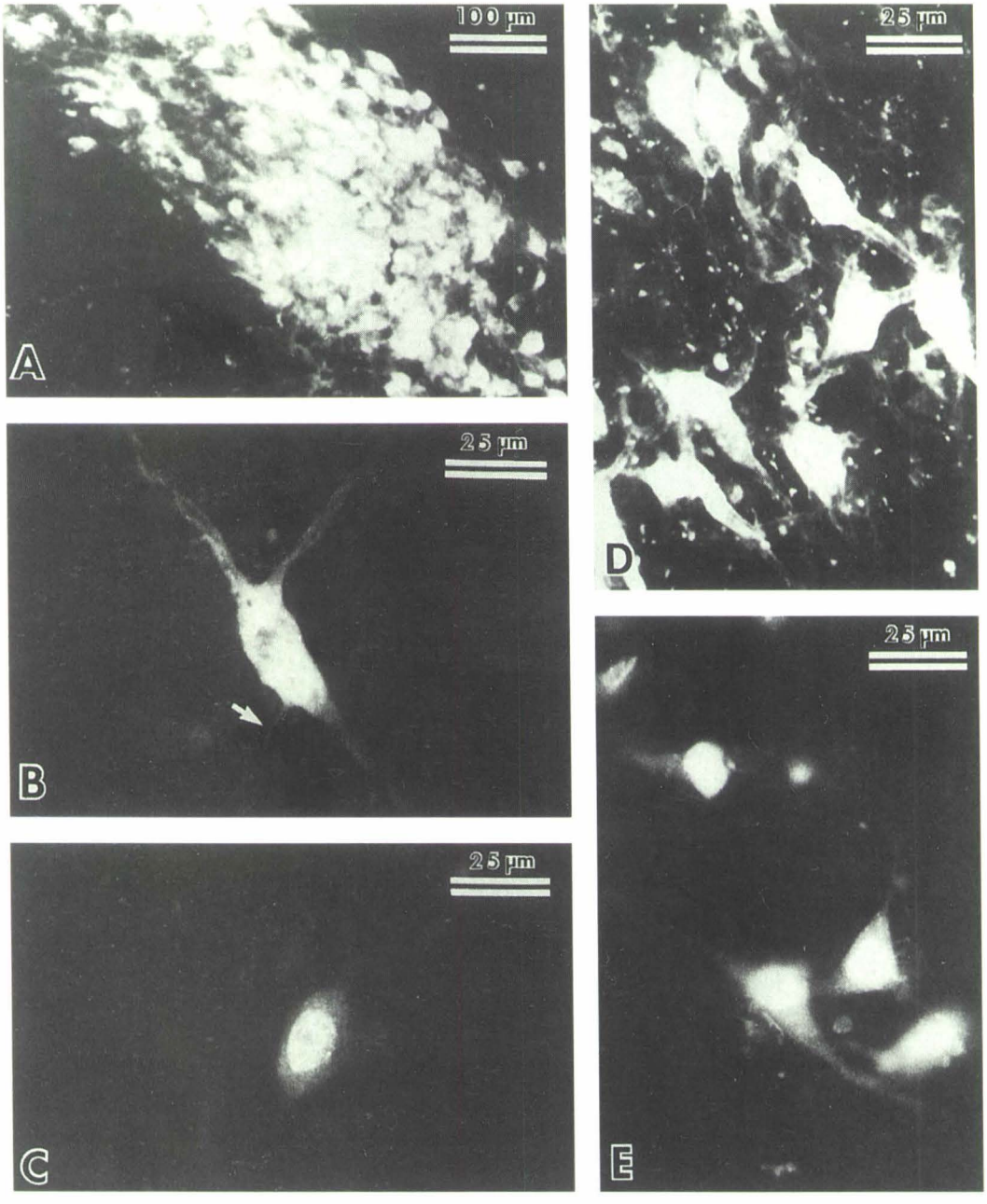


Figure 14.29. Fluorescence photomicrographs showing various features of the retrograde labeling in the substantia nigra of the squirrel monkey after double-labeling experiments. **A.** A typical cluster of pars compacta neurons projecting to the striatum, as seen after injection of Evans blue (*EB*) in the putamen. **B.** One of the few cells in the pars reticulata that was retrogradely labeled after injection of True blue (*TB*) in the putamen. The *arrow* points to the initial axon segment. **C**. One of the rare double-labeled cells visualized in the pars compacta after injection of Nuclear yellow (*NY*) in the putamen and Fast blue (*FB*) in the caudate nucleus. NY is confined to the nucleus, which displays a bright yellow-green fluorescence, whereas TB is revealed by the dull blue appearance of the cytoplasm of the neuron. **D.** High power view of nigrostriatal neurons in the pars compacta retrogradely labeled with *EB* injected into the putamen (same animal as in **A**). **E.** Some of the numerous double-labeled neurons seen in the lateral sector of the pars reticulata after injection of NY into the superior colliculus and FB into the ventral anterior/ventral lateral (VA/VL) thalamic nuclei.

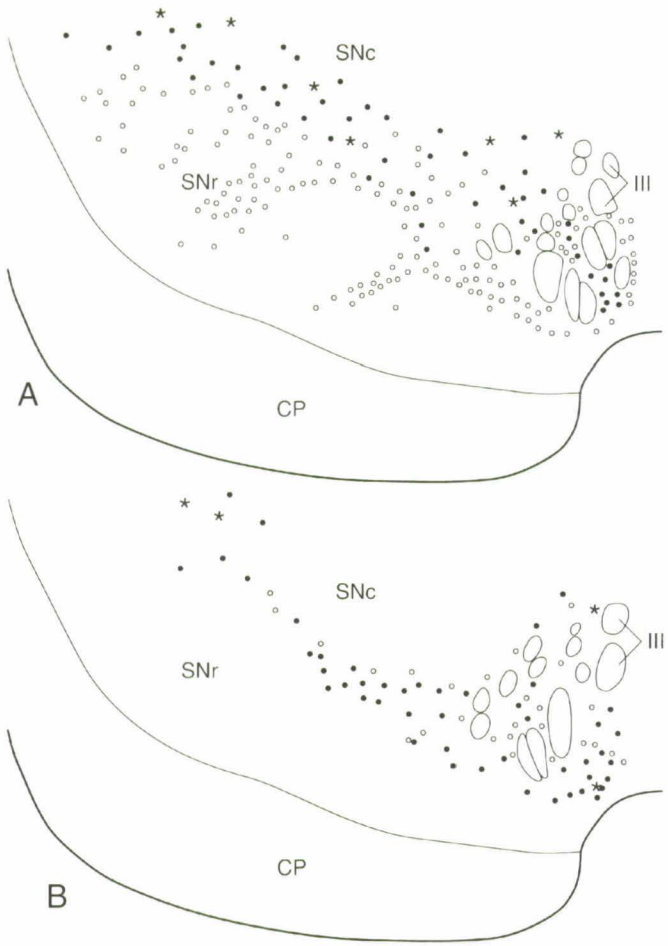


Figure 14.30. Number and distribution of neurons displaying (a) tyrosine hydroxylase (*TH*) immunoreactivity (*open circles*), (b) calbindin (*CaBP*) immunoreactivity (*asterisks*), and (c) both TH and CaBP (*filled circles*) in the middle third of the substantia nigra/ventral tegmental area complex in two cynomolgus monkeys (*Macaca fascicularis*). The animal in **A** was normal, whereas the one in **B** was rendered parkinsonian by the systemic administration of the neurotoxin MPTP. Note the massive loss of TH-immunoreactive neurons in the ventral tier of the substantia nigra pars compacta and the relative sparing of TH/CaBP-immunoreactive neurons in the dorsal tier of the SNc in the parkinsonian monkey. Each symbol represents five cells. *CP*, cerebral peduncle; *SNc*, substantia nigra pars compacta; *SNr*, substantia nigra pars reticulata; *III*, oculomotor nerve rootlets.

424). Fetal nigral neurons can be successfully incorporated into the adult striatum, where they can serve as a permanent intrinsic source of dopamine. Such grafts can alleviate experimentally induced behavioral deficits in rats, but the clinical usefulness of these transplants in humans is still being debated.

Lesions of the substantia nigra in rats, cats, and monkeys result in a marked depletion of striatal dopamine together with motor abnormalities (23, 313, 316, 317, 402). Recently, the discovery that the meperidine analog 1-methyl-4-phenyl-1,2,5,6-tetrahydropyridin (MPTP) is highly toxic to the dopaminergic neurons of the substantia nigra and can produce a typical Parkinsonian syndrome in both human and nonhuman primates (73, 217, 228, 229) gives further support to the hypothesis that an environmental toxin may play a role in the development of Parkinson's disease.

This availability of such a specific neurotoxin has allowed the development of highly valuable primate models of Parkinson's disease (22), as well as the study of molecular mechanisms involved in neuronal cell death. In monkeys rendered Parkinsonian after systemic injection of MPTP, the major loss of ni-

gral dopaminergic neurons occurs in the ventral tier of the SNc, where most pigmented neurons are located (131, 232, 300, 358). By comparison, dopaminergic neurons in the dorsal tier of the SNc and in the VTA are less severely affected. Interestingly, neurons that are less severely affected are those that express both tyrosine hydroxylase and the calcium binding protein calbindin D-28k, whereas neurons that degenerate massively are those that express tyrosine hydroxylase only (Fig. 14.30). Likewise, pigmented neurons devoid of calbindin immunoreactivity degenerate massively, whereas nonpigmented neurons expressing calbindin are relatively spared in cases of human idiopathic Parkinsonism (423). These findings indicate that, by virtue of its capacity of binding large quantities of free calcium ions, calbindin may protect nigral dopaminergic neurons from neurodegenerative processes. Current studies involving animal models of Parkinson's disease should bring novel information regarding the use of various growth factors and different neuroprotective molecules as possible cures for Parkinson's disease and other neurodegenerative disorders.

Other complex interrelationships between dopamine, GABA, and acetylcholine suggest that both the striatum and the substantia nigra may be involved in the neural mechanisms responsible for choreoid dyskinesia in Huntington's disease, which is characterized by a marked striatal atrophy due to a severe loss of GABAergic projection neurons in the striatum (6). Much remains to be learned about neurotransmitter alterations in various multisystemic disorders, such as progressive supranuclear palsy and striatonigral degeneration, which are characterized by motor deficits similar to those encountered in Parkinson's disease.

CRUS CEREBRI

The most ventral part of the midbrain contains a massive band of descending corticofugal fibers, the *crus cerebri*. According to Dejerine (87), the medial three-fifths of the crus cerebri contain somatotopically arranged *corticospinal* and *corticobulbar fibers*. Other authors (105, 323, 408) indicate that much smaller portions of the central part of the crus cerebri contain these fibers. In the classic view, fibers in the most lateral part of the central region are concerned with the lower extremity; the larger middle region contains fibers concerned with the upper extremity; and the most medial fibers of the central region are associated with the musculature of the face, pharynx and larynx. The extreme medial and lateral portions of the crus cerebri contain *corticopontine fibers*. Frontopontine fibers are medial, while corticopontine fibers from the temporal, parietal, and occipital cortices are located laterally (Fig. 14.1).

The corticospinal fibers in the internal capsule are largely confined to a compact region in the caudal part of the posterior limb of the internal capsule (34, 101, 135, 164, 363). Somatotopical organization of fibers destined for particular segmental levels appears relatively crude. These data suggest that the somatotopic arrangement of corticospinal fibers in the crus cerebri probably is much less precise than commonly depicted. In humans, corticospinal fibers probably account for only 1 million of the 20 million fibers in the crus cerebri; the remaining fibers are largely corticopontine (397).

Besides these named tracts, there often are two fiber bundles which descend partly within the crus cerebri and partly in the region of the medial lemniscus, known as *pes lemnisci*. The *medial* or *superficial pes lemniscus* detaches itself from the lateral portion of the crus cerebri, winds ventrally around the crus, and forms a semilunar fiber bundle medial to the frontal corticopontine tract (Fig. 14.1). At lower levels, the fibers leave the crus cerebri, pass dorsally through the substantia nigra, and descend in or near the ventromedial portion of the medial lemniscus. The *lateral* or *deep pes lemniscus* detaches itself from the dorsal surface of the crus, runs for some distance in the lateral portion of the substantia nigra, then turns dorsally and descends in the region of the medial lemniscus (Fig. 14.1). Certain authors (87, 409) regarded these bundles as aberrant corticospinal fibers which during phylogenesis became separated from the main tract by the increasing development of the dorsal pontine nuclei. According to Kuypers (224), fibers of the pes lemnisci can be traced caudally through the pons to the level of the pyramidal decussation. A number of these fibers are distributed to the tegmentum of the pons and medulla. These fibers, undoubtedly corticobulbar, appear to project mainly into the reticular formation. Few, if any, of these fibers pass directly to motor cranial nerve nuclei (Fig. 12.27).

References

1. Afifi A, Kaelber WW. Efferent connections of the substantia nigra in the cat. Exp Neurol 1965;11: 474–482.
2. Aghajanian GK, Kuhar MJ, Roth RH. Serotonin-containing neuronal perikarya and terminals: differential effects of p-chlorophenylalanine. Brain Res 1973;54:85–101.
3. Agid Y, Javoy-Agid F, Ruberg M. Biochemistry of neurotransmitters in Parkinson's disease. In: Marsden CD, Fahn S, eds. Movement disorders. Vol. 2. London: Butterworths, 1987:166–230.
4. Aitkin LM, Gates GR, Phillips SC. Responses of neurons of the inferior colliculus to variations in sound-source azimuth. J Neurophysiol 1984;52:1–17.
5. Aitkin LM, Webster WR, Veale JL, Crosby DC. Inferior colliculus. I. Comparison of response properties of neurons in central, pericentral and external nuclei of adult cat. J Neurophysiol 1975;38: 1196–1207.
6. Albin RL, Young AB, Penney JB Jr. The functional anatomy of basal ganglia disorders. Trends Neurosci 1989;12:366–375.
7. Alley KR, Baker R, Simpson JI. Afferents to the vestibulocerebellum and the origin of the visual climbing fibers in the rabbit. Brain Res 1975;98:582–589.
8. Altman J, Carpenter MB. Fiber projections of the superior colliculus in the cat. J Comp Neurol 1961; 116:157–178.
9. Andén N-E, Carlsson A, Dahlström A, Fuxe K, Hillarp N-A, Larsson K. Demonstration and mapping out of nigro-neostriatal dopamine neurons. Life Sci 1964; 3:523–530.
10. Andén N-E, Dahlström A, Fuxe K, Larsson K, Olson L, Ungerstedt U. Ascending monoamine neurons to the telencephalon and diencephalon. Acta Physiol Scand 1966;67:313–326.
11. Anderson ME, Yoshida M. Electrophysiological evidence for branching nigral projections to the thalamus and the superior colliculus. Brain Res 1977;137:361–364.
12. Anderson ME, Yoshida M. Axonal branching patterns and location of nigrothalamic and nigrocollicular neurons in the cat. J Neurophysiol 1980;43:883–895.
13. Apter JT. Eye movements following strychninization of the superior colliculus of cats. J Neurophysiol 1946;9:73–86.
14. Aronson LR, Papez JW. Thalamic nuclei of Pithecus (Macacus) rhesus. II. Dorsal thalamus. Arch Neurol Psychiatry 1934;32:27–44.
15. Arsenault M-Y, Parent A, Séguéla P, Descarries L. Distribution and morphological characteristics of dopamine-immunoreactive neurons in the midbrain of the squirrel monkey (*Saimiri sciureus*). J Comp Neurol 1988;267:489–506.
16. Azmitia EC, Gannon PJ. The primate serotoninergic system: A review of human and animal studies and a report on *Macaca fascicularis*. In: Fahn S, Marsden CD, Van Woert MH, eds. Myoclonus. Advances in neurology. Vol. 43. New York: Raven Press, 1986:407–468.
17. Bak IJ, Choi WB, Hassler R, Usunoff KG, Wagner A. Fine structural synaptic organization of the corpus striatum and substantia nigra in rat and cat. In: Caine C, Chase TN, Barbeau A, eds. Dopaminergic mechanisms. Advances in neurology. Vol. 9. New York: Raven Press, 1975:15–41.
18. Baker R. Anatomical and physiological organization of brain stem pathways underlying the control of gaze. In: Baker R, Berthoz A, eds. Control of gaze by brain stem neurons: developments in neuroscience. Vol. 1. Amsterdam: Elsevier, 1977;207–222.
19. Bard P. Regulation of the systemic circulation. In: Mountcastle VB, ed. Medical physiology. 12th ed. Vol. I, Ch. 11. St. Louis: C.V. Mosby, 1968:178–208.
20. Beckstead RM. Long collateral branches of the substantia nigra pars reticulata axons to thalamus, superior colliculus and reticular formation in monkey and cat. Multiple neuronal labeling with fluorescent dies. Neuroscience 1983; 10:767–779.
21. Beckstead RM, Domesick VB, Nauta WJH. Efferent connections of the substantia nigra and ventral tegmental area in the rat. Brain Res 1979;175:191–217.
22. Bédard PJ, Boucher R, Gomez-Mancilla B, Blanchette P. Primate models of Parkinson's disease. In: Boulton A, Baker G, Butterworth R, eds. Neuromethods. Vol. 21. Animal models of neurological disease, I. Totowa, NJ: Humana Press, 1992:159–173.
23. Bédard PJ, Larochelle L, Parent A, Poirier LJ. The nigrostriatal pathway: a correlative study based on neuroanatomical and neurochemical criteria in the cat and monkey. Exp Neurol 1969;25:365–377.
24. Beitz AJ. The midbrain periaqueductal gray in the rat. I. Nuclear volume, cell number, density, orientation and regional subdivisions. J Comp Neurol 1985;237:445–459.
25. Beitz AJ, Shepard RD. The midbrain periaqueductal gray in the rat. II. A Golgi analysis. J Comp Neurol 1985;237:460–475.
26. Benevento LA, Fallon JH. The ascending projections of the superior colliculus in the rhesus monkey (*Macaca mulatta*). J Comp Neurol 1975;160:339–362.
27. Benevento LA, Rezak M. The cortical projections of the inferior pulvinar and adjacent lateral pulvinar in the rhesus monkey (*Macaca mulatta*): an autoradiographic study. Brain Res 1976;108:1–24.
28. Benevento LA, Standage GP. The organization of the projection of the retinorecipient nuclei of the pretectal complex and layers of the superior colliculus to the lateral pulvinar and medial pulvinar in the macaque monkey. J Comp Neurol 1983;217:307–336.
29. Benson CG, Chase MC, Potashner SJ. Decreased release of D-aspartate in the guinea pig spinal cord after lesions of the red nucleus. J Neurochem 1991;56:1174–1183.
30. Bentivoglio M, Van Der Kooy D, Kuypers HGJM. The organization of the efferent projections of the substantia nigra in the rat: a retrograde fluorescent double-labeling study. Brain Res 1979;174:1–17.
31. Berger H. Ueber das Elektrenkephalogramm des Menschen. Arch Psychiatr Nervenkr 1929;87: 527–570.
32. Berger H. Ueber das Elektrenkephalogramm des Menschen. J Psychol Neurol 1930;40:160–179.
33. Bernheimer H, Birkmayer W, Hornykiewicz O, Jellinger K, Seitelberger F. Brain dopamine and the syndromes of Parkinson and Huntington. J Neurol Sci 1973; 20:415–455.
34. Bertrand GL, Blundell J, Musella R. Electrical exploration of the internal capsule and neighboring structures during stereotaxic procedures. J Neurosurg 1965;22: 333–343.
35. Bianchi R, Gioia M. Accessory oculomotor nuclei of man. II. The interstitial nucleus of Cajal: a Nissl and Golgi study. Acta Anat (Basel) 1991;142:357–365.
36. Billard JM, Daniel H, Pumain R. Sensitivity of rubrospinal neurons to excitatory amino acids in the rat red nucleus in vivo. Neurosci Lett 1991;134:49–52.
37. Björklund A, Lindvall O. Dopamine-containing systems in the CNS. In: Björklund A, Hökfelt T, eds. Handbook of chemical neuroanatomy. Vol. 2. Part 1: Classical transmitters in the CNS. Ch. 3. Amsterdam: Elsevier, 1984:55–122.
38. Bobillier P, Petitjean F, Salvert D, Ligier M, Seguin S. Differential projections of the nucleus raphe dorsalis and nucleus raphe centralis as revealed by autoradiography. Brain Res 1975;85:205–210.
39. Bobillier P, Seguin S, Petitjean F, Salvert D, Touret M, Jouvet M. The raphe nuclei of the cat brain stem: a topographical atlas of their efferent projections as revealed by autoradiography. Brain Res 1976; 113:449–486.
40. Bolam JP, Francis CM, Henderson Z. Cholinergic input to dopaminergic neurones in the substantia nigra: a double immunocytochemical study. Neuroscience 1991;41: 483–494.
41. Bolam PJ, Smith Y. The GABA and

substance P input to dopaminergic neurones in the substantia nigra of the rat. Brain Res 1990;529:57–78.
42. Braak H, Braak E. Nuclear configuration and neuronal types of the nucleus niger in the brain of the human adult. Hum Neurobiol 1986;5:71–82.
43. Bremer F. L'activité cérébrale au cours du sommeil et de la narcose: contribution à l'étude du mécanisme du sommeil. Bull Acad R Med Belg 1937;2:68–86.
44. Bremer F, Terzuolo C. Contribution à l'étude des mécanismes physiologiques du maintien de l'activité vigile du cerveau: interaction de la formation réticulée et de l'écorce cérébrale dans le processus du réveil. Arch Int Phsyiol Biochim 1954;62:157–178.
45. Brodal A. The reticular formation of the brain stem. Anatomical aspects and functional correlations. Springfield, IL: Charles C. Thomas, 1957.
46. Brodal A, Jansen J. The ponto-cerebellar projection in the rabbit and cat. J Comp Neurol 1946;84:31–118.
47. Brodal A, Rossi GF. Ascending fibers in brain stem reticular formation of cat. Arch Neurol Psychiatry 1955;74:68–87.
48. Brodal P. The corticopontine projection from the visual cortex in the cat. I. The total projection and the projection from area 17. Brain Res 1972;39:297–317.
49. Bunney BS, Aghajanian GK. The precise localization of nigral afferents in the rat as determined by a retrograde tracing technique. Brain Res 1976;117:423–435.
50. Burde RM, Loewy AD. Central origin of oculomotor parasympathetic neurons in the monkey. Brain Res 1980;198:434–439.
51. Burton H, Jones EG. The posterior thalamic region and its cortical projection in new world and old world monkeys. J Comp Neurol 1976;168:249–302.
52. Büttner U, Büttner-Ennever JA, Henn V. Vertical eye movement related unit activity in the rostral mesencephalic reticular formation of the alert monkey. Brain Res 1977;130:239–252.
53. Büttner-Ennever J. Pathways from the pontine reticular formation to structures controlling horizontal and vertical eye movements in the monkey. In: Baker R, Berthoz A, eds. Control of gaze by brain stem neurons: developments in neuroscience. Vol. 1. Amsterdam: Elsevier, 1977:89–98.
54. Büttner-Ennever JA, Henn V. An autoradiographic study of the pathways from the pontine reticular formation involved in horizontal eye movements. Brain Res 1976;108:155–164.
55. Carpenter MB. A study of the red nucleus in the rhesus monkey. Anatomic degenerations and physiologic effects resulting from localized lesions of the red nucleus. J Comp Neurol 1956;105:195–250.
56. Carpenter MB. Functional relationships between the red nucleus and the brachium conjunctivum. Physiologic study of lesions of the red nucleus in monkeys with degenerated superior cerebellar brachia. Neurology 1957;7:427–437.
57. Carpenter MB. Central oculomotor pathways. In: Bach-y-Rita P, ed. The control of eye movements. Ch. 4. New York: Academic Press, 1971:67–103.
58. Carpenter MB. Anatomy of the corpus striatum and brainstem integrating systems. In: Brooks VB, ed. Handbook of physiology. Sec. 1: The Nervous System. Vol. II: Motor control. Ch. 19. Washington, DC: American Physiological Society, 1981:947–995.
59. Carpenter MB, Batton RR III. Abducens internuclear neurons and their role in conjugate horizontal gaze. J Comp Neurol 1980;189: 191–209.
60. Carpenter MB, Carleton SC, Keller JT, Conte P. Connections of the subthalamic nucleus in the monkey. Brain Res 1981;224:1–29.
61. Carpenter MB, Harbison JW, Peter P. Accessory oculomotor nuclei in the monkey. Projections and effects of discrete lesions. J Comp Neurol 1970;140:131–154.
62. Carpenter MB, McMasters RE. Lesions of the substantia nigra in the rhesus monkey: efferent fiber degeneration and behavioral observations. Am J Anat 1964;114: 293–320.
63. Carpenter MB, Nakano K, Kim R. Nigrothalamic projections in the monkey demonstrated by autoradiographic techniques. J Comp Neurol 1976;165:401–416.
64. Carpenter MB, Peter P. Accessory oculomotor nuclei in the monkey. J Hirnforsch 1970/71;12:405–418.
65. Carpenter MB, Peter P. Nigrostriatal and nigrothalamic fibers in the rhesus monkey. J Comp Neurol 1972;144:93–116.
66. Carpenter MB, Pierson RJ. Pretectal region and the pupillary light reflex: an anatomical analysis in the monkey. J Comp Neurol 1973;149:271–300.
67. Carpenter MB, Strominger NL. Efferent fibers of the subthalamic nucleus in the monkey: a comparison of the efferent projections of the subthalamic nucleus, substantia nigra and globus pallidus. Am J Anat 1967;121:41–72.
68. Casagrande VA, Harting JK, Hall WC, Diamond IT. Superior colliculus of the tree shrew: a structural and functional subdivision into superficial and deep layers. Science 1972;177:444–447.
69. Castiglioni AJ, Gallaway MC, Coulter JD. Spinal projections from the midbrain in the monkey. J Comp Neurol 1978;178:329–346.
70. Charara A, Smith Y, Parent A. Glutamatergic inputs from the pedunculopontine nucleus to the midbrain dopaminergic neurons in primates: a light and electron microscopic study. Soc Neurosci Abstr 1993;19:1437.
71. Cheney PD, Fetz EE, Mewes K. Neural mechanisms underlying corticospinal and rubrospinal control of limb movements. Prog Brain Res 1991;87:213–252.
72. Cheramy A, Leviel V, Glowinski J. Dendritic release of dopamine in the substantia nigra. Nature 1981; 289:537–542.
73. Chiueh CC, Burns RS, Markey SP, Jacabowitz DM, Kopin IJ. Primate model of Parkinsonism: selective lesion of nigrostriatal neurons by 1-methyl-4-phenyl-1,2,3,6-tetrahydropyridine produces an extrapyramidal syndrome in rhesus monkeys. Life Sci 1985;36:213–218.
74. Clark WEL. The mammalian oculomotor nucleus. J Anat 1926;60: 426–448.
75. Clements JR, Grant S. Glutamate-like immunoreactivity in neurons of the laterodorsal tegmental and pedunculopontine nuclei in the rat. Neurosci Lett 1990;120:70–73.
76. Cogan DG. Neurology of the ocular muscles. 2d ed. Springfield, IL: Charles C. Thomas, 1956.
77. Collins P, Woolam DHM. The ventricular surface of the subcommisural organ: a scanning and transmission electron microscopic study. J Anat 1979;129:623–631.
78. Cooper JR, Bloom FE, Roth RH. The biochemical basis of neuropharmacology. 6th ed. New York: Oxford University Press, 1991.
79. Côté L, Crutcher MD. The basal ganglia. In: Kandel ER, Schwartz JH, Jessell TM, eds. Principles of neural science. 3rd ed. Ch. 42. New York: Elsevier, 1991:647–659.
80. Courville J. Rubrobulbar fibres to the facial nucleus and the lateral reticular nucleus (nucleus of the lateral funiculus): an experimental study in the cat with silver impregnation methods. Brain Res 1966; 1:317–337.
81. Courville J. Somatotopical organization of the projection from the nucleus interpositus anterior of the cerebellum to the red nucleus: an experimental study in the cat with silver impregnation methods. Exp Brain Res 1966;2:191–215.
82. Courville J. The nucleus of the facial nerve: the relation between cellular groups and peripheral branches of the nerve. Brain Res 1966;1:338–354.
83. Courville J, Brodal A. Rubro-cerebellar connections in the cat: an experimental study with silver impregnation methods. J Comp Neurol 1966;126:471–485.
84. Creese I, Fraser CM. Receptor biochemistry and methodology: dopamine receptors. Vol. 8. New York: Liss, 1987;1–245.

85. Cynader M, Berman N. Receptive-field organization of monkey superior colliculus. J Neurophysiol 1972;35:187–201.
86. Dahlström A, Fuxe K. Evidence for the existence of monoamine-containing neurons in the central nervous system. I. Demonstration of monoamines in the cell bodies of brain stem neurons. Acta Physiol Scand 1964;62(Suppl 232):1–55.
87. Dejerine J. Anatomie des centres nerveux. Vol. 2. Paris: J. Rueff, 1901.
88. Descarries L, Berthelet F, Garcia S, Beaudet A. Dopaminergic projection from nucleus raphe dorsalis to neostriatum in the rat. J Comp Neurol 1986;249:511–520.
89. DeVito JL, Anderson ME, Walsh KE. A horseradish peroxidase study of afferent connections of the globus pallidus in *Macaca mulatta*. Exp Brain Res 1980;38:65–73.
90. Diamond IT, Jones EG, Powell TPS. The projection of the auditory cortex upon the diencephalon and brain stem in the cat. Brain Res 1969;15:305–340.
91. Dray A. Serotonin in the basal ganglia: Functions and interactions with other neuron pathways. J Physiol (Paris) 1981;77:393–403.
92. Dray A, Davies J, Oakley NR, Tongroach P, Vellucci S. The dorsal and medial raphe projections to the substantia nigra in the rat: electrophysiological, biochemical and behavioural observations. Brain Res 1978;151:431–442.
93. Dunnett SB, Björklund A. Mechanisms of function of neuronal grafts in the adult mammalian brain. J Exp Biol 1987;132: 265–289.
94. Edwards SB. The ascending and descending projections of the red nucleus in the cat: an experimental study using an autoradiographic tracing method. Brain Res 1972; 48:45–63.
95. Edwards SB. Autoradiographic studies of the projections of the midbrain reticular formation: descending projections of the nucleus cuneiformis. J Comp Neurol 1975; 161:341–358.
96. Edwards SB. The commissural projection of the superior colliculus in the cat. J Comp Neurol 1977;173: 23–40.
97. Edwards SB, Ginsburgh CL, Henkel CK, Stein BE. Sources of subcortical projections to the superior colliculus in the cat. J Comp Neurol 1979;184:309–330.
98. Edwards SB, De Olmos JS. Autoradiographic studies of projections of the midbrain reticular formation: ascending projections of nucleus cuneiformis. J Comp Neurol 1976;165:417–432.
99. Ehringer H, Hornykiewicz D. Verteilung von Noradrenalin und Dopamin (3-hydroxytyramin) im Gehirn des Menschen und ihr Verhalten bei Erkrangkungen des Extrapyramidalen Systems. Klin Wochensch 1960;38:1236–1239.
100. Emson PC, Arregui A, Clement-Jones V, Sandberg BEB, Rossor M. Regional distribution of methionine enkephalin and substance P-like immunoreactivity in normal human brain and in Huntington's disease. Brain Res 1980;199: 147–160.
101. Englander RN, Netsky MG, Adelman LS. Location of human pyramidal tract in the internal capsule—anatomical evidence. Neurology 1975;25:823–826.
102. Fallon JH, Loughlin SE. Substantia nigra. In: Paxinos G, ed. The Rat nervous system. Vol. 1. Sydney, Australia: Academic Press, 1985: 353–374.
103. Ferraro A. Contributa sperimentale allo studio della substantia nigra normale e dei suoi rapporti con la corteccia cerebrale e con il corpo striato. Arch Gen Neurol Psychiatry 1925;6:26–117.
104. Finlay BL, Schneps SE, Wilson FG, Schneider GE. Topography of visual and somatosensory projections to the superior colliculus of the golden hamster. Brain Res 1978;142:223–235.
105. Flechsig P. Einige Bemerkungen über die Untersuchungsmethoden der Grosshirnrinde, insbesondere des Menschen. Arch Anat Entwickl Gesch 1905;337–444.
106. Flumerfelt BA. An ultrastructural investigation of afferent connections of the red nucleus in the rat. J Anat 1980;131:621–633.
107. Flumerfelt BA, Otabe S, Courville J. Distinct projections to the red nucleus from the dentate and interposed nuclei in the monkey. Brain Res 1973;50:408–414.
108. Foix C. Les lésions anatomiques de la maladie de Parkinson. Rev Neurol (Paris) 1921;37:593–600.
109. Foix C, Nicolesco J. Les noyaux gris centraux et la région mésencéphalo-sous-optique suivi d'un appendice sur l'anatomie pathologique de la maladie de Parkinson. Paris: Masson, 1925.
110. Forno LS. The Lewy body in Parkinson's disease. In: Yahr MD, Bergmann KJ, eds. Parkinson's Disease. Advances in neurology. Vol. 45. New York: Raven Press, 1986:35–43.
111. François C, Percheron G, Yelnik J. Localization of nigrostriatal, nigrothalamic and nigrotectal neurons in ventricular coordinates in macaques. Neuroscience 1984;13: 61–76.
112. François C, Percheron G, Yelnik J, Heyner S. Demonstration of the existence of small local circuit neurons in the Golgi-stained substantia nigra. Brain Res 1979;172: 160–164.
113. François C, Percheron G, Yelnik J, Heyner S. A histological atlas of the macaque (*Macaca mulatta*) substantia nigra in ventricular coordinates. Brain Res Bull 1985;14: 349–367.
114. French JD, Hernández-Peon R, Livingston RB. Projections from cortex to cephalic brain stem (reticular formation) in monkey. J Neurophysiol 1955;18:74–95.
115. French JD, Magoun HW. Effects of chronic lesions in central cephalic brain stem of monkeys. Arch Neurol Psychiatry 1952;68:591–604.
116. French JD, Verzeano M, Magoun HW. An extralemniscal sensory system in the brain. Arch Neurol Psychiatry 1953;69:505–518.
117. Freund TF, Powell JF, Smith AD. Tyrosine hydroxylase-immunoreactive boutons in synaptic contacts with identified striatonigral neurons, with particular reference to dendritic spines. Neuroscience 1984;13:1189–1216.
118. Fuchs A. Role of the vestibular and reticular nuclei in the control of gaze: reticular, prepositus and other internuclear neuronal activity. In: Baker R, Berthoz A, eds. Control of gaze by brain stem neurons: developments in neuroscience. Amsterdam: Elsevier, 1977:341–348.
119. Fujito Y, Imai T, Aoki M. Monosynaptic excitation of motoneurons innervating forelimb muscles following stimulation of the red nucleus in cats. Neurosci Lett 1991;127:137–140.
120. Fukushima K. The interstitial nucleus of Cajal and its role in the control of movements of head and eyes. Prog Neurobiol 1987;29: 107–192.
121. Fuxe K. Evidence for the existence of monoamine neurons in the central nervous system. IV. Distribution of monoamine nerve terminals in the central nervous system. Acta Physiol Scand 1965;64(Suppl 247): 37–120.
122. Gacek RR. Location of brain stem neurons projecting to the oculomotor nucleus in the cat. Exp Neurol 1977;57:725–749.
123. Garcia-Rill E. The pedunculopontine nucleus. Prog Neurobiol 1991;36:363–389.
124. Garey LJ. Visual system. In: Paxinos G, ed. The human nervous system. Ch. 28. New York: Academic Press, 1990:945–977.
125. Garey LJ, Jones EG, Powell TPS. Interrelationships of striate and extrastriate cortex with the primary relay sites of the visual pathway. J Neurol Neurosurg Psychiatry 1968;31:135–157.
126. Geniec P, Morest DK. The neuronal architecture of the human posterior colliculus. Acta Otolaryngol [Suppl] (Stockh) 1971;295:1–33.
127. Gerfen CR. The neostriatal mosaic: I. Compartmental organization of projections from the neostriatum to the substantia nigra in the rat. J Comp Neurol 1985;236:454–476.
128. Gerfen CR. The neostriatal mosaic: Multiple levels of compartmental

organization in the basal ganglia. Annu Rev Neurosci 1992;15: 285–320.
129. Gerfen CR, Engber TM, Mahan LC, et al. D_1 and D_2 dopamine receptor-regulated gene expression of striatonigral and striatopallidal neurons. Science 1990;250: 1429–1492.
130. Gerfen CR, Herkenham M, Thibault J. The neostriatal mosaic. II. Patch- and matrix-directed mesostriatal dopaminergic and non-dopaminergic systems. J Neurosci 1987;7:3915–3934.
131. German DC, Dubach M, Askari S, Speciale SG, Bowden DM. 1-methyl-4-phenyl-1,2,3,6-tetrahydropyridine-induced Parkinsonian syndrome in *Macaca fascicularis*: which midbrain dopaminergic neurons are lost? Neuroscience 1988;24:161–174.
132. Geyer MA, Puerto A, Dawsey WJ, Knap S, Bullard WP, Mandell AJ. Histologic and enzymatic studies of the mesolimbic and mesostriatal serotoninergic pathways. Brain Res 1976;106:241–256.
133. Gilbert GJ. The subcommissural organ. Neurology 1960;10:138–142.
134. Gilbert GJ, Glaser GH. On the nervous system integration of water and salt metabolism. Arch Neurol 1961;5:179–196.
135. Gillingham FJ. Small localized surgical lesions of the internal capsule in the treatment of dyskinesia. Confin Neurol 1962;22:385–392.
136. Giolli RA, Guthrie MD. Organization of subcortical projections of visual areas I and II in the rabbit: an experimental degeneration study. J Comp Neurol 1971;142:351–376.
137. Giolli RA, Tigges J. The primary optic pathways and nuclei of primates. In: Noback CR, Montagna W, eds. The primate brain, advances in primatology. Vol. 1. Ch. 2. New York: Appleton-Century-Crofts, 1970:29–54.
138. Giuffrida R, Li Volsi G, Perciavalle V. Influences of cerebral cortex and cerebellum on the red nucleus of the rat. Behav. Brain Res 1988; 28:109–111.
139. Giuffrida R, Palmeri A, Raffaele R, Ricca G, Sapienza S. Convergence pattern of cortical and interposital influences on rubrospinal neurons of the cat. Behav Brain Res 1988;28:113–116.
140. Glendenning KK, Hall JA, Diamond IT, Hall WC. The pulvinar nucleus of *Galago senegalensis*. J Comp Neurol 1975;161:419–458.
141. Goldberg ME, Eggers HM, Gouras P. The ocular motor system. In: Kandel ER, Schwartz JH, Jessell TM, eds. Principles of neural science. 3rd ed. Ch. 43. New York: Elsevier, 1991:660–678.
142. Gordon B. The superior colliculus of the brain. Sci Am 1972; 227:72–82.
143. Gould E, Woolf NJ, Butcher LL. Cholinergic projections to the substantia nigra from the pedunculopontine and laterodorsal tegmental nuclei. Neuroscience 1989;28: 611–623.
144. Grace AA, Bunney BS. Intracellular and extracellular electrophysiology of nigral dopaminergic neurons. 3. Evidence for electrotonic coupling. Neuroscience 1983;10: 333–348.
145. Graham J. An autoradiographic study of the efferent connections of the superior colliculus in the cat. J Comp Neurol 1977;173:629–654.
146. Granit R. Receptors and sensory perception. New Haven, CT: Yale University Press, 1955.
147. Granit R, Kaada BR. Influence of stimulation of central nervous structures on muscle spindles in cat. Acta Physiol Scand 1952;27: 130–160.
148. Graybiel AM. Some extrageniculate visual pathways in the cat. Invest Ophthalmol 1972;11:322–332.
149. Graybiel AM. Anatomical organization of retinotectal afferents in the cat: an autoradiographic study. Brain Res 1975;96:1–24.
150. Graybiel AM. A satellite system of the superior colliculus: The parabigeminal nucleus and its projection to the superficial collicular layers. Brain Res 1978;145:365–374.
151. Graybiel AM, Hartwieg EA. Some afferent connections of the oculomotor complex in the cat: an experimental study with tracer techniques. Brain Res 1974;81:543–551.
152. Graybiel AM, Ragsdale C Jr. Histochemically distinct compartments in the striatum of human, monkey and cat demonstrated by acetylcholinesterase staining. Proc Natl Acad Sci USA 1978;75:5723–5726.
153. Graybiel AM, Sciascia TR. Origin and distribution of nigrotectal fibers in the cat. Neurosci Abstr 1975;1:271.
154. Grofova I. The identification of striatal and pallidal neurons projecting to substantia nigra: an experimental study by means of retrograde axonal transport of horseradish peroxidase. Brain Res 1975;91:286–291.
155. Guillery RW. Degeneration in the posterior commissural fornix and the mammillary peduncle of the rat. J Anat 1956;90:350–370.
156. Gulley RL, Wood RL. The fine structure of the neurons in the rat substantia nigra. Tissue Cell 1971; 3:675–690.
157. Haber SN, Groenewegen HJ. The interrelationship of the distribution of neuropeptides and tyrosine hydroxylase immunoreactivity in the human substantia nigra. J Comp Neurol 1989;290:53–68.
158. Haber SN, Nauta WJH. Ramifications of the globus pallidus in the rat as indicated by patterns of immunohistochemistry. Neuroscience 1983;9:245–260.
159. Haber SN, Lynd E, Klein C, Groenewegen HJ. Topographic organization of the ventral striatal efferent projection in the rhesus monkey: an anterograde tracing study. J Comp Neurol 1990;293: 282–298.
160. Hagbarth KE, Kerr DIB. Central influences on spinal afferent conduction. J Neurophysiol 1954;17: 295–307.
161. Hallanger AE, Wainer BH. Ascending projections from the pedunculopontine tegmental nucleus and the adjacent mesopontine tegmentum in the rat. J Comp Neurol 1988;274:483–515.
162. Halliday GM, Törk J. Comparative anatomy of the ventromedial mesencephalic tegmentum in the rat, cat, monkey and human. J Comp Neurol 1986;252:423–445.
163. Hamill GS, Olschowska JA, Lenn NJ, Jacobowitz DM. The subnuclear distribution of substance P, cholecystokinin, vasoactive intestinal peptide, somatostatin, leuenkephalin, dopamine—hydroxylase, and serotonin in the rat interpeduncular nucleus. J Comp Neurol 1984;226:580–596.
164. Hanaway J, Young RR. Localization of the pyramidal tract in the internal capsule of man. J Neurol Sci 1977;34:63–70.
165. Harris NC, Davies J. Cortically evoked excitatory synaptic transmission in the cat red nucleus is antagonized by D-AP5 but not by D-AP7. Brain Res 1992;594: 176–180.
166. Harting JK. Descending pathways from the superior colliculus: an autoradiographic analysis in the rhesus monkey (*Macaca mulatta*). J Comp Neurol 1977;173:583–612.
167. Harting JK, Casagrande VA, Weber JT. The projection of the primate superior colliculus upon the dorsal lateral geniculate nucleus: autoradiographic demonstration of intralaminar distribution of tectogeniculate axons. Brain Res 1978; 150:593–599.
168. Harting JK, Guillery RW. Organization of the retinocollicular pathway in the cat. J Comp Neurol 1976;166:133–144.
169. Harting JK, Hall WC, Diamond IT, Martin GF. Anterograde degeneration study of the superior colliculus in *Tupaia glis*: evidence for a subdivision between superficial and deep layers. J Comp Neurol 1973;148:361–386.
170. Hartmann-Von Monakow K, Akert K, Künzle H. Projections of the precentral and premotor cortex to the red nucleus and other midbrain areas in *Macaca fascicularis*. Exp Brain Res 1979;34:91–105.
171. Hassler R. Zur Pathologie der Paralysis agitans und der postenenzephalitischen Parkinsonismus. J Psychol Neurol 1938; 48:387–476.
172. Hatschek R. Zur vergleichenden Anatomie des Nucleus ruber tegmenti. Arb Neurol Inst Wiener Univ 1907;15:89–135.

173. Hazrati L-N, Parent A. Projection from the deep cerebellar nuclei to the pedunculopontine nucleus in the squirrel monkey. Brain Res 1992;585:267–271.
174. Heckers S, Geula C, Mesulam M-M. Cholinergic innervation of the human thalamus: dual origin and differential nuclear distribution. J Comp Neurol 1992;325:68–82.
175. Hedreen JC, DeLong MR. Organization of the striatopallidal, striatonigral, and nigrostriatal projections in the macaque. J Comp Neurol 1991;304:569–595.
176. Hendrickson AM, Wilson ME, Toyne MJ. The distribution of optic nerve fibers in *Macaca mulatta*. Brain Res 1970;23:425–427.
177. Hervé D, Pickel VM, Joh TH, Beaudet A. Serotonin axon terminals in the ventral tegmental area of the rat: Fine structure and synaptic input to dopaminergic neurons. Brain Res 1987;435:71–83.
178. Hikosaka O, Wurtz RH. Visual and oculomotor functions of monkey substantia nigra pars reticulata. I. Relation of visual and auditory responses to saccades. J Neurophysiol 1983;49:1230–1252.
179. Hikosaka O, Wurtz RH. Visual and oculomotor functions of monkey substantia nigra pars reticulata. II. Visual responses related to fixation of gaze. J Neurophysiol 1983; 49:1254–1267.
180. Hikosaka O, Wurtz RH. Visual and oculomotor functions of monkey substantia nigra pars reticulata. III. Memory-contingent visual and saccade responses. J Neurophysiol 1983;49:1268–1284.
181. Hikosaka O, Wurtz RH. Visual and oculomotor functions of monkey substantia nigra pars reticulata. IV. Relation of substantia nigra to superior colliculus. J Neurophysiol 1983;49:1285–1301.
182. Houk JC. Red nucleus: role in motor control. Curr Opin Neurobiol 1991;1:610–615
183. Hopkins DA, Niessen LW. Substantia nigra projections to the reticular formation, superior colliculus and central gray in rat, cat, and monkey. Neurosci Lett 1976; 2:253–259.
184. Hornykiewicz O. Dopamin (3-Hydroxytyramin) in Zentralnervensystem und seine Beziehung zum Parkinson-Syndrom des Menschen. Dtsch Med Wochensch 1962;87:1807–1810.
185. Hornykiewicz O. Dopamine (3-Hydroxytyramine) and brain functions. Pharmacol Rev 1966;18: 925–964.
186. Hornykiewicz O, Kish SJ. Biochemical pathophysiology of Parkinson's disease. In: Yahr MD, Bergmann KJ, eds. Parkinson's Disease. Advances in neurology. Vol. 45. New York: Raven Press, 1986:19–34.
187. Hubel DH, Le Vay S, Wiesel TN. Mode of termination of retino-tectal fibers in macaque monkey: an autoradiographic study. Brain Res 1975;96:25–40.
188. Huerta MF, Harting JK. The mammalian superior colliculus: studies of its morphology and connections. In: Vanegas H, ed. Comparative neurology of the optic tectum. New York: Plenum, 1984:687–733.
189. Hunsperger RW. Affektreaktionen auf elektrische Reizung im Hirnstamm der Kartze. Helv Physiol Pharmacol Acta 1956;14:70–92.
190. Hutchins B, Weber JT. The pretectal complex of the monkey: a reinvestigation of the morphology and retinal terminations. J Comp Neurol 1985;232:425–442.
191. Ilinsky IA, Jouandest MJ, Goldman-Rakic PS. Organization of the nigrothalamocortical system in the rhesus monkey. J Comp Neurol 1985;256:315–330.
192. Ilinsky IA, Kultas-Ilinsky K. Sagittal cytoarchitectonic maps of the *Macaca mulatta* thalamus with a revised nomenclature of the motor related nuclei validated by observation on their connectivity. J Comp Neurol 1987;262:331–364.
193. Ilinsky IA, Tourtelotte WG, Kultas-Ilinsky F. Anatomical distinctions between the two basal ganglia afferent territories in the primate motor thalamus. Stereotact Funct Neurosurg 1993;60:62–69.
194. Inagaki S, Parent A. Distribution of substance P and enkephalin-like immunoreactivity in the substantia nigra of rat, cat and monkey. Brain Res Bull 1984;13:319–329.
195. Ingram WR, Ranson SW. Effects of lesions in the red nuclei in cats. Arch Neurol Psychiatry 1932;28: 483–512.
196. Jackson A, Crossman AR. Basal ganglia and other afferent projections to the peribrachial region in the rat: a study using retrograde and anterograde transport of horseradish peroxidase. Neuroscience 1981;6:1537–1549.
197. Jackson A, Crossman AR. Nucleus tegmenti pedunculopontinus: efferent connections with special references to the basal ganglia, studied in the rat by anterograde and retrograde transport of horseradish peroxidase. Neuroscience 1983; 10:725–765.
198. Jacobs BL, Azmitia EC. Structure and functions of the brain serotonin systems. Physiol Rev 1992; 72:165–229.
199. Jacobs BL, Trulson ME. Mechanisms of action of LSD. Am Sci 1979;67:396–404.
200. Jasper HH, Ajmone-Marsan C, Stoll J. Corticofugal projections to the brain stem. Arch Neurol Psychiatry 1952;67:155–171.
201. Jayaraman A, Batton RR III, Carpenter MB. Nigrotectal projections in the monkey: an autoradiographic study. Brain Res 1977; 135:147–152.
202. Jellinger K. The pathology of Parkinson's disease. In: Marsden CD, Fahn S, eds. Movement disorders. Vol. 2. London: Butterworths, 1987:124–165.
203. Jenny AB, Smith JM, Bernardo KL, Woolsey TA. Distribution of motor cortical neuron synaptic terminals on monkey parvocellular red nucleus neurons. Somatosens Mot Res 1991;8:23–26.
204. Jiménez-Castellanos J, Graybiel AM. Evidence that histochemically distinct zones of the primate substantia nigra pars compacta are related to patterned distributions of nigrostriatal projection neurons and striatonigral fibers. Exp Brain Res 1989;74:227–238.
205. Johansson H. Rubrospinal and rubrobulbospinal influences on dynamic and static gamma motoneurones. Behav Brain Res 1988; 28:97–107.
206. Jones EG. The thalamus. New York: Plenum, 1985.
207. Kabebian JW, Calne DB. Multiple receptors for dopamine. Nature 1979;277:93–96.
208. Kanaseki T, Sprague JM. Anatomical organization of pretectal nuclei and tectal laminae in the cat. J Comp Neurol 1974;158:319–338.
209. Kanazawa I, Emson PC, Cuello AC. Evidence for the existence of substance P-containing fibers in striato-nigral and pallido-nigral pathways in rat brain. Brain Res 1977;119:447–453.
210. Kawamura K, Brodal A. The tectopontine projection in the cat: an experimental anatomical study with comments on pathways for teleceptive impulses to the cerebellum. J Comp Neurol 1973;149:371–390.
211. Kelly DD. Disorders of sleep and consciousness. In: Kandel ER, Schwartz JH, Jessell TM, eds. Principles of neural science. 3rd ed. Ch. 52. New York: Elsevier, 1991: 805–819.
212. Kety S. Sleep and the energy metabolism of the brain. In: Woltenholme GEW, O'Connor M, eds. The nature of sleep. Boston: Little, Brown, 1960:375–381.
213. Kim R, Nakano K, Jayaraman A, Carpenter MB. Projections of the globus pallidus and adjacent structures: an autoradiographic study in the monkey. J Comp Neurol 1976;169:263–289.
214. King JS, Bowman MH, Martin GF. The red nucleus of the opossum (*Didelphis marsupialis virginiana*): a light and electron microscopic study. J Comp Neurol 1971; 143:157–184.
215. King JS, Schwyn RC, Fox CA. The red nucleus in the monkey (*Macaca mulatta*): a Golgi and an electron microscopic study. J Comp Neurol 1971;142:75–108.
216. Kita H, Kitai ST. Efferent projections of the subthalamic nucleus in the rat: a light and electron microscopic analysis. J Comp Neurol 1987;260:435–452.

217. Kopin IJ, Markey SP. MPTP toxicity: implications for research in Parkinson's disease. Annu Rev Neurosci 1988;11:81–96.
218. Kornhuber J, Kim J-S, Kornhuber ME, Kornhuber HH. The corticonigral projection: reduced glutamate content in the substantia nigra following frontal cortex ablation in the rat. Brain Res 1984; 322:124–126.
219. Kudo M, Niimi K. Ascending projections of the inferior colliculus on the medial geniculate body in the cat studied by anterograde and retrograde tracing techniques. Brain Res 1978;155:113–117.
220. Kuffler SW. Discharge patterns and functional organization of mammalian retina. J Neurophysiol 1953;16:37–68.
221. Kuhlenbeck H, Miller RN. The pretectal region of the human brain. J Comp Neurol 1949;91:369–408.
222. Künzle H, Akert K. Efferent connections of cortical Area 8 (frontal eye field) in *Macaca fascicularis*: a reinvestigation using the autoradiographic technique. J Comp Neurol 1977;173:147–164.
223. Künzle H, Akert K, Wurtz RH. Projections of area 8 (frontal eye field) to superior colliculus in monkey: an autoradiographic study. Brain Res 1976;117:487–492.
224. Kuypers HGJM. Corticobulbar connexions to the pons and lower brain stem in man: an anatomical study. Brain 1958;81:364–388.
225. Kuypers HGJM, Lawrence DG. Cortical projections to the red nucleus and the brain stem in the rhesus monkey. Brain Res 1967; 4:151–188.
226. Kuypers HGJM, Maisky VA. Retrograde axonal transport of horseradish peroxidase from spinal cord to brain stem cell groups in the cat. Neurosci Lett 1975;1:9–14.
227. Langer AF, Graybiel AM. Distinct nigrostriatal projection systems innervates striosomes and matrix in the primate striatum. Brain Res 1989;498:344–350.
228. Langston JW, Forno LS, Rebert CS, Irwin I. Selective nigral toxicity after systemic administration of 1-methyl-4-phenyl-1,2,5,6-tetrahydropyridine (MPTP) in the squirrel monkey. Brain Res 1983;292: 390–394.
229. Langston JW, Irwin I. MPTP: Current concepts and controversies. Clin Neuropharmacol 1986;9: 485–507.
230. Lavoie B, Parent A. Immunohistochemical study of the serotoninergic innervation of the basal ganglia in the squirrel monkey. J Comp Neurol 1990;299:1–16.
231. Lavoie B, Parent A. Serotoninergic innervation of the thalamus in the primate: an immunohistochemical study. J Comp Neurol 1991; 312:1–18.
232. Lavoie B, Parent A. Dopaminergic neurons expressing calbindin in normal and Parkinsonian monkeys. Neuroreport 1991;2:601–604.
233. Lavoie B, Parent A. The pedunculopontine nucleus in the squirrel monkey. Topographical organization of cholinergic, monoaminergic and glutamatergic neurons in the mesopontine tegmentum. J Comp Neurol 1994;344:190–209.
234. Lavoie B, Parent A. The pedunculopontine nucleus in the squirrel monkey. Projections to the basal ganglia as revealed by anterograde tract-tracing methods. J Comp Neurol 1994;344:210–231.
235. Lavoie B, Parent A. The pedunculopontine nucleus in the squirrel monkey. Cholinergic and glutamatergic projections to the substantia nigra. J Comp Neurol 1994;344:232–241.
236. Lavoie B, Smith Y, Parent A. Dopaminergic innervation of the basal ganglia in the squirrel monkey as revealed by tyrosine hydroxylase immunohistochemistry. J Comp Neurol 1989;288:36–52.
237. Lewy FH. Zur pathologischen Anatomie der Paralysis agitans. Dtsch Z Nervenheilkd 1913;50: 50–55.
238. Llinás R, Greenfield SA, Jahsen H. Electrophysiology of pars compacta cells in the in vitro substantia nigra—a possible mechanism for dendritic release. Brain Res 1984; 294:355–373.
239. Loewy AD, Saper CB. Edinger-Westphal nucleus: projections to the brain stem and spinal cord in the cat. Brain Res 1978;150:1–27.
240. Loewy AD, Saper CB, Yamodis ND. Re-evaluation of the efferent projections of the Edinger-Westphal nucleus. Brain Res 1978; 121:153–159.
241. Lowenstein O. Clinical pupillary symptoms in lesions of the optic nerve, optic chiasm and optic tract. Arch Opthalmol 1954;52:385–403.
242. Maffel L, Pompeiano O. Cerebellar control of flexor motoneurons. Arch Ital Biol 1962;100:467–500.
243. Magoun HW. An ascending reticular activating system in the brain stem. Arch Neurol Psychiatry 1952;67:145–154.
244. Magoun HW. The waking brain. 2d ed. Springfield, IL: Charles C. Thomas, 1963.
245. Magoun HW, Ranson SW. The central path of the light reflex: a study of the effect of lesions. Arch Opthalmol 1935;13:791–811.
246. Magoun HW, Ranson SW. The afferent path of the light reflex: a review of the literature. Arch Opthalmol 1935;13:862–874.
247. Magoun HW, Ranson SW, Mayer LL. The pupillary light reflex after lesions of the posterior commissure in the cat. Am J Opthalmol 1935;18:624–630.
248. Magoun HW, Rhines R. An inhibitory mechanism in the bulbar reticular formation. J Neurophysiol 1946;9:165–171.
249. Magoun HW, Rhines R. Spasticity: the stretch-reflex and extrapyramidal systems. Springfield, IL: Charles C. Thomas, 1947.
250. Marburg O, Warner FJ. The pathways of the tectum (anterior colliculus) of the midbrain in cats. J Nerv Ment Dis 1947;106:415–446.
251. Marsden CD. Pigmentation in the nucleus substantiae nigrae of mammals. J Anat 1961;95:256–261.
252. Martin GF, Dom R. Rubrobulbar projections of the opossum (*Didelphia virginiana*). J Comp Neurol 1970;139:199–214.
253. Martin JB, Reichlin S, Brown GM. Clinical neuroendocrinology. Philadelphia: F.A. Davis, 1977: 229–246.
254. Martin JH, Ghez C. Red nucleus and motor cortex: parallel motor systems for the initiation and control of skilled movement. Behav Brain Res 1988;28:217–223.
255. Martinez-Murillo R, Villalba RM, Rodrigo J. Electron microscopic localization of cholinergic terminals in the rat substantia nigra: an immunocytochemical study. Neurosci Lett 1989;96:121–126.
256. Martinez-Murillo R, Villalba RM, Montero-Calballero MI, Rodrigo J. Cholinergic somata and terminals in the rat substantia nigra: an immunohistochemical study with optical and electron microscopic techniques. J Comp Neurol 1989; 281:397–416.
257. Mehler WR, Feferman ME, Nauta WJH. Ascending axon degeneration following anterolateral cordotomy: an experimental study in the monkey. Brain 1960;83:718–750.
258. Merzenich MM, Reid MD. Representation of the cochlea within the inferior colliculus of the cat. Brain Res 1974;77:397–415.
259. Mesulam M-M, Marsh D, Hersh L, Bothwell M, Geula C. Cholinergic innervation of the human striatum, globus pallidus, subthalamic nucleus, substantia nigra and red nucleus. J Comp Neurol 1992;323: 252–268.
260. Mesulam M-M, Mufson EJ, Levey AI, Wainer BH. Atlas of cholinergic neurons in the forebrain and upper brainstem of macaque based on monoclonal choline acetyltransferase immunohistochemistry and acetylcholinesterase histochemistry. Neuroscience 1984;12: 669–686.
261. Mettler FA. Relation between pyramidal and extrapyramidal function. Proc Assoc Res Nerv Ment Dis 1942;21:150–227.
262. Mettler FA. Extensive unilateral cerebral removals in the primate: physiologic effects and resultant degeneration. J Comp Neurol 1943;79:185–243.
263. Miller RA, Strominger NL. Efferent connections of the red nucleus in the brainstem and spinal cord of the rhesus monkey. J Comp Neurol 1973;152:327–346.

264. Mingazzini G. Sulla fina struttura della substantia nigra Sömmeringii. Vol. 5. Atti R Acad Lincei 1888.
265. Moon Edley S, Graybiel AM. The afferent and efferent connections of the feline nucleus tegmenti pedunculopontinus, pars compacta. J Comp Neurol 1983;217:187–215.
266. Moore RY, Bhatnagar RK, Heller A. Anatomical and chemical studies of a nigro-neostriatal projection in the cat. Brain Res 1971; 30:119–135.
267. Moore RY, Goldberg JM. Ascending projections of the inferior colliculus in the cat. J Comp Neurol 1963;121:109–136.
268. Moore RY, Halaris AE, Jones BE. Serotonin neurons of the midbrain raphe: ascending projections. J Comp Neurol 1978;180:417–438.
269. Morest DK, Oliver DL. The neuronal architecture of the inferior colliculus in the cat: defining the functional anatomy of the auditory midbrain. J Comp Neurol 1984; 222:209–236.
270. Morgan LR. The corpus striatum. Arch Neurol Psychiatry 1927;18: 495–548.
271. Mori S, Matsumura T, Takino T, Sano Y. Light and electron microscopic studies of serotonin nerve fibers in the substantia nigra of the rat, cat and monkey. Anat Embryol 1987;176:13–18.
272. Morrison JH, Foote SL. Noradrenergic and serotonergic innervation of cortical, thalamic, tectal visual structures in old and new world monkeys. J Comp Neurol 1986; 243:117–138.
273. Moruzzi G, Magoun HW. Brain stem reticular formation and activation of the EEG. Electroencephalogr Clin Neurophysiol 1949;1:455–473.
274. Mugnaini E, Oertel WH. Atlas of the distribution of GABAergic neurons and terminals in the rat CNS as revealed by GAD immunohistochemistry. In: Björklund A, Hökfelt T, eds. Handbook of chemical neuroanatomy. Vol. 4. Part 1: GABA and neuropeptides in the CNS. Ch. 10. Amsterdam: Elsevier, 1985: 436–595.
275. Mussen AT. Experimental investigations on the cerebellum. Brain 1927;50:313–349.
276. Naus CG, Flumerfelt BA, Hrycyshyn AW. An HRP-TMB ultrastructural study of rubral afferents in the rat. J Comp Neurol 1985;239:453–465.
277. Nauta HJW, Cole M. Efferent projections of the subthalamic nucleus: an autoradiographic study in monkey and cat. J Comp Neurol 1978;180:1–16.
278. Nauta HJW, Kaiserman-Abramof IR, Lasek RJ. Electron microscopic observations of horseradish peroxidase transported from the caudoputamen to the substantia nigra in the rat: possible involvement of the granular reticulum. Brain Res 1975;85:373–384.
279. Nauta WJH. Hippocampal projections and related neural pathways to the midbrain in the cat. Brain 1958;81:319–340.
280. Nauta WJH, Kuypers HGJM. Some ascending pathways in the brain stem reticular formation. In: Jasper HH, Proctor LP, Knighton RS, et al., eds. Reticular formation of the brain. Henry Ford Hospital International Symposium. Ch. 1. Boston: Little, Brown, 1958:3–30.
281. Nauta WJH, Mehler WR. Projections of the lentiform nucleus in the monkey. Brain Res 1966;1:3–42.
282. Nedergaard S, Bolam JP, Greenfield SA. Facilitation of a dendritic calcium conductance by 5-hydroxytryptamine in the substantia nigra. Nature 1988;333:174–177.
283. Nieuwenhuys R. Chemoarchitecture of the brain. Berlin: Springer-Verlag, 1985.
284. Niijima K, Yoshida M. Activation of mesencephalic dopamine neurons by chemical stimulation of the nucleus tegmenti pedunculopontinus pars compacta. Brain Res 1988;451:163–171.
285. Nyberg-Hansen R. Functional organization of descending supraspinal fibre systems to the spinal cord: anatomical observations and physiological correlations. Ergeb Anat Entwickl-Gesch 1966;39:1–48.
286. Oertel WH, Tappaz ML, Berod A, Mugnaini E. Two-color immunohistochemistry for dopamine and GABA neurons in rat substantia nigra and zona incerta. Brain Res Bull 1982;9:463–474.
287. Oeth KM, Lewis DA. Cholecystokinin- and dopamine-containing mesencephalic neurons provide distinct projections to monkey prefrontal cortex. Neurosci Lett 1992;145:87–92.
288. Oliver DL, Morest DK. The central nucleus of the inferior colliculus in the cat. J Comp Neurol 1984; 222:237–264.
289. Olpe H-R, Koella WP. The response of striatal cells upon stimulation of the dorsal and median raphe nuclei. Brain Res 1977;122: 357–360.
290. Olszewski J. Cytoarchitecture of the human reticular formation. In: Delafresnaye JF, ed. Brain mechanisms and consciousness. Oxford: Blackwell, 1954:54–80.
291. Olszewski J, Baxter D. Cytoarchitecture of the human brain stem. Philadelphia: J.B. Lippincott, 1954.
292. Papez JW, Freeman GL. Superior colliculi and their fiber connections in the rat. J Comp Neurol 1930;51:409–439.
293. Paré D, Smith Y, Parent A, Steriade M. Projections of brainstem core cholinergic and non-cholinergic neurons of cat to intralaminar and reticular thalamic nuclei. Neuroscience 1988;25:69–86.
294. Parent A.. Comparative neurobiology of the basal ganglia. New York: Wiley, 1986.
295. Parent A, De Bellefeuille L. Organization of efferent projections from the internal segment of the globus pallidus in primate as revealed by fluorescence retrograde labeling method. Brain Res 1982;245: 201–213.
296. Parent A, Descarries L, Beaudet A. Organization of ascending serotonin systems in the adult rat brain. A radioautographic study after intraventricular administration of [^{3}H] 5-hydroxytryptamine. Neuroscience 1981;6:115–138.
297. Parent A, Bouchard C, Smith Y. The striatopallidal and striatonigral projections: two distinct systems in primate. Brain Res 1984; 303:385–390.
298. Parent A, Hazrati L-N. Multiple striatal representation at substantia nigra level in primate. J Comp Neurol 1994;344:305–320.
299. Parent A, Hazrati L-N, Lavoie B. The pallidum as a dual structure in primates. In: Bernardi G, Carpenter MB, Di Chiara G, Morelli M, Stanzione P, eds. The basal ganglia III. New York: Plenum, 1991;81–88.
300. Parent A, Lavoie B. The heterogeneity of the mesostriatal dopaminergic system as revealed in normal and parkinsonian monkeys. In: Narabayashi H, Nagatsu T, Yanagisawa Y, Mizuno Y, eds. Parkinson's disease: from basic research to treatment. Advances in neurology. Vol. 60. New York: Raven Press, 1993:25–33.
301. Parent A, Mackey A, De Bellefeuille L. The subcortical afferents to caudate nucleus and putamen in primate: a fluorescence retrograde double labeling study. Neuroscience 1983;10:1137–1150.
302. Parent A, Mackey A, Smith Y. The output organization of the substantia nigra in primate as revealed by a retrograde double labeling method. Brain Res Bull 1983; 10:529–537.
303. Parent A, Smith Y. Organization of efferent projections of the subthalamic nucleus in primate as revealed by retrograde labeling methods. Brain Res 1987;436: 296–310.
304. Pasik P, Pasik T, Holstein GR, Saavedra JP. Serotoninergic innervation of the monkey basal ganglia: an immunocytochemical light and electron microscopic study. In: McKensie JS, Kemn RE, Wilcock LN, eds. The basal ganglia: structure and function. New York: Plenum, 1984:115–129.
305. Pazos A, Probst A, Palacios JM. Serotonin receptors in the human brain. III. Autoradiographic mapping of serotonin-1 receptors. Neuroscience 1987;21:97–122.
306. Pazos A, Probst A, Palacios JM. Serotonin receptors in the human brain. IV. Autoradiographic map-

ping of serotonin-2 receptors. Neuroscience 1987;21:123–139.
307. Percheron G. The thalamic territory of cerebellar afferents and the lateral region of the macaque thalamus in stereotaxic ventricular coordinates. J Hirnforsch 1977;18: 375–400.
308. Pickel VM, Chan J, Sesack SR. Cellular substrates for interaction between dynorphin terminals and dopamine dendrites in rat ventral tegmental area and substantia nigra. Brain Res 1993;602: 275–289.
309. Pierson RJ, Carpenter MB. Anatomical analysis of pupillary reflex pathways in the rhesus monkey. J Comp Neurol 1974;158:121–143.
310. Pioro EP, Hughes JT, Cuello AC. Loss of substance P and enkephalin immunoreactivity in the human substantia nigra after striatopallidal infarction. Brain Res 1984;292:339–347.
311. Pioro EP, Mai JK, Cuello AC. Distribution of substance P- and enkephalin-immunoreactive neurons and fibers. In: Paxinos G, ed. The human nervous system. Ch. 32. New York: Academic Press, 1990:1051–1094.
312. Plum F, Posner JB. The diagnosis of stupor and coma. 3rd ed. New York: Plenum, 1980.
313. Poirier LJ. Experimental and histological study of midbrain dyskinesias. J Neurophysiol 1960;23: 534–551.
314. Poirier LJ, Bouvier G. The red nucleus and its efferent nervous pathways in the monkey. J Comp Neurol 1966;128:223–244.
315. Poirier LJ, Giguère M, Marchand R. Comparative morphology of the substantia nigra and ventral tegmental area in the monkey, cat and rat. Brain Res Bull 1983; 11:371–397.
316. Poirier LJ, Singh P, Boucher R, Bouvier G, Olivier A, Larochelle P. Effect of brain lesions on striatal monoamines in the cat. Arch Neurol 1967;17:601–608.
317. Poirier LJ, Sourkes TL. Influence of the substantia nigra on catecholamine content of the striatum. Brain 1965;88:181–192.
318. Pompeiano O. Organizzazione somatotopica delle riposte flessorie alla stimolazione elettrica del nucleo interposito nel gatto decerebrato. Arch Sci Biol (Bologna) 1959;43:163–176.
319. Pompeiano O. Localizzazione delle risposte estensorie alla stimolazione elettrica del nucleo interposito nel gatto decerebrato. Arch Sci Biol (Bologna) 1960;44:473–496.
320. Pompeiano O, Brodal A. Experimental demonstration of a somatotopical origin of rubrospinal fibers in the cat. J Comp Neurol 1957; 108:225–251.
321. Pompeiano O, Walberg F. Descending connections to the vestibular nuclei: an experimental study in the cat. J Comp Neurol 1957;108:465–502.
322. Powell EW, Hatton JB. Cingulosептal projections in the squirrel monkey. Brain Res 1969;96: 310–316.
323. Quensel F. Über den Stabkranz des menschlichen Stirnhirns. Folio Neuro-biol 1910;4:319–334.
324. Rademaker GGT. Die Bedeutung der roten Kerne und des übrigen Mittehirns für Muskeltonus, Körperstellung, und Labyrinthreflexe. Berlin: Springer-Verlag, 1926: 64–222.
325. Ralston DD, Milroy AM. Inhibitory synaptic input to identified rubrospinal neurons in *Macaca fascicularis*: an electron microscopic study using a combined immuno-GABA-gold technique and the retrograde transport of WGA-HRP. J Comp Neurol 1992;320:97–109.
326. Ramón y Cajal S. Histologie du Système Nerveux de l'Homme et des Vertébrés. (Azoulay L, trans.), Paris: Maloine, 1909, 1911. (Reprinted, Consejo Superior de Investigaciones Cientificas, Instituto Ramón y Cajal, Madrid, 1972.)
327. Ranson SW, Magoun HW. The central path of the pupillo-constrictor reflex in response to light. Arch Neurol Psychiatry 1933;30: 1193–1204.
328. Ranson SW, Ranson SW Jr, Ranson M. Corpus striatum and thalamus of a partially decorticate monkey. Arch Neurol Psychiatry 1941;46: 402–415.
329. Rasmussen AT. Tractus tectospinalis in the cat. J Comp Neurol 1936;63:501–525.
330. Reiner A, Albin RL, Anderson KD, D'Amato CJ, Penney JB Jr, Young AB. Differential loss of striatal projection neurons in Huntington's disease. Proc Natl Acad Sci USA 1988;85:5733–5737.
331. Richfield EK, Young A, Penny JB Jr. Comparative distribution of dopamine D_1 and D_2 receptors in the basal ganglia of turtles, pigeons, rats, cats and monkeys. J Comp Neurol 1987;262:446–463.
332. Rinvik E. The cortico-nigral projection in the cat: an experimental study with silver impregnation methods. J Comp Neurol 1966; 126:241–254.
333. Rinvik E. Demonstration of nigro-thalamic connections in the cat by retrograde axonal transport of horseradish peroxidase. Brain Res 1975;90:313–318.
334. Rinvik E, Grofova I. Observations on the fine structure of the substantia nigra in the cat. Exp Brain Res 1970;11:229–248.
335. Rinvik E, Grofova I, Ottersen OP. Demonstration of the nigrotectal and nigroreticular projections in the cat by axonal transport of protein. Brain Res 1976;112:388–394.
336. Rinvik E, Ottersen OP. Terminals of subthalamonigral fibres are enriched with glutamate-like immunoreactivity: an electron microscopic, immunogold analysis in the cat. J Chem Neuroanat 1993; 6:19–30.
337. Rinvik E, Walberg F. Demonstration of a somatotopically arranged cortico-rubral projection in the cat: an experimental study with silver methods. J Comp Neurol 1963; 120:393–407.
338. Rinvik E, Walberg F. Is there a cortico-nigral tract? A comment based on experimental electron microscopic observations in the cat. Brain Res 1969;14:742–744.
339. Roberts RC, Ribak CE. GABAergic neurons and axon terminals in the brainstem auditory nuclei of the gerbil. J Comp Neurol 1987;258: 267–280.
340. Robinson DA. Eye movements evoked by collicular stimulation in the alert monkey. Vision Res 1972;12:1795–1808.
341. Robinson RC, Houk JC, Gibson AR. Limb specific connections of the cat magnocellular red nucleus. J Comp Neurol 1987;257:553–577.
342. Rockel AJ, Jones EG. The neuronal organization of the inferior colliculus of the adult cat. I. The central nucleus. J Comp Neurol 1973; 147:11–60.
343. Rockel AJ, Jones EG. The neuronal organization of the inferior colliculus of the adult cat. II. The pericentral nucleus. J Comp Neurol 1973;149:301–334.
344. Role LW, Kelly JP. The brain stem: Cranial nerve nuclei and the monoaminergic systems. In: Kandel ER, Schwartz JH, Jessell TM, eds. Principles of neural science. 3rd ed. Ch. 44. New York: Elsevier, 1991:683–699.
345. Rose JE, Greenwood DB, Goldberg JM, Hind JE. Some discharge characteristics of single neurons in the inferior colliculus of the cat. I. Tonotopical organization, relation of spike-counts to tone intensity, firing patterns of single elements. J Neurophysiol 1963;26:293–320.
346. Rosegay H. An experimental investigation of the connections between the corpus striatum and the substantia nigra in the cat. J Comp Neurol 1944;80:293–310.
347. Rossi GF, Brodal A. Corticofugal fibers to the brain stem reticular formation. An experimental study in the cat. J Anat 1956;90:42–62.
348. Roth GL, Aitkin LM, Anderson RA, Merzenich MM. Some features of the spatial organization of the central nucleus of the inferior colliculus of the cat. J Comp Neurol 1978;182:661–680.
349. Rundles RW, Papez JW. Connections between the striatum and the substantia nigra in a human brain. Arch Neurol Psychiatry 1937;38: 550–563.
350. Rye DB, Saper CB, Lee HJ, Wainer BH. Pedunculopontine tegmental nucleus of the rat: cytoarchitecture, cytochemistry, some extrapyrami-

dal connections of the mesopontine tegmentum. J Comp Neurol 1987;259:483–528.
351. Sakai ST. Corticonigral projections from area 6 in the raccoon. Exp Brain Res 1988;73:498–504.
352. Sano T. Beitrag zur vergleichenden Anatomie der Substantia nigra, des Corpus luysii und der Zona incerta. Mschr Psychiat Neurol 1910;27:110–127.
353. Scalia F. The termination of retinal axons in the pretectal region of mammals. J Comp Neurol 1972; 145:223–257.
354. Scarnati E, Proia A, Campana E, Pacitti C. Pedunculopontine-evoked excitation of the substantia nigra neurons in the rat. Brain Res 1984;304:351–361.
355. Scheibel ME, Scheibel AB. Structural substrates for integrative patterns in the brain stem reticular core. In: Jasper HH, Proctor LP, Knighton RS, et al., eds. Reticular formation of the brain. Ch. 2. Boston: Little Brown, 1958:31–55.
356. Schiller PH, Stryker M. Single-unit recording and stimulation in superior colliculus of the alert rhesus monkey. J Neurophysiol 1972;35: 915–924.
357. Schmied A, Almaric M, Dormont JF, Farin D. GABAergic mechanisms in the cat red nucleus: effects of intracerebral microinjections of muscimol and bicuculline on a conditioned motor task. Exp Brain Res 1990;81:523–532.
358. Scheneider JS, Yuwiler A, Markam CH. Selective loss of subpopulations of ventral mesencephalic dopaminergic neurons in the monkey following exposure to MPTP. Brain Res 1987;411:144–150.
359. Schwyn RC, Fox CA. The primate substantia nigra: a Golgi and electron microscopic study. J Hirnforsch 1974;15:95–126.
360. Seroogy KB, Dangaran K, Haycock JW, Fallon JH. Ventral mesencephalic neurons containing both cholecystokinin- and tyrosine-hydroxylase-like immunoreactivities project to forebrain regions. J Comp Neurol 1989;279:397–414.
361. Sheard MH, Flynn JP. Facilitation of attack behavior by stimulation of the midbrain of cats. Brain Res 1967;4:324–333.
362. Sherk H. Visual response properties and visual field topography in the cats parabigeminal nucleus. Brain Res 1978;145:375–379.
363. Smith MC. Stereotaxic operations for Parkinson's disease—anatomical observations. In: Williams D, ed. Modern trends in neurology. Vol. 4. London: Butterworths, 1967:21–52.
364. Smith Y, Bolam JP. Convergence of synaptic inputs from the striatum and globus pallidus onto identified nigrocollicular cells in the rat: a double anterograde labelling study. Neuroscience 1991;44:45–73.
365. Smith Y, Hazrati L-N, Parent A. Efferent projections of the subthalamic nucleus in the squirrel monkey as studied with the PHA-L anterograde tracing method. J Comp Neurol 1990;294:306–323.
366. Smith Y, Lavoie B, Dumas J, Parent A. Evidence for a separate nigropallidal dopaminergic projection in the squirrel monkey. Brain Res 1989;482:381–386.
367. Smith Y, Parent A. Differential connections of caudate nucleus and putamen in squirrel monkey (*Saimiri sciureus*). Neuroscience 1986;18:178–182.
368. Smith Y, Parent A, Séguéla P, Descarries L. Distribution of GABA-immunoreactive neurons in the basal ganglia of the squirrel monkey (*Saimiri sciureus*). J Comp Neurol 1987;259:50–65.
369. Snider RS. Recent contributions to the anatomy and physiology of the cerebellum. Arch Neurol Psychiatry 1950;64:196–219.
370. Sousa-Pinto A. Cortical projections of the medial geniculate body in the cat. Adv Anat Embryol Cell Biol 1973;48:1–42.
371. Spann BM, Grofova I. Nigropeduncolopontine projection in the rat: an anterograde tracing study with *Phaseolus vulgaris* leucoagglutinin (PHA-L). J Comp Neurol 1991;311:375–388.
372. Spann BM, Grofova I. Cholinergic and non-cholinergic neurons in the rat pedunculopontine tegmental nucleus. Anat Embryol 1992;186: 215–227.
373. Sparks DL, Holland R, Guthrie BL. Size and distribution of movement fields in the monkey superior colliculus. Brain Res 1976;113:21–34.
374. Sprague JM. The superior colliculus and pretectum in visual behavior. Invest Ophthalmol 1972;11: 473–482.
375. Sprague JM, Meikle TH Jr. The role of the superior colliculus in visually guided behavior. Exp Neurol 1965;11:115–146.
376. Starzl TE, Whitlock DG. Diffuse thalamic projection system in monkey. J Neurophysiol 1952;15: 449–468.
377. Steiger H-J, Büttner-Ennever JA. Oculomotor nucleus afferents in the monkey demonstrated with horseradish peroxidase. Brain Res 1979;160:1–15.
378. Stein BE, Magalhaes-Castro B, Kruger L. Relationships between visual and tactile representation in cat superior colliculus. J Neurophysiol 1976;39:401–419.
379. Steinbusch HWM. Distribution of serotonin-immunoreactivity in the central nervous system of the rat—cell bodies and terminals. Neuroscience 1981;6:557–618.
380. Steinbusch HWM, Nieuwenhuys R, Verhofstad AAJ, Van der Kooy D. The nucleus raphe dorsalis of the rat and its projection upon the caudatoputamen. A combined cytoarchitectonic, immunohistochemical and retrograde transport study. J Physiol (Paris) 1980; 77:157–174.
381. Steriade M, Biesold D. Brain cholinergic systems. New York: Oxford University Press, 1990.
382. Steriade M, McCarley RW. Brainstem control of wakefulness and sleep. New York: Plenum, 1990.
383. Sterling P, Wickelgren BG. Visual receptive fields in the superior colliculus of the cat. J Neurophysiol 1969;32:1–15.
384. Stryker MP, Schiller PH. Eye and head movements evoked by electrical stimulation of monkey superior colliculus. Exp Brain Res 1975;23:103–112.
385. Stuart AM, Mitchell IJ, Slater P, Unwin HLP, Crossman AR. A semi-quantitative atlas of 5-hydroxytryptamine-1 receptors in the primate brain. Neuroscience 1986; 18:619–639.
386. Sugimoto T, Itoh K, Mizuno H. Direct projections from the Edinger-Westphal nucleus to the cerebellum and spinal cord in the cat: a HRP study. Neurosci Lett 1978; 9:17–22.
387. Szabo J. Topical distribution of the striatal efferents in the monkey. Exp Neurol 1962;5:21–36.
388. Szabo J. The efferent projections of the putamen in the monkey. Exp Neurol 1967;19:463–476.
389. Szabo J. Projections from the body of the caudate nucleus in the rhesus monkey. Exp Neurol 1970; 27:1–15.
390. Szabo J. Distribution of striatal afferents from the mesencephalon in the cat. Brain Res 1980;188:3–21.
391. Szabo J. Organization of the ascending striatal afferents in monkeys. J Comp Neurol 1980;189: 307–321.
392. Szentagothai J. The elementary vestibulo-ocular reflex arc. J Neurophysiol 1950;13:395–407.
393. Tarlov EC, Moore RY. The tectothalamic connections in the brain of the rabbit. J Comp Neurol 1973;126:403–422.
394. Ternaux JP, Héry F, Bourgoin S, Adrien J, Glowinski J, Hamon M. The topographical distribution of serotoninergic terminals in the neostriatum of the rat and the caudate nucleus of the cat. Brain Res 1977;121:311–326.
395. Terzuolo C, Terzian H. Cerebellar increase of postural tonus after deafferentation and labyrinthectomy. J Neurophysiol 1953;16: 551–561.
396. Tokuno H, Morizami T, Kudo M, Nakamura Y. A morphological evidence for monosynaptic projections from the nucleus tegmenti pedunculopontine pars compacta (TPC) to nigrostriatal projection neurons. Neurosci Lett 1988;85: 1–4.
397. Tomasch J. The numerical capacity of the human cortico-ponto-cere-

bellar system. Brain Res 1969; 13:476–484.
398. Törk I, Hornung J-P. Raphe nuclei and the serotoninergic system. In: Paxinos G, ed. The human nervous system. Ch. 30. New York: Academic Press, 1990:1001–1022.
399. Torvik A, Brodal A. The origin of reticulospinal fibers in the cat: an experimental study. Anat Rec 1957;128:113–137.
400. Toyama K, Tsukahara N, Udo M. Nature of the cerebellar influences upon the red nucleus neurons. Exp Brain Res 1968;4:292–309.
401. Tretiakoff C. Contribution à l'étude de l'anatomopathologie du locus niger de Sommering. Thèse, Université de Paris, Number 293. Paris: Jouve et Cie, 1919.
402. Ungerstedt U. Stereotaxic mapping of the monoamine pathways in the rat brain. Acta Physiol Scand (Suppl) 1971;367:1–48.
403. Van der Kooy D, Hattori T. Single subthalamic nucleus neurons project to both the globus pallidus and substantia nigra in rat. J Comp Neurol 1980;192:751–768.
404. Van der Kooy D, Hattori T. Bilaterally situated dorsal raphe cell bodies have only unilateral forebrain projections in rat. Brain Res 1980;192:550–554.
405. Van Domburg PHMF, Ten Donkelaar HJ. The human substantia nigra and ventral tegmental area. Adv Anat Embryol Cell Biol 1991;121:1–132.
406. Von Economo CF, Karplus JP. Zur Physiologie und Anatomie des Mittelhirn. Arch Psychiatr Nervenkr 1909;46:275–356.
407. Von Monakow C. Experimentelle und pathologisch-anatomische Untersuchunger über die Haubenregion, den Sehhügel und die Regio subthalamica. Arch Psychiatr Nervenkr 1895;27:1–219.
408. Von Monakow C. Gehirnpathologie. 2d ed. Wien: Hölde, 1905.
409. Verhaart WJC. Die aberrierenden Pyramidenfasern bei Menschen und Afen. Schweiz Arch Neurol Neurochir Psychiatr 1935;36: 170–190.
410. Verhaart WJC. Fiber analysis of the basal ganglia. J Comp Neurol 1950;93:425–440.
411. Voneida TJ. An experimental study of the course and destination of fibers arising in the head of caudate nucleus in the cat and monkey. J Comp Neurol 1960;115: 75–87.
412. Walberg F. On the termination of rubrobulbar fibers: experimental observations in the cat. J Comp Neurol 1958;110:66–73.
413. Warwick R. Representation of the extraocular muscles in the oculomotor nuclei of the monkey. J Comp Neurol 1953;98:449–504.
414. Warwick R. The identity of the posterocentral nucleus of Panegrossi. J Comp Neurol 1953;99: 599–612.
415. Warwick R. The ocular parasympathetic nerve supply and its mesencephalic sources. J Anat 1954; 88:71–93.
416. Warwick R. The so-called nucleus of convergence. Brain 1955;78: 92–114.
417. Webster WR, Garey LJ. Auditory system. In: Paxinos G, ed. The human nervous system. Ch. 27. New York: Academic Press, 1990: 889–944.
418. Webster WR, Servière J, Crewther D, Crewther S. Iso-frequency 2–DG contours in the inferior colliculus of the awake monkey. Exp Brain Res 1984;56:427–437.
419. Wickelgren BG, Sterling P. Influence of visual cortex on receptive fields in the superior colliculus of the cat. J Neurophysiol 1969; 32:16–32.
420. Wilson ME, Toyne MJ. Retino-tectal and cortico-tectal projections in *Macaca mulatta*. Brain Res 1970; 24:395–406.
421. Wislocki GB, Leduc E. The cytology and histochemistry of the subcommissural organ and Reissner's fibers in rodents. J Comp Neurol 1953;97:515–543.
422. Woolf NJ, Harrison JB, Buchwald JS. Cholinergic neurons of the pontomesencephalon. II. Ascending anatomical projections. Brain Res 1990;520:55–72.
423. Yamada T, McGeer PL, Baimbridge KG, McGeer EG. Relative sparing in Parkinson's disease of substantia nigra dopamine neurons containing calbindin-D_{28K}. Brain Res 1990;526:303–307.
424. Yurek DM, Sladek JR Jr. Dopamine cell replacement: Parkinson's disease. Annu Rev Neurosci 1990; 13:415–440.
425. Houk JC, Gibson AR, Harvey CF, Kennedy PR, van Kan PL. Activity of primate magnocellular red nucleusd related to hand and finger movements. Behav Brain Res 1988;28:201–206.

15
Cerebellum

REGIONAL ORGANIZATION

The *cerebellum* derives its name from the diminutive of the word *cerebrum*. It was considered by the ancient anatomists as a second, smaller brain in its own right (173). The cerebellum forms the roof of the fourth ventricle and is the only region of the central nervous system that spans the midline without interruption. This structure has expanded during the course of human evolution (142, 227), but its basic neuronal circuits remained relatively similar to what they are in all vertebrates. The cerebellar cortex in humans has a total area of 50,000 cm^2 versus 12 mm^2 in the frog (26). This cortex folds into very deep folia (leafs), allowing this enormous surface to be packed into a 300 cm^3 volume. Because the cerebellar cortex is very long in the rostrocaudal direction (up to 1 meter in humans), most of the folding occurs in that direction.

The cerebellum occupies approximately 10% of the total brain volume, but contains approximately half of all the neurons in the brain. These neurons form multiple, identical modules that compute neural information in a similar way throughout the cerebellum. The functional heterogeneity of the cerebellum derives from the fact that modules located in distinct areas of the structure process different types of neural information deriving from specific sets of inputs (104). The cerebellum is concerned with the coordination of somatic motor activity, the regulation of muscle tone and mechanisms that influence and maintain equilibrium. It acts as a "comparator" that compensates for error in movement by comparing intention with performance. The cerebellum receives (a) information about plans for movement (corollary discharge or internal feedback), (b) information about motor performance (reafference or external feedback), and (c) it projects to descending motor system. The cerebellar afferents play a crucial role in the functional organization of the cerebellum as certain classes of inputs can modify cerebellar circuits for long periods of time. It is currently thought that the function of the cerebellum is modified by experience and that this structure plays an important role in the learning of motor tasks.

The cerebellum is derived from ectodermal thickening about the cephalic borders of the fourth ventricle, known as the rhombic lip (Figs. 3.12 and 3.14). Although the cerebellum is derived from portions of the embryonic neural tube dorsal to the sulcus limitans and receives sensory inputs from virtually all receptors, it is not concerned with conscious sensory perception. Sensory information transmitted to the cerebellum is used in the automatic coordination of somatic motor function, the regulation of muscle tone, and the maintenance of equilibrium. This metencephalic derivative functions in a suprasegmental manner in that its integrative influence affects activities at all levels of the neuraxis. The major influences of the cerebellum on segmental levels of the neuraxis are mediated indirectly by relay nuclei of the brainstem.

Structurally, the cerebellum consists of (a) a superficial gray mantle, the *cerebellar cortex*, (b) an internal white mass, the *medullary substance*, and (c) four pairs of *intrinsic nuclei* embedded in the white matter (Figs. 13.7, 13.26, and 15.19). The cerebellum is divided into a median portion, the *cerebellar vermis*, and two lateral lobes, referred to as the *cerebellar hemispheres*. In spite of a wealth of histologic detail concerning the structural organization of the cerebellum, precise anatomic localization within various lobules is difficult except in gross specimens. Likewise, the precise identification of cerebellar lobules, laminae, and folia in microscopic sections is difficult even in serial sections. Detailed atlases of the cerebellum in human (12) and nonhuman primates (179) facilitate the microscopic study of cerebellar sections (272).

The cerebellar cortex is composed of numerous narrow *laminae* or *folia*, most of which

are oriented transversely. Five deep fissures divide the cerebellum into lobes and lobules. All of these fissures can be identified in gross specimens as well as in midsagittal section (Figs. 2.30–2.33). The cerebellar fissures are (a) the *primary*, (b) the *posterior superior*, (c) the *horizontal*, (d) the *prepyramidal*, and (e) the *posterolateral* (prenodular). The primary fissure is the deepest of all cerebellar fissures. These fissures form the basis for all subdivisions of the cerebellum (169) (Fig. 15.1). Portions of the cerebellar vermis and hemispheres located rostral to the primary fissure form the anterior lobe, whereas those between the primary and the posterolateral fissures constitute the posterior lobe. Portions of the cerebellum caudal to the posterolateral fissure represent the flocculonodular lobe. The various portions of the cerebellar vermis are labeled by names and serial *Roman numerals*. The portion of the cerebellar hemispheres between the primary and the posterior superior fissures is known as the *simple lobule*. The *ansiform lobule* lies between the posterior superior fissure and the gracile lobule and is divided by the horizontal fissure into *crus I* (superior semilunar lobule) and *crus II* (inferior semilunar lobule). The *biventer lobule* and the *cerebellar tonsil* lie between the prepyramidal and the posterolateral fissures in the cerebellar hemispheres. The posterolateral fissure separates the nodulus from the uvula in the cerebellar vermis.

Embryologically, hodologically, and functionally the cerebellum can be divided into three parts: the archicerebellum (or vestibulocerebellum), the paleocerebellum (or spinocerebellum), and the neocerebellum (also termed cerebrocerebellum or pontocerebellum).

The *archicerebellum*, represented largely by the *nodulus*, the paired *flocculi*, and their peduncular connections (i.e., the *flocculonodular lobe*), is believed to be the oldest part of the cerebellum. This division of the cerebellum is most closely related to the vestibular system and is often related to as the *vestibulocerebellum* (169) (Fig. 15.1). The flocculonodular lobe is separated from the corpus cerebelli by the posterolateral fissure, the first fissure to develop in the cerebellum.

The *paleocerebellum* (i.e., the anterior lobe

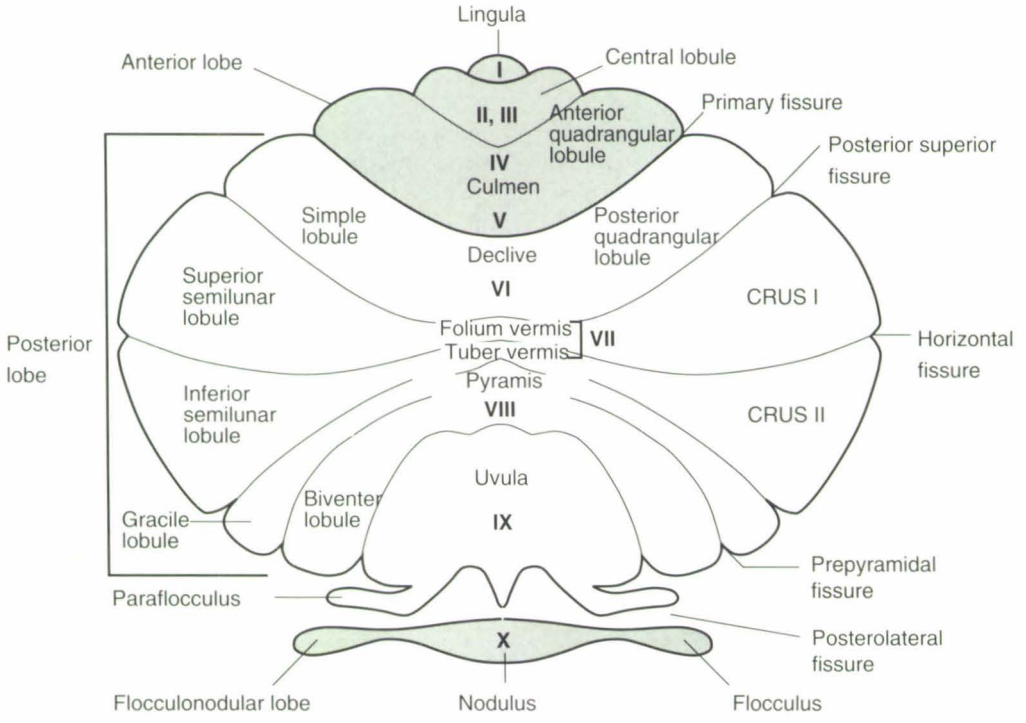


Figure 15.1. Fissures and lobules of the cerebellum. Portions of the cerebellum caudal to the posterolateral fissure (*shaded area*) represent the flocculonodular lobule (archicerebellum or vestibulocerebellum), while portions of the cerebellum rostral to the primary fissure (*shaded area*) constitute the anterior lobe (paleocerebellum or spinocerebellum). The neocerebellum (or cerebrocerebellum) lies between the primary and posterolateral fissure. *Roman numerals* refer to portions of the cerebellar vermis only.

of the cerebellum) lies rostral to the primary fissure (169) (Fig. 15.1). In nonmammalian vertebrates, the paleocerebellum forms the largest part of the cerebellum, while in humans it constitutes a small subdivision which receives impulses primarily from stretch receptors via the spinocerebellar tract. It is the part of the cerebellum most concerned with the regulation of muscle tone (184). Because of its intimate connections with the spinal cord, it is often referred to as the *spinocerebellum*.

The *neocerebellum* (i.e., the posterior lobe), phylogenetically the newest and the largest portion, includes all parts of the cerebellum between the primary and posterolateral fissures in both the vermis and the hemispheres (Fig. 15.1). This division of the cerebellum receives major inputs from the contralateral cerebral cortex via relays in the pontine nuclei, and is the part most concerned with coordination of somatic motor function. Because of its massive corticopontine input, it is often referred to as the *cerebrocerebellum* (104) or *pontocerebellum* (32).

The cerebellum is attached to the medulla, the pons, and the midbrain by three paired cerebellar peduncles (see Chapter 2 for further details on the gross anatomy of the cerebellum). These compact fiber bundles interconnect the archicerebellum, paleocerebellum, and neocerebellum with the spinal cord, brainstem, and higher levels of the neuraxis. The extensive nature of these connections indicates that the cerebellum serves as a major integrative center for the coordination of muscular activity. Before examining the afferent and efferent fiber systems of the cerebellum, the structure of the cerebellar cortex is considered.

CEREBELLAR CORTEX

The cerebellar cortex is uniformly structured in all parts and extends across the midline without evidence of a median raphe. The cortex is composed of three well-defined layers containing five different types of neurons. These layers from the surface are (a) the molecular layer, (b) the Purkinje cell layer, and (c) the granular layer (Figs. 15.2–15.4).

Molecular Layer

The molecular layer contains two types of neurons, dendritic arborizations of cells in deeper layers, and numerous thin axons coursing parallel to the long axis of the folia (Figs. 15.2, 15.4, and 15.5). This layer, whose cell density is relatively low, contains the basket cells in its inner portion and the stellate cells in its outer portion (Figs. 15.4 and 15.5). Dendrites of these two types of neurons are confined to the molecular layer, as are the axons of the stellate cells. Processes of both cells are oriented in a sagittal plane; that is, transversely to the long axis of the folia. Axons of the *stellate cells* make synaptic con-

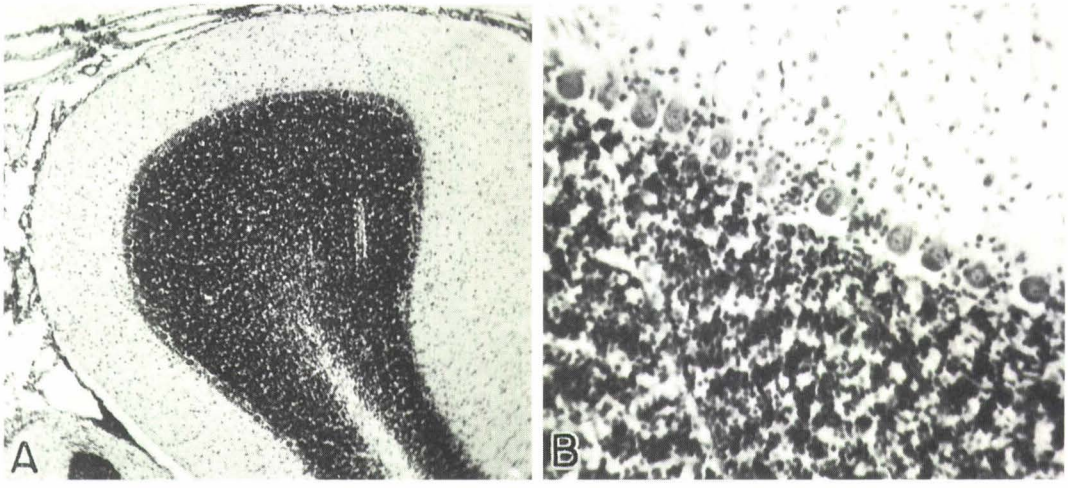


Figure 15.2. Sections through a folium of a rhesus monkey cerebellar cortex. **A.** In this figure, the relative thickness of the three cerebellar layers can be appreciated. Light spaces in the dark staining granular layer are the "cerebellar islands" containing the glomeruli. **B.** A single row of Purkinje cells above the granular layer is shown (Nissl stain, ×20, ×50).

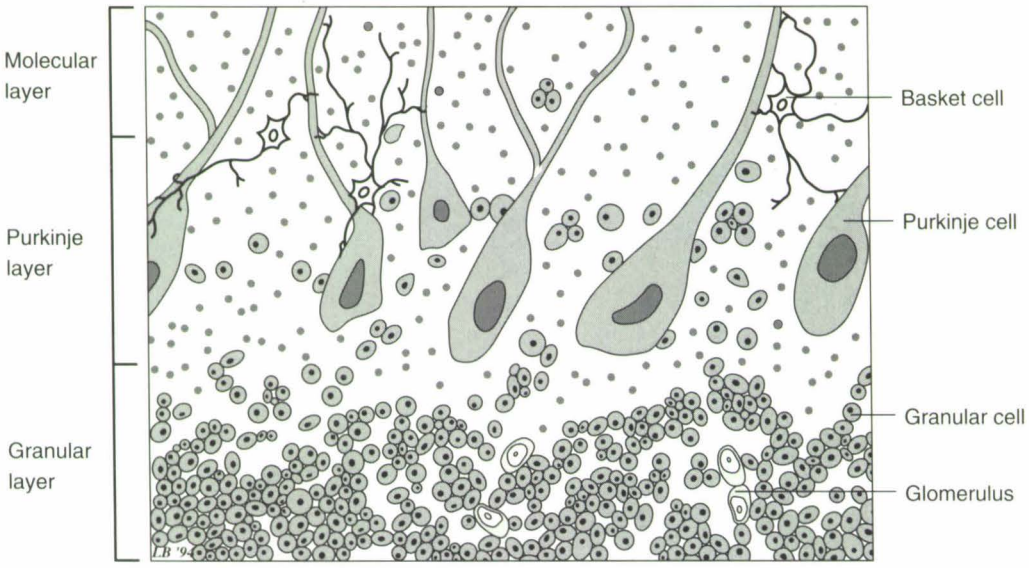


Figure 15.3. Portions of the three layers of the human cerebellar cortex.

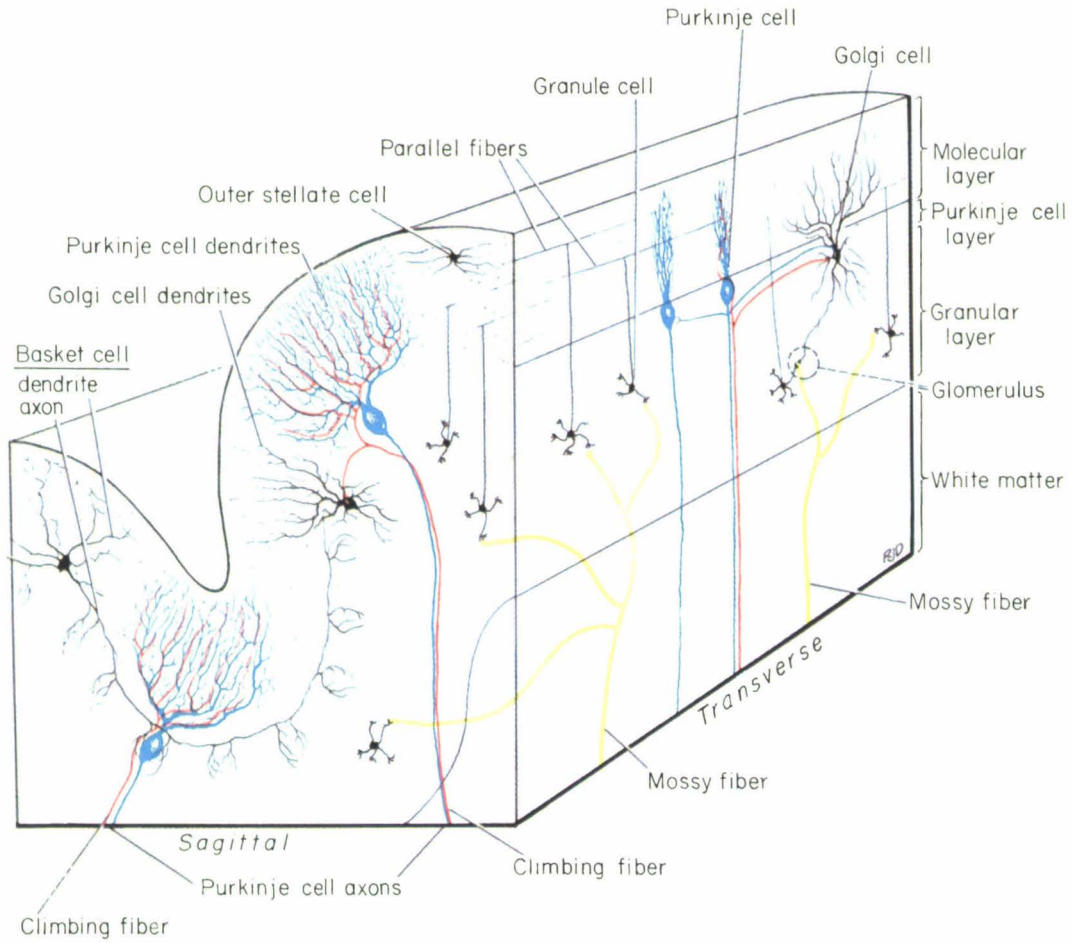


Figure 15.4. Cerebellar cortex in sagittal and transverse planes showing cell and fiber arrangements. Purkinje cells and cell processes (i.e., axons and dendrites) are shown in *blue*. Mossy fibers are in *yellow* and climbing fibers are shown in *red*. Golgi cells, basket cells, and outer stellate cells are in *black*. While the dendritic arborizations of Purkinje cells are oriented in a sagittal plane, dendrites of Golgi cells show no such arrangement. Layers of the cerebellar cortex are indicated.

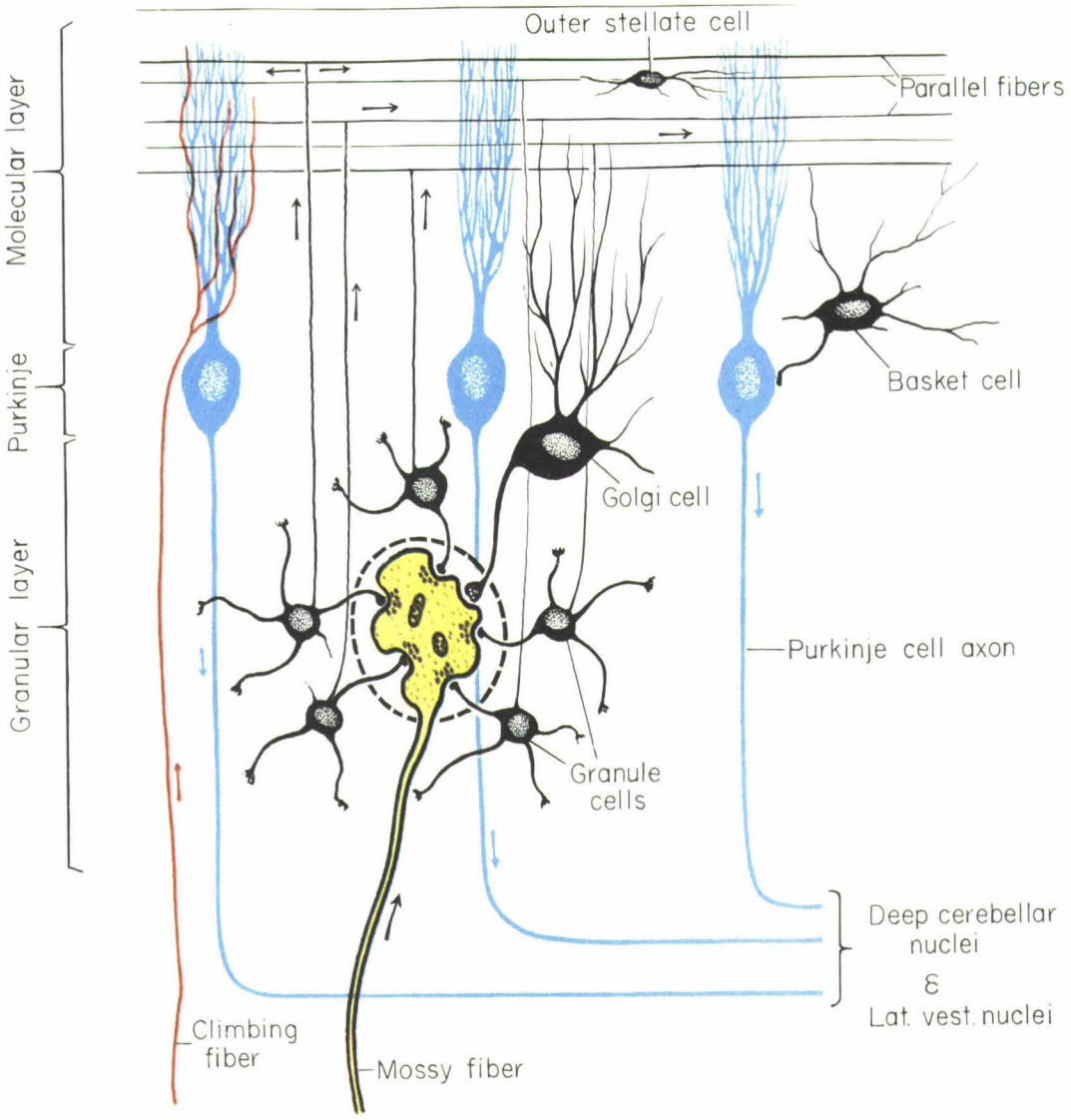


Figure 15.5. Cellular and fiber elements of the cerebellar cortex in the longitudinal axis of a folium. Excitatory (glutamatergic) inputs to the cerebellar cortex are conveyed by the mossy fibers (*yellow*) and the climbing fibers (*red*). The *broken line* represents a glia lamella ensheathing a glomerulus that contains (a) a mossy fiber rosette, (b) several granule cell dendrites, and (c) one Golgi cell axon. Axons of granule cells ascend to the molecular layer, bifurcate, and form an extensive system of parallel fibers which synapse on the spiny processes of the Purkinje cells. Purkinje cells and their processes are shown in *blue*. Climbing fibers traverse the granular layer and ascend the dendrites of the Purkinje cells where they synapse on smooth branchlets. *Arrows* indicate the directions of impulse conduction. Outer stellate and basket cells are shown in the molecular layer, but the axons of the basket cells that ramify around Purkinje cell somata are not shown.

tacts with Purkinje cell dendrites (Figs. 15.4 and 15.5). *Basket cells*, located in the deep parts of this layer near the Purkinje cell bodies (Figs. 15.3–15.5), give rise to dendrites that ascend in the molecular layer in some instances as far as 300 μm. The axons of basket cells extend along the Purkinje cell layer at right angles to the direction of the parallel fibers. They may spread over a distance equal to 20 Purkinje cell widths and may contact as many as 150 Purkinje cell bodies. Along its course, the horizontal segment of a basket cell axon emits groups of collaterals that descend and embrace Purkinje cell soma and its initial segment. As many as 20–30 different basket cells are believed to wrap their axon terminals around each Purkinje cell soma, forming a typical basket-like meshwork (20, 173) (Fig.

15.4). The stellate and basket cells (mean diameter 5–9 μm) may in fact belong to a single class of neurons. It is estimated that stellate and basket cells are respectively 16 and 6 times more numerous than Purkinje cells (173).

Both cells are known to exert an inhibitory action upon the Purkinje cells, and γ-aminobutyric acid (GABA) is likely to serve as the neurotransmitter of basket cells. The basket cells also contain the enzyme that is responsible for synthesizing nitric oxide (NO), a highly toxic gas that is now believed to act as a neurotransmitter in several brain areas, including the cerebellum (269). This enzyme, NO synthase, is identical to nicotinamide adenine dinucleotide phosphate diaphorase (NADPH-diaphorase), an enzyme that has been known for over 30 years and that can be easily visualized with a simple histochemical technique. The target for NO action is the soluble enzyme guanylyl cyclase. By activating this enzyme, NO induces marked increases in cGMP levels in the cerebellum, as elsewhere in the brain. The cGMP formed may then regulate protein kinases, phosphodiesterases, and ion channels in Purkinje cells (269). Although the inhibitory neurotransmitter of stellate cells has not been decisively established, it could be taurine (173, 201). In addition to stellate and basket cells, the molecular layer contains the dendrites of Purkinje and Golgi type II cells and the transversely oriented axons of granule cells (i.e., parallel fibers).

Purkinje Cell Layer

This single-cell layer consists of great numbers of large flask-shaped cells relatively uniformly arranged along the upper margin of the granular layer (Figs. 15.2–15.5). Purkinje cells have a clear vesicular nucleus with a deep-staining nucleolus and irregularly distributed Nissl granules (212). They are among the largest (about 50–80 μm in diameter) and most numerous (approximately 15×10^6) neurons in the central nervous system. A quantitative study of the human cerebellum with stereologic techniques has estimated the number of Purkinje cells to be as high as 30.5×10^6 (6). Each cell gives rise to an elaborate flattened, fan-like, dendritic tree oriented at right angles to the long axis of the folia (Figs. 15.4 and 15.5) (177). The dendritic tree arises from the neck of the cell as two or three large primary dendrites which branch repeatedly. In the depth of a furrow, the dendritic branches form a broad angle approximating 180°, while near the crest of a folium, dendritic branches form more acute angles (89). The full extent of the dendritic arborization can be appreciated only in sagittal sections. Primary and secondary dendritic branches are smooth, but tertiary dendritic branches have spines that are short, thick, and rough. These thick dendritic spines are referred to as *spiny branchlets* or *gemmules* (98) (Figs. 5.9 and 15.6). Larger dendritic processes bear stubbier thorns or spines known as *smooth branchlets*. The combined surface area of the dendritic branchlets and spines of one Purkinje cell in monkeys is said to be about 200,000 μm^2 (98). A synaptic area of such magnitude on each of 15 million cells indicates the complexity and magnitude of the neural computation that occurs in the cerebellar cortex.

Purkinje cell axons are myelinated, pass through the granular layer and white matter, and establish synaptic contacts with the cerebellar nuclei. Purkinje cell axons project to the cerebellar nuclei by the shortest direct route. These axons also give rise to recurrent collaterals (Figs. 15.4 and 15.5), which establish axosomatic contacts with Golgi type II cells in the granular layer (117). Purkinje cell axons represent the sole output pathway of the cerebellar cortex.

The unique feature of Purkinje cells is their monoplanar shape. Both the dendritic arbors and the axonal projections of Purkinje cells lie in a single plane perpendicular to the major axis of the folia. Moreover, the planes of all Purkinje cell dendrites in a given region are parallel, so that the dendritic arrays of the cells stack up in a highly ordered fashion. This remarkable orderly array determines, to a large extent, the nature and number of contacts made with other kind of cells. Thus, parallel fibers running perpendicular to the plane of the dendrites intersect a multitude of Purkinje cells, by the very manner in which these elements are organized (173). In Japan, Masao Ito made the crucial discovery that the Purkinje cells are inhibitory (134), and immunohistochemical studies indicate that GABA is the neurotransmitter released at the synapse of these cells (96, 97, 201, 210). Purkinje cells also express various polypeptides, including motilin (67), nerve growth factor receptor (197), insulin-like growth factor I (IGF-I) (2), β-thyroid receptor (222), and cal-



Figure 15.6. A single Purkinje cell and its rich dendritic arborizations in the molecular layer. Golgi preparation (×300).

bindin D-28k (128). Some of these peptides may play a crucial role in Purkinje cell maturation and maintenance.

The Purkinje cells of the cerebellum were the first neurons to be identified (294) and the first neurons to be analyzed in microscopic detail. They are also the first class of neurons for which a specific immunologic marker, not related to the biosynthesis of a neurotransmitter, has been identified. Guanosine 3′,5′-phosphate-dependent protein kinase (cGK) antiserum is a specific marker for Purkinje cells (79, 284) (Fig. 15.7). Other immunologic markers for Purkinje cells have been characterized and many of these markers stain only subsets of Purkinje cells organized in parasagittal microzones separated by nonimmunoreactive interzones (67, 119, 188, 272, 284, 295). One intrinsic molecular marker of particular interest is the polypeptide antigen zebrin I that is recognized by monoclonal (mab) antibody Q113. Zebrin I immunohistochemistry reveals an array of parasagittal Purkinje cell compartments that are similar in rodents, monkeys, and humans (24, 119, 171, 219) (Fig. 15.8). This peculiar pattern of immunostaining has been shown to be congruent with the parasagittal zones of termination of the olivocerebellar projections (119) and spinocerebellar projections arising from the central cervical nucleus (188). These findings suggest the existence of widespread chemical and anatomic heterogeneity in the cerebellar cortex, particularly among the Purkinje cells.

Granular Layer

This layer is composed of a vast number densely packed small neurons, mostly small granule cells (Figs. 15.2–15.5 and 15.9). The number of these small neurons, about 10^{11}, exceeds that of the entire cerebral cortex (104). Granule cells are so tightly packed (3–7 million cells per cm^3 (26)) that residual space seems insufficient to accommodate their processes and fibers of passage. These cells

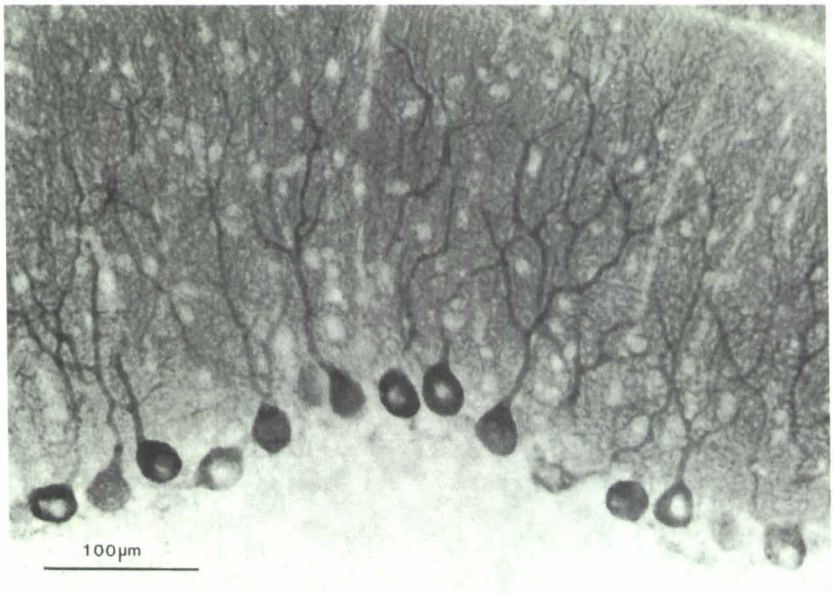


Figure 15.7. Sagittal section of the rat cerebellar cortex immunostained with an antibody to guanosine 3',5'-phosphate-dependent protein kinase (cGK), a specific molecular marker for Purkinje cells. This immunologic marker is not related to the biosynthesis of any neurotransmitters, but specifically labels all parts of the Purkinje cells.

are round or oval, 5–8 μm in diameter, with aggregated chromatin granules near the nuclear membrane. Granule cell nuclei appear as naked nuclei because of the thinness of the rimming cytoplasm and the absence of discrete Nissl granules (99). Each granule cell gives rise to four or five short dendrites with claw-like endings which terminate in the "glomeruli" (Figs. 15.5 and 15.9). The so-called cerebellar islands are irregularly dispersed spaces, which are free of granule cells but contain complex synaptic structures known as "glomeruli" (Fig. 15.12). Axons of granule cells are unmyelinated fibers that ascend vertically into the molecular layer and bifurcate into two branches which run parallel to the long axis of the folium. These fibers, referred to as *parallel fibers*, are found throughout the molecular layer where they are oriented perpendicular to the sagittal fan-shaped dendritic expansions of the Purkinje cells (212) (Fig. 15.4).

Parallel fibers make multiple synapses on the spiny branchlets of Purkinje cells, principally on the head of the spines. This type of synaptic contact has been referred to as the "cross-over" synapse (100, 114, 117). It is estimated that each Purkinje cell bears more than 100,000 dendritic spines and that about 200,000 parallel fibers projected through its dendritic domain (98, 99). This represents, by far, the largest synaptic input to any given central neuron. Each parallel fiber, extending about 3 mm from its bifurcation, has been estimated to traverse the dendritic trees of up to 500 Purkinje cells (173, 255). The parallel fibers of the granule cells also make "crossing-over" synaptic contacts with the dendrites of stellate, basket, and Golgi type II cells in the molecular layer (Fig. 15.5). The granule cells are known to exert a glutamate-mediated excitatory influence upon its target cells (106, 209, 210). They also contain significant levels of nitric oxide synthase or NADPH-diaphorase (269).

Golgi type II cells, found mainly in the upper parts of the granular layer, have vesicular nuclei, and definite chromophilic bodies. They are as numerous as the Purkinje cells and their cell bodies have a diameter that ranges from 6–11 μm. Dendrites of these cells extend throughout all layers of the cerebellar cortex, and arborizations are not restricted to a single plane (Figs. 15.4 and 15.5). Golgi cell dendrites are contacted by parallel fibers in the molecular layer, while their cell bodies receive inputs from collaterals of climbing fibers and recurrent collaterals of Purkinje cells (117, 233). Golgi cells located in the deep portion of the molecular layer tend to be

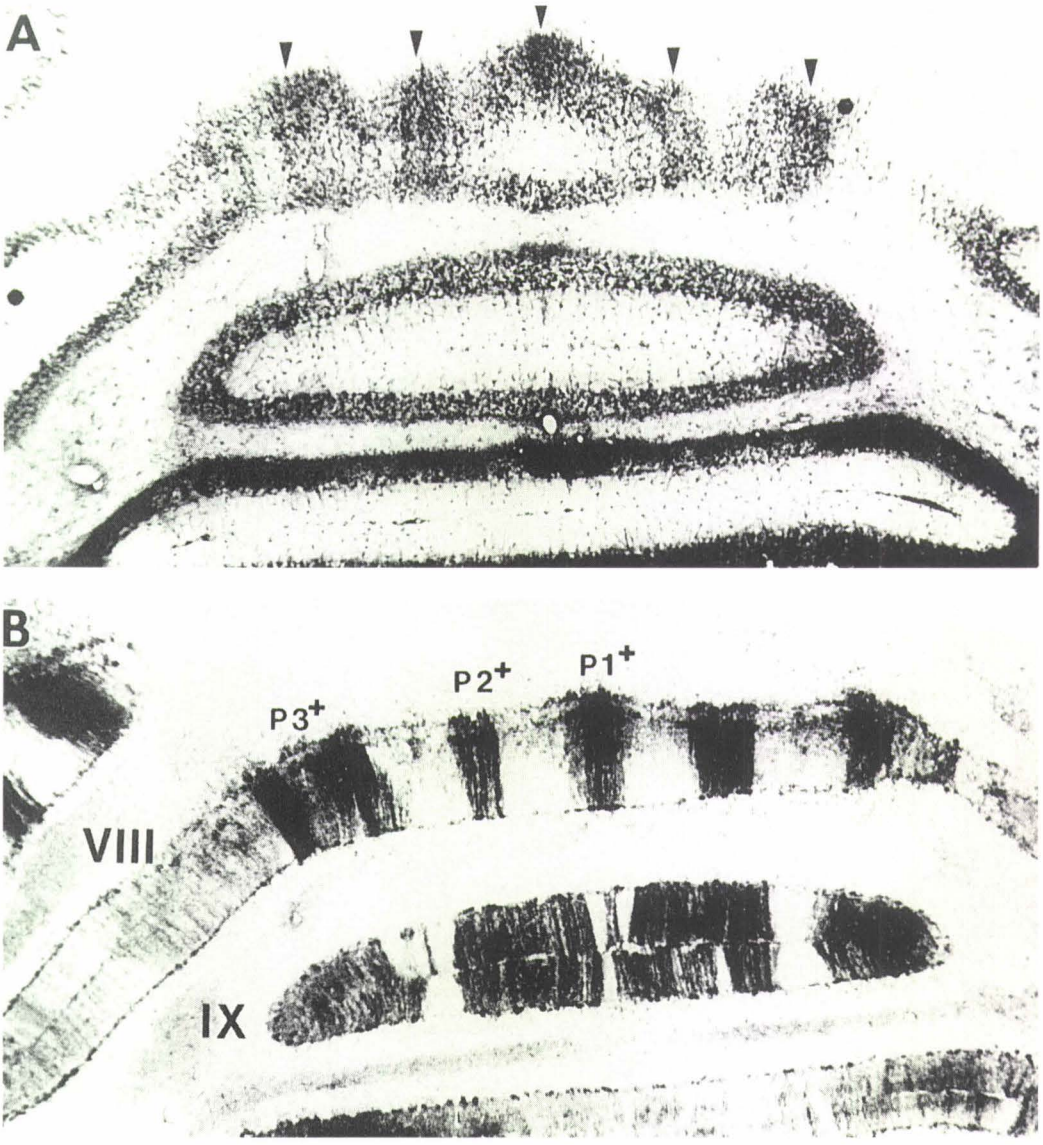


Figure 15.8. Comparison of the band-like distribution of (**A**) acetylcholinesterase (AChE) and (**B**) zebrin I on adjacent frontal sections from the posterior lobe vermis of an adult rat. The presence of the antigen zebrin I was revealed with the monoclonal antibody (mab) Q113. Only Purkinje cells are stained and they are aligned to form a series of parasagittal bands (P1-P7) in both the vermis and the hemispheres. The zebrin-positive bands alternate with bands devoid of immunostaining. This intrinsic molecular marker stains the soma, entire dendritic arbor, and axons of distinct subsets of Purkinje cells that form typical parasagittal microzones that are congruent with the termination patterns of spinocerebellar and olivocerebellar fibers, as well as with the distribution of AChE. The pattern of zebrin-positive bands is particularly obvious in lobule VIII: the *P1*$^{+}$, *P2*$^{+}$, and *P3*$^{+}$ bands are labeled in **B**, and their AChE equivalent in **A** are indicated with *arrowheads*.

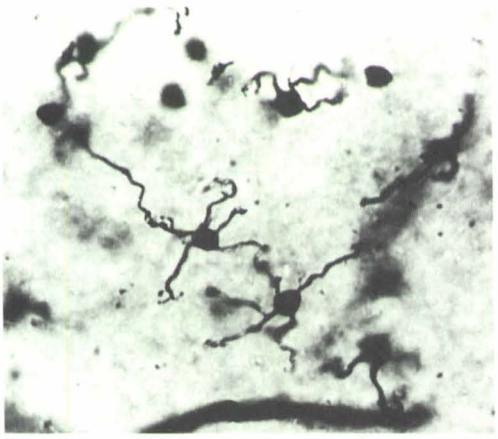


Figure 15.9. Granule cells in the cerebellar cortex displaying short dendrites with claw-like endings. Golgi preparation (×200).



Figure 15.10. Golgi (type II) neuron in the superficial granular layer of the cerebral cortex immunostained for GABA. These interneurons display more intense immunostaining with antiserum to GABA than Purkinje cells.

smaller than those located more superficially and they have dendrites that are largely confined to the granular layer (89). Axons of Golgi cells arborize profusely in the granular layer and terminate on granule cell dendrites in cerebellar glomeruli, where they exert a GABA-mediated inhibitory action (173, 201) (Fig. 15.10).

Cortical Inputs

Afferent fibers to the cerebellum convey impulses primarily to the cerebellar cortex. These afferents form various tracts that enter mainly via the inferior and middle cerebellar peduncles and include the spinocerebellar, cuneocerebellar, olivocerebellar, vestibulocerebellar, and pontocerebellar tracts, as well as numerous smaller bundles. Additionally, there are cerebellar association fibers that pass from one folium to adjacent folia and others that connect different cortical regions on the same side (86, 87, 208). Long- and short-association fibers in the cerebellar cortex are regarded as myelinated axonal collaterals of Purkinje cells (99). Within the cerebellar cortex, the afferent fibers lose their myelin sheath and end either as mossy fibers or climbing fibers. These two inputs use glutamate as a neurotransmitter (173, 201, 209, 210, 211), and their excitatory action determines the activity of the only cortical output system, the Purkinje cells. Despite differences in origin, sites of termination, and functional roles, the mossy and climbing fibers both project to the cerebellar nuclei, most likely via axon collaterals of fibers that terminate in the cerebellar cortex (195, 268). These projections activate neurons in the cerebellar nuclei and represent the *primary cerebellar circuit* (104). This primary circuit is then modulated by the inhibitory action of the cerebellar cortex, which is mediated by the Purkinje cells and driven by the same excitatory inputs.

MOSSY FIBERS

The *mossy fibers*, so-called because of the appearance of their terminations in the embryo, constitute the largest contingent of cerebellar afferents. They originate from a variety of central nervous system regions, including the vestibular nuclei, spinal cord, cerebellar nuclei, and the cerebral cortex via the pontocerebellar projection system, which is one of the most massive pathways in the brain (78, 173). These coarse fibers bifurcate repeatedly in the white matter, give off fine axon collaterals to cerebellar nuclei, enter the granular

layer, and often provide branches to adjacent folia. In the granular layer, fibers lose their myelin sheath and emit many thin collaterals. Fine lobulated enlargements occur along the course of the branches and at their terminals and are referred to as *mossy fiber rosettes* (114). A single mossy fiber may have as many as 44 rosettes along its many branches (Figs. 15.4, 15.5, and 15.11) (99). Each mossy fiber rosette forms the center of a cerebellar glomerulus. In Golgi preparations, mossy fiber rosettes appear as coiled, convoluted fibers (Fig. 15.11) (99). At the ultrastructural level, numerous synaptic vesicles, concentrations of mitochondria, neurofilaments and neurotubules are visualized within single rosettes (Fig. 15.13) (198, 212).

A cerebellar *glomerulus* is a complex synaptic structure contained within the "cerebellar islands" of the granular layer (Figs. 15.4, 15.5, and 15.12). The glomerular complex is a nodular structure formed by (a) one mossy fiber rosette, (b) the claw-like dendritic terminals of numerous granule cells, (c) the terminals of Golgi cell axons, and (d) proximal parts of Golgi cell dendrites. The center of the glomerulus contains a single mossy fiber rosette with which the dendrites of about 20 different granule cells interdigitate (Figs. 15.11–15.13). Axons of Golgi cells form a plexus on the outer surface of the granule cell dendrites. The entire structure is ensheathed in a single glial lamella (20, 89). In the glomerulus, the mossy fiber-granule cell synapse is excitatory, while the Golgi axon-granule cell junction is inhibitory (91). Thus, a cerebellar glomerulus is a synaptic cluster in which two types of presynaptic fibers, mossy fibers, and Golgi cell axons, enter into a complex relationship with one postsynaptic element, the granule cell dendrites. Golgi cells function as a negative feedback to the mossy fiber-granule cell relay. The main excitatory input to the Golgi cell is derived from the parallel fibers (Fig. 15.5).

CLIMBING FIBERS

The *climbing fibers*, whose name derives from the morphology of their terminations

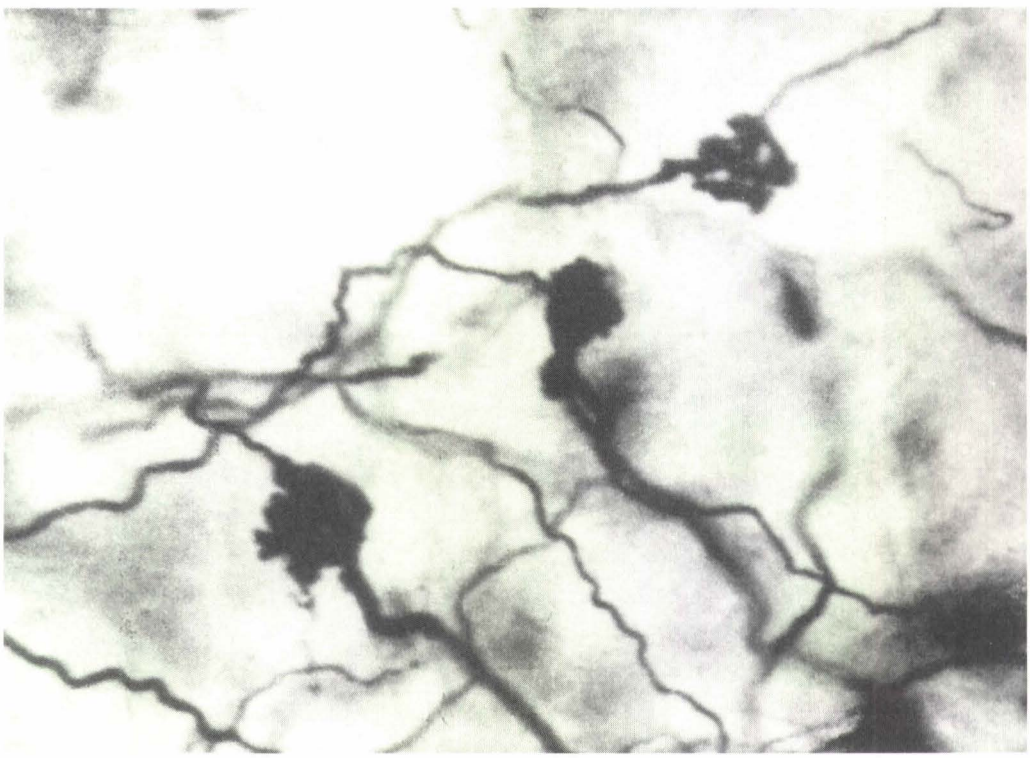


Figure 15.11. Mossy fiber rosettes in the granular layer of the monkey cerebellum as seen in a Golgi preparation. Mossy fiber rosettes look like solid structures at a low magnification, but appear as coiled convoluted fibers at a higher magnification (×850).

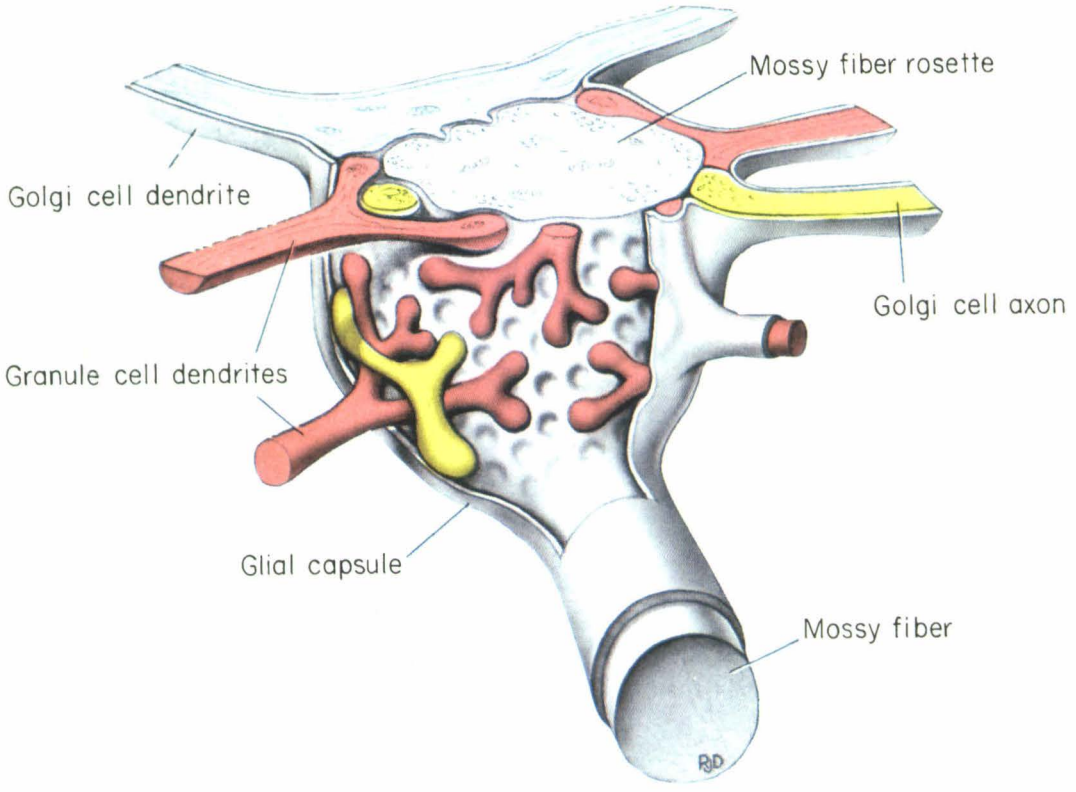


Figure 15.12. Reconstructioin of a cerebellar glomerulus based upon electron microscopic studies. A cerebellar glomerulus is formed by one mossy fiber rosette, the claw-like dendritic terminals of numerous granule cells (*red*), and terminals of Golgi cell axons (*yellow*). Proximal parts of Golgi dendrites (*blue*) also enter the glomerulus and establish broad synaptic contacts with the mossy fiber rosette. The entire nodular structure is ensheathed in a glial capsule. In this reconstruction, the glomerulus is shown in horizontal section, and in a schematic three-dimensional view.

upon Purkinje cells, have been the center of great interest since their discovery by Ramón y Cajal in 1888, because of their remarkable one-to-one relationship with dendritic branches of the Purkinje cell. These fibers have been thought to be recurrent axonal collaterals of Purkinje cells (175) or recurrent axons of the cerebellar nuclei (62). There is now general agreement that climbing fibers, like mossy fibers, have exogenous origins (i.e., from nuclei outside of the cerebellum). Silver impregnation techniques originally suggested that most climbing fibers originated from the inferior olivary complex (251). This view was strengthened by electrophysiologic results which concluded that climbing fibers originated only from the inferior olivary complex (63, 89, 254). Anterograde labeling studies indicate that nearly all climbing fibers arise from the inferior olive and that these fibers terminate in the contralateral cerebellar cortex in the form of thin sagittal strips that interdigitate with unlabeled strips (17, 73, 78).

The climbing fibers ascend undivided through the white matter of the cerebellum and the medullary lamina of the folia, traverse the granular layer, and project beyond the Purkinje cell somata to reach the dendrites of the Purkinje cells. These unmyelinated fibers divide into numerous branches and climb the dendritic arborization of the Purkinje cell (Figs. 15.4 and 15.5). Climbing fibers contact only the smooth branchlets of Purkinje cell dendrites; they do not contact the spiny branchlets on which parallel fibers synapse (99). Many climbing fibers form infraganglionic plexuses immediately beneath the Purkinje cell layer before turning upward to be deployed over the dendritic arbor of a single Purkinje cell. Although collaterals of climbing fibers may established contacts with as many as 10 adjacent Purkinje cells, each Purkinje cell receives synaptic connections

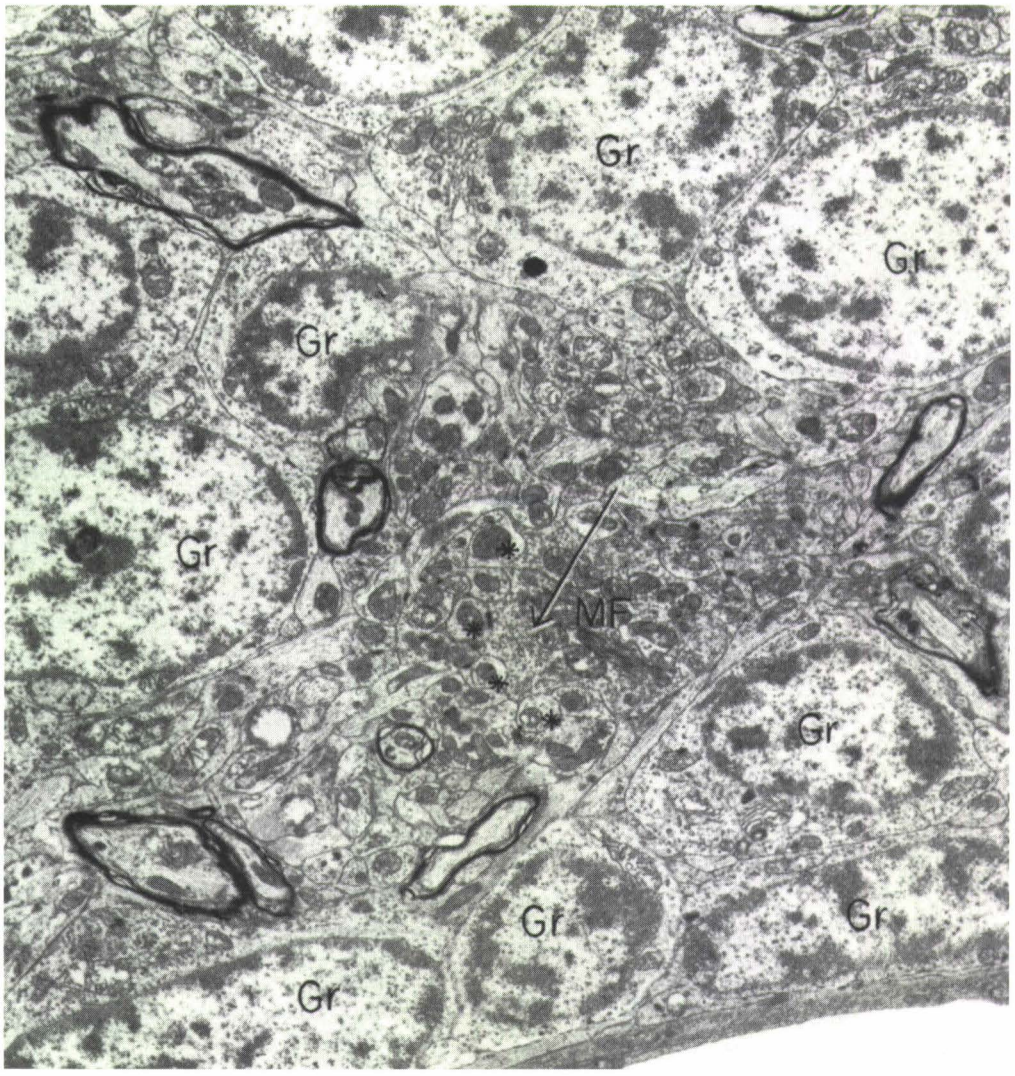


Figure 15.13. Cerebellar glomerulus in the monkey. A mossy fiber rosette (*MF*) with dispersed synaptic vesicles (*arrow*) is surrounded by granule cells (*Gr*). Granule cell dendrites are indicated by *asterisks* (×5600).

from only a single climbing fiber. In fact, the arborization of these thin collaterals (233) appears insignificant when compared with the repeated and abundant synaptic contacts that a climbing fiber makes with the dendrites of its own Purkinje cell (89). Collaterals of the climbing fiber also make contact with stellate, basket, and Golgi cells (117, 233). Electron microscopic evidence indicates that although climbing fibers and basket cell axons partially overlap in their contact with portions of the Purkinje cell dendritic tree, there are no synaptic junctions between these fibers (68). Climbing fibers articulate primarily with the smooth branchlets of the dendritic tree, while basket cell axons are restricted to dendritic shafts. Furthermore, collaterals of climbing fibers given off in the granular layer synapse directly upon the shafts of granule cell dendrites and the somata of Golgi cells (69).

MONOAMINERGIC AND CHOLINERGIC INPUTS

Fluorescence histochemistry has revealed a hitherto unrecognized fiber system in the cerebellar cortex that contains norepinephrine (or noradrenaline) (124). These noradrenergic fibers extend from the white matter into all layers of the cortex, are not restricted to

any particular plane, and are moderately concentrated in the Purkinje cell layer. This fiber system arises chiefly from the locus coeruleus (Figs. 13.33–13.35, and 14.3) and less abundantly from catecholaminergic neurons in the ventrolateral medulla and the rostral pons (296). Cells in the caudal half of the locus coeruleus were shown to arborize in the entire cerebellar vermis, the flocculus, and the ventral paraflocculus (244). The brainstem noradrenergic fibers appear to exert their influence primarily on Purkinje cells (23, 202, 218), but also on GABAergic interneurons (289, 290). Their activation produces a widespread release of norepinephrine that hyperpolarizes the Purkinje cells. This form of inhibition can be mimicked by the application of cyclic adenosine-3′,5′-monophosphate (AMP), and implies that norepinephrine may function by the activation of an electrogenic sodium pump similar to those in other central neurons (173). An additional independent action at low threshold is the enhancement of GABA-mediated inhibition in the cerebellar cortex, an effect that appears mediated through β-1 noradrenergic receptors (289, 290). Hence, norepinephrine seems to exert multiple modulatory functions in the cerebellar cortex.

There is also evidence for dopaminergic afferents to the cerebellar nuclei and to all layers of the cerebellar cortex (213, 236). Dopamine binding sites also exist in the cerebellum as revealed by autoradiographic binding studies undertaken with tritiated spiperone as ligand (213). The role of these dopaminergic afferents, which appear to originate from neurons located in the substantia nigra-ventral tegmental area complex of the ventral midbrain, is still unknown.

The raphe nuclei, which synthesize and release serotonin (5-hydroxytryptamine, 5-HT), project to all parts of the cerebellar nuclei and cortex (66, 152, 253, 265). The largest number of serotonergic fibers appear to arise from the raphe nuclei of the pons and medulla (110, 252, and 296), although serotoninergic neurons located more laterally in the brainstem reticular formation also contribute to the cerebellar innervation (152). All parts of the cerebellar cortex receive afferents from the raphe nuclei, with the most profuse projections passing to lobules VII and X of the vermis and to crus I and II (110). Axons of raphe neurons (a) terminate as mossy fiber rosettes in the granular layer, (b) terminate diffusely throughout all cortical layers without specialized junctions, and (c) pass directly to the molecular layer where they bifurcate like parallel fibers and synapse with cerebellar interneurons (66). Serotonergic fibers differ from noradrenergic afferents in the molecular layer in that they do not synapse upon Purkinje cells.

Evidence for a cerebellar cholinergic innervation derives from immunohistochemical studies with antibodies raised against the acetylcholine synthesizing enzyme, choline acetyltransferase (ChAT), in various species including humans (19, 130, 133, 148, 149). Thin, finely beaded axons that display ChAT-immunoreactivity occurs in all cortical layers. Furthermore, a selective ChAT labeling of some large mossy fibers rosettes is observed in the granular layer, particularly in cerebellar regions (lobules I, II, IX, and X, as well as flocculus-ventral paraflocculus area), which are known to receive primary and secondary vestibular afferents (19). These findings suggest that a subset of vestibular projections to the cerebellar cortex is cholinergic. Retrograde labeling studies have also identified the pedunculopontine nucleus of the mesopontine tegmentum as a potential source of cerebellar afferents (296). As seen in the preceding chapter, this nucleus is topographically related to the superior cerebellar peduncle and is markedly enriched with cholinergic neurons (group Ch 5). Hence, the pedunculopontine nucleus could be a major source of cholinergic input to the cerebellum.

Basic Circuit Organization

Geometric relationships of elements within the cerebellar cortex have furnished many hypotheses concerning the functions of individual neurons. Physiologic studies indicate that (a) climbing fibers exert a powerful excitatory influence on Purkinje cell dendrites, (b) parallel fibers excite Purkinje cells via "cross-over" synapses, and (c) stellate, basket, and Golgi cells are inhibitory interneurons in the cerebellar cortex. Stellate cells exert inhibitory influence of dendrites of Purkinje cells, whereas basket cell inhibition is affected by axosomatic synapses on many Purkinje cells in a sagittal plane. Golgi cells inhibit afferent input to the cerebellar cortex at the mossy fiber-granule cell relay in the glomeruli. Because Golgi cell axons reach glomeruli throughout the depth of the cere-

bellar cortex, they can inhibit mossy fiber input to parallel fibers.

The Purkinje cells are the sole output elements of the cerebellar cortex. They are under the influence of three inhibitory interneurons (the stellate, basket, and Golgi cells) and one excitatory interneurons (the granule cells). This relatively simple basic circuit is driven by two major excitatory inputs, the climbing and the mossy fibers. Climbing fibers have a direct, all-or-none, excitatory action on single Purkinje cell (90, 92). This synaptic connection is one of the most powerful in the nervous system. A single action potential in a climbing fiber elicits a gigantic excitatory postsynaptic potential, which produces high frequency burst of action potentials, called a complex spike, in the Purkinje cell. In contrast, the mossy fiber input transmitted by parallel fibers results in smaller excitatory postsynaptic potentials. Spatial and temporal summation of these smaller postsynaptic potentials is required for the Purkinje cell to produce a single action potential, called a simple spike (104). The mossy and climbing fibers are modulated differently during natural behaviors. Mossy fibers fire spontaneously at high rates, producing 50–100 simple spikes per second in Purkinje cells. Sensory stimuli or voluntary movements increase this firing even further. These mossy fiber inputs are essential for controlling the firing of the Purkinje cell. In contrast, the neurons of the inferior olive that give rise to the climbing fibers fire at low and irregular rates, and, on average, produce only one complex spike per second. Sensory stimuli or movements elicit only one or two complex spikes, suggesting that the climbing fibers are not involved in the direct control of motor behavior (104). Instead, because they can modulate the responsiveness of Purkinje cells to mossy fiber inputs, the climbing fibers are likely to be involved in the learning aspect of cerebellar functions (134).

Climbing fibers reaching a given Purkinje cell also have synaptic articulations with inhibitory interneurons, the Golgi, stellate, and basket cells. Excitation of basket cells results in inhibition of Purkinje cells on both sides of a single Purkinje cell receiving the main branches of a climbing fiber. A single basket cell theoretically could inhibit 7 rows of about 10 Purkinje cells. The excitation of Golgi cells via climbing fibers results in the inhibition of impulses reached by the ramifications of the Golgi cell axon. This mechanism depresses the activity in Purkinje cells on both sides of the single Purkinje cell excited by the climbing fiber. The widespread inhibitory influence exerted by a single climbing fiber appears to be a device to silence the background for a single Purkinje cell activated by a climbing fiber volley (89).

Mossy fiber impulses exert their synaptic excitatory action solely within the cerebellar glomerulus, where they excite granule cells whose axons (the parallel fibers) excite all cells with dendrites in the molecular layer (i.e., Purkinje, basket, stellate, and Golgi cells). Impulses conveyed to dendrites in the molecular layer result in excitation of (a) a narrow band of Purkinje and Golgi cells in the longitudinal axis of the folia, and (b) basket and stellate cells whose axons extend sagittally (transverse to the folia) on each side of the exited beam of parallel fibers (Fig. 15.14). This geometric configuration results in excitation of a narrow band of Purkinje cells, flanked on each side by Purkinje cells inhibited by basket and stellate cells (89, 93). By analogy to the surround inhibition in sensory systems, the stellate and basket cell inhibition is thought to sharpen the boundaries between active clusters of Purkinje cells, whereas Golgi inhibition provides temporal focusing of the excitation (104).

The net result of the complex neural computation that occurs in the cerebellar cortex is a GABA-mediated inhibition conveyed by the axon of Purkinje cells (89, 134, 136–139). Thus, axons of Purkinje cells exert inhibitory influence on cells with which they synapse, namely the cerebellar nuclei and portions of the vestibular nuclei (82, 83, 85, 277). Collaterals originating from proximal portions of the axon of Purkinje cells (Fig. 15.4) exert inhibitory influences on Golgi cells, which in turn inhibit granule cells. This disinhibition tends to release granule cells whose axons excite Purkinje cells.

Neuroglia

While most of the neuroglial elements in the cerebellar cortex are similar to those in other parts of the central nervous system, the architectonics of the neuroglia bear definite relationships to the three-layered neuronal structure (Fig. 15.15). Each cortical layer has a different population of neuroglial cell types, and one type, the Golgi epithelial cell, is

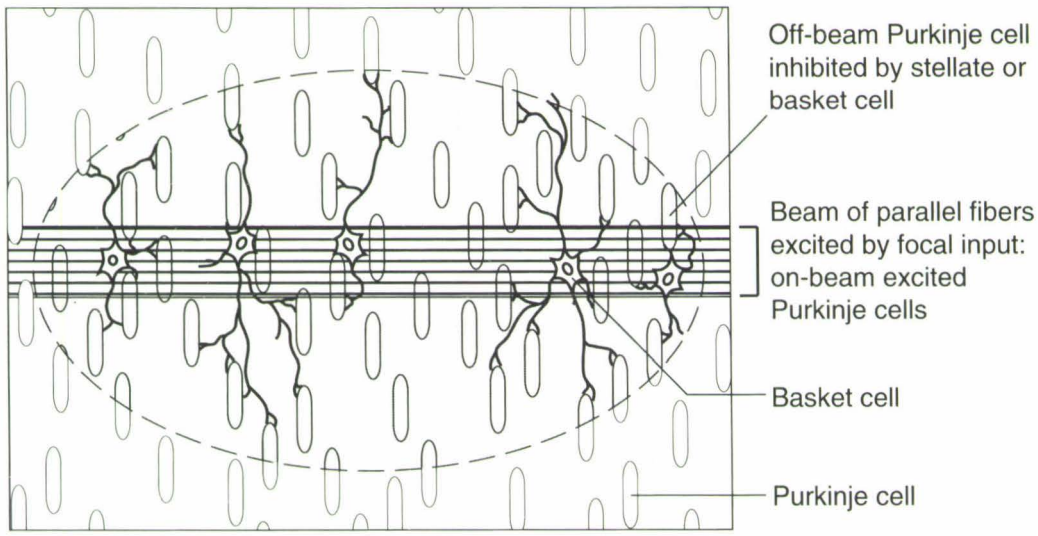


Figure 15.14. Dorsal surface of a folium showing that excitation of a beam of parallel fibers leads to excitation of a central (on-beam) region of Purkinje cells and inhibition of surrounding (off-beam) Purkinje cells. This type of inhibition is mediated via the excitation of the inhibitory basket and stellate cells. The dark area surrounding the excited beam of parallel fibers indicates inhibitory effect.

unique to the cerebellar cortex (Fig. 15.16). The cerebellar cortex contains both astrocytes and oligodendrocytes. Astrocytes are primarily protoplasmic and have been divided into three classes: (a) the Golgi epithelial cell, (b) the lamellar or velate astrocyte, and (c) the smooth astrocyte (212). The Purkinje cell layer contains modified astrocytes known as the *Golgi epithelial cells* (223), or *Bergmann cells*. These neuroglial cells are true satellites of Purkinje cells in that they lie directly against the surface of Purkinje cells and form a nearly complete sheath around them (Fig. 15.16). Purkinje cells also are surrounded by Fañanas cells (Fig. 15.15), which are similar to the Golgi epithelial cells and protoplasmic astrocytes (212, 248). Each Bergmann cell gives rise to two or more processes which bifurcate and ascend in almost parallel lines to the pial surface. These processes course perpendicularly in the molecular layer and terminate at the surface of the cortex (i.e., limiting glial membrane) in conical expansions. These cells resemble miniature candelabra with their branches either clustered or spread out in parasagittal planes. The neuroglial processes of these cells lie between the dendritic arborizations of consecutive Purkinje cells (223). Electron micrographs indicate that the ascending processes of neighboring Bergmann cells are interdigitated to form a dense forest, rather than alternating palisades. Processes of Bergmann cells insulate the smooth branchlets of Purkinje cell dendrites from passing parallel fibers (99). This insulation appears absent only where climbing fibers come into synaptic relationship with the smooth branchlets. These specialized glial processes also may serve to confine transmitter substances to a particular synaptic site and in this way promote neuronal specificity (217). The Golgi epithelial cell is characteristic of the Purkinje and molecular layers and is not found elsewhere. Golgi epithelial cells, Fañanas cells and protoplasmic astrocytes of the cerebellar cortex probably are all variants of a single cell type (212).

The lamellar astrocyte is found chiefly in the granular layer, while the smooth astrocyte may be found in any layer, but is most common in the granular layer. Lamellar astrocytes are about the same size as granule cells, have a bean-shaped nucleus and may contain one or two nucleoli. The distribution and form of the glial processes of these cells are unusual in that numerous lamellar neuroglial processes pass between adjacent granule cells, dendrites, and axons, forming open and confluent compartments. The number and extent of these processes is greater than might be expected. The lamellar processes separate one glomerulus from another in the cerebellar islands, and interweave with the dendrites and Golgi cell axons on the periphery of the glomeruli (212).

Smooth astrocytes with long radiating

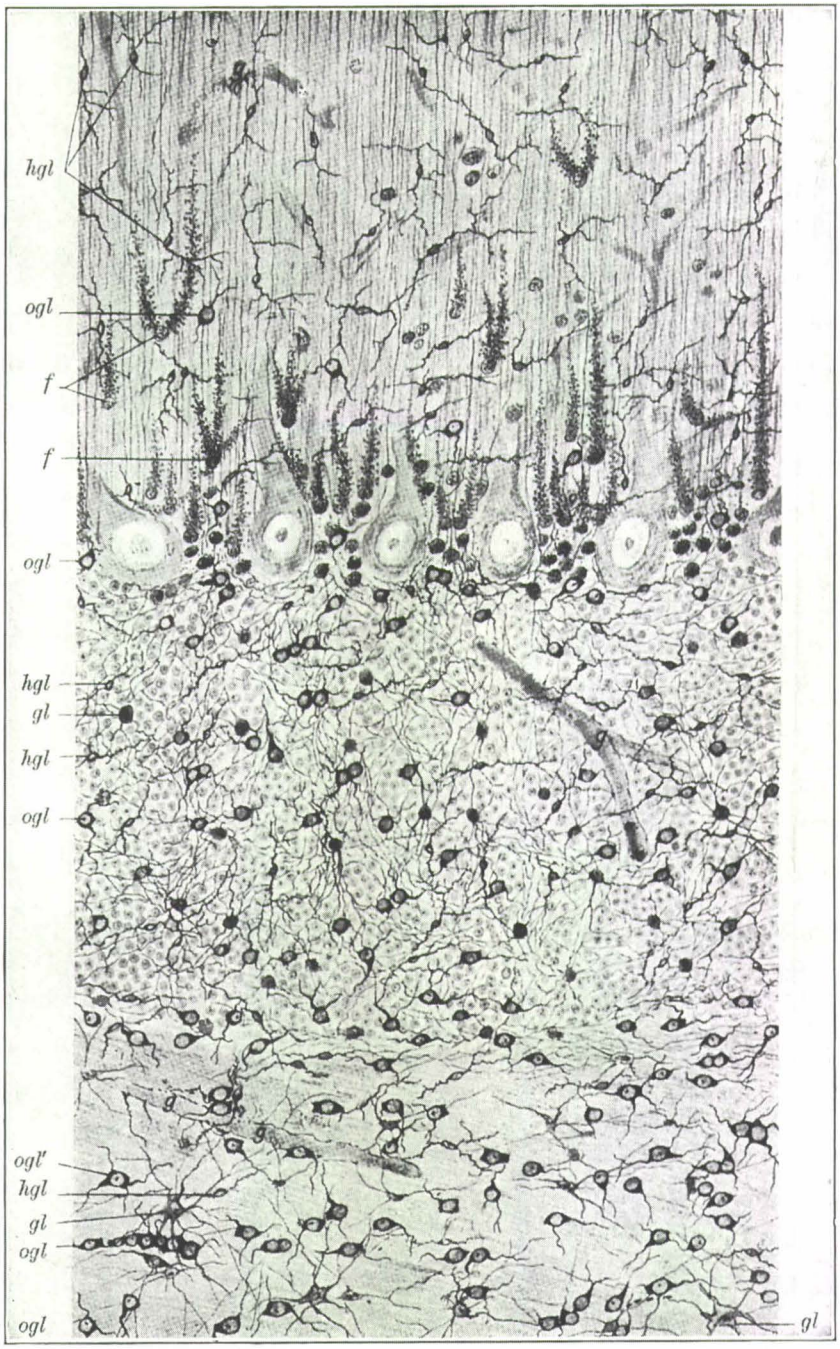


Figure 15.15. Arrangement of neuroglia cells in human cerebellar cortex: *f*, cells of Fañanas; *gl*, astroglia; *hgl*, microglia; *ogl*, *ogl'*, oligodendrocytes.

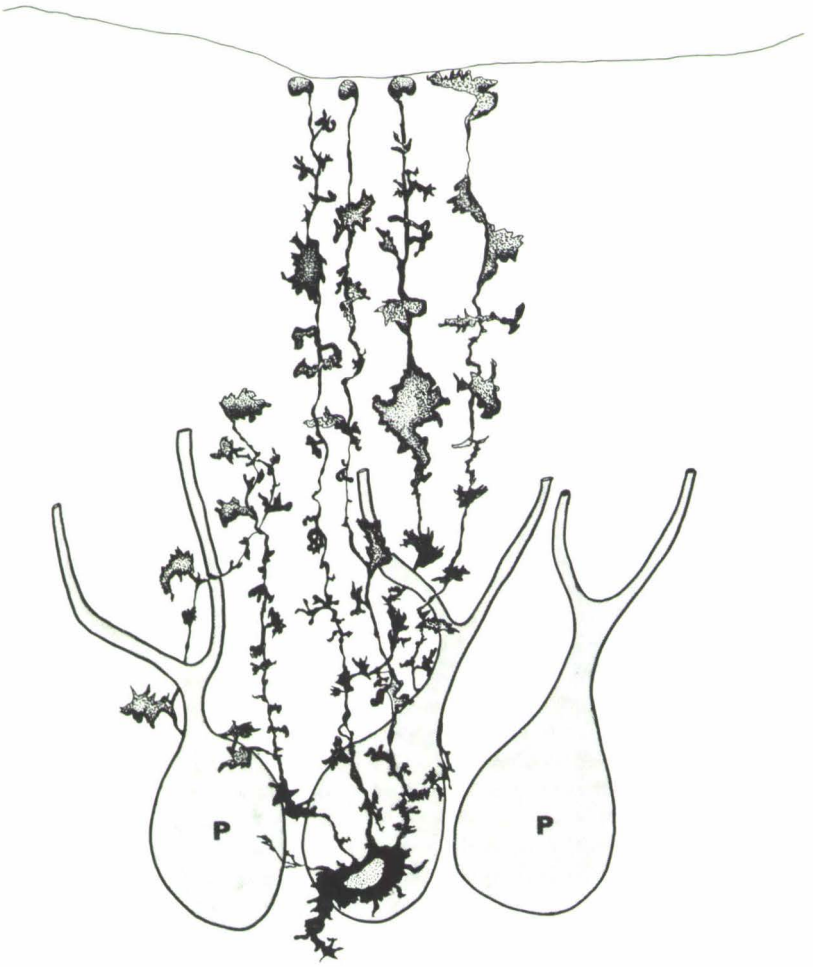


Figure 15.16. Golgi epithelial cells in the rat cerebral cortex. Purkinje cells are surrounded by Golgi epithelial cells whose somata bear ragged irregular appendages. Multiple processes of these glial cells extending upwards to the pial surface in candelabra-fashion bear irregular leaf-like appendages which project horizontally. These cells cannot be distinguished from Fañanas cells.

processes, found in the molecular and granular layers, resemble stellate neuroglial cells, but are much smaller. Processes of these cells are kinky, contorted, and branch repeatedly. Oligodendrocytes, seen throughout the cerebellar cortex, are most numerous in the granular layer and in the depths of the molecular layer where myelinated fibers are found.

CEREBELLAR NUCLEI

Major Features

CORPUS MEDULLARE

It is a compact mass of white matter, which is continuous from one hemisphere to the other and covered everywhere by the cerebellar cortex. It consists of afferent projections to the cerebellar cortex, efferent fibers from the cerebellar cortex and, to a lesser extent, association fibers connecting the various portions of the cerebellum. The corpus medullare is continuous with the three peduncles which connect the cerebellum with the brain stem: (a) the *inferior cerebellar peduncle*, which connects with the medulla; (b) the *middle cerebellar peduncle*, which connects with the pons; and (c) the *superior cerebellar peduncle*, which connects with the midbrain (Figs. 2.26 and 2.32). Medially and ventrally, near the roof of the ventricle, the corpus medullare splits into two white laminae, inferior and superior, which separate at an acute angle to form a tent-like recess (i.e., fastigium) in the roof of the fourth ventricle (Figs. 2.27, 2.28, and 2.33). The inferior medullary lamina (or

velum) passes caudally over the nodulus and becomes continuous with the tela choroidea and the choroid plexus of the fourth ventricle. Laterally, the inferior medullary velum extends to the flocculi, forming a narrow bridge connecting these structures with the nodulus. The largest part of the medullary substance is continued rostrally, forming the superior medullary velum (Figs. 2.28 and 2.32). The latter is a thin white plate joining the two superior cerebellar peduncles. Together, these structures form the roof and lateral walls of the upper part of the fourth ventricle.

CEREBELLAR NUCLEI

Imbedded in the white matter of each half of the cerebellum are four nuclear masses, the cerebellar nuclei (Figs. 13.7, 13.26, 15.18, and 15.19). These cellular aggregates are often referred to as the "deep cerebellar nuclei," but because there exist no superficial cerebellar nuclei, the qualificative "deep" is avoided in the present account. All cerebellar nuclei originate from condensations of cells that migrate outward from the germinal neuroepithelium of the fourth ventricle (155). The four cerebellar nuclei start to differentiate simultaneously at early developmental stages and there is no evidence that individual cerebellar nuclei differ with respect to ontogenetic origin or age. Although four distinct cerebellar nuclei are recognized in most mammals, prior to the investigations of Snider (239) most authors described these nuclei as a capriciously indented cell mass divisible into three nuclei: (a) the medial (fastigial), (b) the interposed, and (c) the lateral (dentate). Studies in the monkey distinguish four cerebellar nuclei on the basis of fiber patterns, cellular morphology, and the size, shape, and orientation of cells (76). The strongest arguments supporting the existence of four individual cerebellar nuclei are observations indicating that each nucleus has unique connections. The four cerebellar nuclei in humans, from medial to lateral, are the fastigial, globose (posterior interposed), emboliform (anterior interposed), and the dentate.

NEUROTRANSMITTERS

Unlike Purkinje cells, neurons of the cerebellar nuclei are excitatory and project beyond the cerebellum. Immunohistochemical data suggest that glutamate and/or aspartate may be the excitatory transmitter of most cells in the cerebellar nuclei (201, 210, 228). Additionally, a significant proportion of the small neurons in the cerebellar nuclei are GABAergic (101). Virtually all of these small GABAergic, presumably inhibitory, cells are projection neurons, and a significant proportion of them project to the inferior olivary nucleus (101). Purkinje cells, which provide the only output from the cerebellar cortex, project in an orderly manner to the cerebellar nuclei, where they inhibit the excitatory (and partly inhibitory) output system that originates from the nuclear masses within the white matter of the cerebellum.

DENTATE NUCLEUS

This nucleus, the largest of the cerebellar nuclei, lies in the white matter of the cerebellar hemisphere close to the vermis (Fig. 15.17). In transverse sections, this large nucleus appears as a convoluted band of gray matter having the shape of a folded bag with the opening or hilus directed medially and dorsally (Fig. 15.19). Its resemblance to the inferior olivary nucleus is obvious (Fig. 15.18). It is found as a definite nucleus only in mammals, and it becomes greatly enlarged in humans and the anthropoid apes. In both anthropoid apes and humans, the dentate nucleus can be divided into an older dorsomedial portion (paleodentate) and a larger, newer ventrolateral portion (neodentate). Cells in the ventrolateral region of the dentate nucleus are smaller than those located dorsomedially (170, 261). The nucleus is composed mainly of large multipolar cells with branching dendrites. Axons of these cells acquire a myelin sheath while still in the nucleus and emerge from the cerebellum in the superior cerebellar peduncle (170). Between these large cells are small stellate cells whose axons arborize within the nucleus. Golgi studies of the dentate nucleus in rats and monkeys reveal several varieties of large and small neurons and a segmentation of the nucleus into zones (66). Large dentate nucleus neurons have radiating tortuous dendrites bearing occasional thorns. Large columnar neurons have elliptical cell bodies with long twisting dendritic branches, which arise from a primary trunk, and occur only in the two major zones of the nucleus. Afferent fibers from the

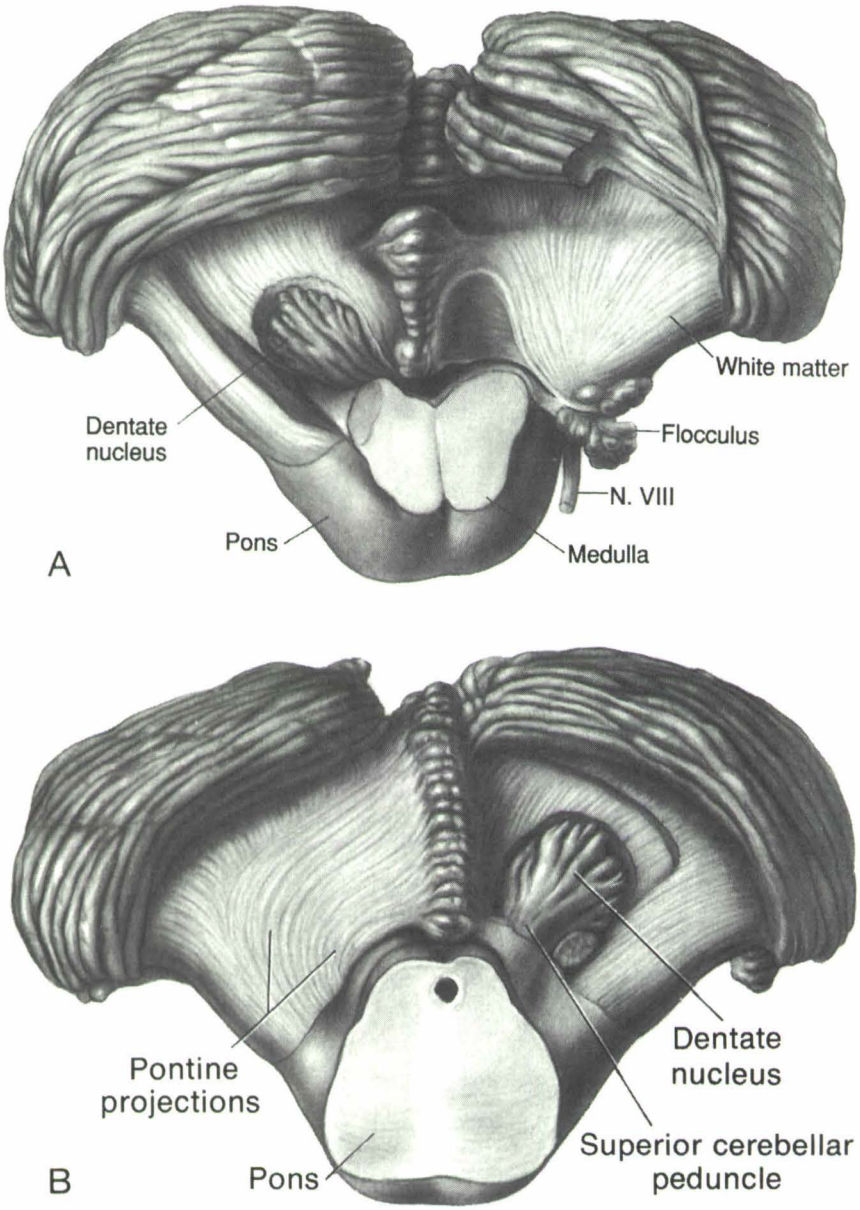


Figure 15.17. Dissections of the left dentate nucleus with portions of the cerebellar cortex and vermis intact. **A**. Dissection of the posterior surface of the cerebellum exposing the dentate nucleus. **B**. Dissection of the superior surface of the cerebellum from above showing the left dentate nucleus in relationship to the isthmus (upper portion) of the pons.

Purkinje cells enter laterally and form a dense fiber plexus, the amiculum, around the nucleus.

EMBOLIFORM NUCLEUS

This nucleus is a wedge-shaped gray mass situated close to the hilus of the dentate nucleus and often is difficult to delimit from the latter. It is composed of clumps of cells resembling those of the dentate nucleus (Figs. 13.26 and 15.19). In most nonprimate mammals, the globose and emboliform nuclei form a continuous nuclear mass referred to as the *nucleus interpositus*. Two parts of the nucleus interpositus have been distinguished: (a) an anterior nucleus interpositus, located rostrally close to the dentate nucleus, and be-

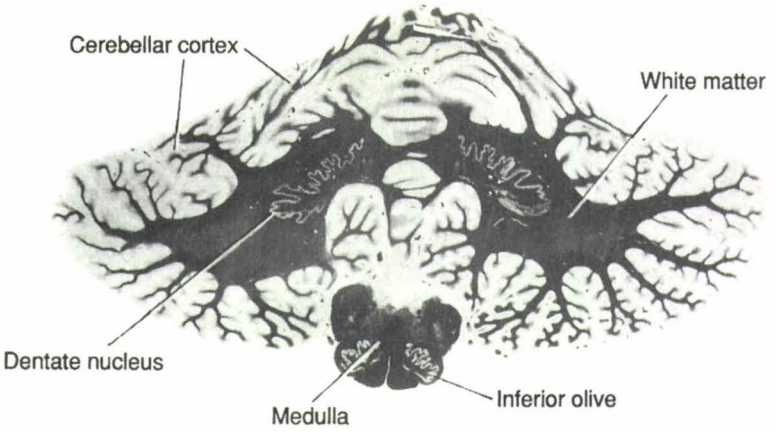


Figure 15.18. Transverse Weigert-stained section through the cerebellum and the medulla. This photomicrograph provides a comparison of the size and shape of the dentate nucleus and the inferior olivary nuclear complex.

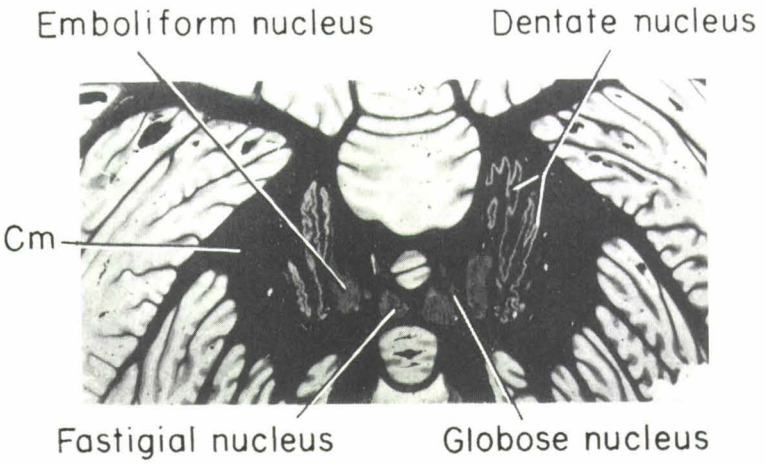


Figure 15.19. Horizontal section through adult cerebellum showing portions of the cerebellar nuclei and the corpus medullare (*Cm*) (Weigert's myelin stain).

lieved to be homologous to the emboliform nucleus in humans, and (b) a posterior nucleus interpositus, located more medially and caudally, and considered as the homologue of the globose nucleus (76).

GLOBOSE NUCLEUS

This nucleus consists of one or more rounded gray masses lying medial to the emboliform nucleus and lateral to the fastigial nucleus (Fig. 15.19). This nucleus contains both large and small multipolar cells.

FASTIGIAL NUCLEUS

This nucleus, the most medial of the cerebellar nuclei, lies near the midline in the roof of the fourth ventricle, and, in humans, is second in size to the dentate nucleus (Figs. 13.26 and 15.19). The fastigial nucleus is characterized by a population of densely packed cells of varying sizes. Large, medium, and small cells are intermingled in dorsal parts of the nucleus, while small cells predominate ventrally (76). Cell strands emerging from the lateral border of the nucleus extend ventrolaterally towards the vestibular nuclei. Both large and small cells have dendrites radiating in all directions which bear spines on distal branches (187). Dendritic fields of neurons within the nucleus show extensive overlap, but there are no Golgi type II cells. Unlike the other cerebellar nuclei, cells of the fastigial nucleus give rise to both crossed and uncrossed axons; axons crossing to the opposite

side are most numerous in rostral regions of the nucleus (57).

Connections

CORTICONUCLEAR PROJECTIONS

The largest number of afferent fibers to cerebellar nuclei arise from Purkinje cells in the cerebellar cortex and have GABA as their neurotransmitter. All parts of the cerebellar cortex project upon the intrinsic nuclei. The work of Jan Jansen and Alf Brodal in Norway revealed that cerebellar cortical projections to the cerebellar nuclei form three rostrocaudal longitudinal zones: (a) a medial or vermal zone projecting to the fastigial nucleus; (b) a paravermal zone projecting to the interposed nuclei; and (c) a lateral or hemispheric zone projecting to the dentate nucleus (85, 143–145, 156, 272, 273). As seen earlier, these longitudinal corticonuclear zones can be further subdivided into numerous parasagittal zones on the basis of patterns of termination of various brainstem afferents and on the heterogeneous distribution of different molecular markers (32, 119, 145, 272).

The *medial cortical zone*, comprising the vermis proper, projects in a strictly unilateral manner to the fastigial nucleus (77, 115). Fibers from the cortical lobules of the vermis project to the nearest region of the fastigial nucleus which results in a sequential representation of the cerebellar vermis in the fastigial nucleus. Each fastigial nucleus receives afferents from a narrow band of Purkinje cells in the ipsilateral vermis in folia of lobules I through X (57, 230). Information concerning the paravermal and lateral longitudinal cerebellar zones is less complete, but the same principle appears to apply. Anterograde tract tracing studies support the concept of three mediolateral zones projecting respectively to the fastigial, interposed and dentate nuclei (22, 32, 80, 258).

NUCLEOCORTICAL PROJECTIONS

The conceptual subdivision of the cerebellum into three sagittal zones (270), each consisting of a longitudinal strip of cerebellar cortex and the cerebellar nucleus to which its Purkinje cells project, has been strengthened by the observation that cells in the cerebellar nuclei send collaterals to the cortex in a specific manner. While it has long been suspected that the cerebellar nuclei provided collaterals to the cerebellar cortex (62, 223), conclusive evidence of this intrinsic cerebellar pathway was provided only with the advent of axonal transport techniques (66, 109, 111, 260). Retrograde neuronal tracers injected into a localized region of the cerebellar cortex resulted in a profuse labeling of cells in a single cerebellar nucleus, whereas injections of anterograde tracer into the cerebellar nuclei labeled fibers terminating into the cerebellar cortex. Nucleocortical and corticonuclear projections are reciprocally organized. Neurons in the cerebellar nuclei project back to the cerebellar cortical regions from which they receive input (66, 80, 109, 111, 259, 262). These reciprocal projections do not appear to be organized in a strict point-to-point manner because projections from the cortex may not terminate on cells that give rise to return cortical projections (258). In primates, the nucleocortical projections from the distinctive parts of the dentate nucleus are more complex than in nonprimates. The neodentate (ventrolateral) projects to the lateral hemisphere, while the paleodentate (dorsomedial) has projections to the vermis (262). Axons of the cerebellar nuclei projecting to the cerebellar cortex arise from a heterogeneous population of cells, similar to those that project to the thalamus and brainstem. Some cells in the dentate and interposed nuclei have collateral axons that project via the superior cerebellar peduncle to the thalamus and inferior olive, as well as to the cerebellar cortex (261). Nucleocortical collaterals terminate in the granular layer of the cerebellar cortex (260). Since the nucleocortical projection arises from axon collaterals of cerebellar neurons, the same signals projected to brainstem nuclei are fed back to the cerebellar cortex. These collateral projections from the cerebellar nuclei represent a major afferent system to the cerebellar cortex.

EXTRACEREBELLAR INPUTS

Although the Purkinje cells exert inhibitory influences on the cerebellar nuclei, these nuclei maintain a high frequency excitatory discharge (134, 139, 140). It is presumed that excitatory inputs from extracerebellar sources overcome the tonic inhibitory output from the cerebellar cortex. The current thesis is that extracerebellar inputs to the cerebellar nuclei provide the tonic facilitation which, at times, predominates over the cortical inhibition and maintains the discharge of impulses directed towards brainstem nuclei (89).

The dentate nucleus receives afferents from (a) the pontine nuclei, (b) the principal inferior olivary nucleus, (c) the trigeminal sensory nuclei, (d) the reticulotegmental nucleus, (e) the locus coeruleus, and (f) the raphe nuclei (66, 94). The largest number of afferent fibers appear to arise from the pontine nuclei, the inferior olivary nucleus, and the reticulotegmental nucleus. Both ipsilateral and contralateral pontine nuclei project to the dentate nucleus, but the largest number of fibers arise from the opposite side (94). Olivocerebellar fibers, comprising one of the largest cerebellar afferent systems, pass to all parts of the cerebellar cortex and to the cerebellar nuclei (29). Afferent projections to the dentate nucleus are crossed and arise from cells of the principal inferior olivary nucleus (74). The interposed nuclei receive crossed fibers from the medial and dorsal accessory olivary nuclei, and the fastigial nucleus receives fibers from the dorsomedial cell column and nucleus *Beta*, which are caudal subdivisions of the medial accessory olive (31, 32). These projections to the cerebellar nuclei probably are collaterals of climbing fibers. The dentate nucleus and the interposed nuclei also receive bilateral projections from the reticulotegmental nucleus (94). The anterior interposed nucleus (i.e., the emboliform nucleus) receives a projection from the red nucleus which is crossed (74), and is reciprocal to the major projection from this nucleus.

The fastigial nucleus receives an input from caudal and dorsal regions of the medial and inferior vestibular nuclei and from cells of group x, located along the lateral borders of the inferior vestibular nucleus. These afferents are bilateral and fairly symmetric in origin (230). The fastigial nucleus also receives small inputs from the nucleus prepositus, the dorsal paramedian reticular nuclei, the reticulotegmental nucleus and the locus coeruleus (57, 244, and 245). Although no primary vestibular afferents have been found to terminate in the fastigial nucleus, these fibers have been shown to end in the small-celled ventrolateral part of the dentate nucleus (36, 60).

These findings suggest that practically all information transmitted to the cerebellar cortex also is conveyed to one or more of the cerebellar nuclei.

SOMATOTOPIC LOCALIZATION

Afferent systems conveying sensory information from various kinds of receptors in different parts of the body are localized to particular parts of the cerebellum. As first shown in the 1940s by Edgar Adrian in England and by Ray Snider in the United States, exteroceptive impulses (e.g., tactile sense, audition, and vision) give rise to action potentials in specific regions of the cerebellum which are organized somatotopically (1, 240, 242). The entire body is mapped in two different areas of the cerebellar cortex: one map lies mainly in the anterior lobe and the other lies in the posterior lobe. These two maps are inverted relative to one another. Tactile stimulation evokes potentials ipsilaterally in the anterior lobe and simple lobule, and bilaterally in the paramedian lobules. The leg area is represented in the central lobule, the arm in the culmen, and the head and face in the simple lobule. The somatotopic localization is the reverse in the paramedian lobules, with the leg represented caudally and the head represented rostrally. Responses in this pattern were most easily obtained from skin receptors or cutaneous nerves. The head area partially overlaps the middle region of the vermis (i.e., simple lobule, folium and tuber, and adjacent areas) where action potentials were recorded following auditory and visual stimuli (Fig. 15.20).

The pioneering studies of Adrian and Snider were based on recording surface potentials evoked in a population of neurons by peripheral stimuli. Although two apparently continuous body maps were revealed by this technique, more refined studies using single cell recordings have led to a more complicated view of the cerebellar somatotopic localization. It was shown that inputs from restricted peripheral sites diverge to influence several independent patches of granule cells that excite a small array of Purkinje neurons (297). Thus, even though input from a given site activates a small, sharply demarcated area, adjacent regions may receive afferents from distant body parts, an arrangement referred to as *fractured somatotopy*. The apparent conflict with earlier studies based on recording of surface potentials can be resolved because the peripheral area giving rise to the largest potential represents only the predominant input to a particular region of the cerebellar cortex (104).

In addition to receiving sensory information directly from the periphery, the cerebellum also receives information from the somatic sensory and motor cortices, and this information is mapped to correspond with

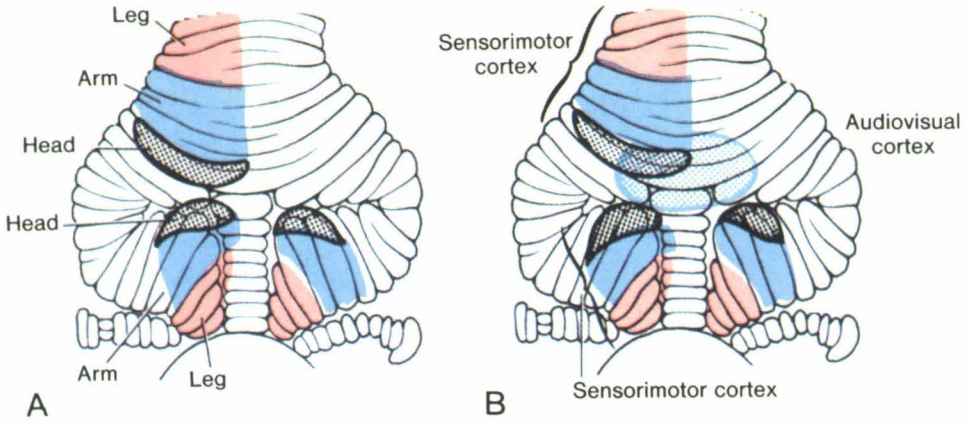


Figure 15.20. Somatotopic localization in the cerebellar cortex of a monkey. **A.** Tactile receiving areas of the cerebellum mapped by surface potentials recorded in response to movement of hairs on the left side of the body. **B.** Cerebellar cortical areas responding to stimulation of the sensorimotor, auditory and visual cortex in the right hemisphere. The leg (*red*), arm (*blue*) and head (*black stipple*) are represented ipsilaterally in the anterior lobe and bilaterally in reversed fashion in the paramedian lobules. The auditory and visual cortex (*blue stipple*) are represented in the simple lobule, folium, tuber and adjacent cortex.

the peripheral body representation (241). Similarly, information from visual and auditory cortical regions reaches the audiovisual receiving areas of the posterior vermis (118). The entire vermis also receives input from primary and secondary vestibular axons.

CEREBELLAR CONNECTIONS

Afferent Fibers

The cerebellum receives inputs generated in virtually all kinds of receptors in all parts of the body. Most afferents enter the cerebellum through the inferior and middle cerebellar peduncles, although a small number enter in association with the superior cerebellar peduncle. Afferent fibers exceeds efferent fibers by an estimated ratio of 40:1 (120). The principal input and output pathways of the cerebellum are summarized in Table 15.1.

The *inferior cerebellar peduncle* consists of a larger, entirely afferent portion, the restiform body, and a smaller medial juxtarestiform portion that contains both afferent and efferent fibers. The juxtarestiform body contains primary and secondary vestibulocerebellar fibers and cerebellovestibular fibers originating from the nodulus, uvula, and the fastigial nuclei (Fig. 13.26). Brainstem nuclei project fibers directly to the cerebellar nuclei. Quantitatively, the largest number of cerebellar afferents terminate in the cerebellar cortex as climbing or mossy fibers. Most of the afferent inputs to the cerebellar cortex are relayed by brainstem nuclei, such as the pontine nuclei, the inferior olivary nuclei, and a number of smaller nuclei located in the medulla and pons. Nuclei in the brainstem that project to the cerebellum are referred to as *precerebellar nuclei*. The precerebellar nuclei receive afferents from a variety of sources and differ greatly with respect to size, cytoarchitecture and cerebellar connections.

VESTIBULOCEREBELLAR FIBERS

These fibers enter the cerebellum largely through the juxtarestiform body and are classified as both primary and secondary. The primary afferent fibers originate both in the semicircular canals, which signal changes in head position, and in the otoliths, which signal the orientation of the head with respect to gravity, whereas the secondary afferent fibers arise from the vestibular nuclei.

Primary vestibulocerebellar fibers arise from the vestibular ganglion and project to the ipsilateral nodulus, uvula, and flocculus (36). Fibers from all parts of the ganglion project to parts of the nodulus and uvula, while fibers from ganglion cells innervating the cristae of the semicircular ducts and the maculae of the utricle and saccule project to different folia of the flocculus (60). Primary vestibulocerebellar fibers end within nearly the entire vermis (159). Among the multiple sources of input to reach the cerebellar cortex, primary vestibu-

Table 15.1. Principal Input and Output Pathways of the Cerebellum

FUNCTIONAL REGION	ANATOMIC REGION	PRINCIPAL INPUT	NUCLEUS	PRINCIPAL DESTINATION	FUNCTION
Vestibulocerebellum (archicerebellum)	Flocculonodular lobe	Vestibular labyrinth	Lateral vestibular	Medial systems: axial motor neurons	Axial control and vestibular reflexes
Spinocerebellum (paleocerebellum)	Vermis	Vestibular labyrinth, proximal body parts; facial, visual, and auditory inputs to posterior lobe only	Fastigial	Medial systems: vestibular nucleus, reticular formation, and motor cortex	Axial and proximal motor control; ongoing execution of movement
Spinocerebellum (paleocerebellum)	Intermediate part of hemisphere	Spinal afferents (distal body parts)	Interposed	Lateral systems: red nucleus (magnocellular part) and distal regions of motor cortex	Distal motor control; ongoing execution
Cerebrocerebellum (neocerebellum)	Lateral part of hemisphere	Cortical afferents	Dentate	Integration areas: red nucleus (parvocellular part) and premotor cortex (area 6)	Initiation, planning, and timing

lar afferents are the only ones that can do so directly from ganglion cells in the periphery without an intervening relay.

Secondary vestibular fibers originate from the inferior vestibular nucleus and, to a lesser extent, from parts of the medial vestibular nucleus. Although primary and secondary vestibulocerebellar fibers have similar distributions, the number of secondary fibers is much greater. Additionally, secondary vestibular fibers pass bilaterally to the nodulus, uvula, and the fastigial nuclei (41, 52, 54–56, 160).

SPINOCEREBELLAR TRACTS

The spinocerebellar tracts arise from cell groups within the spinal cord and pass directly to the cerebellum. Their cells of origin receive primary dorsal root afferents. Included in this group are the posterior, anterior, and rostral spinocerebellar tracts, as well as the cuneocerebellar tract which arises from the accessory cuneate nucleus (291).

The *posterior spinocerebellar tract* enters the inferior cerebellar peduncle (292) and projects upon the rostromedial part of the anterior lobe (lobules I to IV; Fig. 15.1) and the lateral part of the pyramis and the paramedian lobule (112, 170, 205, 207). Most of these fibers terminate ipsilaterally in longitudinally arranged zones in what corresponds to hindlimb regions. The posterior spinocerebellar tract conveys impulses from stretch receptors via group Ia and Ib muscle afferents, exteroceptive impulses from touch and pressure receptors in the skin, and slow adapting pressure receptors (205).

The *anterior spinocerebellar tract* ascends in the brainstem to rostral pontine levels and enters the cerebellum in association with the superior cerebellar peduncle (Figs. 11.9 and 13.24). Fibers initially located dorsolateral to the superior cerebellar peduncle arch medially over this largely efferent bundle to enter the cerebellum. These fibers pass to essentially the same cortical areas as those of the posterior spinocerebellar tract. However, the main area of termination is in the anterior lobe with only a few fibers reaching the pyramis and paramedian lobule (112). The majority of the fibers of this tract terminate in the cerebellum contralaterally with respect to the tract in the spinal cord (and ipsilateral to the cells of origin); about 15% of the fibers terminate bilaterally (112, 170, 205, 237). The ante-

rior spinocerebellar tract conveys impulses from group Ib and flexor reflex afferent fibers from the hindlimb and lower trunk.

Cuneocerebellar fibers arise from the accessory cuneate nucleus in the lower medulla, enter the inferior cerebellar peduncle (292), and pass to the posterior part of the anterior lobe (lobule V; Fig. 15.1), the anterior folia of the simple lobule, the paramedian lobule, and the depths of the prepyramidal fissure in the posterior vermis (113, 226, 247). Fibers of this afferent system are ipsilateral. The accessory cuneate nucleus is regarded as the medullary equivalent of the dorsal nucleus of Clarke, and the cuneocerebellar tract is regarded as the forelimb equivalent of the posterior spinocerebellar tract. This tract conveys impulses from group Ia and Ib muscle afferents and exteroceptive impulses from cutaneous afferents (Fig. 11.9). Receptive fields for cutaneous impulses are smaller than those associated with the posterior spinocerebellar tract (205).

The *rostral spinocerebellar tract*, identified in the cat (204, 205), is the forelimb functional equivalent of the anterior spinocerebellar tract, but is uncrossed. This tract arises from cells rostral to the dorsal nucleus of Clarke, ascends in the anterior part of the spinal cord and enters the cerebellum via both the inferior and superior cerebellar peduncles. Fibers of this tract are distributed almost exclusively to the anterior lobe of the cerebellum in lobules I to V (Fig. 15.1). Fiber terminations are predominantly ipsilateral (205, 206). This tract is activated monosynaptically by group Ib muscle afferents and polysynaptically by flexor reflex afferents.

OLIVOCEREBELLAR FIBERS

These fibers form the largest component of the inferior cerebellar peduncle. They arise from the contralateral inferior olivary nucleus and are distributed to all parts of the cerebellar cortex in an orderly pattern (Figs. 15.21 and 15.27**A**). In humans, fibers from the medial portion of the principal olive and the accessory olives go to all portions of the vermis. A much larger component from the lateral portion of the principal olivary nucleus is distributed to the cerebellar hemisphere. The dorsal part of the olive projects to the superior surface of the cerebellum, while the ventral part projects to its inferior surface (127). The intracerebellar nuclei, as well as all parts of the cortex, receive olivary fibers, and the distribution is localized exquisitely, each portion of the olive projecting to a specific cerebellar area (231).

Anterograde and retrograde axonal transport techniques have demonstrated that the olivocerebellar projection is more complex than revealed by degeneration studies (29). These investigations indicate that cerebellar lobules receive afferents from more than one region of the inferior olivary complex (31, 42, 44, 278). It has further been shown that olivocerebellar fibers terminate in a pattern of thin sagittal strips that alternate with unlabeled strips which are supplied by fibers from another region of the inferior olive (73, 78). Each of these parasagittal zones of terminations appears to originate from small, well-defined, rostrocaudally oriented cell columns in the inferior olivary nucleus (14). The inferior olive also sends fibers to the cerebellar nuclei that are crossed and believed to be collaterals of fibers projecting to the cortex (31, 74).

The inferior olivary nucleus, a highly developed complex in humans (Fig. 15.18), is the major source of climbing fibers that have potent excitatory synapses on Purkinje cell dendrites (73, 78, 90, 91, 117, 251). The principal olivary nucleus receives descending fibers from the central tegmental tract, a composite bundle originating from multiple brainstem nuclei. Descending fibers in this tract passing to the principal part of the inferior olivary nucleus arise from the red nucleus, the central gray substance, and the midbrain tegmentum. Fibers from the sensorimotor cortex pass to the ventral lamella of the principal olive via the crus cerebri and the pyramid (274).

The most important afferents to the inferior olivary complex arise from the spinal cord. Spino-olivary fibers project to specific parts of the medial and dorsal accessory olivary nuclei, and spinal pathways belonging to the olivary system have been identified physiologically by their climbing fiber responses in the anterior lobe of the cerebellum (194). Fibers arising in the spinal cord and ascending in the anterior funiculus form the anterior spino-olivary tract that terminates upon cells of the medial and dorsal accessory olivary nuclei (25). Fibers ascending in the posterior columns synapse upon the posterior column nuclei and project contralaterally to the same olivary nuclei (88, 147), and form a dorsal (funicular) spino-olivary pathway.

Additional spino-olivocerebellar pathways have been described, all of which project to

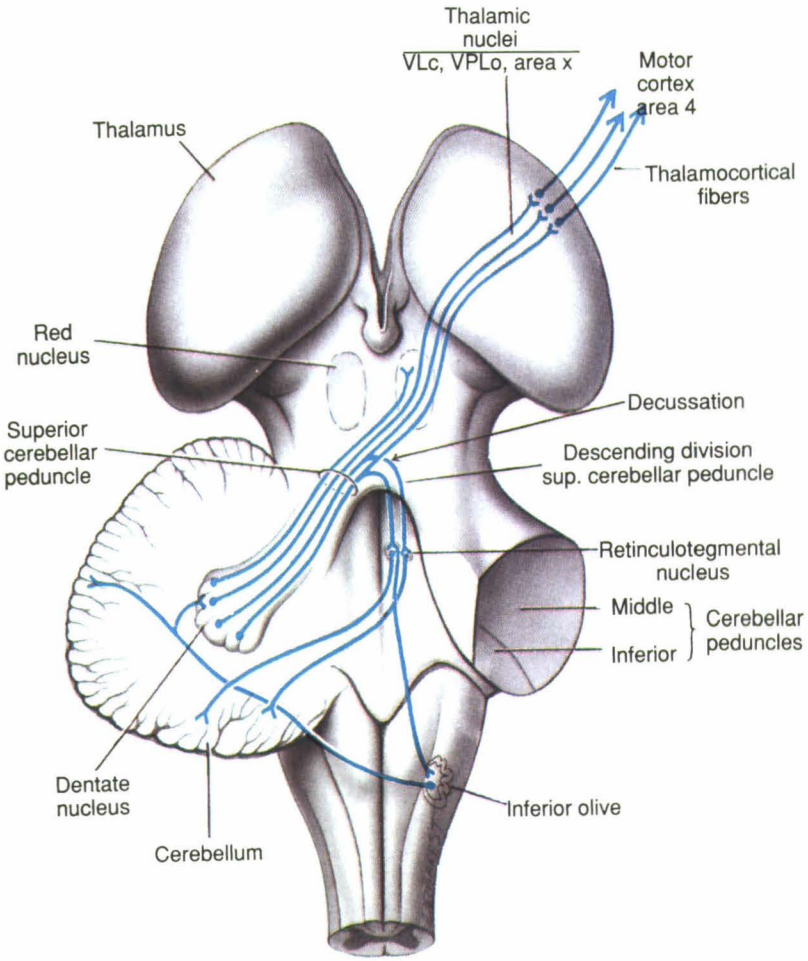


Figure 15.21. Efferent fibers from the dentate nucleus. These fibers emerge as the major constituent of the superior cerebellar peduncle (*blue*) and decussates completely in the caudal portion of the midbrain. Ascending fibers project to rostral parts of the contralateral red nucleus and to the cell sparse zone of the thalamus (i.e., ventral lateral nucleus, pars caudalis (VLc), the ventral posterolateral nucleus, pars oralis (VPLo), and the so-called area X). Fibers from the dentate nucleus terminate somatotopically in these thalamic nuclei, which in turn project upon the primary motor cortex (area 4). Fibers forming the descending division of the superior cerebellar nucleus project to reticular nuclei and the inferior olivary nucleus (*blue*), which project back to the cerebellar cortex of the opposite hemisphere.

parasagittal zones in the anterior lobe. These parasagittal projection zones display a somatotopic pattern in lobules IV and V of the vermis (208). Spino-olivocerebellar pathways resemble the spinocerebellar tracts (43). Responses in these systems are evoked by stimuli activating group II and III muscle afferents, cutaneous afferents, and high threshold joint afferents with wide receptive fields. These impulses, referred to as *flexor reflex afferents*, also have actions upon segmental reflexes and are transmitted by several other ascending tracts. There is difficulty in interpreting the information transmitted by these pathways because it lacks modality specificity and permits only crude spatial discrimination. Certain evidence suggests that olivary neurons may convey specific information related to interneuronal activities at spinal and brainstem levels (194). The spino-olivary systems may be activated by either flexor reflex afferents or by the corticospinal tract through a common set of interneurons, which are assumed to influence motor neurons and to be part of the segmental reflex arc. Thus, the spino-olivocerebellar system may monitor the activity of interneurons at spinal levels and transmit such signals to the cerebellum.

The inferior olivary nucleus also receives afferent fibers from the contralateral cerebellar nuclei which are topographically orga-

nized (263). The dentate nucleus projects to the principal olivary nucleus and the interposed nuclei project to the medial and dorsal accessory olivary nuclei. Projections from the cerebellar nuclei to the inferior olive appear reciprocal to olivonuclear fibers, except that no fibers from the fastigial nucleus terminate in the inferior olive. These observations suggest that the activities of the inferior olivary nucleus may be modulated by feedback from the cerebellar nuclei.

RETICULOCEREBELLAR FIBERS

Three nuclei of the reticular formation project fibers to the cerebellum and can be regarded as precerebellar nuclei: (a) the reticulotegmental nucleus, (b) the lateral reticular nucleus of the medulla, and (c) the paramedian reticular nucleus (296).

The *reticulotegmental nucleus* (Figs. 13.28 and 13.33) receives afferents from the cerebral cortex and the cerebellar nuclei (39, 59, 163, 229). Projections from the frontal and parietal cortex are bilateral, but mainly ipsilateral, and end in ventral parts of the nucleus (33). A larger and more important group of afferent fibers arises from the dentate and anterior interposed nuclei, enter the superior cerebellar peduncle, cross in its decussation, and descend as the crossed descending limb of the superior cerebellar peduncle (37). Cerebellar projections from this nucleus pass via the middle cerebellar peduncle to vermal regions, particularly lobules VI and VII, and to the flocculus, but all parts of the cortex receive some fibers (123). Projections of the reticulotegmental nucleus are bilateral and end as mossy fibers in the granular layer. This nucleus participates in a cerebellar-reticular feedback system, but its efferent fibers do not project back to the cerebellar nuclei that supply it.

The *lateral reticular nucleus* of the medulla (Figs. 12.8 and 12.13), consisting of three cytologically distinct subdivisions, receives inputs from a variety of sources including the spinal cord (30, 161), the cerebral cortex (50), the red nucleus (275), and the fastigial nucleus (279). Spinal afferents contained in the anterolateral funiculus terminate in a specific manner upon the small-celled part of the nucleus and appear to transmit exteroceptive impulses somatotopically (71).

Cerebellar projections of the lateral reticular nucleus arise from cells in all subdivisions, and enter the cerebellum via the inferior cerebellar peduncle. Degeneration and autoradiographic studies indicate that projections of the lateral reticular nucleus terminate as mossy fibers in the anterior lobe, in both vermal and intermediate parts, in the paramedian lobule, and in lobule VII of the vermis (162, 186). The projection is bilateral with ipsilateral predominance. Although there is a topographic projection from the nucleus to the anterior lobe and the paramedian lobule, the entire cerebellar cortex appears to receive some fibers (48, 81, 110).

The *paramedian reticular nuclei* of the medulla (Fig. 12.13) receives afferent fibers from the spinal cord (34), the fastigial nucleus (18), the cerebral cortex (34, 249), and the vestibular nuclei (164). Projections from these nuclei are mostly uncrossed, terminate principally in the vermis of the anterior lobe and in the pyramis and uvula (40, 244), and, less abundantly, in the fastigial nucleus (230). The dorsal paramedian reticular nucleus appears to be connected with a somewhat wider region of the cerebellar cortex than other nuclei of this group. These nuclei, like others in the reticular formation projecting to the cerebellum, are involved in feedback systems.

PONTOCEREBELLAR PROJECTIONS

The pontine nuclei represent the largest collection of precerebellar nuclei and constitute the most important relay in the conduction of impulses from the cerebral cortex to the cerebellum (195). Corticopontine fibers arise from all of the four major lobes of the cerebrum, descend in the internal capsule and crus cerebri, and terminate on the ipsilateral pontine nuclei. The most massive cortical projections arise from the sensorimotor cortex and project in a somatotopical fashion onto longitudinally oriented cell columns within the pontine nuclei (32, 45). Each part of the cerebral cortex projects to several well-defined areas within the pontine nuclei (46, 47, 49). Fibers from the temporal cortex terminate in the caudal pons and those from the frontal cortex end in the rostral pons. Although projections from the motor and somatosensory cortical areas are somatotopically organized, they are separated from each other.

All cells of the pontine nuclei project their axons to the cerebellum via the middle cerebellar peduncle and most, but not all, of these

fibers are crossed. Fibers projecting to the cerebellar hemisphere are mainly crossed, while projections to the vermis are bilateral (32). The nodulus appears to be the only part of the cerebellum that does not receive a pontine projection. Most of the pontocerebellar fibers terminate as mossy fibers (192, 238). The pontocerebellar projection are precisely organized and most cerebellar lobules receive afferents from two or more different sites within the pontine nuclei (35, 42, 122). This pattern of termination suggests that impulses from different regions of the pontine nuclei that receive inputs from various cortical areas converge onto a particular cerebellar lobule (28).

The pontine nuclei also receive afferents from the superior and inferior colliculi (5, 150, 196) and from the cerebellar nuclei (18, 273). The dorsolateral pontine nuclei, which receive fibers from the tectum, project to regions of the cerebellum where visual and auditory impulses have been recorded.

OTHER PRECEREBELLAR AFFERENTS

A number of other brainstem nuclei project smaller numbers of fibers to the cerebellar cortex. These precerebellar nuclei include the perihypoglossal nuclei, the trigeminal sensory nuclei, the nucleus of the solitary tract, the locus coeruleus and the raphe nuclei.

The *perihypoglossal nuclei* (Fig. 12.13) project to the vermis and fastigial nucleus (264), the flocculus, paraflocculus, and nodulus (4, 157), as well as the fastigial nucleus and the anterior interposed nucleus (178, 230). The nucleus prepositus, the largest of the perihypoglossal nuclei, also gives rise to ascending fibers that terminate in the oculomotor nuclei.

Trigeminocerebellar fibers, both primary and secondary, derive from different subdivisions of the trigeminal nuclear complex. Although primary trigeminocerebellar fibers have been observed in nonmammalian vertebrates (121, 166, 167, 288), their areas of termination in the cerebellum have not been established. Trigeminocerebellar fibers from the mesencephalic nucleus of N. V, studied in human fetal material (214, 215), enter the cerebellum in association with the superior cerebellar peduncle and are distributed to the dentate and the emboliform nuclei. These fibers are believed to conduct impulses from stretch receptors in the muscles of mastication and possibly also from the facial muscles. Secondary trigeminocerebellar fibers from the principal sensory and spinal trigeminal nuclei (168, 288, 298) enter the cerebellum via the inferior cerebellar peduncle and terminate in the upper culmen and declive (170, 242, 285, 298).

Studies based upon retrograde transport techniques indicate trigeminocerebellar fibers arising from the spinal and principal trigeminal nuclei are exclusively ipsilateral and project mainly to the simple lobule and the dorsal part of the paramedian lobule (129, 131, 243). Most of the efferent fibers originate from the nuclei interpolaris and oralis of the spinal trigeminal complex and terminate as mossy fibers in the form of typical parasagittal bands (131). According to some studies the motor trigeminal nucleus projects some fibers to the dentate nucleus (94, 158). A small number of the cells in the nucleus of the solitary tract and a number of motor cranial nerve nuclei also project to the cerebellum (158, 232, 243, 246).

Projections from the raphe nuclei, which contain serotoninergic neurons, have been traced to all parts of the cerebellar cortex, except lobule VI, by retrograde transport techniques (252). The most profuse projections are to vermal lobules VII and X and to crus I and II (110). According to Chan-Palay (66), axons of serotoninergic neurons (a) terminate as mossy fiber rosettes, and (b) traverse the molecular layer like parallel fibers, but terminate on cortical interneurons, rather than on Purkinje cells.

Projections from the locus coeruleus, convey noradrenergic input to the cerebellum via the middle and superior cerebellar peduncles (180, 218). In the cerebellar cortex, noradrenergic fibers terminate massively around Purkinje cell somata (70). The extent of the distribution of these fibers in the cerebellum is unclear. According to Somana and Walberg (245), most fibers project to the cerebellar vermis, although a few project to the fastigial nucleus.

Efferent Fibers

Cerebellar efferent fibers arise from all of the cerebellar nuclei and from specific regions of the cerebellar cortex. Direct projections from the cortex of the vermis and from vestibulocerebellum (regions of the cerebellar cortex receiving vestibular inputs) pass to the

ipsilateral vestibular nuclear complex and collectively constitute the cerebellovestibular projection (271). The largest and most widely distributed cerebellar efferent fibers arise from the cerebellar nuclei and are organized into two major systems contained in three separate bundles. The major efferent systems are the superior cerebellar peduncle and the fastigial efferent projection.

SUPERIOR CEREBELLAR PEDUNCLE

This is the largest cerebellar efferent bundle. It is formed by fibers from the dentate, emboliform, and globose nuclei (Figs. 2.26, 13.26, 13.32, and 15.21). These fibers emerge from the hilus of the dentate nucleus and pass rostrally into the upper pons where they form a compact bundle along the dorsolateral wall of the fourth ventricle (Figs. 2.25 and 2.26). At isthmus levels, fibers of the superior cerebellar peduncle sweep ventromedially into the tegmentum and all fibers decussate at levels through the inferior colliculus (Figs. 13.32 and 14.2). Most of these crossed fibers ascend to enter and surround the contralateral red nucleus. A relatively small part of the fibers from the dentate nucleus terminate in the rostral third of the red nucleus (9, 72). The bulk of these fibers project to the thalamus and end in parts of the ventral lateral (VL) and ventral posterolateral thalamic (VPL) nuclei (Fig. 15.21) (53, 66, 132, 146, 190, 193, 216, 225). Fibers from the dentate nucleus terminate somatotopically in the ventral posterolateral pars oralis (VPLo) and the ventral lateral pars caudalis (VLc) thalamic nuclei. Although somatotopic features of the cerebellar nuclei are not compelling, the pattern of termination of these fibers in thalamic nuclear subdivisions appears similar to that of the somatosensory relay nuclei. In this arrangement, the head is represented medially and caudal parts of the body are lateral; the extremities lie ventrally and the back lies dorsally (15, 16, 256). A small number of fibers from the dentate nucleus project to the rostral intralaminar thalamic nucleus, mainly the central lateral (Cl) nucleus (15, 16, 191, 224, 256). Furthermore, recent axonal transport studies indicate that the cerebellar nuclei also project to ventrolateral parts of the mediodorsal thalamic nucleus, where they terminate upon thalamic neurons projecting to the prefrontal cortex (293). These findings suggest that neurons in ventrolateral parts of the mediodorsal nucleus serve as relays in a cerebelloprefrontal connection. Other studies with retrograde double-labeling methods in the rat revealed that single neurons in the cerebellar nuclei provide axon collaterals to thalamic, brainstem, and spinal cord levels (21).

The ventral lateral (VLc) and the ventral posterolateral (VPLo) nuclei of the thalamus project in a topical fashion on the primary motor cortex (203, 280–282). Thus, impulses from the dentate nucleus are conveyed via contralateral thalamic nuclei to the motor cortex (203, 267). In this manner, signals from the dentate nucleus can influence activity of motor neurons in the cerebral cortex. Impulses from the motor cortex are transmitted to spinal levels via the corticospinal tract. This system, concerned primarily with the coordination of somatic motor function, also provides the explanation for occurrence of ipsilateral asynergic disturbances with unilateral cerebellar lesions.

A relatively small number of cerebellar efferent fibers from the ventrocaudal dentate nucleus decussate in the caudal mesencephalon, pass dorsally, and are distributed differentially within the lateral somatic cell columns of the contralateral oculomotor nuclear complex (61, 66, 183, 193). Most of these fibers terminate about cells that innervate the superior rectus muscle on the opposite side (Fig. 14.14). The part of the dentate nucleus from which these fibers arise receives primary vestibular fibers (36, 60). Thus, this dentato-oculomotor projection may constitute a link in a vestibulo-oculomotor pathway (116).

Another small group of fibers in the superior cerebellar peduncle decussate with the main bundle and descend in the ventromedial tegmentum of the brain stem near the median raphe. These fibers, constituting the descending division of the superior cerebellar peduncle, project to the reticulotegmental, the paramedian reticular nuclei, and portions of the inferior olivary nucleus (39, 59, 183, 263). Because these nuclei are known to project to the cerebellum, this component of the superior cerebellar peduncle is a part of both a cerebelloreticular and a cerebello-olivary feedback system (Fig. 15.21).

Fibers from the interposed nuclei (i.e., the emboliform and globose nuclei) project primarily to cells in the caudal two-thirds of the red nucleus. A smaller number of fibers pass beyond the red nucleus to the same thalamic

nuclei as fibers from the dentate nucleus. Fibers from the interposed nuclei end in an interdigitate fashion in VPLo and VLc, but do not overlap those from the dentate nucleus. Fibers from the interposed nuclei project somatotopically on cells of the red nucleus, and rostral parts of the interposed nucleus project to hindlimb regions of the red nucleus (ventral and ventrolateral areas), while caudal parts of the nucleus project to forelimb regions of the red nucleus (dorsal and dorsomedial areas; Fig. 15.22) (72, 184, 221). These fibers form part of a somatotopic linkage extending from the paravermal cortex to the spinal levels. In this pathway, fibers from the paravermal cortex pass to the interposed nuclei. Fibers from the interposed nuclei project via the superior cerebellar peduncle to the opposite red nucleus. Somatotopically organized rubrospinal fibers cross in the midbrain and descend to spinal levels. This small system involved two decussations, that of the superior cerebellar peduncle and that of the rubrospinal tract (Fig. 15.22). Thus, impulses conveyed from the paravermal cortex to the spinal cord end on the same side. This system appears to be primarily concerned with mechanisms that facilitate ipsilateral flexor muscle tone.

A number of studies indicate that axons from cells of the interposed nuclei also project to the VLc nucleus of the thalamus after giving off collaterals to the red nucleus (8, 13, 89, 261).

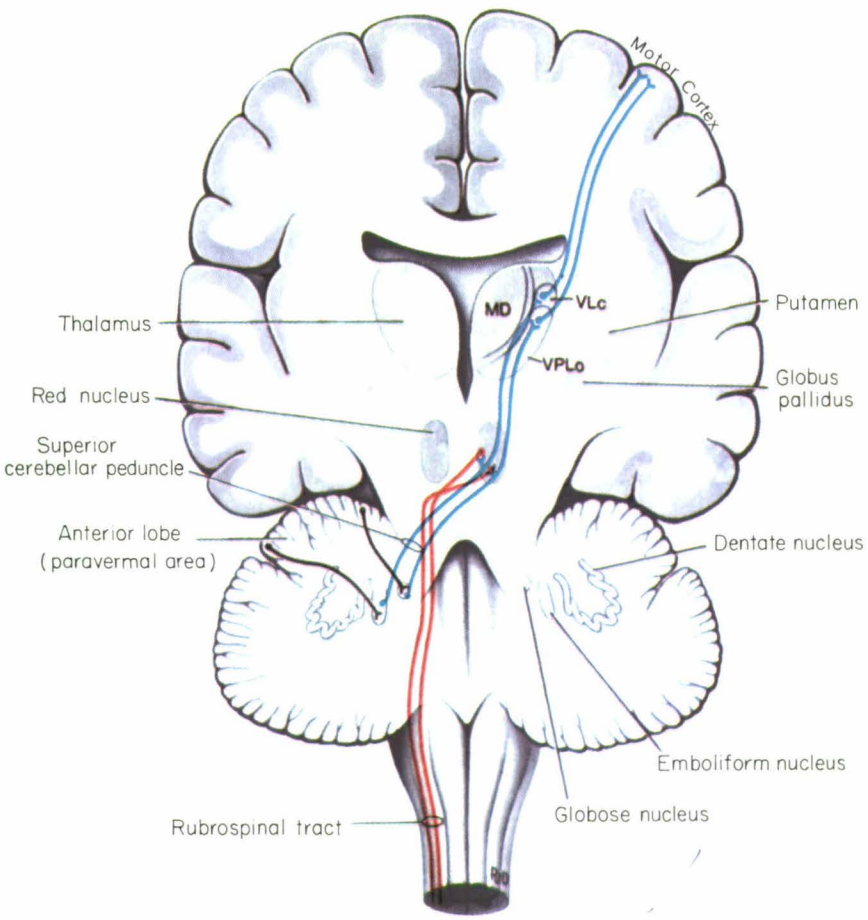


Figure 15.22. Projections from the interposed nuclei of the cerebellum (i.e., emboliform and globose nuclei) via the superior cerebellar peduncle (*blue*). The interposed nuclei receive afferents from the paravermal cortex (*black*) and project somatotopically (*blue*) upon cells in caudal portions of the contralateral red nucleus. Cells in caudal portions of the red nucleus give rise to the crossed rubrospinal tract (*red*), which influence flexor motor tone. Thalamic projections from the interposed nuclei (*blue*) terminate in the cell sparse zone of the thalamus (VLc, VPLo, and area X) contralaterally. Thalamic terminations interdigitate with those of the dentate nucleus without overlap. Thalamic neurons receiving input from the interposed nuclei project to the primary motor cortex (*blue*).

FASTIGIAL EFFERENT PROJECTIONS

Efferent projections of the fastigial nucleus are unique in that (a) they do not emerge via the superior cerebellar peduncle, (b) a large part of the efferent fibers cross within the cerebellum, and (c) they project to nuclei at all levels of the brainstem (57). Crossed fibers from the fastigial nucleus emerge from the cerebellum via the *uncinate fasciculus (Russell)*, which arches around the superior cerebellar peduncle (Figs. 15.23 and 15.24). Uncrossed fastigial efferent fibers project to the brainstem in the *juxtarestiform body* (Figs. 13.7 and 15.24). Crossed efferent fibers contained in the uncinate fasciculus arise from cells in all parts of the fastigial nucleus and outnumber uncrossed efferents in the juxtarestiform body. The largest number of fastigial efferent fibers project to structures in the lower brainstem. Fastigial projections to the vestibular nuclei are bilateral, symmetric, and terminate in ventral parts of the lateral and inferior vestibular nucleus (18). Fastigioreticular fibers arise predominantly from rostral parts of the nucleus, are mainly crossed, and project to (a) medial regions of the nucleus reticularis gigantocellularis, (b) parts of the caudal pontine reticular formation, (c) the dorsal paramedian reticular nucleus, and (d) portions of the lateral reticular nucleus (57). Crossed fastigiopontine fibers separate from the uncinate fasciculus and pass ventrally to terminate in the dorsolateral pontine nuclei.

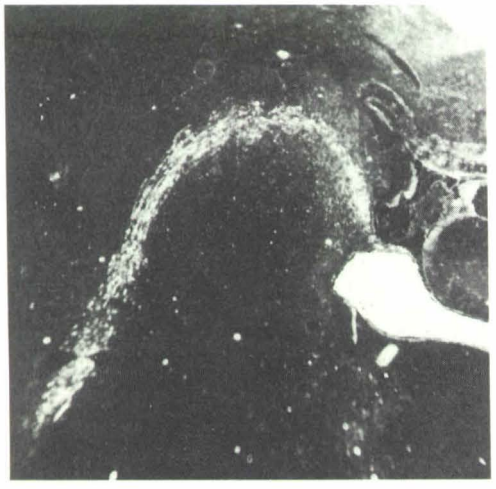


Figure 15.23. Darkfield photomicrograph of (^{3}H)-labeled amino acids transported by fibers of the uncinate fasciculus as seen in an autoradiograph.

A small number of crossed fastigiospinal fibers descend into the upper cervical spinal cord where they contact anterior horn cells (102, 185). Physiologic evidence based upon antidromic stimulation of the upper cervical spinal cord and direct stimulation of the fastigial nucleus indicate that axons of fastigial neurons make monosynaptic contacts with motoneurons at the C2-C3 level (286, 287).

Small numbers of fastigial fibers ascending in the dorsolateral region of the brainstem provide collaterals to the superior colliculus and the nuclei of the posterior commissure (7, 10) and terminate bilaterally in the cell sparse zone of the thalamus (VLc and VPLo) (10, 18, 58, 153, 257). These terminations do not overlap those of the dentate and interposed nuclei. In the superior colliculus, fastigial fibers terminate principally within the intermediate gray layer, which contains neurons giving rise to the tectospinal pathway (189). The cerebellocollicular fibers, together with other cerebellar efferent fibers terminating in various brainstem regions containing premotor, saccade-related neurons, indicate that cerebellar output is involved in saccade-programming neural circuits (189, 200).

CEREBELLOVESTIBULAR PROJECTIONS

Certain regions of the cerebellar cortex project to the vestibular nuclei. These projections are composed of axons of Purkinje cells and arise from the cerebellar vermis and the vestibulocerebellum (i.e., the flocculonodular lobule). Thus, the vestibular nuclei receive cerebellar afferents bilaterally from the fastigial nucleus and ipsilaterally from specific cortical regions. Direct projections from the cerebellar vermis terminate in dorsal regions of the ipsilateral lateral and inferior vestibular nuclei, are somatotopically organized (115, 276, 277), and have GABA as neurotransmitter. Efferent fibers from the anterior lobe establish synaptic contacts of the symmetric type on somata and dendrites of cells of all sizes in the lateral vestibular nucleus (199). Stimulation of the anterior lobe of the cerebellum produces a monosynaptic inhibition of neurons of the lateral vestibular nucleus (134, 138).

The regions of the cerebellum that receive primary and secondary vestibular fibers constitute the "vestibulocerebellum." This designation includes ventral parts of the uvula in addition to the flocculonodular lobule. All

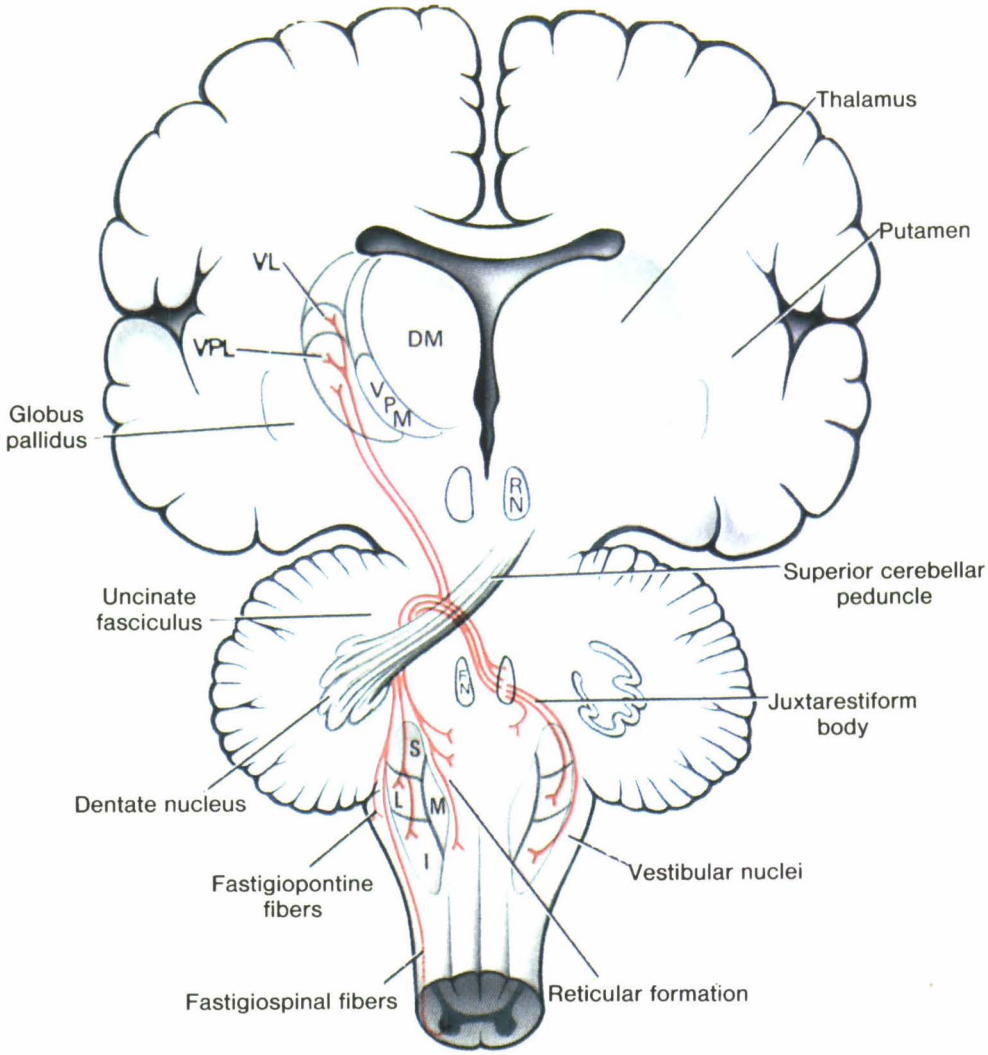


Figure 15.24. Fastigial efferent projections. Crossed fastigial efferent fibers contained in the uncinate fasciculus arise from cells in all parts of the fastigial nucleus (*FN*) and outnumber uncrossed efferent fibers that emerge in the juxtarestiform body. Fastigiovestibular fibers project bilaterally and symmetrically upon ventral portions of the lateral (*L*) and inferior (*I*) vestibular nuclei. Fastigioreticular fibers arise predominantly from rostral parts of the fastigial nucleus. Crossed fastigiopontine fibers separate from the uncinate fasciculus and pass to the dorsolateral pontine nuclei. Crossed fastigiospinal fibers pass to upper cervical spinal segments and exert excitatory effects upon motoneurons. Ascending fastigial projections arise from caudal parts of the nucleus, are entirely crossed, and course in dorsolateral parts of the midbrain tegmentum. These fibers project to parts of the superior colliculus, the nuclei of the posterior commissure, and to the ventral posterolateral (*VPL*) and ventral lateral (*VL*) thalamic nuclei. *DM*, dorsomedial nucleus; *FN*, fastigial nucleus; *RN*, red nucleus; *VL*, *VPL*, and *VPM*, ventral lateral, ventral posterolateral, and ventral posteromedial thalamic nuclei; vestibular nuclei: *I*, inferior, *L*, lateral, *M*, medial, and *S*, superior.

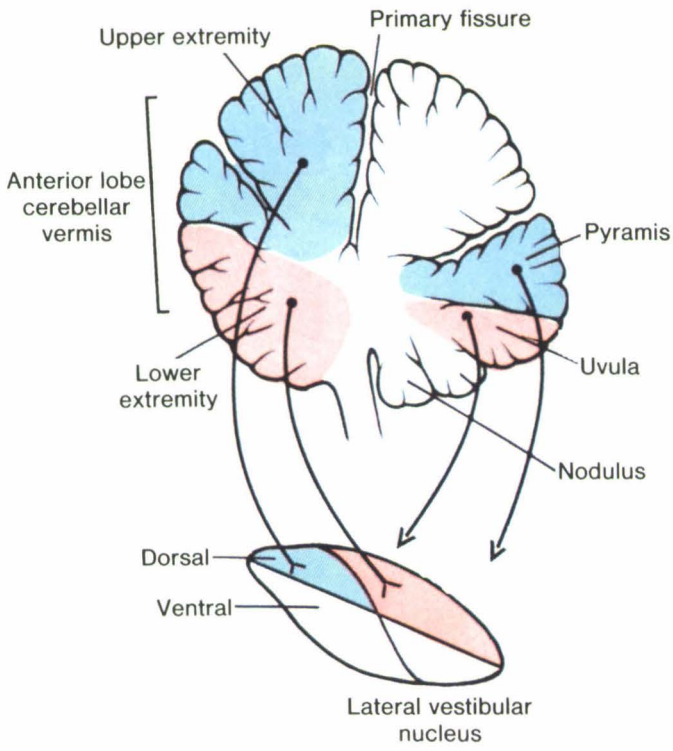


Figure 15.25. Cerebellovestibular projections from the anterior and posterior vermis. Purkinje cell axons from the anterior vermis project somatotopically upon dorsal regions of the lateral vestibular nucleus and exert inhibitory influences. Similar direct projections from the pyramis and parts of the uvula which are not somatotopically arranged are shown by *arrows*.

parts of the vestibulocerebellum project fibers to the vestibular nuclei (11). The flocculus projects to the superior and medial vestibular nuclei, while the nodulus and uvula project fibers to the superior, medial, and inferior vestibular nuclei. All of these cerebellovestibular projections are ipsilateral (Fig. 15.25).

By its action on the vestibular nuclei, the vestibulocerebellum plays a critical role in equilibrium and in the control of axial muscles that are used to maintain balance. Additionally, the vestibulocerebellum functions to control eye movement and to coordinate movements of the head with those of the eye (104).

FUNCTIONAL ORGANIZATION

On the basis of cortical projections to the cerebellar nuclei and projections from the nuclei to the cerebellar cortex, the cerebellum has been divided into three sagittal zones of cortex and their connecting nuclei (22, 77, 80, 85, 109, 111, 115, 143, 144, 156, 258–260, 270, 272, an 273). This zonation provides an elementary view of the functional organization of the cerebellum. In this simplified scheme, the cerebellar efferent systems are related to three longitudinal (sagittal) zones referred to as vermal, paravermal, and lateral (Fig. 15.28).

The *vermal zone* is the midline, unpaired portion of the cerebellum related to fastigial nuclei, and is concerned primarily with mechanisms that modify extensor muscle tone. Direct projections from the anterior and posterior vermis exert inhibitory influences upon the vestibular nuclei which could result in a reduction of extensor muscle tone. The projections of the fastigial nucleus which receive strictly ipsilateral afferents from the vermis (77) are bilateral, although crossed fibers are more numerous (57). These excitatory fibers terminate in the vestibular nuclei and in broad regions of the reticular formation of the pons and medulla. A small number of crossed fastigiospinal fibers descend directly to the upper cervical spinal cord and have excitatory influences upon motoneurons

(286). Ascending fastigial efferents projecting to thalamic nuclei bilaterally contribute to coordinated somatic motor activity. The vermal zone of the cerebellum is particularly concerned with control of posture, muscle tone, locomotion, and equilibrium for the entire body (64, 65).

The *paravermal zone* relates the paravermal cortex with the emboliform and globose nuclei, which have connections predominantly with the contralateral red nucleus. The interposed nuclei project somatotopically on the caudal two-thirds of the red nucleus (8, 72, 95). This somatotopically organized system is concerned with mechanisms that can facilitate ipsilateral flexor muscle tone via the rubrospinal tract (Fig. 15.22). Additionally, the interposed nuclei have modest projections to the contralateral thalamic nuclei.

The *lateral zone* relates the cortex of the cerebellar hemisphere with the dentate nucleus which has the most extensive thalamic projections (Fig. 15.21). These efferent fibers project somatotopically on the cell sparse zone of the thalamus (VLc and VPLo). This is the largest cerebellar efferent system and it appears to be concerned with the coordination of ipsilateral somatic motor activity. Neurons in the cell sparse zone of the thalamus project somatotopically upon the primary motor cortex where they can modify the activity of neurons projecting to spinal and pontine levels.

Some relay nuclei at all brainstem levels, receiving part of the cerebellar output, project fibers back to the cerebellum. The motor cortex, in turn, gives rise to frontopontine fibers, which convey impulses back to the contralateral cerebellar hemisphere via the pontine nuclei and the middle cerebellar peduncle (Fig. 15.26). Other areas of the cerebral cortex also influence the activity of the cerebellum via corticopontine and pontocerebellar pathways. The central tegmental tract conveys impulses from the red nucleus and the midbrain tegmentum which reach the contralateral cerebellar hemisphere by way of parts of the inferior olivary nuclear complex. Certain fibers of the superior cerebellar peduncle that descend in the brainstem terminate upon reticular and olivary nuclei, which project fibers back to the cerebellum (Fig. 15.21). Efferent fibers from the red nucleus also project directly to the interposed nucleus (75). All these feedback pathways help the cerebellum to play its role as a comparator, that is, a neural device that compensates for errors in motor behavior by comparing intention with performance (104).

Some of the neocerebellar connections in humans are especially evident in Figure 15.27, which shows sections through the medulla, pons, and isthmus from an individual in whom the left cerebellar hemisphere failed to develop (250). There was also a correlated agenesis of all the afferent and efferent pathways to and from the left cerebellar hemisphere. The left dentate nucleus was represented by a minute structure, the right inferior olive was greatly reduced, and the right red nucleus (not shown) and pontine nuclei were practically absent. All of the cerebellar peduncles on the left were greatly reduced in size. These preparations emphasize that in humans the middle cerebellar peduncle and the olivocerebellar fibers are practically all crossed.

CLINICAL CONSIDERATIONS

The cerebellum is concerned with the coordination of somatic motor activity, the regulation of muscle tone, and mechanisms that influence and maintain equilibrium. Afferent cerebellar pathways convey impulses from a variety of different receptors including the organs of special sense. Among these afferent systems, the input from stretch receptors (i.e., muscle spindle and Golgi tendon organ) is especially prominent. These impulses are conveyed by the spinocerebellar and cuneocerebellar tracts. The principal function of stretch receptors appears to be the unconscious neural control of muscle tone. The cerebellum, which receives a major afferent input from the stretch receptors, is an integral part of the neural mechanism that (a) effects gradual alterations of muscle tone for proper maintenance of equilibrium and posture, and (b) assures the smooth and orderly sequence of muscular contractions that characterize skilled voluntary movement (205).

Each movement requires the coordinated action (synergy) of a group of muscles. The *agonist* is the muscle that provides the actual movement of the part, while the *antagonist* is the opposing muscle which must relax to permit movement. Other muscles must fix, or stabilize, certain joints in order to produce the desired movement. Such synergistic motor activity requires not only complex reciprocal innervation but coordinated control of

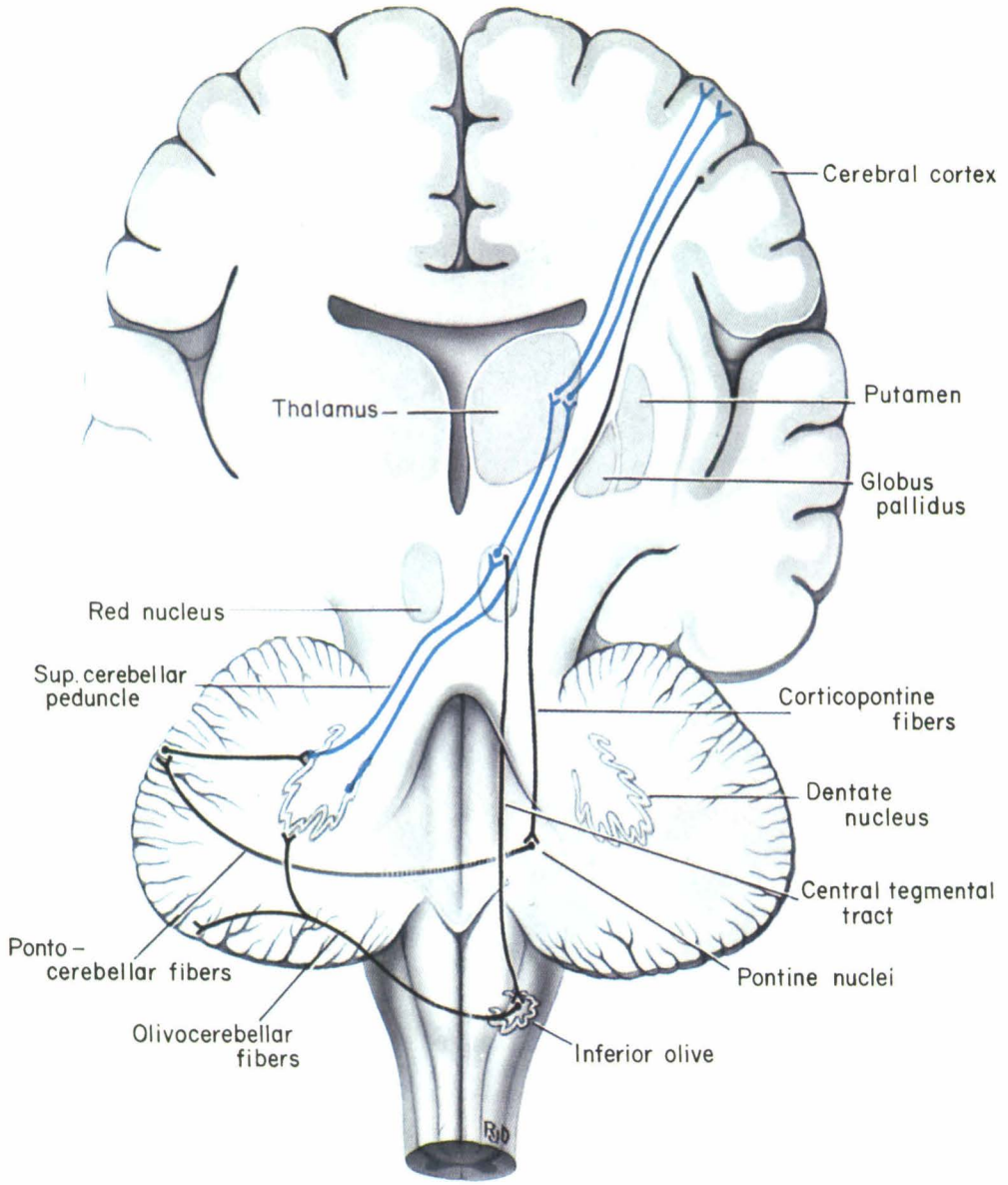


Figure 15.26. Principal afferent and efferent cerebellar connections. Cerebellar efferent fibers from the dentate nucleus are shown in *blue*. Corticopontine and pontocerebellar fibers (*black*) represent the most massive cerebellar afferent system. The principle inferior olivary nucleus receives uncrossed descending fibers from the red nucleus and periaqueductal gray via the central tegmental tract. Cortico-olivary fibers (not shown) to the principal inferior olivary nucleus pass via the medullary pyramids. Olivocerebellar fibers (*black*) cross, enter the restiform body (largest component of the superior cerebellar peduncle), and are distributed to (a) the cerebellar cortex as climbing fibers, and (b) the cerebellar nuclei, most likely as collaterals of fibers terminating in the cerebellar cortex

muscle tone and movement. The cerebellum provides this control for the somatic motor system in an efficient, automatic manner without our being aware of it.

There are certain general principles that pertain to most of the disturbances resulting from cerebellar lesions. These principles are: (a) cerebellar lesions produce ipsilateral disturbances; (b) cerebellar disturbances usually occur as a constellation of intimately related phenomena; (c) cerebellar disturbances due to nonprogressive pathologic changes show a gradual but definite attenuation with time; and (d) cerebellar disturbances resulting from cerebellar lesions probably are the physiologic expression of intact neural structures

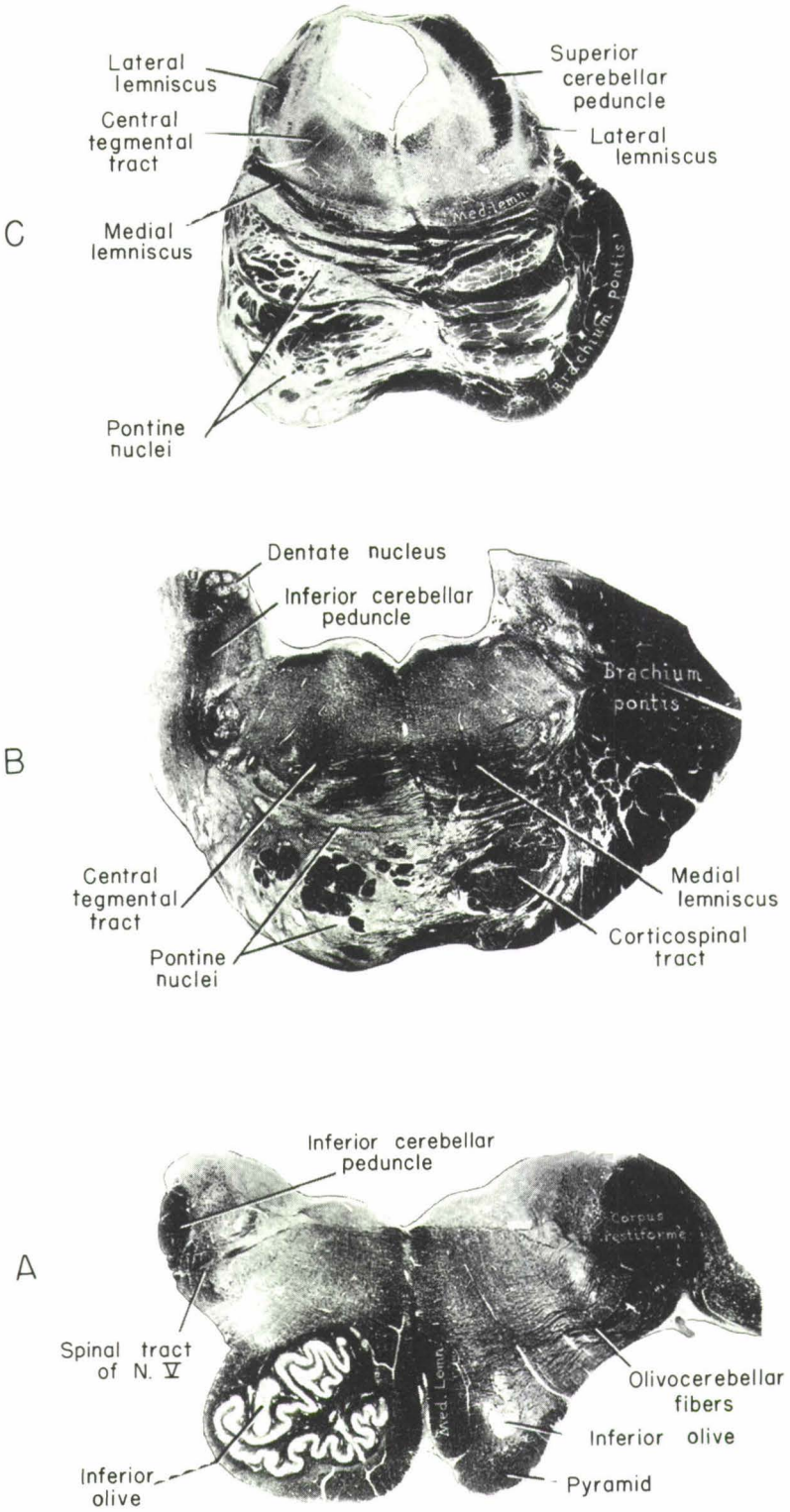


Figure 15.27. Transverse sections through (**A**) the medulla, (**B**), midpons, and (**C**) upper pons or isthmus from a case of left cerebellar agenesis. These sections clearly demonstrate the crossed nature of olivocerebellar and pontocerebellar fibers (Weigert's myelin stain)

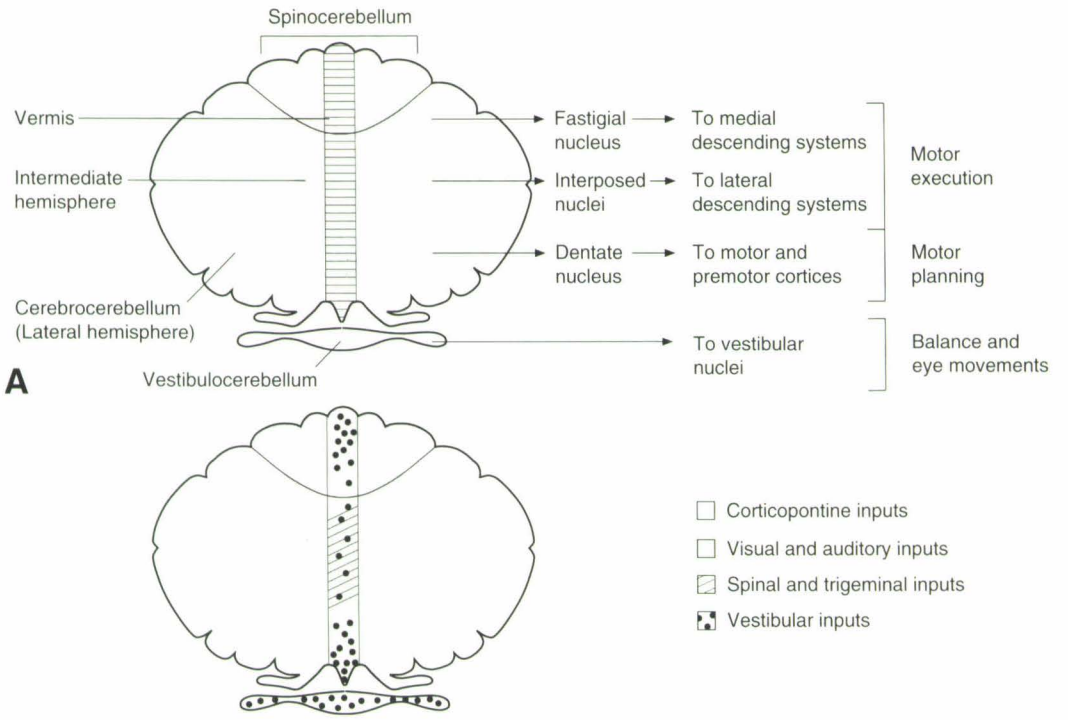


Figure 15.28. Three major functional compartments of the cerebellum with their major (**A**) output and (**B**) input systems.

deprived of the controlling and regulating influences of the cerebellum. Lesions involving the dentate nuclei or the superior cerebellar peduncle produce the most severe and enduring disturbances. The distinctive symptoms and signs that result from cerebellar disorders were comprehensively described by Gordon Holmes in 1939 (51, 105).

NEOCEREBELLAR LESIONS

Lesions involving the cerebellar hemispheres and the dentate nucleus affect primarily skilled voluntary and associated movements (i.e., movements related to the corticospinal system). The muscles become *hypotonic* (flabby) and tire easily. The deep tendon reflexes tend to be sluggish and often have a pendular quality. There are severe disturbances of coordinated movement, referred to as *asynergia*, in which the range, direction, amplitude, and force of muscle contractions are inappropriate. Cerebellar asynergia can be demonstrated by many tests. Among these are tests of precise movements to a point; distances frequently are improperly gauged *(dysmetria)* and fall short of the mark or exceed it *(pastpointing)*. Rapid successive movements, such as alternately supinating and pronating the hands and forearms, are poorly performed *(dysdiadochokinesis)*. The patient is unable to adjust to changes of muscle tension. When the forearm is flexed at the elbow and held flexed against resistance, a sudden release of resistance causes the forearm to strike the chest. This is an example of the *rebound phenomenon*. These patients also demonstrate a *decomposition of movement* in which phases of complex movements are performed as a series of successive single simple movements.

The *tremor* seen in association with neocerebellar lesions occurs primarily during voluntary and associated movements (125, 126). This tremor is referred to as *intention tremor* because it is not present at rest. It involves especially the proximal appendicular musculature, but is transmitted mechanically to distal parts of the extremities. Tremor is most evident in the upper extremities because weight-bearing masks the disturbance in the lower extremities.

Ataxia is an asynergic disturbance associated with neocerebellar lesions which result

in a bizarre distortion of voluntary and associated movements. It involves particularly the axial muscles, and groups of muscles around the shoulder and pelvic girdles. This disturbance is evident during walking and is characterized by muscle contractions which are highly irregular in force, amplitude, and direction, and which occur asynchronously in different parts of the body. Frequently, there is unsteadiness in standing, especially if the feet are close together. The gait is broad-based and the patient reels, lurches, and stumbles.

Nystagmus is commonly seen in association with cerebellar disease. It is most pronounced when the patient deviates the eyes laterally toward the side of the lesion. This disturbance consists of an oscillatory pattern in which the eyes slowly drift in one direction and then rapidly move in the opposite direction to correct the drift. Although nystagmus seen in association with cerebellar disease is considered as an expression of asynergic phenomena in the extraocular muscles, many pathologic processes which affect the cerebellum also involve the underlying brainstem and the vestibular nuclei located in the floor of the fourth ventricle.

Speech disturbances are common in association with cerebellar lesions of long-standing. Speech often is slow, monotonous, and some syllables are unnaturally separated. There is a slurring of speech and some words are uttered in an explosive manner.

ARCHICEREBELLAR LESIONS

Lesions involving portions of the posterior cerebellar vermis (i.e., nodulus and uvula), and probably portions of the flocculus, produce what has been called the *archicerebellar syndrome*. These lesions produce disturbances of locomotion and equilibrium bilaterally. The patient is unsteady in the standing position and shows considerable swaying of the body. When attempts are made to walk, there is staggering and a tendency to fall to one side or backwards. The gait is jerky, uncoordinated, and resembles that of a drunk individual. Muscle tone is not significantly altered and no tremor or asynergic disturbances are seen in the extremities. This syndrome is primarily a truncal ataxia that frequently occurs in children with tumors in the posterior cerebellar vermis. This particular syndrome is frequently a consequence of a midline cerebellar tumor (medulloblastoma) that arises from cell-rests in the inferior medullary velum at the base of the nodulus.

ANTERIOR LOBE OF THE CEREBELLUM

There is no established paleocerebellar syndrome in humans, but lesions of the anterior lobe of the cerebellum in experimental animals produce severe disturbances of posture and greatly increased extensor muscle tone. These animals exhibit many of the features seen in association with decerebration (e.g., extreme opisthotonus, tight closure of the jaw, and hyperactive deep tendon reflexes), but in time regain the ability to walk and perform voluntary movements (27, 103).

Sherrington (235), in a classic experiment, demonstrated that electrical stimulation of the anterior lobe of the cerebellum could inhibit extensor muscle tone in a decerebrate animal. This experiment, confirming the early work of Loewenthal and Horsley (174), showed that both inhibitory and facilitatory effects upon muscle tone could be obtained by stimulating the anterior lobe of the cerebellum depending on the parameters of stimulation (84). Stimulations at low repetitive rates (2–10 cycles/sec) cause a slow increase in ipsilateral extensor muscle tone, while rapid stimulation (30–300 cycles/sec) produces a relaxation of muscle tone. Inhibitory influence obtained by stimulating the anterior lobe appears to be mediated by (a) cerebellovestibular fibers of cortical origin which project to the lateral vestibular nucleus, and (b) fastigial efferent projections to the reticular formation. Facilitatory influence obtained from stimulating the anterior lobe of the cerebellum is mediated by projections from the fastigial nucleus acting on the lateral vestibular nucleus (38, 89, 136, 138).

Other cerebellar mechanisms which can influence muscle tone involve the paravermal cortex, the interposed nuclei, and the contralateral red nucleus (184). All of these structures are somatotopically interconnected. Stimulation of the rostral part of the interposed nuclei in the cat produces flexion in the ipsilateral hindlimb, while stimulation of the caudal part of these nuclei produces flexion in the ipsilateral forelimb (181, 220). These responses are ipsilateral because fibers of both the superior cerebellar peduncle and the rubrospinal tract are crossed (Fig. 15.22). Intracellular recordings in the red nucleus demonstrate that stimulation of the interposed nuclei produces excitatory postsynap-

tic potentials with a monosynaptic latency (184, 266). The pathway between the interposed nucleus and the red nucleus is regarded as purely excitatory and impulses conveyed by this system have an important facilitatory influence upon flexor muscle tone. These impulses are conveyed to spinal levels by the rubrospinal tract. Although the Purkinje cell output from the cerebellar cortex is inhibitory, variations in the activity of those cells are responsible for the inhibition, or activation, of cells in the interposed nucleus, which directly affects cells of the contralateral red nucleus.

INFORMATION PROCESSING AT CEREBELLAR LEVEL

The functional organization of the cerebellar cortex suggests that the cerebellum processes information related to the regulation and control of movement as a computer-like neural device (89, 212). The cerebellum organizes and integrates in a modular fashion the information that flows to it via numerous neural pathways. The cerebellar output participates in the control of motor function by conveying impulses to (a) brainstem nuclei (i.e., lateral vestibular and red nuclei) that project to spinal levels, and (b) thalamic nuclei which can modify the activity of cortical regions concerned with motor function.

Every part of the cerebellar cortex receives two different excitatory inputs, that of the mossy fibers and that of the climbing fibers. Although these inputs differ in their structural characteristics, they appear to convey similar "sensory" information to particular areas of the cerebellar cortex. The only output of the cerebellar cortex is conveyed by Purkinje cell axons. This output, entirely inhibitory, is exerted on the cerebellar nuclei and the lateral vestibular nucleus. The output of the cerebellar nuclei is largely excitatory, which implies that both excitatory and inhibitory impulses must reach these nuclei. Excitatory impulses passing to the cerebellar nuclei, derived from extracerebellar sources, is conveyed via collaterals of both climbing and mossy fibers (154, 173, 178).

The fact that the cerebellar cortex transforms all inputs into inhibition, suggests that there is probably no dynamic storage of information. The cerebellum processes its input information rapidly and conveys its output indirectly to specific brainstem nuclei. This type of organization allows the cerebellum to provide a rapid and clear response to any "sensory" input.

CEREBELLUM AND LEARNING

On the basis of mathematic models they independently developed to simulate the operation of cerebellar circuitry, David Marr (182) and James Albus (3) proposed that the cerebellum plays a crucial role in the learning of motor skills. They both suggested that the function of the climbing fiber input is to modify, for prolonged periods of time, the response of Purkinje cells to mossy fiber inputs (107). Electrophysiologic studies by Ito and colleagues had already led to the suggestion that the cerebellum consists of an excitatory loop circuit in which specific information is processed in the nuclei, and that this process is regulated by changing Purkinje cell inhibition (89, 134). In accordance with Ito's findings, Marr and Albus suggested that the climbing fiber input on specific Purkinje cells could alter the effectiveness of the mossy fibers.

The idea that cerebellar circuits are modified by experience and that these changes are important in motor learning is supported by the results of many experimental studies on the control of eye movement when the visual world is experimentally altered, particularly experiments dealing with the vestibulo-ocular reflex (VOR) and the optokinetic eye movement response (OKR) (151). There is also direct electrophysiologic evidence that climbing fiber activity modifies the response of Purkinje cells to mossy fiber inputs for long periods of time and this modification is responsible for learned changes in the VOR (135). Other investigators further suggested that the role of the cerebellum in motor adaptation may be the expression of a more general role in certain forms of Pavlovian conditioning (176). In the rabbit, lesions of the cerebellum both prevent the acquisition and selectively disrupt the retention of a conditioned eye blink reflex. All these findings suggest that the cerebellum has functions that go beyond its contribution to the control of movement. The role of the cerebellum in motor learning is crucial to movement because even normal motor behavior requires constant adaptation as circumstances change (104, 107, 108, 255).

Neuropsychologic experiments in humans have led to the suggestion that the cerebellum is able to contribute not only to motor

skills but also to higher cognitive functions (165, 172, 234, 283). It is suggested that the cerebellum can function at two different hierarchic levels. At a lower level, the cerebellum can supply signals to the frontal motor areas for effecting the manipulation of muscles. At a higher level, the cerebellum can supply signals to some prefrontal areas for affecting the manipulation of symbols (172). In the same manner as cerebellar programs are used in the primary motor cortex to control the execution of movement, cerebellar programs acting in different prefrontal areas (e.g., area 8 and the inferior frontal convolution) are believed to contribute to various mental and language manipulations. As is the case for its contribution to motor functions, the cerebellum could serve as an adaptive mechanism whose signals enable the frontal cortex to execute learned procedures optimally. In the absence of such cerebellar signals, the frontal cortex would have to perform these procedures less rapidly and fluently (172). Although very attractive and certainly supported by some clinical and experimental data (165, 234, 283), the issue of cerebellar involvement in higher cognitive functions is still a matter of much controversy.

References

1. Adrian ED. Afferent areas in the cerebellum connected with the limbs. Brain 1943;66:289–315.
2. Aguado F, Sánchez-Franco F, Cacidedo L, Fernández T, Rodrigo J, Martinez-Murillo R. Subcellular localization of insulin-like growth factor I (IGF-I) in Purkinje cells of the adult rat: an immunocytochemical study. Neurosci Lett 1992;135:171–174.
3. Albus JS. A theory of cerebellar function. Math Biosci 1971; 10:25–61.
4. Alley KR, Baker R, Simpson JI. Afferents to the vestibulocerebellum and the origin of the visual climbing fibers in the rabbit. Brain Res 1975;98:582–589.
5. Altman J, Carpenter MB. Fiber projections of the superior colliculus in the cat. J Comp Neurol 1961; 116:157–178.
6. Andersen BB, Korbo L, Pakkenberg B. A quantitative study of the human cerebellum with unbiased stereological techniques. J Comp Neurol 1992;326:549–560.
7. Angaut P. The fastigio-tectal projections: an anatomical experimental study. Brain Res 1969;13: 186–189.
8. Angaut P. The ascending projections of the nucleus interpositus posterior of the cat cerebellum: an experimental anatomical study using silver impregnation methods. Brain Res 1970;24:377–394.
9. Angaut P, Bowsher D. Cerebellorubral connexions in the cat. Nature 1965;208:1002–1003.
10. Angaut P, Bowsher D. Ascending projections of the medial (fastigial) nucleus: an experimental study in the cat. Brain Res 1970;24:49–68.
11. Angaut P, Brodal A. The projection of the "vestibulocerebellum" onto the vestibular nuclei in the cat. Arch Ital Biol 1967;105:441–479.
12. Angevine JB Jr, Mancall EL, Yakovlev PI. The human cerebellum. An atlas of gross topography in serial sections. Boston: Little, Brown & Company, 1961.
13. Appelberg B. Localization of focal potentials evoked in the red nucleus and ventrolateral nucleus of the thalamus by electrical stimulation of the cerebellar nuclei. Acta Physiol Scand 1960;51:356–370.
14. Apps R. Columnar organization of the inferior olive projection to the posterior lobe of the rat cerebellum. J Comp Neurol 1990;302: 236–254.
15. Asanuma C, Thach WT, Jones EG. Distribution of cerebellar terminations and their relation to other afferent terminations in the ventral lateral thalamic region of the monkey. Brain Res Rev 1983;5:237–265.
16. Asanuma C, Thach WT, Jones EG. Anatomical evidence for segregated focal groupings of efferent cells and their terminal ramifications in the cerebellothalamic pathway of the monkey. Brain Res Rev 1983;5:267–297.
17. Batini C, Corvisier J, Destombes J, Gioanni H, Everett J. The climbing fibers of the cerebellar cortex, their origin and pathway in cat. Exp Brain Res 1976;26:407–422.
18. Batton RR III, Jayaraman A, Ruggiero D, Carpenter MB. Fastigial efferent projections in the monkey: an autoradiographic study. J Comp Neurol 1977;174:281–306.
19. Barmack NH, Baughman RW, Eckenstein FP, Shojaku H. Secondary vestibular cholinergic projection to the cerebellum of rabbit and rat as revealed by choline acetyltransferase immunohistochemistry, retrograde and orthograde tracers. J Comp Neurol 1992;317:250–270.
20. Bell CC, Dow RS. Cerebellar circuitry. Neurosci Res Program Bull 1967;5:121–222.
21. Bentivoglio M, Kuypers HGJM. Divergent axon collaterals from rat cerebellar nuclei to diencephalon, mesencephalon, medulla oblongata and cervical cord. Exp Brain Res 1982;46:339–356.
22. Bishop GA, McCrea RA, Lighthall JW, Kitai ST. An HRP and autoradiographic study of the projection from the cerebellar cortex to the nucleus interpositus anterior and nucleus interpositus posterior of the cat. J Comp Neurol 1979; 185:735–756.
23. Bloom FE, Hoffer BJ, Siggins GR. Studies on norepinephrine-containing afferents to Purkinje cells of rat cerebellum. I. Localization of the fibers and their synapses. Brain Res 1971;25:501–521.
24. Boegman RJ, Parent A, Hawkes R. Zonation in the rat cerebellar cortex: patches of high acetylcholinesterase activity in the granular layer are congruent with Purkinje cell compartments. Brain Res 1988;448:237–251.
25. Boesten AJP, Voogd J. Projections of the dorsal column nuclei and the spinal cord on the inferior olive in the cat. J Comp Neurol 1975; 161:215–238.
26. Braitenberg V, Atwood RP. Morphological observations on the cerebellar cortex. J Comp Neurol 1958;109:1–27.
27. Bremer F. Contributions à l'étude de la physiologie du cervelet. La fonction inhibitrice du paleo-cérébellum. Arch Int Physiol Biochim 1922;19:189–226.
28. Broch-Smith T, Brodal P. Organization of the cortico-ponto-cerebellar pathway to the dorsal paraflocculus. An experimental study with anterograde and retrograde transport of WGA-HRP in the cat. Arch Ital Biol 1990;128:249–271.
29. Brodal A. Experimentelle Untersuchungen über die olivocerebellare Lokalisation. Z Gesamte Neurol Psychiatry 1940;169:1–153.
30. Brodal A. Spinal afferents to the lateral reticular nucleus of the medulla oblongata in the cat: an experimental study. J Comp Neurol 1949;91:259–295.
31. Brodal A. The olivocerebellar projection in the cat as studied with the method of retrograde axonal transport of horseradish peroxidase. II. The projection of the uvula. J Comp Neurol 1976;166: 417–426.
32. Brodal A. Neurological anatomy in relation to clinical medicine. 3rd ed. New York: Oxford University Press, 1981.

33. Brodal A, Brodal P. The organization of the nucleus reticularis tegmenti pontis in the cat in the light of experimental anatomical studies of its cerebral cortical afferents. Exp Brain Res 1971;13:90–110.
34. Brodal A, Gogstad AC. Afferent connexions of the paramedian reticular nucleus of the medulla oblongata in the cat: an experimental study. Acta Anat (Basel) 1957; 30:133–151.
35. Brodal A, Hoddevik GH. The pontocerebellar projection to the uvula in the cat. Exp Brain Res 1978; 32:105–116.
36. Brodal A, Hoivik B. Site and mode of termination of primary vestibulo-cerebellar fibres in the cat. Arch Ital Biol 1964;102:1–21.
37. Brodal A, Lacerda AM, Destombes J, Angaut P. The pattern of the projection of the intracerebellar nuclei onto the nucleus reticularis tegmenti pontis in the cat: an experimental anatomical study. Exp Brain Res 1972;16:140–160.
38. Brodal A, Pompeiano O, Walberg F. The vestibular nuclei and their connections, anatomy and functional correlations. Springfield, IL: Charles C. Thomas, 1962.
39. Brodal A, Szikla G. The termination of the brachium conjunctivum descendens in the nucleus reticularis tegmenti pontis: an experimental study in the cat. Brain Res 1972;39:337–351.
40. Brodal A, Torvik A. Cerebellar projection of paramedian reticular nucleus of medulla oblongata in the cat. J Neurophysiol 1954;17: 484–495.
41. Brodal A, Torvik A. Über den Ursprung der sekundären vestibulocerebellaren Fasern bei der Katze. Eine experimentelle-anatomische. Studie Arch Psychiatr 1957;195: 550–567.
42. Brodal A, Walberg F. The olivocerebellar projection in the cat studied with the method of retrograde axonal transport of horseradish peroxidase. IV. The projection to the anterior lobe. J Comp Neurol 1977;172:85–108.
43. Brodal A, Walberg F, Blackstad T. Termination of spinal afferents to inferior olive in cat. J Neurophysiol 1950;13:431–454.
44. Brodal A, Walberg F, Hoddevik EG. The olivocerebellar projection in the cat studied with the method of retrograde axonal transport of horseradish peroxidase. J Comp Neurol 1975;164:449–470.
45. Brodal P. The corticopontine projection in the cat. I. Demonstration of a somatotopically organized projection from the primary sensorimotor cortex. Exp Brain Res 1968;5:212–237.
46. Brodal P. The corticopontine projection from the visual cortex in the cat. I. The total projection and the projection from area 17. Brain Res 1972;39:297–317.
47. Brodal P. The corticopontine projection from the visual cortex in the cat. II. The projection from areas 18 and 19. Brain Res 1972;39:319–335.
48. Brodal P. Demonstration of a somatotopically organized projection onto the paramedian lobule and the anterior lobe from the lateral reticular nucleus: an experimental study with the horseradish peroxidase method. Brain Res 1975; 95:221–239.
49. Brodal P. Principles of organization of the monkey corticopontine projection. Brain Res 1978;148: 214–218.
50. Brodal P, Marsala J, Brodal A. The cerebral cortical projection to the lateral reticular nucleus in the cat, with special reference to the sensorimotor cortical area. Brain Res 1967;6:252–274.
51. Brooks VB, Thach WT. Cerebellar control of posture and movement. In: Brooks VB, ed. Handbook of physiology. Section I: The nervous system. Vol II: Motor control. Part 2. Bethesda, MD: American Physiological Society, 1981:877–946.
52. Carleton SC, Carpenter MB. Afferent and efferent connections of the medial, inferior and lateral vestibular nuclei in the cat and monkey. Brain Res 1983;278:29–51.
53. Carpenter MB. Ventral tier thalamic nuclei. In: Williams D, ed. Modern trends in neurology. Vol. 4. London: Butterworths, 1967: 1–20.
54. Carpenter MB. Vestibular nuclei: afferent and efferent projections. In: Pompeiano O, Allum JHJ, eds. Vestibulospinal control of posture and movement. Progress in brain research. Amsterdam: Elsevier, 1988:76:5–15.
55. Carpenter MB. Connectivity patterns of thalamic nuclei implicated in dyskinesia. Stereotact Funct Neurosurg 1989;58:79–119.
56. Carpenter MB, Bard DS, Alling FA. Anatomical connections between the fastigial nuclei, the labyrinth and the vestibular nuclei in the cat. J Comp Neurol 1959;111:1–26.
57. Carpenter MB, Batton RR III. Connections of the fastigial nucleus in the cat and monkey. In: Palay SL, Chan-Palay V, eds. The cerebellum—new vistas. Experimental brain research (Suppl 6). Berlin: Springer-Verlag 1982:250–295.
58. Carpenter MB, Brittin GM, Pines J. Isolated lesions of the fastigial nuclei in the cat. J Comp Neurol 1958;109:65–90.
59. Carpenter MB, Nova HR. Descending division of the brachium conjunctivum in the cat: a cerebelloreticular system. J Comp Neurol 1960;114:295–305.
60. Carpenter MB, Stein BM, Peter P. Primary vestibulocerebellar fibers in the monkey: distribution of fibers arising from distinctive cell groups of the vestibular ganglia. Am J Anat 1972;135:221–250.
61. Carpenter MB, Strominger NL. Cerebello-oculomotor fibers in the rhesus monkey. J Comp Neurol 1964;123:211–230.
62. Carrea RME, Reissig M, Mettler FA. The climbing fibers of the simian and feline cerebellum. J Comp Neurol 1947;87:321–365.
63. Carrea R, Volkind R, Folins JC, Cosarinsky D, Suarez AM, Alfonso J. Some physiological and statistical observations on single unit activity of the feline inferior olive. In: Fields WS, Willis WD, eds. The cerebellum in health and disease. Ch. 7. St. Louis: Warren H. Green, Inc., 1970:201–216.
64. Chambers WW, Sprague JM. Functional localization in the cerebellum. I. Organization in longitudinal corticonuclear zones and their contribution to the control of posture, both extrapyramidal and pyramidal. J Comp Neurol 1955; 103:105–130.
65. Chambers WW, Sprague JM. Functional localization in the cerebellum. II. Somatotopic organization in cortex and nuclei. Arch Neurol Psychiatry 1955;74:653–680.
66. Chan-Palay V. Cerebellar dentate nucleus: organization, cytology and transmitters. Berlin: Springer-Verlag, 1977.
67. Chan-Palay V, Nilaver G, Palay S, et al. Chemical heterogeneity in cerebellar Purkinje cells: existence and coexistence of glutamic acid decarboxylase-like and motilin-like immunoreactivities. Proc Natl Acad Sci USA 1981;78:7787–7791.
68. Chan-Palay V, Palay SL. Interrelations of basket cell axons and climbing fibers in the cerebellar cortex of the rat. Z Anat Entwickl-Gesch 1970;132:191–227.
69. Chan-Palay V, Palay SL. Tendril and glomerular collaterals of climbing fibers in the granular layer of the rat's cerebellar cortex. Z Anat Entwickl-Gesch 1971; 133:247–273.
70. Chu NS, Bloom FE. The catecholamine-containing neurons in the cat dorsolateral pontine tegmentum: distribution of the cell bodies and some axonal projections. Brain Res 1974;66:1–21.
71. Combs CN. Bulbar regions related to localized cerebellar afferent impulses. J Neurophysiol 1956; 19:285–300.
72. Courville J. Somatotopical organization of the projection from the nucleus interpositus anterior of the cerebellum to the red nucleus: an experimental study in the cat with silver impregnation methods. Exp Brain Res 1966;2:191–215.
73. Courville J. Distribution of olivocerebellar fibers demonstrated by a radioautographic tracing method. Brain Res 1975;95:253–263.
74. Courville J, Augustine JR, Martel P. Projections from the inferior olive to the cerebellar nuclei in the cat demonstrated by retrograde transport of horseradish peroxidase. Brain Res 1977;130:405–419.

75. Courville J, Brodal A. Rubrocerebellar connections in the cat: an experimental study with silver impregnation methods. J Comp Neurol 1966;126:471–485.
76. Courville J, Cooper CW. The cerebellar nuclei of *Macaca mulatta*: a morphological study. J Comp Neurol 1970;140:241–254.
77. Courville J, Diakiw N. Cerebellar corticonuclear projection in the cat: the vermis of the anterior and posterior lobes. Brain Res 1976; 110: 1–20.
78. Courville J, Faraco-Cantin F. On the origin of the climbing fibers of the cerebellum: an experimental study in the cat with an autoradiographic tracing method. Neuroscience 1978;3:797–809.
79. De Camilli P, Miller PE, Levitt P, Walter U, Greengard P. Anatomy of cerebellar Purkinje cells in the rat determined by a specific immunohistochemical marker. Neuroscience 1984;11:761–817.
80. Dietrichs E, Walberg F. The cerebellar corticonuclear and nucleocortical projections in the cat as studied with anterograde and retrograde transport of horseradish peroxidase. I. The paramedian lobule. Anat Embryol (Berl) 1979; 158:13–39.
81. Dietrichs E, Walberg F. The cerebellar projection from the lateral reticular nucleus as studied with retrograde transport of horseradish peroxidase. Anat Embryol (Berl) 1979;155:273–290.
82. Dow RS. The fiber connections of the posterior parts of the cerebellum in the rat and cat. J Comp Neurol 1936;63:527–548.
83. Dow RA. Efferent connections of the flocculonodular lobe in *Macaca mulatta*. J Comp Neurol 1938; 68: 297–305.
84. Dow RS, Moruzzi G. The physiology and pathology of the cerebellum. Minneapolis: University of Minnesota Press, 1958.
85. Eager RP. Efferent cortico-nuclear pathways in the cerebellum of the cat. J Comp Neurol 1963;120: 81–103.
86. Eager RP. Cortical association pathways in the cerebellum of the cat. J Comp Neurol 1963;121: 381–393.
87. Eager RP. The mode of termination and temporal course of degeneration of cortical association pathways in the cerebellum of the cat. J Comp Neurol 1965;124:243–257.
88. Ebbesson SOE. A connection between the dorsal column nuclei and the dorsal accessory olive. Brain Res 1968;8:393–397.
89. Eccles JC, Ito M, Szentagothai J. The cerebellum as a neuronal machine. New York: Springer-Verlag, 1967.
90. Eccles JC, Llinás R, Sasaki K. Excitation of cerebellar Purkinje cells by the climbing fibers. Nature 1964;203:245–246.
91. Eccles JC, Llinás R, Sasaki K. The inhibitory interneurones within the cerebellar cortex. Exp Brain Res 1966;1:1–16.
92. Eccles JC, Llinás R, Sasaki K. The excitatory synaptic action of climbing fibres on the Purkinje cells of the cerebellum. J Physiol (Lond) 1966;182:268–296.
93. Eccles JC, Llinás R, Sasaki K. Parallel fibre stimulation and responses induced thereby in the Purkinje cells of the cerebellum. Exp Brain Res 1966;1:17–39.
94. Eller T, Chan-Palay V. Afferents to the cerebellar lateral nucleus: evidence from retrograde transport of horseradish peroxidase after pressure injections through micropipettes. J Comp Neurol 1976;166: 285–301.
95. Flumerfelt BA, Otabe S, Courville J. Distinct projections to the red nucleus from the dentate and interposed nuclei in the monkey. Brain Res 1973;50:408–414.
96. Fonnum F, Storm-Mathisen J, Walberg F. Glutamate decarboxylase in inhibitory neurons: a study of the enzyme in Purkinje cell axons and boutons in the cat. Brain Res 1970;20:259–275.
97. Fonnum F, Walberg F. An estimate of the concentration of γ-aminobutyric and glutamate decarboxylase in the inhibitory Purkinje axon terminals in the cat. Brain Res 1973;54:115–127.
98. Fox CA, Barnard JW. A quantitative study of the Purkinje cell, dendritic branchlets and their relationship to afferent fibres. J Anat 1957;91:299–313.
99. Fox CA, Hillman DE, Siegesmund KA, Dutta CR. The primate cerebellar cortex: a Golgi and electron microscope study. In: Fox CA, Snider RS, eds. The cerebellum, progress in brain research. Vol. 25. Amsterdam: Elsevier, 1967:174–225.
100. Fox CA, Siegesmund KA, Dutt CR. The Purkinje cell dendritic branchlets and their relation with the parallel fibers: light and electron microscopic observations. In: Cohen MM, Snider RS, eds. Morphological and biochemical correlates of neural activity. Ch. 7. New York: Harper & Row, 1964:112–141.
101. Fredette BJ, Mugnaini E. The GABAergic cerebello-olivary projection in the rat. Anat Embryol (Berl) 1991;184:225–243.
102. Fukushima K, Peterson BW, Uchino Y, Coulter JD, Wilson VJ. Direct fastigiospinal fibers in the cat. Brain Res 1977;126:538–542.
103. Fulton JF. Functional localization in the frontal lobes and cerebellum. Oxford: Clarendon Press, 1949.
104. Ghez C. The cerebellum. In: Kandel ER, Schwartz JH, Jessell TM, eds. Principles of neural science. 3rd ed. Ch. 41. New York: Elsevier, 1991:626–646.
105. Gilman S. The cerebellum: its role in posture and movement. In: Swasch M, Kennard C, eds. Scientific basis of clinical neurology. New York: Churchill Livingstone, 1985.
106. Glaum SR, Slater NT, Rossi DJ, Miller RJ. Role of metabotropic glutamate (ACPD) receptors at the parallel fiber-Purkinje cell synapse. J Neurophysiol 1992;68:1453–1462.
107. Glickstein M. The cerebellum and motor learning. Curr Opin Neurobiol 1992;2:802–806.
108. Glickstein M, Yeo C. The cerebellum and motor learning. J Cogn Neurosci 1990;2:69–80.
109. Gould BB. The organization of afferents to the cerebellar cortex in the cat: projections from the cerebellar nuclei. J Comp Neurol 1979; 184:27–42.
110. Gould BB. Organization of afferents from the brain stem nuclei to the cerebellar cortex in the cat. Adv Anat Embryol Cell Biol 1980;62: 1–90.
111. Gould BB, Graybiel AM. Afferents to the cerebellar cortex in the cat: evidence for an intrinsic pathway leading from the nuclei to the cortex. Brain Res 1976;110:601–611.
112. Grant G. Spinal course and somatotopically localized termination of the spinocerebellar tracts: an experimental study in the cat. Acta Physiol Scand 1962;56(Suppl 193): 1–45.
113. Grant G. Projection of the external cuneate nucleus onto the cerebellum in the cat: an experimental study using silver methods. Exp Neurol 1962;5:179–195.
114. Gray EG. The granule cells, mossy synapses and Purkinje spine synapses of the cerebellum: light and electron microscopic observations. J Anat 1961;95:345–356.
115. Haines DE. Cerebellar corticonuclear and corticovestibular fibers of the anterior lobe vermis in a prosimian primate (*Galago senegalensis*). J Comp Neurol 1976; 170:67–96.
116. Haines DE. A proposed functional significance of parvicellular regions of the lateral and medial cerebellar nuclei. Brain Behav Evol 1977;14:328–340.
117. Hamori J, Szentagothai J. Identification under the electron microscope of climbing fibers and their synaptic contacts. Exp Brain Res 1966;1:65–81.
118. Hampson JL, Harrison CR, Woolsey CN. Cerebro-cerebellar projections and the somatotopic localization of motor function in the cerebellum. Proc Assoc Res Nerv Ment Dis 1952;30:299–316.
119. Hawkes R, Gravel C. The modular cerebellum. Prog Neurobiol 1991; 36:309–327.
120. Heidary H, Tomasch J. Neuron numbers and perikaryon areas in the human cerebellar nuclei. Acta Anat (Basel) 1969;74:290–296.
121. Herrick CJ. The brain of the tiger salamander. Chicago: University of Chicago Press, 1948.
122. Hoddevik GH. The pontocerebel-

lar projection onto the paramedian lobule in the cat: an experimental study with the use of horseradish peroxidase as a tracer. Brain Res 1975;95:291–307.
123. Hoddevik GH. The projection from nucleus reticularis tegmenti pontis onto the cerebellum in the cat: a study using the methods of anterograde degeneration and retrograde axonal transport of horseradish peroxidase. Anat Embryol (Berl) 1978;153:227–242.
124. Hökfelt T, Fuxe K. Cerebellar monoamine nerve terminals: a new type of afferent fiber to the cerebellar cortex. Exp Brain Res 1969; 9:63–72.
125. Holmes G. The Croonian Lectures on the clinical symptoms of cerebellar disease and their interpretation. Lancet 1922;1:1177–1182.
126. Holmes JG. The cerebellum of man. Brain 1939;62:1–30.
127. Holmes G, Stewart TG. On the connections of the inferior olive with the cerebellum in man. Brain 1908;31:125–137.
128. Iacopino AM, Rhoten WB, Christakos S. Calcium binding protein (calbindin-D28k) gene expression in the developing and aging mouse cerebellum. Mol Brain Res 1990;8:283–290.
129. Ikeda M. Projections from the spinal and the principal sensory nuclei of the trigeminal nerve to the cerebellar cortex in the cat, as studied by retrograde transport of horseradish peroxidase. J Comp Neurol 1979;184:567–585.
130. Ikeda M, Houtani T, Ueyama T, Sugimoto T. Choline acetyltransferase immunoreactivity in the cat cerebellum. Neuroscience 1991;45: 671–690.
131. Ikeda M, Matsushita M. Trigeminocerebellar projections to the posterior lobe in the cat, as studied by anterograde transport of wheat germ agglutinin-horseradish peroxidase. J Comp Neurol 1992; 316:221–237.
132. Ilinsky IA, Kultas-Ilinsky K. Sagittal cytoarchitectonic maps of the *Macaca mulatta* thalamus with a revised nomenclature of the motor-related nuclei validated by observations on their connectivity. J Comp Neurol 1987;262:331–364.
133. Illing RB. A subtype of cerebellar Golgi cells may be cholinergic. Brain Res 1990;522:267–274.
134. Ito M. The cerebellum and neural control. New York: Raven Press, 1984.
135. Ito M. Long-term depression. Annu Rev Neurosci 1989;12: 85–102.
136. Ito M, Obata K, Ochi R. The origin of cerebellar-induced inhibition of Deiters neurones. II. Temporal correlation between the trans-synaptic activation of Purkinje cells and the inhibition of Deiters neurones. Exp Brain Res 1966;2:350–364.
137. Ito M, Yoshida M. The cerebellar-evoked monosynaptic inhibition of Deiters neurones. Experientia 1964;20:515.
138. Ito M, Yoshida M. The origin of cerebellar-induced inhibition of Deiters neurones. I. Monosynaptic initiation of the inhibitory postsynaptic potentials. Exp Brain Res 1966;2:330–349.
139. Ito M, Yoshida M, Obata K. Monosynaptic inhibition of the intracerebellar nuclei induced from the cerebellar cortex. Experientia 1964; 20:575–576.
140. Ito M, Yoshida M, Obata K, Kawai N, Udo M. Inhibitory control of intracerebellar nuclei by the Purkinje cell axons. Exp Brain Res 1970; 10:64–80.
141. Jakob A. Das Kleinhirn. In: von Möllendorff W, ed. Handbuch der mikroskopishen Anatomie des Menschen. Vol. IV. Berlin: Julius Springer, 1928:674–916.
142. Jansen J. Vertebrate history with special reference to factors related to cerebellar evolution. In: Llinás R, ed. On cerebellar evolution and organization from the point of view of a morphologist. Chicago: American Medical Association, 1969:881–893.
143. Jansen J, Brodal A. Experimental studies on the intrinsic fibers of the cerebellum. II. The corticonuclear projection. J Comp Neurol 1940; 73:267–321.
144. Jansen J, Brodal A. Experimental studies on the intrinsic fibers of the cerebellum. The cortico-nuclear projection in the rabbit and in the monkey (*Macaca rhesus*). Norske Vid-Akad Avh Mat-Naturv 1942; 3:1–50.
145. Jansen J, Brodal A, eds. Aspect of cerebellar anatomy. Oslo: J.G. Tanum, 1954.
146. Jansen J, Brodal A. Das Kleinhirn. In: Von Möllendorff W, ed. Handbuch der mikroskopischen Anatomie des Mensche. Vol. III. Berlin: Julius Springer, 1958:1–323.
147. Kalil K. Projections of the cerebellar and dorsal column nuclei upon the inferior olive in the rhesus monkey: an autoradiographic study. J Comp Neurol 1979; 188: 43–62.
148. Kan KSK, Chao LP, Eng LF. Immunohistochemical localization of choline acetyltransferase in rabbit spinal cord and cerebellum. Brain Res 1978;146:221–229.
149. Kan KSK, Chao LP, Forno LS. Immuno-histochemical localization of choline acetyltransferase in the human cerebellum. Brain Res 1980;193:165–171.
150. Kawamura K. The pontine projection from the inferior colliculus in the cat: an experimental anatomical study. Brain Res 1975;95: 309–322.
151. Kawato M, Gomi H. The cerebellum and VOR/OKR learning models. Trends Neurosci 1992;15: 445–453.
152. Kerr CW, Bishop GA. Topographical organization in the origin of serotoninergic projections to different regions of the cat cerebellar cortex. J Comp Neurol 1991; 304:502–515.
153. Kievit J, Kuypers HGJM. Fastigial cerebellar projections to the ventrolateral nucleus of the thalamus and the organization of the descending pathways. In: Frigyesi TL, Rinvik E, Yard MD, eds. Corticothalamic projections and sensorimotor activities. New York: Raven Press, 1972:91–111.
154. Kitai ST, McCrea RA, Preston RJ, Bishop GA. Electrophysiological and horseradish peroxidase studies of precerebellar afferents to the nucleus interpositus anterior. I. Climbing fiber system. Brain Res 1977;122:197–214.
155. Korneliussen HK. On the ontogenetic development of the cerebellum nuclei, fissures and cortex of the rat with special reference to regional variations in corticogenesis. J Hirnforsch 1968;10:379–412.
156. Korneliussen HK. Histogenesis of the cerebellar cortex and cortical zones. In: Larsell O, Jansen J, eds. The comparative anatomy and histology of the cerebellum: the human cerebellum, cerebellar connections and cerebellar cortex. Minneapolis: University of Minnesota Press, 1972:164–174.
157. Kotchabhakdi N, Hoddevik GH, Walberg F. Cerebellar afferent projections from the perihypoglossal nuclei: an experimental study with the method of retrograde transport of horseradish peroxidase. Exp Brain Res 1978;31:13–29.
158. Kotchabhakdi N, Walberg F. Cerebellar afferent from neurons in motor nuclei of cranial nerves demonstrated by retrograde axonal transport of horseradish peroxidase. Brain Res 1977;137: 158–163.
159. Kotchabhakdi N, Walberg F. Primary vestibular afferent projections to the cerebellum as demonstrated by retrograde axonal transport of horseradish peroxidase. Brain Res 1978;142:142–146.
160. Kotchabhakdi N, Walberg F. Cerebellar afferent projections from the vestibular nuclei in the cat: an experimental study with the method of retrograde transport of horseradish peroxidase. Exp Brain Res 1978;31:591–604.
161. Künzle H. The topographical organization of spinal afferents to the lateral reticular nucleus of the cat. J Comp Neurol 1973;149:103–117.
162. Künzle H. Autoradiographic tracing of the cerebellar projections from the lateral reticular nucleus in the cat. Exp Brain Res 1975;22: 255–266.
163. Kuypers HGJM, Lawrence DG. Cortical projections to the red nucleus and the brain stem in the rhesus monkey. Brain Res 1967;4: 151–188.
164. Ladpli R, Brodal A. Experimental studies of commissural and reticu-

lar projections from the vestibular nuclei in the cat. Brain Res 1968;8:65–96.
165. Lalonde R, Botez MI. The cerebellum and learning process in animals. Brain Res Rev 1990;15: 325–332.
166. Larsell O. The cerebellum of the frog. J Comp Neurol 1923;36: 89–122.
167. Larsell O. The cerebellum of myxinoids and petromyzonts, including developmental stages in the lampreys. J Comp Neurol 1947;86: 395–446.
168. Larsell O. The development of the cerebellum in man in relation to its comparative anatomy. J Comp Neurol 1947;87:85–129.
169. Larsell O. Anatomy of the nervous system. 2d ed. New York: Appleton-Century-Crofts, 1951.
170. Larsell O, Jansen J, eds. The comparative anatomy and histology of the cerebellum: the human cerebellum, cerebellar connections and cerebellar cortex. Minneapolis: University of Minnesota Press, 1972.
171. Leclerc N, Doré L, Parent A, Hawkes R. The compartmentalization of the monkey and rat cerebellar cortex: zebrin I and cytochrome oxidase. Brain Res 1990;506:70–78.
172. Leiner HC, Leiner AL, Dow RS. Reappraising the cerebellum: What does the hindbrain contribute to the forebrain. Behav Neurosci 1989;103:998–1008.
173. Llinás R, Walton KD. Cerebellum. In: Shepherd GM, ed. The synaptic organization of the brain. Chap. 7. New York: Oxford University Press, 1990:214–245.
174. Loewenthal M, Horsley V. On the relations between the cerebellum and other centres (namely cerebral and spinal) with special reference to the action of antagonistic muscles. Proc R Soc Ser B 1897: 61:20–25.
175. Lorente De Nó R. Etudes sur le cerveau postérieur. Trav Lab Rech Biol Univ Madrid 1924;22:51–65.
176. McCormick DA, Thompson RF. Cerebellum: Essential involvement in the classically conditioned eyelid response. Science 1984;223: 296–299.
177. McCrea RA, Bishop GA, Kitai ST. Intracellular staining of Purkinje cells and their axons with horseradish peroxidase. Brain Res 1976;118:132–136.
178. McCrea RA, Bishop GA, Kitai ST. Electrophysiological and horseradish peroxidase studies of precerebellar afferents to the nucleus interpositus anterior. II. Mossy fiber system. Brain Res 1977;122: 215–228.
179. Madigan JC Jr, Carpenter MB. Cerebellum of the rhesus monkey: atlas of lobules, laminae, and folia, in sections. Baltimore: University Park Press, 1971.
180. Maeda T, Pin C, Salvert D, Ligier M, Jouvet M. Les neurones contenant des catécholamines du tegmentum pontique et leurs voies de projection chez le chat. Brain Res 1973;57:119–152.
181. Maffel L, Pompeiano O. Cerebellar control of flexor motoneurons. Arch Ital Biol 1962;100:476–509.
182. Marr D. A theory of cerebellar cortex. J Physiol (Lond) 1969; 202:437–470.
183. Martin GF, King JS, Dom R. The projections of the cerebellar nuclei of the opossum *Didelphis Marsupialis Virginiana*. J Hirnforsch 1974; 15:545–573.
184. Massion J. The mammalian red nucleus. Physiol Rev 1967;47:383–436.
185. Matsushita M, Hosoya Y. The location of spinal projection neurons in the cerebellar nuclei (cerebellospinal tract neurons) of the cat: a study with the horseradish peroxidase technique. Brain Res 1978; 142:237–248.
186. Matsushita M, Ikeda M. Projections from the lateral reticular nucleus to the cerebellar nucleus to the cerebellar cortex and nuclei in the cat. Exp Brain Res 1976; 24:403–422.
187. Matsushita M, Iwahori N. Structural organization of the fastigial nucleus. I. Dendrites and axonal pathways. Brain Res 1971;25: 597–610.
188. Matsushita M, Ragnarson B, Grant G. Topographic relationship between sagittal Purkinje cell bands revealed by a monoclonal antibody to zebrin I and spinocerebellar projections arising from the central cervical nucleus in the rat. Exp Brain Res 1991;84:133–141.
189. May PJ, Hartwich-Young R, Nelson J, Sparks DL, Porter JD. Cerebellotectal pathways in the macaque: implications for collicular generation of saccades. Neuroscience 1990;36:305–324.
190. Mehler WR, Nauta WJH. Connections of the basal ganglia of the cerebellum. Confin Neurol 1974;36:205–222.
191. Mehler WR, Verier VG, Nauta WJH. Efferent projections from the dentate and interpositus nuclei in primates. Anat Rec 1958;30: 430–431.
192. Mettler FA, Lubin AJ. Termination of the brachium pontis. J Comp Neurol 1942;77:391–397.
193. Miller RA, Strominger NL. An experimental study of the efferent connections of the superior peduncle in the rhesus monkey. Brain Res 1977;133:237–250.
194. Miller S, Oscarsson O. Termination and functional organization of spino-olivocerebellar paths. In: Fields WS, Willis WD, eds. The cerebellum in health and disease. Ch. 6. St. Louis: W.H. Green, 1970:172–200.
195. Mihailoff GA. Cerebellar nuclear projections from the basilar pontine nuclei and nucleus reticularis tegmenti pontis as demonstrated with PHA-L tracing in the rat. J Comp Neurol 1993;330:130–146.
196. Mihailoff GA, Kosinski RJ, Border BG, Azizi SA. A survey of non-cortical afferent projections to the basilar pontine nuclei, a retrograde tracing study in the rat. J Comp Neurol 1989;282:617–643.
197. Mufson EJ, Higgins GA, Kordower JH. Nerve growth factor receptor immunoreactivity in the new world monkey (*Cebus apella*) and human cerebellum. J Comp Neurol 1991;308:555–575.
198. Mugnaini E. The histology and cytology of the cerebellar cortex. In: Larsell O, Jansen J, eds. The comparative anatomy and histology of the cerebellum. The human cerebellum, cerebellar connections, and cerebellar cortex. Minneapolis: University of Minnesota Press, 1972:201–262.
199. Mugnaini E, Walberg F. An experimental electron microscopical study on the mode of termination of cerebellar corticovestibular fibres in the cat lateral vestibular nucleus (Deiters' nucleus). Exp Brain Res 1967;4:212–236.
200. Noda H. Cerebellar control of saccadic eye movements: its neural mechanisms and pathways. Jpn J Physiol 1991;41:351–368.
201. Oertel WH. Neurotransmitters in the cerebellum. Scientific aspects and clinical relevance. Adv Neurol 1993;61:33–75.
202. Olsen L, Fuxe K. On the projections from the locus coeruleus noradrenaline neurons: the cerebellar innervation. Brain Res 1971;28: 165–171.
203. Orioli PJ, Strick PL. Cerebellar connections with the motor cortex and the arcuate premotor area: an analysis employing retrograde transneuronal transport of WGA-HRP. J Comp Neurol 1989;288: 612–626.
204. Oscarsson O. Integrative organization of the rostral spinocerebellar tract in the cat. Acta Physiol Scand 1964;64:154–166.
205. Oscarsson O. Functional organization of the spino-and cuneocerebellar tracts. Physiol Rev 1965;45: 495–522.
206. Oscarsson O. Functional significance of information channels from the spinal cord to the cerebellum. In: Yahr MD, Purpura DP, eds. Neurophysiological basis of normal and abnormal motor activities. New York: Raven Press, 1967:93–113.
207. Oscarsson O. Functional organization of spinocerebellar paths. In: Iggo A, ed. Handbook of sensory physiology. Vol. 2. Berlin: Springer-Verlag, 1973:339–380.
208. Oscarsson O, Sjölund B. The central spino-olivocerebellar system in the cat. I. Identification of five paths and their terminations in the cerebellar anterior lobe. Exp Brain Res 1977;28:469–486.
209. Ottersen OP, Laake JH, Storm-Mathisen J. Demonstration of a releasable pool of glutamate in cere-

bellar mossy and parallel fibre terminals by means of light and electron microscopic immunocytochemistry. Arch Ital Biol 1990;128: 111–125.
210. Ottersen OP, Storm-Mathisen J. Glutamate- and GABA-containing neurons in the mouse and rat brain, as demonstrated with a new immunocytochemical technique. J Comp Neurol 1984;229:374–392.
211. Ottersen OP, Zhang N, Walberg F. Metabolic compartmentation of glutamate and glutamine: morphological evidence obtained by quantitative immunocytochemistry in rat cerebellum. Neuroscience 1992; 46:519–534.
212. Palay SL, Chan-Palay V. Cerebellar cortex: cytology and organization. Berlin: Springer-Verlag, 1974.
213. Panagopoulos NT, Papadopoulos GC, Matsokis NA. Dopaminergic innervation and binding in the rat cerebellum. Neurosci Lett 1991; 130:208–212.
214. Pearson AA. The development and connections of the mesencephalic root of the trigeminal nerve in man. J Comp Neurol 1949;90:1–46.
215. Pearson AA. Further observations on the mesencephalic root of the trigeminal nerve. J Comp Neurol 1949;91:147–194.
216. Percheron G. The thalamic territory of cerebellar afferents and the lateral region of the thalamus of the macaque in stereotaxic coordinates. J Hirnforsch 1977;18: 375–400.
217. Peters A, Palay SL, Webster H deF. The fine structure of the nervous system: neurons and their supporting cells. 3rd ed. New York: Oxford University Press, 1991.
218. Pickel VM, Segal M, Bloom FE. A radioautographic study of the efferent pathways of the nucleus locus coeruleus. J Comp Neurol 1974;155:15–42.
219. Plioplys AV, Thibault J, Hawkes R. Selective staining of a subset of Purkinje cells in the human cerebellum with monoclonal antibody mabQ113. J Neurol Sci 1986; 70:245–256.
220. Pompeiano O. Organizzazione somatotopica delle risposte flessorie alla stimolazione elettrica del nucleo interposito nel gatto decerebrato. Arch Sci Bio (Bologna) 1959;43:163–176.
221. Pompeiano O, Brodal A. Experimental demonstration of a somatotopical origin of rubrospinal fibers in the cat. J Comp Neurol 1957;108:225–251.
222. Puymirat J, Marchand R, Dussault JH. Immunocytochemical localization of beta thyroid receptor in the rat cerebellum. Neurosci Lett 1992;135:239–242.
223. Ramón y Cajal S. Histologie du Système Nerveux de l'Homme et des Vertébrés. (Azoulay L, trans.) Paris: Maloine, 1909, 1911. (Reprinted, Consejo Superior de Investigaciones Cientificas, Instituto Ramón y Cajal, Madrid, 1972.)
224. Ranson SW, Ingram WR. The diencephalic course and termination of the medial lemniscus and brachium conjunctivum. J Comp Neurol 1932;56:257–275.
225. Rinvik E, Grofova I. Cerebellar projections to the nuclei ventralis lateralis and ventralis anterior thalami. Anat Embryol (Berl) 1974; 146:95–111.
226. Rinvik E, Walberg F. Studies on the cerebellar projections from the main and external cuneate nuclei in the cat by means of retrograde axonal transport of horseradish peroxidase. Brain Res 1975;95: 371–381.
227. Romer AS. Vertebrate history with special reference to factors related to cerebellar evolution. In: Llinás R, ed. Neurobiology of cerebellar evolution and development. Chicago: American Medical Association, 1969:1–18.
228. Ross CA, Bredt D, Snyder SH. Messenger molecules in the cerebellum. Trends Neurosci 1990;13: 216–222
229. Rossi GF, Brodal A. Corticofugal fibers to the brain stem reticular formation: an experimental study in the cat. J Anat 1956;90:42–62.
230. Ruggiero D, Batton RR III, Jayaraman A, Carpenter MB. Brainstem afferents to the fastigial nucleus in the cat demonstrated by transport of horseradish peroxidase. J Comp Neurol 1977;172:189–210.
231. Ruigrok TJ, Osse RJ, Voogd J. Organization of inferior olivary projections to the flocculus and ventral paraflocculus of the rat cerebellum. J Comp Neurol 1992;316:129–150.
232. Saigal RP, Karamanlidis AN, Voogd J, Michaloud H, Mangana O. Cerebellar afferents from motor nuclei of cranial nerves, the nucleus of the solitary tract and nuclei coeruleus and parabrachialis in sheep, demonstrated with retrograde transport of horseradish peroxidase. Brain Res 1980;197:20–206.
233. Scheibel ME, Scheibel AB. Observations on the intracortical relations of the climbing fibers of the cerebellum: a Golgi study. J Comp Neurol 1954;101:733–764.
234. Schmahmann JD. An emerging concept. The cerebellar contribution to higher function. Arch Neurol 1991;48:1178–1187.
235. Sherrington CS. Decerebrate rigidity, and reflex co-ordination of movements. J Physiol (Lond) 1898;22:319–322.
236. Simon H, Le Moal M, Calas A. Efferents and afferents of the ventral tegmental-A-10 region studied after local injections of [^{3}H] leucine and horseradish peroxidase. Brain Res 1979;175:1–23.
237. Smith MC. The anatomy of the spino-cerebellar fibers in man. II. The distribution of the fibers in the cerebellum. J Comp Neurol 1961; 117:329–354.
238. Snider RS. Alterations which occur in mossy terminals of the cerebellum following transection of the brachium pontis. J Comp Neurol 1936;64:417–435.
239. Snider RS. Morphology of the cerebellar nuclei in rabbit and cat. J Comp Neurol 1940;72:399–415.
240. Snider RS. Recent contributions to the anatomy and physiology of the cerebellum. Arch Neurol Psychiatry 1950;64:196–219.
241. Snider RS, Eldred E. Cerebro-cerebellar relationships in the monkey. J Neurophysiol 1952;15:27–40.
242. Snider RS, Stowell A. Receiving areas of the tactile, auditory, and visual systems in the cerebellum. J Neurophysiol 1944;7:331–357.
243. Somana R, Kotchabhakdi N, Walberg F. Cerebellar afferents from the trigeminal sensory nuclei in the cat. Exp Brain Res 1980;38:57–64.
244. Somana R, Walberg F. Cerebellar afferents from the paramedian reticular nucleus studied with retrograde transport of horseradish peroxidase. Anat Embryol (Berl) 1978;154:353–368.
245. Somana R, Walberg F. The cerebellar projection from locus coeruleus as studied with retrograde transport of horseradish peroxidase in the cat. Anat Embryol (Berl) 1978;155:87–94.
246. Somana R, Walberg F. Cerebellar afferents from the nucleus of the solitary tract. Neurosci Lett 1979; 11:41–47.
247. Somana R, Walberg F. A re-examination of the cerebellar projections from the gracile, main and external cuneate nuclei in the cat. Brain Res 1980;186:33–42.
248. Sotelo C. Cerebellar neuroglia: morphological and histochemical aspects. In: Fox CA, Snider RS, eds. Progress in brain research. Vol. 25: The cerebellum. Amsterdam: Elsevier, 1967:226–250.
249. Sousa-Pinto A. Cortical projections of the medial geniculate body in the cat. Adv Anat Embryol Cell Biol 1973;48:1–42.
250. Strong OS. A case of unilateral cerebellar agenesia. J Comp Neurol 1915;25:361–391.
251. Szentagothai J, Rajkovits K. Über den Ursprung der Kletterfasern des Kleinhirn. Z Anat Entwickl-Gesch 1959;121:130–141.
252. Taber-Pierce E, Hoddevik GH, Walberg F. The cerebellar projection from the raphe nuclei in the cat as studied with the method of retrograde transport of horseradish peroxidase. Anat Embryol (Berl) 1977;152:73–87.
253. Takeuchi Y, Kimura H, Sano Y. Immunohistochemical demonstration of serotonin-containing fibers in the cerebellum. Cell Tissue Res 1982;226:1–12.
254. Thach WT. The behavior of Purkinje and cerebellar nuclear cells during two types of voluntary arm movement in the monkey. In: Fields WS, Willis WD, eds. The

cerebellum in health and disease. Ch. 8. St. Louis: Warren H. Green, Inc., 1970:217–230.
255. Thach WT, Goodkin HP, Keating JG. The cerebellum and the adaptive coordination of movement. Annu Rev Neurosci 1992;15: 403–442.
256. Thach WT, Jones EG. The cerebellar dentatothalamic connection: Terminal field, lamellae, rods and somatotopy. Brain Res 1979;169: 168–172.
257. Thomas DM, Kaufman RP, Sprague JM, Chambers WW. Experimental studies of the vermal cerebellar projections in the brain stem of the cat (fastigiobulbar tract). J Anat 1956;90:371–385.
258. Tolbert DL, Bantli H. An HRP and autoradiographic study of cerebellar corticonuclear-nucleocortical reciprocity in the monkey. Exp Brain Res 1979;36:563–571.
259. Tolbert DL, Bantli H, Bloedel JR. Anatomical and physiological evidence for a cerebellar nucleocortical projection in the cat. Neuroscience 1976;1:205–217.
260. Tolbert DL, Bantli H, Bloedel JR. The intracerebellar nucleocortical projection in a primate. Exp Brain Res 1977;30:425–434.
261. Tolbert DL, Bantli H, Bloedel JR. Multiple branching of cerebellar efferent projections in cats. Exp Brain Res 1978;31:305–316.
262. Tolbert DL, Bantli H, Bloedel JR. Organization features of the cat and monkey cerebellar nucleocortical projection. J Comp Neurol 1978;182:39–56.
263. Tolbert DL, Massopust LC, Murphy MG, Young PA. The anatomical organization of the cerebelloolivary projection in the cat. J Comp Neurol 1976;170:525–544.
264. Torvik A, Brodal A. The cerebellar projection of the peri-hypoglossal nuclei (nuclei intercalatus, nucleus praepositus hypoglossia and nucleus of Roller) in the cat. J Neuropathol Exp Neurol 1954;13: 515–527.
265. Triarhou LC, Ghetti B. Serotonin-immunoreactivity in the cerebellum of two neurological mutant mice and the corresponding wild-type genetic stocks. J Chem Neuroanat 1991;4:421–428.
266. Tsukahara N, Toyama K, Kosaka K. Intracellular recorded responses of the red nucleus neurons during antidromic and orthodromic activation. Experientia 1964;20:632–637.
267. Uno M, Yoshida M, Hirota I. The mode of cerebello-thalamic relay transmission investigated with intracellular recordings from cells of the ventrolateral nucleus of cat's thalamus. Exp Brain Res 1970; 10:121–139.
268. Van der Want JJL, Voogd J. Ultrastructural identification and localization of climbing fiber terminals in the fastigial nucleus of the cat. J Comp Neurol 1987;258:81–90.
269. Vincent SR, Hope BT. Neurons that say NO. Trends Neurosci 1992;15:108–113.
270. Voogd J. The morphology of the cerebellum the last 25 years. Eur J Morphol 1992;30:81–96.
271. Voogd J, Epema AH, Rubertone JA. Cerebello-vestibular connections of the anterior vermis. A retrograde tracer study in different mammals including primates. Arch Ital Biol 1991;129:3–19
272. Voogd J, Feirabend HKP, Schoen JHR. The cerebellum and precerebellar nuclei. In: Paxinos G, ed. The human nervous system. Ch. 14. New York: Academic Press, 1990: 321–386.
273. Voogd J. The cerebellum of the cat. Structure and fibre connexions. Assen, The Netherlands: Gorcum, 1964.
274. Walberg F. Descending connections to the inferior olive: an experimental study in the cat. J Comp Neurol 1956;104:77–173.
275. Walberg F. On the termination of rubrobulbar fibers: experimental observations in the cat. J Comp Neurol 1958;110:66–73.
276. Walberg F. Cerebellovestibular relations: anatomy. Prog Brain Res 1972;37:361–376.
277. Walberg F, Jansen J. Cerebellar corticovestibular fibers in the cat. Exp Neurol 1961;3:32–52.
278. Walberg F, Kotchabhakdi H, Hoddevik GH. The olivocerebellar projections to the flocculus and paraflocculus in the cat, compared to the rabbit: a study using horseradish peroxidase as a tracer. Brain Res 1979;161:389–398.
279. Walberg F, Pompeiano O. Fastigiofugal fibers to the lateral reticular nucleus. An experimental study in the cat. Exp Neurol 1960; 2:40–53.
280. Walker AE. The thalamus of the chimpanzee. IV. Thalamic projections to the cerebral cortex. J Anat 1938;73:37–93.
281. Walker AE. Afferent connections. In: Bucy PC, ed. The precentral motor cortex. 2d ed. Ch. 4. Urbana: University of Illinois, 1949: 112–132.
282. Walker AE. Internal structure and afferent-efferent relations of the thalamus. In: Purpura DP, Yahr MD, eds. The thalamus. New York: Columbia University Press, 1966: 1–12.
283. Wallesch CW, Horn A. Long-term effect of cerebellar pathology on cognitive functions. Brain Cogn 1990;14:19–25.
284. Wassef M, Sotelo C. Asynchrony in the expression of guanosine 3′,5′-phosphate-dependent protein kinase by clusters of Purkinje cells during the perinatal development of rat cerebellum. Neuroscience 1984;13:1217–1241.
285. Whitlock DG. A neurohistological and neurophysiological investigation of the afferent fiber tracts and the receptive areas of the avian cerebellum. J Comp Neurol 1952; 97:567–636.
286. Wilson VJ, Uchino Y, Maunz RA, Susswein A, Fukushima K. Properties and connections of cat fastigiospinal neurons. Exp Brain Res 1978;32:1–17.
287. Wilson VJ, Uchino Y, Susswein A, Fukushima K. Properties of direct fastigiospinal fibers in the cat. Brain Res 1977;126:543–546.
288. Woodburne RT. A phylogenetic consideration of the primary and secondary centers and connections of the trigeminal complex in a series of vertebrates. J Comp Neurol 1936;65:403–501.
289. Woodward DJ, Moises HC, Waterhouse BD, Yeh HH, Cheun JE. The cerebellar norepinephrine system: inhibition, modulation, and gating. Prog Brain Res 1991;88:331–341
290. Woodward DJ, Moises HC, Waterhouse BD, Yeh HH, Cheun JE. Modulatory actions of norepinephrine on neural circuits. Adv Exp Med Biol 1991;287:193–208.
291. Yaginuma H, Matsushita M. Spinocerebellar projections from the upper lumbar segments in the cat, as studied by anterograde transport of wheat germ agglutinin-horseradish peroxidase. J Comp Neurol 1989;281:298–319.
292. Yamada J, Shirao K, Kitamura T, Sato H. Trajectory of spinocerebellar fibers passing through the inferior and superior cerebellar peduncles in the rat spinal cord: a study using horseradish peroxidase with pedunculotomy. J Comp Neurol 1991;304:147–160.
293. Yamamoto T, Yoshida K, Yoshikawa H, Kishimoto Y, Oka H. The medial dorsal nucleus is one of the thalamic relays of the cerebellocerebral responses to the frontal association cortex in the monkey: horseradish peroxidase and fluorescent dye double staining study. Brain Res 1992;579: 315–320.
294. Purkinje JE. Neuste untersuchungen aus der nerven—und Hirn—Anatomie. In: Sternberg K, Krombliotz JV, eds. Bericht über die versammlung deutsches Naturforscher und Ärtze in Prag, 1837:177–180.
295. Ingram VI, Ogren MP, Chatot CL, Gossels JM, Owens BB. Diversity among Purkinje cells in the monkey cerebellum. Proc Natl Acad Sci USA 1985;82:7131–7135.
296. Newman DB, Ginsburg CY. Brainstem reticular nuclei that project to the cerebellum in rats: a retrograde tracer study. Brain Behav Evol 1992;39:24–68.
297. Shambles GM, Gibson JM, Welker W. Fractured somatography in granule cell tactile areas of rat cerebellar hemispeheres revealed by micromapping. Brain Behav Evol 1978;15:94–140.
298. Carpenter MB, Hanna GR. Fiber projections from the spinal trigeminal nucleus in the cat. J Comp Neurol 1961;117:117–132.

Section VI

Forebrain

16
Thalamus

REGIONAL ORGANIZATION OF THE DIENCEPHALON

The thalamus is the gateway to the cerebral cortex and, as such, it has evolved phylogenetically in close parallel with the cerebral cortex. Thus, although present in all vertebrate groups, the thalamus is most highly developed in mammals and especially so in primates. Virtually all sensory systems pass through the thalamus on their way to the cerebral cortex and, in turn, each part of the thalamus receives projections from the cortical area to which it projects (173). Our conscious perception of the world around us is critically dependent on the information that reaches the cerebral cortex to be analyzed there, and the thalamus represents a key-link in this process (393). As we shall see, the thalamus is much more than a passive relay of information to the cortex. It actively filters the flow of information to the cortex and thus is an important neuronal substrate for many forms of the attention phenomenon (397).

The thalamus represents the major portion of the diencephalon, which is a nuclear complex located at the rostral end of the brainstem (130, 263) (Figs. 16.1, 16.2, and 16.6). The smaller and most ventral portion of the diencephalon is represented by the hypothalamus, which is considered in detail in Chapter 17. The thalamus extends caudorostrally from the region of the posterior commissure to the region of the interventricular foramen. It is bounded laterally by the posterior limb of the internal capsule, the tail of the caudate nucleus, and the stria terminalis (Figs. 16.4, 16.6, and 16.7). The third ventricle separates the thalamus into two symmetric halves, except in the region of the interthalamic adhesion (massa intermedia) where the medial surfaces of the thalami may be in continuity. The thalamus can be divided on developmental, comparative, and connectional bases into (a) the epithalamus, (b) the dorsal thalamus or thalamus proper, and (c) the ventral thalamus. The epithalamus is composed principally of the pineal gland and the habenular nuclei. It neither sends fibers to nor receives fibers from the cerebral cortex, but has closer affinity with the hypothalamus (173). The dorsal thalamus, currently referred to simply as the thalamus, is by far the largest thalamic division. It has massive and reciprocal connections with the cerebral cortex and striatum and comprises most of the nuclei described in this chapter. The ventral thalamus includes the reticular nucleus, ventral lateral geniculate nucleus, the zona incerta, and the nucleus of the fields of Forel. The latter two structures are often regrouped in what is known as the subthalamus or subthalamic region, which is described in detail in connection with the basal ganglia (Chapter 19). The ventral thalamic structures, principally the reticular thalamic nucleus, receive inputs from the cerebral cortex, but do not, themselves, project to the cortex (173).

MIDBRAIN-THALAMIC JUNCTION

Several nuclear masses of the caudal thalamus closely surround the posterior and lateral surfaces of the midbrain. These structures include the *medial* and *lateral geniculate nuclei* and the *pulvinar*. External to all of these is the *retrolenticular* portion of the internal capsule (Figs. 16.3, 16.4, and A.12 in the atlas of the human brain, section VII). The pineal gland lies dorsally between the superior colliculi, while portions of he hypothalamic mammillary bodies can be seen in the interpeduncular fossa (Fig. 16.3). Projections from thalamic nuclei pass laterally into the internal capsule, through which they are distributed to various parts of the cerebral cortex. The internal capsule also contains corticofugal fibers projecting to thalamic nuclei. *Thalamocortical* and *corticothalamic fibers* constitute a large part of the internal capsule referred to as the *thalamic radiations* (Fig. 16.39).

The pulvinar is a large nuclear mass dorsal to the medial and lateral geniculate nuclei. Its dorsal surface is covered by a thin plate of fibers, the *stratum zonale* (Figs. 16.3–16.5). Fibers passing laterally from this nucleus

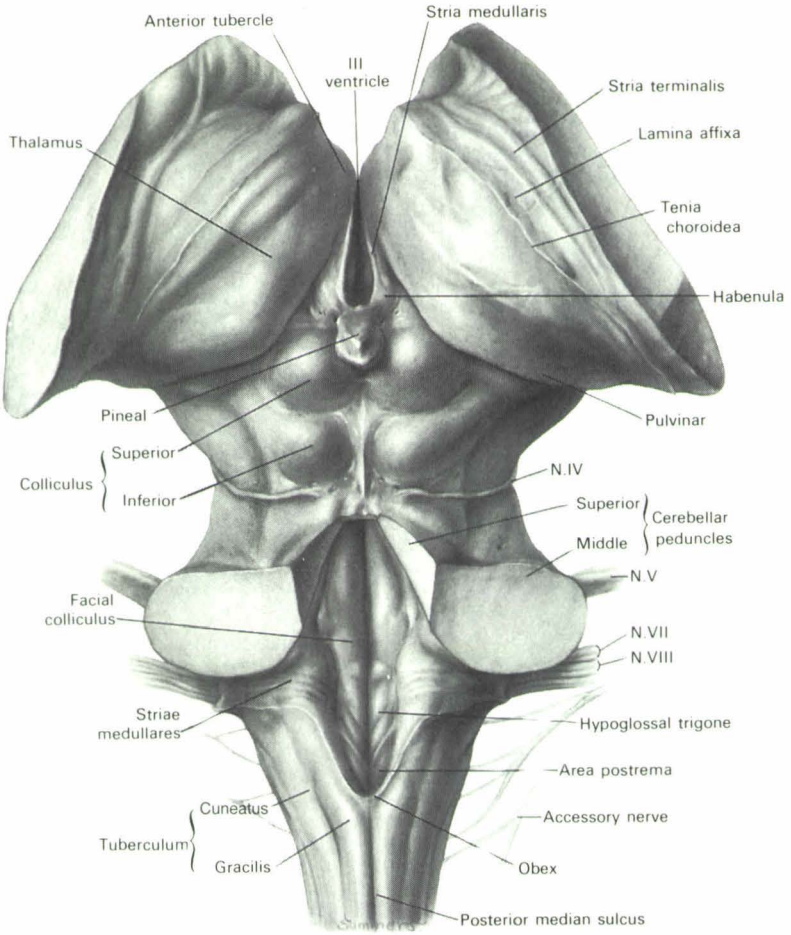


Figure 16.1. Posterior aspect of the brainstem with the cerebellum removed to show the epithalamus and the pulvinar.

contribute to the retrolenticular portion of the internal capsule (Figs. 16.3 and 16.39). The innermost portion of the internal capsule, wedged between the pulvinar and lateral geniculate body, forms a triangular area known as the *zone of Wernicke.* This zone, composed of a mixture of transverse and longitudinal fibers (Fig. 16.3), includes the optic radiations and fibers from the pulvinar and the medial geniculate nucleus.

At more rostral levels, the pulvinar is larger, the medial geniculate nucleus is smaller, and some fibers of the optic tract can be seen entering the lateral geniculate body. Lateral to the pulvinar is the body of the caudate nucleus, separated from the pulvinar by fibers of the *stria terminalis* (Figs. 16.3–16.5). The cerebral aqueduct expands into the deeper third ventricle and the posterior commissure marks the midline dorsal boundary between midbrain and diencephalon. Superior to the posterior commissure is the stalk of the pineal gland, enclosing the pineal recess of the third ventricle (Fig. 16.4). The superior colliculi are replaced by the pretectal region, considered to be a center for the pupillary light reflex (see Chapter 14). The area lateral to the posterior commissure and ventral to the pretectum contains the *nuclei of the posterior commissure* (Fig. 14.10).

Transverse sections through the habenular nuclei (Fig. 16.5) reveal the structural organization of the caudal thalamus. The *habenular nuclei* are two small gray masses forming triangular eminences on the dorsomedial surfaces of the thalami. These nuclei receive fibers mainly from the septal nuclei and the preoptic area via the striae medullares (Figs. 2.29, 16.1, 16.2, and 17.14). Some fibers cross to the opposite side in the *habenular commissure.* Axons from the habenular nuclei form a well-defined bundle, the *fasciculus retroflexus* or *habenulo-interpeduncular tract,* which passes ventrally and

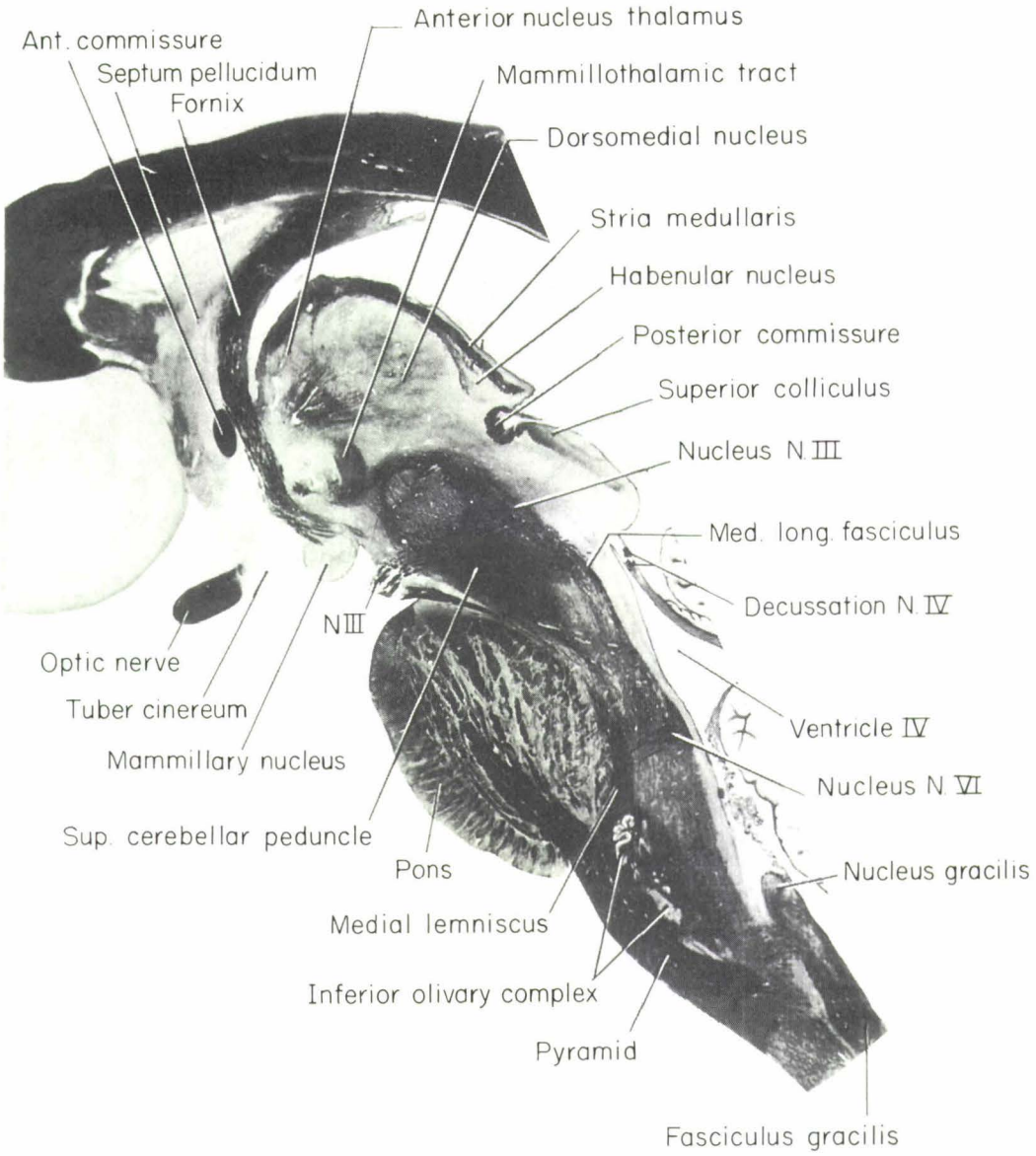


Figure 16.2. Sagittal section of the brainstem and thalamus through the pillar of fornix and root of the third nerve (Weigert's myelin stain).

caudally to terminate in the interpeduncular nuclei. The third ventricle is enlarged (Figs. 16.5 and A.13), and its major portion occurs dorsally, where it is covered by a thin roof extending between the habenular nuclei and the striae medullares. The margins of this attachment on each side constitute the *tenia thalami.*

EPITHALAMUS

Habenula

The epithalamus comprises the pineal body, the habenular trigones, the striae medullares, and the epithelial roof of the third ventricle (Figs. 2.29 and 16.7). In humans, the habenula consists of a smaller medial and a larger lateral nucleus (Figs. 16.5 and 17.14). The medial nucleus consists of small, closely packed, deeply staining round cells. In the lateral nucleus, the cells are larger, paler, and more loosely arranged. These nuclei receive the terminals of the stria medullaris (Figs. 16.2 and 16.7) and give origin to the habenulo-interpeduncular tract or fasciculus retroflexus. Fibers arising from the medial habenular nucleus course within the core of the habenulo-interpeduncular tract and terminate exclusively in the interpedun-

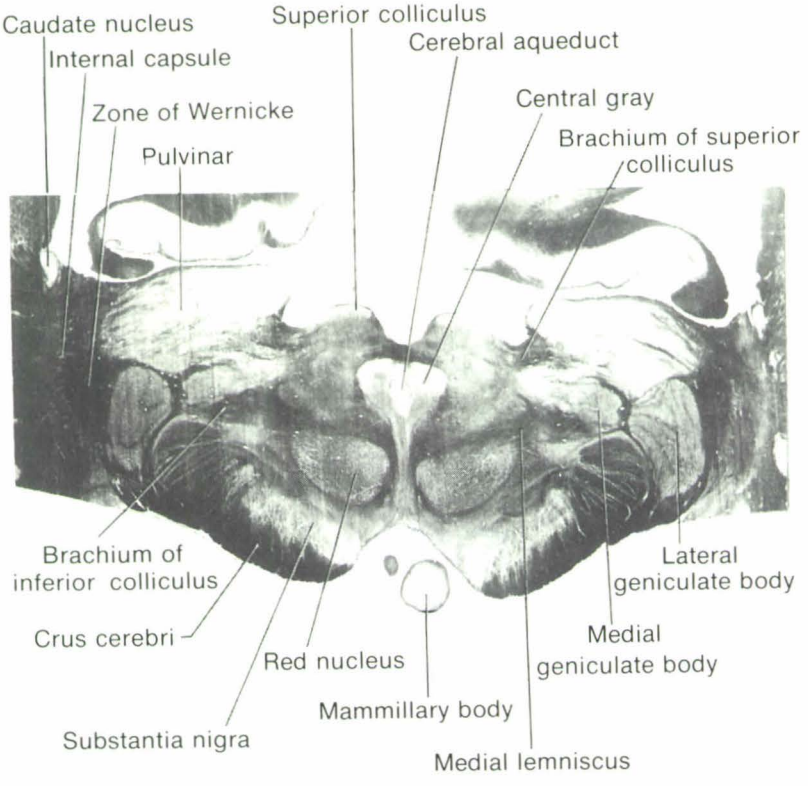


Figure 16.3. Transverse section through the rostral midbrain demonstrating relationship of midbrain and caudal portions of the thalamus (Weigert's myelin stain).

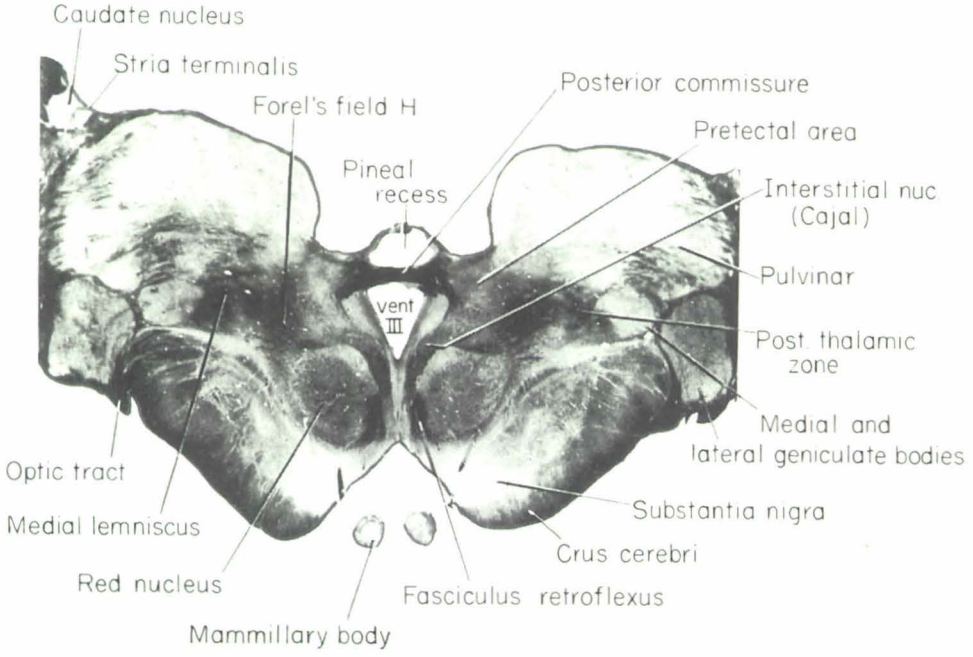


Figure 16.4. Transverse section of the brainstem at the junction of mesencephalon and diencephalon. The posterior nuclear group, which receives collaterals from the spinothalamic tract, lies medial to the medial geniculate body (or nucleus). This cell group lies caudal to the ventral posterior thalamic nucleus (Weigert's myelin stain).

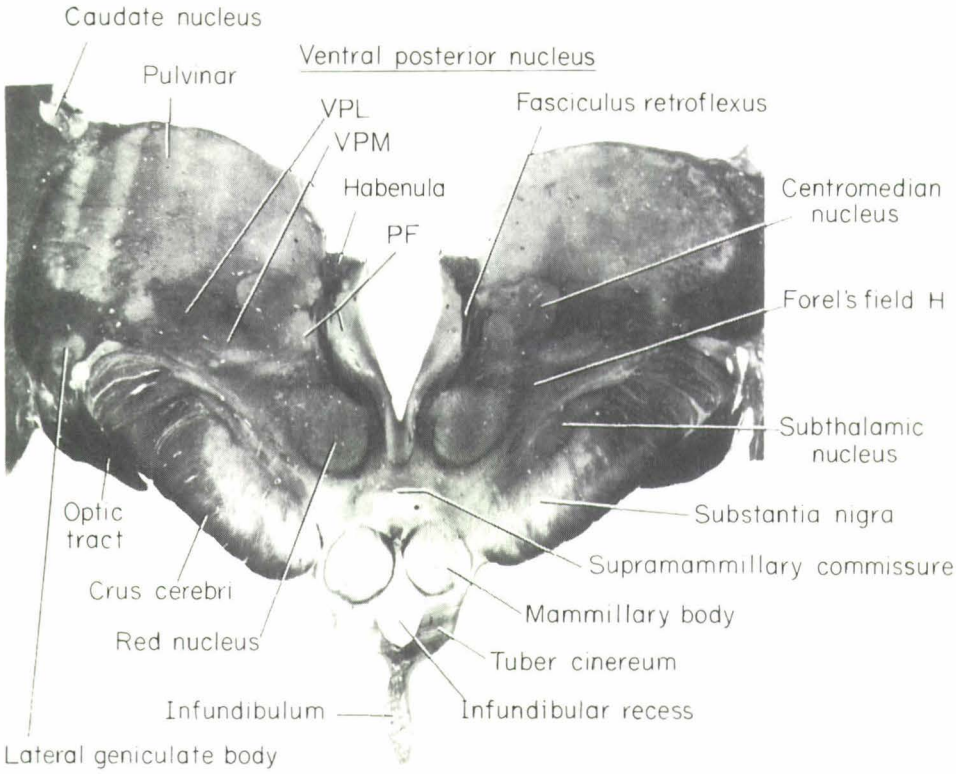


Figure 16.5. Transverse section of the diencephalon through levels of the habenula, the fasciculus retroflexus, the mammillary bodies, and the infundibulum. *VPL*, ventral posterolateral nucleus; *VPM*, ventral posteromedial nucleus; *PF*, parafascicular nucleus (Weigert's myelin stain).

cular nucleus. Fibers originating in the lateral habenular nucleus lie predominantly at the periphery of the habenulo-interpeduncular tract and terminate in the raphe nuclei, as well as in a large region of the reticular formation adjoining the median raphe nucleus (141) (Figs. 16.5 and 17.14). The *stria medullaris* is a complex bundle composed of fibers arising from (a) the septal nuclei, (b) the lateral preoptico-hypothalamic region (292), and (c) the anterior thalamic nuclei. Some fibers of the stria medullaris cross to the opposite side in the habenular commissure. Both the hippocampal formation and the amygdaloid nuclear complex project profusely to the septal nuclei, which, in turn, project to the medial habenular nucleus. Thus, inputs from structures belonging to the limbic system appear to converge onto the medial habenular nucleus, whereas inputs to the lateral habenular nucleus are more diversified.

The lateral habenular nucleus receives afferents from the internal segment of the globus pallidus (or the entopeduncular nucleus, its homologue in nonprimates), the lateral hypothalamus, the substantia innominata, and the lateral preoptic area, as well as from the ventral tegmental area and the midbrain raphe nuclei (140, 216, 290, 295). Because inputs from limbic and basal ganglia structures have been shown to converge upon single neurons in the lateral habenular nucleus of the rat (98), the lateral habenular nucleus is considered as a functional interface between limbic and motor systems (269). In primates, however, the pallidohabenular projection is much less prominent than in nonprimates, and it arises from pallidal neurons distinct from those projecting to other thalamic nuclei (322, 324, 326). The lateral habenular nucleus in the rat has also been shown to project to the substantia nigra pars compacta (141) and to receive, in turn, a dopaminergic input from neurons of the ventral tegmental area (28, 343). The latter projection is known as the mesohabenular dopaminergic pathway (28).

The medial habenular nucleus contains cholinergic neurons (i.e., group Ch 7 of Mesulam et al. (260)) that receive afferents from posterior parts of the septal nuclei and the midbrain raphe nuclei. Serotoninergic

projections from the midbrain raphe nuclei and adrenergic innervation from the superior cervical ganglion reach the medial habenular nucleus (28, 29, 217). Although the habenular nuclei are adjacent to each other, they do not appear to have interconnections. As a whole, the habenula may be viewed as a site of convergence of limbic forebrain pathways that convey impulses to rostral portions of the midbrain.

Pineal Gland

The pineal gland, or *epiphysis*, is a small, cone-shaped body attached to the roof of the third ventricle in the region of the posterior commissure (Figs. 16.1 and 16.4). It appears as a rudimentary gland consisting of a network of richly vascular connective tissue containing glial cells and *pinealocytes* or *epiphysial cells*. Pinealocytes in monkeys contain serotonin and cholecystokinin (CCK). Mammalian pinealocytes are phylogenetically related to the neurosensory photoreceptor elements that become predominantly secretory cells, but they remain indirectly photosensitive (9). The mammalian pineal gland is regarded as an indirectly photosensitive neuroendocrine organ derived from embryonic neuroepithelium. The pinealocyte has one or more processes of variable length which from ultrastructural studies appear adapted for secretory function (248). The club-shaped endings of these processes terminate close to the perivascular space surrounding capillaries that have fenestrations. Pinealocytes receive a direct innervation from sympathetic neurons which form recognizable synapses (395).

The best known pineal secretions are the biogenic amines serotonin, norepinephrine and melatonin, but the gland also contains significant concentrations of identified hypothalamic peptides such as thyrotropin releasing hormone (TRH), luteinizing hormone-releasing hormone (LHRH), and somatostatin (248). Serotonin synthesis from tryptophan involves two enzymes, tryptophan hydroxylase and aromatic amino acid decarboxylase, both of which are found in pinealocytes (197). Only the raphe nuclei of the brainstem have higher levels of tryptophan hydroxylase. Serotonin is synthesized in pinealocytes and released into the extracellular space. Norepinephrine is synthesized in sympathetic neurons which terminate on pineal parenchymal cells (355).

The pineal gland synthesizes melatonin from serotonin by the action of two enzymes sensitive to variations of diurnal light, *N*-acetyltransferase and hydroxyindole-*O*-methyltransferase (15, 199). Daily fluctuations in melatonin synthesis are rhythmic and in direct response to the daily cycle of photic input. Light entrains the circadian rhythm to the environmental light cycle (199, 276) and also acts by an unidentified pathway to rapidly block the transmission of neural signals to the pineal gland (200). *N*-acetyltransferase activity is elevated during the night, but exposure to light turns off enzyme activity (198). Exposure of a rat to constant light for 30 days results in a reduction of hydroxyindole-*O*-methyltransferase and the disappearance of the rhythm in *N*-acetyltransferase activity. If animals are blinded, the suppressive effects of light on hydroxyindole-*O*-methyltransferase are abolished, but the rhythm of *N*-acetyltransferase activity persists (15, 199, 273). Bilateral lesions of the suprachiasmatic nucleus of the hypothalamus (Fig. 17.1), which receives the retinohypothalamic tract, abolish the rhythm in pineal *N*-acetyltransferase activity, and result in low levels of hydroxyindole-*O*-methyltransferase activity (198). Such lesions abolish the circadian rhythms of spontaneous locomotor activity and of both feeding and drinking (286, 436). In female rats, the normal estrous cycle is abolished by lesions of the suprachiasmatic nuclei (286). These studies indicate that photoregulation of pineal *N*-acetyltransferase and hydroxyindole-*O*-methyltransferase is via the retinohypothalamic tract and suggest that the suprachiasmatic nuclei are the endogenous sources of signals which generate the circadian rhythms in pineal *N*-acetyltransferase activity and tonically elevate hydroxyindole-*O*-methyltransferase activity (198). The retinohypothalamic projection alters pineal function by directly interacting with structures in the suprachiasmatic nucleus. Environmental light can be regarded as having an entraining function and a transmission function. The effect of light in entraining the endogenous oscillator to the light cycle is slow, but the effect of light on signal transmission is rapid and probably accounts for the rapid "turn off" of *N*-acetyltransferase by light and the blocking of circadian rhythm by constant light.

Although a single neural pathway from the suprachiasmatic nucleus regulates both

enzymes involved in the formation of melatonin by the pineal gland, details concerning these connections are not known. Indirect evidence suggests that the pathway from the suprachiasmatic nucleus to the pineal involves relays to the tuberal region of the hypothalamus, the medial forebrain bundle, and spinal pathways that reach the intermediolateral cell column and cells of the superior cervical ganglion (201, 276, 278). Thus, the pineal gland appears to be a neuroendocrine transducer that converts neural signals into an endocrine output, melatonin.

Pineal secretions that alter hypothalamic functions do so after they enter the general circulation or the cerebrospinal fluid (86, 248). Daily fluctuations in pineal serotonin and melatonin are rhythmic in response to the cycle of photic input. These rhythmic changes in pineal activity suggest that this gland functions as a biologic clock delivering signals that regulate both physiologic and behavioral processes. Fluctuations, called *circadian rhythms*, have a period of exactly 24 hours in the presence of environmental cues, while in the absence of such cues they only approximate the 24-hour cycle (26).

Parenchymatous pinealomas are associated with depression of gonadal function and delayed pubescence, while lesions which destroyed the pineal frequently are associated with precocious puberty (366). These observations are consistent with experimental studies indicating that the pineal gland exerts an inhibitory influence on the gonads and the reproductive system (86). After the age of 16, calcareous bodies, consisting of calcium and magnesium phosphates and carbonates, frequently are present in the pineal gland. These calcareous bodies form large conglomerations that often are visible in skull radiography. Identification and measurements of the position of the pineal gland in skull films can provide useful information, especially in the diagnosis of space-occupying intracranial lesions.

TOPOGRAPHICAL ORGANIZATION OF THE THALAMUS

The narrow third ventricle, extending from the region immediately ventral to the striae medullares to the optic chiasm, completely separates the thalami. A shallow groove on the ventricular surface, the hypothalamic sulcus (Fig. 16.6), separates the thalamus from the hypothalamus. The dorsal surface of the thalamus is covered by the stratum zonale. At the junction of the dorsal and medial thalamic surfaces, fibers of the striae medullares are cut transversely and appear as small bundles of myelinated fibers.

The thalamus is commonly divided by the fibers of the *internal medullary lamina* into three major nuclear masses that correspond to the anterior, medial, and lateral nuclear groups (Fig. 2.29 and Table 16.1). The anterior nuclear group of the thalamus forms a rostromedial swelling known as the anterior tubercle and is separated from other thalamic nuclei by a myelinated capsule (Figs. 16.1, 16.2, and 16.8). At slightly more caudal levels, the internal medullary lamina becomes more prominent and contains several cellular aggregates, collectively referred to as the intralaminar nuclear group. The lateral nuclear mass is further divided into ventral and lateral (dorsal) nuclear groups (Figs. 16.6, 16.13, and Table 16.1).

The ventral nuclear group, extending nearly the entire length of the thalamus, is divisible into three separate nuclei: (a) a caudal, *ventral posterior nucleus* (VP); (b) an intermediate, *ventral lateral nucleus*; and (c) a rostral, *ventral anterior nucleus*. The ventral posterior nucleus is subdivided into a ventral posterolateral nucleus, located laterally, and a ventral posteromedial nucleus, located medially (Figs. 16.6, 16.11, 16.13, and Table 16.1). These are the ventral tier thalamic nuclei. Caudal to the VP is the posterior nuclear group, which includes (a) the posterior nucleus, (b) the limitans nucleus, and (c) the suprageniculate nucleus (Table 16.1).

The lateral nuclear group of the thalamus, located dorsal to the ventral nuclear group discussed earlier, also is divided into three separate nuclei: (a) a greatly expanded caudal part, the *pulvinar*; (b) an intermediate part, the *lateral posterior nucleus*; and (c) a more rostral part, the *lateral dorsal nucleus*. (Figs. 16.12, 16.13, and Table 16.1). These are the dorsal tier thalamic nuclei.

The medial nuclear group of the thalamus, located medial to the internal medullary lamina, contains the *mediodorsal (or dorsomedial) nucleus*, a nuclear mass intimately related to the cortex of the frontal lobe (Fig. 16.6). Wedged between the dorsomedial nucleus and the ventral nuclei caudally is the *centromedian nucleus*, the largest component of the intralaminar nuclear group (Figs. 16.5, 16.6,

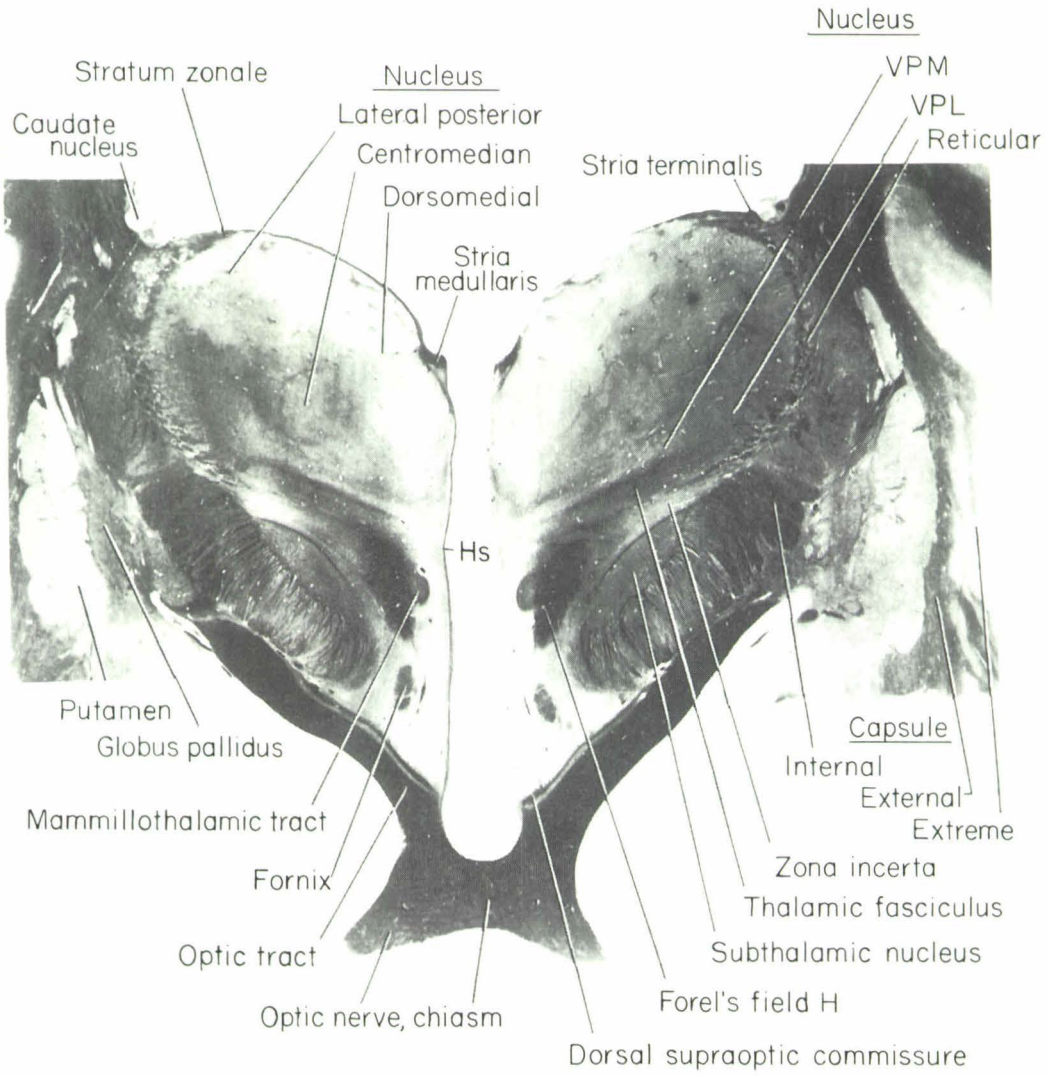


Figure 16.6. Transverse section through the diencephalon and basal ganglia at the level of the optic chiasm. *Hs* indicates the hypothalamic sulcus in the wall of the third ventricle, whereas *VPM* and *VPL* refer to the ventral posteromedial and ventral posterolateral nuclei of the thalamus (Weigert's myelin stain).

16.11–16.13, and Table 16.1). The internal medullary lamina partially splits to surround this nucleus. The two halves of the mediodorsal nucleus are separated by more or less distinct cell clusters which lie in the periventricular gray matter of the dorsal half of the ventricular wall and in the interthalamic adhesion. These nuclei are part of the midline nuclear group (Table 16.1).

Along the lateral border of the thalamus, near the internal capsule, is a narrow band of myelinated fibers, the *external medullary lamina* of the thalamus. Cells located external to these fibers form a thin outer envelope, the reticular nucleus of the thalamus (Figs. 16.6, 16.10, 16.11, 16.13, and Table 16.1). Ventrally, the reticular nucleus becomes continuous with the zona incerta (Fig. 16.7), and both structures are believed by some to be part of the ventral thalamus (173). The medial and lateral geniculate nuclei lie in the caudal portion of the thalamus in a region that is sometimes referred to as the *metathalamus*.

NUCLEAR ORGANIZATION OF THE THALAMUS

The thalamic nuclei, many of which are microscopic subdivisions, are particularly difficult to visualize in three dimensions (Fig. 16.13). The nomenclature of the thalamus is complex, and in some instances the fiber con-

Table 16.1. Classification of Thalamic Nuclei

A. ANTERIOR NUCLEAR GROUP	
Anteroventral nucleus	(AV) *R*
Anterodorsal nucleus	(AD) *R*
Anteromedial nucleus	(AM) *R*
B. MEDIAL NUCLEAR GROUP	
Dorsomedial nucleus	(DM)
parvicellular part	(DMpc) *A*
magnocellular part	(DMmc) *SC*
paralaminar part	(DMpl)
C. MIDLINE NUCLEAR GROUP	
Paratenial nucleus	(pt) *A, SC*
Paraventricular nucleus	(pv) *A, SC*
Reuniens nucleus	(Re) *A, SC*
Rhomboidal nucleus	(Rh) *A, SC*
Median central nucleus	(Mc) *A, SC*
D. INTRALAMINAR NUCLEAR GROUP	
Centromedian nucleus	(CM) *SC, DC*
Parafascicular nucleus	(Pf) *SC, DC*
Subparafascicular nucleus	(sPf) *SC*
Paracentral nucleus	(Pc) *SC, DC*
Central lateral nucleus	(Cl) *SC, DC*
Central median nucleus	(cm) *SC, F*
E. LATERAL NUCLEAR GROUP	
Lateral dorsal nucleus	(LD) *A*
Lateral posterior nucleus	(LP) *A*
Pulvinar	(P) *A*
medial part	
lateral part	
inferior part	

F. VENTRAL NUCLEAR GROUP	
Ventral anterior nucleus	(VA)
parvicellular part	(VApc) *R, SC, DC*
magnocellular part	(VAmc) *R, SC*
Ventral lateral nucleus	(VL)
oral part	(VLo) *R*
caudal part	(VLc) *R*
medial part	(VLm) *R*
Ventral posterior nucleus	(VP) *R*
ventral posterolateral	
oral part	(VPLoP) *R*
caudal part	(VPLc) *R*
ventral posteromedial	(VPM) *R*
parvicellular part	(VPMpc) *R*
ventral posterior inferior	(VPI) *R*
G. POSTERIOR NUCLEAR GROUP	
Posterior nucleus	(PO)
Suprageniculate nucleus	(SG)
Limitans nucleus	(LI)
H. GENICULATE NUCLEAR GROUP	
Medial geniculate nucleus	(MGN) *R*
parvicellular part	(MGpc) *R*
magnocellular part	(MGmc) *R*
dorsal part	*R*
Lateral geniculate nucleus	(LGN) *R*
dorsal part	*R*
ventral part	*SC*
I. RETICULAR NUCLEUS	(RN)

nections and the significance of the smaller thalamic nuclei are unknown. Depending upon their connections, most of the major (principal) thalamic nuclei can be classified either as specific relay nuclei (*R*) or as association nuclei (*A*). The specific relay nuclei project to, and receive fibers from, well-defined cortical areas related to specific functions. The association nuclei of the thalamus do not receive prominent inputs from single specific ascending systems, but project to association areas of the cortex. Other thalamic nuclei have predominantly, or exclusively, subcortical (*SC*) connections. Physiologic and anatomic studies suggest that certain thalamic nuclei may have diffuse cortical (*DC*) connections.

Jones (173) has questioned the validity and usefulness of subdividing the thalamic nuclei into relay nuclei and association nuclei. He aptly pointed out that this subdivision is based, at least in part, upon the erroneous assumption that association nuclei, though projecting to the cortex, receive their input from other thalamic nuclei. Since there appears to be no foundation for this assertion, he proposed that every thalamic nucleus be considered as a relay nucleus (173). This objection is certainly valid, but the terms association and specific nuclei are useful as they allow us to distinguish between (a) thalamic nuclei that receive a unimodal and highly specific input and project to cortical areas that process the same type of information, and (b) thalamic nuclei that receive multimodal inputs and project to cortical regions involved in the complex computation of several types of information (association cortices).

The classification of thalamic nuclei used in this chapter is based upon functional and morphologic data drawn from many sources, but especially from the works of Le Gros Clark (219), Walker (445, 446, 449), Olszewski (314), Russell (381), Van Buren and Borke (435), as well as from more recent investigations (173, 309). This classification is pre-

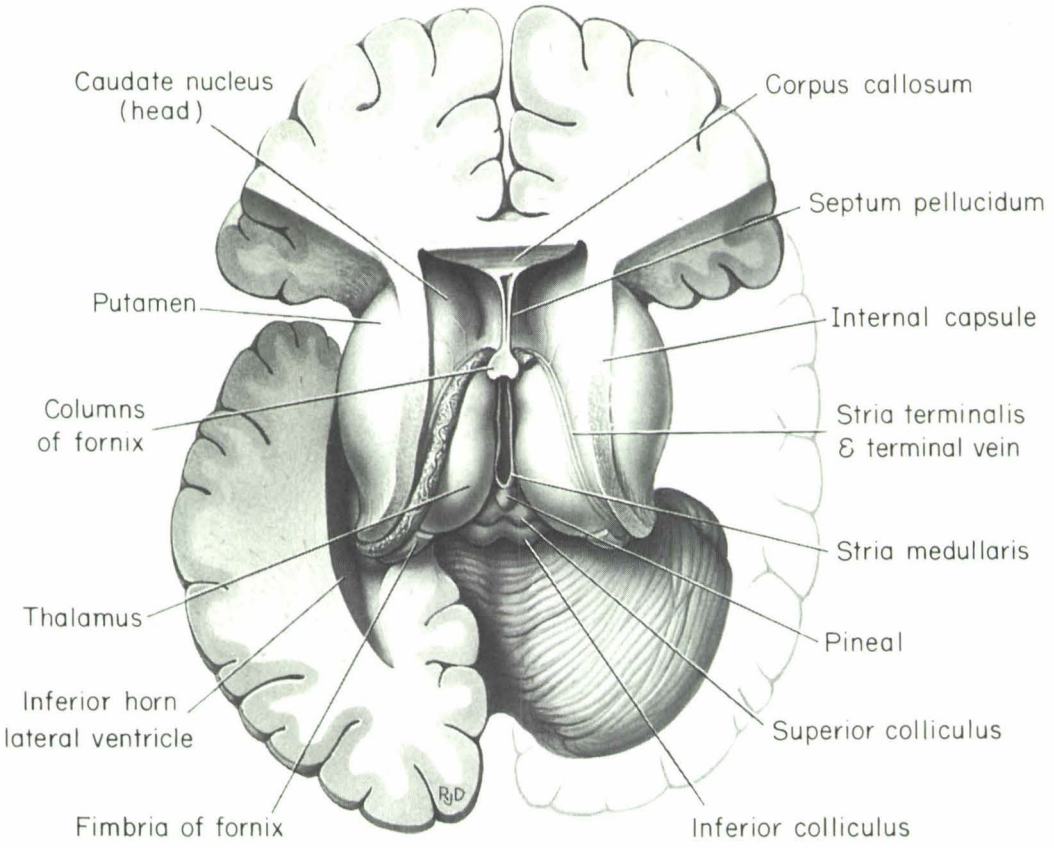


Figure 16.7. Brain dissection showing gross relationships of the thalamus, internal capsule, basal ganglia, and the ventricular system.

sented in Table 16.1, which regroups the major thalamic nuclei into distinct functional entities, indicates in parentheses the abbreviations most frequently used to designate these nuclear subdivisions, and identifies by letters in italics specific relay nuclei (*R*), association nuclei (*A*), and nuclei with subcortical (*SC*) or diffuse cortical (*DC*) projections.

Anterior Nuclear Group

The anterior nuclear group lies beneath the dorsal surface of the most rostral part of the thalamus, where it forms a distinct swelling, the anterior tubercle (Figs. 2.26, 16.1, 16.2, 16.8, 16.10, 16.13, A.16, and A.17). It consists of three nuclei: (a) the *anteroventral nucleus* (AV), (b) the *anterodorsal nucleus* (AD), and (c) the *anteromedial nucleus* (AM). These nuclei can be identified easily in most mammals and their names date back to Nissl (302). Their relative development in the different species varies with the development of the limbic cortical regions to which they are reciprocally connected. The anteroventral and anteromedial nuclei are particularly well-developed in apes and humans (10). Cells composing the anterior group nuclei in humans are of medium size (average cell volume 3000 μm^3), they have little chromophilic substance, moderate amounts of yellow pigment, and are surrounded by a capsule of myelinated fibers.

Approximately 25–30% of human anterior nuclei neurons are interneurons (10). The anterior nuclei receive both direct and indirect projections from the hippocampal formation, essentially from the pre- and parasubiculum. The direct hippocampal projection is formed by fibers that leave the fornix as they course through the thalamus, whereas the indirect projection is mediated via the hypothalamic mammillary bodies and the mammillothalamic tract (222, 352) (Fig. 16.13**B**). Fibers from the medial mammillary nucleus project to the ipsilateral anteroventral and anteromedial nuclei, while the lateral mammillary nucleus projects bilaterally to the anterodorsal nu-

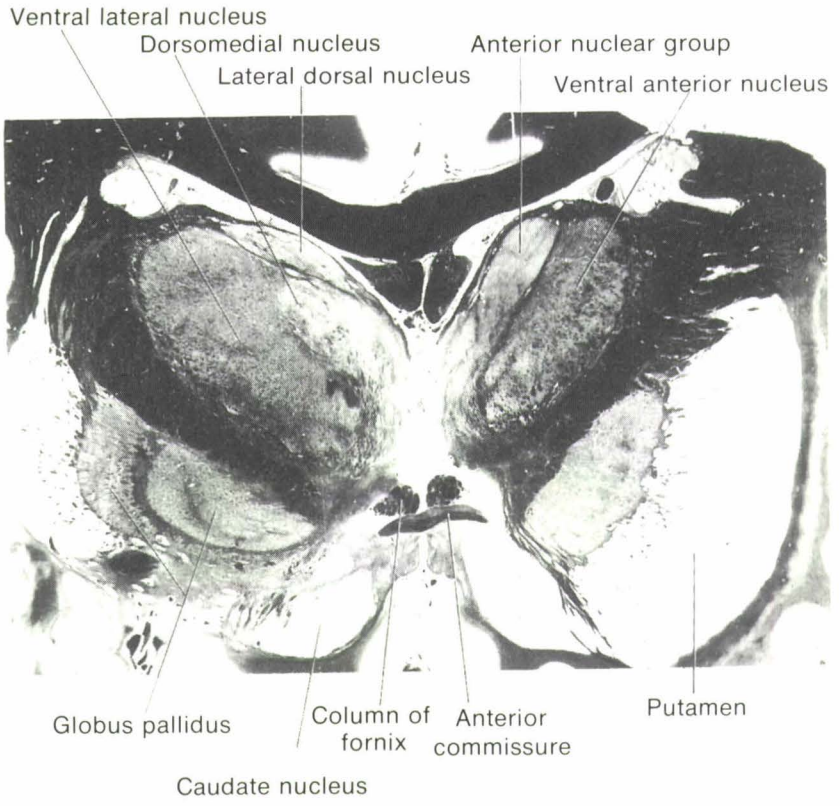


Figure 16.8. Asymmetric transverse section through rostral portions of the thalamus and basal ganglia. The right side reveals the most rostral level (Weigert's myelin stain).

cleus, but not to other subdivisions of the nuclear group (91, 439). These observations were confirmed by fluorescent retrograde double-labeling techniques, which also indicate that cells of the lateral mammillary nucleus project fibers to both the thalamus and the midbrain tegmentum (437).

The cortical projections of the anterior nuclei are to the cingulate gyrus (areas 23, 24, and 32) via the anterior limb of the internal capsule (Figs. 16.14 and 20.10). The anterodorsal nucleus sends fibers to the posterior cingulate gyrus, including the retrosplenial area, while the anteroventral nucleus projects to the middle and posterior cingulate cortex (301). The anteromedial nucleus projects largely to the anterior cingulate cortex, but its diffuse projections extend into the entire limbic cortex and the orbitofrontal region. Although there is considerable overlap, the cingulate cortex receives most of its input from the anteroventral and anteromedial nuclei (299). These cortical areas were considered to project back to the anterior thalamic nuclei (88, 264), but the bulk of the projections are via the cingulum to the entorhinal cortex (Fig. 18.16) (357, 358). The anterior nuclei also receive prominent projections from various brainstem structures, including the serotoninergic dorsal raphe nucleus and the cholinergic pedunculopontine and laterodorsal tegmental nuclei. These brainstem nuclei innervate several other thalamic nuclei and their organization is discussed later in the section dealing with the chemical anatomy of the thalamus.

Because of their connections with various cortical and subcortical limbic areas, the anterior nuclei (together with the mediodorsal nucleus) are often considered as limbic thalamic nuclei (10, 442). The functions of the anterior nuclei, however, are not known with any degree of certainty. Stimulation and lesion experiments in laboratory animals suggest that the anterior nuclei modulate states of alertness and attack, and are also involved in memory and learning (10). Little is known functionally about the anterior nuclei in humans. Analysis of diencephalic lesions and behavioral deficits suggests that the mammil-

lothalamic tract and the anterior nuclei may be critical for encoding memory and for sustained attention. Whether the anterior nuclei have a more central role in mnemonic and attentional processes than the mediodorsal nucleus is still a matter of controversy (10). Interestingly, the nuclei of the anterior group are believed to undergo marked cell degeneration in cases of Alzheimer's disease, which is characterized by severe memory losses (39).

Medial Nuclear Group

Although some authors include parataenial and reuniens nuclei as members of the medial nuclear group (173), the *mediodorsal nucleus* (MD), or dorsomedial nucleus (DM), is by far the most prominent component of this group. The mediodorsal nucleus occupies most of the area between the internal medullary lamina and the periventricular gray matter (Figs. 16.2, 16.6, 16.11–16.13**A**, and A.16). It is the second largest complex in the human thalamus; only the pulvinar has more neurons (10). Three cytologically distinct regions of the nucleus are recognized: (a) a magnocellular portion (MDmc), located rostrally and dorsomedially and consisting of fairly large, polygonal, deeply staining cells, (b) a larger dorsolateral and caudal parvicellular portion (MDpc) made up of small, pale-staining cells that tend to occur in clusters, and (c) a paralaminar portion (MDpl, pars multiformis) characterized by very large cells occupying a narrow band adjacent to the internal medullary lamina (10, 69, 173, 211, 227, 309, 314, 394). The medial magnocellular division of the mediodorsal nucleus receives fibers from the amygdaloid complex, basal forebrain, temporal neocortex, and the caudal orbitofrontal cortex (Fig. 16.13) (5, 293, 350, 351, 365, 450). The medial subdivision of the mediodorsal nucleus also receives projections from the piriform cortex, olfactory tubercle, as well as direct projections from the olfactory bulb (173, 203, 227, 353). The caudal orbitofrontal cortex also has connections with the medial division of the dorsomedial nucleus (294). Most of these fibers constitute components of the *ansa peduncularis*, which consists of the inferior thalamic peduncle (Fig. 16.9), plus fibers interconnecting the amygdaloid complex and the preopticohypothalamic region (295).

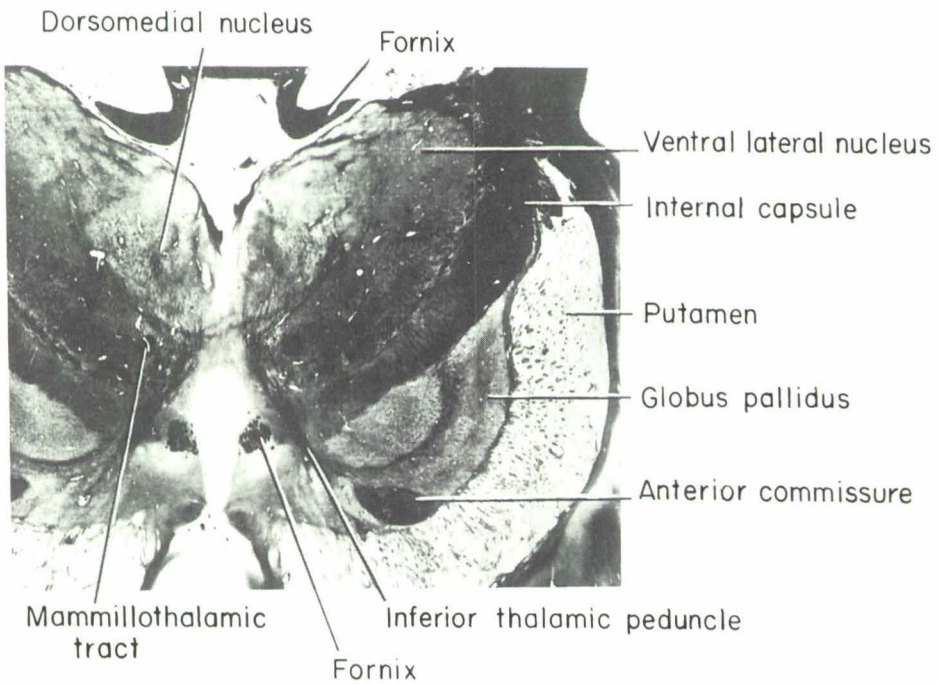


Figure 16.9. Transverse section through the diencephalon and basal ganglia demonstrating fibers of the inferior thalamic peduncle. This peduncle consists of fibers from the amygdaloid complex, temporal neocortex, and possibly the substantia innominata which project to the dorsomedial nucleus of the thalamus. The inferior thalamic peduncle plus amygdaloid projections to the hypothalamus and preoptic regions constitute the ansa peduncularis (Weigert's myelin stain).

The amygdaloid afferent projection to the mediodorsal nucleus, which is not reciprocated (256), is topographically organized. The medial basal amygdaloid nucleus makes the greatest contribution and projects to dorsal portions of MDmc, while the more lateral amygdaloid nuclei supply the anteroventral and central regions of MDmc (5). Furthermore, the medial portion of the mediodorsal nucleus projects to the nucleus basalis of Meynert in the basal forebrain (176). One of the major sources of basal forebrain afferents to the mediodorsal nucleus is the ventral pallidum, which refers to that portion of the pallidum that plunges beneath the anterior commissure within the area of the substantia innominata (120, 460). The ventral pallidum appears to project to large portions of the mediodorsal nucleus, and this projection is believed to play a crucial role in the transfer of information from the ventral striatopallidal system to the cerebral cortex (120, 460). The ventral striatopallidal system is considered as the portion of the basal ganglia more specifically concerned with limbic types of information (460). Recent anatomic investigations, however, revealed that the ventral pallidal input to the mediodorsal nucleus is much less prominent in primates that it is in rodents (121). The paralaminar part of the mediodorsal nucleus receives a substantial projection from the pars reticulata of the substantia nigra (52, 53, 156), and thus can be considered as an additional locus of interaction between the mediodorsal nucleus and the basal ganglia.

The large parvicellular portion of the mediodorsal nucleus is connected by a massive projection with practically the entire frontal cortex rostral to areas 6 and 32 (Figs. 16.13 and 16.14). After extensive prefrontal cortical lesions (i.e., prefrontal lobotomy), or lesions interrupting fibers to this region (i.e., prefrontal leucotomy), nearly all small cells of the mediodorsal nucleus degenerate (88, 241, 264, 394, 444). Axoplasmic transport studies indicate that cells of the mediodorsal nucleus project to all parts of the prefrontal cortex (i.e., rostral to the premotor area (area 6)) including the cortex on the medial aspect of the hemisphere and the orbitofrontal cortex (427). More specifically, the parvicellular and paralamellar parts of the mediodorsal nucleus project to the anterior and posterior dorsolateral prefrontal cortex, respectively, while the magnocellular part projects to the orbital and ventral surface (101, 110). Recent studies, however, indicate that the relationship between the mediodorsal nucleus and the prefrontal cortex is not an exclusive one, because the mediodorsal nucleus projects to other areas of the premotor, limbic, and association cortex as well (101, 110). There are reciprocal connections between the mediodorsal nucleus and the granular frontal cortex (i.e., prefrontal cortex). Particularly profuse reciprocal connections exist between area 8 (i.e., frontal eye field) and the paralaminar part of the mediodorsal nucleus (7, 211, 392).

The results of several behavioral analyses are in keeping with those of the tract-tracing studies mentioned earlier. Both sets of data suggest that the mediodorsal nucleus mediates principally limbic and cognitive processes. Lesions within the mediodorsal nucleus are reported to decrease the emotional responsiveness of nonhuman primates, so that they are placid and do not withdraw from the human experimenter (104). Such lesions also produce problems in executing delayed response tasks, implicating the mediodorsal nucleus with learning and memory (4). In both human and nonhuman primates, lesions in the mediodorsal nucleus result in transient losses of memory, particularly anterograde amnesia (405, 461). Humans with lesions confined to the left portion of the mediodorsal nucleus, as confirmed by axial tomography scanning, showed a deficiency in learning verbal, rather than nonverbal material (405). The verbal nature of the deficit with a left-sided lesion is of particular interest in view of Ojeman's demonstration of functional asymmetry in the human thalamus (310). In studies involving intrathalamic electrical stimulation, Ojeman has found that the left thalamus is specialized for verbal skills and the right thalamus for nonverbal skills. It is unlikely, however, that this functional asymmetry is entirely attributable to the mediodorsal thalamus (173).

Midline Nuclear Group

The midline nuclei are less distinct cell clusters which lie in the periventricular gray matter of the dorsal half of the ventricular wall and in the interthalamic adhesion (Figs. 16.10 and 16.11). These nuclei are small and difficult to delimit in humans, and some are included in other thalamic groups (173). In nonprimate species, however, these nuclei, together with some of the intralaminar nuclei, form a significant portion of the thala-

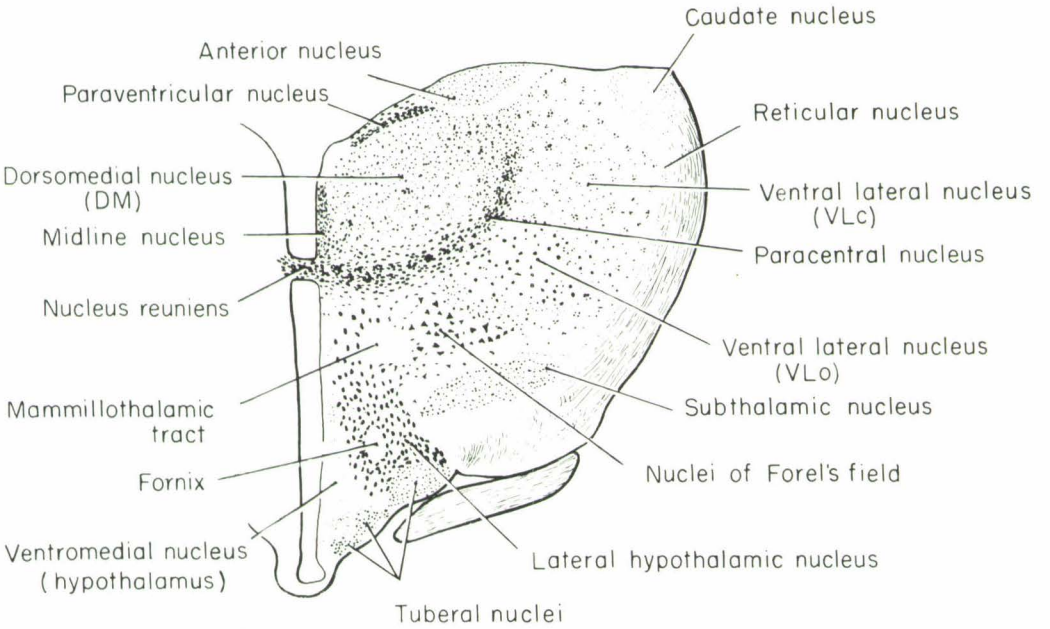


Figure 16.10. Transverse Nissl-stained section through the diencephalon at the level of the tuber cinereum showing nuclei of the thalamus and hypothalamus.

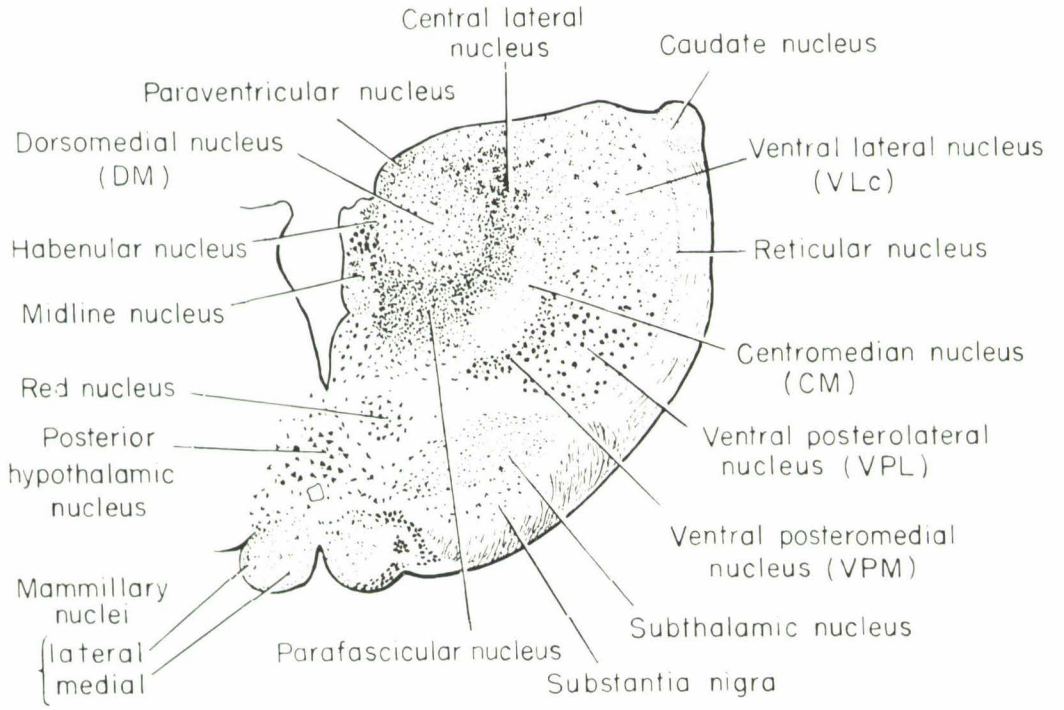


Figure 16.11. Transverse Nissl-stained section through the diencephalon at the level of the habenular nuclei and the mammillary bodies showing the nuclei of the thalamus and hypothalamus.

mus that is sometimes referred to as the paleothalamus.

The most distinct midline cell groups include the *paratenial nucleus* (pt), near the stria medullaris, and the *paraventricular nucleus* (pv), in the dorsal ventricular wall (Fig. 16.10). In an attempt to homologize these ill-defined nuclei with the more developed nuclei of nonprimates, some authorities recognize several cell groups in this periventricular gray matter: (a) the *nucleus reuniens* (Re), (b) the *rhomboidal nucleus* (Rh), and (c) the *median central nucleus* (Mc). The reuniens, rhomboidal, and median central nuclei all bear close relationships with the interthalamic adhesion (massa intermedia), when present. The latter structure is reported to be absent in about 30% of human brains (279). Most midline nuclei are composed of small, fusiform, rather darkly staining cells (246), and are believed to be concerned principally with visceral activities. Efferent fibers from the paraventricular nucleus, the central nuclear complex, and the nucleus reuniens, project to the amygdaloid nuclear complex (256), as well as to ventral parts of the striatum (22). Some of the midline thalamic nuclei may also project to the anterior cingulate cortex (441). Fine myelinated and unmyelinated fibers coursing in the periventricular gray matter are thought to relate these nuclei to the hypothalamus.

Intralaminar Nuclear Group

The intralaminar nuclei (Figs. 16.5, 16.6, and 16.10–16.13) are cell groups within the internal medullary lamina, which separates the medial from the lateral thalamic mass. Cells vary in size in the different nuclei, are fusiform and dark staining, and resemble those of the midline nuclei. They are usually regrouped into a rostral division comprising the paracentral, central lateral, and central medial nuclei, and a caudal division composed essentially of the centromedian and parafascicular nuclei.

ROSTRAL INTRALAMINAR NUCLEI

The rostral division of the intralaminar nuclei comprises (a) the *paracentral nucleus* (Pc), (b) the *central lateral nucleus* (Cl), and (c) the *central medial nucleus* (Cnm). These nuclei are

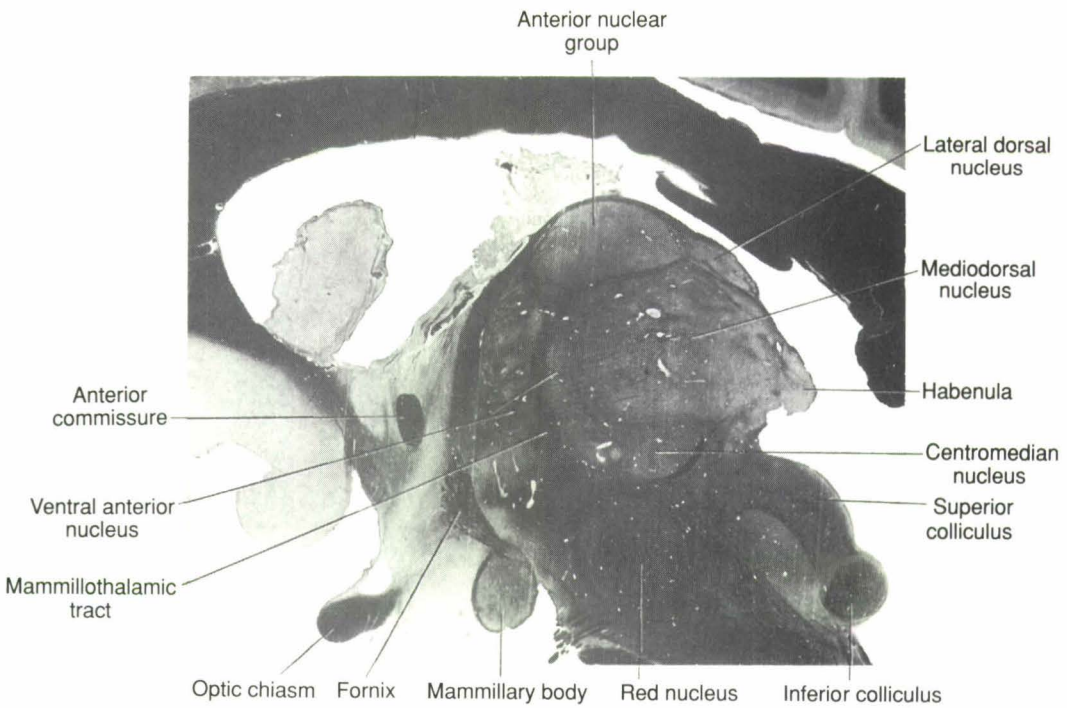


Figure 16.12. Saggital section through medial parts of the thalamus showing the anterior tubercle (anterior nuclear group), the mammillothalamic tract, and the fornix. The relationship of the anterior thalamic nuclei to the lateral dorsal nucleus may also be appreciated. The centromedian nucleus, the largest of the intralaminar thalamic nuclei, lies ventral to the mediodorsal nucleus (Wiegert's myelin stain).

all associated with the internal medullary lamina of the thalamus. The paracentral nucleus lies in the internal medullary lamina adjacent to the rostral part of the dorsomedial nucleus. Cells are large, dark, multipolar, and grouped into clusters. Caudally, the paracentral nucleus appears to fuse with the central lateral nucleus, which borders laterally the dorsomedial nucleus (Figs. 16.10, 16.11, and 16.15). The central lateral nucleus is broader than the paracentral nucleus and composed of similar cells. The central medial nucleus lies adjacent to the medial part of the paracentral nucleus (173, 314, 429).

CAUDAL INTRALAMINAR NUCLEI

The caudal division of the intralaminar nuclei comprises (a) the *centromedian nucleus* (CM), (b) the *parafascicular nucleus* (Pf), and (c) the *subparafascicular nucleus* (sPf).

The centromedian nucleus was first identified in the human thalamus in 1865 by the French anatomist Jules Bernard Luys who named it the "centre médian" (or centrum medianum). The term centre médian is still widely used (173), but is currently being replaced, at least in the American nomenclature, by the name centromedian nucleus. The centromedian nucleus is the largest and most easily defined of the intralaminar thalamic nuclei (Figs. 16.5, 16.6, and 16.13). It is located in the caudal third of the thalamus between the dorsomedial nucleus and the ventral posterior nucleus (Figs. 16.5, 16.6, 16.11, and 16.12). The centromedian nucleus is almost completely surrounded by fibers of the internal medullary lamina, except along its medial border, where it merges by interdigitations with the parafascicular nucleus (Figs. 16.5, 16.11, and 16.15). It is composed of small, loosely arranged, ovoid or round cells containing a considerable amount of yellow pigment (lipofuscin). Cells in the lateral portion of the nucleus are small, while those in more medial regions bordering the dorsomedial nucleus are larger and more densely arranged. There has been considerable controversy concerning precise delimitation of the centromedian nucleus, particularly with respect to the border separating it from the parafascicular nucleus. According to Mehler (253), only the ventrolateral small-celled region should be identified as the centromedian nucleus.

The parafascicular nucleus lies medial to the centromedian nucleus and ventral to the caudal part of the dorsomedial nucleus (Figs. 16.5, 16.11, and 16.15). The most distinguishing feature of the parafascicular nucleus is that its more deeply stained cells surround the dorsomedial part of the fasciculus retroflexus (446). The two major components of the posterior division of the intralaminar nuclei are often considered as a single entity, referred to as the centromedian-parafascicular (CM-Pf) nuclear complex.

The subparafascicular nucleus is an ill-defined structure that lies between the CM-Pf complex and the midbrain tegmentum (11). It is partly intercalated within the fiber capsule surrounding the CM-Pf complex, and it impinges upon this complex at various points along its rostrocaudal extent. The subparafascicular nucleus can be divided into parvicellular and magnocellular parts occupying, respectively, the lateral and medial sector of the nucleus. Laterally, neurons of the parvicellular portion are interspersed among fibers of the medial lemniscus and extend between the CM-Pf complex dorsally and the zona incerta ventrally. Medially, neurons of the magno-cellular portion of the subparafascicular nucleus merge imperceptibly with those of the parafascicular nucleus at various points along the rostrocaudal extension of the subparafascicular nucleus (16.16).

CONNECTIONS AND FUNCTIONAL ORGANIZATION

The intralaminar nuclei receive a topographically organized input from the cerebral cortex. This projection originates principally from smaller pyramidal cells of layer V, some of which send a collateral to the striatum (380). Overall, the prefrontal granular cortex and the limbic cortex on the medial surface of the hemisphere project to the paracentral and central medial nuclei, the premotor cortex (area 6) to the central lateral and parafascicular nuclei, and the motor cortex (area 4) to the centromedian nucleus and/or adjacent central lateral nucleus. The somatic sensory and anterior parietal areas project to the posterior part of the central lateral nucleus. Few fibers reach the intralaminar nuclei from more posteriorly and laterally situated areas of the cortex such as the visual and temporal areas (7, 173, 209, 210, 253, 339, 341).

The intralaminar nuclei also receive affer-

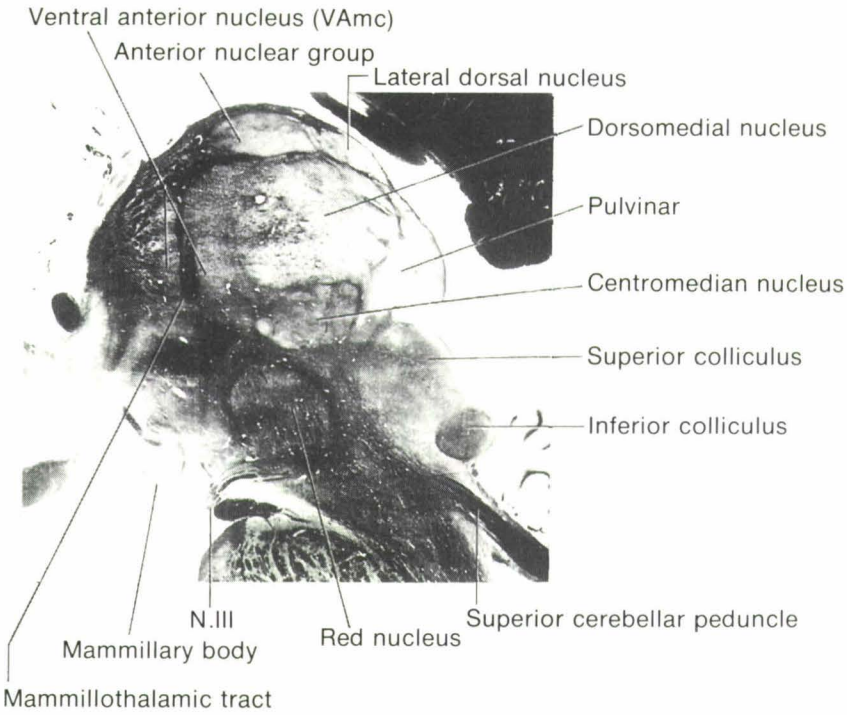


Figure 16.13. Major thalamic nuclei. An oblique dorsolateral view of the thalamus and its major subdivisions is shown in **A**. A transverse section of the thalamus at level of *arrows*, shown on the right in **A**, indicates (a) the relationships between *VPM* and *VPL*, and (b) the location of *CM* with respect to the internal medullary lamina of the thalamus. In **B**, the principal afferent and efferent projections of particular thalamic subdivisions are indicated. While most cortical areas project fibers back to the thalamic nuclei from which fibers are received, not all of these are shown. *CM*, centoromedian nucleus; *DM*, dorsomedial (or mediodorsal) nucleus; *LD*, lateral dorsal nucleus; *LP*, lateral posterior nucleus; *VA*, ventral anterior nucleus; *VLc*, ventral lateral nucleus pars caudalis; *VLo*, ventral lateral nucleus pars oralis; *VPL*, ventral posterolateral nucleus; *VPM*, vental posteromedial nucleus.

ents from subcortical structures, including the basal ganglia, the cerebellum, the spinal cord, and various parts of the brainstem reticular formation. The centromedian nucleus receives a heavy projection from the internal (medial) segment of the globus pallidus, and this input is largely made up of collaterals of pallidal fibers terminating in the ventral lateral thalamic nucleus (196, 212, 216, 295, 325) (Figs. 16.13, 19.36, and 19.38). The central lateral nucleus and the adjoining part of the parafascicular nucleus are major targets of the deep cerebellar nuclei (13, 49, 138, 254, 258, 406, 424). Most of the intralaminar nuclei also receive fibers from the spinal cord and the caudal nucleus of the trigeminal nerve, and some of these appear to be branches of fibers terminating in the ventral posterior nucleus (99, 257). Other afferents arise in the reticular formation of the medulla oblongata and pons, parabrachial nucleus of the pons, nucleus cuneiformis of the midbrain reticular formation, pedunculopontine tegmental nucleus, deep layer of the superior colliculus, pretectum, substantia nigra, and dorsal raphe nucleus (173, 380). The fibers from most of these sites appear to arborize rather diffusely throughout the intralaminar nuclei.

The intralaminar nuclei project heavily and in a highly ordered fashion upon the striatum, and more lightly and diffusely upon widespread areas of the cerebral cortex. Earlier studies have identified the striatum as the primary target of the CM-Pf complex (78, 87, 178, 202, 240, 253, 261, 291, 296, 349, 363, 388). These thalamostriatal fibers follow a wide curved path through the ventral anterior and rostral reticular nuclei of the thalamus, but do not appear to establish terminal connections within the ventral anterior nucleus (253). Some of these fibers, however, may terminate in portions of the thalamic reticular nucleus (169).

More recent studies in primates have shown that the thalamostriatal projection is topographically organized and complemen-

tary. The centromedian nucleus projects specifically to the region of the putamen receiving input from sensorimotor cortices, while the parafascicular nucleus sends fibers to large sectors of the caudate nucleus innervated by association cortices (242, 243, 327, 382, 383). Additionally, the parafascicular nucleus projects more discretely to the nucleus accumbens and the olfactory tubercle, which represent the limbic portion of the striatum. Therefore, the projections from the centromedian and parafascicular nuclei cover the entire striatum, with those from the centromedian arborizing in the "sensorimotor" striatal territory and the ones from the parafascicular nucleus terminating in the "associative-limbic" striatal territory (382). Furthermore, the CM-Pf complex sends fibers to other components of the basal ganglia, namely the subthalamic nucleus, globus pallidus, and substantia nigra, where they also terminate in a complementary fashion. The subparafascicular nucleus gives rise to both ascending and descending projections, the former terminating in various limbic forebrain areas, including the substantia innominata, the amygdala, and the hypothalamus, and the latter arborizing in different brainstem structures, particularly the inferior olivary nucleus (Fig. 16.16). Thus, each component of caudal intralaminar nuclei appears to be involved in different, but complementary, aspects of the basal ganglia function.

Neurons of the anterior intralaminar nuclei, as well as neurons scattered on each side of the internal medullary lamina within the territories of the medial, lateral, and ventral nuclear groups, also participate in the thalamostriatal projections (327, 380, 382). The intralamino-striatal projections terminate in a highly patchy manner. Thalamofugal fibers arborize profusely in the matrix compartment of the striatum, and much less in the striosome or patch compartment (383). The thalamostriatal fibers terminate principally on the dendritic shafts of the medium spiny projection neurons located in the extrastriosomal matrix of the striatum (383).

The intralaminar nuclei of the thalamus were long regarded as having no cortical projections. This conclusion is based on the absence of retrograde cell changes in these nuclei following virtually complete decortication (62, 348, 394, 445, 446) and the absence of degeneration traceable from lesions in the centromedian nucleus to any part of the cortex (222, 223, 296). Retrograde transport of the enzyme horseradish peroxidase (HRP) suggested that thalamostriatal fibers gave rise to collateral systems that project to broad cortical regions. Electrophysiologic studies, however, have shown that neurons in the rostral intralaminar nuclei do not have such bifurcating axons and conduction velocities of fibers projecting to cortex and striatum are different (412). Likewise, retrograde double-labeling methods reveal that neurons in the caudal intralaminar nuclei projecting to cortex are distinct from those projecting to striatum (382). At CM-Pf levels, neurons projecting to the cortex are mostly confined to the lateral aspect of the CM, while those projecting to the striatum are more numerous and centrally located in CM (Fig. 16.16).

This intralaminocortical projection is principally concentrated in frontal, medial, and dorsolateral cortex, although cells can be retrogradely labeled from virtually every cortical area, including that of the piriform lobe and occipital pole (173). Although projecting rather widely upon the cerebral cortex, each intralaminar nucleus appears to have a particular region upon which most of its cortical projection is focused (242, 243). Thus, the intralaminar nucleus-to-cortex projection cannot be regarded as totally diffuse or nonspecific (173, 412). The topography of the intralaminocortical projection conforms to the pattern of "nonspecific" thalamocortical connections demonstrated earlier following electrical stimulation of the intralaminar or midline nuclei (71, 72, 164, 285, 408). These connections were thought to be part of a diffuse cortical activating system that mediates the cortical *recruiting response* via axons terminating in layer I of the cerebral cortex (234). The recruiting response is a surface negative response evoked by repetitive low frequency stimulation of the midline, intralaminar, and ventral anterior thalamic nuclei that waxes and wanes and can be recorded over broad areas of the cerebral cortex. The question of the laminar site of termination of the intralaminocortical fibers is still unresolved. Some data obtained from cats suggest that these fibers terminate exclusively in layer I (170), while other findings in rats point to layer VI as their main target (139).

The intralaminar thalamic nuclei show a striking development in human and nonhuman primates, in relation to thalamic relay nuclei, suggesting that they constitute a com-

plex intrathalamic-regulating mechanism concerned with diverse functions. The intralaminar thalamic nuclei have been considered to serve as the thalamic pacemaker, controlling in a state-dependent manner the electrocortical activities. For example, in relaying activity from the midbrain reticular formation to the cerebral cortex, the rostral intralaminar nuclei play an important role in processes that characterize wakefulness and desynchronized sleep. The posterior intralaminar nuclei (i.e., the large CM-Pf complex) appear more closely related to motor functions in that they receive inputs from the motor and premotor cortex and from the globus pallidus, and, in turn, project to the striatum. The intralaminar nuclei are believed to also be involved in the processing of diffuse sensory inputs, particularly those pertaining to pain.

Lateral Nuclear Group

The lateral nuclear group begins as an oblique narrow strip on the dorsomedial surface of the thalamus caudal to the anterior nuclear group. This group consists of three nuclear masses arranged in rostrocaudal sequence: (a) the *lateral dorsal nucleus* (LD), (b) the *lateral posterior nucleus* (LP), and (c) the *pulvinar* (P) (Figs. 16.12 and 16.13).

LATERAL DORSAL NUCLEUS

This nucleus, which lies on the dorsal surface of the thalamus, extends along the upper margin of the internal medullary lamina and is surrounded by a myelin fiber capsule, similar to that of the anterior nuclear group (Fig. 16.12). The nucleus achieves its largest size dorsal to the paracentral and central lateral nuclei (Figs. 16.8, 16.13, and 16.15) and sometimes is considered as a posterior extension of the anterior nuclear group (173, 232, 449). While many authors believe that this nucleus sends fibers to the posterior parietal cortex (Fig. 16.13), recent data indicate that the lateral dorsal nucleus projects mainly to posterior parts of the cingulate gyrus. It also sends fibers to the supralimbic cortex of the parietal lobe (173, 233, 297, 299, 438). Although afferent fibers to this nucleus are poorly understood, it is believed that the lateral dorsal nucleus receives inputs that are similar to those terminating in the anterior thalamic nuclei (173).

LATERAL POSTERIOR NUCLEUS

This nucleus lies caudal, lateral, and ventral to the lateral dorsal nucleus (Figs. 16.13 and 16.22), and is composed of medium-sized cells evenly distributed. This irregularly shaped nucleus lies dorsal to the ventral posterolateral nucleus and adjacent to the lateral medullary lamina. Caudally, the nucleus merges with the oral and medial parts of the pulvinar, from which it is not easily distinguished (314). Unlike the lateral dorsal nucleus, it has no myelin capsule. The input to this thalamic nucleus is similar to that of the pulvinar, and both structures are often considered as a single functional entity (173). In the cat, the lateral posterior nucleus receives inputs from the superficial layers of the superior colliculus, the pretectal region, and from the superior and inferior parietal lobules (112, 187, 342, 373, 434). Some of these thalamic neurons appear to have reciprocal cortical connections. Retrograde transport studies indicate that the lateral posterior nucleus projects to areas 5 and 7, as well as to various cortical regions involved in the processing of visual information (173, 334).

PULVINAR

This large nuclear mass, forming the most caudal portion of the thalamus, overhangs the geniculate bodies and the dorsolateral surface of the midbrain (Figs. 16.3–16.5 and 16.13). Because the pulvinar exhibits considerable cytologic uniformity, it is subdivided on a topographic basis into four parts: (a) a pars oralis, located between the ventral posterolateral and centromedian nuclei, (b) a pars inferior, located ventrally between the medial and lateral geniculate bodies, (c) a pars medialis forming the medial half of the pulvinar, and (d) a pars lateralis extending along the external medullary lamina which is traversed by fibers (314). The basic element of the pulvinar is a lightly stained, medium-sized, multipolar cell, whose density and pattern of arrangement varies in the different subdivisions. Cells in the oral division of the pulvinar are small, light-staining, and loosely arranged. The pars inferior, separated from the main body of the pulvinar by fibers of the brachium of the superior colliculus, is composed of large dark-staining cells scattered among medium-sized elements. The lateral pulvinar is traversed by oblique fiber bundles

extending from the external medullary lamina and among which small cells are scattered. The medial nucleus contains evenly distributed medium-sized cells and very few fibers.

The nuclei of the pulvinar do not receive inputs from long ascending sensory pathways, but the inferior division receives a projection from the superficial layers of the superior colliculus (19, 128, 330). Topographically, this projection represents the contralateral visual field, with the lower visual field lying dorsomedially and the upper field ventrolaterally. Both the inferior pulvinar and the adjacent portion of the lateral pulvinar have reciprocal connections with occipital cortex, including striate cortex (173, 307, 434). The inferior pulvinar and the adjacent lateral pulvinar each contain a representation of the contralateral visual hemifield and project retinotopically on (a) cortical areas 18 and 19, where fibers end in layers IV, III and I (20), and (b) the striate cortex (area 17), where fibers terminate upon the supragranular layers (367). In contrast, the dorsal lateral geniculate nucleus projects retinotopically largely upon the striate cortex (area 17), where fibers end upon cells in layer IV. These findings indicate three visuotopically organized inputs from the thalamus—the lateral geniculate nucleus, inferior pulvinar, and adjacent lateral pulvinar—to the primary visual cortex that terminates upon different layers. Projections from the inferior pulvinar to cortical areas 17, 18, and 19 constitute the final link in an extrageniculate visual pathway.

The lateral nucleus of the pulvinar (other than that portion adjacent to the inferior pulvinar) projects to the temporal cortex and receives reciprocal projections from the same region (398, 399, 432). The medial pulvinar appears to project to the superior temporal gyrus and to the inferior parietal lobule (126).

Ventral Nuclear Group

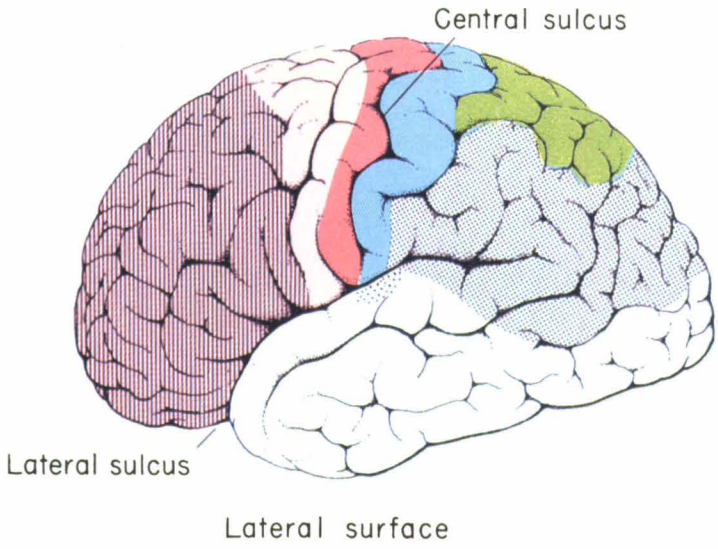
The ventral nuclear group of the thalamus is composed of three nuclei: (a) the *ventral anterior nucleus* (VA), (b) the *ventral lateral nucleus* (VL), and (c) the *ventral posterior nucleus* (VP). The ventral anterior nucleus is the most rostral and the smallest nucleus of this group. The ventral posterior nucleus, the largest and most posterior nucleus of the group, is further subdivided into the ventral posterolateral and ventral posteromedial nuclei (Figs. 16.11, 16.13, 16.15, and 16.21). Although the medial and lateral geniculate bodies together constitute the geniculate nuclear group or metathalamus, these well-defined nuclear masses may be considered as a caudal continuation of the ventral nuclear group (Figs. 16.3, 16.4, and 16.13). The ventral and geniculate nuclear groups constitute the largest division of the thalamus concerned with relaying impulses from other portions of the neuraxis to specific parts of the cerebral cortex. Caudal parts of this complex are concerned with relaying impulses of specific sensory systems to cortical regions, while more rostral nuclei (ventral anterior and ventral lateral nuclei) relay impulses from the basal ganglia and cerebellum.

VENTRAL ANTERIOR NUCLEUS

This thalamic nucleus occupies the extreme rostral part of the ventral nuclear group and is bounded anteriorly and ventrolaterally by the thalamic reticular nucleus (Fig. 16.13). Rostrally the ventral anterior nucleus occupies the entire thalamic region lateral to the anterior nuclear group (Fig. 16.8), but caudally it becomes restricted to a more medial region. The mammillothalamic tract passes through the ventral anterior nucleus but does not form its medial border. The nucleus is composed of large and medium-sized multipolar cells arranged in clusters. The clustering of cells is particularly evident in rostrolateral parts of the nucleus where thick myelinated fiber bundles course longitudinally within the nucleus.

Parts of the nucleus adjacent to the mammillothalamic tract and along the ventral border of the nucleus are composed of large, dark, densely arranged cells. This subdivision, called the magnocellular part (VAmc) (314), extends further caudal than the principal part of the ventral anterior nucleus (VApc). Thus, there are two distinctive cytologic subdivisions of the ventral anterior nucleus. Each of these subdivisions receives fibers from different sources without overlap. The principal part of the nucleus is innervated by fibers from the internal segment of the globus pallidus, while the magnocellular part receives input from the substantia nigra (159).

Afferent fibers from the medial segment of the globus pallidus (Figs. 19.36 and 19.38) reach the nucleus via the lenticular fasciculus and ansa lenticularis (131, 196, 216, 295, 318, 324, 361, 387). These fibers enter the thalamic



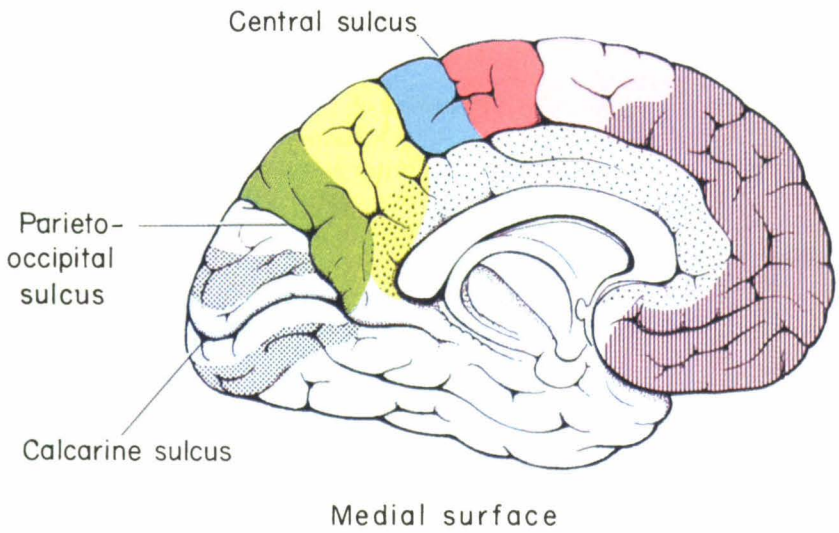


Figure 16.14. Left cerebral hemisphere showing the cortical projection areas of thalamic nuclei. The color code is the same as in Figure 16.13. The diffuse projection of the ventral anterior nucleus (*VApc*) to the frontal lobe appears to largely overlap the projection of the dorsomedial nucleus (*DM*). Information concerning the cortical projection areas of some thalamic nuclei is incomplete.

fasciculus, turn dorsolaterally, and are distributed in a rostrolateral direction within the ventral anterior nucleus. Pallidothalamic fibers projecting to the rostral ventral tier thalamic nuclei (i.e., VApc and VLo) appear organized in a specific manner (50, 212). Rostral parts of the medial pallidal segment project most profusely to VApc. More caudal parts of the medial pallidal segment project fibers to parts of the ventral lateral nucleus (VLo). In nonhuman primates, most pallidal fibers that arborize in the ventral nuclear group were shown to be collaterals of those that project to the centromedian nucleus and the brainstem pedunculopontine tegmental nucleus (324). Furthermore, up to 20% of the pallidothalamic fibers cross the midline at the level of the central medial nucleus and arborize within the contralateral ventral anterior nucleus according to a pattern similar to

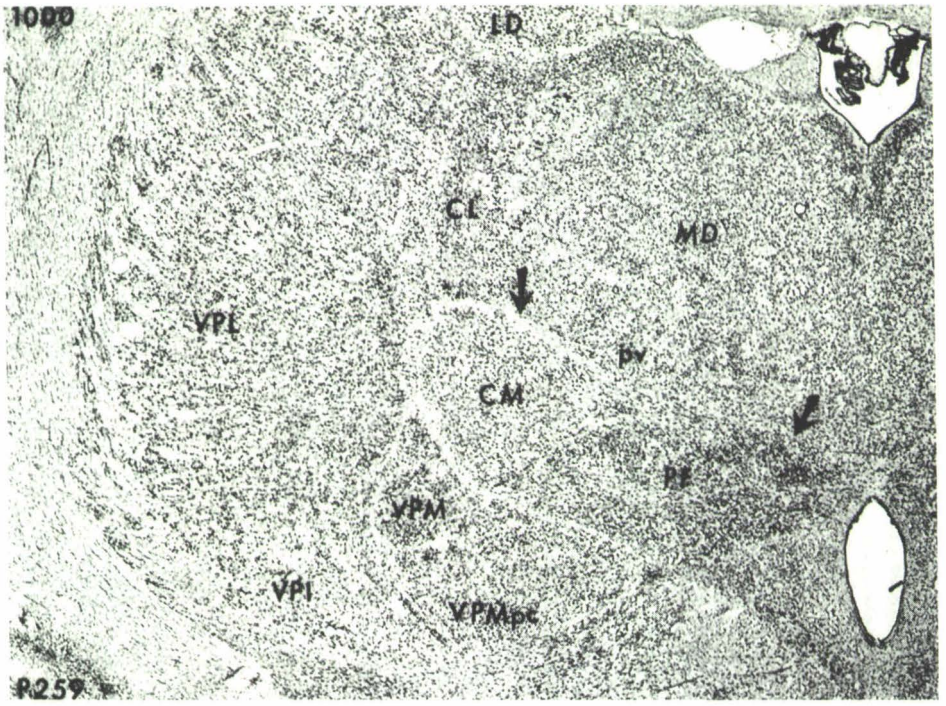


Figure 16.15. Transverse section of the thalamus through the ventrobasal complex and the intralaminar nuclei in a monkey. *CL*, central lateral nucleus; *CM*, centromedian nucleus; *LD*, lateral dorsal nucleus; *MD*, mediodorsal nucleus; *PF*, parafascicular nucleus; *pv*, ventral paralaminar part of dorsomedial nucleus; *VPI*, ventral posterior inferior nucleus; *VPL*, ventral posterolateral nucleus; *VPM*, ventral posteromedial nucleus; *VPMpc*, parvicellular part of VPM. *Arrows* on superior border of the internal medullary lamina define limits of pv. Numbers refer to animal and sequential section (cresyl violet, ×22).

one observed ipsilaterally (Fig. 16.17) (131, 158, 289, 324). Despite the fact that most of them originate from the same neurons in the internal globus pallidus, pallidothalamic fibers display significantly different patterns of arborization within the different thalamic territories. Pallidal fibers in the ventral anterior nucleus form several characteristic glomerulus-like terminal fields, while those in the centromedian course in a more linear fashion giving off only a few thin collaterals throughout the nucleus (131) (Fig. 16.18). Pallidal fibers reaching the habenula form a dense field composed of numerous thin and closely packed terminals, while those reaching the brainstem pedunculopontine tegmental nucleus remain poorly branched (131).

The magnocellular part of the ventral anterior nucleus receives a significant fiber projection from the substantia nigra (3, 50, 52, 54, 60, 84, 156, 157). Nigrothalamic fibers arise from the pars reticularis, pass medially and rostrally through Forel's field H, and follow a course parallel to that of the mammillothalamic tract (Figs. 16.2 and 16.9) (50, 53). Nigrothalamic fibers form a dense terminal felt about groups of cells in the magnocellular part of the ventral anterior nucleus.

Cortical area 6 projects primarily to the principal part, while fibers from area 8 terminate in the magnocellular part of the ventral anterior nucleus (210, 211). Fibers from the primary motor area do not reach any part of the nucleus (209).

Information concerning the efferent projections of the ventral anterior nucleus is incomplete and conflicting (16, 47, 87, 317, 348, 446, 457). Efferent fibers from this nucleus are distributed to widespread areas of the frontal cortex (195). Rostrally projecting cells in the magnocellular part of the ventral anterior nucleus have been described as terminating in localized regions of the caudal and medial orbital cortex (47, 387).

Results from pioneering electrophysiologic studies (165, 166, 407) indicate that the ventral anterior nucleus may be functionally related to the intralaminar nuclei of the thalamus in that recruiting responses in widespread cortical areas can be evoked by repeated low frequency stimulation of the nucleus. Other authors demonstrated that the

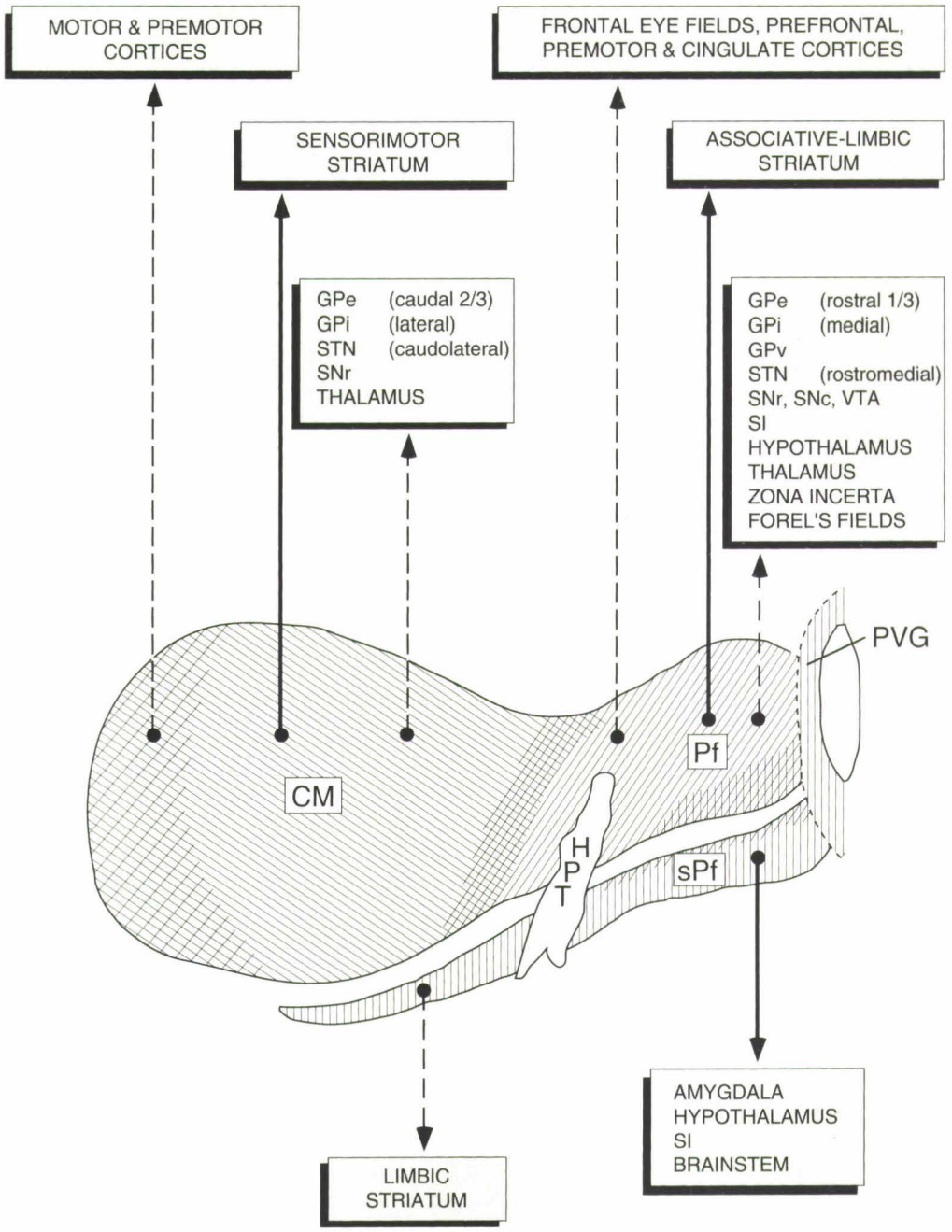


Figure 16.16. Output organization of the centromedian-parafascicular-subparafascicular (CM-Pf-sPf) complex in primates. The major efferent projections are indicated by *uninterrupted lines*, whereas *broken lines* represent less prominent projections. *Cross-hatched* regions in the CM-Pf-sPf complex indicate areas of overlap of cells bearing efferent characteristics of CM, Pf, or sPf.

ventral anterior nucleus is essential for the recruiting response and that lesions in this nucleus block the responses elicited by the stimulation of the intralaminar thalamic nuclei (400). The ventral anterior nucleus appears to be the preeminent site among thalamic nuclei for production of the recruiting response.

VENTRAL LATERAL NUCLEUS

This nucleus, caudal to the ventral anterior nucleus, is composed of small and large neurons that show considerable differences in various parts of the nucleus (Figs. 16.10 and 16.11). It has been subdivided into three main

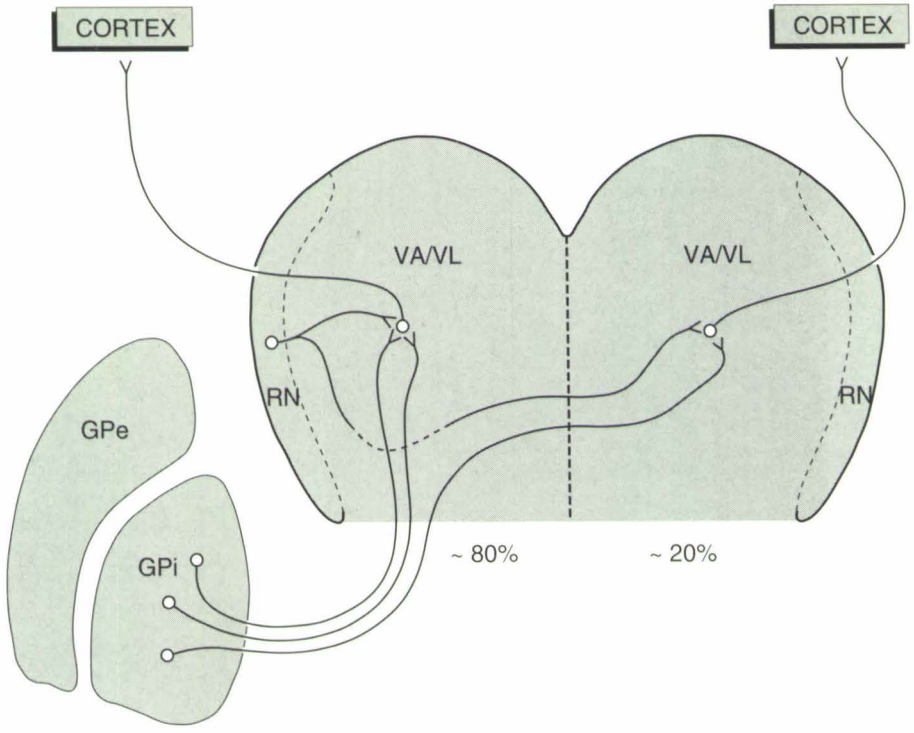


Figure 16.17. Crossed and uncrossed pallidothalamic fibers. The number of contralateral fibers amounts to approximately 20% of the ipsilateral fibers. These fibers arise from the internal segment of the globus pallidus (*GPi*) and terminate within specific regions of the ventral anterior (*VA*) and ventral lateral (*VL*) thalamic nuclei. In turn VA/VL neurons project to the cerebral cortex. Also shown is a decussating fiber from one neuron in the reticular thalamic nucleus (*RN*). The location of the external segment of the globus pallidus (*GPe*) is indicated.

parts (314): (a) pars oralis (VLo), (b) pars caudalis (VLc), and (c) pars medialis (VLm). The pars oralis is the largest subdivision and consists of numerous deep-staining cells arranged in clusters. The pars caudalis is composed of a smaller number of scattered large cells. The pars medialis begins ventral to the ventral anterior nucleus and extends caudally toward the subthalamic region. A crescent-shaped thalamic area in nonhuman primates caudal to VAmc and medial to VLo, designated as "area x" (314), appears, on the basis of connectivity, to be an integral part of the ventral lateral nuclear complex (47, 254, 337, 338). Nuclear subdivisions designated as VLc, "area x," and the oral part of the ventral posterolateral nucleus (VLPo) have been referred to as the "cell-sparse" zone, and cytologically are distinct from VLo, VPLc, and VPM. A recent investigation indicates that the various subdivisions of the ventral lateral nucleus disclosed in monkeys are largely valid for the ventral lateral thalamic mass in humans (145).

Pallidofugal fibers arising from the internal pallidal segment project to the ventral lateral nucleus of the thalamus via the thalamic fasciculus. The major pallidal projection is to VLo and the lateral part of VLm (50, 159, 196, 212, 295). Pallidofugal fibers also project rostrally to ventral anterior nucleus (VApc) and give off collateral fibers to the centromedian nucleus (CM) (Figs. 19.37 and 19.38). These pallidal projections are topographically organized (50, 52, 53, 196, 212, 431).

Efferent fibers, originating in the deep cerebellar nuclei and ascending beyond the contralateral red nucleus, enter the thalamic fasciculus and project to nuclei composing the "cell-sparse" zone of the ventral lateral thalamus (VLc, VPLo, and area x) (50, 56, 138, 191, 254, 265, 406). Single-unit recordings have not revealed a sharp somatotopic organization within the deep cerebellar nuclei, but thalamic nuclei receiving these efferents have a somatotopic representation similar to that of thalamic somatosensory relay nuclei. Different parts of the body are systematically represented with rostral body regions medial and caudal parts of the body lateral. The ex-

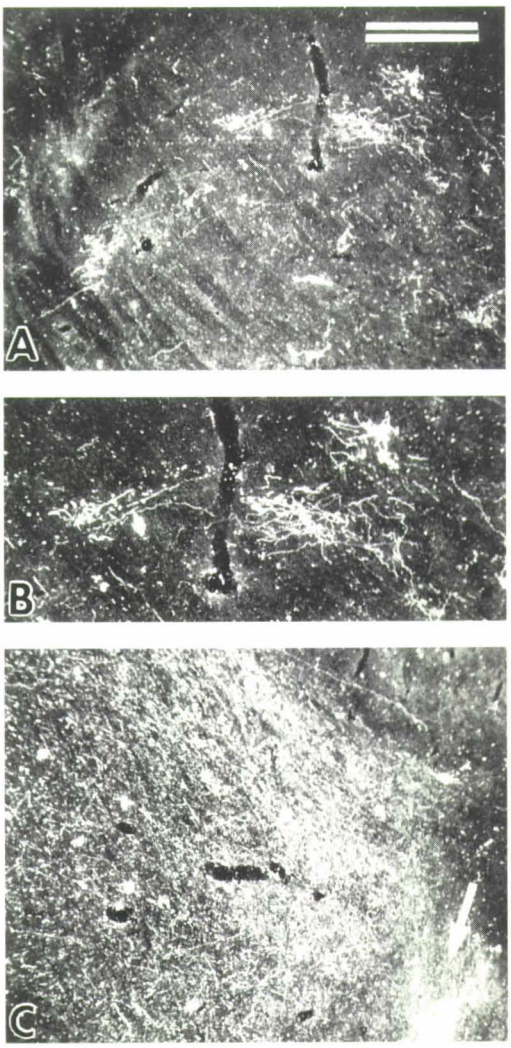


Figure 16.18. Darkfield photomicrographs comparing two forms of terminal arborizations of pallidothalamic fibers that were anterogradely labeled with the lectin *Phaseolus vulgaris*-leucoagglutinin (PHA-L) in the squirrel monkey. **A** and **B.** Terminal arborizations in the form of glomeruli in the ventral lateral thalamic nucleus. **C.** Numerous thin fibers forming a dense and relatively homogeneous terminal field in the centromedian nucleus. The *arrow* indicates the habenulo-interpeduncular tract. Scale bar = 200 μm (**A**) and 360 μm (**B**, **C**).

tremities are represented ventrally. Although dentatothalamic and interpositothalamic fibers appear to end in the same region, terminations are in an interdigitating pattern without overlap. Fastigiothalamic fibers are bilateral with fibers crossing the region of the posterior commissure and/or the internal medullary lamina of the thalamus (158).

The ventral lateral nucleus of the thalamus has long been known to receive a considerable number of fibers from the precentral cortex (219, 229, 230, 262, 440). Studies in monkeys demonstrate that area 4 projects to VLo, VLc, and VPLo, as well as to the centromedian, the paracentral nucleus, and the central lateral nucleus (14, 114, 209, 339, 340, 341, 368). The projection from area 4 to VLc is not as impressive as that from area 6, which also projects to "area x" (210). A systematic analysis indicates that the "cell-sparse" zone of the ventral lateral thalamic region, consisting of VPLo and VLc, projects topographically upon area 4. Medial parts of the zone send fibers to the face area, lateral parts send fibers to the leg area, and fibers from intermediate portions of the zone pass to cortical regions representing the arm and trunk (195, 418, 445, 447) (Fig. 16.14). Thus, the thalamic termination zones for the dentate, interposed, and fastigial nuclei are nearly identical and relay impulses to the primary motor area. The cortical projection zone for the VLo, which receives input from the internal pallidal segment, appears different in that VLo projects to the supplementary motor area and the lateral premotor area (167, 389). The distinctive cytoarchitectural subdivisions of the ventral lateral thalamic region project to separate cortical areas concerned with different aspects of motor function.

VENTRAL POSTERIOR NUCLEUS

The ventral posterior nucleus (VP), whose cells are among the largest in the thalamus, is composed of two major divisions, the *ventral posteromedial nucleus* (VPL) and the *ventral posterolateral nucleus* (VPM), and a smaller intermediate division, the *ventral posterior inferior nucleus* (VPI) (Figs. 16.6, 16.11, 16.13, and 16.15). The VP is the largest primary somatic sensory relay nucleus of the thalamus and is referred to as the ventrobasal complex.

VENTRAL POSTEROLATERAL NUCLEUS

This nucleus has been subdivided into a pars oralis (VPLo), characterized by very large, sparsely distributed cells, and a pars caudalis (VPLc), containing large, evenly dispersed cells and a high density of small cells. Both divisions of the nucleus contain medium-sized fiber bundles radiating in an oblique dorsal direction.

As described earlier, VPLo constitute a distinctive part of the "cell-sparse" zone of

the ventral thalamic region, which receives inputs from the contralateral deep cerebellar nuclei and projects to the primary motor cortex.

Thalamic inputs to VPLc convey somesthetic impulses from the spinal cord and somatosensory relay nuclei in the medulla via (a) the medial lemniscus, and (b) the spinothalamic tracts (24, 35–37, 220, 251, 257, 364, 446, 452). Fibers of the medial lemniscus course through the brainstem, without supplying collateral or terminal fibers to the reticular formation, and terminate exclusively in VPLc (Fig. 16.13) (32, 191, 431, 452). Fibers arising from the nucleus gracilis terminate lateral to those of the nucleus cuneatus (191, 220, 431, 446, 452). Terminals of the medial lemniscus establish predominantly axodendritic contacts throughout VPLc.

Results from single-unit recording studies in VP in a large number of species (287, 288, 377, 378, 345, 346) have revealed somatotopic features in which the contralateral limbs, trunk, and tail are represented in VPLc, and the head, face, and intraoral structures in VPM (Fig. 16.19). Each large body part is represented by a curved lamella with adjacent lamellae related to neighboring body parts (173, 187). Lamellae representing large divisions of the body contain labeled axons arising from cell groups in the dorsal column nuclei that are in register with retrogradely thalamic neurons projecting to corresponding regions of the somesthetic cortex. Representation of the body in VP is continuous, but distorted in a fashion that reflects the greater innervation density of receptors in peripheral parts of the extremities and in the oral region. The distribution of individual, medial lemniscus axons in the VPLc suggests that all axons have terminal ramifications at one level, are focal, and none are sufficiently long to occupy more than one-half of the anteroposterior extent of the nucleus. Terminal ramifications are compressed into narrow sagittal slabs 200–300 μm wide. Axonal ramifications end in either an anterodorsal shell or in the central core of VPLc. Cells in the anterodorsal shell respond to stimulation of deep tissue and largely terminate in cortical areas 3b and 1 (80, 171, 173, 174, 177, 185, 188).

The spinothalamic tracts form a far less discrete ascending sensory pathway than the medial lemniscus. The spinothalamic tract,

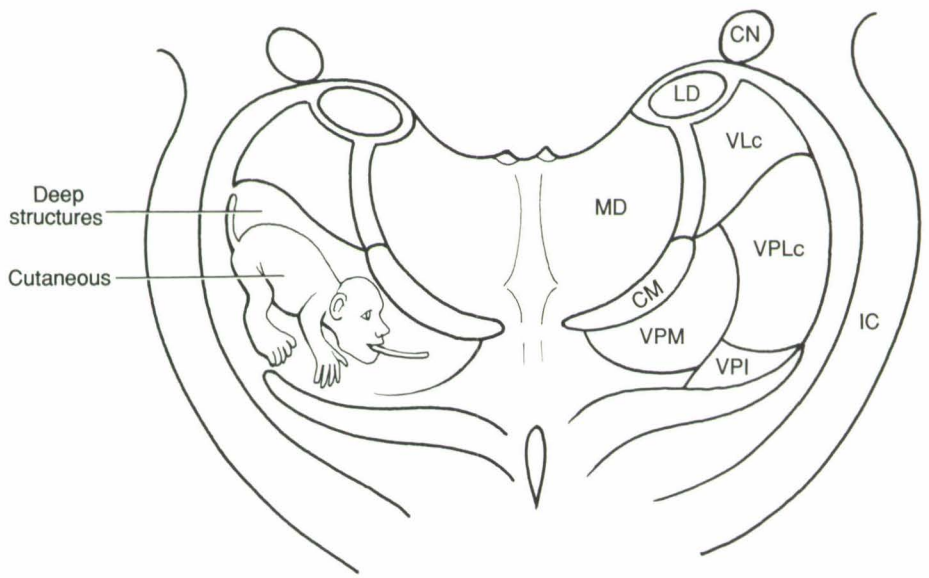


Figure 16.19. Ventrobasal complex in the monkey indicating the cutaneous somatotopic representation of the body surface on the left. Neurons responsive to stimulation of deep receptors lie in a dorsal shell. Areas representing the head, face, and tongue lie in the ventral posteromedial nucleus (*VPM*). The body is represented in the ventral posterolateral nucleus pars caudalis (*VPLc*) with the trunk dorsal and the extermities ventral. Nuclear subdivisions of the thalamus are shown on the right. *CM*, centromedian nucleus; *CN*, caudate nucleus; *IC*, internal capsule; *LD*, laterodorsal nucleus; *MD*, mediodorsal nucleus; *VLc*, ventral lateral nucleus, pars caudalis; *VPI*, ventral posteroinferior nucleus.

and fiber systems ascending with it, contributes a large number of projections and collaterals to the brainstem reticular formation at all levels.

Physiologic studies indicate the precise and orderly fashion in which the contralateral body is represented in VPLc and the spinothalamic tracts. There is a complete, though distorted, image of the body and volume representation of a given part of the body is related to its effectiveness as a tactile organ (i.e., to its innervation density). Cervical spinal cord segments are represented most medially and sacral segments most laterally. The thoracic and lumbar regions are represented only dorsally, while the regions concerned with the distal parts of the limbs extend ventrally. Each neuron of this complex is related to a restricted, specific, and unchanging receptive field on the contralateral side of the body. The neurons are regarded as place specific, modality specific, and concerned almost exclusively with the perception of tactile sense and position sense (kinesthesia). Only a few cells of VP appear to be activated by noxious stimuli.

VENTRAL POSTEROMEDIAL NUCLEUS

This crescent-shaped nucleus with a relatively light-staining neuropil lies medial to VPL and lateral to the curved boundary of the centromedian nucleus (Figs. 16.5, 16.6, 16.11, 16.13, and 16.15). The ventral posteromedial nucleus (VPM) consists of two distinct parts: (a) a principal part composed of both small and large cells, designated simply as VPM, and (b) a small-celled, light-staining part, which occupies the medial apex of this arcuate-shaped nucleus, referred to as the pars parvicellularis (VPMpc). The principal part of VPM receives somatic afferent fibers from receptors in the head, face, and intraoral structures, while VPMpc is concerned with taste (Fig. 16.21). Ascending secondary trigeminal fibers terminating in VPM include (a) crossed fibers from the spinal and principal sensory trigeminal nuclei, which ascend in association with the medial lemniscus (51), and (b) uncrossed fibers of the dorsal trigeminal tract (43, 48, 430), originating from the dorsal part of the principal sensory nucleus of the trigeminal nerve. Tactile impulses from the face and intraoral structures are transmitted bilaterally to parts of the VPM (23, 288, 377).

Secondary gustatory fibers arising from the nucleus solitarius ascend ipsilaterally in the central tegmental tract to terminate in VPMpc (18) (Figs. 16.21). The VPMpc also receives indirect ipsilateral gustatory fibers via a relay in the parabrachial nuclei of the brainstem (304, 305).

VENTRAL POSTERIOR INFERIOR NUCLEUS

This smallest subdivision of the ventral posterior nucleus lies ventrally between VPL and VPM (Fig. 16.15). The ventral border of the nucleus is adjacent to the reticular nucleus and the thalamic fasciculus. Cells of the nucleus are medium-sized and light-staining. Inputs to VPI are not fully understood, but cells in this nucleus appear to provide the major projection to somatic sensory area II (S-II). It has been suggested that a population of sensory neurons of VP with projections to S-II become progressively segregated in VPI.

CORTICAL CONNECTIONS OF THE VENTRAL POSTERIOR NUCLEUS

The ventral posterior nucleus has a precise topical projection to the cortex of the postcentral gyrus (204, 224, 226, 446) (Figs. 16.13 and 16.14). Portions of the gyrus high on the lateral convexity receive fibers from VPLc, while inferior portions of the gyrus near the lateral sulcus are supplied by fibers from VPM (118, 180, 182–184). This thalamocortical projection forms a large part of the superior thalamic radiation. Neurons in the large central core of VPLc, responsive to cutaneous stimuli, project to cortical area 3b on the posterior surface of the central sulcus and to area 1 on the lip of the sulcus. Cells in the thinner peripheral shell of VPLc, responsive to stimulations of deep tissues, project to cortical area 3a in the depths of the central sulcus and to area 2, which forms the posterior part of the postcentral gyrus (Fig. 16.20). Collectively, VPLc and VPM project somatotopically upon the primary somesthetic cortex with a modality segregation. Cells of VPMc that receive ascending gustatory fibers project upon the parietal operculum, area 43. Study of the processing of somatosensory information in the brain has led to the important concept of *parallel processing* (79), whereby each of the pathways that composed the complex somatosensory neural system analyses and treats somewhat different aspects of the somes-

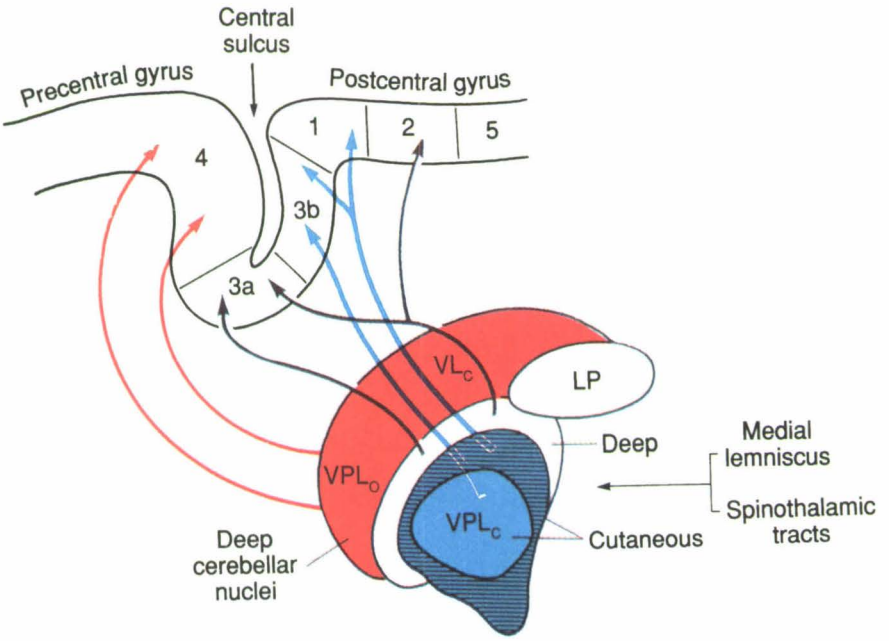


Figure 16.20. Saggital plane showing projections of thalamic subdivisions to the sensorimotor cortex. Neurons in the ventral posterolateral pars caudalis (*VPLc*) and ventral posteromedial (*VPM*) nuclei form a central core (*blue*) consisting of two parts responsive to cutaneous stimuli and an outer shell (*white*) composed of neurons responsive to deep stimuli. Inputs to VPLc are via the medial lemniscus and the spinothalamic projections. Cells in the outer shell project to cortical area 3a (muscle spindles) and to area 2 (deep receptors). Cells in the central core project to areas 3b and 1 (cutaneous). These projections are somatotopic. Inputs to the ventral posterolateral nucleus, pars oralis (*VPLo*), and the ventral lateral nucleus pars caudalis (*VLc*) (*red*) are from the contralateral cerebellar nuclei. Cerebellar input to these thalamic nuclei is considered to be somatotopically organized in nearly the same way as in VPLc and VPM. VPLo and VLc project somatotopically on the primary motor area (area 4).

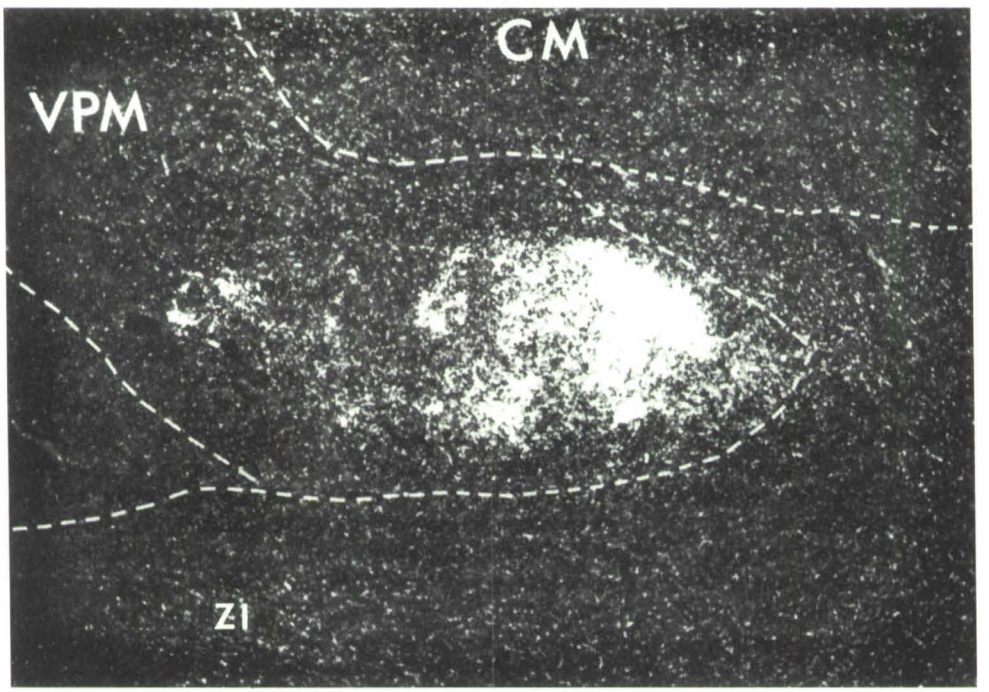


Figure 16.21. Autoradiograph demonstrating transport of isotope from the rostrolateral nucleus of the solitary fasciculus to the ipsilateral ventral posteromedial nucleus (pars parvicellularis). *CM*, centromedian nucleus; *VPM*, somatic part of the ventral posteromedial nucleus, *ZI*, zona incerta.

thetic scene. Parallel processing seems to be a feature of all sensory systems (79, 173).

Posterior Nuclear Group

Caudal to the VPL there is a transitional diencephalic zone with a complex and varied cellular morphology that has been referred to as the posterior thalamic nuclear group (379). The posterior nuclear group (zone) lies caudal to VPLc, medial to the rostral part of the pulvinar, and dorsal to the medial geniculate body (Fig. 16.4). This nuclear complex consists of (a) the *supra-geniculate nucleus*, (b) the *nucleus limitans*, and (c) an ill-defined region of heterogeneous cell types that extends rostrally toward the caudal pole of VPLc, referred to as the *posterior nucleus* (44, 173). The suprageniculate nucleus is a pyramid-shaped cell mass that extends dorsomedially from the dorsal part of the principal division of the medial geniculate body (Fig. 16.22). The nucleus limitans is a narrow band of oval or spindle-shaped cells that separates the pretectum and medial nucleus of the pulvinar (314). These cells merge laterally with those of the suprageniculate nucleus. The posterior nucleus, composed of small- and medium-sized cells which lie rostral to the suprageniculate nucleus, extends rostrally toward VPLc and becomes continuous with VPI. The dorsal part of the posterior nucleus is difficult to distinguish from overlying regions of the pulvinar and the small-celled part of the suprageniculate nucleus. The magnocellular part of the medial geniculate nucleus lies ventral to the rostral part of the suprageniculate nucleus and ventral to the posterior nucleus (Fig. 16.22).

Functionally, the posterior nucleus is of particular interest because it receives spinothalamic medial lemniscal fibers and appears involved, at least in part, in the nociception (13, 30, 32, 33, 35, 37, 173, 193, 194, 252, 253, 255, 257, 359). The medial part of the posterior nucleus may also receive projections from the primary (S-I) somatosensory cortex (136, 180, 181). Studies in cats and monkeys indicate that cells in the medial division of the posterior nucleus project to the retroinsular cortex, and cells in the lateral division of this nucleus project to postauditory cortex (44). Neither of these cortical projections overlap recognized somatosensory or auditory areas. The suprageniculate-limitans nuclear complex receives inputs from the deep layers of the superior colliculus and from the insular cortex and, in turn, projects to the insular cortex (173, 175, 372).

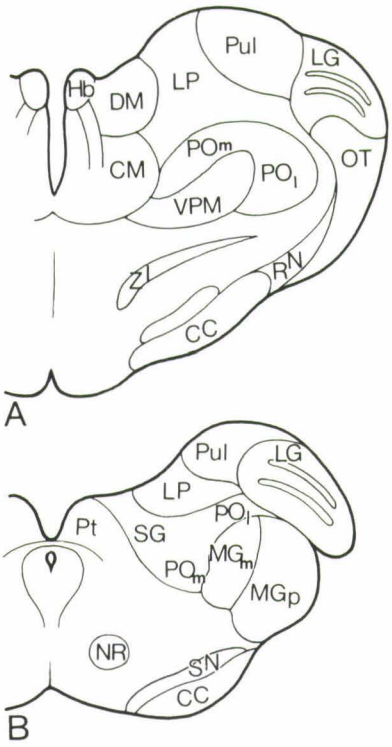


Figure 16.22. Two levels of the caudal thalamus in the cat showing relationships of the nuclei of the posterior thalamic complex to other thalamic nuclei. Two divisions of the posterior thalamic nuclei are recognized, a medial (PO_m) and a lateral (PO_l). In **B**, the posterior thalamic nuclei lie medial and dorsal to the magnocellular part of the medial geniculate nucleus (MG_m); the medial nucleus, PO_m appears continuous with the suprageniculate nucleus (SG). In **A**, PO_m and PO_l lie dorsal and lateral to the ventral posterior medial nucleus (*VPM*) and immediately caudal to the ventral posterolateral nucleus (*VPL*). *CC*, crus cerebri; *CM*, centromedian nucleus; *DM*, dorsomedial (mediodorsal) nucleus; *Hb*, habenula; *LG*, lateral geniculate body; *LP*, lateral posterior nucleus; *MGp*, medial geniculate nucleus, parvicellular part; *NR*, red nucleus; *OT*, optic tract; *Pt*, pretectum; *Pul*, pulvinar; *RN*, reticular nucleus of thalamus; *SN*, substantia nigra; *ZI*, zone incerta.

Recent studies make it clear that the posterior nuclei cannot be thought of as a single functional entity. The only common denominators are their intimate topographic relationship with other thalamic nuclei and their projections to cortical fields in and around the insula. These nuclei are clearly multimodal as they integrate information of the visual, auditory, and somesthetic types. There is a slight preponderance of visual influences in the suprageniculate-limitans complex, while the posterior nucleus appears to be more under

auditory influence. None of the posterior nuclei, however, appear to have the specificity of organization of a typical thalamic relay nucleus.

Geniculate Nuclear Group

MEDIAL GENICULATE NUCLEUS

The medial geniculate nucleus (MGN) lies on the caudal ventral aspect of the thalamus, medial to the lateral geniculate nucleus (LGN) and dorsal to the crus cerebri (Figs. 16.3, 16.4, and 16.13). This large nuclear mass is the thalamic auditory relay nucleus, receiving fibers from the inferior colliculus via its brachium and giving rise to the auditory radiation (Fig. 13.13). Unlike auditory relay nuclei at lower brainstem levels, there are no commissural connections between the medial geniculate nuclei. The medial geniculate nucleus consists of several subdivisions with distinctive cytoarchitecture and connections (127, 280, 311). The three main divisions of the MGN are referred to as medial, dorsal, and ventral (280, 311) (Fig. 16.23). These subdivisions of the medial geniculate nucleus, not easily distinguished in ordinary histologic preparations, become apparent in Golgi preparations (280–282).

The ventral nucleus extends throughout most of the rostrocaudal length of the MGN and is bounded medially by the brachium of the inferior colliculus. Unlike all other major subdivisions of the MGN, the ventral nucleus has a distinct laminar organization. Cells of the ventral division are fairly constant in size and shape and have tufted dendrites. The lamination, produced by the dendritic pattern of tufted cells and fibers of the brachium of the inferior colliculus, is in the form of spirals or curved vertical sheets (Fig. 16.23). Afferent fibers from the inferior colliculus enter particular laminae and remain continuously associated with the same layers. The lamina-

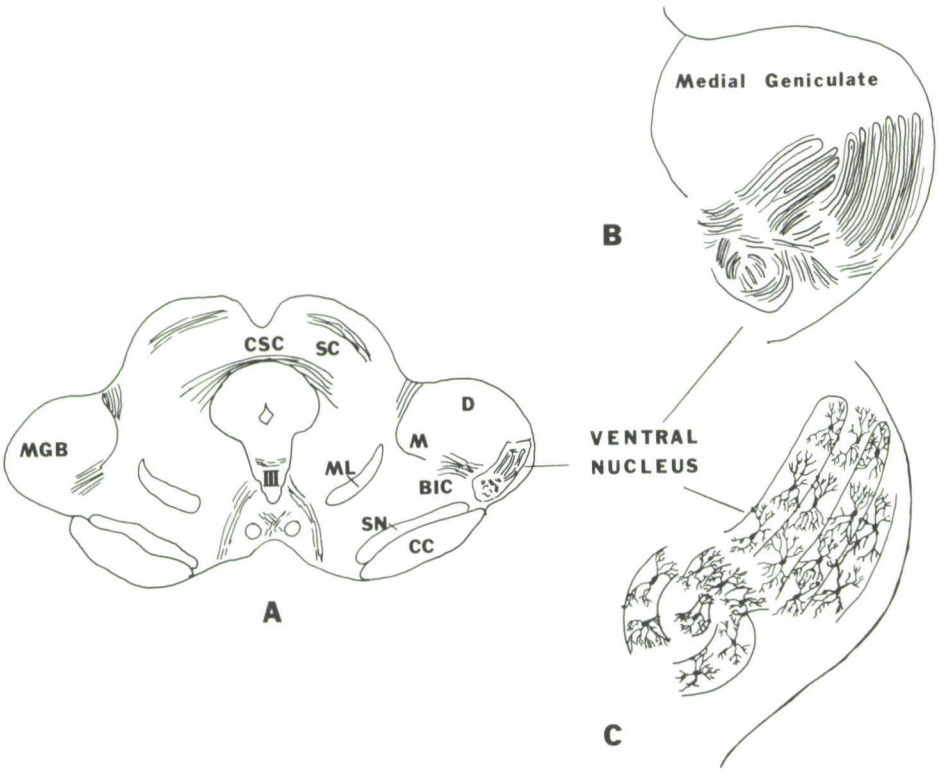


Figure 16.23. Transverse reconstructions of the fibrodendritic laminations in the ventral nucleus of the medial geniculate body in the cat based on Golgi preparations. **A.** Transverse section of midbrain through the superior colliculus (*SC*) and medial geniculate body (*MGB*) or nucleus; *M* and *D* indicate the magnocellular and dorsal nuclei of the MGB. The laminated ventral nucleus of MGB is shown in **A**, **B**, and **C**. The lamination in the ventral nucleus, produced by the arrangement of dendrites of geniculate neurons and fibers in the brachium of the inferior colliculus (*BIC*), occurs in spirals and vertical sheets (**B**, **C**). *CC*, crus cerebri; *CSC*, commissure of the superior colliculus; *ML*, medial lemniscus; *SN*, substantia nigra; *III*, oculomotor nucleus.

tion in the ventral division of the MGN is analogous to that in the lateral geniculate nucleus, except the cellular laminae are not separated by bands of myelinated fibers. The laminar organization of the ventral division of the MGN resembles that of the ventrolateral division of the central nucleus of the inferior colliculus from which it receives its major input (55, 205, 274, 280, 311, 375). Physiologic mapping of the ventral division of the MGN reveals that the cellular laminae are related to the tonotopic organization in which high frequencies are represented medially and low frequencies laterally (6, 93, 115). Neurons in the ventral division of the MGN give rise to the auditory radiation which terminates in the primary auditory cortex (Figs. 13.13, 20.29, and 20.30) where there is a spatial representation of tonal frequencies (55, 298, 312, 356, 453). The primary auditory cortex gives rise to reciprocal corticothalamic fibers that terminate in the ventral division of the MGB (75, 85, 312). Both geniculocortical and corticogeniculate fibers are ipsilateral.

In humans, the MGN projects principally to the superior temporal convolution (transverse gyrus of Heschl) via the geniculo-temporal or auditory radiations (Figs. 13.13, 16.13, and 16.39). This cortical projection area (area 41) has a tonotopic localization in which high tones are appreciated in medial regions and low tones are represented laterally and anteriorly (Fig. 20.10) (160, 259).

The dorsal division of the MGN contains several nuclei, among which are the suprageniculate and the dorsal nuclei (311). The dorsal nucleus, prominent at caudal levels of the MGN (Fig. 16.23), receives projections from a broad lateral tegmental area that extends from the deep layers of the superior colliculus to the area adjacent to the lateral lemniscus (205, 311). The suprageniculate nucleus (Fig. 16.22) appears to receive projections from deep layers of the superior colliculus and the dorsal midbrain tegmentum (44, 311). This nucleus was considered earlier as part of the posterior nuclear group.

The medial division, containing the largest cells in the MGN and lying dorsomedial to the ventral division, is known as the magnocellular part (Figs. 16.22 and 16.23). Rostrally, the magnocellular part of the MGN borders the suprageniculate nucleus and the posterior thalamic nucleus. This division of the MGN receives inputs from the inferior colliculus, lateral tegmentum, and spinal cord (31, 55, 185, 253, 274, 275, 282, 311). All nonlaminated portions of MGN (i.e., the dorsal and medial divisions) send fibers ipsilaterally to at least five cytoarchitectonically distinct areas which form a cortical belt surrounding the primary auditory area (311, 356, 453). There is very little overlap in the cortical projections of these MGN subdivisions. One exception to the foregoing concerns the caudal magnocellular part of the medial division which projects to most, if not all, of the cortical target areas of MGN. Thus, the cortical projection of the magnocellular MGN overlaps terminations of the ventral laminated part of the MGN in the primary auditory area and the terminations of all nuclei in other subdivisions projecting to the secondary auditory cortex. However, there is a difference in the cortical terminations of these fibers in that fibers from the magnocellular division terminate mainly in layer I of the cortex, while all other parts of the MGN send fibers primarily to cortical layer IV and/or III (173).

Although ascending pathways in the auditory system are paralleled by descending fiber linkages which can facilitate or inhibit transmission of impulses at numerous relay nuclei, or in the hair cells of the cochlea, the MGN does not participate in this descending system. Cortical projections from the primary and secondary auditory areas are back to the subdivisions of the MGB from which they receive afferents (55, 312).

LATERAL GENICULATE NUCLEUS

In most species, the lateral geniculate nucleus is a nuclear complex rather than a single nucleus, since two or more components can be recognized (173). One of these, the dorsal lateral geniculate nucleus (LGNd), projects to the cortex and is the major relay nucleus for the visual system. The other component, the ventral lateral geniculate nucleus (LGNv), is developmentally a part of the ventral thalamus and does not project to the cortex. In primates, probably because of the descent and rotation of the dorsal lateral geniculate nucleus during development (219), the ventral lateral geniculate nucleus lies above the dorsal nucleus. In this position, it is often referred to as the pregeniculate nucleus (173). This component is not considered further here.

The (dorsal) lateral geniculate nucleus (LGN), the thalamic relay nucleus for the visual system, lies rostral and lateral to the medial geniculate nucleus (MGN), lateral to the



Figure 16.24. Cellular lamination of the lateral geniculate nucleus with laminae numbered from the hilus. The magnocellular laminae (1 and 2) constitute the ventral subdivision. Parvicellular laminae 3 through 6 are referred to as the dorsal subdivision. Crossed fibers of the optic tract terminate in laminae 1, 4, and 6; uncrossed optic fibers terminate on other laminae.

crus cerebri, and ventral to the pulvinar (Figs. 2.26, 16.3, 16.4, 16.13, and 16.24). This laminated cellular structure has a horseshoe-shaped configuration in transverse sections, with the hilus directed ventromedially. Crossed and uncrossed fibers of the optic tract enter via the hilus and are distributed in a precise pattern. In human and nonhuman primates, the LGN consists of six cellular layers or laminae arranged in two major subdivisions (142, 221, 225). The six concentric cell layers, separated by intervening fiber bands, customarily are numbered from 1 to 6, beginning from the hilar region (Fig. 16.24). Subdivisions of the LGN are magnocellular (layers 1 and 2) and parvicellular (layers 3 to 6) (246). Both divisions of LGN receive afferents from the ganglion cells of the retina (384).

The parvicellular layers of LGN, consisting of layers 3, 4, 5, and 6 in ventro-dorsal sequence, are easily distinguished in caudal parts of the nucleus (Fig. 16.25). As these layers are traced laterally they fuse in pairs: layer 4 with layer 6, and layer 3 with layer 5 (142). In rostral parts of LGN, the individual layers are more difficult to identify because layer 3 does not extend as far rostrally as layer 5, and layers 4 and 6 fuse medially as well as laterally. The projection from the retina onto LGN is precise, and crossed and uncrossed fibers in the optic tract end upon separate layers. Anterograde and retrograde degeneration studies, as well as more recent autoradiographic studies have revealed that crossed fibers of the optic tract end upon layers 1, 4 and 6, while uncrossed fibers terminate in layers 2, 3 and 5 (106, 107, 117, 137, 142, 168, 190, 215, 250, 266, 425, 426).

The monocular crescent of the visual field is subserved by receptor elements in the most medial part of the nasal retina (Fig. 16.27). Ganglion cells in this part of the retina project crossed fibers to the bilaminar segment of opposite LGN, located laterally where parts of layers 4 and 6 fuse (142, 189) (Fig. 16.25). The optic disc, located in the nasal half of the retina and representing optic nerve fibers, has no photoreceptors and is responsible for the blind spot detectable on perimetry. The optic disc, represented in the contralateral LGN by cellular discontinuities in layers 4 and 6, is a constant feature (142) (Fig. 16.25).

Nissl preparations through the human lateral geniculate nucleus reveal a linear cellular organization in which the long axis of the cells tend to run perpendicular to the laminae. This linear cellular orientation corresponds to the orientation of small blood vessels running through the nucleus from its ventral surface (142). Perikarya of the parvicellular layers are oriented perpendicular to laminae so that the long axis of the cells parallel "lines of projection" which indicate isorepresentation of points in the visual field (27, 189) (Fig. 16.26).

The topographic representation of the retinal surface within the LGN is highly organized and precise. The contralateral half of the binocular visual field is represented in each of the six layers of the LGN, even though crossed and uncrossed fibers end in different layers. The projection loci in the six layers lie in perfect register so that any small area in the contralateral binocular visual field can be shown to correspond to a dorsoventral column of cells extending radially through all six layers parallel to the "lines of projection," which indicate identical points in the visual field (Fig. 16.27) (189). The LGN consists of six sheets of cells bent in a horseshoe configuration, but in exact registration, so that columns of cells in the "lines of projection" receive inputs from corresponding points in the retina of each eye related to the contralateral binocular visual field. Binocular fusion does not occur in the LGN because retinogeniculate fibers end on different layers. Following section of the optic nerve, anterograde degeneration or transneuronal degeneration (after long survival) occurs in three layers of the LGN on each side. The layers in which

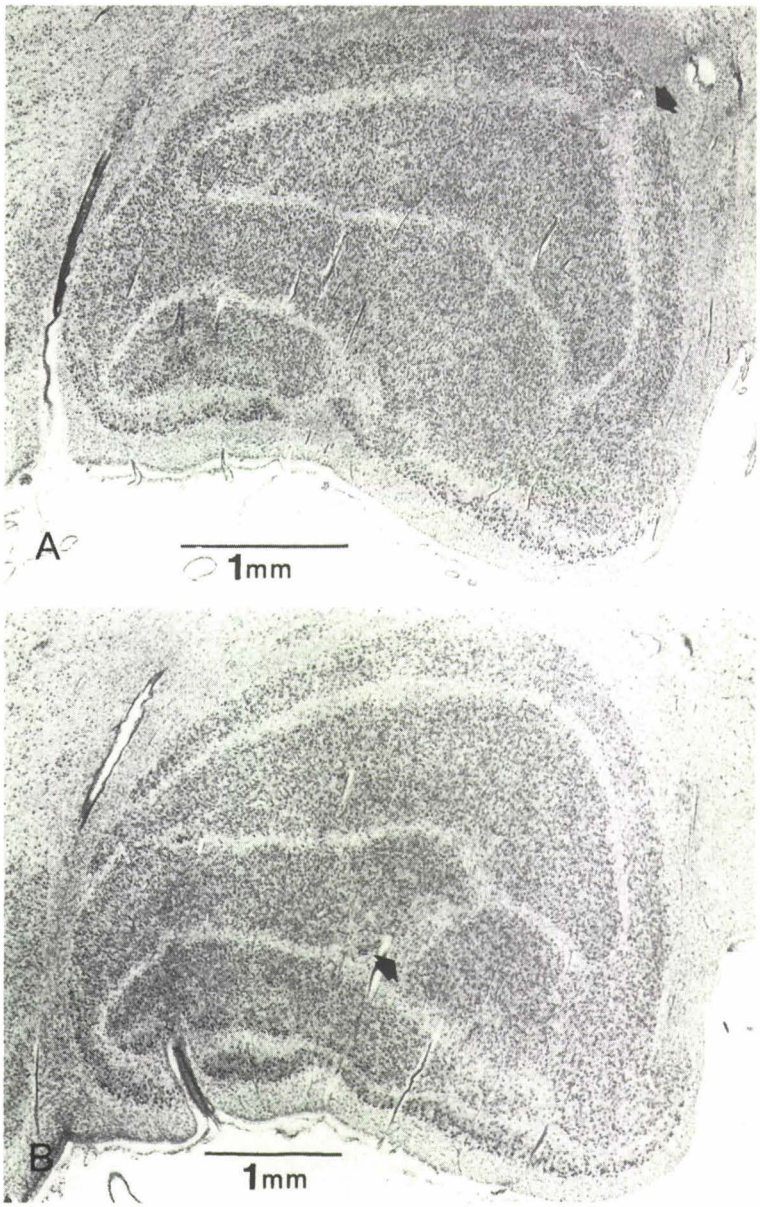


Figure 16.25. Sections through the human lateral geniculate nucleus. The blind spot is represented by discontinuities in layers 6 (**A**, *arrow*) and 4 (**B**, *arrow*). Layers 4 and 6 fuse laterally (*right*) in both **A** and **B**, producing the bilaminar segment ventrally. The bilaminar segment receive an input from the most medial contralateral nasal retina that subserves the monocular visual field (i.e., the monocular crescent).

degeneration of fibers or cells occur differs in accordance with the disposition of crossed (layers 1, 4, and 6) and uncrossed (layers 2, 3, and 5) retinal fibers (107, 117, 142, 250, 347). Small lesions of the retina produce transneuronal degeneration in localized clusters of cells in three different layers on each side aligned according to the "lines of projection" (96, 225, 347). The contralateral monocular visual field (monocular crescent) related to receptor elements in the most medial nasal retina, is represented by crossed fibers terminating in the only bilaminar segment (Figs. 16.25 and 16.27) (142, 189).

The "lines of projection" in the LGN also can be demonstrated by the study of retrograde cell degeneration in the LGN following small lesions in the striate cortex (95, 119, 142,



Figure 16.26. Lateral geniculate nucleus of a baboon that sustained several lesions in the striate cortex. Retrograde degeneration in a large V-shaped sector of the lateral geniculate nucleus demonstrate the lines of projection. Lines of projection represent points of isorepresentation in the visual field.

189, 376). Since one-half of the visual field is represented topographically in the striate cortex of each hemisphere, the zone of retrograde cell degeneration in the LGN is bounded on each side by lines of projections. Cortical projection zones in geniculate segments involve cells of LGN in all layers, and neurons in the LGN with identical receptive fields form a column of cells extending through all laminae. Cells in each of these columns in LGN project to the same region of the striate cortex.

In the LGN, the horizontal meridian of the visual field corresponds to an oblique dorsoventral plane that divides the nucleus into medial and lateral segments. Fibers from the superior retinal quadrants of both eyes project to the medial half of LGN while the inferior retinal quadrants send fibers to the lateral half of the nucleus. The retinal projection from the macula is represented in a wedge-shaped sector in the caudal part of LGN on both sides. The macular representation account for about 12% of the total volume of LGN. The vertical meridian of the visual field, corresponding to the line separating temporal and nasal parts of the retina, is represented along the caudal margin of the nucleus from its medial to lateral borders (41, 142, 149, 150, 189, 213, 225, 247, 347) (Figs. 16.28 and 16.29).

Retinofugal fibers entering various lami-

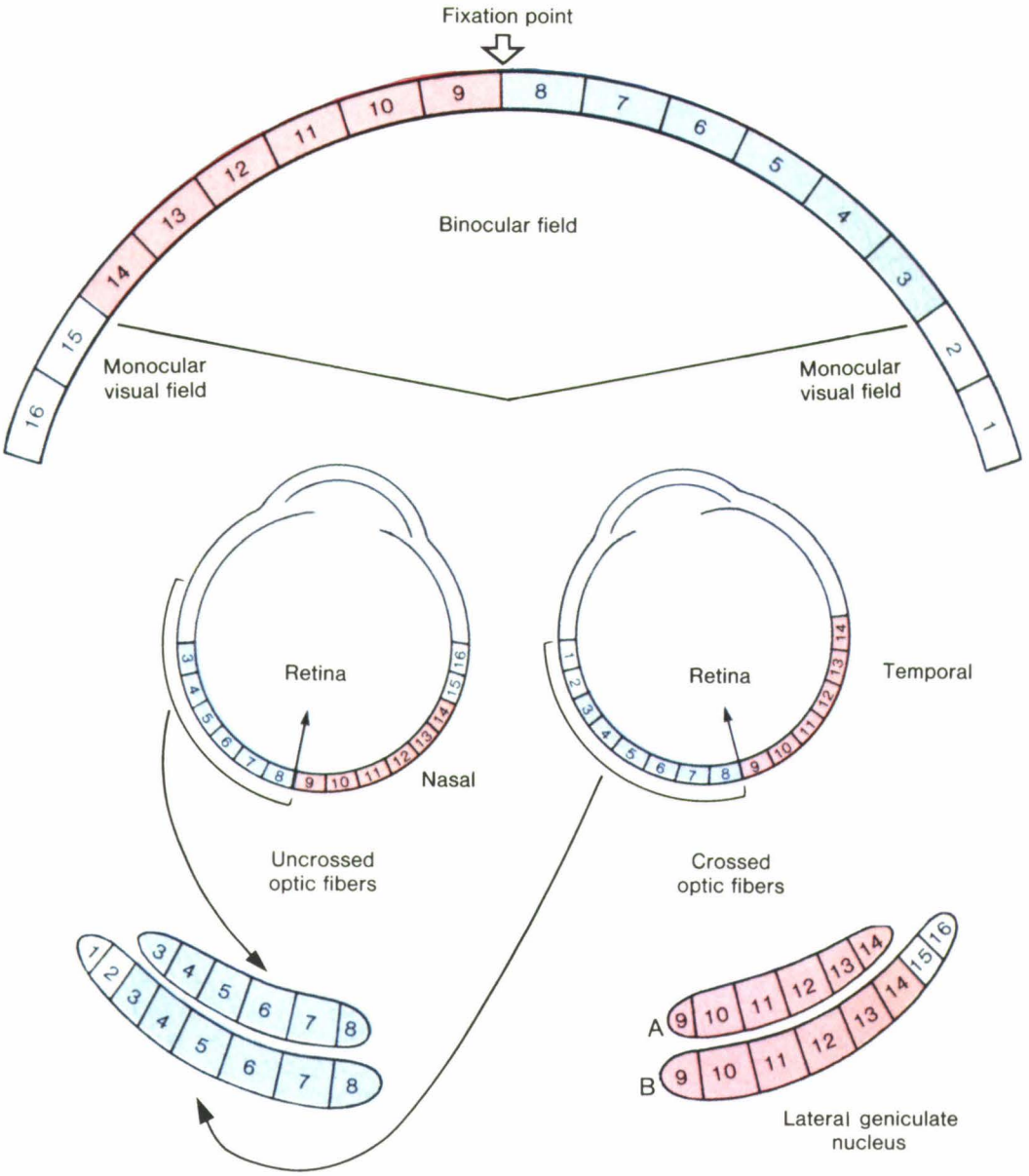


Figure 16.27. Representation of the visual field in the retinae and in the layers of the lateral geniculate nucleus. Portions of the binocular visual field are shown in *red* (*left*) and *blue* (*right*), while the monocular visual fields are *white*. Light from numbered sectors of both the binocular and monocular visual fields falls upon corresponding numbered sectors of the retinae. Crossed and uncrossed retinofugal fibers project upon columns of cells in different laminae of the lateral geniculate nucleus which are in exact registration, represented here by corresponding numbers. **A** represents laminae receiving uncrossed fibers (i.e., laminae 2, 3, and 5). **B** represents laminae receiving crossed fibers (i.e., laminae 1, 4, and 6). Light from the right monocular visual field (sectors 1 and 2) falls upon retinal receptors of the corresponding number in the most medial ipsilateral nasal retina. Crossed retinofugal fibers project to cell columns of the left lateral geniculate nucleus (1, 2). Cell columns 1 and 2 are best developed in laminae 4 and 6 which fuse to form the bilaminar segment.

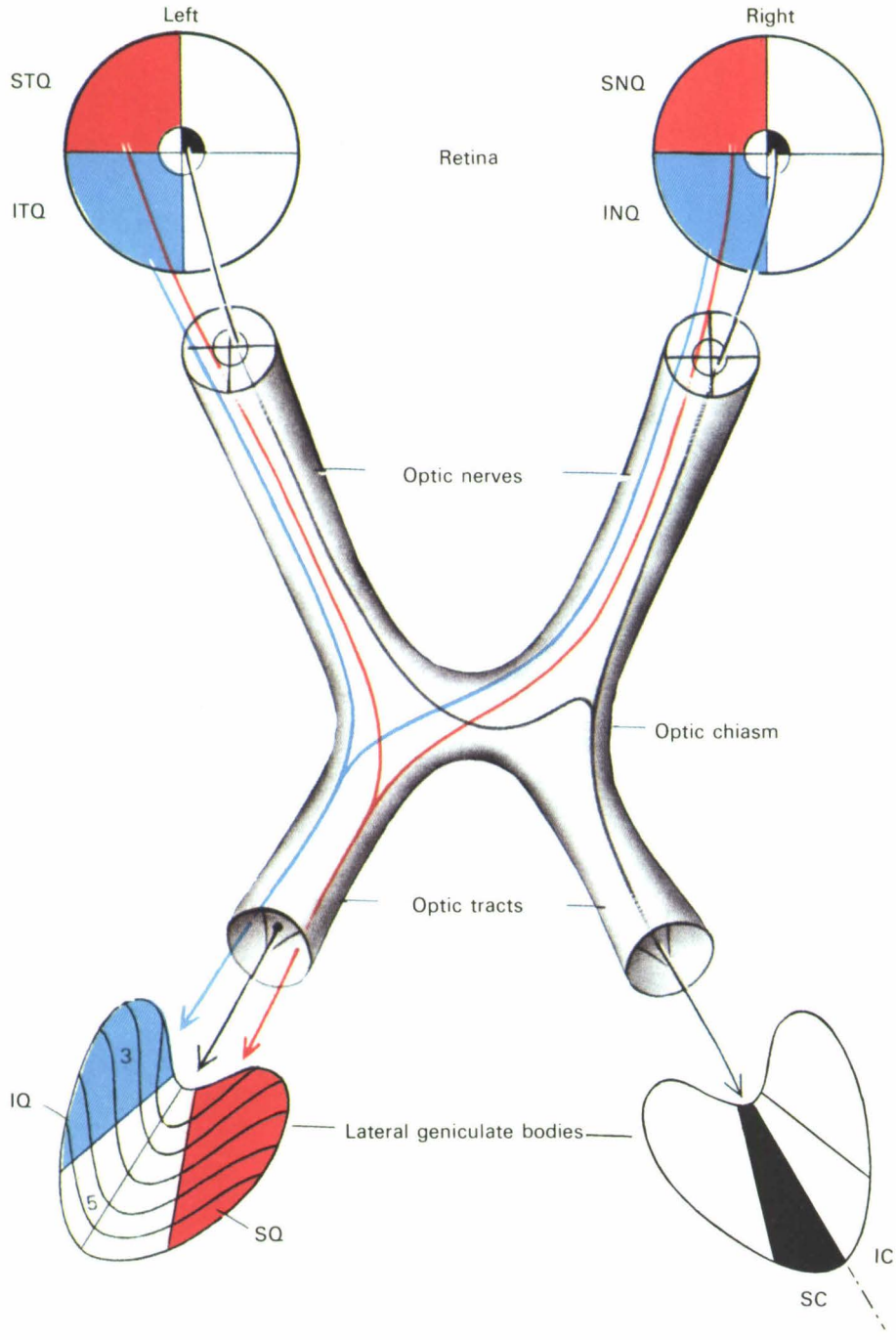


Figure 16.28. Retinal ganglion cell projections through the optic nerves, optic chiasm, and optic tracts to terminations within the lateral geniculate nuclei. Superior peripheral quadrants of the retina on both sides (*SNQ*, superior nasal quadrant, and *STQ*, superior temporal quadrant), shown in *red*, project to the medial part (*SQ*) of the left lateral geniculate nucleus (*red*). Inferior peripheral quadrants of the retina (*INQ*, inferior nasal quadrant, and *ITQ*, inferior temporal quadrant), shown in *blue*, project to the lateral part (*IQ*) of the left lateral geniculate nucleus (*blue*). Superior central regions of the retina on nasal and temporal sides (*black*) on the opposite side project to the region of the right lateral geniculate nucleus indicated by *SC*. Inferior central regions of the retina (*white*) project in the same fashion to the region of the right lateral geniculate body indicated by *IC*. The macular projection to the lateral geniculate is in the caudal region of the nucleus. Numbers in the left lateral geniculate body indicate two of the six laminae.

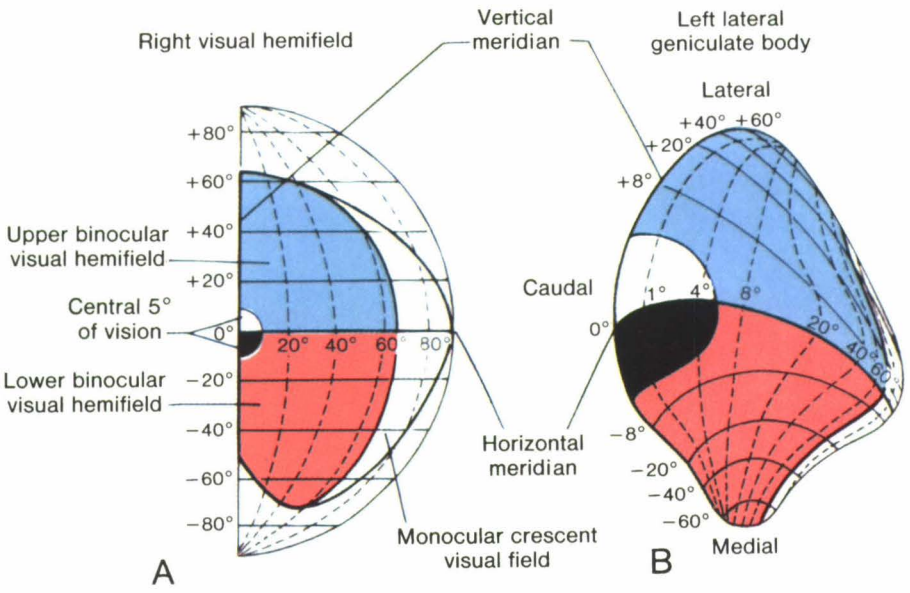


Figure 16.29. Right visual hemifield of the monkey (**A**) and its projection onto the dorsal surface of the unfolded left lateral geniculate body (*LGB*) or nucleus (**B**). The vertical meridian is represented by the *heavy black line* on the left in both **A** and **B**; visual field zones of increasing eccentricity are represented serially in degrees by *dashed lines*. In the left lateral geniculate nucleus, visual field zones (*dashed lines*) are represented serially among the caudorostral axis of the nucleus in degrees. The horizontal meridian of the hemifield at zero degrees is represented by a *curved line* in the caudorostral axis of the LGB (**B**). *Thin lines* above and below the horizontal meridian indicate positive or negative elevations in degrees. Upper (*blue*) and lower (*red*) portions of the binocular visual hemifield indicated in **A** are represented by the same colors in **B**. The central 5° of vision, a generous estimate of the angle subtended by the fovea centralis, are shown in *black* and *white* at the intersection of the vertical and horizontal meridians. The monocular crescent (*white*) in **A** is represented along the rostral border of the LGB.

nae of LGN establish synaptic contact with dendrites of geniculate neurons which are distributed within their particular lamina (45, 61, 116, 422). Cells in LGN exhibit both convergence and divergence: retinal afferent fibers may synapse with several neurons in LGN (divergence), and each neuron of the LGN may receive inputs from several retinofugal fibers (convergence).

Laminae of LGN also contain substantial numbers of Golgi type II neurons that play an important role in processing visual information (116, 124, 214, 331, 332, 422). Electron microscopic observations reveal a synaptic arrangement in which retinal axon terminals establish synaptic contact with both relay neurons and Golgi type II cells (124, 331). This pattern of synaptic articulation, termed *triadic synaptic arrangement*, is a fundamental ultrastructural feature of LGN as well as of other thalamic sensory nuclei. This synaptic arrangement consists of a retinal axon terminating upon dendrites of both a LGN relay neuron and a Golgi type II interneuron. The Golgi type II neuron is presynaptic to the same relay neuron that received a direct retinal ending. These "triads" are found throughout the LGN, as well as in characteristic glial encapsulated synaptic complexes known as *glomeruli*. This triadic synaptic arrangement serves as a mechanism for phasic inhibition of geniculate relay neurons. In this action it is assumed that the retinal axon excites both the geniculate relay neuron and the interneuron. The discharge of the interneuron, in turn, inhibits the same relay neuron excited by the retina afferent.

Glomeruli in the LGN constitute a synaptic complex of interlocking nerve processes of various origins, are arranged in a specific manner, and separated from the environment by a capsule of glial processes (Fig. 16.30) (421). The axon terminals of retinal afferents occupy the central position in these glomeruli. Unlike the cerebellar glomeruli, which contain only one mossy fiber rosette, several club-shaped retinal afferents may occur in a LGN glomerulus. Other contributions to the glomeruli arise from Golgi type II cells and corticofugal fibers (Fig. 16.30). Glomeruli often are located at the bifurcation of stem dendrites of a LGN neuron. Axons of

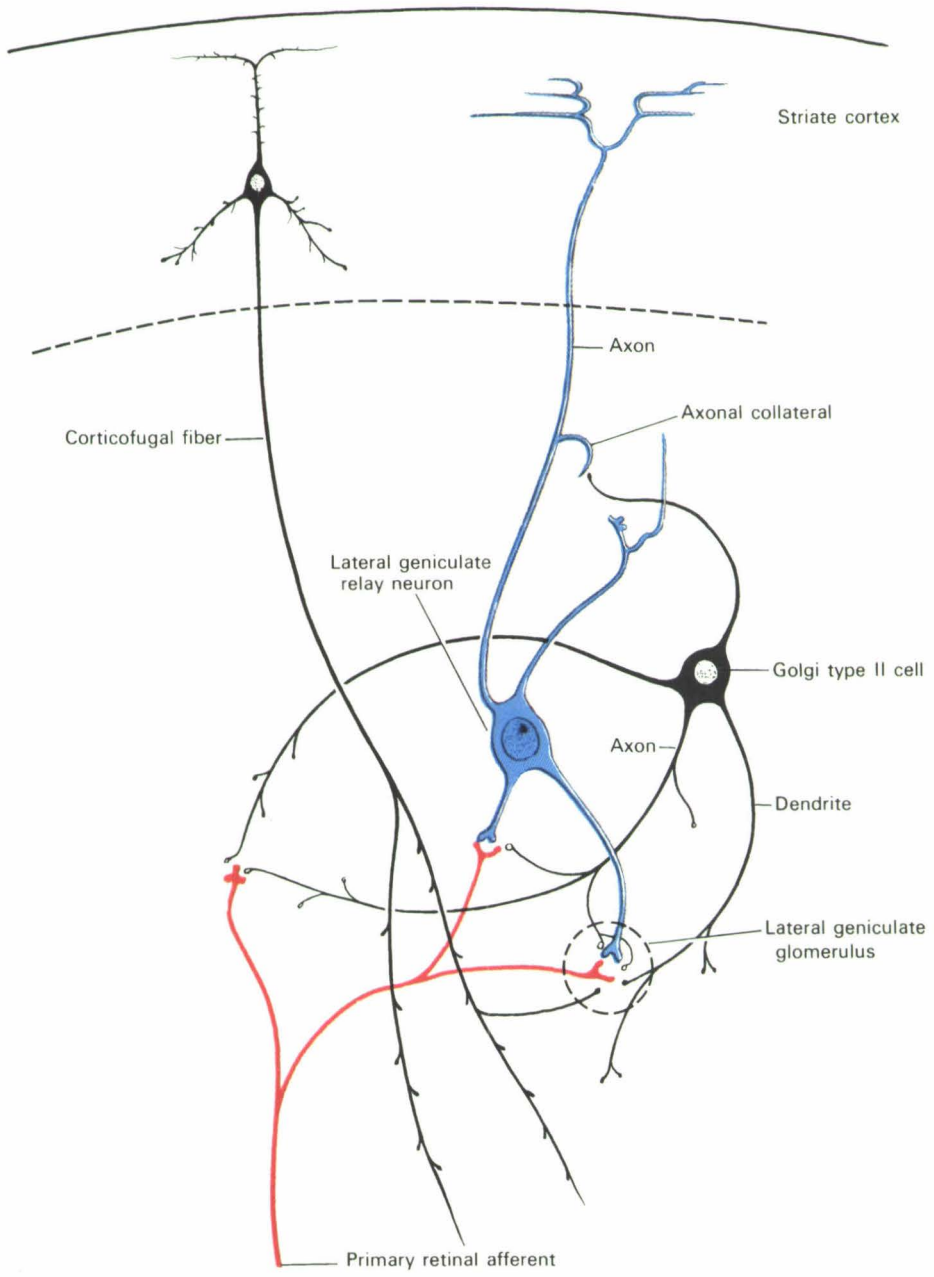


Figure 16.30. Neuronal arrangements in a glomerulus of the lateral geniculate nucleus. A primary retinal afferent is indicated in *red*, while the lateral geniculate nucleus relay neuron is in *blue*. A corticofugal fiber and a Golgi type II cell are shown in *black*. The glomerulus contains a terminal of a primary retinal afferent, several club-shaped terminals of a relay neuron of the lateral geniculate nucleus, and contributions from both Golgi type II neurons and corticofugal fibers. This synaptic complex is enclosed in a capsule of glial processes, indicated by the *dashed line*.

Golgi type II cells enter the glomeruli and establish synapses with relay cell (LGN neuron) dendrites. These cells exert a GABAergic inhibitory influence upon these dendrites. The LGN glomerular complex contains (a) axodendritic synapses on stem, secondary, and peripheral dendrites, and (b) axoaxonic synapses in which the presynaptic portion is contributed by terminals of the retinofugal fibers. The most remarkable feature of these glomeruli is the frequent occurrence of axoaxonic synapses. Some glomeruli of the LGN contain the triadic synaptic arrangement previously described. In the triadic arrangement, the participating neural elements remain the same, but the receptive sur-

faces on geniculate relay neurons or Golgi type II cell may be either the soma or a dendrite (124). Among the participating elements, terminals from corticogeniculate fibers and those from fibers originating in the reticular thalamic nucleus are functionally important.

The complex synaptic arrangements within LGN glomeruli are effective in the versatile processing of visual information (393). The LGN is not a simple cortical relay nucleus, but a structure in which important transformations of visual information occur through physiologic processes involving inhibition from a variety of sources that change the pattern and strength of neuronal responses. It is worth noting that the corticogeniculate fibers outnumber the geniculocortical fibers by a factor of 2 (393). Thus, corticogeniculate fibers are likely to play an important role in the complex internal processing of visual information that occur at LGN level.

The lateral geniculate nucleus is the main end station of the optic tract and, in turn, the nucleus projects massively to the visual (calcarine) cortex via the geniculocalcarine tract or visual radiations (Fig. 16.42). Cells of LGN project retinotopically, primarily upon the striate cortex (area 17), but also upon the parastriate (area 18) and peristriate (area 19) cortex (82, 97, 102, 109, 148, 300, 433, 451, 454). The striate cortex has reciprocal connections with the LGN and also projects to the superior colliculus and the pretectum (102, 147, 236).

Reticular Nucleus

The thalamic reticular nucleus is a thin neuronal shell which surrounds the lateral, superior, and anteroinferior aspects of the thalamus (Figs. 16.6, 16.10, 16.11, and 16.13). This thalamic nuclear envelope is a derivative of the ventral thalamus that has migrated dorsally and lies between the external medullary lamina of the thalamus and the internal capsule (70, 207). Morphologically, the reticular nucleus is closely related to the zona incerta and the ventral lateral geniculate nucleus. The anterior part of the nucleus completely surrounds the rostral pole of the thalamus. It becomes thinner more posteriorly as it curves around the lateral and ventral aspects of the thalamus. Still more caudally, the reticular nucleus is displaced laterally by the dorsal lateral geniculate nucleus. At these caudal levels, the reticular nucleus is continuous with the perigeniculate nucleus that surrounds the lateral geniculate nucleus. Morphologically and physiologically the two structures are alike and may be part of a single entity (173).

Neurons of the reticular nucleus belong to several single classes, but the majority of them are large, fusiform, or triangular, with long dendrites mainly disposed parallel to the surface of the underlying thalamus and at right angles to the fibers entering and leaving the thalamus (169, 173, 235, 360, 386, 404). The axons of reticular neurons penetrate deeply into the thalamus where they ramify over wide areas (386, 459). The axons of reticular neurons arborize at least twice in the thalamus. They usually give off several collaterals that branch profusely within a proximal thalamic nucleus and then continue its course toward more remote thalamic nuclei where they arborize again (Fig. 16.31). In between these two, or more, terminal fields, the axons of reticular neurons remain relatively poorly branched. Terminal of reticular nucleus, axons in the thalamus contain flattened or pleomorphic synaptic vesicles and make symmetric synapses, primarily on dendrites of relay neurons. There appear to be no interneurons in the reticular nucleus. The intranuclear communication is ensured by local axon collaterals of reticular neurons.

Inputs to the reticular nucleus are derived from the principal thalamic nuclei and from the cerebral cortex (46, 169). Fibers emanating from a nucleus of the thalamus and destined for a specific cortical area give collateral branches that terminate in a particular part of the reticular nucleus. Corticothalamic fibers passing toward a particular nucleus of the thalamus give collaterals to the same portions of the reticular nucleus as the target nucleus to the thalamus. Cells in restricted sectors of the reticular nucleus project back to the thalamic nucleus from which it receives an input. The consequence of this pattern of organization is that a particular sector of the reticular nucleus can be dominated by a particular sensory (or other) system (173). Both the intralaminar and relay nuclei of the thalamus project to the reticular thalamic nucleus and both receive fibers from it. The only thalamic nuclei that appear to be devoid of input from the reticular nucleus are those of the anterior nuclear group (414).

The reticular nucleus probably also receives collaterals from the pallidothalamic

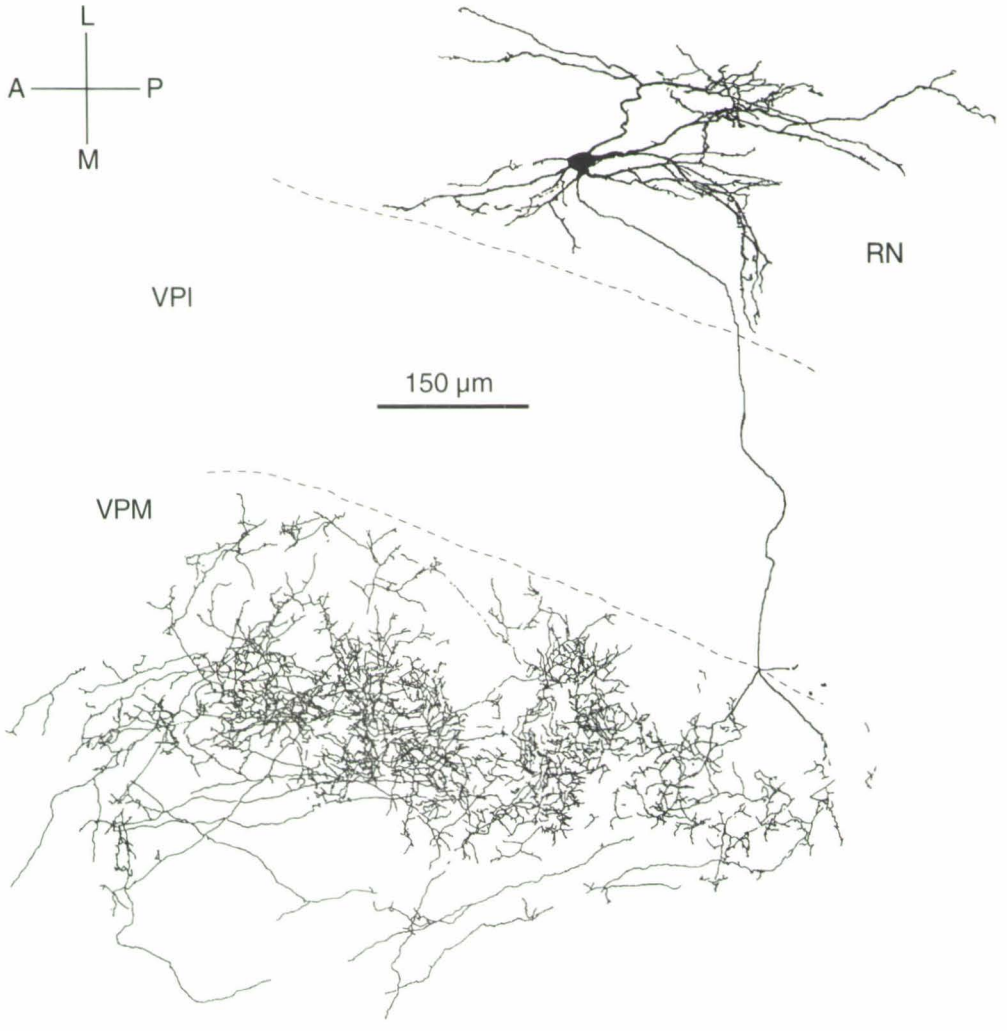


Figure 16.31. Camera lucida drawing of a neuron of the rat reticular thalamic nucleus (*RN*) that has been intracellularly labeled with biocytin. The drawing shows both the dendritic and the profuse axonal arborization, as seen on a horizontal section. The axons of this particular neuron traverse the ventral posterolateral nucleus (*VPL*) and aborize profusely within the ventral posteromedial nucleus (*VPM*).

and thalamostriatal fibers (173). Furthermore, it is innervated by cholinergic fibers originating in the pedunculopontine and laterodorsal tegmental nuclei of the brainstem (groups Ch 5 and Ch 6) (122, 320), as well as in the basal forebrain (group Ch 4) (122, 328, 415). In turn, as predicted by the Scheibels on the basis of Golgi studies (386), the reticular nucleus sends some descending fibers that arborize principally in the midbrain reticular formation, the superior colliculus, and the periaqueductal gray (329, 371). The chemospecific inputs from the brainstem tegmentum are believed to play an important role in the entrainment of reticular neuron activity in accordance with various state-dependent brain conditions (410).

Recent tract-tracing studies revealed that the reticular nucleus receives sparse fibers from the substantia nigra pars reticulata (319) and from the external (lateral) pallidal segment (132). These projections indicate that the two main output nuclei of the basal ganglia have a dual entry into the thalamus: (a) a major direct input, whereby pallidal and nigral neurons can affect specific groups of thalamocortical neurons in the ventral lateral and ventral anterior nuclei, and (b) a minor indirect input via the reticular nucleus, whereby pallidal and nigral neurons can influence diffusely vast collections of thalamocortical neurons. Other studies showed that axons of some reticular neurons traverse the midline to innervate the contralateral nuclei

of the thalamus (131, 321, 362, 369) (Fig. 16.17). An important role is attributed to this projection in the bilateral functioning of the thalamus in rodents (362). In primates, however, fibers from the reticular nucleus that crossed the midline are very sparse by comparison with those that arborize ipsilaterally (131). Thus, this small contralateral projection is unlikely to play a major role in the functional organization of the thalamus in primates. A particularly interesting feature of the morphologic organization of the reticular thalamus is the occurrence of multiple dendrodendritic synapses (73). Such dendrodendritic contacts are believed to be responsible for the synchronization of thalamic spindling, that is, the synchronization of low-frequency (7–14 Hz) rhythmic hyperpolarizations that underlie the highly characteristic repetitive spike bursts ("spindles") that reticular neurons display during anesthesia or slow-wave sleep (73).

The reticular nucleus is an important functional interface between the thalamus and the cerebral cortex. This nucleus is ideally situated so as to sample neural activity passing the cerebral cortex and nuclei of the thalamus, but it has no projection to the cerebral cortex (46, 169, 173, 386). Cortical projections to portions of the reticular nucleus arise from the entire cerebral cortex and are topographically organized. Since the major projections of the thalamic reticular nucleus are to specific and nonspecific thalamic nuclei, it probably serves to integrate and "gate" activities of thalamic neurons (74, 90, 173, 354, 390, 411).

CHEMICAL ANATOMY OF THE THALAMUS

The subdivision of the thalamus presented earlier is largely based on cytoarchitectural and hodologic criteria. The recent development of ever more powerful methods for the localization of various molecules involved in neuronal communication has yielded a large amount of new findings on the chemospecific neuronal systems related to the thalamus. Although our knowledge of the chemoarchitecture of the thalamus is still limited, the chemical anatomy approach has already provided new insights on the functional organization of the thalamus (143, 144, 172, 237). The following section provides a brief review of some of the new findings on the distribution of different transmitters and/or transmitter-related molecules in the thalamus of various species, with emphasis on data relevant to human and nonhuman primates.

Acetylcholine

Histochemical techniques allowing the visualization of acetylcholinesterase (AChE), the enzyme that catabolyzes acetylcholine (ACh), as well as various nonspecific cholinesterases, has been the first approach to be used for the study of the chemoarchitecture of the thalamus (313, 396). A moderate to strong AChE staining was found in the intralaminar nuclei, the anterior nuclei, the lateral and medial geniculate nuclei, and the reticular nucleus, and part of the midline nuclei (313, 323, 382, 396) (Fig. 16.32). Since this AChE staining disappeared after destruction of parts of the midbrain reticular formation, Shute and Lewis (396) concluded that the thalamic cholinergic innervation was part of the ascending reticular cholinergic system, particularly its dorsal tegmental portion, which arises in the nucleus cuneiformis and extends up through the tectum to the thalamus and possibly beyond. The thalamic AChE staining was largely confined to the neuropil and, since the presence of AChE does not necessary imply cholinergic transmission, the significance of these regional thalamic concentrations in AChE remained unclear. The pattern of thalamic AChE distribution, however, appears to follow quite well that of the distribution of cholinergic receptors of both muscarinic and nicotinic types (2, 155, 172). Thus, the presence of AChE at thalamic levels may be indicative of cholinoceptive rather than cholinergic neurons.

Studies combining immunohistochemistry for choline acetyltransferase (CHAT), the enzyme that synthesizes ACh, with retrograde tracer methods confirmed, at least in part, Shute's and Lewis's insights, by demonstrating that the thalamic cholinergic innervation derive largely from brainstem mesopontine reticular nuclei, principally the pedunculopontine (group Ch 5) and laterodorsal tegmental (group Ch 6) nuclei (122, 161, 320, 403, 415, 455). The parabigeminal nucleus (group Ch 8) also provides thalamic inputs, particularly to the pulvinar regions (462). Furthermore, neurons of the nucleus basalis of Meynert (group Ch 4) in the basal forebrain contribute to the cholinergic innervation of certain thalamic nuclei, particularly the reticular and mediodorsal nuclei (122,

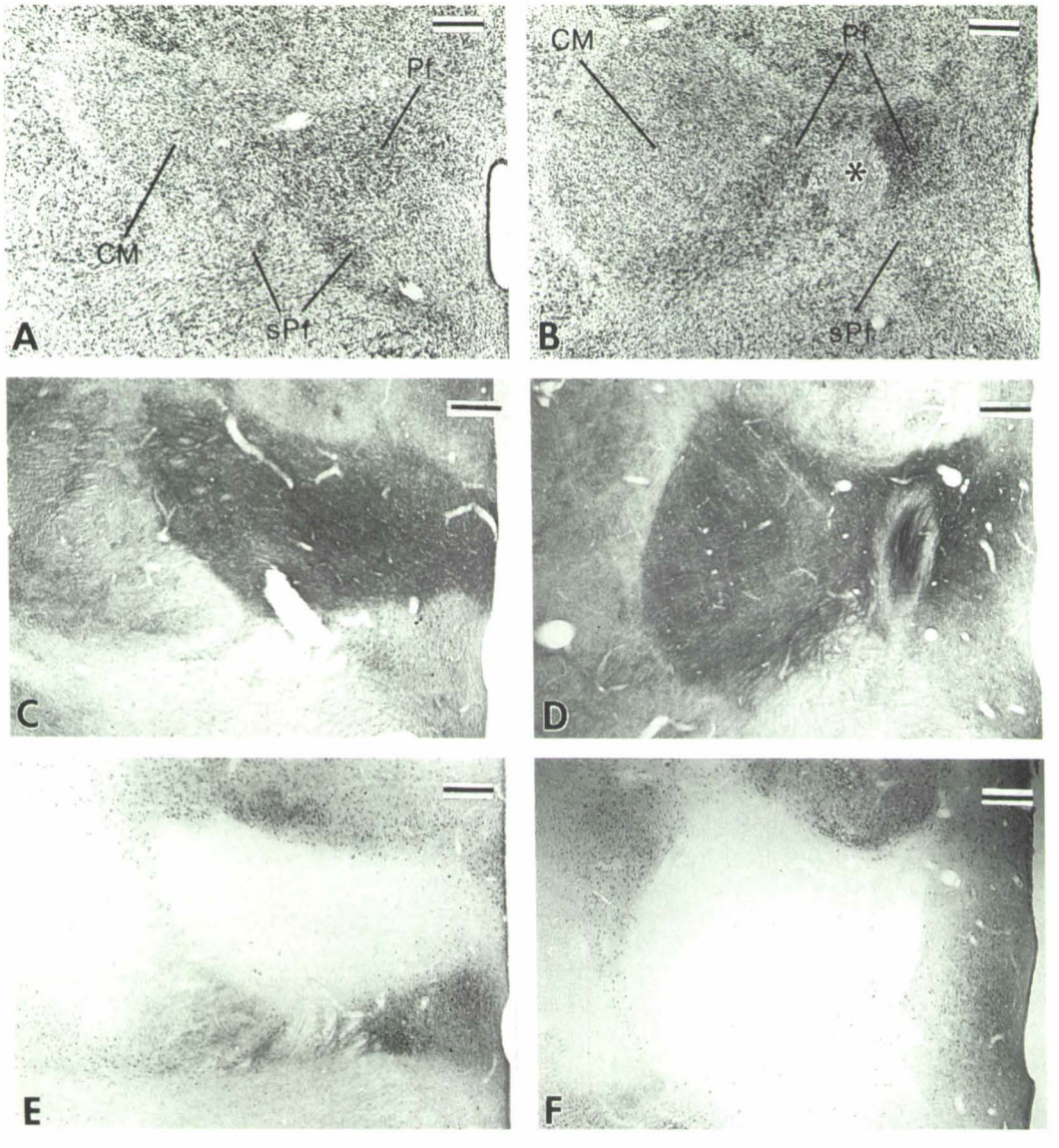


Figure 16.32. Transverse sections at rostral (**A**, **C**, **E**) and middle (**B**, **D**, **F**) thirds of the centromedian(CM)-parafascicular (Pf) complex of the squirrel monkey. Sections show Nissl cell staining (**A**, **B**), acetylcholinesterase (AChE) histochemical staining (**C**, **D**), and calbindin D-28k immunostaining (**E**, **F**). *Asterisk* (**B**) indicates the habenulo-interpeduncular tract and *sPf* indentifies the location of the subparafascicular nucleus (**A**, **B**).

328, 415). The ascending cholinergic projection from the brainstem appears divergent in that single ChAT-positive axons provide collaterals to several thalamic nuclei (34).

The distribution of ChAT-immunoreactive fibers has been studied in detail in rodents (228) and in humans (133). These studies revealed that the only group of cholinergic (ACh producing) neurons in the mammalian thalamus is found in the medial habenular nucleus. In humans, some intralaminar nuclei (central medial, central lateral, and paracentral), the reticular nucleus, midline nuclei (paraventricular and reuniens nuclei), some nuclei associated with the limbic system (anterodorsal nucleus and medially situated patches in the mediodorsal nucleus), and the lateral geniculate nucleus displayed the highest density of ChAT-positive axon terminals. The remaining sensory relay nuclei and the nuclei interconnected with the motor and association cortex are less densely innervated. Since cholinergic neurons of the basal forebrain display immunoreactivity for the nerve

growth factor receptor (NGFr) while those in the brainstem do not, it was possible to specify the contribution of these two sources to the cholinergic innervation of the human thalamus. This indirect approach revealed that the anterior intralaminar nuclei, the reticular nucleus, and medially situated patches in the mediodorsal nucleus receive a projection from the nucleus basalis. The other thalamic nuclei contain only scarce NGFr-positive axons (133). These observations suggest that thalamic nuclei affiliated with limbic structures and with the ascending reticular activating system are under particularly intense cholinergic influence.

The thalamic cholinergic innervation was also investigated at the ultrastructural level (123, 162, 391). These studies have demonstrated the presence of cholinergic synapses of the asymmetric type onto dendrites of both relay projection neurons and interneurons in the mediodorsal nucleus (391). This finding indicates that cholinergic input to thalamic nuclei influence relay cell activity both directly and indirectly vial local circuit neurons. In the reticular nucleus, cholinergic synapses were found on the dendrites of intrinsic neurons but not on cortical and thalamic fibers passing through the reticular nucleus (123). The occurrence of cholinergic synapses on identified intralaminostriatal neurons has been documented (162).

These findings indicate that thalamic nuclei are under a strong cholinergic influence originating principally in the brainstem reticular formation and less abundantly in the basal forebrain. This chemospecific projection could directly modulate the neural activity of thalamic neurons according to various state-dependent activities (410).

Gamma-Aminobutyric Acid

The presence of γ-aminobutyric acid (GABA)-producing neurons in the thalamus has been documented in various species with antibodies directed either against the synthesizing enzyme, glutamate acid decarboxylase (GAD), or GABA itself (129, 308, 370, 402), as well as with *in situ* hybridization methods that reveal the expression of the gene coding for GAD (21). Furthermore, both $GABA_A$ and $GABA_B$ receptor types occur at thalamic levels, some of these receptors being localized directly on thalamocortical projection neurons (63, 208). Virtually all cells in the reticular nucleus are strongly GABA-positive in all species (Fig. 16.35). GABA-immunoreactive neurons in the thalamus, other than the reticular nucleus, appear more numerous in primates than in nonprimates. Most of these GABAergic neurons in monkeys are small and are regarded as interneurons. In nonhuman primates, GABAergic neurons occur in virtually all thalamic nuclei (Figs. 16.33 and 16.34). In the anterior nuclear group, GABA-immunoreactive cell bodies abound particularly in the anterodorsal nucleus. In the anterior group, GABA-positive neurons tend to cluster rostrally while they are more uniformly distributed caudally. In the intralaminar nuclei, GABA-immunoreactive cells prevail in dorsal parts of the central lateral and paracentral nuclei, as well as in the entire parafascicular nucleus. In the mediodorsal nucleus, GABA-positive neurons are more heterogeneously distributed in the lateral parvicellular part than in the medial magnocellular part. GABA-immunoreactive neurons are uniformly distributed in the nuclei of the posterior group, except in the pulvinar where they abound in the pars inferior and oralis of this nucleus. In the lateral geniculate nucleus, GABAergic cell bodies occur in all laminae but are more abundant in the magnocellular laminae (Figs. 16.33 and 16.34).

In addition to GABAergic cell bodies, numerous GABA-immunoreactive axon terminals occur in the various thalamic nuclei (Figs. 16.33 and 16.34). A significant proportion of these axon terminals derive from the neurons of the reticular nucleus, but extrathalamic sources also exist. The major projections of the internal pallidal segment to VApc and VLo and the projection from the pars reticulata of the substantia nigra to VAmc and MDpl are GABAergic (57). These projections are considered to play a major role in aspects of motor function. Furthermore, in addition to GABAergic axon terminals of intrinsic origin (65), the reticular nucleus contains numerous GABAergic terminals that arise from caudal parts of the basal forebrain (12).

Neuroactive Peptides

Immunohistochemical studies have revealed the presence of numerous neuroactive peptides belonging to several distinct families in the thalamus. Among those are (a) the brain-gut peptides substance P (SP), chole-

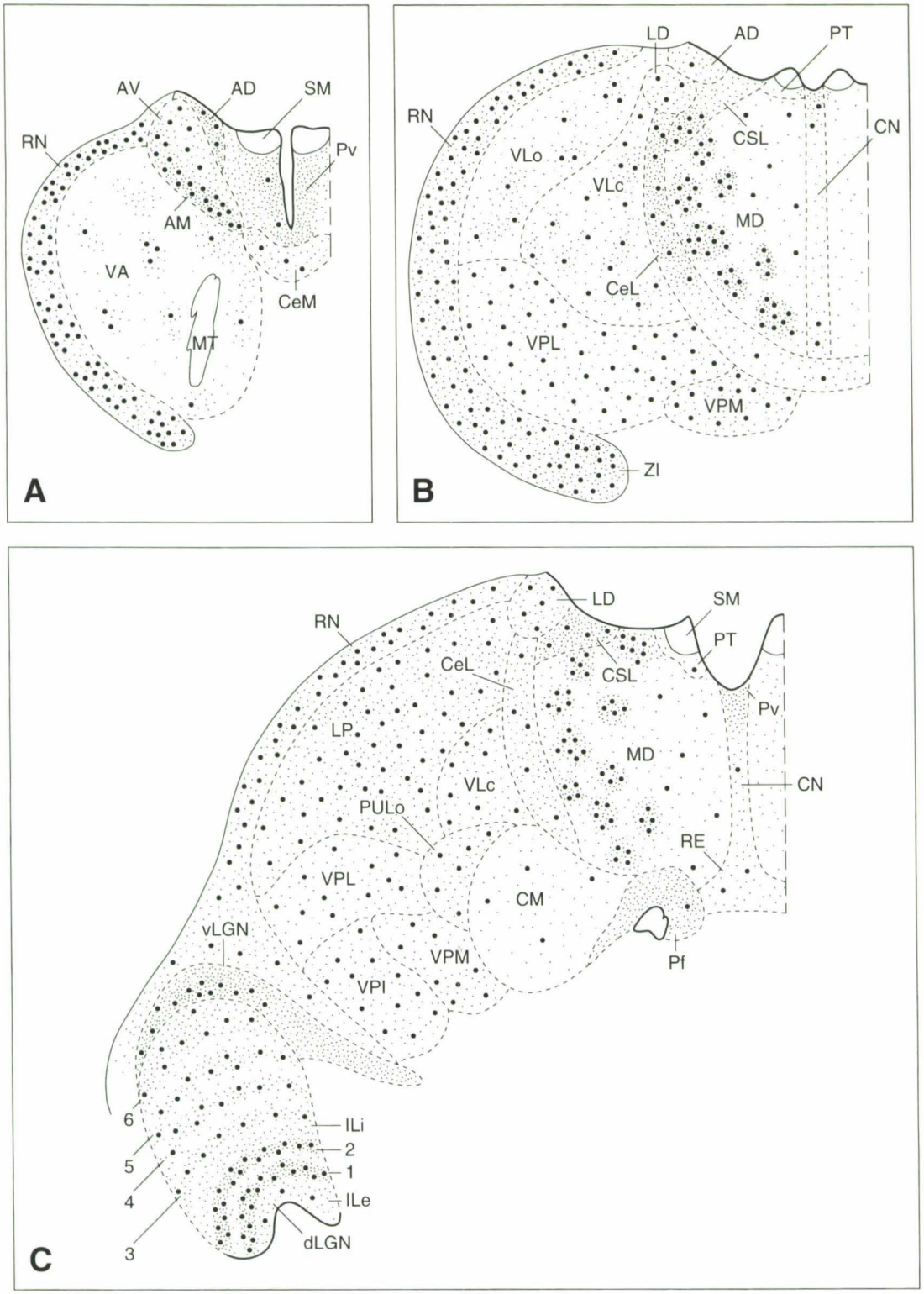


Figure 16.33. Transverse sections through rostral (**A**), middle (**B**), and caudal (**C**) portions of the thalamus in the squirrel monkey illustrating the distribution and relative density of GABA-immunoreactive cell bodies (*large dots*) and axon terminals (*fine dots*), as visualized with an antibody raised directly against GABA. *AD,* anterodorsal nucleus; *AM,* anteromedial nucleus; *AV,* anteroventral nucleus; *CeL,* centrolateral nucleus; *CeM,* centromedial nucleus; *CM,* centromedian nucleus; *CN,* central nucleus; *CSL,* central superior lateral nucleus; *dLGN,* dorsal lateral geniculate nucleus (layers 1 to 6); *ILe,* external intercalated layer of dLGN; *ILi,* internal intercalated layer of dLGN; *LD,* laterodorsal nucleus; *LP,* lateroposterior nucleus; *MD,* mediodorsal nucleus; *MT,* mammillothalamic tract; *Pf,* parafascicular nucleus; *PULo,* pulvinar, oral part; *PT,* parataenial nucleus; *Pv,* paraventricular nucleus; *RE,* nucleus reuniens; *RN,* reticular nucleus; *SM,* stria medullaris; *VLc,* ventral lateral nucleus, caudal part; *VA,* ventral anterior nucleus; *VLo,* ventral lateral nucleus, oral part; *vLGN,* ventral lateral geniculate nucleus; *VPI,* ventral posteroinferior nucleus; *VPL,* ventral posterolateral nucleus; *VPM,* ventral posteromedial nucleus; *ZI,* zona incerta.

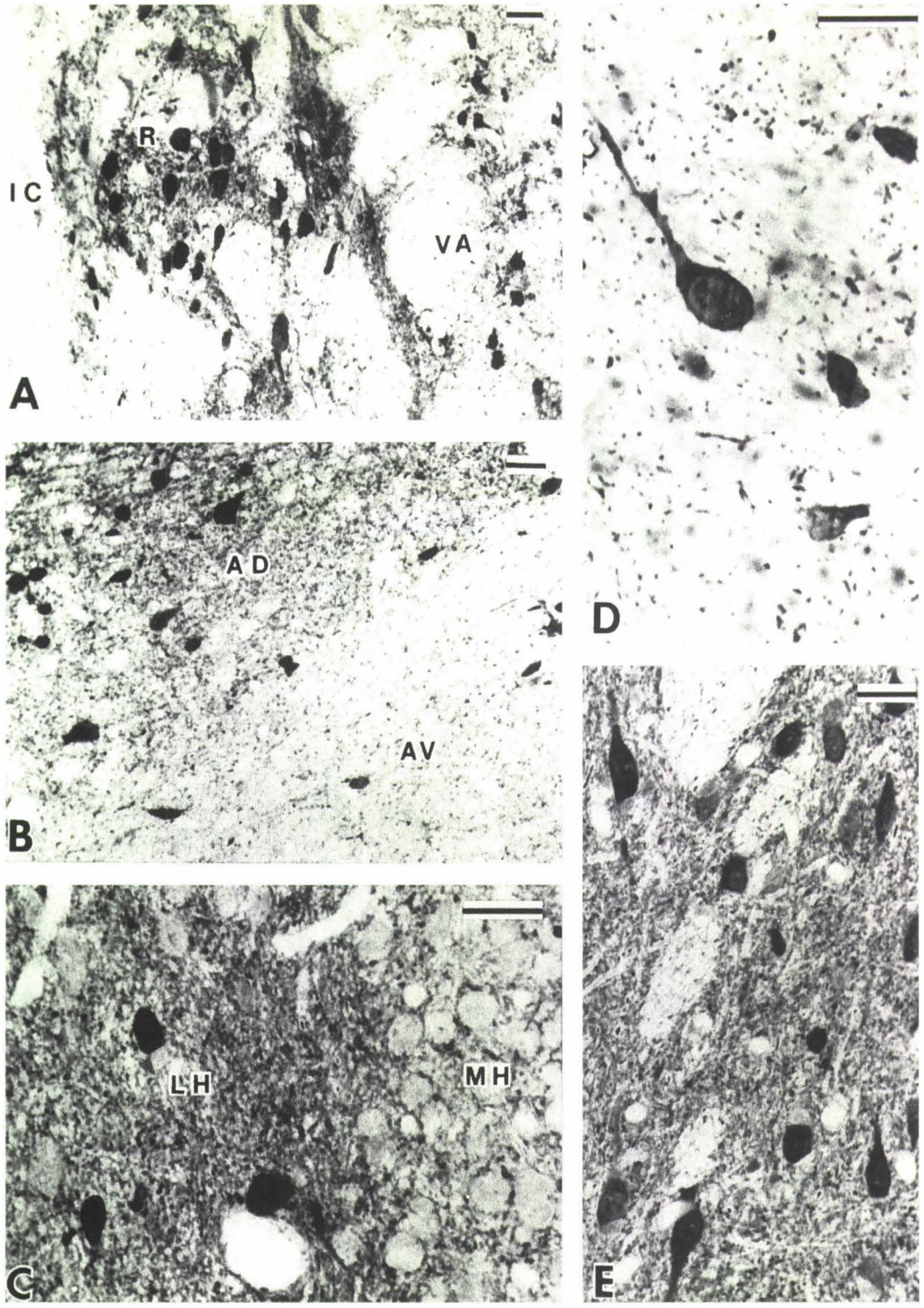


Figure 16.34. Features of the GABA-immunoreactive neuronal profiles disclosed in some rostral and lateral thalamic nuclei and in the zona incerta of the squirrel monkey. **A.** Some GABA-positive cells in the reticular nucleus (*R*) bordering the internal capsule (*IC*) and in the adjoining ventral anterior (*VA*) nucleus. Note that the immunoreactive cells in the reticular nucleus are larger than those in the ventral anterior nucleus. **B.** Some GABA-immunoreactive neuronal elements in the anterodorsal (*AD*) and anteroventral (*AV*) nuclei. The GABA-positive puncta, indicative of GABAergic axon terminals, are particularly numerous in the anterodorsal nucleus. **C.** Distribution of GABA-immunoreactive profiles in the habenula. Note the absence of GABA-positive cell bodies in the medial habenular nucleus (*MH*) and the numerous GABA-immunoreactive terminals with a few cell bodies in the lateral habenular nucleus (*LH*). **D.** Some of the numerous small GABA-positive neurons and one of the few larger positive cells present in the anteroventral nucleus. **E.** Numerous small GABA-immunoreactive cell bodies and axon terminals in the zona incerta. Scale bars = 25 μm.



Figure 16.35. Darkfield autoradiograph showing neurons of the rat reticular nucleus that express glutamic acid decarboxylase (GAD), the enzyme that synthesizes GABA, as revealed by *in situ* hybridization technique. The results were obtained with a cDNA probe that encodes the 67k form of the enzyme.

cystokinin (CCK), neurotensin (NT), vasoactive intestinal peptide (VIP), and neuro-peptide Y (NPY); (b) the opiate peptide leu- and met-enkephalins (ENK) and dynorphin (DYN); (c) the hypophysiotropic peptides somatostatin (SOM) and corticotropin-releasing factor (CRF); (d) angiotensin; (e) calcitonin gene-related peptide; and (f) the calcium binding proteins calbindin D-28k (CaBP), parvalbumin (PV), and calretinin (CR). Largely because of species variations and/or differences in the methodologic approach used, it is not possible at present to provide a general picture of the distribution of all these peptides for the mammalian thalamus. Only the most salient features are discussed here.

Relatively few thalamic cell bodies were found to contain neuroactive peptides in the thalamus of primates. In nonprimate species, however, neurons of the CM-Pf complex projecting to the striatum were found to contain SP (419), CCK (1), and CGRP (458). Many of the fibers and axon terminals containing neuroactive peptides in the thalamus are of extrinsic origin. Several neurons of the brainstem tegmentum that project massively to the thalamus contains SP, CGRP, CCK, and, less abundantly, NPY, DYN, and ENK (218). These peptides are either coexpressed with ChAT in cholinergic neurons of pedunculopontine and lateral tegmental nuclei, or are present in various combinations in noncholinergic neurons of the same nuclei and in the locus coeruleus, periaqueductal gray, parabrachial, and paragigantocellularis nuclei (218). Other peptides, such as SP and ENK, occur in spinothalamic fibers together with glutamate and/or aspartate as the major small molecule transmitter (17). In humans, SP- and ENK-immunoreactive fibers were seen to enter the thalamus anteromedially from the hypothalamus, and posterolaterally from the midbrain tegmentum (143). These fibers arborize principally in the nuclei of the posterior group and in the intralaminar nuclei, except the centromedian nucleus. All these structures have been implicated in pain phenomena. No SP- and ENK-immunoreactive cell bodies were disclosed in the human thalamus.

In nonhuman primates, SOM, NPY, SP, and ENK of extrinsic origin innervate the dorsal and ventral thalami and the epithalamus (270). They reach the thalamus via a rostral and a caudal route. Fibers that follow the rostral route course along the classic periventricular system that links the hypothalamus with the epithalamus, while those in the caudal route ascend within the lateral midbrain tegmentum. Some NPY- and SOM-positive fibers were also seen to enter the thalamus in association with the ansa peduncularis, whereas SP-positive fibers appeared to ascend from the substantia nigra. The four types of fibers arborize densely within the intralaminar nuclei and in the reticular nucleus (270). Another immunohistochemical study has revealed the presence of cell bodies immunoreactive for neurotensin (NT) in the midline and mediodorsal nuclei, and less prominently in the intralaminar nuclei of monkeys (245). Neurotensin-immunoreactive fibers arborize profusely in the midline nuclei, particularly in the nucleus rhomboidalis. Some NT-positive fibers were also encountered in the inferior thalamic peduncle (245).

The two calcium binding proteins cal-

bindin D-28k (CaBP) and parvalbumin (PV) are distributed in the primate thalamus according to a strikingly complementary pattern, and this has been used for providing a new parcellation of the thalamus (144). For example, in the posterior intralaminar nuclei, PV labels intensely the CM-Pf complex, whereas this complex is virtually devoid of CaBP immunoreactivity (144) (Fig. 16.32). The subparafascicular nucleus, however, is intensely stained for CaBP. In the reticular nucleus of cats and monkeys, GABAergic neurons coexpress somatostatin (SOM), but such is not the case in the reticular nucleus of rats, whose neurons appear to coexpress VIP (113, 306). The GABAergic neurons of the reticular nucleus in most species display PV but not CaBP immunoreactivity (59, 267). The comparative study of the immunoreactivity for each of these two calcium binding proteins and for GABA has led to a new functional parcellation of the reticular nucleus in rodents (268).

Excitatory Amino Acids

Pharmacologic and electrophysiologic studies have revealed that excitatory amino acids (EAA) play a crucial role in the functional organization of the thalamus (393). In keeping with such a view, recent immunohistochemical studies have shown that most principal afferent and efferent connections of the thalamus use glutamate and/or aspartate as a neurotransmitter. Glutamate and/or aspartate was shown to mediate the excitatory effect of corticofugal fibers upon neurons of the reticular nucleus, as well as those of most dorsal thalamic nuclei (66, 67, 105). Combined retrograde transport techniques and immunohistochemical methods clearly reveal that corticothalamic neurons in lamina VI are positive for these EAA. Approximately 90% of corticothalamic neurons are immunoreactive for either glutamate or aspartate, and about 25% of these neurons are positive for both (105). The excitatory action of the corticothalamic fibers is mediated via both *N*-methyl-D-aspartate (NMDA) and non-NMDA receptors (81, 238, 385). There is also ample evidence to support the fact that thalamocortical neurons also use glutamate and/or aspartate as neurotransmitter (100, 237, 271, 393). For example, anatomic and physiologic studies in the rat suggest that the thalamic projection from the mediodorsal nucleus to anterior cingulate cortex is glutamatergic and that its excitatory action is mediated by AMPA (α-methyl propionic acid) type receptor (100). The same investigations revealed that the response of cingulate cortex neurons to thalamic stimulation is regulated by GABA acting at both $GABA_A$ and $GABA_B$ receptors.

Glutamate immunoreactivity is also present in the axon terminals of various other thalamic afferent systems, including (a) the medial lemniscal fibers terminating in the VP nucleus (66, 385), (b) the cervicothalamic fibers (40), (c) the retinogeniculate fibers (271), and (d) the trigeminothalamic fibers (244).

Monoamines

The thalamus receives a profuse monoaminergic innervation that derives principally from the noradrenergic neurons of the locus coeruleus and from the serotoninergic neurons of the dorsal raphe nucleus. A smaller contribution from the noradrenergic neurons of the subcoeruleus region and from the serotoninergic neurons of the median and pontine raphe nuclei has also been noted. Except for a projection originating in the ventral tegmental area and terminating in the habenula (the so-called mesohabenular dopaminergic pathway), the midbrain dopaminergic neurons do not contribute significantly to the innervation of the thalamus (28).

The noradrenergic innervation of the thalamus has been studied in detail in rodents with antibodies raised against the enzyme dopamine-β-hydroxylase (DBH) that transforms dopamine into noradrenaline (146, 420). The noradrenergic fibers terminating in the thalamus form part of the large dorsal catecholamine bundle that courses in the dorsomedial part of the midbrain tegmentum. The fibers ascend beneath the thalamus in close association with the superior cerebellar peduncle. The fibers enter the thalamus through the zona incerta and the reticular nucleus. The noradrenergic innervation of the anteroventral nucleus is dense, whereas that of the other anterior nuclei, as well as that of the ventral and dorsal lateral geniculate nuclei and the intralaminar nuclei, is moderate. Only a few noradrenergic fibers are scattered within the other nuclei of the thalamus. In the epithalamus, concentrations of fibers, entering from behind, appear in the paraventricu-

lar and medial habenular nuclei. The main bundle of noradrenergic fibers that give rise to the thalamic innervation continues rostrally into the septum, medial cortical areas, and hippocampal formation (146, 420).

Electron microscopic studies of the catecholaminergic (and serotoninergic) terminals in the ventral posterior nucleus in monkeys revealed that only 7–10% of the immunoreactive terminals form conventional synaptic contacts in this region of the thalamus (231). The dendritic shaft and somata of relay neurons appear to be the major target of these synaptic contacts that were mostly of the asymmetric type. The vast majority of the immunoreactive terminals made intimate membrane associations with relay cell dendrites and somata or presynaptic dendrites of interneurons, but no obvious membrane specializations could be found. These findings suggest that the modulation of thalamocortical relay function by brainstem monoaminergic pathways in the somatosensory thalamus may occur by release of transmitter at atypical contact sites (231).

The serotoninergic innervation of the thalamus in monkeys has been studied in detail with antibodies raised directly against serotonin (217) (Figs. 16.36 and 16.37). As in the rat, the serotoninergic innervation of the thalamus derives from extrinsic fibers arising mostly from the midbrain raphe nuclei and forming the transtegmental system (326). Most of the fibers destined to the thalamus collect into a major bundle that sweeps dorsoventrally within the midbrain tegmentum and courses beneath the thalamus along its entire caudorostral extent. Several fiber fascicles break off from this main bundle at different levels and ascend dorsally to innervate the various thalamic nuclei. Overall, the 5-HT innervation of the primate thalamus is more massive than would have been expected based on earlier studies in nonprimate species. Marked differences in the regional density of innervation can be noted both between the various nuclei and within single nuclei.

The most densely innervated nuclei are those delineating the principal subdivisions of the thalamic mass, that is the midline, rostral intralaminar, limitans, and reticular nuclei, where very dense fields of isolated axonal varicosities occur. In contrast to the rostral intralaminar nuclei, which are rather uniformly innervated, the CM-Pf complex contains immunoreactive fibers and isolated varicosities that are distributed according to a mediolateral gradient. The habenula and the ventral anterior nucleus are among the most weakly innervated nuclei. In the latter nucleus, as well as in more densely innervated nuclei, thin varicose fibers form numerous pericellular contacts on cell bodies and proximal dendrites of thalamic neurons. The serotoninergic innervation of the lateral nuclear group, as well as that of the medial and lateral geniculate nuclei, ranges from very weak to dense. The mediodorsal nucleus displays a highly heterogeneous serotoninergic innervation that varies from weak in its central portion to moderate or dense in its medial and lateral borders. A moderate serotoninergic innervation is observed in the anterior nuclear group. The surprisingly dense and heterogeneous serotoninergic innervation of the thalamus noted here, suggests that this neurotransmitter is involved in several specific functions of the primate thalamus (217).

The presence of numerous serotoninergic receptors heterogeneously distributed in the thalamus of rats and primates strongly supports the hypothesis of a specific role of serotonin in thalamic functions. The serotoninergic receptors in the CNS are divided into four subtypes: 5-HT_1, 5-HT_2, 5-HT_3, and 5-HT_4 (108). In most species, the serotoninergic receptors disclosed at thalamic levels are mainly of the 5-HT_1 subtype. Different subclasses of 5-HT_1 receptors have been described and termed 5-HT_{1A}, 5-HT_{1B}, 5-HT_{1C}, 5-HT_{1D}, and 5-HT_{1E} (108). The distribution of the 5-HT_{1C} receptor subclass at thalamic levels has been described in detail in several species, and the presence of 5-HT_{1B} and 5-HT_{1D} receptor subclasses has also been reported in the thalamus (217). In nonhuman primates, high levels of 5-HT_1 binding sites are observed in most of the midline nuclei as well as in the parafascicular nucleus, whereas moderate levels are noted in the central medial and anteroventral nuclei and in the ventral lateral geniculate nucleus. The remaining thalamic nuclei display low binding levels. In humans, a similar distribution of 5-HT_1 receptors, mainly 5-HT_{1A} subclass, is observed (333).

The involvement of serotonin in pain modulation is one of the most well-documented roles of this indolamine at thalamic levels. Several studies in the rat have demonstrated that stimulation of the dorsal raphe

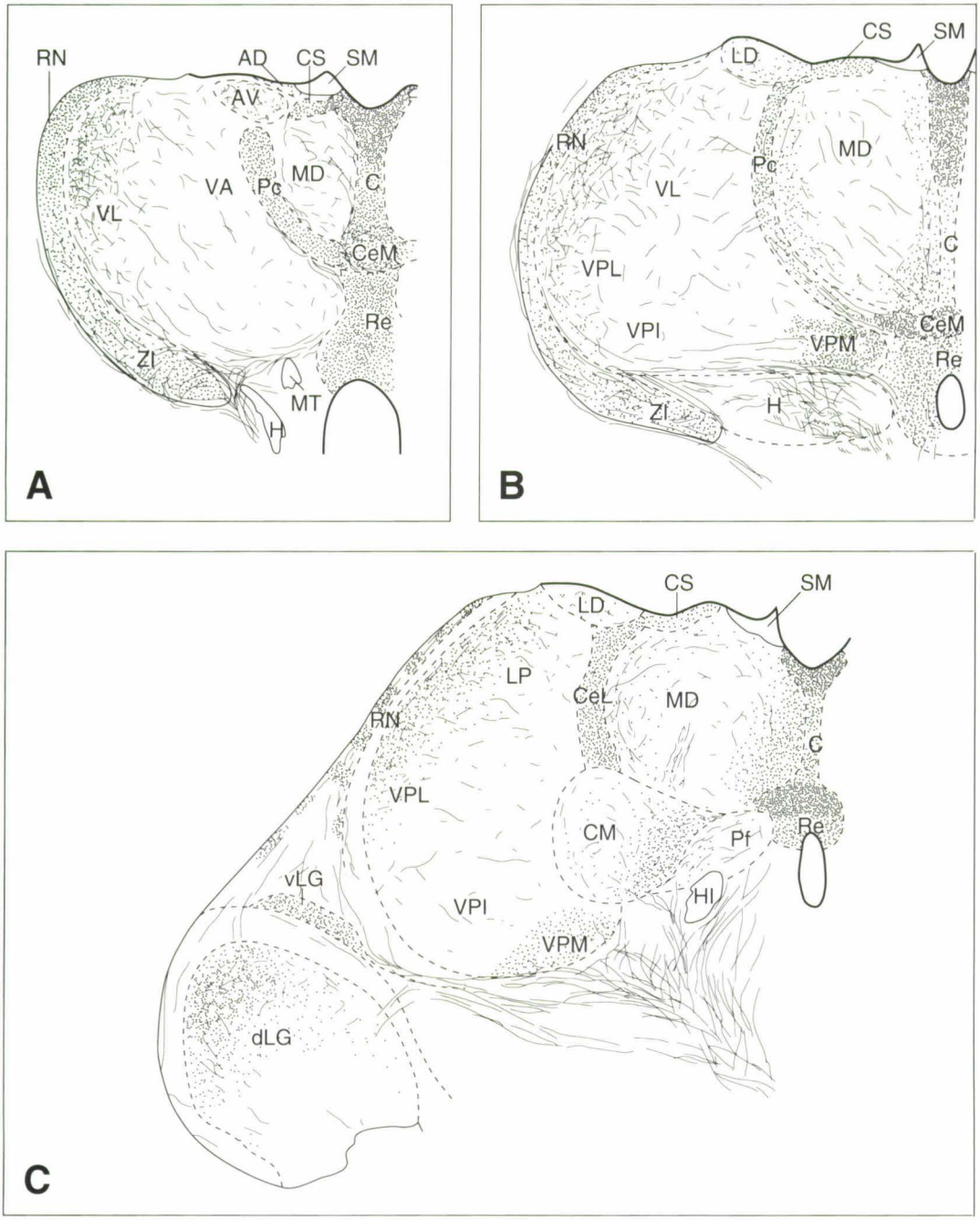


Figure 16.36. Camera lucida drawings of transverse sections through rostral (**A**), middle (**B**), and caudal (**C**) portions of the thalamus in the squirrel monkey illustrating the distribution and relative density of serotonin-munoreactive fibers (*lines*) and axon terminals (*dots*), as visualized with an antibody raised directly against serotonin. *AD,* anterodorsal nucleus; *AV,* anteroventral nucleus; *C,* central nucleus; *CeM,* centromedial nucleus; *CM,* centromedian nucleus; *CS,* central superior lateral nucleus; *dLG,* dorsal lateral geniculate nucleus; *H,* Forel's field *H*; *HI,* habenulo-interpeduncular tract; *LD,* lateral dorsal nucleus; *LP,* lateral posterior nucleus; *MD,* mediodorsal nucleus; *MT,* mammillothalamic tract; *Pc,* paracentral nucleus; *Pf,* parafascicular nucleus; *RN,* reticular nucleus; *RE,* nucleus reuniens; *SM,* stria medullaris; *VA,* ventral anterior nucleus; *VL,* ventral lateral nucleus; *vLG,* ventral lateral geniculate nucleus; *VPI,* ventral posteroinferior nucleus; *VPL,* ventral posterolateral nucleus; *VPM,* ventral posteromedial nucleus; *ZI,* zona incerta.

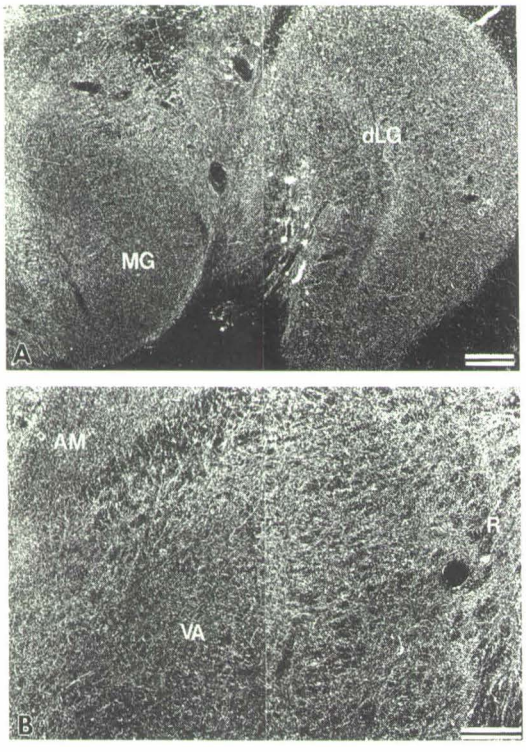


Figure 16.37. Darkfield photomontages showing the distribution of serotonin-immunoreactive fibers and axon terminals in lateral (*dLG*) and medial (*MG*) geniculate nuclei (**A**), and in different rostral thalamic nucleis, including the reticular (*R*), ventral anterior (*VA*), anteromedial (*AM*), and central nuclei (**B**). Scale bar: 500 μm.

nucleus attenuates the increase in the firing rate of the parafascicular neurons induced by noxious stimuli. In serotonin-depleted rats, both the stimulation of the dorsal raphe nucleus and noxious stimuli elicited an increase in the firing rate of the parafascicular neurons. The fact that this effect was not additive indicates that the serotoninergic projection to the parafascicular nucleus has a tonic inhibitory influence on the response to noxious stimuli (8). Likewise, iontophoretic application of serotonin upon neurons of the parafascicular nucleus reduced their response to noxious stimuli (64).

Interesting information has been obtained on the possible role of serotonin at thalamic levels by in vitro experiments. For instance, it has been shown that serotonin reduces the ability to generate burst firing in lateral geniculate neurons (316). A similar effect was observed in the reticular and suprageniculate nuclei (239). Furthermore, local serotonin applications resulted in a pronounced and prolonged neuronal excitation associated with the occurrence of single spike activity (239). This excitation was specifically blocked by 5-HT_2 and 5-HT_{1C} antagonists, and appeared to be mediated through a decrease in potassium current. The same study showed that noradrenaline produces a similar excitation and that both noradrenaline and serotonin converge onto the same potassium conductance. In contrast, application of acetylcholine on the same neurons results in a brief period of inhibition (239). These results indicate that serotonin exerts a specific excitation on thalamic neurons and that this neurotransmitter is also involved in complex interactions with other neurotransmitters, particularly noradrenaline and acetylcholine, that are used by well-characterized brainstem ascending systems.

THALAMIC RADIATIONS AND INTERNAL CAPSULE

Fibers that reciprocally connect the thalamus and the cortex constitute the thalamic radiations. Thalamocortical and corticothalamic fibers form a continuous fan that emerges along the whole lateral extent of the caudate nucleus. Fiber bundles radiating forward, backward, upward, and downward form large portions of various parts of the internal capsule (Figs. 2.12, 2.14, 16.38, and 16.39). Though the radiations connect with practically all parts of the cortex, the richness of connections varies in different cortical areas. Most abundant are the projections to the frontal granular cortex, the precentral and postcentral gyri, the calcarine area, and the gyrus of Heschl. The posterior parietal region and adjacent portions of the temporal lobe also have rich thalamic connections, but relatively scanty radiations go to other cortical areas (448).

The thalamic radiations are grouped into four subradiations designated as the thalamic peduncles (Fig. 16.39). The *anterior* or *frontal peduncle* connects the frontal lobe with the medial and anterior thalamic nuclei. The *superior* or *centroparietal peduncle* connects the Rolandic area and adjacent portions of the frontal and parietal lobes with the ventral tier thalamic nuclei. Fibers, carrying general sensory impulses from the body and head, form part of this radiation and terminate in the postcentral gyrus (Figs. 16.13, 16.14, and 16.39). The *posterior* or *occipital peduncle* con-

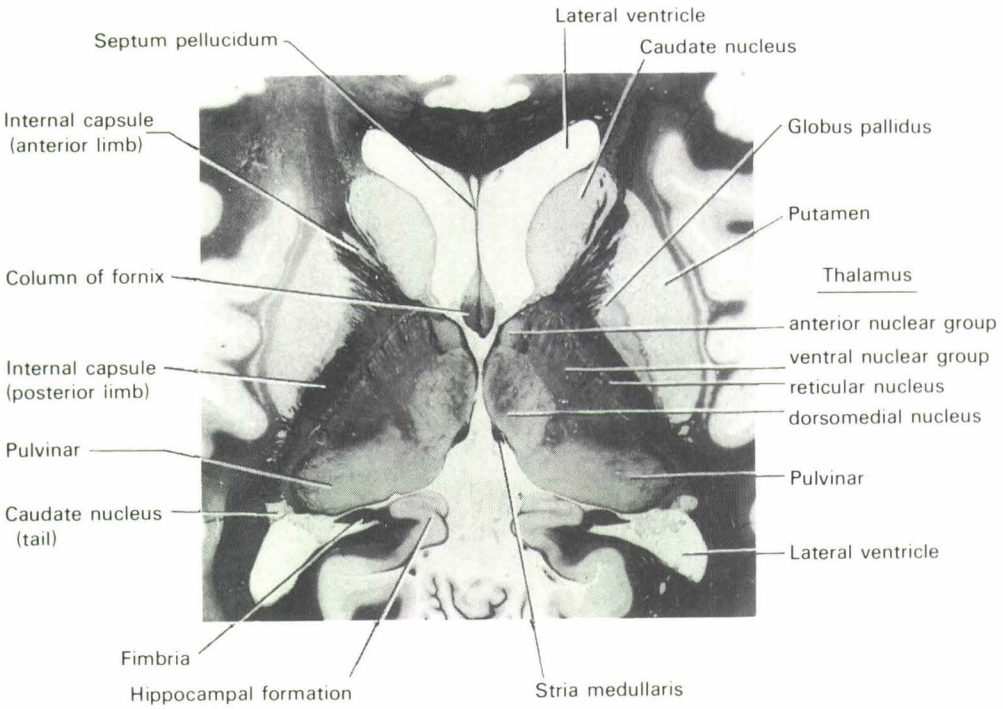


Figure 16.38. Horizontal section through thalamus, internal capsule, and basal ganglia (Weigert's myelin stain).

nects the occipital and posterior parietal convolutions with the caudal portions of the thalamus. It includes the optic radiations from the lateral geniculate nucleus and claustrocortical projections to the calcarine cortex (striate area). The *inferior* or *temporal peduncle* is small and includes the connections of the thalamus with the temporal lobe and the insula. Included in this peduncle are the auditory radiations from the medial geniculate nucleus to the transverse temporal gyrus of Heschl (Fig. 16.39).

The cerebral hemispheres are connected with the thalamus, brainstem, and spinal cord by an extensive projection system. These fibers arise from the whole extent of the cortex, enter the white substance of the hemisphere, and appear as a radiating mass of fibers, the *corona radiata*, which converges toward the thalamus (Fig. 2.12). On reaching the latter, they form a broad, compact fiber band, the *internal capsule*, flanked medially by the thalamus and caudate nucleus and laterally by the lentiform nucleus (Figs. 2.14, 16.38, and 16.39). Thus, the internal capsule is composed of all the fibers, afferent and efferent, which go to, or come from, the cerebral cortex. A large part of the capsule is composed of the thalamic radiations described earlier. The rest is composed mainly of cortical efferent fiber systems (i.e., corticofugal fibers), which descend to the brainstem and to the spinal cord. These include the corticospinal, corticobulbar, corticoreticular, and corticopontine tracts (Fig. 16.39).

The internal capsule, as seen in a horizontal section, is composed of a shorter *anterior* and a longer *posterior limb*, which meet at an obtuse angle. The junctional zone is known as the *genu* (Figs. 2.13, 2.14, 16.38, 16.39, and 16.42). The anterior limb lies between the lentiform and caudate nuclei. The posterior limb of the internal capsule *(lenticulothalamic portion)* lies between the lentiform nucleus and the thalamus. A *retrolenticular part* of the internal capsule extends caudally for a short distance behind the lentiform nucleus. In this caudal region, a number of fibers passing beneath the lentiform nucleus to reach the temporal lobe collectively form the *sublenticular portion* of the internal capsule.

The *anterior limb* of the internal capsule contains the anterior thalamic radiation or peduncle, and the prefrontal corticopontine tract. The *genu* contains corticobulbar and corticoreticular fibers.

The *posterior limb* of the internal capsule contains (a) corticospinal fibers, (b) fronto-

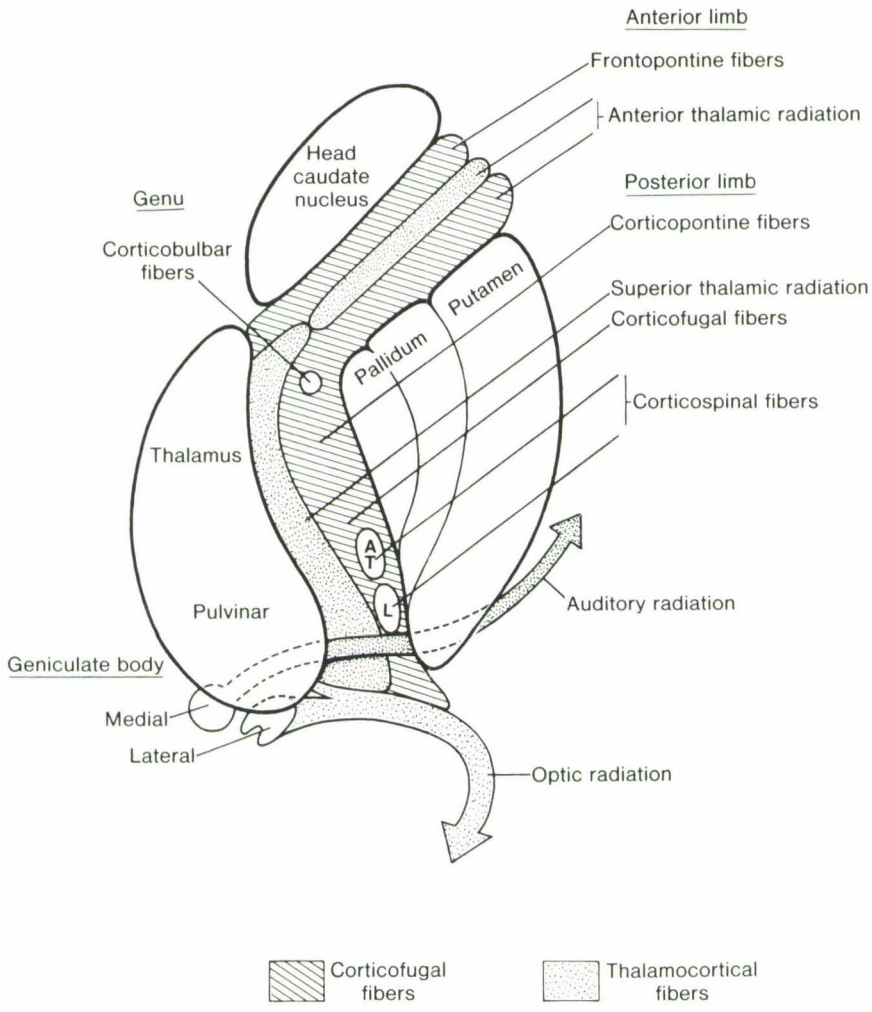


Figure 16.39. Right internal capsule as seen in a horizontal section similar to that shown in Figure 16.38. Corticospinal fibers in humans occupy the caudal third of the posterior limb of the internal capsule.

pontine fibers, (c) the superior thalamic radiation, and (d) relatively smaller numbers of corticotectal, corticorubral, and corticoreticular fibers. Corticospinal fibers in humans have classically been considered to lie in the posterior limb of the internal capsule relatively close to the genu (68). Results from electrical stimulation and neuropathologic analyses suggest that corticospinal fibers are largely confined to a compact region in the posterior half of the posterior limb of the internal capsule (25, 83, 103, 125, 401). Fibers of the corticospinal tract are somatotopically arranged in this part of the internal capsule, with those destined for cervical, thoracic, lumbar, and sacral spinal cord segments arranged in a rostrocaudal sequence. The classic view that corticospinal fibers occupy the medial three-fifths of the crus cerebri appears unreasonable on the basis of the number of fibers in this structure. Corticospinal fibers in humans account for only 1 million of the 20 million fibers in this massive-bundle (428). The somatotopic arrangement of corticospinal fibers in the crus cerebri is much less precise than commonly depicted. Fibers of the superior thalamic radiation, located caudal to the corticospinal fibers, project signals concerned with general somatic sense to the postcentral gyrus.

The *retrolenticular portion* of the posterior limb contains the posterior thalamic radiations, including the optic radiations, parietal and occipital corticopontine fibers, and fibers from the occipital cortex to the superior colliculi and pretectal region (Figs. 16.3 and

16.42). The *sublenticular portion*, difficult to separate from the retrolenticular, contains the *inferior thalamic peduncle* (Fig. 16.9), the auditory radiations (Figs. 2.11 and 16.39), and corticopontine fibers from the temporal and the parieto-occipital areas.

Thalamocortical and *corticofugal* fibers within the internal capsule occupy a comparatively small, compact area (Fig. 16.39). Lesions in this area produce more widespread disability than lesions of comparable size in any other region of the nervous system. Thrombosis or hemorrhage of the anterior choroidal, striate, or capsular branches of the middle cerebral arteries (Fig. 4.14) are responsible for most lesions in the internal capsule. Vascular lesions in the posterior limb of the internal capsule may result in contralateral hemianesthesia due to injury of thalamocortical fibers *en route* to the sensory cortex. If the genu of the internal capsule is included in the injury, corticobulbar fibers may be destroyed. Lesions in the posterior region of the posterior limb may include the optic and auditory radiations. In such instances, there may be a contralateral triad consisting of hemianesthesia, hemianopsia, and hemihypacusis (Figs. 2.11, 16.39, and 16.42). More extensive vascular lesions may include the thalamus or corpus striatum, so that affective changes and symptoms due to injury of the basal ganglia may be added to those characteristic to the internal capsule.

VISUAL PATHWAYS

Retina

The rods and cones of the retina are visual receptors that react specifically to physical light. The cones, numbering some 7 million in the human eye, have a higher threshold of excitability and are stimulated by light of relatively high intensity. They are responsible for sharp visual definition and for color discrimination in adequate illumination. The rods, whose number is estimated at more than 100 million, react to low intensities of illumination and subserve twilight and night vision. Close to the posterior pole of the eye, the retina shows a small, circular, yellowish area, the *macula lutea*. The macula represents the retinal area for central vision, and the eyes are fixed in such a manner that the retinal image of any object is always focused on the macula. The rest of the retina is concerned with paracentral and peripheral vision. In the macular region, the inner layers of the retina are pushed apart, forming a small central pit, the *fovea centralis*, which constitutes the point of sharpest vision and most acute color discrimination. Here the retina is composed entirely of closely packed slender cones (76, 94, 423).

The rods and cones are composed of an outer segment, a narrow neck, an inner segment, a cell body, and a synaptic base (Fig. 16.40). Photopigments are present in the outer segments, where the photochemical reactions to light take place that give rise to the generator potential. The outer segment is composed of a series of laminated discs derived from the infolding of the plasma membrane. The photopigments, bound to the membranes of the discs, are constantly renewed. Rhodopsin is the photopigment of the rods in primates, and three pigments with maximum absorptions for blue, green, and red are present in the cones (443). The synaptic base of the cone is called a *pedicle*, while that of the rod is referred to as a *spherule*. Each cone pedicle has several invaginations which contain terminals of horizontal, midget bipolar, and flat bipolar cells in a specific arrangement. Rod spherules have a single invagination containing multiple processes of horizontal and rod bipolar cells (Fig. 16.40) (303). Each midget ganglion cell makes several synaptic contacts with a single midget bipolar cell. Diffuse ganglion cells establish synaptic contacts with all types of bipolar cells (77). Horizontal cells and amacrine cells constitute retinal interneurons. It is difficult to determine whether processes of horizontal cells are axons or dendrites, and it is possible that each process may be capable of both receiving and transmitting signals. Amacrine cells in the inner plexiform layer have no axon, but make synaptic contacts with all types of bipolar cells, other amacrine cells, and the dendrites and somata of ganglion cells. The axons of ganglion cells, at first unmyelinated, are arranged in fine radiating bundles which run parallel to the retinal surface and converge at the optic disc to form the optic nerve. On emerging from the eyeball the fibers immediately acquire a myelin sheath, and there is a consequent increase in the size of the optic nerve.

In the retina, the transformation from optical to neural image involves three stages: (a) phototransduction by a layer of receptor neu-

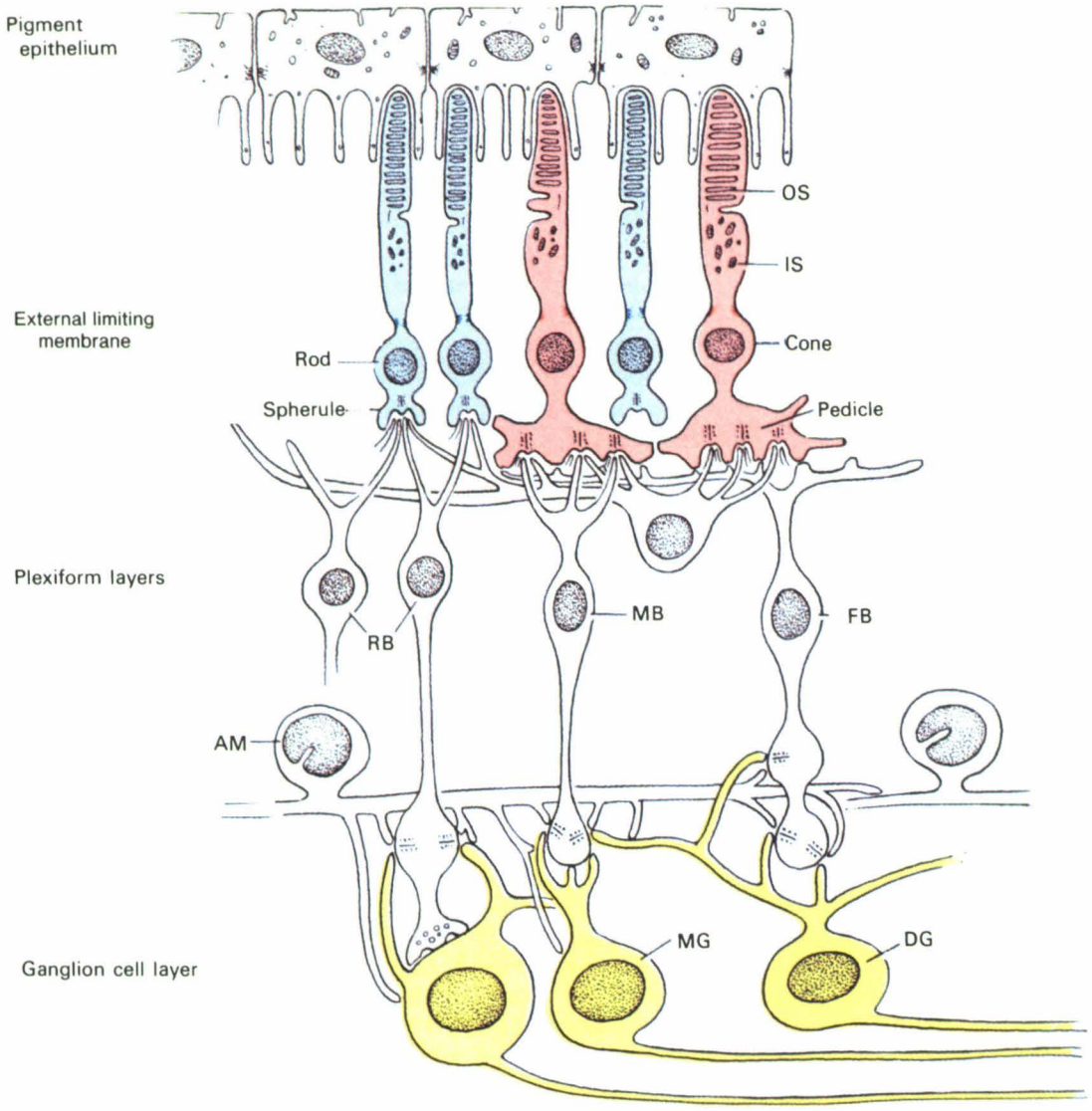


Figure 16.40. Ultrastructural organization of the retina. Rods (*blue*) and cones (*red*) are composed of an outer segment (*OS*), an inner segment (*IS*), a cell body, and a synaptic base. Photopigments are present in the outer segments, which are composed of laminated discs. The synaptic base of the rod is called a spherule, while the synaptic base of the cone is called a pedicle. In the plexiform, layers *RB* indicate rod bipolar cells, *MB* a midget bipolar cell, and *FB* a flat bipolar cell. *AM* indicates an amacrine cell. Ganglion cells (*MG*, midget ganglion cell; *DG*, diffuse ganglion cell) and retinal afferents are in *yellow*.

rons; (b) transmission of their signals by chemical synapses to a layer of "bipolar" cells; and (c) transmission of these signals, also by chemical synapses, to the ganglion cells, which are the output elements of the retina (416, 423). At both synaptic stages (i.e., receptors to bipolar cells and bipolar to ganglion cells) the horizontal and amacrine cells serve to modify the transmission across the synaptic layers. There are also interplexiform cells that convey signals from the inner synaptic layer back to the outer one (94, 416, 423).

Retinal ganglion cells are of different sizes, project to different sites and form at least three functional classes (38, 42, 92, 173, 192, 416, 417). Distinct classes of ganglion cells are referred to as *X*, *Y*, and *W* cells. The X class cells have slower conduction velocities than Y cells, exhibit sustained or tonic responses,

and project to the dorsal lateral geniculate nucleus and the pretectum. The Y cells have rapidly conducting axons, exhibit transient or phasic responses, and project to both the dorsal lateral geniculate nucleus and the superior colliculus. The W ganglion cells have either tonic or phasic responses, very slow axonal conduction velocities, and project to the superior colliculus and the pretectum. It has been suggested that (a) the largest ganglion cells correspond to the Y cells, (b) the medium-sized cells with narrow dendritic arborizations correspond to the X cells, and (c) the smallest ganglion cells with the widest dendritic arborizations correspond to the W cells. Because the central projections of these classes of retinal ganglion cells differ, it is presumed that their functional roles also differ. Both X and Y cells possess properties that contribute to the highly discriminative aspects of vision. The smaller receptive field of the X cells permit resolving higher spatial frequencies than Y cells, but Y cells are more sensitive to moving stimuli. The X cells tend to be concentrated near the central retina, whereas Y cells occur in all parts of the retina. The Y cells are much less numerous than either X or W cells. Since W cells do not project to the dorsal lateral geniculate nucleus, it is presumed that X-type ganglion cells must be concerned with central vision (92).

Optic Nerves

These nerves enter the cranial cavity through the optic foramina and unite to form the optic chiasm, beyond which they are continued as the optic tracts. Within the chiasm a partial decussation occurs, the fibers from the nasal halves of the retina crossing to the opposite side, and those from the temporal halves of the retina remaining uncrossed (Fig. 16.41). In binocular vision, each visual field, right and left, is projected upon portions of both retinae. Thus, the images of objects in the right field of vision (*red* in Fig. 16.41) are projected on the right nasal and the left temporal half of the retina. The right monocular crescent of the visual field projects upon retinal receptors only in the most medial part of the right nasal retina (Fig. 16.27). In the chiasm, the fibers from these two retinal portions are combined to form the left optic tract. By this arrangement, the whole right field of vision is projected upon the left hemisphere, and the left visual field upon the right hemisphere (94, 249).

Optic Tract

On each side, the optic tract partially encircles the hypothalamus and the rostral portions of the crus cerebri. Most of its fibers terminate in the lateral geniculate nucleus, though small portions continue as the brachium of the superior colliculus to the superior colliculi and pretectal area (Fig. 16.41). The lateral geniculate nucleus gives rise to the geniculocalcarine tract, which forms the last relay of the visual pathway. The pretectal area is concerned with light reflex, and the superior colliculi with reflex movement of the eyes and head and tracking of visual stimuli. Retinohypothalamic fibers terminate bilaterally in the suprachiasmatic nucleus of the hypothalamus (272, 277, 344, 425). This direct retinal projection is functionally relevant to neuroendocrine regulation (249).

Geniculocalcarine Tract

This tract arises from cells of the dorsal lateral geniculate nucleus, passes through the retrolenticular portion of the internal capsule, and forms the optic radiations. Its fibers terminate on both sides of the calcarine sulcus in the striate cortex (area 17) (Figs. 2.6, 16.14, 16.41, and 16.42). All fibers of the optic radiation do not reach the cortex by the shortest route (Figs. 16.41 and 16.42). The most dorsal fibers pass almost directly backward to the striate area. More ventral fibers first turn forward and downward into the temporal lobe, and spread out over the rostral part of the inferior horn of the lateral ventricle, and then loop backward. These fibers pass close to the outer wall of the lateral ventricle (external sagittal stratum) to reach the occipital cortex (Fig. 2.22). The most ventral fibers make the longest loop (Figs. 16.41 and 16.42). These fibers, which are referred to as the *temporal* or *Meyer's loop* of the geniculocalcarine tract, terminate in the visual cortex below the calcarine sulcus. Lesions in the temporal lobe involving Meyer's loop causes a defect in the upper visual field on the side opposite to the lesions. Lesions in the parietal lobe, on the other hand, involving the more direct geniculocalcarine fibers that terminate above the calcarine sulcus, may produce a defect in the lower visual field on the side opposite to the lesions.

The retinal areas have a precise point-to-point relationship with the lateral geniculate

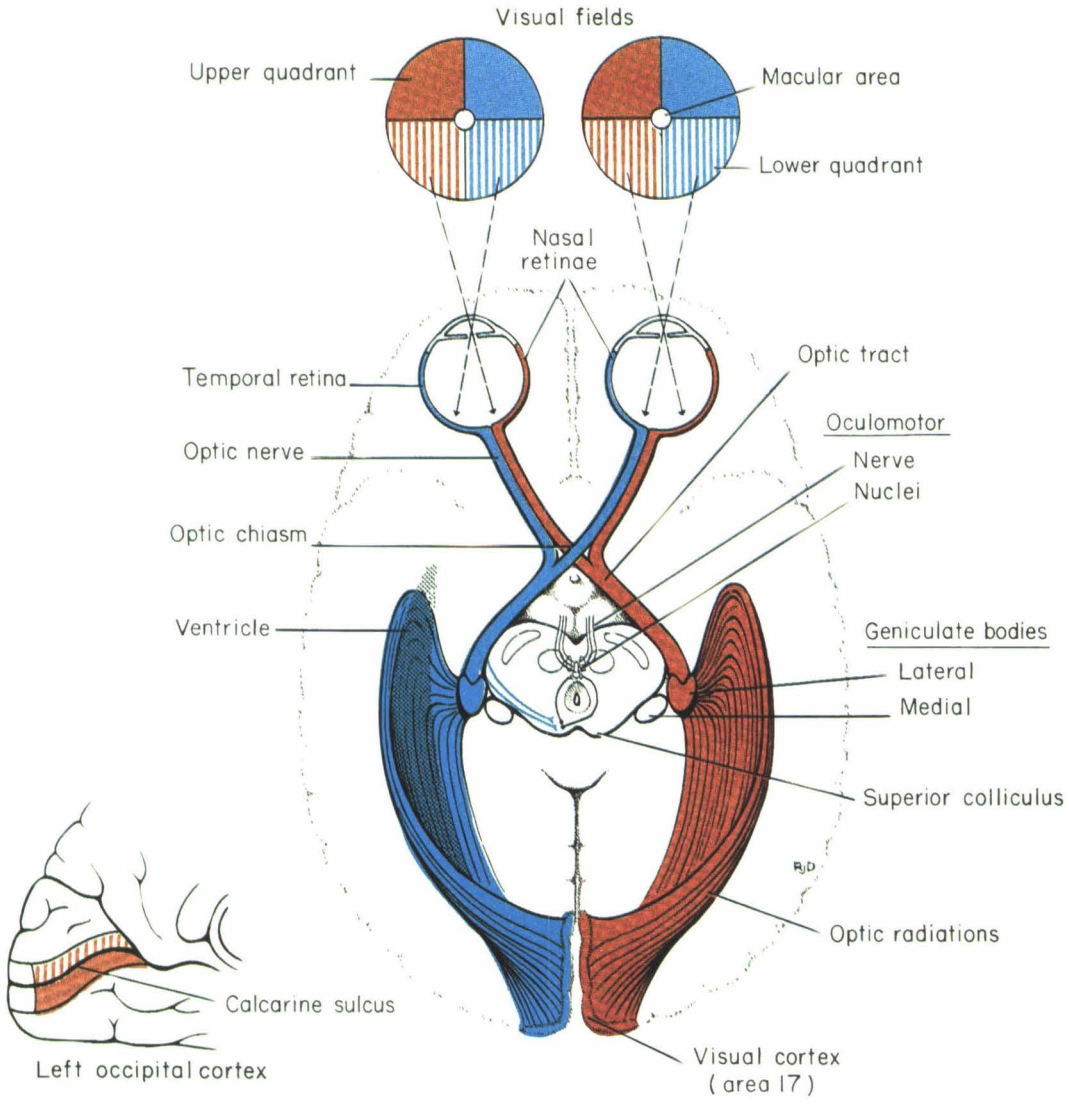


Figure 16.41. Visual pathways viewed from the ventral surface of the brain. Light from the upper half of the visual field falls on the inferior half of the retina. Light from the temporal half of the visual field falls on the nasal half of the retina, while light from the nasal half of the visual field falls on the temporal half of the retina. The visual pathways from the retina to the striate cortex are shown. The plane of the visual fields has been rotated 90° toward the reader. The insert shows the projection of the quadrants of the visual field upon the left calcarine (striate) cortex. The macular area of the retina is represented nearest the occipital pole. Fibers mediating the pupillary light reflex leave the optic tract and project to the pretectal region; other fibers relay impulses indirectly to the visceral nuclei of the oculomotor complex.

nucleus, each portion of the retina projecting on specific and topographically limited portions of the layers of the lateral geniculate nucleus (Figs. 16.27, 16.28, and 16.29). The fibers from the upper retinal quadrants (representing the lower visual field) terminate in the medial half, while those from the lower quadrants terminate in the lateral half of the lateral geniculate nucleus. The macula is represented by a wedge-shaped sector in the caudal part of the lateral geniculate nucleus on both sides of the plane representing the horizontal meridian (247). The peripheral field, including the monocular crescent, is represented rostrally in the lateral geniculate nucleus and is continuous across the horizontal meridian (Fig. 16.29). A similar point-to-point relation exists between the lateral geniculate nucleus and the striate cortex. The medial half of the lateral geniculate nucleus, repre-

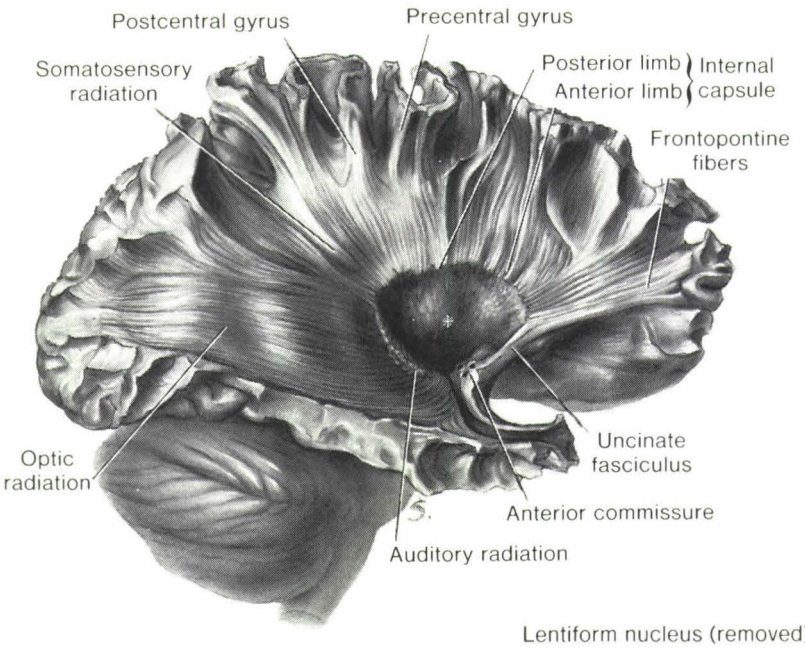


Figure 16.42. Brain dissection showing the corona radiata. The lentiform nucleus has been removed and its position marked by an *asterisk*. The visual, auditory, and somatosensory radiations are identified.

senting the upper retinal quadrants (lower visual fields), projects to the superior lip of the calcarine sulcus. These fibers form the superior portion of the optic radiation (Fig. 16.41). The lateral half of the lateral geniculate nucleus, representing the lower retinal quadrants (upper visual field), projects to the inferior lip of the calcarine sulcus. These fibers form the inferior portion of the optic radiation. The macular fibers, which constitute the intermediate part of the optic radiation, terminate in the caudal third of the calcarine cortex. Those from the paracentral and peripheral retinal areas end in respectively more rostral portions.

Experimental studies with stationary spots of light have revealed important information regarding the organization of the receptive fields of retinal ganglion cells and collicular neurons (151, 154, 206). In the retina, the receptive field is related to those receptors, rods and cones, and other retinal neurons which influence the excitability of a single ganglion cell (163). The retina is a composite of as many receptive fields as there are ganglion cells. Each receptive field is organized into two zones: (a) a small circular central zone, and (b) a surrounding concentric zone referred to as the periphery, or surround. These two zones are functionally antagonistic. Two general types of receptive fields have been described: (a) those with an "on" center and an "off" surround, and (b) those with an "off" center and an "on" surround. If a light stimulus illuminates an "on" center, or an "on" surround the ganglion cell will fire vigorously. If the light stimulus strikes an "off" center, or an "off" surround, the ganglion cell is inhibited until the light is turned off. When the light is withdrawn, the ganglion cell will fire (Fig 20.22). If the light stimulus illuminates both "on" and "off" zones, mutual inhibition cancels the stimulus. Retinal connections account for the concentric circular receptive fields at the ganglion cell level (76, 77). Impulses from the central zone are said to be mediated by direct connections between receptor cells, bipolar cells and ganglion cells, while the antagonistic surround zone has interposed connections with amacrine cells (i.e., between bipolar and ganglion cells).

The receptive fields of neurons in the lateral geniculate nucleus appear similar with stationary spots of light (151, 154, 249), but lateral geniculate neurons show a greater suppression of the receptive field periphery (163). Cells in the different laminae of the lateral geniculate nucleus are driven from receptive fields in one eye, either ipsilaterally or contralaterally. No cells in the lateral

geniculate nucleus are influenced binocularly. An important transformation of the receptive field properties occur between the lateral geniculate nucleus and cells in the striate cortex. Cells in the striate cortex respond to "slits" of light, or moving visual patterns oriented in specific directions (Fig. 20.23) (152–154). The transformation that occurs in the striate cortex is based upon columns of cortical cells of different functional types that encode a wide variety of variables in vertical and horizontal systems (173, 249).

Clinical Notes

Injury to any part of the optic pathway produces visual defects whose nature depends on the location and extent of the injury. During examination, each eye is covered in turn as the retinal quadrants of the opposite eye are tested. Visual defects are said to be *homonymous* when restricted to a single visual field, right or left, and *heteronymous* when parts of both fields are involved. It is evident that homonymous defects are caused by lesions on one side anywhere behind the chiasm (i.e., optic tract, lateral geniculate nucleus, optic radiations, and visual cortex). Complete destruction of any of these structures results in a loss of the whole opposite field of vision *(homonymous hemianopsia)* (Fig. 16.43**C**). Partial injury may produce *quadrantic homonymous* defects. Lesions of the temporal lobe, destroying the looping fibers in the lower portion of the optic radiations, are likely to produce homonymous quadrantic defects in the upper visual field. Injury to the parietal lobe may involve the most superiorly placed fibers of the radiations and cause similar defects in the lower field of vision.

Lesions of the chiasm may cause several kinds of heteronymous defects. Most commonly, crossing fibers from the nasal portions of the retina are involved, with consequent loss of the two temporal fields of vision *(bitemporal hemianopsia)* (Fig. 16.43**D**). Visual defects of this type result from pituitary adenomas that expand out of the sella turcica.

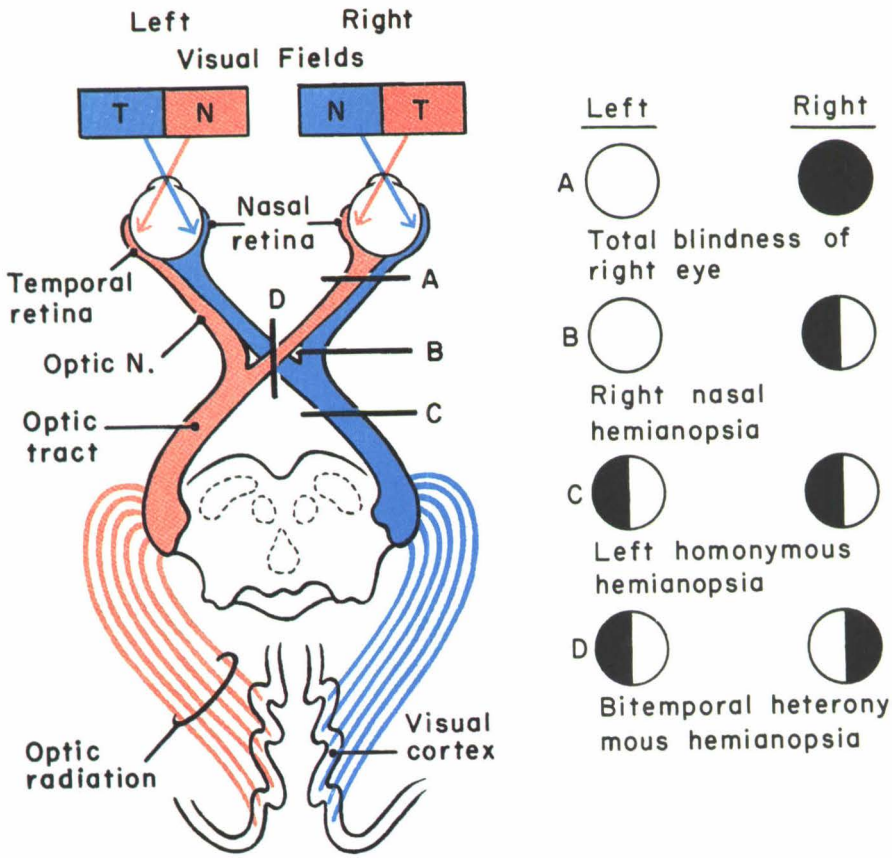


Figure 16.43. Common lesions within the visual pathway. On the left, **A** through **D** indicate lesions. Corresponding visual field defects are shown on the right.

Rarely, both lateral angles of the chiasm may be compressed. In such cases, the nondecussating fibers from the temporal retinae are affected, which results in loss of the nasal visual fields (*binasal hemianopsia*). Injury of one optic nerve naturally produces blindness in the corresponding eye with loss of the pupillary light reflex (Fig. 16.43**A**). The pupil will, however, contract consensually to light entering the other eye, since the pretectal reflex center is related to both Edinger-Westphal nuclei. The pupillary light reflex will not be affected by lesions of the visual pathway above the brachium of the superior colliculus (Fig. 16.41).

FUNCTIONAL CONSIDERATIONS

All sensory impulses, with the sole exception of the olfactory ones, terminate in the gray masses of the thalamus, from which they are projected to specific cortical areas by the thalamocortical radiations. Some fibers from the olfactory tubercle, piriform and entorhinal cortex, and basolateral amygdaloid nuclei project to the mediodorsal nucleus, but this nucleus does not relay impulses to the primary olfactory cortex (203, 227, 353). While portions of the thalamus serve as primary relay nuclei in various sensory pathways in which impulses are projected to specific regions of the cerebral cortex, the structure and organization of the thalamus indicate that its function is more complex and elaborate than that of a simple relay station. The thalamus is obviously one of the chief sensory integrating mechanisms of the neuraxis, but its functions are not limited to this. There is abundant evidence that specific parts of the thalamus play a dominant role in the maintenance and regulation of the state of consciousness, alertness, and attention, but also with the emotional correlates that accompany most sensory experiences. Other data suggest that some thalamic nuclei serve as integrative centers for motor and limbic functions, since their principal afferent projections are from the cerebellum and the basal ganglia, on one hand, and from various limbic structures on the other.

Thalamic Relay Functions

THALAMUS AS A SPECIFIC SENSORY RELAY

Thalamic nuclei involved in the relay of specific sensory information to the cerebral cortex lie in the ventral tier of the lateral nuclear group. The so-called specific sensory relay nuclei include the medial and lateral geniculate nuclei and the major divisions of the ventral posterior nucleus, known as the ventrobasal complex. The medial geniculate nucleus receives fibers from the inferior colliculus. The laminated, tonotopically organized parvicellular part of the nucleus projects fibers via the geniculotemporal radiation to the transverse temporal gyrus of Heschl, the *primary auditory area* (Figs. 13.13 and 16.13). The lateral geniculate nucleus, receiving both crossed and uncrossed fibers of the optic tract, gives rise to the geniculocalcarine fibers, which project in a specific way to the cortex surrounding the calcarine sulcus. This cortex represents the *primary visual area* (Fig. 16.41).

The divisions of the ventral posterior nucleus (VPLc, VPM, and VPMpc) project to the cortex of the postcentral gyrus. In the postcentral gyrus, all parts of the body are represented in a definite sequence (336). This cortical region is referred to as the *primary somesthetic area* (somatic sensory area I). The sensory representation of the body in the primary somesthetic area (S-I) is duplicated in a different sequence in the second somatic area (S-II), which lies buried along the superior bank of the lateral sulcus (335, 456). Somatic sensory area II receives fibers ipsilaterally from VPI and bilaterally from S-I (44, 89, 181, 182, 184, 186), and responds mainly to cutaneous stimuli (374).

Signals from peripheral receptors do not pass through the thalamus without modification. Many of the impulses are modified and integrated at the thalamic level before being projected to specific cortical areas. The thalamocortical projection, which represents one of the most massive fiber collections of the entire neuraxis, is likely to play a very active role in the modulation of the information it receives from the thalamus. It is through this cortico-thalamo-cortical loop that the cerebral cortex can direct its attention to certain sensory experiences and amplify specific sensory messages at the expense of others. In certain lesions of the thalamus or of the thalamocortical connections, after a brief initial stage of complete contralateral anesthesia, pain, crude touch, and some thermal sense return. However, tactile localization, two-point discrimination, and the sense of position and movement remain severely impaired (134, 135).

The sensations recovered are poorly localized and are accompanied by a great increase in "feeling tone," most commonly of an unpleasant character. This condition is referred to as the "thalamic syndrome" (Dejerine-Roussy syndrome). Though the threshold of excitability is raised on the affected side, tactile and thermal stimuli, previously not unpleasant, evoke disagreeable sensations (dysesthesias).

There are two aspects to sensation: the discriminative and the affective. In the former, stimuli are compared with respect to intensity, locality, and relative position in space and time. These impulses are integrated into perceptions of form, size, and texture; movements are judged as to direction, amplitude, and sequence. These aspects of somatic sensation are related to VPLc and VPM and their restricted cortical projection areas. There is a complete, though distorted, representation of the body in VPLc and VPM, and VP neurons are modality specific, being concerned mainly with tactile and position sense, and responding to either superficial mechanical stimulation of the skin, mechanical distortion of deep tissues, or joint rotation, but not more than one of these (58, 111). Some impulses arising from primary endings in muscle spindles (group Ia fibers), conveyed to the outer shell of the ventrobasal complex, are relayed to the depths of the central sulcus (area 3a) (179, 315, 431). These responses from muscle spindles reach the thalamus via the posterior column nuclei and VPLc.

The visual and auditory thalamic nuclei are organized in a very specific manner in which point-for-point relationships exist between the receptor organ, thalamic nuclei, and the thalamocortical projections. Columns of cells in all layers of the lateral geniculate nucleus receive inputs from corresponding points in the retina and, in turn, project to the striate cortex in a retinotopic fashion. No binocular fusion occurs in the lateral geniculate nucleus. This visual input to the cortex is transformed in a manner that gives individual cortical neurons properties different from the lateral geniculate neurons, but better suited to detect shapes and patterns, and to provide binocular vision (Figs. 20.22 and 20.23). The auditory thalamic relay nuclei are organized in a similar specific manner. The cellular laminae in the medial geniculate nucleus, evident only in Golgi preparation, forms the basis for the tonotopic organization. Neurons in the ventral division of the medial geniculate nucleus project to the primary auditory cortex, while those in other cytologic subdivisions of the medial geniculate nucleus project to a belt of secondary auditory cortex surrounding the primary auditory area.

The "affective" side of sensation is concerned with pain, agreeableness, and disagreeableness. Pain is a subjective sensation that often is difficult to describe and almost impossible to measure. The localization of different types of pain is often inexact and clinical judgment of its intensity must take into account the personality of the patient. Temperature and many tactile sensations likewise have a marked affective tone. This is especially true for visceral sensations, in which the discriminative element is practically absent. This affective quality, which forms the basis of general bodily well-being or *malaise*, and of the more intense emotional states, is believed to be "appreciated" at the thalamic rather than the cortical level, though it may be profoundly modified and controlled by the latter.

THALAMUS AS A LIMBIC-MOTOR RELAY

The so-called cortical relay nuclei of the thalamus (or specific thalamic relay nuclei) receive impulses from specific subcortical structures and project to well-defined cortical regions. These nuclei include (a) the anterior nuclei, (b) the ventral posterolateral nucleus, pars oralis (VPLo), and the ventral lateral nucleus, pars caudalis (VLc), and (c) the ventral lateral nucleus, pars oralis (VLo) and the ventral anterior nucleus, pars parvicellularis (VApc). The anterior nuclei of the thalamus receive the largest efferent fiber bundle from the hypothalamus—the mammillothalamic tract—and direct projections from the hippocampal formation via the fornix (Figs. 16.2, 16.8, and 17.14). These nuclei, in turn, project to the cingulate gyrus, a cortical area demonstrated to produce a variety of visceral and limbic functions.

The contralateral deep cerebellar nuclei project most of their ascending fibers to nuclei of the "cell-sparse" thalamic region (VPLo, VLc, and "area x"), which in turn projects somatotopically on the primary motor (M-I, area 4). Furthermore, the "cell-sparse" zone in the ventral lateral thalamic region receives projection from the two major output structures of the basal ganglia, namely the internal pallidal segment and the substantia

nigra pars reticulata. The termination fields of cerebellar, pallidal, and nigral projection to the thalamus do not overlap. Pallidal fibers terminate in VLo and VApc that in turn project to the supplementary motor area (M-II), whereas nigral fibers arborize in VAmc and MDpl that project to the prefrontal cortex. The pallidal and nigral fibers exert a GABAergic inhibitory action on thalamic relay neurons, while the effect of cerebellar fibers is a glutamatergic excitation. Each of three neuronal systems (cerebellar, pallidal, and nigral) form parallel segregated channels that are concerned with unique and different aspects of motor function.

Low frequency electrical stimulation of individual specific sensory relay nuclei, and certain cortical relay nuclei (i.e., the ventral lateral nucleus), evokes a primary surface potential followed by an augmenting sequence which is limited to the cortical projection area. This response is called the *augmenting response*. Characteristically, the augmenting responses (a) have a short latency, (b) are dysphasic and increase in magnitude during the initial four or five stimuli of a repetitive train, and (c) are localized to the primary cortical projection area of the specific thalamic nucleus stimulated (71).

Thalamic Gating Functions

Thalamic relay cells exhibit two response modes: a *relay* mode and a nonrelay *burst* mode (393). If a cell is at rest or slightly depolarized, it is in a relay mode. In such a condition, a suprathreshold excitatory postsynaptic potential (EPSP) will induce a train of action potentials. The frequency of action potentials monotonically rises with increasing EPSP amplitude. Under these conditions, transmission through the thalamic relay neuron to the cortex will lead to a pattern of input to the cortex that faithfully reflects the pattern of retinal or lemniscal input to the thalamus. However, once a thalamic neuron becomes hyperpolarized sufficiently long to deinactivate a low threshold spike, it enters the burst mode. In such a state, a suprathreshold EPSP will trigger a low-threshold spike, and many such spikes may ensue as the cell bursts rhythmically. Until this bursting cycle is broken, the neuron no longer relays sensory input to the cortex because its firing pattern bears no resemblance to the pattern of its retinal or lemniscal inputs (393).

Although thalamic neurons may switch between relay and burst modes at any time, the relay mode appears to be the state of most thalamic neurons in the awake, alert animal, whereas the burst mode dominates during less alert periods, including drowsiness and quiet or non-REM sleep (413). During such inattentive periods, the electroencephalogram (EEG) in all animals, including humans, becomes highly synchronized and fast. Rhythmic, spike-like electrical phenomena known as *spindles* can be seen. These spindles have a frequency of 7–14 Hz.

This dominant feature of the synchronized EEG is generated in the thalamus (413). Electrophysiologic studies of thalamic neurons have shown that all neurons of the reticular nucleus can spontaneously generate rhythmic discharges at a rate of approximately 10 Hz. The low-threshold spike appears to be the underlying cause of this endogenous bursting behavior, and the oscillations can be generated within individual reticular nucleus neurons. Dendrodendritic synapses between reticular nucleus neurons could serve to synchronize the entire reticular nucleus region and, hence, influence in a highly coordinated fashion the neuronal activity of virtually all thalamic nuclei (73). Neurons of the reticular nucleus can generate such synchronized oscillatory activity in the absence of external inputs, whereas neurons of thalamic nuclei deprived of their reticular nucleus input fail to display spindling activity (74, 411, 413). These findings suggest that the reticular nucleus acts as a kind of pacemaker for thalamic relay cells. Since it can induce synchronized bursts in thalamic neurons, the reticular nucleus can markedly affect the gating functions of the thalamic neurons. Hence, the reticular nucleus appears capable of modulating thalamic neural activity, particularly in relation to the passage of afferent volleys through the thalamus. It also appears involved in the modulation of thalamic activity during sleep and arousal, and this may reflect its own underlying control by brainstem cholinergic, noradrenergic, and serotoninergic afferents.

Thalamic Association Functions

The so-called association nuclei of the thalamus are those nuclei that are not governed by a single sensory modality and project largely to association areas of the cerebral cortex in the frontal and parietal lobes and, to a lesser extent, in the occipital and temporal

lobes. The principal association nuclei include the mediodorsal nucleus (MD), the lateral dorsal nucleus (LD), the lateral posterior nucleus (LP), and the pulvinar (P) (Fig. 16.12). The mediodorsal nucleus, the most prominent gray mass of the medial thalamus, is highly developed in primates, especially humans (Fig. 16.13). This nucleus is characterized by its massive and reciprocal connections with the granular frontal cortex. Large bilateral injuries to the frontal lobes cause defects in complex associations, as well as changes in behavior, expressed by loss of acquired inhibitions and excessive, and sometimes inappropriate, emotional responses. These alterations in emotional behavior are produced when the pathways between the dorsomedial nucleus and the frontal cortex are severed (e.g., in frontal lobotomy).

The lateral dorsal nucleus projects upon portions of the limbic and precuneal cortex. The larger lateral posterior nucleus has extensive connections with the association cortex of the superior and inferior parietal lobules, concerned with cognitive and symbolic functions. The pulvinar develops as a huge nuclear mass concerned with the integration of general and special somatic senses, particularly vision and audition. The inferior and parts of the adjacent lateral pulvinar are involved in extrageniculate projections to the secondary visual area.

Thalamic State-Dependent Functions

Stimulation of the ascending reticular activating system and various kinds of sensory stimuli result in a generalized desynchronization and activation of the electroencephalogram, and behavioral arousal. The EEG arousal response, which produces dramatic effects upon cortical activity, is mediated, in large part, by the intralaminar thalamic nuclei. Physiologic studies presumed that impulses producing these changes in cortical activity reached the cortex via a diffuse, nonspecific thalamic projection system (164, 166, 284, 285, 407). The more rostral intralaminar thalamic nuclei (CL and PCN), which receive fibers from the midbrain reticular formation, project directly to widespread cortical regions.

Stimulation of the so-called nonspecific thalamic nuclei, produces widespread and pronounced effects on the electrocortical activity. The *nonspecific*, or *diffuse*, thalamic nuclei include the intralaminar and midline nuclei and part of the ventral anterior nucleus. Repetitive stimulation of these thalamic nuclei alters spontaneous electrocortical activity over large areas and, under certain conditions, resets the frequency of brain waves by eliciting responses that are time-locked to the thalamic stimulus (71, 72, 283). The most characteristic effect of stimulating the nonspecific thalamic nuclei is the *recruiting response*. When the frequency of stimulation is in the range of 6 to 12 cycles per second, predominantly surface negative cortical responses rapidly increase to a maximum (by the fourth to sixth stimulus of the train) and then decrease over a broad area. Continued stimulation causes the evoked responses to wax and wane. Stimulation of one of the nonspecific thalamic nuclei causes all others to be activated in a mass excitation (407). Although stimulating the nonspecific thalamic nuclei produces changes in electrocortical activity over broad areas, these effects are not indiscriminate or equal in all cortical areas. Responsive cortical zones appear to be relatively specific in the frontal, cingulate, orbital, parietal and occipital association areas. This diffuse thalamic projection system appears capable of exerting a massive influence mainly upon large regions of associate cortex, but the most profound effects are upon the frontal association cortex (409).

The original observation of Moruzzi and Magoun (285) that cortical recruiting responses induced by low frequency stimulation of the nonspecific thalamic nuclei could be reduced, or blocked, by stimulation of the bulbar reticular formation provides evidence that the nonspecific nuclei of the thalamus are within the sphere of influence of the ascending reticular formation. The cholinergic, noradrenergic, and serotoninergic systems represent some of the brainstem ascending neuronal systems that can modulate neurons of the nonspecific thalamic nuclei and hence exert a profound influence upon the electrocortical activity according to various state-dependent conditions. Some of these long ascending chemospecific systems (i.e., noradrenergic and serotoninergic systems) also have straight access to the cerebral cortex, where they can directly modulate the activity of vast cortical neuronal assemblies.

The largest component of the intralaminar nuclei, the centromedian-parafascicular (CM-Pf) nuclear complex receives its input mainly from forebrain derivatives. The precentral and premotor cortex project profusely upon

these nuclei (7, 209, 210). The centromedian nucleus (CM) also receives collaterals of pallidofugal fibers arising in the internal pallidal segment. The principal projection of the CM-Pf complex is to the striatum, with cells in Pf projecting to the caudate nucleus (associative striatal territory) and those in CM projecting to the putamen (sensorimotor striatal territory). These connections suggest that the CM-Pf complex plays an important role in motor integration.

The thalamus is played upon by two great streams of afferent fibers, one peripheral and one central. Signals are generated in receptors in all parts of the body and convey information concerning changes in the external environment. Additionally, the thalamus receives significant subcortical inputs from the cerebellar nuclei, the internal pallidal segment, and the pars reticulata of the substantia nigra concerned with different aspects of motor function. Massive cortical projections bring thalamic nuclei under the influence of sensory, motor, and association areas of the cortical mantle. Most of the sensory and motor systems converge on thalamic nuclei in a very specific manner without overlap. The thalamus integrates these systems and distributes projections to specific areas of the cerebral cortex. The thalamus is a neural center where highly complex neural integration occurs, involving sensory, motor, limbic, and state-dependent neuronal systems. The result of such high-level integration will markedly influence the activity of the entire brain.

References

1. Adams CE, Fisher RS. Sources of neostriatal cholecystokinin in the cat. J Comp Neurol 1990;292: 563–574.
2. Adem A, Jossan SS, d'Argy R, Brandt I, Winblad B, Nordberg A. Distribution of nicotinic receptors in human thalamus as visualized by [^{3}H] nicotine and [^{3}H] acetylcholine receptor autoradiography. J Neural Transm 1988;73:77–83.
3. Afifi A, Kaelber WW. Efferent connections of the substantia nigra in the cat. Exp Neurol 1965;11: 474–482.
4. Aggleton JP, Miskin M. Memory impairments following restricted medial thalamic lesions in monkey. Exp Brain Res 1983;52: 199–209.
5. Aggleton JP, Miskin M. Projections of the amygdala to the thalamus in the cynomolgus monkey. J Comp Neurol 1984;222:56–68.
6. Aitkin LM, Webster WR. Medial geniculate body of the cat: organization and responses to tonal stimuli of neurons in the ventral division. J Neurophysiol 1972;35: 365–380.
7. Akert K, Hartmann-von Monakow K. Relationships of precentral, premotor and prefrontal cortex to the mediodorsal and intralaminar nuclei of the monkey thalamus. Acta Neurobiol Exp (Warsz) 1980;40: 7–25.
8. Andersen E, Dafny N. Microiontophoretically applied 5-HT reduces responses to noxious stimulation in the thalamus. Brain Res 1982;241:176–178.
9. Ariëns Kappers J. The pineal organ: an introduction. In: Wolstenholme GEW, Knight J, eds. The pineal gland. Edinburgh: Churchill Livingston, 1971:1–23.
10. Armstrong E. Limbic thalamus: anterior and mediodorsal nuclei. In: Paxinos G, ed. The human nervous system. Ch. 18. New York: Academic Press, 1990:469–481.
11. Aronson LR, Papez JW. The thalamic nuclei of Pithecus (Macacus) Rhesus. II. Dorsal thalamus. Arch Neurol Psychiatr 1934;32:27–44.
12. Asanuma C, Porter LL. Light and electron microscopic evidence for a GABAergic projection from the caudal basal forebrain to the thalamic reticular nucleus in rats. J Comp Neurol 1990;302:159–172.
13. Asanuma C, Thach WT, Jones EG. Anatomical evidence for segregated focal groupings of efferent cells and their terminal ramifications in the cerebellothalamic pathway of the monkey. Brain Res Rev 1983;5:219–235.
14. Auer J. Terminal degeneration in the diencephalon after ablation of frontal cortex in the cat. J Anat 1956;90:30–41.
15. Axelrod J, Wurtman RJ, Snyder SH. Control of hydroxyindole-*o*-methyl transferase activity in the rat pineal gland by environmental lighting. J Biol Chem 1965;240: 949–955.
16. Bard P, Rioch DM. A study of 4 cats deprived of neocortex and additional portions of the forebrain. Bull Johns Hopkins Hosp 1937; 60:73–147.
17. Battaglia G, Colacitti C, Bentivoglio M. The relationship of calbindin-containing neurons with substance P, leu-enkephalin and cholecystokinin fibres: an immunohistochemical study in the rat thalamus. J Chem Neuroanat 1992; 5:453–464.
18. Beckstead RM, Morse JR, Norgren R. The nucleus of the solitary tract in the monkey: projections to the thalamus and brain stem nuclei. J Comp Neurol 1980;190:259–282.
19. Benevento LA, Fallon JH. The ascending projections of the superior colliculus in the rhesus monkey (*Macaca mulatta*). J Comp Neurol 1975;160:339–362.
20. Benevento LA, Rezak M. The cortical projections of the inferior pulvinar and adjacent lateral pulvinar in the rhesus monkey (*Macaca mulatta*): an autoradiographic study. Brain Res 1976;108:1–24.
21. Benson DL, Isackson PJ, Hendry SH, Jones EG. Differential gene expression for glutamic acid decarboxylase and type II calcium-calmodulin-dependent protein kinase in basal ganglia, thalamus, and hypothalamus of the monkey. J Neurosci 1991;11:1540–1564.
22. Berense HW, Groenewegen HJ. Organization of the thalamostriatal projection in the rat, with special emphasis on the ventral striatum. J Comp Neurol 1990;299:1 87–228.
23. Berry CM, Anderson FD, Brooks DC. Ascending pathways of the trigeminal nerve in cat. J Neurophysiol 1956;19:144–153.
24. Berry CM, Karl RS, Hinsey JC. Course of spinothalamic and medial lemniscal pathways in the cat and rhesus monkey. J Neurophysiol 1950;13:149–156.
25. Bertrand GL, Blundell J, Musella R. Electrical exploration of the internal capsule and neighboring structures during stereotaxic procedures. J Neurosurg 1965;22: 333–343.
26. Binkley S. A timekeeping enyme in the pineal gland. Science 1979;240:66–71.
27. Bishop PO, Kozak W, Levick WR, Vakkur GJ. The determination of the projection of the visual field on to the lateral geniculate nucleus in the cat. J Physiol (Lond) 1962;163: 503–539.
28. Björklund A, Lindvall O. Dopamine-containing systems in the CNS. In: Björklund A, Hökfelt T, eds. Handbook of chemical neuroanatomy. Vol. 2. Part 1: Classical

transmitters in the CNS. Ch. 3. Amsterdam: Elsevier, 1984:55–122.
29. Björklund A, Owman C, West KA. Peripheral sympathetic innervation and serotonin cells in the habenular region of the rat brain. Z Zellforsch Mikrosk Anat 1972;127: 570–579.
30. Boivie J. Terminations of the cervicothalamic tract in the cat: an experimental study with silver impregnation methods. Brain Res 1970;19:333–360.
31. Boivie J. The terminations of the spinothalamic tract in the cat: an experimental study with silver impregnation methods. Exp Brain Res 1971;12:331–353.
32. Boivie J. Anatomical observations on the dorsal column nuclei, their thalamic projection and the cytoarchitecture of some somatosensory thalamic nuclei in the monkey. J Comp Neurol 1978;178: 17–48.
33. Boivie J. An anatomical reinvestigation of the termination of the spinothalamic tract in the monkey. J Comp Neurol 1979;186:343–370.
34. Bolton RF, Cornwall J, Phillipson OT. Collateral axons of cholinergic pontine neurones projecting to midline, mediodorsal and parafascicular thalamic nuclei in the rat. J Chem Neuroanat 1993;6:101–114.
35. Bowsher D. Termination of the central pain pathway: the conscious appreciation of pain. Brain 1957;80:606–622.
36. Bowsher D. Projections of the gracile and cuneate nuclei in *Macaca mulatta*: an experimental degeneration study. J Comp Neurol 1958;110:135–155.
37. Bowsher D. The termination of secondary somatosensory neurons within the thalamus of *Macaca mulatta*: an experimental degeneration study. J Comp Neurol 1961;17: 213–227.
38. Boycott BB, Wässle H. The morphological types of ganglion cells of the domestic cat's retina. J Physiol (Lond) 1974;240:397–419.
39. Braak H, Braak E. Alzheimer's disease affects limbic nuclei of the thalamus. Acta Neuropathol (Berl) 1991;81:261–268.
40. Broman J, Ottersen OP. Cervicothalamic tract terminals are enriched in glutamate-like immunoreactivity: an electron microscopic double-labeling study in the cat. J Neurosci 1992;12:204–221.
41. Brouwer B, Zeeman WPC. The projection of the retina in the primary optic neuron in monkeys. Brain 1926;49:1–35.
42. Bunt AH, Hendrickson AE, Lund JS, Lund RD, Fuchs AF. Monkey retinal ganglion cells: morphometric analysis and tracing of axonal projections with a consideration of the peroxidase technique. J Comp Neurol 1975;164:265–286.
43. Burton H, Craig AD Jr. Distribution of trigeminothalamic projection cells in the cat and monkey. Brain Res 1979;161:515–521.
44. Burton H, Jones EG. The posterior thalamic region and its cortical projection in new world and old world monkeys. J Comp Neurol 1976;168:249–302.
45. Campos-Ortega JA, Glees P, Neuhoff V. Ultrastructural analysis of individual layers in the lateral geniculate body of the monkey. Z Zellforsch Mikrosck Anat 1968;87: 82–100.
46. Carman JB, Cowan WM, Powell TPS. Cortical connections of the thalamic reticular nucleus. J Anat 1964;98:587–598.
47. Carmel PW. Efferent projections of the ventral anterior nucleus of the thalamus in the monkey. Am J Anat 1970;128:159–184.
48. Carpenter MB. The dorsal trigeminal tract in the rhesus monkey. J Anat 1957;91:82–90.
49. Carpenter MB. Ventral tier thalamic nuclei. In: Williams D, ed. Modern trends in neurology. Vol. 4. London: Butterworths, 1967:1–20.
50. Carpenter MB. Anatomy of the corpus striatum and brainstem integrating systems. In: Brooks VB, ed. Handbook of physiology. Sec. 1. The nervous system. Vol. II. Motor control. Ch. 19. Washington, DC: American Physiological Society, 1981:947–995.
51. Carpenter MB, Hanna GR. Fiber projections from the spinal trigeminal nucleus in the cat. J Comp Neurol 1961;117:117–132.
52. Carpenter MB, Nakano K, Kim R. Nigrothalamic projections in the monkey demonstrated by autoradiographic techniques. J Comp Neurol 1976;165:401–416.
53. Carpenter MB, Peter P. Nigrostriatal and nigrothalamic fibers in the rhesus monkey. J Comp Neurol 1972;144:93–116.
54. Carpenter MB, Strominger NL. Efferent fibers of the subthalamic nucleus in the monkey: a comparison of the efferent projections of the subthalamic nucleus, substantia nigra and globus pallidus. Am J Anat 1967;121:41–72.
55. Casseday JH, Diamond IT, Harting JK. Auditory pathways to the cortex in *Tupaia glis*. J Comp Neurol 1976;166:303–340.
56. Chan-Palay V. Cerebellar dentate nucleus: organization, cytology and transmitters. Berlin: Springer-Verlag 1977.
57. Chevalier G, Deniau M. Disinhibition as a basic process in the expression of striatal functions. Trends Neurosci 1990;13:277–280.
58. Clark FJ, Burgess PR. Slowly adapting receptors in cat knee joint: can they signal angle? J Neurophysiol 1975;38:1448–1463.
59. Clemence AE, Mitrofanis J. Cytoarchitectonic heterogeneities in the thalamic reticular nucleus of cats and ferrets. J Comp Neurol 1992; 322:167–180.
60. Cole M, Nauta WJH, Mehler WR. The ascending efferent projections of the substantia nigra. Trans Am Neurol Assoc 1964;89:74–78.
61. Colonnier ML, Guillery RW,. Synaptic organization in the lateral geniculate nucleus of the monkey. Z Zellforsch Mikrosk Anat 1964; 62:333–355.
62. Combs CM. Fiber and cell degeneration in the albino rat brain after hemidecortication. J Comp Neurol 1949;90:373–402.
63. Crunelli V, Leresche N. A role for GABAB receptors in excitation and inhibition of thalamocortical cells. Trends Neurosci 1991;14:16–21.
64. Dafny N, Reyes-Vazquez C, Qiao JT. Modification of nociceptively identified neurons in thalamic parafascicularis by chemical stimulation of the dorsal raphe with glutamate, morphine, serotonin and focal dorsal raphe electrical stimulation. Brain Res Bull 1990;24: 717–723.
65. De Biasi S, Frassoni C, Spreafico R. GABA immunoreactivity in the thalamic reticular nucleus of the rat. A light and electron microscopical study. Brain Res 1986; 399:143–147.
66. De Biasi S, Rustioni A. Ultrastructural immunocytochemical localization of excitatory amino acids in the somatosensory system. J Histochem Cytochem 1990;38:1745–1754.
67. De Curtis M, Spreafico R, Avanzini G. Excitatory amino acids mediate responses elicited in vitro by stimulation of cortical afferents to reticularis thalami neurons of the rat. Neuroscience 1989;33:275–283.
68. Dejerine J. Anatomie des centres nerveux. Vol. 2. Paris: J. Rueff, 1901.
69. Dekaban A. Human thalamus. An anatomical, developmental and pathological study. I. Division of the human adult thalamus into nuclei by use of the cyto-myelo-architectonic method. J Comp Neurol 1953;99:639–683.
70. Dekaban A. Human thalamus. An anatomical developmental and pathological study. II. Development of the human thalamic nuclei. J Comp Neurol 1954;100: 63–97.
71. Dempsey EW, Morison RS. The production of rhythmically recurrent cortical potentials after localized thalamic stimulation. Am J Physiol 1942;135:293–300.
72. Dempsey EW, Morison RS. The electrical activity of a thalamocortical relay system. Am J Physiol 1943;138:283–298.
73. Deschênes M, Madariaga-Domich A, Steriade M. Dendrodendritic synapses in the cat reticularis thalami nucleus: a structural basis for thalamic spindle synchronization. Brain Res 1985;334:165–168.
74. Deschênes M, Roy JP, Steriade M. Nature of 7–14 Hz rhythmic hyper-

polarizations in thalamic relay neurons. Neurosci Abstr 1983; 9:678.
75. Diamond IT, Jones EG, Powell TPS. The projection of the auditory cortex upon the diencephalon and brain stem in the cat. Brain Res 1969;15:305–340.
76. Dowling JE. The retina: an approachable part of the brain. Cambridge: Harvard University Press, 1987.
77. Dowling JE, Boycott BB. Organization of the primate retina: electron microscopy. Proc R Soc Lond (Biol) 1966;166:80–111.
78. Droogleever-Fortuyn J, Stefens R. On the anatomical relations of the intralaminar and midline cells of the thalamus. Electroencephalogr Clin Neurophysiol 1951;3:393–400.
79. Dykes RW. Parallel processing of somatosensory information: a theory. Brain Res Rev 1983;6:47–115.
80. Dykes RW, Herron P, Lin CS. Ventroposterior thalamic regions projecting to cytoarchitectonic areas 3a and 3b in the cat. J Neurophysiol 1986;56:1521–1541.
81. Eaton SA, Salt TE. Membrane and action potential responses evoked by excitatory amino acids acting at N-methyl-D-aspartate receptors and non-N-methyl-D-aspartate receptors in the rat thalamus in vivo. Neuroscience 1991;44:277–286.
82. Edwards SB, Rosenquist AC, Palmer LA. An autoradiographic study of ventral lateral geniculate projections in the cat. Brain Res 1974;72:282–287.
83. Englander RN, Netsky MG, Adelman LS. Location of human pyramidal tract in the internal capsule: anatomical evidence. Neurology 1975;25:823–826.
84. Faull RLM, Carman JB. Ascending projections of the substantia nigra in the rat. J Comp Neurol 1968; 132:73–92.
85. Forbes BF, Moskowitz N. Projections of auditory responsive cortex in the squirrel monkey. Brain Res 1974;67:239–254.
86. Fraschini F, Collu R, Martini L. Mechanisms of inhibitory action of pineal principles on gonadotropin secretion. In: Wolstenholme GEW, Knight J, eds. The pineal gland. Edinburgh: Churchill Livingstone, 1971:259–272.
87. Freeman W, Watts JW. Retrograde degeneration of the thalamus following prefrontal lobotomy. J Comp Neurol 1947;86:65–93.
88. Freeman W, Watts JW. The thalamic projection to the frontal lobe. Proc Assoc Res Nerv Ment Dis 1948;27:200–209.
89. Friedman DP, Jones EG, Burton H. Representation pattern in the second somatic sensory area of the monkey cerebral cortex. J Comp Neurol 1980;192:21–41.
90. Frigyesi TL, Schwartz R. Cortical control of thalamic sensorimotor relay activities in the cat and squirrel monkey. In: Frigyesi TL, Yahr MD, eds. Corticothalamic projections and sensorimotor activities. New York: Raven Press, 1972: 161–195.
91. Fry WJ, Krumins R, Fry FJ, Thomas G, Borbely S, Ades H. Origins and distribution of some efferent pathways from the mammillary nuclei of the cat. J Comp Neurol 1963; 120:195–258.
92. Fukuda Y, Stone J. Retinal distribution and central projections of Y, X and W cells of the cat's retina. J Neurophysiol 1974;37:749–772.
93. Galambos R, Rose JE. Microelectrode studies on medial geniculate body of the cat. III. Response to pure tone. J Neurophysiol 1952; 15:381–400.
94. Garey LJ. Visual system. In: Paxinos G, ed. The human nervous system. Ch. 28. New York: Academic Press, 1990:945–977.
95. Garey LJ, Powell TPS. The projection of the lateral geniculate nucleus upon the cortex in the cat. Proc R Soc B 1967;169:107–126.
96. Garey LJ, Powell TPS. The projection of the retina in the cat. J Anat 1968;102:189–222.
97. Garey LJ, Powell TPS. An experimental study of the termination of the lateral geniculo-cortical pathway in the cat and monkey. Proc R Soc Lond (Biol) 1971;179:41–63.
98. Garland JC, Mogenson GJ. An electrophysiological study of convergence of entopeduncular and lateral preoptic inputs on lateral habenular neurons projecting to the midbrain. Brain Res 1983;263: 33–41.
99. Giesler GJ Jr, Spiel HR, Willis WD. Organization of spinothalamic tract axons within the rat spinal cord. J Comp Neurol 1981;195: 243–252.
100. Gigg J, Tan AM, Finch DM. Glutamatergic excitatory responses of anterior cingulate neurons to stimulation of the mediodorsal thalamus and their regulation by GABA: an in vivo iontophoretic study. Cereb Cortex 1992;2: 477–484.
101. Giguère M, Goldman-Rakic PS. Mediodorsal nucleus: areal, laminar, and tangential distribution of afferents and efferents in the frontal lobe of rhesus monkeys. J Comp Neurol 1988;277:195–213.
102. Gilbert CD, Kelly JP. The projection of cells in different layers of the cat's visual cortex. J Comp Neurol 1975;163:81–106.
103. Gillingham FJ. Small localized surgical lesions of the internal capsule in the treatment of dyskinesia. Confin Neurol 1962;22:385–392.
104. Girgis M. The role of the thalamus in the regulation of aggressive behavior. Int J Neurol 1971;8:327–351.
105. Giuffrida R, Rustioni A. Glutamate and aspartate immunoreactivity in corticothalamic neurons of rats. In: Macchi G, Bentivoglio M, Spreafico R, eds. Cellular thalamic mechanisms. Amsterdam: Elsevier, 1988: 311–320.
106. Glees P. Experimental neurology. London: Oxford University Press, 1961.
107. Glees P, Le Gros Clark WE. The termination of optic fibers in the lateral geniculate body of the monkey. J Anat 1941;75:295–310.
108. Glennon RA. Serotonin receptors: clinical implications. Neurosci Biobehav Rev 1990;14:35–47.
109. Glickstein M, King RA, Miller J, Berkley M. Cortical projection from the dorsal lateral geniculate nucleus of cats. J Comp Neurol 1967;130:55–76.
110. Goldman-Rakic PS, Porrino LJ. The primate mediodorsal (MD) nucleus and its projection to the frontal lobe. J Comp Neurol 1985;242: 535–560.
111. Goodwin GM, McCloskey DI, Matthews PBC. Proprioceptive illusions induced by muscle vibration: contribution by muscle spindles to perception? Science 1972; 175:1382–1384.
112. Graybiel AM, Berson DM. Histochemical identification and afferent connections of subdivisions in the lateralis posterior-pulvinar complex and related thalamic nuclei in the cat. Neuroscience 1980; 5:1175–1238.
113. Graybiel AM, Elde RP. Somatostatin-like immunoreactivity characterizes neurons of the nucleus reticularis thalami in the cat and monkey. J Neurosci 1983;3: 1308–1321.
114. Grofova I, Rinvik E. Cortical and pallidal projections to the nucleus ventralis lateralis thalami: electron microscopically studies in the cat. Anat Embryol (Berl) 1974;146: 113–132.
115. Gross NB, Lifschitz WS, Anderson DJ. The tonotopic organization of the auditory thalamus of the squirrel monkey (*Saimiri sciureus*). Brain Res 1974;65:323–332.
116. Guillery RW. A study of Golgi preparations from the dorsal lateral geniculate nucleus of the adult cat. J Comp Neurol 1966;128:21–50.
117. Guillery RW. The laminar distribution of retinal fibres in the dorsal lateral geniculate nucleus of the cat: a new interpretation. J Comp Neurol 1970;138:339–369.
118. Guillery RW, Adrian HO, Woolsey CN, Rose JE. Activation of somotosensory areas I and II of the cat's cerebral cortex by focal stimulation of the basoventral complex. In: Purpura DP, Yahr MD, eds. The thalamus. New York: Columbia University Press, 1966:197–204.
119. Guillery RW, Stelzner DJ. The differential effects of unilateral lid closure upon the monocular and binocular segments of the dorsal lateral geniculate nucleus in the cat. J Comp Neurol 1970;139: 413–422.

120. Haber SN, Groenewegen HJ, Grove EA, Nauta WJH. Efferent connections of the ventral pallidum: evidence of a dual striatopallidofugal pathway. J Comp Neurol 1985;235:322–335.
121. Haber SN, Lynd-Balta E, Mitchell SJ. The organization of the descending ventral pallidal projections in the monkey. J Comp Neurol 1993;329:111–128.
122. Hallanger AE, Levey AI, Lee HJ, Rye DB, Wainer BH. The origins of cholinergic and other subcortical afferents to the thalamus in the rat. J Comp Neurol 1987;262:105–124.
123. Hallanger AE, Wainer BH. Ultrastructure of ChAT-immunoreactive synaptic terminals in the thalamic reticular nucleus of the rat. J Comp Neurol 1988;278:486–497.
124. Hamori J, Pasik T, Pasik P, Szentagothai J. Triadic synaptic arrangements and their possible significance in the lateral geniculate nucleus of the monkey. Brain Res 1974;80:379–393.
125. Hanaway J, Young RR. Localization of the pyramidal tract in the internal capsule of man. J Neurol Sci 1977;34:63–70.
126. Hardy SG, Lynch JC. The spatial distribution of pulvinar neurons that project to two subregions of the inferior parietal lobule in the macaque. Cereb Cortex 1992;2: 217–230.
127. Harrison JM, Howe ME. Anatomy of the afferent auditory nervous system in mammals. In: Keidel WD, Neff WD, eds. Handbook of sensory physiology. Vol. III. Berlin: Springer-Verlag, 1974:283–336.
128. Harting JK, Hall WC, Diamond IT, Martin GF. Anterograde degeneration study of the superior colliculus in *Tupaia glis*: evidence for a subdivision between superficial and deep layers. J Comp Neurol 1973;148:361–386.
129. Houser CR, Vaughn JE, Barber RP, Roberts E. GABA neurons are the major cell type of the nucleus reticularis thalami. Brain Res 1980;200: 341–354.
130. Haymaker W. Bing's local diagnosis in neurological diseases. St. Louis: C.V. Mosby Company, 1956:57–62 and 105–112.
131. Hazrati L-N, Parent A. Contralateral pallidothalamic and pallidotegmental projections in primates: an anterograde and retrograde labeling study. Brain Res 1991;567:212–223.
132. Hazrati L-N, Parent A. Projection from the external pallidum to the reticular thalamic nucleus in the squirrel monkey. Brain Res 1991; 550:142–146.
133. Heckers S, Geula C, Mesulam M-M. Cholinergic innervation of the human thalamus: dual origin and differential nuclear distribution. J Comp Neurol 1992;325:68–82.
134. Head H. Studies in neurology. London: Oxford University Press, 1920.
135. Head H, Holmes G. Sensory disturbances from cerebral lesions. Brain 1911;34:102–254.
136. Heath CJ, Jones EG. An experimental study of ascending connections from the posterior group of thalamic nuclei in the cat. J Comp Neurol 1971;141:397–426.
137. Hendrickson AM, Wilson ME, Toyne MJ. The distribution of optic nerve fibers in *Macaca mulatta*. Brain Res 1970;23:425–427.
138. Hendry SH, Jones EG, Graham J. Thalamic relay nuclei for cerebellar and certain related fiber systems in the cat. J Comp Neurol 1979;185: 679–713.
139. Herkenham M. Laminar organization of thalamic projections to rat neocortex. Science 1980;207:532–534.
140. Herkenham M, Nauta WJH. Afferent connections of the habenular nuclei in the rat: a horseradish peroxidase study, with a note on the fiber-of-passage problem. J Comp Neurol 1977;173:123–145.
141. Herkenham M, Nauta WJH. Efferent connections of the habenular nuclei in the rat. J Comp Neurol 1979;187:19–48.
142. Hickey TL, Guillery RW. Variability of laminar patterns in the human lateral geniculate nucleus. J Comp Neurol 1979;183:221–246.
143. Hirai T, Jones EG. Distribution of tachykinin- and enkephalin-immunoreactive fibers in the human thalamus. Brain Res Rev 1989; 14:35–52
144. Hirai T, Jones EG. A new parcellation of the human thalamus on the basis of histochemical staining. Brain Res Rev 1989;14:1–34
145. Hirai T, Jones EG. Comparative anatomical study of ventrolateral thalamic mass in humans and monkeys. Stereotact Funct Neurosurg 1993;60:6–16.
146. Hökfelt T, Johansson O, Goldstein M. Central catecholamine neurons as revealed by immunohistochemistry with special reference to adrenaline neurons. In: Björklund A, Hökfelt T, eds. Handbook of chemical neuroanatomy. Vol. 2. Part 1: Classical transmitters in the CNS. Ch. 5. Amsterdam: Elsevier, 1984:157–276.
147. Holländer H. Projections from the striate cortex to the diencephalon in the squirrel monkey (*Saimiri sciureus*): a light microscopic radioautographic study following intracortical injection of [^{3}H] leucine. J Comp Neurol 1974;155:424–440.
148. Holländer H, Vanegas H. The projection from the lateral geniculate nucleus onto the visual cortex in the cat: a quantitative study with horseradish peroxidase. J Comp Neurol 1977;173:519–636.
149. Hoyt WF, Luis O. Visual fiber anatomy in the infrageniculate pathway of the primate. Arch Ophthalmol 1962;68:94–106.
150. Hoyt WF, Luis O. The primate chiasm: details of visual fiber organization studied by silver impregnation techniques. Arch Ophthalmol 1963;70:69–85.
151. Hubel DH, Wiesel TN. Integrative action in the cat's lateral geniculate body. J Physiol (Lond) 1961;155: 385–398.
152. Hubel DH, Wiesel TN. Receptive fields, binocular interaction and functional architecture in the cat's visual cortex. J Physiol (Lond) 1962;160:106–154.
153. Hubel DH, Wiesel TN. Shape and arrangement of columns in cat's striate cortex. J Physiol (Lond) 1963;165:559–568.
154. Hubel DH, Wiesel TN. Brain mechanisms of vision. Sci Amer 1979; 241:150–162.
155. Hunt SP, Schmidt J. Some observations on the binding patterns of α-bungarotoxine in the central nervous system of the rat. Brain Res 1978;157:213–232.
156. Illinsky IA, Jouandet M, Goldman-Rakic PS. Organization of the nigrothalamocortical system in rhesus monkey. J Comp Neurol 1985;36:315–330.
157. Ilinsky IA, Kultas-Ilinsky K. Sagittal cytoarchitectonic maps of the *Macaca mulatta* thalamus with a revised nomenclature of the motor-related nuclei validated by observations on their connectivity. J Comp Neurol 1987;262:331–364.
158. Ilinsky IA, Kultas-Ilinsky K, Rosina A, Haddy M. Quantitative evaluation of crossed and uncrossed projections from basal ganglia and cerebellum to the cat thalamus. Neuroscience 1987;21: 207–227.
159. Ilinsky IA, Tourtellotte WG, Kultas-Ilinsky K. Anatomical distinctions between the two basal ganglia afferent territories in the primate motor thalamus. Stereotact Funct Neurosurg 1993;60: 62–69.
160. Imig TJ, Ruggero MA, Kitzes LM, Javel E, Brugge JF . Organization of auditory cortex in the owl monkey (*Aotus trivirgatus*). J Comp Neurol 1977;171:111–128.
161. Isaacson LG, Tanaka D Jr. Cholinergic and non-cholinergic projections from the canine pontomesencephalic tegmentum (Ch5 area) to the caudal intralaminar thalamic nuclei. Exp Brain Res 1986;62: 179–188.
162. Isaacson LG, Tanaka D Jr. Cholinergic innervation of canine thalamostriatal projection neurons: an ultrastructural study combining choline acetyltransferase immunocytochemistry and WGA-HRP retrograde labeling. J Comp Neurol 1988;277:529–540.
163. Jacobs GH. Receptive fields in visual systems. Brain Res 1969;14: 553–573.
164. Jasper HH. Diffuse projection systems: the integrative action of the thalamic reticular system. Elec-

troencephalogr Clin Neurophysiol 1949;1:405–420.
165. Jasper HH. Functional properties of the thalamic reticular system. In: Delafresnaye JF, ed. Brain mechanisms and consciousness (symposium). Oxford: Blackwell Scientific Publications, 1954:374–395.
166. Jasper HH, Ajmone-Marsan C, Stoll J. Corticofugal projections to the brain stem. AMA Arch Neurol Psychiatry 1952;67:155–171.
167. Jinnai K, Nambu A, Tanibuchi I, Yoshida S. Cerebello-and pallidothalamic pathways to areas 6 and 4 in the monkey. Stereotact Funct Neurosurg 1993;60:70–79.
168. Jones AE. The lateral geniculate nucleus of *Ateles ater*. J Comp Neurol 1964;123:205–210.
169. Jones EG. Some aspects of the organization of the thalamic reticular complex. J Comp Neurol 1975; 162:285–308.
170. Jones EG. Possible determinants of the degree of retrograde neuronal labeling with horseradish peroxidase. Brain Res 1975;85:249–253.
171. Jones EG. Distribution patterns of individual medial lemniscus axons in the ventrobasal complex of the monkey thalamus. J Comp Neurol 1983;215:1–16.
172. Jones EG. The thalamus. In: Emson PC, ed. Chemical neuroanatomy. New York: Raven Press, 1983: 257–293.
173. Jones EG. The thalamus. New York: Plenum, 1985.
174. Jones EG, Burton H. Cytoarchitecture and somatic sensory connectivity of thalamic nuclei other than the ventrobasal complex in the cat. J Comp Neurol 1974;154:395–432.
175. Jones EG, Burton H. Areal difference in the laminar distribution of thalamic afferents in cortical fields of the insular, parietal and temporal regions of primates. J Comp Neurol 1976;168:197–247.
176. Jones EG, Burton H, Saper CB, Swanson LW. Midbrain, diencephalic and cortical relationships of the basal nucleus of Meynert and associated structures in primates. J Comp Neurol 1976;167: 385–420.
177. Jones EG, Friedman DP. Projection pattern of functional components of thalamic ventrobasal complex on monkey somatosensory cortex. J Neurophysiol 1982;48:521–544.
178. Jones EG, Leavitt RY. Retrograde axonal transport and the demonstration of non-specific projections to the cerebral cortex and striatum from thalamic intralaminar nuclei in the cat, rat and monkey. J Comp Neurol 1974;154:349–378.
179. Jones EG, Porter R. What is area 3a? Brain Res Rev 1980;2:1–43.
180. Jones EG, Powell TPS. Projections of the somatic sensory cortex upon the thalamus in the cat. Brain Res 1968;10:369–391.
181. Jones EG, Powell TPS. Connexions of the somatic sensory cortex of the rhesus monkey. I. Ipsilateral cortical connexions. Brain 1969;92: 477–502.
182. Jones EG, Powell TPS. Connexions of the somatic cortex of the rhesus monkey. II. Contralateral cortical connexions. Brain 1969;92:717–730.
183. Jones EG, Powell TPS. The cortical projections of the ventroposterior nucleus of the thalamus in the cat. Brain Res 1969;13:298–318.
184. Jones EG, Powell TPS. Connexions of the somatic sensory cortex of the rhesus monkey. III. Thalamic connexions. Brain 1970;93:37–56.
185. Jones EG, Powell TPS. An analysis of the posterior group of thalamic nuclei on the basis its afferent connections. J Comp Neurol 1971; 143:185–216.
186. Jones EG, Powell TPS. Anatomical organization of the somatosensory cortex. In: Iggo A, ed. Handbook of sensory physiology. Vol. 2. Berlin: Springer-Verlag, 1973:579–620.
187. Jones EG, Wise SP, Coulter JD. Differential thalamic relationships of sensory-motor and parietal cortical fields in monkeys. J Comp Neurol 1979;183:833–881.
188. Kaas JH. How the somatosensory thalamus is subdivided and interconnected with areas of the somatosensory cortex in monkeys. In: Bentivoglio M, Spreafico R, eds. Cerebellar thalamic mechanisms. Amsterdam: Excerpta Medica, 1988: 143–150.
189. Kaas JH, Guillery RW, Allman JM. Some principles of organization in the dorsal lateral geniculate nucleus. Brain Behav Evol 1972;6: 253–299.
190. Kaas JH, Huerta MF, Weber JT, Harting JK. Patterns of retinal terminations and laminar organization of the lateral geniculate nucleus of primates. J Comp Neurol 1977;182:517–554.
191. Kalil K. Projections of the cerebellar and dorsal column nuclei upon the thalamus of the rhesus monkey. J Comp Neurol 1981;195:25–50.
192. Kelly JP, Gilbert CD. The projection of different morphological types of ganglion cells in the cat's retina. J Comp Neurol 1975;163:65–80.
193. Kerr FWL. Neuroanatomical substrates of nociception in the spinal cord. Pain 1975;1:325–356.
194. Kerr FWL, Lippan HH. The primate spinothalamic tract as demonstrated by anterolateral cordotomy and commissural myelotomy. Adv Neurol 1974;4:147–156.
195. Kievit J, Kuypers HGJM. Organization of the thalamo-cortical connexions to the frontal lobe in the rhesus monkey. Exp Brain Res 1977;29:299–322.
196. Kim R, Nakano K, Jayaraman A, Carpenter MB. Projections of the globus pallidus and adjacent structures: an autoradiographic study in the monkey. J Comp Neurol 1976;169:263–289.
197. Klein DC, Auerbach DA, Namboodiri AA, Wheler GHT. Indole metabolism in the mammalian pineal gland. In: Reiter RJ, ed. The pineal gland. Ch. 8. Boca Raton, FL: CRC Press, 1981:199–227.
198. Klein DC, Moore RY. Pineal N-acetyltransferase and hydroxyindole-*o*-methyltransferase: control by the retinohypothalamic tract and the suprachiasmatic nucleus. Brain Res 1979;174:245–262.
199. Klein DC, Weller JL. Indole metabolism in the pineal gland: a circadian rhythm in N-acetyltransferase. Science 1970;169:1093–1095.
200. Klein DC, Weller JL. A rapid light-induced decrease in pineal serotonin N-acetyltransferase activity. Science 1972;177:532–533.
201. Klein DC, Weller JL, Moore RY. Melatonin metabolism: neurol regulation of pineal serotonin N-acetyltransferase. Proc Natl Acad Sci USA 1971;68:3107–3110.
202. Kocsis JD, Sugimori M, Kitai ST. Convergence of excitatory synaptic inputs to caudate spiny neurons. Brain Res 1977;124:403–413.
203. Krettek JE, Price JL. A direct input from the amygdala to the thalamus and the cerebral cortex. Brain Res 1974;67:169–174.
204. Kruger L, Porter P. A behavioral study of the functions of the Rolandic cortex in the monkey. J Comp Neurol 1958;109:439–469.
205. Kudo M, Niimi K. Ascending projections of the inferior colliculus on the medial geniculate body in the cat studied by anterograde and retrograde tracing techniques. Brain Res 1978;155:113–117.
206. Kuffler SW. Discharge patterns and functional organization of mammalian retina. J Neurophysiol 1953;16:37–68.
207. Kuhlenbeck H. The derivatives of the thalamus ventralis in the human brain and their relation to the so-called subthalamus. Milit Surg 1948;102:433–447.
208. Kultas-Ilinsky K, Hughes B, Fogarty JD, Ilinsky IA. GABA and benzodiazepine receptors in the cat motor thalamus after lesioning of nigro- and pallidothalamic pathways. Brain Res 1990;511:197–208.
209. Künzle H. Thalamic projections from the precentral motor cortex in *Macaca fascicularis*. Brain Res 1976;105:253–267.
210. Künzle H. An autoradiographic analysis of the efferent connections from premotor and adjacent prefrontal regions (areas 6 and 9) in *Macaca fascicularis*. Brain Behav Evol 1978;15:185–234.
211. Künzle H, Akert K. Efferent connections of cortical Area 8 (frontal eye field) in *Macaca fascicularis*: a reinvestigation using the autoradiographic technique. J Comp Neurol 1977;173:147–167.
212. Kuo J-S, Carpenter MB. Organization of pallidothalamic projections in the rhesus monkey. J Comp Neurol 1973;151:201–236.

213. Kupfer C. The projection of the macula in the lateral geniculate nucleus of man. Am J Ophthalmol 1962;54:597–609.
214. Laemle LK. Cell populations of the lateral geniculate nucleus of the cat as determined with horseradish peroxidase. Brain Res 1975;100: 650–656.
215. Laemle LK, Noback CR. The visual pathways of the lorisid lemurs (*Nycticebus concang* and *Galago crassicaudatus*). J Comp Neurol 1970;138:49–62.
216. Larsen KD, McBride RL. The organization of feline entopeduncular nucleus projections: anatomical studies. J Comp Neurol 1979; 184:293–308.
217. Lavoie B, Parent A. Serotoninergic innervation of the thalamus in the primate: an immunohistochemical study. J Comp Neurol 1991; 312:1–18.
218. Lechner J, Leah JD, Zimmermann M. Brainstem peptidergic neurons projecting to the medial and lateral thalamus and zona incerta in the rat. Brain Res 1993;603:47–56.
219. Le Gros Clark WE. The structure and connections of the thalamus. Brain 1932;55:406–470.
220. Le Gros Clark WE. The termination of ascending tracts in the thalamus of the macaque monkey. J Anat 1936;71:1–40.
221. Le Gros Clark WE. The laminar organization and cell content of the lateral geniculate body in the monkey. J Anat 1941;75:419–433.
222. Le Gros Clark WE, Boggon RH. On the connections of the anterior nucleus of the thalamus. J Anat 1933;67:215–226.
223. Le Gros Clark WE, Boggon RH. On the connections of the medial cell group of the thalamus. Brain 1933; 56:83–98.
224. Le Gros Clark WE, Boggon RH. The thalamic connections of the parietal and frontal lobes of the brain in the monkey. Philos Trans R Soc Lond (Biol) 1935;224: 313–359.
225. Le Gros Clark WE, Penman GG. The projection of the retina in the lateral geniculate body. Proc R Soc B 1934;114:291–313.
226. Le Gros Clark WE, Powell TPS. On the thalamocortical connexions of the general sensory cortex of Macaca. Proc R Soc Lond (Biol) 1953;141:467–487.
227. Leonard CM. The connections of the dorsomedial nuclei. Brain Behav Evol 1972;6:524–541.
228. Levey AI, Hallanger AE, Wainer BH. Choline acetyltransferase immunoreactivity in the rat thalamus. J Comp Neurol 1987;257: 317–332.
229. Levin PM. The efferent fibers of the frontal lobe of the monkey (*Macaca mulatta*). J Comp Neurol 1936;63: 369–419.
230. Levin PM. Efferent fibers. In: Bucy PC, ed. The precentral motor cortex. 2d ed. Ch. 5. Urbana: University of Illinois Press, 1949:133–148.
231. Liu X-B, Jones EG. The fine structure of serotonin and tyrosine hydroxylase immunoreactive terminals in the ventral posterior thalamic nucleus of cat and monkey. Exp Brain Res 1991;85:507–518.
232. Locke S, Angevine JB Jr, Yakovlev PI. Limbic nuclei of thalamus and connections of limbic cortex. I. Thalamo-cortical projections of the lateral dorsal nucleus in man. Arch Neurol 1961;4:355–364.
233. Locke S, Angevine JB Jr, Yakovlev PI. Limbic nuclei of thalamus and connections of limbic cortex. VI. Thalamo-cortical projection of lateral dorsal nucleus in cat and monkey. Arch Neurol 1964;11:1–12.
234. Lorente de Nó R. The structure of the cerebral cortex. In: Fulton JF, ed. Physiology of the nervous system. 3rd ed. New York: Oxford University Press, 1949:288–330.
235. Lübke J. Morphology of neurons in the thalamic reticular nucleus (TRN) of mammals as revealed by intracellular injections into fixed brain slices. J Comp Neurol 1993; 329:458–471.
236. Lund JS, Lund RD, Hendrickson AE, Bunt AH, Fuchs AF. The origin of efferent pathways from the primary visual cortex, area 17 of the macaque monkey as shown by retrograde transport of horseradish peroxidase. J Comp Neurol 1975; 164:287–303.
237. McCormick DA. Neurotransmitter actions in the thalamus and cerebral cortex and their role in neuromodulation of thalamocortical activity. Prog Neurobiol 1992;39: 337–388.
238. McCormick DA, von Krosigk M. Corticothalamic activation modulates thalamic firing through glutamate "metabotropic" receptors. Proc Natl Acad Sci USA 1992;89: 2774–2778.
239. McCormick DA, Wang Z. Serotonin and noradrenaline excite GABAergic neurones of the guinea pig and the cat nucleus reticularis thalami nucleus. J Physiol (Lond) 1991;442:235–255.
240. McLardy T. Projection of the centromedian nucleus of the human thalamus. Brain 1968;71:290–303.
241. McLardy T. The thalamic projection to frontal cortex in man. J Neurol Neurosurg Psychiatry 1950;13:198–202.
242. Macchi G, Bentivoglio M. The thalamic intralaminar nuclei and the cerebral cortex. In: Jones EG, Peters A, eds. Cerebral cortex. Vol. 5. New York: Plenum Press, 1986: 355–401.
243. Macchi G, Bentivoglio M, Molinari M, Minciacchi D. The thalamo-caudate versus thalamo-cortical projections as studied in the cat with fluorescent retrograde double labeling. Exp Brain Res 1984;54: 225–239.
244. Magnusson KR, Clements JR, Larson AA, Madl JE, Beitz AJ. Localization of glutamate in trigeminothalamic projection neurons: a combined retrograde transport-immunohistochemical study. Somatosens Res 1987;4:177–190.
245. Makino S, Okamura H, Morimoto N, Abe J, Yanaihara N, Ibata Y. Distribution of neurotensin-like immunoreactivity in the diencephalon of the Japanese monkey (*Macaca fuscata*). J Comp Neurol 1987;260:552–563.
246. Malone EF. Über die Kerne des menschlichen Diencephalon: Abhandlungen der könighl preuss. Akademie der Wissenschaften 1910;92.
247. Malpeli JG, Baker FH. The representation of the visual field in the lateral geniculate nucleus of the *Macaca mulatta*. J Comp Neurol 1975;161:569–594.
248. Martin JB, Reichlin S, Brown GM. Clinical neuroendocrinology. Philadelphia: F.A. Davis Company, 1977:229–246.
249. Mason C, Kandel ER. Central visual pathways. In Kandel ER, Schwartz JH, Jessell TM, eds. Principles of neural science. Ch. 29. New York: Elsevier, 1991:420–439.
250. Matthews MR, Cowan WM, Powell TPS. Transneuronal cell degeneration in the lateral geniculate nucleus of the macaque monkey. J Anat 1960;94:145–169.
251. Matzke HA. The course of fibers arising from the nucleus gracilis and cuneatus of the cat. J Comp Neurol 1951;94:439–452.
252. Mehler WR. The anatomy of the so-called "pain tract" in man: an analysis of the course and distribution of the ascending fibers of the fasciculus anterolateralis. In: French JD, Porter RW, eds. Basic research in paraplegia. Springfield, IL: Charles C. Thomas, 1962:26–55.
253. Mehler WR. Further notes on the center median nucleus of Luys. In: Purpura DP, Yahr MD, eds. The thalamus. New York: Columbia Unversity Press, 1966:109–127.
254. Mehler WR. Idea of a new anatomy of the thalamus. J Psychiatr Res 1971;8:203–217.
255. Mehler WR. Central pain and the spinothalamic tract. Adv Neurol 1974;4:127–146.
256. Mehler WR. Subcortical afferent connections of the amygdala in the monkey. J Comp Neurol 1980; 190:733–762.
257. Mehler WB, Feferman ME, Nauta WJH. Ascending axon degeneration following anterolateral cordotomy: an experimental study in the monkey. Brain 1960;83:718–750.
258. Mehler WR, Vernier VG, Nauta WJH. Efferent projections from the dentate and interpositus nuclei in primates. Anat Rec 1958;130: 430–431.
259. Merzenich MM, Brugge JF. Representation of the cochlear partition on the superior temporal plane of the Macaque monkey. Brain Res 1973;50:275–296.

260. Mesulam MM, Mufson EJ, Levey AI, Wainer BH. Atlas of cholinergic neurons in the forebrain and upper brainstem of the macaque based on monoclonal choline acetyltransferase immunohistochemistry and acetylcholinesterase histochemistry. Neuroscience 1984; 12:669–686.
261. Mettler FA. The non-pyramidal motor projections from the frontal cerebral cortex. Proc Assoc Res Nerv Ment Dis 1947;26:162–199.
262. Mettler FA. Extracortical connections of the primate frontal cerebral cortex. I. Thalamo-cortical connections. J Comp Neurol 1947;86:95–117.
263. Mettler FA. Neuroanatomy. St. Louis: C.V. Mosby, 1948.
264. Meyer A, Beck E, McLardy T. Prefrontal leucotomy: a neuroanatomical report. Brain 1947;70:18–49.
265. Miller RA, Strominger NL. An experimental study of the efferent connections of the superior peduncle in the rhesus monkey. Brain Res 1977;133:237–250.
266. Minkowski M. Über den Verlauf, die Endigung und die zentrale Repräsentation von gekreutzten and ungekreutzten. Sehnervenfastern bei einigen beim menschen. Schweiz Arch Neurol Psychiatr 1920;6:201–252.
267. Mitrofanis J. Calbindin immunoreactivity in a subset of cat thalamic reticular neurons. J Neurocytol 1992;21:495–505.
268. Mitrofanis J, Guillery RW. New views of the thalamic reticular nucleus in the adult and the developing brain. Trends Neurosci 1993; 16:240–245.
269. Mogenson GJ, Jones DL, Yim CY. From motivation to action: functional interface between the limbic system and the motor system. Prog Neurobiol 1980;14:69–97.
270. Molinari M, Hendry SH, Jones EG. Distributions of certain neuropeptides in the primate thalamus. Brain Res 1987;426:270–289.
271. Montero VM. Quantitative immunogold analysis reveals high glutamate levels in synaptic terminals of retino-geniculate, cortico-geniculate, and geniculo-cortical axons in the cat. Vis Neurosci 1990;4:437–443.
272. Moore BW. Brain-specific proteins. In: Schneider DJ, ed. Proteins of the nervous system. New York: Raven Press, 1973:1–12.
273. Moore RY. The innervation of the mammalian pineal gland. In: Reiter RJ, ed. The pineal and reproduction. Basel: S. Karger, 1978: 1–29.
274. Moore RY, Goldberg JM. Ascending projections of the inferior colliculus in the cat. J Comp Neurol 1963;121:109–136.
275. Moore RY, Goldberg JM. Projections of the inferior colliculus in the monkey. Exp Neurol 1966; 14:429–438.
276. Moore RY, Klein DC. Visual pathways and the central neural control of a circadian rhythm in pineal serotonin N-acetyltransferase activity. Brain Res 1974;71:17–33.
277. Moore RY, Lenn NJ. A retinohypothalamic projection in the rat. J Comp Neurol 1972;146:1–14.
278. Moore RY, Rapport RL. Pineal and gonadal function in the rat following cervical sympathectomy. Neuroendocrinology 1970;7:361–374.
279. Morel F. La massa intermedia ou commisure grise. Acta Anat (Basel) 1947;4:203–207.
280. Morest DK. The neuronal architecture of the medial geniculate body of the cat. J Anat 1964;98:611–638.
281. Morest DK. The laminar structure of the medial geniculate body of the cat. J Anat 1965;99:143–159.
282. Morest DK. The lateral tegmental system of the midbrain and the medial geniculate body: study with Golgi and Nauta methods in the cat. J Anat 1965;99:611–634.
283. Morison RS, Dempsey EW. A study of thalamocortical relations. Am J Physiol 1942;135:281–292.
284. Moruzzi G. Active processes in the brain stem during sleep. Harvey Lect Ser 1963;58:233–297.
285. Moruzzi G, Magoun HW. Brain stem reticular formation and activation of the EEG. Electroencephalogr Clin Neurophysiol 1949; 1:455–479.
286. Mosko SS, Moore RY. Neonatal suprachiasmatic nucleus lesions: effects on the development of circadian rhythms in the rat. Brain Res 1979;164:17–38.
287. Mountcastle VB, Henneman E. Pattern of tactile representation in thalamus of cat. J Neurophysiol 1949;12:85–100.
288. Mountcastle VB, Henneman E. The representation of tactile sensibility in the thalamus of the monkey. J Comp Neurol 1952;97:409–440.
289. Nakano K, Kohno M, Kawahira J, Tokushige A. Entopeduncular nucleus projections to the contralateral thalamic nuclei. Brain Res 1983;262:283–287.
290. Nauta HWJ. Evidence of a pallidohabenular pathway in the cat. J Comp Neurol 1974;156:19–28.
291. Nauta HJW, Pritz MB, Lasek RJ. Afferents to the rat caudoputamen studied with horseradish peroxidase: an evaluation of a retrograde neuroanatomical research method. Brain Res 1974;67:219–238.
292. Nauta WJH. Hippocampal projections and related neural pathways to the midbrain in the cat. Brain 1958;81:319–340.
293. Nauta WJH. Fibre degeneration following lesions of the amygdaloid complex in the monkey. J Anat 1961;95:151–531.
294. Nauta WJH. Neural associations of the amygdaloid complex in the monkey. Brain 1962;85:505–520.
295. Nauta WJH, Mehler WR. Projections of the lentiform nucleus in the monkey. Brain Res 1966;1:3–42.
296. Nauta WJH, Whitlock DG. An anatomical analysis of the non-specific thalamic projection system. In: Delafresnaye JF, ed. Brain mechanisms and consciousness (symposium). Oxford: Blackwell Scientific Publications, 1954:81–98.
297. Niimi K, Inoshita H. Cortical projections of the lateral thalamic nuclei in the cat. Proc Jpn Acad 1971;47:664–669.
298. Niimi K, Matsuoka H. Thalamocortical organization of the auditory system in the cat studied by retrograde axonal transport of horseradish peroxidase. Adv Anat Embryol Cell Biol 1979;57:1–56.
299. Niimi K, Niimi M, Okada Y. Thalamic afferents to the limbic cortex in the cat studied with the method of retrograde axonal transport of horseradish peroxidase. Brain Res 1978;145:225–238.
300. Niimi K, Sprague JM. Thalamocortical organization of the visual system in the cat. J Comp Neurol 1970;138:219–250.
301. Niimi M. Cortical projections of the anterior thalamic nuclei in the cat. Exp Brain Res 1978;31:403–416.
302. Nissl F. Die Kerne des Thalamus beim Kaninchen. Neurol Zentralbl 1889;8:549–550.
303. Noback CR, Laemle LK. Structural and functional aspects of the visual pathways of primates. In: Noback CR, Montagna W, eds. Advances in primatology. Vol. 1: The primate brain. Ch. 3. New York: Appleton-Century-Crofts, 1970:55–81.
304. Norgren R, Leonard CM. Ascending central gustatory pathways. J Comp Neurol 1973;150:217–238.
305. Norgren R, Pfaffman C. The pontine taste area in the rat. Brain Res 1975;91:99–117.
306. Oertel WH, Graybiel AM, Mugnaini E, Elde RP, Schmechel DE, Kopin IJ. Coexistence of glutamic acid decarboxylase- and somatostatin-like immunoreactivity in neurons of the feline nucleus reticularis thalami. J Neurosci 1983;3: 1322–1332.
307. Ogren MP, Hendrickson AE. Pathways between striate cortex and subcortical regions in *Macaca mulatta* and *Saimiri sciureus*: evidence for a reciprocal pulvinar connection. Exp Neurol 1976;53:780–800.
308. Ohara PT, Lieberman AR, Hunt SP, Wu J-Y. Neural elements containing glutamic acid decarboxylase (GAD) in the dorsal lateral geniculate nucleus of the rat: immunohistochemical studies by light and electron microscopy. Neuroscience 1983;8:189–212.
309. Ohye C. Thalamus. In: Paxinos G, ed. The human nervous system. Ch. 17. New York: Academic Press, 1990:439–469.
310. Ojeman G. Interrelationship in the localization of language, memory and motor mechanisms in human cortex and thalamus. In: Thompson R, ed. New perspectives in cerebral localization. New York: Raven Press, 1981:157–175.

311. Oliver DL, Hall WC. The medial geniculate body of the tree shrew, *Tupaia glis*. I. Cytoarchitecture and midbrain connections. J Comp Neurol 1978;182:423–458.
312. Oliver DL, Hall WC. The medial geniculate body of the tree shrew, *Tupaia glis*. II. Connections with the neocortex. J Comp Neurol 1978; 182:459–494.
313. Olivier A, Parent A, Poirier LJ. Identification of the thalamic nuclei on the basis of their cholinesterase content in the monkey. J Anat 1970;106:37–50.
314. Olszewski J. The thalamus of the *Macaca mulatta*. Basel: S. Karger, 1952.
315. Oscarsson O, Rosén I. Short-latency projections to the cat's cerebral cortex from skin and muscle afferents in the contralateral forelimb. J Physiol (Lond) 1966;182: 164–184.
316. Pape H-C, McCormick DA. Noradrenaline and serotonin selectively modulate thalamic burst firing by enhancing a hyperpolarization-activated cation current. Nature 1989;340:715–718.
317. Papez JW. Thalamic connections in a hemidecorticate dog. J Comp Neurol 1938;69:103–119.
318. Papez JW. A summary of fiber connections of the basal ganglia with each other and with other portions of the brain. Proc Assoc Res Nerv Ment Dis 1942;21:21–68.
319. Paré D, Hazrati L-N, Parent A, Steriade M. Substantia nigra pars reticulata projects to the reticular thalamic nucleus of the cat: a morphological and electrophysiological study. Brain Res 1990;535: 139–146.
320. Paré D, Smith Y, Parent A, Steriade M. Projections of brainstem core cholinergic and non-cholinergic neurons of cat to intralaminar and reticular thalamic nuclei. Neuroscience 1988;25:69–86.
321. Paré D, Steriade M. The reticular thalamic nucleus projects to the contralateral dorsal thalamus in macaque monkey. Neurosci Lett 1993;154:96–100.
322. Parent A. Identification of the pallidal and peripallidal cells projecting to the habenula in monkey. Neurosci Lett 1979;15:159–164.
323. Parent A, Butcher LL. Organization and morphologies of acetylcholinesterase-containing neurons in the thalamus and hypothalamus of the rat. J Comp Neurol 1976; 170:205–226.
324. Parent A, De Bellefeuille L. Organization of efferent projections from the internal segment of globus pallidus in primate as revealed by fluorescence retrograde labeling method. Brain Res 1982;245: 201–214.
325. Parent A, De Bellefeuille L. The pallidointralaminar and pallidonigral projections in primate as studied by retrograde double-labeling method. Brain Res 1983; 278:11–27.
326. Parent A, Descarries L, Beaudet A. Organization of ascending serotonin systems in the adult rat brain. A radioautographic study after intraventricular administration of [^{3}H] 5-hydroxytryptamine. Neuroscience 1981;6:115–138.
327. Parent A, Mackey A, De Bellefeuille L. The subcortical afferents to caudate nucleus and putamen in primate: a fluorescence retrograde double-labeling study. Neuroscience 1983;10:1137–1150.
328. Parent A, Paré D, Smith Y, Steriade M. Basal forebrain cholinergic and non-cholinergic projections to the thalamus and brainstem in cats and monkeys. J Comp Neurol 1988;277:281–301.
329. Parent A, Steriade M. Midbrain tegmental projections of nucleus reticularis thalami of cat and monkey: a retrograde transport and antidromic invasion study. J Comp Neurol 1984;229:548–558.
330. Partlow GD, Colonnier M, Szabo J. Thalamic projections of the superior colliculus in the rhesus monkey, *Macaca mulatta*: a light and electron microscopic study. J Comp Neurol 1977;171:285–318.
331. Pasik P, Pasik T, Hamori J. Synapses between interneurons in the lateral geniculate nucleus of monkeys. Exp Brain Res 1976; 25:1–13.
332. Pasik P, Pasik T, Hamori J, Szentagothai J. Golgi type II interneurons in the neuronal circuit of the monkey lateral geniculate nucleus. Exp Brain Res 1973;17:18–34.
333. Pazos A, Probst A, Palacios JM. Serotonin receptors in the human brain. III. Autoradiographic mapping of serotonin-1 receptors. Neuroscience 1987;21:97–122.
334. Pearson RC, Brodal P, Powell TPS. The projection of the thalamus upon the parietal lobe in the monkey. Brain Res 1978;144:143–148.
335. Penfield W, Boldrey E. Somatic motor and sensory representation in the cerebral cortex of man as studied by electrical stimulation. Brain 1937;60:389–443.
336. Penfield W, Rasmussen T. The cerebral cortex of man: a clinical study of localization of function. New York: MacMillan Company, 1950.
337. Percheron G. The thalamic territory of cerebellar afferents and the lateral region of the thalamus of the macaque in stereotaxic ventricular coordinates. J Hirnforsch 1977;18:375–400.
338. Percheron G, François C, Talbi B, Meder JF, Fénelon G, Yelnik J. The primate motor thalamus analysed with reference to subcortical afferent territories. Stereotact Funct Neurosurg 1993;60:32–41.
339. Petras JM. Some fiber connections of the precentral cortex (areas 4 and 6) with the diencephalon in the monkey (*Macaca mulatta*). Anat Rec 1964;148:322.
340. Petras JM. Fiber degeneration in the basal ganglia and diencephalon following lesions in the precentral and postcentral cortex of the monkey (*Macaca mulatta*): with additional observations in the chimpanzee. In: Proceedings of the VI International Congress on Anatomy, Wiesbaden, 1966.
341. Petras JM. Some efferent connections of the motor and somatosensory cortex of simian primates and Felid, Canid and Procyonid carnivores. Ann NY Acad Sci 1969; 167:469–505.
342. Petras JM. Connections of the parietal lobe. J Psychiatr Res 1971; 8:189–201.
343. Phillipson OT, Griffith AC. The neurones of origin for the mesohabenular dopamine pathway. Brain Res 1980;197:213–218.
344. Pierson RJ, Carpenter MB. Anatomical analysis of pupillary reflex pathways in the rhesus monkey. J Comp Neurol 1974;158: 121–143.
345. Poggio GF, Mountcastle VB. A study of the functional contributions of the lemniscal and spinothalamic systems to somatic sensibility. Bull Johns Hopkins Hosp 1960;106:266–316.
346. Poggio GF, Mountcastle VB. The functional properties of ventrobasal thalamic neurons studied in unanesthetized monkeys. J Neurophysiol 1963;26:775–806.
347. Polyak SL. The vertebrate visual system. Chicago: Unversity of Chicago Press, 1957:1390
348. Powell TPS. Residual neurons in the human thalamus following hemidecortication. Brain 1952;75: 571–584.
349. Powell TPS, Cowan WM. A study of thalamo-striate relations in the monkey. Brain 1956;79:364–390.
350. Powell TPS, Cowan WM, Raisman G. Olfactory relationship of the diencephalon. Nature 1963;199: 710–712.
351. Powell TPS, Cowan WM, Raisman G. The central olfactory connexions. J Anat 1965;99:791–813.
352. Powell TPS, Guillery RW, Cowan WM. A quantitative study of the fornix-mammillo-thalamic system. J Anat 1957;91:419–432.
353. Price JL. Olfactory system. In: Paxinos G, ed. The human nervous system. Ch. 29. New York: Academic Press, 1990:979–999.
354. Purpura DP. Intracellular studies of synaptic organization in the mammalian brain. In: Pappas GD, Purpura DP, eds. Structure and function of synapses. New York: Raven Press, 1972:257–302.
355. Quay WB. Pineal chemistry in the cellular and physiological mechanisms. Springfield, IL: Charles C. Thomas, 1974.
356. Raczkowski D, Diamond IT, Winer J Jr. Organization of thalamocorti-

cal auditory system in the cat studied with horseradish peroxidase. Brain Res 1976;101:345–354.
357. Raisman G. Neural connexions of hypothalamus. Br Med Bull 1966; 22:197–210.
358. Raisman G, Cowan WM, Powell TPS. The extrinsic afferent, commisural and association fibres of the hippocampus. Brain 1965;88: 963–996.
359. Ralston HJ 3d, Ralston DD. The primate dorsal spinothalamic tract: evidence for a specific termination in the posterior nuclei (Po/SG) of the thalamus. Pain 1992;48: 107–118.
360. Ramón y Cajal S. Histologie du Système Nerveux de l'Homme et des Vertébrés. (Azoulay L, trans.), Paris: Maloine, 1909, 1911. (Reprinted, Consejo Superior de Investigaciones Cientificas, Instituto Ramón y Cajal, Madrid, 1972.)
361. Ranson SW, Ranson SW Jr. Efferent fibers of the corpus striatum. Proc Assoc Res Nerv Ment Dis 1942;21:69–76.
362. Raos V, Bentivoglio M. Crosstalk between the two sides of the thalamus through the reticular nucleus: a retrograde and anterograde tracing study in the rat. J Comp Neurol 1993;332:145–154.
363. Rasminsky M, Mauro AJ, Albe-Fessard D. Projections of medial thalamic nuclei to putamen and cerebral frontal cortex in the cat. Brain Res 1973;61:69–77
364. Rasmussen AT, Peyton WT. The course and termination of the medial lemniscus in man. J Comp Neurol 1948;88:411–424.
365. Ray JP, Price JL. The organization of the thalamocortical connections of the mediodorsal thalamic nucleus in the rat, related to the ventral forebrain-prefrontal cortex topography. J Comp Neurol 1992;323:167–197.
366. Relkin R. The pineal. Montréal: Eden Press, 1976.
367. Rezak M, Benevento LA. A comparison of the organization of the projections of the dorsal lateral geniculate nucleus, the inferior pulvinar and adjacent lateral pulvinar to primary visual cortex (area 17) in the macaque monkey. Brain Res 1979;167:19–40.
368. Rinvik E. The corticothalamic projection from the pericruciate and coronal gyri in the cat: an experimental study with silver-impregnation methods. Brain Res 1968; 10:79–119.
369. Rinvik E. Thalamic commissural connections in the cat. Neurosci Lett 1984;44:311–316.
370. Rinvik E, Ottersen OP, Storm-Mathisen J. Gamma-aminobutyrate-like immunoreactivity in the thalamus of the cat. Neuroscience 1987;21:781–805.
371. Rinvik E, Wiberg M. Demonstration of a reciprocal connection between the periaqueductal gray matter and the reticular nucleus of the thalamus. Anat Embryol 1990; 181:577–584.
372. Roberts TS, Akert K. Insular and opercular cortex and its thalamic projection in *Macaca mulatta*. Schweiz Arch Neurol Neurochir Psychiat 1963;92:1–43.
373. Robertson RT, Rinvik E. The corticothalamic projections from parietal regions of the cerebral cortex: experimental degeneration studies in the cat. Brain Res 1973; 51:61–79.
374. Robinson CJ, Burton H. The organization of somatosensory receptive fields in cortical area 7b, retroinsular, postauditory and granular of *M. fascicularis*. J Comp Neurol 1980;192:69–92.
375. Rockel AJ, Jones EG. The neuronal organization of the inferior colliculus of the adult cat. I. The central nucleus. J Comp Neurol 1973; 147:11–60.
376. Rose JE, Malis LI. Geniculostriate connections in the rabbit. II. Cytoarchitectonic structure of the striate region and of the dorsal lateral geniculate body: organization of the geniculo-striate projections. J Comp Neurol 1965;125:121–140.
377. Rose JE, Mountcastle VB. The thalamic tactile region in rabbit and cat. J Comp Neurol 1952;97:441–490.
378. Rose JE, Mountcastle VB. Touch and kinesthesis. In: Fields J, ed. Handbook of physiology. Section I, Vol. I: Neurophysiology. Ch. 17. Washington, DC: American Physiological Society, 1959:387–429.
379. Rose JE, Woolsey CN. Cortical connections and functional organization of the thalamic auditory system of the cat. In: Harlow HF, Woolsey CN, eds. Biological and biochemical bases of behavior. Madison: University of Wisconsin Press, 1958:127–150.
380. Royce GJ. Recent research on the centromedian and parafascicular nuclei. In: Carpenter MB, Jayaraman A, eds. The basal ganglia. II: Structure and function—current concepts. New York: Plenum Press, 1987:293–319.
381. Russell GV. A schematic presentation of thalamic morphology and connections. Tex Rep Biol Med 1955;13:989–992.
382. Sadikot AF, Parent A, François C. Efferent connections of the centromedian and parafascicular thalamic nuclei in primates. A PHA-L study of subcortical projections. J Comp Neurol 1992;315:137–159.
383. Sadikot AF, Parent A, Smith Y, Bolam JP. Efferent connections of the centromedian and parafascicular thalamic nuclei in the squirrel monkey: a light and electron microscopic study of the thalamostriatal projection in relation to striatal heterogeneity. J Comp Neurol 1992;320:228–242.
384. Sanides D. The retinal projection to the ventral lateral geniculate nucleus of the cat. Brain Res 1975; 85:313–316.
385. Salt TE. Electrophysiological studies of excitatory amino acid neurotransmission in the ventrobasal thalamus. In: Macchi G, Bentivoglio M, Spreafico R, eds. Cellular thalamic mechanisms. Amsterdam: Elsevier, 1988:297–310.
386. Scheibel ME, Scheibel AB. The organization of the nucleus reticularis thalami: a Golgi study. Brain Res 1966;1:43–62.
387. Scheibel ME, Scheibel AB. The organization of the ventral anterior nucleus of the thalamus: a Golgi study. Brain Res 1966;1:250–268.
388. Scheibel ME, Scheibel AB. Structural organization of nonspecific thalamic nuclei and their projection toward cortex. Brain Res 1967;6:60–94.
389. Schell GR, Strick PL. The origin of thalamic input to the arcuate, premotor and supplementary areas. J Neurosci 1984;4:539–560.
390. Schlag J, Waszak M. Characteristics of unit responses in nucleus reticularis thalami. Brain Res 1970; 21:286–288.
391. Schwartz ML, Mrzljak L. Cholinergic innervation of the mediodorsal thalamic nucleus in the monkey: ultrastructural evidence supportive of functional diversity. J Comp Neurol 1993;327:48–62.
392. Scollo-Lavizzari G, Akert K. Cortical area 8 and its thalamic projection in *Macaca mulatta*. J Comp Neurol 1963;121:259–267.
393. Sherman SM, Koch C. Thalamus. In G.M Shepherd, ed. The synaptic organization of the brain. Ch. 8. New York: Oxford University Press, 1990:246–278.
394. Sheps JG. The nuclear configuration and cortical connections of the human thalamus. J Comp Neurol 1945;83:1–56.
395. Sheridan MN, Sladek JR Jr. Histofluorescence and ultrastructural analysis of hamster and monkey pineal. Cell Tissue Res 1975;164: 145–152.
396. Shute CCD, Lewis PR. The ascending cholinergic reticular system: neocortical, olfactory and subcortical projections. Brain 1967;90: 497–520.
397. Singer W. Control of thalamic transmission by corticofugal and ascending reticular pathways in the visual system. Physiol Rev 1977;57:386–420.
398. Simpson DA. The projection of the pulvinar to the temporal lobe. J Anat 1952;86:20–28.
399. Siqueira EB. The cortical connections of the nucleus pulvinaris of the dorsal thalamus in the rhesus monkey. J Hirnforsch 1971;10: 487–498.
400. Skinner JE, Lindsley DB. Electrophysiological and behavioral effects of blockage on the nonspecific thalamocortical system. Brain Res 1967;6:95–117.

401. Smith MC. Stereotaxic operations for Parkinson's disease—anatomical observations. In: Williams D, ed. Modern trends in neurology. Vol. 4. London: Butterworths, 1967:21–52.
402. Smith Y, Parent A, Séguéla P, Descarries L. Distribution of GABA-immunoreactive neurons in the basal ganglia of the squirrel monkey (*Saimiri Sciureus*). J Comp Neurol 1987;259:50–65.
403. Sofroniew MV, Priestley JV, Consolazione A, Eckenstein F, Cuello AC. Cholinergic projections from the midbrain and pons to the thalamus in the rat, identified by combined retrograde tracing and choline acetyltransferase immunohistochemistry. Brain Res 1985; 329:213–223.
404. Spreafico R, Battaglia G, Frassoni C. The reticular thalamic nucleus (RTN) of the rat: cytoarchitectural, Golgi, immunocytochemical, and horseradish peroxidase study. J Comp Neurol 1991;304:478–490.
405. Squire LR. Mechanisms of memory. Science 1986;232:1612–1619.
406. Stanton GB. Topographical organization of ascending cerebellar projections from the dentate and interposed nuclei in *Macaca mulatta*: an anterograde degeneration study. J Comp Neurol 1980;190:699–731.
407. Starzl TE, Magoun HW. Organization of the diffuse thalamic projection system. J Neurophysiol 1951;14:133–146.
408. Starzl TE, Taylor CW, Magoun HW. Ascending conduction in reticular activating system, with special reference to the diencephalon. J Neurophysiol 1951; 14:461–477.
409. Starzl TE, Whitlock DG. Diffuse thalamic projection system in monkey. J Neurophysiol 1952;15: 449–468.
410. Steriade M, Biesold D. Brain cholinergic systems. Oxford: Oxford University Press, 1990.
411. Steriade M, Deschêne M. The thalamus as a neuronal oscillator. Brain Res 1984;320:1–63.
412. Steriade M, Glenn LL. Neocortical and caudate projections of intralaminar thalamic neurons and their synaptic excitation from midbrain reticular core. J Neurophysiol 1982;48:352–371.
413. Steriade M, Llinás RR. The functional states of the thalamus and the associated neuronal interplay. Physiol Rev 1988;68:649–742.
414. Steriade M, Parent A, Hada J. Thalamic projections of nucleus reticularis thalami of cat: a study by using retrograde transport of HRP and fluorescent tracers. J Comp Neurol 1984;229:531–547.
415. Steriade M, Parent A, Paré D, Smith Y. Cholinergic and noncholinergic neurons of cat basal forebrain project to reticular and mediodorsal thalamic nuclei. Brain Res 1987;408:372–376.
416. Sterling P. Retina. In: Shepherd GM, ed. The synaptic organization of the brain. Ch. 6. New York: Oxford University Press, 1990: 170–213.
417. Stone J, Fukuda Y. Properties of cat retinal ganglion cells: a comparison of W cells with X and Y cells. J Neurophysiol 1974;37:722–748.
418. Strick PL. Anatomical analysis of ventrolateral thalamic input to primate motor cortex. J Neurophysiol 1976;39:1020–1031.
419. Sugimoto T, Takada M, Kaneko T, Mizuno N. Substance P-positive thalamocaudate neurons in the center median-parafascicular complex in the cat. Brain Res 1984; 323:181–184.
420. Swanson LW, Hartman BK. The central adrenergic system: an immunofluorescence study of the location of cell bodies and their efferent connections in the rat utilizing dopamine-beta-hydroxylase as a marker. J Comp Neurol 1975; 163:467–506.
421. Szentagothai J. Glomerular synapses, complex synaptic arrangements, and their operational significance. In: Schmitt FO, ed. The neurosciences. Second study program. Ch. 40. New York: Rockefeller University Press, 1970: 427–443.
422. Szentagothai J. Neuronal and synaptic architecture of the lateral geniculate nucleus. In: Jung R, ed. Handbook of sensory physiology. Vol 7: Central processing of visual information. Part B: Morphology and function of visual centers in the brain. Berlin: Springer-Verlag, 1973:141–176.
423. Tessier-Lavigne M. Phototransduction and information processing in the retina. In: Kandel ER, Schwartz JH, Jessell TM, eds. Principles of neural science. Ch. 28. New York: Elsevier, 1991:400–417.
424. Thach WT, Jones EG. The cerebellar dentatothalamic connection: terminal field, lamellae, rods and somatotopy. Brain Res 1979;169: 168–172.
425. Tigges J, O'Steen WK. Terminations of retinofugal fibers in squirrel monkey: a re-investigation using autoradiographic methods. Brain Res 1974;79:489–495.
426. Tigges M, Tigges J. The retinofugal fibers and their terminal nuclei in *Galago crassicaudatus* (primates). J Comp Neurol 1970;138:87–102.
427. Tobias TJ. Afferents to prefrontal cortex from the thalamic mediodorsal nucleus in the rhesus monkey. Brain Res 1975;83:191–212.
428. Tomasch J. The numerical capacity of the human cortico-ponto-cerebellar system. Brain Res 1969; 13:476–484.
429. Toncray JE, Krieg WJS. The nuclei of the human thalamus: a comparative approach. J Comp Neurol 1946;85:421–459.
430. Torvik A. The ascending fibers from the main trigeminal sensory nucleus: an experimental study in the cat. Am J Anat 1957;100:1–15.
431. Tracey DJ, Asanuma C, Jones EG, Porter R. Thalamic relay to motor cortex: afferent pathways from brain stem, cerebellum, and spinal cord in monkeys. J Neurophysiol 1980;44:532–553.
432. Trojanowski JJ, Jacobson S. A combined horseradish peroxidase-autoradiographic investigation of reciprocal connections between superior temporal gyrus and pulvinar in squirrel monkey. Brain Res 1975;85:347–353.
433. Tusa RJ, Rosenquist AC, Palmer LA. Retinotopic organization of areas 18 and 19 in the cat. J Comp Neurol 1979;185:657–678.
434. Updyke BV. A reevaluation of the functional organization and cytoarchitecture of the feline lateral posterior complex, with observations on adjoining cell groups. J Comp Neurol 1983;219:143–181.
435. Van Buren JM, Borke RC. Variations and connections of the human thalamus. New York: Springer-Verlag, 1972.
436. Van den Pol AN, Powley T. A fine-grained anatomical analysis of the role of the rat suprachiasmatic nucleus in circadian rhythms of feeding and drinking. Brain Res 1979;160:307–326.
437. Van der Kooy D, Kuypers HGJM, Catsman-Berrevoets CE. Single mamillary body cells with divergent axon collaterals: demonstration by a simple fluorescent retrograde double labeling technique in the rat. Brain Res 1978;158:189–196.
438. Van Groen T, Wyss JM. Projections from the laterodorsal nucleus of the thalamus to the limbic and visual cortices in the rat. J Comp Neurol 1992;324:427–448.
439. Veazey RB, Amaral DG, Cowan WM. The morphology and connections of the posterior hypothalamus in the cynomolgus monkey (*Macaca fascicularis*). II. Efferents connections. J Comp Neurol 1982; 207:135–156.
440. Verhaart WJC, Kennard MA. Corticofugal degeneration following thermocoagulation of areas 4, 6 and 4S in *Macaca mulatta*. J Anat 1940;74:239–254.
441. Vogt BA, Rosene DL, Pandya DN. Thalamic and cortical afferents differentiate anterior from posterior cingulate cortex in the monkey. Science 1979;204:205–207.
442. Vogt LJ, Vogt BA, Sikes RW. Limbic thalamus in rabbit: architecture, projections to cingulate cortex and distribution of muscarinic acetylcholine, GABAA, and opioid receptors. J Comp Neurol 1992; 319:205–217.
443. Wald G. Molecular basis of visual excitation. Science 1968;162: 230–239.
444. Walker AE. An experimental study of the thalamocortical projection of

the macaque monkey. J Comp Neurol 1936;64:1–39.
445. Walker AE. The thalamus of the chimpanzee. IV. Thalamic projections to the cerebral cortex. J Anat 1938;73:37–93.
446. Walker AE. The primate thalamus. Chicago: University of Chicago Press, 1938.
447. Walker AE. Afferent connections. In: Bucy PC, ed. The precentral motor cortex. 2d ed. Ch. 4. Urbana: University of Illinois, 1949: 112–132.
448. Walker AE. Normal and pathological physiology of the thalamus. In: Schaltenbrand G, Bailey P, eds. Introduction to stereotaxis with an atlas of the human brain. Vol. I. Stuttgart: Georg Thieme Verlag, 1959:291–330.
449. Walker AE. Internal structure and afferent-efferent relations of the thalamus. In: Purpura DP, Yahr MD, eds. The thalamus. New York: Columbia University Press, 1966: 1–12.
450. Whitlock DG, Nauta WJH. Subcortical projections from the temporal neocortex in the *Macaca mulatta*. J Comp Neurol 1956;106:183–212.
451. Wilson ME, Cragg BG. Projection from the lateral geniculate nucleus in the cat and monkey. J Anat 1967;101:677–692.
452. Willis WD Jr. Nociception neurons in the primate ventral posterior lateral (VPL) neucleus. In: Bentivoglio M, Spreafico R, eds. Cerebellar thalamic mechanisms. Amsterdam: Excerpta Medica, 1988:77–92.
453. Winer JA, Diamond IT, Raczkowski D. Subdivisions of the auditory cortex in the cat: the retrograde transport of horseradish peroxidase to the medial geniculate body and posterior thalamic nuclei. J Comp Neurol 1977; 176:387–418.
454. Wong-Riley MTT. Projections from the dorsal lateral geniculate nucleus to prestriate cortex in the squirrel monkey as demonstrated by retrograde transport of horseradish peroxidase. Brain Res 1976; 109:595–600.
455. Woolf NJ, Butcher LL. Cholinergic systems in the rat brain: III. Projections from the pontomesencephalic tegmentum to the thalamus, tectum, basal ganglia, and basal forebrain. Brain Res Bull 1986;16: 603–637.
456. Woolsey CN. Organization of somatic sensory and motor areas of the cerebral cortex. In: Harlow HF, Woolsey CN, eds. Biological and biochemical bases of behavior. Madison: University of Wisconsin, 1958:63–81.
457. Yakovlev PI, Locke S, Angevine JB Jr. The limbus of the cerebral hemisphere, limbic nuclei of the thalamus and the cingulum bundle. In: Purpura DP, Yahr MD, eds. The thalamus. New York: Columbia University Press, 1966:77–97.
458. Yasui Y, Saper CB, Cechetto DF. Calcitonin gene-related peptide (CGRP) immunoreactive projections from the thalamus to the striatum and amygdala in the rat. J Comp Neurol 1991;308:293–310.
459. Yen C-T, Jones EG. Intracellular staining of physiologically identified neurons and axons in the somatosensory thalamus of the cat. Brain Res 1983;280:148–154.
460. Zahm DS, Zaborszky L, Alheid GF, Heimer L. The ventral striatopallidothalamic projection: II. The ventral pallidothalamic link. J Comp Neurol 1987;255:592–605.
461. Zola-Morgan S, Squire LR. Amnesia in monkeys after lesions of the mediodorsal nucleus of the thalamus. Ann Neurol 1985;17:558–564.
462. Diamond IT, Fitzpatrick D, Conley M. A projection from the parabigerminal nucleus (Pbg) to the pilvinar nucleus in *Galago*. J Comp Neurol 1992;316:375–382.

17
Hypothalamus

At the end of the 19th Century, the French physiologist Claude Bernard drew attention to the importance of maintaining a constant internal environment ("milieu interne") for the survival of the organism (8). This notion was further emphasized by Walter Cannon, who first coined the term *homeostasis* to refer to the condition that results from various mechanisms acting to limit the variability of the body's internal states (22). The internal environment of the body is maintained constant through the interplay of three major classes of mechanisms: neuroendocrine, autonomic, and motivational. The hypothalamus, together with a group of highly heterogeneous structures referred to as the limbic system, are key neuronal elements involved in maintaining homeostasis. The hypothalamus and closely related structures in the limbic system receive information directly from the internal environment and act directly on the internal environment. Other brain structures affect the internal environment indirectly through action on the external environment, and both the direct and indirect ways of regulating the internal environment function largely in parallel (81, 161). In this chapter, we examine the anatomic organization of the hypothalamus and its role in controlling the neuroendocrine and autonomic functions. Structures of the limbic system and their roles in organizing motivational and emotional behaviors are examined in Chapter 18.

More than half a century ago, the English anatomist Wilfrid Le Gros Clark noted that the hypothalamus accounts for only about 4 g of the total 1200–1400 g of adult human brain weight, or less than 1% of the total volume of the human brain (83). Despite its small size, the hypothalamus is known to contain the integrative neural systems critical for basic life support, including activities such as fluid and electrolytic balance, food ingestion and energy metabolism, thermoregulation, reproduction, and emotional responses (161). The hypothalamus is also the key structure of the brain for the control of the regulation of hormone release from the pituitary gland or hypophysis. The involvement of the hypothalamus in the control of neuroendocrine, autonomic, and motivational output systems has been documented by experimental studies undertaken principally in rodents. By comparison, little is known of the anatomic and functional organization of these hypothalamic control systems in primates, particularly humans. Nevertheless, the fact that the structural organization of the hypothalamus in rodents differs only slightly from that in primates allows interesting interspecies comparisons that can shed light on the functional organization of the hypothalamus in humans.

The hypothalamus represents the most ventral portion of the diencephalon. The thalamus lies dorsal to the hypothalamus, and the subthalamic region is lateral and caudal (Figs. 2.29 and 16.6). The hypothalamus is located in the walls of the third ventricle below the hypothalamic sulci and is continuous across the floor of this ventricle (Figs. 2.29 and 17.1). On the ventral surface of the brain, the *infundibulum*, to which the hypophysis is attached, emerges posterior to the optic chiasm (Figs. 2.9, 2.10, and 17.1). A slightly bulging region posterior to the infundibulum is the *tuber cinereum* (Figs. 2.10, 17.12, and 17.13). The *mammillary bodies* lie posteriorly near the interpeduncular fossa (Figs. 2.9 and 2.28).

Externally, the hypothalamus is bounded rostrally by the optic chiasm, laterally by the optic tracts, and posteriorly by the mammillary bodies. This region is roughly diamond-shaped, and its surface is irregular because of several small eminences. The zone forming the floor of the third ventricle is called the *median eminence* of the tuber cinereum. The portion rostral to the infundibular stem is the *anterior median eminence*. The portion posterior to the infundibular stem forms the *posterior median eminence*, which is better developed in humans (Fig. 2.9). Paired lateral eminences

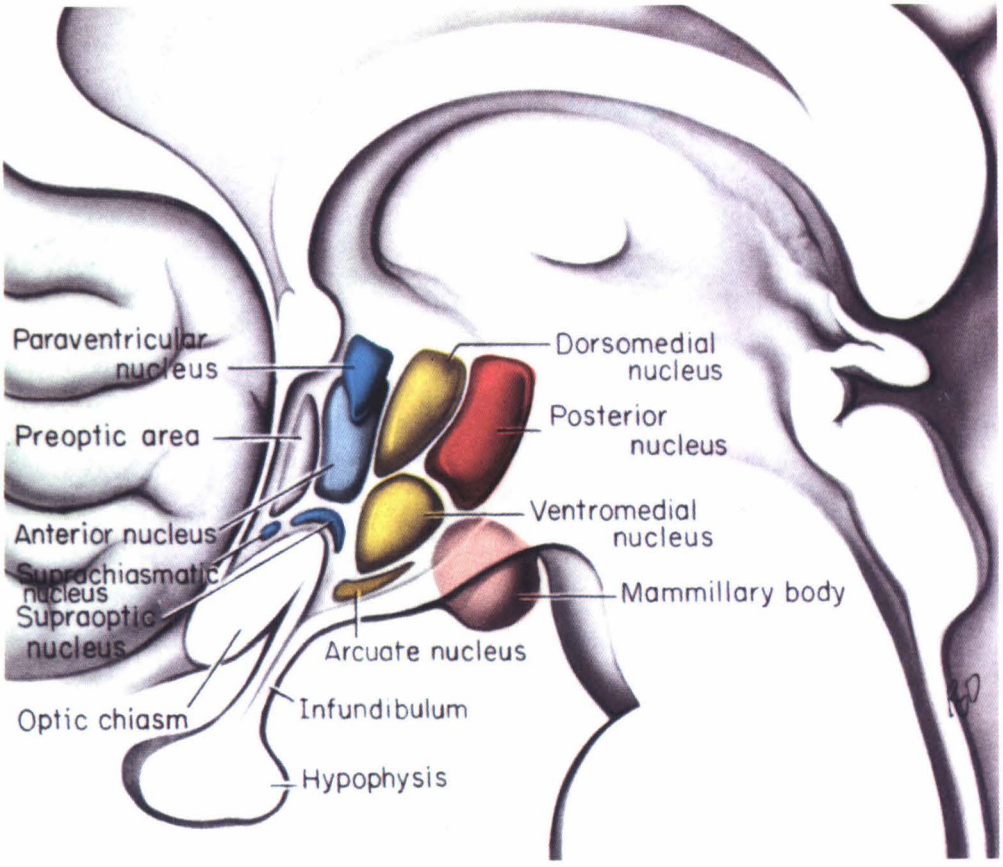


Figure 17.1. Major hypothalamic nuclei. Nuclei in the supraoptic region are in *blue*. Nuclei of the middle or tuberal region of the hypothalamus are *yellow*. Nuclei of the caudal or mammillary region are shades of *red*. The preoptic area (*gray*) lies rostral to the supraoptic region.

form well-defined landmarks. The ventral protrusion of the hypothalamus and the third ventricular recess form the infundibulum. The most distal portion of the infundibular process is the neurohypophysis. Tissue joining the infundibular process to the median eminence is called the *infundibular stem*. The median eminence represents the final point of convergence of pathways from the central nervous system upon the peripheral endocrine system. The median eminence is the anatomic site of the interface between brain and the anterior pituitary. Primary capillaries of the hypophysial portal vessels vascularize the median eminence. Ependymal cells lining the floor of the third ventricle have processes that traverse the width of the median eminence and terminate near the portal perivascular space. These cells, called tanycytes, provide a structural and functional link between the cerebrospinal fluid (CSF) and the perivascular space of the pituitary portal vessels.

HYPOTHALAMIC NUCLEI

The cytoarchitectural organization of the human hypothalamus is largely similar to that found in other primate and nonprimate species. It was described in detail by Le Gros Clark (82), Rioch, et al. (155), Brockhaus (14), and, more recently, by Nauta and Haymaker (118), and Saper (161). The nomenclature used in this chapter is largely based on the results of the two latter studies. The nuclear masses in the adult human hypothalamus are not as distinct as their counterparts in other mammalian species. Nevertheless, as in other species, the human hypothalamus is usually divided in Nissl-stained material into three rostrocaudal regions and three mediolateral zones or areas.

Rostrocaudally, the most anterior region of the hypothalamus is bordered rostrally by the lamina terminalis and caudally by the posterior edge of the optic chiasm. This region can

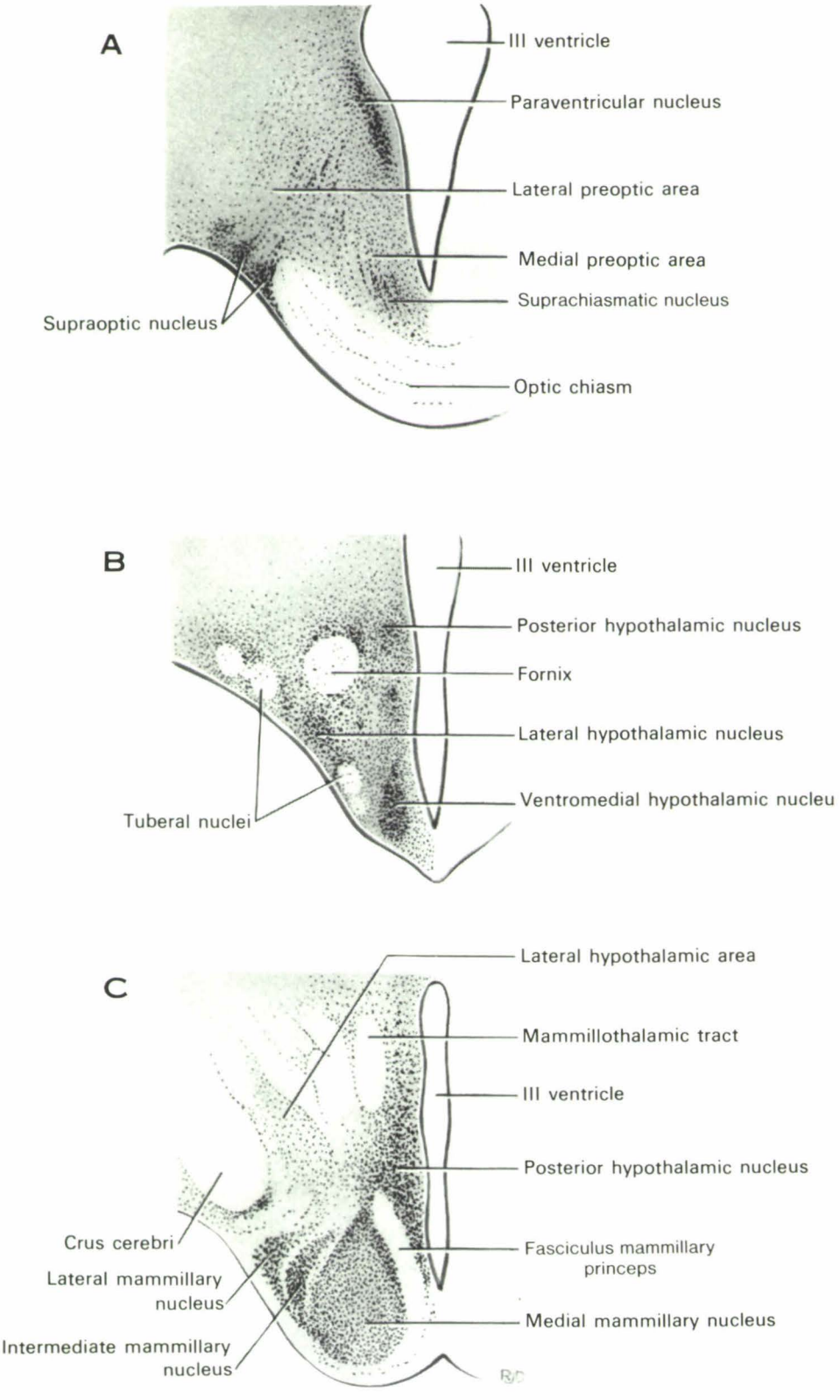


Figure 17.2. Transverse sections through portions of the human hypothalamus: **A**, supraoptic region; **B**, infundibular region; **C**, mammillary region.

be further subdivided into a *preoptic region* located between the lamina terminalis and the optic chiasm, and a *supraoptic region* lying above the optic chiasm (Figs. 17.2 and 17.3). The middle hypothalamic region gives rise medially to the pituitary stalk and is often referred to as the *infundibular* or *tuberal region*. The lateral surface of the tuberal region often displays several small protuberances, representing the external protrusions of the lateral tuberal nuclei. The posterior hypothalamic region is characterized by the presence of the mammillary bodies and is referred to as the *mammillary region*. A small portion of the third ventricle, the mammillary recess, is often trapped ventrally between the mammillary bodies and the midline. Caudally, the hypothalamus merges imperceptibly into the central gray matter and tegmentum of the midbrain.

Mediolaterally, the hypothalamus can be subdivided into (a) a thin and relatively un-

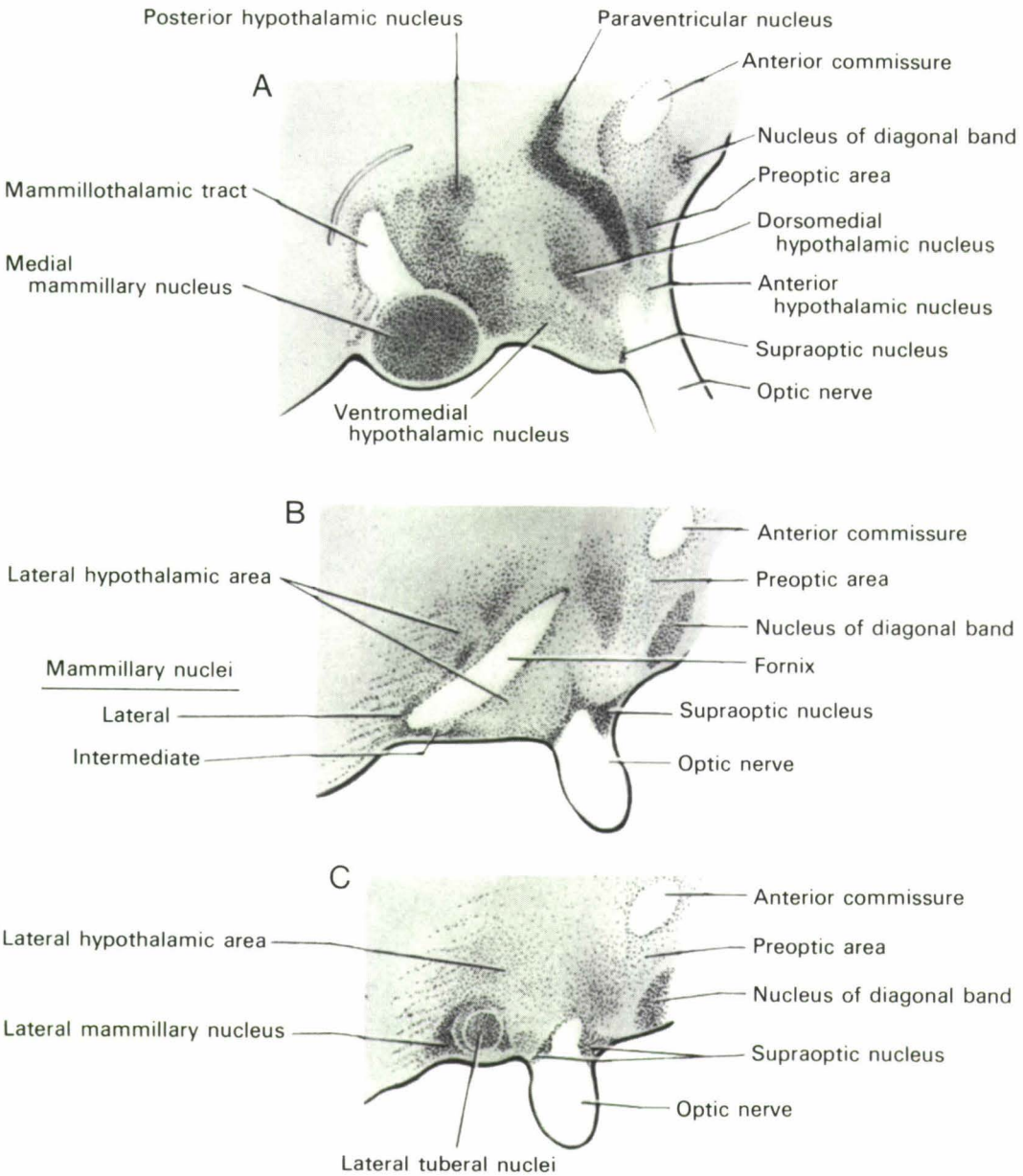


Figure 17.3. Sagittal sections through portions of the human hypothalamus: **A**, near ventricular surface; **B**, through the anterior column of the fornix; **C**, near lateral border of hypothalamus.

differentiated periventricular area, (b) a large medial hypothalamic area, which contains most well-defined hypothalamic nuclear masses, and (c) a large lateral hypothalamic area, which contains large neurons scattered among numerous ascending and descending fibers. The anterior columns of the fornix can be used as a landmark to separate the medial and lateral hypothalamic areas on sagittal sections (Figs. 17.2 and 17.3). The boundary between the periventricular and medial hypothalamic areas is much more discrete, and neurons in these two zones appear to contribute in the formation of certain hypothalamic nuclei.

Lateral Hypothalamic Area

This area is bounded medially by the mammillothalamic tract and the anterior column of the fornix. The medial edge of the internal capsule and the subthalamic region form its lateral boundary (Figs. 17.2 and 17.3). Rostrally, this area is continuous with the lateral preoptic nucleus, while caudally it merges with the ventral tegmental area of the midbrain. Rostral and caudal portions of this area are narrow, but the tuberal region is expanded. The pattern of organization of the lateral hypothalamic area is similar throughout the three principal hypothalamic regions. It is composed of a relatively small number of large, darkly-staining, multipolar cells scattered among numerous nonmyelinated or weakly myelinated fibers. The neurons present in the lateral hypothalamic area form the *lateral hypothalamic nucleus*. Most of the fibers that course within the lateral hypothalamic area are part of the so-called *medial forebrain bundle*. This bundle can be followed as far rostrally as the *lateral preoptic nucleus*, which is regarded by some authors as the interstitial nucleus of the median forebrain bundle (80) (Figs. 17.2 and 17.3).

The lateral hypothalamic area also contains some well-delineated groups of cells, the largest of which is the *tuberomammillary nucleus*. This nucleus is particularly well-developed in the tuberal region, but it extends caudolaterally and caudoventrally to the mammillary body (118). The *lateral tuberal nuclei* (nuclei tuberales) consists of two or three sharply delimited cell groups that often produce small visible eminences on the basal surface of the hypothalamus (Fig. 16.10). They consist of small, pale, multipolar cells surrounded by a delicate fiber capsule about which are found the large cells of the lateral hypothalamic nucleus (Figs. 17.2 and 17.3). The tuberal nuclei are particularly well-developed in humans, but similar nuclei also exist in a much less developed state in nonprimates. In rodents, the tuberal nuclei contain several neuroactive peptides, small-molecule transmitters such as GABA, as well as acetylcholinesterase, and they are known to project to the cerebral cortex (130, 131, 133, 161). The most prominent of these nuclei, the tuberomammillary nucleus, is enriched with histamine and projects widely to the cerebral cortex. In humans, there are acetylcholinesterase-positive neurons in locations similar to those of the hypothalamocortical groups in the rat, and the fact that the cerebral cortex is so greatly enlarged in humans compared to rodents may explain the prominence of the tuberal nuclei in the former group. Interestingly, the tuberal nuclei in humans undergo neurofibrillary degeneration, as is the case for the basal nucleus of Meynert which projects widely to the cerebral cortex (160, 162). Also of interest is the demonstration of a well-organized network of histamine-immunoreactive fibers that covers the frontal temporal cortex in humans (129). This prominent fiber system appears to originate in the hypothalamus, where numerous histamine-immunoreactive nerve cells occur.

Medial and Periventricular Hypothalamic Areas

The medial hypothalamic area lies medial to the fibers of the fornix and the mammillothalamic tract, whereas the periventricular area borders the ependymal lining of the third ventricle. The medial hypothalamic area is the most differentiated zone of the hypothalamus. Its nuclear composition is described according to the pattern it displays in the anterior, tuberal, and mammillary regions.

Anterior Region

PREOPTIC REGION

The preoptic region has long been regarded as a forebrain derivative and, as such, has often been treated as a distinct entity (83). Detailed developmental studies, however, show that the preoptic area arises from a rostral hypothalamic anlage (75, 80). Thus, the preoptic region is currently believed to be

structurally and functionally a part of the hypothalamus (7).

The preoptic region constitutes the periventricular gray matter of the most rostral part of the third ventricle (Figs. 17.1–17.3). The periventricular area at this level contains the *preoptic periventricular nucleus,* which surrounds the walls of the third ventricle in the region of the preoptic recess. The diffusely arranged small cells of this nucleus are poorly differentiated from the ependymal lining. The *medial preoptic nucleus,* composed of predominantly small cells, lies lateral to the preoptic periventricular nucleus and extends ventrally to the optic chiasm (Fig. 17.3). It is part of the medial area of the preoptico-hypothalamic complex. The lateral area contains the lateral preoptic nucleus, which is composed of diffusely dispersed medium-sized cells.

The preoptic region plays a role in regulating the release of gonadotropic hormones from the anterior lobe of the hypophysis. In the human female, pituitary gonadotropins are released in a cyclic manner, and the duration of the cycle determines the length of the menstrual cycle. In the male, the gonadotropins are released tonically without regularly occurring fluctuations. It is, therefore, not surprising that there are differences in the functional organization of the preoptic region in the male and female of the species. A morphologic expression of this difference was observed in the preoptic area of the rat, where a nucleus of densely stained cells was larger in the male (49, 50). This nucleus represents a specialized portion of the medial preoptic nucleus that is termed the "sexually dimorphic nucleus of the preoptic area" (Fig. 17.22). The full ontogenetic development of this nucleus, as well as the male pattern of tonic gonadotropic release, depends upon the presence of testosterone in the circulation during the first week of life. If the testes are removed from the newborn rat, the genetic male fails to develop the sexually dimorphic nucleus of the preoptic region and has a female pattern of gonadotropin release at puberty. Conversely, a newborn female given exogenous testosterone will, as an adult, show the male pattern of gonadotropin release. A sexually dimorphic nucleus, which was identified in the human preoptic area (68, 177), contains approximately twice as many neurons in men as in women. Further evidence is required, however, to determine whether this nucleus is homologous to the sexually dimorphic part of the medial preoptic nucleus in rodents.

The vascular organ of the lamina terminalis (organum vasculosum laminae terminalis (OVLT)) is a vascular midline circumventricular organ located in the rostral wall of the third ventricle superior to the optic chiasm (Fig. 1.17). The subfornical organ (SFO) is another highly vascularized circumventricular organ that develops from the dorsal extremity of the lamina terminalis and lies at the confluence of the two interventricular foramina and ventral to the junction of the two fornix columns in the adult (52, 96). These two circumventricular organs are made up of neural, glial, and ependymal elements, combined with leptomeningeal and vascular tissue of mesodermal origin. The blood-brain barrier is absent at these levels due to fenestrations in the capillary endothelium (96). The SFO and the OVLT are reciprocally connected with a wide variety of structure, principally the hypothalamus, brainstem, and subcortical and cortical areas of the limbic system. They receive a particularly dense serotoninergic innervation from the dorsal raphe nucleus (Fig. 17.5**A**). The SFO and OVLT are believed to be involved in the control of body fluid balance and are sites at which the circulating octapeptide angiotensin II binds to receptors and initiates water drinking and vasopressin secretion (96, 136). In the rat, intravenous injection of angiotensin II induces the expression of the proto-oncogene *c-fos* in the OVLT (95). Binding sites in the SFO of rats for other circulating hormones, such as somatostatin, atrial natriuretic peptide, or calcitonin, have also been demonstrated, suggesting that angiotensin II may not be the only blood-borne agent acting at this site. In addition to being a receptor zone, morphologic evidence suggests that hormones such as luteinizing hormone-releasing hormone (LHRH), somatostatin, or angiotensin II of central origin are released by neurosecretion into the blood stream by the SFO (96). Furthermore, the OVLT is believed to be involved in the production of the pyrogenic cytokin interleukin-1 (IL-1), which acts on the central nervous system to produce the fever response in the presence of circulating pyrogens (111).

SUPRAOPTIC REGION

This region contains two of the most striking and sharply defined hypothalamic nuclei,

the *paraventricular nucleus* and the *supraoptic nucleus*. Cells of the paraventricular nucleus form a vertical plate of densely packed cells immediately beneath the ependyma of the third ventricle, the dorsal part of which extends laterally toward the fornix (Figs. 17.1–17.4). The paraventricular nucleus consists of several distinct cell groups, among which are a medial predominantly parvicellular group and a prominent lateral magnocellular group (161). The supraoptic nucleus caps the optic chiasm and straddles the optic tract laterally (Figs. 17.1–17.4). This nucleus is composed mainly of uniformly large cells. Large cells in both the paraventricular and supraoptic nucleus appear similar with peripherally distributed Nissl substance and colloidal cytoplasmic inclusions, regarded as neurosecretory products. These cells are considered as magnocellular neurosecretory elements. The concept of *neurosecretion* was developed in the first half of this century by Ernst and Berta Scharrer (167). This concept implies that certain neurons function in two ways: (a) as nerve cells that receive and transmit electrical information, and (b) as endocrine cells that release their secretory products into the blood stream. The magnocellular elements of the paraventricular and supraoptic nuclei are perfect examples of neuroendocrine transducers that convert neural information into hormonal information (154).

Immunocytochemically large cells in both nuclei contain either oxytocin or vasopressin (antidiuretic hormone), each being associated with a distinctive neurophysin. Although they contain several neuroactive peptides (16, 70), it is generally accepted that one large cell produces only one hormone, either oxytocin or vasopressin (190). Oxytocin and vasopressin contain nine amino acid residues (37). As with most peptide hormones, both oxytocin and vasopressin are cleaved from a larger prohormone. The prohormone for oxytocin and vasopressin are synthesized in the cell bodies of the magnocellular neurons, and cleaved within the vesicles during their transport down the axons. The peptide neurophysin is a cleavage product of both oxytocin and vasopressin. However, the neurophysin formed in neurons that secrete oxytocin differs slightly from that produced in neurons that release vasopressin (170, 171). Each neurophysin is released along with its hormone at the terminals of the magnocellular supraoptico-hypophysial tract in the neural lobe of the hypophysis (posterior lobe of the pituitary gland) (17). A small projection from the magnocellular neurons reaches the external zone of the median eminence, whereas

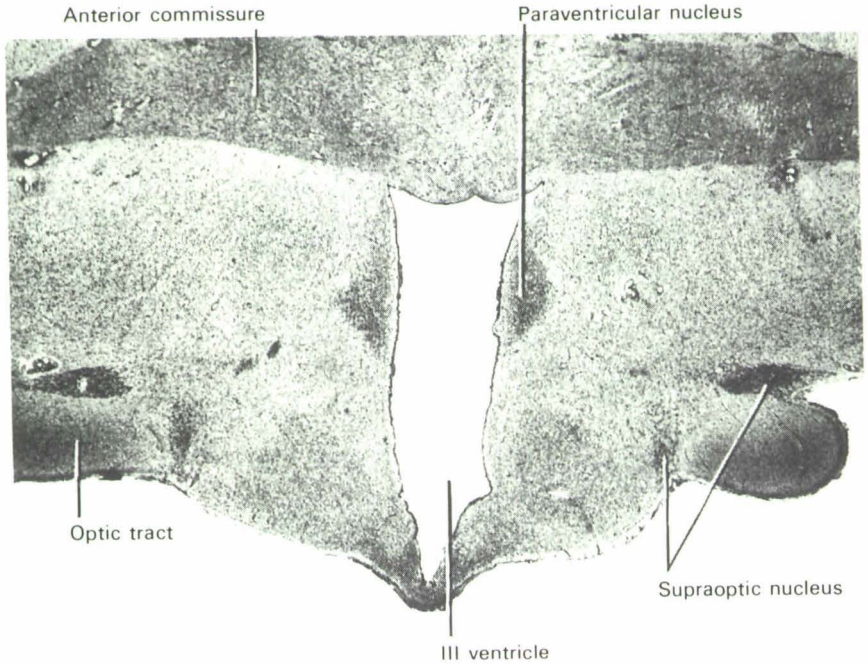


Figure 17.4. Human hypothalamus at the level of the anterior commissure demonstrating the paraventricular and supraoptic nuclei (Nissl stain).

other neurons containing oxytocin or vasopressin project as far down as the spinal cord (20).

Neurons in the parvicellular portion of the paraventricular nucleus contain a multitude of neuroactive peptides such as enkephalin, neurotensin, cholecystokinin, somatostatin, vasoactive intestinal polypeptide. Each of these peptides occurs alone or in various combinations in single parvicellular neurons (81). The parvicellular neurons in the paraventricular nucleus give rise to descending axons projecting to the brainstem and all levels of the spinal cord (181). These projections are involved in the mediation of the hypothalamic influence upon lower autonomic nerve centers (161).

The less differentiated central gray in the supraoptic region constitutes an *anterior hypothalamic nucleus*. This nucleus merges imperceptibly with the preoptic area (Figs. 17.1 and 17.3).

The *suprachiasmatic nucleus* forms a group of small round cells immediately dorsal to the optic chiasm and close to the ventral part of the third ventricle (Figs. 17.1 and 17.2). These small nuclei receive direct bilateral projections from the retina (Fig. 17.8) (103, 105, 137, 139), as well as indirect retinal input via the geniculohypothalamic pathway (24, 108, 180). The direct retinal input appears to exert a glutamate-mediated excitatory effect on the suprachiasmatic nucleus, whereas the indirect pathway exerts a GABA-mediated inhibitory effect (106). Neurons of the indirect geniculohypothalamic projection, which arises mainly from the so-called intergeniculate leaflet of the lateral geniculate complex, also express neuropeptide Y (106).

The well-defined role of the suprachiasmatic nucleus is that of biologic clock. Retinohypothalamic projections to the suprachiasmatic nucleus provide the anatomic link between a cyclical environment and the internal clock (104). Neurons in the suprachiasmatic nucleus use GABA as small-molecule transmitter (106), and also express one or more specific neuroactive peptides or hormones such as vasopressin, somatostatin, vasoactive intestinal peptide, neurotensin, thyrotropin hormone, and angiotensin II (161, 189). The cellular levels of some of these peptides are regulated by photic stimulation while others are not (123). The suprachiasmatic nucleus also receive a dense serotoninergic projection from the midbrain raphe nuclei (132) (Fig. 17.5**B**). This projection exerts a marked regulatory effect on circadian rhythmicity (107). This complex circadian timing system is believed to coordinate the activities of a series of homeostatic mechanisms with the control of behavioral state in a temporal pattern that facilitate adaptive behavior, including reproduction (104). Thus, this system appears to provide the appropriate physiologic and behavioral background to facilitate adaptation and survival.

Tuberal Region

In this region, the hypothalamus reaches its widest extent. The fornix separates the medial and the lateral hypothalamic areas (Figs. 17.2 and 17.12). The medial portion forms the central gray substance of the ventricular wall, in which there may be distinguished a ventromedial and a dorsomedial nucleus.

The *ventromedial nucleus*, the largest cell group in the tuberal region, has a round or oval shape and is surrounded by a cell-poor zone that helps to delineate its boundaries (Figs. 17.1–17.3). Neurons of the ventromedial nucleus typically have dendrites that extend beyond the borders of the nucleus (102). The cell-free capsular zone around the nucleus is formed by a dense ring of axons and terminals (Fig. 17.9). The *dorsomedial nucleus* is a less distinct aggregation of cells that borders the third ventricle (Fig. 17.3).

The *arcuate nucleus* (infundibular nucleus) is located in the most ventral part of the third ventricle near the entrance to the infundibular recess, and extends into the median eminence (Fig. 17.1). The small cells of this nucleus are in close contact with the ependyma lining the ventricle. In frontal sections, the nucleus has an arcuate shape (118). The efferent projections of the arcuate nucleus have been traced to the external layer of the median eminence. This projection is of great importance to adenohypophysial function. It is composed of axons of neurons producing various neuropeptides that are released into the hypophysial portal system where they act as inhibiting or releasing factor for the different hormones produced in the anterior lobe of the hypophysis. Additionally, neurons of the arcuate nucleus are immunoreactive for the adrenocorticotrophic hormone (ACTH), β-lipotrophic hormone (β-LPH), and β-endorphin (β-END). Chemical substances from the arcuate nucleus play a major role in the regulation of hormonal output from the anterior pituitary.

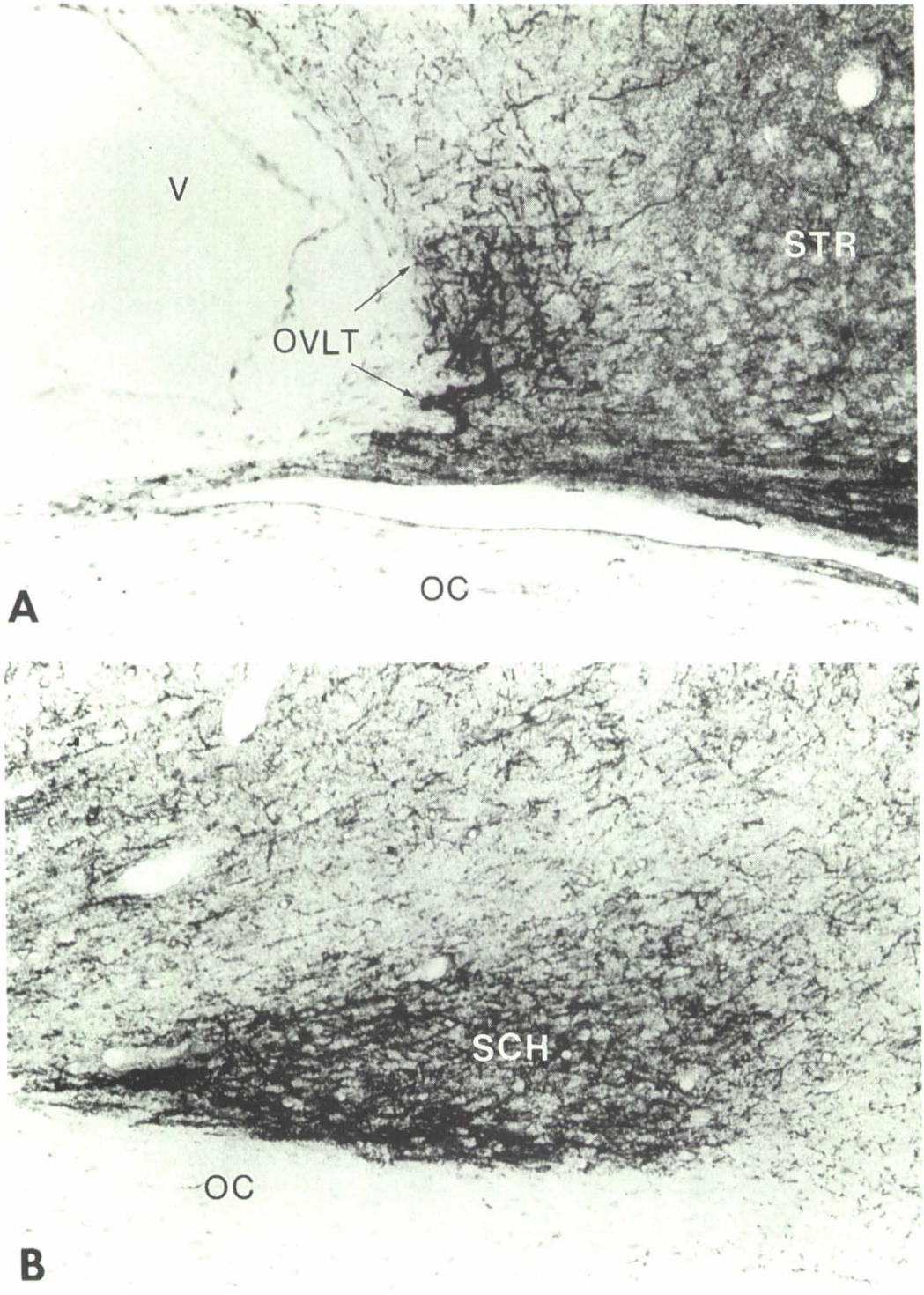


Figure 17.5. Radioautographs showing the dense serotoninergic innervation of (**A**) the organum vasculosum laminae terminalis (OVLT), and (**B**) the suprachiasmatic nucleus (SCH) in the rat, as seen on parasagittal sections. The serotoninergic fibers and axon terminals are darkly labeled because they have taken up a large amount of (^{3}H)serotonin that was injected intraventricularly. *OC*, optic chiasm; *STR*, striatum; *V*, third ventricle.

Mammillary Region

This region consists of the mammillary bodies and the dorsally located cells of the posterior hypothalamic nucleus (Figs. 17.1–17.3 and 17.12). In humans, the mammillary body consists almost entirely of the large, spherical *medial mammillary nucleus*, composed of relatively small cells invested by a capsule of myelinated fibers. Lateral to this is the small *intermediate (intercalated) mammillary nucleus* composed of smaller cells (Fig. 17.2). Even further lateral is a well-defined group of large cells, the *lateral mammillary nucleus*.

The *posterior hypothalamic nucleus* lies dorsal to the mammillary body and caudal to portions of the ventromedial nucleus (Figs. 17.1–17.3). This nucleus consists of a matrix of small cells in which large round or oval cells are scattered. The large cells are especially numerous in humans and extend caudally over the mammillary body to become continuous with the periaqueductal gray.

General descriptions may suggest that all hypothalamic nuclei are sharply circumscribed, but the cellular matrix of the hypothalamus is broadly continuous with the surrounding gray matter. Tissue continuities with surrounding gray matter contain the major afferent and efferent hypothalamic pathways. Rostrally and laterally, the hypothalamus is continuous with the *basal olfactory region*, a large gray mass beneath the rostral part of the lentiform nucleus and the head of the caudate nucleus (Figs. 18.6 and A.24 in the atlas of the human brain, section VII). Near the median plane, this region extends dorsally, rostral to the anterior commissure, where it becomes the *septal region* (Figs. 18.10 and A.23). Beneath the lentiform nucleus, the gray mass extends toward the amygdaloid complex. This region contains cell islands and groups referred to as the substantia innominata (Fig. A.22). The *substantia innominata* contains clusters of large cholinergic neurons, which includes the basal nucleus of Meynert (group Ch4 of Mesulam, et al. (100)). These large cholinergic neurons have widespread projections to the cortex and the amygdala. Neurons in the basal nucleus constitute the major source of cholinergic innervation of the entire cerebral cortex. The base of the septal region (i.e., the part ventral to the anterior commissure) is continuous with the substantia innominata laterally and with the preoptic region caudally. The septal region contains (a) the *medial septal nucleus*, composed of fairly large cholinergic neurons (group Ch1 of Mesulam, et al. (100)) that project to the hippocampal formation, (b) the *lateral septal nucleus*, which consists of smaller noncholinergic neurons, and (c) the *nucleus accumbens septi* (Fig. A.24), which leans against the base of the septum and is situated medially at the junction of caudate nucleus and putamen.

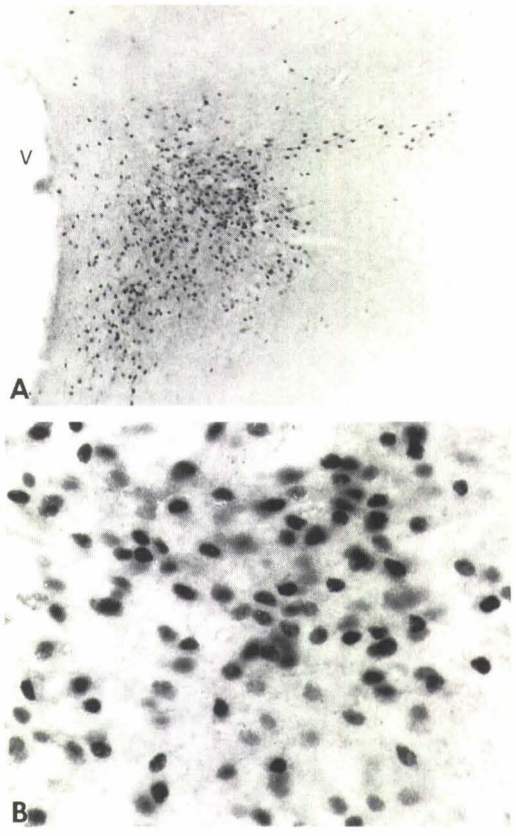


Figure 17.6. Neurons of the paraventricular nucleus in the rat that express the early proto-oncogene *c-fos* following a pharmacologic treatment that leads to a profuse release of serotonin. The animal was injected intraperitoneally with the serotonin releasing agent fenfluramine (15 mg/kg) and sacrificed 1 hour following the injection. *V*, third ventricle.

HYPOTHALAMIC CONNECTIONS

The hypothalamus has extensive and complex fiber connections. Some fibers are organized into definite and conspicuous bundles, while others are diffuse and difficult to trace.

Afferent Connections

The major afferent connections of the hypothalamus are (a) the medial forebrain bundle, (b) the hippocampo-hypothalamic fibers, (c) the amygdalo-hypothalamic fibers, (d) brainstem afferents, (e) the retino-hypothalamic fibers, (f) the cortico-hypothalamic fibers, and (g) forebrain afferents, including olfactory inputs.

MEDIAL FOREBRAIN BUNDLE

This bundle is a complex group of fibers arising from the basal olfactory regions, the septal nuclei, the periamygdaloid region, and the subiculum that pass to, and through, the lateral preoptic and hypothalamic regions (Figs. 17.14 and 17.15). At levels rostral to the anterior commissure, the bundle is formed mainly of fibers from the septal region, and in its parasagittal course receives contributions from the substantia innominata and amygdaloid complex. In humans, the bundle consists of a loose association of pathways, of variable degree of myelination, composed of short and long fibers that course both rostrally and caudally. This tract is well-developed in nonmammalian vertebrates, but is relatively small in humans. In most species, the ascending dopaminergic, serotoninergic, and noradrenergic fibers systems all course in the medial forebrain bundle.

HIPPOCAMPO-HYPOTHALAMIC FIBERS

The projection from the hippocampal formation to the hypothalamus in monkeys arises somewhat more widely than in rats including cells in the CA1 field as well as the subiculum (99, 149, 151, 161, 178, 179). These fibers form the fornix, which is one of the most prominent and heavily myelinated fiber bundles in the human hypothalamus (Figs. 17.7, 17.12, 17.15, and 18.10). The development of the temporal lobe in the primate brain carries the hippocampal formation, which is located medially in the embryonic brain, far from its site of origin near the lamina terminalis. As a result, the fimbria of the fornix is left behind as a long, arching reminder of the migration of the hippocampal



Figure 17.7. Paraventricular nuclei in the mouse hypothalamus immunostained with an antiserum to bovine neurophysin I demonstrating cells and their processes.

formation during development (161). In the septal region, just dorsal to the anterior commissure, fibers of the fornix divide into two distinct bundles: (a) a compact fornix column, or postcommissural fornix, which arches caudal to the anterior commissure, and (b) a more diffuse precommissural fornix (32, 145).

The *precommissural fibers* of the fornix are distributed to the septal nuclei, the lateral preoptic region, the nucleus of the diagonal band, and the dorsal hypothalamic area (114, 161). The *postcommissural fibers* of the fornix project principally to the medial mammillary nucleus. However, many of the fibers that form the columns of the fornix lose their myelination as they course within the hypothalamus and several of them peel off the fornix to innervate several medial hypothalamic nuclei (Fig. 17.9), the lateral hypothalamic area, as well as the anterior thalamic nuclei (161).

AMYGDALO-HYPOTHALAMIC FIBERS

The projections from the amygdaloid nuclear complex to the hypothalamus follows two distinctive pathways: (a) a long, looping fiber system through the stria terminalis (Figs. 16.6 and 16.7), and (b) a short, direct fiber system beneath the lentiform nucleus, which is a component of the ansa peduncularis termed the ventral amygdalofugal pathway (47, 146, 161). The *stria terminalis* arises principally from the corticomedial group of the amygdaloid nuclei (Fig. 18.19) and distributes terminals in the medial preoptic area, medial parts of the anterior hypothalamic area, and in the ventromedial and arcuate nuclei (36, 56, 63, 114, 116, 118, 161). This pathway has been implicated in the olfactory influence on reproductive behavior (84). The *ventral amygdalofugal pathway* arises from the basolateral amygdaloid nuclei and the piriform cortex and spread medially and rostrally under the lentiform nucleus to reach the lateral hypothalamic nucleus and the medial forebrain bundle region (Fig. 17.17) (28, 56, 147, 161, 188). The amygdalofugal fibers that reach the lateral hypothalamic area have been implicated in the amygdaloid influence on the autonomic nervous system (169).

BRAINSTEM AFFERENTS

Fibers from the brainstem reticular formation ascend to the hypothalamus principally via the *mammillary peduncle* and the *dorsal longitudinal fasciculus*. The mammillary peduncle arises from the dorsal and ventral tegmental nuclei in the midbrain and projects mainly to the lateral mammillary nucleus (29) (Fig. 17.14). It passes rostrally through the rootlets of the third nerve and courses lateral to the interpeduncular nucleus. A few fibers ascend in the medial forebrain bundle beyond the level of the mammillary bodies. The mammillary peduncle is not very well differentiated in humans. It corresponds to a rather discrete myelinated bundle that lies medial to the cerebral peduncle and caudal to the mammillary body. Its fibers appear to enter the capsule of the mammillary bodies, although it is not possible to trace them caudally to their origin (161). The *dorsal longitudinal fasciculus* (of Schutz) is the main fiber system that runs longitudinally through the periventricular and periaqueductal gray matter, connecting the hypothalamus with structures in the midbrain and pontine tegmentum. Fibers in this bundle spread out over caudal and dorsal regions of the hypothalamus where they become part of a periventricular system (118). Like the medial forebrain bundle, the dorsal longitudinal fasciculus is composed largely of unmyelinated or poorly myelinated fibers. Since fibers of the dorsal longitudinal fasciculus conduct impulses both rostrally and caudally, this fiber tract may be regarded as a reciprocally organized association system between the hypothalamus and the midbrain central gray (Fig. 17.16).

Brainstem afferents to the hypothalamus also arise from neurons in the raphe nuclei of the midbrain, the locus coeruleus, and from the lateral parabrachial nucleus in the pons (5, 93, 132). Serotoninergic fibers arising mainly from the median raphe nucleus (superior central nucleus), ascend in the medial forebrain bundle to, and through, the lateral hypothalamus. Terminals of these fibers are distributed preferentially to the preoptic region, the lateral hypothalamic area, the paraventricular nucleus, and the suprachiasmatic nucleus (Fig. 17.5**B**). Noradrenergic fibers originating in the locus coeruleus ascend in the dorsal tegmental bundle, which distributes terminals in the dorsomedial, supraoptic, and paraventricular hypothalamic nuclei (130). The brainstem monoaminergic afferents are known to exert a profound modulatory effect on the activity of various subsets of hypothalamic neurons. For exam-

ple, a pharmacologic increase in the release of serotonin can readily induce the expression of the immediate gene *c-fos* (Fig. 17.6). The early and transient expression of this proto-oncogene can be used to study the topography and time course of the metabolic activation in different groups of neurons. A similar expression of *c-fos* can be induced in oxytocin-immunoreactive neurons in the supraoptic and paraventricular neurons following osmotic stress in the rat (46).

Afferents from different parts of the nucleus solitarius project to the medial and lateral parabrachial nuclei. Portions of the nucleus solitarius that receive general visceral afferents (located caudally) project primarily to the lateral parabrachial nuclei. The lateral parabrachial nuclei innervate the medial preoptic region, the paraventricular and dorsomedial hypothalamic nuclei, and the lateral hypothalamic area. The rostral portion of the nucleus solitarius that receives special visceral afferents (taste) projects to the medial parabrachial nuclei. The medial parabrachial nuclei project to the substantia innominata, the amygdala, and the posterolateral regions of the hypothalamus. Afferent fibers to the hypothalamus from the brainstem and other sources are shown in Figures 17.15 and 17.17.

RETINOHYPOTHALAMIC FIBERS

These fibers arise from the ganglion cells of the retina and project bilaterally to the suprachiasmatic nuclei via the optic nerve and chiasm (156) (Fig. 17.8). The retinal axons terminate principally on dendrites of the suprachiasmatic nucleus cells (61, 65, 105). The suprachiasmatic nuclei also receive inputs from extrahypothalamic sources, such as the ventral lateral geniculate nucleus and the paraventricular nuclei of the thalamus. The suprachiasmatic nucleus is the pacemaker for circadian rhythms (104).

CORTICOHYPOTHALAMIC FIBERS

Corticohypothalamic fibers are believed to arise principally from portions of the frontal, parietal, and occipital cortices (118). Medial prefrontal cortex lesions in monkeys reportedly produce terminal degeneration throughout the rostrocaudal extent of the lateral hypothalamus and in the lateral mammillary nucleus (87), whereas frontal granular cortex lesions result in anterograde degeneration in the lateral, dorsal, and posterior hypothalamic areas (117). Furthermore, fibers from the cingulate gyrus vocalization area, identified by electrical stimulation, appear to project to

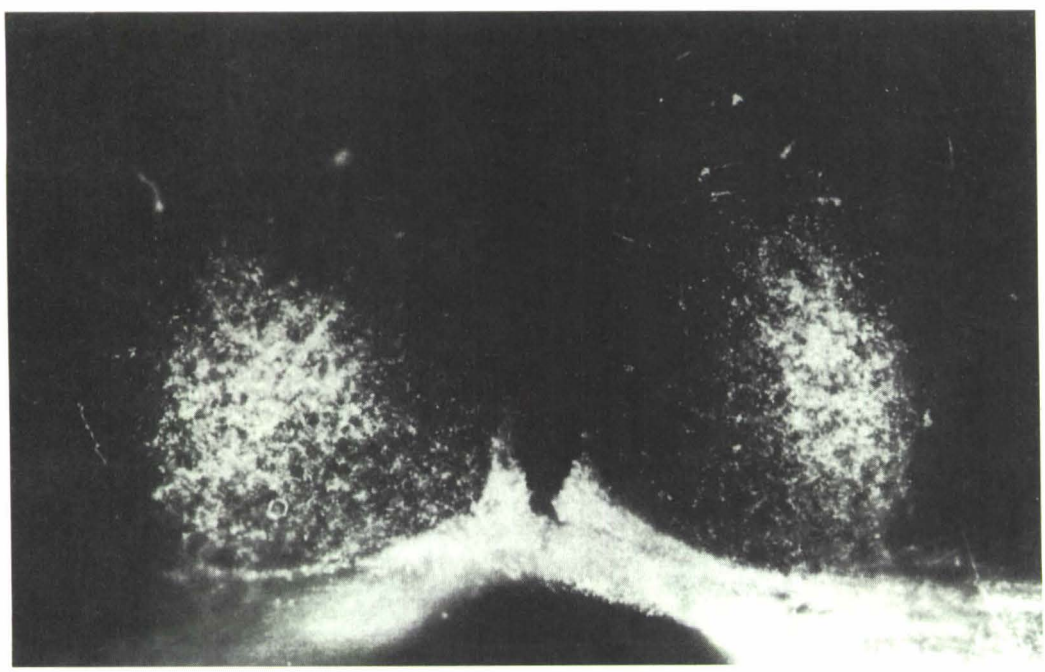


Figure 17.8. Darkfield photomicrograph of retinal fibers and terminals in the suprachiasmatic nuclei of the hamster demonstrated by transport of horseradish peroxidase (HRP).

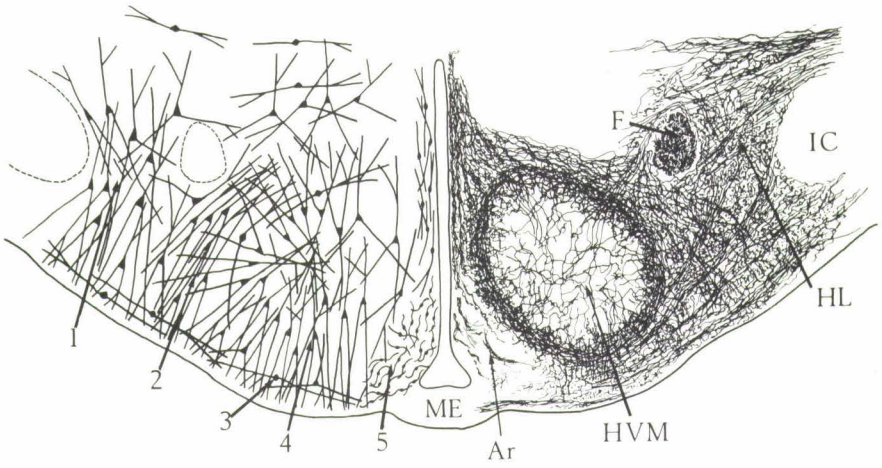


Figure 17.9. Tuberal region of the rodent hypothalamus based upon Golgi preparations. On the reader's left the general arrangement of dendrites and axons is shown. (*1*) Dendrites of neurons in the lateral hypothalamus (*HL*) radiate in the mediolateral and dorsoventral directions. (*2*) There is a compression of the dendritic fields of neurons located between the fornix (*F*) and the hypothalamic ventromedial nucleus (*HVM*). (*3*) The dendritic fields of neurons along the hypothalamic surface are generally parallel with the pia. (*4*) The long dendrites of HVM extend in all directions from the nucleus. (*5*) Small bipolar neurons of the arcuate nucleus (*Ar*) nestle against the ventricle wall, adjacent to the median eminence (*ME*). *IC*, internal capsule.

the hypothalamus where they terminate principally in the preoptic region and the dorsomedial hypothalamus along its whole extent (110). In rodents, direct corticohypothalamic inputs have been documented following tract-tracing studies (77, 158, 186). These afferents arise primarily from insular, lateral frontal, infralimbic, and prelimbic areas, and terminate principally in the lateral hypothalamic area.

FOREBRAIN AFFERENTS

Broadly stated, the principal forebrain afferents to the hypothalamus arise from the two phylogenetically oldest cortical areas, the piriform cortex and the hippocampal formation (Fig. 17.17) (147). In each instance, the cortical projection is reinforced by a corresponding subcortical projection, the amygdala in the case of the piriform cortex, and the septum in the case of the hippocampal formation. Each of these subcortical nuclei is reciprocally connected with the overlying cortical area. Of the phylogenetically newer cortical areas, the cingulate gyrus appears particularly favored to influence the hypothalamus indirectly through the entorhinal cortex and the hippocampal formation. The cingulate cortex can, in turn, be influenced by hypothalamic projections to the anterior nuclear group of the thalamus.

Both the senses of taste and olfaction are directly involved in the arousal and consummatory phases of behavior. Gustatory projections to the hypothalamus are mediated via the parabrachial nuclei, whereas the olfactory projections are relayed through the cortical and medial amygdaloid nuclei and the periamygdaloid piriform cortex (33, 63, 165, 172).

Efferent Connections

The efferent connections of the hypothalamus appear, in part, to be reciprocal to the afferent systems. There are reciprocal connections in the medial forebrain bundle which provide indirect connections between the lateral hypothalamus and the hippocampal formation (148). Additionally, there are hypothalamic projections to the amygdaloid nuclear complex via both the stria terminalis (Fig. 18.10) and the ventral pathway (93). Reciprocal connections with the midbrain tegmentum and central gray matter are conducted by the dorsal longitudinal fasciculus and via pathways projecting to and from the mammillary bodies. There also are several efferent hypothalamic pathways which have no counterpart among afferent systems.

MEDIAL FOREBRAIN BUNDLE

This bundle consists of a loose association of poorly myelinated or nonmyelinated fibers that run longitudinally through the lateral

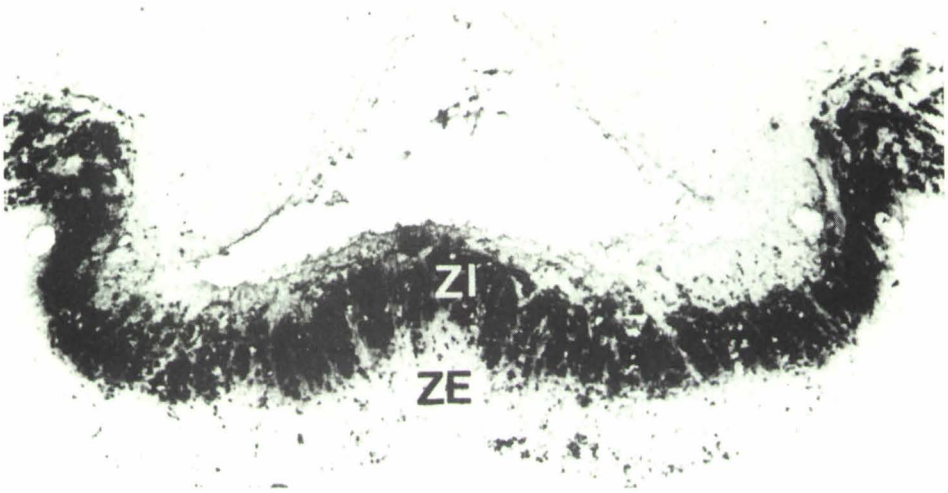


Figure 17.10. Transverse section through the rat median eminence immunostained with antiserum to neurophysin demonstrating the zona interna (*ZI*) and the zona externa (*ZE*). Fibers of the hypothalamo-neurophysiologic tract are abundant in ZI and a few positive fibers are evident in ZE.

hypothalamus to connect the forebrain autonomic and limbic regions with the hypothalamus and brainstem (161). Because the degree of myelination in the medial forebrain bundle is so low, it is not possible to reliably trace any of its components to their origins or terminations in myelin-stained material from the human brain. Experiments in laboratory animals revealed that this bundle conveys impulses from the lateral hypothalamus rostrally to the nuclei of the diagonal band and to the medial septal nuclei (55, 148), which in turn send fibers to the hippocampal formation via the fimbria of the fornix (32). Descending hypothalamic efferents in the medial forebrain bundle project through the ventral tegmental area to the superior central nucleus, the ventral tegmental nucleus, and to parts of the central gray matter (Fig. 17.14) (28, 55, 115, 176, 183). Fibers from the lateral hypothalamic region follow the ventral pathway through the substantia innominata to the amygdala, while those that pass via the stria terminalis arise from more medial cells (118).

DORSAL LONGITUDINAL FASCICULUS

Together with the medial forebrain bundle, the dorsal longitudinal bundle is a major pathway of communication between the hypothalamus and the brainstem. It contains poorly myelinated fibers that originate mostly from medial and periventricular portions of the hypothalamus and project to the central gray matter, tectum, and midbrain tegmentum. Some descending fibers in this system may extend to the dorsal tegmental nucleus (Fig. 17.16). The ascending component of the dorsal longitudinal bundle includes noradrenergic and serotoninergic fibers that arborize within various hypothalamic nuclei.

MAMMILLARY EFFERENT FIBERS

These fibers arise from the medial mammillary nucleus, and to a lesser extent from the lateral and intermediate mammillary nuclei, forming a well-defined bundle, the *fasciculus mamillaris princeps* (Figs. 17.2 and 17.14). This bundle passes dorsally for a short distance and divides into two components—the *mammillothalamic tract* and the *mamillotegmental tract* (Figs. 17.12, 17.14, and A.20). The mammillothalamic tract contains fibers from the medial mammillary nucleus which project to the ipsilateral anteroventral and anteromedial thalamic nuclei, and fibers from the lateral mammillary nucleus that pass bilaterally to the anterodorsal nucleus (30, 42, 191). Superimposed upon this hypothalamic relay to the thalamus are projections from the hippocampal formation via the fornix to the anterior thalamic nuclei (54, 187). Each of the anterior thalamic nuclei in turn projects to subdivisions of the cingulate cortex (Figs. 2.6, 18.1, and 18.10). Thus, the main neocortical projection of impulses from the hippocampal formation and subiculum is to the cingulate cortex via postcommissural fibers of the

fornix to (a) the anterior thalamic nuclei, and (b) the mammillary body which relays impulses to the anterior thalamic nuclei (Fig. 17.17). Impulses from the cingulate cortex pass back to the hippocampal formation via the entorhinal cortex (150) (Fig. 17.15). These connections appear to form a closed anatomic circuit often referred to as the Papez circuit. The *mamillotegmental tract* arches caudally into the midbrain tegmentum. Fibers of this tract terminate in the dorsal and ventral tegmental nuclei (Fig. 17.14).

DESCENDING HYPOTHALAMIC PROJECTIONS

Hypothalamic fibers descending to the brainstem and spinal cord constitute pathways whereby cells of the hypothalamus exert regulatory influences on central autonomic neurons (161, 163). Parvicellular elements of the paraventricular nucleus, cells of the lateral hypothalamic area, and cells in the posterior hypothalamus project fibers directly to the dorsal motor nucleus of the vagus, the medial nucleus solitarius, portions of the nucleus ambiguus, and into ventrolateral regions of the medulla. Fibers from the same hypothalamic nuclei enter the spinal cord, descend in the lateral funiculus, and terminate in the intermediolateral cell column at all levels (Figs. 11.23 and 17.17). These direct hypothalamic fibers influence autonomic functions in the lower brainstem and at all spinal levels. The existence of these pathways in humans can be inferred from the presence of an ipsilateral sympathetic deficit following injury to the hypothalamus, lateral brainstem tegmentum, or spinal lateral funiculus (113).

Descending fibers from the paraventricular nucleus, which forms a part of this system, appear to contain both oxytocin and vasopressin (119). Paraventricular nucleus cells projecting to the spinal cord are largely distinct from those sending axons to the posterior lobe of the pituitary gland (71, 121). Another descending projection to the spinal cord

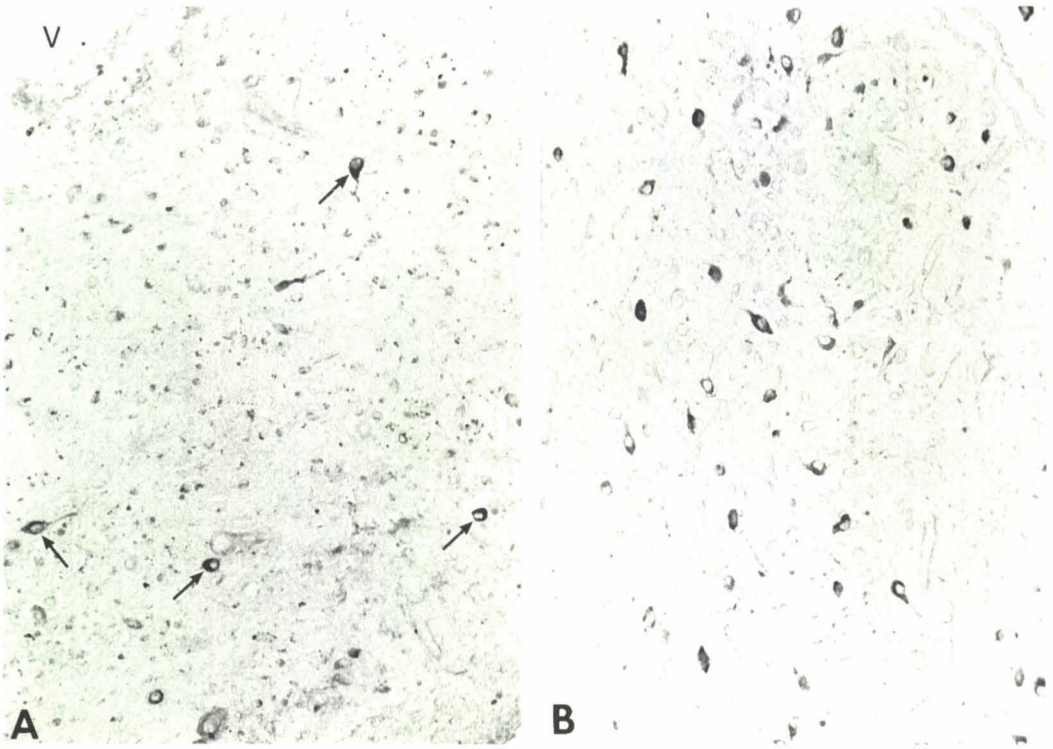


Figure 17.11. **A**. The immunocytologic localization of somatostatin-14 (SRIF-14) in the infundibular (arcuate) nucleus of the human hypothalamus. The *arrows* point to a few cell bodies which are dispersed among weakly immunolabeled nerve fibers. *V*, third ventricle. ×220. **B**. The localization of corticotrophin releasing factor (*CRF*) immunoreactivity in the paraventricular nucleus of the human hypothalamus. Several immunostained neurons can be observed (×280).

arises from the dopaminergic neurons in the dorsomedial hypothalamus and zona incerta (5, 6, 10, 163).

HYPOTHALAMOCORTICAL FIBERS

Hypothalamic projections to the cerebral cortex have been examined with retrograde transport methods in both rats and monkeys (76, 78, 101, 143, 159, 184). In the rat, tuberal lateral hypothalamic nuclei and the posterior hypothalamic nucleus project to the entire cerebral cortex (161). In monkeys, retrogradely-labeled neurons have been visualized in the lateral tuberal nuclei and in the posterior hypothalamic nucleus following injections into the frontal, parietal, and occipital cortex (76, 101, 143, 184). Unfortunately, no attempt has been made to examine the topographic organization of these projections.

SUPRAOPTIC DECUSSATIONS

Dorsal to the optic chiasm, several bundles of fine fibers cross the midline. These fiber bundles constitute the supraoptic decussa-

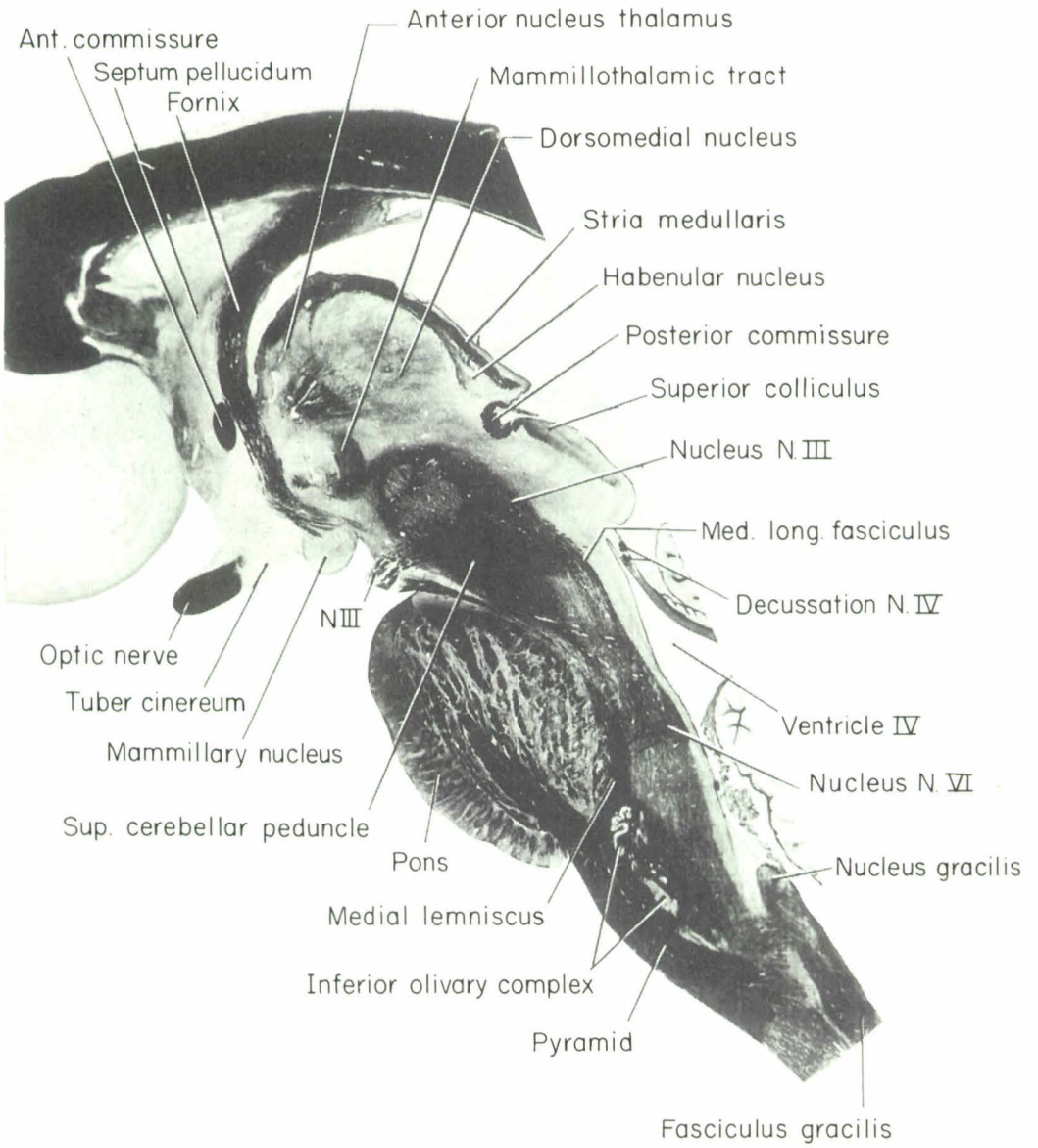


Figure 17.12. Sagittal section of brainstem through the pillar of fornix, the mammillothalamic tract, and the stria medullaris (Weigert's myelin stain).

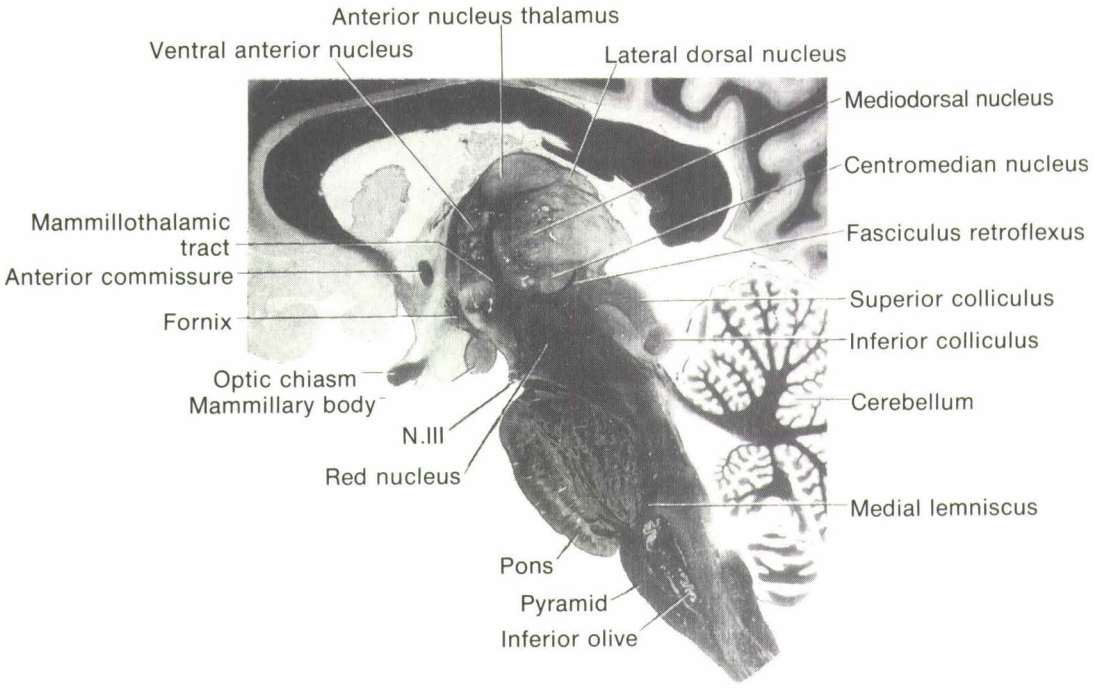


Figure 17.13. Sagittal section of the brainstem demonstrating the mammillothalamic tract, the anterior thalamic nuclei, and thalamic nuclei lateral to those shown in Figure 17.12. (Weigert's stain).

tions. Three decussations or commissures are recognized, although little is known concerning their origin, course, termination or function. The most rostral of these decussations is the *anterior hypothalamic commissure* (Ganser) (Figs. 17.12 and 17.13). Fibers of this commissure are most readily identified as they project ventromedially from Forel's field H and arch over the fibers of the fornix. These fibers pass ventrally in the hypothalamus, cross the midline ventral to the third ventricle, and contralaterally fan out into the lateral preopticohypothalamic area (118). Fibers of the anterior hypothalamic commissure are considered to arise from the reticular formation of the rostral pons and to ascend in association with fibers of the medial longitudinal fasciculus (18). Two decussations lie along the dorsal aspect of the optic chiasm, the *dorsal supraoptic decussation* (Meynert) and the *ventral supraoptic decussation* (Gudden) (Fig. 16.6). The precise origin of both of these bundles is obscure.

Supraopticohypophysial Tract

This tract consists of fibers arising from the magnocellular elements of the supraoptic and paraventricular nuclei that project to the posterior lobe of the hypophysis (81, 161) (Figs. 17.4, 17.16, and 17.18). The peptides specific for these large neurons, oxytocin and vasopressin, were the first brain peptides to be isolated and characterized (37). These peptides are always present in conjunction with a class of larger peptides, known as neurophysins. As mentioned earlier, the neurophysins are part of a large precursor (prohormone) molecule, whose cleavage gives rise to both oxytocin and vasopressin—neurophysin I is associated with oxytocin and neurophysin II with vasopressin (Figs. 17.7 and 17.10). Neurons containing oxytocin or vasopressin and their associated neurophysins are present in both supraoptic and paraventricular nuclei, but each hormone is synthesized in a distinct set of neurons in each nucleus (190). Cells of the supraoptic and paraventricular nuclei are *neurosecretory neurons*. Secretory products are synthesized within the cell bodies, transported along the axonal flow down the axons, and liberated by axon terminals near capillaries in the neurohypophysis. The neurosecretory material is contained within granules 50–200 nm in diameter (12, 13, 126). Oxytocin and vasopressin are stored in dense core vesicles present in different axonal profiles. The content of these dense core vesicles

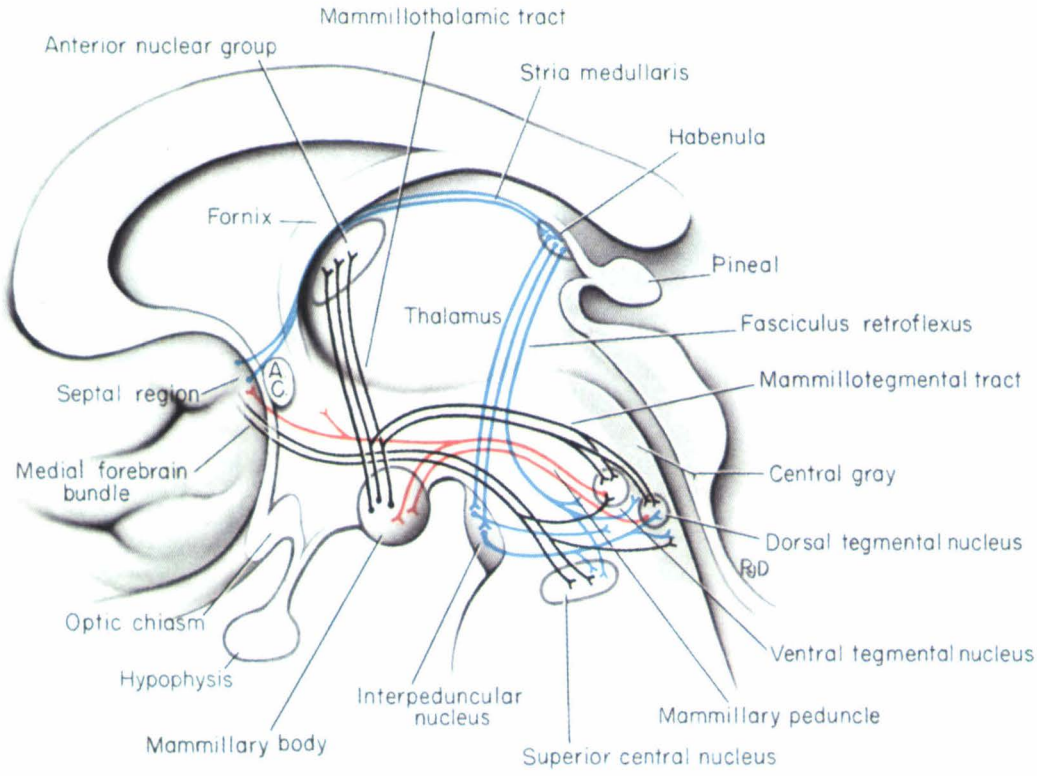


Figure 17.14. Limbic pathways interrelating the telencephalon and diencephalon with medial midbrain structures. The medial forebrain bundle and efferent fibers of the mammillary body are shown in *black*. The medial forebrain bundle originates from the septal and lateral preoptic regions, traverses the lateral hypothalamic area and projects into the midbrain tegmentum. It also includes many ascending fibers. The fasciculus mammillary princeps divides into two bundles, the mammillothalamic tract and the mammillotegmental tract. Ascending fibers of the mammillary peduncle, arising from the dorsal and ventral tegmental nuclei, are shown in *red*. Most of these fibers pass to the mammillary body, but some continue rostrally to the lateral hypothalamus, the preoptic region, and the medial septal nucleus. Fibers arising from the septal nuclei project caudally in the medial part of the stria medullaris (*blue*) to terminate in the medial habenular nucleus. Impulses conveyed to the habenular nucleus are distributed to midbrain tegmental nuclei via the fasciculus retroflexus (habenulo-interpeduncular bundle) (*blue*).

is released into perivascular space containing fenestrated capillaries (168).

A second efferent projection from the magnocellular elements of the paraventricular nucleus has been described in the external zone of the median eminence. Additionally, high levels of vasopressin have been demonstrated in the hypophysial portal system. The role of vasopressin in the zona externa of the median eminence is unresolved, but it may act as a regulator for adrenocorticotropic hormone (ACTH) release. Cells of the supraoptic and paraventricular nuclei also contain other biologically active substances, such as enkephalin, cholecystokinin, glucagon, dynorphin, angiotensin, and corticotrophin releasing factor (CRF) (134) (Fig. 17.11).

Neurosecretory cells in the hypothalamus retain their capacity to conduct electrical impulses. Stimulation of the cell bodies in the hypothalamus gives rise to action potentials conducted in axons that trigger the release of the hormones.

Tuberohypophysial Tract

The tuberohypophysial or tuberoinfundibular tract arises from the tuberal region, mainly from the arcuate (or infundibular) nucleus (Figs. 17.1 and 17.21), and can be traced only to the median eminence and the infundibular stem (Figs. 17.10, 17.16, and 17.18) (62, 79, 161, 183). Cells of the arcuate nucleus are situated in the uppermost part of the infundibulum (i.e., the median eminence) and lie directly upon the ependymal lining. Axons of these cells form the tuberoinfundibular tract,

which projects to the internal and external zones of the median eminence, where they collateralize (Figs. 17.10 and 17.21). Some cells in the arcuate nucleus have projections, or collaterals, that extend to other parts of the hypothalamus, the thalamus, and the amygdala. Although these fibers accompany those of the supraoptic hypophysial tract in part of their course, they end on capillary loops near the sinusoids of the hypophysial portal system (Figs. 17.18 and 17.19). These are fine fibers, but secretory granules can be demonstrated in their axons. Fibers of the tuberoinfundibular tract convey "releasing" or "releasing-inhibiting" hormones, which are transported via the hypophysial portal vessels to the anterior lobe of the hypophysis where they modulate the synthesis and release of adenohypophysial hormones (62, 144, 166). Functionally, the tuberoinfundibular tract and the hypophysial portal system establish the neurohumoral link between the hypothalamus and the anterior pituitary.

Dopamine was the first of many substances identified in the arcuate nucleus (Fig. 17.21) (31, 44). Dopaminergic neurons innervate the external zone of the median eminence and dopamine is released into the portal capillaries. Dopamine in the hypophysial portal system inhibits the release of prolactin from the anterior pituitary. A short feedback loop suggests that pituitary prolactin inhibits dopamine release from the median eminence. Increases in dopamine occur in the arcuate nucleus in pregnancy, pseudopregnancy, and lactation, suggesting there is little release of the inhibiting factor in these conditions. Physiologic stimuli of major importance in the release of prolactin from the anterior lobe are estrogens and suckling. Dopamine neurons in the arcuate nucleus represents the group A12 of Dahlström and Fuxe (31). Dopamine neurons are also present in other regions of the hypothalamus, including (a) the periventricular zone of the posterior hypothalamus (group A11), (b) the periventricular zone of the anterior hypothalamus (group A14), and the dorsomedial hypothalamus and zona incerta (group A13) (5, 69, 127, 130, 133, 140, 141) (see Fig. 17.21 and Table 17.1).

In addition to dopamine, the arcuate nucleus contains a number of peptides similar to hormones in the anterior pituitary, such as ACTH, β-lipotrophin (β-LPH), and β-endor-

TABLE 17.1. Location of Principal Catecholamine Cell Groups[a]

MEDULLA	Ventrolateral medulla and lateral reticular nucleus	A1	NE+E
	Dorsomedial medulla: dorsal vagal nucleus and solitary nucleus	A2	NE+E
	Ventrolateral medulla and lateral reticular nucleus	A3	NE
PONS	Lateral pontine	A3	NE
	Periventricular region		
	Ventrolateral pons medial to N. VII, also dorsolateral to superior olive	A5	NE
	Locus coeruleus	A6	NE
	Nucleus subcoeruleus	A7	NE
MIDBRAIN	Retrorubral midbrain tegmental area	A8	DA
	Substantia nigra pars compacta	A9	DA
	Ventral tegmental area	A10	DA
HYPOTHALAMUS	Periventricular zone of posterior hypothalamus	A11	DA(+NE ?)
	Median eminence	A12	DA
	Dorsomedial hypothalamus and zona incerta	A13	DA
	Periventricular zone of anterior hypothalamus	A14	DA
	Olfactory bulb	A15	DA

[a] These major groups of catecholamine-containing cell bodies and the corresponding alphanumeric designation were given by the investigators who first described them in fluorescence histochemical study. The letter A in the second column refers to "adrenergic" cells numbered according to their position in ascending caudorostral levels of the brainstem, diencephalon, and olfactory bulb. In the third column, the subsequent identification of the catecholamine is shown. DA, dopamine; NE, norepinephrine (or noradrenaline); and E, epinephrine (or adrenaline). Cells containing the indolamine serotonin (5-hydroxytryptamine) are not included in this table.

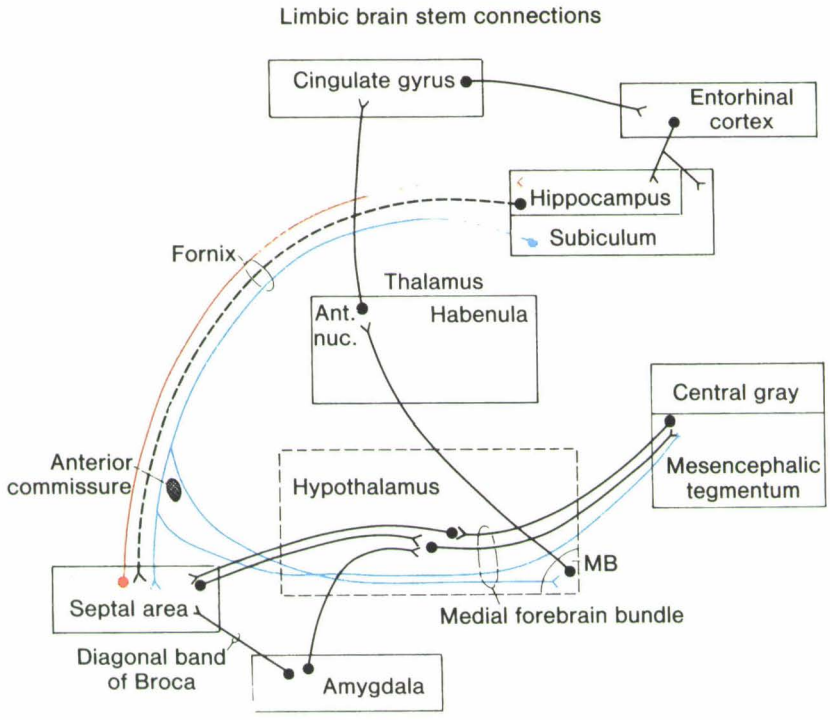


Figure 17.15. Major interconnections of structures comprising the limbic system. Projection fibers arising from the subiculum (*blue*) project via the fornix to the septal area, hypothalamus and mesencephalic tegmentum. Fibers projecting in the fornix from the hippocampus are shown in *black-dashed* lines. Projections from the septal area to the hippocampus are shown in red. *MB* indicates mammillary body.

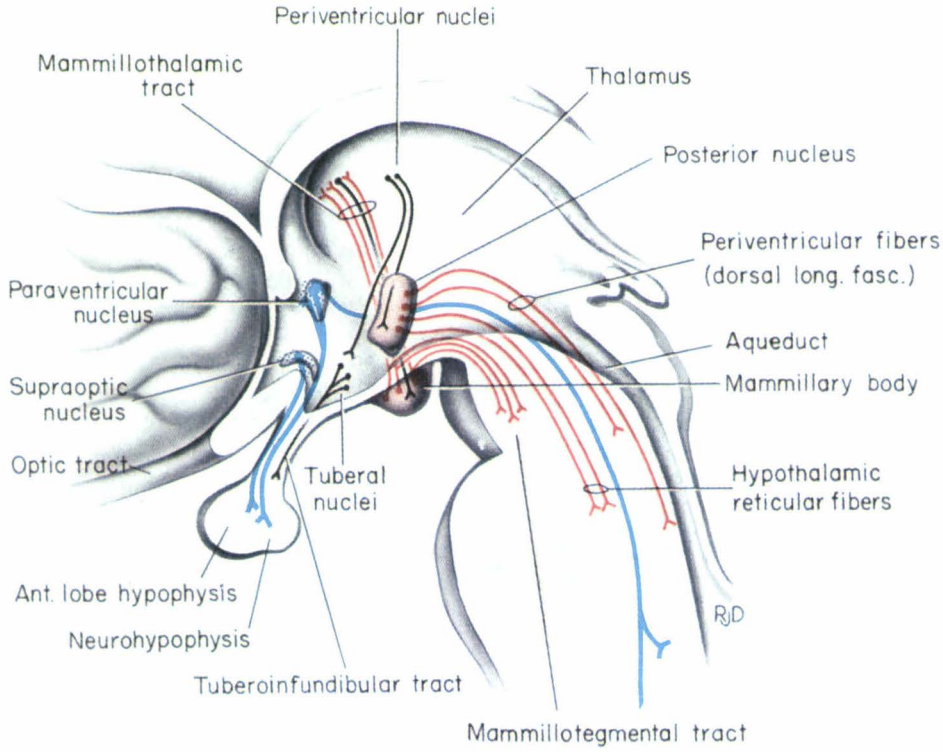


Figure 17.16. Efferent hypothalamic pathways. Nuclei in the supraoptic region are in *blue*. Nuclei of the middle or tuberal region of the hypothalamus are *gray*. Nuclei of the caudal or mammillary region are shades of *red*. The preoptic area (*gray*) lies rostral to the supraoptic region. Terminations of the mammillotegmental tract are shown in Figure 17.14.

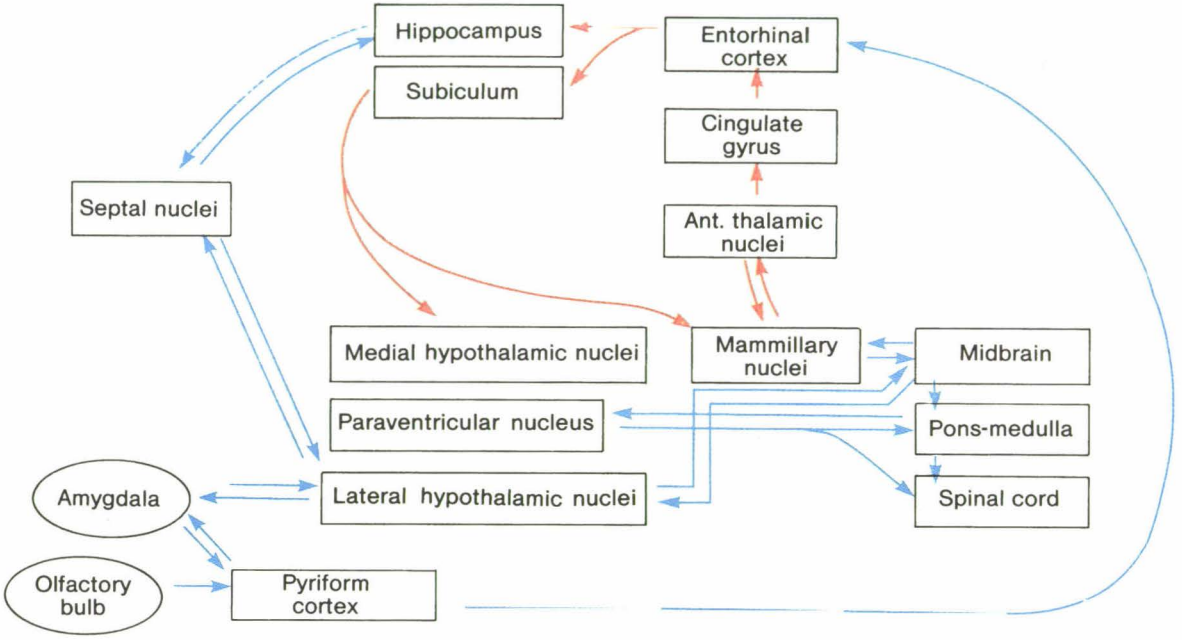


Figure 17.17. Principal fiber connections of the hypothalamus. The principal afferents to the hypothalamus from the forebrain arise from two phylogenetically older cortical areas, the piriform cortex, and the hippocampal formation. Each of these projections is reinforced by a second projection from a related subcortical nuclear mass. This secondary projection arises from the amygdaloid complex in the case of the piriform cortex, and from the septal nuclei in the case of the hippocampal formation. Reciprocal connections exist between the hypothalamus and these subcortical structures. The cingulate gyrus and the piriform cortex can exert influences upon the hypothalamus via the entorhinal area and the hippocampal formation. The mammillary nuclei and the hippocampal formation project to the anterior thalamic nuclei which in turn influence activities in the cingulate gyrus. Projection pathways from the mammillary nuclei to the cortex and from the hippocampus and subiculum to the hypothalamus are in *red*. Other connections are shown in *blue*.

phin (β-END). ACTH and β-LPH in the arcuate nucleus do not appear to coexist in neurons with dopamine. The heterogeneity of the substances found in the arcuate nucleus, and the presence of releasing factors beyond the limits of this nucleus, suggest it is not the sole hypophysiotrophic center in the hypothalamus.

Hypothalamic efferent projections fall into five main categories: (a) fibers that emerge via the medial forebrain bundle, (b) neurosecretory neurons that convey hormones to the neurohypophysis, (c) fibers concerned with releasing hormones into the hypophysial portal system, (d) fibers that arise from the mammillary nuclei that project to the anterior nuclear group of the thalamus and to nuclei in the midbrain tegmentum, and (e) fibers that project to the lower brain stem and spinal cord.

HYPOPHYSIAL PORTAL SYSTEM

The hypophysis is supplied by two sets of arteries, both of which arise from the internal carotid artery. The superior hypophysial artery forms an arterial ring around the upper part of the hypophysial stalk, while the inferior hypophysial artery forms a ring about the posterior lobe and gives branches to the lower infundibulum (Figs. 17.18 and 17.19). Both of these arteries enter the hypophysial stalk and break up into a number of sinusoids (124, 125). Both arteries are innervated by postganglionic sympathetic fibers. Blood from these sinusoids collects into vessels that pass into the anterior lobe of the hypophysis, which receives almost all of its blood supply via these vessels. These vessels are referred to as the hypophysial portal vessels (142). Anatomic and physiologic evi-

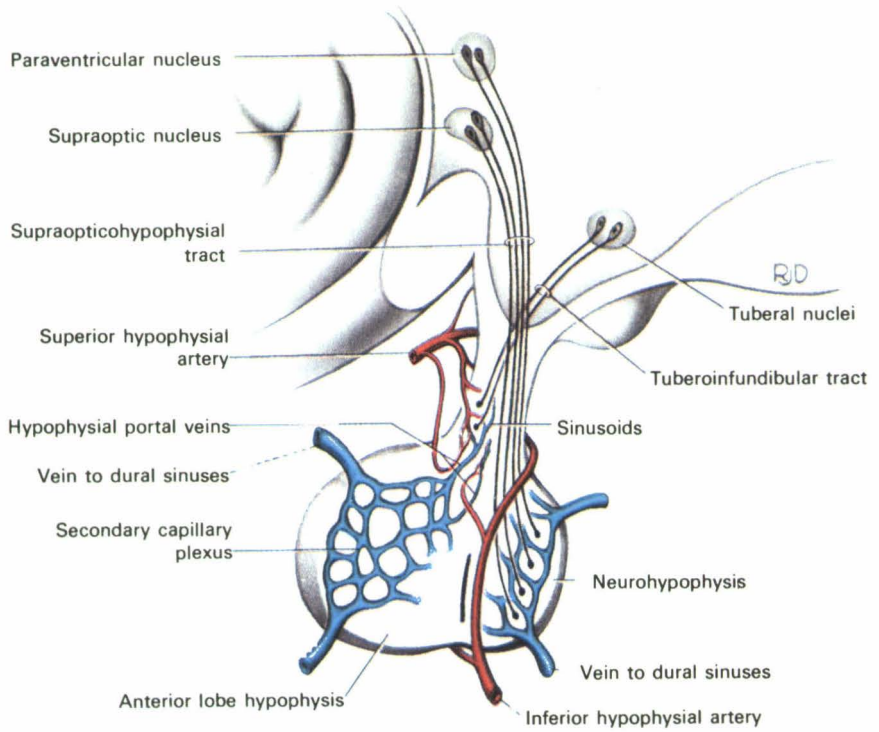


Figure 17.18. Hypophysial portal system, the tuberoinfundibular tract, and the supraopticohypophysial tract. The hypophysis is supplied by the superior and inferior hypophysial arteries. Branches of these arteries form sinusoidal capillaries about the infundibulum. Blood from the sinusoids passes to the anterior lobe of the hypophysis via the portal vessels which give rise to a second capillary plexus in the anterior lobe. The tuberoinfundibular tract ends in the sinusoids of the infundibular stem and transports neurosecretory substances, called releasing/inhibiting hormones or releasing/inhibiting factors, which enter the sinusoids. The supraopticohypophysial tract contains fibers from the supraoptic and paraventricular nuclei which pass to the neurohypophysis. Neurosecretory products of cells in these hypothalamic nuclei are conveyed directly to the neurohypophysis. The supraoptic and paraventricular nuclei are the main source of the hormones vasopressin and oxytocin.

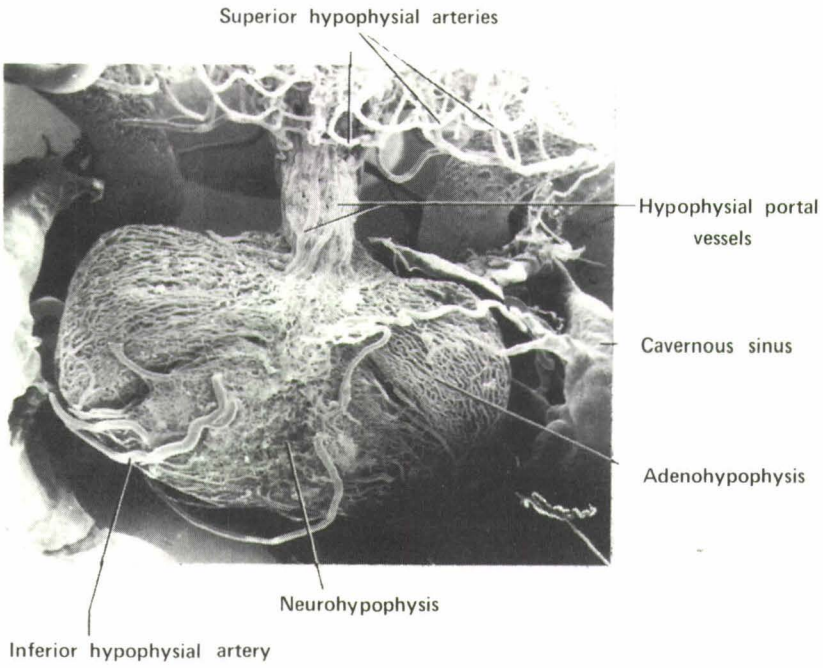


Figure 17.19. Scanning electron micrograph of vascular casts of the pituitary gland, infundibular stalk, and median eminence in a monkey. The gland is viewed from its posterior aspect. The hypophysial arteries and the portal system of vessels shown in this figure should be compared with the schematic diagram showing a sagittal view in Figure 17.18.

dence indicate that hypothalamic influences on the anterior lobe of the hypophysis are conveyed by humoral substances transported via the tuberoinfundibular tract to the sinusoids and the anterior lobe via the portal system. The pattern of blood flow in living animals is not easily deduced from anatomic studies of blood vessels. Observations in living animals leave no doubt that blood in the portal system flows from the median eminence to the anterior lobe (51). Hypophysiotrophic releasing factors in neuronal terminals in the median eminence are carried to the adenohypophysis via this restricted vascular route.

The hypothalamus is intimately concerned with the synthesis and transmission of factors that stimulate and inhibit the secretion of hormones by the anterior pituitary (58, 59). Electrical stimulation of the hypothalamus can increase the discharges of gonadotrophic hormone and ACTH. Stimulation of the tuberal region in the rabbit has produced ovulation. Direct stimulation of the anterior lobe does not elicit these responses, because the humoral part of this pathway is not electrically excitable. The neurosecretory substances acting on cells of the anterior lobe are called *hypophysiotrophic agents* or *releasing hormones* and are named according to the hormone they release.

HYPOPHYSIOTROPHIC AGENTS

These releasing factors have most of the attributes of hormones and most appear to be neuropeptides. Hypophysiotrophic agents include corticotrophin-releasing factor (CRF) (Fig. 17.11**B**), growth hormone-releasing factor (GHRF), gonadotrophin hormone-releasing factor (or luteinizing hormone-releasing hormone (LRH)), thyrotrophin-releasing factor (TRF), prolactin-inhibiting factor (PIF), somatostatin (somatic inhibiting releasing factor (SRIF)), melanocyte-releasing hormone (MSH), as well as β-lipotrophin (β-LPH), and β-endorphin (β-END). Neurons of the arcuate nucleus are immunocytochemically positive for ACTH, β-LPH, and β-END. These peptides are derived from a common precursor glycosylated molecule called pro-opiomelanocortin (POMC) (27). Under stressful conditions CRF is present in the plasma of the portal vessels, but it is suspected that all of these peptides are released. Secretion of growth hormone (GH) is regulated by neural

influences both stimulatory and inhibitory. This is achieved by two hypothalamic releasing factors, growth hormone-releasing factor (GHRF) and growth hormone-inhibiting factor (GHIF), or somatostatin (41). Secretion of these hormones is regulated by monoamines, dopamine (DA), norepinephrine (NE), and serotonin (5-HT), all of which appear to have stimulating effects. Growth hormone measured in the plasma is age-dependent and occurs in surges from early puberty to adolescence. Somatostatin, which also inhibits secretion of thyrotropin, has been recognized in many locations other than the hypothalamus from which it was originally isolated. Clinical studies confirm the powerful inhibitory effects of somatostatin on growth hormone, as well as on insulin and glucagon.

Thyrotropin-releasing factor (TRF) has been isolated and synthesized. The synthetic compound has an action greater than the natural secretion on the thyroid-stimulating hor-

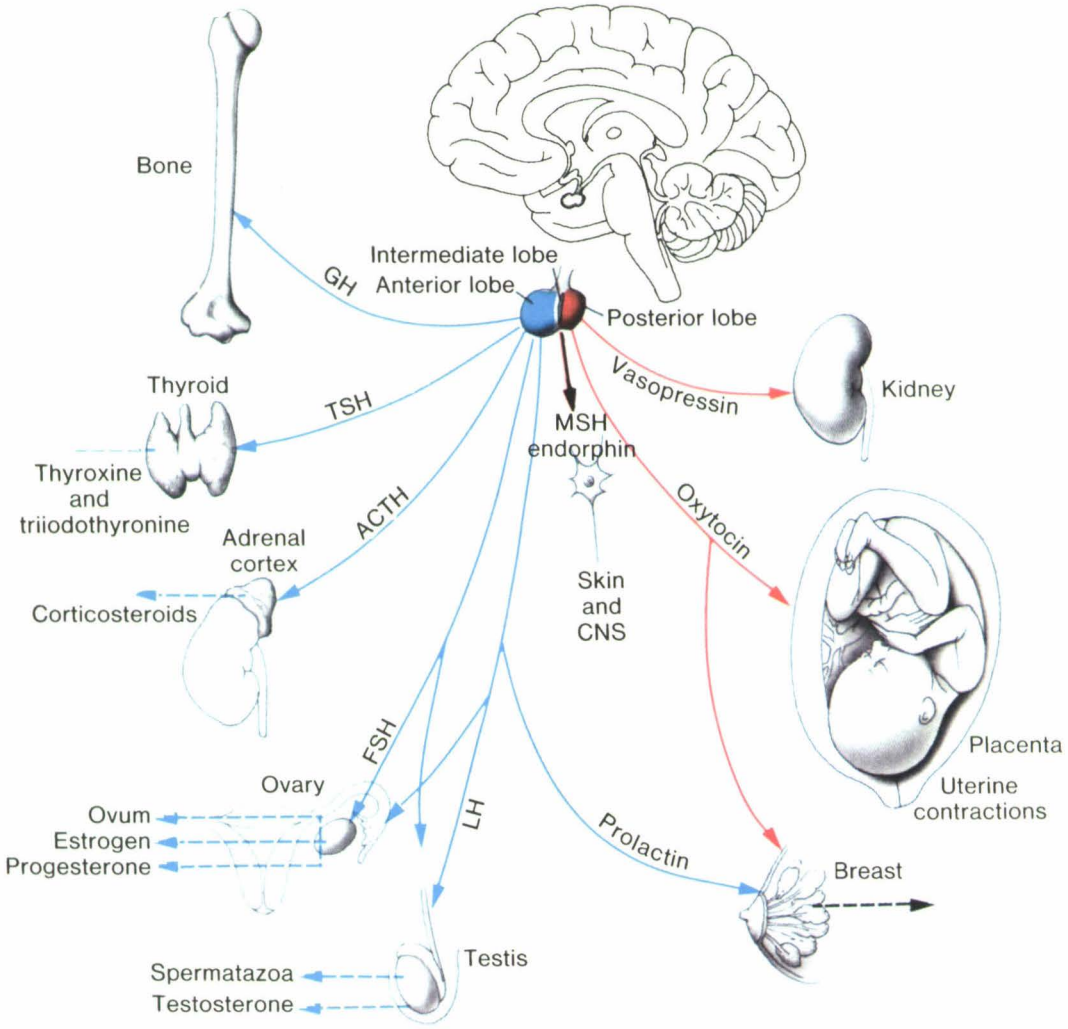


Figure 17.20. Target organs upon which pituitary hormones act. Pituitary (hypophysial) hormones are either secreted or controlled by neurons of the hypothalamus. Hormones secreted by cells in the anterior (*blue*) and intermediate lobes (*black*) of the pituitary are regulated by hypothalamic hypophysiotrophic peptides conveyed by the hypophysial portal system. Hormones of the anterior lobe include (a) growth hormone (*GH*), (b) thyrotropin (*TSH*), (c) corticotrophin (*ACTH*), (d) follicle stimulating hormone (*FSH*), (e) luteinizing hormone (*LH*), and (f) prolactin. Melanocyte stimulating hormone (*MSH*) is derived from cells of the intermediate lobe (*black*) of the pituitary. The posterior (*neural*) lobe (*red*) of the pituitary contains vasopressin and oxytocin secreted by cells of the supraoptic and paraventricular nuclei of the hypothalamus. These hormones act upon the kidney tubules, the smooth muscle of the uterus and glandular tissue of the breast.

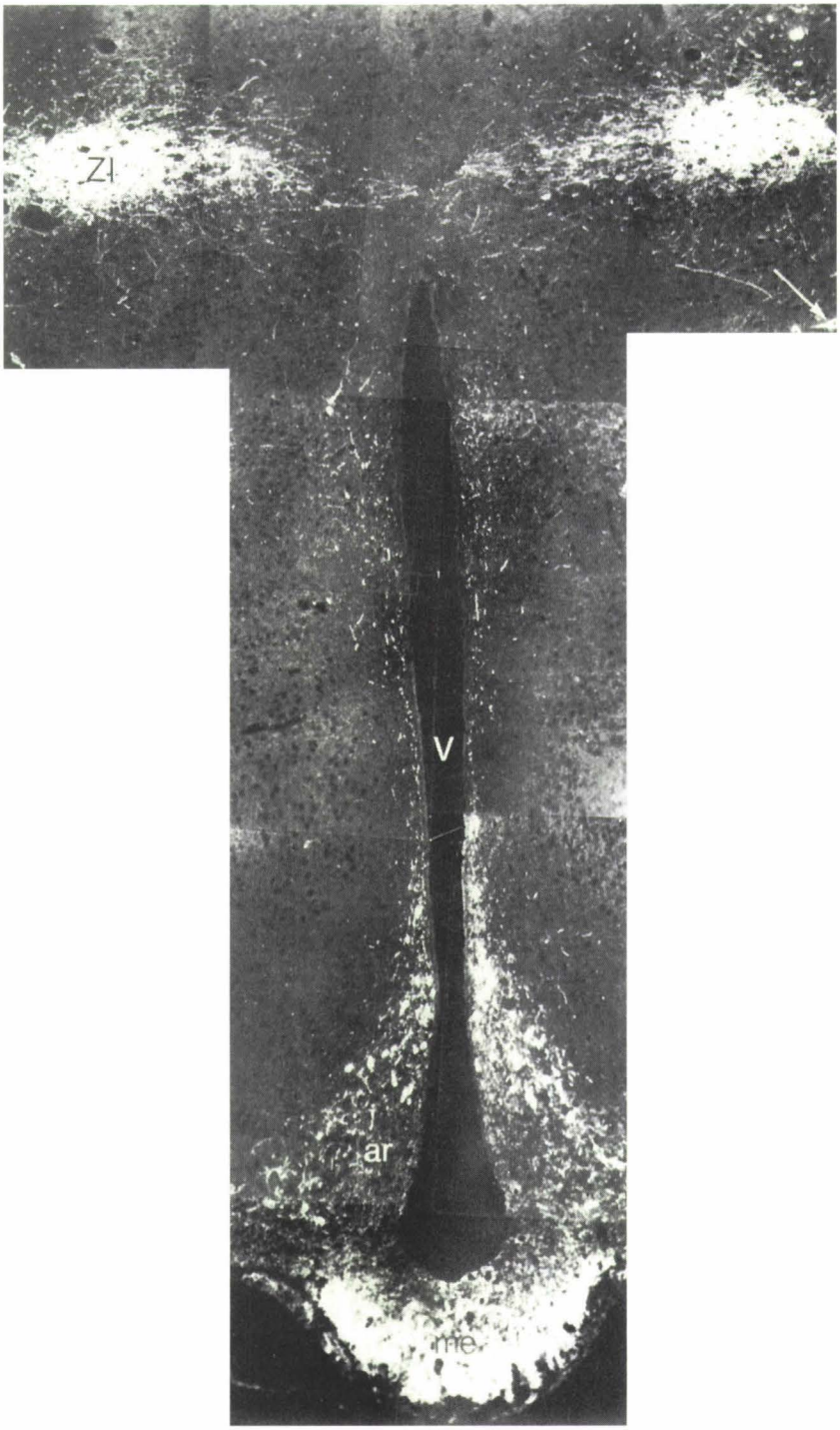


Figure 17.21. Frontal section of the rat hypothalamus showing the localization of dopaminergic neurons revealed by their immunoreactivity for the enzyme tyrosine hydroxylase (*TH*). The section is oblique in the frontal plane with the ventral part more cranial than the dorsal part. Immunofluorescent cell bodies are seen in the arcuate nucleus (*ar*) (A12 cell group) and in the zona incerta (*ZI*) (A13 cell group). Note the dense plexus of TH-positive fibers in the median eminence (*me*), especially the external layer. At this level the TH-positive fibers are present in the whole external layer, whereas at a more caudal level the highest concentrations are found in the lateral parts. Note single cell bodies (*arrow*) ventral to the A13 cell group. *V*, third ventricle (magnification ×170).

mone (TSH) (Fig. 17.20). No true antagonist of TRF has been reported, but thyroxin is known to inhibit TSH. The luteinizing hormone-releasing hormone (LHRH) and the follicle-stimulating-releasing factor (FRH) appear to be parts of the same molecule. FRH causes the release of the follicle-stimulating hormone (FSH) from the anterior pituitary, which initiates cyclical changes in the ovaries and the production of estrogens. The discharge of LHRH liberates the luteinizing hormone, which produces ovulation and the development of the corpus luteum. Ovulation appears to require both FSH and LH. Neuropeptide Y (NPY) acts at the level of the median eminence to stimulate the release of LH. This peptide also activates postsynaptic messenger pathways that complement and reinforce those affected by noradrenaline, which as another major neuroregulator of LHRH secretion is released as a cotransmitter with NPY (74). The medial preoptic area is considered responsible for the cyclical nature of the female reproductive system.

The prolactin-inhibiting factor (PIF) appears to be dopamine, which has been identified in the arcuate nucleus, the portal vessels, and in pituitary receptors (Fig. 17.21). Thyrotropin-releasing factor (TRF) also appears to potentiate the release of prolactin. Prolactin secretion increases as the effective dopamine concentrations at receptor site in the anterior pituitary are reduced.

The naturally occurring opioid peptide β-endorphin is found in rat anterior and intermediate lobes of the pituitary. Cells in the arcuate nucleus of the hypothalamus contain a common 31,000-Dalton precursor (pro-opiomelanocortin or POMC) of ACTH, β-lipotrophin (β-LPH), and β-endorphin (β-END), which is cleaved in the anterior and intermediate lobes. β-LPH has no opioid activity but may be a prohormone for opioid-like peptides. β-endorphin has 5–10 times the analgesic potency of morphine, but its effects are seen mainly after intracerebral administration and β-endorphin-labeled axons are distributed along the ventricular wall to the supraoptic, periventricular, paraventricular, and suprachiasmatic nuclei, and some fibers may reach the thalamus. In severe stress, there is a coordinated release of ACTH, β-LPH, and β-END from the anterior pituitary. In syndromes characterized by hypersecretion of ACTH, the peptides that form part of the precursor molecule also are increased. There is, as yet, no well-defined physiologic role for β-END, but it would appear to be involved in maintaining homeostasis. The enkephalins are not derived from β-lipotrophin or β-endorphin and the cells and fibers labeled for β-endorphin are distinct from those labeled by antisera specific for enkephalins.

The localization and axonal projections of neurons synthesizing the peptides vasopressin and oxytocin were described earlier. The role of these peptides in memory is a subject of active investigation which has already led to the development of new approaches to the cell biology of higher mental function. In a number of behavioral tests, vasopressin facilitates and oxytocin diminishes memory consolidation and retrieval (19, 35, 45). These actions appear to involve different regions of the peptide, for the covalent ring portion of the molecule affects mainly consolidation and the linear part is implicated in memory retrieval (34). Indirect evidence indicates that vasopressin may interact with noradrenergic synapses to influence memory consolidation.

Some of the releasing hormones or factors mentioned earlier, as well as several pituitary pro-opiomelanocortin-derived peptides, have also been identified in extrahypothalamic regions of the brain. Their functional significance as possible neurotransmitters or modulators is not yet established (79).

The naturally occurring opioid peptide β-endorphin is found in the rat intermediate lobe and adenohypophysis and in the brain. Hypophysectomy does not reduce brain β-endorphin, suggesting an endogenous synthesis within the CNS. β-Endorphin-labeled cell bodies are at the base of the tuberal region of the hypothalamus, and labeled axons are distributed along the ventricular wall extending anteriorly to the level of the anterior commissure. The supraoptic, periventricular, paraventricular, and suprachiasmatic nuclei receive abundant β-endorphin-labeled fibers (11, 27). The cells and fibers labeled for β-endorphin are distinct from those labeled by antisera specific for the enkephalins (see Chapter 5).

FUNCTIONAL CONSIDERATIONS

Coordination of the Autonomic Nervous System

The hypothalamus and immediately adjoining regions are related to all kinds of vis-

ceral activities. The most diverse disturbances of autonomic functions, involving water balance, internal secretion, sugar and fat metabolism, and temperature regulation, all can be produced by stimulation or destruction of hypothalamic areas. Even the mechanism for normal sleep may be altered profoundly by such lesions.

The hypothalamus is the chief subcortical center for the regulation of both sympathetic and parasympathetic activities. These dual activities are integrated into coordinated responses that maintain adequate internal conditions in the body. It is improbable that each of the autonomic activities has its own discrete center in the hypothalamus. However, a specific function has been established for the supraoptic and paraventricular nuclei. There is also a fairly definite topographic organization with regard to the two main divisions of the autonomic system. Control of parasympathetic activities is related to the anterior and medial hypothalamic regions (supraoptic and preoptic areas) and the ventricular portion of the tuber cinereum. Stimulation of this region results in increased vagal and sacral autonomic responses, characterized by reduced heart rate, peripheral vasodilation, and increased tonus and motility of the alimentary and vesical walls.

The lateral and posterior hypothalamic regions are concerned with the control of sympathetic responses. Stimulation of this region, especially the posterior portion from which many descending efferents arise, activates the thoracolumbar outflow. This results in increased metabolic and somatic activities characteristic of emotional stress, combat or flight. These responses are expressed by dilatation of the pupil, piloerection, acceleration of the heart rate, elevation of blood pressure, increase in the rate and amplitude of respiration, somatic struggling movements, and inhibition of the gut and bladder. All these physiologic correlates of emotional excitement can be elicited when the hypothalamus is released from cortical control. Removal of the cortex, or interruption of the cortical connections with the hypothalamus, induces many of these visceral symptoms, collectively designated as "sham rage" (4, 43). On the other hand, destruction of the posterior hypothalamus produces emotional lethargy, abnormal sleepiness, and a fall in temperature due to general reduction of visceral and somatic activities.

The intermediolateral cell column of the thoracic cord is the major origin of sympathetic preganglionic neurons. There is a dense innervation of the intermediolateral column by catecholamine containing terminals, but their source in the medulla and pons has not been definitely established (91). Descending serotonin (5-HT) containing axons from the raphe nuclei also reach the intermediolateral cell column. Anatomic studies emphasized the close association between visceral receptive cells in the solitary nucleus of the medulla and the hypothalamus (25, 26, 91, 182) and between the hypothalamus and the spinal cord (161, 182). Oxytocin immunoreactivity is seen in terminals of laminae I and II of the dorsal horn and in the intermediolateral cell column (119). This information about connectivity and putative transmitters in visceroceptive and visceromotor regions of the central nervous system is leading to new experimental approaches in the physiologic study of cardiovascular regulatory mechanisms.

REGULATION OF BODY TEMPERATURE

The coordination of sympathetic and parasympathetic responses is strikingly shown in the regulation of body temperature. This complex function, involving widespread physical and chemical processes, is mediated by two hypothalamic mechanisms, one concerned with the dissipation of heat and the other with its production and conservation. Experimental evidence indicates that the anterior hypothalamus is sensitive to increases in blood temperature and sets in motion the mechanisms for dissipating excess heat. In humans, this consists mainly of profuse sweating and vasodilatation of the cutaneous blood vessels. These actions permit the rapid elimination of heat by convection and radiation from the surface of the engorged blood vessels, and by the evaporation of sweat. In animals, heat loss is effected mainly by the rapid warming of successive streams of inspired air (panting). Lesions involving the anterior part of the hypothalamus abolish the neural mechanisms concerned with the dissipation of heat and result in hyperthermia. Thus, hyperthermia (hyperpyrexia) may result from tumors in, or near, the anterior hypothalamus.

The posterior hypothalamus, on the other hand, is sensitive to conditions of decreasing body temperature and controls mechanisms for the conservation and increased produc-

tion of heat. The cutaneous blood vessels are constricted and sweat secretion ceases, so that heat loss is reduced. Simultaneously there is augmentation of visceral activities, and the somatic muscles exhibit shivering. All these activities tremendously increase the process of oxidation, with a consequent production and conservation of heat. Bilateral lesions in posterior regions of the hypothalamus usually produce a condition in which body temperature varies with the environment (poikilothermia), since such lesions effectively destroy descending pathways concerned with both heat conservation and dissipation.

These two intrinsically antagonistic mechanisms do not function independently but are continually interrelated and balanced against each other to meet changing needs of the body. The coordinated responses always are directed to the maintenance of a constant optimum temperature.

MAINTENANCE OF WATER BALANCE

The supraoptic and paraventricular nuclei are specifically concerned with the maintenance of body water balance (Figs. 17.2–17.4, 17.16, and 17.18). Destruction of these nuclei, or their hypophysial connections, invariably is followed by the condition known as *diabetes insipidus*, in which there is increased secretion of urine (polyuria) without an increase in the sugar content. The antidiuretic hormone, vasopressin, is secreted directly by the cells of the supraoptic and paraventricular nuclei. Vasopressin is transported by the unmyelinated axons of the supraopticohypophysial tract and is stored in terminals in the posterior lobe of the pituitary (88). The production of antidiuretic hormone varies in accordance with changes in the osmotic pressure of the blood. An increase in the osmotic pressure of the blood that supplies the magnocellular hypothalamic nuclei increases the activity of these neurons and the release of antidiuretic hormone. In states of dehydration, there is a depletion of the hormone in the posterior lobe and increased secretory activity in the supraoptic nuclei. After reestablishment of water balance, there is a reaccumulation of the hormone in the posterior lobe. The antidiuretic hormone is considered to act specifically on the kidneys (138), although the exact mechanism by which vasopressin brings about the reabsorption of renal water is not clear. Reabsorption of sodium chloride and bicarbonate ions is followed by passive reabsorption of water. This hormone also appears to alter the osmotic permeability of water in the distal and collecting tubules of the kidney.

There is evidence that a region of the hypothalamus is responsible for the regulation of water intake. Electrical stimulation of anterior regions on the hypothalamus in goats creates fantastic "thirst" and results in consumption of large volumes of water (3). This is probably part of a more extensive system which regulates the consumption of both food and water. An increase in the osmotic pressure of body fluids may be an effective stimulus for water intake. Osmoreceptors probably are situated close to the cells of the supraoptic nucleus which have an abundant blood supply (192). Localized lesions in the lateral hypothalamus at the level of the ventromedial nucleus in rats cause a reduction in water intake without affecting food intake. Larger lesions in the lateral hypothalamus may cause adipsia as well as aphagia. The lateral hypothalamic area can excite cells of the supraoptic nucleus, which in turn inhibit the lateral hypothalamic area in a negative feedback circuit (38).

The paraventricular and supraoptic nuclei also produce oxytocin, which causes contractions of uterine muscle and myoepithelial cells surrounding the alveoli of the mammary gland (Fig. 17.20) (64, 120, 161). Surprisingly, the role of oxytocin in the male is still unknown (27).

CONTROL OF ANTERIOR PITUITARY

The important role of the hypothalamus in maintaining and regulating the activity of the anterior lobe of the hypophysis has been described in relation to the hypophysial portal system (59) (Figs. 17.18 and 17.20). This is a humoral control mechanism in which releasing hormones are transmitted via the portal system (128). There are no hypothalamic efferent fibers that reach the anterior lobe of the pituitary. The anterior pituitary stands in marked contrast to other endocrine organs, such as the ovary, testis, thyroid, and adrenal cortex, which may be transplanted to distant sites and still retain their endocrine functions. The anterior lobe of the pituitary cannot be transplanted to distant locations and retain its function, because it is dependent upon its

close relationships with the hypothalamus. The essential hypothalamic features are the tuberoinfundibular tract and the hypophysial portal system.

The hypothalamus is considered the site of elaboration of releasing or releasing-inhibiting hormones (peptides) related to gonadotrophic, adrenocorticotrophic (ACTH), thyrotrophic (TSH), and growth hormones (Figs. 17.18 and 17.20). Attempts to determine the loci within the hypothalamus concerned with particular releasing factors suggest that the neural area related to TSH appears to lie on either side of the midline between the paraventricular nucleus and the median eminence. Electrical stimulation of the anterior median eminence appears to be the most effective site for increasing thyroid activity (60). Similarly, electrical stimulation of the hypothalamus in the rabbit can cause the discharge of gonadotrophic hormone and ACTH (53, 57, 97). While bilateral lesions in almost any region near the base of the hypothalamus reduce ACTH release, the median eminence-tuberal region has the most important controlling influence.

Hypothalamic neurons that produce releasing and releasing-inhibiting factors are regulated by various hypothalamic afferents, as well as by hormones of the target organs or pituitary hormones. For example, when the concentration of triodothyroxine in the blood is high, hypothalamic neurons that produce thyrotropin-releasing factor (TRF) are inhibited. Conversely, if the levels of thyroid hormones are low, the hypothalamic neurons produce more TRF. This stimulates increased output of thyroid-stimulating hormone (TSH) from the pituitary, and the thyroid gland, in turn, is induced to synthesize and release more of its hormone. This hormonal negative feedback plays a crucial role in the control of hypothalamic neurons that produce releasing or releasing-inhibiting factors.

CONTROL OF REPRODUCTIVE FUNCTIONS

The hypothalamus plays an important role in the initiation and coordination of reproductive functions, and these functions are different in the two sexes. The tuberal region of the hypothalamus appears essential for the maintenance of basal levels of gonadotrophic hormone, but the integrity of the preoptic area is necessary for the cyclic surge of gonadotropin which precedes ovulation (Fig. 17.20) (40, 152, 164). Electrical stimulation of the preoptic area, or the corticomedial nuclear group of the amygdaloid complex, produces ovulation in rabbits and cats. The effects of preoptic stimulation are abolished by lesions separating this area from the tuberal region of the hypothalamus, while the effects of amygdaloid stimulation are blocked by a section of the stria terminalis. These observations suggest a functional linkage between the amygdala and the medial preoptic area via the stria terminalis, and fiber systems from the medial preoptic area to the tuberal region of the hypothalamus. However, the amygdaloid input to the preoptic area is not essential for ovulation, for bilateral destruction of the stria terminalis does not prevent ovulation (15).

Tumors and other pathologic processes involving the hypothalamus frequently modify sexual development. Such lesions may be associated with precocious puberty or hypogonadism associated with underdevelopment of secondary sex characteristics. Although hypergonadism has been attributed to tumors of the pineal, most tumors of the brain associated with precocious puberty actually involve, or impinge on, the hypothalamus. These lesions frequently destroy the posterior hypothalamus and leave the anterior hypothalamus intact. The intact hypothalamic regions functioning in the absence of inhibitory influences from posterior regions leads to increased pituitary function.

The preoptic region plays an important role in regulating the release of gonadotrophic hormones from the anterior lobe of the hypophysis (Fig. 17.20). In the female, pituitary gonadotropins are released in a cyclic manner, the duration of the cycle corresponding to the menstrual period. In the male, the gonadotropins are released topically without regularly occurring fluctuations. Therefore, it is not surprising that there are differences in the functional organization of the preoptic region in the male and female. A morphologic expression of this difference has been observed in the preoptic region of the rat, where a nucleus of densely stained cells is larger in the male. This nucleus has been termed the "sexually dimorphic nucleus of the preoptic area" (Fig. 17.22) (49, 50). The full ontogenetic development of this nucleus, as well as the male pattern of tonic gonadotrophic release, depends on the presence in the circulation of

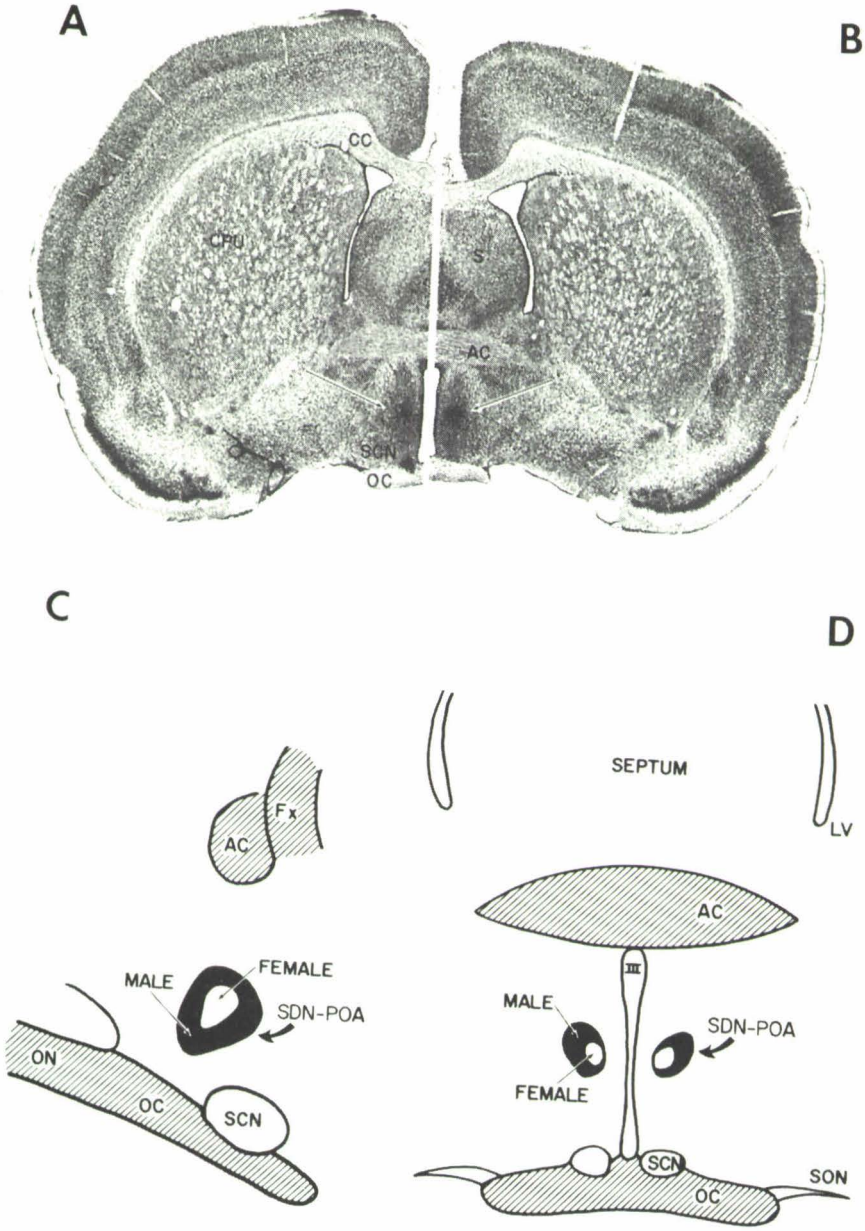


Figure 17.22. Frontal sections through the brain of adult female (**A**) and male (**B**) rat sacrificed 2 weeks after gonadectomy (thionine stain). The *arrows* indicate that portion of the medial preoptic nucleus which exhibits a marked sexual dimorphism, both at the same magnification. The absence of the suprachiasmatic nucleus (*SCN*) in **B** is an artifact of the plane of tissue sectioning. The localization and magnitude of the sexually dimorphic nucleus of the preoptic area (*SDN-POA*) is shown in the parasagittal (**C**) and frontal (**D**) planes. *AC*, anterior commissure; *CC*, corpus callosum; *CPU*, caudate-putamen; *FX*, fornix; *LV*, lateral ventricle; *OC*, optic chiasm; *S*, septum; *SCN*, suprachiasmatic nucleus; *SON*, supraoptic nucleus; *III*, third ventricle.

testosterone during the first week of life (92). If the testes are removed from the newborn animal, the genetic male will fail to develop the sexually dimorphic nucleus of the preoptic region. Conversely, a newborn female given exogenous testosterone will, as an adult, show the male pattern of gonadotropin release. As mentioned earlier, a probable homologue of the sexually dimorphic nucleus was identified in the human preoptic area (68, 177). It is a nucleus that contains approximately twice as many neurons in men as in

women. In the male, the equivalent of luteinizing hormone promotes the growth and development of interstitial testicular cells (Leydig cells), which convert steroid precursors to testosterone. The role of gonadotrophins in spermatogenesis is complex and unclear, but a high level of testosterone appears essential (Fig. 17.20).

Morphologic features in hypothalamic nuclei other than the sexually dimorphic nucleus can also be affected by fetal or neonatal exposure to androgens. These morphologic features include changes in the size of neuronal nuclei and nucleoli, types of synaptic vesicles and terminals, synaptic organization, and dendritic branching patterns (92). The mechanisms whereby steroid hormones affect the brain to determine sexual behavior and patterns of gonadotropin release are complex. For example, implantation of small quantities of estradiol into the hypothalamic ventromedial nucleus (HVM) of the rat activates feminine sexual behavior. Estradiol has been shown to alter a number of cellular properties in the HVM, including induction of progestin receptors, decrease of the inhibitory neurotransmitter synthetic enzyme glutamic acid decarboxylase (GAD), increased muscarinic cholinergic receptor binding, and a decrease in the type A monoamine oxidase activity. This example illustrates estrogen regulation of a neurotransmitter, synthetic and degradative enzymes, and neurotransmitter receptors (94). Neurons endowed with specific steroid hormone receptors are widely distributed in the hypothalamus (135, 175). These receptors are particularly abundant in neuronal nuclei, where hormones can exert profound genomic effects. The presence of immunoreactivity for estrogen receptors on dendrites and axon terminals (9) suggests the possibility that steroid hormones may influence other aspects of neuronal functioning by acting at nongenomic sites.

CONTROL OF GROWTH

Growth hormone-releasing factor acts on acidophilic cells of the anterior pituitary that produce the growth hormone (39, 109). Growth hormone functions synergistically with thyroxin, and blood levels fluctuate widely. A large part of the daily output of growth hormone is secreted in bursts following the onset of sleep. Strenuous exercise, hypoglycemia, and testosterone also appear to stimulate growth hormone secretion. Somatostatin, which inhibits the release of growth hormone, is present in the hypothalamus and in a variety of other tissues. Chronic hypersecretion of growth hormone leads to an overgrowth of bones and soft tissues, which produce a highly characteristic syndrome (acromegaly).

Tumors of the adenohypophysis may produce symptoms due to their increasing size or because they result in alterations of pituitary functions (185). Expanding tumors cause a ballooning of the sella turcica, may compress fibers in the optic chiasm or optic tract, and frequently produce headaches due to traction on the meninges. The most typical visual field defect is a bitemporal hemianopsia due to involvement of the decussating fibers in the optic chiasm, but visual field defects take many forms dependent on the growth pattern of the tumor. Endocrinopathy may take the form of hypersecretion or hyposecretion depending on the type of tumor. The pituitary syndrome may be associated with excess prolactin (amenorrhea-galactorrhea), growth hormones (acromegaly), or adrenocorticotrophic hormone (Cushing's syndrome). Patients with prolactin-secreting tumors have been successfully treated with dopamine agonists, particularly bromocriptine. Dopamine synthesized in the arcuate and periventricular nuclei of the hypothalamus and transported via the portal system inhibits prolactin release.

CONTROL OF FOOD INTAKE

It has been known for a long-time that certain lesions near the base of the brain are associated with obesity. Localized bilateral lesions in the hypothalamus involving primarily, or exclusively, the ventromedial nucleus in the tuberal region produce *hyperphagia* (67, 73, 173, 174). Such animals eat voraciously, consuming two or three times the usual amount of food. Obesity appears to be the direct result of increased food intake. Bilateral lesions destroying portions of the lateral hypothalamic nucleus impair, or abolish, the desire to feed in hyperphagic and normal animals (1, 2, 174). These data suggest that the ventromedial nucleus of the hypothalamus is concerned with *satiety*, while the lateral hypothalamic nucleus may be regarded as a feeding center. This concept, though useful, has proved too simplistic to incorporate all of the information available about the appetitive and consummatory phases of ingestive behavior. The study of α-

and β-adrenergic receptor mechanisms in feeding (85, 86) and electrophysiologic studies in alert, behaving animals (122), have extended the concepts based exclusively upon lesions or knife cuts, and suggest that neural models that can explain feeding behavior may be similar in principle to those used to explain the regulation of blood pressure and respiration.

CONTROL OF EMOTIONAL BEHAVIOR

The hypothalamus is regarded as one of the principal centers concerned with emotional expression. It is acknowledged that the physiologic expression of emotion is dependent on both sympathetic and parasympathetic components of the autonomic nervous system. The hypothalamus, intimately relating both of these, probably is involved directly or indirectly in most emotional reactions. Stimulation of the hypothalamus in unanesthetized cats with implanted electrodes provokes responses resembling rage and fear, which can be increased by graded stimuli of different intensities (48, 66, 98). These reactions, referred to as "pseudoaffective," are "stimulus-bound" in that they are present only during the period of stimulation. Different types of responses are elicited from different parts of the hypothalamus: flight responses are most readily evoked from lateral regions of the anterior hypothalamus, while aggressive responses characterized by hissing, snarling, baring of teeth, and biting are seen with stimulation of the region of the ventromedial nucleus. Because the emotional reactions provoked by electrical stimulation of the hypothalamus are directed, it seems likely that the cerebral cortex and thalamus play important roles in these responses. In these reactions, the hypothalamus cannot be regarded as a simple efferent mechanism influencing only lower levels of the neuraxis.

Observations that selective stimulation and lesions of the ventromedial nucleus of the hypothalamus both produce aggressive behavior (48, 112) raise questions concerning the mechanism. Savage behavior after bilateral lesions of the ventromedial nucleus (48, 193) cannot be assumed to result from release of inhibitory influences. Because animals with such lesions never show spontaneous outburst of aggressive behavior and this hyperirritable state develops slowly, it has been postulated that destruction of these nuclei leads to a state of supersensitivity (23). Further secondary lesions involving the periaqueductal gray and the reticular formation may have a "taming" effect on this savage behavior (72). Hypothalamic-induced rage reactions may be blocked by midbrain lesions, indicating that structures at this level play a role in the expression of savage and aggressive behavior.

It is generally accepted that morphophysiologic substrates of abnormal and aggressive behavior involve, in some differential and selective fashion, predominantly structures of the forebrain. This part of the central nervous system contains the neural structures concerned with goal-directed behavior, and the motivational and emotional concomitants that make such behavior possible. Impulses generated in sensory systems, the cerebral cortex, and still undetermined neural structures may trigger mechanisms that excite visceral and somatic systems whose activities in concert provide the physiologic expression of aggressive behavior.

HYPOTHALAMUS AND SLEEP

Although hypothalamic lesions produce somnolence resembling normal sleep (21, 153), the fact that sleep and sleep-like states can be produced by electrical and chemical stimulation in a variety of structures within the brainstem makes it clear that there is no single "sleep center." The intralaminar and reticular thalamic nuclei also seem to be concerned with the modulation of vigilance states. Sleep induced by thalamic stimulation lasts for long periods of time and is comparable to that occurring naturally. The pontine reticular formation and the raphe nuclei constitute a lower center concerned with the triggering of paradoxical sleep. Nevertheless, the idea that the hypothalamus may be involved in some aspects of the sleep-waking cycle has received support from recent studies by Michel Jouvet and his colleagues in Lyon, France. Following pharmacologic and electrophysiologic experiments in freely moving cats, these investigators suggested that neurons in the posterior hypothalamus, including the tuberomammillary nucleus, play an important role in the arousal mechanism. Principally involved are neurons that contain histamine, project widely upon the cerebral cortex, and receive prominent afferents from the forebrain and brainstem tegmentum (89, 90, 157).

References

1. Anand BK, Brobeck JR. Hypothalamic control of food intake in rats and cats. Yale J Biol Med 1951; 24:123–140.
2. Anand BK, Brobeck JR. Localization of a "feeding center" in the hypothalamus of the rat. Proc Soc Exp Biol Med 1951;77:323–324.
3. Andersson B. Polydipsia, antidiuresis and milk ejection caused by hypothalamic stimulation. In: Heller H, ed. Neurohypophysis. London: Butterworths, 1957:131–140.
4. Bard P. Central nervous mechanisms for emotional behavior patterns in animals. Proc Assoc Res Nerv Ment Dis 1939;19:190–218.
5. Björklund A, Lindvall O. Dopamine-containing systems in the CNS. In: Björklund A, Hökfelt T, eds. Handbook of chemical neuroanatomy. Vol. 2. Part 1: Classical transmitters in the CNS. Ch. 3. Amsterdam: Elsevier, 1984:55–122.
6. Björklund A, Skagerberg G. Evidence for a major spinal cord projection from the diencephalic A-11 dopamine cell group in the rat using transmitter-specific fluorescent retrograde tracing. Brain Res 1979;177:170–175.
7. Bleier R, Cohn P, Siggelkow IR. A cytoarchitectonic atlas of the hypothalamus and hypothalamic third ventricle of the rat. In: Morgane P, Panksepp J, eds. Handbook of the hypothalamus. Vol. I: Anatomy of the hypothalamus. New York: Marcel Dekker, 1979:137–220.
8. Bernard C. Leçons sur les phénomènes de la vie commune aux animaux et aux végétaux. Paris: Baillière, 1878, 1879.
9. Blaustein JD, Lehman MN, Turcotte JC, Greene G. Estrogen receptors on dendrites and axon terminals in the guinea pig hypothalamus. Endocrinology 1992; 131:281–290.
10. Blessing WW, Chalmers JP. Direct projection of catecholamine (presumably dopamine) containing neurons from hypothalamus to spinal core. Neurosci Lett 1979; 11:35–40.
11. Bloom FE, Battenberg E, Rossier J, Ling N, Guillemin R. Neurons containing β-endorphin in rat brain exist separately from those containing enkephalin: immunocytochemical studies. Proc Natl Acad Sci USA 1978;75:1591–1595.
12. Bodian D. Cytological aspects of neurosecretion in opossum neurohypophysis. Bull Johns Hopkins Hosp 1963;113:57–93.
13. Bodian D. Herring bodies and neuro-apocrine secretion in the monkey: an electron microscopic study of the fate of the neurosecretory product. Bull Johns Hopkins Hosp 1966;118:282–326.
14. Brockhaus H. Beitrage zur normalen Anatomie des Hypothalamus und der Zona incerta beim Menschen. J Psychol Neurol 1942; 51:96–196.
15. Brown-Grant K, Raisman G. Reproductive function in the rat following selective destruction of afferent fibres to the hypothalamus from the limbic system. Brain Res 1972;46:23–42.
16. Brownstein MJ, Mezey E. Multiple chemical messengers in hypothalamic magnocellular neurons. Prog Brain Res 1986;68:161–168.
17. Brownstein MJ, Russell JT, Gainer H. Synthesis, transport and release of posterior pituitary hormones. Science 1980;207:373–378.
18. Bucher VM, Bürgi SM. Some observations on the fiber connections of the di- and mesencephalon in the cat. III. The supraoptic decussations. J Comp Neurol 1953;98: 355–379.
19. Buijs RM. Vasopressin and oxytocin localization and putative functions in the brain. Acta Neurochir (Wien) 1990;47:86–89.
20. Cachetto DF, Saper CB. Neurochemical organization of the hypothalamic projection to the spinal cord in the rat. J Comp Neurol 1988;272:579–604.
21. Cairns H. Disturbances of consciousness with lesions of the brain-stem and diencephalon. Brain 1952;75:109–146.
22. Cannon WB, Britton SW. Studies on the conditions of activity in endocrine glands. XV. Pseudoaffective medulliadrenal secretion. Am J Physiol 1925;72:283–294.
23. Cannon WB, Rosenblueth A. The supersensitivity of denervated structures. New York: Macmillan, 1949.
24. Card JP, Moore RY. Organization of the lateral geniculate-hypothalamic connections in the rat. J Comp Neurol 1989;284:135–147.
25. Ciriello J, Calaresu FR. Autoradiographic study of ascending projections from cardiovascular sites in the nucleus tractus solitarii in the cat. Brain Res 1980;180:448–453.
26. Ciriello J, Calaresu FR. Monosynaptic pathway from cardiovascular neurons in the nucleus tractus solitarii to the paraventricular nucleus in the cat. Brain Res 1980; 193:529–533.
27. Cooper JR, Bloom RE, Roth RH. The biochemical basis of neuropharmacology. 6th ed. New York: Oxford University Press, 1991.
28. Cowan WM, Raisman G, Powell TPS. The connections of the amygdala. J Neurol Neurosurg Psychiatry 1965;28:137–151.
29. Cowan WM, Guillery RW, Powell TPS. The origin of the mammillary peduncle and the hypothalamic connexions from the midbrain. J Anat 1964;98:345–363.
30. Cruce JAF. An autoradiographic study of the projection of the descending connections of the mammillothalamic tract in the rat. Brain Res 1975;85:211–219.
31. Dahlström A, Fuxe K. Evidence for the existence of monoamine-containing neurons in the central nervous system. I. Demonstration of monoamines in the cell bodies of brain stem neurons. Acta Physiol Scand 1964;62(Suppl 232):1–55.
32. Daitz HM, Powell TPS. Studies of the connections of the fornix system. J Neurol Neurosurg Psychiatry 1954;17:75–82.
33. De Olmos JS. The amygdaloid projection field in the rat as studied with cupric-silver method. In: Eleftheriou BE, ed. The neurobiology of the amygdala. New York: Plenum Press, 1972:145–204.
34. De Wied D. Behavioral actions of neurohypophyseal peptides. Proc R Soc Lond (Biol) 1980;210: 183–195.
35. De Wied D. The importance of vasopressin in memory. Trends Neurosci 1984;7:62–63.
36. Dreifuss JJ, Murphy JT, Gloor P. Contrasting effect of two identified amygdaloid efferent pathways on single hypothalamic neurons. J Neurophysiol 1968;31:237–248.
37. Du Vigneaud V. Hormones of the posterior pituitary gland: oxytocin and vasopressin. Harvey Lect 1956;50:1–26.
38. Emmers R. Interaction of neural systems which control body water. Brain Res 1973;49:323–347.
39. Epelbaum J. Intrahypothalamic neurohormonal interactions in the control of growth hormone secretion. Ciba Found Symp 1992;168: 54–64.
40. Everett JW. Central neural control of reproductive functions of the adenohypophysis. Physiol Rev 1964;44:373–431.
41. Frohman LA, Jansson JO. Growth hormone-releasing hormone. Endocr Rev 1986;7:223–253.
42. Fry WJ, Krumins R, Fry FJ, Thomas G, Borbely S, Ades H. Origins and distribution of some efferent pathways from the mammillary nuclei of the cat. J Comp Neurol 1963;120:195–258.
43. Fulton JF, Ingraham FD. Emotional disturbances following experimental lesions of the base of the brain (pre-chiasmal). J Physiol (Lond) 1929;67:27–28.
44. Fuxe K, Hökfelt T. Central monoaminergic systems and hypothalamic function. In: Martini L, Motta M, Fraschini F, eds. The hypothalamus. New York: Academic Press, 1970:123–138.
45. Gash DM, Thomas GJ. What is the importance of vasopressin in memory processes? Trends Neurosci 1983;6:197–198.
46. Giovannelli L, Shiromani PJ, Jirikowski GF, Bloom FE. Expression of *c-fos* protein by immunohistochemically identified oxytocin neurons in the rat hypothalamus upon osmotic stimulation. Brain Res 1992;588:41–48.
47. Gloor P. Electrophysiological studies on the connections of the amyg-

daloid nucleus in the cat. Electroencephalogr Clin Neurophysiol 1955;7:243–264.
48. Glusman M. The hypothalamic "savage" syndrome. Proc Assoc Res Nerv Ment Dis 1974;52:52–92.
49. Gorski RA, Gordon JH, Shryne JE, Southam AM. Evidence for a morphological sex difference within the medial preoptic area of the rat brain. Brain Res 1978;148:333–346.
50. Gorski RA, Harlan RE, Jacobson DC, Shryne JE, Southam AM. Evidence for the existence of a sexually dimorphic nucleus in the preoptic area of the rat. J Comp Neurol 1980;193:529–539.
51. Green JD, Harris GW. Observation of the hypophysioportal vessels of the living rat. J Physiol (Lond) 1949;108:359–361.
52. Gross PM, ed.. Circumventricular organs and body fluids. Boca Raton, FL: CRC Press, 1987.
53. De Groot J, Harris GW. Hypothalamic control of the anterior pituitary gland and blood lymphocytes. J Physiol (Lond) 1950;111: 335–346.
54. Guillery RW. Degeneration in the posterior commissural fornix and the mammillary peduncle of the rat. J Anat 1956;90:350–370.
55. Guillery RW. Degeneration in the hypothalamic connections of the albino rat. J Anat 1957;91:91–115.
56. Hall EA. Efferent connections of the basal and lateral nuclei of the amygdala in the cat. Am J Anat 1963;113:139–151.
57. Harris GW. Electrical stimulation of the hypothalamus and the mechanism of neural control of the adenohypophysis. J Physiol (Lond) 1948;107:418–427.
58. Harris GW. Neural control of the pituitary gland. London: Edward Arnold and Company, 1955.
59. Harris GW, George R. Neurohumoral control of the adenohypophysis and regulation of the secretion of TSH, ACTH and growth hormone. In: Haymaker W, Anderson E, Nauta WJH, eds. The hypothalamus. Ch. 10. Springfield, IL: Charles C. Thomas, 1969:326–388.
60. Harris GW, Woods JW. The effect of electrical stimulation of the hypothalamus or pituitary gland on thyroid activity. J Physiol (Lond) 1958;143:246–274.
61. Hartwig HG. Electron microscopic evidence for a retinohypothalamic projection to the suprachiasmatic nucleus of *Passer domesticus*. Cell Tissue Res 1974;153:88–99.
62. Haymaker W. Hypothalamo-pituitary neural pathways and the circulatory system of the pituitary. In: Haymaker W, Anderson E, Nauta WJH, eds. The hypothalamus. Ch. 6. Springfield, IL: Charles C. Thomas, 1969:219–250.
63. Heimer L, Nauta WJH. The hypothalamic distribution of the stria terminalis in the rat. Brain Res 1969;13:284–297.
64. Heller H. The hormone content of the vertebrate hypothalamo-neurohypophysial system. Br M Bull 1966;22:227–231.
65. Hendrickson AE, Wagoner N, Cowan WM. An autoradiographic and electron microscopic study of retino-hypothalamic connections. Z Zellforsch Mikrosk Anat 1972; 135:1–26.
66. Hess WR. Diencephalon, autonomic and extrapyramidal functions. New York: Grune & Stratton, 1954.
67. Hetherington AW, Ranson SW. Hypothalamic lesions and adiposity in the rat. Anat Rec 1940;78: 149–172.
68. Hofman MA, Swaab DF. The sexually dimorphic nucleus of the preoptic area in the human brain: a comparative morphometric study. J Anat 1989;164:55–72.
69. Hökfelt T, Johansson O, Fuxe K, Goldstein M, Park D. Immunohistochemical studies on the localization and distribution of monoamine neuron systems in the rat brain. I. Tyrosine hydroxylase in the mes- and diencephalon. Med Biol 1976;54:427–453.
70. Hökfelt T, Meister B, Villar MJ, et al. Hypothalamic neurosecretory systems and their messenger molecules. Acta Physiol Scand 1989; 583:105–111.
71. Hosoya Y, Matsushita M. Identification and distribution of the spinal and hypophyseal projection neurons in the paraventricular nucleus of the rat: a light and electron microscopic study with the horseradish peroxidase method. Exp Brain Res 1979;35:315–331.
72. Hunsperger RW. Affektreaktionen auf elektrische Reizung im Hirnstamm der Katze. Helv Physiol Pharmacol Acta 1956;14:70–92.
73. Ingram WR. Brain stem mechanisms in behavior. Electroencephalogr Clin Neurophysiol 1952; 4:397–406.
74. Kalra SP, Crowley WR. Neuropeptide Y: a novel neuroendocrine peptide in the control of pituitary hormone secretion, and its relation to luteinizing hormone. Front Neuroendocrinol 1992;13:1–46
75. Keyser A. Development of the hypothalamus in mammals: an investigation into its morphological position during ontogenesis. In: Morgane PJ, Panksepp J, eds. Handbook of the hypothalamus. New York: Marcel Dekker, 1979: 65–136.
76. Kievit J, Kuypers HGJM. Basal forebrain and hypothalamus connections to frontal and parietal cortex in the rhesus monkey. Science 1975;187:660–663.
77. Kita H, Oomura Y. An HRP study of the afferent connections to the rat hypothalamic region. Brain Res Bull 1982;8:63–71.
78. Köhler C, Swanson LW. Acetylcholinesterase-containing cells in the lateral hypothalamic area are immunoreactive for alpha-melanocyte stimulating hormone (alpha-MSH) and have cortical projections in the rat. Neurosci Lett 1984;49:39–43.
79. Krieger DT, Liotta AS. Pituitary hormones in brain: where, how and why? Science 1979;205: 366–372.
80. Kuhlenbeck H. Derivation and boundaries of the hypothalamus, with atlas of hypothalamic grisea. In: Haymaker W, Anderson E, Nauta WJH, eds. The hypothalamus. Ch. 2. Springfield, IL: Charles C. Thomas, 1969;13–60.
81. Kupfermann I. Hypothalamus and limbic system: peptidergic neurons, homeostasis, and emotional behavior. In: Kandel ER, Schwartz JH, Jessell TM, eds. Principles of neural science. Ch. 47. New York: Elsevier, 1991:735–749.
82. Le Gros Clark WE. The topography and homologies of the hypothalamic nuclei in man. J Anat 1936;70:203–216.
83. Le Gros Clark WE, Beattie J, Riddoch G, Dott NM, eds. The hypothalamus. Edinburgh: Oliver and Boyd, 1938.
84. Lehman MN, Winans SS. Vomeronasal and olfactory pathways to the amygdala controlling male hamster sexual behavior: autoradiographic and behavioral analyses. Brain Res 1982;240:27–41.
85. Leibowitz SF. Brain catecholaminergic mechanisms for control of hunger. In: Novein D, Wyriecka W, Bray GA, eds. Hunger: brain mechanisms and clinical implications. New York: Raven Press, 1976:1–18.
86. Leibowitz SF. Hypothalamic neurotransmitters in relation to normal and disturbed eating patterns. Ann NY Acad Sci 1987;499: 137–143.
87. Leichnetz GR, Astruc J. The efferent projections of the medial prefrontal cortex in the squirrel monkey (*Saimiri sciureus*). Brain Res 1976;109:455–472.
88. Leng G, Dyball RE, Luckman SM. Mechanisms of vasopressin secretion. Horm Res 1992;37:33–38.
89. Lin JS, Sakai K, Jouvet M. Evidence for histaminergic arousal mechanism in the hypothalamus of cat. Neuropharmacology 1988;27: 111–122.
90. Lin JS, Sakai K, Vannier-Mercier G, Jouvet M. A critical role of the posterior hypothalamus in the mechanisms of wakefulness determined by microinjection of muscimol in freely moving cats. Brain Res 1989; 479:225–240.
91. Loewy AD. Descending pathways to sympathetic and parasympathetic preganglionic neurons. J Auton Nerv Syst 1981;3:265–275.
92. MacLusky NJ, Naftolin F. Sexual differentiation of the central nervous system. Science 1981;211: 1294–1302.
93. McBride RL, Sutin J. Amygdaloid and pontine projections to the ven-

tromedial nucleus of the hypothalamus. J Comp Neurol 1977;174: 377–396.
94. McEwen BS. Neural gonadal steroid actions. Science 1981; 211:1303–1311.
95. McKinley MJ, Badoer E, Oldfield BJ. Intravenous angiotensin II induces Fos-immunoreactivity in circumventricular organs of the lamina terminalis. Brain Res 1992;594: 295–300.
96. McKinley MJ, Oldfield BJ. Circumventricular organs. In: Paxinos G, ed. The human nervous system. Ch. 16. New York: Academic Press, 1990:415–438.
97. Markee JE, Sawyer CH, Hollinshead WH. Activation of the anterior hypophysis by electrical stimulation in the rabbit. Endocrinology 1946;38:345–357.
98. Masserman JH. Behavior and neurosis. Chicago: University of Chicago Press, 1943.
99. Meibach RC, Siegel A. Efferent connections of the hippocampal formation in the rat. Brain Res 1977;124:197–224.
100. Mesulam M-M, Geula C, Bothwell MA, Hersh LB. Human reticular formation: cholinergic neurons of the pedunculopontine and laterodorsal tegmental nuclei and some cytochemical comparisons to forebrain cholinergic neurons. J Comp Neurol 1989;283:611–633.
101. Mesulam M-M, Mufson EJ, Levey AI, Wainer BH. Cholinergic innervation of cortex by the basal forebrain: cytochemistry and cortical connections of the septal area, diagonal band nuclei, nucleus basalis (substantia innominata) and hypothalamus in the rhesus monkey. J Comp Neurol 1983; 214:170–197.
102. Millhouse OE. A Golgi anatomy of the rodent hypothalamus. In: Morgane P, Panksepp J, eds. Handbook of the hypothalamus. Vol. I: Anatomy of the hypothalamus. New York: Marcel Dekker, 1979: 221–265.
103. Moore RY. Retinohypothalamic projection in mammals: a comparative study. Brain Res 1973;49: 403–409.
104. Moore RY. The fourth C.U. Ariëns Kappers lecture. The organization of the human circadian timing system. Prog Brain Res 1992;93: 99–115.
105. Moore RY, Lenn NJ. A retinohypothalamic projection in the rat. J Comp Neurol 1972;146:1–14.
106. Moore RY, Speh JC. GABA is the principal neurotransmitter of the circadian system. Neurosci Lett 1993;150:112–116.
107. Morin LP, Michels KM, Smale L, Moore RY. Serotonin regulation of circadian rhythmicity. Ann NY Acad Sci 1990;600:418–426.
108. Morin LP, Blanchard J, Moore RY. Intergeniculate leaflet and suprachiasmatic nucleus organization and connections in the golden hamster. Vis Neurosci 1992;8: 219–230.
109. Müller EE. Neural control of somatotropic function. Physiol Rev 1987;67:962–1053.
110. Müller-Preuss P, Jürgens U. Projections from the "cingular" vocalization area in the squirrel monkey. Brain Res 1975;103:29–43.
111. Nakamori T, Morimoto A, Yamaguchi K, Watanabe T, Long NC, Murukami N. Organum vasculosum laminae terminalis (OVLT) is a brain site to produce interleukin-1β during fever. Brain Res 1993;618:155–159.
112. Nakao H. Emotional behavior produced by hypothalamic stimulation. Am J Physiol 1958;194: 411–418.
113. Nathan PW, Smith MC. The location of descending fibres to sympathetic neurons supplying the eye and sudomotor neurons supplying the head and neck. J Neurol Neurosurg Psychiatry 1986;49:187.
114. Nauta WJH. An experimental study of the fornix in the rat. J Comp Neurol 1956;104:247–272.
115. Nauta WJH. Hippocampal projections and related neural pathways to the midbrain in the cat. Brain 1958;81:319–340.
116. Nauta WJH. Fibre degeneration following lesions of the amygdaloid complex in the monkey. J Anat 1961;95:515–531.
117. Nauta WJH. Some efferent connections of the prefrontal cortex in the monkey. In: Warren JM, Akert K, eds. The frontal granular cortex and behavior. New York: McGraw-Hill, 1964:397–409.
118. Nauta WJH, Haymaker W. Hypothalamic nuclei and fiber connections. In: Haymaker W, Anderson E, Nauta WJH, eds. The hypothalamus. Ch. 4. Springfield, IL: Charles C. Thomas, 1969:136–209.
119. Nilaver G, Zimmerman EA, Wilkins J, Michaels J, Hoffman D, Silverman AJ. Magnocellular hypothalamic projections to the lower brain stem and spinal cord of the rat. Neuroendocrinology 1980;30:150–158.
120. Olivecrona H. Paraventricular nucleus and the pituitary gland. Acta Physiol Scand 1957;40:(Suppl 136):1–178.
121. Ono T, Nichino H, Sasaka K, Muramoto K, Yano I, Simpson A. Paraventricular nucleus connections to spinal cord and pituitary. Neurosci Lett 1978;10:141–146.
122. Ono T, Oomura Y, Sugimori M, et al. Hypothalamic unit activity related to lever pressing and eating in the chronic monkey. In: Novin D, Wyrwicka WR, Bray GA, eds. Hunger: basic mechanisms and clinical implications. New York: Raven Press, 1976:159–170.
123. Otori Y, Tominaga K, Fukuhara C, et al. Substance P-like immunoreactivity in the suprachiasmatic nucleus of the rat. Brain Res 1993; 619:271–277.
124. Page RB. The anatomy of the hypothalamo-hypophyseal complex. In: Knobil KH, ed. The physiology of reproduction. New York: Raven Press, 1988:1161–1233.
125. Page RB, Bergland RM. The neurohypophyseal capillary bed. I. Anatomy and arterial supply. Am J Anat 1977;148:345–357.
126. Palay SL. The fine structure of the neurohypophysis. In: Waelsch H, ed. Ultrastructure and cellular chemistry of neural tissue. New York: Paul B. Hoeber, 1957:31–344.
127. Palkovits M. Catecholamines in the hypothalamus: an anatomical review. Neuroendocrinology 1981; 33:123–128.
128. Palkovits M. Peptidergic neurotransmitters in the endocrine hypothalamus. Ciba Found Symp 1992;168:3–10.
129. Panula P, Airaksinen MS, Pirvola U, Kotilainen E. A histamine-containing neuronal system in human brain. Neuroscience 1990;34: 127–132.
130. Parent A. Anatomical organization of monoamines- and acetylcholinesterase-containing neuronal systems in the vertebrate hypothalamus. In: Morgane PJ, Panksepp J, eds. Handbook of the hypothalamus. Vol. I: Anatomy of the hypothalamus. New York: Marcel Dekker, 1979:511–554.
131. Parent A, Butcher LL. Organization and morphologies of acetylcholinesterase-containing neurons in the thalamus and hypothalamus of the rat. J Comp Neurol 1976; 170:205–226.
132. Parent A, Descarries L, Beaudet A. Organization of ascending serotonin systems in the adult rat brain. A radioautographic study after intraventricular administration of [^{3}H] 5-hydroxytryptamine. Neuroscience 1981;6:115–138.
133. Parent A, Poirier LJ, Boucher R, Butcher LL. Morphological characteristics of acetylcholinesterase-containing neurons in the CNS of DFP-treated monkeys. Part II. Diencephalic and medial telencephalic structures. J Neurol Sci 1977;32:9–28.
134. Pelletier G, Désy L, Côté J, Vaudry H. Immunocytochemical localization of corticotropin-releasing-factor-like immunoreactivity in the human hypothalamus. Neurosci Lett 1983;41:259–263.
135. Pfaff DW, Keiner M. Estradiol-concentrating cells in the rat amygdala as part of a limbic-hypothalamic hormone-sensitive system. In: Eleftheriou BE, ed. The neurobiology of the amygdala. New York: Plenum Press, 1972:775–785.
136. Phillips MI, Felix D, Hoffman WE, Ganten A. Angiotensin-sensitive sites in the brain ventricular system. Neurosci Symp 1977;2: 308–339.
137. Pickard GE, Silverman A-J. Direct retinal projection to the hypothalamus, piriform cortex, and acces-

sory optic nuclei in the golden hamster as demonstrated by a sensitive anterograde horseradish peroxidase technique. J Comp Neurol 1981;196:155–172.
138. Pickford M. Neurohypophysis-antidiuretic (vasopressor) and oxytocic hormones. In: Haymaker W, Anderson E, Nauta WJH, eds. The hypothalamus. Ch. 13. Springfield, IL: Charles C. Thomas, 1969: 463–505.
139. Pierson RJ, Carpenter MB. Anatomical analysis of pupillary reflex pathways in the rhesus monkey. J Comp Neurol 1974;158: 121–143.
140. Poitras D, Parent A. A fluorescence microscopic study of the distribution of monoamines in the hypothalamus of the cat. J Morphol 1975;145:387–408.
141. Poitras D, Parent A. Atlas of the distribution of monoamine-containing nerve cell bodies in the brain stem of the cat. J Comp Neurol 1978;179:699–718.
142. Popa GT, Fielding U. A portal circulation from the pituitary to the hypothalamic region. J Anat 1930; 65:88–91.
143. Porrino LJ, Goldman-Rakic PS. Brainstem innervation of prefrontal and anterior cingulate cortex in the rhesus monkey revealed by retrograde transport of HRP. J Comp Neurol 1982;205:63–76.
144. Porter JC, Jones JC. Effect of plasma from hypophyseal-portal vessel blood on adrenal ascorbic acid. Endocrinology 1956;58:62–67.
145. Powell TPS, Guillery RW, Cowan WM. A quantitative study of the fornix-mammillo-thalamic system. J Anat 1957;91:419–432.
146. Price JL, Amaral DG. An autoradiographic study of the projections of the central nucleus of the monkey amygdala. J Neurosci 1981;1: 1242–1259.
147. Raisman G. Neural connections of hypothalamus. Br Med Bull 1966; 22:197–201.
148. Raisman G. The connexions of the septum. Brain 1966;89:317–348.
149. Raisman G. An evaluation of the basic pattern of connections between the limbic system and the hypothalamus. Am J Anat 1972; 129:197–202.
150. Raisman G, Cowan WM, Powell TPS. The extrinsic afferent, commissural and association fibres of the hippocampus. Brain 1965;88: 963–996.
151. Raisman G, Cowan WM, Powell TPS. An experimental analysis of the efferent projections of the hippocampus. Brain 1966;89:83–108.
152. Raisman G, Field PM. Sexual dimorphism in the neuropil of the preoptic area of the rat and its dependence on neonatal androgen. Brain Res 1973;54:1–29.
153. Ranson SW. Somnolence caused by hypothalamic lesions in the monkey. Arch Neurol Psychiatry 1939; 41:1–23.
154. Renaud LP, Allen AM, Cunningham JT, et al. Synaptic and neurotransmitter regulation of activity in mammalian hypothalamic magnocellular neurosecretory cells. Prog Brain Res 1992;92:277–288.
155. Rioch DM, Wislocki GB, O'Leary JL. A precis of preoptic, hypothalamic and hypophyseal terminology with atlas. In: Fulton JF, ed. The hypothalamus and central levels of autonomic function. Assoc Res Nerv Ment Dis 1939;20:3–30.
156. Sadum AA, Schaechter JD, Smith LEH. A retinohypothalamic pathway in man: light mediation of circadian rhythms. Brain Res 1984; 302:371–377.
157. Sakai K, Yoshimoto Y, Luppi PH, et al. Lower brainstem afferents to the cat posterior hypothalamus: a double-labeling study. Brain Res Bull 1990;24:437–55
158. Saper CB. Convergence of autonomic and limbic connections in the insular cortex of the rat. J Comp Neurol 1982;210:163–173.
159. Saper CB. Organization of cerebral cortical afferent system in the rat. II. Hypothalamocortical projections. J Comp Neurol 1985;237: 21–46.
160. Saper CB. Chemical neuroanatomy of Alzheimer's disease. In: Iversen SD, Snyder SH, eds. Handbook of psychopharmacology. Vol. 20. New York: Plenum Press, 1988: 131–156.
161. Saper CB. Hypothalamus. In: Paxinos G, ed. The human nervous system. Ch. 15. New York: Academic Press, 1990:389–413.
162. Saper CB, German DC. Hypothalamic pathology in Alzheimer's disease. Neurosci Lett 1987;74:364–370.
163. Saper CB, Loewy AD, Swanson LW, Cowan WM. Direct hypothalamo-autonomic connections. Brain Res 1976;117:305–312.
164. Sawyer CH. Nervous control of ovulation. In: Lloyd CW, ed. Endocrinology of reproduction. New York: Academic Press, 1959:1–18.
165. Scalia F, Winans SS. The differential projections of the olfactory bulb and accessory olfactory bulb in mammals. J Comp Neurol 1975; 161:31–56.
166. Schally AV, Kastin AJ, Arimura A. Hypothalamic hormones: the link between brain and body. Am Sci 1977;65:712–719.
167. Scharrer E, Scharrer B. Hormones produced by neurosecretory cells. Recent Prog Horm Res 1954;10: 183–232.
168. Scheithauer BW, Horvath E, Kovacs K. Ultrastructure of the neurohypophysis. Microsc Res Tech 1992;20:177–186.
169. Schwaber JS, Kapp BS, Higgins GA, Rapp PR. Amygdaloid and basal forebrain direct connections with the nucleus of the solitary tract and the dorsal motor nucleus. J Neurosci 1982;2:1424–1438.
170. Silverman AJ, Zimmerman EA. Magnocellular neurosecretory system. Annu Rev Neurosci 1983;6: 357–380.
171. Silverman AJ, Pickard GE. The hypothalamus. In: Emson PC, ed. Chemical neuroanatomy. New York: Raven Press, 1983:295–336.
172. Skeen LC, Hall WC. Efferent projections of the main and the accessory olfactory bulb in the tree shrew (*Tupaia glis*). J Comp Neurol 1977;172:1–36.
173. Stevenson JAF. Effects of hypothalamic lesions on water and energy metabolism in the rat. Recent Prog Horm Res 1949;4:363–394.
174. Stevenson JAF. Neural control of food and water intake. In: Haymaker W, Anderson E, Nauta WJH, eds. The hypothalamus. Ch. 15. Springfield, IL: Charles C. Thomas, 1969:524–621.
175. Stumpf WE. Estrogen-neurons and estrogens-neuron systems in the periventricular brain. Am J Anat 1970;129:207–217.
176. Sutin J. The periventricular structures of the hypothalamus. Int Rev Neurobiology 1966;9:263–300.
177. Swaab DF, Fliers E. A sexually dimorphic nucleus in the human brain. Science 1985;228: 1112–1115.
178. Swanson LW, Cowan WM. A note on the connections and development of the nucleus accumbens. Brain Res 1975;92:324–330.
179. Swanson LW, Cowan WM. An autoradiographic study of the organization of the efferent connections of the hippocampal formation in the rat. J Comp Neurol 1977;172: 49–84.
180. Swanson LW, Cowan WM, Jones EG. An autoradiographic study of the efferent connections of the ventral lateral geniculate nucleus in the albino rat and the cat. J Comp Neurol 1974;156:143–163.
181. Swanson LW, Kuypers HGJM. The paraventricular nucleus of the hypothalamus: cytoarchitectonic subdivisions and organization of projections to the pituitary, dorsal vagal complex, and spinal cord as demonstrated by retrograde fluorescence double-labeling methods. J Comp Neurol 1980;194:555–570.
182. Swanson LW, Sawchenko PE. Paraventricular nucleus: a site for the integration of neuroendocrine and autonomic mechanisms. Neuroendocrinology 1980;31:410–417.
183. Szentagothai J, Flerko B, Mess B, Halasz B. Hypothalamic control of the anterior pituitary: an experimental-morphological study. Budapest: Akademiai Kiado, 1968.
184. Tigges J, Walker LC, Tigges M. Subcortical projections to the occipital and parietal lobes of the chimpanzee brain. J Comp Neurol 1983;220:106–115.
185. Tindall GT, McLanahan CS. Hyperfunctional pituitary tumors: pre- and postoperative management considerations. Clin Neurosurg 1980;27:48–82.

186. Tucker DC, Saper CB. Neural connections of an infralimbic cortical pressor area. Soc Neurosci Abst 1984;10:606.
187. Valenstein ES, Nauta WJH. A comparison of the distribution of the fornix system in the rat, guinea pig, cat and monkey. J Comp Neurol 1959;113:337–363.
188. Valverde F. Studies on the piriform lobe. Cambridge: Harvard University Press, 1965.
189. Van den Pol AN, Tsujimoto KL. Neurotransmitters of the hypothalamic suprachiasmatic nucleus: immunohistochemical analysis of 25 neuronal antigens. Neuroscience 1985;15:1049–1086.
190. Vandesande F, Dierickx K. The activated hypothalamic magnocellular neurosecretory system and the one neuron–one neurohypophysial hormone concept. Cell Tissue Res 1979;200:29–33.
191. Veazey RB, Amaral DG, Cowan WM. The morphology and connections of the posterior hypothalamus in the cynomolgus monkey (*Macaca fascicularis*). II. Efferent connections. J Comp Neurol 1982; 207:135–156.
192. Verney EB. The antidiuretic hormone and factors which determine its release. Proc R Soc Lond (Biol) 1947;135:25–106.
193. Wheatley MD. Hypothalamus and affective behavior in cats. Arch Neurol Psychiatry 1944;52: 296–316.

18
Limbic System

LIMBIC LOBE VERSUS LIMBIC SYSTEM

On the medial surface of the cerebral hemisphere, a large arcuate convolution, formed primarily by the cingulate and parahippocampal gyri, surrounds the rostral brainstem and interhemispheric commissures. These gyri, which encircle the upper brainstem, constitute what the French neurologist Paul Broca referred to as the "grand lobe limbique" (*limbus* is Latin for "border") (Fig. 18.1) (38). Interest in the limbic lobe was heightened in 1937 when James Papez, a neuroanatomist at Cornell University, suggested that limbic structures form a complex neuronal network involved in emotional behavior (193). Since that time, the bulk of experimental data has revealed that the limbic lobe has profuse connections with the olfactory system, the hypothalamus (Chapter 17), the thalamus (Chapter 16), and various areas of the neocortex (Chapter 20). It is intimately implicated in the higher integration of visceral, olfactory, and somatic information, as well as the patterning of complex long and short term homeostatic responses. These responses include various types of fundamental behaviors that ensure the survival of the individual and the species (e.g., feeding, mating, emotional responses, and motivational states) (284).

The concept of the limbic lobe was later expanded by Paul MacLean to include other structures functionally and anatomically related to those described by Papez (142). MacLean considered the hypothalamus, the septal area, the nucleus accumbens (a part of the striatum), neocortical areas such as the orbitofrontal cortex, and the amygdala, as part of what he called the "limbic system" (142, 145).

The terminology applied to structures belonging to the limbic lobe is extremely complex and there is still much controversy regarding the rational basis for defining the limbic lobe or limbic system (109, 121). However, the remarkable increase over the past ten years in the use of the concept of limbic system in both experimental and clinical literature indicate that such collective terms serve a useful purpose (109).

Limbic Lobe

The limbic lobe includes the subcallosal, cingulate, and parahippocampal gyri, as well as the underlying hippocampal formation and dentate gyrus (Fig. 18.1). The limbic lobe consists of *archicortex* (hippocampal formation and dentate gyrus), *paleocortex* (piriform cortex of the anterior parahippocampal gyrus), and *juxtallocortex* or *mesocortex* (cingulate gyrus). The *juxtallocortex* or *mesocortex* represents a type of cortex that is transitional between allocortex and neocortex. Some authors have additionally included the cortex of the posterior orbital surface of the frontal lobe, the anterior insular region, and the temporal polar region. The striking feature of the limbic lobe is that it appears early in phylogenesis and possesses a certain constancy in gross and microscopic structure. As mentioned, the extent to which these various cortical areas form a functional unit is not fully understood (109, 121).

Limbic System

An even more extensive and inclusive designation is the *limbic system*. This term is used to include all of the limbic lobe (Fig. 18.1) as well as associated subcortical nuclei (Fig. 18.10), such as the amygdaloid complex, septal nuclei, hypothalamus, epithalamus, various thalamic nuclei, and part of the basal ganglia (142, 145). The medial tegmental region of the midbrain also is regarded as a part of the limbic system since this region contains both ascending and descending pathways which directly or indirectly are related to the hippocampal formation and the amygdaloid nuclear complex (Figs. 18.2 and

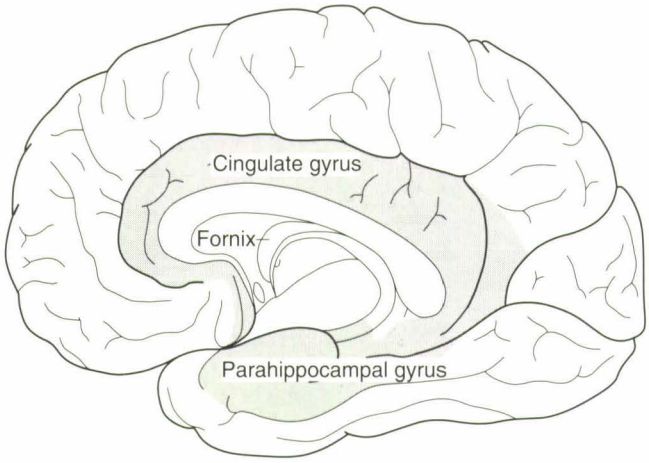


Figure 18.1. Medial surface of the hemisphere. *Shading* indicates the limbic lobe that encircles the upper brainstem. Although the cortical areas designated as the limbic lobe have some common structural characteristics, the extent to which they form a functional unit is not clear.

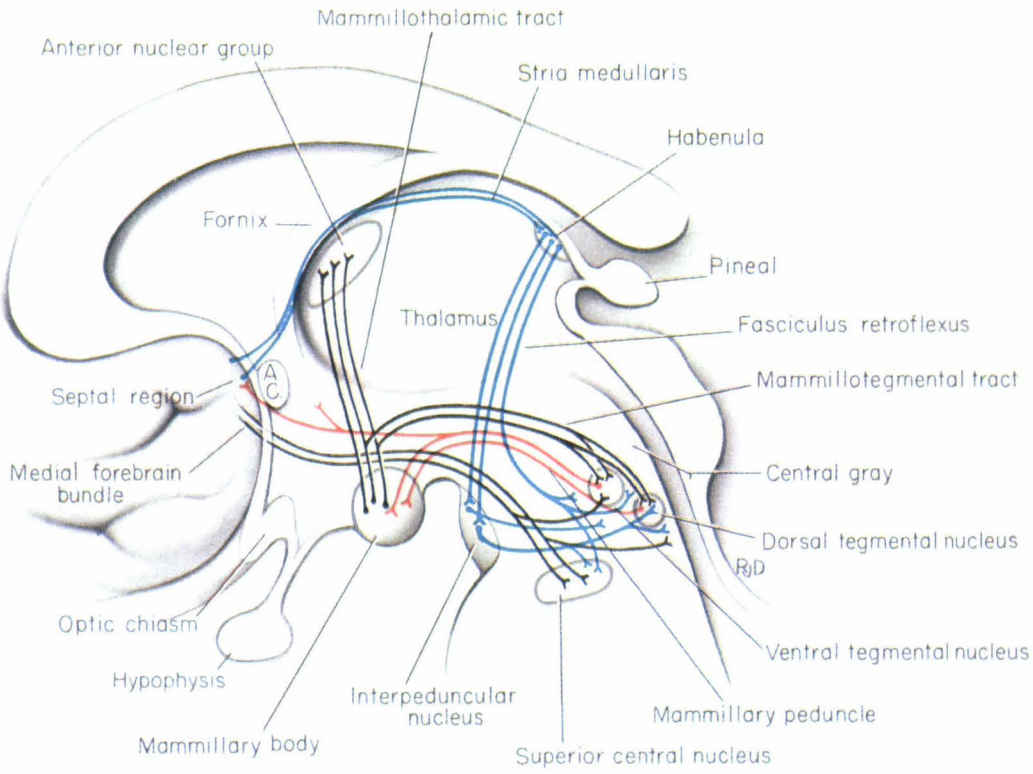


Figure 18.2. Limbic pathways interrelating the telencephalon and diencephalon with medial midbrain structures. The medial forebrain bundle and efferent fibers of the mammillary body are shown in *black*. The medial forebrain bundle originates from the septal and lateral preoptic regions, traverses the lateral hypothalamic area, and projects into the midbrain tegmentum. Fibers from the midbrain also ascend in the medial forebrain bundle. The mammillary princeps fasciculus divides into two bundles, the mammillothalamic tract and the mammillotegmental tract. Ascending fibers of the mammillary peduncle, arising from the dorsal and ventral tegmental nuclei (of Gudden), are shown in *red*. Most of these fibers pass to the mammillary body, but some continue rostrally to the lateral hypothalamus, the preoptic regions, and the medial septal nucleus via the medial forebrain bundle. Fibers arising from the septal nuclei project caudally in the medial part of the stria medullaris (*blue*) to terminate in the medial habenular nucleus. Impulses conveyed by this bundle are distributed to midbrain tegmental nuclei via the fasciculus retroflexus.

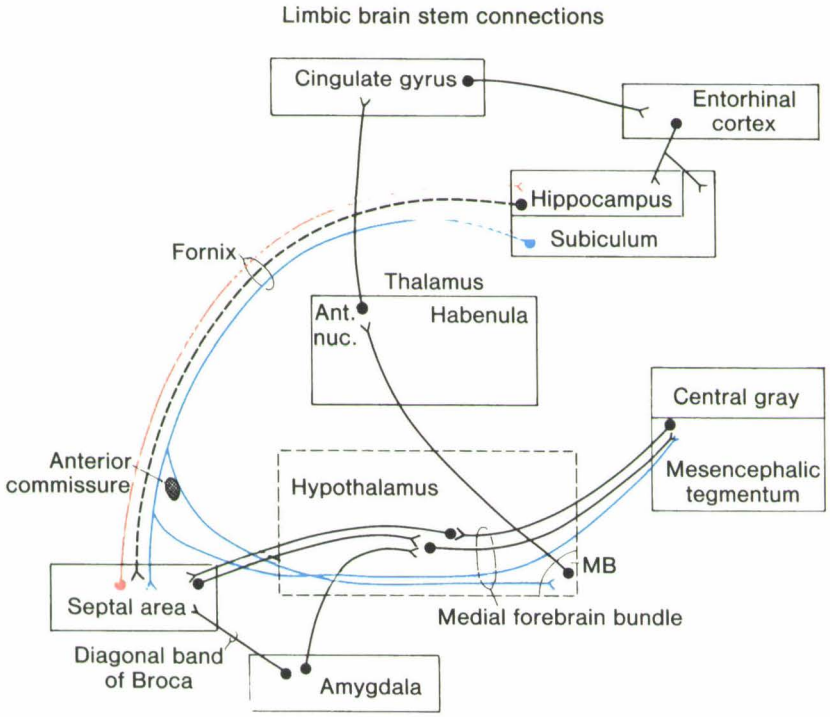


Figure 18.3. Major interconnections of structures that form the limbic system. Projection fibers arising from the subiculum (*blue*) project via the fornix to the septal area, hypothalamus, and mesencephalic tegmentum. Fibers projecting in the fornix from the hippocampal formation are shown in *black-dashed* lines. Projections from the septal area to the hippocampus are shown in *red*. *MB* indicates mammillary body.

18.3) (176). Despite the heterogeneity and diffuse nature of the limbic system, there are compelling observations that structures comprising this system are involved in neural circuitry that gives rise to a subcortical continuum that begins in the septal area and extends in a paramedian zone through the preoptic region and hypothalamus into the rostral mesencephalon (179). This longitudinal continuum has extensive reciprocal connections with the amygdala and the substantia innominata.

Molecular biologic studies revealed that structures belonging to the limbic system possess a distinct chemical phenotype (134). These neurons contain the *limbic system-associated membrane protein* (LAMP), which is a cell surface glycoprotein that is expressed early in development (105). Transplantation studies in the rat suggest that cells in the cerebral wall are committed to a limbic or nonlimbic molecular phenotype by embryonic day 14 (E14) (23). Furthermore, in vitro experiments have shown that after 4 days in culture, up to 75% of the progenitor cells from presumptive limbic cortex (perirhinal area) express LAMP upon differentiation. In contrast, only 20–30% of the differentiated cells from presumptive sensorimotor cortex express LAMP. Thus, most cortical progenitors are fated to a limbic or nonlimbic phenotype early in development, and the decision by neuronal stem cells to differentiate into neurons exhibiting this molecular phenotype occurs prior to the completion of neurogenesis in the absence of subcortical environmental cues (67). LAMP is also a valuable marker for limbic structures in monkeys. As shown in Figure 18.4, the hippocampal formation, the hypothalamus, as well as the amygdaloid complex and its dorsal extension, all display a strong immunoreactivity for this protein.

The role of the cerebral cortex in the subjective aspects of emotion has been emphasized repeatedly, yet the neocortex appears to have relatively few hypothalamic connections. Both the amygdala and the substantia innominata have reciprocal connections with regions of the cerebral cortex, although projections from these structures to the cortex are most extensive. These nuclear masses appear to represent the principal interface between visceral and autonomic centers in the hypothalamus and brainstem and broad expanses

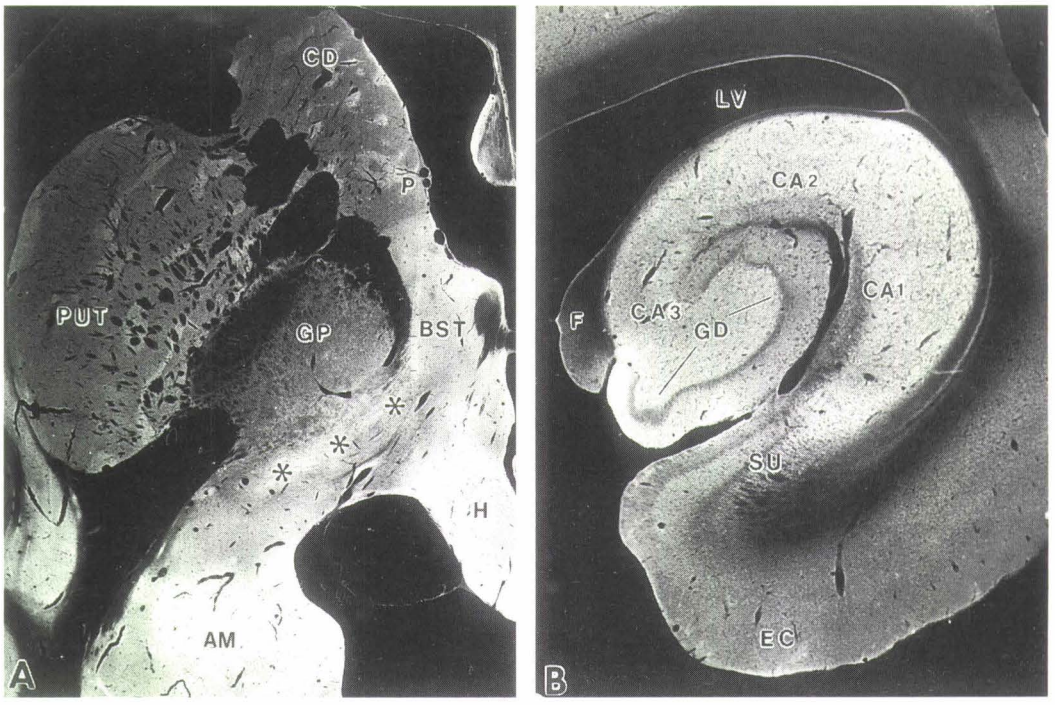


Figure 18.4. Darkfield photographs of transverse sections through (**A**) the basal forebrain and (**B**) the hippocampal formation in a cynomolgus monkey, illustrating the distribution of the limbic system-associated membrane protein (LAMP). This membrane surface glycoprotein, which is specifically expressed in limbic regions of the brain, was visualized with highly specific monoclonal antibodies. **A**. Note the intense labeling in the amygdala (*AM*), hypothalamus (*H*), bed nucleus of the stria terminalis (*BST*), and the so-called extended amygdala (*asterisks*), which includes significant portions of the substantia innominata and dorsal amygdaloid region. Patches showing moderate LAMP immunostaining are seen in both caudate nucleus (*CD*) and putamen (*PUT*), but not in the globus pallidus (*GP*). **B**. Note the intense LAMP immunostaining in all three sectors of the hippocampus (*CA1, CA2,* and *CA3*), and in the dentate gyrus (*GD*). The immunostaining is moderate in the subiculum (*SU*) and virtually absent in the entorhinal cortex (*EC*). The letters *F* and *LV* indicate fimbria and lateral ventricle, respectively.

of the cortical mantle. These extensive cortical connections of forebrain nuclei appear to provide part of the mechanism by which sensory stimuli and psychic phenomena influence emotional aspects of behavior. These connections may also explain the close adjustment of visceral and somatic activities in emotional expression.

Various visceral, somatic, and behavioral responses can be obtained by electrical stimulation of the anterior cingulate cortex and the orbital-insular-temporal cortex. Earlier studies demonstrated that elevation, as well as depression, of arterial blood pressure results from electrical stimulation of these regions in experimental animals (21, 114). Points from which pressor and depressor effects can be obtained, frequently are only a few millimeters apart. Effects on arterial pressure do not appear to be secondary to respiratory changes. Other autonomic responses obtained in experimental animals include inhibition of peristalsis, pupillary dilatation, salivation, and bladder contraction. Perhaps the most striking effect of stimulating these regions is profound inhibition of respiratory movements (245), which involves mainly the inspiratory phase, occurs almost instantaneously, and cannot be held in abeyance for long.

Somatic effects of stimulating the anterior cingulate and the orbital-insular-temporal cortex resemble those obtained by stimulating the amygdala in awake animals. These responses include (a) inhibition of spontaneous movements, (b) chewing, licking, and swallowing movements, and (c) the "arrest" reaction. The arrest reaction consists of an immediate cessation of other activities, an expression of attention or surprise, and movements of the head and eyes to the opposite side. Animals remain alert during stimulations and respond to external stimuli. Stimulation of posterior cingulate areas may

induce enhanced grooming and seemingly pleasurable reactions. Neither unilateral nor bilateral ablations of the cingulate cortex, or of the cortex of the orbital-insular-temporal polar region, appear to disturb basic somatomotor or autonomic functions.

Electrical stimulation of certain subcortical structures via implanted electrodes in unanesthetized rats, cats, and monkeys produces a patterned self-stimulation behavior (35, 185, 186). In these studies, the experimental arrangement is such that the animals can deliver an electrical stimulus to localized areas of their own brains by pressing a pedal. Self-stimulations of the septal region, the anterior preoptic area, and the posterior hypothalamus by bar pressing may be at rates as high as 5000 per hour in the rat. The compulsive behavior seen in these situations, where the only reward is an electric shock to a localized region of the brain, suggests that the stimulus may provide a primary reinforcement for drives related to food or sex. Repeated self-stimulation may occur in the monkey from electrodes implanted in a variety of subcortical sites, such as the head of the caudate nucleus, the amygdaloid complex, the medial forebrain bundle, and the midbrain reticular formation. Self-stimulation of certain regions of the thalamus and hypothalamus may produce unpleasant or avoidance reactions, but these regions appear relatively small in number compared to those from which some gratification appears to result.

The limbic lobe and system occupy central positions in the neural mechanisms that govern behavior and emotion. Components of the limbic system appear to have their main afferent and efferent relationships with two great functional realms, the neocortex, and the visceroendocrine periphery. The amygdala with complex connections, to and from the cerebral cortex and with subcortical autonomic centers, appears to represent the key structure of the system.

OLFACTORY SYSTEM

The term *rhinencephalon* refers to the olfactory brain. Although some authors use this term broadly to include those regions of the brain concerned with both the reception and integration of olfactory information, not all regions of the brain in which responses can be recorded upon olfactory stimulation are concerned exclusively with olfactory sense. Higher order pathways of the olfactory system are complex and subject to modifying influences from many sources. Some of these regions have lost their original olfactory specificity. For this reason use of the term "rhinencephalon" should be restricted to those structures of the central nervous system that receive fibers from the olfactory bulb (40). In this strict sense, the rhinencephalon includes the olfactory bulb, tract, tubercle and striae, the anterior olfactory nucleus, parts of the amygdaloid complex, and parts of the piriform cortex. The term rhinencephalon, in this restricted sense, is equivalent to the *paleopallium* or primitive olfactory lobe (270).

Although the rhinencephalon is large and conspicuous in nonprimate species, including many macrosmatic mammals, in humans it is overshadowed and comparatively reduced by the tremendous development of the *neopallium*. The *archipallium*, the oldest cortical derivative, is represented by the hippocampus, the dentate gyrus, the fasciolar gyrus, and the indusium griseum (supracallosal gyrus). The hippocampal formation reaches its greatest development in microsmatic man and is well-formed in certain anosmatic aquatic mammals (e.g., porpoise, whale).

Olfactory Receptors

The olfactory membrane is a yellowish brown patch of specialized epithelium in the upper posterior part of the nasal cavity. Olfactory receptors are located in this membrane (Fig. 18.5). Slender sensory cells scattered among supporting cells in the olfactory epithelium have two processes, a coarse peripheral one, passing to the surface, and a fine central one, projecting through the basement membrane. From the coarse peripheral processes a variable number of fine olfactory hairs arise. The delicate central processes, which constitute the unmyelinated *olfactoria fila*, converge to form small fascicles and pass from the nasal cavity via foramina in the cribriform plate of the ethmoid bone. These exceedingly small fibers (mean diameter 0.2 μm) are unmyelinated, they have a very slow conduction rate, and enter the ventral surface of the olfactory bulb (Figs. 18.5 and 18.6). The olfactory fila, representing the central processes of bipolar cells in the olfactory epithelium, collectively constitute the olfactory nerve (N I). The incoming olfactory axons are gathered into bundles of 100–200 axons con-

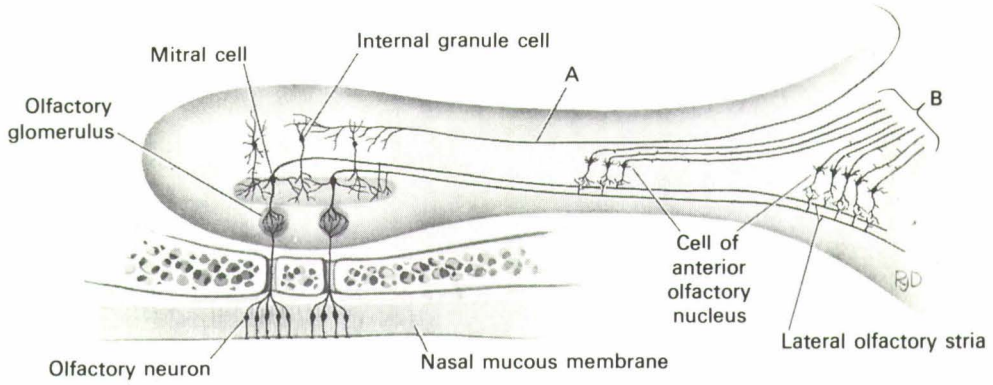


Figure 18.5. Olfactory bulb and tract showing relationship of the olfactory receptors and neurons in the nasal mucosa with cells in the olfactory bulb. Cells of the anterior olfactory nucleus form scattered groups caudal to the olfactory bulb. Centrally projecting fibers from the anterior olfactory nucleus are labeled *B*, while a fiber from the contralateral anterior olfactory nucleus is labeled *A*.

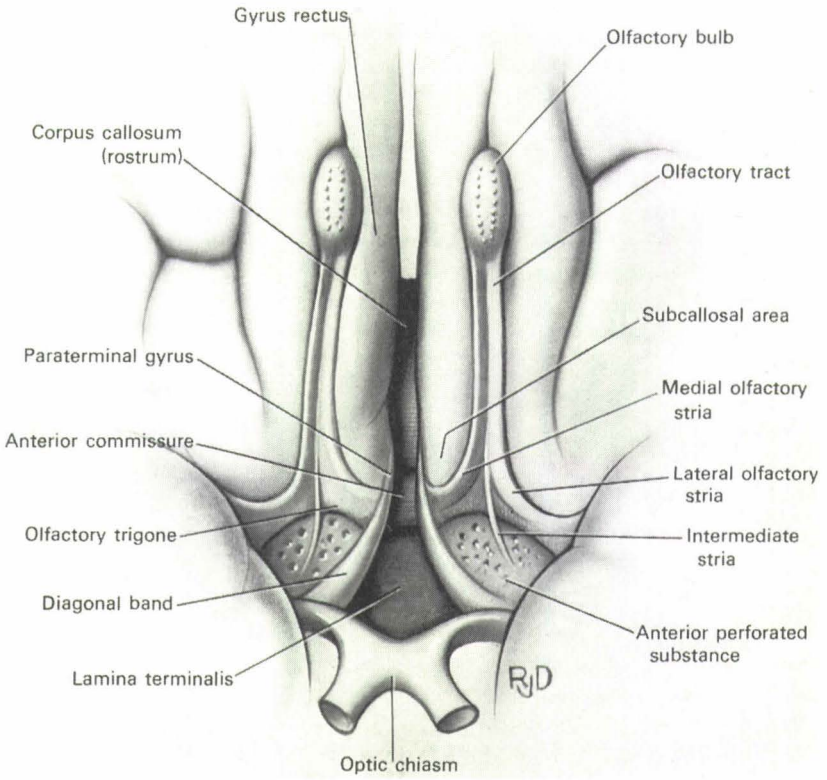


Figure 18.6. Olfactory structures on the inferior surface of the brain. The optic nerves and chiasm have been retracted caudally to expose the olfactory area.

tained within one glial (Schwann) cell. These glial cells contain glial fibrillary acidic protein (GFAP), like central astrocytes but unlike Schwann cells of peripheral nerves (244).

A notable feature of the sensory neurons of the olfactory epithelium is that they are continuously replaced from stem cells throughout adult life (81). The olfactory receptor is a bipolar neuron with a lifespan of 30–40 days, depending upon the species. New axons are continually growing into the olfactory bulb and forming new synapses. When the olfactory fibers are surgically cut as they enter the olfactory bulb (164), olfactory receptor axons can regenerate and form new synapses in the glomeruli of the olfactory

bulb. The normal cyclic loss and formation of olfactory receptor axons and their synapses upon mitral cells, and the demonstration of posttraumatic regeneration in primates, offers hope that a means can be devised to minimize scar tissue formation and permanent deafferentation of the bulb in humans with anosmia due to fractures of the cribriform plate.

The constant turnover of sensory olfactory neurons is one of the rare examples in mammals of continued genesis of neurons that make synaptic connections in the central nervous system. The molecular basis of this phenomenon is not completely known, but most likely involves the complex interplay of several guiding molecules. The olfactory sensory neurons contain a special peptide [olfactory marker protein (OMP)] and are enriched with the dipeptide carnosine (β-alanyl-L-histidine) (151, 152). The olfactory axons are known on the basis of electrophysiologic experiments to be excitatory, but neither OMP nor carnosine have been shown to be neuroactive at their synapses (102, 244). Numerous studies have generated monoclonal antibodies to all parts of the sensory neuronal population, indicating the presence of molecules that may be involved in the sensory transduction of the olfactory signals as well as the specificity of synaptic connections (166, 167, 244). Some of these molecules appear to be unique to subsets of olfactory neurons (8). The calcium-binding proteins calbindin D-28k, parvalbumin, and calretinin, are known to occur in various combination in the olfactory sensory neurons of the main olfactory epithelium and that of the vomeronasal organ (118).

Olfactory Bulb

This flattened, ovoid body, resting on the cribriform plate of the ethmoid bone, is the terminal "nucleus" of the olfactory nerve (Figs. 18.5 and 18.6). The olfactory bulb is the first processing station in the olfactory pathway. Most of the fibers of the olfactory nerve enter the anterior tip of the olfactory bulb. Structurally, the olfactory bulb has a laminar organization arranged in both radial and tangential fashion. From the surface progressing toward the central core, the olfactory bulb consists of (a) the olfactory nerve fiber layer, (b) the layer of synaptic glomeruli, (c) the external plexiform layer, (d) the mitral cell layer, (e) the granule cell layer, and (f) the fibers of the olfactory tract (Fig. 18.7). Although obvious in fetal stages of development, the layers are irregular and indistinct in the adult human olfactory bulb. The principal cells of the olfactory bulb are the *mitral cells*, so named because of their resemblance to a bishop's miter (Figs. 18.5, 18.6, and 18.8). Their dendrites extend into the glomeruli, where they are contacted by axons of sensory olfactory cells (215, 243, 244) (Fig. 18.7), and in the external plexiform layer, where they receive input from fibers originating in various brain centers (centrifugal fibers) that ascend along the olfactory tract. The axons of the mitral cells descend along the olfactory tract and constitute the main output of the olfactory bulb and are recognized as *secondary olfactory fibers* (Figs. 18.5 and 18.8). *Tufted cells* are similar to the mitral cells, but their smaller somata lie more rostrally in the plexiform layer. Both the mitral and tufted cells exert an excitatory effect upon neurons they contact. This excitatory action appears to be mediated by glutamate (243, 244).

The olfactory bulb contains two type of interneurons—the periglomerular cells and the granule cells. The *periglomerular cells* have dendrites that receive synaptic input from olfactory sensory neurons and from centrifugal fibers. The dendrites also form dendrodendritic synapses with the mitral cells. The axons of the periglomerular cells course in the external plexiform layer to contact dendrites of mitral cells associated with other glomeruli, which they may excite or inhibit depending on the postsynaptic receptors (25). Periglomerular cells use dopamine and γ-aminobutyric acid (GABA) as neurotransmitters, and they are also enriched with various neuroactive peptides and enzyme, such as nitric oxide synthase (37). A large variety of neuropeptides (substance P, neuropeptide Y, corticotrophic releasing factor, vasoactive intestinal peptide, enkephalin, and somatostatin) occur in the olfactory bulb, but their functional significance remains to be elucidated. The *granule cells* are the most numerous interneurons in the olfactory bulb. These cells have no axons (amacrine cells), are located in the deepest part of the bulb (Fig. 18.7) (214), and use GABA as inhibitory neurotransmitter (96, 149, 223, 244). Their dendrites receive axodendritic contacts from mitral cells and from centrifugal fibers. Other dendrites form dendrodendritic synapses with mitral cell dendrites. The morphologic

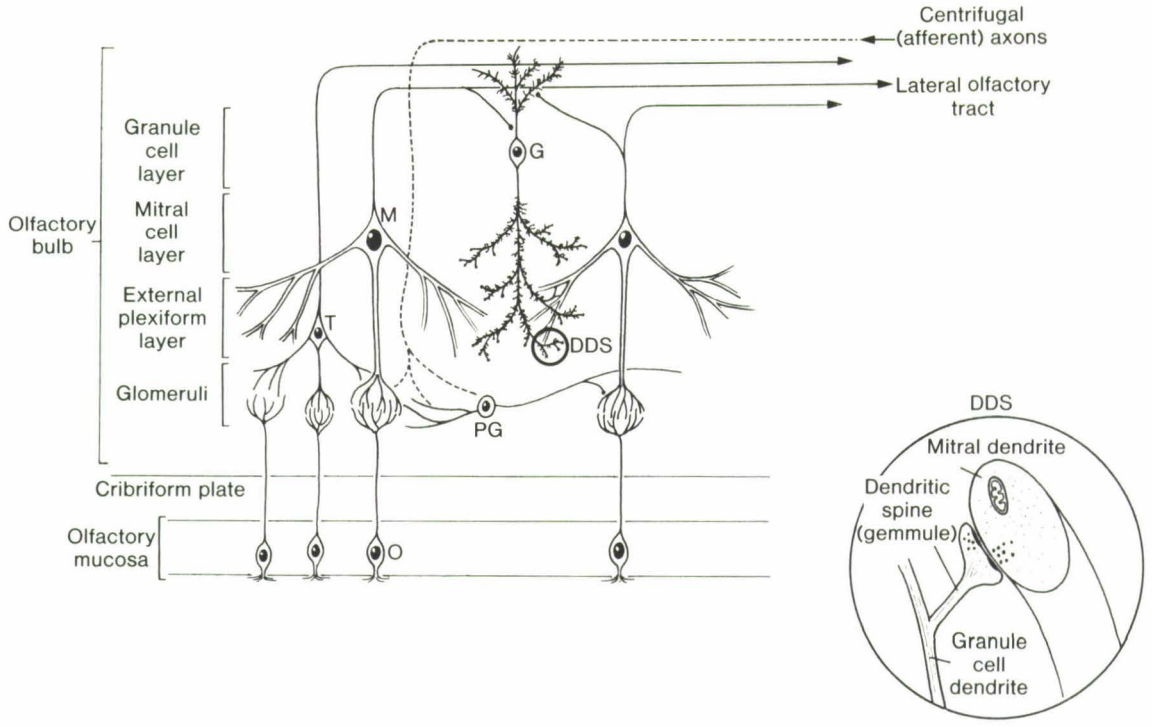


Figure 18.7. Major classes of cells in the olfactory bulb. The sensory receptors (*O*) in the olfactory mucosa are illustrated at the bottom of the Figure. The central process of the receptor enters the olfactory bulb and synapses upon a dendritic tuft of a mitral cell to form a complex called a glomerulus. Axons of mitral cells (*M*) pass centrally to form the lateral olfactory tract. Mitral axons also have recurrent collaterals which synapse upon granule cells. The granule cells (*G*) have no axons. Their external dendrites have dendritic spines which form reciprocal dendrodendritic synapses (*DDS* and *insert*) on mitral dendrites. Periglomerular cells (*PG*) represent several morphologic types of cells linking mitral cell glomeruli. Tufted cells (*T*) are morphologically similar to mitral cells, but their cell bodies are dispersed throughout the external plexiform layer.

features of these junctions suggest reciprocal synapses—one from granule cell to mitral cell, and one from mitral cell to granule cell (Fig. 18.7). Granule cells inhibit mitral cells, and the mitral cells appear to excite the granule cells (76, 244). The complex circuitry of the olfactory bulb recalls that of the retina and suggests that, as is the case with visual images, the olfactory information is partially analyzed and modulated before reaching the cerebral olfactory areas (25).

Olfactory sensory neurons in one side of the nose amount to approximately 50×10^6 in the rabbit, giving rise to as many axons entering each olfactory bulb. This large array of sensory input channels converge onto approximately 2000 glomeruli, to which are connected about 50,000 mitral cells and 100,000 tufted cells (11, 12, 14, 244). Thus, the convergence ratios in the olfactory system are very high: (a) 25,000:1 onto glomeruli; (b) 1000:1 onto mitral cells; and (c) 500:1 onto tufted cells (244).

The *olfactory glomeruli* are the most characteristic feature of the olfactory bulb in all vertebrates. They represent the reception site as well as the first stage in the analysis and modulation of olfactory information. Within these spherical acellular islands, three neuronal elements interact: (a) the olfactory axon, which represents the input fiber; (b) the mitral/tufted cell, which represents the principal neuron; and (c) the periglomerular cell, which represents the intrinsic neuron. These three basic elements form a *synaptic triad* that is characteristic of most brain regions involved in sensory processing (244). The synapse between the input and principal elements provides the necessary basis for input-output transmission, whereas synapses between the principal and intrinsic elements allow for elaboration and control of the input-output transfer. The synaptic triad in the olfactory glomerulus involves synapses from the input onto both the principal and the intrinsic elements. After this initial inter-

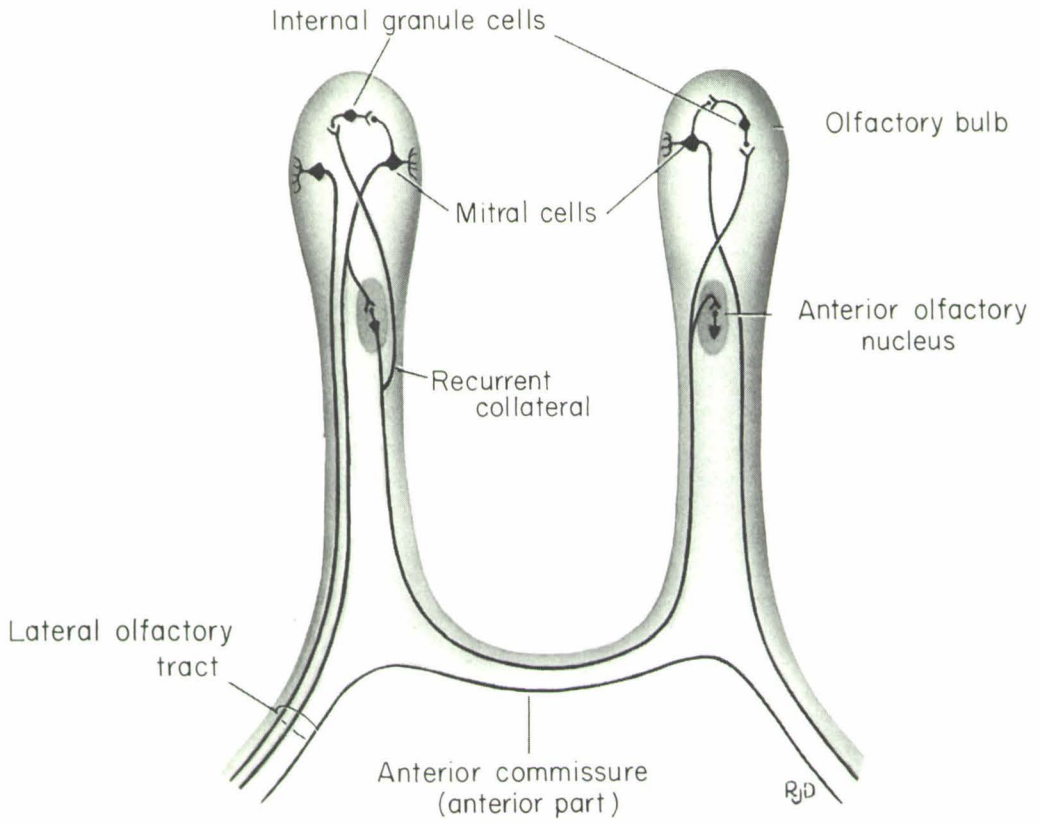


Figure 18.8. Interconnections of the olfactory bulbs and anterior olfactory nuclei. Collaterals of mitral cell axons synapse upon apical dendrites of pyramidal-shaped cells of the anterior olfactory nucleus. These cells give rise to fibers that cross in the anterior part of the anterior commissure and synapse upon cells in the contralateral anterior olfactory nucleus and internal granule cells in the olfactory bulb. Recurrent collaterals of axons of the anterior olfactory nuclei project back to the ipsilateral olfactory bulb to terminate upon internal granule cells, which can, in turn, activate mitral cells. The principal axons of mitral cells enter the lateral olfactory tract.

action, further processing takes place within the glomerulus through the dendrodendritic microcircuits. Moreover, the activity in one glomerulus can affect that in other glomeruli through interglomerular connections mediated chiefly by the axons of periglomerular cells. If glomeruli function as units, then one effect of the interglomerular microcircuits could be to enhance the contrast between glomeruli of different specificities, much like intercolumnar interactions in the cerebral cortex (243, 244). A second level of organization in the olfactory bulb involves interactions between mitral/tufted cells and granule cells, which play a crucial role in the control of the output of the olfactory bulb. Finally, it must be noted that the complex neuronal computation that occurs at various levels in the olfactory bulb is directly under the modulatory influence of different chemospecific centrifugal fiber systems. The most prominent of these centrifugal fiber systems are the serotoninergic fibers of the dorsal raphe nucleus (196), the noradrenergic fibers of the locus coeruleus (32, 95), and the cholinergic fibers that arise from the large neurons of the basal forebrain (202).

Olfactory glomeruli are among the clearest examples in the brain of the principle of grouping of neuronal elements and synapses. They are, in some ways, analogous to "barrels" and "clumps" in the cerebral cortex, representing a higher level of organization than the synaptic glomeruli in the thalamus or the cerebellum (244). Although the arrangement of afferent fibers in the olfactory bulb does not appear to be localized in any patterned way (133), a regional organization of olfactory nerve projections to the olfactory bulb has been demonstrated in mammals (3, 130, 131). Localized lesions in different regions of the olfactory epithelium produce degeneration in specific regions of the glomerular layer (127). Groupings of glomeruli show

marked variations in the intensity of degeneration and some normal glomeruli are present in regions containing degeneration. It has been suggested that a selective projection from receptors in small regions of the olfactory epithelium to specific glomeruli, or groups of glomeruli, could provide the anatomic basis for selective responses to odors. Functional mapping studies with the 2-deoxyglucose (2-DG) method indicate that there are groups of glomeruli with similar specificities for a given odor. This implies that the group of mitral, tufted, and periglomerular cells whose dendrites are connected to a given subset of "specific" glomeruli will all share this specificity, in a manner analogous to the functional columns in the cerebral cortex (243, 244). Such a view is supported by the results of studies that have employed the proto-oncogene *c-fos* as a physiologic marker (92). These investigations revealed that the presentation of specific odors to alert rats for as little as 5 minutes increased *c-fos* mRNA in radially distributed neuronal ensembles that spanned the lamina of the main olfactory bulb. The complementary RNA (cRNA)-labeled neuronal groups consisted of cells in the glomerular layer that precisely defined the borders of individual glomeruli and underlying tufted, mitral, and granule cells. The activated fields were much broader in the granule cell layer than in the overlying glomerular layer, and thus exhibited a flask-like, as opposed to a columnar, contour (92).

Caudal to the olfactory bulb are scattered groups of neurons, intermediate in size between mitral and granule cells, that form the *anterior olfactory nucleus* (Figs. 18.5 and 18.8). Some cells of this loosely organized nucleus are found along the olfactory tract near the base of the hemisphere. Dendrites of these cells pass among the fibers of the olfactory tract, from which they receive impulses. Collateral branches of axons of mitral and tufted cells terminate in the anterior olfactory nucleus. Axons of the cells in this nucleus pass centrally, cross in the anterior part of the an-

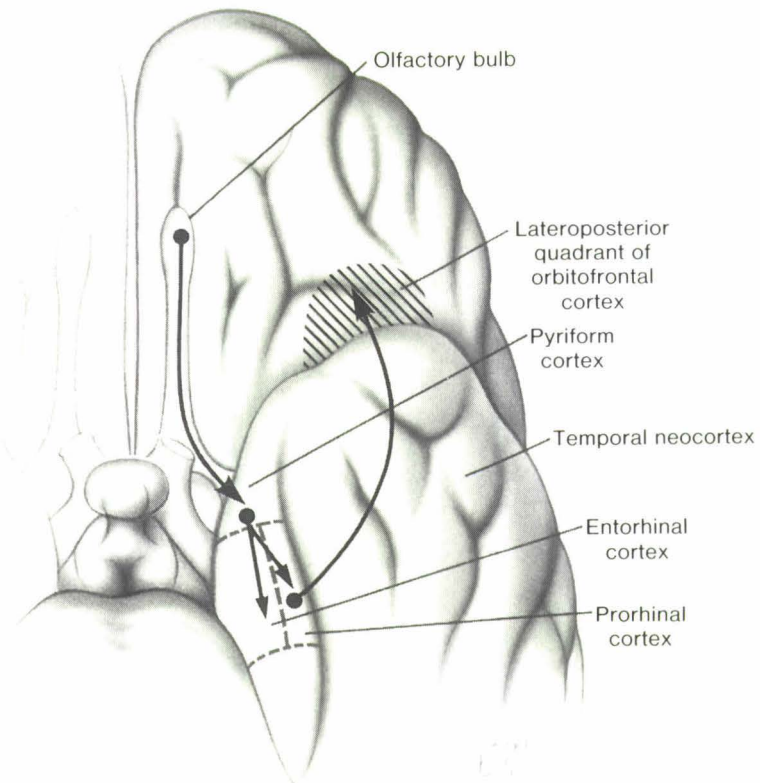


Figure 18.9. Inferior surface of the frontal and temporal lobes of a primate brain showing olfacto-frontal connections. The lateroposterior quadrant of the orbitofrontal cortex receives olfactory information which is relayed from the lateral entorhinal area (perirhinal cortex). The lateral entorhinal area receives olfactory information indirectly from the piriform cortex.

terior commissure and enter the contralateral anterior olfactory nucleus and olfactory bulb (Fig. 18.8) (25, 139, 209, 270). As seen earlier, this is only one of the populations of centrifugal fibers that project to the olfactory bulb. Centrifugal fibers synapse principally with dendrites of the interneurons.

Olfactory Tract

This tract passes toward the anterior perforated substance and divides into well-defined *lateral* and *medial olfactory striae*. A thin covering of gray substance over the olfactory striae composes the *lateral* and *medial olfactory gyri*. The lateral olfactory stria and gyrus pass along the lateral margin of the anterior perforated substance to reach the piriform region (124) (Figs. 18.9 and 18.10). Fibers of the lateral olfactory stria arising in the olfactory bulb give collaterals to the anterior olfactory nucleus and the anterior perforated substance, which corresponds to the olfactory tubercle in macrosmatic animals. These fibers terminate in the piriform cortex (also termed prepiriform cortex) and in the corticomedial part of the amygdaloid nuclear complex (11, 12, 93, 132, 209, 213, 216). Terminations of these fibers also are present in the nucleus of the lateral olfactory tract and in parts of the anterior amygdaloid nucleus.

Olfactory Lobe

This lobe develops as a longitudinal bulge on the basal surface of the hemisphere, where it is separated from the neocortex by the rhinal sulcus (Fig. 2.10). It soon differentiates into anterior and posterior portions. The anterior portion, at first containing an extension of the lateral ventricle, elongates into a tubular stalk which becomes solid by the end of the third month, and forms the rudiment of the olfactory tract and bulb. The posterior

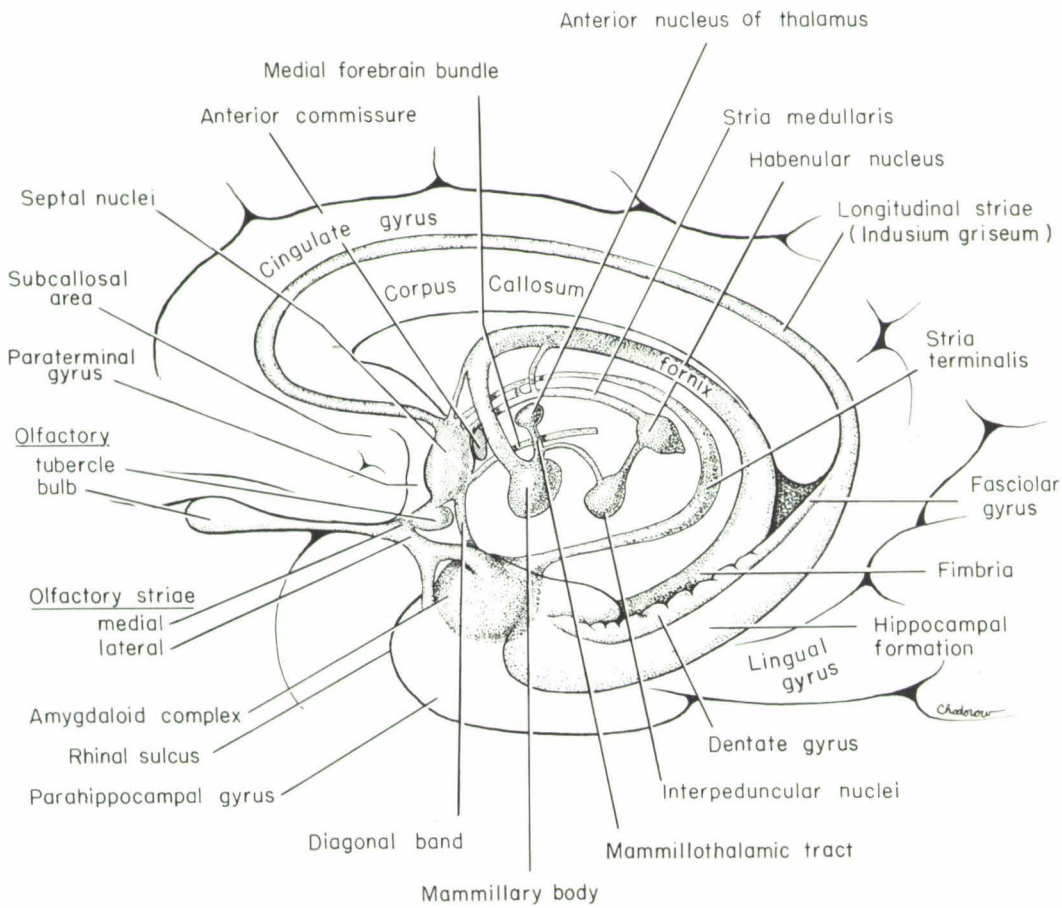


Figure 18.10. "Rhinencephalic" structural relationships as seen in medial view of the right hemisphere. Both deep and superficial structures are indicated.

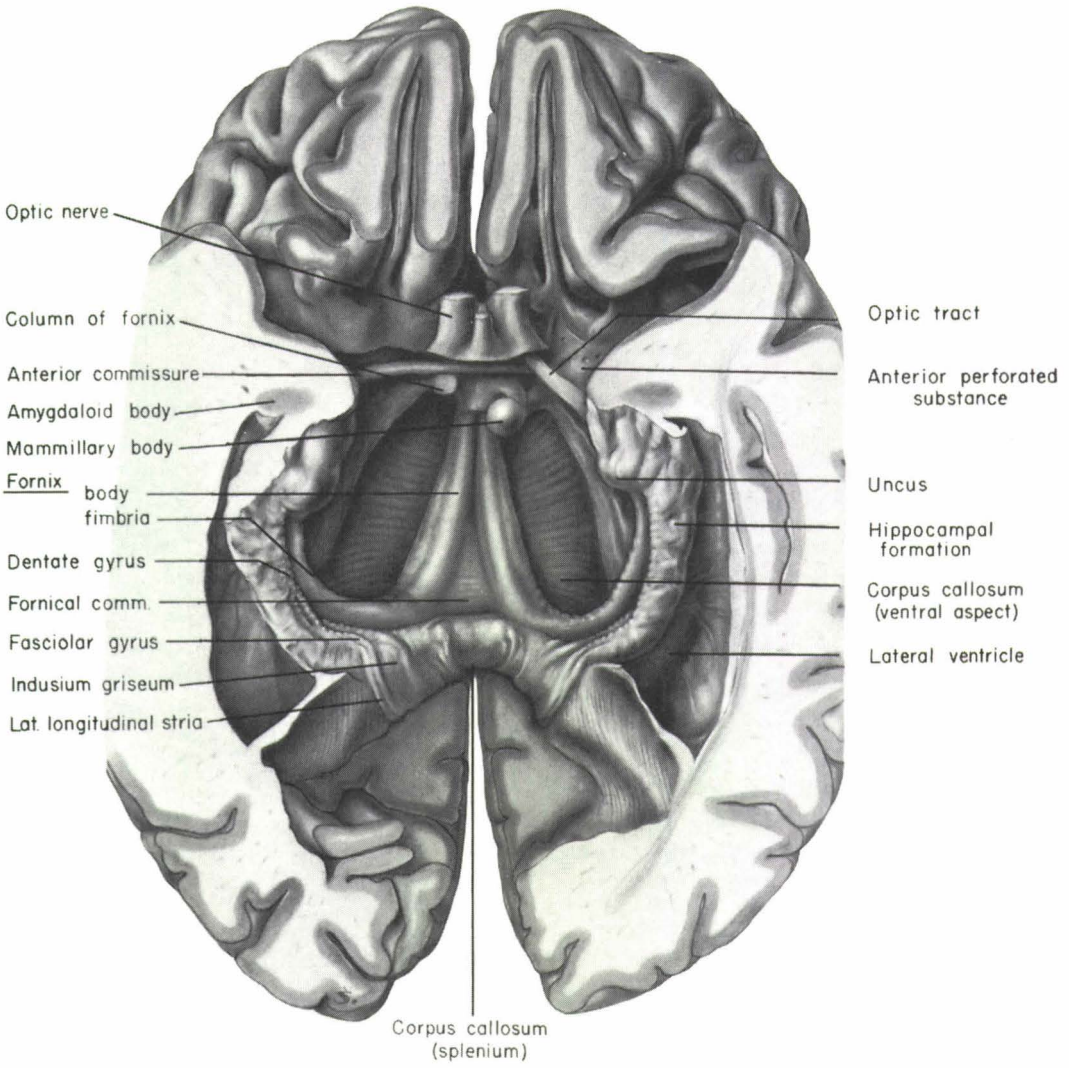


Figure 18.11. Dissection of the inferior surface of the brain showing the configuration of the fornix, the hippocampus, the dentate gyrus, and related structures.

portion differentiates into the olfactory area (anterior perforated substance) and certain other olfactory structures closely related to the anteromedial portion of the temporal lobe, collectively known as the piriform lobe.

The *piriform lobe*, so named because of its pear shape in certain species, is divided into several regions (Fig. 18.9). These include the *piriform*, the *periamygdaloid*, and the *entorhinal areas*. The piriform area, often referred to as the lateral olfactory gyrus, extends along the lateral olfactory stria to the rostral amygdaloid region (Figs. 18.9 and 18.10). Since its afferent fibers are derived from the lateral olfactory stria, it is regarded as an olfactory relay center. The periamygdaloid area is a small region dorsal and rostral to the amygdaloid nuclear complex. The entorhinal area, the most posterior part of the piriform lobe, corresponds to area 28 of Brodmann and constitutes a major portion of the anterior parahippocampal gyrus in humans (Figs. 18.9 and 18.10). The rostral part of the parahippocampal gyrus is rolled inward and upward as a consequence of the tremendous development of the neocortex. The rostromedial protrusion of this gyrus is the *uncus* (160) (Figs. 2.10 and 18.11). Fibers of the lateral olfactory stria, arising in the olfactory bulb, give collaterals to the anterior olfactory nucleus and the olfactory tubercle, and terminate in the piriform cortex and in parts of the amygdaloid nuclear complex (93, 94, 213, 216, 235, 273).

The piriform cortex and the periamygdaloid area, which receive fibers from the lateral olfactory stria, constitute the *primary olfactory cortex*. Olfaction appears to be unique among the sensory systems, in that impulses in this system project to the cortex without being relayed by thalamic nuclei. The piriform cortex projects fibers to the entorhinal cortex (area 28), the basal and lateral amygdaloid nuclei, the lateral preoptic area, the nucleus of the diagonal band, and parts of the mediodorsal nucleus of the thalamus (93, 216, 244). The entorhinal cortex is the *secondary olfactory cortical area* (Figs. 18.9). Efferent fibers from the entorhinal cortex are projected to the hippocampal formation, and to the anterior insular and frontal cortex via the uncinate fasciculus (Fig. 2.18). No fibers from the piriform cortex pass to the hippocampal formation.

The lateroposterior quadrant of the orbitofrontal cortex receives olfactory information via relays in the piriform and entorhinal cortex (207) (Fig 18.9). Additionally, the piriform cortex projects to the magnocellular portion of the mediodorsal nucleus (MDmc) of the thalamus (209), which in turn projects to the orbitofrontal cortex (see Chapter 16).

Different parts of the amygdaloid nuclear complex receive olfactory inputs. Direct projections from the olfactory bulb pass to the cortical and medial amygdaloid nuclei, while indirect olfactory impulses pass to the basal and lateral amygdaloid nuclei, via relays in the piriform cortex. Direct and indirect olfactory pathways to the amygdaloid complex terminate in different components that probably influence almost the entire complex.

Fibers originating from the cells of the anterior olfactory nucleus project (a) peripherally to internal granule cells of the ipsilateral olfactory bulb, and (b) via the anterior part of the anterior commissure to the contralateral anterior olfactory nucleus and olfactory bulb. Projections from the anterior olfactory nucleus on one side thus reach internal granule cells of the olfactory bulb on both sides and the contralateral anterior olfactory nucleus (Fig. 18.8).

The medial olfactory stria becomes continuous with the subcallosal area and the paraterminal gyrus (Figs. 18.6 and 18.10). Some of the fibers in this stria may reach the olfactory tubercle, a prominent structure in macrosmatic species located immediately above the anterior perforated substance. The *anterior perforated substance* is a rhomboid-shaped region bounded by the medial and lateral olfactory striae and the optic tract (Figs. 2.10, 18.6, and 18.11). This region is studded with perforations made by penetrating blood vessels (Fig. 4.11). The posterior border of this region is formed by the *diagonal band of Broca* (Fig. 18.6).

The *subcallosal area* and the *paraterminal gyrus* together constitute the septal area. The term *septal area* refers to the cortical part of this region, beneath which are the septal nuclei. The *medial* and *lateral septal nuclei* lie rostral to the anterior commissure and the preoptic area near the base of the septum pellucidum (Figs. 18.10 and 18.11). The medial septal nucleus becomes continuous with the nucleus and tract of the diagonal band and has connections with the hippocampal formation. Cells of the medial septal nuclei and the nuclei of the diagonal band are strongly cholinergic (Fig. 18.23). The septal nuclei receive afferents from the hippocampal formation via the fornix (175, 176, 217). Afferents to the medial septal nucleus ascend in the medial forebrain bundle and mammillary peduncle (90, 91, 180) (Figs. 18.2 and 18.3). Efferent fibers from the septal nuclei project via (a) the stria medullaris to the medial habenular nucleus, (b) the medial forebrain bundle to the lateral hypothalamus and midbrain tegmentum, and (c) the fornix to the hippocampal formation (52, 217) (Figs. 17.17 and 18.3).

Vomeronasal System and Terminal Nerve

VOMERONASAL SYSTEM

In addition to receptors in the olfactory epithelium, chemosensory receptor cells are found in most mammalian species in the *vomeronasal organ* (of Jacobson), which is a bilateral, blind-ended tube in the ventral part on each side of the nasal septum. The receptor neurons are similar to those in the olfactory epithelium, except that they have microvilli rather than cilia at their apical pole. Vascular connective tissue with sympathetic vasomotor innervation separates the vomeronasal epithelium from the rigid cartilaginous wall of the tube. The central processes of vomeronasal sensory cells form the *vomeronasal nerve*, which passes through the cribriform plate alongside the olfactory nerves and ends in the so-called *accessory ol-*

factory bulb located along the dorsal aspect of the main olfactory bulb. In the accessory olfactory bulb, the axons of the vomeronasal nerve contact mitral/tufted cells whose axons course in the lateral olfactory tract and terminate in sectors of the amygdala involved in the control of sexual behavior (see later). In several nonprimate mammals, as well as in reptiles, the entrance of the vomeronasal organ is immediately dorsal to the nasopalatine foramen, through which the oral and nasal cavities communicate (25). Activity of the sympathetic nervous system causes constriction of the blood vessels of the vomeronasal organ, making the connective tissue layer thinner because it contains less blood. The resulting enlargement of the lumen sucks in tiny drops of liquid that have been either sniffed into the nostrils or placed by the tongue into the nasopalatine foramen.

The vomeronasal system plays an important role in the detection of chemical messages from other members of the same species. The compounds (*pheromones*) used as sexual attractants and for delineating territory may be secreted by specialized sweat or sebaceous glands, or they may be excreted in the urine (25). In animals with well-developed vomeronasal systems, such as snakes and rodents, transection of the vomeronasal nerves impairs reproductive behavior (158, 211, 289).

In humans, there is no accessory olfactory bulb, and the vomeronasal organ has been assumed to be vestigial or absent and without functional significance (288). However, recent studies in humans revealed the presence of vomeronasal pits in all individuals except those with pathologic conditions affecting the septum (165, 249). Electron microscopy of the adult human vomeronasal organ indicates the presence of two potential receptor elements in the pseudostratified epithelial lining: microvillar cells, and unmyelinated, intraepithelial axons. Additionally, unmyelinated axons are common in the lamina propria surrounding the organ. They appear to constitute the components essential for a functional chemosensory system, and may thus provide the basis for a pheromone detection system as in other animals (211, 249, 288). In some nonhuman primates, the involvement of the vomeronasal system in the detection of urinary signals has been demonstrated with the use of the 2-deoxyglucose (2-DG) method (233). This study has revealed that urine in the volatile phase specifically activates the main olfactory bulb, whereas urine in the liquid phase activates the accessory olfactory bulb only. Thus, the vomeronasal system may play an important role that is complementary to that of the principal olfactory system.

TERMINAL NERVE

The fibers of the tiny terminal nerve (*nervus terminalis*) lie along the medial side of the olfactory bulb and olfactory tract. The bipolar neurons that give rise to the terminal nerve occur in small ganglia scattered along the course of the nerve. Their distal processes pass through the cribriform plate and are distributed to the nasal septum (25). In experimental animals, the proximal processes have been traced to the septal and preoptic areas. Evidence obtained in various species indicate that the terminal nerve exerts a strong influence on the reproductive system during development and in the adult. This influence could be mediated, at least in part, by luteinizing hormone-releasing hormone (LHRH) because immunoreactivity for this peptide has been visualized in both cell bodies and fibers associated with this nerve (182).

The terminal nerve is present, although in microscopic size, in adult humans. It is often called nerve zero because it lies medial, and, therefore, perhaps rostral, to the olfactory nerves (25). Both the terminal and the vomeronasal nerves were discovered after the 12 main cranial nerves were given their numbers.

Clinical Considerations

The ability of the human nose, in concert with the brain, to discriminate thousands of different odors is well-known, but the physiologic and psychologic bases for such discriminations are not yet entirely known. Olfactory discrimination is not based on morphologically distinct types of receptors, but there is some evidence that certain odors may be distinguished by their effectiveness in stimulating particular regions of the olfactory epithelium (92, 127, 171, 244). Current theories suggest that spatial and temporal factors probably play important roles in coding of olfactory responses (170). Functional mapping studies with either 2-DG or *c-fos* methods revealed that stimulation with one odor (e.g., amylacetate, which has a fruity smell) activates glomeruli in certain regions of the olfac-

tory bulb, whereas stimulation with a different odor (e.g., camphor) activates glomeruli in other regions of the olfactory bulb (92, 244).

Other evidence indicates that the sense of smell is based on molecular geometry (19, 22). Molecules identical in every respect, except that one is the mirror image of the other, may have different odors. Seven primary odors (i.e., camphoraceous, musky, floral, pepperminty, ethereal (ether-like), pungent, and putrid) are considered to be equivalent to the three primary colors, because every known odor can be produced by appropriate mixtures of primary odors. Molecules with the same primary odor appear to have particular configurations, and these configurations are thought to fit appropriately shaped receptors. Molecules that may fit more than one receptor are considered to signal complex odors.

Odor discrimination is mediated via dendritic cilia of olfactory receptor neurons. Odorants traverse the aqueous mucous interphase that lines the surface of the olfactory neuroepithelium and interact with odorant receptors, which are members of the superfamily of G-protein-linked receptors. These interactions trigger synthesis of second messengers, including adenosine 3′,5′-cyclic monophosphate (cAMP) and inositol triphosphate (IP_3). Cyclic AMP opens a cation channel to elicit the generator current, which depolarizes the cell and, ultimately, leads to action potentials. Inositol triphosphate opens a calcium channel in the ciliary plasma membrane. Calcium entering through both this channel and the cyclic nucleotide-gated channel modulates the response to odorants by amplifying the generation of cyclic AMP after binding to calmodulin. Calcium is also essential for desensitization of olfactory receptor neurons. Differential expression of odorant receptors of diverse ligand specificities by different olfactory neurons, ensures that the structures and concentrations of odorants that reach the chemosensory surface are encoded as distinct patterns of neuronal activity. These are relayed to the brain where they take shape as characteristic odor sensations (22). Recently, the interplay between guanosine 3′,5′-cyclic monophosphate (cGMP) and nitric oxide (NO) synthase was involved in the triggering of molecular mechanisms, including adaptation processes, which enable the olfactory neuroepithelium to cope with strong stimuli (37).

It is estimated that the nose of macrosmatic mammals can detect and discriminate 10,000 different odor-bearing molecules in the environment. These constitute by far the largest single class of ligands detected by any neuronal signal-transducing system. Whether this gigantic task of detection and recognition is accomplished by the presence of a large number of peripheral receptors with high affinity and specificity for odor ligands or is the result from central processing of the input from only a few receptors with overlapping specificities is still unclear. Recent molecular biologic studies, however, have led to the identification of large multigene family, which comprises at least 100 distinct gene encoding specific odorant receptors (43). This finding suggests that the receptor neurons are the main site of odor discrimination and that considerable stimulus information can be encoded at the peripheral level.

From a clinical viewpoint valuable information can be obtained by testing olfactory sense by appropriate methods. Olfaction is tested in each nostril separately by having the patient inhale or sniff nonirritating volatile oils or liquids with characteristic odors. Substances which stimulate gustatory end organs, or peripheral endings of the trigeminal nerve in the nasal mucosa, are not appropriate for testing olfaction. Comparisons between the two sides are of great importance.

While the olfactory nerves are rarely the seat of disease, they frequently are involved by disease or injury of adjacent structures. Fractures of the cribriform plate of the ethmoid bone or hemorrhage at the base of the frontal lobes may cause tearing of the olfactory filaments. The same injury may result in leakage of the cerebrospinal fluid from the subarachnoid space into the nasal cavity, so that the fluid runs from the nose (cerebrospinal fluid rhinorrhea). This abnormal communication with the external environment is dangerous because it provides a route whereby bacteria and viruses may attack the meninges and the brain. Even in normal conditions, the olfactory nerve appears to be a privileged route for viral infection and dissemination (24, 281). The olfactory nerves may be involved as a consequence of meningitis or abscess of the frontal lobe.

Unilateral loss of the olfaction sense or *anosmia* may be of important diagnostic significance in localizing intracranial neoplasms, especially meningiomas of the sphenoidal ridge or olfactory groove. Hypophysial tu-

mors affect the olfactory bulb and tract only when they extend above the sella turcica. Olfactory "hallucinations" frequently are a consequence of lesions involving or irritating the parahippocampal gyrus, the uncus or adjoining areas around the amygdaloid nuclear complex. The olfactory sensations which these patients experience usually are described as disagreeable in character and may precede a generalized convulsion. Such seizures are referred to as "uncinate fits."

Olfactory deficits and degenerative changes in central olfactory pathways are prominent in patients with Alzheimer's disease. Degenerative changes occur in the olfactory bulb, olfactory cortices, as well as in the olfactory neuroepithelium. Immunohistochemical studies of nasal tissue taken at autopsy reveal extensive degeneration in the sensory epithelium as well as abnormal neurites that share immunoreactive epitopes with dystrophic neurites and neurofibrillary tangles of the brains of Alzheimer patients (129, 261). The neuritic masses can be stained with well-characterized monoclonal antibodies that do not normally stain olfactory neurons but which are very reactive with dystrophic neuritic structures and neurofibrillary tangles in the brains of Alzheimer patients. These include antibodies to phosphorylated and nonphosphorylated neurofilament subunits, tau, and also Alz 50, which is characteristically reactive in Alzheimer's disease but not in normal conditions. Such accumulations of ectopic neurites are present in 81% of Alzheimer's disease patients (261).

ANTERIOR COMMISSURE

The anterior commissure crosses the midline as a compact fiber bundle immediately in front of the anterior columns of the fornix (Figs. 2.14, 2.15, 16.2, 18.2, 18.10, 18.11, and A.25 in the atlas of the human brain, section VII). Proceeding laterally, it splits into two portions. The small anterior, or olfactory portion, greatly reduced in man, loops rostrally and connects the gray substance of the olfactory tract on one side with the olfactory bulb of the opposite side (Fig. 18.12). Fibers in this part of the anterior commissure arise from the anterior olfactory nucleus, cross to the opposite side and project to the contralateral anterior olfactory nucleus and to granule cells in the olfactory bulb (Fig. 18.8). It has been suggested (208) that these centrifugal fibers may subserve reflex control of activity in the olfactory bulb, and in principle may be com-

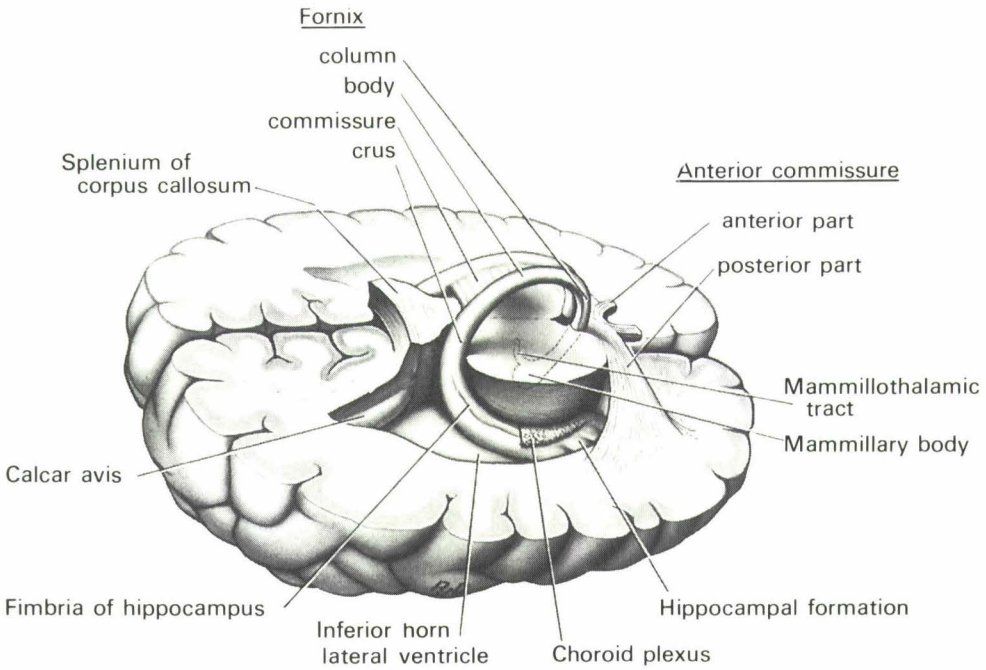


Figure 18.12. Brain dissection showing the hippocampal formation, the fornix system and the anterior and posterior parts of the anterior commissure. Postcommissural fibers of the fornix are here shown projecting only to the mammillary body.

parable to the efferent system to sensory nuclei at spinal levels.

The larger posterior portion forms the bulk of the anterior commissure. From its central region, fibers of the anterior commissure pass laterally and backward through the most inferior parts of the lateral segment of the globus pallidus and putamen, a relationship most obvious in sagittal sections of the brain (Figs. 19.6, A.31, and A.32). Further laterally, the fibers of the anterior commissure enter the external capsule and come into apposition with the inferior part of the claustrum. On entering the external capsule the fibers of the commissure twist so that posterior fibers pass ventrally. Fibers of the posterior portion of the anterior commissure mainly interconnect the middle temporal gyri, although some pass into the inferior temporal gyrus (72, 282).

Anatomic and physiologic investigations in experimental animals indicate that olfaction is subserved by several cortical regions, but the areas implicated in the human olfactory system have not been definitively identified by functional criteria. Behavioral evidence has suggested that laterally specialized mechanisms for odor processing may exist, but the neuroanatomic substrate remains unknown. The cortical representation of human olfactory processing was recently investigated by comparing cerebral blood flow changes evoked during olfactory stimulation with those of a control task with positron emission tomography (PET) (292). Significant cerebral blood flow increases were observed during olfactory stimulation at the junction of the inferior frontal and temporal lobes bilaterally, corresponding to the piriform cortex, and unilaterally, in the right orbitofrontal cortex. The results complement and extend previous data implicating these regions in olfactory processing, and indicate that a functional asymmetry exists in the human brain favoring the right orbitofrontal area in olfaction (292).

HIPPOCAMPAL FORMATION

Topographic Organization

The hippocampal formation is laid down in the embryo on the medial wall of the hemisphere along the hippocampal fissure. This fissure lies immediately above and parallel to the choroidal fissure, which marks the invagination of the choroid plexus into the ventricle (Fig. 3.15). With the formation of the tempo-

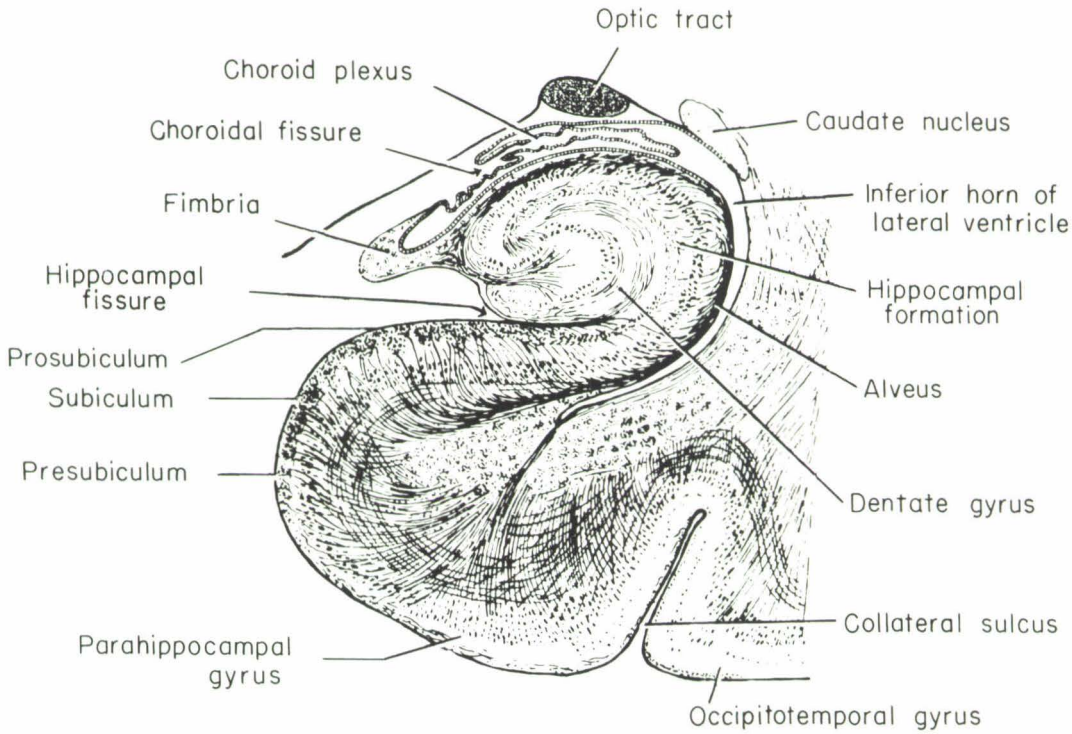


Figure 18.13. Transverse section through the human hippocampal formation and parahippocampal gyrus.

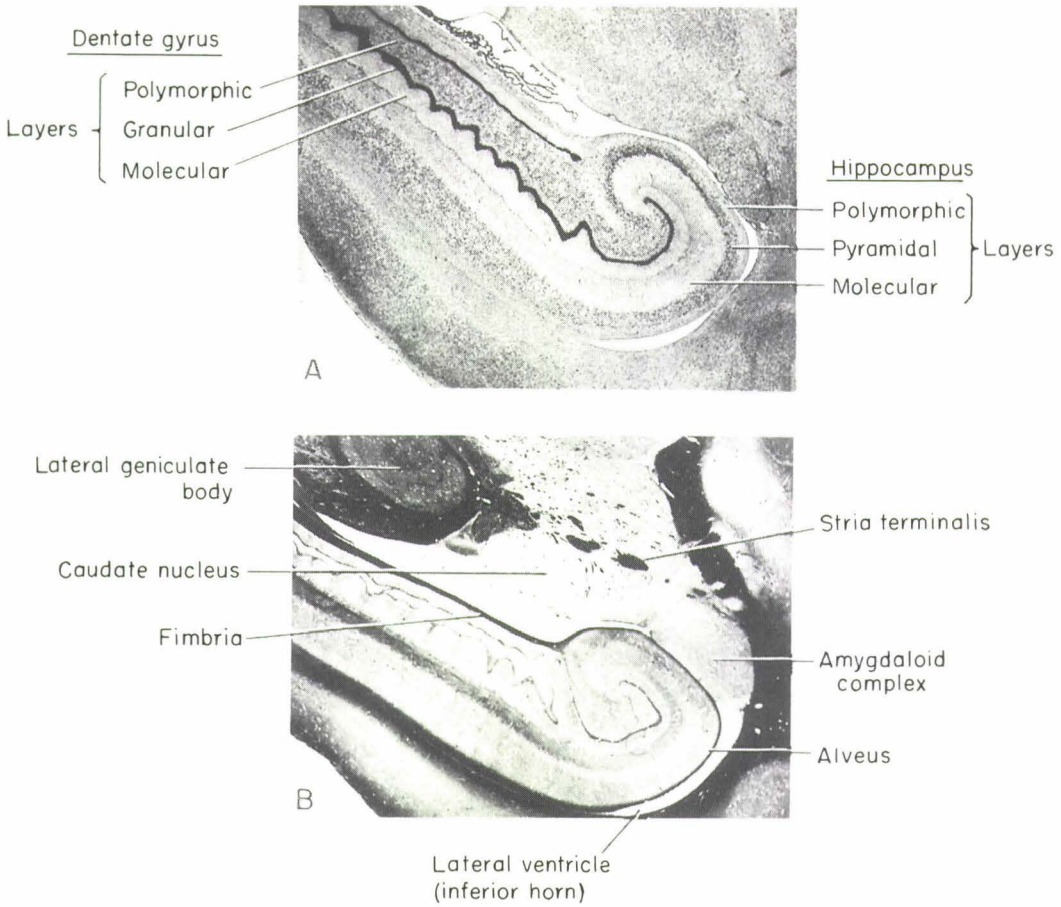


Figure 18.14. Sagittal sections through the hippocampal formation in the rhesus monkey showing the relationships of the hippocampus and dentate gyrus to the inferior horn of the lateral ventricle, the striatum, and the amygdaloid nuclear complex. In **A**, the cellular layers of the hippocampus and dentate gyrus are identified, whereas in **B**, the alveus, fimbria, tail of the caudate nucleus, stria terminalis, amygdaloid complex, and part of the lateral geniculate body are indicated (**A**, Nissl stain, ×8; **B**, Weil stain, ×9).

ral lobe, both these fissures are carried downward and forward, each forming an arch extending from the region of the interventricular foramen to the tip of the inferior horn of the lateral ventricle (Fig. 3.17). The various parts of the hippocampal arch do not develop to the same extent. The dorsal portion of the hippocampal fissure is invaded by commissural fibers of the corpus callosum and ultimately becomes the callosal fissure. The part of the hippocampal formation that remains above the corpus callosum, undergoes little differentiation; in the adult, it forms a thin vestigial convolution, the *indusium griseum* (Figs. 18.10 and 18.11).

The temporal part of the arch, which is not affected by the corpus callosum, differentiates into the hippocampal formation. As the hippocampal fissure deepens, the invaginated portion bulges deeply into the inferior horn of the lateral ventricle and becomes the *hippocampus*. The lips of the fissure give rise to the *dentate* and the *parahippocampal gyri*. The relationships between the three major components of the hippocampal formation, that is, the hippocampus proper (or Ammon's horn), the dentate gyrus, and the subicular cortex, are best illustrated in frontal sections or in special dissections (Figs. 18.11–18.13). Proceeding from the collateral sulcus, the *parahippocampal gyrus* extends to the hippocampal fissure, where it dips into the lateral ventricle to form the *hippocampus*. The latter curves dorsally and medially and, on reaching the medial surface, curves inward again to form a semilunar convolution, the *dentate gyrus* or *fascia dentata* (Figs. 18.14 and 18.15). The whole ventricular surface of

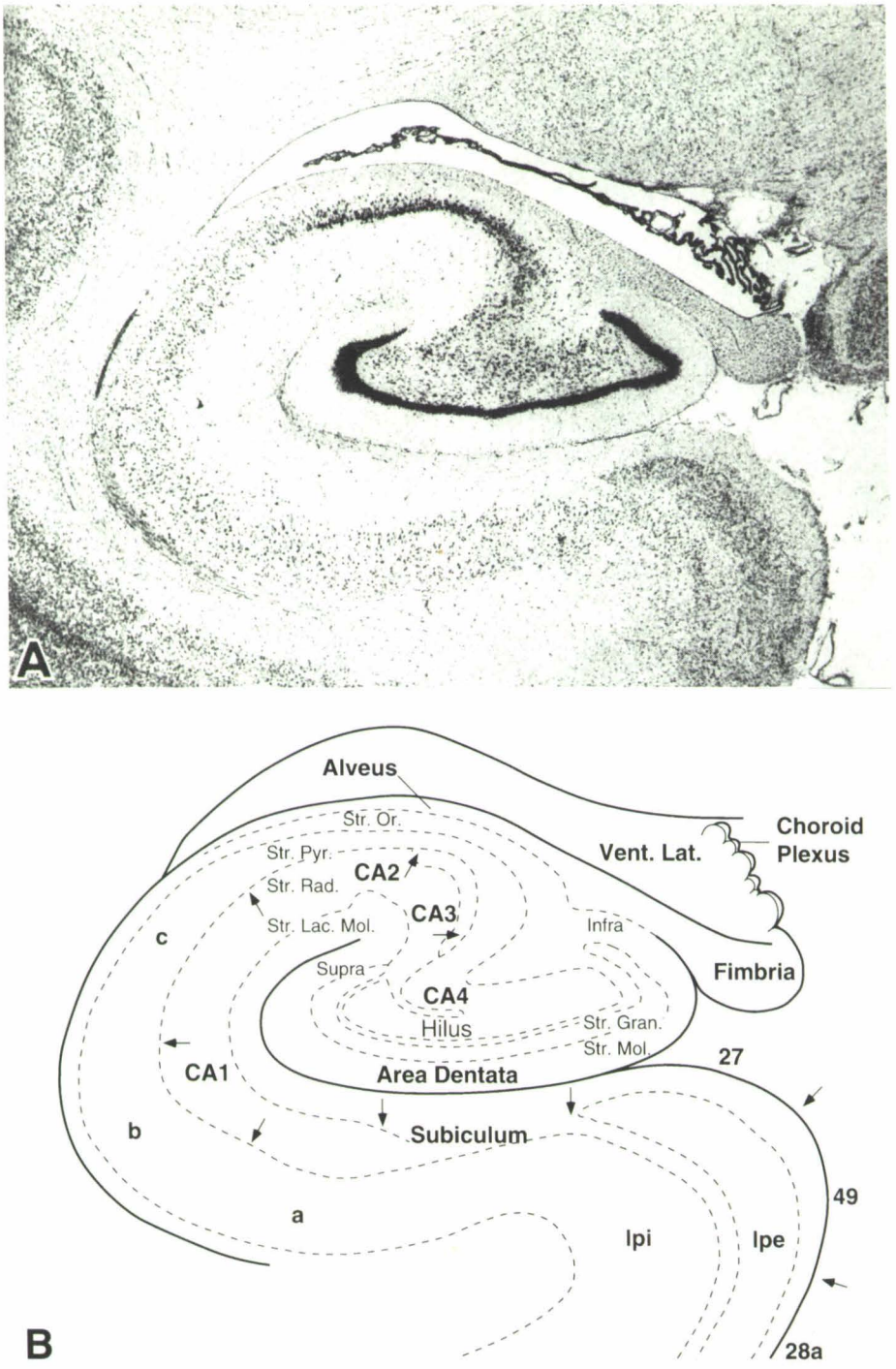


Figure 18.15. Hippocampal region in the rhesus monkey in horizontal section showing the respective layers of the hippocampal formation and dentate gyrus, as seen on a photograph (×20) of a Nissl stained section (**A**) and a corresponding drawing (**B**). The borders of the layers and sectors of the hippocampal formation are designated according to Lorente de Nó. *28a*, entorhinal area; *area 49*, parasubiculum; *area 27*, presubiculum; *Str. gran.*, stratum granulosum; *Str. Lac-Mol.*, stratum lacunosum moleculare; *Str. Mol.*, stratum moleculare; *Str. Or.*, stratum oriens; *Str. Pyr.*, stratum pyramidale; *Str. Rad.*, stratum radiatum; *supra* and *infra*, suprapyramidal and infrapyramidal limbs of the stratum granulosum; *lpi*, lamina principalis interna; *lpe*, lamina principalis externa.

the hippocampal formation is covered by a white layer, the *alveus*, which is composed of axons from cells of the hippocampus and subicular cortex (Figs. 18.13–18.15). These fibers converge on the medial surface of the hippocampus to form a flattened band, the *fimbria*, lying medial to the hippocampus and the dentate gyrus. Fibers from the alveus entering the fimbria constitute the beginning of the fornix system (Figs. 18.10–18.12). The free, thin border of the fimbria is directly continuous with the epithelium of the choroidal fissure, which lies immediately above it. The choroid plexus, invaginated into the ventricle along this fissure, partly covers the hippocampus (Fig. 18.13). The superior portion of the parahippocampal gyrus adjoining the hippocampal fissure is known as the *subiculum*, and the area of transition between it and the parahippocampal gyrus, is known as the *presubiculum* (Fig. 18.13).

On the basis of phylogenetic observations, the cerebral cortex can be divided into an older portion, the *allocortex*, and a newer part, the *isocortex* or *neocortex*. The allocortex consists, in turn, of the *archicortex* and *paleocortex*. The presubiculum, subiculum, prosubiculum, hippocampus, and dentate gyrus have an archicortical structure, while the piriform cortex is paleocortical. The larger inferior portion of the parahippocampal gyrus near the collateral sulcus (Figs. 2.6 and 2.10) has a six-layered transitional lamination resembling the isocortex.

When the hippocampal fissure is opened up, the *dentate gyrus* is seen as a narrow, notched band of cortex between the hippocampal fissure below and the fimbria above (Fig. 18.11). In sagittal sections (Fig. 18.14), the relationships between the hippocampal formation, the dentate gyrus, the amygdaloid nucleus and the inferior horn of the lateral ventricle are readily appreciated. Traced backward, the dentate gyrus accompanies the fimbria almost to the splenium of the corpus callosum. There it separates from the fimbria, loses its notched appearance, and, as the delicate *fasciolar gyrus*, passes on to the superior surface of the corpus callosum (Fig. 18.11). It spreads out into a thin gray sheet representing a vestigial convolution, the *indusium griseum or supracallosal gyrus* (Figs. 18.10 and 18.11). Imbedded in the indusium griseum are two slender bands of myelinated fibers, which appear as narrow longitudinal ridges on the superior surface of the corpus callosum. These are the *medial* and *lateral longitudinal striae* (of Lancisii), which constitute the white matter of these vestigial convolutions (Figs. 2.11 and 18.11). The indusium griseum and the longitudinal striae extend the whole length of the corpus callosum, pass over the genu, and become continuous with the paraterminal gyrus, which is in turn prolonged into the diagonal band of Broca (Fig. 18.6). Traced forward, the dentate gyrus extends into the notch between the uncus and hippocampal gyrus. Here it makes a sharp dorsal bend and passes as a smooth band across the inferior surface of the uncus. This terminal portion is known as the *band of Giacomini*, and the part of the uncus lying posterior to it often is designated as the *intralimbic gyrus*.

Subicular Cortex and Hippocampus

The cortical zones from the parahippocampal gyrus through the presubiculum, the subiculum, and the prosubiculum to the hippocampus and the dentate gyrus show a gradual transition from a six- to three-layered cellular organization (Figs. 18.13 and 18.15). Although the entorhinal region (area 28) is six-layered cortex, it represents a transitional form not typical of neocortex. In more medial cortical areas, certain layers of the entorhinal cortex drop out and undergo rearrangement, so that the cortex of the hippocampus has only three fundamental layers. These are the *polymorphic layer*, the *pyramidal layer*, and the *molecular layer* (Fig. 18.14). Several secondary laminae are formed by the arrangement of axons and dendrites of cells within the fundamental layers. Immediately beneath the ependyma of the lateral ventricle is the alveus. Recognized laminae passing inward from the alveus are (a) the stratum oriens, (b) the stratum pyramidale, (c) the stratum radiatum, (d) the stratum lacunosum, and (e) the stratum moleculare (Figs. 18.15 and 18.18). The last three laminae are considered to correspond to the molecular layer of the neocortex (140, 141, 199).

The most characteristic layer of the hippocampal formation is the pyramidal layer consisting of large and small pyramidal and Golgi type II cells (Fig. 18.16). *Large* and *small pyramidal cells* exhibit many morphologic differences, especially in dendritic development. Some of the cells are described as double pyramids because of the rich dendritic

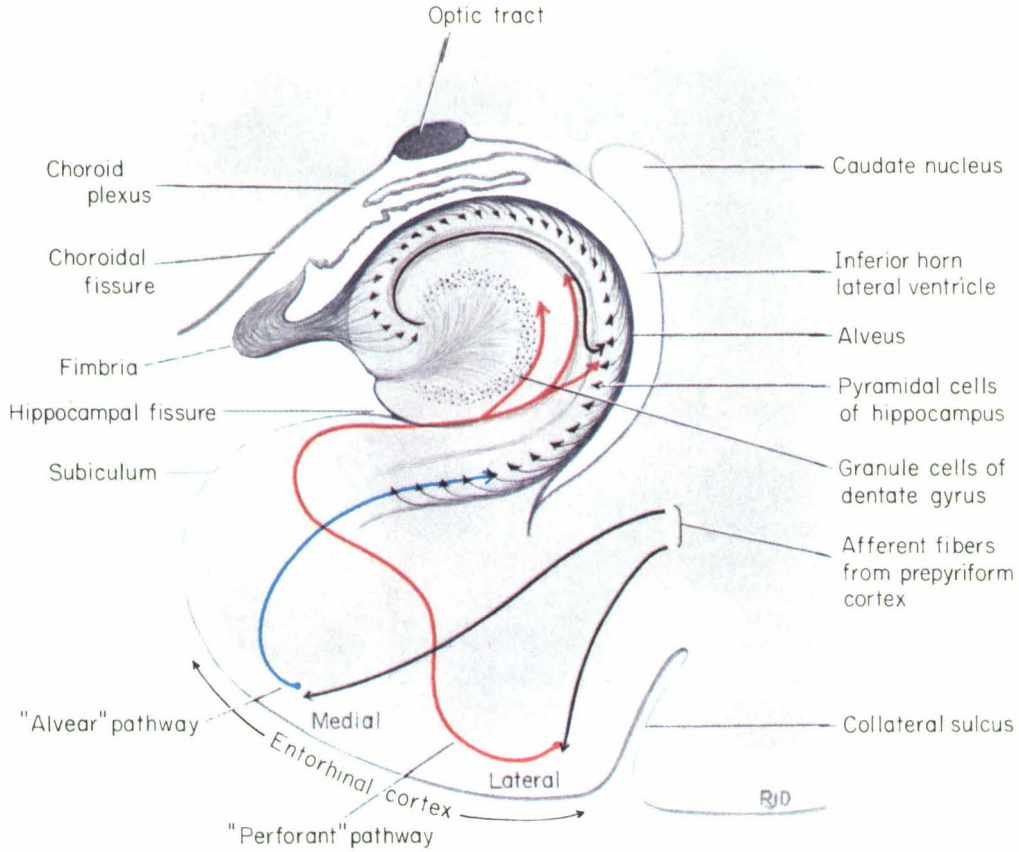


Figure 18.16. Hippocampal formation, dentate gyrus, and entorhinal area. In the dentate gyrus, only the granular layer is indicated. In the hippocampus, only pyramidal cells and their axons projecting into the alveus are shown. Afferent fibers from the prepiriform cortex projecting to the entorhinal cortex are shown in *black*. Projections of the entorhinal cortex to the hippocampal formation follow two pathways: (a) the lateral region gives rise to fibers which follow the so-called "perforant" pathway (*red*), and (b) the medial region gives rise to fibers which follow the so-called "alvear" pathway (*blue*). Axons of pyramidal cells in the hippocampal formation, including those in the subiculum, enter the alveus, and pass to the fimbria of the hippocampal formation. The dentate gyrus gives rise to fibers that remain within the confines of the hippocampal formation.

plexuses arising from both poles (Fig. 5.8J). Basal and apical dendrites of the pyramidal cells enter adjacent layers, while axons of these cells pass through the stratum oriens to enter the alveus (Fig. 18.16). On their way to the fornix, branches of pyramidal cell axons, called *Schaffer collaterals*, pass through the polymorphic and pyramidal cell layers to synapse in the molecular layer with the dendrites of other pyramidal neurons. *Hippocampal basket cells*, similar to the pyramidal cells, are found mainly near the border between the stratum pyramidale and the stratum oriens (219). Their axons do not enter the alveus, but loop back through the stratum radiatum to form a dense basket plexus about pyramidal cell bodies. The stratum oriens, containing fibers and polymorphic cells, has been divided into outer and inner zones. Cells of the outer zone distribute axons to the molecular layer. Cells of the inner zone send some axons into the alveus, while others ramify within this layer or pass into the pyramidal layer. The stratum radiatum is made up largely of interlacing and branching processes which appear to radiate from the bordering pyramidal layer. The stratum lacunosum and stratum moleculare, sometimes considered as a single lamina, contain a rich plexus of fibers from other layers.

Although the architectonics of the hippocampal formation is uniform throughout its extent, there are variations in cell morphology, differences in the relative development of various cortical regions, and differences in the pathways followed by various

fiber systems. On the basis of these differences Lorente de Nó (141) subdivided the hippocampal formation into sectors designated as CA1, CA2, CA3, and CA4. The letters "CA" are derived from *cornu ammonis*, an older descriptive term applied to the hippocampus because of its resemblance, when seen in cross-section, to the horns of an Egyptian deity that is represented by a ram's head (161). The position of these various sectors is shown in Figure 18.15. In humans, the CA4 sector merges imperceptibly with the dentate gyrus and often is not recognized as a distinct entity (16, 59). It has been estimated that there are about 2.1×10^6 neurons in the CA3 sector and approximately 0.22×10^6 pyramidal cells in the CA2 sector of the human hippocampus (241).

Dentate Gyrus

Like the hippocampus, the dentate gyrus consists of three layers—a *molecular layer*, a *granular layer*, and a *polymorphic layer* (Figs. 18.14 and 18.15). Layers of the dentate gyrus are arranged in a U- or V-shaped configuration in which the open portion is directed toward the fimbria in transverse sections (Figs. 18.13 and 18.16). Thus, layers are present on both sides of sector CA3 of the hippocampus, which extends into the hilus of the dentate gyrus. The molecular layer of the dentate gyrus is continuous with that of the hippocampus in the depths of the hippocampal fissure. The granular layer is made up of closely arranged spherical or oval neurons that are termed granule cells and whose axons pass through the polymorphic layer to terminate upon dendrites of pyramidal cells in the hippocampus. Dendrites of granule cells enter mainly the molecular layer. It has been estimated that the human dentate gyrus contains 9×10^6 granules cells (241). Cells of the polymorphic layer are of several types, including modified pyramidal cells and so-called basket cells. The dentate gyrus does not give rise to fibers passing beyond the hippocampal formation (220).

Intrinsic Connections

The dentate gyrus can be considered as the first step in the intrinsic hippocampal circuitry. Its major input comes from cells located primarily in layers II and III of the entorhinal cortex (area 28) that give rise to the so-called *perforant path* and *alvear path* (16, 140, 141, 221, 286, 287). Fibers of the perforant path originate principally in the lateral part of the entorhinal area and follow a complex trajectory through the subiculum and across the base of the hippocampal sulcus to terminate in the outer two-thirds of the molecular layer of the dentate gyrus (Fig. 18.16) (16). Fibers of the alvear path originate mainly from the medial aspect of the entorhinal area and traverse the subcortical white matter and the alveus to enter the hippocampus from its ventricular surface (Fig. 18.16). The perforant and alvear pathways are often referred to simply as lateral and medial perforant pathways (41). Both pathways innervate chiefly the dentate gyrus, but also provide direct projection to the subiculum, which could be of great functional importance (286).

Cells of the dentate gyrus do not project outside of the hippocampal formation, but send their distinctive axons (the mossy fibers) to cells of the dentate gyrus own polymorphic layer and to proximal dendrites of pyramidal cells of the CA3 sector of the hippocampus (16). Collaterals of single CA3 pyramidal cells project to other levels of CA3, to CA1, and to subcortical regions, especially the septal nuclei. The CA3 cells contribute the major input system to CA1 (the Scheffer collaterals), which terminate throughout the stratum radiatum and stratum oriens (110). In contrast to CA3 cells, CA1 pyramidal cells do not project significantly to other levels of CA1. Instead, CA1 pyramidal cells predominantly project to the subicular cortex, which in turn projects to the deep layers (layers V and VI) of the entorhinal cortex (Fig. 18.17). Cells in the deep layers of the entorhinal cortex in turn project to the superficial layers, and the latter give rise to the perforant pathway fibers.

The intrinsic circuitry of the hippocampal formation appears to be organized into a closed loop that enables unidirectional flow of information (16, 41). This unidirectional feedforward neuronal system involves the classic trisynaptic pathway, which consists of successive excitatory projections from the entorhinal cortex to the dentate gyrus, from granule cells of the dentate gyrus to the CA3 pyramidal cell region, and from CA3 to the CA1 pyramidal cell region. Results of more recent studies, however, provide a different conceptualization of the functional organization of the hippocampus with respect to the

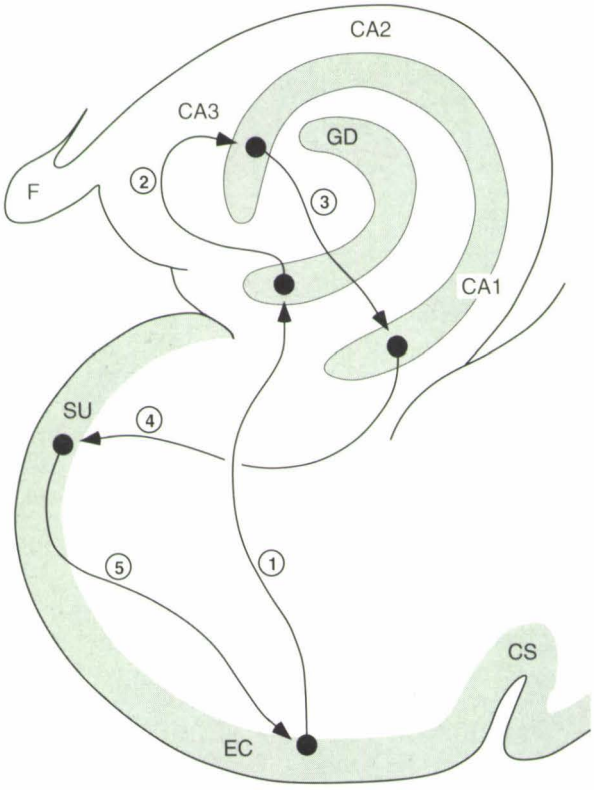


Figure 18.17. Transverse section of the hippocampal formation showing the anatomic circuitry allowing information to flow in a serial, unilinear manner in this structure so as to form a closed loop. This loop involves a series of projections leading from (1) the entorhinal cortex to the dentate gyrus, (2) the dentate gyrus to the CA3 sector, (3) the CA3 sector to the CA1 sector, (4) the CA1 sector to the subiculum, and (5) the subiculum back to the entorhinal cortex. The first three segments of this loop constitute the classic trisynaptic pathway that has been extensively studied in regard to learning and memory functions and their physiologic correlate, long-term potentiation (*LTP*). *CA*, cornu ammonis; *CS*, collateral sulcus; *EC*, entorhinal cortex; *F*, fimbria; *GD*, dentate gyrus; *SU*, subiculum.

propagation of activity through its intrinsic pathways. This novel scheme underlines the fact that input from the entorhinal cortex initiates a two-phase feedforward excitation of pyramidal cells, with the dentate gyrus providing feedforward excitation of CA3, and with both the dentate and CA3 providing feedforward excitation of CA1 (290). Other studies emphasized the multiple similarities that exist between the hippocampus (Ammon's horn) and dentate gyrus with regard to the organization of the intrinsic circuitry, and pointed out the importance of local interactions and parallel processing (234). The idea of serial processing of afferent information, from one hippocampal subregion to the next, appears to be inadequate and based on an oversimplification of the circuitry. Information processing undoubtedly occurs over parallel, as well as serial pathways, with an important contribution from multiple populations of specific local circuit neurons (234).

The hippocampal formation has a unique and highly distributed network of intrinsic connections, and much remains to be known about the principles of organization that govern information flow through this system. The notion that information processing in the hippocampal formation is segregated in autonomous chips or lamellae, however, appears to be inconsistent with the extremely divergent nature of many of the intrinsic connections (15).

Extrinsic Connections

The *fornix* constitutes the main efferent fiber system of the hippocampal formation. This bundle contains about 1.2 million fibers in humans (210). It includes both projection and commissural fibers (Figs. 18.11 and

18.12). It is composed of axons of cells of the subicular cortex (presubiculum, subiculum, and prosubiculum) and of pyramidal cells of the hippocampus (16, 156, 157, 229, 255–257), which spread over the ventricular surface as the *alveus* and then converge to form the *fimbria*. Proceeding backward, the fimbriae of the two sides increase in thickness. On reaching the posterior end of the hippocampus, they arch under the splenium of the corpus callosum as the *crura* of the fornix, at the same time converging toward each other. In this region, a number of fibers pass to the opposite side, forming a thin sheet of crossing fibers, the *fornical commissure* (hippocampal commissure, or psalterium) a structure rather poorly developed in humans (Figs. 18.11 and 18.12). In nonhuman primates, only the rostral (or uncal) part of the hippocampus and associated dentate gyrus are connected by commissural fibers. The presubiculum in monkeys gives rise to a substantial commissural projection, which terminates in layer III of the contralateral entorhinal cortex (16). The two crura then join to form the *body of the fornix*, which runs forward under the corpus callosum to the rostral margin of the thalamus (Fig 16.2). Here the bundles separate again, and, as the *anterior columns of the fornix*, arch ventrally in front of the interventricular foramina and caudal to the anterior commissure. The fimbriae, thin bands of fibers situated laterally, accompany the fornices throughout most of their extent (Figs. 18.11 and 18.12), but rostrally they become incorporated within the anterior columns of the fornix. The largest number of the fibers descend caudal to the anterior commissure as the *postcommissural fornix* (52, 210). Remaining fibers of the fornix pass rostral to the anterior commissure as the *precommissural fornix*.

Postcommissural fornix fibers, originating from the subicular cortex, traverse the hypothalamus en route to the mammillary body. In their course, they give off fibers to the thalamus (16, 157, 256). Fibers leaving the postcommissural fornix in the rostral hypothalamus are distributed to the lateral septal nuclei and the anterior and lateral dorsal thalamic nuclei (16, 90, 175, 269). The anterior nuclei of the thalamus receive as many direct fibers from the fornix as from the mammillothalamic tract (210). Presubicular fibers innervate the anteromedial, anteroventral, and lateral dorsal nuclei of the thalamus, and fibers originating in the subiculum and presubiculum provide the major extrinsic input to the mammillary nuclei. The lateral mammillary nucleus is innervated by the subiculum and presubiculum and the median mammillary nucleus is innervated by the subiculum (16). Other efferent fibers from the subicular cortex project directly to the medial frontal cortex, the caudal cingulate gyrus, and the parahippocampal gyrus. Some postcommissural fornix fibers descend caudally beyond the mammillary bodies to enter the midbrain tegmentum (16, 90, 175, 176). Caudally continuing fibers of the fornix are joined by numerous fibers from the septal nuclei to form a large part of one of the most massive roots of the medial forebrain bundle (Zuckerkandl's "olfactory bundle of Ammon's horn").

Precommissural fornix fibers constitute a smaller, less compact group of fibers that cannot be detected grossly. These fibers originate from pyramidal cells in the hippocampus proper and to a lesser extent from the subiculum and entorhinal cortex. They are distributed principally to the septal nuclei, the lateral preoptic area, the anterior part of the hypothalamus, and the nucleus of the diagonal band (175, 176).

The nucleus accumbens also receives a projection through the fornix that arises in the subicular and entorhinal cortex. The subiculum and entorhinal cortex give rise to additional projections to the caudate nucleus and the putamen (16, 88). The hippocampal formation is also reciprocally connected with the amygdala and the claustrum through the subicular and entorhinal cortex (4, 16, 122). The septal and surpramammillary areas also project to the hippocampal formation. The septohippocampal projection, first demonstrated in the early 1950s (52, 168), arises from cholinergic and, to a lesser extent, GABAergic neurons in the medial septal nucleus and the nucleus of the diagonal band of Broca. The axons of these neurons course in either the fimbria, dorsal fornix, supracallosal striae, or along a ventral route through the amygdala, and arborize in virtually all fields of the hippocampal formation, but are most prominent in the dentate gyrus and the CA3 field of the hippocampus (16). The entorhinal cortex also is innervated by cholinergic neurons of the medial septal nucleus and the nucleus of the diagonal band of Broca.

The major hypothalamic projection to the hippocampal formation arises from a popula-

tion of large neurons located dorsal and lateral to the mammillary bodies in the so-called supramammillary area. This projection terminated principally in sectors CA2 and CA3 of the hippocampus, and in the rostral entorhinal cortex (16, 108). This projection could provide a reciprocal link between the mammillary bodies and the subiculum, which projects heavily upon the medial and lateral mammillary nuclei.

Recent tract-tracing studies have revealed hitherto unknown projections from the thalamus to the hippocampal formation (108). These projections arise from all divisions of the anterior thalamic nuclear complex and associated lateral dorsal nucleus, as well as from the midline thalamic nuclei (e.g., parataenial, centralis medialis, and reuniens nuclei). The nucleus reuniens projects primarily to the stratum lacunosum-moleculare of CA1, in portions of the subicular cortex, and in the entorhinal cortex (16, 108). Projections to the entorhinal cortex from the dorsomedial portion of the pars medialis of the pulvinar nucleus have also been documented (108).

The neuronal activity in the hippocampal formation is also modulated by inputs originating in various brainstem nuclei, principally the ventral tegmental area, the locus coeruleus, and the midbrain raphe nuclei. The locus coeruleus gives rise to the major noradrenergic input to the hippocampal formation (198), whereas the midbrain raphe nuclei, chiefly the median (or central superior) nucleus, provides a prominent serotoninergic innervation (265). Both of these nuclei project to most of the hippocampal formation, with a particularly dense innervation of the dentate gyrus. There is also experimental evidence for the existence of a dopaminergic projection to the hippocampus that appears to originate in the midbrain ventral tegmental areas (16).

The entorhinal and subicular cortex are in close reciprocal relationship with the surrounding cerebral neocortex. In monkeys, the entorhinal cortex receives prominent projections from (a) several areas of the temporal lobe, particularly areas TF and TH of the parahippocampal gyrus, the perirhinal cortex (area 35), the temporal polar cortex (area TG), the dorsal bank of the superior temporal gyrus, (b) the ventral or agranular insular cortex, (c) the posterior orbitofrontal cortex, (d) the dorsolateral frontal cortex (areas 9, 10, and 46), (e) the infralimbic and prelimbic portions of the medial frontal cortex (areas 25 and 32) and the cingulate cortex (area 24), and (f) the retrosplenial cortex (107). In turn, the entorhinal cortex appears to project back to most of these cortical areas (16). Through these connections, the hippocampal formation is able to influence widespread areas of the temporal, parietal, and frontal lobes. The parahippocampal gyrus, in particular, projects to virtually all association cortices of the brain (272).

While the entorhinal cortex is the major anatomic interface between the hippocampal formation and the cerebral cortex, the subicular cortex is also reciprocally linked to the neocortex. The various regions of the subicular complex in nonhuman primates receive projections from, and project to, the perirhinal cortex, the parahippocampal gyrus, the cingulate gyrus, and the medial frontal and medial orbitofrontal cortices.

All the extrinsic anatomic connections described earlier indicate the complex pathways whereby signals from the hippocampal formation can be projected to different parts of the neuraxis. Both direct and indirect pathways connect the hippocampal formation with the septal nuclei, the thalamus, the hypothalamus, and widespread regions of the cerebral cortex and the midbrain reticular formation (Figs. 18.3 and Fig. 18.10).

Chemical Anatomy

Studies of the localization of neurotransmitters with histochemical and immunohistochemical methods provide important clues concerning the neural computation that occurs in the hippocampal formation (104). A large variety of small-molecule transmitters and neuroactive peptides have been detected at the hippocampal level. GABA is believed to be the main inhibitory transmitter, whereas noradrenaline, serotonin, and acetylcholine are widely distributed neuromodulators. Glutamate is the most important excitatory neurotransmitter in this region (41). A multitude of neuroactive peptides are also present in the hippocampal formation (e.g., somatostatin, galanin, substance P, enkephalin, histamine, cholecystokinin, neuropeptide Y, dynorphin, angiotensin, vasoactive intestinal peptide, and corticotropin-releasing factor), but their exact functional significance is still uncertain. Enkephalin oc-

curs in some axons that emerge from the hilar region of the dentate gyrus and terminate as mossy fibers on proximal apical dendrites of hippocampal pyramidal cells, as well as in other axons of the lateral perforant pathway (74).

GABA is believed to be the primary transmitter released by inhibitory interneurons that synapse onto both the soma and dendrites of pyramidal and granule cells. As elsewhere in the brain, its action depends on the class of postsynaptic receptors to which it binds. The two main GABA receptor subtypes, $GABA_A$ and $GABA_B$, are differentially distributed in the hippocampus. The $GABA_A$ subtype, which is coupled to a slow potassium conductance, is preferentially found on the soma of hippocampal neurons, whereas $GABA_B$, which is coupled to a fast chloride conductance, is preferentially located on dendrites of hippocampal neurons (111). GABA can interact with other neurotransmitters or neuromodulators in the hippocampus. For example, glutamate enhances the $GABA_A$ response, and serotonin and $GABA_B$ can interact via potassium channels that are coupled to the same G-protein. Inhibitory postsynaptic potentials evoked by both $GABA_A$ and $GABA_B$ can be reversibly blocked by enkephalin (41). GABA is not confined to hippocampal interneurons, but is also present in some hippocampal afferent fibers, particularly those from the septal region (162). Additionally, this inhibitory neurotransmitter appears to coexist with the excitatory neurotransmitter glutamate in mossy fiber terminals (232).

Acetylcholine exerts various modulatory effects in the hippocampus. As mentioned earlier, the cholinergic fibers to the hippocampus arise mainly from neurons in the medial septal nucleus and the nucleus of the diagonal band of Broca. They terminate in all hippocampal regions, but are most prominent in the dentate gyrus and the CA3 sector of the hippocampus. Lesions of the fimbria/fornix system produce a substantial loss of the cholinergic innervation of the hippocampus, as shown by the pioneering studies of Lewis and Shute (135, 136). This loss of cholinergic input can be alleviated by transplantation of embryonic cholinergic neurons from the septal area into the hippocampus of adult animals, a brain grafting procedure that also restores learning ability in monkeys with fornix lesions (224). Cholinergic septal afferents and serotoninergic input from the median raphe nucleus converge onto distinct classes of hippocampal interneurons. These interneurons can be differentiated from one another by the type of calcium binding protein they contain; some are enriched with calbindin D-28k, while others contain parvalbumin (163). At the synaptic level, the action of acetylcholine on hippocampal neurons appears to be mediated by the muscarinic subtype of cholinergic receptor.

The noradrenergic input from the locus coeruleus is also known to play an important modulatory role at the hippocampal level, principally at the hilus of the dentate gyrus and the stratum lucidum of the CA3 sector, where the innervation is most dense (240). Noradrenaline applied to the CA1 region has at least two different effects: (a) a decrease of pyramidal cell inhibition, possibly through an inhibitory effect on the inhibitory interneurons mediated via an α_1 receptor, and (b) a direct effect on pyramidal neurons mediated through β_1 receptor, probably to enhance the response to excitation and reduce accommodation. Although noradrenaline plays an important role in the control of cell excitability in the CA1 sector, there is no evidence that it has any direct effect on long-term potentiation (discussed later) at the Schaffer collateral synapse in this region (41).

Glutamate is known to exert its excitatory action at the hippocampal level by activating two distinct conductances, one mediated by *N*-methyl-D-aspartate (NMDA) receptors and the other by non-NMDA (kainate-quisqualate) receptors. In contrast to ionic channels associated with non-NMDA receptors, the NMDA receptor-gated channels have a high permeability to calcium, and it is the calcium current through these channels that appears to trigger long-term potentiation induction (41). The molecular properties of the NMDA receptor-gated channels are especially important in regard to the activity-dependent neuronal modifications that occurs at the hippocampal level during learning and information storage procedures.

Functional Considerations

Anatomic and physiologic evidence indicate that the hippocampus has no significant olfactory function (39). The hippocampus and dentate gyrus are well-developed in cetaceans that are said to be completely anos-

matic and lack olfactory bulbs and nerves (1, 225). Although not directly involved in the processing of olfactory information, the hippocampal formation is believed to play important roles in learning and memory, as well as in the control of emotional behaviors and neuroendocrine functions.

Our knowledge of the functions of the hippocampal formation is largely based upon the results of lesion studies in experimental animals and on clinical observations of patients with hippocampal lesions. Bilateral damage to the hippocampus can occur when a head injury causes the temporal poles to strike the greater wings of the sphenoid bone, which form the anterior wall of the middle cranial fossa. Loss of hippocampal function can also occur as a result of cerebral anoxia. The large pyramidal cells of the CA1 sector of the hippocampus are exceptionally sensitive to oxygen deprivation and die after only a few minutes without a supply of fresh arterial blood. Pathologists refer to area CA1 as the *Sommer's sector*. Many patients resuscitated after cardiac arrest of more than a few minutes' duration are left with defective memory for this reason (25). Degenerative changes, including neurofibrillary tangles, neuritic plaques, and amyloid deposits, are particularly prominent in this hippocampal area in patients suffering from Alzheimer's disease, which is initially characterized by the inability to form new memories.

Localized lesions in the hippocampus and local stimulation of this structure in conscious experimental animals tend to produce similar phenomena (83, 84). Behavioral changes observed in these animals resemble those occurring in psychomotor epilepsy, and it seems likely that the abnormal fears, hyperesthesia, and pupillary dilatation seen may represent fragments of a seizure. The behavioral changes noted initially after lesions tend to disappear but recur at a later time. The hippocampus has an exceedingly low threshold for seizure activity (83, 86, 143, 144), and seizure discharges tend to spread from the hippocampus to other parts of the limbic lobe and ultimately to the neocortex. Amygdalohippocampectomy is a surgical procedure that is often used for the treatment of temporal lobe epilepsy (187). It allows removal of an ample amount of epileptogenic tissue and is not accompanied by significant intellectual deficit. It takes into account the fact that temporal seizures usually arise in the limbic structures but, in most instances, quickly recruit the whole anterior cortex. Selective amygdalo-hippocampectomy is an alternative approach when a clear mediobasal limbic focus has been repeatedly demonstrated by intracranial recording (187).

The hippocampus appears to be concerned particularly with recent memory (86). Relatively large bilateral lesions of the hippocampus (58, 77, 239, 278, 279) are associated with profound impairment of memory for recent events (short-term memory) and with relatively mild behavioral changes. Memory for remote events (long-term memory) usually is unaffected. Although general intellectual functions may remain at a fairly high level, these patients demonstrate an inability to learn new facts and skills. These findings are in accord with those found after bilateral resection of the medial parts of the temporal lobe in cases of epilepsy (187). According to Scoville and Milner (239), lesions of the most anterior portion of the temporal lobe do not impair memory, which occurs only when the lesions extend far enough posteriorly to involve the hippocampal formation, the dentate gyrus, and parts of the parahippocampal gyrus. It is generally believed that loss of memory occurs only if lesions of the hippocampal formation and parahippocampal gyrus are bilateral (200), but some patients may show mild verbal disorders or disturbances of memory following resections of parts of the temporal lobe of the dominant hemisphere.

Experimental studies in the monkey indicate that bilateral removals of the amygdaloid complex and portions of the hippocampal formation, including perirhinal and parahippocampal cortices, impair memory and learning that depend upon visual, auditory, and tactile discriminations (189, 248, 250, 253, 294). The type of behavioral test used to measure retention following temporal lobe lesions is very important. When rhesus monkeys are tested for their ability to discriminate between pairs of visual stimuli presented concurrently, anterior inferotemporal cortex lesions impair learning. This is also true when the lesions extend more deeply to include the hippocampus. With the extension of the lesions into the hippocampus, the animals show an additional impairment of learning for tactile stimuli (169, 253). These complexities in analyzing the involvement of the hippocampus and other temporal

lobe structures in mechanisms of memory make it difficult to draw broad generalizations from the experimental and clinical literature related to lesions (103, 248, 294).

Even though the fornix contains most of the efferent fibers from the hippocampal formation, evidence that interruption of these fibers produces memory loss is still controversial (6, 7, 57, 75, 169, 258). The mammillary bodies, like the fornix, seem to be implicated in memory, but available experimental data do not always concur with such a view. Recent clinical and experimental findings, however, suggest that the fornix system is indeed involved in mnemonic functions in both humans (73) and monkeys (224). Furthermore, it seems that the hippocampal connections with the entorhinal cortex (16, 229) are important for associative learning involving more than one modality (169).

In rats, bilateral destruction of the hippocampus, the fornix, and mammillary bodies produces a severe disturbance in maze learning (115). Chronic single hippocampal neuron recordings in freely behaving rats indicate that these cells encode the animals' specific position in its environment (183). It has been hypothesized that the hippocampus contains an internal "cognitive map" of behaviorally significant features of the environment (184). Single unit recordings in the rabbit hippocampus show a high correlation between pyramidal cell discharge in CA1 and CA3 and the acquisition of a conditioned response (31).

Much more information is needed about the location of neurons that are essential for learning a specific task before it will be possible to understand the mechanisms of learning. It can be reasonably argued from the available literature that memory and learning are distributed processes, involving neuron assemblies in many regions of the brain. If this is true, progress on the problem of memory will require new strategies to relate biophysic and biochemical events at the cellular level to the properties of distributed neuronal networks (45, 116, 117).

It has been hypothesized that short- and long-term learning and memory is related to morphologic or functional changes in synapses. The association of the hippocampal formation with learning, together with its highly ordered arrangement of cells and input axons (Fig. 18.18), has led to a large number of experiments dealing with neuronal plasticity. From these studies emerge the idea that *long-term potentiation* (LTP) could be the synaptic mechanism responsible for rapid learning in mammals (33). This fascinating form of synaptic plasticity has been most thoroughly studied in the mossy-fiber synaptic input to CA3 sector and the Schaffer collateral synaptic input to CA1 sector (41). LTP is an increase in synaptic efficiency that follows a few seconds of high-frequency activity of presynaptic terminals. For example, brief repetitive stimulations of fornix or entorhinal afferent axons leads to a prolonged increase in the responsivity of hippocampal pyramidal cells or dentate granule cells (33). The concept of increased synaptic efficiency referred to a reduction in the number of afferent impulses and, therefore, of the amount of neurotransmitter needed to depolarize the postsynaptic cells. Depending upon the conditions of stimulation, the effect may last several hours or days and typically lead to increased activity of affected postsynaptic neurons. In normal conditions, LTP can be induced at the level of certain pyramidal and granule cells following a suitable pattern of activity in hippocampal afferent axons. The affected recipient cells will continue to transmit impulses more frequently than before, even though the original external stimuli have ceased (25, 41).

Although LTP is likely to serve as a mechanism for the storage of recent memories by the hippocampus, the formation of permanent memory traces is likely to involve the synthesis of new proteins and the formation of new synapses (42, 117). The consolidation of recent memories may occur during sleep, when the serotoninergic raphe neurons that project to the hippocampus are active. In deep sleep, when the electroencephalogram (EEG) recorded over the neocortex displays regular, synchronized rhythms, the hippocampal EEG is desynchronized. In the waking state, the neocortical record is desynchronized and the hippocampus generates a typical, slow regular rhythm, that is termed the theta rhythm. The *theta rhythm* is a 5–12 Hz pattern of electrical activity observed in the hippocampal region that is correlated with certain behavioral states in the freely moving animal. It is most pronounced when the animal is alert and interested by what is happening in its immediate environment; it fades when external stimuli are repeated. The theta rhythm is believed to reflect the "gat-

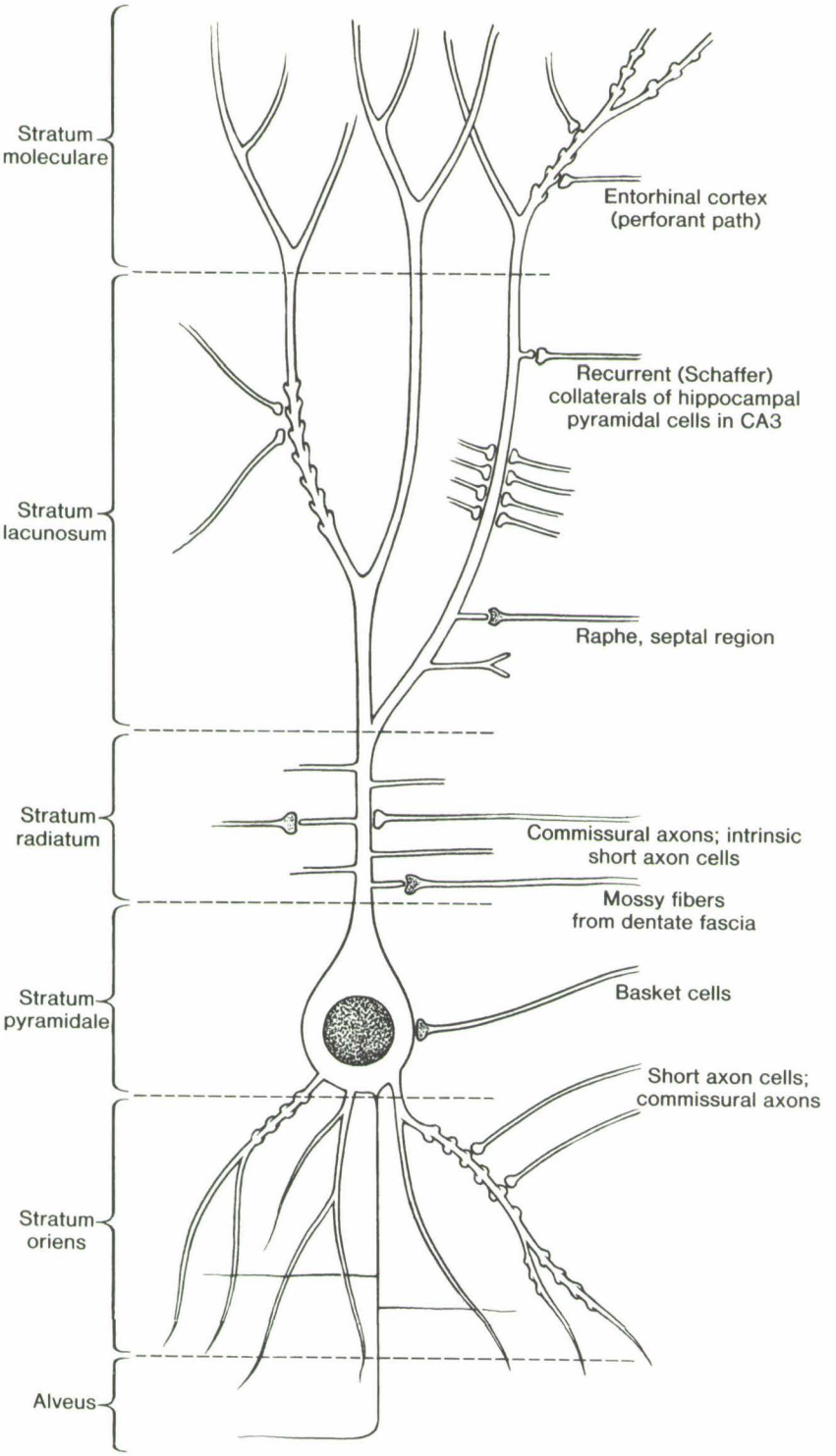


Figure 18.18. CA1 sector hippocampal pyramidal neuron indicating the regions of the cell that receive specific afferent inputs. Specific cell layers of the hippocampal formation can be related to specific parts of the pyramidal cell and are shown on the *left*. Afferent inputs from several sources are indicated on the *right*. Afferent fibers synapse in specific locations upon dendritic shafts, dendritic spines, the cell body, and the basal dendrites of the pyramidal cell.

ing" of information through the hippocampal circuits (41).

The hippocampal circuitry displays a remarkable degree of morphologic plasticity. This feature renders the hippocampal formation particularly suitable for playing a role in memory and learning. The hippocampus shows reactive synaptogenesis following interruption of some of its afferent fiber systems. This morphologic plasticity has been studied extensively in the dentate gyrus following interruption of perforant pathway fibers from the entorhinal cortex (46, 47). Unilateral entorhinal cortical ablation leads, over a period of weeks, to the formation of new synapses in the denervated area of the ipsilateral dentate gyrus. Many of the new synapses are formed by growth of collaterals from axons originating in the contralateral entorhinal cortex, and by sprouting of septohippocampal axons. Like the original perforant pathway projection, the newly formed synapses may sustain long-term potentiation following repetitive stimulation (285).

Korsakoff's syndrome (amnestic confabulatory syndrome) appears as a sequel to Wernicke's encephalopathy and probably is related to a thiamine deficiency associated with alcoholism. This syndrome is characterized by severe impairment of memory without clouding of consciousness, confusion, and confabulatory tendencies. Lesions in this syndrome almost always involve the mammillary bodies and adjacent areas (259). Patients suffering from the Korsakoff's syndrome, insert remembered events from the remote past into fluent, but blatantly untrue, stories, attempting to compensate for the absence of more recent memories (25). Amnesia is said to be present in this syndrome, especially if there is additional involvement of certain thalamic nuclei, chiefly the mediodorsal nucleus (277, 280).

Particularly prominent among concepts relating the hippocampal formation to emotion is the theory proposed by James Papez in 1937 (193). Realizing that the term "emotion" denotes both subjective feelings and the appropriate autonomic and somatic responses, Papez concluded that (a) the cortex is essential for subjective emotional experience, and (b) emotional expression must be dependent on the integrative actions of the hypothalamus. The hippocampal formation and its principal projection system, the fornix, provides the main pathway by which impulses from the cortex reach the hypothalamus. Impulses reaching the hypothalamus are projected caudally through the brainstem to effector structures, as well as rostrally to thalamic and cortical levels. The "central emotive process of cortical origin" is considered by Papez to be formed in the hippocampal formation and transmitted to the mammillary bodies, the anterior nuclei of the thalamus, and the cingulate gyrus. The cingulate cortex is regarded as the receptive cortical region for impulses concerned with emotion. Signals transmitted from the cingulate gyrus to other cortical regions are believed to add emotional coloring to the psychic process (193).

AMYGDALA

Nuclear Organization

The amygdala (or amygdaloid nuclear complex) is a gray mass situated in the dorsomedial portion of the temporal lobe, in front of, and partly above the tip of the inferior horn of the lateral ventricle (Figs. 2.10, 2.16, 18.10, 18.11, 18.14, 18.19, and 18.20). It is covered by a rudimentary cortex and caudally is continuous with the uncus of the parahippocampal gyrus (Figs. 2.6, 2.10, and 18.19).

The amygdaloid complex is divided into two main nuclear masses: (a) a corticomedial nuclear group and (b) a basolateral nuclear group (50, 51, 79, 270). A central nucleus, which can be divided into a medial and a lateral part, is regarded as a separate subdivision, but sometimes is included as part of the corticomedial group, basolateral nuclear group, or the so-called extended amygdala. The extended amygdala concept is based on recent evidence that supports the view held by Johnston (112) that the bed nucleus of the stria terminalis and the central and medial amygdaloid nuclei constitute a single anatomic entity. This concept, which is supported by the strikingly uniform staining of this group of structures with various neuronal molecular markers, particularly the limbic system-associated membrane protein (LAMP) (Fig. 18.4), has gained wide acceptance (55).

In humans, the *corticomedial nuclear group* occupies the dorsomedial aspect of the amygdaloid complex due to a medial rotation of the temporal lobe. Nuclear subdivisions of the corticomedial group include (a) the ante-

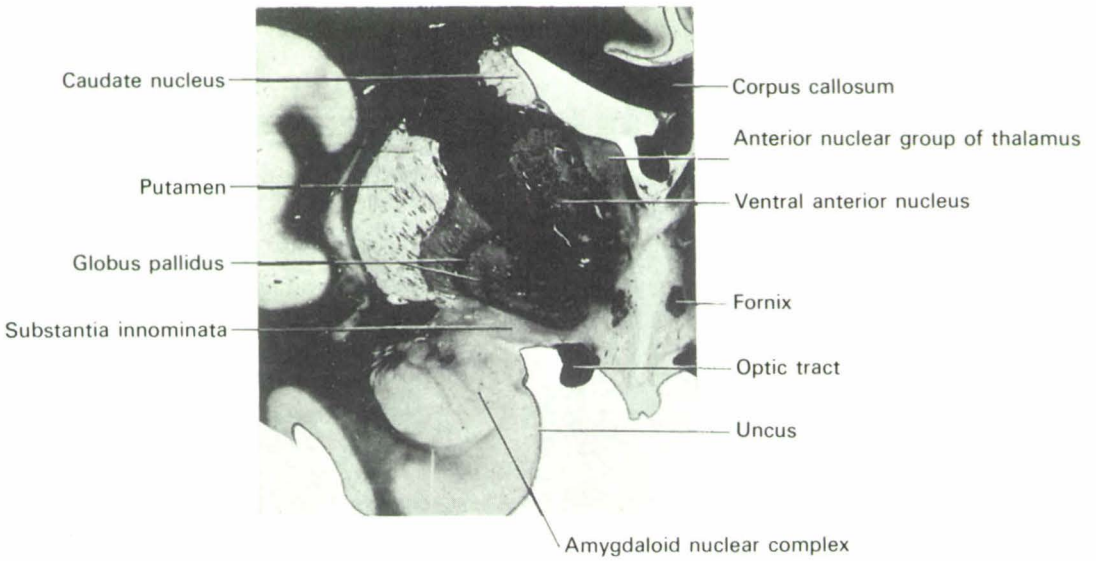


Figure 18.19. Transverse section through the thalamus, basal ganglia, and amygdaloid nuclear complex. The substantia innominata lies ventral to the globus pallidus and dorsal to the amygdala. Human brain, Weil stain.

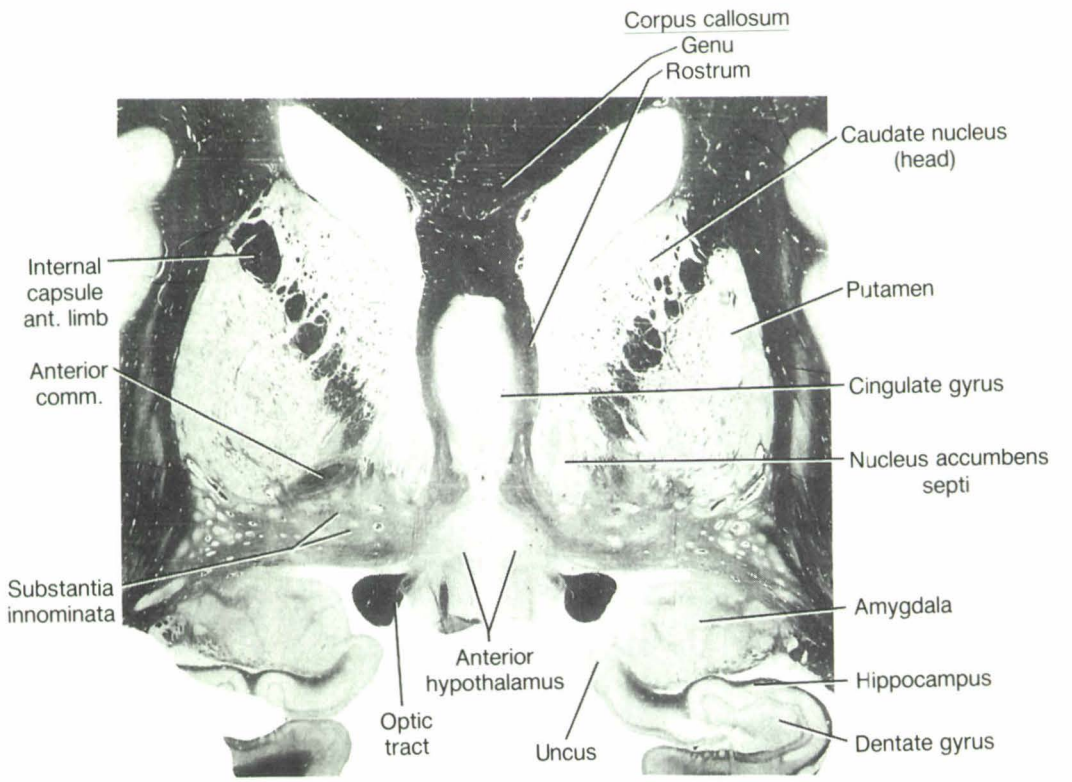


Figure 18.20. Section cut parallel to the longitudinal axis of the brainstem through the genu of the corpus callosum, the head of the caudate nucleus, the putamen, the substantia innominata, the amygdala, and the hippocampal formation. The sections reveal the nucleus accumbens, ventromedial to the head of the caudate nucleus. The substantia innominata lies in the subcommissural region, ventral to the basal ganglia, and contains the large hyperchromic neurons known as the basal nucleus of Meynert. Cells of the basal nucleus are the major source of cholinergic innervation of the entire cerebral cortex and the amygdala. Human brain, Weigert's myelin stain.

rior amygdaloid area, (b) the nucleus of the lateral olfactory tract, (c) the medial amygdaloid nucleus, and (d) the cortical amygdaloid nucleus, whose dorsalmost portion is termed periamygdaloid cortex. The nucleus of the lateral olfactory tract is the least well-developed of the amygdaloid nuclei in humans. The anterior amygdaloid area, representing the most rostral part of the amygdaloid complex, is rather poorly differentiated (70). The corticomedial amygdaloid nuclear group lies closest to the putamen and tail of the caudate nucleus.

The largest and best differentiated part of the amygdaloid complex in humans is the *basolateral nuclear group*. Subdivisions of this nuclear group are (a) the lateral amygdaloid nucleus, (b) the basal amygdaloid nucleus, which can be divided into magno-and parvicellular parts, and (c) the accessory basal amygdaloid nucleus, which can also be divided into magno- and parvicellular parts. Caudally, the amygdala is in contact with the tail of the caudate nucleus, which sweeps rostrally in the roof of the inferior horn of the lateral ventricle (Figs. 2.13,18.14 , and 19.57).

The *extended amygdala*, a term that was coined by Alheid and Heimer (9), includes principally (a) the central amygdaloid nucleus, (b) the bed nucleus of the stria terminalis, and (c) the sublenticular portion of the substantia innominata, through which the medial and central amygdaloid nuclei are linked with the bed nucleus of the stria terminalis. In some descriptions, the medial amygdaloid nucleus also is considered as part of the extended amygdala (55).

Major Fiber Bundles

The amygdala is commonly regarded as having two major extrinsic fiber systems—the ventral amygdalofugal pathway and the stria terminalis. Fibers forming the *ventral amygdalofugal pathway* emerge from the dorsomedial edge of the amygdala and spread medially and rostrally beneath the lentiform nucleus (48, 78, 177). They pass through the substantia innominata (Figs. 18.19 and A.22) and enter the lateral preoptic and hypothalamic areas, the septal region, and the nucleus of the diagonal band (of Broca). Amygdalofugal fibers, bypassing the preoptic region and hypothalamus, enter the inferior thalamic peduncle (Fig. 16.9) and project to the magnocellular part of the dorsomedial nucleus of the thalamus (71, 122, 177, 206). In contrast, fibers of the *stria terminalis* (stria semicircularis) collect at the ventromedial portion of the caudal amygdala and arch along the entire medial border of the caudate nucleus near its junction with the thalamus (Fig. 16.7). Rostrally, these fibers pass into and terminate in the bed nuclei of the stria terminalis located lateral to the columns of the fornix and dorsal to the anterior commissure (54, 99). Other fibers of the stria terminalis end in the anterior hypothalamic area, and some may join the medial forebrain bundle.

In contrast to previous beliefs (48, 54, 70, 97, 125, 220, 270), these two bundles do not carry distinct sets of fibers, and fibers from one bundle appear to join fibers in the other bundle throughout their trajectory. For example, fibers which initially run in the ventral amygdalofugal pathway have been observed to run into the internal capsule to join the stria terminalis. Efferents from most of the amygdaloid nuclei generally exit the amygdala via both the stria terminalis and the amygdalofugal pathway (18). These two well-delineated pathways are primarily subcortical fiber systems. The amygdalocortical interconnections, which are prominent in primates, are established mostly via the internal capsule. In primates, this fiber system is as prominent as the subcortical fiber systems. The amygdala also contains several small intrinsic fiber bundles. Most of them are part of what Johnston (112) described as "longitudinal association bundles."

Cytochemical Features

The amygdala contains a multitude of neurotransmitters and neurotransmitter-related molecules. A detailed review of the enormous amount of literature on the chemical anatomy of the amygdala is beyond the scope of this chapter. The interested reader is referred to the comprehensive reviews on this topic by de Olmos (55) and, principally, Amaral, et al. (18). In the following section, a brief description of the localization of the major classes of neuromediators is provided because this type of information is crucial for understanding the functional organization of the amygdala.

AMINO ACIDS

The primate amygdala contains high levels of the inhibitory transmitter GABA, and the distribution of GABA-immunoreactive

neurons in the amygdaloid complex of monkeys were recently documented (148). GABAergic neuronal subpopulations appear to exist in each amygdaloid nucleus in monkeys. The pattern of GABA immunoreactivity varies in different amygdaloid regions and is very similar to that described in the rat. In both basolateral and corticomedial nuclear groups, GABA-positive cells are of the nonpyramidal type and often arranged in clusters. These GABA-positive nonpyramidal neurons represent about 25% of the total neuronal population of the basolateral and corticomedial amygdaloid nuclei. Numerous GABA-positive puncta, resembling axon terminals, are scattered in the neuropil, while others closely surround the perikarya of GABA-negative pyramidal cells. A very dense field of GABA-positive puncta occur in the central and medial amygdaloid nuclei. There are numerous GABA-positive neurons in the lateral subdivision of the central nucleus and fewer cells in the medial nucleus and medial subdivision of the central nucleus. Many immunoreactive puncta contact the perikarya and dendrites of GABA-positive cells in these regions (148). It is worth noting the presence of benzodiazepine/$GABA_A$ receptor complex in the primate amygdala (18). Benzodiazepines are the most widely used anxiolytic drugs and the presence of receptors for such molecules in the amygdala is in agreement with the concept that this structure is involved in the control of emotional behavior. Also worth mentioning is the recent demonstration of intrinsic GABAergic neurons in the extended amygdala of the rat (251).

The amygdala in monkeys also contains high concentrations of the excitatory transmitters glutamate and aspartate, but our knowledge of the nuclear distribution and specific origin of these amino acids is still limited. Studies with tritiated aspartate as a retrograde tracer have identified the sources of some amygdaloid afferents that may use aspartate and/or glutamate as an excitatory neurotransmitter in monkeys (17). These include (a) neurons in layers III and V of the frontal, cingulate, insular and temporal cortices, (b) neurons in the CA1 region of the hippocampus and in the deep layers of the entorhinal cortex, and (c) neurons in the claustrum and the midbrain peripeduncular nucleus. These findings suggest the existence of numerous extrinsic excitatory inputs to the amygdala. Glutamate-immunoreactive terminals that make asymmetric synaptic contacts with dendritic shafts and spines of pyramidal neurons have been visualized in the lateral amygdaloid nucleus of the rat (65), but similar information is not yet available in primates.

MONOAMINES

The primate amygdala contains moderate levels of noradrenaline and serotonin, which arise respectively from the locus coeruleus and the midbrain raphe nuclei (155, 181). The central, medial, and cortical (or periamygdaloid cortex) nuclei receive a moderate noradrenergic innervation, whereas nuclei of the basolateral group contain relatively few noradrenergic fibers (Fig. 18.21) (231). A substantial intranuclear variability in the density of innervation exists within several of the amygdaloid nuclei. The serotoninergic innervation of primate amygdala is overall more massive than the noradrenergic innervation. Fairly dense serotonin-immunoreactive fiber plexuses occur in the lateral nucleus, parvicellular division of the basal nucleus, magnocellular division of the basal accessory nucleus, central nucleus, and the amygdalohippocampal transition area (Fig. 18.21) (231). The serotoninergic receptor of the 5-HT_1 subtype is particularly abundant in the lateral, basal, and cortical amygdaloid nuclei (18).

The dopaminergic innervation of the monkey amygdala overall is moderate, but a particularly dense innervation can be noted in the lateral and central nuclei (231). In the basal nucleus, the most profuse innervation occurs in the lateral part of the parvicellular division. The dopaminergic innervation of the amygdala in primates arises principally from neurons in the ventral tegmental area and in the dorsal tier of the substantia nigra pars compacta (138, 155, 181, 268, 274). The dopaminergic axons reach the amygdala through the stria terminalis, as well as via ventral sublenticular pathways.

Some of the adrenergic neurons located in the lower medulla project to the central nucleus of the amygdala in the rat (191), but this projection is rather weak in primates (231).

ACETYLCHOLINE

High levels of the cholinergic enzymes acetylcholinesterase (AChE) and choline

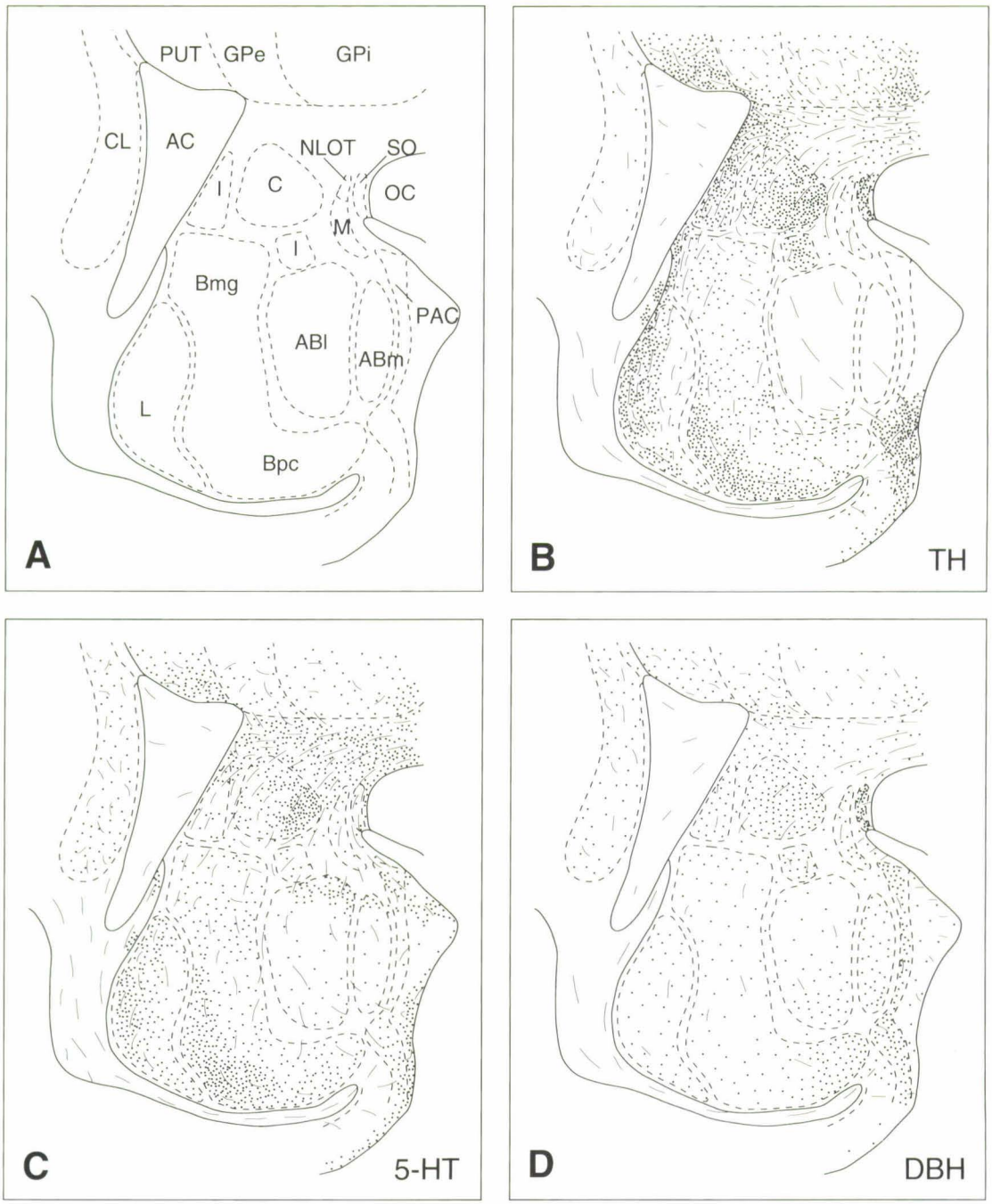


Figure 18.21. Transverse section through the middle third of the amygdala in the squirrel monkey illustrating the distribution of monoaminergic fibers and terminals. **A.** Principal subdivisions of the amygdala. **B**, **C,** and **D.** Fibers (*sinuous lines*) and terminals (*dots*) displaying immunoreactivity respectively for (**B**) tyrosine hydroxylase ((*TH*) indicative of dopaminergic elements); (**C**) serotonin (5-hydroxytryptamine, 5-HT); and (**D**) dopamine-β—hydroxylase (*DBH*) indicative of noradrenergic elements)) *AAA*, anterior amygdaloid area; *ABl*, accessory basal nucleus, lateral part; *ABm*, accessory basal nucleus, medial part; *AC*, anterior commissure; *Bmg*, basal nucleus, magnocellular part; *Bpc*, basal nucleus, parvicellular part; *C*, central nucleus; *CL*, claustrum; *GPi*, globus pallidus, internal part; *GPe*, globus pallidus external part; *I*, intercalated nuclei; *L*, lateral nucleus; *M*, medial nucleus; *NLOT*, nucleus of the lateral olfactory tract; *OC*, optic chiasm; *PAC*, periamygdaloid cortex; *PUT*, putamen; *SO*, supraoptic nucleus.

acetyltransferase (ChAT) are found in the amygdala of monkeys, and these two enzymes are heterogeneously distributed throughout the various nuclei (18, 194). A high density of ChAT-immunoreactive fibers and terminals is observed in the basal nucleus, parvicellular division of the accessory basal nucleus, amygdalo-hippocampal area, and the nucleus of the olfactory tract. These cholinergic fibers originate in the basal nucleus of Meynert, specifically in the anterolateral portion of the nucleus (18). A smaller number of cholinergic inputs arise from neurons in the anteromedial and intermediate portions of the basal nucleus and in the horizontal limb of the diagonal band. In human amygdala, the basolateral nucleus and the lateral part of the central nucleus receive the most prominent cholinergic innervation (62). The lateral nucleus displays a relatively low density of ChAT-positive fibers, and there are only rare ChAT-immunoreactive fibers in the medial nucleus. The other amygdaloid nuclei contain a moderate number of ChAT-positive fibers. The cholinergic innervation of the amygdaloid complex in humans is severely affected in cases of Alzheimer's disease (62). The action of acetylcholine at the level of the amygdala is most likely mediated through a muscarinic (M_1) receptor subtype, but the distribution of this receptor does not exactly correspond to the distribution of the ChAT-immunoreactive fibers.

NEUROACTIVE PEPTIDES

A plethora of neuroactive peptides occur at the amygdala level in primates. Among the most abundant ones are (a) somatostatin, (b) neuropeptide Y, (c) neurosecretory peptides (vasopressin, neurophysin, and oxytocin), (d) opiate peptides (enkephalin and dynorphin), (e) corticotropin-releasing factor, (f) vasoactive intestinal peptide, (g) cholecystokinin, (h) galanin, (i) neurotensin, and (j) calcitonin gene-related peptide (18).

The levels of somatostatin in the primate amygdala are among the highest in the brain and appear to have an intrinsic origin. The distribution of somatostatin immunoreactivity shows both internuclear and intranuclear variability (Fig. 18.22). In the lateral nucleus, the density of immunoreactive fibers is highest in the ventrolateral part, whereas the number of immunoreactive cells is greater in the dorsomedial portion. In the basal nucleus, a ventrodorsal decreasing gradient of fiber density is observed. In the central nucleus, the lateral division contains more somatostatin immunoreactive cells and fibers than the medial division (Fig. 18.22) (18, 56).

Neuropeptide Y (NPY) is also present in high concentrations in the amygdala and immunoreactive cell bodies, fibers, and terminals displaying immunoreactivity for this peptide were shown to be widely distributed in this structure (247). Since somatostatin and neuropeptide Y are colocalized in several cortical and striatal neurons (246), it is likely, although not yet demonstrated, that these two peptides are also colocalized in neurons of the amygdala. Regarding the role of the amygdala in the control of emotions, it is worth noting that neuropeptide Y exerts an anxiolytic action at the amygdala level (98).

Vasopressin-immunoreactive fibers, which are likely to arise from the magnocellular neurosecretory nuclei of the hypothalamus, terminate in the medial amygdaloid nucleus, whereas enkephalin-immunoreactive fibers and terminals abound in the central amygdaloid nucleus (27, 28, 60, 63, 89, 106, 126). In the rhesus monkey, opiate receptors are distributed widely throughout the amygdala (126). The locations of enkephalin and opiate receptors generally parallel each other, but there are some regions, such as the amygdala, in which differences (mismatches) occur.

Numerous neurotensin-immunoreactive fibers and terminals occur in the human amygdala (30). The neurotensin-immunoreactive elements are particularly abundant in the central nucleus followed by the medial nucleus and intercalated masses. The anterior amygdaloid area, basal nuclear complex, cortical nucleus, cortical-amygdaloid transition area, and amygdalo-hippocampal area contain moderate densities of immunoreactivity. The accessory basal and lateral nuclei exhibited scant neurotensin-positive fibers and terminals. Immunoreactive cell bodies were found only within the anterior amygdaloid area and the central, medial, and intercalated nuclei. The distribution of neurotensin-immunoreactive processes and cell bodies within selected regions of the amygdala provides an anatomic substrate that may explain, in part, the neuromodulatory actions of neurotensin upon autonomic, endocrine, and memory systems. Of particular interest is the finding that neurotensin-immunoreactivity is

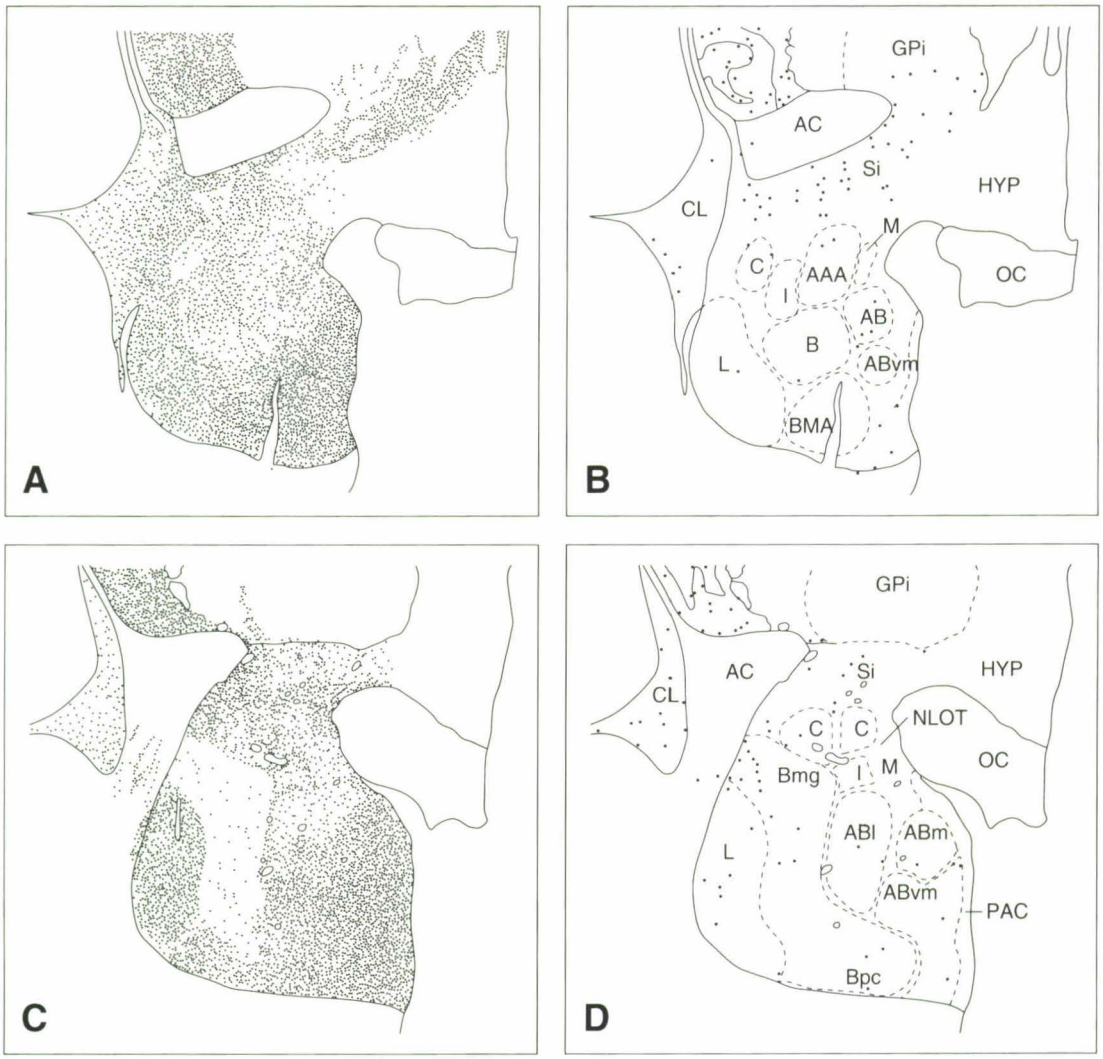


Figure 18.22. Camera lucida drawings of transverse section through the rostral (**A, B**) and middle (**C, D**) third portions of the amygdala in the squirrel monkey illustrating the distribution of somatostatin (SRIF)-immunoreactive terminals (*small dots on the right*) and cells bodies (*filled circles on the left*). Specific polyclonal antibodies raised against somatostatin-28 and somatostatin 28 (1–12) were used and both antibodies gave similar results. *AAA*, amygdaloid anterior area; *AC*, anterior commissure; *AB*, accessory basal nucleus; *ABl*, accessory basal nucleus, lateral part; *ABm*, accessory basal nucleus, medial part; *ABvm*, accessory basal nucleus, ventromedial part; *B*, basal nucleus; *BMA*, basal medial nucleus; *Bmg*, basal nucleus, magnocellular part; *Bpc*, basal nucleus, parvicellular part; *C*, central nucleus; *CL*, claustrum; *GPi*, globus pallidus, internal segment; *HYP*, hypothalamus; *I*, intercalated nuclear masses; *L*, lateral nucleus; *M*, medial nucleus of amygdala; *NLOT*, nucleus of lateral olfactory tract; *OC*, optical chiasm; *PAC*, periamygdaloid cortex; *SI*, substantia innominata.

markedly decreased in the amygdala in cases of Alzheimer's disease (29).

OTHER SUBSTANCES

The amygdala in monkeys and humans contains numerous cell bodies and fibers that express the enzyme nicotinamide adenine dinucleotide phosphate diaphorase (NADPH-d) (18, 36, 266). In the human amygdaloid complex, NADPH-d cells and processes occur in large number in the basolateral group and in moderate number in the corticomedial group. The central amygdaloid area is characterized by minimal NADPH-d histochemical staining (36). In contrast to several other types of amygdaloid neurons, those that stain for NADPH-d do not appear to be affected in cases of Alzheimer's disease. Furthermore, colocalization experiments re-

veal that numerous amygdaloid neurons that contain NADPH-d also express neuropeptide and/or somatostatin in humans (266).

The enzyme NADPH-d is a nitric oxide synthase that produces the highly toxic molecule nitric oxide (NO) in response to changes in intracellular free calcium levels. In the amygdala, calcium levels appear to be controlled by two calcium-binding proteins, namely calbindin D-28k and parvalbumin. Immunohistochemical studies have revealed the presence of parvalbumin (203) or calbindin D-28k (204) in distinct sets of amygdaloid neurons in monkeys.

Intrinsic Connections

The complexity and functional importance of the inter-and intranuclear amygdaloid connections have been underestimated in the past largely because of the lack of adequate methodologic procedures to study the intrinsic microcircuitry of the amygdala. The relatively recent use of neuronal tracers that are not taken up, at least in significant amount, by fibers of passage (e.g., tritiated amino acids and various plant lectins), has allowed the gathering of some new information regarding the intrinsic circuitry of the amygdala.

In monkeys, as in nonprimates species, the major intra-amygdaloid connections arise in the lateral and basal nuclei and terminate in the more medially located nuclei. The accessory basal nucleus also projects to the central, medial, and cortical nuclei and the amygdalohippocampal area. By comparison, the projection from the medial, cortical, or central nuclei back to the nuclei of the basolateral group are relatively weak. This pattern of connectivity indicates that the processing of information within the amygdala is basically unidirectional and follows a lateromedial direction (18).

Subcortical Connections

OLFACTORY SYSTEM

The amygdala in primates is not dominated by olfaction as in some macrosmatic nonprimate species (e.g., rodents). Nonetheless, it has substantial interconnections with several components of the olfactory system. Fibers originating in the olfactory bulb and coursing in the lateral olfactory tract terminate principally in the corticomedial nuclear group, including the nucleus of the lateral olfactory tract (2, 13, 18, 55, 79, 132, 209). Fibers concerned with the vomeronasal organ that originate in the accessory olfactory bulb also terminate in the corticomedial nuclear group (218). No fibers from the lateral olfactory tract appear to enter the basolateral nuclear group, but this group receives an indirect olfactory input via relays in the piriform cortex (18, 55, 209, 270). Thus, nearly all parts of the primate amygdaloid nuclear complex receive either direct or indirect olfactory pathways. In turn, neurons in the nucleus of the olfactory tract and in other components of the corticomedial nuclear group send fibers to the olfactory bulb (18, 55).

BASAL FOREBRAIN

The amygdala is reciprocally linked with the basal forebrain. This projection is directed principally, although not exclusively, toward the magnocellular basal forebrain nuclei, including the basal nucleus of Meynert and the nucleus of the diagonal band (of Broca). The efferent projection from the amygdala arises primarily from the parvicellular division of the basal nucleus, the magnocellular division of the accessory basal nucleus, and the central nucleus. Many of these amygdalofugal fibers appear to contact only *en passant* the magnocellular nuclei on their way to the thalamus, hypothalamus, and brainstem (230). In turn, neurons in the anterolateral part of the basal nucleus of Meynert project to the amygdala where they terminate massively in the magnocellular division of the basal nucleus and less abundantly in the magnocellular division of the accessory basal nucleus. As mentioned earlier, this projection arises in large part from cholinergic neurons of the basal nucleus of Meynert (Fig. 18.23), with a smaller contribution from GABAergic neurons in the same nucleus. The cholinergic projection to the magnocellular division of the amygdaloid basal nucleus is, in fact, considered to be one of the most massive cholinergic projections of any forebrain region (18).

STRIATUM

The existence of a substantial projection to the ventral part of the striatum, principally to the nucleus accumbens and deep layers of the olfactory tubercle (collectively termed the

ventral striatum), has been known for some time (87, 178). More recent studies, however, revealed that the amygdala projects much more profusely to the striatum than previously believed. Amygdalostriatal fibers terminate in the ventral and medial parts of the caudate nucleus and putamen that border the nucleus accumbens, but also in the ventral part of the putamen and in the sector of the body and tail of the caudate nucleus that borders the stria terminalis (230). The amygdalostriatal projection arises mainly, if not solely, from the basal and accessory basal nuclei (197, 230). The parvicellular division of the basal nucleus projects preferentially to the medial part of the nucleus accumbens, while the magnocellular division projects more extensively to the body and tail of the caudate nucleus and to the ventral putamen (230). Thus, the amygdalostriatal projection should be considered as one of the most substantial efferents of the amygdala in primates (18).

HIPPOCAMPUS

As mentioned in the earlier section dealing with the hippocampal formation, there are prominent interconnections between the amygdala and the hippocampus. The amygdalo-hippocampal projection arises principally from the lateral nucleus, the parvicellular division of the basal nucleus, and the magnocellular division of the accessory basal nucleus. The main projection arises from the lateral nucleus and terminates in the rostral entorhinal cortex. Other, less massive, projections are directed to the hippocampus and the proximal portion of the subiculum.

By comparison, the hippocampo-amygdaloid projection is meager, consisting essentially of a projection from the CA1/subiculum border zone and the entorhinal cortex to the parvicellular division of the basal nucleus (18). The fact that amygdalo-hippocampal projections are more prominent than hippocampo-amygdaloid projections suggests that the amygdala exerts a more powerful influence upon the hippocampal formation than vice versa.

THALAMUS

The amygdala projection to the magnocellular portion of the mediodorsal thalamic nucleus (MDmc) is particularly well-documented (18, 155, 206). In turn, the MDmc projects to the region of the orbitofrontal cortex that receive direct amygdalocortical projections (122). Besides this prominent projection, there is a projection from the central and medial amygdaloid nuclei that terminates in the midline thalamic nuclei, particularly the nucleus reuniens and the caudal part of the centralis nuclear complex. A light projection from the central amygdaloid nucleus to the medial part of the pulvinar has also been identified (18).

Surprisingly, the main thalamic recipient of the amygdala projection, the MDmc, does not project back to the amygdala. The midline thalamic nuclei, however, do project back to the amygdala, particularly to the central nucleus and adjoining portion of the basal nucleus (155, 190, 275). In the rat and cat, cells surrounding the medial geniculate nucleus in the posterior thalamus project to the lateral, accessory basal, medial, and central amygdaloid nuclei. Since these posterior thalamic areas receive auditory inputs from the inferior colliculus, their projections to the amygdala have been implicated in conditioned emotional responses to auditory stimuli (128).

HYPOTHALAMUS

As mentioned earlier, the bed nucleus of the stria terminal is considered by many investigators as forming a morphologic and functional continuum termed the extended amygdala (154). Like the central and medial amygdaloid nuclei, the bed nucleus of the stria terminalis forms a relay for projections from the amygdala to the hypothalamus. Caudal to the bed nucleus, fibers originating in the corticomedial nuclear group terminate in the anterior hypothalamus, with some of them appearing to contact the dendrites of cells in the supraoptic and paraventricular hypothalamic nuclei. A more substantial amygdalohypothalamic projection terminates in and around the ventromedial hypothalamic nucleus. Fibers originating in the amygdalo-hippocampal transitional area and the adjacent ventral subiculum terminate in the cell-sparse shell around the ventromedial nucleus, whereas other fibers arising from the medial and accessory amygdaloid basal nuclei terminate in the cellular core of the nucleus (99, 147). Fibers originating in the central amygdaloid nucleus also arborize throughout the rostrocaudal extent of the lateral hypothalamus. Some fibers of the central

nucleus also innervate the tuberomammillary and supramammillary nuclei, before continuing into the midbrain tegmentum.

Hypothalamoamygdaloid projections are not particularly prominent. Most of them arise in the ventromedial nucleus and the more caudal parts of the lateral hypothalamic area, and terminate in the central, medial, and accessory basal nuclei and parvicellular division of the basal nucleus (18, 48, 222, 260).

BRAINSTEM

The central amygdaloid nucleus is the major source of inputs to the brainstem, but the bed nucleus of the stria terminalis has essentially similar projections. Fibers from the central nucleus descend through the midbrain, pons, and medulla, with some fibers extending as far down as the spinal cord. Along their course these fibers distribute numerous collaterals within structures implicated in autonomic control, including the periaqueductal gray, the parabrachial nucleus, the dorsal nucleus of the vagus nerve, and the reticular formation. Many of these structures send reciprocal ascending projections to the central nucleus (155, 181).

In the midbrain, fibers from the central amygdaloid nucleus arborize in the ventral tegmental areas and in the lateral part of the substantia nigra pars compacta, thus reciprocating the dopaminergic mesoamygaloid projection described earlier. In the pons, fibers from the central amygdaloid nucleus terminate massively in the medial and lateral parabrachial nuclei bordering the superior cerebellar peduncle, whereas in the medulla the amygdalofugal fibers terminate most heavily in the nucleus of the solitary tract and dorsal motor nucleus of the vagus nerve. The parabrachial nuclei send direct reciprocal fibers to the central amygdaloid nucleus (155, 181, 190, 291), but the nucleus of the solitary tract projects only indirectly to the central nucleus via a relay in the parabrachial nuclei (18, 26)

The central nucleus of the amygdala, as well as other amygdaloid nuclei, receive ascending prominent monoaminergic inputs, besides the dopaminergic projections just described. These include (a) adrenergic projections from neurons in the lower medulla, (b) noradrenergic projections from the locus coeruleus, and (c) serotoninergic projections from the midbrain raphe nuclei, principally the dorsal raphe nucleus. In contrast to the mesoamygdaloid dopaminergic projections, the adrenergic, noradrenergic, and serotoninergic amygdaloid afferents do not appear to have reciprocal amygdalofugal projections.

Amygdalocortical Connections

The primate amygdala is massively interconnected with the neocortex (100, 123, 125, 150, 177, 192, 270, 271, 282), and a detailed review on the organization of the amygdalocortical connections has been published (18). In brief, the amygdala can be said to receive unimodal sensory input from the visual, auditory, and somatosensory cortices, the afferents arising from high stages in the hierarchy of sensory processing (5). For example, the amygdala is not innervated by the primary visual cortex or even by the peristriate cortex but receives input primarily from the inferotemporal cortex (area TE). There exist prominent return projections from the amygdala to unimodal sensory cortices, and these projections are surprisingly much more widespread than the corticoamygdaloid projections. In the visual system, the amygdala projects to virtually all visually related areas of the temporal and occipital cortex. This finding suggests that the amygdala could modulate sensory processing at every stage in the cortical hierarchy (18). It is interesting to note that the reciprocal connections between the cerebral cortex and the amygdala are not organized in a cell-to-cell manner. For example, visual inputs to the amygdala terminate principally in the lateral nucleus, whereas projections back to the visual cortex originate chiefly in the basal nucleus. Thus, one or more stages of intrinsic neuronal processing in the amygdala are needed to close the amygdala-cortex-amygdala loop.

There are also substantial interconnections between the amygdala and polysensory and limbic association areas, including the cingulate gyrus, temporal pole, superior temporal sulcus, insula, perirhinal and frontal cortices. These projections arise from the lateral and basal amygdaloid nuclei (18).

These findings on the amygdalocortical projections reveal that the amygdala receives an enormous array of convergent sensory information. Given its numerous subcortical projections to regions such as the hypothalamus, basal forebrain, ventral striatum, and various autonomic centers in the brainstem,

the amygdala represents an important relay whereby external stimuli can influence and activate emotions. Furthermore, through its extensive projections back to the cortex, the amygdala can modulate sensory processing according to affective states (5).

Functional Considerations

Even though the amygdaloid complex receives an olfactory input, the exact role of this structure in the processing of olfactory information is still not clear. Early observations that the amygdaloid complex is well-developed in anosmatic aquatic mammals and that bilateral destruction of this complex does not impair olfactory discrimination (10, 254), led to the conclusion that the amygdala is not closely related to olfaction. Detailed functional studies are obviously needed before any conclusion can be drawn about the involvement of the amygdala in olfaction.

Pronounced behavioral changes are elicited by stimulation of the amygdala in unanesthetized animals. The most common response to amygdaloid stimulation under such conditions is an "arrest" reaction in which all spontaneous ongoing activities cease as the animal assumes an attitude of aroused attention (79, 113, 146). The "arrest" reaction appears as the initial phase of flight or defense reactions. Flight (fear) and defensive (rage and aggression) reactions, termed agonistic behavior, have been elicited from different regions of the amygdaloid complex (53). In the amygdaloid complex, the intensity of the stimulus determines the magnitude of the response, which builds gradually and outlasts the period of stimulation (293). The fact that long-term potentiation can be induced in the amygdala (44) could explain the long-lasting aspect of this response. Intense reactions of fear and rage are associated with pupillary dilatation, piloerection, growling, hissing, unmistakable signs of emotional involvement, and activity of the autonomic nervous system. Electrical stimulation of the stria terminalis, or of the ventral amygdalofugal fibers, produces components of the defense reaction, but lesions of the stria terminalis do not alter the response obtained by stimulating the amygdala (101). After completely interrupting the ventral amygdalofugal projections, defense reactions can no longer be obtained by stimulating the amygdaloid complex (293).

Stimulation of the amygdaloid region in humans produces feelings of fear, confusional states, disturbances of awareness, and amnesia for events taking place during the stimulation (53, 66, 80, 172). Although rage is the most common behavioral response to amygdaloid stimulation in animals, it rarely is associated with temporal lobe seizures (80).

Bilateral lesions of the amygdaloid complex in animals consistently produce disturbances of emotional behavior (5, 20, 79, 82, 85, 113, 205, 212, 228, 264). Animals become placid and display no reactions of fear, rage, or aggression. Previously dominant and abusive animals became tame and did not retaliate to the threats or molestations of other animals. Hypersexuality has been noted as a prominent feature in some experimental studies. Hypersexual behavior may occur only when the lesions concomitantly involve the piriform cortex, since amygdaloid lesions sparing this region do not alter sexual behavior.

The *Klüver-Bucy syndrome* is characterized by conversion of wild intractable monkeys to docile beasts, which show no evidence of fear, rage, or aggression (119, 120). These animals display apparent "psychic blindness," a compulsion to examine objects visually, tactually, and orally, bizarre sexual behavior, and certain changes in dietary habits. Almost all objects are examined, smelled, and mouthed, and if the object is not edible, it is discarded. Hypersexuality is characterized by the indiscriminate partnerships sought with both male and female animals, animals of other species, and even inanimate objects.

Observations in humans concerning the effects of bilateral lesions in the amygdaloid complex indicate that these lesions cause a decrease of aggressive and assaultive behavior (137, 153, 262, 263). Stereotaxic lesions in the amygdaloid complex in humans produce a marked reduction in emotional excitability and tend to normalize social behavior in individuals with severe behavior disturbances (173, 174, 228). Unilateral lesions in some cases proved sufficient to bring about improvement. Bilateral lesions did not produce the signs and symptoms suggestive of the Klüver-Bucy syndrome.

Visceral and autonomic responses include alterations of respiratory rate, rhythm, and amplitude, as well as inhibition of respiration. The most common response of amygdaloid stimulation in unanesthetized animals

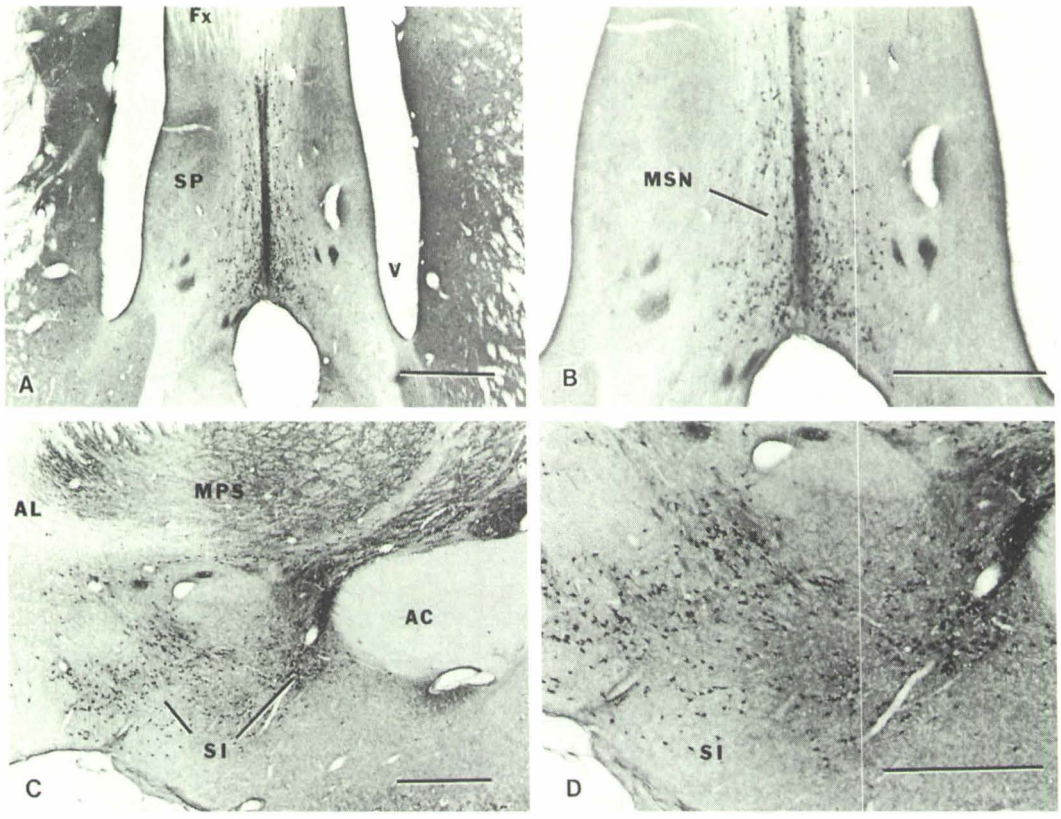


Figure 18.23. Cells in the septal nuclei and the substantia innominata immunoreactive to choline acetyltransferase (ChAT) in the rhesus monkey. **A** and **B**. Cells in the medial septal nucleus (MSN). **C** and **D**. ChAT immunoreactive cells in portions of the substantia innominata (*SI*) ventral to the medial (internal) pallidal segment (*MPS*). Collections of large cholinergic neurons in this complex constitute the basal nucleus of Meynert. The substant a innominata extends rostrally beneath the anterior commissure. *AC*, anterior commissure; *AL*, ansa lenticularis; *Fx*, fibers of the fornix; *SP*, septum pellucidum; *V*, anterior horn of the lateral ventricle. Scale bars represent 1 mm.

is an acceleration of the respiratory rate associated with a reduction in amplitude (113). Cardiovascular responses involve both increases and decreases in arterial blood pressure and alterations in heart rate. Pressor responses appear to predominate following amygdaloid stimulation in the unanesthetized animal. Gastrointestinal motility and secretion may be inhibited or activated, and both defecation and micturition may be induced. Piloerection, salivation, pupillary changes, and alterations of body temperature can occur. These responses may be either sympathetic or parasympathetic in nature.

Somatic responses obtained by stimulation of the amygdaloid complex include turning of the head and eyes to the opposite side, and complex rhythmic movements related to chewing, licking, and swallowing. The varied somatic and autonomic effects of electrical stimulation of the amygdaloid complex constitute an insignificant part of the syndrome produced by lesions in this complex.

Endocrine responses to stimulation of the amygdaloid nuclear complex include the release of adrenocorticotropin (ACTH) and gonadotrophic hormone, and lactogenic responses. Stimulation of the amygdaloid areas that produce arousal and emotional responses also produce increased adrenocortical output (113, 295). Bilateral lesions in the medial amygdaloid nuclei produce an elevation of serum levels of ACTH, presumably due to release of an inhibitory influence on the secretion of ACTH (61). Stimulation of the corticomedial division of the amygdala may induce ovulation, but this response is abolished by transection of the stria terminalis (64, 242, 276). The corticomedial amygdaloid nuclei in the female appear to have estrogen concentrating neurons which are part of a system of similar cells extending into hypo-

thalamic and limbic structures (201). The amygdala also is concerned with the luteinizing (LH) and follicle-stimulating (FSH) hormones (113). It is quite clear that the amygdala participates with the hypothalamus in the control and regulation of hypophysial secretions.

The amygdaloid complex also plays a role in food and water intake (238). Bilateral ablations of the amygdala may result in striking hyperphagia, or in hypophagia. Lesions of the basolateral nucleus of the amygdala result in hyperphagia (68), while stimulation of this part of the amygdala produces an arrest of feeding behavior (69). It has been postulated that this part of the amygdaloid complex inhibits the lateral hypothalamic area, which is regarded as the feeding center of the hypothalamus (113, 188). The corticomedial part of the amygdaloid complex is a facilitatory area concerned with food intake. Stimulation of this region produces increases in food intake (226, 227). The amygdala receives projections from the primary taste cortex in monkeys, offering a route whereby it could gain access to the gustatory information required to guide feeding behavior. Neurons in the amygdala are implicated in mediating hedonic appreciation, emotional expression, and conditioning, particularly as these relate to feeding (238). The amygdala appears to exert its influence upon feeding by modulating the activity of hypothalamic mechanisms (147, 250) (Fig. 18.24).

The role of the amygdala as an integrator of autonomic and visceral functions through its reciprocal connections with the hypothalamus and visceral nuclei of the brainstem is widely accepted. It has become increasingly evident that the amygdala also is involved in complex cognitive functions that influence emotion and behavior in a global fashion (5, 228). These functions appear to involve virtually all regions of the cerebral cortex and all sensory modalities. Cortical inputs to the amygdala derived from modality specific as-

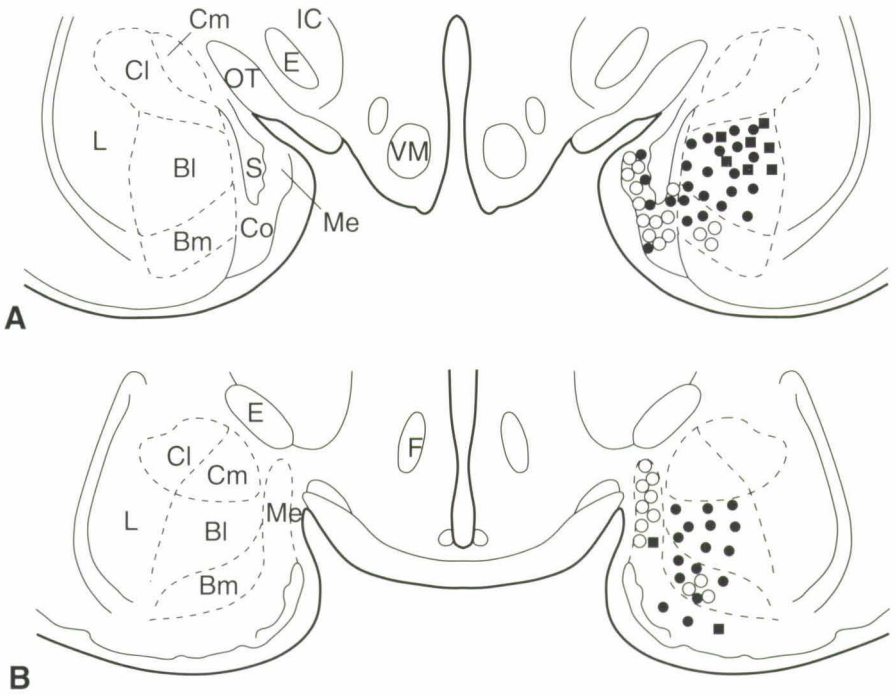


Figure 18.24. Amygdala of the cat at the level of the tuberal region (**A**) and the optic chiasm (**B**). The major nuclear boundaries are shown with *dashed lines*. On the right side are the locations of cell bodies labeled by retrograde transport of horseradish peroxidase injected into three locations in the hypothalamus: *open circles*, ventromedial nucleus; *filled squares*, lateral hypothalamus; *filled circles*, preoptic area. *Bl*, basolateral amygdaloid nucleus (magnocellular part); *Bm*, basomedial amygdaloid nucleus (parvicellular part); *Cl*, central amygdaloid nucleus, lateral part; *Cm*, central amygdaloid nucleus, medial part; *Co*, cortical amygdaloid nucleus; *E*, entopeduncular nucleus (homologue of the internal pallidal segment of primates); *F*, fornix; *IC*, internal capsule; *L*, lateral amygdaloid nucleus; *Me*, medial amygdaloid nucleus; *VM*, ventromedial hypothalamic nucleus; *S*, stria terminalis.

sociation areas appear unique among central limbic structures. It has been suggested that the amygdala represents the interface between the hypothalamus and brainstem visceral centers, and regions of the cerebral cortex concerned with cognitive functions. The Klüver-Bucy syndrome provides an example of this interrelationship. In the presence of lesions in the amygdala, monkeys respond to visual stimuli in a bizarre fashion because the visual stimuli have no meaning. This may also apply to other sensory modalities whose cortical inputs to the amygdala are disconnected by destruction of the amygdalae. Broadly stated, impulses generated in sensory systems, the cerebral cortex, and probably still-undetermined neural structures, trigger mechanisms that excite visceral and somatic systems whose activities in concert provide the physiologic expression of emotion and goal-directed behavior. Reciprocal connections between areas of the cerebral cortex and the amygdala appear essential to the correlation of emotional expression and meaningful behavior.

The involvement of the amygdala in emotion may have an important bearing on several forms of dementia. In Alzheimer's disease, the amygdala suffers from severe neuronal loss and displays numerous neurofibrillary tangles and senile plaques (237, 267). There is also a marked volumetric decrease of the amygdala in Alzheimer's disease (236). These changes are severe and occur early in the course of the disease. Besides a marked memory impairment, dementia of the Alzheimer type is characterized by changes in emotional behaviors (e.g., increases in passivity and in agitated and self-centered behavior, and a loss in spontaneity and esthetic appreciation) (5). These negative mood changes associated with dementia are somewhat similar to the hypoemotionality noted in monkeys with amygdala damage. Furthermore, the emotional changes can be unrelated to the memory loss, a finding that suggests a clear dissociation between amygdala (emotion) and hippocampus (memory) functions (5).

The amygdala may also be involved in the emotional changes observed in schizophrenia. Patients suffering from schizophrenia often display inappropriate mood or lack of affect, and they also have difficulty identifying the emotional status of other people. It is also known that the volume of the amygdala (together with that of the hippocampal formation) is markedly reduced in schizophrenics (34). Further evidence comes from the connectivity between the amygdala and the other brain regions that show pathologic changes in schizophrenia, that is, the hippocampus, entorhinal cortex, parahippocampal gyrus, cingulate gyrus, and frontal cortex (159).

The connections between the amygdala and the frontal cortex appear particularly relevant here because frontal lobe dysfunction is believed to be a central feature of schizophrenia (5). Results of various neurochemical studies also suggest a possible involvement of the amygdala in schizophrenia. For example, the therapeutic action of most neuroleptic drugs given to schizophrenics depends on their action as antagonist of dopamine D_2 receptors. It is, therefore, relevant that the amygdala is reciprocally connected with midbrain dopaminergic neurons giving rise to the mesolimbic dopaminergic pathway. It has been hypothesized that an increase in the activity of this mesolimbic dopaminergic pathway, which innervates also the ventral striatum and the frontal cortex, is a key neurochemical feature of schizophrenia. While it is unlikely that the malfunctioning of any one brain region will prove sufficient to produce the complex array of cognitive, emotional, and attentional disorders associated with schizophrenia, the link between the amygdala and emotional changes in schizophrenia is worth further study.

SUBSTANTIA INNOMINATA

The substantia innominata is part of a heterogeneous group of telencephalic structures on the medial and ventral aspect of the cerebral hemispheres, which collectively are referred to as the basal forebrain. Despite the location of these structures near the surface of the brain, they lack a cortical organization. The basal forebrain extends from the olfactory tubercle rostrally to the hypothalamic region caudally and overlaps the area known as the anterior perforated substance (Fig. 18.6). Although the precise boundaries of the basal forebrain are not clearly defined, it is generally agreed to include the septal area, the olfactory tubercle, parts of the amygdala, and the area under the anterior commissure known as the *substantia innominata* (Figs. 18.19 and 18.20). The large neurons scattered

within the basal forebrain are often referred to as the magnocellular basal forebrain neurons. The subcommissural region contains a number of cell groups in contact with fiber bundles traversing the region, which include the diagonal band (of Broca), the anterior commissure, the medial forebrain bundle, the ansa lenticularis, the ansa peduncularis, and the inferior thalamic peduncle.

In the subcommissural region, the most conspicuous cells are a group of magnocellular hyperchromic neurons, known as the *basal nucleus* (of Meynert) or *nucleus basalis* (Fig. 18.23). The term substantia innominata is

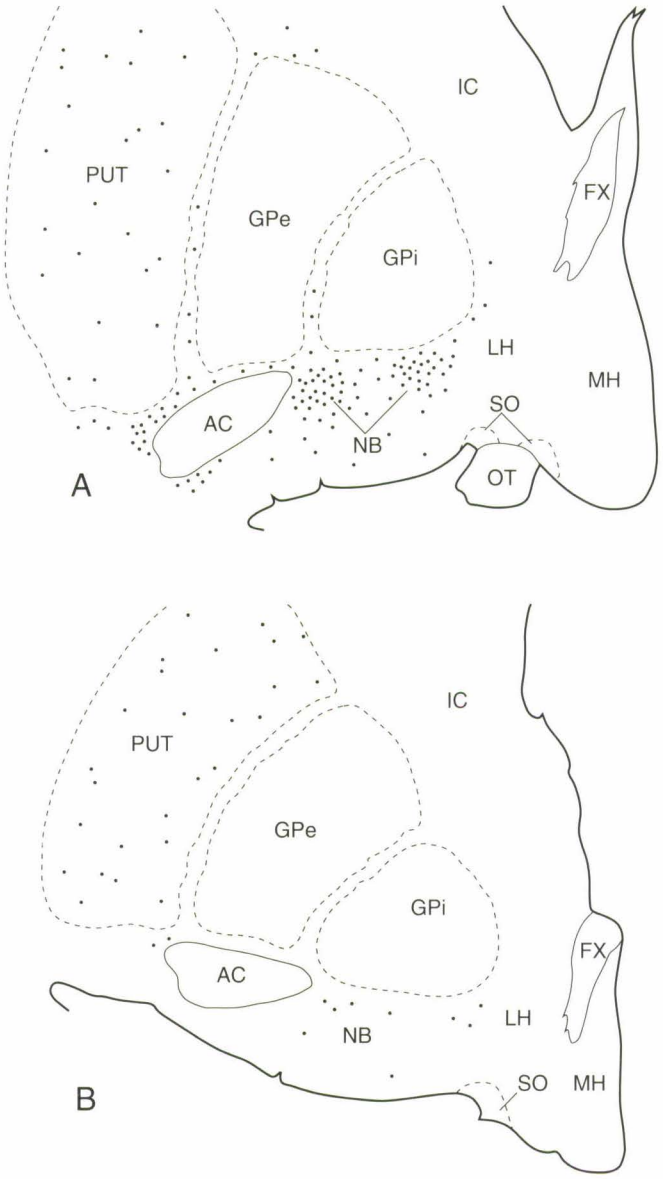


Figure 18.25. Transverse section through the basal forebrain showing the distribution of neurons intensely stained for acetylcholinesterase (*dots*) in a normal human brain (**A**; age 84) and in a typical case of senile dementia of the Alzheimer type (**B**; age 75). Note that the basal nucleus in the Alzheimer diseased brain (**B**) displays a marked cell loss, whereas the actetylcholinesterase-rich neurons in the putamen are not affected. This indicates that cholinergic neurons in the basal nucleus are specifically altered in Alzheimer's disease. *AC*, anterior commissure; *FX*, fornix; *GPe*, external pallidum; *GPi*, internal pallidum; *IC*, internal capsule; *LH*, lateral hypothalamus; *MH*, medial hypothalamus; *NB*, basal nucleus of Meynert; *OT*, optic tract; *PUT*, putamen; *SO*, supraoptic nucleus.

used inconsistently and frequently as a synonym for the basal nucleus, but the term "basal nucleus" should be restricted specifically to the clusters of magnocellular elements that are scattered throughout the substantia innominata. Large basophilic neurons with morphologic characteristics similar to those of the basal nucleus of Meynert are present in the medial septum, vertical and horizontal parts of the nucleus of the diagonal band, and in largest numbers along the ventral and lateral margins of the pallidal segments (Fig. 18.23). Similar cells are present in parts of the medullary laminae of the globus pallidus. In the basal nucleus, most neurons are cholinergic. Clusters of small GABA-immunoreactive cells are scattered among the large cholinergic neurons of the basal nucleus. Afferents to the substantia innominata and the basal nucleus arise mainly from the amygdala, portions of the insular and temporal cortex, and from the piriform and entorhinal cortices. About 90% of the cholinergic neurons in the basal nucleus project to widespread regions of the cerebral cortex. It has been suggested that the basal nucleus may be the single major source of cholinergic innervation of the entire cerebral cortex. In this sense, the basal nucleus appears analogous to the raphe nuclei and the locus coeruleus, which constitute the major sources of serotonergic and noradrenergic innervation, respectively, to widespread regions of the cerebral cortex.

Interest in the basal nucleus is related to the discovery that neurons in this nucleus selectively degenerate in Alzheimer's disease and its variant, senile dementia of the Alzheimer's type, the most common dementia occurring in middle and late life (Fig. 18.25) (49, 195, 283). The loss of cholinergic input from neurons in the basal nucleus appears to be a highly significant factor in the well-documented cortical cholinergic deficiency that occurs in these patients (49). Alzheimer's disease usually develops between the ages of 40 and 60 and is characterized by progressive dementia with apraxia and speech disturbances. There is loss of memory, slurred speech, and disorientation. The pathologic picture is associated with diffuse degeneration of the cerebral cortex involving all layers, senile amyloid plaques in the cortex, intraneuronal fibrillary tangles, and selective degeneration of the cells in the basal nucleus.

References

1. Addison WHF. On the rhinencephalon of *Delphinus delphis*. J Comp Neurol 1915;25:497–522.
2. Adey WR, Meyer M. Hippocampal and hypothalamic connexions of the temporal lobe in the monkey. Brain 1952;75:358–384.
3. Adrian ED. Olfactory reactions in the brain of the hedgehog. J Physiol (Lond) 1942;100:459–473.
4. Aggleton JP. A description of the amygdalo-hippocampal interconnections in the macaque monkey. Exp Brain Res 1986;64:515–526.
5. Aggleton JP. The contribution of the amygdala to normal and abnormal emotional states. Trends Neurosci 1993;16:328–333.
6. Akelaitis AJ. Study of language function (tactile and visual lexia and graphia) unilaterally following section of the corpus callosum. J Neuropathol Exp Neurol 1943; 2:226–262.
7. Akelaitis AJ, Risteen WA, Herren RY, Van Wagenen WP. Studies on corpus callosum: Contribution to study of dyspraxia and apraxia following partial and complete section of corpus callosum. Arch Neurol Psychiatry 1942;47:971–1008.
8. Akeson RA. Primary olfactory neuron subclasses. In: Margolis FL, Gretchell TV, eds. Molecular neurobiology of the olfactory system. New York: Plenum Press, 1988:297–318.
9. Alheid GF, Heimer L. New perspectives in basal forebrain organization of special relevance for neuropsychiatric disorders: the striatopallidal, amygdaloid, and corticopetal components of substantia innominata. Neuroscience 1988;27:1–39.
10. Allen WF. Effect of ablating the pyriform-amygdaloid areas and hippocampi on positive and negative olfactory conditioned reflexes and on conditioned olfactory differentiation. Am J Physiol 1941; 132:81–92.
11. Allison AC. The structure of the olfactory bulb and its relationship to the olfactory pathways in the rabbit and the rat. J Comp Neurol 1953;98:309–353.
12. Allison AC. The morphology of the olfactory system in the vertebrates. Biol Rev 1953;28:195–244.
13. Allison AC. The secondary olfactory areas in the human brain. J Anat 1954;88:481–488.
14. Allison AC, Warwick R. Quantitative observations on the olfactory system of the rabbit. Brain 1949;72:186–197.
15. Amaral DG. Emerging principles of intrinsic hippocampal organization. Curr Opin Neurobiol 1993;3:225–229.
16. Amaral DG, Insausti R. Hippocampal formation. In: Paxinos G, ed. The human nervous system. Ch. 21. New York: Academic Press, 1990:711–755.
17. Amaral DC, Insausti R. Retrograde transport of D-[^{3}H]-aspartate injected into the monkey amygdaloid complex. Exp Brain Res 1992;88:375–388.
18. Amaral DG, Price JL, Pitkänen A, Carmichael ST. Anatomical organization of the primate amygdaloid complex. In: Aggleton JP, ed. The amygdala: neurobiological aspects of emotion, memory, and mental dysfunction. New York: Wiley-Liss, 1992:1–66.
19. Amoore JE, Johnston JW Jr, Rubin M. The stereochemical theory of odor. Sci Am 1964;210:42–49.
20. Anand BK, Brobeck JR. Food intake and spontaneous activity or rats with lesions in the amygdaloid nuclei. J Neurophysiol 1952;15:421–430.
21. Anand BK, Dua S. Circulatory and respiratory changes induced by electrical stimulation of limbic system (visceral brain). J Neurophysiol 1956;19:393–400.
22. Anholt RR. Molecular neurobiology of olfaction. Crit Rev Neurobiol 1993;7:1–22.
23. Barbe MF, Levitt P. The early commitment of fetal neurons to the limbic cortex. J Neurosci 1991;11: 519–533.

24. Barnett EM, Perlman S. The olfactory nerve and not the trigeminal nerve is the major site of CNS entry for mouse hepatitis virus, strain JHM. Virology 1993;194: 185–191.
25. Barr ML, Kiernan JA. The human nervous system. 6th ed. Philadelphia: J.B. Lippincott, 1993.
26. Beckstead RM, Morse JR, Norgren R. The nucleus of the solitary tract in the monkey: Projections to the thalamus and brainstem. J Comp Neurol 1980;190:259–282.
27. Ben-Ari Y, Le Gal La Salle G, Kanazawa I. Regional distribution of substance P within the amygdaloid complex and bed nucleus of the stria terminalis. Neurosci Lett 1977;4:299–302.
28. Ben-Ari Y, Zigmond RE, Shute CCD, Lewis PR. Regional distribution of choline acetyltransferase and acetylcholinesterase within the amygdaloid complex and stria terminalis system. Brain Res 1977; 120:435–445.
29. Benzing WC, Mufson EJ, Jennes L, Armstrong DM. Reduction of neurotensin immunoreactivity in the amygdala in Alzheimer's disease. Brain Res 1990;537:298–302.
30. Benzing WC, Mufson EJ, Jennes L, Stopa EG, Armstrong DM. Distribution of neurotensin immunoreactivity within the human amygdaloid complex: a comparison with acetylcholinesterase- and Nissl-stained tissue sections. J Comp Neurol 1992;317:283–297.
31. Berger TW, Thompson RF. Identification of pyramidal cells as critical elements in hippocampal neuronal plasticity during learning. Proc Natl Acad Sci USA 1978;75: 1572–1576.
32. Björklund A, Lindvall O. Dopamine-containing systems in the CNS. In: Björklund A, Hökfelt T, eds. Handbook of chemical neuroanatomy. Vol. 2. Part 1: Classical transmitters in the CNS. Ch. 3. Amsterdam: Elsevier, 1984:55–122.
33. Bliss T, Lomo T. Long lasting potentiation of synaptic transmission in the dentate area of the anesthetized rabbit following stimulation of the perforant path. J Physiol (Lond) 1973;232:331–356.
34. Bogerts B, Lieberman JA, Ashtari M, et al. Hippocampus-amygdala volumes and psychopathology in chronic schizophrenia. Biol Psychiatry 1993;33:236–246.
35. Brady JV. Temporal and emotional effects related to intracranial electrical self-stimulation. In: Ramey SR, O'Doherty DS, eds. Electrical studies on the unanesthetized brain. Ch. 3. New York: Paul B. Hoeber, 1960:52–77.
36. Brady DR, Carey RG, Mufson EJ. Reduced nicotinamide adenine dinucleotide phosphate-diaphorase (NADPH-d) profiles in the amygdala of human and New World monkey (*Saimiri sciureus*). Brain Res 1992;577:236–248.
37. Breer H, Shepherd GM. Implications of the NO/cGMP system for olfaction. Trends Neurosci 1993;16:5–9.
38. Broca P. Anatomie comparée des circonvolutions cérébrales: le grand lobe limbique et la scissure limbique dans la série des mammifères. Rev Anthropol (Ser 2) 1878;1:384–498.
39. Brodal A. The hippocampus and the sense of smell. Brain 1947; 70:179–222.
40. Brodal A. General discussion of the terminology of the rhinencephalon. In: Bargmann W, Schadé JP, eds. The rhinencephalon and related structures. Progress in brain research. Vol. 3. Amsterdam: Elsevier, 1963:237–244.
41. Brown TH, Zador AM. Hippocampus. In: Shepherd GM, ed. The synaptic organization of the brain. 3rd ed. Ch. 11. New York: Oxford University Press, 1990:346–388.
42. Browning M, Dunwiddie T, Bennett W, Gispen W, Lynch G. Synaptic phosphoproteins: Specific changes after repetitive stimulation of the hippocampal slice. Science 1979;203:60–62.
43. Buck L, Axel R. A novel multigene family may encode odorant receptors: a molecular basis for odor recognition. Cell 1991;65:175–187.
44. Chapman PF, Kairiss EW, Keenan CL, Brown TH. Long-term synaptic potentiation in the amygdala. Synapse 1990;6:271–278.
45. Cooper LN. Distributed memory in the central nervous system: possible test of assumptions in visual cortex. In: Schmitt FO, Worden FG, Adelman G, Dennis SG, eds. The organization of the cerebral cortex. Cambridge, MA: MIT Press, 1981:479–503.
46. Cotman C, Gentry C, Steward O. Synaptic replacement in dentate gyrus after unilateral entorhinal lesion: electron microscopic analysis of extent of replacement of synapses by remaining entorhinal cortex. J Neurocytol 1977;6:455–464.
47. Cotman CW, Nadler JV. Reactive synaptogenesis in the hippocampus. In: Cotman CW, ed. Neuronal plasticity. New York: Raven Press, 1978;227–265.
48. Cowan WM, Raisman G, Powell TPS. The connexions of the amygdala. J Neurol Neurosurg Psychiatry 1965;28:137–151.
49. Coyle JT, Price DL, DeLong MR. Alzheimer's disease: a disorder of cortical cholinergic innervation. Science 1983;219:484–1190.
50. Crosby EC, Humphrey T. Studies of the vertebrate telencephalon. II. The nuclear pattern of the anterior olfactory nucleus, tuberculum olfactorum and the amygdaloid complex in adult man. J Comp Neurol 1941;74:309–352.
51. Crosby EC, Humphrey T, Lauer EW. Correlative anatomy of the nervous system. New York: Macmillan Company, 1962.
52. Daitz HM, Powell TPS. Studies of the connections of the fornix system. J Neurol Neurosurg Psychiatry 1954;17:75–82.
53. Davis M. The role of the amygdala in fear and anxiety. Annu Rev Neurosci 1992;15:353–375.
54. De Olmos JS. The amygdaloid projection field in the rat as studied with the cupric-silver method. In: Eleftheriou BE, ed. The neurobiology of the amygdala. New York: Plenum Press, 1972:145–204.
55. De Olmos JS. Amygdala. In: Paxinos G, ed. The human nervous system. Ch. 20. New York: Academic Press, 1990:583–710.
56. Desjardins C, Parent A. Distribution of somatostatin immunoreactivity in the forebrain of the squirrel monkey. Basal ganglia and amygdala. Neuroscience 1992;47: 115–133.
57. Dott NM. Surgical aspects of the hypothalamus. In: Le Gros Clark WE, ed. The hypothalamus. Edinburgh: Oliver and Boyd, 1938: 131–185.
58. Drachman DA, Arbit J. Memory and the hippocampal complex. II. Is memory a multiple process? Arch Neurol 1966;15:52–61.
59. Duvernoy HM. The human hippocampus. München: J.G. Bergman Verlag, 1988.
60. Elde R, Hökfelt T, Johansson O, Terenius L. Immunohistochemical studies using antibodies to leucine-enkephalin: initial observations on the nervous systems of the rat. Neuroscience 1976;1:349–351.
61. Eleftheriou BE, Zolovick AJ, Pearse R. Effects of amygdaloid lesions on pituitary-adrenal axis in the deermouse. Proc Soc Exp Biol Med 1966;122:1259.
62. Emre M, Heckers S, Mash DC, Geula CG, Mesulam M-M. Cholinergic innervation of the amygdaloid complex in the human brain and its alteration in old age and Alzheimer's disease. J Comp Neurol 1993;336:117–134.
63. Epelbaum J, Arancibia LT, Kordon C, Ottersen OP, Ben-Ari Y. Regional distribution of somatostatin within the amygdaloid complex of the rat brain. Brain Res 1979; 174:172–174.
64. Everett JW. Neuroendocrine mechanisms in control of the mammalian ovary. In: Gorbman A, ed. Comparative endocrinology. New York: John Wiley & Sons, 1959: 168–174.
65. Farb C, Aoki C, Milner T, Kaneko T, LeDoux J. Glutamate immunoreactive terminals in the lateral amygdaloid nucleus: a possible substrate for emotional memory. Brain Res 1992;593: 145–158.
66. Feindel W, Penfield W. Localization of discharge in temporal lobe automatism. Arch Neurol Psychiatry 1954;72:605–639.
67. Ferri RT, Levitt P. Cerebral cortical progenitors are fated to produce

region-specific neuronal populations. Cereb Cortex 1993;3: 187–198.
68. Fonberg E. The role of the amygdaloid nucleus in animal behaviour. Prog Brain Res 1968; 22: 273–281.
69. Fonberg E, Delgado JMR. Avoidance and alimentary reactions during amygdala stimulation. J Neurophysiol 1961;24:651–664.
70. Fox CA. Certain basal telencephalic centers in the cat. J Comp Neurol 1940;72:1–62.
71. Fox CA. The stria terminalis, longitudinal association bundle and precommissural fornix fibres in the cat. J Comp Neurol 1943;79: 277–295.
72. Fox CA, Fisher RR, DeSalva SJ. The distribution of the anterior commissure in the monkey (*Macaca mulatta*). Experimental studies. J Comp Neurol 1948;89:245–277.
73. Gaffan D, Gaffan EA. Amnesia in man following transection of the fornix. A review. Brain 1991;114: 2611–2618.
74. Gall C, Brecha N, Karten HJ, Chang K-J. Localization of enkephalin-like immunoreactivity to identified axonal and neuronal populations of the rat hippocampus. J Comp Neurol 1981;198: 335–350.
75. Garcia-Bengochea F, Corrigan R, Morgane P, Russell D, Heath R. Studies on the function of the temporal lobes. I. The section of the fornix. Trans Am Neurol Assoc 1951;76:238–239.
76. Getchell TV, Shepherd GM. Short-axon cells in the olfactory bulb: dendrodendritic synaptic interactions. J Physiol (Lond) 1975;251: 523–548.
77. Glees P, Griffith HB. Bilateral destruction of the hippocampus (cornu ammonis) in a case of dementia. Monatsschr Psychiatr Neurol 1952;123:193–204.
78. Gloor P. Electrophysiological studies on the connections of the amygdaloid nucleus in the cat. Electroencephalogr Clin Neurophysiol 1955;7:243–264.
79. Gloor P. Amygdala. In: Field J, ed. Handbook of physiology. Vol. II, Sec. 1. Ch. 57. Washington, DC: American Physiological Society, 1960:1395–1420.
80. Gloor P. Temporal lobe epilepsy: its possible contribution to the understanding of the functional significance of the amygdala and of its interaction with neocortical-temporal mechanisms. In: Eleftheriou BE, ed. The neurobiology of the amygdala. New York: Plenum Press, 1972:423–457.
81. Graziadei PPC, Monti Graziadei GA. Neurogenesis and neuron regeneration in the olfactory system of mammals. 1. Morphological aspects of differentiation and structural organization of the olfactory sensory neurons. J Neurocytol 1979;8:1–18.
82. Green JD. The rhinencephalon: aspects of its relation to behavior and the reticular activating system. In: Jaspers HH, Proctyoror LP, Knighton RS, et al., eds. Reticular formation of the brain. Henry Ford Hospital International Symposium. Boston: Little, Brown and Company, 1958:607–619.
83. Green JD. The hippocampus. In: Field J, ed. Handbook of physiology. Vol. II, Sec. I. Ch. 56. Washington, DC: American Physiological Society, 1960:1373–1389.
84. Green JD. The hippocampus. Physiol Rev 1964;44:561–608.
85. Green JD, Clemente CA, De Groot J. Rhinencephalic lesions and behavior in cats. J Comp Neurol 1957;108:505–545.
86. Green JD, Shimamoto T. Hippocampal seizures and their propagation. Arch Neurol Psychiatry 1953;70:687–702.
87. Groenewegen HJ, Becker NEHM, Lohman AHM. Subcortical afferents of the nucleus accumbens septi in the cat, studied with retrograde axonal transport of horseradish peroxidase and bisbenzimid. Neuroscience 1980;5: 1902–1916.
88. Groenewegen HJ, Room P, Witter MP, Lohman AHM. Cortical afferents of the nucleus accumbens in the cat, studied with anterograde and retrograde transport techniques. Neuroscience 1982;7: 977–995.
89. Gros C, Pradelles P, Dray F, Le Gal La Salle G, Ben-Ari Y. Regional distribution of met-enkephalin within the amygdaloid complex and bed nucleus of the stria terminalis. Neurosci Lett 1978;10: 193–196.
90. Guillery RW. Degeneration in the posterior commissural fornix and the mammillary peduncle of the rat. J Anat 1956;90:350–370.
91. Guillery RW. Degeneration in the hypothalamic connexions of the albino rat. J Anat 1957;91:91–115.
92. Guthrie KM, Anderson AJ, Leon M, Gall C. Odor-induced increases in c-fos mRNA expression reveal an anatomical "unit" for odor processing in olfactory bulb. Proc Natl Acad Sci USA 1993;90:3329–3333.
93. Haberly LB. Olfactory cortex. In: Shepherd GM, ed. The synaptic organization of the brain. 3rd ed. Ch. 11. New York: Oxford University Press, 1990:317–345.
94. Haberly LB, Price JL. The axonal projection patterns of the mitral and tufted cells of the olfactory bulb in the rat. Brain Res 1977; 129:152–157.
95. Halasz N, Ljungdahl A, Hökfelt T. Transmitter histochemistry of the rat olfactory bulb. II. Fluorescence histochemical, autoradiographic and electron microscopic localization of monoamines. Brain Res 1978;154:253–272.
96. Halasz N, Parry DM, Blackett NM, Ljungdahl A, Hökfelt T. [^{3}H]γ-aminobutyrate autoradiography of the rat olfactory bulb: hypothetical grain analysis of the distribution of silver grains. Neuroscience 1981;6: 473–479.
97. Hall EA. Efferent connections of the basal and lateral nuclei of the amygdala in the cat. Am J Anat 1963;113:139–151.
98. Heilig M, McLeod S, Brot M, et al. Anxiolytic-like action of neuropeptide Y: mediation by Y1 receptors in amygdala, and dissociation from food intake effects. Neuropsychopharmacology 1993;8: 357–363.
99. Heimer L, Nauta WJH. The hypothalamic distribution of the stria terminalis in the rat. Brain Res 1969;13:284–297.
100. Herzog AG, Van Hoesen GW. Temporal neocortical afferent connections to the amygdala in the rhesus monkey. Brain Res 1976; 115:57–70.
101. Hilton SM, Zbrozyna A. Defense reaction from the amygdala and its afferent connections. J Physiol (Lond) 1963;165:160–173.
102. Hirsch JD, Grillo M, Margolis FL. Ligand binding studies in the mouse olfactory bulb: identification and characterization of a L-[^{3}H]carnosine binding site. Brain Res 1978;158:407–422.
103. Horel J. The neuroanatomy of amnesia: a critique of the hippocampal memory hypothesis. Brain 1978;101:403–445.
104. Hörtnagl H, Berger ML, Sperk G, Pifl C. Regional heterogeneity in the distribution of neurotransmitter markers in the rat hippocampus. Neuroscience 1991;45: 261–272.
105. Horton HL, Levitt P. A unique membrane protein is expressed on early developing limbic system axons and cortical targets. J Neurosci 1988;8:4653–4661.
106. Inagaki S, Parent A. Distribution of enkephalin-immunoreactive neurons in the forebrain and upper brainstem of the squirrel monkey. Brain Res 1985;359:267–280.
107. Insausti R, Amaral DG, Cowan WM. The entorhinal cortex of the monkey. II. Cortical afferents. J Comp Neurol 1987;264:356–395.
108. Insausti R, Amaral DG, Cowan WM. The entorhinal cortex of the monkey. III. Subcortical afferents. J Comp Neurol 1987;264:396–408.
109. Isaacson RL. A fuzzy limbic system. Behav Brain Res 1992;52: 129–131.
110. Ishizuka N, Weber J, Amaral DG. Organization of intrahippocampal projections originating from CA3 pyramidal cells in the rat. J Comp Neurol 1990;295:580–623.
111. Janigro D, Schwartzkroin PA. Effects of GABA on CA3 pyramidal cell dendrites in rabbit hippocampal slices. Brain Res 1988;453: 265–274.
112. Johnston JB. Further contributions to the study of the evolution of the

forebrain. J Comp Neurol 1923;35: 337–481.
113. Kaada BR. Stimulation and regional ablation of the amygdaloid complex with reference to functional representations. In: Eleftheriou BE, ed. The neurobiology of the amygdala. New York: Plenum Press, 1972:205–281.
114. Kaada BR, Pribram KH, Epstein JA. Respiratory and vascular responses in monkeys from temporal pole, insula, orbital surface and cingulate gyrus. J Neurophysiol 1949;12:347–356.
115. Kaada BR, Rasmussen EW, Kveini O. Effects of hippocampal lesions on maze learning and retention in rats. Exp Neurol 1961;3:333–355.
116. Kandel E. Cellular insights into behavior and learning. In: The Harvey Lectures, Series 73. New York: Academic Press, 1979:19–92.
117. Kandel ER. Cellular mechanisms of learning and biological basis of individuality. In: Kandel ER, Schwartz JH, Jessell TM, eds. Principles of neural science. Ch. 65. New York: Elsevier, 1991: 1009–1031.
118. Kishimoto J, Keverne EB, Emson PC. Calretinin, calbindin-D28k and parvalbumin-like immunoreactivity in mouse chemoreceptor neurons. Brain Res 1993;610: 325–329.
119. Klüver H. Brain mechanisms and behavior with special reference to the rhinencephalon. Lancet 1952;72:567–574.
120. Klüver H, Bucy P. Preliminary analysis of functions of the temporal lobes in monkeys. Arch Neurol Psychiatry 1939;42:979–1000.
121. Kötter R, Meyer N. The limbic system: A review of its empirical foundation. Behav Brain Res 1992;52:105–127.
122. Krettek JE, Price JL. Projections from the amygdaloid complex to the cerebral cortex and thalamus in the rat and cat. J Comp Neurol 1977;172:687–722.
123. Krettek JE, Price JL. Projections from the amygdaloid complex and adjacent olfactory structures to the entorhinal cortex and to the subiculum in the rat and cat. J Comp Neurol 1977;172:723–752.
124. Krieg WJS. Functional neuroanatomy. New York: Blakiston Company, 1953.
125. Lammers HJ. The neural connections of the amygdaloid complex in mammals. In: Eleftheriou BE, ed. The neurobiology of the amygdala. New York: Plenum Press, 1972:123–144.
126. La Motte CC, Snowman A, Pert CB, Snyder SH. Opiate receptor binding in rhesus monkey brain: Association with limbic structures. Brain Res 1978;155:374–379.
127. Land LJ. Localized projection of olfactory nerves to rabbit olfactory bulb. Brain Res 1973;63:153–166.
128. LeDoux JE. Brain mechanisms of emotion and emotional learning. Curr Opin Neurobiol 1992;2: 191–197.
129. Lee JH, Goedert M, Hill WD, Lee VM, Trojanowski JQ. Tau proteins are abnormally expressed in olfactory epithelium of Alzheimer patients and developmentally regulated in human fetal spinal cord. Exp Neurol 1993;121:93–105.
130. Le Gros Clark WE. The projection of the olfactory epithelium on the olfactory bulb in the rabbit. J Neurol Neurosurg Psychiatry 1951; 14:1–10.
131. Le Gros Clark WE. Inquiries into the anatomical basis of olfactory discrimination. Proc R Soc Lond (Biol) 1957;146:299–319.
132. Le Gros Clark WE, Meyer M. The terminal connexions of the olfactory tract in the rabbit's brain. Brain 1947;70:304–328.
133. Le Gros Clark WE, Warwick RT. The pattern of olfactory innervation. J Neurol Neurosurg Psychiatry 1946;9:101–111.
134. Levitt P. A monoclonal antibody to limbic system neurons. Science 1984;223:299–301.
135. Lewis PR, Shute CCD. The cholinergic limbic system: projections to hippocampal formation, medial cortex, nuclei of the ascending cholinergic reticular system, and the subfornical organ and supraoptic crest. Brain 1967;90:521–540.
136. Lewis PR, Shute CCD, Silver A. Confirmation of choline acetylase analyses of massive cholinergic innervation to the rat hippocampus. J Physiol (Lond) 1967;191:215–224.
137. Lilly R, Cummings JL, Benson F, Frankel M. The human Klüver-Bucy syndrome. Neurology 1983; 33:1141–1145.
138. Lindvall O, Björklund A. Organization of catecholamine neurons in the rat central nervous system. In: Iversen LL, Iversen SD, Snyder SH, eds. Handbook of psychopharmacology. Vol. 9. New York: Plenum Press, 1978:139–231.
139. Lohman AHM. The anterior olfactory lobe of the guinea pig. Acta Anat (Basel) 1963;53:(Suppl 49): 1–109.
140. Lorente De Nó R. Studies on the structure of the cerebral cortex. I. The area entorhinalis. J Psychol Neurol 1933;45:381–438.
141. Lorente de Nó, R. 1934. Studies on the structure of the cerebral cortex. II. Continuation of the study of the ammonic system. J Psychol Neurol 46:113–177.
142. MacLean PD. Some psychiatric implications of physiological studies on frontotemporal portions of limbic system (visceral brain). Electroencephalogr Clin Neurophysiol 1952;4:407–418.
143. MacLean PD. Chemical and electrical stimulation of the hippocampus in unrestrained animals. I. Methods and electroencephalographic findings. AMA Arch Neurol Psychiatry 1957;78:113–127.
144. MacLean PD. Chemical and electrical stimulation of the hippocampus in unrestrained animals. II. Behavioral findings. AMA Arch Neurol Psychiatry 1957;78:128–142.
145. MacLean PD. The triune brain in evolution. New York: Plenum Press, 1989.
146. MacLean PD, Delgado JMR. Electrical and chemical stimulation of fronto-temporal portion of limbic system in the waking animal. Electroencephalogr Clin Neurophysiol 1953;5:91–100.
147. McBride RL, Sutin J. Amygdaloid and pontine projections to the ventromedial nucleus of the hypothalamus. J Comp Neurol 1977;174: 377–396.
148. McDonald AJ, Augustine JR. Localization of GABA-like immunoreactivity in the monkey amygdala. Neuroscience 1993;52: 281–294.
149. McLennan H. The pharmacology of inhibition of mitral cells in the olfactory bulb. Brain Res 1971;29: 177–184.
150. Macchi G, Bentivoglio M, Rossini P, Tempesta E. The basolateral amygdaloid projections to the neocortex in the cat. Neurosci Lett 1978;9:347–352.
151. Margolis FL. Carnosine in the primary olfactory pathway. Science 1974;84:909–911.
152. Margolis FL. Molecular cloning of olfactory-specific gene products. In: Margolis FL, Getchell TV, eds. Molecular neurobiology of the olfactory system. New York: Plenum Press, 1988:237–265.
153. Marlowe WB, Mancall EL, Thomas JJ. Complete Klüver-Bucy syndrome in man. Cortex 1975;11:53–59.
154. Martin LJ, Spicer DM, Lewis MH, Gluck JP, Cork LC. Social deprivation of infant rhesus monkeys alters the chemoarchitecture of the brain: I. Subcortical regions. J Neurosci 1991;11:3344–3358.
155. Mehler WR. Subcortical afferent connections of the amygdala in the monkey. J Comp Neurol 1980;190: 733–762.
156. Meibach RC, Siegel A. The origin of fornix fibers which project to the mammillary bodies in the rat: a horseradish peroxidase study. Brain Res 1975;88:508–512.
157. Meibach RC, Siegel A. Efferent connections of the hippocampal formation in the rat. Brain Res 1977;124:197–224.
158. Meredith M. Sensory processing in the main and accessory olfactory systems: comparisons and contrasts. J Steroid Biochem Mol Biol 1991;39:601–614.
159. Mesulam M-M, Geschwind N. On the possible role of neocortex and its limbic connections in the process of attention and schizophrenia: clinical cases of inattention in man and experimental anatomy in monkey. J Psychiatr Res 1978;14:249–260.
160. Mettler FA. Neuroanatomy. 2d ed. St. Louis: C.V. Mosby, 1948.

161. Meyer A. Historical aspects of cerebral anatomy. London: Oxford University Press, 1971.
162. Miettinen R, Freund TF. Neuropeptide Y-containing interneurons in the hippocampus receive synaptic input from median raphe and GABAergic septal afferents. Neuropeptides 1992;22:185–193.
163. Miettinen R, Freund TF. Convergence and segregation of septal and median raphe inputs onto different subsets of hippocampal inhibitory interneurons. Brain Res 1992;594:263–272.
164. Monti Graziadei GA, Karlan MS, Bernstein JJ, Graziadei PPC. Reinnervation of the olfactory bulb after section of the olfactory nerve in monkey (*Saimiri sciureus*). Brain Res 1980;189:343–355.
165. Moran DT, Jafek BW, Rowley JC 3d. The vomeronasal (Jacobson's) organ in man: Ultrastructure and frequency of occurrence. J Steroid Biochem Mol Biol 1991;39:545–552.
166. Morgan JI. Monoclonal antibody mapping of the rat olfactory tract. In: Margolis FL, Gretchell TV, eds. Molecular neurobiology of the olfactory system. New York: Plenum Press, 1988:269–296.
167. Mori K. Molecular and cellular properties of mammalian primary olfactory axons. Microsc Res Tech 1993;24:131–141.
168. Morin F. An experimental study of hypothalamic connections in the guinea pig. J Comp Neurol 1950;92:193–213.
169. Moss M, Mahut H, Zola-Morgan S. Concurrent discrimination learning of monkeys after hippocampal, entorhinal, or fornix lesions. J Neurosci 1981;1:227–240.
170. Moulton DG, Beidler LM. Structure and function in the peripheral olfactory system. Physiol Rev 1967;47:1–52.
171. Mozell MM. Olfactory discrimination: electrophysiological spatiotemporal basis. Science 1964;143: 1336–1337.
172. Mullan S, Penfield W. Illusions of comparative interpretation and emotion. AMA Arch Neurol Psychiatry 1959;81:269–284.
173. Narabayashi H. Stereotaxic amygdalotomy. In: Eleftheriou BE, ed. The neurobiology of the amygdala. New York: Plenum Press, 1972: 459–483.
174. Narabayashi H, Nagao T, Saito Y, Yoshida M, Nagahata M. Stereotaxic amygdalotomy for behavior disorders. Arch Neurol 1963; 9:1–16.
175. Nauta WHJ. An experimental study of the fornix in the rat. J Comp Neurol 1956;104:247–272.
176. Nauta WJH. Hippocampal projections and related neural pathways to the midbrain in the cat. Brain 1958;81:319–340.
177. Nauta WJH. Fibre degeneration following lesions of the amygdaloid complex in the monkey. J Anat 1961;95:319–340.
178. Nauta WJH. Neural associations of the amygdaloid complex in the monkey. Brain 1962;85:505–520.
179. Nauta WJH. The central visceromotor system: a general survey. In: Hockman CH, ed. Limbic system mechanisms and autonomic function. Ch. 2. Springfield, IL: Charles C. Thomas, 1972:21–33.
180. Nauta WJH, Kuypers HGJM. Some ascending pathways in the brain stem reticular formation. In: Jasper HH, Proctor LP, Knighton RS, et al., eds. Reticular formation of the brain. Henry Ford Hospital International Symposium. Ch. 1. Boston: Little, Brown and Company, 1958:3–30.
181. Norita M, Kawamura K. Subcortical afferents to the monkey amygdala: an HRP study. Brain Res 1980;190:225–230.
182. Oelschläger HA, Northcutt RG. Immunocytochemical localization of luteinizing hormone-releasing hormone (LHRH) in the nervus terminalis and brain of the big brown bat, *Eptesicus fuscus*. J Comp Neurol 1992;315:344–363.
183. O'Keefe J, Conway DH. Hippocampal place units in the freely moving rat: why they fire where they fire. Exp Brain Res 1978; 31:573–590.
184. O'Keefe J, Nadel L. The hippocampus as a cognitive map. Oxford: Oxford University Press, 1978.
185. Olds J. Differentiation of reward systems in the brain by self-stimulation technics. In: Ramey SR, O'Doherty DS, eds. Electrical studies on the unanesthetized brain. Ch. 2. New York: Paul B. Hoeber, 1960: 17–51.
186. Olds J, Milner P. Positive reinforcement produced by electrical stimulation of septal area and other regions of the rat brain. J Comp Physiol Psychol 1954;47:419–427.
187. Olivier A. Temporal resections in the surgical treatment of epilepsy. Epilepsy Res (Suppl) 1992;5:175–88
188. Oomura Y, Ono T, Ooyama H. Inhibitory action of the amygdala on the lateral hypothalamic area in rats. Nature 1970;228:1108–1110.
189. Orbach J, Milner B, Rasmussen T. Learning and retention in monkeys after amygdala-hippocampus resection. Arch Neurol 1960;3: 230–251.
190. Ottersen OP, Ben-Ari Y. Pontine and mesencephalic afferents to the central nucleus of the amygdala of the rat. Neurosci Lett 1978; 8:329–34.
191. Palkovits M, Mezey E, Skirboll LR, Hökfelt T. Adrenergic projections from the lower brainstem to the hypothalamic paraventricular nucleus, the lateral hypothalamic area and the central nucleus of the amygdala in rats. J Chem Neuroanat 1992;5:407–415.
192. Pandya DN, Van Hoesen GW, Domesick VB. A cingulo-amygdaloid projection in the rhesus monkey. Brain Res 1973;61: 369–373.
193. Papez JW. A proposed mechanism of emotion. Arch Neurol Psychiatry 1937;38:725–743.
194. Parent A. Comparative histochemical study of the amygdaloid complex. J Hirnforsch 1971;13:89–96.
195. Parent A, Csonka C, Étienne P. The occurrence of large acetylcholinesterase-containing neurons in human neostriatum as disclosed in normal and Alzheimer-diseased brains. Brain Res 1984;291:154–158.
196. Parent A, Descarries L, Beaudet A. Organization of ascending serotonin systems in the adult rat brain. A radioautographic study after intraventricular administration of [^{3}H] 5-hydroxytryptamine. Neuroscience 1981;6:115–138.
197. Parent A, Mackey A, De Bellefeuille L. The subcortical afferents to caudate nucleus and putamen in primate: a fluorescence retrograde double-labeling study. Neuroscience 1983;10:1137–1150.
198. Pearson J, Halliday G, Sakamoto N, Michel JP. Catecholaminergic neurons. In: Paxinos G, ed. The human nervous system. Ch. 31. New York: Academic Press, 1990: 1023–1049.
199. Peele TL. The neuroanatomical basis for clinical neurology. New York: McGraw Hill, 1961.
200. Penfield W, Milner B. Memory deficit produced by bilateral lesions in the hippocampal zone. AMA Arch Neurol Psychiatry 1958;79:475–497.
201. Pfaff DW, Keiner M. Atlas of estradiol concentrating cells in the central nervous system of the female rat. J Comp Neurol 1973;151: 121–159.
202. Phelps PE, Houser CR, Vaughn JE. Small cholinergic neurons within fields of cholinergic axons characterize olfactory-related regions of rat telencephalon. Neuroscience 1992;48:121–136.
203. Pitkänen A, Amaral DG. Distribution of parvalbumin-immunoreactive cells and fibers in the monkey temporal lobe: The amygdaloid complex. J Comp Neurol 1993;331: 14–36.
204. Pitkänen A, Amaral DG. Distribution of calbindin-D28k immunoreactivity in the monkey temporal lobe: the amygdaloid complex. J Comp Neurol 1993;331:199–224.
205. Poirier LJ. Anatomical and experimental studies on the temporal pole of the macaque. J Comp Neurol 1952;96:209–248.
206. Porrino LJ, Crane AM, Goldman-Rakic PS. Direct and indirect pathways from the amygdala to the frontal lobe in rhesus monkeys. J Comp Neurol 1981;198:121–136.
207. Potter H, Nauta WJH. A note on the problem of olfactory associations of the orbitofrontal cortex in the monkey. Neuroscience 1979;4: 361–369.
208. Powell TPS, Cowan WM. Centrifugal fibers in the lateral olfactory tract. Nature 1963;199:1296–1297.

209. Powell TPS, Cowan WM, Raisman G. The central olfactory connexions. J Anat 1965;99:791–813.
210. Powell TPS, Guillery RW, Cowan WM. A quantitative study of the fornix-mammillo-thalamic system. J Anat 1957;91:419–432.
211. Powers JB, Fields RB, Winans SS. Olfactory and vomeronasal system participation in male hamsters attraction to female vaginal secretions. Physiol Behav 1979;22:77–84.
212. Pribram KH, Bagshaw M. Further analysis of the temporal lobe syndrome utilizing fronto-temporal ablations. J Comp Neurol 1953; 99:347–375.
213. Price JL. The central olfactory and accessory olfactory systems. In: Finger TE, Silver WL, eds. Neurobiology of taste and smell. New York: John Wiley, 1987:179–203.
214. Price JL, Powell TPS. The morphology of the granule cells of the olfactory bulb. J Cell Sci 1970;7: 91–124.
215. Price JL, Powell TPS. The mitral and short axon cells of the olfactory bulb. J Cell Sci, 1970;7: 631–652.
216. Price JL, Russchen FT, Amaral DG. The limbic region. II: The amygdaloid complex. In: Björklund A, Hökfelt T, Swanson LW, eds. Handbook of chemical neuroanatomy. Vol. 5, Part 1: Integrated Systems in the CNS. Amsterdam: Elsevier, 1987:279–381.
217. Raisman G. Neural connexions of hypothalamus. Br Med Bull 1966; 22:197–201.
218. Raisman G. An experimental study of the projection of the amygdala to the accessory olfactory bulb and its relationship to the concept of a dual olfactory system. Exp Brain Res 1972;14:395–408.
219. Raisman G, Cowan WM, Powell TPS. The extrinsic afferent, commissural and association fibres of the hippocampus. Brain 1965;88: 963–996.
220. Raisman G, Cowan WM, Powell TPS. An experimental analysis of the efferent projections of the hippocampus. Brain 1966;89:83–108.
221. Ramón y Cajal S. Histologie du Système Nerveux de l'Homme et des Vertébrés. (Azoulay L, trans.) Paris: Maloine, 1909, 1911. (Reprinted Consejo Superior de Investigaciones Cientificas, Instituto Ramón y Cajal, Madrid, 1972.)
222. Renaud LP, Hopkins DA. Amygdala afferents from the mediobasal hypothalamus: an electrophysiological and neuroanatomical study in the rat. Brain Res 1977;121: 201–213.
223. Ribak CE, Vaughn JE, Saito L, Barber R, Roberts E. Glutamate decarboxylase in neurons of the olfactory bulb. Brain Res 1977;126:1–18.
224. Ridley RM, Thornley HD, Baker HF, Fine A. Cholinergic neural transplants into hippocampus restore learning ability in monkeys with fornix transections. Exp Brain Res 1991;83:533–538.
225. Ries EA, Langworthy OR. A study of the surface structure of the brain of the whale (*Balaenopter physolus* and *Physter catadon*). J Comp Neurol 1937;68:1–47.
226. Robinson BW, Mishkin M. Alimentary responses evoked from forebrain structures in *Macaca mulatta*. Science 1962;136:260–261.
227. Robinson BW, Mishkin M. Alimentary responses to forebrain stimulation in monkeys. Exp Brain Res 1968;4:330–366.
228. Rolls ET. Neurophysiology and functions of the primate amygdala. In: Aggleton JP, ed. The amygdala: neurobiological aspects of emotion, memory, and mental dysfunction. New York: Wiley-Liss, 1992:143–165.
229. Rosene DL, Van Hoesen GW. Hippocampal efferents reach widespread areas of cerebral cortex and amygdala in the rhesus monkey. Science 1977;198:315–317.
230. Russchen FT, Amaral DG, Price JL. The afferent connections of the substantia innominata in the monkey, *Macaca fascicularis*. J Comp Neurol 1985;242:1–27.
231. Sadikot A, Parent A. The monoaminergic innervation of the amygdala in the squirrel monkey: an immunohistochemical study. Neuroscience 1990;36:431–447.
232. Sandler R, Smith AD. Coexistence of GABA and glutamate in mossy fiber terminals of the primate hippocampus: an ultrastructural study. J Comp Neurol 1991;303: 177–192.
233. Schilling A, Serviere J, Gendrot G, Perret M. Vomeronasal activation by urine in the primate *Microcebus murinus*: a 2-DG study. Exp Brain Res 1990;81:609–618.
234. Schwartzkroin PA, Scharfman HE, Sloviter RS. Similarities in circuitry between Ammon's horn and dentate gyrus: local interactions and parallel processing. Prog Brain Res 1990;83:269–286.
235. Scott JW, McBride RL, Schneider SP. The organization of projections from the olfactory bulb to the piriform cortex and olfactory tubercle in the rat. J Comp Neurol 1980; 194:519–534.
236. Scott SA, DeKosky ST, Scheff SW. Volumetric atrophy of the amygdala in Alzheimer's disease: quantitative serial reconstruction. Neurology 1991;41:351–356.
237. Scott SA, DeKosky ST, Sparks DL, Knox CA, Scheff SW. Amygdala cell loss and atrophy in Alzheimer's disease. Ann Neurol 1992;32:555–563.
238. Scott TR, Karadi Z, Oomura Y, et al. Gustatory neural coding in the amygdala of the alert macaque monkey. J Neurophysiol 1993;69: 1810–1820.
239. Scoville WB, Milner B. Loss of recent memory after bilateral hippocampal lesions. J Neurol Neurosurg Psychiatry 1957;20:11–21.
240. Segal M, Markram H, Richter-Levin G. Actions of norepinephrine in the rat hippocampus. Prog Brain Res 1991;88:323–330.
241. Seress L. Interspecies comparison of the hippocampal formation shows increased emphasis on the regio superior in the Ammon's horn of the human brain. J Hirnforsch 1988;29:335–340.
242. Shealy CN, Peele TL. Studies on amygdaloid nucleus of cat. J Neurophysiol 1957;20:125–139.
243. Shepherd GM. Principles of specificity and redundancy underlying the organization of the olfactory system. Microsc Res Tech 1993; 24:106–112.
244. Shepherd GM, Greer CA. Olfactory Bulb. In: Shepherd GM, ed. The synaptic organization of the brain. 3rd ed. Ch. 5. New York: Oxford University Press, 1990; 133–169.
245. Smith WK. The functional significance of the rostral cingular cortex as revealed by its responses to electrical excitation. J Neurophysiol 1945;8:241–255.
246. Smith Y, Parent A. Neuropeptide Y-immunoreactive neurons in striatum of cats and monkeys: morphological characteristics, intrinsic organization and co-localization with somatostatin. Brain Res 1986;372:241–252.
247. Smith Y, Parent A, Kerkerian L, Pelletier G. Distribution of neuropeptide Y-immunoreactivity in the basal forebrain and upper brainstem of the squirrel monkey (*Saimiri sciureus*). J Comp Neurol 1985;236:71–89.
248. Squire LR, Zola-Morgan S. The medial temporal lobe memory system. Science 1991;253:1380–1386.
249. Stensaas LJ, Lavker RM, Monti-Bloch L, Grosser BI, Berliner DL. Ultrastructure of the human vomeronasal organ. J Steroid Biochem Mol Biol 1991;39:553–560.
250. Stepien LS, Cordeau JP, Rasmussen T. The effect of temporal lobe and hippocampal lesions on auditory and visual recent memory in monkeys. Brain 1960; 83:470–489.
251. Sun N, Cassell MD. Intrinsic GABAergic neurons in the rat central extended amygdala. J Comp Neurol 1993;330:381–404.
252. Sutin J, McBride RL. Anatomical analysis of neuronal connectivity. In: Myers RD, ed. Methods in psychobiology. Vol. 3. New York: Academic Press, 1977:1–26.
253. Suzuki WA, Zola-Morgan S, Squire LR, Amaral DG. Lesions of the perirhinal and parahippocampal cortices in the monkey produce long-lasting memory impairment in the visual and tactual modalities. J Neurosci 1993;13:2430–2451.
254. Swann HG. The function of the brain in olfaction. II. The results of destruction of olfactory and other nervous structures upon the discrimination of odors. J Comp Neurol 1934;59:175–201.

255. Swanson LW, Cowan WM. Hippocampal-hypothalamic connections: Origin in subicular cortex, not Ammon's horn. Science 1975;189:303–304.
256. Swanson LW, Cowan WM. An autoradiographic study of the organization of the efferent connections of the hippocampal formation in the rat. J Comp Neurol 1977; 172:49–84.
257. Swanson LW, Sawchenko PE, Cowan WM. Evidence for collateral projections by neurons in Ammon's horn, the dentate gyrus and the subiculum: a multiple retrograde labeling study in the rat. J Neurosci 1981;1:548–559.
258. Sweet WH, Talland GA, Ervin FR. Loss of recent memory following section of the fornix. Trans Am Neurol Assoc 1959;84:76–82.
259. Symonds C. Disorders of memory. Brain 1966;89:625–644.
260. Szentagothai J, Flerko B, Mess B, Halasz B. Hypothalamic control of the anterior pituitary: an experimental-morphological study. Budapest: Akademiai Kiado, 1968.
261. Talamo BR, Feng WH, Perez-Cruet M, et al. Pathologic changes in olfactory neurons in Alzheimer's disease. Ann NY Acad Sci 1991; 640:1–7.
262. Terzian H. Observations on the clinical symptomatology of bilateral partial or total removal of the temporal lobe in man. In: Baldwin M, Bailey P, eds. Temporal lobe epilepsy. Springfield, IL: Charles C. Thomas, 1958:510–529.
263. Terzian H, Ore GD. Syndrome of Klüver and Bucy reproduced in man by bilateral removal of the temporal lobes. Neurology 1955;5:373–380.
264. Thomson AF, Walker AE. Behavioral alterations following lesions of the medial surface of the temporal lobe. AMA Arch Neurol Psychiatry 1951;65:251–252.
265. Törk I, Hornung JP. Raphe nuclei and the serotonergic system. In: Paxinos G, ed. The human nervous system. Ch. 30. New York: Academic Press, 1990;1001–1022.
266. Unger JW, Lange W. NADPH-diaphorase-positive cell populations in the human amygdala and temporal cortex: neuroanatomy, peptidergic characteristics and aspects of aging and Alzheimer's disease. Acta Neuropathol (Berl) 1992;83:636–646.
267. Unger JW, Lapham LW, McNeill TH, Eskin TA, Hamill RW. The amygdala in Alzheimer's disease: neuropathology and Alz 50 immunoreactivity. Neurobiol Aging 1991;12:389–399.
268. Ungerstedt U. Stereotaxic mapping of the monoamine pathways in the rat brain. Acta Physiol Scand (Suppl) 1971;367:1–48.
269. Valenstein ES, Nauta WJH. A comparison of the distribution of the fornix system in the rat, guinea pig, and monkey. J Comp Neurol 1959;113:337–369.
270. Valverde F. Studies on the piriform lobe. Cambridge: Harvard University Press, 1965.
271. Van Alphen HAW. The anterior commissure of the rabbit. Acta Anat (Basel) 1969;74(Suppl 57): 9–111.
272. Van Hoesen GW. The parahippocampal gyrus. New observations regarding its cortical connections in the monkey. Trends Neurosci 1982;5:345–350.
273. Van Hoesen G, Mesulam M-M, Haaxma R. Temporal cortical projections to the olfactory tubercle in the rhesus monkey. Brain Res 1976;109:375–381.
274. Vankova M, Arluison M, Leviel V, Tramu G. Afferent connections of the rat substantia nigra pars lateralis with special reference to peptide-containing neurons of the amygdalo-nigral pathway. J Chem Neuroanat 1992;5:39–50.
275. Veening JG. Subcortical afferents of the amygdaloid complex in the rat: an HRP study. Neurosci Lett 1978;8:197–202.
276. Velasco ME, Taleisnik S. Release of gonadotropins induced by amygdaloid stimulation in the rat. Endocrinology 1969;84:132–139.
277. Victor M. Functions of memory and learning in man and their relationship to lesions in the temporal lobe and diencephalon. In: Brazier MAB, ed. Brain function. Vol. III: RNA in brain function: memory and learning. Washington, DC: American Institute of Biological Sciences, 1964.
278. Victor M, Angevine JB Jr, Mancall EL, Fisher CM. Memory loss with lesions of hippocampal formation. Arch Neurol 1961;5:244–263.
279. Von Bechterew WV. Demonstration eines Gehirns mit Zerstörung der vorderen und inneren Theile der Hirnrinde beider Schläfenlappen. Neurol Zentrabl 1900;19: 990–991.
280. Von Cramon DY, Hebel N, Schuri U. A contribution to the anatomical basis of thalamic amnesia. Brain 1985;108:993–1008.
281. Wada Y, Fujinami RS. Viral infection and dissemination through the olfactory pathway and the limbic system by Theiler's virus. Am J Pathol 1993;143:221–229.
282. Whitlock DG, Nauta WJH. Subcortical projections from the temporal neocortex in the *Macaca mulatta*. J Comp Neurol 1956;106:183–212.
283. Whitehouse PJ, Price DL, Clark AW, Coyle JT, DeLong MR. Alzheimer disease: Evidence for selective loss of cholinergic neurons in the nucleus basalis. Ann Neurol 1981;10:122–126.
284. Williams PL, Warwick R. Functional neuroanatomy of man. Philadelphia: W.B. Saunders, 1975.
285. Wilson RC, Levy WB, Steward O. Functional effects of lesion-induced plasticity: long-term potentiation in normal and lesion-induced temporodentate connections. Brain Res 1979;176: 65–78.
286. Witter MP, Griffioen AW, Jorritsma-Byham B, Krijnen JOM. Entorhinal projections to the hippocampal CA1 region in the rat: an underestimated pathway. Neurosci Lett 1988;85:193–198.
287. Witter MP, Van Hoesen GW, Amaral DG. Topographical organization of the entorhinal projection to the dentate gyrus of the monkey. J Neurosci 1989;9:216–228.
288. Wysocki CJ. Neurobehavioral evidence for the involvement of the vomeronasal system in mammalian reproduction. Neurosci Behav Rev 1979;3:301–341.
289. Wysocki CJ, Meredith M. The vomeronasal system. In: Finger TE, Silver WL, eds. Neurobiology of taste and smell. New York: Wiley-Interscience, 1987:125–150.
290. Yeckel MF, Berger TW. Feedforward excitation of the hippocampus by afferents from the entorhinal cortex: redefinition of the role of the trisynaptic pathway. Proc Natl Acad Sci USA 1990;87: 5832–5836.
291. Zaborsky L, Feminger A, Palkovits M. Afferent brain stem connections of the central amygdaloid nucleus. Verh Anat Ges 1979;73: 1117–1120.
292. Zatorre RJ, Jones-Gotman M, Evans AC, Meyer E. Functional localization and lateralization of human olfactory cortex. Nature 1992;360:339–340.
293. Zbrozyna AW. The organization of the defense reaction elicited from amygdala and its connections. In: Eleftheriou BE, ed. The neurobiology of the amygdala. New York: Plenum Press, 1972:597–606.
294. Zola-Morgan S, Squire LR. The neuropsychology of memory. Parallel findings in humans and nonhuman primates. Ann NY Acad Sci 1990;608:434–450.
295. Zolovick AJ. Effects of lesions and electrical stimulation of the amygdala on hypothalamic-hypophyseal regulation. In Eleftheriou BE, ed. The neurobiology of the amygdala. New York: Plenum Press, 1972:643–683.

19
Basal Ganglia

NOMENCLATURE

The basal ganglia are large subcortical structures classically considered to be derived largely, but not exclusively, from the telencephalon. These huge nuclear masses are in close relationship to the diencephalon, but separated from it by the internal capsule (Figs. 19.1 and 19.2). The anatomic nomenclature applied to the basal ganglia is confused and reflects much uncertainty and inconsistency. The situation is due in part to the fact that, much like the limbic system, terms such as "basal ganglia" or "extrapyramidal system" have no precise limits. The use and abuse of the epithet "striatum" has also contributed to the inconsistency, particularly in the comparative neurology literature, which is cluttered with terms such as "archistriatum," "paleostriatum," "hyperstriatum," and "epistriatum," whose intended meanings vary markedly (273). In the following account, the terms archi-, paleo-, and neostriatum will be avoided when referring to the human basal ganglia because these names, so commonly used in neuroanatomic textbooks, are based on a misinterpretation of the phylogenetic evolution of the basal ganglia.

The term *basal ganglia*, as generally used by anatomists, refers to some or all of the major telencephalic subcortical nuclear masses lying at the base of the forebrain [see the excellent historical review by Lewy (223)]. These nuclei include (a) the caudate nucleus and the putamen (together referred to as the neostriatum or simply the striatum), (b) the globus pallidus or the pallidum (the paleostriatum of older literature), (c) the amygdaloid complex (or archistriatum of older literature), and (d) the claustrum. The putamen and the globus pallidus together form a topographic unit that is often designated the lentiform or lenticular (lens-shaped) nucleus. The lentiform nucleus, as well as the globus pallidus, claustrum, and amygdala, were first clearly identified by the German anatomist Karl Friedrich Burdach (37), whose contribution to this area of neuroanatomy was particularly important (247).

In primates, the globus pallidus is divided into an internal and an external segment by the fibers of the internal medullary lamina (Fig. 19.3). In nonprimate species, the term globus pallidus refers to the equivalent of the external pallidal segment only, while the entopeduncular nucleus is generally regarded as the homologue of the internal pallidal segment (see Table 19.1). The term "corpus striatum," first defined by Willis in 1664 (371), has survived to the present day, although its original meaning changed considerably through the years. It is now occasionally used to designate the caudate nucleus, putamen, and globus pallidus together (43, 124) or the caudate nucleus and the putamen without the globus pallidus (239).

In the following account we have adapted the nomenclature commonly used by clinicians, in which the term basal ganglia is restricted to a few key structures whose involvement in psychomotor behavior is well-established or strongly suspected. This restricted definition of the basal ganglia includes the caudate nucleus and putamen, which together are referred to as the striatum, the globus pallidus or pallidum, and the closely related subthalamic nucleus and substantia nigra. Other nuclei in the thalamus and mesopontine tegmentum can also be considered as important links in the basal ganglia circuitry. The striatum and pallidum form the core structures of the basal ganglia. The other nuclei are reciprocally connected with these core structures through closed ancillary loops that are typical of the basal ganglia circuitry. These structures are thought to exert a profound modulatory influence on the core structure of the basal ganglia; thus, they are referred to here as control structures (see Table 19.1).

Lennart Heimer and his colleagues introduced the terms ventral striatum and ventral

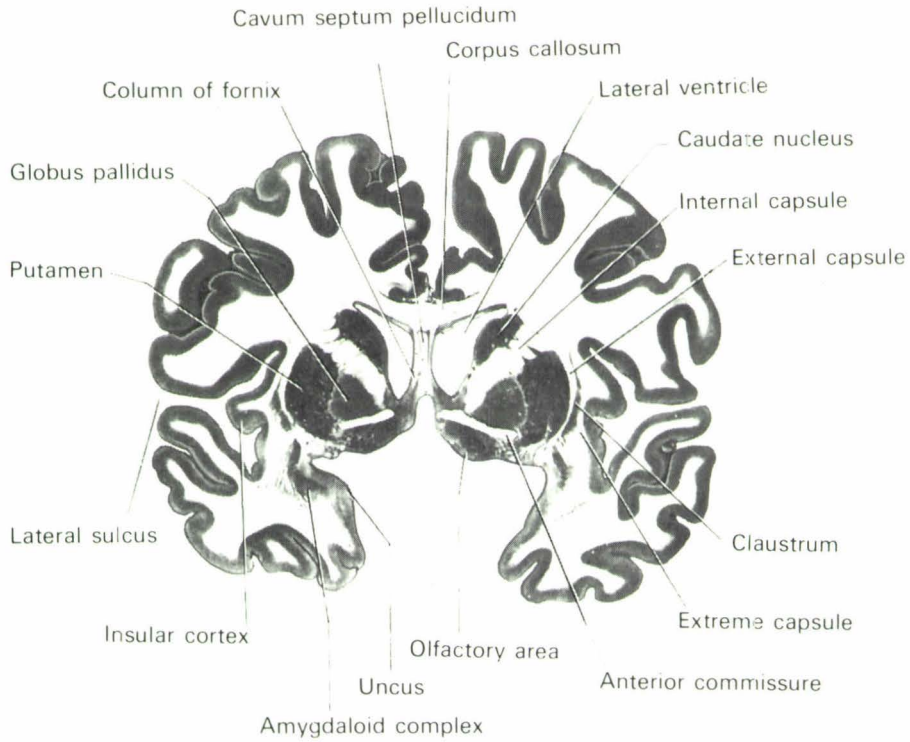


Figure 19.1. Frontal section of the human brain passing through the columns of the fornix and the anterior commissure. At this level the putamen and the external (lateral) pallidal segment lie beneath the insular cortex.

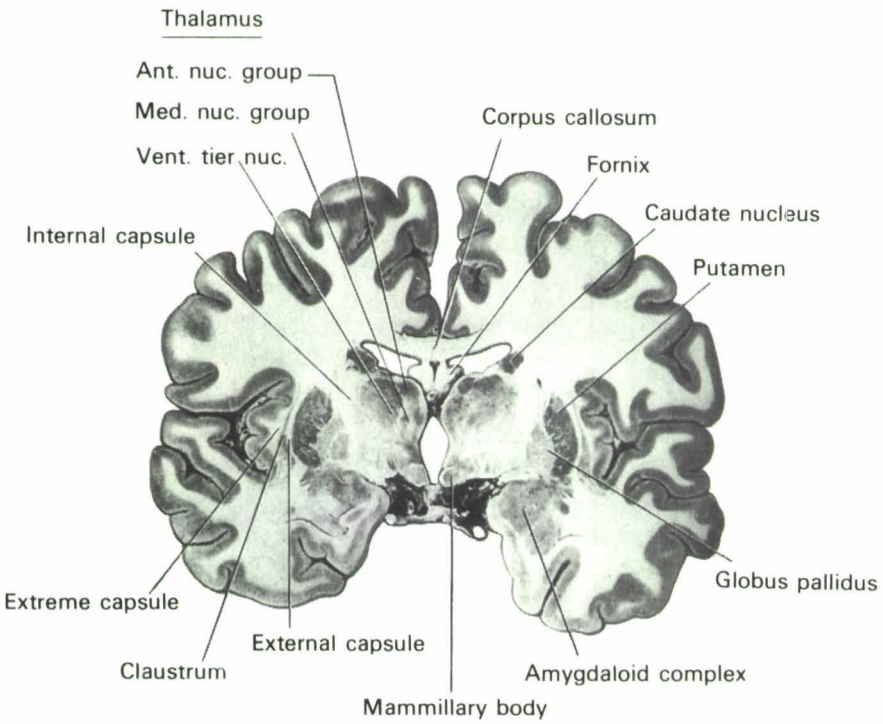


Figure 19.2. Frontal section of the human brain at the level of the mammillary bodies. In this section, the main nuclear groups of the thalamus are identified, and portions of all components of the basal ganglia are present. The amygdaloid nuclear complex lies in the temporal lobe internal to the uncus and ventral to the lentiform nucleus.

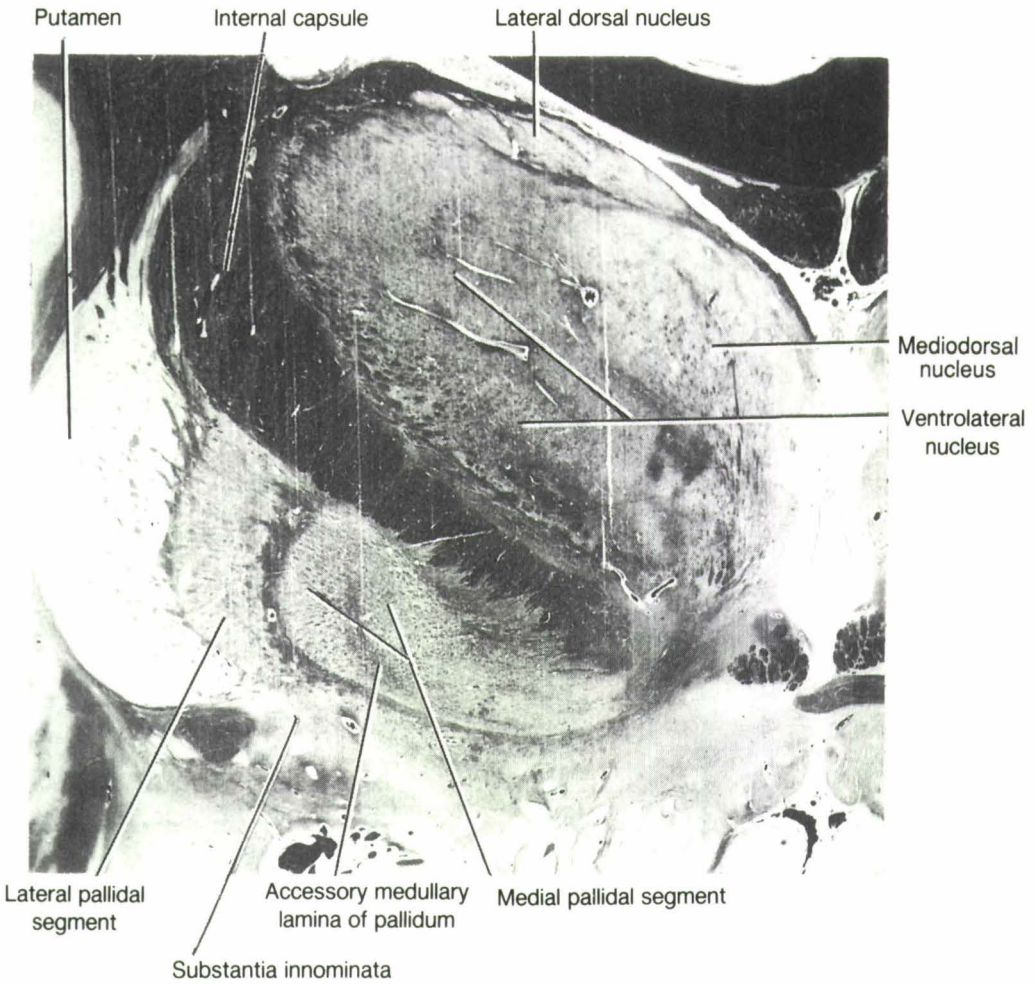


Figure 19.3. Frontal section of the human brain through the basal ganglia, internal capsule, and thalamus. Segments of the globus pallidus are separated by the internal medullary lamina and the accessory medullary lamina divides the internal or medial pallidal segment into inner and outer parts. The substantia innominata lies ventral to the globus pallidus and extends rostrally. Wiegert's myelin stain.

Table 19.1. The Basal Ganglia: A Synopsis of the Nomenclature used in the Present Account

CORE STRUCTURES		CONTROL STRUCTURES
A. STRIATUM		A. SUBSTANTIA NIGRA (Reciprocal connection with striatum)
Caudate nucleus Putamen	Forming a single entity in rodents	Pars compacta Pars recticulata Pars lateralis
Ventral striatum	(comprising nucleus accumbens or fundus striati)	
B. PALLIDUM or GLOBUS PALLIDUS		B. VENTRAL TEGMENTAL AREA (Reciprocal connection with ventral striatum)
External segment	(or globus pallidus in non-primates)	C. SUBTHALAMIC NUCLEUS (Reciprocal connection with pallidum)
Internal segment	(or entopeduncular nucleus in non-primates)	D. THALAMUS and BRAINSTEM Centromedian / parafascicular complex Midbrain dorsal raphe nucleus Pedunculopontine tegmental nucleus
Ventral pallidum	(comprising part of the substantia innominata)	

pallidum to designate the ill-defined ventralmost portions of the striatum and pallidum which encroach upon the basal forebrain limbic structures (11, 132, 158, 159). The ventral striatum of Heimer and coworkers comprises the nucleus accumbens septi (the fundus striati of Hassler (143)) and the deepest part of the olfactory tubercle (anterior perforated substance in humans), while the ventral pallidum refers to part of the substantia innominata, which these authors consider a ventral extension of the pallidum. These terms are retained here because of their usefulness in describing these poorly known regions of the basal ganglia.

The claustrum and the amygdala are part of the basal ganglia by the extended topologic definition. As far as we know, however, the claustrum has no major connections with the core structures of the basal ganglia as defined earlier, and it has never been directly involved in any of the characteristic diseases of the basal ganglia. Essential knowledge about this structure will, nevertheless, be reviewed briefly. The amygdala, on the other hand, is generally regarded as part of the limbic system and was examined in detail in Chapter 18. This structure occupies a crucial position at the interface between the basal ganglia and the limbic system and may play an important role in the integration of these two sets of neural structures. This possibility is explored to a certain extent in the present chapter.

The striatum is the major receptive component of the basal ganglia. In rodents, the striatum forms a single mass striated by the dispersed corticofugal and corticipetal fibers. In primates, it is separated into two distinct entities—the caudate nucleus and the putamen—by the corticofugal and corticipetal fibers that form the internal capsule (Fig. 19.4). The striatum receives massive inputs from (a) broad regions of the cerebral cortex, (b) the centromedian-parafascicular (CM-Pf) nuclear complex, (c) the substantia nigra, (d) several smaller mesencephalic nuclei, and (e) portions of the lateral amygdala. Most of the striatal afferent systems are associated with specific neurotransmitters. The neural activities of the striatum involve a large number of distinctive cell types and a multitude of different neurotransmitters, which include acetylcholine, monoamines, peptides, and amino acids. The striatum is reciprocally linked with individual cytologic subdivisions of the substantia nigra. Impaired synthesis and transmission of neurotransmitters involved in striatal functions constitute one important feature of metabolic disturbances associated with two relatively common forms of dyskinesia (disturbances of movement), namely, Parkinson's disease and Huntington's chorea.

The globus pallidus forming the smaller, most medial part of the lentiform nucleus consists of two cytologically similar segments that have input systems with both common and distinctive neurotransmitters. Each pallidal segment gives rise to different projections. The projections of the internal pallidal segment are principally to ipsilateral thalamic nuclei, which in turn have access to motor regions of the cerebral cortex. The external pallidal segment projects massively to the subthalamic nucleus. Reciprocal connections interrelate portions of the external pallidal segment and the subthalamic nucleus. The output systems of the corpus striatum arise from the internal pallidal segment and from the pars reticulata of the substantia nigra.

STRIATUM

Topographic Organization

The striatum consists of two distinctive parts, the caudate nucleus and putamen, which are partially separated by fibers of the anterior limb of the internal capsule. These two striatal components represent a single anatomic and functional entity, which for embryologic reasons has a particular configuration. Both portions of the striatum arise from a thickening of the lateral telencephalic vesicle known as the striatal ridge (Fig. 3.15).

CAUDATE NUCLEUS

The caudate nucleus is an elongated, arched gray mass related throughout its extent to the surface of the lateral ventricle. Its enlarged anterior portion, or *head*, lies rostral to the thalamus and bulges into the anterior horn of the lateral ventricle (Figs. 2.13, 2.14, 19.5, and 19.6). The head of the caudate nucleus and the putamen are separated by fibers of the anterior limb of the internal capsule, except rostroventrally where continuity is maintained. The *body* of the caudate nucleus extends along the dorsolateral border of the thalamus, from which it is separated by the stria terminalis and the terminal vein (Figs. 19.2 and 19.5). This part of the caudate nu-

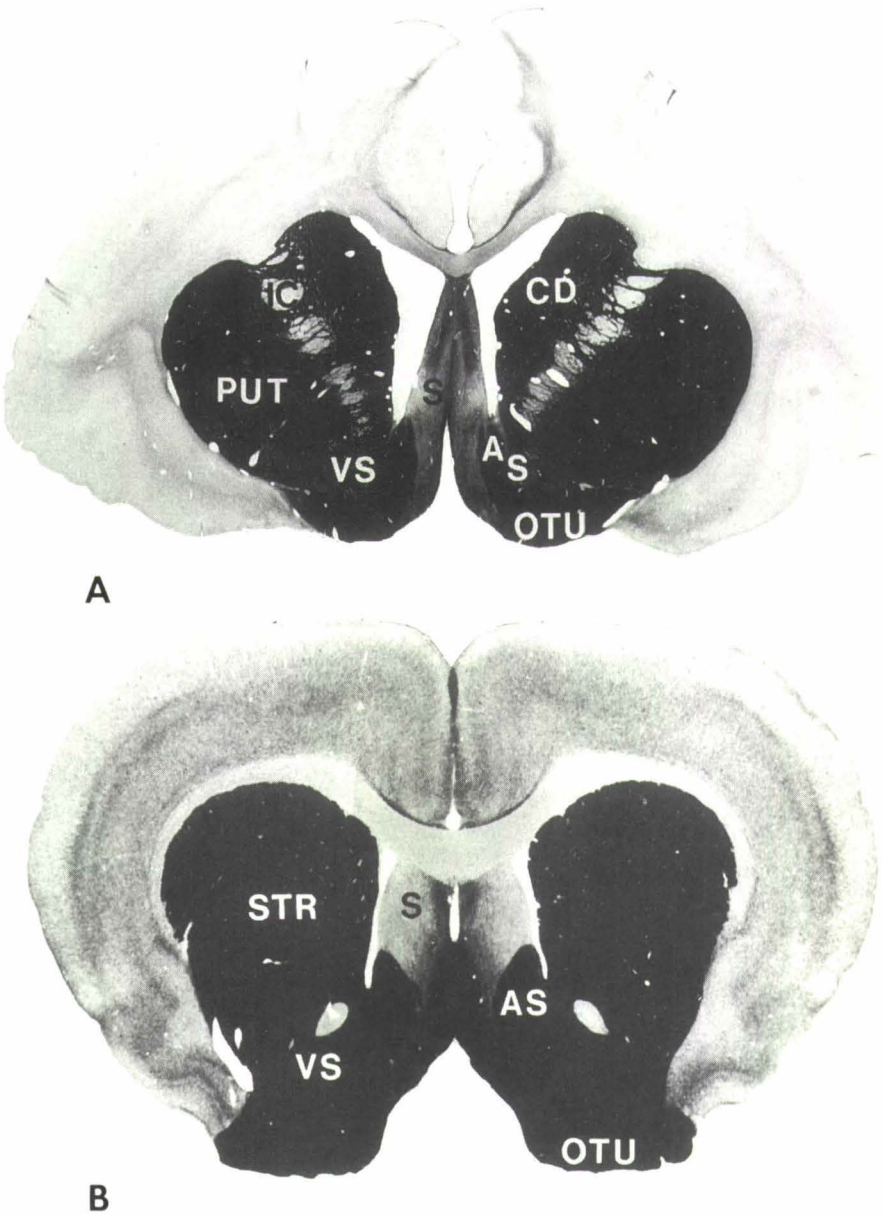


Figure 19.4. Frontal sections of the brain of the squirrel monkey (*Saimiri sciureus*) (**A**) and the rat (**B**) showing the relative proportion of the striatum (*dark areas*) in material prepared for the demonstration of acetylcholinesterase (AChE). Note that in monkeys the striatum is divided into two parts, the caudate nucleus (*CD*) and the putamen (*PUT*), by the fibers of the internal capsule (*IC*), while in rodents it forms a single mass. In both primates and rodents, the striatum has a ventral extension, the ventral striatum (*VS*), which comprises the nucleus accumbens (*AS*), ventral to the septum (*S*), and the deep portions of the olfactory tubercle (*OTU*).

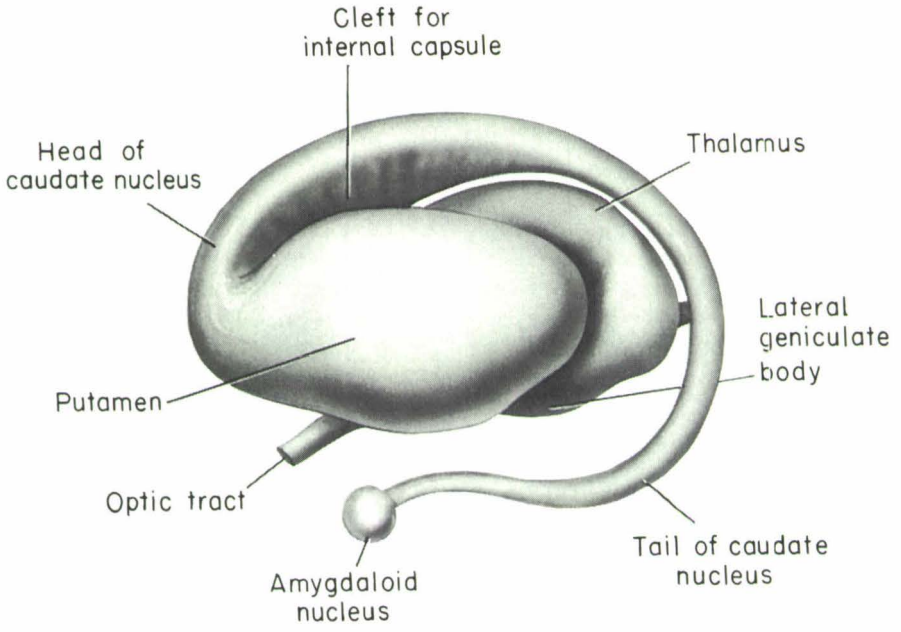


Figure 19.5. Isolated striatum, thalamus, and amygdaloid complex showing (a) the continuity of the putamen and head of the caudate nucleus rostrally, and (b) the relationships between the tail of the caudate nucleus and the amygdaloid nuclear complex. The cleft occupied by fibers of the internal capsule is indicated. The anterior limb of the internal capsule is situated between the caudate nucleus and the putamen, while the posterior limb of the internal capsule lies between the lentiform nucleus and the thalamus.

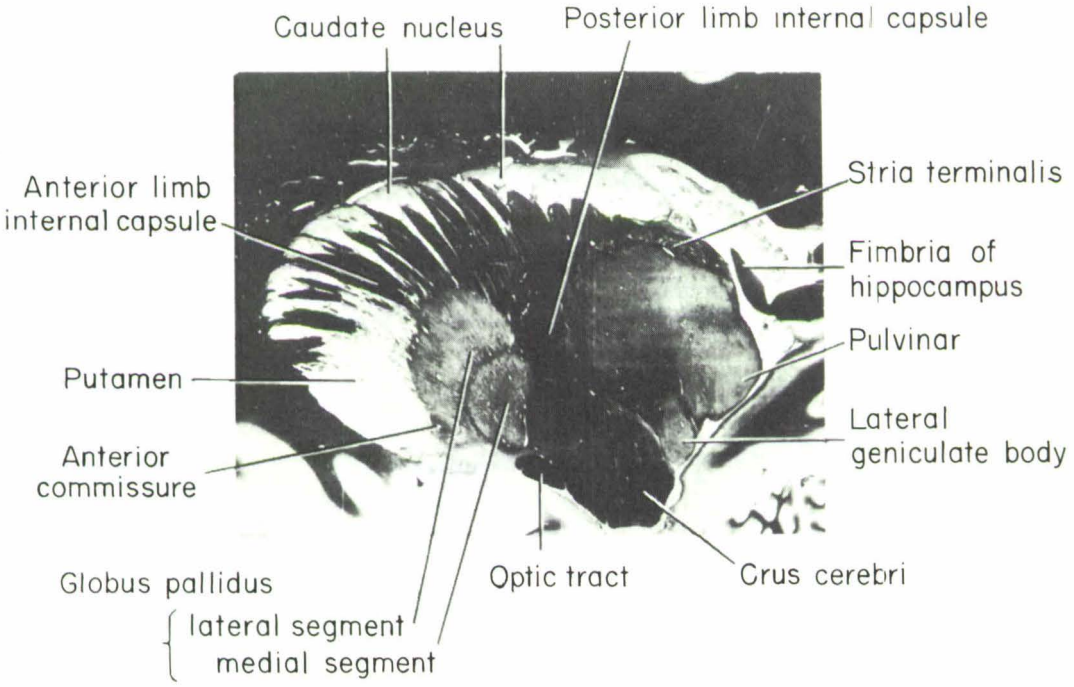


Figure 19.6. Sagittal section through the basal ganglia, internal capsule, and thalamus in a human brain. Note the relationship of the caudate nucleus to the fibers of the anterior limb of the internal capsule. Weigert's myelin stain.

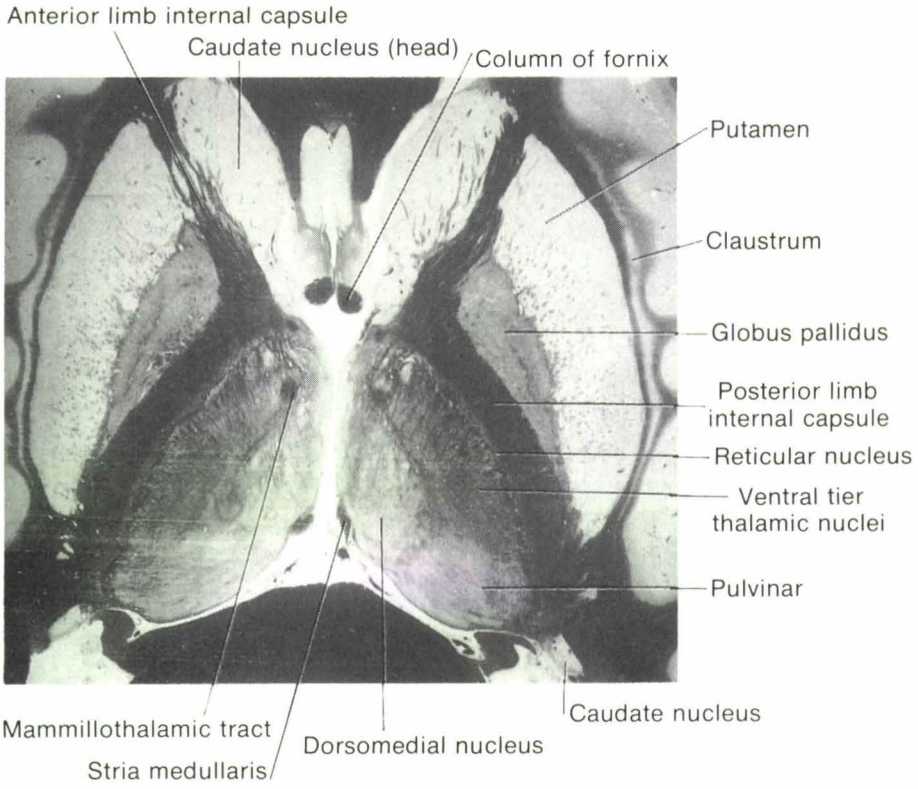


Figure 19.7. Horizontal section of the thalamus internal capsule and basal ganglia in a human brain. Weigert's myelin stain.

cleus is regarded as suprathalamic. The *tail* of the caudate nucleus is the attenuated caudal portion that sweeps into the temporal lobe in the roof of the inferior horn of the lateral ventricle and comes into relationship with the central nucleus of the amygdaloid complex (Figs. 2.13, 16.38, 18.19, and 19.5).

PUTAMEN

The putamen, the largest and most lateral portion of the corpus striatum, lies between the external capsule and the lateral medullary lamina of the globus pallidus (Figs. 2.13, 16.38, 19.1, 19.2, and 19.5–19.7). Most of the putamen is situated medial to the insular cortex and is separated from it by the extreme capsule, the claustrum, and the external capsule. In transverse sections, the lightly stained putamen is traversed by myelinated fibers coursing ventromedially, which are bundles of striatopallidal fibers (Figs. 16.8 and 19.2). The caudate nucleus and putamen are continuous rostroventrally, beneath the anterior limb of the internal capsule, and in dorsal regions where slender gray cellular bridges pass across the posterior limb of the internal capsule (Figs. 16.8, 19.3, and 19.4) At levels of the septum pellucidum, the nucleus accumbens (or fundus striati of Hassler (143)) lies adjacent to medial and ventral portions of the striatum. The nucleus accumbens is ontogenetically more closely related to the caudate nucleus and putamen than to the septal nuclei, and has projections to both the globus pallidus and the substantia nigra (341).

Intrinsic Organization

Cytologically, the caudate nucleus and the putamen appear identical and are composed of enormous numbers of cells that exhibit no lamination. However, the striatum is not as uniform as it appears because in its development cells of different types migrate in clusters, histochemical activity has a patchy distribution, and efferent neurons show some segregation (384, 385).

Although small cells were considered to outnumber large cells by ratios of 20:1 or 60:1 (99, 364), a morphometric and statistical

analysis of the human striatum indicated that (a) the mean numerical density of small striatal neurons is approximately 11,000 cells per mm^3, while the mean numerical density of the large striatal neurons is about 65 cells/mm^3, and (b) the ratio of small to large striatal neurons averages about 170:1, with a range from 130:1 to 258:1 (323). On average, the putamen is about 13% larger than the caudate nucleus in humans. Golgi and electron microscopic observations indicate that striatal neurons fall into two categories: (a) those with spiny dendrites, and (b) those with smooth dendrites (1, 82, 101, 103, 190, 194, 195, 288).

SPINY NEURONS

The spiny neurons are by far the most numerous striatal cells. They are round or oval medium-sized cells, emit multiple primary dendrites covered with spines, and have long axons (Fig. 19.8). Two types of spiny striatal

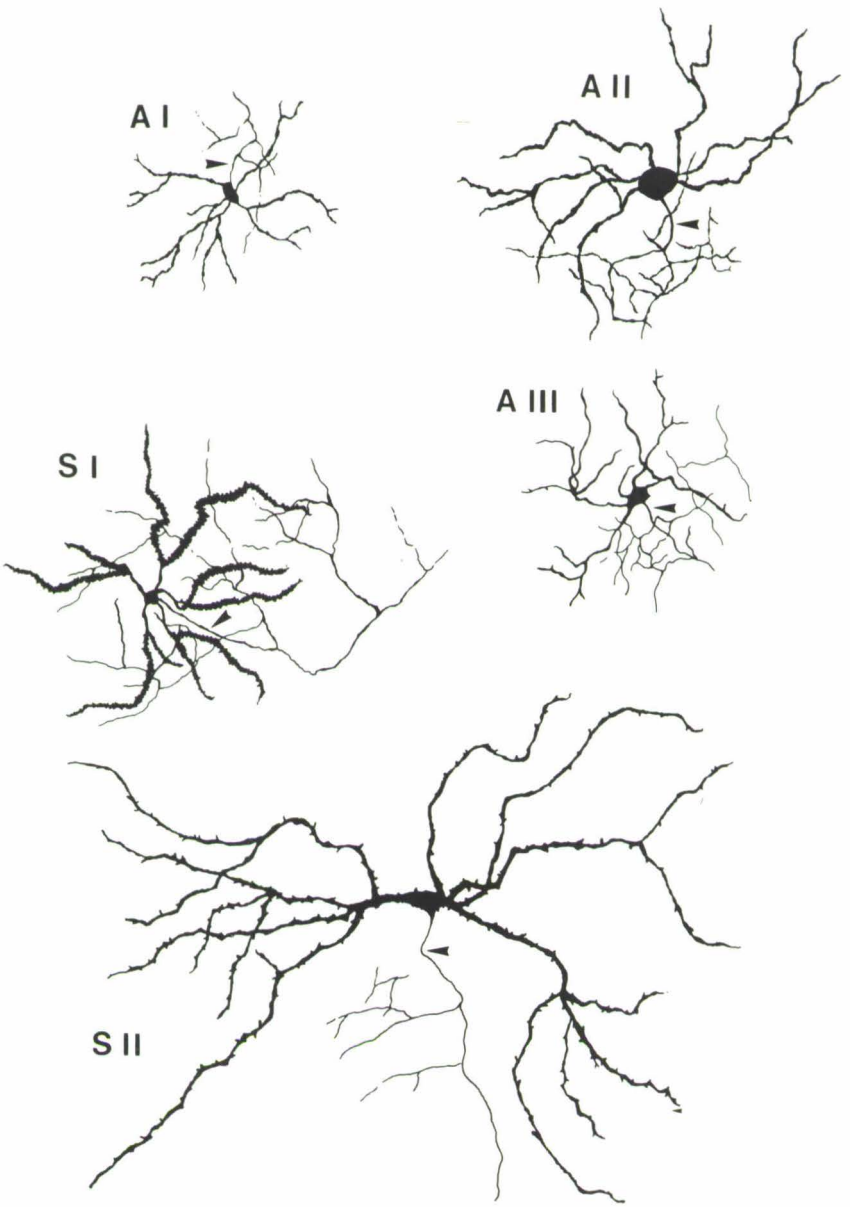


Figure 19.8. Major types of striatal neurons such as seen in Golgi preparations of the brain of rhesus monkeys. Three types of aspiny neurons (*AI, AII,* and *AIII*) and two types of spiny cells are illustrated. There exist several other classifications of striatal neurons (see text). *Arrowheads* indicate the initial segment of the axons.

neurons are recognized (82). Type I spiny neurons, present in very large numbers, have smooth somata and proximal dendrites that distally become laden with spines. The dendrites radiate into spherical space of about 200 μm (Figs. 19.9 and 19.10). Long axons of these cells give rise to both proximal and distal collaterals. Spiny type II striatal neurons commonly are larger neurons with spiny dendrites that extend 600 μm from the somata. Axons of spiny II neurons are long and give off collaterals near the somata. Spiny striatal neurons serve as both receptive and projection neurons. Most afferents from various sources terminate on spiny processes of these neurons (189, 192, 193, 196), and all fibers projecting beyond the striatum arise from spiny striatal neurons (126, 205, 206, 288).

Virtually all medium spiny neurons use γ-aminobutyric acid (GABA) as their main neurotransmitter (307) (Fig. 19.11), but also coexpress a number of neuroactive peptides (16, 122, 292) such as substance P (SP), enkephalin (ENK), dynorphin (DYN), and neurotensin (NT) (Fig. 19.12). Not all of these peptides are found in every spiny striatal neuron. Instead, specific combinations of neuropeptides and GABA characterize particular subsets of striatal projection neurons. In individual medium spiny neurons, GABA coexists with either ENK or SP and/or DYN (122, 127). The coexistence of GABA with a given peptide in a spiny striatal neuron is in correlation with its target site. Compared to the well-documented inhibitory action of GABA, the physiologic role of the different peptides remains to be established. Also worth noting is the presence of the calcium-binding protein calbindin D-28k in virtually all medium spiny projection neurons of the striatum (Fig. 19.13). In contrast, striatal interneurons are devoid of calbindin, but many of them contain parvalbumin, another calcium-binding protein.

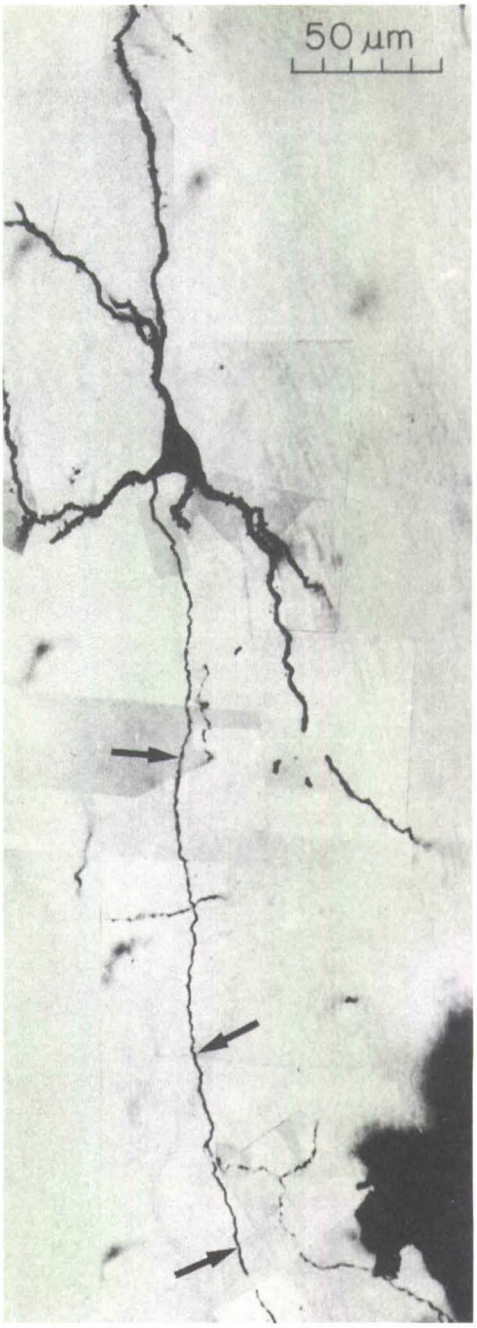


Figure 19.9. Spiny type II striatal neuron in a Golgi preparation of the rhesus monkey. These pyramidal cells give rise to four to six primary dendrites with relatively low spine densities, and have an axon which emerges from the soma or a proximal dendrite. Axons of these neurons take a straight course and have been followed for 300 μm without narrowing or forming terminal arborizations. The axon (*arrows*) is directed toward the globus pallidus and appears to give rise to collaterals. (Full scale, 50 μm.)

ASPINY NEURONS

These neurons are intrinsic striatal elements with short axons (82, 103) (Fig. 19.7). Golgi studies revealed a great diversity of interneurons in the striatum, but most of these interneurons share a common characteristic, that is the absence or rarity of spines on their dendrites. This is in striking contrast with the highly spinous dendrites of the projection neurons. The striatal interneurons can be

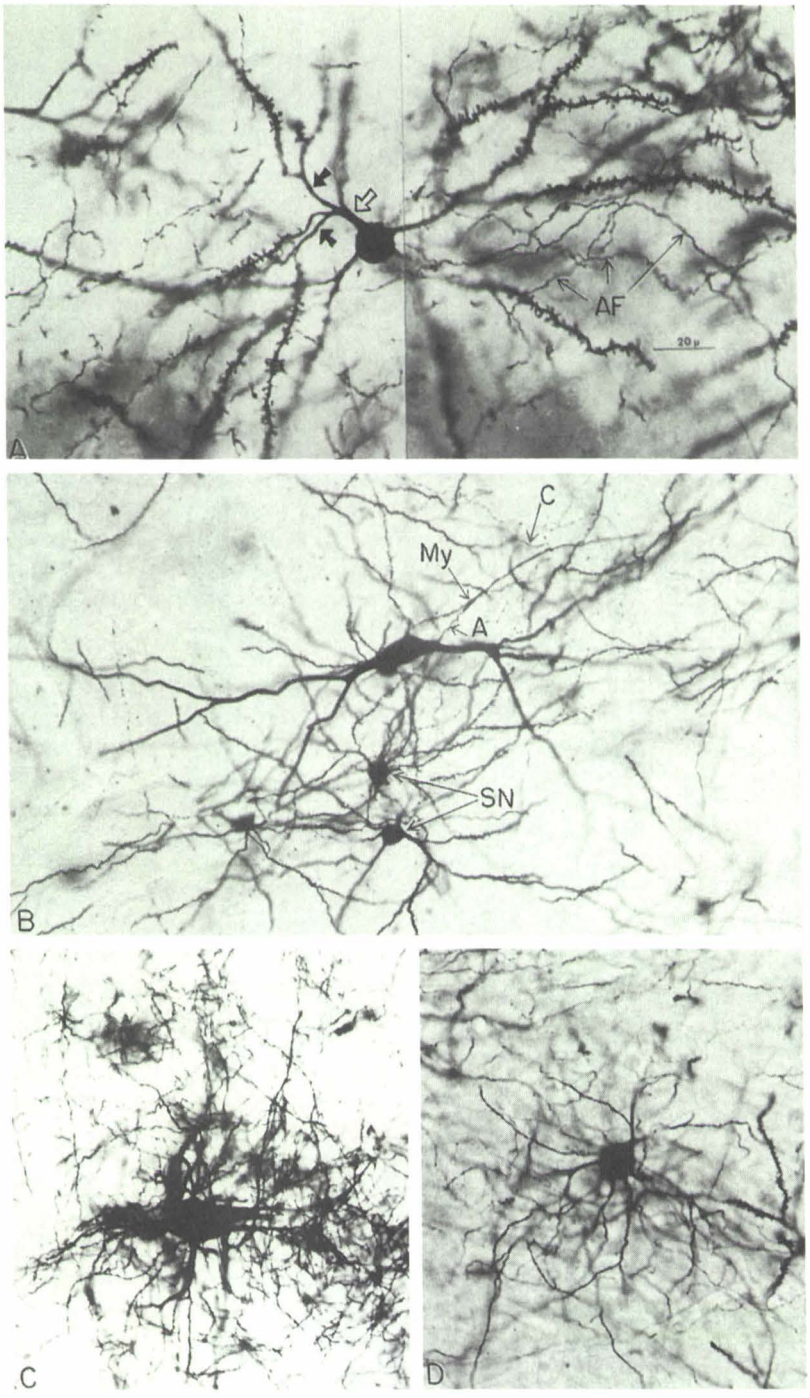


Figure 19.10. **A.** Spiny striatal neuron in a Golgi preparation of the rhesus monkey. "Boutons en passage" of afferent fibers (*AF*) cross over its dendrites. The *open arrow* and the *closed arrows* indicate the spine-free dendritic trunk and the initial, spine-free dendritic branches, respectively. (Golgi, ×700.) **B.** A large aspiny striatal neuron. *A*, axon; *My*, initial segment of myelin sheath; *C*, axon collateral; *SN*, spiny striatal neurons. (Golgi, ×300.) **C.** A large aspiny neuron in the putamen. (Golgi, ×300.) **D.** A spidery aspiny neuron in the putamen. (Golgi, ×300.)

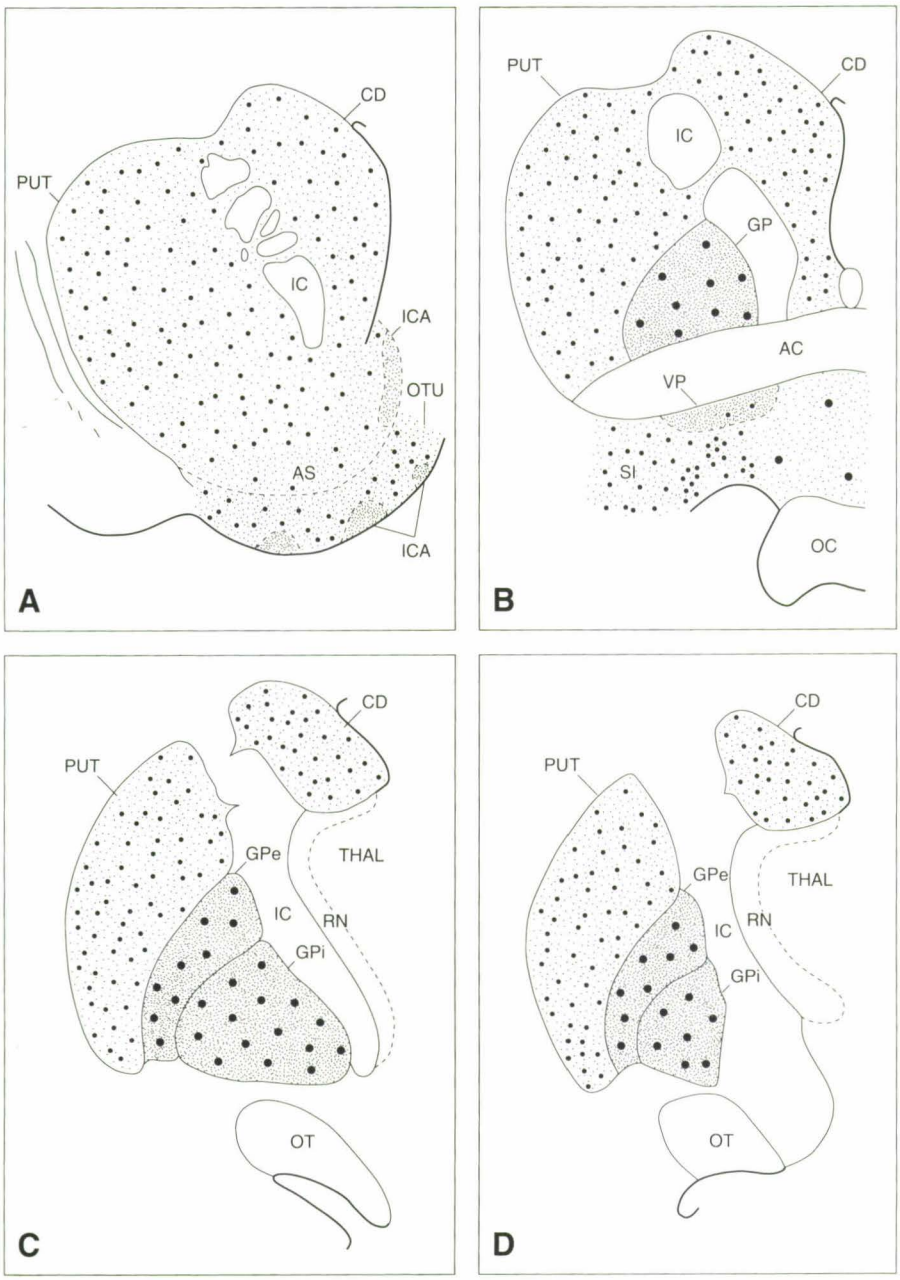


Figure 19.11. Frontal half sections through the forebrain of the squirrel monkey illustrating the distribution of γ-aminobutyric acid (GABA)-immunoreactive neurons (*filled circles*) in the core structures of the basal ganglia. In the striatum and pallidum, the GABA-containing neurons are scattered among innumerable GABA-immunoreactive axon terminals (*dots*). The sections are displayed in a rostrocaudal order. *AC*, anterior commissure; *AS*, nucleus accumbens; *CD*, caudate nucleus; *GP*, globus pallidus; *GPe*, external segment of GP; *GPi*, internal segment of GP; *IC*, internal capsule; *ICA*, islands of Calleja; *OC*, optic chiasm; *OT*, optic tract; *OTU*, olfactory tubercle; *PUT*, putamen; *RN*, reticular thalamic nucleus; *SI*, substantia innominata; *THAL*, thalamus; *VP*, ventral pallidum.

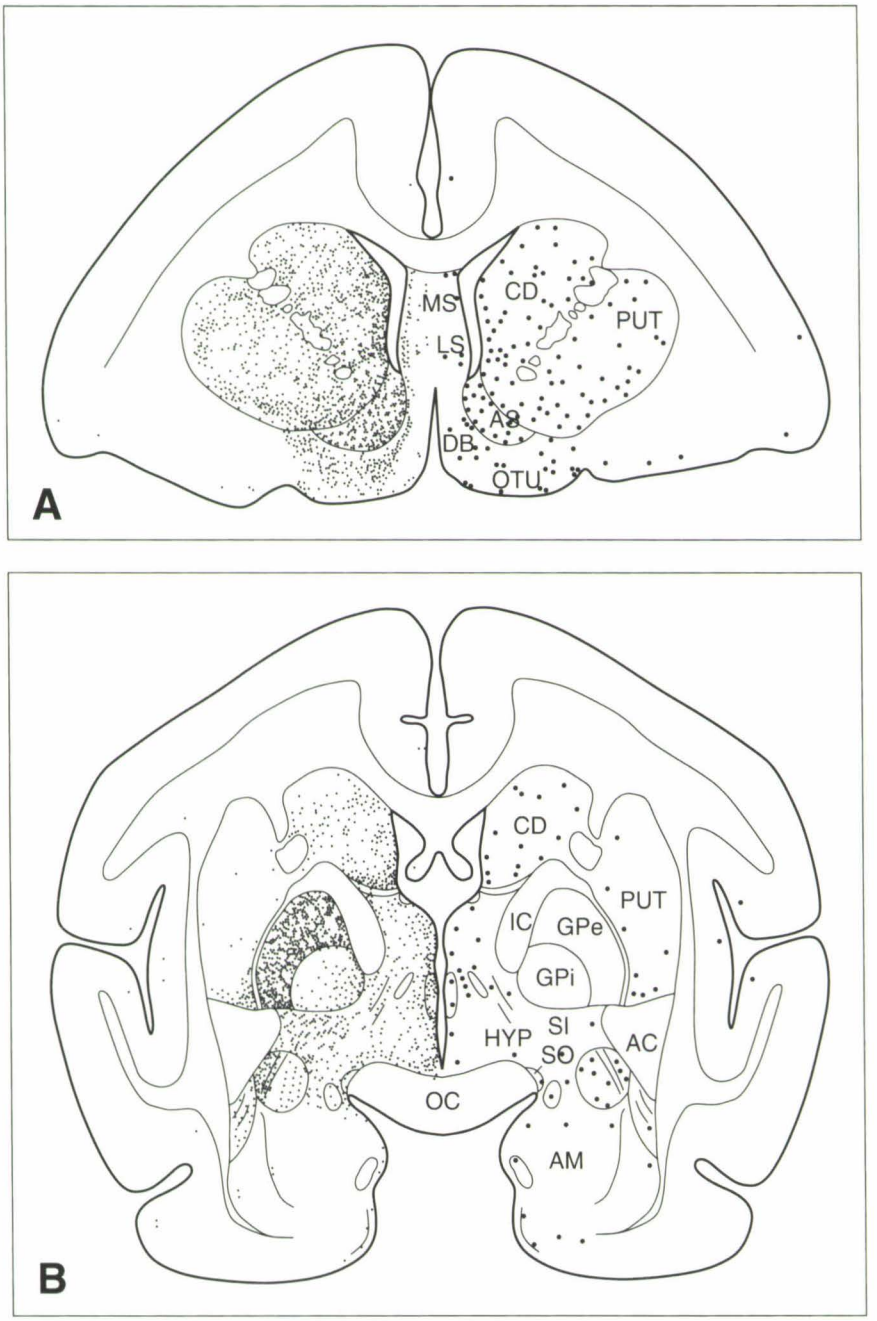


Figure 19.12. Frontal sections through the forebrain of the squirrel monkey illustrating the distribution of enkephalin-immunoreactive axon terminals (*dots on the left*) and cell bodies (*filled circles on the right*). Note the dense enkephalinergic innervation of the external segment of the globus pallidus. The sections are displayed in a rostrocaudal order. *AM*, amygdaloid nuclear complex; *AS*, nucleus accumbens; *CD*, caudate nucleus; *DB*, diagonal band of Broca; *GPe*, external segment of globus pallidus; *GPi*, internal segment of globus pallidus; *HYP*, hypothalamus; *IC*, internal capsule; *LS*, lateral septal nucleus; *MS*, medial septal nucleus; *OC*, optic chiasm; *OTU*, olfactory tubercle; *PUT*, putamen; *SI*, substantia innominata; *SO*, supraoptic nucleus.

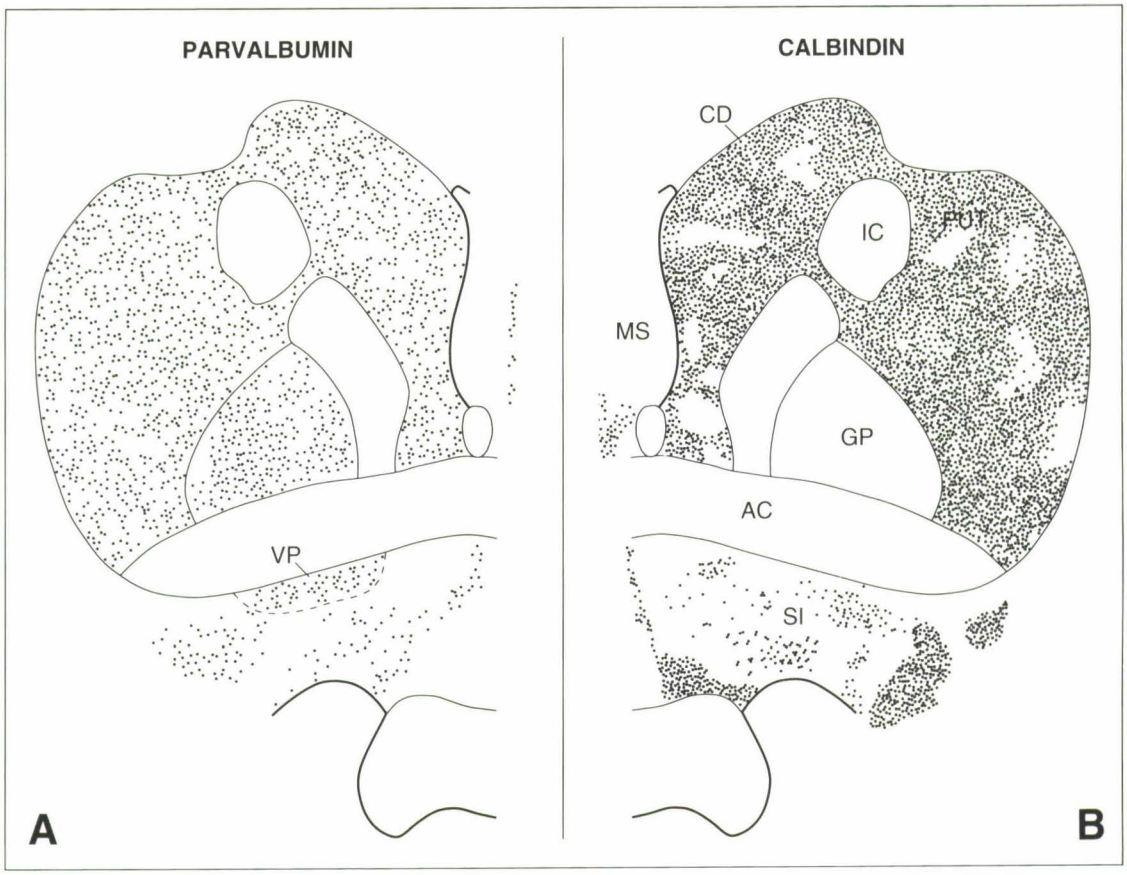


Figure 19.13. Frontal half sections through the basal ganglia of the squirrel monkey illustrating the distribution of parvalbumin (**A**) and calbindin D-28k (**B**) in the striatum and pallidum. These two calcium-binding proteins have a striking complementary distribution in the basal ganglia. Calbindin specifically labels the multitude of striatal projection neurons, whereas parvalbumin marks subsets of striatal interneurons. At pallidal levels, virtually all neurons contain parvalbumin but are devoid of calbindin. *AC,* anterior commissure; *CD,* caudate nucleus; *GP,* globus pallidus; *IC,* internal capsule; *MS,* medial septal nucleus; *PUT,* putamen; *SI,* substantia innominata; *VP,* ventral pallidum.

grouped in two broad categories: the giant aspiny interneurons [corresponding to the aspiny II cells of DiFiglia, et al. (82)], and the medium-sized interneurons [corresponding to the aspiny I and III cells of DiFiglia, et al. (82)].

The giant aspiny interneurons have elongated cell bodies (50 or 60 μm × 15–25 μm) from which emerge a few stout dendrites that branch radially with some dendrites extending up to 750 μm from the soma. The axon arises from the dendritic trunk, branches extensively, with the resulting arborization consisting of a dense plexus of extremely fine axonal branches that fill the region of the dendritic field and sometimes go beyond. These giant neurons, which were demonstrated to be the striatal cholinergic neurons (Fig. 19.14) (30, 200, 222, 295), represent less than 2% of all striatal cells (295). Originally thought to be projection neurons (101, 194, 195), they were later shown by retrograde labeling techniques not to project to the major recipient structures of the striatum (126, 284, 374).

The medium-sized interneurons are usually divided into two categories on the basis of their neurotransmitter content. The first type displays intense GABA immunoreactivity and also contains parvalbumin (Fig. 19.13) (62, 63, 188, 204, 208). These intrinsically organized cells, which represent approximately 1% of the striatal neuronal population, are characterized by a round cell body (14–15 μm) with five to eight varicose and often curved dendrites that branch close to the cell body. Their axon is short and beaded and form a rich local plexus. These interneurons

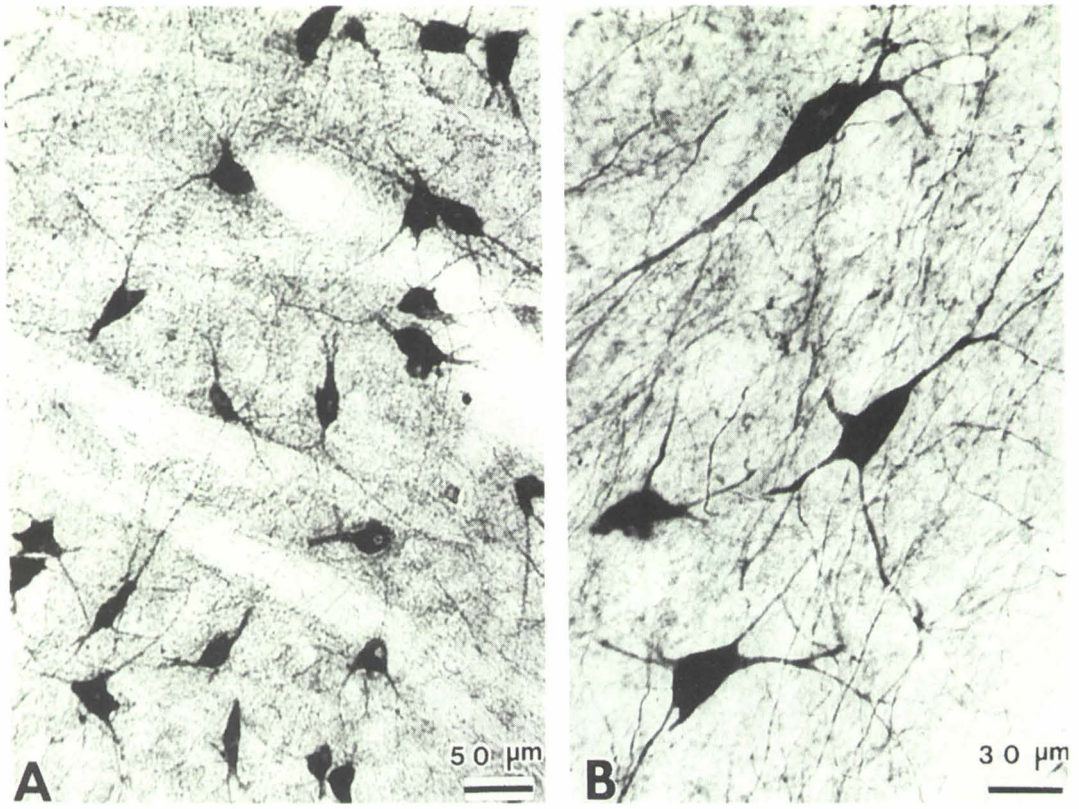


Figure 19.14. Striatal cholinergic interneurons in the squirrel monkey as seen at two different magnifications. The neurons were visualized with a pharmacohistochemical technique for acetylcholinesterase (AChE) (**A**) and immunohistochemical methods for choline acetyltransferase (ChAT) (**B**). These cholinergic neurons are the largest striatal elements. They have a triangular or ovoid cell body from which emerge 3–5 thick primary dendrites. Their axon remains confined to the striatum.

correspond to spiny type I of DiFiglia, et al. (82). The second type of interneuron displays immunoreactivity for both somatostatin (78, 81, 348) and neuropeptide Y (333), but they do not contain mRNA coding for GABA decarboxylase (GAD) (55) (Figs. 19.15 and 19.16). The neurons also contain the enzyme nicotinamide adenine dinucleotide phosphate (NADPH)-diaphorase (358, 359), which is a nitric oxide synthase involved in the production of nitric oxide (NO), a short-lived radical believed to be a novel messenger molecule (32, 165). The somatostatinergic interneurons have a spheroid cell body with a mean diameter of approximately 12 μm. They possess three or four rather straight and relatively long (150 μm) dendrites that exhibit spine-like appendages and fine tufted terminations. Their axon is relatively short, but displays extensive local arborization. They correspond to the aspiny III neurons of DiFiglia, et al. (82).

Striatal Compartments

There is considerable evidence that the striatal neuropil is organized into a mosaic of chemically distinct compartments related to the organization of afferent and efferent connections and to particular transmitter substances (118, 122, 123) (Figs. 19.15**A**, **B**, 19.16, and 19.17). Every major striatal afferent system studied has been shown to terminate in a patchy fashion. A histochemical compartmentalization of the striatum was demonstrated for a variety of neuropeptides and transmitter-related enzymes. Acetylcholinesterase (AChE) staining has been particularly useful in dramatically demonstrating these compartments (122, 123) (Fig. 19.17). The two major compartments of the striatum are referred to as "striosomes" (or patches) and extrastriosomal "matrix." Striosomes (or striatal bodies) are characterized by high levels of opiate receptors, substance P (SP), neu-

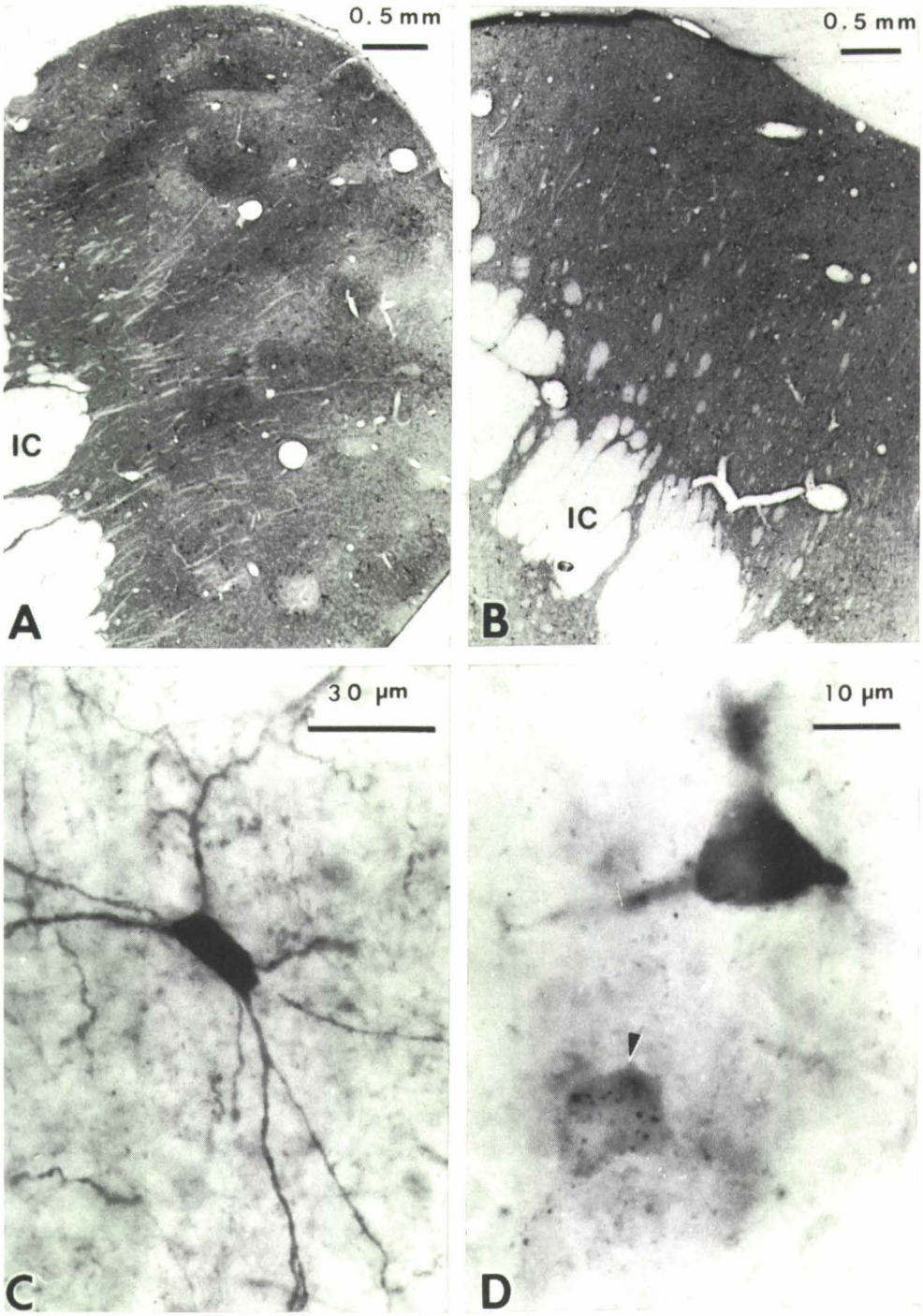


Figure 19.15. Striatal interneurons displaying neuropeptide Y (NPY) immunoreactivity. **A**, **B**. Comparison of the distribution of NPY-immunoreactive cell bodies and fibers in the caudate nucleus of the cat (**A**) and the squirrel monkey (**B**). Note that NPY-immunoreactive profiles are more heterogeneously distributed in the caudate nucleus of the cat than in the monkey. **C**. Typical example of a NPY-positive neuron in the putamen of the squirrel monkey. **D**. A NPY-immunoreactive neuron and a retrogradely labeled neuron (*arrowhead*) in the caudate nucleus of the squirrel monkey as seen after injection of wheat germ agglutinin-conjugated horseradish peroxidase (WGA-HRP) into the substantia nigra. Note the absence of black WGA-HRP granules in the NPY-positive neuron, which displays only a diffuse, light brown immunostaining. This finding indicates that striatal NPY-immunoreactive neurons do not send their axon to the substantia nigra. *IC* indicates the internal capsule.



Figure 19.16. Distribution of somatostatin immunoreactivity in the basal ganglia of the squirrel monkey in a rostrocaudal sequence. **A** and **C** represent the immunoreactive terminals (*fine dots*), whereas **B** and **D** show the distribution of immunoreactive cell bodies (*filled circles*) as seen on the same section. *AC,* anterior commissure; *CC,* corpus callosum; *CD,* caudate nucleus; *GPe,* external segment of globus pallidus; *GPi,* internal segment of globus pallidus; *HYP,* hypothalamus; *IC,* internal capsule; *OC,* optic chiasm; *OTU,* olfactory tubercle; *PUT,* putamen; *SI,* substantia innominata; *THAL,* thalamus.

rotensin (NT) and tyrosine hydroxylase (TH) (122). The extrastriosomal matrix is identified with high levels of AChE, calbindin somatostatin (SRIF), neurotensin receptors, and terminals of thalamic projections. Prefrontal, cingulate, and motor cortical areas project to both patches and matrix.

Striking changes occur in organization of striatal compartments during early development. In the fetus, AChE and dopamine are in register in the patches, but postnatally AChE is largely in the matrix (122, 350) (Fig. 19.17). Opiate receptors, diffusely distributed prenatally, are found postnatally in the patches. Chemical compartmentalization of the striatum appears to be a mammalian evolutionary phenomenon that expresses functional differences in groups of striatal neurons.

A further subdivision of the dual striosome/matrix system has been proposed on the basis that cortico-striatal fibers (as well as

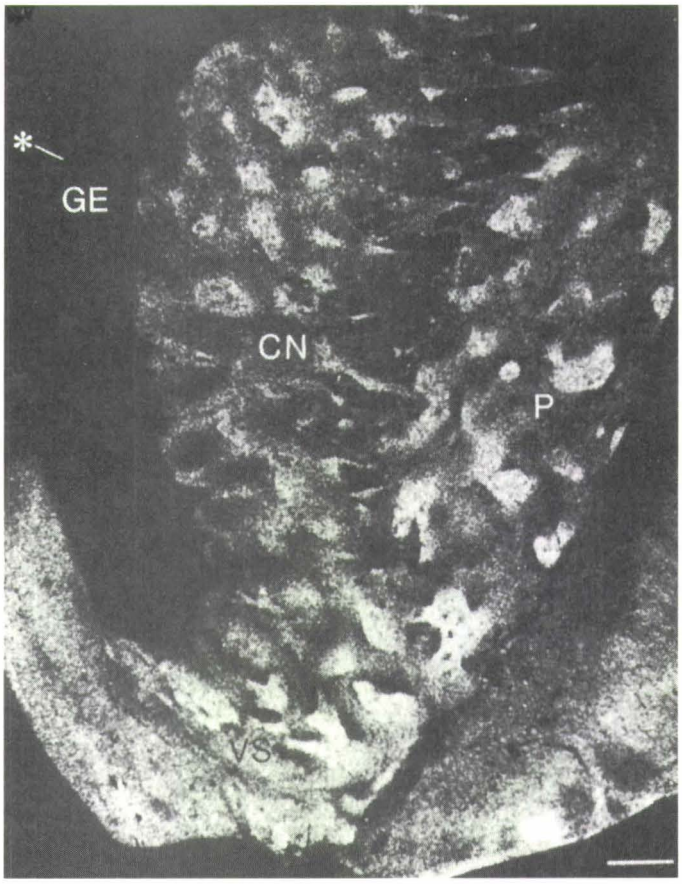


Figure 19.17. Muscarinic cholinergic receptor binding sites in the caudate nucleus (*CN*) and putamen (*P*) of a 22-week-old human fetus. Areas rich in binding sites appear as light patches (striosomes). *GE* indicates the ganglionic eminence. Scale bar = 1.0 mm.

other striatal afferents) form distinct clusters within the neurochemically homogeneous matrix (122, 230). Interestingly, the output cells of the matrix have also been shown to be grouped in clusters in relation to the different projection systems leading from the striatum to the external and internal segment of the globus pallidus, as well as to the substantia nigra (75, 96, 97, 116, 122, 180). These clusters are termed "matrisomes" (122) and are considered as functional modules that could be related to the physiologically defined microexcitable zones described by Alexander and DeLong (6, 7).

Afferent Connections

Because it receives dense projections from a wide variety of sources, the striatum is considered to be the major receptive and integrative component of the basal ganglia. Afferent systems arising from the cerebral cortex, the intralaminar thalamic nuclei, and the substantia nigra are profuse and topographically organized (Fig. 19.18). Additionally, the striatum, or parts of it, receive projections from cells of the amygdala and dorsal nucleus of the raphe (384, 385).

CORTICOSTRIATAL PROJECTIONS

Among the various striatal afferents, those arising from the cerebral cortex are by far the most prominent. The corticostriatal projections are of utmost importance, as they impose on the striatum a pattern of functional regionalization that is maintained throughout the whole basal ganglia.

The entire cerebral cortex is known to project topographically to the striatum. Input from the sensorimotor cortex is extensive and bilateral, whereas that from the visual cortex is minimal. Earlier degeneration studies emphasized the high degree of overlap of corti-

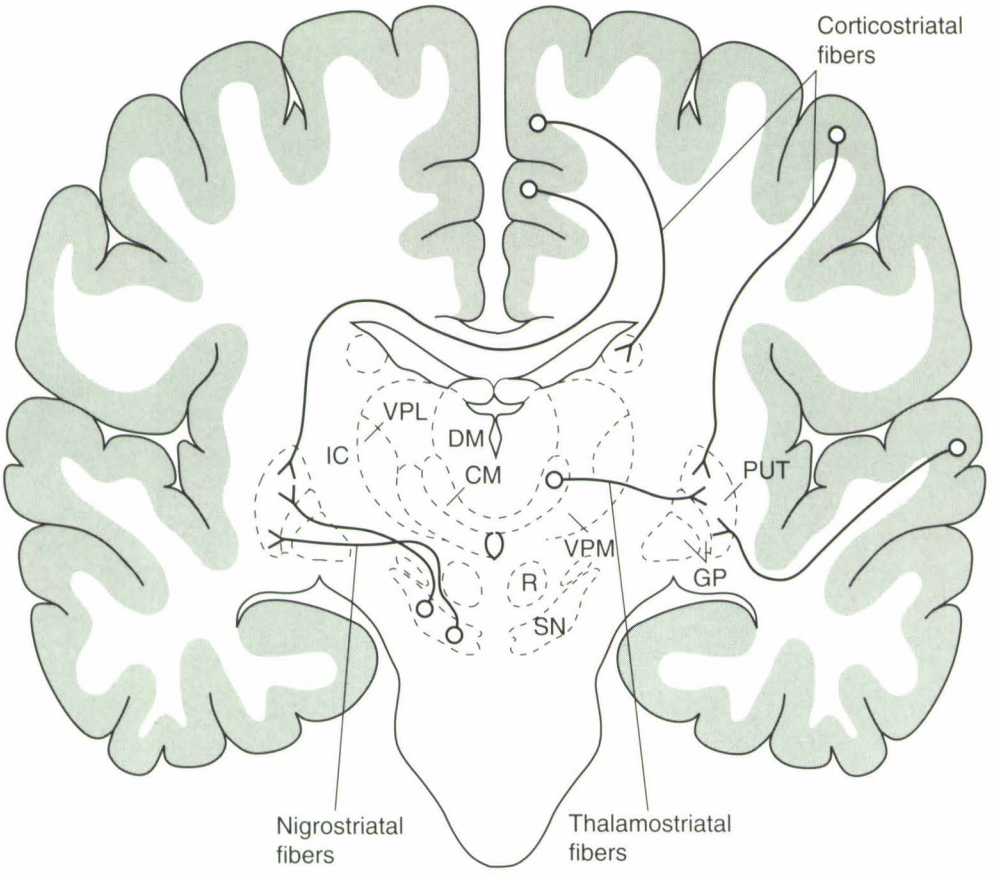


Figure 19.18. Major striatal afferent systems. Corticostriatal projections arise from broad regions of the cerebral cortex, are topographically organized, and are distributed to both the caudate nucleus and the putamen. Corticostriatal fibers arise mostly from pyramidal cells in the upper half of lamina V, and those from area 4 project bilaterally and somatotopically upon the putamen. These projections have glutamate as their neurotransmitter. Nigrostriatal fibers arise from cells of the pars compacta of the substantia nigra and convey dopamine to terminals in the caudate nucleus and putamen. Thalamostriatal fibers arise largely from the centromedian-parafascicular nuclear complex. Not shown are striatal afferents from serotoninergic cell groups in the midbrain dorsal raphe nucleus. *CM*, centromedian thalamic nucleus; *DM* dorsomedial (or mediodorsal) thalamic nucleus; *GP*, globus pallidus; *IC*, internal capsule; *PUT*, putamen; *R*, red nucleus; *SN*, substantia nigra; *VPL* and *VPM*, ventral posterolateral and ventral posteromedial thalamic nuclei.

costriatal projections (39, 193, 366, 367). However, the results of more recent autoradiographic studies reveal that the sensorimotor cortex in monkeys projects exclusively to the putamen, where a somatotopic representation of the leg, arm, and face occurs in the form of obliquely arranged strips (71, 72, 211, 224). In contrast, associative areas of the prefrontal, temporal, parietal, and anterior cingulate cortices appear to project almost exclusively to the caudate nucleus in monkeys (117, 303, 325). These findings suggest that the caudate nucleus in primates is more closely related to complex and associative types of behavior, whereas the putamen appears more directly involved in sensorimotor aspects of forebrain mechanisms. Afferents from limbic and paralimbic cortical areas terminate largely in the ventral portion of the striatum, including the deep layers of the olfactory tubercle, and the ventral part of both the caudate nucleus and the putamen.

Based on the organization of its cortical afferents, the striatum can be subdivided into three major functional sectors termed the associative, sensorimotor, and limbic striatal territories (274) (Fig. 19.19). The associative territory comprises most of the head of the caudate nucleus and a large portion of the rostral, precommissural putamen. The sensorimotor territory includes most of the postcommissural putamen, the dorsolateral rim of the head of the caudate nucleus, and the lateral aspect of the body of the caudate nu-

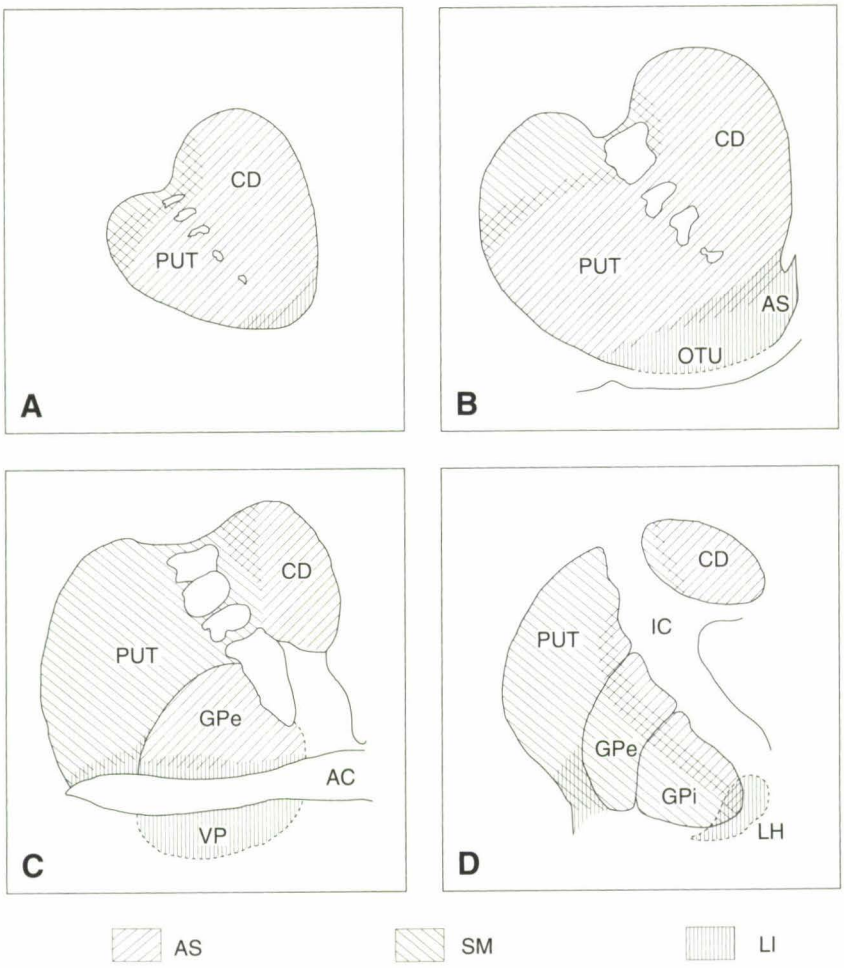


Figure 19.19. Localization of the associative (*AS*), sensorimotor (*SM*), and limbic (*LI*) striatal territories in primates. The drawings are set out in a rostrocaudal order and *double hatched* areas indicate zone of overlap. *AC,* anterior commissure; *AS,* nucleus accumbens; *CD,* caudate nucleus; *GPe,* external segment of globus pallidus; *GPi,* internal segment of globus pallidus; *IC,* internal capsule; *LH,* lateral hypothalamic area; *OTU,* olfactory tubercle; *PUT,* putamen; *VP,* ventral pallidum.

cleus, whereas the limbic territory comprises the ventral striatum (274). Neurons in the associative, sensorimotor, and limbic territories are concerned with the treatment of information deriving from association, sensorimotor, and limbic/paralimbic cortices, respectively. Since overlap exists among the different cortical projections, these three territories should be viewed more as a functional continuum rather than striatal subdivisions with strict boundaries.

Terminals from corticostriatal axons are not uniformly distributed in striatal tissue, but appear as patches or clusters of various sizes (211). Furthermore, the cortical areas reciprocally connected via corticocortical connections tend to share common zones of fiber termination in the striatum (357, 379, 380). The latter finding supports the view that the corticostriatal system is organized according to general functional affiliation of cortical areas rather than their topographic location (124). However, it appears that many reciprocally connected areas of the association cortex project to spatially distinct, rather than overlapping, areas of the striatum (119). In monkeys, various areas of the association cortex project to longitudinal sectors that occupy restricted mediolateral domains of the striatum. Convergence of inputs within these elongated parasagittal bands is not governed by reciprocity of corticocortical connectivity but ranges from complete segregation to overlap. Even in areas where overlap occurs, the ter-

minal fields of different association cortices do not intermix but form complex interdigitation patterns (325).

The first successful attempts to label the cells of origin of the corticostriatal projection by retrograde transport of horseradish peroxidase (HRP) led to the conclusion that these fibers arise from a neuronal population distinct from those giving rise to other corticofugal systems (183, 185). This massive projection was believed to arise almost exclusively from small pyramidal cells in the upper half of layer V in all cortical areas. In contrast, intracellular recording studies suggest that larger pyramidal cells in layer V, which can be activated antidromically by stimulation of the thalamus or cerebral peduncle, have a collateral that terminates in the striatum (83, 181), as originally suggested by Ramón y Cajal (304). Such branched neurons have been identified by means of intracellular HRP injection (83) or retrograde double-labeling experiments (316).

Other findings suggest that the corticostriatal fibers arise from both supragranular (laminae I, II, III) and infragranular (laminae V, VI) cortical layers (205, 206, 267, 315). Neurons located in lamina VI are reported to project principally to the striosomes (patches), whereas neurons in other cortical layers project chiefly to the matrix compartment (113). Retrograde double-labeling studies reveal that cortical neurons projecting bilaterally to the striatum are few in number compared to those projecting ipsilaterally or contralaterally (95, 316).

The massive striatal afferents from the cerebral cortex terminate principally on the head of the dendritic spines of the spiny projection neurons, where they make asymmetric synapses (108, 337). The corticostriatal fibers exert an excitatory influence on striatal projection neurons, most probably through the use of glutamate as a neurotransmitter (100, 198, 338).

THALAMOSTRIATAL PROJECTIONS

The thalamostriatal projection is the second most prominent striatal group of afferents (Figs. 19.18 and 19.34). Its existence was first detected in human material by Cécile and Oskar Vogt in Germany, who suggested that the intralaminar nucleus known as the centromedian projects densely and selectively to the putamen (361). The authors were referring to the small-celled part of the centromedian-parafascicular (CM-Pf) complex which, along with the putamen, is very enlarged in monkeys and humans and receives a massive projection from the motor cortex (238, 243, 262). The Vogts' suggestion was confirmed by a cell degeneration study (300) that showed that virtually all intralaminar nuclei in primates project to the striatum, the parafascicular and central lateral nuclei providing input to the caudate nucleus and the anterior intralaminar nuclei to the nucleus accumbens. Anterograde labeling studies revealed that the projections from the centromedian nucleus terminate principally in the sensorimotor striatal territory, whereas those from the parafascicular nucleus terminate in the associative territory (283, 319, 320). In both of these territories, fibers from the intralaminar nuclei form distinct patches or elongated bands whose exact relationship with the mosaic-like arrangements of the corticostriatal projection is not yet known (Fig. 19.20) (160, 320, 321).

Single- and double-retrograde labeling studies confirmed that the CM-Pf complex is the major source of thalamic afferents to the striatum (182, 184, 283). These studies further showed that the thalamostriatal projection is topographically organized, with a rostrocaudal and dorsoventral correspondence between the intralaminar nuclei and their main termination sites in the striatum. It was also demonstrated that, in addition to prominent afferents from the "nonspecific" intralaminar nuclei, the striatum receives a significant input from "specific" thalamic nuclei such as the ventral anterior, ventral lateral, and lateral posterior nuclei (273).

Earlier electrophysiologic and HRP studies suggested that the thalamostriatal fibers issue collateral to the cerebral cortex (184, 306). The existence of such collaterals was confirmed by retrograde double-labeling and antidromic invasion studies (181, 229). These branched neurons abound in rostral intralaminar nuclei, but are rather few in number in the centromedian nucleus, where neurons projecting to the cerebral cortex are confined to the lateralmost portion of the nucleus (320). Collaterals of thalamostriate fibers projecting to broad cortical areas end in laminae V and VI.

The thalamostriatal fibers terminate principally on the shafts and, less abundantly, on the dendritic spines of the medium spiny

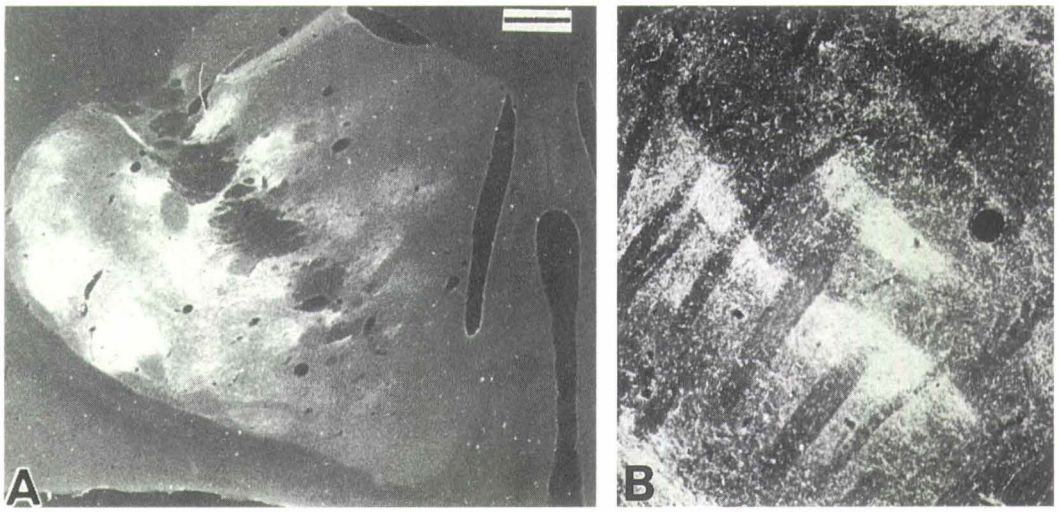


Figure 19.20. Patch-like terminal fields of the thalamostriatal projection in the squirrel monkey, as seen at low (**A**) and high power (**B**) magnifications. The pathway was traced following injection of the highly sensitive anterograde tracer *Phaseolus vulgaris*-leucoagglutinin (PHA-L) in the centromedian nucleus. As seen at low power (**A**), the thalamostriatal fibers terminate in a highly heterogeneous manner in the putamen and mediodorsal border of the caudate nucleus. These areas correspond to the sensorimotor striatal territory. At higher magnification (**B**), thalamostriatal fibers can be seen to form elongated bands in the dorsolateral portion of the putamen. Scale bar = 1 mm in **A** and 300 μm in **B**.

projection neurons (Fig. 19.21) (101, 321). These fibers form asymmetric synapses and are thought to exert an excitatory influence that is mediated probably through glutamate.

NIGROSTRIATAL PROJECTIONS

Evidence concerning nigrostriatal fibers has, for a long time, been based almost entirely upon retrograde cell changes produced in the substantia nigra following large striatal lesions (93, 94, 242, 363). Attempts to trace fiber degeneration from lesions in the substantia nigra to the striatum in Marchi preparations and silver-impregnated material (2, 49, 57, 90) either failed to demonstrate these fibers or indicated that they were sparse. However, the histofluorescence technique for the demonstration of monoamines (38, 88) revealed that cells in the pars compacta of the substantia nigra send axons to the striatum that convey dopamine to their terminals (12, 13, 23, 67, 109, 164, 167, 354). Striatal dopamine is stored in regularly spaced swellings or varicosities along the terminal portions of the axons. Dopaminergic fibers appear as a distinct matrix of fine varicose axons which form thick sworls around both small and large striatal neurons (330).

Dopamine is synthesized in the pigmented cells of the pars compacta [SNc, group A9 of Dahlström and Fuxe (66)]. Other neurons located in the ventral tegmental area [(VTA, group A10 of Dahlström and Fuxe (66))] and in the retrorubral area [(RRA, group A8 of Dahlström and Fuxe (66))] also contribute to the nigrostriatal projection. Neurons in the VTA give rise to the mesolimbocortical system, whose fibers terminate principally in the ventral striatum (limbic striatal territory) and the frontal cortex, whereas those in the SNc and RRA project via the nigrostriatal pathway to the bulk of the striatum (48). The nigrostriatal pathway is partially crossed but the number of nigrostriatal neurons projecting contralaterally does not exceed 5% of those projecting ipsilaterally and there are apparently very few neurons in the SNc and VTA that project bilaterally (273). Furthermore, some 10% of nigrostriatal fibers are said to be nondopaminergic, but their cells of origin are uncertain (130)

Neuroanatomic data from various sources indicate that the nigrostriatal projection is topographically organized in different species. In monkeys, the rostral two-thirds of the substantia nigra is related to the head of the caudate nucleus, whereas nigral neurons projecting to the putamen are more caudally located and display a rostrocaudal topography

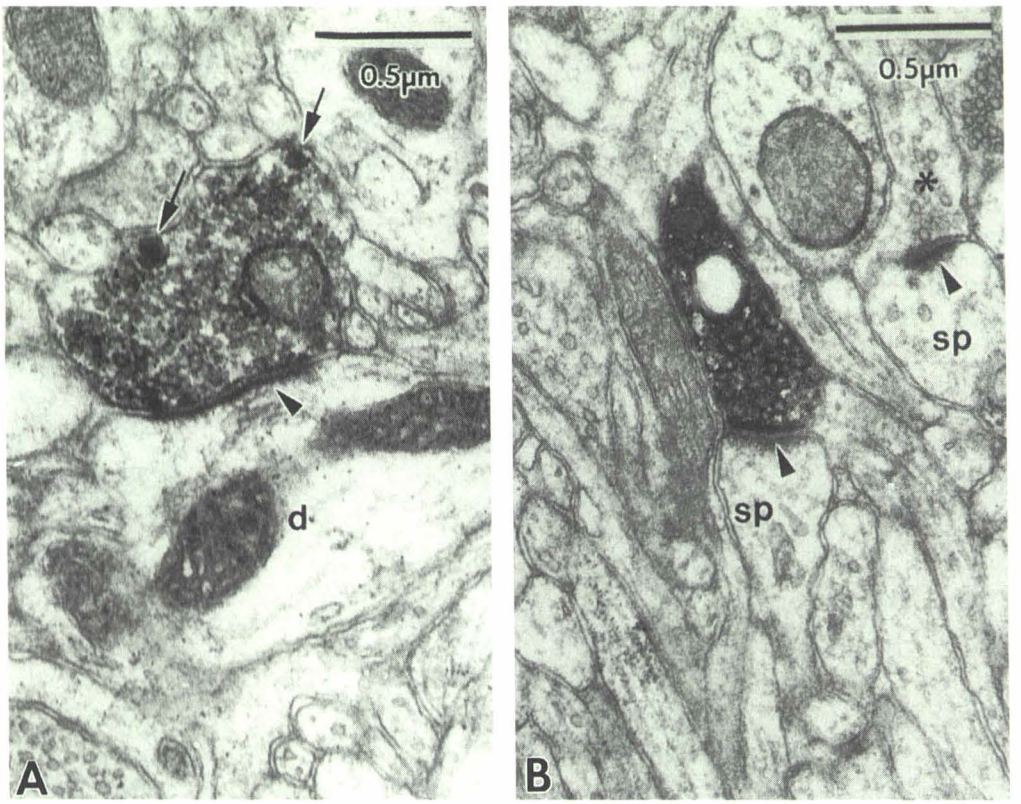


Figure 19.21. Ultrastructural features of PHA-L anterogradely labeled elements in the caudate nucleus (**A**) and putamen (**B**) following PHA-L injections in the parafascicular nucleus and the centromedian nucleus, respectively. PHA-L-labeled boutons (containing a dark precipitate) form asymmetric synapses (*arrowheads*) with dendritic shafts (*d*) (**A**) and, more rarely, with spines (*SpP*) (**B**). Note the presence of two large dense-core vesicles (*arrows*) in the PHA-L-labeled boutons in **A**, and a nonimmunoreactive bouton (*asterisk*) that forms an axospinous synapse (*arrowhead*) in **B**.

(259, 347) (Fig. 19.22). A mediolateral topographic relationship between the SNc and the striatum is also proposed, with an apparent inverse relationship along the dorsoventral axis (346, 347). Additionally, projection fields of the nigrostriatal pathway are purported to overlap significantly in all planes, possibly accounting for the apparent lack of precise organization of the nigrostriatal system (347).

In contrast, retrograde double-labeling studies in primates revealed that nigral neurons projecting to the caudate nucleus and those projecting to the putamen are organized in the form of closely intermingled clusters of various sizes and distributed throughout the entire SNc in a complex and precise mosaic-like pattern (Fig. 19.23) (283). Only a few nigral neurons appear to project to both the caudate nucleus and the putamen. The functional significance of the complex intrinsic organization of the SNc remains to be investigated, but it may reflect the highly heterogeneous and mosaic-like arrangement of the various neuronal elements within the striatum itself.

Autoradiographic studies have revealed that nigrostriatal fibers terminate in patches, although these patches are less distinct in adults than those of the corticostriatal and thalamostriatal projections (115, 375). The patches of nigrostriatal axons are closely intermingled with the patches of the thalamostriatal projection (20). Immunohistochemical studies with antibodies raised against tyrosine hydroxylase (TH), the rate-limiting enzyme in the synthesis of catecholamines, showed that the striosomes are rather

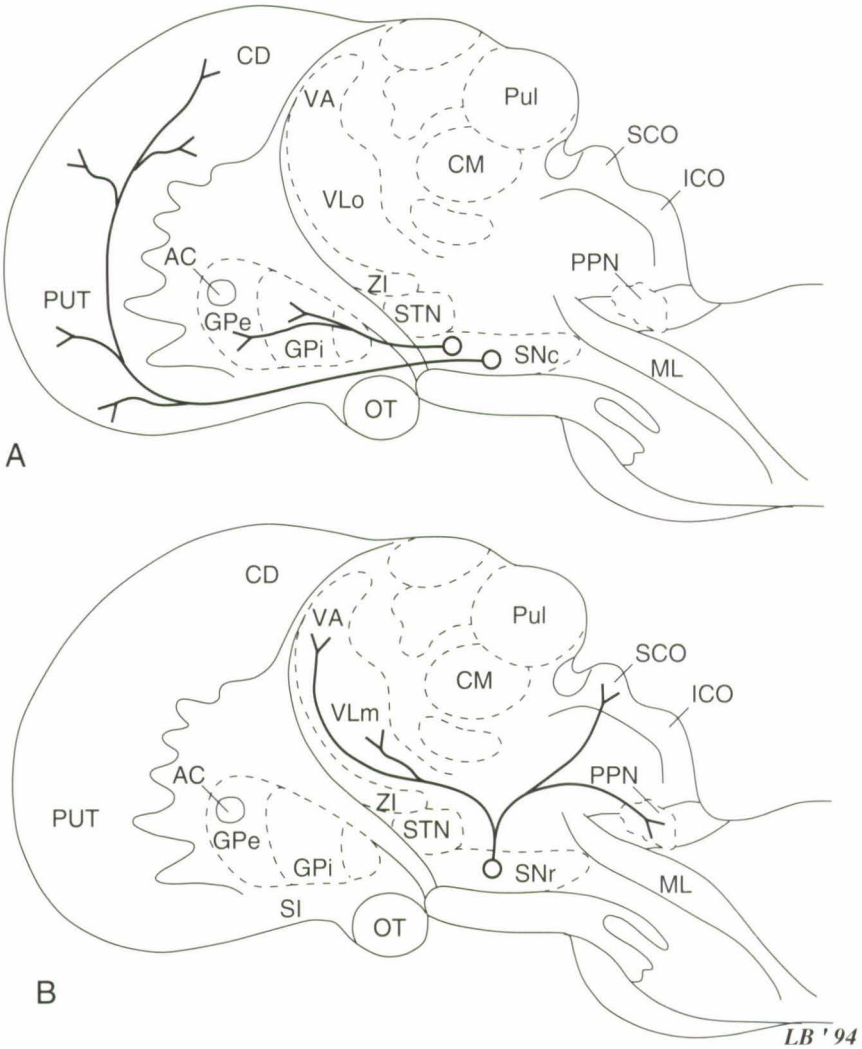


Figure 19.22. Comparison of the efferent projections of the substantia nigra pars compacta (SNc) (**A**) and the substantia nigra pars reticulata (SNr) (**B**), as seen in the sagittal plane. Fibers from dopaminergic neurons of the SNc form a feedback projection to the caudate nucleus (*CD*) and putamen (*PUT*). Distinct neurons in the SNc also project to the globus pallidus, where they arborize more extensively in the internal (*GPi*) than in the external (*GPe*) pallidal segment. By contrast, the SNr is a major output nucleus of the basal ganglia. Fibers from SNr neurons branch profusely to (a) the ventral tier thalamic nuclei (*VA*, nucleus ventral anterior and *VLm/VLo*, nucleus ventral lateral pars magnocellular and oralis), (b) the superior colliculus (*SCO*), and (c) the pedunculopontine nucleus (*PPN*). *AC*, anterior commissure; *CM*, centromedian thalamic nucleus; *ICO*, inferior colliculus; *ML*, medial lemniscus; *OT*, optic tract; *Pul*, pulvinar; *STN*, subthalamic nucleus; ZI, zona incerta.

poorly innervated in adult monkeys by comparison to the extrastriosomal matrix (Fig. 19.24**A**) (220).

Lesions in the substantia nigra cause conspicuous reductions in striatal dopamine ipsilaterally (13, 109, 164, 298, 354), whereas large striatal lesions produce distinct increases in dopamine in the SNc cells which decrease as the cells undergo chromatolysis.

It is generally accepted that dopamine has an inhibitory action on striatal neurons (28, 162, 228, 330). However, the effect of dopamine can be multifarious as it is mediated through a family of dopaminergic receptors that contains at least five members. The two most well-characterized dopaminergic receptors in the striatum are designated as D_1 and D_2 subtypes. The pattern of binding for

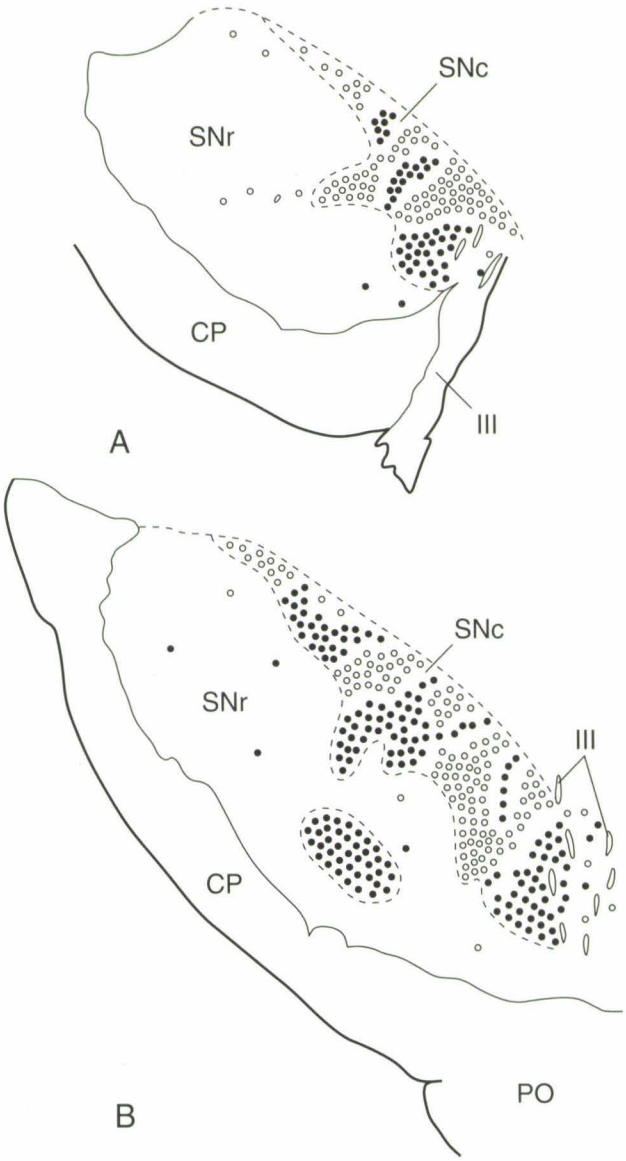


Figure 19.23. Frontal sections through the rostral (**A**) and middle (**B**) thirds of the substantia nigra of the squirrel monkey illustrating the mosaic-like distribution of the pars compacta (*SNc*) neurons projecting to the caudate nucleus (*open circles*) and putamen (*filled circles*), as seen after injection of one retrograde fluorescent tracer in the caudate nucleus and the other in the putamen on the same side of the brain. *CP*, cerebral peduncle; *PO*, pontine gray; *SNr*, substantia nigra pars reticulata; *III*, oculomotor nerve root fibers.

both D_1 and D_2 receptors in the striatum does not match the patchy heterogeneity seen with acetylcholinesterase staining, but areas of greatest receptor density are found in the matrix. Activation of D_1 receptors reduces membrane excitability, while activation of D_2 receptors causes a decrease in the release of transmitter substance at synaptic terminals. Although D_1 and D_2 receptors can be distinguished, these receptors appear to function synergistically to modulate neuronal activities.

Ultrastructural studies revealed that nerve terminals containing dopamine have small clear vesicles, with a few large dense-core vesicles (76, 164). The dopaminergic nerve terminals make symmetric synapses with the dendritic shafts and spines of striatal spiny neurons (31, 107). A large proportion of the dopaminergic synapses occur on the neck of

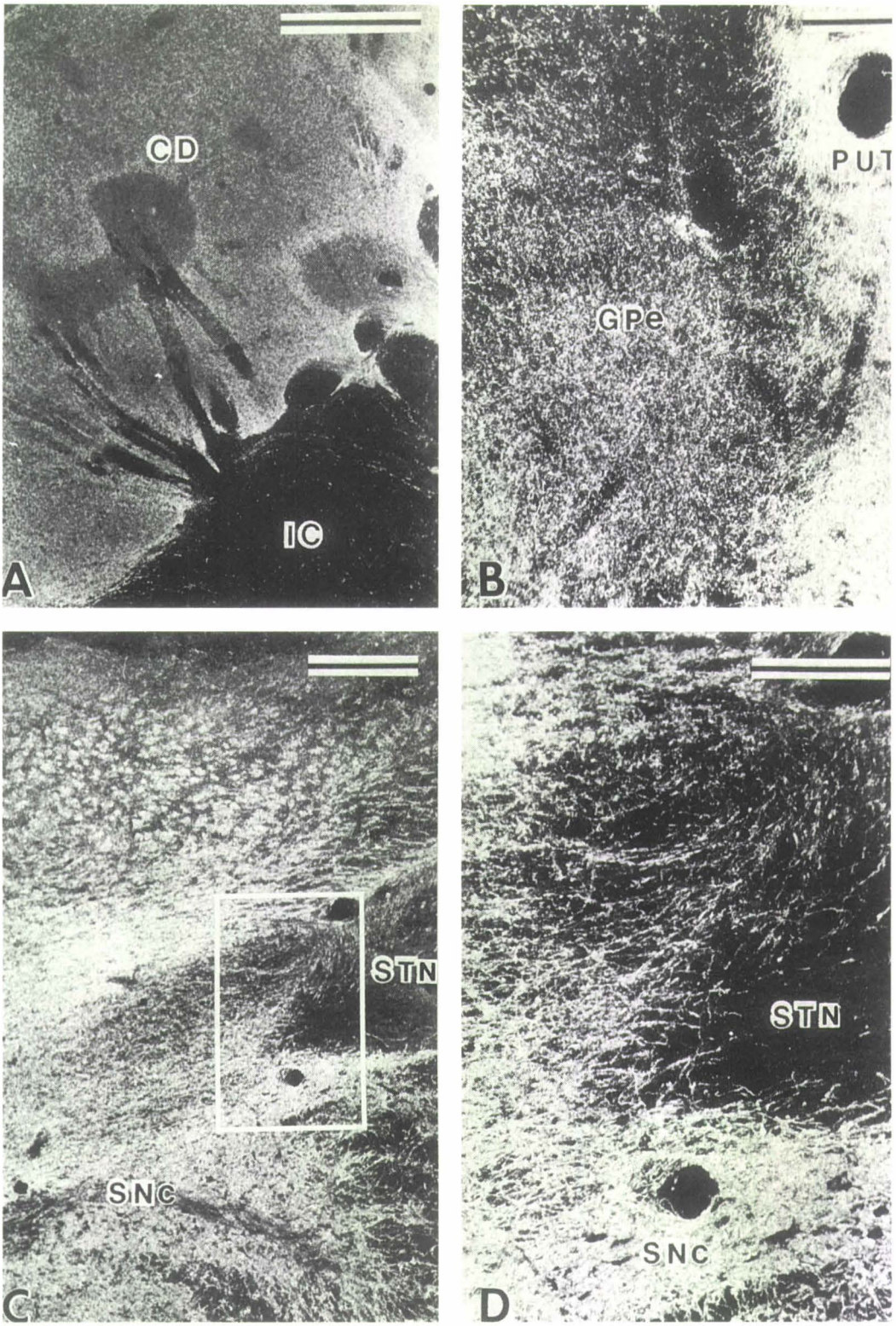


Figure 19.24. Features of the dopaminergic innervation of the basal ganglia in the squirrel monkey as revealed with immunohistochemical staining for the enzyme tyrosine hydroxylase (*TH*). **A**. Patches of poor TH immunostaining surrounded by zones of intense immunoreactivity in the caudate nucleus (*CD*) near the internal capsule (*IC*). **B**. Numerous TH-positive fibers in the external pallidum (*GPe*) and innumerable TH axon terminals in the adjoining putamen (*PUT*). **C**. Dense TH-immunoreactive fiber bundles emerging from the substantia nigra pars compacta (*SNc*) and coursing within the zona incerta near the subthalamic nucleus (*STN*). **D**. Higher power view of the TH-positive fiber bundles located dorsal to the SNc corresponding to the insert in **C**. Scale bars = 500 μm (**A**, **C**) and 300 μm (**B**, **D**).

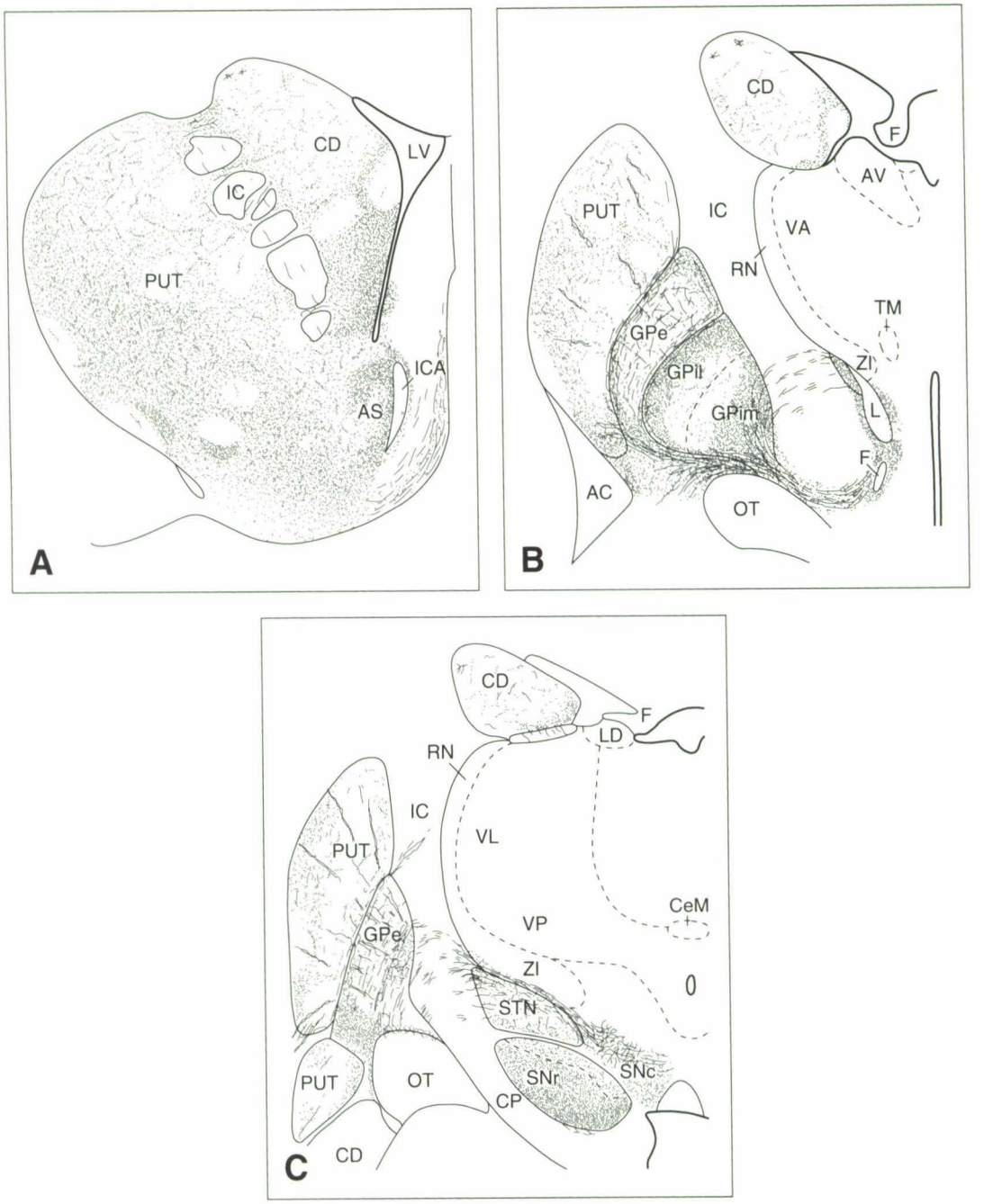


Figure 19.25. Frontal sections through the rostral (**A**), middle (**B**), and caudal (**C**) thirds of the basal ganglia of the squirrel monkey illustrating the distribution of serotonin-immunoreactive fibers (*sinuous lines*) and axon terminals (*dots*). Note the highly heterogeneous distribution of serotonin-positive profiles in the striatum and the dense serotoninergic innervation of the internal pallidal segment and the substantia nigra. *AC*, anterior commissure; *AS*, nucleus accumbens; *AV*, anterior ventral thalamic nucleus; *CD*, caudate nucleus; *CeM*, centromedial thalamic nucleus,; *CP*, cerebral peduncle; *F*, fornix; *GPe*, external segment of globus pallidus; *GPl*, internal segment of globus pallidus; *IC*, internal capsule; *ICA*, island of Calleja; *L*, lenticular fasciculus; *LD*, laterodorsal thalamic nucleus; *LV*, lateral ventricle; *OT*, optic tract; *PUT*, putamen; *RN*, reticular thalamic nucleus; *SNnr*, substantia nigra pars reticulata; *SNnc*, substantia nigra pars compacta; *STN*, subthalamic nucleus; *TM*, mammillothalamic nucleus; *VA*, *VL*, and *VP*, ventral anterior, ventral lateral, and ventral posterior thalamic nuclei; *ZI*, zona incerta.

spines whose head receives asymmetric contacts from what appears to be corticostriatal fibers. Thus, dopamine terminals are ideally positioned to control or modulate the excitatory information from the cerebral cortex as it flows through the striatal spiny projection neurons (Fig. 19.26) (107).

Dopamine also may influence the activity of intrinsic and extrinsic striatal neuronal elements through nonjunctional appositions (31, 76, 135, 296, 350). Furthermore, in addition to its ionotropic action mediated through classic axospinous or axodendritic synapses, dopamine can alter neuronal membrane properties and exert a marked metabotropic and genomic influence on striatal projection neurons. For example, dopamine plays an important role in the regulation of peptide expression in striatal spiny neurons. Destruction of the dopaminergic nigrostriatal projection results in a marked increase in the level of mRNA coding for enkephalin and concomitant decrease in levels of mRNA coding for substance P (17, 122).

AFFERENTS FROM THE RAPHE NUCLEI

These afferents originate principally from the dorsal raphe nucleus and use serotonin [5-hydroxytryptamine (5-HT)] as a neurotransmitter (19, 29, 58, 162, 173, 218, 278, 351). The dorsal raphe-striatal projection is mainly ipsilateral and arborizes profusely within the entire striatum, but slightly more heavily in the ventrocaudal region (Fig. 19.25). Retrograde double-labeling studies in rodents showed that dorsal raphe neurons projecting to the striatum also send axon collaterals to

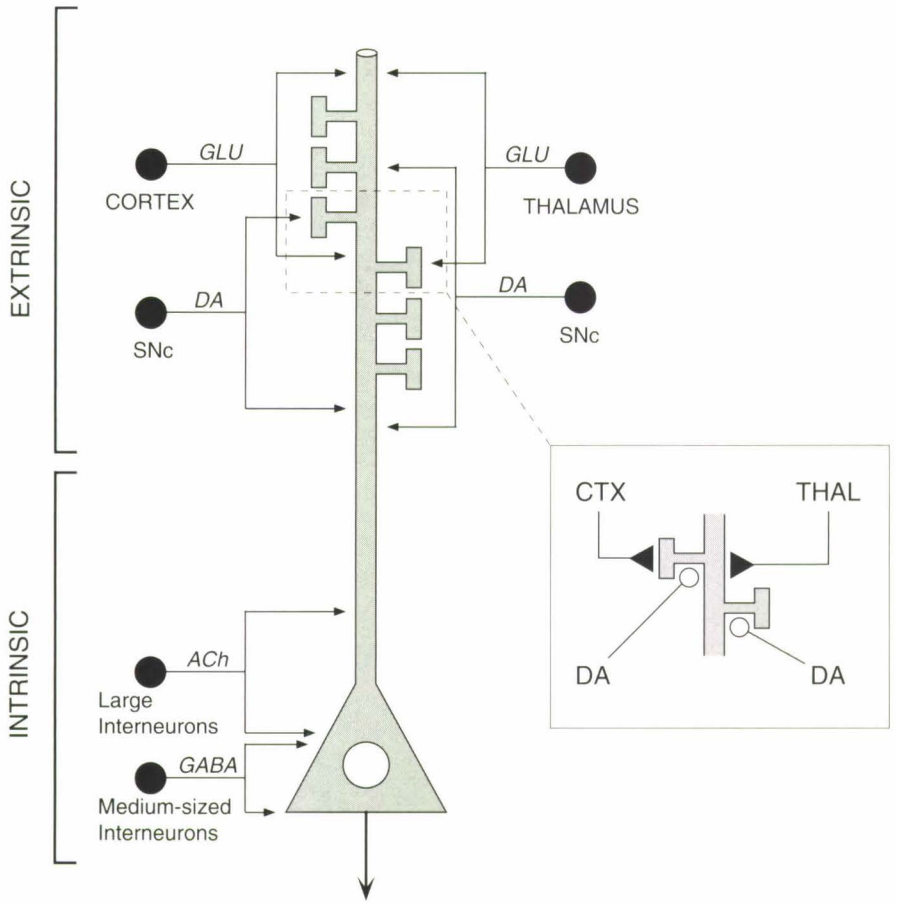


Figure 19.26. Hierarchy of the various intrinsic and extrinsic inputs to the medium spiny projection neuron of the striatum. Note that extrinsic inputs tend to terminate on the distal dendritic tree while intrinsic inputs favor the proximal somatodendritic domain. The insert illustrates the crucial position occupied by the dopaminergic input (*DA*) on spines that receive cortical afferent. The spiny striatal neuron is the major integrative element, as well as the principal output cell of the striatum. *ACh*, acetylcholine; *CTX*, cerebral cortex; *DA*, dopamine; *GABA*, γ-aminobutyric acid; *GLU*, glutamate; *SNc*, substantia nigra pars compacta; *THAL*, thalamus.

the substantia nigra (355). Serotoninergic striatal afferents form asymmetric synapses on dendritic spines or shafts of medium spiny striatal neurons (15, 289, 290, 336). Only 10–15% of 5-HT varicosities, however, exhibit a typical synaptic junction in the striatum of rats (15, 336). Although 5-HT terminals display asymmetric synapses, which is usually indicative of excitatory effect, the electrical stimulation of the dorsal raphe nucleus was reported to produce inhibitory, as well as excitatory, responses on spiny neurons (248, 269, 287, 340). This wide variety of responses may be explained by the existence of junctional and nonjunctional modes of innervation, as well as by a wide variety of 5-HT receptors (218). Of particular interest is the existence of important functional and anatomic interactions between 5-HT and dopaminergic afferents and the cholinergic system in the striatum (19, 77, 173, 175, 263).

AMYGDALOSTRIATAL PROJECTIONS

Although the amygdala and the striatum are parts of anatomically and functionally distinct basal forebrain neuronal systems (i.e., the limbic system and basal ganglia), experimental data suggest a close functional relationship between parts of these structures. Projections from the basolateral amygdala terminate massively in the ventral striatum and less abundantly in the head of the caudate nucleus and the rostral portion of the putamen (318). The densest terminal field of the amygdalostriatal projection overlaps that of the limbic and paralimbic cortical areas and corresponds to the limbic striatal territory. Neurons in this striatal sector are believed to be chiefly concerned with the control of the emotional and motivational aspects of various types of motor behavior.

Efferent Connections

The striatum receives input from a wide variety of sources, including the cerebral cortex, thalamus, and brainstem. In contrast, this major receptive component of the basal ganglia is much more limited in its efferent projections, as the vast majority of striatofugal fibers terminate only in the pallidum and substantia nigra (Figs. 19.27 and 19.28).

Different populations of spiny striatal neurons containing different combinations of the same neurotransmitters (GABA, SP, and ENK) project to both the globus pallidus and the pars reticulata of the substantia nigra (SNr). Striatonigral projections that establish synaptic relationships with cells of the SNr and the GABAergic neurons of the SNr together constitute part of the output system from the basal ganglia. Striatopallidal fibers terminating in the internal pallidal segment (GPi) and the GABAergic pallidal neurons that project to the thalamus form the largest output system from the basal ganglia. Major projections from the SNr and the GPi are to different rostral ventral tier thalamic nuclei, which have projections to different regions of the cortex concerned with motor function.

STRIATOPALLIDAL PROJECTIONS

Striatopallidal fibers are topographically organized in both dorsoventral and rostrocaudal sequences and radiate into various parts of the pallidum like spokes of a wheel (64, 260, 344) (Figs. 16.8 and 19.6). Striatopallidal fibers originating from the caudate nucleus and the rostral part of the putamen (i.e., the associative striatal territory) pierce the internal capsule and penetrate the globus pallidus through its dorsal surface. These caudatopallidal fibers arborize in the form of dense plexuses principally in the rostral pole of the external pallidal segment and, more caudally, in the dorsomedial third of both the external (GPe) and internal pallidal segment (GPi) (Fig. 19.27). Striatopallidal fibers arising from the postcommissural putamen (i.e., the sensorimotor striatal territory) form several distinct fascicles [termed Wilson's pencils after Kinnier Wilson (372)], that pierce the external medullary lamina to reach the globus pallidus through its lateral border. In both segments of the pallidum, the putamenopallidal fibers arborize in elongated bands aligned parallel with the medullary laminae. These bands are confined to the ventrolateral two-thirds of both pallidal segments and do not significantly overlap the areas containing the plexuses formed by caudatopallidal fibers. These findings indicate that axons of striatal neurons located in the associative or sensorimotor striatal territory remain rather well-segregated from one another at pallidal levels (274, 384, 385).

Anterograde labeling studies in monkeys reveal that the axons emerging from a small group of striatal neurons form several band-like terminal fields (or plexuses) that are distributed according to a highly specific rostrocaudal sequence in the globus pallidus (150). Furthermore, anterograde double-labeling studies show that the band-like terminal fields

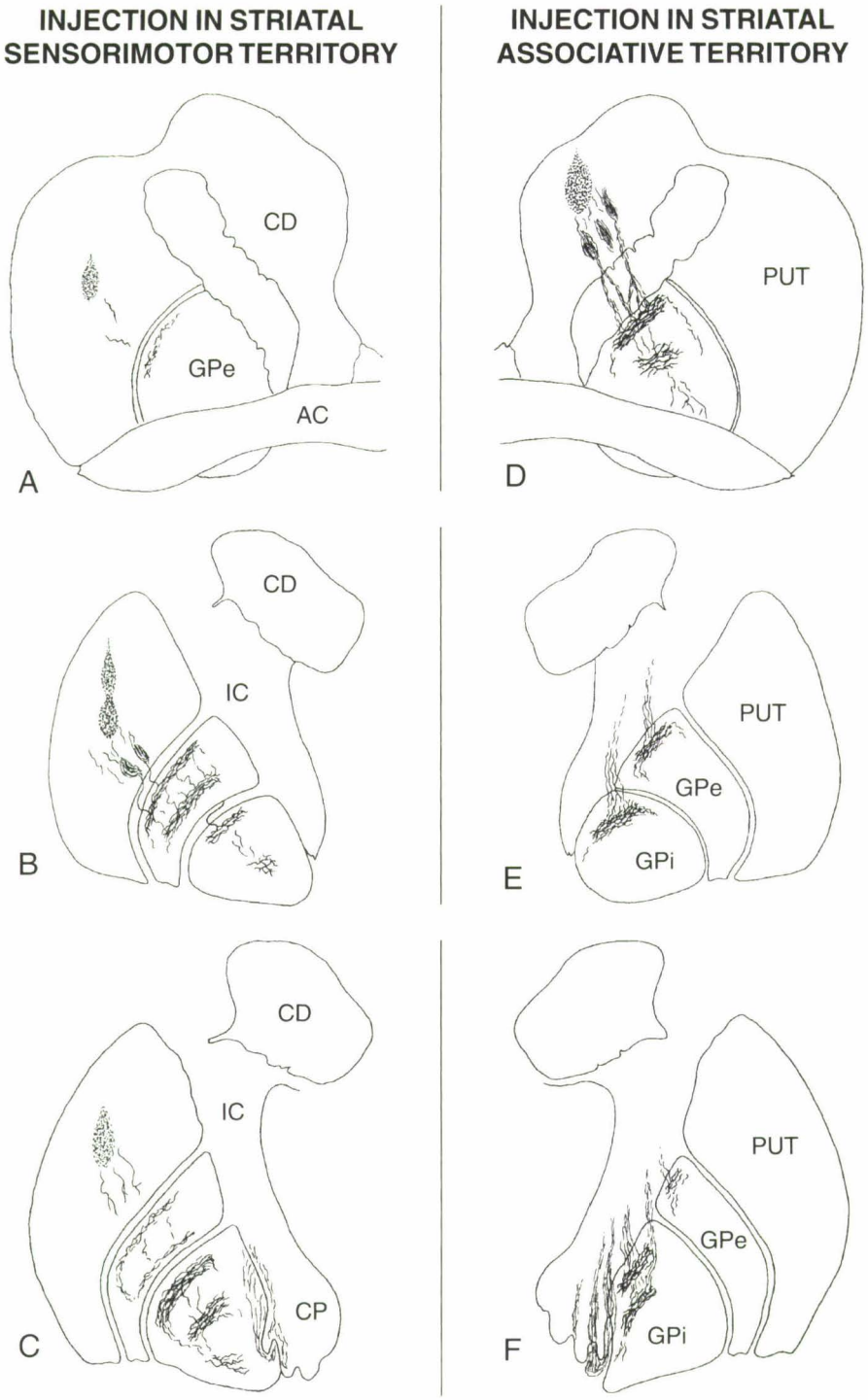


Figure 19.27. Frontal half-sections through the rostral (**A**, **D**), middle (**B**, **E**), and caudal (**C**, **E**) thirds of the striatopallidal complex of the squirrel monkey comparing the distribution of anterogradely labeled fibers resulting from injections of PHA-L in the sensorimotor (**A**–**C**) and associative (**D**–**F**) striatal territories. Fibers emerging from the head of the caudate nucleus terminate in the form of plexuses in the dorsolateral portion of the globus pallidus, whereas those from the postcommissural putamen form bands in the ventrolateral two-thirds of the pallidum. *AC*, anterior commissure; *CD*, caudate nucleus; *GPe*, external segment of globus pallidus; *GPi*, internal segment of globus pallidus; *IC*, internal capsule; *PUT*, putamen.

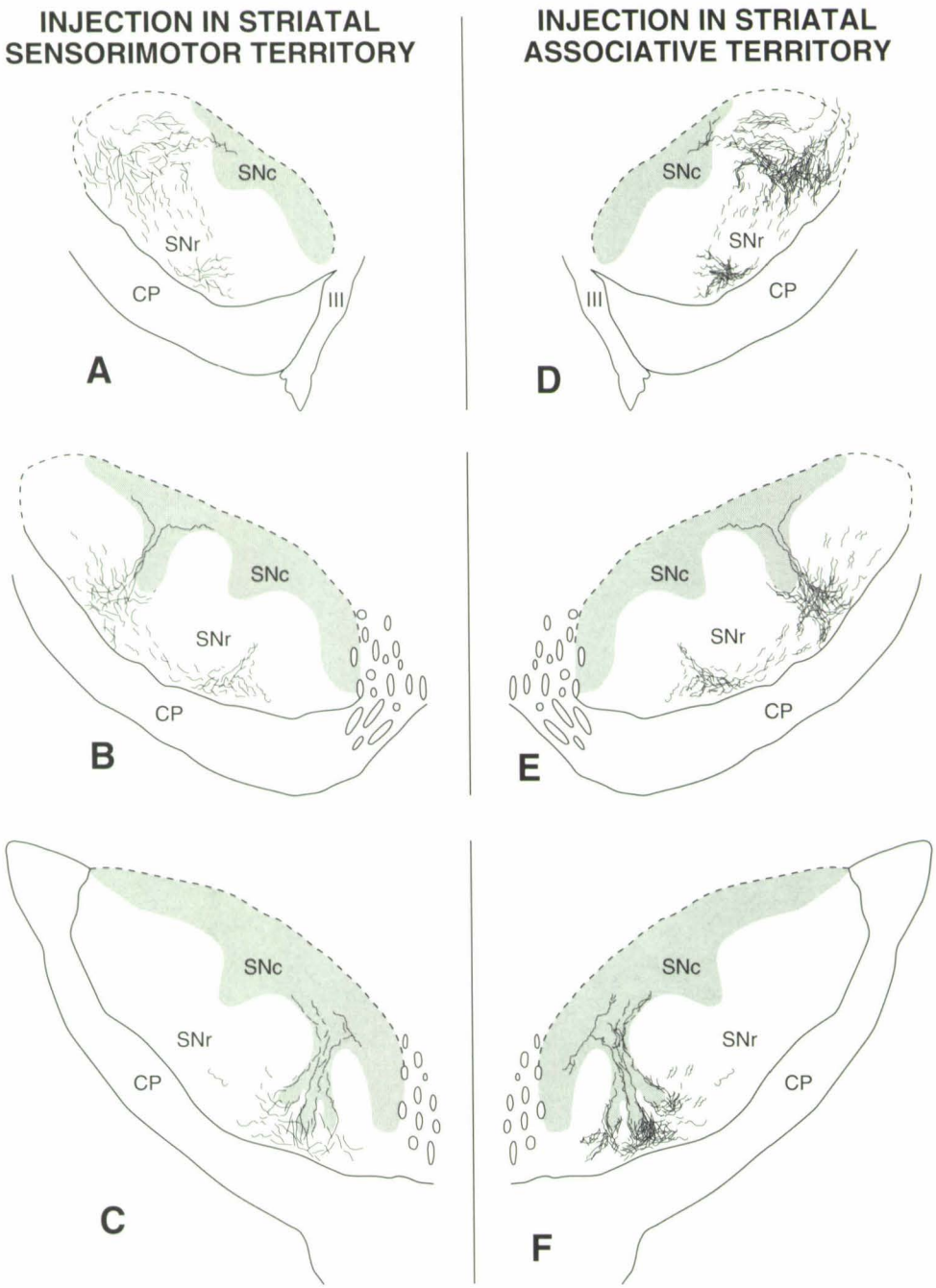


Figure 19.28. Frontal half-sections through the rostral (**A**, **D**), middle (**B**, **E**), and caudal (**C**, **E**) third of the substantia nigra of the squirrel monkey comparing the distribution of anterogradely labeled fibers resulting from injections of PHA-L in the sensorimotor (**A**–**C**) and associative (**D**–**F**) striatal territories. Note that fibers emerging from the head of the caudate nucleus are much more abundant than those from the postcommissural putamen. Both types of fibers form dense plexuses that are distributed along the lateromedial extent of the substantia nigra according to a precise sequence. Many of these plexuses lie at the basis of the pars compacta cell columns that impinge deeply upon the pars reticulata. *CP*, cerebral peduncle; *SNc*, substantia nigra pars compacta; *SNr*, substantia nigra pars reticulata; *III*, oculomotor nerve root fibers.

arising from two adjacent striatal neuronal groups do not overlap but remain well-segregated at pallidal levels (Fig. 19.29) (150). These findings indicate that the striatopallidal projection is a highly patterned neuronal system whereby information from the striatum can be conveyed and integrated in a remarkably precise and ordered manner (281, 384, 385).

The band-like terminal fields formed by putamenopallidal fibers are composed of striatopallidal fibers and their axon collaterals, many of which closely entwine the dendrites of pallidal neurons. The resulting profile, which is typically composed of several thin striatopallidal axons wrapped around an unstained core (the pallidal dendrite), has often

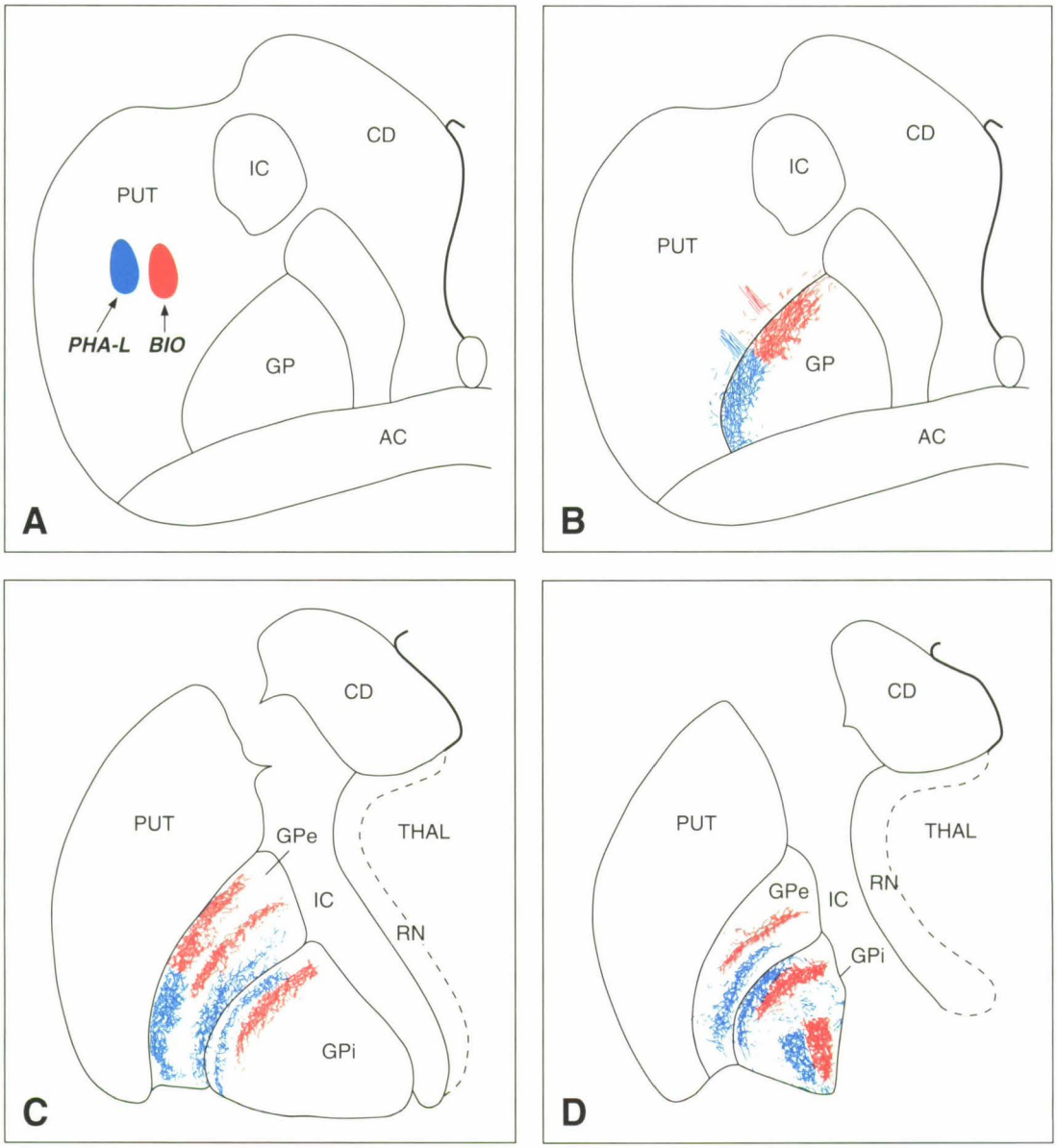


Figure 19.29. Frontal half-sections through the striatopallidal complex of the squirrel monkey illustrating the distribution of anterogradely labeled fibers originating from two adjacent sites in the putamen, one injected with PHA-L (*blue*) and the other with biocytin (*red*). The two types of anterogradely labeled fibers remain segregated at pallidal levels. They form elongated terminal fields that often lie close to one another but do not intermix. This finding underlines the high degree of specificity in the organization of the striatopallidal projection system in primates. *AC*, anterior commissure; *CD*, caudate nucleus; *GP*, globus pallidus; *GPe*, external segment of GP; *GPi*, internal segment of GP; *IC*, internal capsule; *PUT*, putamen; *RN*, reticular thalamic nucleus; *THAL*, thalamus.

been referred to as "woolly" fibers (133). Studies of the termination of striatopallidal fibers at the ultrastructural level indicate that pallidal dendrites are studded with axonal terminals ensheathed with glia. Less frequent axosomatic synapses are seen. Cell bodies have a wrapping of glial processes except over axon terminals (191, 194, 195). The striatopallidal fibers form GABA-positive synapses of the symmetric type with higher order dendrites of pallidal neurons.

It has long been assumed that a single striatal efferent system supplies both the globus pallidus and the substantia nigra through axon collaterals (104, 105, 197). Retrograde double-labeling studies in primates, however, have revealed that striatal projections to the GPe, the GPi, and the substantia nigra arise principally from separate neurons (Fig. 19.30) (91, 275, 286). These findings reveal that the striatofugal system is not a monolithic entity but, instead, appears to be composed of distinct striato-GPe, striato-GPi, and striatonigral subsystems. These findings are in agreement with data on the distribution of various neuropeptides at both pallidal and nigral levels.

As mentioned earlier, all striatal spiny neurons use GABA as an inhibitory neurotransmitter (227, 301, 335). These projection neurons can, nevertheless, be distinguished from each other by their neuroactive peptide content. For instance, striatal neurons projecting to the GPe contain enkephalin, whereas striatal cells projecting to the GPi are enriched with substance P (and dynorphin) (Figs. 19.31 and 19.32**A**, **B**). Regional differences in the distribution and concentration of these two peptides are evident in both pallidal segments. Substance P immunoreactivity in fibers is particularly dense in the apical region of the GPi and enkephalin (ENK) immunoreactive fibers appear most numerous in ventral regions of the GPe caudally (Fig. 19.32**A**, **B**). The ventral pallidum contains numerous SP-, ENK-, and DYN-immunoreactive fibers (131, 134). It is believed that SP, ENK, and DYN fibers, distributed differentially in the two segments of the globus pallidus, play different roles in modifying the distinctive efferent systems of these segments, which arise from intrinsic GABAergic neurons. Comparisons of normal human brains with those from patients with Huntington's disease indicate substantial reductions of SP and ENK in the globus pallidus and substantia nigra (86).

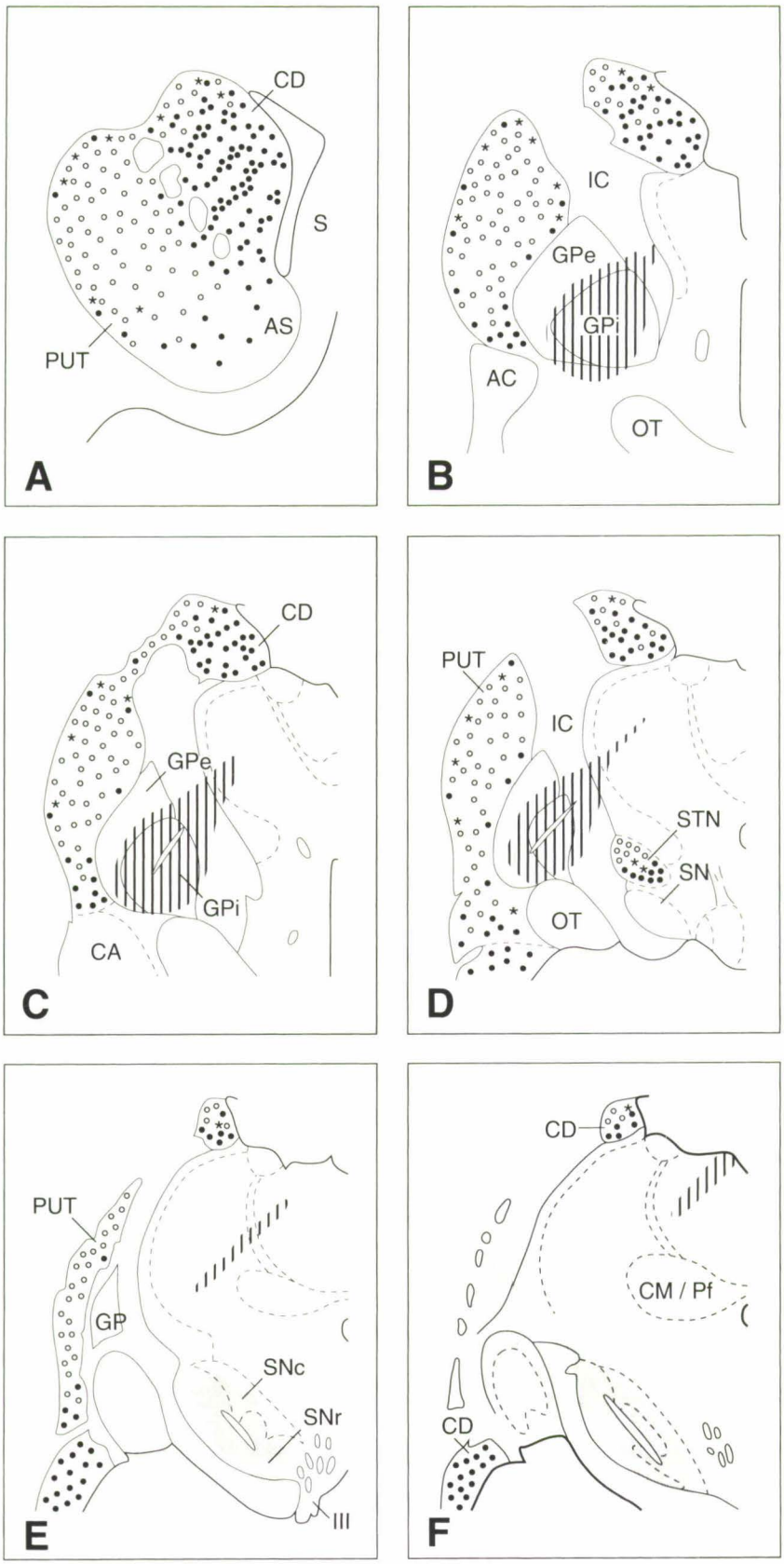
STRIATONIGRAL PROJECTIONS

These fibers originate from spiny striatal neurons and project topographically, mainly on cells of the pars reticulata of the substantia nigra (SNr) (36, 126, 199, 260, 343, 344, 345). Fibers from the head of the caudate nucleus project to rostral parts of the substantia nigra. Putamenonigral fibers passing to more caudal parts of the substantia nigra are arranged so that dorsal parts of the putamen project to lateral parts of the SNr and ventral parts of the putamen are related to medial parts of the SNr. Striatonigral fibers arise from a different population of spiny neurons than striatopallidal fibers but have the same neurotransmitters, namely, GABA, SP, ENK, DYN, and NT (51, 68, 87, 110, 113, 122, 171, 186, 268, 273) (Figs. 19.30–19.32**A**, **B**). Almost all striatonigral fibers terminate in the SNr, but fibers immunoreactive for SP have been identified in both the SNr and the SNc. Neurons in the pars reticulata have smooth dendrites radiating rostrocaudally. Virtually all cells of the SNr are GABAergic (335) and GABAergic fibers and terminals occur in all parts of the SNr. These GABAergic striatonigral fibers form a synapse of the symmetric type with the dendrites of either GABAergic SNr neurons or dopaminergic SNc cells.

Anterograde double-labeling studies in monkeys revealed that the striatonigral fibers terminate in the form of clusters uniformly scattered throughout the SNr (Fig. 19.28) (282). These plexuses are often located at the basis of the dopaminergic cell columns of the SNc. As for the band-like terminal fields formed by putamenopallidal fibers, the striatonigral fiber plexuses are multiple and distributed according to a very precise rostrocaudal sequence. This finding underlines the highly ordered nature of the organization of the striatonigral projection (282, 384, 385).

The GABAergic neurons of the SNr give

Figure 19.30. Injection sites (*hatched* and *stippled* areas) and the rostrocaudal distribution of the retrogradely labeled cells observed in the striatum after injections of fast blue in the substantia nigra and nuclear yellow in the globus pallidus of the squirrel monkey. The striatal neurons containing the tracer injected in the pallidum are represented by *open circles*, those containing the tracer injected in the substantia nigra by *filled circles*, and the double-labeled neurons by *asterisks*. The small number of double-labeled cells encountered after such a double-injection experiment indicates that striatopallidal and striatonigral projections arise largely from distinct striatal populations in primates.


CD
S
AS
PUT
A
IC
GPe
GPi
AC
OT
B
CD
GPe
GPi
CA
C
PUT
IC
STN
SN
OT
D
PUT
GP
SNc
SNr
III
E
CD
CM / Pf
CD
F

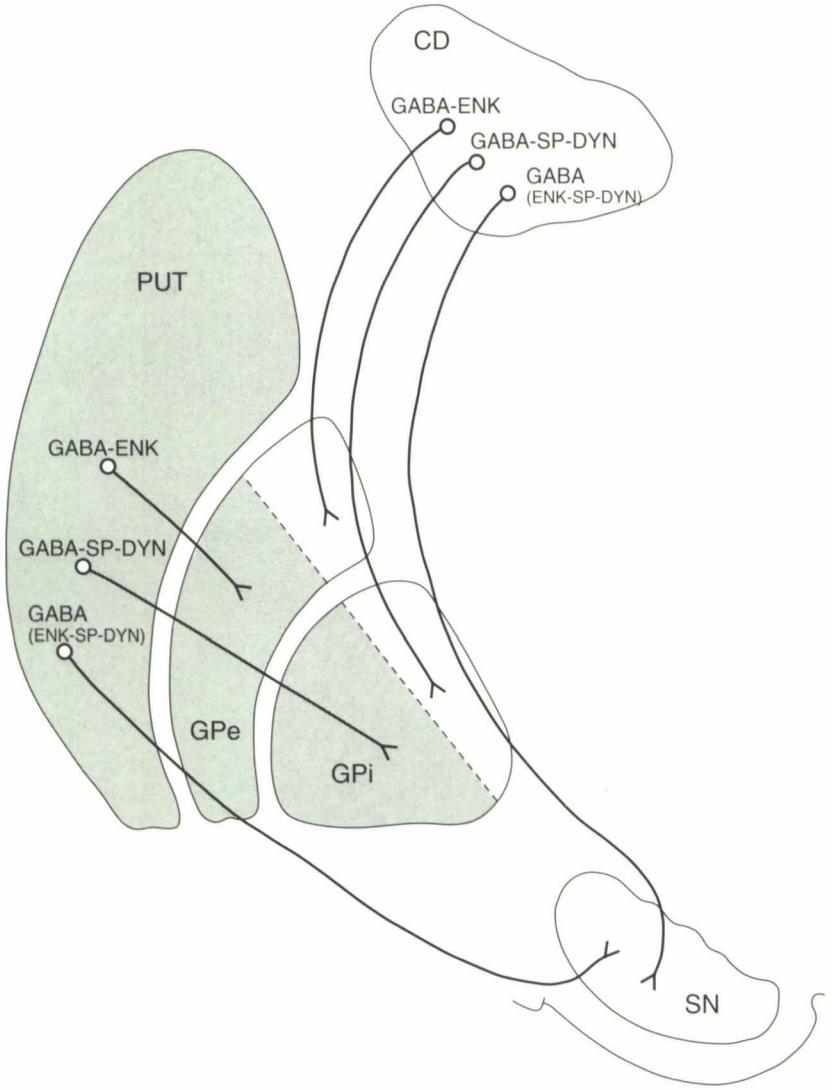


Figure 19.31. Neurochemical content of the striatopallidal and striatonigral pathways. Virtually all striatofugal neurons use γ-aminobutyric acid (*GABA*) as inhibitory neurotransmitter. Several subsets of striatal neurons can nevertheless be distinguished on the basis of their content in neuroactive peptides and their site of termination. At pallidal levels, GABAergic striatal neurons containing enkephalin (*ENK*) project principally to the external pallidal segment (*GPe*), whereas those containing substance P (*SP*) and dynorphin (*DYN*) project mainly to the internal pallidal segment (*GPi*). GABAergic striatonigral neurons are of several sorts, some containing enkephalin, substance P, or dynorphin, or combinations of these peptides. The *dotted line* in the pallidum traces the limit between the associative pallidal sector dorsomedially and the sensorimotor pallidal sector ventrolaterally. *CD*, caudate nucleus; *PUT*, putamen; *SN*, substantia nigra.

rise to nigrothalamic projections that have large numbers of collaterals terminating in middle layers of the superior colliculus and in the midbrain tegmentum. Nigrothalamic fibers terminate in the ventral anterior nucleus (VAmc), parts of the ventral lateral nucleus (VLm), and in parts of the mediodorsal nucleus (MDpl). These thalamic nuclei do not receive afferents from any other part of the basal ganglia.

GLOBUS PALLIDUS

Topography, Development and Intrinsic Organization

This nuclear complex, forming the smaller and inner part of the lentiform nucleus, lies medial to the putamen throughout most of its extent. The dorsomedial margin of the pallidum borders the posterior limb of the inter-

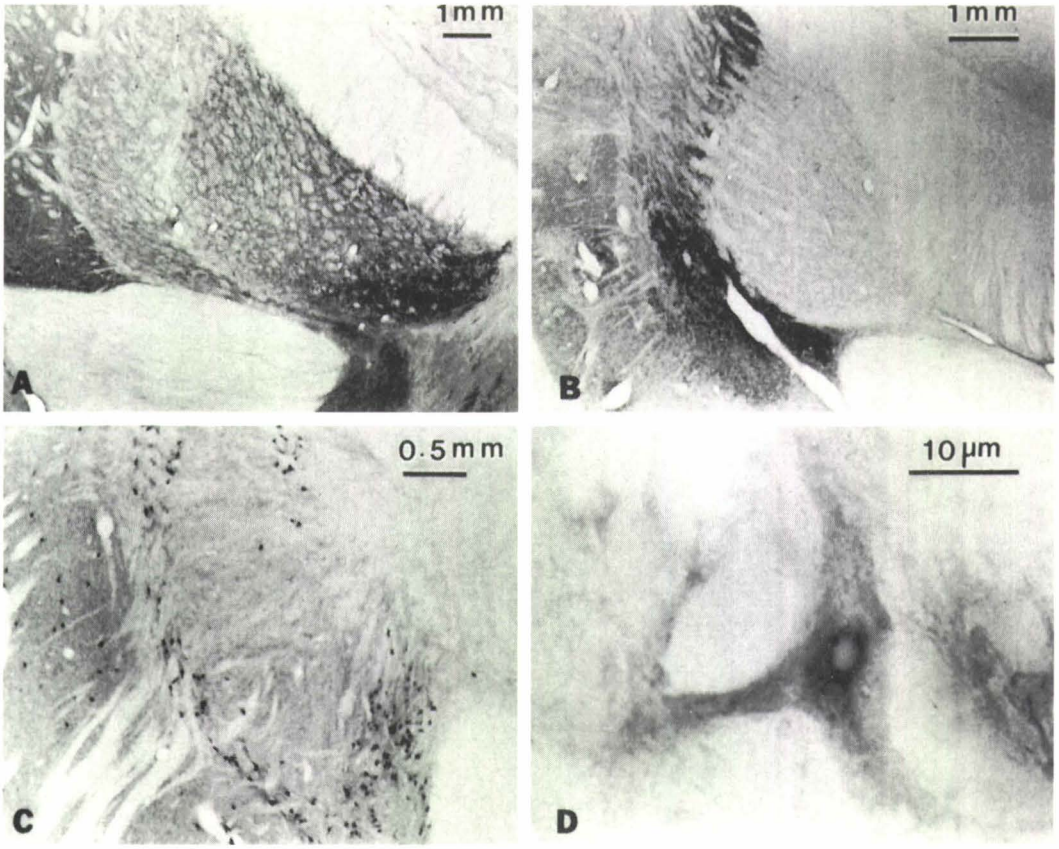


Figure 19.32. Immunohistochemical features of the globus pallidus in the rhesus monkey. **A**. Substance P-immunoreactive fibers confined to the internal pallidal segment are more intensely stained in the apical region. **B**. Enkephalin-immunoreactive fibers and terminals are limited to the external pallidal segment. In the middle third of the external pallidum, immunoreactive fibers are most intense ventrally and near the medullary lamina. **C**. Large cholinergic neurons (choline acetyltransferase (ChAT)-immunoreactive) are abundant in the medullary lamina caudally. These neurons represent a dorsal extension of the basal nucleus of Meynert. ChAT-positive aspiny cells are evenly distributed in the striatum. **D**. A large GABA-immunoreactive neuron characteristic of virtually all pallidal neurons in both segments.

nal capsule. A thin *lateral medullary lamina* lies on the external surface of the pallidum at its junction with the putamen. A *medial medullary lamina* divides the globus pallidus into internal (GPi) and external (GPe) segments (Figs. 19.2, 19.6, 19.33, and 19.34). The two major pallidal subdivisions are also termed medial and lateral segments by some authors. A less distinct *accessory medullary lamina* (214) divides the internal (or medial) pallidal segment into outer and inner portions, which appear to give rise to efferent fibers that have distinctive courses (Fig. 19.33).

Classically, the globus pallidus is considered to be a telencephalic derivative (136). Studies of the ontogenetic development of the globus pallidus and subthalamic nucleus, however, suggest that these structures are diencephalic derivatives (309). During early development the anlage of the corpus subthalamicum and both segments of the pallidum are arranged in a linear fashion with the anlage of the external (or lateral) pallidal segment most rostral, that of the subthalamic nucleus most caudal, and that of the internal pallidal segment (or entopeduncular nucleus in nonprimates) in an intermediate position. In the third month of fetal life, the external pallidal segment migrates rostrolaterally to contact the medial surface of the putamen. The entopeduncular nucleus follows the external pallidal segment rostrolaterally and assumes an adjacent medial or internal position, where it is called the internal (or medial) pallidal segment. The most caudal anlage in this longitudinal hypothalamic zone, the subthalamic nucleus, is pushed medially by invading fibers of the hemispheric stalk and becomes separated from the pallidum by the

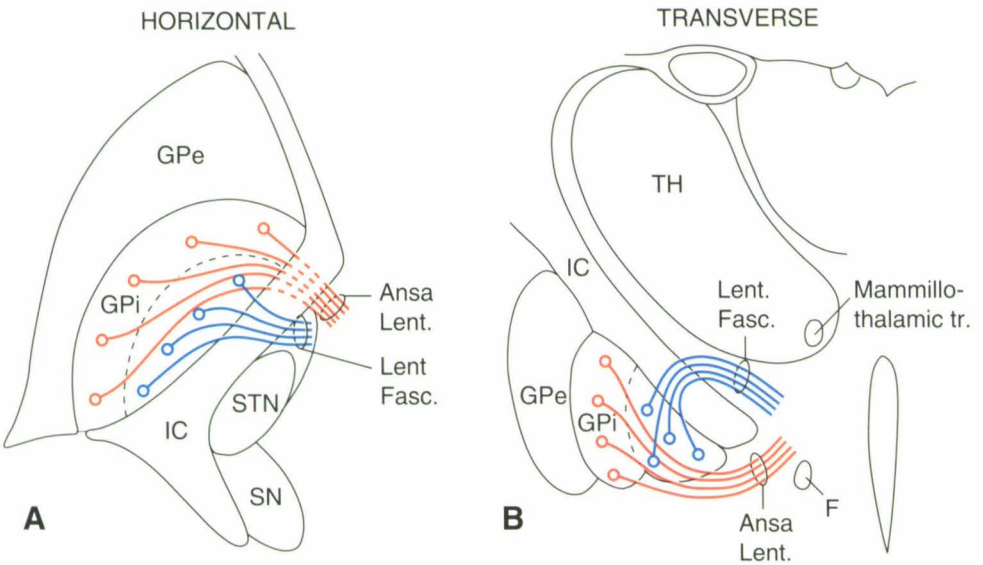


Figure 19.33. Origin and course of pallidothalamic fibers forming the ansa lenticularis and lenticular fasciculus as seen in horizontal (**A**) and transverse (**B**) sections. Fibers of the ansa lenticularis (*red*) arise from the outer portion of the internal pallidal segment (lateral to the accessory medullary lamina, *dashed line*) and course rostrally, ventrally, and medially. Fibers of the lenticular fasciculus (*blue*) arise from the inner portion of the internal pallidal segment (medial to the accessory medullary lamina, *dashed line*) and course dorsally and medially through the fibers of the internal capsule. *F,* fornix; *IC,* internal capsule; *GPe,* external pallidal segment; *GPi,* internal pallidal segment; *SN,* substantia nigra; *STN,* subthalamic nucleus; *TH,* thalamus.

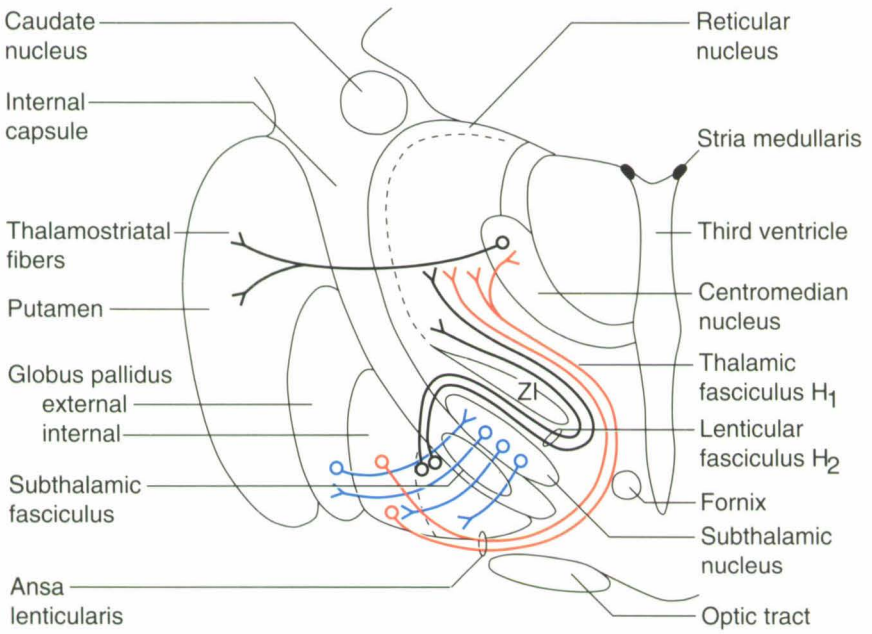


Figure 19.34. Pallidofugal fiber systems in a transverse plane. Fibers of the ansa lenticularis (*red*) arise from the outer portion of the internal pallidal segment, pass ventrally, medially and rostrally around the internal capsule and enter the prerubral field. Fibers of the lenticular fasciculus (H_2, *black*) issue from the dorsal surface of inner part of the internal pallidal segment, traverse the posterior limb of the internal capsule, and pass medially dorsal to the subthalamic nucleus to enter the prerubral field. The ansa lenticularis and the lenticular fasciculus merge in the prerubral field (field H of Forel, not labeled here) and project dorsolaterally as components of the thalamic fasciculus (H_1). Fibers of the thalamic fasciculus (H_1) pass dorsal to the zona incerta (*ZI*). The subthalamic fasciculus (*blue*) consists of pallidosubthalamic fibers arising from the lateral pallidal segment, and subthalamopallidal fibers that terminate in arrays parallel to the medullary lamina in the two pallidal segments. Both components of the subthalamic fasciculus traverse the internal capsule. Thalamostriatal fibers from the centromedian nucleus (*black*) project to the putamen, as part of a feedback system.

internal capsule. Anatomic connections between the subthalamic nucleus and the pallidum are maintained during these migrations by fibers which traverse the peduncular part of the internal capsule.

Many bundles of myelinated fibers traverse the globus pallidus, which in fresh preparations give it a paler appearance than the putamen or caudate nucleus. A morphometric analysis of the human globus pallidus indicates that the GPe constitutes 70% of the total volume of the pallidum and has cell densities which are greater than those for the GPi (323). However, the mean volume of nerve cells in the GPi is 10% higher than in the GPe. Estimates of the total number of pallidal neurons indicate a range of 465,000 to 540,000 for the GPe and 143,000 to 171,000 for the GPi. Golgi studies reveal that pallidal neurons are large ovoid or polygonal cells, 35–50 μm in their long axis, with long, thick, relatively smooth dendrites (102).

The dendrites of the large (principal) pallidal neurons are sparsely branched and often have complex appendages, referred to as "thin processes" or "complex endings" (106). The mean value for the total dendritic length of the large pallidal neurons is about 7600 μm (139, 378). The dendritic arborization of the pallidal neurons in primates is characteristically discoidal, with a mean dimension of 1500×1000×250 μm (378). These large neurons with disk-like dendritic fields are particularly numerous laterally near the medullary laminae, while the more medial pallidal neurons display an oval dendritic field (287). These dendritic disks lie parallel to the border of the pallidum, that is, with their largest surface perpendicular to the incoming striatal axons. They are ideally positioned to intercept the entire proximal arborization of the striatopallidal axons (287, 378).

A rich plexus of afferent fibers invests the long dendrites with an array of longitudinal fibers that bear "boutons en passage." The most prevalent synaptic endings contain large pleomorphic vesicles and a few large dense-core vesicles. These endings make symmetric contacts on dendrites of pallidal neurons (144). No morphologic or chemical differences are evident in the large neurons of the GPi and the GPe—all large neurons within both segments of the globus pallidus are GABAergic (Fig. 19.32**D**). Axons of the pallidal neurons have few collaterals. Large cholinergic neurons in portions of the medial and lateral medullary laminae constitute extensions of the basal nucleus of Meynert, which lies ventral to the globus pallidus (Fig. 19.32**C**) (120, 246, 280).

Afferent Connections

Major afferent fibers to the globus pallidus arise from the striatum and the subthalamic nucleus. Unlike the striatum, the globus pallidus does not receive massive projections from the cerebral cortex or the thalamus.

STRIATOPALLIDAL PROJECTIONS

The striatopallidal fiber system is by far the most massive afferent projection to the globus pallidus. As seen earlier, this projection is topographically organized: efferents from the caudate nucleus occupy the dorsomedial third and those from the putamen the entire ventrolateral two-thirds of the pallidum. The pallidal region receiving putamenal afferents contain neurons whose activity is closely related to body movement (8, 14, 71). The striatopallidal fibers are arranged in the form of bands, parallel to the medullary laminae, a pattern that reflects the discoidal organization of the dendritic domain of pallidal neurons. The remarkable length of the disk-like dendritic fields in planes perpendicular to the striatopallidal border suggest that there is a large degree of convergence in the striatopallidal system (287, 294). However, the fact that efferents from the caudate nucleus and those from the putamen occupy distinct pallidal sectors would indicate that output from the associative striatal territory and that from the sensorimotor territory are processed largely independently in the globus pallidus (274, 281).

SUBTHALAMOPALLIDAL PROJECTIONS

Subthalamopallidal fibers are topographically organized and project to both segments of the pallidum in arrays parallel to the medullary laminae (44, 45, 49, 258, 331) (Fig. 19.41**C**, **D**). The largest number of fibers arise from cells in the lateral two-thirds of the subthalamic nucleus and project to well-defined laminae in dorsal regions of the GPe. Terminals in the GPe closely surround arrays of neurons that project back to the subthalamic nucleus. Reciprocal relationships appear to exist between rostral and central portions of the GPe and the lateral two-thirds of the subthalamic nucleus. A much smaller number of cells in medial regions of the subthalamic nucleus project to the GPi.

Anterograde double-labeling studies in monkeys indicate that the band-like terminal fields formed by the subthalamopallidal fibers are in register with those of the striatopallidal fibers. Furthermore, both inputs converge upon the same pallidal neurons (151, 152, 154) (Fig. 19.43). In contrast to the striatopallidal fibers whose inhibitory action is mediated through GABAergic synapses of the symmetric type, the subthalamopallidal fibers exert an excitatory influence that is mediated through glutamatergic synapses of the asymmetric type (Fig. 19.41**E**, **F**) (334). Thus, the firing pattern of pallidal neurons is the result of a complex interplay between these two functionally opposite inputs (281).

Retrograde double-labeling studies and intracellular labeling experiments in the rat suggested that virtually all neurons of the subthalamic nucleus project to both the globus pallidus and the SNr (202, 356). Similar studies in the primate indicate that only about 10% of the cells in the subthalamic nucleus project to both the globus pallidus and the substantia nigra (Figs. 19.41**A**, **B**, and 19.42) (285).

OTHER PALLIDAL AFFERENTS

The globus pallidus of the monkey receives a dense innervation of dopaminergic fibers that arborize mainly in the GPi. These dopaminergic fibers appear to originate from cells throughout the SNc (220). This projection to the GPi is considered distinct from that of dopaminergic neurons projecting to the striatum (Fig. 19.22) (332). The GPi also receives a serotonergic projection derived from ascending 5-HT fiber bundles (Fig. 19.25) (53, 218). Although cells of the two pallidal segments are morphologically and chemically similar, the activities of GABAergic neurons in each segment appear subject to modulations by different chemospecific afferents.

Efferent Connections

Because they are composed of neurons that are morphologically and chemically identical and receive similar inputs, the two pallidal segments cannot be readily distinguished from another. However, the two pallidal segments markedly differ on the basis of their efferent projections. Fibers arising from cells of the GPi project to thalamic nuclei, the lateral habenular nucleus, and via a descending tegmental bundle to a cell group in the mesopontine tegmentum (Figs. 19.36**B**, 19.37, and 19.38). Thus, the GPi can be viewed, together with the SNr, as a major output component of the basal ganglia. In contrast, the GPe has long been considered as having more limited efferent projections than the GPi. It is reciprocally linked with the subthalamic nucleus, thus forming part of the well-known pallido-subthalamo-pallidal loop, one of the many closed ancillary systems that are so characteristic of the basal ganglia circuitry (273). Anterograde and retrograde labeling studies, however, have shown that the GPe project to a wide variety of structures, including the substantia nigra (277, 283), the striatum (285), the reticular thalamic nucleus (148), and the GPi (Fig. 19.39) (155). The latter projection forms large, GABAergic, symmetric synapses around the cell bodies and proximal dendrites of pallidal neurons (Fig. 19.40). The GPe is thus in an ideal position to modulate and even shunt the activity of the output neurons of the GPi. Moreover, this GPe-GPi projection allows the striatum to exert a double effect on GPi neurons (a) a direct inhibitory effect upon the distal dendrites of pallidal neurons mediated through the direct striatopallidal projection, and (b) an indirect disinhibitory effect upon the soma and proximal dendrites of pallidal neurons mediated through a relay in the GPe (281) (Fig. 19.43). In light of these findings, the GPe can no longer be considered as a mere relay in the pallido-subthalamo-pallidal loop. Instead, it should be regarded as a structure that exerts an important control upon the information that flows along the main axis of the basal ganglia.

The efferent fibers from the two pallidal segments can be divided into four main bundles: (a) the *ansa lenticularis*, (b) the *lenticular fasciculus*, (c) the *pallidotegmental fibers*, and (d) the *pallidosubthalamic fibers*. The first three of these arise exclusively from the GPi (Figs. 19.33–19.35) (42, 49, 199, 244, 260, 305). Pallidosubthalamic fibers arise exclusively from the GPe (Figs. 19.33 and 19.36**A**) (44, 45, 226). Pallidofugal fibers are arranged in a rostrocaudal sequence with the ansa lenticularis most rostral, the lenticular fasciculus in an intermediate position and pallidosubthalamic fibers most caudal.

ANSA LENTICULARIS

Fibers of the ansa lenticularis arise from lateral portions of the GPi and form a well-defined bundle on the ventral surface of the pallidum (Figs. 19.33–19.35). Fibers sweep

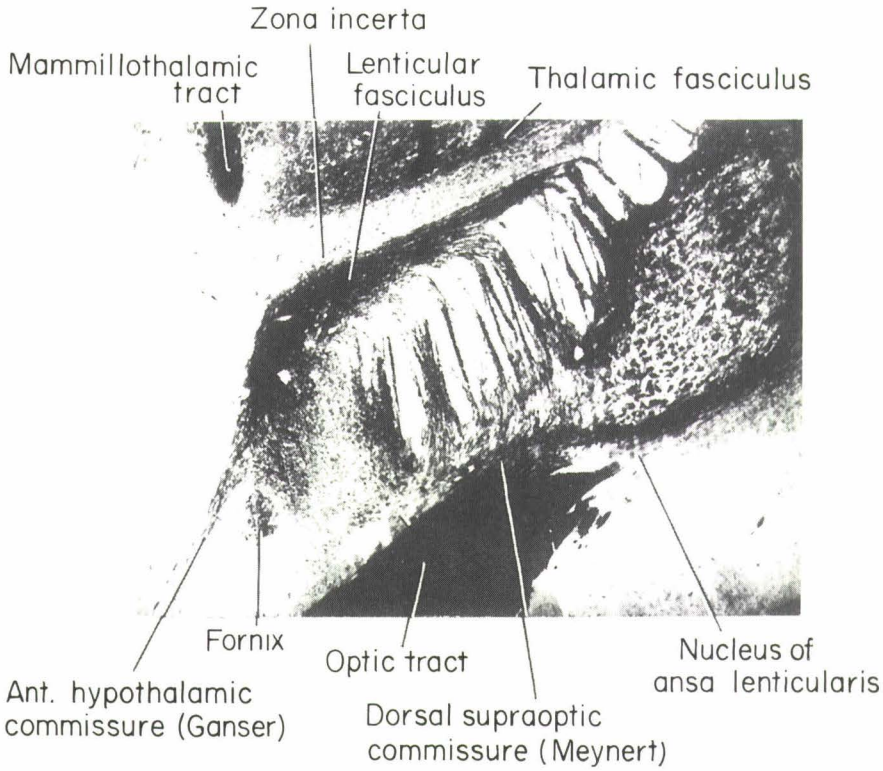


Figure 19.35. Lenticular fasciculus in a decorticate rhesus monkey. Fibers of this bundle can be seen passing through the degenerated internal capsule. At this level, immediately rostral to the subthalamic nucleus, the lenticular fasciculus lies on the inner aspect of the internal capsule ventral to the zona incerta. (Weigert's myelin stain.)

ventromedially and rostrally around the posterior limb of the internal capsule and then course posteriorly to enter Forel's field H.

LENTICULAR FASCICULUS

These fibers arise from inner portions of the GPi, emerge from the dorsomedial margin of the pallidum, slightly caudal to the ansa lenticularis, and traverse ventral parts of the internal capsule in a number of small fascicles (Figs. 19.33–19.35). Fibers cross through the internal capsule immediately rostral to the subthalamic nucleus and form a discrete bundle ventral to the zona incerta (Fig. 19.35). Although most of the lenticular fasciculus lies rostral to the subthalamic nucleus, some fibers of this bundle course along its dorsal border. Fibers of the lenticular fasciculus are referred to as Forel's field H2. While fibers of the lenticular fasciculus pursue a distinctive course through the internal capsule, they pass medially and caudally to join fibers of the ansa lenticularis in Forel's field (H) (prerubral field). Fibers of the lenticular fasciculus (H2) and the ansa lenticularis, which merge in Forel's field H, ultimately enter the thalamic fasciculus (Forel's field H1) located dorsal to the zona incerta (Figs. 19.34 and 19.35).

Investigations of the origin of pallidothalamic fibers in the monkey indicate that fibers emerging via the ansa lenticularis and the lenticular fasciculus arise from specific portions of the GPi (42, 214). These data indicate that fibers of the ansa lenticularis arise predominantly from the outer part of the GPi (i.e., from that part of the GPi lateral to the accessory medullary lamina). These fibers course rostrally, ventrally and medially, and traverse portions of the GPi (Fig. 19.33). Fibers of the lenticular fasciculus arise largely from the inner part of the GPi (i.e., from the portion medial to the accessory medullary lamina). These fibers course dorsally, rostrally and medially and traverse the peduncular part of the internal capsule (Fig. 19.33).

THALAMIC FASCICULUS

Pallidofugal fibers from Forel's field H pass rostrally and laterally along the dorsal surface of the zona incerta where they form part of the thalamic fasciculus (Figs. 19.34 and 19.35). Some of the fibers of the lenticular

fasciculus merely make a C-shaped loop around the medial part of the zona incerta and enter the thalamic fasciculus (Figs. 19.34 and 19.36**B**). The thalamic fasciculus contains pallidothalamic fibers, as well as ascending fibers from the contralateral deep cerebellar nuclei. This composite bundle projects dorsolaterally over the zona incerta to terminate in specific nuclear subdivisions of the rostral ventral tier thalamic nuclei (260). In the region dorsal to the zona incerta, where fibers of this bundle are distinct and separate from those of the lenticular fasciculus (Figs. 19.34 and 19.35), the thalamic fasciculus is designated as bundle H1 of Forel.

PALLIDOTHALAMIC PROJECTIONS

Pallidothalamic fibers project to the ventral anterior (VApc, pars principalis) and ventral lateral (VLo, pars oralis) thalamic nuclei (Figs. 16.13, 19.36**B**, and 19.38**A**) and give off collaterals to the centromedian (CM) nucleus (Figs. 19.34 and 19.38**B**). Pallidal projections to the rostral ventral tier thalamic nuclei are topographically organized (199, 214). Pallidothalamic terminations do not overlap the crossed projections from the deep cerebellar nuclei or the ascending projections from the substantia nigra (169, 170, 293, 352, 353). Each of these ascending systems terminates in separate divisions of the thalamic nuclei. The ventral lateral thalamic nucleus, particularly the pars oralis (VLo), projects to the supplementary motor area on the medial aspect of the hemisphere and to the lateral premotor area (area 6).

Retrograde labeling studies in monkeys confirmed that pallidal projections to the ventral tier nuclei of the thalamus and the CM nucleus arise largely from the axon collaterals of the same neurons in the GPi (276). These branched neurons are located in the central portion of the GPi (Fig. 19.37). Anterograde labeling studies in nonhuman primates showed that the pallidothalamic fibers that reach the ventral tier nuclei arborize according to a pattern that is strikingly different from that of the fibers terminating in the CM nucleus (149). Pallidothalamic fibers form multiple small clusters in the VA/VL nuclei, whereas they display a much more linear pattern, indicative of terminals *en passant*, in the CM nucleus. Furthermore, there is a significant proportion (approximately 10–20%) of the GPi efferent fibers that cross the midline to reach the contralateral ventral tier nuclei (149, 384, 385). These contralateral pallidothalamic fibers arborize in patterns that are similar to those disclosed ipsilaterally (see Chapter 16).

PALLIDOHABENULAR PROJECTIONS

Fibers from the GPi projecting to the lateral habenular nucleus separate from the ansa lenticularis and the lenticular fasciculus in Forel's field H and course through and around the medial part of the internal capsule to enter the stria medullaris (47, 260). Autoradiographic studies in the cat stress the substantial nature of this bundle and the diverse routes followed by different components (217, 257). Injections of HRP confined to the lateral habenular nucleus in the rat label large numbers of cells in the entopeduncular nucleus (the homologue of the primate GPi) and lesser numbers of cells in the lateral hypothalamus, the nuclei of the diagonal band, the substantia innominata and the lateral preoptic area (161, 217). In primates, however, the pallidohabenular projection is much less prominent than in rats and cats (272, 279). It arises from a small subset of pallidal neurons distributed peripherally in the Gpi (Fig. 19.37). These neurons are distinct from those giving rise to the pallidothalamic fibers (276).

The habenular nuclear complex is an epithalamic structure considered to be an integral part of the limbic system (see Chapters 16 and 18). In the habenular complex, the enzyme glutamic acid decarboxylase (GAD) is contained in terminals about cells of the lateral nucleus (121). Sources of GABAergic fibers projecting to the lateral habenular nucleus are multiple and include pallidohabenular fibers and fibers in the stria medullaris. Histofluorescent, histochemical, and sensitive biochemical microassay techniques reveal several neurotransmitters and their synthesizing enzymes in the habenular nuclei, including catecholamines, serotonin, choline acetyltransferase, acetylcholine, and substance P, in addition to GAD. It has been suggested that projections of the GPi to the lateral habenular nucleus may be involved in a circuitry that functions in conjunction with the limbic system (257).

PALLIDONIGRAL PROJECTIONS

Most of the evidence supporting a pallidonigral pathway has been based upon the retrograde transport of HRP from the substantia nigra to the GPe (36, 126, 187, 226, 277,

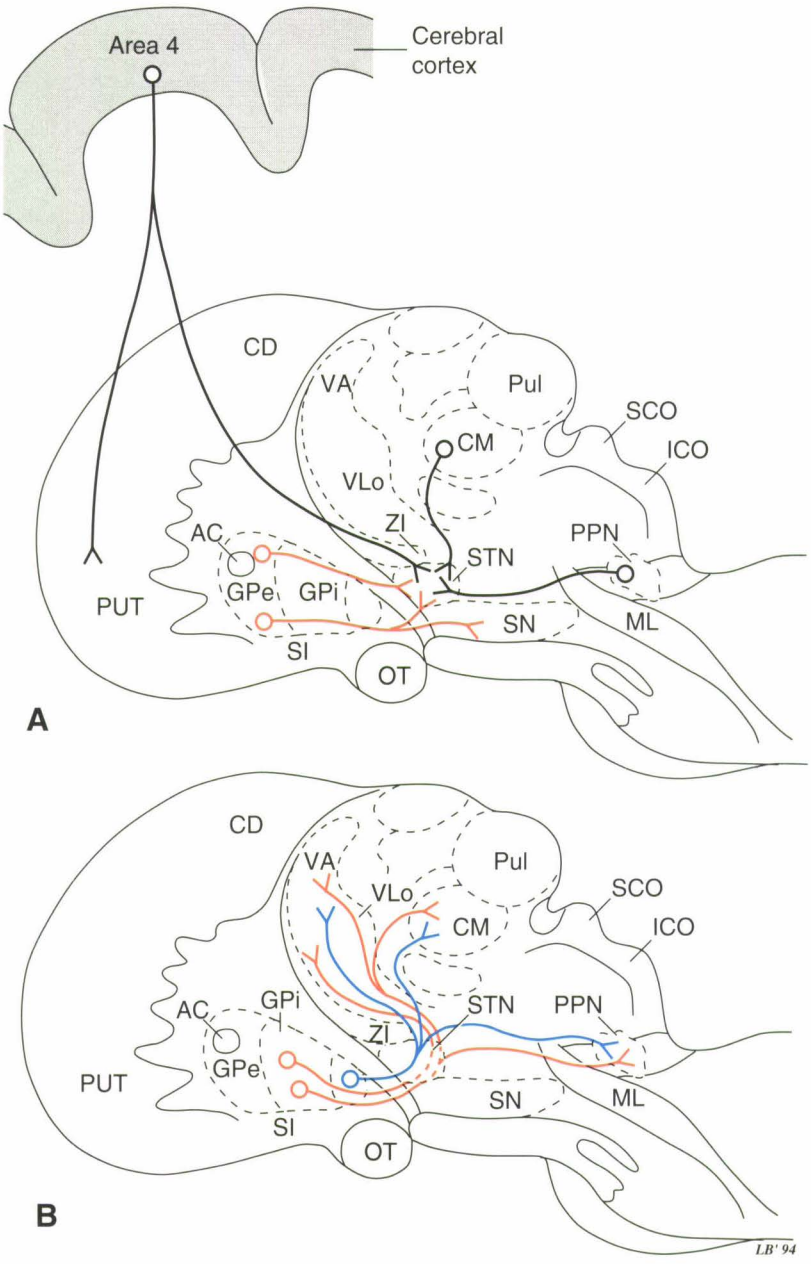


Figure 19.36. Afferent projections of the subthalamic nucleus (**A**) and efferent projections of the internal pallidal segment (**B**) shown in a sagittal plane. The subthalamic nucleus (*STN*) receives afferents from a wide variety of sources, including the motor areas of the cerebral cortex (*black*) and the external segment of the globus pallidus (*GPe*) (*red*). The internal segment of the globus pallidus (*GPi*) is, together with the substantia nigra pars reticulata, a major output nucleus of the basal ganglia. Its neurons send axons (*red* and *blue*) that branch to the ventral tier and centromedian thalamic nuclei (*VA, VLo,* and *CM*), and to the pedunculopontine nucleus (*PPN*). *AC,* anterior commissure; *CD,* caudate nucleus; *GPe,* external segment of globus pallidus; *IC,* internal capsule; *ICO,* inferior colliculus; *ML,* medial lemniscus; *OT,* optic tract; *Pul,* pulvinar; *PUT,* putamen; *SCO,* superior colliculus; *SI,* substantia innominata; *SN,* substantia nigra; *ZI,* zona incerta.

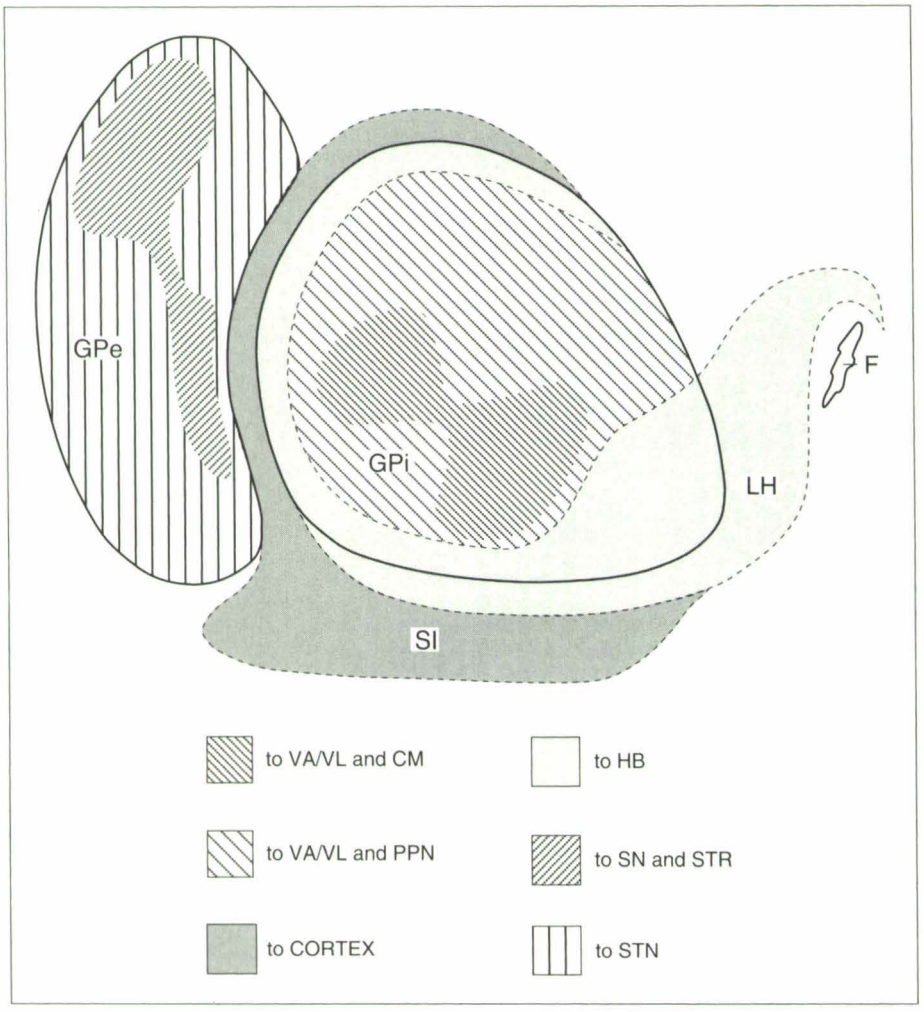


Figure 19.37. Output organization of the globus pallidus in primates based on its main efferent projections as revealed by fluorescent retrograde double-labeling studies. The various *stippled* and *hatched* areas indicate the zones of origin of the major pallidal efferents. *CM,* centromedian thalamic nucleus; *F,* fornix; *GPe,* external segment of globus pallidus; *GPi,* internal segment of globus pallidus; *HB,* habenula; *LH,* lateral hypothalamus; *PPN,* pedunculopontine nucleus; *SI,* substantia innominata; *SN,* substantia nigra; *STN,* subthalamic nucleus; *STR,* striatum; *VA* and *VL,* ventral anterior and ventral lateral thalamic nuclei.

283). Retrograde transport studies suggest that most pallidonigra fibers terminate in the SNr. Autoradiographic studies in the rat employing 6-hydroxydopamine (6-0HDA) to produce degeneration in cells of the SNc suggest that pallidonigral fibers terminate preferentially upon dopaminergic cells in the substantia nigra (146). Pallidonigral fibers are considered to have GABA as their neurotransmitter (147, 227). These fibers are distinguished from striatonigral fibers, which also have GABA as their neurotransmitter, by their termination mainly upon cells of the SNr.

PALLIDOTEGMENTAL PROJECTIONS

These fibers (Fig. 19.39**B**), derived from the GPi (214, 260), become identifiable as a separate bundle dorsomedial to the subthalamic nucleus. The fibers of this bundle descend along the ventrolateral border of the red nucleus and, in the caudal midbrain tegmentum, they sweep dorsolaterally to terminate principally upon large cells of the pedunculopontine nucleus (PPN). This nucleus is partially embedded in fibers of the superior cerebellar peduncle (271). Studies in monkeys indicate that cells in the GPi have di-

chotomizing axons that project the same signal to thalamic nuclei and to the PPN (277).

Although the pedunculopontine nucleus receives its largest input from the medial pallidal segment, it also receives projections from the cerebral cortex (142, 215) and the substantia nigra (21, 44, 45, 157, 166, 174, 252). Projections of the PPN appear to be mainly ascending, with the largest number of ascending fibers projecting to the SNc, although a significant number of fibers project to the GPi and the subthalamic nucleus (Fig. 19.20) (21, 44, 45, 79, 174, 219, 252, 264). Connections between the pedunculopontine nucleus and the substantia nigra are not reciprocal in the strict sense, since nigrotegmental fibers arise from cells of the SNr and ascending projections from the pedunculopontine nucleus end upon cells of the SNc (21, 219, 252).

Large cells in the PPN are strongly cholinergic. In the rat, cholinergic cells of PPN are considered to project mainly to the ventrolateral thalamic nuclei. Noncholinergic neurons in and around this nucleus are described as projecting to the basal ganglia and related nuclei (221). In monkeys, the major projection of the PPN is to the ipsilateral substantia nigra and this projection is at least in part cholinergic (219). Glutamate is also present in neurons of the PPN, including the cholinergic neurons (219). Thus, the PPN may exert a dual cholinergic and glutamatergic excitatory effect upon nuclei of the basal ganglia. Special interest in the PPN region centers around locomotor activity produced by electrical stimulation. Also worth noting is the demonstration of a direct projection from the deep cerebellar nuclei to the PPN in monkeys (153). This projection indicates that the PPN may act as an important functional interface between the two major subcortical systems involved in the control of motor behavior, that is, the cerebellum and the basal ganglia.

SUBTHALAMIC FASCICULUS

The subthalamic fasciculus consists of pallidofugal fibers that pass through the internal capsule to enter the subthalamic nucleus, and of fibers from the subthalamic nucleus that project back to the globus pallidus.

Pallidosubthalamic fibers, arising only from the GPe, project upon cells of the subthalamic nucleus (44, 45, 47, 49, 260, 305). These fibers are topographically organized. Rostral parts of the GPe project to medial and rostral parts of the subthalamic nucleus. Cells in the central division of the GPe (flanking the GPi) project to the lateral third of the subthalamic nucleus throughout most of its rostrocaudal extent. Pallidosubthalamic fibers traverse ventromedial and caudal parts of the internal capsule, caudal to both the ansa lenticularis and the lenticular fasciculus (Fig. 19.34). Pallidal neurons projecting to the subthalamic nucleus are GABAergic. Sensitive anterograde tracing techniques indicate that neurons in the GPe projecting to the subthalamic nucleus emit collaterals that arborize in lateral parts of the SNr.

Subthalamopallidal fibers also traverse the ventromedial and caudal parts of the internal capsule but in the opposite direction. They are distributed to both pallidal segments where they terminate in the form of vertically

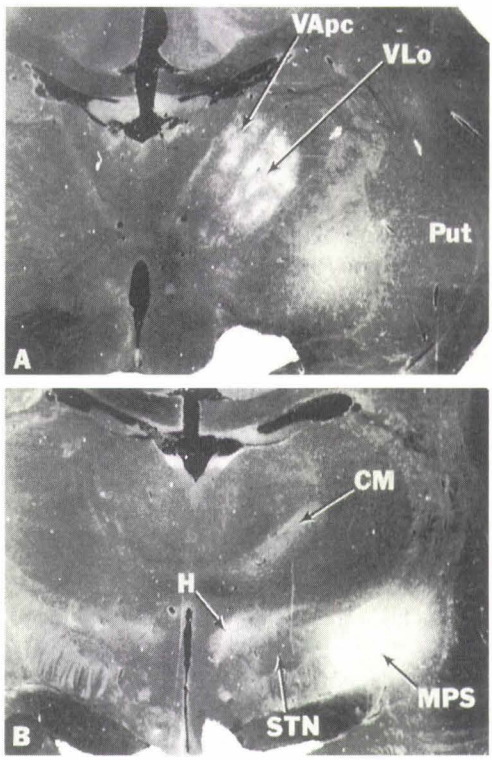


Figure 19.38. Sections through the diencephalon in a rhesus monkey demonstrating transport of (^{3}H) amino acids from the internal (or medial) pallidal segment (*MPS*) to thalamic nuclei. **A.** Transported radioactive label is distributed in a patchy fashion to the pars oralis of the ventral lateral (*VLo*) and to the principal part of the ventral anterior nuclei (*VApc*) of the thalamus. **B.** The central region of the injection in the medial pallidal segment and modest transport of the label to the centromedian nucleus (*CM*) of the thalamus. Radioactive label also is seen in Forel's field H and in lateral parts of the subthalamic nucleus (*STN*). *Put* indicates putamen. Cresyl violet, ×3.5.

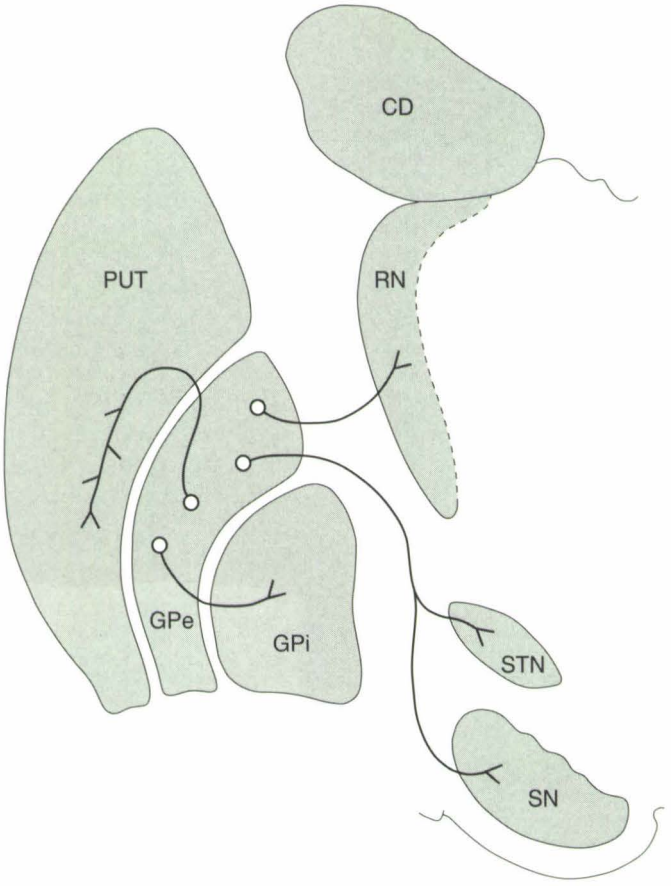


Figure 19.39. Efferent projections of the external pallidal segment (*GPe*). This structure, once believed to be locked in a closed loop with the subthalamic nucleus (STN), is now known to be the source of projections to the substantia nigra (*SN*), striatum (putamen (*PUT*) and caudate nucleus (*CD*)), reticular thalamic nucleus (*RN*), *STN*, and the internal segment of the globus pallidus (*GPi*).

elongated bands (44, 45, 49, 258, 331). As mentioned earlier, the band-like terminal fields formed by the subthalamopallidal fibers are in register with those of the striatopallidal fibers, and both subthalamopallidal and striatopallidal fibers converge upon the same pallidal neurons (151, 152, 281).

SUBTHALAMIC REGION

The subthalamic region lies ventral to the thalamus, medial to the internal capsule, and lateral and caudal to the hypothalamus (Figs. 2.29, 16.5, 16.6, and 19.34). Nuclei found within the subthalamic region include the subthalamic nucleus, the zona incerta, and the nuclei of the tegmental fields of Forel (nucleus campi Foreli, Forel's field H). Fiber bundles passing through this region include the ansa lenticularis, the lenticular fasciculus (Forel's field H2), the thalamic fasciculus (Forel's field H1), and the subthalamic fasciculus (Fig. 19.34).

Subthalamic Nucleus

The subthalamic nucleus *(corpus Luysi)*, located on the inner surface of the peduncular portion of the internal capsule, has the shape of a thick biconvex lens (Figs. 2.29, 16.5, 16.6, 16.10, 16.11, 19.34, 19.38, and A.20). Caudally, the medial part of the nucleus overlies rostral portions of the substantia nigra .

The subthalamic nucleus is considered to be derived from the dorsocaudal part of the lateral hypothalamic cell column (209, 210). Richter (309) describes the subthalamic nucleus as arising from the "subthalamic longitudinal zone," along with both segments of the pallidum. The anlage of the subthalamic

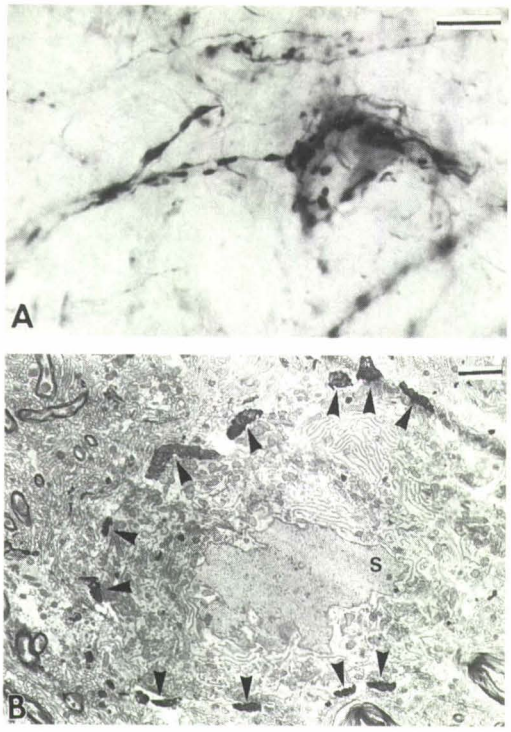


Figure 19.40. Dense pericellular innervation formed by the pallido (*GPe*)-pallidal (*GPi*) projection at light (**A**) and electron microscopic (**B**) levels. Axons of neurons in the external segment of the globus pallidus (*GPe*) give rise to large terminal boutons that closely surround the soma and proximal dendrites of neurons in the internal segment of the globus pallidus (*GPi*). These large terminal boutons (*arrowheads* in **B**) can be seen to be closely apposed to the soma (*S*) of a GPi neuron at the electron microscopic level. Scale bars = 10 μm (**A**) and 4 μm (**B**).

nucleus, caudal to that of both pallidal segments, is said to mature before either the globus pallidus or the substantia nigra.

Cells of the subthalamic nucleus are spindle-shaped, pyramidal, or round with branching processes, but form a single population of neurons (377). Fusiform cells are seen near the margins of the nucleus, oriented parallel to capsular fibers. All cells contribute to an extremely rich neuropil, and there are mediolateral differences in cell size and concentrations (99, 207). The principal elements of the subthalamic nucleus are long-axoned projection neurons whose sparsely spined dendrites extend for more than 750 μm (302). In some ways, they resemble nigral and pallidal neurons except that their dendrites are much thinner (106, 294, 302). Each neuron of the subthalamic nucleus gives rise to six or seven stem dendrites that branch successively in an ellipsoidal domain parallel with the rostrocaudal axis of the nucleus (302, 377). While subthalamic nucleus neurons in rat and primate are similar, their relationships to the nucleus as a whole have evolved to confer upon the primate the potential for a much more specific organization.

The subthalamic nucleus receives a rich blood supply derived from branches of the posterior communicating, posterior cerebral, and anterior choroidal arteries (98). It has a consistent distribution in mammals, being rudimentary in rodents and carnivores, but well-developed in primates. While the nucleus is small in monkeys, its relative size is essentially the same as in humans (362, 369).

Cells of the subthalamic nucleus were shown to contain glutamate and to exert excitatory effects on pallidal and nigral neurons (Fig. 19.41**E**, **F**) (334). This structure is considered as one of the "driving forces" of the basal ganglia (203, 384, 385).

Connections of the Subthalamic Nucleus

AFFERENT CONNECTIONS

The major afferent projections to the subthalamic nucleus are derived from (a) the precentral motor cortex and other regions of the frontal lobe, (b) the GPe, and (c) the pedunculopontine nucleus. Other less prominent afferents arise from the midbrain raphe nuclei and the CM-Pf complex of the thalamus (Fig. 19.36).

Autoradiographic studies in the monkey reveal that the precentral motor cortex projects somatotopically upon a restricted lateral part of the subthalamic nucleus (3, 141). In this projection, fibers from the face area terminate laterally within the nucleus, while fibers from the leg area end in a more medial region. Less substantial projections from the premotor and prefrontal cortex end in more medial parts of the subthalamic nucleus (168, 212, 213, 339). Thus, as is the case for the striatum, the topographically organized corticosubthalamic projection imposes upon the subthalamic nucleus a specific functional subdivision. Indeed, this nucleus can be divided into a large dorsolateral sector corresponding to the sensorimotor territory and a smaller ventromedial sector corresponding to the associative territory (Fig. 19.42). Cells in the dorsolateral sector of the subthalamic nucleus

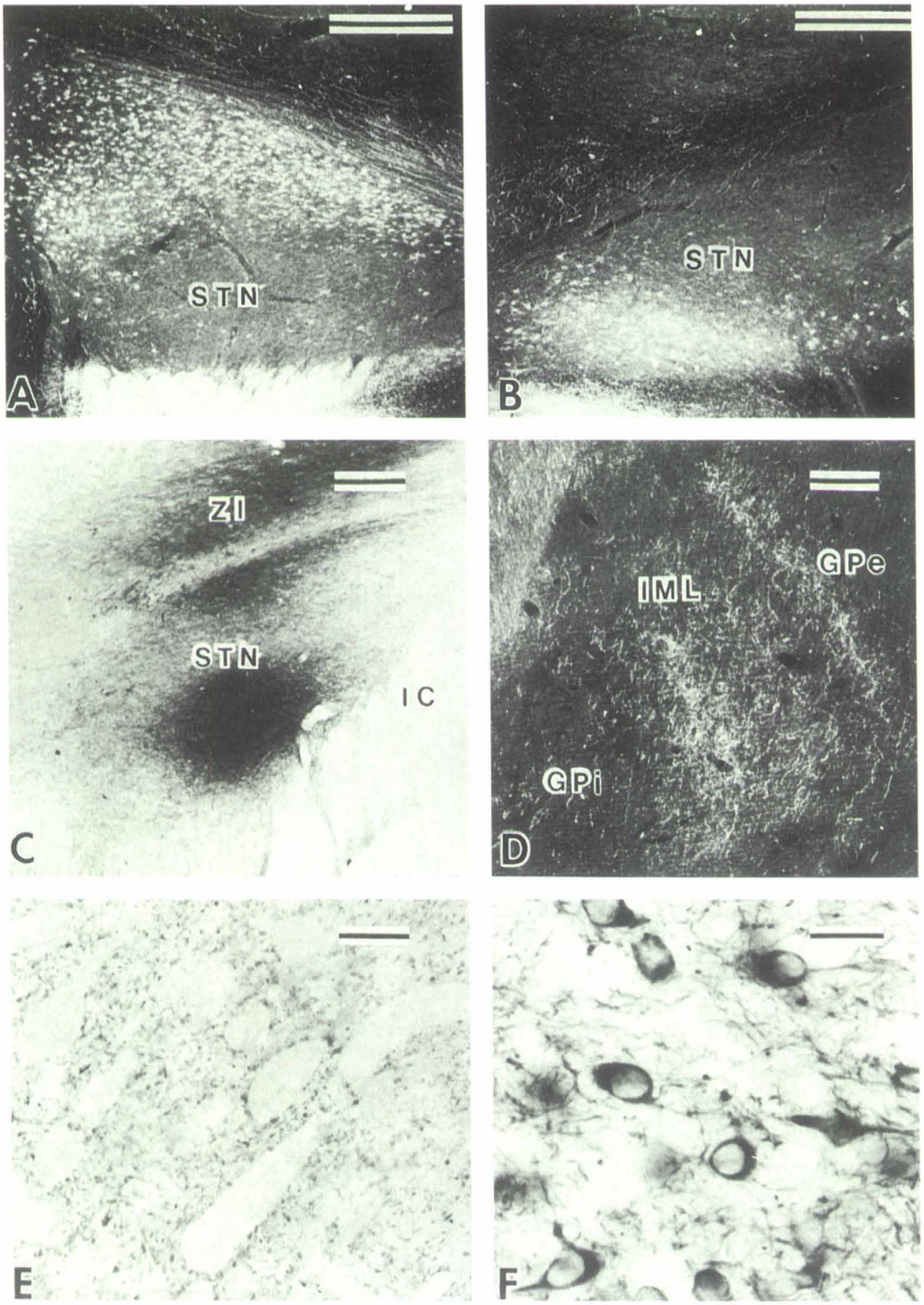


Figure 19.41. **A, B.** Darkfield photomicrographs showing the large number of retrogradely labeled cells observed in the dorsolateral (sensorimotor) sector subthalamic nucleus (*STN*) after WGA-HRP injections in the left putamen (**A**) compared to a much smaller number of labeled cells in the ventromedial (associative) portion of the nucleus after injection in the right caudate nucleus (**B**) in the squirrel monkey. **C, D.** Examples of PHA-L injection site in the core of the subthalamic nucleus (**C**) and of the type of anterograde fiber labeling it has produced in the internal (*GPi*) and external (*GPe*) pallidal segments (**D**). **E, F.** Examples of immunohistochemical staining for GABA (**E**) and for glutamate (**F**) in the subthalamic nucleus. Note that cell of the subthalamic nucleus are closely surrounded by numerous GABA-immunoreactive terminals but do not themselves display GABA immunoreactivity (**E**). By contrast, cells of the subthalamic nucleus are strongly immunoreactive for glutamate (**F**). *IC,* internal capsule; *IML,* internal medullary lamina; *ZI,* zona incerta. Scale bars = 500 μm (**A–C**), 50 μm (**D**), and 30 μm (**E, F**).

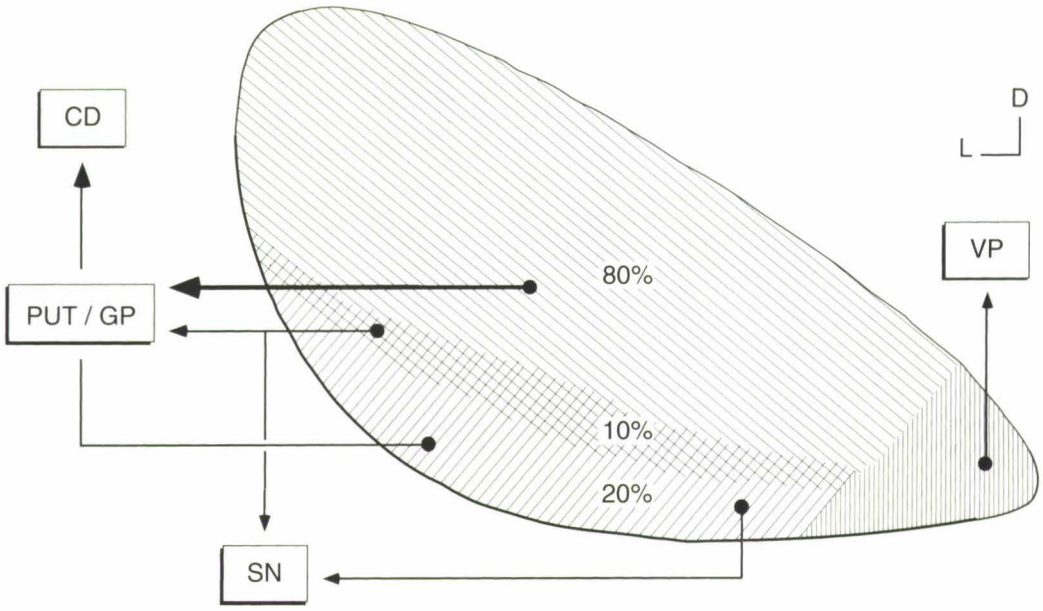


Figure 19.42. Major organizational features of the subthalamic nucleus in primates as revealed after study of the efferent projections of this nucleus with retrograde double-labeling methods. The relative proportion (%) occupied by each major sector of the subthalamic nucleus, including the area of overlap between the sensorimotor and associative territories, is indicated. The medial tip of the nucleus is believed to represent the limbic territory. *CD,* caudate nucleus; *GP,* globus pallidus; *PUT,* putamen; *SN,* substantia nigra; *VP,* ventral pallidum.

change their discharge rate during skeletal movements and in response to somatosensory stimulation (70, 114), whereas those in the ventromedial sector are activated principally during visuo-oculomotor tasks (237). Thus, the dorsolateral sector (sensorimotor territory) of the subthalamic nucleus appears more specifically involved in the control of skeletomotor behavior, whereas the ventromedial sector (associative territory) is more concerned with oculomotor and associative aspects of motor behavior (237). The medial tip of the nucleus, which receives projections from limbic cortices and ventral (subcommissural) pallidum (125), could represent the limbic territory of this structure.

Electron microscopic studies indicate that cortical influences upon subthalamic nucleus neurons are mediated by thin myelinated and unmyelinated axons that terminate in small round boutons on spines and small dendrites (314). Attempts to determine the lamina of origin of corticosubthalamic projections in the cat and monkey by retrograde transport of HRP have been inconclusive (226, 311), but the corticosubthalamic projection appears to be composed mainly of collaterals of fibers destined to other loci.

The GPe is the source of the largest number of subcortical afferents to the subthalamic nucleus (44, 45, 47, 79, 226, 260). Cells in the GPe are arranged in arrays parallel to the lateral medullary lamina and in monkeys have a rostrocaudal organization in which fibers from (a) the rostral division of the GPe (i.e., the part rostral to the medial medullary lamina) project to the medial two-thirds of the subthalamic nucleus, and (b) the central division of the GPe (i.e., the part lateral to the medial medullary lamina) project to the lateral third of the nucleus (44, 45, 47). These fibers traverse the GPi and the peduncular part of the internal capsule en route to the subthalamic nucleus. Retrograde transport studies using HRP in the cat suggest a mediolateral topographic relationship between the subthalamic nucleus and the GPe (226).

The pedunculopontine nucleus (PPN), which receives inputs from the cerebral cortex, the internal pallidal segment, and the SNr, projects directly to the subthalamic nucleus (Fig. 19.36**A**) (44, 45, 219, 252, 264, 311). This projection is rather massive in monkeys and involves the entire subthalamic nucleus (219). The presence of numerous cholinergic fibers in the human subthalamic nucleus (240) indicates that cholinergic neurons of the PPN may participate in this projection.

The subthalamic nucleus also receives a dense serotoninergic innervation in monkeys. Numerous serotonin-immunoreactive fibers and axon terminals occur throughout the entire subthalamic nucleus in primates (218). These fibers most likely belong to neurons of the midbrain dorsal raphe nucleus. In contrast, the subthalamic nucleus in monkeys is only poorly innervated by catecholaminergic neurons (220).

A relatively small, but definite, projection from the centromedian/parafascicular nuclear complex (CM-Pf) has been established in the monkey, cat, and rat (92, 317, 319, 320). These thalamosubthalamic fibers appear to exert a glutamate-mediated excitatory effect upon neurons of the subthalamic nucleus (253).

EFFERENT PROJECTIONS

Efferent fibers from the subthalamic nucleus traverse the internal capsule, enter caudal parts of the GPi, and radiate into all parts of the globus pallidus. This massive projection is composed of fibers that are arranged in arrays parallel to the medullary laminae of the pallidum (Fig. 19.41**C**, **D**) (44, 45, 258, 331). Retrograde transport studies using HRP indicate the topographic organization of this

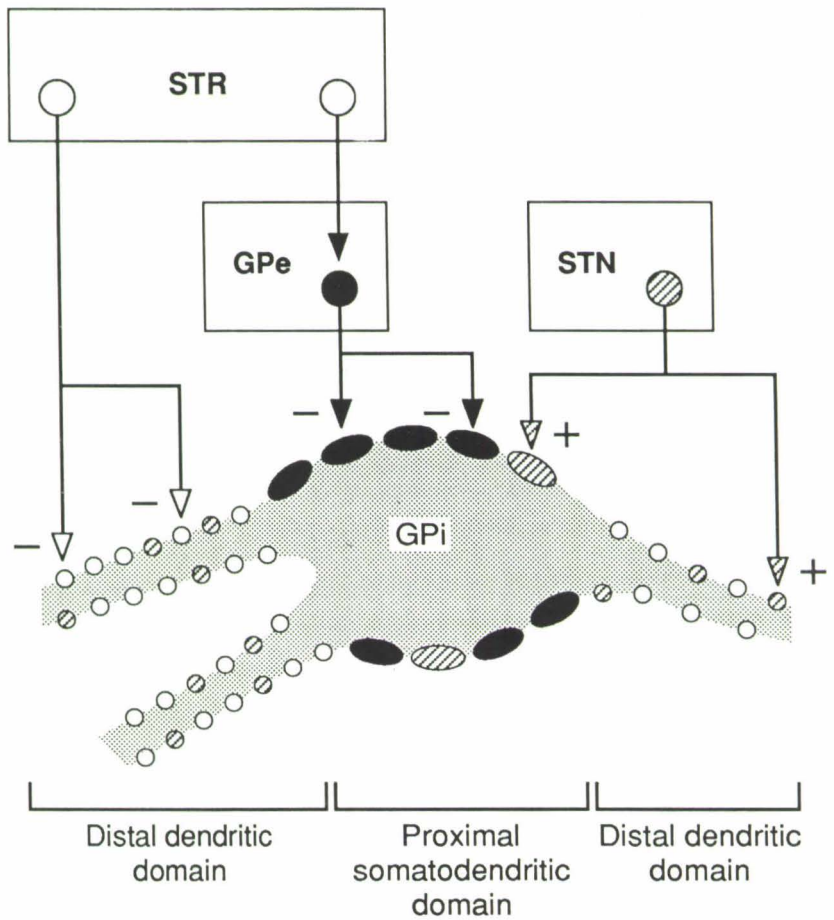


Figure 19.43. Location of terminal boutons deriving from various sources and apposed to different regions of an internal pallidal (*GPi*) neuron that can be regarded as a typical output element of the basal ganglia. The inputs from the striatum (*STR*), the external pallidum (*GPe*), and the subthalamic nucleus (*STN*) are illustrated in *white*, *black*, and *hatched black*, respectively. The net effects of each of these inputs upon the output neuron are indicated by plus (glutamate-mediated excitation) and minus (GABA-mediated inhibition) signs. The drawing emphasizes the complex interplay between the opposite actions of STN and STR inputs on the same basal ganglia output neuron. It also indicates the crucial position occupied by the GPe-GPi projection, which could modulate or even shunt the effects of other inputs to the GPi neuron. Some important connections between various basal ganglia components, such as the massive and reciprocal relation between STN and GPe, are deliberately omitted from the diagram to keep it readable.

projection (44, 45). Cells in medial and caudal parts of the subthalamic nucleus project mainly to the GPi, while cells in the central third of the nucleus project to the GPe. Few cells in the lateral third of the subthalamic nucleus project to any part of the globus pallidus. The observation that subthalamic afferent and efferent fibers terminate and arise in different parts of the nucleus suggest that this relatively small structure is not homogeneous and that reciprocal circuits between the GPe and the subthalamic nucleus probably involve interneurons.

Subthalamic nucleus neurons also project fibers to the SNr (73, 137, 187, 258, 331, 369). A fluorescent retrograde double-labeling study in the rat suggests that single subthalamic nucleus neurons project fibers to both the globus pallidus and the substantia nigra (356). In monkeys, however, subthalamic projections to the pallidum and the substantia nigra appear to originate from distinct cell populations in the subthalamic nucleus (285, 286). Ultrastructural studies in rats reveal that the subthalamic nucleus terminals in the substantia nigra form asymmetric synapses mainly with dendritic shafts and, to a lesser extent, with the soma of SNr neurons. Synaptic boutons of subthalamic origin contain small pleomorphic vesicles and display glutamate immunoreactivity (52, 203, 312). Because the subthalamic nucleus projects to both the globus pallidus and the SNr, it is believed to modulate the activities of neurons which collectively constitute the output system of the entire basal ganglia. Electrophysiologic studies in the rat have suggested that the efferent projections of the subthalamic nucleus control the initiation of movement by setting the physiologic conditions (i.e., membrane potential or modulatory effects on synaptic transmission) of pallidal and nigral neurons to the appropriate level prior to the arrival of striatal signals (201, 384, 385).

The subthalamic nucleus also gives rise to efferents that arborize within the striatum. The subthalamostriatal projection is relatively scarce by comparison with the subthalamopallidal and subthalamonigral projections (203, 331). In monkeys, neurons of the subthalamic nucleus that project to the caudate nucleus and the putamen lie respectively within the associative and sensorimotor territories of the subthalamic nucleus (Fig. 19.42). Anterograde tract-tracing studies with the plant lectin *Phaseolus vulgaris* (PHA-L) reveal that, despite their relatively low density, subthalamostriatal axons are scattered over wide areas of both the caudate nucleus and the putamen. These fibers are long, varicose, and poorly branched. In rodents, subthalamostriatal fibers appear to target specifically the somatostatinergic cells of the striatum. This glutamatergic input may play a role in the regulation of the activity of striatal neurons, in conjunction with the more massive cortical and thalamic excitatory afferents.

In humans, relatively discrete lesions in the subthalamic nucleus, usually hemorrhagic, give rise to violent, forceful, and persistent choroid movements, referred to as *hemiballismus*. These unusually violent involuntary movements occur contralateral to the lesion and involve primarily axial and proximal musculature of the upper and lower extremities, although they may involve the facial and cervical musculature as well (65, 176, 232, 249, 365, 368).

Zona Incerta

The zona incerta is a strip of gray matter situated between the thalamic and lenticular fasciculi (Figs. 16.6, and 19.34–19.36). It is composed of diffuse cell groups that laterally are continuous with the thalamic reticular nucleus. Neurons of the zona incerta can be distinguished from those of the reticular thalamic nucleus by the fact that they display immunoreactivity for the calcium-binding protein calbindin D-28k (250). Neurons of the reticular thalamic nucleus are immunoreactive for the calcium-binding protein parvalbumin but not for calbindin. The zona incerta receives corticofugal fibers from the precentral cortex.

Prerubral Field (Forel's Field H)

Forel's field H *(prerubral field)* contains pallidofugal fibers and scattered cells that constitute the nucleus of the prerubral field (nucleus campi Foreli). The nuclei of the prerubral field (Figs. 16.6 and 16.10), together with similar cells scattered along pallidofugal pathways, are collectively referred to as the *subthalamic reticular nucleus.*

The lenticular fasciculus, ansa lenticularis, and thalamic fasciculus constitute the largest and best-defined fibers of passage in the subthalamic region. Scattered along and between the fibers of the ansa lenticularis are strands of cells which collectively constitute the so-called *nucleus of the ansa lenticularis* (310).

VENTRAL STRIATOPALLIDAL COMPLEX

Ventral Striatum

During the last few years, it became well-established that both the striatum and pallidum extend to the ventral surface of the brain in the region of the olfactory tubercle or the anterior perforated substance in primates (10, 11). Taking into account the fact that both the nucleus accumbens and the olfactory tubercle have striking embryologic, cytologic, histochemical, and hodologic features in common with the striatum, Lennart Heimer and colleagues proposed that the two structures be referred to as the ventral striatum (10, 11, 132, 158, 159). Because of a similar pattern of extrinsic connections, the ventromedial portion of the striatum proper is also included in the concept of the ventral striatum.

Ventral Pallidum

The ventral pallidum was originally defined on the basis of its cytologic and ultrastructural features, and delimited by mapping the terminal fields of its afferents from the two major components of the ventral striatum—the nucleus accumbens and the olfactory tubercle (158, 159). The ventral pallidum occupies a rather extensive area beneath the anterior commissure, which is generally referred to as the substantia innominata. The results of histochemical and immunohistochemical studies in the rat clearly demonstrate that the globus pallidus extends in a rostral and ventral direction toward the surface of the brain in the region of the olfactory tubercle (89, 342). Thus, the ventral extension of the striatum (ventral striatum) is accompanied by a ventral extension of the pallidum (ventral pallidum), and the topographic relationship between the striatum and the pallidum at dorsal levels is maintained throughout the ventral extension of the striatopallidal complex in the olfactory tubercle and the substantia innominata (158). Although the concept of a striatopallidal complex was formulated following observations and experiments on the rat brain, the ventral striatum and ventral pallidum appear to exist in all mammals, including human and nonhuman primates (11, 132).

Connections

There is a remarkable parallel between the neuronal connections of the ventral striatopallidal complex and those of the striatum and pallidum (Fig. 19.44). For instance, inputs from the cerebral cortex, thalamus, and midbrain converge on the ventral striatum, which is thus the major receptive component of the ventral striatopallidal complex. The ventral striatum largely corresponds to the limbic striatal territory defined earlier.

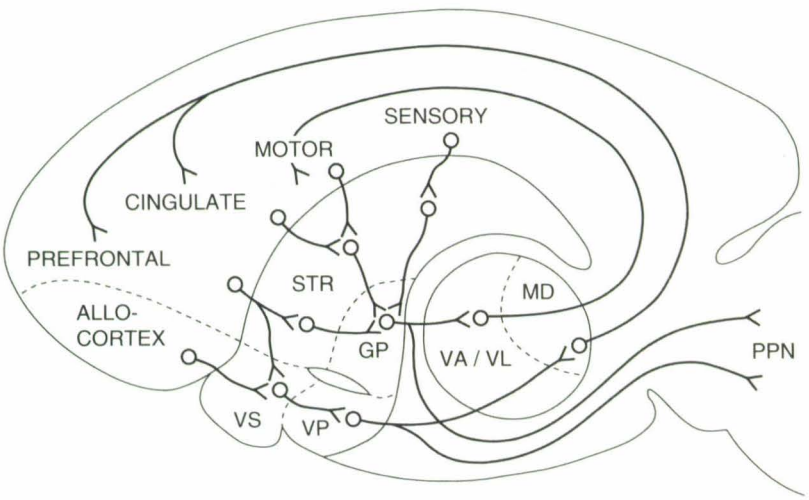


Figure 19.44. Sagittal view of the circuitry of the ventral striatopallidal complex, which parallels that of the dorsal striatopallidal system (see text for further details). *GP*, globus pallidus; *MD*, mediodorsal thalamic nucleus; *PPN*, pedunculopontine nucleus; *STR*, striatum; *VA* and *VL*, ventral anterior and ventral lateral thalamic nuclei; *VP*, ventral pallidum; *VS*, ventral striatum.

Cortical projection to the ventral striatum, that is, the olfactory tubercle and the nucleus accumbens, are complementary to those terminating in the striatum proper. They arise mostly from the prefrontal, insular, primary olfactory, perirhinal, entorhinal, subicular, and hippocampal cortices (11). Hence, the inputs that are channeled through the ventral striatum come not only from the hippocampus and olfactory cortex, but also from other limbic cortices and the temporal association cortex. These projections are thus part of a more global corticostriatal system that includes the entire cortical mantle (158). As seen earlier, the olfactory tubercle and the nucleus accumbens also receive projections from the basolateral amygdaloid nuclei.

Thalamic projections to the ventral striatum arise principally from the paraventricular and medial parafascicular nuclei and from various midline nuclei (178). The major midbrain afferent to the ventral striatum originates from the dopaminergic neurons of the ventral tegmental area. A smaller contribution from neurons of the medial substantia nigra, the retrorubral area, and the dorsal raphe nucleus has also been reported.

In turn, the ventral striatum projects massively to the ventral pallidum, substantia nigra, ventral tegmental area, and mesopontine tegmentum. The efferent projections of the ventral striatum, particularly those of the nucleus accumbens, are said to largely avoid the GPi, except its medial tip, and to terminate in a region of the substantia nigra-ventral tegmental area complex considerably larger than that from which it receives nigrostriatal fibers (261). This suggests that the nigro-striato-nigral loop associated with the ventral striatum may not be organized in a mode of point-to-point reciprocity.

As noted earlier, the ventral pallidum receives a massive projection from the ventral striatum. Like the GPi, the ventral pallidum projects to the thalamus (381). Its major termination site, however, is not the ventral tier nuclei but the mediodorsal nucleus, which in turn projects to the prefrontal cortex and other limbic cortical areas known to send inputs to the ventral striatum (360). Furthermore, there is evidence for descending projections from the ventral pallidum, similar to the prominent pallidotegmental system arising from the GPi and terminating in the pedunculopontine nucleus (Fig. 19.44) (251). In rats, descending projections from the ventral pallidum are known to reach the so-called mesencephalic locomotor region (MLR) located in the pedunculopontine area (111, 112, 251). This projection supports the hypothesis that limbic structures, such as the hippocampus, can influence somatomotor activities by way of the nucleus accumbens and its efferent projections to the ventral pallidal area (376).

Chemical Anatomy

The concept of the ventral striatopallidal complex has received strong support from studies of neurotransmitter localization within the basal forebrain. These investigations reveal that the ventral striatum and ventral pallidum are distinct among basal forebrain structures in their high content of neurochemicals. For example, the ventral striatum displays among the highest levels of acetylcholinesterase and dopamine of the entire forebrain (89). Additionally, high levels of the enzyme choline acetyltransferase (ChAT), glutamic acid decarboxylase (GAD), the neuropeptide cholecystokinin (CCK), and neurotensin occur in the ventral striatum (273). Neurotensin and CCK are largely related to the ascending neuronal systems in the ventral tegmental area.

The ventral pallidum is characterized by high iron content, and the distribution of ferric iron in the basal forebrain of rats provides evidence that the globus pallidus indeed extends rostroventrally beneath the anterior commissure and into the olfactory tubercle (342). The presence of dense plexuses of GAD, substance P, and enkephalin-immunoreactive fibers is also highly characteristic of the ventral pallidum (133, 342). It is believed that these immunoreactive fibers originate from the adjoining ventral striatum (133). Furthermore, there is both pharmacologic and electrophysiologic evidence supporting the GABAergic nature of projections from the ventral striatum to the ventral pallidum and substantia nigra.

Possible Roles

The corticosubcortical loop through the ventral striatopallidal complex and the mediodorsal thalamus closely parallels the more classic loops through the main dorsal part of the basal ganglia and ventral tier thalamic nuclei. This input to the ventral stri-

atopallidal system is largely related to the olfactory and limbic systems, while the rest of the striatopallidal system is more closely linked to the sensorimotor and association cortices (11, 158). The ventral striatopallidal system is believed to exist in parallel with the dorsal striatopallidal system for the planning and initiation of movements. More specifically, the dorsal striatopallidal system is thought to play a prominent role in initiating motor behavior that stems from cognitive activities, while the ventral striatopallidal system is involved in initiating movements in response to stimuli that are motivationally and emotionally significant (158).

CLAUSTRUM

The claustrum is a thin strip of gray matter that lies in the white matter of the hemisphere between the lentiform nucleus and the insular cortex. It is separated from these structures by the external capsule medially and the extreme capsule laterally (Figs. 2.13, 19.1, and 19.2). Although situated close to the striatum, its principal connections are with the cerebral cortex and this structure bears striking resemblance with the thalamus. Two distinct parts of the claustrum are recognized: (a) an insular part composed of large cells underlying the insular cortex, and (b) a temporal part located between the putamen and the temporal lobe (33, 256).

The cerebral cortex projects in a gross topographic fashion upon the claustrum (84, 85, 256) and may be the site of convergence of polymodal afferents from the sensory cortex. Observations based upon the retrograde transport of HRP indicate that cells in the claustrum project to widespread regions of the cerebral cortex (265, 308). These observations suggest a reciprocal relationship between the claustrum and sensory areas of the cortex. Studies indicate that projections from the striate and peristriate cortex end in restricted dorsolateral regions of the claustrum with evidence of a retinotopic organization (179, 327, 383). Comparison of the receptive field properties of claustral neurons with those of visual cortical neurons indicates that most claustral neurons respond best to appropriately oriented bars of light, have little spontaneous activity and respond poorly to stationary light stimuli (326, 327). Claustral neurons respond equally well to stimulation of either eye, and those dominated by the contralateral eye have receptive fields in the monocular segment of the visual field.

The corticoclaustral projection arises from pyramidal cells in cortical layer VI, and fibers projected by the claustrum terminate most densely in layer IV of the cortex (270, 291, 326, 327). Cells of layer VI of the visual cortex projecting to the claustrum are distinct from those projecting to the lateral geniculate nucleus. Much like the reticular nucleus of the thalamus, the claustrum is composed of discrete somesthetic, visual, and auditory zones. The claustrum also receives projections from the lateral hypothalamus, the centromedian thalamic nucleus, and the locus coeruleus (383).

FUNCTIONAL CONSIDERATIONS

Disinhibition in Basal Ganglia Functions

The basal ganglia and related nuclei exert their influences on motor activities by way of thalamic neurons that project on regions of the frontal cortex that influence motor function. Motor cortical neurons, whose activities are modulated by thalamic neurons, project fibers to, and exert motor control, at all levels of the neuraxis, mainly contralaterally. Neither the basal ganglia nor anatomically related brainstem nuclei project directly to spinal levels.

The striatum, pallidum, subthalamic nucleus, substantia nigra, and pedunculopontine nucleus are interrelated with each other by an orderly linkage and with specific parts of the neuraxis that can modulate somatic motor activities. The striatum, representing the receptive component of the basal ganglia, receives inputs from broad regions of the cerebral cortex, the intralaminar thalamic nuclei, the substantia nigra, and the midbrain raphe nuclei, mediated by a variety of neurotransmitters. Striatal output originates from different populations of spiny neurons that project selectively to the GPe, GPi, and SNr. GABA is the principal neurotransmitter in striatopallidal and striatonigral fiber systems, but fibers in both projections contain enkephalin or substance P.

The output systems of the basal ganglia arise from morphologically similar cells in the GPi and the SNr. Thalamic projections of the GPi and the SNr are distinctive without overlap. Nuclear subdivisions of the thalamus receiving these outputs do not exert their major effects on the primary motor cor-

tex. The output of the GPi appears to project to the premotor and supplementary motor areas. Most physiologic data suggest that pallidothalamic and nigrothalamic projections exert primarily inhibitory effects on thalamic neurons. The inhibitory influences of neurons in the GPi and SNr projecting to the thalamus may result in disinhibition of thalamic neurons that act on the cortical neurons.

Disinhibition has been proposed as the basic mechanism in the expression of striatal functions (Fig. 19.45) (56). Medium spiny neurons, which are the main striatal efferents, are GABAergic and inhibit the nigro- and pallidofugal neurons, which are themselves GABAergic and inhibitory. An important clue to the understanding of this system is the striking contrast in activity between the two constituents of this double inhibitory chain. When animals are at rest, most striatal neurons (90%) are mute, while SNr and GPi neurons emit a regular and sustained flow of impulses up to 100 spikes per second. Increased firing of striatal cells inhibits GPi and SNr neurons and produces disinhibition in thalamic, collicular, and tegmental neurons. For example, pharmacologically induced striatal activity readily produces a phasic silencing of the tonically active nigral neurons, accompanied by a robust firing in the superior colliculus and ventral tier thalamic nuclei (Fig. 19.45). This disinhibitory process does not, of itself, excite, but merely releases a tonic hyperpolarization and allows convergent excita-

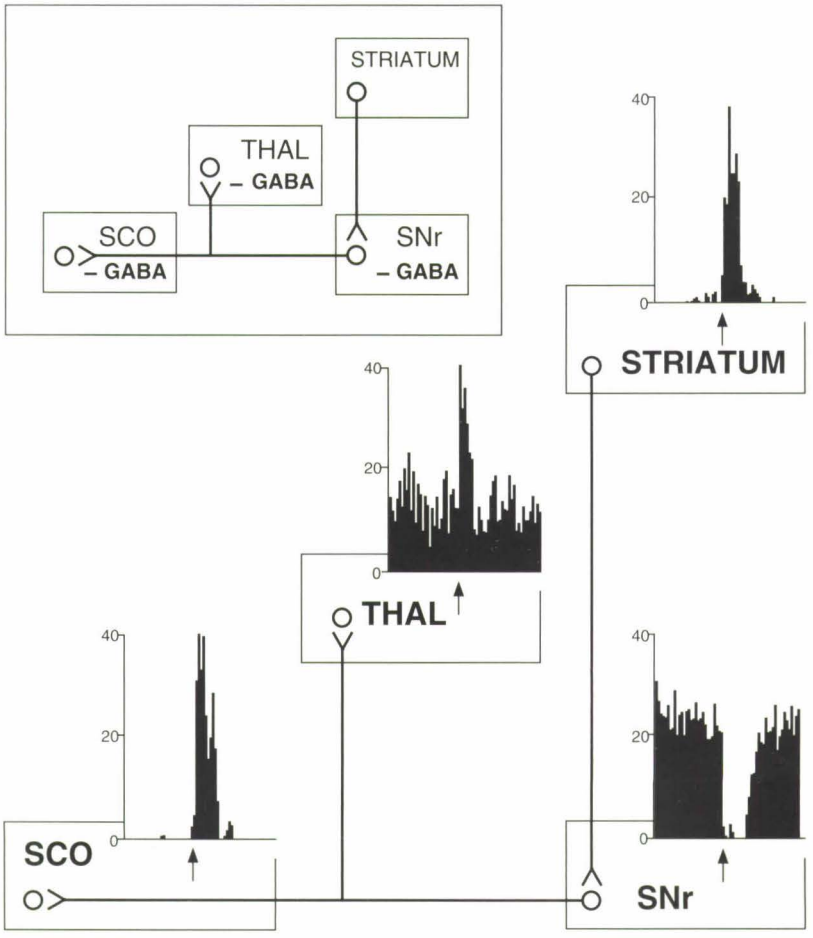


Figure 19.45. Disinhibition mechanism involved in the functional organization of the striatonigrofugal pathway to the ventral tier thalamic nuclei (*THAL*) and the superior colliculus (*SCO*). These circuits are composed of two serial GABAergic inhibitory links (*inset*). Frequency histograms in the main diagram illustrate the sequence of electrophysiologic events underlying the disinhibitory influence of the striatum. A striatal spike discharge, evoked by local application of glutamate, induces a silencing of the tonically active nigral (*SNr*) neurons. Released from the potent nigral inhibition, collicular and thalamic cells discharge vigorously in response to various incoming inputs and exert a strong excitatory effect upon tectospinal and cortical motor neurons.

tory inputs to control cell firing. During nigral silencing produced by intranigral application of GABA, a procedure that mimics the consequence of a striatal discharge, the reactivity of thalamocortical and colliculospinal neurons to their cerebellar and sensory inputs is considerably increased. Thus, the arousing message that the striatum sends to the motor system must be regarded as a gating signal. By using a disinhibitory mechanism instead of a direct synaptic excitation to arouse premotor networks, the striatum exerts a dual influence on them. When striatal cells are silent, which is the case for long periods of time, premotor systems are kept under an inhibitory constraint, shielding them from any disturbing noise. In contrast, when active, striatal cells enable premotor circuits to work (56).

The substantia nigra receives inputs from the two core structures of the basal ganglia (i.e., striatum and pallidum) and from all closely related subcortical nuclei (i.e., the subthalamic nucleus, the pedunculopontine nucleus, and the dorsal nucleus of the raphe). Dopaminergic neurons in the SNc provide a major feedback to the striatum and also have a small projection to the GPi. The output system of the substantia nigra arises from GABAergic neurons in the SNr, which projects to thalamic nuclei and via collaterals to the tectum and the pedunculopontine nucleus.

The subthalamic nucleus, in contrast to the substantia nigra, receives major inputs from only two sources, the GPe and the motor cortex. Cortical projections to the subthalamic nucleus probably represent collaterals of corticofugal fibers destined for other structures. A single type of subthalamic nucleus neuron projects fibers to both pallidal segments, but a small number of these cells project collaterals to the SNr. The cells in the subthalamic nucleus contain glutamate and are regarded as exerting excitatory influences on their projection targets.

Movement disorders associated with basal ganglia dysfunction comprise a spectrum of abnormalities that ranges from *hypokinetic disorders* (of which Parkinson's disease is the best known example) at one extreme to the *hyperkinetic disorders* exemplified by Huntington's disease and ballism at the other (69). Hypokinetic disorders are characterized by significant impairments in movement initiation (akinesia) and reduction in the amplitude and velocity of voluntary movement (bradykinesia). Hypokinetic disorders are usually accompanied by muscular rigidity and tremor at rest. By contrast, hyperkinetic disorders are characterized by excessive motor activity in the form of involuntary movements (dyskinesia) and varying degrees of hypotonia. Types of dyskinesia occurring in association with basal ganglia diseases include *tremor, athetosis, chorea,* and *ballism* (or *hemiballismus*). These and other forms of dyskinesia occur with a constellation of related somatic, visceral, and behavioral disturbances resulting from progressive degenerative disease, genetic defects, and vascular lesions. The metabolic disturbances associated with these disease processes often result in deficiencies in one or more neurotransmitters essential for normal function.

Dyskinesia

TREMOR

Tremor, the most common form of dyskinesia, is a rhythmic, alternating, abnormal, involuntary activity having a relatively regular frequency and amplitude. A major clinical criterion used to describe and classify different tremors is whether the tremor occurs "at rest" or during voluntary movement. The type of tremor commonly seen in paralysis agitans (Parkinsonism), involves primarily the digits, the head, and the lips, and occurs during the absence of voluntary movement. During voluntary movements the tremor ceases. Tremor classically associated with cerebellar lesions becomes evident during voluntary and associated movements, and ceases when the patient is "at rest." Although this criterion is of importance in clinical neurology, it is acknowledged that tremor "at rest" and tremor during voluntary movement sometimes occur together in various degrees in association with diseases involving primarily either the basal ganglia or the cerebellum. Tremor also is seen in association with weakness (paresis), emotional excitement, and as a side effect of a variety of drugs. In general, tremor is exaggerated when the patient is anxious, self-conscious, or exposed to cold. Tremor disappears during sleep and under general anesthesia.

ATHETOSIS

This term (140) is used to designate slow, writhing, vermicular involuntary movements involving particularly the extremities. It may

also involve axial muscle groups and the muscles of the face and neck. The movements blend with each other to give the appearance of a continuous mobile spasm. Athetoid movements involving primarily the axial musculature produce severe torsion of the neck, shoulder girdle, and pelvic girdle. This form of the disturbance, referred to as *torsion spasm* or *torsion dystonia,* is considered as a variant (9, 177) of athetosis. Differences between torsion dystonia and athetosis are considered to be due largely to inherent mechanical differences between axial and appendicular musculature.

CHOREA

Chorea is a brisk, graceful series of successive involuntary movements of considerable complexity that resemble fragments of purposeful voluntary movements. These movements involve primarily the distal portions of the extremities, the muscles of facial expression, the tongue, and the deglutitional musculature. Most forms of choreoid activity are associated with hypotonus. *Sydenham's chorea* occurs in childhood in association with rheumatic heart disease, and most patients recover from the chorea in a relatively short time. *Huntington's chorea* is inherited through an autosomal-dominant gene localized on chromosome 4. The symptoms usually do not begin until adult life, are progressive, and are characterized by choreiform activity in the face and hands and severe behavioral disturbances with dementia. Not every family member carries the defective gene.

BALLISM

Ballism, a violent, forceful, flinging movement, involves primarily the proximal appendicular musculature and muscles about the shoulder and pelvic girdles. It represents the most violent form of dyskinesia known. Ballism is almost invariably associated with discrete lesions in the subthalamic nucleus or its connections. In cases of unilateral lesion of the subthalamic nucleus, the dyskinesia occurs contralateral to the lesion and the condition is referred to as *hemiballism* or *hemiballismus.* Ballism is always associated with marked hypotonus.

Although athetosis, chorea and ballism each present distinguishing features, basic resemblances among these forms of dyskinesia are greater than their differences (41, 54, 245, 373). Characteristics common to these dyskinesias include (a) variable amplitude and frequency, (b) occurrence of movements in immediate and delayed sequence, (c) variations in the duration of single movements, and (d) a highly integrated, complex activity pattern. While each of these types of involuntary motor activity is specialized to a degree, there are indications that athetosis, chorea, and ballism may form a spectrum of choreoid activity in which athetosis and ballism represent extreme forms.

Although it is customary to associate increased muscle tonus with most syndromes of the basal ganglia, this is not always found. The initial symptom of Parkinsonism is frequently a rigidity of the muscles, which gradually increases over a period of years. The augmentation of muscle tone is not selective, as in hemiplegia, but is present to a nearly equal degree in antagonistic muscle groups (i.e., in both flexor and extensor muscles). The rigidity in the early stages can be demonstrated by passively flexing or extending the muscles of the extremities, or by attempting to rotate the hand in a circular fashion at the wrist. These movements are interrupted by a series of jerks, referred to as the *cogwheel phenomenon.* In later stages of the disease, rigidity may be so severe as to completely incapacitate the patient.

Athetosis usually is associated with variable degrees of paresis and spasticity. It is suggested that the slow, writhing character of this dyskinesia may be due in part to the spasticity. Although muscle tone is increased greatly during athetoid movements and persists after the completion of the movement, muscle tone may thereafter gradually diminish (163). Chorea and ballism usually are associated with variable degrees of hypotonus (232).

Neural Mechanisms Involved in Dyskinesia

The various types of dyskinesia and excesses of muscle tone associated with diseases of the basal ganglia are regarded as positive disturbances, since they involve an excess of neural activity and the expenditure of energy (233). Such disturbances cannot arise directly from destruction of specific neural structures, but must represent the functional capacity of surviving intact structures. Accordingly, positive disturbances, such as tremor, athetosis, chorea, and ballism,

are believed to be the result of *release phenomena*. This theory implies that a lesion in one structure removes the controlling and regulating influences which that structure previously exerted upon another neural mechanism. This concept forms the basis for neurosurgical attempts to alleviate dyskinesia and excesses of muscle tone without producing paresis. However, not all of the disturbances associated with diseases of the basal ganglia can be regarded as positive phenomena. Patients with Parkinson's disease (paralysis agitans) also exhibit a mask-like face, infrequent blinking of the eyes, a slow dysarthric speech, a stooped posture, a slow shuffling gait, loss of associated movements (e.g., swing of the arms while walking), slowness of movement (bradykinesia), and general poverty of movement. These disturbances can be regarded as negative symptoms. The negative symptoms of Parkinsonism largely concern disorders of postural fixation, equilibrium, locomotion, phonation, and articulation, and are considered to be deficits due to destroyed structures (232, 234).

In most forms of dyskinesia categorized as "extrapyramidal," the basal ganglia suffer severe pathologic alterations, but specific brainstem nuclei and parts of the cerebral cortex may be affected also.

PARKINSONISM

In Parkinson's disease, pathologic changes most consistently affect the substantia nigra, but significant alterations may be found also in the globus pallidus, the cerebral cortex, and the brainstem reticular formation (4, 25, 74, 156). In this syndrome, the synthesis and transmission of dopamine from cells of the SNc is greatly impaired. Terminals containing dopamine synapse mainly on dendrites and dendritic spines of spiny striatal neurons, and their effect is mediated by a variety of specific receptors (e.g., D_1 and D_2 receptor subtypes). Spiny striatal neurons also receive extrinsic excitatory inputs from the cortex and thalamus (Fig. 19.26). Intrinsic cholinergic striatal neurons form symmetric synaptic endings on all parts of spiny striatal neurons. The special importance of intrinsic cholinergic neurons concerns their modulating influences on spiny striatal neurons known to project to the substantia nigra. Dopamine tonically inhibits the release of acetylcholine (ACh) in the striatum, whereas ACh, or cholinomimetic drugs, enhance the release of GABA. In Parkinson's disease, there is an imbalance between ACh and dopamine that favors ACh. This imbalance can be modified by elevating dopamine levels by giving L-dihydroxyphenylalanine (L-dopa), a precursor of dopamine that passes the blood-brain barrier (Fig. 1.15), or by reducing the action of ACh with cholinergic receptor antagonists. This rationale forms the basis for giving L-dopa in Parkinson's disease. The effectiveness of L-dopa can be enhanced by the use of a peripheral decarboxylase inhibitor, which prevents systemic decarboxylation of L-dopa to dopamine. Recently, the implantation of fetal nigral cells within the denervated striatum of Parkinsonian patients has been used as a source of dopamine (225). Animal experiments reveal that this grafting procedure can restore dopaminergic functions in the striatum and alleviate the motor deficits caused by dopamine loss (Fig. 5.42). Despite claims of improvement in some Parkinsonian patients, however, the usefulness of this novel approach for the treatment of idiopathic Parkinsonism remains to be demonstrated.

ATHETOSIS

Athetosis most frequently is associated with pathologic processes involving the striatum and cerebral cortex, though lesions are sometimes found in the globus pallidus and thalamus (40). Hemiathetosis may develop after a hemiparesis, or in association with it, as a consequence of a necrotizing cerebrovascular lesion destroying portions of the internal capsule and striatum. Athetoid activity occurs contralateral to the lesion.

CHOREA

With respect to chorea, there is relatively little information available, except that concerning chronic progressive chorea, or Huntington's chorea. This hereditary disease, due to a gene defect on chromosome 4 (129), is characterized by an insidious onset in adult life. Pathologic changes are widespread but have a special predilection for the cerebral cortex and striatum. In brains of patients dying with Huntington's chorea, it was demonstrated that striatal neurons reduced concentrations of the enzymes GAD, GABA, and ChAT (27). GAD is the enzyme responsible for the biosynthesis of GABA and is localized mainly in inhibitory neurons that release GABA as their neurotransmitter (5, 172). In

these same patients, concentrations of tyrosine hydroxylase (TH) and dopamine were normal in the striatum. The most consistent neurotransmitter disturbance in Huntington's chorea appears to be a loss of GABA-containing neurons in the striatum, which causes an imbalance in striatal levels of GABA and dopamine in favor of dopamine. The large cholinergic striatal neurons are involved in this imbalance because dopamine inhibits ACh and ACh enhances the release of GABA. It is well-known that L-dopa given in large doses to patients with Parkinson's disease may cause choreiform movements to appear. L-dopa also tends to exacerbate choreiform activity in patients with Huntington's chorea. The most effective drugs for ameliorating choreiform dyskinesia are those which deplete catecholamines, such as reserpine and dopamine receptor antagonists. The presence of normal dopaminergic systems in association with reduced availability of GABA and acetylcholine may be the key neuropharmacologic feature of Huntington's disease (5, 27). Clinical attempts to overcome deficiencies of GABA and acetylcholine by administering GABA-mimetic drugs or inhibitors of acetylcholine hydrolysis have so far met with limited success (328, 329). This has been explained by the inability of GABA or the GABA agonists to cross the blood-brain barrier in sufficient concentrations (324).

The biochemical changes that characterize Huntington's chorea in humans can be mimicked in the rat by striatal injections of kainic acid, an analogue of glutamate (80, 231, 236, 324). After injections of kainic acid, the GAD and ChAT activities were reduced, whereas the activity of TH was increased. The striatal content of dopamine was unchanged. The neurotoxic effects of kainic acid appear related to the excessive stimulation of glutamate receptors that result in degeneration (80, 147, 231, 324). The long-term effects of striatal kainic acid lesions and the reduction in activities of GABAergic and cholinergic neurons are not as severe as those in Huntington's disease (382).

BALLISM OR HEMIBALLISMUS

This neurologic disorder appears to be the only form of dyskinesia resulting from a discrete, destructive lesion. Small lesions confined to the subthalamic nucleus, or its immediate connections, usually are vascular in nature and occur mainly in elderly hypertensive individuals (368). The dyskinesia has a sudden onset, occurs contralateral to the lesion, usually involves both upper and lower extremities, and displays a forceful, flinging, repetitive pattern. Affected limbs exhibit a marked hypotonus.

Animal Models of Basal Ganglia Disorders

SUBTHALAMIC DYSKINESIA

Attempts to produce dyskinesia in experimental animals by creating lesions in parts of the basal ganglia have been notoriously unsuccessful (241, 372). The principal form of dyskinesia, aside from cerebellar tremor, produced in an experimental animal is that resulting from discrete lesions in the subthalamic nucleus. This dyskinesia closely resembles that which occurs in humans with lesions in the same nucleus. In the monkey, violent choreoid and ballistic activity occurs contralateral to localized lesions in the subthalamic nucleus that (a) destroy approximately 20% of the nucleus, and (b) preserve the integrity of surrounding pallidofugal fiber systems (50, 369). This abnormal involuntary activity has been called *subthalamic dyskinesia* and becomes apparent immediately upon recovery from anesthesia. Subthalamic dyskinesia in the monkey is enduring, associated with distinct hypotonus, and can be ameliorated or abolished contralaterally by subsequent stereotaxic lesions in the GPi, the ventral lateral nucleus of the thalamus, and the motor cortex. Similar subthalamic dyskinesia has been produced in the monkey by kainic acid lesions involving the subthalamic nucleus, but its onset usually is delayed (138). A transitory form of similar dyskinesia has been produced in the awake primate by injections of GABA antagonists (picrotoxin and bicuculline methiodide) into the subthalamic region (65, 249). The site of action of these antagonists remains unclear. Original studies of subthalamic dyskinesia in the monkey suggested that lesions of the subthalamic nucleus resulted in a removal of inhibitory influences acting on cells of the GPi. Physiologic observations indicating that subthalamic nucleus efferents are excitatory suggest more complex neural mechanisms. There is general agreement that the cells of the subthalamic nucleus do not contain GABA but that GABAergic terminals of pallidal projec-

tions closely surround individual cells (Fig. 19.41).

Surgical attempts to ameliorate and abolish various forms of dyskinesia and excesses of muscle tone are based on the thesis that these disturbances are the physiologic expression of release phenomena. This implies that disease or pathologic alterations of certain neural structures have removed inhibitory influences normally acting on other intact neural structures, and that this overactivity, or excessive function, is responsible for the dyskinesia. Attention has focused mainly on the globus pallidus and the ventral lateral nucleus of the thalamus, since these structures appear to be of greatest importance in the subcortical integration of nonpyramidal motor function. In some instances, localized lesions produced by different techniques in these structures have abolished, or significantly reduced, various forms of dyskinesia (46, 50, 59–61, 145, 235, 254, 255, 266, 313, 349). Stereotaxic surgery in humans is often unpredictable, unless carefully controlled by physiologic studies and sophisticated imaging techniques.

The cerebral cortex is acknowledged to play an important role in the neural mechanisms of all forms of dyskinesia. Almost all forms of abnormal involuntary movement cease during sleep and are abolished by general anesthesia. Most forms of dyskinesia are exaggerated in situations where the patient becomes self-conscious, overly anxious, or excited. The fact that ablations of the motor cortex or interruption of the corticospinal tract at various locations abolish dyskinesia suggests that impulses responsible for the dyskinesia probably are transmitted to segmental levels via the corticospinal tract (35, 46).

EXPERIMENTAL PARKINSONISM

Symptoms of Parkinsonism, particularly tremor, can be produced by electrolytic lesions of the ventromedial portion of the midbrain tegmentum in monkeys (297, 299). However, the deficits observed after such lesions are highly variable and the different neural structures involved are difficult to identify. A more faithful model of Parkinsonism has became available following the discovery of the neurotoxin MPTP (1-methyl-4-phenyl-4-1,2,5,6-tetrahydropyridine). MPTP is a meperidine-analogue that can be found in some illicit drugs (cocaine, meperidine). When given intravenously in concentrations of 2.5–3%, this neurotoxin produces a chronic form of Parkinsonism in both humans and nonhuman primates (216). This compound was first identified as the product of a clandestine laboratory attempting to synthesize 1-methyl-4-phenyl-4-propionoxypiperdine (MPPP). Individuals taking this drug presented with a classic picture of Parkinson's disease. In a patient who died of a drug overdose, destruction within the substantia nigra was comparable in severity with that seen in idiopathic Parkinsonism. All patients exhibiting this syndrome responded to L-dopa and carbidopa. MPTP is converted in the brain to the highly toxic compound MPP^+, which is then taken up into nigrostriatal neurons. How MMP^+ selectively destroys nigral dopaminergic neurons is still uncertain, but there is evidence for interference with mitochondrial oxidation and redox reactions. Monkeys treated with MPTP develop signs virtually identical to those in humans with Parkinson's disease, including akinesia, bradykinesia, flexed posture, muscular rigidity, and postural tremor (22).

In recent years, the use of such animal models has yielded data that clarify some of the pathophysiologic mechanisms underlying hypokinetic (as well as hyperkinetic) disorders. These disorders can be explained using a functional model of the basal ganglia-thalamocortical "motor" circuit that incorporates current data from several experimental fields (Fig. 19.46) (5, 8, 69, 128, 322). The so-called motor circuit, like other basal ganglia-thalamocortical circuits, is viewed as a reentrant pathway through which influences emanating from sensorimotor areas of the cortex are returned to some of the same cortical areas after intermediate processing within the basal ganglia and thalamus (Fig. 19.46) (69, 370). Parts of the putamen constitute the input stage of the basal ganglia, receiving projection from the precentral motor areas. The GPi and the SNr are the major output nuclei of the basal ganglia circuitry. Between input and output structures, two major projection systems—the so-called direct and indirect pathways—have been identified, arising from separate populations of putamen neurons. The inhibitory *direct pathway* arises from putamen neurons that contain GABA and substance P and project monosynaptically to the motor portion of the GPi and SNr.

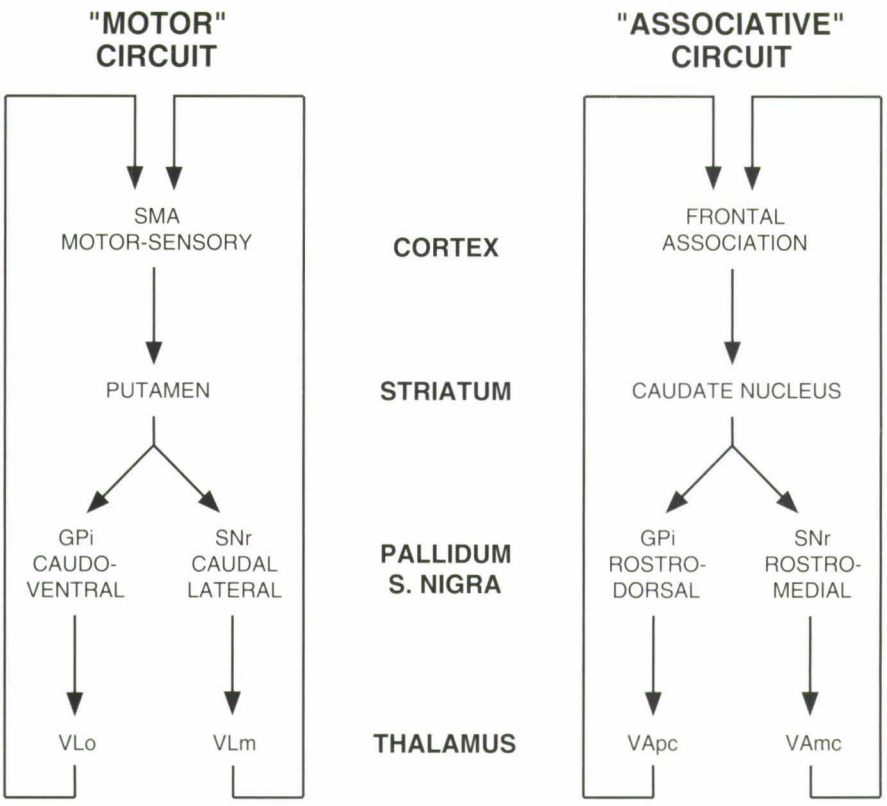


Figure 19.46. Comparison of the organization of the so-called sensorimotor and associative circuits of the basal ganglia, which can be distinguished electrophysiologically and anatomically. *GP*, internal pallidal segment; *SMA*, supplementary motor area; *SNr*, substantia nigra pars reticulata; *VAmc*, ventral anterior nucleus pars magnocellular; *VApc*, ventral anterior nucleus pars parricellular; *VLm* ventral lateral nucleus pars medialis; *VLo*, ventral lateral nucleus pars oralis.

The *indirect pathway*, on the other hand, arises from putamen neurons that contain GABA and enkephalin and whose influence is conveyed to GPi/SNr polysynaptically through a sequence of connections involving the GPe and the subthalamic nucleus. This sequence of connections comprises (a) an inhibitory connection between the putamen and the GPe, (b) an inhibitory connection between the GPe and the STN, and (c) an excitatory connection between the STN and GPi/SNr (Fig. 19.47).

In the striatum, dopamine appears to have differential effects on the activity of the direct and the indirect pathway, facilitating transmission via the direct pathway and decreasing the activity of the indirect pathway. These opposite actions of dopamine are believed to be mediated by different types of dopamine receptors, with D_2 receptors located on neurons projecting to the GPe and D_1 receptors on neurons projecting to GPi/SNr (113). Balance between the activity in the direct and indirect pathways and the resulting alterations in the GPi/SNr are thought to account for the hypo- and hyperkinetic features of basal ganglia disorders (69). It appears that enhanced conduction through the indirect pathway leads to hypokinesia by increasing the GABAergic pallidothalamic inhibition. By contrast, reduced conduction through the direct pathway results in hyperkinesia by reduction of pallidothalamic inhibition (Fig. 19.47).

According to the proposed functional model of the motor circuit, the motor disturbances of Parkinson's disease are postulated to result in large part from increased thalamic inhibition due to excessive excitatory drive from the STN to the output nuclei of the basal ganglia (GPi/SNr). It may, therefore, be predicted that a lesion or inactivation of the STN in Parkinsonian subjects would improve some of the motor impairments. This hypothesis has been tested by selective lesioning of the STN with the fiber-sparing excitotoxin

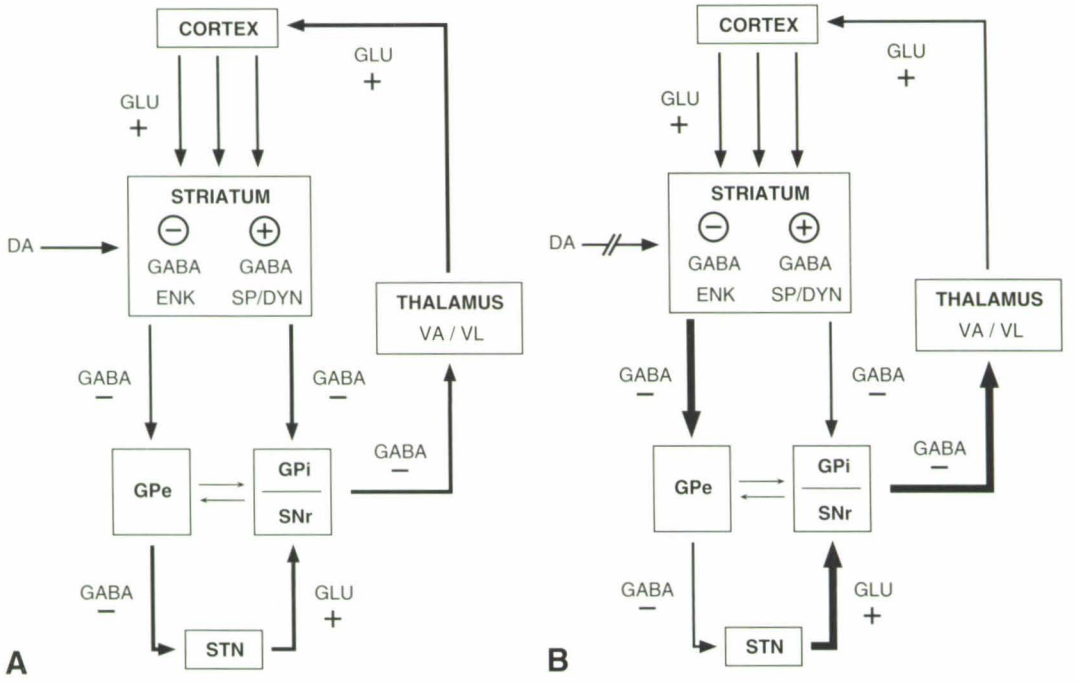


Figure 19.47. Major basal ganglia circuits, particularly the indirect and direct striatofugal pathways, and their activity under normal conditions (**A**) and following lesion of the substantia nigra pars compacta (**B**). In normal conditions, the balance between the effects of the direct and indirect pathways is maintained by the opposite action that dopamine (*DA*) exerts upon neurons giving rise to each of these two pathways. The loss of striatal dopamine (*DA*) causes a release of the inhibition on the GABA/enkephalin striatal neurons that project to the external pallidum (*GPe*). The GPe thus comes under a strong striatal inhibition and is no longer able to exert its inhibitory action on the subthalamic nucleus (*STN*). This results in a marked increase of the excitatory action of the STN on the two output structures of the basal ganglia, namely the internal pallidum (*GPi*) and the pars reticulata of the substantia nigra (*SNr*). In turn, the GPi/SNr augment their inhibitory constraint upon the premotor neurons of the thalamus (*VA/VL*, ventral anterior and ventral lateral nuclei). The net effect of this cascade of events is a marked decrease of the excitatory influence that thalamocortical neurons exert upon cortical neurons involved in the initiation and execution of movements. Clinically, this leads to bradykinesia or akinesia.

ibotenate in monkeys rendered Parkinsonian after MPTP administration. Such lesions reportedly produce an immediate and dramatic reduction of akinesia and bradykinesia, as well as tremor and rigidity in the contralateral limbs (18, 26). Improvements in motor functions of Parkinsonian monkeys also can be obtained by high frequency stimulation (100–130 Hz) of the subthalamic nucleus (24), which is believed to produce a reversible physiologic lesion of the nucleus, and after injection of antagonisms of excitotoxic amino acids in the GPi (34). These results provide a direct support for the postulated positive role of the STN and the indirect pathway in the pathogenesis of hypokinetic disorders.

References

1. Adinolfi AM, Pappas GD. The fine structure of the caudate nucleus of the cat. J Comp Neurol 1968;133: 167–184.
2. Afifi A, Kaelber WE. Efferent connections of the substantia nigra in the cat. Exp Neurol 1965;1:474–482.
3. Afsharpour S. Topographical projections of the cerebral cortex to the subthalamic nucleus. J Comp Neurol 1985;236:14–28.
4. Agid Y. Parkinson's disease: pathophysiology. Lancet 1991;337: 1321–1324.
5. Albin RL, Young AB, Penney JB. The functional anatomy of basal ganglia disorders. Trends Neurosci 1989;12:366–375.
6. Alexander GE, DeLong MR. Microstimulation of the primate neostriatum. I. Physiological properties of striatal microexcitable zones. J Neurophysiol 1985;53: 1401–1416.
7. Alexander GE, DeLong MR. Microstimulation of the primate neostriatum. II. Somatotopic organization of striatal microexcitable zones and their relation to neuronal response properties. J Neurophysiol 1985;53:1417–1430.
8. Alexander GE, DeLong MR, Strick PL. Parallel organization of functionally segregated circuits linking basal ganglia and cortex. Ann Rev Neurosci 1986;9:357–381.
9. Alexander L. The vascular supply of the striopallidum. Proc Assoc Res Nerve Ment Dis 1942;21: 77–132.
10. Alheid GF, Heimer L. New perspective in basal forebrain organization of special relevance for neuropsychiatric disorders: the striatopallidal, amygdaloid, and corticopetal components of the substantia innominata. Neuroscience 1988;27:1–39.

11. Alheid GF, Heimer L, Switzer RC III. Basal ganglia. In: Paxinos G, ed. The human nervous system. Ch. 19. New York: Academic Press, 1990:483–582.
12. Andén N-E, Carlsson A, Dahlström A, Fuxe K, Hillarp N-A, Larsson K. Demonstration and mapping out of nigro-neostriatal dopamine neurons. Life Sci 1964; 3:523–530.
13. Andén N-E, Dahlström A, Fuxe K, Larsson K, Olson L, Ungerstedt U. Ascending monoamine neurons to the telencephalon and diencephalon. Acta Physiol Scand 1966;67:313–326.
14. Anderson ME, Horak FB. Influence of the globus pallidus on arm movements in monkeys. III. Timing of movement-related information. J Neurophysiol 1985;53: 1417–1430.
15. Arluison M, De la Manche IS. High-resolution radioautographic study of the serotonin innervation of the rat corpus striatum after intraventricular administration of [^{3}H] 5-hydroxytryptamine. Neuroscience 1980;5:229–240.
16. Aronin N, DiFiglia M, Graveland GA, Schwartz WJ, Wu J-Y. Localization of immunoreactive enkephalins in GABA synthesizing neurons of the rat neostriatum. Brain Res 1984;300:376–380.
17. Augood SJ, Emson PC. Pertussis toxin administration increases the expression of proneurotensin and preproenkephalin A mRNAs in rat striatum. Neuroscience 1992;47: 317–324.
18. Aziz TZ, Peggs D, Sambrook MA, Crossman AR. Lesion of the subthalamic nucleus for the alleviation of 1-methyl-4-phenyl-1,2,3,6-tetrahydropyridine (MPTP)- induced Parkinsonism in the primate. Mov Disord 1991;6:288–293.
19. Azmitia EC, Gannon PJ. The primate serotonergic system: A review of human and animal studies and a report on *Macaca fascicularis*. In: Fahn S, ed. Advances in neurology. New York: Raven Press, 1986:407–468.
20. Beckstead RM. Complementary mosaic distribution of thalamic and nigral axons in the caudate nucleus of the cat: double anterograde labeling combining autoradiography and wheat germ-HRP histochemistry. Brain Res 1985;335: 153–159.
21. Beckstead RM, Domesick VB, Nauta WJH. Efferent connections of the substantia nigra and ventral tegmental area in the rat. Brain Res 1979;175:191–217.
22. Bédard PJ, Boucher R, Gomez-Mancilla B, Blanchette P. Animal models of Parkinson's disease. In: Boulton A, Baker G, Butterworth R, eds. Animal models of neurological disease. Totowa, NJ: Humana Press, 1992:159–173.
23. Bédard P, Larochelle L, Parent A, Poirier LJ. The nigrostriatal pathway: a correlative study based on neuroanatomical and neurochemical criteria in the cat and monkey. Exp Neurol 1969;25:365–377.
24. Benazzouz A, Gross CH, Féger J, Boraud T, Bioulac B. Reversal of rigidity and improvement in motor performance by subthalamic high frequency stimulation in MPTP-treated monkeys. Eur J Neurosci 1993;5:382–389.
25. Benda CE, Cobb S. On the pathogenesis of paralysis agitans (Parkinson's disease). Medicine 1942;21:95–142.
26. Bergman H, Wichmann T, DeLong MR. Reversal of experimental Parkinsonism by lesion of the subthalamic nucleus. Science 1990;249: 1436–1438.
27. Bird ED, Iversen LL. Huntington's chorea: Post-mortem measurements of glutamic acid decarboxylase, choline acetyltransferase and dopamine in the basal ganglia. Brain 1974;97:457–472.
28. Bloom FE, Costa E, Salmoiraghi GC. Anesthesia and responsiveness of individual neurons of the caudate nucleus of the cat to acetylcholine, norepinephrine and dopamine administered by microelectrophoresis. J Pharmacol Exp Ther 1965;150:244–252.
29. Bobillier P, Petitjean F, Salvert D, Ligier M, Seguin S. Differential projections of the nucleus raphe dorsalis and nucleus raphe centralis as revealed by autoradiography. Brain Res 1975;85:205–210.
30. Bolam JP, Ingham CA, Smith AD. The section-Golgi-impregnation procedure-3. Combination of Golgi-impregnation with enzyme histochemistry and electron microscopy to characterize acetylcholinesterase-containing neurons in the rat neostriatum. Neuroscience 1984;12:687–709.
31. Bouyer JJ, Park DH, Joh TH, Pickel VM. Chemical and structural analysis of the relation between cortical inputs and tyrosine hydroxylase-containing terminals in rat neostriatum. Brain Res 1984; 302:267–275.
32. Bredt DS, Hwang PM, Snyder S H. Localization of nitric oxide synthase indicating a neural role for nitric oxide. Nature 1990;347: 768–770.
33. Brockhaus H. Die Cyto-und Myeloarchitektonik des Cortex claustralis und des Claustrum beim menschen. J Psychol Neurol 1940;49:249–348.
34. Brotchie JM, Mitchell IJ, Sambrook MA, Crossman AR. Alleviation of parkinsonism by antagonism of excitatory aminoacid transmission in the medial pallidal segment of the globus pallidus in the rat and primate. Mov Disord 1991;6: 133–138.
35. Bucy PC. The cortico-spinal tract and tremor. In: Fields WS, ed. Pathogenesis and treatment of Parkinsonism. Ch. 11. Springfield, IL: Charles C. Thomas, 1958: 271–293.
36. Bunney BS, Aghajanian GK. The precise localization of nigral afferents in the rat as determined by a retrograde tracing technique. Brain Res 1976;117:423–435.
37. Burdach KF. Vom Bau und Leben des Gehirns. Leipzig: Dyksche Buchhandlung, 1819–1824.
38. Carlsson A, Falck B, Hillarp NA. Cellular localization of brain monoamines. Acta Physiol Scand 1962;56(Suppl 196):1–28.
39. Carman JB, Cowan WM, Powell TPS. The organization of corticostriate connexions in the rabbit. Brain 1963;86:525–562.
40. Carpenter MB. Athetosis and the basal ganglia. Arch Neurol Psychiatry 1950;63:875–901.
41. Carpenter MB. The neuroanatomical basis of dyskinesia. In: Fields WS, ed. Pathogenesis and treatment of Parkinsonism. Ch. 2. Springfield, IL: Charles C. Thomas, 1958:50–85.
42. Carpenter MB. Anatomical organization of the corpus striatum and related nuclei. In: Yahr MD, ed. The basal ganglia. New York: Raven Press, 1976:1–36.
43. Carpenter MB. Anatomy of the corpus striatum and brain stem integrating systems. In: Brooks V, ed. Handbook of physiology. Vol. II, Sec. 1. Motor control. Ch. 19. Washington, DC: American Physiological Society, 1981:947–995.
44. Carpenter MB, Batton RR III, Carleton SC, Keller JT. Interconnections and organization of pallidal and subthalamic nucleus neurons in the monkey. J Comp Neurol 1981;197:579–603.
45. Carpenter MB, Carleton SC, Keller JT, Conte P. Connections of the subthalamic nucleus in the monkey. Brain Res 1981;224:1–29.
46. Carpenter MB, Correll JW, Hinman A. Spinal tracts mediating subthalamic hyperkinesia. Physiological effects of partial selective cordotomies upon dyskinesia in the rhesus monkey. J Neurophysiol 1960;23:288–304.
47. Carpenter MB, Fraser RAR, Shriver JE. The organization of pallidosubthalamic fibers in the monkey. Brain Res 1968;11:522–559.
48. Carpenter MB, Peter P. Nigrostriatal and nigrothalamic fibers in the rhesus monkey. J Comp Neurol 1972;144:93–116.
49. Carpenter MB, Strominger NL. Efferent fibers of the subthalamic nucleus in the monkey: a comparison of the efferent projections of the subthalamic nucleus, substantia nigra and globus pallidus. Am J Anat 1967;121:41–72.
50. Carpenter MB, Whittier JR, Mettler FA. Analysis of choreoid hyperkinesia in the rhesus monkey: surgical and pharmacological analysis of hyperkinesia resulting from lesions in the subthalamic nucleus of Luys. J Comp Neurol 1950;92:293–332.

51. Castel MN, Morino P, Frey P, Terenius L, Hökfelt T. Immunohistochemical evidence for a neurotensin striatonigral pathway in the rat brain. Neuroscience 1993;55:833–847.
52. Chang HT, Kita H, Kitai ST. The ultrastructural morphology of the subthalamo-nigral axon terminals intracellularly labeled with horseradish peroxidase. Brain Res 1984;299:182–185.
53. Charara A, Parent A. Brainstem dopaminergic, cholinergic and serotoninergic afferents to the pallidum in the squirrel monkey. Brain Res 1994;640:155–170.
54. Charcot JM. Lectures on the diseases of the nervous system. Sigerson G, trans. Philadelphia: Henry C. Lea, 1879.
55. Chesselet MF, Robbins E. Characterization of striatal neurons expressing high levels of glutamic acid decarboxylase messenger RNA. Brain Res 1989;492:237–244.
56. Chevalier G, Deniau JM. Disinhibition as a basic process in the expression of striatal functions. Trends Neurosci 1990;13:277–280.
57. Cole M, Nauta WJH, Mehler WR. The ascending efferent projections of the substantia nigra. Trans Am Neurol Assoc 1964;89:74–78.
58. Conrad LCA, Leonard CA, Pfaff DW. Connections of the median and dorsal raphe nuclei in the rat: an autoradiographic and degeneration study. J Comp Neurol 1974;156:170–206.
59. Cooper IS. Neurosurgical alleviation of Parkinsonism. Springfield, IL: Charles C. Thomas, 1956.
60. Cooper IS. Neurosurgical relief of intention tremor due to cerebral disease and multiple sclerosis. Arch Phys Med Rehabil 1960;41: 1–4.
61. Cooper IS, Bravo GJ. Anterior choroidal artery occlusion, chemopallidectomy and chemothalamectomy in parkinsonism: a consecutive series of 700 operations. In: Fields WS, ed. Pathogenesis and treatment of Parkinsonism. Ch. 15. Springfield, IL: Charles C. Thomas, 1958:325–352.
62. Côté P-Y, Sadikot AF, Parent A. Complementary distribution of calbindin D-28k and parvalbumin in the basal forebrain and midbrain of the squirrel monkey. Eur J Neurosci 1991;3:1316–1329.
63. Cowan RL, Wilson CJ, Emson PC, Heizmann CW. Parvalbumin-containing GABAergic interneurons in the rat neostriatum. J Comp Neurol 1990;302:197–205.
64. Cowan WM, Powell TPS. Striopallidal projection in the monkey. J Neurol Neurosurg Psychiatry 1966;29:426–439.
65. Crossman AR, Féger J, Hammond C, Jackson A, Sambrook MA. Studies on site specificity of intracerebral injection in the production of experimental hemiballismus. J Physiol (London) 1981;319:109–110.
66. Dahlström A, Fuxe K. Evidence for the existence of monoamine-containing neurons in the central nervous system. I. Demonstration of monoamines in the cell bodies of brain stem neurons. Acta Physiol Scand 1964;62(Suppl 232):1–55.
67. Dahlström A, Fuxe K. Evidence for the existence of monoamines in the central nervous system. II. Experimentally induced changes in the intraneuronal amine levels of bulbospinal neuron systems. Acta Physiol Scand 1965;64(Suppl 247):1–36.
68. Davies J, Dray A. Substance P in the substantia nigra. Brain Res 1976;107:623–627.
69. DeLong MR. Primate models of movement disorders of the basal ganglia. Trends Neurosci 1990;13: 281–285.
70. DeLong MR, Crutcher MD, Georgopoulos AP. Primate globus pallidus and subthalamic nucleus: functional organization. J Neurophysiol 1985;53:530–543.
71. DeLong MR, Georgopoulos AP. Motor functions of the basal ganglia. In: Brookhart JM, Mountcastle VB, Brooks VB, Geiger SR, eds. Handbook of physiology. Sec. 1: The nervous system. Vol. II: Motor control. Part 2. Bethesda, MD: American Physiological Society, 1981:1017–1061.
72. DeLong MR, Georgopoulos AP, Crutcher MD. Cortico-basal ganglia relations and coding of motor performance. Exp Brain Res Suppl 1983;7:30–40.
73. Deniau JM, Hammond C, Chevalier G, Féger J. Evidence for branched subthalamic nucleus projections to substantia nigra, entopeduncular nucleus and globus pallidus. Neurosci Lett 1978;9: 117–121.
74. Denny-Brown D. The basal ganglia and their relation to disorders of movement. London: Oxford University Press, 1962.
75. Desban M, Gauchy C, Kemel ML, Besson MJ, Glowinski J . Three-dimensional organization of the striosomal compartment and patchy distribution of striatonigral projections in the matrix of the cat caudate nucleus. Neuroscience 1989;29:551–566.
76. Descarries L, Bossler O, Berthelet F, Desrosiers MH. Dopaminergic nerve endings visualized by high resolution autoradiography in adult rat neostriatum. Nature 1980;284:620–622.
77. De Simoni MG, Dal Toso G, Fodritto F, Sokola A, Algeri S. Modulation of striatal dopamine metabolism by the activity of dorsal raphe serotoninergic afferents. Brain Res 1987;411:81–88.
78. Desjardins C, Parent A. Distribution of somatostatin immunoreactivity in the forebrain of the squirrel monkey: basal ganglia and amygdala. Neuroscience 1992;47: 115–133.
79. DeVito JL, Anderson ME, Walsh RE. A horseradish peroxidase study of afferent connections of the globus pallidus in *Macaca mulatta*. Exp Brain Res 1980;38:65–73.
80. DiFiglia M. Excitotoxic injury of the neostriatum: a model for Huntington's disease. Trends Neurosci 1990;13:286–289.
81. DiFiglia M, Aronin N. Ultrastructural features of immunoreactive somatostatin neurons in the rat caudate nucleus. J Neurosci 1982;2: 1267–1274.
82. DiFiglia M, Pasik P, Pasik T. A Golgi study of neuronal types in the neostriatum of monkeys. Brain Res 1976;114:245–256.
83. Donoghue JP, Kitai ST. A collateral pathway to the neostriatum from corticofugal neurons of the rat sensory-motor cortex: An intracellular HRP study. J Comp Neurol 1981;201:1–13.
84. Druga R. Cortico-claustral connections. I. Fronto-claustral connections. Folia Morphol (Praha) 1966;14:391–399.
85. Druga R. Cortico-claustral connections. II. Connections from the parietal, temporal and occipital cortex to the claustrum. Folia Morphol (Praha) 1968;16:142–149.
86. Emson PC, Arregui A, Clement-Jones V, Sandberg BEB, Rossor M. Regional distribution of methionine-enkephalin and substance P-like immunoreactivity in normal human brain and in Huntington's disease. Brain Res 1980;199: 147–160.
87. Fahn S, Côté LJ. Regional distribution of γ-aminobutyric acid (GABA) in brain of the rhesus monkey. J Neurochem 1968;15: 209–213.
88. Falck B. Observations on the possibilities of the cellular localization of monoamines by a fluorescence method. Acta Physiol Scand 1962;56(Suppl 197):1–25.
89. Fallon JH, Loughlin SE, Ribak CE. The island of Calleja complex of the rat basal forebrain. III. Histochemical evidence for a striatopallidal system. J Comp Neurol 1983;218:91–120.
90. Faull RLM, Carman JB. Ascending projections of the substantia nigra in the rat. J Comp Neurol 1968;132:73–92.
91. Féger J, Crossman AR. Identification of different subpopulations of neostriatal neurones projecting to globus pallidus and substantia nigra in the monkey: a retrograde fluorescence double-labeling study. Neurosci Lett 1984;49: 7–12.
92. Féger J, Mouroux M. Mise en évidence de l'effet excitateur de l'efférence thalamo-subthalamique issue du noyau parafasciculaire. CR Acad Sci III 1991;313:447–452.
93. Ferraro A. Contributa sperimentale allo studio della substantia nigra normale e dei suoi rapporti con la corteccia cerebrale e con il corpo

striato. Arch Gen Neurol Psychiatry 1925;6:26–117.
94. Ferraro A. The connections of the pars suboculomotoria of the substantia nigra. Arch Neurol Psychiatry 1928;19:177–180.
95. Fisher RS, Shiota C, Levine MS, Hull CD, Buchwald NA. Interhemispheric organization of corticocaudate projections in the cat: a retrograde double-labeling study. Neurosci Lett 1984;48:369–373.
96. Flaherty AW, Graybiel AM. Two input systems for body representations in the primate striatal matrix: experimental evidence in the squirrel monkey. J Neurosci 1993;13: 1120–1137.
97. Flaherty AW, Graybiel AM. Output architecture of the primate putamen. J Neurosci 1993;13: 3222–3237.
98. Foix C, Hillemand J. Irrigation de la couche optique. CR Soc Biol (Paris) 1925;92:52–54.
99. Foix C, Nicolesco J. Les noyaux gris centraux et la région mésencephalo-sous-optique. Paris: Masson, 1925.
100. Fonnum F, Storm-Mathisen J. High affinity uptake of glutamate in terminals of corticostriate axons. Nature 1977;266:377–378.
101. Fox CA, Andrade AN, Hillman DE, Schwyn RC. The spiny neurons in the primate striatum: a Golgi and electron microscopic study. J Hirnforsch 1971;13: 181–201.
102. Fox CA, Andrade AN, Lu Qui I, Rafols JA. The primate globus pallidus: A Golgi and electron microscopic study. J Hirnforsch 1974;15: 75–93.
103. Fox CA, Andrade AN, Schwyn RC, Rafols JA. The aspiny neurons and the glia in the primate striatum: a Golgi and electron microscopic study. J Hirnforsch 1971/1972: 13:341–362.
104. Fox CA, Rafols JA. The radial fibers in the globus pallidus. J Comp Neurol 1975;159:177–200.
105. Fox CA, Rafols JA, Cowan WM. Computer measurements of axis cylinder diameters of radial fibers and "comb" bundle fibers. J Comp Neurol 1975;159:201–224.
106. François C, Percheron G, Yelnik J. A Golgi analysis of the primate globus pallidus. I. Inconstant processes of large neurons, other neuronal types, and afferent axons. J Comp Neurol 1984;227: 182–189.
107. Freund TF, Powell JF, Smith AD. Tyrosine hydroxylase-immunoreactive boutons in synaptic contacts with identified striatonigral neurons, with particular reference to dendritic spines. Neuroscience 1984;13:1189–1216.
108. Frotscher M, Rinne V, Hassler R, Wagner A. Termination of cortical afferents on identified neurons in the caudate nucleus of the cat. Exp Brain Res 1981;41:329–337.
109. Fuxe K, Andén NE. Studies on the central monoamine neurons with special reference to the nigro-neostriatal dopamine neuron system. In: Costa E, ed. Biochemistry and pharmacology of the basal ganglia. New York: Raven Press, 1966: 123–129.
110. Gale K, Hong J-S, Guidotti A. Presence of substance P and GABA in separate striatonigral neurons. Brain Res 1977;36:371–375.
111. Garcia-Rill E. The basal ganglia and the locomotor regions. Brain Res Rev 1986;11:47–63.
112. Garcia-Rill E. The pedunculopontine nucleus. Prog Neurobiol 1991; 36:363–389.
113. Gerfen CR. The neostriatal mosaic: Multiple levels of compartmental organization in the basal ganglia. Annu Rev Neurosci 1992;15: 285–320.
114. Georgopoulos AP, DeLong MR, Crutcher MD. Relations between parameters of step-tracking movements and single cell discharge in the globus pallidus and subthalamic nucleus of the behaving monkey. J Neurosci 1983;3:1586–1598.
115. Giguère M, Marchand R, Poirier LJ. The nigrostriatal nervous pathway in the brain of the cat: An autoradiographic study. In: Hassler RG, Christ JF, eds. Advances in neurology. New York: Raven Press, 1984:77–83.
116. Giménez-Amaya JM, Graybiel AM. Compartmental origins of the striatopallidal projection in the primate. Neuroscience 1990;34:111–126.
117. Goldman PS, Nauta WJH. Columnar distribution of cortico-cortical fibres in the frontal association, limbic and motor cortex of the developing Rhesus monkey. Brain Res 1977;122:393–413.
118. Goldman-Rakic PS. Cytoarchitectonic heterogeneity of the primate neostriatum: subdivision into island and matrix cellular compartments. J Comp Neurol 1982;205: 398–413.
119. Goldman-Rakic PS. Modular organization of prefrontal cortex. Trends Neurosci 1984;7:419–424.
120. Gorry JD. Studies on the comparative anatomy of the ganglion basale of Meynert. Acta Anat (Basel) 1963;55:51–104.
121. Gottesfeld A, Massari VJ, Muth EA, Jacobowitz DM. Stria medullaris: a possible pathway containing GABAergic afferents to the lateral habenula. Brain Res 1977;130:184–189.
122. Graybiel AM. Neurotransmitters and neuromodulators in the basal ganglia. Trends Neurosci 1990;13: 244–254.
123. Graybiel AM, Ragsdale CW Jr. Histochemically distinct compartments in the striatum of human, monkey and cat demonstrated by acetylcholinesterase staining. Proc Natl Acad Sci USA 1978;75: 5723–5726.
124. Graybiel AM, Ragsdale CW Jr. Fiber connections of the basal ganglia. In: Cuenod M, Kreutzberg GW, Bloom FE, eds. Development and chemical specificity of neurons. Amsterdam: Elsevier, 1979: 239–283.
125. Groenewegen HJ, Berendse HW. Connections of the subthalamic nucleus with ventral striatopallidal parts of the basal ganglia in the rat. J Comp Neurol 1990;294:607–622.
126. Grofova I. The identification of striatal and pallidal neurons projecting to substantia nigra: an experimental study by means of retrograde axonal transport of horseradish peroxidase. Brain Res 1975;91:286–291.
127. Guevara Guzman R, Kendrick KM, Emson PC. Effect of substance P on acetylcholine and dopamine release in the rat striatum: a microdialysis study. Brain Res 1993; 622:147–154.
128. Guridi J, Luquin MR, Herrero MT, Obeso JA. The subthalamic nucleus: a possible target for stereotaxic surgery in Parkinson's disease. Mov Disord 1993;8:421–429.
129. Gusella JF, Waxler NS, Conneally P-M, et al. A polymorphic DNA marker genetically linked to Huntington's disease. Nature 1983; 306:234–238.
130. Guyenet PG, Crane JK. Nondopaminergic nigrostriatal pathway. Brain Res 1981;213:291–305.
131. Haber SN, Elde R. Correlation between met-enkephalin and substance P immunoreactivity in primate globus pallidus. Neuroscience 1981;6:1291–1297.
132. Haber SN, Lynd-Balta E, Mitchell SJ. The organization of the descending ventral pallidal projections in the monkey. J Comp Neurol 1993;329:111–128
133. Haber SN, Nauta WJH. Ramifications of the globus pallidus in the rat as indicated by patterns of immunohistochemistry. Neuroscience 1983;9:245–260.
134. Haber SN, Watson SJ. The comparative distribution of enkephalin, dynorphin and substance P in the human globus pallidus and basal forebrain. Neuroscience 1985;14: 1011–1024.
135. Hamel E, Beaudet A. Opioid receptors in rat neostriatum: Radioautographic distribution at the electron microscopic level. Brain Res 1987; 401:239–257.
136. Hamilton WJ, Mossman HW. Human embryology. Baltimore: Williams & Wilkins, 1972.
137. Hammond C, Deniau JM, Rizk A, Féger J. Electrophysiological demonstration of an excitatory subthalamonigral pathway in the rat. Brain Res 1978;151:235–244.
138. Hammond C, Féger J, Bioulac B, Souteyrand JP. Experimental hemiballism in the monkey produced by unilateral kainic acid lesion in corpus Luysii. Brain Res 1979;171:577–580.
139. Hammond C, Yelnik J. Intracellu-

lar labelling of rat subthalamic neurones with horseradish peroxidase: Computer analysis of dendrites and characterization of axon arborization. Neuroscience 1983;8: 781–790.
140. Hammond WA. A treatise on diseases of the nervous system. New York: D. Appleton, 1871:655–662.
141. Hartmann-von Monakow K, Akert K, Künzle H. Projections of the precentral motor cortex and other cortical areas of the frontal lobe to the subthalamic nucleus in the monkey. Exp Brain Res 1978;33: 395–403.
142. Hartmann-von Monakow K, Akert K, Künzle H. Projections of the precentral and premotor cortex to the red nucleus and other midbrain areas in *Macaca fascicularis*. Exp Brain Res 1979;34:91–105.
143. Hassler R. Striatal control of locomotion, intentional actions and of integrating and perceptive activity. J Neurol Sci 1978;36:187–224.
144. Hassler R, Chung Y-M. Identification of eight types of synapses in the pallidum externum and internum in the squirrel monkey (*Saimiri sciureus*). Acta Anat (Basel) 1984;118:65–81.
145. Hassler R, Reichert T, Mundinger F, Umbach W, Gangleberger JA. Physiological observations in stereotaxic operations in extrapyramidal motor disturbances. Brain 1960;83:337–350.
146. Hattori T, Fibiger HC, McGeer PL. Demonstration of a pallidonigral projection innervating dopaminergic neurons. J Comp Neurol 1975;162:487–504.
147. Hattori T, McGeer PL, Fibiger HC, McGeer EG. On the source of GABA-containing terminals in the substantia nigra: electron microscopic autoradiographic and biochemical studies. Brain Res 1973; 54:103–114.
148. Hazrati L-N, Parent A. Projection from the external pallidum to the reticular thalamic nucleus in the squirrel monkey. Brain Res 1991; 550:142–146.
149. Hazrati L-N, Parent A. Contralateral pallidothalamic and pallidotegmental projections in primates: an anterograde and retrograde labeling study. Brain Res 1991;567:212–223.
150. Hazrati L-N, Parent A. The striatopallidal projection displays a high degree of anatomical specificity in the primate. Brain Res 1992;592:213–227
151. Hazrati L-N, Parent A. Convergence of subthalamic and striatal afferents at pallidal level in primates: an anterograde double-labeling study with biocytin and PHA-L. Brain Res 1992;569: 336–340.
152. Hazrati L-N, Parent A. Differential patterns of arborization of striatal and subthalamic fibers in the two pallidal segments in primates. Brain Res 1992;598:311–315.
153. Hazrati L-N, Parent A. Projection from the deep cerebellar nuclei to the pedunculopontine nucleus in the squirrel monkey. Brain Res 1992;585:267–271.
154. Hazrati L-N, Parent A. Striatal and subthalamic afferents to the primate pallidum: interactions between two opposite chemospecific neuronal systems. In: Arbuthnott GW, Emson PC, eds. Chemical signalling in the basal ganglia. Vol. 6. Prog Brain Res 1993;99:89–104.
155. Hazrati L-N, Parent A, Mitchell S, Haber SN. Evidence for interconnections between the two segments of the globus pallidus in primates: a PHA-L anterograde tracing study. Brain Res 1990;533: 171–175.
156. Heath JW. Clinicopathologic aspects of Parkinsonian states. Arch Neurol Psychiatry 1947;58:484–497.
157. Hedreen JC. Separate demonstration of dopaminergic and nondopaminergic projections of the substantia nigra in the cat. Anat Rec 1971;169:338.
158. Heimer, L., Switzer, R.C., III, and Van Hoesen, G.W. 1982. Ventral striatum and ventral pallidum: Components of the motor system? Trends Neurosci 5:83–87.
159. Heimer, L, Wilson, R.D. 1975. The subcortical projections of the allocortex: Similarities in the neural association of the hippocampus, the pyriform cortex, and the neocortex. In M. Santini, ed. Golgi Centennial Symposium. New York: Raven Press, 177–193.
160. Herkenham, M. 1978. Intralaminar and parafascicular efferents to the striatum and cortex in the rat: An autoradiographic study. Anat Rec 190:420.
161. Herkenham M, Nauta WJH. Afferent connections of the habenular nuclei in the rat: a horseradish peroxidase study, with a note on the fiber-of-passage problem. J Comp Neurol 1977;173:123–145.
162. Herz A, Zieglgänsberger W. The influence of microelectrophoretically applied biogenic amines, cholinomimetics and procaine on synaptic excitation in the corpus striatum. Int J Neuropharmacol 1968;7:221–230.
163. Herz E. Die amyostatischen Unruheerschelnungen. J Psychol Neurol 1931;43:3–182.
164. Hökfelt T, Ungerstedt U. Electron and fluorescence microscopical studies on the nucleus caudatus putamen of the rat after unilateral lesions of ascending nigro-neostriatal dopamine neurons. Acta Physiol Scand 1969;76:415–426.
165. Hope BT, Michael G, Knigge KM, Vincent SR. Neuronal NADPH diaphorase is a nitric oxide synthase. Proc Natl Acad Sci USA 1991;88:2811–2814.
166. Hopkins DA, Niessen LW. Substantia nigra projections to the reticular formation, superior colliculus and central gray in rat, cat, and monkey. Neurosci Lett 1976;2: 253–259.
167. Hornykiewicz O. Metabolism of brain dopamine in human parkinsonism: neurochemical and clinical aspects. In: Costa E, ed. Biochemistry and pharmacology of the basal ganglia. New York: Raven Press, 1966:171–185.
168. Huerta MF, Krubitzer LA, Kaas JH. Frontal eye field as defined by intracortical microstimulation in squirrel monkeys, owl monkeys, and macaque monkeys. I. Subcortical connections. J Comp Neurol 1986;253:415–439.
169. Ilinsky IA, Kultas-Ilinsky K. Sagittal cytoarchitectonic maps of the *Macaca mulatta* thalamus with a revised nomenclature of the motor-related nuclei validated by observations on their connectivity. J Comp Neurol 1987;262:331–364.
170. Ilinsky IA, Tourtellotte WG, Kultas-Ilinsky K. Anatomical distinctions between the two basal ganglia afferent territories in the primate motor thalamus. Stereotact Funct Neurosurg 1993;60: 62–69.
171. Inagaki S, Parent A. Distribution of substance P and enkephalin-like immunoreactivity in the substantia nigra of rat, cat and monkey. Brain Res Bull 1984;13:319–329.
172. Iversen LL. The uptake, storage, release and metabolism of GABA in inhibitory nerves. In: Snyder SH, ed. Perspectives in neuropharmacology. London: Oxford University Press, 1972:75–111.
173. Jacobs BL, Azmitia EC. Structure and function of the brain serotonin system. Physiol Rev 1992;72: 165–229.
174. Jackson A, Crossman AR. Basal ganglia and other afferent projections to the peribrachial region in the rat: a study using retrograde and anterograde transport of horseradish peroxidase. Neuroscience 1983;6:1537–1549.
175. Jackson D, Bruno JP, Stachowiak MK, Zigmond MJ. Inhibition of striatal acetylcholine release by serotonin and dopamine after the intracerebral administration of 6-hydroxydopamine to neonatal rats. Brain Res 1988;457:267–273.
176. Jakob A. Die Extrapyramidalen Erkrankungen. Berlin: Julius Springer, 1923.
177. Jakob A. The anatomy, clinical syndromes and physiology of the extrapyramidal system. Arch Neurol Psychiatry 1925;13:596–620.
178. Jayaraman A. Organization of thalamic projections to the nucleus accumbens and the caudate nucleus in cats and its relation with hippocampal and other subcortical afferents. J Comp Neurol 1985;231: 396–420.
179. Jayaraman A, Updyke BV. Organization of visual cortical projections to the claustrum in the cat. Brain Res 1979;178:107–115.
180. Jiménez-Castellanos J, Graybiel

AM. Compartmental origins of striatal efferent projections in the cat. Neuroscience 1989;32:297–321.
181. Jinnai K, Matsuda Y. Neurons of the motor cortex projecting commonly on the caudate nucleus and the lower brain stem in the cat. Neurosci Lett 1979;26:95–99.
182. Jones EG. The thalamus. New York: Plenum, 1985.
183. Jones EG, Coulter JD, Burton H, Porter R. Cells of origin and terminal distribution of corticostriatal fibers arising in the sensory-motor cortex of monkeys. J Comp Neurol 1977;173:53–80.
184. Jones EG, Leavitt RY. Retrograde axonal transport and the demonstration of non-specific projections to the cerebral cortex and striatum from thalamic intralaminar nuclei in the cat, rat and monkey. J Comp Neurol 1974;154:349–378.
185. Jones EG, Wise SP. Size, laminar and columnar distribution of efferent cells in the sensory-motor cortex of monkeys. J Comp Neurol 1977;175:391–438.
186. Kanazawa I, Emson PC, Cuello AC. Evidence for the existence of substance P-containing fibers in striato-nigral and pallido-nigral pathways in rat brain. Brain Res 1977;119:447–459.
187. Kanazawa I, Marshall GR, Kelly JS. Afferents to the rat substantia nigra studied with horseradish peroxidase, with special reference to fibers from the subthalamic nucleus. Brain Res 1976;115: 485–491.
188. Kawaguchi Y. Physiological, morphological, and histochemical characterization of three classes of interneurons in rat neostriatum. J Neurosci 1993;13:4908–4923.
189. Kemp J. An electron microscopic study of the termination of afferent fibres in the caudate nucleus. Brain Res 1968;11:464–467.
190. Kemp J. Observations on the caudate nucleus of the cat impregnated with the Golgi method. Brain Res 1968;11:467–470.
191. Kemp JM. The termination of striopallidal and strionigral fibers. Brain Res 1970;17:125–128.
192. Kemp JM. The site of termination of afferents fibers on the neurones of the caudate nucleus. J Physiol (Lond) 1970;210:17–18.
193. Kemp JM, Powell TPS. The corticostriate projection in the monkey. Brain 1970;93:525–546.
194. Kemp JM, Powell TPS. The structure of the caudate nucleus of the cat: light and electron microscopy. Phil Trans R Soc Lond (Biol) 1971;262:383–401.
195. Kemp JM, Powell TPS. The synaptic organization of the caudate nucleus. Phil Trans R Soc Lond (Biol) 1971;262:403–412.
196. Kemp JM, Powell TPS. The termination of fibres from the cerebral cortex and thalamus upon dendritic spines in the caudate nucleus: a study with the Golgi method. Phil Trans R Soc Lond (Biol) 1971;262:429–439.
197. Kemp JM, Powell TPS. The connexions of the striatum and globus pallidus: synthesis and speculation. Phil Trans R Soc Lond (Biol) 1971;262:441–457.
198. Kim J-S, Hassler R, Haug P, Paik KS. Effect of frontal cortical ablation on striatal glutamic acid levels in rat. Brain Res 1977;132:370–374.
199. Kim R, Nakano K, Jayaraman A, Carpenter MB. Projections of the globus pallidus and adjacent structures: an autoradiographic study in the monkey. J Comp Neurol 1976;169:263–289.
200. Kimura H, McGeer PL, Peng JH, McGeer EG. The central cholinergic system studied by choline acetyltransferase immunohistochemistry in the cat. J Comp Neurol 1981;200:151–201.
201. Kita H. Responses of globus pallidus neurons to cortical stimulation: intracellular study in the rat. Brain Res 1992;589:84–90.
202. Kita H, Chang HT, Kitai ST. The morphology of intracellularly labeled rat subthalamic neurons: a light microscopic analysis, J Comp Neurol 1983;215:245–257.
203. Kita H, Kitai ST. Efferent projections of the subthalamic nucleus in the rat: light and electron microscopic analysis with the PHA-L method. J Comp Neurol 1987;260: 435–452.
204. Kita H, Kosaka T, Heizmann CW. Parvalbumin-immunoreactive neurons in the rat neostriatum: a light and electron microscopic study. Brain Res 1990;536:1–15.
205. Kitai ST, Koscis JD, Preston RJ, Sugimori M. Monosynaptic inputs to caudate neurons identified by intracellular injection of horseradish peroxidase. Brain Res 1976; 109:601–606.
206. Kitai ST, Kocsis JD, Wood J. Origin and characteristics of the corticocaudate afferents: an anatomical and electrophysiological study. Brain Res 1976;118:137–141.
207. Kodama S. Über die sogenannten Basalganglien. II. Pathologischanatomische Untersuchungen mit Bezug auf die sogenannten Basalganglien and ihre Adnexe. Schweiz Arch Neurol Psychiatr 1928;23:38–100;179–265.
208. Kubota Y, Kawaguchi Y. Spatial distributions of chemically identified intrinsic neurons in relation to patch and matrix compartments of rat neostriatum. J Comp Neurol 1993;332:499–513.
209. Kuhlenbeck H. The derivatives of the thalamus ventralis in the human brain and their relation to the so-called subthalamus. Milit Surg 1948;102:433–447.
210. Kuhlenbeck H, Haymaker W. The derivatives of the hypothalamus in the human brain: their relation to the extrapyramidal and autonomic systems. Milit Surg 1949;105:25–52.
211. Künzle H. Bilateral projections from precentral motor cortex to the putamen and other parts of the basal ganglia: an autoradiographic study in *Macaca fascicularis*. Brain Res 1975;88:195–209.
212. Künzle H. An autoradiographic analysis of the efferent connections from premotor and adjacent prefrontal regions (areas 6 and 9) in *Macaca fascicularis*. Brain Behav Evol 1978;15:185–234.
213. Künzle H, Akert K. Efferent connections of cortical area 8 (frontal eye field) in *Macaca fascicularis*: a reinvestigation using the autoradiographic technique. J Comp Neurol 1977;173:147–164.
214. Kuo J-S, Carpenter MB. Organization of pallidothalamic projections in the rhesus monkey. J Comp Neurol 1973;151:201–236.
215. Kuypers HGJM, Lawrence DG. Cortical projections to the red nucleus and the brain stem in the rhesus monkey. Brain Res 1967;4: 151–188.
216. Langston JW, Ballard P, Tetrud JW, Irwin I. Chronic parkinsonism in humans due to a product of meperidine-analog synthesis. Science 1983;249:979–980.
217. Larsen KD, McBride RL. The organization of feline entopeduncular nucleus projections: anatomical studies. J Comp Neurol 1979;184: 293–308.
218. Lavoie B, Parent A. Immunohistochemical study of the serotoninergic innervation of the basal ganglia in the squirrel monkey. J Comp Neurol 1990;299:1–16.
219. Lavoie B, Parent A. The pedunculopontine nucleus in the squirrel monkey. Cholinergic and glutamatergic projections to the substantia nigra. J Comp Neurol 1994;344:232–241.
220. Lavoie B, Smith Y, Parent A. Dopaminergic innervation of the basal ganglia in the squirrel monkey as revealed by tyrosine hydroxylase immunohistochemistry, J Comp Neurol 1989;289:36–52.
221. Lee HJ, Rye DB, Hallanger AE, Levey AI, Wainer BH. Cholinergic vs noncholinergic efferents from the mesopontine tegmentum to the extrapyramidal motor system nuclei. J Comp Neurol 1988;275: 469–492.
222. Levey AI, Wainer BH, Mufson EJ, Mesulam M-M. Co-localization of acetylcholinesterase and choline acetyltransferase in the rat cerebrum. Neuroscience 1983;9:9–22.
223. Lewy FH. Historical introduction. In: The basal ganglia and their Diseases. Res Publ Ass Nerv Ment Dis 1942;21:1–20.
224. Liles SL, Updyke BV. Projection of the digit and wrist area of precentral gyrus to the putamen: relation between topography and physiological properties of neurons in the putamen. Brain Res 1985;339:245–255.
225. Lindvall O, Brudin P, Widner H, et al. Grafts of fetal dopamine neurons survive and improve motor

function in Parkinson's disease. Science 1990;247:574–577.
226. McBride RL, Larsen KD. Projections of the feline globus pallidus. Brain Res 1980;198:3–14.
227. McGeer PL, Fibiger HC, Maler L, Hattori T, McGeer EG. Evidence for descending pallido-nigral GABA-containing neurons. Adv Neurol 1974;5:153–160.
228. McLennan H, York DH. The action of dopamine on neurons of the caudate nucleus. J Physiol (Lond) 1967;189:393–402.
229. Macchi G, Bentivoglio M, Molinari M, Minciacchi D. The thalamo-caudate versus thalamo-cortical projections as studied in the cat with fluorescent retrograde double-labeling. Exp Brain Res 1984;54: 225–239.
230. Malach R, Graybiel AM. Mosaic architecture of the somatic sensory-recipient sector of the cat's striatum. J Neurosci 1986;6:3436–3458.
231. Martin JB, Beal MF. Huntington's disease and neurotoxins. Ann NY Acad Sci 1992;648:169–175.
232. Martin JP. Hemichorea resulting from a local lesion of the brain. (The syndrome of body of Luys.) Brain 1927;50:637–651.
233. Martin JP. Remarks on the functions of the basal ganglia. Lancet 1959;1:999–1005.
234. Martin JP, Hurwitz LJ. Locomotion and the basal ganglia. Brain 1962;85:261–276.
235. Martin JP, McCaul IR. Acute hemiballismus treated by ventrolateral thalamolysis. Brain 1959;82: 104–108.
236. Mason ST, Fibiger HC. Kainic acid lesions of the striatum: behavioral sequelae similar to Huntington's chorea. Brain Res 1978;155: 313–329.
237. Matsumura M, Kojima J, Gardiner TW, Hikosaka O. Visual and oculomotor functions of monkey subthalamic nucleus. J Neurophysiol 1992;67:1615–1632
238. Mehler WR. Further notes on the center median nucleus of Luys. In: Purpura DP, Yahr MD, eds. The thalamus. New York: Columbia University Press, 1966:109–127.
239. Mehler WR. The basal ganglia—circa 1982. Appl Neurophysiol 1981;44:261–290.
240. Mesulam M-M, Mash D, Hersh L, Bothwell M, Geula C. Cholinergic innervation of the human striatum, globus pallidus, subthalamic nucleus, substantia nigra, and red nucleus. J Comp Neurol 1992;323: 252–268.
241. Mettler FA. Relation between pyramidal and extrapyramidal function. Proc Assoc Res Nerv Ment Dis 1942;21:150–227.
242. Mettler FA. Extensive unilateral cerebral removals in the primate: physiologic effects and resultant degeneration. J Comp Neurol 1943;79:185–243.
243. Mettler FA. Extracortical connections of the primate frontal cerebral cortex. I. Thalamo-cortical connections. J Comp Neurol 1947;86:95–117.
244. Mettler FA. Neuroanatomy. St. Louis: C.V. Mosby, 1948.
245. Mettler FA. The experimental anatomo-physiologic approach to the study of diseases of the basal ganglia. J Neuropathol Exp Neurol 1955;14:115–141.
246. Mettler FA. Anatomy of the basal ganglia. In: Vinken PJ, Bruyn GW, eds. Handbook of clinical neurology. Vol. 6. Amsterdam: North-Holland Publishing Company, 1968:1–55.
247. Meyer A. Karl Friedrich Burdach and his place in the history of neuroanatomy. J Neurol Neurosurg Psychiat 1970;33:553–561.
248. Miller JJ, Richardson TL, Fibiger HC, McLennan H. Anatomical and electrophysiological identification of a projection from the mesencephalic raphe to the caudate putamen in the rat. Brain Res 1975;97:133–138.
249. Mitchell IJ, Jackson A, Sambrook MA, Crossman AR. Common neural mechanisms in experimental chorea and hemiballismus in the monkey. Evidence from 2-deoxyglucose autoradiography. Brain Res 1985;339:346–350.
250. Mitrofanis J. Calbindin immunoreactivity in a subset of cat thalamic reticular neurons. J Neurocytol 1992;21:495–505.
251. Mogenson GJ, Swanson LW, Wu M. Evidence that projections of the substantia innominata to zona incerta and mesencephalic locomotor region contribute to locomotor activity. Brain Res 1985;334:65–76.
252. Moon Edley S, Graybiel AM. The afferent and efferent connections of the feline nucleus tegmenti pedunculopontinus, pars compacta. J Comp Neurol 1983;217:187–215.
253. Mouroux M, Féger J. Evidence that the parafascicular projection to the subthalamic nucleus is glutamatergic. Neuroreport 1993;4:613–615.
254. Narabayashi H. Role of stereotaxic surgery in treatment of Parkinson's disease. In: Nagatsu T, Narabayashi H, Yoshida M, eds. Parkinson's disease: from clinical aspects to molecular basis. Wien: Springer-Verlag, 1991:187–199.
255. Narabayashi H, Okuma T, Shikiba S. Procain oil blocking of the globus pallidus. AMA Arch Neurol Psychiatry 1956;75:36–48.
256. Narkiewicz O. Degenerations in the claustrum after regional neocortical ablations in the cat. J Comp Neurol 1964;123:335–356.
257. Nauta HJW. Evidence of a pallidohabenular pathway in the cat. J Comp Neurol 1974;156:19–28.
258. Nauta HJW, Cole M. Efferent projections of the subthalamic nucleus: An autoradiographic study in monkey and cat. J Comp Neurol 1978;180:1–16.
259. Nauta HJW, Pritz MB, Lasek RJ. Afferents to the rat caudoputamen studied with horseradish peroxidase: an evaluation of a retrograde neuroanatomical research method. Brain Res 1974;67:219–238.
260. Nauta WJH, Mehler WR. Projections of the lentiform nucleus in the monkey. Brain Res 1966;1:3–42.
261. Nauta WJH, Smith GP, Faull RLM, Domesick VB. Efferent connections and nigral afferents of the nucleus accumbens septi in the rat. Neuroscience 1978;3:385–401.
262. Nauta WJH, Whitlock DG. An anatomical analysis of the non-specific thalamic projection system. In: Delafresnaye JF, ed. Brain mechanisms and consciousness. Oxford: Blackwell Scientific Publications, 1954:81–98.
263. Nicolaou NM, Garcia-Munoz M, Arbuthnott GW, Eccleston D. Interactions between serotoninergic and dopaminergic systems in rat brain demonstrated by small unilateral lesions of the raphe nuclei. Europ J Pharmacol 1979;57: 295–305.
264. Nomura S, Mizuno N, Sugimoto T. Direct projections from the pedunculopontine tegmental nucleus to the subthalamic nucleus in the cat. Brain Res 1980;196:223–227.
265. Norita M. Demonstration of bilateral claustro-cortical connections in the cat with the method of retrograde axonal transport of horseradish peroxidase. Arch Histol Jpn 1977;40:1–10.
266. Ohye C. Dynamic aspects of the striatothalamic connection studied in cases with movement disorders. In: Narabayashi H, Nagatsu T, Yanagisawa N, Mizuno Y, eds. Advances in neurology. New York: Raven Press, 1993:78–83.
267. Oka H. Organization of the cortico-caudate projections. A horseradish peroxidase study in the cat. Exp Brain Res 1980;40:203–208.
268. Okada Y, Nitch-Hassler C, Kim JS, Bak IJ, Hassler R . The role of γ-aminobutyric acid (GABA) in the extrapyramidal motor system. I. Regional distribution of GABA in rabbit, rat and guinea pig brain. Exp Brain Res 1971;13:514–518.
269. Olpe H-R, Koella WP. The response of striatal cells upon stimulation of the dorsal and median raphe nuclei. Brain Res 1977; 122:357–360.
270. Olson CR, Graybiel AM. Sensory maps in the claustrum of the cat. Nature 1980;288:479–481.
271. Olszewski J, Baxter D. Cytoarchitecture of the human brain stem. Philadelphia: J.B. Lippincott, 1954.
272. Parent A. Identification of the pallidal and peripallidal cells projecting to the habenula in monkey. Neurosci Lett 1979;15:159–164.
273. Parent A. Comparative neurobiology of the basal ganglia. New York: John Wiley & Sons, 1986.
274. Parent A. Extrinsic connections of the basal ganglia. Trends Neurosci 1990;13:254–258.
275. Parent A, Bouchard C, Smith Y.

The striatopallidal and striatonigral projections: two distinct fiber systems in primate. Brain Res 1984;303:385–390.
276. Parent A, De Bellefeuille L. Organization of efferent projections from the internal segment of the globus pallidus in primates as revealed by fluorescent retrograde labeling method. Brain Res 1982;245: 201–214.
277. Parent A, De Bellefeuille L. The pallidointralaminar and pallidomigral projections in primate as studied with retrograde double-labeling method. Brain Res 1983; 278:11–27.
278. Parent A, Descarries L, Beaudet A. Organization of ascending serotonin systems in the adult rat brain. A radioautographic study after intraventricular administration of [^{3}H]5-hydroxytryptamine. Neuroscience 1981;6:115–138.
279. Parent A, Gravel S, Boucher R. The origin of forebrain afferents to the habenula in rat, cat and monkey. Brain Res Bull 1981;6:23–38.
280. Parent A, Gravel S, Olivier A. The extrapyramidal and limbic systems relationship at the globus pallidus level: a comparative histochemical study in the rat, cat, and monkey. In: Poirier LJ, Sourkes TL, Bédard PJ, eds. Advances in neurology. New York: Raven Press, 1978:1–11.
281. Parent A, Hazrati L-N. Anatomical aspects of information processing in primate basal ganglia. Trends Neurosci 1993;16:111–116.
282. Parent A, Hazrati L-N. Multiple striatal representation in primate substantia nigra. J Comp Neurol 1994;344:305–320.
283. Parent A, Mackey A, De Bellefeuille L. The subcortical afferents to caudate nucleus and putamen in primate: a fluorescence retrograde double labeling study. Neuroscience 1983;10:1137–1150.
284. Parent A, O'Reilly-Fromentin J, Boucher R. Acetylcholinesterase-containing neurons in cat neostriatum: a morphological and quantitative analysis. Neurosci Lett 1980;20:271–276.
285. Parent A, Smith Y. Organization of efferent projections of the subthalamic nucleus in the squirrel monkey as revealed by retrograde labeling methods. Brain Res 1987;436:296–310.
286. Parent A, Smith Y, Filion M, Dumas J. Distinct afferents to internal and external pallidal segments in the squirrel monkey. Neurosci Lett 1989;96:140–144.
287. Park MR, Falls WM, Kitai ST. An intracellular HRP study of the rat globus pallidus. I. Responses and light microscopic analysis. J Comp Neurol 1982;211:284–294.
288. Pasik P, Pasik T, Di Figlia M. Quantitative aspects of neuronal organization in the neostriatum of the Macaque monkey. Proc Assoc Res Nerv Ment Dis 1976;55:57–89.
289. Pasik P, Pasik T, Holstein GR, Saavedra JP. Serotonergic innervation of the monkey basal ganglia: an immunocytochemical study. In: McKenzie JS, Kemm RE, Wilcock LN, eds. The basal ganglia: structure and function. Plenum Press, New York, 1984:115–129.
290. Pasik P, Pasik T, Saavedra JP. Immunocytochemical localization of serotonin at the ultrastructural level. J Histochem Cytochem 1982;30:760–764.
291. Pearson RCA, Brodal P, Gatter KC, Powell TPS. The organization of the connections between the cortex and the claustrum in the monkey. Brain Res 1982;234:435–441.
292. Penney JB Jr, Young AB. Striatal inhomogeneities and basal ganglia function. Mov Disord 1986;1:3–15.
293. Percheron G. The thalamic territory of cerebellar afferents and the lateral region of the thalamus of the macaque in stereotaxic ventricular coordinates. J Hirnforsch 1977;18:375–400.
294. Percheron G, Yelnik J, François C. A Golgi analysis of the primate globus pallidus. III. Spatial organization of the striatopallidal complex. J Comp Neurol 1984;227: 214–227.
295. Phelps PE, Houser CR, Vaughn JE. Immunocytochemical localization of choline acetyltransferase within the rat neostriatum: A correlated light and electron microscopic study of cholinergic neurons and synapses. J Comp Neurol 1985; 238:286–307.
296. Pickel VM, Beckley SC, Joh TH, Reis DJ. Ultrastructural immunocytochemical localization of tyrosine hydroxylase in the neostriatum. Brain Res 1981;225: 373–385.
297. Poirier LJ, Parent A, Roberge AG. The striopallidal system: its implication in motor disorders. In: Ioachim HL, ed. Pathobiology annual. New York: Appleton-Century-Crofts, 1975:339–367.
298. Poirier LJ, Sourkes TL. Influence of the substantia nigra on catecholamine content of the striatum. Brain 1965;88:181–192.
299. Poirier LJ, Sourkes TL, Bouvier G, Boucher R, Scarabin S. Striatal amines, experimental tremor and the effect of harmaline in the monkey. Brain 1966;89:37–52.
300. Powell TPS, Cowan WM. A study of thalamo-striate relations in the monkey. Brain 1956;79:364–390.
301. Pycock C, Horton RW, Marsden CD. The behavioural effects of manipulating GABA function in the globus pallidus. Brain Res 1976;116:353–359.
302. Rafols J, Fox CS. The neurons of the primate subthalamic nucleus: a Golgi and electron microscopic study. J Comp Neurol 1976;168: 75–112.
303. Ragsdale CW Jr, Graybiel AM. The fronto-striatal projection in the cat and monkey and its relationship to inhomogeneities established by acetylcholinesterase histochemistry. Brain Res 1981;208: 259–266.
304. Ramón y Cajal S. Histologie du Système Nerveux de l'Homme et des Vertébrés. (Azoulay L, trans.) Paris: Maloine, 1909, 1911. (Reprinted, Consejo Superior de Investigaciones Cientificas, Instituto Ramón y Cajal, Madrid, 1972.)
305. Ranson SW, Ranson SW Jr. Efferent fibers of the corpus striatum. Proc Assoc Res Nerv Ment Dis 1942;21:69–76.
306. Rasminsky M, Mauro A, Albe-Fessard D. Projections of medial thalamic nuclei to the putamen and frontal cerebral cortex in the cat. Brain Res 1973;61:69–77.
307. Ribak CE, Vaughn JE, Roberts E. The GABA neurons and their axon terminals in the rat corpus striatum as demonstrated by GAD immunocytochemistry. J Comp Neurol 1979;187:261–284.
308. Riche D, Lanoir J. Some claustrocortical connections in the cat and baboon as studied by retrograde horseradish peroxidase transport. J Comp Neurol 1978;177:434–444.
309. Ritcher E. Die Entwicklung des Globus Pallidus und des Corpus Subthalamicum. Berlin: Springer-Verlag, 1965.
310. Riley HA. An atlas of the basal ganglia, brain stem and spinal cord. Baltimore: Williams & Wilkins, 1943.
311. Rinvik E, Grofova I, Hammond C, Féger J, Deniau JM. A study of the afferent connections of the subthalamic nucleus in the monkey and cat using the HRP technique. In: Poirier LJ, Sourkes TL, Bédard PJ, eds. Advances in neurology. New York: Raven Press, 1979:53–70.
312. Rinvik E, Ottersen OP. Terminals of subthalamonigral fibres are enriched with glutamate-like immunoreactivity: an electron microscopic, immunogold analysis in the cat. J Chem Neuroanat 1993;6: 19–30.
313. Roeder F, Orthner H. Erfahrungen mit stereotaktischen Eingriffen. I. Mitteilung: Zur Pathogenese und Therapie extrapyramidal-motorischer Bewegungsstörungen. Erfolgreiche Behandlung eines Falles schwerem Hemiballismus mit gezielter Electrokoagulation des Globus pallidus. Dtsch Z Nervenh 1956;175:419–434.
314. Romansky KV, Usunoff KG, Ivanov DP, Galabov GP. Corticosubthalamic projection in the cat: an electron microscopic study. Brain Res 1979;163:319–322.
315. Royce GJ. Laminar origin of cortical neurons which project upon the caudate nucleus: a horseradish peroxidase investigation in the cat. J Comp Neurol 1982;205:8–29.
316. Royce GJ, Bromley S. Fluorescent double labeling studies of thalamostriatal and corticostriatal neurons. In: McKenzie JS, Kemm RE, Wilcox LN, eds. The basal ganglia: structure and function. New York: Plenum Press, 1984:131–146.

317. Royce GJ, Mourey RJ. Efferent connections of the centromedian and parafascicular thalamic nuclei: an autoradiographic investigation in the cat. J Comp Neurol 1985; 235:277–300.
318. Russchen FT, Bask I, Amaral DG, Price DL. The amygdalostriatal projection in the monkey. An anterograde tracing study. Brain Res 1985;329:249–257.
319. Sadikot AF, Parent A, François C. The centre médian and parafascicular thalamic nuclei project respectively to the sensorimotor and associative-limbic striatal territories in the squirrel monkey. Brain Res 1990;510:161–165.
320. Sadikot AF, Parent A, François C. Efferent connections of the centromedian and parafascicular thalamic nuclei in the squirrel monkey: a PHA-L study of subcortical projections. J Comp Neurol 1992;315: 137–159.
321. Sadikot AF, Parent A, Smith Y, Bolam JP. Efferent connections of the centromedian and parafascicular thalamic nuclei in the squirrel monkey: a light and electron microscopic study of the thalamostriatal projection in relation to striatal heterogeneity. J Comp Neurol 1992;320:228–242.
322. Scheel-Kruger J. Dopamine-GABA interaction: evidence that GABA transmits, modulates and mediates dopaminergic functions in the basal ganglia and the limbic system. Acta Neurol Scand 1986; 73(Suppl 107):1–49.
323. Schröder KF, Hopf A, Lange H, Thörner G. Morphometrisch-statische Strukturanalysen des Striatum, Pallidum und Nucleus subthalamicus beim Menschen. J Hirnforsch 1975;16:333–350.
324. Schwarcz R, Coyle JT. Striatal lesions with kainic acid: Neurochemical characteristics. Brain Res 1977;127:235–249.
325. Selemon LD, Goldman-Rakic PS. Longitudinal topography and interdigitation of corticostriatal projections in the rhesus monkey. J Neurosci 1985;5:776–794.
326. Sherk H. The claustrum and the cerebral cortex. In: Jones EG, Peters A, eds. Cerebral cortex. Vol. 5. New York: Plenum Press, 1984: 467–499.
327. Sherk H, Levay S. Visual claustrum: topography and receptive field properties in the cat. Science 1981;212:87–89.
328. Shoulson I, Chase TN. Huntington's disease. Annu Rev Med 1975;26:419–426.
329. Shoulson I, Kartzinel R, Chase TN. Huntington's disease: treatment with dipropylacetic acid and gamma-aminobutyric acid. Neurology 1976;26:61–63.
330. Siggins GR, Hoffer BJ, Bloom FE, Ungerstedt U. Cytochemical and electrophysiological studies of dopamine in the caudate nucleus. In: Yahr MD, ed. The basal ganglia. Proc Assoc Res Nerv Ment Dis 1976;55:227–247.
331. Smith Y, Hazrati LN, Parent A. Efferent projections of the subthalamic nucleus in the squirrel monkey as studied by the PHA-L anterograde tracing method. J Comp Neurol 1990;294:306–323.
332. Smith Y, Lavoie B, Dumas J, Parent A. Evidence for a separate nigropallidal dopaminergic projection in the squirrel monkey. Brain Res 1989;482:381–386.
333. Smith Y, Parent A. Neuropetide Y-immunoreactive neurons in the striatum of cat and monkey: morphological characteristics, intrinsic organization and co-localization with somatostatin. Brain Res 1986;372:241–252.
334. Smith Y, Parent A. Neurons of the subthalamic nucleus in primates display glutamate but not GABA immunoreactivity. Brain Res 1988; 453:353–356.
335. Smith Y, Parent A, Séguéla P, Descarries L. Distribution of GABA immunoreactive neurons in the basal ganglia of the squirrel monkey (*Saimiri sciureus*). J Comp Neurol 1987;259:50–65.
336. Soghomonian J-J, Descarries L, Watkins KC. Serotonin innervation in adult rat neostriatum. II. Ultrastructural features: a radioautographic and immunocytochemical study. Brain Res 1989;481:67–86.
337. Somogyi P, Bolam JP, Smith AD. Monosynaptic cortical input and local axon collaterals of identified striatonigral neurons. A light and electron microscopic study using the Golgi-peroxidase transport-degeneration procedure. J Comp Neurol 1981;195:567–584.
338. Spencer HJ. Antagonism of cortical excitation of striatal neurons by glutamic acid diethyl ester: evidence for glutamic acid as an excitatory transmitter in the rat striatum. Brain Res 1976;102:91–101.
339. Stanton GB, Goldberg ME, Bruce CJ. Frontal eye field efferents in the macaque monkey. II: Topography of terminal fields in midbrain and pons. J Comp Neurol 1988;271: 493–506.
340. Stefani A, Surmeier DJ, Kitai ST. Serotonin enhances excitability in neostriatal neurons by reducing voltage-dependent potassium currents. Brain Res 1990;529:354–357.
341. Swanson LW, Cowan WM. A note on the connections and development of the nucleus accumbens. Brain Res 1975;92:324–330.
342. Switzer RC III, Hill J, Heimer L. The globus pallidus and its rostroventral extension into the olfactory tubercle of the rat: a cyto- and chemoarchitectural study. Neuroscience 1982;7:1891–1904.
343. Szabo J. Topical distribution of the striatal efferents in the monkey. Exp Neurol 1962;5:21–36.
344. Szabo J. The efferent projections of the putamen in the monkey. Exp Neurol 1967;19:463–476.
345. Szabo J. Projections from the body of the caudate nucleus in the rhesus monkey. Exp Neurol 1970; 27:1–15.
346. Szabo J. Distribution of striatal afferents from the mesencephalon in the cat. Brain Res 1980;188:3–21.
347. Szabo J. Organization of the ascending striatal afferents in monkeys. J Comp Neurol 1980;189: 307–321.
348. Takagi H, Somogyi P, Somogyi J, Smith AD. Fine structural studies on a type of somatostatin-immunoreactive neuron and its synaptic connections in the rat neostriatum: a correlated light and electron microscopic study. J Comp Neurol 1983;214:1–16.
349. Talairach J, Paillas JE, David M. Dyskinésie de type hémiballique traitée par cortectomie frontale limitée, puis par coagulation de l'anse lenticulaire et de la portion interne du globus pallidus. Rev Neurol (Paris) 1950;83:440–451.
350. Tennyson VM, Barrett RE, Cohen G, Côté L, Heikkila R, Mytilineou C. The developing neostriatum of the rabbit: correlation of fluorescence histochemistry, electron microscopy, endogenous dopamine levels, and [^{3}H] dopamine uptake. Brain Res 1972;46:251–285.
351. Ternaux JP, Héry F, Bourgoin S, Adrien J, Glowinski J, Hamon M. The topographical distribution of serotoninergic terminals in the neostriatum of the rat and the caudate nucleus of the cat. Brain Res 1977;121:311–326.
352. Thach WT, Jones EG. The cerebellar dentatothalamic connection: terminal field, lamellae, rods and somatotopy. Brain Res 1979;169: 168–172.
353. Tracey DJ, Asanuma C, Jones EG, Porter R. Thalamic relay to motor cortex: afferent pathways from brain stem, cerebellum, and spinal cord in monkeys. J Neurophysiol 1980;44:532–553.
354. Ungerstedt U. Stereotaxic mapping of the monoamine pathways in the rat brain. Acta Physiol Scand (Suppl) 1971;367:1–48.
355. Van der Kooy D, Hattori T. Dorsal raphe cells with collateral projections to the caudate-putamen and substantia nigra: a fluorescent retrograde double labeling study in the rat. Brain Res 1980;186:1–7.
356. Van der Kooy D, Hattori T. Single subthalamic nucleus neurons project to both the globus pallidus and substantia nigra in rat. J Comp Neurol 1980;192:751–768.
357. Van Hoesen GW, Yeterian EH, Lavizzo-Mourey R. Widespread corticostriate projection from temporal cortex of the rhesus monkey. J Comp Neurol 1981;199:205–219.
358. Vincent SR, Johansson O, Hökfelt T, et al. NADPH-diaphorase: A selective histochemical marker for striatal neurons containing both somatostatin- and avian pancreatic polypeptide (APP)-like immunore-

activities. J Comp Neurol 1983; 217:252–263.
359. Vincent SR, Staines WA, Fibiger HC. Histochemical demonstration of separate populations of somatostatin and cholinergic neurons in the rat striatum. Neurosci Lett 1983;35:111–114.
360. Vives F, Mogenson GJ. Electrophysiological evidence that the mediodorsal nucleus of the thalamus is a relay between the ventral pallidum and the medial prefrontal cortex in the rat. Brain Res 1985;344:320–337.
361. Vogt C, Vogt O. Thalamusstudien I-III. I. Zur Einfurung, II. Homoginät und Grenzgestaldung der Grisea des Thalamus, III. Das Griseum centrale (centrum medianum Luys). J Psychol Neurol (Leipzig) 1941;50:31–154.
362. Von Bonin G, Shariff GA. Extrapyramidal nuclei among mammals. J Comp Neurol 1951;94: 427–438.
363. Von Monakow C. Experimentelle und pathologisch-anatomische Untersuchunger über die Haubenregion, den Sehhügel und die Regio subthalamica. Arch Psychiatr Nervenkr 1895;27:1–219.
364. Von Namba M. Cytoarchitektonische Untersuchungen am Striatum. J Hirnforsch 1957;3:24–48.
365. Von Santha K. Zur Klinik und Anatomie des Hemiballismus. Arch Psychiatr Nervenkr 1928;84: 664–678.
366. Webster KE. Cortico-striate interrelations in the albino rat. J Anat 1961;95:532–544.
367. Webster KE. The cortico-striatal projection in the cat. J Anat 1965;99:329–337.
368. Whittier JR. Ballism and the subthalamic nucleus (nucleus hypothalamicus; corpus Luysi). Arch Neurol Psychiatry 1947;58:672–692.
369. Whittier JR, Mettler FA. Studies on the subthalamus of the rhesus monkey. II. Hyperkinesia and other physiologic effects of subthalamic lesions with special reference to the subthalamic nucleus of Luys. J Comp Neurol 1949;90: 319–372.
370. Wichmann T, DeLong MR. Pathophysiology of parkinsonian motor abnormalities. In: Narabayashi H, Nagatsu T, Yanagisawa N, Mizuno Y, eds. Advances in neurology. New York: Raven Press, 1993; 60:53–61.
371. Willis T. Cerebri Anatome, cui Accessit Nervorum Descriptio et Usus. London: Martyn and Allestry, 1664.
372. Wilson SAK. An experimental research into the anatomy and physiology of the corpus striatum. Brain 1914;36:427–492.
373. Wilson SAK. Disorders of motility and muscle tone with special reference to the corpus striatum (Croonian lectures). Lancet 1925; 2:215–291.
374. Woolf NJ, Butcher LL. Cholinergic neurons in the caudate-putamen complex proper are intrinsically organized: a combined Evans blue and acetylcholinesterase analysis. Brain Res Bull 1981;7:487–507.
375. Wright AK, Arbuthnott GW. The pattern of innervation of the corpus striatum by the substantia nigra. Neuroscience 1981;6: 2063–2067.
376. Yang CR, Mogenson GJ. An electrophysiological study of the neural projection from the hippocampus to the ventral pallidum and subpallidal area by way of the nucleus accumbens. Neuroscience 1985;15:1015–1024.
377. Yelnik J, Percheron G. Subthalamic neurons in primates: A quantitative and comparative analysis. Neuroscience 1979;4:1717–1743.
378. Yelnik J, Percheron G, François C. A Golgi analysis of the primate globus pallidus. II. Quantitative morphology and spatial orientation of dendritic arborizations. J Comp Neurol 1984;227:200–213.
379. Yeterian EH, Pandya DN. Prefrontostriatal connections in relation to cortical architectonic organization in rhesus monkeys. J Comp Neurol 1991;312:43–67.
380. Yeterian EH, Van Hoesen GW. Cortico-striate projections in the rhesus monkey: the organization of certain cortico-caudate connections. Brain Res 1978;139:43–63.
381. Young WS, Alheid GF, Heimer L. The ventral pallidal projection to the mediodorsal thalamus: a study with fluorescent retrograde tracers and immunofluorescence. J Neurosci 1984;4:1626–1638.
382. Zaczek R, Schwarcz R, Coyle JT. Long term sequelae of striatal kainate lesion. Brain Res 1978; 152:626–632.
383. Garey LJ. Visual system. In: Paxinos G, ed. The human nervous system. Ch. 28. New York: Academic Press, 1990:945–977.
384. Parent A, Hazrati LN. Functional anatomy of the basal ganglia. I. The cortico-basal ganglia-thalamocortical loop. Brain Res Rev 1995; 20:91–127.
385. Parent A, Hazrati LN. Functional anatomy of the basal ganglia. II. The place of subthalmic nucleus and external pallidum in basal ganglia circuitry. Brain Res Rev 1995;20:128–154.

20
Cerebral Cortex

STRUCTURE OF THE CORTEX

The cerebral cortex develops from the telencephalon, which in early stages of histogenesis resembles other parts of the embryonic neural tube. The suprastriatal portion of the early telencephalic vesicle is composed of three concentric zones in its smooth-surfaced (lissencephalic) stage: (a) a *germinal zone* surrounding the lateral ventricle, (b) the *intermediate zone,* which becomes the white matter of the cerebral hemispheres, and (c) a *marginal zone,* which becomes the cortical zone or plate. The original columnar epithelial cells extend through all zones (338). At the end of the second month, cells migrate from the intermediate zone into the marginal zone, where they form a superficial gray layer, the *cerebral cortex.* As the cerebral cortex gradually thickens by the addition and differentiation of the migrating cells, as well as by the arrival of afferent fibers, it assumes a laminated appearance. As cells become organized into horizontal layers, between the sixth and eighth months, six such layers may be distinguished (44). The deeper pyramidal layer, rich in cells, forms layers II to VI, while the outermost layer, composed mostly of fibers, becomes the molecular layer (I). Cells formed at the same time tend to remain in the same layer, and newly formed cells migrate through these layers to more superficial locations (10). This "inside-out" sequence of neuronal migration applies to the majority of cortical cells (see Chapter 3 for details on the migration of cortical cells during development). This six-layered cellular arrangement is characteristic of the entire neopallial cortex, which is referred to as *neocortex, isocortex* (371), or *homogenetic cortex* (44). The *paleopallium* (olfactory cortex) and the *archipallium* (hippocampal formation and dentate gyrus) do not show six layers in either the developing or adult stage. The paleopallium and archipallium together constitute the *allocortex* or *heterogenetic cortex.*

The cerebral cortex in humans has an area of approximately 2200 cm^2 (2.5 square feet), and a total volume of about 500,000 mm^3. Only one-third of the cerebral cortex is found on the free surface of the brain; the remaining cerebral cortex is hidden in the depths of the sulci. The thickness of the cortex varies from about 4.5 mm in the precentral gyrus to about 1.5 mm in the depths of the calcarine sulcus. The cortex is always thickest over the crest of a convolution and thinnest in the depth of a sulcus. It has been estimated that besides nerve fibers, neuroglia, and blood vessels, the cerebral cortex contains about 15–20 billion neurons (368). With a mean incidence of 0.6×10^9 synapses per mm^3, there are roughly 3×10^{14} morphologically differentiated interneuronal contacts in human cerebral cortex. This number corresponds to the number of milliseconds that have elapsed in the last 10,000 years, that is, since the beginning of the Neolithic period (60).

The cerebral cortex contains (a) *afferent* fibers and *terminals* from other parts of the nervous system (e.g., thalamocortical fibers), (b) *association* and *commissural neurons* whose axons interrelate cortical regions of the same or opposite hemisphere, and (c) *projection neurons* whose axons conduct impulses to other parts of the neuraxis (e.g., corticospinal, corticoreticular, or corticopontine fibers). Most projection fibers arise from the deeper layers of the cortex, while the association and commissural fibers arise mainly from the more superficial ones (179). A striking feature of pallial structure is the relatively small number of projection fibers compared with the enormous number of cortical neurons.

Cortical Cells and Fibers

Although the cerebral cortex contains an enormous number of cells, the number of cell types is small (59, 80, 381, 414). The principal types of neurons found in the cortex are pyramidal cells and the stellate or granule cells

(Figs. 5.8, 20.1, and 20.2). The pyramidal cells (including a variant form, the fusiform cell) are the major projection neurons of the cerebral cortex, whereas the stellate cells act as interneurons.

The pyramidal cells, which are most characteristic of the cortex, have the form of an isosceles triangle whose upper pointed end is continued toward the surface of the brain as the *apical dendrite* (Fig. 20.2). Besides the apical dendrite, a number of more or less horizontally running *basal dendrites* spring from the cell body and arborize in its vicinity. The axon emerges from the base of the cell and descends toward the medullary substance, either terminating in the deeper layers of the cortex, or entering the white matter as a projection, or association fiber. Pyramidal cells have large vesicular nuclei, prominent Nissl granules, and usually are classified as small, medium, and large. The height of the cell body varies from 10–12 μm for the smaller neurons to 45–50 μm for the larger ones. The giant pyramidal cells of Betz, found in the precentral gyrus may be more than 100 μm in height.

Stellate or *granule cells* are small, polygonal or triangular, and have dark-staining nuclei and scanty cytoplasm. These cells, ranging from 4–8 μm, have a number of dendrites passing in all directions and a short axon which ramifies close to the cell body (Golgi type II) (Fig. 20.2). Other larger stellate cells have longer axons that may enter the medullary substance. Some resemble pyramidal cells in that they have an apical dendrite that extends to the surface. These cells are known as *stellate* or *star pyramidal cells* (239). Stellate cells are found throughout all layers of the cortex but are especially numerous in layer IV.

The *fusiform* or *spindle cells* are found mainly in the deepest cortical layer, with their long axis vertical to the surface (Fig. 20.2). The two poles of the cell are continued into dendrites, with the lower dendrites arborizing within the layer, while the upper ones ascend toward the surface. The axon arises from the middle or lower part of the cell body, and enters the white matter as a projection fiber. The large fusiform cells have been classified as "modified pyramidal" cells (337).

Other cell types found in the cortex are the *horizontal cells of Cajal,* and the cells with ascending axons, known as the *cells of Martinotti* (Fig. 20.4). The former are small fusiform cells found in the most superficial cortical layer and their long axons run horizontally for considerable distances and arborize within that layer. Martinotti cells, present in practically all cortical layers, are small triangular cells whose axons are directed toward the surface. Some fibers arborize in the same layer, while others send collaterals to a number of layers.

Apart from the subdivision of cortical cells into projection neurons (Golgi type I) and interneurons (Golgi type II), there exists another classification based on the presence or absence of spines on the dendrites of cortical neurons (80, 381). Spiny pyramidal cells are found in most cortical layers, except layer I, whereas stellate spiny cells occur principally in layer IV. The aspiny cortical cells comprise several types of interneurons distributed throughout the different layers of the cortex. Spiny and aspiny cortical neurons are believed to be respectively excitatory and inhibitory, but there could be some exceptions to this generalization (80).

Fibers in the cerebral cortex are disposed both radially and tangentially. Radially arranged fiber bundles run vertically from the medullary substance toward the cortical surface (Fig. 20.1). They include axons of pyramidal, fusiform, and stellate cells, which leave the cortex as projection or association fibers, and the entering afferent and association fibers, which terminate within the cortex. Ascending axons of the Martinotti cells likewise have a vertical course. Tangential fibers run parallel to the cortical surface. These fiber bundles are composed of (a) the terminal branches of the afferent and association fibers, (b) the axons of the horizontal and granule cells, and (c) the terminal branches of collaterals from the pyramidal and fusiform cells. Horizontal fibers in large part represent terminal portions of radial fibers that bend horizontally to come into synaptic relation with cortical cells. Tangential fibers are not distributed evenly throughout the cortex but are concentrated at varying depths into horizontal bands separated by layers with relatively few fibers (Fig. 20.1). The two most prominent bands are known as the *bands of Baillarger,* which form delicate white stripes in sections of the fresh cortex (Fig. 20.1).

Cortical Layers

In Nissl-stained sections the cell bodies are arranged in superimposed horizontal layers.

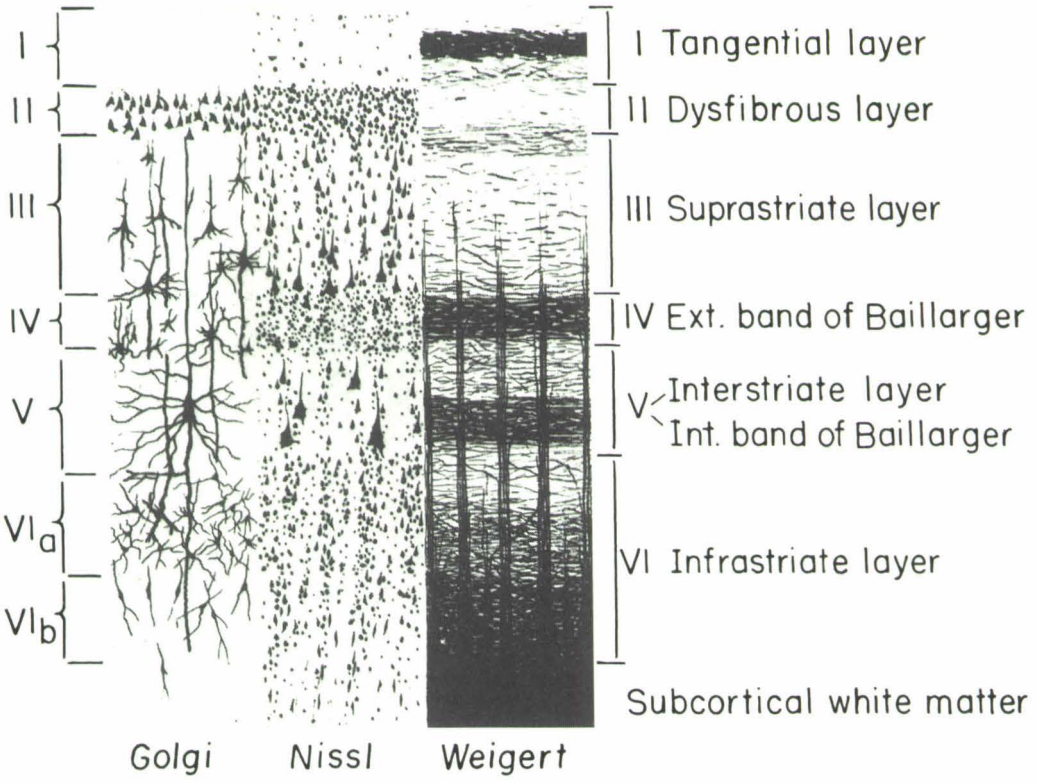


Figure 20.1. Cell layers and fiber arrangement of the human cerebral cortex.

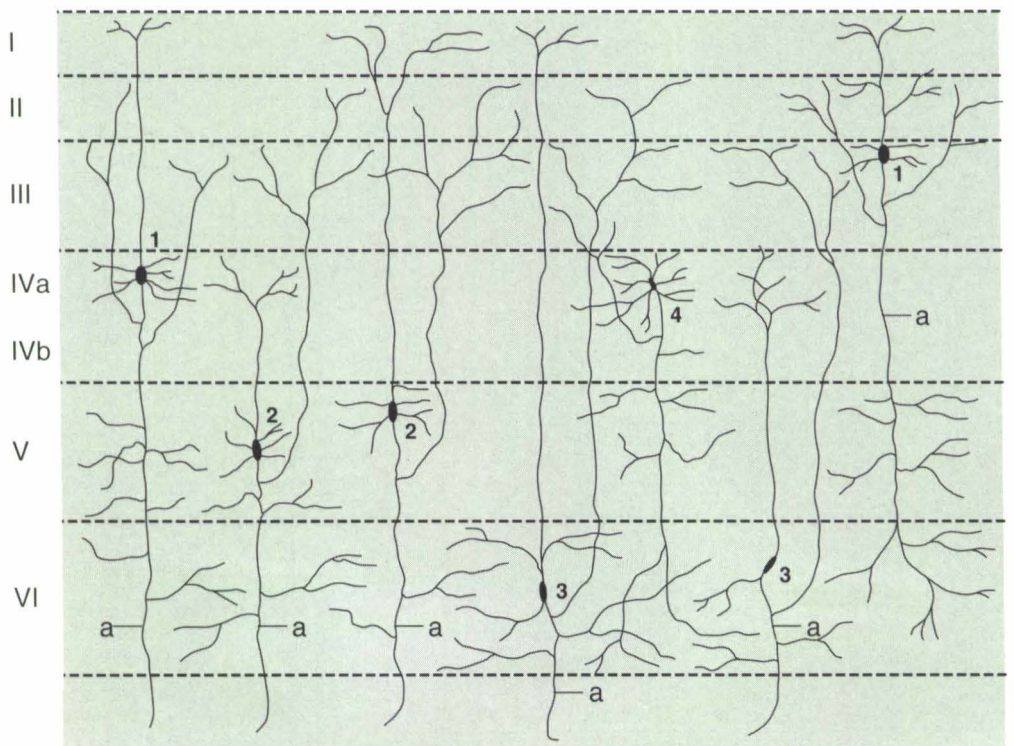


Figure 20.2. Dendritic and axonal branchings of several types of cortical neurons with descending axons. **1**, Pyramidal cells of superficial layers; **2**, pyramidal cells from ganglionic layer; **3**, spindle cells; **4**, stellate cells; *a*, axon.

Each layer is distinguished by the types, density, and arrangements of their cells. The lamination seen in myelin sheath-stained sections is determined primarily by the disposition of the horizontal fibers, which vary in the different layers (Figs. 20.1, 20.2, and 20.4). The neopallium (neocortex or isocortex), which forms 90% of the hemispheric surface, has six fundamental layers (44). Some of these layers are divided into sublayers.

The following layers are distinguished in the neocortex in passing from the pial surface to the underlying white matter: I, molecular; II, external granular; III, external pyramidal; IV, internal granular; V, internal pyramidal; and VI, multiform (Figs. 20.1, 20.3, and 20.4).

I. The *molecular layer* containing cells with horizontal axons and Golgi type II cells. Within it are the terminal dendritic ramifications of the pyramidal and fusiform cells from the deeper layers, and the axonal endings of Martinotti cells. These dendritic and axonal branches form a fairly dense tangential fiber plexus (Fig. 20.1).

II. The *external granular layer* consisting of numerous closely packed small granule cells whose apical dendrites terminate in the molecular layer and whose axons descend to the deeper cortical layers. This layer is poor in myelinated fibers.

III. The *external pyramidal layer* comprising two sublayers of pyramidal neurons: a superficial layer of medium cells and a deeper layer of large ones. Their apical dendrites go to the first layer, while most of their axons enter the white matter, chiefly as association or commissural fibers (164, 165, 179, 355). Intermingled with the pyramidal neurons are granule and Martinotti cells. In the most superfi-

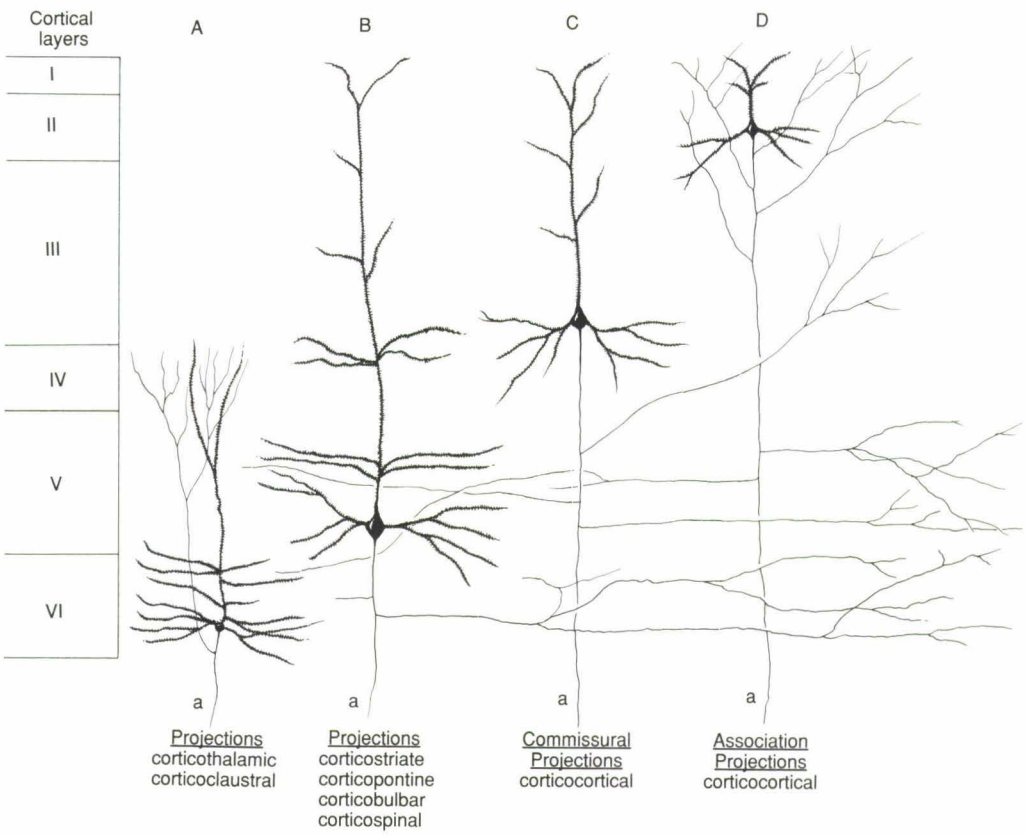


Figure 20.3. Major projection neurons in different layers of the cerebral cortex. Cortical layers are indicated on the left by *Roman numerals* and columns *A, B, C,* and *D* depict individual projection neurons in different layers which have separate targets. Subcortical projections of neurons in column B arise from pyramidal cells located in different parts of layer V, with corticostriatal neurons most superficial, and corticospinal neurons in the deepest part. Intracortical ramifications of dendrites and axonal collaterals are shown. Projections axons (*a*) are indicated as they enter the white matter.

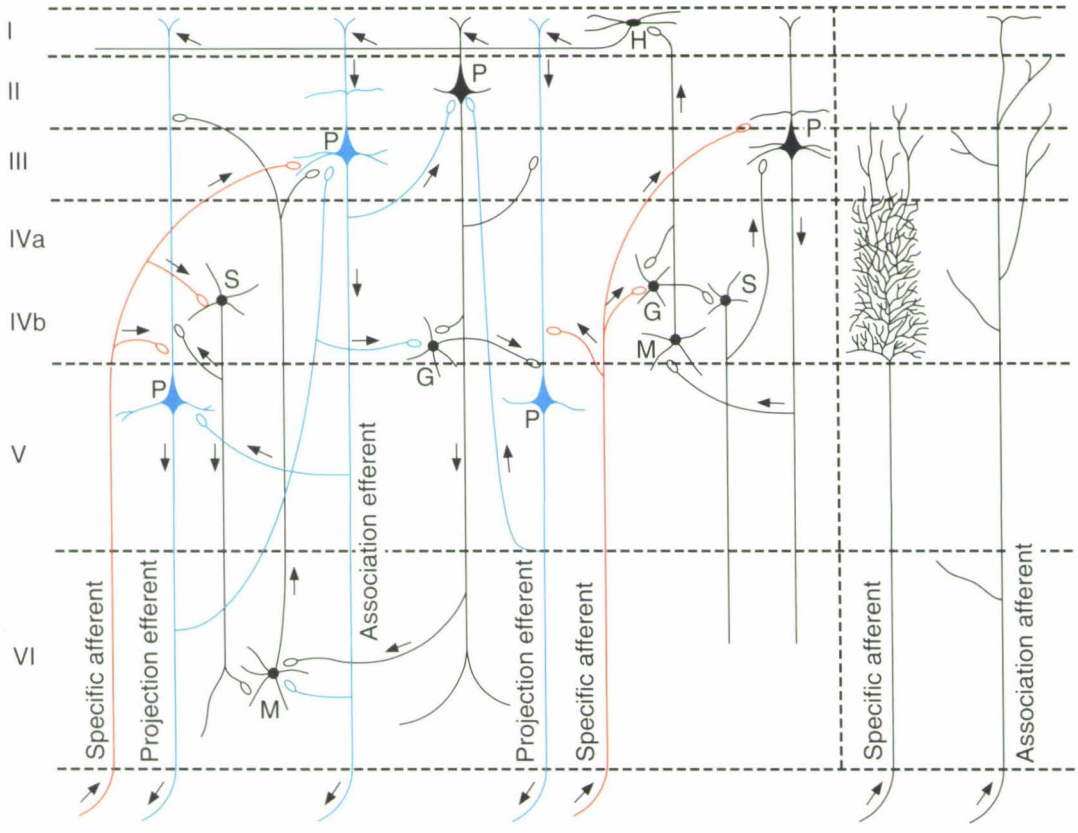


Figure 20.4. Intracortical circuits. Synaptic junctions are indicated by loops. *Red,* afferent thalamocortical fibers; *blue,* efferent cortical neurons; *black,* intracortical neurons; *G,* granule cell; *H,* horizontal cell; *M,* Martinotti cell; *P,* pyramidal cell; *S,* stellate cell. Mode of termination of afferent cortical fibers are shown on the right.

cial part of the layer, a number of horizontal myelinated fibers constitute the *band of Kaes-Bechterew.*

IV. The *internal granular layer* composed of closely packed stellate cells, many of which have short axons ramifying within the layer. Other larger cells have descending axons that terminate in deeper layers, or may enter the white substance. The whole layer is permeated by a dense horizontal plexus of myelinated fibers, forming the external band of Baillarger (Fig. 20.1).

V. The *internal pyramidal layer* consisting of medium and large-size pyramidal neurons intermingled with granule and Martinotti cells. Apical dendrites of large pyramidal cells ascend to the molecular layer, while dendrites of small pyramidal cells ascend only to layer IV, or may even arborize within this layer (Figs. 20.2 and 20.4). Axons of these cells enter the white matter chiefly as projection fibers, although a small number of callosal fibers are furnished by the smaller pyramidal cells. The horizontal fiber plexus in the deeper portion of this layer constitutes the internal band of Baillarger.

VI. The *multiform* or *fusiform layer* containing predominantly spindle-shaped cells whose long axes are perpendicular to the cortical surface. Like pyramidal neurons of layer V, the spindle cells vary in size. The larger ones send dendrites into the molecular layer, while the dendrites of the smaller ones ascend only to layer IV, or arborize within the fusiform layer. The dendrites of many pyramidal and spindle cells from layers V and VI come into direct relation with the endings of sensory thalamocortical fibers, which ramify chiefly in the internal granular layer. Axons of the spindle cells enter the white substance mainly as projection fibers. Some of the short arcuate association fibers connecting adjacent convolutions are furnished by the deep stellate cells of layer VI (239). The multiform layer may be divided into an upper sublayer of densely packed large cells, and a lower

one of loosely arranged small cells. The whole layer is pervaded by fiber bundles which enter or leave the medullary substance (Fig. 20.4).

Besides the horizontal cellular lamination, the cortex also exhibits a vertical or radial arrangement of the cells, which gives the appearance of slender vertical cell columns extending the whole thickness of the cortex (Figs. 20.14 and 20.15). These vertical columns are quite distinct in the parietal, occipital, and temporal lobes, but are practically absent in the frontal lobe. The columnar arrangement of cells in the cerebral cortex appears to be determined largely by the mode of termination of corticocortical afferents rather than specific sensory afferents (355). Corticocortical afferents are distributed throughout all layers of the cortex in columnar modules 200–300 μm in diameter, while terminals of specific sensory afferents usually are restricted to layer IV. It is remarkable that columnar units of corticocortical afferents are all nearly the same size and have dimensions similar to physiologically identified columnar units in the specific sensory cortex (122, 123, 140, 266, 276, 355). The arrangement into vertical cell columns is produced by the radial fibers of the cortex, just as the horizontal lamination is largely determined by the distribution of the tangential fibers.

The internal granular layer, which receives the main specific afferent projections and is best developed in the primary sensory areas, has been used to distinguish supragranular and infragranular layers. The *supragranular layers* (II and III) are the last to arise, the most highly differentiated, and the most extensive in humans (184). These layers are considered to be concerned mainly with associative cortical functions. The *infragranular layers* (V and VI), well-developed in all mammals, give rise to subcortical projection fibers concerned with efferent mechanisms. The supragranular layers are not present in the archipallium or paleopallium.

Interrelation of Cortical Neurons

The structure of the cerebral cortex as seen in Nissl or myelin sheath-stained sections is incomplete. These stains show only the type and arrangement of cell bodies, or the course and distribution of myelinated fibers. These methods give no information regarding terminal dendritic and axonal arborizations, which contain the synaptic junctions through which nerve impulses are transmitted. An understanding of the neuronal relationships, and of intracortical circuits, can be obtained from (a) classic Golgi studies, (b) intracellular injection experiments, (c) electron microscopic studies of various types of synaptic relationships, and (d) electron microscopic reconstruction of clearly identified Golgi-stained neurons. The distribution of dendritic and axonal terminals has been studied with the Golgi technique by a number of investigators, notably Ramón y Cajal (312) and Lorente de Nó (239). The latter author gave a detailed account for the elementary pattern of cortical organization that is applicable to the parietal, temporal, and occipital isocortex. The arrangement of the axonal and dendritic branching forms one of the most constant features of cortical organization. Most cortical interneurons also are highly specific with respect to their pattern of axonal arborizations and their synaptic contacts with other cortical neurons which form local networks (24, 80).

The afferent fibers to the cortex include projection fibers from the thalamus, association fibers from other cortical areas of the same hemisphere, and commissural fibers from the opposite side. The thalamocortical fibers, especially the specific afferent ones from the ventral tier thalamic nuclei and the geniculate bodies, pass unbranched to layer IV (Figs. 11.1, 11.6, 11.7, 13.30, 15.22, 16.13, and 16.14). These axons form a dense terminal plexus in layer IV (59, 165) and some of them extend to layer III where they arborize (Fig. 20.4). Specific afferent fibers in layer IV establish both axodendritic and axosomatic synapses upon stellate neurons, which are remarkably profuse on some cells (Fig. 20.5) (59). Estimates of the number of synaptic contacts upon neurons in the motor and visual cortex in the monkey indicate as many as 60,000 synapses per neuron in the motor area and 5,600 in the striate cortex (65). Additionally, these cells receive synaptic contacts from intracortical neurons.

Fibers of the so-called nonspecific thalamocortical system, related to the intralaminar thalamic nuclei and indirectly to the ascending reticular activating system, project to broad regions of the cerebral cortex (172). The potent effects of the stimulation of the intralaminar thalamic and the brainstem reticular formation upon electrocortical activity probably are mediated by these diffuse pro-

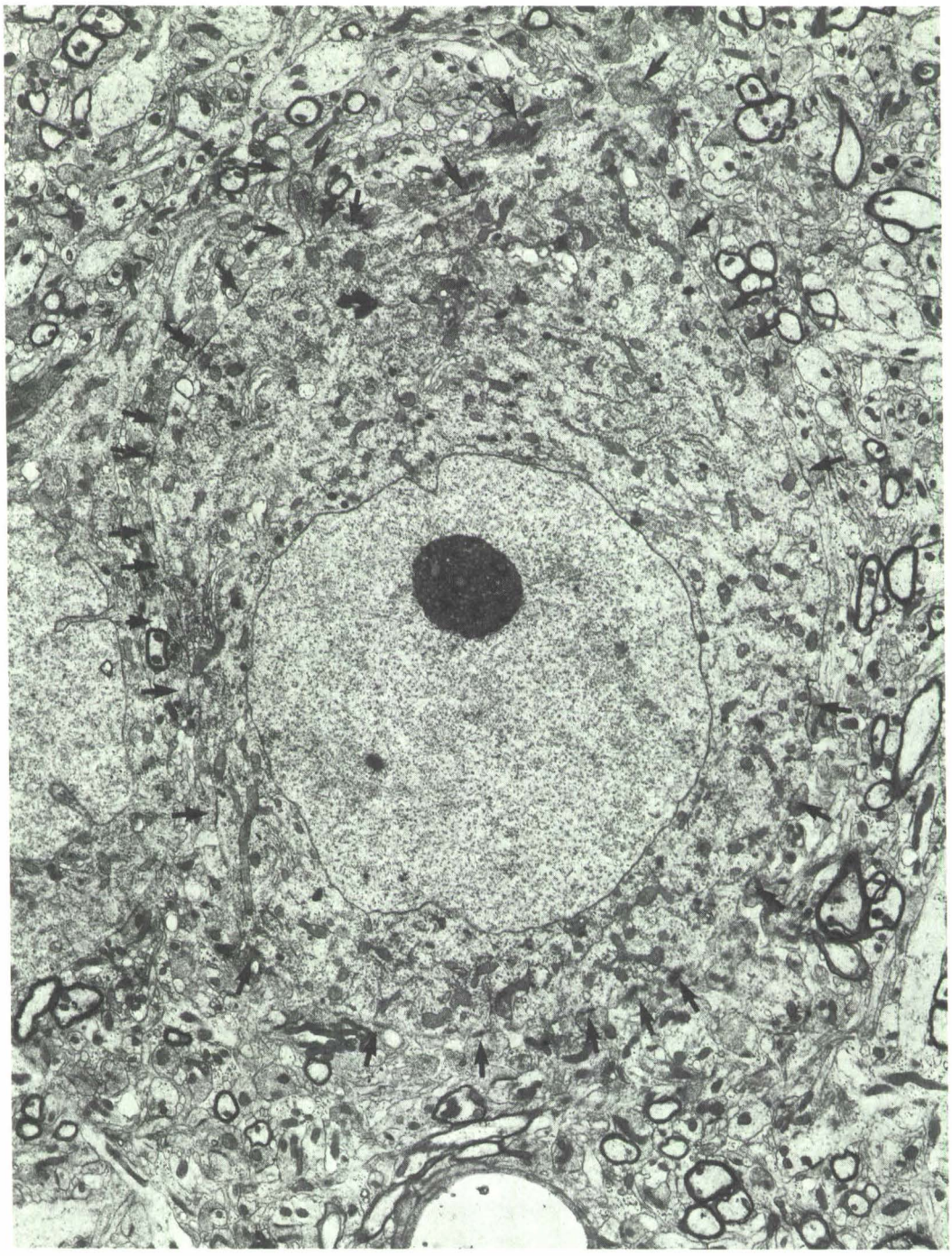


Figure 20.5. Stellate cell in the fourth layer of the striate cortex of the cat. *Arrows* indicate the large number of synaptic contacts (×5000).

jections. According to Jasper (161), the synaptic termination of fibers of this nonspecific system in the cortex is chiefly axodendritic and widely distributed in all layers, but the principal physiologic effects appear to be within the superficial layers. The recruiting response, recorded from the surface of the cerebral cortex, is regarded as a reflection of dendritic electrical activity, which implies that it is a graded response not dependent on the all-or-none firing of cortical cells (310).

Commissural fibers arise from cells in all cortical regions and interconnect homologous cortical areas via the corpus callosum. Exceptions to this generalization are found in the regions of the primary motor (area 4) and somesthetic cortex (S-I) that represent the hand and foot (171, 179, 186), in the visual cortex (area 17) (146, 401, 402, 413), and parts of the auditory cortex (77). Commissural cells are large pyramidal cells in deep parts of layer III (179). Cortical afferents from commissural neurons extend throughout all cortical layers and fill a column about 200–300 μm in diameter (355). Not all callosal fibers terminate in the entire columnar space and some collaterals terminate preferentially in particular layers. Association fibers in the same hemisphere arise from the supragranular layers (179). Ipsilateral corticocortical fibers arise from cells in more superficial parts of layer III and from parts of layer II. Terminal branches of association fibers are distributed mainly to layers III and IV but they have been identified in deeper layers as well (174).

The cortical neurons may be grouped into cells with descending, ascending, horizontal, and short axons. The last three types provide only intracortical connections (Fig. 20.4). The cells with descending axons (pyramidal, fusiform, and larger stellate cells) furnish all the efferent projection and association fibers, and their axonal collaterals form extensive intracortical connections. Some descending axons that do not reach the medullary substance have only intracortical branches.

The pyramidal cells of layers II, III, and IV have a similar pattern of dendritic and axonal branchings (Fig. 20.2). They have a number of basilar dendrites that arborize in the same layer, and an apical dendrite that ends in the molecular layer. Their descending axons in part terminate in the deeper layers of the cortex and, in part, are continued as association or callosal fibers. They give off a few recurrent collaterals to their own layers, chiefly II and III, and numerous horizontal collaterals to layers V and VI, where they contribute to the horizontal plexuses.

The pyramidal and fusiform cells of layers V and VI have a characteristic pattern of dendritic and axonal branchings. All the pyramidal cells of layer V give off basilar dendrites to their own layer and an apical dendrite extending to the molecular layer. There are, however, medium-sized pyramidal neurons, whose apical dendrites terminate in layer IV, and short pyramidal cells, whose dendrites all ramify in layer V (Fig. 20.2). The spindle cells of layer VI have similar branches. The axons of pyramidal and spindle neurons, and some axons of deep stellate cells are continued as projection fibers. All of these axons send horizontal collaterals to layers V and VI, where they contribute to the horizontal plexuses, especially those of layer V (internal band of Baillarger). Additionally, one or more recurrent collateral ascends unbranched to arborize in layers II and III, and some even extend to the molecular layer (Fig. 20.2).

The horizontal laminar arrangement of the cerebral cortex has served as a major criteria to map the distinctive cytoarchitectonic areas. This lamination also serves to segregate different efferent projections from the cortex. Each of the major efferent pathways emanating from sensory-motor cortex has a specific laminar or sublaminar origin (179). The somata of the majority of cells whose axons are distributed intracortically (both ipsilaterally and contralaterally) lie in the supragranular layers (layers II and III). Most of the cortical neurons whose axons project to subcortical structures lie in the infragranular layers, particularly layer V and VI. In the supragranular layers, cells whose axons are distributed ipsilaterally as corticocortical fibers lie superficial to cells projecting axons to the cortex of the opposite hemisphere, and cells with shorter axons tend to lie superficial to those with longer axons. In the infragranular layers (layers V and VI), the majority of the somata of corticostriate neurons lie in the most superficial part of layer V while somata giving rise to corticospinal and corticotectal fibers are in the deepest part of the same layer. Somata of neurons giving rise to corticorubral, corticopontine, and corticobulbar fibers lie in intermediate regions of layer V, between corticostriate and corticospinal neurons. Cells in layer VI of the cortex give rise to corticothalamic projections. Cells giving rise to a particular set of efferent connections are of nearly the same size and do not vary in their laminar distribution. Only neurons giving rise to corticospinal fibers show great variation in cell size. Cells of particular efferent systems occur in single or multiple strips oriented mediolaterally across the cortex.

Functional Columnar Organization

Although the most striking feature of Nissl-stained sections of the cerebral cortex is

its horizontal lamination, physiologic studies of the somatosensory and visual cortex indicate that a vertical column of cells, extending across all cellular layers, constitutes the elementary functional cortical units (24, 123, 124, 142, 143, 266, 268, 309). This conclusion in the somatosensory cortex is supported by these facts: (a) neurons of a particular vertical column are all related to the same, or nearly the same, peripheral receptive field; (b) neurons of the same vertical column are activated by the same peripheral stimulus; and (c) all cells of a vertical column discharge at more or less the same latency following a brief peripheral stimulus. The topographic pattern present on the cortical surface extends throughout its depth. Studies of the visual (striate) cortex demonstrate similar discrete functional columns extending from the pial surface to the white matter that are responsive to a specific kind of retinal stimulation in the form of long narrow rectangles of light ("slits"), dark bars against a light background, or straight-line borders, all of which have a particular axis of orientation (142, 143). Functional columns are arranged radially, perpendicular to the cortical layers and display variations in size and cross-sectional area, but most fall within the 200–500 μm range (143). The receptive field axis of orientation varies in a continuous manner as the surface of the cortex is traversed. Columns of cells in the striate cortex are of two types, ocular dominance columns and orientation columns (386, 387). Ocular dominance columns receive their input predominantly from one eye, while orientation columns are concerned with the receptive field axis (Fig. 20.26).

Anatomically, an elementary functional unit of the cortex, represented by a column of cells, must contain the afferent, efferent, and internuncial fiber systems necessary for the formation of a complete cortical circuit (276). In the basic columnar units, the internal circuitry must vary with differences in cytoarchitecture. The convergence of specific afferents upon cells in the columnar unit appears to imprint a specific sensory modality which is relayed by intracortical connections to other cells in the column. The complex axonal branching suggests that intracortical circuits involve cells in all parts of the column. These vertical circuits are interconnected by short neuronal links, represented primarily by the short axons of granule cells. Through these short links cortical excitation may spread horizontally and involve a progressively larger number of vertical units (Fig. 20.4). Thus, a specific afferent fiber may not only fire vertical columns of cells in its immediate vicinity, but may reach other units through Golgi type II cell relays. These vertical units are fundamentally similar in all mammals. However, the columns of cells with short relays increase in complexity in primates, especially humans. According to Ramón y Cajal, the unique morphologic feature of the human cortex is the enormous number of Golgi type II cells, considered to interrelate vertical cell columns.

The cerebral cortex has been envisaged as a mosaic of columnar units of remarkably similar internal structure (355). In addition to the functional columnar arrangement described in the sensory cortical areas, there are corticocortical columns delineated primarily by the pattern of termination of association and commissural fibers. Columnar units of corticocortical afferents and the functional columns of the sensory cortex are roughly the same size. In the corticocortical columns, there is a convergence of afferent fibers from multiple modular units that create a vast mosaic of cortical connections. Neurons within the cortical column are conceived of as being arranged in microcolumns, smaller than the larger units, concerned primarily with the vertical connectivity within each column. Excitatory inputs from the thalamus and other cortical areas are considered to be processed through a column-oriented circuitry composed of both excitatory and inhibitory neurons. Most interneurons in the cerebral cortex are highly specific with respect to (a) the neurons from which they receive inputs, (b) the arborization pattern of their axons, and (c) the specific sites at which they establish synapses on other neurons. The vast majority of stellate or granular cells belong to the heterogeneous group, referred to as Golgi type II cells, which do not project fibers beyond the cerebral cortex. Many unresolved problems remain concerning synaptic relationships of cells within the cortex, but electron microscopic evidence, based upon the types of synaptic contact, suggests that the majority of cortical interneurons are excitatory, forming synapses of the asymmetric type with spherical synaptic vesicles. Interneurons identified as putative inhibitory cells in the cortex constitute only a minority of the known interneuron types. Both excitatory and inhibitory influences within the cerebral cortex

are exerted upon selected segments of pyramidal cells that represent the principal cortical output neurons.

CHEMICAL ANATOMY OF THE CORTEX

Excitatory Amino Acids

Glutamate (Glu) and aspartate (Asp) are the two major excitatory neurotransmitters in the central nervous system. Although Glu is involved in basic cellular metabolism, it satisfies the criteria for classification as a neurotransmitter (91, 288, 346). When exogenously applied, they both evoke a rapid spiking activity associated with membrane depolarization. There are strong indications that Glu and Asp are the principal neurotransmitters of most cortical projection neurons, forming corticospinal, corticostriate, corticothalamic, and corticopontine pathways (Fig. 20.6) (120, 121). Glutamatergic synapses are all symmetric and the vast majority of them contact dendritic spines and shafts. Axon collaterals of pyramidal cells are likely also to be part of the cortical glutamatergic system. At the synaptic level, glutamate acts via several pharmacologically characterized receptors, including NMDA (*N*-methyl-D-aspartate), kainate, AMPA (α-amino-3-hydroxy-5 methyl-4-isoxazolepropionic acid), AP4 (L-amonophosphonobutyric acid), and metabo-tropic receptors (80). These receptors have a differential distribution in the cerebral cortex: kainate receptors are denser in layer V-VI, whereas AMPA and NMDA receptors are concentrated within layers I and III.

The pyramidal cell is the key excitatory neuronal class in the neocortex. All cortical output is mediated through pyramidal cells, and, as such, the intrinsic neocortical activities can be viewed simply as a means to regulate pyramidal cell activity (264). The glutamate/aspartate excitatory inputs to the pyramidal cells can be divided into intrinsic afferents such as recurrent collaterals from other pyramidal cells and excitatory interneurons, and extrinsic afferents which derive from the thalamus and other cortical regions.

Recurrent collaterals of pyramidal cells give rise to both a vertical and horizontal system of excitatory fibers that appears to parallel the vertical and horizontal system of inhibitory projections that arise from cortical interneurons and use γ-aminobutyric acid (GABA) as a neurotransmitter. One of the major sites of termination of the recurrent collaterals is the spines of other pyramidal cells in layers III and V, the two major output layers of the cortex (197). The vertically oriented recurrent collaterals appear to set up local excitatory patterns and play a recruitment role (117, 118), while the horizontally oriented ones serve to integrate the activity of columnar modules.

The excitatory interneurons are often referred to as spiny stellate cells. They abound in layer IV of the visual cortex and are infrequent or even absent in other cortical areas, particularly the primary motor cortex. The axon of the spiny stellate cell forms a radial link between layer IV, the major thalamorecipient layer, and layers III, V, and VI, the major projection layers. The spiny stellate cell appears to be specialized in the reception and local dissemination of thalamic inputs (80, 264).

The thalamocortical and corticocortical projections provide the major excitatory input to the neocortex and are believed to use glutamate and/or aspartate as their neurotransmitter. These amino acids are quick acting, potent, excitatory neurotransmitters that are well-suited for neuronal systems such as thalamocortical circuits that convey precise, topographically organized information that requires a high degree of synaptic security to maintain the level of fidelity necessary for the transmission of sensory information. As seen earlier, thalamocortical input terminates principally in layer IV, while corticocortical projections are mainly to layers II and IV if they are characterized as forward projections, and layers more superficial and deep if they are characterized as feedback projections. The thalamocortical and corticocortical fibers form asymmetric synapses principally on spines of pyramidal and stellate cells, as well as on inhibitory interneurons.

γ-Aminobutyric Acid

While there are multiple excitatory inputs to drive a pyramidal cell, there are also several inhibitory afferents that regulate the firing rate of pyramidal cells. These inhibitory influences come almost entirely from local interneurons that lack spines and utilize γ-aminobutyric acid (GABA) as their neurotransmitter (129, 137). The GABAergic neuronal population comprises a wide variety of intrinsic nonpyramidal cortical neu-

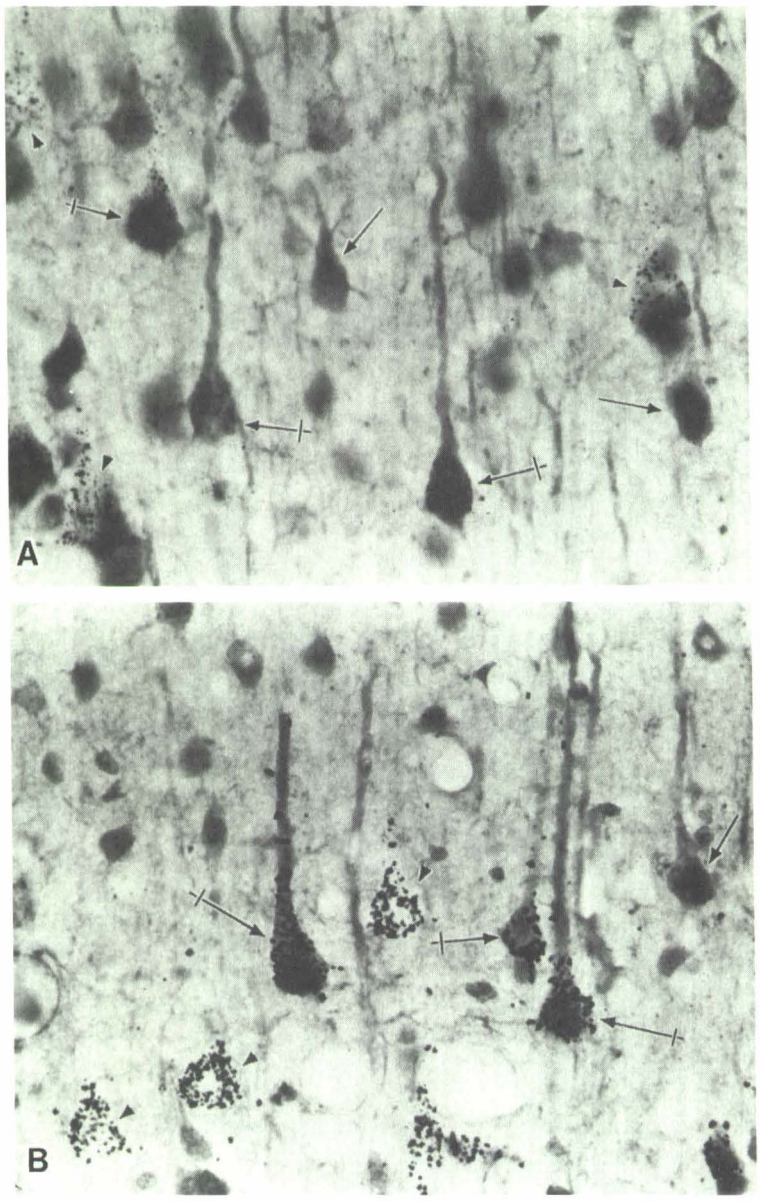


Figure 20.6. Layer V of the primary motor cortex (M-I) in the rat processed immunocytochemically for glutamate (**A**) and aspartate (**B**). Colloidal gold coupled with enzymatically inactive horseradish peroxidase conjugated to wheat germ agglutinin (WGAapoHRP-Au) injected into the spinal cord retrogradely labels corticospinal neurons (*black granules*). Three types of neurons can be seen: (a) cells immunoreactive for glutamate or aspartate only (*arrows*), (b) cells retrogradely labeled only with WGAapoHRP-Au (*arrowheads*), and (c) cells retrogradely labeled with WGAapoHRP-Au and immunoreactive for either glutamate or aspartate (*tailed arrows*). Calibration bar: 50 μm.

rons (e.g., basket cell, chandelier or axoaxonic cell, bitufted cell, and clutch cell) whose aspiny dendrites form both vertical and horizontal arborizations. The unique feature of GABAergic cortical interneurons is their extensive synaptic contacts with receptive surfaces of pyramidal neurons (Fig. 20.7). These intrinsic neurons are organized to inhibit pyramidal output neurons irrespective of their sources of excitation. Thus, the inhibitory nature of GABA action can be understood in terms of control of the cortical integration and regulation of information processing with small cortical domains (80, 241).

The various types of GABAergic interneu-



Figure 20.7. Glutamic acid decarboxylase (GAD)-immunoreactive terminals (*arrows*) on the soma and proximal dendrites of a pyramidal neuron in the motor cortex of a rhesus monkey. The material was photographed with Nomarski optics. Calibration bar: 20 μm.

rons act at specific levels on the pyramidal cell via synapses of the symmetric type. Some of these neurons (e.g., basket cells) are the principal source of horizontally directed inhibitory inputs to the soma, proximal dendrites, and apical shafts of pyramidal neurons, while others (e.g., chandelier cells) synapse exclusively on the initial axon segment of pyramidal cells. A large proportion of the GABAergic interneurons contain the calcium-binding protein parvalbumin, as well as a variety of neuroactive peptides such as cholecystokinin, somatostatin, neuropeptide Y, substance P, and corticotrophin releasing factor. The action of GABA in the neocortex is mediated by two types of receptors $GABA_A$ and $GABA_B$. The $GABA_A$ receptor is characterized by a competitive site and by a benzodiazepine modulatory site. The action of minor tranquilizers of the benzodiazepine family on cortical neuronal activity is largely mediated by the $GABA_A$ receptor subtype (80). Cortical sites identified as the focus of chronic epileptiform activity, demonstrate significant loss of GABA in cells and terminals. Barbiturates and anticonvulsant drugs are considered to potentiate GABAergic inhibition.

Neuroactive Peptides

Peptides present in the cerebral cortex include cholecystokinin (CCK), vasoactive intestinal polypeptide (VIP), neuropeptide Y (NPY), somatostatin (SS), substance P (SP), and corticotrophin releasing factor (CRF) (84). Many of these peptides are colocalized with GABA in cortical interneurons. The cellular action of the peptides is poorly understood, but they are presumed to function as modulators of excitatory amino acids, GABA, and/or monoamine effects. For example, when iontophoretically applied on cortical neurons, SS appears to increase acetylcholine excitatory action through the inhibition of second messengers (e.g., adenylate cyclase and G protein). Another example is the interaction between VIP and noradrenaline. VIP-containing neurons in the cortex form a homogeneous population of intracortical, bipolar neurons, that are devoid of GABA. Noradrenaline and VIP act synergistically to increase cAMP levels in neocortex. Noradrenaline, by activating specific α1 receptor subtype, potentiates the increases in cAMP elicited by VIP. When VIP and noradrenergic neurons are simultaneously active, they may act in a functionally coordinated manner to generate a "cortical hot-spot" where cAMP levels are drastically increased in comparison to surrounding regions to activate those intracellular processes that are regulated by cAMP-dependent phosphorylation. Thus, sensory stimulation within certain contexts (i.e., heightened vigilance) could trigger the synergistic interaction between VIP and noradrenaline within the terminal field of thalamocortical afferents in primary sensory cortex (84, 264).

Besides their role in neurotransmission, some of the neuroactive peptides present in the cerebral cortex may play a role in the control of local metabolism and blood flow. Such is the case for neurons containing NPY or

VIP, which are found in superficial layers close to capillaries. VIP is a potent vasodilator and NPY is a vasoconstrictor (Fig. 20.8).

Monoamines

There are distinct noradrenergic (NA), serotoninergic (5-HT), and dopaminergic (DA) projections to the cerebral cortex. Together with the cholinergic cortical projections, these monoaminergic neurons form an important extrathalamic afferent system that circumvents the presumed obligatory synapse in the thalamus to directly reach the cerebral cortex. The NA projection originates in the locus coeruleus (LC) located in the dorsomedial portion of the pontine tegmentum (Figs. 13.35 and 13.36). The 5-HT projection arises from the dorsal and median raphe nuclei in the medial portion of the caudal midbrain tegmentum. The DA projection originates from the substantia nigra (SN) and ventral tegmental area (VTA) complex at the base of the midbrain.

The ascending monoaminergic projections are highly divergent systems in that a given nucleus or individual neuron can innervate a vast expanse of neocortex (92, 237, 241, 261, 293). The cortical termination patterns of these extrathalamic systems differs fundamentally from that of thalamocortical and cortical afferents. The well-known columnar, radial organization of the neocortex that is driven by the thalamo- and corticocortical afferents, differs markedly from the tangentially organized extrathalamic afferents in which single axons may innervate not only different columns within a functional region but different functional areas (264). The thalamo- and corticocortical projections are involved in both serial and parallel processing of information through precise excitatory actions on specific subsets of cortical neurons. In contrast, the monoaminergic ascending

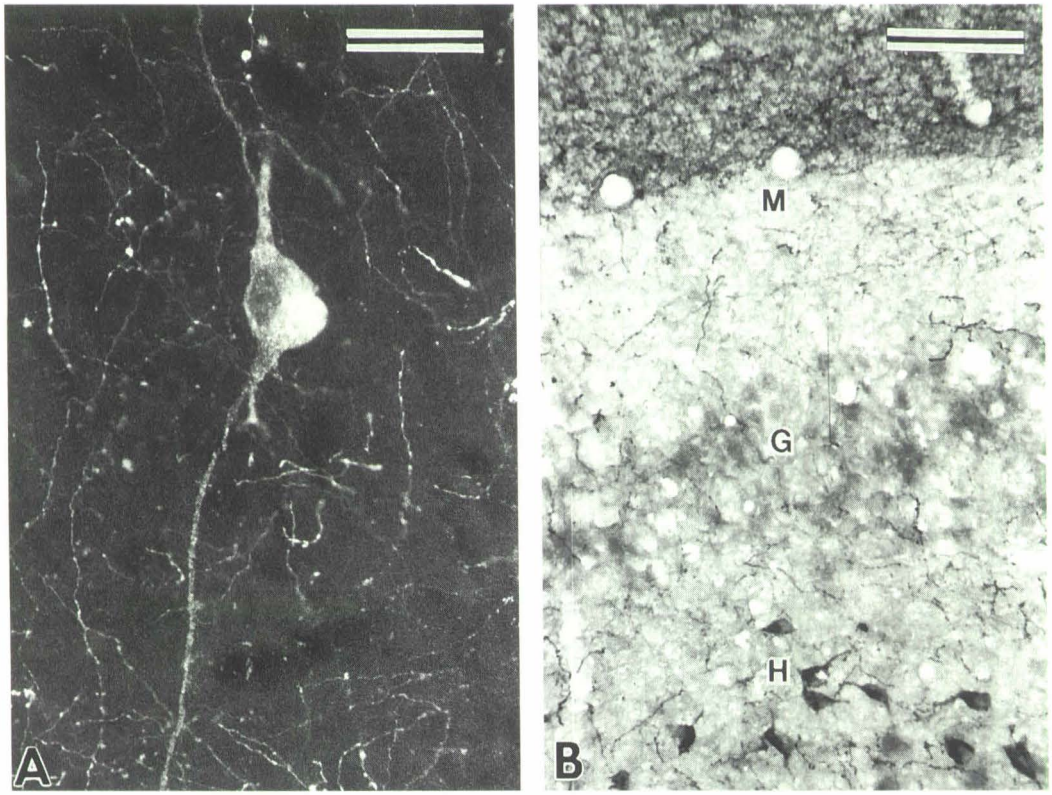


Figure 20.8. Neuropeptide Y (NPY)-immunoreactive neurons in the deep layers of the frontal cortex (**A**) and in the hilus (*H*) of the dentate gyrus (**B**) of the squirrel monkey. In **B**, note the dense NPY-immunoreactive terminal field in the external portion of the molecular layer (*M*), which contrasts with the relatively poor innervation of the granular layer (*G*). NPY has been shown to coexist with somatostatin in some cortical neurons in the rat and humans. Calibration bars: 50 μm (**A**) and 100 μm (**B**). **A** and **B** are darkfield and brightfield photomicrographs, respectively.

projections are able to modulate various state-dependent cortical activities through their general effect on vast neuronal assemblies.

NORADRENERGIC INNERVATION

Axons from individual LC neurons arborize within multiple cortical areas that are often distributed over widely separate regions. These highly divergent axons run principally in layer VI where they form a continuous sheet of longitudinal fine fibers overlying the white matter (Fig. 20.9). Along their rostrocaudal trajectory through the cortical hemisphere, these noradrenergic axons provide numerous collateral branches to various cortical areas. In primates, the NA innervation of the cortex is much more prominent in primary motor and somatosensory cortices, and their related association regions in the frontal and parietal lobes, than in prefrontal, temporal, and occipital lobe areas (92, 237, 241, 261). Furthermore, detailed analysis of cortical areas subserving a particular modality such as vision indicates that functional related regions tend to share common and distinguishable densities of NA innervation (264).

Locus coeruleus neurons are most active during waking, less active during slow-wave sleep, and silent during rapid-eye-movement (REM) sleep. Within the waking state, the mean discharge rates of LC neurons increases proportionally with increases in the level of behavioral arousal or vigilance. Electrophysiologic studies indicate that noradrenaline enhances evoked activity relative to spontaneous activity such that it increases the "signal-to-noise" characteristics of cortical neurons. Noradrenaline can also enhance the effect of iontophoretically applied GABA or

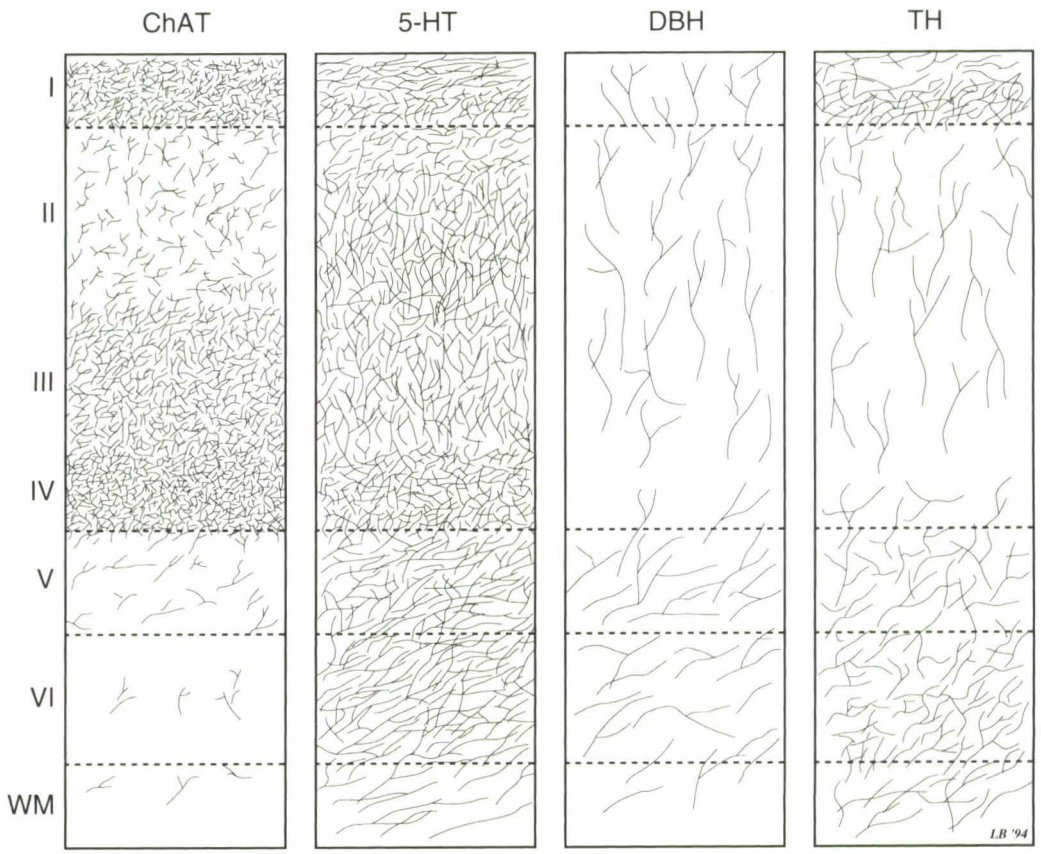


Figure 20.9. Cholinergic and monoaminergic innervation of the primary auditory cortex of a macaque monkey. Antisera against choline acetyltransferase (ChAT), serotonin (5-HT), dopamine-β-hydroxylase, and tyrosine hydroxylase were used to visualized immunohistochemically the cholinergic, serotoninergic, noradrenergic, and dopaminergic fibers, respectively.

ACh, suggesting that it can enhance both inhibitory and excitatory inputs. Coactivity of LC terminals appears to "enable" other systems converging on the same target neuron to transmit more effectively during the period of simultaneous activity regardless of whether the primary effect is inhibition or excitation (13, 92, 241, 264).

Four types of adrenergic receptors have been pharmacologically characterized in the primate brain: α1, α2, β1, and β2. In the human cerebral cortex, α1 receptors abound in the external layers (I-II) and layer VI. Receptors of the β subtype have a lower concentration than α receptors, but they also predominate in the superficial layers. Overall, adrenergic receptors are more abundant in prefrontal, motor, and somatosensory regions than in parietal, temporal, and occipital areas.

SEROTONINERGIC INNERVATION

The 5-HT innervation of the cerebral cortex is more profuse than the noradrenergic innervation and involves all cortical layers. In primates, the regional and laminar specialization of the 5-HT innervation is greater than in nonprimates. This has been demonstrated by detailed studies of the primary visual cortex. The 5-HT innervation is particularly dense in layer IV, which is the primary recipient of thalamocortical afferents (Fig. 20.9). Two classes of 5-HT fibers can be found in the neocortex: very fine, highly tortuous fibers with very small varicosities, and larger caliber fibers with larger, more beaded varicosities. Each type of fiber appears to originate from distinct raphe subnuclei and has differential vulnerability to amphetamine derivatives (242). In primary visual cortex, serotoninergic fibers terminate principally on distal dendrites of both pyramidal and nonpyramidal neurons. Thus, the 5-HT system is well-situated to modulate the activity of both interneurons and projection neurons that subserve visuospatial analysis.

In unanesthetized, behaving animals, 5-HT neurons in the dorsal raphe nucleus exhibit slow, regular discharge patterns during quiet waking, and increases in firing with phasic arousal. Furthermore, mean discharge rates decrease during slow-wave sleep and raphe neurons become almost silent during REM sleep (16, 159, 241, 261). Different responses can be obtained from cortical neurons following iontophoretic application of 5-HT. These various effects of 5-HT may be explained by the existence of up to seven distinct serotoninergic receptors (5-HT_1 to 5-HT_7 subtypes) (282). The most common response to iontophoretically applied 5-HT or electrical stimulation of the median raphe nucleus, however, is marked inhibition of spontaneous activity. Additionally, it has been suggested that 5-HT, like NA, may have primarily a modulatory role, rather than a classical inhibitory or excitatory action. Serotoninergic neurons exhibit activity that is most strongly correlated with behavioral "state" while noradrenergic neurons display more phasic fluctuations, associated with "attentiveness" (241, 264).

DOPAMINERGIC INNERVATION

Earlier biochemical and fluorescent histochemical studies in rodents emphasized the propensity for midbrain dopaminergic (DA) neurons to terminate more massively in frontal cortex than in other cortical regions. Immunohistochemical studies using antibodies against tyrosine hydroxylase (TH) suggested that the DA innervation extends throughout the four lobes of the primate neocortex, with striking regional variations that coincide with cytoarchitectonic and functional subdivisions. In both New World and Old World monkeys, the density of TH-immunoreactive fibers is greatest in primary motor cortex and decreases in the more rostral prefrontal regions. It decreases markedly across the central sulcus from motor to primary somatosensory cortex, but increases again caudally in the parietal and temporal cortices. The primary visual cortex possesses the lowest density of TH-positive fibers. Overall, The DA innervation of the primate cerebral cortex is such that fibers preferentially innervate motor relative to sensory regions, limbic and high level sensory association relative to primary sensory areas, and auditory association relative to visual association areas (264).

The laminar pattern of fibers in a given region is correlated with fiber density. In very sparsely innervated regions, DA fibers are limited to layer I, and areas of an intermediate density have DA fibers in layers I, II, superficial III, and deep V-VI layers (Fig. 20.9). The primary motor cortex displays fibers in all layers, while layer IV has the lowest density of innervation throughout the neocortex. Thus, the DA ascending system appears to be in a position to influence the activity of corti-

cocortical and possibly corticostriatal circuits rather than thalamocortical circuits, and high-order integrative processes rather than the more analytic aspects of sensory processing (232, 233).

The action of dopamine is mediated through a large family of specific receptors (D_1 to D_5), the most well-characterized members of which are the D_1 and D_2 receptor subtypes. Ligand binding studies suggest that the D_1 receptor is far more abundant than the D_2 receptor in monkey neocortex, and that D_1 binding is generally highest in layers I-III and D_2 is generally highest in layer V (80, 234). Because of the lack of cellular resolution of the current ligand binding methods, there remains much uncertainty regarding the exact cellular location (on pre- or postsynaptic neural elements, or even on glial cells) of these receptors. It is, nevertheless, believed that different dopamine receptor subtypes may predominate on different classes of pyramidal neurons. This is supported by data from molecular biology showing, for example, that virtually all of the giant Betz cells of the monkey and human motor cortex express mRNA coding for D_1, D_2, and D_5 receptor subtypes.

In unanesthetized behaving animals, DA neurons in the substantia nigra pars compacta-ventral tegmental area complex (SN-VTA) discharge more rapidly during heightened motor activity, but unlike NA and 5-HT neurons, they do substantially decrease their activity during or after various stressful or arousing stimuli. The most striking change is a prolonged suppression of activity that accompanies orientation toward and fixation of a novel or meaningful stimulus. Iontophoretically applied dopamine elicit both excitation and inhibition of cortical neurons while electrical stimulations of SN-VTA neurons attenuate the excitatory effect on cortical neurons of thalamic stimulation.

The regional and laminar distribution of DA fibers suggest that the pyramidal cells of origin of both corticocortical and corticostriatal systems are likely targets of DA innervation (232, 233). Indeed, DA synapses on spines of layer III pyramidal cells in the prefrontal cortex have been visualized by using a combined Golgi-EM-immunohistochemical approach (125). Such layer II pyramidal cells are very likely to be corticocortical projection neurons, suggesting that dopamine may be in a position to modulate the activity of circuits linking association cortices. Furthermore, the overall density of innervation in motor cortex of primates suggests that cells of origin of major descending motor pathways are also innervated by dopamine.

Dopamine is also likely to play an important role in cognitive and affective brain functions. For instance, psychopharmacologic studies reveal that performance on cognitive tasks dependent on the integrity of the prefrontal cortex are affected by manipulation of the DA system (45, 124). Furthermore, following a suggestion by the Scandinavian pharmacologist Arvid Carlsson (53), several studies found that, despite their differences in chemical structure, antipsychotic agents (neuroleptics) block dopamine receptors. It was, therefore, thought that an excess of dopamine transmission underlies at least some aspects of the pathogenesis of schizophrenia. Schizophrenia is a devastating mental illness that comprises both positive and negative symptoms. The positive symptoms characterize the psychotic period of the disease and include distinctive behaviors, such as bizarre delusions, prominent hallucinations, and disordered thoughts. The negative or residual symptoms are encountered in the nonpsychotic phase and refer to the absence of normal social and interpersonal function.

The introduction of antipsychotic drugs in the 1950s has markedly improved the treatment of the psychotic phase of schizophrenia. Antipsychotics can be divided into two major groups that act on different dopamine receptors. The first group is termed *typical antipsychotics* and include phenothiazine derivatives (e.g., chlorpromazine), butyrophenones (haloperidol), and thioxanthene derivatives (e.g., chlorprothixene). The typical antipsychotic drugs bind to D_2 receptors and produce basal ganglia side effects such as tardive dyskinesia. The second group is referred to as *atypical antipsychotics* and include principally the dibenzodiazepines (e.g., clozapine). The atypical antipsychotic drugs bind to D_3 and D_4 receptors and do not produce tardive dyskinesia. The D_1 and D_5 receptors are expressed in neurons of the cortex and hippocampus and have a low affinity for most types of antipsychotic drugs. The D_2 receptors are expressed by neurons of the striatum and limbic structures such as the nucleus accumbens, the amygdala, the hippocampus, as well as the cerebral cortex. They have a high affinity for typical antipsychotic drugs. The D_3 and D_4 dopamine receptors are restricted in their expression to limbic structures and

cerebral cortex, and are only weakly expressed in the basal ganglia. This selective distribution may explain why atypical antipsychotic agents, such as clozapine, that bind selectively to D_3 and D_4 receptors, do not produce basal ganglia side effects (340, 366).

The "dopamine hypothesis" of schizophrenia has received support from two sets of findings in humans. First, drugs that increase the level of dopamine (e.g., L-DOPA, cocaine, and amphetamine) cause a psychosis that resembles the paranoid subtype of schizophrenia. Second, the brains of schizophrenic patients studied at autopsy contain an increased number of D_2 receptors in the caudate nucleus and the ventral striatum. This increase is particularly prominent in patients with positive symptoms and has been demonstrated in positron emission tomography (PET) scans of living patients (185). However, these changes in D_2 receptors might be secondary to disturbances elsewhere in the brain that are mediated by dopamine receptor mechanisms. Moreover, there is still no evidence that excessive activity of DA cells actually contributes to the defect underlying schizophrenia.

The most widely accepted version of the DA hypothesis of schizophrenia suggests that there are two different disturbances in dopaminergic transmission: (a) an increase in activity of the mesolimbic subcortical component of the dopaminergic system, which accounts for the positive symptoms and responds to antipsychotic drugs that probably act via D_2, D_3, and D_4 receptors, and (b) a decrease in the activity of the mesocortical component of the DA system, which accounts for the negative symptoms and does not respond effectively to antipsychotic drugs (376). It is proposed that the mesocortical DA pathway to the prefrontal cortex normally inhibits the mesolimbic component by feedback inhibition, and that the primary defect in schizophrenia is a reduction in prefrontal activation by the mesocortical pathway, which leads to disinhibition and overactivity in the mesolimbic pathway (376).

The DA hypothesis of schizophrenia is obviously of great interest and appears to be supported, at least in part, by data derived from animal studies. However, there is a clear lack of evidence from human studies to fully support this theory. The involvement of dopamine in schizophrenia could be secondary to, or strongly linked, to a more fundamental cellular pathology of the cerebral cortex. However, a clear and reproducible cellular pathology as impressive as that found in Parkinson's disease, Alzheimer's dementia, or Huntington's chorea has not yet emerged from studies of schizophrenic brains. Dopamine may also act in conjunction with several other chemospecific neuronal systems. In this perspective, it is worth noting that the addictive drug phencyclidine (PCP, also known as angel dust) produces psychotic behavior by binding to NMDA receptors. Furthermore, a reduction in the number of 5-HT_2 receptors and 5-HT reuptake sites has been found in the prefrontal cortex of schizophrenic patients (282). These findings indicate that psychotic behavior can probably be produced by interfering with several transmitter systems other than dopamine, either alone or in combination (54).

Acetylcholine

Cholinergic axons in the cerebral cortex have been visualized by both acetylcholinesterase (AChE) histochemistry and choline acetyltransferase (ChAT) immunohistochemistry (204). Although ChAT is considered a more reliable marker than AChE for cholinergic neurons, both procedures reveal a similar pattern of innervation by cortical cholinergic fibers (253). In primates, cholinergic fibers innervating the cortex arise principally from neurons in the basal nucleus of Meynert (252) (group Ch 4 of Mesulam, et al. (254)), which lies ventral to the globus pallidus, and less abundantly from neurons in the vertical limb of the diagonal band of Broca in the septal area (group Ch 2). The cholinergic neurons in the medial septal nucleus project specifically to the hippocampal formation (254) (see Chapter 18). Like the noradrenergic and serotoninergic systems, the cholinergic fibers innervate virtually the entire cortical mantle in a highly divergent manner. However, different subdivisions of the basal nucleus project preferentially to major regions of the cortex, revealing the existence of a crude topography in the organization of the cholinergic cortical afferents.

The cholinergic cortical innervation displays specific regional patterns. There is a high density of cholinergic innervation of the limbic cortex, less dense but very substantial innervation of primary sensory and motor cortex, and still less dense innervation of association cortex. In all cortical areas, layer I is

the most densely innervated, followed by layers II and III. In association cortex, the deep layers (V and VI) are more densely innervated than the deep portion of layers III and IV. This is not the case in densely innervated primary sensory areas such as primary auditory and visual cortices, where there is a very dense innervation of layers I and IV, relatively dense innervation of layers II and III, and sparse innervation of layers V and VI. This laminar pattern suggests that in primary sensory areas cholinergic neurons are able to modulate activity in the same layer and perhaps on the same neurons as those receiving direct thalamic input.

The action of acetylcholine at the cortical level is mediated by both muscarinic and nicotinic cholinergic receptors (204, 241, 244). In the human cerebral cortex, the two subtypes of muscarinic receptors (M_1 and M_2) are relatively uniformly distributed among the different cortical regions, with higher density in layer IV. The cortex shows higher densities of M_1 binding sites, but the deep layers show relatively higher M_2 sites than the upper layers. Furthermore, the M_2 receptor subtype is preferentially associated with the primary sensory areas and is much denser in these areas than the M_1 sites (244, 264). Immunohistochemical studies have shown the presence of either muscarinic or nicotinic receptors on the soma and apical dendrites of pyramidal cells in layers II-III and V. Knowledge about the exact location of these two types of cholinergic receptors on cortical neurons is important functionally, since muscarinic and nicotinic receptors have different effectors at the molecular level and could thus differentially influence the activity of specific subgroups of pyramidal projection cells. The nicotinic response is mostly ionotropic (i.e., glutamate-like), whereas the muscarinic site is linked to second messengers.

Although data on receptors suggest that pyramidal cells are the prominent target of cholinergic fibers, both pyramidal and nonpyramidal cells were seen to receive cholinergic synapses. These synapses are predominantly of the asymmetric type and occur on dendritic spines and shafts of cortical cells. The light and electron microscopic data currently available indicate that the primary synaptic target of the cholinergic fibers are distal dendritic shafts in the superficial layers (particularly layer I) and the more proximal dendrites of layer IV neurons in primary sensory areas.

Electrophysiologic recordings from neurons of the basal nucleus of Meynert in behaving monkeys, reveal that some neurons exhibit a phasic change in discharging during delivery of food reward or show a short latency of response when the monkey is given a food stimulus (72). These and other findings suggest that, in contrast to the overlying pallidal neurons whose neuronal activity is tightly coupled to body movement, neurons of the basal nucleus may play a role in reward, learning, and attentional mechanisms.

The basal nucleus of Meynert has attracted much attention because of its possible involvement in the pathophysiologic mechanisms underlying the severe memory and cognitive function disorders that occur in senile dementia of the Alzheimer type. Two major lines of evidence support this involvement: (a) compared to age-matched controls, the cerebral cortex and hippocampus in patients with Alzheimer's disease (AD) show 60–90% reduction of the cholinergic markers ChAT and AChE (69, 303); and (b) compared to age-matched controls, the basal nucleus in AD patients show a 70–95% cell loss (64, 382). These two lines of evidence led to the development of a model for the pathogenesis of neuritic (or senile) plaques (64). The abundance of neuritic plaques, as well as the presence of neurofribillary tangles and granulovacuolar degeneration, are neuropathologic hallmarks of Alzheimer's disease. In this model, a neuron of the basal nucleus would first show cytoskeletal abnormalities in the distal intracortical axons due to an unidentified pathologic factor or process. The axon then deteriorates toward the cell body (dying-back phenomenon), and clusters of dystrophic AChE-rich neurites form the immature plaques. With time some of the neurites degenerate and eventually disappear, leaving an amyloid plaque as the only evidence of this process. Ultimately, the entire neuron would degenerate (64). This complex sequence of events, involving the death of multiple neurons over time, can indeed lead to serious impairment of memory and cognition, a high density of plaques in the cortex, a marked reduction of the cholinergic markers at cortical levels, and severe loss of cells in the nucleus basalis.

Although the loss of cholinergic neurons in the basal nucleus in cases of AD appears highly specific (292), it is far too simplistic to consider this disease exclusively a cholinergic dysfunction. In fact, other neurotransmitters

or neuromodulators, particularly noradrenaline, serotonin, somatostatin, and neuropeptide Y, are also depleted in AD. Furthermore, attempts to develop cholinergic pharmacotherapies to alleviate the cognitive and behavioral deficits in AD have been largely unsuccessful (87). It appears that, both structurally and functionally, AD is predominantly a disease of the cerebral cortex, in which specific cortical cell populations are affected. There is evidence that the pyramidal cells that furnish the corticocortical projections and use glutamate as their neurotransmitter are particularly vulnerable in AD. Data from several sources support the notion that AD involves a global cortical disconnection syndrome, in which each cortical region functions in isolation rather than in a cohesive and synthetic manner. Such a condition would be particularly devastating in the human brain, given the dependence on corticocortical connections of functions such as cognition (264).

CORTICAL AREAS

The cerebral cortex does not have a uniform structure. It has been mapped and divided into a number of distinctive areas that differ from each other in total thickness, in the thickness and density of individual layers, and in the arrangement of cells and fibers. Structural variations are so extreme in some areas that the basic six-layered pattern is practically obscured. Such areas are termed *heterotypical cortex*, as opposed to *homotypical*, which refers to cortex in which the six layers are easily distinguished (44). Differences in the arrangements and types of cells, as well as the patterns of myelinated fibers, have been used to construct several fundamentally similar maps of the cortex composed of distinctive cytologic areas (Fig. 20.10). Campbell (52) described some 20 cortical areas, whereas Brodmann (44) increased the number to 47 and von Economo (368) to 109. The Vogts (371) parceled the human cerebral cortex into more than 200 areas. Even the last number is apparently insufficient, since other investigators have found a number of distinctive cytoarchitectural areas in regions previously considered homogeneous (20, 325). The brain map of Bailey and von Bonin (18) utilizes various colors to distinguish distinctive cytoarchitectural features. These authors felt that the concept of absolutely sharp areal boundaries was carried to absurd lengths and that most brain maps failed to properly represent transitional areas. Brodmann's chart, which is the most widely used for reference, is shown in Figure 20.10. This cytoarchitectural map of the human cortex can be compared with the lateral view of the brain shown in Figure 20.11.

According to von Economo (368), all cortical structure is reducible to five fundamental types, based primarily on the relative development of granule and pyramidal cells. Types 2, 3, and 4, known respectively as the frontal, parietal, and polar types, are homotypical and constitute by far the largest part of the cortex. Types 1 (agranular) and 5 (granular) are heterotypical and limited to smaller specialized regions (Figs. 20.12 and 20.13).

Agranular type cortex (type 1) is distinguished by its thickness and the virtual ab-

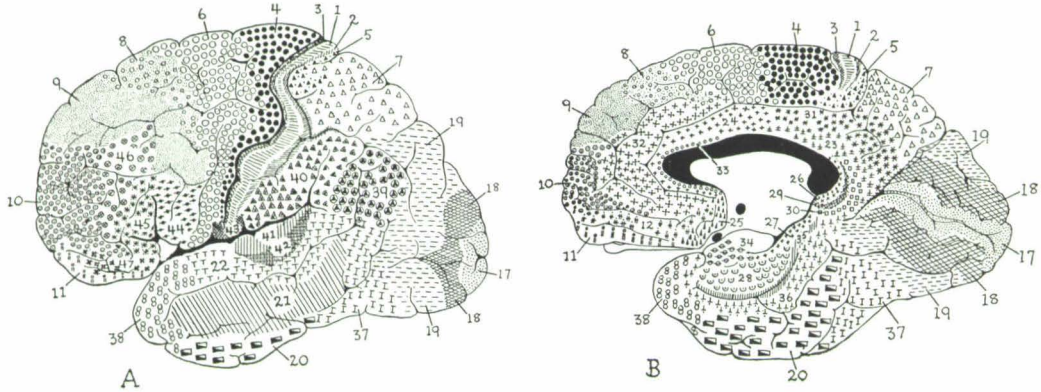


Figure 20.10. Cytoarchitectural map of human cortex. **A.** Convex surface; **B.** medial surface.

sence of granule cells (Figs. 20.12 and 20.14). Pyramidal cells of layers III and V are well-developed and large. Even the smaller cells in layers II and IV are predominantly pyramidal-shaped, making it difficult to distinguish individual layers. The agranular type cortex is represented classically by the cortex of the precentral gyrus.

Frontal type cortex (type 2) is relatively thick and shows six distinct layers (Fig. 20.14). Pyramidal cells of layers III and V are large and well-developed, as are the spindle cells of layer VI (Fig. 20.12). Although the granular layers are distinct, they are narrow and composed of loosely arranged small triangular cells.

Parietal type cortex (type 3) is characterized by even more distinctive cortical layers due to the greater thickness and cell density of the granular layers (Figs. 20.12 and 20.15). In this type of cortex, the pyramidal layers are thinner and their cells are smaller and more irregularly arranged.

Polar type cortex (type 4), found near the frontal and occipital poles, is characterized by its thinness, its well-developed granular layers, and its comparative wealth of cells.

Granular type cortex or *koniocortex* (type 5) is extremely thin and is composed mainly of densely packed granule cells (Figs. 20.12 and 20.15). These are found not only in layers II and IV, but the other layers, especially layer III, show large numbers of such small cells and a consequent reduction of the pyramidal cells. The most striking example of this type is the calcarine cortex (Fig. 20.15).

The general distribution of these five types of cortex is shown in Figure 20.13. The agranular type cortex covers the caudal part of the frontal lobe in front of the central sulcus, the anterior half of the cingulate gyrus, and the anterior portion of the insula. A narrow strip also is found in the retrosplenial region of the cingulate gyrus and is continued along the parahippocampal gyrus and uncus. Since the chief efferent fiber systems arise from these regions, especially from the precentral gyrus, the agranular cortex may be considered as efferent or motor type cortex (Figs. 11.13 and 12.27). The koniocortex may be re-

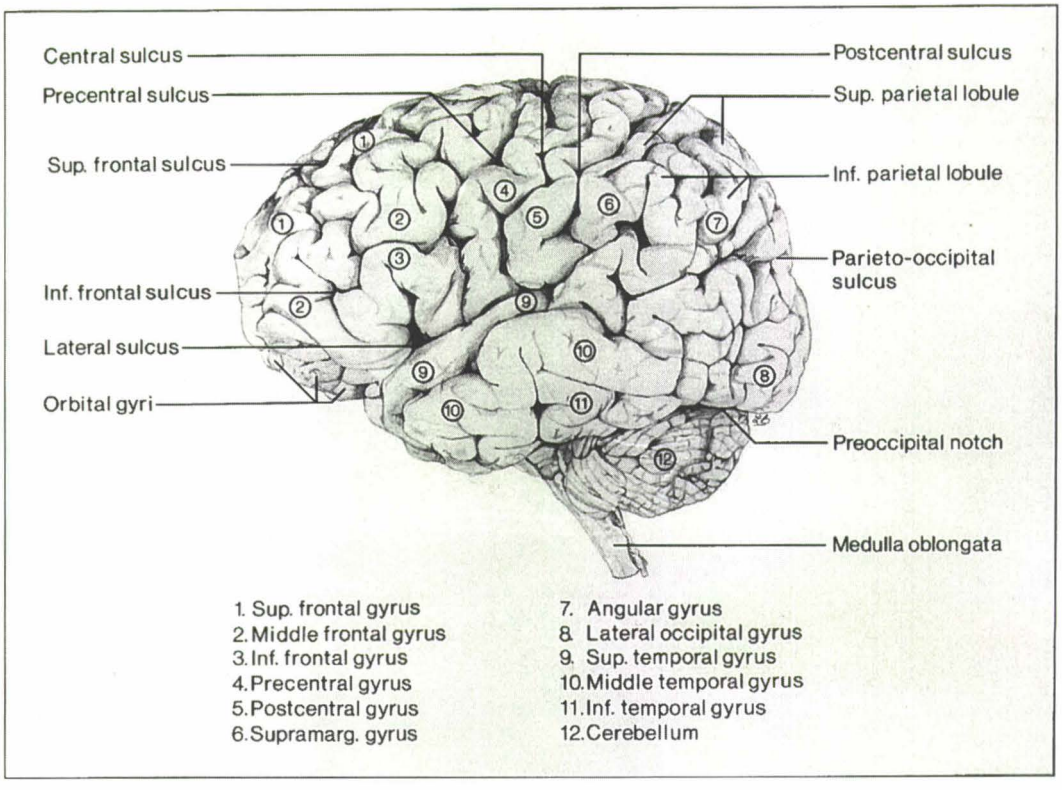


Figure 20.11. Lateral view of human brain with identification of the major gyri and sulci.

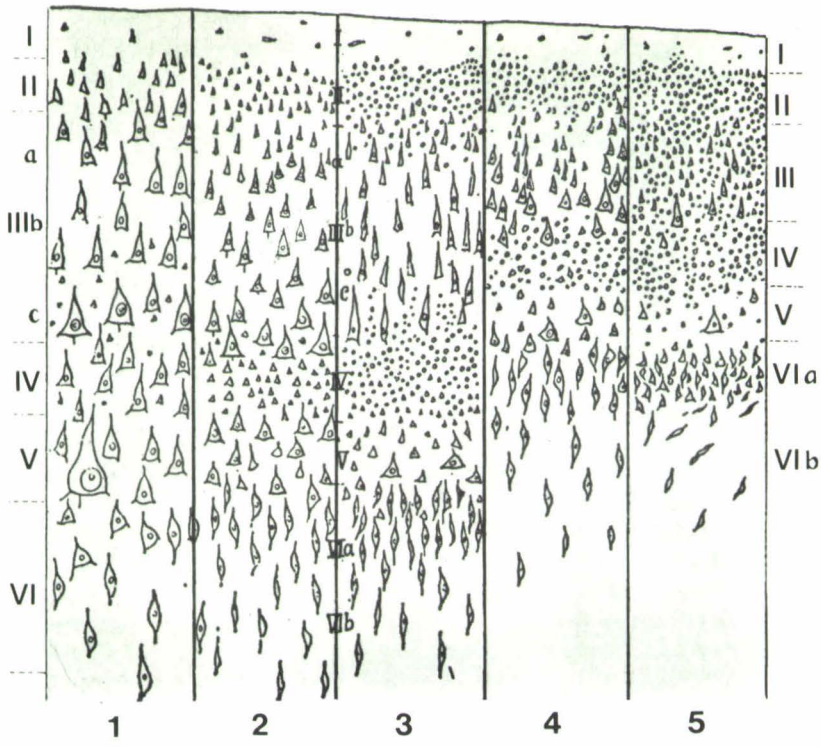
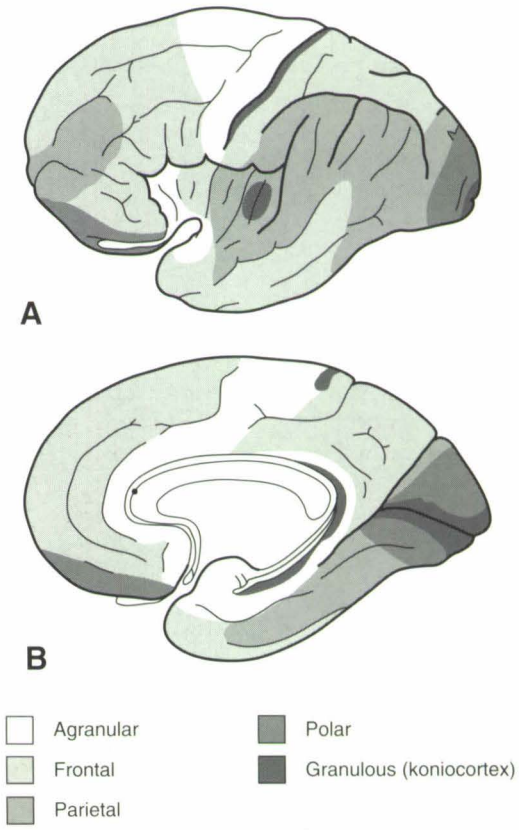


Figure 20.12. The five fundamental types of cortical structure: **1**, agranular; **2**, frontal; **3**, parietal; **4**, polar; and **5**, granulous (koniocortex).

Figure 20.13. Distribution of the five fundamental types of cortex (Fig. 20.12) over the convex (**A**) and the medial (**B**) surfaces of the hemisphere. The agranular, frontal, parietal, polar, and granulous (koniocortex) type of cortex are indicated by various shades of gray.



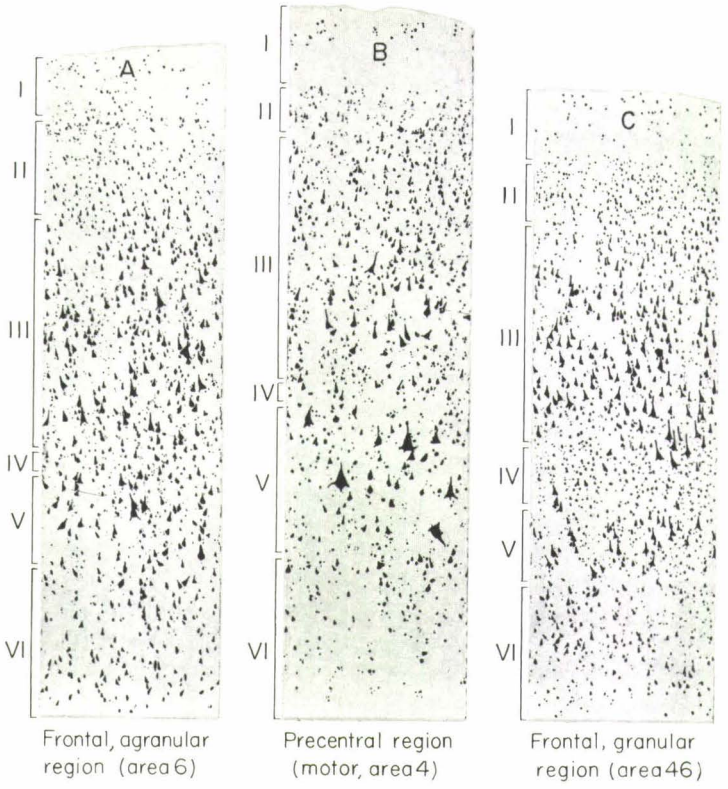


Figure 20.14. Cytoarchitectural pictures of several representative cortical areas.

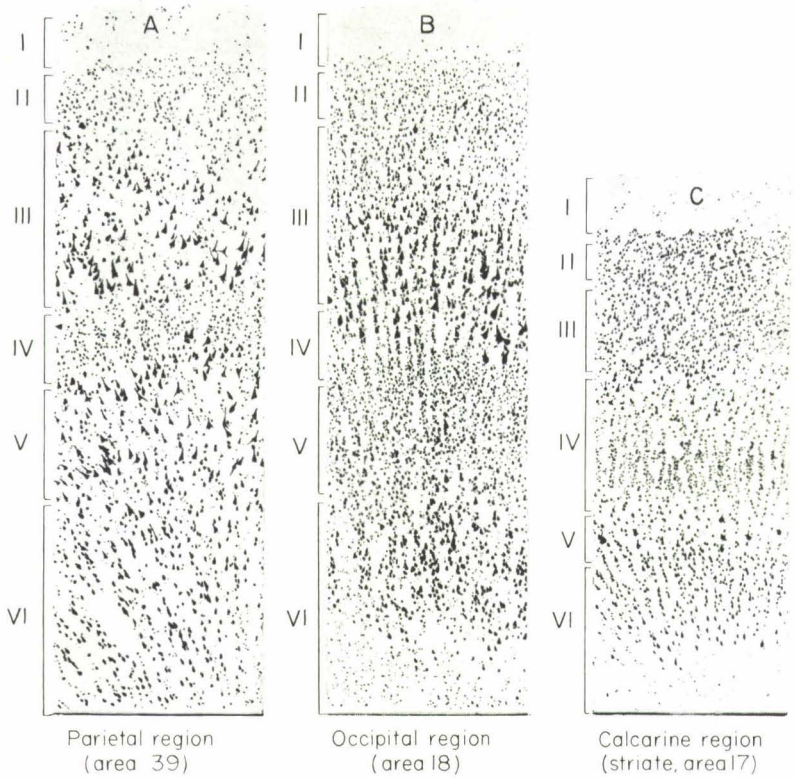


Figure 20.15. Cytoarchitectural pictures of several representative cortical areas.

garded as primarily sensory in character, since it is found only in the areas receiving the specific sensory thalamocortical projections. These areas include the anterior wall of the postcentral gyrus, the banks of the calcarine sulcus, and the transverse temporal gyri (Heschl, Figs. 2.11 and 13.13).

By far the largest part of the hemispheric surface is covered by homotypical cortex. Frontal type cortex is spread over the larger anterior part of the frontal lobe, the superior parietal lobe, the precuneus, and most of the middle and inferior temporal gyri. Parietal type cortex includes chiefly the inferior parietal lobule, the superior temporal gyrus, the occipitotemporal gyrus, and the anterior convex parts of the occipital lobe. Polar type cortex, as the name implies, covers the frontal and occipital poles. The thalamic connections of these areas are mainly with the association nuclei, such as the dorsomedial, lateral dorsal, lateral posterior, and the pulvinar.

Practically every part of the cerebral cortex is connected with subcortical centers by afferent and efferent projections. Strictly speaking, there are no circumscribed cortical areas which are purely associative or projective in character. However, there are regions from which the more important descending tracts arise, which directly or through intercalated centers reach the lower motor neurons for the initiation and control of both somatic and visceral activities (298). These primarily efferent or motor areas, from which muscular movements can be elicited by electrical stimulation, are concentrated chiefly in the precentral part of the frontal lobe. Similarly, cortical regions that receive direct thalamocortical sensory fibers from the ventral tier thalamic nuclei and from the geniculate bodies represent the primary receptive or sensory areas. The remaining cortical areas, which constitute the largest part of the cerebral cortex in humans, are referred to as "association areas." Although the primary sensory and motor areas are predominant in nonprimates in that they constitute unusually large parts of the neocortex, there is considerable intermingling of functions. In primates, the primary sensory and motor areas become more specific, and there is an absolute increase in the association cortex (404). Afferent fibers to the association areas are derived from association nuclei of the thalamus and from primary sensory areas of the cortex.

SENSORY AREAS OF THE CORTEX

Primary Sensory Areas

The localized cortical regions to which impulses concerned with specific sensory modalities are projected constitute the primary sensory areas of the cerebral cortex. Although certain aspects of sensation probably enter consciousness at thalamic levels, the primary sensory areas are concerned especially with the integration of sensory experience and with the discriminative qualities of sensation. With the exception of olfaction, impulses involved in all forms of sensation reach localized areas of the cerebral cortex via thalamocortical projections. The organization of the thalamus is such that all of the specific sensory relay nuclei are located caudally in the ventral tier (Figs. 16.13 and 16.14). The cortical projections of the specific sensory relay nuclei are to localized areas in the parietal, occipital, and temporal lobes. Although there is probably a primary cortical receptive area for each sensory modality, each modality is not represented separately, and the primary sensory areas for some forms of sensation are poorly defined. Established primary sensory areas in the cerebral cortex are (a) the *somesthetic area* (somesthetic area I, S-I), consisting of the postcentral gyrus and its medial extension in the paracentral lobule (areas 3, 1, and 2), (b) the *visual* or *striate area* (visual area I, V-I), located along the lips of the calcarine sulcus (area 17), and (c) the *auditory area* (auditory area I, A-I), located on the two transverse gyri (Heschl; areas 41 and 42; see Figs. 2.6, 2.8, 2.11, 13.13, 16.14, and 20.10). The *gustatory area* is localized to the most ventral part (opercular) of the postcentral gyrus (area 43). The primary *olfactory area,* consisting of the allocortex of the prepiriform and periamygdaloid regions, is not assigned numbers under the Brodmann parcellation.

Secondary Sensory Areas

The primary sensory areas of the cerebral cortex undoubtedly receive the principal projections of the specific sensory relay nuclei of the thalamus, and are the focal regions in the cerebral cortex where specific sensory modalities are most extensively and critically represented. Evidence suggests that near each primary receptive area there are cortical zones which may receive sensory inputs directly

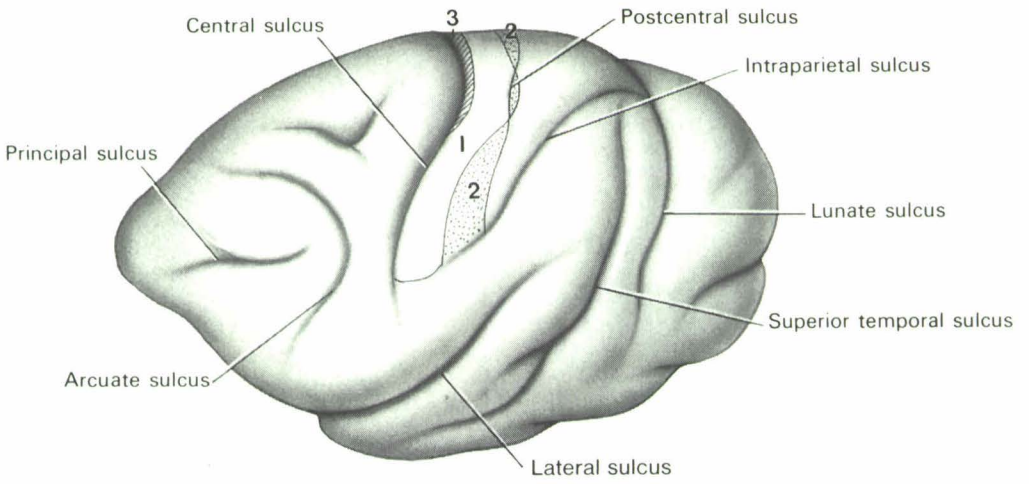
from the thalamus, from the primary sensory area, or from both (49, 98, 145). Cortical zones, adjacent to primary sensory areas, but outside of the principal projection area of the specific sensory relay nuclei of the thalamus, are referred to as the *secondary sensory areas.* Secondary sensory areas have been defined primarily in animals by recording evoked potentials in response to sensory stimuli (3, 49, 145, 165, 305, 359, 379, 407, 409). Secondary sensory areas are smaller than the primary sensory areas, and the sequence of representation is the reverse, or different from that found in the primary areas. Ablations of secondary sensory areas produce relatively minor sensory disturbances compared with those resulting from ablations of primary sensory areas.

Secondary sensory areas, defined primarily in experimental animals, include (a) a *second somatic sensory area* (somatic sensory area II, S-II), located ventral to the primary sensory and motor areas along the superior lip of the lateral sulcus (49, 319, 384, 404) (Figs. 20.19 and 20.20), (b) a *secondary auditory area* (auditory area II, A-II), located ventral to the primary auditory area (A-I) in the cat (1, 251, 275, 324), and (c) a *secondary visual area* (visual area II, V-II), described in the rabbit, cat, and monkey (9, 145, 356, 359, 365, 403) as anterolateral to visual area I (V-I), and identical to the area defined anatomically as area 18 (Fig. 20.19). The primary and secondary visual areas are often termed striate and extrastriate areas, respectively. A second somatic sensory area has been demonstrated in humans (299), stimulation of which produces various sensations in the upper and lower extremities. Representation of the extremities is chiefly contralateral, although ipsilateral representation also is present. In humans, no cortical representation for the face, tongue, mouth, or throat has been found in S-II. Because of the intimate functional relationships between the primary and secondary sensory areas, these are discussed together.

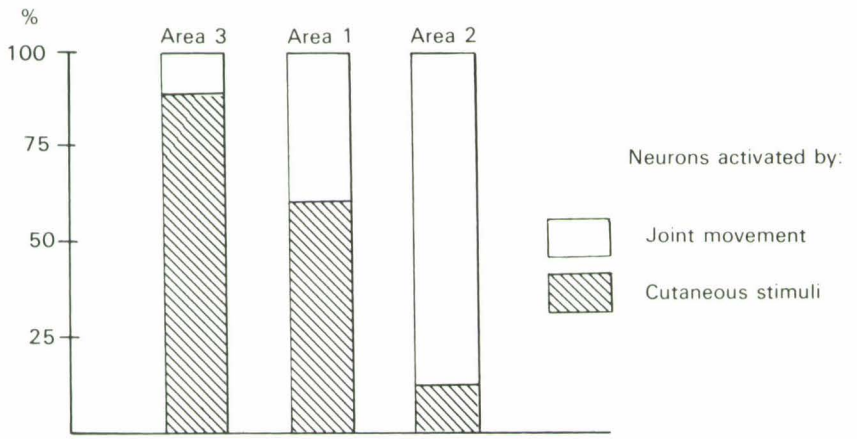
Primary Somesthetic Area (S-I)

The cortical area subserving general somatic sensibility, superficial as well as deep, is located in the postcentral gyrus and in the posterior part of the paracentral lobule. Histologically, the gyrus is composed of three narrow strips of cortex (areas 3, 1, 2) which differ in their architectural structure (Figs. 20.10 and 20.16) (49, 173). In the postcentral region, there is a definite anteroposterior gradient of morphologic change, but the gradient is not uniformly gradual. The anterior part, area 3, is clearly distinguishable from the posterior part, while areas 1 and 2 show more gradual morphologic changes. Area 3 lies along the posterior wall of the central sulcus. Its transition with area 4 anteriorly is not sharp and most of it lies in the depths of the central sulcus (Fig. 20.16). Cortical area 3 is characterized by its thinness and by the fact that layers II, III, and IV tend to fuse with each other (308) and are composed of densely packed granule cells (368). It lies along the posterior wall of the central sulcus and is divided into two parts, 3b on the posterior wall of the sulcus and 3a in the depths of the central sulcus (Fig. 20.17). Areas 1 and 2 forming, respectively, the crown and posterior wall of the postcentral gyrus, have a six-layered structure characteristic of homogenetic cortex (Fig. 20.16). The most marked differences between area 3 and area 1 are found in layer III where cells all become pyramidal in shape and there is a reduction in cell density. The transition from area 1 to area 2 is not sharply defined, but is characterized by an increase in the thickness of the cortex and an increase in the number of large pyramidal cells in layers III and V. The transition from area 2 to areas 5 and 7 is gradual. In the latter areas, layers II and IV are sharply demarcated and a pronounced columnar arrangement of cells is seen.

The postcentral gyrus receives the thalamic projections from the ventral posterior nuclei (VPLc and VPM), which relay impulses from the medial lemniscus, the spinothalamic tracts, the secondary trigeminal tracts, and ascending gustatory pathways from the nucleus of the solitary tract. The majority of the cells of the ventral posterior nuclei project to area 3. In the ventrobasal complex (VB) of the thalamus (VPLc and VPM), the central core region receives cutaneous input and a thinner outer shell receives input from receptors in deep tissues. The inner part of the central core project to area 3b, while the outer part of the central core (cutaneous) projects to areas 3b and 1 (Fig. 20.17). The narrower outer shell concerned with input from deep receptors projects to areas 3a and 2. All thalamocortical projections from the VB complex to the primary somesthetic cortex are somatotopically organized (170). Cortical area 3a in the depths



A



B

Figure 20.16. **A.** Lateral surface of the macaque monkey cerebral hemisphere showing the extent of areas 3, 1, and 2, which compose the primary somesthetic cortex. Area 3, which forms the posterior wall of the central sulcus, is hidden, except for a small dorsomedial region indicated in the diagram. Areas 1 and 2 form the crown and posterior wall of the postcentral gyrus. **B.** Bar graph indicating the relative prevalence of neurons activated by cutaneous stimuli and joint movement in each cytoarchitectural area of the postcentral gyrus.

of the central sulcus receives input from group Ia muscle afferents (muscle spindles). In the somatosensory cortex, most of the thalamic afferents terminate in layer IV. Area 1, however, receives exclusive projections of about 30% of the cells in these nuclei, but it also receives collaterals of fibers passing to area 3. Most of the fibers projecting to area 2 appear to be collaterals of fibers passing primarily to areas 3 and 1.

Although most of the information concerning thalamocortical projections is based upon retrograde cellular degeneration (225, 226, 318, 372), studies of discrete lesions in the ventral posterior thalamic nuclei reveal that coarse fibers project profusely to area 3 while fibers projecting to areas 1 and 2 are of fine caliber and distribute terminals sparsely throughout these two areas (177, 178). Autoradiographic studies of the projections of

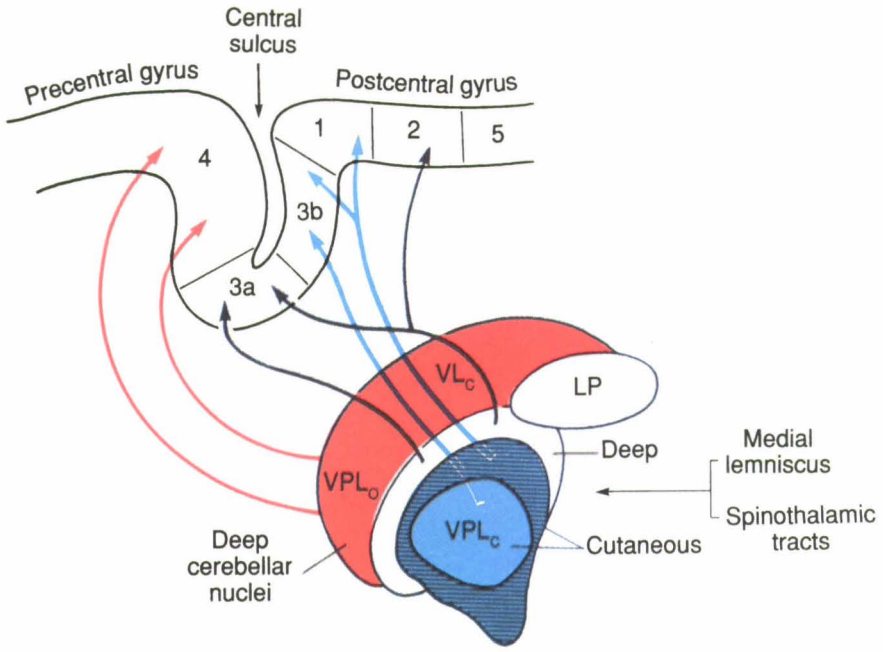


Figure 20.17. Sagittal plane showing projections of thalamic subdivisions to the sensorimotor cortex. Neurons in the ventral posterolateral nucleus (*VPLc*) (and the ventral posteromedial nucleus, VPM, not shown) form a central core (*blue*) responsive to cutaneous stimuli. An outer shell (*white*) of neurons in these nuclei is responsive to deep stimuli. Input to VPLc is via the medial lemniscus and the spinothalamic tracts, while input to VPM is via trigeminothalamic projections (not illustrated). These thalamic afferents terminate somatotopically. Cells in the outer shell project to cortical area 3a (muscle spindles) and to area 2 (deep receptors). Cells in the inner central core (*blue*) project to areas 3b (cutaneous). Cells in the outer central core (*lined blue*) project to areas 3b and 1 (cutaneous). Input to the ventral posterolateral nucleus, pars oralis (*VPLo*), and the ventral lateral nucleus, pars caudalis (*VLc*) (*red*), is from the contralateral deep cerebellar nuclei. Cerebellar input to these thalamic nuclei is considered to terminate somatotopically in the same fashion as sensory input in VPLc and VPM. VPLo and VLc project somatotopically upon the primary motor area (area 4).

the ventral posterior thalamic nuclei confirm the substantial projection to area 3, but do not resolve the question concerning collateral projections to areas 1 and 2 (163–165). Because neurons in area 3 respond preferentially to light tactile stimuli and cells in areas 1 and 2 are excited mainly by deep stimuli and joint movement, it is expected that different populations of thalamic neurons will project to areas 3, 1 and 2 (308, 378). In the somatosensory cortex most of the thalamic afferents terminate in layer IV, but some end in deep parts of layer III (163).

Studies in monkeys by V.B. Mountcastle and T.P.S. Powell indicate that the majority of neurons in the postcentral gyrus are activated by mechanical stimulation, and are selectively excited by stimulation of receptors within either skin or deep tissues, but not by stimulation of both (Fig. 20.16) (268, 270, 271). Over 90% of the neurons in area 2 are related to receptors in deep tissues of the body (joint receptors), while the majority of neurons in area 3 are activated only by cutaneous stimuli. Different neurons in area 1 are related to either cutaneous or deep receptors. This differential representation of sensory modalities is closely correlated with the gradient of morphologic change that characterizes these three cytoarchitectural areas. Afferent impulses from receptors in joint capsules and pericapsular tissues, stimulated by joint movement, are conveyed by the posterior columns, the medial lemniscus, and thalamic relay neurons to particular cell columns in the postcentral gyrus (Fig. 11.1) (271). Impulses conveyed by this system subserve position sense and kinesthesis. Cell columns of the postcentral gyrus responsive to cutaneous stimuli have constant unchanging receptive fields on the body surface. The majority of cortical neurons driven by cutaneous stimuli adapt quickly to steady stimuli. This is a system of great synaptic security, poised for ac-

tion at high frequency levels, and possessing the neural attributes required for discriminative functions.

Stretch receptors in muscles and tendons probably do not provide information useful in perception of joint position. Although most of the afferent impulses from stretch receptors are projected to the cerebellum (284, 285), the margin of the primary somesthetic area, designated as area 3a, receives impulses from Ia muscle afferents via the ventrobasal complex (286). The medullary relay centers for group I muscle afferents are in the rostral part of the nuclei gracilis and cuneatus and project only to the ventral posterolateral nucleus pars caudalis (VPLc) (362). This region is considered a part of the somesthetic cortex.

Although fibers of the spinothalamic tract project to the ventral posterolateral nucleus (VPLc) of the thalamus, fibers of this system also project bilaterally upon portions of the intralaminar and posterior thalamic nuclei (27, 28, 31, 50, 164, 165, 167, 194, 247, 383). Cells of the VPLc project to areas 3, 1 and 2 (S-I), as well as to the second somatic area (S-II) (Figs. 20.19 and 20.20) (175–178). Both of these cortical projections are topographically organized. Studies in monkeys disclose that S-I and S-II are reciprocally and topographically connected with each other within the same hemisphere. The remarkable feature of these somatic sensory areas is the interlocking of topographic subdivisions. Parts of S-I, S-II, and motor cortex related to the same periphery are interconnected. Commissural connections also exist for the somatic sensory cortex. The S-I has connections with its counterpart and with S-II on the opposite side. S-II projects to its counterpart on the opposite side, but only to the region of S-I that represents perioral regions (176). Only S-I projects to parietal cortex and this projection is restricted to area 5.

The various regions of the body are represented in specific portions of the postcentral gyrus, the pattern corresponding to that of the motor area (Fig. 20.18) (86, 306, 354). Thus, the face area lies in the most ventral part of the postcentral gyrus, while above it are the sensory areas for the hand, arm, trunk, leg, and foot in the order named. The lower extremity extends into the paracentral lobule or the medial surface of the brain (Fig. 2.6). The cortical areas representing the hand, face and mouth regions are disproportionally large. The digits of the hand, particularly the thumb and index finger, are well-represented. The cortical area related to sensations from the face occupies almost the entire lower half of the postcentral gyrus. The upper part of the face is represented above, while the lips and mouth are represented below. The tongue and pharyngeal region are localized in more ventral areas. The distorted representation of the body surface in the primary sensory area is said to reflect the pe-

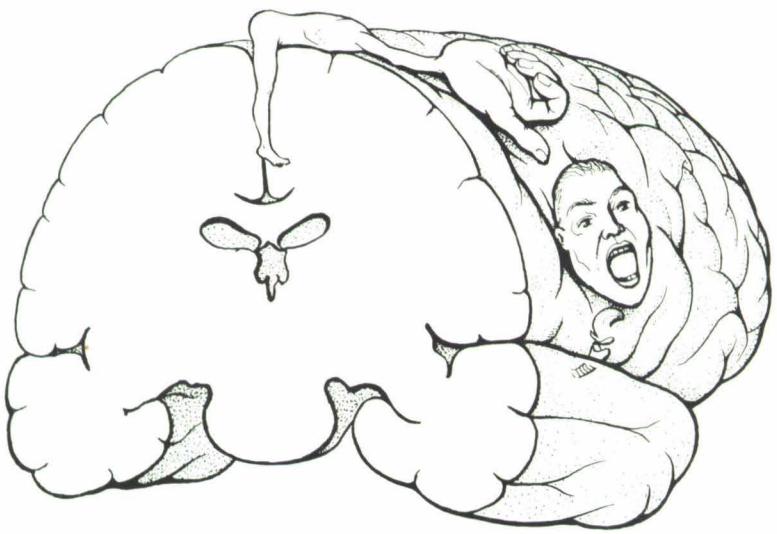


Figure 20.18. Somatotopic localization of parts of the body in the motor cortex. Parts of the body are drawn in proportion to the extent of their cortical representation. The resulting disproportionate figure is called the motor "homunculus." A similar pattern of localization with respect to somesthetic sense is found in the postcentral gyrus.

ripheral innervation density. Those regions of the body with higher densities of receptor elements have extensive cortical representation, while those regions with relatively few receptors have a minimal representation. According to Penfield, sensations from intra-abdominal structures are represented near the opercular surface of the postcentral gyrus. Most of our information concerning the pattern of representation in the somesthetic cortex in humans was obtained from stimulating this region in patients operated upon under local anesthesia (297–299). In attempts to present a readily apparent visual pattern of the sequence of sensory representation in the cerebral cortex, Penfield has drawn the "sensory homunculus" relating different parts of the body to appropriate areas of the cortex. The "sensory homunculus" corresponds to the "motor homunculus" (Fig. 20.18).

Stimulation of the postcentral gyrus in humans produces sensations described by the patient as numbness, tingling, or a feeling of electricity. Occasionally, the patient may report a sensation of movement in a particular part of the body, though no actual movement is observed. A sensation of pain is rarely produced by these stimulations. Sensations are referred to contralateral parts of the body, except in response to stimulation of the face area. The face and tongue are represented bilaterally. Position sense and kinesthetics are represented only contralaterally in the cerebral cortex. Sensory deficits caused by lesion in the postcentral gyrus are detectable only on the opposite side.

Some neurons in the primary motor cortex (area 4) respond to sensory stimuli, particularly proprioceptive inputs, at short latency. The finding that section of the posterior columns of the spinal cord in monkeys causes disappearance of peripheral receptive fields of motor cortex neurons (34, 35) led to the view that the medial lemniscal system could gain direct access to the motor cortex (11). However, the distribution of medial lemniscus in the thalamus is such that the possibility of its fibers gaining synaptic access to thalamocortical neurons projecting to area 4 is quite remote (165) (see Chapter 16). It is possible that lemniscal inputs reach the motor cortex via corticocortical connections from areas 1 and 2, but such projections have not yet been identified anatomically.

The primary somesthetic cortex is not concerned primarily with the recognition of crude sensory modalities, such as pain, thermal sense, and mere contact. In regard to pain perception, experiments in animals have revealed that the number of neurons in S-I that can be activated from nociceptors is relatively low, considering that no other cortical area appears to contain more of them then S-I. Although pain sensation was elicited by electrical stimulation of S-I in humans, this is an infrequent effect of such stimulation. Ablation of S-I does not necessarily reduce pain perception, and only occasionally has it been reported to relieve chronic pain. The central processing from nociceptors is far less understood than the processing of signals from other kind of receptors. The massive and reciprocal thalamocortical connections, as well as the thalamus itself, may play a crucial role in the perception of nociceptive and thermal sensory modalities.

Microelectrode multiunit mapping of the S-I cortex in monkeys suggests that the representation of the body surface may be far more complex than indicated by earlier studies (249). These earlier studies suggest two large systematic representations of the body surface, each of which is activated by low threshold stimuli. One representation of the body surface is coextensive with area 3 and the other with area 1. Each of these somatotopic transformations of the skin surface has some discontinuities. While the two fields of cutaneous representation are basically similar and are approximate mirror images of each other, they differ in size and in the relative proportion of cortex devoted to the representation of various body parts. Because the proportions in each representation differ, both cannot be simple reflections of peripheral innervation density. Area 2 is considered to contain a systematic representation of deep body structures. Studies in monkeys suggest that the somatotopic organization of area 2 only roughly parallels area 1, and some parts of the body are represented in more than one location. The three distinctive cytoarchitectonic areas that compose the postcentral gyrus may each represent different aspects of somatic sensation.

Many neurons in S-I are activated only or most easily from one receptor type, that is, they are *modality-specific*. There are also neurons in S-I with more complex properties such as large receptive fields, indicating that they receive convergent inputs from many primary sensory neurons. For example, many

neurons are activated by movement of just one joint in one direction, while others are activated by several joints. Some neurons in S-I require a specific combination of receptor inputs to be activated. Thus, some processing of the raw sensory information has already taken place in S-I, which appears to be more than a simple receiver of sensory information.

Secondary Somesthetic Area (S-II)

This area lies along the superior bank of the lateral sulcus and extends posteriorly into the parietal lobe (404). In monkeys, the greater part of S-II lies buried in the lateral sulcus (165, 175–177). Representation of the various parts of the body is depicted in reverse sequence to that found in the primary somesthetic area with the two face areas adjacent (Fig. 20.19). Representation of the body is bilateral in S-II, although contralateral representation predominates. In unanesthetized monkeys, two distinct portions of S-II were identified physiologically: (a) an anterior part described as responding to bilateral low threshold somatic stimuli in which body regions were arranged in the sequence of their dermatomes, and (b) a posterior region responding to nociceptive stimuli, related to asymmetric receptive fields and lacking a definite topographic organization (384).

The boundaries of S-II in different animals are not easily defined physiologically (49, 165, 319–321, 384). Anatomically, S-II is the area on the superior bank of the lateral sulcus (or buried in it) that receives afferents from (a) the ventral posterior nucleus of the thalamus (49, 50, 177, 178), and (b) both the ipsilateral and contralateral S-I (49, 98, 175, 176). Anatomic and physiologic studies of the somatotopic organization of S-II in primates indicate that the different body regions are represented in successive, obliquely oriented, cortical strips parallel with the lateral sulcus (49, 98, 165, 319). Neurons with trigeminal receptive fields were found rostrally in S-II and responded to bilateral stimuli (Fig. 20.20). Regions representing the hand were posterior to the face area and formed the largest component. Regions related to the arm, trunk, and hindlimbs follow in a rostrocaudal sequence. These cortical strips representing various parts of the body in S-II do not form a topologic map of the body surface as depicted in the figurines for S-I. The efferent cortical connections of S-II are with S-I and with the primary motor area within the same hemisphere (165, 174, 175).

In addition to the S-II, there are a number of small areas in the parietal and insular cortex that respond in various ways to cutaneous stimulation (320). Of these, the retroinsular area seems especially significant because it receives projections from the medial part of the posterior thalamic nucleus (50). Physiologic observations indicate that cells in the retroinsular cortex are activated only from small, well-defined, contralateral receptive fields located in the hand and foot (319). These findings raise important questions concerning the notion that cells in the posterior thalamic nucleus may be specifically involved in relaying impulses concerned with pain and noxious stimuli to regions of the cerebral cortex (165, 305). They cast doubt upon the concept that impulses concerned with painful and noxious stimuli are relayed to S-II or the retroinsular cortex via the posterior thalamic nucleus. It was suggested that some of the response characteristics attributed to neurons in S-II may be those of cells in neighboring cortical areas, perhaps the area referred to as 7b in the inferior parietal lobule (319).

The S-II has been described in humans, but face, mouth, and tongue regions have not been identified, presumably because of proximity to the primary face area (299). Stimulation of S-II in the unanesthetized patient produces sensations in the extremities similar to those obtained by stimulating S-I.

Primary Visual Area (V-I)

Area 17 (primary visual area or V-I) is located in the walls of the calcarine sulcus. It occasionally extends around the occipital pole on to the lateral surface of the hemisphere (Figs. 16.14 and 20.10). The exceedingly thin cortex of this area (1.5–2.5 mm) is the most striking example of the heterotypical granulous cortex (type 5). Layers II and III are narrow and contain numerous small pyramidal cells that are hardly larger than typical granule cells (Fig. 20.15**C**). A thick layer IV is subdivided by a light band into three sublayers (Fig 20.26). The upper and lower sublayers are packed with small granule cells. In the middle, lighter layer, fewer small cells are scattered between the large

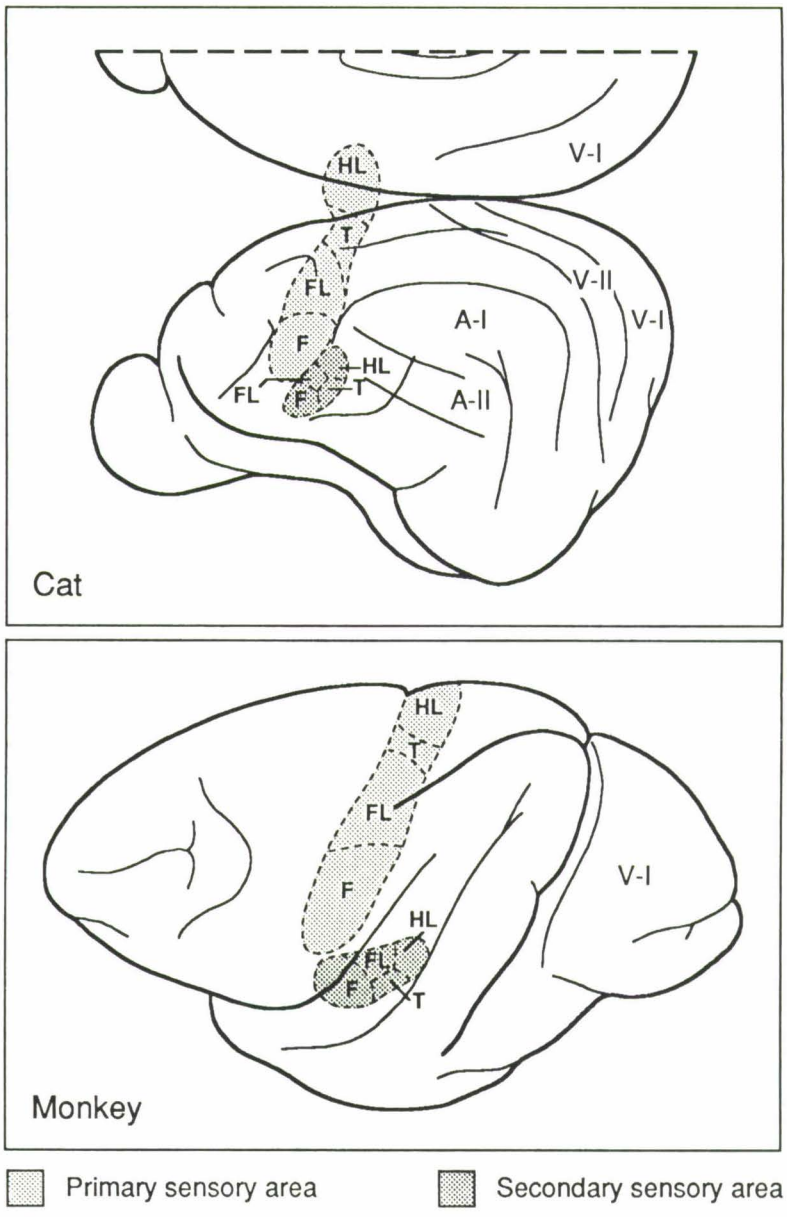


Figure 20.19. Primary and secondary sensory areas in the cortex of the cat and monkey. Somatotopic representation of different parts of the body are indicated in the primary and secondary somatic sensory areas: *F*, face area; *T*, trunk; *FL*, forelimb; *HL*, hindlimb. Primary and secondary auditory (A-I and A-II) and visual (V-I and V-II) areas in the cat brain are shown. The medial aspect of the cat brain is represented above.

stellate cells (giant stellate cells of Meynert). The middle layer contains the greatly thickened outer band of Baillarger, here known as the *band of Gennari*, and is visible to the naked eye in sections of the fresh cortex (Fig. 20.21). The band of Gennari has given to this region the name *area striata* (or striate cortex). Layer V is relatively narrow and poor in small cells, but scattered among these cells are isolated large pyramidal neurons whose cell bodies may reach a height of 60 μm (Fig. 20.15C).

The visual cortex contains numerous GABAergic interneurons and fibers in layers II and III which exhibit a periodicity suggesting a correlation with the functional columnar subdivision (129, 137, 339). These small neurons make symmetric, inhibitory,

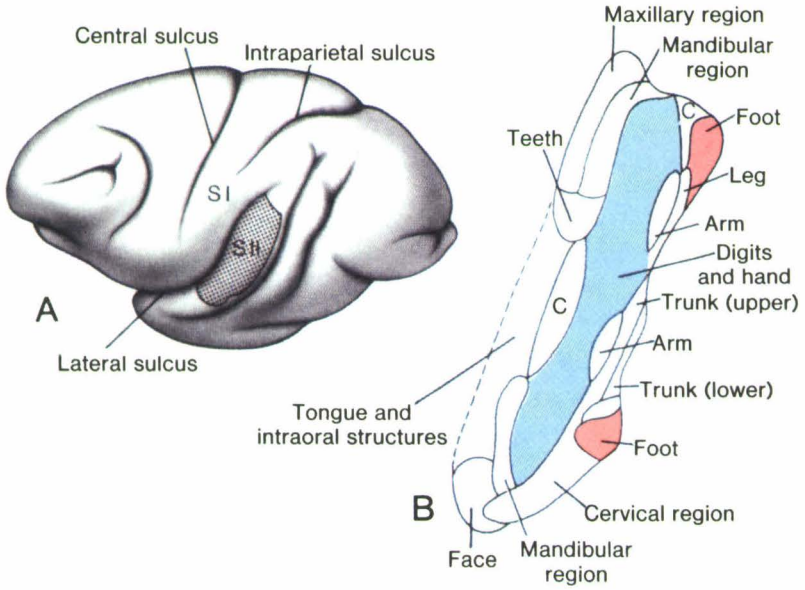


Figure 20.20. Position and somatotopic organization of the secondary somesthetic area (S-II) in the cynomolgus monkey (*Macaca fascicularis*). Most of S-II lies buried in the depths of the lateral sulcus and has been identified on the basis of its cytoarchitecture and connections with the ventrobasal complex and projections from the primary somesthetic cortex (S-I). In **A**, S-II is shown in a flattened view on the cortical surface. In **B**, the body representation in S-II is outlined as determined from recordings in awake monkeys. Different regions of the body are represented by a series of oblique strips parallel to the lateral sulcus, with the face and intraoral structures most rostral. The area in *blue* represents the digits and hand, while the areas in *red* represent the foot. Areas designated *C* are regions with poorly defined receptive fields.

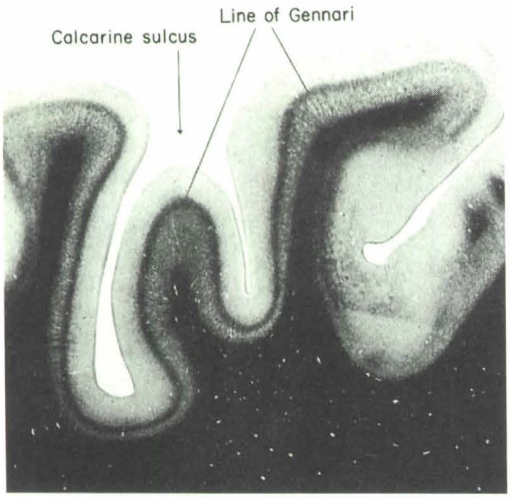
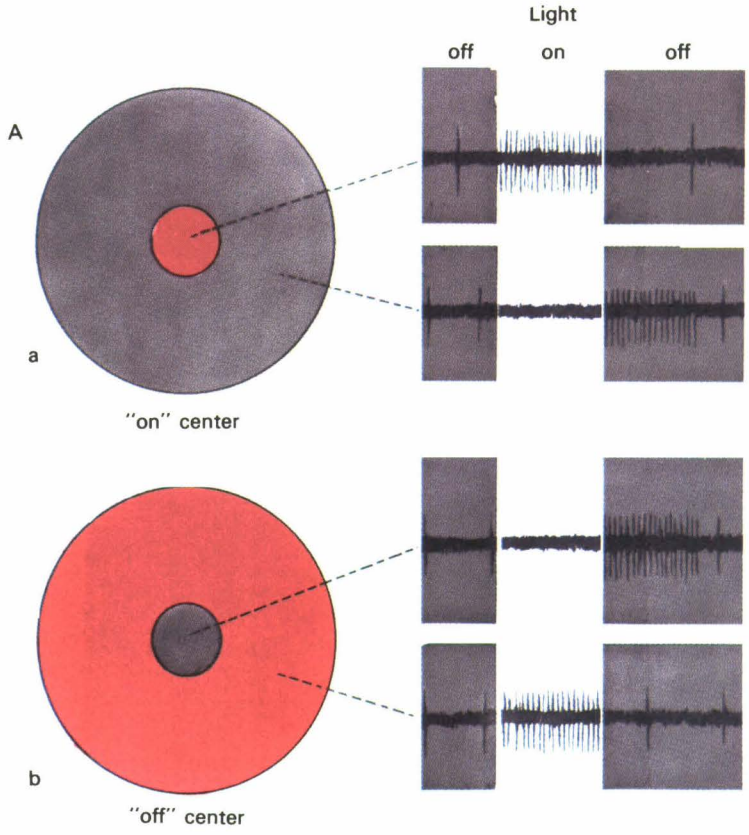


Figure 20.21. Frontal section through calcarine cortex (striate cortex) showing extent of line of Gennari. Weigert's myelin stain.

synapses with the apical and basilar dendrites of pyramidal cells.

The striate cortex (V-I) receives the geniculocalcarine tract, whose course and exact projection were discussed in Chapter 16 (Fig. 16.41). Geniculocalcarine fibers pass in the *external sagittal stratum*, separated from the wall of the inferior and posterior horns of the lateral ventricle by the *internal sagittal stratum*, and by fibers of the corpus callosum designated as the *tapetum* (Fig. 2.22). Fibers of the internal sagittal stratum are corticofugal fibers passing from the occipital lobe to the superior colliculus and the lateral geniculate nucleus or lateral geniculate body (LGB) (102, 103, 135, 187, 392, 400). The optic radiation projects topographically upon the striate cortex so that cells in (a) the medial half of the LGB, representing upper retinal quadrants (lower quadrants of the visual field) project to the superior bank of the calcarine sulcus, and (b) the lateral half of the LGB, representing lower retinal quadrants (upper quadrants of the visual field) project to the inferior bank of the calcarine sulcus (Figs. 16.28 and 16.41).

The macular fibers terminate in the caudal third of the calcarine area, and those from the paracentral and peripheral retinal areas end in respectively more rostral portions. Parts of each macular area are represented only in the visual cortex of one hemisphere. The representation of the macular area in the occipital



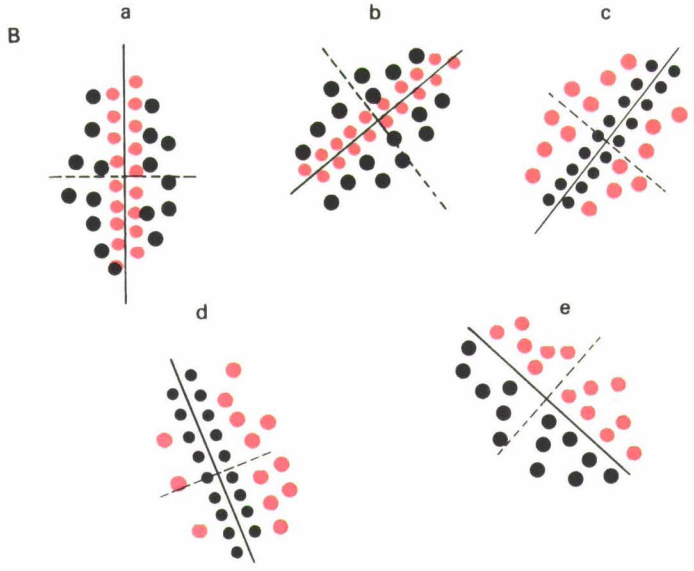


Figure 20.22. **A.** Receptive fields of retinal ganglion cells and lateral geniculate neurons are concentric with either an "on" (excitatory) center and an "off" (inhibitory) surround, or the reverse. In *a*, a spot of light (*red*) filling the "on" center causes the cell to fire vigorously. If the spot of light strikes the surrounding "off" zone, firing of the neuron is suppressed until the light is turned off. In *b*, the responses of a cell with an "off" center and an "on" surround are the reverse. **B.** Simple cells of striate cortex receive their input from sets of lateral geniculate neurons whose "on" or "off" centers are arranged in straight lines. The receptive field axis of orientation varies for simple cells, as in *a*, *b*, and *c*, with excitatory areas represented by *red dots* and inhibitory areas by *black dots*. Although simple cells always have excitatory and inhibitory areas parallel and in a straight line, these areas may be asymmetric as in *d* and *e*.

cortex appears relatively large compared with the macular area of the LGB (Figs. 16.28, 16.29, and 16.41). Clinically, sparing of macular vision associated with vascular lesions involving the occipital cortex usually is attributed to collateral circulation provided by branches of the middle cerebral artery (Fig. 4.8). Following occlusion of the posterior cerebral artery, these collateral vessels may be sufficient to preserve some macular vision. Similar collateral circulation apparently is not present in the cortical area representing paracentral and peripheral parts of the retina.

Complete unilateral destruction of the visual cortex in man produces a contralateral homonymous hemianopia in which there is blindness in the ipsilateral nasal field and the contralateral temporal field. Thus, a lesion in the right visual cortex produces a left homonymous hemianopsia (Fig. 16.43). Lesions involving portions of the visual cortex, such as the inferior calcarine cortex, produce an *homonymous quadrantanopsia,* in which blindness results in the superior half of the visual field contralaterally. Homonymous hemianopsia can result from lesions involving all fibers of either the optic tract or the optic radiations (Fig. 16.43**C**), but lesions in these locations tend to be incomplete and the visual field defects in the two eyes are rarely identical. Patients frequently are unaware of an existing homonymous hemianopsia and complain of bumping into people and objects on the side of the visual field defect.

An image falling upon the retina initiates a tremendously complex process that results in vision. The transformation of a retinal image into a perceptual image occurs partly in the retina but mostly in the brain. An impressive series of studies by David Hubel and Torsten Wiesel in cats and monkeys provided the first real insight into the functional organization of the visual cortex (140, 142, 143, 147).

The receptive field of a cell in the visual system is defined as the region of the retina (or visual field) over which one can influence the firing of that cell. In the retina, the receptive field comprises those receptor sets (i.e., rods and cones) and other retinal neurons which influence the firing of one retinal ganglion cell. Receptive fields of retinal ganglion cells are circular, vary somewhat in size, and are of two types: (a) those with an "on" (excitatory) center and an "off" (inhibitory) surround, and (b) those with an "off" (inhibitory) center and an "on" (excitatory) surround (205). Retinal ganglion cells fire at a fairly steady rate even in the absence of stimulation. An "on" response is characterized by an increased firing rate of the cell to a light stimulus. In an "off" response, the cell's firing rate diminishes when the light stimulus decreases. The physiologic basis for the "on" and "off" retinal responses are the concentric receptive fields with either an "on" or "off" center and the reverse type of surround (Fig. 20.22). Lighting the entire retina diffusely does not affect retinal ganglion cells as strongly as a small circular spot of light that covers only the excitatory center of the receptive field.

Cells of the LGB have physiologic characteristics similar to retinal ganglion cells, in that (a) each cell is driven from a circumscribed retinal region (receptive field), and (b) each receptive field has either an "on" or "off" center with an opposing surround (141). Lateral geniculate neurons are more specialized than retinal ganglion cells in that they are more sensitive to the differences in retinal illumination than to the illumination itself. Cells in different laminae of the LGB are driven from receptive fields in one eye, either ipsilaterally or contralaterally, depending upon the uncrossed or crossed connections (141). Visual processing by the brain begins in the LGB.

The striate cortex, anatomically far more complex than the retina or LGB, does not have cells with concentric receptive fields. Cells of the striate cortex show marked specificity in their responses to restricted retinal stimulation (140, 142, 143, 147). The most effective stimulus shapes are long, narrow rectangles of light ("slits"), dark bars against a light background ("dark bars"), and straight-line borders separating areas of different brightness ("edges"). A given cell responds vigorously when an appropriate stimulus is shone on its receptive field or moves across it, provided the stimulus is presented in a specific orientation. This orientation is referred to as the *"receptive field axis of orientation"* and it is critical and constant for any particular cell, but it differs for other cells in the locations. Cells with the same receptive field axis of orientation are arranged in columns extending from the cortical surface to the white matter.

The cortical columns of the striate cortex may be looked upon as the structural expression of the necessity to encode more than two variables. The two surface coordinates (ec-

centricity from fovea and distance above or below the horizontal meridian) encode topographic representation in the visual fields. Engrafted upon this representation are two more variables in columnar form concerned with receptive-field orientation and ocular dominance. The topographic representation of the retinae upon the striate cortex is primary and for each position in the visual field there is neuronal machinery for each orientation and for each eye (150). In the striate cortex, there exist two independent and overlapping systems of columns referred to as orientation columns and ocular dominance columns (147). Ocular dominance columns are parallel sheets or slabs arranged perpendicular to the cortical surface which are subdivided into a mosaic of alternating left eye and right eye stripes 250–500 μm in width (149). Orientation columns are an order of magnitude smaller than the ocular dominance columns (Fig. 20.26). The horizontal distance corresponding to a complete cycle of orientation columns, representing a rotation through 180°, is roughly equal to a set of left plus right ocular dominance columns with a thickness of 0.5–1 mm (151).

ORIENTATION COLUMNS

The visual cortex is subdivided into discrete columns extending from the surface to the white matter, with all cells within each column having the same receptive field axis of orientation. The many varieties of cells in the striate cortex have been grouped into two main functional types, but it is apparent that other subtypes or varieties also exist. The main functional cell types are referred to as *"simple"* and *"complex."*

"Simple"-type cells respond to slits of light having the proper receptive field axis of orientation. A slit of light, oriented vertically in the visual field, may activate a given "simple" cell, whereas the same cell will not respond, though other cells will, if the orientation of the slit of light is moved out of the vertical position. The retinal region over which a "simple" type cell can be influenced is, like the receptive fields of retinal and geniculate cells, divided into "on" and "off " areas (Fig. 20.22). In "simple" cells, these "on" areas are not circular but are narrow rectangles, adjoined on each side by larger "off" regions. The magnitude of the "on" response depends upon how much of the "on" region is covered by the stimulus light. A narrow slit of light that just fills the elongated "on" region produces a powerful "on" response. Stimulation with a slit of light having a different orientation produces a weaker response, because it includes part of the antagonistic "off" regions. A slit of light at right angles to the optimum orientation for a particular cell usually produces no response (Fig. 20.23) (138). Thus, a large spot of light covering the whole retina evokes no response in "simple" cortical cells, because "on" and "off" effects balance. A particular cortical cell's optimum receptive field axis of orientation appears to be a functional property built into the cells by its anatomic connections. The receptive field axis of orientation differs from one cell column to the next, and may be vertical, horizontal, or oblique. There is no evidence that any one orientation is more common than any other.

"Simple" cells, located in layer IV, receive their impulses directly from the LGB (142). A typical "simple" cell receives an input from a large number of lateral geniculate neurons whose "on" centers are arranged in a straight line which corresponds to the receptive field orientation of the "simple" cell (Fig. 20.22**B**). Thus, for each area of the retina stimulated, each line, and each orientation of the stimulus, there is a particular set of "simple" striate cells to respond. Changing any of the stimulus arrangements will cause an entirely new and different population of "simple" striate cells to respond.

"Complex" type cells, like "simple" cells, respond best to "slits," "bars," or "edges," provided the orientation is suitable. Unlike "simple" cells, these cells respond with sustained firing as the slits of light are moved across the retina, preserving the same receptive field axis of orientation (142). These cells have peculiar characteristics in that a slit of light with the appropriate receptive field axis of orientation can cause cells to fire vigorously as it moves across the retina in one direction, but reversing the direction of movement of the light stimulus may produce a diminished, or different, response.

Although "complex" cells in the striate cortex have some characteristics similar to those of "simple" cells, their receptive fields cannot be mapped into antagonistic "on" and "off" regions. A "complex" cell receives its input from a large number of "simple" cells, all of which have the same receptive field axis of orientation. Most "simple" cells in the striate cortex are stellate cells located in layer IV

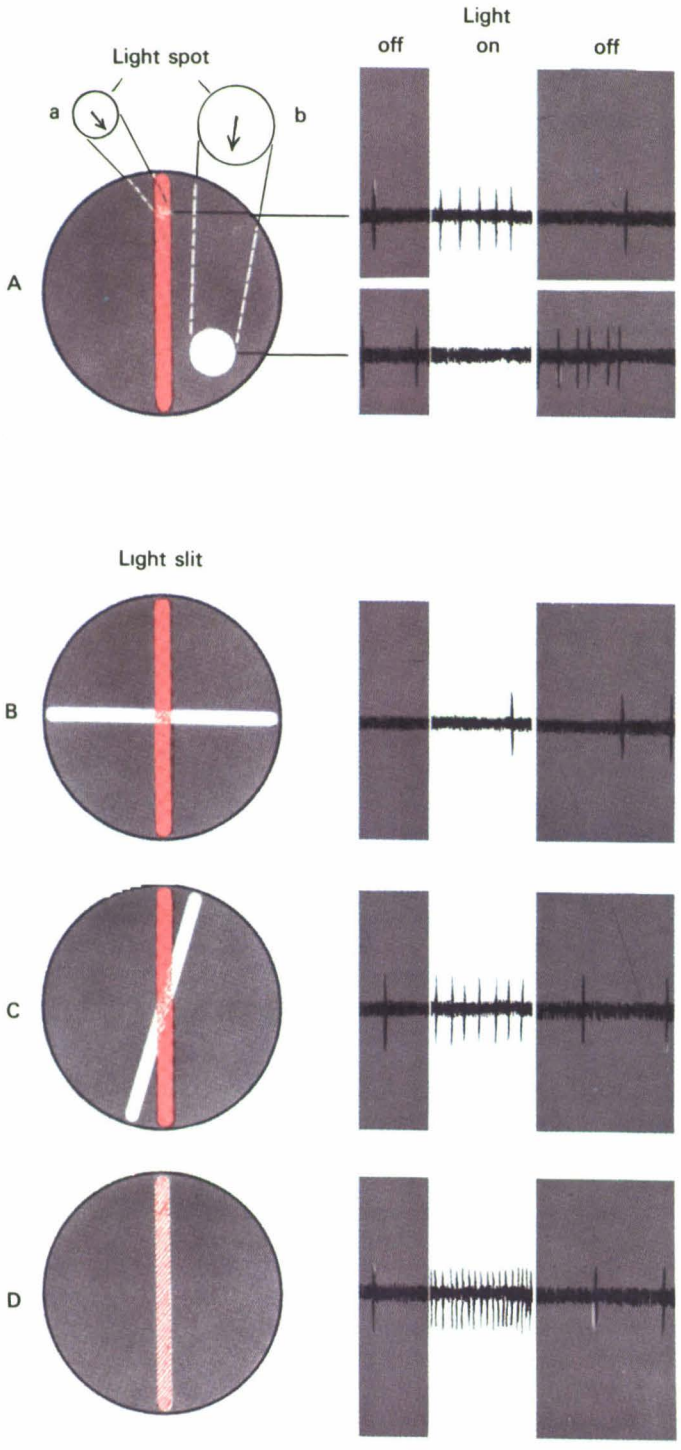


Figure 20.23. Functional characteristics of "simple" cells in the striate cortex. In **A**, a small circular spot of light (*a*) shone on the excitatory part of the receptive field (*red*) of a simple cortical cell produces a weak response. A larger spot of light (*b*) shone on the inhibitory surround produces no response. Small spots of light (*a*) produce vigorous responses in retinal ganglion cells and lateral geniculate neurons. The receptive field of the simple cell shown above is similar to *a* in Figure 20.22**B**. In **B**, a narrow slit of light shone perpendicular to the receptive field axis of orientation (*red*) produces virtually no response. In **C**, tilting the slit of light produces a weak response. In **D**, a vertical slit of light, which corresponds to receptive field axis of the simple striate cell, produces a vigorous response.

(Fig. 20.26). The majority of "complex" and "hypercomplex" cells are pyramidal neurons lying in layers superficial or deep to layer IV (147, 188). "Hypercomplex" cells have the properties of two or more "complex" cells from which they are believed to receive their input. Most cells in layer IV are driven by only one eye while cells in other layers are driven binocularly (147). There are a few cells in layer III of the striate cortex that have a center-surround field organization, but their behavior is much more complex than cells in the LGB.

These findings imply that a vast network of intracortical connections relate "simple" and "complex" cells in the striate cortex in a very specific fashion, and that similar arrangements must exist for all receptive field axes of orientations. Since columns of cells constitute the fundamental functional units of the cortex, each small region of the visual field must be represented in the striate cortex many times, in column after column of cells with different receptive field orientations.

Attempts have been made to determine the geometry and sequence of the orientation columns in the primate striate cortex (150). Orientation columns appear to have the form of narrow slabs, as do ocular dominance columns. The arrangement of the columns is highly ordered and recordings made along a tangential microelectrode penetration show that the preferred orientations of cells change in a systematic fashion, in either a clockwise or counter-clockwise direction with advancement of the electrode (Fig. 20.26). There is a continuous variation in the preferred orientation with horizontal distance along the cortex. When the electrode crosses from a left-eye region to a right-eye region, there is no noticeable disturbance in the sequence of orientation columns, which suggests a degree of independence for the two systems (Fig. 20.26). The horizontal distance along the cortex corresponding to a complete cycle of orientation columns, representing rotations through 180°, is said to be of the same size as a set of left and right ocular dominance

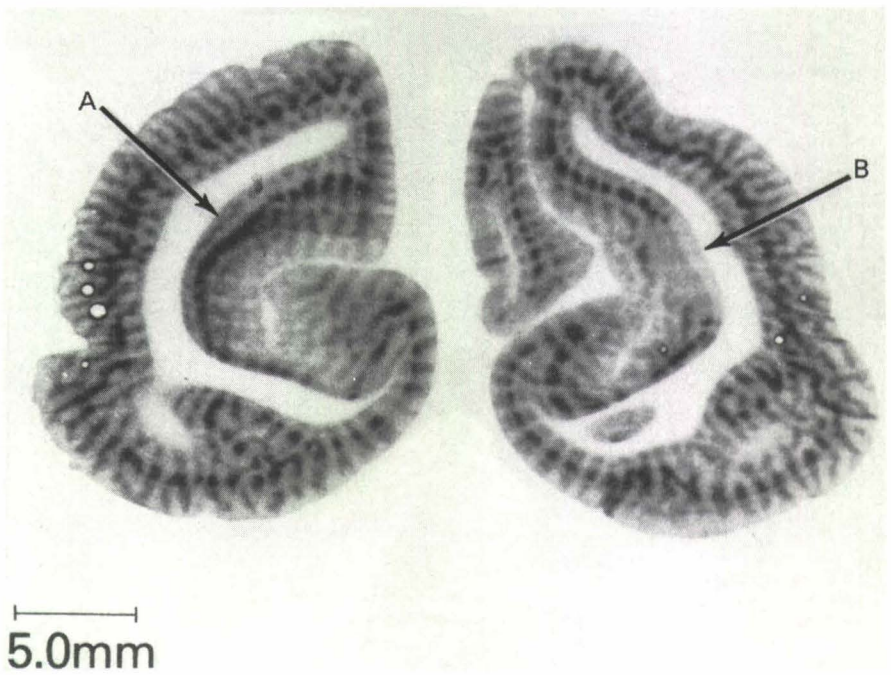


Figure 20.24. Autoradiographic mapping of the visual system in a monkey using 2-(^{14}C)deoxyglucose. Coronal sections of the striate cortex in an animal with the right eye occluded. The alternate dark and light striations, each 0.3–0.4 mm in width, represent ocular dominance columns. These columns are darkest in a band which corresponds to layer IV, but they extend the entire thickness of the cortex. *Arrows A* and *B* point to regions without ocular dominance columns. These regions receive only monocular input. The region indicated by *arrow A* is contralateral to the occluded eye. The region indicated by *arrow B* is ipsilateral to the occluded eye and shows no evidence of radioactivity. Both arrows indicate loci believed to be the cortical representation of the blind spots.

columns (0.5–1 mm). Orientation columns are arranged with great regularity so that a probe moving along the cortex horizontally generally can be expected to encounter all values of orientation in a regular sequence before any one value is repeated (151). In young monkeys deprived of vision by suturing the eyelids closed, the same highly ordered sequence of orientation columns is found in the striate cortex (150). This finding indicates that the orientation column system is innately determined and not the result of early visual experience.

OCULAR DOMINANCE COLUMNS

Recording from single cells at various levels of the visual system offers a direct means of determining the site of convergence of impulses from the two eyes. In the LGB, the first point at which convergence is possible, no binocularly influenced cells have been observed (141). No crossed and uncrossed optic tract fibers overlap in layers of the LGB (102, 104, 128, 131). It has long been recognized that the primary visual cortex receives projections via the LGB from both eyes. The receptive fields of all binocularly influenced cortical cells occupy corresponding sites in the two retinas (Fig. 16.27). About 80% of cells in the striate cortex are influenced independently by the two eyes (142). In a binocularly influenced cell, the two receptive fields have the same organization and axis of orientation, and a summation occurs when corresponding parts of the two retinas are stimulated simultaneously.

In monkeys, binocular convergence in area 17 is delayed beyond the first and second synaptic stages (147, 152). Projections of the LGB terminate in deep parts of layer IV where they are segregated into a series of parallel alternating stripes, one set connected with the left eye and the other to the right eye. Although input to deep parts of layer IV is essentially monocular, ocular dominance columns extend vertically from the pial surface to the white matter, and show alternate preference for left and right eyes (Figs. 20.24 and 20.26). This columnar arrangement is demonstrated by vertical electrode penetrations of the striate cortex in which there is no change in eye preference (Fig. 20.26). In tangential penetrations of the striate cortex, the electrode moves from a region in which one eye gives the best response to an adjacent region where the other eye dominates (152). In layer IV the responses are monocular, while cells in other layers respond binocularly, but with definite dominance by one eye. The widths of the ocular dominance columns innervated by the ipsilateral or contralateral eye are the same (0.5–1 mm) (151). Iontophoretic application of the GABA antagonist bucucullin to the visual cortex cancels the "on" and "off" subregions of "simple" cells and abolishes orientation selectivity. It also produces a shift in ocular dominance columns from one eye to the other. These effects are reversible and appear correlated with the loss of GABAergic inhibition.

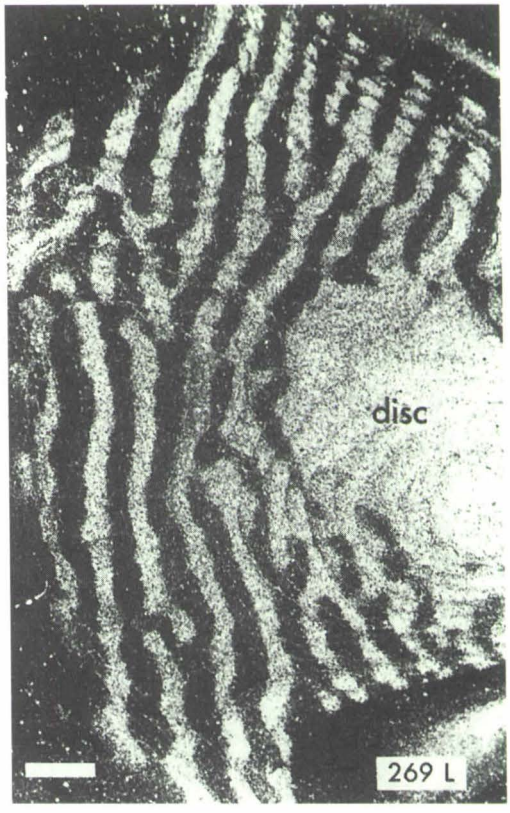


Figure 20.25. Autoradiographic montage of tangential sections of area 17 on the left in a monkey whose right eye was removed as an adult. The left eye was injected 4 months later with (^{3}H)proline. The montage shows the normal mosaic pattern of ocular dominance columns with uniformly labeled bands alternating with unlabeled bands. The uniformly labeled area (disc) represents the monocular area which covers the blind spot (optic disc) of the enucleated right eye. Calibration bar: 1 mm.

The striate cortex is organized into both vertical and horizontal systems. The vertical or columnar system is concerned with retinal position, line orientation, ocular dominance,

and perhaps detection of direction of movement. These functional features are mapped in sets of superimposed, but independent mosaics (Figs. 20.24 and 20.25). The horizontal system segregates cells of different orders of complexity. Cells of the lowest order (simple cells), located in layer IV, are driven monocularly, while those of higher orders (complex and hypercomplex cells), located in the other layers, are driven by impulses from both eyes (Fig. 20.26).

Ocular dominance columns in the striate cortex have been demonstrated by a variety of neuroanatomic techniques. After a discrete lesion in a single layer of the LGB, degenerated fibers can be traced to a region of the striate cortex where bands of degenerated fibers in layer IV (250–500 μm) are separated from interbands of the same extent free of degeneration (149). Combined physiologic studies and a reduced silver staining method show that the boundaries of ocular dominance columns correspond with a mosaic pattern of dark bands seen in tangential sections of the striate cortex (227). Autoradiographic methods, using the principle of transneuronal transport or 2-[^{14}C]deoxyglucose (2-DG) as a metabolic marker to measure glucose utilization, also reveal the characteristic pattern of ocular dominance columns (Figs. 20.24 and 20.25) (193, 387). Two regions of the striate cortex do not contain ocular dominance columns: (a) the region representing the blind spot of the retina, and (b) the cortical region representing the monocular temporal crescent of the visual field. These regions of striate cortex, receiving only monocular visual inputs, have been identified with the 2-DG

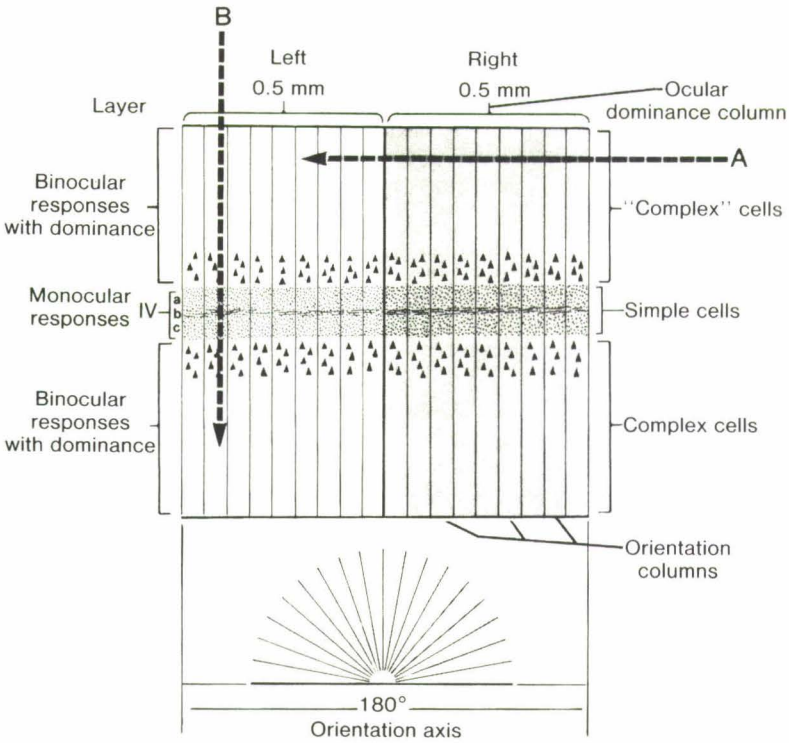
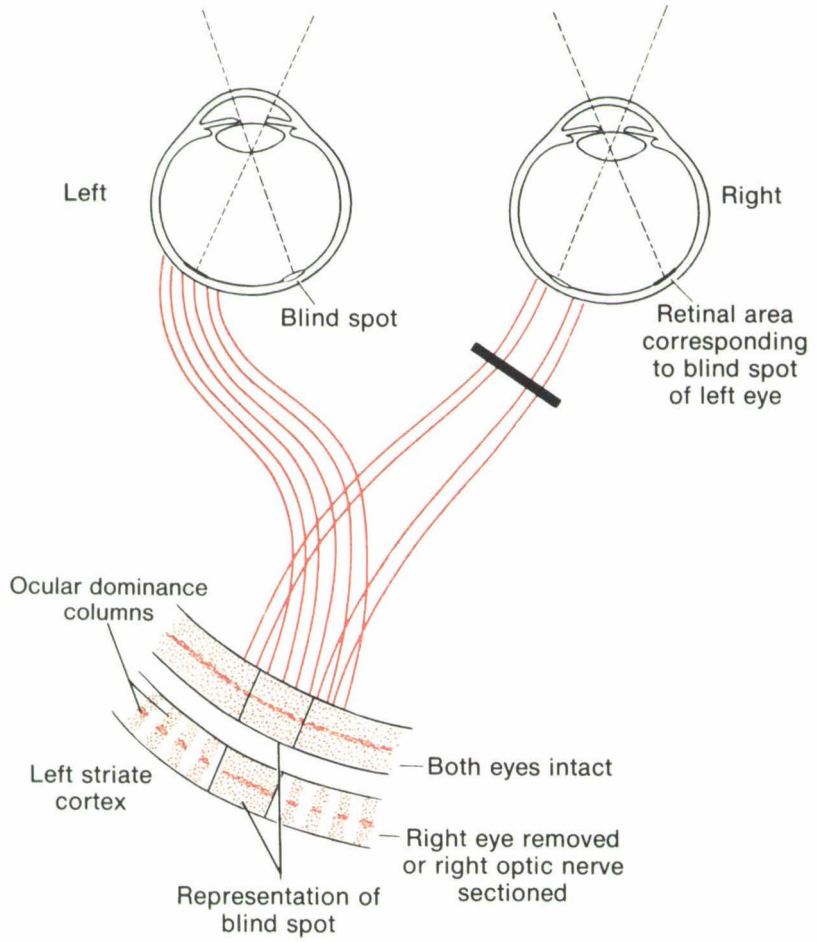


Figure 20.26. Organization of ocular dominance and orientation columns in the striate cortex. Ocular dominance columns (0.25–0.5 mm) are an order of magnitude larger than orientation columns and a pair of left-right ocular dominance columns (0.5–1 mm) are roughly equal to a set of orientation columns representing a complete cycle of orientations through 180°. Input from the lateral geniculate body to layer IV is strictly monocular and consists of a series of parallel and alternating stripes, one for the left eye and one for the right eye. Most of the cells in layer IV are "simple" cells. Binocularly influenced cells are predominantly "complex" cells in layers above and below layer IV. A recording electrode inserted tangential to the pial surface, as in *arrow A*, will detect responses to successive stimuli with different orientations, first with right eye dominance and then with left eye dominance. A recording electrode inserted vertically, as in *B*, will indicate responses only to stimuli presented in one axis of orientation. About 50% of the cells above and below layer IV will respond to binocular stimuli, but with consistent left dominance. When the electrode is in layer IV, monocular responses will be recorded.



Figures 20.27 and 20.28. Ocular dominance columns and the blind spot in the striate cortex with the 2-(^{14}C)-deoxyglucose metabolic mapping technique in macaque monkeys. In the animal with an intact visual system, silver grains are distributed throughout the striate cortex with greatest concentrations in layer IV. Neither the blind spot or ocular dominance columns can be demonstrated. Following removal of the right eye or section of the right optic nerve (*heavy black line*), silver grains are distributed evenly in the representation of the blind spot on the left (Figs. 20.24**A** and 20.27) but no isotope is evident in the blind spot on the right (Figs. 20.24**B** and 20.28). Other regions of the striate cortex demonstrated ocular dominance columns on both sides. Fibers from the ipsilateral temporal retina normally cover the blind spot of the opposite eye.

metabolic mapping technique and other autoradiographic methods (Figs. 20.24, 20.25, 20.27, and 20.28). The area of the optic disc in the nasal half of each retina transmits no visual impulses to the contralateral striate cortex. This region of striate cortex receives its sole input from the temporal half of the ipsilateral retina.

When an animal is deprived of vision in the right eye and the 2-DG method is employed as a metabolic marker (a) the left striate cortex shows the striped pattern of ocular dominance columns, except in the representation of the blind spot where metabolic activity is evidenced by a continuous band of isotope uptake, and (b) the right striate cortex shows a similar pattern of striped columns but no evidence of metabolic activity in the cortical area representing the blind spot (Figs. 20.24, 20.27, and 20.28). The cortical area representing the monocular crescent of the right visual field, which lies in the left striate cortex, would not contain isotope because all of its afferent input is crossed.

VISUAL DEPRIVATION

Studies in very young, visually inexperienced kittens and monkeys, deprived of all vision from birth by visual occluders, have shown that responses in the striate cortex indicate that orientation columns are as highly

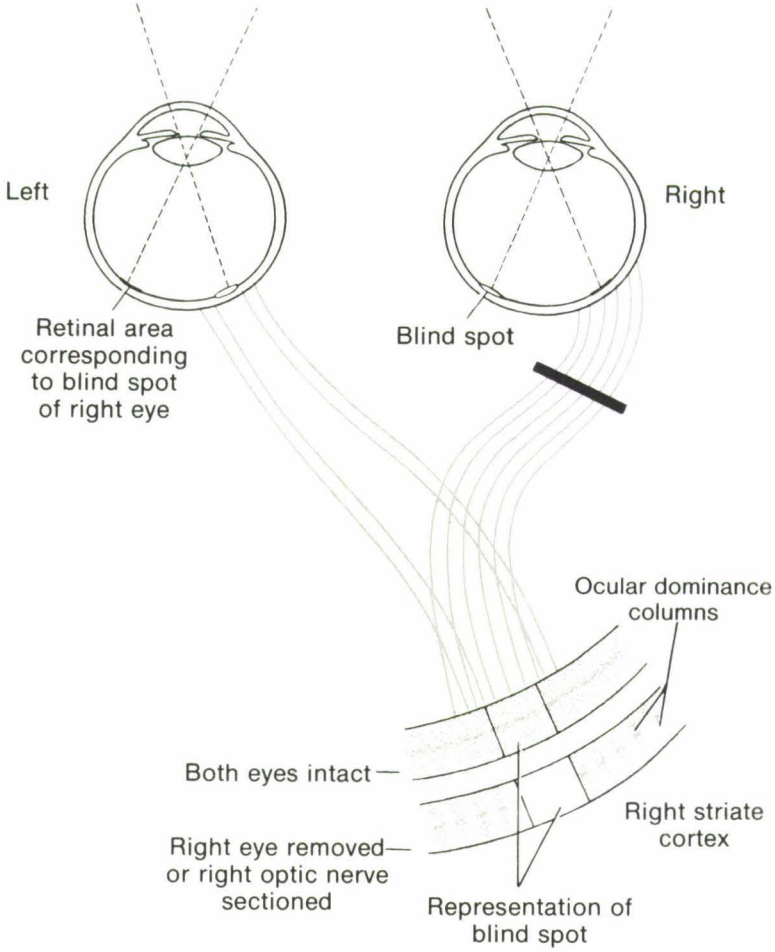


Figure 20.28. *Continued.*

ordered as in the adult (144, 386). The connections responsible for the highly organized function of the visual cortex must be present at birth and appear to be genetically determined. The surprising finding in young monkeys deprived of binocular vision for a few weeks after birth was the marked reduction in number of cells in the striate cortex that could be influenced by both eyes. Deprivation of binocular vision for a few weeks after birth may result in deterioration of innate cortical connections subserving binocular vision.

Unilateral visual deprivation, accomplished by suturing the eyelids closed or placing a contact occluder over the cornea, in very young kittens results in marked histologic changes in the layers of the LGB receiving fibers from the deprived eye, but no obvious histologic changes in the retina, optic nerves, superior colliculi, or striate cortex (385). Similar visual deprivation in older kittens or in adult animals produced less severe, or no detectable, histologic changes in the LGB. In young kittens, most of the geniculate neurons with inputs from the deprived eye had abnormal receptive fields, and the overall activity of cells in these layers was diminished. Single unit recordings from the striate cortex in these animals indicated that the majority of cortical cells were driven only from the normal eye (385). Kittens deprived from birth for 2–3 months showed profound visual defects in the deprived eye, although pupillary light reflexes were normal. Thus, monocular visual deprivation in kittens from birth can result in severe visual defects and unresponsiveness of cortical neurons to stimulation of the deprived eye. Physiologic defects following unilateral visual deprivation appear to result from disruption of cortical connections present from birth.

Ocular dominance columns in monkeys are only partially formed at birth and undergo rapid development during the first 6 weeks of life (152, 228). The process of left and right eye segregation of afferent fibers in layer IV of the striate cortex occurs in the presence or absence of visual experience. Monocular visual deprivation during the first six postnatal weeks causes ocular dominance columns in the deep parts of layer IV related to the open eye to be greatly expanded, while dominance columns related to the closed eye appear to shrink. Thus, monocular visual deprivation in very young monkeys causes a redirection of cortical afferents into sets of columns of unequal width. The eye preference of neurons in layers of the striate cortex superficial and deep to layer IV also changes as a consequence of monocular deprivation. In young animals deprived of vision bilaterally, cells in upper and lower layers of the striate cortex responding binocularly are greatly reduced (386). Monocular eyelid suture in the adult animal does not result in detectable anatomic or physiologic defects in the striate cortex (228). These studies indicate normal visual binocular experience, particularly in the first 6 weeks of life, is necessary for the maintenance of cortical connections beyond the deep parts of layer IV of the striate cortex that subserve binocular vision.

Secondary Visual Areas (V-II and V-III)

A second visual area (visual area II) has been mapped in a number of different animals by recording the potentials evoked by photic stimulation of the retina (356, 359, 403). Visual area II is a smaller mirror image representation of the primary visual area (V-I) and is identified as area 18 (Fig. 20.19). Lateral to V-I and V-II is a third systematic projection of the contralateral visual field (visual area III, V-III), which corresponds to area 19 (145). Areas 18 and 19 are often collectively termed extrastriate cortex (Fig. 20.10).

Cells in V-II and V-III respond to slits, dark bars, and edges that have a specific receptive-field orientation. The majority of cells (about 90%) in V-II are "complex," whereas in V-III, only about half of the cells are complex (145). Other cells in the extrastriate cortex are referred to as "hypercomplex" cells because of more elaborate properties. These cells, however, differ in the precise position and arrangement of receptive fields. Hypercomplex cells have been divided into two types: (a) lower order hypercomplex cells that behave as though their input was derived from two sets of complex cells, one excitatory and one inhibitory, and (b) higher order hypercomplex cells that behave as though they receive their input from a large number of lower order hypercomplex cells. In visual area II, 5–10% of the cells are lower order hypercomplex cells, while in visual area III they comprised about half of the cells.

Area 18 is a six-layered granular cortex which lacks the band of Gennari and rostrally merges with area 19 without distinct demarcation (Figs. 20.10 and 20.15). Large pyramidal cells in the third layer of area 18 are useful in establishing its medial and lateral borders, and coarse, irregular, often oblique, fibers are seen in the deep cortical layers in myelin-stained sections (145). Otsuka and Hassler (287) have provided a comprehensive study of the visual areas in the cat. Area 18 interrelates areas 17 and 19 of the same and opposite hemispheres by association and commissural fibers.

The retinotopic organization of area 18 indicates that the border between areas 17 and 18 corresponds to the representation of the vertical meridian of the visual hemifield (contralateral half of the visual field). Thus, as successive recordings are made moving from area 17 to area 18 there is a reversal of the receptive fields (i.e., from peripheral to central followed by a central to peripheral sequence) about the vertical meridian. The isoelevation lines running through both areas 17 and 18 are roughly perpendicular to the representation of the vertical meridian (145, 365). Visual area II (area 18) represents roughly the central 50° of the visual hemifield which corresponds to the binocular overlap zone. In area 19 (V-III), the visual hemifield is represented basically as a mirror image of area 18 with the vertical meridian for area 19 on its lateral border. If a recording electrode were moved laterally from the border of areas 17 and 18, successive lateral positions in area 18 would represent more peripheral regions of the visual field. When the medial border of area 19 is reached, the visual receptive fields would begin to move centrally toward the vertical meridian. The manner in which the contralateral visual hemifield is represented in areas 18 and 19 has been referred to as a second order transformation, which means that some adjacent points in the visual field are not represented by adjacent points on the cortex (8, 9).

Cells of the six layers of the dorsal division of the LGB project mainly upon area 17 but some fibers also reach areas 18 and 19 (102). Larger cells in the dorsal nucleus of the LGB project to area 18, while cells of all sizes project to area 17. Some of the larger cells may project collaterals to both areas 17 and 18. The inferior pulvinar and the adjacent part of the lateral pulvinar, each containing a representation of the contralateral visual hemifield, project retinotopically upon areas 18 and 19. Pulvinar fibers end upon cortical layers IV, III, and I in the extrastriate cortex, and in the supragranular layers of the striate cortex (313). Fibers projecting to area 18 and 19 from these parts of the pulvinar appear to constitute important links in the extrageniculate visual projection. Additionally, area 17 has been demonstrated to project association fibers to areas 18 and 19 (145, 243). Although there are few commissural connections between areas 17 in the two hemispheres, both anatomic and physiologic findings indicate that commissural fibers interconnect the junctional region at the border between areas 17 and 18 (146, 243, 401, 402, 413). These fibers arise mainly from the cells in layer III. Cells situated at the boundary between areas 17 and 18 functionally represent the vertical meridian of the visual hemifield. Thus, the vertical meridian of the visual field is bilaterally represented in the visual cortex. This bilateral representation ensures a uniform visual field free of interruptions along the vertical midline (146, 401).

In V-III there are columns in which some cells have one receptive field orientation, others with an orientation at 90° to the first, and still others that respond to both of these orientations. The majority of cells in V-II and V-III are driven from both eyes. Thus, there appears to be as much binocular representation in V-II and V-III as in V-I.

A separate representation of the contralateral visual hemifield (V-II) adjacent to the primary visual (striate) cortex and with a common vertical meridian (junction of areas 17 and 18) has been found in every mammalian species studied (365). The fact that all mammals appear to have an area 18 suggests that this area may be homologous in different species, although all connections may not be identical. In contrast, representation of the contralateral visual hemifield in V-III (area 19) has not been found in all species and its organization differs from species to species. Although the function(s) of area 19 are elusive, area 18 appears ideally suited for processing visual information concerned with stereoscopic depth perception and may play a special role in the analysis of retinal disparities (148, 365). Area 18 contains a representation of the entire binocular visual field.

Auditory Areas (A-I and A-II)

In humans, the primary auditory area (areas 41 and 42) is located on the two transverse temporal gyri (Heschl) which lie on the dorsal surface of the superior temporal gyrus and is buried in the floor of the lateral sulcus (Figs. 2.8, 2.11, and 20.10). The middle part of the anterior transverse temporal gyrus constitutes the principal auditory receptive area (area 41). Remaining parts of the posterior transverse gyrus and adjacent portions of the superior temporal gyrus compose area 42, largely an auditory association area. To visualize these gyri in an intact brain, it is necessary to separate widely the banks of the lateral sulcus (Fig. 2.8). Area 41 is a typical koniocortex (primary sensory cortex), resembling that of areas 3 and 17. Granular cells are arranged in perpendicular columns. Area 42 is a six-layered cortex of the parietal type (type 3) (Fig. 20.12), distinguished by a number of large pyramidal cells in layer III.

The cortical auditory area receives geniculotemporal fibers (auditory radiation) from the medial geniculate body (MGB) (Fig. 2.11). The auditory radiation reaches its cortical projection site by passing through the sublenticular portion of the internal capsule (Fig. 16.39). The greater part of the auditory radiation projects to area 41.

The ventral laminated part of the MGB has a tonotopic organization with high frequencies represented medially and low frequencies laterally (4, 5, 46, 101, 127, 157). The auditory radiation arises from the ventral laminated nucleus of the MGB (Fig. 16.23) and projects to the primary auditory cortex where there is a spatial representation of tonal frequencies (4, 46, 57, 275, 283, 311, 393). These fibers, passing to the primary auditory cortex, constitute the *core projection* (Figs. 20.29 and 20.30).

The medial geniculate body also has two nonlaminated divisions which receive auditory inputs. These divisions of the MGB, referred to as dorsal and medial (magnocellular) (263), project ipsilaterally via the auditory radiation to at least five cytoarchitectonic areas forming a cortical belt around the pri-

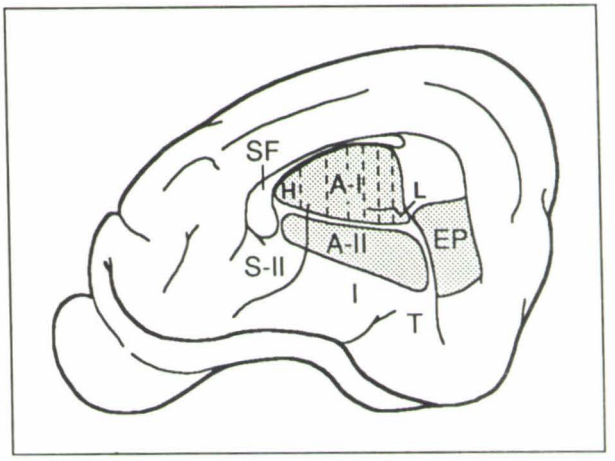


Figure 20.29. Auditory areas in the cat. The primary auditory area A-I has a tonotopic organization with high frequencies (*H*) represented rostrally and low frequencies (*L*) caudally. The *dashed vertical lines* represent isofrequency bands. The primary auditory area is surrounded by a belt of secondary auditory cortex designated as *SF*, suprasylvian fringe, partially in the depth of the suprasylvian sulcus, *EP*, the posterior ectosylvian area, *A-II*, the secondary auditory area, *S-II*, the secondary somesthetic area, *I*, the insular area, and *T*, the temporal area.

mary auditory area (4, 46, 275, 283, 311, 393). Fibers arising from the nonlaminated parts of the MGB passing to the secondary auditory areas constitute the *belt projection* (38, 311, 393). There appears to be very little overlap of the auditory projections to the belt area surrounding the primary auditory cortex, except for the projection arising from the caudal part of the medial division of the MGB (283). The medial magnocellular division appears to project to the entire cortical area receiving fibers from the MGB, although the laminar distribution of fibers in the cortex is different. The caudal part of the medial nucleus projects primarily upon layer VI, while other subdivisions of the MGB project primarily upon cells in layer IV and to parts of layer III.

In the cat, two auditory areas were defined originally on the lateral aspect of the hemisphere below the suprasylvian sulcus, designated auditory area I (A-I) and auditory area II (A-II) (4, 46, 409) (Fig. 20.29). Frequency representation in A-I indicates a series of isofrequency strips oriented vertically, in which high frequencies are represented rostrally and low frequencies caudally (250, 251). In A-II, no clear tonotopic representation has been established because of the broad tuning curve of its neurons. Auditory area II receives most of its fibers from the medial magnocellular nucleus of the MGB. The other secondary auditory areas receive their inputs via the belt projection from the nonlaminated parts of the MGB.

The primary auditory cortex in monkeys lies caudal to the superior surface of the superior temporal gyrus and can be exposed by resection of the overlying parietal cortex (Fig. 20.30). Best frequencies in the full auditory range for the monkey were represented in an orderly fashion in the primary auditory area. This is a cytoarchitectonic field coextensive with the koniocortex. Lowest frequencies were represented rostrally and laterally, whereas highest frequencies were found caudally and medially (Fig. 20.30). A cortical region immediately rostral to A-I has a cytoarchitecture similar to that of A-I and appears to respond as vigorously to acoustic stimulation (158). This rostral field, smaller than A-I, contains a complete and orderly representation of the audible frequency spectrum with lower frequencies represented rostrally and higher frequencies represented in progressively more caudal and medial regions (Fig. 20.30). The A-I and the field rostral to it, designated R, appear to constitute the central core of the auditory cortex in primates. The primary auditory cortex in monkeys is surrounded by a belt of auditory cortex which is not cytoarchitectonically uniform. This cortical belt, which represents the secondary auditory areas, has been divided topographically into three or more auditory fields (Fig. 20.30). In the fields which form this cortical belt, units are less responsive to acoustic stimulation and the frequency organization is more complex than in A-I or R. The organization and tonotopic localization in the A-I appears to be very similar in monkeys, apes, and humans. Within this field low frequencies are represented rostrolaterally and higher frequencies extend caudomedially.

The functional architecture of the auditory cortex appears similar to that of the visual and somesthetic cortex in that cells in the

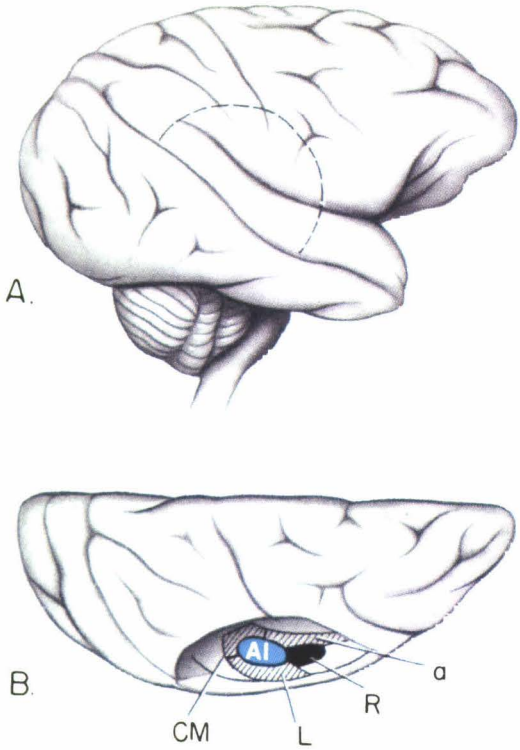


Figure 20.30. **A.** Lateral aspect of the rhesus monkey brain with *dashed line* indicating region excised to expose the superior temporal plane. **B.** Dorsal view of the right hemisphere exposing the auditory region in the superior temporal plane. In the primary auditory area, A-I (*blue*), low frequencies are represented rostrally and laterally and high frequencies are represented caudally and medially. The area designated R (*black*) has a cytoarchitecture similar to A-I, an orderly representation of the auditory spectrum, and responds vigorously to auditory stimuli. Auditory areas A-I and R are surrounded by a belt of secondary auditory cortex (*shaded*) designated as *a, L,* and *CM.*

same column share the same functional properties (5405). The functional columns in the auditory cortex appear less discrete, do not have sharp boundaries, and are considered to be much smaller units than in other sensory areas. The isofrequency strips oriented across the primary auditory cortex probably represent, or are composed of, isofrequency cell columns (248, 251). In these columns, units throughout the depth of the cortex respond to the same frequency. Both binaural and monaural cell columns have been described (156). With the exception of some neurons responding only to binaural stimulation, monaural responses were classified as contralateral dominant, ipsilateral dominant, or equidominant. Most neurons in the same perpendicular column display the same aural dominance and binaural interaction.

Electrical stimulation of the cortical areas in the temporal lobe near the A-I (i.e., areas 42 and 22) in humans produces sounds described as the noise of a cricket, a bell, or a whistle. These sounds are elementary tones that may be high or low pitched, continuous or interrupted, but always are devoid of complicated or changing qualities (299). Most of these auditory responses are referred to the contralateral ear.

One of the distinctive features of the auditory system, in contrast to other sensory systems, is the large number of actual and potential sites at which impulses from one side can be transmitted to contralateral relay nuclei. The largest and most important fiber crossing is in the trapezoid body, but others also are present (Fig. 13.13), including fibers from auditory cortical areas that cross in the corpus callosum (255). The commissural connections of the auditory cortex in the cat project to homologous areas in the opposite hemisphere (77). Auditory area I projects contralaterally to A-I and A-II, while A-II sends fibers only to A-II. Within each subdivision of the auditory cortex there are some areas which receive only small numbers of terminal fibers, the region of A-I representing the low frequency range being a clear example. Auditory commissural connections differ greatly from those of the visual cortex (area 17) which are absent except near the border of area 18. Association fibers in the auditory cortex of the cat reciprocally interconnect primary and secondary areas with each other (78).

Each cochlea is represented bilaterally in the auditory cortex, although some slight differences exist between the two sides (2, 4, 46,

327, 409, 410). The cortical effects of sound stimulating each ear separately are nearly the same, but significant differences occur when the position of the stimulus is varied with respect to both ears (327). When sound is presented on one side, the cortical response is greatest contralaterally. If sound is presented in a median plane, the cortical activity in the two hemispheres is equal. Although these observations suggest that localization of sound in space is dependent upon the relative amounts of neural activity at higher levels of the auditory system, this conclusion is not correct. Localization of sound in space involves a two-stage process: (a) convergence and comparison of auditory input from the two ears, and (b) a distribution of this computerized analysis to the appropriate side of the system (199, 245). The trapezoid body is the only auditory commissure essential to sound localization (162, 273); above this level mechanisms for detecting sound localization are present only on one side (contralateral to the source). Attempts to physiologically identify a place map for sound direction have been elusive, but most evidence suggest it is likely to be in the deep layers of the superior colliculus, or the brainstem tegmentum.

Because audition is represented bilaterally at a cortical level, unilateral lesions of the auditory cortex cause only a partial deafness. The deficits, however, are bilateral, and the greatest loss is contralateral. Brodmann's area 22, bordering the primary auditory area (Fig. 20.10) and representing typical six-layered isocortex, receives fibers from areas 41 and 42 and has connections with areas of the parietal, occipital, and insular cortex (19, 352, 353). Lesions in Brodmann's area 22 in the dominant hemisphere produce word deafness or sensory aphasia. Although hearing is unimpaired by such lesions, patients cannot interpret the meaning of the sounds. In humans, there are considerable variations in the size and convolutional patterns of Heschl's gyrus in the two hemispheres—the gyrus on the left is frequently unpaired, larger, and longer than on the right side (369, 399).

Gustatory Area

Taste sensibility is represented in the parietal operculum (area 43) and in the adjacent parainsular cortex (Fig. 20.10) (17, 29, 30, 299). Gustatory representation in the parietal operculum is adjacent to the somesthetic area for the tongue, but separate from the nongustatory lingula area.

In cats and monkeys, the taste pathway ascends ipsilaterally. Taste impulses arising in the nucleus of the solitary fasciculus, which receives primary gustatory afferents, are conveyed by the chorda tympani and glossopharyngeal nerves and projected to the ventral posteromedial nucleus, pars parvicellularis (VPMpc) of the thalamus (25, 81, 83). Cells in rostral regions of the nucleus of the solitary fasciculus project fibers ipsilaterally to the VPMpc, while cells in more caudal regions project ascending fibers to both the VPMpc and parabrachial nuclei in the rostral pons (the so-called "pontine taste area") (Figs. 12.19 and 16.21) (22, 278, 279). Cells in the parabrachial nuclei, in turn, project upon VPMpc, as well as to regions of the hypothalamus and ventral forebrain structures (277, 279, 314). Thalamic cell groups subserving taste in the VPMpc are distinct from neurons related to other sensory modalities of the tongue (25, 82, 83, 280). The VPMpc projects to both the insular and parietal opercular cortex (318).

Lesions in either VPMpc or the parietal operculum cause loss of gustatory sensation. Ablations of the precentral and postcentral opercula in the monkey and chimpanzee reportedly cause a loss of taste (26, 295). Similar lesions involving the anterior insular cortex, the postcentral operculum, and the anterior supratemporal cortex in the monkey impair taste sensibility (17). Stimulation of the parietal operculum (297) and adjacent insular cortex (299) in conscious patients produces gustatory sensations.

Vestibular Representation

In the cerebral cortex vestibular sense is poorly defined in comparison with other sensory modalities. In humans, electrical stimulation of portions of the superior temporal gyrus, particularly regions rostral to the auditory area, provoke sensations of turning movements and dizziness (299). These sensations are mild compared with the vertigo produced by direct stimulation of the labyrinth. Less distinct illusions of body movement have been reported following stimulation of parietal cortex (296).

Two cortical areas have been identified as receiving vestibular input in cats and monkeys (94, 96, 200). These are area 3a and the

posterior margin of area 2, which is designated as area 2v (95). The common feature of these areas is the convergence of vestibular inputs and signals from deep somatic receptors. Area 3a also receives inputs from muscle spindles and area 2v receives inputs from joint receptors (96, 334). Thalamic projections to these cortical areas originate from portions of the ventrobasal complex and are not localized to a single division (i.e., VPLc, VPM, and VPI) (235). Vestibular projections to the cortex are bilateral with contralateral dominance. Regions of the vestibular complex projecting to the thalamus are poorly understood (51, 70, 235).

MOTOR AREAS OF THE CORTEX

Corticofugal fibers arise from all regions of the cerebral cortex. These projections convey impulses concerned with motor function, modifications of muscle tone and reflex activity, modulation of sensory input, and alterations of awareness. Corticofugal fibers, originating mainly from the deeper cortical layers, can be grouped under these designations: (a) corticospinal, (b) corticobulbar, (c) corticoreticular, (d) corticopontine, (e) corticothalamic, (f) corticostriate, and (g) corticonuclear, a composite grouping of fibers that project to brainstem nuclei at different levels (e.g., corticosubthalamic, corticorubral, corticotectal, and projections to various sensory and cerebellar relay nuclei).

The somata of the cells of origin of particular corticofugal fiber systems have a specific laminar or sublaminar distribution (Fig. 20.3) (179). Corticospinal neurons lie in the deepest part of layer V, occur in clusters, and show great variation in cell size, particularly in area 4. Corticostriate fibers principally form the smallest group of pyramidal cells in superficial regions of layer V. Corticopontine, corticobulbar, and corticorubral neurons lie in middle regions of layer V. The majority of corticothalamic cells are found in layer VI, but some of these neurons are located in deep parts of layer V. The somata of cortical association and commissural neurons lie in the supragranular layers of the cortex. Association neurons giving rise to ipsilateral corticocortical projections are superficial (layers II and III) to neurons giving rise to commissural connections (layer III). These observations based upon retrograde transport of HRP indicate that cells contributing to distinctive fiber systems occur in single or multiple strips 0.5–1 mm wide oriented mediolaterally across the cortex.

Three principal motor areas are recognized in the cerebral cortex: (a) the *primary* (precentral) *motor area*, (b) the *premotor area*, and (c) the *supplementary motor area* (Figs. 20.32 and 20.33). The primary motor area (M-I) is preeminently concerned with voluntary motor activity. The premotor area, rostral to M-I, is concerned with voluntary motor function dependent upon sensory stimuli. The supplementary motor area, on the medial aspect of the frontal lobe, participates in the programming and planning of motor activities, and perhaps their initiation. The premotor and supplementary motor areas are somatotopically organized and are interconnected with each other and with M-I. Still further rostral, in Brodmann's area 8, are the *frontal eye fields* which, as their name implies, are concerned with movements of the eyes. Finally, the *posterior parietal cortex*, comprising Brodmann's areas 5 and 7, appears to be involved in programming directed movements of the limbs and eyes to targets in space.

Primary Motor Area (M-I)

Area 4 of Brodmann, commonly designated as the primary motor area (M-I), is located on the anterior wall of the central sulcus and adjacent portions of the precentral gyrus (Figs. 20.10 and 20.11). This area is broad at the superior margin of the hemisphere, but near the inferior frontal gyrus, it is practically limited to the anterior wall of the central sulcus. On the medial surface of the hemisphere, it comprises the anterior portion of the paracentral lobule (Fig. 2.6). The unusually thick cortex of M-I (3.5–4.5 mm) is agranular in structure, and its ganglionic layer contains the giant pyramidal cells of Betz, whose cell bodies may reach a height of 60–120 μm (Figs. 5.9 and 20.14**B**). These cells are largest in the paracentral lobule, and smallest inferiorly in the opercular region. The density of Betz cells also varies in different parts of area 4 (214). Approximate percentages of Betz cells in different topographic subdivisions of area 4 are 75% in the leg area, 18% in the arm area, and 7% in the face area. Approximately 34,000 giant pyramidal cells with cross-sectional areas between 900 and 4100 μm^2 have been counted in area 4 in the human brain (214, 215). Cytoarchitecturally,

area 4 represents a modification of the typical six-layered isocortex in which the pyramidal cells in layers III and V are increased in number and the internal granular layer is obscured. For this reason the cortex is called agranular.

The corticospinal tract, considered to transmit impulses for highly skilled volitional movements to lower motor neurons, arises in large part from area 4. The larger corticospinal fibers are the axons of giant pyramidal cells as these cell undergo chromatolysis following section of the pyramids (136, 231). Since the number of fibers in the human corticospinal tract at the level of the pyramid is approximately 1,000,000, axons of the giant cells of Betz could account for only a little over 3% of these fibers, assuming that each cell gives rise to a single corticospinal fiber (214). The fiber spectrum of the human corticospinal tract indicates about 30,000 fibers with diameters between 9 and 22 μm (217, 219, 220), supporting the view that these fibers are the parent axons of the giant pyramidal cells. Approximately 90% of the fibers of the corticospinal tract range from 1–4 μm in diameter. Of the total number of fibers in the tract, about 40% are poorly myelinated.

Earlier retrograde and anterograde degeneration studies have revealed that virtually all fibers of the corticospinal tract arise from area 4, area 6, and parts of the parietal lobe (329). Approximate percentages of corticospinal fibers arising from these areas, as determined in earlier retrograde degeneration studies, are (a) area 4, 31%, (b) area 6, 29%, and (c) parietal lobe, 40%. Complete decortication, or hemispherectomy, causes all fibers of the corticospinal tract to degenerate in humans (216, 218) and nonhuman primates (256, 329). More recent retrograde HRP transport studies in monkeys indicate that corticospinal fibers arise from cells widely distributed in the sensorimotor cortex, all of which are located in layer V (62, 179). Labeled corticospinal neurons in the deep parts of layer V are found in areas 6, 4, 3a, 3, 1, 2, and 5, and in S-II. Although these neurons show great variation in size, all are pyramidal cells. The largest cells are seen in area 4, while smaller cells are evident in other areas. Cells giving rise to corticospinal projections occur in clusters aligned to form strips oriented mediolaterally across the cortex. Anterograde autoradiographic tract-tracing studies suggest that major differences exist in the pattern of terminal labeling in the spinal gray matter following injections of different cytoarchitectonic areas (63). Isotope injected into cortical areas 3, 1, 2, and 5 label terminals in parts of the posterior horn which correspond to Rexed's laminae III and IV, while injections into areas 4 and 3a label terminals largely in Rexed's lamina VII, but with extensions into regions of spinal motor neurons. No corticospinal neurons project into Rexed's laminae I and II. Some corticospinal neurons in area 4 end directly upon anterior horn cells in the brachial and lumbosacral enlargements in the monkey (212, 238). Some corticospinal axons innervate more than one spinal segment, but axons supplying motor pools innervating distal limb muscles have fewer collaterals (336). This arrangement is considered to be related to discrete contraction of individual distal limb muscles. Anatomically, the corticospinal tract is not somatotopically organized. Pyramidal tract cells located posterior to the central sulcus tend to terminate more dorsally in the spinal cord among interneurons relaying peripheral input from afferent fibers to motoneurons and higher centers. This postcentral component of the pyramidal tract may be involved in regulating sensory function by presynaptic modulation of transmission of afferent impulses.

Electrical stimulation of M-I evokes discrete isolated movements on the opposite side of the body. Contractions usually involve functional muscle groups concerned with specific movements, but individual muscles may be contracted separately. While the general pattern of excitable foci is nearly the same for all mammals, the number of such foci, and hence the number of discrete movements, is increased in humans. Thus, flexion or extension at a single finger joint, twitching at the corners of the mouth, elevation of the palate, protrusion of the tongue, and even vocalization, all may be evoked by careful stimulation of the proper areas. Charts of motor representation have been furnished by a number of investigators (89, 90, 297, 298, 299, 331). Data concerning the human brain were collected during neurosurgical procedures in which patients were operated upon under local anesthesia (Fig. 20.31). The location of centers for specific movements may vary from individual to individual, but the orderly sequence of motor representation appears constant. Ipsilateral movements have not been observed in hu-

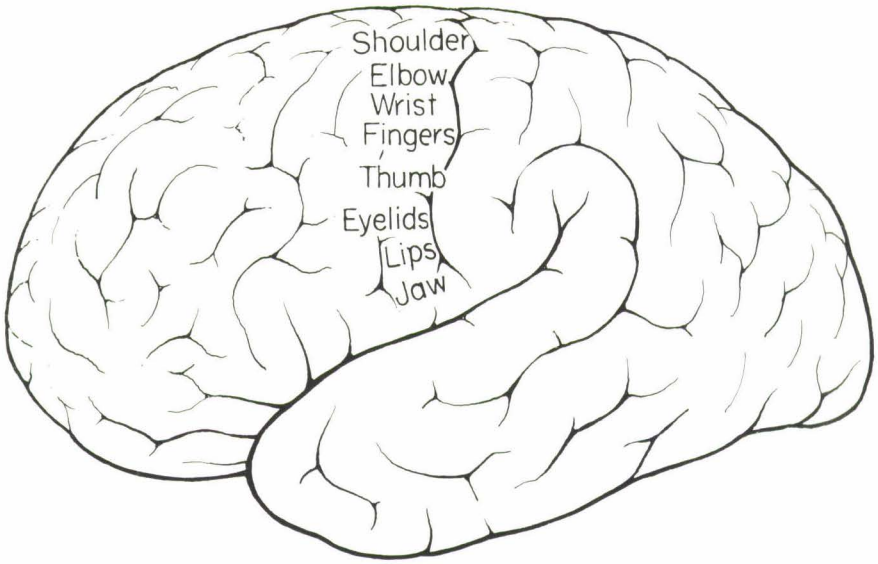


Figure 20.31. Representation of parts of the body in the motor area on the lateral surface of the hemisphere. The leg usually is represented only in the anterior part of the paracentral lobule.

mans, but bilateral responses occur in the muscles of the eyes, face, tongue, jaw, larynx, and pharynx. The center for the pharynx (swallowing) lies in the most inferior opercular portion of the precentral gyrus (297), followed, from below upward, by centers for the tongue, jaw, lips, larynx, eyelid, and brow, in the order named (Fig. 20.18). Next come the extensive areas for finger movements, the thumb being lowest and the little finger highest, followed by areas for the hand, wrist, elbow, and shoulder. Finally, in the most superior part are the centers for the hip, knee, ankle, and toes. The last named are situated at the medial border of the hemisphere and extend into the paracentral lobule, which also contains the centers for the anal and vesicle sphincters (Fig. 20.18).

The movements elicited by electrical stimulation of M-I probably are not equivalent to voluntary movements, although they are interpreted by the patient as "volitional." Responses are never skilled movements, comparable to complex acquired movements, but consist largely of either simple flexions or extensions at one or more joints. The threshold in different topographic parts of area 4 varies. The thumb region appears to have the lowest threshold, while the face area has the highest. Excessive stimulation of area 4 produces either a focal seizure, or one resembling a Jacksonian convulsion.

The classical view of the somatotopic organization in the motor cortex is a single continuous, distorted representation of the body parts within M-I. This pattern of organization, represented by the motor homunculus or its equivalent (Fig. 20.18), has been extrapolated from studies in which movements have been produced by surface stimulation in a variety of animals and in humans (Fig. 20.31). The summation of cortical representation depicted in a single line drawing is regarded as an oversimplification because it rarely takes into account the extent of overlap of various body regions, which is a characteristic feature of the motor cortex (408). Studies indicating a double representation of the body surface within cytoarchitectonic areas 3 and 1 in monkeys (249) have raised questions concerning multiple representations of body parts in the regions of overlap in M-I (350). The possibility of multiple representation of the body in motor cortex was explored in the squirrel monkey in which none of M-I is buried in the central sulcus (350). Microstimulation at depths coincident with layer V revealed a discrete double representation of the hand and wrist with the second hand zone located rostrally. Although all regions of the motor cortex have not been explored in detail, the possibility of dual representation of motor function appears to have some foundation. However, it seems unlikely that these systems could be entirely independent. Earlier physiologic studies indicated that repeti-

tive microstimulation at various depths in the motor cortex can either facilitate or inhibit monosynaptic reflexes (12). Although there is little evidence that cells in the motor cortex are organized into functional cell columns as in the somesthetic and visual cortex, microstimulation in a vertical column produces the same response in all layers (164–166).

Ablations of the motor cortex in mammals produce greater neurologic deficits in primates than in nonprimates (373). In cats, removal of the motor cortex, or even hemidecortication, does not impair the animal's ability to walk upon recovery from anesthesia. Ablations of area 4 in monkeys produce a contralateral flaccid paralysis, marked hypotonia, and areflexia. Within a relatively short time myotatic reflexes reappear, along with withdrawal responses to nociceptive stimuli (99). There is recovery of some motor function in both proximal and distal musculature, but skilled movements are performed slowly with deliberation (363). No significant spasticity developed in these animals.

Because the precentral gyrus gives rise to a large number of nonpyramidal fibers, and is the source of only a part of the corticospinal tract, it is instructive to compare the motor deficits described earlier with those which follow surgical section of the pyramids. Selective pyramidotomy in monkeys and apes, accomplished by an anterior approach, produces a contralateral paresis which is somewhat more severe in apes than in monkeys (360, 361). In neither animal group is the paresis so severe that the effected limbs are useless. The relatively stereotyped movements of progression are impaired, and there is a severe poverty of movement. The usage which survives is stripped of all the finer qualities which contribute to the skill, precision, and versatility of motor performance. Although remaining stereotyped movements are useful, execution of purposeful movements appears to require deliberation and critical attention. Pyramidotomy is associated with hypotonia and loss of superficial abdominal and cremasteric reflexes. The myotatic reflexes are increased in threshold and somewhat pendular. Tonic neck reflexes are absent, and clonus does not occur. A forced grasp reflex is prominent and may be so severe as to interfere with climbing. In apes, a persistent and enduring Babinski sign can be elicited. Observations by Donald Lawrence and Hans Kuypers (222) of monkeys with bilateral pyramidal lesions also indicate that considerable recovery of independent limb movement occurs, but recovery of individual finger movement never returns. All movements are slower and the muscle fatigue is more rapid than in normal animals. These findings indicate that corticospinal pathways conduct impulses concerned with speed and agility of movement, and fractionation of movements, as exemplified by individual finger movements. Motor function remaining after bilateral pyramidotomy must be mediated by brainstem pathways projecting to spinal levels. These findings have been confirmed in young monkeys (221). Relatively independent finger movements are not present in young monkeys until approximately 8 months of age, as such finger movements develop gradually in parallel with the spinal connections of the corticospinal system. Following bilateral pyramidal tract lesions a few weeks after birth, relatively independent finger movements failed to develop in a 3-year period of observation.

Lesions of the motor cortex in humans produce neurologic deficits similar to those described in primates. Ablations limited to the "arm" or "leg" area of the precentral gyrus result in a paralysis of a single limb (i.e., monoplegia). The ultimate loss of movement is always greatest in the distal muscle groups, but motor recovery in the affected limb usually is more complete than that associated with nearly total lesions of the motor area (48). Immediately after complete or partial lesions of the precentral gyrus, there is a flaccid paralysis of the contralateral limbs or limb, marked hypotonia, and loss of superficial and myotatic reflexes. Within a relatively short time, the Babinski sign can be elicited. The myotatic reflexes generally return early in an exaggerated form.

Premotor Area

The region designated as 6aα on the lateral convexity of the hemisphere is considered the premotor area. The part of area 6aα on the medial aspect of the hemisphere is the supplementary motor area (M-II) (Figs. 20.10 and 20.32) (90, 377). Histologically, the premotor area resembles the M-I. It is composed principally of large pyramidal cells, but there are no giant cells of Betz (Fig. 20.14**A**). Pyramidal cells in layers III and V and the narrowness of

layer IV make it difficult to distinguish an internal granular layer. For this reason area 6, like area 4, is referred to as agranular frontal cortex.

The premotor area has a specific role in sensory guided movements. Units of the premotor area are activated in response to visual, auditory, and somatosensory stimuli. Like the M-I, units are clearly related to voluntary motor function. The premotor area differs from M-I in that it has a higher threshold and its neurons are activated by visuospatial signals (88, 89, 377). The premotor area discharges via the corticospinal tract. Unilateral ablations of area 6, not involving the primary or supplementary motor areas, do not produce paresis, grasp reflex, or hypertonia.

Supplementary Motor Area (M-II)

Observations by early investigators indicated that motor responses in different parts of the body could be elicited by electrical stimulation of a portion of the frontal lobe rostral to M-I and termed the supplementary motor area (M-II) (299, 301). In human and nonhuman primates, M-II occupies the medial surface of the superior frontal gyrus rostral to area 4 and corresponds to the medial part of area 6 (area 6aβ) (Fig. 20.32). Detailed descriptions of somatotopic representation within M-II of monkeys have been provided by the pioneering studies of C.N. Woolsey and his colleagues (406, 408). The sequential representation of body parts in M-II is shown in Figure 20.33. The main features of the anatomic and physiologic organization of this cortical area were reviewed recently (34, 183, 389, 390).

Movement-related neurons in M-II (cells firing during movement) are of three types: (a) cells related to proximal movement, (b) cells related to distal movement, and (c) cells activated throughout a motor task. The majority of cortical neurons in this area (94%) exhibit movement-related activity regardless of whether the motor task is performed with the contralateral or ipsilateral limbs (394). The threshold for stimulation of M-II in human and nonhuman primates is slightly higher than for the precentral region. Motor responses obtained by stimulating M-II are abolished by ablation of M-I. The somatotopic features of M-II also are distinct after ablation of M-I.

Unilateral ablations of M-II in human and nonhuman primates produce no permanent deficit in the maintenance of posture or the capacity for movement. In monkeys, removal of M-II in combination with M-I on the same side results in a contralateral spastic hemiparesis in which marked hypertonus develops in both proximal and distal muscles (100, 132, 190, 191, 192, 364). Combined ablations of M-II and M-I in monkeys with longitudinal

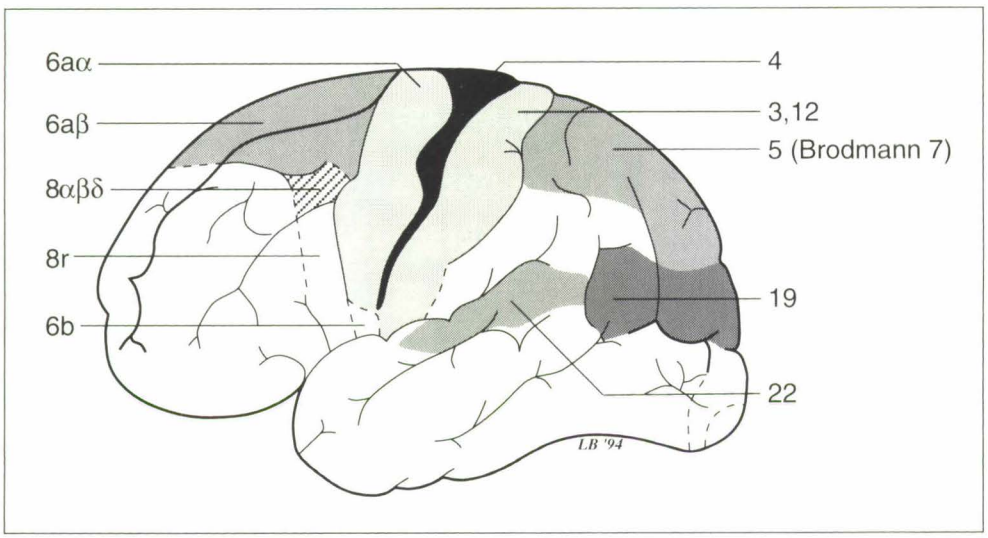


Figure 20.32. The areas of electrically excitable cortex on the lateral surface of the human brain. The motor area is shown in *black*, and the so-called "extrapyramidal areas" of the frontal lobe are *gray stippled* areas of different intensities, except for the eye fields, which are hatched.

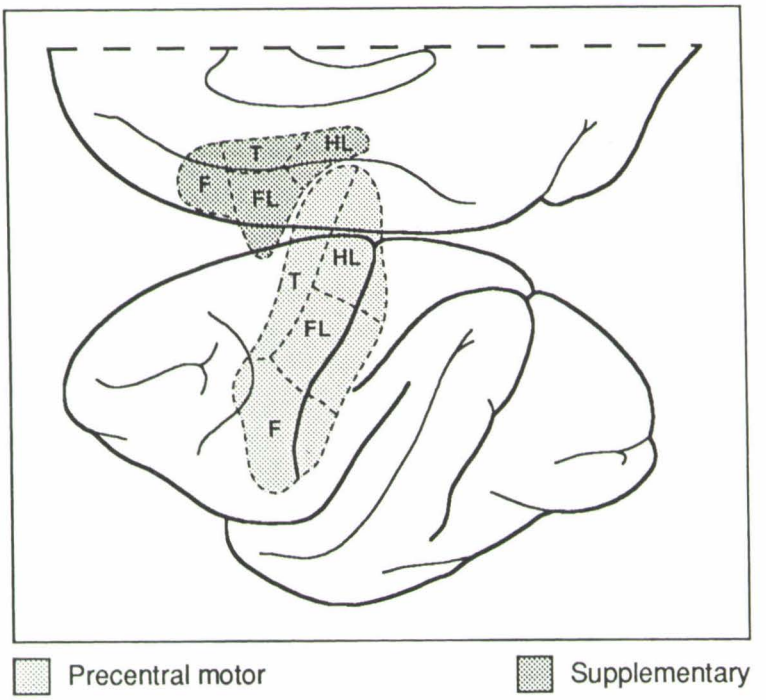


Figure 20.33. Precentral and supplementary motor areas in a macaque monkey. The somatotopic representation of different parts of the body are shown: *F*, face area; *T*, trunk; *FL*, forelimb; *HL*, hindlimb. The precentral motor area on the lateral convexity extends over onto the medial aspect of the hemisphere. The *outlined area* shown posterior to the central sulcus represents cortex hidden in the depths of the central sulcus. The supplementary motor area, largely on the medial aspect of the hemisphere, is shown above.

section of the corpus callosum (i.e., split-brain preparations) result in more pronounced spasticity, suggesting that part of the bilateral influences of M-II involve fibers that cross in the corpus callosum.

Cortical projections from M-II are ipsilateral to areas 4, 6 (lateral part), 5, and 7, and to contralateral M-II (164–166, 169, 175, 394). Connections between M-II and these cortical areas are almost completely reciprocal (289, 370). Approximately 5% of the neurons in M-II project directly to the spinal cord with a bilateral disposition (23, 33, 34, 394). Subcortical projections of M-II are profuse to parts of the caudate nucleus and putamen (168, 189) and to thalamic nuclei (ventral anterior, VApc, ventral lateral, VLO, and mediodorsal, MD) (76, 390, 391). Afferents to M-I, the premotor area, and M-II have distinctive features and are discussed together in the section "Inputs to Motor Cortical Areas."

Studies in conscious, behaving monkeys indicate that neurons in M-II are related to movements on both sides of the body and involve distal and proximal musculature equally. Most of the neurons in M-II increase their activity before the onset of movement and large numbers of neurons in this area discharge during movement of either arm. Only a small number of cells in this area respond to peripheral stimuli and the responses are weaker than in M-I (33, 34, 357, 394, 395).

While M-II, as described in humans and monkeys, is recognized as a distinct and separate motor area with striking bilateral influences upon both proximal and distal musculature, it precise contribution to motor function has not been defined. The supplementary motor area (M-II) is considered to be involved in mechanisms that influence muscle tone and modify posture, the automatic grasp reflex response, bimanual coordination, and voluntary movement. There appears to be general agreement that neurons in M-II modify the activities of cells in M-I and probably are involved in the programming of learned skilled motor sequences. Some evidence suggests that M-II may play a role in initiating voluntary movement. Studies in humans indicate that lesions in M-II are associated with a reduction of voluntary motor

activity (akinesis) and poverty of spontaneous speech.

Inputs to Motor Cortical Areas

Although impulses generated in neurons of M-I are responsible for movement, changes in muscle tone, and certain cortical reflex responses, these motor activities are initiated by inputs that arise from the thalamus, other cortical regions, and peripheral receptors. Particular potent drives on the motor cortical areas are derived from all divisions of the ventral lateral (VLc and VLo), and the ventral posterolateral, pars oralis (VPLo) thalamic nuclei (73, 317, 347, 348, 362). Crossed projections from the deep cerebellar nuclei terminate somatotopically in VPLo and in the cell-sparse region of the ventral lateral thalamic nuclear complex, which includes the ventral lateral nucleus (VLc) and area X (155, 166, 196, 210, 272, 302, 358, 362). The M-I is the major target of the VPLo and cell-sparse region of the ventral lateral thalamic nuclear complex (56, 195, 318, 347).

The pallidothalamic fibers, originating from the internal pallidal segment, project to the ventral anterior (VApc), ventral lateral (VLo), and the centromedian (CM) thalamic nuclei (see Chapter 19). Pallidal puts to the rostral ventral tier thalamic nuclei do not overlap cerebellothalamic terminations. The cortical projections of VLo are to M-II and the lateral premotor area (area 6aα) (Figs. 20.32 and 20.33). The thalamic terminations of projections from the substantia nigra are distinct from those arising from the deep cerebellar nuclei and the globus pallidus. The cortical projections of the magnocellular division of the ventral anterior (VAmc) and the mediodorsal (MDpl) thalamic nuclei, which receive nigral terminations, appear to exclude area 4, and probably project to frontal areas rostral to area 6 (see Chapter 19).

Neurons of the ventral posterolateral nucleus (VPLo) and the cell sparse zone of the ventral lateral nucleus (VLc) show increased activity prior to any movement (348). This finding suggests that these neurons may play a role in initiating activity in muscles that effect discrete movements and control posture. Thalamic neurons that project to M-I, M-II, and the premotor cortex are distinct and separate from those that terminate in somatic sensory areas. Electron microscopic evidence in the cat indicates that fibers from VLc and VPLo projecting to the motor cortex make synaptic terminations largely in three cortical layers: (a) layer 1(18%), (b) layer III (66%), and (c) layer VI (13%) (351). Fibers terminating directly in layer V were relatively sparse (3%). The majority of thalamocortical projections synapse on dendrite spines of cells in layer III, the apical dendrites of motor neurons (Betz cells of layer V), and on interneurons in layer III (163).

The primary motor area (M-I) also receives inputs from S I and M-II (174, 175, 178). Area 4 has reciprocal connections with areas 1, 2, and parts of area 5 (164–166, 169, 349, 370, 412). These cortical inputs to M-I are of an interlocking nature in that somatotopic subdivisions are connected with each other. The supplementary motor area (M-II) receives input from the same sensory areas (areas 1, 2, and parts of area 5), but has reciprocal connections only with area 4 (M-I). Neither M-I nor M-II receives input from any part of area 3.

It has been postulated that area 5 contains the "command apparatus" for limb and hand movements in immediate extrapersonal space (268, 269). Neurons in area 5 have been observed to discharge only when an animal moves its arm toward a desired object or manipulates an object with its hand. The "command" hypothesis suggests that the cortical pathway from area 5 to area 4 is involved in initiating limb and hand movements.

Physiologic studies indicate that M-I receives inputs from both cutaneous and deep receptors (326, 388). Impulses from joint receptors projecting to areas 1 and 2 appear to have access to M-I and M-II directly and via area 5. Inputs from cutaneous receptors may be involved in instinctive grasping as well as in the startle reaction (388).

Cortical Eye Fields

Rostral to the premotor area is a cortical region particularly concerned with voluntary eye movements. The *frontal eye field* in humans occupies principally the caudal part of the middle frontal gyrus (corresponding to parts of area 8, shown in Figs. 20.10 and 20.32). The entire frontal eye field does not lie within a single cytoarchitectonic area. Cytoarchitecturally, area 8 is typical six-layered isocortex of the frontal type in which the granular layers are distinct (Fig. 20.12). Electrical stimulation of the frontal eye field in humans causes conjugate deviation of the eyes, usually to the opposite side (88, 299).

This cortical field is believed to be a center for voluntary eye movements, independent of visual stimuli. The conjugate eye movements commonly are called "movements of command," since they can be elicited by instructing the patient to look to the right or left (58). The frontal eye field participates in the initiation of purposeful saccades (rapid eye movements to targets of behavioral importance) and is implicated in the coordination of eye movement necessary for accurate gaze changes.

The concept of an *occipital eye center* for conjugate eye movements is based on the fact that stimulation of occipital cortex produces conjugate eye movements to the opposite side, and lesions in this area are associated with transient deviation of the eyes to the side of the lesion. Unlike the frontal eye field, the occipital eye center is not localized to a small area. Eye responses can be obtained from a wide region of the occipital lobe in monkeys, but the lowest threshold is found in area 17 (374). The occipital eye centers subserve movements of the eyes induced by visual stimuli, such as following moving objects. These pursuit eye movements are largely involuntary, although they are not present in young infants. Parts of the occipital eye centers are interconnected by fibers passing in the splenium of the corpus callosum. The threshold for excitation is higher in the occipital eye center than in the frontal eye fields, the latency of responses is longer, and eye movements tend to be smoother. With a lesion of the occipital eye field the patient may have difficulty following a slow moving object, but on command can direct the eyes to a particular location. Eye movements on command are impaired by lesions in the frontal eye field, particularly in the dominant hemisphere.

The pathways by which responses from the frontal eye fields are mediated involve multiple subcortical loci, chief among which are the rostral interstitial nucleus of the medial longitudinal fasciculus (RiMLF), the interstitial nucleus of Cajal, the pontine paramedian reticular formation (PPRF), and layer IV of the superior colliculus (139, 153, 154, 208, 209). These structures are known to have direct and indirect influences on eye movements (see Chapter 14). The occipital eye center appears to influence eye movements via substantial and highly organized direct projections from the visual cortex to the superior colliculus, even though this projection is to the superficial layers (67, 102, 104, 153, 154, 392).

NONPYRAMIDAL CORTICOFUGAL FIBERS

These cortical *projection fibers* consist largely of corticoreticular, corticopontine, corticothalamic, and corticonuclear fibers.

Corticoreticular Fibers

These fibers originate from all parts of the cerebral cortex, but the largest number arise from the motor and premotor areas (328). Inferior cortical areas (basal) and parts of the cortex on the medial surface of the hemisphere also contribute to the corticoreticular projection, but few fibers arise from the auditory and visual areas. Corticoreticular fibers descend in association with fibers of the corticospinal tract, but they leave this bundle to enter specific areas of the brainstem reticular formation. The number of corticoreticular fibers is not large, and most of these fibers terminate in two fairly well circumscribed brainstem areas: (a) the nucleus reticularis gigantocellularis in the medulla, and (b) the nucleus reticularis pontis oralis in the pons (Fig. 11.22). Unilateral cerebral lesions produce an approximately equal distribution of degenerated corticoreticular fibers on both sides of the reticular formation. Some corticoreticular fibers also reach reticular cerebellar relay nuclei, such as the reticulotegmental nucleus, the lateral reticular nucleus, and the paramedian reticular nuclei of the medulla.

Corticopontine Fibers

These fibers arise from frontal, temporal, parietal, and occipital regions of the cerebral cortex (21, 39–41, 281). In monkeys, the largest number of corticopontine fibers arise from areas 4, 3, 1, 2, 5, and parts of the visual areas (42, 43, 179). This contingent of corticofugal fibers, which originate from pyramidal cells in layer V lying superficial to the giant pyramidal cells, is larger than other cortical efferent systems except the corticospinal projection. Corticopontine fibers arising from the visual cortex are from regions representing the peripheral visual field. Contributions to this system from temporal and prefrontal cortex are relatively modest. Most of the fibers from the prefrontal areas arise from areas 9 and 8 (14, 39). On reaching the midbrain, the frontopontine tract forms the most

medial part of the crus cerebri, and is distributed to the medial pontine nuclei (Fig. 14.1 and 15.26). In cats, corticopontine fibers from sensorimotor areas project in a somatotopic manner onto two longitudinally oriented cell columns in the pontine nuclei (37, 39). One cell column is located medial and one is lateral. Within the medial column, the hindlimb is represented ventrally and the face dorsally, while in the lateral column, the hindlimb is represented caudally and the forelimb rostrally. Thus, fibers from particular regions of the cerebral cortex end within columnar zones of pontine nuclei which are separated from each other. Although the synaptic relationships of corticopontine fibers are incompletely known, most of these fibers appear to end only upon dendrites of pontine neurons (61). There appears to be considerable overlap in the terminations of corticopontine fibers from some cortical areas. Most corticopontine fibers exert a monosynaptic excitatory action upon pontine neurons (7).

Through the synaptic linkage of corticopontine and pontocerebellar fibers, impulses from the cerebral cortex are brought into association with the regulating influences of the cerebellum. The patterns of this disynaptic linkage are complex, but there is no doubt that this is the most massive input system to the cerebellum.

Corticothalamic Fibers

A large and impressive group of corticofugal fibers arise from specific regions of the cortex and project upon particular thalamic nuclei. In general, cortical areas receiving projections from particular thalamic nuclei give rise to reciprocal fibers which pass back to the same nuclei. The granular frontal cortex has reciprocal connections with the dorsomedial nucleus pars parvicellularis (MDpc) of the thalamus (6, 195, 224). Particularly prominent among these fibers are those arising from frontal areas 9 and 10. The frontal eye field (area 8) has reciprocal connections with the paralaminar part of the mediodorsal (MDpl) and the magnocellular part of the ventral anterior (VAmc) thalamic nuclei (208, 209, 335). Area 6 projects fibers to the ventral anterior (VA), ventral lateral (VLc), ventral posterolateral (VPLo), and mediodorsal (MDpl) nuclei, as well as to "area X" and the parafascicular nucleus of the thalamus. In general, the premotor area shows projections to thalamic nuclei related to either the precentral or prefrontal cortex. Corticothalamic fibers from the precentral gyrus are widespread and include projections to VLo, VLc, and VPLo, as well as to portions of the intralaminar thalamic nuclei (133, 223, 229, 230, 257, 258, 316, 317, 367). Cortical projections from area 4 to parts of VL and VPLo are reciprocal and topographically arranged. Projections from area 4 to VLc are not as impressive as those from area 6 (207). These data indicate that corticofugal fibers from the precentral gyrus project to thalamic nuclei which receive selective inputs from the deep cerebellar nuclei, the globus pallidus, and the substantia nigra.

Efferent fibers from the parietal cortex pass via the sensory radiations to the ventral posterolateral (VPLc) and posteromedial (VPM) thalamic nuclei. Corticothalamic fibers from the primary somesthetic cortex project to the ventral posterolateral (VPL) and posteromedial (VPM) nuclei, and are described as ending in a somatotopic fashion within these nuclei (174, 203). Corticothalamic projections from areas 3, 1, and 2 are confined to the ventrobasal complex, except for small projections to the reticular and central lateral thalamic nuclei (180). No fibers from parietal areas project to VPLo. It is considered likely that reciprocating corticothalamic fibers involving the ventrobasal complex may influence the transmission of impulses to the cortex in a way similar to that exerted by corticofugal fibers upon the posterior column nuclei and neurons of the trigeminal nuclear complex.

Parts of the auditory cortex project back to the medial geniculate body nucleus or medial geniculat4e body (MGB) via the sublenticular segment of the internal capsule (202, 291, 315, 375). The cortical projections from the primary and secondary auditory areas are back to the subdivisions of the MGB from which they receive inputs (57, 283). The primary auditory cortex has reciprocal connections with the ventral laminated part of the MGB, both geniculocortical and corticogeniculate fibers being ipsilateral (79, 93). Although cortical projections to the MGB do not participate in the descending auditory pathways that influence auditory relay nuclei at lower levels of the brainstem, projections from auditory cortex to the inferior colliculus (pericentral nucleus) are involved in this activity (57, 79, 283, 322).

The striate cortex (area 17) sends fibers to the LGB, the superior colliculus, the pretec-

tum, and the inferior pulvinar (119, 135, 240). Corticofugal fibers from area 17 project to all layers of the LGB. Fibers from area 17, projecting retinotopically to all layers of the LGB, arise from small and medium-sized pyramidal cells in layer VI (135, 240). Cells in layer V of the striate cortex project to the superior colliculus and the inferior pulvinar. Although corticogeniculate and geniculocortical fibers are topographically organized, they are not reciprocal in the true sense since they arise and terminate in different layers of the striate cortex. Cells in the magnocellular layers of the LGB have no cortical projection.

While reciprocal relationships exist between the principal thalamic nuclei and their cortical projection sites, a different relationship pertains to the reticular and intralaminar thalamic nuclei. The reticular nucleus of the thalamus receives afferents from all areas of the cerebral cortex but does not project back to the cortex (55, 163, 333). Collaterals of thalamocortical fibers destined for specific cortical areas, however, terminate in particular parts of the reticular nucleus (55, 163). Also, corticothalamic fibers give collaterals to the same portions of the reticular nucleus as the thalamic nucleus which receives the main cortical projection. Thus, the reticular nucleus of the thalamus is strategically situated to sample activities passing in both directions between the cerebral cortex and thalamic relay nuclei. This complex arrangement suggests that the reticular nucleus of the thalamus, composed of heterogeneous cell types, may serve to integrate and modulate intrathalamic activities.

The intralaminar thalamic nuclei, like the thalamic reticular nucleus, receive corticofugal fibers. The prefrontal cortex project on the rostral intralaminar nuclei, while the premotor and motor cortex send fibers respectively, to the parafascicular (Pf) and centromedian (CM) nuclei (6, 15, 206, 207, 274, 304, 307, 316). The parietal and occipital cortex do not project fibers to the intralaminar nuclei. Thus, the intralaminar thalamic nuclei, particularly the CM-Pf complex, receive substantial projections from the precentral and premotor cortex, but these nuclei project diffusely upon broad regions of the cortex in a fashion that cannot be regarded as reciprocal (6, 172, 195).

ASSOCIATION FIBERS

In addition to projection fibers, the white matter of the cerebral cortex also contains commissural fibers and association fibers. The *commissural fibers* interconnect different regions of the two cerebral hemispheres across the medial plane. These fibers comprising the corpus callosum are discussed later in the section pertaining to interhemispheric transfer. The *association fibers*, also referred to as the *arcuate fibers*, interconnect different cortical regions of the same hemisphere. There are both short and long arcuate fibers. The short arcuate fibers comprise intracortical as well as subcortical axons. The intracortical short arcuate fibers are entirely confined to the cortical gray matter. They form bands of both myelinated and unmyelinated fibers within certain cortical layers that interconnect adjacent gyri. The subcortical short arcuate fibers leave the cortical gray matter to invade the white matter where they form U-shaped loops that curve upward to join the gray matter of an adjacent gyrus. The long arcuate fibers form bundles of various sizes that course deeply in the subcortical white matter and link widely separated gyri. The most prominent of these association bundles are (a) the uncinate fasciculus, (b) the cingulum, (c) the superior longitudinal fasciculus, and (d) the inferior longitudinal fasciculus.

The *uncinate fasciculus* can be divided into a ventral and a dorsal component. The ventral component links the orbital gyri of the frontal lobe to the parahippocampal gyrus and other gyri of the medial surface of the temporal lobe. The dorsal component connects other gyri on the superolateral aspect of the frontal lobe with gyri on located the more lateral aspect of the temporal lobe near the temporal pole. The uncinate fasciculus arches around the lateral sulcus and this trajectory gives to this bundle a hook-shaped appearance.

The *cingulum* is a prominent collection of association fibers that courses along the medial aspect of the hemisphere and forms much of the white matter of the cingulate gyrus. It courses along the corpus callosum and links the subcallosal and paraolfactory gyri rostrally with the parahippocampal gyrus caudally.

The *superior longitudinal fasciculus* lies deep within the white matter of the cerebral hemisphere and courses along the dorsolateral border of the lentiform nucleus. Along the rostrocaudal axis, fibers of this prominent bundle emerge from the frontal lobe and extend backward over the insula and through

the parietal lobe to the occipital lobe, where they arch downward and forward to disperse within the temporal lobe. As it is the case with all association bundles, however, the superior longitudinal fasciculus contains fibers that course in both rostrocaudal and caudorostral directions. The superior longitudinal fasciculus is often referred to as the *arcuate fasciculus* because of the arching nature of the caudal portion of the this bundle.

The *inferior longitudinal fasciculus* joins the primary and secondary visual cortices (areas 18 and 19) in the occipital lobe with the superior, middle, and inferior temporal gyri, and the parahippocampal gyrus of the temporal lobe. It runs near the lateral walls of the temporal and occipital horns of the lateral ventricle and is separated from them by the optic radiation. Like other arcuate or association bundles, the inferior longitudinal fasciculus ensures interconnections between several distinct functional cortical areas in the same hemisphere. Lesions of such bundles lead to serious impairment of cognitive functions.

FUNCTIONAL CONSIDERATIONS

Cerebral Dominance

Although the two cerebral hemispheres appear as mirror images of each other, many functions are not represented equally at cortical levels. This appears true even though (a) impulses from receptors on each side of the body seem to project nearly equally, though largely contralaterally, to symmetric cortical areas, and (b) information received in the cortex of one hemisphere can be transferred to the other via interhemispheric commissures (114, 115, 260).

In certain higher functions, believed to be cortical in nature, one hemisphere appears to be the "most competent" and, in this sense, is referred to as the *dominant hemisphere*. With respect to most of the higher functions, cerebral dominance appears to be one of degree (411). Cerebral dominance probably is most complete in relation to highly evolved aspects of language (112–115, 130). Handedness also is related to cerebral dominance, though its relationship is less clear-cut than has been assumed. It seems likely that handedness is a graded characteristic. Left-handedness, in particular, is less definite than right-handedness, and less regularly associated with dominance in either hemisphere. There also appears to be a group of disturbances related to language that are said to be commonly associated with imperfectly developed cerebral dominance. These include improper development of reading, writing, and drawing abilities, poor spatial judgment, and imperfect directional control (411). In true right-handed individuals, it is nearly always the left hemisphere that is dominant and governs language and related processes. Even in left-handed individuals, the left hemisphere is most often dominant for language, but this function may be represented bilaterally. The degree of cerebral dominance appears to vary widely, not only among individuals, but with respect to different functions.

Although a degree of "cerebral ambilaterality" would appear to be a distinct advantage with respect to recovery of speech following a unilateral cerebral injury, it carries the risk, or possibility, of difficulty in learning to read, spell, and draw. The relationship between handedness and speech is perhaps a more natural one than is commonly realized, since gesturing often accompanies speech and in certain situations may substitute for it. Most clinicians relate handedness and speech to the dominant hemisphere.

The dominant hemisphere, usually the left, is primarily concerned with processing language, arithmetic, and analytic functions, while the nondominant hemisphere is concerned with spatial concepts, recognition of faces, some elements of music, and many aspects of emotion (343). Ideographic (pictographic) languages (e.g., Japanese Kanji) may be processed by the nondominant hemisphere because of its spatial and pictorial features, while grammatic languages (e.g., Japanese Kana) using script depend upon the dominant hemisphere. Visual sign language used by deaf persons appears to be processed primarily in the left hemisphere.

It has been suggested that the normal neonate in a sense has a split-brain because the corpus callosum is incompletely developed and not fully functional (105, 106). Thus, interhemispheric communication at birth probably is slight, but it increases with development of the corpus callosum which becomes reasonably complete about the second or third year of life. Until this level of development is reached, each hemisphere may process and record some linguistic information. Hand use probably reinforces hemisphere use, and the development of a special competence in one hemisphere results in a mutual reinforcement that establishes a life

pattern. The major differences between the right and left hemispheres concern the analysis of language and the ability to speak. The fact that large left hemisphere lesions in young children do not cause total disruption of speech indicates that the right hemisphere has some linguistic competence. Surgical section of the interhemispheric commissure sheds light on certain problems of cerebral dominance, and indicates that in the adult the left hemisphere speaks for both hemispheres.

Cerebral dominance is considered to have a genetic basis, but its hereditary determination probably is not absolute. Pathologic and psychologic factors also influence handedness, but most determining factors remain unknown. Theoretic arguments suggest that variations in levels of testosterone, and perhaps other hormones, during pregnancy may alter the patterns of migrations of cortical neurons. Every neuron in the cerebral cortex has migrated during fetal life from the germinal zone of the neural tube to its final location. The brain of the male matures later than in the female and the left hemisphere matures later than the right. If fetal levels of testosterone are altered by maternal stress or other factors, the right hemisphere may become more developed and assume functions for language and handedness which the left hemisphere cannot support. The effects of testosterone on brain development is most pronounced in the male, which may account for the higher incidence of left-handedness, dyslexia (reading problems), and stuttering in the male. Anomalous cerebral dominance appears to be a major factor in learning disorders, even in individuals not totally left-handed. The left dominant hemisphere is particularly concerned with ability to handle sequential information, such as language, musical rhythms, Morse code, and complex spatial tasks.

Many cortical functions are concerned only with contralateral regions of the body, and unilateral lesions affecting these areas produce contralateral disturbances, regardless of cerebral dominance. This appears particularly true of the primary motor and sensory areas. It is also the case with lesions of the parietal cortex which result in *astereognosis*, or inability to recognize the form, size, texture, and identity of an object by touch alone. In lesions of the inferior parietal lobule, particular deficits occur more commonly in the nondominant hemisphere. One such syndrome is characterized by a disorder of the body image in which the patient (a) fails to recognize parts of his or her own body, (b) fails to appreciate the existence of hemiparesis, and (c) neglects the part of the body that is denied (66). Lesions of the angular and supramarginal gyri in the dominant hemisphere produce devastating neurologic disturbances of a curious nature. Disturbances in the *Gerstmann syndrome* include (a) finger agnosia (inability to name and identify individual fingers), (b) agraphia (inability to write), (c) acalculia (impaired ability to make simple mathematical calculations), and (d) right-left disorientation. Patients with this syndrome can copy written material and write their name but cannot convert spoken words to script.

Positron emitting tomography (PET) can be of great help in the study of the functional organization of the human brain in living individuals and in identifying brain regions involved in specific higher cognitive and affective functions. The use of ^{18}F-labeled deoxyglucose reveals the patterns of utilization of glucose in different brain regions when a given individual is at rest or while performing various complex tasks (e.g., talking, reading, or listening to music). The brain regions most active during these tasks become readily visible with PET scans because they utilize more glucose than quiescent brain regions. This method has been extensively applied by Per Roland and his colleagues in Sweden to identify cortical regions involved in various complex cognitive tasks (323). The same procedure can be used to detect various brain pathologies that interfere with higher mental functions.

Interhemispheric Transfer

Although the corpus callosum is the largest of the interhemispheric commissures, relatively little was known of its functions until recently. The first convincing evidence regarding its function was the demonstration of its importance in interhemispheric transfer of visual discrimination learning in cats with longitudinal section of the optic chiasm (260). Following section of the optic chiasm and corpus callosum, cats trained with one eye masked were unable to remember simple visual discriminations learned with the first eye. The untrained eye could be trained to make a reverse type of discrimination without interfering with the patterned discrimination learned on the opposite side. This func-

tional independence of the surgically separated cerebral hemispheres with respect to learning, memory, and other gnostic activity is the stimulus for considerable investigation (267). The results originally suggested that section of the corpus callosum prevented the spread of learning and memory from one hemisphere to the other. It was as if each hemisphere existed independently and had a complete amnesia for the experience of the other (342). Extension of these transfer studies in monkeys from visual to somesthetic and motor learning (105, 106, 341, 342) have indicated that the independence of the surgically separated hemispheres may be less clear-cut than originally supposed. In humans and monkeys, a subcallosal route may be active in transmitting high-order tactile information. Furthermore, both hemispheres may learn to discriminate simultaneously, one via a contralateral sensory system and the other by an ipsilateral sensory system (105).

Observations of the functional effects of surgical separation of the hemispheres in humans (106–108) by complete transection of the corpus callosum, anterior and hippocampal commissures, and separation of the thalamic adhesion (massa intermedia) have been reported. These "split-brain" patients show a striking functional independence of the gnostic activities of the two hemispheres. Perceptual, cognitive, mnemonic, learned, and volitional activities persist in each hemisphere, but each can proceed outside the realm of awareness of the other hemisphere. Subjective experiences of each hemisphere are known to the other only indirectly through lower level and peripheral effects. Disconnection of the hemispheres produces little disturbance of ordinary, daily behavior, temperament, or intellect. Functional deficits tend to be compensated for by development of bilateral motor control from each hemisphere, as well as by the bilaterality of some sensory pathways. Information perceived exclusively, or generated exclusively, in the nondominant (right) hemisphere could not be communicated in speech or in writing; it was expressed entirely by nonverbal responses. There was no detectable impairment of speech or writing with reference to information processed in the dominant (left) hemisphere. Linguistic expression was found to be organized almost exclusively in the dominant hemisphere (106, 113).

In contrast to this, comprehension of language, both spoken and written, was found to be represented in both hemispheres, with the nondominant hemisphere less proficient. In an analysis of the visual fields, with fixation assured, subjects verbally described only those small spots of light presented in the right half of the visual field (105). A similar light stimulus present in the left half of the visual field produced no verbal responses. With double field stimulation, only spots of light falling in the right visual field were reported. In these subjects, the visual fields stopped exactly in the midline and no macular sparing was evident. Thus, it would appear that no visual information can be transferred from one hemisphere to the other after section of the corpus callosum.

Certain lesions involving portions of the corpus callosum, or association areas of the cortex which give rise to commissural fibers, produce disturbances of higher brain functions collectively recognized as *disconnection syndromes* (110–113). Word blindness without agraphia presumably results from lesions which interrupt fibers from the visual association areas which cross in the splenium of the corpus callosum and project to the left angular gyrus. Pure word deafness may result from subcortical lesions in the left temporal lobe which interrupt the left auditory radiation, as well as callosal fibers from the contralateral auditory region. Similar syndromes manifested by various forms of agnosia or apraxia may result from lesions involving portions of the corpus callosum and association fiber systems.

Recent postmortem studies undertaken by Sandra Witelson and her colleagues have shown variations in the morphology of the corpus callusum associated with hand preference and sex in humans (397, 398). In these studies, the size of the corpus callosum was measured along the sagittal plane in relationship to (a) hand preference, that is, consistent-right-hand preference versus nonconsistent-right-hand preference, and (b) sex. Individuals with nonconsistent-right-hand preference were found to have a larger overall callosal area, with the greatest difference occurring in the posterior body segments, especially the isthmus. The isthmus is the narrow segment of the most posterior part of the body of the corpus callosum, just anterior to the splenium. This callosal segment includes fibers whose neurons of origin and termination are in posterior parietal and superior temporal cortical gyri (74, 290), that is, re-

gions of the human brain which are involved in the asymmetric representation of language, motor, and spatial cognitive skills (47). These findings are in keeping with the fact that left-handers, who are believed to have greater bihemispheric representation of cognitive functions than do right-handers (47), display a larger callosal area that may account for greater interhemispheric communication (396).

Interestingly, sex differences were found in several aspects of callosal anatomy. For example, the foregoing studies revealed that the callosal size was greater in individuals with nonconsistent-right-hand preference in men only—there was almost no difference between hand groups in women (397). The latter result was said to be consistent with the general hypothesis of females having less clear lateralization than males (397). The lack of relationship between callosal size and handedness in women also suggests that the developmental mechanisms leading to callosal anatomic variation in relation to lateralization and brain functional asymmetry are influenced by sex hormones (397, 398).

Sleep

Sleep has been considered a unique passive state, interpreted physiologically as the expression of functional deafferentation of the ascending reticular activating system. The awake state was explained in terms of increased activity of this ascending activating system, while sleep was correlated with passive dampening of this system. Recent advances indicate that sleep is an active, complex neural phenomenon initiated by sleep-inducing structures and mediated, in part, by chemospecific neuronal systems. Sleep is not a single phenomenon, but a series of successive functionally related states, which depend upon different active mechanisms, some of which can be selectively modified or suppressed (181, 182, 198, 236). In mammals, two recurring, distinctive, and related sleep states can be readily recognized. These are referred to as slow-wave sleep and paradoxical sleep.

Slow-wave sleep is characterized in the electroencephalogram (EEG) by synchronized cortical activity consisting of spindles (11–16 cycles/sec) and high voltage slow waves. There are no specific behavioral criteria for slow-wave sleep because the relationship between synchronized, or slow cortical activity, and sleep behavior is not absolute. During slow-wave sleep, tone remains in the neck muscles, spinal reflex activity is present, and changes in autonomic activity are minimal. After a time, this state is succeeded by a totally different sleep state, known as paradoxical sleep.

Paradoxical sleep is characterized by an EEG pattern with low-voltage fast-activity which resembles that of the alert, waking state. This sleep state occurs intermittently after variable periods of slow-wave sleep and has precise behavioral criteria: (a) abolition of antigravity muscle tone (especially in cervical muscles), (b) depression of spinal reflex activity, (c) characteristic autonomic changes (i.e., reduction in blood pressure, bradycardia, and irregular respiration), and (d) bursts of rapid eye movements (REM). The fact that paradoxical sleep is "deeper" than slow-wave sleep, but associated with an EEG pattern similar to that of the waking state, gave rise to the term paradoxical sleep. Rapid eye movements of 50–60 per minute occur in a stereotypical pattern different from that seen in the waking state. These rapid eye movements are associated with subcortical and cortical activity, which have been termed *pontogeniculo-occipital* (PGO) *activity.* These high voltage phasic activities can be recorded from the pontine reticular formation, the LGB, and the occipital cortex. This activity occurs transiently during slow-wave sleep, and always precedes paradoxical sleep. During paradoxical sleep, PGO waves are fairly constant (about 60 waves/min), and it has been suggested that electrical events are triggering both these activities and REM (182). In fact, pontine-generated phasic activity is thought to be a pacemaker that drives many of the phasic events of REM sleep, including muscle twitches, changes in respiration, and surges in heart rate and coronary blood flow, in addition to eye movements. The REM sleep (paradoxical sleep) occurs periodically during a night of sleep, with longer periods during the latter part of the night. If the subject is awakened during or immediately after a period of rapid eye movements, 80% of the subjects will report that they have been dreaming, and can relate the content of the dream (236).

Despite innumerable studies, anatomic structures and physiologic mechanisms involved in the control of the sleep-waking cycle are still uncertain. The pioneering investigations of Giuseppe Moruzzi and

Horace Magoun in the late 1950s refuted the passive view of sleep as a functional deafferentation regulated by the ascending reticular activating system. Their studies clearly established that sleep is an active process that involves (a) a population of neurons in the rostral brainstem reticular formation whose activity is required for wakefulness, and (b) a group of neurons in the caudal brainstem whose activity is necessary for the induction of sleep (265).

Early studies suggested that the sleep-inducing "center" in the brainstem might be the serotoninergic raphe nuclei, while the noradrenergic neurons of the locus coeruleus could play a role in paradoxical sleep (181, 182). In support of this concept, is the demonstration that reserpine, which depletes both serotonin and norepinephrine, produces a tranquil state and suppresses both-slow wave and paradoxical sleep for different periods of time. Furthermore, pharmacologic inhibition of serotonin synthesis at the level of tryptophane hydroxylase leads to total insomnia which is reversible. Injections of the immediate precursor of serotonin (5-hydroxytryptophan) causes a return to normal sleep. Likewise, nearly total destruction of serotonin-containing neurons in the raphe system also produces insomnia. One of the problems with the "monoaminergic hypothesis" of sleep is that serotoninergic neurons in the dorsal raphe nucleus and noradrenergic neurons in the locus coeruleus fire maximally during waking, drastically reduce their firing rate during slow-wave, and become totally silent during REM sleep (16, 159). Thus, these structure are unlikely to play a crucial role in sleep induction.

The firing pattern of serotoninergic neurons nevertheless fits with the suggestion that these cells may normally suppress PGO waves. In the transition from slow-wave to REM sleep, most raphe neurons specifically cease firing prior to PGO spikes, and remain silent throughout REM episodes. It was suggested that these neurons normally inhibit phasic REM events and that their silence during REM sleep indicates a termination of this inhibition.

Recent studies by Mircea Steriade, Allan Hobson, Robert McCarley, and their colleagues, led to the suggestion that an intrinsic pattern of alternating activity between noradrenergic and cholinergic cells in the brainstem might account for the cyclicity of REM and slow-wave sleep (134, 345). The cholinergic neurons thought to be involved in the control of sleep-waking cycle lie in the area of the pedunculopontine tegmental nucleus. The cholinergic neurons of the pedunculopontine tegmental nucleus project massively to the intralaminar nuclei of the thalamus, which are known to send profuse projections to widespread areas of the cerebral cortex. There is strong physiologic evidence for a role of this disynaptic pathway, which comprises a cholinergic pedunculothalamic and a glutamatergic thalamocortical segment, in the control of the sleep-waking cycle (344). Furthermore, the cholinergic neurons of the basal forebrain, particularly those of the basal nucleus of Meynert which project diffusely upon the cortex, may also contribute to the modulation of vigilance states. The complex neuropharmacologic events which underlie paradoxical and slow-wave sleep involve a variety of neurotransmitters and neural structures, not all of which are known.

Integrated Cortical Functions

One of the most striking and unique features of the human brain is its elaborate neural mechanisms for complex correlations, sensory discriminations, and the utilization of former experiences and reactions. These mechanisms involve *associative memory* and *mnemonic reactions*. The ability to retain, modify, and reuse neuronal circuits probably provides the basis of conscious and unconscious memory.

In a general way, the central sulcus divides the cerebral cortex into a posterior receptive portion and an anterior part related to motor functions. The posterior part contains all the primary receptive areas that receive specific sensory signals from the brainstem and spinal cord. Hence, this large region receives inputs indirectly from the peripheral sensory receptors. Impulses entering these primary areas produce sensations of a sharply defined character, such as distinct vision and hearing, sharply localized touch and accurate sensations of position and movement. These sensations, however, probably have not attained the perceptual level necessary for the recognition of an object. This requires the integration of primary stimuli with other neural information. Regions immediately adjacent to the receptive centers, known as *parasensory areas*, serve for the combination and elaboration of the primary impulses into more complex sensory perceptions which can

be recalled under appropriate conditions. In the more distant *association areas*, the various sensory fields overlap (e.g., the inferior parietal lobule) and form the basis for multisensory perceptions. The interaction of different sensory modalities initiated by "feeling" and "seeing" an object or person excite memory constellations which lead to recognition. The arousal of associative mnemonic complexes has been termed "gnosis," and it forms the basis of understanding and knowledge. Disorders of these mechanisms caused by lesions in association areas of the cerebral cortex are known as gnostic disturbances, or *agnosias*. In these conditions, tactile, visual, or auditory stimuli may no longer evoke appropriate memory constellations. When these gnostic disturbances involve the associative mechanisms underlying the comprehension of language, they form part of the complex known as the *aphasias*.

Closely related to both agnosia and aphasia is another group of disorders characterized by difficulty in performing skilled, learned movements even though no paralysis or sensory loss is present. Disorders that affect the motor side of sensory-motor integration are referred to as the *apraxias*. There are only two ways a patient can show that he or she recognizes an object: (a) by naming or describing the object, or (b) by demonstrating its use. If the patient can demonstrate the use of an object but is unable to name it, the individual has an aphasia. If the patient can name the object, or describe it, but does not know how to use it, he or she has an apraxia. The above examples demonstrate that agnosia partially underlies both aphasia and apraxia.

AGNOSIA

Agnosia means a failure to recognize. Various types of agnosias have been defined according to the particular sensory modality effected. Of the many types of agnosia classified on this basis with respect to both objects and space, three may properly be considered here, namely *tactile agnosia*, *visual agnosia*, and *auditory agnosia*.

Tactile agnosia is a failure to recognize objects by means of tactile and kinesthetic sensibilities when both of these sensory modalities are normal in the part of the body being tested. Astereognosis is the inability to recognize objects owing to sensory impairment at a cortical level. According to Brain (32), tactile agnosia is associated especially with lesions of the supramarginal gyrus in the left cerebral hemisphere, which probably is the dominant hemisphere for tactile recognition.

Visual agnosia is a failure to recognize objects that cannot be attributed to a defect of visual acuity or to intellectual impairment. Although a patient with visual agnosia is unable to recognize an object by sight, he or she may recognize it by other sensibilities, and he or she can still recognize people. The disability usually is limited to small objects and varies somewhat from day to day. In some instances, the visual agnosia may extend to surroundings, in which case it is associated with spatial disorientation. Lesions associated with visual agnosia involve the lateral visual association areas in the dominant hemisphere. The term *alexia* denotes a special form of visual agnosia in which the patient is unable to read because he or she fails to recognize written or printed words. Lesions in this syndrome interrupt pathways conveying impulses from the visual cortex of both sides to the angular gyrus of the left hemisphere.

Auditory agnosia is the term to describe the condition in which a patient with unimpaired hearing fails to recognize or distinguish what he or she hears. This type of agnosia may involve speech, musical sounds, or familiar noises, such as the telephone bell or running water. One form of auditory agnosia, known as word deafness, constitutes a type of receptive aphasia. Lesions associated with auditory agnosia involve parts of the superior temporal gyrus posteriorly (area 22) in the dominant hemisphere; these disturbances are more severe when the injury is bilateral.

APHASIA

This disorder is characterized by receptive and expressive disturbances in the use of symbols and signs to communicate. It results from organic neural lesions involving cerebral memory mechanisms for language, without impairment of cortical or subcortical structures essential for the relay of impulses or the innervation of speech organs (i.e., the muscles of the larynx, tongue, and lips). The three major types of aphasia are (a) receptive or sensory aphasia, (b) expressive or motor aphasia, and (c) conduction aphasia (68). Receptive aphasia was characterized by the German neurologist Carl Wernicke in 1908 (380), while motor aphasia was first described by the French neurologist Paul Broca as early as 1865 (36). Thus, sensory and motor aphasias

are often termed Wernicke's and Broca's aphasias.

Receptive or *Wernicke's aphasia* involves impairments in the appreciation of the meanings of both spoken and written words. The lesion primarily affects Wernike's area, that is, the left portion of the temporal lobe, or Brodmann's area 22, although it often extends to the superior portion of the temporal lobe (areas 39 and 40) and inferiorly to area 37 (Fig. 20.10). When the lesion is extensive, comprehension of both visual and auditory language input is severely impaired. In contrast, speech is fluent but often "empty." Language is normal in rate, rhythm, and melody, although patients may use wrong words (*paraphasia*).

In *expressive* or *Broca's aphasia* the language is not fluent but comprehension is usually preserved. Patients have damage to the motor association cortex in the frontal lobe, usually extending to the posterior portion of the third frontal gyrus (Brodmann's areas 44 and 45) which forms part of the pars opercularis and triangularis (Broca's area). In severe cases, there is also damage to the surrounding premotor and prefrontal regions (areas 6, 8, 9, 10, and 46). The deficit in language production ranges from almost muteness to a slowed, deliberate speech constructed from very simple grammatic structures. Patients with Broca's aphasia use only key words (246).

Conduction aphasia involves lesions in the arcuate or superior longitudinal fasciculus, which is composed of association fibers that link Broca's and Wernicke's areas. This bundle can be injured with lesions involving the supramarginal gyrus of the parietal lobe, or, less frequently, the posterior and superior parts of the left temporal lobe (68). Patients with conduction aphasia are fluent and their comprehension is relatively good. The major deficit concerns the ability to repeat words. These patients also make many paraphasic errors, substituting incorrect sounds or words for correct ones. Naming is also severely impaired. Reading aloud is abnormal, but patients can read silently with good comprehension.

The division of the aphasias into three types is an oversimplification since common disturbances of memory and language must be involved in both types. While relatively pure receptive or expressive forms of aphasia do occur, mixed varieties are the most common. Clinical experience reveals that the symptoms of aphasic patients rarely fall into one category or another simply because lesions producing cortical damage are rarely coextensive with a functional site (32, 300).

APRAXIA

The inability to perform certain learned complex movements, in the absence of paralysis, sensory loss, or disturbance of coordination, is known as apraxia. Since complex voluntary movements require the utilization of cerebral processes in formulating the nature of the act to be performed, movements of this nature are considered separate from those which are more or less automatic. Formulation of these movement complexes is largely unconscious and appears to depend upon memory constellations of similar acts previously performed. Complex learned movement patterns are organized in space and time, and follow sequences requiring close attention. Multiple sensory systems contribute to the skill of these movement patterns. Apraxia has been regarded as a disorganization of the underlying complex movement patterns. Many varieties of apraxia have been proposed as distinct entities, although some tend to have common features.

Kinetic apraxia is characterized by an inability to execute fine acquired motor movements; there is no paresis, and automatic and associated movements can be carried out. This disturbance may be confined to one limb. It has been interpreted as an expressive defect, most frequently associated with lesions of the precentral gyrus. The defect usually occurs contralateral to the lesion (71).

Ideomotor apraxia is caused by an interruption of pathways between the centers for formulation of a motor act and the motor areas necessary for its execution. Although patients may know what they want to do, they are unable to do it. Patients can perform many complex acts automatically, but may fail to perform the same acts on command. Spontaneous gestures may be normal. Ideomotor apraxia is often bilateral and affects the extremities equally. It is said to be associated with lesions of the parietal lobe, particularly the supramarginal gyrus, in the dominant hemisphere.

Ideational apraxia is the term used to describe loss of ability to formulate the ideational plan for the execution of the components of a complex act. While simple isolated movements may be performed nor-

mally, the component movements of a complex act are not synthesized into a purposeful plan and individual movements may be performed in a faulty sequence. Since kinesthetic memory and appreciation of the act to be performed are defective, ideational apraxia may be a variety of agnosia. This form of apraxia has been considered to result from lesions in the dominant parietal lobe, or in the corpus callosum (116), but frequently it is associated with rather diffuse pathologic processes.

Constructional apraxia is a disorder characterized by loss of visual guidance, impairment of the visual image, and disturbances of revisualization. A patient suffering from this form of apraxia is unable to reproduce simple geometric figures by drawing or by the arrangement of blocks. Although constructional apraxia is included with expressive disorders of motor function, it is rarely a pure motor disorder. As a rule the patient is unaware of his inability to perceive spatial relationships. This variety of apraxia appears to be related to interruption of pathways between the occipital and parietal cortex (66).

Curious combinations of agnosia and apraxia occur as a consequence of lesions involving primarily the inferior parietal lobule, usually in the dominant hemisphere (66, 109). This syndrome (*Gerstmann's syndrome*) is characterized by (a) finger agnosia, (b) right-left disorientation, (c) agraphia or dysgraphia, and (d) acalculia or dyscalculia. Patients suffering from Gerstmann's syndrome have difficulty in differentiating their fingers, in naming the individual fingers, and in pointing to particular fingers. Right-left disorientation, unlike finger agnosia, may affect all parts of the body, as well as inanimate objects and other individuals. The disturbance in writing does not extend to copying, which can be accomplished without difficulty. Inability to solve arithmetic problems is most evident with written figures, but it involves mental calculations as well.

Prefrontal Cortex

The frontal lobe rostral to area 6 is particularly well-developed in primates, especially in humans. These areas of cortex, including that on the orbital surface, are referred to as the prefrontal cortex. They consist of association areas whose major function is related to the capacity of the organism to weigh the consequences of future actions and to plan accordingly. The frontal lobes integrate the interoceptive and exteroceptive information they receive so as to select appropriate motor responses from many available (211).

The frontal lobe can be subdivided into multiple functional subregions. However, experimental studies in monkeys suggest that it is composed of two main regions: (a) the *prefrontal cortex* proper, located on the dorsolateral surface of the frontal lobe, and (b) the *orbitofrontal cortex*, located on the medial and ventral surface of the brain. Both regions receive a massive input from the mediodorsal thalamic nucleus, whose fibers terminate in layer IV. The prefrontal and orbitofrontal cortices are sometimes referred together as frontal granular cortex, in distinction to the agranular cortex of the motor and premotor areas. The frontal granular cortex is connected by the cingulum and the uncinate fasciculus with anterior portions of the temporal lobe and, directly or indirectly, with parietal and adjacent occipitotemporal association areas. It was recently discovered that the pattern of termination of intercortical connections between regions of association cortex of the parietal lobe and frontal lobe is organized into distinct, vertically oriented columns (123). These columns are 200–500 μm wide and extend across all layers of cortex. Thus, columnar organization is not unique to sensory or motor cortices, but appears to be a general feature of all neocortex.

The two major parts of the frontal lobe have somewhat distinct functions. Whereas the prefrontal cortex is involved in the strategic planning of higher motor actions, including cognitive tasks, the orbitofrontal cortex appears mainly concerned with emotional behavior. The orbitofrontal cortex is part of the limbic association cortex; it has direct connection with limbic structures, such as the amygdala. The functions of the premotor cortex appear largely dependent upon various forms of short-term memories, such as the working memory, a temporary storing of information used to guide a future action (123). Pioneering investigations in the 1930s by Carlyle Jacobsen have greatly helped our understanding of the frontal lobe functions in primates. These studies revealed, among other things, that lesions involving the prefrontal cortex impair the ability to perform a task involving delayed spatial response. In contrast, frontal lobe lesions involving the orbitofrontal and anterior cingulate cortex produce a marked alteration of the emotional responsiveness of monkeys, in addition to a deficit

in delayed responses. In cases where damage is limited to the orbitofrontal cortex, the normal aggressiveness and emotional responsiveness of primates is reduced (160).

A procedure known as frontal *lobotomy* or *leucotomy* was used widely some years ago in attempts to modify the behavior of severely psychotic patients. The basic operation involved bilateral sectioning of the fiber connections to and from the prefrontal area. The frontal lobotomy, introduced by the Portuguese neuropsychiatrist Egas Moniz (262), was performed in the United States and elsewhere in the 1940s (97). This neurosurgical procedure permitted many institutionalized patients to return home and even to resume their former activities. Moreover, a considerable number of lobotomies were performed for the relief of chronic intractable pain of organic origin when other measures, such as massive doses of narcotics and even cordotomy, had proved of no avail (85, 97, 332). After the operation, the patient no longer complained spontaneously of pain and no longer appeared to be in distress, although when asked patients acknowledged that pain was still present. Relief apparently was due to removal of the anxiety and fear usually associated with pain. Since frontal lobotomy, and numerous technical variations of it (126, 259), was performed on a large number of patients, it afforded an opportunity to study the associated intellectual and behavioral effects of these lesions.

The results of numerous lobotomies have been critically reviewed in a number of publications (75, 97, 294). These studies are difficult to evaluate because of lack of agreement concerning the extent of the changes in behavior and intellect. Most striking are the alterations in emotional behavior, which were characterized by Freeman and Watts as a lessening of "consciousness of the self," and a narrowing of the patient's mental horizon to the immediate present and to his own person. The patient was easily amused, careless in personal habits, unconcerned in social relations, and affected little by criticism. His emotional reactions were abrupt, transient, and superficial, and they often were accompanied by outspoken tactlessness. Pain and hardship were not associated with anxiety, nor was there much concern about financial or domestic difficulties. There was inability to gauge or appreciate the gravity of a situation and to maintain a responsible attitude toward it. These were the most enduring changes which could be attributed to the operation, and they probably were responsible for the successful abolition of morbid anxiety and obsessional states (97).

Intellectual damage is especially difficult to evaluate. General memory returns rapidly, and standard psychometric tests are accurately performed. Capacity for abstract thought is reduced and patients develop a more concrete attitude. Easy distractibility is common, judgment is poor, and initiative is reduced. Mental concentration and the capacity for sustained intellectual effort are impaired, especially with respect to solving complex problems. The most reliable data concerning the effects of lobotomy upon intelligence are those obtained from nonpsychotic patients in whom this procedure was done for relief of pain. On the basis of thorough studies of patients before and after operation, Rylander (330) concluded that intellectual and emotional deterioration may be severe. The results of the operation necessarily depend upon the intelligence of the patient and the extent of the operative procedure. This conclusion appears to be supported by others (201). Other forms of frontal (or prefrontal) lobe surgery, such as topectomy and orbitofrontal lobotomy, were not reported to produce such severe impairment of intellectual function (126, 213). The fact that the extent of intellectual deterioration following prefrontal lobotomy cannot be measured in specific terms, reflects the exceedingly complex nature of what is called intellect, and suggests that the criteria used to evaluate it may not be adequate. The unpredictable effects of the procedure upon intellect and severe personality changes associated with the irreversible nature of surgery caused this procedure to be rarely used.

Despite the difficulties in evaluating the behavior changes and the intellectual alterations of prefrontal lobotomy, some patients were considered to have benefited from the operation. Perhaps the greatest problem, and one of the reasons why this form of psychosurgery is now rarely done, was the difficulty in determining preoperatively which patients might be expected to be improved by it. Another important factor in the decline of psychosurgery was the introduction of tranquilizing drugs which facilitated the treatment of severe behavioral disorders.

The human nervous system has evolved slowly, and although many of the details of its anatomic structure appear firmly estab-

lished, concepts concerning the functional significance and interrelation of its various subdivisions change as a result of continuing research. Many so-called "electronic brains" or "artificial intelligence" devices have been constructed which can perform certain functions faster and more efficiently than the human brain. The more complex the performed function, the more elaborate the programming of the computer must be. Such computerized networks are impressive in appearance and function, yet they do not approach in versatility or scope the fantastic potentialities of the human brain. The human brain is unique in that it provides its own programming. In fact, it is programmed throughout life by daily experiences. It seems likely that manmade neuronal machines will in the future perform many more of the functions now performed by human brains, but this change must be regarded as a redistribution of labor. These computerized versions of the brain are, after all, only one of the expressions of the ingenuity of the human brain.

References

1. Ades HW. Central auditory mechanisms. In: Field J, ed. Handbook of physiology. Vol. I, Sect. 1. Ch. 24. Washington, DC: American Physiological Society, 1959: 585–613.
2. Ades HW, Brookhart JM. The central auditory pathway. J Neurophysiol 1950;13:189–205.
3. Adrian ED. Afferent discharges to the cerebral cortex from peripheral sense organs. J Physiol (Lond) 1941;100:159–191.
4. Aitkins LM, Irvine DRF, Webster WR. Central neural mechanisms of hearing. In: Darian-Smith I, ed. Handbook of physiology. Sect. I: the nervous system. Vol. III. Bethesda, MD: American Physiological Society, 1984:675–737.
5. Aitkins LM, Webster WR. Medial and geniculate body of the cat: organization and responses to tonal stimuli of neurons in the ventral division. J Neurophysiol 1972;35: 365–380.
6. Akert K, Hartmann-von Monakow K. Relationships of precentral, premotor and prefrontal cortex to the mediodorsal and intralaminar nuclei of the monkey thalamus. Acta Neurobiol Exp (Warsz) 1980;40: 7–25.
7. Allen GI, Korn H, Oshima T, Toyama K. The mode of synaptic linkage in the cerebroponto-cerebellar pathway of the cat. II. Responses of single cells in the pontine nuclei. Exp Brain Res 1975; 24:15–36.
8. Allman JM. Evolution of the visual system in the early primates. In: Sprague JM, Epstein A, eds. Progress in physiological psychology. Vol. 7. New York: Academic Press, 1977:1–53.
9. Allman JM, Kaas JH. The organization of the second visual area (VII) in the owl monkey: a second order transformation of the visual hemifield. Brain Res 1974;76:247–265.
10. Angevine JB Jr, Sidman RL. Autoradiographic study of cell migration during histogenesis of the cerebral cortex in the mouse. Nature 1961;192:766–768.
11. Asanuma H. Functional role of sensory inputs to the motor cortex. Prog Neurobiol 1981;16:241–262.
12. Asanuma H, Sakata H. Functional organization of a cortical efferent system examined with focal depth stimulation in cats. J Neurophysiol 1967;30:35–54.
13. Aston-Jones G, Bloom FE. Activity of norepinephrine-containing locus coeruleus neurons in behaving rats exhibit pronounced responses to non-noxious environmental stimuli. J Neurosci 1981;1:887–900.
14. Astruc J. Corticofugal connections of area 8 (frontal eye field) in *Macaca mulatta*. Brain Res 1971; 33:241–256.
15. Auer J. Terminal degeneration in the diencephalon after ablation of frontal cortex in the cat. J Anat 1956;90:30–41.
16. Azmitia EC, Gannon PJ. The primate serotonergic system: a review of human and animal studies and a report on *Macaca fascicularis*. In: Fahn S, ed. Advances in neurology. New York: Raven Press, 1986:407–468.
17. Bagshaw MH, Pribram KH. Cortical organization in gustation (*Macaca mulatta*). J Neurophysiol 1953;16:499–508.
18. Bailey P, von Bonin G. The isocortex of man. Urbana: University of Illinois Press, 1951.
19. Bailey P, von Bonin G, Garol HW, McCulloch WS. Functional organization of temporal lobe of monkey (*Macaca mulatta*) and chimpanzee (*Pan satyrus*). J Neurophysiol 1943; 6:121–128.
20. Beck E. Die myeloarchitektonische Felderung in der Sylvischen Furche gelegenen Teiles des menschlichen Schläfenlappens. J Psychol Neurol 1929;36:1–21.
21. Beck E. The origin, course and termination of the prefronto-pontine tract in the human brain. Brain 1950;73:368–391.
22. Beckstead RM, Morse JR, Norgren R. The nucleus of the solitary tract in the monkey: projections to the thalamus and brain stem nuclei. J Comp Neurol 1980;190:259–282.
23. Bertrand G. Spinal efferent pathways from the supplementary motor area. Brain 1956;79:461–473.
24. Bindman L, Lippold RL. The neurophysiology of the cerebral cortex. Austin: University of Texas Press, 1981.
25. Blomquist AJ, Benjamin RM, Emmers R. Thalamic localization of afferents from the tongue in squirrel monkey (*Saimiri sciureus*). J Comp Neurol 1962;118:77–87.
26. Blum M, Walker AE, Ruch TC. Localization of taste in the thalamus of *Macaca mulatta*. Yale J Biol Med 1943;16:175–182.
27. Boivie J. Terminations of the cervicothalamic tract in the cat: an experimental study with silver impregnation methods. Brain Res 1970;19:333–360.
28. Boivie J. An anatomical reinvestigation of the termination of the spinothalamic tract in the monkey. J Comp Neurol 1979;186:343–370.
29. Börnstein WS. Cortical representation of taste in man and monkey. I. Functional and anatomical relations of taste, olfaction and somatic sensibility. Yale J Biol Med 1940; 12:719–736.
30. Börnstein WS. Cortical representation of taste in man and monkey. II. Localization of cortical taste area in man and method of measuring impairment of taste in man. Yale J Biol Med 1940;13:133–156.
31. Bowsher D. The termination of secondary somatosensory neurons within the thalamus of *Macaca mulatta*: an experimental degeneration study. J Comp Neurol 1961;177: 213–227.
32. Brain R. Speech disorders. Aphasia, apraxia and agnosia. London: Butterworths, 1961.
33. Brinkman C, Porter R. Supplementary motor area in the monkey: activity of neurons during performance of a learned motor task. J Neurophysiol 1979;42:681–709.
34. Brinkman C, Porter R. Supplementary motor area and premotor area of monkey cerebral cortex: functional organization and activities of single neurons during performance of a learned movement. In: Desmedt JC, ed. Motor control mechanisms in health and disease. New York: Raven Press, 1983: 393–420.
35. Brinkman J, Bush BM, Porter R. Deficient influences of peripheral

stimuli on precentral neurones in monkeys with dorsal column lesions. J Physiol (Lond) 1978;276: 27–48.
36. Broca P. Sur le siège de la faculté du langage articulé. Bull Soc Anthropol 1865;6:377–393.
37. Brodal A. The olivocerebellar projection in the cat as studies with the method of retrograde axonal transport of horseradish peroxidase. II. The projection of the uvula. J Comp Neurol 1976;166: 417–426.
38. Brodal A. Neurological anatomy in relation to clinical medicine. 3rd ed. New York: Oxford University Press, 1981.
39. Brodal P. The corticopontine projection in the cat. I. Demonstration of a somatotopically organized projection from the primary sensorimotor cortex. Exp Brain Res 1968; 5:212–237.
40. Brodal P. The corticopontine projection from the visual cortex in the cat. I. The total projection and the projection from area 17. Brain Res 1972;39:297–317.
41. Brodal P. The corticopontine projection from the visual cortex in the cat. II. The projection from areas 18 and 19. Brain Res 1972;39:319–335.
42. Brodal P. Principles of organization of the monkey corticopontine projection. Brain Res 1978;148: 214–218.
43. Brodal P. The corticopontine projection in the rhesus monkey: origin and principles of organization. Brain 1978;101:251–283.
44. Brodmann K. Vergleichende Lokalisation lehre der Grosshirnrinde in ihren Prinzipien dargestellt auf Grund des Zellenbaues. Leipzig: J.A. Barth, 1909.
45. Brozoski TJ, Brown RM, Rosvold HE, Goldman PS. Cognitive deficit cause by regional depletion of dopamine in prefrontal cortex of rhesus monkey. Science 1979;205: 929–932.
46. Brugge JF, Reale RA. Auditory cortex. In: Peters A, Jones EG, eds. Cerebral cortex. Vol. 4. New York: Plenum Press, 1985:229–271.
47. Bryden MP. Laterality: functional asymmetry in the intact brain. New York: Academic Press, 1982.
48. Bucy PC. Effects of extirpation in man. In: Bucy PC, ed. The precentral motor cortex. 2d ed. Ch. 14. Urbana: University of Illinois Press, 1949:353–394.
49. Burton H. Second somatosensory cortex and related areas. In: Jones EG, Peters A, eds. Cerebral cortex. Vol. 5. New York: Plenum Press, 1986:31–98.
50. Burton H, Jones EG. The posterior thalamic region and its cortical projection in new world and old world monkeys. J Comp Neurol 1976;168:249–302.
51. Büttner U, Henn V. Thalamic unit activity in the alert monkey during natural vestibular stimulation. Brain Res 1976;103:127–132.
52. Campbell AW. Histological studies on the localization of cerebral function. New York: Cambridge University Press, 1905.
53. Carlsson A. Antipsychotic drugs and catecholamine synapses. J Psychiat Res 1974;11:57–64.
54. Carlsson M, Carlsson A. Interactions between glutamatergic and monoaminergic systems within the basal ganglia: implications for schizophrenia and Parkinson's disease. Trends Neurosci 1990;13: 272–276.
55. Carman JB, Cowan WM, Powell TPS. Cortical connexions of the thalamic reticular nucleus. J Anat 1964;98:587–598.
56. Carmel PW. Efferent projections of the ventral anterior nucleus of the thalamus in the monkey. Am J Anat 1970;128:159–184.
57. Casseday JH, Diamond IT, Harting JK. Auditory pathways to the cortex in *Tupaia glis*. J Comp Neurol 1976;166:303–340.
58. Cogan DG. Neurology of the ocular muscles. 2d ed. Springfield, IL: Charles C. Thomas, 1956.
59. Colonnier M. The fine structural arrangement of the cortex. Arch Neurol 1967;16:651–657.
60. Colonnier M. The electron microscopic analysis of the neuronal organization of the cerebral cortex. In: Schmitt FO, Worder FG, Adelman G, Dennis SG, eds. The organization of the cerebral cortex. Cambridge, MA: MIT Press, 1981: 125–152.
61. Cooper MH, Beal JA. The neurons and the synaptic endings in the primate basilar pontine gray. J Comp Neurol 1978;180:17–42.
62. Coulter JD, Ewing L, Carter C. Origin of primary sensorimotor cortical projections to lumbar spinal cord of cat and monkey. Brain Res 1976;103:366–372.
63. Coulter JD, Jones EG. Differential distribution of corticospinal projections from individual cytoarchitectonic fields in the monkey. Brain Res 1977;129:335–340.
64. Coyle JT, Price DL, DeLong MR. Alzheimer's disease: a disorder of cortical cholinergic innervation. Science 1983;219:1184–1190.
65. Cragg BG. The density of synapses and neurones in the motor and visual areas of the cerebral cortex. J Anat 1967;101:639–654.
66. Critchley M. The parietal lobes. London: Edward Arnold, 1953.
67. Cynader M, Berman N. Receptive-field organization of monkey superior colliculus. J Neurophysiol 1972;35:187–201.
68. Damasio AR, Geschwind N. The neural basis of language. Annu Rev Neurosci 1984;7:127–147.
69. Davies P, Maloney AJR. Selective loss of central cholinergic neurons in Alzheimer's disease. Lancet 1976;2:1403.
70. Deecke L, Schwarz DWF, Fredrickson JM. Vestibular responses in the rhesus monkey ventroposterior thalamus. II. Vestibuloproprioceptive convergence at thalamic neurons. Exp Brain Res 1977;30: 219–232.
71. DeJong RN. The neurological examination. 4th ed. New York: Harper & Row, 1979.
72. DeLong MR. Activity of pallidal neurons during movement. J Neurophysiol 1971;34:414–427.
73. Dekker JJ, Kievit J, Jacobson S, Kuypers HGJM. Retrograde axonal transport of horseradish peroxidase in the forebrain of the rat, cat and rhesus monkey. In: Santini M, ed. Prospectives in neurobiology. Golgi centennial symposium. New York: Raven Press, 1975: 201–208.
74. De Lacoste MC, Kirkpartrick JB, Ross ED. Topography of the human corpus callosum. J Neuropath Exp Neurol 1985;44: 578–591.
75. Denny-Brown D. The frontal lobes and their functions. In: Feiling A, ed. Modern trends in neurology. New York: Paul B. Hoeber, 1951: 13–89.
76. DeVito JL, Smith OA Jr. Projections from the mesial frontal cortex (supplementary motor area) to the cerebral hemispheres and brain stem of the *Macaca mulatta*. J Comp Neurol 1959;111:261–277.
77. Diamond IT, Jones EG, Powell TPS. Interhemispheric fiber connections of the auditory cortex in the cat. Brain Res 1968;11:177–193.
78. Diamond IT, Jones EG, Powell TPS. The association connections of the auditory cortex of the cat. Brain Res 1968;11:560–579.
79. Diamond IT, Jones EG, Powell TPS. The projection of the auditory cortex upon the diencephalon and brain stem in the cat. Brain Res 1969;15:305–340.
80. Douglas RJ, Martin KA. Neocortex. In: Shepherd GM, ed. The synaptic organization of the brain. Chap. 12. New York: Oxford University Press, 1990:389–438.
81. Emmers R. Localization of thalamic projection of afferents from the tongue in the cat. Anat Res 1964; 148:67–74.
82. Emmers R. Separate relays of tactile, thermal and gustatory modalities in the cat thalamus. Proc Soc Exp Biol Med 1966;121:527–531.
83. Emmers R, Benjamin RM, Blomquist AJ. Thalamic localization of afferents from the tongue in albino rat. J Comp Neurol 1962; 118:43–48.
84. Emson PC, Hunt SP. Peptide-containing neurons of the cerebral cortex. In: Jones EG, Peters A, eds. Cerebral cortex. Vol. 2. New York: Plenum Press, 1984;145–169.
85. Falconer MA. Relief of intractable pain of organic origin by frontal lobotomy. Proc Assoc Res Nerv Ment Dis 1948;27:706–722.
86. Felleman DJ, Nelson RJ, Kaas JH. Representations of the body surface in areas 3b and I of postcentral

cortex of cebus monkeys. Brain Res 1983:268:15–26.
87. Fibiger HC. Cholinergic mechanisms in learning, memory and dementia: a review of recent evidence. Trends Neurosci 1991;14: 220–223.
88. Foerster O. The cerebral cortex in man. Lancet 1931;2:309–312.
89. Foerster O. Motor cortex in man in the light of Hughlings Jackson's doctrines. Brain 1936;59:135–159.
90. Foerster O. Symptomatologie der Erkrankungen des Grosshirns. Motorische Felder und Bahnen. In: Bumke O, Foerster O, eds. Handbuch der Neurologie. Vol. 6. Berlin: Julius Springer, 1936:1–357.
91. Fonnum F. Glutamate: a neurotransmitter in mammalian brain. J Neurochem 1984;42:1–11.
92. Foote SL, Morrison JH. Extrathalamic modulation of cortical function. Ann Rev Neurosci 1987;10: 67–95.
93. Forbes BF, Moskowitz N. Projections of auditory responsive cortex in the squirrel monkey. Brain Res 1974;67:239–254.
94. Fredrickson JM, Figge U, Scheid P, Kornhuber HH. Vestibular nerve projection to the cerebral cortex of the rhesus monkey. Exp Brain Res 1966;2:318–327.
95. Fredrickson JM, Kornhuber HH, Schwarz DWF. Cortical projections of the vestibular nerve. In: Kornhuber H, ed. Handbook of sensory physiology. Vol. 6. Berlin: Springer-Verlag, 1974:565–582.
96. Fredrickson JM, Rubin AM. Vestibular cortex. In: Jones EG, Peters A, eds. Cerebral cortex. Vol. 5. New York: Plenum Press, 1986: 99–111.
97. Freeman W, Watts JW. Psychosurgery. Intelligence, emotion and social behavior following prefrontal lobotomy for mental disorders. 2d ed. Springfield, IL: Charles C. Thomas, 1949.
98. Friedman DP, Jones EG, Burton H. Representation pattern in the second somatic sensory area of the monkey cerebral cortex. J Comp Neurol 1980;192:21–41.
99. Fulton JF, Keller AD. The sign of Babinski. A study of the evolution of cortical dominance in primates. Springfield, IL: Charles C. Thomas, 1932.
100. Fulton JF, Kennard MA. A study of flaccid and spastic paralysis produced by lesions of the cerebral cortex in primates. Proc Assoc Res Nerv Ment Dis 1934;13:158–210.
101. Galambos R, Rose JE. Microelectrode studies on medial geniculate body of the cat. III. Response to pure tone. J Neurophysiol 1952; 15:381–400.
102. Garey LJ. Visual system. In: Paxinos G, ed. The human nervous system. Ch. 28. New York: Academic Press, 1990:945–977.
103. Garey LJ, Jones EG, Powell TPS. Interrelationships of striate and extrastriate cortex with the primary relay sites of the visual pathway. J Neurol Neurosurg Psychiatry 1968; 31:135–157.
104. Garey LJ, Powell TPS. The projection of the retina in the cat. J Anat 1968;102:189–222.
105. Gazzaniga MS. The bisected brain. New York: Appleton-Century-Crofts, 1970.
106. Gazzaniga MS. Organization of the human brain. Science 1989;245: 947–952.
107. Gazzaniga MS, Bogen JE, Sperry RW. Observations on visual perception after disconnexion of the cerebral hemispheres in man. Brain 1965;88:221–236.
108. Gazzaniga MS, Sperry RW. Language after section of the cerebral commissures. Brain 1967;90:131–148.
109. Gerstmann J. Syndrome of finger agnosia: disorientation for right and left, agraphia and acalculia. Arch Neurol Psychiatry 1940;44: 398–408.
110. Geschwind N. Disconnexion syndromes in animals and man. I. Brain 1965;88:237–294.
111. Geschwind N. Disconnexion syndromes in animals and man. II. Brain 1965;88:585–644.
112. Geschwind N. The organization of language and the brain. Science 1970;170:940–944.
113. Geschwind N. Specialization of the human brain. Sci Am 1979;241: 180–199.
114. Geschwind J, Galaburda AM. Cerebral dominance: the biological foundation. Cambridge, MA: Harvard University Press, 1984.
115. Geschwind N, Galaburda AM. Cerebral lateralization: biological mechanisms, associations and pathology. Cambridge, MA: MIT Press, 1987.
116. Geschwind N, Kaplan E. A human cerebral deconnection syndrome. Neurology 1962;12:675–685.
117. Gilbert CD. Horizontal integration in the visual cortex. Trends Neurosci 1985;8:160–165.
118. Gilbert CD. Horizontal integration and cortical dynamics. Neuron 1992;9:1–13.
119. Gilbert CD, Kelly JP. The projection of cells in different layers of the cat's visual cortex. J Comp Neurol 1975;163:81–106.
120. Giuffrida R, Rustioni A. Glutamate and aspartate immunoreactivity in corticothalamic neurons of rats. In: Bentivoglio M, Spreafico R, eds. Cellular thalamic mechanisms. Amsterdam: Elsevier, 1988:311–320.
121. Giuffrida R, Rustioni A. Glutamate and aspartate immunoreactivity in corticospinal neurons of rat. J Comp Neurol 1989;288:154–164.
122. Goldman PS, Nauta WJH. Columnar distribution of cortico-cortical fibres in the frontal association, limbic and motor cortex of the developing Rhesus monkey. Brain Res 1977;122:393–413.
123. Goldman-Rakic PS. Circuitry of primate prefrontal cortex and regulation of behavior by representational memory. In: Plum F, Mountcastle VB, eds. Handbook of physiology. Vol. V: Higher functions of the brain. Part I, Sect. 1: The nervous system. Bethesda, MD: American Physiological Society, 1987:373–417.
124. Goldman-Rakic PS. Topography of cognition: parallel distributed networks in primate association cortex. Annu Rev Neurosci 1988;11: 137–156.
125. Goldman-Rakic PS, Leranth C, Williams SM. Dopamine synaptic complex on pyramidal neurons in primate cerebral cortex. Proc Natl Acad Sci USA 1989;86: 9015–9019.
126. Green JR, Duisberg REH, McGrath WB. Orbitofrontal lobotomy with reference to effects on 55 psychotic patients. J Neurosurg 1952;9: 579–587.
127. Gross NB, Lifschitz WS, Anderson DJ. The tonotopic organization of the auditory thalamus of the squirrel monkey (*Saimiri sciureus*). Brain Res 1974;65:323–332.
128. Hayhow WR. The cytoarchitecture of the lateral geniculate body in the cat in relation to the distribution of crossed and uncrossed optic fibers. J Comp Neurol 1958;110:1–64.
129. Hendrickson AE, Hunt SP, Wu J-Y. Immunocytochemical localization of glutamic acid decarboxylase in monkey striate cortex. Nature 1981;292:605–607.
130. Henschen SE. On the function of the right hemisphere of the brain in relation to the left in speech, music and calculation. Brain 1926; 49:110–123.
131. Hickey TL, Guillery RW. An autoradiographic study of retinogeniculate pathways in the cat and the fox. J Comp Neurol 1974; 156:239–254.
132. Hines M. The "motor" cortex. Bull Johns Hopkins Hosp 1937;60: 313–336.
133. Hines M. Significance of the precentral motor cortex. In: Bucy PC, ed. The precentral motor cortex. Ch. 18. Urbana: University of Illinois Press, 1949:461–494.
134. Hobson JA, Steriade M. Neuronal basis of behavioral state control. In: Bloom FE, ed. Handbook of physiology. Vol. IV: Intrinsic regulatory system of the brain. Sect. I: The nervous system. Bethesda, MD: American Physiological Society, 1986:701–823.
135. Holländer H. Projections from the striate cortex to the diencephalon in the squirrel monkey (*Saimiri sciureus*): a light microscopic radioautographic study following intracortical injection of ^{3}H leucine. J Comp Neurol 1974;155:424–440.
136. Holmes G, May WP. On the exact origin of the pyramidal tract in man and other mammals. Brain 1909;32:1–43.
137. Houser CR, Vaughn JE, Hendry

SHC, Jones EG, Peters A. GABA neurons in the cerebral cortex. In: Jones EG, Peters A, eds. Cerebral cortex. Vol. 2. New York: Plenum Press, 1984:63–89.
138. Hubel DH. The visual cortex of the brain. Sci Am 1963;209:54–62.
139. Hubel DH, LeVay S, Wiesel TN. Mode of termination of retino-tectal fibers in macaque monkey: an autoradiographic study. Brain Res 1975;96:25–40.
140. Hubel DH, Wiesel TN. Receptive fields of single neurons in the cat's striate cortex. J Physiol (Lond) 1959;148:574–591.
141. Hubel DH, Wiesel TN. Integrative action in the cat's lateral geniculate body. J Physiol (Lond) 1961;155: 385–398.
142. Hubel DH, Wiesel TN. Receptive fields, binocular interaction and functional architecture in the cat's visual cortex. J Physiol (Lond) 1962;160:106–154.
143. Hubel DH, Wiesel TN. Shape and arrangement of columns in cat's striate cortex. J Physiol (Lond) 1963;165:559–568.
144. Hubel DH, Wiesel TN. Receptive fields of cells in striate cortex of very young, visually inexperienced kittens. J Neurophysiol 1963;26: 994–1002.
145. Hubel DH, Wiesel TN. Receptive fields and functional architecture in two non-striate visual areas (18 and 19) of the cat. J Neurophysiol 1965;28:229–289.
146. Hubel DH, Wiesel TN. Cortical and callosal connections concerned with the vertical meridian of visual fields in the cat. J Neurophysiol 1967;30:1561–1573.
147. Hubel DH, Wiesel TN. Receptive fields and functional architecture of monkey striate cortex. J Physiol (Lond) 1968;195:215–243.
148. Hubel DH, Wiesel TN. Stereoscopic vision in macaque monkey. Nature 1970;225:41–42.
149. Hubel DH, Wiesel TN. Laminar and columnar distribution of geniculo-cortical fibers in the Macaque monkey. J Comp Neurol 1972;146:421–450.
150. Hubel DH, Wiesel TN. Sequence regularity and geometry of orientation columns in the monkey striate cortex. J Comp Neurol 1974; 158:267–294.
151. Hubel DH, Wiesel TN. Uniformity of monkey striate cortex: a parallel relationship between field size, scatter and magnification factor. J Comp Neurol 1974;158:295–306.
152. Hubel DH, Wiesel TN, LeVay S. Plasticity of ocular dominance columns in monkey striate cortex. Phil Trans R Soc Lond (Biol) 1977; 278:377–409.
153. Huerta MF, Krubitzer LA, Kaas JH. Frontal eye field as defined by intracortical microstimulation in squirrel monkeys, owl monkeys and macaque monkeys. I. Subcortical connections. J Comp Neurol 1986;253:415–439.
154. Huerta MJ, Krubitzer LA, Kaas JH. Frontal eye field as defined by intracortical microstimulation in squirrel monkeys, owl monkeys and macaque monkeys. II. Cortical connections. J Comp Neurol 1987; 265:332–361.
155. Ilinsky IA, Tourtellotte WG, Kultas-Ilinsky K. Anatomical distinctions between the two basal ganglia afferent territories in the primate motor thalamus. Stereotact Funct Neurosurg 1993;60: 62–69.
156. Imig TJ, Adrian HO. Binaural columns in the primary field (AI) of cat auditory cortex. Brain Res 1977;138:241–257.
157. Imig TJ, Morel A. Tonotopic organization of the ventral nucleus of the medial geniculate body in the cat. J Neurophysiol 1985;53:309–340.
158. Imig TJ, Ruggero MA, Kitzes LM, Javel E, Brugge JF. Organization of auditory cortex in the owl monkey (*Aotus trivirgatus*). J Comp Neurol 1977;171:111–128.
159. Jacobs BL, Azmitia EC. Structure and function of the brain serotonin system. Physiol Rev 1992;72: 165–229.
160. Jacobsen CF. Functions of frontal association area in primates. Arch Neurol Psychiat 1935;33:558–569.
161. Jasper HH. Unspecific thalamocortical relations. In: Field J, ed. Handbook of physiology. Vol. II, Sect. I, Ch. 53. Washington, DC: American Physiological Society, 1960:1307–1326.
162. Jerger JF. Observations on auditory behavior in lesions of the central auditory pathways. AMA Arch Otolaryngol 1960;71:797–806.
163. Jones EG. Some aspects of the organization of the thalamic reticular complex. J Comp Neurol 1975;162: 285–308.
164. Jones EG. Anatomy of cerebral cortex: columnar input-output organization. In: Schmitt FO, Worden FG, Adelman G, Dennis SG, eds. The organization of the cerebral cortex. Cambridge, MA: MIT Press, 1981: 199–235.
165. Jones EG. Connectivity of primate sensory-motor cortex. In: Jones EG, Peters A, eds. Cerebral cortex. Vol. 5. New York: Plenum Press, 1986: 113–183.
166. Jones EG. Ascending inputs to, and internal organization of, cortical motor areas. In: Motor areas of the cerebral cortex. CIBA Foundation symposium. Chichester: John Wiley & Sons, 1987:132:21–39.
167. Jones EG, Burton H. Cytoarchitecture and somatic sensory connectivity of thalamic nuclei other than the ventrobasal complex in the cat. J Comp Neurol 1974;154:395–432.
168. Jones EG, Coulter JD Burton H, Porter R. Cells of origin and terminal distribution of corticostriatal fibers arising in the sensory-motor cortex of monkeys. J Comp Neurol 1977;173:53–80.
169. Jones EG, Coulter JD, Hendry SHC. Intracortical connectivity of architectonic fields in the somatic sensory, motor and parietal cortex of monkeys. J Comp Neurol 1978;181:291–348.
170. Jones EG, Friedman DP. Projection pattern of functional components of thalamic ventrobasal complex on monkey somatosensory cortex. J Neurophysiol 1982;48:521–544.
171. Jones EG, Hendry SHC. Distribution of callosal fibers around the hand representation in monkey somatic sensory cortex. Neurosci Lett 1980;19:167–172.
172. Jones EG, Leavit RY. Retrograde axonal transport and the demonstration of non-specific projections to the cerebral cortex and striatum from thalamic intralaminar nuclei in the cat, rat and monkey. J Comp Neurol 1974;154:349–378.
173. Jones EG, Porter R. What is area 3a? Brain Res Rev 1980;2:1–43.
174. Jones EG, Powell TPS. The ipsilateral cortical connexions of the somatic sensory areas in the cat. Brain Res 1968;9:71–94.
175. Jones EG, Powell TPS. Connexions of the somatic sensory cortex of the rhesus monkey. I. Ipsilateral cortical connexions. Brain 1969;92: 477–502.
176. Jones EG, Powell TPS. Connexions of the somatic cortex of the rhesus monkey. II. Contralateral cortical connexions. Brain 1969;92:717–730.
177. Jones EG, Powell TPS. Connexions of the somatic sensory cortex of the rhesus monkey. II. Thalamic connexions. Brain 1970;93:37–56.
178. Jones EG, Powell TPS. Anatomical organization of the somatosensory cortex. In: Iggo A, ed. Handbook of sensory physiology. Vol. 2. Berlin: Springer-Verlag, 1973:579–620.
179. Jones EG, Wise SP. Size, laminar and columnar distribution of efferent cells in the sensory-motor cortex of monkeys. J Comp Neurol 1977;175:391–438.
180. Jones EG, Wise SP, Coulter JD. Differential thalamic relationships of sensory-motor and parietal cortical fields in monkey. J Comp Neurol 1979;183:833–881.
181. Jouvet M. Neurophysiology of the states of sleep. Physiol Rev 1967; 47:117–177.
182. Jouvet M. Biogenic amines and the states of sleep. Science 1969;163: 32–41.
183. Jürgens J. The efferent and afferent connections of the supplementary motor area. Brain Res 1984;300: 63–81.
184. Kaes T. Die Grosshirnrinde des Menschen in ihren Massen und in ihrem Fasergehalt. Vol. I. Jena: Gustav Fischer, 1907.
185. Kandel ER. Disorders of thought: schizophrenia. In: Kandel ER, Schwartz JH, Jessell TM, eds. Principles of neural science. Ch. 55. New York: Elsevier, 1991:853–868.
186. Karol EA, Pandya DN. The distribution of the corpus callosum in the

rhesus monkey. Brain 1971;94: 471–486.
187. Kawamura S, Sprague JN, Niimi K. Corticofugal projections from the visual cortices to the thalamus in the cat. J Comp Neurol 1974;158: 339–362.
188. Kelly JP, van Essen DC. Cell structure and function in the visual cortex of the cat. J Physiol (Lond) 1974;238:515–547.
189. Kemp JM, Powell TPS. The corticostriate projection in the monkey. Brain 1970;93:525–546.
190. Kennard MA. Somatic functions. In: Bucy PC, ed. The precentral motor cortex. 2d ed. Ch. 9. Urbana: University of Illinois Press, 1949: 243–276.
191. Kennard MA, Fulton JF. The localizing significance of spasticity, reflex grasping and the signs of Babinski and Rossolimo. Brain 1933;56:213–225.
192. Kennard MA, Viets HR, Fulton JF. The syndrome of the premotor cortex in man: impairment of skilled movement, forced grasping, spasticity and vasomotor disturbances. Brain 1934;57:69–84.
193. Kennedy C, Des Rosiers MH, Sakurada O, et al. Metabolic mapping of the primary visual system of the monkey by means of the autoradiographic [^{14}C] deoxyglucose technique. Proc Natl Acad Sci USA 1976;73:4230–4234.
194. Kerr FWL, Lippman HH. The primate spinothalamic tract as demonstrated by anterolateral cordotomy and commissural myelotomy. Adv Neurol 1974;4:147–156.
195. Kievet J, Kuypers HGJM. Organization of the thalamo-cortical connexions to the frontal lobe in the rhesus monkey. Exp Brain Res 1977;29:299–322.
196. Kim R, Nakano K, Jayaraman A, Carpenter MB. Projections of the globus pallidus and adjacent structures: an autoradiographic study in the monkey. J Comp Neurol 1976;169:263–289.
197. Kisvárday ZF, Martin KAC, Freund TF, Maglóczy Z, Whitteridge D, Somogyi P. Synaptic targets of HRP-filled layer III pyramidal cells in the cat striate cortex. Exp Brain Res 1986;64:541–552.
198. Kleitman N. Sleep and wakefulness. Chicago: University of Chicago Press, 1963.
199. Konishi M, Knudsen EI. A theory of neural auditory space. In: Woolsey CN, ed. Cortical sensory organization. Vol. 3. Clifton, NJ: Humana Press, 1982:219–229.
200. Kornhuber HH, Fredrickson JM, Figge U. Die korticale Projektion der vestibulären Afferenz Beim Rhesusaffen. Pfluegers Arch 1965; 283:20.
201. Koskoff YD, Dennis W, Lazovik D, Wheeler ET. The psychological effects of frontal lobotomy performed for alleviation of pain. Proc Assoc Res Nerv Ment Dis 1948; 27:723–753.
202. Krieg WJS. Connections of the cerebral cortex. I. The albino rat. C. Extrinsic connections. J Comp Neurol 1947;86:267–394.
203. Krieg WJS. Connections of the cerebral cortex. II. The macaque. E. The postcentral gyrus. J Comp Neurol 1954;101:101–165.
204. Krnjević K. Neurotransmitters in cerebral cortex. In: Jones EG, Peters A, eds. Cerebral cortex. Vol. 2. New York: Plenum Press, 1984: 39–61.
205. Kuffler SW. Discharge patterns and functional organization of mammalian retina. J Neurophysiol 1953;16:37–68.
206. Künzle H. Thalamic projections from the precentral motor cortex in *Macaca fascicularis*. Brain Res 1976; 105:253–267.
207. Künzle H. An autoradiographic analysis of the efferent connections from premotor and adjacent prefrontal regions (areas 6 and 9) in *Macaca fascicularis*. Brain Behav Evol 1978;15:185–234.
208. Künzle H, Akert K. Efferent connections of cortical Area 8 (frontal eye field) in *Macaca fascicularis*: a reinvestigation using the autoradiographic technique. J Comp Neurol 1977;173:147–164.
209. Künzle H, Akert K, Wurtz RH. Projections of area 8 (frontal eye field) to superior colliculus in the monkey: an autoradiographic study. Brain Res 1976;117:487–492.
210. Kuo J-S, Carpenter MB. Organization of pallidothalamic projections in the rhesus monkey. J Comp Neurol 1973;151:201–236.
211. Kupfermann I. Localization of higher cognitive and affective functions: the association cortices. In: Kandel ER, Schwartz JH, Jessell TM, eds. Principles of neural science. Ch. 53. New York: Elsevier, 1991:823–838.
212. Kuypers HGJM. Central cortical projections to motor and somatosensory cell groups. Brain 1960; 83:161–184.
213. Landis C, Zubi J, Mettler FA. The functions of the human frontal lobe. J Psychol 1950;30:123–138.
214. Lassek AM. The human pyramidal tract. II. A numerical investigation of the Betz cells of the motor area. Arch Neurol Psychiatry 1940;44: 718–724.
215. Lassek AM. The human pyramidal tract. IV. A study of the mature, myelinated fibers of the pyramid. J Comp Neurol 1942;76:217–225.
216. Lassek AM. The pyramidal tract. The effect of pre- and postcentral cortical lesions on the fiber components of the pyramids in monkey. J Nerv Ment Dis 1942;95:721–729.
217. Lassek AM. The pyramidal tract: its status in medicine. Springfield, IL: Charles C. Thomas, 1954.
218. Lassek AM, Evans JP. The human pyramidal tract. XII. The effect of hemispherectomies on the fiber components of the pyramids. J Comp Neurol 1945;83:113–119.
219. Lassek AM, Rasmussen GL. The human pyramidal tract: a fiber and numerical analysis. Arch Neurol Psychiatry 1939;42:872–876.
220. Lassek AM, Rasmussen GL. A comparative fiber and numerical analysis of the pyramidal tract. J Comp Neurol 1940;72:417–428.
221. Lawrence DG, Hopkins DA. The development of motor control in the rhesus monkey: evidence concerning the role of corticomotorneuronal connections. Brain 1976;99:235–254.
222. Lawrence DG, Kuypers HGJM. The functional organization of the motor system in the monkey. I. The effects of bilateral pyramidal lesions. Brain 1968;91:1–14.
223. Le Gros Clark WE. The structure and connections of the thalamus. Brain 1932;55:406–470.
224. Le Gros Clark WE. The connections of the frontal lobes of the brain. Lancet 1948;1:353–356.
225. Le Gros Clark WE, Boggon RH. The thalamic connections of the parietal and frontal lobes of the brain in the monkey. Phil Trans R Soc Lond (Biol) 1935;224:313–359.
226. Le Gros Clark WE, Powell TPS. On the thalamocortical connexions of the general sensory cortex of Macaca. Proc R Soc Lond (Biol) 1953;141:467–487.
227. LeVay S, Hubel D, Wiesel TN. The pattern of ocular dominance columns in Macaque visual cortex revealed by reduced silver stain. J Comp Neurol 1975;159:559–576.
228. LeVay S, Wiesel TN, Hubel DH. The development of ocular dominance columns in normal visually deprived monkeys. J Comp Neurol 1980;191:1–51.
229. Levin PM. The efferent fibers of the frontal lobe of the monkey (*Macaca mulatta*). J Comp Neurol 1936;63: 369–419.
230. Levin PM. Efferent fibers. In: Bucy PC, ed. The precentral motor cortex. 2d ed. Ch. 5. Urbana: University of Illinois Press, 1949:133–148.
231. Levin PM, Bradford FK. The exact origin of the corticospinal tract in the monkey. J Comp Neurol 1938; 68:411–422.
232. Lewis DA, Campbell MJ, Foote SL, Goldstein M, Morrison JH. The distribution of tyrosine hydroxylase-immunoreactive fibers in primate neocortex is widespread but regionally specific. J Neurosci 1987; 7:279–290.
233. Lewis DA, Campbell MJ, Foote SL, Morrison JH. The monoaminergic innervation of the primate neocortex. Human Neurobiol 1986;5: 181–186.
234. Lidov MS, Goldman-Rakic PS, Gallager DW, Geschwind DH, Rakic P. Distribution of major neurotransmitter receptors in the motor and somatosensory cortex of the rhesus monkey. Neuroscience 1989;32:609–627.
235. Liedgren SRC, Milne AC, Rubin AM, Schwarz DWF, Tomlinsen

RD. Representation of vestibular afferents in somatosensory thalamic nuclei of the squirrel monkey (*Saimiri sciureus*). J Neurophysiol 1976;39:601–612.
236. Lindsley DB. Attention, consciousness, sleep and wakefulness. In: Field J, ed. Handbook of physiology. Vol. III, Sect. 1. Washington, DC: American Physiological Society, 1960:1553–1593.
237. Lindvall O, Björklund A. General organization of cortical monoamine systems. In: Descarries L, Reader TR, Jasper HH, eds. Monoamine innervation of cerebral cortex. New York: Alan Liss, 1984:9–40.
238. Liu CN, Chambers WW. An experimental study of the corticospinal system in the monkey (*Macaca mulatta*): the spinal pathways and preterminal distribution of degenerating fibers following discrete lesions of the pre- and postcentral gyri and bulbar pyramid. J Comp Neurol 1964;123:257–284.
239. Lorente de Nó R. The structure of the cerebral cortex. In: Fulton JF, ed. Physiology of the nervous system. 3rd ed. New York: Oxford University Press, 1949:288–330.
240. Lund JS, Lund RD, Hendrickson AE, Bunt AH, Fuchs AF. The origin of efferent pathways from the primary visual cortex, area 17, of the macaque monkey as shown by retrograde transport of horseradish peroxidase. J Comp Neurol 1975; 164:287–303.
241. McCormick DA. Neurotransmitter actions in the thalamus and cerebral cortex and their role in neuromodulation of thalamocortical activity. Prog Neurobiol 1992;39: 337–388.
242. Mamounas LA, Mullen CA, O'-Hearn E, Molliver ME. Dual serotoninergic projections to forebrain in the rat: morphologically distinct 5-HT axon terminals exhibit differential vulnerability to neurotoxic amphetamine derivatives. J Comp Neurol 1991;314:558–586.
243. Martinez-Millan L, Holländer H. Cortico-cortical projections from striate cortex of the squirrel monkey (*Saimiri sciureus*): a radioautographic study. Brain Res 1975;3: 405–417.
244. Mash DC, White WF, Mesulam M-M. Distribution of muscarinic receptor subtypes within architectonic subregions of the primate cerebral cortex. J Comp Neurol 1988;278:265–274.
245. Masterton RB, Imig TJ. Neural mechanisms for sound localization. Annu Rev Physiol 1984;46: 275–287.
246. Mayeux R, Kandel ER. Disorders of language: the aphasia. In: Kandel ER, Schwartz JH, Jessell TM, eds. Principles of neural science. Ch. 54. New York: Elsevier, 1991: 839–851.
247. Mehler WR, Feferman ME, Nauta WJH. Ascending axon degeneration following anterolateral cordotomy: an experimental study in the monkey. Brain 1960;83:718–750.
248. Merzenich MM, Brugge JF. Representation of the cochlear partition on the superior temporal plane of the Macaque monkey. Brain Res 1973;50:275–296.
249. Merzenich MM, Kaas JH, Sur M, Lin CS. Double representation of the body surface within cytoarchitectonic Areas 3b and 1 in "S1" in the owl monkey (*Aotus trivigatus*). J Comp Neurol 1978;181:41–74.
250. Merzenich MM, Knight PL, Roth GL. Cochleotopic organization of primary auditory cortex in the cat. Brain Res 1973;63:343–346.
251. Merzenich MM, Knight PL, Roth GL. Representation of cochlea within the primary auditory cortex in the cat. J Neurophysiol 1975; 38:231–249.
252. Mesulam M-M, Geula C. Nucleus basalis (Ch4) and cortical cholinergic innervation in the human brain: observations based on the distribution of acetylcholinesterase and choline acetyltransferase. J Comp Neurol 1988;275:216–240.
253. Mesulam M-M, Geula C. Overlap between acetylcholinesterase-rich and choline acetyltransferase-positive (cholinergic) axons in human cerebral cortex. Brain Res 1992; 577:112–120.
254. Mesulam M-M, Mufson EJ, Levey AI, Wainer BH. Cholinergic innervation of the cortex by the basal forebrain: cytochemistry and cortical connections of the septal area, diagonal band nuclei, nucleus basalis (substantia innominata), and hypothalamus in the rhesus monkey. J Comp Neurol 1983; 214:170–197.
255. Mettler FA. Connections of the auditory cortex of the cat. J Comp Neurol 1932;55:139–183.
256. Mettler FA. On the origin of the fibers in the pyramid of the primate brain. Proc Soc Exp Biol Med 1944;57:111–113.
257. Mettler FA. The non-pyramidal motor projections from the frontal cerebral cortex. Proc Assoc Res Nerv Ment Dis 1947;267:162–199.
258. Mettler FA. Extracortical connections of the primate frontal cerebral cortex. II. Corticofugal connections. J Comp Neurol 1947;86: 119–154.
259. Mettler FA. Selective partial ablation of the frontal cortex: a correlative study of the effects on human psychotic subjects. New York: Paul B. Hoeber, 1949.
260. Meyers RE. Function of corpus callosum in interocular transfer. Brain 1956;79:358–363.
261. Molliver ME, Grzanna R, Lidow HGW, Morrison JH, Olschowka JA. Monoamine systems in the cerebral cortex. In: Chan-Palay J, Palay SL, eds. Cytochemical methods in neuroanatomy. New York: Alan Liss, 1983:255–277.
262. Moniz E. Tentative opératoire dans le traitement de certaines psychoses. Paris: Masson, 1936.
263. Morest DK. The neuronal architecture of the medial geniculate body of the cat. J Anat 1964;98:611–638.
264. Morrison JH, Hof PR. The organization of the cerebral cortex: from molecules to circuits. In: Magistretti PJ, ed. Discussions in neuroscience. Vol. 9. Amsterdam: Elsevier, 1992:11–79.
265. Morruzi G, Magoun HW. Brain stem reticular formation and activation of the EEG. Electroencephalogr Clin Neurophysiol 1949; 1:455–473.
266. Mountcastle VB. Modality and topographic properties of single neurons of cat's somatic sensory cortex. J Neurophysiol 1957;20: 408–434.
267. Mountcastle VB. Interhemispheric relations and cerebral dominance. Baltimore: Johns Hopkins University Press, 1974.
268. Mountcastle VB. Central nervous mechanisms in mecanoreceptive sensibility. In: Darian-Smith I, ed. Handbook of physiology. Vol. III: Sensory processes. Part 2, Sect. I: The nervous system. Bethesda, MD: American Physiological Society, 1984;789–878.
269. Mountcastle VB, Lynch JC, Georgopoulos A, Sakata H, Acuna C. Posterior parietal association cortex of the monkey: command functions for operation within extrapersonal space. J Neurophysiol 1975;38:871–908.
270. Mountcastle VB, Powell TPS. Central nervous mechanisms subserving position sense and kinesthesis. Bull Johns Hopkins Hosp 1959; 105:173–200.
271. Mountcastle VB, Powell TPS. Neural mechanisms subserving cutaneous sensibility with special reference to the role of afferent inhibition in sensory perception and discrimination. Bull Johns Hopkins Hosp 1959;105:201–232.
272. Nauta WJH, Mehler WR. Projections of the lentiform nucleus in the monkey. Brain Res 1966;1:3–42.
273. Neff WD, Diamond IT. The neural basis of auditory discrimination. In: Harlow HF, Woolsey CN, eds. Biological and biochemical bases of behavior. Madison: University of Wisconsin Press, 1958:101–126.
274. Niimi K, Katayama K, Kanaseki T, Morimoto K. Studies on the derivation of the centre median nucleus of Luys. Tokushima J Exp Med 1960;6:261–268.
275. Niimi K, Matsuoka H. Thalamocortical organization of the auditory system in the cat studied by retrograde axonal transport of horseradish peroxidase. Adv Anat Embryol Cell Biol 1979;57:1–56.
276. Noback CR, Demarest RJ. The human nervous system. 3rd ed. New York: McGraw-Hill, 1981.
277. Norgren R. Gustatory afferents to ventral forebrain. Brain Res 1974; 81:285–295.

278. Norgren R, Leonard CM. Ascending central gustatory pathways. J Comp Neurol 1973;150:217–238.
279. Norgren JR, Pfaffman C. The pontine taste area in the rat. Brain Res 1975;91:99–117.
280. Norgren R, Wolf G. Projection of thalamic gustatory and lingual areas in the rat. Brain Res 1975; 92:123–129.
281. Nyby O, Jansen J. An experimental investigation of the corticopontine projection in *Macaca mulatta*. Norsk Vidensk Akad Avh Mat-Naturv 1951;3:1–47.
282. Ohuoha DC, Hyde TM, Kleinman JE. The role of serotonin in schizophrenia: an overview of the nomenclature, distribution and alteration of serotonin receptors in the central nervous system. Psychopharmacology 1993;112:5–15.
283. Oliver DL, Hall WC. The medial geniculate body of the tree shrew, *Tupaia glis*. II. Connections with the neocortex. J Comp Neurol 1978; 182:459–494.
284. Oscarsson O. Functional organization of the spino- and cuneocerebellar tracts. Physiol Rev 1965; 45:495–522.
285. Oscarsson O. Functional organization of spinocerebellar paths. In: Iggo A, ed. Handbook of sensory physiology. Vol. 2. Berlin: Springer-Verlag, 1973:339–380.
286. Oscarsson O, Rosén I. Short-latency projections to the cat's cerebral cortex from skin and muscle afferents in the contralateral forelimb. J Physiol (Lond) 1966;182: 164–184.
287. Otsuka R, Hassler R. Über Aufbau und Gliederung der corticalen Sehsphäre bei der Katze. Arch Psychiatr Nervenk 1962;203:212–234.
288. Ottersen OP, Storm-Mathisen J. Glutamate- and GABA-containing neurons in the mouse and rat brain as demonstrated with a new immunocytochemical technique. J Comp Neurol 1984;229:374–392.
289. Pandya DN, Vignolo LA. Intra- and interhemispheric projections of the precentral, premotor and arcuate areas in the rhesus monkey. Brain Res 1971;26:217–233.
290. Pandya DN, Seltzer B. The topography of commissural fibers. Neurol Neurobiol 1986;17:47–73.
291. Papez JW. Evolution of the medial geniculate body. J Comp Neurol 1936;64:41–61.
292. Parent A, Csonka C, Etienne P. The occurrence of large acetylcholinesterase-containing neurons in human neostriatum as disclosed in normal and Alzheimer-diseased brains. Brain Res 1984;291:154–158.
293. Parnavelas JG, McDonald JK. The cerebral cortex. In: Emson PC, ed. Chemical neuroanatomy. New York: Raven Press, 1983:505–549.
294. Partridge M. Prefrontal leucotomy: a survey of 300 cases personally followed over 11/2–3 years. Oxford: Blackwell Scientific Publications, 1950.
295. Patton HD, Ruch TC, Walker AE. Experimental hypogeusia from Horsley-Clarke lesions of the thalamus in *Macaca mulatta*. J Neurophysiol 1944;7:171–184.
296. Penfield W. Vestibular sensation and the cerebral cortex. Ann Otol Rhinol 1957;66:691–698.
297. Penfield W, Boldrey E. Somatic motor and sensory representation in the cerebral cortex of man as studied by electrical stimulation. Brain 1937;60:389–443.
298. Penfield W, Jasper HH. Epilepsy and the functional anatomy of the human brain. Boston: Little Brown & Company, 1954.
299. Penfield W, Rasmussen T. The cerebral cortex of man: a clinical study of localization of function. New York: MacMillan, 1950.
300. Penfield W, Roberts L. Speech and brain mechanisms. Princeton, NJ: Princeton University Press, 1959.
301. Penfield W, Welch K. The supplementary motor area of the cerebral cortex: a clinical and experimental study. AMA Arch Neurol Psychiatry 1951;66:289–317.
302. Percheron G. The thalamic territory of cerebellar afferents and the lateral region of the thalamus of the macaque in stereotaxic ventricular coordinates. J Hirnforsch 1977;18:375–400.
303. Perry EK, Tomlinson BE, Blessed G, Bergmann K, Gibson PH, Perry RH. Correlation of cholinergic abnormalities with senile plaques and mental test scores in senile dementia. Br Med J 1977;2:1457–1459.
304. Petras JM. Some efferent connections of the motor and somatosensory cortex of simian primates and felid, canid and procyonid carnivores. Ann NY Acad Sci 1969; 167:469–505.
305. Poggio GF, Mountcastle VB. A study of the functional contributions of the lemniscal and spinothalamic systems to somatic sensibility. Bull Johns Hopkins Hosp 1960;106:266–316.
306. Pons TP, Garraghty PE, Cusik CG, Kaas JH. The somatotopic organization of area 2 in macaque monkeys. J Comp Neurol 1985; 241:445–466.
307. Powell TPS, Cowan WM. The interpretation of the degenerative changes in the intralaminar nuclei of the thalamus. J Neurol Neurosurg Psychiatry 1967;30:140–153.
308. Powell TPS, Mountcastle VB. The cytoarchitecture of the postcentral gyrus of the monkey *Macaca mulatta*. Bull Johns Hopkins Hosp 1959;105:18–131.
309. Powell TPS, Mountcastle VB. Some aspects of the functional organization of the cortex of the postcentral gyrus of the monkey: a correlation of findings obtained in a single unit analysis with cytoarchitecture. Bull Johns Hopkins Hosp 1959; 105:133–162.
310. Purpura DP, Grundfest H. Nature of dendritic potentials and synaptic mechanisms in cerebral cortex of cat. Neurophysiol 1956;19: 573–595.
311. Raczkowski D, Diamond IT, Winer J Jr. Organization of thalamocortical auditory system in the cat studied with horseradish peroxidase. Brain Res 1976;101:345–354.
312. Ramón y Cajal S. Histologie du Système Nerveux de l'Homme et des Vertébrés. (Azoulay L, trans.) Paris: Maloine, 1909, 1911. (Reprinted Consejo Superior de Investigaciones Cientificas, Instituto Ramón y Cajal, Madrid, 1972.)
313. Rezak M, Benevento LA. A comparison of the organization of the projections of the dorsal lateral geniculate nucleus, the inferior pulvinar and adjacent lateral pulvinar to primary visual cortex (area 17) in the macaque monkey. Brain Res 1979;167:19–40.
314. Ricardo JA, Koh ET. Anatomical evidence of direct projections from the nucleus of the solitary tract to the hypothalamus, amygdala and other forebrain structures in the rat. Brain Res 1978;153:1–26.
315. Riley HA. An atlas of the basal ganglia, brain stem and spinal cord. Baltimore: Williams & Wilkins, 1943.
316. Rinvik E. The corticothalamic projection from the pericruciate and coronal gyri in the cat: an experimental study with silver-impregnation methods. Brain Res 1968; 10:79–119.
317. Rispal-Padel L, Massion J, Grangetto A. Relations between the ventrolateral thalamic nucleus and motor cortex and their possible role in the central organization of motor control. Brain Res 1973; 60:1–20.
318. Roberts TS, Akert K. Insular and opercular cortex and its thalamic projection in *Macaca mulatta*. Schweiz Arch Neurol Neurochir Psychiatr 1963;92:1–43.
319. Robinson CJ, Burton H. Somatotopographic organization in the second somatosensory area of *M. fascicularis*. J Comp Neurol 1980; 192:43–67.
320. Robinson CJ, Burton H. The organization of somatosensory receptive fields in cortical area 7b, retroinsular, postauditory and granular insular of *M. fascicularis*. J Comp Neurol 1980;192:69–92.
321. Robinson CJ, Burton H. Somatic submodality distribution within the second somatosensory (SII), 7b, retroinsular, postauditory and granular insular cortical areas of *M. fascicularis*. J Comp Neurol 1980;192:93–108.
322. Rockel AJ, Jones EG. The neuronal organization of the inferior colliculus of the adult cat. II. The pericentral nucleus. J Comp Neurol 1973; 149:301–334.
323. Roland PE. Brain activation. New York: Wiley-Liss, 1993.
324. Rose JE, Woolsey CN. Cortical connections and functional organiza-

tion of the thalamic auditory system of the cat. In: Harlow HF, Woolsey CN, eds. Biological and biochemical bases of behavior. Madison: University of Wisconsin Press, 1958:127–150.
325. Rose M. Cytoarchitektonik und myeloarchitektonik der Grosshirnrinde. In: Bumke O, Foerster O, eds. Handbuch der Neurologie. Vol. 1. Berlin: Springer-Verlag, 1935:588–778.
326. Rosén I, Asanuma H. Peripheral afferents inputs to the forelimb area of the monkey motor cortex: input-output relations. Exp Brain Res 1972;14:257–273.
327. Rosenzweig MR. Cortical correlates of auditory localization and of related perceptual phenomena. J Comp Physiol Psychol 1954;47: 269–276.
328. Rossi GF, Brodal A. Corticofugal fibers to the brain stem reticular formation: an experimental study in the cat. J Anat 1956;90:42–62.
329. Russell JR, Demyer W. The quantitative cortical origin of pyramidal axons of *Macaca rhesus*. Neurology 1961;11:96–108.
330. Rylander G. Personality analysis before and after frontal lobotomy. Proc Assoc Nerv Ment Dis 1948; 27:691–705.
331. Scarff JE. Primary cortical centers for movement of upper and lower limbs in man. Arch Neurol Psychiatry 1940;44:243–299.
332. Scarff JE. Unilateral prefrontal lobotomy for relief of intractable pain and termination of narcotic addiction. Surg Gynecol Obstet 1949;89:385–392.
333. Scheibel ME, Scheibel AB. The organization of the nucleus reticularis thalami: a Golgi study. Brain Res 1966;1:43–62.
334. Schwarz DWF, Fredrickson JM. Rhesus monkey vestibular cortex: a binodal primary projection field. Science 1971;171:280–281.
335. Scollo-Lavizzari JG, Akert K. Cortical area 8 and its thalamic projection in *Macaca mulatta*. J Comp Neurol 1963;121:259–267.
336. Shinoda Y, Zarzecki P, Asanuma H. Spinal branching of pyramidal tract neurons in the monkey. Exp Brain Res 1979;34:59–72.
337. Sholl DA. The organization of the cerebral cortex. New York: John Wiley & Sons, 1956.
338. Sidman RL. Cell proliferation, migration and interaction in the developing mammalian central nervous system. In: Schmitt FO, ed. The neurosciences. Second study program. New York: Rockefeller University Press, 1970:100–116.
339. Sillito AM. Functional consideration of the operation of GABAergic inhibitory processes in the visual cortex. In: Jones EG, Peters A, eds. Cerebral cortex. Vol. 2. New York: Plenum Press, 1984:91–117.
340. Sokoloff P, Giros B, Martres M-P, Bouthenet M-L, Schwartz J-C. Molecular cloning and characterization of a novel dopamine receptor (D_3) as a targets for neuroleptics. Nature 1990;347:146–151.
341. Sperry RW. Cerebral organization and behavior. Science 1961;133: 1749–1757.
342. Sperry RW. Some general aspects of interhemispheric integration. In: Mountcastle VB, ed. Interhemispheric relations and cerebral dominance. Ch. 3. Baltimore: Johns Hopkins University Press, 1962: 43–49.
343. Sperry RW. Lateral specialization in the surgically separated hemispheres. In: Schmitt FO, Worden FG, eds. The neurosciences, third study program. Cambridge, MA: MIT Press, 1974:5–19.
344. Steriade M, Biesold D. Brain cholinergic systems. New York: Oxford University Press, 1990.
345. Steriade M, McCarley RW. Brainstem control of wakefulness and sleep. New York: Plenum Press, 1990.
346. Streit P. Glutamate and aspartate as transmitter candidates for systems of the cerebral cortex. In: Jones EG, Peters A, eds. Cerebral cortex. Vol. 2. New York: Plenum Press, 1984;119–143.
347. Strick PL. Anatomical analysis of ventrolateral thalamic input to primate motor cortex. J Neurophysiol 1976;39:1020–1031.
348. Strick PL. Activity of ventrolateral thalamic neurons during arm movement. J Neurophysiol 1976; 39:1032–1044.
349. Strick PL, Kim CC. Input to primate motor cortex from posterior parietal cortex (area 5). I. Demonstration by retrograde transport. Brain Res 1978;157:325–330.
350. Strick PL, Preston JB. Multiple representation in the primate motor cortex. Brain Res 1978;154:366–370.
351. Strick PL, Sterling P. Synaptic terminations of afferents from the ventrolateral nucleus of the thalamus in the cat motor cortex: a light and electron microscope study. J Comp Neurol 1974;153:77–106.
352. Sugar O, Amador LV, Griponissiotes B. Corticocortical connections of the walls of the superior temporal sulcus in the monkey (*Macaca mulatta*). J Neuropathol Exp Neurol 1950;9:179–185.
353. Sugar O, French JD, Chusid JG. Corticocortical connections of the superior surface of the temporal operculum in the monkey (*Macaca mulatta*). J Neurophysiol 1948;11: 175–184.
354. Sur M, Nelson RJ, Kaas JH. Representations of the body surface in cortical areas 3b and 1 of squirrel monkeys: comparisons with other primates. J Comp Neurol 1982; 211:177–192.
355. Szentagothai J. The neuron network of the cerebral cortex: a functional interpretation. Proc R Soc Lond (Biol) 1978;201:219–248.
356. Talbot SA, Marshall WH. Physiological studies on neuronal mechanisms of visual localization and discrimination. Am J Ophthalmol 1941;24:1255–1263.
357. Tanji J, Wise SP. Submodality distribution in sensorimotor cortex of the unanesthetized monkey. J Neurophysiol 1981;45:467–481.
358. Thach WT, Jones EG. The cerebellar dentatothalamic connection: terminal field, lamellae, rods and somatotopy. Brain Res 1979;169: 168–172.
359. Thompson JM, Woolsey CN, Talbot SA. Visual areas I and II of cerebral cortex of rabbit. J Neurophysiol 1950;13:277–288.
360. Tower SS. Pyramidal lesion in the monkey. Brain 1940;63:36–90.
361. Tower SS. The pyramidal tract. In: Bucy PC, ed. The precentral motor cortex. 2d ed. Ch. 6. Urbana: University of Illinois Press, 1949: 149–172.
362. Tracey DJ, Asanuma C, Jones EG, Porter R. Thalamic relay to motor cortex: afferent pathways from brain stem, cerebellum, and spinal cord in monkeys. J Neurophysiol 1980;44:532–555.
363. Travis AM. Neurological deficiencies after ablation of the precentral motor area in *Macaca mulatta*. Brain 1955;78:155–173.
364. Travis AM. Neurological deficiencies following supplementary motor area lesions in *Macaca mulatta*. Brain 1955;78:174–198.
365. Tusa RJ, Rosenquist AC, Palmer LA. Retinotopic organization of areas 18 and 19 in the cat. J Comp Neurol 1979;185:657–678.
366. Van Tol HHM, Bunzow JR, Guan H-C, et al. Cloning of the gene for a human dopamine D_4 receptor with high affinity for the antipsychotic clozapine. Nature 1991;350: 610–614.
367. Verhaart WJC, Kennard MA. Corticofugal degeneration following thermocoagulation of areas 4, 6, and 4S in *Macaca mulatta*. J Anat 1940;74:239–254.
368. von Economo CF. The cytoarchitectonics of the human cerebral cortex. London: Oxford Medical Publications, 1929.
369. von Economo C, Horn L. Über Windungsrelief, Masse und Rindenarchitektonik der Supratemporalfläche, ihre individuellen und ihre Seitenunterschiede. Z Gesamte Neurol Psychiatry 1930; 130:678–757.
370. Vogt BA, Pandya DN. Cortico-cortical connections of somatic sensory cortex (areas 3, 1, and 2) in the rhesus monkey. J Comp Neurol 1978;177:170–192.
371. Vogt C, Vogt O. Allgemeine Ergebnisse unserer Hirnforschung. Vierte Mitteilung: Die physiologische Bedeutung der architektonischen Rindenreizungen. J Psychol Neurol 1919;25:279–462.
372. Walker AE. The primate thalamus. Chicago: University of Chicago Press, 1938.
373. Walker AE, Fulton JF. Hemidecor-

tication in chimpanzee, baboon, macaque, potto, cat and coati: a study in encephalization. J Nerv Ment Dis 1938;87:677–700.
374. Walker AE, Weaver TA Jr. Ocular movements from the occipital lobe in the monkey. J Neurophysiol 1940;3:353–357.
375. Walther JB, Rasmussen GL. Descending connections of auditory cortex and thalamus of the cat. Fed Proc 1960;19:291.
376. Weinberger DR. Implications of normal brain development for the pathogenesis of schizophrenia. Arch Gen Psychiat 1987;44: 660–669.
377. Weinrich M, Wise SP. The premotor cortex in the monkey. J Neurosci 1982;2:1329–1345.
378. Werner GW, Whitsel BL. The topology of the body representation in somatosensory area I of primates. J Neurophysiol 1968;31: 856–869.
379. Werner GW, Whitsel BL. Functional organization of the somatosensory cortex. In: Iggo A, ed. Handbook of sensory physiology. Vol. 2. Berlin: Springer-Verlag, 1973:621–700.
380. Wernicke C. The symptom-complex of aphasia. In: Chuich A, ed. Diseases of the nervous system. New York: Appleton, 1908: 265–324.
381. White EL. Cortical circuits. Synaptic organization in the cerebral cortex: structure, function, and theory. Boston: Birkhaäser, 1989.
382. Whitehouse PJ, Price DL, Clark AW, Coyle JT, DeLong MR. Alzheimer's disease: evidence for selective loss of cholinergic neurons in the nucleus basalis. Ann Neurol 1981;10:122–126.
383. Whitlock DG, Perl ER. Thalamic projections of spinothalamic pathways in monkey. Exp Neurol 1961;3:240–255.
384. Whitsel BL, Petrucelli LM, Werner G. Symmetry and connectivity in the map of the body surface in somatosensory area II of primates. J Neurophysiol 1969;32:170–183.
385. Wiesel TN, Hubel DH. Effects of visual deprivation on morphology and physiology of cells in the cat's lateral geniculate body. J Neurophysiol 1963;26:978–993.
386. Wiesel TN, Hubel DH. Ordered arrangement of orientation columns in monkeys lacking visual experience. J Comp Neurol 1974; 158:307–318.
387. Wiesel TN, Hubel DH, Lam DMK. Autoradiographic demonstration of ocular-dominance columns in the monkeys striate cortex by means of transneuronal transport. Brain Res 1974;79:273–279.
388. Wiesendanger M. Input from muscle and cutaneous nerves of the hand and forearm to neurones of the precentral gyrus of baboons and monkeys. J Physiol (Lond) 1973;228:203–219.
389. Wiesendanger M. Recent developments in studies of the supplementary motor area of primates. Rev Physiol Biochem Pharmacol 1986; 103:1–57.
390. Wiesendanger M, Hummelsheim H, Bianchetti M, et al. Input and output organization of the supplementary motor area. In: Motor areas of the cerebral cortex. CIBA Foundation symposium. Chichester: John Wiley & Sons, 1987: 132:40–62.
391. Wiesendanger M, Séguin JJ, Künzle H. The supplementary motor area: a control system for posture. Adv Behav Biol 1974;7:331–346.
392. Wilson ME, Toyne MJ. Retino-tectal and cortico-tectal projections in *Macaca mulatta*. Brain Res 1970; 243:395–406.
393. Winer JA, Diamond IT, Raczkowski D. Subdivisions of the auditory cortex in the cat: the retrograde transport of horseradish peroxidase to the medial geniculate body and posterior thalamic nuclei. J Comp Neurol 1977;176: 387–418.
394. Wise SP, Strick PL. Anatomical and physiological organization of the nonprimary motor cortex. Trends Neurosci 1984;7:442–446.
395. Wise SP, Tanji J. Supplementary and precentral motor cortex: contrast in responsiveness to peripheral input in the hindlimb area of the unanesthetized monkey. J Comp Neurol 1981;195:433–451.
396. Witelson SF. The brain connection: the corpus callosum is larger in left handers. Science 1985;229:665–668.
397. Witelson SF. Hand and sex difference in the isthmus and genu of the human corpus callosum: a postmortem morphological study. Brain 1989;112:799–835.
398. Witelson SF, Goldsmith CH. The relationship of hand preference to anatomy of the corpus callosum in men. Brain Res 1991;545:175–182.
399. Witelson SF, Pollie W. Left hemisphere specialization for language in the newborn: neuroanatomical evidence of asymmetry. Brain 1973;96:541–646.
400. Wong-Riley MTT. Changes in the dorsal lateral geniculate nucleus of the squirrel monkey after unilateral ablation of the visual cortex. J Comp Neurol 1972;146:519–548.
401. Wong-Riley MTT. Demonstration of geniculocortical and callosal projection neurons in the squirrel monkey by means of retrograde axonal transport of horseradish peroxidase. Brain Res 1974;79: 267–272.
402. Wong-Riley MTT. Columnar cortico-cortical interconnections within the visual system of the squirrel and macaque monkeys. Brain Res 1979;162:201–217.
403. Woolsey CN. Patterns of sensory representation in the cerebral cortex. Fed Proc 1947;6:437–441.
404. Woolsey CN. Organization of somatic sensory and motor areas of the cerebral cortex. In: Harlow HF, Woolsey CN, eds. Biological and biochemical bases of behavior. Madison: University of Wisconsin, 1958:63–81.
405. Woolsey CN. Organization of cortical auditory system: a review and synthesis. In: Rasmussen GL, Windle WF, eds. Neural mechanisms of the auditory and vestibular systems. Springfield, IL: Charles C. Thomas, 1960:165–180.
406. Woolsey CN. Cortical motor map of *Macaca mulatta* after chronic section of the medullary pyramid. In: Zulch KJ, Creutzfeldt O, Galbraith GC, eds. Cerebral localization. Berlin: Springer-Verlag, 1975: 19–31.
407. Woolsey CN, Fairman D. Contralateral, ipsilateral and bilateral representation of cutaneous receptors in somatic areas I and II of the cerebral cortex of pigs, sheep and other mammals. Surgery 1946;19: 684–702.
408. Woolsey CN, Settlage PH, Meyer DR, Sencer W, Hamuy TP, Travis AM. Patterns of localization in precentral and "supplementary" motor areas and their relation to the concept of a premotor area. Proc Assoc Nerv Ment Dis 1951; 30:238–264.
409. Woolsey CN, Walzl EM. Topical projection of nerve fibers from local regions of the cochlea to the cerebral cortex of the cat. Bull Johns Hopkins Hosp 1942;71: 315–344.
410. Woolsey CN, Walzl EM. Cortical auditory area of *Macaca mulatta* and its relation to the second somatic sensory area (SMII): determination by electrical excitation of auditory nerve fibers in the spiral osseous lamina and by click stimulation. In: Woolsey CN, ed. Cortical sensory organization. Vol. 3. Clifton, NJ: Humana Press, 1982: 231–256.
411. Zangwill OL. Cerebral dominance and its relation to psychological function. Springfield, IL: Charles C. Thomas, 1969.
412. Zarzecki P, Strick PL, Asanuma H. Input to primate motor cortex from posterior parietal cortex (area 5). II. Identification by antidromic activation. Brain Res 1978;157:331–335.
413. Zeki SM. Interhemispheric connections of prestriate cortex in monkeys. Brain Res 1971;19:63–75.
414. Zilles. Cortex. In: Paxinos G, ed. The human nervous system. Ch. 22. New York: Academic Press, 1990:757–802.

Atlas of Brain and Brain Stem

Section I

Transverse sections of Brain Stem (A-1 to A-13).

Section II

Frontal sections cut transverse to the longitudinal axis of the diencephalon (A-14 to A-18).

Section III

Frontal sections of diencephalon and basal ganglia (A-19 to A-24).

Section IV

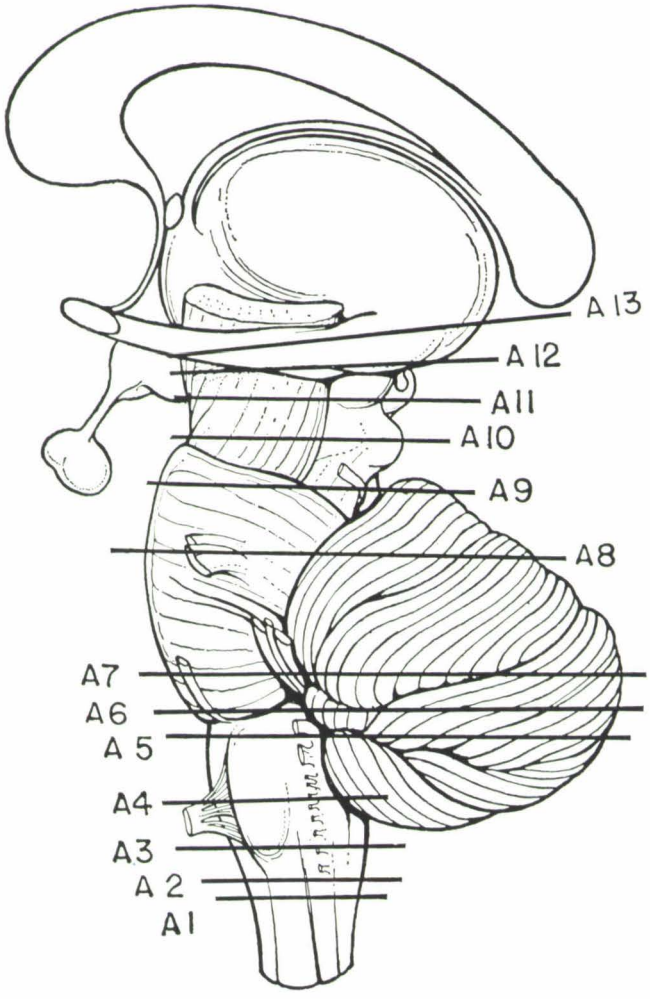
Sagittal sections of brain and brain stem (A-25 to A-32).

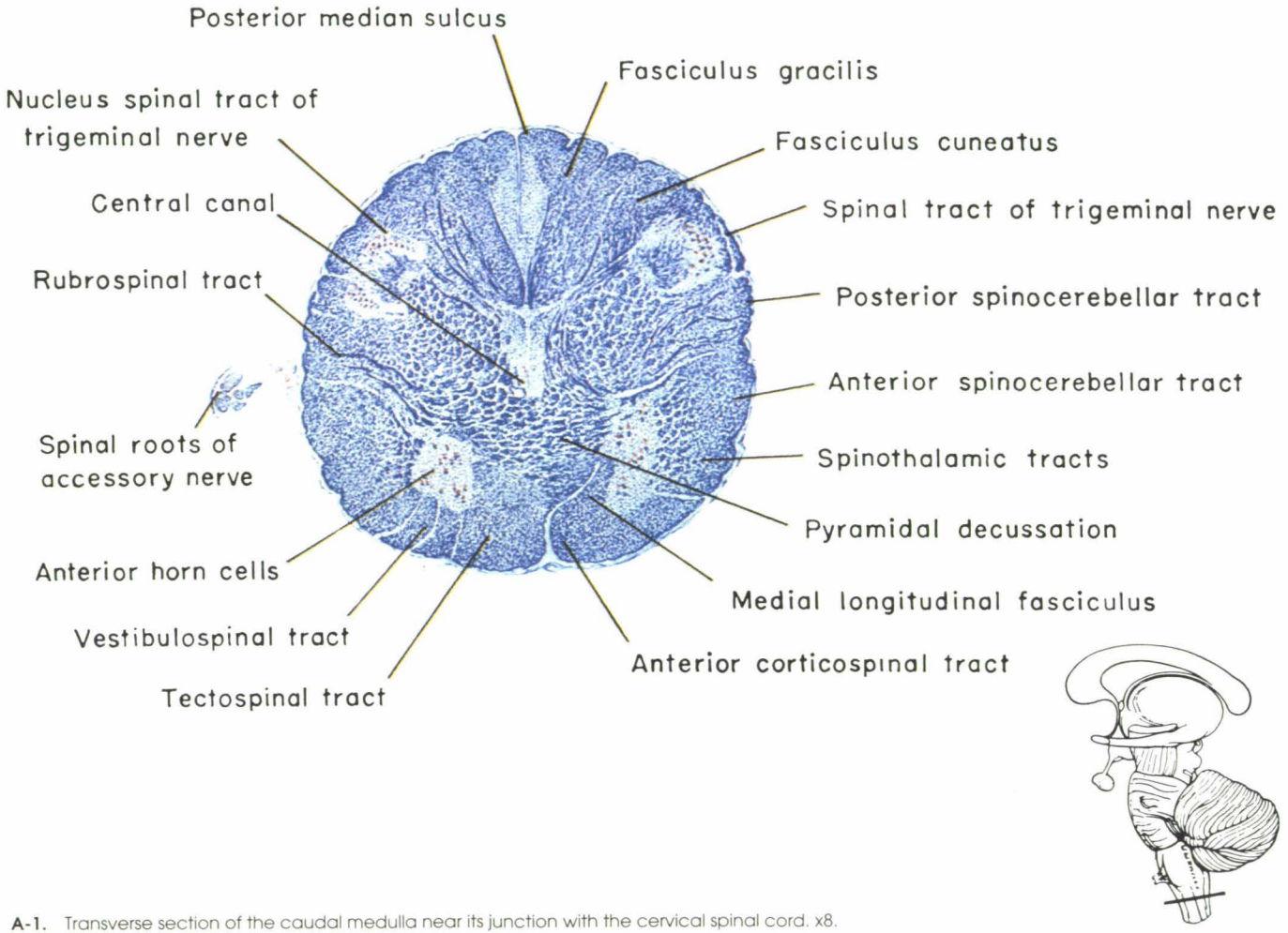
The following series of drawings of transverse sections of the brain stem taken at critical levels are reproduced in colors that faithfully reveal the definition of fiber tracts and cellular groupings characteristic of the original preparations. These sections, stained with luxol fast blue and counterstained with cresyl violet (1334), appear particularly appropriate for laboratory instruction since the student is presented with a complete picture of cellular configurations in relationship with the myelinated fiber tracts in a single microscopic slide. The outline drawing of the brain stem indicates the levels and planes of section of the individual figures and should be used as a key. The magnification of the figures is noted in the legends.

Illustrations used in Sections I, II and III were prepared by Miss Marjorie Stodgell, Medical Artist, of the Hahnemann Medical College and Hospital of Philadelphia. Photographs used in Section IV were made from original Weigert preparations of the late Professor Andrew T. Rasmussen of the University of Minnesota.

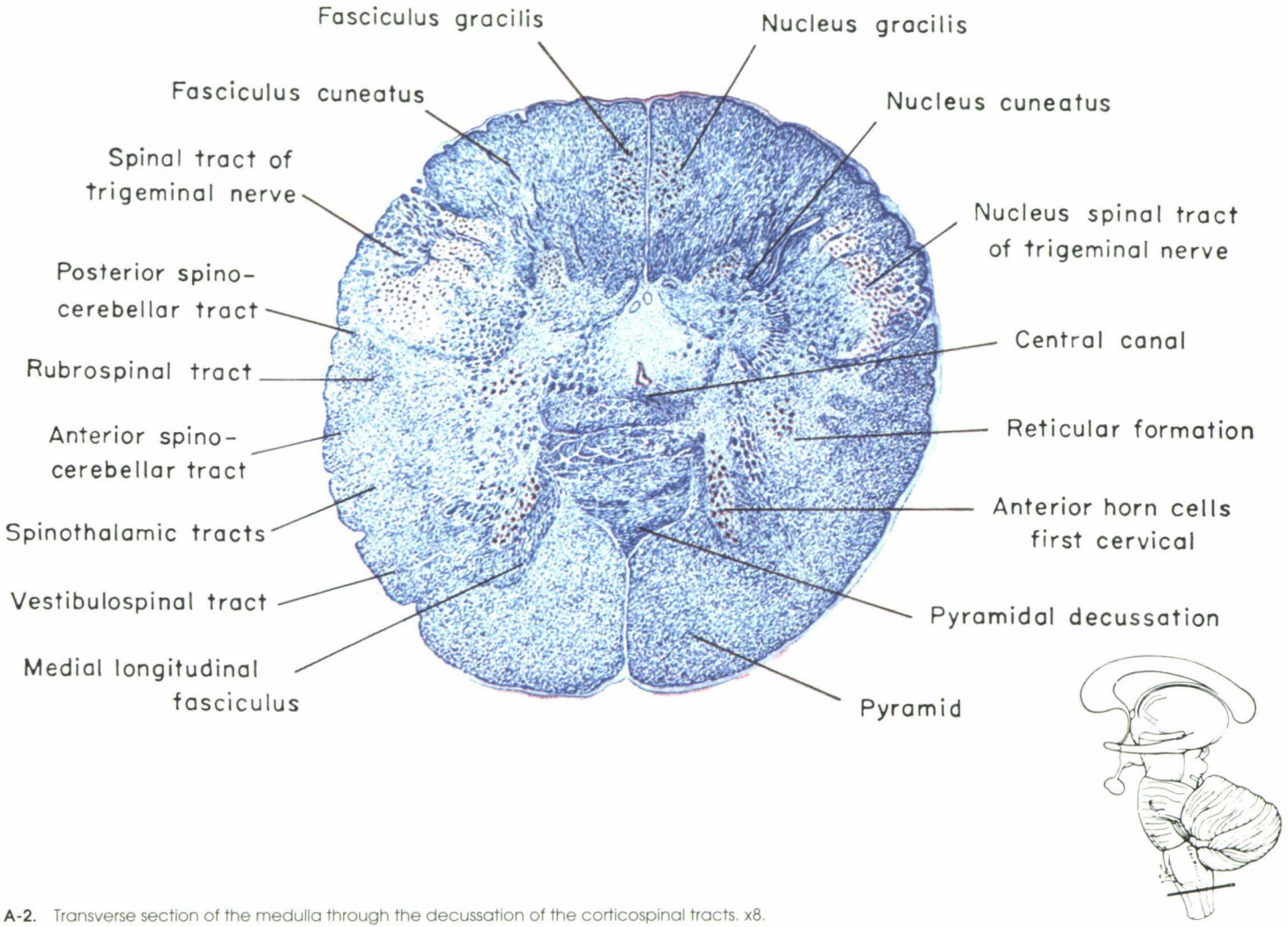
Brain Stem Atlas

Drawing of the brain stem indicating the level and plane of sections A-1 through A-13.

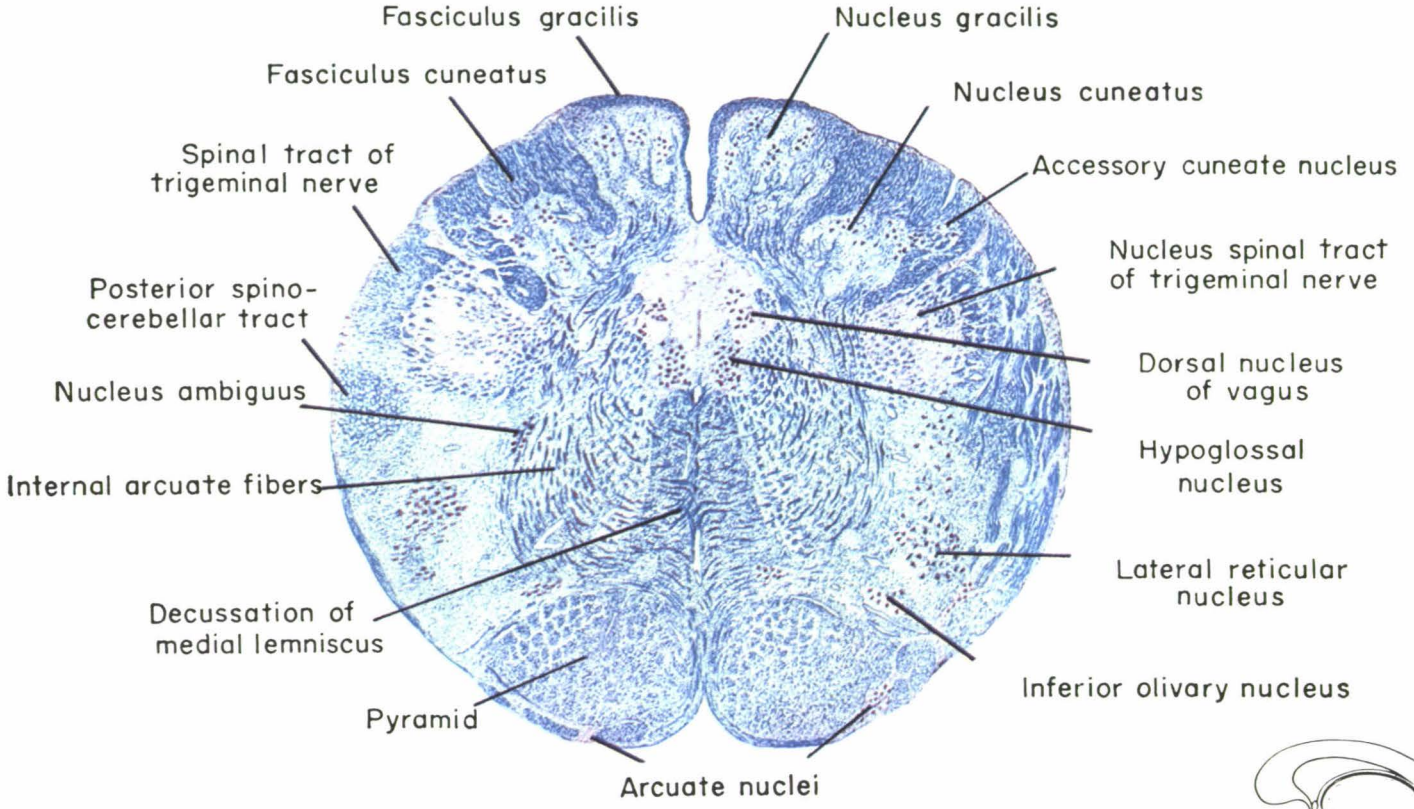




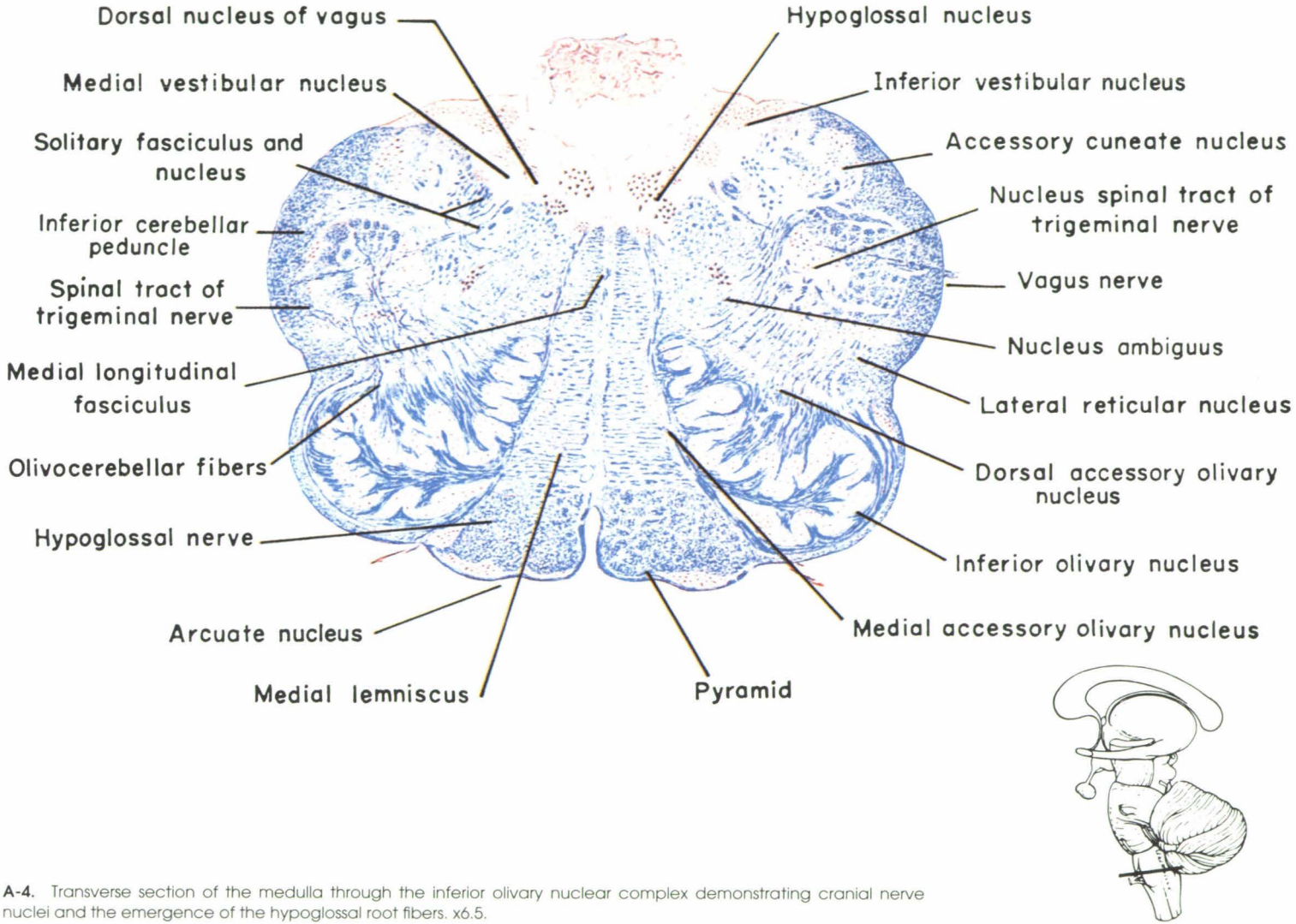
A-1. Transverse section of the caudal medulla near its junction with the cervical spinal cord. x8.



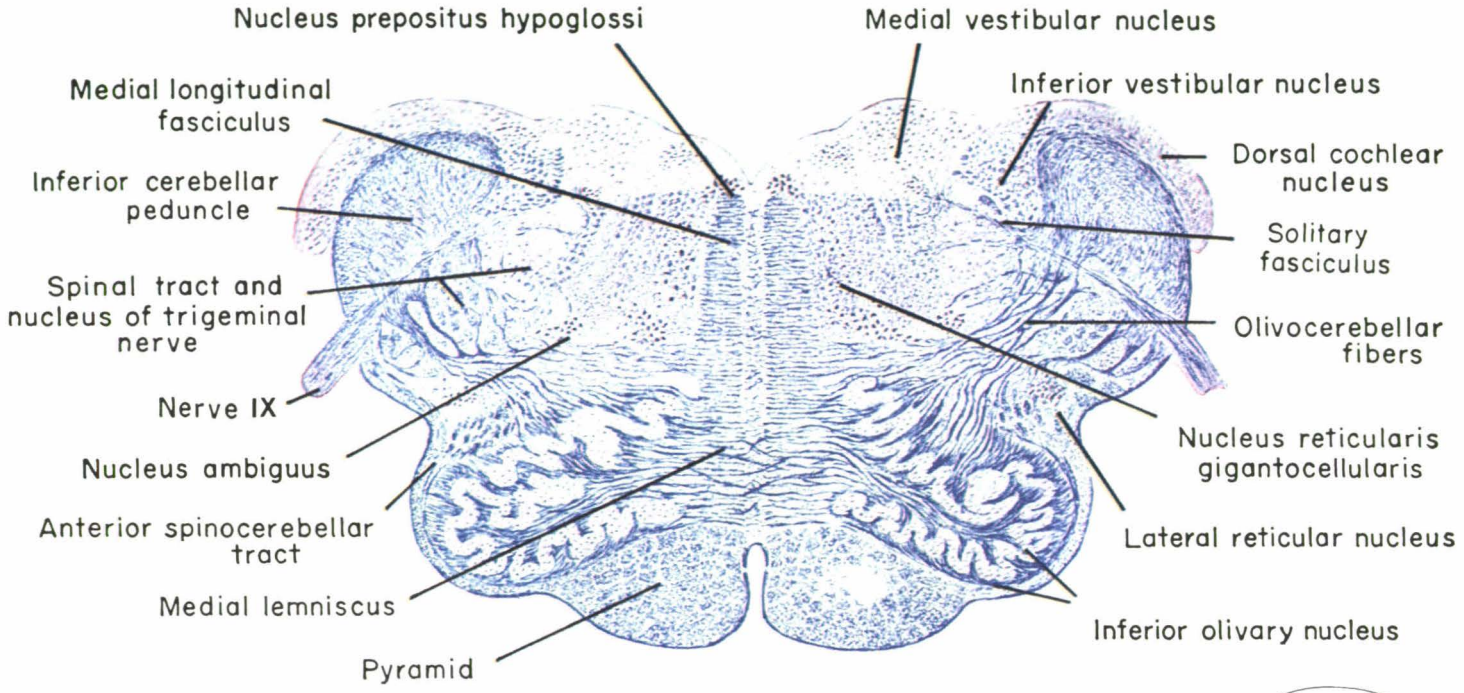
A-2. Transverse section of the medulla through the decussation of the corticospinal tracts. x8.

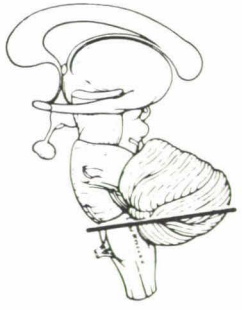


A-3. Transverse section of the medulla at the level of the decussation of the medial lemniscus showing the nuclei of the posterior columns and the course of the internal arcuate fibers. x8.

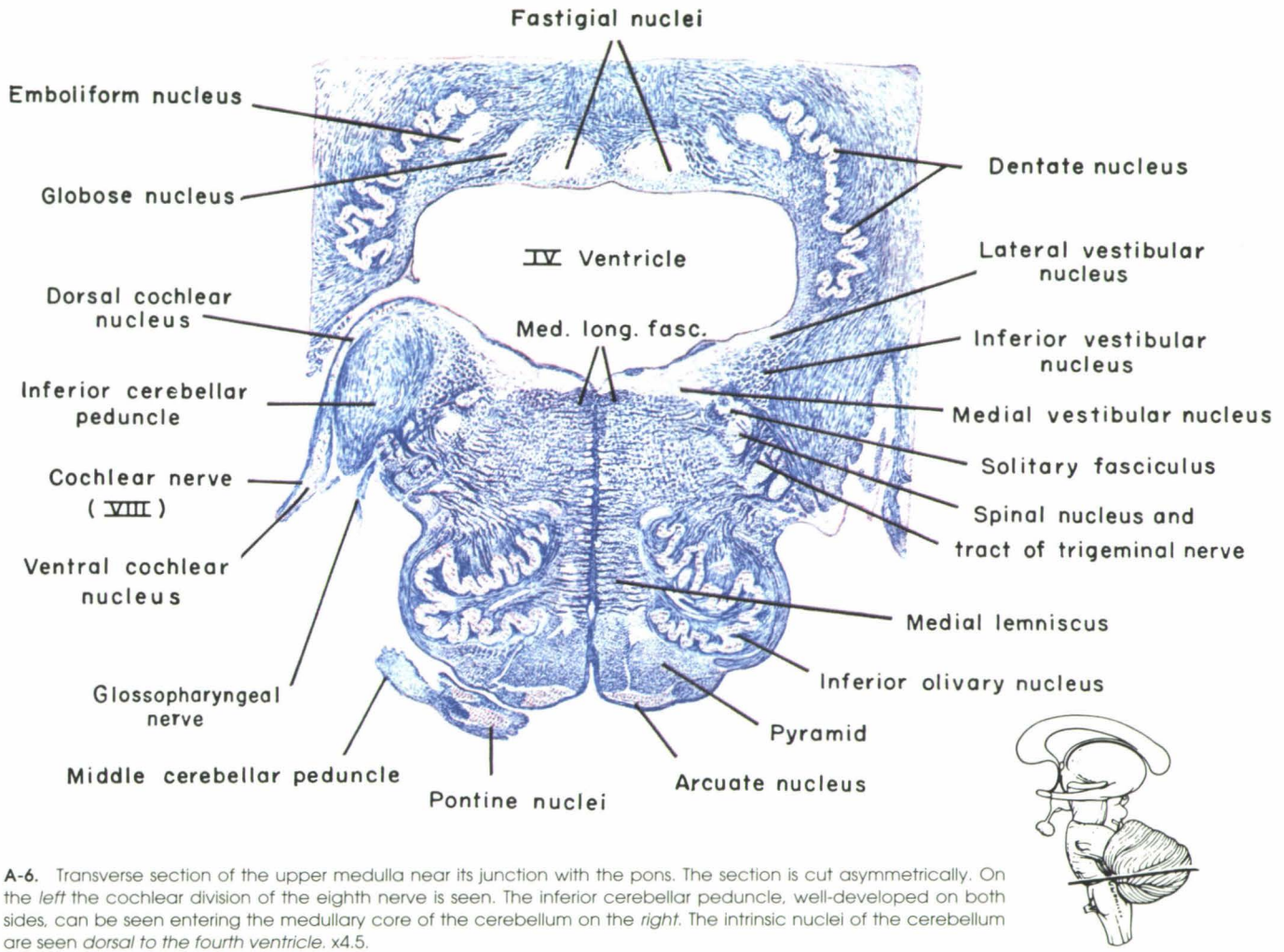


A-4. Transverse section of the medulla through the inferior olivary nuclear complex demonstrating cranial nerve nuclei and the emergence of the hypoglossal root fibers. x6.5.

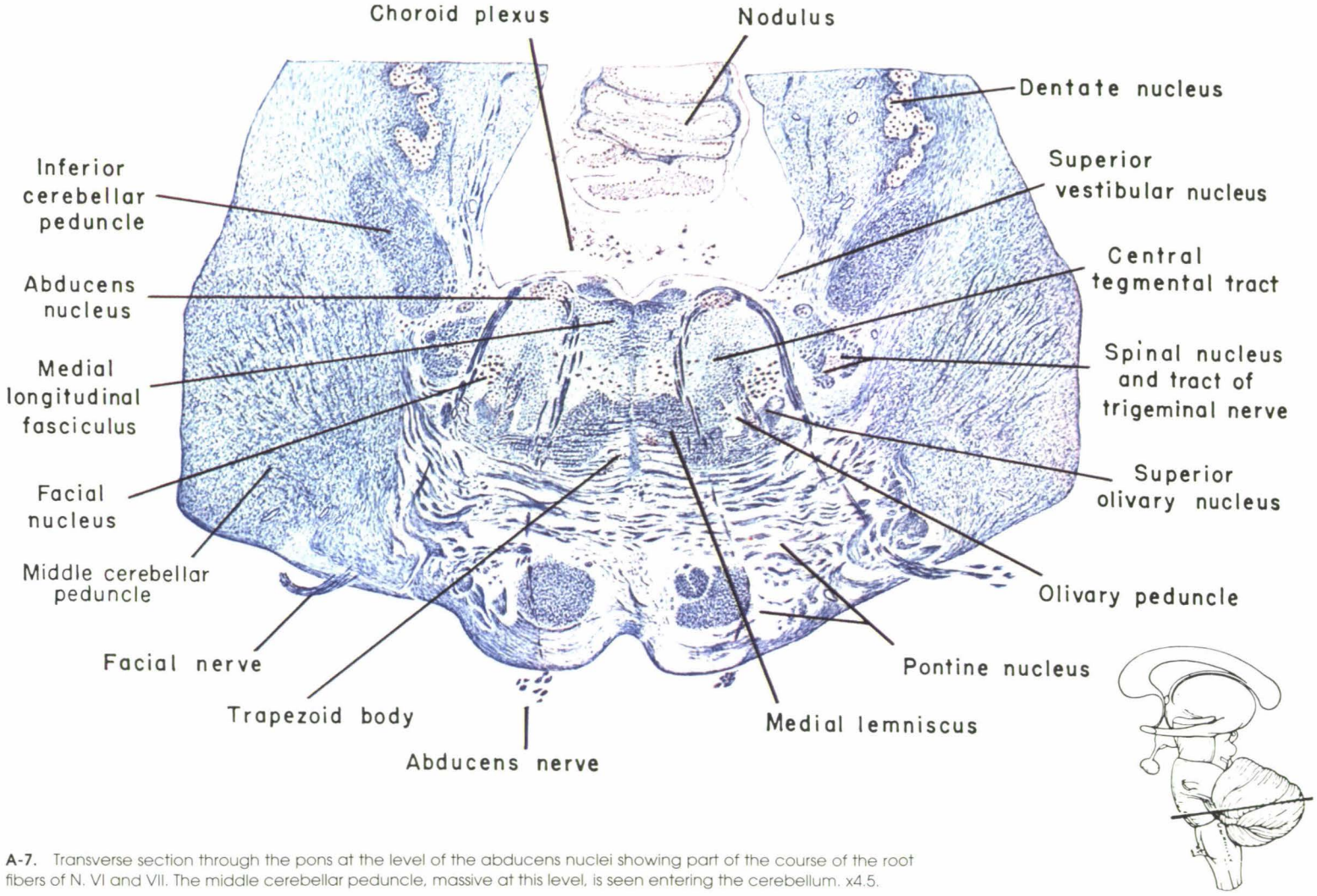




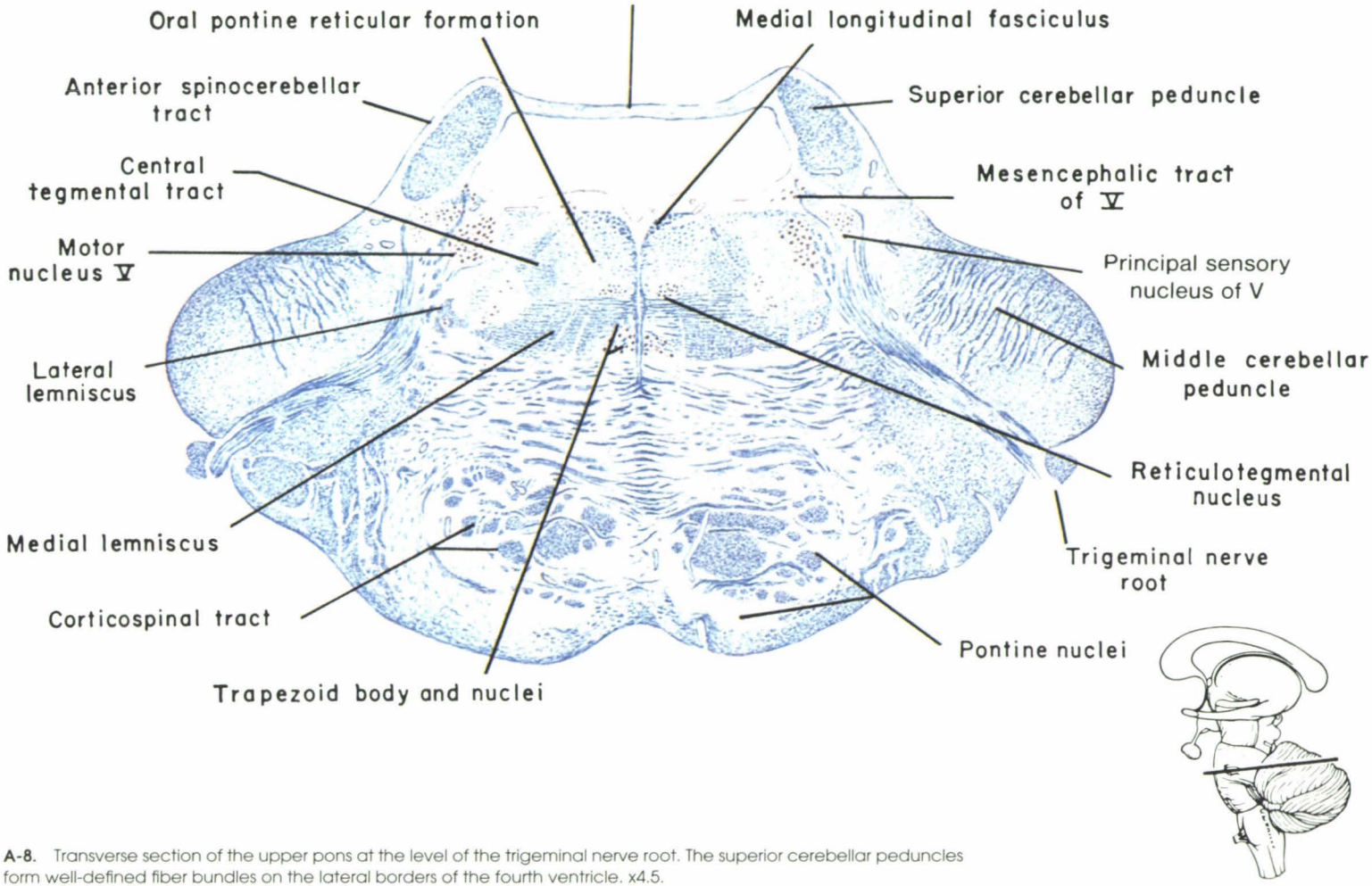
A-5. Transverse section of the full development of the medulla showing the glossopharyngeal nerve, the vestibular nuclei in the floor of the fourth ventricle, and the dorsal cochlear nuclei. x6.5.



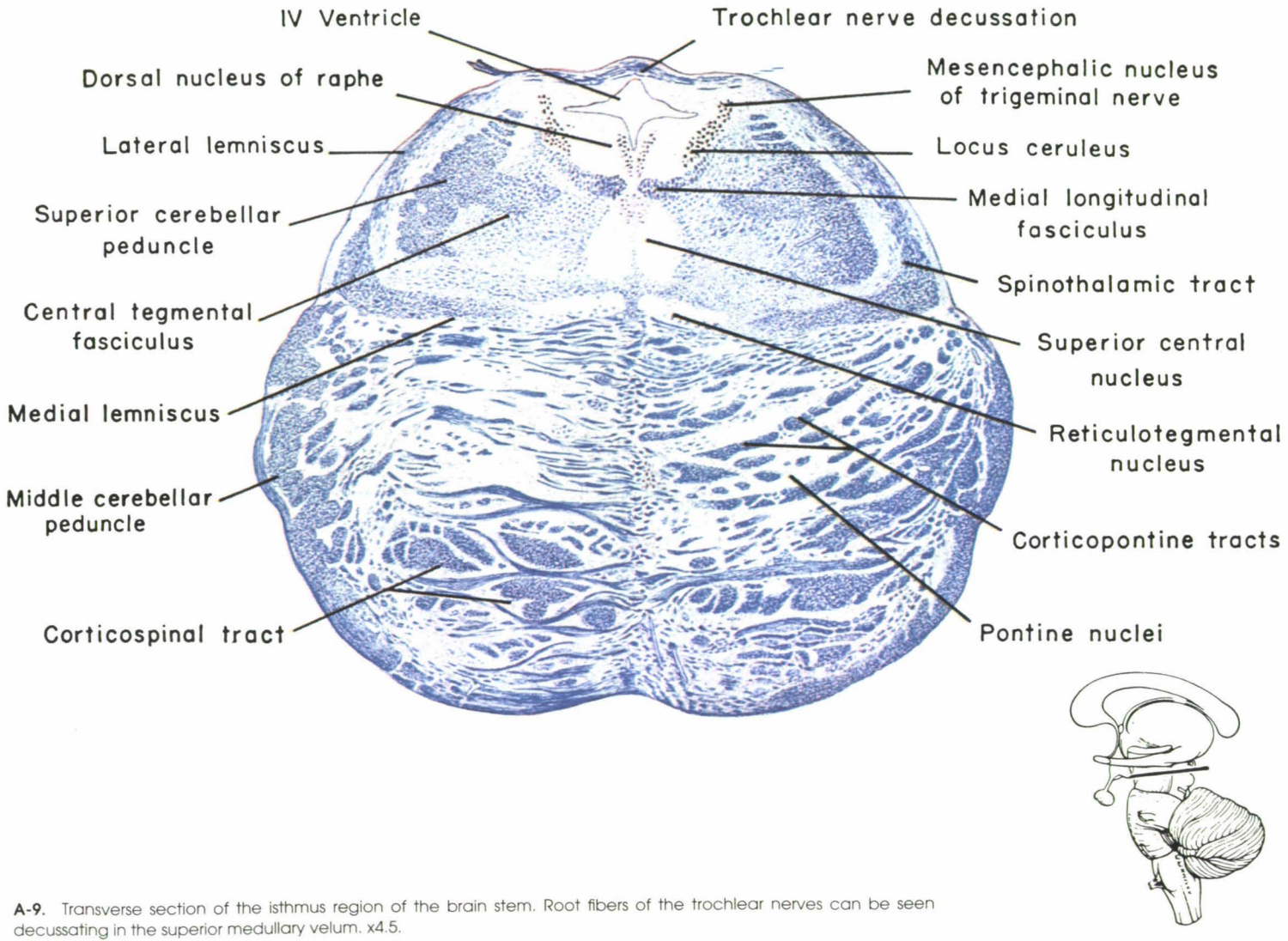
A-6. Transverse section of the upper medulla near its junction with the pons. The section is cut asymmetrically. On the *left* the cochlear division of the eighth nerve is seen. The inferior cerebellar peduncle, well-developed on both sides, can be seen entering the medullary core of the cerebellum on the *right*. The intrinsic nuclei of the cerebellum are seen *dorsal to the fourth ventricle*. x4.5.



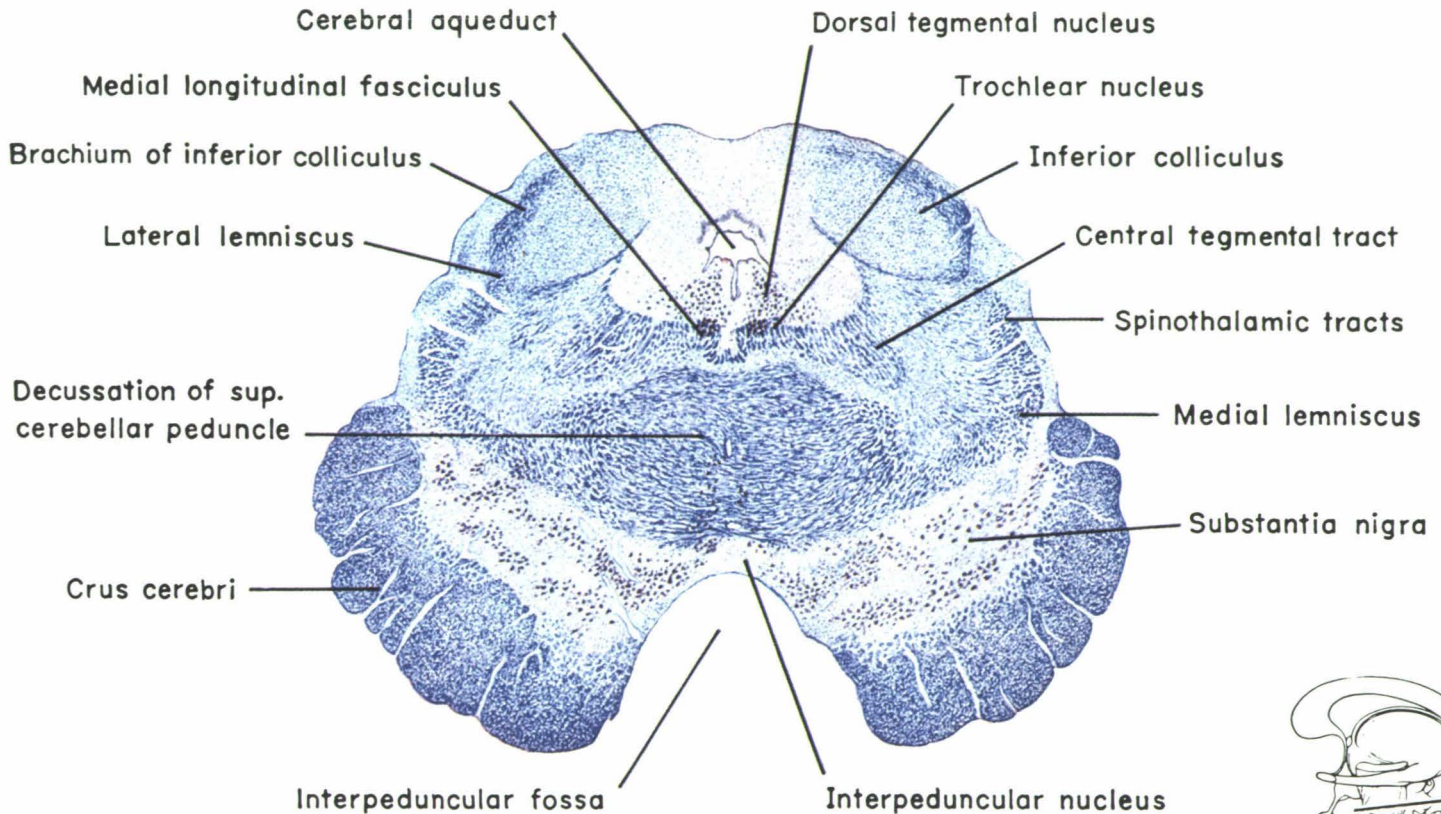
A-7. Transverse section through the pons at the level of the abducens nuclei showing part of the course of the root fibers of N. VI and VII. The middle cerebellar peduncle, massive at this level, is seen entering the cerebellum. x4.5.

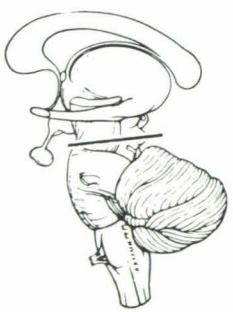


A-8. Transverse section of the upper pons at the level of the trigeminal nerve root. The superior cerebellar peduncles form well-defined fiber bundles on the lateral borders of the fourth ventricle. x4.5.

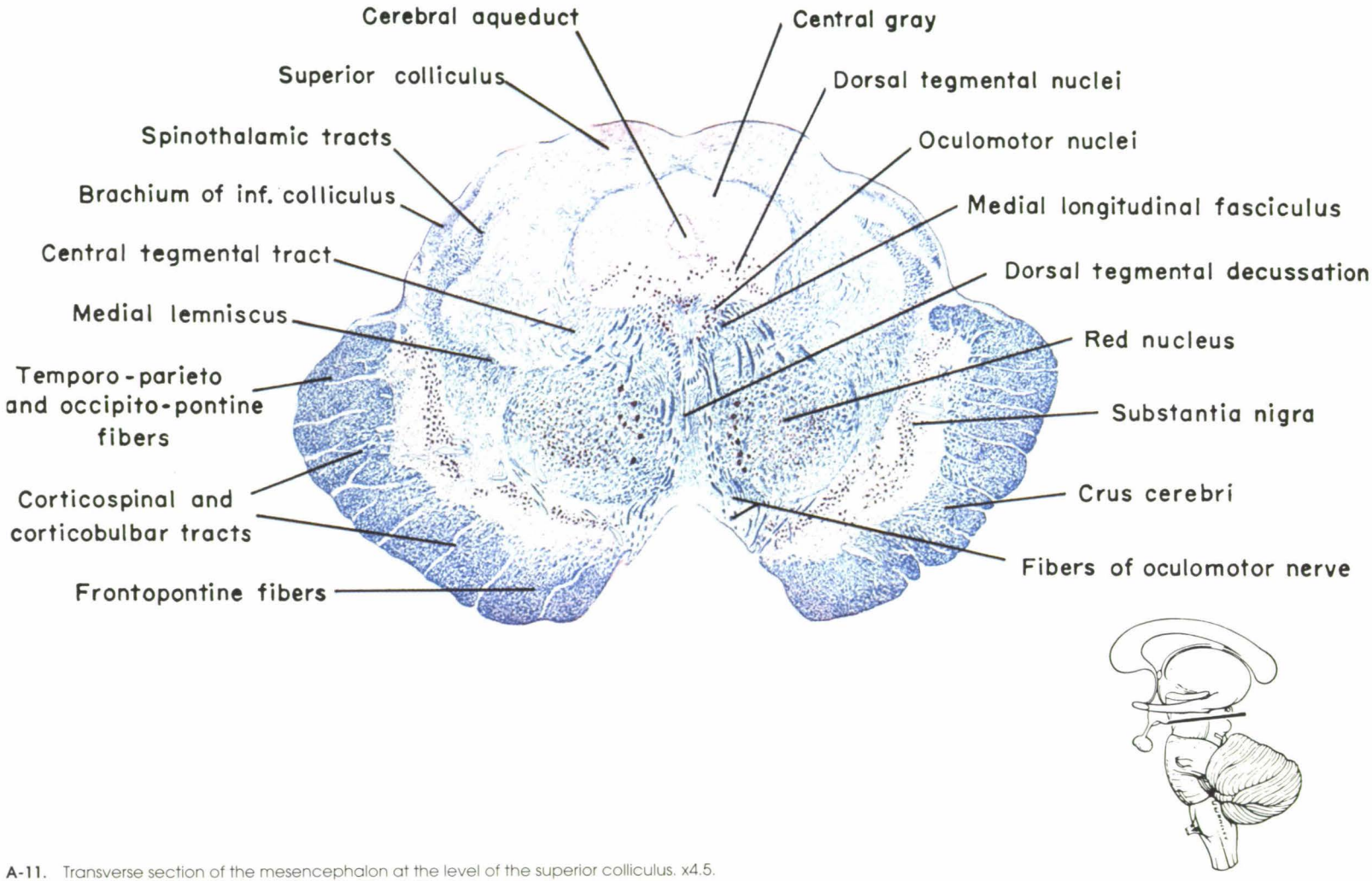


A-9. Transverse section of the isthmus region of the brain stem. Root fibers of the trochlear nerves can be seen decussating in the superior medullary velum. x4.5.

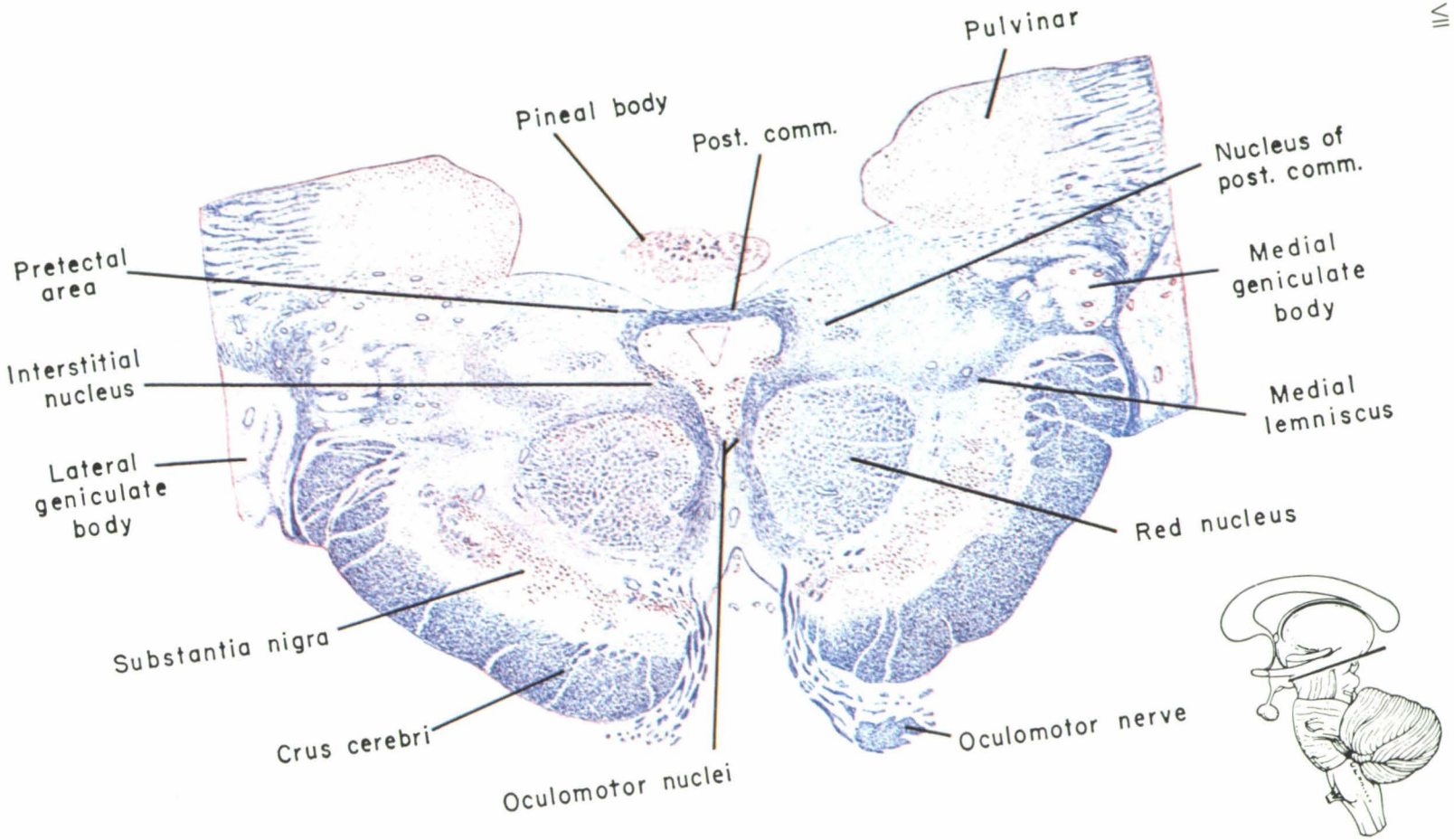




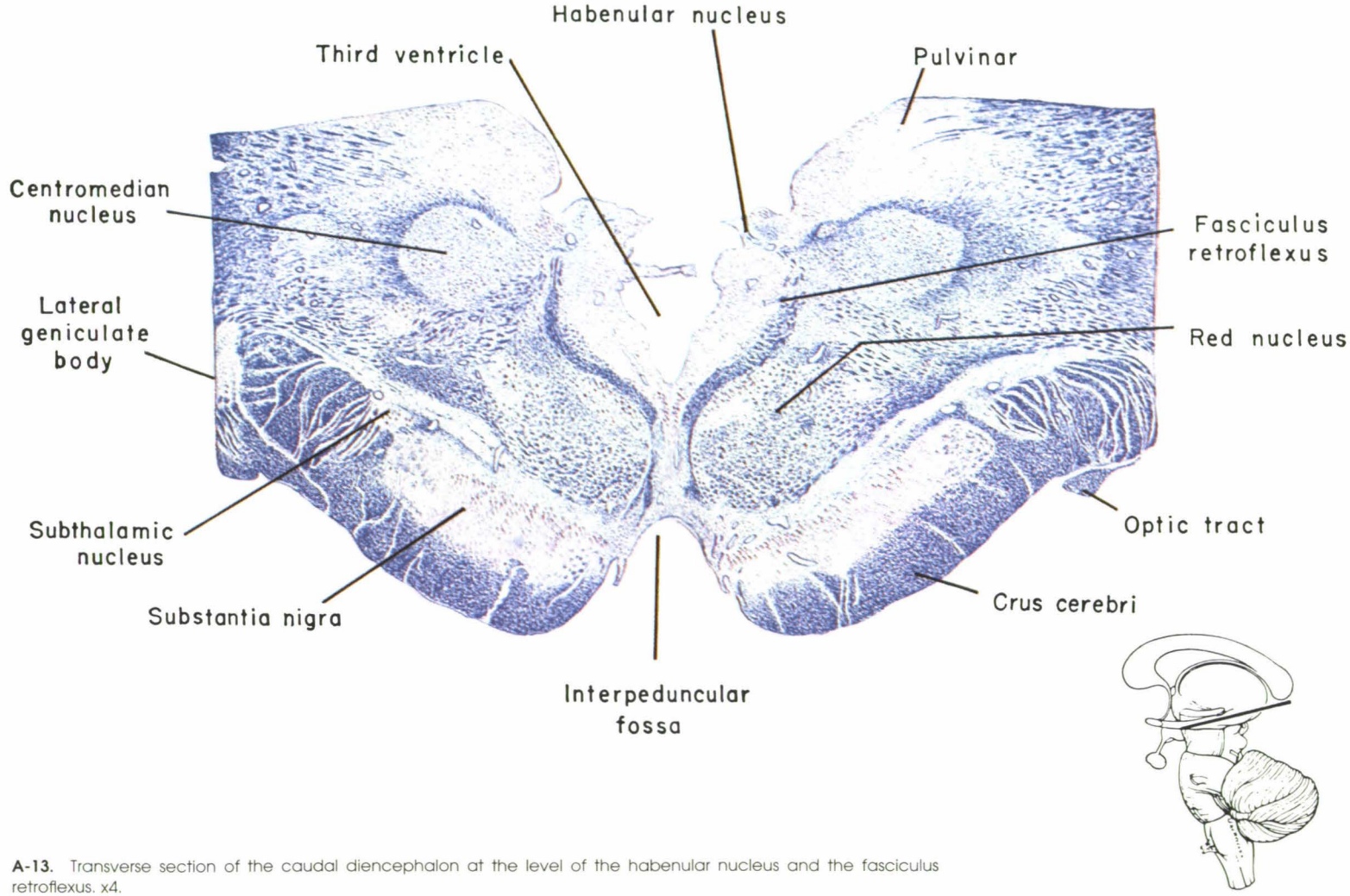
A-10. Transverse section of the caudal mesencephalon passing through the inferior colliculus, the decussation of the superior cerebellar peduncle, and the crus cerebri. x4.5.



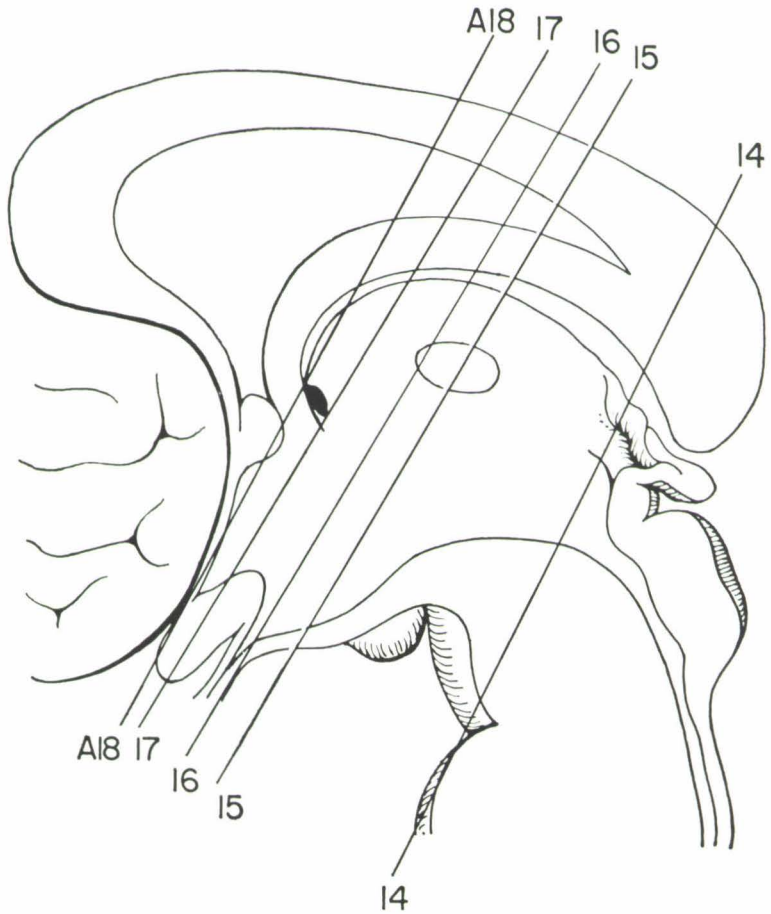
A-11. Transverse section of the mesencephalon at the level of the superior colliculus. x4.5.



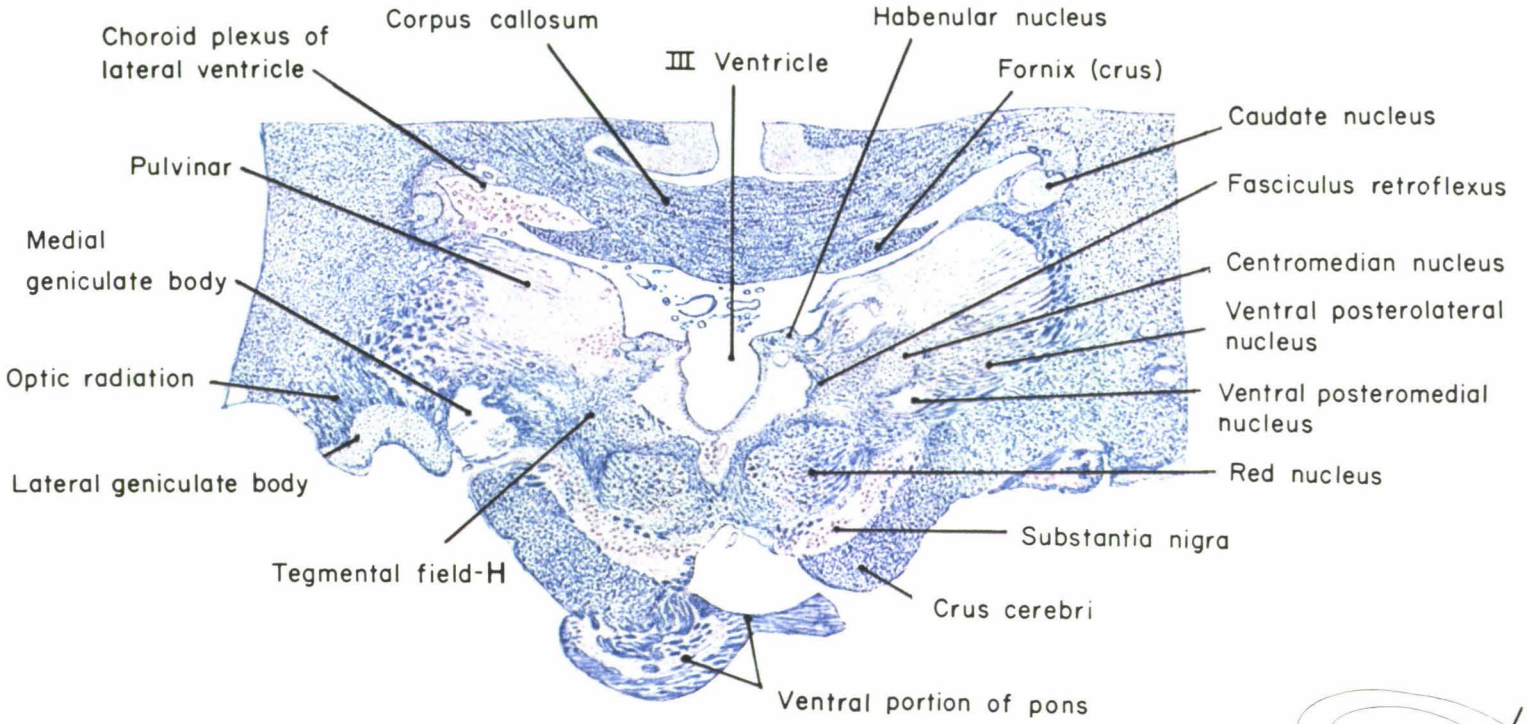
A-12. Transverse section of the brain stem at the junction of the mesencephalon and diencephalon. x4.



A-13. Transverse section of the caudal diencephalon at the level of the habenular nucleus and the fasciculus retroflexus. x4.

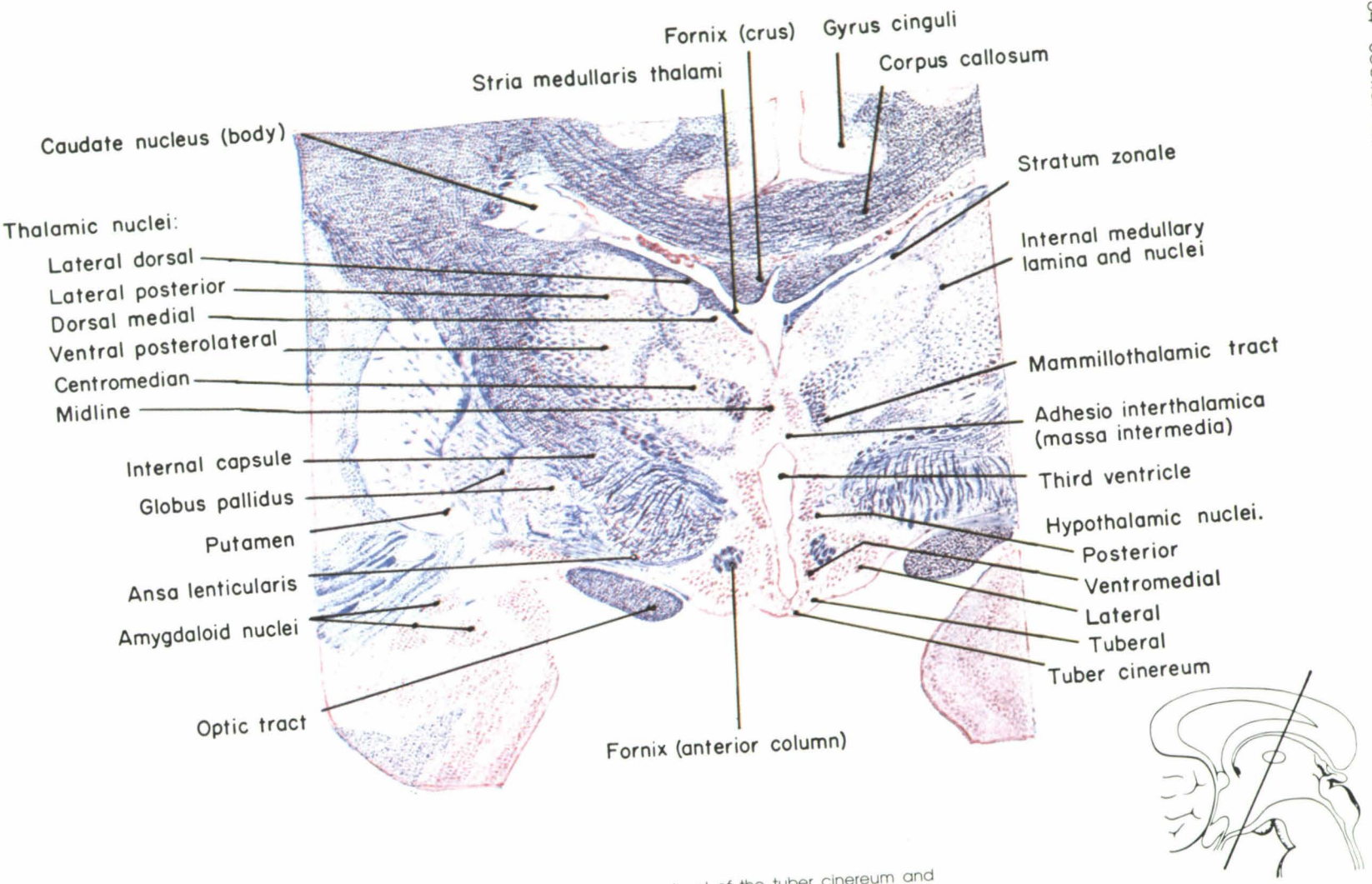


Outline of median sagittal surface of brain indicating level and plane of frontal sections A-14 to A-18.

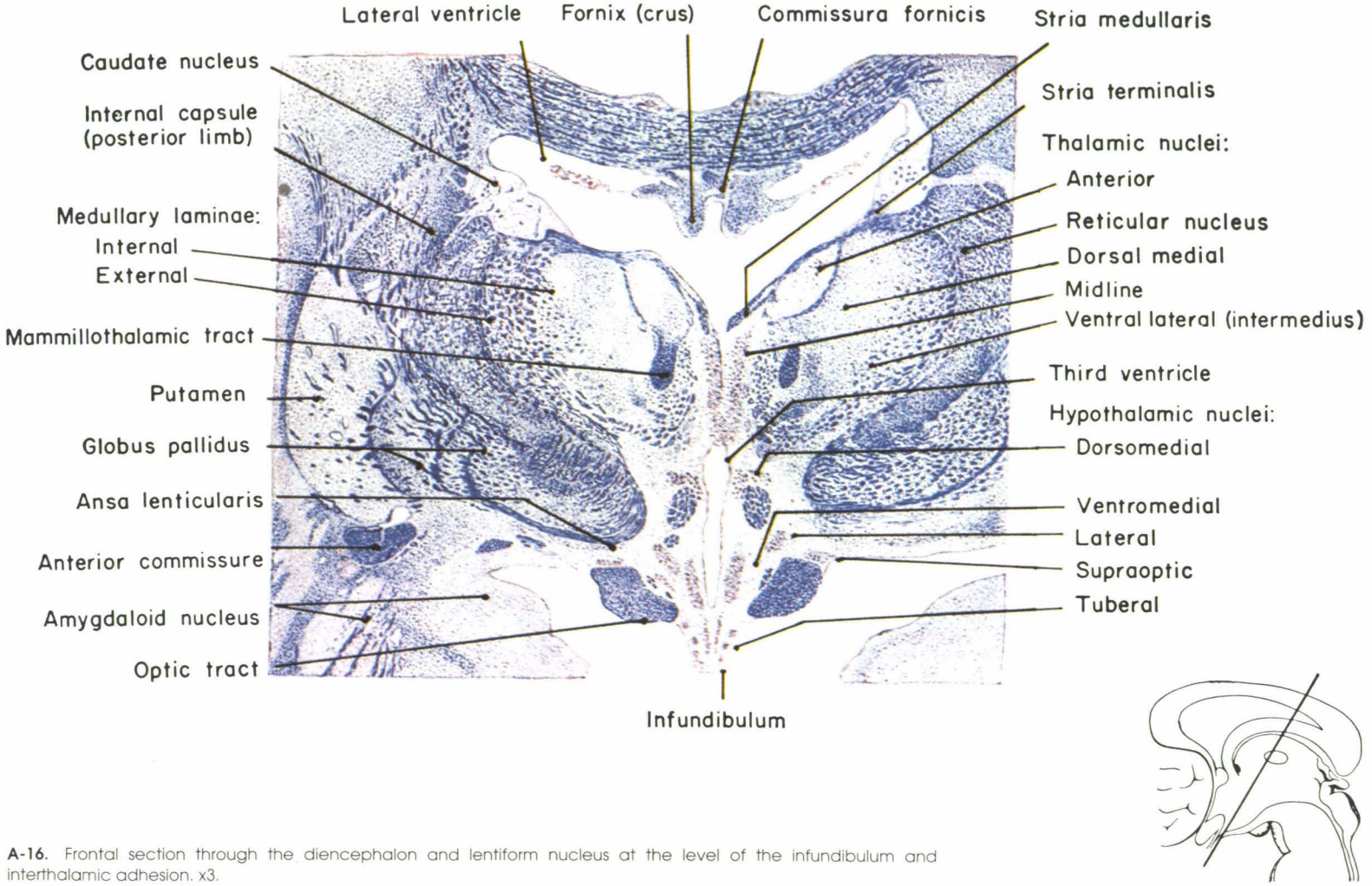




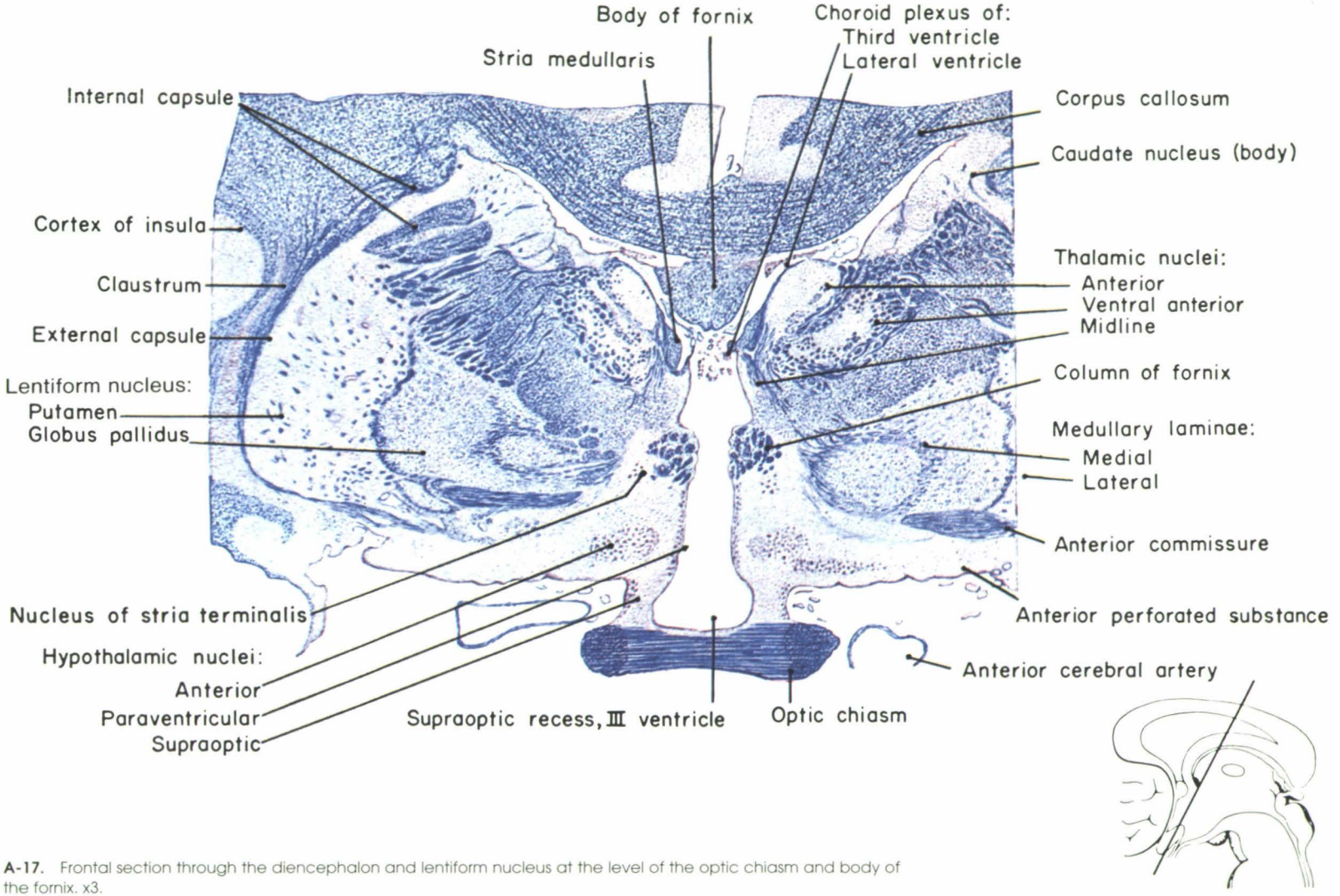
A-14. Frontal section through the junction of the midbrain and the diencephalon at the level of the habenular nucleus. x2.5.



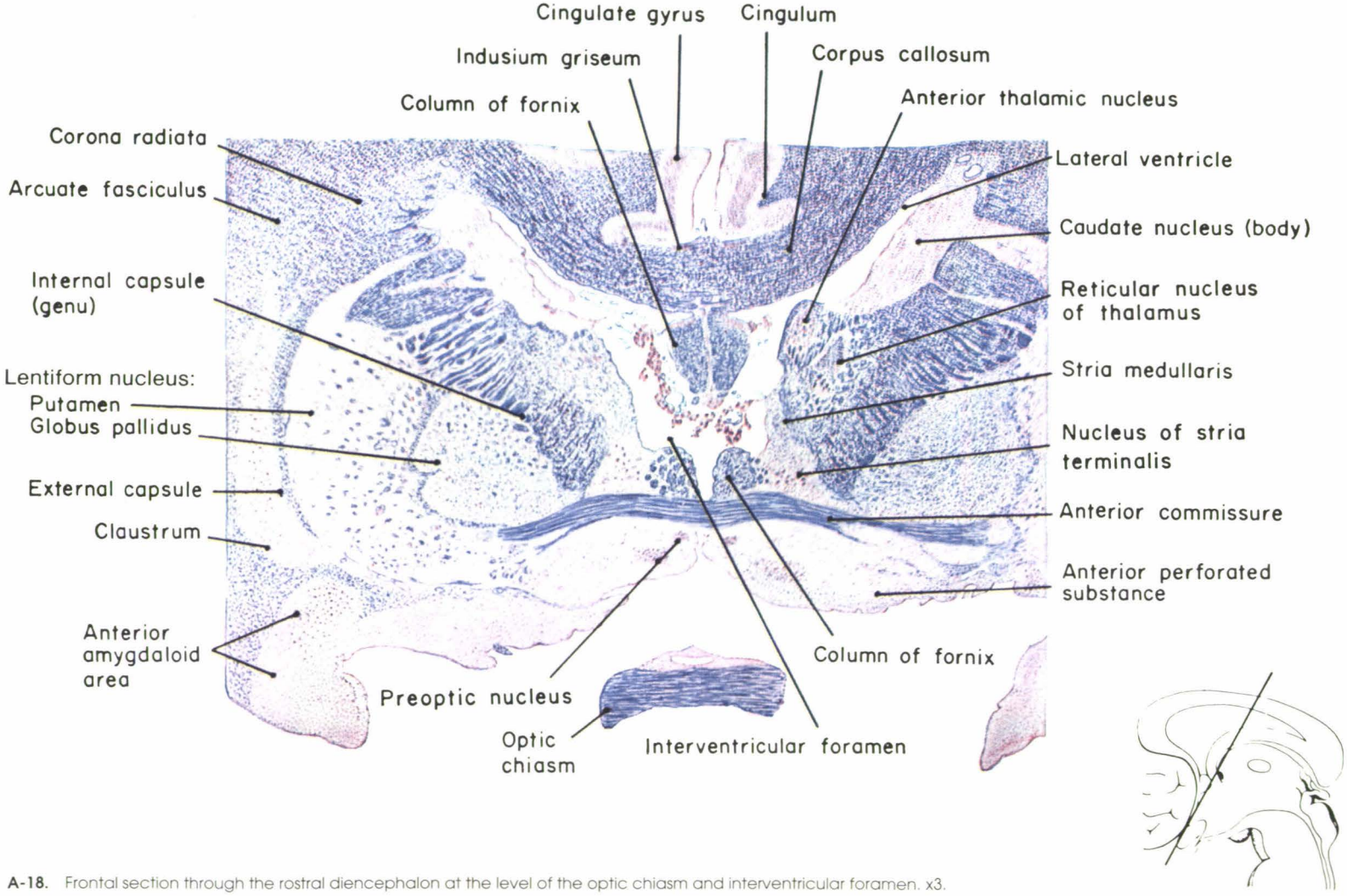
A-15. Frontal section through the diencephalon and lentiform nucleus at the level of the tuber cinereum and interthalamic adhesion. x3.



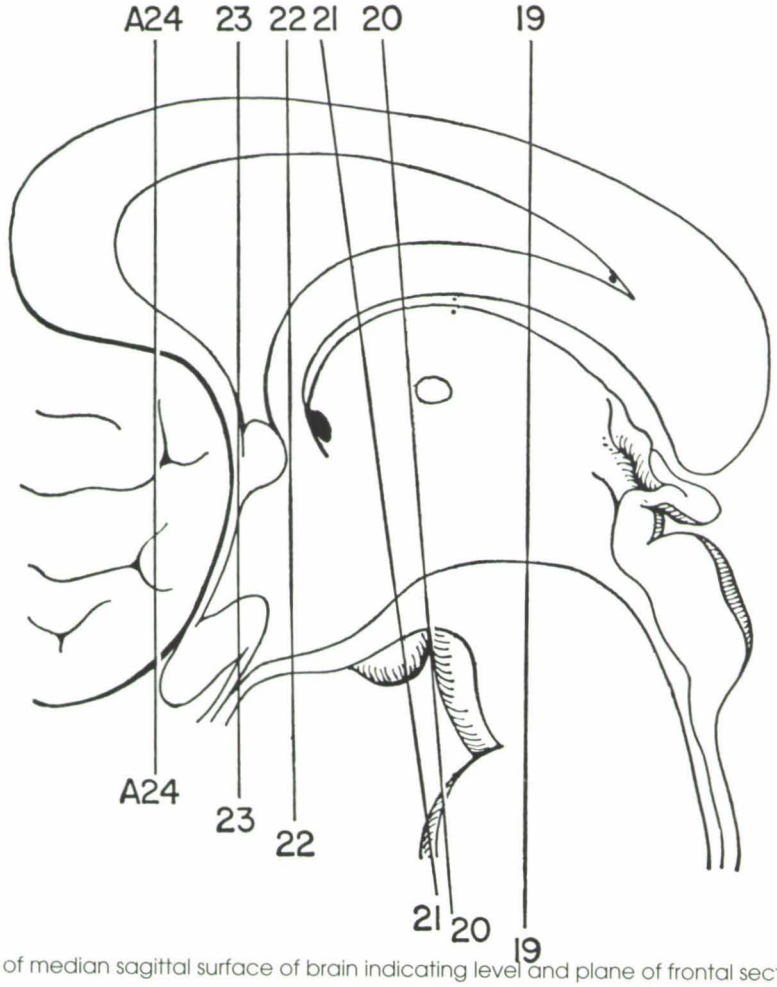
A-16. Frontal section through the diencephalon and lentiform nucleus at the level of the infundibulum and interthalamic adhesion. x3.



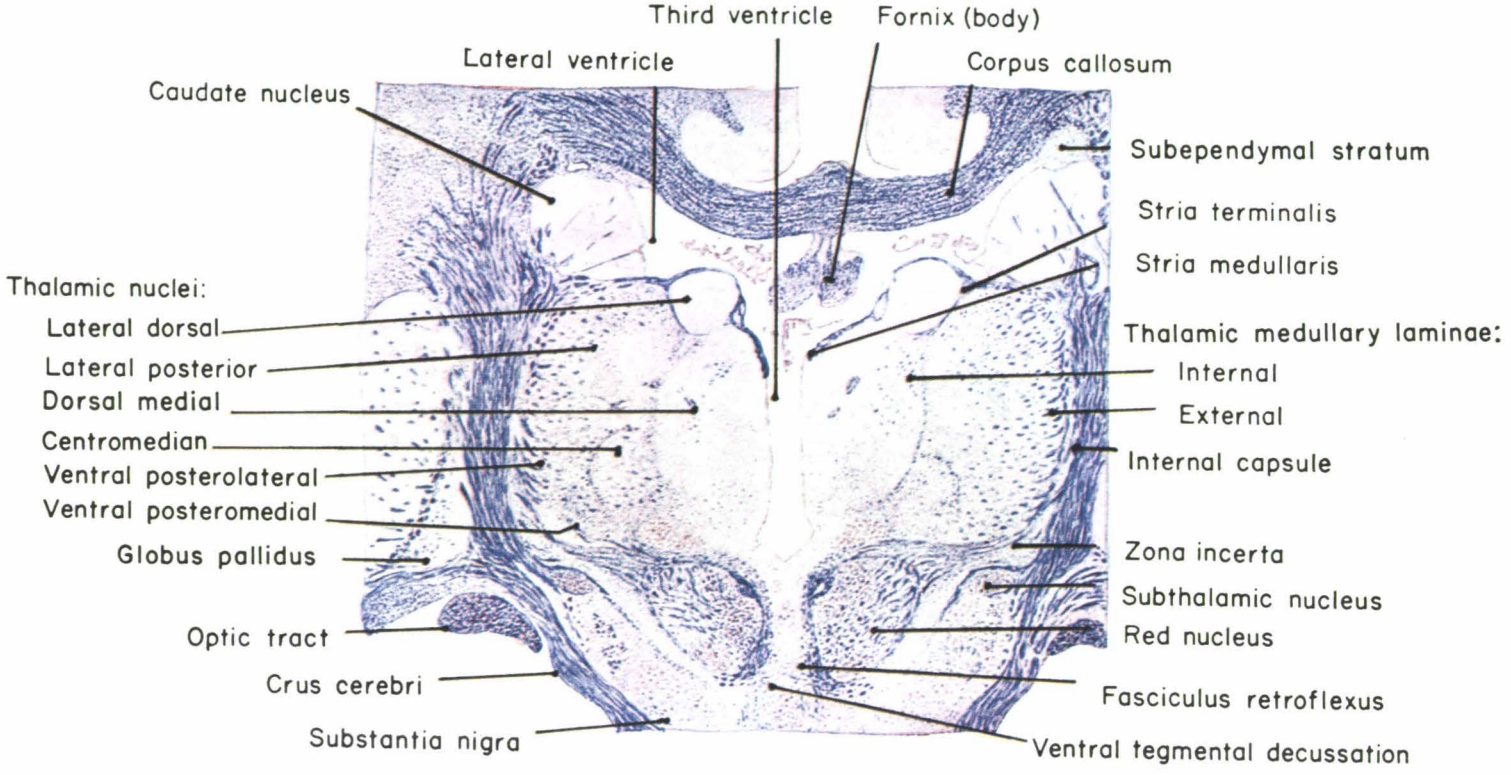
A-17. Frontal section through the diencephalon and lentiform nucleus at the level of the optic chiasm and body of the fornix. x3.

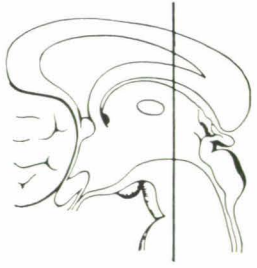


A-18. Frontal section through the rostral diencephalon at the level of the optic chiasm and interventricular foramen. x3.

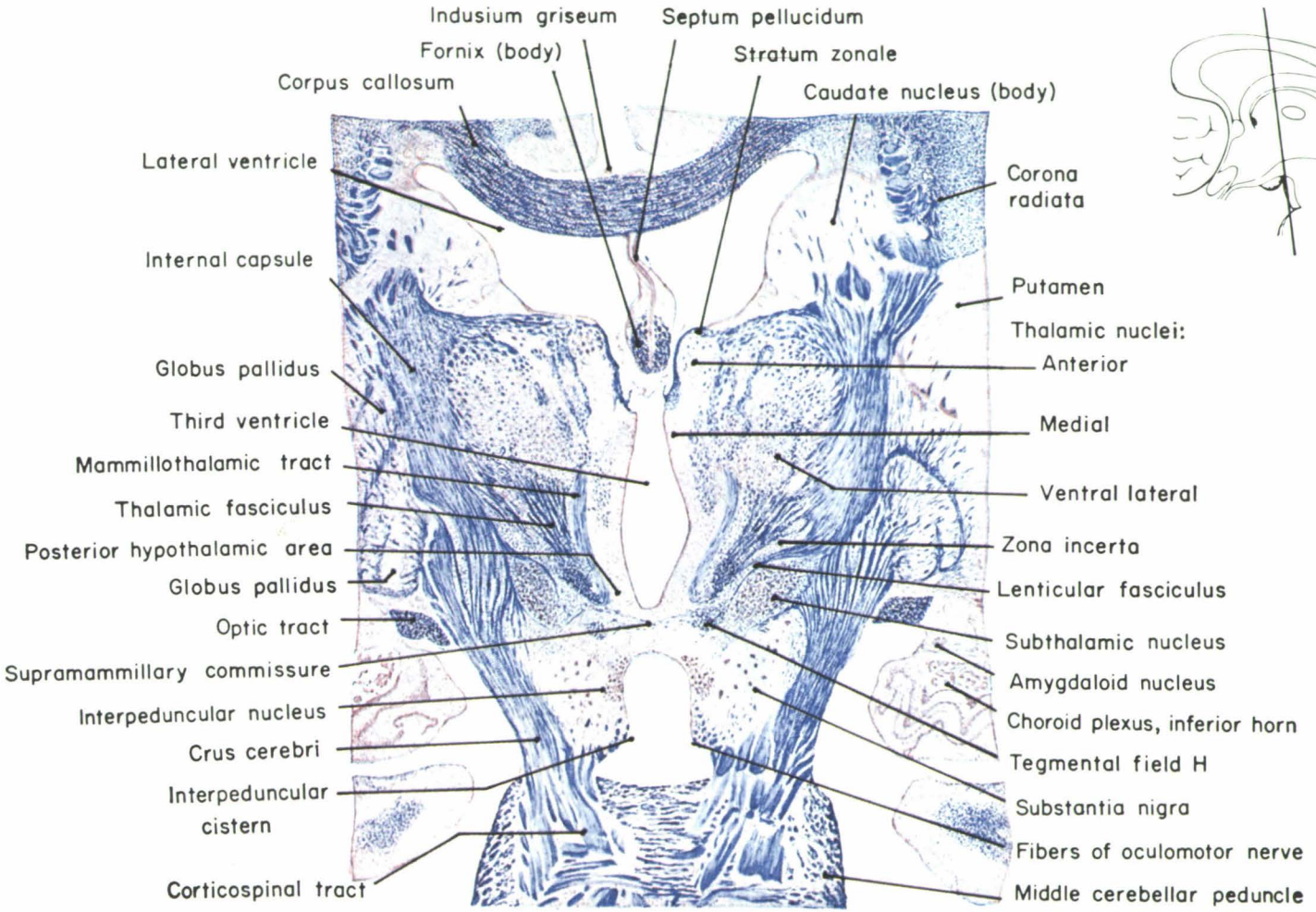


Outline of median sagittal surface of brain indicating level and plane of frontal sections A-19 to A-24.

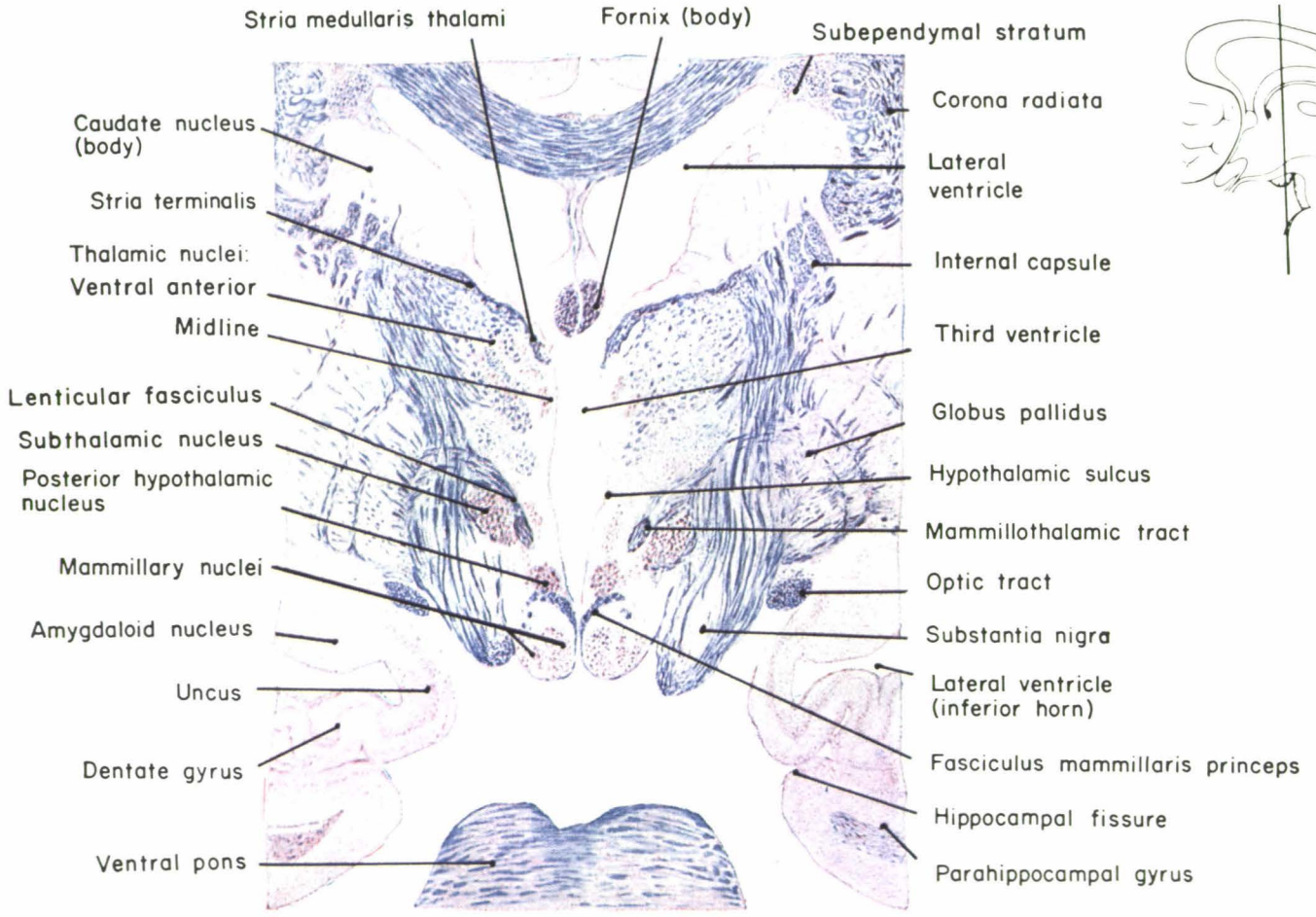




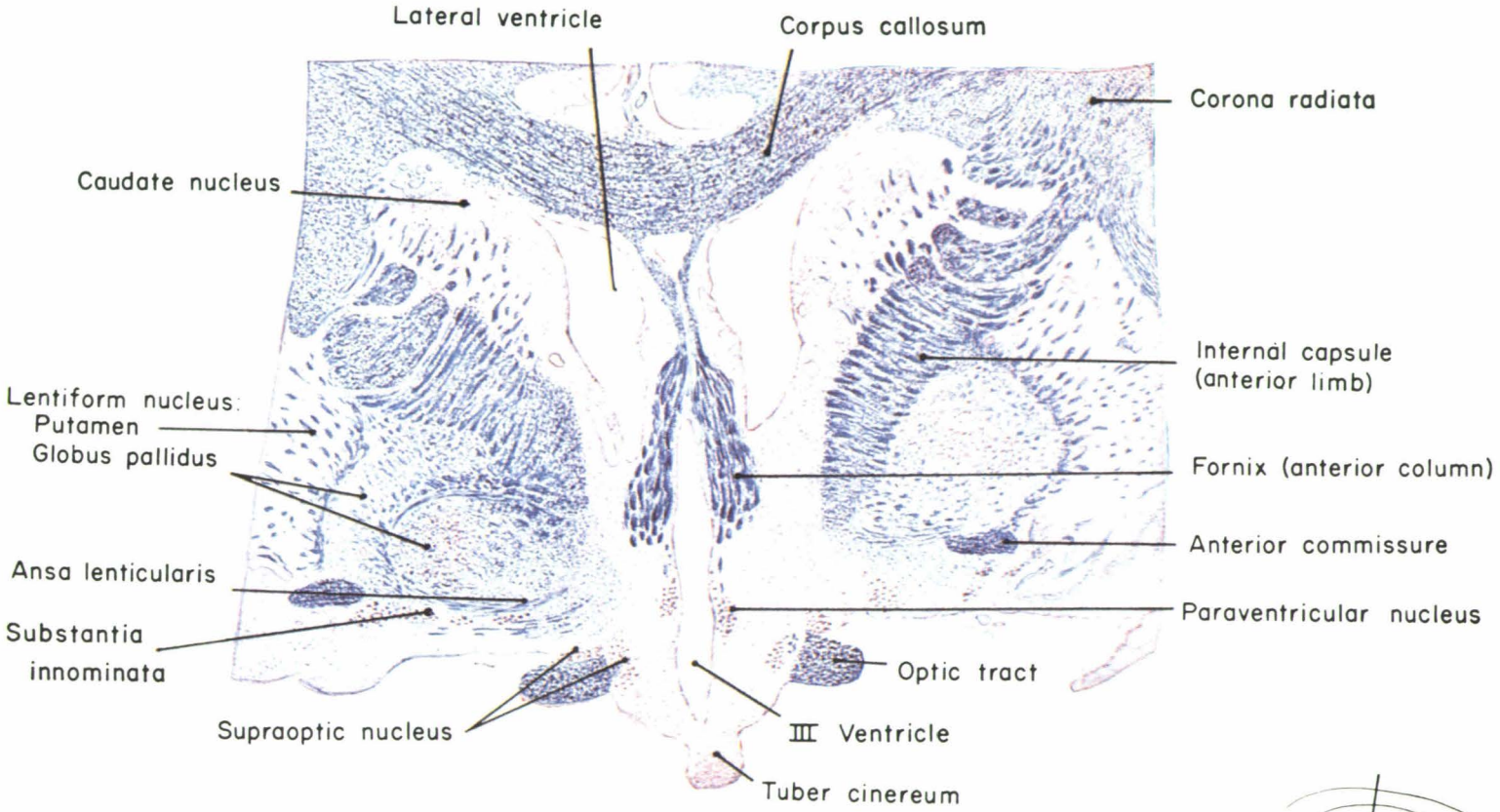
A-19. Frontal section through midbrain and diencephalon at the level of red nucleus and posterior thalamic nuclei. x2.5.



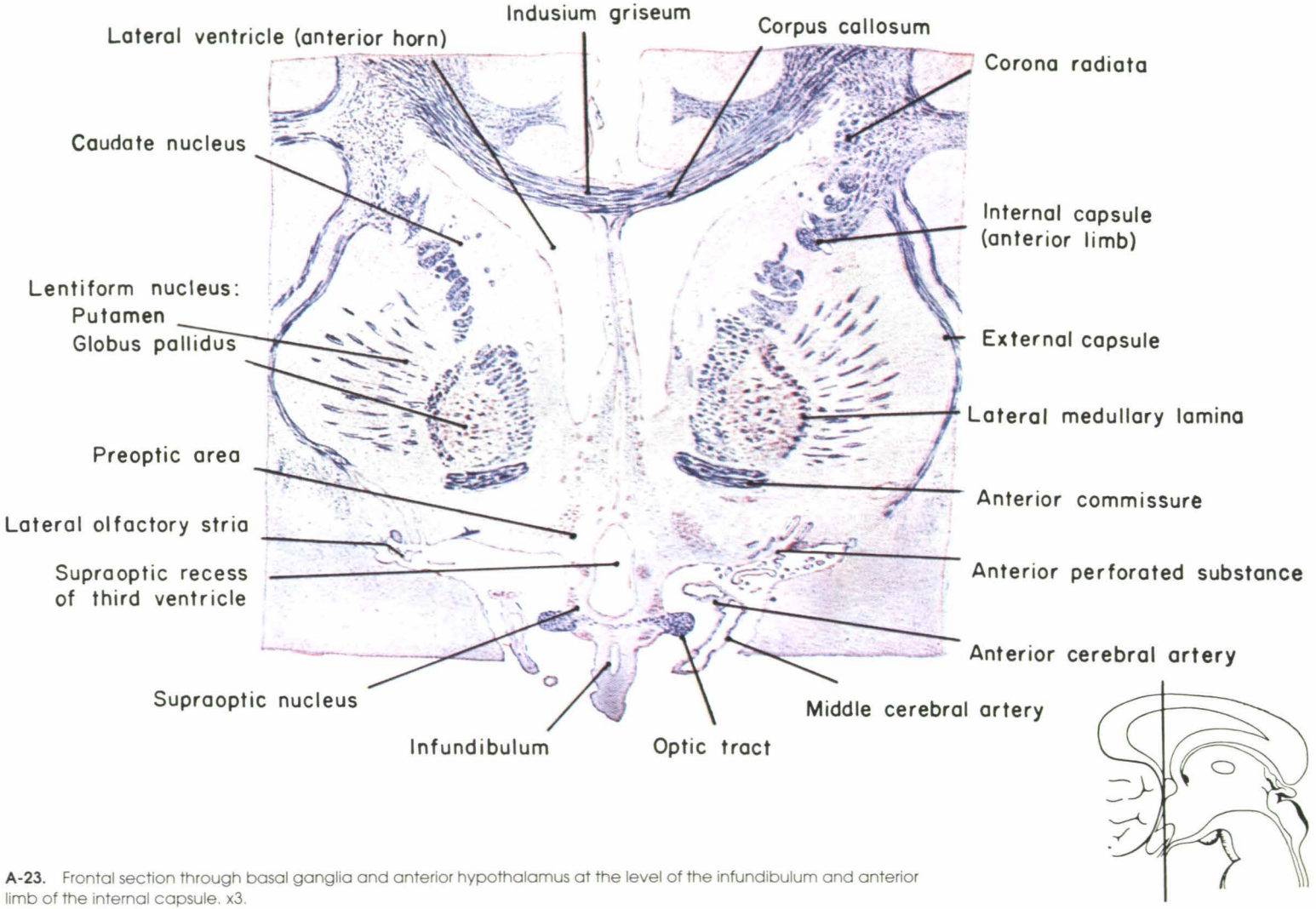
A-20. Frontal section through ventral pons, midbrain, and diencephalon at the level of the interpeduncular fossa and posterior hypothalamus. x3.



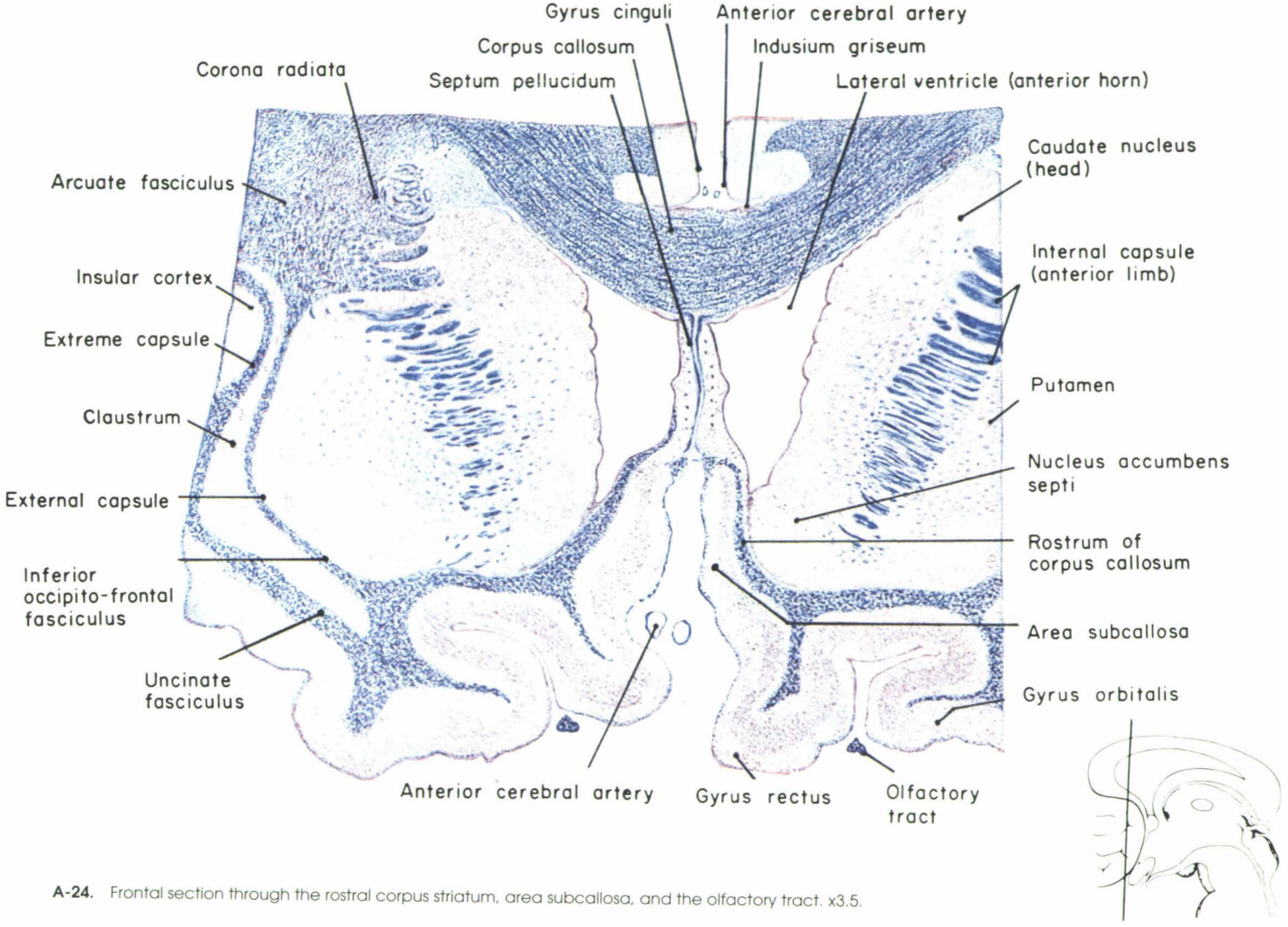
A-21. Frontal section through diencephalon at the level of the mammillary body. x3.



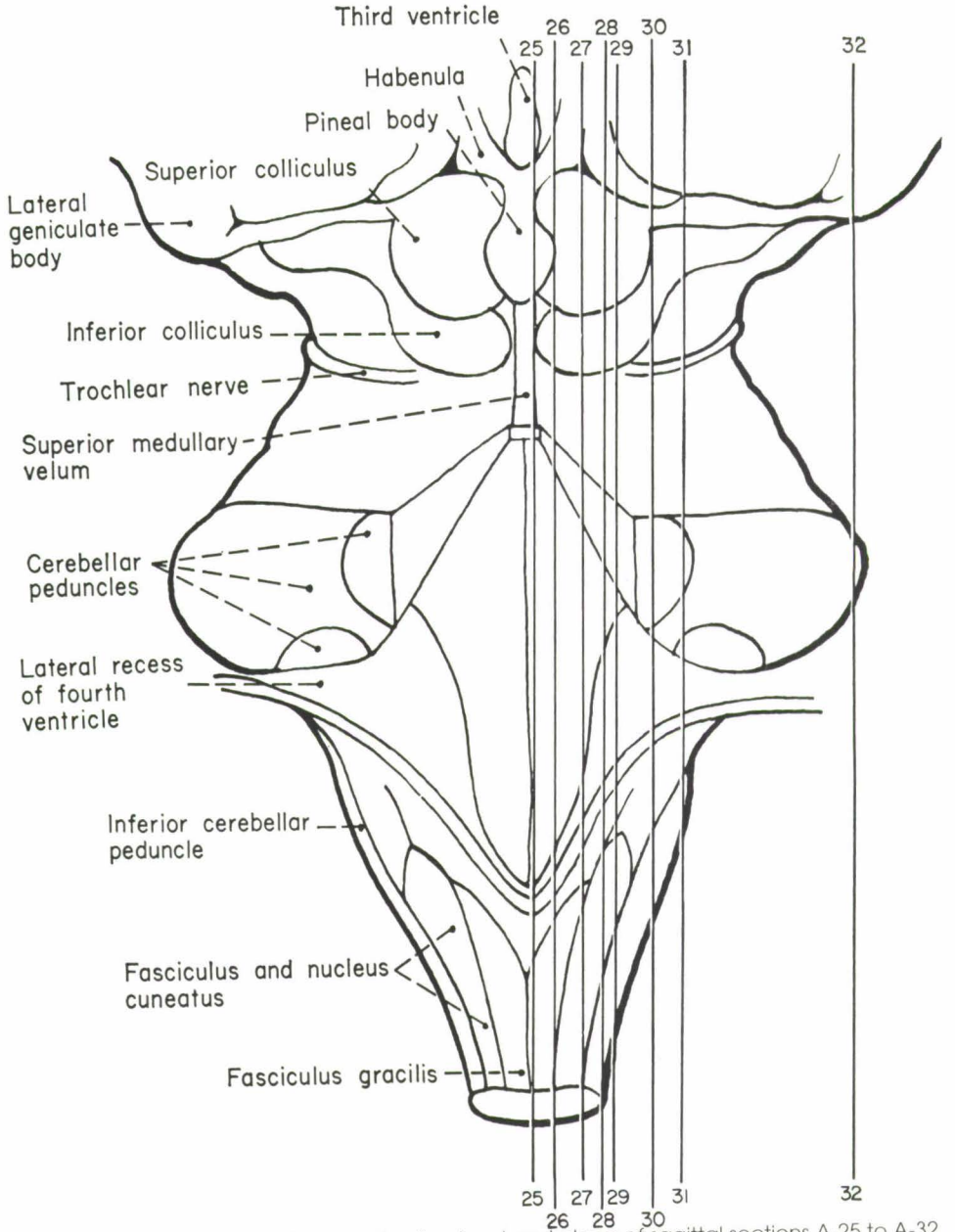
A-22. Frontal section through rostral hypothalamus and lentiform nucleus at the level of the tuber cinereum and columns of the fornix. x3.



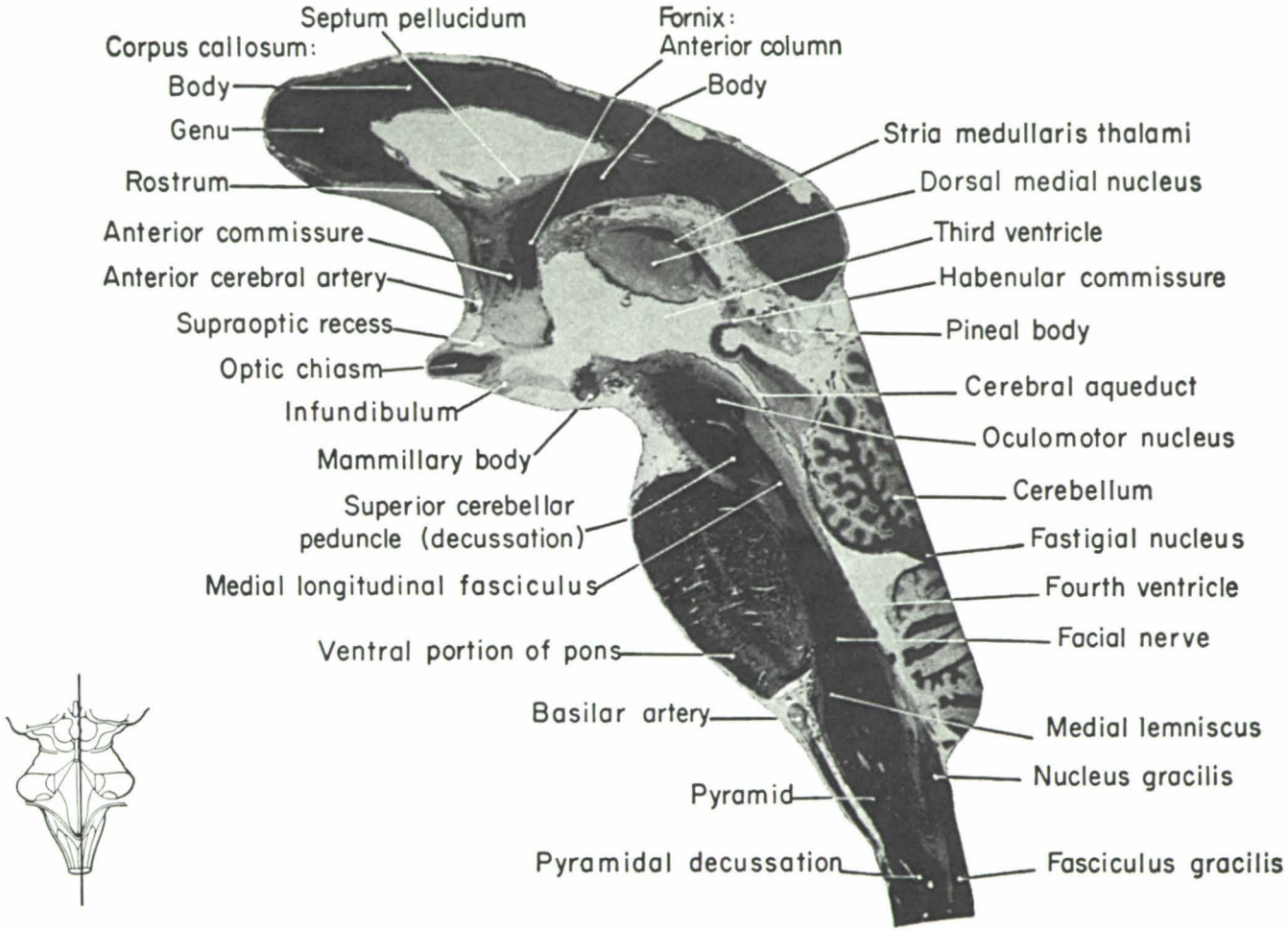
A-23. Frontal section through basal ganglia and anterior hypothalamus at the level of the infundibulum and anterior limb of the internal capsule. x3.



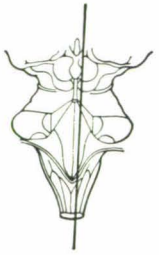
A-24. Frontal section through the rostral corpus striatum, area subcallosa, and the olfactory tract. x3.5.

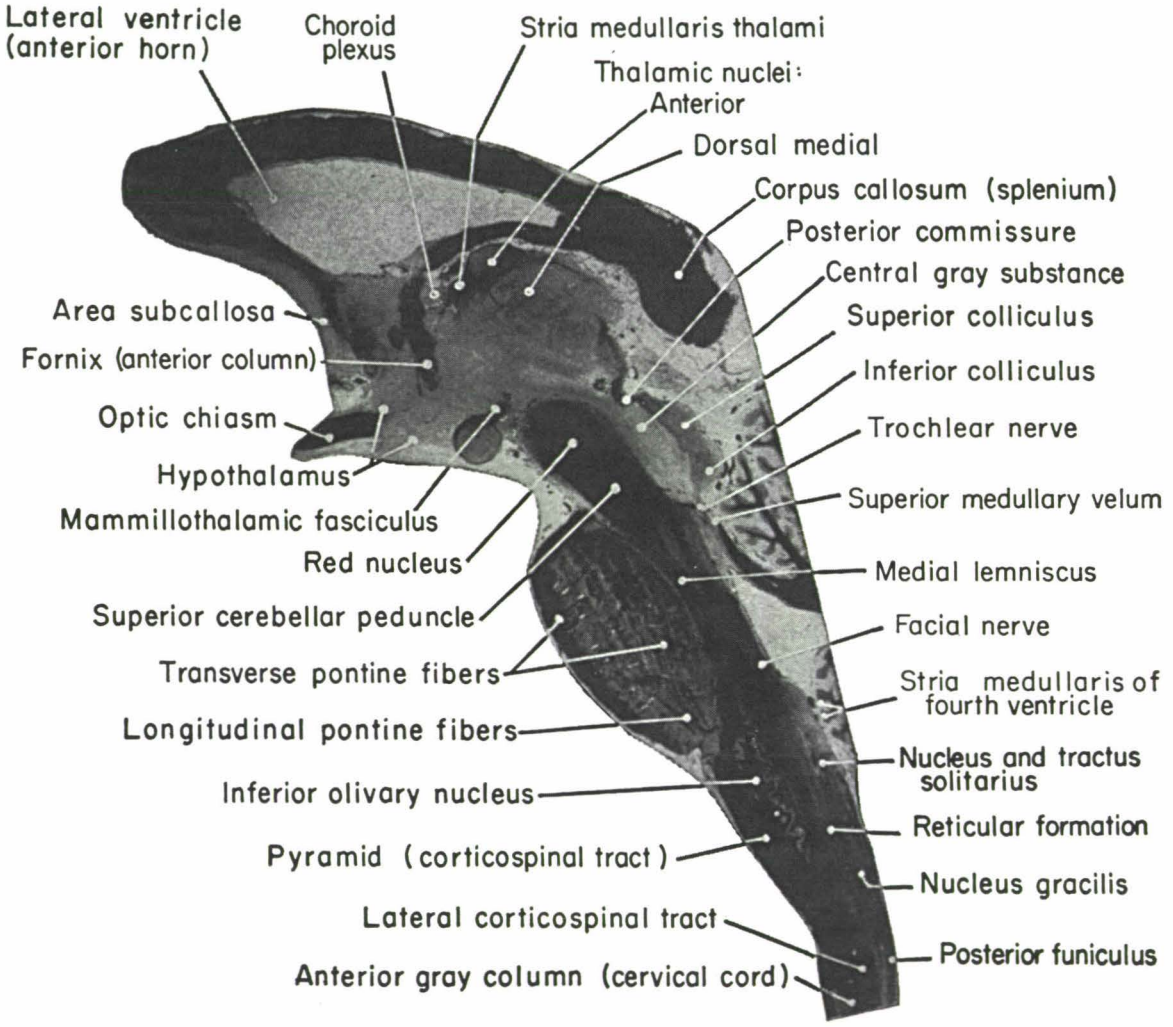


Outline of dorsal surface of brain indicating level and plane of sagittal sections A-25 to A-32.

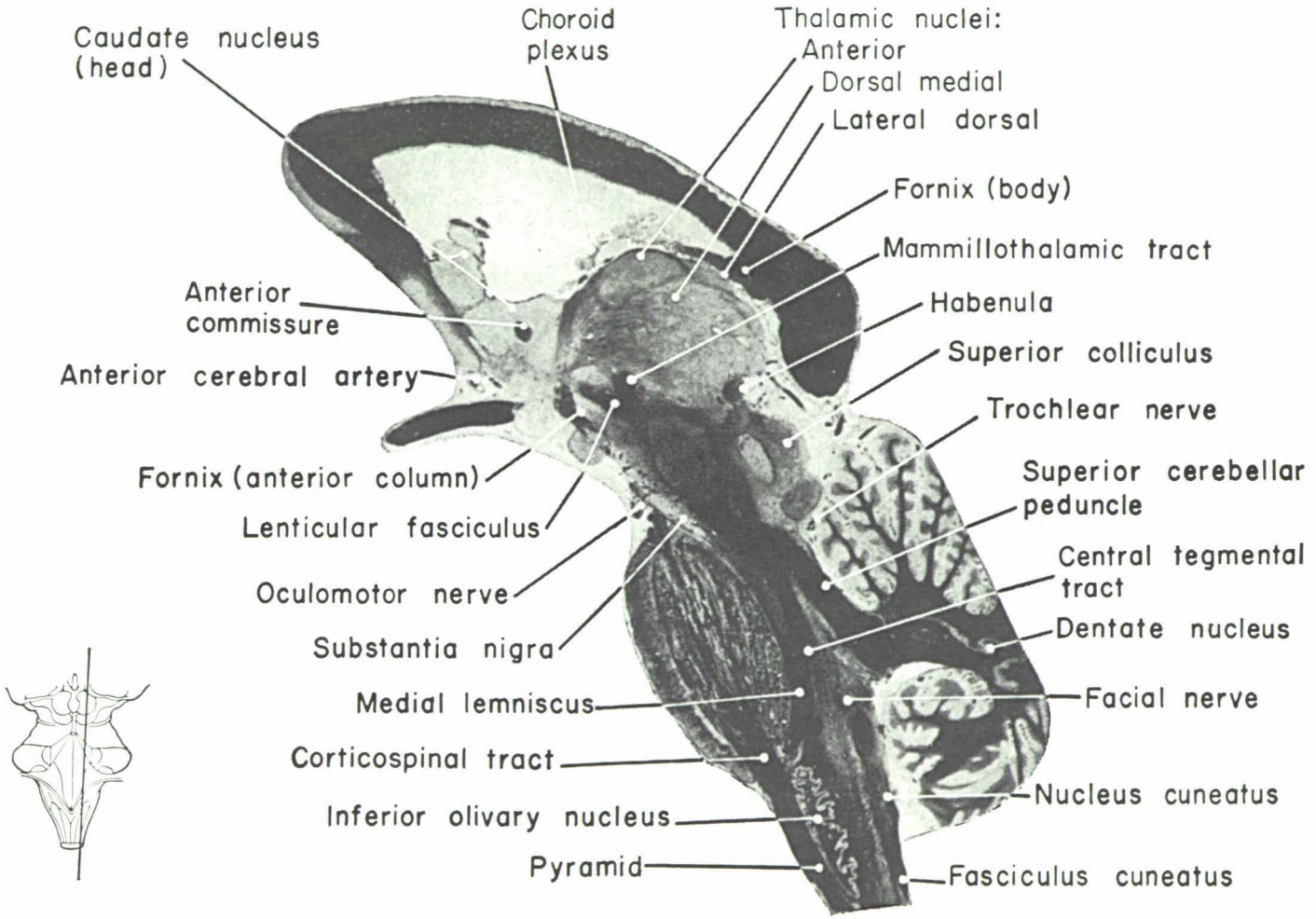


A-25. Sagittal section through the ventricular system and brain stem at the level of the pineal body. x15.

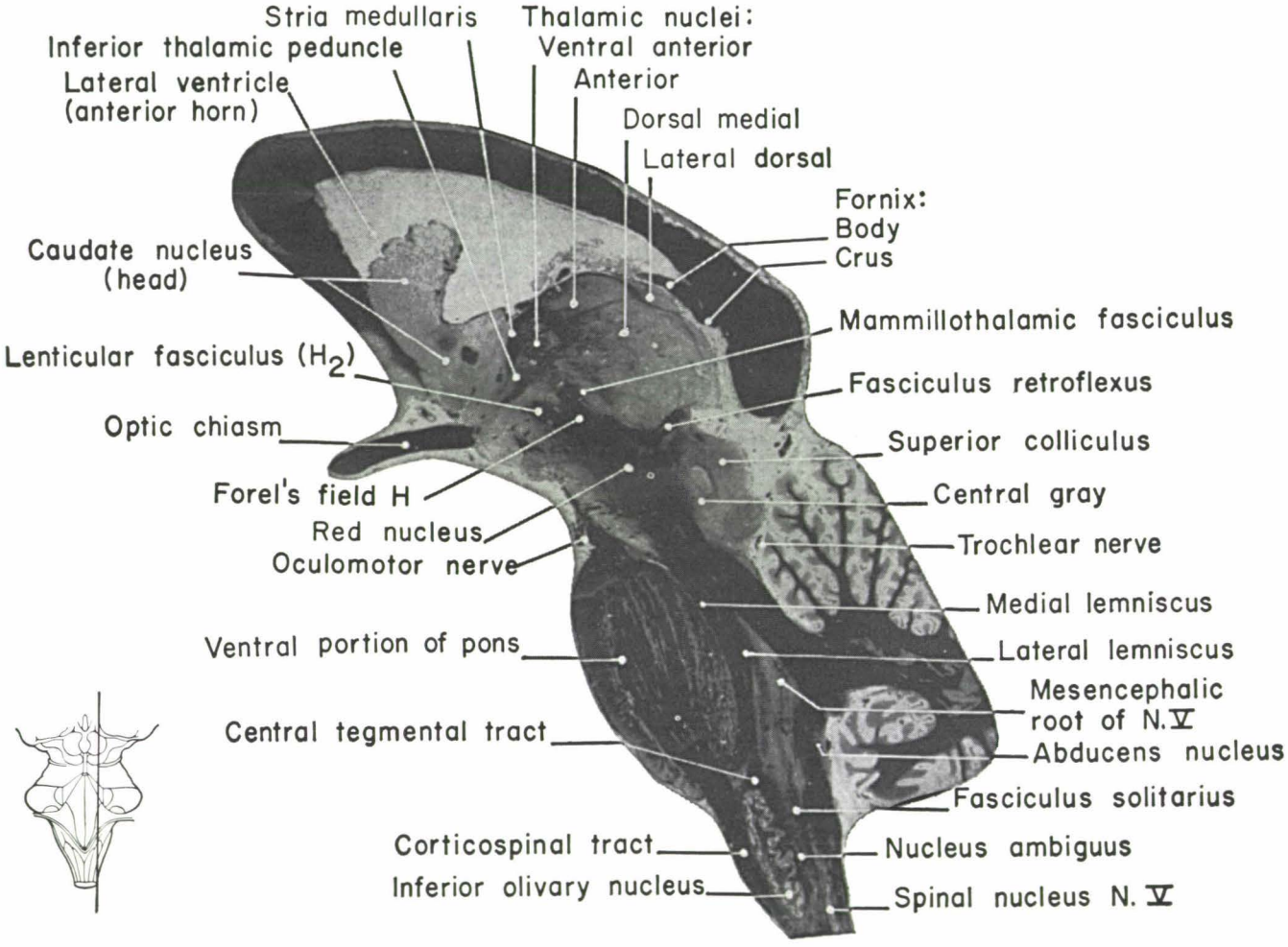




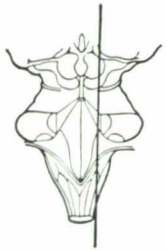
A-26. Sagittal section through brain stem at the level of the nucleus gracilis and emergence of the trochlear nerve. x1.3.

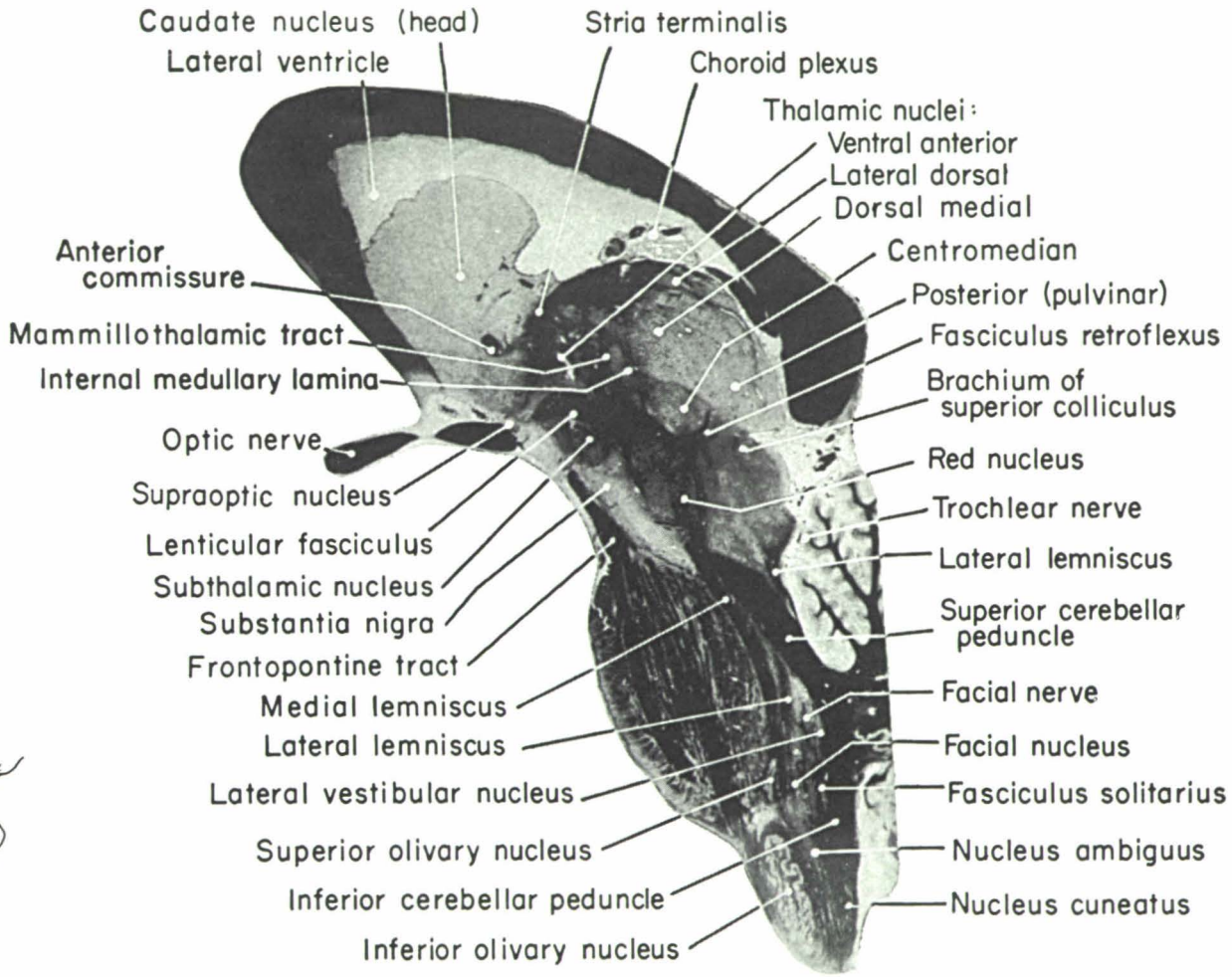


A-27. Sagittal section through the brain stem at the level of the nucleus cuneatus and habenula. x1.3.

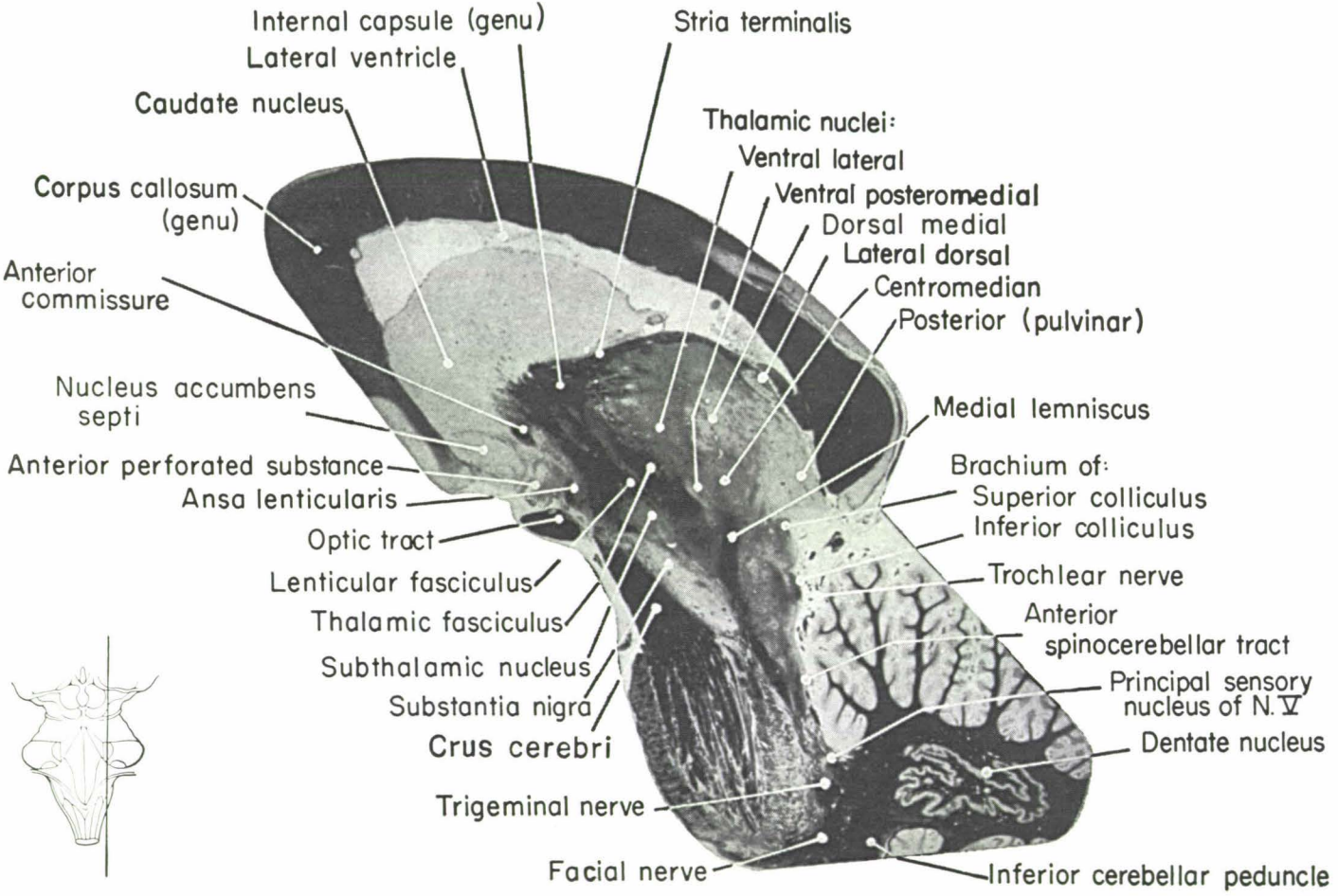


A-28. Sagittal section through the brain stem at the level of the nucleus ambiguus, lateral lemniscus, and fasciculus retroflexus. x1.3.

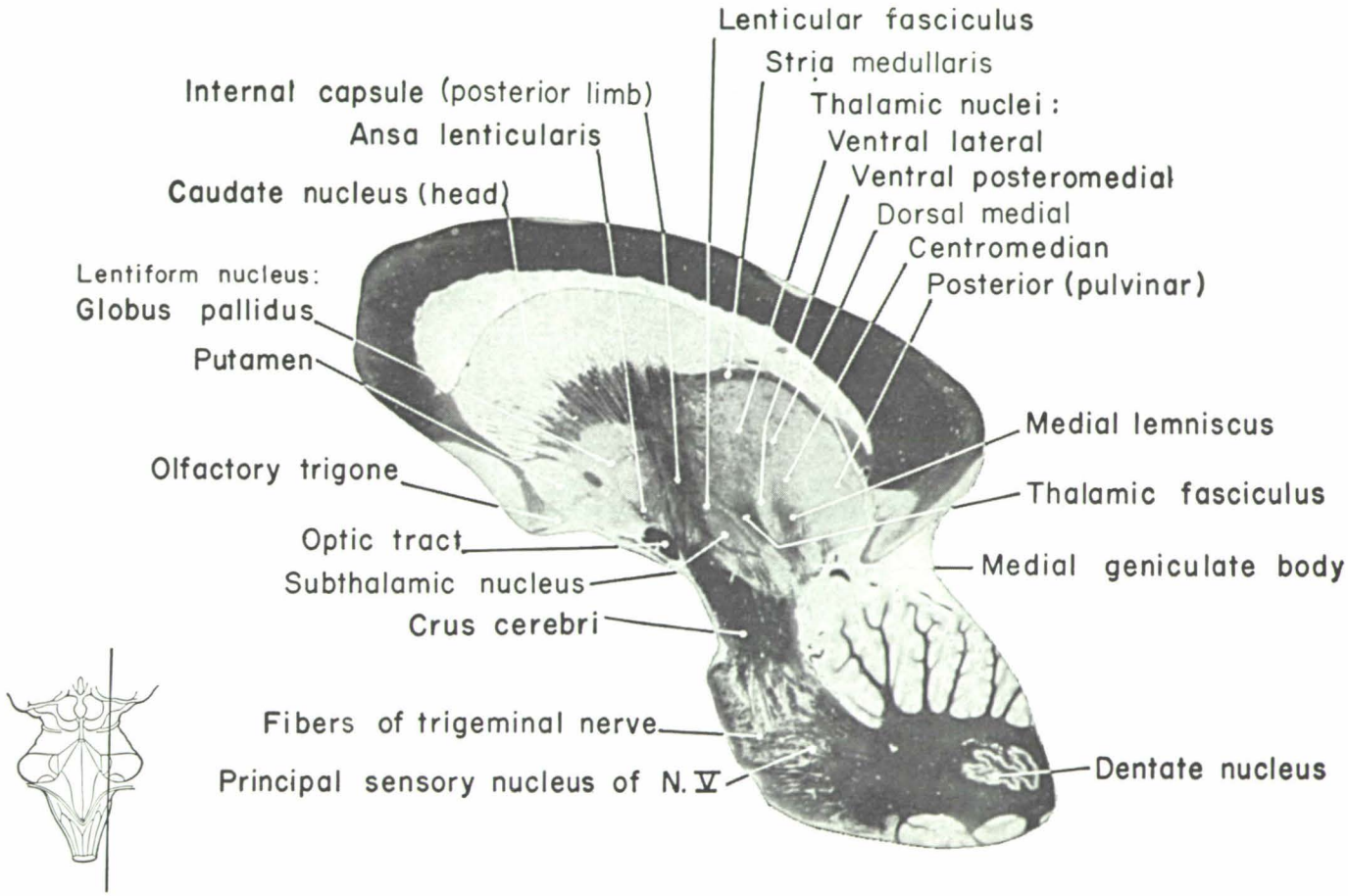




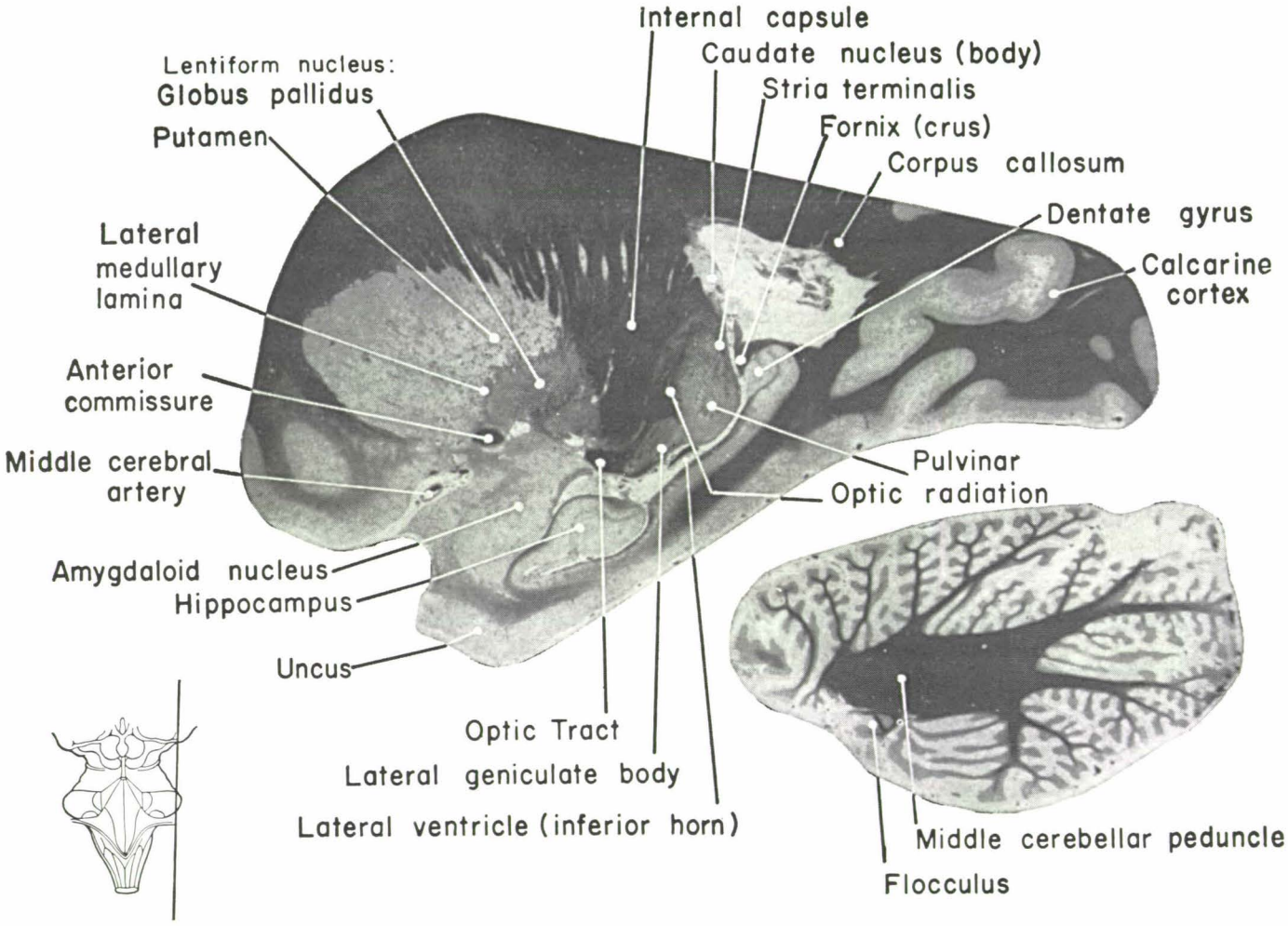
A-29. Sagittal section through the brain stem at the level of the facial, subthalamic and centromedian nuclei. x1.3.



A-30. Sagittal section through the brain stem at the level of the trigeminal nerve, brachia of the colliculi, and thalamic nuclei. x1.5.



A-31. Sagittal section through upper brain stem at the level of the trigeminal nerve and the medial geniculate body. x1.3.



A-32. Sagittal section of the brain at the level of the flocculus, lateral geniculate body, and inferior horn of the lateral ventricle. x65.

Figure/Table Credits

FIGURES

Figure 1.1 from Mettler FA. Neuroanatomy 2d ed. St. Louis: C.V. Mosby Co., 1948.

Figure 1.2 from Mettler FA. Neuroanatomy 2d ed. St. Louis: C.V. Mosby Co., 1948.

Figure 1.3 from Mettler FA. Neuroanatomy 2d ed. St. Louis: C.V. Mosby Co., 1948.

Figure 1.4 from Mettler FA. Neuroanatomy 2d ed. St. Louis: C.V. Mosby Co., 1948.

Figure 1.5 from Mettler FA. Neuroanatomy 2d ed. St. Louis: C.V. Mosby Co., 1948.

Figure 1.8 from Mettler FA. Neuroanatomy 2d ed. St. Louis: C.V. Mosby Co., 1948.

Figure 1.14 from Fenstermacher JD, Rall DP. Physiology and pharmacology of cerebrospinal fluid. In: Fenstermacher JD, ed. Pharmacology of the cerebral circulation. Vol. 1. Oxford: Pergamon Press, 1973:35–79.

Figure 1.16 modified from Weindl A, Sofroniew MV. Relation of neuropeptides to mammalian circumventricular organs. In: Martin JB, Reichlin S, Bick KL, eds. Advances in biochemical psychopharmacology. Vol 28. Neurosecretion and brain peptides. New York: Raven Press, 1981;303–320.

Figure 2.2 from Mettler FA. Neuroanatomy 2d ed. St. Louis: C.V. Mosby Co., 1948.

Figure 2.4 from Mettler FA. Neuroanatomy 2d ed. St. Louis: C.V. Mosby Co., 1948.

Figure 2.5 from Mettler FA. Neuroanatomy 2d ed. St. Louis: C.V. Mosby Co., 1948.

Figure 2.6 from Mettler FA. Neuroanatomy 2d ed. St. Louis: C.V. Mosby Co., 1948.

Figure 2.7 from Mettler FA. Neuroanatomy 2d ed. St. Louis: C.V. Mosby Co., 1948.

Figure 2.9 from Truex RC, Kellner CE. Detailed atlas of the head and neck. New York: Oxford University Press, 1948.

Figure 2.10 from Mettler FA. Neuroanatomy 2d ed. St. Louis: C.V. Mosby Co., 1948.

Figure 2.11 from Mettler FA. Neuroanatomy 2d ed. St. Louis: C.V. Mosby Co., 1948.

Figure 2.17 from Mettler FA. Neuroanatomy 2d ed. St. Louis: C.V. Mosby Co., 1948.

Figure 2.18 from Mettler FA. Neuroanatomy 2d ed. St. Louis: C.V. Mosby Co., 1948.

Figure 2.19 from Mettler FA. Neuroanatomy 2d ed. St. Louis: C.V. Mosby Co., 1948.

Figure 2.20 from Mettler FA. Neuroanatomy 2d ed. St. Louis: C.V. Mosby Co., 1948.

Figure 2.26 from Mettler FA. Neuroanatomy 2d ed. St. Louis: C.V. Mosby Co., 1948.

Figure 2.30 from Mettler FA. Neuroanatomy 2d ed. St. Louis: C.V. Mosby Co., 1948.

Figure 2.31 from Mettler FA. Neuroanatomy 2d ed. St. Louis: C.V. Mosby Co., 1948.

Figure 2.32 from Mettler FA. Neuroanatomy 2d ed. St. Louis: C.V. Mosby Co., 1948.

Figure 2.33 from Mettler FA. Neuroanatomy 2d ed. St. Louis: C.V. Mosby Co., 1948.

Figure 2.34 from Hanaway J, Scott WR, Strother CM. Atlas of the human brain and the orbit for computed tomography. St. Louis: Warren H. Green, Inc., 1980.

Figure 2.35 from Hanaway J, Scott WR, Strother CM. Atlas of the human brain and the orbit for computed tomography. St. Louis: Warren H. Green, Inc., 1980.

Figure 2.36 from Hanaway J, Scott WR, Strother CM. Atlas of the human brain and the orbit for computed tomography. St. Louis: Warren H. Green, Inc., 1980.

Figure 2.37 images were kindly provided by Drs. Denis Melançon and Donatella Tampieri, Montreal Neurological Institute, McGill University.

Figure 2.38 images were kindly provided by Drs. Denis Melançon and Donatella Tampieri, Montreal Neurological Institute, McGill University.

Figure 2.39 images were kindly provided by Drs. Denis Melançon and Donatella Tampieri, Montreal Neurological Institute, McGill University.

Figure 2.40 images were kindly provided by Dr. David Li, Division of Neurology, Department of Medicine, and Dr. Brian C. Pate, Professor at the Faculty of Medicine of the University of British Columbia.

Figure 2.41 images were kindly provided by Dr. Donald B. Calne, Division of Neurology, Department of Medicine, University of British Columbia, and Dr. Brian C. Pate, Professor at the Faculty of Medicine of the University of British Columbia.

Figure 2.42 images were kindly provided by Dr. Donald B. Calne, Division of Neurology, Department of Medicine, University of British Columbia, and Dr. Brian C. Pate, Professor at the Faculty of Medicine of the University of British Columbia.

Figure 3.2A from Davis CL. Description of a human embryo having 20 paired somites. Contrib Embryol 1923;15:1–51.

Figure 3.2B from Ingalls NW. A human embryo at the beginning of segmentation with special reference to the vascular system. Contrib Embryol 1920;11:61–90.

Figure 3.3C from Payne F. General description of a 7-somite human embryo. Contrib Embryol 1924;16: 115–124.

Figure 3.4 from Sauer FC. Mitosis in the neural tube. J Comp Neurol 1935;62:377–405.

Figure 3.5 from Keibel F, Mall FP. Manual of Human Embryology, Vol. II, Ch. XIV. Philadelphia: J.P. Lippincott, 1912:1–144.

Figure 3.10 from Hochstetter F. Beiträge zur Entwicklungsgeschichte des menschlichen Gehirns. Vol. I. Vienna and Leipzig: F. Deutcke, 1919.

Figure 3.11 from Hochstetter F. Beiträge zur Entwicklungsgeschichte des menschlichen Gehirns. Vol. I. Vienna: F. Deutcke, 1919.

Figure 3.14 from Prentiss CW, Arey LB. A laboratory manual and textbook of embryology. Ch. XII. Philadelphia: W.B. Saunders Company, 1920:321–352.

Figure 3.15 from Hamilton WJ, Boyd JD, Mossman HW. Human embryology. Prenatal development of form and function. Ch. XII. Baltimore: Williams & Wilkins, 1962:315–388.

Figure 3.17 from Keibel F, Mall FP. Manual of Human Embryology, Vol. II, Ch. XIV. Philadelphia: J.P. Lippincott, 1912:1–144.

Figure 3.19 modified from Tuchman-Duplessis H, Auronx M, Haegel P. Illustrated human embryology. Vol. 3. Nervous system and endocrine glands (translated from French). New York: Springer-Verlag, 1974.

Figure 4.1 based on Bolton B. The blood supply of the human spinal cord. J Neurol Psychiatry 1939; 2:137–148; Suh TH, Alexander L. Vascular system of the human spinal cord. Arch Neurol Psychiatry 1939;41:659–677; and Zülch KJ. Mangeldurchblutung an der Grenzzone zweier Gefässgebiete als Ursache bisher ungeklärter Rückenmarksschädigungen. Dtsch Z Nervenheilk 1954;172:81–101.

Figure 4.3 courtesy of Drs. Daniel Hottenstein and Keith Himes, Holy Spirit Hospital, Camp Hill, PA.

Figure 4.4 from Truex RC, Kellner CE. Detailed atlas of the head and neck. New York: Oxford University Press, 1948.

Figure 4.9 from Taveras JM, Wood EH. Diagnostic neuroradiology. 2d ed. Baltimore: Williams & Wilkins, 1976.

Figure 4.10 courtesy of Dr. Harry A Kaplan.

Figure 4.12 courtesy of Dr. Harry A Kaplan.

Figure 4.13 modified from Aitken HF. A report on the circulation of the lobar ganglia made to Dr. James B. Ayer (with a postscript by JB Ayer, MD). Boston Med Surg J 1909;160(Suppl):18.

Figure 4.14 based on Alexander L. The vascular supply of the striopallidum. Proc Assoc Res Nerv Ment Dis 1942;21:77–132.

Figure 4.15 courtesy of Drs. Daniel Hottenstein and Keith Himes, Holy Spirit Hospital, Camp Hill, PA.

Figure 4.16 courtesy of Drs. Daniel Hottenstein and Keith Himes, Holy Spirit Hospital, Camp Hill, PA.

Figure 4.17 courtesy of Dr. Abbas F. Sadikot, Montreal Neurological Institute, McGill University.

Figure 4.19 from Hassler O. Venous anatomy of human hindbrain. Arch Neurol 1967a;16: 404–409.

Figure 4.20 based on Stopford JSB. The arteries of the pons and medulla oblongata. Part I. J Anat Physiol 1915;50:131–164; and Stopford JSB. The arteries of the pons and medulla oblongata. Part II. J Anat Physiol 1916;51:255–280.

Figure 4.21 from Hassler O. Venous anatomy of human hindbrain. Arch Neurol 1967a;16: 404–409.

Figure 4.23 from Mettler FA. Neuroanatomy. St. Louis: C.V. Mosby Co., 1948.

Figure 4.26 modified from Schwartz P, Fink L. Morphologie und Entstehung der geburstraumatischen Blutungenim Gehirn und Schädel des Neugeborenen. Z Kinder heilk 1926;40:427–474.

Figure 4.27 modified from Schlesinger B. Venous drainage of the brain, with special reference to galenic system. Brain 1939;62: 274–291.

Figure 4.28 from Hassler O. Deep cerebral venous system in man: a microangiographic study on this areas of drainage and its anastomoses with the superficial cerebral veins. Neurology 1966a;16: 505–511.

Figure 4.29 modified from Schlesinger B. Venous drainage of the brain, with special reference to galenic system. Brain 1939;62: 274–291.

Figure 4.30 from Hassler O. Deep cerebral venous system in man: a microangiographic study on this areas of drainage and its anastomoses with the superficial cerebral veins. Neurology 1966a;16:505–511.

Figure 5.4 from the work of L.N. Hazrati and A. Parent, Neurobiology Research Center, Laval University, Québec, Canada.

Figure 5.5 courtesy of Drs. Y. Soltesz and M. Deschênes, Neurobiology Research Center, Laval University, Québec, Canada.

Figure 5.6 courtesy of Dr. J-J Soghomonian, Neurobiology Research Center, Laval University, Québec, Canada.

Figure 5.7 based on Bodian D. The generalized vertebrate neuron. Science 1962;137:323–326.

Figure 5.8 courtesy of the late Dr. Clement Fox, Wayne State University.

Figure 5.9 courtesy of the late Dr. Clement Fox, Wayne State University.

Figure 5.11 from Barr ML, Bertram LF, Lindsay HA. The morphology of the nerve cell nucleus according to sex. Anat Rec 1950;107:283–297.

Figure 5.13 courtesy of H.J. Ralston III, University of California School of Medicine, San Francisco.

Figure 5.14 courtesy of Drs. Sandford L. Palay and Victoria Chan-Palay, Harvard Medical School; from Cerebellar cortex: cytology and organization. Berlin: Springer-Verlag, 1974.

Figure 5.15 courtesy of Drs. Alan Peters, Henry de Webster, and Sandford Palay, Harvard Medical School, Boston, MA.

Figure 5.17 courtesy of Dr. C. Sotelo, Laboratoire d'Histologie Normale et Pathologique du Système Nerveux, Paris; from Sotelo C, Palay SL. The fine structure of the lateral vestibular nucleus in the rat. I. Neurons and neuroglial cells. J Cell Biol 1968;36:151–179.

Figure 5.18 from the work of A. F. Sadikot, and A. Parent, Neurobiology Research Center, Laval University, Québec, Canada.

Figure 5.19 from the work of L-N Hazrati, A. Charara, and A. Parent, Neurobiology Research Center, Laval University, Québec, Canada.

Figure 5.21 from Copenhaver WM, Bunge RP, Bunge MB. Bailey's textbook of histology. 16th ed. Baltimore: Williams & Wilkins, 1971.

Figure 5.22 from Bunge RP. Glial cells and the central myelin sheath. Physiol Rev 1968;48:197–251.

Figure 5.23 courtesy of H.J. Ralston III, University of California School of Medicine, San Francisco.

Figure 5.24 courtesy of Drs. M.B. Bunge and R.P. Bunge, Washington University School of Medicine, St. Louis.

Figure 5.26 courtesy of Dr. R.P. Bunge.

Figure 5.27 courtesy of Dr. J. Rhodin, School of Medicine, University of South Florida, Tampa.

Figure 5.29 modified from Standaert FG, Dretchen KL. Cyclic nucleotides and neuromuscular transmission. Fed Proc 1979;38: 2183–2192.

Figure 5.30 courtesy of Dr. J. Francis Hartmann, Presbyterian-St. Luke's Hospital, Chicago.

Figure 5.31 courtesy of Dr. Ray C. Hendrikson, Albany College of Medicine of Union University, Albany, NY.

Figure 5.32 based on Greengard P. Cyclic nucleotides, phosphorylated proteins and neuronal structure. New York: Raven Press, 1978; Greengard P. Cyclic nucleotides, phosphorylated proteins and the nervous system. Fed Proc 1979; 38:2208–2217.

Figure 5.34 based on Kandel E. Cellular insights into behavior and learning. In: The Harvey Lectures, series 73. New York: Academic Press, 1979:19–92; Greengard P. Possible role for cyclic nucleotides and phosphorylated membrane proteins in postsynaptic actions of neurotransmitters. Nature 1976; 260:101–108.

Figure 5.35 from Young JZ. The functional repair of nervous tissue. Physiol Rev 1942;23:318–374.

Figure 5.38 based on Ramón y Cajal, S.. Histologie du Système Nerveux de l'Homme et des Vertébrés. (Azoulay L, trans.) Paris: Maloine, 1909, 1911 (Reprinted, Consejo Superior de Investigaciones Cientificas, Instituto Ramón y Cajal, Madrid, 1972).
Figure 5.39 from Young JZ. Factors influencing the regeneration of nerves. Adv Surg 1949;1:165–220.
Figure 5.41 based on Weiss P, Hiscoe HB. Experiments on the mechanism of nerve growth. J Exp Zool 1948;107:315–396; Young JZ. Factors influencing the regeneration of nerves. Adv Surg 1949;1:165–220.
Figure 5.42 courtesy of Dr. P.J. Bédard, Neurobiology Research Center, Laval University, Québec, Canada.
Figure 6.1 from Bodian D. The neurosciences. In: Quarton GC, ed. A study program. New York: Rockefeller University Press, 1967:6–24.
Figure 6.3 from Penfield W. Cytology and cellular pathology of the nervous system. New York: Paul B. Hoeber, 1932.
Figure 6.5 courtesy of Dr. James E. Vaughn, City of Hope Medical Center, Duarte, CA.
Figure 6.8 courtesy of Dr. James E. Vaughn, City of Hope Medical Center, Duarte, CA.
Figure 6.9 courtesy of Dr. R.P. Bunge; from Copenhaver WM, Bunge RP, Bunge MB, et al. Bailey's textbook of histology. 16th ed. Baltimore: Williams & Wilkins, 1971.
Figure 6.12 based on Ramón y Cajal S. Histologie du Système Neveux de l'Homme et des Vertébrés. (Azoulay L, trans.) Paris: Maloine, 1909, 1911. (Reprinted, Consejo Superior de Investigaciones Cientificas, Instituto Ramón y Cajal, Madrid, 1972.)
Figure 6.14 courtesy of Dr. Virginia Tennyson, College of Physicians and Surgeons, Columbia University, New York.
Figure 6.15 from Brightman MW, Palay SL. The fine structure of ependyma in the brain of the rat. J Cell Biology 1963;19:415–439.
Figure 6.16 from Page RB, Rosenstein JM, Dovey BJ, et al. Ependymal changes in experimental hydrocephalus. Anat Rec 1979;194: 67–82.
Figure 6.19 courtesy of Dr. Virginia Tennyson, College of Physicians and Surgeons, Columbia University, New York.
Figure 6.20 courtesy of Dr. R. Marchand, Neurobiology Research Center, Laval University, Québec, Canada.
Figure 7.1 modified from Tuchmann-Duplessis H, Auronx M, Haegel P. Illustrated human embryology. Vol. 3: Nervous system and endocrine glands (translated from French) New York: Springer-Verlag, 1974.
Figure 7.2 from Ramón y Cajal S. Histologie du Système Nerveux de l'Homme et des Vertébrés. (Azoulay L, trans.) Paris: Maloine, 1909, 1911. (Reprinted, Consejo Superior de Investigaciones Cientificas, Instituto Ramón y Cajal, Madrid, 1972.)
Figure 7.4A based on De Castro F. Contribution à la connaissance de l'innervation du pancréas. Y a t-il des conducteurs spécifiques pour les îlots de Langerhans, pour les acini glandulaires et pour les vaisseaux. Trav Lab Rech Biol Univ Madrid 1923;21:423–457.
Figure 7.4B based on Smirnow A. Über die sensiblen Nervenendigungen im Herzen bei Amphibien und Saügetieren. Anat Anz 1895;10:737–749.
Figure 7.4C based on Larsell O, Dow RS. Innervation of the human lung. Am J Anat 1933;52:414–438.
Figure 7.4D based on Carpenter FW. Nerve endings of sensory type in the muscular coat of the stomach and small intestine. J Comp Neurol 1918;29:553–560.
Figure 7.5 modified from Cauna N. The effects of aging on the receptor organs of the human dermis. In: Montagna W, ed. Advances in biology of skin. Vol. 6. Aging. New York: Pergamon Press, 1965:63–69.
Figure 7.6 from Merkel F. Tastzellen und Tastkörperchen beiden Hausthieren und beim Menschen. Arch Mikrosk Anat Entwick Mech 1975;11:636–652.
Figure 7.7 based on Ralston HJ III, Miller MR, Kasahara M. Nerve endings in human fasciae, tendons, ligaments, periosteum, and joint synovial membrane. Anat Rec 1960;136:137–148.
Figure 7.9A based on Dogiel AS. Die Nervenendkörperchen (Endkolben. W. Krause) in der Cornea und Conjunctiva Bulbi des Menschen. Arch Mikrosk Anat Entwickl-Gesch 1891;37:602–619.
Figure 7.9B from Ruffini A. Sur un nouvel organe nerveux terminal et sur la présence des corpuscules Golgi-Mazzoni dans le conjonctif sous-cutané de la pulpe des doigts de l'homme. Arch Ital Biol 1894;21:249–265.
Figure 7.10 based on from Ramón y Cajal S. Histologie du Système Nerveux de l'Homme et des Vertébrés. (Azoulay L, trans.) Paris: Maloine, 1909, 1911. (Reprinted, Consejo Superior de Investigaciones Cientificas, Instituto Ramón y Cajal, Madrid, 1972.)
Figure 7.11 after Barker D. The innervation of the muscle-spindle. QJ Microscop Sci 1948;89:143–186.
Figure 7.12 courtesy of Dr. W.R. Kennedy, University of Minnesota, Minneapolis, MN.
Figure 7.13 courtesy of Dr. W.R. Kennedy, University of Minnesota, Minneapolis, MN.
Figure 7.14 courtesy of Dr. W.R. Kennedy, University of Minnesota, Minneapolis, MN.
Figure 7.15 modified from Schoultz TW, Swett JE. The fine structure of the Golgi tendon organ. J Neurocytol 1972;1:1–26.
Figure 7.16 from Schoultz TW, Swett JE. The fine structure of the Golgi tendon organ. J Neurocytol 1972;1:1–26.
Figure 7.17 modified from Robertson JD. The ultrastructure of a reptilian myoneural junction. J Biophys Biochem Cytol 1956;2: 381–394; Robertson JD. Electron microscopy of the motor end-plate and the neuromuscular spindle. Am J Phys Med 1960;39:1–43; and Couteaux R. Morphological and cytochemical observations on the postsynaptic membrane at motor endplates and ganglionic synapses. Exp Cell Res 1958;5:294–322.
Figure 7.18 from Larsell O, Dow RS. Innervation of the human lung. Am J Anat 1933;52:414–438.
Figure 8.2 from Carmel PW, Stein, BM. J Comp Neurol 1969;135: 145–166.
Figure 8.3 after Ramón y Cajal S. Histologie du Système Nerveux de l'Homme et des Vertébrés. (Translated by L. Azoulay), Paris: Maloine, 1909, 1911. (Reprinted, Consejo Superior de Investigaciones Cientificas, Instituto Ramón y Cajal, Madrid, 1972.)
Figure 8.4 from Truex RC. Morphological alterations in the Gasserian ganglion cells and their association with senescence in man. Am J Pathol 1940;16:255–268.
Figure 8.5 from Carmel PW, Stein BM. Cell changes in sensory ganglia following proximal and distal nerve section in the monkey. J Comp Neurol 1969;135:145–166.
Figure 8.7 from Copenhaver WM. Bailey's textbook of histology. 15th ed. Baltimore: Williams & Wilkins, 1964.
Figure 8.8 modified from Haymaker W, Woodhall B. Peripheral nerve injuries: principles of diagnosis. Philadelphia: W.B. Saunders, 1945.

Figure 8.9 modified from Haymaker W, Woodhall B. Peripheral nerve injuries: principles of diagnosis. Philadelphia: W.B. Saunders, 1945.

Figure 8.10 modified from Haymaker W, Woodhall B. Peripheral nerve injuries: principles of diagnosis. Philadelphia: W.B. Saunders, 1945.

Figure 8.16 after Haymaker W. Bing's local diagnosis in neurological diseases. St. Louis: C.V. Mosby, 1956.

Figure 8.17 after Haymaker W. Bing's local diagnosis in neurological diseases. St. Louis: C.V. Mosby, 1956.

Figure 8.18 after Haymaker W. Bing's local diagnosis in neurological diseases. St. Louis: C.V. Mosby, 1956.

Figure 9.4 adapted from Furness JB, Costa M. Types of nerves in the enteric nervous system. Neuroscience 1980;5:1–20.

Figure 9.6A after Ramón y Cajal S. Histologie du Système Nerveux de l'Homme et des Vertébrés. (Azoulay L, Trans.) Paris: Maloine, 1909, 1911. (Reprinted, Consejo Superior de Investigaciones Cientificas, Instituto Ramón y Cajal, Madrid, 1972.)

Figure 9.6B after Ranson SW, Billingsley PR. The superior cervical ganglion and the cervical portion of the sympathetic trunk. J Comp Neurol 1918;29:313–358.

Figure 9.7 courtesy of Dr. Torbjörn Malmfors, Karolinska Institutet, Sweden.

Figure 9.8 courtesy of Dr. Michael D. Gershon, College of Physicians and Surgeons, Columbia University, New York.

Figure 9.10 modified from White JC, Okelberry AM, Whitelaw GP. Vasomotor tonus of the denervated artery. Arch Neurol and Psychiatry 1936;36:1251–1276.

Figure 10.20 adapted from Cullheim S, Kellerth J-O. Morphological study of the axons and recurrent axon collaterals of cat sciatic a motoneurons after intracellular staining with horseradish peroxidase. J Comp Neurol 1978;178: 537–558; and Cullheim S, Kellerth J-O, Conradi S. Evidence for direct synaptic interconnections between cat spinal gamma-motoneurons via the recurrent axon collaterals: A morphological study using intracellular injection of horseradish peroxidase. Brain Res 1977;132: 1–10.

Figure 10.21 based on Sterling P, Kuypers HGJM. Anatomical organization of the brachial spinal cord of the cat. II. The motoneuron plexus. Brain Res 1967;4:16–32.

Figure 10.26 based on Cummings JF, Petras JM. The origin of spinocerebellar pathways. I. The nucleus cervicalis centralis of the cranial cervical spinal core. J Comp Neurol 1977;173:655–692.

Figure 10.28 from Jessell TM, Iversen LL. Opiate analgesics inhibit substance P release from rat trigeminal nucleus. Nature 1977; 268:549–551; and courtesy of Professor Stephen Hunt, Cambridge University.

Figure 12.18 based on Kalia M, Mesulam M-M. Brain stem projections of sensory and motor components of the vagus complex in the cat. I. The cervical vagus and nodose ganglion. J Comp Neurol 1980;193:435–465; Loewy AD, Burton H. Nuclei of the solitary tract: efferent projections to the lower brain stem and spinal cord of the cat. J Comp Neurol 1978;181: 421–450; and Beckstead RM, Norgren R. An autoradiographic examination of the central distribution of the trigeminal, facial, glossopharyngeal and vagal nerves in the monkey. J Comp Neurol 1979;184:455–472.

Figure 12.20 based on Ramón y Cajal S. Histologie du Système Nerveux de l'Homme et des Vertébrés. (Azoulay L, trans.), Paris: Maloine, 1909, 1911. (Reprinted, Consejo Superior de Investigaciones Cientificas, Instituto Ramón y Cajal, Madrid, 1972.)

Figure 12.21 reproduced from Kalia M, Mesulam M-M. Brain stem projections of sensory and motor components of the vagus complex in the cat. I. The cervical vagus and nodose ganglion. J Comp Neurol 1980;193:435–465.

Figure 12.22 from Kalia M, Mesulam M-M. Brain stem projections of sensory and motor components of the vagus complex in the cat. I. The cervical vagus and nodose ganglion. J Comp Neurol 1980;193: 435–465.

Figure 12.23 reproduced from Kalia M, Mesulam M-M. Brain stem projections of sensory and motor components of the vagus complex in the cat. I. The cervical vagus and nodose ganglion. J Comp Neurol 1980;193:435–465.

Figure 12.24 modified from Loewy AD, McKellar S. The neuroanatomical basis of central cardiovascular control. Fed Proc 1980;39: 2495–2503.

Figure 12.27 modified from Kuypers HGJM. Pericentral cortical projections to motor and sensory nuclei. Science 1958;128: 662–663.

Figure 13.6 from Mettler FA. Neuroanatomy. St. Louis: C.V. Mosby Co., 1948.

Figure 13.11 from Rivera-Dominguez M, Agate FJ Jr, Noback CR. Scanning electron microscopy of the spiral organ of Corti of the adult rhesus monkey. Brain Res 1973;65:159–164.

Figure 13.12 from Rose JE, Galambos R, Hughes JR. Organization of frequency sensitive neurons in the cochlear complex of the cat. In: Rasmussen GL, Windle WF, eds. Neural mechanisms of the auditory and vestibular systems. Springfield, IL: Charles C. Thomas, 1960;116–136.

Figure 13.12 from Carpenter MB. Core text of neuroanatomy. Baltimore: Williams & Wilkins, 1991.

Figure 13.14 modified from Rasmussen GL. Efferent fibers of the cochlear nerve and cochlear nucleus. In: Rasmussen GL, Windle WF, eds. Neural mechanisms of the auditory and vestibular systems. Ch. 8. Springfield, IL: Charles C. Thomas, 1960:105–115.

Figure 13.15 from Carpenter MB, Chang L, Pereira AB, Hersh LB, Bruce G, Wu JY. Vestibular and cochlear efferent neurons in the monkey identified by immunocytochemical methods. Brain Res 1987;408:275–280.

Figure 13.16 from Stein BM, Carpenter MB. Central projections of portions of the vestibular ganglia innervating specific part of the labyrinth in the rhesus monkey. Am J Anat 1967;120:281–318.

Figure 13.17 from Stein BM, Carpenter MB. Central projections of portions of the vestibular ganglia innervating specific part of the labyrinth in the rhesus monkey. Am J Anat 1967;120:281–318.

Figure 13.21 from Carpenter MB, Chang L, Pereira AB, Hersh LB, Bruce G, Wu JY. Vestibular and cochlear efferent neurons in the monkey identified by immunocytochemical methods. Brain Res 1987;408:275–280.

Figure 13.25 from Carpenter MB, Carleton SC. Comparison of vestibular and abducens projections to the medial rectus subdivision of the oculomotor complex in the monkey. Brain Res 1983;274: 144–149.

Figure 13.29 from Carpenter MB. Core text of neuroanatomy. Baltimore: Williams & Wilkins, 1991.

Figure 13.31 modified from Ramón y Cajal S. Histologie du Système Nerveux de l'Homme et des Vertébrés. (Azoulay L, Trans.) Paris: Maloine, 1909, 1911. (Reprinted, Consejo Superior de Investigaciones Cientificas, Instituto Ramón y Cajal, Madrid, 1972.)
Figure 13.35 courtesy of Drs. Jacqueline McGinty and Floyd Bloom, Salk Institute, La Jolla, CA.
Figure 14.10 from Carpenter MB, Pierson RJ. Pretectal region and the pupillary light reflex: an anatomical analysis in the monkey. J Comp Neurol 1973;149:271–300.
Figure 14.11 from Carpenter MB, Pierson RJ. Pretectal region and the pupillary light reflex: an anatomical analysis in the monkey. J Comp Neurol 1973;149:271–300.
Figure 14.14 based on Warwick R. Representation of the extraocular muscles in the oculomotor nuclei of the monkey. J Comp Neurol 1953;98:449–504; and Warwick R. The identity of the posterocentral nucleus of Panegrossi. J Comp Neurol 1953;99:599–612.
Figure 14.15 from Carpenter MB, Peter P. Accessory oculomotor nuclei in the monkey. J Hirnforsch 1970/71;12:405–418.
Figure 14.16 from Carpenter MB, Pierson RJ. Pretectal region and the pupillary light reflex: an anatomical analysis in the monkey. J Comp Neurol 1973;149:271–300.
Figure 14.17 from Carpenter MB, Harbison JW, Peter P. Accessory oculomotor nuclei in the monkey. Projections and effects of discrete lesions. J Comp Neurol 1970;140: 131–154.
Figure 14.18 after Ramón y Cajal S. Histologie du Système Nerveux de l'Homme et des Vertébrés. (Azoulay L, trans.), Paris: Maloine, 1909, 1911. (Reprinted, Consejo Superior de Investigaciones Cientificas, Instituto Ramón y Cajal, Madrid, 1972.)
Figure 15.3 modified from Ramón y Cajal S. Histologie du Système Nerveux de l'Homme et des Vertébrés. (Azoulay L, trans.), Paris: Maloine, 1909, 1911. (Reprinted, Consejo Superior de Investigaciones Cientificas, Instituto Ramón y Cajal, Madrid, 1972.)
Figure 15.5 based on Eccles JC, Ito M, Szentagothai J. The cerebellum as a neuronal machine. New York: Springer-Verlag, 1967; and Gray EG. The granule cells, mossy synapses and Purkinje spine synapses of the cerebellum: light and electron microscopic observations. J Anat 1961;95:345–356.
Figure 15.6 courtesy of the late Dr. C.A. Fox, School of Medicine, Wayne State University.
Figure 15.7 courtesy of Dr. P. De Camilli, Department of Cell Biology, School of Medicine, Yale University.
Figure 15.8 from Boegman RJ, Parent A, Hawkes R. Zonation in the rat cerebellar cortex: patches of high acetylcholinesterase activity in the granular layer are congruent with Purkinje cell compartments. Brain Res 1988;448:237–251.
Figure 15.9 courtesy of Dr. D.B. Newman, Uniformed Service University, Bethesda, MD.
Figure 15.11 courtesy of the late Dr. C.A. Fox, School of Medicine, Wayne State University.
Figure 15.12 based on Eccles JC, Ito M, Szentagothai J. The cerebellum as a neuronal machine. New York: Springer-Verlag, 1967.
Figure 15.13 courtesy of Dr. R.C. Henrikson, Albany Medical College, Albany, NY.
Figure 15.14 modified from Eccles JC, Ito M, Szentagothai J. The cerebellum as a neuronal machine. New York: Springer-Verlag, 1967.
Figure 15.15 from Jakob A. Das Kleinhirn. In: von Möllendorff W, ed. Handbuch der mikroskopishen Anatomie des Menschen. Vol. IV. Berlin: Julius Springer, 1928: 674–916.
Figure 15.16 based on Palay SL, Chan-Palay V. Cerebellar cortex: cytology and organization. Berlin: Springer-Verlag, 1974.
Figure 15.17 from Mettler FA. Neuroanatomy. St. Louis: C.V. Mosby, 1948.
Figure 15.20 based on Snider RS. Recent contributions to the anatomy and physiology of the cerebellum. Arch Neurol Psychiatry 1950;64:196–219.
Figure 15.23 from Batton RR III, Jayaraman A, Ruggiero D, Carpenter MB. Fastigial efferent projections in the monkey: an autoradiographic study. J Comp Neurol 1977;174:281–306.
Figure 15.25 modified from Brodal A, Pompeiano O, Walberg F. The vestibular nuclei and their connections, anatomy and functional correlations. Springfield, IL: Charles C. Thomas, 1962.
Figure 16.1 from Mettler FA. Neuroanatomy. St. Louis: C.V. Mosby Co., 1948.
Figure 16.8 from Carpenter MB. Core text of neuroanatomy. Baltimore: Williams & Wilkins, 1978.
Figure 16.10 modified from Malone EF. Über die Kerne des menschlichen Diencephalon: Abhandlungen der könighl preuss. Akademie der Wissenschaften 1910;92.
Figure 16.11 modified from Malone EF. Über die Kerne des menschlichen Diencephalon: Abhandlungen der könighl preuss. Akademie der Wissenschaften 1910;92.
Figure 16.15 from Roberts TS, Akert K. Insular and opercular cortex and its thalamic projection in Macaca mulatta. Schweiz Arch Neurol Neurochir Psychiat 1963; 92:1–43.
Figure 16.16 modified from Sadikot AF, Parent A, François C. Efferent connections of the centromedian and parafascicular thalamic nuclei in primates. A PHA-L study of subcortical projections. J Comp Neurol 1992;315:137–159.
Figure 16.18 modified from Hazrati L-N, Parent A. Contralateral pallidothalamic and pallidotegmental projections in primates: an anterograde and retrograde labeling study. Brain Res 1991;567:212–223.
Figure 16.19 based on Jones EG, Friedman DP. Projection pattern of functional components of thalamic ventrobasal complex on monkey somatosensory cortex. J Neurophysiol 1982;48:521–544.
Figure 16.20 based on Jones EG, Friedman DP. Projection pattern of functional components of thalamic ventrobasal complex on monkey somatosensory cortex. J Neurophysiol 1982;48:521–544.
Figure 16.21 from Beckstead RM, Morse JR, Norgren R. The nucleus of the solitary tract in the monkey: projections to the thalamus and brain stem nuclei. J Comp Neurol 1980;190:259–282.
Figure 16.22 modified from Jones EG, Powell TPS. An analysis of the posterior group of thalamic nuclei on the basis its afferent connections. J Comp Neurol 1971;143: 185–216.
Figure 16.23 based on Morest DK. The laminar structure of the medial geniculate body of the cat. J Anat 1965;99:143–159.
Figure 16.25 from Hickey TL, Guillery RW. Variability of laminar patterns in the human lateral geniculate nucleus. J Comp Neurol 1979;183:221–246.
Figure 16.26 from Kaas JH, Guillery RW, Allman JM. Some principles of organization in the dorsal lateral geniculate nucleus. Brain Behav Evol 1972;6:253–299.
Figure 16.27 modified from Kaas

JH, Guillery RW, Allman JM. Some principles of organization in the dorsal lateral geniculate nucleus. Brain Behav Evol 1972;6:253–299.

Figure 16.28 based on Hoyt WF, Luis O. Visual fiber anatomy in the infrageniculate pathway of the primate. Arch Opthalmol 1962;68: 94–106; and Noback CR, Laemle LK. Structural and functional aspects of the visual pathways of primates. In: Noback CR, Montagna W, eds. Advances in primatology. Vol. 1: The primate brain. Ch. 3. New York: Appleton-Century-Crofts, 1970:55–81.

Figure 16.29 based on Malpeli JG, Baker FH. The representation of the visual field in the lateral geniculate nucleus of the Macaca mulatta. J Comp Neurol 1975;161: 569–594.

Figure 16.30 modified from Szentagothai J. Glomerular synapses, complex synaptic arrangements, and their operational significance. In: Schmitt FO, ed. The neurosciences. Second study program. Ch. 40. New York: Rockefeller University Press, 1970:427–443.

Figure 16.31 courtesy of Drs. M. Deschênes and D. Pinault, Neurobiology Research Center, Laval University, Québec, Canada.

Figure 16.32 modified from Sadikot AF, Parent A, François C. Efferent connections of the centromedian and parafascicular thalamic nuclei in primates. A PHA-L study of subcortical projections. J Comp Neurol 1992;315:137–159.

Figure 16.33 modified from Smith Y, Parent A, Séguéla P, Descarries L. Distribution of GABA-immunoreactive neurons in the basal ganglia of the squirrel monkey (*Saimiri Sciureus*). J Comp Neurol 1987;259:50–65.

Figure 16.34 modified from Smith Y, Parent A, Séguéla P, Descarries L. Distribution of GABA-immunoreactive neurons in the basal ganglia of the squirrel monkey (*Saimiri Sciureus*). J Comp Neurol 1987;259:50–65.

Figure 16.35 courtesy of Dr. J.-J. Soghomonian, Neurobiology Research Center, Laval University, Québec, Canada.

Figure 16.36 modified from Lavoie B, Parent A. Serotoninergic innervation of the thalamus in the primate: an immunohistochemical study. J Comp Neurol 1991;312: 1–18.

Figure 16.37 modified from Lavoie B, Parent A. Serotoninergic innervation of the thalamus in the primate: an immunohistochemical study. J Comp Neurol 1991;312: 1–18.

Figure 16.40 modified from Dowling JE, Boycott BB. Organization of the primate retina: electron microscopy. Proc R Soc Lond (Biol) 1966;166:80–111; and Noback CR, Laemle LK. Structural and functional aspects of the visual pathways of primates. In: Noback CR, Montagna W, eds. Advances in primatology. Vol. 1: The primate brain. Ch. 3. New York: Appleton-Century-Crofts, 1970:55–81.

Figure 16.42 from Mettler FA. Neuroanatomy. St. Louis: C.V. Mosby Co., 1948.

Figure 16.43 modified from Haymaker W. Bing's local diagnosis in neurological diseases. St. Louis: C.V. Mosby Company, 1956:57–62 and 105–112.

Figure 17.2 based on Le Gros Clark WE, Beattie J, Riddoch G, Dott NM, eds. The hypothalamus. Edinburgh: Oliver and Boyd, 1938.

Figure 17.3 based on Le Gros Clark WE, Beattie J, Riddoch G, Dott NM, eds. The hypothalamus. Edinburgh: Oliver and Boyd, 1938.

Figure 17.5 modified from Parent A, Descarries L, Beaudet A. Organization of ascending serotonin systems in the adult rat brain. A radioautographic study after intraventricular administration of [^{3}H] 5-hydroxytryptamine. Neuroscience 1981;6:115–138.

Figure 17.6 courtesy of S. Bovetto, C. Rouillard, and D. Richard of the Neurobiology Research Center and Physiology Department, Laval University, Québec, Canada.

Figure 17.7 from Silverman AJ, Pickard GE. The hypothalamus. In: Emson PC, ed. Chemical neuroanatomy. New York: Raven Press, 1983:295–336.

Figure 17.8 from Pickard GE, Silverman A-J. Direct retinal projection to the hypothalamus, piriform cortex, and accessory optic nuclei in the golden hamster as demonstrated by a sensitive anterograde horseradish peroxidase technique. J Comp Neurol 1981;196:155–172.

Figure 17.9 from Millhouse OE. A Golgi anatomy of the rodent hypothalamus. In: Morgane P, Panksepp J, eds. Handbook of the hypothalamus. Vol. I: Anatomy of the hypothalamus. New York: Marcel Dekker, 1979:221–265.

Figure 17.10 from Silverman AJ, Pickard GE. The hypothalamus. In: Emson PC, ed. Chemical neuroanatomy. New York: Raven Press, 1983:295–336.

Figure 17.11 courtesy of Dr. Georges Pelletier, Molecular Endocrinology Laboratory, CHUL, Québec, Canada.

Figure 17.14 based on Nauta WJH. Hippocampal projections and related neural pathways to the midbrain in the cat. Brain 1958;81: 319–340.

Figure 17.17 modified from Raisman G. Neural connections of hypothalamus. Br Med Bull 1966; 22:197–201.

Figure 17.19 from Page RB, Bergland RM. The neurohypophyseal capillary bed. I. Anatomy and arterial supply. Am J Anat 1977; 148:345–357.

Figure 17.20 modified from Schally AV, Kastin AJ, Arimura A. Hypothalamic hormones: The link between brain and body. Am Sci 1977;65:7122–719.

Figure 17.21 from Hökfelt T, Johansson O, Fuxe K, Goldstein M, Park D. Immunohistochemical studies on the localization and distribution of monoamine neuron systems in the rat brain. I. Tyrosine hydroxylase in the mes- and diencephalon. Med Biol 1976;54: 427–453.

Figure 17.22 from Gorski RA, Gordon JH, Shryne JE, Southam AM. Evidence for a morphological sex difference within the medial preoptic area of the rat brain. Brain Res 1978;148:333–346.

Figure 18.2 based on Nauta WJH. Hippocampal projections and related neural pathways to the midbrain in the cat. Brain 1958;81: 319–340.

Figure 18.4 from the work of P-Y Côté, P. Levitt, and A. Parent, Neurobiology Research Center, Laval University, Québec, Canada, and Robert Johnson Wood School of Medicine, Piscataway, NJ.

Figure 18.5 after Ramón y Cajal S. Histologie du Système Nerveux de l'Homme et des Vertébrés. (Azoulay L, trans.) Paris: Maloine, 1909, 1911. (Reprinted Consejo Superior de Investigaciones Cientificas, Instituto Ramón y Cajal, Madrid, 1972.)

Figure 18.8 based on Valverde F. Studies on the piriform lobe. Cambridge: Harvard University Press, 1965.

Figure 18.9 based on Potter H, Nauta WJH. A note on the problem of olfactory associations of the orbitofrontal cortex in the monkey. Neuroscience 1979;4:361–369.

Figure 18.10 modified from Krieg WJS. Functional neuroanatomy. New York: Blakiston Company, 1953:658.

Figure 18.11 from Mettler FA. Neuroanatomy. 2d ed. St. Louis: C.V. Mosby, 1948.

Figure 18.15 The assistance of Dr. J.B. Angevine of the University of Arizona, College of Medicine, and Dr. R.S. Nowakowski, University of Mississippi Medical Center, is acknowledged for delimiting the cytoarchitectonic boundaries.

Figure 18.16 based on Lorente de Nó, R. 1934. Studies on the structure of the cerebral cortex. II. Continuation of the study of the ammonic system. J Psychol Neurol 46:113–177; and Peele TL. The neuroanatomical basis for clinical neurology. New York: McGraw Hill, 1961.

Figure 18.21 modified from Sadikot A, Parent A. The monoaminergic innervation of the amygdala in the squirrel monkey: an immunohistochemical study. Neuroscience 1990;36:431–447.

Figure 18.22 modified from Desjardins C, Parent A. Distribution of somatostatin immunoreactivity in the forebrain of the squirrel monkey. Basal ganglia and amygdala. Neuroscience 1992;47:115–133.

Figure 18.24 modified from Sutin J, McBride RL. Anatomical analysis of neuronal connectivity. In: Myers RD, ed. Methods in psychobiology. Vol. 3. New York: Academic Press, 1977:1–26.

Figure 18.25 modified from Parent A, Csonka C, Étienne P. The occurrence of large acetylcholinesterase-containing neurons in human neostriatum as disclosed in normal and Alzheimer-diseased brains. Brain Res 1984;291:154–158.

Figure 19.9 from DiFiglia M, Pasik P, Pasik T. A Golgi study of neuronal types in the neostriatum of monkeys. Brain Res 1976;114: 245–256.

Figure 19.10 courtesy of the late Dr. C.A. Fox, Wayne State University, Detroit, MI.

Figure 19.17 courtesy of Prof. Ann M. Graybiel, Massachusetts Institute of Technology, Amherst, MA.

Figure 19.24 and 19.25 based on the work of B. Lavoie and A. Parent, Neurobiology Research Center, Laval University, Québec, Canada.

Figure 19.26, 19.27, 19.28, and 19.29 based on the work of LN Hazrati and A. Parent, Neurobiology Research Center, Laval University, Québec, Canada.

Figure 19.35 from Mettler FA. Neuroanatomy. St. Louis: C.V. Mosby, 1948.

Figure 19.45 based on Chevalier G, Deniau JM. Disinhibition as a basic process in the expression of striatal functions. Trends Neurosci 1990; 13:277–280.

Figure 19.46 based on DeLong MR, Georgopoulos AP, Crutcher MD. Cortico-basal ganglia relations and coding of motor performance. Exp Brain Res Suppl 1983;7:30–40.

Figure 19.47 based on Albin RL, Young AB, Penney JB. The functional anatomy of basal ganglia disorders. Trends Neurosci 1989; 12:366–375; Alexander GE, DeLong MR, Strick PL. Parallel organization of functionally segregated circuits linking basal ganglia and cortex. Ann Rev Neurosci 1986;9: 357–381; DeLong MR. Primate models of movement disorders of the basal ganglia. Trends Neurosci 1990;13:281–285; and Guridi J, Luquin MR, Herrero MT, Obeso JA. The subthalamic nucleus: a possible target for stereotaxic surgery in Parkinson's disease. Mov Disord 1993;8:421–429.

Figure 20.1 after Brodmann K. Vergleichende Lokalisation lehre der Grosshirnrinde in ihren Prinzipien dargestellt auf Grund des Zellenbaues. Leipzig: J.A. Barth, 1909.

Figure 20.2 based on Ramón y Cajal S. Histologie du Système Nerveux de l'Homme et des Vertébrés. (Azoulay L, trans.) Paris: Maloine, 1909, 1911. (Reprinted Consejo Superior de Investigaciones Cientificas, Instituto Ramón y Cajal, Madrid, 1972.); and Lorente de Nó R. The structure of the cerebral cortex. In: Fulton JF, ed. Physiology of the nervous system. 3rd ed. New York: Oxford University Press, 1949:288–330.

Figure 20.3 redrawn from Jones EG. Connectivity of primate sensory-motor cortex. In: Jones EG, Peters A, eds. Cerebral cortex. Vol. 5. New York: Plenum Press, 1986: 113–183.

Figure 20.4 based on Lorente de Nó R. The structure of the cerebral cortex. In: Fulton JF, ed. Physiology of the nervous system. 3rd ed. New York: Oxford University Press, 1949:288–330.

Figure 20.5 courtesy of Dr. Marc Colonnier, Neurobiology Research Center, Laval University, Québec, Canada, and Elsevier Publishing Company, Amsterdam.

Figure 20.6 courtesy of Dr. R. Giuffrida, Istituto di Fisiologia Umana, Catania, Italy, and Dr. A. Rustioni, University of North Carolina, and from Giuffrida R, Rustioni A. Glutamate and aspartate immunoreactivity in corticospinal neurons of rat. J Comp Neurol 1989;288: 154–164, with permission of the authors and Alan R. Liss, Inc., New York.

Figure 20.7 from Houser CR, Vaughn JE, Hendry SHC, Jones EG, Peters A. GABA neurons in the cerebral cortex. In: Jones EG, Peters A, eds. Cerebral cortex. Vol. 2. New York: Plenum Press, 1984: 63–89; and courtesy of Dr. Carolyn R. Houser, Brain Research Institute, UCLA, Los Angeles, CA.

Figure 20.9 based on Morrison JH, Hof PR. The organization of the cerebral cortex: from molecules to circuits. In: Magistretti PJ, ed. Discussions in neuroscience. Vol. 9. Amsterdam: Elsevier, 1992:11–79.

Figure 20.10 after Brodmann K. Vergleichende Lokalisation lehre der Grosshirnrinde in ihren Prinzipien dargestellt auf Grund des Zellenbaues. Leipzig: J.A. Barth, 1909.

Figure 20.12 after von Economo CF. The cytoarchitectonics of the human cerebral cortex. London: Oxford Medical Publications, 1929.

Figure 20.13 after von Economo CF. The cytoarchitectonics of the human cerebral cortex. London: Oxford Medical Publications, 1929.

Figure 20.14 after Campbell AW. Histological studies on the localization of cerebral function. New York: Cambridge University Press, 1905.

Figure 20.15 after Campbell AW. Histological studies on the localization of cerebral function. New York: Cambridge University Press, 1905.

Figure 20.16 based on Powell TPS, Mountcastle VB. The cytoarchitecture of the postcentral gyrus of the monkey Macaca mulatta. Bull Johns Hopkins Hosp 1959;105: 18–131; and Powell TPS, Mountcastle VB. Some aspects of the functional organization of the cortex of the postcentral gyrus of the monkey: a correlation of findings obtained in a single unit analysis with cytoarchitecture. Bull Johns Hopkins Hosp 1959;105:133–62.

Figure 20.17 based on, and redrawn from, Jones EG, Friedman DP. Projection pattern of functional components of thalamic ventrobasal complex on monkey somatosensory cortex. J Neurophysiol 1982;48:521–544.

Figure 20.18 after Penfield W, Rasmussen T. The cerebral cortex of man: a clinical study of localization of function. New York: MacMillan, 1950.

Figure 20.19 after Woolsey CN. Organization of somatic sensory and

motor areas of the cerebral cortex. In: Harlow HF, Woolsey CN, eds. Biological and biochemical bases of behavior. Madison: University of Wisconsin, 1958:63–81.

Figure 20.20 after Robinson CJ, Burton H. The organization of somatosensory receptive fields in cortical area 7b, retroinsular, postauditory and granular insular of *M. fascicularis*. J Comp Neurol 1980;192:69–92.

Figure 20.22 after Hubel DH, Wiesel TN. Receptive fields, binocular interaction and functional architecture in the cat's visual cortex. J Physiol (Lond) 1962;160:106–154.

Figure 20.23 after Hubel DH. The visual cortex of the brain. Sci Am 1963;209:54–62.

Figure 20.24 courtesy of Dr. Louis Sokoloff, Laboratory of Cerebral Metabolism, National Institute of Mental Health, Bethesda, MD; and from Kennedy C, Des Rosiers MH, Sakurada O, et al. Metabolic mapping of the primary visual system of the monkey by means of the autoradiographic [^{14}C] deoxyglucose technique. Proc Natl Acad Sci USA 1976;73:4230–4234.

Figure 20.25 courtesy of Dr. David Hubel and Allan R. Liss, Inc., New York; from LeVay S, Wiesel TN, Hubel DH. The development of ocular dominance columns in normal visually deprived monkeys. J Comp Neurol 1980;191:1–51.

Figure 20.26 after Hubel DH, Wiesel TN. Uniformity of monkey striate cortex: a parallel relationship between field size, scatter and magnification factor. J Comp Neurol 1974;158:295–306; and Hubel DH, Wiesel TN, LeVay S. Plasticity of ocular dominance columns in monkey striate cortex. Phil Trans R Soc Lond (Biol) 1977;278:377–409.

Figures 20.27 and 20.8 courtesy of Dr. Louis Sokoloff, National Institute of Mental Health, N.I.H.

Figure 20.29 after Woolsey CN. Organization of cortical auditory system: a review and synthesis. In: Rasmussen GL, Windle WF, eds. Neural mechanisms of the auditory and vestibular systems. Springfield, IL: Charles C. Thomas, 1960:165–180; and Merzenich MM, Knight PL, Roth GL. Representation of cochlea within the primary auditory cortex in the cat. J Neurophysiol 1975;38: 231– 249.

Figure 20.30 after Merzenich MM, Brugge JF. Representation of the cochlear partition on the superior temporal plane of the Macaque monkey. Brain Res 1973;50: 275–296.; and Imig TJ, Ruggero MA, Kitzes LM, Javel E, Brugge JF. Organization of auditory cortex in the owl monkey (*Aotus trivirgatus*). J Comp Neurol 1977; 171:111–128.

Figure 20.32 after Foerster O. Symptomatologie der Erkrankungen des Grosshirns. Motorische Felder und Bahnen. In: Bumke O, Foerster O, eds. Handbuch der Neurologie. Vol. 6. Berlin: Julius Springer, 1936:1–357.

Figure 20.33 after Travis AM. Neurological deficiencies after ablation of the precentral motor area in *Macaca mulatta*. Brain 1955;78: 155–173.

TABLES

Table 7.1 from Horch KW, Tuckett RP, Burgess PR. A key to the classification of cutaneous mechanoreceptors. J Invest Dermatol 1977; 69:75–82.

Index

Page numbers in *italics* indicate figures; those followed by t indicate tables.

Abdominal aorta plexus, characteristics, 301
Abdominal superficial reflexes, spinal innervation, 273
Abducens nerve
  amino acid transport, *499*
  lesions, 499
  neuron types, 498–499
  root fibers, transverse section, *496*
Abducens nucleus
  afferent input, 499
  lesions, 499–500
  transverse section, *470*
Accessory cuneate nucleus, 371
  anatomic and functional features, 428
Accessory oculomotor nuclei
  interstitial nucleus, 544
  nucleus of Darkschewitsch, 545
  posterior commissure nuclei, 545
Accessory olfactory bulb, characteristics, 756–757
Accommodation-convergence reaction, process, 548
Acetylcholine, (*see also* Cholinergic neurons)
  autonomic nervous system, 306
  cerebral cortex, 880–882
  enteric neurons, 302
  hippocampus, 769
  motoneuron effects, 77
  muscle contraction, 257
  in primate amygdala, 776, 778
  receptors, types, 307
  spinal cord transmitter, 352–353
  storage in motor endplates, 255
  synaptic excitation, 177
  thalamus, 673–675
Acetylcholinesterase
  cholinergic neurons, 353
  function, 307
  inhibitory drugs, 307
  myasthenia gravis, 258
  presence in thalamus, 673–674
ACh, (*see* Acetylcholine)
AChE, *see* Acetylcholinesterase (x)
Achilles tendon reflex, spinal innervation, 273
Acoustic reflex, mechanisms, 482–483
Acoustic striae, types, 480
Acoustic tubercle, 476
Acousticofacial reflex, secondary auditory fiber regulation, 497
ACTH, (*see* Adrenocorticotrophic hormones)
Action potential
  definition, 132
  purpose, 133
  single, climbing fiber, 597
Adenohypophysis, tumors, 737
Adrenergic blocking agent, definition, 310
Adrenergic fibers, overactivity, 311
Adrenergic neurons
  characteristics, 458
  storage granules, functions, 308
  transmission inactivation, 308
Adrenergic receptors, types, 310
Adrenergic transmission, autonomic nervous system, 307–310
Adrenocorticotrophic hormones, 735
Afferent fibers
  abducens nucleus, 499
  amygdaloid, medial nuclear group, 645
  cerebellar cortex, 596
  cerebellar nuclei
    corticonuclear fibers, 604
    extracerebellar fibers, 604–605
    nucleocortical fibers, 604
  cerebellum, *618*
    olivocerebellar fibers, 608–610
    pontocerebellar fibers, 610–611
    precerebellar nuclei, 611
    reticulocerebellar fibers, 610
    spinocerebellar tracts, 607–608
    vestibulocerebellar fibers, 606–607
  cerebral cortex, 869
  dentate nucleus, 605
  facial nerve, 496–497
  globus pallidus
    other types, 832
    striatopallidal fibers, 831
    subthalamopallidal fibers, 831–832
  golgi tendon organ, 252
  hypothalamus, 716–719
    schematic, *727*
  intralaminar nuclei, 649
  lamina I, 339
  lamina II, 340
  lamina III, 341
  lamina IV, 341–342
  lower motor neurons, 402
  medullary reticular formation, 435
  oculomotor complex, 545–547
  olfactory bulb, 752–753
  primary
    topographic organization, 351
    zone of Lissauer, 351–352
  raphe nuclei, 821–822
  red nucleus, 550
  striatum, 798
    amygdalostrial, 822
    corticostriatal, 811–814
    nigrostriatal, 815–818, 821
    thalamostriatal, 814–815
  substantia nigra
    corticonigral, 563
    pallidonigral, 562
    pedunculonigral, 563
    raphe-nigral, 563
    striatonigral, 560–562
    subthalamonigral, 562
  subthalamic nucleus, *835*, 839, 841–842
  superior colliculus, 535–536
  thalamus, 695
  trigeminal nerve, mesencephalic nucleus, 506
  types, in visceral structures, *240*
  vagus nerve, 443
  ventral anterior nucleus, 652–653
  vestibular nuclei, 489
  visceral, 293, 303–304
Afferent neurons, function, 144
Agnosia
  definition, 924
  types, 924
Agonist, definition, 617
Akinetic mutism, 556
Alar plate, 73
  ventromedial portions, 81
Alexia, definition, 924
Alvear path, dentate gyrus, 765
Alveus
  characteristics, 763
  inward laminae, 763
Alzheimer's disease
  amygdala destruction, 786
  basal nucleus, 788
  basal nucleus of Meynert, 881
  microglia, 218
  olfactory deficits and degenerative changes, 759
Amiculum olivae, 433
Amine precursor uptake and decarboxylation cells, amine retention, 68
Amino acids
  in amygdala, 776
  aspartate, spinal cord, 355–356
  excitatory
    cerebral cortex, 873
    thalamus, 679
  glutamate
    cerebral cortex, 973
    hippocampal formation, 768
    neurotransmitter, 161
    regulation, astrocytes, 207
    spinal cord, 355
    subthalamic nucleus, *840*
  glycine, 356
  transport, diencephalon, *837*
γ-Aminobutyric acid
  basal ganglia core structures, *805*
  cerebral cortex, 873–875
  enteric neurons, 302
  hippocampus receptors, 769
  inhibitory transmitter in spinal cord, 356
  neocortex, receptors, 875
  striatofugal neurons, *828*
  subthalamic nucleus, *840*
  thalamus, 675, *676–677*
Amygdala, *774*
  amygdalocortical connections, 782–783
  camera lucida drawing, in monkey
  central nucleus, dopaminergic projections, 782
  cytochemical features
    acetylcholine, 776, 778
    amino acids, 775–776
    monoamines, 776
    neuroactive peptides, 778–779
    other substances, 779–780

Amygdala—*continued*
fiber bundles, *775*
frontal cortex and, connections, 786
functional considerations, 783–786
hippocampus and, relationship, 781
hypothalamus and, relationship, 781–782
intrinsic connections, 780
monoaminergic fibers and terminals, *777*
nuclear organization, 773, *775*
role in emotion, 786
subcortical connections
basal forebrain, 780
olfactory system, 780
striatum, 780–781
thalamus and, relationship, 781
tuberal region and optic chiasm, in cat, *785*
Amygdalocortical connections, structures, 782–783
Amygdaloid afferent fibers, medial nuclear group, 645
Amygdaloid nuclear complex, *37*
autonomic and visceral functions, 785–786
bilateral lesions, 783
brain stem input, 782
characteristics, 42
fiber projections, hypothalamus, 717
food and water intake, 785
frontal section, *796*
illustration, *761*
olfactory inputs, 756
stimulation, endocrine responses, 784–785
transverse section, *774*
Amygdalostriatal fibers, characteristics, 822
Amyotrophic lateral sclerosis
fasciculations, 289
spinal cord pathology, *409*
Anal reflex, spinal innervation, 273
Anastomoses, cerebral veins, 123
Aneurysms
cerebral, 93
anterior communicating artery, *110*
characteristics, 109
saccular cerebral, cerebral arterial circle occurrence, 102
Angiograms
cerebral, *102*
limitations, 109
vessel imaging, 109
principles, 54
Anisocoria, 548
Anisomorphic gliosis, definition, 209
Anosmia, 758
Ansa cervicalis, 275
Ansa lenticularis
characteristics, 832–833
fiber organization, *830*
nucleus, 843
Ansa peduncularis, 644
Antagonist, definition, 617
Anterior commissure
characteristics, 41
development, 89
frontal section, *37*, *796*
horizontal section, *35*, *36*
hypothalamus, *712*
structures, *759*, 759–760
Anterior gray horn, characteristics, 328
Anterior horn cells
activation, 363
amyotrophic lateral sclerosis, 409
injury, 402
spinomedullary transition, 423
structures, 42
syringomyelia, *411*
Anterior median nucleus, 543
Anterior neuropore, 66
Anterior nuclear group, *647*
thalamus
functions, 643–644
illustration, *649*
nuclei classifications, 642
Anterograde axonal transport
fast and slow components, 182
features, *190*
Anterograde degeneration, axon and myelin, 184–186
Anterograde double-labeling technique
example, *139*
neuronal imaging, *158*
substantia nigra, *566*
Anterograde transport
axons, 182
components, *190*
substances transported, *183*
Antipsychotic drugs, schizophrenia, 879
Aphasia
characteristics, 924–925
types, 924–925
Apraxia
characteristics, 925
types, 925–926
APUD cells, (*see* Amine precursor uptake and decarboxylation cells)
Arachnoid
characteristics, 9
granulations
characteristics, 11
illustration, *13*
villi, 11
Arbor vitae, 53
Archicerebellum
characteristics, 584
lesions, 621
Archipallium, 748
Arcuate fasciculus, characteristics, 40–41
Arcuate fibers, internal, 428
Arcuate nucleus
characteristics, 430, 713
dopamine presence, 725
somatostatin-14 localization, *721*
Area postrema, *445*
characteristics, 23, 432
Areflexia, definition, 403
Argyll-Robertson pupil, 548
Argyrophilia, 134
Arterial vasocorona, 96
Arteries
anterolateral, 111
anteromedial, 111
basilar, 116
branches, 113
brain
lateral surface, *101*
medial surface, *101*
callosomarginal, 104–105
carotid, internal, characteristics, 98
central
characteristics, 103
groups, 111
cerebellar, characteristics, 118–119
cerebral, 99
cortical branches, 103
middle, 106–107
posterior, 107, 109
radiopaque imaging, *103–104*
choroidal, anterior and posterior, 112
circumferential, long and short, 116
communicating
aneurysms, *110*
anterior and posterior, 99
dura mater, 6
hypophysial portal system, 728
intercostal, occlusion, 96
lenticulostriate, 107
medial striate, characteristics, 104
meningeal, 119–120
occipital, internal, 107
ophthalmic, dura mater, 6
paramedian, 116
pericallosal, 105
posterolateral, 111
posteromedial, 111
quadrigeminal, 118
radicular, characteristics, 95
spinal, anterior and posterior, 94–95, 114
temporo-occipital, 107
thalamogeniculate, 111
thalamoperforating, 111
vertebral
branches, 113
characteristics, 98
Artery of Adamkiewicz, 95
Ascending fiber systems
locus coeruleus, 513
spinopontine, 383
spinoreticular, *382*
spinovestibular, 383
Ascending spinal tracts
function, 368
spinotectal, 378
spinothalamic
anterior, 373–374
lateral, 375, *376*
Aspartate, presence in spinal cord, 355–356
Association fibers
cerebral cortex, 918–919
interconnection to cortical regions, *39*
long and short groups, 39–40
Associative memory, 923
Astereognosis, definition, 920
Astrocytes
Bergman, 82
biochemical markers
glial fibrillary acidic protein, 206
glutamine synthetase, 206
biogenic amine regulation, 207
blood-brain barrier formation, 208–209
characteristics, 203–204
classes, 598
distribution and appearance, gray and white matter of spinal cord, *201*
fibrous, *202*, *203*
characteristics, 204
in rat optic nerve, *205*
functions, homeostasis, 206
GABA regulation, 207
glutamate regulation, 207
illustration, *200*
immunoreactivity for glial acidic fibrillary protein, *227*
injury reactions, 209–210
intermediate filament, 206
lamellar, 598
neuronal development, 208
oligodendrocytes and, comparison, 211
plasticity, 208
potassium concentration regulation, 206–207
protoplasmic, *203*
characteristics, 204–205

reaction to hepatic encephalopathy, 209
reactive, *210*
smooth, 598, 600
transmitter receptors, 207–208
Astrocytomas, definition, 210–211
Asymmetric synapses, 174
Asynergia, definition, 620
Ataxia, definition, 620–621
Athetosis, 568
characteristics, 848–849
pathologic changes, 850
Auditory areas
cerebral cortex, 886
actual and potential sites, 907
characteristics, 905–908
Auditory cortex
functional architecture, 906–907
primary, cholinergic and monoaminergic innervation, *877*
unilateral lesions, 908
Auditory fibers
primary, 478, *479*
secondary
acousticofacial reflex regulation, 480
groups, 480
tonotopic localization, 478
Auditory radiation, *33*
Auditory system
cochlea
characteristics, 474–475
in monkey, *477*
radial section, *476*, *477*
structures, *477*
cochlear duct, *476*
cochlear nerve
characteristics, 461–462
destruction, 484
nuclei, 475–476, *478*
fibers
primary, 478, *479*
secondary, groups, 480
tonotopic localization, 478
lesions, 484
Augmenting response, characteristics, 693
Autaptic synapses, 559
Autoimmune diseases, molecules necessary for, 258
Autonomic cells, characteristics, 304
Autonomic ganglia
classifications, 296
description, 295
neuroactive peptides, functions, 311
nicotinic receptors, 306
structure, 304–306
Autonomic nervous system
afferent fibers, visceral structures, 303–304
body functions, 319
central pathways, 314–315
chemical anatomy
adrenergic transmission, 307–310
cholinergic transmission, 306–307
Dale's principle, 310–311
coordination
body temperature regulation, 733–734
overview, 732–733
definition, 293
denervation sensitization, 311–314
enteric
characteristics, 302–303
function, 262
neurons, 302
noradrenergic axon, *309*
preganglionic regulation, 303
structures, 302
ganglia, structure, 304–306
general arrangement, *294*
innervation
eye, 316–317
salivary glands, 316–317
urinary bladder, *317*, 318–319
neuroactive peptides, 310–311
neuronal classifications, 293
norepinephrine varicosities, 308
organization, tract-tracing techniques, 298
parasympathetic
cranial region, 301–302
function, 262
preganglionic fibers, 301–302
sacral region, 302
sympathetic system and, antagonistic effects, 315–316
visceral structures, *312*
pseudorabies virus studies, 298–299
sympathetic
cervical ganglia, 300
function, 262
neural reflex arcs, *295*
parasympathetic system and, antagonistic effects, 315–316
postganglionic fibers, 307, 311, *313*
preganglionic fibers, *313*
projections, *294*
spinal ganglia, 300
topographic organization, 299–300
visceral structures, *312*
vomeronasal organ, 757
Autoradiographic tracing method
examples, *141*
principles, 138
Axial lines, human body, *270*
Axillary nerve, muscle innervation, 281
Axodendritic synapses, 172
cerebral cortex
human, *176*
monkey, *177*
Axolemma, 165
Axons
action potential, 132–133
definition, 132
purpose, 133
axoplasm, 149
axoplasmic transport
anterograde, 181–182, *183*
definition, 181
retrograde, 181–182
breakup, during nerve degeneration, *184–185*
characteristics, 132
connective tissue sheaths
endoneurium, 169
epineurium, 169, 171
perineurium, 169, 171
corticostriatal, terminals, 813
cutaneous, properties, *244–245*
elongation, role of astrocytes, 208
function, 132
fusimotor, types, 247
myelin sheath, 163, *164*
action potential, 168
molecular organization, 167–168
nodes of Ranvier, 168
Schmidt-Lantermann clefts, 168
sheath of Schwann, 168–169
structural organization, 165–167
noradrenergic, enteric system, *309*
regeneration, *188*
spinal nerve ventral root, 264
synapses, 173
unmyelinated, action potential, 168
Axoplasmic transport
anterograde, 181
overview, *183*
purpose, 181
retrograde, 181–182
Axosomatic synapses, 172

Babinski's sign, (*see* Sign of Babinski)
Ballism, 568
characteristics, 849
Band of Gennari, 893
Bands of Baillarger, 865
Basal forebrain
amygdala and, relationship, 780
substantia innominata, *774*
choline acetyltransferase immunoreactivity, *784*
cholinergic neurons, 715
structures, 715, 786–788
transverse section, *747*, *787*
Basal ganglia
γ-aminobutyric acid immunoreactive neurons, *805*
arterial supply, *105*
associative circuits, *853*
blood supply, *106*
caudate nucleus, 41–42
muscarinic cholinergic receptor binding sites, *811*
PHA-L anterograde labeled elements, *816*
circuitry schematic, *854*
claustrum, 41
cerebral cortex projections, 846
characteristics, 798, 846
direct and indirect pathways, 852–853, *854*
diseases, 568
animal models, 851–854
dyskinesias, (*see* Dyskinesias)
dopaminergic innervation, *819*
frontal section, serotonin-immunoreactive fibers, *820*
functional considerations, disinhibition of functions, 846–848
globus pallidus, 41, *106*
afferent fibers, 652–653, 831
characteristics, 41
development, 829, 831
divisions, in primates, 795
efferent fibers, 832–834, *836*, 836–838
immunohistochemical features, *829*
intrinsic organization, 831
output organization, *836*
topography, 828–829
horizontal section, *683*, *801*
internal capsule and, 86
nomenclature, 795, *797*, 798
output nuclei, entry into thalamus, 672–673
placement in brain, *642*
putamen, 41, *106*, *774*
characteristics, 41, 801
frontal section of brain, *796*
illustration, *800*
muscarinic cholinergic receptor binding sites, *811*
sagittal section, *800*
sensorimotor circuits, *853*
somatostatin immunoreactivity, *810*
striatum
γ-aminobutyric acid concentrations, *805*

Basal ganglia—*continued*
amygdala and, relationship, 780–781
caudate nucleus, 798–799
characteristics, 112, 798
illustration, *799*
intrinsic organization, 801–802
neuronal types, *802*, 802–804
putamen, 801
subthalamic region, (*see* Subthalamic region)
telencephalic subcortical nuclear masses, 795
transverse section, *774*
asymmetric, *643*
inferior thalamic peduncle fibers, *644*
optic chiasm level, *640*
ventral striatopallidal complex
chemical anatomy, 845
circuitry, sagittal view, *844*
connections, 844–845
functions, 845–846
ventral pallidum, 844
ventral striatum, 844–845
Basal nucleus of Meynert, involvement in Alzheimer's disease, 881
Basal plate, neuroblasts, 73
Basement membrane, 18
Basilar artery, 116
branches, 113
occlusion, 116–117
Basilar membrane, *476*
Basket cells, cerebellar cortex
characteristics, 587
neurotransmitter, 588
transverse section, *586*
Bell's palsy, etiology, 498
Belt projection, 906
Bergmann cells, characteristics, 598
Biceps tendon reflex, spinal innervation, 273
Bilirubin, unconjugated, blood-brain barrier permeability, 19
Binasal hemianopsia, 690
Biochemical markers, astrocytes, 206
Biocytin, neuronal morphology studies, 138
Biogenic amines, (*see also* Monoamines)
imaging methods, 160
pineal gland, 638
Bipolar neurons, characteristics, 144
Bitemporal hemianopsia, 690
Bladder, (*see* Urinary bladder)
Blocking agents, adrenergic, 310
Blood plasma
cerebrospinal fluid, 15–16
filtration, 15–16
Blood vessels, cerebral, 18
Blood-brain barrier
components, 17
dopamine impermeability, 18
formation, role of astrocytes, 208–209
in newborns, 18–19
purpose, 16–17
regions without, 18–19
schematic, *20*
Blood-CSF barrier
permeability, 17
purpose, 16, 20
schematic, *20*
Bodian method, neuronal morphology studies, 134
Body movement, postcentral gyrus, *890*, 891
Body temperature, regulation, 733–734
Borderzone infarction, 103
Botulinum toxin, 257
Boutons, terminal, types, *156*
Bowel, spinal cord transection effects, 407
Brachial plexus
development, cervical enlargement, 327
formation, *276*
embryologic origins, 277
injuries
Duchenne-Erb syndrome, 283
Klumpke syndrome, 283
structures, 275–277, *277*
Brain
adrenergic receptors, in primates, 878
anterior commissure
characteristics, 41
development, 89
frontal section, *37*, *796*
horizontal section, *35*, *36*
structures, *759*, 759–760
arteries
lateral surface, *101*
medial surface, *101*
barriers
blood-brain, 16–19, *20*, 208–209
blood-CSF, 16–17, 20, *20*, 21
interrelationships, *20*
blood flow measurements, 93
blood supply
carotid artery, internal, 98
vertebral artery, 98–99
capillaries
dopamine impermeability, *21*
general circulation capillaries and, comparison, *17*
structure, *17*
central nervous system, (*see* Central nervous system)
circumventricular organs, midsagittal view, *22*
cranial nerves, *31*
developmental stages, 77–79
dissection, relationship of internal structures, *642*
edema, signs and symptoms, 19–20
fetus, lateral view, *89*
forebrain, (*see* Forebrain)
frontal lobe
convolutions, 31
in monkey, *753*
frontal section
gonadectomy, *736*
striatum, *799*
structures, *796–797*
thalamic nuclear groups, 796
functions, 25
gliomas, 210–211
gray matter removal, lateral view, *39*
hypothalamus, 706
imaging techniques
computerized tomography, 55, *56–57*
magnetic resonance imaging, 55, 57, *58–61*, 60
positron emitting tomography, 60–64, *62*
x-ray, 54
inferior surface, *10*, 38
structures, *755*
insula, characteristics, 34
intracellular fluid compartment, 19
ischemic necrosis, astrocytic reaction, 209
lateral surface, *27*
auditory region, *907*
gyri and sulci, *883*
insula, 34
locus coeruleus, 457
ascending and descending noradrenergic axons, *514*
macrophages, (*see* Brain macrophages)
medial surface
dissection, *40*
limbic lobe, 36
medulla, (*see* Medulla)
meninges, 3
midbrain, (*see* Midbrain)
occipital lobe, components, 34
olfactory structures, *749*
parietal lobe, parts, 32
peripheral nervous system, components, 25
rostral aspect, frontal view, *29*
sagittal view, *4*
cerebrospinal fluid circulation, *12*
sensory receptors, function, 235
subdivisions, 25, 78–79
superior surface, *28*
temporal lobe, components, 34
topographic relationships, *27*
ventricular system, 78–79
Brain macrophages, resident, (*see also* Microglia)
neuronal shaping, 217–218
types, 217
Brain-derived neurotrophic factor, 193
Brain stem
amygdaloid nuclear group, 782
arteries, medial surface, *101*
corticobulbar pathways, *453*
corticoreticular fibers, 452
cranial nerves and, *44*
descending spinal tracts
fastigiospinal fibers, 397
medial longitudinal fasciculus, 396–397
reticulospinal, *394*, 394–396
rubrospinal, *389–390*, 391
tectospinal, 389, *389*, 391
vestibulospinal, 391–392, *392*, 394
development, *87*
fourth ventricle
eminences, 432–433
periventricular gray matter, *511*
structures, 48
transverse section, *431*
vagal nuclei, *444*
lateral surface, *46*
longitudinal axis, *774*
lower portion, lesions, 556
medial forebrain bundle
afferent fibers, 716
efferent fibers, 719–720
medial lemniscus, posterior white column formation and course, *369*
medulla, (*see* Medulla)
midbrain, (*see* Midbrain)
midsagittal view, *47*, *48*
noradrenergic fibers, 596
parts, 25, 47
peripheral ganglia, *441*
pons, (*see* Pons)
posterior surface, *6*, *45*, *423*
epithalamus and pulvinar placement, *634*
raphe nuclei, *455*
reticular formation
hypothalamus, 717
neurotransmitter presence, 556–557
projections to cerebellum, 610
stimulation, 396
roof plate, 47
sagittal section, *635*, *722–723*
structures, 45
subdivisions, 23

transverse section, mesencephalon and diencephalon junction, *636*
upper portion, lesions, 556
venous drainage, 118
Broca's aphasia, characteristics, 925
Broca's speech area, 32
Brodmann's area, unilateral lesions of auditory cortex, 908
Brown-Séquard syndrome, 377
spinal cord degenerative pattern, 408
spinal cord hemisection, 407–408
Bulbocavernous reflex, spinal innervation, 273

Calamus scriptorius, 48
Calcar avis, 44
Calcarine cortex, frontal section, *894*
Calcitonin gene-related peptide, spinal cord laminae, 358
Calmodulin, characteristics, 180
CAM, (*see* Cell adhesion molecules)
cAMP, (*see* Cyclic adenosine monophosphate)
Canal, central, embryonic and adult human spinal cord, *329*
Cannon's law of denervation, precepts, 313
Capillaries
brain
dopamine impermeability, *21*
endothelial cells, *21*
general circulation capillaries and, comparison, *17*
structure, *17*
characteristics, 18
morphologic and enzymatic properties, 18
Capsule cells, autonomic ganglia, 305–306
Carotid artery, internal
branches, 98
segments, 98
Carotid sinus nerve, 450
Carotid sinus reflex, 451
Carpal tunnel syndrome, etiology, 282
Catecholamines
cell groups
hypothalamus, principal locations, *725*
noradrenergic, 457–458
definition, 160
projections
characteristics, 399
descending, *448*
pontine cell group, *400*
Cauda equina, 325
development, 74
sagittal view, *8*
Caudal anesthesia, purpose, 7
Caudal central nucleus, 543
Caudal medulla, cell groups and tracts, *441*
Caudal midbrain
inferior colliculi, 527, 530–531
parabigeminal area, 531
pretectal region, 540–541
tegmental and interpeduncular nuclei, 531–534
trochlear nerve, 531
Caudal pons
dorsal, 469, 473
ventral, *470*
Caudate nucleus, *774*
characteristics, 41–42, 798–799
head, *800*
muscarinic cholinergic receptor binding sites, *811*
nigrostriatal fibers, 816
PHA-L anterograde labeled elements, *816*
Causalgia, definition, 282
Cavenous sinus
characteristics, 120–121
venous connections and related structures, *122*
Cavernous sinus, oblique coronal section, *100*
Celiac plexus, characteristics, 300–301
Cell adhesion molecules, 72
Cells
anterior horn
activation, 363
amyotrophic lateral sclerosis, 409
injury, 402
spinomedullary transition, 423
structures, 42
syringomyelia, *411*
autonomic, characteristics, 304
basket
characteristics, 587
neurotransmitter, 588
transverse section, *586*
Bergmann, characteristics, 598
capsule, autonomic ganglia, 305–306
choroid epithelium, phosphatase activity, 225
chromatolytic, lumbar spinal ganglia, *267*
cuboidal epithelial, choroid plexus, 16, *226*
dopaminergic nigral, examples, *192*
endothelial, blood-brain barrier, *21*
ependyma
characteristics, 218
cytoplasm structures, 223
embryonic and adult human spinal cord, *329*
features, *221*
origins, 202
tanycytes, 223–224
fusiform, *866*
characteristics, 865
ganglion
dorsal root, *153*, *349*
retinal, 686–687, *895*, 896
spinal, 75–76
sympathetic, 305, *306*
gitter, 217
glial
characteristics, 73
macroglia, 201
microglia, 201, 214–216
golgi epithelial
cerebral cortex, *600*
characteristics, 598
granule
cerebellar cortex, *592*
characteristics, 750
illustration, *751*
interfascicular, characteristics, 211
Merkel, 241
mitral, olfactory bulb, 750
neural crest, spinal ganglia creation, *76*
neurilemma, origins, 202
neuroepithelial, sensory nerve cells, 241
neuroglia, histogenesis, *71*
olfactory bulb, *749*
periglomerular
characteristics, 750
illustration, *751*
progenitor
differentiation into type-2 astrocytes, induction factors, 203
oligodendrocyte development, 203
Purkinje, 82, 597
characteristics, 588–589
dendrites, 146
dendritic arborizations, *589*
nucleus, 149, *152*
transverse section, *586*
pyramidal, *866*
characteristics, 865
dendritic pattern, 146
excitatory role in neocortex, 873
hippocampal formation, 763
length, 146
Renshaw
characteristics, 344
types, 345
satellite
development, 265–266
origins, 202
perineuronal, 211, *211*
Schwann, 75
behavior, after anatomic severance, 290
cross section, *170*
nuclear division, 186
role in degeneration and regeneration of neurons, 185–186
sensory receptors, classifications, *236*
simple, functional characteristics, *898*
stellate, 596, *866*
characteristics, 585, 587, 865
striate cortex, in cat, *870*
transverse section, *586*
tufted, 750
Central arteries
characteristics, 103
groups, 111
Central canal, embryonic and adult human spinal cord, *329*, 329–330
Central cervical nucleus, cervical spinal segments, in dog, *350*
Central chromatolysis
in monkey neurons, *187*
principles, 186
Central nervous system
blood supply
basilar artery, 113
carotid artery, internal, 98
central arteries, 109, 111
cerebral arterial circle, 99, 102–103
cerebral arteries, 103–109
cerebral veins, 122–127
choroidal arteries, 112
overview, 93–94
radicular arteries, 95–96
spinal arteries, 94–95
spinal veins, 96–98
vertebral artery, 98–99, 113
brain, (*see* Brain)
components, 25, *26*
determination and differentiation, 65
development
cerebellum, 81–82
congenital abnormalities, 90–91
early stages, *67*
glial cells, 73
mesencephalon, 83
metencephalon, 81–82
neural crest, 67–69
neural tube, 69
neural tube formation, 65–67
telencephalon, 85–86
extracellular space, 200
potassium concentration regulation, 206
intima pia, 12, 14
ionic channels, 214
myelination, oligodendrocytes, 212–214

Central nervous system—*continued*
nerve fibers, size and appearance, histologic staining, *136*
neuroglia, (*see* Neuroglia)
neurons
axons distributed in, *143*
categories, 144
components, 131
intercellular and intracellular communication, 132
nerve growth factor, 193
regenerative processes, 189–190, *191*
nodal regions, *164*
pH regulation, 214
resident macrophages, 217
serotoninergic receptors, subtypes, 680
spinal cord, (*see* Spinal cord)
subdivisions, *26*
vascular lesions, 93
Central sulci, functions, 923
Central tegmental tract, 469
ascending projections, bundle types, 555
impulse transport, 617
Centrobasal nucleus, 342
Centromedian nucleus
afferent fibers, 649
characteristics, 648, *649*
input, 695
Centromedian-parafascicular nuclear complex, 648
fiber projection, 650
formation, 648
input, 694–695
thalamic afferents to striatum, 814
transverse sections, *674*
Centromedian-parafascicular-subparafascicular complex, output organization, *655*
Centrosomes, characteristics, 154, 156
Cerebellar cortex
cell types, *144*
circuit organization, 596–597
connections
corticonuclear fibers, 604
extracerebellar inputs, 604–605
nucleocortical fibers, 604
cortical inputs
climbing fibers, 593–595
monoaminergic and cholinergic inputs, 595–596
mossy fibers, 592–593
interneurons, 82
layers, *586*
granular, 589–590, 592
molecular, 585, 587–588
purkinje cell, 588–589, 598
neuroglia cells, *599*
sagittal and transverse planes, cell and fiber arrangements, *586–587*
sections, folium of rhesus monkey, *585*
somatotopic localization, *606*
Cerebellar peduncles
brain stem projection, 600
inferior
characteristics, 606
fiber organization, 437
in medulla, 463
structures, 437
superior, 509
characteristics, 612–613
fiber organization, 510
Cerebellomedullary cistern, 10
Cerebellopontine angle, 462
formation, 469
lateral view, *472*
Cerebelloreticular fibers, characteristics, 435
Cerebellum
afferent fibers, *618*
cuneocerebellar, 380–381
olivocerebellar, 608–610
other types, 381
pontocerebellar, 610–611
precerebellar nuclei, 611
reticulocerebellar, 610
spinocerebellar, 378, *379*, 380, 607–608
vestibulocerebellar, 606–607
anterior lobe, lesions, 621–622
archicerebellum, 584
arteries
characteristics, 118–119
types, 116
blood supply, arteries, *101*, 118–119
comparator role, 617
cortical inhibition, 550
development, *81*, 81–82
efferent fibers, *618*
cerebellovestibular projections, 614–615
fastigial nucleus, 614
superior cerebellar peduncle, 612–613
fissures, 53, *584*
function, 583, 617
glomerular complex, 593, *594–595*
horizontal section, *603*
inferior surface, *53*
information processing, 622
lateral zone, 617
learning and, relationship, 622
lesions
archicerebellar, 621
neocerebellar, 620–621
lobules, *584*
motor skills, 622–623
neocerebellum, 585
nuclei
corpus medullare, 600–601
corticonuclear fibers, 604
dentate, 601–602, *602*
emboliform, 602–603
fastigial, 603–604
globose, 603
interposed, *613*
neurotransmitters, 601
relay, 617
vestibular fibers, 489
paleocerebellum, 584–585
paravermal zone, 617
pathways
input and output, *607*, *620*
neuronal types, 380
peduncles, (*see* Cerebellar peduncles)
posterior lobe, vermal parts, 53
posterior spinocerebellar tract, 378, *379*
posterior surface, *30*
posteroinferior surface, *52*
regional organization, 583–585
sagittal section, *54*
sensory inputs, 368
somatotopic localization, 605–606
structures, 52–54, 583
superior surface, *52*
transverse section, *473*
veins, characteristics, 119
vermal zone, 616–617
Weigert-stained section, *603*
Cerebral aneurysms, 93
characteristics, 109
limitations, 109
Cerebral angiography, cerebral vessel imaging, 109
Cerebral arterial circle
base of brain, *104*
formation and branches, *100*
structures, 99, 102–103
Cerebral arteries
anterior
anomalies, 105–106
branches, 103–106
middle
branches, 107
characteristics, 106–107
occlusions, 107
posterior, 99
characteristics, 107, 109
occlusion, 109
Cerebral blood flow
blockage, 93
flow amounts, 93
Cerebral cortex
association fibers, 918–919
axodendritic synapse, *176*
cell types, *144*
chemical anatomy
γ-aminobutyric acid, 873–875
cholinergic innervation, 880–882
excitatory amino acids, 873
neuroactive peptides, 875–876
claustrum projections, 846
columnar organization, 871–872
consciousness, 555
cortical areas, 882–883, *884–885*, 886
cortical cells and fibers, 864–865, *866*
cortical layers, 865–866
cortical neurons, interrelation, 869–871
corticopontocerebellar pathway, 474
cytoarchitectonic areas, 871, *882*
development, 86–87
divisions, 763
dyskinesia development, 852
emotion, subjective aspects, 746–747
fibers
afferent, 869
association, 918–919
commissural, 918
5-HT, 878
functions
cerebral dominance, 919–920
integrated cortical functions, 923–926
interhemispheric transfer, 920–922
prefrontal cortex, 926–928
sleep, 922–923
interneurons, 872
monoamines
dopaminergic innervation, 878–880
noradrenergic innervation, 877–878
serotoninergic innervation, 878
motor areas
eye fields, 915–916
inputs, 915
primary, 909–913
supplementary, 913–915
neocortex, layers, 867–868
nonpyramidal corticofugal fibers
corticopontine, 916–917
corticoreticular, 916
corticothalamic, 917
projection neurons, *867*
sensory areas
auditory, 905–908, *906–907*
gustatory, 908
primary, 886–887, *893*
secondary, 887
somesthetic
primary, 887–888, *888*
secondary, 892

vestibular representation, 908–909
visual
primary, 892–893, 896, *899*
secondary, 904–905
six-layered cellular structure, 864
somatotopic localization, body parts, *890*
structure, 864
visual sensory areas, primary, visual deprivation, 902–904
Cerebral dominance, differences in hemispheric functions, 919–920
Cerebral hemispheres
anterior commissure
characteristics, 41
development, 89
frontal section, *37*, *796*
horizontal section, *35*
structures, *759*, 759–760
central branches
central arteries, 109–112
choroidal arteries, 112
cortical branches, anterior cerebral artery, 103–106
crus cerebri, horizontal section, *35*
development, 87, *88*
inferior surface, parts, 38
internal structures and internal capsule, horizontal section, *35*
lateral aspects, *40*
lateral surface, 28, 31
dissection, *39*
frontal lobe, 31–32
occipital lobe, 34
parietal lobe, 32, 34
primary somesthetic area, *888*, 891
temporal lobe, 34
lateral ventricles
anterior horn, 42
inferior horn, 42
lateral and superior views, *43*
posterior horn, 44
structures, 42–45
left, medial surface dissection, *40*
longitudinal fissure, 25
medial surface, *29*
limbic lobe, 36
structures, 34–36
posterior view, *30*
superior surface, *33*
white matter
association fibers, 39–41
astrocytes, distribution and appearance, *201*
commissural fibers, 41
internal arrangement, *331*
projection fibers, 38
spinal cord, *330*
Cerebral veins
deep, 125–127
angiographic appearance, *125–126*
superficial and, connections between, *126*, 127
drainage patterns, 123
illustration, *123*
superficial, 122–123, *124*
deep and, connections between, *126*, 127
Cerebral vesicle, development, *87*
Cerebrospinal fluid
blood plasma filtration, 15–16
buoyancy, 15
characteristics, 14
choroid plexus, 16
molecular substance barrier, 228
circulation, in brain and spinal cord, *12*
composition and pressure, 14
peptides, 23
peripheral endocrine functions, 15
production sites, 14
subarachnoid space, 9
waste removal, 15
water content, 16
Cerebrovascular accident, (*see* Stroke)
Cerebrum
aneurysms, 102–103, 109
arterial circle, (*see* Cerebral arterial circle)
arteries, (*see* Cerebral arteries)
hemispheres, (*see* Cerebral hemispheres)
lobes, 28
veins, (*see* Cerebral veins)
Cervical enlargement
characteristics, 327
section through, *387*
Cervical flexure, 74
Cervical ganglia, related fibers, 300
Cervical plexus, structures, 275
Cervical segments
cell groups, *346*
nuclei
central, *350*
lateral, *377*
spinal cord
characteristics, 330, *331–333*, 334
crush injury, *372–373*
Cervical spinal nerves, cutaneous innervation, *274*
ChAT, (*see* Choline acetyltransferase)
Chemical messengers, putative, criteria for neurotransmitter, 159
Chemical synapses, advantages, 175
Chemical transmission, neurons, receptors, 177–178, 180
Chemoelectric transduction, sensory receptors, 237
Chemoreceptors, function, 238
Cholecystokinin, spinal cord laminae, 358
Choline acetyltransferase, 295
immunoreactive fibers
medulla, *460*
thalamus, 674
Cholinergic fibers, overactivity, 311
Cholinergic neurons, (*see also* Acetylcholine)
genomic regulatory mechanisms, 180
globus pallidus, *829*
identification, 458
medial habenular nucleus, 637–638
substantia innominata, 715
Chorea
characteristics, 849
Huntington's, biochemical changes, 851
pathologic changes, 850–851
types, 849
Choroid epithelium
cells, phosphatase activity, 225
illustration, *224*
Choroid plexus
cerebrospinal fluid, 14, 228
characteristics, 16
development, frontal section, *84*
formation, 44, 223, 224
frontal section, *84*
function, 224
illustration, *223*
purpose, 17
rabbit
dual secretory-absorptive role, 225
illustration, *226*
schematic, *22*
villi, *22*
Choroid point, 112
Choroidal arteries
anterior and posterior, 112
structures supplied by, 112
Choroidal fissure, 85
Chromatin, neuron nucleoproteins, 151
Chromatolysis, 154
Chromatolytic cells, lumbar spinal ganglia, *267*
Chromophilic substances, neurons, 152
Ciliary neurotrophic factor, 193
progenitor cell differentiation, 203
Cingulate cortex, anterior, stimulation, somatic effects, 747
Cingulum, *33*
characteristics, 41, 918
illustration, *40*
Circadian rhythms, 639
Circle of Willis, (*see* Cerebral arterial circle)
Circumferential arteries
blood supply to midbrain, *114*, 118
obstruction, 117
Circumventricular organs
components, 21
median eminence, 23
purpose, 23
vascular casts, *729*
zona interna and externa, *720*
in nonmammalian vertebrates, 23
schematic, *22*
serotoninergic innervation, 711
Cisterns, subarachnoid, 10, *11*
Claustrum, 41
cerebral cortex projections, 846
characteristics, 798, 846
Claw hand, definition, 282
Climbing fibers
characteristics, 593–595
Purkinje cells, 597
Clonus, definition, 405
CM-Pf, (*see* Centromedian-parafascicular nuclear complex)
CM-Pf-sPf, (*see* Centromedian-parafascicular-subparafascicular complex)
CNTF, (*see* Ciliary neurotrophic factor)
Coccygeal ligament, characteristics, *7*
Cochlea, 907
characteristics, 474–475
in monkey, *477*
radial section, *476*, *477*
structures, *477*
Cochlear duct, *476*
Cochlear nerve
characteristics, 461–462
destruction, 484
nuclei, 475–476, *478*
Cogwheel phenomenon, definition, 849
Colchicine, purpose, 147
Collateral eminence, 42
Collateral fibers, characteristics, 435
Collateral trigone, 42
Colliculi
facialis, 498
inferior, *649*
superior, *649*
Coma, sleep and, comparison, 556
Combined system disease
characteristics, 409–410
spinal degenerative pattern, *410*
Commissural fibers, (*see also* Anterior commissure; Posterior commissure)
cerebral cortex, 918
corpus callosum, *33*
characteristics, 89
frontal section, *43*
function, 35, 920–921

Commissural fibers—*continued*
genus, *774*
lesions, 921
morphology, 921–922
parts, 41
structures, 34
structures, 41
Commissural nucleus, 443
Commissures
anterior
characteristics, 41
development, 89
frontal section, *37*, *796*
gray, 328
horizontal section, *35*, *36*
hypothalamus, *712*, 723
structures, *759*, 759–760
fornical, 767
posterior
gray, 328
lesions, 541–542
structures, 541–542
transverse section, *540*, *545*
Common peroneal nerve
muscle innervation, 287
section of, 287
Communicating arteries, anterior and posterior, 99
aneurysm, *110*
Communicating hydrocephalus, definition, 15
Computerized tomography
brain imaging, 55
operation principles, 55
planes, *56*
schematic and illustration, *56–57*
tomographic planes, *56*
Conductance, definition, 132
Conduction aphasia, characteristics, 925
Conduction deafness, 484
Conduction velocity, 171
Cones, characteristics, 685
Confluens of sinuses, structures, 120
Congenital dermal sinus, 91
Conjugate horizontal gaze
characteristics, 493
lesions that affect, *494*
Connective tissue sheaths
characteristics, 267–268
peripheral nerve fibers
endoneurium, 169
epineurium, 171
perineurium, 169, 171
Consciousness, cerebral cortex influences, 555
Conus medullaris, 74, 325
characteristics, 327
sagittal view, *8*
syndrome, 407
Copied deoxyribonucleic acid, *in situ* hybridization and, 141
Corneal reflex, secondary trigeminal fibers, 508
Cornu ammonis, 765
Corona radiata, *33*, *40*
characteristics, 683
illustration, *689*
Corpus callosum, *33*
characteristics, 89
frontal section, *43*
function, 35, 920–921
genus, *774*
lesions, 921
morphology, 921–922
parts, 41
structures, 34
Corpus medullare, characteristics, 600–601
Corpuscle of Meissner, (*see* Meissner's corpuscles)
Corpuscles of Golgi-Mazzoni
characteristics, 247
illustration, from finger tip, *246*
Cortical inputs
climbing fibers, 593–595
monoaminergic and cholinergic, 595–596
mossy fibers, 592–593
Cortical surface, meninges and, relationship, *13*
Cortical zone, medial, 604
Corticobulbar fibers
characteristics, 451, 474
pathways, *453*
unilateral lesions, 454
spinal trigeminal nucleus, 502
Corticofugal fibers
accommodation-convergence reaction, 548
inhibitory effects, 452
internal capsule, 685
nonpyramidal
corticopontine fibers, 916–917
corticoreticular fibers, 916
corticothalamic fibers, 917
origins, 909
Corticohypothalamic fibers, characteristics, 718
Corticomedial nuclear group, characteristics, 773
Corticonigral fibers, characteristics, 563
Corticonuclear fibers, characteristics, 604
Cortico-olivary fibers, origins, 433
Corticopontine fibers
cerebellum, *618*
characteristics, 474, 916–917
Corticoreticular fibers
brain stem, 452
reticular formation, 555
characteristics, 435, 916
Corticorubral fibers, precentral and premotor cortex, 550
Corticospinal decussation
characteristics, 422
illustration, *424–425*
Corticospinal fibers, characteristics, 474
Corticospinal neurons, characteristics, 385
Corticospinal system
decussation, 383–384, *385*
lateral and anterior sections, 384, *384*, *386*
structures, 383
Corticospinal tract
effect of lesions, 388
primary motor area, 910
Corticostriatal axons, terminals, 813
Corticostriatal fibers
characteristics, 811–814
origins, 814
Corticotectal fibers, characteristics, 536
Corticothalamic fibers, 633
characteristics, 917–918
excitatory action, methods to mediate, 679
Cotranslational modification, proteins, 159
Cranial fossae
anterior, 3
middle, 3
posterior, 3
Cranial nerves
emergence and entrance, in brain stem, *44*
frontal view, *29*
inferior view, *10*
infratentorial, *440*
medulla, 47–48, 437
midsagittal view, *439*
midbrain, 49
peripheral ganglia, *441*
pons, 49
root fiber origins, *532*
schematic, *31*
Cranial outflow, preganglionic fibers, 296
Cranial region, ganglia, 301
Cranium, base, *121*
Cremasteric superficial reflex, spinal innervation, 273
Cribiform plate, fractures, effect on smell, 758
Crista ampullaris, 484
Crus cerebri, *33*, 45, 47, 49, 527
projections, 49–50
structures, 572
CSF, (*see* Cerebrospinal fluid)
CT, (*see* Computerized tomography)
Cuboidal epithelial cells, choroid plexus, 16, *226*
Cuneate nucleus, accessory, 371
anatomic and functional features, 428
Cuneate tubercle, 46
Cuneocerebellar fibers, characteristics, 428, 608
Cuneocerebellar tract, schematic, *379*
Cuneus, *29*
Cupula, 484
Cutaneous axons, properties, *244–245*
Cutaneous fields, innervation
peripheral nerve, *271*
segmental, *270*
Cutaneous nerves
antebrachial and brachial branches, 283
femoral
lateral, 285–286
posterior, 287
Cutaneous receptive fields, 235
Cutaneous receptors
mechanical stimuli sensitivity, classification criteria, 242–243
peritrichal endings, 241
Cutaneous sensibility
effect of dorsal root sectioning, 406
elemental qualities, 236
Cutaneous somatotopic representation, body surface, *658*
Cyclic adenosine monophosphate, synaptic transmission, *179*
Cytokeratins, neurofilaments, 148

Dale's principle, precepts, 310
Decerebrate rigidity, characteristics, 493–494
Decussations
medial lemniscus, 427–428
supraoptic, 722–723
Deglutition, (*see* Swallowing)
Dejerine-Roussy syndrome, 692
Dementia, characteristics, 786
Dendrites
action potential, 133–134
expansion illustration, *155*
Purkinje cells, 14
Dendritic zone, definition, 132
Denervation, Cannon's law, 313
Dentate gyrus
characteristics, 763
illustration, *755*, *761*, *764*
intrinsic connections, 765–766
three layers, 765
Dentate nucleus
afferent fibers, 605
characteristics, 601–602

dissections, *602*
efferent fibers, *609*, 612, *618*
Denticulate ligaments, characteristics, 9
2-Deoxyglucose
neuronal metabolism, 142
PET scans, 61
Dermatomes
function, 268
mapping, 270
peripheral nerve innervation
anterior, *271*
posterior, *272*
Descending spinal tracts, brain stem
fastigiospinal fibers, 397
medial longitudinal fasciculus, 396–397
reticulospinal, *394*, 394–396
rubrospinal, *389–390*, 391
tectospinal, 389, *389*, 391
vestibulospinal, 391–392, *392*, 394
Determination, central nervous system, 65
Diabetes insipidus, causes, 734
Diaphragm, movements, spinal innervation, 273
Diaphragma sellae, characteristics, 3
Diencephalon
amino acid transport, *837*
development, 83–85
epithalamus, 50
frontal section, *84*
hypothalamus, (*see* Hypothalamus)
lateral view, *46*
midsagittal view, *47*, *48*
pathways, 554–555
limbic, *724*, *745*
posterior surface, *45*, *51*
regional organization, 633
structures, 50–51
subthalamus, structures, 51–52
thalamus, (*see* Thalamus)
transverse section, *637*
habenular nuclei and mammillary bodies, *646*
inferior thalamic peduncle fibers, *644*
optic chiasm level, *640*
thalamic and hypothalamic nuclei, *646*
zones, 84
Differentiation, central nervous system, 65
Diplopia
definition, 499
trochlear nerve lesion, 531
Directly-gated transmission, 178
Disconnection syndrome, types, 921
Discriminative sensibility, 377
Disinhibition, basal ganglia functions, 846–848
Dominance cells, ocular, striate cortex, 900–902
Dopamine
arcuate nucleus, 725
basal ganglia
effect on direct and indirect pathways, 852–853
innervation, *819*
blood-brain barrier impermeability, 18
cerebral cortex innervation, 878–880
effect on striatal neurons, 817
PET visualization, 64
receptor subtypes, 565
synthesis, in nigrostriatal fibers, 815
visualization, immunocytochemical methods, 140
Dopaminergic neurons, hypothalamus, *731*
Dopaminergic nigral cells, examples of, *192*
Dorsal accessory olivary nucleus, 433
Dorsal cochlear nucleus, cell divisions, 476
Dorsal longitudinal fasciculus, 532
characteristics, 717
Dorsal motor nucleus, vagus nerve, 446
Dorsal nucleus of Clarke, 334
anatomic and functional features, 428
characteristics, 349–350
dorsal root fiber termination, 352
Dorsal rami
divisions, *267*
muscle innervation, 274
Dorsal raphe nuclei
circumventricular organ innervation, 711
serotonin-containing neurons, *517*
Dorsal roots
ganglion cells
cytoplasm, *153*
major branches and collaterals, *349*
nerve fibers, *268*
spinal cord
arrangement, *348*
degenerated image, *350*
lesions, *403*, 405–406
termination sites, 352
spinal nerve, *327*
characteristics, 262–263
schematic, *326*
Dorsal tegmental decussation, 389
Dorsal tegmental nucleus, characteristics, 531–532
Dorsal thalamus, characteristics, 633
Duchenne-Erb syndrome, characteristics, 283
Dura mater
arteries, 119–120
base view, *5*
blood supply, 6
components, 3
innermost layer
spinal dura, 6
subdural space, 6
posterior surface, *4*
venous sinuses, 120–122
Dural sinus
extracranial veins and, relationship, *117*, 121–122
venous
characteristics, 120
sagittal view, *121*
Dynorphin immunoreactivity, 358
Dysdiadochokinesis, definition, 620
Dyskinesias
athetosis, 848–849
ballism, 849
chorea, 849
choreiform, drug therapy, 851
neural mechanisms, 849–851
Parkinson's disease
causes, 18
characteristics, 850
experimental animal models, 852–853
initial symptoms, 849
motor disturbances, 853–854
neural mechanisms, 850
neuropathologic features, 568
treatments, 569
sterotaxic surgery effects, 314–315
subthalamic, animal models, 851–852
tremor, 848
Dysmetria, definition, 620
Dystonia, 568

EAA, (*see* Excitatory amino acids)
Edinger-Westphal nucleus, 543
EEG, (*see* Electroencephalogram)
Effectors
somatic, 255–257
motor endplates, 255, *256*, 257, 295
visceral, 259
Efferent fibers
central nucleus of inferior colliculus, 531
cerebellum, *618*
superior cerebellar peduncle, 612–613
cochlear, 482–484
in cat, *483*
dentate nucleus, *609*
descending rubral, 550
external pallidal segment, *838*
facial nerve, 496
fastigial nucleus, 614, *615*
globus pallidus, *836*
lenticular fasciculus, 833, *833*
pallidohabenular fibers, 834
pallidonigral fibers, 834, 836
pallidotegmental fibers, 836–837
pallidothalamic fibers, 834
subthalamic fasciculus, 837–838
thalamic fasciculus, 833–834
hypothalamus
descending projections, 721–722
hypothalamocortical fibers, 722
medial forebrain bundle, 719–720, *724*
supraoptic decussations, 722–723
locus coeruleus, 513
mammillary, 720–721
medullary reticular formation, 435–436
parietal cortex, 917
pars compacta and pars reticulata, comparison, *817*
striatum, striatopallidal, 822, *823*, 825–826
substantia nigra
nigrostriatal fibers, 564–566
nigrotectal and nigrotegmental fibers, 567–568
nigrothalamic fibers, 566–567
subthalamic nucleus, 842–843
superior colliculus, 538–539
ventral nuclei
anterior, 654
lateral, 656–657
ventral striatum, 845
vestibular, labyrinth hair cells and, relationship, *491*
Efferent neurons, visceral
intermediolateral nucleus, 347
sacral autonomic nuclei, 347
Efferent vestibular system
characteristics, 491–492
labyrinth hair cells and, relationship, *491*
Electrical synapse, definition, 175
Electroencephalogram, brain stem reticular formation, procedures, 554
Electron microscopy, neuronal cytology, 137
Emboliform nucleus, characteristics, 602–603
Embryonic disk, schematic, *66*
Embryonic neural crest, spinal ganglia development, 265
Emissaries, dural sinus, 121–122

Emotion
  amygdala influences, 786
  subjective aspects, role of cerebral cortex, 746–747
Emotional behavior, control, hypothalamus, 738
En grappe endings, 257
En plaque endings, 257
Encapsulated endings
  end bulbs, characteristics, 243
  Meissner's corpuscles
    characteristics, 243
    illustration, *243*
  pacinian corpuscles, characteristics, 243, 246–247
Encephalopathy, hepatic, protoplasmic astrocyte reaction, 209
End bulbs
  characteristics, 243
  Krause, from conjunctiva, *246*
End feet, 204
Endocytosis, 177
Endoneurium, 268
  characteristics, 169
Endothelial cells, blood-brain barrier, *21*
Enkephalin fibers, 459
  lamina I and II, 357
Enteric system
  function, 262
  neurons, 302
  noradrenergic axon, *309*
  preganglionic regulation, 303
  structures, 302
Entorhinal area
  characteristics, 768
  illustration, *764*
Ependyma
  cells
    characteristics, 218
    cytoplasm structures, 223
    embryonic and adult human spinal cord, *329*
    features, *221*
    origins, 202
  illustration, *219–220*
  scanning electron micrographs, *222*
Epidural space, 7
Epidural venogram, *97*
Epineurium
  characteristics, 169, 171
  peripheral nerve fibers, 267
Epipial layer, characteristics, 8
Epithalamus, 45
  characteristics, 633
  habenula, characteristics, 635
  illustration, *634*
  pineal gland
    characteristics, 638–639
    development, 83
    secretions, 638–639
    structure, *638*
  structures, *50*
EPSP, (*see* Fast excitatory synaptic potential)
Equilibrium, governing mechanisms, 493
Estradiol, effect on sexual behavior, 737
Excitatory amino acids
  cerebral cortex, 873
  thalamus, 679
Exteroceptive impulses, trigeminal nerve, 500
Exteroceptors, function, 237
Extracellular space
  central nervous system, 200
  potassium concentration, 206
Extracranial veins, dural sinuses and, relationship, *117*, 121–122
Extrafusal muscle fibers
  Golgi tendon organ and muscle spindle, anatomic and functional relationships, *361*
  innervation by spinal nerve ventral roots, 263
Extraocular muscles
  localization in oculomotor nuclear complex, *543*
  origin of root fibers to, *532*
Eye
  autonomic innervation, 316–317
  movement
    horizontal and vertical, 500
    secondary vestibular fibers, 492
Eye fields, cerebral cortex, 915–916

Facial colliculus, 46
Facial nerve
  functional components, 495
  lesions, 497–498
  motor nuclei, 495
    afferent fiber source, 496–497
  muscle innervations, 495
  overview, *495*
  parasympathetic fibers, group division, 497
Facial palsies, central types, 498
Falx cerebelli, 52
  characteristics, 3
  sagittal view, *4*
Falx cerebri
  characteristics, 3
  sagittal view, *4*
Familial dysautonomia, characteristics, 315
Fasciculi
  amyotrophic lateral sclerosis, 409
  cuneatus, 330, 368
  definition, 289
  dorsal longitudinal, characteristics, 717
  gracilis, 330, 368
  interfascicularis, 371
  lower motor neurons, 404
  proprii, 401
  retroflexus, 634
  solitarus, 443–444
Fast excitatory synaptic potential, presynaptic fiber stimulation, 307
Fastigial nucleus
  afferent fibers, 605
  characteristics, 603–604
  efferent fibers, 614, *615*
Fastigiospinal fibers, characteristics, 397
Fastigium, 48
Femoral nerve
  injury, 285
  muscle innervation, 285
Fibrillary gliosis, definition, 209
Fibrillation, definition, 289, 404
Fibroblast growth factor, 193
Filum terminale, 325
  characteristics, 327
Fimbria, 42
Fissures, cerebellum, 53, 584, *584*
FITC, (*see* Fluorescein isothiocyanate)
Flexor muscle spasms, spinal cord recovery, 406–407
Flexor reflex afferents, 609
Flocculonodular lobe, 82
Fluorescein isothiocyanate, antibody visualization, 140
Folium, dorsal surface, *598*
Follicle-stimulating-releasing factor, hypothalamus, 732
Food intake, control, hypothalamus, 737–738
Foramen cecum posterior, 463
Foramen of Magendie, 48
  cerebrospinal fluid transportation, 14
Foramina of Luschka, 48
  cerebrospinal fluid transportation, 14
Forearm
  innervation, 281
  peripheral nerves, 276
Forebrain, (*see also* Brain)
  basal, (*see* Basal forebrain)
  frontal sections, enkephalin-immunoreactive axons terminals and cell bodies, *806*
  serotoninergic innervation, 533
Forel's field H, (*see* Prerubral field)
Formalin fixation, neuronal morphology, 134
Fornix, *647*
  columns, frontal section of brain, *796*
  fiber projections
    divisions, 717
    efferent, 766
  illustration, *755*, *759*
  pillar of, *722*
Fossae
  dural blood supply, 120
  interpeduncular, 49
  posterior, *5*
  rhomboid, 48
Fourth ventricle
  choroid plexus, *226*
  eminences, 432–433
  periventricular gray matter, *511*
  structures, 48
  transverse section of medulla through, *431*
  vagal nuclei, *444*
Fovea centralis, definition, 685
Fractured somatotopy, 605
Free nerve endings
  afferent, *240*
  characteristics, 239–240
  in skin and hair follicle, *239*
Freeze-etch apparatus, 137
FRH, (*see* Follicle-stimulating-releasing factor)
Frontal cortex, amygdala and, connections, 786
Frontal lobe
  convolutions, 31
  functional divisions, 926–927
Frontal lobotomy
  function, 927
  intellectual damage, 927
  origins, 927
Funiculi
  spinal cord
    posterior, 425
    white matter, 328
  spinospinal, 401
Fusiform cells, *866*
  characteristics, 865
Fusiform layer, dorsal cochlear nucleus, 476

GABA, (*see* γ-Aminobutyric acid)
Ganglia
  autonomic, 295
    structure, 304–306
  basal
    associative circuits, *853*
    circuitry schematic, *854*
    disinhibition of functions, 846–848
    dopaminergic innervation, *819*
    horizontal section, *683*, *801*
    nomenclature, 795, 798
    optic chiasm level, *640*
    output nuclei, entry into thalamus, 672–673

placement in brain, *642*
sensorimotor circuits, *853*
serotonin-immunoreactive fibers, *820*
somatostatin immunoreactivity, *810*
thalamic peduncle fibers, inferior, *644*
transverse section, *640, 643, 644, 774*
cervical, 299
related fibers, 300
ciliary, 301
dorsal root, major branches and collaterals, *349*
geniculate, lesions, 498
inferior, nerve X, *447*
otic, 301
peripheral, brain stem and cranial nerves, *441*
prevertebral, 296, 299
pterygopalatine, 301
spinal
related nerves, 300–301
schematic, *326*
stellate, 299
submandibular, 301
sympathetic
amine production, 67–68
preganglionic fibers, 299–300
terminal, 296
trigeminal, divisions, 501
vestibular, *475*
characteristics, 485
labyrinth innervation, *485*
Ganglion cells
retinal
characteristics, 686–687
receptive fields, *895*, 896
spinal, processes, 75–76
Gap junction channels, definition, 175
Gate control theory of pain, principles, 360
Gating
definition, 178
role of thalamus, 693
Gaze paralysis, lateral, *494*
etiology, 500
Gene expression, role in neuronal protein synthesis, 157
General efferent fibers, 80
General somatic afferent fibers, 80, 437, *438–440*, 450
intermediate nerve, 497
General somatic efferent fibers, 80, 437, *438–440*
General somatic sense, glossopharyngeal nerve, 450
General visceral afferent fibers, 80, 437, *438–440*, 450
General visceral efferent fibers, 437, *438–440*, 450
facial nerve, *495*
intermediate nerve, 497
Geniculate bodies
lateral, 50
secondary visual area, 905
medial, 50
auditory area, 905–906
Geniculate ganglia, lesions, effect on taste, 498
Geniculate nuclei
lateral
cellular lamination, *664*
components, 663–664
cross-section, *665*
glomeruli, neuronal arrangements, *670*
laminae, 669
lesions, in baboon, *666*
parvicellular layers, 664
retinae, representation of visual field, *667*
retinal ganglion cell terminations, *668*
retinal surface, topographic representation, 664–665
right visual hemifield, *669*
serotonin-immunoreactive fibers, *682*
medial, 662–663
serotonin-immunoreactive fibers, *682*
thalamus, medial nucleus, 662–663
Geniculocalarine fibers, striate cortex, 894
Geniculocalcarine tract, characteristics, 687–690
Genital corpuscles, 243
Germinal zone
neural tube histogenesis, 69
oscillatory movements in, *70*
Gerstmann's syndrome
characteristics, 926
definition, 920
GFAP, (*see* Glial fibrillary acidic protein)
Gitter cells
characteristics, 217
formation stages, *216*, 217
Glial acidic fibrillary protein, immunoreactivity, astrocytic processes, *227*
Glial cells
characteristics, 73
macroglia, (*see* Macroglia)
microglia, (*see* Microglia)
Glial fibrillary acidic protein, intermediate filament, 206
Glial membrane, 223
Gliomas, astrocytes and, 210
Gliosomes, 204
Globose nucleus, characteristics, 603
Globus pallidus, *106*
afferent fibers
striatopallidal, 831
subthalamopallidal, 831–832
ventral anterior thalamic nuclei, 652–653
characteristics, 41
development, 829, 831
divisions, in primates, 795
efferent fibers, *836*
ansa lenticularis, 832–833
pallidonigral, 834, 836
pallidotegmental, 836–837
pallidothalamic, 834
subthalamic fasciculus, 837–838
thalamic fasciculus, 833–834
immunohistochemical features, *829*
intrinsic organization, 831
output organization, *836*
topography, laminae, 828–829
Glomeruli
complex formation, 593, *594–595*
sympathetic ganglion cell dendrites, *306*
lateral geniculate nucleus, 669
Glossopharyngeal nerve
characteristics, 449–451
effect on swallowing, 451
functional components, 450
lesions, 451
Glutamate
cerebral cortex, 973
hippocampal formation, 768
neurotransmitter, 161
regulation, astrocytes, 207
spinal cord, 355
subthalamic nucleus, *840*
Glutamic acid decarboxylase expression, in reticular nucleus, *678*
Glutamine synthetase, astrocyte marker, 206
Gluteal nerves, muscle innervation, 287
Gluteal superficial reflex, spinal innervation, 273
Glycine, inhibitory transmitter in spinal cord, 356
Golgi apparatus, characteristics, 156
Golgi epithelial cells
cerebral cortex, *600*
characteristics, 598
Golgi technique
advantages, 137
neuronal morphology studies, 134, 137
Golgi tendon organ
afferent fibers, 252, 363
anatomic and functional relationships, to extrafusal muscle fibers, *361*
axonal branches and collagen bundles, relationship, *253*
capsule, 251
illustration, *252*
Gonadotropic hormones, regulation, 735
Gracilis tubercle, 46
Grafting experiments, peripheral nerve fibers, 192–193
Granule cells
cerebellar cortex, *592*
characteristics, 750
illustration, *751*
Gray horns, spinal cord
anterior, 328
activation, 363
cell groups in cervical spinal segment, *346*
motor neuron groupings, 345–346
motor nuclei, in cervical segment, *344*
posterior, 328, 347–349
cutaneous input, *336*
Gray matter
astrocytes, distribution and appearance, *201*
cytoarchitectural lamination
lamina I, 339
lamina II, 340–341
lamina III, 341
lamina IV, 341–342
lamina IX, 343–344
lamina V, 342
lamina VI, 342
lamina VII, 342–343
lamina VIII, 343
internal arrangement, *331*
spinal cord, characteristics, 329, *330*
Gray ramus communicans, 300
Great cerebral vein (Galen), 122
characteristics, 127
Growth cones, 71
direction of, influences, 72
Growth hormones
control, role of hypothalamus, *737*
hypothalamic releasing factors, 729–730
Growth promoting factors, neurons, 193
Guamanian syndrome, characteristics, 62–63
Gustatory areas, cerebral cortex, 886
characteristics, 908
Gustatory nucleus, 444
Gyri
angular, 34
brain, *27–28*
lateral view, *883*

Gyri—*continued*
definition, 28
frontal lobe, *29*, 31
hippocampal, 36, 761
limbic lobe, 36
occipital lobe, 34
orbital, *29*
parahippocampal, transverse section, *760*
postcentral
activation, by cutaneous stimuli and joint movement, *888*
characteristics, 887
neuronal activation, 889–890
somatotopic localization, body parts, *890*
stimulation, effects, 891
thalamic projections, 887–888
ventral posterior nucleus projection, 659
temporal lobe, *29*, 34
Gyrus rectus, 32

Habenula, characteristics, 635
Habenular nuclei
characteristics, 634
transverse section, *646*
Hair follicles
characteristics, 241
nerves and nerve endings, *239*
Head
cutaneous fields, *274*
movements, spinal innervation, 273
Hearing, unilateral loss, 484
Hemianopsia, types, 690–691
Hemiparesis, contralateral, causes, 116–117
Hemiplegia
alternating
inferior, 114, 442
middle, 499
superior, 118, 548–549
definition, 389
motor function recovery, 405
Hepatic encephalopathy, protoplasmic astrocyte reaction, 209
Herpes zoster, dermatome mapping, 270
Herring bodies, 161
Hindbrain, (*see* Brain stem)
Hip, segmental innervation, *280*
Hippocampal formation, 42, 85
anatomic circuitry, *766*
chemical anatomy, 768–769
dentate gyrus
characteristics, 763
illustration, *755*, *761*, *764*
intrinsic connections, 765–766
three layers, 765
extrinsic connections, 766–768
functional considerations, 769–773
illustration, *759*, *764*
layers, *76*
neuronal activity, 768
Papez's theory, 773
pyramidal layer, 763
sagittal section, *761*
subicular cortex
efferent fibers, 767
hippocampus and, 763–765
thalamic projections, 768
topographic organization, 760–763
transverse section, *747*, *760*
Hippocampus
amygdala and, relationship, 781
basket cells, 764
bilateral damage, 770
CA-1 sector pyramidal neurons, 772
fiber projection, hypothalamus, 716–717
formation, (*see* Hippocampal formation)
fundamental layers, 763
GABA receptors, 769
illustration, *755*
localized lesions, 770
memory functions, 770–771
morphologic plasticity, 773
Histochemical techniques, neurotransmitters, 140–141
Histologic techniques, neuronal morphology studies, 134–137
examples, *135*
Homeostasis
definition, 706
enteric system, 302
role of neuroglia, 199–200
Homonymous hemianopsia, 690
Homonyous quadrantanopia, definition, 896
Homotypical cortex
characteristics, 886
definition, 882
Hormone-releasing factors, cerebrospinal fluid transportation, 15
Hormones
cerebrospinal regulation, 15
gonadotropic, regulation, 711, 735
hypothalamic-releasing, *162*
neurohypophyseal, (*see* Neurohypophyseal hormones)
pituitary, *730*
Horner's syndrome, 316
causes, 548
characteristics, 283
definition, 406
Horseradish peroxidase method
principles, 138
retrograde transport studies, 182
HRP, (*see* Horseradish peroxidase method)
Huntington's disease
characteristics, 209–210
role of astrocytes, 209–210
Hydrocephalus
causes, 15
communicating, 15
Hyperacusis, definition, 498
Hyperkinetic disorders
characteristics, 848
pathophysiologic mechanisms, 852
Hyperphagia, definition, 737
Hyperpolarizing potential, 133
Hypertonicity, 404
Hypoglossal eminence, 46, 432
Hypoglossal nerve
characteristics, 438, 440, 442
lesions, 442
perihypoglossal nuclei, 442
Hypokinetic disorders
characteristics, 848
pathophysiologic mechanisms, 852
Hypophysectomy, 732
Hypophysial portal system
artery supply, 728
schematic, *728*
Hypophysiotrophic agents, hypothalamus, types, 729–730, 732
Hypophysis, *29*
Hyporeflexia, definition, 288
Hypothalamic sulcus, 84
Hypothalamocortical fibers, characteristics, 722

Hypothalamus
afferent connections
hippocampo-hypothalamic fibers, 716–717
medial forebrain bundle, 716, 719
schematic, *727*
amygdala and, relationship, 781–782
anterior commissure, 723
anterior region
preoptic, 710–711
supraoptic, 711–713
arcuate nucleus, somatosatin-14 localization, *721*
autonomic nervous system regulation, 314
blood supply, 113
dopaminergic neurons, *731*
efferent connections
descending projections, 721–722
dorsal longitudinal fasciculus, 720
hypothalamocortical fibers, 722
main categories, 728
mammillary fibers, 720–721
medial forebrain bundle, 719–720, *724*
pathways, *726*
supraoptic decussations, 722–723
external structures, 707
fiber connections, *727*
functions
anterior pituitary control, 734–735
body temperature regulation, 733
control of growth, 737
emotional behavior, 738
food intake, 737–738
reproduction control, 735–737
water balance maintenance, 734
hormone release, 735
hypophysial portal system, structures, 728–729
hypophysiotrophic agents, 729
types, 729–730, 732
input to mesencephalon, pathways, 314
lateral surface, 710
lesions, 734
lesions, effect on thalamus, 638
mammillary region, nuclei, 715
medial and periventricular areas, 710
median eminences, 706–707
mediolateral divisions, 709–710
neurosecretory, 162
nuclei
illustration, *707*
paraventricular, *712*, *716*
sexual dimorphism, 737
supraoptic, *712*
posterior
functions, 733–734
lesions, 734
releasing factors, 730
role in homeostasis, 706
rostrocaudal regions, 51
sagittal section, *709*
sleep and, relationship, 738
structures, 51
supraopticohypophysial tract, characteristics, 723–724
sympathetic responses, 733
transverse section, *774*
infundibular region, *708*
mammillary region, *708*
supraoptic region, *708*
tuberal region
overview, *719*
structures, 713

tuberohypophysial tract, characteristics, 724–725, 728
ventromedial nucleus, lesions, effect on aggressive behavior, 738
visceral reflexes, 315
Hypotonia, definition, 288, 403, 620

Imaging techniques
angiogram, 54
computerized tomography, 55
brain imaging, 55
operation principles, 55
schematic and illustration, *56–57*
tomographic planes, *56*
magnetic resonance imaging
frontal sections, *59*
horizontal sections, *58*
operation principles, 55, 57
parasagittal sections, *60*
positron emitting tomography
brain imaging, 93
imaging examples, *62*
microglia, 218
neurotransmitter presence in brain, 63–64
operation principles, 60–61
scanning electron microscopy, ependymal cells, *222*
x-ray, 54
Immunocytochemical methods
neuronal imaging examples, *158*
principles, 140
Impulse transmission, central nervous system to viscera, 296
In situ hybridization, principles, 141
Inclusion bodies, characteristics, 156–157
Induction factors
ciliary neurotrophic factor, progenitor cell differentiation, 203
platelet-derived growth factor, progenitor cell differentiation, 203
Indusium griseum, 761
Infarction, definition, 93
Inferior cerebellar peduncle
fiber arrangement, 437
medulla, 463
structures, 437
Inferior colliculi
fiber organization, 530
neurons, 481
nuclei
central, 527
external, 530
pericentral, 530
rostral part, *532*
sagittal section, *529*
tonotopic organization, 530–531
transverse section
midbrain of 3-month infant, *529*
through adult midbrain, *528*
Inferior frontal gyrus, parts, 31
Inferior horn, structures, 42
Inferior olivary complex, 80
characteristics, 432–434
gray band of cells, 433
medullo-pontine junction, 462
transverse section of medulla through, *431*
Inferior olive, *29*
Inferior salivatory nucleus, 451
Information processing, cerebellum, 622
Infratentorial dura, 3
innervation, 6
Infundibulum, 706
stalk, vascular casts, *729*
stem, 707
transverse section, *708*
Inhibitory factors, nerve regeneration, 193
Inhibitory transmitters, spinal cord
γ-aminobutyric acid, 356
glycine, 356
Initial glomerulus, 265
Insula, *30*
characteristics, 34
definition, 28
Intention tremor, definition, 620
Intercostal arteries, occlusion, 96
Interfascicular cells, characteristics, 211
Interhemispheric transfer, effect of hemispheric separation, 921
Interleukin-1
nerve growth factor production, 218
neuronal shaping, 218
Intermediate filaments, astrocyte reactions, 206, 209
Intermediate gray zone, structures
dorsal nucleus of Clarke, 349–350
intermediomedial nucleus, 350
Intermediate nerve, characteristics, 497
Internal arcuate fibers, 428
Internal capsule, *33*
basal ganglia and, 86
blood supply, *106*
characteristics, 112
composition, 683
corticofugal fibers, 685
horizontal section, *683*, *801*
parts, 38
placement in brain, *642*
posterior limb, structures, 683–684
retrolenticular portion, 684–685
right portion, *684*
sagittal section, *800*
thalamocortical fibers, 685
Internal mesaxon, 167
Interneurons, (*see also* Neurons)
anterior nuclei, 642
cerebral cortex, 82, 872
function, 144
Renshaw cells, 344
striatal cholinergic, *808–809*
types, 144
Internuclear ophthalmoplegia
causes, 500
characteristics, 493
Interoceptors, function, 238
Interossei, paralysis, 282
Interpeduncular nucleus, structures, 533
Interposed nuclei
cerebellum, *613*
projections, 612–613
Interstitial nucleus of Cajal
degeneration from lesion in, *546*
nucleus of Darkschewitsch and, relationship, *547*
Interthalamic adhesion, 50
Intima pia
characteristics, 8
purpose, 12, 14
Intrafusal muscle fibers
illustration, *247–248*
size variations, 247
spinal nerve innervation, 263
Intralaminar nuclear group
caudal, 648
connections and functional organization, 648–651
cortical projections, 650
rostral, 647
thalamostriatal projections, 649–650
thalamus, *654*
Ionic channels, expression in oligodendrocytes, 214
Iron, in ventral pallidum, 845
Ischemia, definition, 93
Ischemic necrosis, astrocytic reaction, 209
Isotopes, positron-emitting, half-life, 61
Isthmus, transition to midbrain, 527
Isthmus rhombencephali, regions, 509–510

Jaw-jerk reflex, 509
Juxtarestiform body, 437

Karyosomes, 151
Kernicterus, characteristics, 19
Kernig's sign, 286
Kinesin, 182
Kinesthesia, effects of posterior white column lesions, 371
Kinesthetic sense, definition, 238
Klumpke syndrome, characteristics, 283
Kluver-Bucy syndrome, characteristics, 783
Knife-clasp phenomenon, definition, 407
Kölliker-Fuse nucleus, 511
Korsakoff's syndrome, characteristics, 773

Labyrinth
amino acid transport, *488*
equilibrium, 493
hair cells, vestibular efferent fibers and, relationship, *491*
structures, 484
vestibular ganglia, 485, *485*
vestibular nuclei, 485–486
Labyrinthine, anatomic orientation, *475*
Lacrimal reflex, 508
Lamina affixa, 50
Lamina I
afferent fibers, 339
characteristics, 339
enkephalin fibers, 357
nociceptor input, 339
substance P localization, *357*
Lamina II
afferent fibers, 340
enkephalin fibers, 357
GABA receptors, 356
glutamate receptors, 356
horseradish peroxidase studies, 340
neuronal classification, 340
substance P localization, *357*
Lamina III
afferent fibers, 341
characteristics, 341
neuronal types, 341
Lamina IV
afferent fibers, 341–342
neuron types, 341
Lamina IX
characteristics, 343–344
motor neuron types, 343
Lamina terminalis, 67
Lamina V
characteristics, 342
neuron types, 342
Lamina VI, centrobasal nucleus, 342
Lamina VIII, characteristics, 343
Laminin, nerve regeneration, 193
LAMP, (*see* Limbic system-associated membrane protein)
Lateral cervical nucleus
characteristics, 377
illustration, *377*
Lateral geniculate body, secondary visual area, cell projections, 905
Lateral geniculate neurons, receptive fields, *895*, 896

Lateral geniculate nucleus
cellular lamination, *664*
components, 663–664
cross-section, *665*
glomeruli
neuronal arrangements, *670*
synaptic organization, 671
laminae, 669
lesions, illustration, in baboon, *666*
neurons, receptive fields, 689–690
parvicellular layers, 664
retinal ganglion cell terminations, *668*
retinal surface
topographic representation, 664–665
visual field representation, *667*
serotonin-immunoreactive fibers, *682*
visual hemifield, right, *669*
Lateral lemniscus
nuclei, 481, 509
pathways, 481
Lateral medullary syndrome
characteristics, 463
dorsolateral structures, 463
Lateral nuclear group
serotoninergic innervation, 680
thalamus
components, 651–652
nuclei types, 639
Lateral reticular nucleus, cytoarchitectural parts, 434
Lateral tegmental system, formation, 399–400
Lateral ventricles
anterior horn, 42
inferior horn, 42
lateral and superior views, *43*
posterior horn, 44
Lateral vestibular nucleus, reflex activity of spinal cord, 394
L-Dopa
blood-brain barrier passage, *21*, 64
Parkinson's disease, 18, 569
Learning, cerebellum and, relationship, 622
Lenticular fasciculus
characteristics, 833
fiber organization, *830*
illustration, *833*
Lesions
cerebellum
anterior lobe, 621–622
archicerebellar, 621
neocerebellar, 620–621
corticospinal tract, 388–389
posterior white columns, 371
visual pathway, *690*
LGB, (*see* Lateral geniculate body)
LGN, (*see* Lateral geniculate nucleus)
LHRH, (*see* Luteinizing hormone-releasing hormone)
Ligaments
coccygeal, characteristics, 7
denticulate, 9
Limb bud, upper extremity, developmental stages, *269*
Limbic lobe
characteristics, 36
schematic, *745*
structures, 36, 744
Limbic pathways
diencephalon, *724*
telencephalon, *724*
Limbic system
diencephalon, *745*
limbic lobe, structures, 744
major interconnections, *746*
telencephalon, *745*
Limbic system-associated membrane protein, 746, *747*
Limen insula, *30*, 34
Lipochrome, 156
Lobotomy, frontal
function, 927
intellectual damage, 927
origins, 927
Lock-in syndrome, 117
Locus coeruleus
ascending and descending noradrenergic axons, *514*
brain stem innervation, 514
cell types, *511*, 513
characteristics, 457, 513
neurons, norepinephrine, 399, *512*
noradrenergic input
cerebellum, 611
hypothalamus, 769
Longitudinal fasciculus
medial, head position regulation, 397
superior, characteristics, 918–919
Longitudinal fissure, 25
Longitudinal striae, *33*
Long-term potentiation, definition, 771
Lower extremity
movements, spinal innervation, 273
segmental innervation, *280*
Lower motor neurons
characteristics, 402
effect of lesions, 289
fasciculations, 404
LSD, (*see* Lysergic acid diethylamide)
Lumbar cistern
cerebrospinal fluid pressure, 15
characteristics, 10
diagrammatic representation, *8*
Lumbar enlargement, characteristics, 327
Lumbar plexus
anterior division, 285
development, lumbar enlargement, 327
illustration, *284*
posterior division, 285
Lumbar segments
spinal cord, *334*, 335, *337*
crush injury, section, *388*
transverse section, *347*
Lumbosacral plexus
illustration, *284*
lower extremity innervation, 283
Luteinizing hormone-releasing hormone
hypothalamus, 732
organum vasculosum laminae terminalis, 23
release by neuropeptide Y, 732
Lysergic acid diethylamide
characteristics, 516
effect on serotoninergic system, 557

Macroglia
astrocytes
Bergman, 82
biochemical markers, 205–206
biogenic amine regulation, 207
blood-brain barrier formation, 208–209
characteristics, 203–204
classes, 598
distribution and appearance, *201*
fibrous, *202*, *203*, 204, *205*
GABA regulation, 207
glial fibrillary acidic protein, 206
glutamate regulation, 207
glutamine synthetase, 206
homeostasis, 206
illustration, *200*
immunoreactivity for glial acidic fibrillary protein, *227*
inducing factors, 203
intermediate filament, 206
ionic channels, 206–207
lamellar, 598
neuronal development, 208
oligodendrocytes and, comparison, 211
pathologic conditions, 209–210
plasticity, 208
potassium concentration regulation, 206–207
protoplasmic, *203*, 204–205, 209
reactive, *210*
smooth, 598, 600
transmitter receptors, 207–208
oligodendrocytes
astrocytes and, comparison, 211
discovery, 211
electrical properties, 214
illustration, *202*
ionic channels, 214
myelin sheath formation, *212*, *214*
spinal cord, *211*
types, 211–212
Macula, 484
afferent fibers, 484–485
Macula lutea, characteristics, 685
MAG, (*see* Myelin-associated glycoprotein)
Magnetic resonance imaging
brain imaging, 55, 57, 60
frontal sections, *59*
horizontal sections, *58*
multiple sclerotic patient, *61*
operation principles, 55, 57
parasagittal sections, *60*
Mammillary bodies, 85, *649*, 706
frontal section, *37*
transverse section, *646*
Mammillary fibers, hypothalamus, 720–721
Mammillary peduncle, 533
Mammillary region, hypothalamus
efferent fibers, 720–721
nuclei, 715
substantia innominata, 715
transverse section, *708*
Mammillotegmental tract, 721
Mammillothalamic tract, *647*, *649*, *722–723*
Mandibular branch, trigeminal ganglia, 501
MAO, (*see* Monoamine oxidase)
MAPs, (*see* Microtubule-associated proteins)
Marchi technique, neuronal morphology studies, 134
Marginal layer, 69
Mass reflex, definition, 407
Maxillary branch, trigeminal ganglia, 501
Mechanoelectric transduction, sensory receptors, 237
Mechanoreceptors, function, 238
Medial accessory olivary nucleus, 433
Medial forebrain bundle
hypothalamus, afferent projections, 716
illustration, *724*, *745*
Medial geniculate body, auditory area of cerebral cortex, 905–906
Medial geniculate nucleus
serotonin-immunoreactive fibers, *682*
ventral nucleus
fibrodendritic laminations, *662*
laminar organization, 663

Medial lemniscus
  ascending fibers, 436
  decussation, 427–428
    transverse section, *426*
  fiber organization, in brain, 658
  pons, dorsal part, 509
  posterior white column formation and course, *369*, 370
  upper medulla, 462
Medial longitudinal fasciculi, 469
  ascending and descending fibers, 490
  internuclear ophthalmoplegia, 493
  lesions, 493
Medial nuclear group
  amygdaloid afferent fibers, 645
  lesions, 645
  parvicellular portion, 645
  thalamus
    nuclei types, 639
    regions, 644
Medial tegmental region, midbrain, 744–745
Median eminence
  purpose, 23
  in rat, zona interna and externa, *720*
  vascular casts, in monkey, *729*
Median fissure, anterior, 325
Median nerve
  injury, 282
  lesion, sensory loss, 282
  muscle innervation, 281–282
Median septum, posterior, 325
Median sulcus, posterior, 325
Mediodorsal nucleus, (*see* Medial nuclear group)
  thalamus, characteristics, 694
Medulla
  anterior aspect, *422*
  arteries, 115, *115*
  ascending tracts, 436–437
  basic features, transverse section, *438*
  blood supply, 113
    microangiogram, *114*
  caudal, cell groups and tracts, *441*
  characteristics, 79
  chemical anatomy
    acetylcholine, 457
    catecholamines, 457–457
    neuroactive peptides, 458–461
    neuromediators, 454–455
    serotonin, 455–457
  choline acetyltransferase
    immunoreactivity, transverse section, *460*
  corticobulbar fibers
    corticoreticular, 452
    pathways, *453*
    sensory relay nuclei, 451–452
  cranial nerves
    glossopharyngeal, 449–451
    hypoglossal, 438, 440, 442
    midsagittal view, *439*
    overview, 437–438
    spinal accessory, 442
    vagus, 442–446, 448–449
  descending tracts, 436–437
  development, *80*
  horizontal section, *445*
  horseradish peroxidase studies, *446–447*
  inferior olivary complex, 80, 432–434
    characteristics, 432–434
    gray band of cells, 433
    medullo-pontine junction, 461–463
    transverse section of medulla through, *431*
  lateral medullary syndrome, 116
  lesions, 463
  midolivary region, transverse section, *432*
  midsagittal section, microangiogram, *116*
  noradrenergic cells, 457
  olivocerebellar and pontocerebellar fibers, transverse section, *619*
  raphe nuclei, 515
  respiratory regulation, 446
  reticular formation
    afferent fibers, 435
    cytoarchitecture, 434
    divisions, 436
    efferent fibers, 435–436
    major subdivisions, 434–435
    nuclear masses, 435
  spinomedullary transition
    corticospinal decussation, 422–423, 425
    medial lemniscus decussation, 427–428
    overview, 421
    posterior column nuclei, 425–427
    trigeminal tract, 428–432
  spinoreticular fibers, 381
  structures, 47–48
  transverse section, *424*
    fourth ventricle, caudal, *431*
    inferior olivary complex, *431*
    medial lemniscus decussation, *426*
    1-month infant, *427*, *449*
    pons, caudal border, *462*
    upper portion, *450*
  vestibulospinal tract, 490
  Weigert-stained section, *603*
  zones, 552
Medulla oblongata, *27*
Medullary lamina
  external, thalamus, 640
  internal, 639
Medullary pyramid, *33*, 45, 47
  vascular lesion, transverse section through cervical enlargement, *387*
Medullary syndrome, lateral
  causes, 116
  characteristics, 430, 463
  dorsolateral structures, 463
Medullary-pontine junction
  characteristics, 462
  overview, 461
  transverse section, *461*
Meissner's corpuscles
  characteristics, 243
  dermal papilla, *241*
  illustration, *243*
Melanin, presence in substantia nigra, 157
Melatonin
  inhibitory effects, 84
  pineal gland synthesis, 638
Membrane proteins, in neurons, types, 159
Memory
  regulation by hippocampus, 770–771
  role of vasopressin and oxytocin, 732
Meningeal layer, dura mater, 3
Meninges
  arachnoid, characteristics, 9
  cortical surface and, relationship, *13*
  dura mater
    arteries, 119–120
    base view, *5*
    blood supply, 6
    characteristics, 3
    components, 3
    innermost layer, 6
    posterior surface, *4*
    venous sinuses, 120–122
  inferior view, *10*
  pia mater, characteristics, 8–9
  posterior view, *6*
  spinal cord coverings, *9*
  subarachnoid and perivascular spaces, *13*
Meningitis, acute bacterial
  detection using cerebrospinal fluid, 14
  pencillin treatment, 19
Meningocele, characteristics, 91
Meningomyelocele, associated complications, 91
Merkel cell, characteristics, 241
Mesencephalic nucleus
  characteristics, 503–504
  illustration, *506*
  sensory neuron presentation, 508
Mesencephalon, (*see* Midbrain)
Messenger ribonucleic acid
  methods for detecting, 141
  neuronal protein synthesis, 157
Metabotropic receptors, 178
Metencephalon
  caudal, *80*
  developmental stages, 81–82
1-Methy-4-phenyl-4-1,2,5,6,-tetrahydropyridine
  Guamanian syndrome, 64
  Parkinsonism, 852
MGB, (*see* Medial geniculate body)
M-I, (*see* Primary motor cortex)
Microfilaments, characteristics, 148
Microglia, (*see also* Brain macrophages)
  characteristics, 214–216
  illustration, *215*, *216*
  imaging studies, 218
  neuronal shaping, 217–218
  origins, 201
  pathologic processes, 218
  role in Alzheimer's disease, 218
Microtubule-associated proteins, types, 147
Microtubules, characteristics, 147
Micturition
  innervation
    autonomic, 318
    sympathetic, 318
  vesical capacity and frequency, 319
Midbrain
  anterior aspect, *422*
  autonomic pathways, 314
  blood supply
    arteries, 117
    microangiogram, *114*
  caudal
    inferior colliculi, 527, 530–531
    parabigeminal area, 531
    pretectal region, 540–541
    tegmental and interpeduncular nuclei, 531–534
    trochlear nerve, 531
  cranial nerves, 49
  crus cerebri, structures, 572
  development, 83
  divisions, 527
  hypothalamic input, pathways, 314
  isthmic transition, 527
  medial tegmental region, 744–745
  midsagittal section, microangiogram, *116*
  oculomotor nerve, nuclear complex, 542–544, *544*
  posterior commissure, structures, 541–542
  pupillary reflexes, types, 547–548
  reticular formation
    caudal transections, 553
    cytoarchitectonic divisions, 552

Midbrain—*continued*
functional considerations, 552–553
inhibitory and facilitatory regions, stimulation, 554
neuronal systems
ascending, 554–556
descending, 553
rostral
oculomotor nerve, 542–547
posterior commissure, 541–542
pretectal region, 540–541
pupillary reflexes, 547–549
superior colliculi, 535–540
transverse section, *528*, 534–535, *549*
structures, 49
substantia nigra, (*see* Substantia nigra)
tegmentum, (*see* Midbrain tegmentum)
thalamic junction, 633–635, *636*
transection, inferior view, *32*
transverse section
level of oculomotor nerve, *534*
posterior commissure, *545*
Midbrain periaqueductal gray, characteristics, 533
Midbrain tegmentum
lesions, 551–552
red nucleus
cerebellum, *618*
connections, 550–551
cytoarchitecture, 549–550
fiber organization, 391
functional considerations, 551
illustration, *649*
lesions, 551–552
neurons, 391
neurotransmitters, 551
rubrospinal tract, 391
topography, 549
Middle alternating hemiplegia, 499
Middle cerebellar peduncle, 49
Midline nuclear group
cell groups, 647
characteristics, 645, 647
Midolivary region, medulla, transverse section, *432*
M-II, (*see* Supplementary motor cortex)
Mitochondria, *155*
characteristics, 154
Mitral cells, olfactory bulb, 750
Mixed nerve
branches, 267
lesions, 402
MLF, (*see* Medial longitudinal fasciculi)
Mnemonic reactions, 923
Molecular layer
cerebellar cortex, 585, 587–588
dorsal cochlear nucleus, 476
Monoamine oxidase, intraneuronal enzyme, 308
Monoaminergic systems, spinal cord
catecholaminergic projections, 399–400
serotoninergic projections, 399
Monoamines, (*see also* Biogenic amines)
amygdala, *776*
neuronal activity, 307–308
spinal cord innervation, 353
thalamus, 679–680, 682
Mossy fibers
characteristics, 592–593
granular layer, *593*
synaptic excitatory action, 597
transverse section, *586*
Motor cortex
primary
electrical stimulation, 910–911
somatotopic organization, 911, *911*
body parts, *890*
supplementary, characteristics, 913–915
Motor deficits, causes, 402
Motor endplates
extraocular muscles, 257
skeletal muscle fibers, *256*
smooth muscle fibers, *256*
striated muscle, 295
structural features, 255
Motor nerve terminal, neuromuscular transmission, *175*
Motor neurons
α, 345–346
acetylcholine use, 353
anterior gray horn, 345–346
muscle innervation, 346
axons, trajectories, *345*
function, 144
lower
fasciculations, 404
lesions, 289
segmental input, 402
muscle fiber innervation, 257
recurrent inhibition, 344
somatic, involvment in bladder function, 318
spinal cord, *154*
upper
lesions, 404
paralysis, 405
Motor nuclei
cranial nerves
skeletal muscle innervation, 452
supranuclear innervation, 452–453
trigeminal nerve, 507
Motor skills, cerebellum influences, 622–623
Motor unit
functional components, 257
myasthenia gravis, 258
MPTP, (*see* 1-Methyl-4-phenyl-4-1,2,5,6,-tetrahydropyridine)
MRI, (*see* Magnetic resonance imaging)
mRNA, (*see* Messenger ribonucleic acid)
Multiple sclerosis
characteristics, 15, 412
detection using cerebrospinal fluid, 15
spin-echo MRI imaging, *61*
Multipolar neurons, characteristics, 146
Muscarinic receptors, presence in spinal cord, 353
Muscle
α motor neuron innervation, 346
extraocular
localization in oculomotor nuclear complex, *543*
root fiber origins, *532*
progressive atrophy, 291
skeletal
afferent fibers, *348*
efferent fibers, *348*
motor cranial nerve nuclei innervation, 452
motor endplates, *256*
smooth
efferent axon, 295–296
innervation, 295
motor endplates, *256*
norepinephrine effects, 310
paralysis, 313
urinary bladder, 318
stretch receptors, 890
striated
innervation, 295
motor endplate, 295
trunk, segmental innervation, *278*
Muscle atrophy, causes, 404
Muscle end plate, neuromuscular transmission, *175*
Muscle spasms, flexor, spinal cord recovery, 406–407
Muscle tone
cerebellar influence, 621–622
pontine reticular formation effects, 493
Muscle tonus, reflex regulation, neuromuscular spindles, 251
Musculocutaneous nerve, muscle innervation, 281
Myasthenia gravis, characteristics, 258
Myelencephalon, (*see* Medulla)
Myelin sheath
basic protein, 167–168
breakup, during nerve degeneration, *184–185*
central, oligodendrocytes and, relationship, *124*
cross section, *170*
formation
jelly-roll theory, 166, *167*
molecular organization, 167–168
neuroglia function, 201
oligodendrocytes, 212–214
stages, *167*
structural organization, 165–167
nodes of Ranvier, 168
Schmidt-Lantermann clefts, 168
Myelin-associated glycoprotein, role in myelination, 167
Myotactic reflex, 361
methods to elicit, 363
Myotomes, innervation
segmental, 273
ventral root, 268

Nauta-Gygax method, neuronal morphology studies, 137–140
Neck, cutaneous fields, *274*
Neocerebellum
characteristics, 585
lesions
characteristics, 620
tremors, 620
Neocortex
γ-aminobutyric acid regulation, receptors, 875
layers
granular, 867–868
molecular, 867
multiform, 868–869
pyramidal, 867–868, *874*
Neopallium, 748
Nerve cell body, (*see* Soma)
Nerve compression, effect on spinal roots, 288
Nerve constriction, consequences of, *191*
Nerve endings
afferent, visceral structures, *240*
encapsulated
end bulbs, 243
Meissner's corpuscles, 243, *243*
pacinian corpuscles, 243, 246–247
free, in skin and hair follicle, *239*
unencapsulated, in deep somatic tissues of humans, *242*
Nerve fibers
degeneration
anterograde, 184–186
axons, *184*
myelin sheath, *184*
myelinated
conductance speed, 171
size variations, 171

peripheral
classification table, *173*
connective tissue sheaths, 169, 171
severed portion, transverse section, *189*
regeneration, stages, *191*
three types, 172
unmyelinated, characteristics, 171
Nerve growth factor
nerve regenerative ability, 193
production, effect of interleukins-1 and -6, 218
purpose, 72
Nerve section, regeneration, 290
Nerves
abducens
neuron types, 498–499
root fibers, transverse section, *496*
accessory, spinal, 442
auricular, great, 275
axillary, 277
muscle innervation, 281
cochlear, 461–462
nuclei, 475–476, *478*
common peroneal, muscle innervation, 287
cranial, (*see* Cranial nerves)
root fiber origins, *532*
cutaneous
femoral
lateral, 285–286
posterior, 287
medial branches, 277, 283
facial
functional components, 495
overview, *495*
root fibers, transverse section, *496*
glossopharyngeal
characteristics, 449–451
effect on swallowing, 451
lesions, 451
gluteal, 287
greater occipital, 274
hypoglossal, 438, 440, 442
injury, types, 289
intermediate, 497
long thoracic, 276
median, muscle innervation, 281
mixed, characteristics, 267
musculocutaneous, 277
muscle innervation, 281
obturator, muscle innervation, 285
occipital, lesser, 275
oculomotor
nuclear complex, 542–544, *544*, 545–547
root fiber pathway, 544
transverse section, *534*
pectoral, medial and lateral, 276
peripheral, dermatome and cutaneous innervation, *271–272*
phrenic, 275
radial, 277
muscle innervation, 281
scapular, dorsal, 276
sciatic, cross-section, drawing, *269*
spinal
dorsal roots, 262
general organization, 262
splanchnic, 300
suboccipital, 274
subscapular, 276
supraclavicular, 275
suprascapular, 276
terminal, olfactory system, 757
third, lesions, 548–549
thoracodorsal, 276
tibial, muscle innervation, 286
trigeminal
exteroceptive and proprioceptive impulses, 500–501
supratentorial dura innervation, 6
trochlear, characteristics, 531
ulnar, 277
muscle innervation, 282
vagus
characteristics, 442–443
dorsal motor nucleus, 446
infratentorial dura innervation, 6
lesions, 449
vestibulocochlear, cochlea and related nerve and nuclei, 474–478
Nervous system
central, (*see* Central nervous system)
peripheral, (*see* Peripheral nervous system)
Neural connections, composition stages, 72
Neural crest
cell differentiation, *76*
characteristics, 67
derivatives, 67
embryonic, spinal ganglia development, 265
Neural crest cells, spinal ganglia creation, *76*
Neural fold, 66
Neural groove, 66
Neural induction, 65
Neural plate, 66
Neural tube
dividing cells of germinal zone, *70*
formation, 65–67
histogenesis, 69
Neurilemma cells, origins, 202
Neurite growth inhibitory proteins, function, 193
Neuroactive peptides
autonomic ganglia, functions, 311
autonomic nervous system, 310–311
calcitonin gene-related, spinal cord laminae, 358
cerebral cortex, 875–876
cholecytokinin, spinal cord laminae, 358
list, *162–163*
locus coeruleus, 513
medulla, 454
opioid peptides, 458–459
oxytocin, 460–461
substance P, 460
vasopressin, 460–461
neuropeptide Y, 358
in amygdala, 778
cerebral cortex, *876*
luteinizing hormone release, 732
spinal cord laminae, 358
opioid, presence in spinal cord, 357–358
oxytocin, spinal cord laminae, 359
purpose, 161
somatostatin
in amygdala, 778–779
immunoreactivity in basal ganglia, *810*
spinal cord laminae, 358–359
subcoeruleus, 513
thalamus, 675, 678
thyrotropin releasing hormone, spinal cord laminae, 359
vasopressin, spinal cord laminae, 359
Neuroblasts, differentiation into neurons, 69
Neuroectoderm, capillary production, 18
Neuroepithelial cells, sensory nerve cells, 241
Neurofilaments, characteristics, 147–148
Neuroglia, (*see also* Glial cells)
astrocytes
characteristics, 203–204
fibrous, *202*, *205*
protoplasmic, *203*
biochemical investigations, 199
cell lineage, 200–203
cerebellar cortex, *599*
function, 199
general features, 200
macroglia, (*see* Macroglia)
microglia, (*see* Microglia)
myelin sheath formation, 201
oligodendrocytes
astrocytes and, comparison, 211
discovery, 211
illustration, *202*
structures, 597–598, 600
Neuroglia cells, histogenesis, *71*
Neurohypophyseal hormones
oxytocin
effect on memory, 732
function, *162*
medulla, 460
production, 712
spinal cord laminae, 359
vasopressin
function, *162*
medulla, 460
memory, 732
production, 712
spinal cord laminae, 359
Neurohypophysis, 23, 707
Neurokeratin network, 168
Neurolemma sheath, 169
Neuromediators
pain control, 456
types, in medulla, 454
Neuromuscular spindles
characteristics, 247
intercostal, *248*
fusiform axons, *250*
sensory nerve endings, *249*
intrafusal and extrafusal fibers, *247*
proprioceptive impulses, 254
Neuron doctrine, principles, 131
Neuronal systems, reticular
ascending, 554–556
descending, 553–554
Neurons, (*see also* Interneurons)
abducens nerve, 498
adrenergic, 458
arborization pattern, 146
auditory pathway, 481–482
axons, *143*
myelin, 165–168
overview, 162–163
catecholaminergic, noradrenergic cell group, 457–458
cerebellum pathway, 380
cholinergic, 458
globus pallidus, *829*
immunohistochemical studies, 353
medial habenular nucleus, 637–638
substantia innominata, 715
classification, chemospecificity, 306
claustral, receptive field properties, 846
cochlear efferent, *483*
components, 131
cortical
dendritic and axonal branchings, *866*
interrelations, in cerebral cortex, 869–871

Neurons—*continued*
corticospinal, characteristics, 385
cytoplasm, 149
cytoskeleton
centrosomes, 154, 156
chromophilic substances, 151–154
Golgi apparatus, 156
illustration, *151*
inclusion bodies, 156–157
microfilaments, 147–148
microtubules, 147
mitochondria, 154
neurofilaments, 147–148
nucleolus, 150–151
peroxisomes, 154
polymerization, 148
Dale's principle, 310
degeneration
anterograde, 184–186
retrograde, 186
dendrites, *143*
development
astrocytes, 208
resident brain macrophage presence, 217–218
differentiation stages, 69
dopaminergic, *158*
hypothalamus, *731*
tuberohypophysial tract, 724–725
enteric, 302
description, 293
ganglia, differentiation, 75
growth
peripheral and central grafting experiments, 192–193
promoting and inhibiting factors, 193
histogenesis, *71*
histologic staining, *135*
hypothalamic, 397
internal pallidal, terminal boutons, *842*
intracellular and intercellular communication, *133*
lamina II, 340
lamina III, 341
lamina IV, 341–342
lamina IX, 343
lateral geniculate, receptive fields, *895*, 896
locus coeruleus, *512*
metabolic activity, visualization methods, 141, 144
morphology, histologic study techniques, 134–137
motor, (*see* Motor neurons)
multipolar
characteristics, 146
histologic staining, *135*
neurosecretory, 161–162, 723
nucleus, characteristics, 149–150
olfactory, 750
pallidal, dendrites of, 831
parasympathetic, *145*
description, 293
postganglionic, characteristics, 296
preganglionic, characteristics, 296
proteins
synthesis, 157, 159
types, 157
pyramidal, *140*
glutamic acid decarboxylase-immunoreactive terminals, *875*
in hippocampus, afferent input, *772*
red nucleus, 391
regeneration, 186–189
resting, (*see* Resting neuron)
reticular nucleus, 671, *672*
sensory, *145*
impulse site, *142*
trigeminal ganglion, *266*
serotoninergic, *158*
effects of LSD, 516
medulla, 455–456
raphe nuclei, 515, *517*
soma, (*see* Soma)
spinal
immunocytochemical staining, in monkey, *354*
posterior horn, 347–349
somatic efferent, 345–347
visceral efferent, 347
spinothalamic tracts, 373
stapedius reflex, 497
striatal, *802*
aspiny, 803, 807–808
effect of dopamine, 817
neurotransmitter use, 826
spiny, 802–803, *803–804*, *821*
substantia nigra, 208, 557
sympathetic, *145*
description, 293
illustration, *305*
synapses
chemical, 175–176
electrical, 174–175
overview, 172–173
receptors, 177–178, 180
ultrastructural classifications, 173–174
vesicle recycling, 176–177
thalamic, gating functions, 693
types, 144
unipolar, histologic staining, *135*
varying lengths, 146
visceral efferent, *492*
types, 347
Neuropeptide Y
amygdala, 778
cerebral cortex, *876*
luteinizing hormone release, 732
spinal cord laminae, 358
Neuropeptides, solitary nuclear complex, 445
Neurophysins, supraopticohypophysial tract, 723
Neuropil, 329
Neurosecretion, concept development, 712
Neurosecretory neurons, 723
Neurotendinous organs
characteristics, 251
Golgi tendon organ
afferent fibers, 252, 363
anatomic and functional relationships, *361*
axonal branches and collagen bundles, relationship, *253*
capsule, 251
illustration, *252*
Neurotoxins, effect on motor neurons, 257, *257*
Neurotransmitters
acetylcholine, 160, 353
autonomic nervous system, 306
cerebral cortex, 880–882
enteric neurons, 302
hippocampus, 769
motoneuron effects, 77
muscle contraction, 257
in primate amygdala, 776, 778
receptor types, 307
spinal cord transmitter, 352–353
storage in motor endplates, 255
thalamus, 673–675
γ-aminobutyric acid, 160
basal ganglia core structures, *805*
cerebral cortex, 873–875
enteric neurons, 302
hippocampus receptors, 769
inhibitory transmitter in spinal cord, 356
neocortex, receptors, 875
striatofugal neurons, *828*
subthalamic nucleus, *840*
thalamus, 675, *676–677*
aspartate
cerebral cortex, 873, *874*
presence in spinal cord, 355–356
biogenic amines, 160
pineal gland, 638
cerebellar nuclei, 601
chemical synapses, 176
enteric neurons, 302
glutamate, 161
cerebral cortex, 873, *874*, 973
hippocampal formation, 768
neurotransmitter, 161
presence in spinal cord, 355
regulation, astrocytes, 207
subthalamic nucleus, *840*
ion channel gating, 178
neuronal communication, 133
PET scan, 663–664
putative chemical messengers, classification criteria, 159
receptor localization, 141
visualization methods, 141
red nucleus, 551
ventral striatopallidal complex, 845
visualization
histochemical techniques, 140–141
immunocytochemical techniques, 140–141
Neurulation, stages, 65–66
NGF, (*see* Nerve growth factor)
Nicotinic receptors, 306
Nigrostriatal dopaminergic system, PET visualization, 64
Nigrostriatal fibers
characteristics, 815–818, 821
feedback loop, 565
substantia nigra, 564–566
termination locations, 565
Nigrotectal fibers
origins, 567
terminations, *568*
Nigrotegmental fibers, origins, 568
Nigrothalamic fibers, characteristics, 566–567
Nissl bodies
characteristics, 152
retrograde degeneration, 186
Nitric oxide synthase, 588
NMDA, (*see* N-methyl-D-aspartate)
N-methyl-D-aspartate, conductance in hippocampal formation, 769
NO synthase, (*see* Nitric oxide synthase)
Nocioceptors
fiber types, 359
function, 239
lamina I input, 339
Node of Ranvier
characteristics, 165, 168
illustration, *165*
Nodulus, 53
Nonpyramidal corticofugal fibers
corticopontine fibers, 916–917
corticoreticular fibers, 916
corticothalamic fibers, 917
Noradrenaline
axons
ascending and descending, *514*

enteric system, *309*
fibers, thalamic innervation, 679–680
postganglionic sympathethic nerve release, 307
Norepinephrine
chemical transmission, 306
content in terminals, 308
effects on smooth muscle, 310
synthesis, 638
Notochord, 65
Nuclear membrane, soma, 149, *150*
Nuclei
hypothalamic
illustration, *707*
paraventricular and supraoptic, *712*
tuberal region, 713
intermediate gray zone
central cervical, 350–351
intermediomedial, 350
posterior gray horn
posteromarginal, 348
proper sensory, 348–349
thalamus
anterior, 642–644, *649*
classification, *641*
intralaminar, 647–648
lateral, 651–652
medial, 644–645
midline, 645, 647
overview, 640–642
ventral, 652–660
visceral efferent neurons
intermediolateral, 347
sacral autonomic, 347
Nucleocortical projections, characteristics, 604
Nucleolus, characteristics, 150–151
Nucleus, neurons, characteristics, 149–150
Nucleus ambiguus
caudal parts, 448–449
characteristics, 448
Nucleus basalis, 787
Nucleus cornucommissurales, posterior and anterior, 351
Nucleus cuneatus, 370
cytoarchitecture, 427
dorsal root projections, 427
pathways, 371
Nucleus cuneiformis, 552
Nucleus gracilis, 370
characteristics, 425
cytological regions, 426
dorsal root organization, 427
neuronal appearance, 426
pathways, 371
terminal arborization, 427
Nucleus intercalatus, 442
Nucleus interpositus, divisions, 602–603
Nucleus of Darkschewitsch, interstitial nucleus of Cajal and, relationship, *547*
Nucleus of Onuf, 347
Nucleus pericornualis anterior, 346, 380
Nucleus prepositus, 442
Nucleus raphe magnus
efferent innervation, 516
neurons, retrogradely labeled, *515*
spinal serotoninergic projections, *456*
stimulation, 456
Nucleus reticularis gigantocellularis, 396
Nucleus reticularis pontis, 469
Nucleus solitarius
cytoarchitecture divisions, 444
projections, 718
Nucleus subcuneiformis, 552
Nystagmus
characteristics, 621
definition, 492

Obturator nerve, muscle innervation, 285
Occipital eye center, 916
Occipital lobe, components, 34
Ocular dominance columns
primary visual sensory areas, 900–902
striate cortex, *901–902*, 904
Oculomotor nerve
accessory oculomotor nuclei, 544–545
nuclear complex, 542–544
afferent connections, 545–547
extraocular muscle locations, *543*
sagittal section, *544*
visceral nuclei, 543–544
root fiber pathway, 544
transverse section, *534*
Odor discrimination, (*see* Smell)
OKR, (*see* Optokinetic eye movement response)
Olfaction, overview, 756
Olfacto-frontal connections, in primate brain, *753*
Olfactoria fila, 748
Olfactory area, cerebral cortex, 886
Olfactory bulb
accessory, characteristics, 756–757
afferent fibers, 752–753
anterior olfactory nucleus, 753
cells, *749*
functional organization, 752
interconnections, *752*
interneuron types, 750
mitral cells, 750
striae, 754
structures, 750
Olfactory glomeruli
characteristics, 751
localized lesions, 752–753
Olfactory inputs, amygdaloid nuclear complex, 756
Olfactory lobe, structures, 754–755
Olfactory nerves, lesions, 758
Olfactory neurons, 750
Olfactory nuclei, anterior
characteristics, 753
fiber projections, 756
interconnections, *752*
Olfactory receptors, characteristics, 748–750
Olfactory striae, brain inferior surface, 38
Olfactory sulcus, 32
Olfactory system
amygdala and, relationship, 780
brain, *749*
clinical considerations, 757–759
convergence ratios, 751
olfactory bulb, accessory, 756–757
olfactory lobe, structures, 754–755
olfactory receptors, characteristics, 748–750
olfactory tract, structures, 754
rhinencephalon, 748
septal area, structures, 756
terminal nerve, structures, 757
vomeronasal system, structures, 756–757
Oligodendrocytes
astrocytes and, comparison, 211
discovery, 211
electrical properties, 214
illustration, *202*
ionic channels, 214
myelin sheath formation, *212*, *214*
spinal cord, *211*
types, 211–212
Olivary complex, inferior
afferent input, 608
characteristics, 432–434
climbing fibers, 594
gray band of cells, 433
Olivary eminences, 45
Olivary nucleus, inferior
afferent input, 609–610
climbing fibers, 608
Olivocerebellar fibers
cerebellum, 605, *618*
characteristics, 608–609
Olivocochlear bundle, fiber origins, 482
Opercular portions, 28
Ophthalmic artery, dura mater, 6
Ophthalmic branch, trigeminal ganglia, 501
Opiate receptors, pain mechanisms, 361
Opioid peptides
in medulla, 458–459
nociceptive transmission, 361
presence in spinal cord, 357–358
Opioids, endogenous
pain mechanisms, 360
pain regulation, 358
Optic chiasm, 45
lesions, 690
Optic nerves, characteristics, 687
Optic radiations, *33*, 38, *40*, *43*
Optic tract
characteristics, 687
nucleus, 540
Optokinetic eye movement response, 622
Orbitofrontal cortex, lateroposterior quadrant, olfactory information, *756*
Organ of Corti, *476*
characteristics, 475
Organum vasculosum laminae terminalis, 23
characteristics, 711
serotoninergic innervation, *714*
Orientation columns
primary visual sensory areas, simple and complex cells, 897, 899–900
striate cortex, *901*
Otolith organ, 484
Otosclerosis, definition, 484
OVLT, (*see* Organum vasculosum lamina terminalis); (see Organum vasculosum laminae terminalis)
Oxytocin
function, *162*
medulla, 460
memory, 732
production, 712
spinal cord laminae, 359

Pacinian corpuscles
characteristics, 243, 246–247
function, 254
illustration, *246*
PAG, (*see* Midbrain periaqueductal gray)
Pain
aspects of, 239
endogenous opioids, 358
gate control theory, 360
mechanisms to control, 360
neuromediators, 456
nociceptive afferent fibers, 359
phantom, 290
primary somesthetic area, 891
referred, (*see* Referred pain)
serotonin involvement, 680–681

Paleocerebellum, characteristics, 584
Paleopallium, 748
Pallidal fibers, ventral anterior nucleus, 654
Pallidal segments
  external, *796*
    efferent projections, *838*
  internal
    amino acid transport, to thalamic nuclei, *837*
    efferent fibers, *835*
Pallidonigral fibers, characteristics, 562, 834, 836
Pallidosubthalamic fibers, characteristics, 837
Pallidotegmental fibers, characteristics, 836–837
Pallidothalamic fibers
  characteristics, 834
  crossed and uncrossed, *656*
  origin and course, *830*
  terminal arborizations, *657*
Pallidum, γ-aminobutyric acid concentrations, *805*
Palsies
  Bell's, 498
  facial, 498
  pseudobulbar, 454
  right lateral rectus, *494*
Parabigeminal area, cells, 531
Parabrachial nuclei, 509
  structures, 511
Paracusis, definition, 484
Paradoxical sleep, characteristics, 518
Parafascicular nucleus, characteristics, 648
Parahippocampal gyrus, transverse section, *760*
Parallel processing, definition, 659
Paramedian arteries
  blood supply to midbrain, 118
  characteristics, 116
Paramedian pontine reticular formation, 499
  caudal regions, stimulation, 500
Paramedian reticular nuclei, 435
Paraphysis, 84
Paraplegia, definition, 389
Parasympathetic nervous system
  cranial region, 301–302
  effect on visceral structures, *312*
  function, 262
  preganglionic fibers, 301–302
  sacral region, 302
  sympathetic system and, antagonistic effects, 315–316
Parasympathetic responses, role in body temperature regulation, 733
Paratrigeminal nucleus, 430
Paraventricular nucleus
  descending fibers, 721–722
  hypothalamus, in mouse, *716*
  neurons, 713
    c-fos expression, *715*
Parietal lobe, parts, 32
Parietal operculum, *30*
Parkinson's disease
  animal models, experimental, 852–853
  causes, 18
  characteristics, 850
  initial symptoms, 849
  motor disturbances, causes, 853–854
  neural mechanisms, 850
  neuropathologic features, 568
  treatments, L-dopa, 569
Parotid gland, innervation, 311
Pars caudalis, 469, 502, 519
  cytologic lamination, 429
Pars compacta, 557
  dopaminergic neurons, *558*
    ascending projections, *560*
  lesions, effect on basal ganglia circuitry, *854*
  pars reticulata and, efferent connections comparison, *817*
Pars interpolaris, 502
  characteristics, 429
Pars lateralis, 557
Pars oralis, 502, 519
  characteristics, 429
Pars ovalis, 469
Pars parvicellularis, lesions, 908
Pars reticulata, 557
  dynorphin, 559
  efferent projections, *564*
  pars compacta and, efferent connections comparison, *817*
  subthalamic nucleus neuron projections, 843
Parvicellular reticular nucleus, 435
Pastpointing, definition, 620
Patellar tendon reflex
  schematic, *362*
  spinal innervation, 273
PCP, (*see* Phencyclidine)
PDGF, (*see* Platelet-derived growth factor)
Pedicle, definition, 685
Peduncle of the flocculus, 461
Peduncle of the superior olive, 480
Peduncles
  cerebellar
    brain stem, 600
    inferior, 437, 463, 606
    superior, 509, 510, 612–613
  thalamus, anterior, posterior, and superior, 682–683
Pedunculonigral fibers, characteristics, 563
Pedunculopontine nucleus
  afferent fibers, 552
  cholinergic cells, 836
  definition, 836
  projection to subthalamic nucleus, 841
  projections, 836
Pedunculopontine tegmental nucleus, 510
  cholinergic neurons, role in sleep, 923
Penicillin, blood-brain barrier permeability, 19
Peptides
  in cerebrospinal fluid, 23
  heart-derived, *162*
  neuroactive, 161, 310–311
    in amygdala, 778–779
    cerebral cortex, 875–876
    neuropeptide Y, (*see* Neuropeptide Y)
    opioid, 357–358
    somatostatin, (*see* Somatostatin)
    substance P, 356–357
    in thalamus, 675, 678
  pineal gland, 638
  pituitary, *162*
Perforant path, dentate gyrus, 765
Pericytes, 18
Periglomerular cells
  characteristics, 750
  illustration, *751*
Perikarya, postganglionic, denervation hypersensitivity, 312–313
Perineurium, 268
  characteristics, 169, 171
Perineuronal satellite cells, characteristics, 211, *211*
Periosteal layer, dura mater, 3
Peripeduncular nucleus, 557
Peripheral fibers
  somatic efferent, characteristics, 255–257
  visceral efferent, characteristics, 255–257
Peripheral innervation
  brachial plexus, 275–276
  cervical plexus, 275
  dorsal rami, 274
  ventral rami, 274–275
Peripheral nerve fibers
  classification table, *173*
  degenerated myelin, macrophage removal, 217
  grafting experiments, 192–193
  injured, regeneration, 289–291
Peripheral nervous system
  autonomic division, (*see* Autonomic nervous system)
    responsibilities, 262
  components, 25
  connective tissue sheaths
    characteristics, 267–268
    endoneurium, 169
    epineurium, 171
    perineurium, 169, 171
  cutaneous fields
    anterior view, *271*
    posterior view, *272*
  dermatome innervation
    anterior view, *271*
    posterior view, *272*
  fiber types, *77*
  mixed nerve, 267
  myelin sheath, 166
  neurons, axons distributed in, *145*
  nodal regions, *164*
  peripheral innervation
    dorsal rami, 274
    overview, 273–274
    ventral rami, 274
  plexuses
    brachial, 275–277, 281–283
    cervical, 275
  regenerative processes, 186–189
  Schwann cells, 75
    behavior of, after anatomic severance, 290
    cross section, *170*
    nerve fiber degeneration and regeneration, 185–186
  segmental arrangement, 75, *77*
  segmental innervation, 268–273
  somatic division
    connective tissue sheaths, 267–268
    mixed nerve, 267
    responsibilities, 262
    spinal ganglia, 264–266
  spinal ganglia
    cell types, 264, 265
    characteristics, 264–266
    lumbar, *264*, *267*
    neuron differentiation, 75
    related nerves, 300–301
    schematic, *326*
    sensory neurons, *266*
    superior glossopharyngeal, *264*
    transverse section, *74*
    vagus, *265*
  spinal nerves
    cutaneous innervation, *274*
    dorsal roots, 262–263, *327*
    functional categories, *76*
    functions, 287–288, *437*
    general organization, 262
    injuries, 288
    lesions, 288, *403*
    thoracic, *263*, *348*

ventral roots, 263–264, *327*
vertebral canal emergence, 325
Peripheral receptive field, definition, 235
Peritrichal endings, cutaneous receptors, 241
Perivascular space
membranes and, relationship, *13*
relationship of membranes to, *13*
Periventricular gray matter, cell groups, 647
Peroxisomes, characteristics, 154
Pes lemnisci, 572
PET, (*see* Positron emitting tomography)
pH, regulation in central nervous system, 214
Phagocytosis, 218
neuronal shaping, 218
PHA-L, (*see Phaseolus vulgaris*-leucoagglutinin)
Phantom pain, 290
Phaseolus vulgaris-leucoagglutinin, neuronal morphology studies, 138
Phencyclidine, psychotic behavior production, 880
Phenylethanolamine-*n*-methyltransferase, immunoreactivity in medulla, 457–458
Pheromones, vomeronasal organ, *757*
Phosphatase, activity in choroid epithelial cells, 225
Phosphorylation, definition, 159
Photoelectric transduction, sensory receptors, 237
Photoreceptors, function, 238
Pia mater, *9*
characteristics, 8–9
Pia-glia, (*see* Intima pia)
PICA, (*see* Posterior inferior cerebellar artery)
PIF, (*see* Prolactin-inhibiting factor)
Pigment granules, types, in autonomic cells, 156–157
Pineal gland, 23
development, 83
secretions, 638–639
structure, 638
Pinealocytes, characteristics, 638
Pinocytosis
choroid epithelial cells, 225
role in blood-brain barrier, *20*
Piriform lobe, divisions, 755
Pituitary gland
anterior, control by hypothalamus, 734–735
β-endorphin, 732
vascular casts, in monkey, *729*
Pituitary hormones, target organs, *730*
Pituitary peptides
adrenocorticotrophic hormones, 735
growth hormones
control, 737
hypothalamic releasing factors, 729–730
Plantar superficial reflex, spinal innervation, 273
Plasmalemma, soma, characteristics, 148–149
Platelet-derived growth factor, progenitor cell differentiation, 203
Plexuses
abdominal aorta, 301
adrenergic ground, *308*
brachial
development, 327
Duchenne-Erb syndrome, 283
formation, *276*, 277
Klumpke syndrome, 283
structures, 275–277, *277*
celiac, characteristics, 300–301
cervical, structures, 275
choroid, (*see* Choroid plexus)
lumbosacral, lower extremity innervation, 283, *284*
mucosal, cross-section, *303*
myenteric, 302–303
cross-section, *303*
sacral, 283
submucosal, 302
cross-section, *303*
venous
basilar, 121
internal vertebral, 97
PNMT, (*see* Phenylethanolamine-*n*-methyltransferase)
Polymerization, neuronal cytoskeleton, processes, 148
Polymorphic layer, dorsal cochlear nucleus, 476
Polyneuritis, definition, 289
Polyuria, definition, 734
Pons
abducens nerve
characteristics, 498
horizontal and vertical eye movements, 500
lesions, 499
abducens nucleus, lesions, 499–500
anterior aspect, *422*
arterial supply, *115*
auditory fiber systems
cochlear bundle, efferent, 482, *483*, 484
pathways, 478, *479*, 480–482
primary, 478, *479*
secondary, 478–482, *479*
autonomic pathways, 314
blood supply, 113
microangiogram, *114*
caudal
dorsal, 469, 473
ventral, *470*
caudorostral segments, 469
cranial nerves, 49
facial nerve
lesions, 497–498
structures, 495–497
longitudinal fiber bundles, 473–474
mid, olivocerebellar and pontocerebellar fibers, transverse section, *619*
midsagittal section, microangiogram, *116*
principal nucleus, 503
reticular formation
effect on muscle tone, 493
structures, 469, 519
rostral pons-isthmus level
locus coeruleus, 511, 513–515
parabrachial nuclei, 511
raphe nuclei, 515–516, 518
superior cerebellar peduncle, 510–511
tegmentum, 509–510
secondary pathways, characteristics, 498
structures, 49
transverse section, *471*
abducens nerve, *496*
abducens nuclei, *470*, *473*
asymmetric, *470*
facial nerve root, *471*, *496*
reticular formation, *470*
trigeminal nerve level, *501*, *503–504*
3-year-old child, *472*
trigeminal ganglion, divisions, 501
trigeminal nerve
cutaneous innervation, *274*
mesencephalic nucleus, 503, 506–507
motor nucleus, 507
reflexes, 508–509
secondary pathways, 507–508
spinal trigeminal tract and nucleus, 502–503
upper
olivocerebellar and pontocerebellar fibers, transverse section, *619*
transverse section, *507*, *510*
ventral portion, 473–474
vestibulocochlear nerve
cochlea and related nerve and nuclei, 474–476, 478
functions, 492–495
labyrinth and related nerve and nuclei, 484–488
vestibular fiber systems, 488–492
zones, 552
Pontine tegmentum
characteristics, 469
transverse section, *471*
abducens nuclei level, *473*
trigeminal nerve level, *501*, *503–504*
3-year-old child, *472*
trapezoid body, 481
Pontobulbar nucleus, 437
Pontocerebellar fibers
cerebellum, *618*
characteristics, 610–611
Ponto-geniculo-occiptal activity, 922
Positron emitting tomography
brain imaging, 93
examples, *62*
neurotransmitters, 63–64
microglia, 218
operation principles, 60–61
Postcentral gyrus
activation, by cutaneous stimuli and joint movement, *888*
neuronal activation, 889–890
somatotopic localization, body parts, *890*
stimulation, effects, 891
Postcommissural fornix, fiber projection, *767*
Posterior column nuclei
overall appearance, 425
somatotropic lamination, 426–427
Posterior commissure
brain stem transverse section, *540*
lesions, 541–542
structures, 541–542
transverse section, through midbrain, *545*
Posterior gray horn
characteristics, 328
structures, 44
posteromarginal nucleus, 348
proper sensory nucleus, 348–349
substantia gelatinosa, 348
Posterior inferior cerebellar artery, occlusion, 463
Posterior nuclear group
brain stem, *636*
thalamus
functions, 661
structures, 661–662
Posterior white columns
ascending fibers, function, 370–371
dorsal column fibers, 371
dorsal root fibers, 371
formation and course, *369*
lesions, 371

Posterior white columns—*continued*
spino-olivary fibers, 433
structures, 368–369
Posteromarginal nucleus, posterior gray horn, 348
Posteroventral cochlear nucleus, 478
Postganglionic fibers
cervical ganglia, 300
sympathetic, types, 311
Postganglionic neurons
characteristics, 296
visceral locations, *297*
Postjunctional effectors, nicotinic and muscarinic, 306–307
Potassium, regulation, role of astrocytes, 206
PPN, (*see* Pedunculopontine nucleus)
PPRF, (*see* Paramedian pontine reticular formation)
Precentral gyrus, corticothalamic fibers, 917
Precerebellar nuclei, types, 611
Precommissural fornix, fiber projection, *767*
Prefrontal cortex, functional subregions, 926
Preganglionic fibers
parasympathetic system, 301–302
regulation of enteric system, 303
sacral region, 302
sympathetic ganglion cells and, relationship, 305, *306*
sympathetic system, 299–300, 316
Preganglionic neurons
characteristics, 296
divisions, 298
outflow regions, 296–297
parasympathetic system, 316
visceral innervation, 298
visceral locations, *297*
Preoptic region, hypothalamus
function, 711
structures, 711
Prerubral field, characteristics, 843–844
Pretectal region, nuclei, 540
Prevertebral ganglia, characteristics, 296
Primary motor cortex
electrical stimulation, 910–911
inputs to, 915
parts body in, *911*
Primary somesthetic area, 32, 691
Principal inferior olivary nucleus, 433
Principal sensory nucleus
characteristics, 503
illustration, *506*
Progenitor cells
differentiation into type-2 astrocytes, induction factors, 203
oligodendrocyte development, 203
Prolactin-inhibiting factor, hypothalamus, 732
Proprioceptive receptors, position and movement, 254
Proprioceptors, function, 237
Proteins
GAP-43, 193
membrane, 159
modification procedure, 159
neurite growth inhibitory, 193
receptor, 178
secretory, 161
synthesis, in neurons, 157–159
Proto-oncogenes, c-*fos*, neuronal activity studies, 142
Psammoma bodies, 225
Pseudobulbar palsy, characteristics, 454
Pseudorabies virus, autonomic nervous system studies, 298–299
Pulvinar, 50
characteristics, 651–652
illustration, *634*
nuclei, 652
Pupillary dilatation, 58
Pupillary reflexes
light, 541
types, 547–548
Purkinje cells, 82
cerebellar cortex, 597
characteristics, 588–589
dendritic arborizations, *589*
dendrites, 146
nucleus, 149, *152*
transverse section, *586*
Putamen, *106*, *774*
characteristics, 41, 801
frontal section of brain, *796*
illustration, *800*
muscarinic cholinergic receptor binding sites, *811*
nigrostriatal fibers, 816
PHA-L anterograde labeled elements, *816*
Pyramidal cells, *866*
characteristics, 865
dendritic pattern, 146
excitatory role in neocortex, 873
hippocampal formation, 763
length, 146
Pyramidal neurons, in hippocampus, afferent input, *772*

Quadrigeminal plate, 47, 527
Quadriplegia, definition, 389

Rachischisis, 91
Radial nerve, injuries, 281
Radial periosteal reflex, spinal innervation, 273
Radicular arteries, characteristics, 95
Rami
dorsal, muscle innervation, 274
ventral, muscle innervation, 274
Ramus communicans, 75, 77, 267
gray, sympathetic system, 300
Ranvier nodes, (*see* Node of Ranvier)
Raphe nuclei
afferents, 821–822
brain stem, *455*
caudal, ascending fibers, 516
cerebellar cortex, 596
dorsal
circumventricular organ innervation, 711
descending fibers, 516
median, serotoninergic innervation to hypothalamus, 717–718
precerebellar nuclei, 611
serotonin, 455
ascending and descending axons, *518*
role in sleep, 923
Raphe-nigral fibers, collateralization, 563
Rapid eye movements, 923
Rathke's pouch, 85
Raynaud's disease, characteristics, 313–314
Reactive gliosis, definition, 209
Rebound phenomenon, example, 620
Receptive fields
lateral geniculate neurons, *895*, 896
retina
ganglion cells, *895*, 896
general types, 689
Receptors
chemical transmission in neurons, 177–178, 180–181
ion channel gating, 178
neurotransmitters, 207–208
visualization methods, 141
sensory
classifications, embryonic origin, *236*
diversity, 237–239
exteroceptors, 237
function, 235
introceptors, 237
physiological classifications, 238–239
proprioceptors, 237
terminations in corneal epithelium, *237*
transduction process, 237
stretch
function, 617
neuromuscular spindles, 247–251
neurotendinous organs, 251–252
Recruiting response, 694
Rectus palsy, right lateral, *494*
Recurrent inhibition, motor neuron firing, 344
Red nucleus
cerebellum, *618*
connections, 550–551
cytoarchitecture, 549–550
fiber organization, 391
functional considerations, 551
illustration, *649*
lesions, 551–552
neurons, 391
neurotransmitters, 551
rubrospinal tract, 391
topography, 549
Referred pain
diseased viscus, 254
etiology, 254
Reflex arcs, visceral, neuronal involvement, 296
Reflexes
brain stem reticular formation, 553
corneal, secondary trigeminal fibers, 508
mass, 407
pupillary
light, 541
types, 547–548
vomiting, 509
Regeneration, peripheral nerves, 290–291
Relaxation
magnetic resonance imaging, 57
MRI imaging, 57
Release phenomenon, dyskinesias, 849–850
REM, (*see* Rapid eye movements)
Renshaw cells
characteristics, 344
types, 345
Reproduction, control, hypothalamus regulation, 735–737
RER, (*see* Rough endoplasmic reticulum)
Reserpine, effect on sleep, 923
Resident brain macrophages
neuronal shaping, 217–218
response to injury and edema, 217
types, 217
Respiration regulation, brain stem, 446
Restiform body, 437
Resting membrane potential, 132
Resting neuron, membrane potential, 132
Reticular formations
brain stem
cerebellar projections, 610
hypothalamus, 717

medulla
afferent fibers, 435
cytoarchitecture, 434
divisions, 436
efferent fibers, 435–436
major subdivisions, 434–435
nuclear masses, 435
midbrain tegmentum
cytoarchitectonic divisions, 552
functions, 552–553
lesions, 556
neurotransmitters, 556–557
reticular neuronal systems, 553–556
pontine
muscle tone, 493
structures, 519
Reticular nuclei
glutamic acid decarboxylase expression, *678*
lateral, characteristics, 610
paramedian, characteristics, 610
thalamus
function, 673
neuronal classifications, 671
Reticular process, 334
Reticulospinal tract
medullary, components, 396
overview, *395*
pathways, 395–396
termination sites, 396
Reticulotegmental nucleus, characteristics, 610
Retina
optical to neural image transformation, stages, 685–686
receptive field zones, 689
rods and cones, 685
ultrastructural organization, *686*
Retinal ganglion cells
characteristics, 686–687
receptive fields, *895*, 896
Retinohypothalamic fibers, characteristics, 718
Retinotectal fibers, characteristics, 536
Retrograde axonal transport
features, *190*
function, 182–183
speed of, 182
Retrograde degeneration, neurons, 186
Retrograde double-labeling methods
example, *139*
principles, 138
substantia nigra, *566*, *570*
Retrograde transport
axons, 182–183
components, *190*
substances, *183*
Retroinsular cortex, cutaneous stimulation, 892
Retrorubral area, 557
Rhinencephalon, 748
Rhizotomy, dorsal, spinal cord degeneration, 406
Rhodopsin, definition, 685
Rhombencephalon, 25
Rhomboid fossa, 78
Riley-Day syndrome, (*see* Familial dysautonomia)
RiMLF, (*see* Rostral interstitial nucleus of the MLF)
Rods, characteristics, 685
Rostral interstitial nucleus of the MLF, 500, 547
Rostral midbrain, transverse sections, 534–535
Rostral pons-isthmus level
locus coeruleus, 511, 513–515
ascending and descending noradrenergic axons, *514*
brain stem innervation, 514
cell types, *511*, 513
characteristics, 457, 513
neurons, norepinephrine, 399, *512*
noradrenergic input, 611, 769
parabrachial nuclei, 511
raphe nuclei, 515–516, 518
superior cerebellar peduncle, 510–511
tegmentum, 509–510
Rough endoplasmic reticulum, 153
Rubrobulbar fibers, 436
in medulla, 551
Rubro-olivary fibers, origins, 433
Rubrospinal tract
course of, *390*
schematic, *389*

Saccule, 484
Sacral outflow, characteristics, 298
Sacral plexus, 285
Sacral segments, spinal cord, 335, *337–338*
Salivary glands, autonomic innervation, 317–318
Salivary reflexes, secondary trigeminal fiber involvement, 509
Salivatory nucleus, superior, 497
Satellite cells
development, 265–266
origins, 202
perineuronal, characteristics, 211, *211*
Scanning electron micrographs, ependyma, *222*
Schaffer collaterals, 764
Schizophrenia
dopamine
hypothesis, 880
transmission, 879
emotional changes, role of amygdala, 786
Schmidt-Lantermann clefts
characteristics, 168
illustration, *169*
Schwann cells, 75
behavior of, after anatomic severance, 290
cross section, *170*
nerve fiber degeneration and regeneration, 185–186
Sciatic nerve
cross-section, drawing, *269*
divisions, 286
Sclerotome, function, 268
SCO, (*see* Subcommissural organ)
Secondary trigeminal pathways, characteristics, 507–508
Secondary vestibular fibers
role in eye movement, 492
types, 489–490
Segmental innervation
hip, *280*
lower extremity, *280*
shoulder, *279*
skeletal muscle, 273
spinal cord, cutaneous fields, *270*
trunk muscles, *278*
Semicircular ducts, 484
Sensation
affective, 692
discriminative, thalamic projections, 692
protopathic and epicritic, 238
receptors, 235
Sensibility
affective, body variations, 253
discriminative, 238
body variations, 253
superficial and deep, 238
Sensorimotor cortex, thalamic subdivisions, sagittal view, *660*, *889*
Sensory areas, cerebral cortex
auditory, 905–908
gustatory, 908
primary, 886–887
primary somesthetic, 887–888, *888*
primary visual, 892–893, *899*
secondary, 887, *893*
secondary somesthetic, 892
secondary visual, 904–905
vestibular representation, 908–909
Sensory ganglia, cell changes, 266–267
Sensory impulses, organization in spinal cord, *377*
Sensory modality, definition, 235
Sensory receptors
classifications
embryonic origin, *236*
physiological, 238–239
rapidly and slowly adapting, 236
corneal epithelium terminations, *237*
diversity, 237–239
encapsulated endings
corpuscles of Meissner, 243, *243*
end bulbs, characteristics, 243
pacinian corpuscles, characteristics, 243, 246–247
exteroceptors, function, 237
free nerve endings
afferent, *240*
characteristics, 239–240
in skin and hair follicle, *239*
function, 235
introceptors, function, 237
morphologic types, 239
overall view, 252–254
proprioceptors, function, 237
transduction process, 237
Sensory relay nuclei
corticobulbar fibers, 451
electrical stimulation, 693
Sensory unit, characteristics, 235
Septa, falx cerebri, 3
Septal nuclei, choline acetyltransferase immunoreactivity, *784*
Septal region
olfactory system, 756
substantia innominata, *774*
choline acetyltransferase immunoreactivity, *784*
cholinergic neurons, 715
structures, 715, 786–788
Septomarginal fasciculus, 371
Septum pellucidum, *29*, 42
Serotonin, 556–557
circumventricular organs, 23
immunoreactive fibers
basal ganglia, *820*
thalamus, *681*
innervation
amygdala, 776
cerebral cortex, 878
thalamic, 680
neurons
effects of LSD, 516
medulla, 455–456
raphe nuclei, 515
pinealocyte synthesis, 638
projections
characteristics, 399
function, 399
raphe nuclei, 455

Serotonin—*continued*
receptors, types in central nervous system, 680
spinal cord
fibers, 355
neurotransmission, 355
visualization, immunocytochemical methods, 140
Sexual development, hypothalamus, 735
Sexual dimorphism, hypothalamic nuclei, morphologic features, 737
SFO, (*see* Subfornical organ)
Sheath of Schwann, 163
characteristics, 168–169
Shoulder
innervation, 276
segmental innervation, *279*
Sign of Babinski, definition, 388
Sign of Lasègue, 286
Signaling molecules
characteristics, 159
neuroactive peptides, 161
neurosecretion, 161–162
small, 160–161
Silver impregnation technique, connectivity studies, 137–138
Simian hand, 282
Simple cells, striate cortex, functional characteristics, *898*
Simple crush, definition, 290
Sinuses
cavernous, 120–121
oblique coronal section, *100*
structures, *122*
circular, 121
confluens of, 120–121
dura venous
characteristics, 120
sagittal view, *121*
occipital, 120
rectus, *124*
sagittal, 120
sphenoid, 121
sphenoparietal, 121
transverse, 120
Skeletal muscle
afferent fibers, *348*
efferent fibers, *348*
motor cranial nerve nuclei innervation, 452
motor endplates, *256*
Skin
mechanical stimulation, cutaneous axon properties, *244–245*
nerves and nerve endings, *239*
Sleep
brain stem reticular formation, 555
coma and, comparison, 556
hypothalamus and, relationship, 738
paradoxical, 922
process, 923
serotonin and norepinephrine-containing neurons, 518
slow-wave, 518, 922
Small-molecule transmitters, characteristics, 454
Smell
characteristics, 758
primary odors, 758
Smooth muscle
denervation, paralysis, 313
efferent axon, 295–296
innervation, 295
motor endplates, *256*
norepinephrine effects, 310
urinary bladder, activity types, 318
SNc, (*see* Pars compacta)
Sneezing, secondary trigeminal fiber involvement, 508
SNr, (*see* Pars reticulata)
Solitary nuclear complex
ascending projections, *443*
neuropeptides, 445
secondary fiber system, 445
Soma
action potential, 133–134
function, 132
organelles, *150*
structures
centrosomes, 154
chromophilic substance, 151–154
golgi apparatus, 156
inclusion bodies, 156–157
mitochondria, 154
nucleolus, 150–151
nucleus, 149–150
overview, 148–149
peroxisomes, 154
Somatic cell columns, lateral, 543
Somatic division, spinal nerve
dorsal roots, 262–263
general organization, 262
Somatic effectors, motor endplates, 255
extraocular muscles, 257
muscle fibers, *256*, 295
myasthenia gravis, 258
structural features, 255
Somatic efferent neurons, medial and lateral nuclear group, 246–247
Somatic motor neurons, involvement in bladder function, 318
Somatic voluntary motor system, visceral motor system and, comparison, 296
Somatostatin
in amygdala, 778
immunoreactivity in basal ganglia, *810*
spinal cord laminae, 358–359
Somatotopic localization
cerebellar cortex, *606*
cerebellum, 605–606
Somatotopic representation, cutaneous, body surface, *658*
Somesthetic areas
cerebral cortex, 886
primary, function, 891
secondary, position and somatotopic organization, *894*
Sommer's sector, 770
Sound
cortical effects, 908
localization, 908
Spasticity
characteristics, 405
definition, 405
spinal cord transection, 407
Spatial buffering, definition, 206
Special efferent fibers, 80
Special somatic afferent fibers, 80, 437, *438–440*
Special visceral afferent fibers, 80, 437, *439–440*
facial nerve, *495*
Special visceral efferent fibers, 437, *438–440*
facial nerve, *495*
muscle innervation, 438
Spermatogenesis, gonadotrophins, 737
Sphenoid sinus, structures, 121
Spherule, definition, 685
Spike potential, 171
Spina bifida occulta, 91
Spinal accessory nerve, spinal portion, 442
Spinal arteries, anterior and posterior, 94–95
characteristics, 114
Spinal bifida, characteristics, *90*
Spinal cord
afferent fibers, primary
termination sites, 352
topographic organization, 351
zone of Lissauer, 351–352
ascending tracts, *401*
cerebellar afferents, 378, *379*, 380–381
posterior white columns, 368, *369*, 370–371, 373
spinoreticular fibers, 381, 383
spinotectal, 378
spinothalamic, 373–378
blood supply
anterior and posterior spinal arteries, 94–95
occlusion, 96
radicular arteries, 95–96
schematic, *94*
spinal veins, 96–98
caudal portion, diagrammatic representation, *8*
cerebrospinal fluid circulation, *12*
cervical enlargement, section through, *387*
cervical segments
crush injury, *372–373*
lateral cervical nucleus, *377*
upper, posterior view, *6*
chemoarchitecture
acetylcholine, 352–353
amino acids, 355–356
monoamines, 353–355
neuroactive peptides, 356–359
cross-section, drawing, *327*
crushed portions, transverse section, *370*
descending tracts
autonomic pathways, 397–399
catecholaminergic projections, 399–400
corticospinal system, 383–389
fastigiospinal, 397
medial longitudinal fasciculus, 396–397
reticulospinal, 394–396
rubrospinal, *390*, 391
serotoninergic projections, 399
tectospinal, 389, *390*, 391
vestibulospinal, 391–392, *393*, 394
developmental stages, *68*, 73–75
differentiating layers, *70*
dopaminergic input, 353–354
dorsal roots, *326*
lesions, 405–406
embryonic, ependymal cells and central canal, *329*
ependyma
characteristics, 218
human and rabbit brains, *219*
illustration, *219–220*
scanning electron micrographs, *222*
functions, 328–329
gray matter
astrocytes, *201*, 204
characteristics, *330*
internal arrangement, *331*
hemisection, 407–409
degenerative pattern, *408*
internal structure
cytoarchitectural lamination, 338–345
efferent neurons, 345–347
gray and white matter, 329–330
intermediate gray zone, 349–351

posterior horn, 347–349
segmental variations, 330–338
intrinsic fibers, 400–402
length, 325
lesions, degenerative effects, *403*
longitudinal furrows, 325–326
lumbar segments, *334*, 335, *337*
crush injury, section, *388*
transverse section, *347*
medulla and, transitional steps, 421
meningeal coverings, *9*
microglial cells, *215*
monoaminergic innervation, 353
motor activities, 273
motor neurons
lower, 402–404
upper, 404–405
neuroactive peptides, substance P, 356–357
neurotransmitters
acetylcholine, 353–354
γ-Aminobutyric acid, 356
glutamate and aspartate, 355–356
glycine, 356
norepinephrine, 355
serotonin, 355
pain mechanisms, 359–361
posterior view, *326*
receptors, muscarinic, 353
reflexes, 273, 361–363
sacral segments, *334*, 335, *337–338*
segmental innervation
cutaneous fields, *270*
hip, *280*
lower extremity, *280*
overview, 268–269
shoulder, *279*
trunk muscles, *278*
upper extremity, *279*
segments, 325
cervical, 330, *331–333*, 334
schematic, *328*
thoracic, 334–335, *336*
sensory impulse conveyance, 377
serotoninergic innervation, 355
spinal reflexes, 361–362
syndromes
amyotrophic lateral sclerosis, 409
combined system disease, 409–410
multiple sclerosis, 412
syringomyelia, 410–411
tabes dorsalis, 411–412
topographic organization, 325–329
transection, complete
degenerative pattern, 407
neural function recovery, 406
patient status at 1 year, 407
transverse section, *74*, *76*
structures, 327–328
upper thoracic, posterior view, *7*
venous drainage, *95*
ventral root, lesions, 406
visceral activities, 273
white matter
astrocytes, distribution and appearance, *201*
characteristics, *330*
fibrous astrocytes presence, 204
funiculi, 328
internal arrangement, *331*
Spinal dura, 6
coccygeal ligament, 7
Spinal ganglia
cell types, 264, 265
characteristics, 264–266
lumbar
chromatolytic cells, *267*
in monkeys, *264*
neuron differentiation, 75
related nerves, 300–301
schematic, *326*
superior glossopharyngeal, in monkeys, *264*
transverse section, *74*
trigeminal, sensory neurons, *266*
vagus, in cat, *265*
Spinal ganglion cells, central processes, 75–76
Spinal nerves
cervical, cutaneous innervation, *274*
dorsal roots, 262–263, *327*
functions, 287–288, 437
general organization, 262
injuries, 288
lesions, 288
degenerative effects, *403*
thoracic, *263*
functional components, *348*
transverse section, *76*
ventral roots, characteristics, 263–264
vertebral canal emergence, 325
Spinal neurons, immunocytochemical staining, in monkey, *354*
Spinal reflexes, essential elements for, 361–362
Spinal shock, 406
Spinal trigeminal nucleus
characteristics, 423
corticobulbar fibers, 502
cytoarchitectural divisions, 429–430, 502
laminar organization, *429*, 429–430
Spinal trigeminal tract, 423
characteristics, 428
fibers
origin, 430
topographic arrangement, *429*, 502, *504*
illustration, *424–426*
immunocytochemical features, *459*
lesions, 502
sensory conveyance, 430
Spinal veins, characteristics, 96–98
Spine, stress and strain effects, 287–288
Spinocerebellar tracts
anterior, 380, 607–608
fiber organization, 510
cervicospinocerebellar, 381
posterior, 378, *379*, 607
rostral, 381, 608
spino-olivary pathway, 381
Spinocervicothalamic tracts, characteristics, 377–378
Spinomedullary transition
area postrema, 432
corticospinal decussation, 422–424
overview, 421
posterior column nuclei, 425–427
transverse section, *424–425*
Spino-olivary pathway, two types, 381
Spinoreticular fibers
anterior and posterior, *382*
characteristics, 381, 383, 435
Spinospinal fasciculi, 401
Spinospinal fibers, characteristics, 401–402
Spinotectal fibers
characteristics, 378, 538
schematic, *374*
Spinothalamic tracts
anterior, 373, *374*
fiber projection, in thalamus, 658–659
lateral
characteristics, 375
schematic, *376*
sectioning effects, 375
Spontaneous remyelination, definition, 212, 214
Stapedius reflex, neuronal involvement, 497
Stellate cells, *866*
cerebellar cortex, 596
characteristics, 585, 587
transverse section, *586*
characteristics, 865
striate cortex, *870*
Sternocleidomastoid
corticofugal innervation, 454
innervation, 275
Storage granules, in adrenergic neurons, functions, 308
Stratum cinerale, composition, 535
Stratum lemnisci, composition, 535
Stratum opticum, composition, 535
Stratum zonale, 633
composition, 535
Stretch corpuscles, neuromuscular spindles, characteristics, 247–251
Stretch receptors, function, 617
Stretch reflex, clonus, 405
Stria medullaris, 48, *722*
fiber organization, 637
Stria terminalis, 50, 634, 717
characteristics, 775
Striate cortex
blind spot, *902*
columnar organization, 897
fiber projection, 917–918
geniculocalarine fibers, 894
ocular dominance, *901–902*
orientation columns, *901*
receptive fields, 896
simple cells
functional characteristics, *898*
inputs, *895*
stellate cells, *870*
vertical and horizontal systems, 901–902
Striated muscle
innervation, 295
motor endplate, 295
Striatonigral fibers
anterograde tract-tracing imaging, *158*
characteristics, 826, 828
feedback loop, 565
neurochemical content, *828*
sagittal section, *562*
topographic organization, 560–562
Striatonigrofugal fibers, functional organization, role of disinhibition, *847*
Striatopallidal fibers
characteristics, 822, *823*, 825–826
frontal half-sections, fiber organization, *825*
globus pallidus, 831
neurochemical content, *828*
Striatum
afferent fibers
amygdalostriatal, 822
corticostriatal, 811–814
nigrostriatal, 815–818, 821
raphe nuclei, 821–822
thalamostriatal, 814–815
γ-aminobutyric acid concentrations, *805*
amygdala and, relationship, 780–781
caudate nucleus, *774*
characteristics, 41–42, 798–799
head, *800*
muscarinic cholinergic receptor binding sites, *811*
nigrostriatal fibers, 816
PHA-L anterograde labeled elements, *816*

Striatum—*continued*
characteristics, 112, 798
efferent fibers
striatonigral, 826, 828
striatopallidal, 822, *823*, 825–826
illustration, *799*
intrinsic organization, 801–802
major compartments, 808, 810–811
neuronal types, *802*
aspiny, 803–804
spiny, 802–803, *821*, 826
spiny cholinergic interneurons, *808–809*
putamen, *106*, *774*
characteristics, 41, 801
frontal section, *796*
illustration, *800*
muscarinic cholinergic receptor binding sites, *811*
nigrostriatal fibers, 816
PHA-L anterograde labeled elements, *816*
rostrocaudal distribution of retrogradely labeled cells, *827*
subthalamic nucleus projections, 843
territories, 812–813
topographic organization, 798–799, 801
veins, 126–127
Stroke, types, 93
Stupor, definition, 556
Subarachnoid cisternae
components, 10
midsagittal view, *11*
Subarachnoid space
arachnoid granulations, 11
hemorrhages, 93–94
membranes and, relationship, *13*
purpose, 9–10
relationship of membranes to, *13*
Subcommissural organ
characteristics, 542
in monkey, *541*
purpose, 23
Subdural space, 6
Subfornical organ, 23
characteristics, 711
Subicular cortex
efferent fibers, 767
hippocampus and, 763–765
Subiculum
definition, 763
projection fibers, *726*
Subparafascicular nucleus, characteristics, 648
Substance P
lamina I and II, *357*
medulla, 460
presence in spinal cord, 357
Substantia gelatinosa
cells, 146
lamina II, 340
oxytocin receptor binding sites, 359
posterior gray horn, 348
spinomedullary transition, 421, 423
Substantia gliosa, 328
Substantia innominata, *774*
choline acetyltransferase immunoreactivity, *784*
cholinergic neurons, 715
structures, 715, 786–788
Substantia nigra, 49
afferent fibers, 560–563
chemoarchitecture, neurotransmitter variations, 559–560
cytoarchitecture, divisions, 557–559
development, 83
efferent fibers, 563–568
frontal sections
caudal third, *824*
middle third, *818*, *824*
rostral third, *818*, *824*
inputs, 848
lesions, 571
melanin presence, 157
neuronal types, 557, *558*
neuropathology, 568–572
pars compacta
lesions, effect on basal ganglia circuitry, *854*
pars reticulata and, efferent connection comparison, *817*
pars reticulata, pars compacta and, efferent connection comparison, *817*
retrograde labeling, *570*
transverse sections
middle third, *561*, *567*, *569*
rostral third, *567*
Subthalamic fasciculus, characteristics, 837–838
Subthalamic nucleus, 86
fibers
afferent, *835*, 839, 841–842
cortical, 848
efferent, 842–843
striatum, 843
GABA and glutamate staining, *840*
inputs, 848
organizational features, *841*
PHA-L injection site, *840*
retrograde labeled cells, *840*
topographic organization, 838–839
Subthalamic region
prerubral field, characteristics, 843–844
subthalamic nucleus, 86, 838–839
afferent fibers, *835*, 839, 841–842
cortical fibers, 848
efferent fibers, 842–843
GABA and glutamate staining, *840*
inputs, 848
organizational features, *841*
PHA-L injection site, *840*
retrograde labeled cells, *840*
striatal projections, 843
topographic organization, 838–839
zona incerta, 843
Subthalamonigral fibers, characteristics, 562
Subthalamopallidal fibers, characteristics, 831–832, 837
Subthalamus, structures, 51–52
Sulci
anterolateral, 326
brain, *27–28*
lateral view, *883*
calcarine, *29–30*
callosal, *29*, 35
central, 28–29, 923
cingulate, *29*, 35
collateral, *29*, 36
corpus callosum, 35
hippocampal, *29*, 35
intraparietal, *30*, 34
lateral, 28
frontal lobe, 31
marginal, 35
occipital lobe, 34
olfactory, 32
parahippocampal, *29*
posterior intermediate, 326–327
posterolateral, 326
rhinal, 36
Sulcus limitans, 73
Superficial glial membrane, 330
Superior cerebellar peduncle, 509
fiber organization, 510
Superior cistern, purpose, 10
Superior colliculi
afferent fibers, 536, 538
cellular lamination and organization, *534*
efferent fibers, 538–539
function, 535, 539–540
layers, 535
lesions, 539
myelinated fiber structure, *535*
receptive fields, 539
retinae projections, 536, *537*
striate cortex projections, 536, *537*
superficial layers, 536
tectum junction, myelin-stained section, *541*
transverse section, 3-month infant, *542*
Superior olivary complex, nuclei, 480–481
Superior olivary nucleus, *448*
Supplementary motor cortex, characteristics, 913–913
Suprachiasmatic nucleus
bilateral lesions, effect on thalamus, 638
function, 713
retinal fibers and terminals, *718*
serotoninergic innervation, *714*
Supraoptic nuclei, water balance maintenance, 734
Supraoptic region
hypothalamus, neurosecretion, 712
nuclei, *707*, *726*
suprachiasmatic nucleus, 713
serotoninergic innervation, *714*
transverse section, *708*
Supraopticohypophysial tract
hypothalamus, characteristics, 723–724
schematic, *728*
Supraspinal nucleus, 421
Supratentorial compartment, characteristics, 3
Supratentorial dura, 3
innervation, 6
Swallowing, neuroregulatory systems involved, 451
Sweat gland, innervation, 311
Sylvian triangle
cerebral angiogram, *102*
characteristics, 106
Symmetric synapses, 174
Sympathetic ganglia, 75
amine production, 67–68
cells, preganglionic fibers and, relationship, 305, *306*
Sympathetic nervous system
cervical ganglia, and related fibers, 300
function, 262
neural reflex arcs, *295*
parasympathetic system and, antagonistic effects, 315–316
postganglionic fibers
types, 311
upper and lower extremity projection, *313*
postganglionic nerves, noradrenaline release, 307
preganglionic fibers, upper and lower extremity projection, *313*
spinal ganglia, (*see* Spinal ganglia)
topographic organization, 299–300
visceral structures, *312*
vomeronasal organ, 757

Sympathetic neurons, illustration, *305*
Sympathetic responses, role in body temperature regulation, 733
Sympathetic trunks, 296
Synapses
  catecholaminergic, *180*
  central nervous system neurons, *174*
  cholinergic, *180*
  definition, 172
  neuronal
    chemical, 175–176
    electrical, 174
    function, 132
    types, 174
    ultrastructural characteristics, 173–174
  second messenger mediation, *181*
  transmission, role of cAMP, *179*
Synaptic potentials, definition, 133
Synaptic triad, structures, 751
Syndrome of Benedikt, 551
Syndromes
  Brown-Séquard, 377
    spinal cord degenerative pattern, 408
    spinal cord hemisection, 407–408
  carpal tunnel, etiology, 282
  disconnection, 921
  spinal cord
    amyotrophic lateral sclerosis, 409
    combined system disease, 409–410
    multiple sclerosis, 15, *61*, 412
    syringomyelia, 410–411
    tabes dorsalis, 411–412
Syringomyelia
  characteristics, 410–411
  spinal degenerative pattern, *411*

Tabes dorsalis, characteristics, 411–412
Tactile discs of Merkel
  characteristics, 241
  illustration, *241*
Tactile impulses, ascending spinal fibers, 370–371
Tactile sense, lesions of posterior white columns, 371
Tangential fibers, cerebral cortex, 865
Tanycytes, function, 223–224
Tapetum, 41
Taste
  geniculate ganglia lesions, 498
  impulses, pathways, 908
Taste bud, circumvallate papilla, *242*
Tectobulbar fibers
  crossed, characteristics, 539
  uncrossed, characteristics, 538
Tectofugal fibers, descending, characteristics, 538
Tectogeniculate fibers, characteristics, 538
Tectopontine fibers
  crossed, characteristics, 539
  uncrossed, characteristics, 538
Tectoreticular fibers, characteristics, 538
Tectorial membrane, *476*
Tectospinal tract
  characteristics, 389
  course, *390*
  schematic, *389*
Tectothalamic fibers, characteristics, 538
Tectum, 527
Tegmental tract, central, ascending projections, bundle types, 555
Tegmentum, 527
  midbrain
    lesions, 551–552
    red nucleus, 391, 549–552, *618*, *649*
  pontine
    characteristics, 469
    transverse section, *471*, *472*, *473*, *501*, *503–504*
    trapezoid body, 481
Tela choroidea, 48
  characteristics, 9
  formation, 223
Telaxons, function, 132
Telencephalon
  basal ganglia, (*see* Basal ganglia)
  cerebral cortex, (*see* Cerebral cortex)
  characteristics, 85–86
  limbic pathways, *724*, *745*
  suprastriatal portion, structures, 864
Temporal lobe, components, 34
Tenai thalami, 635
Tendon reflex, patellar, schematic, *362*
Tendons, stretch receptors, 890
Tenia choroidea, definition, 223
Tentorial incisure, 3
Tentorium cerebelli
  characteristics, 3
  sagittal view, *4*
Terminal boutons, types, *156*
Terminal ganglia, characteristics, 296
Terminal nerve, olfactory system, structures, *757*
Tetrodotoxin, 257
Thalamic fasciculus, characteristics, 833–834
Thalamic nuclei
  anterior, *723*
  cortical projection, in left cerebral hemisphere, *653*
  illustration, *649*
  lateral, *723*
  nonspecific, characteristics, 694–695
  sensory relay function, 691
  transverse section, *646*
Thalamic peduncle, inferior, fiber organization, *644*
Thalamic radiations
  postcentral gyri, 887–888
  subgroups, 682–683
Thalamocortical fibers, 38, 633
  cerebral cortex, 889
  characteristics, 869
  information modulation from thalamus, 691–692
  internal capsule, 685
Thalamostriatal fibers, *812*
  characteristics, 814–815
  terminal fields, 814, *815*
Thalamus, 45
  afferent fibers, 695
  amygdala and, relationship, 781
  arterial supply, *105*
  association functions, 693–694
  asymmetric transverse section, *643*
  blood supply, 112–113
  caudal, *661*
  characteristics, 50
  chemical anatomy
    acetylcholine, 673–675
    γ-aminobutyric acid, 675, *676–677*
    excitatory amino acids, 679
    monoamines, 679–680, 682
    neuroactive peptides, 675, 678–679
  divisions, 633
  epithalamus, (*see* Epithalamus)
  functions
    association, 693–694
    gating, 693
    limbic-motor relay, 692–693
    sensory relay, 691–692
    state-dependent, 694–695
  geniculate bodies, 50
  horizontal section, *683*
  internal capsule, (*see* Internal capsule)
  mediodorsal nucleus, 694
  midbrain junction, 633–635, *636*
  noradrenergic innervation, 679
  nuclei
    afferent terminations, 918
    anterior, 642–644
    classifications, *641*
    geniculate, 662–666, 669–671
    intralaminar, 647–651
    lateral, 639, 651–652
    medial, 639–640
    midline, 645, 647
    nonspecific, 694–695
    overview, 640–642
    posterior, 661–662
    reticular, 671–673
    ventral, 639, 652–660
  placement in brain, *642*
  radiations, subgroups, 682–683
  sagittal section, *635*, *647*, *800*
  sensorimotor cortex, subdivisional projections, sagittal view, *660*
  serotoninergic innervation, 680
  subcortical input, 695
  topographic organization, 639–640
  transverse sections, serotonin-immunoreactive fibers, *681*
  visual pathways
    defects, 690–691
    geniculocalcarine tract, 687–690
    optic nerves, 687
    optic tract, 687
    retina, 685–687
    ventral surface representation, *688*
Thermoreceptors, function, 238
Third nerve, lesions, 548–549
Thoracic segments, spinal cord, 334–335, *336*
Thoracolumbar outflow, preganglionic fibers, 296–297
Thyrotropin releasing hormone, spinal cord laminae, 359
Tibial nerve
  branches, 286
  muscle innervation, 286
Tic douloureux, 503
Tongue, taste bud receptors, *242*
Torsion spasm, definition, 849
Torticollis, 275
Touch, nerve endings, 253
Tract-tracing techniques
  anterograde, neuronal imaging examples, *158*
  autonomic nervous system organization, 298
  horseradish peroxidase method
    principles, 138
    retrograde transport studies, 182
  neuronal morphology studies
    double-labeling methods, 138
    Nauta-Gygax silver impregnation method, 137–138
  spinal tracts, organization, 371
Tractus solitarius, 444
Transcytosis, 177
Transection, spinal cord
  neural function recovery, 406
  patient status at 1 year, 407
Transmitter transporters, 177
Trapezius
  innervation, 275
  upper part, paralysis, 442
Trapezoid body, characteristics, 481
Traumatic neuroma, definition, 290

Tremor, 568
  characteristics, 848
  intention, 620
Triadic synaptic arrangement, definition, 669
Triceps
  innervation, 281
  tendon reflex, spinal innervation, 273
Trigeminal fibers
  secondary
    corneal reflex, 508
    impulse transmission to cranial nerve nuclei, 508
  termination, in ventral posteromedial nucleus, 659
Trigeminal ganglion, divisions, 501
Trigeminal nerve
  cutaneous innervation, *274*
  exteroceptive impulses, 500
  motor nucleus, characteristics, 507
  secondary pathways, 507–508
Trigeminal nucleus, spinal, cytoarchitectural parts, 502
Trigeminal reflex arcs, illustration, *506*
Trigeminal tract, spinal
  dorsal portion, 508
  lesions, 502
  root fibers, topographic appearance, 502
  secondary, *505*
  ventral, *505*
  ventral portion, 507–508
Trigeminospinal fibers, origins, 508
Trigeminothalamic fibers, 507
Trigonum lemnisci, 509
Triple flexion of Sherrington, definition, 407
Trochlear nerve, characteristics, 531
Trunk
  movements, spinal innervation, 273
  muscles, segmental innervation, *278*
Tuber cinereum, *646*, 706
Tuberal region, hypothalamus, structures, 713
Tuberculum acusticum, 462
Tuberohypophysial tract, hypothalamus, characteristics, 724–725, 728
Tuberoinfundibular tract, schematic, *728*
Tuberomammillary nucleus, 710
Tufted cells, 750
Type A nerve fibers, characteristics, 172
Type B nerve fibers, characteristics, 172

Ubiquitination, purpose, 159
Ulnar nerve
  injuries, 282
  muscle innervation, 282
Uncinate fasciculus, 614, *614*
  characteristics, 40, 918
  fastigial efferent fibers, *615*
Uncus, *29*, 36, 755
Unipolar neurons, characteristics, 144
Upper extremity
  innervation
    movements, 273
    segmental, *279*
  limb bud developmental stages, *269*
  peripheral nerve distribution, 281–283
Urinary bladder
  autonomic innervation
    characteristics, 318
    schematic, *317*
  spinal cord transection effects, 407
  status of, sensory information, 319
Urine retention, spinal innervation, 273
Utricle, 484

Vagal trigone, 48
Vagus nerve
  afferent fibers, 443
  characteristics, 442–443
  dorsal motor nucleus, 446
  lesions, 449
  nuclei, in fourth ventricle, *444*
Vallecula cerebelli, 53
Vascular lesions, of central nervous system, 93
Vasopressin
  function, *162*
  in medulla, 460
  memory, 732
  production, 712
  spinal cord laminae, 359
Vegetative nervous system, discovery, 293
Veins
  basal, 127
  caudate, transverse and longitudinal, 125
  cerebellar, characteristics, 119
  cerebral
    deep, *125–126*, 125–127
    drainage patterns, 123
    illustration, *123*
    superficial, 122–123, *124*, *126*, 127
  choroidal, 126
  epithalamic, 126
  occipital, 127
  septal, 126
  spinal, characteristics, 96–98
  striate, 126–127
  thalamostriate, 125
  ventricular, lateral, 126–127
Velum interpositum, 9
Vena radicularis magna, 96
Venogram, epidural, *97*
Venous plexus
  basilar, 121
  internal vertebral, 97
Venous sinus, dura
  characteristics, 120
  sagittal view, *121*
Venous vasocoronal, 96
Ventral anterior nucleus
  efferent fibers, 654–655
  magnocellular portion, 654
  thalamus, pallidal fibers, 654
Ventral cochlear nucleus, divisions, 476–477
Ventral lateral nucleus, divisions, 656
Ventral nuclear group, thalamus
  anterior nucleus, 652
  lateral nucleus, 655–657
  nuclei types, 639
  posterior nucleus, 657
Ventral pallidum, characteristics, 645, 844
Ventral posterior nucleus
  cortical connections, 659–661
  projections, 691
  thalamus
    posterior inferior portion, 659
    posterolateral portion, 657–659
    posteromedial portion, 659
Ventral posterolateral nucleus
  divisions, 657–659
  input to motor cortical areas, 915
Ventral posteromedial nucleus
  divisions, 659
  isotope transport, from rostrolateral nucleus of solitary fasciculus, *660*
Ventral rami
  brachial plexus, 276
  divisions, 267
  muscle innervation, 274
Ventral reticular nucleus, 434
Ventral roots
  nerve fibers, *268*
  spinal cord, lesions, *403*, 406
  spinal nerves, *327*
    characteristics, 263–264
    lesions, 288
    myotome innervation, 268
    sensory fibers, 264
Ventral striatopallidal complex
  chemical anatomy, 845
  circuitry, sagittal view, *844*
  connections, 844–845
  functions, 845–846
  ventral pallidum, 844
  ventral striatum, 844–845
Ventral striatum
  characteristics, 844
  cortical projections, 845
  efferent projections, 845
  thalamic projections, 845
Ventral tegmental area
  ascending projections, *560*
  definition, 557
  dopaminergic neurons, 559
Ventral tegmental decussation, 391, 550
Ventral thalamus, characteristics, 633
Ventricular system
  development, *78*
  frontal section, *84*
Ventrobasal complex
  cutaneous somatotopic representation, *658*
  thalamus, *654*
Vermal zone, cerebellum, 616–617
Vermis, 52
  cerebellovesticular projections, *616*
Vertebral angiogram, vertebral basilar system, *108*
Vertebral arteries
  branches, 113–114
  characteristics, 98–99
Vertebral basilar system, structures
  basilar artery, 113
  medulla and pons, 113–117
  vertebral artery, 113
Vertigo, definition, 492
Vesicle recycling
  endocytosis, 177
  transcytosis, 177
Vestibular fibers
  efferent, characteristics, 491–492
  medial longitudinal fasciculus, characteristics, 490–491
  primary, characteristics, 488–489
  secondary, 489–490
    role in eye movement, 492
  vestibular nuclei, afferent projections, 489
Vestibular ganglia
  characteristics, 485
  vestibular nuclear complex and, relationship, *486*
Vestibular nuclei
  afferent fibers, 489
  amino acid transport to labyrinth, *488*
  fibers, *487*
  inferior, 486, *487*
  lateral, 486–487
  medial, 488
    ascending fibers, 490
  superior, 487
  vestibular ganglia and, relationship, *486*
Vestibular sense, cortical areas, 908–909
Vestibulocerebellar fibers
  primary, 489, 606–607, 614
  secondary, 489–490, 606–607, 614

Vestibulocochlear nerve, cochlea, 474–475
Vestibulo-ocular reflex, 622
Vestibulospinal tract
  characteristics, 391–392
  fiber organization, *393*
  function, 394
  spinal projections, *392*
Vibratory sense, 371
  definition, 238
Villi
  arachnoid, 11
  choroid plexus, *22*
Virchow-Robin space
  astrocytes, 204
  purpose, 14
Visceral afferent fibers, description, 293
Visceral effectors, characteristics, 259
Visceral innervation, sympathetic and parasympathetic systems, antagonistic effects, 315–316
Visceral motor system, somatic voluntary motor system and, comparison, 296
Visceral muscle, fiber innervation, *348*
Visceral organs, diffuse nerve endings, 240
Visceral pain, sympathetic nerves, 304
Visceral reflex arc, neuronal involvement, 296
Visceral reflexes
  control of, 295
  hypothalamus regulation, 315
Visceral structures, sympathetic and parasympathetic effects, *312*
Viscus, diseased, contribution to referred pain, 254
Visual areas
  cerebral cortex, 886
  secondary
    area 18, 904
    cell types, 904
    contralateral visual hemifield, 905
Visual deprivation, experiments, 902–904
Visual pathways, thalamus
  common lesions, *690*
  geniculocalcarine tract, 687–690
  optic nerves, 687
  optic tract, 687
  retina, 685–687
  ventral surface representation, *688*
Visual sensory areas, primary, cerebral cortex
  autoradiographic mapping, *899*
  characteristics, 892–893
  ocular dominance, 900–902
  orientation columns, 897, 899–900
  unilateral destruction, 896
  visual deprivation, 902–904
Vomeronasal organ, 756
Vomeronasal system, olfactory system, structures, 756–757
Vomiting, secondary trigeminal fiber involvement, 509
VOR, (*see* Vestibulo-ocular reflex)
VPLo, (*see* Ventral posterolateral nucleus)
VPMpc, (*see* Pars parvicellularis)

Wallenberg's syndrome, (*see* Medullary syndrome, lateral)
Water balance, maintenance, supraoptic nuclei, 734
Watershed zones, 103
Weber's syndrome, 118
Wernicke's aphasia, characteristics, 925
WGA, (*see* Wheat germ agglutinin)
Wheat germ agglutinin, neuronal morphology studies, 138
White matter
  astrocytes, distribution and appearance, *201*
  commissural fibers, structures, 41
  fibers
    association, 39–41
    projection, 38
  internal arrangement, *331*
  spinal cord, characteristics, *330*
White rami communicantes, characteristics, 197
Wrist tendon reflex, spinal innervation, 273

X-ray imaging, principles, 54

Zona incerta, 52, 843
Zona intermedia, 342
Zone of Lissauer, 377
  structures, 351–352
Zone of Wernicke, 634